AUGMENTATION OF BRAIN FUNCTION: FACTS, FICTION AND CONTROVERSY

VOLUME I: BRAIN-MACHINE INTERFACES

EDITED BY: Mikhail Lebedev, Ioan Opris and Manuel F. Casanova
PUBLISHED IN: Frontiers in Systems Neuroscience and Frontiers in Neuroscience

frontiers Research Topics

ISSN 1664-8714
ISBN 978-2-88945-614-7
DOI 10.3389/978-2-88945-614-7

About Frontiers

Frontiers is more than just an open-access publisher of scholarly articles: it is a pioneering approach to the world of academia, radically improving the way scholarly research is managed. The grand vision of Frontiers is a world where all people have an equal opportunity to seek, share and generate knowledge. Frontiers provides immediate and permanent online open access to all its publications, but this alone is not enough to realize our grand goals.

Frontiers Journal Series

The Frontiers Journal Series is a multi-tier and interdisciplinary set of open-access, online journals, promising a paradigm shift from the current review, selection and dissemination processes in academic publishing. All Frontiers journals are driven by researchers for researchers; therefore, they constitute a service to the scholarly community. At the same time, the Frontiers Journal Series operates on a revolutionary invention, the tiered publishing system, initially addressing specific communities of scholars, and gradually climbing up to broader public understanding, thus serving the interests of the lay society, too.

Dedication to Quality

Each Frontiers article is a landmark of the highest quality, thanks to genuinely collaborative interactions between authors and review editors, who include some of the world's best academicians. Research must be certified by peers before entering a stream of knowledge that may eventually reach the public - and shape society; therefore, Frontiers only applies the most rigorous and unbiased reviews.
Frontiers revolutionizes research publishing by freely delivering the most outstanding research, evaluated with no bias from both the academic and social point of view. By applying the most advanced information technologies, Frontiers is catapulting scholarly publishing into a new generation.

What are Frontiers Research Topics?

Frontiers Research Topics are very popular trademarks of the Frontiers Journals Series: they are collections of at least ten articles, all centered on a particular subject. With their unique mix of varied contributions from Original Research to Review Articles, Frontiers Research Topics unify the most influential researchers, the latest key findings and historical advances in a hot research area! Find out more on how to host your own Frontiers Research Topic or contribute to one as an author by contacting the Frontiers Editorial Office: researchtopics@frontiersin.org

AUGMENTATION OF BRAIN FUNCTION: FACTS, FICTION AND CONTROVERSY
VOLUME I: BRAIN-MACHINE INTERFACES

Topic Editors:
Mikhail Lebedev, Duke University Durham, United States
Ioan Opris, University of Miami, United States
Manuel F. Casanova, University of South Carolina, United States

Volume I, entitled "Augmentation of Brain Functions: Brain-Machine Interfaces", is a collection of articles on neuroprosthetic technologies that utilize brain-machine interfaces (BMIs). BMIs strive to augment the brain by linking neural activity, recorded invasively or noninvasively, to external devices, such as arm prostheses, exoskeletons that enable bipedal walking, means of communication and technologies that augment attention. In addition to many practical applications, BMIs provide useful research tools for basic science. Several articles cover challenges and controversies in this rapidly developing field, such as ways to improve information transfer rate. BMIs can be applied to the awake state of the brain and to the sleep state, as well. BMIs can augment action planning and decision making. Importantly, BMI operations evoke brain plasticity, which can have long-lasting effects. Advanced neural decoding algorithms that utilize optimal feedback controllers are key to the BMI performance. BMI approach can be combined with the other augmentation methods; such systems are called hybrid BMIs. Overall, it appears that BMI will lead to many powerful and practical brain-augmenting technologies in the future.

Citation: Lebedev, M., Opris, I., Casanova, M. F., eds (2018). Augmentation of Brain Function: Facts, Fiction and Controversy. Volume I: Brain-Machine Interfaces. Lausanne: Frontiers Media. doi: 10.3389/978-2-88945-614-7

Table of Contents

frontiers in Systems Neuroscience

EDITORIAL
published: 12 September 2018
doi: 10.3389/fnsys.2018.00045

Editorial: Augmentation of Brain Function: Facts, Fiction and Controversy

Mikhail A. Lebedev[1]*, *Ioan Opris*[2] *and Manuel F. Casanova*[3]

[1] School of Medicine, Duke University, Durham, NC, United States, [2] Leonard M. Miller School of Medicine, Miami, FL, United States, [3] School of Medicine Greenville, University of South Carolina, Greenville, SC, United States

Keywords: neuroprosthesis, implants, microcircuits, nootropics, tDCS—transcranial direct current stimulation, TMS, Brain machine interface (BMI), neural networks

Editorial on the Research Topic

Augmentation of Brain Function: Facts, Fiction and Controversy

BRAIN AUGMENTATION: THE MAJOR TRENDS

This research topic consists of 148 articles on various aspects of brain augmentation contributed by more than 600 authors. At the time of writing, the articles have been viewed online more than 1.3 million times and received plentiful citations in the scientific literature. The topic won the 2017 Frontiers Spotlight Award.

The topic theme, "Augmentation of brain function," is an umbrella term for the approaches from different disciplines, aimed at the improvement of brain performance in both healthy people and patients suffering from neurological disabilities. Functions of the brain that scientists hope to augment belong to sensory, motor and cognitive domains. Brain enhancements could be achieved pharmacologically or using neurostimulation. Functional improvements can be also achieved with brain training techniques that employ modern technologies like computer games and virtual reality. Furthermore, brain performance can be augmented using brain-machine interfaces (BMIs), the pathways that connect neuronal circuits to external assistive devices, such as limb prostheses, exoskeletons, and communication aids. In addition to sending commands to external devices, BMIs can enable bidirectional communications, where artificial sensory signals are delivered to the brain while information is being decoded from neural recordings.

Even though many of the brain-augmenting ideas sound like science fiction, the topic authors feel optimistic about most of them. The overall consensus is that brain performance can be improved with artificial components, and this approach will lead to practical applications in the not-too-distant future. Many of the techniques covered in the topic, for example BMIs and noninvasive stimulation, have already experienced an explosive development. While expectations are high for the augmentation approaches, philosophers are warning about the ethical issues related to technologies that interfere with the mind, possibly in unpredictable ways. Although some of these concerns seem far-fetched, it is important that ethical standards are kept high as these revolutionary brain-augmenting methods are being developed.

The 10 most viewed articles in the topic ("1" is the highest rank) highlight the major trends in brain augmentation research:

OPEN ACCESS

Edited and reviewed by:
Maria V. Sanchez-Vives, Institut d'Investigacions Biomèdiques August Pi i Sunyer (IDIBAPS), Spain

***Correspondence:**
Mikhail A. Lebedev
mikhail.a.lebedev@gmail.com

Received: *04 September 2018*
Accepted: *10 September 2018*
Published: *12 September 2018*

Citation:
Lebedev MA, Opris I and Casanova MF (2018) Editorial: Augmentation of Brain Function: Facts, Fiction and Controversy. Front. Syst. Neurosci. 12:45. doi: 10.3389/fnsys.2018.00045

1. *Performance enhancement at the cost of potential brain plasticity: neural ramifications of nootropic drugs in the healthy developing brain* (Urban and Gao). This a review of the main classes of drugs potentially capable of the enhancement of cognitive functions in healthy individuals. The authors warn, however, about the unwanted consequences of these pharmacological approaches, such as the development of addictive behaviors and detrimental effects related to drug overdose. These drugs could induce brain plasticity that interferes with normal brain functions and their development, particularly in young individuals.
2. *"Non-invasive" brain stimulation is not non-invasive* (Davis and Koningsbruggen). This opinion article critically evaluates the methods known as "noninvasive brain stimulation," such as transcranial magnetic stimulation (TMS) and transcranial direct current stimulation (tDCS). Although these approaches do not require physical penetration of an instrument in the body (i.e., the medical definition of "noninvasive"), they could affect the brain in profound ways, for example by causing long-lasting plasticity that extends beyond the intended augmentation effect. Therefore, safety is an important concern, and perhaps the terminology should be changed so that non- expert users are not misled that the effects of these methods are mild.
3. *Augmentation of cognitive brain functions with transcranial lasers* (Gonzalez-Lima and Barrett). This article suggests that transcranial stimulation with infrared lasers could affect brain bioenergetics in a positive way, and that frontal cortex functions, such as attention, working memory, and affective state, could be augmented with such stimulation.
4. *Increased intelligence is a myth (so far)* (Haier). This article points to the problem of quantifying the effects of cognitive training. Haier argues that it is difficult to evaluate the enhancement of mental abilities with tests such as intelligence scores, which are prone to errors. These scores have high test-retest reliability but their standard error across subjects is high. A better estimate of intelligence could be provided with a battery of intelligence tests instead of a single test.
5. *Attitudes toward pharmacological cognitive enhancement—a review* (Schelle et al.). This article analyzes 40 published studies on public attitude toward using drugs to achieve cognitive enhancement. The authors conclude that the public concerns regarding pharmacological enhancement – medical safety, coercion, and fairness – match the agenda of academic debates.
6. *Sleep for cognitive enhancement* (Diekelmann). This article reviews the potential of sleep for augmenting such cognitive functions as attention, language, reasoning, decision making, learning and memory. The article also discusses the role of sleep in memory consolidation and the acquisition of new memories after sleep, the role of sleep-specific brain oscillations in these processes, and the neurotransmitters involved. Diekelmann describes how memory processing during sleep can be augmented by cueing memory reactivation with olfactory and auditory cues, electrically inducing sleep-specific brain oscillations, and modulating specific neurotransmitter systems pharmacologically.
7. *Transcranial direct current stimulation: five important issues we aren't discussing (but probably should be)* (Horvath et al.). This article discusses several key issues related to the usage of tDCS as a cognitive enhancement approach: (1) inter-subject variability and the need for an individualized approach, (2) intra-subject reliability, such as reliability over time, (3) the importance of proper controls in tDCS studies, such as sham stimulation and blinding, (4) interference of motor and cognitive activities with the tDCS effects, and (5) changes in electric current related to hair thickness and electrode attachment methods.
8. *Donor/recipient enhancement of memory in rat hippocampus* (Deadwyler et al.). This article reports an augmentation approach, where the memory content of one subject is transferred to the brain of another subject using electrical stimulation. The study was conducted in rats. The information was read out from the hippocampus of a "donor" rat performing a difficult long-delay behavioral task. This signal was then processed by a multiple-input multiple-output model and delivered to the hippocampus of the "recipient" animal that utilized this memory trace to reproduce the task performance.
9. *Enhancement of cognitive and neural functions through complex reasoning training: evidence from normal and clinical populations* (Chapman and Mudar). This article describes an approach, where enhancement in higher-order brain functions, such as reasoning, is achieved through cognitive training. The training includes such strategies as strategic attention, integrated reasoning, and innovation. The authors argue that cognitive training can be efficient in both healthy subjects and patients.
10. *When is diminishment a form of enhancement? Rethinking the enhancementdebate in biomedical ethics* (Earp et al.). This article discusses cases where a diminishment of certain functions could have a positive effect on an individual's well-being and thus act as a form of enhancement. For example, TMS could disrupt one brain function but by doing so enhance another function.

These and other articles in the research topic express three main ideas regarding the approaches to brain augmentation. The first is the idea of *decoding* information from brain activity. Neural signals can be sampled with various recording methods. The decoded brain signals could be processed by a BMI and utilized to augment motor, sensory, and cognitive functions. The second idea is the proposal that the brain could be augmented by *stimulation*; for example, modulating neural circuits by the application of electrical/optogenetic stimulation or using pharmacological agents to affect neural processing. The third idea is a *futuristic* vision of radical improvements of individual humans and mankind, such as revolutionary clinical approaches, immortality of consciousness, and even brain-to-brain communications. We used these themes to group the articles into three volumes. Volume I covers the approaches for recording and decoding neural signals with BMIs; Volume II is a collection of articles on neurostimulation and pharmacological methods; and Volume III describes clinical applications of brain-augmenting methods, futuristic ideas, and ethical issues.

VOLUME I: BRAIN-MACHINE INTERFACES

BMIs are the major theme of Volume I. The articles cover a wide range of BMI applications, including the traditional ones and BMIs those that have emerged relatively recently. The notable new developments in this field are the BMIs for controlling bipedal walking (Wall et al.; Lisi et al.; Zarka et al.; Bouyarmane et al.; Li W. et al., Solopova et al.; Song W. et al.; Onose et al.), BMIs that modulate attention (Astrand et al.; Ordikhani-Seyedlar et al.), and technologies that enhance the human ability to predict future events (Pezzulo et al.). As any rapidly developing field of science, the BMI field is not without challenges and controversies (Vassanelli and Mahmud; Serruya; Bauer and Gharabaghi). To this end, several articles critically evaluate the current state of the field and propose improvements for the future (Waldert; Zehr; Deca and Koene; Serruya). One pressing issue is the relatively low information transfer rate (ITR) of current BMIs. Baranauskas discusses the major factors limiting the ITR and proposes that a better understanding of neural mechanisms is needed to improve BMI accuracy and versatility. Several articles describe the specific neural mechanisms that could be utilized in BMIs and other brain-augmenting approaches to improve their efficiency. Thus, Opris and Casanova highlight the need for better understanding of brain microcircuits in healthy people and neurologically impaired patients. Mandonnet and Duffau propose that the cerebral circuitry engaged in cognition and action should be thoroughly investigated for the BMI methods to be effective, and Taya et al. argue that connectome approach should be combined with cognitive enhancement methods. Furthermore, Hales and Pockett argue that a better understanding is needed of the electrical fields produced by brain circuits, and Saniotis et al. discuss evolutionary challenges related to using BMIs and other augmenting methods.

When designing brain-augmenting systems, it is important to understand the brain states targeted by these technologies. Sleep is one such state to which augmenting methods could be applied. As mentioned above, one of the articles (Diekelmann) discusses at length how sleep mechanisms could be employed for brain augmentation. Additionally, Pigarev and Pigareva highlight two sleep-related phenomena that are relevant to brain-augmenting approaches: partial sleep and visceral processing during sleep.

Action planning and decision making are the other neural functions where augmenting methods could be applied. To this end, Mirabella reviews neuronal mechanisms of goal-directed actions and links them to the research on brain augmentation. Furthermore, Opris et al. report that the relationship between neostriatal activity and movement kinematics is affected by the degree of certainty about the reward that could result from the motor act. Therefore, BMIs that decode kinematic parameters of movements should incorporate a model of reward representation. As a matter of fact, reward (or reinforcement) is an integral part of any BMI system, and operation of some of these systems is explicitly described as self-regulation of brain activity based on reinforcement learning. Yet, Wood et al. clarify that self-control of neural activity should be distinguished from the broader concept of BMI control and propose a framework that considers the interplay of automatic and controlled information processing. Moreover, Deepeshwar et al. and Telles et al. advocate meditation as a self-control paradigm for augmenting the brain.

For a brain-augmenting method to be efficient, it should properly accommodate mechanisms of brain plasticity. Several Volume I articles discuss such mechanisms. Di Pino et al. and Sakurai review brain plasticity caused by the use of artificial augmenting effectors. Sakurai et al. describe operant conditioning of neural circuits that could cause plasticity Without a change in behavior? Benyamini and Zacksenhouse present evidence showing that brain circuits act very much like an optimal feedback controller during the adaptation to BMI control. Additionally, Qi et al. report that the somatosensory system in mature primates is capable of plasticity that compensates for unilateral lesions of dorsal column afferents. Finally, Frye et al. suggest that brain-augmentation research should not be limited to the brain tissue because the peripheral organs also play a role in modulating and augmenting brain functions. In support of this suggestion, they have found a liver factor involved in neural plasticity.

BMI performance critically depends on the type of neural signal being recorded and decoded. Invasive and noninvasive BMIs are the two major classes of BMIs defined by the recording method. Waldert discusses the pros and cons of invasive and noninvasive recordings and the future of these approaches. Among the noninvasive methods, electroencephalography (EEG) is the most popular approach utilized in BMIs. Obeid and Picone report an EEG database collected by Temple University Hospital. This database could be useful for the exploration of neural representation of information and development of BMI decoding algorithms. Callan et al. assess the efficiency of dry EEG recordings; they argue that this method is useful for decoding of auditory events from EEG data, even when substantial acoustic noise, and mechanical and physiological artifacts, interfere with the recordings during simulated and real flight conditions. Blankertz at al. review different usages of EEG-based BMIs, including practically oriented applications and employing BMIs as research tools.

While EEG-based BMIs are easy to implement and safe to use, their information transfer rate (ITR) is limited. ITR can be improved if electrical activity is recorded from the surface of the brain using electrocorticography (ECoG), a minimally invasive method. Kapeller et al. report a high-performing ECoG BMI based on visual evoked potentials, and Zippo et al. describe a novel epicortical grid with wireless recordings, tested in rhesus monkeys.

Functional magnetic resonance imaging is the other noninvasive recording method suitable for BMI implementations. Caria discusses the neurophysiological mechanisms involved in self-regulation of blood oxygenation level monitored with fMRI.

Intracranial recordings hold the promise of radically improving the quality of neural signals utilized in BMIs. However, this potential has not yet been realized because of safety and longevity issues with brain implants. Technologies are developing rapidly for making invasive implants more efficient. Among such technologies, nanostructure-based recording

sensors are particularly promising (Vidu et al.). Additionally, Agorelius et al. describe a new multichannel implant composed of flexible electrodes to minimize damage to the brain tissue.

In addition to "pure" BMIs (i.e., the ones based on the recordings from the brain only) additional types of bioelectric recordings may be useful for brain-augmenting methods. Shishkin et al. report a hybrid BMI that, in addition to extracting motor intentions from EEG activity, utilizes recordings of eye position EEG markers of gaze fixation to improve BMI performance. Interfaces based on electromyographic (EMG) recordings are another class of augmenting devices that could operate a myoelectric hand prostheses for amputees (Atzori and Müller) or convert forearm electromyographic (EMG) activity into traces for handwriting (Okorokova et al.; Okorokova et al.).

The choice of sensory feedback is another important factor that fundamentally affects BMI performance. Several articles investigate different types of feedback. Alimardani et al. report manipulations with visual feedback that improve the operation of motor-imagery BMIs. BMI performance can be further improved using multisensory stimuli as the feedback (Thurlings et al.), such as combining visual feedback with haptic (Honeine and Schieppati; Bouchard et al.) and auditory (Tonelli et al.) inputs. Oei and Patterson describe the feedback provided by action videogames; they show that videogames have similar demands as many other perceptual and attention tasks, which explains transfer of functional enhancements resulting from playing these games. Wright examines the visual feedback provided by virtual reality; the article discusses how virtual reality could be used as a brain-augmenting approach. Alfaro et al. report the results of a neuroimaging study, in which they examined plasticity in visual and auditory areas of a color-blind subject with eight years of training to utilize a device called "Eyeborg" that transforms colors into sounds. Finally, Bravi et al. report improvements of somatosensory feedback with elastic therapeutic tape.

BMI performance can be improved with better decoding algorithms. The article by Li reviews the current state of research in this field. Rouse and Schieber argue that BMI decoders should incorporate non-linear characteristics to advance BMIs to better match natural motor performance. Lebedev discusses how different BMI decoders could be assessed using neuron-dropping curves.

VOLUME II: NEUROSTIMULATION AND PHARMACOLOGICAL APPROACHES

In Volume II, one group of articles covers a variety of neurostimulation methods (Balan et al.), while the other group describes pharmacological approaches. Electrical stimulation is a conventional method for inducing brain activity. The types of electrical stimulation include intracortical microstimulation (ICMS), transcranial direct current stimulation (tDCS), and transcranial magnetic stimulation (TMS) that induces electrical currents in the nervous tissue. Electrical stimulation can be also be applied to muscles (Talis et al.).

Noninvasive stimulation methods have gained popularity in recent years as a means of augmenting brain function, yet many unknowns and controversies still remain. Krause and Cohen Kadosh and Horvath et al. examine the role of inter-subject differences in responsiveness to tDCS. McKendrick et al. propose an approach in which wearable devices are used that combine tDCS with a new generation of miniaturized fNIRS systems. Blumberg et al. and Foroughi et al. report that performance on spatial tasks can be enhanced by tDCS applied to the posterior parietal cortex. Younger et al. demonstrate that tDCS applied to the left inferior parietal lobe can augment reading subskills. Luft et al. propose that a connectome approach can be combined with brain stimulation. Horschig et al. discuss neurostimulation methods that could be used to manipulate cortical oscillations. Koganemaru et al. and Tsagaris et al. suggest that the efficiency of neurostimulation can be improved if it is combined with the appropriate task patterns.

As mentioned above, Davis and Koningsbruggen do not think that the term "noninvasive" is appropriate to describe noninvasive stimulation methods that strongly affect the brain and evoke long- lasting consequences. Therefore, these approaches should be used with great caution. Among the effects of noninvasive stimulation the authors of the topic name biasing network dynamics (Wokke et al.) and influencing brain hemodynamics (Pulgar; Dutta). Additionally, brain functions can be affected even with transcranial lasers (Gonzalez-Lima and Barrett). Duecker et al. discuss the potential of noninvasive stimulation as a research tool in the studies of perception, cognition, and behavior. Additionally, Luber argues that brain augmentation with noninvasive stimulation cannot be explained by a net zero sum proposition; i.e., the mechanism where brain resources are reallocated: gains in one function are balanced by costs elsewhere.

Among the invasive approaches to neurostimulation, optogenetic methods have received particular attention in recent years, and several articles in Volume II cover different aspects of this approach (Kwon et al., Jarvis and Schultz). While the optogenetic methods are being developed, the classical electrical stimulation approach has already resulted in clinically relevant applications like the vestibular implant (van der Berg et al.) and tactile neuroprosthesis that utilizes intracortical microstimulation (Kim et al.).

Memory prostheses represent a recent trend in stimulation-based BMIs. Volume II covers several memory-augmenting approaches. Madan, Bennabi et al., Deveau et al., Moreau, Mallow et al., and Takeuchi et al. discuss different ways to implement neuroprosthetic memory. Song D. et al. report a memory prosthesis, where memory content is extracted from hippocampal activity using a multiple-input, multiple-output non-linear dynamical model. In addition to neurostimulation, pharmacological approaches have been developed for augmenting memory and cognition (Lynch et al.). Brain training techniques can be also used to improve memory and cognition (Chapman and Mudar; Ben-Soussan et al.; Haier). In particular, Beatty et al. investigate several working memory tasks where training could be transferred from one task to another. Additionally, Rabinovich et al. propose a computational model

to explore the ways of augmenting memory. The model is based on recurrent inhibitory-excitatory networks with heterogeneous inhibition.

As far as pharmacological approaches to brain augmentation are concerned, Urban and Gao and Lynch et al. discuss the pros and cons of using nootropic drugs to augment brain performance. The concern regarding nootropic drugs is significant and is shared by general public (Schelle, Faulmüller et al.; Schelle, Olthof, et al.; Garasic and Lavazza). Using an individual-oriented approach, Jellen et al. propose a method for screening and personalizing nootropic drugs; the method utilizes gene expression data to evaluate affected signaling pathways. Piermacino et al. review the effects of pharmacological interventions on cognition in the elderly, while Kang et al. review the effects of acetylcholine in the primary visual cortex that could be used to alter and augment visual perception.

VOLUME III: FROM CLINICAL APPLICATIONS TO ETHICAL ISSUES AND FUTURISTIC IDEAS

Developing clinical applications is perhaps the most important direction of the brain- augmentation field (Schicktanz et al.), and many Volume III articles demonstrate the progress that has been achieved already in clinical solutions for such conditions as epilepsy (Höller and Trinka; DeMarse and Carney; Zeitler and Tass), stroke (Grimm et al.), Parkinson's disease (Lebedev et al.; Lee et al.), Huntington's disease (Nagel et al.), dementia (Garriga et al.; Franco), Alzheimer's disease (Yegla and Parikh), autism spectral disorders (ASD) (Billeci et al.), traumatic brain injury (Alwis and Rajan; Tajiri et al.), and disorders of consciousness (Bai et al.). Evidence is growing that noninvasive stimulation can be employed to treat a range of neurological conditions (Vicario and Nitsche). Thus, Sokhadze et al. report that TMS applied to dorso-lateral prefrontal cortex improves executive function in ASD, which is evident from the improvements in behavioral reactions and event-related EEG potentials. Additionally, according to the case report by Brem et al., tDCS can be applied to treat visuospatial neglect. Krawinkel et al. provide insights on how noninvasive stimulation could treat such conditions as schizophrenia and Parkinson's disease by modulating brain oscillations. Additionally, Kubera et al. review the application of noninvasive brain stimulation to the treatment of auditory verbal hallucinations in schizophrenia. Moreover, Ayache et al. report that prefrontal tDCS can decrease pain in patients suffering from multiple sclerosis. Charvet et al. propose that therapeutic noninvasive stimulation can be administered remotely under the supervision of medical personnel, which removes the need for the patients to travel to the hospital, and Thibeault argues that efficiency of therapeutic neurostimulation can be improved by neuromorphic components.

The articles that we call futuristic examine the prospects for augmentation methods that only recently migrated from science fiction to scientific theory and research. Thus, Kennedy argues that advances in BMI technologies could help mankind cope with the "moment of singularity", the time when artificial intelligence surpasses human intelligence. Brain-to-brain interfaces that enable communications between several individual brains are another futuristic idea implemented in several studies (Hildt). For example, Deadwyler et al. demonstrate that brain-to-brain communications can be employed to transfer memories (see also the summary of this article above). Kyriazis extends the idea of brain-to-brain interface even further by proposing a global brain, a self-organizing system that connects many humans. Additionally, Sexton and Lukinova and Myagkov, discuss the role of social interactions in the operations of augmenting technologies. Finally, augmenting methods could be applied to modulate consciousness (Berry and Parker), even though its neural mechanisms are poorly understood (Pockett).

The topic attracted a considerable number of the articles on ethical issues related to the brain- augmenting methods (Glannon; Glannon; Attiah and Farah; Nagel; Clark; Maslen et al.), including the relationship between the diminishment and enhancement following the application of brain-augmenting technologies (Earp et al.), the problem of "mind control" with BMI technologies (Koivuniemi and Otto), free will (Glannon; Glannon), the duty to use cognitive enhancers in high-responsibility professions (Santoni et al.), determining the population of people in need of brain enhancement (Schleim), informed public policy (Shook et al.), cognitive biases (Caviola et al.), and the hype caused by the development of brain-augmenting approaches (Rusconi and Mitchener-Nissen).

AUTHOR CONTRIBUTIONS

All authors listed have made a substantial, direct and intellectual contribution to the work, and approved it for publication.

ACKNOWLEDGMENTS

To the always helpful Frontiers team whose organizational skills and understanding made this Research Topic possible.

Conflict of Interest Statement: The authors declare that the research was conducted in the absence of any commercial or financial relationships that could be construed as a potential conflict of interest.

frontiers in Systems Neuroscience

MINI REVIEW
published: 26 March 2015
doi: 10.3389/fnsys.2015.00048

Clinical application of the Hybrid Assistive Limb (HAL) for gait training—a systematic review

Anneli Wall[1,2]*, *Jörgen Borg*[1,2] *and Susanne Palmcrantz*[1,2]

[1] Department of Rehabilitation Medicine, Danderyd University Hospital, Stockholm, Sweden, [2] Department of Clinical Sciences, Karolinska Institute, Stockholm, Sweden

Objective: The aim of this study was to review the literature on clinical applications of the Hybrid Assistive Limb system for gait training.

Methods: A systematic literature search was conducted using Web of Science, PubMed, CINAHL and clinicaltrials.gov and additional search was made using reference lists in identified reports. Abstracts were screened, relevant articles were reviewed and subject to quality assessment.

Results: Out of 37 studies, 7 studies fulfilled inclusion criteria. Six studies were single group studies and 1 was an explorative randomized controlled trial. In total, these studies involved 140 participants of whom 118 completed the interventions and 107 used HAL for gait training. Five studies concerned gait training after stroke, 1 after spinal cord injury (SCI) and 1 study after stroke, SCI or other diseases affecting walking ability. Minor and transient side effects occurred but no serious adverse events were reported in the studies. Beneficial effects on gait function variables and independence in walking were observed.

Conclusions: The accumulated findings demonstrate that the HAL system is feasible when used for gait training of patients with lower extremity paresis in a professional setting. Beneficial effects on gait function and independence in walking were observed but data do not allow conclusions. Further controlled studies are recommended.

Keywords: rehabilitation, robotics, gait, walking, locomotion, paresis, review, gait machine

OPEN ACCESS

Edited by:
Mikhail Lebedev, Duke University, USA

Reviewed by:
Jun Morimoto, ATR Computational Neuroscience Labs, Japan
Mukul Talaty, Moss, USA
Antoinette Domingo, San Diego State University, USA

***Correspondence:**
Anneli Wall, Department of Rehabilitation Medicine, Danderyd University Hospital, Danderyds Sjukhus, Rehabiliteringsmedicinska Universitetskliniken, Hus 39, plan 3, Stockholm 18288, Sweden
anneli.wall@ds.se

Received: *23 December 2014*
Accepted: *10 March 2015*
Published: *26 March 2015*

Citation:
Wall A, Borg J and Palmcrantz S (2015) Clinical application of the Hybrid Assistive Limb (HAL) for gait training—a systematic review. Front. Syst. Neurosci. 9:48. doi: 10.3389/fnsys.2015.00048

Background

Normal gait depends on the functional integrity and interactions in sensory-motor neural networks at spinal and supraspinal levels (Bowden et al., 2013). This complex system may be disturbed in many neurological conditions such as stroke or spinal cord injury (SCI) resulting in limited mobility and impaired gait function, which are major challenges in neuro rehabilitation. Intensive, repetitive task specific training may drive beneficial neuroplasticity, enhance functional restitution and improve final outcome (Kwakkel et al., 2004; Langhorne et al., 2009, 2011; Peurala et al., 2014). However, there is a need for further development of training methods in response to an increasing understanding of the individual capacity for regaining functioning (Krakauer et al., 2012; Bowden et al., 2013).

Approaches to improve gait function after stroke and SCI include treadmill training with or without use of partial body weight support (BWS), yet the evidence to support this is

inconclusive (Schwartz and Meiner, 2013; Dobkin et al., 2014). Gait machines (GM) may allow more reproducible gait movements compared to conventional training and reduce the burden on the therapist. GM work according to the end-effector principle (foot plates move the feet in a controlled gait pattern) or as exoskeletons, which have joints matching the limb joints and motors that drive movements over these joints to assist, e.g., leg movements (Hesse et al., 2010). A recent Cochrane review concluded that electromechanically assisted gait training in combination with physiotherapy after stroke increases the odds of achieving independent walking and most so when applied for severely impaired patients in the first 3 months after stroke (Mehrholz et al., 2013) but less clear after SCI (Mehrholz et al., 2012).

The importance of incorporating more active participation than allowed by gait machines to enhance training effects and the need for new concepts and devices are recognized (Dobkin, 2009; Pennycott et al., 2012). One new approach is represented by the Hybrid Assistive Limb system (HAL). HAL is an exoskeleton with a hybrid system allowing both a voluntary and an autonomous mode of action to support training of gait. HAL comprises a control algorithm and supporting devices, where each knee and hip joint can be controlled separately. Key features of the HAL system have been reported in detail (Kawamoto, 2002; Suzuki et al., 2007; Kawamoto et al., 2010). Movements are triggered by use of either the "Cybernic Voluntary Control" (CVC), which is based on the users voluntary activation of gait muscles as recorded by surface electromyography (EMG), or by the "Cybernic Autonomous Control" (CAC), which is based on the users weight shifting and input from force pressure sensors in the shoes. The CVC mode allows the operator to adjust the degree of support for each joint and reduce the support as training progress and to adjust settings to achieve a gait pattern that is as close as possible to normal gait. In case of complete loss of voluntary activation of gait muscles the CAC mode may be used. Gait is then initiated and sustained by input from force-pressure sensors in the shoes. HAL is manufactured in single-leg and double-leg versions and training with HAL may be performed with or without BWS.

A number of clinical studies with HAL have been conducted and there is a need for an evaluation of available data to guide further trials. The aim of this report was to provide a systematic review in order to evaluate current evidence with regard to feasibility (i.e., usability and safety) and effects and to make recommendations for further studies.

Methods

A systematic search of the literature was conducted using the databases Web of Science, PubMed, and CINAHL. Both MeSH (Medical Subject Headings for Medline) terms and free text relevant for the subject were used and detected synonyms were added to the search. Search terms were (MeSH terms in bold): ((((robot OR robots OR robotic OR robotics OR robot-assisted OR exoskeleton OR machine-assisted OR electro-mechanic OR DGO OR "driven gait orthosis"))) AND (gait OR gaits OR walking OR walk OR walks OR locomotion OR "motor activity")) AND (HAL OR "hybrid assistive limb" OR "wearable robot"). Search limitations were "Humans" and "English," while publication date was unlimited. Using the same search terms, a search was also performed at clinicaltrials.gov, in order to identify ongoing studies and/or unpublished papers (Clinicaltrials, online). Abstracts identified were screened and studies were considered relevant if they addressed any clinical application of the HAL system regardless of study design. If needed the full text article was retrieved and assessed. Relevant studies were exported to EndNote where duplicates were identified and removed. Reference lists of these studies were manually searched for further articles. Studies were included if they were primary research articles, concerned gait training with the Hybrid Assistive Limb. Studies only reporting technology data, including only healthy subjects, single subjects or reviews were excluded. Thirty-seven articles were identified, 20 were retrieved in full text for assessment of eligibility and 13 of these did not fulfill inclusion criteria (see **Figure 1**). Overall 7 studies met the inclusion criteria and were subject to data extraction and analyses (Maeshima et al., 2011; Kawamoto et al., 2013; Kubota et al., 2013; Ueba et al., 2013; Aach et al., 2014; Nilsson et al., 2014; Watanabe et al., 2014). Included studies were subject to critical review by two independent reviewers.

The quality of the included studies, regarding risk of confounding and bias, was evaluated in accordance with the Scottish Intercollegiate Guidelines Network (SIGN) criteria (SIGN, online[1]). According to SIGN the methodological quality can be coded (++) meaning *all or most of criteria fulfilled*, (+) *some of the criteria fulfilled* or (−) *few or no criteria fulfilled*. The evaluation was performed independently by two investigators and in case of disagreement, a third reviewer was consulted. Since two investigators are authors of one of the included studies (Nilsson et al., 2014) this study was assessed by a fourth investigator.

Data extraction was performed by one investigator and checked by the two additional investigators. The extracted data comprised; characteristics of participants, intervention protocols and settings, outcome measures and effects and feasibility.

Results

The 7 studies included 8–38 participants each, 6 were single group studies and 1 was a randomized controlled trial (RCT). In total, the studies involved 140 participants of whom 118 completed the intervention protocols and 107 used HAL for gait training. Extracted study data and results of the quality evaluation are presented in the **Table 1**. All included studies were found to have a high risk of bias and confounding according to the SIGN criteria and do not provide data for a meta-analysis.

Characteristics of Participants Included in the Studies

The most frequent diagnosis reported was stroke ($n = 106$) followed by complete or incomplete SCI ($n = 16$) and other disorders ($n = 18$). Five of the studies included solely persons with stroke, 1 study included solely persons with SCI (Aach et al., 2014) and 1 study included persons with stroke ($n = 12$) and SCI

[1]SIGN. Scottish Intercollegiate Guidelines Network. Available online at: http://www.sign.ac.uk/methodology/checklists.html [Accessed Dec 2014].

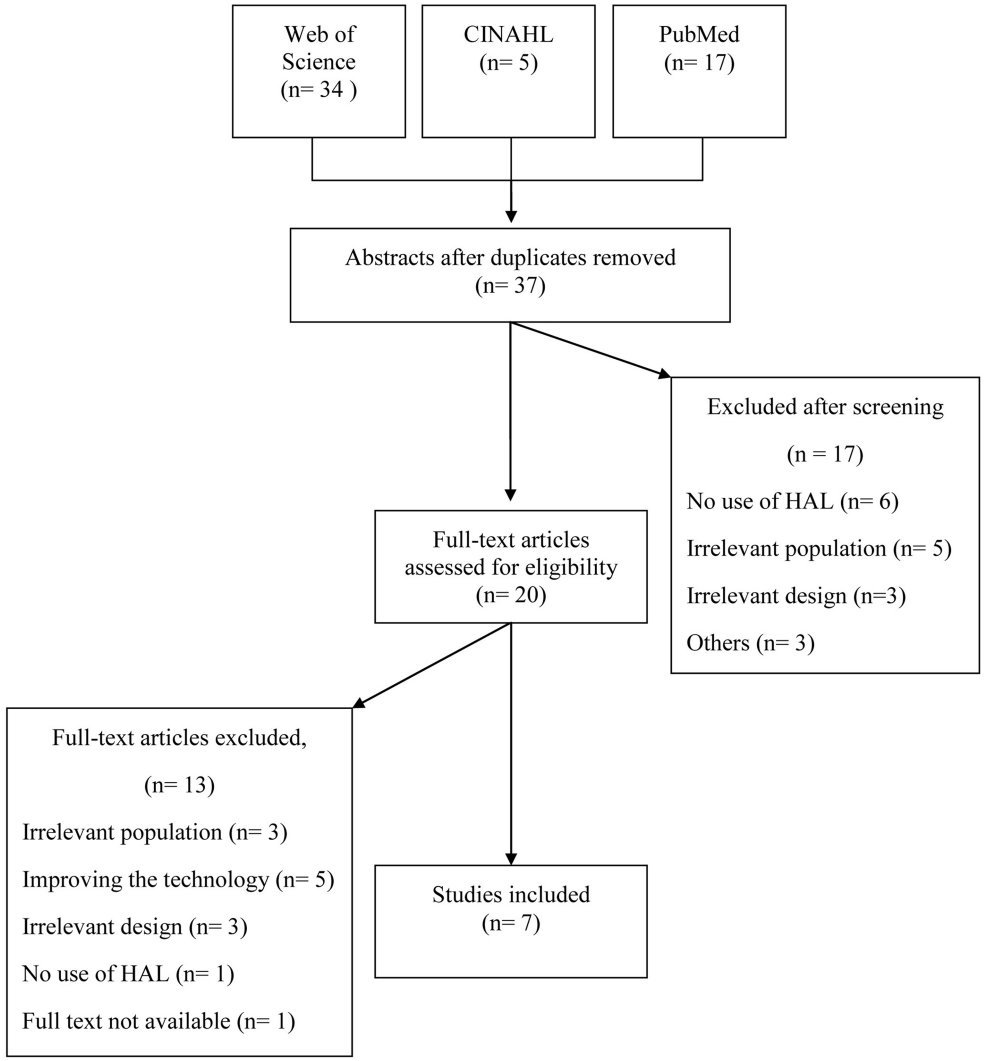

FIGURE 1 | Presentation of the results of the systematic search of the literature.

($n = 8$) as well as other disorders ($n = 18$) (Kubota et al., 2013). Mean age of the participants ranged from 48 to 67 years with a total range of 18–90 years.

In 6 of the included studies a total of 65.7% ($n = 67$) of the participants who completed the study intervention were men and 34.3% ($n = 35$) were women. Ueba et al. (2013) did not report gender for participants completing the study but among the included 32% ($n = 7$) were men and 68% ($n = 15$) were women.

The total time from disease onset to inclusion ranged from 6 days to 54 years. For persons with SCI the time from injury ranged from 1 to 19 years and for persons with stroke this time ranged from approximately 6 days to 16 years. Three studies (Maeshima et al., 2011; Nilsson et al., 2014; Watanabe et al., 2014) included persons early after stroke, with a mean range of 31–59 days since stroke onset. Two other studies included persons later than 1 year and up to 16 years after stroke onset (Kawamoto et al., 2013; Kubota et al., 2013).

The number of reported dropouts during the study interventions ranged from 6 to 10 and was 22, in total (18 with stroke, 1 with SCI and 3 participants with other diagnosis,). Reported reasons for dropouts were medical ($n = 5$), technical ($n = 1$), discharge ($n = 2$), personal ($n = 4$) and withdrawal of consent ($n = 4$). Another 6 participants dropped out due to inappropriate size of shoes, lumbar spondylosis which prevented correct fitting and/or depressive status.

Intervention Protocols and Settings

All except 1 (Ueba et al., 2013) of the 7 studies specifically addressed gait training. The HAL training protocols showed a great variation with regard to frequency, intensity and number of sessions performed. Most studies applied HAL training ≥2 times per week during ≥4 weeks with durations of ≥20 min per session. In the studies involving persons with stroke, the total number of sessions per participant training with HAL ranged from 1 (Maeshima et al., 2011) to 31 (Nilsson et al., 2014). In studies

TABLE 1 | Extracted study data.

First author	Kawamoto et al., 2013	Maeshima et al., 2011	Nilsson et al., 2014	Ueba et al., 2013	Watanabe et al., 2014	Aach et al., 2014	Kubota et al., 2013
Aim	To investigate the feasibility of locomotor training with the HAL in chronic stroke patients and to examine differences between two functional ambulation subgroups	To evaluate the effects of the HAL suit on the gait of stroke patients undergoing rehabilitation	To explore the safety and feasibility of the HAL system when used for early onset, intensive gait training as part of an inpatient rehabilitation program for patients with hemiparetic stroke	To investigate the feasibility and safety of the HAL suit in the rehabilitation of patients in the acute phase after stroke	To examine the effects of gait rehabilitation using the HAL for patients in the recovery phase of stroke to test the feasibility of intervention and outcome assessment protocols for a future randomized controlled trial on a larger scale	To evaluate the possibilities of exoskeletal locomotor training with HAL under voluntary control and identify beneficial effects on functional mobility of the patients Hypothesis: that exoskeleton treadmill training is feasible and safe in application and capable of improving ambulatory mobility in chronic SCI patients	To investigate the feasibility of 16-session (8 week) HAL rehabilitation training for patients with limited mobility
Study design and setting	Single group study Out-patient setting	Single group study Inpatient rehabilitation setting	Single group study Inpatient rehabilitation setting	Single group study Inpatient rehabilitation setting	Randomized controlled study (outcome assessment not blinded) Inpatient rehabilitation setting	Single group study Out-patient setting	Single group study Out-patient setting
Inclusion criteria	1. Requirement of physical assistance or assistive devices for standing up sitting down, and/or walking; 2. Understanding study protocol and expressing voluntary consent 3. A body shape that could fit in the robotic suit HAL 4. Concurrent use of physical and occupational therapies	Not reported	1. <7 weeks since stroke 2. Able to sit 5 min 3. Unable to walk due to paresis 4. Postural control to allow standing with assistance 5. Understand instructions 6. Express informed consent 7. Body size that fits HAL	1. Hemiplegi or ataxia after stroke 2. Height >120 cm weight <100 kg 3. Glascow coma scale >9 4. Systolic BP 100–160 mmHg 5. Saturation > 90% 6. Heart rate between 40 and 120 beats/min 7. Body temperature <37.5°C	1. Hemiparesis from unilateral ischemic/hemorrhagic stroke 2. Time since onset <6 months	1. Traumatic SCI with cronic incomplete or complete paraplegia 2. Present motor functions of hip and knee extensor and flexor muscle groups	1. Musculoskeletal disability affecting ambulation 2. Physical assistance or assistive devices in at least one of following daily activities: standing up, sitting down, and walking 3. Ability to understand study and to express consent 4. Body size that fit HAL 5. Ability to undergo usual physical and occupational therapies
Diagnosis and number of patients	Stroke Divided into two subgroups based on FAC-score FAC 2–3 (dependent ambulatory) FAC 4–5 (independent ambulatory) Included $n = 16$ Completed $n = 16$	Stroke Patients were divided in 3 groups: 1. Assisted group 2. Handrail group 3. Quad cane group included $n = 16$ completed $n = 16$	Stroke Included $n = 8$ Completed $n = 8$	Stroke Included $n = 22$ Completed $n = 16$	Stroke Included $n = 32$ Completed $n = 22$ (11 in each group)	SCI Included $n = 8$ Completed $n = 8$	Stroke $n = 12$ SCI $n = 8$ Musculoskeletal diseases $n = 4$ Other diseases $n = 14$ Included $n = 38$ Completed $n = 32$

(Continued)

TABLE 1 | Continued

First author	Kawamoto et al., 2013	Maeshima et al., 2011	Nilsson et al., 2014	Ueba et al., 2013	Watanabe et al., 2014	Aach et al., 2014	Kubota et al., 2013
Time since event/disease onset	Months, mean: 47.1 ± 37.6 Months, range: 13–132	Days, mean: 52 Days, range: 29–116	Days, range: 6–46	Days, mean: Group 1: 12.7 ± 7.6 Group 2: 9.5 ± 2.4 (divided into two groups based on occurrence of orthostatic hypotension)	Days, mean: HAL group 58.9 ± 46.5 Control group 50.6 ± 33.8	Months, mean: 97.2 ± 88.4 Years, range: 1–19	Years, range: 1–54
Age	Years, mean: 61 Years, range: 18–84	Years, mean: 63 Years, range: 53–78	Years, mean: 53 Years, range: 39–64	Years, mean: 66.6 Years, range: ?-90 (min not reported)	Years, mean: HAL group 67 Control group 75.6 Years, range: not reported	Years, mean: 48 Years, range: 36–63	Years, mean: 53.2 Years, range: 18–81
Gender	Men $n = 12$ Women $n = 4$	Men $n = 9$ Women $n = 7$	Men $n = 8$ Women $n = 0$	Men $n = 7$ Women $n = 15$ (included, completed not reported)	Men $n = 11$ Women $n = 11$ HAL group, men $n = 7$, women $n = 4$ Control group, men $n = 4$, women $n = 7$	Men $n = 6$ Women $n = 2$	Men $n = 21$ Women $n = 11$
Intervention	HAL-training: with use of mobile suspension system and harness. Sit-to-stand and walking No of sessions: $n = 16$ Times/week: approximately $n = 2$ (individualized) Duration, weeks, mean: 10.8 ± 3.5 HAL version: double leg Training lasted 90 min/session HAL training was 20–30 min/session	HAL-training: walking (overground), stair climbing No of sessions: $n = 1$ Times/week: NA Duration: NA HAL version: double leg	HAL-training: with use of treadmill and body weight support No of sessions: median 16, range 6–31 Times/week: $n = 5$ Duration, weeks: approximately $n = 3$ (individualized) HAL version: double leg Training lasted 90 min/session, max 60 min (effective time)	HAL-training: not reported No of sessions, mean: 3.8 ± 3.1 Times/week: not reported Duration, days, mean: 12.1 ± 7 HAL version: double leg	HAL training: with use of mobile suspension system and harness if necessary HAL group: no of sessions: $n = 12$ Times/week: $n = 3$ Duration, weeks: $n = 4$ HAL version: single leg Control group receiving conventional training: no of sessions: $n = 12$ Times/week: $n = 3$ Duration, weeks: $n = 4$ Training lasted 20 min per session	HAL-training: with use of treadmill and body weight support. Included some regular physiotherapy No of sessions, mean: 51.75 ± 5.6 Times/week: $n = 5$ Duration, days: $n = 90$ HAL version: double leg Training lasted 90 min/session	HAL-training: with use of mobile suspension system and harness, or treadmill and body weight support No of sessions: $n = 16$ Times/week: $n = 2$ Duration, weeks: $n = 8$ HAL version: double leg Training lasted 90-min/session (including all). Net walking time was approximately 20 min
Assessments	10 m walk test* (walk speed, number of steps, cadence) Timed up and go Berg balance scale	10 m walk test (stride length, speed) Physiological cost index Assessed before, during, after HAL training and the next day	10 m walk test Timed up and go Berg balance scale Functional ambulation categories NIH stroke scale Fugl-Meyer-LE Clinical outcome variable scale Falls-efficacy scale Barthel index Functional independence measure EQ-5D	Orthostatic hypotension and several medical and functional variables were assessed	10 m walk test (Max walking speed) Timed up and go Functional ambulation categories* 6 min walk test Fugl-Meyer-LE Short physical performance battery Isometric muscle strength	10 m walk test (time, number of steps, assistance) Timed up and go 6 min walk test Walking index for SCI II (WISCI II) Lower extremity motor score Muscle volume ASIA impairment scale	10 m walk test* Timed up and go* Berg balance scale*

(Continued)

TABLE 1 | Continued

First author	Kawamoto et al., 2013	Maeshima et al., 2011	Nilsson et al., 2014	Ueba et al., 2013	Watanabe et al., 2014	Aach et al., 2014	Kubota et al., 2013
Results	Dependent ambulators: improvements in 10 m walk test (speed, cadence and number of steps) and berg balance scale. statistically significant differences ($p < 0.05$) Independent ambulators: improvements in Berg Balance Scale. Statistically significant differences ($p < 0.05$) Whole group: improvements in 10 m walk test and berg balance scale. Statistically significant differences ($p < 0.05$) Adverse events reported as: no training-related serious adverse events were observed	During HAL training physiological cost index (PCI) increased in $n = 11$ participants. PCI was associated with ability to ambulate ($p < 0.05$) Walking speed decreased during training in $n = 12$ participants. Speed was associated with ability to ambulate ($p < 0.05$) Stride length increased during training in $n = 4$ participants. Stride length was not associated with ability to ambulate (p-value not reported) Adverse events: not reported	Improvements in FAC, Fugl-Meyer-LE, 10 m walk test, and berg balance scale Statistically significant differences: not reported Adverse events reported as: no serious adverse events occurred	Improved walking and torso posture $n = 2$ Standing with HAL $n = 12$ No change $n = 2$ Withdrew $n = 6$ Statistically significant differences ($p < 0.05$): not reported Adverse events reported as: orthostatic hypotension ($n = 4$)	HAL group: improvements in independent walking (FAC), walking speed, timed up and go, 6 min walk test and Fugl-Meyer LE. Statistically significant differences ($p < 0.05$) Control group: improvements in independent walking (FAC), short physical performance and timed Up and go. Statistically significant differences ($p < 0.05$) Between groups: improvements in independent walking (FAC) greater in HAL group. Statistically significant differences ($p < 0.04$) Adverse events reported as: no participants withdrew because of adverse effects	All patients improved in treadmill training with HAL. Mean walking speed and average walking time increased Improvements in 10 m walk test (gait speed, number of steps), lower extremity motor score, timed up and go, 6 min walk test statistically significant differences ($p < 0.05$) Improvements in walking index for SCI II. No statistically significant differences ($p < 0.05$) Adverse events reported as: neither adverse nor severe adverse events occurred during the intervention	Improvements in gait speed, steps and cadence based on 10 m walk test, (27 participants) Statistically significant differences ($p < 0.05$) Improvements according to timed up and go and berg balance scale. No statistically significant differences ($p < 0.05$) Adverse events reported as: no serious training-related adverse events
Quality according to SIGN criteria	(–)	(–)	(–)	(–)	(–)	(–)	(–)

**Indicated as the primary outcome in the study.*

involving persons with SCI, Aach et al. (2014) used a mean of 51.75 sessions while the number of sessions for persons with SCI in the study by Kubota et al. (2013) was 16. Data on the use of the active CVC mode and the autonomous CAC mode was not consistently reported. Based on the information provided, we anticipate that 6 of the studies used the CVC mode during training but the extent is not clear. One study (Ueba et al., 2013) did not report on modes used. Four studies reported the total length of each training sessions to be approximately 90 min including assessments, donning, doffing and effective walking time. The effective training time in these studies was approximately 20–30 min per session. Training with HAL was performed by use of BWS and/or a mobile suspension system in 5 studies, by over ground training in 1 study and was not defined in 1 study. Four studies were conducted in inpatient rehabilitation settings and 3 in out-patient care (see **Table 1**).

Outcome Measures and Effects

All assessments were performed without wearing HAL except for one study (Maeshima et al., 2011) where measurements were performed both with and without HAL. Outcome measures mainly related to walking ability. Most frequently used were the 10 m walking test ($n = 6$) (Wade et al., 1987), Timed up and Go ($n = 5$) (Podsiadlo and Richardson, 1991), and Berg Balance Scale ($n = 3$) (Berg et al., 1992). Assessments performed at baseline and after the training period were reported in all studies except 1 (Ueba et al., 2013). No study reported on a long-term follow up. The explorative RCT (Watanabe et al., 2014) compared the effect of HAL-training to the effect of conventional training in the subacute phase after stroke and included 11 participants in each group. The study shows a significant differences ($p = 0.04$) according to the Functional Ambulation Categories (FAC) (Holden et al., 1984) between groups, in favor for the HAL training group. This study has several limitations with regard to study sample size, varying time after stroke and lack of blinding of outcome assessments, as recognized by the authors. One other study (Nilsson et al., 2014) also used FAC and observed improvements suggesting a beneficial effect in a single group. Other studies also report on varying effects such as improvements in walking- and torso posture, gait speed, number of steps and cadence, functional ambulation/independent walking, motor function in lower extremity, activity performance and/or balance (see **Table 1**).

Adverse Events

All studies except 1 (Maeshima et al., 2011) explicitly reported on adverse events. Except for transient complaints related to pressure of the suit, irritated skin, training related pain etc., no adverse events during training with HAL were reported.

Discussion

The aim of this review was to explore existing evidence regarding gait training with the exoskeleton HAL (Hybrid Assistive Limb). We included 7 studies, each with small study samples but comprising a total of 140 patients. Of these, 118 completed the intervention and 107 used HAL. Studies differed in terms of aim, design, duration of intervention, patients/diagnosis, setting and participant characteristics as well as allocation, randomization, blinding and outcome measures. Only 1 study compared training with HAL with other training (Watanabe et al., 2014) but outcome assessment in that study was not blinded. Although no study provides conclusive data on the effects of gait training with HAL as compared to other training and the risk of confounding and bias was considered high, the experiences of training with HAL and the responses that were observed will be useful in the design of further studies.

Feasibility

In total, adult subjects within a broad age range (18–90 years) participated. Both genders were represented, however two thirds were men. Since the majority of subjects had a stroke diagnosis and gender proportions are fairly similar in this diagnostic group, the uneven distribution is surprising but only scarcely commented on in the studies.

Study participants in both post-acute and long-term after stroke onset were represented and 88 out of 106 included subjects completed the study interventions. One small experimental study included subjects with paraplegia 1–19 years after spinal cord injury where all completed the intervention (Aach et al., 2014) while no study addressed effects of training with HAL in the post-acute phase after SCI. The severity of paresis and gait problems varied both within and between the included studies, from severe (only able to maintain sitting balance) to moderate (independent walkers) and a corresponding use of HAL mode and BWS. Reasons for training of independent walkers were not stated or discussed in the included studies although plausible beneficial effects may be, e.g., an increase in walking speed and/or distance or level of independence. The reported numbers of dropouts were low and a total of 107 participants, representing a broad spectrum of motor impairments completed >1500 training sessions with the HAL system without any reported serious adverse events.

Thus, the accumulated results of the included studies demonstrate that training with the HAL system is feasible when applied in professional settings, irrespective of the patients age and sex and the severity of the lower extremity paresis. The feasibility of training with HAL in the post-acute phase after SCI will need to be explored further.

Intervention Protocols and Settings

Even though not stated, the variability in applied frequency, intensity and duration of the reported training sessions and evaluations of outcome, probably reflect both theoretical and practical considerations of, e.g., training needed to achieve significant effects, participants' functional level and study resources. Reasonably, the optimal design would allow training programs to be on the edge for each participant's capacity with regard to the intensity and length of each training session. The intensity and length of the training periods must also consider the patient's functional level as well as the capacity and aims with regard to, e.g., on neuroplasticity, musculoskeletal function, cardiovascular function, gait pattern or independence in walking. Three or more sessions weekly during the training period would probably be justified

from a neuroplasticity and relearning perspective (Bowden et al., 2013).

Both single- and double-leg versions of HAL were used even though not specified in all studies. Reasonably the double-leg version is most relevant for subjects with paraparesis and the single-leg version most often appropriate for subjects with one sided paresis.

Only 2 of the studies included patients early after stroke when the potential to utilize beneficial neuroplasticity processes is higher (Bowden et al., 2013) and there is a need for controlled HAL studies in this area. Post-acute studies are more challenging as they have to consider both the impact of spontaneous recovery early after the event as well as other post-acute health problems.

Outcome Measures and Effects

Outcome measures in the included studies primarily relate to aspects of gait function and walking. Most frequently used was the 10 m walking test, which is a measure of over ground walking speed. Six studies report a positive impact on gait function after HAL training, 5 of these specifically on walking speed and 2 studies report increased level of independence in walking according to the FAC (Nilsson et al., 2014; Watanabe et al., 2014). FAC is the most commonly used outcome measure in studies of walking after robotic training for patients with severe to moderate walking limitations in both the acute and chronic phase after stroke (Geroin et al., 2013). FAC takes the persons level of independence and amount of personal assistance required into account, which from the individuals' perspective is more important than walking speed. However, gait speed may be associated with functional ambulation ability (Perry et al., 1995; Dobkin et al., 2014) and a gait speed improvement may generate improved function and quality of life (Schmid et al., 2007). Therefore, we suggest both the FAC and the 10 m walking test to be used in further studies. In studies including participants with severely impaired gait function at baseline and who are unable to walk 10 m, the 2 min walk test (Kosak and Smith, 2005) is an option to be considered in order to achieve baseline data also when participants cannot walk (i.e., 0 m in 2 min). The potential effect of HAL training on movement related function such as gait pattern is poorly addressed in the included studies. Future studies should consider using assessments that cover also these aspects, for example by use of 3-dimensional motion analysis.

Data on self-perceived aspects of the training were scarce and we found no data on perceived activity performance, participation in everyday life, health or cost-effectiveness that need to be approached in future studies. Further, no study reported on potential effects on cardiovascular, metabolic, emotional or cognitive functions of training with the HAL system. The possible additional value of training with HAL in these areas should be of interest in future studies.

Further, controlled studies should compare training with the HAL system with the most relevant alternative training method. As pointed out, gait machines such as the Lokomat differs from the HAL system in terms of the degree of active patient participation. Comparison studies of these gait machines would be of interest. However, until now, studies using Lokomat have not consistently demonstrated effects, regarding sensory-motor function, gait speed, balance and/or mobility, that are superior to those achieved with conventional training (Swinnen et al., 2010; Ucar et al., 2014; van Nunen et al., 2014) although there might be other advantages such as less therapist burden. Thus, further studies that compare the effects of training with the HAL system to the effects of well designed "conventional training" are justified. Moreover, studies combining robotics with other therapeutic interventions with increasing evidence support, such as Fluoxetine (Chollet et al., 2011), BMI (Brain-Machine Interface) (Shindo et al., 2011; Noda et al., 2012) or brain stimulation (Liew et al., 2014) are also of great interest.

Currently, there are a number of exoskeletons at various stages of development or clinical applications. In addition to differences in mechanical design and control strategies existing exoskeletons uses different activation systems to produce movement of the limb. The most common are hydraulic, pneumatic, and electric motor actuator. In a recent review by Chen et al. (2013) focused on lower extremity robots, the authors divides exoskeletons in different subgroups depending on their functioning and design and conclude that real-time control strategies with timely assistance are a new promising area in rehabilitation therapy. The importance of incorporating more active participation in electromechanical gait training (Dobkin, 2009; Pennycott et al., 2012) as well as of allowing variation of the task during training to promote adequate motor learning (Hidler and Sainburg, 2011) has also been addressed previously.

Some recently developed designs of exoskeletons have taken this into account by establishing intention-based control strategies. In the Ekso (Ekso Bionics, online[2]), ReWalk (Rewalk, online[3]), and in Indego (Indego, online[4]) stepping is initiated by shifting of bodyweight. In Indego, shifting of body weight is used in combination with functional electric stimulation (FES). Another exoskeleton the MINDWALKER (Mindwalker, online[5]) uses EEG and EMG based control.

Recent studies using Ekso for patients in different stages after SCI conclude that the system is safe and show improvements in walking while wearing Ekso (Ekso Clinical Research, online[6]). For inpatient rehabilitation after stroke the authors find Ekso safe to use and indicate that the training may have an effect on cadence as a result of training with Ekso (Ekso Clinical Research, online). However, the number of participant in these studies are limited and do not allow any further conclusions. Ongoing studies after both SCI and severe stroke (Clinicaltrials, online) will evaluate potential effects on ambulation and mobility.

Indego has been introduces in single-subject clinical trials in SCI patients (Quintero et al., 2011; Farris et al., 2014). An ongoing study will evaluate the safety and effectiveness of using Indego

[2]Ekso Bionics. Available online at: http://intl.eksobionics.com/ekso. [Accessed March 2015].

[3]ReWalk. Available online at: http://www.rewalk.com/products/rewalk-rehabilitation/. [Accessed March 2015].

[4]Indego. Available online at: http://www.indego.com/indego/en/home. [Accessed March 2015].

[5]Mindwalker. Available online at: https://mindwalker-project.eu/. [Accessed March 2015].

[6]Ekso Clinical Research, Summary of Findings. Available online at: http://intl.eksobionics.com/clinical-research-summary-download. [Accessed March 2015].

for non-ambulatory or poorly ambulatory SCI patients during standing and walking (Clinicaltrials, online[7]).

In a study by Zeilig et al. (2012) ReWalk was found to be well tolerated and did not cause any adverse events among persons with SCI. This was repeated in a study by Spungen et al. (ReWalk Peer Reviewed Publications, online[8]) where persons with motor-complete paraplegia performed different community-based activities while wearing ReWalk. Several ongoing studies where ReWalk is used after SCI are registered at Clinicaltrials.gov.

Like the HAL, exoskeletons such as the powered knee-ankle-foot-orthosis (KAFO) (Sawicki and Ferris, 2009) and NEUROExos (Cain et al., 2007) use EMG activity to detect a person's intended movement. In both KAFO and NEUROExos EMG activity is used to control the activation of a pneumatic power system to provide torque over the ankle and/or knee joint. In HAL the wearer's joint torque is estimated from the EMG signals on both hip and knee muscles and an electrical motor actuator is used to generate power over these joints (Suzuki et al., 2007).

[7]Clinicaltrials.gov. Available online at: https://www.clinicaltrials.gov/ [Accessed Dec 2014].

[8]ReWalk, Peer Reviewed Publications. Available online at: http://www.rewalk.com/technology/peer-reviewed-publications-copy/. [Accessed March 2015].

This brief survey of other exoskeletons points to a general need for randomized controlled studies where exoskeletons that allow active participation are compared to other types of interventions as well as for studies with larger study populations.

Study Limitations

Since the Hybrid Assistive Limb was developed and is most frequently used in Japan there might be studies published in Japanese journals that were not included in this review. Of note, in 6 of the included studies, the inventor and CEO of the company, Professor Y. Sankai, behind the Hybrid Assistive Limb system is one co-author. No studies using qualitative approach were discovered, which could have been due to the search strategy used. However, even when a broader search was performed, no qualitative studies appeared.

Conclusions and Recommendations

This review identified consistent evidence that the use of the HAL system is feasible when used for gait training in hospital and rehabilitation settings. Data suggest that such training may have beneficial effects on gait function and independence in walking after stroke and after spinal cord injury, but do not allow any conclusions in this respect. Further, well designed controlled studies in these areas are recommended to explore effect sizes and to be followed by larger, confirmatory studies.

References

Aach, M., Cruciger, O., Sczesny-Kaiser, M., Hoffken, O., Meindl, R. C., Tegenthoff, M., et al. (2014). Voluntary driven exoskeleton as a new tool for rehabilitation inchronicspinal cord injury: a pilot study. *Spine J.* 14, 2847–2853. doi: 10.1016/j.spinee.2014.03.042

Berg, K. O., Maki, B. E., Williams, J. I., Holliday, P. J., and Wood-Dauphinee, S. L. (1992). Clinical and laboratory measures of postural balance in an elderly population. *Arch. Phys. Med. Rehabil.* 73, 1073–1080.

Bowden, M. G., Woodbury, M. L., and Duncan, P. W. (2013). Promoting neuroplasticity and recovery after stroke: future directions for rehabilitation clinical trials. *Curr. Opin. Neurol.* 26, 37–42. doi: 10.1097/WCO.0b013e32835c5ba0

Cain, S. M., Gordon, K. E., and Ferris, D. P. (2007). Locomotor adaptation to a powered ankle-foot orthosis depends on control method. *J. Neuroeng. Rehabil.* 4:48. doi: 10.1186/1743-0003-4-48

Chen, G., Chan, C. K., Guo, Z., and Yu, H. (2013). A review of lower extremity assistive robotic exoskeletons in rehabilitation therapy. *Crit. Rev. Biomed. Eng.* 41, 343–363. doi: 10.1615/CritRevBiomedEng.2014010453

Chollet, F., Tardy, J., Albucher, J. F., Thalamas, C., Berard, E., Lamy, C., et al. (2011). Fluoxetine for motor recovery after acute ischaemic stroke (FLAME): a randomised placebo-controlled trial. *Lancet Neurol.* 10, 123–130. doi: 10.1016/S1474-4422(10)70314-8

Dobkin, B. H. (2009). Motor rehabilitation after stroke, traumatic brain, and spinal cord injury: common denominators within recent clinical trials. *Curr. Opin. Neurol.* 22, 563–569. doi: 10.1097/WCO.0b013e3283314b11

Dobkin, B. H., Nadeau, S. E., Behrman, A. L., Wu, S. S., Rose, D. K., Bowden, M., et al. (2014). Prediction of responders for outcome measures of locomotor Experience Applied Post Stroke trial. *J. Rehabil. Res. Dev.* 51, 39–50. doi: 10.1682/JRRD.2013.04.0080

Farris, R. J., Quintero, H. A., Murray, S. A., Ha, K. H., Hartigan, C., and Goldfarb, M. (2014). A preliminary assessment of legged mobility provided by a lower limb exoskeleton for persons with paraplegia. *IEEE Trans. Neural Syst. Rehabil. Eng.* 22, 482–490. doi: 10.1109/TNSRE.2013.2268320

Geroin, C., Mazzoleni, S., Smania, N., Gandolfi, M., Bonaiuti, D., Gasperini, G., et al. (2013). Systematic review of outcome measures of walking training using electromechanical and robotic devices in patients with stroke. *J. Rehabil. Med.* 45, 987–996. doi: 10.2340/16501977-1234

Hesse, S., Waldner, A., and Tomelleri, C. (2010). Innovative gait robot for the repetitive practice of floor walking and stair climbing up and down in stroke patients. *J. Neuroeng. Rehabil.* 7:30. doi: 10.1186/1743-0003-7-30

Hidler, J., and Sainburg, R. (2011). Role of Robotics in Neurorehabilitation. *Top. Spinal Cord Inj. Rehabil.* 17, 42–49. doi: 10.1310/sci1701-42

Holden, M. K., Gill, K. M., Magliozzi, M. R., Nathan, J., and Piehl-Baker, L. (1984). Clinical gait assessment in the neurologically impaired. Reliability and meaningfulness. *Phys. Ther.* 64, 35–40.

Kawamoto, H. (2002). "Power assist system HAL-3 for gait disorder person," in *Lecture Notes in Computer Science, ICCHP 2002, LNCS 2398*, eds K. Miesenberger, J. Klaus, and W. Zagler (Berlin; Heidelberg: Springer-Verlag), 196–203.

Kawamoto, H., Kamibayashi, K., Nakata, Y., Yamawaki, K., Ariyasu, R., Sankai, Y., et al. (2013). Pilot study of locomotion improvement using hybrid assistive limb in chronic stroke patients. *BMC Neurol.* 13:141. doi: 10.1186/1471-2377-13-141

Kawamoto, H., Taal, S., Niniss, H., Hayashi, T., Kamibayashi, K., Eguchi, K., et al. (2010). "Voluntary motion support control of Robot Suit HAL triggered by bioelectrical signal for hemiplegia," in *Conference Proceedings:Annual International Conference of the IEEE Engineering in Medicine and Biology Society. IEEE Engineering in Medicine and Biology Society. Annual Conference* (Buenos Aires), 462–466.

Kosak, M., and Smith, T. (2005). Comparison of the 2-, 6-, and 12-minute walk tests in patients with stroke. *J. Rehabil. Res. Dev.* 42, 103–107. doi: 10.1682/JRRD.2003.11.0171

Krakauer, J. W., Carmichael, S. T., Corbett, D., and Wittenberg, G. F. (2012). Getting neurorehabilitation right: what can be learned from animal models? *Neurorehabil. Neural Repair* 26, 923–931. doi: 10.1177/1545968312440745

Kubota, S., Nakata, Y., Eguchi, K., Kawamoto, H., Kamibayashi, K., Sakane, M., et al. (2013). Feasibility of rehabilitation training with a newly developed wearable robot for patients with limited mobility. *Arch. Phys. Med. Rehabil.* 94, 1080–1087. doi: 10.1016/j.apmr.2012.12.020

Kwakkel, G., van Peppen, R., Wagenaar, R. C., Wood Dauphinee, S., Richards, C., Ashburn, A., et al. (2004). Effects of augmented exercise therapy time after stroke: a meta-analysis. *Stroke* 35, 2529–2539. doi: 10.1161/01.STR.0000143153.76460.7d

Langhorne, P., Bernhardt, J., and Kwakkel, G. (2011). Stroke rehabilitation. *Lancet* 377, 1693–1702. doi: 10.1016/S0140-6736(11)60325-5

Langhorne, P., Coupar, F., and Pollock, A. (2009). Motor recovery after stroke: a systematic review. *Lancet Neurol.* 8, 741–754. doi: 10.1016/S1474-4422(09)70150-4

Liew, S. L., Santarnecchi, E., Buch, E. R., and Cohen, L. G. (2014). Non-invasive brain stimulation in neurorehabilitation: local and distant effects for motor recovery. *Front. Hum. Neurosci.* 8:378. doi: 10.3389/fnhum.2014.00378

Maeshima, S., Osawa, A., Nishio, D., Hirano, Y., Takeda, K., Kigawa, H., et al. (2011). Efficacy of a hybrid assistive limb in post-stroke hemiplegic patients: a preliminary report. *BMC Neurol.* 11:116. doi: 10.1186/1471-2377-11-116

Mehrholz, J., Elsner, B., Werner, C., Kugler, J., and Pohl, M. (2013). Electromechanical-assisted training for walking after stroke: updated evidence. *Stroke* 44, e127–e128. doi: 10.1161/STROKEAHA.113.003061

Mehrholz, J., Kugler, J., and Pohl, M. (2012). Locomotor training for walking after spinal cord injury. *Cochrane Database Syst. Rev.* 11:CD006676. doi: 10.1002/14651858.CD006676.pub3

Nilsson, A., Vreede, K. S., Haglund, V., Kawamoto, H., Sankai, Y., and Borg, J. (2014). Gait training early after stroke with a new exoskeleton—the hybrid assistive limb: a study of safety and feasibility. *J. Neuroeng. Rehabil.* 11:92. doi: 10.1186/1743-0003-11-92

Noda, T., Sugimoto, N., Furukawa, J., Sato, M., Sang-Ho, H., and Morimoto, J. (2012). "Brain-controlled exoskeleton robot for BMI rehabilitation. Humanoid Robots (Humanoids)," in *12th IEEE-RAS International Conference* (Osaka), 21–27. doi: 10.1109/HUMANOIDS.2012.6651494

Pennycott, A., Wyss, D., Vallery, H., Klamroth-Marganska, V., and Riener, R. (2012). Towards more effective robotic gait training for stroke rehabilitation: a review. *J. Neuroeng. Rehabil.* 9:65. doi: 10.1186/1743-0003-9-65

Perry, J., Garrett, M., Gronley, J. K., and Mulroy, S. J. (1995). Classification of walking handicap in the stroke population. *Stroke* 26, 982–989. doi: 10.1161/01.STR.26.6.982

Peurala, S. H., Karttunen, A. H., Sjogren, T., Paltamaa, J., and Heinonen, A. (2014). Evidence for the effectiveness of walking training on walking and self-care after stroke: a systematic review and meta-analysis of randomized controlled trials. *J. Rehabil. Med.* 46, 387–399. doi: 10.2340/16501977-1805

Podsiadlo, D., and Richardson, S. (1991). The timed "Up & Go": a test of basic functional mobility for frail elderly persons. *J. Am. Geriatr. Soc.* 39, 142–148.

Quintero, H. A., Farris, R. J., Hartigan, C., Clesson, I., and Goldfarb, M. (2011). A powered lower limb orthosis for providing legged mobility in paraplegic individuals. *Top Spinal Cord Inj. Rehabil.* 17, 25–33. doi: 10.1310/sci1701-25

Sawicki, G. S., and Ferris, D. P. (2009). A pneumatically powered knee-ankle-foot orthosis (KAFO) with myoelectric activation and inhibition. *J. Neuroeng. Rehabil.* 6:23. doi: 10.1186/1743-0003-6-23

Schmid, A., Duncan, P. W., Studenski, S., Lai, S. M., Richards, L., Perera, S., et al. (2007). Improvements in speed-based gait classifications are meaningful. *Stroke* 38, 2096–2100. doi: 10.1161/STROKEAHA.106.475921

Schwartz, I., and Meiner, Z. (2013). The influence of locomotor treatment using robotic body-weight-supported treadmill training on rehabilitation outcome of patients suffering from neurological disorders. *Harefuah* 152, 166–171, 182, 181.

Shindo, K., Kawashima, K., Ushiba, J., Ota, N., Ito, M., Ota, T., et al. (2011). Effects of neurofeedback training with an electroencephalogram-based brain-computer interface for hand paralysis in patients with chronic stroke: a preliminary case series study. *J. Rehabil. Med.* 43, 951–957. doi: 10.2340/16501977-0859

Suzuki, K., Mito, G., Kawamoto, H., Hasegawa, Y., and Sankai, Y. (2007). Intention-based walking support for paraplegia patients with Robot Suit HAL. *Adv. Robot.* 21, 1441–1469. doi: 10.1163/156855307781746061

Swinnen, E., Duerinck, S., Baeyens, J. P., Meeusen, R., and Kerckhofs, E. (2010). Effectiveness of robot-assisted gait training in persons with spinal cord injury: a systematic review. *J. Rehabil. Med.* 42, 520–526. doi: 10.2340/16501977-0538

Ucar, D. E., Paker, N., and Bugdayci, D. (2014). Lokomat: a therapeutic chance for patients with chronic hemiplegia. *NeuroRehabilitation* 34, 447–453. doi: 10.3233/NRE-141054

Ueba, T., Hamada, O., Ogata, T., Inoue, T., Shiota, E., and Sankai, Y. (2013). Feasibility and safety of acute phase rehabilitation after stroke using the hybrid assistive limb robot suit. *Neurol. Med. Chir. (Tokyo)* 53, 287–290. doi: 10.2176/nmc.53.287

van Nunen, M. P., Gerrits, K. H., Konijnenbelt, M., Janssen, T. W., and De Haan, A. (2014). Recovery of walking ability using a robotic device in subacute stroke patients: a randomized controlled study. *Disabil. Rehabil. Assist. Technol.* 10, 141–148. doi: 10.3109/17483107.2013.873489

Wade, D. T., Wood, V. A., Heller, A., Maggs, J., and Langton Hewer, R. (1987). Walking after stroke. Measurement and recovery over the first 3 months. *Scand. J. Rehabil. Med.* 19, 25–30.

Watanabe, H., Tanaka, N., Inuta, T., Saitou, H., and Yanagi, H. (2014). Locomotion improvement using a hybrid assistive limb in recovery phase stroke patients: a randomized controlled pilot study. *Arch. Phys. Med. Rehabil.* 95, 2006–2012. doi: 10.1016/j.apmr.2014.07.002

Zeilig, G., Weingarden, H., Zwecker, M., Dudkiewicz, I., Bloch, A., and Esquenazi, A. (2012). Safety and tolerance of the ReWalk™ exoskeleton suit for ambulation by people with complete spinal cord injury: a pilot study. *J. Spinal Cord Med.* 35, 96–101. doi: 10.1179/2045772312Y.0000000003

Conflict of Interest Statement: The authors declare that the research was conducted in the absence of any commercial or financial relationships that could be construed as a potential conflict of interest.

frontiers in
SYSTEMS NEUROSCIENCE

ORIGINAL RESEARCH ARTICLE
published: 14 May 2014
doi: 10.3389/fnsys.2014.00085

Decoding the ERD/ERS: influence of afferent input induced by a leg assistive robot

***Giuseppe Lisi*[1,2]*, *Tomoyuki Noda*[1] *and Jun Morimoto*[1]**

[1] *ATR Computational Neuroscience Laboratories, Department of Brain Robot Interface, ATR, Kyoto, Japan*
[2] *Mathematical Informatics Laboratory, Department of Information Science, Nara Institute of Science and Technology, Nara, Japan*

Edited by:
Mikhail Lebedev, Duke University, USA

Reviewed by:
Yuri P. Ivanenko, IRCCS Fondazione Santa Lucia, Italy
Marta Gandolla, Politecnico di Milano, Italy

***Correspondence:**
Giuseppe Lisi, ATR Computational Neuroscience Laboratories, Department of Brain Robot Interface, ATR, 2-2-2 Hikaridai, Seika-cho, Soraku-gun, Kyoto, 619-0288, Japan
e-mail: beppelisi@gmail.com

This paper investigates the influence of the leg afferent input, induced by a leg assistive robot, on the decoding performance of a BMI system. Specifically, it focuses on a decoder based on the event-related (de)synchronization (ERD/ERS) of the sensorimotor area. The EEG experiment, performed with healthy subjects, is structured as a 3 × 2 factorial design, consisting of two factors: "finger tapping task" and "leg condition." The former is divided into three levels (BMI classes), being left hand finger tapping, right hand finger tapping and no movement (Idle); while the latter is composed by two levels: leg perturbed (*Pert*) and leg not perturbed (*NoPert*). Specifically, the subjects' leg was periodically perturbed by an assistive robot in 5 out of 10 sessions of the experiment and not moved in the remaining sessions. The aim of this study is to verify that the decoding performance of the finger tapping task is comparable between the two conditions *NoPert* and *Pert*. Accordingly, a classifier is trained to output the class of the finger tapping, given as input the features associated with the ERD/ERS. Individually for each subject, the decoding performance is statistically compared between the *NoPert* and *Pert* conditions. Results show that the decoding performance is notably above chance, for all the subjects, under both conditions. Moreover, the statistical comparison do not highlight a significant difference between *NoPert* and *Pert* in any subject, which is confirmed by feature visualization.

Keywords: brain robot interface, assistive exoskeleton robot, ERD/ERS of the sensorimotor hand area, lower limb afferent input, ICA/CSP, wavelet, PCA/LDA, sparse logistic regression

1. INTRODUCTION

Brain-machine interfaces (BMI) have recently raised much interest in that they can help improve the quality of life of people with severe motor disabilities. In previous studies, the brain signal has been used to control devices that affect the surrounding environment such as wheelchairs or neuroprosthesis (Mussa-Ivaldi, 2000; Daly and Wolpaw, 2008; Pfurtscheller and Solis-Escalante, 2008). Regarding the nature of ERD/ERS, movement or preparation for movement is typically accompanied by a decrease in mu and beta rhythms, particularly contralateral to the movement (Wolpaw et al., 2002). This phenomenon has been named event-related desynchronization or ERD (Babiloni et al., 1999). Its opposite, rhythm increase, or event-related synchronization (ERS), occurs after movement and with relaxation (Pfurtscheller and Lopes da Silva, 1999). To note that similar ERD/ERS patterns in the sensorimotor area can be elicited also by motor imagery (Pfurtscheller and Neuper, 1997; Pfurtscheller and Lopes da Silva, 1999; McFarland et al., 2000). These features make it possible to use a BMI system based on ERD/ERS for the control of an external device (Pfurtscheller et al., 2000b; Wolpaw et al., 2003; Babiloni et al., 2007). If this is done irrespectively of any system cues, the control paradigm is called asynchronous and allows the subject to make self-paced decisions (Müller-Putz et al., 2006; Zhao et al., 2009; Solis-Escalante et al., 2010).

A similar control paradigm has yet to be carefully investigated for a lower limb exoskeleton robot. Of particular interest would be a BMI system, based on the ERD/ERS of the sensorimotor area, able to control an assistive robot (downward arrow of **Figure 1**). Similarly, Tsui et al. (2011); Huang et al. (2012) have succeeded in controlling a wheelchair by means of a BMI based on event-related (de)synchronization (ERD/ERS). Nonetheless, one of the differences between a wheelchair and a lower limb assistive robot is that the latter induces movements of the legs. In this context, the ERD/ERS phenomenon is not only related to active movements or motor imagery, but also to passive movements (upward arrow of **Figure 1**; Cassim et al., 2001; Müller et al., 2003; Müller-Putz et al., 2007; Wagner et al., 2012). Especially, Müller-Putz et al. (2007) highlighted that passive movements of the feet produce a significant ERD/ERS not only at the vertex, but over the whole sensorimotor cortex. This raises the question whether the somatosensory afferent input, induced by the periodic leg perturbation, interferes with the decoding ability of a BMI system based on the ERD/ERS of the sensorimotor hand area (horizontal arrow of **Figure 1**).

Specifically, in this paper, we investigate whether the periodic perturbation of lower limbs produces a significant decrease in the classification performance of actual right and left hand finger movements. The reason for decoding the right and left sensorimotor hand area stands in the reliability of the contralateral ERD/ERS spatial distribution (Wang et al., 2007) and in the fact that this approach is exhaustively discussed in literature (Guger et al., 2000; Pfurtscheller et al., 2000b; Blankertz et al.,

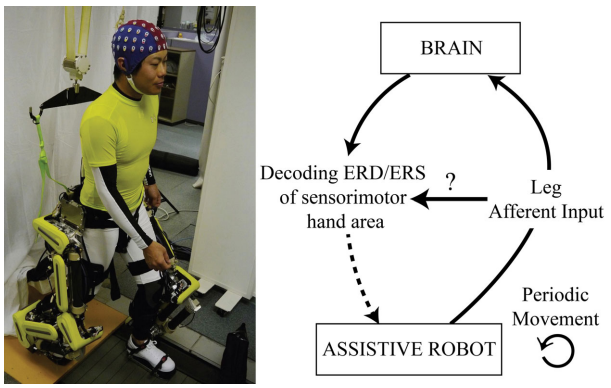

FIGURE 1 | Conceptual representation of the problem. Understanding how the leg afferent input, induced by a leg assistive robot, influences the decoding of the ERD/ERS of the sensorimotor hand area. The paper focuses on the concepts represented by the solid arrows of this figure.

2008a). Moreover, the *Idle* class is considered in order to simulate the behavior of the system in an online asynchronous setup (Müller-Putz et al., 2006).

Furthermore, the motivation for using real movements instead of motor imagery, is that the latter cannot be mechanically measured nor visually assessed by the experiment operator. As such, in case of misclassification, there is no certainty about whether the subject failed in generating a significant ERD/ERS by motor imagery or if the somatosensory afferent input of the leg actually affected the decoding. On the other hand, for real upper limb movements, the motor output is visible; therefore, we are certain that the motor cortex has produced a control command.

To note that even though patterns of mu and beta de/synchronization associated with actual movements are similar to those with motor imagery, they differ in magnitude (McFarland et al., 2000). Specifically, the spectral perturbations associated with motor imagery are considerably smaller than the ones of actual movements (Solis-Escalante et al., 2010). Nonetheless, according to Pfurtscheller et al. (1998), the beta ERS is significantly larger with hand as compared to finger movement. Therefore, the latter is chosen in this experiment, so as to deal with a spectral perturbation that is as close as possible to the one associated with motor imagery, while preserving the necessary property of objective measurability by the experiment operator.

Previous studies have dealt with EEG-based neuroprosthesis control (Pfurtscheller et al., 2000a; Müller-Putz et al., 2005, 2006, 2009), but to our knowledge this is the first time that the possibility of interference between the rhythms associated with passive and active movements is investigated.

2. METHODS

Five healthy subjects were asked to perform real right/left-hand brisk finger tapping, or not to move (idle), while their brain activity was recorded by EEG. Each task lasted 2 s and was instructed by visual cues, interleaved by periods of rest of 8 s. Simultaneously, the subjects' leg was *perturbed by a periodic swing movement of a lower limb assistive robot* in 5 out of 10 sessions of the experiment. In this way, the experiment is characterized by two conditions: leg perturbed (*Pert*) and leg not perturbed (*NoPert*).

Therefore, the main question regarding the influence of the leg afferent input on the decoding of the sensorimotor area ERD/ERS can be stated as follows: *is the performance of finger tapping decoding significantly different between the NoPert and Pert conditions, for one or more subjects?* To answer this question, a classifier is trained to output the class of the finger tapping (*Idle, Left, Right*), given as input the features associated with the ERD/ERS. Cross-validated Kappa score (see section 2.3) is used to assess the decoding performance separately for *NoPert* and *Pert*. Then, individually for each subject, the Kappa scores of the two conditions are statistically compared by the Z-test (see Appendix). Moreover, it is important to perform an analysis that is as independent as possible from the characteristics of a specific decoder. For this reason, two types of feature extraction methods are used separately: *Unsupervised feature extraction* (ICA, Wavelet and PCA) and *Supervised feature extraction* (CSP, Wavelet, LDA).

As discussed in the introduction, actual left/right hand finger tapping and idle were chosen because of the following reasons:

1. the contralateral ERD/ERS spatial distribution associated with left or right hand movements can be reliably decoded;
2. actual movements are observable by the experiment operator, or mechanically measurable, therefore we are certain that an ERD/ERS activation must have been elicited by the motor task (with motor imagery the subject may fail to produce ERD/ERS);
3. finger movements are characterized by a significantly smaller ERS as compared to hand movements (Pfurtscheller et al., 1998), which makes the task as close as possible to a motor imagery one, while preserving the properties at point 1 and 2;
4. the idle class is used to simulate an online asynchronous setup.

2.1. EXPERIMENTAL SETUP

2.1.1. Assistive robot specifications

Our custom made one degree of freedom robot (oneDOF, Noda et al., 2012) was used as assistive robot (**Figure 2A**). OneDOF is actuated using a pneumatic-electric hybrid strategy. In detail, two antagonistic pneumatic artificial muscles (PAM) generate large force by converting pressured gas energy into contraction force through their rubber tube. The advantage of using a PAM is that it can exert very large torques (maximal 70 Nm), while generating insignificant electromagnetic noise from the point of view of the EEG system. Moreover, an electric motor generates parallel small torque (maximal 5 Nm) in order to make fast and precise corrections to the torque generated by PAM. This strategy allows for both a powerful and precise actuation of the robot.

For this specific experiment, OneDOF was mounted on a custom made support in order to allow subjects to sit near to the robot (**Figure 2B**). Moreover a leg-shaped thermoplastic polymer was anchored to OneDOF in order to secure the subject's leg (**Figure 2C**).

2.1.2. Data acquisition

The experiment, which was carried out with five healthy subjects aged 23–27, can be represented by a 3×2 factorial design

(**Figure 3**) consisting of two factors: "finger tapping task" and "leg condition." The former is divided into three levels, being left tapping, right tapping and idle; while the latter is composed by two levels: *NoPert* and *Pert*.

With regard to the "leg condition" factor, five sessions of the experiment were performed while the assistive robot was stopped (*NoPert*) and other five while the robot continuously swung up and down at a frequency of 0.5 Hz between 5° and 50° of the knee joint (*Pert*).

During all the 10 sessions of the experiment the finger tapping task was carried out as follows: an hyphen was shown on the screen for 8 s to indicate that the subject should not move (rest). After this period, a left or right arrow randomly appeared, or the hyphen was maintained on the screen, for 2 s, indicating respectively that the subject should perform left or right hand brisk continuous finger tapping, or keep not moving (idle). Within one session, each of the three tasks, Left/Right tapping and Idle, was performed 10 times, resulting in 30 trials per session. After each session, subjects rested for about 5 min. Moreover, the EEG signal was recorded at a sampling rate of 2048 Hz with a 64-electrode cap and a Biosemi Active Two system for amplification and analog-to-digital conversion.

In order to confirm that to each visual cue corresponds a motor action, the finger tapping performance was visually

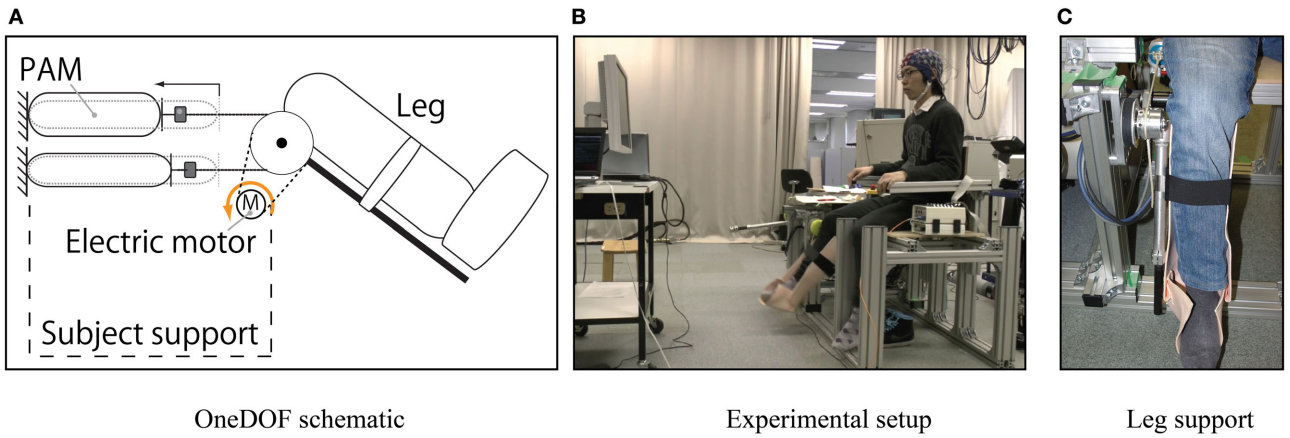

FIGURE 2 | Robot used during the experiment. (A) PAM and electric actuators can exert parallel torques to move the leg. **(B)** Representation of the experimental setup. **(C)** Representation of the thermoplastic polymer leg support anchored to the robot and holding up the subject's leg.

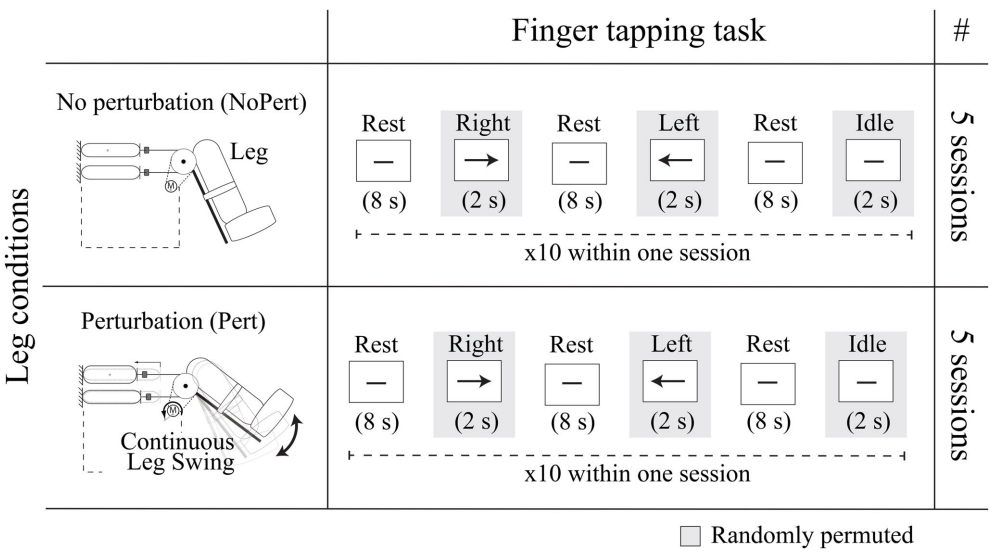

FIGURE 3 | Experimental design. The experiment is structured as a 3 × 2 factorial design, consisting of two factors "finger tapping task" and "leg condition." The former is divided into three levels, being left hand finger tapping (Left), right hand finger tapping (Right) and Idle, whose temporal representation is visualized in the "Finger tapping task" column. The "leg condition" factor is divided into two levels *NoPert* and *Pert*, which are represented, respectively, in the first and second rows of the table. To note that *Rest* is the resting period between tasks and that the visual cues of the tasks are randomly permuted within a session. Moreover, in the last column, the number of sessions performed for each experimental condition are visualized.

observed by the experiment operator. Moreover, for the first three subjects the experiment was recorded on video, while for the other two subjects the index finger angle was measured by means of a goniometer sensor (Biometrics Ltd).

Subjects gave written informed consent for the experimental procedures, which were approved by the ATR Human Subject Review Committee.

2.2. DECODER TRAINING

In this section, we introduce the methodology to train and test the decoder that is used in the cross-validation procedure described in section 2.3. Moreover, we refer to "training set" and "test set," detailed as well in section 2.3, but for the time being it is sufficient to think of them as two independent datasets that are used to, respectively, fit the parameters of a model (decoder) and evaluate the predictive power of the trained (fitted) model.

The six steps of the training algorithm (**Figure 4**) are: *1. preprocessing* (section 2.2.1), *2. spatial filter identification* (section 2.2.2), *3. wavelet transform for time-frequency feature extraction* (section 2.2.3), *4. spatial filter selection* (section 2.2.4), *5. feature dimensionality reduction* (section 2.2.5) and *6. training of a classifier* (section 2.2.6). In order to produce results that are independent from the characteristics of a specific feature extraction method, two types of decoder are used separately:

- *Unsupervised feature extraction*-based: the spatial filter identification step is performed by Independent Component Analysis (ICA) and feature dimensionality reduction by Principal Component Analysis (PCA);
- *Supervised feature extraction*-based: the spatial filter identification is carried out by Common Spatial Patterns (CSP) and feature dimensionality reduction by Linear Discriminant Analysis (LDA).

It is important to stress that the *Unsupervised feature extraction*-based decoder is trained and tested independently from the *Supervised feature extraction*-based one.

2.2.1. Preprocessing

This step is common to both the *Unsupervised* and *Supervised feature extraction*-based decoders. Only a subset of 35 electrodes, centered at the motor cortex, is used: all the electrodes positioned within the ranges F5-F6, FC5-FC6, C5-C6, CP5-CP6, P5-P6. The training and test sets are resampled at 128 Hz and bandpass filtered (FIR filter implemented in EEGLAB, Delorme and Makeig, 2004) in the range from 8 to 30 Hz, encompassing the mu and beta frequency bands, which have been shown to be most important for movement classification. Epochs are extracted with respect to the visual cues presented to the subjects. In particular, the epoch starts 0.5 s before the cue onset and ends 2.5 s after the offset, for a total of 5 s. The time window after the movement offset is needed to capture completely the ERS, also considering that, sometimes, this is slightly delayed due to the subject's reaction time. In the following subsections $\mathbf{E}_j \in \mathbb{R}^{c \times t}$ represents the single-trial EEG signals of the training set, where c is the number of channels, t is the number of time samples and $j = 1 \ldots n$ where n is the number of training trials.

2.2.2. Spatial filter identification (ICA and CSP)

Previous studies have demonstrated that spatial filters are useful in single-trial analysis, in order to improve the signal-to-noise ratio (Blankertz et al., 2008b). For this purpose, Independent Component Analysis (ICA) is implemented in the *Unsupervised feature extraction*-based decoder, while Common Spatial Patterns (CSP) is used in the *Supervised feature extraction*-based one. Both ICA and CSP transform the observed EEG signals as:

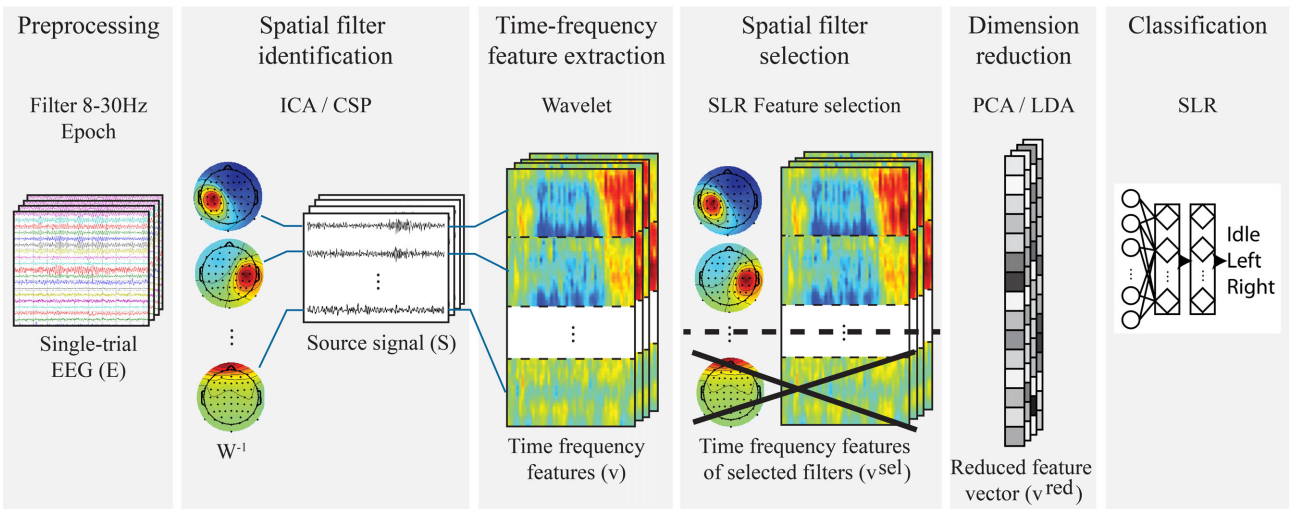

FIGURE 4 | Decoder training in a single fold of the cross-validation. In the *Unsupervised feature extraction*-based version, ICA and PCA are used, respectively, for spatial filter selection and dimension reduction, while CSP and LDA are, respectively, employed in the *Supervised feature extraction*-based one. Important to note that the transformation matrices of spatial filter identification, spatial filter selection and dimensionality reduction are computed only on the training set of each cross-validation fold. Moreover, the time-frequency features are vectorized in the algorithm, while in figure they are kept in matrix form for a visualization purpose: the horizontal axis represents the time, and the vertical axis represents the frequency.

$$\mathbf{S}_j = \mathbf{W}\mathbf{E}_j \quad (1)$$

where $\mathbf{E}_j$ represents the observed single-trial EEG signals, $\mathbf{W}$ the unmixing matrix, $\mathbf{S}_j$ the recovered single-trial sources and $j = 1 \ldots n$, where n is the number of training trials.

2.2.2.1. Independent Component Analysis (ICA). ICA is an unsupervised method that finds a linear transformation (W) of non-gaussian data ($\mathbf{E}$), so that the resulting components ($\mathbf{S}$) are as statistically independent as possible (Hyvärinen and Oja, 2000). Hence, the EEG signal is separated into Independent Components (ICs) accounting for different neural activities, but also stereotyped non-brain artifact signals including eye movements, line noise and muscle activities (Makeig et al., 2004). In this study, the logistic infomax ICA algorithm, implemented in the EEGLAB function *binica* (Delorme and Makeig, 2004), is executed on the preprocessed training set. This yields an unmixing matrix $\mathbf{W} \in \mathbb{R}^{s \times c}$ and source signals (independent components) $\mathbf{S}_j \in \mathbb{R}^{s \times t}$, where s is the number of sources, c the number of channels, t is the number of time samples and $j = 1 \ldots n$, where n is the number of training trials.

2.2.2.2. Common Spatial Patterns (CSP). CSP computes the unmixing matrix $\mathbf{W}$ to yield features whose variances are optimal for discriminating two classes of EEG measurements (Ramoser et al., 1998; Blankertz et al., 2008a) by solving the eigenvalue decomposition problem

$$\boldsymbol{\Sigma}_1 \boldsymbol{W} = (\boldsymbol{\Sigma}_1 + \boldsymbol{\Sigma}_2)\boldsymbol{W}\boldsymbol{D} \quad (2)$$

where $\boldsymbol{\Sigma}_1$ and $\boldsymbol{\Sigma}_2$ represent the estimates of the covariance matrices of the EEG signal associated with two different tasks, the diagonal matrix $\mathbf{D}$ contains the eigenvalues of $\boldsymbol{\Sigma}_1$ and the column vectors of $\mathbf{W}^{-1}$ are the filters for the CSP projections. The best contrast is provided by those filters with the highest and lowest eigenvalues, therefore the common practice is to retain e eigenvectors from both ends of the eigenvalue spectrum (Blankertz et al., 2008a). CSP is applied in a One-vs-Rest (OvR) fashion, in order to cope with the multi-class nature of the problem, separately (Dornhege et al., 2004) for three different frequency bands 8–13 Hz (μ), 15–25 Hz (β), 8–30 Hz (μ and β), in the time segment starting 1 s after the cue (Blankertz et al., 2008b). Moreover, $e = 2$ eigenvectors from the top and from the bottom of the eigenvalue spectrum are retained. This procedure is performed only on the preprocessed training dataset, yielding the unmixing matrix $\mathbf{W} \in \mathbb{R}^{s \times c}$ and source signals $\mathbf{S}_j \in \mathbb{R}^{s \times t}$, where $s = 2 \times e \times 3$ (frequency bands)$\times 3$ (classes) is the number of sources (CSP projections), c is the number of channels, t is the number of time samples and $j = 1 \ldots n$, where n is the number of training trials.

It is important to note that, with both ICA and CSP, the unmixing matrix $\mathbf{W}$ is computed *only using the training set*.

2.2.3. Time-frequency analysis: the wavelet transform

In both the *Unsupervised* and *Supervised feature extraction*-based decoders, the Morlet Wavelet transform (Daubechies, 1990) is employed to extract time-frequency features, representing the subject-specific ERD/ERS patterns, from the source signals $\mathbf{S}$. For each trial, a wavelet coefficient matrix with 50 time samples and 20 frequency bins is computed for the i-th source signal. The resulting coefficients are squared to get the spectral power and the $10 \log_{10}$ transformation is computed to obtain a final time-frequency representation ($\mathbf{c}_i$). Therefore, the feature vector of the j-th trial ($\mathbf{v}_j$) is obtained by the concatenation of the time-frequency coefficients $\mathbf{c}_i$ computed from the i-th source signal inside $\mathbf{S}_j$:

$$\mathbf{v}_j = \begin{bmatrix} \mathbf{c}_1 \\ \mathbf{c}_i \\ \vdots \\ \mathbf{c}_s \end{bmatrix}, \mathbf{c}_i = \begin{bmatrix} c_{11}, \ldots, c_{f1}, c_{12}, \ldots, c_{f2}, \ldots, c_{1t}, \ldots, c_{ft} \end{bmatrix}^\top \quad (3)$$

In the equations above, $\mathbf{v}_j$ represents the j-th feature vector, $j = 1 \ldots n$, where n is the number of training trials, $\mathbf{c}_i$ is the time-frequency coefficients vector of the i-th source, $i = 1 \ldots s$ where s is the number of sources in $\mathbf{S}_j$, t is the number of time samples and f is the number of frequency bins.

2.2.4. Spatial filter selection based on SLR

Not all the spatial filters that have been previously identified by ICA or CSP are related to the neural processes of the tapping task. In particular, ICA identifies a large number of independent components that account for artifacts and other neural sources, while CSP might return some spatial patterns that over-fit the training set. Therefore, in order to avoid over-fitting and to obtain results that are not influenced by artifacts, it is necessary to reduce the number of spatial filters to the ones that are strictly indispensable for the classification of the tapping task.

For this purpose, Sparse Logistic Regression (SLR) is used to select the most important spatial filters based on their time-frequency features. SLR is a Bayesian extension of logistic regression, which simultaneously performs feature selection and training of model parameters for classification. It utilizes automatic relevance determination (ARD) to determine the importance of each parameter while estimating its values. This process selects only a few parameters as important and prunes away others. The resulting model has a sparse representation with a small number of estimated parameters (Yamashita et al., 2008). In this work we apply the OvR version of the algorithm to cope with the multi-class problem. Moreover, prior to training, each feature of the training set is normalized using its mean across trials and scaled using the respective standard deviation. Furthermore, the mean and standard deviation of the training features are used to normalize also the feature vectors of the test set.

SLR can be used to assign scores to spatial filters based on the classification performance and selection recurrence of their time-frequency features. In the current study we were inspired by the method proposed by Yamashita et al. (2008), which selects features on the basis of their selection recurrence. Given the fact that our goal is not to select single features, but spatial filters which are, in turn, represented by a set of time-frequency features we had to modify the original algorithm. The revised method considers the recurrence of the group of time-frequency features belonging

to each spatial filter. The basic idea is that spatial filters whose time-frequency features are repeatedly selected with good classification performance among a variety of training data sets could be important.

Specifically, the selection of spatial filters is implemented by estimating SLR weight parameters on 80% of the *training set* and evaluating the classification performance on the remaining 20% of the *training set*. This process is *repeated five times* so that each trial of the training set is used once to evaluate the performance. Therefore, we can define a score value for each i-th spatial filter ($i = 1 \dots s$ where s is the number of sources in $\mathbf{S}_j$) based on the number of selected features that belong to it. More precisely, let $\overline{\theta}_j$ and p_j denote the estimated parameter vector and classification performance (percent) resulting from the j-th repetition of SLR ($j = 1 \dots R$, where R is the number of SLR repetitions). Moreover, $\overline{\theta}_j(k) = 0$ if the k-th feature is not selected ($k = 1 \dots |\overline{\theta}|$ where $|\overline{\theta}|$ is the length of the feature vector) . Then the score value (SC) for the i-th spatial filter (SF) is defined by:

$$SC_i = \sum_{j}^{R} \sum_{k \in SF_i}^{|\overline{\theta}|} I(\overline{\theta}_j(k) \neq 0) \times p_j \tag{4}$$

where $I(\cdot)$ denotes an indicator function that takes the value of 1 if the condition inside the brackets is satisfied, 0 otherwise. $R = 5$ is the number of SLR repetitions, $|\overline{\theta}|$ is the length of the feature vector and $\overline{\theta}_j(k)$ is the estimate of the k-th parameter belonging to the i-th spatial filter (SF), with respect to the j-th repetition. Once SC has been computed for all the spatial filters, we retain only those whose SC is above a given threshold. Specifically for selecting independent components the threshold is $\mu_{SC} + \sigma_{SC}$, while for CSP the threshold is simply μ_{SC}, where μ and σ represent respectively mean and standard deviation of the SC values. The reason for having two different thresholds is that ICA returns a large number of independent components, not related to the classification, that need to be removed, such as artifacts and other neural sources. On the other hand, being CSP a supervised method, it selects mainly spatial filters that are important for the classification, and we only remove the few ones that would cause over-fitting.

Supposing that the set D of selected filters contains $d < s$ components (s total number of sources in $\mathbf{S}_j$), the new feature vector $\mathbf{v}_j^{sel}$ is obtained by concatenating the time-frequency features of the selected filters $\mathbf{c}_{i \in D}$:

$$\mathbf{v}_j^{sel} = \begin{bmatrix} \mathbf{c}_1 \\ \mathbf{c}_i \\ \vdots \\ \mathbf{c}_d \end{bmatrix}, \mathbf{c}_{i \in D} = \begin{bmatrix} c_{11}, \dots, c_{f1}, c_{12}, \dots, c_{f2}, \dots, c_{1t}, \dots, c_{ft} \end{bmatrix}^{\top} \tag{5}$$

In the equations above, $\mathbf{v}_j^{sel}$ represents the feature vector associated with the selected spatial filters of the j-th trial, $\mathbf{c}_{i \in D}$ the time-frequency coefficient vector of the i-th source belonging to the set of selected filters D, $j = 1 \dots n$ where n is the number of training trials, $i = 1 \dots d$ where d is the cardinality of D, t is the number of time samples and f is the number of frequency bins. Therefore, the j-th feature vector $\mathbf{v}_j^{sel}$ is composed by $l = d \times f \times t$ elements. Moreover, the spatial filter unmixing matrix takes the following form $\mathbf{W}^{sel} \in \mathbb{R}^{d \times c}$, where c is the number of channels and d the number of selected spatial filters. To note that the SLR-based spatial filter selection is performed *only on the training set*.

2.2.5. Dimensionality reduction (PCA and LDA)

Even though the spatial filter selection method reduces the number of sources, the dimensionality of the concatenated time-frequency feature vector is in the order of thousands elements. Moreover, *the time-frequency features are somewhat redundant, because the values of adjacent points in the spectrogram are highly correlated*. Therefore, it is important to perform dimensionality reduction. For this purpose, Principal Component Analysis (PCA) is employed in the *Unsupervised feature extraction*-based decoder, while Linear Discriminant Analysis (LDA) in the *Supervised feature extraction*-based one.

PCA and LDA are, respectively, the most popular unsupervised and supervised dimensionality reduction methods in literature (Wang and Paliwal, 2003) and they both reduce the features dimension by projecting the original feature vector into a new feature space through a linear transformation matrix. Nonetheless, they optimize the transformation matrix with different intentions: PCA optimizes the transformation matrix by finding the largest variations in the original unlabeled feature space, while LDA pursues the largest ratio of between-class variation and within-class variation when projecting the original labeled features to a subspace (Wang and Paliwal, 2003). In this study PCA is implemented by Singular Value Decomposition (SVD), while LDA is executed by means of the algorithm proposed by Cai et al. (2008). To note that prior to performing PCA or LDA the mean of the training set is subtracted, and that in the case of PCA the mean of the training set is also subtracted from the test set.

The dimensionality reduction step yields a linear transformation matrix $\mathbf{A} \in \mathbb{R}^{p \times l}$ that projects the original feature vector $\mathbf{v}_j^{sel} \in \mathbb{R}^l$ to the reduced vector $\mathbf{v}_j^{red} \in \mathbb{R}^p$, where l is the length of the original feature vector and p the number of projections (reduced features, $p < l$). When dimensionality reduction is performed by PCA, the number of retained principal components (p) is set so as to achieve 90% of variance (Jolliffe, 2002), bringing the length of the feature vector from the order of thousands to the order of hundreds elements. On the other hand, when using LDA, the number of projections $p = 2$ since the number of non-zero eigenvalues is bounded by $g - 1$, where g is the number of classes (Cai et al., 2008). Once again, it is important to note that, with both PCA and LDA, the projection matrix A is computed only using the training set.

2.2.6. Classification

Once the feature vectors of all the trials in the training dataset ($\mathbf{v}_j^{red}$) are obtained, it is possible to compute the ones of the test dataset ($\hat{\mathbf{v}}_k^{red}$), by the following steps:

1. to generate the source signal matrix of the k-th trial in the test set ($\mathbf{S}_k^{test}$), multiply the preprocessed k-th single-trial EEG of

the *test dataset* ($k = 1 \ldots m$, where m is the number of test trials) by the spatial filter unmixing matrix $\mathbf{W}^{sel}$, obtained on the training set by *spatial filter selection* (section 2.2.4);
2. to generate the test feature vectors $\hat{\mathbf{v}}_k^{sel}$, compute the time-frequency matrix for each trial k and source in $\mathbf{S}_k^{test}$;
3. to generate the reduced feature vector $\hat{\mathbf{v}}_k^{red}$, multiply $\hat{\mathbf{v}}_k^{sel}$ by the projection matrix $\mathbf{A}$, obtained on the training set by *dimensionality reduction* (section 2.2.5).

The reduced feature vectors of the training set $\mathbf{v}_j^{red}$ and the one of the test set $\hat{\mathbf{v}}_k^{red}$ are used, with the respective labels, to train and evaluate a SLR classifier (introduced in section 2.2.4). To note that the SLR classifier used to decode the finger tapping task is trained and tested on features and datasets that differ from to the ones used to select spatial filters in section 2.2.4.

2.3. PERFORMANCE ASSESSMENT

The main objective of this study is to verify that the decoding performance of the upper limb tasks is not affected by the lower limb periodic perturbation. To do so, we compare the performance of the finger tapping decoding under the two conditions *NoPert* and *Pert*. In other words, from a factorial point of view, the goal is to assess the main effect of leg perturbation on the decoding of finger tapping. Given the fact that the leg perturbation might influence each subject's performance in a different way, an intra-subject analysis is carried out.

Individually for each subject, the datasets of 9 out of 10 sessions are used as "training set," to train the decoder described in section 2.2, and the dataset of the remaining session is used as "test set." This procedure is repeated 10 times so as to use each session as test set once and only once , where a repetition is named "fold" and the whole operation is called 10-fold cross validation. Therefore, 5 out of 10 folds are characterized by a test set which belongs to the *NoPert* condition and the remaining 5 folds are characterized by a test set belonging to the *Pert* condition. In this way, the decoding performance of the test sets belonging to the *NoPert* condition is computed separately from the one of the *Pert* condition, in order to carry out a statistical comparison of the two.

Specifically, performance is evaluated by Cohen's Kappa (Cohen, 1960), also employed in the BCI Competitions (Tangermann et al., 2012):

$$k = \frac{Pr(a) - Pr(e)}{1 - Pr(e)} \tag{6}$$

where $Pr(a)$ is the proportion of observed agreements, and $Pr(e)$ is the proportion of agreements expected by chance. The range of possible values of Kappa is between -1 and 1, though it usually falls between 0 and 1. Perfect agreement between the true target labels and the predicted ones is represented by $k = 1$. Agreement no better than that expected by chance is indicated by $k = 0$. A negative kappa would indicate agreement worse than that expected by chance (Sim and Wright, 2005). An advantage of using the Kappa coefficient is the possibility to perform a Z-test to compare two classifications and determine if the accuracy level between the two is significantly different (Congalton et al., 1983, see Appendix for details).

3. RESULTS

3.1. DECODING PERFORMANCE

Table 1 represent the results obtained, respectively, by the *Unsupervised feature extraction*-based decoder and by the *Supervised feature extraction*-based one. The table contain the Kappa values for each subject, relative to the conditions *NoPert* and *Pert*, and the associated intra-subject comparison (Z-score). We observe that all the Kappa scores are above chance level ($K = 0$). Importantly, the comparisons between *NoPert* and *Pert* has always a Z-score <1.96, therefore, for every subject, the two conditions are not significantly different from a classification performance point of view.

3.2. FEATURE VISUALIZATION

In order to interpret the results, the features used in the decoding process are visualized separately for each subject. Specifically, we focus on the features of the *Unsupervised feature extraction*-based decoder, since ICA yields unmixing matrices ($\mathbf{W}$) that are similar along cross-validation folds. This means that ICA components can be clustered along folds, and for each cluster, topographies and time-frequency patterns can be averaged. Nonetheless, CSP patterns differ along cross-validation folds, given the supervised nature of CSP and the fact that the training set varies from fold to fold. Therefore, it is not possible to cluster and average the CSP features. For these reasons we decided to focus on the feature visualization of the *Unsupervised feature extraction*-method. Nonetheless, we report that, for each fold and subject, CSP filters and the associated ERD/ERS activations are compatible with the ones related to the *Unsupervised feature extraction* method.

3.2.1. Topographic maps

The spatial filters extracted after ICA and SLR spatial filter selection ($\mathbf{W}^{sel}$) are visualized in this section. In order to obtain a compact representation, they are clustered across folds, separately for each subject. Specifically, the rows of $\mathbf{W}^{sel}$ are clustered by means of hierarchical clustering, in such a way that only rows with a small Euclidean distance are grouped together. Moreover,

Table 1 | Intra-subject comparison of Kappa associated with *NoPert* and *Pert*, and the relative *Z*-score.

a. Unsupervised feature extraction				b. Supervised feature extraction			
Sbj	**K(NoPert)**	**K(Pert)**	**Z-score**	**Sbj**	**K(NoPert)**	**K(Pert)**	**Z-score**
S1	0.95	0.81	1.47	S1	0.97	0.85	1.23
S2	0.85	0.75	1.24	S2	0.79	0.67	1.47
S3	0.59	0.58	0.02	S3	0.58	0.48	1.16
S4	0.79	0.64	1.75	S4	0.63	0.67	0.42
S5	0.68	0.75	0.90	S5	0.76	0.76	0.02

Two conditions are significantly different ($\alpha = 0.05$) if Z-score is > 1.96. The table shows the results of the Unsupervised and Supervised feature extraction-based decoders. To note that chance level is $K = 0$.

for each cluster C we compute the selection ratio, representing how frequently a member of the cluster is selected along cross-validation folds: $r = |C|/k$, where $|C|$ represents the cardinality of C and k is the total number of cross-validation folds. In **Figure 5** the topographic maps of the average of each cluster and the respective selection ratio r are displayed separately for every subject. The figure shows that spatial filters with a selection ratio $r \geq 50\%$ represent, for every subject, either the activation of the left or right hemisphere. Moreover, it is important to note that the selected spatial filters cover areas of the EEG electrode space that are different from subject to subject.

3.2.2. Time-frequency features

In order to visualize the time-frequency features of the *Unsupervised feature extraction*-based decoder, the event-related spectral perturbation (ERSP, Grandchamp and Delorme, 2011) is employed:

$$ERSP(f,t) = 10log_{10}\left(\frac{ERS(f,t)}{\mu_B(f)}\right),$$

$$ERS(f,t) = \frac{1}{n}\sum_{k=1}^{n}\left|F_k(f,t)\right|^2 \quad (7)$$

where *ERS* is the event related spectrum and is obtained by averaging across trials the time-frequency power estimate computed by wavelet (F), $\mu_B(f)$ is the mean spectral estimate at baseline, n is the total number of trials, $F_k(f,t)$ is the spectral estimate at frequency f and time point t for trial k.

The ERSP is computed separately for the test datasets of *NoPert* and *Pert*, for each subject and class (Idle, Left trapping, Right tapping). Thus, **Figure 6** is organized so that it is possible to compare the spectral perturbation associated with the two conditions (*NoPert*, *Pert*), while appreciating the features that characterize each class, individually for each subject. To note that only the ERSP of the spatial filters with a selection ratio $r = 100\%$, discussed in the previous section, are visualized. The ERSP visualization does not highlight differences in the ERD/ERS pattern between *NoPert* and *Pert* conditions. Moreover, we observe that the spectral perturbations are actually informative for the classification. In particular, the ERSP of the *Idle* class does not contain ERD/ERS, while the remaining two classes are characterized by strong spectral perturbations. Furthermore, we note subject-specific differences in the ERSP of the *Left* and *Right* classes as well. Subject 1 (S1) is characterized by a stronger beta ERS of the right hemisphere when left tapping is performed and by beta ERS of the left hemisphere in case of right tapping (contralateral activation); S2 displays a similar class-specific contralateral mu and beta ERS; for S3 we observe a stronger mu ERD of the left hemisphere when left tapping is executed (ipsilateral activation), compared to the mu ERD of the right hemisphere associated with the right tapping; for S4 we observe a stronger contralateral mu ERD and, lastly, for S5 we note a stronger contralateral beta ERS.

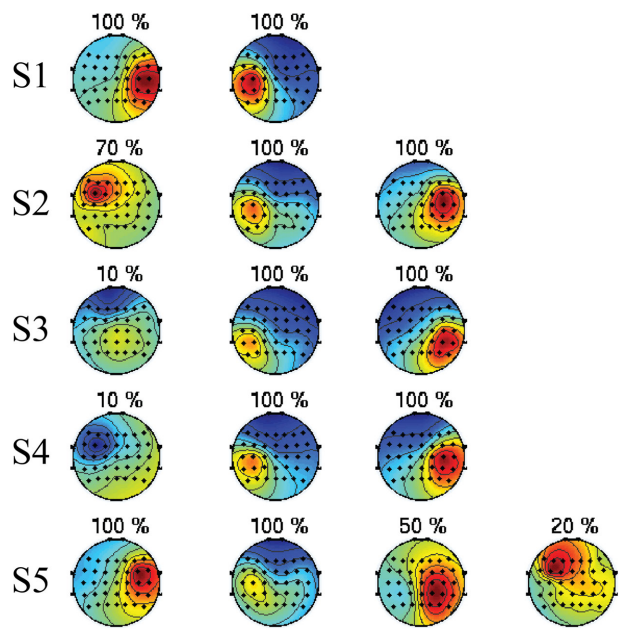

FIGURE 5 | Topographies of the automatically selected ICA components. Each row represents one subject, and each topographic map represents a cluster of ICA components obtained by hierarchical clustering along cross-validation folds. On top of each map there is the selection ratio r representing how frequently a member of the cluster is selected along folds. Spatial filters with a selection ratio $r \geq 50\%$ represent, for every subject, either the activation of the left or right hemisphere. Moreover, it is important to note that the selected spatial filters cover areas of the EEG electrode space that are different from subject to subject.

4. DISCUSSION

The aim of this study is to investigate the main effect of the leg afferent input, induced by a lower limb assistive robot, on the decoding performance of the sensorimotor hand area ERD/ERS. To do so, we devised an experiment to compare the finger tapping decoding performance under the conditions of leg perturbation (*Pert*) and no perturbation (*NoPert*). From the experimental results we find that the classification performance is always above chance ($K > 0$) and we do not observe intra-subject significant difference (Z-score <1.96, p-value >0.05) between the conditions *NoPert* and *Pert*.

To note that, in each cross-validation fold, a decoder is trained on both conditions. This is motivated by the fact that it is important to evaluate the performance on a common model. Training and testing a decoder separately for *NoPert* and *Pert* wouldn't allow for a sound comparison, since the underlying models would be different. Moreover, the datasets representing the two conditions might differ due to non-stationarities that are not related to the leg perturbations (e.g., electrode impedance variation, Wojcikiewicz et al., 2011). Training across both conditions should minimize the effect of those non-stationarities, while testing separately between *NoPert* and *Pert* should highlight the actual differences caused by leg perturbations.

In order to corroborate the interpretation of the quantitative analysis carried out so far, we visualize only the features of the *Unsupervised feature extraction*-based decoder in **Figures 5**, **6**. This is motivated by the fact that spatial filters obtained by ICA are more stable along cross-validation folds. Therefore, they can be clustered and the ERSP of each cluster can be computed in a

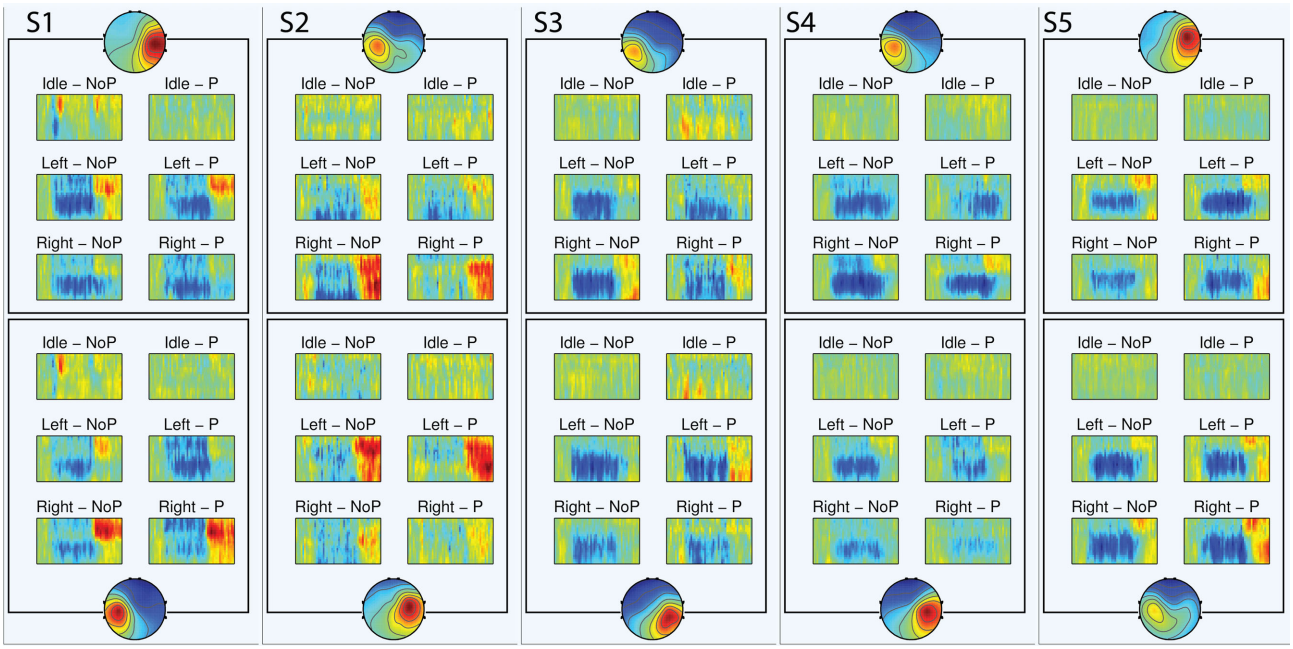

FIGURE 6 | ERSP visualization. In each ERSP image, the abscissa represents the time (−0.3 to +4.3 s), while the ordinate represents the frequency (from 8 to 30 Hz), the red color portrays power increase with respect to the baseline (dB), while the blue color power decrease (dB). For each subject, only the ERSP of the spatial filters with a selection ratio $r = 100\%$ are visualized. The figure is organized so that it is possible to compare the ERSP of *NoPert* (NoP) and *Pert* (P), while appreciating the features that characterize each class. To note that the ERD/ERS patterns are subjects-specific and informative for the classification. Moreover this representation do not highlight differences between the two conditions *NoPert* and *Pert*, confirming the quantitative results of the *Z*-test.

meaningful way. From this analysis we confirm that the spatial patterns with high selection ratio ($r \geq 50\%$) are compatible with the spatial mapping of the sensorimotor hand area ERD/ERS suggested by (Pfurtscheller and Lopes da Silva, 1999). Moreover, the fact that spatial topographies are different from subject to subject is in line with the thesis of Blankertz et al. (2008b), asserting that subject-specific spatial filters are important to enhance the decoding performance. Not only spatial patterns, but also the ERD/ERS patterns are highly subject-specific (Pfurtscheller and Neuper, 2006): compatibly with Pfurtscheller and Lopes da Silva (1999), for some subjects the discriminability between the three classes is to be inputed to strong post movement mu and/or beta ERS (S1, S2, and S5), while for other subjects we observe a predominance of mu ERD (S3 and S4). Importantly, the ERSP visualization does not highlight differences in the ERD/ERS pattern between *NoPert* and *Pert* conditions, which confirms the quantitative results of the *Z*-test.

One possible explanation to the fact that the ERD/ERS patterns associated with upper limb movements are not significantly changed by lower limb afferent input is that periodic lower limb passive movements do not produce EEG perturbation that are as significant as the ones of active movements. This is in line with other studies (Wagner et al., 2012; Jain et al., 2013) reporting a significant mu and beta desynchronization, at the primary motor cortex, associated with active periodic movements as opposed to passive periodic movements of the lower limbs. Nonetheless, in Müller-Putz et al. (2007) it is observed that for *non-periodic* passive and active movements, the beta ERD/ERS have similar levels of significance at the central sensorimotor and surrounding areas (electrodes Cz, C2, and Fcz). Therefore, it is possible that in the current study, being the leg perturbations periodic, they did not elicit ERD/ERS significant enough to interfere with the EEG perturbations associated with the upper limb task.

This paper focuses on one of the many aspects regarding the implementation of a brain-controlled assistive robot. Especially, it is important to highlight that, even though EEG topographies and ERD/ERS patterns are shared between actual movements and motor imagery (Pfurtscheller and Lopes da Silva, 1999; McFarland et al., 2000), the latter is characterized by a significantly smaller ERD/ERS magnitude (McFarland et al., 2000; Solis-Escalante et al., 2010). This raises the question, whether the EEG decoding of a motor imagery task might be affected by the leg afferent input. This issue will be investigated in future studies. Nonetheless, we need to stress the necessity of the current study, which establishes a "ground truth" understanding of the possible interference between the ERD/ERS of the sensorimotor area and the lower limb afferent input. In this context, the term "ground truth" is related to the fact that actual movements are observable by the experiment operator, or mechanically measurable, therefore we are certain that a motor command is elicited for every cue presented to the subject. On the other hand, motor imagery cannot be visually observed by the experiment operator, therefore, in case of misclassification it is impossible to say whether the subject

failed to elicit motor imagery ERD/ERS or the leg perturbation actually inhibited it.

Moreover, it is important to note that finger movements are characterized by a significantly smaller EEG power perturbation as compared to hand movements (Pfurtscheller et al., 1998). This means that the finger tapping task is a good compromise in order to keep the spectral perturbation magnitude as close as possible to the one of motor imagery, while preserving the necessary property of mechanical measurability, or observability by the experiment operator.

Another issue, that must be addressed in future studies, regards the influence of a multi-DoF assistive robot on the ERD/ERS decoding. Especially, it remains an open question how the afferent input, induced by the passive movement of the whole lower limbs, affects the EEG decoding. An fMRI study by Newton et al. (2008) found a substantial overlap of the motor representations of ankle dorsiflexion, ankle plantarflexion and knee extension. This supports the notion that the afferent input induced by a multi-DoF robot should not differ significantly from the one induced by OneDOF robot. Nonetheless, further investigations are required to clarify this point.

Additionally, it is of interest whether reflex responses of the major leg muscles could influence the EEG patterns. For this purpose, in future experiments the electromyographic (EMG) signal will be recorded from the lower limbs. In this way, it would be possible to detect the onsets of possible reflex muscle activations at the leg, and further analyze the EEG signal based on this information.

Moreover, another concern regarding the application of our approach to a multi-DoF assistive robot is represented by the mechanical artifacts affecting the EEG signal. However, other researchers have shown that artifacts during walking (Gwin et al., 2010) and robotic-assisted treadmill walking (Wagner et al., 2012) can be significantly reduced by means of ICA, encouraging further studies with the multi-DoF assistive robot.

In conclusion, this study does not find a main effect of the leg afferent input, induced by a lower limb assistive robot, on the decoding performance of the sensorimotor area ERD/ERS. This establishes a solid ground for future experiments and studies aimed at controlling a multi-DoF assistive robot by motor imagery. A possible future application of such a Brain Robot Interface (BRI) system would be to modulate, by left or right motor imagery, the walking speed of an exoskeleton robot once it started moving.

ACKNOWLEDGMENTS

This research reflects the results of the "Brain Machine Interface Development" carried out under the auspeces of the Strategic Research Program for Brain Sciences by the Ministry of Education, Culture, Sports, Science, and Technology of Japan. Part of this research was supported by MIC-SCOPE and a contract with the Ministry of Internal Affairs and Communications entitled "Novel and innovative R&D making use of brain structures." This research was also partially supported by MEXT KAKENHI grant Number 23120004, JSPS KAKENHI Grant Number 24700203 and Strategic International Cooperative Program, Japan Science and Technology Agency (JST) and by JSPS and MIZS: Japan–Slovenia research Cooperative Program.

REFERENCES

Babiloni, C., Carducci, F., Cincotti, F., Rossini, P. M., Neuper, C., Pfurtscheller, G., et al. (1999). Human movement-related potentials vs desynchronization of EEG alpha rhythm: a high-resolution EEG study. *Neuroimage* 10, 658–665. doi: 10.1006/nimg.1999.0504

Babiloni, F., Cichocki, A., and Gao, S. (2007). Brain-computer interfaces: towards practical implementations and potential applications. *Comput. Intell. Neurosci.* 2007, 62637. doi: 10.1155/2007/62637

Blankertz, B., Losch, F., Krauledat, M., Dornhege, G., Curio, G., and Muller, K.-R. (2008a). The berlin brain–computer interface: accurate performance from first-session in BCI-naive subjects. *IEEE Trans. Biomed. Eng.* 55, 2452–2462. doi: 10.1109/TBME.2008.923152

Blankertz, B., Tomioka, R., Lemm, S., Kawanabe, M., and Muller, K.-R. (2008b). Optimizing spatial filters for robust EEG single-trial analysis. *IEEE Signal Process. Mag.* 25, 41–56. doi: 10.1109/MSP.2008.4408441

Cai, D., He, X., and Han, J. (2008). SRDA: an efficient algorithm for large-scale discriminant analysis. *IEEE Trans. Knowl. Data Eng.* 20, 1–12. doi: 10.1109/TKDE.2007.190669

Cassim, F., Monaca, C., Szurhaj, W., Bourriez, J. L., Defebvre, L., Derambure, P., et al. (2001). Does post-movement beta synchronization reflect an idling motor cortex? *Neuroreport* 12, 3859–3863. doi: 10.1097/00001756-200112040-00051

Cohen, J. (1960). A coefficient of agreement for nominal scales. *Educ. Psychol. Measur.* 20, 37–46. doi: 10.1177/001316446002000104

Congalton, R. G., Oderwald, R. G., and Mead, R. A. (1983). Assessing landsat classification accuracy using discrete multivariate analysis statistical techniques. *Photogramme. Eng. Remote Sens.* 49, 1671–1678.

Daly, J. J., and Wolpaw, J. R. (2008). Brain-computer interfaces in neurological rehabilitation. *Lancet Neurol.* 7, 1032–1043. doi: 10.1016/S1474-4422(08)70223-0

Daubechies, I. (1990). The wavelet transform, time-frequency localization and signal analysis. *IEEE Trans. Inform. Theor.* 36, 961–1005. doi: 10.1109/18.57199

Delorme, A., and Makeig, S. (2004). Eeglab: an open source toolbox for analysis of single-trial EEG dynamics including independent component analysis. *J. Neurosci. Methods* 134, 9–21. doi: 10.1016/j.jneumeth.2003.10.009

Dornhege, G., Blankertz, B., Curio, G., and Muller, K. (2004). Boosting bit rates in noninvasive EEG single-trial classifications by feature combination and multiclass paradigms. *IEEE Trans. Biomed. Eng.* 51, 993–1002. doi: 10.1109/TBME.2004.827088

Grandchamp, R., and Delorme, A. (2011). Single-trial normalization for event-related spectral decomposition reduces sensitivity to noisy trials. *Front. Psychol.* 2:236–236. doi: 10.3389/fpsyg.2011.00236

Guger, C., Ramoser, H., and Pfurtscheller, G. (2000). Real-time EEG analysis with subject-specific spatial patterns for a brain-computer interface (BCI). *IEEE Trans. Rehabil. Eng.* 8, 447–456. doi: 10.1109/86.895947

Gwin, J. T., Gramann, K., Makeig, S., and Ferris, D. P. (2010). Removal of movement artifact from high-density EEG recorded during walking and running. *J. Neurophysiol.* 103, 3526–3534. doi: 10.1152/jn.00105.2010

Huang, D., Qian, K., Fei, D.-Y., Jia, W., Chen, X., and Bai, O. (2012). Electroencephalography (EEG)-based brain-computer interface (BCI): a 2-d virtual wheelchair control based on event-related desynchronization/synchronization and state control. *IEEE Trans. Neural Syst. Rehabil. Eng.* 20, 379–388. doi: 10.1109/TNSRE.2012.2190299

Hyvärinen, A., and Oja, E. (2000). Independent component analysis: algorithms and applications. *Neural Netw.* 13, 411–430.

Jain, S., Gourab, K., Schindler-Ivens, S., and Schmit, B. D. (2013). EEG during pedaling: evidence for cortical control of locomotor tasks. *Clin. Neurophysiol.* 124, 379–390. doi: 10.1016/j.clinph.2012.08.021

Jolliffe, I. T. (2002). *Principal Component Analysis, 2nd Edn*. New York: Springer.

Makeig, S., Debener, S., Onton, J., and Delorme, A. (2004). Mining event-related brain dynamics. *Trends Cogn. Sci.* 8, 204–210. doi: 10.1016/j.tics.2004.03.008

McFarland, D. J., Miner, L. A., Vaughan, T. M., and Wolpaw, J. R. (2000). Mu and beta rhythm topographies during motor imagery and actual movements. *Brain Topogr.* 12, 177–186. doi: 10.1023/A:1023437823106

Müller, G. R., Neuper, C., Rupp, R., Keinrath, C., Gerner, H. J., and Pfurtscheller, G. (2003). Event-related beta EEG changes during wrist movements induced by

functional electrical stimulation of forearm muscles in man. *Neurosci. Lett.* 340, 143–147. doi: 10.1016/S0304-3940(03)00019-3

Müller-Putz, G. R., Scherer, R., Pfurtscheller, G., Neuper, C., and Rupp, R. (2009). Non-invasive control of neuroprostheses for the upper extremity: temporal coding of brain patterns. *Conf. Proc. IEEE Eng. Med. Biol. Soc.* 2009, 3353–3356. doi: 10.1109/IEMBS.2009.5333185

Müller-Putz, G. R., Scherer, R., Pfurtscheller, G., and Rupp, R. (2005). EEG-based neuroprosthesis control: a step towards clinical practice. *Neurosci. Lett.* 382, 169–174. doi: 10.1016/j.neulet.2005.03.021

Müller-Putz, G. R., Scherer, R., Pfurtscheller, G., and Rupp, R. (2006). Brain-computer interfaces for control of neuroprostheses: from synchronous to asynchronous mode of operation. *Biomed. Tech. (Berl)* 51, 57–63. doi: 10.1515/BMT.2006.011

Müller-Putz, G. R., Zimmermann, D., Graimann, B., Nestinger, K., Korisek, G., and Pfurtscheller, G. (2007). Event-related beta EEG-changes during passive and attempted foot movements in paraplegic patients. *Brain Res.* 1137, 84–91. doi: 10.1016/j.brainres.2006.12.052

Mussa-Ivaldi, S. (2000). Neural engineering: real brains for real robots. *Nature* 408, 305–306. doi: 10.1038/35042668

Newton, J. M., Dong, Y., Hidler, J., Plummer-D'Amato, P., Marehbian, J., Albistegui-Dubois, R. M., et al. (2008). Reliable assessment of lower limb motor representations with fMRI: use of a novel MR compatible device for real-time monitoring of ankle, knee and hip torques. *Neuroimage* 43, 136–146. doi: 10.1016/j.neuroimage.2008.07.001

Noda, T., Sugimoto, N., Furukawa, J., Sato, M., Hyon, S., and Morimoto, J. (2012). "Brain-controlled exoskeleton robot for BMI rehabilitation," in *Proceedings of IEEE-RAS International Conference on Humanoid Robots* (Osaka). doi: 10.1109/HUMANOIDS.2012.6651494

Pfurtscheller, G., Guger, C., Müller, G., Krausz, G., and Neuper, C. (2000a). Brain oscillations control hand orthosis in a tetraplegic. *Neurosci. Lett.* 292, 211–214. doi: 10.1016/S0304-3940(00)01471-3

Pfurtscheller, G., and Lopes da Silva, F. H. (1999). Event-related EEG/MEG synchronization and desynchronization: basic principles. *Clin. Neurophysiol.* 110, 1842–1857. doi: 10.1016/S1388-2457(99)00141-8

Pfurtscheller, G., and Neuper, C. (1997). Motor imagery activates primary sensorimotor area in humans. *Neurosci. Lett.* 239, 65–68. doi: 10.1016/S0304-3940(97)00889-6

Pfurtscheller, G., and Neuper, C. (2006). Future prospects of ERD/ERS in the context of brain-computer interface (BCI) developments. *Prog. Brain Res.* 159, 433–437. doi: 10.1016/S0079-6123(06)59028-4

Pfurtscheller, G., Neuper, C., Guger, C., Harkam, W., Ramoser, H., Schlogl, A., et al. (2000b). Current trends in Graz brain-computer interface (BCI) research. *IEEE Trans. Rehabil. Eng.* 8, 216–219. doi: 10.1109/86.847821

Pfurtscheller, G., and Solis-Escalante, T. (2008). Could the beta rebound in the EEG be suitable to realize a brain switch? *Clin. Neurophysiol.* 120, 24–29. doi: 10.1016/j.clinph.2008.09.027

Pfurtscheller, G., Zalaudek, K., and Neuper, C. (1998). Event-related beta synchronization after wrist, finger and thumb movement. *Electroencephalogr. Clin. Neurophysiol.* 109, 154–160. doi: 10.1016/S0924-980X(97)00070-2

Ramoser, H., M§ller-Gerking, J., and Pfurtscheller, G. (1998). Optimal spatial filtering of single trial EEG during imagined hand movement. *IEEE Trans. Rehabil. Eng* 8, 441–446. doi: 10.1109/86.895946

Sim, J., and Wright, C. C. (2005). The kappa statistic in reliability studies: use, interpretation, and sample size requirements. *Phys. Ther.* 85, 257–268.

Solis-Escalante, T., Müller-Putz, G., Brunner, C., Kaiser, V., and Pfurtscheller, G. (2010). Analysis of sensorimotor rhythms for the implementation of a brain switch for healthy subjects. *Biomed. Signal Process. Control* 5, 15–20. doi: 10.1016/j.bspc.2009.09.002

Tangermann, M., Müller, K.-R., Aertsen, A., Birbaumer, N., Braun, C., Brunner, C., et al. (2012). Review of the BCI competition IV. *Front. Neurosci.* 6:55. doi: 10.3389/fnins.2012.00055

Tsui, C. S. L., Gan, J. Q., and Hu, H. (2011). A self-paced motor imagery based brain-computer interface for robotic wheelchair control. *Clin. EEG Neurosci.* 42, 225–229. doi: 10.1177/155005941104200407

Wagner, J., Solis-Escalante, T., Grieshofer, P., Neuper, C., Müller-Putz, G., and Scherer, R. (2012). Level of participation in robotic-assisted treadmill walking modulates midline sensorimotor EEG rhythms in able-bodied subjects. *Neuroimage* 63, 1203–1211. doi: 10.1016/j.neuroimage.2012.08.019

Wang, X., and Paliwal, K. K. (2003). Feature extraction and dimensionality reduction algorithms and their applications in vowel recognition. *Pattern Recogn.* 36, 2429–2439. doi: 10.1016/S0031-3203(03)00044-X

Wang, Y., Hong, B., Gao, X., and Gao, S. (2007). "Implementation of a brain-computer interface based on three states of motor imagery," in *Engineering in Medicine and Biology Society, 2007. EMBS 2007. 29th Annual International Conference of the IEEE* (IEEE), 5059–5062.

Wojcikiewicz, W., Vidaurre, C., and Kawanabe, M. (2011). "Stationary common spatial patterns: towards robust classification of non-stationary EEG signals," in *IEEE International Conference on Acoustics, Speech and Signal Processing (ICASSP), 2011* (Prague), 577–580. doi: 10.1109/ICASSP.2011.5946469

Wolpaw, J. R., Birbaumer, N., McFarland, D. J., Pfurtscheller, G., and Vaughan, T. M. (2002). Brain-computer interfaces for communication and control. *Clin. Neurophysiol.* 113, 767–791. doi: 10.1016/S1388-2457(02)00057-3

Wolpaw, J. R., McFarland, D. J., Vaughan, T. M., and Schalk, G. (2003). The wadsworth center brain-computer interface (BCI) research and development program. *IEEE Trans. Neural Syst. Rehabil. Eng.* 11, 204–207. doi: 10.1109/TNSRE.2003.814442

Yamashita, O., Sato, M. A., Yoshioka, T., Tong, F., and Kamitani, Y. (2008). Sparse estimation automatically selects voxels relevant for the decoding of fMRI activity patterns. *Neuroimage* 42, 1414–1429. doi: 10.1016/j.neuroimage.2008.05.050

Zhao, Q. B., Zhang, L. Q., and Cichocki, A. (2009). EEG-based asynchronous BCI control of a car in 3D virtual reality environments. *Chin. Sci. Bull.* 54, 78–87. doi: 10.1007/s11434-008-0547-3

Conflict of Interest Statement: The authors declare that the research was conducted in the absence of any commercial or financial relationships that could be construed as a potential conflict of interest.

Received: 03 March 2014; accepted: 22 April 2014; published online: 14 May 2014.
Citation: Lisi G, Noda T and Morimoto J (2014) Decoding the ERD/ERS: influence of afferent input induced by a leg assistive robot. Front. Syst. Neurosci. ***8****:85. doi: 10.3389/fnsys.2014.00085*
This article was submitted to the journal Frontiers in Systems Neuroscience.

A. APPENDIX

A.1 *Z*-TEST

Being k_N and k_P the Kappa scores, respectively, of the *NoPert* and *Pert* conditions, the Z-score of their difference can be computed as:

$$z_{NP} = \frac{|k_N - k_P|}{\sqrt{var(k_N) + var(k_P)}} \quad \text{(A1)}$$

where $var(k)$, the variance of k, can be computed according to the original formula in Congalton et al. (1983). Thus, two Kappa values are considered significantly different, with a significance level of p-value <0.05 if their Z-score is bigger than 1.96.

frontiers in
SYSTEMS NEUROSCIENCE

ORIGINAL RESEARCH ARTICLE
published: 18 September 2014
doi: 10.3389/fnsys.2014.00169

Neural rhythmic symphony of human walking observation: *Upside-down* and *Uncoordinated* condition on cortical theta, alpha, beta and gamma oscillations

David Zarka[1], Carlos Cevallos[1], Mathieu Petieau[1], Thomas Hoellinger[1], Bernard Dan[1,2] and Guy Cheron[1,3]*

[1] *Laboratory of Neurophysiology and Movement Biomechanics, Université Libre de Bruxelles, Brussels, Belgium*
[2] *Department of Neurology, Hopital Universitaire des Enfants reine Fabiola, Université Libre de Bruxelles, Bruxelles, Belgium*
[3] *Laboratory of Electrophysiology, Université de Mons-Hainaut, Bruxelles, Belgium*

Edited by:
Mikhail Lebedev, Duke University, USA

Reviewed by:
Daniel P. Ferris, University of Michigan, USA
Lewis A. Wheaton, Georgia Tech, USA
Miguel Escudero, University of Seville, Spain

***Correspondence:**
Guy Cheron, Laboratory of Neurophysiology and Movement Biomechanics, Université Libre de Bruxelles, CP 640, 50 Av. F. Roosevelt, 1050 Brussels, Belgium
e-mail: gcheron@ulb.ac.be

Biological motion observation has been recognized to produce dynamic change in sensorimotor activation according to the observed kinematics. Physical plausibility of the spatial-kinematic relationship of human movement may play a major role in the top-down processing of human motion recognition. Here, we investigated the time course of scalp activation during observation of human gait in order to extract and use it on future integrated brain-computer interface using virtual reality (VR). We analyzed event related potentials (ERP), the event related spectral perturbation (ERSP) and the inter-trial coherence (ITC) from high-density EEG recording during video display onset (−200–600 ms) and the steady state visual evoked potentials (SSVEP) inside the video of human walking 3D-animation in three conditions: *Normal*; *Upside-down* (inverted images); and *Uncoordinated* (pseudo-randomly mixed images). We found that early visual evoked response P120 was decreased in *Upside-down* condition. The N170 and P300b amplitudes were decreased in *Uncoordinated* condition. In *Upside-down* and *Uncoordinated* conditions, we found decreased alpha power and theta phase-locking. As regards gamma oscillation, power was increased during the *Upside-down* animation and decreased during the *Uncoordinated* animation. An SSVEP-like response oscillating at about 10 Hz was also described showing that the oscillating pattern is enhanced 300 ms after the heel strike event only in the *Normal* but not in the *Upside-down* condition. Our results are consistent with most of previous point-light display studies, further supporting possible use of virtual reality for neurofeedback applications.

Keywords: ERP, ERSP, ITC, SSVEP, walking, observation, virtual reality

INTRODUCTION

Neuronal processing of the visual system allows us to perceive objects, movements, colors, contrasts, and to represent the space around us with a very high resolution. In addition to the classical dichotomy between the ventral stream (the "What" pathway) supporting object vision and a dorsal stream (the "Where" pathway), a more recent conception based on clinical evidence (Kravitz et al., 2011) divides the dorsal stream into three sub-pathways projecting on to the premotor (supporting visually-guided actions), the prefrontal and the medial temporal lobes (supporting spatial working memory) both directly and through the posterior cingulate and retrosplenial areas (supporting navigation). This emphasizes the contribution of numerous functionally specialized, hierarchically organized visual areas giving rise to a conscious perception of the different attributes of the visual scene (Zeki et al., 1991; Singer, 1999). The discovery of the phase-locking mechanism at the level of the cortical neurons producing gamma oscillation (Gray et al., 1989) constitutes a strong scientific foundation for the binding by synchrony hypothesis (Singer, 1999) and has also paved the way for non-invasive investigation of the implicated mechanisms by electroencephalography (EEG) and event-related potentials (ERP) (Makeig et al., 2002; Cheron et al., 2007, 2014; Cebolla et al., 2009, 2014). New approaches of signal analysis (Delorme and Makeig, 2004) have permitted to better understand the genesis of the sensory evoked responses including visual motion in VR environment (Gramann et al., 2009; Cheron et al., 2014) and the origin of the movement gating of sensory evoked responses (Cebolla et al., 2009).

The discovery of mirror neurons responding similarly when the monkey performs an action and when it observes the experimenter performing the same action (Rizzolatti et al., 1996) has led to human studies of visual processes involved in recognition (Blake and Shiffrar, 2007; Avanzini et al., 2013; Di Dio et al., 2013), prediction of others' movements (Csibra, 2007; Kilner et al., 2007), and their implication in social cognition (Jacob and Jeannerod, 2005; Schütz-Bosbach and Prinz, 2007; Heyes, 2010; Press et al., 2011). Behavioral, neuroimaging and

neurophysiological data have demonstrated a high sensitivity to reference frame (Pavlova and Sokolov, 2000; Pavlova et al., 2004; McGlothlin et al., 2012), human body form (Downing et al., 2001), kinematics of human movement (Avanzini et al., 2012; McAleer et al., 2014), gender and personal traits (Pollick et al., 2005; Troje et al., 2005; McGlothlin et al., 2012). Several studies demonstrated that shape and motion information are treated separately by ventral and dorsal visual streams, and converge to the posterior portion of superior temporal sulcus (Vaina et al., 2001; Giese and Poggio, 2003; Blake and Shiffrar, 2007). Moreover, the motor theory of perception, based on the fact that movement perception is influenced by the implicit knowledge about the working principles of the motor control system (Viviani and Stucchi, 1992; Rizzolatti and Craighero, 2004), give a critical place to ventral premotor cortex in biological motion perception processes (Saygin et al., 2004).

By extending Darwin's evolutionary perspective about face emotion (Darwin, 1872) to human locomotion, we may advance that the recognition of the human primate by its bipedal locomotion already present in early hominid before stone tools and large brains (Leakey and Walker, 1997) is probably one of the most vital activities of human in a selection retrospective view. Moreover, such human gestures may represent a constitutive element of the emotional body language (De Gelder, 2006, for a review). This whole body movement of *homo sapiens* is characterized by distinctive patterns of smooth, regular, alternated lower and upper limbs movements performed around a relatively fixed and erected posture of the head and trunk segment (Pozzo et al., 1990). Another remarkable element is the heel-strike considered as an acquired character of African and Asian apes linked closely to knuckle walking quadrupedalism (Thorpe et al., 2007; Crompton et al., 2010). These highly recognizable elements would implicate that human mirror neuron systems should be active when watching somebody else walk (Cheng et al., 2005).

Thanks to dynamics analysis of high-density EEG associating event-related potential (ERP), event-related spectral perturbation (ERSP) and inter-trial coherency (ITC), it has become possible to identify electrophysiological mechanisms related to recognition processes (Engel et al., 1997; Singer, 2009). In this context, coherent stimulus representation, including biological motion (Pavlova et al., 2004), are thought to result from binding of widely distributed cell ensembles by synchronizing their high-frequency oscillation activity (Tallon-Baudry and Bertrand, 1999; Singer, 2009). In parallel, other oscillatory processes may be activated following a motor template as suggested for mu rhythm (Ulloa and Pineda, 2007; Arnstein et al., 2011; Braadbaart et al., 2013; Urgen et al., 2013; Frenkel-Toledo et al., 2014). Point-light display of human locomotion has been used to characterized the cortical activity involved in recognition of locomotion either through MEG (Pavlova et al., 2004, 2006) or ERP studies (Hirai et al., 2003, 2005, 2013; Jokisch et al., 2005; Hirai and Hiraki, 2006; Krakowski et al., 2011; Buzzell et al., 2013).

Here, we studied the ERP and dynamics of theta, alpha, beta and gamma oscillations induced by the observation of an animated avatar in a virtual reality (VR). We hypothesized that physical plausibility of the spatial-kinematic of human locomotion plays a major role in different modes of neural processing (bottom-up and top-down) implicated in locomotion recognition: we expect that these processes will be reflected in different contributions of rhythmic power and phase-locked perturbation in different frequency bands and cortical areas. To address this question, we used an animation representing a human mannequin during walking action performed in normal, *Uncoordinated* kinematics and in *Upside-down* views. This will offer the possibility to extract the dynamic signature of human walking observation with respect to the neural activity evoked by the same image content but in an unusual frame of reference (*Upside-down* view) or without respect to normal kinematics (*Uncoordinated* walk) from the EEG signals.

MATERIALS AND METHODS

ARTICIPANTS

Sixteen healthy volunteers took part in this study (ten males, mean age 25.9 years, range 18–35 years). All subjects were right-handed, had *Normal* or corrected-to-*Normal* vision, were naive with respect to the purpose of the experiment, and gave informed consent. The experiment was performed with the approval of the ethics committee of Université Libre de Bruxelles and realized in accordance with the ethical standards of the 1964 Declaration of Helsinki.

STIMULI

Visual stimuli consisted of an animation in the center of the screen representing human walking mannequin (from Cal3D Library) that was presented in three different ways: *Normal* walking (N), *Upside-down* (U), and *Uncoordinated* (J) (**Figure 1**). Each animation was organized in 22 blocks of 10 s duration interspersed by 7–12 s of random periods of gray screen. This allowed us to obtain a repetitive control of the baseline state throughout the whole recording session and facilitated the recording of the averaged responses (see below). For the *Normal* walking condition, each block was initiated by an image representing the heel strike event of the right leg and was ended by the last image preceding the next heels strike of the right leg picture (**Figure 1A**). The animation had a 10 Hz frequency. In the *Upside-down* condition the same successive pictures were merely inverted, keeping the same kinematics sequences. In the *Uncoordinated* condition the first image remained the same as the *Normal* condition while all the others were randomly mixed giving rise to an incoherent *Uncoordinated* movement. The random sequence was conserved for each trial and each subject (**Figure 1B**).

We have calculated the luminosity of each image in the three colors (RGB) by using "imread" MATLab function. This function stores in a matrix the composition in red, green and blue of each pixel of an image. For each frame of the animation, we subtracted this matrix to that of the previous frame. We have then computed the mean of the resulting matrix and called this composition "dynamic contrast." This represents overall change between two successive frames of the composition in luminosity of the same located pixels.

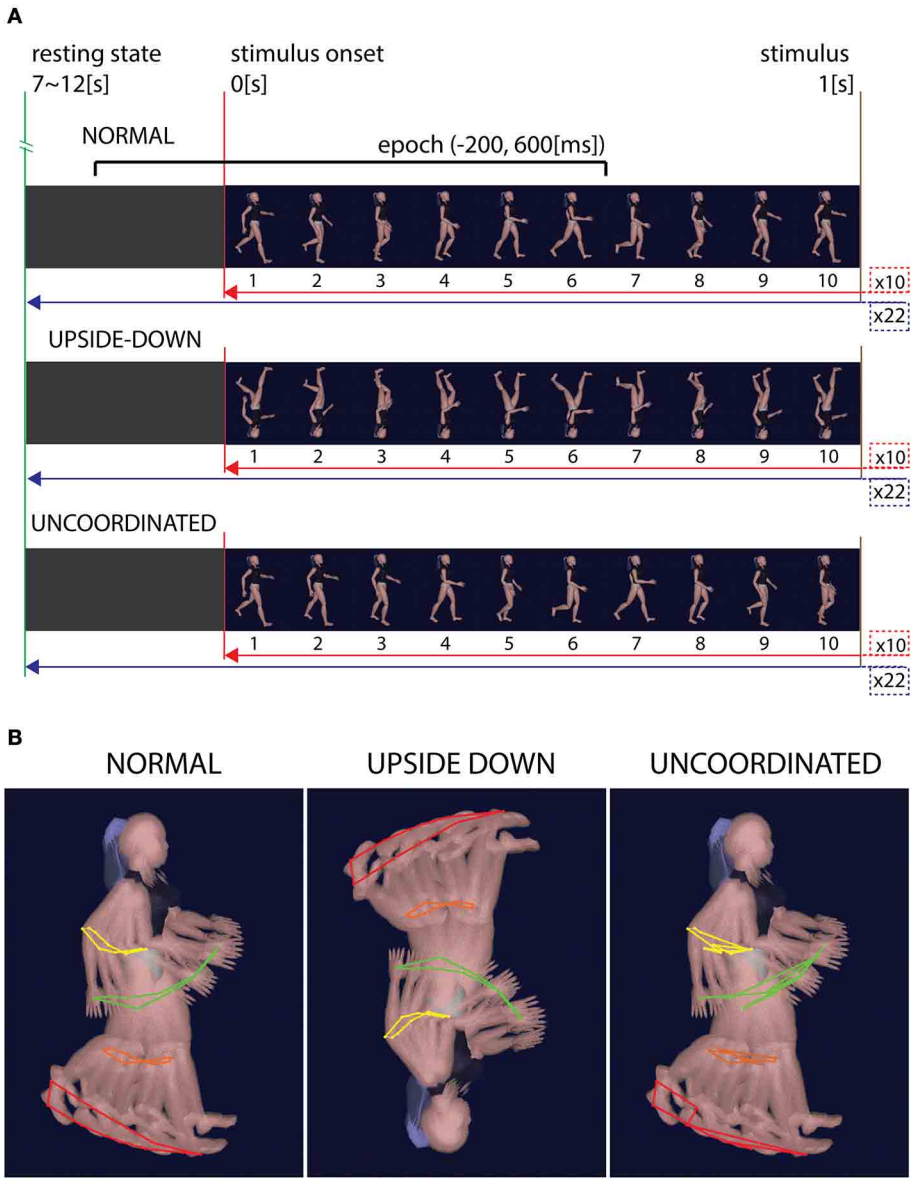

FIGURE 1 | Condition's stimuli. (A) Time representation of the stimuli in each three conditions. *Normal* condition shows ten successive gait cycles of 1 s each. Trials were separated by 7–12 s of gray screen and repeated 22 times. *Upside-down* condition show the same images sequence, rotated to 180° in the image plane. *Uncoordinated* condition show the same first image as the *Normal* condition while all the others images were mixed. **(B)** Kinematics representation of the gait in the three conditions. While *Normal* and *Upside-down* conditions have the same coherent kinematic sequence, *Uncoordinated* condition show an incoherent kinematic sequence.

EXPERIMENTAL SETUP

The recording was realized in a single session. EEG was recorded in 128 channels (ANT system, *The Netherlands*) at a sampling frequency of 2048 Hz and with a resolution of 22 bits (71.5 nV per bit). An active-shield cap using 128 Ag/AgCl sintered ring electrodes and shielded co-axial cables (5–10 electrode system placements) was comfortably adjusted to subject head. All electrodes were referred to left earlobe. Impedance was lowered below 10 kΩ for each electrode and checked before each recording. Displays were presented on a 17″ Dell computer screen. Participants looked straight ahead at the computer screen through a form-fitting facemask and a circular barrel (cylinder). The screen was centered on the line of gaze at a distance of ∼30 cm from the eyes. Viewing through the barrel removed any external visual references. In addition, subjects had earplugs to isolate from external hearing disturbance. For eight subjects, we presented in three successive sessions the *Normal* walking condition, then *Upside-down* walking and then *Uncoordinated* one *(No-Random group)*. For eight other subjects, conditions were presented randomly in three successive sessions (*Random* group). We made a pause between each session in order to limit the effect of fatigue. As the aim of this study was to evaluate the effect of

purposeless perception on the brain rhythms, no particular attentional task was required. However, the state of awareness was continuously checked by online EEG (absence of slow rhythm linked to drowsiness) and EOG, for which we placed electrodes above, below, right and left of the right eye. In particular, we checked that the blink number and configuration remained unchanged throughout the experimental session. We used an in-house script that counts the number of blinks by incrementing an index for each potential higher than 250 μV, and calculates the interval between blinks to provide a view of their configuration over time. We then calculated the number of saccades by EOG derived function. The results show there is no difference between conditions for blink (means by subject for *Normal*: 81 ± 33.3; *Upside-down*: 99.8 ± 27.2; *Uncoordinated*: 120.4 ± 34.6) and saccades (means by subject for *Normal*: 316 ± 137.8; *Upside-down*: 455.4 ± 98.3; *Uncoordinated*: 385.2 ± 136.6).

DATA TREATMENT

Off-line data treatment and analysis was performed by means of EEGLAB software (Delorme and Makeig, 2004; Brunner et al., 2013) and in-house MATLAB-based tools (Cheron et al., 2014). DC offset was removed, then band pass filter 0.1–80 Hz and notch filter around 50 Hz (47.5–52.5 Hz) were applied to attenuate electrical artifacts. Portions of data and defective electrodes (max. 6%) were removed by careful visual inspection. Ocular (blink and saccade) and any other remaining artifacts (muscular, cardiac) were isolated by ICA algorithm decomposition. We used the scalp topography, temporal activity localization and spectra magnitude criterion to identify ICA related to artifact. In case of doubt the rejection occurred only if all experimenters involved in data treatment reached agreement. After ICA rejection, defective electrodes were spherically interpolated.

Two analyses were performed: animation onset analysis and SSVEP analysis. In the animation onset analysis, data were organized in epochs corresponding to intervals [−1000; 3000] ms, centered on animation onset. We rejected epochs according to ±100 μV threshold criterion, and we made a visual review to confirm epoch rejection. In total, we obtained 17 ± 5 epochs per subject ($n = 16$) and per condition ($n = 3$). A study design was used to average data from subjects for each condition. A time window of 1000 ms before stimulus onset was used as baseline.

In SSVEP analysis, data were organized in epochs corresponding to intervals [−200; 600] ms, centered on each heel strike except for the first and the last one. As in preceding analysis, we applied ±100 μV threshold criterion confirmed by a visual review. In total, we obtained 159 ± 16) epochs per subject ($n = 16$) and per condition ($n = 3$). We performed a grand average study including 2065 ± 26 trials for each condition. The interval [−200; 0] ms was used as baseline, and the first and last heel strikes were excluded from the analysis In this case, the SSVEP analysis was independent of the neutral black screen periods allowing to join mixed *Random* and *Non-Random* groups.

A subset of 32 electrodes was explored for each measure analysis: O2, Oz, O1, POz, P8, P4, Pz, P3, P7, CP6, CP2, CP1, CP5, T8, C4, Cz, C3, T7, FC6, FC2, FC1, FC5, F8, F4, Fz, F3, F7, Fp2, Fpz, Fp1. We first checked ERP and ERSP of [−1000; 3000] ms epoch, and then we focused on events related to animation onset, and SSVEP centered on heel strike between −200 and 600 ms. ERP, ERSP, and ITC analysis was performed. Difference between *Random* and *No-Random* groups and between *Normal* and both *Upside-down* and *Uncoordinated* condition were performed by EEGLab non-parametric permutation test ($n = 2000$) at each trial latency of the average ERPs and every time-frequency point for ERSP and ITC.

RESULTS

EVENT-RELATED POTENTIAL

The first noticeable ERP component referenced to the earlobe elicited after the onset of the VR-animation was the P120 component recorded in occipito-parietal electrodes. Analysis revealed a peak reduction in *Upside-down* condition with respect to *Normal* condition over occipito-parietal regions. The next component was the N170 mainly recorded over the occipito-parietal regions (**Figure 2**). We observed a significant decrease in *Uncoordinated* condition over occipital and parieto-lateral regions. This was followed by a large P300 component ending at about 500 ms in occipital regions and 400 ms in frontal regions. In order to simplify the description of condition effect, we subdivided P300 in the two classical P300a and P300b components (**Figure 2**). The P300a component was significantly smaller in the *Upside-down* condition over parietal regions with respect to the *Normal* situation, whereas the P300b component remained the same. On the contrary in the *Uncoordinated* condition, the P300a component was not modified whereas the P300b showed a significant decrease in occipital and parietal regions (**Table 1**). Comparison between *Random* and *No-Random* group revealed no significant difference between their respective conditions except in the P300 amplitude in parietal region which was greater for the *No-Random* group for the 3 conditions.

EVENT-RELATED SPECTRAL PERTURBATION AND INTER-TRIAL COHERENCE

Whatever the observed condition (**Figures 3–5**), the video onset triggered throughout the scalp a theta ERS in the [0; 500] ms interval followed by an alpha ERD initiated at about 200 ms and maintained during all the duration of the video. This alpha ERD was accompanied by a beta ERD which was more pronounced in the *Uncoordinated* condition (**Figure 5**). The *Normal* presentation induced a gamma ERD at about 700 ms and maintained for all the duration of the video in the left sensori-motor region (**Figure 3**, CP5 electrode). This gamma ERD was not present in the two others conditions (**Figures 4**, **5**).

In the [−200;600] ms time-window, the *Normal* condition was characterized by the following observations (**Figures 6–9**): (1) at the latency of the P120, ERSP plots showed an earlier alpha ERS reaching maximal value in the parietal region and extending to the beta band in the parieto-central region. (2) This was sustained by theta activation and phase-locking presenting its maximal value at about 200 ms. (3) ERD in the upper alpha band at about 200 ms in the occipito-parietal regions. (4) ERS clusters in the gamma range (30–70 Hz) in the parieto-occipital and centro-frontal regions.

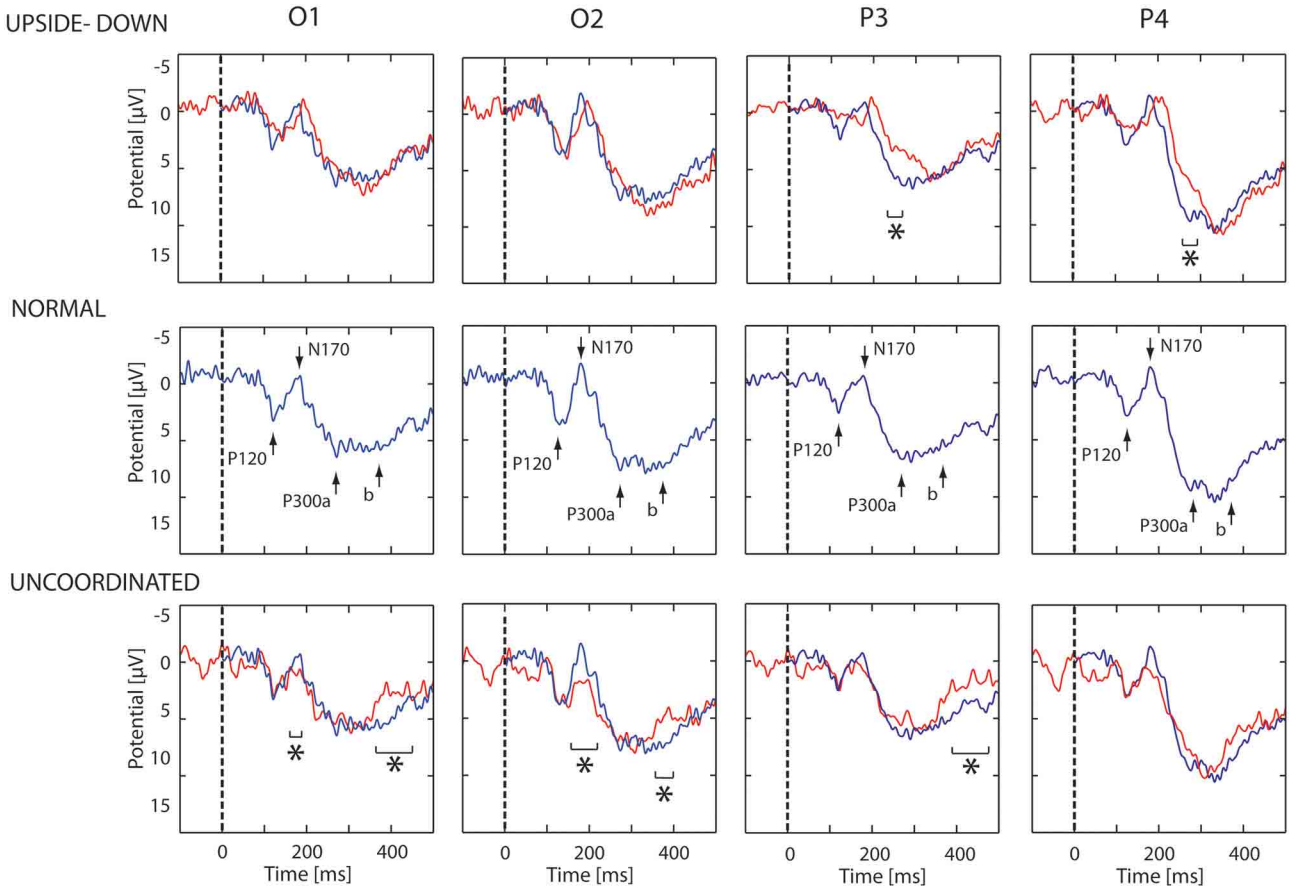

FIGURE 2 | ERP evoked by animation onset in each condition. ERP recorded in O1, O2, P3, and P4 electrodes. In middle part, the ERP evoked by the normal animation onset show three successive potentials: P120, N170, and P300a,b. In upper part, the blue and red lines show respectively the ERP response in the *Normal* and *Upside-down* condition. In lower part, the blue and red lines show respectively the ERP response in the *Normal* and *Uncoordinated* conditions. Significant differences are mark by asterisks ($p < 0.05$).

With respect to the *Normal* condition, in the *Upside-down* condition, three significant changes were noted (**Figures 6–9**): (1) a decrease in alpha-beta power between 100 and 500 ms over occipital to frontal regions, resulting in a lack of ERS in alpha bands at the latency of the P120, and an increased alpha-beta ERD at about 200–500 ms; (2) a decrease of the theta phase-locking in the parieto-central regions; (3) an increase in (gamma) 40 and 60 Hz ERS over occipito-central regions, respectively at about 150 and 350 ms latency (**Table 1**).

With respect to the *Normal* condition, in the *Uncoordinated* condition the following was observed (**Figures 6–9**): (1) a decrease of alpha-beta band at the latency of the P120, followed by an earlier and greater alpha-beta ERD over the occipito-parietal region; (2) a reduction of theta phase-locking. However, in contrast to the *Upside-down* and *Normal* condition, (3) the *Uncoordinated* animation produced a gamma 40–60 Hz ERD at about 200–500 ms over occipito-central regions (**Table 1**). The analysis of the dynamic contrast of the image showed that the *Uncoordinated* condition presented an increased contrast between the third and the fourth image (400 ms after the onset) with respect to the two other conditions.

STEADY STATE VISUAL EVOKED POTENTIALS

When the heel strike of the right leg was used as trigger, the average trace corresponded to an oscillatory pattern peaking at about 9 Hz. (8.86 Hz). This was observed for all subjects and conditions and may be considered as a SSVEP induced by the frequency of the video. **Figure 10** illustrates the SSVEP traces resulting from a grand average of all the 16 subjects which conserve the 9 Hz oscillating pattern presented in each single subject. However, the amplitude of the grand average oscillation was not constant throughout the time period. The first negative peak occurred close to 100 ms after the heel strike in any of the 3 different conditions (**Figure 10A**). For *Normal* and *Upside-Down* condition the SSVEP amplitude increased after the heel strike and culminated at a latency of 300 ms (negative peak) only in the *Normal* condition. Thereafter, the oscillating pattern decreased in *Normal* and *Upside-down* condition but was maintained in the *Uncoordinated* condition.

The *Upside-down* condition showed a significant decrease of the third negative SSVEP component at 300 ms with respect to the *Normal* condition over parieto-occipital regions (**Figure 10A**,

Table 1 | Summary of statistical analysis about the 32 selected electrodes for both conditions *Upside-down* (U) and *Uncoordinated* (J) vs. Normal (N).

A

Conditions	**U–N**		**J–N**	
ERP	**P120**	**P300a**	**N170**	**P300b**
Frontal				
Central				
Temporal			***T8	
Parietal	**P3, *P7, ***Pz, *P4	*P3, *Pz, **P4, ***P8, ***CP6	**P7, **P8	*P3, *Pz
Occipital	**O1		**O1, **Oz, ***O2	**O1, **Oz, **POz, *O2

B

ERSP/U-N	**Alpha-Beta ERS/ERD**	**Gamma (40 Hz) ERS**	**Gamma (60 Hz) ERS**
Frontal	***Fz		
Central	***C3, ***Cz, ***FC1, ***FC2		
Temporal			
Parietal	***P3, ***CP1, ***CP5, ***Pz	***P3, ***P7, ***CP5, ***P4	***P3, ***P7, ***CP1, ***CP5, ***P4, ***CP2, ***CP6
Occipital	***O1, ***O2	***O1, ***POz, ***O2	***O1, ***Oz, ***O2, ***POz

C

ERSP/J–N	**Alpha-Beta ERS/ERD**	**Gamma (40–60 Hz) ERD**
Frontal		
Central	***C3, ***Cz	***C3, ***C4
Temporal		
Parietal	***P3, ***P7, ***CP1, ***CP5, ***Pz, **P4, ***P8, ***CP2	***P3, ***P7, **Pz, ***CP1, ***CP5, ***CP2, ***CP6
Occipital	***O1, ***Oz, ***POz, ***O2	***O1, ***Oz, ***POz, ***O2

D

SSVEP	**U–N 300 ms**	**J–N 400 ms**
Frontal		
Central	***C3, **Cz	
Temporal		
Parietal	***CP1, **P3, ***Pz, **P4, **CP2	***CP5, **CP1, ***P3, ***Pz, **P4, **CP2
Occipital	***O1, ***Oz, ***POz, ***O2	***O1, ***Oz, ***POz, ***O2

*(A) ERP for P120, N170, P300a, and P300b amplitudes. (B) ERSP and ITC for U vs. N. (C) ERSP and ITC for J vs. N. Only the electrodes showing significant results are represented (***0.001, **0.01). The reduction in theta phase locking (ITC) is indexed by gray shading (dark $p < 0.001$, light $p < 0.01$). (D) SSVEP behavior differences.*

left part; **Table 1**). The reduction of the ascending phase slope of this negativity in the *Upside-Down* condition was accompanied over parieto-occipital regions by a power increase in beta-gamma band at about 250 ms and later by a power increase in gamma band (60 Hz) at about 400 ms (**Figure 10B**, *left part*). These effects were preceded by a decrease of theta-alpha bands ITC at about 120 ms with respect to the *Normal* condition (**Figure 10B**, *left part*).

The *Uncoordinated* condition showed a significant increase of the SSVEP negativity at about 400 ms with respect to the *Normal* condition (**Figure 10A**, *right part*; **Table 1**). This was preceded by an ERD in the theta–alpha band (**Figure 10B**) over parieto-occipital regions. While the higher amplitude of the first negative peak recorded in this condition remained under the significance level (**Figure 10A**, *right part*) it was accompanied by a significant increase of theta-alpha bands power at about 100 ms with respect to the *Normal* condition. These effects were followed by successive decrease and then increase of theta-alpha ITC respectively at about 350 and 450 ms (**Figure 10B**, *right part*).

DISCUSSION

To our knowledge, this work represents the first study on the dynamic neural response elicited by VR-animation of human walking. The presentation of the VR-animation elicits ERP components classically described in response to a visual stimulation (Jeffreys, 1996). We demonstrate significant changes in the amplitude of the P120 and P300a when the avatar

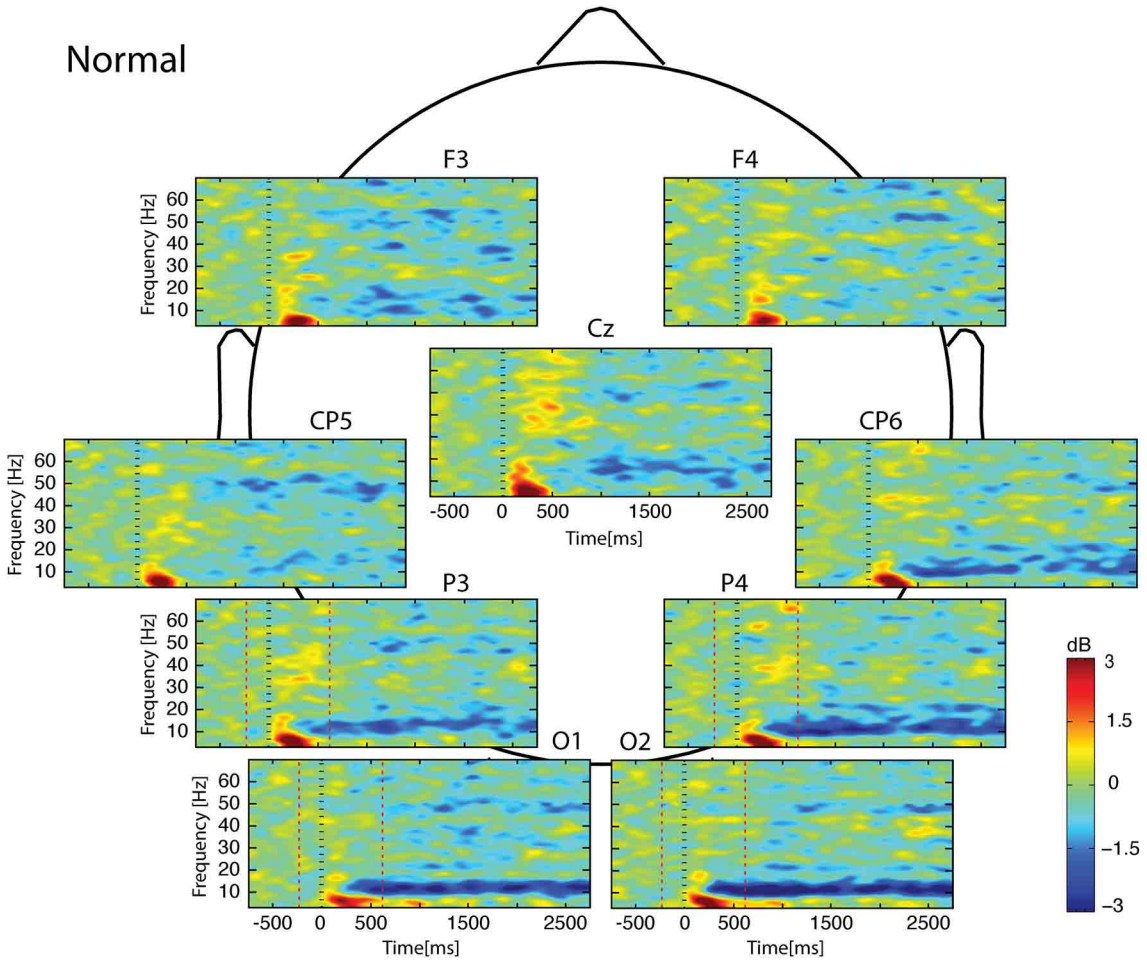

FIGURE 3 | Scalp ERSP on [−1000; 3000] ms in *Normal* condition. Rhythmic activity can be splits in two parts: [0; 500] ms which contains responses evoked by animation onset; and [500; 3000] ms of maintaining task. Note that bilateral alpha-beta ERD was continue from 200 to 3000 ms, and gamma ERD at about 700 ms, maintained for the 3000 ms in the left sensori-motor region. Red lines delimit epochs analyzed: [−200; 600] ms.

was upside-down, and the N170 and P300b when the walking sequence was perturbed (*Uncoordinated*) with respect to the *Normal* condition.

The presence of the early alpha ERS characterize the *Normal* condition. The alpha-beta ERD was reinforced and the theta phase-locking was disturbed in *Upside-down* and *Uncoordinated* condition. As regards gamma oscillation, a contrasting situation was seen as its power was increased in association with the *Upside-down* animation and decreased with the *Uncoordinated* animation.

An SSVEP-like response oscillating at about 9 Hz was also described when the heel strike event was used as trigger, showing that the oscillating pattern is enhanced 300 ms after the heel strike event only in the *Normal* but not in the *Upside-Down* condition.

ERP

The present ERP components evoked by avatar observation are in accordance with those recorded in previous studies using point-light paradigm (Johansson, 1973). The timing of P120, N170, and P300 are commonly regarded as corresponding to the main three components P1 around 130 ms, N1 at 200 ms and N2 (P3 depending of the type and the placement of reference electrode) at 300–400 ms described in point-light walking studies (Hirai et al., 2003, 2005, 2009, 2013; Jokisch et al., 2005; Krakowski et al., 2011; Buzzell et al., 2013).

Although point-light and VR displays concern the same biological motion, VR display induced a stronger visual representation, including form and color than point-light walking. VR display conserved body structure in the *Normal*, *Upside-down,* and *Uncoordinated* conditions. This was not the case in point-light studies, where inverted condition associate form recognition to motion, and scramble condition deconstruct body form. In this context, the present VR-paradigm offers the possibility to dissociate recognition of body form occurring at the first video frame, and motion coherence (smoothness, coordination, speed, etc.) produced by the successive frames. This allows to focus specifically on the effect induced by changing the frame of reference in *Upside-down* and the global coherency of the walking motion in *Uncoordinated*.

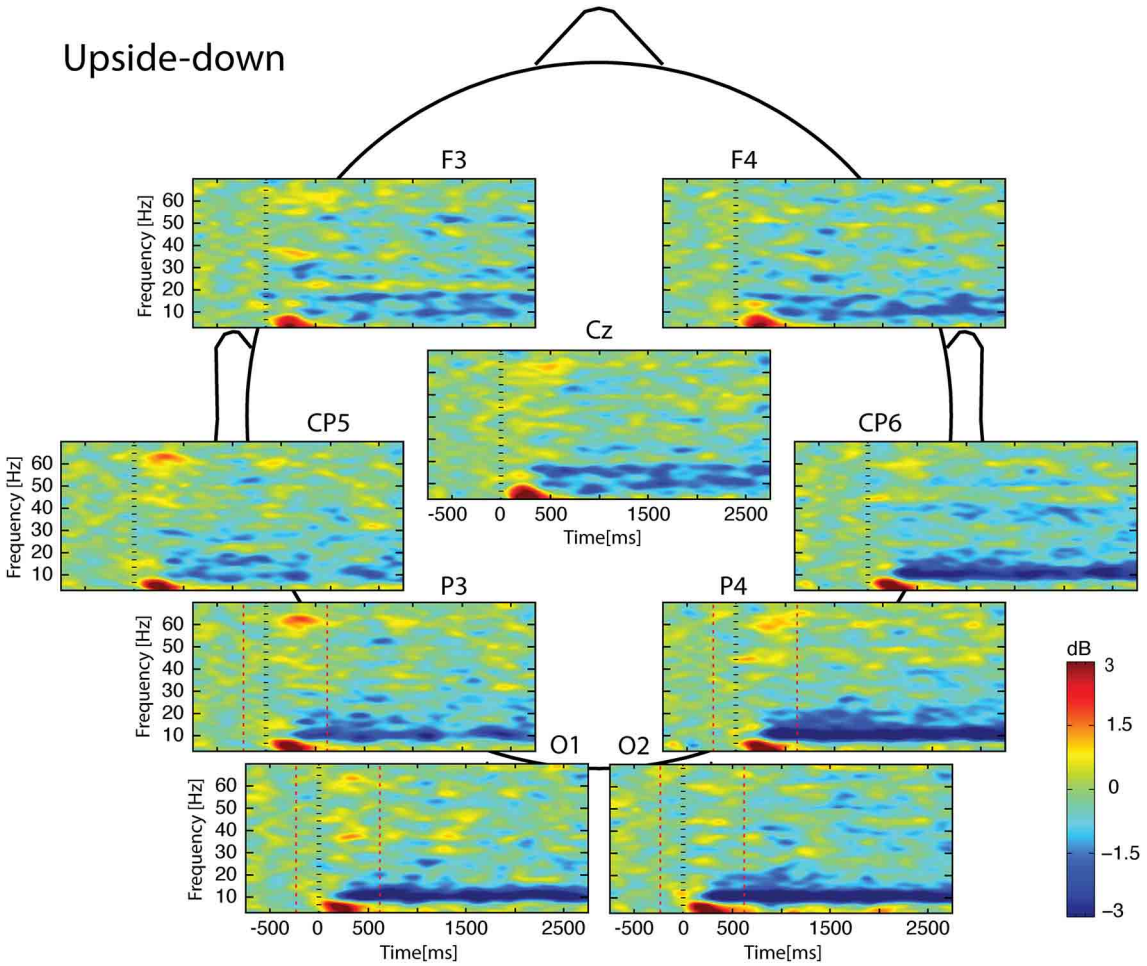

FIGURE 4 | Scalp ERSP on [−1000; 3000] ms in *Upside-down* condition. Rhythmic activity can be splits in two parts: [0; 500] ms which contains responses evoked by animation onset; and [500; 3000] ms of maintaining task. Note that bilateral alpha-beta ERD was continue from 200 to 3000 ms. Red lines delimit epochs analyzed: [−200; 600] ms.

The similarity of P120 evoked by the *Normal* and the *Uncoordinated* conditions is consistent with the fact that the first image is the same in these conditions. In contrast, point-light studies showed a delay and a decrease in P1 response elicited by scramble condition with respect to upright condition (Hirai et al., 2009, 2013; Krakowski et al., 2011). These results support common interpretation that first component reflects a global representation coding of form (Baccus et al., 2009; Buzzell et al., 2013; White et al., 2014). However, the finding of decrease P120 in the *Upside-down* condition with respect to the *Normal* condition was not reported by previous point-light studies. The origin of this early alteration can be explained by both bottom-up and/or top-down process. Distinctions between these influences are not easy. The *Normal* presentation of the avatar may unconsciously induce an easy visual representation than the *Upside-down* mannequin which implies a mental transformation of the reference frame. In parallel, the repeated presentation of normal or inverted locomotion can predictively influence this early response by a top-down effect exerted by the frontal cortex to the primary visual cortex (Peyrin et al., 2010; Cardin et al., 2011; Zanto et al., 2011; Ramalingam et al., 2013). However, previous studies suggest that explicitly attended tasks process does not appear to influence the earlier activity at about 100 ms (Krakowski et al., 2011; Buzzell et al., 2013).

Concerning later activation, N1 and N2 were generally related to integration of form and motion (Baccus et al., 2009; Buzzell et al., 2013; White et al., 2014). It is interesting to note that the effects of *Uncoordinated* condition on N170 (analogous to N1 in point-light studies) and of point-light scramble on N1 are comparable, as N170 was reduced in *Uncoordinated* condition as N1 in scramble condition (Hirai et al., 2003, 2013; Jokisch et al., 2005). This result suggests that N170 was mainly related to motion. In contrast, P300a (analogous to N2 in point-light studies) amplitude was the same in *Normal* and *Uncoordinated* conditions, whereas N2 was larger in upright point-light walker than point-light scramble (Jokisch et al., 2005; Hirai et al., 2013). Moreover, P300a amplitude was smaller in *Upside-down* than in *Normal*. This could also be related to the alteration of the SSVEP pattern occurring at this latency in the

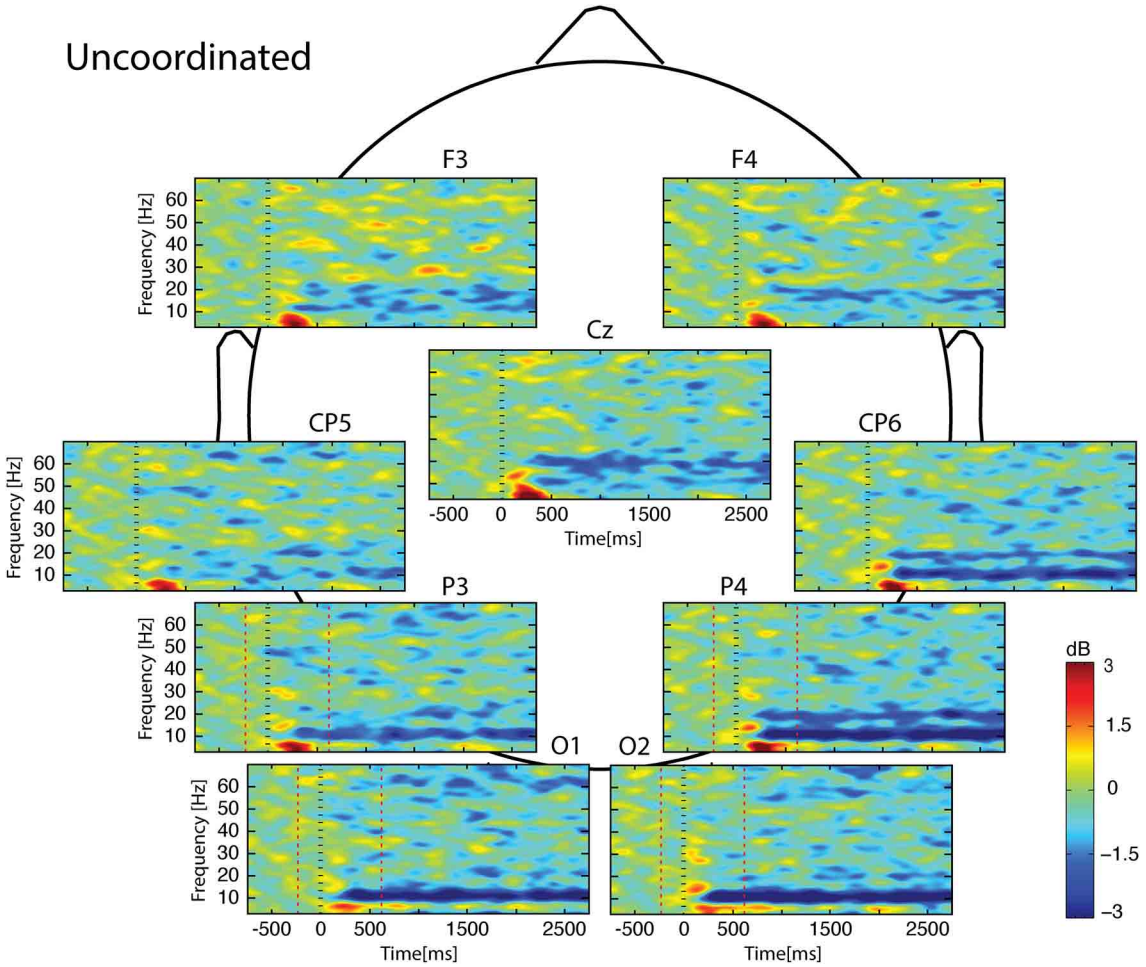

FIGURE 5 | Scalp ERSP on [−1000; 3000] ms in *Uncoordinated* condition. Rhythmic activity can be splits in two parts: [0; 500] ms which contains responses evoked by animation onset; and [500; 3000] ms of maintaining task. Note bilateral that alpha-beta ERD was continue from 200 to 3000 ms. Red lines delimit epochs analyzed: [−200; 600] ms.

Upside-down vs. *Normal* condition. Taken together these results suggest that P300a was mainly related to the global form of walking.

Finally, the effect we recorded on P300b and in the SSVEP at about the same latency in the *Uncoordinated* condition is comparable to the late phase describe by Krakowski et al. (2011), which was characterized by a greater positivity in response to upright and inverted point-light walker than point-light scramble. This last phase after 400 ms is generally considered as indexing a high-order representation coding (Krakowski et al., 2011). This effect observed in *Uncoordinated* suggests that P300b component is sensitive to coherence of motion rather to mere recognition of walking.

ERSP AND ITC

Alpha ERS/ERD

The significant alpha ERS occurring at about 120 ms in the occipito-parietal regions characterized the *Normal* walking observation. It was followed by an alpha-beta ERD at 200 ms, which extends throughout the video. This was significantly more pronounced in *Upside-down* and *Uncoordinated* conditions than in *Normal*.

The first alpha ERS is in accordance with recent studies showing similar transient alpha increase in response to upright facial motion (Girges et al., 2014). The suppression of the early alpha ERS in *Upside-down* suggest that the inversion of the body presentation rapidly affect the early visual process. However, similar alteration found for the *Uncoordinated* condition while the first image was exactly the same suggests a top-down influence. Alpha oscillation has been interpreted as reflecting global inhibition of the cortex, improving behavioral performance by facilitation of the cognitive control (Klimesch et al., 1996, 2003, 2007; Klimesch, 1999, 2012; Cheron et al., 2006; Haegens et al., 2010). Thus, increase in alpha power (ERS) may participate to a general clearance of noise or distracting event in order to selectively update relevant incoming information (Sadaghiani et al., 2012), and access to memory (Klimesch, 2012). In this context, suppression of alpha ERS in *Upside-down* and *Uncoordinated* conditions would be correlated with increase of attention to motion cue and involvement of cognitive resources.

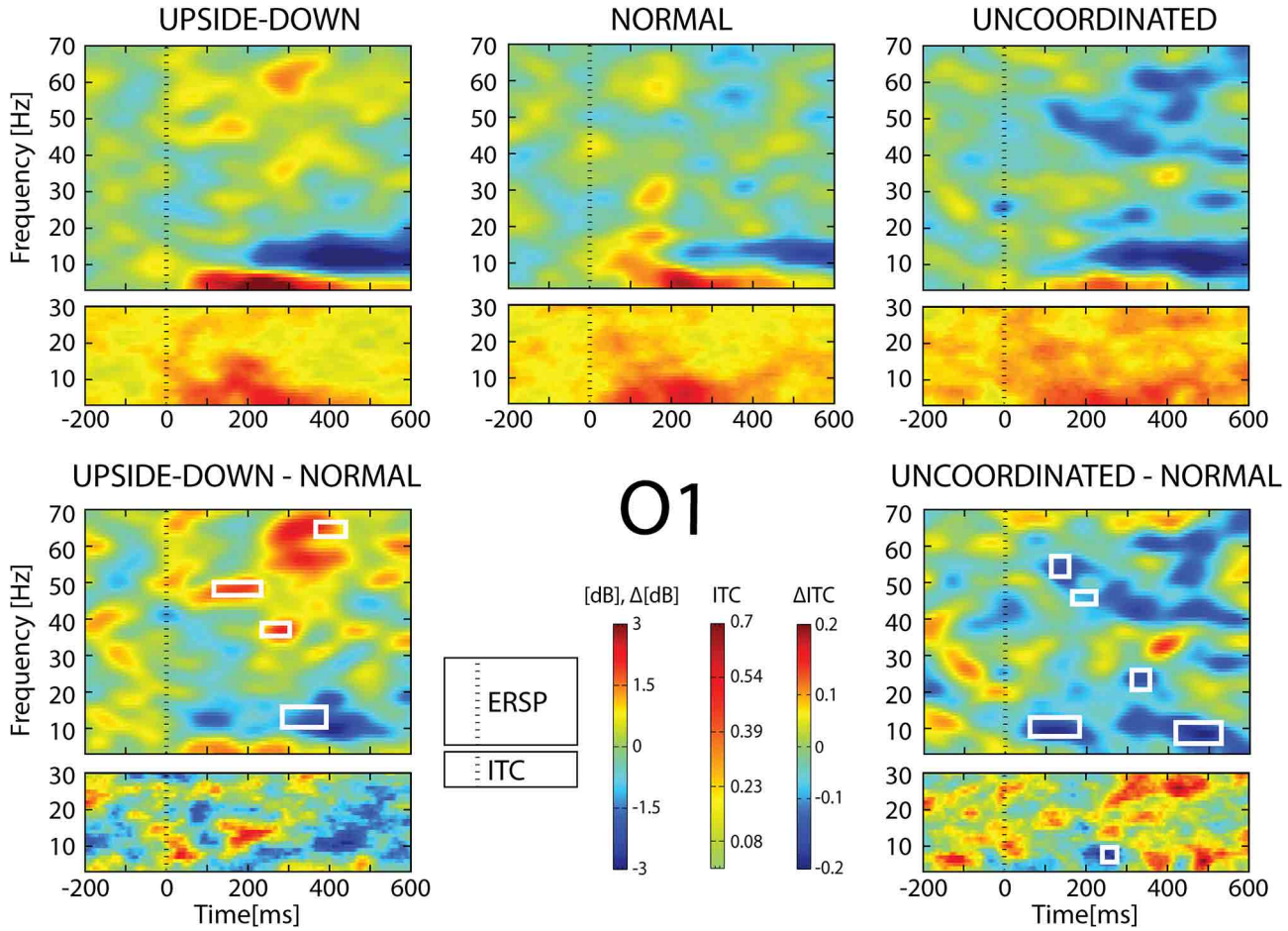

FIGURE 6 | ERSP and ITC from O1 electrode. The upper panel shows the ERSP and ITC in each three conditions. The lower panel shows difference *Upside-down-Normal* (left), and *Uncoordinated-Normal* (right) for ERSP and ITC. Areas of statistical significances ($p < 0.001$) are marked by white squares.

The next alpha ERD are in line with previous research showing decrease in alpha band power during perception of human motion (Cochin et al., 1998; Ulloa and Pineda, 2007). This was generally related to the desynchronization of mirror neurons activity as studied with EEG and fMRI combination (Arnstein et al., 2011), and would reflect a release from inhibition. However, it is interesting to note that our results are in contrast to studies of face perception (Girges et al., 2014), which report a greater alpha ERD in response to upright facial motion than in inverted condition. This difference between face and body motion recognition may be explain by high specialization of the brain to face recognition, and in particular to treatment of semantic content of facial gesture (Rojas et al., 2011). According to Klimesch et al. (1997, 1999, 2012), the alpha ERD increased as a function of the semantic content of retrieved information from the storage system. In our study, each stimulus has the same semantic content as a walking avatar. In this context, amplification of alpha ERD would indicate a recruitment of the mirror neurons system in order to recognize or predicted observed motion, by transformation of reference frame (in *Upside-down*) and reconstruction of motion (in *Uncoordinated*). The enhancement of the alpha ERD in *Upside-down* and *Uncoordinated* condition might then facilitate a dynamical process throughout the neural network involved in alpha rhythm generation evoked by the *Normal* walking avatar.

Theta ERS

The present ITC analysis shows that phase locking occur mainly in the theta range (peaked at ∼5 Hz). However, as it is classically the case, this is not a pure phase locking because it was accompanied by theta ERS throughout all electrodes. Indeed, the visual evoked potentials (P100-N200) elicited by the classical checkerboard pattern or by more complex visual stimuli were accompanied by a clear theta ERS and related ITC (Klimesch et al., 2004; Cheron et al., 2014). Although present in each of the three present conditions in the 100–400 ms time period, the theta ITC was significantly perturbed in both *Upside-down* and *Uncoordinated* condition, while theta ERS were not significantly different. This indicates that the recognition of *Normal* walking is accompanied by a stronger theta phase locking peaking between 200 and 300 ms.

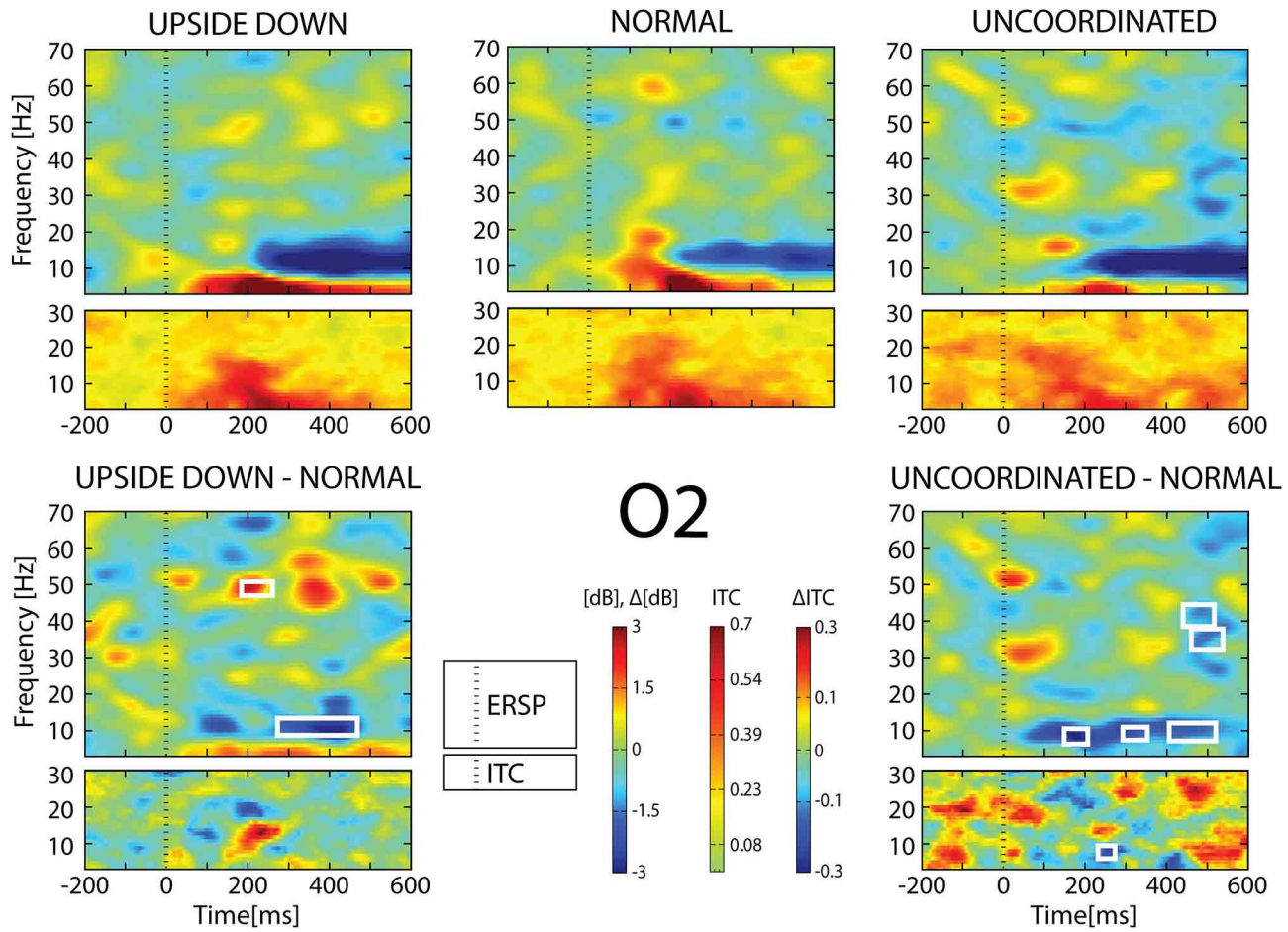

FIGURE 7 | ERSP and ITC from O2 electrode. The upper panel shows the ERSP and ITC in each three conditions. The lower panel shows difference *Upside-down-Normal* (left), and *Uncoordinated-Normal* (right) for ERSP and ITC. Areas of statistical significances ($p < 0.001$) are marked by white squares.

In humans the theta EEG rhythm (4–7 Hz) was initially defined as an intermediate rhythm between delta and alpha (Walter and Dovey, 1944; Mitchell et al., 2008). Later, the term FM-theta (FM for fronto-midline) was introduced by Ishihara and Yoshi (1972) when EEG was recorded during arithmetic task (Ishihara and Yoshi, 1972). Later, the presence of FM-theta during arithmetic and musical activities was demonstrated with MEG (Sasaki et al., 1996a,b,c). The midline frontal areas, such as the anterior cingulate cortex encompassing the lateral part of the prefrontal cortex are commonly cited as potential generators of the FM-theta (Gevins et al., 1997; Mizuhara et al., 2004; Sauseng et al., 2007).

In rat hippocampal regions, theta oscillation (3–9 Hz) is recognized to play an important role in the phase precession of the place cells firing assuming cued recall of the coming positions along the locomotion path of the rat (O'Keefe and Recce, 1993). The intrinsic theta generator of the hippocampal cortex is reinforced by the extrinsic theta pacemaker situated in the medial septal nucleus and allows a large-scale synchronization of theta oscillations in the hippocampus (Kocsis et al., 1999; Buzsáki, 2002). Theta oscillation is not restricted to the hippocampus but also emerges in different cortical areas in the rat (Leung and Borst, 1987; Silva et al., 1991). The ability of different cortical regions to produce theta is supported by slice recording demonstrating that theta oscillation may be produced by the activation of the NMDA receptors of the layer 5 (Silva et al., 1991; Flint and Connors, 1996) as well as by cholinergic activation of interneurons (Blatow et al., 2003).

Although human theta rhythm is not as robust as in the rat hippocampus, the ability of the human cortex to produce theta oscillation is now well recognized. It has been related to sensorimotor integration (Caplan et al., 2001), navigation (Kahana et al., 1999), memory load (Howard et al., 2003) and working memory (Raghavachari et al., 2001, 2006; Liebe et al., 2012). Interestingly, all the different phases of virtual movement during a navigation game induced an increase of 4–8 Hz oscillation in both the hippocampus and neocortex in human (Ekstrom et al., 2005). Although the present experiment involves the observation of human locomotion it cannot be assumed that the recorded theta oscillations are specifically related to locomotion *per se*. Indeed, theta oscillations are now considered as a basic physiological element involved in global oscillatory synchronization processes

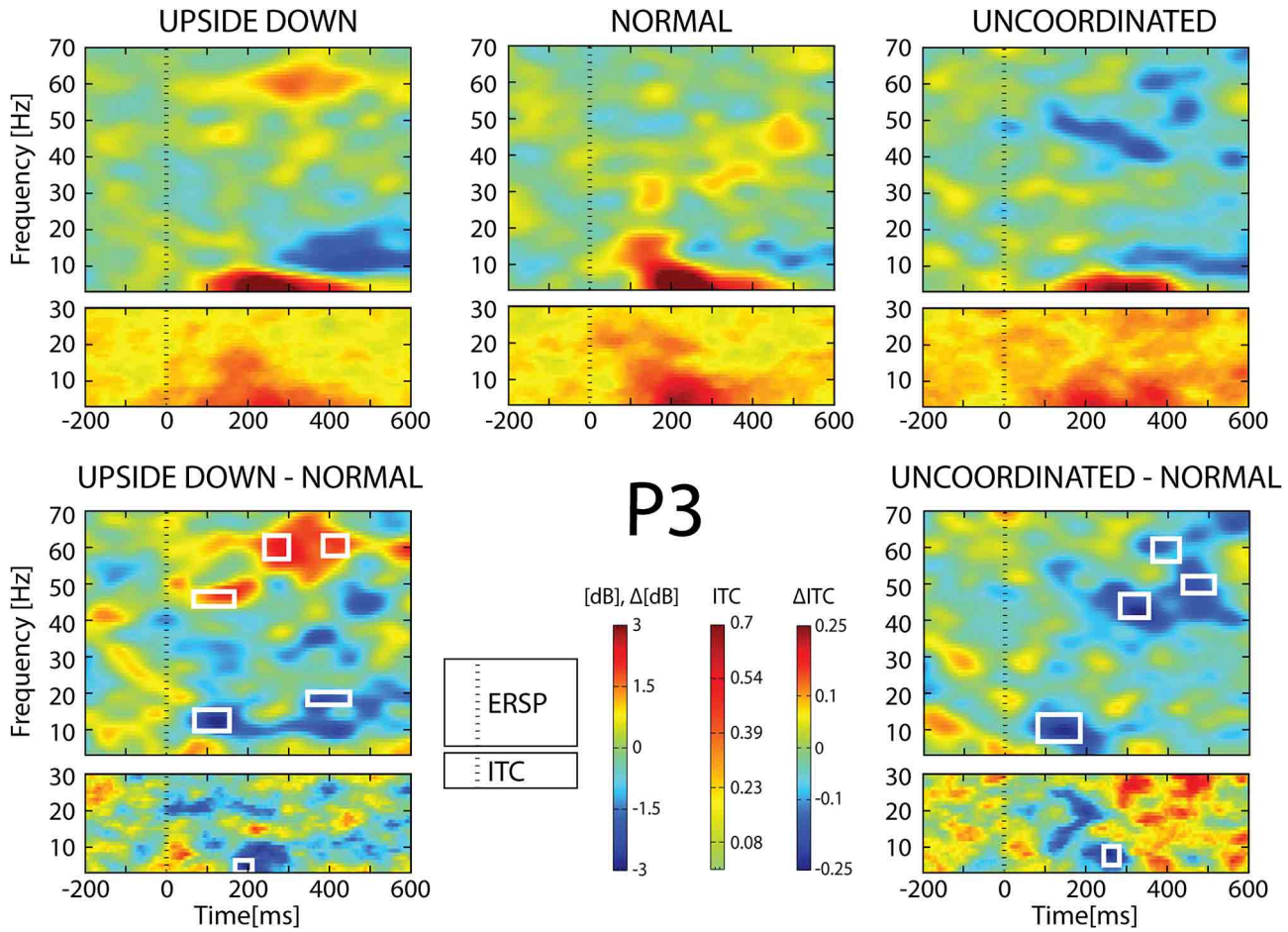

FIGURE 8 | ERSP and ITC from P3 electrode. The upper panel shows the ERSP and ITC in each three conditions. The lower panel shows difference *Upside-down-Normal* (left), and *Uncoordinated-Normal* (right) for ERSP and ITC. Areas of statistical significances ($p < 0.001$) are marked by white squares.

linking together multiple brain regions (Buzsáki and Draguhn, 2004; Fries, 2005). For example, the multiplicity of functional roles for this oscillation was demonstrated by the fact that the amplitude of theta power recorded over the temporal and frontal cortex predicted the behavioral performance of the subject (Sederberg et al., 2003). A recent MEG study demonstrated that hippocampal-prefrontal theta synchronization plays a mnemonic guidance in human decision-making (Guitart-Masip et al., 2013). Single neurons and local field potential recordings in the human medial temporal lobe show that theta phase locking reflects a global activation providing a temporal window for the conscious recognition (Rey et al., 2014). At a lower hierarchical level closer to the present observational task, theta oscillation is related to the perception of color shape of object and visual attention (Fries et al., 2001b). It is also involved in different sensory modalities to provide meaningful chunks of neuronal signals allowing subsequent decoding for an enhanced perception. In our case, such theta oscillation may thus be viewed as taking part of time-division multiplexing mechanism representing sequential information upon which a neuronal code may emerge by cross-frequency interaction with faster (gamma) oscillation (Akam and Kullmann, 2014).

Gamma modulation

Gamma oscillation (30–100 Hz) occupies a privileged position in cognitive neuroscience. The current understanding of gamma oscillation points to its emergence from the synchronous activity of a large ensemble of firing neurons (Eckhorn et al., 1988; Gray et al., 1989; Jensen and Colgin, 2007). It is central to the binding theory, in which gamma oscillations combine different features in a visual scene to form a coherent percept (Singer, 1999). Unexpectedly, our results show that *Upside-down* condition elicited gamma power increase at about 150 and 400 ms and a gamma ERD at the same latency in the *Uncoordinated* condition. This contrasting behavior of gamma oscillation is interesting because these oscillations are considered to underlie perception of coherent stimuli. These data are in accordance to previous MEG study showing enhancements in gamma rhythm at 100 ms after display onset in upright and inverted point-light walker (Pavlova et al., 2004). However, in the latter study additional gamma peak appeared only for upright point-light walker at 130 and 170 ms. Another study of the same group reported increased gamma activity in the left parieto-occipital region at 80 ms, with additional peaks in attended point-light walker on the right parietal and temporal cortex at 120 and

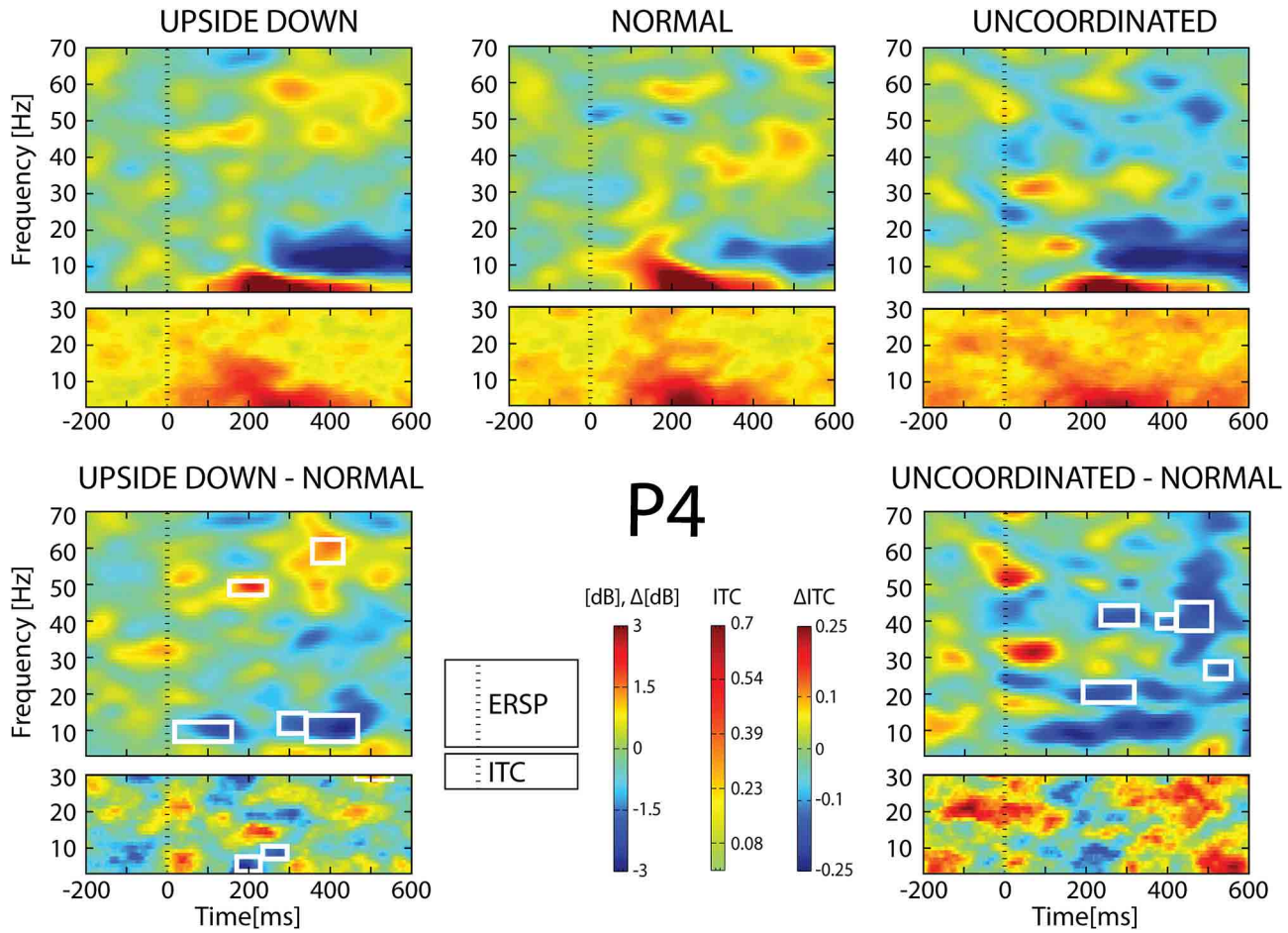

FIGURE 9 | ERSP and ITC from P4 electrode. The upper panel shows the ERSP and ITC in each three conditions. The lower panel shows difference *Upside-down-Normal* (left), and *Uncoordinated-Normal* (right) for ERSP and ITC. Areas of statistical significances ($p < 0.001$) are marked by white squares.

155 ms, respectively (Pavlova et al., 2006). The present results are in agreement with the data of Tallon-Baudry et al. (1996), where they demonstrated the presence of non-phase-locked gamma activation (60 Hz) at about 300–400 ms after the presentation of an illusory Kanizsa triangle figure (Tallon-Baudry et al., 1996). In this experiment, the gamma activity was stronger when the recognition task required additional mental reconstruction (stronger gamma oscillation for illusory triangle than normal triangle). In our present study, a non-phase-locked 60 Hz power increase occurred at the same latency only when the walking avatar was presented in *Upside-down* configuration. The subject was not instructed to perform any mental task but implicit recognition can recruit gamma activity for unconscious and conscious neuronal process (Aru et al., 2012; Vidal et al., 2014). The complex interplay between these neuronal qualia occupies a central position in cognitive neuroscience (Kandel, 2013). In the context of the Global Workspace Theory, serial and parallel processing take part from the widespread treatment of unconscious information to the emergence of consciousness (Baars, 1997; Dehaene and Naccache, 2001; Baars et al., 2013; Dehaene et al., 2014).

From a physiological perspective, experiments and modeling have demonstrated that gamma rhythms emerge from the interaction between local excitation and inhibition (Traub et al., 1997; Brunel and Wang, 2003; Kang et al., 2010), in which the gap junctions between interneurons play a pivotal role in ensuring gamma oscillation coherence (Traub et al., 2003; Whittington and Traub, 2003). In macaque, high density electrocorticography recording (Brunet et al., 2013) demonstrated that natural viewing induced a strong gamma oscillation (50–80 Hz) over most of the recorded visual cortex including V1 and V4 but not over most of the remaining cortex extending from superior temporal sulcus to the anterior part of the arcuate sulcus. The functional link between neuronal spikes and local field potential oscillation has been well documented in different preparations, demonstrating that spike-field coherence in the gamma-band frequency is accompanied by power enhancement of the gamma rhythm (Fries et al., 2001a,b, 2002, 2008). It was also demonstrated that when visual stimuli are moving smoothly, the visual cortex produces neuronal synchronization in the gamma-frequency band (Friedman-Hill et al., 2000). This gamma synchronization is considered as a key element for signal transmission to

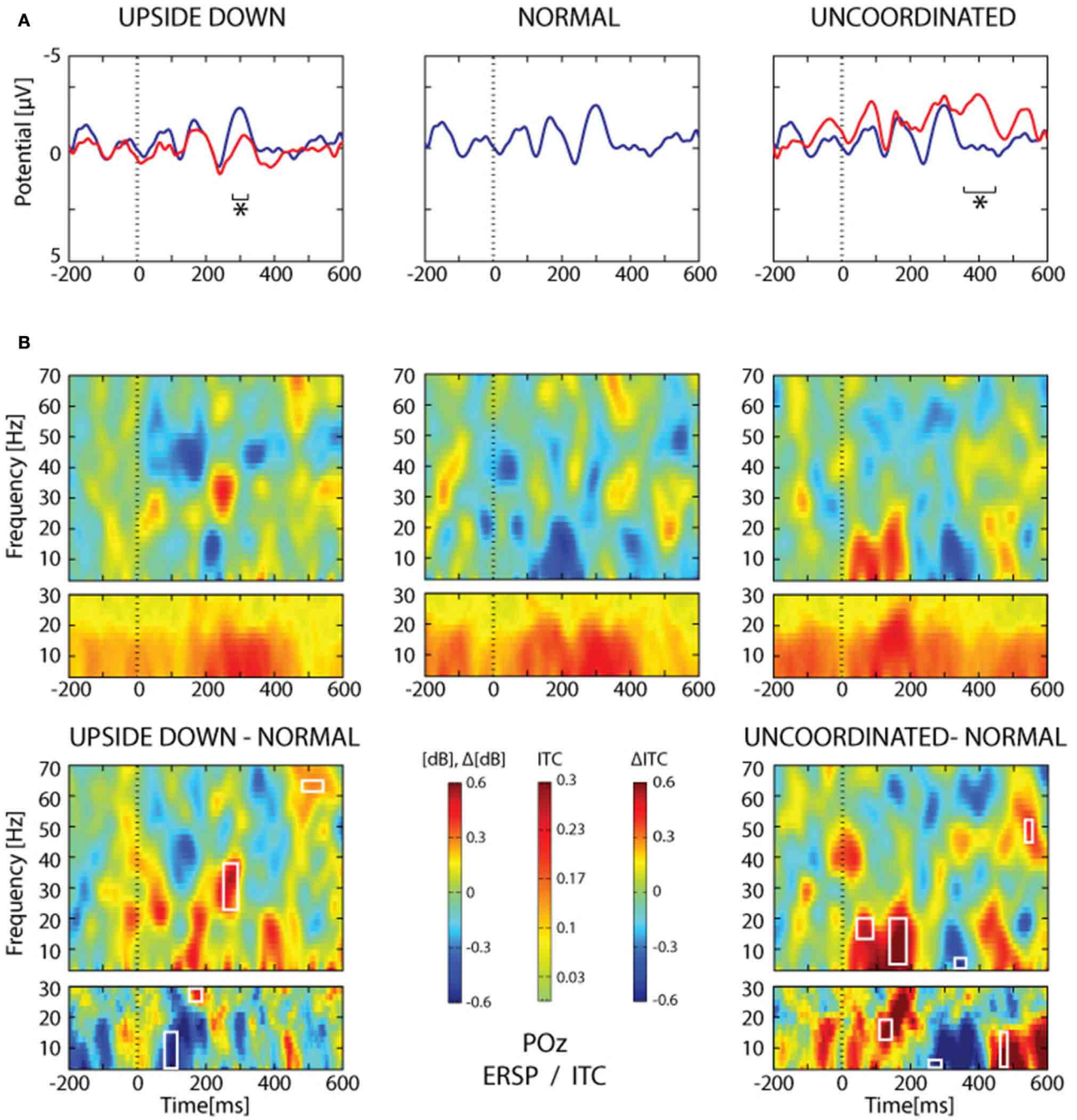

FIGURE 10 | SSVEP analysis from POz electrode. (A) Grand average trace corresponding to 16 subjects and about 2065 ± 26 trials for each condition. The heel strike of the right leg was used as trigger. Note the oscillating pattern at about 9 Hz and the superimposition of the *Normal* condition (blue trace) over the *Upside-down* (red trace, left part) and the *Uncoordinated* condition (red trace, right part). Areas of statistical significance ($p < 0.001$) are indicated by an asterisk. **(B)** The upper panel shows ERSP and ITC analysis of the same SSVEP data for the three respective conditions presented in **(A)**. The lower panel shows, ERSP and ITC differences *Upside-down-Normal* (left), and *Uncoordinated-Normal* (right). Areas of statistical significance ($p < 0.001$) are marked by white squares.

postsynaptic targets and to assume the continuity of the visual message (Fries, 2009).

In this context, the gamma ERD recorded during the *Uncoordinated* condition could be explained by a previous experience of Kruse and Eckhorn (1996) realized in the primary visual cortex of the cat. When a smooth movement of the visual field was presented it induced gamma oscillation, but when the smooth movement was intermingled with sudden random acceleration in and against the original direction of the smooth movement the gamma oscillations disappeared (Kruse and Eckhorn, 1996). This

latter situation corresponds to the present *Uncoordinated* condition where gamma ERD replace gamma ERS present in *Normal* and *Upside-down* condition. The smoothness aspect of the walking video for both *Normal* and *Upside-down* presentations induces gamma oscillation while the sudden "*Uncoordinated*" image desynchronizes the neuronal population responsible for the gamma oscillation. In addition, Kruse and Eckhorn (1996) have demonstrated an inverse relationship between the decrease in gamma power and an increase in the stimulus-locked responses in lower frequency band (Kruse and Eckhorn, 1996).

Following the canonical microcircuit model (Bastos et al., 2012) based on intracellular recordings in cat visual cortex incorporating the neuronal sources of forward and backward connections in cortical hierarchies, it was proposed that the superficial pyramidal neurons generate gamma responses whereas deep pyramidal neurons generate alpha and beta dynamics. The visual cortex has been suggested to act as a dynamic filter of the visual input where stimulus properties like movement, contrast, localization and size of visual cues may modify the configuration of gamma oscillation (Gray et al., 1989; Ray and Maunsell, 2010; Brunet et al., 2013; Roberts et al., 2013). Among these stimulus properties, contrast is able to enhanced the signal-to-noise ratio of the sensory input inducing an increase in the postsynaptic gain of superficial pyramidal cells implicate in gamma oscillation (Feldman and Friston, 2010). Although, the same avatar was used here in the three different conditions the kinematic change of the *Uncoordinated* condition induced a significant increase in the dynamic contrast at the latency of 400 ms and may thus explain the late gamma ERD present in this condition. The spatial summation and the receptive field organization in V1 depend on contrast stimulus (Sceniak et al., 2002). The effects of contrast on the induced rhythms are complex and specifically influence the postsynaptic gain of neuronal populations, the strength of intrinsic and horizontal connectivity which can be differentially engaged depending on stimulus properties (Pinotsis et al., 2014). These authors have reported that the increase in visual contrast induces an increase of gamma peak frequency (from 46 to 58 Hz) accompanied by a decrease in gamma power. This contrast effect on the gamma power must be taken in account in the present gamma ERD and is complementary to the previous Kruse and Eckhorn's (1996) reported effect on the gamma power when the visual movement is *Uncoordinated*.

SSVEP

In order to strengthen the ERP, ERSP, and ITC studies of the transient presentation of the walking video, a SSVEP approach was made by using the heel strike events as the synchronized item of the video images occurring at every 100 ms. SSVEP offer many advantages in comparison to ERP, including better signal-to-noise ratio with a clear peak in the FFT occurring at the frequency of interest and some of its harmonics, and greater number of averaged items in a shorter period of time. SSVEP are classically obtained by using neutral LED or LCD image flashing between 1 and 100 Hz inducing resonance phenomena. In the present study, the SSVEP was not obtained by directly triggering all of the images occurring at 10 Hz but by using a specific event of the avatar locomotion corresponding to the initiation of the step cycle.

SSVEP is classically considered as an oscillatory response of the visual cortex evoked by contrast or luminance-modulated stimuli that drive the neural response at the imposed frequency of the constant peripheral stimulation (Regan, 1966; Müller et al., 1998). SSVEP are not only imposed by the physical properties of the stimulus but also depends on the brain state, task related-process, bottom-up and top-down influences (Müller et al., 1998; Keil et al., 2003; Andersen and Müller, 2010). This oscillatory pattern is a strong steady state potential that mainly arises from the occipital area, with strong contribution from the early visual cortex but also from more extended parts of the visual system including higher visual areas (Müller et al., 1997; Di Russo et al., 2007). This partly explains why SSVEP approach is increasingly used in cognitive and affective neurosciences to study face processing including face identification and decoding of facial emotional expressions (McTeague et al., 2011; Ales et al., 2012; Gruss et al., 2012; Rossion et al., 2012). To our knowledge, the present study is the first to use a walking avatar video for inducing SSVEP-like response. It showed specific amplitude enhancement of the oscillatory pattern and the related spectral perturbation at a precise time in relation to a kinematic event. Although no direct comparison can be made between SSVEP and ERP results, it is interesting to highlight the convergence of both types of results with regard to significant changes in the EEG brain rhythms at about the latency of 300 ms when the same avatar video was presented in *Upside-down* vs. *Normal* condition. The reported differences in the SSVEP configuration and rhythmic alteration (early theta-alpha ERS and late gamma ERS) in the *Uncoordinated* condition can be due to the higher dynamic contrast of this condition with respect to the other two conditions.

ACKNOWLEDGMENTS

We wish to thank Cal3D team for providing us with the original stimuli. We thank all volunters for their participation. This work was funded by the Belgian Federal Science Policy Office, the European Space Agency (AO-2004,118), the Belgian National Fund for Scientific Research (FNRS), the research funds of the Université Libre de Bruxelles and of the Université de Mons (Belgium), the FEDER support (BIOFACT), the MINDWALKER project (FP7–2007–2013) supported by the European Commission, and the NeuroAtt BIOWIN project supported Walloon Country. The scientific responsibility rests with its author(s).

REFERENCES

Akam, T., and Kullmann, D. M. (2014). Oscillatory multiplexing of population codes for selective communication in the mammalian brain. *Nat. Rev. Neurosci.* 15, 111–122. doi: 10.1038/nrn3668

Ales, J. M., Farzin, F., Rossion, B., and Norcia, A. M. (2012). An objective method for measuring face detection thresholds using the sweep steady-state visual evoked response. *J. Vis.* 12:18. doi: 10.1167/12.10.18

Andersen, S. K., and Müller, M. M. (2010). Behavioral performance follows the time course of neural facilitation and suppression during cued shifts of feature-selective attention. *Proc. Natl. Acad. Sci. U.S.A.* 107, 13878–13882. doi: 10.1073/pnas.1002436107

Arnstein, D., Cui, F., Keysers, C., Maurits, N. M., and Gazzola, V. (2011). μ-suppression during action observation and execution correlates with BOLD in dorsal premotor, inferior parietal, and SI cortices. *J. Neurosci.* 31, 14243–14249. doi: 10.1523/JNEUROSCI.0963-11.2011

Aru, J., Axmacher, N., Do Lam, A. T. A., Fell, J., Elger, C. E., Singer, W., et al. (2012). Local category-specific gamma band responses in the visual cortex do not reflect conscious perception. *J. Neurosci.* 32, 14909–14914. doi: 10.1523/JNEUROSCI.2051-12.2012

Avanzini, P., Fabbri-Destro, M., Campi, C., Pascarella, A., Barchiesi, G., Cattaneo, L., et al. (2013). Spatiotemporal dynamics in understanding hand-object interactions. *Proc. Natl. Acad. Sci. U.S.A.* 110, 15878–15885. doi: 10.1073/pnas.1314420110

Avanzini, P., Fabbri-Destro, M., Dalla Volta, R., Daprati, E., Rizzolatti, G., and Cantalupo, G. (2012). The dynamics of sensorimotor cortical oscillations during the observation of hand movements: an EEG study. *PLoS ONE* 7:e37534. doi: 10.1371/journal.pone.0037534

Baars, B. J. (1997). Spatial brain coherence during the establishment of a conscious event. *Conscious. Cogn.* 6, 1–2. doi: 10.1006/ccog.1996.0289

Baars, B. J., Franklin, S., and Ramsoy, T. Z. (2013). Global workspace dynamics: cortical "binding and propagation" enables conscious contents. *Front. Psychol.* 4:200. doi: 10.3389/fpsyg.2013.00200

Baccus, W., Mozgova, O., and Thompson, J. C. (2009). Early integration of form and motion in the neural response to biological motion. *Neuroreport* 20, 1334–1338. doi: 10.1097/WNR.0b013e328330a867

Bastos, A. M., Usrey, W. M., Adams, R. A., Mangun, G. R., Fries, P., and Friston, K. J. (2012). Canonical microcircuits for predictive coding. *Neuron* 76, 695–711. doi: 10.1016/j.neuron.2012.10.038

Blake, R., and Shiffrar, M. (2007). Perception of human motion. *Annu. Rev. Psychol.* 58, 47–73. doi: 10.1146/annurev.psych.57.102904.190152

Blatow, M., Rozov, A., Katona, I., Hormuzdi, S. G., Meyer, A. H., Whittington, M. A., et al. (2003). A novel network of multipolar bursting interneurons generates theta frequency oscillations in neocortex. *Neuron* 38, 805–817. doi: 10.1016/S0896-6273(03)00300-3

Braadbaart, L., Williams, J. H. G., and Waiter, G. D. (2013). Do mirror neuron areas mediate mu rhythm suppression during imitation and action observation? *Int. J. Psychophysiol.* 89, 99–105. doi: 10.1016/j.ijpsycho.2013.05.019

Brunel, N., and Wang, X.-J. (2003). What determines the frequency of fast network oscillations with irregular neural discharges? I. Synaptic dynamics and excitation-inhibition balance. *J. Neurophysiol.* 90, 415–430. doi: 10.1152/jn.01095.2002

Brunet, N., Bosman, C. A., Roberts, M., Oostenveld, R., Womelsdorf, T., De Weerd, P., et al. (2013). Visual cortical gamma-band activity during free viewing of natural images. *Cereb. Cortex*. doi: 10.1093/cercor/bht280. [Epub ahead of print].

Brunner, C., Delorme, A., and Makeig, S. (2013). Eeglab—an open source matlab toolbox for electrophysiological research. *Biomed. Tech. (Berl)*. doi: 10.1515/bmt-2013-4182. [Epub ahead of print].

Buzsáki, G. (2002). Theta oscillations in the hippocampus. *Neuron* 33, 325–340. doi: 10.1016/S0896-6273(02)00586-X

Buzsáki, G., and Draguhn, A. (2004). Neuronal oscillations in cortical networks. *Science* 304, 1926–1929. doi: 10.1126/science.1099745

Buzzell, G., Chubb, L., Safford, A. S., Thompson, J. C., and McDonald, C. G. (2013). Speed of human biological form and motion processing. *PLoS ONE* 8:e69396. doi: 10.1371/journal.pone.0069396

Caplan, J. B., Madsen, J. R., Raghavachari, S., and Kahana, M. J. (2001). Distinct patterns of brain oscillations underlie two basic parameters of human maze learning. *J. Neurophysiol.* 86, 368–380.

Cardin, V., Friston, K. J., and Zeki, S. (2011). Top-down modulations in the visual form pathway revealed with dynamic causal modeling. *Cereb. Cortex* 21, 550–562. doi: 10.1093/cercor/bhq122

Cebolla, A. M., De Saedeleer, C., Bengoetxea, A., Leurs, F., Balestra, C., d' Alcantara, P., et al. (2009). Movement gating of beta/gamma oscillations involved in the N30 somatosensory evoked potential. *Hum. Brain Mapp.* 30, 1568–1579. doi: 10.1002/hbm.20624

Cebolla, A. M., Palmero-Soler, E., Dan, B., and Cheron, G. (2014). Modulation of the N30 generators of the somatosensory evoked potentials by the mirror neuron system. *Neuroimage* 95C, 48–60. doi: 10.1016/j.neuroimage.2014.03.039

Cheng, Y.-W., Tzeng, O. J. L., Hung, D., Decety, J., and Hsieh, J.-C. (2005). Modulation of spinal excitability during observation of bipedal locomotion. *Neuroreport* 16, 1711–1714. doi: 10.1097/01.wnr.0000183325.13618.5f

Cheron, G., Cebolla, A. M., De Saedeleer, C., Bengoetxea, A., Leurs, F., Leroy, A., et al. (2007). Pure phase-locking of beta/gamma oscillation contributes to the N30 frontal component of somatosensory evoked potentials. *BMC Neurosci.* 8:75. doi: 10.1186/1471-2202-8-75

Cheron, G., Leroy, A., De Saedeleer, C., Bengoetxea, A., Lipshits, M., Cebolla, A., et al. (2006). Effect of gravity on human spontaneous 10-Hz electroencephalographic oscillations during the arrest reaction. *Brain Res.* 1121, 104–116. doi: 10.1016/j.brainres.2006.08.098

Cheron, G., Leroy, A., Palmero-Soler, E., De Saedeleer, C., Bengoetxea, A., Cebolla, A.-M., et al. (2014). Gravity influences top-down signals in visual processing. *PLoS ONE* 9:e82371. doi: 10.1371/journal.pone.0082371

Cochin, S., Barthelemy, C., Lejeune, B., Roux, S., and Martineau, J. (1998). Perception of motion and qEEG activity in human adults. *Electroencephalogr. Clin. Neurophysiol.* 107, 287–295. doi: 10.1016/S0013-4694(98)00071-6

Crompton, R. H., Sellers, W. I., and Thorpe, S. K. S. (2010). Arboreality, terrestriality and bipedalism. *Philos. Trans. R. Soc. Lond. B Biol. Sci.* 365, 3301–3314. doi: 10.1098/rstb.2010.0035

Csibra, G. (2007). "Action mirroring and action interpretation: an alternative account," in *Sensorimotor Foundations of Higher Cognition. Attention and Performance XXII*, eds P. Haggard, Y. Rosetti, and M. Kawato (Oxford; New York, NY: Oxford University Press), 435–459.

Darwin, C. (1872). *The Expression of the Emotions in Man and Animals*. 1st Edn. London: John Murray.

De Gelder, B. (2006). Towards the neurobiology of emotional body language. *Nat. Rev. Neurosci.* 7, 242–249. doi: 10.1038/nrn1872

Dehaene, S., Charles, L., King, J.-R., and Marti, S. (2014). Toward a computational theory of conscious processing. *Curr. Opin. Neurobiol.* 25C, 76–84. doi: 10.1016/j.conb.2013.12.005

Dehaene, S., and Naccache, L. (2001). Towards a cognitive neuroscience of consciousness: basic evidence and a workspace framework. *Cognition* 79, 1–37. doi: 10.1016/S0010-0277(00)00123-2

Delorme, A., and Makeig, S. (2004). EEGLAB: an open source toolbox for analysis of single-trial EEG dynamics including independent component analysis. *J. Neurosci. Methods* 134, 9–21. doi: 10.1016/j.jneumeth.2003.10.009

Di Dio, C., Di Cesare, G., Higuchi, S., Roberts, N., Vogt, S., and Rizzolatti, G. (2013). The neural correlates of velocity processing during the observation of a biological effector in the parietal and premotor cortex. *Neuroimage* 64, 425–436. doi: 10.1016/j.neuroimage.2012.09.026

Di Russo, F., Pitzalis, S., Aprile, T., Spitoni, G., Patria, F., Stella, A., et al. (2007). Spatiotemporal analysis of the cortical sources of the steady-state visual evoked potential. *Hum. Brain Mapp.* 28, 323–334. doi: 10.1002/hbm.20276

Downing, P. E., Jiang, Y., Shuman, M., and Kanwisher, N. (2001). A cortical area selective for visual processing of the human body. *Science* 293, 2470–2473. doi: 10.1126/science.1063414

Eckhorn, R., Bauer, R., Jordan, W., Brosch, M., Kruse, W., Munk, M., et al. (1988). Coherent oscillations: a mechanism of feature linking in the visual cortex? Multiple electrode and correlation analyses in the cat. *Biol. Cybern.* 60, 121–130. doi: 10.1007/BF00202899

Ekstrom, A. D., Caplan, J. B., Ho, E., Shattuck, K., Fried, I., and Kahana, M. J. (2005). Human hippocampal theta activity during virtual navigation. *Hippocampus* 15, 881–889. doi: 10.1002/hipo.20109

Engel, A. K., Roelfsema, P. R., Fries, P., Brecht, M., and Singer, W. (1997). Role of the temporal domain for response selection and perceptual binding. *Cereb. Cortex* 7, 571–582. doi: 10.1093/cercor/7.6.571

Feldman, H., and Friston, K. J. (2010). Attention, uncertainty, and free-energy. *Front. Hum. Neurosci.* 4:215. doi: 10.3389/fnhum.2010.00215

Flint, A. C., and Connors, B. W. (1996). Two types of network oscillations in neocortex mediated by distinct glutamate receptor subtypes and neuronal populations. *J. Neurophysiol.* 75, 951–957.

Frenkel-Toledo, S., Bentin, S., Perry, A., Liebermann, D. G., and Soroker, N. (2014). Mirror-neuron system recruitment by action observation: effects of focal brain damage on mu suppression. *Neuroimage* 87, 127–137. doi: 10.1016/j.neuroimage.2013.10.019

Friedman-Hill, S., Maldonado, P. E., and Gray, C. M. (2000). Dynamics of striate cortical activity in the alert macaque: I. Incidence and stimulus-dependence of gamma-band neuronal oscillations. *Cereb. Cortex* 10, 1105–1116. doi: 10.1093/cercor/10.11.1105

Fries, P. (2005). A mechanism for cognitive dynamics: neuronal communication through neuronal coherence. *Trends Cogn. Sci.* 9, 474–480. doi: 10.1016/j.tics.2005.08.011

Fries, P. (2009). Neuronal gamma-band synchronization as a fundamental process in cortical computation. *Annu. Rev. Neurosci.* 32, 209–224. doi: 10.1146/annurev.neuro.051508.135603

Fries, P., Neuenschwander, S., Engel, A. K., Goebel, R., and Singer, W. (2001a). Rapid feature selective neuronal synchronization through correlated latency shifting. *Nat. Neurosci.* 4, 194–200. doi: 10.1038/84032

Fries, P., Reynolds, J. H., Rorie, A. E., and Desimone, R. (2001b). Modulation of oscillatory neuronal synchronization by selective visual attention. *Science* 291, 1560–1563. doi: 10.1126/science.1055465

Fries, P., Schröder, J.-H., Roelfsema, P. R., Singer, W., and Engel, A. K. (2002). Oscillatory neuronal synchronization in primary visual cortex as a correlate of stimulus selection. *J. Neurosci.* 22, 3739–3754.

Fries, P., Womelsdorf, T., Oostenveld, R., and Desimone, R. (2008). The effects of visual stimulation and selective visual attention on rhythmic neuronal synchronization in macaque area V4. *J. Neurosci.* 28, 4823–4835. doi: 10.1523/JNEUROSCI.4499-07.2008

Gevins, A., Smith, M. E., McEvoy, L., and Yu, D. (1997). High-resolution EEG mapping of cortical activation related to working memory: effects of task difficulty, type of processing, and practice. *Cereb. Cortex* 7, 374–385. doi: 10.1093/cercor/7.4.374

Giese, M. A., and Poggio, T. (2003). Neural mechanisms for the recognition of biological movements. *Nat. Rev. Neurosci.* 4, 179–192. doi: 10.1038/nrn1057

Girges, C., Wright, M. J., Spencer, J. V., and O'Brien, J. M. D. (2014). Event-related alpha suppression in response to facial motion. *PLoS ONE* 9:e89382. doi: 10.1371/journal.pone.0089382

Gramann, K., El Sharkawy, J., and Deubel, H. (2009). Eye-movements during navigation in a virtual tunnel. *Int. J. Neurosci.* 119, 1755–1778. doi: 10.1080/00207450903170361

Gray, C. M., König, P., Engel, A. K., and Singer, W. (1989). Oscillatory responses in cat visual cortex exhibit inter-columnar synchronization which reflects global stimulus properties. *Nature* 338, 334–337. doi: 10.1038/338334a0

Gruss, L. F., Wieser, M. J., Schweinberger, S., and Keil, A. (2012). Face-evoked steady-state visual potentials: effects of presentation rate and face inversion. *Front. Hum. Neurosci.* 6:316. doi: 10.3389/fnhum.2012.00316

Guitart-Masip, M., Barnes, G. R., Horner, A., Bauer, M., Dolan, R. J., and Duzel, E. (2013). Synchronization of medial temporal lobe and prefrontal rhythms in human decision making. *J. Neurosci.* 33, 442–451. doi: 10.1523/JNEUROSCI.2573-12.2013

Haegens, S., Osipova, D., Oostenveld, R., and Jensen, O. (2010). Somatosensory working memory performance in humans depends on both engagement and disengagement of regions in a distributed network. *Hum. Brain Mapp.* 31, 26–35. doi: 10.1002/hbm.20842

Heyes, C. (2010). Where do mirror neurons come from? *Neurosci. Biobehav. Rev.* 34, 575–583. doi: 10.1016/j.neubiorev.2009.11.007

Hirai, M., Fukushima, H., and Hiraki, K. (2003). An event-related potentials study of biological motion perception in humans. *Neurosci. Lett.* 344, 41–44. doi: 10.1016/S0304-3940(03)00413-0

Hirai, M., and Hiraki, K. (2006). The relative importance of spatial versus temporal structure in the perception of biological motion: an event-related potential study. *Cognition* 99, B15–B29. doi: 10.1016/j.cognition.2005.05.003

Hirai, M., Senju, A., Fukushima, H., and Hiraki, K. (2005). Active processing of biological motion perception: an ERP study. *Brain Res. Cogn. Brain Res.* 23, 387–396. doi: 10.1016/j.cogbrainres.2004.11.005

Hirai, M., Watanabe, S., Honda, Y., and Kakigi, R. (2009). Developmental changes in point-light walker processing during childhood and adolescence: an event-related potential study. *Neuroscience* 161, 311–325. doi: 10.1016/j.neuroscience.2009.03.026

Hirai, M., Watanabe, S., Honda, Y., and Kakigi, R. (2013). Developmental changes in point-light walker processing during childhood: a two-year follow-up ERP study. *Dev. Cogn. Neurosci.* 5, 51–62. doi: 10.1016/j.dcn.2013.01.002

Howard, M. W., Rizzuto, D. S., Caplan, J. B., Madsen, J. R., Lisman, J., Aschenbrenner-Scheibe, R., et al. (2003). Gamma oscillations correlate with working memory load in humans. *Cereb. Cortex* 13, 1369–1374. doi: 10.1093/cercor/bhg084

Ishihara, T., and Yoshi, N. (1972). Multivariate analytic study of EEG and mental activity in juvenile delinquents. *Electroencephalogr. Clin. Neurophysiol.* 33, 71–80. doi: 10.1016/0013-4694(72)90026-0

Jacob, P., and Jeannerod, M. (2005). The motor theory of social cognition: a critique. *Trends Cogn. Sci.* 9, 21–25. doi: 10.1016/j.tics.2004.11.003

Jeffreys, D. A. (1996). Simple methods of identifying the independently generated components of scalp-recorded responses evoked by stationary patterns. *Exp. Brain Res.* 111, 100–112. doi: 10.1007/BF00229559

Jensen, O., and Colgin, L. L. (2007). Cross-frequency coupling between neuronal oscillations. *Trends Cogn. Sci.* 11, 267–269. doi: 10.1016/j.tics.2007.05.003

Johansson, G. (1973). Visual perception of biological motion and a model for its analysis. *Percept. Psychophys.* 14, 201–211. doi: 10.3758/BF03212378

Jokisch, D., Daum, I., Suchan, B., and Troje, N. F. (2005). Structural encoding and recognition of biological motion: evidence from event-related potentials and source analysis. *Behav. Brain Res.* 157, 195–204. doi: 10.1016/j.bbr.2004.06.025

Kahana, M. J., Sekuler, R., Caplan, J. B., Kirschen, M., and Madsen, J. R. (1999). Human theta oscillations exhibit task dependence during virtual maze navigation. *Nature* 399, 781–784. doi: 10.1038/21645

Kandel, E. (2013). The new science of mind and the future of knowledge. *Neuron* 80, 546–560. doi: 10.1016/j.neuron.2013.10.039

Kang, J., Robinson, H. P. C., and Feng, J. (2010). Diversity of intrinsic frequency encoding patterns in rat cortical neurons—mechanisms and possible functions. *PLoS ONE* 5:e9608. doi: 10.1371/journal.pone.0009608

Keil, A., Gruber, T., Müller, M. M., Moratti, S., Stolarova, M., Bradley, M. M., et al. (2003). Early modulation of visual perception by emotional arousal: evidence from steady state visual evoked brain potentials. *Cogn. Affect. Behav. Neurosci.* 3, 195–206. doi: 10.3758/CABN.3.3.195

Kilner, J. M., Friston, K. J., and Frith, C. D. (2007). Predictive coding: an account of the mirror neuron system. *Cogn. Process.* 8, 159–166. doi: 10.1007/s10339-007-0170-2

Klimesch, W. (1999). EEG alpha and theta oscillations reflect cognitive and memory performance: a review and analysis. *Brain Res. Brain Res. Rev.* 29, 169–195. doi: 10.1016/S0165-0173(98)00056-3

Klimesch, W. (2012). Alpha-band oscillations, attention, and controlled access to stored information. *Trends Cogn. Sci.* 16, 606–617. doi: 10.1016/j.tics.2012.10.007

Klimesch, W., Doppelmayr, M., Pachinger, T., and Russegger, H. (1997). Event-related desynchronization in the alpha band and the processing of semantic information. *Brain Res. Cogn. Brain Res.* 6, 83–94. doi: 10.1016/S0926-6410(97)00018-9

Klimesch, W., Doppelmayr, M., Schimke, H., and Pachinger, T. (1996). Alpha frequency, reaction time, and the speed of processing information. *J. Clin. Neurophysiol.* 13, 511–518.

Klimesch, W., Sauseng, P., and Gerloff, C. (2003). Enhancing cognitive performance with repetitive transcranial magnetic stimulation at human individual alpha frequency. *Eur. J. Neurosci.* 17, 1129–1133. doi: 10.1046/j.1460-9568.2003.02517.x

Klimesch, W., Sauseng, P., and Hanslmayr, S. (2007). EEG alpha oscillations: the inhibition-timing hypothesis. *Brain Res. Rev.* 53, 63–88. doi: 10.1016/j.brainresrev.2006.06.003

Klimesch, W., Schack, B., Schabus, M., Doppelmayr, M., Gruber, W., and Sauseng, P. (2004). Phase-locked alpha and theta oscillations generate the P1-N1 complex and are related to memory performance. *Brain Res. Cogn. Brain Res.* 19, 302–316. doi: 10.1016/j.cogbrainres.2003.11.016

Kocsis, B., Bragin, A., and Buzsáki, G. (1999). Interdependence of multiple theta generators in the hippocampus: a partial coherence analysis. *J. Neurosci.* 19, 6200–6212.

Krakowski, A. I., Ross, L. A., Snyder, A. C., Sehatpour, P., Kelly, S. P., and Foxe, J. J. (2011). The neurophysiology of human biological motion processing: a high-density electrical mapping study. *Neuroimage* 56, 373–383. doi: 10.1016/j.neuroimage.2011.01.058

Kravitz, D. J., Saleem, K. S., Baker, C. I., and Mishkin, M. (2011). A new neural framework for visuospatial processing. *Nat. Rev. Neurosci.* 12, 217–230. doi: 10.1038/nrn3008

Kruse, W., and Eckhorn, R. (1996). Inhibition of sustained gamma oscillations (35-80 Hz) by fast transient responses in cat visual cortex. *Proc. Natl. Acad. Sci. U.S.A.* 93, 6112–6117. doi: 10.1073/pnas.93.12.6112

Leakey, M., and Walker, A. (1997). Early hominid fossils from Africa. *Sci. Am.* 276, 74–79. doi: 10.1038/scientificamerican0697-74

Leung, L. W., and Borst, J. G. (1987). Electrical activity of the cingulate cortex. I. Generating mechanisms and relations to behavior. *Brain Res.* 407, 68–80. doi: 10.1016/0006-8993(87)91220-0

Liebe, S., Hoerzer, G. M., Logothetis, N. K., and Rainer, G. (2012). Theta coupling between V4 and prefrontal cortex predicts visual short-term memory performance. *Nat. Neurosci.* 15, 456–462, S1–S2. doi: 10.1038/nn.3038

Makeig, S., Westerfield, M., Jung, T. P., Enghoff, S., Townsend, J., Courchesne, E., et al. (2002). Dynamic brain sources of visual evoked responses. *Science* 295, 690–694. doi: 10.1126/science.1066168

McAleer, P., Pollick, F. E., Love, S. A., Crabbe, F., and Zacks, J. M. (2014). The role of kinematics in cortical regions for continuous human motion perception. *Cogn. Affect. Behav. Neurosci.* 14, 307–318. doi: 10.3758/s13415-013-0192-4

McGlothlin, B., Jiacoletti, D., and Yandell, L. (2012). The inversion effect: biological motion and gender recognition. *Psi Chi J. Psychol. Res.* 17, 68–72.

McTeague, L. M., Shumen, J. R.,Wieser, M. J., Lang, P. J., and Keil, A. (2011). Social vision: sustained perceptual enhancement of affective facial cues in social anxiety. *Neuroimage* 54, 1615–1624. doi: 10.1016/j.neuroimage.2010.08.080

Mitchell, D. J., McNaughton, N., Flanagan, D., and Kirk, I. J. (2008). Frontal-midline theta from the perspective of hippocampal "theta." *Prog. Neurobiol.* 86, 156–185. doi: 10.1016/j.pneurobio.2008.09.005

Mizuhara, H., Wang, L.-Q., Kobayashi, K., and Yamaguchi, Y. (2004). A long-range cortical network emerging with theta oscillation in a mental task. *Neuroreport* 15, 1233–1238. doi: 10.1097/01.wnr.0000126755.09715.b3

Müller, M. M., Teder-Salejarvi, W., and Hillyard, S. A. (1998). The time course of cortical facilitation during cued shifts of spatial attention. *Nat. Neurosci.* 1, 631–634. doi: 10.1038/2865

Müller, M. M., Teder, W., and Hillyard, S. A. (1997). Magnetoencephalographic recording of steady-state visual evoked cortical activity. *Brain Topogr.* 9, 163–168. doi: 10.1007/BF01190385

O'Keefe, J., and Recce, M. L. (1993). Phase relationship between hippocampal place units and the EEG theta rhythm. *Hippocampus* 3, 317–330.

Pavlova, M., Birbaumer, N., and Sokolov, A. (2006). Attentional modulation of cortical neuromagnetic gamma response to biological movement. *Cereb. Cortex* 16, 321–327. doi: 10.1093/cercor/bhi108

Pavlova, M., Lutzenberger, W., Sokolov, A., and Birbaumer, N. (2004). Dissociable cortical processing of recognizable and non-recognizable biological movement: analysing gamma MEG activity. *Cereb. Cortex* 14, 181–188. doi: 10.1093/cercor/bhg117

Pavlova, M., and Sokolov, A. (2000). Orientation specificity in biological motion perception. *Percept. Psychophys.* 62, 889–899. doi: 10.3758/BF03212075

Peyrin, C., Michel, C. M., Schwartz, S., Thut, G., Seghier, M., Landis, T., et al. (2010). The neural substrates and timing of top-down processes during coarse-to-fine categorization of visual scenes: a combined fMRI and ERP study. *J. Cogn. Neurosci.* 22, 2768–2780. doi: 10.1162/jocn.2010.21424

Pinotsis, D. A., Brunet, N., Bastos, A., Bosman, C. A., Litvak, V., Fries, P., et al. (2014). Contrast gain control and horizontal interactions in V1: a DCM study. *Neuroimage* 92C, 143–155. doi: 10.1016/j.neuroimage.2014.01.047

Pollick, F. E., Kay, J. W., Heim, K., and Stringer, R. (2005). Gender recognition from point-light walkers. *J. Exp. Psychol. Hum. Percept. Perform.* 31, 1247–1265. doi: 10.1037/0096-1523.31.6.1247

Pozzo, T., Berthoz, A., and Lefort, L. (1990). Head stabilization during various locomotor tasks in humans. I. Normal subjects. *Exp. Brain Res.* 82, 97–106. doi: 10.1007/BF00230842

Press, C., Heyes, C., and Kilner, J. M. (2011). Learning to understand others' actions. *Biol. Lett.* 7, 457–460. doi: 10.1098/rsbl.2010.0850

Raghavachari, S., Kahana, M. J., Rizzuto, D. S., Caplan, J. B., Kirschen, M. P., Bourgeois, B., et al. (2001). Gating of human theta oscillations by a working memory task. *J. Neurosci.* 21, 3175–3183.

Raghavachari, S., Lisman, J. E., Tully, M., Madsen, J. R., Bromfield, E. B., and Kahana, M. J. (2006). Theta oscillations in human cortex during a working-memory task: evidence for local generators. *J. Neurophysiol.* 95, 1630–1638. doi: 10.1152/jn.00409.2005

Ramalingam, N., McManus, J. N. J., Li, W., and Gilbert, C. D. (2013). Top-down modulation of lateral interactions in visual cortex. *J. Neurosci.* 33, 1773–1789. doi: 10.1523/JNEUROSCI.3825-12.2013

Ray, S., and Maunsell, J. H. R. (2010). Differences in gamma frequencies across visual cortex restrict their possible use in computation. *Neuron* 67, 885–896. doi: 10.1016/j.neuron.2010.08.004

Regan, D. (1966). Some characteristics of average steady-state and transient responses evoked by modulated light. *Electroencephalogr. Clin. Neurophysiol.* 20, 238–248. doi: 10.1016/0013-4694(66)90088-5

Rey, H. G., Fried, I., and Quian Quiroga, R. (2014). Timing of single-neuron and local field potential responses in the human medial temporal lobe. *Curr. Biol.* 24, 299–304. doi: 10.1016/j.cub.2013.12.004

Rizzolatti, G., and Craighero, L. (2004). The mirror-neuron system. *Annu. Rev. Neurosci.* 27, 169–192. doi: 10.1146/annurev.neuro.27.070203.144230

Rizzolatti, G., Fadiga, L., Gallese, V., and Fogassi, L. (1996). Premotor cortex and the recognition of motor actions. *Brain Res. Cogn. Brain Res.* 3, 131–141. doi: 10.1016/0926-6410(95)00038-0

Roberts, M. J., Lowet, E., Brunet, N. M., Ter Wal, M., Tiesinga, P., Fries, P., et al. (2013). Robust gamma coherence between macaque V1 and V2 by dynamic frequency matching. *Neuron* 78, 523–536. doi: 10.1016/j.neuron.2013.03.003

Rojas, M., Masip, D., Todorov, A., and Vitria, J. (2011). Automatic prediction of facial trait judgments: appearance vs. structural models. *PLoS ONE* 6:e23323. doi: 10.1371/journal.pone.0023323

Rossion, B., Prieto, E. A., Boremanse, A., Kuefner, D., and Van Belle, G. (2012). A steady-state visual evoked potential approach to individual face perception: effect of inversion, contrast-reversal and temporal dynamics. *Neuroimage* 63, 1585–1600. doi: 10.1016/j.neuroimage.2012.08.033

Sadaghiani, S., Scheeringa, R., Lehongre, K., Morillon, B., Giraud, A.-L., D'Esposito, M., et al. (2012). α-band phase synchrony is related to activity in the fronto-parietal adaptive control network. *J. Neurosci.* 32, 14305–14310. doi: 10.1523/JNEUROSCI.1358-12.2012

Sasaki, K., Gemba, H., Nambu, A., Kyuhou, S., Matsuzaki, R., and Tsujimoto, T. (1996a). Studies on integrative functions of the human frontal association cortex by use of MEG. *Electroencephalogr. Clin. Neurophysiol. Suppl.* 47, 181–190.

Sasaki, K., Nambu, A., Tsujimoto, T., Matsuzaki, R., Kyuhou, S., and Gemba, H. (1996b). Studies on integrative functions of the human frontal association cortex with MEG. *Brain Res. Cogn. Brain Res.* 5, 165–174. doi: 10.1016/S0926-6410(96)00053-5

Sasaki, K., Tsujimoto, T., Nishikawa, S., Nishitani, N., and Ishihara, T. (1996c). Frontal mental theta wave recorded simultaneously with magnetoencephalography and electroencephalography. *Neurosci. Res.* 26, 79–81. doi: 10.1016/0168-0102(96)01082-6

Sauseng, P., Hoppe, J., Klimesch, W., Gerloff, C., and Hummel, F. C. (2007). Dissociation of sustained attention from central executive functions: local activity and interregional connectivity in the theta range. *Eur. J. Neurosci.* 25, 587–593. doi: 10.1111/j.1460-9568.2006.05286.x

Saygin, A. P., Wilson, S. M., Hagler, D. J. Jr., Bates, E., and Sereno, M. I. (2004). Point-light biological motion perception activates human premotor cortex. *J. Neurosci.* 24, 6181–6188. doi: 10.1523/JNEUROSCI.0504-04.2004

Sceniak, M. P., Hawken, M. J., and Shapley, R. (2002). Contrast-dependent changes in spatial frequency tuning of macaque V1 neurons: effects of a changing receptive field size. *J. Neurophysiol.* 88, 1363–1373.

Schütz-Bosbach, S., and Prinz, W. (2007). Perceptual resonance: action-induced modulation of perception. *Trends Cogn. Sci.* 11, 349–355. doi: 10.1016/j.tics.2007.06.005

Sederberg, P. B., Kahana, M. J., Howard, M. W., Donner, E. J., and Madsen, J. R. (2003). Theta and gamma oscillations during encoding predict subsequent recall. *J. Neurosci.* 23, 10809–10814.

Silva, L. R., Amitai, Y., and Connors, B. W. (1991). Intrinsic oscillations of neocortex generated by layer 5 pyramidal neurons. *Science* 251, 432–435. doi: 10.1126/science.1824881

Singer, W. (1999). Neuronal synchrony: a versatile code for the definition of relations? *Neuron* 24, 49–65, 111–125. doi: 10.1016/S0896-6273(00)80821-1

Singer, W. (2009). Distributed processing and temporal codes in neuronal networks. *Cogn. Neurodyn.* 3, 189–196. doi: 10.1007/s11571-009-9087-z

Tallon-Baudry, C., and Bertrand, O. (1999). Oscillatory gamma activity in humans and its role in object representation. *Trends Cogn. Sci.* 3, 151–162. doi: 10.1016/S1364-6613(99)01299-1

Tallon-Baudry, C., Bertrand, O., Delpuech, C., and Pernier, J. (1996). Stimulus specificity of phase-locked and non-phase-locked 40 Hz visual responses in human. *J. Neurosci.* 16, 4240–4249.

Thorpe, S. K. S., Holder, R. L., and Crompton, R. H. (2007). Origin of human bipedalism as an adaptation for locomotion on flexible branches. *Science* 316, 1328–1331. doi: 10.1126/science.1140799

Traub, R. D., Cunningham, M. O., Gloveli, T., LeBeau, F. E. N., Bibbig, A., Buhl, E. H., et al. (2003). GABA-enhanced collective behavior in neuronal axons underlies persistent gamma-frequency oscillations. *Proc. Natl. Acad. Sci. U.S.A.* 100, 11047–11052. doi: 10.1073/pnas.1934854100

Traub, R. D., Jefferys, J. G., and Whittington, M. A. (1997). Simulation of gamma rhythms in networks of interneurons and pyramidal cells. *J. Comput. Neurosci.* 4, 141–150. doi: 10.1023/A:1008839312043

Troje, N. F., Westhoff, C., and Lavrov, M. (2005). Person identification from biological motion: effects of structural and kinematic cues. *Percept. Psychophys.* 67, 667–675. doi: 10.3758/BF03193523

Ulloa, E. R., and Pineda, J. A. (2007). Recognition of point-light biological motion: mu rhythms and mirror neuron activity. *Behav. Brain Res.* 183, 188–194. doi: 10.1016/j.bbr.2007.06.007

Urgen, B. A., Plank, M., Ishiguro, H., Poizner, H., and Saygin, A. P. (2013). EEG theta and Mu oscillations during perception of human and robot actions. *Front. Neurorobotics* 7:19. doi: 10.3389/fnbot.2013.00019

Vaina, L. M., Solomon, J., Chowdhury, S., Sinha, P., and Belliveau, J. W. (2001). Functional neuroanatomy of biological motion perception in humans. *Proc. Natl. Acad. Sci. U.S.A.* 98, 11656–11661. doi: 10.1073/pnas.191374198

Vidal, J. R., Perrone-Bertolotti, M., Levy, J., De Palma, L., Minotti, L., Kahane, P., et al. (2014). Neural repetition suppression in ventral occipito-temporal cortex occurs during conscious and unconscious processing of frequent stimuli. *Neuroimage* 95C, 129–135. doi: 10.1016/j.neuroimage.2014.03.049

Viviani, P., and Stucchi, N. (1992). Biological movements look uniform: evidence of motor-perceptual interactions. *J. Exp. Psychol. Hum. Percept. Perform.* 18, 603–623. doi: 10.1037/0096-1523.18.3.603

Walter, W. G., and Dovey, V. J. (1944). Electro-encephalography in cases of sub-cortical tumour. *J. Neurol. Neurosurg. Psychiatry* 7, 57–65. doi: 10.1136/jnnp.7.3-4.57

White, N. C., Fawcett, J. M., and Newman, A. J. (2014). Electrophysiological markers of biological motion and human form recognition. *Neuroimage* 84, 854–867. doi: 10.1016/j.neuroimage.2013.09.026

Whittington, M. A., and Traub, R. D. (2003). Interneuron diversity series: inhibitory interneurons and network oscillations *in vitro*. *Trends Neurosci.* 26, 676–682. doi: 10.1016/j.tins.2003.09.016

Zanto, T. P., Rubens, M. T., Thangavel, A., and Gazzaley, A. (2011). Causal role of the prefrontal cortex in top-down modulation of visual processing and working memory. *Nat. Neurosci.* 14, 656–661. doi: 10.1038/nn.2773

Zeki, S., Watson, J. D., Lueck, C. J., Friston, K. J., Kennard, C., and Frackowiak, R. S. (1991). A direct demonstration of functional specialization in human visual cortex. *J. Neurosci.* 11, 641–649.

Conflict of Interest Statement: The authors declare that the research was conducted in the absence of any commercial or financial relationships that could be construed as a potential conflict of interest.

Received: 30 May 2014; accepted: 31 August 2014; published online: 18 September 2014.

*Citation: Zarka D, Cevallos C, Petieau M, Hoellinger T, Dan B and Cheron G (2014) Neural rhythmic symphony of human walking observation: Upside-down and Uncoordinated condition on cortical theta, alpha, beta and gamma oscillations. Front. Syst. Neurosci. **8**:169. doi: 10.3389/fnsys.2014.00169*

This article was submitted to the journal Frontiers in Systems Neuroscience.

frontiers in
SYSTEMS NEUROSCIENCE

ORIGINAL RESEARCH ARTICLE
published: 05 August 2014
doi: 10.3389/fnsys.2014.00138

Brain-machine interfacing control of whole-body humanoid motion

Karim Bouyarmane[1]*, Joris Vaillant[2,3], Norikazu Sugimoto[4], François Keith[2,3], Jun-ichiro Furukawa[1,5] and Jun Morimoto[1]

[1] Computational Neuroscience Laboratories, Department of Brain Robot Interface, Advanced Telecommunications Research Institute International (ATR), Kyoto, Japan
[2] Laboratoire d'Informatique de Robotique et de Micro-électronique de Montpellier, CNRS-University of Montpellier 2, Montpellier, France
[3] CNRS-AIST Joint Robotics Laboratory, UMI3218/CRT, National Intitute of Advanced Industrial Science and Technology, Tsukuba, Japan
[4] National Institute of Information and Communications Technology, Osaka, Japan
[5] Graduate School of Frontier Biosciences, Osaka University, Osaka, Japan

Edited by:
Mikhail Lebedev, Duke University, USA

Reviewed by:
Randal A. Koene, Boston University, USA
M. Van Der Meulen, University of Luxembourg, Luxembourg

***Correspondence:**
Karim Bouyarmane, ATR Computational Neuroscience Laboratories, Department of BRI, 2-2-2 Hikaridai, Seika-cho Soraku-gun, Kyoto 619-0288, Japan
e-mail: karim.bouyarmane@lirmm.fr

We propose to tackle in this paper the problem of controlling whole-body humanoid robot behavior through non-invasive brain-machine interfacing (BMI), motivated by the perspective of mapping human motor control strategies to human-like mechanical avatar. Our solution is based on the adequate reduction of the controllable dimensionality of a high-DOF humanoid motion in line with the state-of-the-art possibilities of non-invasive BMI technologies, leaving the complement subspace part of the motion to be planned and executed by an autonomous humanoid whole-body motion planning and control framework. The results are shown in full physics-based simulation of a 36-degree-of-freedom humanoid motion controlled by a user through EEG-extracted brain signals generated with motor imagery task.

Keywords: humanoid whole-body control, brain-machine interfacing, motor imagery, motion planning, semi-autonomous humanoid, contact support planning

1. INTRODUCTION

Due to their design that allows them to be readily used in an environment that was initially arranged to accommodate the human morphology, that makes them more acceptable to the users, and easier to interact with, it is generally admitted that humanoid robots are an appropriate choice as living assistants for the everyday tasks, for instance for the elderly and/or reduced-mobility people. The problem that naturally arises is that of the control of such an assistant and how to communicate the wills and intentions of the user to the robot. This problem is of course general but becomes more challenging when addressing the above-mentioned category of users for which communication capabilities can also be impaired (stroke patients for example). This brings our initial idea of considering brain-machine interfaces (BMI) as the possible communication tool between the human and the humanoid assistant. Notwithstanding, brought along with this reflection was the more general question, non-necessarily application-directed, of a human using its brain motor functions to control a human-like artificial body the same way they control their own human body. This question becomes our main motivation and concern in the present work since solving it would pave the way of the discussed applicative perspectives. We thus propose our solution to it in this paper.

The approach we choose to investigate deals with the following constraints of the problem. First, we only consider easy-and-ready-to-use non-invasive BMI technologies. Among this class of technologies, we aim more specifically at the one that would align best and most intuitively with our expressed desire of mimicking human motor-control function, namely motor-imagery-based BMI, consisting ideally for the human user of imagining a movement of their own body for it to be replicated in the humanoid body, though we do not reach that ideal vision restricting our study for the sake of feasibility demonstration to the use of a generic motor-imagery task (imagining arm movement) that we re-target to the specific motion of the robot at hand (leg motion of the robot). Finally, the control paradigm for the humanoid robot we set as objective in our study is that of low-level joint/link-level control, to keep as general behavior and class of movements as possible for the user to replicate at the robot, without restriction of the class of movements allowed by particular higher-level humanoid motion controllers.

We address the related work and existing proposed solutions for this problem or approaching ones in the next section (Section 2). We then detail our own solution, based on the integration of, for the humanoid motion control part, an autonomous contact-based planning and control framework (Section 3), and for the BMI part, a motor-imagery-task-generated brain-signal classification method (Section 4). The integration of these two originally independent components is discussed in Section 5, 6 presents an example proof-of-concept experiment with a fully physics-simulated humanoid robot. Section 7 concludes the paper with discussion and future work.

2. RELATED WORK AND PROPOSED SOLUTION

Various approaches have been proposed to solve the problem we stated in the introduction of controlling a humanoid robot with

BMI (Bell et al., 2008; Bryan et al., 2011; Chung et al., 2011; Finke et al., 2011; Gergondet et al., 2011; Ma et al., 2013). All approaches, ours included, are based on the integration of a BMI technology with a humanoid controller, and can thus be categorized according to which strategy is followed for each of these two components. See **Figure 1** for an overview.

From the BMI point-of-view, all these works do abide by our posed constraint of using non-invasive BMIs that rely on electroencephalography (EEG), generally utilizing the well-established frameworks of visual-stimulation-based event-related potentials (ERP) such as P300 in Bell et al. (2008), evoked potentials (EP) such as the steady state visually evoked potential (SSVEP) in Bryan et al. (2011); Chung et al. (2011); Gergondet et al. (2011), or hybrid approaches combining electrooculogram (EOG) with ERP such as in Ma et al. (2013), or P300 with motor-imagery-evoked event-related desynchronization (ERD) (Finke et al., 2011; Riechmann et al., 2011). None, however, investigated a solely motor-imagery-based BMI as stated in our motivations of replicating intuitive human motor-control strategies. Hence our first contribution in the integration initiative.

We adapt in this work a motor-imagery decoding scheme that we previously developed for the control of a one-degree-of-freedom robot and for sending standing-up/sitting-down commands to a wearable exoskeleton (Noda et al., 2012). It allows us to generate a three-valued discrete command that we propose to map to a one-dimensional subspace of the multi-dimensional whole-body configuration space motion of the humanoid, and more precisely the motion along a generalized notion of "vertical axis" of the moving end-limb, such as the foot of the swing leg in a biped motion for instance. As we detail in the course of the paper (Section 5), the motivation behind this strategy is to allow the user to assist the autonomous motion that might lead the moving limb to be "blocked" in potential field local minima while trying to avoid collision. The strategy can in future work be developed into a more sophisticated two-dimensional continuous command one as proven possible by recent and ongoing studies on motor-imagery control (Wolpaw and McFarland, 2004; Miller et al., 2010).

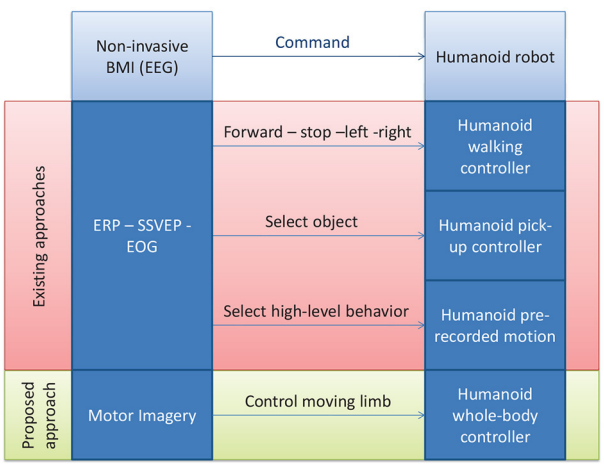

FIGURE 1 | A schematic illustration of the proposed approach vs. the existing ones for controlling a humanoid robot with non-invasive BMI.

From the humanoid controller point-of-view now, the most standard retained solution consists in using available humanoid high level controllers. These can be either walking controllers with the commands "walk forward" "stop" "turn left" "turn right" sent to a walking humanoid, effectively reducing the problem of humanoid motion control to that of walk steering control (Bell et al., 2008; Chung et al., 2011; Finke et al., 2011; Gergondet et al., 2011), or an object selecton/pick-up controller, where the user selects an object in the scene and then the arm reaching/grasping controller of the robot picks up the desired object (Bryan et al., 2011). Finally Ma et al. (2013) use a hybrid control strategy where both walk steering and selecting a high-level behavior among a finite library can be done by switching between EOG and ERP control. With these strategies, a humanoid can be seen as an arm-equipped mobile robot, with wheels instead of legs (as it is actually the case in Bryan et al., 2011 where only the upper body is humanoid), and consequently the considerable amount of work done on BMI wheelchair control, for example, can be readily adapted. However, in doing so, the advantages of using a legged device over a wheeled one are partially lost, and we can no longer claim the need for the humanoid design nor defend the argument of the possibility of using the robot in everyday living environment which would present non-flat structures, such as stairs for example, with which the walking controllers are not efficient to deal.

While we admit that these strategies relying on walking pattern generators can in the long term benefit from the developments in these techniques that would allow them to autonomously cope with unstructured terrain (variable height stairs, rough terrain) (Takanishi and Kato, 1994; Hashimoto et al., 2006; Herdt et al., 2010; Morisawa et al., 2011), and that they can as well use the hierarchical architectures in which they are embedded as it is the case in Chung et al. (2011); Bryan et al. (2011); Ma et al. (2013) for switching, for example, to an appropriate stair-climbing controller when facing stairs, we choose in this work to investigate an entirely different approach that does not incorporate any kind of walking or high-level controller. Instead, we propose to allow the user to perform lower-level joint/link level control of the whole-body motion of humanoid, driven again by the desire of replicating the human low-level motor-control strategies into the humanoid, but also by the belief that a generic-motion generating approach will allow the robot assistant to deal more systematically with unpredictable situations that inevitably occur in everyday living scenarios and for which the discussed hierarchical architectures would not have exhaustively accounted. This is our second contribution. To achieve this goal, we rely on the contact planning paradigm that we previously proposed for fully autonomous robot (Bouyarmane and Kheddar, 2012), adapting it here to the instance of a BMI-controlled robot.

3. HUMANOID CONTROLLER

Our humanoid controller is based on the multi-contact planning paradigm, introduced in Hauser et al. (2008); Bouyarmane and Kheddar (2012). This controller allows for autonomously planning and executing the complex high-degree-of-freedom motion

of the humanoid from a high-level objective expressed in terms of a desired contact state to reach. The controller works in two stages: an off-line planning stage and an on-line execution stage.

At the planning stage (Bouyarmane and Kheddar, 2011a), a search algorithm explores all the possible contact transitions that would allow the robot to go from the initial contact state to the desired goal contact state. What we mean by contact transition is either removing one contact from the current contact state (e.g., removing the right foot from a double-support state to transition to a left-foot single-support one) or adding one contact to the current contact state (e.g., bringing the swing right foot in contact with the floor to transition from a left-foot single-support phase to a double support phase). One must however note that a contact is defined as a pairing between any surface designated on the cover of the links of the robot and any surface on the environment, and is not restricted to be established between the soles of the feet and the floor surface. For instance, a contact can be defined between the forearm of the robot and the arm of an armchair, or between the palm of the hand of the robot and the top of a table. This strategy stems from the observation that all motions of humans can be broken down to such a succession of contact transitions, be it cyclic motions such as walking where these transitions occur between the feet and the ground, or more complex maneuvers such as standing up from an armchair were contacts transitions occur between various parts of the body (hands, forearms feet, tights, etc.) and various parts the environment objects (armchair, table floor, etc.). This feature makes our planning paradigm able to cope with situations that are broader than the ones classically tackled by humanoid motion planner that either plan for the motion assuming a given contact state (e.g., planning a reaching motion with the two feet fixed on the ground) (Kuffner et al., 2002; Yamane et al., 2004; Yoshida et al., 2006, 2008), or planning footprint placements assuming a cyclic walking pattern will occur on these footprints (Kuffner et al., 2001; Chestnutt et al., 2003, 2005). This aligns well with our initially expressed objective of controlling whole-body motion of any kind without restriction to a subclass of taxonomically identified motions.

At the above-described contact-transition search stage, every contact state that is being explored is validated by running an inverse-kinematics solver which finds an appropriate whole-body configuration (posture) of the robot that meets the desired contact state, while at the same time satisfying physics constraints to make the posture physically realizable within the mechanical limits of the robots (Bouyarmane and Kheddar, 2010). At the end of the offline-contact planning stage, we are provided with a sequence of feasible contact transitions and associated transition postures, that go from the initial contact state to the the goal.

The second stage of the controller is an on-line real-time low-level controller (Bouyarmane and Kheddar, 2011b) that will successively track each of the intermediate postures fed by the off-line planning stage, until the last element of the planned sequence is reached. The controller is formulated as a multi-objective quadratic program optimization scheme, the objectives being expressed in terms of the moving link of the robot involved in the current contact transition being tracked along the sequence (e.g., the foot if the contact transition is a sole/floor one), the center of mass (CoM) of the robot to keep balance, and the whole configuration of the robot to solve for the redundancies of the high-DOF motion. These objectives are autonomously decided by a finite-state machine (FSM) that encodes the current type of transition among the following two types:

- Removing-contact transition: the motion of the robot is performed on the current contact state, and the step is completed when the contact forces applied on the contact we want to remove vanish. This is done by shifting the weight of the robot away from the being-removed contact, tracking the CoM position of the following configuration in the sequence. There is no end-link motion in this kind of step. The corresponding FSM state is labeled "Shift CoM."
- Adding-contact transition: the motion of the robot is performed on the current contact state, and the motion of the link we want to add as a contact is guided to its desired contact location. There is thus an end-link motion (contact link) in this kind of step. Balance is ensured by also tracking the CoM position of the following configuration in the sequence. The corresponding FSM state is labeled "Move contact link."

As an example, a cyclic walking FSM state transition sequence will look like: Move contact link (left foot) → Shift CoM (on the left foot) → Move contact link (right foot) → Shift CoM (on the right foot) → Move contact link → ... But non-cyclic behaviors are also possible and allowed, for example when standing up from an armchair where contacts between the hands of the robot and arms of chair can be added in succession and removed in succession.

The final output of the quadratic program optimization scheme is a torque command that is sent to the robot at every control iteration, after the execution of which the state of the robot is fed-back to the controller.

4. BMI DECODING

Our aim is for the humanoid system to be controlled by using brain activities in the similar brain regions that are used to control the user's own body. Therefore, we asked a subject to control the simulated humanoid system by using motor imagery of arm movements so that brain activities in motor-related regions such as the primary motor cortex can be used.

As non-invasive brain signal acquisition device we use an electroencephalogram (EEG) system (64 channels and sampling rate of 2048 Hz). The brain signals are decoded and classified using the method that was applied and presented in our previous work (Noda et al., 2012), based on the spectral regularization matrix classifier described in Tomioka and Aihara (2007); Tomioka and Muller (2010). We recall the method here.

The EEG signals, of covariance matrices $\mathbf{C}$ considered as input, are classified into two classes, labeled with the variable k, with the following output probabilities (at sampled time t):

$$P(k_t = +1|\mathbf{C}_t) = \frac{1}{1 + \exp(-a_t)}, \quad (1)$$

$$P(k_t = -1|\mathbf{C}_t) = \frac{\exp(-a_t)}{1 + \exp(-a_t)}, \quad (2)$$

with the logit being modeled as a linear function of $\mathbf{C}$

$$a_t = \mathrm{tr}[\mathbf{W}^\top \mathbf{C}_t] + b\,, \tag{3}$$

and where $\mathbf{W}$ is the parameter matrix to be learned (b is a constant-valued bias).

To learn $\mathbf{W}$ the following minimization problem is solved

$$\min \sum_{t=1}^{n} \ln\left(1 + \exp\left(-k_t a_t\right)\right) + \lambda \|\mathbf{W}\|_1\,, \tag{4}$$

λ being the regularization variable ($\lambda = 14$ in the application below) and

$$\|\mathbf{W}\|_1 = \sum_{i=1}^{r} \sigma_i[\mathbf{W}] \tag{5}$$

being the spectral l_1-norm of $\mathbf{W}$ (r is the rank of $\mathbf{W}$ and $\sigma_i[\mathbf{W}]$ its i-th singular value).

Once the classifier learned, the 7–30 Hz band-pass-filtered measured EEG signals are decoded online, by down-sampling them from 2048 to 128 Hz, and applying Laplace filtering and common average substraction to remove voltage bias. Their covariance matrix, initialized at $\mathbf{C}_t = \mathbf{x}_t^\top \mathbf{x}_t$ for the first time step $t = 1$, where $\mathbf{x}_t \in \mathbb{R}^{1\times 64}$ denotes the filtered EEG signals, are updated at every time step as follows

$$\mathbf{C}_t = \frac{1}{N}\mathbf{x}_t^\top \mathbf{x}_t + \frac{N-1}{N}\mathbf{C}_{t-1}\,, \tag{6}$$

and used to compute the probabilities in Equations (1) and (2).

Finally, the three-valued discrete command c_t that is sent to the robot is selected from these probabilities through the following hysteresis

$$c_t = \begin{cases} +1 & \text{if } P(k_t = +1|\mathbf{C}_t) > P_{\text{thresh}} \text{ and } c_{t-1} \neq +1\,, \\ -1 & \text{if } P(k_t = -1|\mathbf{C}_t) > P_{\text{thresh}} \text{ and } c_{t-1} \neq -1\,, \\ 0 & \text{otherwise}\,, \end{cases} \tag{7}$$

where the threshold is set at $P_{\text{thresh}} = 0.6$.

5. COMPONENT INTEGRATION

The command c_t devised in Equation (7) is sent to the online humanoid whole-body controller via UDP protocol at 128 Hz frequency and used to modify the planned and autonomously executed motion of the humanoid robot as described below and as schematically represented in **Figure 2**.

When the robot is executing a step that requires moving a link to a planned contact location (contact-adding step, executed by the state "Move contact link" of the FSM, see Section 3), then instead of tracking directly the goal contact location, we decompose the motion of the end-link (the contact link, for instance the foot) into two phases:

- Lift-off phase: The link first tracks an intermediate position located at a designated way-point.
- Touch-down phase: The link then tracks its goal location in the planned contact state sequence.

This two-phase decomposition allows the link to avoid unnecessary friction with the environment contact surface and to avoid colliding with environment features such as stairs.

Each of these two phases correspond to a sub-state of the meta-state "Move contact link" of the FSM, namely:

- State "Move contact link to way-point"
- State "Move contact link to goal"

Additionally, in order to avoid stopping the motion of the contact link at the way-point and to ensure a smooth motion throughout the step, we implemented a strategy that makes the transition from the former to the latter sub-state triggered when the contact link crosses a designated threshold plan along the way, before reaching the tracked way-point.

A default position of the intermediate way-point is automatically pre-set by the autonomous framework using the following heuristic (see **Figure 2**, left): Let P_s denote the start position of the contact link (at the beginning of the contact-adding step) and P_g denote its goal position (its location in the following contact state

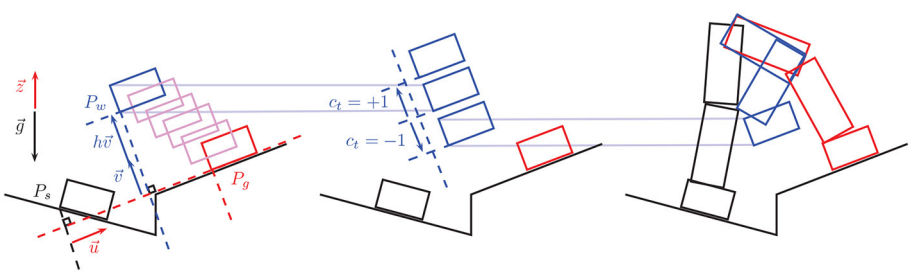

FIGURE 2 | The way-point moving strategy. The rectangles in the left and middle figures represent positions of the moving foot (say the right foot, supposing the left foot is the support foot that is fixed and not represented here). In the right figure the whole leg motion is reconstructed from the foot motion. In all three figures, in black is the initial position of the foot/leg at the beginning of the step, in blue the controlled way-point position of the foot/leg at the middle of the step, and in red is the planned final foot/leg position at the end of the step. The left figure shows how a default position of the way point is initialized autonomously by a translation of the final planned position. $\vec{g}$ is the gravity vector, $\vec{z}$ the vertical unit vector (opposite to $\vec{g}$), $\vec{u}$ is the unit vector from the initial to the goal position along the goal planned-contact surface plane, $\vec{v}$ is the generalized vertical direction unit vector, i.e., the unit vector normal to $\vec{u}$ and in the plane defined by $\vec{u}$ and $\vec{z}$, finally, h is a pre-set default height. The middle figure shows how the way-point position is controlled via the command c_t sent through the motor imagery interface. Finally the left figure shows how the resulting motion of the leg actually looks like with the foot going through the desired way-point that was translated downwards via the command $c_t = -1$.

along the planned sequence). Let $\vec{g}$ denote the gravity vector, $\vec{z}$ the unit vector opposite to $\vec{g}$, i.e., $\vec{z} = -\vec{g}/\|\vec{g}\|$, and $\vec{u}$ the unit vector from $P_{s,g}$ (P_s projected on the goal-contact surface plane) to P_g, i.e., $\vec{u} = \overrightarrow{P_{s,g}P_g}/\|\overrightarrow{P_{s,g}P_g}\|$. Finally let $\vec{v} = \vec{u} \times (\vec{z} \times \vec{u})$ be the unit vector normal to $\vec{u}$ that lies in the plan defined by $\vec{u}$ and $\vec{z}$. The default way-point P_w is defined as

$$P_w = P_g - \frac{1}{2}\overrightarrow{P_{s,g}P_g} + h\,\vec{v}\,, \tag{8}$$

where h is the hand-tuned user-defined parameter that specifies the height of the steps. The command c_t in Equation (7) that comes from the BMI decoding system is finally used to modify in real-time this way-point position P_w by modifying its height h (see **Figure 2**, middle). Let δh denote a desired height control resolution, then the modified position of the way-point through the brain command c_t becomes

$$P_w(c_t) = \begin{cases} P_g - \frac{1}{2}\overrightarrow{P_{s,g}P_g} + (h + c_t\,\delta h)\,\vec{v} & \text{if } t = 1\,, \\ P_w(c_{t-1}) + c_t\,\delta h\,\vec{v} & \text{if } t > 1\,. \end{cases} \tag{9}$$

The command c_t could have been used in other ways, however we identified two principles that should in our view stand in a BMI low-level control endeavor of humanoid motion such as ours:

- Principle 1: The full detailed motion, that cannot be designed joint-wise by the BMI user, should be autonomously planned and executed from high-level (task-level) command.
- Principle 2: The brain command can then be used to locally correct or bias the autonomously planned and executed motion, and help overcome shortcomings inherent to full autonomy.

The way-point is a key feature to be controlled according to these two principles as it helps surmount the main limitation of the autonomous collision-avoidance constraint expressed in the on-line quadratic-program-formulated controller described in Section 3. This collision-avoidance constraint, that had to be formulated as a linear constraint in the joint acceleration vector of the robot in order to fit within the quadratic-program formulation [adapting to this end the velocity-damper formulation (Faverjon and Tournassoud, 1987)], acts as a repulsive field, with the tracked way-point acting as an attractive field, on the contact link. The resultant field (from the superposition of these two fields) can display local extrema corresponding to equilibrium situations in which the link stops moving though without having completed its tracking task (see **Figure 9**). Manual user intervention, here through the brain command, is then necessary to un-block the motion of the link by adequately moving the tracked way-point. The brain command is thus used here for low-level correction of a naturally limitation-affected full-autonomy strategy.

6. PROOF-OF-CONCEPT EXPERIMENT

The experiment we designed (see **Figure 3** and video that can be downloaded at http://www.cns.atr.jp/~xmorimo/videos/frontiers.wmv) to test the whole framework is described as follows.

An initial and goal configurations (**Figure 4**) are pre-specified manually by the user among a finite number of locations in the environment. In this case the initial configuration is standing in front of a stair and the goal task is to go up on the stair. This selection is for now done manually, but it can later also be selected through a brain command by embedding the strategy described in this work within a hierarchical framework such as the ones suggested in Chung et al. (2011); Bryan et al. (2011), that will switch between the behavior of selecting the high-level goal task and the low-level motion control.

Off-line, the framework autonomously plans the sequence of contact transitions and associated intermediate static postures to reach that goal (**Figure 5**), then the on-line controller is executed.

The user is wearing an EEG cap and is trained with 3 training sessions of approximately 5 min each to learn the parameter of the classifier described in Section 4, through a motor imagery task

FIGURE 3 | Experiment setup. The user is wearing an EEG cap. The laptop on his left side is used for decoding the motor imagery task signal, the computer on his right runs the real-time physics simulation allowing him to control the position of the moving foot through the visual feedback he gets from the simulator window.

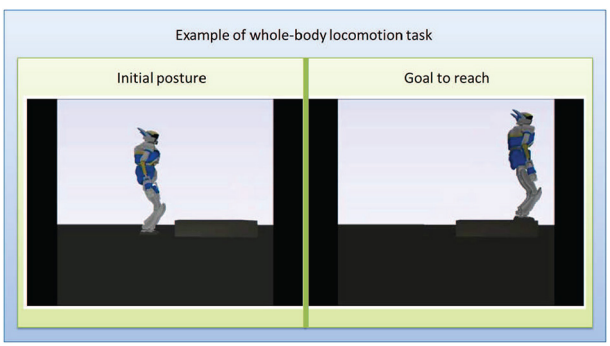

FIGURE 4 | Intial and goal positions for the experiment. Left: initial configuration with the robot standing in front of the stair. **Right**: goal configuration with the robot standing at the extremity up on the srair.

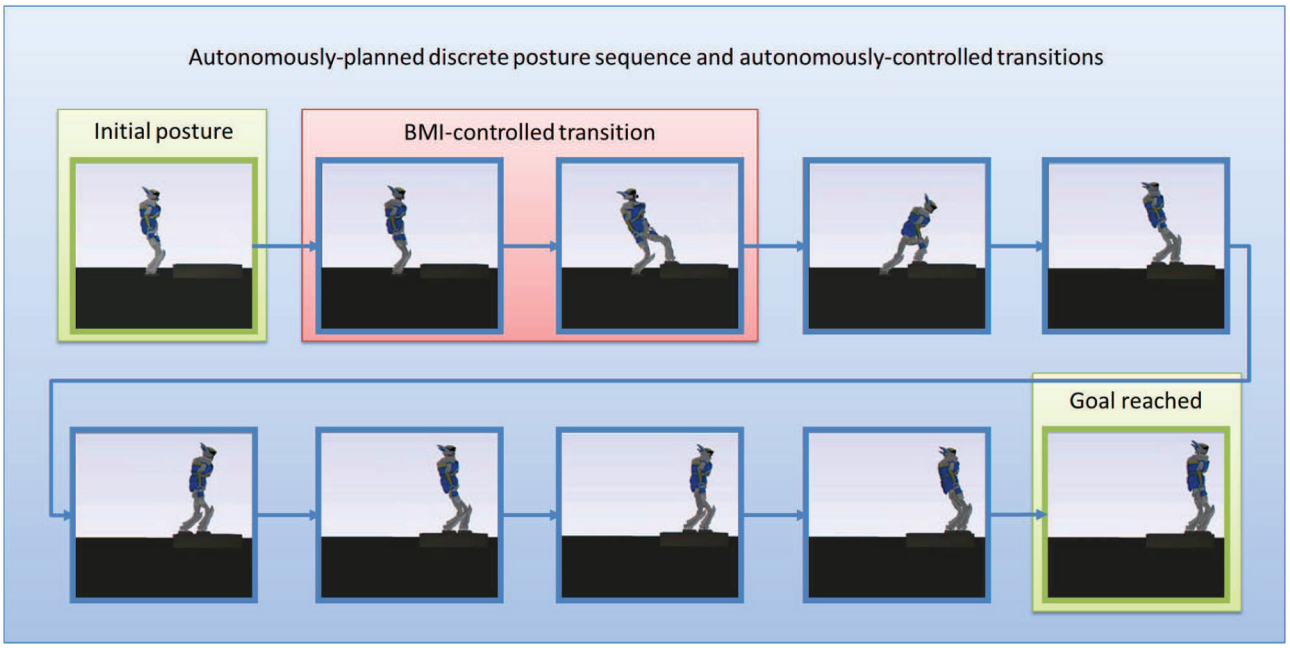

FIGURE 5 | The sequence of static postures planned autonomously. The first posture is the initial posture. The second posture which looks like the first one keeps both feet on the ground but puts all the weight of the robot on the right foot so as to zero the contact forces on the right left to release it for the next posture. The third posture moves the now free left foot and puts it on the stair, but still without any contact force applied on it (all the weith of the robot is still supported by the right foot). the fourth postures keeps both feet at their current locations but shifts all the weight of the robot away from the right foot to put it entirely on the left foot, the right foot becomes free of contact forces, and so on.

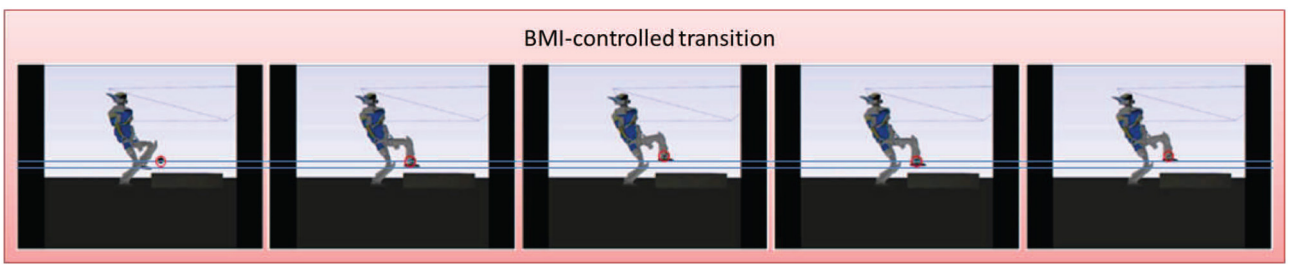

FIGURE 6 | The controlled motion. The figures represent successive snapshots from the real-time controlled motion in the physics simulator. The controlled position of the way point appears in the simulator as a black sphere that we circle here in red for clarity. This position is tracked by the foot (more precisely at the ankle joint) throught the simulation. The two horizontal lines represent the level of the sole of the foot at the two positions sent as a command by the user through the BMI. These lines do not appear in the simulator we add them here only as common visualization reference lines for all the snapshots. In the first two frames the robot tracks the default position of the way point. In the third frame the user decides to move that position up, then down in fourth frame, and finally up again in the fifth frame.

consisting of imagining respectively left arm and right arm circling movements for going up and down. This task is generic and we retained it since it gave us in our experiment better decoding performances than some other tasks (e.g., leg movements). The user has visual feed-back from the simulator on the desktop computer screen (on his right in **Figure 3**) and from a bar-diagram representing in real-time the decoded probability of the motor-imagery task classification on the laptop computer screen (on his left in **Figure 3**). The experiment was successfully completed on the first effective trial, which was the overall third trial (the first two trials were canceled after their respective training sessions since we encountered and fixed some minor implementation bugs before starting the control phase). The subject had prior experience with the same motor-imagery classifier in our previously-cited study (Noda et al., 2012). We only experimented with that one subject as we considered that we reached our aim of testing our framework and providing its proof-of-concept experiment.

The decoding of the BMI command is done in real-time and implemented in Matlab, and the brain command is then sent via UDP protocol to the physics simulator process implemented in C++.

We tested the way-point control strategy in the second step of the motion (the first contact-adding step along the sequence, the highlighted transition in **Figure 5**). **Figure 6** focuses on this

controlled part of the motion. The user controlled the position of a black sphere that represents the position of the targeted way-point, that the foot of the robot tracks in real-time, while autonomously keeping balance and avoiding self-collisions, joint limits, and collision with the environment. A total of 8 commands ("up"/"down") were sent during this controlled transition phase, that we voluntarily made last around 300 s (5 min) in order to allow the user to send several commands. We then externally (manually) triggered the FSM transition to the following step along the sequence and left the autonomous controller complete the motion without brain control. That autonomous part was completed in about 16 s. See the accompanying video.

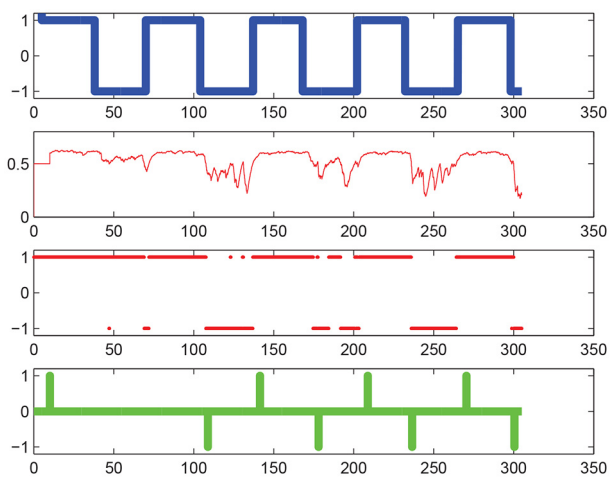

FIGURE 7 | Motor imagery decoding performances. On the horizontal axis is iteration number. From top to bottom: the thick blue line represents the command cue given as an input to the user, the thin red line represents the decoded brain activities [the probability $P(k_t = +1|\mathbf{C}_t)$], the thick red point markers represent the estimated classified label [$P(k_t = +1|\mathbf{C}_t) \geq 0.5$ or < 0.5], finally the thick green line represents the command c_t sent to the robot (based on the threshold $P_{\text{thres}} = 0.6$). Note that this green command does not represent the position of the way-point but the instantaneous rate of change in this position between two successive time steps t and $t + 1$, according to Equation (9), line 2 (i.e., the "derivative" were we talking of a continuous and differentiable function rather than the time-discretized one at hand).

Figure 7 illustrates the decoding performances of the BMI system, while **Figure 8** shows the tracking performance of the humanoid whole-body controller. The table below gives computation time figures executed on a Dell Precision T7600 Workstation equipped with a Xeon processor E5-2687W (3.1 GHz, 20 M). Full details on the physics simulator, including contact modeling and resolution, and collision detection, can be found in Chardonnet et al. (2006); Chardonnet (2012).

Offline planning	2.7 s
Average online control command (QP) (@ 200 Hz)	2.661 ms
Average online simulation step (@ 1 kHz)	0.389 ms
BCI classifier training and learning session	$\sim$ 30 min
Average online BCI signal buffering (@ 2048 Hz)	0.137 ms
Avg online BCI classification (@ 128 Hz) no control signal sent ($c_t = 0$)	0.204 ms
Avg BCI classification (@ 128 Hz) control signal sent ($c_t = +1$ or -1)	6.20 ms

From this experiment, we confirmed that the autonomous framework can be coupled with the BMI decoding system in real-time in simulation and that the simulated robot can safely realize the task while receiving and executing the brain command.

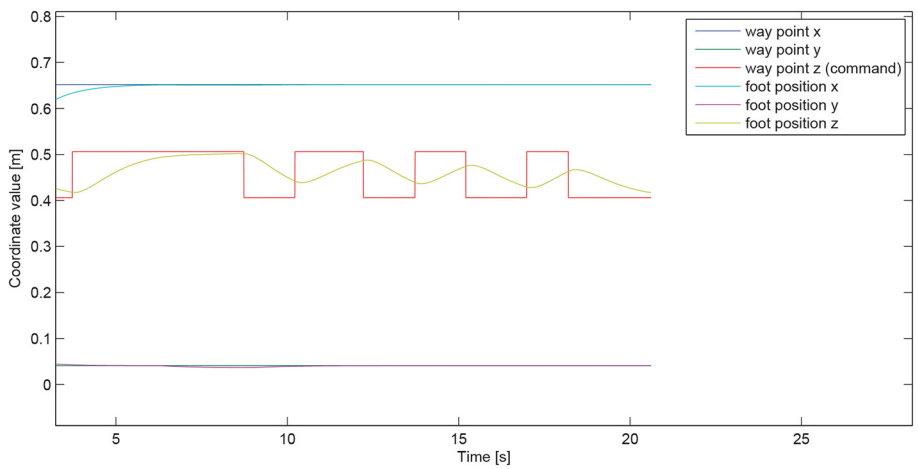

FIGURE 8 | Way-point tracking performance. The user-controlled quantity, that happens to be in the particular case demonstrated here the z-coordinate of the tracked way-point (the "generalized" vertical direction being reduced in this case to the "conventional" vertical direction, meaning $\vec{v} \equiv \vec{z}$ in **Figure 2**, since the goal-contact surface on the stair is horizontal), is represented by the piecewise-constant red curve. The corresponding motion of the foot, that tracks this command-induced way-point position, is shown in yellow curve. the two other coordinates of the foot (x and y) are auonomously maintained by the controller at the corresponding ones of the way-point and stay at their desired values throught the command phase.

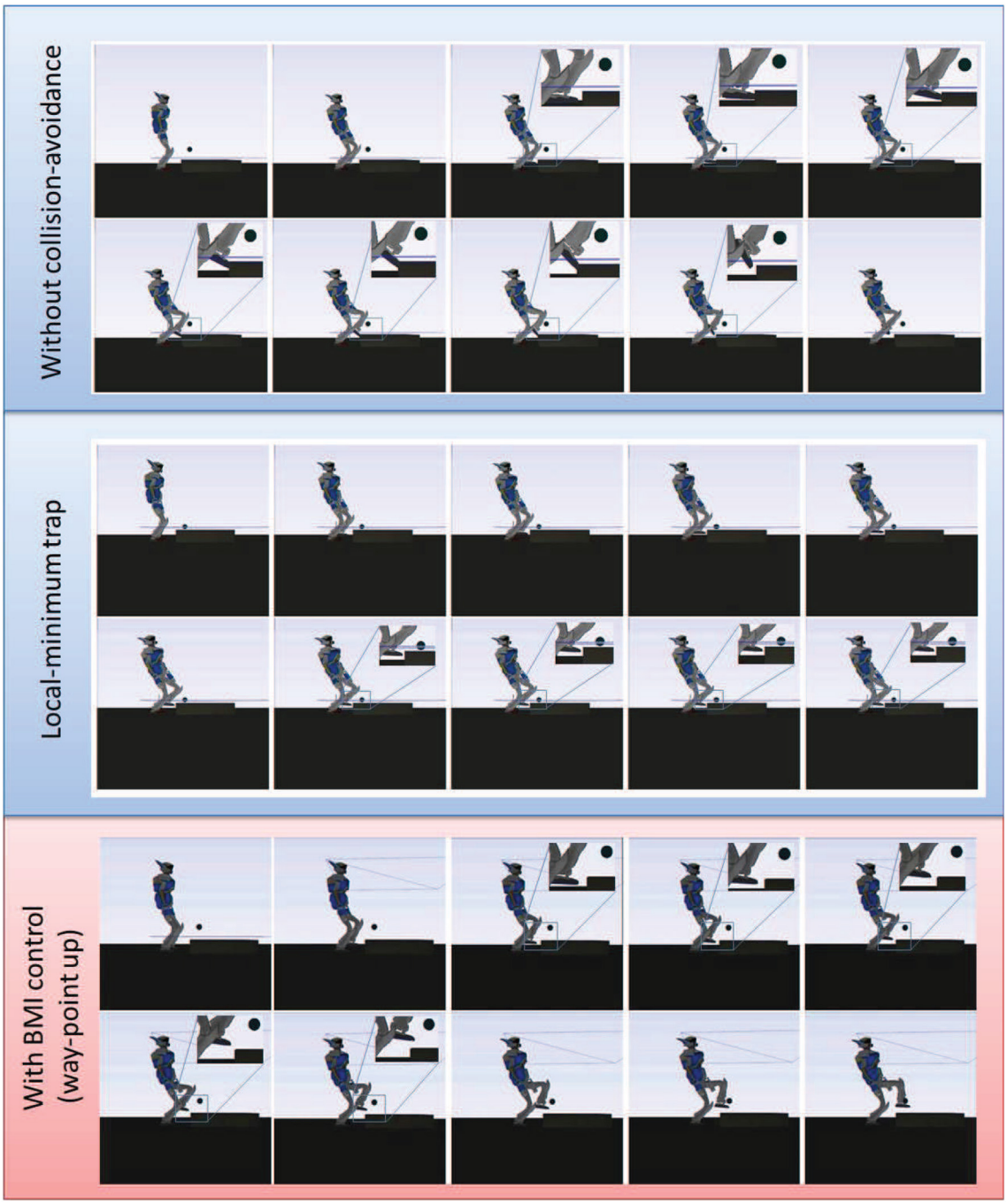

FIGURE 9 | Comparison of the controlled transition motion in three instances. Top: without collision-avoidance constraint, the foot of the robot collides with the stair while targeting its goal, and the simulation stops. **Middle**: with autonomous collision-avoidance constraint that happens to create in this case a local-minimum trap, the robot reaches an equilibrium situation and stays idle for as long as we let the simulation run (infinite time). **Bottom**: The autonomous collision-avoidance strategy combined with the proposed BMI-control approach helps reposition the way-point and overcome the local-minimum problem. The robot safely reaches the goal contact location and the motion along the sequence can be completed.

7. DISCUSSION AND FUTURE WORK

This work demonstrated the technical possibility of real-time online low-level control of whole-body humanoid motion using motor-imagery-based BMI.

We achieved it by coupling an existing EEG decoder and whole-body multi-contact acyclic planning and control framework. In particular, this coupling allowed us to control a one-dimensional feature of the high-DOF whole-body motion,

designed as the generalized height of moving link way-point, in a discrete way. Though the motor-imagery task used in our proof-of-concept experiment was a generic one (left-arm vs. right-arm circling movement), we plan in the future to investigate more specific motor-imagery tasks that are in tighter correspondence with the limb of the robot being controlled, along the longer-term user's-mind-into-robot's-body "full embodiment" quest that motivates our study as expressed in our introductory section. Since previous studies reported that imagery of gait and actual gait execution have been found to recruit very similar cerebral networks (Miyai et al., 2001; La Fougère et al., 2010), we may be able to expect that a human can control a humanoid the same way they control their own human body through motor imagery.

We also aim now at continuous control of two-dimensional feature of this whole-body motion, allowing not only the control of the tracked way point but also of a corresponding threshold plan that decides when to trigger the transition between the lift-off and touch-down phases. We believe this can be achieved based on the previous work done for example on motor-imagery two-dimensional cursor control (Wolpaw and McFarland, 2004). Other previous studies also discussed the possibilities of using EEG for such continuous control (Yoshimura et al., 2012). In addition, for the continuous two-dimensional feature control, explicit consideration of individual differences in cerebral recruitment during motor imagery may be necessary (Meulen et al., 2014). As a future study, we may consider using transfer learning approaches (Samek et al., 2013) to cope with this individual difference problem.

Finally, we aim at porting this framework from the simulation environment to the real robot control, so that in future study we may possibly use the proposed framework in a rehabilitation training program to enhance recovery of motor-related nervous system of stroke patients.

ACKNOWLEDGMENTS

This work is supported with a JSPS Postodoctoral Fellowship for Foreign Researchers, ID No. P12707. This study is the result of "Development of BMI Technologies for Clinical Application" carried out under the Strategic Research Program for Brain Sciences by the Ministry of Education, Culture, Sports, Science and Technology of Japan. Part of this research was supported by MIC-SCOPE and a contract with the Ministry of Internal Affairs and Communications entitled "Novel and innovative R&D making use of brain structures." This research was also partially supported by MEXT KAKENHI grant Number 23120004, Strategic International Cooperative Program, Japan Science and Technology Agency (JST) and by JSPS and MIZS: Japan-Slovenia research Cooperative Program Joris Vaillant and François Keith were partially suported by grants from the RoboHow.Cog FP7 www.robohow.eu, Contract N288533. The authors would like to thank Abderrahmane Kheddar for valuable use of the AMELIF dynamics simulation framework.

REFERENCES

Bell, C. J., Shenoy, P., Chalodhorn, R., and Rao, R. P. N. (2008). Control of a humanoid robot by a noninvasive brain-computer interface in humans. *J. Neural Eng.* 5, 214–220. doi: 10.1088/1741-2560/5/2/012

Bouyarmane, K., and Kheddar, A. (2010). "Static multi-contact inverse problem for multiple humanoid robots and manipulated objects," in *10th IEEE-RAS International Conference on Humanoid Robots* (Nashville, TN), 8–13. doi: 10.1109/ICHR.2010.5686317

Bouyarmane, K., and Kheddar, A. (2011a). "Multi-contact stances planning for multiple agents," in *IEEE International Conference on Robotics and Automation* (Shanghai), 5546–5353.

Bouyarmane, K., and Kheddar, A. (2011b). "Using a multi-objective controller to synthesize simulated humanoid robot motion with changing contact configurations," in *IEEE/RSJ International Conference on Intelligent Robots and Systems* (San Fransisco, CA), 4414–4419.

Bouyarmane, K., and Kheddar, A. (2012). Humanoid robot locomotion and manipulation step planning. *Adv. Robot.* 26, 1099–1126. doi: 10.1080/01691864.2012.686345

Bryan, M., Green, J., Chung, M., Chang, L., Scherery, R., Smith, J., et al. (2011). "An adaptive brain-computer interface for humanoid robot control," in *11th IEEE-RAS International Conference on Humanoid Robots* (Bled), 199–204.

Chardonnet, J.-R. (2012). Interactive dynamic simulator for multibody systems. *Int. J. Hum. Robot.* 9, 1250021:1–1250021:24. doi: 10.1142/S0219843612500211

Chardonnet, J.-R., Miossec, S., Kheddar, A., Arisumi, H., Hirukawa, H., Pierrot, F., et al. (2006). "Dynamic simulator for humanoids using constraint-based method with static friction," in *Robotics and Biomimetics, 2006. ROBIO'06. IEEE International Conference on* (Kunming), 1366–1371.

Chestnutt, J., Kuffner, J., Nishiwaki, K., and Kagami, S. (2003). "Planning biped navigation strategies in complex environments," in *IEEE-RAS International Conference on Humanoid Robots* (Munich).

Chestnutt, J., Lau, M., Kuffner, J., Cheung, G., Hodgins, J., and Kanade, T. (2005). "Footstep planning for the ASIMO humanoid robot," in *IEEE International Conference on Robotics and Automation* (Barcelona), 629–634.

Chung, M., Cheung, W., Scherer, R., and Rao, R. P. N. (2011). "A hierarchical architecture for adaptive brain-computer interfacing," in *Proceedings of the Twenty-Second International Joint Conference on Artificial Intelligence Vol. 2* (Barcelona), 1647–1652.

Faverjon, B., and Tournassoud, P. (1987). "Planning of manipulators with a high number of degrees of freedom," in *IEEE International Conference on Robotics and Automation* (Raleigh, NC).

Finke, A., Knoblauch, A., Koesling, H., and Ritter, H. (2011). "A hybrid brain interface for a humanoid robot assistant," in *33rd Annual International Conference of the IEEE Engineering in Medicine and Biology Society (EMBC2011)* (Boston, MA).

Gergondet, P., Druon, S., Kheddar, A., Hintermuller, C., Guger, C., and Slater, M. (2011). "Using brain-computer interface to steer a humanoid robot," in *IEEE International Conference on Robotics and Biomimetics* (Phuket), 192–197.

Hashimoto, K., Sugahara, Y., Kawase, M., Ohta, A., Tanaka, C., Hayashi, A., et al. (2006). "Landing pattern modification method with predictive attitude and compliance control to deal with uneven terrain," in *Proceedings of the IEEE-RSJ International Conference on Intelligent Robots and Systems* (Beijing).

Hauser, K., Bretl, T., Latombe, J.-C., Harada, K., and Wilcox, B. (2008). Motion planning for legged robots on varied terrain. *Int. J. Robot. Res.* 27, 1325–1349. doi: 10.1177/0278364908098447

Herdt, A., Diedam, H., Wieber, P.-B., Dimitrov, D., Mombaur, K., and Diehl, M. (2010). Online walking motion generation with automatic footstep placement. *Adv. Robot.* 24, 719–737. doi: 10.1163/016918610X493552

Kuffner, J., Kagami, S., Nishiwaki, K., Inaba, M., and Inoue, H. (2002). Dynamically-stable motion planning for humanoid robots. *Auton. Robots* 12, 105–118. doi: 10.1023/A:1013219111657

Kuffner, J., Nishiwaki, K., Kagami, S., Inaba, M., and Inoue, H. (2001). "Footstep planning among obstacles for biped robots," in *IEEE/RSJ International Conference on Intelligent Robots and Systems - Vol. 1* (Maui, HI), 500–505.

La Fougère, C., Zwergal, A., Rominger, A., Förster, S., Fesl, G., Dieterich, M., et al. (2010). Real versus imagined locomotion: an intraindividual [18F]-FDG PET - fMRI comparison. *Neuroimage* 50, 1589–1598. doi: 10.1016/j.neuroimage.2009.12.060

Ma, J., Zhang, Y., Nam, Y., Cichocki, A., and Matsuno, F. (2013). "EOG/ERP hybrid human-machine interface for robot control," in *IEEE-RAS International Conference on Intelligent Robots and Systems* (Tokyo), 859–864.

Meulen, M. V. D., Allali, G., Rieger, S., Assal, F., and Vuilleumier, P. (2014). The influence of individual motor imagery ability on cerebral recruitment during gait imagery. *Hum. Brain Mapp.* 35, 455–470. doi: 10.1002/hbm.22192

Miller, K. J., Schalk, G., Fetza, E. E., den Nijs, M., Ojemanne, J., and Rao, R. (2010). Cortical activity during motor execution, motor imagery, and imagery-based online feedback. *Proc. Natl. Acad. Sci. U.S.A.* 107, 4430–4435. doi: 10.1073/pnas.0913697107

Miyai, I., Tanabe, H., Sase, I., Eda, H., Oda, I., Konishi, I., et al. (2001). Cortical mapping of gait in humans: a near-infrared spectroscopic topography study. *Neuroimage* 14, 1186–1192. doi: 10.1006/nimg.2001.0905

Morisawa, M., Kanehiro, F., Kaneko, K., Kajita, S., and Yokoi, K. (2011). "Reactive biped walking control for a collision of a swinging foot on uneven terrain," in *Proceedings of the IEEE-RAS International Conference on Humanoid Robots* (Bled).

Noda, T., Sugimoto, N., Furukawa, J., Sato, M., Hyon, S., and Morimoto, J. (2012). "Brain-controlled exoskeleton robot for bmi rehabilitation," in *12th IEEE-RAS International Conference on Humanoid Robots* (Osaka), 21–27.

Riechmann, H., Hachmeister, N., Ritter, H., and Finke, A. (2011). "Asynchronous, parallel on-line classification of P300 and ERD for an efficient hybrid BCI," in *5th IEEE EMBS Conference on Neural Engineering (NER2011)* (Cancun).

Samek, W., Meinecke, F. C., and Muller, K.-R. (2013). Transferring subspaces between subjects in brain-computer interfacing. *IEEE Trans. Biomed. Eng.* 60, 2289–2298. doi: 10.1109/TBME.2013.2253608

Takanishi, A., and Kato, I. (1994). "Development of a biped walking robot adapting to a horizontally uneven surface," in *Proceedings of the IEEE-RSJ International Conference on Intelligent Robots and Systems* (Munich).

Tomioka, R., and Aihara, K. (2007). "Classifying matrices with a spectral regularization," in *24th International Conference on Machine Learning* (New York, NY), 895–902.

Tomioka, R., and Muller, K. (2010). A regularized discriminative framework for EEG analysis with application to brain-computer interface. *Neuroimage* 49, 415–432. doi: 10.1016/j.neuroimage.2009.07.045

Wolpaw, J. R., and McFarland, D. J. (2004). Control of a two-dimensional movement signal by a noninvasive brain-computer interface in humans. *Proc. Natl. Acad. Sci. U.S.A.* 101, 17849–17854. doi: 10.1073/pnas.0403504101

Yamane, K., Kuffner, J., and Hodgins, J. K. (2004). Synthesizing animations of human manipulation tasks. *ACM Trans. Graph.* 23, 532–539. doi: 10.1145/1015706.1015756

Yoshida, E., Kanoun, O., Esteves, C., and Laumond, J. P. (2006). "Task-driven support polygon reshaping for humanoids," in *6th IEEE-RAS International Conference on Humanoid Robots* (Genova), 208–213.

Yoshida, E., Laumond, J.-P., Esteves, C., Kanoun, O., Sakaguchi, T., and Yokoi, K. (2008). "Whole-body locomotion, manipulation and reaching for humanoids," in *Motion in Games*, Volume 5277 of *LNCS*, eds A. Egges, A. Kamphuis, and M. Overmars (Berlin; Heidelberg: Springer), 210–221.

Yoshimura, N., Dasalla, C., Hanakawa, T., Sato, M., and Koike, Y. (2012). Reconstuction of flexor and extensor muscle activity from electroencephalography cortical currents. *Neuroimage* 59, 1324–1337. doi: 10.1016/j.neuroimage.2011.08.029

Conflict of Interest Statement: The authors declare that the research was conducted in the absence of any commercial or financial relationships that could be construed as a potential conflict of interest.

Received: 28 May 2014; accepted: 15 July 2014; published online: 05 August 2014.
Citation: Bouyarmane K, Vaillant J, Sugimoto N, Keith F, Furukawa J and Morimoto J (2014) Brain-machine interfacing control of whole-body humanoid motion. Front. Syst. Neurosci. ***8****:138. doi: 10.3389/fnsys.2014.00138*
This article was submitted to the journal Frontiers in Systems Neuroscience.

frontiers in
SYSTEMS NEUROSCIENCE

MINI REVIEW ARTICLE
published: 16 July 2014
doi: 10.3389/fnsys.2014.00129

Decoding methods for neural prostheses: where have we reached?

Zheng Li [1,2]*

[1] State Key Laboratory of Cognitive Neuroscience and Learning and IDG/McGovern Institute for Brain Research, Beijing Normal University, Beijing, China
[2] Center for Collaboration and Innovation in Brain and Learning Sciences, Beijing Normal University, Beijing, China

Edited by:
Ioan Opris, Wake Forest University, USA

Reviewed by:
Gytis Baranauskas, Neuroscience Institute at Lithuanian University of Health Sciences, Lithuania
David Sussillo, Stanford University, USA

***Correspondence:**
Zheng Li, State Key Laboratory of Cognitive Neuroscience and Learning and IDG/McGovern Institute for Brain Research, Beijing Normal University, 19 Xin Jie Kou Wai Da Jie, Beijing 100875, China
e-mail: lz@bnu.edu.cn

This article reviews advances in decoding methods for brain-machine interfaces (BMIs). Recent work has focused on practical considerations for future clinical deployment of prosthetics. This review is organized by open questions in the field such as what variables to decode, how to design neural tuning models, which neurons to select, how to design models of desired actions, how to learn decoder parameters during prosthetic operation, and how to adapt to changes in neural signals and neural tuning. The concluding discussion highlights the need to design and test decoders within the context of their expected use and the need to answer the question of how much control accuracy is good enough for a prosthetic.

Keywords: brain-machine interface, brain computer interface, decoding, neural prosthetic, neural engineering, multichannel recordings, signal processing

INTRODUCTION

The field of brain-machine interfaces (BMIs) for control of motor prostheses is quickly growing (Baranauskas, 2014, for other reviews, see Tehovnik et al., 2013; Kao et al., 2014). Research in decoders, the algorithms which translate neural signals to movement commands, has largely switched focus from improving control accuracy to resolving practical considerations of future clinical deployments of prostheses. The goal of this mini-review is to briefly highlight recent (2013 to mid-2014) advances in decoding methodology for extracellular signals recorded from motor areas of the brain. The review sections are organized by main research themes, corresponding to important questions and practical considerations. At the end, the importance of developing and testing decoders in realistic contexts and the question of how much control accuracy is "good enough" for a prosthetic are discussed.

ALGORITHMS FOR DECODING

Which algorithmic framework should we use for decoding? Different algorithms offer different benefits. **Figure 1** illustrates three commonly-used methods. The Kalman filter and point process filter are state-based (modeling temporal evolution) and probabilistic (modeling and estimating uncertainty). The linear filter, in contrast, is a linear transformation of neural data to the decoded variables, with the advantages of simplicity and execution speed.

The Kalman filter's Gaussian noise model clearly does not match the data (spike counts), yet due to its accuracy and execution speed the method has remained popular since its first use by Wu et al. (2003) (Aggarwal et al., 2013; Chen et al., 2013; Dangi et al., 2013a,c; Homer et al., 2013; Ifft et al., 2013; Jarosiewicz et al., 2013; Kao et al., 2013; Merel et al., 2013; Wong et al., 2013; Zhang and Chase, 2013; Fan et al., 2014; Golub et al., 2014; Gowda et al., 2014; Homer et al., 2014). While point process filters (for a review, see Koyama et al., 2010) offer a more realistic noise model, their use in decoding is still relatively rare (Shanechi et al., 2013; Velliste et al., 2014; Xu et al., 2014), due in part to their heavier computational burden. Recently, Citi et al. (2013) extend point process methods to model refractory periods of neurons and allow for coarser time discretization by a factor of 10, which may ease this burden. However, one feature which current point process decoders lack is the ability to assign different amounts of noise or weights to different neurons.

Linear filtering, or discrete Wiener filtering, is fading in popularity. It is still used by some research groups, either because of its computational form (Badreldin et al., 2013) or when the research focuses on other aspects of decoding (Chen et al., 2013; Chhatbar and Francis, 2013; Philip et al., 2013; Suminski et al., 2013; Willett et al., 2013). A variant of the Wiener filter method, which passes the Wiener filter output through a fitted non-linear function to compute the final output, is also used (Flint et al., 2013; Scheid et al., 2013).

Several other methods have been used in the recent literature: kernel autoregressive moving average (KARMA; Wong et al., 2013), quantized kernel least mean square (Li et al., 2014), support vector machines (Cao et al., 2013; Xu et al., 2013; Wang et al., 2014), K-nearest neighbors (Brockmeier et al., 2013; Ifft et al., 2013; Xu et al., 2013), naïve Bayes (Bishop et al., 2014), and artificial neural networks (Chen et al., 2013; Mahmoudi et al., 2013; Pohlmeyer et al., 2014). All of these methods allow highly non-linear neural models.

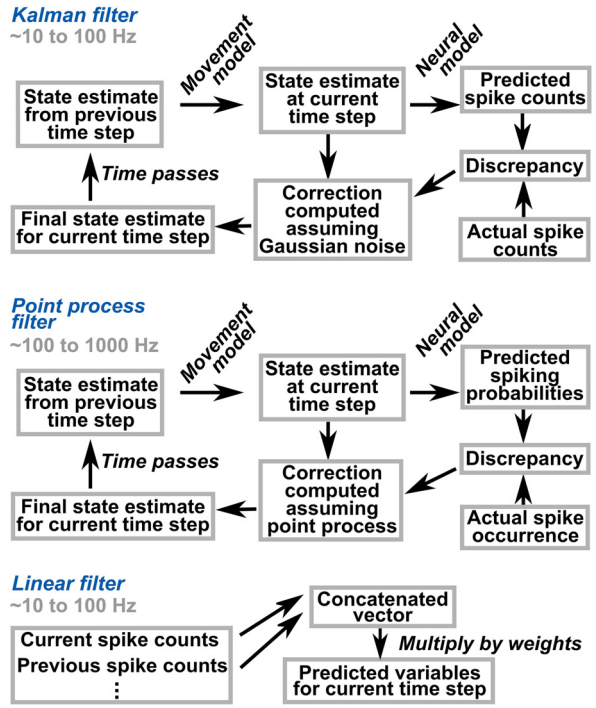

FIGURE 1 | Schematic illustration of popular decoding algorithms. The Kalman and point process filters are based on the notion of a state, which holds the current estimates of the variables of interest. The state is related to neural activity through a neural model. Bayesian computations on the neural model, assuming a distribution for noise, permit probabilistic tracking of the state based on neural activity. In contrast, the linear filter is state-less; it linearly maps the recent history of neural activity to estimates of the variables of interest.

VARIABLES TO DECODE

What values should a decoder predict? Ideally, a prosthetic should offer accurate, intuitive control that works under all likely usage contexts. In most prior work, desired positions or velocities of end-effectors were decoded. Homer et al. (2013) proposed a method for combining decoded position and velocity, to avoid choosing between the two. The method defines a quantity Δr as the difference between the decoded cursor position and the previous cursor position. The cursor position's update is a linear combination of the decoded velocity and the decoded velocity vector rotated to the direction of Δr.

Decoders aim to predict user intentions, and it is possible that intentions may be slightly different from the observed limb movements used for parameter fitting. Fan et al. (2014) showed that the heuristic for guessing user intention during online recalibration proposed by Gilja et al. (2012), and tested with human users in a study by Jarosiewicz et al. (2013), could also be applied to the initial training data for fitting decoder parameters. This method rotates the cursor's velocity vector towards the target and zeroes the velocity when the cursor is in the target. Fitting Kalman filter parameters on these estimates of intended movements, instead of actual limb movements, could achieve comparable gains in accuracy as online recalibration using the same scheme (Fan et al., 2014).

Two recent studies have explored decoding torque values, to allow a prosthetic to interact with objects with mass more naturally. Chhatbar and Francis (2013) showed that hybrid neural control by both torque and position produced more natural movements in novel dynamic environments. Decoding of position and torque was performed via a Wiener filter applied to the largest 20 principal components of neural activity. The final angular accelerations of the prosthetic joints were calculated by a weighted sum of the accelerations implied by the predicted positions and torques. Suminski et al. (2013) decoded position and velocity as well as torques of a two-link virtual arm with a Wiener filter. The kinematic variables were converted to torques using a position-derivative controller and the results were combined linearly with the directly decoded torques to produce the final torque output.

Besides kinematics and forces, the target location of a reach may be directly decoded to improve the trajectory of the reach. Shanechi et al. (2013) presented a real-time, two-stage decoder which first decoded target location during an instructed delay period and then decoded reach trajectory during the reach period. The decoded target location served as the goal position for an optimal feedback controller that acted as the movement model of the point process trajectory decoder.

To address the need for BMI control of limbs with many degrees of freedom, an important consideration for clinical deployment, Wong et al. (2013) used principal component analysis to reduce the dimensions of limb movements. They showed that decoding principal-component-space kinematic variables with KARMA or Kalman filtering was more accurate than decoding canonical-space kinematic variables. Ifft et al. (2013) decoded the kinematics of both arms during a bimanual reaching task using an unscented Kalman filter which included variables for both arms in its state.

Besides the biomimetic approach of designing a prosthetic so that it can be controlled like a natural limb, another approach is to use operant conditioning of neuron ensembles (for a review, see Sakurai et al., 2014) to let the user learn to control a new, synthetic actuator. Though more initial training may be required, greater final control accuracy may be possible using this paradigm. Balasubramanian et al. (2013) used two groups of neurons from M1 to control reach and grasp, which were simplified to one dimension each. The neuron groups were chosen based on their stability and functional connectivity, and algorithmic assistance was given during the operant conditioning process to assist neuronal learning. Badreldin et al. (2013) developed an unsupervised method for non-biomimetic linear filter initialization. The method performs an eigendecomposition of the sample covariance matrix of the neural data. The eigenvectors provide a basis for the space of all possible linear filters that could be fitted from the data. They designed a cost function to choose a particular linear filter from this space, which probably differs from the filter which would have been fitted by supervised linear regression. Their cost function optimizes for characteristics such as low jitter and evenly distributed weights among neurons.

NEURAL MODELS

How should we model neural activity? Recent studies have explored the aspects of neural models beyond movement tuning, with the hope of improving user-friendliness. Considering that a system with high latency is difficult to control, Willett et al. (2013) trained a decoder to predict intended future movements to compensate for BMI system latency and shorten the feedback loop. To predict intended future movements, they fitted a linear filter using kinematic values which were temporally offset from the neural data.

In a clinical setting, it is important that a prosthetic can be turned off when not used, to avoid undesired movements. Aggarwal et al. (2013) classified behavioral states into baseline, reaction, movement, and hold using linear discriminant analysis (LDA) on local field potentials (LFPs), and then decoded arm, hand, and finger kinematics using a Kalman filter on spike signals. The position outputs were held constant when the behavioral state decoder predicted the baseline or hold state. Similarly, Velliste et al. (2014) used LDA to detect idle (resting) arm states and set velocity to zero during idle. The baseline or idle states in these studies could serve as the "off" mode for a prosthetic.

Xu et al. (2014) included ensemble firing history, in addition to the standard tuning to kinematic variables, in the neural model. This paradigm helps model the background activity that is unrelated to movements. They used parallel computation on graphics processing units to achieve real-time execution of a point process particle filter that used this model.

NEURON SELECTION

Which neurons should we include in decoding? BMI researchers have long sought ways to reduce computational load to decoders and noise in neural data by excluding irrelevant neurons. Several recent studies have provided tools for finding relevant neurons. Chen et al. (2013) used variational Bayesian inference to fit parameters for a linear filter, a state-space model, and a non-linear echo state network. Using priors which favor small parameters, the inference procedure generated sparse parameter fits, and the zeroes in the fitted parameters can be interpreted as the absence of tuning.

Cao et al. (2013) determined which neurons modulated for reach direction versus hand configuration during grasping by using mutual information. In another study from the same group, Xu et al. (2013) proposed a supervised metric learning algorithm to optimize decoding of hand grasp configuration. Their gradient descent algorithm maximizes the difference between inter-class and intra-class distances while regularizing by the L1 norm, resulting in sparse weights which indicate relevance.

Also using a supervised approach, Brockmeier et al. (2013) proposed a method for computing a linear dimensionality reduction which maximizes the information between the class labels and the projected neural data. The low dimensional data can be used for visualization or decoding via distance-based methods such as K-nearest neighbors. Brockmeier et al. (2013) proposed an improved method that only uses inner products between inputs, allowing non-linear dimensionality reduction via the kernel trick. Their kernel metric learning algorithm aims to make data points with the same class labels lay close together in the output space.

MOVEMENT MODELS

How can we design movement models to assist decoding? Kalman and point process filters include movement models which can encode prior beliefs about how variables change over time. Cleverly engineering these models may make prostheses easier to control. Two studies examined how to improve the user's ability to stop a BMI cursor when desired. Golub et al. (2014) designed a speed-dampening Kalman filter which modifies the movement model to decrease speed when fast changes in movement direction are detected, with the goal of allowing a quick change in direction to signal the desire to stop (a "hockey stop"). Using a different approach, Velliste et al. (2014) added a separate speed variable, independent of the Cartesian velocity variables, to the state space of a point process filter. This speed term dynamically adjusts the filter's movement model error covariance so that smaller changes in position and velocity are allowed when the decoded speed is smaller.

In a general examination of movement models, Gowda et al. (2014) analyzed the linear models typically used in past studies and found that some may harbor hidden attractor points, to the detriment of controllability. They also point out that specific coefficients in movement model matrices parameterize the speed-accuracy tradeoff.

LEARNING

How can we improve decoder parameters during decoding? To handle poor initial parameter fits or changes in neural tuning after practice, continuous learning of decoder parameters may be required in a clinical device. There has been much recent work, mostly from Jose Carmena's Lab (for a review, see Carmena, 2013), on improving decoder parameter fits during BMI operation, called closed-loop decoder adaptation. They adapted Kalman filter parameters via stochastic updates based on the likelihood gradient (Dangi et al., 2013a), provided tools for analysis of adaptive methods (Dangi et al., 2013b), and applied adaptation to decoding of LFPs (Dangi et al., 2013c).

Information about the target locations of reaches can help improve the parameter learning process. Kowalski et al. (2013) proposed an algorithm which uses the joint estimation paradigm (augmenting tuning parameters into the state space), combined with the "reach state equation" (Srinivasan et al., 2006) as a way to incorporate target location in decoder recalibration. Similarly, Shanechi and Carmena (2013) designed a dual filtering method which uses the target location to assist movements towards the target. The method provides the target location, assumed known, to a linear-quadratic-Gaussian optimal feedback controller which acts as the movement model of the point process decoder. A second point process filter updates the decoder parameters.

In Suminski et al.'s (2013) study, incongruence between decoded kinematics and torques were used as an error signal for recalibration. The differences between the decoded position (and velocity) and the virtual arm's endpoint position (and velocity), as computed via the decoded torques, were used as an error signal to update torque decoder parameters via gradient descent.

Merel et al. (2013) modeled co-adaptation in BMIs as two agents (encoder and decoder) optimizing with respect to each other, under linear-quadratic-Gaussian assumptions. They derive

a novel decoder update step which anticipates what the future encoder will be and updates with respect to that, instead of the current encoder. They show that this "one step ahead" update rule reduces error faster in simulations.

SIGNAL STABILITY AND ADAPTATION

Are neural signals stable over long time periods? There has been controversy as to whether updating of decoder parameters is required for long-term prosthetic usability. Recent studies have analyzed stability of signals over long time spans. Flint et al. (2013) and Scheid et al. (2013) showed that multiunit spiking activity can be stable over more than six months and LFPs can be stable for almost a year. Wang et al. (2014) found signal instability and concluded that LFPs allowed more accurate offline reconstruction than single- and multi-unit signals 1–2 years post implantation. Perge et al. (2013) found significant intra-day changes in neural firing rates and concluded that 85% of these changes were likely due to physiological mechanisms.

If decoder updates are needed, how can we improve the accuracy of updates? Recent studies have proposed heuristics to improve adaptation. Zhang and Chase (2013) used two extensions to a dual-Kalman filter. First, they updated baseline firing rates of neurons using a moving window. Second, they normalized the velocity provided to the parameter updater so that the median absolute velocity matches that of the initial training data. Kao et al. (2013) proposed a firing rate normalization that also includes a regularization term that penalizes neurons with low firing rates. They also showed that dimensionality reduction via principal component analysis improves robustness to neuron loss.

Besides updating baseline firing rates via windowed estimates, other methods for tracking baseline changes have been proposed. Bishop et al. (2014) found that most changes occur between days. They designed a classifier for movement direction using the naïve Bayes algorithm and a hierarchical model; baseline firing rates are inferred each day while the class-specific parameters and the prior distributions for the baseline firing rates are learned once on initial training data. Homer et al. (2014) designed a probabilistic algorithm for detecting infrequent, rapid changes in baseline firing rates under the Kalman filtering framework. Their method first performs a forward stepwise search for neurons which have changed in baseline firing rate and then determines the magnitude of changes.

Using a reinforcement learning approach to adaptation, two studies from the same group (Mahmoudi et al., 2013; Pohlmeyer et al., 2014) showed that an actor-critic reinforcement learning BMI that uses Hebbian learning on an artificial neural network decoder's weights could learn weights from scratch and maintain decoding accuracy despite shuffling, loss, or gain of neurons, using only a one-bit feedback signal. In another study from the same group, Prins et al. (2013) decoded a one-bit reward signal from nucleus accumbens by clustering spike counts with *k*-means.

DISCUSSION

As researchers focus more on practical hurdles to clinical deployment of neural prostheses, it becomes more and more important to develop and test BMI decoders in the contexts in which actual prostheses will be used, i.e., to control artificial limbs, natural limbs via functional electrical stimulation (Moritz et al., 2008; Ethier et al., 2012; Nishimura et al., 2013), or computer cursors in graphical user interfaces. By using more realistic contexts, questions such as which variables to decode or which algorithms are sufficiently fast can be answered empirically. Realistic contexts may also uncover new considerations and obstacles to overcome.

An important question which has been thus far neglected in the field is how much control accuracy is enough? Full restoration of human ability in terms of movement accuracy may come at computational and other costs, e.g., number of recording channels, which likely trade off against other figures of merit of a prosthetic system. While we should continually endeavor to improve BMI technology, from a practical standpoint, we should also answer the question of how much control is good enough, so that engineers can design systems with clear requirements in mind.

ACKNOWLEDGMENTS

The author is grateful to Joseph E. O'Doherty, Mikhail A. Lebedev, and the reviewers for their helpful comments. This work was supported by the National Key Basic Research Program of China (2014CB846101) and the Fundamental Research Funds for the Central Universities.

REFERENCES

Aggarwal, V., Mollazadeh, M., Davidson, A. G., Schieber, M. H., and Thakor, N. V. (2013). State-based decoding of hand and finger kinematics using neuronal ensemble and LFP activity during dexterous reach-to-grasp movements. *J. Neurophysiol.* 109, 3067–3081. doi: 10.1152/jn.01038.2011

Badreldin, I., Southerland, J., Vaidya, M., Eleryan, A., Balasubramanian, K., Fagg, A., et al. (2013). "Unsupervised decoder initialization for brain-machine interfaces using neural state space dynamics," in *2013 6th International IEEE/EMBS Conference on Neural Engineering (NER)* (San Diego, CA), 997–1000. doi: 10.1109/NER.2013.6696104

Balasubramanian, K., Southerland, J., Vaidya, M., Qian, K., Eleryan, A., Fagg, A. H., et al. (2013). Operant conditioning of a multiple degree-of-freedom brain-machine interface in a primate model of amputation. *Conf. Proc. IEEE Eng. Med. Biol. Soc.* 303–306. doi: 10.1109/EMBC.2013.6609497

Baranauskas, G. (2014). What limits the performance of current invasive brain machine interfaces? *Front. Syst. Neurosci.* 8:68. doi: 10.3389/fnsys.2014.00068

Bishop, W., Chestek, C. C., Gilja, V., Nuyujukian, P., Foster, J. D., Ryu, S. I., et al. (2014). Self-recalibrating classifiers for intracortical brain-computer interfaces. *J. Neural Eng.* 11:026001. doi: 10.1088/1741-2560/11/2/026001

Brockmeier, A. J., Sanchez Giraldo, L. G., Emigh, M. S., Bae, J., Choi, J. S., Francis, J. T., et al. (2013). Information-theoretic metric learning: 2-D linear projections of neural data for visualization. *Conf. Proc. IEEE Eng. Med. Biol. Soc.* 5586–5589. doi: 10.1109/EMBC.2013.6610816

Cao, Y., Hao, Y., Liao, Y., Xu, K., Wang, Y., Zhang, S., et al. (2013). Information analysis on neural tuning in dorsal premotor cortex for reaching and grasping. *Comput. Math. Methods Med.* 2013:730374. doi: 10.1155/2013/730374

Carmena, J. M. (2013). Advances in neuroprosthetic learning and control. *PLoS Biol.* 11:e1001561. doi: 10.1371/journal.pbio.1001561

Chen, Z., Takahashi, K., and Hatsopoulos, N. G. (2013). Sparse Bayesian inference methods for decoding 3D reach and grasp kinematics and joint angles with primary motor cortical ensembles. *Conf. Proc. IEEE Eng. Med. Biol. Soc.* 2013, 5930–5933. doi: 10.1109/EMBC.2013.6610902

Chhatbar, P. Y., and Francis, J. T. (2013). Towards a naturalistic brain-machine interface: hybrid torque and position control allows generalization to novel dynamics. *PLoS One* 8:e52286. doi: 10.1371/journal.pone.0052286

Citi, L., Ba, D., Brown, E. N., and Barbieri, R. (2013). Likelihood methods for point processes with refractoriness. *Neural Comput.* 26, 237–263. doi: 10.1162/NECO_a_00548

Dangi, S., Gowda, S., and Carmena, J. (2013a). Likelihood gradient ascent (LGA): a closed-loop decoder adaptation algorithm for brain-machine interfaces. *Conf. Proc. IEEE Eng. Med. Biol. Soc.* 2013, 2768–2771. doi: 10.1109/EMBC.2013.6610114

Dangi, S., Orsborn, A. L., Moorman, H. G., and Carmena, J. M. (2013b). Design and analysis of closed-loop decoder adaptation algorithms for brain-machine interfaces. *Neural Comput.* 25, 1693–1731. doi: 10.1162/NECO_a_00460

Dangi, S., So, K., Orsborn, A., Gastpar, M., and Carmena, J. (2013c). Brain-machine interface control using broadband spectral power from local field potentials. *Conf. Proc. IEEE Eng. Med. Biol. Soc.* 2013, 285–288. doi: 10.1109/EMBC.2013.6609493

Ethier, C., Oby, E. R., Bauman, M. J., and Miller, L. E. (2012). Restoration of grasp following paralysis through brain-controlled stimulation of muscles. *Nature* 485, 368–371. doi: 10.1038/nature10987

Fan, J. M., Nuyujukian, P., Kao, J. C., Chestek, C. A., Ryu, S. I., and Shenoy, K. V. (2014). Intention estimation in brain-machine interfaces. *J. Neural Eng.* 11:016004. doi: 10.1088/1741-2560/11/1/016004

Flint, R. D., Wright, Z. A., Scheid, M. R., and Slutzky, M. W. (2013). Long term, stable brain machine interface performance using local field potentials and multiunit spikes. *J. Neural Eng.* 10:056005. doi: 10.1088/1741-2560/10/5/056005

Gilja, V., Nuyujukian, P., Chestek, C. A., Cunningham, J. P., Yu, B. M., Fan, J. M., et al. (2012). A high-performance neural prosthesis enabled by control algorithm design. *Nat. Neurosci.* 15, 1752–1757. doi: 10.1038/nn.3265

Golub, M. D., Yu, B. M., Schwartz, A. B., and Chase, S. M. (2014). Motor cortical control of movement speed with implications for brain-machine interface control. *J. Neurophysiol.* doi: 10.1152/jn.00391.2013. [Epub ahead of print].

Gowda, S., Orsborn, A., Overduin, S., Moorman, H., and Carmena, J. (2014). Designing dynamical properties of brain-machine interfaces to optimize task-specific performance. *IEEE Trans. Neural Syst. Rehabil. Eng.* doi: 10.1109/tnsre.2014.2309673. [Epub ahead of print].

Homer, M., Harrison, M., Black, M., Perge, J., Cash, S., Friehs, G., et al. (2013). "Mixing decoded cursor velocity and position from an offline Kalman filter improves cursor control in people with tetraplegia," in *2013 6th International IEEE/EMBS Conference on Neural Engineering (NER)* (San Diego, CA), 715–718. doi: 10.1109/NER.2013.6696034

Homer, M., Perge, J., Black, M., Harrison, M., Cash, S., and Hochberg, L. (2014). Adaptive offset correction for intracortical brain-computer interfaces. *IEEE Trans. Neural Syst. Rehabil. Eng.* 22, 239–248. doi: 10.1109/TNSRE.2013.2287768

Ifft, P. J., Shokur, S., Li, Z., Lebedev, M. A., and Nicolelis, M. A. L. (2013). A brain-machine interface enables bimanual arm movements in monkeys. *Sci. Transl. Med.* 5:210ra154. doi: 10.1126/scitranslmed.3006159

Jarosiewicz, B., Masse, N. Y., Bacher, D., Cash, S. S., Eskandar, E., Friehs, G., et al. (2013). Advantages of closed-loop calibration in intracortical brain-computer interfaces for people with tetraplegia. *J. Neural Eng.* 10:046012. doi: 10.1088/1741-2560/10/4/046012

Kao, J., Nuyujukian, P., Stavisky, S., Ryu, S., Ganguli, S., and Shenoy, K. (2013). Investigating the role of firing-rate normalization and dimensionality reduction in brain-machine interface robustness. *Conf. Proc. IEEE Eng. Med. Biol. Soc.* 2013, 293–298. doi: 10.1109/EMBC.2013.6609495

Kao, J., Stavisky, S., Sussillo, D., Nuyujukian, P., and Shenoy, K. (2014). Information systems opportunities in brain-machine interface decoders. *Proc. IEEE* 102, 666–682. doi: 10.1109/jproc.2014.2307357

Kowalski, K. C., He, B. D., and Srinivasan, L. (2013). Dynamic analysis of naive adaptive brain-machine interfaces. *Neural Comput.* 25, 2373–2420. doi: 10.1162/NECO_a_00484

Koyama, S., Eden, U., Brown, E., and Kass, R. (2010). Bayesian decoding of neural spike trains. *Ann. Inst. Stat. Math.* 62, 37–59. doi: 10.7551/mitpress/9780262042383.003.0004

Li, L., Brockmeier, A. J., Choi, J. S., Francis, J. T., Sanchez, J. C., and Príncipe, J. C. (2014). A tensor-product-kernel framework for multiscale neural activity decoding and control. *Comput. Intell. Neurosci.* 2014:870160. doi: 10.1155/2014/870160

Mahmoudi, B., Pohlmeyer, E. A., Prins, N. W., Geng, S., and Sanchez, J. C. (2013). Towards autonomous neuroprosthetic control using Hebbian reinforcement learning. *J. Neural Eng.* 10:066005. doi: 10.1088/1741-2560/10/6/066005

Merel, J. S., Fox, R., Jebara, T., and Paninski, L. (2013). "A multi-agent control framework for co-adaptation in brain-computer interfaces," in *Advances in Neural Information Processing Systems*, (vol. 26) eds C. Burges, L. Bottou, M. Welling, Z. Ghahramani and K. Weinberger (Red Hook, NY: Curran Associates, Inc.), 2841–2849.

Moritz, C. T., Perlmutter, S. I., and Fetz, E. E. (2008). Direct control of paralysed muscles by cortical neurons. *Nature* 456, 639–642. doi: 10.1038/nature07418

Nishimura, Y., Perlmutter, S. I., and Fetz, E. E. (2013). Restoration of upper limb movement via artificial corticospinal and musculospinal connections in a monkey with spinal cord injury. *Front. Neural Circuits.* 7:57. doi: 10.3389/fncir.2013.00057

Perge, J. A., Homer, M. L., Malik, W. Q., Cash, S., Eskandar, E., Friehs, G., et al. (2013). Intra-day signal instabilities affect decoding performance in an intracortical neural interface system. *J. Neural Eng.* 10:036004. doi: 10.1088/1741-2560/10/3/036004

Philip, B., Rao, N., and Donoghue, J. (2013). Simultaneous reconstruction of continuous hand movements from primary motor and posterior parietal cortex. *Exp. Brain Res.* 225, 361–375. doi: 10.1007/s00221-012-3377-0

Pohlmeyer, E. A., Mahmoudi, B., Geng, S., Prins, N. W., and Sanchez, J. C. (2014). Using reinforcement learning to provide stable brain-machine interface control despite neural input reorganization. *PLoS One* 9:e87253. doi: 10.1371/journal.pone.0087253

Prins, N. W., Geng, S., Pohlmeyer, E. A., Mahmoudi, B., and Sanchez, J. C. (2013). Feature extraction and unsupervised classification of neural population reward signals for reinforcement based BMI. *Conf. Proc. IEEE Eng. Med. Biol. Soc.* 5250–5253. doi: 10.1109/EMBC.2013.6610733

Sakurai, Y., Song, K., Tachibana, S., and Takahashi, S. (2014). Volitional enhancement of firing synchrony and oscillation by neuronal operant conditioning: interaction with neurorehabilitation and brain-machine interface. *Front. Syst. Neurosci.* 8:11. doi: 10.3389/fnsys.2014.00011

Scheid, M., Flint, R., Wright, Z., and Slutzky, M. (2013). Long-term, stable behavior of local field potentials during brain machine interface use. *Conf. Proc. IEEE Eng. Med. Biol. Soc.* 2013, 307–310. doi: 10.1109/EMBC.2013.6609498

Shanechi, M., and Carmena, J. (2013). "Optimal feedback-controlled point process decoder for adaptation and assisted training in brain-machine interfaces," in *2013 6th International IEEE/EMBS Conference on Neural Engineering (NER)* (San Diego, USA), 653–656. doi: 10.1109/NER.2013.6696019

Shanechi, M. M., Williams, Z. M., Wornell, G. W., Hu, R. C., Powers, M., and Brown, E. N. (2013). A real-time brain-machine interface combining motor target and trajectory intent using an optimal feedback control design. *PLoS One* 8:e59049. doi: 10.1371/journal.pone.0059049

Srinivasan, L., Eden, U. T., Willsky, A. S., and Brown, E. N. (2006). A state-space analysis for reconstruction of goal-directed movements using neural signals. *Neural Comput.* 18, 2465–2494. doi: 10.1162/neco.2006.18.10.2465

Suminski, A., Fagg, A., Willett, F., Bodenhamer, M., and Hatsopoulos, N. (2013). Online adaptive decoding of intended movements with a hybrid kinetic and kinematic brain machine interface. *Conf. Proc. IEEE Eng. Med. Biol. Soc.* 2013, 1583–1586. doi: 10.1109/EMBC.2013.6609817

Tehovnik, E., Woods, L., and Slocum, W. (2013). Transfer of information by BMI. *Neuroscience* 255, 134–146. doi: 10.1016/j.neuroscience.2013.10.003

Velliste, M., Kennedy, S. D., Schwartz, A. B., Whitford, A. S., Sohn, J.-W., and McMorland, A. J. (2014). Motor cortical correlates of arm resting in the context of a reaching task and implications for prosthetic control. *J. Neurosci.* 34, 6011–6022. doi: 10.1523/JNEUROSCI.3520-13.2014

Wang, D., Zhang, Q., Li, Y., Wang, Y., Zhu, J., Zhang, S., et al. (2014). Long-term decoding stability of local field potentials from silicon arrays in primate motor cortex during a 2D center out task. *J. Neural Eng.* 11:036009. doi: 10.1088/1741-2560/11/3/036009

Willett, F. R., Suminski, A. J., Fagg, A. H., and Hatsopoulos, N. G. (2013). Improving brain-machine interface performance by decoding intended future movements. *J. Neural Eng.* 10:026011. doi: 10.1088/1741-2560/10/2/026011

Wong, Y., Putrino, D., Weiss, A., and Pesaran, B. (2013). Utilizing movement synergies to improve decoding performance for a brain machine interface. *Conf. Proc. IEEE Eng. Med. Biol. Soc.* 2013, 289–292. doi: 10.1109/EMBC.2013.6609494

Wu, W., Black, M. J., Gao, Y., Bienenstock, E., Serruya, M., Shaikhoun, A., et al. (2003). "Neural decoding of cursor motion using a Kalman filter," in *Advances*

in Neural Information Processing Systems (Vol. 15), eds S. Becker, S. Thrun and K. Obermayer (Boston: MIT Press), 133–140.

Xu, K., Wang, Y., Wang, F., Liao, Y., Zhang, Q., Li, H., et al. (2014). Neural decoding using a parallel sequential Monte Carlo method on point processes with ensemble effect. *Biomed Res. Int.* 2014:685492. doi: 10.1155/2014/685492

Xu, K., Wang, Y., Wang, Y., Wang, F., Hao, Y., Zhang, S., et al. (2013). Local-learning-based neuron selection for grasping gesture prediction in motor brain machine interfaces. *J. Neural Eng.* 10:026008. doi: 10.1088/1741-2560/10/2/026008

Zhang, Y., and Chase, S. (2013). A stabilized dual Kalman filter for adaptive tracking of brain-computer interface decoding parameters. *Conf. Proc. IEEE Eng. Med. Biol. Soc.* 2013, 7100–7103. doi: 10.1109/EMBC.2013.6611194

Conflict of Interest Statement: The author declares that the research was conducted in the absence of any commercial or financial relationships that could be construed as a potential conflict of interest.

Received: 29 May 2014; accepted: 29 June 2014; published online: 16 July 2014.
Citation: Li Z (2014) Decoding methods for neural prostheses: where have we reached? Front. Syst. Neurosci. ***8****:129. doi: 10.3389/fnsys.2014.00129*
This article was submitted to the journal Frontiers in Systems Neuroscience.

frontiers in
SYSTEMS NEUROSCIENCE

REVIEW ARTICLE
published: 18 February 2015
doi: 10.3389/fnsys.2015.00014

Tapping into rhythm generation circuitry in humans during simulated weightlessness conditions

Irina A. Solopova[1], Victor A. Selionov[1], Francesca Sylos-Labini[2,3], Victor S. Gurfinkel[4], Francesco Lacquaniti[2,3,5] and Yuri P. Ivanenko[2]*

[1] *Laboratory of Neurobiology of Motor Control, Institute for Information Transmission Problems, Russian Academy of Science, Moscow, Russia*
[2] *Laboratory of Neuromotor Physiology, IRCCS Fondazione Santa Lucia, Rome, Italy*
[3] *Centre of Space Bio-medicine, University of Rome Tor Vergata, Rome, Italy*
[4] *Biomedical Engineering Department, Oregon Health and Science University, Portland, OR, USA*
[5] *Department of Systems Medicine, University of Rome Tor Vergata, Rome, Italy*

Edited by:
Ioan Opris, Wake Forest University, USA

Reviewed by:
E. Paul Zehr, Centre for Biomedical Research, Canada
Maria Knikou, City University of New York, USA
Elena Yu. Shapkova, State Research Institute for Phthysiopulmonology, Russia

***Correspondence:**
Yuri P. Ivanenko, Laboratory of Neuromotor Physiology, IRCCS Fondazione Santa Lucia, 306 via Ardeatina, 00179 Rome, Italy
e-mail: y.ivanenko@hsantalucia.it

An ability to produce rhythmic activity is ubiquitous for locomotor pattern generation and modulation. The role that the rhythmogenesis capacity of the spinal cord plays in injured populations has become an area of interest and systematic investigation among researchers in recent years, despite its importance being long recognized by neurophysiologists and clinicians. Given that each individual interneuron, as a rule, receives a broad convergence of various supraspinal and sensory inputs and may contribute to a vast repertoire of motor actions, the importance of assessing the functional state of the spinal locomotor circuits becomes increasingly evident. Air-stepping can be used as a unique and important model for investigating human rhythmogenesis since its manifestation is largely facilitated by a reduction of external resistance. This article aims to provide a review on current issues related to the "locomotor" state and interactions between spinal and supraspinal influences on the central pattern generator (CPG) circuitry in humans, which may be important for developing gait rehabilitation strategies in individuals with spinal cord and brain injuries.

Keywords: central pattern generator, sensory input, rhythmogenesis, locomotion, humans

INTRODUCTION

It is now largely accepted that the neural circuitry controlling locomotion involves a central pattern generator (CPG; Grillner, 1981). CPG functioning depends on supraspinal inputs and sensory feedback (Shik, 1997; Orlovsky et al., 1999; Pearson, 2004; Jordan et al., 2008). Most CPGs are quiescent under resting condition and become recruited by supraspinal pathways with command function (Grillner, 2006). Sensory activity establishes the timing of major phase transitions and contributes to the production of motoneuronal drive (Nielsen and Sinkjaer, 2002; Pearson, 2004), and may also trigger a stepping-like output (Sherrington, 1910; Gurfinkel et al., 1998; Gerasimenko et al., 2010).

The capacity of the mammalian lumbosacral spinal cord to generate rhythmic activity in the absence of input from the brain is firmly established in animal models (Sherrington, 1910; Graham Brown, 1912; Grillner, 1981) and there is indirect evidence that CPGs may also be a feature of the human spinal cord (Bussel et al., 1996; Minassian et al., 2004; Shapkova, 2004; Dominici et al., 2011; Hubli and Dietz, 2013; Ivanenko et al., 2013). The available evidence suggests that many locomotor-related movements that humans perform routinely (walking, running, cycling, swimming, crawling, backward walking, etc.) use similar rhythm circuitry but additionally require specialized control circuits (Zehr, 2005; Patrick et al., 2009; Hoogkamer et al., 2014). In fact, the capacity of neural circuits to generate rhythmic activity represents the common core for various locomotor tasks (Zehr, 2005). The aim of this article is to provide a review on current issues related to the excitability of spinal CPG circuitry in humans. Under normal conditions, it is sometimes difficult to investigate impairments in the CPG functioning due to interference with the ongoing task of body weight and balance control (including intense feedback). Therefore, one might examine the rhythmogenesis capacity of spinal circuitry in conditions not-complicated by these two factors.

Body weight support systems coupled with robotic devices or pharmacologic treatments are now often used in the rehabilitation practice to assist locomotor recovery in individuals with neuromotor disorders (Dietz, 2009; Sale et al., 2012; Hubli and Dietz, 2013; Valentin-Gudiol et al., 2013; Meyns et al., 2014; Moraru and Onose, 2014). There is still limited evidence of the efficacy of treadmill interventions with body weight support in some injured populations due to the complex nature of the control of locomotion, compensatory strategies, and plasticity of neuronal networks (Grasso et al., 2004; Picelli et al., 2013; Valentin-Gudiol et al., 2013; Swinnen et al., 2014; Sylos-Labini et al., 2014b). We will not review here any detailed analysis of clinical outcomes for ambulation when using locomotor training with body weight support systems and refer to other reviews (e.g.,

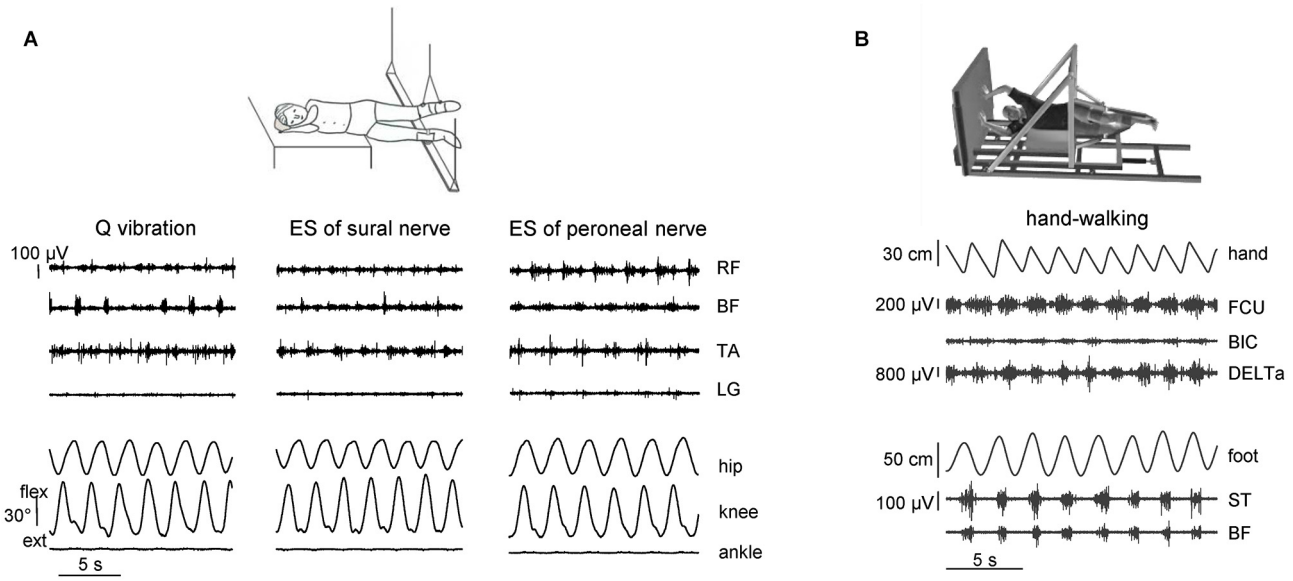

FIGURE 1 | Eliciting non-voluntary limb stepping movements in simulated weightlessness (gravity neutral) conditions. **(A)** examples of non-voluntary rhythmic movements of the suspended legs induced by quadriceps (Q) muscle vibration and electrical stimulation (ES) of sural and peroneal nerves in one representative subject from the study of Selionov et al. (2009). An upward deflection of traces denotes flexion in the hip and knee joint angles and dorsiflexion in the ankle joint. Note the absence of ankle joint rotations during evoked air-stepping. **(B)** An example of evoked rhythmic leg movements during hand walking in one subject from the study of Sylos-Labini et al. (2014a). RF, rectus femoris, BF, biceps femoris, TA, tibialis anterior, LG, lateral gastrocnemius, FCU, flexor carpi ulnaris, BIC, biceps brachii, DELTa, anterior deltoid, ST, and semitendinosus. Hand and foot denote anterior-posterior displacements of the left hand and foot.

Wirz et al., 2005; Sale et al., 2012; Valentin-Gudiol et al., 2013; Scivoletto et al., 2014). The main focus here is to give emphasis to a facilitatory effect of simulated weightlessness on rhythmogenesis and its potential for assessing the state of the CPG circuits and for gait recovery after spinal cord injury and other neuromotor disorders.

LOCOMOTOR "STATE" OF THE SPINAL CIRCUITY

Historically, Goltz and Freusberg (1874) were the first to report spontaneous air-stepping of the hindlimbs of the spinal dog before voiding the distended bladder, presumably due to some excitatory state of the spinal circuitry. In decerebrated animals exhibiting spontaneous fluctuations in their level of rigidity, rhythmic movements can be evoked by peripheral stimulation, provided there is an appropriate level of background extensor tonus and that the tonus is neither too low nor too high (Beritoff, 1915). In addition, an increase in tonus precedes the initiation of locomotion (Mori et al., 1982). The excitability status or state of the spinal network is thus of particular importance (Edgerton et al., 2008). Air-stepping can be used as a unique and important model for investigating human rhythmogenesis since its manifestation is largely facilitated by a reduction of external resistance, such as that resulting from body weight unloading (Gurfinkel et al., 1998; Selionov et al., 2009). Below we consider various experiments and observations in conditions of reduced gravity effects that help revealing the intrinsic properties of locomotor pattern generators and making evident the facilitation of non-voluntary limb stepping in humans.

The spinal CPG circuitry can be activated in healthy humans by applying tonic central or peripheral sensory inputs. As we previously mentioned, in addition to the control of the timing of major phase transitions and muscle activity production (Nielsen and Sinkjaer, 2002; Pearson, 2004), sensory activity has access to the functional state of CPG and may initiate a stepping-like output (Sherrington, 1910; Gurfinkel et al., 1998; Gerasimenko et al., 2010). **Figure 1A** illustrates different examples of stimulation techniques that were explored for eliciting non-voluntary air-stepping: continuous muscle vibration (40–60 Hz, ∼1 mm amplitude), and electrical stimulation of the superficial peroneal or sural nerves (0.3 ms duration pulses, 2–3 mA, 60 Hz) (Selionov et al., 2009). To minimize interference with the ongoing task of body weight and balance control, stepping movements are elicited during air-stepping in the absence of gravity influences and reduced external resistance. The subjects were tested while lying on their side with the legs supported using long ropes attached to the ceiling (**Figure 1A**) or using an exoskeleton (**Figure 1B**) so that they provided low-friction pendulum-like leg motion in the horizontal plane with a limited vertical motion component. The afferent signals due to vibration or electrical stimulation of peripheral nerves may increase the excitability of several segments of the spinal cord, which may facilitate triggering of locomotor-like movements. The latency of the elicited cyclic movements varied significantly across subjects and conditions (range 1–25 s). The delay in the onset of leg movement likely reflects the general property of the pattern generation circuitry and transition from tonic activation to

the phasic CPG output. Generally, cyclic movements increased monotonically for 2–10 cycles until they reached a relatively constant amplitude of angular oscillations (Gurfinkel et al., 1998; Selionov et al., 2009; Gerasimenko et al., 2010). The characteristics of non-voluntary air-stepping (amplitude, cycle duration) were similar to the voluntary stepping in the same conditions.

In addition to peripheral sensory stimulation, central tonic facilitatory influences may be used for eliciting rhythmic leg movements, such as the Jendrassik maneuver and the Kohnstamm phenomenon (Gurfinkel et al., 1998; Selionov et al., 2009). An intriguing approach related to the role of tonic influences is the Kohnstamm phenomenon (Kohnstamm, 1915), which consists in the appearance of involuntary tonic activity and a particular sensation of "lightness" after the cessation of a long-lasting (30–40 s) isometric effort. Post-activation phenomena can therefore be used as a tool to study tonic influences. After-effects of a voluntary, long-lasting contraction in the leg muscles featured alternating rhythmic leg movements that lasted for about 20–40 s (Selionov et al., 2009), corresponding roughly to a typical duration of the post-contraction activity (Craske and Craske, 1986; Duclos et al., 2004; Ivanenko et al., 2006b). The difference in the effects of the two techniques (the post-contraction phenomenon and the Jendrassik maneuver) may point to the importance of tonic activation of the lumbosacral enlargement, since voluntary arm contractions (due to the Jendrassik maneuver) are weaker in evoking stepping movements: they act primarily on the cervical spinal cord and are not sufficient to evoke air-stepping unless the experimenter triggers them (Selionov et al., 2009).

Other techniques for triggering stepping movements are based on the more direct stimulation of the spinal cord by electromagnetic (Gerasimenko et al., 2010), transcutaneous or epidural electrical stimulation (Shapkova and Schomburg, 2001; Gorodnichev et al., 2012), which can initiate and sustain movements more robustly than by stimulation of sensory afferent fibers. Transcutaneous electrical spinal cord stimulation (at 5–40 Hz) is applied over T11-T12 vertebrae and presumably activates the locomotor circuitry through the dorsal roots (Gorodnichev et al., 2012; Gerasimenko et al., 2014), while epidural stimulation is based on an implanted array of electrodes directly placed over the back portion of the lower thoracic-upper lumbar spinal cord (**Figure 4A**, upper panel). Rhythmic locomotor-like leg movements in a gravity neutral position can be evoked in ∼10–50% of healthy subjects, and the degree of activation may depend on supraspinal influences and the state and the rhythmogenesis capacity of the spinal circuitry (Gurfinkel et al., 1998; Selionov et al., 2009; Gerasimenko et al., 2010). The common feature of all stimulations described above is that they are tonic. In this respect, they corroborate earlier pioneering observations in decerebrate cats that stepping can be induced using a simple tonic stimulation pattern applied to the mesencephalic locomotor region (Shik et al., 1966), but they also show that this type of control can be initiated at the lumbosacral spinal cord level. Overall, the findings suggest that nonspecific tonic excitability may elicit or facilitate CPG activity.

Finally, automatic, alternating movements of the legs can be initiated by upper limb movements by asking participants to move their arms rhythmically, as in hand-walking (**Figure 1B**; Sylos-Labini et al., 2014a). The idea is grounded on the evidence that the coordination between arms and legs during human locomotion shares many features with that in quadrupeds (Falgairolle et al., 2006; Zehr et al., 2007; Patrick et al., 2009; Dietz, 2011; Kuhtz-Buschbeck and Jing, 2012). For instance, inter-limb coupling in humans has previously been demonstrated by evoking reflexes in one limb and observing the extent to which the movement of another limb modulates reflex expression during walking (Haridas and Zehr, 2003; Mezzarane et al., 2011; Massaad et al., 2014). The coupling between the activity of cervical motoneurons underlying hand-walking and the activity of lumbosacral motoneurons underlying leg movements (**Figure 1B**) is presumably indirect, delayed and asynchronous (e.g., leg stepping is often characterized by a non-integer ratio between arm and leg movements frequency). These variable features suggest that signals related to arm movements do not directly entrain the motor commands to leg muscles, but affect the state of the lumbosacral locomotor circuitry, consistent with a facilitatory effect of arm swinging on cyclic leg muscle activity (de Kam et al., 2013). In addition, it has been recently shown that cervical transcutaneous stimulation of the spinal cord significantly facilitates non-voluntary air-stepping leg movements and the lumbosacral locomotor-related neuronal circuitry (Gerasimenko et al., 2014). One possible route for these trigger signals is through the intrinsic spinal pathways (propriospinal interneurons) linking cervical to lumbosacral regions in humans (Nathan et al., 1996). However, considering the latency of the leg responses relative to arm oscillations, supraspinal contributions cannot be excluded. Rhythmic arm movements imitating those during running or walking can also evoke prominent modulation of leg muscle EMGs during standing (Danna-Dos-Santos et al., 2009). Whatever the exact mechanism, these findings (**Figure 1B**) reinforce the idea that there exists a functional coupling between arm and leg CPGs.

INTERACTION BETWEEN RHYTHM-GENERATION ACTIVITY AND SENSORY INPUT

The previous studies, which aimed to activate the CPG circuits using the "air-stepping" paradigm (Gurfinkel et al., 1998; Selionov et al., 2009; Gerasimenko et al., 2010, 2014; Sylos-Labini et al., 2014a), also revealed some essential features of the intrinsic rhythm generation in humans. The evoked cyclic movements share many of their characteristics with animals. For instance, given the extensive evidence for the presence of commissural interneurons driving the contralateral locomotor circuitry (Kiehn, 2011), oscillator mechanisms and tonic influences may not be limb-specific. We found, for example, that treating one limb (e.g., applying electrical stimulation of the peroneal or sural nerves of one leg) can have its output transferred to another limb, even if the treated limb is kept stationary (Selionov et al., 2009). Also, although pattern generators for each limb have the potential to produce relatively autonomous rhythmic patterns (Forssberg et al., 1980; Yang et al., 2005), right

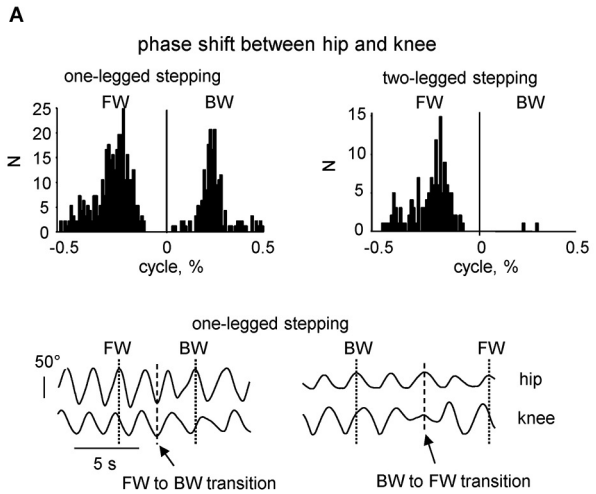

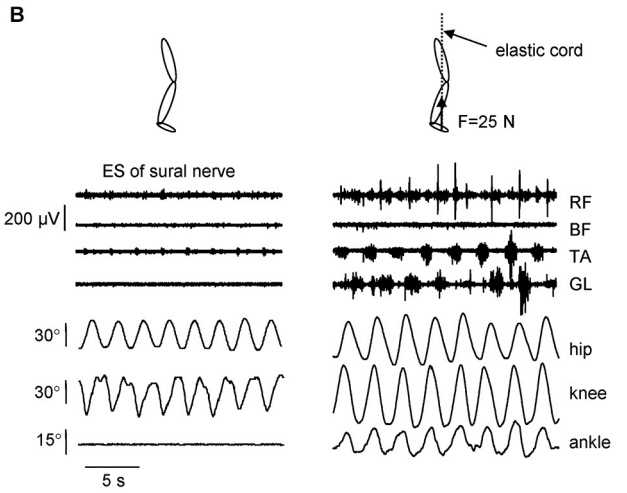

FIGURE 2 | Kinematic features of non-voluntary air-stepping movements. **(A)** one-legged vs. two-legged air-stepping evoked by quadriceps muscle vibration. Upper panels—histogram of the phase shift between hip and knee joints across subjects and probes. Note similar occurrence of forward and backward one-legged air-stepping and predominantly forward 2-legged stepping. Low panels—examples of transitions (in the middle of the record) from FW to BW stepping and vice versa in 2 subjects. **(B)** examples of rhythmic leg movements evoked by continuous electrical stimulation (ES) of the sural nerve in the absence (left) and presence (right) of small (25 N) force applied to the forefoot part of the foot. The force was applied approximately in the direction of the longitudinal axis of the body using a long elastic thread cord. The length of the thread cord was about 5 m so that fluctuations in its force due to the length changes were minimal (<10%) during air-stepping. Eight consecutive cycles are shown for each condition. Note the appearance of noticeable oscillations in the ankle joint angle and activity in the distal muscles in the presence of small load force (adapted from Selionov et al., 2009).

and left sides are strongly coupled under most natural conditions (Orlovsky et al., 1999; Ivanenko et al., 2006a; Maclellan et al., 2014). Further evidence of the importance of bilateral coupling is demonstrated by the finding that two-legged stepping was more stable (and predominantly forward, **Figure 2A**, upper panels), whereas one-legged stepping in some subjects displayed frequent spontaneous transitions from forward to backward direction and vice versa (**Figure 2A**, lower panels).

Air-stepping tends to involve prominent movements in the hip and knee joints, whereas the ankle joint is typically not involved, unless minimal loading forces are applied to the foot (**Figure 2B**). The facilitatory effect of forces is often accompanied by modulation of the EMG activity, consistent with phase-dependent contribution of sensory activity to the pre-programmed motoneuronal drive of the distal muscles during human walking (Duysens et al., 2000; Nielsen and Sinkjaer, 2002). Even individuals with clinically motor complete paralysis demonstrate modulated activity of distal leg muscles during assisted stepping with body weight support (during locomotion with 100% body unloading, no EMG activity was present) (Harkema et al., 1997; Dietz et al., 2002). It can be concluded that afferent input from load-related receptors (including Golgi tendon organs, spindles, cutaneous receptors, and various load mechanoreceptors in the foot arch, Duysens et al., 2000; Pearson, 2004; Gravano et al., 2011) contributes to the generation of locomotor activity in the isolated human spinal cord. Therefore, the sacral pattern generation circuitry (Cazalets and Bertrand, 2000) might be inactivated when the input from the support surface is lacking. The more direct stimulation of the spinal cord locomotor circuitry using repetitive electromagnetic stimuli can evoke ankle joint oscillations (Gerasimenko et al., 2010). However, in this case it likely involves stimulation of the dorsal roots, and thus load-related afferents. Overall, the lack of ankle joint movements during non-voluntary air-stepping (**Figures 1A**, **2B**) supports the hypothesis that the upper lumbar pattern generator activity may constitute the major oscillator "pacemaker," whereas the sacral generator could play a subordinator role for adaptation to specific foot-support interactions. Also, minimal contact forces during air-stepping may significantly improve accurate foot trajectory control, suggesting that the support surface represents an importance reference frame and is included in the locomotor body scheme (Ivanenko et al., 2002).

ENGAGEMENT OF SUPRASPINAL MOTOR AREAS

Better understanding of interactions between spinal and supraspinal influences on the state of CPG circuitry may be important for developing gait rehabilitation strategies in individuals with spinal cord and brain injuries. In addition, there is an increasing consensus that motor centers in the brain, and the motor cortex in particular, play an essential and greater role in human walking compared to other mammals (Capaday, 2002; Yang and Gorassini, 2006; Petersen et al., 2012; Beloozerova et al., 2013). For instance, the coherence analysis demonstrated significant coupling between EEG recordings over the leg motor area and EMG from the tibialis anterior muscle prior to heel strike during the swing phase of walking, suggesting that the motor cortex and corticospinal

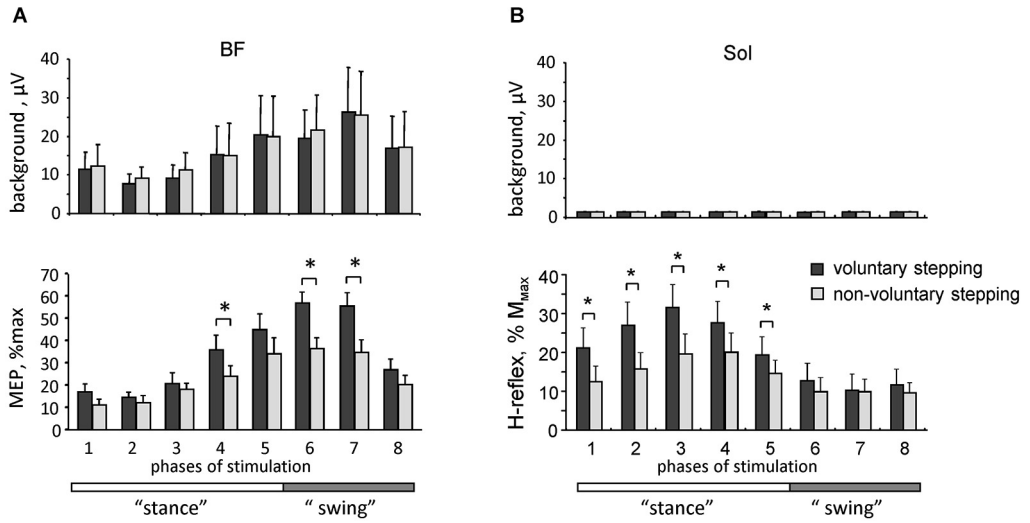

FIGURE 3 | Motor responses during voluntary and non-voluntary air-stepping in healthy subjects. **(A)** background EMG activity (upper panel) and motor evoked potentials (lower panel) in response to transcranial magnetic stimulation of the motor cortex (MEPs, mean ± SE, *n* = 8 subjects) in the BF muscle during different phases of the step cycle. **(B)** background soleus EMG activity (upper panel) and H-reflex (lower panel) modulation. Asterisks denote significant differences. Note facilitation of motor responses during voluntary stepping. Adapted from Solopova et al. (2014).

tract contribute directly to the muscle activity observed in steady-state human walking (Petersen et al., 2012). Recently, we compared motor evoked potentials (MEP) in response to transcranial magnetic stimulation of the motor cortex and the H-reflex during voluntary and vibration-induced air-stepping movements in healthy humans (Solopova et al., 2014). Both the MEPs and H-reflex were significantly smaller during vibration-induced cyclic leg movements at matched amplitudes of angular motion and muscle activity (**Figure 3**). One may suppose that in both cases the locomotor-like leg movements are evoked via activation of the spinal pattern generation circuitry. The greater responsiveness to central inputs during voluntary CPG activation (**Figure 3**) may be related to facilitation of transcortical reflex pathways (Christensen et al., 1999), increased depolarization of motoneurons, and/or an overall facilitatory effect on spinal motoneurons and interneurons. Interestingly, modulation of the H-reflex was observed in the absence of noticeable background EMG activity of the soleus and tibialis anterior muscles (likely due to the absence of limb loading and ankle joint movements), and occurred during the hypothetical stance phase of the step cycle (**Figure 3**), consistent with a CPG phase-related modulation of spinal reflexes.

These findings highlight differences between voluntary and non-voluntary activation of the spinal pattern generator circuitry, presumably due to an extra facilitatory effect of voluntary control of stepping on spinal motoneurons and interneurons. It has been argued that the engagement of supraspinal motor areas may be beneficial for gait recovery (van den Brand et al., 2012), and there is a link between facilitation of segmental reflexes and the ability to recover gait (Dietz et al., 2009; Thompson and Wolpaw, 2014). Our results (**Figure 3**) support this hypothesis, and show an overall facilitatory effect of supraspinally mediated stepping on reflex responses. Such investigations may contribute to the clinical development of CPG-modulating therapies (Guertin, 2014).

TAPPING INTO RHYTHM GENERATION CIRCUITRY IN NEUROMOTOR DISORDERS

During the last decade, there has been a growing interest in understanding an appropriate state of the spinal circuitry for performing locomotor movements (Hultborn, 2001; Edgerton et al., 2008; van den Brand et al., 2012; Selionov et al., 2013). In particular, to trigger the CPG by neurons with command function (Grillner, 2006), the physiological state of the spinal network needs to be properly prepared (Edgerton et al., 2008) since the same interneurons and motoneurons may contribute to a vast repertoire of motor actions (Hultborn, 2001).

A facilitatory effect of simulated weightlessness can be used for investigating rhythmogenesis of the spinal cord in injured populations and for entraining the spinal locomotor circuitry. Epidural stimulation is a technique that has been used for a number of years to treat individuals with a spinal cord injury, and various experiments emphasized a significant complementary effect of epidural stimulation when combined with pharmacological facilitation, e.g., serotonergic agonists, and step training (Shapkova and Schomburg, 2001; Minassian et al., 2007; Gerasimenko et al., 2008). The existence of a spinal locomotor generator circuitry in humans has been confirmed based on observations in patients with a severe spinal cord injury implanted with an array of electrodes directly placed over the back portion of the lower thoracic-upper lumbar spinal cord (Minassian et al., 2004; Shapkova, 2004). In these experiments, stepping-like movements were produced in patients who were supine with the legs in the resting position (**Figure 4A**) or suspended in the air (**Figure 4B**). Epidural stimulation could

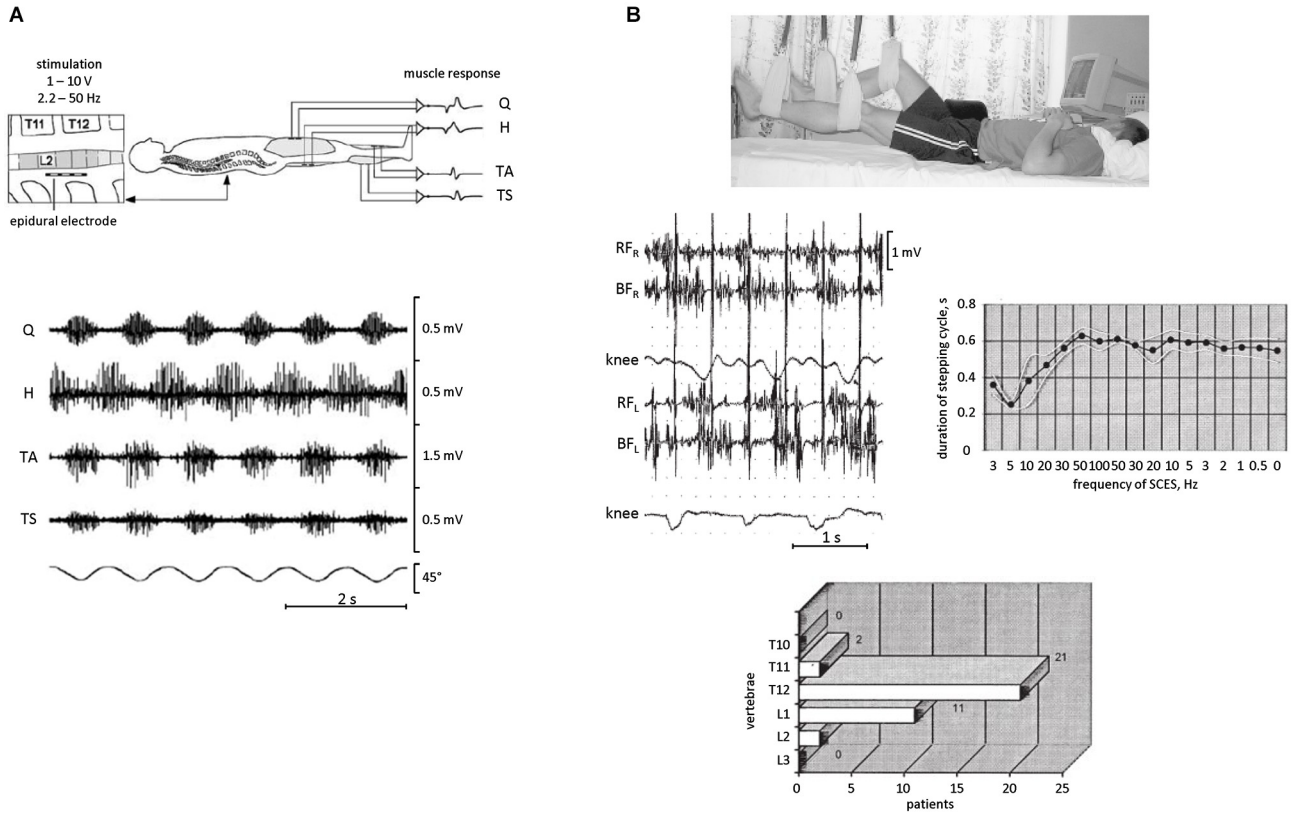

FIGURE 4 | EMG activity and rhythmic leg movements induced by epidural spinal cord electrical stimulation (SCES) in SCI patients in a supine position. **(A)** epidural SCES (upper panel) and an example of EMG recordings (bottom panel) obtained from quadriceps (Q), hamstrings (H), tibialis anterior (TA), and triceps surae (TS) during SCES at 31 Hz. The goniometer traces of the knee joint angle illustrate the corresponding induced rhythmical movements of the lower limbs. Adapted from Minassian et al. (2004). **(B)** SCES-induced rhythmic leg movements in SCI patients. During SCES, the patient was lying supine and the legs were suspended on elastic straps in a position such that the hip and knee joints were in semi-flexion (top panel). Middle panels: an example of stepping-like movements at ∼1 Hz evoked with 2 Hz SCES in one SCI patient. On the right—duration of stepping cycle in relationship to the frequency of SCES in this patient. The frequency gradually increased from 3 to 100 Hz and then decreased from 100 to 0.5 Hz. Bottom panel: location of the effective zone for initiating alternating stepping-like movements with SCES in a group of paraplegic patients (n = 29). Adapted from Shapkova (2004).

even produce rhythmic EMG activities without step-related sensory feedback (stationary legs) or with a rhythm frequency independent of that of passive treadmill stepping (Minassian et al., 2013). Nevertheless, leg suspension significantly facilitates the manifestation of rhythmic motion (**Figure 4B**) and permits to reveal its characteristics. For instance, depending on the exact location of the stimulating electrodes, the stimulation could produce different patterns of rhythmic leg movements with different involvements of leg joints (Shapkova, 2004), consistent with the idea that there exist individual CPGs for each limb and/or each segment, and are coordinated during natural locomotion to produce a coherent interlimb pattern (Graham Brown, 1912; Grillner, 1981). Epidural stimulation can also transform the CPG circuitry into the active functional state which persists even after a significant decrease of stimulation frequency (**Figure 4B**, right panel). Interestingly, non-voluntary (evoked by epidural stimulation) air-stepping movements in incomplete spinal cord injury individuals can be sustained for more than 1 h with increasing EMG activity, while voluntarily initiated rhythmic leg movements in these patients demonstrate progressive fatigue after several minutes (Shapkova, 2004). Thus, even though supraspinally mediated activation of stepping has an overall facilitatory effect on reflex responses (**Figure 3**) and pattern generation (Solopova et al., 2014), it may also contribute to the development of "central" fatigue (Taylor et al., 2006). Furthermore, daily sessions with epidural stimulation evoking air-stepping rhythmic movements were effective in restoring the locomotor function in some children with a severe spinal cord injury (Shapkova, 2004).

The residual sensory pathways may be critical in regaining voluntary movement. Moreover, the neuromodulation and activation of the "locomotor state" of the spinal circuitry below the lesion may enable completely paralyzed individuals to process conceptual, auditory and visual inputs, and to regain some voluntary control of paralyzed muscles (Angeli et al., 2014). In this study, a stimulation protocol was developed to allow the individuals to stimulate for ∼1 h while practicing intentional movement in the supine position. Four individuals diagnosed

with clinically motor complete paralysis (classified as AIS-B and AIS-A before implantation) and implanted with a lumbrosacral spinal cord stimulator at least 2.2 years post injury were able to generate EMG activity and movement during ankle dorsiflexion in the presence of epidural stimulation following a verbal command. No motor activity was present when attempting to move without epidural stimulation. Furthermore, daily training resulted in the generation of voluntary efforts with higher forces and lower stimulation voltages to reach the thresholds that enabled voluntary motor responses that could be modulated by visual and/or auditory input (Angeli et al., 2014). Hence, it is essential to discern how the spinal pattern generation circuitry is controlled by sensory input and supraspinal networks to design new rehabilitation devices that involve modulation of the physiological state of the spinal cord during training. A degradation of spinal neuronal activity takes place following a spinal cord injury, suggesting that a continuous training approach starting early after injury is necessary to maintain neuronal activity below the level of the lesion (Dietz and Müller, 2004). Future studies may focus on the mechanisms underlying the manifestation of early motor symptoms, muscle tone, impaired sensory feedback and their relation to rhythmogenesis investigated under simulated weightlessness conditions. This may also help facilitating the application of neurophysiological analyses as quantification tools for evaluating new medications useful to assess or augment the rhythmogenesis capacity and gait recovery in neurological disorders.

CONCLUDING REMARKS

Novel pharmacological strategies (Roy et al., 2012; Borton et al., 2014; Guertin, 2014) and electromagnetic stimulation techniques (Shapkova and Schomburg, 2001; Minassian et al., 2007; Gerasimenko et al., 2008; Selionov et al., 2009; Angeli et al., 2014) are being developed aimed at modulating spinal activity and restoring the locomotor function. Even though electrochemical or sensory stimulations do not necessarily induce automated stepping by activating CPG networks, they may transform lumbosacral circuits from non-functional to functional states, enabling the information-processing interface in the spinal cord to utilize multifaceted sensory input as a source of control for locomotion (Courtine et al., 2009). Overall, recent findings highlight the importance of investigating the tonic "state" of the spinal circuits. Since the air-stepping is free from many of the mechanical constraints of normal walking, it may provide an effective model for studying how peripheral inputs influence CPG behavior in human adults (Gurfinkel et al., 1998; Shapkova and Schomburg, 2001; Selionov et al., 2009; Gerasimenko et al., 2010; Solopova et al., 2014; Sylos-Labini et al., 2014a). Thus, the beneficial effect of simulated weightlessness on rhythmogenesis may enhance the utility of spinal cord stimulation techniques for developing CPG-modulating therapies and augmentation of function for disabled people.

ACKNOWLEDGMENTS

The work was supported by the Russian Foundation for Basic Research grants #13-04-12076 and #15-04-02825, Italian Health Ministry and Italian Space Agency (COREA Grant).

REFERENCES

Angeli, C. A., Edgerton, V. R., Gerasimenko, Y. P., and Harkema, S. J. (2014). Altering spinal cord excitability enables voluntary movements after chronic complete paralysis in humans. *Brain* 137, 1394–1409. doi: 10.1093/brain/awu038

Beloozerova, I. N., Stout, E. E., and Sirota, M. G. (2013). Distinct Thalamo-cortical controls for shoulder, elbow and wrist during locomotion. *Front. Comput. Neurosci.* 7:62. doi: 10.3389/fncom.2013.00062

Beritoff, J. S. (1915). On the mode of originating of labyrinthine and cervical tonic reflexes and on their part in the reflex reactions of decerebrate preparation. *Q. J. Exp. Physiol.* 6, 199–229. doi: 10.1113/expphysiol.1915.sp000204

Borton, D., Bonizzato, M., Beauparlant, J., DiGiovanna, J., Moraud, E. M., Wenger, N., et al. (2014). Corticospinal neuroprostheses to restore locomotion after spinal cord injury. *Neurosci. Res.* 78, 21–29. doi: 10.1016/j.neures.2013.10.001

Bussel, B., Roby-Brami, A., Néris, O. R., and Yakovleff, A. (1996). Evidence for a spinal stepping generator in man. Electrophysiological study. *Acta Neurobiol. Exp. (Wars)* 56, 465–468.

Capaday, C. (2002). The special nature of human walking and its neural control. *Trends Neurosci.* 25, 370–376. doi: 10.1016/s0166-2236(02)02173-2

Cazalets, J. R., and Bertrand, S. (2000). Coupling between lumbar and sacral motor networks in the neonatal rat spinal cord. *Eur. J. Neurosci.* 12, 2993–3002. doi: 10.1046/j.1460-9568.2000.00169.x

Christensen, L. O., Morita, H., Petersen, N., and Nielsen, J. (1999). Evidence suggesting that a transcortical reflex pathway contributes to cutaneous reflexes in the tibialis anterior muscle during walking in man. *Exp. Brain Res.* 124, 59–68. doi: 10.1007/s002210050600

Courtine, G., Gerasimenko, Y., van den Brand, R., Yew, A., Musienko, P., Zhong, H., et al. (2009). Transformation of nonfunctional spinal circuits into functional states after the loss of brain input. *Nat. Neurosci.* 12, 1333–1342. doi: 10.1038/nn.2401

Craske, B., and Craske, J. D. (1986). Oscillator mechanisms in the human motor system: investigating their properties using the aftercontraction effect. *J. Mot. Behav.* 18, 117–145. doi: 10.1080/00222895.1986.10735374

Danna-Dos-Santos, A., Shapkova, E. Y., Shapkova, A. L., Degani, A. M., and Latash, M. L. (2009). Postural control during upper body locomotor-like movements: similar synergies based on dissimilar muscle modes. *Exp. Brain Res.* 193, 565–579. doi: 10.1007/s00221-008-1659-3

de Kam, D., Rijken, H., Manintveld, T., Nienhuis, B., Dietz, V., and Duysens, J. (2013). Arm movements can increase leg muscle activity during submaximal recumbent stepping in neurologically intact individuals. *J. Appl. Physiol. (1985)* 115, 34–42. doi: 10.1152/japplphysiol.00510.2012

Dietz, V. (2009). Body weight supported gait training: from laboratory to clinical setting. *Brain Res. Bull.* 78, I–VI. doi: 10.1016/s0361-9230(08)00410-3

Dietz, V. (2011). Quadrupedal coordination of bipedal gait: implications for movement disorders. *J. Neurol.* 258, 1406–1412. doi: 10.1007/s00415-011-6063-4

Dietz, V., Grillner, S., Trepp, A., Hubli, M., and Bolliger, M. (2009). Changes in spinal reflex and locomotor activity after a complete spinal cord injury: a common mechanism? *Brain* 132, 2196–2205. doi: 10.1093/brain/awp124

Dietz, V., and Müller, R. (2004). Degradation of neuronal function following a spinal cord injury: mechanisms and countermeasures. *Brain* 127, 2221–2231. doi: 10.1093/brain/awh255

Dietz, V., Müller, R., and Colombo, G. (2002). Locomotor activity in spinal man: significance of afferent input from joint and load receptors. *Brain J. Neurol.* 125, 2626–2634. doi: 10.1093/brain/awf273

Dominici, N., Ivanenko, Y. P., Cappellini, G., d'Avella, A., Mondì, V., Cicchese, M., et al. (2011). Locomotor primitives in newborn babies and their development. *Science* 334, 997–999. doi: 10.1126/science.1210617

Duclos, C., Roll, R., Kavounoudias, A., and Roll, J. P. (2004). Long-lasting body leanings following neck muscle isometric contractions. *Exp. Brain Res.* 158, 58–66. doi: 10.1007/s00221-004-1871-8

Duysens, J., Clarac, F., and Cruse, H. (2000). Load-regulating mechanisms in gait and posture: comparative aspects. *Physiol. Rev.* 80, 83–133.

Edgerton, V. R., Courtine, G., Gerasimenko, Y. P., Lavrov, I., Ichiyama, R. M., Fong, A. J., et al. (2008). Training locomotor networks. *Brain Res. Rev.* 57, 241–254. doi: 10.1016/j.brainresrev.2007.09.002

Falgairolle, M., de Seze, M., Juvin, L., Morin, D., and Cazalets, J.-R. (2006). Coordinated network functioning in the spinal cord: an evolutionary perspective. *J. Physiol. Paris* 100, 304–316. doi: 10.1016/j.jphysparis.2007.05.003

Forssberg, H., Grillner, S., and Halbertsma, J. (1980). The locomotion of the low spinal cat. I. Coordination within a hindlimb. *Acta Physiol. Scand.* 108, 269–281. doi: 10.1111/j.1748-1716.1980.tb06533.x

Gerasimenko, Y., Gorodnichev, R., Machueva, E., Pivovarova, E., Semyenov, D., Savochin, A., et al. (2010). Novel and direct access to the human locomotor spinal circuitry. *J. Neurosci.* 30, 3700–3708. doi: 10.1523/JNEUROSCI.4751-09.2010

Gerasimenko, Y. P., Gorodnichev, R., Puhov, A., Moshonkina, T., Savochin, A., Selionov, V. A., et al. (2014). Initiation and modulation of locomotor circuitry output with multi-site transcutaneous electrical stimulation of the spinal cord in non-injured humans. *J. Neurophysiol.* doi: 10.1152/jn.00609.2014. [Epub ahead of print].

Gerasimenko, Y., Roy, R. R., and Edgerton, V. R. (2008). Epidural stimulation: comparison of the spinal circuits that generate and control locomotion in rats, cats and humans. *Exp. Neurol.* 209, 417–425. doi: 10.1016/j.expneurol.2007.07.015

Goltz, F., and Freusberg, A. (1874). Uber die Funktionen des Lendenmarkes des Hundes. *Pflugers Physiol.* 8, 460–498. doi: 10.1007/BF01612308

Gorodnichev, R. M., Pivovarova, E. A., Pukhov, A., Moiseev, S. A., Savokhin, A. A., Moshonkina, T. R., et al. (2012). Transcutaneous electrical stimulation of the spinal cord: non-invasive tool for activation of locomotor circuitry in human. *Fiziol. Cheloveka* 38, 46–56.

Graham Brown, T. (1912). The factors in rhythmic activity of the nervous system. *Proc. R. Soc. B Biol. Sci.* 85, 278–289. doi: 10.1098/rspb.1912.0051

Grasso, R., Ivanenko, Y. P., Zago, M., Molinari, M., Scivoletto, G., Castellano, V., et al. (2004). Distributed plasticity of locomotor pattern generators in spinal cord injured patients. *Brain* 127, 1019–1034. doi: 10.1093/brain/awh115

Gravano, S., Ivanenko, Y. P., Maccioni, G., Macellari, V., Poppele, R. E., and Lacquaniti, F. (2011). A novel approach to mechanical foot stimulation during human locomotion under body weight support. *Hum. Mov. Sci.* 30, 352–367. doi: 10.1016/j.humov.2010.01.002

Grillner, S. (1981). "Control of locomotion in bipeds, tetrapods and fish," in *Handbook of Physiology: Section 1: The Nervous System, volume II, Part.1 Motor Control*, eds V. B. Brooks, J. M. Brookhart and V. B. Mountcastle (Bethesda, MD: Am. Physiol. Soc.), 1179–1236.

Grillner, S. (2006). Biological pattern generation: the cellular and computational logic of networks in motion. *Neuron* 52, 751–766. doi: 10.1016/j.neuron.2006.11.008

Guertin, P. A. (2014). Preclinical evidence supporting the clinical development of central pattern generator-modulating therapies for chronic spinal cord-injured patients. *Front. Hum. Neurosci.* 8:272. doi: 10.3389/fnhum.2014.00272

Gurfinkel, V. S., Levik, Y. S., Kazennikov, O. V., and Selionov, V. A. (1998). Locomotor-like movements evoked by leg muscle vibration in humans. *Eur. J. Neurosci.* 10, 1608–1612. doi: 10.1046/j.1460-9568.1998.00179.x

Haridas, C., and Zehr, E. P. (2003). Coordinated interlimb compensatory responses to electrical stimulation of cutaneous nerves in the hand and foot during walking. *J. Neurophysiol.* 90, 2850–2861. doi: 10.1152/jn.00531.2003

Harkema, S. J., Hurley, S. L., Patel, U. K., Requejo, P. S., Dobkin, B. H., and Edgerton, V. R. (1997). Human lumbosacral spinal cord interprets loading during stepping. *J. Neurophysiol.* 77, 797–811.

Hoogkamer, W., Meyns, P., and Duysens, J. (2014). Steps forward in understanding backward gait: from basic circuits to rehabilitation. *Exerc. Sport Sci. Rev.* 42, 23–29. doi: 10.1249/JES.0000000000000000

Hubli, M., and Dietz, V. (2013). The physiological basis of neurorehabilitation - locomotor training after spinal cord injury. *J. Neuroeng. Rehabil.* 10:5. doi: 10.1186/1743-0003-10-5

Hultborn, H. (2001). State-dependent modulation of sensory feedback. *J. Physiol.* 533, 5–13. doi: 10.1111/j.1469-7793.2001.0005b.x

Ivanenko, Y. P., Dominici, N., Cappellini, G., Di Paolo, A., Giannini, C., Poppele, R. E., et al. (2013). Changes in the spinal segmental motor output for stepping during development from infant to adult. *J. Neurosci.* 33, 3025a–3036a. doi: 10.1523/JNEUROSCI.2722-12.2013

Ivanenko, Y. P., Grasso, R., Macellari, V., and Lacquaniti, F. (2002). Control of foot trajectory in human locomotion: role of ground contact forces in simulated reduced gravity. *J. Neurophysiol.* 87, 3070–3089.

Ivanenko, Y. P., Poppele, R. E., and Lacquaniti, F. (2006a). Motor control programs and walking. *Neuroscientist* 12, 339–348. doi: 10.1177/1073858406287987

Ivanenko, Y. P., Wright, W. G., Gurfinkel, V. S., Horak, F., and Cordo, P. (2006b). Interaction of involuntary post-contraction activity with locomotor movements. *Exp. Brain Res.* 169, 255–260. doi: 10.1007/s00221-005-0324-3

Jordan, L. M., Liu, J., Hedlund, P. B., Akay, T., and Pearson, K. G. (2008). Descending command systems for the initiation of locomotion in mammals. *Brain Res. Rev.* 57, 183–191. doi: 10.1016/j.brainresrev.2007.07.019

Kiehn, O. (2011). Development and functional organization of spinal locomotor circuits. *Curr. Opin. Neurobiol.* 21, 100–109. doi: 10.1016/j.conb.2010.09.004

Kohnstamm, O. (1915). Demonstration einer katatonieartigen Erscheinung beim Gesunden (Katatonusversuch). *Neurol Zent. Bl* 34S, 290–291.

Kuhtz-Buschbeck, J. P., and Jing, B. (2012). Activity of upper limb muscles during human walking. *J. Electromyogr. Kinesiol.* 22, 199–206. doi: 10.1016/j.jelekin.2011.08.014

Maclellan, M. J., Ivanenko, Y. P., Massaad, F., Bruijn, S. M., Duysens, J., and Lacquaniti, F. (2014). Muscle activation patterns are bilaterally linked during split-belt treadmill walking in humans. *J. Neurophysiol.* 111, 1541–1552. doi: 10.1152/jn.00437.2013

Massaad, F., Levin, O., Meyns, P., Drijkoningen, D., Swinnen, S. P., and Duysens, J. (2014). Arm sway holds sway: locomotor-like modulation of leg reflexes when arms swing in alternation. *Neuroscience* 258, 34–46. doi: 10.1016/j.neuroscience.2013.10.007

Meyns, P., Van de Crommert, H. W. A. A., Rijken, H., van Kuppevelt, D. H. J. M., and Duysens, J. (2014). Locomotor training with body weight support in SCI: EMG improvement is more optimally expressed at a low testing speed. *Spinal Cord* 52, 887–893. doi: 10.1038/sc.2014.172

Mezzarane, R., Klimstra, M., Lewis, A., Hundza, S., and Zehr, E. (2011). Interlimb coupling from the arms to legs is differentially specified for populations of motor units comprising the compound H-reflex during "reduced" human locomotion. *Exp. Brain Res.* 208, 157–168. doi: 10.1007/s00221-010-2467-0

Minassian, K., Hofstoetter, U. S., Danner, S. M., Mayr, W., McKay, W. B., Tansey, K., et al. (2013). Mechanisms of rhythm generation of the human lumbar spinal cord in response to tonic stimulation without and with step-related sensory feedback. *Biomed. Eng. Biomed. Tech.* Available online at: http://www.degruyter.com/view/j/bmte.2013.58.issue-s1-A/bmt-2013–4013/bmt-2013–4013.xml;jsessionid=AF92C08F8D31046DE80E9B1BB68DC420. Accessed on December 15, 2014.

Minassian, K., Jilge, B., Rattay, F., Pinter, M. M., Binder, H., Gerstenbrand, F., et al. (2004). Stepping-like movements in humans with complete spinal cord injury induced by epidural stimulation of the lumbar cord: electromyographic study of compound muscle action potentials. *Spinal Cord* 42, 401–416. doi: 10.1038/sj.sc.3101615

Minassian, K., Persy, I., Rattay, F., Pinter, M. M., Kern, H., and Dimitrijevic, M. R. (2007). Human lumbar cord circuitries can be activated by extrinsic tonic input to generate locomotor-like activity. *Hum. Mov. Sci.* 26, 275–295. doi: 10.1016/j.humov.2007.01.005

Moraru, E., and Onose, G. (2014). Current issues and considerations about the central role of rehabilitation therapies in the functional recovery of neurological impairments after stroke in adults. *J. Med. Life* 7, 368–372.

Mori, S., Kawahara, K., Sakamoto, T., Aoki, M., and Tomiyama, T. (1982). Setting and resetting of level of postural muscle tone in decerebrate cat by stimulation of brain stem. *J. Neurophysiol.* 48, 737–748.

Nathan, P. W., Smith, M., and Deacon, P. (1996). Vestibulospinal, reticulospinal and descending propriospinal nerve fibres in man. *Brain* 119, 1809–1833. doi: 10.1093/brain/119.6.1809

Nielsen, J. B., and Sinkjaer, T. (2002). Afferent feedback in the control of human gait. *J. Electromyogr. Kinesiol.* 12, 213–217. doi: 10.1016/s1050-6411(02)00023-8

Orlovsky, G. N., Deliagina, T. G., Grillner, S., Orlovskii, G. N., and Grillner, S. (1999). *Neuronal Control of Locomotion: From Mollusc to Man.* Oxford, UK: Oxford University Press.

Patrick, S. K., Noah, J. A., and Yang, J. F. (2009). Interlimb coordination in human crawling reveals similarities in development and neural control with quadrupeds. *J. Neurophysiol.* 101, 603–613. doi: 10.1152/jn.91125.2008

Pearson, K. G. (2004). Generating the walking gait: role of sensory feedback. *Prog. Brain Res.* 143, 123–129. doi: 10.1016/s0079-6123(03)43012-4

Petersen, T. H., Willerslev-Olsen, M., Conway, B. A., and Nielsen, J. B. (2012). The motor cortex drives the muscles during walking in human subjects. *J. Physiol.* 590, 2443–2452. doi: 10.1113/jphysiol.2012.227397

Picelli, A., Melotti, C., Origano, F., Neri, R., Waldner, A., and Smania, N. (2013). Robot-assisted gait training versus equal intensity treadmill training in patients

with mild to moderate Parkinson's disease: a randomized controlled trial. *Parkinsonism Relat. Disord.* 19, 605–610. doi: 10.1016/j.parkreldis.2013.02.010

Roy, R. R., Harkema, S. J., and Edgerton, V. R. (2012). Basic concepts of activity-based interventions for improved recovery of motor function after spinal cord injury. *Arch. Phys. Med. Rehabil.* 93, 1487–1497. doi: 10.1016/j.apmr.2012.04.034

Sale, P., Franceschini, M., Waldner, A., and Hesse, S. (2012). Use of the robot assisted gait therapy in rehabilitation of patients with stroke and spinal cord injury. *Eur. J. Phys. Rehabil. Med.* 48, 111–121.

Scivoletto, G., Tamburella, F., Laurenza, L., Torre, M., and Molinari, M. (2014). Who is going to walk? A review of the factors influencing walking recovery after spinal cord injury. *Front. Hum. Neurosci.* 8:141. doi: 10.3389/fnhum.2014.00141

Selionov, V. A., Ivanenko, Y. P., Solopova, I. A., and Gurfinkel, V. S. (2009). Tonic central and sensory stimuli facilitate involuntary air-stepping in humans. *J. Neurophysiol.* 101, 2847–2858. doi: 10.1152/jn.90895.2008

Selionov, V. A., Solopova, I. A., Zhvansky, D. S., Karabanov, A. V., Chernikova, L. A., Gurfinkel, V. S., et al. (2013). Lack of non-voluntary stepping responses in Parkinson's disease. *Neuroscience* 235, 96–108. doi: 10.1016/j.neuroscience.2012.12.064

Shapkova, E. Y. (2004). "Spinal locomotor capability revealed by electrical stimulation of the lumbar enlargement in paraplegic patients," in *Progress in Motor Control*, eds M. Latash and M. Levin (Champaign, IL: Human Kinetics), 253–289.

Shapkova, E. Y., and Schomburg, E. D. (2001). Two types of motor modulation underlying human stepping evoked by spinal cord electrical stimulation (SCES). *Acta Physiol. Pharmacol. Bulg.* 26, 155–157.

Sherrington, C. S. (1910). Flexion-reflex of the limb, crossed extension-reflex and reflex stepping and standing. *J. Physiol.* 40, 28–121. doi: 10.1113/jphysiol.1910.sp001362

Shik, M. L. (1997). Recognizing propriospinal and reticulospinal systems of initiation of stepping. *Motor Control* 1, 310–313.

Shik, M. L., Severin, F. V., and Orlovskiĭ, G. N. (1966). Control of walking and running by means of electric stimulation of the midbrain. *Biofizika* 11, 659–666.

Solopova, I. A., Selionov, V. A., Kazennikov, O. V., and Ivanenko, Y. P. (2014). Effects of transcranial magnetic stimulation during voluntary and non-voluntary stepping movements in humans. *Neurosci. Lett.* 579, 64–69. doi: 10.1016/j.neulet.2014.07.015

Swinnen, E., Baeyens, J.-P., Pintens, S., Van Nieuwenhoven, J., Ilsbroukx, S., Buyl, R., et al. (2014). Trunk kinematics during walking in persons with multiple sclerosis: the influence of body weight support. *NeuroRehabilitation* 34, 731–740. doi: 10.3233/NRE-141089

Sylos-Labini, F., Ivanenko, Y. P., Maclellan, M. J., Cappellini, G., Poppele, R. E., and Lacquaniti, F. (2014a). Locomotor-like leg movements evoked by rhythmic arm movements in humans. *PloS One* 9:e90775. doi: 10.1371/journal.pone.0090775

Sylos-Labini, F., La Scaleia, V., d' Avella, A., Pisotta, I., Tamburella, F., Scivoletto, G., et al. (2014b). EMG patterns during assisted walking in the exoskeleton. *Front. Hum. Neurosci.* 8:423. doi: 10.3389/fnhum.2014.00423

Taylor, J. L., Todd, G., and Gandevia, S. C. (2006). Evidence for a supraspinal contribution to human muscle fatigue. *Clin. Exp. Pharmacol. Physiol.* 33, 400–405. doi: 10.1111/j.1440-1681.2006.04363.x

Thompson, A. K., and Wolpaw, J. R. (2014). Operant conditioning of spinal reflexes: from basic science to clinical therapy. *Front. Integr. Neurosci.* 8:25. doi: 10.3389/fnint.2014.00025

Valentin-Gudiol, M., Bagur-Calafat, C., Girabent-Farrés, M., Hadders-Algra, M., Mattern-Baxter, K., and Angulo-Barroso, R. (2013). Treadmill interventions with partial body weight support in children under six years of age at risk of neuromotor delay: a report of a Cochrane systematic review and meta-analysis. *Eur. J. Phys. Rehabil. Med.* 49, 67–91.

van den Brand, R., Heutschi, J., Barraud, Q., DiGiovanna, J., Bartholdi, K., Huerlimann, M., et al. (2012). Restoring voluntary control of locomotion after paralyzing spinal cord injury. *Science* 336, 1182–1185. doi: 10.1126/science.1217416

Wirz, M., Zemon, D. H., Rupp, R., Scheel, A., Colombo, G., Dietz, V., et al. (2005). Effectiveness of automated locomotor training in patients with chronic incomplete spinal cord injury: a multicenter trial. *Arch. Phys. Med. Rehabil.* 86, 672–680. doi: 10.1016/j.apmr.2004.08.004

Yang, J. F., and Gorassini, M. (2006). Spinal and brain control of human walking: implications for retraining of walking. *Neuroscientist* 12, 379–389. doi: 10.1177/1073858406292151

Yang, J. F., Lamont, E. V., and Pang, M. Y. C. (2005). Split-belt treadmill stepping in infants suggests autonomous pattern generators for the left and right leg in humans. *J. Neurosci.* 25, 6869–6876. doi: 10.1523/jneurosci.1765-05.2005

Zehr, E. P. (2005). Neural control of rhythmic human movement: the common core hypothesis. *Exerc. Sport Sci. Rev.* 33, 54–60.

Zehr, E. P., Balter, J. E., Ferris, D. P., Hundza, S. R., Loadman, P. M., and Stoloff, R. H. (2007). Neural regulation of rhythmic arm and leg movement is conserved across human locomotor tasks. *J. Physiol.* 582, 209–227. doi: 10.1113/jphysiol.2007.133843

Conflict of Interest Statement: The authors declare that the research was conducted in the absence of any commercial or financial relationships that could be construed as a potential conflict of interest.

Received: 05 November 2014; accepted: 27 January 2015; published online: 18 February 2015.

Citation: Solopova IA, Selionov VA, Sylos-Labini F, Gurfinkel VS, Lacquaniti F and Ivanenko YP (2015) Tapping into rhythm generation circuitry in humans during simulated weightlessness conditions. Front. Syst. Neurosci. ***9****:14. doi: 10.3389/fnsys.2015.00014*

This article was submitted to the journal Frontiers in Systems Neuroscience.

frontiers in
SYSTEMS NEUROSCIENCE

ORIGINAL RESEARCH ARTICLE
published: 28 May 2014
doi: 10.3389/fnsys.2014.00097

Extraction and restoration of hippocampal spatial memories with non-linear dynamical modeling

Dong Song[1]*, Madhuri Harway[1], Vasilis Z. Marmarelis[1], Robert E. Hampson[2], Sam A. Deadwyler[2] and Theodore W. Berger[1]

[1] *Department of Biomedical Engineering, University of Southern California, Los Angeles, CA, USA*
[2] *Department of Physiology and Pharmacology, School of Medicine, Wake Forest University, Winston-Salem, NC, USA*

Edited by:
Mikhail Lebedev, Duke University, USA

Reviewed by:
Mikhail Lebedev, Duke University, USA
Yoshio Sakurai, Kyoto University, Japan
Yu Liu, The University of Tennessee Health Science Center, USA

***Correspondence:**
Dong Song, Department of Biomedical Engineering, University of Southern California, 403 Hedco Neuroscience Building, Los Angeles, CA 90089, USA
e-mail: dsong@usc.edu

To build a cognitive prosthesis that can replace the memory function of the hippocampus, it is essential to model the input-output function of the damaged hippocampal region, so the prosthetic device can stimulate the downstream hippocampal region, e.g., CA1, with the output signal, e.g., CA1 spike trains, predicted from the ongoing input signal, e.g., CA3 spike trains, and the identified input-output function, e.g., CA3-CA1 model. In order for the downstream region to form appropriate long-term memories based on the restored output signal, furthermore, the output signal should contain sufficient information about the memories that the animal has formed. In this study, we verify this premise by applying regression and classification modelings of the spatio-temporal patterns of spike trains to the hippocampal CA3 and CA1 data recorded from rats performing a memory-dependent delayed non-match-to-sample (DNMS) task. The regression model is essentially the multiple-input, multiple-output (MIMO) non-linear dynamical model of spike train transformation. It predicts the output spike trains based on the input spike trains and thus restores the output signal. In addition, the classification model interprets the signal by relating the spatio-temporal patterns to the memory events. We have found that: (1) both hippocampal CA3 and CA1 spike trains contain sufficient information for predicting the locations of the sample responses (i.e., left and right memories) during the DNMS task; and more importantly (2) the CA1 spike trains predicted from the CA3 spike trains by the MIMO model also are sufficient for predicting the locations on a single-trial basis. These results show quantitatively that, with a moderate number of unitary recordings from the hippocampus, the MIMO non-linear dynamical model is able to extract and restore spatial memory information for the formation of long-term memories and thus can serve as the computational basis of the hippocampal memory prosthesis.

Keywords: hippocampus, spatio-temporal pattern, spike, classification, regression, memory

INTRODUCTION

Cortical prosthesis is an emerging technology seeking to restore cognitive functions lost in diseases or injuries (Berger et al., 2005, 2010, 2011, 2012). It is achieved by bi-directional, closed-loop communications between the prosthetic device and the brain regions. This is distinct from sensory or motor prostheses, where one side of the communication is an external entity such as the sensory input (Loeb, 1990; Humayun et al., 1999) or the motor output (Mauritz and Peckham, 1987; Taylor et al., 2002; Nicolelis, 2003; Shenoy et al., 2003; Wolpaw and McFarland, 2004; Hochberg et al., 2006). Therefore, a cortical prosthesis must deal exclusively with the internal brain signals, in which sensory or motor information is embedded, by re-encoding the upstream (input) brain signals into the downstream (output) signals (**Figure 1A**).

For the past decade, we have been working on developing a hippocampal-cortical prosthesis for restoring the memory functions. Hippocampus is a brain region responsible for the creation of new long-term episodic memories (Milner, 1970; Squire and Zola-Morgan, 1991; Eichenbaum, 1999). Damage to the hippocampal areas can result in a permanent loss of such cognitive functions. In a normal hippocampus, short-term memories are encoded in the spatio-temporal patterns of spikes (i.e., spike trains) as the input from the entorhinal cortex. Memory information is then processed by the hippocampal feed-forward tri-synaptic pathway, which consists of dentate gyrus, CA3, and CA1 regions, and eventually transformed into the output spike trains to the subiculum, that is appropriate for the formation of long-term memories (**Figure 1B**). Although the exact nature of such a transformation or the underlying mechanisms is still largely unclear, it must be the neural signal (i.e., spike trains) flow from entorhinal cortex to dentate gyrus, to CA3, to CA1, and to subiculum, that enables the re-encoding of short-term memories into long-term memories. Maintaining the normal signal flow with a prosthetic device that bypasses a damaged or diseased hippocampal region provides a feasible way of restoring the lost long-term memory functions (**Figure 1A**).

For example, in our first-generation hippocampal memory prosthesis applications, we (a) record input spike trains from the

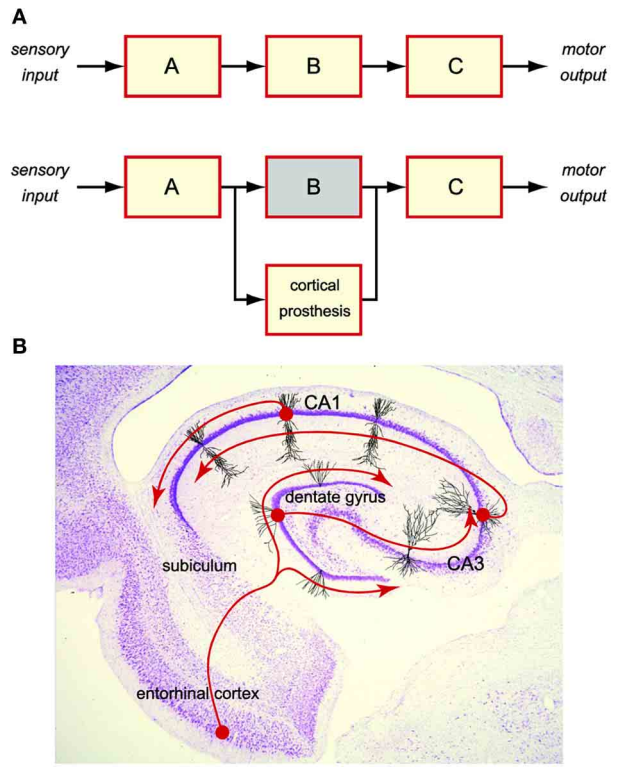

FIGURE 1 | Cortical prosthesis restores cognitive functions by bypassing the damaged brain region to maintain the brain signal flow. **(A)** Schematic diagram of a cortical prosthesis. **(B)** Intrinsic tri-synaptic pathway of the hippocampus.

CA3 region, (b) process them with a multi-input, multi-output (MIMO) non-linear dynamical model to predict the desired CA1 output spike trains, and (c) electrically stimulate the CA1 region with the predicted CA1 output patterns. Previous results have shown that, (a) the MIMO model can accurately predict the output spike trains in real time based on the ongoing input spike trains (Song et al., 2007, 2009a, 2013), and (b) the electrical stimulation can restore or even enhance the memory functions performed by the hippocampal CA3-CA1 system (Berger et al., 2011, 2012; Hampson et al., 2012a,b).

However, despite the success of demonstrating such a prosthesis, how the external behavioral events (i.e., memory events) are encoded in the two hippocampal regions and, more importantly, re-encoded by the prosthesis has not been clearly revealed, precisely due to the internal nature of the cortical prosthesis. In this study, we propose a new framework of modeling and representing the re-encoding process performed by a brain region at the *memory representation level*, as opposed to the *signal level* in our previous studies. In addition to ask the question, "What should the output signal be?" We further ask the question, "What do the signals mean?" Specifically, we combine our previously developed MIMO signal model (Song et al., 2007, 2009a, 2013), which predicts the output signal based on the input signal, with an additional memory decoding model that relates the input and/or output signals to the behaviors (memories) of the animal (**Figure 2**). The MIMO signal model is essentially a time-series regression model non-linear dynamically mapping the multiple output (CA1) signals to the multiple input (CA3) signals. On the other hand, the memory decoding model is a multi-input, signal-output (MISO) classification model identifying to which of a set of memory categories the spatio-temporal patterns of the input and/or output signals belong. The former model quantifies the input-output signal transformation, while the latter model decodes the memory by predicting the behavior.

The paper is organized as the follows. In section Materials and Methods, we formally formulate the modeling problem and provide the mathematical expressions. In section Results, we apply the methods to the modeling of the hippocampus during a memory-dependent task in rodents.

MATERIALS AND METHODS

BEHAVIORAL TASK AND ELECTROPHYSIOLOGICAL PROCEDURES

All animal procedures are reviewed and approved by the Institutional Animal Care and Use Committee of Wake Forest University, in accordance with US Department of Agriculture, International Association for the Assessment and Accreditation of Laboratory Animal Care and National Institutes of Health guidelines. Two male Long-Evans rats are trained to criterion on a two-lever, spatial delayed-non-match-to-sample (DNMS) task with random delay intervals (Deadwyler et al., 1996; Hampson et al., 1999). Animals perform the task by pressing (sample response) a single lever presented in one of the two positions in the sample phase (left or right). This event is called the "sample response." The lever is then retracted and the delay phase initiates; for the duration of the delay phase, the animal is required to nose-poke into a lighted device on the opposite wall. When the delay is ended, nose-poke light is extinguished, both levers are extended, and the animal is required to press the lever *opposite* to the sample lever. This event is called the "non-match response." If the correct lever is pressed, the animal is rewarded (**Figure 3**, top). A session includes approximately 100 successful DNMS tasks that each consists of two of the four behavioral events, i.e., right sample (RS) and left non-match (LN), or left sample (LS) and right non-match (RN).

Spike trains are obtained with multi-site recordings from different septo-temporal regions of the hippocampus of rats performing the DNMS task (**Figure 3**, bottom). For each hemisphere of the brain, a microwire multi-electrodes array (MEA) is surgically implanted into the hippocampus, with 8 electrodes in the CA3 (input) region and 8 electrodes in the CA1 (output) region. Spike trains are pre-screened based on mean firing rate and perievent histogram. Perievent (-2 to $+2$ s) spike trains of the four behavioral events are extracted from each trial and then concatenated to form the datasets (**Figure 3**, bottom). The spike train data are discretized with a 2 ms bin size.

MIMO SIGNAL MODEL OF INPUT-OUTPUT SPIKE TRAIN TRANSFORMATION

The MIMO signal model of input-output spike train transformation takes the form of the sparse generalized Laguerre-Volterra model (SGLVM) we previously developed (Song et al., 2009a,b,

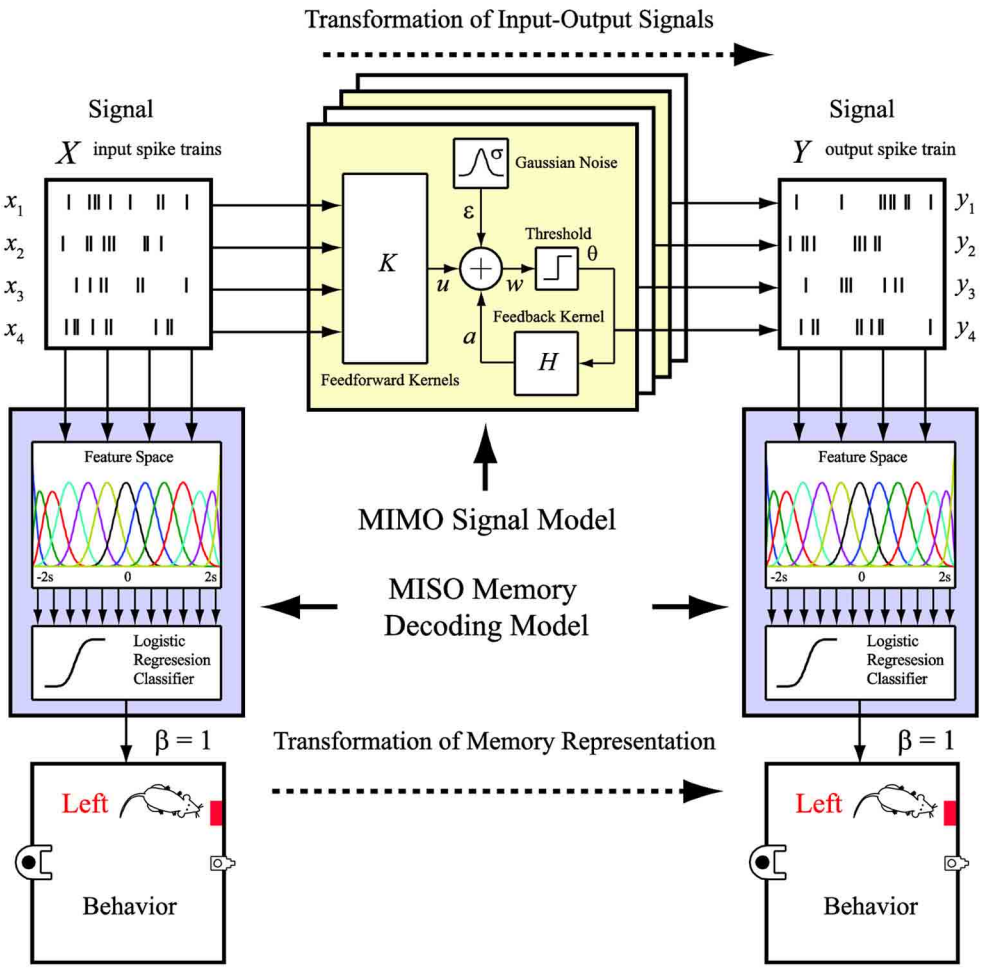

FIGURE 2 | MIMO signal model and MISO memory decoding model. The MIMO signal model predicts the output spatio-temporal patterns of spikes based on the ongoing input spatio-temporal patterns of spikes. The MISO memory decoding model predicts the memory (behavioral) events based on the input or output spatio-temporal patterns of spikes.

2013). In this approach, a MIMO model is a concatenation of a series of MISO models (not to be confused with the MISO classification model), that each can be considered a spiking neuron model (Song et al., 2006, 2007) (**Figure 2**). In this study, each MISO model consists of (a) MISO second-order Volterra kernels k transforming the input spike trains x to the synaptic potential u, (b) a Gaussian noise term ε capturing the stochastic properties of spike generation, (c) a threshold θ for generating output spikes y, (e) an adder generating the pre-threshold membrane potential w, and (d) a single-input, single-output first-order Volterra kernel h transforming the preceding output spikes to the spike-triggered feedback after-potential a. The model can be mathematical expressed as:

$$w = u(k, x) + a(h, y) + \varepsilon(\sigma) \tag{1}$$

$$y = \begin{cases} 0 \text{ when } w < \theta \\ 1 \text{ when } w \geq \theta \end{cases} \tag{2}$$

$$u(t) = k_0 + \sum_{n=1}^{N} \sum_{\tau=0}^{M_k} k_1^{(n)}(\tau) x_n(t-\tau) + \sum_{n=1}^{N} \sum_{\tau_1=0}^{M_k} \sum_{\tau_2=0}^{M_k} k_{2s}^{(n)}(\tau_1, \tau_2) x_n(t-\tau_1) x_n(t-\tau_2) \tag{3}$$

$$a(t) = \sum_{\tau=1}^{M_h} h(\tau) y(t-\tau) \tag{4}$$

The zeroth-order kernel, k_0, is the value of u when the input is absent. First-order kernels $k_1^{(n)}$ describe the first-order linear relation between the n^{th} input x_n and u, as functions of the time intervals τ between the present time and the past time. Second-order self kernels $k_{2s}^{(n)}$ describe the second-order non-linear interaction between pairs of spikes in the n^{th} input x_n as they affect u. N is the number of inputs. M_k and M_h denote the memory lengths of the feedforward process and feedback process,

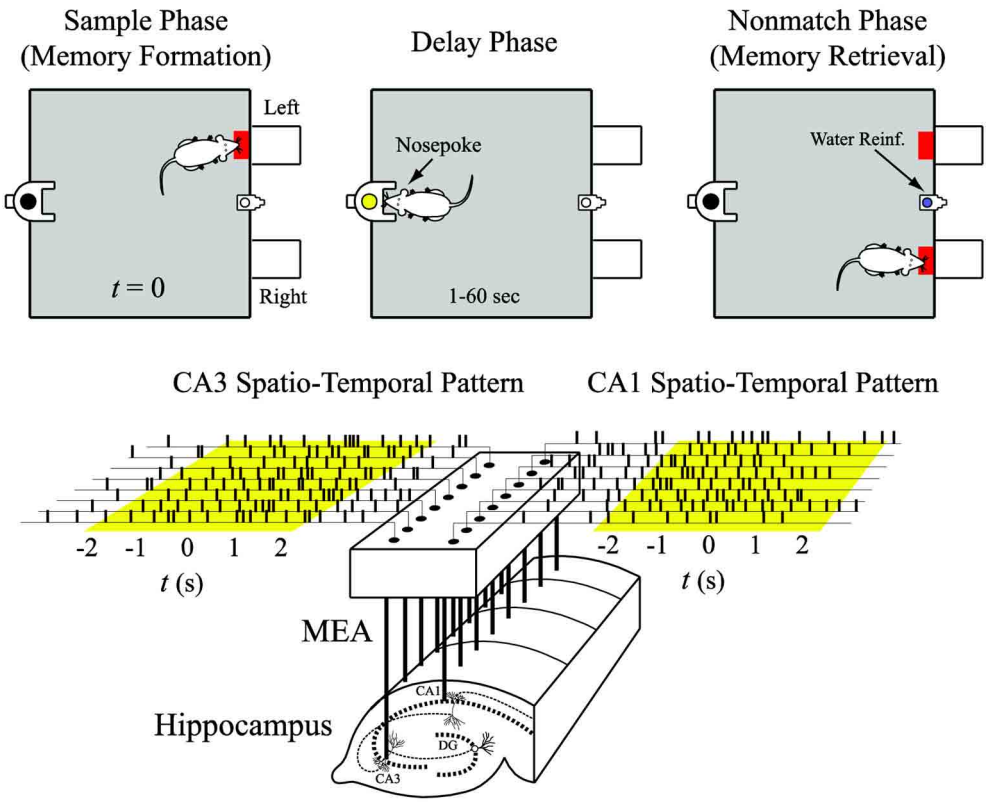

FIGURE 3 | Input (CA3) and output (CA1) spatio-temporal patterns of spikes recorded with a multi-electrode array (MEA) during the sample phase of the delayed-non-match-to-sample (DNMS) task.

respectively. They are chosen to be 2 s in this study. Second-order cross kernels and higher-order (e.g., third-order) kernels are not included in this study.

To facilitate model estimation and avoid overfitting, the Volterra kernels are expanded with Laguerre basis functions b as in Song et al. (2009c,d):

$$u(t) = c_0 + \sum_{n=1}^{N}\sum_{j=1}^{J} c_1^{(n)}(j) v_j^{(n)}(t) + \sum_{n=1}^{N}\sum_{j_1=1}^{J}\sum_{j_2=1}^{j_1} c_{2s}^{(n)}(j_1, j_2) v_{j_1}^{(n)}(t) v_{j_2}^{(n)}(t) \quad (5)$$

$$a(t) = \sum_{j=1}^{L} c_h(j) v_j^{(h)}(t) \quad (6)$$

where $v_j^{(n)}(t) = \sum_{\tau=0}^{M_k} b_j(\tau) x_n(t-\tau)$, $v_j^{(h)}(t) = \sum_{\tau=1}^{M_h} b_j(\tau) y(t-\tau)$; $c_1^{(n)}$, $c_{2s}^{(n)}$, and c_h are the sought Laguerre expansion coefficients of $k_1^{(n)}$, $k_{2s}^{(n)}$, and h, respectively (c_0 is equal to k_0); J is the number of basis functions.

To achieve model sparsity, the coefficients are estimated with a composite penalized likelihood estimation method, i.e., group LASSO (Song et al., 2013). In maximum likelihood estimation (MLE), model coefficients are estimated by minimizing the negative log likelihood function $-l(c)$. In group LASSO, the composite penalized criterion is written as

$$\begin{aligned} S(c) &= -l(c) + \lambda\left(\sum_{n=1}^{N} ||c_1^{(n)}(j)||_2^1 + \sum_{n=1}^{N} ||c_{2s}^{(n)}(j_1, j_2)||_2^1\right) \\ &= -l(c) + \lambda\left(\sum_{n=1}^{N}\left(\sum_{j=1}^{J} c_1^{(n)}(j)^2\right)^{\frac{1}{2}} + \sum_{n=1}^{N}\left(\sum_{j_1=1}^{J}\sum_{j_2=1}^{j_1} c^{(n)}(j_1, j_2)^2\right)^{\frac{1}{2}}\right) \end{aligned} \quad (7)$$

where $\lambda \geq 0$ is a tuning parameter that controls the relative importance of the likelihood and the penalty term. When λ takes on a larger value, the estimation yields sparser result of the coefficients. λ is optimized with a two-fold cross-validation method.

MISO MEMORY DECODING MODEL OF SPATIO-TEMPORAL PATTERN OF SPIKES

The MISO memory decoding model of spike spatio-temporal patterns takes the form of the sparse generalized B-spline linear classification model (Song et al., 2013). In this approach, the feature space is defined as a set of B-spline basis functions for each neuron (input and/or output neurons depending on the application). The classifier is essentially the logistic regression (**Figure 2**).

B-splines are piecewise polynomials with smooth transitions between the adjacent pieces at a set of interior *knot* points. A polynomial spline of degree $d \geq 0$ on $[0, M]$ with $m > 0$ interior knot points and the knot sequence $\eta_0 = 0 < \eta_1 < \ldots < \eta_m < \eta_{m+1} = M$ is a function that is a polynomial of degree d between each pair of adjacent knots, and has d-1 continuous derivatives for $d = 1$. B-spline basis functions of degree d can be defined in a recursive fashion as

$$B_{j,d}(\tau) = \frac{\tau - \eta_j}{\eta_{j+d-1} - \eta_j} B_{j,d-1}(\tau) + \frac{\eta_{j+d} - \tau}{\eta_{j+d} - \eta_{j+1}} B_{j+1,d-1}(\tau) \tag{8}$$

where

$$B_{j,0}(\tau) = \begin{cases} 1 & \text{if } \eta_j < \tau < \eta_{j+1} \\ 0 & \text{otherwise} \end{cases} \tag{9}$$

For a given sequence of m knots and a fixed degree d, the total number of B-spline basis functions is $J = m + d + 1$.

Spatio-temporal patterns of spikes are projected to the B-spline feature space via inner product to yield the feature vectors as

$$z^{(n)}(j) = \sum_{\tau=0}^{M} B_j(\tau) x_n(\tau) \tag{10}$$

where M is the time widow for inner product. It is chosen to be from −2 to +2 s of the sample events (**Figure 3**, bottom). x_n is the nth neuron of the total N neurons included in analysis. Different from in the regression model, x can be CA3 and/or CA1 neurons depending on the context. $z^{(n)}(j)$ denotes the feature value of the nth neuron using the jth B-spline function. Therefore, z is a 1-by-JN vector. J is optimized in the range of 5–100 based on the out-of-sample prediction accuracy. In most of the cases, $J = 20$ is found to be optimal.

Since there are two possible behavioral outcomes, i.e., left or right position, the model output can be represented as a binary variable β. The classification model assumed by logistic regression is

$$P(\beta = 1|x) = \left[1 + \exp\left\{ -w_0 - \sum_{n=1}^{N} \sum_{j=1}^{J} w^{(n)}(j) z^{(n)}(j) \right\} \right]^{-1} \tag{11}$$

$$P(\beta = 0|x) = 1 - P(\beta = 1|x) \tag{12}$$

where w are the sought model coefficients; 1 and 0 represent left and right positions, respectively.

The linear classification rule is simply

$$\beta = \begin{cases} 1 & \text{if } \left\{ -w_0 - \sum_{n=1}^{N} \sum_{j=1}^{J} w^{(n)}(j) z^{(n)}(j) \right\} < 0 \\ 0 & \text{otherwise} \end{cases} \tag{13}$$

Compared with the MIMO regression model, the MISO classification model may suffer even more serious overfitting problem due to the high dimensional input (typically with hundreds of features) and the relatively small number of data points (typically 100 trials in this study). Therefore, $L1$ regularization (Lasso) is applied to achieve model sparsity and avoid overfitting as

$$S(c) = -l(c) + \lambda \left(\sum_{n=1}^{N} \sum_{j=1}^{J} ||w^{(n)}(j)||_2^1 \right) \tag{14}$$

Where $-l(c)$ and $\lambda = 0$ are the negative log likelihood function and the tuning parameter of the classification model, respectively. In this study, λ is optimized with a four-fold cross-validation method. By minimizing S, sparse weight matrix w are estimated and further used to reconstruct the classification feature matrix F with the B-spline basis functions as

$$F^{(n)}(\tau) = \sum_{j=1}^{J} B_j(\tau) w^{(n)}(j) \tag{15}$$

F can be directly used in the logistic regression along with the spatio-temporal pattern x as

$$P(\beta = 1|x) = \left[1 + \exp\left\{ -w_0 - \sum_{n=1}^{N} \sum_{t=1}^{M} F^{(n)}(\tau) x^{(n)}(t) \right\} \right]^{-1} \tag{16}$$

RESULTS

HIPPOCAMPAL CA3 AND CA1 ACTIVITIES CONTAINS SUFFICIENT INFORMATION FOR DECODING SPATIAL MEMORIES DURING THE DNMS TASK

First, we apply the MISO memory decoding model to the CA3 spike trains recorded during the sample phase of the DNMS tasks. For each sample event (left or right), we take the perievent spikes 2 s before and after the event with a 2 ms bin size. The spatio-temporal patterns of spikes are then N-by-2000 matrices, where N is the number of neurons. A session typically consists of 80–100 trials with roughly half being left sample trials and half being right sample trials. The spatio-temporal patterns are labeled with 1 for the left trials and 0 for the right trials. **Figure 4** (case #1) and **Figure 5** (case #2) show the spatio-temporal patterns from two animals with 26 and 43 CA3 neurons, respectively. For each position, four representative patterns and the overall patterns are shown. The overall patterns are obtained by smoothing the spike trains with B-spline functions and then summing across all trials for the specific position. It is evident that the two positions show different spatio-temporal patterns and the differences exist in specific time ranges of specific neurons (**Figures 4**, **5**). The task

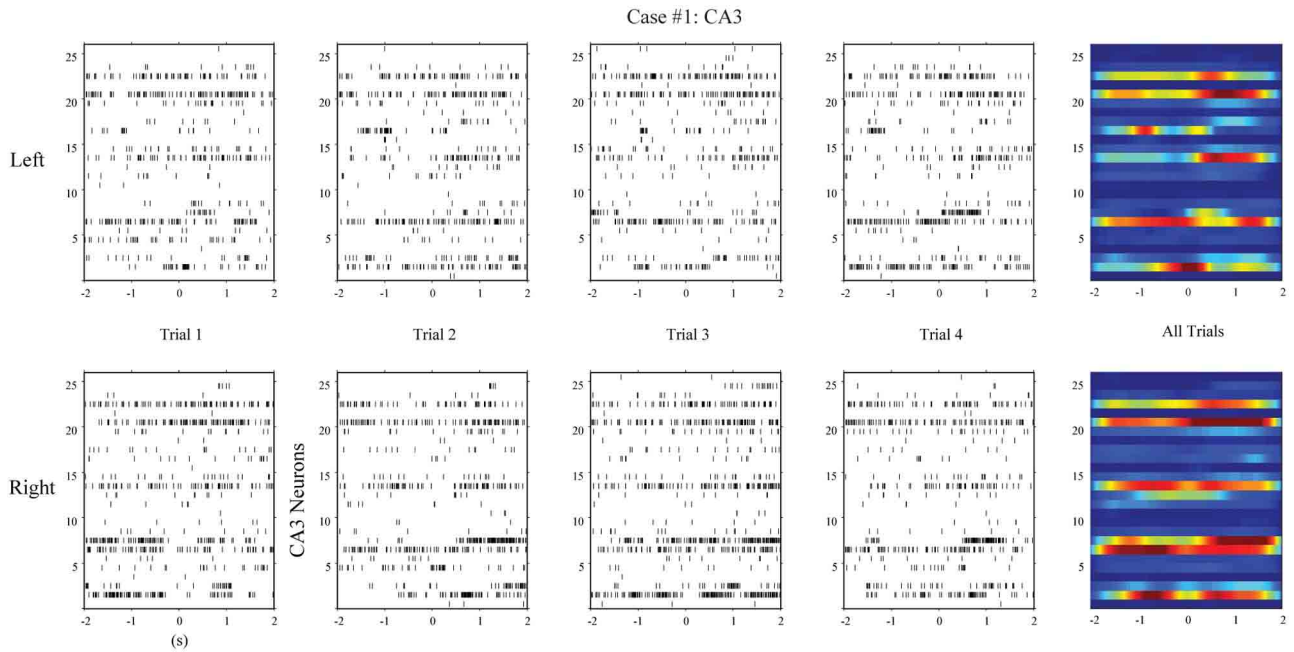

FIGURE 4 | Spatio-temporal patterns of spikes in the hippocampal CA3 (input) region during left and right sample events of the DNMS (case #1).

of the MISO memory decoding model is to identify these sparsely distributed differences from single trials of the spatio-temporal pattern and then predict the positions of the animal. Results show that the MISO memory decoding model can achieve a 100% out-of-sample prediction accuracy using the CA3 spatio-temporal patterns in both cases (**Figure 8**, top row).

Using the same method, we build MISO memory decoding models for the CA1 spike trains. **Figure 6** (case #1) and **Figure 7** (case #2) show the spatio-temporal patterns of CA1 during left and right trials (row 1 and 3) from the same two animals. There are 19 and 17 CA1 neurons recorded from these two animals, respectively. Similar to CA3, CA1 also show different spatio-temporal patterns during left and right trials. The prediction accuracy is 100% in one case and 91.3% in the other (**Figure 8**, middle row).

HIPPOCAMPAL CA1 ACTIVITIES CAN BE ACCURATELY PREDICTED BY THE MIMO SIGNAL MODEL BASED ON THE HIPPOCAMPAL CA3 ACTIVITIES

In the second step, we build MIMO signal models for the transformations from the CA3 spatio-temporal patterns to the CA1 spatio-temporal patterns. To build such a model, we concatenate CA3 perievent spike trains across all trials to form the input data and the corresponding CA1 spike trains to form the output data, and then apply our MIMO modeling method. The resulting SGLVM non-linear dynamically predicts the CA1 spikes based on the ongoing and past (within the memory window) CA3 spikes (Song et al., 2007, 2009a; Song and Berger, 2010). Results show that in both cases (**Figures 6**, **7**, row 2 and 4), the MIMO signal model can accurately predict the CA1 spatio-temporal patterns at both the single trial level (**Figures 6**, **7**, column 1–4) and the overall level (**Figures 6**, **7**, column 5). Importantly, a single set of the model coefficients are used for both the left and right trials. In other words, the estimated MIMO signal models are memory-invariant and can be used to predict the output signals without explicitly knowing what the events are (Song et al., 2011).

HIPPOCAMPAL CA1 ACTIVITIES PREDICTED BY THE MIMO SIGNAL MODEL CAN BE USED TO ACCURATELY DECODE THE SPATIAL MEMORY

Lastly, we build MISO memory decoding models for the CA1 spatio-temporal patterns predicted by the MIMO signal model, as opposed to the actual CA1 spatio-temporal patterns. Results show that the MISO memory decoding models can accurately predict the spatial memory based on the predicted CA1 patterns (**Figure 8**, bottom). The prediction accuracies are 91% and 87.5 for the two cases, respectively. Importantly, the MISO memory decoding model coefficients remain the same for the actual CA1 patterns and the predicted CA1 patterns. This indicates that the MIMO signal model has successfully transmitted the spatial information from CA3 to CA1 in the same form as it is encoded in the actual CA1 patterns. The MIMO signal model has not only *restored the signal*, but also *re-encoded the memory representations*.

SPATIAL INFORMATION IS SPARSELY DISTRIBUTED IN THE HIPPOCAMPAL CA1 AND CA3 SPATIO-TEMPORAL PATTERNS OF SPIKES

In order to gain more insights into how hippocampal CA3 and CA1 spike trains encode spatial information, we calculate Equation (15) and plot the classification weight matrices. These matrices have the same dimensions as their corresponding spatio-temporal patterns. In order to perform classification, we can simply calculate the dot products of the weight matrices and

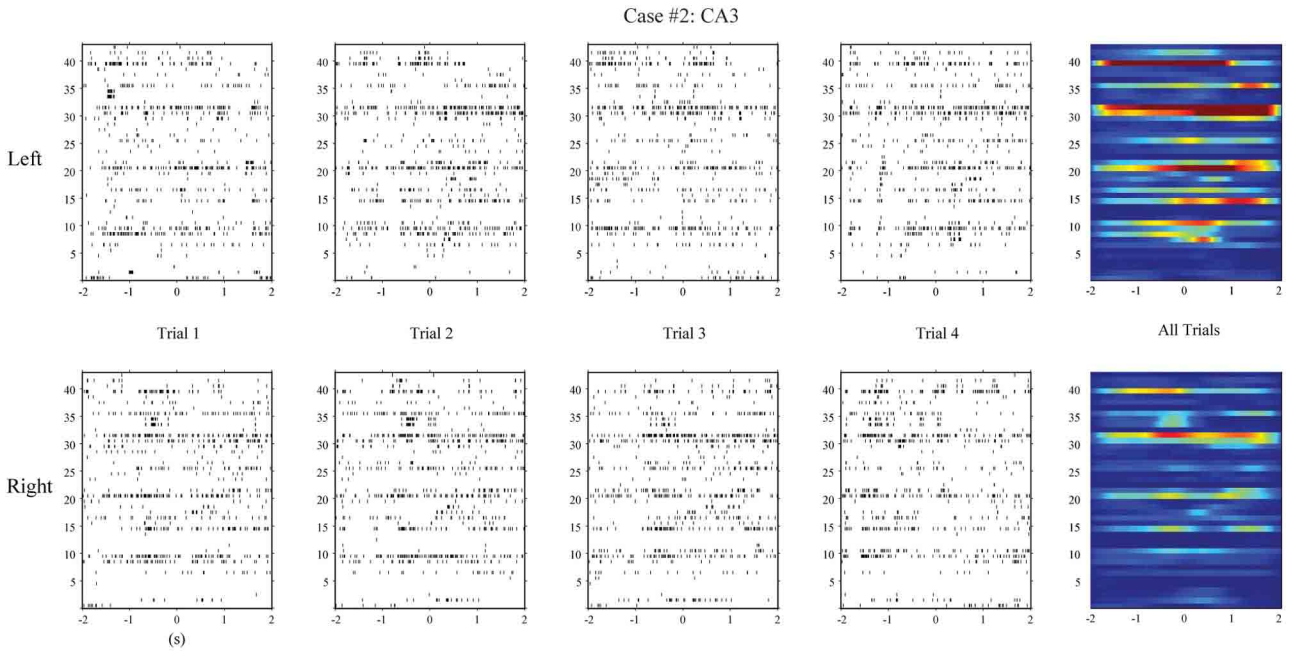

FIGURE 5 | Hippocampal CA3 spatio-temporal patterns from a different animal (case #2).

the corresponding spatio-temporal patterns (strictly speaking, the dot products of vectorized matrices), add the bias (i.e., w_0), and then use Equation (16) to predict the probability of the animal having left or right memories. **Figure 9** show results of CA3 and CA1 from the two animals. The CA1 weight matrices are for both the actual and MIMO predicted CA1 spatio-temporal patterns. In both cases, non-zero values (warm and cold colors represent positive and negative values, respectively) are sparsely distributed in the weight matrices. These results indicate that the spatial information exists in a redundant fashion in multiple ranges of the perievent intervals of multiple neurons. The MIMO signal model and the MISO memory decoding model jointly describe the re-encoding of the memory representations from CA3 to CA1.

DISCUSSIONS

Brain regions process and transmit information with spatio-temporal patterns of spikes. In order to build a cortical prosthesis to bypass a damaged brain region, it is necessary to restore the output signals of the damaged region and send it to the downstream region, so the information flow is maintained. We have shown intensively that non-linear dynamical MIMO models can predict accurately the output spatio-temporal patterns based on the ongoing input spatio-temporal patterns, and electrical stimulations of the output region following the predicted patterns can effectively restore and even enhance the memory function (Berger et al., 2011, 2012; Hampson et al., 2012a,b, 2013). The unique contribution of this paper is to combine the MIMO models with a new set of MISO memory decoding models so that the input and output signals can be related to the memory (behavioral) events and thus explain why it is possible for the downstream hippocampal region to correctly decode the MIMO model generated signals.

In our previous publications on the MIMO signal model (Song et al., 2006, 2007, 2009a,b, 2011, 2013; Song and Berger, 2010), the model goodness-of-fit are validated with a Kolmogorov-Smirnov (KS) test based on the time-rescaling theorem (Brown et al., 2002; Haslinger et al., 2010). This KS test is a powerful tool that allows the firing probability intensity function predicted by the MIMO model to be directly validated with the actual output spike train, and the model goodness-of-fit to be quantified statistically with confidence bounds. However, the KS test does not necessarily indicate whether the model goodness-of-fit is sufficient for decoding the behavior or restoring the cognitive function since it is developed only for quantifying the accuracy of the predicted point-process output signal. The typically used 95 or 99% confidence bounds will not guarantee a successful MIMO model for building the prosthesis. For example, a perfectly predicted output signal may contain no information about a specific memory of interest; on the other hand, a less accurately predicted output signal may still contain some or even sufficient information about the memory. The MISO memory decoding model described here directly quantifies the relations between output signals and memories, and provides a more functionally relevant measure to the model performance that is complementary to the KS test.

In hippocampal prosthesis applications, MISO memory decoding models are estimated with input-output data during the sample phase (−2 to 2 s). The reason is that, in the DNMS task, animals form the spatial memory (i.e., left or right level position) during the sample phase, retain the memory during the delay phase, and recall the memory during the non-match phase. Previous results have shown that MIMO model-based

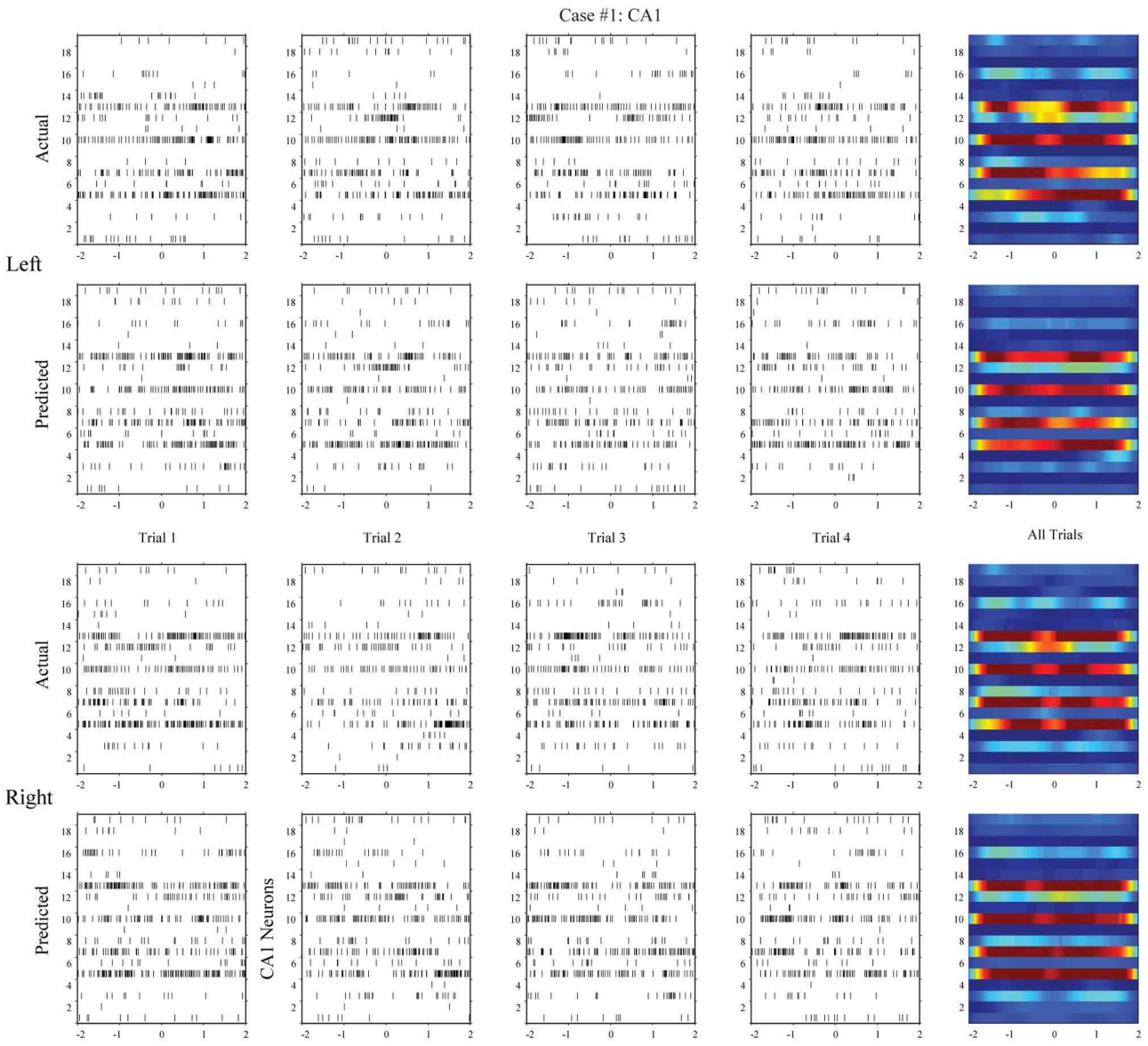

FIGURE 6 | Spatio-temporal patterns of spikes in the hippocampal CA1 (output) region during left and right events of the DNMS. For each position, the top row shows the actual CA1 spatio-temporal patterns; the bottom row shows the CA1 spatio-temporal patterns predicted by the MIMO model based on the ongoing CA3 spiking activities (case #1).

electrical stimulation restores and enhances the spatial memory during sample phases but not non-match phases (Berger et al., 2011, 2012; Hampson et al., 2012a), despite that the MIMO signal model is able to predict accurately the output signal during both sample and non-match phases (Song et al., 2011).

Hippocampus is a mainly feedforward network consisting of a large number of neurons. There are approximately 1 million, 330 thousand, and 420 thousand principal neurons in the rodent dentate gyrus, CA3, and CA1 regions, respectively (Amaral et al., 1990). However, despite the small number (tens to a hundred) of recorded neurons allowed by the current MEA technology, our hippocampal prosthesis has shown impressive success in both rodents and non-human primates during the spatial memory tasks. The main reason is that, at least during the DNMS task or the delayed match-to-sample (DMS) task, spatial memories (e.g., locations of the levels) are encoded in a highly redundant and distributed fashion in a large portion of the hippocampal neurons. As shown in this study, sampling a small number of neurons from the whole population still allows accurate extraction of spatial information.

The DNMS task is a highly restricted experimental paradigm that involves only two positions. Under normal conditions, however, the animal needs to form much more complex memories to maintain its normal life (Eichenbaum, 1999). A practical

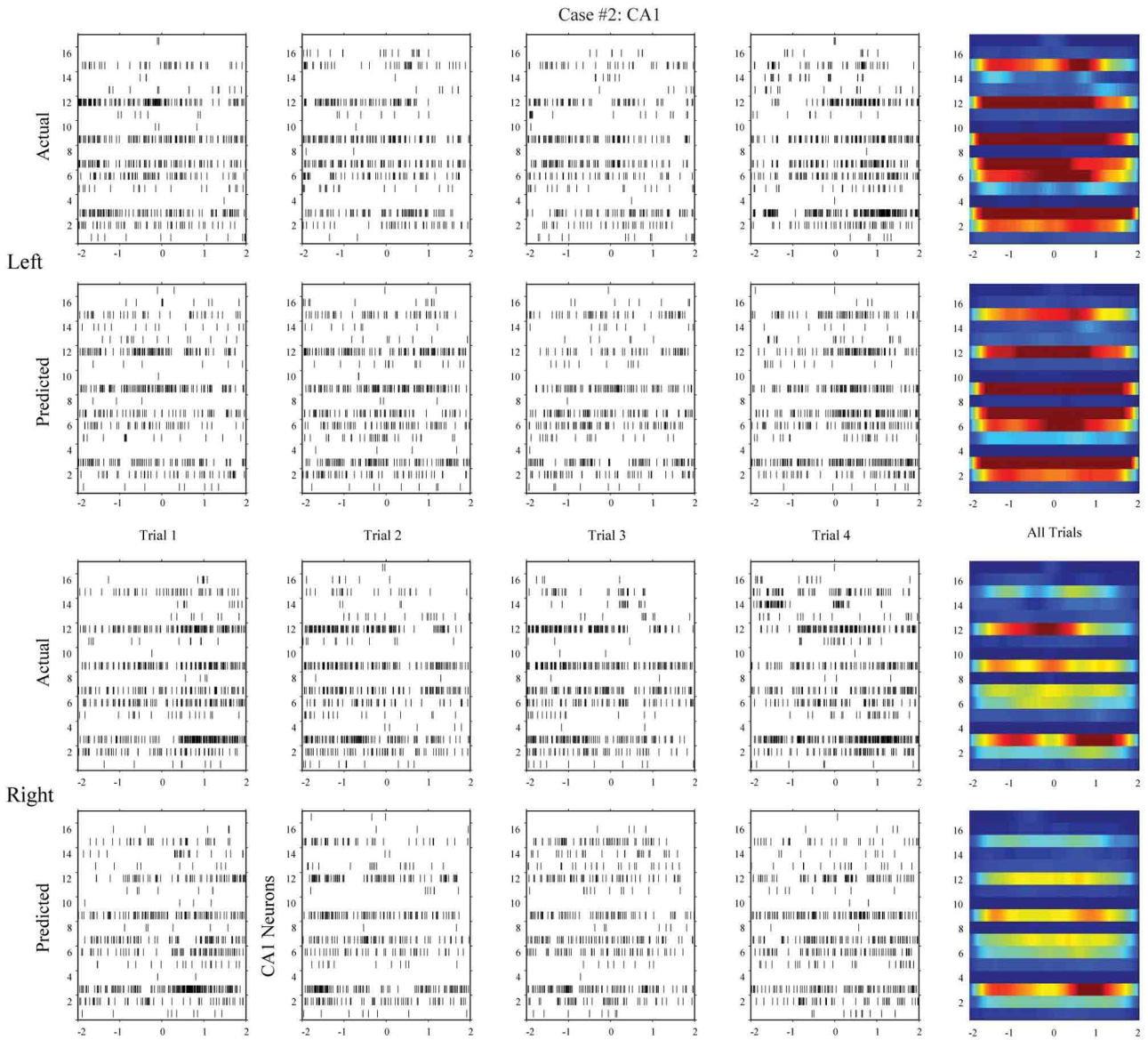

FIGURE 7 | Hippocampal CA1 spatio-temporal patterns (actual and MIMO model predicted) from a different animal (case #2).

hippocampal prosthesis should be able to extract and restore a large number of memories with the MIMO signal model and MISO memory decoding model. This will likely require (1) recording a larger number of hippocampal neurons to obtain more information necessary for decoding the episodic memories, (2) stimulating with more electrodes for generating richer output patterns to the downstream hippocampal region, and (3) developing more powerful MIMO signal model and MISO memory decoding model to more accurately restore the output signal and decode the memories. For example, the current MISO memory decoding model has binary (left or right) output; in order to decode more memories, it needs to be extended to handle multiple-category output. A natural solution is to use multinomial logistic regression (McCullagh and Nelder, 1989), instead of the standard binary-output logistic regression used in this study. Besides, other forms of discriminative models, e.g., support vector machine, or generative models, e.g., naive Bayes classifier, may be considered for their specific advantages. In addition, to collect input-output data for building multiple-memory models, new experimental paradigms involving multiple forms of behavioral events and sensory modalities need to be utilized (Hampson et al., 2012b). Nonetheless, the study described in the paper for the first time combines the regression model with the classification model to illustrate how memory-related information is encoded and re-encoded in the hippocampus, and has made a critical step toward building a hippocampal memory prosthesis.

Interestingly, in both cases in this study, the MISO memory decoding model shows higher prediction accuracy in the CA3

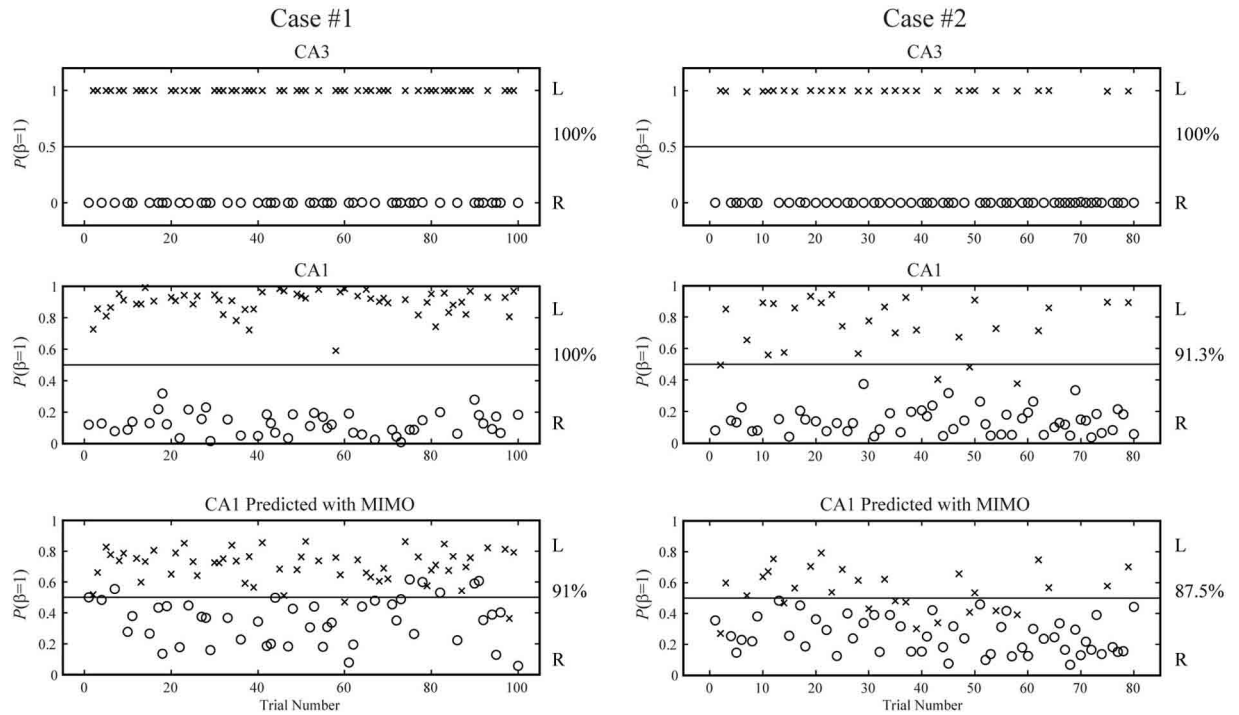

FIGURE 8 | Predicting spatial memory events based on inputs (CA3), outputs (CA1), or outputs predicted by the MIMO models (case #1 and #2). The horizontal lines in the middle represent the decision boundaries ($P = 0.5$).

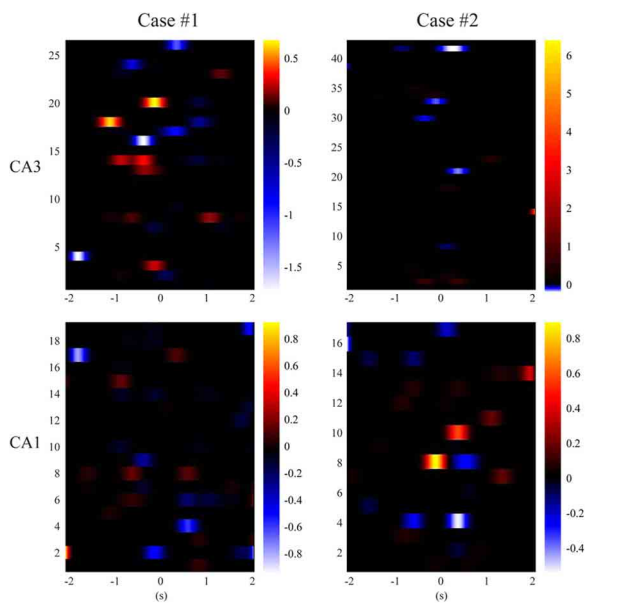

FIGURE 9 | Sparse classification feature matrices of the MISO memory decoding models (case #1 and #2). Black color represents zero-valued weights.

than in the actual CA1, and higher accuracy in the actual CA1 than in the predicted CA1. The latter is unsurprising since the predicted CA1 patterns are calculated with the MIMO signal model using the actual CA1 patterns as target signals, although the real-time calculation is driven by the ongoing CA3 patterns. It is thus unlikely for the predicted CA1 patterns to contain more memory-related information than the actual CA1 patterns. The former observation can be caused by two factors. First, it is possible that CA3 neurons contain more spatial information than CA1 neurons as suggested by previous studies (Lee et al., 2004). Second, it could simply due to the fact that we have recorded more CA3 units than CA1 units in the two cases included in this study. A more systematic, comparative study of CA3 and CA1 patterns needs to be performed to draw further conclusions.

In this study, the MISO memory decoding model takes the form of a B-spline, logistic regression model. The B-spline basis functions are utilized to reduce the model dimensionality and introduce a continuous metric for the similarities between spike trains. The optimal number of basis functions provides an estimate to the relevant temporal resolution of the spike trains. The logistic regression maps the spatio-temporal features to the probability of having a certain behavioral outcome. Despite the rather general model structure and the high prediction accuracy, however, this study does not necessarily suggest that the downstream hippocampal region decodes the CA1 spatio-temporal patterns in the same way. Instead, the main biological implications of this study are: first, the CA1 spatio-temporal patterns can be accurately predicted from the CA3 spatio-temporal patterns using a non-linear dynamical MIMO signal model; second, both CA3 and CA1 patterns contains sufficient information for decoding the memory events; third, the MIMO-model predicted CA1 patterns also contain sufficient information of the memory, and it must be this fact that makes the successful implementation of the hippocampal memory prostheses possible.

ACKNOWLEDGMENTS

This work was supported by the Defense Advanced Research Projects Agency (DARPA) through the Restorative Encoding Memory Integration Neural Device (REMIND) Program.

REFERENCES

Amaral, D. G., Ishizuka, N., and Claiborne, B. (1990). "Neurons, numbers and the hippocampal network," in *Progress in Brian Research,* Vol 83, eds J. Storm-Mathisen, J. Zimmer, and O. P. Ottersen (Amsterdam: Elsevier), 1–11.

Berger, T. W., Ahuja, A., Courellis, S. H., Deadwyler, S. A., Erinjippurath, G., Gerhardt, G. A., et al. (2005). Restoring lost cognitive function. *IEEE Eng. Med. Biol. Mag.* 24, 30–44. doi: 10.1109/MEMB.2005.1511498

Berger, T. W., Hampson, R. E., Song, D., Goonawardena, A., Marmarelis, V. Z., and Deadwyler, S. A. (2011). A cortical neural prosthesis for restoring and enhancing memory. *J. Neural Eng.* 8, 046017. doi: 10.1088/1741-2560/8/4/046017

Berger, T. W., Song, D., Chan, R. H. M., and Marmarelis, V. Z. (2010). The neurobiological basis of cognition: identification by multi-input, multioutput nonlinear dynamic modeling. *Proc. IEEE* 98, 356–374. doi: 10.1109/JPROC.2009.2038804

Berger, T. W., Song, D., Chan, R. H. M., Marmarelis,V. Z., LaCoss, J., Wills, J., et al. (2012). A hippocampal cognitive prosthesis: multi-input, multi-output nonlinear modeling and VLSI implementation. *IEEE Trans. Neural Syst. Rehabil. Eng.* 20, 198–211. doi: 10.1109/TNSRE.2012.2189133

Brown, E. N., Barbieri, R., Ventura, V., Kass, R. E., and Frank, L. M. (2002). The time-rescaling theorem and its application to neural spike train data analysis. *Neural Comput*. 14, 325–346. doi: 10.1162/08997660252741149

Deadwyler, S. A., Bunn, T., and Hampson, R. E. (1996). Hippocampal ensemble activity during spatial delayed-nonmatch-to-sample performance in rats. *J. Neurosci*. 16, 354–372.

Eichenbaum, H. (1999). The hippocampus and mechanisms of declarative memory. *Behav. Brain Res*. 103, 123–133. doi: 10.1016/S0166-4328(99)00044-3

Hampson, R. E., Gerhardt, G. A., Marmarelis, V. Z., Song, D., Opris, I., Santos, L., et al. (2012b). Facilitation and restoration of cognitive function in primate prefrontal cortex by a neuroprosthesis that utilizes minicolumn-specific neural firing. *J. Neural Eng.* 9, 056012. doi: 10.1088/1741-2560/9/5/056012

Hampson, R. E., Simeral, J. D., and Deadwyler, S. A. (1999). Distribution of spatial and nonspatial information in dorsal hippocampus. *Nature* 402, 610–614. doi: 10.1038/45154

Hampson, R. E., Song, D., Chan, R. H. M., Sweatt, A. J., Fuqua, J., Gerhardt, G. A., et al. (2012a). A nonlinear model for cortical prosthetics: memory facilitation by hippocampal ensemble stimulation. *IEEE Trans. Neural Syst. Rehabil. Eng.* 20, 184–197. doi: 10.1109/TNSRE.2012.2189163

Hampson, R. E., Song, D., Opris, I., Santos, L., Shin, D., Gerhardt, G. A., et al. (2013). Facilitation of memory encoding in primate hippocampus by a neuroprosthesis that promotes task specific neural firing. *J. Neural Eng.* 10, 066013. doi: 10.1088/1741-2560/10/6/066013

Haslinger, R., Pipa, G., and Brown, E. (2010). Discrete time rescaling theorem: determining goodness of fit for discrete time statistical models of neural spiking. *Neural Comput*. 22, 2477–2506. doi: 10.1162/NECO_a_00015

Hochberg, L. R., Serruya, M. D., Friehs, G. M., Mukand, J. A., Saleh, M., Caplan, A. H., et al. (2006). Neuronal ensemble control of prosthetic devices by a human with tetraplegia. *Nature* 442, 164–171. doi: 10.1038/nature04970

Humayun, M. S., de Juan, E., Weiland, J. D., Dagnelie, G., Katona, S., Greenberg, R., et al. (1999). Pattern electrical stimulation of the human retina. *Vision Res*. 39, 2569–2576. doi: 10.1016/S0042-6989(99)00052-8

Lee, I., Yoganarasimha, D., Rao, G., and Knierim, J. J. (2004). Comparison of population coherence of place cells in hippocampal subfields CA1 and CA3. *Nature* 430, 456–459. doi: 10.1038/nature02739

Loeb, G. E. (1990). Cochlear Prosthetics. *Annu. Rev. Neurosci*. 13, 357–371. doi: 10.1146/annurev.ne.13.030190.002041

Mauritz, K. H., and Peckham, H. P. (1987). Restoration of grasping functions in quadriplegic patients by Functional Electrical Stimulation (FES). *Int. J. Rehabil. Res*. 10, 57–61. doi: 10.1097/00004356-198712005-00010

McCullagh, P., and Nelder, J. A. (1989). *Generalized Linear Models*. Boca Raton, FL: Chapman & Hall/CRC. doi: 10.1007/978-1-4899-3242-6

Milner, B. (1970). "Memory and the medial temporal regions of the brain," in *Biology of Memory* eds K. H. Pribram and D. E. Broadbent (New York, NY: Academic Press), 29–50.

Nicolelis, M. A. L. (2003). Brain-machine interfaces to restore motor function and probe neural circuits. *Nat. Rev. Neurosci*. 4, 417–422. doi: 10.1038/nrn1105

Shenoy, K. V., Meeker, D., Cao, S. Y., Kureshi, S. A., Pesaran, B., Buneo, C. A., et al. (2003). Neural prosthetic control signals from plan activity. *Neuroreport* 14, 591–596. doi: 10.1097/00001756-200303240-00013

Song, D., and Berger, T. W. (2010). "Identification of nonlinear dynamics in neural population activity," in *Statistical Signal Processing for Neuroscience and Neurotechnology* ed K. G. Oweiss (Amsterdam: Elsevier), 103–128. doi: 10.1016/B978-0-12-375027-3.00004-1

Song, D., Chan, R. H., Marmarelis, V. Z., Hampson, R. E., Deadwyler, S. A., and Berger, T. W. (2007). Nonlinear dynamic modeling of spike train transformations for hippocampal-cortical prostheses. *IEEE Trans. Biomed. Eng.* 54, 1053–1066. doi: 10.1109/TBME.2007.891948

Song, D., Chan, R. H. M., Marmarelis, V. Z., Hampson, R. E., Deadwyler, S. A., and Berger, T. W. (2006). Physiologically plausible stochastic nonlinear kernel models of spike train to spike train transformation. *Conf. Proc. IEEE Eng. Med. Biol. Soc.* 1, 6129–6132. doi: 10.1109/IEMBS.2006.259253

Song, D., Chan, R. H. M., Marmarelis, V. Z., Hampson, R. E., Deadwyler, S. A., and Berger, T. W. (2009a). Nonlinear modeling of neural population dynamics for hippocampal prostheses. *Neural Netw*. 22, 1340–1351. doi: 10.1016/j.neunet.2009.05.004

Song, D., Chan, R. H. M., Marmarelis, V. Z., Hampson, R. E., Deadwyler, S. A., and Berger, T. W. (2009b). Sparse generalized Laguerre-Volterra model of neural population dynamics. *Conf. Proc. IEEE Eng. Med. Biol. Soc.* 2009, 4555–4558. doi: 10.1109/IEMBS.2009.5332719

Song, D., Chan, R. H. M., Marmarelis, V. Z., Hampson, R. E., Deadwyler, S. A., and Berger, T. W. (2011). Estimation and statistical validation of event-invariant nonlinear dynamic models of hippocampal CA3-CA1 population activities. *Conf. Proc. IEEE Eng. Med. Biol. Soc.* 2011, 3330–3333. doi: 10.1109/IEMBS.2011.6090903

Song, D., Marmarelis, V. Z., and Berger, T. W. (2009d). Parametric and nonparametric modeling of short-term synaptic plasticity. Part II: experimental study. *J. Comput. Neurosci*. 26, 21–37. doi: 10.1007/s10827-008-0098-2

Song, D., Wang, H., Tu, C. Y., Marmarelis, V. Z., Hampson, R. E., Deadwyler, S. A., et al. (2013). Identification of sparse neural functional connectivity using penalized likelihood estimation and basis functions. *J. Comput. Neurosci*. 35, 335–357. doi: 10.1007/s10827-013-0455-7

Song, D., Wang, Z., Marmarelis, V. Z., and Berger, T. W. (2009c). Parametric and non-parametric modeling of short-term synaptic plasticity. Part I: computational study. *J. Comput. Neurosci*. 26, 1–19. doi: 10.1007/s10827-008-0097-3

Squire, L. R., and Zola-Morgan, S. (1991). The medial temporal lobe memory system. *Science* 253, 1380–1386. doi: 10.1126/science.1896849

Taylor, D. M., Tillery, S. I. H., and Schwartz, A. B. (2002). Direct cortical control of 3D neuroprosthetic devices. *Science* 296, 1829–1832. doi: 10.1126/science.1070291

Wolpaw, J. R., and McFarland, D. J. (2004). Control of a two-dimensional movement signal by a noninvasive brain-computer interface in humans. *Proc. Natl. Acad. Sci. U.S.A.* 101, 17849–17854. doi: 10.1073/pnas.0403504101

Conflict of Interest Statement: The authors declare that the research was conducted in the absence of any commercial or financial relationships that could be construed as a potential conflict of interest.

Received: 26 February 2014; accepted: 06 May 2014; published online: 28 May 2014.
Citation: Song D, Harway M, Marmarelis VZ, Hampson RE, Deadwyler SA and Berger TW (2014) Extraction and restoration of hippocampal spatial memories with non-linear dynamical modeling. Front. Syst. Neurosci. ***8****:97. doi: 10.3389/fnsys.2014.00097*
This article was submitted to the journal Frontiers in Systems Neuroscience.

frontiers in Neuroscience

REVIEW
published: 29 September 2016
doi: 10.3389/fnins.2016.00343

Mechatronic Wearable Exoskeletons for Bionic Bipedal Standing and Walking: A New Synthetic Approach

Gelu Onose[1,2], Vladimir Cârdei[3], Ştefan T. Crăciunoiu[3], Valeriu Avramescu[3], Ioan Opriş[4], Mikhail A. Lebedev[5] and Marian Vladimir Constantinescu[6]*

[1] Department of Physical and Rehabilitation Medicine, University of Medicine and Pharmacy "Carol Davila", Bucharest, Romania, [2] Teaching Emergency Hospital "Bagdasar-Arseni", Bucharest, Romania, [3] Research and Technological Design Institute for Machines Construction, Bucharest, Romania, [4] Miller School of Medicine, University of Miami, Miami, FL, USA, [5] Department of Neurobiology, Duke University, Durham, NC, USA, [6] Holistic Dental Medicine Institute – ROPOSTURO, Bucharest, Romania

During the last few years, interest has been growing to mechatronic and robotic technologies utilized in wearable powered exoskeletons that assist standing and walking. The available literature includes single-case reports, clinical studies conducted in small groups of subjects, and several recent systematic reviews. These publications have fulfilled promotional and marketing objectives but have not yet resulted in a fully optimized, practical wearable exoskeleton. Here we evaluate the progress and future directions in this field from a joint perspective of health professionals, manufacturers, and consumers. We describe the taxonomy of existing technologies and highlight the main improvements needed for the development and functional optimization of the practical exoskeletons.

Keywords: mechatronic, portable/wearable exoskeletons, bipedal standing, bionic walk assistance, models

OPEN ACCESS

Edited by:
Mircea Dragoman, National Institute for Research and Development in Microtechnologies, Romania

Reviewed by:
Giuseppe D'Avenio, Istituto Superiore di Sanità, Italy
Giovanni Stellin, Telerobot Labs Srl, Italy

****Correspondence:***
Gelu Onose
geluonose@gmail.com

Specialty section:
This article was submitted to Neural Technology, a section of the journal Frontiers in Neuroscience

Received: *09 April 2016*
Accepted: *08 July 2016*
Published: *29 September 2016*

Citation:
Onose G, Cârdei V, Crăciunoiu ŞT, Avramescu V, Opriş I, Lebedev MA and Constantinescu MV (2016) Mechatronic Wearable Exoskeletons for Bionic Bipedal Standing and Walking: A New Synthetic Approach. Front. Neurosci. 10:343. doi: 10.3389/fnins.2016.00343

HUMAN POSTURE AND WALKING, AND THEIR RESTORATION TO THE DISABLED

Vertical posture and bipedal gait are two hallmarks of human biomechanics and motor physiology, which emerged over the millions of years of evolution. While our body size and overall physical performance are not particularly impressive compared to other animal species, having our hands relieved from body support against gravity gives us a number of advantages, dexterity being one of the most important ones. In addition to motor physiology, virtually any human physiological function is adapted to the bipedal posture and walking, for example breathing, digestion, and excretion (Uebelhart et al., 2000)[1]. Moreover, human bipedalism has had a great influence on our daily social interactions and the manmade habitat.

While the surrounding objects and structure of the buildings all fit the needs of healthy humans, the conditions are quite different for disabled, wheelchair bound people. No matter how many facilities would be made in order to overcome their numberless structural barriers, new hurdles are always to be expected. Wheelchair users will never be able to completely adapt to the habitat built for the people who walk bipedally and stand upright. By contrast, the cartoon of a person in the wheelchair is the worldwide used symbol for handicap.

[1]http://www.sci-info-pages.com/other_issues.html#Osteoporosis

Although there is no cure for many lesions of the spinal cord and the brain (Talley Watts et al., 2015)—the major causes of paralysis—essential improvements can be made to the quality of life of handicapped people using devices that assist vertical stance and bipedal walking (Louie et al., 2015). These assistive technologies are based on mechatronic, robotic, and bionic exoskeletons (Chen et al., 2013). Such devices clearly represent one of the most important developments in rehabilitation of paralysis, even though they are currently not expected to deliver a truly spectacular, translational progress. Rather, they are considered as viable intermediary solutions, which bring us closer to the long-awaited recovery of posture and gait to the paralyzed patients. While much work is still needed to improve these external aids, they already have shown effective daily use capabilities.

ASSISTIVE TECHNOLOGIES: MANUFACTURER AND CONSUMER PERSPECTIVES

In the last decade and mostly in its second half, a series of exoskeletons have been designed, built, clinically tested in small groups of subjects, and reviewed in the literature[2−9]. These previous publications have fulfilled the promotional and marketing objectives of the manufacturers, and several exoskeletons are currently commercially available. Yet, an optimal, fully functional assistive device has not yet emerged from this research and development[10,11] (Chen et al., 2013; Arazpour et al., 2015b; Lajeunesse et al., 2015; Louie et al., 2015).

An optimal, practical exoskeleton should fulfill the following requirements:

- The system should be safe.
- It should be effectively wearable[11] in the common sense of the term, mainly regarding don and doff issues. Additionally, it should be psychologically acceptable in terms of self-esteem, miniaturization, and esthetics. Ideally, the exo-suit should be thin and wearable like clothes or underwear.
- The exoskeleton should be appropriate for long time performance, including the performance in community (Louie et al., 2015).
- It should produce very low, practically imperceptible noise when functioning.
- The assistive device should be truly affordable and cost effective.

We believe that achieving these requirements should be the main goal of the field, so we focus on these practical, consumer-oriented objectives in this article. We start with proposing a taxonomy of exoskeletons. We then discuss the improvements of these assistive devices that need to be achieved in near-term and long-term. Our views reflect both the professional, multi-disciplinary expertise of the authors and consumer perspective. The first author (**Figure 1**) sees both sides of the coin: he is an academic physician in Physical and Rehabilitation Medicine (with special focus on Neurorehabilitation) and in Gerontology and Geriatrics, and also a chronic, complete paraplegic, dependent on the wheelchair.

Our multidisciplinary approach intends—without underestimating the legitimate competition between different technical solutions and producers—to foster the optimization of assistive and rehabilitation devices, so that they could eventually become suitable and available to as many people in need as possible. Being one of the consumers too, the first author is looking forward to welcome this long awaited accomplishment, no matter which exoskeleton model meets the expectations first.

MAIN INDICATIONS

The currently available wearable powered exoskeletons serve two main functions. The first function is medical: providing assistive and rehabilitation technology for disabled people[12]. The second function is non-medical: augmenting normal human physical capabilities.

As to the non-medical domain, we are covering it here only briefly. Noteworthy, non-medical exoskeletons have indirect linkages to medical issues, such as contributions to technology development and prevention of occupational injuries. The other uses encompass military devices for enhancement of soldier speed, power, and interactions with the equipment[13−15]; exoskeletons for people professionally involved in critical rescue situations, such transportation of wounded individuals to safety from the war or civil disaster areas[13−16]; civil applications for lifting and carrying heavy objects and patients[17]; and exoskeletons that augment human gait by assisting leg muscles and supporting a comfortable orthostatic posture. The target population for these applications includes the elderly with weak legs, personnel engaged in long-distance walking and/or performing flexion and extension movements with their lower limbs, and people utilizing exoskeleton appliances for entertainment[18].

[2]http://www.cyberdyne.jp/company/download/20160212_financialresultssummary.pdf
[3]http://www.digitaltrends.com/cool-tech/rewalk-6-0-exoskeleton/
[4]http://www.rexbionics.com/investors/
[5]http://www.engadget.com/2011/05/02/new-zealand-paralympian-buys-first-rex-bionics-exoskeleton-take/
[6]http://www.fastcompany.com/1822791/eksos-exoskeletons-let-paraplegics-walk-will-anyone-actually-wear-one
[7]http://world.honda.com/news/2015/p150721eng.html
[8]http://www.indego.com/indego/en/Product
[9]http://www.fastcodesign.com/3056049/a-budget-exoskeleton-allows-parapalegics-to-walk-for-the-price-of-a-car7
[10]http://www.b-temia.com/category/press_releases/
[11]https://www.cadth.ca/sites/default/files/pdf/htis/july-2015/RA0784%20Powered%20Wearable%20Walking%20Assistive%20Devices%20Final.pdf
[12]http://www.keeogo.com/biomechatronics/
[13]http://bleex.me.berkeley.edu/research/exoskeleton/bleex/
[14]http://bleex.me.berkeley.edu/research/exoskeleton/exohiker/
[15]http://bleex.me.berkeley.edu/research/exoskeleton/hulc/
[16]http://www.b-temia.com/defense-security-soldier-protection/
[17]http://www.cyberdyne.jp/english/products/Lumbar_LaborSupport.html
[18]http://asimo.honda.com/innovations/feature/body-weight-support-assist/

FIGURE 1 | The picture of the first author Prof. Dr. Gelu Onose in wheelchair visiting patients in the NeuroRehabilitation Clinic Division of the 'Bagdasar-Arseni' Teaching Emergency Hospital, Bucharest, Romania. Reproduced with permission of the TV producer, Romanian Television.

The medical domain includes wearable devices utilized for prophylactic, rehabilitation, and assistance to disabled people. Taxonomy of these devices reflects the needs of different types of patients. A complete paraplegic would need a device that performs a set of sophisticated tasks, and there is currently no device with these capabilities. Such a device would require no effort from the paralyzed patient, and would do almost everything for the patient.

The device for a complete paraplegic would have to ensure:

- Complete assistance to orthostatic posture and walking, including the very difficult task of maintaining balance in order to avoid falls with severe consequences (Kannape and Lenggenhager, 2016).
- Prevention of spasticity and contractures (Arazpour et al., 2013) and related articular stiffness and pain.
- Prevention of venous and lymphatic stasis in the lower limbs, which could result in lower extremity edema and related complications due to prolonged standing (Louie et al., 2015).
- Partial compensation of the body weight to avoid injuries, such as fracture of the talus (Louie et al., 2015).

The complete paraplegia is classified by the scales of American Spinal Injury Association (ASIA) and International Spinal Cord Society (ISCoS) ("Standard Neurological Classification of Spinal Cord Injury"[19], Frankel et al., 1969). Mechatronic wearable exoskeletons can be very useful as assistive devices in these cases because in complete chronic lesions of the spinal cord, as a rule, there are not enough remaining neural-muscular units to be trained. The possibility that exoskeletons could be used for rehabilitation in such cases, for example for rehabilitation of muscle activity, is still unclear (Arazpour et al., 2015b). The use of exoskeletons still can induce neuroplasticity (Muresanu et al., 2012; Bryce et al., 2015; Louie et al., 2015) that improved patient interaction with the device[20]. Additionally, a supplementary input from the patient's collected and decoded cortical activity might improve the man-machine interaction and the overall functional outcome.

The indications are different for incomplete paraplegics classified as AIS/ Frankel B-D, tetraplegics with low cervical spinal cord lesions classified as AIS/ Frankel C, and for hemiplegics and hemiparetics with fully preserved functionality of the non-affected hemi-body and limbs, and no sensorial, cognitive and balance serious impairments. The other potential beneficiaries of such exoskeletons are patients with neuromuscular and somatic impairments, including patients with polyneuropathia in lower limbs (Zeilig et al., 2012), multiple sclerosis, Parkinson's disease, hip or knee osteoarthritis[21], limb fractures, and amputated limbs (Chen et al., 2013).

In hemiplegia cases, an H2 (Technaid S.L., Spain) robotic exoskeleton is more appropriate for gait rehabilitation (Bortole et al., 2015)—an exoskeleton based on two control strategies: (i) adaptive trajectory control for guiding the patient's limb within a desired path, the strategy that facilitates patient interaction with the device, and (ii) admittance control strategy that captures the user's movements during assistive training phase and reproduces it during active training phase (Bortole et al., 2013). The main feature of the wearable exoskeletons indicated to approach these kinds of patients is usually not an assistive control of the trunk. An essential feature of using such devices is training induced rehabilitation, where the exercise outcomes are compared to the time spent exercising (Louie et al., 2015).

[19]http://www.scribd.com/doc/37064936/2006-Classif-Worksheet

[20]http://who.int/disabilities/policies/actionplan/disability_action_plan_en.docx

[21]http://www.keeogo.com/keeogo-in-action/

The choice of the exoskeleton system and training regime critically depend on the extent of neurological impairment, the affected neural site (central, peripheral, or both), and the state of muscles (which can change with training). Additionally, it is important to take into account and correct by training such conditions as pain, contracture, osteoporosis, bed sores, and edema (Arazpour et al., 2013).

In the disabled elderly, the degree and characteristics of multimorbidity should be considered (Salive, 2013), particularly balance disorders, cardio-respiratory impairments, and para-physiological sarcopenia (Morley, 2012). The assistive and rehabilitation devices should be adjusted to these conditions. For instance, if an older adult has preserved, although altered, ability to stand-up and walk, extended trunk stabilization may not be needed. However, if the senior beneficiary has marked sensory and/or balance impairment, a maximally assistive devices might be more appropriate, in order to avoid frequent falls in the older population[22]. The frequency of falls is variable (6–34%) in different countries and regions: (Kalache et al., 2007). Falls represent some of the most serious negative events with considerable pathological consequences, including disabilities and life threatening conditions. Such negative events result in economic burden for the patients, their families, and the society[22] (Kalache et al., 2007). These considerations will become progressively more important in the future, as the global process of demographic ageing intensifiers[22] (Kalache et al., 2007; Chen et al., 2013).

CURRENT TECHNOLOGIES

Currently popular wearable powered exoskeletons include Isocentric Reciprocating Gait Orthosis (IRGO), Hybrid Assistive Leg/Limb (HAL), ReWalk, Ekso, Mina, Wearable Power-Assist Locomotor (WPAL), Rex, Indego, Keeogo, Kickstart, Stride Management Assist, and ExoAtlet[23]. These devices have been recently reviewed[11] (Arazpour et al., 2013, 2015a,b; Chen et al., 2013; Lajeunesse et al., 2015; Louie et al., 2015). These review articles documented the following characteristics of the existing systems:

- Benefits, including compared to the robotic exoskeletons fixed to treadmills (Chen et al., 2013; Louie et al., 2015).
- Safety (Lajeunesse et al., 2015).
- Efficacy in restoring walking[11] (Louie et al., 2015), including the performense in community settings (Lajeunesse et al., 2015).
- Clinical effectiveness outcomes, imcluding such parameters as stair climbing performance, speed, mobility, quaility of life, and independence[11] (Chen et al., 2013; Lajeunesse et al., 2015; Louie et al., 2015; Arazpour et al., 2015a,b; Lajeunesse et al., 2015).
- Walking distance (Benson et al., 2016).
- Vertical ground reaction force (vGRF) that quantifies the pattern and magnitude of mechanical loading (Fineberg et al., 2013). This characteristic is particularly important for exoskeletons used by completely paralyzed persons.
- Training protocols (Lajeunesse et al., 2015; Louie et al., 2015).
- User satisfaction and secondary benefits and skills achieved with the exoskeleton (Lajeunesse et al., 2015).
- Level of scientific evidence (Lajeunesse et al., 2015).
- Cost-effectiveness outcomes[11].

Overall, the current literature reports both successes of exoskeleton technology and remaining problems. One important achievement is that wearable exoskeletons enable patients with complete paralysis of the lower part of the body to stand and walk. The speed of walking is modest; it varies with the level of injury and training duration (Louie et al., 2015). In addition to paraplegics, wearable exoskeletons can be used by patients with post-stroke hemiparesis (Bortole et al., 2015), as well as non-stroke neurological pathologies[24] (Esquenazi et al., 2012), such as cerebral palsy, myelome-ningocele, traumatic brain injury and Guillain Barré syndrome (Zeilig et al., 2012).

Wearable exoskeletons have advantages compared to Hip-Knee-Ankle-Foot-Orthoses (KHAFO). For example, powered gait orthosis (PGO) and the IRGO outperform HKAFO, as evident from the improvements in physiological cost index (PCI), distance walked, and walking speed (Arazpour et al., 2013). Additionally, wearable exoskeletons have certain advantages compared to the treadmill-based ones. With wearable exoskeletons, patients get much greater autonomy. The autonomy in turn facilitates rehabilitative training because the device can be used at home in addition to specialized facilities (Chen et al., 2013; Louie et al., 2015). Yet, autonomous use of wearable exoskeletons in community settings still has to be demonstrated (Lajeunesse et al., 2015). Overall, there is still a discrepancy between the consumer high expectations of autonomy and versatility and the actual effectiveness of using wearable exoskeletons (Benson et al., 2016).

A critical analysis of the assessments of exoskeletons as health technology[11] indicates the need for more research, particularly regarding long-term performance (Lajeunesse et al., 2015), assessment of training (Louie et al., 2015), randomized controlled trials, and economic analysis[11]. Overall, the level of scientific evidence remains low in clinical trials of exoskeletons (Lajeunesse et al., 2015). Prevention and detection of medical complications in the exoskeleton users is yet another area that needs more research (Benson et al., 2016). A unified framework is needed for assessment of exoskeleton performance (Bryce et al., 2015). Such a framework is needed to make different clinical trials comparable. The framework should include at least six modules: functional applications, personal factors, device factors, external factors, activities, and health outcomes (Bryce et al., 2015).

Current exoskeletons (**Figure 2**) provide several secondary skills and benefits (Lajeunesse et al., 2015). Exoskeleton with compact design and small backpacks are particularly useful

[22]http://www.cdc.gov/Features/OlderAmericans/
[23]http://www.exoatlet.com/
[24]http://www.parker.com/literature/Exoskeleton/Parker%20Indego%20Brochure.pdf

FIGURE 2 | Images of several types of exoskeletons. (A) Mindwalker mind-controlled exoskeleton could help the disabled walk again. With courtesy from Professor van der Kooij at University of Twente, NL. **(B)** The Keeogo^{TM} exoskeleton from B- TEMIA reveals the latest in an increase of the human systems (human augmentation systems) designed to help people walk more and better. Keeogo^{TM} eliminates several problems in patients with Parkinson's disease. With courtesy from Danielle Beaudoin at b-termia.com. **(C,D)** The ExoAtlet is a powered exoskeleton designed to assist patients during their rehabilitation after stroke, injury, or unsuccessful operation. ExoAtlet automatically repeats the natural patterns of walking, has electrical stimulation system, and physiological sensors. The control system of the ExoAtlet is unique: it collects data from body angles, allows to set the height and length of the step, which provides: (i) standing still; (ii) classic walking; (iii) walking on angled surface; (iv) stepping over obstacles; and (v) comfortable walking up & down stairs. ExoAtlet can be used in rehabilitation centers and at home[24]. ExoAtlet can be controlled with the app on tablet when used in clinics. Experienced user of ExoAtlet use "thinking" crutch for control. With courtesy from Ekaterina Bereziy at exoatlet.ru.

in this respect (Chen et al., 2013) because they allow don, doff and wearing an exoskeleton while sitting in a wheelchair. These operations are possible using electrically actuated ReWalk and ExoAtlet, hydraulically actuated Ekso, and Indego, which combines electriaclly actuated hip and knee joints for both legs (Chen et al., 2013) with functional electrical stimulation (FES) of paralyzed, yet responsive muscles[23] (Chen et al., 2013). This combination of the exoskeleton action with FES training improves rehabilitation results.

FUTURE DIRECTIONS

Notwithstanding significant technological advancements in the field, the current exoskeleton systems still need much improvement for them to become practically efficient. The areas that need improvement remain almost the same as about one decade ago. Accordingly, our assessment made 8 years ago (Onose et al., 2008) remains of current interest: exoskeletons need further miniaturization, optimization of actuators and sensors. Ideally, exoskeletons should become robotic orthotic suits wearable beneath the clothes.

In our perspectives from 2007 to 2008 (**Figures 3**, **5**, **6**), we conceived a soft cable-driven exo-suit device that can apply forces to the body to assist walking. Unlike traditional exoskeletons which contain rigid framing elements, the soft exosuit is worn like clothing and uses geared motors to pull on Bowden cables connected to the suit near the ankle (Asbeck et al., 2013).

Some of the authors of this article have been involved in extensive scientific research on this topic for almost 15 years (Onose et al., 2008, 2012a), and were awarded with the Gold Medal at the Inventions Saloon, in Genève, Switzerland, in 2008 (**Figure 4**).

We have not finished all the necessary tests and improvements of our prototype (**Figure 5**). Because of this delay, several

mechatronic wearable powered exoskeletons are in overall more advanced stage of development, including the clinical trials.

We re-emphasize ichnographically two important requirements to exoskeletons: (i) prevention of venous-lymphatic stasis in the lower limbs, and (ii) skin protection at the interface with the rigid structure of the exoskeleton.

Both issues can cause serious hurdles, especially during the long-time wearing of the assistive devices. Regarding the former issue, because of an impaired venous-lymphatic outflow in paralyzed persons (as well as patients with cardiovascular problems) (Guyton and Hall, 2006), regaining vertical posture with the aid of a wearable exoskeleton provokes regional stasis. This may cause discomfort and edema, including the risk of venous thrombosis, associated trophic somatic lesions, and secondary reactive heart conditions. As for the latter, an improper interface between the exoskeleton and the limb can result in mechanically generated lesions of the heel, respectively of the skin and subjacent soft tissue, which thus need for protection at the interface with the rigid structure of such devices (compressive, friction and tensile forces), as determined through performance metrics (van der Kooij et al., 2006). Therefore, we have conceived—for counteracting these problems—two components of our MOD.

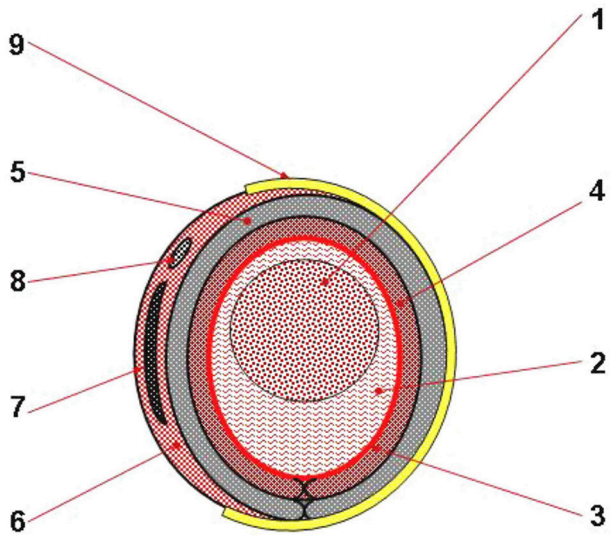

FIGURE 3 | Concept design of a cross section through lower limb(s)'module of the MOD. 1, Bony area; 2, Muscle area; 3, Skin and sucutaneous soft tissues; 4, Textile material for contact with the skin; 5, Pulsed air flow textile structure; 6, (Eeach) exoskeleton's external part, made of composite material; 7, Metallic insertion; 8, Tubular seating for pull and respectively, electric cables; 9, Fasten system. Reproduced with permission from the publisher (Onose et al., 2012a, pp. 1–99).

Furthermore, regarding the underwear exoskeleton, we consider it ambitious and difficult, but worth trying developmental direction. Such an underwear exoskeleton would require a soft supporting structure actuated by strengthening/relaxing device. Specifically, we have foreseen, since 2006–2007 (Onose, 2007) the usage of electro-active polymers (EAPs). EAP materials seem to be the most applicable because of their large actuation forces and highest robustness (Bar-Cohen, 2005). These materials could be improved to act as artificial muscles (Bar-Cohen, 2005; Mirfakhrai et al., 2007).

The development of such a device would be a revolutionary breakthrough, since the soft support structure in cadence with the artificial muscle contraction could not only move the lower limbs but also apply thrusts to the user's calf and thighs, thus mimicking a "muscle pump" and compensating for the returning, venous-lymphatic circulation (Onose, 2007; Onose et al., 2012a). However, during the last decade not enough progress has been made in the development and subsequent translational implementation of EAPs. We still need to improve the safety, controllability and energy supply for EAPs[25].

Another extremely challenging and still incompletely solved item, as mentioned above, is the problem of balance maintenance using advanced mechatronic wearable exoskeletons. Reliable balance is needed for prevention of falls during exoskeleton usage.

At least regarding the most difficult and demanding—in need for total assistance from the apparatus—but, at the same time, an essential category of potential beneficiaries, *the complete paraplegics*, all current devices require supplementary aids for securing the balance: walkers, crutches or—at

[25]http://sbdi.co.kr/cart/data/info/IDTechEx_Electroactive_Polymers_and_Devices_2013-2018_Sample.pdf?ckattempt=1

FIGURE 4 | Mechatronic Orthotic Device (MOD) Left: some relevant images of exoskeletons. Right: Award Diploma by the Geneva International Inventions Fair. Reproduced with permission from the publisher (Onose et al., 2012a, pp. 1–99).

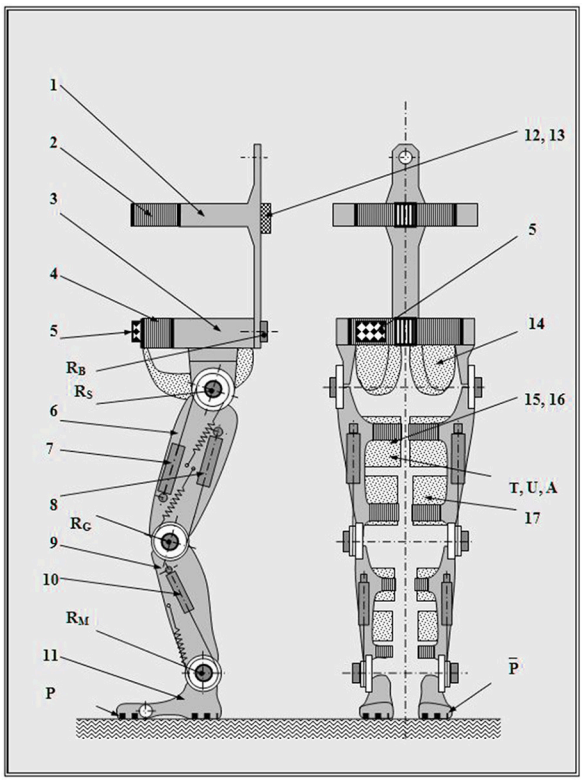

FIGURE 5 | General concept design of the MOD. 1, Back segment; 2, Chest belt; 3, Pelvis segment; 4, Pelvis belt; 5, Programs command box; 6, Thigh segment; 7, Hip actuator; 8, Knee actuator; 9, Ankle segment; 10, Foot actuator; 11, Foot segment; 12, Connections box; 13, Pneumatic connect fitting; 14, Bottom holder; 15, Drawer panty hose; 16, Pulsed air flow textile structure; 17, Attachment belt; R, Angular transducers (B, lumbar sacral; S, hip; G, knee; M, ankle); P, Pressure sensor; T, Temperature sensor; U, Humidity sensor; A, Compressed air pressure sensor. Reproduced with permission from the publisher (Onose et al., 2012a, pp. 1–99).

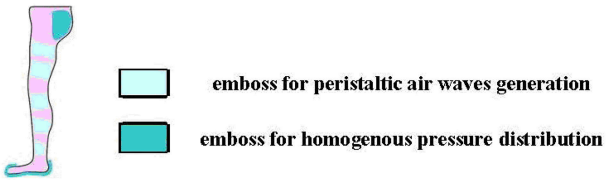

FIGURE 6 | MOD: plantar skin protection and pulsed air flow to mimic the "muscles' pump"—thus compensating the returning, venous-lymphatic circulation, in the lower limbs—concepts. Reproduced with permission from the publisher (Onose et al., 2012a, pp. 1–99).

best—canes. In sum, the powered exoskeletons that assist over-ground walking require the user to maintain balance (Swinnen et al., 2014; Yoshimoto et al., 2015; Louie and Eng, 2016).

As an illustration of the current state of this problem, it is worth mentioning a study that reported loss of balance (LOB) and falls as the primary safety outcomes (Kolakowsky-Hayner et al., 2013). Additionally, the EU FP7 "BALANCE" project (Veneman, 2014) made an observation that "none of the devices available on the market use the exoskeleton itself to support postural balance." Therefore, the goal of the BALANCE project is to research the possibility of using the exoskeleton to maintain balance and prevent falls. The project is organized as a 4 year Specific Targeted Research Project (STREP)[26] and has the practical objectives to "create a human-cooperative robotic postural balance controller framework," in order to "implement the human-cooperative postural balance controller on a real exoskeleton" and to "evaluate the developed concepts in subjects walking with the exoskeleton."[27]

Lastly, one more direction to improve the performances of a mechatronic wearable exoskeleton, is to empower it with brain's voluntary motor commands using a brain-machine-interface (BMI) (Onose et al., 2012b; Lebedev, 2014). The feasibility of such a BMI has been demonstrated in an experiment conducted in rhesus monkeys (Fitzsimmons et al., 2009). In this study, monkeys were implanted with invasive multielectrode arrays in the leg representation of the sensorimotor cortex. The animals were trained to walk bipedally on a treadmill. Activity of several hundred cortical neurons was recorded and converted into the kinematics of lower limb movements. This BMI was able to extract lower limb kinematics when monkeys walked both forward and backward on the treadmill.

These results justified the foundation of the Walk Again Project with the goal of the advancement of BMI-controlled exoskeletons (Nicolelis and Lebedev, 2009). An European project, called Mindwalker (**Figure 2A**), declared the goal of controlling an exoskeleton with electroencephalographic (EEG) and electromyographis (EMG) recordings (Cheron et al., 2012). Decoding of leg movements from EEGs have been demonstrated in humans walking on a treadmill (Presacco et al., 2012). Moreover, a BMI that decoded steady-state visual evoked potentials (SSVEP) from EEGs was employed to operate a lower-limb exoskeleton by healthy human subjects (Kwak et al., 2015).

The progress in BMIs for bipedal walking opens the perspective of neural control of exoskeleton-assisted walking by a completely paralyzed subject. While a slow control of walking could be provided by EEG-based BMIs, invasive BMIs hold promise to enable faster and more accurate control. However, invasive recordings are risky, so there have been no studies of invasive BMIs for walking control in humans. Additionally, it is unclear whether patients could become proficient enough to efficiently control an exoskeleton through an invasive or noinvasive BMI (Onose et al., 2012b). In this respect, we are satisfied of having deployed a clinical trial in the motor imagery BMI domain, by enrolling nine chronic tetraplegics volunteers (the largest lot for such type of trial, at that time), to control

[26]http://balance-fp7.eu/project_structure.php

[27]http://balance-fp7.eu/objectives.php

wirelessly a robotic arm by EEG commands (Onose et al., 2012b).

We have foreseen also the possibility of empowering MOD's actuating systems by voluntary commands extracted from EEGs (Onose et al., 2008). From this point of view, we have expressed our confidence in the success of the Walk Again[28] and Mindwalker projects[29] (**Figure 2**).

CONCLUSION

We suggest that the joint perspective of health professionals, manufacturers and consumers on the mechatronic wearable exoskeletons should contribute to a comprehensive agenda regarding the development of devices that assist and rehabilitate bipedal posture and walking to severely impaired people. The technological advances, together with collaborative endeavors of multidisciplinary teams of researchers, could foster the progress and pave the way to the long awaited optimized and practical exoskeleton.

[28]http://virtualreality.duke.edu/project/walk-again-project/

[29]https://www.utwente.nl/ctw/bw/research/projects/MINDWALKER/

AUTHOR CONTRIBUTIONS

All authors listed, have made substantial, direct and intellectual contribution to the work, and approved it for publication.

ACKNOWLEDGMENTS

The authors thank to: Florin Alexiuc, Ioana Andone, Aurelian Anghelescu, Cornel Baluţă, Ana Maria Bumbea, Eftalea Cărpuş, Crenguţa Coman, Cristina Daia, Alexandru Vlad Ciurea, Jean Ciurea, Radu Stefan Craciunoiu, Ionut Catalin Dimache, Constantin Dogariu, Angela Dorogan, Condurache Dumitru, Maria Gratiela Epureanu, Eva Gheorghiţă, Carmen Giuglea, Roxana Grejdanescu, Monica Haras, Gheorghe Huian, Noela Ionescu, Andrada Mirea, Marius Modreanu, Alexandru Moldovanu, Cristian Nicolau, Raluca Magdalena Niţă, Liliana Onose, Horia Catalin Orasanu, Loredana Theodora Păun, Vergil Racicovschi, Dorin Roşu, Aura Spînu, Olga Surdu, Emilia Visileanu, and Tudor Ursu—for their contribution to the inter-/multi-disciplinary scientific research project that has resulted in the achievement of the MOD and/or to the afferent monography (Onose et al., 2012a), which constitutes a valuable background resource, including for this article.

REFERENCES

Arazpour, M., Bani, M. A., Hutchins, S. W., and Jones, R. K. (2013). The physiological cost index of walking with mechanical and powered gait orthosis in patients with spinal cord injury. *Spinal Cord* 51, 356–359. doi: 10.1038/sc.2012.162

Arazpour, M., Hutchins, S. W., and Bani, M. A. (2015a). The efficacy of powered orthoses on walking in persons with paraplegia. *Prosthet. Orthot. Int.* 39, 90–99. doi: 10.1177/0309364613520031

Arazpour, M., Samadian, M., Bahramizadeh, M., Joghtaei, M., Maleki, M., Bani, M. A., et al. (2015b). The efficiency of orthotic interventions on energy consumption in paraplegic patients: a literature review. *Spinal Cord* 53, 168–175. doi: 10.1038/sc.2014.227

Asbeck, A. T., Dyer, R. J., Larusson, A. F., and Walsh, C. J. (2013). Biologically-inspired soft exosuit. *IEEE Int. Conf. Rehabil. Robot*. 2013:6650455. doi: 10.1109/icorr.2013.6650455

Bar-Cohen, Y. (2005). Current and future developments in artificial muscles using electroactive polymers. *Expert Rev. Med. Devices* 2, 731–740. doi: 10.1586/17434440.2.6.731

Benson, I., Hart, K., Tussler, D., and van Middendorp, J. J. (2016). Lower-limb exoskeletons for individuals with chronic spinal cord injury: findings from a feasibility study. *Clin. Rehabil.* 30, 73–84. doi: 10.1177/0269215515575166

Bortole, M., del Ama, A., Rocon, E., Moreno, J. C., Brunetti, F., and Pons, J. L. (2013). "A robotic exoskeleton for overground gait rehabilitation," in *Proceedings of 2013 IEEE International Conference on Robotics and Automation* (Karlsruhe), 3356–3361.

Bortole, M., Venkatakrishnan, A., Zhu, F., Moreno, J. C., Francisco, G. E., Pons, J. L., et al. (2015). The H2 robotic exoskeleton for gait rehabilitation after stroke: early findings from a clinical study. *J. Neuroeng. Rehabil.* 12:54. doi: 10.1186/s12984-015-0048-y

Bryce, T. N., Dijkers, M. P., and Kozlowski, A. J. (2015). Framework for assessment of the usability of lower-extremity robotic exoskeletal orthoses. *Am. J. Phys. Med. Rehabil.* 94, 1000–1014. doi: 10.1097/PHM.0000000000000321

Chen, G., Chan, C. K., Guo, Z., and Yu, H. (2013). A review of lower extremity assistive robotic exoskeletons in rehabilitation therapy. *Crit. Rev. Biomed. Eng.* 41, 343–363 doi: 10.1615/critrevbiomedeng.2014010453

Cheron, G., Duvinage, M., De Saedeleer, C., Castermans, T., Bengoetxea, A., Petieau, M., et al. (2012). From spinal central pattern generators to cortical network: integrated BCI for walking rehabilitation. *Neural Plast.* 2012:375148. doi: 10.1155/2012/375148

Esquenazi, A., Talaty, M., Packel, A., and Saulino, M. (2012). The ReWalk powered exoskeleton to restore ambulatory function to individuals with thoracic-level motor-complete spinal cord injury. *Am. J. Phys. Med. Rehabil.* 91, 911–921. doi: 10.1097/PHM.0b013e318269d9a3

Fineberg, D. B., Asselin, P., Harel, N. Y., Agranova-Breyter, I., Kornfeld, S. D., Bauman, W. A., et al. (2013). Vertical ground reaction force-based analysis of powered exoskeleton-assisted walking in persons with motor-complete paraplegia. *J. Spinal Cord Med.* 36, 313–321. doi: 10.1179/2045772313Y.0000000126

Fitzsimmons, N. A., Lebedev, M. A., Peikon, I. D., and Nicolelis, M. A. L. (2009). Extracting kinematic parameters for monkey bipedal walking from cortical neuronal ensemble activity. *Front. Integr. Neurosci.* 3:3. doi: 10.3389/neuro.07.003.2009

Frankel, H. L., Hancock, D. O., Hyslop, G., Melzak, J., Michaelis, L. S., Ungar, G. H., et al. (1969). The value of postural reduction in the initial management of closed injuries of the spine with paraplegia and tetraplegia. I. *Paraplegia* 7, 179–192. doi: 10.1038/sc.1969.30

Guyton, A. C., and Hall, J. E. (eds.). (2006). *Textbook of Medical Physiology 11th (International) Edition – Chap. 15 (Vascular Distensibility and Functions of the Arterial and Venous Systems) and 20 (Cardiac Output, Venous Return, and Their Regulation)*. Philadelphia, PA: Elsevier Inc.

Kalache, A., Fu, D., and Yoshida, S. (2007). *WHO Global Report on Falls Prevention in Older Age*. Geneva: WHO Press.

Kannape, O. A., and Lenggenhager, B. (2016). Engineered embodiment: Comment on "The embodiment of assistive devices—from wheelchair to exoskeleton" by M. Pazzaglia and M. Molinari Oliver. *Phys. Life Rev.* 16, 181–183. doi: 10.1016/j.plrev.2016.01.011

Kolakowsky-Hayner, S. A., Crew, J., Moran, S., and Shah, A. (2013). Safety and feasibility of using the EksoTM bionic exoskeleton to aid ambulation after spinal cord injury. *J. Spine S*4:003. doi: 10.4172/2165-7939.S4-003

Kwak, N. S., Müller, K. R., and Lee, S. W. (2015). A lower limb exoskeleton control system based on steady state visual evoked potentials. *J. Neural Eng.* 12:056009. doi: 10.1088/1741-2560/12/5/056009

Lajeunesse, V., Vincent, C., Routhier, F., Careau, E., and Michaud, F. (2015). Exoskeletons' design and usefulness evidence according to a systematic review of lower limb exoskeletons used for functional mobility by people with spinal cord injury. *Disabil. Rehabil. Assist. Technol.* 4, 1–13. doi: 10.3109/17483107.2015.1080766

Lebedev, M. (2014). Brain-machine interfaces: an overview. *Transl. Neurosci.* 5, 99–110. doi: 10.2478/s13380-014-0212-z

Louie, D. R., and Eng, J. J. (2016). Powered robotic exoskeletons in post-stroke rehabilitation of gait: a scoping review. *J. Neuroeng. Rehabil.* 13, 53. doi: 10.1186/s12984-016-0162-5

Louie, D. R., Eng, J. J., Lam, T., and Spinal Cord Injury Research Evidence (SCIRE) Research Team (2015). Gait speed using powered robotic exoskeletons after spinal cord injury: a systematic review and correlational study. *J. Neuroeng. Rehabil.* 12, 82. doi: 10.1186/s12984-015-0074-9

Mirfakhrai, T., Madden, J. D. W., and Baughman, R. H. (2007). Polymer artificial muscles. *Mater. Today* 10, 30–38. doi: 10.1016/S1369-7021(07)70048-2

Morley, J. E. (2012). Sarcopenia in the elderly. *Fam. Pract.* 29(Suppl. 1), i44–i48. doi: 10.1093/fampra/cmr063

Muresanu, D. F., Buzoianu, A., Florian, S. I., and von Wild, T. (2012). Towards a roadmap in brain protection and recovery. *J. Cell. Mol. Med.* 16, 2861–2871. doi: 10.1111/j.1582-4934.2012.01605.x

Nicolelis, M. A., and Lebedev, M. A. (2009). Principles of neural ensemble physiology underlying the operation of brain-machine interfaces. *Nat. Rev. Neurosci.* 10, 530–540. doi: 10.1038/nrn2653

Onose, G. (2007). *Manual de Recuperare, Medicină Fizică şi Balneoclimatologie – Noţiuni de Baza şi Actualităşi*, Vol. I. Bucureşti: Editura Medicalã.

Onose, G., Cârdei, V., Ciurea, A. V., Ciurea, J., Onose, L., Anghelescu, A., et al. (2008). "Achievement of an experimental mechatronic orthotic device to assist/rehabilitate orthostatism and walk in patients with complete paraplegia and other specific severe disabling conditions (short form)," in *Proceedings of the 7th Mediterranean Congress of Physical and Rehabilitation Medicine* (Portorose; Torino: Edizioni Minerva Medica), 40–42.

Onose, G., Cârdei, V., Crăciunoiu, Ş T., and Avramescu, V. (eds.). (2012a). *Mechatronic Orthotic Device. Concept, Sumptions and Functional-Construction Aspects*. Bucureşti: Editura ICTCM.

Onose, G., Grozea, C., Anghelescu, A., Daia, C., Sinescu, C. J., Ciurea, A. V., et al. (2012b). On the feasibility of using motor imagery EEG-based brain-computer interface in chronic tetraplegics for assistive robotic arm control: a clinical test and long-term post-trial follow-up. *Spinal Cord* 50, 599–608. doi: 10.1038/sc.2012.14

Presacco, A., Forrester, L. W., and Contreras-Vidal, J. L. (2012). Decoding intralimb and inter-limb kinematics during treadmill walking from scalp electroencephalographic (EEG) signals, IEEE Trans. *Neural Syst. Rehabil. Eng.* 20, 212–219. doi: 10.1109/TNSRE.2012.2188304

Salive, M. E. (2013). Multimorbidity in older adults. *Epidemiol. Rev.* 35, 75–83. doi: 10.1093/epirev/mxs009

Swinnen, E., Beckwée, D., Meeusen, R., Baeyens, J. P., and Kerckhofs, E. (2014). Does robot-assisted gait rehabilitation improve balance in stroke patients? A systematic review. *Top Stroke Rehabil.* 21, 87–100. doi: 10.1310/tsr2102-87

Talley Watts, L., Long, J. A., Manga, V. H., Huang, S., Shen, Q., and Duong, T. Q. (2015). Normobaric oxygen worsens outcome after a moderate traumatic brain injury. *J. Cereb. Blood. Flow. Metab.* 35, 1137–1144. doi: 10.1038/jcbfm.2015.18

Uebelhart, D., Bernard, J., Hartmann, D. J., Moro, L., Roth, M., Uebelhart, B., et al. (2000). Modifications of bone and connective tissue after orthostatic bedrest. *Osteoporos. Int.* 11, 59–67 doi: 10.1007/s001980050007

van der Kooij, H., Veneman, J. F., Ekkelenkamp, R., (2006)."Compliant actuation of exoskeletons," in *Robots Towards New Applications*, ed A. Lazinica (Source: ISBN 978-3-86611-314-5, pp. 784, ARS/plV. I-Tech Education and Publishing; DOI: 10.5772/33). Available online at: https://core.ac.uk/download/files/363/11473533.pdf

Veneman, J. F. (2014). "Chapter: exoskeletons supporting postural balance – the balance project," in *Replace, Repair, Restore, Relieve – Bridging Clinical and Engineering Solutions in Neurorehabilitation. Vol. 7 of the Series Biosystems and Biorobotics*, eds W. Jensen, O. K. Andersen, and M. Akay (San Sebastian: Springer International Publishing Switzerland), 203–208.

Yoshimoto, T., Shimizu, I., Hiroi, Y., Kawaki, M., Sato, D., and Nagasawa, M. (2015). Feasibility and efficacy of high-speed gait training with a voluntary driven exoskeleton robot for gait and balance dysfunction in patients with chronic stroke: nonrandomized pilot study with concurrent control. *Int. J. Rehabil. Res.* 38, 338–343. doi: 10.1097/MRR.0000000000000132

Zeilig, G., Weingarden, H., Zwecker, M., Dudkiewicz, I., Bloch, A., and Esquenazi, A. (2012). Safety and tolerance of the ReWalk™ exoskeleton suit for ambulation by people with complete spinal cord injury: a pilot study. *J. Spinal Cord Med.* 35, 96–101. doi: 10.1179/2045772312Y.0000000003

Disclosures: GO, VC, ŞC, and VA have been the main researchers involved in achieving the aforementioned Romanian original experimental prototype of mechatronic orthotic device (MOD), but as it could be determined throughout this article, there hasn't been any intention at all to favor in description this model of device, including with the fact that it has been honestly acknowledged in the body text that currently, there are a series of other such models significantly closer to reach the optimal, desired form.

Conflict of Interest Statement: The authors declare that the research was conducted in the absence of any commercial or financial relationships that could be construed as a potential conflict of interest.

frontiers in
SYSTEMS NEUROSCIENCE

REVIEW ARTICLE
published: 12 August 2014
doi: 10.3389/fnsys.2014.00144

Selective visual attention to drive cognitive brain–machine interfaces: from concepts to neurofeedback and rehabilitation applications

Elaine Astrand, Claire Wardak and Suliann Ben Hamed*

CNRS, Cognitive Neuroscience Center, UMR 5229, University of Lyon 1, Bron Cedex, France

Edited by:
Mikhail Lebedev, Duke University, USA

Reviewed by:
Guilherme Wood, Karl-Franzens-University of Graz, Austria
Georgia Gregoriou, University of Crete, Greece

***Correspondence:**
Suliann Ben Hamed, CNRS, Cognitive Neuroscience Center, UMR 5229, University of Lyon 1, 67 Boulevard Pinel, 69675 Bron Cedex, France
e-mail: benhamed@isc.cnrs.fr

Brain–machine interfaces (BMIs) using motor cortical activity to drive an external effector like a screen cursor or a robotic arm have seen enormous success and proven their great rehabilitation potential. An emerging parallel effort is now directed to BMIs controlled by endogenous cognitive activity, also called cognitive BMIs. While more challenging, this approach opens new dimensions to the rehabilitation of cognitive disorders. In the present work, we focus on BMIs driven by visuospatial attention signals and we provide a critical review of these studies in the light of the accumulated knowledge about the psychophysics, anatomy, and neurophysiology of visual spatial attention. Importantly, we provide a unique comparative overview of the several studies, ranging from non-invasive to invasive human and non-human primates studies, that decode attention-related information from ongoing neuronal activity. We discuss these studies in the light of the challenges attention-driven cognitive BMIs have to face. In a second part of the review, we discuss past and current attention-based neurofeedback studies, describing both the covert effects of neurofeedback onto neuronal activity and its overt behavioral effects. Importantly, we compare neurofeedback studies based on the amplitude of cortical activity to studies based on the enhancement of cortical information content. Last, we discuss several lines of future research and applications for attention-driven cognitive brain-computer interfaces (BCIs), including the rehabilitation of cognitive deficits, restored communication in locked-in patients, and open-field applications for enhanced cognition in normal subjects. The core motivation of this work is the key idea that the improvement of current cognitive BMIs for therapeutic and open field applications needs to be grounded in a proper interdisciplinary understanding of the physiology of the cognitive function of interest, be it spatial attention, working memory or any other cognitive signal.

Keywords: brain–machine interfaces, brain–computer interfaces, cognition, spatial attention, neurofeedback, neural training, frontal eye field, prefrontal cortex

INTRODUCTION

Only a couple of decades ago imagining an interface between the human brain and a machine was more of a science fiction than of a scientific endeavor. Chapin et al. (1999) pioneered the field with the first demonstration of a real time motor brain–machine interface (BMI) that is the demonstration that brain activity from the rat motor cortex can be used to control a robotic arm. This achievement brought about the realization of the enormous potential of the field, which up to this day has not ceased to expand.

The main objective of motor BMIs is the rehabilitation of patients with major motor deficits yet preserved cortical motor functions. Applications involve for example controlling a screen cursor using motor or premotor cortex brain activity in monkeys (Serruya et al., 2002; Taylor et al., 2002; Santhanam et al., 2006; Kim et al., 2011) and in tetraplegic human patients (Hochberg et al., 2006) which has been proven feasible with a remarkable spatial accuracy. As computer-assisted aids continue to permeate our everyday life environments, this approach is expected to grant patients who have difficulties moving their arms or hands an increased autonomy and freedom of action. Pushing BMIs yet a step further, several studies show that motor cortical activities can also be used to control robotic arms in their reaching and grasping components with an impressive degree of precision, both in monkeys (Carmena et al., 2003; Tillery et al., 2003; Lebedev et al., 2005; Velliste et al., 2008; Ifft et al., 2013) and in humans. This has for example allowed a tetraplegic patient to help herself with a drink with the aid of an artificial arm controlled by her motor cortex activity (Hochberg et al., 2012).

Several new directions are currently being explored by BMI research. For example, a recent study demonstrates that incorporating sensory feedback to a motor brain-computer interface (BCI) improves its performance (Suminski et al., 2010). Along another line, Shanechi et al. (2014) demonstrate that the signals decoded from the motor cortical activity recorded in a monkey performing a sensorimotor task can be used to stimulate the spinal cord and muscles of a second anesthetized monkey giving rise to directed movements of its limb toward distinct targets. This study opens new rehabilitation perspectives for paralyzed patients. The

exhaustive review of the major advances in motor BMIs and their novel perspectives is however beyond the scope of the present review.

BASIC PRINCIPLES UNDERLYING BRAIN–MACHINE INTERFACES

The basic concept behind BMIs is the interpretation, in real time, of cortical neuronal population activities and their translation into a goal directed action through a diversity of external effectors (**Figure 1A**). Developing a BMI includes two distinct phases (**Figure 1B**): (1) a learning or training phase during which a classifier learns to associate the observed instantaneous simultaneous activity of a neuronal population with the actual state of the variable of interest (the position of a stimulus in space, the direction of an intended motor plan, the spatial location of visuospatial attention, or the content of short term memory etc.); (2) a testing phase during which the classifier defined in the learning phase is used to define the most probable state of the variable of interest, given the observed instantaneous simultaneous activity of the recorded neuronal population. Above-chance decoding accuracy indicates that the neuronal population contains reliable information about the variable of interest.

In its simplest form, the mapping between the neuronal code and the desired output relies on the interpretation of the subject's endogenous neuronal codes. For example identifying the neuronal codes with which a set of movements is encoded in the motor cortex allows to associate a given neuronal population activity (e.g., corresponding to moving one's arm left) with a specific spatially congruent external effector output (e.g., moving a cursor left, **Figure 1B**). More complex designs are further based on the adaptive capabilities of the primate cortex and rely on learning and positive reinforcement procedures. In these designs, subjects learn to produce the neuronal population activities that best control the effector output, thanks to a sensory feedback (e.g., seeing the cursor's trajectory) that allows them to assess how well they are successful at controlling the external effector (**Figure 1C**).

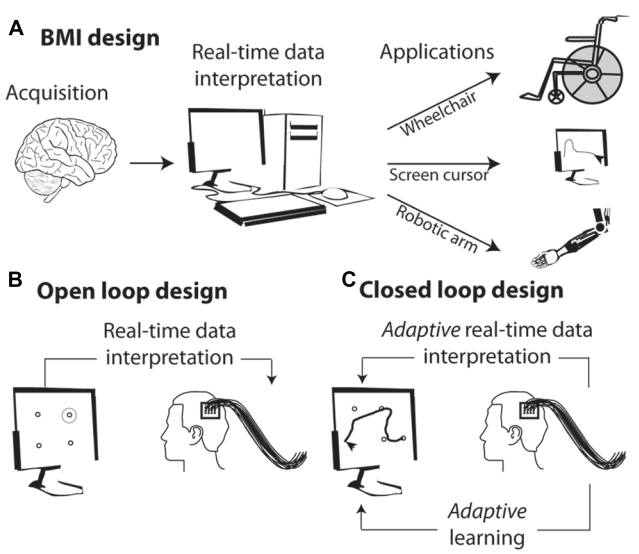

FIGURE 1 | From brain signals to controlled external effectors. **(A)** Schematic representation of the workings behind brain–machine interfaces (BMI). **(B)** Open loop BMI. The subject is here implanted with intracortical electrodes in the primary motor cortex. The activity of this cortical region is used to select a target on the screen without the subject being required to adjust his or her neuronal activity. **(C)** Closed loop design. The activity of the motor cortex is used to guide a cursor on the screen. The subject sees the screen cursor in real time and is required to adapt his or her brain activity in order to increase the precision of the cursor's trajectory.

COGNITIVE BRAIN–MACHINE INTERFACES (cBMI)

While most of the research effort in neural prosthetics has concentrated on the use of motor signals to drive external devices, new directions in the field of BMIs are also emerging. For example, Musallam et al. (2004) have shown, in the context of motor behavior, that cognitive signals such as the expected value of a reward, i.e., the subject's motivation, can be decoded, at the single trial time scale, from parietal neural activity. Jerbi et al. (2009) show that such signals as attention orientation signals and mental calculation signals can be used to drive a cognitive BCI. Instead of decoding movement-related signals from motor specific cortical activity, these cognitive BMIs (cBMIs) seek to access the content of cognitive processes. One of their principal long-term goals is to develop therapeutic tools for the treatment of cognitive disorders.

In healthy subjects, motor cortical commands can be objectified and time-locked to overt limb displacements. In contrast, cognitive processes, such as planning, holding information in short-term memory or orienting one's attention in the environment, are essentially internal subjective processes. From a behavioral point of view, their content is covert and can be inferred only indirectly from their effects on other overt measures (e.g., oral report, reaction time measures, detection rates etc.). From a neurophysiological point of view, their neural bases are increasingly understood and clear neuronal signatures can be assigned to them. However, unlike sensory or motor processes, these cognitive processes cannot be precisely time-locked to objective external events. In addition, they are often multiplexed with sensory, motor as well as other cognitive signals. As a result, cBMIs currently appear as more challenging than motor BMIs. The present review focuses on a major cognitive function, namely visuospatial attention (**Figure 2A**), which is known to enhance visual processing both at the behavioral (**Figure 2B**) and neurophysiological levels (**Figure 2C**, see below). It proposes a precisely quantified comparative overview of the different cBMI approaches that have been developed to decode this cognitive signal at the scale of the single trial (**Figure 2D**). It also explores the initial steps at using such cBMIs for cognitive rehabilitation purposes. These studies are discussed in the light of the accumulated knowledge about the psychophysics, anatomy, and neurophysiology of visual spatial attention. The core motivation of the present review is the key idea that the improvement of current cBMIs for therapeutic and open field applications needs to be grounded in a proper interdisciplinary understanding of the physiology of the cognitive function of interest, be it spatial attention, working memory or any other cognitive signal.

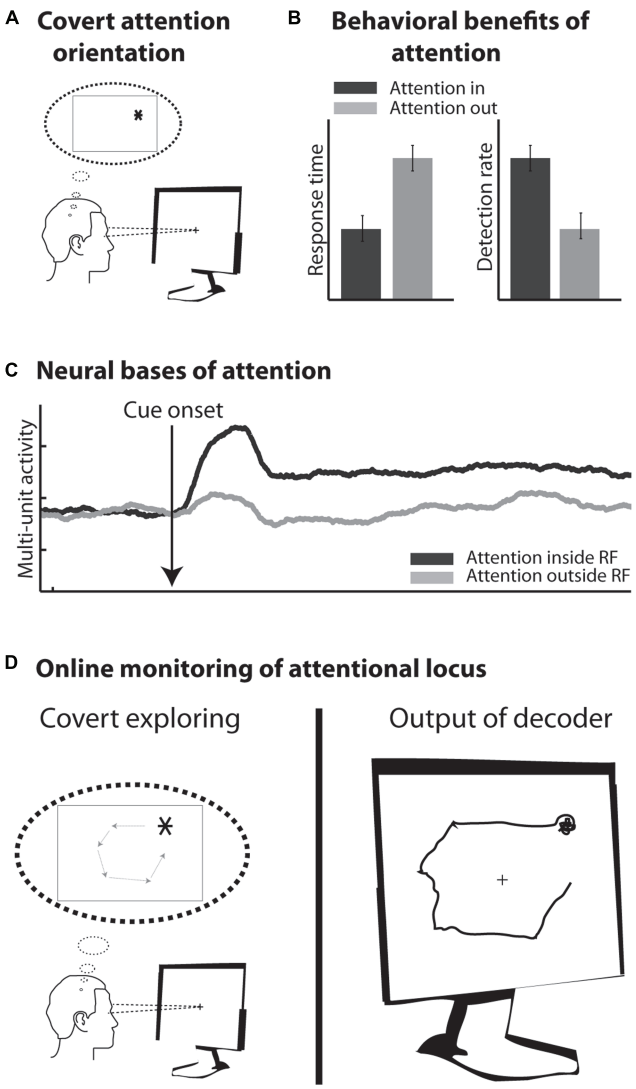

FIGURE 2 | (A) Covert orienting of attention involves selecting a peripheral location in space (here *) while the eyes remain at the center of the screen. **(B)** Attention orientation results in faster response times and higher detection rates in response to visual stimuli presented at the attended location, as compared to the non-attended location. **(C)** Attention orientation enhances both the phasic and tonic neuronal response components in several cortical areas including the frontal eye fields (FEF). Schematic representation of this effect onto multi-unit neuronal activity. **(D)** Online monitoring of the spatial locus of attention. On the left: the subject is covertly moving his attention to covertly explore the screen. On the right: the decoder interprets in real time the activity related to the subject's attention orientation.

VISUOSPATIAL ATTENTION AND ITS NEURAL CORRELATES

Orienting one's attention toward a given location in space enhances visual processing at that location (**Figure 2B**). Reaction times are faster (Posner et al., 1980, but see also Albares et al., 2011), spatial processing (Bashinski and Bacharach, 1980; Prinzmetal et al., 2005; Ibos et al., 2009) and spatial resolution are enhanced at the attended location (Yeshurun and Carrasco, 1998; Gobell and Carrasco, 2005; Carrasco and Yeshurun, 2009; Anton-Erxleben and Carrasco, 2013) and spatial representation is distorted up to several degrees away from the attended location (Wardak et al., 2011a). At the neuronal level, attention is described to modulate both the baseline (e.g., Armstrong et al., 2009; Ibos et al., 2013) and the visual responses (e.g., McAdams and Maunsell, 1999), to decrease neuronal response latency (Lee et al., 2007), as well as to modify the neurons' spatial selectivity profiles (Ben Hamed et al., 1997, 2002; Anton-Erxleben et al., 2009). At the neuronal population level, attention is also thought to decrease interneuronal correlations (Cohen and Maunsell, 2009).

Spatial orienting of attention can be achieved through two different mechanisms. It can either be driven by external stimuli that capture attention. This mechanism is referred to as exogenous, bottom-up or involuntary attention. Alternatively, attention can be voluntarily driven by internal goals. This mechanism is referred to as endogenous, top-down or voluntary attention. Early on, Posner et al. (1980) and Jonides (1981) suggested that a single cortical system controls both the endogenous and the exogenous orientation of attention. In contrast with this proposal, Müller and Rabbitt (1989) postulated that the endogenous and exogenous orienting of attention are functionally distinct and constitute separate mechanisms in constant competition with each other (e.g., Zénon et al., 2008, 2009). Confirming this view, recent functional magnetic resonance imaging (fMRI)-studies demonstrate the co-existence of two distinct frontoparietal networks involved in orienting attention (Corbetta and Shulman, 2002): a dorsal network that is active during top-down attentional control, i.e., when attention is internally maintained or voluntarily driven (Kastner et al., 1999; Shulman et al., 1999; Corbetta et al., 2000; Hopfinger et al., 2000; Kincade et al., 2005), and a ventral network that is activated when attention is reoriented both voluntarily and by relevant but unexpected stimuli (Arrington et al., 2000; Corbetta et al., 2000; Macaluso et al., 2002; Kincade et al., 2005; Vossel et al., 2006). In the non-human primate, a bilateral frontoparietal attentional network involving the frontal eye fields (FEF; Bruce and Goldberg, 1985) and the lateral intraparietal area (LIP; Barash et al., 1991; Ben Hamed et al., 2001) is described. These areas are activated by both endogenously driven attention and exogenously driven attention to task-relevant stimuli (Gottlieb et al., 1998; Armstrong et al., 2009; Gregoriou et al., 2009; Suzuki and Gottlieb, 2013). Interestingly, during endogenous top-down driven attention, FEF neurons tend to respond earlier than LIP neurons whereas during exogenous bottom-up driven attention, the inverse is observed (Buschman and Miller, 2007; Ibos et al., 2013). The distinction between a dorsal and a ventral frontoparietal network is still unclear in the macaque monkey. The FEF possibly belongs to a putative monkey dorsal attentional network while area 45, ventral to area FEF, possibly belongs to a putative monkey ventral attentional network (Wardak et al., 2011b).

VISUOSPATIAL ATTENTIONAL SIGNALS FROM A cBMI PERSPECTIVE

TIME-LOCKING

The feasibility of cBMIs based on visuospatial attention signals as compared to motor or sensory BMIs depends on the existence of neuronal population activity patterns that distinguish between whether the subject is orienting its attention say to the left or to the

right of the visual field. The P300 speller is an example of a successful non-invasive cBMI driven by the decoding of visuospatial attentional locus as inferred from the modulation of neuronal responses to a visual stimulus presented at the specific locus of attention. Another approach is to decode sustained attentional brain correlates toward different spatial positions from neuronal population activities. This approach is different because decoding such sustained information cannot be precisely time-locked to an external event. As a result, identifying its precise neuronal activation pattern during the training phase of the decoding is in itself a challenge.

DECODING ATTENTION-RELATED CORTICAL INFORMATION

One important question is whether such attentional information, because of its self-initiated endogenous nature, can be decoded with an accuracy that is comparable to that obtained from sensory and motor related activities. Two studies are interesting in this respect. Armstrong et al. (2009) recorded neuronal responses from the macaque FEF while the animals were involved in a cued target detection task. The cue was an exogenous cue, having the same spatial location as the target. Astrand et al. (2014a) also recorded neuronal responses from the macaque FEF while the animals were involved in a cued target detection task, except that in this case, the cue was calling for an endogenous orienting of attention toward the cued location (FarbodKia et al., 2011; Astrand et al., 2014a). An exogenous cue is thought to involuntarily shift the subject's attention to its location whereas to shift attention to a location indicated by an endogenous cue, the subject needs to voluntarily orient its attention toward it (Jonides, 1981). Both studies thus manipulate spatial attention but the cue that was used called for different orientation processes. Armstrong et al. (2009) show that both visual and sustained attention information can be decoded from a macaque FEF population of neurons modulated both by visual stimuli and attention orientation. Specifically, they report 100% accuracy for the decoding of the spatial location of a visual peripheral stimulus and up to 90% accuracy for the decoding of the spatial locus of sustained attention. They also describe a lower decoding variability for a visual stimulus than for sustained attention. Astrand et al. (2014a) report a similar trend on a random neuronal population selection including both attention-selective neurons and attention non-selective neurons. They further quantify the sensitivity of decoding accuracy to neuronal population size and trial number. In addition, they show that, using populations of visual-selective and attention-related neurons of the exact same size, comparable decoding accuracies are obtained for both variables. This is a strong indication that both exogenous (visual) and endogenous (attention-related) information are encoded in the cortex with a similar reliability. As a result, cognitive variables such as attention can be expected to be decoded from neuronal population activities with similar accuracies as those achieved when decoding sensory or motor variables (for example, see Ben Hamed et al., 2003, 2007).

USING ATTENTION-RELATED SIGNALS TO CONTROL A BRAIN–MACHINE INTERFACE

In the following, we will present an overview of recent studies evaluating the accuracy with which attention-related cortical information can be decoded. These range from non-invasive recording studies in humans [MagnetoEncephaloGraphic recordings (MEG), Electroencephalographic (EEG) recordings and fMRI] to invasive recording studies in human (ECoG) and non-human primate [ECoG, multi-unit neuronal activity (MUA) recordings and single-unit neuronal activity (SUA) recordings] subjects (**Figure 3**). Whenever possible, we document for each study the following information (**Table 1**): (1) the type of signal component each study relies on, (2), whether attention is driven endogenously or exogenously, (3) how well each method succeeds at decoding attentional engagement signals (i.e., the fact that the subject is focusing its attention as compared to no attentional focus), (4) how well each method allows to distinguish between left and right attentional orientation, (5) how well each method allows to distinguish between attentional loci situated in the same visual hemifield, and (6) how visual distractors interfere with the decoding of attention. Points 4 and 5 reflect the spatial resolution with which attention-related signals can be accessed. All this comparative information is presented in **Table 1**. Importantly, to be considered as robust, it has been proposed that BCI performance needs to be above 70% (Kübler et al., 2004, 2006), a threshold accuracy to keep in mind while analyzing **Table 1**.

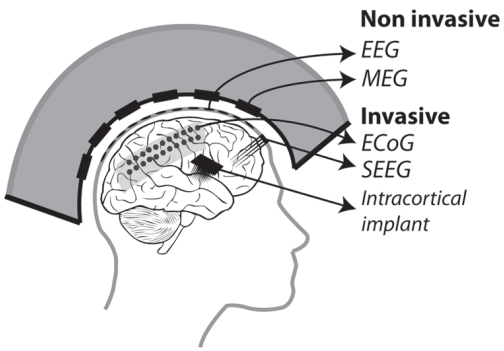

FIGURE 3 | Different recording methods used to control BMIs. Invasive methods includes: ECoG electrodes placed on the dura, SEEG electrodes placed through the skull into the cortex and intracortical electrodes implanted in the cortex. Non-invasive methods include: EEG electrodes placed on the scalp and MEG squids placed around the head.

NON-INVASIVE STUDIES IN HUMANS (MEG, EEG, AND fMRI)

The first attempt at decoding attention orientation at the single trial level is that of van Gerven and Jensen (2009). The authors recorded the cortical activity using MEG while subjects were covertly attending to one amongst four possible locations in space, previously indicated by an endogenous central cue. Analyzing these signals offline, and specifically the alpha-band power (8–14 Hz) of the parieto-occipital captors, they report an average decoding performance of 69% when discriminating between two possible spatial locations (chance being at 50%). They observe better decoding performances at discriminating *left/right* locations (78%, average calculated over their best subjects) than *up/down* locations (58%, *ibid*). They additionally report an average decoding performance of 41% when discriminating between four possible spatial locations (chance being at 25%). This study

Table 1 | Comparative overview of the non-invasive EEG and MEG and invasive ECoG, SEEG and neuronal recording studies, in humans and non-human primates, that have aimed at decoding attention-related information from the ongoing neuronal activity in a perspective of using these signals to drive BMIs.

	Study	Signal	Attention	Atentional engagement	Average decoding performance	Left/right attention	Up/down attention	Distracters
Non-invasive	van Gerven and Jensen (2009)	MEG/Alpha power (8–14 Hz) occipito-parietal channels	Endogenous	–	*2 positions*: 69% ($n = 15$ subjects, chance at 50%) *4 positions*: 41% ($n = 15$ subjects, chance at 25%)	Five best subjects: 78%	Five best subjects: 58%	–
	Treder et al. (2011)	EEG/Alpha power	Endogenous	–	*2 positions*: 75% ($n = 8$ subjects, chance at 50%)	–	–	–
	Morioka et al. (2014)	EEG/Alpha and Beta Power guided by NIRS	*Exogenous*	–	*2 positions*: 79% ($n = 8$ subjects, chance at 50%)	79%	–	–
	Andersson et al. (2011)	fMRI/7T	Endogenous	–	–	*Online fixed threshold:* L: 41%/R: 25% ($n = 7$) *Offline fixed threshold*: L: 89%/R: 88% ($n = 7$) *Online adaptive threshold*: L: 75%/R: 85% ($n = 2$)	–	–
	Andersson et al. (2012)	fMRI	Endogenous	–	*2 positions*: 79% ($n = 9$ subjects, chance at 50%)	77%	82%	–
Invasive in humans	Gunduz et al. (2012)	ECoG/Power from all frequency bands	Endogenous	84% (chance 50%)	*3 positions*: 48% (35% during motor engagement) (chance at 33%)	–	–	–
	Andersson et al. (2011)	ECoG/High gamma power	Endogenous	–	*3 positions*: 70% (chance at 33%)	Left: 55%/Right: 60%/Center: 82%	–	–
Invasive in non-human primates	Rotermund et al. (2013)	ECoG/Power, phase coherence and difference	*Exogenous*	–	*2 positions*: 96% (chance at 50%)	94%	99%	Present but not quantified
	Astrand et al. (2014a)	SUA/average spiking rate	Endogenous	–	–	82%	–	Present but not quantified
	Astrand et al. (2014b)	MUA/average spiking rate	Endogenous/ *Exogenous*	90–100%	*4 positions*: 67%/79% (chance at 25%)	–	–	–
	Armstrong et al. (2009)	SUA/average spiking rate	*Exogenous*	–	*2 positions*: 90% (chance at 50%)	–	–	20% drop in performance
	Zhang et al. (2011)	SUA/average spiking rate	Endogenous	–	*3 positions*: 56% (chance at 33%)	–	*3 positions* 56%	10% drop in performance

thus provided the first evidence that endogenous spatial orientation of attention can potentially be monitored in real time. A subsequent EEG study, using a very similar experimental design reports an average performance of 75% (chance being at 50%) based on the alpha power of the recorded signals (Treder et al., 2011). Morioka et al. (2014), report a slightly higher average decoding performance (79%) using near-infrared spectroscopy (NIRS) as prior information for the analysis of the EEG signals. It is however not clear if this improved performance results from using the NIRS prior information or is due to the fact that an exogenous cue was used instead of an endogenous cue. Using fMRI, Andersson et al. (2011, 2012) take the field one step further by decoding, in real time, the spatial orientation of attention between three endogenously cued locations (one central and two peripheral locations, 2011) and five endogenously cued locations (one central and four peripheral locations, 2012).When using an adaptive threshold on the classification of the real-time BOLD signal, thanks to a real-time design, they obtain a decoding performance of attention orientation (79, 75% at decoding attention to the left and 85% at decoding attention to the right) equal to that obtained with EEG. In contrast with van Gerven and Jensen (2009), they demonstrate a slightly better performance at discriminating between up/down attention (82%) than between left/right attention (77%). When reprocessed offline the average decoding performances reported by Andersson et al. (2011, 2012) reaches 88% (89% at decoding attention to the left and 88% at decoding attention to the right).This sets the ground for a promising future in the field of attention cBMI. Importantly, it is to be noted that all of these non-invasive studies aiming at decoding spatial attention signals from human cortical activities report an important intersubject variability, overall attention orientation decoding performance being high in some subjects and almost at chance in other subjects. See **Table 1** for comparison of the above studies.

INVASIVE STUDIES IN HUMANS (ECoG)

Drawing nearer to the source of the cortical signals, ECoG studies in patients implanted for clinical purposes predicted higher performances for decoding spatial attention than non-invasive techniques. Gunduz et al. (2012) report a performance of 84% at decoding whether a subject is engaging its spatial attention or not using the spectral power amplitude from all frequency bands and a performance of only 48% at decoding the location of attention amongst three possible spatial positions (chance at 33%). Andersson et al. (2011) focus on the high gamma power and report an average of performance of 70% in a similar design (chance at 33%). The discrepancy between these two studies most probably reflects the dependence of the decoding performance upon the exact localization of the ECoG electrode arrays in each subject. Interestingly, Andersson et al. (2011) used the exact same design to decode spatial attention both from ECoG implanted patients and from subjects included in the fMRI experiment described in the previous section. Surprisingly enough, the average decoding performance is higher in the fMRI-based non-invasive approach than in the ECoG implanted patient. This is most probably due to the fact that the fMRI-based protocol specifically relies on the analysis of the regions of interest (ROIs) that are specifically activated by attention orientation, while the ECoG recording correspond to an averaged smoothed analog of these signals. See **Table 1** for comparison of the above studies.

INVASIVE STUDIES IN NON-HUMAN PRIMATES (ECoG, SUA, MUA)

These approaches are expected to yield the highest decoding performances as compared to the two previous approaches, due to the fact that the recording are specifically targeted to the cortical regions involved in attention processing (closest to these regions, on the cortical surface for ECoG, and right within these regions for MUA and SUA recordings), though the number of simultaneously recorded signal sources is also a variable to take into account (the higher the number of recording contacts, the higher the expected decoding performance). MUA can be considered as averaged SUA, as MUA represents several neurons at the same time while SUA represents well identified individual neurons. In a very elegant study, Rotermund et al. (2013) demonstrate extremely high accuracies in discriminating between two exogenously driven attentional loci (average 96%), with slightly better performance for two attentional loci situated in the same visual hemifield (99%) as compared to two attentional loci situated in different visual hemifields (94%), in agreement with the non-invasive fMRI driven study by Andersson et al. (2012). Importantly, Rotermund et al. (2013) placed the ECoG array onto the visual areas V1 and V4 the activity of which is known to be strongly modulated by attention, according to a strict topography matching attention allocation. While these areas can functionally be considered as downstream from the parietofrontal network described above, the fact that attention can be decoded with such high performances from these regions is noteworthy given that these areas are not expected to be subjected to eye-movement or motor planning interferences that can possibly degrade the decoding of spatial attention in other cortical regions (see below). This performance is to be compared with the performance of 90% at predicting the location of attentional locus amongst two possible locations (inside or outside the receptive field) following an endogenous cue (Armstrong et al., 2009), when using the SUA of attention-selective cells recorded in the monkey prefrontal cortex (FEF). Astrand et al. (2014a) report that it is possible to predict whether a monkey was orienting its attention to the right or to the left visual field from the activity of a cortical population of mixed selectivities (attentional and non-attentional) with a performance of 82%. Both these studies (Armstrong et al., 2009; Astrand et al., 2014a) correspond to a coarse approximation of real-time decoding of attention orientation, as they involve the artificial concatenation of cells recorded in independent sessions and having different spatial selectivities. More recently, Astrand et al. (2014b) report, in a real-time decoding design, a 67% performance at discriminating between four possible attentional locations from MUA recordings in the FEF, following an endogenous cue (79% when attention is oriented exogenously). The performance with which they can predict whether the monkey has engaged its attention or not is around 90% for endogenous cueing (98% when attention is oriented exogenously).

DEPENDENCE OF DECODING PERFORMANCE ON THE EXPERIMENTAL DESIGN

Classification accuracy increases as a function of the number of recorded signals and as a function of the number of

available training trials (e.g., Armstrong et al., 2009; Astrand et al., 2014a). The impact of these two parameters on classification accuracy depends on the classification algorithm being used. Indeed, regularized linear regression classifiers appear to be more resilient to low number of recorded signals and low number of trials than other decoders (e.g., support vector machine, reservoir, linear regression, see Astrand et al., 2014a). The impact of these two parameters on classification accuracy also depends on how much information about the variable of interest is present in each recorded signal. For example, a 75% decoding performance of spatial attention can be achieved with as few as 15 trials per condition when each recorded signal has been selected on the basis of its high attention-related content (e.g., attention-related cells in SUA decoding studies). When no prior selection is exerted onto the recorded signals, up to 80 trials are required to reach this 75% decoding performance (Astrand et al., 2014a). As the number of recorded signals and/or the number of trials increases, the impact of further increasing any of these two parameters onto the decoding performance decreases (Astrand et al., 2014a). **Table 2** summarizes, for each of the different studies decoding spatial attention discussed above, the number of recorded signals and how they are placed with respect to the brain, the classifier being used as well as the number of available trials for the classification analysis. In general, there appears to be a trade-off between the number of recorded signals and the number of trials required to achieve a high decoding performance (Astrand et al., 2014a). A precise quantification of this trade-off per type of recorded signal, from non-invasive to invasive, is unfortunately missing and would be extremely useful. This would allow a more direct comparison between the different types of studies. But most importantly, this would allow to better adjust the experimental design to the constraints of the method being used. One expects for example that a higher number of trials will significantly improve the decoding performance achieved in implanted patients. Quantifying this trade-off is all the more important if we want to move from a two-class decoding design (e.g., left/right) to a multi-class (e.g., upper left/upper right/lower right/lower left) or to a 2D continuous decoding design (e.g., x, y), in which case, the number of available trials per condition clearly becomes a limitative parameter.

Overall, most of these studies report a decoding performance above the 70% criteria for a robust BMI (Kübler et al., 2004, 2006). However, in spite of the fact that several experimental parameters contribute to the final decoding performance, invasive attention-based approaches in the non-human primate produce the highest decoding performances as compared to both invasive and non-invasive recording approaches in humans. This provides grounds of improvement for the latter. This is most probably due to the fact that the recordings can be performed closest to the source of the attention-related signals. Supporting this hypothesis, fMRI decoding of spatial attention (driven by activations in ROIs specifically identified based on their contribution to spatial attention processes) outperforms all other non-invasive decoding approaches.

CHALLENGES OF ATTENTION-DRIVEN COGNITIVE BRAIN–MACHINE INTERFACES

ENDOGENOUS VERSUS EXOGENOUS ATTENTION

As seen above, attention can be voluntarily controlled by the subject or involuntarily oriented by an external event. An efficient cBMI is expected to be able to infer spatial attention signals independently of how attention has been driven. Given the functionally partially distinct neural bases of endogenous and exogenous attention orientation, it is thus crucial to quantify, from a cBMI perspective, (1) whether both types of attention orientation modes lead to comparable decoding accuracies, i.e., whether the performance of a cBMI driven by endogenous attention signals is comparable to that of a cBMI driven by exogenous attention signals; and (2) whether a cBMI driven by say endogenous attention signals can generalize and also be driven by exogenous attention signals and vice versa. As discussed above, a recent study shows that the decoding of spatial attention during a cued target detection task from MUA recordings in the non-human primate FEF is partially dependent on whether attention is oriented endogenously or exogenously (Astrand et al., 2014b). Importantly, the decoding performance of exogenous attention signals (79%) is higher than that obtained when decoding endogenous attention signals (67%). Most interestingly, they additionally show that a classifier trained at decoding endogenous attention successfully reads out exogenous spatial attention neuronal signals (54%), though significantly less than if the classifier is directly trained on exogenous attention (drop of 13%). The relationship is not symmetrical as a classifier trained at decoding exogenous attention successfully reads out endogenous spatial attention neuronal signals with a performance of 62%, again slightly lower than if the classifier is directly trained on endogenous attention (drop of 5%).

SUSCEPTIBILITY OF ATTENTION-DRIVEN COGNITIVE BRAIN–MACHINE INTERFACES TO SENSORY AND COGNITIVE FACTORS

Neuronal signals collected from the primary motor cortex are only marginally affected by changes in the sensory environment (e.g., changes in the visual or somatosensory information) or by changes in the cognitive context (e.g., changes in what the subject is thinking about or planning to do). As a result, the generalization capabilities of motor BMIs are unaffected by such varying circumstances. It is still unclear whether this is also the case for cBMIs. While the several studies cited above quantified how well a cognitive variable, namely spatial attention, can be predicted from cortical activity response patterns, none directly tested whether and how this prediction was affected by either a change in the sensory environment or in the cognitive context. A recent report by Astrand et al. (2013) shows that the decoding of spatial attention orientation during the delay period of a memory-guided saccade task is affected by the presence of visual noise. Precisely, they report a 62% performance at decoding spatial attention orientation and spatial short-term memory information from MUA activities recorded in the non-human primate FEF during the delay period of a memory-guided saccade task in the absence of any visual noise and a performance of 63% in the presence of visual noise. When a classifier is trained at decoding this spatial attention orientation in the absence of visual noise and is tested

Table 2 | Comparative overview of the type of signals used for the decoding of spatial attention in the studies discussed in Table 1.

	Study	Signal	# Recorded signals	Coverage	Classification	Available trials
Non-invasive	van Gerven and Jensen (2009)	MEG/Alpha power (8–14 Hz) occipito-parietal channels	275 DC Squid axial gradiometers	Full head	Support Vector Machine w. linear kernel	128 trials per condition
	Treder et al. (2011)	EEG/Alpha power	64 channels	Full head	Logistic regression with L2 regularizer	40 trials per position
	Morioka et al. (2014)	EEG/Alpha and Beta Power guided by NIRS	EEG: 64 channels. NIRS: 49 channels.	Full head EEG. Parietal and occipital NIRS	Sparse logistic regression	88 trials per position
	Andersson et al. (2011)	fMRI/7T	Two ROIs: right vs. left and left vs. right	Full head		8 trials (13s) per condition
	Andersson et al. (2012)	fMRI		Full head		9 trials (13s) per position
Invasive in humans	Gunduz et al. (2012)	ECoG/Power from all frequency bands	86, 78, 64, 103, and 88 electrodes	Left hemisphere, 1 subject right hemisphere. No occipital lobe	Stepwise regression and Bayesian classification	40 trials per position (except for one subject: 80)
	Andersson et al. (2011)	ECoG/High gamma power	64 electrodes	Left parietal-occipital cortex		20 left/20 right/39 center
Invasive in non-human primates	Rotermund et al. (2013)	ECoG/Power, phase coherence and difference	36 and 37 electrodes	Extrastriate area V4 and portions of V1/V2 along lunate sulcus	Support Vector Machine w. Gaussian kernel	∼several hundred trials
	Astrand et al. (2014a)	SUA/average spiking rate	131 neurons	Single hemisphere, Right or Left Frontal Eye Fields	Linear Regression with regularization	60 trials per condition
	Astrand et al. (2014b)	MUA/average spiking rate	48 channels	Both hemispheres, Frontal Eye Fields	Linear Regression with regularization	60 trials per position
	Armstrong et al. (2009)	SUA/average spiking rate	40 neurons	Right Frontal Eye Field	Support Vector Machine w. linear kernel	>10 trials per condition (leave-one out procedure)
	Zhang et al. (2011)	SUA/average spiking rate	187 neurons	Anterior Inferior Temporal cortex, single hemisphere	Correlation Coefficient Classifier	12 trials per stimulus (leave-one-out procedure)

This includes the type of recording method, the number of recorded signals, brain coverage, the type of classifier used for the decoding, the available number of trials per condition.

on MUA activities collected in the presence of visual noise (or vice versa) performance drops by 12%, though it remains well above chance. The decoding of spatial attention signals are thus affected by changes in the sensory environment. Astrand et al. (2013) similarly show that the decoding of the spatial position of a visual stimulus from MUA activities recorded in the non-human primate FEF depends on whether the monkey is for example performing a memory-guided saccade task or a simple target detection task (decoding performance across contexts leads to a drop in 18%, Astrand et al., 2013). Last, as described above, the authors also show that the decoding performance of spatial attention depends on whether attention is oriented endogenously or exogenously, a situation that can be seen as a change in the cognitive context (Astrand et al., 2014b).

SUSCEPTIBILITY OF ATTENTION-DRIVEN COGNITIVE BRAIN–MACHINE INTERFACES TO DISTRACTERS

Another important aspect to consider is how distracters affect the spatial location of attention and hence the stability of a cBMI based on spatial attention signals. Such distracters can be considered as a specific case of a sensory change in the subject's environment (cf. above).In an urban environment where we are constantly exposed to salient stimuli, the endogenous attention that corresponds to an internal objective that the subject wishes to achieve will be continually interrupted by a diversity of external stimuli, both relevant (traffic lights, car horns, your children's voice etc.) or irrelevant (christmas lights, traffic flow, strangers passing by etc.).Several behavioral studies show that peripheral cues automatically capture attention (Jonides and Irwing, 1981; Christ and Abrams, 2006; Neo and Chua, 2006; Schreij et al., 2008). However, attentional capture is not constant. For example, when subjects are explicitly instructed to ignore a peripheral cue, attentional capture is reduced, though not completely abolished (Lambert et al., 1987). Similarly, if attention is highly focused, for example when the subject strongly expects a visual event at a certain location (e.g., following a 100% validity cue), the attentional capture as measured from reaction times is extremely weak (Yantis and Jonides, 1990). In contrast, if the subject is expecting a visual event that can take place at an undefined location (its attention is thus diffuse, e.g., following a 25% validity cue), the attentional capture is much stronger (Yantis and Jonides, 1990). The same reduction in attentional capture can also be observed in visual search experiments where subjects need to distribute their attention over the whole search display in order to scan the scene efficiently (Schreij et al., 2008). Last, attentional capture also depends on the complexity of the visual scene (which is the case of our everyday environment). Cosman and Vecera (2009) show that, when subjects need to search for an item in a complex environment, attentional capture declines as the complexity of the visual scene increases.

These behavioral observations are in agreement with single cell recordings in the monkey parietal cortex. For example, the neurons of the LIP (Ben Hamed et al., 2001), an area functionally associated with attentional processes (Wardak et al., 2002, 2004), are specifically activated by behaviorally relevant visual events independently of whether relevance is due to the intrinsic properties of the stimuli (e.g., an abrupt onset high contrast stimulus) or to its extrinsic properties (e.g., a low contrast stimulus, the processing of which is important to the ongoing task, Gottlieb et al., 1998; Kusunoki et al., 2000). Spatial attentional priority is suggested to be encoded by the differential response between the neurons encoding a specific spatial location against the response of the entire LIP population (Bisley and Goldberg, 2003). Consequently, the selection of a spatial location by attention can be biased by focal LIP optogenetic or electrical microstimulation, mimicking an attention interference or capture (Dai et al., 2014). A recent study by Suzuki and Gottlieb (2013) further suggests that these suppression mechanisms might differ between the prefrontal and parietal nodes of the parietofrontal attentional network. Specifically, the neuronal response to distractors is weaker in the prefrontal cortex than in parietal cortex, indicating a stronger suppression. Additionally, the degree of this suppression with behavioral suppression markers is stronger in the prefrontal cortex. Last, reversible inactivation of the prefrontal cortex leads to a more severe distractability than observed following inactivation of the parietal cortex.

From a decoding perspective, Astrand et al. (2014b) show that a distracter interferes with the performance with which spatial attention can be decoded from FEF MUA recordings in the non-human primates performing a cued target detection task. As observed by others (Armstrong et al., 2009; Zhang et al., 2011), distractors interfere with the accuracy with which spatial attention can be decoded on correct trials. Astrand et al. (2014b) further show that this interference is maximal on false alarm trials, i.e., on trials in which the monkey erroneously responded to the distractor instead of waiting for the target. The distractor interference is similar between correct trials and trials on which the monkey missed the target. Remarkably, the accuracy with which spatial attention can be decoded is much lower on incorrect trials than on correct trials, whether attention has been oriented endogenously (25%) or exogenously (40%), a trend also reported by Armstrong et al. (2009).

SUSCEPTIBILITY OF ATTENTION-DRIVEN COGNITIVE BRAIN–MACHINE INTERFACES TO EYE MOVEMENTS

The last constraint that needs to be discussed in the context of attention-driven BMIs is eye movements. Indeed, the attentional frontoparietal network described above is highly overlapping with, though distinct from, the cortical oculomotor network (Corbetta et al., 1998; Wardak et al., 2006). In all of the studies considered above, the subjects are required to maintain eye fixation during the decoding procedure. As a result, they are behaviorally constrained to suppress an oculomotor-related signal. Studies evaluating the impact of eye movements on cBMIs are yet missing. Treder et al. (2011) demonstrate that high accuracy for EEG-based classification is often associated with low accuracy for eye movement electrooculography (EOG)-based classification, and vice versa. This suggests a dissociation between EEG- and EOG-based classification. It also indicates that eye movements disturb the decoding of attention orientation if not taken into account. Gunduz et al. (2012) further show that, in the absence of any prior processing, the performance with which attention orientation can be decoded in ECoG-implanted patients drops from 48 to 35% when the subjects are planning their motor response (i.e., hardly above the

33% chance level). This suggests that a "naïve" attention decoding performance is most probably disrupted by other signals than just eye-movements, including motor planning. The exact location of the recording sensors is expected to highly impact on such interferences. However, generally speaking, real-time denoising algorithms minimizing the impact of eye movement signals over the attention-related signals are potentially promising. Extremely simple strategies such as analyzing cortical signals only at a distance from eye movements might also prove sufficient.

Overall, in spite of the notable progress in the field of attention-driven cBMIs, several challenges need to be faced before large field therapeutical applications can be considered. A tight interaction between the field of real-time decoding of cortical activity and cognitive neurosciences is expected to have a major impact on facing these challenges, the growing understanding of how the brain functions playing a crucial role toward refined machine learning strategies to handle and analyze massive cortical recordings. This being said, prospective therapeutical application for such cBMIs can already be foreseen, as will be described below.

NEUROFEEDBACK AND COGNITIVE CONTROL

The capacity of the brain to restore and ameliorate its functioning after a major trauma or disease is still poorly understood. It is known that after a CNS disease or trauma (such as a stroke), the brain undergoes extensive functional reorganization (Murase et al., 2004; Nudo, 2006; He et al., 2007; Grefkes et al., 2008; Wang et al., 2010). Building on these impressive adaptive capabilities of the brain, researchers have, in the last 50 years, investigated the ability of the brain to modulate its activity and improve overt behavioral performance thanks to neurofeedback techniques. Initially, this technique consisted in continuously providing the patient with a feedback on the level of activity of a specific cortical region (e.g., thanks to an auditory or visual feedback correlating with the intensity of this cortical activity) and instructing the patient to increase or decrease this activity by their own volition. It has been proven efficient in treating patients with attention disorders and in reducing seizures in epileptic patients (reviewed below). More recent feedback techniques are not based on the raw cortical signals but rather use decoding procedures as described above in order to quantify the exact information of interest contained in the neuronal signals and provide this information as a feedback to the subjects. The subject's goal is then to improve this specific information through cognitive control. This is a very promising tool that could be used to target specific functions in order to enhance the activity in the brain, both in patients with cognitive deficits arising from acute brain damage or neurodegenerative or neurodevelopmental conditions, as well as in normal subjects seeking to enhance their own cognitive functions.

NEUROFEEDBACK AND COVERT NEURONAL ACTIVITY

When we are trained on a specific task, our performance often becomes better. Several studies have investigated the underlying neural bases that account for this behavioral improvement. In visual perceptual tasks that involve difficult discriminations, it has been observed that a behavioral improvement in perceptual sensitivity is strongly coupled with improved neural sensitivity in early and intermediate visual areas (Schoups et al., 2001; Yang and Maunsell, 2004; Hua et al., 2010) as well as in higher visual decision areas (Law and Gold, 2008). The idea behind neurofeedback is precisely grounded on such observations. Indeed, if the brain is capable of modulating its activity through learning, why not by voluntary control of the neuronal activity of specific brain areas? Several fMRI studies have approached this question by providing participants with a visual feedback of the level of activity (BOLD signal) in a specific area of the brain and asking them to increase or decrease this level. These studies have all come to the conclusion that brain activity can be regulated and enhanced volitionally by the subject (Weiskopf et al., 2003; deCharms et al., 2004, 2005; Caria et al., 2007; Scharnowski et al., 2014), even when trading the continuous visual feedback for a monetary reward feedback the value of which correlated with the level of activity of the cortical area of interest (Bray et al., 2007). On a neuronal level, electrophysiological studies not only confirm the above results but reveal a remarkable plasticity of individual neurons to modulate their activity under volitional control (Fetz, 1969, 2007; Cerf et al., 2010; Kobayashi et al., 2010; Schafer and Moore, 2011). For example, Fetz performed, in 1969, a visual and auditory feedback experiment where monkeys were rewarded for increasing the activity of newly isolated neurons in the precentral motor cortex. They observe that the activity could be increased with as much as 50–500% above the initial spike rates.

NEUROFEEDBACK AND OVERT BEHAVIORAL PERFORMANCE

The above studies demonstrate the feasibility of modulating the activity of our own brain by voluntary control. The next question is thus whether this neuronal modulation has an impact on overt behavior? Being able to increase or decrease the activity in the brain is amazing but quite useless if it does not lead to a measurable change in cognitive performance. In the field of EEG neurofeedback, it has actually been known for a long time that a voluntary change in the EEG rhythm, i.e., in the frequency content of the scalp EEG signals, can improve behavior (Wyrwicka and Sterman, 1968; Sterman et al., 1969). For example, Sterman and colleagues highlighted the specific impact of the *sensorimotor rhythm* (SMR: 12–14 Hz) on the capacity to inhibit ongoing behavior. They used neurofeedback to regulate this electrophysiological signature and thereby the frequency of the refractory seizures of a female patient. Specifically, after several months of EEG neurofeedback training to enhance the SMR, the authors noted that the seizures essentially ceased at the same time that a significant increase in the 11–15 Hz frequency band and a corresponding decrease in lower frequencies were observed (Sterman and Friar, 1972). This initial study was followed by a wave of studies describing the clinical benefits of using EEG driven neurofeedback over placebo experimental designs on patients with seizure disorders refractory to pharmacological treatments (Sterman et al., 1974; Kaplan, 1975; Seifert and Lubar, 1975; Kuhlman and Allison, 1977; Kuhlman, 1978; Sterman and Macdonald, 1978; Lantz and Sterman, 1988; Andrews and Schonfeld, 1992; Hansen et al., 1996). A different line of research using the same technique has tried to treat attention disorders such as attention deficit/hyperactivity disorder (ADHD). The first study conducted by Lubar and Shouse (1976), showed that SMR training improved inattentive symptoms in an

11-year old boy with hyperactivity. Further studies confirm that neurofeedback training has a significant effect on reducing hyperactivity or impulsivity symptoms in ADHD (Lubar, 1991; Lubar et al., 1995; Lindén et al., 1996; Thompson and Thompson, 1998; Kaiser and Othmer, 2000). Remarkably, this SMR-driven neurofeedback has further been proven as equally effective as medication (Rossiter and La Vaque, 1995).

Several recent fMRI-based neurofeedback studies show that the operant control of cortical activity can also lead to changes in behavior and to interesting therapeutical applications. For example, Rota et al. (2009) show that the self-regulation of the activity of the right inferior frontal gyrus improves the identification of emotional prosodic intonations. Haller et al. (2010) show that the operant control of the activity of the auditory cortex allows to improve chronic tinnitus, a condition in which subjects perceive more or less constantly an aversive tone or noise, in the absence of any objective external sound source. More recently, Subramanian et al. (2011) show that the clinical motor symptoms of Parkinson disease patients can be improved thanks to neurofeedback driven by the fMRI activity of their supplementary motor area.

In a single-cell recording study in the non-human primates, Schafer and Moore (2011) show that monkeys can learn to modulate the firing rate of individual prefrontal neurons (specifically recorded in the FEF). Importantly, they show that during up-regulation sessions (as compared to down-regulation), an increased firing rate leads to enhanced target discrimination in the receptive field of that neuron. This is a nice demonstration that the voluntary control of FEF neuronal activity is specifically associated with an enhancement of selective spatial attention. It is interesting to compare the finding to Schafer and Moore (2011) in the non-human primate to those obtained by Scharnowski et al. (2012) using fMRI-driven neurofeedback in human subjects. In this study, Scharnowski et al. (2014) demonstrate that the control of the ongoing spontaneous activity as estimated by the BOLD fMRI signal in the visual cortex results in improved visual perception. The authors further show that these observations correlated with increased effective connectivity between the visual cortex and the superior parietal lobe, suggesting that the improved visual perception resulted from enhanced top-down attentional control processes. Top-down attention has been repeatedly shown to modulate the activity of early visual areas (Brefczynski and DeYoe, 1999; Kastner et al., 1999; Li et al., 2008; Gregoriou et al., 2009). The fact that operant control of the activity of visual cortex did not exclusively involve local processes restricted to this cortical region but also involved long-distance and large-scale networks is an indication that the behavioral effects of neurofeedback are maximized by the involvement of the adaptive capabilities of higher level associative cortical regions such as the parietal or the prefrontal cortex.

The above studies all have in common to require the subjects to either increase or decrease the cortical activity being recorded. Cerf et al. (2010) use a concept that is completely different. Instead of just modulating the level of activity, they ask the subjects to actually enhance the information content of the recorded population activity. Specifically, they show that by focusing attention on a concept represented by a target image, neurons in the medial temporal lobe (MTL), an area involved in generating memories of fact and events (Squire and Zola-Morgan, 1991), increase their activity. In this study twelve patients implanted with intracranial electrodes were instructed to manipulate the display of two superimposed images by modulating the firing rate of four MTL units in their brain. The initial visibility of the two images was 50% and the patients were instructed to enhance a target image so as to make it 100% visible. The visibility of the two images was continuously updated via a real-time decoding procedure reflecting the information contained in the spiking activity of these four neurons about either images. This nicely designed experiment is yet limited because the authors only used four units in the decoder which leads to a straightforward interpretation of the decoding performance. Indeed, in this configuration, an increased decoding performance directly translates into an increase in the activity of the unit specifically tuned to the target image and/or decreased activity for the other units. A decoding performance based on the increases or decreases in the information content of hundreds of neurons would result in a much more complex pattern of neuronal changes, possibly more based on functional population synergies than on the mere increase in the activity of selective cells associated with a decrease in the activity of the non-selective cells. Shibata et al. (2011) demonstrate the feasibility of such an experimental design. Participants were given feedback based on the real-time decoding of BOLD fMRI activity. The decoder was configured to discriminate between different angles of a Gabor patch (10°/70°/130°) based on the fMRI BOLD signal recorded from V1 and V2 prior to the neurofeedback procedure. During the neurofeedback sessions, the participants were instructed to enlarge a green circle presented on the screen. For each subject, the size of the green circle was manipulated by how well they could encode a given Gabor patch orientation in their fMRI BOLD activity. The specific angle driving the change in the circle's size changed from one subject to the other. All participants succeeded in increasing the circle. They were therefore all able to increase the information content related to the assigned specific angle even though the strategies they overtly reported were far from the true workings of the experiment. Importantly, this led to an increased perceptual sensitivity specific to the angle used during feedback in contrast with the two other angles. The results of this experiment are important in several aspects. First, they prove the feasibility of human subjects voluntarily increasing their cortical information content relative to a specific visual feature. Second, they suggest that training the brain to increase its information content directly leads to an improvement in overt behavior. Third, they indicate that the improvements are specific to the exact feature that is being trained, similarly to what can be obtained through perceptual learning.

FUTURE DIRECTIONS

COGNITIVE BRAIN–MACHINE INTERFACES FOR COGNITIVE REHABILITATION

As covered in the previous section, neurofeedback applications based on the raw or interpreted (decoded) cognitive information have already been proven efficient for several rehabilitation applications ranging from auditory tinnitus to Parkinson's disease, seizures, ADHD. These applications are progressively infusing off the laboratory patient care protocols. For example, several

start-ups are now providing ADHD EEG-based neurofeedback game platforms integrating enriched immersive virtual 3D environment technologies with neurofeedback training. A challenge facing these future directions is constructing neurofeedback environments that are optimally targeted to specific pathologies. In the above discussed examples, Parkinson's disease clinical symptoms were improved using the activity of the supplementary motor area. ADHD was improved using the sensory motor rhythm involved in overt behavior inhibition. These conditions were thus critically improved by targeting the specific cortical nodes of the dysfunction which have been associated with the overt clinical symptoms. The further development of such rehabilitation methods based on neurofeedback will require a tight interaction between fundamental neuroscience research providing an ever growing understanding of the neural bases of cognition and its deficits and clinical neuroscience research evaluating the impact of specific neurofeedback designs on well identified groups of patients (as defined by clear-cut genotypes, functional deficits or behavioral deficits). For example, while SMR-based neurofeedback has been shown to reduce impulsivity in hyperactive ADHD patients, it is expected that ADHD patients with low hyperactivity symptoms but high inattention symptoms will not benefit by this approach, due to a different functional deficit underlying their symptoms.

COGNITIVE BRAIN–MACHINE INTERFACES TO PALLIATE FOR A DEFICIT IN COMMUNICATION

Most of these above foreseen applications will rely on non-invasive cBMI designs. However, in the case of extremely severe cognitive deficits, cost–benefit recommendations will be needed to evaluate whether invasive cBMIs are ethically acceptable. Two such conditions come to mind. The first condition is the case of total locked-in patients, who are unable to move any muscle of their body including their eyes, while they are otherwise aware and awake. The motor recovery is extremely rare and often very minimal. In a recent report, a locked-in patient was able to communicate via sniffing (Plotkin et al., 2010). Using a direct brain-interface, another total locked-in patient was able to answer yes-or-no questions (Parker, 2003; Keiper, 2006).The second condition that could justify invasive cBMIs corresponds to minimally conscious patients. Unlike patients in a persistent vegetative state, these patients have partially preserved conscious awareness. Recent studies indicate that the overall brain metabolism of these patients is 20–40% lower than that of normal subjects, though slightly higher than that of patients in a vegetative state (Schiff et al., 2005). In addition, several studies indicate some degree of preserved cognitive functions. For example, sounds result in a more widespread activation of the primary auditory and prefrontal associative areas in minimally conscious patients than in vegetative state patients (Laureys et al., 2004), more so when narratives were presented as compared to meaningless narratives played backward (Schiff et al., 2002; Coleman et al., 2007). More recently, and in tight relation with the attention-driven cBMIs discussed above, preserved exogenous attention functions and preserved underlying brain processes have been described in these patients, in association with a marked deficit in endogenous attention processes (Chennu et al., 2013). From a therapeutical perspective, deep brain thalamic stimulation has been described to improve the condition of minimally conscious patients (Laureys et al., 2007). Invasive cBMIs are also potentially interesting in this respect. In a first step, cBMIs can serve to assess and quantify the information content of the baseline or stimulus-induced cortical activity of these patients, and possibly serve to interpret part of their phenomenological experience (pain, surprise, attention, etc.). In a second step, cBMIs associated with focal stimulation approaches such as electric or optogenetic stimulations can help increase the information content of specific cortical regions. As soon as consciousness is high enough for the subject to express a preference (e.g., hearing the name of her loved ones instead of the names of strangers), this activity can be used for feedback-cBMI designs that can further help reinforce the weak yet meaningful endogenous cortical activities of minimally conscious patients. While this can seem like science fiction, all the theoretical and experimental grounds are set to make this possible.

OPEN FIELD COGNITIVE BRAIN–MACHINE INTERFACES FOR ENHANCED COGNITION

In addition to rehabilitation, there is a growing social pressure for healthy individuals to increase their cognitive performance or preserve it from aging. Several tools are already being used to this goal, ranging from cognitive training (through a growing range of enriched video game applications, see for example Cardoso-Leite and Bavelier, 2014), to cognitive pharmacological enhancers (i.e., drugs primarily developed to treat people with cognitive or motor function difficulties that are used by healthy subjects to improve memory, attention, concentration, and planning, see for example Greely et al., 2008), to off-the-laboratory brain stimulation (transcranial direct current stimulation – tDCS-kits are now commercially available). In this context, given its consequences on behavioral performance as described above, non-invasive neurofeedback applications can be considered as a safe improved alternative to cognitive training, as compared to cognitive enhancers or brain stimulation.

SHARED COGNITION

In a recent report, Pais-Vieira et al. (2013) describe an astounding brain-to-brain interface (BTBI). The cortical activity of an "encoder" rat, performing a learned sensorimotor task was injected, using intracortical microstimulations, into the matching cortical area of a "decoder" rat that was able to learn to use these alien activity patterns to perform the sensorimotor choices as the "encoder" rat. This opens amazing perspectives. From a rehabilitation point of view, one can think of injecting in target cortical regions of the brain of a patient suffering from a severe cognitive deficit the activity patterns recorded from healthy subjects in well-defined contexts. This is not very different from deep brain stimulation procedures now classically used in Parkinson Disease patients for example or from trans-cranial direct current stimulation applied in severe refractory depression, except that the stimulations would in this case correspond to the cognitive information content of healthy subjects.

CLOSING THE LOOP

Overall, this review brings together several studies that not only demonstrate the feasibility of decoding spatial attention in real

time using a diversity of experimental set-ups, but that also show that this real-time decoding can further be used for rehabilitation purposes. As a concluding note, we would like to highlight the fact that this field of cBMIs, and specifically attention-driven BMIs, is still young and that the reviewed studies mostly represent proofs of concept. We believe that the real-time access to spatial attention signals (and other cognitive information) also has the potential to bring about a novel understanding of the neural bases of these cognitive processes that cannot be accessed by more classical investigation methods. Taking this fundamental neuroscience perspective on cBMI research will also provide a better understanding of why and how neurofeedback improves cognition. These are the crucial challenges the field will need to face in the coming years.

ACKNOWLEDGMENTS

Elaine Astrand was funded by the Fondation pour la recherché médicale (FRM) and the Direction générale des armées (DGA). Suliann Ben Hamed was funded by the French Agence nationale de la recherche (Grant #ANR-05-JCJC-0230-01 and Grant # ANR-11-BSV4-0011), as well as by a CNRS bioinformatics grant.

REFERENCES

Albares, M., Criaud, M., Wardak, C., Nguyen, S. C. T., Ben Hamed, S., and Boulinguez, P. (2011). Attention to baseline: does orienting visuospatial attention really facilitate target detection? *J. Neurophysiol.* 106, 809–816. doi: 10.1152/jn.00206.2011

Andersson, P., Pluim, J. P. W., Siero, J. C. W., Klein, S., Viergever, M. A., and Ramsey, N. F. (2011). Real-time decoding of brain responses to visuospatial attention using 7T fMRI. *PLoS ONE* 6:e27638. doi: 10.1371/journal.pone.0027638

Andersson, P., Ramsey, N. F., Raemaekers, M., Viergever, M. A., and Pluim, J. P. W. (2012). Real-time decoding of the direction of covert visuospatial attention. *J. Neural Eng.* 9:045004. doi: 10.1088/1741-2560/9/4/045004

Andrews, D. J., and Schonfeld, W. H. (1992). Predictive factors for controlling seizures using a behavioural approach. *Seizure* 1, 111–116. doi: 10.1016/1059-1311(92)90008-O

Anton-Erxleben, K., and Carrasco, M. (2013). Attentional enhancement of spatial resolution: linking behavioural and neurophysiological evidence. *Nat. Rev. Neurosci.* 14, 188–200. doi: 10.1038/nrn3443

Anton-Erxleben, K., Stephan, V. M., and Treue, S. (2009). Attention reshapes center-surround receptive field structure in macaque cortical area MT. *Cereb. Cortex* 19, 2466–2478. doi: 10.1093/cercor/bhp002

Armstrong, K. M., Chang, M. H., and Moore, T. (2009). Selection and maintenance of spatial information by frontal eye field neurons. *J. Neurosci.* 29, 15621–15629. doi: 10.1523/JNEUROSCI.4465-09.2009

Arrington, C. M., Carr, T. H., Mayer, A. R., and Rao, S. M. (2000). Neural mechanisms of visual attention: object-based selection of a region in space. *J. Cogn. Neurosci.* 12, 106–117. doi: 10.1162/089892900563975

Astrand, E., Enel, P., Ibos, G., Dominey, P. F., Baraduc, P., and Ben Hamed, S. (2014a). Comparison of classifiers for decoding sensory and cognitive information from prefrontal neuronal populations. *PLoS ONE* 9:e86314. doi: 10.1371/journal.pone.0086314

Astrand, E., Wardak, C., and Ben Hamed, S. (2014b). "Real-time decoding of visual attention from monkey prefrontal population activities: towards context independent high performance cognitive brain computer interfaces," in *FENS Meeting*, Milan.

Astrand, E., Huguet, N., Wardak, C., and Ben Hamed, S. (2013). "Real-time decoding from prefrontal neuronal population activities: how flexible is the decoding?," in *Annual Meeting of the Sociétéfrançaise des neurosciences*, Lyon.

Barash, S., Bracewell, R. M., Fogassi, L., Gnadt, J. W., and Andersen, R. A. (1991). Saccade-related activity in the lateral intraparietal area. II. Spatial properties. *J. Neurophysiol.* 66, 1109–1124.

Bashinski, H. S., and Bacharach, V. R. (1980). Enhancement of perceptual sensitivity as the result of selectively attending to spatial locations. *Percept. Psychophys.* 28, 241–248. doi: 10.3758/BF03204380

Ben Hamed, S., Duhamel, J.-R., Bremmer, F., and Graf, W. (1997). Attentional modulation of visual receptive fields in the posterior parietal cortex of the behaving macaque. *Exp. Brain Res. Series* 25, 371–384.

Ben Hamed, S., Duhamel, J.-R., Bremmer, F., and Graf, W. (2001). Representation of the visual field in the lateral intraparietal area of macaque monkeys: a quantitative receptive field analysis. *Exp. Brain Res.* 140, 127–144. doi: 10.1007/s002210100785

Ben Hamed, S., Duhamel, J.-R., Bremmer, F., and Graf, W. (2002). Visual receptive field modulation in the lateral intraparietal area during attentive fixation and free gaze. *Cereb. Cortex* 12, 234–245. doi: 10.1093/cercor/12.3.234

Ben Hamed, S., Page, W., Duffy, C., and Pouget, A. (2003). MSTd neuronal basis functions for the population encoding of heading direction. *J. Neurophysiol.* 90, 549–558. doi: 10.1152/jn.00639.2002

Ben Hamed, S., Schieber, M. H., and Pouget, A. (2007). Decoding M1 neurons during multiple finger movements. *J. Neurophysiol.* 98, 327–333. doi: 10.1152/jn.00760.2006

Bisley, J. W., and Goldberg, M. E. (2003). Neuronal activity in the lateral intraparietal area and spatial attention. *Science* 299, 81–86. doi: 10.1126/science.1077395

Bray, S., Shimojo, S., and O'Doherty, J. P. (2007). Direct instrumental conditioning of neural activity using functional magnetic resonance imaging-derived reward feedback. *J. Neurosci.* 27, 7498–7507. doi: 10.1523/JNEUROSCI.2118-07.2007

Brefczynski, J. A., and DeYoe, E. A. (1999). A physiological correlate of the "spotlight" of visual attention. *Nat. Neurosci.* 2, 370–374. doi: 10.1038/7280

Bruce, C. J., and Goldberg, M. E. (1985). Primate frontal eye fields. I. Single neurons discharging before saccades. *J. Neurophysiol.* 53, 603–635.

Buschman, T. J., and Miller, E. K. (2007). Top-down versus bottom-up control of attention in the prefrontal and posterior parietal cortices. *Science* 315, 1860–1862. doi: 10.1126/science.1138071

Cardoso-Leite, P., and Bavelier, D. (2014). Video game play, attention, and learning: how to shape the development of attention and influence learning? *Curr. Opin. Neurol.* 27, 185–191. doi: 10.1097/WCO.0000000000000077

Caria, A., Veit, R., Sitaram, R., Lotze, M., Weiskopf, N., Grodd, W., et al. (2007). Regulation of anterior insular cortex activity using real-time fMRI. *Neuroimage* 35, 1238–1246. doi: 10.1016/j.neuroimage.2007.01.018

Carmena, J. M., Lebedev, M. A., Crist, R. E., O'Doherty, J. E., Santucci, D. M., Dimitrov, D. F., et al. (2003). Learning to control a brain–machine interface for reaching and grasping by primates. *PLoS Biol.* 1:E42. doi: 10.1371/journal.pbio.0000042

Carrasco, M., and Yeshurun, Y. (2009). Covert attention effects on spatial resolution. *Prog. Brain Res.* 176, 65–86. doi: 10.1016/S0079-6123(09)17605-7

Cerf, M., Thiruvengadam, N., Mormann, F., Kraskov, A., Quiroga, R. Q., Koch, C., et al. (2010). On-line, voluntary control of human temporal lobe neurons. *Nature* 467, 1104–1108. doi: 10.1038/nature09510

Chapin, J. K., Moxon, K. A., Markowitz, R. S., and Nicolelis, M. A. (1999). Real-time control of a robot arm using simultaneously recorded neurons in the motor cortex. *Nat. Neurosci.* 2, 664–670. doi: 10.1038/10223

Chennu, S., Finoia, P., Kamau, E., Monti, M. M., Allanson, J., Pickard, J. D., et al. (2013). Dissociable endogenous and exogenous attention in disorders of consciousness. *Neuroimage Clin.* 3, 450–461. doi: 10.1016/j.nicl.2013.10.008

Christ, S. E., and Abrams, R. A. (2006). Abrupt onsets cannot be ignored. *Psychon. Bull. Rev.* 13, 875–880. doi: 10.3758/BF03194012

Cohen, M. R., and Maunsell, J. H. R. (2009). Attention improves performance primarily by reducing interneuronal correlations. *Nat. Neurosci.* 12, 1594–1600. doi: 10.1038/nn.2439

Coleman, M. R., Rodd, J. M., Davis, M. H., Johnsrude, I. S., Menon, D. K., Pickard, J. D., et al. (2007). Do vegetative patients retain aspects of language comprehension? Evidence from fMRI. *Brain* 130, 2494–2507. doi: 10.1093/brain/awm170

Corbetta, M., Akbudak, E., Conturo, T. E., Snyder, A. Z., Ollinger, J. M., Drury, H. A., et al. (1998). A common network of functional areas for attention and eye movements. *Neuron* 21, 761–773. doi: 10.1016/S0896-6273(00)80593-0

Corbetta, M., Kincade, J. M., Ollinger, J. M., McAvoy, M. P., and Shulman, G. L. (2000). Voluntary orienting is dissociated from target detection in human posterior parietal cortex. *Nat. Neurosci.* 3, 292–297. doi: 10.1038/73009

Corbetta, M., and Shulman, G. L. (2002). Control of goal-directed and stimulus-driven attention in the brain. *Nat. Rev. Neurosci.* 3, 201–215. doi: 10.1038/nrn755

Cosman, J. D., and Vecera, S. P. (2009). Perceptual load modulates attentional capture by abrupt onsets. *Psychon. Bull. Rev.* 16, 404–410. doi: 10.3758/PBR.16.2.404

Dai, J., Brooks, D. I., and Sheinberg, D. L. (2014). Optogenetic and electrical microstimulation systematically bias visuospatial choice in primates. *Curr. Biol.* 24, 63–69. doi: 10.1016/j.cub.2013.11.011

deCharms, R. C., Christoff, K., Glover, G. H., Pauly, J. M., Whitfield, S., and Gabrieli, J. D. E. (2004). Learned regulation of spatially localized brain activation using real-time fMRI. *Neuroimage* 21, 436–443. doi: 10.1016/j.neuroimage.2003.08.041

deCharms, R. C., Maeda, F., Glover, G. H., Ludlow, D., Pauly, J. M., Soneji, D., et al. (2005). Control over brain activation and pain learned by using real-time functional MRI. *Proc. Natl. Acad. Sci. U.S.A.* 102, 18626–18631. doi: 10.1073/pnas.0505210102

FarbodKia, S., Åstrand, E., Ibos, G., and Ben Hamed, S. (2011). Readout of the intrinsic and extrinsic properties of a stimulus from un-experienced neuronal activities: towards cognitive neuroprostheses. *J. Physiol. Paris* 105, 115–122. doi: 10.1016/j.jphysparis.2011.07.015

Fetz, E. E. (1969). Operant conditioning of cortical unit activity. *Science* 163, 955–958. doi: 10.1126/science.163.3870.955

Fetz, E. E. (2007). Volitional control of neural activity: implications for brain–computer interfaces. *J. Physiol.* 579, 571–579. doi: 10.1113/jphysiol.2006.127142

Gobell, J., and Carrasco, M. (2005). Attention alters the appearance of spatial frequency and gap size. *Psychol. Sci.* 16, 644–651. doi: 10.1111/j.1467-9280.2005.01588.x

Gottlieb, J. P., Kusunoki, M., and Goldberg, M. E. (1998). The representation of visual salience in monkey parietal cortex. *Nature* 391, 481–484. doi: 10.1038/35135

Greely, H., Sahakian, B., Harris, J., Kessler, R. C., Gazzaniga, M., Campbell, P., et al. (2008). Towards responsible use of cognitive-enhancing drugs by the healthy. *Nature* 456, 702–705. doi: 10.1038/456702a

Grefkes, C., Nowak, D. A., Eickhoff, S. B., Dafotakis, M., Küst, J., Karbe, H., et al. (2008). Cortical connectivity after subcortical stroke assessed with functional magnetic resonance imaging. *Ann. Neurol.* 63, 236–246. doi: 10.1002/ana.21228

Gregoriou, G. G., Gotts, S. J., Zhou, H., and Desimone, R. (2009). High-frequency, long-range coupling between prefrontal and visual cortex during attention. *Science* 324, 1207–1210. doi: 10.1126/science.1171402

Gunduz, A., Brunner, P., Daitch, A., Leuthardt, E. C., Ritaccio, A. L., Pesaran, B., et al. (2012). Decoding covert spatial attention using electrocorticographic (ECoG) signals in humans. *Neuroimage* 60, 2285–2293. doi: 10.1016/j.neuroimage.2012.02.017

Haller, S., Birbaumer, N., and Veit, R. (2010). Real-time fMRI feedback training may improve chronic tinnitus. *Eur. Radiol.* 20, 696–703. doi: 10.1007/s00330-009-1595-z

Hansen, L. M., Trudeau, D. L., and Grace, D. L. (1996). Neurotherapy and drug therapy in combination for adult ADHD, personality disorder, and seizure disorder. *J. Neurother.* 2, 6–14. doi: 10.1300/J184v02n01_02

He, B. J., Snyder, A. Z., Vincent, J. L., Epstein, A., Shulman, G. L., and Corbetta, M. (2007). Breakdown of functional connectivity in frontoparietal networks underlies behavioral deficits in spatial neglect. *Neuron* 53, 905–918. doi: 10.1016/j.neuron.2007.02.013

Hochberg, L. R., Bacher, D., Jarosiewicz, B., Masse, N. Y., Simeral, J. D., Vogel, J., et al. (2012). Reach and grasp by people with tetraplegia using a neurally controlled robotic arm. *Nature* 485, 372–375. doi: 10.1038/nature11076

Hochberg, L. R., Serruya, M. D., Friehs, G. M., Mukand, J. A., Saleh, M., Caplan, A. H., et al. (2006). Neuronal ensemble control of prosthetic devices by a human with tetraplegia. *Nature* 442, 164–171. doi: 10.1038/nature04970

Hopfinger, J. B., Buonocore, M. H., and Mangun, G. R. (2000). The neural mechanisms of top-down attentional control. *Nat. Neurosci.* 3, 284–291. doi: 10.1038/72999

Hua, T., Bao, P., Huang, C.-B., Wang, Z., Xu, J., Zhou, Y., et al. (2010). Perceptual learning improves contrast sensitivity of V1 neurons in cats. *Curr. Biol.* 20, 887–894. doi: 10.1016/j.cub.2010.03.066

Ibos, G., Duhamel, J.-R., and Ben Hamed, S. (2009). The spatial and temporal deployment of voluntary attention across the visual field. *PLoS ONE* 4:e6716. doi: 10.1371/journal.pone.0006716

Ibos, G., Duhamel, J.-R., and Ben Hamed, S. (2013). A functional hierarchy within the parietofrontal network in stimulus selection and attention control. *J. Neurosci.* 33, 8359–8369. doi: 10.1523/JNEUROSCI.4058-12.2013

Ifft, P. J., Shokur, S., Li, Z., Lebedev, M. A., and Nicolelis, M. A. L. (2013). A brain–machine interface enables bimanual arm movements in monkeys. *Sci. Transl. Med.* 5:210ra154. doi: 10.1126/scitranslmed.3006159

Jerbi, K., Freyermuth, S., Minotti, L., Kahane, P., Berthoz, A., and Lachaux, J.-P. (2009). Watching brain TV and playing brain ball exploring novel BCI strategies using real-time analysis of human intracranial data. *Int. Rev. Neurobiol.* 86, 159–168. doi: 10.1016/S0074-7742(09)86012-1

Jonides, J. (1981). "Voluntary vs. automatic control over the mind's eye's movement," in *Attention and performance IX*, eds J. B. Long and A. D. Baddely (Hillsdale, NJ: Lawrence Erlbaum Associates), 187–203.

Jonides, J., and Irwing, D. E. (1981). Capturing attention. *Cognition* 145–150. doi: 10.1016/0010-0277(81)90038-X

Kaiser, D. A., and Othmer, S. (2000). Effect of neurofeedback on variables of attention in a large multi-center trial. *J. Neurother.* 4, 5–15. doi: 10.1300/J184v04n01_02

Kaplan, B. J. (1975). Biofeedback in epileptics: equivocal relationship of reinforced EEG frequency to seizure reduction. *Epilepsia* 16, 477–485. doi: 10.1111/j.1528-1157.1975.tb06076.x

Kastner, S., Pinsk, M. A., De Weerd, P., Desimone, R., and Ungerleider, L. G. (1999). Increased activity in human visual cortex during directed attention in the absence of visual stimulation. *Neuron* 22, 751–761. doi: 10.1016/S0896-6273(00)80734-5

Keiper, A. (2006). The age of neuroelectronics. *New Atlantis* 11, 4–41.

Kim, S.-P., Simeral, J. D., Hochberg, L. R., Donoghue, J. P., Friehs, G. M., and Black, M. J. (2011). Point- and-click cursor control with an intracortical neural interface system by humans with tetraplegia. *IEEE Trans. Neural Syst. Rehabil. Eng.* 19, 193–203. doi: 10.1109/TNSRE.2011.2107750

Kincade, J. M., Abrams, R. A., Astafiev, S. V., Shulman, G. L., and Corbetta, M. (2005). An event-related functional magnetic resonance imaging study of voluntary and stimulus-driven orienting of attention. *J. Neurosci.* 25, 4593–4604. doi: 10.1523/JNEUROSCI.0236-05.2005

Kobayashi, S., Schultz, W., and Sakagami, M. (2010). Operant conditioning of primate prefrontal neurons. *J. Neurophysiol.* 103, 1843–1855. doi: 10.1152/jn.00173.2009

Kübler, A., Mushahwar, V. K., Hochberg, L. R., and Donoghue, J. P. (2006). BCI meeting 2005 – workshop on clinical issues and applications. *IEEE Trans. Neural Syst. Rehabil. Eng.* 14, 131–134. doi: 10.1109/TNSRE.2006.875585

Kübler, A., Neumann, N., Wilhelm, B., Hinterberger, T., and Birbaumer, N. (2004). Predictability of brain – computer communication. *J. Psychophysiol.* 18, 121–129. doi: 10.1027/0269-8803.18.23.121

Kuhlman, W. N. (1978). EEG feedback training of epileptic patients: clinical and electroencephalographic analysis. *Electroencephalogr. Clin. Neurophysiol.* 45, 699–710. doi: 10.1016/0013-4694(78)90138-4

Kuhlman, W. N., and Allison, T. (1977). EEG feedback training in the treatment of epilepsy: some questions and some answers. *Pavlov. J. Biol. Sci.* 12, 112–122. doi: 10.1007/BF03004498

Kusunoki, M., Gottlieb, J., and Goldberg, M. E. (2000). The lateral intraparietal area as a salience map: the representation of abrupt onset, stimulus motion, and task relevance. *Vision Res.* 40, 1459–1468. doi: 10.1016/S0042-6989(99)00212-6

Lambert, A., Spencer, E., and Mohindra, N. (1987). Automaticity and the capture of attention by a peripheral display change. *Curr. Psychol.* 6, 136–147. doi: 10.1007/BF02686618

Lantz, D. L., and Sterman, M. B. (1988). Neuropsychological assessment of subjects with uncontrolled epilepsy: effects of EEG feedback training. *Epilepsia* 29, 163–171. doi: 10.1111/j.1528-1157.1988.tb04414.x

Laureys, S., Owen, A. M., and Schiff, N. D. (2004). Brain function in coma, vegetative state, and related disorders. *Lancet Neurol.* 3, 537–546. doi: 10.1016/S1474-4422(04)00852-X

Laureys, S., Perrin, F., and Brédart, S. (2007). Self-consciousness in non-communicative patients. *Conscious. Cogn.* 16, 722–741; discussion 742–745. doi: 10.1016/j.concog.2007.04.004

Law, C.-T., and Gold, J. I. (2008). Neural correlates of perceptual learning in a sensory-motor, but not a sensory, cortical area. *Nat. Neurosci.* 11, 505–513. doi: 10.1038/nn2070

Lebedev, M. A., Carmena, J. M., O'Doherty, J. E., Zacksenhouse, M., Henriquez, C. S., Principe, J. C., et al. (2005). Cortical ensemble adaptation to represent velocity of an artificial actuator controlled by a brain – machine interface. *J. Neurosci.* 25, 4681–4693. doi: 10.1523/JNEUROSCI.4088-04.2005

Lee, J., Williford, T., and Maunsell, J. H. R. (2007). Spatial attention and the latency of neuronal responses in macaque area V4. *J. Neurosci.* 27, 9632–9637. doi: 10.1523/JNEUROSCI.2734-07.2007

Li, X., Lu, Z.-L., Tjan, B. S., Dosher, B. A., and Chu, W. (2008). Blood oxygenation level-dependent contrast response functions identify mechanisms of covert attention in early visual areas. *Proc. Natl. Acad. Sci. U.S.A.* 105, 6202–6207. doi: 10.1073/pnas.0801390105

Lindén, M., Habib, T., and Radojevic, V. (1996). A controlled study of the effects of EEG biofeedback on cognition and behavior of children with attention deficit disorder and learning disabilities. *Biofeedback Self Regul.* 21, 35–49. doi: 10.1007/BF02214148

Lubar, J. F. (1991). Discourse on the development of EEG diagnostics and biofeedback for attention-deficit/hyperactivity disorders. *Biofeedback Self Regul.* 16, 201–225. doi: 10.1007/BF01000016

Lubar, J. F., and Shouse, M. N. (1976). EEG and behavioral changes in a hyperkinetic child concurrent with training of the sensorimotor rhythm (SMR): a preliminary report. *Biofeedback Self Regul.* 1, 293–306. doi: 10.1007/BF01001170

Lubar, J. F., Swartwood, M. O., Swartwood, J. N., and O'Donnell, P. H. (1995). Evaluation of the effectiveness of EEG neurofeedback training for ADHD in a clinical setting as measured by changes in T.O.V.A. scores, behavioral ratings, and WISC-R performance. *Biofeedback Self Regul.* 20, 83–99. doi: 10.1007/BF01712768

Macaluso, E., Frith, C. D., and Driver, J. (2002). Supramodal effects of covert spatial orienting triggered by visual or tactile events. *J. Cogn. Neurosci.* 14, 389–401. doi: 10.1162/089892902317361912

McAdams, C. J., and Maunsell, J. H. (1999). Effects of attention on the reliability of individual neurons in monkey visual cortex. *Neuron* 23, 765–773. doi: 10.1016/S0896-6273(01)80034-9

Morioka, H., Kanemura, A., Morimoto, S., Yoshioka, T., Oba, S., Kawanabe, M., et al. (2014). Decoding spatial attention by using cortical currents estimated from electroencephalography with near-infrared spectroscopy prior information. *Neuroimage* 90, 128–139. doi: 10.1016/j.neuroimage.2013.12.035

Müller, H. J., and Rabbitt, P. M. (1989). Reflexive and voluntary orienting of visual attention: time course of activation and resistance to interruption. *J. Exp. Psychol. Hum. Percept. Perform.* 15, 315–330. doi: 10.1037/0096-1523.15.2.315

Murase, N., Duque, J., Mazzocchio, R., and Cohen, L. G. (2004). Influence of interhemispheric interactions on motor function in chronic stroke. *Ann. Neurol.* 55, 400–409. doi: 10.1002/ana.10848

Musallam, S., Corneil, B. D., Greger, B., Scherberger, H., and Andersen, R. A. (2004). Cognitive control signals for neural prosthetics. *Science* 305, 258–262. doi: 10.1126/science.1097938

Neo, G., and Chua, F. K. (2006). Capturing focused attention. *Percept. Psychophys.* 68, 1286–1296. doi: 10.3758/BF03193728

Nudo, R. J. (2006). Mechanisms for recovery of motor function following cortical damage. *Curr. Opin. Neurobiol.* 16, 638–644. doi: 10.1016/j.conb.2006.10.004

Pais-Vieira, M., Lebedev, M., Kunicki, C., Wang, J., and Nicolelis, M. A. L. (2013). A brain-to-brain interface for real-time sharing of sensorimotor information. *Sci. Rep.* 3:1319. doi: 10.1038/srep01319

Parker, I. (2003). Reading minds. *The New Yorker*, 52–63.

Plotkin, A., Sela, L., Weissbrod, A., Kahana, R., Haviv, L., Yeshurun, Y., et al. (2010). Sniffing enables communication and environmental control for the severely disabled. *Proc. Natl. Acad. Sci. U.S.A.* 107, 14413–14418. doi: 10.1073/pnas.1006746107

Posner, M. I., Snyder, C. R., and Davidson, B. J. (1980). Attention and the detection of signals. *J. Exp. Psychol.* 109, 160–174. doi: 10.1037/0096-3445.109.2.160

Prinzmetal, W., McCool, C., and Park, S. (2005). Attention: reaction time and accuracy reveal different mechanisms. *J. Exp. Psychol. Gen.* 134, 73–92. doi: 10.1037/0096-3445.134.1.73

Rossiter, D. T. R., and La Vaque, T. J. (1995). A comparison of EEG biofeedback and psychostimulants in treating attention deficit/hyperactivity disorders. *J. Neurother.* 1, 48–59. doi: 10.1300/J184v01n01_07

Rota, G., Sitaram, R., Veit, R., Erb, M., Weiskopf, N., Dogil, G., et al. (2009). Self-regulation of regional cortical activity using real-time fMRI: the right inferior frontal gyrus and linguistic processing. *Hum. Brain Mapp.* 30, 1605–1614. doi: 10.1002/hbm.20621

Rotermund, D., Ernst, U., Mandon, S., Taylor, K., Smiyukha, Y., Kreiter, A., et al. (2013). Toward high performance, weakly invasive brain computer interfaces using selective visual attention. *J. Neurosci.* 33, 6001–6011. doi: 10.1523/JNEUROSCI.4225-12.2013

Santhanam, G., Ryu, S. I., Yu, B. M., Afshar, A., and Shenoy, K. V. (2006). A high-performance brain – computer interface. *Nature* 442, 195–198. doi: 10.1038/nature04968

Schafer, R. J., and Moore, T. (2011). Selective attention from voluntary control of neurons in prefrontal cortex. *Science* 332, 1568–1571. doi: 10.1126/science.1199892

Scharnowski, F., Hutton, C., Josephs, O., Weiskopf, N., and Rees, G. (2012). Improving visual perception through neurofeedback. *J. Neurosci.* 32, 17830–17841. doi: 10.1523/JNEUROSCI.6334-11.2012

Scharnowski, F., Rosa, M. J., Golestani, N., Hutton, C., Josephs, O., Weiskopf, N., et al. (2014). Connectivity changes underlying neurofeedback training of visual cortex activity. *PLoS ONE* 9:e91090. doi: 10.1371/journal.pone.0091090

Schiff, N. D., Plum, F., and Rezai, A. R. (2002). Developing prosthetics to treat cognitive disabilities resulting from acquired brain injuries. *Neurol. Res.* 24, 116–124. doi: 10.1179/016164102101199576

Schiff, N. D., Rodriguez-Moreno, D., Kamal, A., Kim, K. H. S., Giacino, J. T., Plum, F., et al. (2005). fMRI reveals large-scale network activation in minimally conscious patients. *Neurology* 64, 514–523. doi: 10.1212/01.WNL.0000150883.10285.44

Schoups, A., Vogels, R., Qian, N., and Orban, G. (2001). Practising orientation identification improves orientation coding in V1 neurons. *Nature* 412, 549–553. doi: 10.1038/35087601

Schreij, D., Owens, C., and Theeuwes, J. (2008). Abrupt onsets capture attention independent of top-down control settings. *Percept. Psychophys.* 70, 208–218. doi: 10.3758/PP.70.2.208

Seifert, A. R., and Lubar, J. F. (1975). Reduction of epileptic seizures through EEG biofeedback training. *Biol. Psychol.* 3, 157–184. doi: 10.1016/0301-0511(75)90033-2

Serruya, M. D., Hatsopoulos, N. G., Paninski, L., Fellows, M. R., and Donoghue, J. P. (2002). Instant neural control of a movement signal. *Nature* 416, 141–142. doi: 10.1038/416141a

Shanechi, M. M., Hu, R. C., and Williams, Z. M. (2014). A cortical–spinal prosthesis for targeted limb movement in paralysed primate avatars. *Nat. Commun.* 5:3237. doi: 10.1038/ncomms4237

Shibata, K., Watanabe, T., Sasaki, Y., and Kawato, M. (2011). Perceptual learning incepted by decoded fMRI neurofeedback without stimulus presentation. *Science* 334, 1413–1415. doi: 10.1126/science.1212003

Shulman, G. L., Ollinger, J. M., Akbudak, E., Conturo, T. E., Snyder, A. Z., Petersen, S. E., et al. (1999). Areas involved in encoding and applying directional expectations to moving objects. *J. Neurosci.* 19, 9480–9496.

Squire, L. R., and Zola-Morgan, S. (1991). The medial temporal lobe memory system. *Science* 253, 1380–1386. doi: 10.1126/science.1896849

Sterman, M. B., and Friar, L. (1972). Suppression of seizures in an epileptic following sensorimotor EEG feedback training. *Electroencephalogr. Clin. Neurophysiol.* 33, 89–95. doi: 10.1016/0013-4694(72)90028-4

Sterman, M. B., and Macdonald, L. R. (1978). Effects of central cortical EEG feedback training on incidence of poorly controlled seizures. *Epilepsia* 19, 207–222. doi: 10.1111/j.1528-1157.1978.tb04483.x

Sterman, M. B., Macdonald, L. R., and Stone, R. K. (1974). Biofeedback training of the sensorimotor electroencephalogram rhythm in man: effects on epilepsy. *Epilepsia* 15, 395–416. doi: 10.1111/j.1528-1157.1974.tb04016.x

Sterman, M. B., Wyrwicka, W., and Roth, S. (1969). Electrophysiological correlates and neural substrates of alimentary behavior in the cat. *Ann. N. Y. Acad. Sci.* 157, 723–739. doi: 10.1111/j.1749-6632.1969.tb12916.x

Subramanian, L., Hindle, J. V., Johnston, S., Roberts, M. V., Husain, M., Goebel, R., et al. (2011). Real-time functional magnetic resonance imaging neurofeedback for treatment of Parkinson's disease. *J. Neurosci.* 31, 16309–16317. doi: 10.1523/JNEUROSCI.3498-11.2011

Suminski, A. J., Tkach, D. C., Fagg, A. H., and Hatsopoulos, N. G. (2010). Incorporating feedback from multiple sensory modalities enhances brain–machine interface control. *J. Neurosci.* 30, 16777–16787. doi: 10.1523/JNEUROSCI.3967-10.2010

Suzuki, M., and Gottlieb, J. (2013). Distinct neural mechanisms of distractor suppression in the frontal and parietal lobe. *Nat. Neurosci.* 16, 98–104. doi: 10.1038/nn.3282

Taylor, D. M., Tillery, S. I. H., and Schwartz, A. B. (2002). Direct cortical control of 3D neuroprosthetic devices. *Science* 296, 1829–1832. doi: 10.1126/science.1070291

Thompson, L., and Thompson, M. (1998). Neurofeedback combined with training in metacognitive strategies: effectiveness in students with ADD. *Appl. Psychophysiol. Biofeedback* 23, 243–263. doi: 10.1023/A:1022213731956

Tillery, S. I. H., Taylor, D. M., and Schwartz, A. B. (2003). "The general utility of a neuroprosthetic device under direct cortical control," in *Proceedings of the 25th Annual International Conference of the IEEE Engineering in Medicine and Biology Society*, Vol. 3, Cancun, 2043–2046.

Treder, M. S., Bahramisharif, A., Schmidt, N. M., van Gerven, M. A., and Blankertz, B. (2011). Brain – computer interfacing using modulations of alpha activity induced by covert shifts of attention. *J. Neuroeng. Rehabil.* 8:24. doi: 10.1186/1743-0003-8-24

van Gerven, M., and Jensen, O. (2009). Attention modulations of posterior alpha as a control signal for two-dimensional brain – computer interfaces. *J. Neurosci. Methods* 179, 78–84. doi: 10.1016/j.jneumeth.2009.01.016

Velliste, M., Perel, S., Spalding, M. C., Whitford, A. S., and Schwartz, A. B. (2008). Cortical control of a prosthetic arm for self-feeding. *Nature* 453, 1098–1101. doi: 10.1038/nature06996

Vossel, S., Thiel, C. M., and Fink, G. R. (2006). Cue validity modulates the neural correlates of covert endogenous orienting of attention in parietal and frontal cortex. *Neuroimage* 32, 1257–1264. doi: 10.1016/j.neuroimage.2006.05.019

Wang, L., Yu, C., Chen, H., Qin, W., He, Y., Fan, F., et al. (2010). Dynamic functional reorganization of the motor execution network after stroke. *Brain* 133, 1224–1238. doi: 10.1093/brain/awq043

Wardak, C., Denève, S., and Ben Hamed, S. (2011a). Focused visual attention distorts distance perception away from the attentional locus. *Neuropsychologia* 49, 535–545. doi: 10.1016/j.neuropsychologia.2010.12.008

Wardak, C., Olivier, E., and Duhamel, J.-R. (2011b). The relationship between spatial attention and saccades in the frontoparietal network of the monkey. *Eur. J. Neurosci.* 33, 1973–1981. doi: 10.1111/j.1460-9568.2011.07710.x

Wardak, C., Ibos, G., Duhamel, J.-R., and Olivier, E. (2006). Contribution of the monkey frontal eye field to covert visual attention. *J. Neurosci.* 26, 4228–4235. doi: 10.1523/JNEUROSCI.3336-05.2006

Wardak, C., Olivier, E., and Duhamel, J.-R. (2002). Saccadic target selection deficits after lateral intraparietal area inactivation in monkeys. *J. Neurosci.* 22, 9877–9884.

Wardak, C., Olivier, E., and Duhamel, J.-R. (2004). A deficit in covert attention after parietal cortex inactivation in the monkey. *Neuron* 42, 501–508. doi: 10.1016/S0896-6273(04)00185-0

Weiskopf, N., Veit, R., Erb, M., Mathiak, K., Grodd, W., Goebel, R., et al. (2003). Physiological self-regulation of regional brain activity using real-time functional magnetic resonance imaging (fMRI): methodology and exemplary data. *Neuroimage* 19, 577–586. doi: 10.1016/S1053-8119(03)00145-9

Wyrwicka, W., and Sterman, M. B. (1968). Instrumental conditioning of sensorimotor cortex EEG spindles in the waking cat. *Physiol. Behav.* 3, 703–707. doi: 10.1016/0031-9384(68)90139-X

Yang, T., and Maunsell, J. H. R. (2004). The effect of perceptual learning on neuronal responses in monkey visual area V4. *J. Neurosci.* 24, 1617–1626. doi: 10.1523/JNEUROSCI.4442-03.2004

Yantis, S., and Jonides, J. (1990). Abrupt visual onsets and selective attention: voluntary versus automatic allocation. *J. Exp. Psychol. Hum. Percept. Perform.* 16, 121–134. doi: 10.1037/0096-1523.16.1.121

Yeshurun, Y., and Carrasco, M. (1998). Attention improves or impairs visual performance by enhancing spatial resolution. *Nature* 396, 72–75. doi: 10.1038/23936

Zénon, A., Ben Hamed, S., Duhamel, J.-R., and Olivier, E. (2008). Spatial and temporal dynamics of attentional guidance during inefficient visual search. *PLoS ONE* 3:e2219. doi: 10.1371/journal.pone.0002219

Zénon, A., Ben Hamed, S., Duhamel, J.-R., and Olivier, E. (2009). Attentional guidance relies on a winner-take-all mechanism. *Vision Res.* 49, 1522–1531. doi: 10.1016/j.visres.2009.03.010

Zhang, Y., Meyers, E. M., Bichot, N. P., Serre, T., Poggio, T. A., and Desimone, R. (2011). Object decoding with attention in inferior temporal cortex. *Proc. Natl. Acad. Sci. U.S.A.* 108, 8850–8855. doi: 10.1073/pnas.1100999108

Conflict of Interest Statement: The authors declare that the research was conducted in the absence of any commercial or financial relationships that could be construed as a potential conflict of interest.

Received: 28 May 2014; accepted: 23 July 2014; published online: 12 August 2014.
Citation: Astrand E, Wardak C and Ben Hamed S (2014) Selective visual attention to drive cognitive brain–machine interfaces: from concepts to neurofeedback and rehabilitation applications. Front. Syst. Neurosci. ***8****:144. doi: 10.3389/fnsys.2014.00144*
This article was submitted to the journal Frontiers in Systems Neuroscience.

frontiers in Neuroscience

REVIEW
published: 03 August 2016
doi: 10.3389/fnins.2016.00352

Neurofeedback Therapy for Enhancing Visual Attention: State-of-the-Art and Challenges

Mehdi Ordikhani-Seyedlar[1]*, *Mikhail A. Lebedev*[2,3], *Helge B. D. Sorensen*[1] and *Sadasivan Puthusserypady*[1]

[1] Division of Biomedical Engineering, Department of Electrical Engineering, Technical University of Denmark, Lyngby, Denmark, [2] Department of Neurobiology, Duke University, Durham, NC, USA, [3] Center for Neuroengineering, Duke University, Durham, NC, USA

We have witnessed a rapid development of brain-computer interfaces (BCIs) linking the brain to external devices. BCIs can be utilized to treat neurological conditions and even to augment brain functions. BCIs offer a promising treatment for mental disorders, including disorders of attention. Here we review the current state of the art and challenges of attention-based BCIs, with a focus on visual attention. Attention-based BCIs utilize electroencephalograms (EEGs) or other recording techniques to generate neurofeedback, which patients use to improve their attention, a complex cognitive function. Although progress has been made in the studies of neural mechanisms of attention, extraction of attention-related neural signals needed for BCI operations is a difficult problem. To attain good BCI performance, it is important to select the features of neural activity that represent attentional signals. BCI decoding of attention-related activity may be hindered by the presence of different neural signals. Therefore, BCI accuracy can be improved by signal processing algorithms that dissociate signals of interest from irrelevant activities. Notwithstanding recent progress, optimal processing of attentional neural signals remains a fundamental challenge for the development of efficient therapies for disorders of attention.

Keywords: visual attention, electroencephalography, brain-computer interface, feature extraction

OPEN ACCESS

Edited by:
Stefano Ferraina,
Sapienza University of Rome, Italy

Reviewed by:
Olivia Carter,
University of Melbourne, Australia
Tomasz Maciej Rutkowski,
University of Tokyo, Japan

***Correspondence:**
Mehdi Ordikhani-Seyedlar
mehdi.ordikhani@gmail.com

Specialty section:
This article was submitted to Neural Technology, a section of the journal Frontiers in Neuroscience

Received: *19 April 2016*
Accepted: *12 July 2016*
Published: *03 August 2016*

Citation:
Ordikhani-Seyedlar M, Lebedev MA, Sorensen HBD and Puthusserypady S (2016) Neurofeedback Therapy for Enhancing Visual Attention: State-of-the-Art and Challenges. Front. Neurosci. 10:352. doi: 10.3389/fnins.2016.00352

INTRODUCTION

The visual system in both human and non-human organisms transforms complex input information into robust neural representation of the visual world. Because the amount of information can only decrease during stochastic neural processing, it is crucial for the visual system to selectively process behaviorally relevant information (Sprague et al., 2015). For instance, when a driver approaches a busy intersection it is important to detect and respond to the relevant traffic light rather than any light source in the visual scene. Attention is the ability to block the irrelevant information to the current task and to enhance the processing of the important information. This key neural function can deteriorate due to some disorders. Patients with disorders of attention are unable to allocate their focus of attention continuously to one task or easily get distracted by irrelevant information. One of the most common disorders of attention, attention deficit hyperactivity disorder (ADHD), is a mental condition characterized by inattention, hyperactivity and impulsivity. ADHD symptoms are dominant in childhood, and extend to adulthood in 15–40%

of cases (Biederman et al., 2000; Faraone et al., 2006). ADHD impairs performance in academic, occupational and social tasks (Fleming and McMahon, 2012). According to a meta-regression analysis of 102 studies, ADHD has 5% prevalence worldwide (Polanczyk and Rohde, 2007; Skounti et al., 2007; Millichap, 2008). Treatment strategies have been mostly pharmacological, such as prescription of psychostimulants. However, long-term treatment with pharmacological agents is hindered by side-effects (Conners et al., 2001; Greenhill et al., 2001). Children develop anxiety symptoms after being treated with psychostimulants for 6 months and longer (Vance et al., 1999). There is also a considerable risk of drug misuse and abuse (Kollins, 2008; Steiner et al., 2014a). Psychological therapy, an alternative approach, relieves ADHD symptoms in 30% of cases (Zarin et al., 1998). Overall, currently available therapies for ADHD are only partially effective.

Here we review a novel strategy for enhancing the attention capability in patients with disorders of attention. This strategy is based on brain-computer interface (BCI) approach (Arns et al., 2009; Lim et al., 2010, 2012). BCIs establish uni- or bidirectional communication between the brain and external devices (Wolpaw et al., 2000; Donoghue et al., 2004; Lebedev and Nicolelis, 2006; Nicolelis and Lebedev, 2009; Lebedev, 2014; Schwarz et al., 2014). BCIs decode neural signals using mathematical algorithms. Such decoding often utilizes templates of neural patterns defined based on prior knowledge of the characteristics of different neural states. A computer algorithm then compares neural activities with the set of templates to find the best match and determine the current neural state. Additionally, the algorithm can evaluate how well the brain signals match certain requirements, and generate a feedback based on the difference. Such feedback can be used to improve neural function in patients: patients observe their own brain activity in real time, and learn to self-regulate this activity in order to bring it to normal state. This paradigm is called "*neurofeedback*" and the corresponding therapeutic approach is called "*neurofeedback therapy*." BCIs for humans most commonly utilize electroencephalographic (EEG) recordings (Kus et al., 2013; Tonin et al., 2013; Bamdadian et al., 2014; De Vos et al., 2014; Kashihara, 2014; Yang et al., 2014). Additionally, BCIs can employ magnetoencephalography (MEG) (Mellinger et al., 2007; Bianchi et al., 2010; Ahn et al., 2013), near infrared spectroscopy (NIRS) (Coyle et al., 2004; Sitaram et al., 2007; Power et al., 2012; Waldert et al., 2012; Khan et al., 2014), functional magnetic resonance imaging (fMRI) (Logothetis, 2003; deCharms et al., 2005; Ruiz et al., 2013; Sato et al., 2013), electrocortigraphy (ECoG) (Freeman et al., 2003; Leuthardt et al., 2004, 2009; Schalk, 2010), and multi-electrode intracranial implants (Nicolelis and Ribeiro, 2002; Carmena et al., 2003; Nicolelis et al., 2003; Lebedev et al., 2005, 2011; Zacksenhouse et al., 2007; Peikon et al., 2009; Ifft et al., 2013; see **Figure 1** for comparison).

Neurofeedback therapy is applicable to a number of neurological disorders of attention (Lofthouse et al., 2012b; Hillard et al., 2013; Gevensleben et al., 2014; Steiner et al., 2014c; Zandi Mehran et al., 2014). Attention-based neurofeedback paradigms for ADHDs are usually based on visual attention (Arns et al., 2014). As to recording methods, some (EEG, NIRS, ECoG) have been already shown effective for attention control and for treatment of ADHDs, whereas the applicability of others, such as MEG and fMRI, is being researched (Ahn et al., 2013; Sulzer et al., 2013; Sokunbi et al., 2014; Stoeckel et al., 2014; Bruhl, 2015; Okazaki et al., 2015). Implementing an attention-based BCI is a challenging task because the neural representation of attention is highly complex (Ming et al., 2009; Rossini et al., 2012). A good understanding of neurophysiology of attention is required to extract attentional signals from neural recordings and dissociate them from the other ongoing activities in the brain (Sanei and Chambers, 2008). Notwithstanding these difficulties, visual-attention based BCI systems have been already developed and applied to ADHD (Christiansen et al., 2014; Heinrich et al., 2014; Holtmann et al., 2014a,b; Micoulaud-Franchi et al., 2014; Steiner et al., 2014b). In this article, we cover the current state of the art and future challenges in this research.

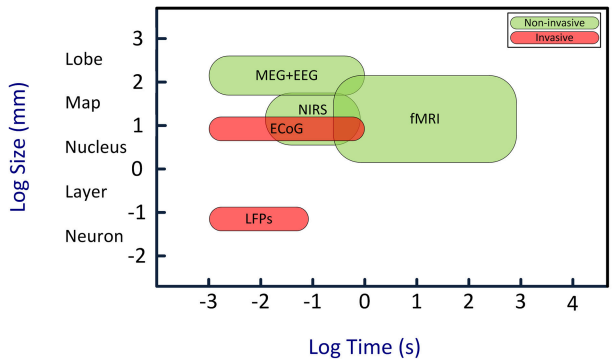

FIGURE 1 | Temporal and spatial resolution of different BCI techniques. Although EEG has a relatively poor spatial resolution, its high temporal resolution is an adequate characteristic for real-time BCIs. Abbreviations: EEG, electroencephalography; MEG, magneto-encephalogram; NIRS, near-infrared spectroscopy; fMRI, functional magnetic resonance imaging; ECoG, electro-corticogram; LFPs, local field potentials. Image is inspired from Van Gerven et al. (2009).

DECODING OF VISUAL ATTENTION FROM NEURAL SIGNALS

Neural Mechanisms of Visual Attention

In everyday life, we constantly deal with multiple sensory streams from our complex and dynamic environment. The brain starts the processing of this incoming information by filtering out irrelevant signals, which are not consciously experienced because of the filtering. Only a tiny amount of the incoming information enters the higher-order processing levels and becomes available to consciousness (Posner, 1994, 2012). Selective attention is a key function that enables the brain to effectively use its limited information processing capability when confronted with an immense number of inputs from all sensory modalities. High-level cortical areas, particularly the areas of the frontal cortex, play a key role in attentional control. It has been long known that damage to prefrontal cortex (PFC) causes mental deficits which are consistent with a loss of attentional control

(Ferrier, 1876). Neurophysiological and functional neuroimaging studies by Posner's group (Fan et al., 2005; Posner and Rothbart, 2007; Petersen and Posner, 2012) have provided a wealth of information on cortical circuitry for attentional control. The main conclusion of these studies is that attention is controlled by a network of interconnected areas that also involved in oculomotor control. These areas include the frontal eye field (FEF), parietal areas and subcortical structures, importantly superior colliculus. This attentional selection network works together with yet another, overlapping network of areas that sustains the focus of attention, called *sustained attention*. The latter system maintains the focus of attention on the selected stimulus. It is composed of the parietal cortex, right frontal cortex and locus coeruleus (Corbetta et al., 2008). Volumetric analysis in ADHD subjects showed that they have smaller frontal cortex compared to healthy subjects (He et al., 2015). This finding explains the deficits in both selective and sustained attention (Pritchard et al., 2008; Avisar and Shalev, 2011; Gomes et al., 2012; Wang et al., 2013). Notably, attention-based BCIs usually require both selecting a visual target and focusing on it (i.e., selective attention) and mental endurance training (i.e., sustained attention).

Selective attention is not a unitary process; it is driven by distinct functional sub-processes associated with different selection criteria (Brosch et al., 2011). Two major sub-processes are: stimulus-driven (exogenous) attention and observer-dependent (endogenous) attention. *Exogenous attention* is driven by intrinsic low-level features of sensory inputs (Egeth and Yantis, 1997; Wolfe and Horowitz, 2004). Low-level properties include such features as stimulus intensity, color and contrast. They all trigger involuntary responses. *Endogenous attention* refers to selection of a target based on an internal state and conscious expectation of a specific object or location (Posner et al., 1980; Desimone and Duncan, 1995). Endogenous selection is performed based on the current aim of the observer. In the classical Posner experiment that dissociated endogenous and exogenous effects, participants were instructed to press a button in response to a visual stimulus that appeared either to the left or right of a central fixation point (Posner, 1980). They were asked to keep their eyes fixed at the center of the screen throughout the task and covertly (i.e., without looking at the target) attend to the peripheral location. To guide this covert attention, a symbolic cue was presented at the center of the screen, which instructed the location to attend. This cue preceded the stimulus onset, and correctly specified the upcoming stimulus location in 80% of the trials. In the remaining 20% of trials, the target appeared at a location that disagreed with the cue. This study showed that the reaction time was significantly shorter when the stimulus was presented at the attended location than when it appeared in the opposite location and there was a misalignment between the endogenous and exogenous attention. Busse et al. investigated neurophysiological mechanisms underlying these two types of attention (Busse et al., 2008). They recorded from single neurons in macaque middle temporal area while monkeys' endogenous and/or exogenous attention was manipulated by the task events. They used a double-cueing paradigm where the first cue instructed the monkey to attend (endogenous attention) to one of three moving random dot patterns (RDPs) until a second cue. The second cue was unpredictable, and therefore captured exogenous attention. It signaled to either shift or maintain the current focus of attention. Findings of this experiment showed that the neural activity was enhanced when attention was endogenously shifted to the first cue. Then, attention was exogenously attracted to the second cue, which was manifested by a transient interruption of neural activity for approximately 70 ms, after which the endogenous attention restored neural representation of the previously relevant stimulus. These results showed that the interruption of endogenous attention by exogenous attention is not a simple refocusing to the new stimulus. Rather, there are separate ongoing processes with distinct neural correlates for endogenous and exogenous effects, as well as an interaction between these mechanisms.

Both endogenous and exogenous attention can be maintained with and without eye movements (i.e., overtly or covertly, respectively). The premotor theory of attention (Rizzolatti et al., 1987) suggests that essentially the same neural circuits in the frontal and parietal areas control the orientation of both overt and covert attention. For overt shifts of attention, eye movements are prepared and executed, whereas for covert shifts they are prepared but not executed. The premotor theory of attention is supported by the fMRI studies showing an overlap between the frontal and parietal regions activated for covert and overt attentional tasks (de Haan et al., 2008). Additionally, neurons in the intermediate layer of superior colliculus which has been long known for their involvement in saccades, are also engaged in the covert attentional shifts (Ignashchenkova et al., 2004). Golla et al. reported a clinical case of impaired overt attention in a cerebellar disorder, and suggested that the cerebellum plays a role in spatial attention (Golla et al., 2005).

Lebedev, Wise and their colleagues compared neural representation of attention with the representation of other behavioral variables, such as spatial memory, target of movement and gaze angle, which often coincide with the orientation of attention, but still can be controlled independently by the brain. In one study (Lebedev and Wise, 2001), they compared neuronal activity in monkey's dorsal premotor cortex (PMd) that reflected the orientation of selective spatial attention with neuronal activities that represented motor preparation, gaze angle, and saccades. The monkeys' attention was attracted by a robot, to which they attended in order to know when to initiate a reaching movement. The target of movement varied. It was either the location of the feeder mounted on the robot or a location of a different feeder. This study showed that approximately 20% of PMd reflected the orientation of selective spatial attention, which could be disengaged from the other spatial variables. These attention-tuned PMd neurons could account for gaze-independent (covert) attentional effects in behaviors with stimulus-response incompatibility. In another study (Lebedev et al., 2004), Lebedev et al. tested the theory that the main function of prefrontal cortex (PF) is the maintenance of working memory. To investigate alternative possibilities, activity of PF neurons was recorded while the monkeys performed an oculomotor task that required remembering one location, but attending to a different location. The largest subpopulation of

PF neurons was linked to attention, not to working memory, which indicated that PF has a major contribution to selective spatial attention. Consistent with these findings, studies in human subjects demonstrated the crucial role of frontal cortex in ADHDs (Praamstra et al., 2005; Dirlikov et al., 2015). Dirlikov et al. (2015) used brain imaging technique to explore the cortical morphology in 93 children with ADHD. They found a reduction in cortical surface of PF and premotor cortex (Dirlikov et al., 2015). Several neuroimaging studies suggested that visual attention is controlled by a network of cortical areas interconnected with the FEF. Gray matter is substantially affected in ADHD in the structures of this network, including dorsal and ventral prefrontal cortices, dorsal anterior cingulate area and inferior parietal cortex (Valera et al., 2007; Szuromi et al., 2011). Jonkman and colleagues suggested that the frontal lobe performs early selective filtering, and disorders of this function cause ADHD (Jonkman et al., 2004). A recent resting-state EEG study also suggested that frontal cortex abnormalities are a reliable marker for ADHD (Keune et al., 2015).

Neural oscillations is another neural marker of attention. Oscillations represent synchronous activity of neuronal populations of different sizes, from local to very large. They can be detected in local field potentials (LFPs) recorded with invasive electrodes, or EEGs recorded non-invasively from the scalp (Kahana, 2006). Oscillations are conventionally classified into five frequency bands: δ (1–4 Hz), θ (4–8 Hz), α (8–12 Hz), β (12–30 Hz), and γ (30–80 Hz). Attentional effects have been reported for each of these bands. For instance, attending to a spatial location and anticipating a stimulus at that location is associated with α rhythm attenuation (Rohenkohl and Nobre, 2011). α oscillations are involved in attentional gating of information flow between brain regions (Fu et al., 2001; ter Huurne et al., 2013). To investigate the relationship between brain oscillations and ADHD, ter Huurne used a motion coherence detection task where subjects were instructed to direct attention to either left or right visual field. The attended stimulus was a random dot kinematogram, a field of chaotically moving dots. Subjects were instructed to respond after the dot pattern started to move coherently in the horizontal, but not vertical dimension in the attended hemifield. Dot movements in the unattended hemifield had to be ignored. In healthy subjects, lateralized and sustained α oscillations were detected in the visual cortex during the period when the subjects prepared to respond. In patients with ADHD, oscillations started, but they were not sustained and often stopped before the stimulus onset. Furthermore, lateralization of α oscillation was highly correlated with the degree of spatial attention in the healthy group, but not in the ADHD group (ter Huurne et al., 2013). In neurofeedback training experiments, children with ADHD were able to increase α-power following 18 training sessions (Escolano et al., 2014). Overall, these studies suggest that brain oscillations can be used to monitor neural regulation of attention and improve it using neurofeedback therapy.

BCIs for Visual Attention

Early attempts to treat disorders of attention using neurofeedback date back to the mid-eighties and nineties (Elbert et al., 1980; Lutzenberger et al., 1980; Wolpaw et al., 1991). Since then, considerable progress has been made in the development of computer algorithms for the decoding of attention-related neural signals. In a typical setting, subjects endeavor to keep their visual attention while playing a video game. Attention related brain signals are extracted from the neural recordings and fed back to the subjects using visual feedback. Successful performance is rewarded. Repeated training sessions with such a BCI system engage brain plasticity mechanisms, and eventually improve attention (Dobkin, 2007; Rossini et al., 2012).

Both invasive and non-invasive recordings have been used in BCIs. Invasive BCIs utilize electrodes that penetrate the brain (LFPs and single-unit recordings) or are placed on the brain surface (ECoG). These systems require an invasive surgical procedure to implant the electrodes. Non-invasive BCIs, on the other hand, do not require any surgery and can be safely and easily implemented. Non-invasive sensors are placed on the scalp (EEG, fNIRS), or in some implementations make no contact with the head (fMRI, MEG) (see **Table 1** for details). Additionally, *hybrid* or *multimodal* BCIs employ combinations of different recording methods in order to improve performance. Fazli et al. (2012) developed a multimodal BCI consisting of the combination of EEG and NIRS that improved the signal classification accuracy in 90% of participants. That multimodal BCI had higher sensitivity and specificity and were resistant to environmental noise. Such combined EEG-NIRS neurofeedback can be used by subjects who cannot operate a BCI solely by their EEG activity (Fazli et al., 2012).

The research on BCIs that improve attention has experienced a steady growth, especially BCIs for ADHD patients. Some of these results are controversial. A number of studies reported positive outcome of neurofeedback training (Leins et al., 2007; Gevensleben et al., 2009; Steiner et al., 2011; Wangler et al., 2011), whereas others questioned these findings. In the camp of neurofeedback advocates, Arns et al. (2009) analyzed literature on neurofeedback therapy for ADHD and concluded that this treatment was "efficient and specific" (Arns et al., 2009). Lofthouse et al. (2012a) called this therapy "probably efficacious" based on their analysis of research conducted from 1994 to 2010, where the majority of studies utilized θ/β ratio (see below) (Lofthouse et al., 2012a). However, Vollebregt et al. (2014a) came to a different conclusion in their systematic review of frequency-band based BCIs for ADHD. They concluded that there was no significant effect of treatment on any neurocognitive variables affected by ADHD (Vollebregt et al., 2014a). This negative result highlights the need for further research on EEG features that would better suit attention-based BCIs. Here we review these features and the ways they could be used to improve neurofeedback therapy for ADHD.

FEATURE EXTRACTION FOR VISUAL-ATTENTION BCIs

Feature extraction is a critical part of BCI implementation and design (Shahid and Prasad, 2011). During this processing stage, a specific characteristics are extracted from brain recordings, which are then decoded and converted into control commands or neurofeedback. Depending on the recording method, different

TABLE 1 | Comparison of different signal acquisition methods used for BCI application.

BCI method (measured signal type)	Advantages	Disadvantages
LFPs (Firing rate of bundles of neurons)	High SNR; low variability during the experiment; targeting the activity in specific brain areas; higher resolution of detecting temporal and spatial features in several parallel-activated brain regions.	Intracranial surgery; very susceptible to signal-loss in long-term implantation (Shain et al., 2003; Donoghue et al., 2004); requires precise source localization in order to implant the electrodes in the right location; less common in human studies.
ECoG (Electrical activity from brain surface)	Supports accurate BCI operation with little training (Leuthardt et al., 2004); higher spatial resolution and amplitude than EEG (Freeman et al., 2000; Leuthardt et al., 2009); far less EMG and EOG artifacts (Freeman et al., 2003; Ball et al., 2009); greater long-term functionality compared to LFPs (Margalit et al., 2003); more stable SNR compared to EEG (Schalk, 2010).	Intracranial surgery; Limited long-term functional stability and signal loss (Schalk and Leuthardt, 2011); very rare research application (Sutter and Tran, 1992).
EEG (Electrical activity from the scalp)	Superior temporal resolution (suitable for real-time experiments); ease of use (non-invasive) even by inexpert individuals; inexpensive (compared to other devices); least ethical concern and medical risks compared to other methods; portable.	Susceptible to noise (EMG, EOG and environmental); Low spatial resolution (harder to localize brain activities); requires a substantial degree of user training in BCI development.
fMRI [Blood oxygenation level dependent (BOLD)]	Superior spatial resolution (deCharms et al., 2005; Lee et al., 2009); signal detection from whole brain including the subcortical structures (Logothetis, 2003; Weiskopf et al., 2004).	Signal drift due to imperfection of magnetic gradient field (Lee et al., 2009); limited to BOLD-signal-based analysis (can be done in ERP experiments but not in frequency-range analysis); less suitable for real-time BCI due to low temporal resolution; strict physical restriction of subjects inside the scanner due to motion artifacts; requires expensive devices and expertise to operate the system.
NIRS (Measure of oxygenated hemoglobin)	Robust when dealing with noise (Coyle et al., 2004; Waldert et al., 2012); superior in detection of stimulation onsets and offsets (reducing the false positive commands) (Tomita et al., 2014); precise parameter setting to extract features is not needed to detect information on the brain (Kanoh et al., 2009).	Lower temporal resolution compared to EEG (Tomita et al., 2014).
MEG (Magnetic field)	Higher spatiotemporal resolution (Mellinger et al., 2007) than EEG; less training sessions than EEG; more robust in detectability of different frequency-band compared to EEG (Mellinger et al., 2007).	Expensive (at least 10 times more expensive than EEG cost) and non-portable; lower spatial resolution compared to fMRI; poorer localization for deeper brain structures compared to fMRI.

features can be used. For example, single-unit recording are usually converted into neuronal firing rates, and EEGs are converted either into the spectral power or parameters of event related potentials. The selection of features depends on the way the user communicates with the BCI system. In the BCI design called endogenous BCI, subjects self-generate neural patterns (Nicolas-Alonso and Gomez-Gil, 2012). Alternatively, in the BCI design called exogenous BCI, neural responses are evoked by an external stimulus, and subjects modulate these responses, usually by focusing attention on relevant stimuli. **Table 2** compares these two BCI types.

Endogenous BCI

Attention-Based BCIs That Utilize Neural Oscillations

Spectral analysis of EEGs recorded at different scalp locations is commonly used to extract features for endogenous BCIs. Here, time-dependent changes in the EEG spectra for different electrodes are detected using EEG time-frequency (TF) analysis. For example, TF analysis can detect the occurrence of brain oscillations that result from transient synchronization of neuronal discharges over a millisecond time scale (Sanei and Chambers, 2008). This method can be applied to measure EEG changes associated with attention, such as synchronization of specific EEG bands associated with attention to an object. Attention-related synchronization of neural activity can be detected using a variety of recording methods, including single-unit recordings from brain neurons. Fries et al recorded from individual neurons in cortical area V4 while macaque monkeys attended to behaviorally relevant stimuli and ignored distractors (Fries et al., 2001). The neurons increased their gamma-band synchrony while decreasing low-frequency (<17 Hz) synchrony when the monkeys attended. Several studies showed attention related effects in ECoGs. Rougeul-Buser and Buser recorded ECoGs in freely moving cats and observed that 10–14 Hz oscillation over sensorimotor cortex, called μ-rhythm or "expectancy rhythm," increased when an animal actively attended

TABLE 2 | Comparison of endogenous and exogenous BCIs and their corresponding protocols.

Category	Protocol	Advantages	Drawbacks
Endogenous BCI	- Source of the brain activity - Frequency bands	- Independent of any specific task - Useful for patients with sensory deficits - Perfect for freely moving operations (since subjects are not instructed to stare at specific stimulus)	- Requires several sessions of trainings - Some patients may not be able to communicate with BCI (BCI illiterate) - Low information transfer rate - Low signal-to-noise ratio - Low spatial resolution of EEG-based BCIs (harder for source localization analysis) - Requires many EEG electrodes
Exogenous BCI	- ERP - SSVEP	- Low training session - High information transfer rate (explained in the next section) - Feasible with a few EEG channels - Higher signal-to-noise ratio	- System failure if the subject is not attending to the stimuli - Fatigue in subjects (especially in SSVEP tasks due to constant flickering objects)

to a place where a mouse was expected to appear (Rougeul-Buser and Buser, 1997). The μ-rhythm epochs were often followed by a brief 20 Hz (β-range) ECoG burst. Thorpe et al reported topographical details of these ECoG patterns. Attention was associated with μ-rhythm increases over parietal regions, whereas, β-band activity increased in motor areas (Thorpe et al., 2012). Daitch et al. suggested that these oscillatory patterns serve to increase functional connectivity between the areas that process relevant information while suppressing unwanted cross-talk within the neural network areas that could be caused by irrelevant stimuli (Daitch et al., 2013).

EEG studies have shown that high-frequency oscillations (>30 Hz) are correlated with increased attention (Kaiser and Lutzenberger, 2005; Koelewijn et al., 2013; Musch et al., 2014). Similar results were obtained using microelectrode recordings in freely behaving monkeys (Fries et al., 2001). Attention-related oscillations can have the frequency higher than the typical γ -band range (30–80 Hz) (Crone et al., 2006). Ray et al. (2008) presented human subjects with a sequence of tactile and auditory stimuli separated by pseudo-random time intervals. The tactile stimuli were delivered using a tactile stimulating cylinder, which the subjects gripped with their hands. The auditory stimuli were delivered through a headset. The subjects were instructed to attend to one of the two modalities (auditory or tactile) and respond to the attended stimulus with a button press (Ray et al., 2008). The attended stimuli enhanced high γ activity (80–150 Hz) in the cortical areas that processed the corresponding modality: attention to auditory stimuli activated auditory cortex, and attention to somatosensory stimuli activated somatosensory cortex. Additionally, these high-gamma oscillations occurred in PFC irrespective of the attended modality. This result is consistent with PFC being involved in the global attentional system (Dirlikov et al., 2015; Keune et al., 2015) regardless of the modalities of input information. Another study reported that attention in humans was associated with high frequency oscillations of approximately 350 Hz that occurred in frontal and centro-parietal regions in response to somatosensory stimuli (Ozaki et al., 2006). Several hypotheses have been proposed to explain the role of high-frequency oscillations in attention. One hypothesis states that low-amplitude, ultra-high frequency activity is a background neural noise that enhances neural processing (Benzi et al., 1982). For example, adding a small amount of noise to a neural circuit makes its component fire more synchronous (Ward et al., 2006). Here, the performance is improved due to stochastic resonance (Benzi et al., 1982), where high-frequency noise lowers detection threshold for the relevant stimulus-. The stochastic resonance driven by γ waves can play a role in high cognitive functions (Ward et al., 2006). A similar resonance can be produced by injecting noise to the brain using electrical stimulation (Medina et al., 2012).

A number of BCIs for controlling attention have been developed based on EEG spectral bands. A recent study showed that healthy subjects can quickly learn to self-modulate their γ-oscillation in superior parietal cortex by alternating between the attentive and rest states (Grosse-Wentrup and Scholkopf, 2014). This BCI system correctly decoded brain state in 70.2% of cases. Several of studies on attention-based BCIs employed the ratio of power in specific spectral bands as the signal feature to be classified. This ratio was calculated as $\beta/(\alpha+\theta)$ in many reports (Nagendra et al., 2015). The higher the ratio, the higher is the level of attention. Other studies used θ/β ratio (Clarke et al., 2013; Dupuy et al., 2013; Heinrich et al., 2014; Vollebregt et al., 2014b) that decreased with enhanced attention. These ratios reflect the fact that θ and α rhythms are stronger in drowsiness and the inattentive states; whereas, β rhythm is stronger in attentive states. For example, spectral EEG composition prior to stimulus presentation is indicative of the level of visual attention (Busch et al., 2009). Several characteristics of EEG rhythms can be also used to assess the level of attention. Instantaneous phase of EEG oscillations is one such characteristic (Busch et al., 2009). In the experiments of Busch et al. (2009), subjects were instructed to detect a brief (6 ms) light flash presented either at an attended or unattended location. Hit and miss rates were found to be correlated with the phase of EEG oscillations at the time of stimulus presentation. Additionally, stimuli preceded by strong α activity were less likely to be detected, an observation reported in the previous literature (Ergenoglu et al., 2004; Babiloni et al., 2006; Thut et al., 2006; Hanslmayr et al., 2007). In the other

study on the relationship between EEG phase and detection of attended and unattended stimuli, Busch and VanRullen (Busch and VanRullen, 2010) analyzed the relationship between the pre-stimulus EEG pattern and the EEG response to the stimulus. They found that EEG responses were higher when EEG was at a certain phase the just prior to the stimulus onset and the EEG response was the lowest for the opposite EEG phase (Busch and VanRullen, 2010). The periodicity of EEG was 100–150 ms in these experiments. Several studies reported similar results (Makeig et al., 2002; Lakatos et al., 2008; Busch and VanRullen, 2010).

Exogenous BCI

Event-Related Potential (ERP) Paradigms

Event-relate potentials (ERPs) represent a compound response to a stimulus of large neuronal populations. An ERP consists of several voltage deflections that occur on a millisecond time scale. Specific ERP components have been linked to different neural origins (Cohen, 2013), including the components that are associated with attention. ERP is one of the most commonly used protocols for attention studies (Wu et al., 2009; Gherri and Eimer, 2011; Jones et al., 2013; Matheson et al., 2014; Zheng et al., 2014). ERPs recorded in primary sensory areas increase when the corresponding stimulus modality is attended to Harter et al. (1984). Selection of the appropriate ERP components and scalp locations to sample is essential to achieve good performance of an ERP-based BCI. The first ERP-based BCI was designed by Farwell and Donchin (1988). Subjects looked at a 6×6 matrix of alphanumeric characters. A single electrode was placed over the Pz (central-parietal) site. Subjects were instructed to attend to a specific character within the matrix while rows and columns periodically flashed. Attended stimuli evoked stronger ERPs and thus could be identified. Averaging over 30 trials was required to improve the signal-to-noise ratio and assure BCI accuracy.

For better design of ERP-based BCIs, it is important to take into consideration the detailed sequence of ERPs components. The first component is the C1-wave which is detected mostly by the posterior midline electrodes in the EEG. The onset of the C1-wave is typically 40–60 ms after the stimulus with the peak at 80–100 ms post-stimulus. C1 is generated in the primary visual cortex (Luck, 2014) and its polarity changes as a function of location of the stimulus in the visual field, i.e., whether the response comes from upper or lower bank of calcarine sulcus. This change in polarity has been identified as a unique feature for C1-wave compared to other components and has been used by many studies as a marker for V1 sources. However, later neuroimaging studies challenged this view. Ales et al. (2010) used fMRI retinotopic mapping to identify the location of V1, V2, and V3 overlaid on the high-resolution structural MRI (Ales et al., 2010). This technique allowed them to acquire a 3D shape of the upper and lower visual field projection in V1 and adjacent areas, V2 and V3. Contrary to previous studies, they found that sources in V1 do not fully conform to the sign reversal. Furthermore, V2 and V3 also showed a polarity change for upper and lower field stimuli. This suggested that the polarity inversion criterion was not a reliable method for source localization. Yet another study challenged this conclusion. Kelly et al. claimed that C1 does initiate from V1 (Kelly et al., 2013). It has been also reported that attention is not important to generate the C1 component (Martinez et al., 1999; Fu et al., 2010). According to Martinez et al., although primary visual cortex is involved in attention, it does not serve as the locus of initial sensory gain control for attended and unattended inputs. Kelly et al. (2008) disagreed with this and proposed that attentional selection occurs at the early visual processing stage reflected by C1 generation in V1 (Kelly et al., 2008). In that study, target brightness and location were adjusted for each participant in order to reduce inter-subjective variability of C1. After this correction, it became clear that C1 was enhanced due to spatial attention, which indicated that this early sensory component was adjusted before the visual information arrived in V1.

The second component is the P1-wave that starts 60–90 ms after the stimulus and peaks at 100–130 ms. It contains an early portion generated from middle occipital gyrus and a late-portion generated more ventrally, from fusiform gyrus (Di Russo et al., 2002). P1 is sensitive to the direction of spatial attention (Hillyard and Anllo-Vento, 1998). Luck and Hillyard (1995) studied attentional modulation of P1 using a stimulus display that consisted of 14 gray items and 2 colored items (Luck and Hillyard, 1995). Subjects were instructed to report presence or absence of specific colored-item (feature detection condition) or the shape of a specific colored-item (conjunction discrimination condition). Just after the onset of the search array, a task-irrelevant stimulus appeared either at the location of relevant or irrelevant items. The irrelevant stimulus evoked larger ERPs for the relevant location compared to irrelevant location. P1-wave was present in that ERP only in the discrimination condition and not in the feature detection condition, indicating that conjunction discrimination recruited additional attentional resources. In the traditional paradigm, where subjects are instructed to pay attention to one direction and ignore the other, Mangun et al. (2001) showed that the P1 magnitude is larger for the attended compared to unattended location. The study of Mangum et al. also showed that P1 response was generated not only by the contralateral hemisphere but also by the ipsilateral one, the observation that was difficult to explain in terms of redistribution of attentional resources between the hemispheres. Klimesch (2011) suggested that these results is due to inhibition effect of the P1 in two different levels. In the task-irrelevant pathways (e.g., ipsilateral hemisphere) inhibition is used to block the information processing, whereas, in the task-relevant pathways it is used to increase the SNR by enabling precisely timed activity in neurons with high level of excitation and suppressing the neurons with low-level of excitation. It seems that the inhibition increased when an attentional demand increases to make the response to the relevant stimulus sharper.

N1-wave contains an early component generated in the frontal (140 ms) and two late components between 150 and 200 ms generated parietal cortex and the lateral occipital cortex, respectively (Clark and Hillyard, 1996; Luck, 2005; Ceballos and Hernandez, 2015). The magnitude of N1-potential is highly influenced by visual spatial attention (Hillyard et al., 1998). N1

is insensitive to the physical properties of the paradigm such as light intensity and the contrast. This point was clarified in the experiment where a 6 × 6 matrix alphanumeric matrix (similar to Farwell and Donchin's paradigm) could be either high-contrast or low-contrast (Shishkin et al., 2009). Although the visual stimuli were designed in a very different contrasts, N1 characteristics between high- and low-contrast tasks remained the same. N1 is an interesting feature from two aspects: first N1 seems to be reproduce robust feature regardless of design on the paradigm which makes it suitable to compare different studies; second, there is no need to make detection paradigm hard to enhance N1 as it works well for clearly visible stimuli, and therefore, N1-based BCIs can be visually comfortable for ADHD subjects. This is important for ADHD subjects as they have higher tendency for fatigue or visual discomfort (Cao et al., 2014; Kooij and Bijlenga, 2014). It has been shown that about two-third of children with ADHD suffer from visual problems such as irritability by light (Kooij and Bijlenga, 2014). If BCIs are intended to be used on a daily basis for training and rehabilitation purposes, the rapid visual fatigue would be a great disadvantage (Sakurada et al., 2015). Therefore, presenting a paradigm with less discomfort effect should enhance the endurance of patients in long-lasting training sessions and consequently increase the chance of successful therapy.

N1 properties are influenced by repetitive training which can be a potential marker for evaluating the effect of neurofeedback therapy. For example, training to play a video game affects N1 (Latham et al., 2013). In that study, checkerboard stimuli appeared for a short time (92 ms) either in the left or right hemifield against a gray background. Subjects were instructed to respond to the flash of checkerboards by pressing a button while EEG was being recorded. Participants were divided into two groups: professional video-game players (VGP) and non-professional VGP. Expert VGPs had significantly shorter N1 latencies compared to inexperienced VGPs, and no other difference in ERP components was found between the groups.

P2-wave, that follows N1, occurs mostly for the anterior and central electrodes. P2 is larger when the stimulus occurs relatively infrequently (*oddball*). From this point of view, the anterior P2 is similar to P3-wave (see below) with the difference that P2 represents simple features (e.g., color) of the stimulus, whereas P3 is related to complex stimulus features (e.g., color and shape). For posterior electrodes, P2 component is often difficult to distinguish from the overlapping N1, N2, and P3 (Luck, 2014). P2 magnitude has been reported to differ between healthy and ADHD individuals (Banaschewski et al., 2003, 2008; Broyd et al., 2005). The P2 component is associated with automatic processing and inhibition of irrelevant information (Barry et al., 2003). Studies have shown that P2 has larger amplitude and different topographical distribution in ADHD (Banaschewski et al., 2003; Broyd et al., 2005; Barry et al., 2009; Ortega et al., 2013). Therefore, P2 amplitude could be used in BCIs as an indicator for improvement scale for ADHDs.

P3 component (also called the P300 since it peaks at 300–500 ms post-stimulus) consists of two sub-components P3a and P3b. The P3b amplitude varies between 5 and 15 μV for the parietal electrodes (Soltani and Knight, 2000). It appears following the occurrence of the oddball stimulus among a sequence of frequently repeating background stimuli. P3a, on the other hand, is distributed more in the fronto-central scalp region and peaks about 60–80 ms prior to P3b for all sensory modalities. An important characteristic of P3a component is its habituation in frontal sites within 5–10 stimulus presentations; i.e., the P3a disappears when the same type of stimulus is repeatedly presented (Lynn and Eysenck, 1966; Sokolov, 1969; Friedman et al., 2001). P3b, in many publications, is simply referred to P3 or P300. It was proposed that P3 is a possible endophenotype for ADHD (Doyle et al., 2005; Szuromi et al., 2011). Patients with ADHD have significantly lower P3 amplitude during the attention task (Szuromi et al., 2011). Szuromi et al. (2011) proposed that the P3 may be used as an ADHD marker that characterizes the deficits in the level of attentional allocation and information processing. P3 magnitude has been reported to represent the effort of attentional allocation, whereas, the latency of P3 indexes the processing speed of stimulus evaluation (Polich, 2007). Yet, P3 should be considered conservatively as a unique indicator for attention deficiency since its characteristics can be affected also by other disorders such as externalizing psychopathology (substance use, conduct disorder and antisocial behavior) (Bertoletti et al., 2014; Burwell et al., 2014).

ERP-based BCIs is one of the early developed methods in the field of BCI (Farwell and Donchin, 1988). ERP-based BCIs have a relatively low information transfer rate (ITR) or bit-rate. Bit-rate in a BCI system is an index of how much information can be communicated between the brain and the computer in the time-unit (van der Waal et al., 2012). In Farwell and Donchin's BCI, the ITR was about 12 bits min^{-1}. Zhang et al developed a visual P300-speller BCI which was able to communicate at 20 bits min^{-1}. BCI performance is substantially higher for visual ERPs compared to auditory (1.54 bit min^{-1}) and tactile (7.8 bit min^{-1}) ERPs (Furdea et al., 2009; van der Waal et al., 2012). Combination of ERP with other protocols such as steady-state visual evoked potential (SSVEP) increases the ITR up to 19.05 bit min^{-1} (Panicker et al., 2011).

ERP-based BCIs increase SNR by performing an ensemble averaging across several responses. Only the time-locked activities survive the averaging and irrelevant activities are canceled out. However, averaging is also considered as a drawback of ERP-based BCIs as the system has to obtain two or more ERP events to improve performance. Collecting data in multiple trials slows down the system speed. Thus, choosing this ERP-BCI method is a trade-off between the speed and accuracy of the system. Another limitation of ERP-based BCI is the across-trial variability in ERP amplitude and timing. The amplitude of P3 decreases if inter-trial intervals are short. To keep P3 amplitude in the standard range (10–20 μV) inter-trial interval should be around 8 s (Polich and Bondurant, 1997). This long interval limits BCI performance. In most experimental designs, intervals between oddball stimuli are random, which introduces ERP variability. Variability in the P3-characteristics makes it an unstable feature in attention experiments where the rigidity of ERP depend both on factors such as the designed paradigm and the mental states of the subjects.

Signal Characteristics in Steady-State Visual Evoked Potential (SSVEP) Paradigms

Another widely used BCI protocol is the SSVEP (Zhang et al., 2010; Palomares et al., 2012; Lesenfants et al., 2014; Wu and Su, 2014; Reuter et al., 2015). Visual evoked potential (VEP) is the brain responses to a visual stimulus such as light flash or flickering of a checker board at a specific frequency (Punsawad and Wongsawat, 2012). Presentation of a flickering visual object leads to VEPs entrained to the stimulus frequency. SSVEP-based BCIs usually detect this entrained response in the EEG of the visual and parietal cortices. These BCIs achieve high SNR over a few seconds of stimulation (Dmochowski et al., 2015). In a typical SSVEP-based BCI, several objects flicker at different frequencies while the subject attends to one the object. The subject usually looks at the attended object. SSVEP-based BCIs can be easily implemented using graphical interfaces such as video games (Leins et al., 2007; Lim et al., 2010, 2012; Bakhshayesh et al., 2011).

SSVEP-based BCIs have good accuracy and resistance to artifacts. As such, they can be used to build practical assistive systems for disabled users (Muller-Putz and Pfurtscheller, 2008). For example, Bin et al reported a SSVEP-based BCI that attained 95.3% accuracy and the ITR of 58 $\pm$ 9.6 bits min^{-1} (Bin et al., 2009). This is a substantially higher ITR compared to other BCI types, such as ERP-based BCIs. Muller and Hillyard (2000) designed a paradigm in which ERPs were embedded within a flicker sequence. They found that the magnitude of SSVEP and that of the N1 and N2 component of ERP varied together (positive correlation), whereas no significant correlation was found with other ERP components (Muller and Hillyard, 2000). SSVEP paradigms usually utilize the flickering frequency greater than 6 Hz. In a recent study (Dreyer and Herrmann, 2015), flickering frequency of up to 100 Hz was used by utilizing a novel technology. High-frequency SSVEPs are of great advantage because subjects do not perceive the flicker and are not annoyed. The flicker is not perceived for stimulus frequencies higher than 40 Hz (Lin et al., 2012). Sakurada et al. (2015) demonstrated that using BCIs with SSVEP frequency above 50–60 Hz enhanced the classification accuracy and decreased visual fatigue (Sakurada et al., 2015). Training time is also improved, particularly in ADHD subjects, as they are less irritated by light flicker (Kooij and Bijlenga, 2014).

SSVEPs can be detected not only in awake subjects, but in anesthetized subjects, as well. Several experiments employed the SSVEP technique in fully or partially anesthetized animals whose eyes were kept open in front of a visual display (Harnois et al., 1984; Xu et al., 2013). The flicker frequency was detected from the occipital electrodes.

Harmonics of the flickering frequency in some cases give a better BCI readout (Muller-Putz and Pfurtscheller, 2008; Allison et al., 2010; Ordikhani-Seyedlar et al., 2014). Müller-Putz and his colleagues reported particularly good results when they used three harmonic peaks (Muller-Putz et al., 2005). In our study (Ordikhani-Seyedlar et al., 2014) that employed a covert attention paradigm, the power of the second harmonic was higher compared to the first harmonic. This result is in agreement with Kim et al. (2011) and others Garcia et al. (2013), Zhang et al. (2015) who also reported that visual spatial attention modulates the second, but not the first harmonic of the SSVEP frequency.

PROSPECTS FOR BCIs IN RESEARCH OF ATTENTION

We are witnessing a rapid development of the BCI field. The number of peer-reviewed articles has been rapidly increasing over the past 20 years. Many of BCIs reported in the literature enable sensorimotor functions (O'Doherty et al., 2011; Ifft et al., 2013; Pais-Vieira et al., 2013; Yoo et al., 2013). While BCIs for cognitive functions are less developed, there has been a growing interest to such systems. In our opinion, the most important future challenges for attention-based BCIs include:

(1) Filtering out noise: Noise can be caused by mechanical and electrical artifacts, and it can be a neural signal that is irrelevant to the function that the BCI enables and/or augments. Noise can be reduced by proper selection of features representing a brain function of interest. Choosing the right features is especially important for therapeutic BCIs because if features are selected incorrectly, unwanted functions could be enhanced instead of the desired alleviation of an individual's disability. For instance, using the α-band to regulate attention has certain caveats. Ideally, the α-band represents suppression of irrelevant information in an attention paradigm. However, if the subject is not attending, such suppression could be confused with the drowsiness state, and the BCI would enhance drowsiness instead of working properly to enhance attention. This problem could be addressed by adding features, such as topographical information about the source of the α-oscillations.

(2) Developing of reliable criteria to quantify BCI training effects: Neurofeedback therapy is usually evaluated using a comparison of specific features before and after the training. However, enhancement in EEG features does not guarantee a behavioral improvement. For example, increase in β-band power is a popular feature indicating high attention level. If the aim is just to increase β-band oscillation, this frequency band might also be increased due to some other brain function unrelated to attention *per se*. For example, the β-band increased when motor movement had to be voluntarily suppressed in macaque monkeys (Zhang et al., 2008). Therefore, we suggest that the evaluation of neurofeedback therapy outcome should include behavioral and psychological tests to that evaluate the target function.

(3) Accounting for intra- and inter-individual variability: Sources of variability include non-stationarity of EEG signals (Vidaurre et al., 2011) as well as non-stationarities induced by the task (Iturrate et al., 2013) and different mental states of different subjects. The BCI algorithms should be able to accommodate individual characteristics of subjects, and to adapt to EEG variability during the neurofeedback therapy.

(4) Developing BCIs for individual use: current methods of NF-training require the presence of an expert to conduct the training session from the installation of scalp electrode to running the programs and maintaining the system. These

procedures impose restrictions on the usage of BCIs by patients. More user-friendly, highly automated BCIs should be developed in the future.

CONCLUSIONS

BCIs offer exciting opportunities for enhancing neural functions and developing therapies for neural disabilities, including BCIs that assist subject to regulate their neural function. Attention is a fundamental brain mechanism for selection of relevant and essential information while suppressing irrelevant signals. Disorders of this mechanism result in dysfunctions, such as ADHD. BCIs hold promise to provide effective rehabilitation strategies for individuals with impairments of attention. Several attention-based BCIs have been already developed whereas many challenges still remain. The main challenge is to combine highly technical knowledge needed to build effective BCIs with the expertise from neuroscience and psychology. Merging these multidisciplinary contributions is key to developing clinically relevant BCIs to treat attentional dysfunctions.

AUTHOR CONTRIBUTIONS

MO, ML: wrote the paper; HS, SP: edited the paper.

ACKNOWLEDGMENTS

The authors gratefully appreciate Karoline B. Doser for her valuable comments on the manuscript and Dr. Sean Bowen for editorial assistance on an earlier version of this manuscript. The original project was supported by the Department of Electrical Engineering (Biomedical Engineering) at the Technical University of Denmark (DTU), the Lundbeck Foundation and Radiometer.

REFERENCES

Ahn, M., Ahn, S., Hong, J. H., Cho, H., Kim, K., Kim, B. S., et al. (2013). Gamma band activity associated with BCI performance: simultaneous MEG/EEG study. *Front. Hum. Neurosci.* 7:848. doi: 10.3389/fnhum.2013.00848

Ales, J. M., Yates, J. L., and Norcia, A. M. (2010). V1 is not uniquely identified by polarity reversals of responses to upper and lower visual field stimuli. *Neuroimage* 52, 1401–1409. doi: 10.1016/j.neuroimage.2010.05.016

Allison, B. Z., Brunner, C., Kaiser, V., Müller-Putz, G. R., Neuper, C., and Pfurtscheller, G. (2010). Toward a hybrid brain-computer interface based on imagined movement and visual attention. *J. Neural Eng.* 7, 1–9. doi: 10.1088/1741-2560/7/2/026007

Arns, M., de Ridder, S., Strehl, U., Breteler, M., and Coenen, A. (2009). Efficacy of neurofeedback treatment in ADHD: the effects on inattention, impulsivity and hyperactivity: a meta-analysis. *Clin. EEG Neurosci.* 40, 180–189. doi: 10.1177/155005940904000311

Arns, M., Feddema, I., and Kenemans, J. L. (2014). Differential effects of theta/beta and SMR neurofeedback in ADHD on sleep onset latency. *Front. Hum. Neurosci.* 8:1019. doi: 10.3389/fnhum.2014.01019

Avisar, A., and Shalev, L. (2011). Sustained attention and behavioral characteristics associated with ADHD in adults. *Appl. Neuropsychol.* 18, 107–116. doi: 10.1080/09084282.2010.547777

Babiloni, C., Brancucci, A., Del Percio, C., Capotosto, P., Arendt-Nielsen, L., Chen, A. C., et al. (2006). Anticipatory electroencephalography alpha rhythm predicts subjective perception of pain intensity. *J. Pain* 7, 709–717. doi: 10.1016/j.jpain.2006.03.005

Bakhshayesh, A. R., Hansch, S., Wyschkon, A., Rezai, M. J., and Esser, G. (2011). Neurofeedback in ADHD: a single-blind randomized controlled trial. *Eur. Child Adolesc. Psychiatry* 20, 481–491. doi: 10.1007/s00787-011-0208-y

Ball, T., Kern, M., Mutschler, I., Aertsen, A., and Schulze-Bonhage, A. (2009). Signal quality of simultaneously recorded invasive and non-invasive EEG. *NeuroImage* 46, 708–716. doi: 10.1016/j.neuroimage.2009.02.028

Bamdadian, A., Guan, C., Ang, K. K., and Xu, J. (2014). The predictive role of pre-cue EEG rhythms on MI-based BCI classification performance. *J. Neurosci. Methods* 235, 138–144. doi: 10.1016/j.jneumeth.2014.06.011

Banaschewski, T., Brandeis, D., Heinrich, H., Albrecht, B., Brunner, E., and Rothenberger, A. (2003). Association of ADHD and conduct disorder–brain electrical evidence for the existence of a distinct subtype. *J. Child Psychol. Psychiatry* 44, 356–376. doi: 10.1111/1469-7610.00127

Banaschewski, T., Yordanova, J., Kolev, V., Heinrich, H., Albrecht, B., and Rothenberger, A. (2008). Stimulus context and motor preparation in attention-deficit/hyperactivity disorder. *Biol. Psychol.* 77, 53–62. doi: 10.1016/j.biopsycho.2007.09.003

Barry, R. J., Clarke, A. R., McCarthy, R., Selikowitz, M., Brown, C. R., and Heaven, P. C. (2009). Event-related potentials in adults with Attention-Deficit/Hyperactivity Disorder: an investigation using an inter-modal auditory/visual oddball task. *Int. J. Psychophysiol.* 71, 124–131. doi: 10.1016/j.ijpsycho.2008.09.009

Barry, R. J., Johnstone, S. J., and Clarke, A. R. (2003). A review of electrophysiology in attention-deficit/hyperactivity disorder: II. Event-related potentials. *Clin. Neurophysiol.* 114, 184–198. doi: 10.1016/S1388-2457(02)00363-2

Benzi, R., Parisi, G., Sutera, A., and Vulpiani, A. (1982). Stochastic resonance in climatic change. *Tellus* 34, 10–16. doi: 10.1111/j.2153-3490.1982.tb01787.x

Bertoletti, E., Michelini, G., Moruzzi, S., Ferrer, G., Ferini-Strambi, L., Stazi, M. A., et al. (2014). A general population twin study of conduct problems and the auditory P300 waveform. *J. Abnorm. Child Psychol.* 42, 861–869. doi: 10.1007/s10802-013-9836-7

Bianchi, L., Sami, S., Hillebrand, A., Fawcett, I. P., Quitadamo, L. R., and Seri, S. (2010). Which physiological components are more suitable for visual ERP based brain-computer interface? A preliminary MEG/EEG study. *Brain Topogr.* 23, 180–185. doi: 10.1007/s10548-010-0143-0

Biederman, J., Mick, E., and Faraone, S. V. (2000). Age-dependent decline of symptoms of attention deficit hyperactivity disorder: impact of remission definition and symptom type. *Am. J. Psychiatry* 157, 816–818. doi: 10.1176/appi.ajp.157.5.816

Bin, G., Gao, X., Wang, Y., Hong, B., and Gao, S. (2009). VEP-based brain-computer interfaces: time, frequency, and code modulations. *IEEE Comput. Intell. Mag.* 4, 22–26. doi: 10.1109/MCI.2009.934562

Brosch, T., Pourtois, G., Sander, D., and Vuilleumier, P. (2011). Additive effects of emotional, endogenous, and exogenous attention: behavioral and electrophysiological evidence. *Neuropsychologia* 49, 1779–1787. doi: 10.1016/j.neuropsychologia.2011.02.056

Broyd, S. J., Johnstone, S. J., Barry, R. J., Clarke, A. R., McCarthy, R., Selikowitz, M., et al. (2005). The effect of methylphenidate on response inhibition and the event-related potential of children with attention deficit/hyperactivity disorder. *Int. J. Psychophysiol.* 58, 47–58. doi: 10.1016/j.ijpsycho.2005.03.008

Bruhl, A. B. (2015). Making sense of real-time functional magnetic resonance imaging (rtfMRI) and rtfMRI neurofeedback. *Int. J. Neuropsychopharmacol.* 18:pyv020. doi: 10.1093/ijnp/pyv020

Burwell, S. J., Malone, S. M., Bernat, E. M., and Iacono, W. G. (2014). Does electroencephalogram phase variability account for reduced P3 brain potential in externalizing disorders? *Clin. Neurophysiol.* 125, 2007–2015. doi: 10.1016/j.clinph.2014.02.020

Busch, N. A., Dubois, J., and VanRullen, R. (2009). The phase of ongoing EEG oscillations predicts visual perception. *J. Neurosci.* 29, 7869–7876. doi: 10.1523/JNEUROSCI.0113-09.2009

Busch, N. A., and VanRullen, R. (2010). Spontaneous EEG oscillations reveal periodic sampling of visual attention. *Proc. Natl. Acad. Sci. U.S.A.* 107, 16048–16053. doi: 10.1073/pnas.1004801107

Busse, L., Katzner, S., and Treue, S. (2008). Temporal dynamics of neuronal modulation during exogenous and endogenous shifts of visual attention in macaque area MT. *Proc. Natl. Acad. Sci. U.S.A.* 105, 16380–16385. doi: 10.1073/pnas.0707369105

Cao, T., Wan, F., Wong, C. M., da Cruz, J. N., and Hu, Y. (2014). Objective evaluation of fatigue by EEG spectral analysis in steady-state visual evoked potential-based brain-computer interfaces. *Biomed. Eng. Online* 13:28. doi: 10.1186/1475-925x-13-28

Carmena, J. M., Lebedev, M. A., Crist, R. E., O'Doherty, J. E., Santucci, D. M., Dimitrov, D. F., et al. (2003). Learning to control a brain-machine interface for reaching and grasping by primates. *PLoS Biol.* 1:E42. doi: 10.1371/journal.pbio.0000042

Ceballos, G. A., and Hernandez, L. F. (2015). Non-target adjacent stimuli classification improves performance of classical ERP-based brain computer interface. *J. Neural Eng.* 12:026009. doi: 10.1088/1741-2560/12/2/026009

Christiansen, H., Reh, V., Schmidt, M. H., and Rief, W. (2014). Slow cortical potential neurofeedback and self-management training in outpatient care for children with ADHD: study protocol and first preliminary results of a randomized controlled trial. *Front. Hum. Neurosci.* 8:943. doi: 10.3389/fnhum.2014.00943

Clark, V. P., and Hillyard, S. A. (1996). Spatial selective attention affects early extrastriate but not striate components of the visual evoked potential. *J. Cogn. Neurosci.* 8, 387–402. doi: 10.1162/jocn.1996.8.5.387

Clarke, A. R., Barry, R. J., Dupuy, F. E., McCarthy, R., Selikowitz, M., and Johnstone, S. J. (2013). Excess beta activity in the EEG of children with attention-deficit/hyperactivity disorder: a disorder of arousal? *Int. J. Psychophysiol.* 89, 314–319. doi: 10.1016/j.ijpsycho.2013.04.009

Cohen, M. X. (ed.). (2013). "Overview of time-domain EEG analyses," in *Analyzing Neural Time Series Data: Theory and Practice* (London: MIT Press), 97–106.

Conners, C. K., Epstein, J. N., March, J. S., Angold, A., Wells, K. C., Klaric, J., et al. (2001). Multimodal treatment of ADHD in the MTA: an alternative outcome analysis. *J. Am. Acad. Child Adolesc. Psychiatry* 40, 159–167. doi: 10.1097/00004583-200102000-00010

Corbetta, M., Patel, G., and Shulman, G. L. (2008). The reorienting system of the human brain: from environment to theory of mind. *Neuron* 58, 306–324. doi: 10.1016/j.neuron.2008.04.017

Coyle, S., Ward, T., Markham, C., and McDarby, G. (2004). On the suitability of near-infrared (NIR) systems for next-generation brain-computer interfaces. *Physiol. Meas.* 25, 815–822. doi: 10.1088/0967-3334/25/4/003

Crone, N. E., Sinai, A., and Korzeniewska, A. (2006). High-frequency gamma oscillations and human brain mapping with electrocorticography. *Prog. Brain Res.* 159, 275–295. doi: 10.1016/S0079-6123(06)59019-3

Daitch, A. L., Sharma, M., Roland, J. L., Astafiev, S. V., Bundy, D. T., Gaona, C. M., et al. (2013). Frequency-specific mechanism links human brain networks for spatial attention. *Proc. Natl. Acad. Sci. U.S.A.* 110, 19585–19590. doi: 10.1073/pnas.1307947110

deCharms, R. C., Maeda, F., Glover, G. H., Ludlow, D., Pauly, J. M., Soneji, D., et al. (2005). Control over brain activation and pain learned by using real-time functional MRI. *Proc. Natl. Acad. Sci. U.S.A.* 102, 18626–18631. doi: 10.1073/pnas.0505210102

de Haan, B., Morgan, P. S., and Rorden, C. (2008). Covert orienting of attention and overt eye movements activate identical brain regions. *Brain Res.* 1204, 102–111. doi: 10.1016/j.brainres.2008.01.105

Desimone, R., and Duncan, J. (1995). Neural mechanisms of selective visual attention. *Annu. Rev. Neurosci.* 18, 193–222. doi: 10.1146/annurev.ne.18.030195.001205

De Vos, M., Kroesen, M., Emkes, R., and Debener, S. (2014). P300 speller BCI with a mobile EEG system: comparison to a traditional amplifier. *J. Neural Eng.* 11:036008. doi: 10.1088/1741-2560/11/3/036008

Dirlikov, B., Shiels Rosch, K., Crocetti, D., Denckla, M. B., Mahone, E. M., and Mostofsky, S. H. (2015). Distinct frontal lobe morphology in girls and boys with ADHD. *Neuroimage Clin.* 7, 222–229. doi: 10.1016/j.nicl.2014.12.010

Di Russo, F., Martinez, A., Sereno, M. I., Pitzalis, S., and Hillyard, S. A. (2002). Cortical sources of the early components of the visual evoked potential. *Hum. Brain Mapp.* 15, 95–111. doi: 10.1002/hbm.10010

Dmochowski, J. P., Greaves, A. S., and Norcia, A. M. (2015). Maximally reliable spatial filtering of steady state visual evoked potentials. *Neuroimage* 109, 63–72. doi: 10.1016/j.neuroimage.2014.12.078

Dobkin, B. H. (2007). Brain-computer interface technology as a tool to augment plasticity and outcomes for neurological rehabilitation. *J. Physiol.* 579, 637–642. doi: 10.1113/jphysiol.2006.123067

Donoghue, J. P., Nurmikko, A., Friehs, G., and Black, M. (2004). Development of neuromotor prostheses for humans. *Suppl. Clin. Neurophysiol.* 57, 592–606. doi: 10.1016/S1567-424X(09)70399-X

Doyle, A. E., Willcutt, E. G., Seidman, L. J., Biederman, J., Chouinard, V. A., Silva, J., et al. (2005). Attention-deficit/hyperactivity disorder endophenotypes. *Biol. Psychiatry* 57, 1324–1335. doi: 10.1016/j.biopsych.2005.03.015

Dreyer, A. M., and Herrmann, C. S. (2015). Frequency-modulated steady-state visual evoked potentials: a new stimulation method for brain-computer interfaces. *J. Neurosci. Methods* 241, 1–9. doi: 10.1016/j.jneumeth.2014.12.004

Dupuy, F. E., Clarke, A. R., Barry, R. J., McCarthy, R., and Selikowitz, M. (2013). EEG differences between the combined and inattentive types of attention-deficit/hyperactivity disorder in girls: a further investigation. *Clin. EEG Neurosci.* 45, 231–237. doi: 10.1177/1550059413501162

Egeth, H. E., and Yantis, S. (1997). Visual attention: control, representation, and time course. *Annu. Rev. Psychol.* 48, 269–297. doi: 10.1146/annurev.psych.48.1.269

Elbert, T., Rockstroh, B., Lutzenberger, W., and Birbaumer, N. (1980). Biofeedback of slow cortical potentials. I. *Electroencephalogr. Clin. Neurophysiol.* 48, 293–301. doi: 10.1016/0013-4694(80)90265-5

Ergenoglu, T., Demiralp, T., Bayraktaroglu, Z., Ergen, M., Beydagi, H., and Uresin, Y. (2004). Alpha rhythm of the EEG modulates visual detection performance in humans. *Brain Res. Cogn. Brain Res.* 20, 376–383. doi: 10.1016/j.cogbrainres.2004.03.009

Escolano, C., Navarro-Gil, M., Garcia-Campayo, J., Congedo, M., and Minguez, J. (2014). The effects of individual upper alpha neurofeedback in ADHD: an open-label pilot study. *Appl. Psychophysiol. Biofeedback* 39, 193–202. doi: 10.1007/s10484-014-9257-6

Fan, J., McCandliss, B. D., Fossella, J., Flombaum, J. I., and Posner, M. I. (2005). The activation of attentional networks. *Neuroimage* 26, 471–479. doi: 10.1016/j.neuroimage.2005.02.004

Faraone, S. V., Biederman, J., and Mick, E. (2006). The age-dependent decline of attention deficit hyperactivity disorder: a meta-analysis of follow-up studies. *Psychol. Med.* 36, 159–165. doi: 10.1017/S003329170500471X

Farwell, L. A., and Donchin, E. (1988). Talking off the top of your head: toward a mental prosthesis utilizing event-related brain potentials. *Electroencephalogr. Clin. Neurophysiol.* 70, 510–523. doi: 10.1016/0013-4694(88)90149-6

Fazli, S., Mehnert, J., Steinbrink, J., Curio, G., Villringer, A., Muller, K. R., et al. (2012). Enhanced performance by a hybrid NIRS-EEG brain computer interface. *Neuroimage* 59, 519–529. doi: 10.1016/j.neuroimage.2011.07.084

Ferrier, D. (1876). *The Function of the Brain*. London: Smith, Elder & Co.

Fleming, A. P., and McMahon, R. J. (2012). Developmental context and treatment principles for ADHD among college students. *Clin. Child Fam. Psychol. Rev.* 15, 303–329. doi: 10.1007/s10567-012-0121-z

Freeman, W. J., Holmes, M. D., Burke, B. C., and Vanhatalo, S. (2003). Spatial spectra of scalp EEG and EMG from awake humans. *Clin. Neurophysiol.* 114, 1053–1068. doi: 10.1016/S1388-2457(03)00045-2

Freeman, W. J., Rogers, L. J., Holmes, M. D., and Silbergeld, D. L. (2000). Spatial spectral analysis of human electrocorticograms including the alpha and gamma bands. *J. Neurosci. Methods* 95, 111–121. doi: 10.1016/S0165-0270(99)00160-0

Friedman, D., Cycowicz, Y. M., and Gaeta, H. (2001). The novelty P3: an event-related brain potential (ERP) sign of the brain's evaluation of novelty. *Neurosci. Biobehav. Rev.* 25, 355–373. doi: 10.1016/S0149-7634(01)00019-7

Fries, P., Reynolds, J. H., Rorie, A. E., and Desimone, R. (2001). Modulation of oscillatory neuronal synchronization by selective visual attention. *Science* 291, 1560–1563. doi: 10.1126/science.1055465

Fu, K. M., Foxe, J. J., Murray, M. M., Higgins, B. A., Javitt, D. C., and Schroeder, C. E. (2001). Attention-dependent suppression of distracter visual input can be cross-modally cued as indexed by anticipatory parieto-occipital alpha-band oscillations. *Brain Res. Cogn. Brain Res.* 12, 145–152. doi: 10.1016/S0926-6410(01)00034-9

Fu, S., Fedota, J. R., Greenwood, P. M., and Parasuraman, R. (2010). Dissociation of visual C1 and P1 components as a function of attentional load: an event-related potential study. *Biol. Psychol.* 85, 171–178. doi: 10.1016/j.biopsycho.2010.06.008

Furdea, A., Halder, S., Krusienski, D. J., Bross, D., Nijboer, F., Birbaumer, N., et al. (2009). An auditory oddball (P300). spelling system for brain-computer interfaces. *Psychophysiology* 46, 617–625. doi: 10.1111/j.1469-8986.2008.00783.x

Garcia, J. O., Srinivasan, R., and Serences, J. T. (2013). Near-real-time feature-selective modulations in human cortex. *Curr. Biol.* 23, 515–522. doi: 10.1016/j.cub.2013.02.013

Gevensleben, H., Holl, B., Albrecht, B., Vogel, C., Schlamp, D., Kratz, O., et al. (2009). Is neurofeedback an efficacious treatment for ADHD? A randomised controlled clinical trial. *J. Child Psychol. Psychiatry* 50, 780–789. doi: 10.1111/j.1469-7610.2008.02033.x

Gevensleben, H., Moll, G. H., Rothenberger, A., and Heinrich, H. (2014). Neurofeedback in attention-deficit/hyperactivity disorder - different models, different ways of application. *Front. Hum. Neurosci.* 8:846. doi: 10.3389/fnhum.2014.00846

Gherri, E., and Eimer, M. (2011). Active listening impairs visual perception and selectivity: an ERP study of auditory dual-task costs on visual attention. *J. Cogn. Neurosci.* 23, 832–844. doi: 10.1162/jocn.2010.21468

Golla, H., Thier, P., and Haarmeier, T. (2005). Disturbed overt but normal covert shifts of attention in adult cerebellar patients. *Brain* 128, 1525–1535. doi: 10.1093/brain/awh523

Gomes, H., Duff, M., Ramos, M., Molholm, S., Foxe, J. J., and Halperin, J. (2012). Auditory selective attention and processing in children with attention-deficit/hyperactivity disorder. *Clin. Neurophysiol.* 123, 293–302. doi: 10.1016/j.clinph.2011.07.030

Greenhill, L. L., Swanson, J. M., Vitiello, B., Davies, M., Clevenger, W., Wu, M., et al. (2001). Impairment and deportment responses to different methylphenidate doses in children with ADHD: the MTA titration trial. *J. Am. Acad. Child Adolesc. Psychiatry* 40, 180–187. doi: 10.1097/00004583-200102000-00012

Grosse-Wentrup, M., and Scholkopf, B. (2014). A brain-computer interface based on self-regulation of gamma-oscillations in the superior parietal cortex. *J. Neural Eng.* 11:056015. doi: 10.1088/1741-2560/11/5/056015

Hanslmayr, S., Aslan, A., Staudigl, T., Klimesch, W., Herrmann, C. S., and Bauml, K. H. (2007). Prestimulus oscillations predict visual perception performance between and within subjects. *Neuroimage* 37, 1465–1473. doi: 10.1016/j.neuroimage.2007.07.011

Harnois, C., Bodis-Wollner, I., and Onofrj, M. (1984). The effect of contrast and spatial frequency on the visual evoked potential of the hooded rat. *Exp. Brain Res.* 57, 1–8. doi: 10.1007/BF00231126

Harter, M. R., Aine, C., and Schroeder, C. (1984). Hemispheric differences in event-related potential measures of selective attention. *Ann. N.Y. Acad. Sci.* 425, 210–211. doi: 10.1111/j.1749-6632.1984.tb23535.x

He, N., Li, F., Li, Y., Guo, L., Chen, L., Huang, X., et al. (2015). Neuroanatomical deficits correlate with executive dysfunction in boys with attention deficit hyperactivity disorder. *Neurosci. Lett.* 600, 45–49. doi: 10.1016/j.neulet.2015.05.062

Heinrich, H., Busch, K., Studer, P., Erbe, K., Moll, G. H., and Kratz, O. (2014). EEG spectral analysis of attention in ADHD: implications for neurofeedback training? *Front. Hum. Neurosci.* 8:611. doi: 10.3389/fnhum.2014.00611

Hillard, B., El-Baz, A. S., Sears, L., Tasman, A., and Sokhadze, E. M. (2013). Neurofeedback training aimed to improve focused attention and alertness in children with ADHD: a study of relative power of EEG rhythms using custom-made software application. *Clin. EEG Neurosci.* 44, 193–202. doi: 10.1177/1550059412458262

Hillyard, S. A., and Anllo-Vento, L. (1998). Event-related brain potentials in the study of visual selective attention. *Proc. Natl. Acad. Sci. U.S.A.* 95, 781–787. doi: 10.1073/pnas.95.3.781

Hillyard, S. A., Vogel, E. K., and Luck, S. J. (1998). Sensory gain control (amplification) as a mechanism of selective attention: electrophysiological and neuroimaging evidence. *Philos. Trans. R. Soc. Lond. B. Biol. Sci.* 353, 1257–1270. doi: 10.1098/rstb.1998.0281

Holtmann, M., Pniewski, B., Wachtlin, D., Worz, S., and Strehl, U. (2014a). Neurofeedback in children with attention-deficit/hyperactivity disorder (ADHD)–a controlled multicenter study of a non-pharmacological treatment approach. *BMC Pediatr.* 14:202. doi: 10.1186/1471-2431-14-202

Holtmann, M., Sonuga-Barke, E., Cortese, S., and Brandeis, D. (2014b). Neurofeedback for ADHD: a review of current evidence. *Child Adolesc. Psychiatr. Clin. N. Am.* 23, 789–806. doi: 10.1016/j.chc.2014.05.006

Ifft, P. J., Shokur, S., Li, Z., Lebedev, M. A., and Nicolelis, M. A. (2013). A brain-machine interface enables bimanual arm movements in monkeys. *Sci. Transl. Med.* 5, 210ra154. doi: 10.1126/scitranslmed.3006159

Ignashchenkova, A., Dicke, P. W., Haarmeier, T., and Their, P. (2004). Neuron-specific contribution of the superior colliculus to overt and covert shifts of attention. *Nat. Neurosci.* 7, 56–64. doi: 10.1038/nn1169

Iturrate, I., Montesano, L., and Minguez, J. (2013). Shared-control brain-computer interface for a two dimensional reaching task using EEG error-related potentials. *Conf. Proc. IEEE Eng. Med. Biol. Soc.* 2013, 5258–5262. doi: 10.1109/embc.2013.6610735

Jones, A., Hughes, G., and Waszak, F. (2013). The interaction between attention and motor prediction. An ERP study. *Neuroimage* 83, 533–541. doi: 10.1016/j.neuroimage.2013.07.004

Jonkman, L. M., Kenemans, J. L., Kemner, C., Verbaten, M. N., and van Engeland, H. (2004). Dipole source localization of event-related brain activity indicative of an early visual selective attention deficit in ADHD children. *Clin. Neurophysiol.* 115, 1537–1549. doi: 10.1016/j.clinph.2004.01.022

Kahana, M. J. (2006). The cognitive correlates of human brain oscillations. *J. Neurosci.* 26, 1669–1672. doi: 10.1523/JNEUROSCI.3737-05c.2006

Kaiser, J., and Lutzenberger, W. (2005). Human gamma-band activity: a window to cognitive processing. *Neuroreport* 16, 207–211. doi: 10.1097/00001756-200502280-00001

Kanoh, S., Murayama, Y. M., Miyamoto, K., Yoshinobu, T., and Kawashima, R. (2009). A NIRS-based brain-computer interface system during motor imagery: system development and online feedback training. *Conf. Proc. IEEE Eng. Med. Biol. Soc.* 2009, 594–597. doi: 10.1109/IEMBS.2009.5333710

Kashihara, K. (2014). A brain-computer interface for potential non-verbal facial communication based on EEG signals related to specific emotions. *Front. Neurosci.* 8:244. doi: 10.3389/fnins.2014.00244

Kelly, S. P., Gomez-Ramirez, M., and Foxe, J. J. (2008). Spatial attention modulates initial afferent activity in human primary visual cortex. *Cereb. Cortex* 18, 2629–2636. doi: 10.1093/cercor/bhn022

Kelly, S. P., Schroeder, C. E., and Lalor, E. C. (2013). What does polarity inversion of extrastriate activity tell us about striate contributions to the early VEP? A comment on Ales et al. (2010). *Neuroimage* 76, 442–445. doi: 10.1016/j.neuroimage.2012.03.081

Keune, P. M., Wiedemann, E., Schneidt, A., and Schonenberg, M. (2015). Frontal brain asymmetry in adult attention-deficit/hyperactivity disorder (ADHD): extending the motivational dysfunction hypothesis. *Clin. Neurophysiol.* 126, 711–720. doi: 10.1016/j.clinph.2014.07.008

Khan, M. J., Hong, M. J., and Hong, K. S. (2014). Decoding of four movement directions using hybrid NIRS-EEG brain-computer interface. *Front. Hum. Neurosci.* 8:244. doi: 10.3389/fnhum.2014.00244

Kim, Y. J., Grabowecky, M., Paller, K. A., and Suzuki, S. (2011). Differential roles of frequency-following and frequency-doubling visual responses revealed by evoked neural harmonics. *J. Cogn. Neurosci.* 23, 1875–1886. doi: 10.1162/jocn.2010.21536

Klimesch, W. (2011). Evoked alpha and early access to the knowledge system: the P1 inhibition timing hypothesis. *Brain Res.* 1408, 52–71. doi: 10.1016/j.brainres.2011.06.003

Koelewijn, L., Rich, A. N., Muthukumaraswamy, S. D., and Singh, K. D. (2013). Spatial attention increases high-frequency gamma synchronisation in human medial visual cortex. *Neuroimage* 79, 295–303. doi: 10.1016/j.neuroimage.2013.04.108

Kollins, S. H. (2008). ADHD, substance use disorders, and psychostimulant treatment: current literature and treatment guidelines. *J. Atten. Disord.* 12, 115–125. doi: 10.1177/1087054707311654

Kooij, J. J., and Bijlenga, D. (2014). High prevalence of self-reported photophobia in adult ADHD. *Front. Neurol.* 5:256. doi: 10.3389/fneur.2014.00256

Kus, R., Duszyk, A., Milanowski, P., Labecki, M., Bierzynska, M., Radzikowska, Z., et al. (2013). On the quantification of SSVEP frequency responses in human EEG in realistic BCI conditions. *PLoS ONE* 8:e77536. doi: 10.1371/journal.pone.0077536

Lakatos, P., Karmos, G., Mehta, A. D., Ulbert, I., and Schroeder, C. E. (2008). Entrainment of neuronal oscillations as a mechanism of attentional selection. *Science* 320, 110–113. doi: 10.1126/science.1154735

Latham, A. J., Patston, L. L., Westermann, C., Kirk, I. J., and Tippett, L. J. (2013). Earlier visual N1 latencies in expert video-game players: a temporal basis of enhanced visuospatial performance? *PLoS ONE* 8:e75231. doi: 10.1371/journal.pone.0075231

Lebedev, M. A. (2014). How to read neuron-dropping curves? *Front. Syst. Neurosci.* 8:102. doi: 10.3389/fnsys.2014.00102

Lebedev, M. A., Carmena, J. M., O'Doherty, J. E., Zacksenhouse, M., Henriquez, C. S., Principe, J. C., et al. (2005). Cortical ensemble adaptation to represent

velocity of an artificial actuator controlled by a brain-machine interface. *J. Neurosci.* 25, 4681–4693. doi: 10.1523/JNEUROSCI.4088-04.2005

Lebedev, M. A., Messinger, A., Kralik, J. D., and Wise, S. P. (2004). Representation of attended versus remembered locations in prefrontal cortex. *PLoS Biol.* 2:e365. doi: 10.1371/journal.pbio.0020365

Lebedev, M. A., and Nicolelis, M. A. (2006). Brain-machine interfaces: past, present and future. *Trends Neurosci.* 29, 536–546. doi: 10.1016/j.tins.2006.07.004

Lebedev, M. A., Tate, A. J., Hanson, T. L., Li, Z., O'Doherty, J. E., Winans, J. A., et al. (2011). Future developments in brain-machine interface research. *Clinics* 66(Suppl. 1), 25–32. doi: 10.1590/s1807-59322011001300004

Lebedev, M. A., and Wise, S. P. (2001). Tuning for the orientation of spatial attention in dorsal premotor cortex. *Eur. J. Neurosci.* 13, 1002–1008. doi: 10.1046/j.0953-816x.2001.01457.x

Lee, J. H., Ryu, J., Jolesz, F. A., Cho, Z. H., and Yoo, S. S. (2009). Brain-machine interface via real-time fMRI: preliminary study on thought-controlled robotic arm. *Neurosci. Lett.* 450, 1–6. doi: 10.1016/j.neulet.2008.11.024

Leins, U., Goth, G., Hinterberger, T., Klinger, C., Rumpf, N., and Strehl, U. (2007). Neurofeedback for children with ADHD: a comparison of SCP and Theta/Beta protocols. *Appl. Psychophysiol. Biofeedback* 32, 73–88. doi: 10.1007/s10484-007-9031-0

Lesenfants, D., Habbal, D., Lugo, Z., Lebeau, M., Horki, P., Amico, E., et al. (2014). An independent SSVEP-based brain-computer interface in locked-in syndrome. *J. Neural Eng.* 11:035002. doi: 10.1088/1741-2560/11/3/035002

Leuthardt, E. C., Freudenberg, Z., Bundy, D., and Roland, J. (2009). Microscale recording from human motor cortex: implications for minimally invasive electrocorticographic brain-computer interfaces. *Neurosurg. Focus* 27:E10. doi: 10.3171/2009.4.FOCUS0980

Leuthardt, E. C., Schalk, G., Wolpaw, J. R., Ojemann, J. G., and Moran, D. W. (2004). A brain-computer interface using electrocorticographic signals in humans. *J. Neural Eng.* 1, 63–71. doi: 10.1088/1741-2560/1/2/001

Lim, C. G., Lee, T. S., Guan, C., Fung, D. S., Zhao, Y., Teng, S. S., et al. (2012). A brain-computer interface based attention training program for treating attention deficit hyperactivity disorder. *PLoS ONE* 7:e46692. doi: 10.1371/journal.pone.0046692

Lim, C. G., Lee, T. S., Guan, C., Sheng Fung, D. S., Cheung, Y. B., Teng, S. S., et al. (2010). Effectiveness of a brain-computer interface based programme for the treatment of ADHD: a pilot study. *Psychopharmacol. Bull.* 43, 73–82.

Lin, F. C., Zao, J. K., Tu, K. C., Wang, Y., Huang, Y. P., Chuang, C. W., et al. (2012). SNR analysis of high-frequency steady-state visual evoked potentials from the foveal and extrafoveal regions of human retina. *Conf. Proc. IEEE. Eng. Med. Biol. Soc.* 2012, 1810–1814. doi: 10.1109/EMBC.2012.6346302

Lofthouse, N., Arnold, L. E., Hersch, S., Hurt, E., and DeBeus, R. (2012a). A review of neurofeedback treatment for pediatric ADHD. *J. Atten. Disord.* 16, 351–372. doi: 10.1177/1087054711427530

Lofthouse, N., Arnold, L. E., and Hurt, E. (2012b). Current status of neurofeedback for attention-deficit/hyperactivity disorder. *Curr. Psychiatry Rep.* 14, 536–542. doi: 10.1007/s11920-012-0301-z

Logothetis, N. K. (2003). MR imaging in the non-human primate: studies of function and of dynamic connectivity. *Curr. Opin. Neurobiol.* 13, 630–642. doi: 10.1016/j.conb.2003.09.017

Luck, S. J. (2005). *An Introduction to the Event-Related Potential Technique*. Cambridge, MA: MIT.

Luck, S. J. (ed.). (2014). "Overview of common ERP components" in *An Introduction to the Event-Related Potential Technique* (London: MIT Press), 71–118.

Luck, S. J., and Hillyard, S. A. (1995). The role of attention in feature detection and conjunction discrimination: an electrophysiological analysis. *Int. J. Neurosci.* 80, 281–297. doi: 10.3109/00207459508986105

Lutzenberger, W., Elbert, T., Rockstroh, B., and Birbaumer, N. (1980). Biofeedback of slow cortical potentials. II. Analysis of single event-related slow potentials by time series analysis. *Electroencephalogr. Clin. Neurophysiol.* 48, 302–311. doi: 10.1016/0013-4694(80)90266-7

Lynn, R., and Eysenck, H. J. (1966). *Attention, Arousal and the Orientation Reaction: International Series of Monographs in Experimental Psychology*. Oxford: Pergamon Press.

Makeig, S., Westerfield, M., Jung, T. P., Enghoff, S., Townsend, J., Courchesne, E., et al. (2002). Dynamic brain sources of visual evoked responses. *Science* 295, 690–694. doi: 10.1126/science.1066168

Mangun, G. R., Hinrichs, H., Scholz, M., Mueller-Gaertner, H. W., Herzog, H., Krause, B. J., et al. (2001). Integrating electrophysiology and neuroimaging of spatial selective attention to simple isolated visual stimuli. *Vision Res.* 41, 1423–1435. doi: 10.1016/S0042-6989(01)00046-3

Margalit, E., Weiland, J. D., Clatterbuck, R. E., Fujii, G. Y., Maia, M., Tameesh, M., et al. (2003). Visual and electrical evoked response recorded from subdural electrodes implanted above the visual cortex in normal dogs under two methods of anesthesia. *J. Neurosci. Methods* 123, 129–137. doi: 10.1016/S0165-0270(02)00345X

Martinez, A., Anllo-Vento, L., Sereno, M. I., Frank, L. R., Buxton, R. B., Dubowitz, D. J., et al. (1999). Involvement of striate and extrastriate visual cortical areas in spatial attention. *Nat. Neurosci.* 2, 364–369. doi: 10.1038/7274

Matheson, H., Newman, A. J., Satel, J., and McMullen, P. (2014). Handles of manipulable objects attract covert visual attention: ERP evidence. *Brain Cogn.* 86, 17–23. doi: 10.1016/j.bandc.2014.01.013

Medina, L. E., Lebedev, M. A., O'Doherty, J. E., and Nicolelis, M. A. (2012). Stochastic facilitation of artificial tactile sensation in primates. *J. Neurosci.* 32, 14271–14275. doi: 10.1523/JNEUROSCI.3115-12.2012

Mellinger, J., Schalk, G., Braun, C., Preissl, H., Rosenstiel, W., Birbaumer, N., et al. (2007). An MEG-based brain-computer interface (BCI). *Neuroimage* 36, 581–593. doi: 10.1016/j.neuroimage.2007.03.019

Micoulaud-Franchi, J. A., Geoffroy, P. A., Fond, G., Lopez, R., Bioulac, S., and Philip, P. (2014). EEG neurofeedback treatments in children with ADHD: an updated meta-analysis of randomized controlled trials. *Front. Hum. Neurosci.* 8:906. doi: 10.3389/fnhum.2014.00906

Millichap, J. G. (2008). Etiologic classification of attention-deficit/hyperactivity disorder. *Pediatrics* 121, e358–e365. doi: 10.1542/peds.2007-1332

Ming, D., Xi, Y., Zhang, M., Qi, H., Cheng, L., Wan, B., et al. (2009). Electroencephalograph (EEG) signal processing method of motor imaginary potential for attention level classification. *IEEE Eng. Med. Biol. Soc.* 2009, 4347–4351. doi: 10.1109/iembs.2009.5332743

Muller, M. M., and Hillyard, S. (2000). Concurrent recording of steady-state and transient event-related potentials as indices of visual-spatial selective attention. *Clin. Neurophysiol.* 111, 1544–1552. doi: 10.1016/S1388-2457(00)00371-0

Muller-Putz, G. R., and Pfurtscheller, G. (2008). Control of an electrical prosthesis with an SSVEP-based BCI. *IEEE Trans. Biomed. Eng.* 55, 361–364. doi: 10.1109/TBME.2007.897815

Muller-Putz, G. R., Scherer, R., Brauneis, C., and Pfurtscheller, G. (2005). Steady-state visual evoked potential (SSVEP)-based communication: impact of harmonic frequency components. *J. Neural Eng.* 2, 123–130. doi: 10.1088/1741-2560/2/4/008

Musch, K., Hamame, C. M., Perrone-Bertolotti, M., Minotti, L., Kahane, P., Engel, A. K., et al. (2014). Selective attention modulates high-frequency activity in the face-processing network. *Cortex* 60, 34–51. doi: 10.1016/j.cortex.2014.06.006

Nagendra, H., Kumar, V., and Mukherjee, S. (2015). Cognitive behavior evaluation based on physiological parameters among young healthy subjects with yoga as intervention. *Comput. Math. Methods Med.* 2015:821061. doi: 10.1155/2015/821061

Nicolas-Alonso, L. F., and Gomez-Gil, J. (2012). Brain computer interfaces, a review. *Sensors* 12, 1211–1279. doi: 10.3390/s120201211

Nicolelis, M. A., Dimitrov, D., Carmena, J. M., Crist, R., Lehew, G., Kralik, J. D., et al. (2003). Chronic, multisite, multielectrode recordings in macaque monkeys. *Proc. Natl. Acad. Sci. U.S.A.* 100, 11041–11046. doi: 10.1073/pnas.1934665100

Nicolelis, M. A., and Lebedev, M. A. (2009). Principles of neural ensemble physiology underlying the operation of brain-machine interfaces. *Nat. Rev. Neurosci.* 10, 530–540. doi: 10.1038/nrn2653

Nicolelis, M. A., and Ribeiro, S. (2002). Multielectrode recordings: the next steps. *Curr. Opin. Neurobiol.* 12, 602–606. doi: 10.1016/S0959-4388(02)00374-4

O'Doherty, J. E., Lebedev, M. A., Ifft, P. J., Zhuang, K. Z., Shokur, S., Bleuler, H., et al. (2011). Active tactile exploration using a brain-machine-brain interface. *Nature* 479, 228–231. doi: 10.1038/nature10489

Okazaki, Y. O., Horschig, J. M., Luther, L., Oostenveld, R., Murakami, I., and Jensen, O. (2015). Real-time MEG neurofeedback training of posterior alpha activity modulates subsequent visual detection performance. *Neuroimage* 107, 323–332. doi: 10.1016/j.neuroimage.2014.12.014

Ordikhani-Seyedlar, M., Sorensen, H. B., Kjaer, T. W., Siebner, H. R., and Puthusserypady, S. (2014). SSVEP-modulation by covert and overt attention: novel features for BCI in attention neuro-rehabilitation. *IEEE Eng. Med. Biol. Soc.* 2014, 5462–5465. doi: 10.1109/embc.2014.6944862

Ortega, R., Lopez, V., Carrasco, X., Anllo-Vento, L., and Aboitiz, F. (2013). Exogenous orienting of visual-spatial attention in ADHD children. *Brain Res.* 1493, 68–79. doi: 10.1016/j.brainres.2012.11.036

Ozaki, I., Yaegashi, Y., Baba, M., and Hashimoto, I. (2006). High-frequency oscillatory activities during selective attention in humans. *Suppl. Clin. Neurophysiol.* 59, 57–60. doi: 10.1016/S1567-424X(09)70012-1

Pais-Vieira, M., Lebedev, M., Kunicki, C., Wang, J., and Nicolelis, M. A. (2013). A brain-to-brain interface for real-time sharing of sensorimotor information. *Sci. Rep.* 3:1319. doi: 10.1038/srep01319

Palomares, M., Ales, J. M., Wade, A. R., Cottereau, B. R., and Norcia, A. M. (2012). Distinct effects of attention on the neural responses to form and motion processing: a SSVEP source-imaging study. *J. Vis.* 12:15. doi: 10.1167/12.10.15

Panicker, R. C., Puthusserypady, S., and Sun, Y. (2011). An asynchronous P300 BCI with SSVEP-based control state detection. *IEEE Trans. Biomed. Eng.* 58, 1781–1788. doi: 10.1109/TBME.2011.2116018

Peikon, I. D., Fitzsimmons, N. A., Lebedev, M. A., and Nicolelis, M. A. (2009). Three-dimensional, automated, real-time video system for tracking limb motion in brain-machine interface studies. *J. Neurosci. Methods* 180, 224–233. doi: 10.1016/j.jneumeth.2009.03.010

Petersen, S. E., and Posner, M. I. (2012). The attention system of the human brain: 20 years after. *Annu. Rev. Neurosci.* 35, 73–89. doi: 10.1146/annurev-neuro-062111-150525

Polanczyk, G., and Rohde, L. A. (2007). Epidemiology of attention-deficit/hyperactivity disorder across the lifespan. *Curr. Opin. Psychiatry* 20, 386–392. doi: 10.1097/YCO.0b013e3281568d7a

Sutter, E. E., and Tran, D. (1992). The field topography of ERG components in man–I. The photopic luminance response. *Vision Res.* 32, 433–446. doi: 10.1016/0042-6989(92)90235-B

Polich, J. (2007). Updating P300: an integrative theory of P3a and P3b. *Clin. Neurophysiol.* 118, 2128–2148. doi: 10.1016/j.clinph.2007.04.019

Polich, J., and Bondurant, T. (1997). P300 sequence effects, probability, and interstimulus interval. *Physiol. Behav.* 61, 843–849. doi: 10.1016/S0031-9384(96)00564-1

Posner, M. I. (1980). Orienting of attention. *Q. J. Exp. Psychol.* 32, 3–25. doi: 10.1080/00335558008248231

Posner, M. I. (1994). Attention: the mechanisms of consciousness. *Proc. Natl. Acad. Sci. U.S.A.* 91, 7398–7403. doi: 10.1073/pnas.91.16.7398

Posner, M. I. (2012). Attentional networks and consciousness. *Front. Psychol.* 3:64. doi: 10.3389/fpsyg.2012.00064

Posner, M. I., and Rothbart, M. K. (2007). Research on attention networks as a model for the integration of psychological science. *Annu. Rev. Psychol.* 58, 1–23. doi: 10.1146/annurev.psych.58.110405.085516

Posner, M. I., Snyder, C. R., and Davidson, B. J. (1980). Attention and the detection of signals. *J. Exp. Psychol.* 109, 160–174. doi: 10.1037/0096-3445.109.2.160

Power, S. D., Kushki, A., and Chau, T. (2012). Automatic single-trial discrimination of mental arithmetic, mental singing and the no-control state from prefrontal activity: toward a three-state NIRS-BCI. *BMC Res. Notes* 5:141. doi: 10.1186/1756-0500-5-141

Praamstra, P., Boutsen, L., and Humphreys, G. W. (2005). Frontoparietal control of spatial attention and motor intention in human EEG. *J. Neurophysiol.* 94, 764–774. doi: 10.1152/jn.01052.2004

Pritchard, V. E., Neumann, E., and Rucklidge, J. J. (2008). Selective attention and inhibitory deficits in ADHD: does subtype or comorbidity modulate negative priming effects? *Brain Cogn.* 67, 324–339. doi: 10.1016/j.bandc.2008.02.002

Punsawad, Y., and Wongsawat, Y. (2012). Motion visual stimulus for SSVEP-based BCI system. *IEEE Eng. Med. Biol. Soc.* 2012, 3837–3840. doi: 10.1109/embc.2012.6346804

Ray, S., Niebur, E., Hsiao, S. S., Sinai, A., and Crone, N. E. (2008). High-frequency gamma activity (80-150Hz) is increased in human cortex during selective attention. *Clin. Neurophysiol.* 119, 116–133. doi: 10.1016/j.clinph.2007.09.136

Reuter, E. M., Bednark, J., and Cunnington, R. (2015). Reliance on visual attention during visuomotor adaptation: an SSVEP study. *Exp. Brain Res.* 233, 2041–2051. doi: 10.1007/s00221-015-4275-z

Rizzolatti, G., Riggio, L., Dascola, I., and Umilta, C. (1987). Reorienting attention across the horizontal and vertical meridians: evidence in favor of a premotor theory of attention. *Neuropsychologia* 25, 31–40. doi: 10.1016/0028-3932(87)90041-8

Rohenkohl, G., and Nobre, A. C. (2011). alpha oscillations related to anticipatory attention follow temporal expectations. *J. Neurosci.* 31, 14076–14084. doi: 10.1523/JNEUROSCI.3387-11.2011

Rossini, P. M., Noris Ferilli, M. A., and Ferreri, F. (2012). Cortical plasticity and brain computer interface. *Eur. J. Phys. Rehabil. Med.* 48, 307–312.

Rougeul-Buser, A., and Buser, P. (1997). Rhythms in the alpha band in cats and their behavioural correlates. *Int. J. Psychophysiol.* 26, 191–203. doi: 10.1016/S0167-8760(97)00764-2

Ruiz, S., Birbaumer, N., and Sitaram, R. (2013). Abnormal neural connectivity in schizophrenia and fMRI-brain-computer interface as a potential therapeutic approach. *Front. Psychiatry* 4:17. doi: 10.3389/fpsyt.2013.00017

Sakurada, T., Kawase, T., Komatsu, T., and Kansaku, K. (2015). Use of high-frequency visual stimuli above the critical flicker frequency in a SSVEP-based BMI. *Clin. Neurophysiol.* 126, 1972–1978. doi: 10.1016/j.clinph.2014.12.010

Sanei, S., and Chambers, J. (2008). "Brain-computer interface," in *EEG Signal Processing*, eds S. Sanei and J. Chambers (Chichester: John Wiley & Sons), 239–261.

Sato, J. R., Basilio, R., Paiva, F. F., Garrido, G. J., Bramati, I. E., Bado, P., et al. (2013). Real-time fMRI pattern decoding and neurofeedback using FRIEND: an FSL-integrated BCI toolbox. *PLoS ONE* 8:e81658. doi: 10.1371/journal.pone.0081658

Schalk, G. (2010). Can electrocorticography (ECoG) support robust and powerful brain-computer interfaces? *Front. Neuroeng.* 3:9. doi: 10.3389/fneng.2010.00009

Schalk, G., and Leuthardt, E. C. (2011). Brain-computer interfaces using electrocorticographic signals. *IEEE Rev. Biomed. Eng.* 4, 140–154. doi: 10.1109/RBME.2011.2172408

Schwarz, D. A., Lebedev, M. A., Hanson, T. L., Dimitrov, D. F., Lehew, G., Meloy, J., et al. (2014). Chronic, wireless recordings of large-scale brain activity in freely moving rhesus monkeys. *Nat. Methods* 11, 670–676. doi: 10.1038/nmeth.2936

Shahid, S., and Prasad, G. (2011). Bispectrum-based feature extraction technique for devising a practical brain-computer interface. *J. Neural Eng.* 8:025014. doi: 10.1088/1741-2560/8/2/025014

Shain, W., Spataro, L., Dilgen, J., Haverstick, K., Retterer, S., Isaacson, M., et al. (2003). Controlling cellular reactive responses around neural prosthetic devices using peripheral and local intervention strategies. *IEEE Trans Neural. Syst. Rehabil. Eng.* 11, 186–188. doi: 10.1109/TNSRE.2003.814800

Shishkin, S. L., Ganin, I. P., Basyul, I. A., Zhigalov, A. Y., and Kaplan, A. Y. (2009). N1 wave in the P300 BCI is not sensitive to the physical characteristics of stimuli. *J. Integr. Neurosci.* 8, 471–485. doi: 10.1142/S0219635209002320

Sitaram, R., Zhang, H., Guan, C., Thulasidas, M., Hoshi, Y., Ishikawa, A., et al. (2007). Temporal classification of multichannel near-infrared spectroscopy signals of motor imagery for developing a brain-computer interface. *Neuroimage* 34, 1416–1427. doi: 10.1016/j.neuroimage.2006.11.005

Skounti, M., Philalithis, A., and Galanakis, E. (2007). Variations in prevalence of attention deficit hyperactivity disorder worldwide. *Eur. J. Pediatr.* 166, 117–123. doi: 10.1007/s00431-006-0299-5

Sokolov, E. N. (1969). *Handbook of Contemporary Soviet Psychology*. New York, NY: Basic Books.

Sokunbi, M. O., Linden, D. E., Habes, I., Johnston, S., and Ihssen, N. (2014). Real-time fMRI brain-computer interface: development of a "motivational feedback" subsystem for the regulation of visual cue reactivity. *Front. Behav. Neurosci.* 8:392. doi: 10.3389/fnbeh.2014.00392

Soltani, M., and Knight, R. T. (2000). Neural origins of the P300. *Crit. Rev. Neurobiol.* 14, 199–224. doi: 10.1615/CritRevNeurobiol.v14.i3-4.20

Sprague, T. C., Saproo, S., and Serences, J. T. (2015). Visual attention mitigates information loss in small- and large-scale neural codes. *Trends Cogn. Sci.* 19, 215–226. doi: 10.1016/j.tics.2015.02.005

Steiner, H., Warren, B. L., Van Waes, V., and Bolanos-Guzman, C. A. (2014a). Life-long consequences of juvenile exposure to psychotropic drugs on brain and behavior. *Prog. Brain Res.* 211, 13–30. doi: 10.1016/B978-0-444-63425-2.00002-7

Steiner, N. J., Frenette, E. C., Rene, K. M., Brennan, R. T., and Perrin, E. C. (2014b). In-school neurofeedback training for ADHD: sustained improvements from a randomized control trial. *Pediatrics* 133, 483–492. doi: 10.1542/peds.2013-2059

Steiner, N. J., Frenette, E. C., Rene, K. M., Brennan, R. T., and Perrin, E. C. (2014c). Neurofeedback and cognitive attention training for children with attention-deficit hyperactivity disorder in schools. *J. Dev. Behav. Pediatr.* 35, 18–27. doi: 10.1097/DBP.0000000000000009

Steiner, N. J., Sheldrick, R. C., Gotthelf, D., and Perrin, E. C. (2011). Computer-based attention training in the schools for children with attention deficit/hyperactivity disorder: a preliminary trial. *Clin. Pediatr.* 50, 615–622. doi: 10.1177/0009922810397887

Stoeckel, L. E., Garrison, K. A., Ghosh, S., Wighton, P., Hanlon, C. A., Gilman, J. M., et al. (2014). Optimizing real time fMRI neurofeedback for therapeutic discovery and development. *Neuroimage Clin.* 5, 245–255. doi: 10.1016/j.nicl.2014.07.002

Sulzer, J., Haller, S., Scharnowski, F., Weiskopf, N., Birbaumer, N., Blefari, M. L., et al. (2013). Real-time fMRI neurofeedback: progress and challenges. *Neuroimage* 76, 386–399. doi: 10.1016/j.neuroimage.2013.03.033

Szuromi, B., Czobor, P., Komlosi, S., and Bitter, I. (2011). P300 deficits in adults with attention deficit hyperactivity disorder: a meta-analysis. *Psychol. Med.* 41, 1529–1538. doi: 10.1017/S0033291710001996

ter Huurne, N., Onnink, M., Kan, C., Franke, B., Buitelaar, J., and Jensen, O. (2013). Behavioral consequences of aberrant alpha lateralization in attention-deficit/hyperactivity disorder. *Biol. Psychiatry* 74, 227–233. doi: 10.1016/j.biopsych.2013.02.001

Thorpe, S., D'Zmura, M., and Srinivasan, R. (2012). Lateralization of frequency-specific networks for covert spatial attention to auditory stimuli. *Brain Topogr.* 25, 39–54. doi: 10.1007/s10548-011-0186-x

Thut, G., Nietzel, A., Brandt, S. A., and Pascual-Leone, A. (2006). Alpha-band electroencephalographic activity over occipital cortex indexes visuospatial attention bias and predicts visual target detection. *J. Neurosci.* 26, 9494–9502. doi: 10.1523/JNEUROSCI.0875-06.2006

Tonin, L., Leeb, R., Sobolewski, A., and Millan Jdel, R. (2013). An online EEG BCI based on covert visuospatial attention in absence of exogenous stimulation. *J. Neural Eng.* 10:056007. doi: 10.1088/1741-2560/10/5/056007

Tomita, Y., Vialatte, F. B., Dreyfus, G., Mitsukura, Y., Bakardjian, H., and Cichocki, A. (2014). Bimodal BCI using simultaneously NIRS and EEG. *IEEE Trans. Biomed. Eng.* 61, 1274–1284. doi: 10.1109/TBME.2014.2300492

Valera, E. M., Faraone, S. V., Murray, K. E., and Seidman, L. J. (2007). Meta-analysis of structural imaging findings in attention-deficit/hyperactivity disorder. *Biol. Psychiatry* 61, 1361–1369. doi: 10.1016/j.biopsych.2006.06.011

Vance, A. L., Luk, E. S., Costin, J., Tonge, B. J., and Pantelis, C. (1999). Attention deficit hyperactivity disorder: anxiety phenomena in children treated with psychostimulant medication for 6 months or more. *Aust. N.Z. J. Psychiatry* 33, 399–406. doi: 10.1046/j.1440-1614.1999.00575.x

van der Waal, M., Severens, M., Geuze, J., and Desain, P. (2012). Introducing the tactile speller: an ERP-based brain-computer interface for communication. *J. Neural Eng.* 9:045002. doi: 10.1088/1741-2560/9/4/045002

Van Gerven, M., Farquhar, J., Schaefer, R., Vlek, R., Geuze, J., Nijholt, A., et al. (2009). The brain-computer interface cycle. *J. Neural Eng.* 6:041001. doi: 10.1088/1741-2560/6/4/041001

Vidaurre, C., Kawanabe, M., von Bunau, P., Blankertz, B., and Muller, K. R. (2011). Toward unsupervised adaptation of LDA for brain-computer interfaces. *IEEE Trans. Biomed. Eng.* 58, 587–597. doi: 10.1109/TBME.2010.2093133

Vollebregt, M. A., van Dongen-Boomsma, M., Buitelaar, J. K., and Slaats-Willemse, D. (2014a). Does EEG-neurofeedback improve neurocognitive functioning in children with attention-deficit/hyperactivity disorder? A systematic review and a double-blind placebo-controlled study. *J. Child Psychol. Psychiatry* 55, 460–472. doi: 10.1111/jcpp.12143

Vollebregt, M. A., van Dongen-Boomsma, M., Slaats-Willemse, D., Buitelaar, J. K., and Oostenveld, R. (2014b). How the individual alpha peak frequency helps unravel the neurophysiologic underpinnings of behavioral functioning in children with attention-deficit/hyperactivity disorder. *Clin. EEG Neurosci.* 46, 285–291. doi: 10.1177/1550059414537257

Waldert, S., Tushaus, L., Kaller, C. P., Aertsen, A., and Mehring, C. (2012). fNIRS exhibits weak tuning to hand movement direction. *PLoS ONE* 7:e49266. doi: 10.1371/journal.pone.0049266

Wang, S., Yang, Y., Xing, W., Chen, J., Liu, C., and Luo, X. (2013). Altered neural circuits related to sustained attention and executive control in children with ADHD: an event-related fMRI study. *Clin. Neurophysiol.* 124, 2181–2190. doi: 10.1016/j.clinph.2013.05.008

Wangler, S., Gevensleben, H., Albrecht, B., Studer, P., Rothenberger, A., Moll, G. H., et al. (2011). Neurofeedback in children with ADHD: specific event-related potential findings of a randomized controlled trial. *Clin. Neurophysiol.* 122, 942–950. doi: 10.1016/j.clinph.2010.06.036

Ward, L. M., Doesburg, S. M., Kitajo, K., MacLean, S. E., and Roggeveen, A. B. (2006). Neural synchrony in stochastic resonance, attention, and consciousness. *Can. J. Exp. Psychol.* 60, 319–326. doi: 10.1037/cjep2006029

Weiskopf, N., Mathiak, K., Bock, S. W., Scharnowski, F., Veit, R., Grodd, W., et al. (2004). Principles of a brain-computer interface (BCI) based on real-time functional magnetic resonance imaging (fMRI). *IEEE Trans. Biomed. Eng.* 51, 966–970. doi: 10.1109/TBME.2004.827063

Wolfe, J. M., and Horowitz, T. S. (2004). What attributes guide the deployment of visual attention and how do they do it? *Nat. Rev. Neurosci.* 5, 495–501. doi: 10.1038/nrn1411

Wolpaw, J. R., Birbaumer, N., Heetderks, W. J., McFarland, D. J., Peckham, P. H., Schalk, G., et al. (2000). Brain-computer interface technology: a review of the first international meeting. *IEEE Trans. Rehabil. Eng.* 8, 164–173. doi: 10.1109/TRE.2000.847807

Wolpaw, J. R., McFarland, D. J., Neat, G. W., and Forneris, C. A. (1991). An EEG-based brain-computer interface for cursor control. *Electroencephalogr. Clin. Neurophysiol.* 78, 252–259. doi: 10.1016/0013-4694(91)90040-B

Wu, J., Li, Q., Bai, O., and Touge, T. (2009). Multisensory interactions elicited by audiovisual stimuli presented peripherally in a visual attention task: a behavioral and event-related potential study in humans. *J. Clin. Neurophysiol.* 26, 407–413. doi: 10.1097/WNP.0b013e3181c298b1

Wu, Z., and Su, S. (2014). A dynamic selection method for reference electrode in SSVEP-based BCI. *PLoS ONE* 9:e104248. doi: 10.1371/journal.pone.0104248

Xu, P., Tian, C., Zhang, Y., Jing, W., Wang, Z., Liu, T., et al. (2013). Cortical network properties revealed by SSVEP in anesthetized rats. *Sci. Rep.* 3, 1–11. doi: 10.1038/srep02496

Yang, L., Leung, H., Peterson, D. A., Sejnowski, T. J., and Poizner, H. (2014). Toward a semi-self-paced EEG brain computer interface: decoding initiation state from non-initiation state in dedicated time slots. *PLoS ONE* 9:e88915. doi: 10.1371/journal.pone.0088915

Yoo, S. S., Kim, H., Filandrianos, E., Taghados, S. J., and Park, S. (2013). Non-invasive brain-to-brain interface (BBI): establishing functional links between two brains. *PLoS ONE* 8:e60410. doi: 10.1371/journal.pone.0060410

Zacksenhouse, M., Lebedev, M. A., Carmena, J. M., O'Doherty, J. E., Henriquez, C., and Nicolelis, M. A. (2007). Cortical modulations increase in early sessions with brain-machine interface. *PLoS ONE* 2:e619. doi: 10.1371/journal.pone.0000619

Zandi Mehran, Y., Firoozabadi, M., and Rostami, R. (2014). Improvement of neurofeedback therapy for improved attention through facilitation of brain activity using local sinusoidal extremely low frequency magnetic field exposure. *Clin. EEG Neurosci.* 46, 100–112. doi: 10.1177/1550059414524403

Zarin, D. A., Suarez, A. P., Pincus, H. A., Kupersanin, E., and Zito, J. M. (1998). Clinical and treatment characteristics of children with attention-deficit/hyperactivity disorder in psychiatric practice. *J. Am. Acad. Child Adolesc. Psychiatry* 37, 1262–1270. doi: 10.1097/00004583-199812000-00009

Zhang, D., Maye, A., Gao, X., Hong, B., Engel, A. K., and Gao, S. (2010). An independent brain-computer interface using covert non-spatial visual selective attention. *J. Neural Eng.* 7:16010. doi: 10.1088/1741-2560/7/1/016010

Zhang, Y., Chen, Y., Bressler, S. L., and Ding, M. (2008). Response preparation and inhibition: the role of the cortical sensorimotor beta rhythm. *Neuroscience* 156, 238–246. doi: 10.1016/j.neuroscience.2008.06.061

Zhang, Y., Guo, D., Cheng, K., Yao, D., and Xu, P. (2015). The graph theoretical analysis of the SSVEP harmonic response networks. *Cogn. Neurodyn.* 9, 305–315. doi: 10.1007/s11571-015-9327-3

Zheng, H. Y., Peng, G., Chen, J. Y., Zhang, C., Minett, J. W., and Wang, W. S. (2014). The influence of tone inventory on ERP without focal attention: a cross-language study. *Comput. Math. Methods Med.* 2014:961563. doi: 10.1155/2014/961563

Conflict of Interest Statement: The authors declare that the research was conducted in the absence of any commercial or financial relationships that could be construed as a potential conflict of interest.

frontiers in Neuroscience

PERSPECTIVE
published: 27 April 2016
doi: 10.3389/fnins.2016.00186

Predictive Technologies: Can Smart Tools Augment the Brain's Predictive Abilities?

Giovanni Pezzulo[1]*, *Alessandro D'Ausilio*[2] and *Andrea Gaggioli*[3,4]

[1] Institute of Cognitive Sciences and Technologies, National Research Council, Rome, Italy, [2] IIT - Istituto Italiano di Tecnologia, CTNSC@UniFe - Center of Translational Neurophysiology for Speech and Communication, Ferrara, Italy, [3] Department of Psychology, Università Cattolica del Sacro Cuore, Milan, Italy, [4] Applied Technology for Neuro-Psychology Lab, I.R.C.C.S. Istituto Auxologico Italiano, Milan, Italy

The ability of "looking into the future"—namely, the capacity of anticipating future states of the environment or of the body—represents a fundamental function of human (and animal) brains. A goalkeeper who tries to guess the ball's direction; a chess player who attempts to anticipate the opponent's next move; or a man-in-love who tries to calculate what are the chances of her saying yes—in all these cases, people are simulating possible future states of the world, in order to maximize the success of their decisions or actions. Research in neuroscience is showing that our ability to predict the behavior of physical or social phenomena is largely dependent on the brain's ability to integrate current and past information to generate (probabilistic) simulations of the future. But could predictive processing be augmented using advanced technologies? In this contribution, we discuss how computational technologies may be used to support, facilitate or enhance the prediction of future events, by considering exemplificative scenarios across different domains, from simpler sensorimotor decisions to more complex cognitive tasks. We also examine the key scientific and technical challenges that must be faced to turn this vision into reality.

Keywords: predictive processing, planning, robotics, augmented reality, brain stimulation

OPEN ACCESS

Edited by:
Mikhail Lebedev,
Duke University, USA

Reviewed by:
Victor Manuel Pulgar,
Wake Forest School of Medicine, USA
Emiliano Macaluso,
Fondazione Santa Lucia, Italy

***Correspondence:**
Giovanni Pezzulo
giovanni.pezzulo@istc.cnr.it

Specialty section:
This article was submitted to Neural Technology, a section of the journal Frontiers in Neuroscience

Received: *23 February 2016*
Accepted: *11 April 2016*
Published: *27 April 2016*

Citation:
Pezzulo G, D'Ausilio A and Gaggioli A (2016) Predictive Technologies: Can Smart Tools Augment the Brain's Predictive Abilities? Front. Neurosci. 10:186. doi: 10.3389/fnins.2016.00186

INTRODUCTION

Modern cognitive neuroscience describes the brain as a predictive device, not a stimulus-response system. In this "predictive brain" perspective, the brain continuously predicts environmental dynamics and anticipates action effects, and this permits animals to be "ahead of time" when it takes decisions, rather than just react to what it currently senses (Pezzulo, 2008; Bar, 2009; Friston, 2010). Predictive abilities range from short-term predictions, which target (say) the few hundreds of milliseconds—the timescale of the sensorimotor loop, which is relevant to predict (say) whether or not to cross a busy road—to medium- or long-term predictions, which are useful for distal decisions such as the road to take to go home or the career to choose.

Recent research is shedding light on the neuronal underpinnings of these diverse abilities. For example, a growing literature studies predictive dynamics in sensorimotor control, highlighting the importance of so-called forward models: internal models that the brain uses to predict action consequences and plan accurate movements (Wolpert and Ghahramani, 2000). Even more interesting, research in "motor cognition" has shown that these forward models can be widely reused outside motor control, in more cognitive such as domains

action recognition, action simulation and imagery (Jeannerod, 2006). Predictive domains, have been widely studied in many other domains of cognition, such as perceptual processing and navigation. For example, growing evidence indicates that internally generated brain dynamics in the (rodent) hippocampus might support navigational planning: in fact, if one registers from the hippocampus of rodents at rest before a decision, one can find neuronal sequences of place cells assembled to form trajectories in T-mazes, which can be predictive of the actual trajectories that they will select immediately afterwards (Johnson and Redish, 2007; Pfeiffer and Foster, 2013; Pezzulo et al., 2014). Based on parallels between neurophysiological evidence and human neuroimaging studies, it has been (speculatively) proposed that the ability to internally generate and "mesh" dynamical events—especially in the hippocampus—might support sophisticated prospective abilities such as the mental simulation of future events and "mental time travel" (Schacter et al., 2012; Buzsáki et al., 2014).

From the "predictive brain" perspective, the ubiquity of predictive components across cognitive domains reflects the fact that brain processing is intrinsically predictive. The most comprehensive attempt to describe formally the "predictive brain" perspective is the *free energy principle* developed by Friston and collaborators (Friston, 2010; Pezzulo et al., 2015). In this perspective, the brain is a statistical machine that learns a so-called *generative model* of external dynamics (especially how the environment changes as a function of the agent's actions) and uses it for continuous prediction. Importantly, prediction can be at multiple timescales, where these timescales map to brain hierarchies (especially cortical hierarchies) and increase from motor and premotor areas to prefrontal areas (Badre, 2008). Here, cognition depends on the interplay of top-down and bottom-up signals across (brain) hierarchical layers, the former propagating predictions and the latter prediction errors. Minimizing prediction errors (the difference from what is expected and what is sensed) across layers—or more formally minimizing free energy—supports both perception (because perceptual hypotheses encoded at higher levels can be revised based on prediction errors) and action (because goals encoded at higher hierarchical layers generate a cascade of exteroceptive and proprioceptive predictions, say on the next desired hand position, and the latter are ultimately suppressed by engaged reflexes that—essentially—guide the hand to the desired position). The same principles of prediction error minimization have been extended to model the planning of action sequences—when, essentially, predictions stemming from the generative model (encoding the agent's knowledge of action-outcome contingencies) are "chained" to covertly simulate and evaluate possible action plans in advance, before the agent performs any actual action or receives external feedback (Friston et al., 2012, 2015).

In sum, the idea of a "predictive brain" is becoming dominant in cognitive neuroscience. In this article, we explore an intriguing technological side of this phenomenon: the possible development of "predictive technologies" that augment human prediction. We address questions such as: is it possible to augment predictive abilities in humans using technologies? Which kind of predictions can be enhanced? Is it possible to use enhanced predictive abilities to improve real-time decisions and actions? What are the key scientific/technological issues for developing predictive technologies? And what are their potential applications?

Of course, prediction-based technologies are already routinely used, for example, in weather or stock market forecast, or in the development of smart (e.g., self-guiding) cars. Here, however, we specifically focus on *predictive technologies that can be seamlessly integrated into real-time human cognition, and augment it*. We discuss, for example, new interfaces that help humans predict the movements of a car in order to decide when to cross a busy road. Below we consider this and other specific examples of predictive technologies that—we will argue—might be soon within our reach.

DOMAINS OF ENHANCED PREDICTION

Human cognitive tasks involve short-, medium- or long-term predictions—and at least in principle, predictive technologies can support all them. Here we focus our analysis on predictive technologies that can support real-time, embodied decisions (Cisek and Pastor-Bernier, 2014; Lepora and Pezzulo, 2015), such as for example those that we continuously face when we drive a car (should I accelerate or press the brake?), which are based on short-term predictions of the order of hundreds of milliseconds (am I risking a collision with a pedestrian?) or sometimes medium-term predictions; but we do not target decisions that unfold over longer-term timescales such as "which University or career should I select?".

It is important to distinguish between two potential outputs of predictive technologies. The first, direct output of a predictive technology is enhancing a person's prediction abilities. For example, the technology might help a goalkeeper predicting the trajectory of a penalty kick, on the basis of (say) statistical information about past penalty kicks and the movements of the attacker. A second, more indirect output of predictive technologies is aiding decision-making and/or planning (based on prediction). For example, the predictive technology might suggest the goalkeeper the action course that maximizes the probability to parry the penalty kick, given the predicted trajectory. Below we provide examples of both kinds.

Consider the case of a person who wants to cross a busy road. Deciding when to cross is a complex embodied decision that has to take into consideration several factors, from cognitive rules and knowledge (e.g., knowledge of traffic rules; presence of traffic lights) to situational facts (e.g., where are the cars and at what velocity they run; what my own velocity is; how long the road to be crossed is). Various predictions can be useful to solve this task, such as the prediction of "where" a car is going, "whether" it will stop or "when" it will arrive at the crossing point. There are cases when an augmentation technology may help, such as when the person who is crossing has impaired perceptual or cognitive abilities, or comes from another culture (think of a Chinese tourist crossing a busy road in Rome).

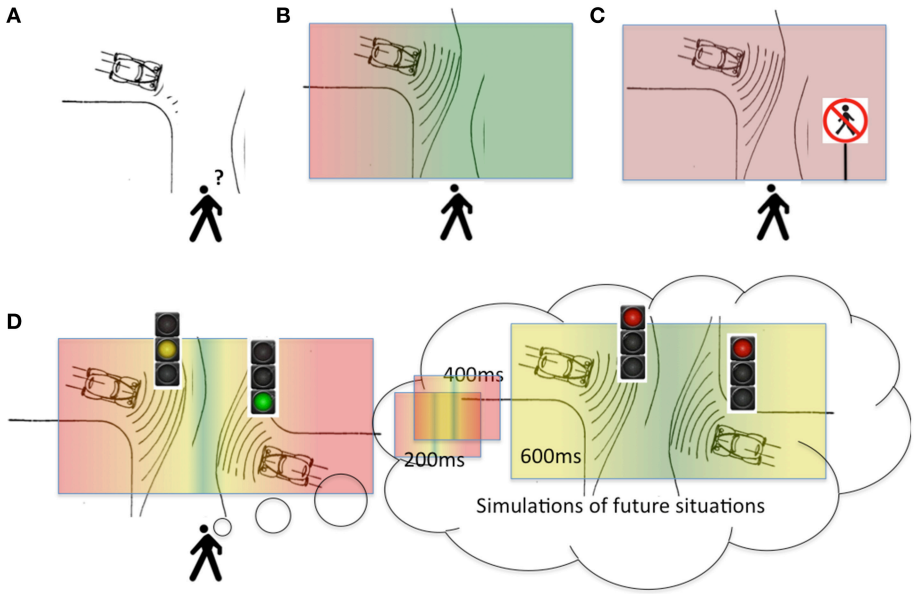

FIGURE 1 | How the affordance landscape changes as an effect of car movements and traffic signs. (A) An example situation: a pedestrian has to cross a road, with a car approaching. **(B)** The same situation, but now with the putative results of a predictive technology superimposed: here, the lines in front of the car represent its predicted future locations, and the colors represent a gradient of the "cross-ability" affordance (red = not crossable; green = crossable) ordered in a continuum. **(C)** The same situation with a traffic panel does not afford cross-ability anymore. **(D)** A more complex scenario, in which the predictive technology might simulate future simulated situations, e.g., display how the affordance landscape will change in the next 200, 400, and 600 ms.

How can we design a predictive technology that augments human cognition in this kind of situation? A useful starting point is the notion of an "affordance," which originates from ecological psychology (Gibson, 1979) but is also used in neuroscience (Cisek and Kalaska, 2010; Pezzulo and Cisek, 2016). In this perspective, an empty street *affords* "cross-ability," whereas a busy road does not. More generally, one can think of a "landscape" of affordances, which changes as an effect of environmental dynamics and our own actions. For example a car approaching fast in our direction (see **Figure 1**) modifies the landscape of "cross-ability" over time: when the car is far, the road is cross-able; but when it approaches, it becomes not cross-able. The concept of a landscape of affordances is dynamical and highly context-sensitive, in the sense that (for example) there is a gradient of "cross-ability" over time and it depends on both our and the car's velocity and direction, as well as the color of the traffic light (see **Figures 1B–D**).

While ecological psychology has often focused on the idea of exploiting available affordances (e.g., use the "sit-ability" of a chair to sit down), here we recast this concept in predictive terms, and discuss how the *prediction* of (for example) car movements permits to foresee how the affordance landscape will change in the immediate future - and to spot in advance the right time window to cross the road. **Figure 2B** exemplifies the potential benefits of a predictive technology: an augmented reality display that shows (predictively) the affordance landscape and signals that a good time frame for crossing the road is approaching (see later for a discussion of the feasibility of this technology and its required components). Coming back to our previous distinction between "prediction" and "prediction-based decision or planning," here the curved lines around the car represent its predicted future locations, while the colored parts represent the future predicted affordances (red = not crossable; green = crossable)—which can be considered as an aid to the decision (when and where to cross) based on the predicted car trajectory.

Another, more complex example concerns the decision of which path to take to cross a crossroad and reach a supermarket. This can be considered analogous to the "travel planning" functionality of Google maps (https://www.google.it/maps), which already takes several factors into account (e.g., length, size of streets, current traffic) to provide an estimate of "the best" or "the faster" road. Predictive technologies can extend these functionalities by considering various contextual factors, such as the current "cross-ability" affordances (as above) and the anticipated effort associated to the different paths (e.g., one path might require climbing stairs)—which in turn might require predicting energy expenditure based on physiological signals (e.g., heart rate) or other information (e.g., age). Here, different from the former example, the predictive technology would not (only) show a field of affordances, but—like Google maps—propose several paths and suggest the best one. Importantly, this exemplifies a medium-term decision, not a short-term decision as in road crossing case, and it can incorporate various elements and various predictions, at short and medium terms.

As a third example, let's consider a professional domain: an aircraft pilot who has to decide which buttons to press, which levers to pull, which indicators to look at, etc. A predictive technology might help pilots predict (for example) the outcome of different maneuver by directing attention to the controls

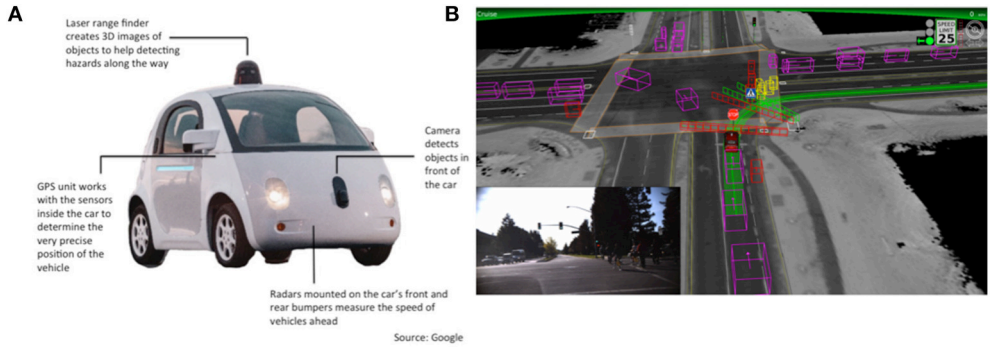

FIGURE 2 | Examples of enabling technologies. (A) Sensors of a self-driving car (source: Google). **(B)** Schematic of how objects are represented (from the self-guiding car's perspective) while approaching a turn; the inset shows what a human driver sees from inside the car. This representation can be used to generate predictions (e.g., of the trajectory of cars and pedestrians) based, for example, on probabilistic mechanisms (Thrun et al., 2006).

that are likely to show the most critical information. These functionalities might be useful for pilots but more critically to those who are learning to fly; the latter might learn faster if their attention is directed to the most relevant displays or controls.

As these examples illustrate, predictive technologies can augment human predictive abilities and be flexibly incorporated into human cognition, providing raw predictions (of car movements), suggestions (of a road to take) or guiding attention (to the most-likely-to-be-useful displays)—just to make a few examples.

ENABLING TECHNOLOGIES

In the previous section we have briefly discussed a few examples of predictive technologies and their use in everyday life. These examples are (on purpose) beyond the scope of the current state of the art. However, some components required by predictive technologies—software or hardware—are already available as components of existing technologies, or are currently studied as part of research programs. Here we provide some examples of enabling technologies that might support the future development of predictive technologies.

Self-driving cars are under development by many companies (e.g., Google, Tesla) and they might enter in the market in the near future. Self-driving cars already use many technologies—from sensors such as laser cameras and radars to dedicated processors—that can be integrated in future predictive technologies, see **Figure 2A**. Furthermore, at the software level, self-driving cars use prediction for control and planning—for example, to predict car trajectories that avoid collisions; and some of the solutions implemented in self-driving cars might be reused within human augmentation systems such as those that we described in the previous section.

Although self-driving cars use a range of diverse mechanisms, some solutions to key problems such as self-localization, path planning, data fusion and trajectory prediction are reused from robot navigation (Thrun et al., 2006) and most can be solved using probabilistic prediction methods (Thrun et al., 2006). Predictive mechanisms, and in particular methods for approximate-but-fast prediction figure prominently in both robot navigation (Montemerlo et al., 2002) and self-driving cars.

Another example of predictive algorithm that was initially developed for robotics but might be reused (or modified) within predictive technologies is the "internal world model" used by Ripley the robot (Roy et al., 2004). The system uses a physical engine to simulate or predict the robot movements, and to keep the "world model" of the robot updated—for example, to keep simulating the trajectory of a moving ball even if the robot is looking somewhere else. In this way, the robot's internal model is continuously "in register" with the external world. This software exemplifies the idea of using a physical engine—of the kind used, for example, in computer games—to run physically realistic simulations. Many widely-used physical engines are very accurate and can afford real-time simulation or prediction. Of course, they cannot simulate everything with the required level of accuracy (and in real time), thus their putative role within a predictive technology can only be evaluated case-by-case.

Physical engines have been also used for simulation in a series of studies on human physical scene understanding, such as how well humans predict how towers of wooden bricks will fall down (Battaglia et al., 2013). This study illustrates that a physical engine simulation can be used to predict in real time a challenging physical event that derives from the interaction of many components (here, many wooden bricks). This method might be extended to predict how other physical events (e.g., movements of objects such as cars) unfold in time.

Another example of a computational solution developed within robotics is the idea of "affordance gradients": a formalism that describes the transformations that can be applied on an object (e.g., how a triangular object rotates when it is pushed or pulled) and permits a robot to plan actions that exploit the affordances to achieve goals (e.g., plan a series of pushing actions that guide the triangular object to a desired or goal position, see Sanchez-Fibla et al., 2011). This method can be potentially reused outside robotics to represent e.g., the affordances of objects and infer their dynamics.

As these examples demonstrate, some component solutions of predictive technologies are available or under development. At the same time, these are still incomplete solutions to the

problems of prediction, planning and decision, especially in real time (Geffner, 2013; Donnarumma et al., 2016). Thus, a key challenge for future research is integrating and extending these (and other) models to deliver predictive technologies that are effective and usable. Another key issue is making predictive technologies *usable*—a theme that we explore next.

REPRESENTING PREDICTIVE INFORMATION

A key challenge of predictive technologies is how to represent the information about an upcoming event (predictive cue). As suggested earlier, augmented reality may provide a viable solution. An augmented reality system allows superimposing digital information on the physical environment in real-time using a smartphone or head-mounted see-through displays coupled with a wearable computer. Thanks to recent progresses, current augmented reality systems afford real-time applications in which the user can interact with synthetic objects, manipulate them and receive additional information about the environment or the task at hand, in the form of images, text, video, audio components, etc.

Predictive information could be represented in augmented reality using various levels of abstraction, ranging from analog models to symbolic cues. For example, consider the question of how to represent the predicted trajectory of a ball. One could either visualize a virtual ball that precedes the actual ball (analog representation) or use a dynamic arrow (symbolic representation). In choosing the most appropriate representation of the predictive cue, a key requirement is the definition of temporal constraints. If the augmentation cue is too complex, its processing time may even exceed the timeframe available to complete the task, thus rendering the augmentation useless. For example, in rallying the pacenotes are a commonly used method of describing a route to be taken, in terms of turnings, junctions, the degree and severity of bends etc. The notes are designed to help the driver anticipating the conditions of the course ahead, but with a fast-moving vehicle, they are encoded to carry maximal information in minimum reading time. Relatedly, the design of AR interface should take into account user's cognitive requirements, i.e., by preventing split-attention between multiple predictive cues while preserving global situation awareness. This translates to the need for optimizing the trade-off between cue's maximal informativity about upcoming event(s) and least cognitive processing effort.

A further issue is whether, and in which ways, the presentation of the predictive cue could affect the course of the predicted event. For example, if a goalkeeper is shown the prediction that the penalty taker is going to place the ball at the lower right corner, he/she will jump as fast as possible to the lower right corner in order to reach the ball. However, if the goalkeeper initiates the movement too early, the penalty taker may notice the goalkeeper's intention and kick the ball in the opposite corner. Thus, in designing augmented predictions, it is necessary to model the complex interdependencies between the user's action and the context of his/her action, in order to prevent the predictive cue triggering behaviors that affect the course of events in (unpredictable) ways.

CONCLUSIONS

We have explored the idea of using technology to augment the human ability of predicting future events, by seamlessly integrating anticipatory information in the perception-action loop. The presentation of predictive cues is meant to facilitate perceptual, decision and action processes. Some key building blocks of predictive technology are available from developments in robotics and machine learning. In these fields, the need of accurately modeling the evolution of complex system has led to the deployment of computational solutions that could be eventually re-adapted to match the requirements of predictive cognition. However, the provision of external cues may not be the only possible approach to augment predictive processing. A rather more ambitious strategy could be to directly stimulating brain areas that are implicated in the computation of future events. Numerous studies have shown the possibility of modulating, and in some cases enhancing, cognitive processes by exciting brain regions involved in working memory and attention through transcranial electrical brain stimulation, including planning ability (Dockery et al., 2009). This approach could be justifiable within rehabilitation domains, where the goal would be to restore or support predictive functions in individuals suffering from neurocognitive impairments.

As the rehabilitation example suggests, predictive technologies hold the promise to enable a wide range of applications based on the extension of our prediction and planning abilities. Such application scenarios may include, but are not be limited to, anticipation of sources of dangers in natural or working environments for enhancing personal safety; support decision making and judgments in emergency situations; optimization of team coordination in complex collaboration tasks. Clearly, the exploitation of these possibilities require to address significant scientific and technological challenges, some of which have been outlined in this contribution. However, as understanding of cognitive mechanisms involved in predicting future progresses, so should the ability of enhancing these processes using advanced technologies.

AUTHOR CONTRIBUTIONS

GP and AG jointly conceived the main idea behind the article. GP drafted the manuscript. AD and AG gave conceptual advice and revised the manuscript critically for important intellectual content. GP and AG edited the manuscript. All authors read and approved the final manuscript.

ACKNOWLEDGMENTS

GP is funded by the EU's FP7 Initiative (grant FP7-270108) and the HFSP (grant RGY0088/2014).

REFERENCES

Badre, D. (2008). Cognitive control, hierarchy, and the rostro–caudal organization of the frontal lobes. *Trends Cogn. Sci.* 12, 193–200. doi: 10.1016/j.tics.2008.02.004

Bar, M. (2009). The proactive brain: memory for predictions. *Philos. Trans. R. Soc. Lond. B Biol. Sci.* 364, 1235–1243. doi: 10.1098/rstb.2008.0310

Battaglia, P. W., Hamrick, J. B., and Tenenbaum, J. B. (2013). Simulation as an engine of physical scene understanding. *Proc. Natl. Acad. Sci. U.S.A.* 110, 18327–18332. doi: 10.1073/pnas.1306572110

Buzsáki, G., Peyrache, A., and Kubie, J. (2014). Emergence of cognition from action. *Cold Spring Harb. Symp. Quant. Biol.* 79, 41–50. doi: 10.1101/sqb.2014.79.024679

Cisek, P., and Kalaska, J. F. (2010). Neural mechanisms for interacting with a world full of action choices. *Annu. Rev. Neurosci.* 33, 269–298. doi: 10.1146/annurev.neuro.051508.135409

Cisek, P., and Pastor-Bernier, A. (2014). On the challenges and mechanisms of embodied decisions. *Philos. Trans. R Soc. Lond. B Biol. Sci.* 369, 20130479. doi: 10.1098/rstb.2013.0479

Dockery, C. A., Hueckel-Weng, R., Birbaumer, N., and Plewnia, C. (2009). Enhancement of planning ability by transcranial direct current stimulation. *J. Neurosci.* 29, 7271–7277. doi: 10.1523/JNEUROSCI.0065-09.2009

Donnarumma, F., Maisto, D., and Pezzulo, G. (2016). Problem solving as probabilistic inference with subgoaling: explaining human successes and pitfalls in the Tower of Hanoi. *PLoS Comput. Biol.* 12:e1004864. doi: 10.1371/journal.pcbi.1004864

Friston, K. (2010). The free-energy principle: a unified brain theory? *Nat. Rev. Neurosci.* 11, 127–138. doi: 10.1038/nrn2787

Friston K., Rigoli, F., Ognibene, D., Mathys, C., Fitzgerald, T., and Pezzulo, G. (2015). Active inference and epistemic value. *Cogn. Neurosci.* 6, 187–214. doi: 10.1080/17588928.2015.1020053

Friston, K., Samothrakis, S., and Montague, R. (2012). Active inference and agency: optimal control without cost functions. *Biol. Cybern.* 106, 523–541. doi: 10.1007/s00422-012-0512-8

Geffner, H. (2013). Computational models of planning. *Wiley Interdiscip. Rev. Cogn. Sci.* 4, 341–356. doi: 10.1002/wcs.1233

Gibson, J. J. (1979). *The Ecological Approach to Visual Perception*. Mahwah, NJ: Lawrence Erlbaum Associates, Inc.

Jeannerod, M. (2006). *Motor Cognition*. Oxford: Oxford University Press.

Johnson, A., and Redish, A. D. (2007). Neural ensembles in CA3 transiently encode paths forward of the animal at a decision point. *J. Neurosci.* 27, 12176–12189. doi: 10.1523/JNEUROSCI.3761-07.2007

Lepora, N., and Pezzulo, G. (2015). Embodied Choice: how action influences perceptual decision making. *PLOS Comput. Biol.* 11:e1004110. doi: 10.1371/journal.pcbi.1004110

Montemerlo, M., Thrun, S., Koller, D., and Wegbreit, B. (2002). "FastSLAM: a factored solution to the simultaneous localization and mapping problem," in *Proceedings of the Eighteenth National Conference on Artificial Intelligence* (Edmonton, AB), 593–598.

Pezzulo, G. (2008). Coordinating with the future: the anticipatory nature of representation. *Minds Mach.* 18, 179–225. doi: 10.1007/s11023-008-9095-5

Pezzulo, G., Rigoli, F., and Friston, K. (2015). Active Inference, homeostatic regulation and adaptive behavioural control. *Prog. Neurobiol.* 134, 17–35. doi: 10.1016/j.pneurobio.2015.09.001

Pezzulo, G., van der Meer, M. A., Lansink, C. S., and Pennartz, C. M. (2014). Internally generated sequences in learning and executing goal-directed behavior. *Trends Cogn. Sci.* 18, 647–657. doi: 10.1016/j.tics.2014.06.011

Pezzulo, G. and Cisek, P. (2016). Navigating the affordance landscape: feedback control as a process model of behavior and cognition. *Trends Cogn. Sci.* doi: 10.1016/j.tics.2016.03.013

Pfeiffer, B. E., and Foster, D. J. (2013). Hippocampal place-cell sequences depict future paths to remembered goals. *Nature* 497, 74–79. doi: 10.1038/nature12112

Roy, D., Hsiao, K. Y., and Mavridis, N. (2004). Mental imagery for a conversational robot. *IEEE Trans. Syst. Man. Cybern. B. Cybern.* 34, 1374–1383. doi: 10.1109/TSMCB.2004.823327

Sanchez-Fibla, M., Duff, A., and Verschure, P. F. (2011). "The acquisition of intentionally indexed and object centered affordance gradients: a biomimetic controller and mobile robotics benchmark," in *Intelligent Robots and Systems (IROS), 2011 IEEE/RSJ International Conference on. IEEE*, (San Francisco, CA), 1115–1121.

Schacter, D. L., Addis, D. R., Hassabis, D., Martin, V. C., Spreng, R. N., and Szpunar, K. K. (2012). The future of memory: remembering, imagining, and the brain. *Neuron* 76, 677–694. doi: 10.1016/j.neuron.2012.11.001

Thrun, S., Montemerlo, M., Dahlkamp, H., Stavens, D., Aron, A., Diebel, J. et al. (2006). Stanley: The robot that won the DARPA Grand Challenge. *J. Field Robot.* 23, 661–692. doi: 10.1002/rob.20147

Wolpert, D. M., and Ghahramani, Z. (2000). Computational principles of movement neuroscience. *Nat. Neurosci.* 3, 1212–1217. doi: 10.1038/81497

Conflict of Interest Statement: The authors declare that the research was conducted in the absence of any commercial or financial relationships that could be construed as a potential conflict of interest.

frontiers in Neuroscience

HYPOTHESIS AND THEORY
published: 23 September 2016
doi: 10.3389/fnins.2016.00438

Trends and Challenges in Neuroengineering: Toward "Intelligent" Neuroprostheses through Brain-"Brain Inspired Systems" Communication

*Stefano Vassanelli * and Mufti Mahmud*

NeuroChip Laboratory, Department of Biomedical Sciences, University of Padova, Padova, Italy

Future technologies aiming at restoring and enhancing organs function will intimately rely on near-physiological and energy-efficient communication between living and artificial biomimetic systems. Interfacing brain-inspired devices with the real brain is at the forefront of such emerging field, with the term "neurobiohybrids" indicating all those systems where such interaction is established. We argue that achieving a "high-level" communication and functional synergy between natural and artificial neuronal networks *in vivo*, will allow the development of a heterogeneous world of neurobiohybrids, which will include "living robots" but will also embrace "intelligent" neuroprostheses for augmentation of brain function. The societal and economical impact of intelligent neuroprostheses is likely to be potentially strong, as they will offer novel therapeutic perspectives for a number of diseases, and going beyond classical pharmaceutical schemes. However, they will unavoidably raise fundamental ethical questions on the intermingling between man and machine and more specifically, on how deeply it should be allowed that brain processing is affected by implanted "intelligent" artificial systems. Following this perspective, we provide the reader with insights on ongoing developments and trends in the field of neurobiohybrids. We address the topic also from a "community building" perspective, showing through a quantitative bibliographic analysis, how scientists working on the engineering of brain-inspired devices and brain-machine interfaces are increasing their interactions. We foresee that such trend preludes to a formidable technological and scientific revolution in brain-machine communication and to the opening of new avenues for restoring or even augmenting brain function for therapeutic purposes.

Keywords: neuroengineering, biohybrid systems, neurobiohybrid systems, neuromimetic systems, brain-chip interfaces, brain machine interfaces, neurorehabilitation, artificial sensory organs

OPEN ACCESS

Edited by:
Mikhail Lebedev,
Duke University, USA

Reviewed by:
Dimiter Prodanov,
IMEC, Belgium
Fabian Kloosterman,
Neuroelectronics Research Flanders, Belgium

****Correspondence:***
Stefano Vassanelli
stefano.vassanelli@unipd.it

Specialty section:
This article was submitted to Neural Technology, a section of the journal Frontiers in Neuroscience

Received: *04 February 2016*
Accepted: *09 September 2016*
Published: *23 September 2016*

Citation:
Vassanelli S and Mahmud M (2016) Trends and Challenges in Neuroengineering: Toward "Intelligent" Neuroprostheses through Brain-"Brain Inspired Systems" Communication. Front. Neurosci. 10:438. doi: 10.3389/fnins.2016.00438

INTRODUCTION TO *NEUROBIOHYBRIDS*

An Overview on Biohybrids

The research field of biohybrid systems (or biohybrids) is capturing increasing interest across various scientific communities. The deepening of our knowledge on the physiology of living organisms –down to the cellular and molecular level– and the progress in the engineering of miniaturized interfaces between living and artificial systems, are driving research toward the

creation of biohybrids where boundaries between living beings and man-made artifacts are collapsed. Classically, individual scientific communities are approaching this type of research from a different perspective. For example, within the "*robotics*" and "*biomimetics*" community, biohybrid systems are generally considered as an opportunity to exploit the unique characteristics of biological systems or their components, refined over millions of years of natural evolution, in order to solve complex or critical problems hampering artificial systems performance (Ricotti and Menciassi, 2012; Wilson et al., 2015). In this "learning from nature" endeavor, biological systems are seen as a source of inspiration for innovative solutions, toward a "soft" and "wet" robotics or "living" systems/technologies characterized by self-organization, evolvability, adaptability, and robustness (Eiben et al., 2012). Thus, biohybrid systems come here into play as workbenches where to experiment how to build "living" artificial systems.

On the other hand, biohybrids are seen by the "*life science*" community as useful tools to explore the physiology of living organisms or even as therapeutic tools. Whenever new and more advanced ways of communication with the living matter are developed, new opportunities arise to extend our capability to measure biological parameters that are relevant for understanding physiological mechanisms. Furthermore, building artificial artifacts emulating physiological operations and interacting with natural systems is a way to assess biological working hypotheses through a "reverse engineering" and reductionist approach. Biohybrids bear a huge and yet unexplored potential also for medical application, through the embodiment of natural "intelligence" and material properties in diagnostic and therapeutic tools. Neuroprostheses (Hochberg et al., 2006) and bioelectronics medicines (Birmingham et al., 2014) represent a typical example and it is easy to assume that much effort will be deployed in the future to implement artificial devices with near-physiological characteristics and communication properties for restoring function in humans. Finally, the "*materials science and engineering*" community is active in investigating fundamentals of interfacing between living matter and inorganic material. This work goes at the root of biohybrid research and has an increasing impact on other classical disciplines, including chemistry and biology. For example, thanks also to the availability of a synthetic toolbox to conjugate biomolecules and synthetic polymers in a controlled fashion, combining biomolecules, and synthetic polymers into a new class of versatile biohybrid materials following a "click" chemistry methodology has gained much interest in recent years (Dirks et al., 2007). The concept of interdisciplinary coverage of biohybrids research is sketched in **Figure 1**.

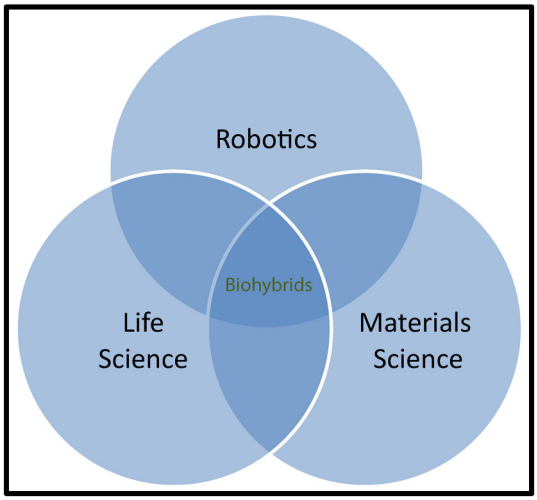

FIGURE 1 | Biohybrids as interdisciplinary research field. Within Information and Communication Technologies (ICT), Robotics, Life science, and Materials science communities are involved in biohybrids research. Scientific cooperation and interaction within the three communities is growing rapidly, although the involvement of the different actors varies by extend and typology depending on the specific research topics.

Biohybrid: A Working Definition

A common definition of biohybrid system that accepted by the scientific community is still missing. Thus, we propose a working definition to be shared with researchers interested to the field and eventually to be further refined in the future. As the term *biohybrids* encompasses a heterogeneous "melting pot" of systems spanning a range from the macro- to the nanoscale, we propose a comprehensive working definition, which highlights the importance of information exchange between living and artificial entities and its processing.

> *Biohybrid: a working definition.* A *biohybrid*, is a system formed by at least one natural and at least one artificial entity that establish close physical interactions at the molecular, cellular, or systems level, eventually leading to information flow and processing in one or both directions.

Neurobiohybrids

Within the world of biohybrids, neurobiohybrids are those where the natural component is represented by neurons. They can be present in the form of individual cells or networks, and either *in vitro* (i.e., cell culture or brain slice preparations) or *in vivo* (i.e., within the nervous system of a living animal). In general, within a neurobiohybrid, the artificial part will be composed by two functional units: (1) a device (or more devices) that have to establish the communication with neurons; (2) an interface, which mediates the physical interaction between neuron(s) and device(s), allowing the transfer of information between biological and artificial components, either in one or both directions, and its processing (**Figure 2**).

In practice, artificial devices, such as computers or bionic neuroprostheses, are communicating with neurons through energy exchange occurring in one or both directions and forming a new system acting as a whole. Whatever the approach adopted to create the neurobiohybrid system, a crucial component is represented by the interface that must include several fundamental elements to operate. First of all, in case of neuron-to-device communication, a sensor is needed, $\mathbf{S_N}$,

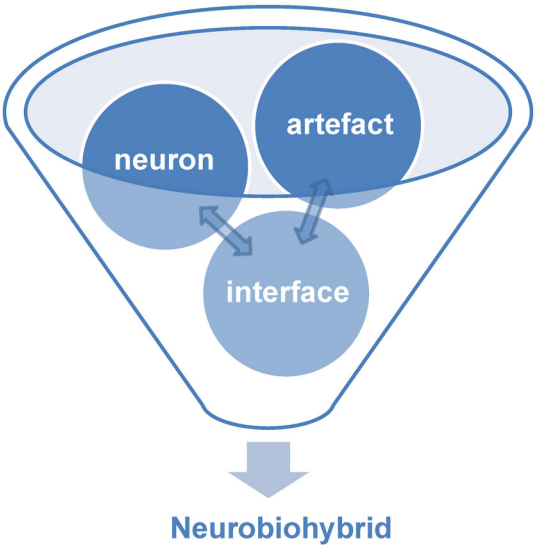

FIGURE 2 | Components of neurobiohybrid. A Neurobiohybrid is formed by three fundamental components: neuron, artifact and an interface, the latter with the function of establishing a uni- or bi-directional communication between the two.

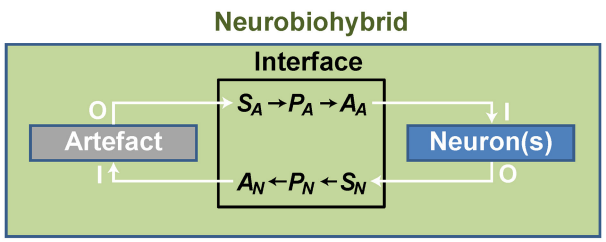

FIGURE 3 | General scheme of a neurobiohybrid. Artificial and natural components, i.e., artifact and neuron(s) respectively, communicate through a bidirectional interface. Here, signals are detected and converted by transducers, the sensor elements $\mathbf{S_A}$ and $\mathbf{S_N}$, processed by processing units, $\mathbf{P_A}$ and $\mathbf{P_N}$, and fed through actuators, $\mathbf{A_A}$ and $\mathbf{A_N}$.

transducing neuronal signals (**Figure 3**); second, a processing unit, $\mathbf{P_N}$, elaborates transduced signals; third, another transducer, the actuator $\mathbf{A_N}$, transforms the output signals from the processing unit into signals suitable to control the device. Similarly, in the opposite direction, signals from the device control the neuronal response through a chain formed by a sensor ($\mathbf{S_A}$), a processing unit ($\mathbf{P_A}$), and an actuator ($\mathbf{A_A}$) (**Figure 3**).
We must clarify how this general description of the interface is wide-ranging:

- Bidirectional communication is not an absolute requirement, as unidirectional communication is sufficient to establish a neurobiohybrid;
- Communication can occur through any type of energy conveying information (electromagnetic, chemical, mechanical). Thus, any possible mechanism allowing information exchange and processing within the neurobiohybrid is included;
- "Processing" is here intended as "operating on time-varying physical quantities." As such, the term does not solely comprise the more conventional digital or analog signal processing, but rather any type of processing that can be operated by any type of suitable processing unit, e.g., from single molecules to electronic computing architectures.

According to this introduction and the definition of biohybrid provided above, we propose a working definition of neurobiohybrid.

> *Neurobiohybrid: working definition.* A *neurobiohybrid* is a system formed by the combination of at least one neuron as natural entity and at least one device as artificial entity. To form a neurobiohybrid system, neuron(s), and device(s) establish physical interactions through an interface at the molecular, cellular, or systems level, eventually leading to information transfer and processing in one or both directions.

Noteworthy, according to such definition, all those implementations that are commonly known as brain-computer-interfaces (BCI) fall under the neurobiohybrids umbrella. Included are also those therapeutic hybrid systems working through stimulation and/or recording of the central or peripheral nervous system, and that are relying on appropriate interfacing for information transfer and processing. Typical examples based on "invasive" interfacing are deep brain stimulation (DBS, McConnell et al., 2016), neuroprosthetic limbs (e.g., Micera, 2016), cochlear implants (Roche and Hansen, 2015; Sato et al., 2016), or artificial retinas (e.g., Zeck, 2016). Interestingly, also "non-invasive" interfacing approaches such as functional electrical stimulation (FES) (for a review see Peckham and Knutson, 2005) or transcranial current stimulation (TCS, Ruffini et al., 2013) should be considered as part of the neurobiohybrids family. Given the obvious relevance of neurobiohybrids in computer science, basic neuroscience, and therapy of neurological disorders, it is no surprise that funding agencies are devoting resources to attack major challenges in the field (e.g., Miranda et al., 2015). However, we believe that, among major challenges, learning how to create functional hybrids between biological neural networks and neuromimetic architectures emulating their processing capabilities has an immense potential, particularly in the perspective of restoring or even augmenting brain function.

NEUROBIOHYBRIDS: STATE-OF-THE-ART, CURRENT TRENDS, AND CHALLENGES

In this section, a brief overview on the state-of-the-art and current trends in neurobiohybrids research is given, with particular emphasis on recent advances originating from the convergence of novel neurotechnologies and neuromimetics research. Specifically, we focus on those paving the way to "intelligent" neuroprosthetics for restoring

and augmenting brain function in living animals. We identify key scientific and technological challenges as also pointed out by Thibeault (2014), and briefly discuss opportunities and threats for the development of the neurobiohybrids research community.

Neurobiohybrids: State-of-the-Art and Main Trends

We recognize in the "dynamic clamp" technique the first fundamental leap into research on neurobiohybrids. Here, although in *in vitro* conditions, artificial neuromimetic systems are physically and functionally coupled to biological neurons with mutual information exchange in a clear manner. The dynamic clamp relies on a closed-loop control over the neuronal intracellular potential and membrane conductances, the controller being an elementary analog or software-based neuronal counterpart (Sharp et al., 1993; Prinz et al., 2004). Although ground-breaking, and despite significant improvements from the time of its introduction, this method is not suited for long-term and large-scale network implementations, as it is intrinsically limited by the interfacing through intracellular electrodes.

Brain processing, instead, deeply relies on neuronal circuits. Therefore, multi-site—and minimally invasive—techniques are necessary, allowing to interface many neurons at once within the neurobiohybrid. Attempts have been made to create network-based neurobiohybrids and in the first instance, in *in vitro* systems. For example, metal multi-electrode arrays (MEA, for a historical review of MEA, see Pine, 2006) were used to interface networks of dissociated neurons to a robot actuator where the processing was taken over by software-based spike encoding/decoding algorithms (Novellino et al., 2007). In addition, parallel progress made on neural interfaces for large-scale high-resolution multi-site recording techniques and neuromimetic nanodevices and architectures, have opened up new avenues. Recording and stimulating *in vitro* with large and dense arrays of voltage transducers (Hutzler et al., 2006; Hierlemann et al., 2011; Ferrea et al., 2012; Lewandowska et al., 2016) and optical imaging techniques (Chemla and Chavane, 2010; Tian et al., 2012) allow the gathering of spiking or sub-threshold signaling events from large neuronal networks.

Studies *in vivo*, instead, have led to implant-based BCIs and brain-machine-interfaces (BMIs) taking advantage of advanced multi-site neural interfaces and real-time software-based processing for neuroprosthetic applications. Numerous examples can be found in literature, from basic research to translational medicine, and ranging from rodents (e.g., Shobe et al., 2015), to non-human primates (Zhang et al., 2016) and even to human subjects (Hochberg et al., 2006). Although constrained in terms of number of recording/stimulation sites in comparison to their *in vitro* counterpart (Csicsvari et al., 2003; Berényi et al., 2014; Vassanelli, 2014; Schroder et al., 2015), their importance for investigating neurons in an intact brain (Buzsáki et al., 2012), or as interfaces for brain-machine communication and neuroprosthetics is well recognized (Nicolelis and Lebedev, 2009; Lebedev and Nicolelis, 2011).

However, a real paradigm shift toward "intelligent" neuroprosthetics and brain augmentation can be expected from the creation of neurobiohybrids where such brain interfaces are functionally coupled to neuromimetic devices and architectures emulating brain circuits (Thibeault, 2014). In fact, in our view, similarly to what happens for cardiac pacemakers (see Miller et al., 2015; Seriwala et al., 2016) or more "classical" prostheses (e.g., orthopedic prostheses, see Goldfarb et al., 2013; Ortiz-Catalan et al., 2014; Raspopovic et al., 2014; Vujaklija et al., 2016), the challenge is to engineer artificial neuronal systems emulating as closely as possible their natural counterpart and interfacing them efficiently to the native organ to restore (or to augment) function. Recent neuromorphic architectures based on very large scale integration (VLSI) technology (Indiveri et al., 2011; Qiao et al., 2015) and the discovery of physical components with synaptic-like plasticity properties such as memristors (Strukov et al., 2008) or carbon nanotubes based circuits (Joshi et al., 2011), have set the foundations for developing such novel generation of neurobiohybrids.

Large improvements and innovations are unquestionably necessary to achieve effective communication between natural and artificial neuronal networks. Two-way (recording and stimulation), high-resolution (down to micrometers), and large-scale (hundreds to thousands of neurons) interfacing is still beyond reach. Particularly, in this context, techniques for large-scale and high-density stimulation (also known as microstimulation) are lagging behind expectations. Although optogenetic platforms may be suitable candidates (Dugue et al., 2012; Buzsáki et al., 2015; Grosenick et al., 2015; Newman et al., 2015), other means of stimulation not requiring neuronal transfection with biological agents are to be taken into account for real clinical applications (e.g., via tuneable and field-shaped electrical stimulation or localized neurotransmitters detection and release).

Scientific and Technological Challenges

Transducers (Sensing and Actuating)

As hinted above, the development of novel sensing and actuating probes is expected to play a fundamental role in the neurobiohybrids field toward application in neuroprosthetics. A wide range of probes with different materials, design, and fabrication processes, and interfacing principles have been developed and reported earlier targeting specific research needs (for reviews see Wheeler and Nam, 2011; Spira and Hai, 2013; Vassanelli, 2014; Vidu et al., 2014; Angle et al., 2015; Fekete, 2015; Giocomo, 2015; Ruther and Paul, 2015; Lee et al., 2016; Patil and Thakor, 2016; Pisanello et al., 2016; Prodanov and Delbeke, 2016). Brain-chip interfaces are among most promising strategies to support such development (Vassanelli et al., 2012) as semiconductor technology allows for integration into a single millimeter scale device of a large number (hundreds to thousands) of microtransducers for recording and stimulation of neuronal signals.

Concerning interfaces based on electrical signaling between neurons and chips (those that are most developed so far), two fundamental approaches exist depending on the nature of the transducer:

1. Neural interfaces based on metal microelectrodes were developed first, and are now available in the form of 2D or 3D arrays that can be implanted in the brain or following a different interfacing philosophy, connected to peripheral nerves (Rutten, 2002; Wise et al., 2004; Stieglitz et al., 2014). The neuroelectronic interface is established when neuron and microelectrode are "close enough," allowing signal detection (from neuron to microelectrode) or stimulation (from microelectrode to neuron). This condition can be met both *in vitro* and *in vivo*, although under different biophysical bases. In the *in vitro* case, neurons are typically cultured on the chip surface where their membrane come into close contact with microelectrodes (i.e., typically in the tens of nanometers range) by adhering to the solid chip substrate (Braun and Fromherz, 2004). Though the original brain network topology is lost, the dissociated neurons reconnect and form a more random-like network (Haider and McCormick, 2009; Kwan and Dan, 2012). Recent technological advances allowed the development of large-scale high-density metal electrode arrays (MEA) for high-resolution recording of such neuronal networks in culture (Eversmann et al., 2011; Maccione et al., 2012; Muller et al., 2015). When a MEA, instead, is implanted in the nervous system (i.e., brain or spinal cord), transducers and neurons are more separated than in *in vitro* conditions, as cell adhesion is not governing neuro-chip interaction in this context. Also, in case of chronic implants, damaged tissue first, and gliosis afterwards are commonly building a separation layer between transducers and neurons. Thus, a volume conductor of tissue surrounds the interface and ionic currents and voltage gradients developing within it are governing recording and stimulation of neurons (Mitzdorf, 1985; Gold et al., 2006; Anastassiou et al., 2010). Other types of microstructured metal electrode-based interfaces exist, as regenerating sieves (Lago et al., 2005) and cone-in-growth electrodes (Rutten, 2002). In addition, alternative to brain implantation, microfabricated cuff or intrafascicular electrodes can be used to interface peripheral nerves (Mailley et al., 2004). Whatever the site of implantation, owing to electrochemical features of the electrolyte-metal electrode interface, faradaic currents are likely to occur, particularly when relatively large potentials come into play, i.e., during stimulation (Vassanelli, 2014).
2. The second fundamental strategy for neuron-chip interfacing aims to solve this problem by using oxide-insulated semiconductor or metal-semiconductor transducers to generate a capacitive coupling with neurons (Fromherz, 2006; Eickenscheidt et al., 2012). The approach has the advantage of relying on non-faradaic currents, at least within wider voltage ranges. Basing on this approach, very high-resolution CMOS chips have been developed for electrical imaging of neurons *in vitro* (Hutzler et al., 2006) and more recently, for *in vivo* applications (Felderer and Fromherz, 2011; Schroder et al., 2015). Noteworthy, as excitatory and inhibitory neurons are expected to respond differently to appropriately selected electrical stimuli (Mahmud and Vassanelli, 2016a), it will be strategically important to achieve a high degree of control over the electrolyte-microelectrode interface to achieve a finely tuned stimulation of neurons.

Finally, it is worth to mention that electrical neural interfaces will be improved also by clever use of novel materials. For example, read-out of neuronal activity from the mammalian brain *in vivo* was achieved by means of injectable free-standing mesh electronics (Liu et al., 2015), thus potentially minimizing tissue damage and reaction and reaching and unprecedented level of intermingling between neural tissue and electronics.

With the advent of optogenetic stimulation (Dugue et al., 2012) new hybrid optoelectronic interfaces are emerging (Park et al., 2011; Armstrong et al., 2013; Wu et al., 2013; Pashaie et al., 2015). With respect to electric stimulation (Mukaino et al., 2014; Tabot et al., 2015), optogenetics offers basically two potential advantages: (i) neuronal type specificity and (ii) the possibility to inhibit and not only to excite target neurons. It is therefore easy to foresee that a considerable amount of work will be deployed to exploit these characteristics in neurobiohybrids for controlling neuronal circuit activities within a closed-loop at cellular rsolution (Packer et al., 2015).

Although invasive interfaces are the most suitable to enable a reliable and high-resolution communication with the brain, several sorts of non-invasive brain-machine interfaces are also available (Waldert, 2016). They can be indeed included within the neurobiohybrids scheme, albeit based on unidirectional communication. They include for example EEG based platforms (Friehs et al., 2004; Norton et al., 2015), but also recent developments on fMRI for real time brain-machine interfacing (Weiskopf et al., 2007; Lee et al., 2009; Ruiz et al., 2014). On the other hand, functional electrical stimulation (FES) or transcranial current (TCS) (Ali et al., 2013) or magnetic (TMS) (Camprodon, 2016) stimulation approaches are to be included as they allow for machine-to-brain communication. Although limited in spatiotemporal resolution, non-invasive interfaces offer undoubtful advantages in terms of clinical application (Ortiz-Rosario and Adeli, 2013). "Hybrid" less-invasive solutions such as high-resolution electrocorticography (ECoG), represent an interesting compromise when cortical areas are to be interfaced for recording and perhaps, stimulation (Girardi et al., 2011; Vassanelli et al., 2012; Berényi et al., 2014; Khodagholy et al., 2015) because of their limited invasiveness with respect to in-brain implants (Pei et al., 2011; Matsushita et al., 2013).

Processing Unit

Fast processing of neuronal signals is essential for real-time performance in neurobiohybrids. When dealing with one or a few neurons, this is achievable also on the basis of conventional software or analog circuits. However, when dealing with larger networks, high-performance approaches must be considered for simultaneous real-time processing of multiple

neuronal signals. A detailed analysis of state-of-the art signal processing tools for brain-machine interfaces goes beyond the scope of this article and is available elsewhere (see, for example, Krusienski et al., 2011; Mahmud et al., 2012, 2014; Mahmud and Vassanelli, 2016b). However, we think that among parallel computing architectures speeding up processing times, "intelligent" neuromorphic analog processors based on artificial neuromorphic neural networks (see for example Qiao et al., 2015) will play a major role in the next generation of neurobiohybrids. As a matter of fact and similarly to other prostheses, in neuroprosthetics the ideal goal is replacing neuronal networks that have undergone injury or degeneration with artificial circuits emulating as closely as possible native functional features. Artificial neurons owning functional properties similar to their natural counterparts such as firing behavior and plasticity-based synaptic integration, will be an ideal replacement or rehabilitation support for injured or degenerating neuronal circuits in neuroprosthetics.

Dynamic Clamp

The dynamic clamp technique offers a prototypic example of such vision, where an artificial brain-inspired computing system drives the excitability of a living neuron establishing a real-time closed-loop control within a neurobiohybrid system. Beginning in the early 90s, researchers started to investigate the interaction of living nerve cells in culture with model neurons in order to understand and emulate the behavior of neural networks (Yarom, 1991; Le Masson et al., 2002). The interface connection between living and model neurons was based on intracellular electrodes, in fact obtaining a two-way artificial-natural communication within a neurobiohybrid. Due to intrinsic limitations of intracellular electrode techniques, such neurobiohybrid setup was limited to only one, or a few, biological neurons. On the other hand, having access to the intracellular potential, it had the advantage of providing high sensitivity for detecting and eliciting neuronal signals. From the neurobiohybrid perspective (see Section Neurobiohybrids), the "device" was here represented by a biomimetic artificial neuron. We may refer to this type of neurobiohybrid, where the interfaced device is a biomimetic artificial neuron, as a Neuron-Neuron Hybrid (NNH). NNH gained interest as a mean to correlate experimental and modeling studies through a sort of reverse-engineering approach, taking advantage of biological neurons to validate their emulators as well as working hypotheses on operational properties of neuronal circuits. Biomimetic neurons and their networks can be digital or analog. Elementary NNHs and their networks have been investigated through the dynamic clamp (Sharp et al., 1993; Prinz, 2004; Yang et al., 2015), which was used to monitor the membrane potential of living neurons and via numerical simulation of model neurons and synapses on a computer, to inject synaptic currents into the living neurons in real-time, as if they were "synaptically" connected to the model neurons. Alternatively, the dynamic clamp could be used to "insert" artificial membrane conductances into living neurons embedded in a network, thus exploring the role of intrinsic conductances in shaping the network's output.

From Single Neurons to Networks

In hybrid NNHs with analog model neurons and synapses, a specially designed microelectronic circuit constitutes the artificial part of the network. Such hardware model neurons and synapses can be connected to living circuits through electrodes, creating a hybrid circuit that consists of a biological network and a dedicated "neuromorphic" (or neuromimetic) silicon chip. With the development of multi-electrode approaches (Rutten, 2002), pioneering work has first succeeded to interface, through dedicated software, cultured neurons and robots, a step toward the creation of "autonomous intelligent biohybrid systems" (Novellino et al., 2007). In other examples of neurobiohybrid network applications, Nowotny et al. (2003) used a hybrid circuit with an Aplysia neuron to show that spike-timing dependent plasticity (STDP) enhances synchronization in neural networks, while Manor and Nadim (2001) demonstrated that synaptic depression in neural networks with recurrent inhibition gives rise to bistability by combining a digital model neuron with a biological pacemaker neuron. In a particular elegant study, Le Masson et al. (2002) reconstructed a thalamocortical circuit by coupling living neurons in the lateral geniculate nucleus to digital and analog model neurons. The researchers showed how feedback inhibition can functionally disconnect the cortex from sensory input in a state reminiscent of sleep, demonstrating the potential of the "Natural-Artificial-Neurohybrid" and/or hybrid NNHs approach in elucidating network function even in large circuits. Overall, when examined from a broader perspective, this sort of pioneering investigations on hybrid networks can be also interpreted as a part of a general effort in the search for novel experimental approaches to investigate neural microcircuits and to develop more efficient brain-machine interfaces for neurological therapy and rehabilitation.

Artificial Neuromorphic Neuronal Networks

Integration into a unique neurobiohybrid system of large (i.e., tens to hundreds of neurons) neuronal networks is a major challenge to be faced. To this endeavor, Very Large Scale Integrated (VLSI) devices come into play. VLSI devices comprise hybrid analog/digital circuits that implement hardware models of biological systems, using computational principles analogous to the ones used by nervous systems (Indiveri and Horiuchi, 2011; Indiveri, 2015). When implemented in VLSI technology, neuromorphic circuits use, to some extent, similar physics used in neural systems (e.g., they transport majority carriers across the channel of transistors by diffusion processes, very much like neurons transport ions inside or outside cell bodies through their ionic channels). Given the analogies at the single device level, neuromorphic circuits are ideal interfacing circuits to real neurons. Moreover, larger scale neuromorphic networks of spiking neurons share the same physical constraints of their biological counterparts (i.e., noise, temperature dependence, inhomogeneities, etc.). As a consequence, to carry out computation in a robust and reproducible manner, these architectures often have to use similar strategies for maximizing compactness, optimizing robustness to noise, minimizing power consumption, and increasing fault tolerance.

In recent years, an interesting class of neuromorphic devices implementing general-purpose computational architectures based on networks of silicon neurons and synapses emerged (Bartolozzi and Indiveri, 2007; Indiveri et al., 2011; Indiveri and Liu, 2015). Such devices range from reconfigurable arrays of basic integrate and fire neuron models to learning architectures implementing detailed models of spike-based synaptic plasticity. Spike-based plasticity circuits enable these systems to adapt to the statistics of their input signals, to learn and classify complex sequences of spatio-temporal patterns (e.g., arising from visual or auditory signals), and eventually to interact with the user and the environment. Typically, the analog circuits implemented on these devices operate in the *weak-inversion* regime, where current amplitudes are of the order of pico-Amperes and operating time-constants are of the order of milliseconds. This is a crucial characteristic that differentiates this approach with other more conventional full custom analog VLSI approaches for implementing spike-based neural networks. Conventional analog VLSI implementations of spike-based neural networks use circuits biased in the *strong-inversion* region, that produce currents of the order of micro-amperes, so the largest time-constants that can be achieved in practice are at least 1000 times smaller than biological ones. The biologically plausible time constants achieved with the neuromorphic approach are crucial, as they allow seamless interactions with real living networks. Given the types of parallel architectures that can be implemented with these silicon neurons and synapses, processing time does not increase with size, and large networks can be fabricated by (e.g., simply using more silicon real-estate) to match the numbers of recording/stimulating electrodes or real targeted neurons that one would like to interact with.

Consistent with the neuromorphic engineering approach, the strategy used to transmit signals across chip boundaries in these types of systems is inspired from the nervous system: output signals are represented by stereotyped digital pulses (spikes), and the analog nature of the signal is typically encoded in the mean frequency of the neuron's pulse sequence (spike rates). Similarly, input signals are represented by spike trains, conveyed to the chip in the form of asynchronous digital pulses, that stimulate their target synapses on the receiving chip. The circuits that generate the on-chip synaptic currents when stimulated by incoming spikes are slow low-power analog circuits. The circuits that generate and manage these streams of input/output digital pulses are fast asynchronous logic elements based on an emerging new communication standard for neuromorphic chips called the "Address-Event Representation" (AER). This representation is ideal for both implementing real-time interfaces with living networks, as well as for allowing reconfigurability of artificial network topology (e.g., via address-event source-destination lookup tables).

Memristive Plasticity

An important advancement in the field of biological networks emulation and with great potential in neuroprosthetics is the development of new nanoelectronic elements with synaptic functional properties. Carbon nanotubes (Cellot et al., 2009; Joshi et al., 2011; Fabbro et al., 2013) and particularly, memristors are emerging as a new class of devices that might serve the purpose. Resistive Random Access Memory (ReRAM) cells are nowadays classified as being memristive in nature (Chua, 2011) and have first being conceptually conceived in 1971 by Chua (1971), with the first neuromimetics applications presented at the same time. Since then, the usage of memristors in simulating artificial synapses has started to be explored (Yang et al., 2013; Kim et al., 2015; Niehrster and Thomas, 2015; Thomas et al., 2015). The functional signature of memristors is a pinched hysteresis loop in the current-voltage (i-v) domain when excited by a bipolar periodic stimulus. Such hysteresis is typically noticed for all kind of devices/materials in support of a discharge phenomenon that possess certain inertia, causing the value of a physical property to lag behind changes in the mechanism causing it, and has been common both to large scale (Prodromakis et al., 2012) as well as nanoscale dissipative devices (Strukov et al., 2008). The analogy of memristors and chemical synapses is thus made on the basis that synaptic dynamics depend upon ions flowing through the postsynaptic membrane in a similar fashion that "ionic species" can be displaced within any inorganic barrier. TiO2-based memristor models (Strukov et al., 2008; Prodromakis et al., 2011) hypothesized that solid-state devices comprise a mixture of TiO2 phases, a stoichiometric and a reduced one (TiO2-x), that can facilitate distinct resistive states via controlling the displacement of oxygen vacancies and thus the extent of the two phases. More recently however it was demonstrated that substantial resistive switching is only viable through the formation and annihilation of continuous conductive percolation channels (Shihong et al., 2012) that extend across the whole active region of a device, shorting the top (TE) and bottom (BE) electrodes; no matter what the underlying physical mechanism is.

The development of such emerging nanoscale synaptic-like computation elements may notably benefit the establishment of neuromorphic architectures and neurobiohybrids. This technology adds substantially on computation functionality, due to the rate-dependency of the underlying physical switching mechanisms. At the same time it can facilitate unprecedented complexity due to the capacity of storing and processing spiking events locally. Moreover, the minuscule dimensions and architectural simplicity of solid-state memristor implementations could be successfully exploited to substantially increase the number of cells per unit area, and effectively enhance the system's tolerance to issues stemming from device mismatch and low-yields (Gelencser et al., 2012; Gupta et al., 2016).

Toward "Intelligent" Neuroprosthetics

In perspective, neurobiohybrids, and particularly NNHs, will represent the basis for creating advanced and "intelligent" neuroprostheses. Novel generations of neuroprostheses or bioelectronic medicines (BM) acting through electrical stimulation of the central or peripheral nervous system bear a huge potential for therapy of numerous diseases, including neurological disorders, metabolic, and autonomic dysfunctions (Hyam et al., 2012; Afshar et al., 2013; Birmingham et al., 2014). In order to exploit the envisaged potential, such devices will have to be "adaptive," i.e., adjust "intelligently" and continuously their stimulation of neurons while monitoring effectiveness in real time. This is needed to counterbalance drift and intrinsic variability of the response to nerve stimulation through time,

and to cope with patient-specific changes of conditions during daily life. Such a vision implies that BM must be also "precise," i.e., allow for a finely tuned control of the nervous system by means of modulating neuronal excitability. Achieving this vision and conferring such a degree of "intelligence" to a miniaturized implantable device is a tremendous challenge. As pointed out above, significant technological progress has been made in artificially emulating neurons, synapses, and neuronal networks by low-power neuromimetic microelectronics. Beyond the capability to "speak the same language" made of nerve impulses and distributed computation, such neuromimetic architectures share with biological neuronal networks other properties, as online learning and reconfigurability based upon internal plastic changes (Qiao et al., 2015). The envisioned challenge toward brain repair and augmentation is to pair neuromorphic architectures with biological neurons *in vivo*, and set it to act as "chaperon or surrogate" of neuronal circuits to intelligently restore function. The neuromorphic devices will communicate bi-directionally (i.e., both receiving and sending nerve impulses) with biological neurons in the central or peripheral nervous system through advanced neural interfaces, enabling precise, and "near-physiological" tuning of neuronal activity within an "intelligent" adaptive closed-loop. In perspective, such approach could support a variety of bioelectronic and neuroprosthetic applications, independent of the physical nature of signals measured and stimuli delivered (i.e., electrical, chemical, etc.). It will set the context and the technological grounds for a true revolution toward "intelligent" neuroprosthetics and augmentation of brain function.

Bibliometrics on Neurobiohybrids Research

The success of neurobiohybrids in neuroprosthetics will depend on community building, paralleling scientific-technological development, and directed to strenghtening of interactions, e.g., between neuroscientists, neurologists, and neurotechnologists and the communities working on brain-inspired computation and microdevices. We analyzed the development of such interactions in recent years by means of bibliometric analysis.

Bibliometrics was performed on publications related to neurobiohybrids to quantify interaction trends within the new interdisciplinary community. The details of the analysis procedure is provided in Section Methods. For the analysis, a total of 5320 journal articles and conference papers were carefully selected from three commercial scientific repositories (IEEE-Xplore, Thompson Reuters Web of Knowledge, and Elsevier's Scopus) through keyword searching for a window of 20 years (1995–2014). After careful selection, 3914 articles from 125 journals and 1406 papers from 93 conferences were taken into consideration for further analysis.

Pie-charts in **Figure 4** report the number of publications appeared in top 20 journals and top 8 conferences. It is interesting to note that the great majority of publications are mostly found in applied physics or engineering journals, with only a few appearances in multidisciplinary journals (e.g., Nature, Science and PLoS One) and even less in neuroscience journals (e.g., Neuron). From this first indications, it is tempting to conclude that the field is still very much biased toward engineering and physics communities rather than neuroscience communities. Additionally, it appears that only a few cutting edge publications have gained visibility to a wider community by publication on prestigious multidisciplinary journals. These results imply that the vast majority of researches in the neurobiohybrid field are not reaching the neuroscientific counterparts, which is a limiting factor for further development of this highly interdisciplinary field of research.

Also conference publications are dominated by engineering meetings. This can be in part explained as in neuroscience it is uncommon to publish results in conference papers, which are conversely well evaluated in the engineering environment. Again,

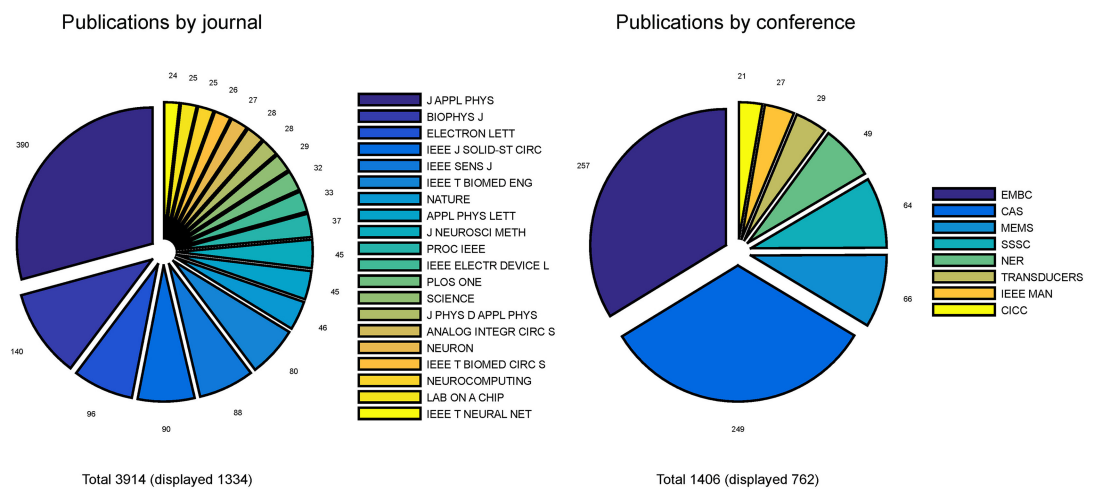

FIGURE 4 | Distribution of publications. Distribution of journal articles **(left)** and conference papers **(right)** per year are reported as slices of pies. Only journals and conferences were considered with more than 20 articles and papers in the neurobiohybrid field.

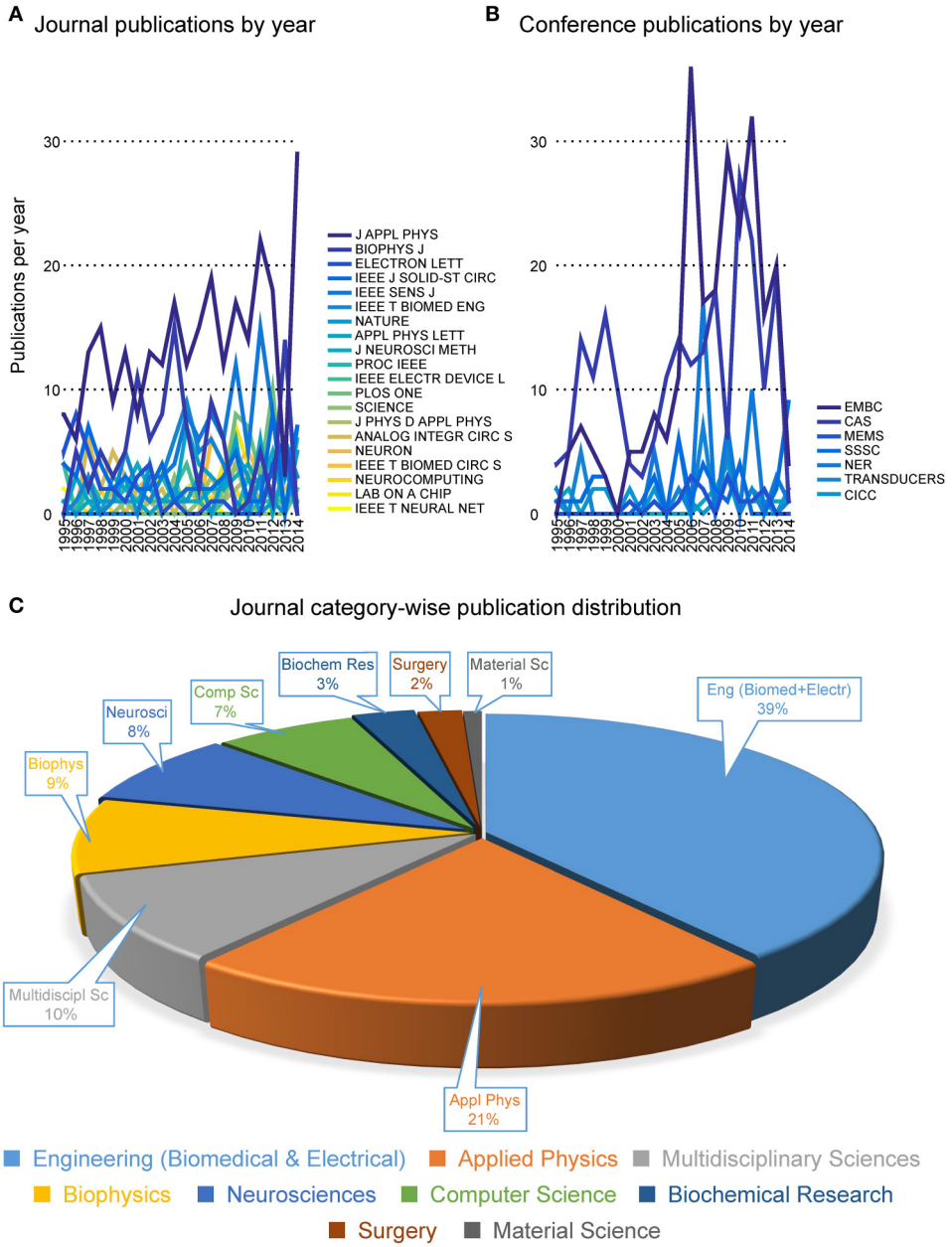

FIGURE 5 | Publication trends. Distribution of the number of publications per year in journals **(A)** and conferences **(B)**. The journal category-wise publication distribution **(C)** shows dominating appearance of publications from the Neurobiohybrid field in journals belonging to the Engineering and Physical Sciences category, in comparison to the Health and Life Sciences category.

efforts should be made to improve homogeneity of dissemination and to reach a wider audience.

Judging from the trend of the number of publications per year (**Figures 5**, **6**), a reasonable growth of the field can be appreciated, although comparable with other research fields.

Most interestingly, an analysis on the impact factor (IF) distribution (**Figures 7**, **8**) reveals that most publications fall within a window below impact factor 5 with a high peak at around 2. While this may be acceptable within the engineering community, it is far below average with respect to publications in the neuroscience community. This discrepancy is playing against the building of a homogeneous community with equal career opportunities for engineers or physicist, on one side, and neuroscientists on the other side. Particularly, neuroscientists working in the neurobiohybrid field seem heavily penalized in terms of IF and will struggle in the competition with colleagues of other neuroscientific disciplines. Thus, in our view, the neurobiohybrid community should invest major

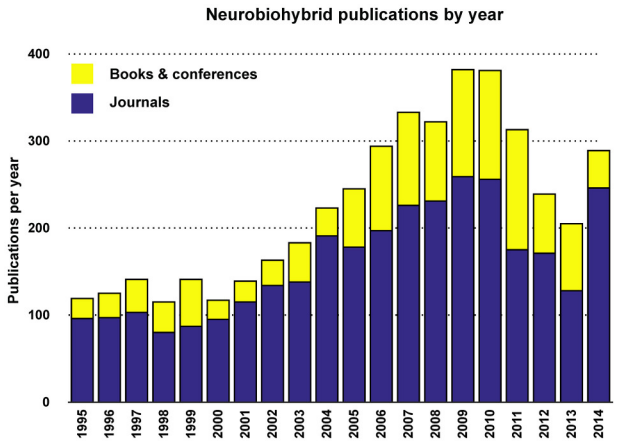

FIGURE 6 | Yearly total publications. Total number of publications appeared in journals, conference proceedings, and books per year.

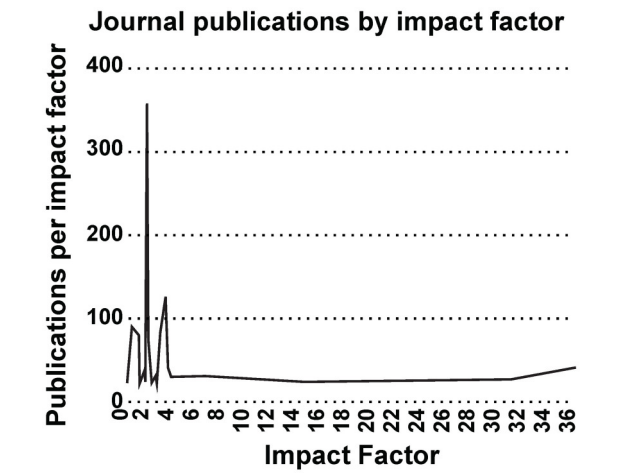

FIGURE 7 | Impact Factor distribution. Impact factor distribution of publications in the neurobiohybrid field shows that majority of the publications appeared in journals with impact factor less than 5.

efforts to improve dissemination efficacy, in particular, by increasing visibility of matured results through publications in interdisciplinary journals that can attract interest from a broader neuroscience community. In fact, as shown in **Figure 5C**, only 10% of the journal publications concerning neurobiohybrids appear in multidisciplinary journals and expanding this share will favor the communities' coalescence given the exemplary increasing interactions between the specialized subcommunities of Neuromimetics and Neuroprosthetics (**Figure 9**). Such efforts should be paralleled by organization of focused workshops and training initiatives in the neurobiohybrid field conceived in a way to attract interdisciplinary audience and to create a new generation of scientists with competences and skills spanning from neurotechnologies to neuromimetic systems and more classical neuroscience.

Word clouds of keywords used for the bibliometric analysis are reported hereafter in **Figure 10**.

DISCUSSION

Biohybrids, that is, biohybrid systems where artificial devices and living organisms establish physical interactions with information exchange, will play a pivotal role in the future development of efficient, sustainable, and powerful information and communication technologies. A clear and well known example of biohybrid application supporting such expectations is represented by cardiac pacemakers, where information needed for restoring physiological heart pacing is provided by artificial rhythm generators through implanted electrodes. Noteworthy, closed-loop bi-directional interaction between organ and artificial pacemaker is seen as an important strategy to effectively restore function through a dynamic control and prevent cardiovascular pathologies (Occhetta et al., 2003). Biohybrids will represent an essential workbench to better investigate living organisms, to assess new principles of communication between natural and artificial world, and to develop novel generations of bio-inspired devices based on non-living matter. From the application perspective, they represent an innovative strategy to improve therapy of a variety of diseases through *in vivo* implants (Nicolelis and Lebedev, 2009). Overall, from a broad perspective, biohybrid technologies may replace artificial ones, leading to higher energy efficiency and performance gain while lowering environmental impact. Among biohybrids, *neurobiohybrids* are of paramount importance. After millions of years of evolution, the nervous system of living animals, and the human brain in particular, is endowed with unique abilities to cope with information processing in an energy effective, adaptable and robust manner, outperforming artificial devices when dealing with "real world" problems. Biohybrid systems of natural and artificial neurons implanted *in vivo* will be central to explore brain operational principles and, on the clinical side, to create novel generations of "intelligent" neuroprostheses.

The Paradigm Shift

In our opinion, we are set to experience a true paradigm shift in neurobiohybrids research thanks to concomitant advances in three highly intertwined disciplines: *neurophysiology of brain microcircuits*, *neural interfaces,* and *neuromimetics* (that is, the creation of physical elements and circuits emulating living neurons and networks). For the first time, and thanks to recent development of physical elements with synaptic-like plasticity, a fascinating challenge is coming within reach: natural and hardware-based neuronal circuits could be integrated into new entities, operating *in vivo* through brain implants, and evolving together on the basis of shared plasticity and processing rules. To this endeavor, non-"von Neumann" brain-inspired architectures will have to be interfaced to their natural counterparts, the brain microcircuits. This will occur, at the physical level, through high-resolution, and bi-directional neural interfaces, and at the algorithmic level, by emulating in artificial architectures those processing rules that are key for the function of real biological brain networks. Noteworthy, however, neurobiohybrids can

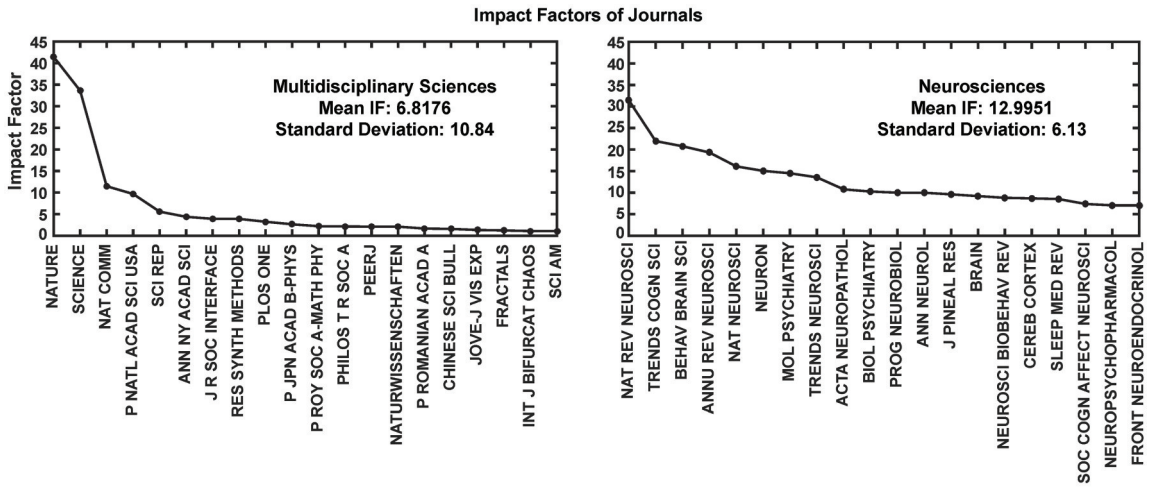

FIGURE 8 | Impact Factor comparison. Two categories of journals were compared for the impact factors (IF) during the year 2014. These journals' IFs were calculated by Thomson Reuters and reported through Journal Citation Reports (https://jcr.incites.thomsonreuters.com/). Average IFs of the journals in the multidisciplinary sciences category (left) is almost half in comparison to the neurosciences category (right). For better representation only top 20 journals from each category are shown in the figure.

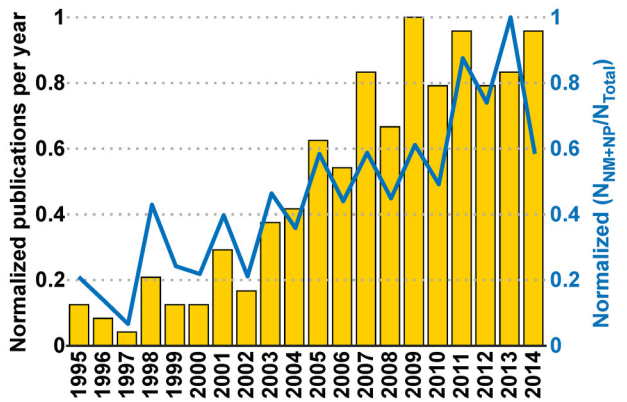

FIGURE 9 | Interaction between communities and its effect on the Neurobiohybird publications. The bar plot (left Y-axis) shows the normalized publication frequencies calculated by extracting relevant publications through "interaction keywords"-based querying (see Section Analysis of Database) of the XML database. The increasing trend of the publication frequencies from two subcommunities ("Neuromimetics" and "Neuroprosthetics") associated to the Neurobiohybrid field demonstrates a growing interaction between them. The interaction effect on the Neurobiohybrid publications is evident in the line plot (right Y-axis) which reports the yearly normalized ratios between subsets of publications resulting from the interactions (N_{NM+NP}) and total number of journal publications in the Neurobiohybrid field (N_{Total}).

involve living networks at various levels of complexity and conditions, ranging from *in vitro* to *in vivo* systems and from "simple" nervous systems of invertebrates to the mammalian brain. Whatever the implementation strategy, the new hybrid systems will represent a technological platform with enormous potential not only for application in neuroscience and healthcare, as discussed below, but also in computer science and robotics. In fact, they will play a key role to understand operational principles of brain microcircuits and to developing new forms of brain-inspired computing devices more energy efficient and robust in dealing with real-world tasks.

From the theoretical point of view, the processing of information following the classical "von Neumann" digital computing paradigms is known to be less efficient compared to the biological counterparts, when dealing with ill-posed problems and noisy data. Though current computing technologies have reached speed and computational power figures that allows them to simulate parts of animal brains and behavior, the energy required by these systems grows exponentially with the increasing hierarchy of animal intelligence. The reason is that the biological brain is configured differently and the keys are the extremely high (∼1015 synapses) connectivity between neurons in a network which offers highly parallel processing power as well as the fact that neurons are plastic and adaptive (i.e., memory dependent) signal processing and computing units. Yet, brain's most striking feature is that it is structured as an evolving system were synapses undergo "birth" and "death" as well as strengthening and weakening, reconfiguring neuronal connectivity in a self-organizing manner and allowing the networked population of neuronal processors to adapt motor and behavioral responses to the ever changing environmental inputs. Thus, by rearranging both the structural and functional topology, brain's neuronal circuits demonstrate unique evolvability, scalability, and adaptability properties that are unmatched by current computing devices. The challenge posed by neurobiohybrids research is to create networks where artificial elements overcome this deficiency by merging data storage and processing into single electronic devices, where topology can be reconfigured in a self-organizing manner, and to interface them to biological nervous systems. On-chip neuromorphic networks have recently emerged that may fulfill the purpose, and whose

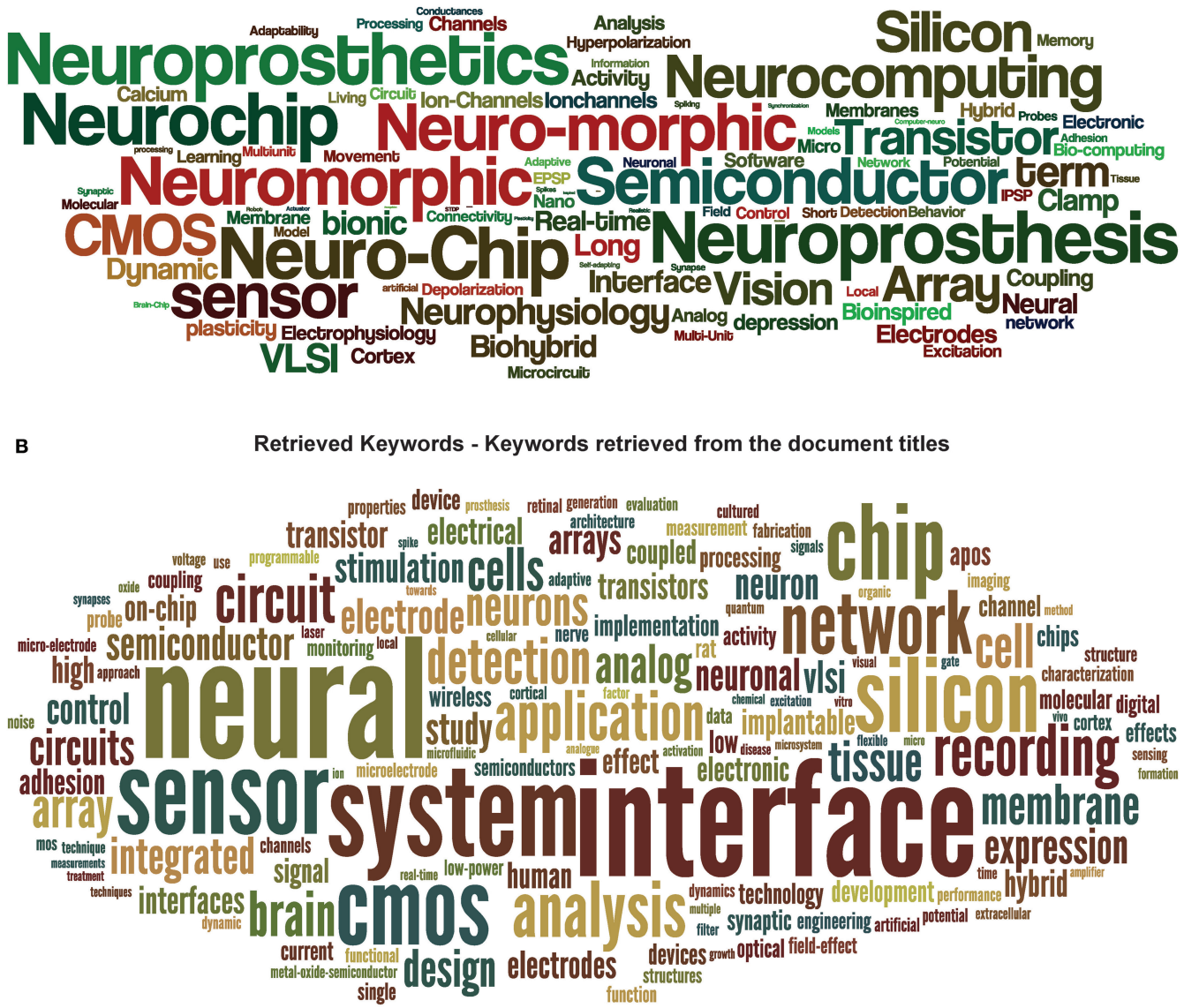

FIGURE 10 | Word cloud of keywords. Word clouds of keywords used in searching the databases **(A)** and retrieved from the publication titles **(B)**. The size of a word in **(A)** denotes the number of times it was used with other search keywords in searching for publications in the database. On the other hand, in **(B)**, the size of a word represents its number of appearances in the publication titles.

development is relying both on established microelectronic technologies (Indiveri et al., 2011; Indiveri and Liu, 2015) and novel approaches to emulate neuronal functions in single nanodevices (Indiveri et al., 2013; Gupta et al., 2016; Serb et al., 2016). Such artificial neural networks could provide the complexity, connectivity, and massive parallel information processing and thus mimic the performance of biological systems including their evolvability, self-organization, adaptability, and robustness. Following this vision, research on neurobiohybrids will on one hand enable significant progress toward novel "autonomous cognitive systems" while, on the other hand, it will promote the understanding of principles behind brain computation. The conception of brain-inspired implantable microdevices acting as "intelligent" neuroprostheses for brain rehabilitation and functional augmentation or as adaptive bioelectronic medicines will be the logical exploitation of such efforts toward clinical application.

In conclusion, we feel that we are at the beginning of a new era, where the fusion of neuromimetics and neurotechnologies

for brain interfacing and creation of neurobiohybrids will lead to a new class of "smart" implantable systems with great potential for neuroscience and particularly for therapy of diseases of the nervous system. However, a process of community building is also necessary to reach the critical mass, which will have to overcome difficulties and hurdles. In particular, having a common and effective dissemination strategy, ensuring high visibility and career opportunities across all disciplines involved will be key aspect.

METHODS

The bibliometrics was performed following standard bibliometric methods as reported in Nathan et al. (2013). In short, a two-step method started with construction of an analysis database by searching and extracting information from three commercial scientific repositories using predefined search terms which was followed by analysis of the extracted publication data.

Construction of Search Terms

As part of the Convergent Science Network's (CSN) road-mapping action, we had supplied questionnaires to experts belonging to the different communities mentioned above. Mining the answers provided to the question "Relevant state-of-the-art in your field of research" we formed a "keywords pool." The unique keywords ($n = 100$) in that pool were then identified, combined and permuted to obtain the search terms ($N = 862$) which were used in querying the scientific repositories.

Construction of Analysis Database

Three commercial scientific repositories were used to gather the publication information: (i) the IEEEXplore repository (http://ieeexplore.ieee.org/), (ii) the Thomson Reuters Web of Knowledge repository (http://apps.webofknowledge.com/), and (iii) Elsevier's Scopus (http://scopus.com/) repository. Out of the three, the IEEEXplore repository was used as source of articles published in IEEE journals and conferences, and the latter two were used for other journals and conferences.

Each of these repositories were searched for priorly defined keywords (or combinations of keywords, referred as "search terms" in the subsequent text, see Section Construction of Search Terms). The search domains were restricted to science, engineering, and life sciences for the Web of knowledge and Scopus repositories. But, the IEEEXplore repository was searched only science and engineering domain articles.

These repositories were queried using their built-in search engines which compared the search terms with the stored metadata (e.g., publication title, abstract, and author-defined keywords) corresponding to each indexed article. The metadata returned by the query as a result of a match with the given search term was appended to a predefined database created in EndNote reference management software (V7.4; Thompson Reuters, Philadelphia, USA; http://endnote.com/). At the end of the querying process, the Endnote database was exported to an extensible markup language (XML, http://www.w3.org/XML/) file (referred as analysis/XML database) and an automated in-house algorithm written in MATLAB (R2015a; Mathworks Inc., Natick, USA, http://www.mathworks.com/) eliminated the redundant entries returned by overlapped queries in different repositories from the XML file. The tagged structure of XML file facilitated the application of MATLAB's standard string-manipulation functions to extract the relevant information (e.g., article title, publication year, and title, etc.) from the metadata pertaining to each publication stored in the XML database. For each unique journals, its impact factor and category were manually retrieved from the Thompson Reuters Journal Citation Reports (JCR, https://jcr.incites.thomsonreuters.com/) and appended to the database.

Analysis of Database

The pre-processed metadata belonging to publication entries in the XML database were then analyzed to extract publication titles, unique journal and conference titles, and year of publication.

The following information were then extracted from the database:

1. Yearly publication frequency in journals or conferences (as reported in **Figures 4–6**), and journal category-wise publication distribution (**Figure 5C**; top 44 journals, from a descendingly ordered list of number of appeared articles, were categorized with a total number of 1200 articles and at least 10 articles in each journal during 1994–2014).
2. Impact factor distribution of the published articles belonging to the Neurobiohybrids (as reported in **Figure 7**) field. Also, comparison of impact factors of various journals belonging to the "Multidisciplinary Sciences" and "Neurosciences" category (see **Figure 8**).

In addition, two subcategories of seven keywords each (termed as "interaction keywords") were defined by selecting popular keywords pertaining to two active subcommunities (Neuromimetics and Neuroprosthetics) in the Neurobiohybrid field. For the Neuromimetics, the selected keywords were: "neuromimetic," "neuro-morphic," "neuromorphic," "neuro-chip," "neurochip," "neurocomputing," and "sensor"; whereas for the Neuroprosthetics they were: "neuroprosthetic," "neuroprosthesis," "interface," "brain machine interface," "tissue," "slice," and "*in-vivo.*" The document titles, abstracts and author-provided keywords present in the XML database were searched for co-occurrence of at least one interaction keyword from each subcategories. The resulting publications along with their publication year were saved. The yearly publication frequency computed from the search results of the interaction keywords (see **Figure 9**) was used as a measure to determine interactions between the two subcommunities belonging to the Neurobiohybrids field.

Finally, the search terms and the retrieved keywords from the publication titles were represented as word clouds (see **Figure 10**) using a web-based free tool (wordle; http://www.wordle.net/) showing the frequencies of usage of each search keyword with another keyword (in case of search keywords cloud) and frequencies of occurrence of

keywords in the publication titles (in case of retrieved keywords cloud).

AUTHOR CONTRIBUTIONS

SV and MM performed the studies reported in the article and wrote the paper. Both authors have contributed to, seen and approved the final manuscript.

FUNDING

Financial support from the 7th Framework Programme of the European Commission through "CSN II" (http://www.csnetwork.eu/, FP7-ICT-601167) and "RAMP" projects (http://www.rampproject.eu/, FP7-ICT-612058) are acknowledged.

ACKNOWLEDGMENTS

The authors are particularly thankful to the following scientists for their help and fruitful discussion: Guenther Zeck, Christian Meier, Michele Giugliano, Marco Fanciulli, Themis Prodromakis, Ralf Zeitler, Giacomo Indiveri, Peter Fromherz, Roland Thewes, Astrid Prinz, Jennifer Hasler, Andrei Zenkevich. Dr. Nathan Lepora's kind help and assistance in performing the bibliometric research is also acknowledged.

REFERENCES

Afshar, P., Khambhati, A., Stanslaski, S., Carlson, D., Jensen, R., Dani, S., et al. (2013). A translational platform for prototyping closed-loop neuromodulation systems. *Front. Neural Circuits* 6:117. doi: 10.3389/fncir.2012.00117

Ali, M. M., Sellers, K. K., and Fröhlich, F. (2013). Transcranial alternating current stimulation modulates large-scale cortical network activity by network resonance. *J. Neurosci.* 33, 11262–11275. doi: 10.1523/JNEUROSCI.5867-12.2013

Anastassiou, C. A., Montgomery, S. M., Barahona, M., Buzsáki, G., and Koch, C. (2010). The effect of spatially inhomogeneous extracellular electric fields on neurons. *J. Neurosci.* 30, 1925–1936. doi: 10.1523/JNEUROSCI.3635-09.2010

Angle, M. R., Cui, B., and Melosh, N. A. (2015). Nanotechnology and neurophysiology. *Curr. Opin. Neurobiol.* 32, 132–140. doi: 10.1016/j.conb.2015.03.014

Armstrong, C., Krook-Magnuson, E., Oijala, M., and Soltesz, I. (2013). Closed-loop optogenetic intervention in mice. *Nat. Protoc.* 8, 1475–1493. doi: 10.1038/nprot.2013.080

Bartolozzi, C., and Indiveri, G. (2007). Synaptic dynamics in analog vlsi. *Neural Comput.* 19, 2581–2603. doi: 10.1162/neco.2007.19.10.2581

Berényi, A., Somogyvári, Z., Nagy, A. J., Roux, L., Long, J. D., Fujisawa, S., et al. (2014). Large-scale, high-density (up to 512 channels) recording of local circuits in behaving animals. *J. Neurophysiol.* 111, 1132–1149. doi: 10.1152/jn.00785.2013

Birmingham, K., Gradinaru, V., Anikeeva, P., Grill, W. M., Pikov, V., McLaughlin, B., et al. (2014). Bioelectronic medicines: a research roadmap. *Nat. Rev. Drug Discov.* 13, 399–400. doi: 10.1038/nrd4351

Braun, D., and Fromherz, P. (2004). Imaging neuronal seal resistance on silicon chip using fluorescent voltage-sensitive dye. *Biophys. J.* 87, 1351–1359. doi: 10.1529/biophysj.104.039990

Buzsáki, G., Anastassiou, C. A., and Koch, C. (2012). The origin of extracellular fields and currents – eeg, ecog, lfp and spikes. *Nat. Rev. Neurosci.* 13, 407–420. doi: 10.1038/nrn3241

Buzsáki, G., Stark, E., Berényi, A., Khodagholy, D., Kipke, D. R., Yoon, E., et al. (2015). Tools for probing local circuits: high-density silicon probes combined with optogenetics. *Neuron* 86, 92–105. doi: 10.1016/j.neuron.2015.01.028

Camprodon, J. A. (2016). "Transcranial Magnetic Stimulation," in *Psychiatric Neurotherapeutics: Contemporary Surgical and Device-Based Treatments*, eds A. J. Camprodon, L. S. Rauch, D. B. Greenberg, and D. D. Dougherty (New York, NY: Springer), 165–186.

Cellot, G., Cilia, E., Cipollone, S., Rancic, V., Sucapane, A., Giordani, S., et al. (2009). Carbon nanotubes might improve neuronal performance by favouring electrical shortcuts. *Nat. Nanotech.* 4, 126–133. doi: 10.1038/nnano.2008.374

Chemla, S., and Chavane, F. (2010). Voltage-sensitive dye imaging: technique review and models. *J. Physiol. Paris* 104, 40–50. doi: 10.1016/j.jphysparis.2009.11.009

Chua, L. (1971). Memristor-the missing circuit element. *IEEE T. Circuit Theory* 18, 507–519. doi: 10.1109/TCT.1971.1083337

Chua, L. (2011). Resistance switching memories are memristors. *Appl. Phys. A* 102, 765–783. doi: 10.1007/s00339-011-6264-9

Csicsvari, J., Henze, D. A., Jamieson, B., Harris, K. D., Sirota, A., Barthó, P., et al. (2003). Massively parallel recording of unit and local field potentials with silicon-based electrodes. *J. Neurophysiol.* 90, 1314–1323. doi: 10.1152/jn.00116.2003

Dirks, A., Cornelissen, J. J. L. M., van Delft, F. L., van Hest, J. C. M., Nolte, R. J. M., Rowan, A. E., et al. (2007). From (bio)molecules to biohybrid materials with the click chemistry approach. *QSAR Comb. Sci.* 26, 1200–1210. doi: 10.1002/qsar.200740085

Dugue, G. P., Akemann, W., and Knopfel, T. (2012). A comprehensive concept of optogenetics. *Prog. Brain. Res.* 196, 1–28. doi: 10.1016/B978-0-444-59426-6.00001-X

Eiben, A. E., Kernbach, S., and Haasdijk, E. (2012). Embodied artificial evolution artificial evolutionary systems in the 21st century. *Evol. Intell.* 5, 261–272. doi: 10.1007/s12065-012-0071-x

Eickenscheidt, M., Jenkner, M., Thewes, R., Fromherz, P., and Zeck, G. (2012). Electrical stimulation of retinal neurons in epiretinal and subretinal configuration using a multicapacitor array. *J. Neurophysiol.* 107, 2742–2755. doi: 10.1152/jn.00909.2011

Eversmann, B., Lambacher, A., Gerling, T., Kunze, A., Fromherz, P., and Thewes, R. (2011). A neural tissue interfacing chip for *in-vitro* applications with 32k recording/stimulation channels on an active area of 2.6 mm2. *Proc. ESSCIRC* 211–214. doi: 10.1109/ESSCIRC.2011.6044902

Fabbro, A., Prato, M., and Ballerini, L. (2013). Carbon nanotubes in neuroregeneration and repair. *Adv. Drug Deliv. Rev.* 65, 2034–2044. doi: 10.1016/j.addr.2013.07.002

Fekete, Z. (2015). Recent advances in silicon-based neural microelectrodes and microsystems: a review. *Sens. Actuator B Chem.* 215, 300–315. doi: 10.1016/j.snb.2015.03.055

Felderer, F., and Fromherz, P. (2011). Transistor needle chip for recording in brain tissue. *Appl. Phys. A* 104, 1–6. doi: 10.1007/s00339-011-6392-2

Ferrea, E., Maccione, A., Medrihan, L., Nieus, T., Ghezzi, D., Baldelli, P., et al. (2012). Large-scale, high-resolution electrophysiological imaging of field potentials in brain slices with microelectronic multielectrode arrays. *Front. Neural Circuits* 6:80. doi: 10.3389/fncir.2012.00080

Friehs, G. M., Zerris, V. A., Ojakangas, C. L., Fellows, M. R., and Donoghue, J. P. (2004). Brain-machine and brain-computer interfaces. *Stroke* 35, 2702–2705. doi: 10.1161/01.STR.0000143235.93497.03

Fromherz, P. (2006). Three levels of neuroelectronic interfacing. *Ann. N.Y. Acad. Sci.* 1093, 143–160. doi: 10.1196/annals.1382.011

Gelencser, A., Prodromakis, T., Toumazou, C., and Roska, T. (2012). Biomimetic model of the outer plexiform layer by incorporating memristive devices. *Phys. Rev. E* 85:041918. doi: 10.1103/physreve.85.041918

Giocomo, L. M. (2015). Large scale *in vivo* recordings to study neuronal biophysics. *Curr. Opin. Neurobiol.* 32, 1–7. doi: 10.1016/j.conb.2014.09.009

Girardi, S., Maschietto, M., Zeitler, R., Mahmud, M., and Vassanelli, S. (2011). "High resolution cortical imaging using electrolyte-(metal)-oxide-semiconductor field effect transistors," in *2011 5th International*

IEEE/EMBS Conference on Neural Engineering (NER) (Cancun, QR), 269–272.

Gold, C., Henze, D. A., Koch, C., and Buzsáki, G. (2006). On the origin of the extracellular action potential waveform: a modeling study. *J. Neurophysiol.* 95, 3113–3128. doi: 10.1152/jn.00979.2005

Goldfarb, M., Lawson, B. E., and Shultz, A. H. (2013). Realizing the promise of robotic leg prostheses. *Sci. Transl. Med.* 5, 210ps15. doi: 10.1126/scitranslmed.3007312

Grosenick, L., Marshel, J. H., and Deisseroth, K. (2015). Closed-loop and activity-guided optogenetic control. *Neuron* 86, 106–139. doi: 10.1016/j.neuron.2015.03.034

Gupta, I., Serb, A., Khiat, A., Zeitler, R., Vassanelli, S., and Prodromakis, T. (2016). Real-time encoding and compression of neuronal spikes by metal-oxide memristors. *Nat. Commun.* doi: 10.5258/SOTON/400411. [Epub ahead of print].

Haider, B., and McCormick, D. A. (2009). Rapid neocortical dynamics: cellular and network mechanisms. *Neuron* 62, 171–189. doi: 10.1016/j.neuron.2009.04.008

Hierlemann, A., Frey, U., Hafizovic, S., and Heer, F. (2011). Growing cells atop microelectronic chips: interfacing electrogenic cells *in vitro* with cmos-based microelectrode arrays. *Proc. IEEE* 99, 252–284. doi: 10.1109/JPROC.2010.2066532

Hochberg, L. R., Serruya, M. D., Friehs, G. M., Mukand, J. A., Saleh, M., Caplan, A. H., et al. (2006). Neuronal ensemble control of prosthetic devices by a human with tetraplegia. *Nature* 442, 164–171. doi: 10.1038/nature04970

Hutzler, M., Lambacher, A., Eversmann, B., Jenkner, M., Thewes, R., and Fromherz, P. (2006). High- resolution multitransistor array recording of electrical field potentials in cultured brain slices. *J. Neurophysiol.* 96, 1638–1645. doi: 10.1152/jn.00347.2006

Hyam, J. A., Kringelbach, M. L., Silburn, P. A., Aziz, T. Z., and Green, A. L. (2012). The autonomic effects of deep brain stimulation-a therapeutic opportunity. *Nat. Rev. Neurol.* 8, 391–400. doi: 10.1038/nrneurol.2012.100

Indiveri, G. (2015). "Neuromorphic engineering," in *Springer Handbook of Computational Intelligence*, eds J. Kacprzyk and W. Pedrycz (Berlin: Springer), 715–725.

Indiveri, G., and Horiuchi, T. K. (2011). Frontiers in neuromorphic engineering. *Front. Neurosci.* 5:118. doi: 10.3389/fnins.2011.00118

Indiveri, G., Linares-Barranco, B., Hamilton, T. J., van Schaik, A., Etienne-Cummings, R., Delbruck, T., et al. (2011). Neuromorphic silicon neuron circuits. *Front. Neurosci.* 5:73. doi: 10.3389/fnins.2011.00073

Indiveri, G., Linares-Barranco, B., Legenstein, R., Deligeorgis, G., and Themistoklis, P. (2013). Integration of nanoscale memristor synapses in neuromorphic computing architectures. *Nanotechnology* 24:384010. doi: 10.1088/0957-4484/24/38/384010

Indiveri, G., and Liu, S. C. (2015). Memory and information processing in neuromorphic systems. *Proc. IEEE* 103, 1379–1397. doi: 10.1109/JPROC.2015.2444094

Joshi, J., Zhang, J., Wang, C., Hsu, C.-C., Parker, A., Zhou, C., et al. (2011). "A biomimetic fabricated carbon nanotube synapse for prosthetic applications," in *Life Science Systems and Applications Workshop (LiSSA) 2011 IEEE/NIH*, eds K. Peterson and E. Sanchez-Sinencio (Bethesda, MD: IEEE), 139–142.

Khodagholy, D., Gelinas, J. N., Thesen, T., Doyle, W., Devinsky, O., Malliaras, G. G., et al. (2015). NeuroGrid: recording action potentials from the surface of the brain. *Nat. Neurosci.* 18, 310–315. doi: 10.1038/nn.3905

Kim, S., Du, C., Sheridan, P., Ma, W., Choi, S., and Lu, W. D. (2015). Experimental demonstration of a second-order memristor and its ability to biorealistically implement synaptic plasticity. *Nano Lett.* 15, 2203–2211. doi: 10.1021/acs.nanolett.5b00697

Krusienski, D. J., Grosse-Wentrup, M., Galn, F., Coyle, D., Miller, K. J., Forney, E., et al. (2011). Critical issues in state-of-the-art brain-computer interface signal processing. *J. Neural Eng.* 8:025002. doi: 10.1088/1741-2560/8/2/025002

Kwan, A. C., and Dan, Y. (2012). Dissection of cortical microcircuits by single-neuron stimulation *in vivo*. *Curr. Biol.* 22, 1459–1467. doi: 10.1016/j.cub.2012.06.007

Lago, N., Ceballos, D., Rodrguez, F. J., Stieglitz, T., and Navarro, X. (2005). Long term assessment of axonal regeneration through polyimide regenerative electrodes to interface the peripheral nerve. *Biomaterials* 26, 2021–2031. doi: 10.1016/j.biomaterials.2004.06.025

Lebedev, M. A., and Nicolelis, M. A. (2011). Toward a whole-body neuroprosthetic. *Prog. Brain. Res.* 194, 47–60. doi: 10.1016/B978-0-444-53815-4.00018-2

Lee, J. H., Kim, H., Kim, J. H., and Lee, S. H. (2016). Soft implantable microelectrodes for future medicine: prosthetics, neural signal recording and neuromodulation. *Lab Chip* 16, 959–976. doi: 10.1039/C5LC00842E

Lee, J. H., Ryu, J., Jolesz, F. A., Cho, Z. H., and Yoo, S. S. (2009). Brain-machine interface via real- time fmri: preliminary study on thought-controlled robotic arm. *Neurosci. Lett.* 450, 1–6. doi: 10.1016/j.neulet.2008.11.024

Le Masson, G., Renaud-Le Masson, S., Debay, D., and Bal, T. (2002). Feedback inhibition controls spike transfer in hybrid thalamic circuits. *Nature* 417, 854–858. doi: 10.1038/nature00825

Lewandowska, M. K., Radivojević, M., Jäckel, D., Müller, J., and Hierlemann, A. R. (2016). Cortical axons, isolated in channels, display activity-dependent signal modulation as a result of targeted stimulation. *Front Neurosci.* 10:83. doi: 10.3389/fnins.2016.00083

Liu, J., Fu, T. M., Cheng, Z., Hong, G., Zhou, T., Jin, L., et al. (2015). Syringe-injectable electronics. *Nat. Nanotechnol.* 10, 629–636. doi: 10.1038/nnano.2015.115

Maccione, A., Garofalo, M., Nieus, T., Tedesco, M., Berdondini, L., and Martinoia, S. (2012). Multiscale functional connectivity estimation on low-density neuronal cultures recorded by high-density CMOS micro electrode arrays. *J. Neurosci. Methods* 207, 161–171. doi: 10.1016/j.jneumeth.2012.04.002

Mahmud, M., Bertoldo, A., Girardi, S., Maschietto, M., and Vassanelli, S. (2012). Sigmate: a matlab-based automated tool for extracellular neuronal signal processing and analysis. *J. Neurosci. Methods* 207, 97–112. doi: 10.1016/j.jneumeth.2012.03.009

Mahmud, M., Pulizzi, R., Vasilaki, E., and Giugliano, M. (2014). Qspike tools: a generic framework for parallel batch preprocessing of extracellular neuronal signals recorded by substrate microelectrode arrays. *Front. Neuroinform.* 8:26. doi: 10.3389/fninf.2014.00026

Mahmud, M., and Vassanelli, S. (2016a). Differential modulation of excitatory and inhibitory neurons during periodic stimulation. *Front. Neurosci.* 10:62. doi: 10.3389/fnins.2016.00062

Mahmud, M., and Vassanelli, S. (2016b). Processing and analysis of multichannel extracellular neuronal signals: state-of-the-art and challenges. *Front. Neurosci.* 10:248. doi: 10.3389/fnins.2016.00248

Mailley, S., Hyland, M., Mailley, P., McLaughlin, J. A., and McAdams, E. T. (2004). Thin film platinum cuff electrodes for neurostimulation: *in vitro* approach of safe neurostimulation parameters. *Bioelectrochemistry* 63, 359–364. doi: 10.1016/j.bioelechem.2003.10.033

Manor, Y., and Nadim, F. (2001). Synaptic depression mediates bistability in neuronal networks with recurrent inhibitory connectivity. *J. Neurosci.* 21, 9460–9470.

Matsushita, K., Hirata, M., Suzuki, T., Ando, H., Ota, Y., Sato, F., et al. (2013). Development of an implantable wireless ECoG 128ch recording device for clinical brain machine interface. *Conf. Proc. IEEE Eng. Med. Biol. Soc.* 2013, 1867–1870. doi: 10.1109/embc.2013.6609888

McConnell, G. C., So, R. Q., and Grill, W. M. (2016). Failure to suppress low-frequency neuronal oscillatory activity underlies the reduced effectiveness of random patterns of deep brain stimulation. *J. Neurophysiol.* 115, 2791–2802. doi: 10.1152/jn.00822.2015

Micera, S. (2016). Staying in touch: toward the restoration of sensory feedback in hand prostheses using peripheral neural stimulation. *IEEE Pulse* 7, 16–19. doi: 10.1109/MPUL.2016.2539760

Miller, M. A., Neuzil, P., Dukkipati, S. R., and Reddy, V. Y. (2015). Leadless cardiac pacemakers back to the future. *J. Am. Coll. Cardiol.* 66, 1179–1189. doi: 10.1016/j.jacc.2015.06.1081

Miranda, R. A., Casebeer, W. D., Hein, A. M., Judy, J. W., Krotkov, E. P., Laabs, T. L., et al. (2015). DARPA-funded efforts in the development of novel brain-computer interface technologies. *J. Neurosci. Methods* 244, 52–67. doi: 10.1016/j.jneumeth.2014.07.019

Mitzdorf, U. (1985). Current source-density method and application in cat cerebral cortex: investigation of evoked potentials and EEG phenomena. *Physiol. Rev.* 65, 37–100.

Mukaino, M., Ono, T., Shindo, K., Fujiwara, T., Ota, T., Kimura, A., et al. (2014). Efficacy of brain- computer interface-driven neuromuscular electrical

stimulation for chronic paresis after stroke. *J. Rehabil. Med.* 46, 378–382. doi: 10.2340/16501977-1785

Muller, J., Ballini, M., Livi, P., Chen, Y., Radivojevic, M., Shadmani, A., et al. (2015). High-resolution CMOS MEA platform to study neurons at subcellular, cellular, and network levels. *Lab Chip* 15, 2767–2780. doi: 10.1039/C5LC00133A

Nathan, F., L., Paul, V., and Tony J, P. (2013). The state of the art in biomimetics. *Bioinspir. Biomim.* 8:013001. doi: 10.1088/1748-3182/8/1/013001

Newman, J. P., Fong, M., Millard, D. C., Whitmire, C. J., Stanley, G. B., and Potter, S. M. (2015). Optogenetic feedback control of neural activity. *eLife* 4:e07192. doi: 10.7554/eLife.07192

Nicolelis, M. A. L., and Lebedev, M. A. (2009). Principles of neural ensemble physiology underlying the operation of brain-machine interfaces. *Nat. Rev. Neurosci.* 10, 530–540. doi: 10.1038/nrn2653

Niehrster, S., and Thomas, A. (2015). "Preparation of Ta-O-Based tunnel junctions to obtain artificial synapses based on memristive switching," in *Methods in Molecular Biology,* Vol. 1260, ed H. Cartwright (New York, NY: Springer), 261–267.

Norton, J. J., Lee, D. S., Lee, J. W., Lee, W., Kwon, O., Won, P., et al. (2015). Soft, curved electrode systems capable of integration on the auricle as a persistent brain-computer interface. *Proc. Natl. Acad. Sci. U.S.A.* 112, 3920–3925. doi: 10.1073/pnas.1424875112

Novellino, A., D'Angelo, P., Cozzi, L., Chiappalone, M., Sanguineti, V., and Martinoia, S. (2007). Connecting neurons to a mobile robot: An *in vitro* bidirectional neural interface. *Comput. Intell. Neurosci.* 2007:12725. doi: 10.1155/2007/12725

Nowotny, T., Zhigulin, V. P., Selverston, A. I., Abarbanel, H. D., and Rabinovich, M. I. (2003). Enhance- ment of synchronization in a hybrid neural circuit by spike-timing dependent plasticity. *J. Neurosci.* 23, 9776–9785.

Occhetta, E., Bortnik, M., Vassanelli, C., and on behalf of the INVASY Italian feasibility study group (2003). The DDDR closed loop stimulation for the prevention of vasovagal syncope: results from the INVASY prospective feasibility registry. *Europace* 5, 153–162. doi: 10.1053/eupc.2002.0292

Ortiz-Catalan, M., Hakansson, B., and Branemark, R. (2014). An osseointegrated human-machine gateway for long-term sensory feedback and motor control of artificial limbs. *Sci. Transl. Med.* 6, 257re6. doi: 10.1126/scitranslmed.3008933

Ortiz-Rosario, A., and Adeli, H. (2013). Brain-computer interface technologies: from signal to action. *Rev. Neurosci.* 24, 537–552. doi: 10.1515/revneuro-2013-0032

Packer, A. M., Russell, L. E., Dalgleish, H. W. P., and Hausser, M. (2015). Simultaneous all-optical manipulation and recording of neural circuit activity with cellular resolution *in vivo*. *Nat. Meth.* 12, 140–146. doi: 10.1038/nmeth.3217

Park, H., Shin, H. J., Cho, I. J., Yoon, E. S., Suh, J. K., Im, M., et al. (2011). The first neural probe integrated with light source (blue laser diode) for optical stimulation and electrical recording. *Conf. Proc. IEEE. Eng. Med. Biol. Soc.* 2011, 2961–2964. doi: 10.1109/IEMBS.2011.6090813

Pashaie, R., Baumgartner, R., Richner, T. J., Brodnick, S. K., Azimipour, M., Eliceiri, K. W., et al. (2015). Closed-loop optogenetic brain interface. *IEEE Trans. Biomed. Eng.* 62, 2327–2337. doi: 10.1109/TBME.2015.2436817

Patil, A. C., and Thakor, N. V. (2016). Implantable neurotechnologies: a review of micro- and nanoelectrodes for neural recording. *Med. Biol. Eng. Comput.* 54, 23. doi: 10.1007/s11517-015-1430-4

Peckham, P. H., and Knutson, J. S. (2005). Functional electrical stimulation for neuromuscular applications. *Ann. Rev. Biomed. Eng.* 7, 327–360. doi: 10.1146/annurev.bioeng.6.040803.140103

Pei, X., Leuthardt, E. C., Gaona, C. M., Brunner, P., Wolpaw, J. R., and Schalk, G. (2011). Spatiotem- poral dynamics of electrocorticographic high gamma activity during overt and covert word repetition. *Neuroimage* 54, 2960–2972. doi: 10.1016/j.neuroimage.2010.10.029

Pine, J. (2006). "A history of MEA development," in *Advances in Network Electrophysiology Using Multi-Electrode Arrays*, eds M. Taketani and M. Baudry (New York, NY: Springer), 3–23.

Pisanello, F., Sileo, L., and De Vittorio, M. (2016). Micro- and nanotechnologies for optical neural interfaces. *Front. Neurosci.* 10:70. doi: 10.3389/fnins.2016.00070

Prinz, A. A. (2004). Neural networks: models and neurons show hybrid vigor in real time. *Curr. Biol.* 14, R661–R662. doi: 10.1016/j.cub.2004.08.012

Prinz, A. A., Abbott, L. F., and Marder, E. (2004). The dynamic clamp comes of age. *Trends Neurosci.* 27, 218–224. doi: 10.1016/j.tins.2004.02.004

Prodanov, D., and Delbeke, J. (2016). Mechanical and biological interactions of implants with the brain and their impact on implant design. *Front. Neurosci.* 10:11. doi: 10.3389/fnins.2016.00011

Prodromakis, T., Peh, B. P., Papavassiliou, C., and Toumazou, C. (2011). A versatile memristor model with nonlinear dopant kinetics. *IEEE T. Electron. Dev.* 58, 3099–3105. doi: 10.1109/TED.2011.2158004

Prodromakis, T., Toumazou, C., and Chua, L. (2012). Two centuries of memristors. *Nat. Mater.* 11, 478–481. doi: 10.1038/nmat3338

Qiao, N., Mostafa, H., Corradi, F., Osswald, M., Stefanini, F., Sumislawska, D., et al. (2015). A reconfigurable on-line learning spiking neuromorphic processor comprising 256 neurons and 128K synapses. *Front. Neurosci.* 9:141. doi: 10.3389/fnins.2015.00141

Raspopovic, S., Capogrosso, M., Petrini, F. M., Bonizzato, M., Rigosa, J., Pino, G. D., et al. (2014). Restoring natural sensory feedback in real-time bidirectional hand prostheses. *Sci. Transl. Med.* 6, 222ra19. doi: 10.1126/scitranslmed.3006820

Ricotti, L., and Menciassi, A. (2012). Bio-hybrid muscle cell-based actuators. *Biomed. Microdevices* 14, 987–998. doi: 10.1007/s10544-012-9697-9

Roche, J. P., and Hansen, M. R. (2015). On the horizon: cochlear implant technology. *Otolaryngol. Clin. North Am.* 48, 1097–1116. doi: 10.1016/j.otc.2015.07.009

Ruffini, G., Wendling, F., Merlet, I., Molaee-Ardekani, B., Mekonnen, A., Salvador, R., et al. (2013). Transcranial Current Brain Stimulation (tCS): models and technologies. *IEEE Trans. Neural Syst. Rehabil. Eng.* 21, 333–345. doi: 10.1109/TNSRE.2012.2200046

Ruiz, S., Buyukturkoglu, K., Rana, M., Birbaumer, N., and Sitaram, R. (2014). Real-time fmri brain computer interfaces: self-regulation of single brain regions to networks. *Biol. Psychol.* 95, 4–20. doi: 10.1016/j.biopsycho.2013.04.010

Ruther, P., and Paul, O. (2015). New approaches for CMOS-based devices for large-scale neural recording. *Curr. Opin. Neurobiol.* 32, 31–37. doi: 10.1016/j.conb.2014.10.007

Rutten, W. L. C. (2002). Selective electrical interfaces with the nervous system. *Annu. Rev. Biomed. Eng.* 4, 407–452. doi: 10.1146/annurev.bioeng.4.020702.153427

Sato, M., Baumhoff, P., and Kral, A. (2016). Cochlear implant stimulation of a hearing ear generates separate electrophonic and electroneural responses. *J. Neurosci.* 36, 54–64. doi: 10.1523/JNEUROSCI.2968-15.2016

Schroder, S., Cecchetto, C., Keil, S., Mahmud, M., Brose, E., Dogan, O., et al. (2015). "Cmos-compatible purely capacitive interfaces for high-density *in-vivo* recording from neural tissue," in *2015 IEEE Biomedical Circuits and Systems Conference (BioCAS)* (Atlanta, GA), 1–4.

Serb, A., Johannes, B., Khiat, A., Berdan, R., Legenstein, R., and Prodromakis, T. (2016). Unsupervised learning in probabilistic neural networks with multi-state metal-oxide memristive synapses. *Nat. Commun.* [Epub ahead of print].

Seriwala, H. M., Khan, M. S., Munir, M. B., Riaz, I. B., Riaz, H., Saba, S., et al. (2016). Leadless pacemakers: a new era in cardiac pacing. *J. Cardiol.* 67, 1–5. doi: 10.1016/j.jjcc.2015.09.006

Sharp, A. A., O'Neil, M. B., Abbott, L. F., and Marder, E. (1993). Dynamic clamp: computer-generated conductances in real neurons. *J. Neurophysiol.* 69, 992–995.

Shihong, M. W., Prodromakis, T., Salaoru, I., and Toumazou, C. (2012). Modelling of current percolation channels in emerging resistive switching elements. *ArXiv e-prints*.

Shobe, J. L., Claar, L. D., Parhami, S., Bakhurin, K. I., and Masmanidis, S. C. (2015). Brain activity mapping at multiple scales with silicon microprobes containing 1,024 electrodes. *J. Neurophysiol.* 114, 2043–2052. doi: 10.1152/jn.00464.2015

Spira, M. E., and Hai, A. (2013). Multi-electrode array technologies for neuroscience and cardiology. *Nat. Nano.* 8, 83–94. doi: 10.1038/nnano.2012.265

Stieglitz, T., Neves, H., and Ruther, P. (2014). Neural probes–microsystems to interface with the brain. *Biomed. Tech. (Berl.)* 59, 269–271. doi: 10.1515/bmt-2012-0094

Strukov, D. B., Snider, G. S., Stewart, D. R., and Williams, R. S. (2008). The missing memristor found. *Nature* 453, 80–83. doi: 10.1038/nature06932

Tabot, G. A., Kim, S. S., Winberry, J. E., and Bensmaia, S. J. (2015). Restoring tactile and proprioceptive sensation through a brain interface. *Neurobiol. Dis.* 83, 191–198. doi: 10.1016/j.nbd.2014.08.029

Thibeault, C. M. (2014). A role for neuromorphic processors in therapeutic nervous system stimulation. *Front. Syst. Neurosci.* 8:187. doi: 10.3389/fnsys.2014.00187

Thomas, A., Niehorster, S., Fabretti, S., Shepheard, N., Kuschel, O., Kupper, K., et al. (2015). Tunnel junction based memristors as artificial synapses. *Front. Neurosci.* 9:241. doi: 10.3389/fnins.2015.00241

Tian, L., Hires, S. A., and Looger, L. L. (2012). Imaging neuronal activity with genetically encoded calcium indicators. *Cold Spring Harb. Protoc.* 2012, 647–656. doi: 10.1101/pdb.top069609

Vassanelli, S. (2014). "Multielectrode and multitransistor arrays for *in vivo* recording," in *Nanotechnology and Neuroscience: Nano-Electronic, Photonic and Mechanical Neuronal Interfacing*, eds M. De Vittorio, L. Martiradonna, and J. Assad (New York, NY: S*pringer)*, 239–267.

Vassanelli, S., Mahmud, M., Girardi, S., and Maschietto, M. (2012). On the way to large-scale and high-resolution brain-chip interfacing. *Cogn. Comput.* 4, 71–81. doi: 10.1007/s12559-011-9121-4

Vidu, R., Rahman, M., Mahmoudi, M., Enachescu, M., Poteca, T. D., and Opris, I. (2014). Nanostructures: a platform for brain repair and augmentation. *Front. Syst. Neurosci.* 8:91. doi: 10.3389/fnsys.2014.00091

Vujaklija, I., Farina, D., and Aszmann, O. (2016). New developments in prosthetic arm systems. *Orthop. Res. Rev.* 8, 31–39. doi: 10.2147/ORR.S71468

Waldert, S. (2016). Invasive vs. Non-invasive neuronal signals for brain-machine interfaces: will one prevail? *Front. Neurosci.* 10:295. doi: 10.3389/fnins.2016.00295

Weiskopf, N., Sitaram, R., Josephs, O., Veit, R., Scharnowski, F., Goebel, R., et al. (2007). Real-time functional magnetic resonance imaging: methods and applications. *Magn. Reson. Imaging* 25, 989–1003. doi: 10.1016/j.mri.2007.02.007

Wheeler, B. C., and Nam, Y. (2011). *In vitro* microelectrode array technology and neural recordings. *Crit. Rev. Biomed. Eng.* 39, 45–61. doi: 10.1615/CritRevBiomedEng.v39.i1.40

Wilson, S. P., Verschure, P. F. M. J., Mura, A., and Prescott, T. J. (eds.). (2015). *Biomimetic and Biohybrid Systems*. Cham: Springer International Publishing.

Wise, K. D., Anderson, D. J., Hetke, J. F., Kipke, D. R., and Najafi, K. (2004). Wireless implantable microsystems: high-density electronic interfaces to the nervous system. *Proc. IEEE* 92, 76–97. doi: 10.1109/JPROC.2003.820544

Wu, F., Stark, E., Im, M., Cho, I. J., Yoon, E. S., Buzsaki, G., et al. (2013). An implantable neural probe with monolithically integrated dielectric waveguide and recording electrodes for optogenetics applications. *J. Neural Eng.* 10:056012. doi: 10.1088/1741-2560/10/5/056012

Yang, J. J., Strukov, D. B., and Stewart, D. R. (2013). Memristive devices for computing. *Nat. Nano.* 8, 13–24. doi: 10.1038/nnano.2012.240

Yang, Y., Adowski, T., Ramamurthy, B., Neef, A., and Xu-Friedman, M. A. (2015). High-speed dynamic-clamp interface. *J. Neurophysiol.* 113, 2713–2720. doi: 10.1152/jn.00543.2014

Yarom, Y. (1991). Rhythmogenesis in a hybrid system - interconnecting an olivary neuron to an analog network of coupled oscillators. *Neuroscience* 44, 263–275. doi: 10.1016/0306-4522(91)90053-Q

Zeck, G. (2016). Aberrant activity in degenerated retinas revealed by electrical imaging. *Front. Cell. Neurosci.* 10:25. doi: 10.3389/fncel.2016.00025

Zhang, S., Song, Y., Wang, M., Zhang, Z., Fan, X., Song, X., et al. (2016). A silicon based implantable microelectrode array for electrophysiological and dopamine recording from cortex to striatum in the non-human primate brain. *Biosens. Bioelectron.* 85, 53–61. doi: 10.1016/j.bios.2016.04.087

Conflict of Interest Statement: The authors declare that the research was conducted in the absence of any commercial or financial relationships that could be construed as a potential conflict of interest.

frontiers in
SYSTEMS NEUROSCIENCE

PERSPECTIVE ARTICLE
published: 02 December 2014
doi: 10.3389/fnsys.2014.00226

Bottlenecks to clinical translation of direct brain-computer interfaces

Mijail D. Serruya*

Department of Neurology, Thomas Jefferson University, Philadelphia, PA, USA

Edited by:
Ioan Opris, Wake Forest University, USA

Reviewed by:
Mikhail Lebedev, Duke University, USA
Dong Song, University of Southern California, USA

****Correspondence:***
Mijail D. Serruya, Department of Neurology, Thomas Jefferson University, 901 Walnut Street, Suite 400, Philadelphia, PA 19107, USA
e-mail: Mijail.Serruya@jefferson.edu

Despite several decades of research into novel brain-implantable devices to treat a range of diseases, only two—cochlear implants for sensorineural hearing loss and deep brain stimulation for movement disorders—have yielded any appreciable clinical benefit. Obstacles to translation include technical factors (e.g., signal loss due to gliosis or micromotion), lack of awareness of current clinical options for patients that the new therapy must outperform, traversing between federal and corporate funding needed to support clinical trials, and insufficient management expertise. This commentary reviews these obstacles preventing the translation of promising new neurotechnologies into clinical application and suggests some principles that interdisciplinary teams in academia and industry could adopt to enhance their chances of success.

Keywords: brain-computer interface, neurotechnology, device approval, commercialization, neuroprosthetic

INTRODUCTION

"Brain-computer interfaces" (BCI) and "brain-machine interfaces" (BMI) comprise a class of medical devices designed to restore independent function lost by neurological disease or injury. The qualifier "direct" implies that some component of the artificial device is physically implanted into the brain. While the BCI terminology usually refers to techniques that sense electrical activity in the brain to determine intended movement with the goal of restoring independent communication and movement in patients with paralysis, in principle any device implanted into the brain that includes electronic components could be considered a BCI, for example systems to detect and arrest seizures (Stacey and Litt, 2008) or to restore episodic memory (Hampson et al., 2013; Sankar et al., 2014). While there has been tremendous interest in BCIs, including several pilot trials in human patients and an explosion of publications in the past few decades, the clinical benefits have remained quite limited. The purpose of this essay is to address the disconnect between hundreds of laboratories around the world toiling on BCIs and the thousands to millions of patients who could benefit from this technology yet are not.

"Motor" BCIs refer to systems that decode intended movement and use this decoded information to control some object in the world: such as a computer to type out text for communication, turn off and on light switches, navigate with a wheelchair, or control one's own body with external powered braces or internal neuromuscular stimulators. Given several decades of work on external scalp-EEG based BCIs and nearly a decade since the first human patient was implanted with a multi-electrode array to decode motor intent (Hochberg et al., 2006; Lebedev, 2014), what are the limitations holding back this promising technology from entering the mainstream for clinical care? Sadly, there is no lack of people paralyzed by spinal cord injury, stroke, brain injury, muscular dystrophy and amyotrophic lateral sclerosis. One possible answer would be to counsel patience: while there are over 300,000 people with sensorineural hearing loss who have been implanted with cochlear implants, it has been over seven decades since Djourno and Eyriès showed in 1957, that an inner ear electrode could elicit sound sensations in a deaf listener (Djourno and Eyries, 1957; Macherey and Carlyon, 2014). Is there any way we can learn from prior mistakes and successes so that the translation cycle may be accelerated to bring these therapies to the clinic faster than seven decades?

TECHNICAL LIMITATIONS

INFLAMMATION/GLIOSIS

Several groups have demonstrated that motor intent can be decoded from the activity of ensembles of neurons recorded by microelectrode arrays implanted into the neocortex of paralyzed people (Hochberg et al., 2012; Collinger et al., 2013). A problem for chronic recording of single units is that the number and quality of recordings fall off with time (Suner et al., 2005; Barrese et al., 2013; Wang et al., 2014). Several explanations have been posited: the foreign body of the array induces a reactive gliosis with scarring or inflammation, the device experiences micromotion relative to the cell bodies it seeks to record quenching signal to noise, or the device itself fails internally such as through mechanical breakage of electrodes or electrolytic changes in surface chemistry altering impedance (Prasad et al., 2014). Certain groups have attempted to address this device-brain interface problem by altering the microscopic geometry or surface chemistry of the devices (Sanchez et al., 2006; Moxon et al., 2007; Sommakia et al., 2009; Frewin et al., 2011; Ceyssens et al., 2013; Edgington et al., 2013) others have attempted to circumvent the problem entirely by focusing analysis on the envelope

of multi-unit activity or analyzing time series in the frequency domain, rather than requiring single units to be discriminated (Dolan et al., 2009; Flint et al., 2013; Lebedev, 2014; Perge et al., 2014).

CHASING THE NOISE

For motor BCIs there are two learning systems: the mathematical algorithm that decodes neural activity into motor commands, and the patient's brain itself. Unlike alpha motor neurons in the spinal cord which are "hard-wired" in motor pools to specific sets of skeletal muscles, the relationship of cortical neurons to external muscular and somatosensory features is fluid. If the calibration routines used are too frequent or extreme, then the two learning systems will fail to converge on a decoding-control solution and instead will chase the noise, and the paralyzed patient will not be able make use of the device (Wu et al., 2004). It would be analogous to attempting to learn to ride a bicycle if the laws of physics changed with every attempt to pedal.

CALIBRATION AND TECHNICIANS

All types of motor BCI, whether non-invasive scalp EEG or direct invasive BCI with implanted electrodes, require considerable set up and calibration with one or more technicians (Sellers et al., 2010; Taherian et al., 2014). Even in the net-connected age with telemedicine, the burden of daily calibration becomes so onerous as to render the motor BCI unfeasible for widespread clinical application (Rupp, 2014).

CHALLENGING PRECONCEPTIONS

PRECONCEPTION: LESS INVASIVE TECHNOLOGY IS SAFER FOR PATIENTS THAN MORE INVASIVE TECHNOLOGY

Just because a technology does not involve a surgical procedure does not mean it is not risky. The balance of risk and benefit must take into account all aspects of a technology, not simply whether one cuts into the skin. As an example, while the heart can be defibrillated and paced by electrodes worn on the chest, this would be completely impractical for patients to use on a daily basis. The system had to be implanted to make it useful. While motor BCIs may not have proved their utility to an equal degree of implanted cardiac pacemakers, the point is that the focus of device development should be on the overall net utility: the greater the potential benefit, the more a given amount of risk could be taken. In terms of risks, there seems to be significant misunderstanding on the part of non-clinicians about what procedures pose risks to patients and what do not. Relative to other neurosurgical procedures, implantation of tiny microelectrode arrays into the surface cortex is less risky than other common neurosurgical procedure. Likewise, the daily scrubbing of a patient's scalp and attachment of electrode pads has its own risks of skin breakdown and even fatal cellulitis in patients who have limited mobility and may be in a constant state of relative immunocompromise (Rupp, 2014). Patients with quadriplegia invariably already have undergone surgeries and have percutaneous devices, such as tracheostomy tubes attached to ventilators and feeding tubes. It would be more useful and safer for quadriplegic patients if scalp EEG systems could be rendered as implantable systems: for example, subdermal grids with wireless telemetry. A minimally invasive approach would simultaneously address several bottlenecks in application: it would decrease the risk of skin infection from repeated scalp electrode application, it would decrease impedance variability that affects device performance, and it would take out the reliance on an external technician to physically affix the electrodes every day to afford useful communication. Conclusion: "Degree of invasiveness" is not a helpful metric of neurotechnology safety or utility. Scientists and engineers developing devices should take a holistic view of how the device affects the patient's overall health.

PRECONCEPTION: BCIs WILL NOT BE CLINICALLY USEFUL UNTIL THEY CAN EXTRACT MORE INFORMATION

Over the past several decades, several groups working on primate motor neurophysiology have found that the single-unit, ensemble and local field potential activity of motor areas in the brain can be "decoded" to yield information about a wide variety of motor parameters: not only two and three-dimensional end-point (i.e., hand) trajectory, but also muscle contraction states, pattern generator and spinal synergy activation states, joint kinematics, velocity and acceleration, attentional states, sequence and planning features and somatosensory fields (Carpenter et al., 1999; Matsuzaka et al., 2007; Stark et al., 2007; Umilta et al., 2007; Scott, 2008; Zach et al., 2008; Griffin et al., 2009; Vargas-Irwin et al., 2010; Pruszynski et al., 2011; Saleh et al., 2012; Addou et al., 2014; Crowe et al., 2014; Kirsch et al., 2014). Information rate, following the conventions initially developed by Claude Shannon, have been one popular way of quantifying BCI performance (Baranauskas, 2014). While elucidating from a basic neurophysiology perspective, these approaches do not axiomatically translate into device development and clinical utility. Information transfer metrics that elucidate how single neurons transform sensory and motor phenomena (Rieke et al., 1997), tend to devolve into unhelpful distortions of more appropriate performance metrics (such as task completion time or validated daily living functional measures; Peckham et al., 2001). From a practical engineering perspective it would be far better to have one or two degrees of freedom that could be decoded in a fast, reliable, technician-free manner, than seven degrees of freedom that were unreliable and required considerable external supervision to derive (Peckham et al., 2001; Rupp, 2014). While entropy rates can be constructed so as to include reliability as a feature, they are usually not considered in this manner. Another important feature to consider in addition to reliability is subjective effort. In principle, even one's heart rate could be used as input to a BCI: clearly such a tactic would require considerable mental focus and would be confounded by environmental distractions (e.g., accidentally launching oneself in a heart-rate driven wheelchair upon hearing a horn honk). The farther one moves from the neocortical areas driving voluntary movement, the more challenging it is for a patient to acquire and sustain control. While direct BCIs have been touted for their ability to yield more degrees-of-freedom and signal complexity, their greatest benefit may in fact be the fact that voluntary modulation of signals recorded intracranially from motor areas is most akin to natural movement and hence is subjectively effortless for the human participant, much as it is for healthy humans moving their intact limbs. Conclusion:

The quantity and complexity of information are limited metrics for BCI translation to clinical application. BCIs will be clinically useful when they can extract information in a reliable and subjectively effortless manner with minimal calibration or technician supervision.

PRECONCEPTION: HUMAN PILOT TRIALS FOR DIRECT BCIs MUST RELY ON VENTURE CAPITAL FUNDING OR RARE FEDERAL OPPORTUNITIES

It usually takes 7 years and costs $40 million to take a final medical device prototype from bench to bedside. It takes two to three years of preparation and nearly $6 million just to launch an initial Investigational Device Exemption (IDE) trial. What exactly does this money pay for? One component is to salary support for consultants with regulatory expertise: this knowledge of the inner workings of the FDA, CE and other foreign equivalents, does not typically "live" inside academia. To have any hope of translational success, investigators must recruit regulatory colleagues who have successful track records of shepherding novel devices through the IDE process. The upfront $6 million also pays for "freezing the design" of the device or fabrication process, establishing clean room Good Manufacturing Practices, and sending off device prototypes to existing, commercial "testing houses" that can systematically test the toxicity and biocompatibility of the device and its electrical safety in the hospital environment. While purposefully incorporating already-approved well-tested materials and fabrication techniques can reassure regulators, these agencies ultimately require these additional tests.

The organizational complexity and financial cost of this process does not fit into the typical R01 or non-NIH equivalents that sustain academic neuroscience laboratories. These leave translational investigators with few options. One is to appeal to special multi-center U01, Veteran's Affairs or other military-based (e.g., DARPA) multi-million dollar requests for applications. The FES Center in Cleveland, has been successful in following this non-commercial multi-center approach for their neuromuscular stimulator system to restore independent voluntary movement in veterans with spinal cord injury (Peckham et al., 1988). The Department of Defense may withdraw funds if performance metrics aren't met rendering it difficult to plan appropriately for multi-year trials. While the National Institutes of Health sponsors intramural clinical trials, there is not as extensive a track record for extramural ones devoted to novel devices. In terms of funding academic-industry partnerships, SBIRs and STTRs are simply not at the scale of $6 million needed.

The other option is to create a startup neurotechnology company and apply for funding from angel investors and venture capitalists. Except for very simple mechanical based neurotechnologies (such as a new kind of shunt), few BCI technologies are at a stage of commercialization potential that render them appropriate for risk-averse investors. A pilot trial for a BCI may simply not make any investment sense for the typical venture capital funding model (Ford and Nelsen, 2014). If anything, a promising BCI would be more ripe for VC funding after a pilot trial demonstrated safety and efficacy.

This investigator therefore proposes that federal agencies create new funding mechanisms that fill this gap. These funds would help investigators set up clean room fabrication facilities and cover the cost of the numerous regulatory-required tests for the device. Ideally, all members on the study sections for this putative new mechanism would have some kind of clinical trial expertise, including physicians, FDA regulators, and scientists or engineers who have already successfully run human trials on their own. Given the scale and duration of the funding, and the fact that sudden withdrawal of funding in the middle of a trial could potentially risk patient health, thought should be given to render this new mechanism "sequester-proof" should political forces slash funding. Since industry investors would be the financial beneficiaries of these trials, one approach would be to set aside transparent pools donated by industry explicitly allocated for this novel translational funding mechanism. Agencies could make this financially worthwhile if they could eliminate waste and streamline the process, thus increasing the amount of return for each dollar invested on pilot trial development. By pulling actual FDA regulatory officials into these novel study sections, investigators and future investors would also reap enormous benefit in the regulatory process with this "insider" knowledge. Rather than have each BCI team muddle through the prototype, clean room, standard biosafety/bioelectrical testing, by itself, this mechanism would have its own streamlined process. Conclusion: Leaders in government, industry and academia should forge new funding mechanisms that can help investigators shepherd promising BCI technologies into pilot clinical trials to a stage where traditional existing VC and industry funding make sense and the chances of commercialization were greater.

PRECONCEPTION: IF A BCI WERE SAFE AND EFFECTIVE, MARKET FORCES WILL AUTOMATICALLY PROPEL IT TOWARDS WIDESPREAD CLINICAL USE

Many good ideas may never end up helping patients due to a variety of reasons as they may not be marketable or may be badly marketed (Vecht et al., 2010). Despite clear demonstration of the safety and efficacy of the FreeHand functional electrical stimulation system to help patients with spinal cord injury (Peckham et al., 1988; Taylor et al., 2002), the small company commercializing it (NeuroControl) went out of business before meeting clinical demand. Scientists seeking to bring a promising neurotechnology from bench to bedside would do well to understand why certain efforts flounder and why others succeed (de Ana et al., 2013; Pisano, 2006; Galloway, 2007; Fletcher and Bourne, 2012). Neurotechnology ventures need to involve business experts early (Leuthardt, 2013) to ensure they can navigate issues of patents, pricing, reimbursement, and multi-year alliances (Pangarkar and Hutmacher, 2003; Bergsland et al., 2014). Inventors must recognize the importance of skilled management (Burns et al., 2009), and have realistic expectations of how commercialization unfolds (Galloway, 2007; Fletcher and Bourne, 2012). Translational scientists must learn that: what drives science does not drive business, there is no single path to commercialization, "research" and "development" are very different phases, the market may not exist at the outset, and that customers are the "ultimate peer review" (Fletcher and Bourne, 2012). Conclusion: While having a strong safety and efficacy profile is necessary

for a medical device, it is not sufficient to reach patients in need. To reach patients, devices must be supported by skilled management in both startup and established biotechnology companies.

PRECONCEPTION: THE MARKET FOR NEUROSCIENCE MEDICAL DEVICE APPLICATIONS IS TOO HETEROGENEOUS AND SMALL TO BE WORTH THE INVESTMENT

Any business from a Fortune 500 company to a corner bodega can be run poorly or well: the fact that there is more than one company manufacturing cochlear implants, for a market of less than a million patients, is testament to the fact that a device with demonstrable safety and efficacy can be financially sustainable. Furthermore, both DBS and cochlear implants are designed to improve quality of life: patients are not expected to die directly from deafness or tremor. Conclusion: To reach and benefit patients, safe and effective technologies must be brought to market by visionary entrepreneurs who have excellent management skills and a deep understanding of the clinical neuroscience landscape.

PRECONCEPTION: THE BRAIN IS TOO COMPLEX: ANY MEDICAL DEVICE CANNOT SUCCEED UNTIL THE BRAIN IS BETTER UNDERSTOOD

While cochlear and auditory-brainstem implants leverage neuroanatomical tonotopy to "play" neural structures, the fundamental mechanism of deep brain stimulators for movement disorders remains a source of controversy. Medicine is replete with countless treatments that are used daily to successfully improve human health despite the mechanism of these treatments not being understood. The efficacy of medical interventions is established empirically rather than mechanistically. Hundreds of medications are used to treat brain-based conditions (such as schizophrenia and epilepsy) despite our limited knowledge about the pathophysiology of these conditions or how particular medications exercise their effects. Conclusion: Neurotechnoloogy that can concretely help people can be financially remunerative even despite our incomplete knowledge of the human brain. Companies can "do well by doing good" by focusing on concrete quality of life outcome measures rather than relying on a mechanistic understanding of neurobiology.

PRECONCEPTION: THE TIME TO APPROACH CLINICIANS AND PATIENTS WHEN CONSIDERING HUMAN APPLICATIONS OF DIRECT BCI OR OTHER NEUROTECHNOLOGIES IS ONLY AFTER THE TECHNOLOGY ITSELF IS FINALIZED AND ANIMAL STUDIES ARE COMPLETED

Development of the Utah array from a research tool restricted to animal investigation to a clinical intervention in a pilot trial for human patients, benefited from close, friendly collaboration between engineers designing the device within industry and academic neurosurgeons. By literally handing prototypes to experienced surgeons to test in animal models and human cadavers, engineers could gain immediate feedback about helpful or limiting design features that no amount of bench work could reveal (Suner et al., 2005; Som et al., 2014). Conclusion: Scientists should engage physicians, surgeons and patients much earlier in the design cycle.

RECOMMENDATIONS FOR IMPROVING NEUROTECHNOLOGY DEVELOPMENT

BCI translation can be accelerated by tightening the design cycle with close collaboration between engineers, scientists, surgeons, regulatory experts, and clinicians.

Basic scientists and engineers are urged to never assume what risk-safety profiles are needed for a device to help a person: they should query physicians, surgeons and even potential beneficiaries and their families, sooner rather than later to ascertain the medical context, and should focus their energies on making the device truly useful.

Engineers and scientists are encouraged to visit the patients whose their technology is intended to help and understand what solutions they have deployed now to inform what the new technology must outperform.

Considerations of safety must be holistic and take into account the overall clinical context: non-invasive devices are not necessarily safer or more practical than invasive ones.

While metrics such as "degrees of freedom" and "entropy bit rate" have their utility, to facilitate clinical translation, device developers should focus on increasing device reliability, decreasing subjective effort, reducing calibration and minimizing technician supervision.

Leadership in government and industry are encouraged to consider alternate funding mechanisms that can shepherd technologies farther towards commercialization.

Scientists, surgeons, engineers and physicians seeking to commercialize promising neurotechnologies should recruit entrepreneurs with considerable management skill and a track record of shepherding devices into profitable commercialization.

ACKNOWLEDGMENTS

The author would like to thank John Donoghue, Mikhail Shapiro, Nandini Murthy, and Kurt Dasse for their helpful input and insights over the past two decades, and to Abdolmohammed Rostami and Thomas Jefferson University for financial support.

REFERENCES

Addou, T., Krouchev, N., and Kalaska, J. F. (2014). Motor cortex single-neuron and population contributions to compensation for multiple dynamic force fields. *J. Neurophysiol.* doi: 10.1152/jn.00094.2014. [Epub ahead of print].

Baranauskas, G. (2014). What limits the performance of current invasive brain machine interfaces? *Front. Syst. Neurosci.* 8:68. doi: 10.3389/fnsys.2014.00068

Barrese, J. C., Rao, N., Paroo, K., Triebwasser, C., Vargas-Irwin, C., Franquemont, L., et al. (2013). Failure mode analysis of silicon-based intracortical microelectrode arrays in non-human primates. *J. Neural Eng.* 10:066014. doi: 10.1088/1741-2560/10/6/066014

Bergsland, J., Elle, O. J., and Fosse, E. (2014). Barriers to medical device innovation. *Med. Devices (Auckl)* 7, 205–209. doi: 10.2147/MDER.S43369

Burns, L. R., Housman, M. G., and Robinson, C. A. (2009). Market entry and exit by biotech and device companies funded by venture capital. *Health Aff. (Millwood)* 28, w76–w86. doi: 10.1377/hlthaff.28.1.w76

Carpenter, A. F., Georgopoulos, A. P., and Pellizzer, G. (1999). Motor cortical encoding of serial order in a context-recall task. *Science* 283, 1752–1757. doi: 10.1126/science.283.5408.1752

Ceyssens, F., van Kuyck, K., Vande Velde, G., Welkenhuysen, M., Stappers, L., Nuttin, B., et al. (2013). Resorbable scaffold based chronic neural electrode arrays. *Biomed. Microdevices* 15, 481–493. doi: 10.1007/s10544-013-9748-x

Collinger, J. L., Wodlinger, B., Downey, J. E., Wang, W., Tyler-Kabara, E. C., Weber, D. J., et al. (2013). High-performance neuroprosthetic control by an individual with tetraplegia. *Lancet* 381, 557–564. doi: 10.1016/S0140-6736(12)61816-9

Crowe, D. A., Zarco, W., Bartolo, R., and Merchant, H. (2014). Dynamic representation of the temporal and sequential structure of rhythmic movements in the primate medial premotor cortex. *J. Neurosci.* 34, 11972–11983. doi: 10.1523/JNEUROSCI.2177-14.2014

de Ana, F. J., Umstead, K. A., Phillips, G. J., and Conner, C. P. (2013). Value driven innovation in medical device design: a process for balancing stakeholder voices. *Ann. Biomed. Eng.* 41, 1811–1821. doi: 10.1007/s10439-013-0779-5

Djourno, A., and Eyries, C. (1957). Auditory prosthesis by means of a distant electrical stimulation of the sensory nerve with the use of an indwelt coiling. *Presse Med.* 65, 1417.

Dolan, K., Martens, H. C., Schuurman, P. R., and Bour, L. J. (2009). Automatic noise-level detection for extra-cellular micro-electrode recordings. *Med. Biol. Eng. Comput.* 47, 791–800. doi: 10.1007/s11517-009-0494-4

Edgington, R. J., Thalhammer, A., Welch, J. O., Bongrain, A., Bergonzo, P., Scorsone, E., et al. (2013). Patterned neuronal networks using nanodiamonds and the effect of varying nanodiamond properties on neuronal adhesion and outgrowth. *J. Neural Eng.* 10:056022. doi: 10.1088/1741-2560/10/5/056022

Fletcher, A. C., and Bourne, P. E. (2012). Ten simple rules to commercialize scientific research. *PLoS Comput. Biol.* 8:e1002712. doi: 10.1371/journal.pcbi.1002712

Flint, R. D., Wright, Z. A., Scheid, M. R., and Slutzky, M. W. (2013). Long term, stable brain machine interface performance using local field potentials and multiunit spikes. *J. Neural Eng.* 10:056005. doi: 10.1088/1741-2560/10/5/056005

Ford, D., and Nelsen, B. (2014). The view beyond venture capital. *Nat. Biotechnol.* 32, 15–23. doi: 10.1038/nbt.2780

Frewin, C. L., Locke, C., Saddow, S. E., and Weeber, E. J. (2011). Single-crystal cubic silicon carbide: an in vivo biocompatible semiconductor for brain machine interface devices. *Conf. Proc. IEEE Eng. Med. Biol. Soc.* 2011, 2957–2960. doi: 10.1109/IEMBS.2011.6090582

Galloway, R. L. (2007). Found in translation; from the laboratory to the operating room to the market. *Conf. Proc. IEEE Eng. Med. Biol. Soc.* 2007, 5162–5165. doi: 10.1109/IEMBS.2007.4353504

Griffin, D. M., Hudson, H. M., Belhaj-Saïf, A., and Cheney, P. D. (2009). Stability of output effects from motor cortex to forelimb muscles in primates. *J. Neurosci.* 29, 1915–1927. doi: 10.1523/JNEUROSCI.4831-08.2009

Hampson, R. E., Song, D., Opris, I., Santos, L. M., Shin, D. C., Gerhardt, G. A., et al. (2013). Facilitation of memory encoding in primate hippocampus by a neuroprosthesis that promotes task-specific neural firing. *J. Neural Eng.* 10:066013. doi: 10.1088/1741-2560/10/6/066013

Hochberg, L. R., Bacher, D., Jarosiewicz, B., Masse, N. Y., Simeral, J. D., Vogel, J., et al. (2012). Reach and grasp by people with tetraplegia using a neurally controlled robotic arm. *Nature* 485, 372–375. doi: 10.1038/nature11076

Hochberg, L. R., Serruya, M. D., Friehs, G. M., Mukand, J. A., Saleh, M., Caplan, A. H., et al. (2006). Neuronal ensemble control of prosthetic devices by a human with tetraplegia. *Nature* 442, 164–171. doi: 10.1038/nature04970

Kirsch, E., Rivlis, G., and Schieber, M. H. (2014). Primary motor cortex neurons during individuated finger and wrist movements: correlation of spike firing rates with the motion of individual digits versus their principal components. *Front. Neurol.* 5:70. doi: 10.3389/fneur.2014.00070

Lebedev, M. (2014). Brain-machine interfaces: an overview. *Transl. Neurosci.* 5, 99–110. doi: 10.2478/s13380-014-0212-z

Leuthardt, E. C. (2013). Developing a new model for the invention and translation of neurotechnologies in academic neurosurgery. *Neurosurgery* 72 (Suppl. 1), 182–192. doi: 10.1227/NEU.0b013e318270cfec

Macherey, O., and Carlyon, R. P. (2014). Cochlear implants. *Curr. Biol.* 24, R878–R884. doi: 10.1016/j.cub.2014.06.053

Matsuzaka, Y., Picard, N., and Strick, P. L. (2007). Skill representation in the primary motor cortex after long-term practice. *J. Neurophysiol.* 97, 1819–1832. doi: 10.1152/jn.00784.2006

Moxon, K. A., Hallman, S., Aslani, A., Kalkhoran, N. M., and Lelkes, P. I. (2007). Bioactive properties of nanostructured porous silicon for enhancing electrode to neuron interfaces. *J. Biomater. Sci. Polym. Ed.* 18, 1263–1281. doi: 10.1163/156856207782177882

Pangarkar, N., and Hutmacher, D. W. (2003). Invention and business performance in the tissue-engineering industry. *Tissue Eng.* 9, 1313–1322. doi: 10.1089/10763270360728224

Peckham, P. H., Keith, M. W., and Freehafer, A. A. (1988). Restoration of functional control by electrical stimulation in the upper extremity of the quadriplegic patient. *J. Bone Joint Surg. Am.* 70, 144–148.

Peckham, P. H., Keith, M. W., Kilgore, K. L., Grill, J. H., Wuolle, K. S., Thrope, G. B., et al. (2001). Efficacy of an implanted neuroprosthesis for restoring hand grasp in tetraplegia: a multicenter study. *Arch. Phys. Med. Rehabil.* 82, 1380–1388. doi: 10.1053/apmr.2001.25910

Perge, J. A., Zhang, S., Malik, W. Q., Homer, M. L., Cash, S., Friehs, G., et al. (2014). Reliability of directional information in unsorted spikes and local field potentials recorded in human motor cortex. *J. Neural Eng.* 11:046007. doi: 10.1088/1741-2560/11/4/046007

Pisano, G. P. (2006). Can science be a business? Lessons from biotech. *Harv. Bus. Rev.* 84, 114–124.

Prasad, A., Xue, Q. S., Dieme, R., Sankar, V., Mayrand, R. C., Nishida, T., et al. (2014). Abiotic-biotic characterization of Pt/Ir microelectrode arrays in chronic implants. *Front. Neuroeng.* 7:2. doi: 10.3389/fneng.2014.00002

Pruszynski, J. A., Kurtzer, I., Nashed, J. Y., Omrani, M., Brouwer, B., and Scott, S. H. (2011). Primary motor cortex underlies multi-joint integration for fast feedback control. *Nature* 478, 387–390. doi: 10.1038/nature10436

Rieke, F., Warland, D., de Ruyter van Stevenick, R., and Bialek, W. (1997). *Spikes. Exploring the Neural Code.* Cambridge, MA: MIT Press.

Rupp, R. (2014). Challenges in clinical applications of brain computer interfaces in individuals with spinal cord injury. *Front. Neuroeng.* 7:38. doi: 10.3389/fneng.2014.00038

Saleh, M., Takahashi, K., and Hatsopoulos, N. G. (2012). Encoding of coordinated reach and grasp trajectories in primary motor cortex. *J. Neurosci.* 32, 1220–1232. doi: 10.1523/JNEUROSCI.2438-11.2012

Sanchez, J. C., Alba, N., Nishida, T., Batich, C., and Carney, P. R. (2006). Structural modifications in chronic microwire electrodes for cortical neuroprosthetics: a case study. *IEEE Trans. Neural Syst. Rehabil. Eng.* 14, 217–221. doi: 10.1109/TNSRE.2006.875581

Sankar, T., Lipsman, N., and Lozano, A. M. (2014). Deep brain stimulation for disorders of memory and cognition. *Neurotherapeutics* 11, 527–534. doi: 10.1007/s13311-014-0275-0

Scott, S. H. (2008). Inconvenient truths about neural processing in primary motor cortex. *J. Physiol.* 586, 1217–1224. doi: 10.1113/jphysiol.2007.146068

Sellers, E. W., Vaughan, T. M., and Wolpaw, J. R. (2010). A brain-computer interface for long-term independent home use. *Amyotroph. Lateral Scler.* 11, 449–455. doi: 10.3109/17482961003777470

Som, A., Charanya, T., Linderman, S. W., and Siegel, J. S. (2014). Bridging the gap between invention and commercialization in medical devices. *Nat. Biotechnol.* 32, 1063–1065. doi: 10.1038/nbt.3041

Sommakia, S., Rickus, J. L., and Otto, K. J. (2009). Effects of adsorbed proteins, an antifouling agent and long-duration DC voltage pulses on the impedance of silicon-based neural microelectrodes. *Conf. Proc. IEEE Eng. Med. Biol. Soc.* 2009, 7139–7142. doi: 10.1109/IEMBS.2009.5332456

Stacey, W. C., and Litt, B. (2008). Technology insight: neuroengineering and epilepsy-designing devices for seizure control. *Nat. Clin. Pract. Neurol.* 4, 190–201. doi: 10.1038/ncpneuro0750

Stark, E., Drori, R., Asher, I., Ben-Shaul, Y., and Abeles, M. (2007). Distinct movement parameters are represented by different neurons in the motor cortex. *Eur. J. Neurosci.* 26, 1055–1066. doi: 10.1111/j.1460-9568.2007.05711.x

Suner, S., Fellows, M. R., Vargas-Irwin, C., Nakata, G. K., and Donoghue, J. P. (2005). Reliability of signals from a chronically implanted, silicon-based electrode array in non-human primate primary motor cortex. *IEEE Trans. Neural Syst. Rehabil. Eng.* 13, 524–541. doi: 10.1109/TNSRE.2005.857687

Taherian, S., Selitskiy, D., Pau, J., Davies, T. C., and Owens, R. G. (2014). Training to use a commercial brain-computer interface as access technology: a case study. *Disabil. Rehabil. Assist. Technol.* 1, 1–6. doi: 10.3109/17483107.2014.967313.

Taylor, P., Esnouf, J., and Hobby, J. (2002). The functional impact of the Freehand System on tetraplegic hand function. Clinical results. *Spinal Cord* 40, 560–566. doi: 10.1038/sj.sc.3101373

Umilta, M. A., Brochier, T., Spinks, R. L., and Lemon, R. N. (2007). Simultaneous recording of macaque premotor and primary motor cortex neuronal populations reveals different functional contributions to visuomotor grasp. *J. Neurophysiol.* 98, 488–501. doi: 10.1152/jn.01094.2006

Vargas-Irwin, C. E., Shakhnarovich, G., Yadollahpour, P., Mislow, J. M., Black, M. J., and Donoghue, J. P. (2010). Decoding complete reach and grasp actions from local primary motor cortex populations. *J. Neurosci.* J30, 9659–9669. doi: 10.1523/JNEUROSCI.5443-09.2010

Vecht, J. A., von Segesser, L. K., Ashrafian, H., Rao, C., Skapinakis, P., Saso, S., et al. (2010). Translation to success of surgical innovation. *Eur. J. Cardiothorac. Surg.* 37, 613–625. doi: 10.1016/j.ejcts.2009.08.032

Wang, D., Zhang, Q., Li, Y., Wang, Y., Zhu, J., Zhang, S., et al. (2014). Long-term decoding stability of local field potentials from silicon arrays in primate motor cortex during a 2D center out task. *J. Neural Eng.* 11:036009. doi: 10.1088/1741-2560/11/3/036009

Wu, W., Black, M. J., Mumford, D., Gao, Y., Bienenstock, E., and Donoghue, J. P. (2004). Modeling and decoding motor cortical activity using a switching Kalman filter. *IEEE Trans. Biomed. Eng.* 51, 933–942. doi: 10.1109/TBME.2004.826666

Zach, N., Inbar, D., Grinvald, Y., Bergman, H., and Vaadia, E. (2008). Emergence of novel representations in primary motor cortex and premotor neurons during associative learning. *J. Neurosci.* 28, 9545–9556. doi: 10.1523/JNEUROSCI.1965-08.2008

Conflict of Interest Statement: The author declares that the research was conducted in the absence of any commercial or financial relationships that could be construed as a potential conflict of interest.

Received: 14 October 2014; accepted: 10 November 2014; published online: 02 December 2014.

Citation: Serruya MD (2014) Bottlenecks to clinical translation of direct brain-computer interfaces. Front. Syst. Neurosci. ***8****:226. doi: 10.3389/fnsys.2014.00226*

This article was submitted to the journal Frontiers in Systems Neuroscience.

frontiers in Neuroscience

PERSPECTIVE
published: 13 March 2017
doi: 10.3389/fnins.2017.00111

Constraints and Adaptation of Closed-Loop Neuroprosthetics for Functional Restoration

Robert Bauer and Alireza Gharabaghi**

Division of Functional and Restorative Neurosurgery, Centre for Integrative Neuroscience, Eberhard Karls University Tuebingen, Tuebingen, Germany

Closed-loop neuroprosthetics aim to *compensate* for lost function, e.g., by controlling external devices such as prostheses or wheelchairs. Such assistive approaches seek to maximize speed and classification accuracy for high-dimensional control. More recent approaches use similar technology, but aim to restore lost motor function in the long term. To achieve this goal, *restorative* neuroprosthetics attempt to facilitate motor re-learning and to strengthen damaged and/or alternative neural connections on the basis of neurofeedback training within rehabilitative environments. Such a restorative approach requires reinforcement learning of self-modulated brain activity which is considered to be beneficial for functional rehabilitation, e.g., improvement of β-power modulation over sensorimotor areas for post-stroke movement restoration. Patients with motor impairments, however, may also have a compromised ability for motor task-related regulation of the targeted brain activity. This would affect the estimation of feature weights and hence the classification accuracy of the feedback device. This, in turn, can frustrate the patients and compromise their motor learning. Furthermore, the feedback training may even become erroneous when unconstrained classifier adaptation—which is often used in assistive approaches—is also applied in this rehabilitation context. In conclusion, the conceptual switch from assistance toward restoration necessitates a methodological paradigm shift from classification accuracy toward instructional efficiency. Furthermore, a constrained feature space, a priori regularized feature weights, and difficulty adaptation present key elements of restorative brain interfaces. These factors need, therefore, to be addressed within a therapeutic framework to facilitate reinforcement learning of brain self-regulation for restorative purposes.

Keywords: assistive technology, neurorehabilitation, stroke, rehabilitation robotics, brain-computer interface, brain-machine interface, brain-robot interface

OPEN ACCESS

Edited by:
Mikhail Lebedev, Duke University, USA

Reviewed by:
ShiNung Ching, Washington University in St. Louis, USA
Aysegul Gunduz, University of Florida, USA

****Correspondence:***
Robert Bauer
robert.bauer@cin.uni-tuebingen.de
Alireza Gharabaghi
alireza.gharabaghi@uni-tuebingen.de

Specialty section:
This article was submitted to Neuroprosthetics, a section of the journal Frontiers in Neuroscience

Received: *05 June 2016*
Accepted: *21 February 2017*
Published: *13 March 2017*

Citation:
Bauer R and Gharabaghi A (2017) Constraints and Adaptation of Closed-Loop Neuroprosthetics for Functional Restoration. Front. Neurosci. 11:111. doi: 10.3389/fnins.2017.00111

RESTORATION INSTEAD OF ASSISTANCE

Brain self-regulation has recently been applied in the context of motor rehabilitation after stroke by providing contingent feedback of motor imagery (Buch et al., 2012; Ang et al., 2014; Morone et al., 2015; Pichiorri et al., 2015). In these approaches, specific brain states (i.e., rest vs. motor imagery) are often separated using an online analysis of sensorimotor power in a cue-paced trial-structure. When used in conjunction with robotic rehabilitation technology, these devices are also referred to as brain-robot interfaces (BRI; Bauer et al., 2015; Naros and Gharabaghi, 2015; Kraus et al., 2016).

While *assistive* BRIs aim to replace lost function by controlling external devices (Hochberg et al., 2012; Collinger et al., 2013), *restorative* BRIs aim to rehabilitate an impaired function (Gharabaghi, 2016; Krucoff et al., 2016). In such a restorative framework, BRIs adhere to an operant conditioning rationale (Sherlin et al., 2011; Bauer and Gharabaghi, 2015b). They provide contingent feedback to facilitate the self-regulation of specific brain activity. This reinforcement learning-based approach is considered to be beneficial for recovery and might ultimately lead to functional gains on the basis of motor re-learning and strengthening of damaged and/or alternative neural connections (Daly and Wolpaw, 2008). Restorative BRIs might be additionally supported by brain state dependent stimulation to strengthen cortico-spinal connectivity (Gharabaghi et al., 2014a; Royter and Gharabaghi, 2016; Kraus et al., 2016).

METHODOLOGICAL ADJUSTMENTS

We propose that, on account of their different goals, these restorative techniques require a different methodological approach than assistive BRIs, i.e., modifying brain physiology vs. controlling extremal devices. We acknowledge that different strategies may be adopted to achieve modified neurophysiology and, ultimately, behavioral gains. However, on the basis of empirical evidence acquired in our lab, we propose the following adjustments: constrained feature space, regularized feature weights, and difficulty adaptation.

Instead of analyzing all acquired signals for optimal classification, we propose that the feature space be intentionally constrained to reinforce a specific oscillatory pattern in accordance with the respective treatment rationale (*constrained feature space*). In a next step, to differentiate between the classes, assistive BRIs use classifier calibration to weight features according to their relevance. However, learning brain self-regulation may lead to non-stationarity of these classes in the course of the training (Vidaurre et al., 2011a; Sugiyama et al., 2013; Naros and Gharabaghi, 2015). Unsupervised adaptation of the feature weights may therefore lead to a switch in the mental strategy (Vidaurre et al., 2011b; Bryan et al., 2013). This approach may even result in artefactual control (Gharabaghi et al., 2014b). We, therefore, propose that *feature weight regularization* be applied to address this issue. Furthermore, cognitive, sensory, and motor impairments may limit the ability to modulate brain activity, perceive, and/or process feedback. This may cause frustration, which, in turn, may be exacerbated due to the low classification accuracy caused by the constrained and regularized feature space (Nijboer et al., 2008; Fels et al., 2015). In this context, we propose that *difficulty adaptation* be applied to overcome cognitive load issues (Bauer and Gharabaghi, 2015a; Bauer et al., 2016a,b). Such an approach may also improve the instructional efficiency of feedback (Bauer and Gharabaghi, 2015b) and maintain motivation (Bauer et al., 2016a,b).

In the following paragraphs, we discuss these methodological adjustments in greater detail.

CONSTRAINED FEATURE SPACE

In high-dimensional feature spaces, some regions may be sparsely populated with data, thereby, impairing the classifier setup (Theodoridis and Koutroumbas, 2009). Under these circumstances, constraining the feature space provides a way of dealing with this *curse of dimensionality*. However, if the feature space is constrained a priori, some useful features for classification may also be discarded. A classifier based on a constrained feature set therefore usually performs less well than a classifier based on a full feature set.

Restorative BRIs, which apply this approach, therefore appear inferior in comparison to their assistive counterparts. The latter use more flexible algorithms to select and weight all available features and to maximize classification accuracy (Ang et al., 2009; Theodoridis and Koutroumbas, 2009). An a priori constraint should therefore be well considered. It is tempting to assume that the brain will find the best combination of features by itself. Such an approach is therefore implicitly followed during standard or robotic neurorehabilitation, when the feedback that is provided by the therapist or the training device is independent of specific brain features. This strategy, however, has not been successful until now, at least when considering severely motor-impaired stroke patients with persistent deficits. Moreover, the features (α-desynchronization) identified as most useful for classification between different states in the post-stroke brain, e.g., rest vs. motor imagery, are not necessarily those that are most therapeutically relevant (β-desynchronization): Synchronization/Desynchronization describe the (often task-induced) increase/reduction in power in specific frequency bands. The α-band usually ranges from 8–14 Hz, while the β-band ranges from 15–30 Hz. Specifically, movement-related β-desynchronization (β-ERD) is compromised in the contralateral primary cortex in comparison to healthy controls; the more severe the patient's motor impairment, the less β-ERD (Rossiter et al., 2014). And so β-ERD remains inferior to other features for classification purposes in stroke patients, e.g., in differentiating movement-related brain states for the control of external devices (Gomez-Rodriguez et al., 2011). In this context, we argue that the fact that β-oscillations are less optimal for classification purposes does not compromise—but rather qualifies—this physiological marker as a therapeutic target (Naros and Gharabaghi, 2015). Here, we see an analogy to the concept of constraint-induced movement therapy in stroke patients, where the affected rather than the healthy side of the body is trained to facilitate restoration instead of compensation of motor function. Notably, such an approach does not exclude the possibility that alternative cortico-spinal pathways which do not originate from the contralateral primary motor cortex take over lost function. These pathways would be facilitated on the basis of cortical disinhibition and coherent interaction with the muscles in the β-band as well (Mima et al., 2001; Kilavik et al., 2012; Aumann and Prut, 2015; Brittain et al., 2014; Rossiter et al., 2014; Kraus et al., 2016).

Furthermore, an approach based on a constrained feature space allows making a direct, hypothesis-driven comparison of different interventions based on specific oscillatory patterns. By

way of example, an increase in the β-modulation range will improve cortico-spinal connectivity (Kraus et al., 2015, 2016) and motor function (Naros et al., 2016). This will enable us to empirically detect functionally relevant markers and mechanisms of restoration and to determine physiology-based strategies for further improvement. Such knowledge will also enable us to develop approaches for treatment matching, e.g., defining feature sets on the basis of specific functional impairments and/or lesion locations (Shelton and Reding, 2001; Stinear et al., 2012). By contrast, an approach based on an unconstrained feature space would be based on the assumption that the most accurate detection of motor intention/imagery and provision of feedback is in itself sufficient to restore function.

REGULARIZED FEATURE WEIGHTS

Regularization can be considered a penalty term to prevent feature weights from reaching implausibly high values (Theodoridis and Koutroumbas, 2009; Bishop, 2013) caused by the empirical estimation of class parameters (e.g., mean and covariance). Such estimates can be biased, especially when the sample size is low. Due to the large variety of classification approaches (Theodoridis and Koutroumbas, 2009), several regularization approaches have been suggested, e.g., pooled covariance estimation (Friedman, 1989), rejection of eigenvectors (Blankertz et al., 2008), shrinkage estimators (Beltrachini et al., 2010), or feature subset selection (Friedman, 1989).

Even when recognizing that a constrained feature space can already be considered a form of regularization, the empirical determination of feature weights during the calibration period may pose a particular challenge for restorative brain-interface approaches, e.g., when estimating mean and covariance of two classes (rest vs. motor imagery). When patients are able to desynchronize sensorimotor oscillations (Pfurtscheller et al., 2005; Neuper et al., 2006; Kaiser et al., 2011), the estimation of feature weights is usually straightforward. In such a case, several approaches for regularization have been discussed (Yuan and Bentler, 1998; Beltrachini et al., 2010). If, however, the volitional modulation of sensorimotor oscillations has not been learned (Brauchle et al., 2015; Bauer and Gharabaghi, 2015b; Naros and Gharabaghi, 2015), or when it is impaired due to the underlying pathology (Buch et al., 2012; Bundy et al., 2012; Rossiter et al., 2014), the estimation might become noisy or even false. More formally, if one class (i.e. motor imagery) is not sufficiently expressed, its parameters (e.g., mean and covariance) cannot be measured. If, however, the mean during motor imagery is not sufficiently different from the mean during rest, a noisy estimate can result in the classifier being calibrated toward the wrong direction of modulation. Subsequently, the patient might receive feedback for synchronizing instead of desynchronizing.

Novelty detection has been suggested as a solution, if no information about a second class is available (Pimentel et al., 2014). Such a one-class approach might base mean and covariance estimation on the rest class only. However, without a priori information about the targeted direction of modulation, data-driven regularization approaches cannot be sufficient.

Furthermore, when a patient alters the mental strategy in the course of the intervention, a classifier trained on the initial strategy can become misaligned. In classical brain-interface approaches, the adaptation of feature weights has been proposed for such cases (Vidaurre et al., 2011b; Bryan et al., 2013; Sugiyama et al., 2013). But such data-driven approaches can be problematic for restorative approaches; classifier adaptation might condition the patients to explore alternative, i.e., therapeutically non-desired strategies (Bauer and Gharabaghi, 2015a,b). When the patient becomes frustrated with motor imagery, he/she may use artifacts for control, e.g., muscle contractions (Gharabaghi et al., 2014b).

Bearing these points in mind, we suggest employing informed regularization determined by a priori selected feature weights, thereby, ensuring the targeted direction of modulation. In our lab, we currently employ a variant of novelty classification by using a linear discriminant analysis with a fixed direction. In that regard, we base the mean and covariance estimation on the rest class only, with the parameter estimation pooled across several electrodes. Thereby, we provide feedback for the reduction of the mean, i.e., desynchronization, only.

DIFFICULTY OF ADAPTATION

Lotte and colleagues have pointed out that most neurofeedback protocols are limited with regard to their instructional design. They suggested adaptive training approaches, i.e., the use of difficulty levels which are challenging, but still achievable (Lotte et al., 2013). A similar idea was postulated by the cognitive load theory (Schnotz and Kürschner, 2007). On the basis of these concepts, both under- and over-challenge must be avoided to facilitate learning (Schnotz and Kürschner, 2007; Bauer and Gharabaghi, 2015a). In classifiers, which are constrained, regularized and linear, item response theory enables us to directly relate the threshold used for classification to the difficulty level (Bauer and Gharabaghi, 2015a). By using a linear discriminant analysis with a fixed direction, thresholding allows us to provide reward for desynchronization only when it is sufficiently strong. Within this framework, the shape of classification accuracy CA across different threshold can be interpreted as the zone of proximal development (ZPD). This argument, with detailed examples, has been clarified elsewhere (Bauer and Gharabaghi, 2015a). The ZPD is an indirect measure of a subject's cognitive resources (Schnotz and Kürschner, 2007). It also constitutes the range of threshold, where learning may occur because subjects are able to compensate for the extraneous load caused by the mismatch of ability and difficulty (Bauer and Gharabaghi, 2015a). Along these lines, two recent studies with healthy subjects provided empirical evidence that dynamic threshold adaptation is instrumental in facilitating learning (Bauer et al., 2016b; Naros et al., 2016).

Unconstrained and unregularized classifiers do not offer an accessible, one-dimensional parameter to fine-tune the difficulty of the task. It might therefore be problematic to adapt

the difficulty within these approaches. In particular, a multi-dimensional or even non-linear theory of difficulty adaptation appears to be challenging. We instead explored the difficulty threshold of a linear, a priori constrained and regularized classifier and found evidence of a direct correlation between the subjects' perceived mental effort and the task difficulty (Bauer et al., 2016b). Further empirical evidence suggests that there is a link between classification accuracy and cognitive load; classification performance has been linked to mood and mastery confidence (Nijboer et al., 2008), as well as to the degree of concentration on the task and the ability to ignore distracting stimuli (Hammer et al., 2012). The sensation of challenge might therefore be linked to the ratio of true to false positives returned by the classifier. This hypothesis is supported by a Bayesian simulation study of reinforcement learning under adaptive changes of true and false positive rates (Bauer and Gharabaghi, 2015b). A generalized concept of difficulty adaptation might, therefore, be based on controlling the relationship between true and false positive rates by asking the patients to self-rate the perceived effort and/or applying non-cued training.

Nonetheless, further factors may affect the difficulty of the training: the challenge of achieving a sense of cognitive and internal control (Burde and Blankertz, 2006; Wood et al., 2014), the appropriate processing of cues to reduce impairments in mental chronometry (Liepert et al., 2012), and to increase the quality of motor imagery (Heremans et al., 2009, 2012), the specific sensory impairments of patients and their interaction with the feedback modality (e.g., visual, haptic, auditory) (Nijboer et al., 2008; Gomez-Rodriguez et al., 2011; Parker et al., 2011; Sollfrank et al., 2015), or the repetitive and fatiguing nature of training (Lee et al., 1991; Page et al., 2011). Dealing with these aspects by proper instructional design is more important for restorative than for assistive approaches (Lotte et al., 2013).

CONCLUSION

We propose that restorative approaches should apply prior information about beneficial features (e.g., β-power desynchronization over sensorimotor areas) to constrain the feature space and regularize their direction. Such an approach may reduce the classification accuracy in comparison to unconstrained or unregularized approaches, particularly in patients who are only partially able to self-regulate the targeted brain state. At the same time, this method would increase the likelihood that feedback is provided for the therapeutically targeted modulation of brain activity only. The threshold selection in restorative approaches should therefore not be misled by the goal of maximum classification accuracy. Instead, it should follow instructional demands to maximize learning.

Accordingly, several methods have been proposed for locating the threshold for maximum learning (Ivanova et al., 2005; Cegarra and Chevalier, 2008; Naros et al., 2016; Bauer et al., 2016a,b). Moreover, physiological parameters, e.g., distributed cortical patterns in the α-range (Vukelić et al., 2014; Vukelić and Gharabaghi, 2015a,b) and the θ-range (Fels et al., 2015) which were linked to β-band self-regulation may also be used in the long term for this purpose.

The conceptual switch from assistive to restorative neuroprosthetics necessitates methodological adjustments (constrained feature space, a priori regularized feature weights, difficulty adaptation) which ultimately represent a paradigm switch from classification accuracy toward instructional efficiency to facilitate reinforcement learning of brain self-regulation.

AUTHOR CONTRIBUTIONS

All authors listed, have made substantial, direct and intellectual contribution to the work, and approved it for publication.

ACKNOWLEDGMENTS

RB was supported by the Graduate Training Centre of Neuroscience, International Max Planck Research School for Cognitive and Systems Neuroscience, Tuebingen, Germany. AG was supported by grants from the German Federal Ministry of Education and Research [BMBF IMONAS 13GW0119B] and the Baden-Württemberg Stiftung [NemoPlast NEU005]. There are no conflicts of interests.

REFERENCES

Ang, K. K., Chin, Z. Y., Zhang, H., and Guan, C. (2009). "Robust filter bank common spatial pattern (RFBCSP) in motor-imagery-based brain-computer interface," in *Conference Proceedings Annual International Conference of the IEEE Engineering in Medicine and Biology Society* (Minneapolis, MN), 578–581. doi: 10.1109/IEMBS.2009.5332817

Ang, K. K., Guan, C., Phua, K. S., Wang, C., Zhou, L., Tang, K. Y., et al. (2014). Brain-computer interface-based robotic end effector system for wrist and hand rehabilitation: results of a three-armed randomized controlled trial for chronic stroke. *Front. Neuroeng.* 7:30. doi: 10.3389/fneng.2014.00030

Aumann, T. D., and Prut, Y. (2015). Do sensorimotor β-oscillations maintain muscle synergy representations in primary motor cortex? *Trends Neurosci.* 38, 77–85. doi: 10.1016/j.tins.2014.12.002

Bauer, R., Fels, M., Royter, V., Raco, V., and Gharabaghi, A. (2016a). Closed-loop adaptation of neurofeedback based on mental effort facilitates reinforcement learning of brain self-regulation. *Clin. Neurophysiol.* 127, 3156–3164. doi: 10.1016/j.clinph.2016.06.020

Bauer, R., Fels, M., Vukelić, M., Ziemann, U., and Gharabaghi, A. (2015). Bridging the gap between motor imagery and motor execution with a brain-robot interface. *Neuroimage* 108, 319–327. doi: 10.1016/j.neuroimage.2014.12.026

Bauer, R., and Gharabaghi, A. (2015a). Estimating cognitive load during self-regulation of brain activity and neurofeedback with therapeutic brain-computer interfaces. *Front. Behav. Neurosci.* 9:21. doi: 10.3389/fnbeh.2015.00021

Bauer, R., and Gharabaghi, A. (2015b). Reinforcement learning for adaptive threshold control of restorative brain-computer interfaces: a Bayesian simulation. *Front. Neurosci.* 9:36. doi: 10.3389/fnins.2015.00036

Bauer, R., Vukelić, M., and Gharabaghi, A. (2016b). What is the optimal task difficulty for reinforcement learning of brain self-regulation? *Clin. Neurophysiol.* 127, 3033–3041. doi: 10.1016/j.clinph.2016.06.016

Beltrachini, L., von Ellenrieder, N., and Muravchik, C. H. (2010). Shrinkage approach for EEG covariance matrix estimation. *Conf. Proc. IEEE Eng. Med. Biol. Soc.* 2010, 1654–1657. doi: 10.1109/iembs.2010.5626668

Bishop, C. M. (2013). *Pattern Recognition and Machine Learning*. New Delhi: Springer.

Blankertz, B., Tomioka, R., Lemm, S., Kawanabe, M., and Muller, K. (2008). Optimizing spatial filters for robust EEG single-trial analysis. *IEEE Signal Process. Mag.* 25, 41–56. doi: 10.1109/MSP.2008.4408441

Brauchle, D., Vukelić, M., Bauer, R., and Gharabaghi, A. (2015). Brain state-dependent robotic reaching movement with a multi-joint arm exoskeleton: combining brain-machine interfacing and robotic rehabilitation. *Front. Hum. Neurosci.* 9:564. doi: 10.3389/fnhum.2015.00564

Brittain, J.-S., Sharott, A., and Brown, P. (2014). The highs and lows of beta activity in cortico-basal ganglia loops. *Eur. J. Neurosci.* 39, 1951–1959. doi: 10.1111/ejn.12574

Bryan, M. J., Martin, S. A., Cheung, W., and Rao, R. P. (2013). Probabilistic co-adaptive brain–computer interfacing. *J. Neural Eng.* 10:66008. doi: 10.1088/1741-2560/10/6/066008

Buch, E. R., Modir Shanechi, A., Fourkas, A. D., Weber, C., Birbaumer, N., and Cohen, L. G. (2012). Parietofrontal integrity determines neural modulation associated with grasping imagery after stroke. *Brain J. Neurol.* 135, 596–614. doi: 10.1093/brain/awr331

Bundy, D. T., Wronkiewicz, M., Sharma, M., Moran, D. W., Corbetta, M., and Leuthardt, E. C. (2012). Using ipsilateral motor signals in the unaffected cerebral hemisphere as a signal platform for brain-computer interfaces in hemiplegic stroke survivors. *J. Neural Eng.* 9:36011. doi: 10.1088/1741-2560/9/3/036011

Burde, W., and Blankertz, B. (2006). "Is the locus of control of reinforcement a predictor of brain-computer interface performance?," in *Proceedings of the 3rd International Brain-Computer Interface Workshop and Training Course* (Graz), 76–77.

Cegarra, J., and Chevalier, A. (2008). The use of Tholos software for combining measures of mental workload: toward theoretical and methodological improvements. *Behav. Res. Methods* 40, 988–1000. doi: 10.3758/BRM.40.4.988

Collinger, J. L., Wodlinger, B., Downey, J. E., Wang, W., Tyler-Kabara, E. C., Weber, D. J., et al. (2013). High-performance neuroprosthetic control by an individual with tetraplegia. *Lancet* 381, 557–564. doi: 10.1016/S0140-6736(12)61816-9

Daly, J. J., and Wolpaw, J. R. (2008). Brain–computer interfaces in neurological rehabilitation. *Lancet Neurol.* 7, 1032–1043. doi: 10.1016/S1474-4422(08)70223-0

Fels, M., Bauer, R., and Gharabaghi, A. (2015). Predicting workload profiles of brain-robot interface and electromyographic neurofeedback with cortical resting-state networks: personal trait or task-specific challenge? *J. Neural Eng.* 12:046029. doi: 10.1088/1741-2560/12/4/046029

Friedman, J. H. (1989). Regularized Discriminant Analysis. *J. Am. Stat. Assoc.* 84, 165–175. doi: 10.1080/01621459.1989.10478752

Gharabaghi, A. (2016). What turns assistive into restorative brain-machine interfaces? *Front. Neurosci.* 10:456. doi: 10.3389/fnins.2016.00456

Gharabaghi, A., Kraus, D., Leão, M. T., Spüler, M., Walter, A., Bogdan, M., et al. (2014a). Coupling brain-machine interfaces with cortical stimulation for brain-state dependent stimulation: enhancing motor cortex excitability for neurorehabilitation. *Front. Hum. Neurosci.* 8:122. doi: 10.3389/fnhum.2014.00122

Gharabaghi, A., Naros, G., Khademi, F., Jesser, J., Spüler, M., Walter, A., et al. (2014b). Learned self-regulation of the lesioned brain with epidural electrocorticography. *Front. Behav. Neurosci.* 8:429. doi: 10.3389/fnbeh.2014.00429

Gomez-Rodriguez, M., Peters, J., Hill, J., Schölkopf, B., Gharabaghi, A., and Grosse-Wentrup, M. (2011). Closing the sensorimotor loop: haptic feedback facilitates decoding of motor imagery. *J. Neural Eng.* 8:36005. doi: 10.1088/1741-2560/8/3/036005

Hammer, E. M., Halder, S., Blankertz, B., Sannelli, C., Dickhaus, T., Kleih, S., et al. (2012). Psychological predictors of SMR-BCI performance. *Biol. Psychol.* 89, 80–86. doi: 10.1016/j.biopsycho.2011.09.006

Heremans, E., Helsen, W. F., De Poel, H. J., Alaerts, K., Meyns, P., and Feys, P. (2009). Facilitation of motor imagery through movement-related cueing. *Brain Res.* 1278, 50–58. doi: 10.1016/j.brainres.2009.04.041

Heremans, E., Nieuwboer, A., Feys, P., Vercruysse, S., Vandenberghe, W., Sharma, N., et al. (2012). External cueing improves motor imagery quality in patients with Parkinson disease. *Neurorehabil. Neural Repair* 26, 27–35. doi: 10.1177/1545968311411055

Hochberg, L. R., Bacher, D., Jarosiewicz, B., Masse, N. Y., Simeral, J. D., Vogel, J., et al. (2012). Reach and grasp by people with tetraplegia using a neurally controlled robotic arm. *Nature* 485, 372–375. doi: 10.1038/nature11076

Ivanova, G., Perez, D., and Both, R. (2005). Threshold adaptation for mean value based operant conditioning. *Conf. Proc. Annu. Int. Conf. IEEE Eng. Med. Biol. Soc.* 4, 3612–3615. doi: 10.1109/iembs.2005.1617263

Kaiser, V., Kreilinger, A., Müller-Putz, G. R., and Neuper, C. (2011). First steps toward a motor imagery based stroke BCI: new strategy to set up a classifier. *Front. Neurosci.* 5:86. doi: 10.3389/fnins.2011.00086

Kilavik, B. E., Zaepffel, M., Brovelli, A., MacKay, W. A., and Riehle, A. (2012). The ups and downs of beta oscillations in sensorimotor cortex. *Exp. Neurol.* 15–26. doi: 10.1016/j.expneurol.2012.09.014

Kraus, D., Naros, G., Bauer, R., Khademi, F., Leão, M. T., Ziemann, U., et al. (2016). Brain state-dependent transcranial magnetic closed-loop stimulation controlled by sensorimotor desynchronization induces robust increase of corticospinal excitability. *Brain Stimul.* 9, 415–424. doi: 10.1016/j.brs.2016.02.007

Kraus, D., Naros, G., Bauer, R., Leão, M. T., Ziemann, U., and Gharabaghi, A. (2015). Brain-robot interface driven plasticity: distributed modulation of corticospinal excitability. *Neuroimage* 125, 522–532. doi: 10.1016/j.neuroimage.2015.09.074

Krucoff, M. O., Rahimpour, S., Slutzky, M. W., Edgerton, V. R., and Turner, D. A. (2016). Enhancing nervous system recovery through neurobiologics, neural interface training, and neurorehabilitation. *Front. Neurosci.* 10:584. doi: 10.3389/fnins.2016.00584

Lee, T. D., Swanson, L. R., and Hall, A. L. (1991). What is repeated in a repetition? Effects of practice conditions on motor skill acquisition. *Phys. Ther.* 71, 150–156.

Liepert, J., Greiner, J., Nedelko, V., and Dettmers, C. (2012). Reduced upper limb sensation impairs mental chronometry for motor imagery after stroke: clinical and electrophysiological findings. *Neurorehabil. Neural Repair* 26, 470–478. doi: 10.1177/1545968311425924

Lotte, F., Larrue, F., and Mühl, C. (2013). Flaws in current human training protocols for spontaneous Brain-Computer Interfaces: lessons learned from instructional design. *Front. Hum. Neurosci.* 7:568. doi: 10.3389/fnhum.2013.00568

Mima, T., Matsuoka, T., and Hallett, M. (2001). Information flow from the sensorimotor cortex to muscle in humans. *Clin. Neurophysiol. Off. J. Int. Fed. Clin. Neurophysiol.* 112, 122–126. doi: 10.1016/S1388-2457(00)00515-0

Morone, G., Pisotta, I., Pichiorri, F., Kleih, S., Paolucci, S., Molinari, M., et al. (2015). Proof of principle of a brain-computer interface approach to support poststroke arm rehabilitation in hospitalized patients: design, acceptability, and usability. *Arch. Phys. Med. Rehabil.* 96, S71–S78. doi: 10.1016/j.apmr.2014.05.026

Naros, G., and Gharabaghi, A. (2015). Reinforcement learning of self-regulated β-oscillations for motor restoration in chronic stroke. *Front. Hum. Neurosci.* 9:391. doi: 10.3389/fnhum.2015.00391

Naros, G., Naros, I., Grimm, F., Ziemann, U., and Gharabaghi, A. (2016). Reinforcement learning of self-regulated sensorimotor β-oscillations improves motor performance. *NeuroImage* 134, 142–152. doi: 10.1016/j.neuroimage.2016.03.016

Neuper, C., Wörtz, M., and Pfurtscheller, G. (2006). ERD/ERS patterns reflecting sensorimotor activation and deactivation. *Prog. Brain Res.* 159, 211–222. doi: 10.1016/S0079-6123(06)59014-4

Nijboer, F., Furdea, A., Gunst, I., Mellinger, J., McFarland, D. J., Birbaumer, N., et al. (2008). An auditory brain–computer interface (BCI). *J. Neurosci. Methods* 167, 43–50. doi: 10.1016/j.jneumeth.2007.02.009

Page, S. J., Dunning, K., Hermann, V., Leonard, A., and Levine, P. (2011). Longer versus shorter mental practice sessions for affected upper extremity movement after stroke: a randomized controlled trial. *Clin. Rehabil.* 25, 627–637. doi: 10.1177/0269215510395793

Parker, J., Mountain, G., and Hammerton, J. (2011). A review of the evidence underpinning the use of visual and auditory feedback for computer technology

in post-stroke upper-limb rehabilitation. *Disabil. Rehabil. Assist. Technol.* 6, 1–8. doi: 10.3109/17483107.2011.556209

Pfurtscheller, G., Neuper, C., Brunner, C., and da Silva, F. L. (2005). Beta rebound after different types of motor imagery in man. *Neurosci. Lett.* 378, 156–159. doi: 10.1016/j.neulet.2004.12.034

Pichiorri, F., Morone, G., Petti, M., Toppi, J., Pisotta, I., Molinari, M., et al. (2015). Brain-computer interface boosts motor imagery practice during stroke recovery. *Ann. Neurol.* 77, 851–865. doi: 10.1002/ana.24390

Pimentel, M. A. F., Clifton, D. A., Clifton, L., and Tarassenko, L. (2014). A review of novelty detection. *Signal Process.* 99, 215–249. doi: 10.1016/j.sigpro.2013.12.026

Royter, V., and Gharabaghi, A. (2016). Brain state-dependent closed-loop modulation of paired associative stimulation controlled by sensorimotor desynchronization. *Front Cell Neurosci.* 10:115. doi: 10.3389/fncel.2016.00115

Rossiter, H. E., Boudrias, M.-H., and Ward, N. S. (2014). Do movement-related beta oscillations change following stroke? *J. Neurophysiol.* 112, 2053–2058. doi: 10.1152/jn.00345.2014

Schnotz, W., and Kürschner, C. (2007). A reconsideration of cognitive load theory. *Educ. Psychol. Rev.* 19, 469–508. doi: 10.1007/s10648-007-9053-4

Shelton, F. N., and Reding, M. J. (2001). Effect of lesion location on upper limb motor recovery after stroke. *Stroke* 32, 107–112. doi: 10.1161/01.STR.32.1.107

Sherlin, L. H., Arns, M., Lubar, J., Heinrich, H., Kerson, C., Strehl, U., et al. (2011). Neurofeedback and basic learning theory: implications for research and practice. *J. Neurother.* 15, 292–304. doi: 10.1080/10874208.2011.623089

Sollfrank, T., Ramsay, A., Perdikis, S., Williamson, J., Murray-Smith, R., Leeb, R., et al. (2015). The effect of multimodal and enriched feedback on SMR-BCI performance. *Clin. Neurophysiol.* 127, 490–498. doi: 10.1016/j.clinph.2015.06.004

Stinear, C. M., Barber, P. A., Petoe, M., Anwar, S., and Byblow, W. D. (2012). The PREP algorithm predicts potential for upper limb recovery after stroke. *Brain* 135, 2527–2535. doi: 10.1093/brain/aws146

Sugiyama, M., Yamada, M., and du Plessis, M. C. (2013). Learning under nonstationarity: covariate shift and class-balance change: learning under nonstationarity. *Wiley Interdiscip. Rev. Comput. Stat.* 5, 465–477. doi: 10.1002/wics.1275

Theodoridis, S., and Koutroumbas, K. (2009). *Pattern Recognition*. Burlington, MA; London: Academic Press.

Vidaurre, C., Kawanabe, M., von Bünau, P., Blankertz, B., and Müller, K. R. (2011a). Toward unsupervised adaptation of LDA for brain-computer interfaces. *IEEE Trans. Biomed. Eng.* 58, 587–597. doi: 10.1109/TBME.2010.2093133

Vidaurre, C., Sannelli, C., Müller, K.-R., and Blankertz, B. (2011b). Co-adaptive calibration to improve BCI efficiency. *J. Neural Eng.* 8:25009. doi: 10.1088/1741-2560/8/2/025009

Vukelić, M., Bauer, R., Naros, G., Naros, I., Braun, C., and Gharabaghi, A. (2014). Lateralized alpha-band cortical networks regulate volitional modulation of beta-band sensorimotor oscillations. *NeuroImage* 87, 147–153. doi: 10.1016/j.neuroimage.2013.10.003

Vukelić M., and Gharabaghi, A. (2015a). Oscillatory entrainment of the motor cortical network during motor imagery is modulated by the feedback modality. *Neuroimage* 1, 1–11. doi: 10.1016/j.neuroimage.2015.01.058

Vukelić, M., and Gharabaghi, A. (2015b). Self-regulation of circumscribed brain activity modulates spatially selective and frequency specific connectivity of distributed resting state networks. *Front. Behav. Neurosci.* 9:181. doi: 10.3389/fnbeh.2015.00181

Wood, G., Kober, S. E., Witte, M., and Neuper, C. (2014). On the need to better specify the concept of "control" in brain-computer-interfaces/neurofeedback research. *Front. Syst. Neurosci.* 8:171. doi: 10.3389/fnsys.2014.00171

Yuan, K. H., and Bentler, P. M. (1998). Robust mean and covariance structure analysis. *Br. J. Math. Stat. Psychol.* 51 (Pt 1), 63–88. doi: 10.1111/j.2044-8317.1998.tb00667.x

Conflict of Interest Statement: The authors declare that the research was conducted in the absence of any commercial or financial relationships that could be construed as a potential conflict of interest.

frontiers in Neuroscience

OPINION
published: 27 June 2016
doi: 10.3389/fnins.2016.00295

Invasive vs. Non-Invasive Neuronal Signals for Brain-Machine Interfaces: Will One Prevail?

Stephan Waldert *

Sobell Department of Motor Neuroscience and Movement Disorders, University College London Institute of Neurology, University College London, London, UK

Keywords: Brain computer interface (BCI), intracortical, action potentials, LFP, EEG, neuroprosthetics, microstimulation, Ethics

Brain-machine interfaces (BMI) translate neuronal activity of the brain into signals driving an external effector or affecting internal body parts and functions. Initially, their applications were seen in the field of rehabilitation and medical care for patients to restore social interaction or movement capabilities. Inspired by their success we can already witness the advent of bidirectional and commercial BMIs.

Contemporary BMIs allow for real-time control of prostheses (Gilja et al., 2015), communication (Chen et al., 2015) and "sensation" (O'doherty et al., 2011), notably, the cochlea implant could be considered as the most successful BMI. These applications exemplify that performance can be high but is far from natural interaction with the environment and success depends on manifold factors.

This Opinion is not about algorithms and paradigms but about possibilities and limitations of invasive vs. non-invasive means to *electrically* interface the brain, argued in the realm of BMIs for direct and intuitive motor control.

Current techniques allow to interface electric neuronal activity *in vivo* ranging from intracellular potentials over extracellular action potentials (APs) up to local field potentials (LFPs). These neurophysiological processes are inherently coupled: neurons can interact ephaptically and via electric synapses, spikes change LFPs via synaptic input which in turn influences spiking activity, electric fields of APs can influence LFPs directly without involvement of synaptic currents. Although the LFP is difficult to interpret (Einevoll et al., 2013), correlations between APs and LFPs vary (Buzsaki et al., 2012) and the information they convey can be independent (Belitski et al., 2008), this coupling may have given rise to discussions I have come across and which have triggered this Opinion: the misconception that, to a certain extent, information conveyed by invasive (APs/LFPs) vs. non-invasive (EEG) signals are similar enough for non-invasive signals, and thus non-invasive BMIs, not to be subject to intrinsic impediments.

Such speculations may have been nourished by studies showing similar performance for intracortical BMIs based on APs vs. LFPs (Mehring et al., 2003) as the latter are detectable by EEG techniques. Similar performance might be evident for multi-unit APs vs. high-frequency LFPs ($>\approx$200 Hz), which contain extracellular fields of APs. However, also low/band-pass filtered LFPs below 8 Hz, generally free of such direct AP influences (Waldert et al., 2013), can show similar BMI performance as APs and are suitable for online BMIs (Stavisky et al., 2015). Importantly, this LFP component also carries information about movement parameters if recorded non-invasively (MEG, EEG; Waldert et al., 2008).

Non-invasive EEG yields lower performance than APs or LFPs (Waldert et al., 2009) but with the findings mentioned above and novel approaches: Could non-invasive BMIs catch up?

The source of neuronal signals extracted from EEG after thorough removal of noise, muscle, eye, and movement artifacts, are post-synaptic extracellular currents; in fact, the same currents that

OPEN ACCESS

Edited by:
Mikhail Lebedev, Duke University, USA

Reviewed by:
Thomas G. Brochier, Centre National de la Recherche Scientifique France, France

***Correspondence:**
Stephan Waldert
s.waldert@ucl.ac.uk

Specialty section:
This article was submitted to Neuroprosthetics, a section of the journal Frontiers in Neuroscience

Received: *04 February 2016*
Accepted: *13 June 2016*
Published: *27 June 2016*

Citation:
Waldert S (2016) Invasive vs. Non-Invasive Neuronal Signals for Brain-Machine Interfaces: Will One Prevail? Front. Neurosci. 10:295. doi: 10.3389/fnins.2016.00295

contribute to spike-free LFPs. Despite this common source, there are several differences, most of which well-documented, between invasive and non-invasive signals.

First, number and type of neurons: As electric fields produced by neurons decay exponentially with distance, the number of neurons that have to be simultaneously active in a confined area for the fields to superimpose and produce a detectable signal, is magnitudes smaller for LFP than EEG. Hence, the activity of small neuronal clusters is undetectable or recorded at a lower SNR with EEG. In addition, EEG signals are dominated by fields of pyramidal neurons as only their morphology (long, parallel dendrites) and high number in the cortex allow fields to add up and reach the scalp. In contrast, LFPs reflect a superposition of a variety of electrophysiological processes, those underlying EEG plus interneurons, APs, etc.

Second, signal composition: Tissue acts as a low-pass filter generally attenuating high-frequency signals to the extent that buries them in background noise. Hence, with the exception of AP bursts in neuronal populations (Waterstraat et al., 2015), non-invasive signals mainly allow analysis of low-frequency neuronal activity ($<\approx$90 Hz, lower for dry EEG electrodes). Invasive signals convey information up to several kHz. Moreover, frequency-dependent phase shifts might be stronger when signals spread across larger distances (EEG) and might disintegrate temporal consistency across signal components.

Third, spatial distortion: The extracellular space is composed of media with different electrophysiological properties, which influence how fields spread before being detected as LFPs. On top of this, fields spread in the cerebrospinal fluid, skull, and scalp, causing further spatial distortion before reaching EEG electrodes. Sophisticated head models and algorithms in combination with high-density EEG montages mitigate distortion (Michel and Murray, 2012) for signals above a certain noise level. To be similar to invasive signals, such models might need to be obtained *in vivo* for each user individually, rely on stable sensor positions, necessitate finite-element analysis and run near real-time (BMI performance depends on small delays, Cunningham et al., 2011).

These limitations are intrinsic to EEG and cannot be practicably (or theoretically) overcome. However, EEG offers the paramount advantage to monitor large-scale neuronal activity of the entire brain adjacent to the neurocranium at a low cost and risk-free. Invasive recordings can be deeper but cannot cover the whole neocortex and are initially more laborious due to surgical interventions.

Invasive electrodes come in many forms: single electrodes, electrodes with multiple contacts at the tip or along the shaft, multi-electrode arrays (MEA), or combinations of these in different designs. Electrodes can have arbitrary lengths up to several cm or, for example, up to 1.5 mm (Utah, Blackrock Microsystems) or 10 mm (FMA, MicroProbes) in a MEA. Intracortical electrodes typically yield LFPs and detectable APs of 0–5 identifiable neurons per intact contact. Electrodes can be specifically targeted at arbitrary cerebral areas although accuracy decreases with implantation depth (unless aided by MRI and/or CT).

Nevertheless, for several reasons high implantation accuracy seems not to be crucial for invasive motor BMIs as long as contacts remain in gray matter. The general aim is to record APs and LFPs. In motor cortex, LFPs are recorded at different depths and convey information about movement parameters; recorded APs are faint at layer 1 and usually increase in amplitude with electrode depth up to layer 5 because the size of pyramidal cell somas tends to increase from layer 3 to 5, possibly to support the longer dendrites necessary to project to superficial (input) layers, and because layer 5 is the place of large corticospinal neurons, a main cortical output to control motor functions. This region may therefore often be targeted in invasive motor BMIs for high performance. Importantly, even MEAs with relatively short electrodes (Utah) should have access to this activity because: layer 4 is very thin in motor cortex (Rockel et al., 1980), floating MEAs sink into cortical tissue and APs of large pyramidal neurons can be recorded at several 100 μm distance (experimental and analytical experiences here in the Sobell Department, UCL). For deeper regions, like the anterior wall of the central sulcus, MEAs with longer electrodes can be used to follow layers into the sulcus.

Overall and in contrast to non-invasive signals, invasive signals reflect input to, local processing and output of cortical areas. They may even allow to deduce on intracellular states of neurons (Henze et al., 2000).

Hence, a main advantage of intracortical over non-invasive approaches are inherently possible higher information transfer rates. This and two further advantages are decisive for the future of motor BMIs: tuning and sensation.

BMI performance is still far from natural. After BMI initiation this is partly due to an undersampling of the neuronal network required for natural motor control. Performance then increases during BMI usage as the neurons' tuning "improves" (Carmena et al., 2003), i.e., plasticity enables the brain to learn to control the BMI (closed-loop). This works with arbitrary neurons (Fetz, 1969) and is facilitated by using already tuned neuronal activity (Ganguly and Carmena, 2009) accompanied by a transition from externally assisted to full brain control (Collinger et al., 2013). LFPs seem to be more stable (Flint et al., 2013; Perge et al., 2014), i.e., less easy to tune; probably as in contrast to spiking activity of some neurons, activity of a neuronal cluster needs to change coherently. Although possible (Okazaki et al., 2015), this holds even more so for EEG.

Feedback in closed-loop BMIs has been mainly visual or acoustic. Such inadequate feedback also accounts for low BMI performance as the absence of direct forms of feedback (touch and proprioception) impoverishes information contained in brain signals (Galan et al., 2014) and can disturb the generation of appropriate motor commands (Galan and Baker, 2015). Researchers have begun to employ intracortical microstimulation to establish a direct BMI input channel (Klaes et al., 2014) with possible long-term stability (Callier et al., 2015). This should eventually improve performance as feedback may be delivered specifically to task-relevant cortical areas, which closes the output-feedback loop adequately. As electrodes may be used for stimulation and recording; stimulation could be adapted to ongoing brain activity to improve efficacy.

In contrast to non-invasive BMIs, the great opportunity offered by invasive BMIs thus lies in accurate control, a prerequisite for user acceptance, combined with restoration

of somatosensation: Prostheses will be controlled using high-dimensional BMI output signals (Wodlinger et al., 2015) while at the same time BMI input signals, obtained from skin prostheses (Kim et al., 2014) during interaction with the environment, will be transmitted to cortical sensory areas. Providing such information may remain far off evoking natural percepts but the brain will learn to make use of such artificial input channels.

User acceptance is lower for invasive than non-invasive BMIs (Blabe et al., 2015). Invasive BMIs will for many years remain to be used in patients, either for research or if no other remedy is available. Present commercial BMIs are all non-invasive.

This lower acceptance mainly arises from medical concerns related to neurosurgery and the implant. Such risks are clearly not negligible but seem to be partly overrated. For example, validation of DBS showed that complications are rare and, with appropriate procedures, are reduced to 0.9% transient and no permanent deficits (Zrinzo et al., 2012). Even if multiple subpial transection, a series of long cuts in gray matter used to treat epilepsy, is performed in the primary motor cortex, patients are left with no permanent motor deficits (Blount et al., 2004). Implanting electrode arrays for invasive motor BMIs should appear innocuous against this procedure. They have been used in many laboratories for years now and also here in the Sobell Department, UCL, we have not experienced any motor deficits after array implantations. Medical concerns might subside with better awareness of such evidence.

It is now crucial to overcome current challenges of invasive BMIs: better understanding of the "neuronal code," implant miniaturization, wireless signal transmission (Borton et al., 2013), implants charged from outside (Ho et al., 2014) or by harvesting energy from the body (Hannan et al., 2014). BMIs need to be asynchronous for unrestricted control, adaptable to unstable signals and require better sensory-motor prostheses. A major challenge of intracortical implants is biocompatibility, time-dependent degradation of recording quality, and eventually implant failure due to tissue damage during implantation, array micromotion, and a breach of the blood-brain-barrier triggering glial scarring, neurodegeneration, and neuronal death. Only few APs are still recorded years after implantation (Hochberg et al., 2012). LFPs also deteriorate but might show better long-term stability (Flint et al., 2013; Perge et al., 2014). To increase longevity and yield, electrodes need to be reduced in size, coated with neurointegrative, anti-inflammatory factors (Gunasekera et al., 2015), and/or redesigned (e.g., carbon nanotubes, Vitale et al., 2015; Lopez et al., 2016).

As an invasive but extracortical technique, miniaturized ECoG causes lesser cortical tissue damage/irritation and allows for epicortical recordings of LFPs at high spatial resolution and, as recently shown, also of spiking activity (Khodagholy et al., 2015). Benefits derivable from such advances, especially regarding increased information transfer rates, biocompatibility, and long-term signal stability (Chao et al., 2010) over years, are being investigated and might be decisive for the development of future BMIs.

Once invasive BMIs are fully body-embeddable and their benefits outweigh concerns, they might become acceptable to the majority (of patients). However, other, non-medical concerns have to be addressed as well. As invasive BMIs allow access to the brain, i.e., the individual as such, it is necessary to discuss (and regulate) socio-ethical issues: privacy, "mind reading," remote control, brain enhancement, which accuracy legitimates control of potentially hazardous devices, liability, and eventually self-perception and perception through others.

This Opinion is not a polemic against EEG. EEG is a prime tool for many applications, e.g., medical, rehabilitation, current BMIs for communication.

The conclusion of this Opinion is that once technical, socio-ethical, and neuroscientific challenges are resolved, user concerns might subside, and invasive BMIs (using primarily intracortical and potentially epicortical recordings) will prevail in most applications; certainly those for restoration of motor functions and perhaps even in applications not medically indicated.

AUTHOR CONTRIBUTIONS

SW conceived and wrote the paper.

FUNDING

This work was supported by the Wellcome Trust (WT102849MA).

REFERENCES

Belitski, A., Gretton, A., Magri, C., Murayama, Y., Montemurro, M. A., Logothetis, N. K., et al. (2008). Low-frequency local field potentials and spikes in primary visual cortex convey independent visual information. *J. Neurosci.* 28, 5696–5709. doi: 10.1523/JNEUROSCI.0009-08.2008

Blabe, C. H., Gilja, V., Chestek, C. A., Shenoy, K. V., Anderson, K. D., and Henderson, J. M. (2015). Assessment of brain-machine interfaces from the perspective of people with paralysis. *J. Neural Eng.* 12:043002. doi: 10.1088/1741-2560/12/4/043002

Blount, J. P., Langburt, W., Otsubo, H., Chitoku, S., Ochi, A., Weiss, S., et al. (2004). Multiple subpial transections in the treatment of pediatric epilepsy. *J. Neurosurg.* 100, 118–124. doi: 10.3171/ped.2004.100.2.0118

Borton, D. A., Yin, M., Aceros, J., and Nurmikko, A. (2013). An implantable wireless neural interface for recording cortical circuit dynamics in moving primates. *J. Neural Eng.* 10:026010. doi: 10.1088/1741-2560/10/2/026010

Buzsaki, G., Anastassiou, C. A., and Koch, C. (2012). The origin of extracellular fields and currents–EEG, ECoG, LFP and spikes. *Nat. Rev. Neurosci.* 13, 407–420. doi: 10.1038/nrn3241

Callier, T., Schluter, E. W., Tabot, G. A., Miller, L. E., Tenore, F. V., and Bensmaia, S. J. (2015). Long-term stability of sensitivity to intracortical microstimulation of somatosensory cortex. *J. Neural Eng.* 12:056010. doi: 10.1088/1741-2560/12/5/056010

Carmena, J. M., Lebedev, M. A., Crist, R. E., O'doherty, J. E., Santucci, D. M., Dimitrov, D. F., et al. (2003). Learning to control a brain-machine interface for reaching and grasping by primates. *PLoS Biol.* 1:e42. doi: 10.1371/journal.pbio.0000042

Chao, Z. C., Nagasaka, Y., and Fujii, N. (2010). Long-term asynchronous decoding of arm motion using electrocorticographic signals in monkeys. *Front. Neuroeng.* 3:3. doi: 10.3389/fneng.2010.00003

Chen, X., Wang, Y., Gao, S., Jung, T. P., and Gao, X. (2015). Filter bank canonical correlation analysis for implementing a high-speed SSVEP-based brain-computer interface. *J. Neural Eng.* 12:046008. doi: 10.1088/1741-2560/12/4/046008

Collinger, J. L., Wodlinger, B., Downey, J. E., Wang, W., Tyler-Kabara, E. C., Weber, D. J., et al. (2013). High-performance neuroprosthetic control by an individual with tetraplegia. *Lancet* 381, 557–564. doi: 10.1016/S0140-6736(12)61816-9

Cunningham, J. P., Nuyujukian, P., Gilja, V., Chestek, C. A., Ryu, S. I., and Shenoy, K. V. (2011). A closed-loop human simulator for investigating the role of feedback control in brain-machine interfaces. *J. Neurophysiol.* 105, 1932–1949. doi: 10.1152/jn.00503.2010

Einevoll, G. T., Kayser, C., Logothetis, N. K., and Panzeri, S. (2013). Modelling and analysis of local field potentials for studying the function of cortical circuits. *Nat. Rev. Neurosci.* 14, 770–785. doi: 10.1038/nrn3599

Fetz, E. E. (1969). Operant conditioning of cortical unit activity. *Science* 163, 955–958. doi: 10.1126/science.163.3870.955

Flint, R. D., Wright, Z. A., Scheid, M. R., and Slutzky, M. W. (2013). Long term, stable brain machine interface performance using local field potentials and multiunit spikes. *J. Neural Eng.* 10:056005. doi: 10.1088/1741-2560/10/5/056005

Galan, F., Baker, M. R., Alter, K., and Baker, S. N. (2014). Degraded EEG decoding of wrist movements in absence of kinaesthetic feedback. *Hum. Brain Mapp.* 36, 643–654. doi: 10.1002/hbm.22653

Galan, F., and Baker, S. N. (2015). Deafferented controllers: a fundamental failure mechanism in cortical neuroprosthetic systems. *Front. Behav. Neurosci.* 9:186. doi: 10.3389/fnbeh.2015.00186

Ganguly, K., and Carmena, J. M. (2009). Emergence of a stable cortical map for neuroprosthetic control. *PLoS Biol.* 7:e1000153. doi: 10.1371/journal.pbio.1000153

Gilja, V., Pandarinath, C., Blabe, C. H., Nuyujukian, P., Simeral, J. D., Sarma, A. A., et al. (2015). Clinical translation of a high-performance neural prosthesis. *Nat. Med.* 21, 1142–1145. doi: 10.1038/nm.3953

Gunasekera, B., Saxena, T., Bellamkonda, R., and Karumbaiah, L. (2015). Intracortical recording interfaces: current challenges to chronic recording function. *ACS Chem. Neurosci.* 6, 68–83. doi: 10.1021/cn5002864

Hannan, M. A., Mutashar, S., Samad, S. A., and Hussain, A. (2014). Energy harvesting for the implantable biomedical devices: issues and challenges. *Biomed. Eng.* 13:79. doi: 10.1186/1475-925X-13-79

Henze, D. A., Borhegyi, Z., Csicsvari, J., Mamiya, A., Harris, K. D., and Buzsaki, G. (2000). Intracellular features predicted by extracellular recordings in the hippocampus *in vivo*. *J. Neurophysiol.* 84, 390–400.

Ho, J. S., Yeh, A. J., Neofytou, E., Kim, S., Tanabe, Y., Patlolla, B., et al. (2014). Wireless power transfer to deep-tissue microimplants. *Proc. Natl. Acad. Sci. U.S.A.* 111, 7974–7979. doi: 10.1073/pnas.1403002111

Hochberg, L. R., Bacher, D., Jarosiewicz, B., Masse, N. Y., Simeral, J. D., Vogel, J., et al. (2012). Reach and grasp by people with tetraplegia using a neurally controlled robotic arm. *Nature* 485, 372–375. doi: 10.1038/nature11076

Khodagholy, D., Gelinas, J. N., Thesen, T., Doyle, W., Devinsky, O., Malliaras, G. G., et al. (2015). NeuroGrid: recording action potentials from the surface of the brain. *Nat. Neurosci.* 18, 310–315. doi: 10.1038/nn.3905

Kim, J., Lee, M., Shim, H. J., Ghaffari, R., Cho, H. R., Son, D., et al. (2014). Stretchable silicon nanoribbon electronics for skin prosthesis. *Nat. Commun.* 5, 5747. doi: 10.1038/ncomms6747

Klaes, C., Shi, Y., Kellis, S., Minxha, J., Revechkis, B., and Andersen, R. A. (2014). A cognitive neuroprosthetic that uses cortical stimulation for somatosensory feedback. *J. Neural Eng.* 11:056024. doi: 10.1088/1741-2560/11/5/056024

Lopez, C. M., Mitra, S., Putzeys, J., Raducanu, B., Ballini, M., Andrei, A., et al. (2016). "A 966-electrode neural probe with 384 configurable channels in 0.13μm SOI CMOS," in *IEEE International Solid-State Circuits Conference (ISSCC)* (San Fransisco, CA), 392–393. doi: 10.1109/ISSCC.2016.7418072

Mehring, C., Rickert, J., Vaadia, E., Cardoso De Oliveira, S., Aertsen, A., and Rotter, S. (2003). Inference of hand movements from local field potentials in monkey motor cortex. *Nat. Neurosci.* 6, 1253–1254. doi: 10.1038/nn1158

Michel, C. M., and Murray, M. M. (2012). Towards the utilization of EEG as a brain imaging tool. *Neuroimage* 61, 371–385. doi: 10.1016/j.neuroimage.2011.12.039

O'doherty, J. E., Lebedev, M. A., Ifft, P. J., Zhuang, K. Z., Shokur, S., Bleuler, H., et al. (2011). Active tactile exploration using a brain-machine-brain interface. *Nature* 479, 228–231. doi: 10.1038/nature10489

Okazaki, Y. O., Horschig, J. M., Luther, L., Oostenveld, R., Murakami, I., and Jensen, O. (2015). Real-time MEG neurofeedback training of posterior alpha activity modulates subsequent visual detection performance. *Neuroimage* 107, 323–332. doi: 10.1016/j.neuroimage.2014.12.014

Perge, J. A., Zhang, S., Malik, W. Q., Homer, M. L., Cash, S., Friehs, G., et al. (2014). Reliability of directional information in unsorted spikes and local field potentials recorded in human motor cortex. *J. Neural Eng.* 11:046007. doi: 10.1088/1741-2560/11/4/046007

Rockel, A. J., Hiorns, R. W., and Powell, T. P. (1980). The basic uniformity in structure of the neocortex. *Brain* 103, 221–244. doi: 10.1093/brain/103.2.221

Stavisky, S. D., Kao, J. C., Nuyujukian, P., Ryu, S. I., and Shenoy, K. V. (2015). A high performing brain-machine interface driven by low-frequency local field potentials alone and together with spikes. *J. Neural Eng.* 12, 036009. doi: 10.1088/1741-2560/12/3/036009

Vitale, F., Summerson, S. R., Aazhang, B., Kemere, C., and Pasquali, M. (2015). Neural stimulation and recording with bidirectional, soft carbon nanotube fiber microelectrodes. *ACS Nano* 9, 4465–4474. doi: 10.1021/acsnano.5b01060

Waldert, S., Lemon, R. N., and Kraskov, A. (2013). Influence of spiking activity on cortical local field potentials. *J. Physiol.* 591, 5291–5303. doi: 10.1113/jphysiol.2013.258228

Waldert, S., Pistohl, T., Braun, C., Ball, T., Aertsen, A., and Mehring, C. (2009). A review on directional information in neural signals for brain-machine interfaces. *J. Physiol. Paris* 103, 244–254. doi: 10.1016/j.jphysparis.2009.08.007

Waldert, S., Preissl, H., Demandt, E., Braun, C., Birbaumer, N., Aertsen, A., et al. (2008). Hand movement direction decoded from MEG and EEG. *J. Neurosci.* 28, 1000–1008. doi: 10.1523/JNEUROSCI.5171-07.2008

Waterstraat, G., Burghoff, M., Fedele, T., Nikulin, V., Scheer, H. J., and Curio, G. (2015). Non-invasive single-trial EEG detection of evoked human neocortical population spikes. *Neuroimage* 105, 13–20. doi: 10.1016/j.neuroimage.2014.10.024

Wodlinger, B., Downey, J. E., Tyler-Kabara, E. C., Schwartz, A. B., Boninger, M. L., and Collinger, J. L. (2015). Ten-dimensional anthropomorphic arm control in a human brain-machine interface: difficulties, solutions, and limitations. *J. Neural. Eng.* 12, 016011. doi: 10.1088/1741-2560/12/1/016011

Zrinzo, L., Foltynie, T., Limousin, P., and Hariz, M. I. (2012). Reducing hemorrhagic complications in functional neurosurgery: a large case series and systematic literature review. *J. Neurosurg.* 116, 84–94. doi: 10.3171/2011.8.JNS101407

Conflict of Interest Statement: The author declares that the research was conducted in the absence of any commercial or financial relationships that could be construed as a potential conflict of interest.

frontiers in Systems Neuroscience

OPINION
published: 19 May 2015
doi: 10.3389/fnsys.2015.00072

Future think: cautiously optimistic about brain augmentation using tissue engineering and machine interface

E. Paul Zehr [1, 2, 3, 4, 5, 6]*

[1] Rehabilitation Neuroscience Laboratory, University Victoria, Victoria, BC, Canada, [2] Human Discovery Science, International Collaboration on Repair Discoveries, Vancouver, BC, Canada, [3] Centre for Biomedical Research, University of Victoria, Victoria, BC, Canada, [4] Division of Medical Sciences, University of Victoria, BC, Canada, [5] School of Exercise Science, Physical, and Health Education, University of Victoria, Victoria, BC, Canada, [6] Zanshin Consulting, Inc., Victoria, BC, Canada

Keywords: rehabilitation, enhancement, transhumanism, stem cell, engraftment, brain machine, neuroprosthetics, Asimov

> *"There is no sensible way in which we must take the possibility of misuse into account before determining that something is an enhancement." —John Harris in "Enhancing Evolution" (Harris, 2007)*

> *"I need to wire the armor directly into my brain. Extremis could do that…I need to be the suit…I need to grow new connections"* —Tony Stark talking about integration with the Iron Man armor in the graphic novel "Extremis" by Warren Ellis (Ellis, 2007)

OPEN ACCESS

Edited by:
Mikhail Lebedev, Duke University, USA

Reviewed by:
Philip Kennedy, Neural Signals Inc., USA
Roni Hogri, Medical University of Vienna, Austria
Marios Kyriazis, ELPIs Foundation for Indefinite Lifespans, UK

***Correspondence:**
E. Paul Zehr, pzehr@uvic.ca

Received: *20 February 2015*
Accepted: *22 April 2015*
Published: *19 May 2015*

Citation:
Zehr EP (2015) Future think: cautiously optimistic about brain augmentation using tissue engineering and machine interface. Front. Syst. Neurosci. 9:72. doi: 10.3389/fnsys.2015.00072

Introduction

Augmentation of brain function can imply restoration of function lost due to pathology or injury. On the other hand, techniques, approaches, and technologies used for brain augmentation in restoration can also amplify the range of human abilities in those without pathology. For example, non-invasive brain stimulation using transcranial magnetic stimulation (TMS) was originally applied for investigative and diagnostic purposes in neurological injury (Nollet et al., 2003). While TMS continues to be used in brain mapping and restoration of functional output (Romero et al., 2011; Bestmann and Krakauer, 2015), recent clinical applications in otherwise "healthy people" are widening. These include enhancing attention and vigilance (Nelson et al., 2014), motor learning (Cantarero et al., 2015) and various methods to "…improve attention, perception, memory and other forms of cognition…" (Clark and Parasuraman, 2014).

Technological augmentation of so-called "normal" human function moves us away from the functional limitations of our species and closer to "super" human function (Zehr, 2015), as with suggestions found in the transhumanist literature (Mcnamee and Edwards, 2006). Future applications of emerging technology can continue to shift us from our subspecies of *homo sapiens sapiens* to the transformative *homo sapiens technologicus*—a species that uses, fuses and integrates technology to enhance its own function (Zehr, 2011, 2015).

While there are many related approaches, this opinion article explores brain augmentation using approaches delimited to internally implanted biological enhancements (e.g. tissue engineering), and internal/external technological hardware [e.g., brain machine interface (BMI)].

Tissue Engineering and Stem Cell Chimeras

The pace of discoveries in the field of tissue engineering in regenerative medicine applications continues to accelerate (Leach et al., 2010; Elliott Donaghue et al., 2014). In 2013, Xiaoning Han and colleagues in the laboratories of Steven Goldman and Maiken Nedergaard at the University of Rochester Medical Center published a paper examining the possibility of augmenting neural processing ability of one species by surgically transplanting cells from the brain of another "more advanced" species (Han et al., 2013).

This research team was concerned with "biocompatability" in the mouse brain with certain evolutionary adaptations in human astroglial cells which are much larger with more complex structure than those found in the mouse. These astrocytes, which don't produce electric signals like neurons, are considered critical as physiological support and protection for the processing neurons, particularly in calcium signaling. This signaling is crucial for overall brain activity and human astrocytes operate threefold faster than those found in the mouse.

This generated the question: what would happen if you grafted human glial progenitor cells—the stem cells in the brain that would normally become astrocytes—into the forebrain of immunosuppressed mice? For how long would human cells survive in the mouse brain, and, critically, would the human astrocytes offer any behavioral advantage to the mice hosting the implanted cells?

Han and colleagues discovered that, in the mouse hippocampus, human glial cells thrived, and propagated calcium signals at the rate usually found in the human brain. Moreover, there was strengthened signal transmission between neurons (that is, long-term potentiation underlying learning and memory formation).

Critically, the functioning transplanted stem cells augmented behavior in the mice, including maze learning, fear conditioning, and enhanced ability to identify and find new objects in the murine habitat. The augmented chimeric mice with engrafted human glial cells essentially had improved all-around performance and this study represented an important test that cross-species grafting techniques could be a useful way to modify and augment (and examine in pathology) brain function.

Later, Martha Windrem and colleagues from the same laboratories, used an expanded protocol to examine the long term effects of engrafting human glial progenitor cells into the forebrains of neonatal mice (Windrem et al., 2014). Quite dramatically, there was a steady fall in murine cells coincident with an in increase in human cell content in the mouse brain. This proportional shift was so strong that after 1 year the glial progenitor cells found in the mouse forebrain populations were almost entirely of human origin.

That implanted human cells "outcompeted" and eventually replaced and "infected" the initial host mouse cells was an unexpected outcome. Windrem et al. "were surprised to note that the forebrains of these animals were often composed primarily of human glia and their progenitors" (Windrem et al., 2014).

External Technological Hardware and Augmentation with Brain Machine Interface

The interface of physiology and engineering represented by brain computer or brain machine interface has a history of success in non-human and human applications for restoration of function (Lebedev and Nicolelis, 2006; Wang et al., 2010; Shih et al., 2012). This tremendous success raises new questions. For example, is it possible to attach a biological brain to an external circuit and establish a functional connection for learning? This question was addressed by Theodore Berger and colleagues who showed that an input/output (stimulation and recording) neuroprosthetic interface enhanced memory function subserved by the rodent hippocampus and could overcome memory deficits mimicking natural damage (Berger et al., 2011). This approach was extended to restoration of cognitive decision making using a neuroprosthetic interfaced into the prefrontal cortex in the rhesus monkey (Hampson et al., 2012).

Simeon Bamford and colleagues established a proof of principle for direct applications of brain-machine neuroprosthetics in motor learning using cerebellar motor control and learning circuitry as the model (Prueckl et al., 2011; Bamford et al., 2012). They envisaged engineering scenarios that could meet the challenge required for truly integrated neuroprosthetics—a closed loop system. Such a system would be able to send to and receive from the brain inputs and processing to control devices that supplement the functionality of the brain itself (Bamford et al., 2012).

Cerebellar circuits are essential to classical conditioning of the eye-blink reflex (Cheron et al., 2013). In this protocol a conditioned stimulus (CS; a neutral stimulus like a sound) is paired with an unconditioned stimulus (US; e.g., an airpuff to the eye to evoke a blink reflex).

Initially only the US causes the blink reflex but over time the CS can evoke the blink in the absence of the US. Bamford and colleagues used the known input and output properties of the cerebellum to guide the development of a prototype chip fabricated as a microcircuit. Real data from anaestethized animals were used calibration and training. The circuit could be "conditioned in a manner very similar to that of a real intact cerebellum" thus establishing partial brain function replication using BMI (Bamford et al., 2012).

Herreros and colleagues successfully connected to the brain of an anesthetized rat as a "step toward the development of neuroprostheses that could recover lost learning functions in animals and, in the longer term, humans" (Herreros et al., 2014). Most recently, this approach was used effectively in interfacing with the rodent brain for testing closed loop motor learning in real time (Hogri et al., 2015). These data lay the groundwork for refining future neuroprosthetics as well as creating a useful system for testing motor learning theories.

Miguel Pais-Vieira and colleagues, part of the Nicolelis and Lebedev groups, demonstrated that brain-machine interface concepts could be extended to brain-to-brain interfaces for shared information processing (Pais-Vieira et al., 2013). In this compelling research, two rats had electrode arrays implanted

into the sensorimotor areas. One rat served as an "encoder" of sensorimotor information during performance of either a tactile or visual task. The cortical activity generated in the brain of the "encoder rat" was monitored and then relayed to a second "receiving" or "decoder" rat, located in a distant laboratory.

The brain of the "decoder rat" was electrically stimulated through the implanted electrode array based on the timing and pattern of activity received from the "encoder rat." The behavior of the "decoder rat" was directed by this activity and subsequently made similar task choices as did the "encoder rat." Thus, the distant "decoder rat" was taught by the neural traffic generated by the initial activity of the "encoder rat" and relayed by the direct brain-to-brain coupling afforded in this novel "artificial communication channel" (Pais-Vieira et al., 2013). This shows that rats linked through brain-to-brain electrode arrays could learn complex, cooperative, goal-directed behaviors.

A related human test of brain-to-brain interaction was conducted by Grau et al. (2014). They used non-invasive methodologies of electroencephalography (EEG) for signal detection at the "source" brain (essentially the "encoder" rat above) and TMS for transmission to the "receiver" brain (the "decoder" rat analog of Pias-Vieira et al.) to establish that direct communication between the brains of conscious humans was possible. This study focused only on transmission of simple language but heralds the future arrival of more complex communication.

Conclusion—Optimism Balanced with Some Cautious Forethought

Stem cell technologies continue to show promise and have the most imminent restorative applications in neurodegenerative disorders such as Alzheimer's disease, Parkinson's disease, and stroke. Critically, tissue engineering may help bootstrap this field while techniques for parallel non-invasive brain monitoring develop. While considerable progress continues, immune response and acute inflammation with implantations and microelectrode insertions into the brain present limitations on long-term viability of some approaches (Richter et al., 2011; Fernandez et al., 2014; Groothuis et al., 2014).

Applications of stem cell technologies in augmenting the "normal" range of human brain function await discovery. Possible avenues discoveries of superior cell function in specialized systems in other animals that may see implantation in humans to augment functions unrelated to processing speed. Assuming improvements in achieving robust and behaviorally-relevant interfaces allowing facile access to discrete input and output pathways, proven, and nascent BMI methodologies have implications for restoration of brain function on a large scale. As the dovetailing of stem cell technology and brain machine interface continues, I suggest we must also pay attention to the issues of security and ethics.

As for security, connecting a machine so the human operator can access the functional capacity of the machine also allows the machine access to the functional capacity of the human. In 1942 the scientist and science fiction writer Isaac Asimov presaged these concerns when describing artificial intelligence and robotics.

In his influential 1942 short story "Runaround," (later found in the book "I, Robot" ;Asimov, 1950) Asimov laid down his "Three Laws of Robotics" which aimed to protect the sanctity of human life. However, such concerns may be rendered moot if future neural interfaces function indistinguishably from the user since it enacts part of the control system that manifests as the will of the user. This means it may actually be impossible to separate between the actions of the neural interface and that of its wearer.

Assuming such convergence, this places a higher order of responsibility on such "augmented" users. I've reworked Asimov's Three Laws below to apply to the complexities of machine-brain-machine interfaces.

An augmented user with a neural interface:

- may not injure a human being or, through inaction, allow a human being to come to harm (Law 1);
- must protect its own existence as long as such protection does not conflict with Law 1 (Law 2).

In fact, this yields Two Laws, since Asimov's declaration (original Law 2) that a robot "must obey order given to it by human beings" is irrelevant. In this future look, the user is the interface and the term human being applies to all and related subspecies (e.g., *homo sapiens sapiens* and *homo sapiens technologicus*; Zehr, 2015).

As for ethical considerations, this sets the stage for complete fusion between trans-species biology and neuroengineering. This will bring us to real life artificial-human brain hybrids and increased applications to enhance and augment innate function rather than simply recover lost function. This includes the extension of the concept of brain augmentation to include the "global brain" suggested by Kyriazis (2015). Future applications to augmentation of otherwise healthy and intact brain function may well be in "the new wave of human enhancement" (Harris, 2007).

Yet, the issue of brain augmentation should proceed with appropriate caution in neurologically intact "normally functioning" people. The comment of Rudolf Jaenisch—in the context of the human gene editing controversy (Baltimore et al., 2015; Cyranoski, 2015; Vogel, 2015)—that "We need some principled agreement that we want to enhance humans in this way or we don't" (Wade, 2015) has resonance here.

Using the examples of brain augmentation discussed above, what other intact cellular interactions in the brain are disrupted by the effect of transpecies implants? What changes in brain structure and function may arise from long-term neuroprosthetic interface? What are the implications for what we now accept as "normal human behavior" and functional capacity?

Especially we need to establish what societal boundaries—if any—we will place on multi-species transplants and what does this mean for the concept of species itself? Many of the related ethical and moral issues are addressed elsewhere in more detail (Clark, 2014; Clark and Parasuraman, 2014; Kennedy, 2014; Hildt, 2015). Along the way forward it remains for us as scientists, engineers, and future users of brain augmentation methodologies

to proceed with conviction and purpose, but also with suitable care and caution. Establishing the context for conviction, care and caution must also include dialogue with all members of our society including the general lay public.

Acknowledgments

I wish to thank those reviewers who provided excellent suggestions for improving this paper.

References

Asimov, I. (1950). *I, Robot*. New York, NY: DoubleDay

Baltimore, B. D., Berg, P., Botchan, M., Carroll, D., Charo, R. A., Church, G., et al. (2015). A prudent path forward for genomic engineering and germline gene modification. *Science* 348, 36–38. doi: 10.1126/science.aab1028

Bamford, S. A., Hogri, R., Giovannucci, A., Taub, A. H., Herreros, I., Verschure, P. F. M. J., et al. (2012). A VLSI field-programmable mixed-signal array to perform neural signal processing and neural modeling in a prosthetic system. *IEEE Trans. Neural Syst. Rehabil. Eng.* 20, 455–467. doi: 10.1109/TNSRE.2012.2187933

Berger, T., W., Robert, E. H., Dong, S., Anushka, G., Vasilis, Z. M., and Sam, A. D. (2011). A cortical neural prosthesis for restoring and enhancing memory. *J. Neural Eng.* 8, 046017. doi: 10.1088/1741-2560/8/4/046017

Bestmann, S., and Krakauer, J. (2015). The uses and interpretations of the motor-evoked potential for understanding behaviour. *Exp. Brain Res.* 233, 679–689. doi: 10.1007/s00221-014-4183-7

Cantarero, G., Spampinato, D., Reis, J., Ajagbe, L., Thompson, T., Kulkarni, K., et al. (2015). Cerebellar direct current stimulation enhances on-line motor skill acquisition through an effect on accuracy. *J. Neurosci.* 35, 3285–3290. doi: 10.1523/JNEUROSCI.2885-14.2015

Cheron, G., Dan, B., and Márquez-Ruiz, J. (2013). Translational approach to behavioral learning: lessons from cerebellar plasticity. *Neural Plast.* 2013:853654. doi: 10.1155/2013/853654

Clark, V. P. (2014). The ethical, moral and pragmatic rationale for brain augmentation. *Front. Syst. Neurosci.* 8:130. doi: 10.3389/fnsys.2014.00130

Clark, V. P., and Parasuraman, R. (2014). Neuroenhancement: enhancing brain and mind in health and in disease. *Neuroimage* 85, 889–894. doi: 10.1016/j.neuroimage.2013.08.071

Cyranoski, D. (2015). Ethics of embryo editing divides scientists. *Nature (London)* 519, 272–272. doi: 10.1038/519272a

Elliott Donaghue, I., Tam, R., Sefton, M. V., and Shoichet, M. S. (2014). Cell and biomolecule delivery for tissue repair and regeneration in the central nervous system. *J. Control. Release* 190, 219–227. doi: 10.1016/j.jconrel.2014.05.040

Ellis, W. (2007). *Invincible Iron Man: Extremis*. New York, NY: Marvel Comics.

Fernandez, E., Greger, B., House, P. A., Aranda, I., Botella, C., Albisua, J., et al. (2014). Acute human brain responses to intracortical microelectrode arrays: challenges and future prospects. *Front. Neuroeng.* 7:24. doi: 10.3389/fneng.2014.00024

Grau, C., Ginhoux, R., Riera, A., Nguyen, T. L., Chauvat, H., Berg, M., et al. (2014). Conscious brain-to-brain communication in humans using non-invasive technologies. *PLoS ONE* 9:e105225. doi: 10.1371/journal.pone.0105225

Groothuis, J., Ramsey, N. F., Ramakers, G. M. J., and Van Der Plasse, G. (2014). Physiological challenges for intracortical electrodes. *Brain Stimulation* 7, 1–6. doi: 10.1016/j.brs.2013.07.001

Hampson, R. E., Greg, A. G., Vasilis, M., Dong, S., Ioan, O., Lucas, S., et al. (2012). Facilitation and restoration of cognitive function in primate prefrontal cortex by a neuroprosthesis that utilizes minicolumn-specific neural firing. *J. Neural Eng.* 9:056012. doi: 10.1088/1741-2560/9/5/056012

Han, X., Chen, M., Wang, F., Windrem, M., Wang, S., Shanz, S., et al. (2013). Forebrain engraftment by human glial progenitor cells enhances synaptic plasticity and learning in adult mice. *Cell Stem Cell* 12, 342–353. doi: 10.1016/j.stem.2012.12.015

Harris, J. (2007). *Enhancing Evolution: the Ethical Case for Making Better People*. Princeton, NJ: Princeton University Press.

Herreros, I., Giovannucci, A., Taub, A. H., Hogri, R., Magal, A., Bamford, S., et al. (2014). A cerebellar neuroprosthetic system: computational architecture and *in vivo* test. *Front. Bioeng. Biotechnol.* 2:14. doi: 10.3389/fbioe.2014.00014

Hildt, E. (2015). What will this do to me and my brain? Ethical issues in brain-to-brain interfacing. *Front. Syst. Neurosci.* 9:17. doi: 10.3389/fnsys.2015.00017

Hogri, R., Bamford, S. A., Taub, A. H., Magal, A., Giudice, P. D., and Mintz, M. (2015). A neuro-inspired model-based closed-loop neuroprosthesis for the substitution of a cerebellar learning function in anesthetized rats. *Sci. Rep.* 5:8451. doi: 10.1038/srep08451

Kennedy, P. (2014). Brain-machine interfaces as a challenge to the 'moment of singularity'. *Front. Syst. Neurosci.* 8:213. doi: 10.3389/fnsys.2014.00213

Kyriazis, M. (2015). Systems neuroscience in focus: from the human brain to the global brain? *Front. Syst. Neurosci.* 9:7. doi: 10.3389/fnsys.2015.00007

Leach, J. B., Achyuta, A. K. H., and Murthy, S. K. (2010). Bridging the divide between neuroprosthetic design, tissue engineering and neurobiology. *Front. Neuroeng.* 2:18. doi: 10.3389/neuro.16.018.2009

Lebedev, M. A., and Nicolelis, M.A. L. (2006). Brain-machine interfaces: past, present and future. *Trends Neurosci.* 29, 536–546. doi: 10.1016/j.tins.2006.07.004

Mcnamee, M. J., and Edwards, S. D. (2006). Transhumanism, medical technology and slippery slopes. *J. Med. Ethics* 32, 513–518. doi: 10.1136/jme.2005.013789

Nelson, J. T., Mckinley, R. A., Golob, E. J., Warm, J. S., and Parasuraman, R. (2014). Enhancing vigilance in operators with prefrontal cortex transcranial direct current stimulation (tDCS). *Neuroimage* 85, Pt 3, 909–917. doi: 10.1016/j.neuroimage.2012.11.061

Nollet, H., Van Ham, L., Deprez, P., and Vanderstraeten, G. (2003). Transcranial magnetic stimulation: review of the technique, basic principles and applications. *Vet. J.* 166, 28–42. doi: 10.1016/S1090-0233(03)00025-X

Pais-Vieira, M., Lebedev, M., Kunicki, C., Wang, J., and Nicolelis, M. A. L. (2013). A brain-to-brain interface for real-time sharing of sensorimotor information. *Sci. Rep.* 3:1319. doi: 10.1038/srep01319

Prueckl, R., Taub, A. H., Herreros, I., Hogri, R., Magal, A., Bamford, S. A., et al. (2011). "Behavioral rehabilitation of the eye closure reflex in senescent rats using a real-time biosignal acquisition system," in *Engineering in Medicine and Biology Society, EMBC, 2011 Annual International Conference of the IEEE*. (Boston, MA).

Richter, A., Kruse, C., Moser, A., Hofmann, U. G., and Danner, S. (2011). Cellular modulation of polymeric device surfaces: promise of adult stem cells for neuroprosthetics. *Front. Neurosci.* 5:114. doi: 10.3389/fnins.2011.00114

Romero, J. R., Ramirez, D. M., Aglio, L. S., and Gugino, L. D. (2011). Brain mapping using transcranial magnetic stimulation. *Neurosurg. Clin. N.Am.* 22, 141–152. doi: 10.1016/j.nec.2010.11.002

Shih, J. J., Krusienski, D. J., and Wolpaw, J. R. (2012). Brain-computer interfaces in medicine. *Mayo Clin. Proc.* 87, 268–279. doi: 10.1016/j.mayocp.2011.12.008

Vogel, G. (2015). Embryo engineering alarm. *Science* 347:1301. doi: 10.1126/science.347.6228.1301

Wade, N. (2015, March 19). Scientists seek ban on method of editing the human genome. *New York Times*.

Wang, W., Collinger, J. L., Perez, M. A., Tyler-Kabara, E. C., Cohen, L. G., Birbaumer, N., et al. (2010). Neural interface technology for rehabilitation: exploiting and promoting neuroplasticity. *Phys. Med. Rehabil. Clin. N.Am.* 21, 157–178. doi: 10.1016/j.pmr.2009.07.003

Windrem, M. S., Schanz, S. J., Morrow, C., Munir, J., Chandler-Militello, D., Wang, S., et al. (2014). A competitive advantage by neonatally engrafted human glial progenitors yields mice whose brains are chimeric for human glia. *J. Neurosci.* 34, 16153–16161. doi: 10.1523/JNEUROSCI.1510-14.2014

Zehr, E. P. (2011). *Inventing Iron Man: the Possibility of a Human Machine.* Baltimore, MD: Johns Hopkins University Press.

Zehr, E. P. (2015). The potential transformation of our species by neural enhancement. *J. Mot. Behav.* 47, 73–78. doi: 10.1080/00222895.2014.916652

Conflict of Interest Statement: The author declares that the research was conducted in the absence of any commercial or financial relationships that could be construed as a potential conflict of interest.

frontiers in
SYSTEMS NEUROSCIENCE

OPINION ARTICLE
published: 08 October 2014
doi: 10.3389/fnsys.2014.00189

Experimental enhancement of neurphysiological function

Diana Deca[1]* and Randal A. Koene[2]

[1] Center for Integrated Protein Science and SyNergy Cluster, Institute of Neuroscience, Technical University Munich, Munich, Germany
[2] Carboncopies.org Foundation, San Francisco, CA, USA
*Correspondence: diana.deca@lrz.tum.de

Edited by:
Mikhail Lebedev, Duke University, USA

Reviewed by:
Mikhail Lebedev, Duke University, USA
Ioan Opris, Wake Forest University, USA

Keywords: experimental enhancement, optogenetics, single cell electrical stimulation, whole brain emulation, artificial general intelligence

Enhancing brain function entails controlling neuronal function. There are several methods available for this which led to some relevant experimental data. Deca (2011) Since methods for connectome (Briggman et al., 2011; Prevedel et al., 2014) and circuit functional analysis (Marblestone et al., 2013) are advancing rapidly (Deca, 2012), it makes sense to consider only the most convincing neurophysiological data in the context of enhancement and their future development.

STIMULATION METHODS: ELECTRICAL AND OPTICAL

The Brecht lab (Houweling and Brecht, 2008) has achieved training of a biological neural network in the living animal through a single neuron leading to enhanced learning speed. Microstimulation of the monkey frontal eye fields (FEF) (Goldberg et al., 1986) and training (Ferrera and Lisberger, 1995) can induce eye fixation and use neuronal activity as a predictor for saccadic eye movements (Shadlen and Newsome, 2001). Schiller and Tehovnik mapped the neurophysiological basis of saccadic eye movements (Tehovnik and Lee, 1993) as a basis for a visual prosthetic (Schiller and Tehovnik, 2008).

Optogenetics is by now a stock neuromodulation technique. The Deisseroth lab used it to enhance neuronal direction selectivity through optical stimulation of interneurons (Lee et al., 2012). Increasing inhibition can promote learning. It was also used to modulate the astroglial activation (Perea et al., 2014) for enhancing both excitatory and inhibitory neurotransmission. Neuronal activity can also be inhibited optogenetically (Zhang et al., 2007) using halorhodopsin.

NEUROFEEDBACK

Romo et al. (2000) used microstimulation as a substitute for sensory stimulation and obtained the same results, showing that sensory input can be replaced in a network by its corresponding electrical input. Furthermore, it was shown that rhesus monkeys can control the activity of their own FEF neurons, when experimenters reinforce visual attention (neurofeedback training Schafer and Moore, 2011).

The finding that rats can press a lever in order to get drugs that interfere with their own dopaminergic system (Yokel and Wise, 1976; Wise et al., 1990) also inspired the invention of an electrode for chronic brain self-stimulation.

NEURAL PROSTHETICS

The discovery of neural population coding of directional motor control signals (Georgopoulos et al., 1982, 1986), plus the discovery of stable cortical maps for motor control (Ganguly and Carmena, 2009), have enabled control of prosthetic limbs through chronic multi-site neural interfaces in non-human primates (Nicolelis, 2001; Graziano et al., 2002; Nicolelis et al., 2003; Gilja et al., 2012) and human experiments with implantable devices that enable control of a cursor, a wheel chair, a TV remote control, and a prosthetic hand by a single neuron or by an ensemble of neurons (Kennedy and Bakay, 1998; Hochberg et al., 2006; Truccolo et al., 2008; Simeral et al., 2011). There are also efforts to use signals from higher-level cognitive processing to instruct devices (Andersen et al., 2004). The FDA has approved clinical trials for cortical motor control of prosthetic arms using Utah arrays (Maynard et al., 1997).

Work from the Schreiner lab (Atencio et al., 2014) shows that an auditory implant in the thalamus can give better results than cochlear implants.

Also, a short-term memory neuroprosthetic in the rodent hippocampus enhanced performance (Berger et al., 2011). It performed real-time diagnosis and stimulation and enhanced cognitive, mnemonic processes. Furthermore, one can transfer performance-related spiking activity from one donor brain and use this pattern to stimulate another and generate the same behavior through BMBI. Deadwyler et al. (2013), Opris et al. (2001, 2013), Opris and Casanova (2014), Berger and Deadwyler made a neuroprosthetic multi-input multi-output (MIMO) model replicating CA3-to-CA3 coding functions which successfully enhanced monkeys' performance on a decision making task (Dibazar et al., 2013; Hampson et al., 2013) and recovered it under pharmacological disruption (Hampson et al., 2012). They are currently starting trials in volunteer human patients. Guggenmos et al. (2013) invented a prosthetic for restoring motor function. Circuit function was also emulated in the cerebellum (Herreros et al., 2014). Using the neuroprosthetic system, a rat underwent acquisition, retention and extinction of the eye-blink reflex even under anesthesia.

Table 1 | Summary of successful neurophysiological enhancements.

Enhanced function	Method	What is modulated	Possible developments
Vision/Stimulus selectivity	Optogenetics	Interneurons	Enhancing other senses and learning by inhibiting the responsible inhibitory circuits
Vision/Stimulus selectivity	Optogenetics	Astrocytes	Speeding up network computation in response to any stimulus by activating the brain's immune response
Learning/Decision making	Single neuron electrical stimulation	Neuronal firing/Behavior	Enhancing a desired behavioral response through electrical stimulation
Oculomotor control	Neurofeedback training	Neuronal firing in the FAF/thalamic	Inducing long-term plasticity and learning through repetitive neurofeedback training
Hearing	Auditory thalamic implant	Thalamic input	Activated auditory cortex at low electrical current levels
Vision/Fixation	Electrical stimulation	Frontal eye fields	Electrically evoked saccadic eye movements
Memory	Neuroprosthetic	Neuronal firing/behavior	Enhanced mnemonic processes through electrical stimulation
Memory	Neuroprosthetic/Emulated firing patterns	Neuronal firing	Induced memory-related processing
Learning	MIMO	Substituted layer 5 neuronal input	Enhanced performance in a primate decision making task
Motor skills	Brain-machine-brain interface (BMBI)	Bridged damaged neural pathways	Promoted LTP, Restored motor function
Learning	Neuroprosthetic	Restored the eye-blink reflex under anesthesia with BMBI	Induced learning in the cerebellum with neuroprosthetic conditioning

TOWARD THE CONNECTOME

The goal of this paper was to present the clearest experimental evidence of neurophysiological enhancement to date, while employing a very conservative definition of enhancement.

The neural mechanisms for the enhancement effects of drugs, deep brain stimulation or transcranial current stimulation are largely unknown. Microstimulation and optogenetics provide means to control specific system components and study their contribution to a particular brain function. Neuroprosthetics, brain implants, MIMO, BMBI, and neurofeedback training do electrophysiological data acquisition, interpretation and reimplementation which, if successful, show a clear direction of causality of the neurophysiological substrate of sensing, learning, memory and decision making. These approaches provide mechanistic explanations together with clear enhancement of brain functions.

In the near future, more mechanistic/causal electrophysiological data showing enhancement in lower animals will enable further exploration of these mechanisms in primate non-human and human subjects. A significant challenge for non-invasive experimental enhancement is getting around the isolating effects of the skull. Lebedev (2014) if this cannot be achieved, then very small invasive implants (Seo et al., 2013) may be an alternative solution.

ACKNOWLEDGMENTS

We would like to thank Anders Sandberg (Oxford University), Leslie Seymour (PersInVitro) and Antje Birkner (Technical University Munich) for their inspiring comments and suggestions.

REFERENCES

Andersen, R. A., Burdick, J. W., Musallam, S., Pesaran, B., and Cham, J. G. (2004). Cognitive neural prosthetics. *Trends Cognit. Sci.* 8, 486–493. doi: 10.1016/j.tics.2004.09.009

Atencio, C. A., Shih, J. Y., Schreiner, C. E., and Cheung, S. W. (2014). Primary auditory cortical responses to electrical stimulation of the thalamus. *J. Neurophysiol.* 111, 1077–1087. doi: 10.1152/jn.00749.2012

Berger, T. W., Hampson, R. E., Song, D., Goonawardena, A., Marmarelis, V. Z., and Deadwyler, S. A. (2011). A cortical neural prosthesis for restoring and enhancing memory. *J. Neural Eng.* 8:046017. doi: 10.1088/1741-2560/8/4/046017

Briggman, K. L., Helmstaedter, M., and Denk, W. (2011). Wiring Specificity in the Direction-Selectivity circuit of the retina. *Nature* 471, 183–188. doi: 10.1038/nature09818

Deadwyler, S. A., Berger, T. W., Sweatt, A. J., Song, D., Chan, R. H. M., Opris, I., et al. (2013). Donor/recipient enhancement of memory in rat hippocampus. *Front. Syst. Neurosci.* 7:120. doi: 10.3389/fnsys.2013.00120

Deca, D. (2011). Available tools for whole brain emulation. *Int. J. Mach. Conscious* 04, 67. doi: 10.1142/S1793843012400045

Deca, D. (2012). The Connectome, WBE and AGI. *Artif. Gen. Intell. Lect. Notes Comp. Sci.* 7716, 41–49. doi: 10.1007/978-3-642-35506-6_5

Dibazar, A. A., Yousefi, A., and Berger, T. W. (2013). "Multi-layer spike-in spike-out representation of Hippocampus circuitry," in *Proceedings of the 6th International IEEE/EMBS Conference on Neural Engineering (NER)* (San Diego, CA), 613–616.

Ferrera, V. P., and Lisberger, S. G. (1995). Attention and target selection for smooth pursuit eye movements. *J. Neurosci.* 15, 7472–7484.

Ganguly, K., and Carmena, J. M. (2009). Emergence of a stable cortical map for neuroprosthetics. *PLoS Biol.* 7, 1–13. doi: 10.1371/journal.pbio.1000153

Georgopoulos, A. P., Kalaska, J. F., Caminiti, R., and Massey, J. T. (1982). On the Relations Between the direction of two-dimensional arm movements and cell discharge in primate motor cortex. *J. Neurosci.* 2, 1527–1537.

Georgopoulos, A. P., Schwartz, A., and Kettner, R. E. (1986). Neuronal population coding of movement direction. *Science* 233, 1416–1419.

Gilja, V., Nuyujukian, P., Chestek, C. A., Cunningham, J. P., Yu, B. M., Fan, J. M., et al. (2012). A high-performance neural prosthesis enabled by control algorithm design. *Nat. Neurosci.* 15, 1752–1757. doi: 10.1038/nn.3265

Herreros, I., Giovannucci, A., Taub, A. H., Hogri, R., Magal, A., Bamford, S. A., et al. (2014). A cerebellar neuroprosthetic system: computational architecture and *in vivo* experiments. *Front. Bioeng. Biotechnol.* 2:14, doi: 10.3389/fbioe.2014.00014

Goldberg, M. E., Bushnell, M. C., and Bruce, C. J. (1986). The effect of attentive fixation on eye movements evoked by electrical stimulation of the frontal eye fields. *Exp. Brain Res.* 61, 579–584.

Graziano, M. S. A., Taylor, C. S. R., and Moore, T. (2002). Complex movements evoked by microstimulation of precentral cortex. *Neuron* 34, 841–851. doi: 10.1016/S0896-6273(02)00698-0

Guggenmos, D. J., Azinc, M., Barbaya, S., Mahnkend, J. D., Dunhama, C., Mohsenic, P., et al. (2013). Restoration of function after brain damage using a neural prosthesis. *Proc. Natl. Acad. Sci. U.S.A.* 110, 21177–21182. doi: 10.1073/pnas.1316885110

Hampson, R. E., Gerhardt, G. A., Marmarelis, V., Song, D., Opris, I., Santos, L., et al. (2012). Facilitation and restoration of cognitive function in primate prefrontal cortex by a neuroprosthesis that utilizes minicolumn-specific neural firing. *J. Neural Eng.* 9:056012. doi: 10.1088/1741-2560/9/5/056012

Hampson, R. E., Song, D., Opris, I., Santos, L. M., Shin, D. C., Gerhardt, G. A., et al. (2013). Facilitation of memory encoding in primate hippocampus by a neuroprosthesis that promotes task-specific neural firing. *J. Neural Eng.* 10:066013. doi: 10.1088/1741-2560/10/6/066013

Hochberg, L. R., Serruya, M. D., Friehs, G. M., Mukand, J. A., Saleh, M., Caplan, A. H., et al. (2006). Neuronal ensemble control of prosthetic devices by a human with tetraplegia. *Nature* 442, 164–171. doi: 10.1038/nature04970

Houweling, A. R., and Brecht, M. (2008). Behavioural report of single neuron stimulation in somatosensory cortex. *Nature* 451, 65–68. doi: 10.1038/nature06447

Kennedy, P. R., and Bakay, R. A. (1998). Restoration of neural output from a paralyzed patient by a direct brain connection. *Neuro Rep.* 9, 1707–1711.

Lebedev, M. (2014). Brain-machine interfaces: an overview. *Transl. Neurosci.* 5, 99–110. doi: 10.2478/s13380-014-0212-z

Lee, S. H., Kwan, A. C., Zhang, S., Phoumthipphavong, V., Flannery, J. G., Masmanidis, S. C., et al. (2012). Activation of specific interneurons improves V1 feature selectivity and visual perception. *Nature* 488, 379–383. doi: 10.1038/nature11312

Marblestone, A. H., Zamft, B. M., Maguire, Y. G., Shapiro, M. G., Cybulski, T. R., Glaser, J. I., et al. (2013). Physical principles for scalable neural recording. *Front. Comput. Neurosci.* 7:137. doi: 10.3389/fncom.2013.00137

Maynard, E. M., Nordhausen, C. T., and Normann, R. A. (1997). The utah intracortical electrode array: a recording structure for potential brain-computer interfaces, electroencephalography and Clinical. *Neurophysiology* 102, 228–239.

Nicolelis, M. A. L. (2001). Actions from Thoughts. *Nature* 409, 403–407. doi: 10.1038/35053191

Nicolelis, M. A. L., Dimitrov, D., Carmena, J. M., Crist, R., Lehew, G., Kralik, J. D., et al. (2003). Chronic, multisite, multielectrode recordings in macaque monkeys. *Proc. Natl. Acad. Sci. U.S.A.* 100, 11041–11046. doi: 10.1073/pnas.1934665100

Opris, I., Barborica, A., and Ferrera, V. P. (2001). A gap effect during microstimulation in the prefrontal cortex of monkey. *Exp. Brain Res.* 138, 1–7. doi: 10.1007/s002210100686

Opris, I., and Casanova, M. F. (2014). Prefrontal cortical minicolumn: from executive control to disrupted cognitive processing. *Brain* 137(Pt 7), 1863–1875. doi: 10.1093/brain/awt359

Opris, I., Santos, L. M., Song, D., Gerhardt, G. A., Berger, T. W., Hampson, R. E., et al. (2013). Prefrontal cortical microcircuits bind perception to executive control. *Sci. Rep.* 3:2285. doi: 10.1038/srep02285

Perea, G., Yang, A., Boyden, E. S., and Sur, M. (2014). Optogenetic astrocyte activation modulates response selectivity of visual cortex neurons *in vivo*. *Nat. Commun.* 5, 3262. doi: 10.1038/ncomms4262

Prevedel, R., Yoon, Y.-G., Hoffmann, M., Pak, N., Wetzstein, G., Kato, S., et al. (2014). Simultaneous whole-animal 3D imaging of neuronal activity using light-field microscopy. *Nat. Methods* 11, 727–730. doi: 10.1038/nmeth.2964

Romo, R., Hernandez, A., Zainos, A., Brody, C. D., and Lemus, L. (2000). Sensing without touching: psychophysical performance based on cortical microstimulation. *Neuron* 26, 273–278. doi: 10.1016/S0896-6273(00)81156-3

Schafer, R. J., and Moore, T. (2011). Selective attention from voluntary control of neurons in prefrontal cortex. *Science* 332, 1568–1571. doi: 10.1126/science.1199892

Schiller, P. H., and Tehovnik, E. J. (2008). Visual prosthesis. *Perception* 37, 1529–1559. doi: 10.1068/p6100

Seo, D., Carmena, J. M., Rabaey, J. M., Alon, E., and Maharbiz, M. M. (2013). *Neural Dust: An Ultrasonic, Low Power Solution for Chronic Brain-Machine Interfaces, arXiv:1307.2196 [q-bio.NC]*.

Shadlen, M. N., and Newsome, W. T. (2001). Neural basis of a perceptual decision in the parietal cortex (area LIP) of the rhesus monkey. *J. Neurophysiol.* 86, 1916–1936.

Simeral, J. D., Kim, S. P., Black, M. J., Donoghue, J. P., and Hochberg, L. R. (2011). Neural control of cursor trajectory and click by a human with tetraplegia 1000 days after implant of an intracortical microelectrode array. *J. Neural Eng.* 8, 1–24. doi: 10.1088/1741-2560/8/2/025027

Tehovnik, E. J., and Lee, K. (1993). The dorsomedial frontal cortex of the rhesus monkey: topographic representation of saccades evoked by electrical stimulation. *Exp. Brain Res.* 96, 430–442. doi: 10.1007/BF00234111

Truccolo, W., Friehs, G. M., Donoghue, J. P., and Hochberg, L. R. (2008). Primary motor cortex tuning to intended movement kinematics in humans with tetraplegia. *J. Neurosci.* 28, 1163–1178. doi: 10.1523/JNEUROSCI.4415-07.2008

Wise, R. A., Murray, A., and Bozarth, M. A. (1990). Bromocriptine self-administration and bromocriptine-reinstatement of cocaine-trained and heroin-trained lever pressing in rats. *Psychopharmacol* 100, 355–360.

Yokel, R. A., and Wise, R. A. (1976). Attenuation of intravenous amphetamine reinforcement by central dopamine blockade in rats. *Psychopharmacology* 48, 311–318.

Zhang, F., Wang, L. P., Brauner, M., Liewald, J. F., Kay, K., Watzke, N., et al. (2007). Multimodal fast optical interrogation of neural circuitry. *Nature* 446, 633–639. doi: 10.1038/nature05744

Conflict of Interest Statement: The authors declare that the research was conducted in the absence of any commercial or financial relationships that could be construed as a potential conflict of interest.

Received: 31 May 2014; accepted: 17 September 2014; published online: 08 October 2014.

*Citation: Deca D and Koene RA (2014) Experimental enhancement of neurphysiological function. Front. Syst. Neurosci. **8**:189. doi: 10.3389/fnsys.2014.00189*

This article was submitted to the journal Frontiers in Systems Neuroscience.

frontiers in Systems Neuroscience

OPINION
published: 14 April 2015
doi: 10.3389/fnsys.2015.00053

As we may think and be: brain-computer interfaces to expand the substrate of mind

Mijail D. Serruya *

Department of Neurology, Thomas Jefferson University, Philadelphia, PA, USA

Keywords: brain-computer interface, neurotechnology, neuroprosthetic

Over a half-century ago, the scientist Vannevar Bush explored the conundrum of how to tap the exponentially rising sea of human knowledge for the betterment of humanity. In his description of a hypothetical electronic library he dubbed the memex, he anticipated internet search and online encyclopedias (Bush, 1945). By blurring the boundary between brain and computer, BCI could lead to more efficient use of electronic resources (Schalk, 2008). The advantage of the well-designed direct interface is not simply the discarding of a cumbersome mouse or keyboard in exchange for whispered thought, but the creation of a new, fundamental language bridging essential brain states to discrete items and functions in computers.

Should we achieve such BCI integration, we would come up against the attentional, multi-tasking and global processing limitations of the brain. Both in terms of overall spatial architecture and in moment-to-moment engagement of the world, we appear to have a limited amount of real-estate or bandwidth to work with (Müller et al., 2003; Busse et al., 2005). Just as a stroke may take away a person's ability to do something- such a perceive half the world, or be able to speak—so too one might wonder whether adding on to the brain, at a direct biological level, might provide us with new abilities. We could expand the substrate of the mind itself rather than merely interfacing it to external computers. Components of brain-computer interfaces (BCI) could be re-arranged to create brain-brain interfaces, or tightly interconnected links between a person's brain and ectopic neural modules (Serruya and Kahana, 2008). Such modules—whether sitting in a bubbling Petri dish, rendered in reciprocally linked integrated circuits, or implanted in our belly—would mark the first step on to a path of breaking out of the limitations imposed by our phylogenetic past (O'Doherty et al., 2011; Deadwyler et al., 2013; Vidu et al., 2014). Constructed properly, this system could allow us to experience sensations and movements here fore only granted to other animals—perceiving in true infrared or ultraviolet rather than false-color extrapolations—and we could begin building an architecture to interface with abstract data forms, and indeed with other people, otherwise not possible in 2015. We could extend our nervous systems beyond being a puppeteer of individual vehicles toward being a conductor of swarms of robots, flocks of mechanical birds and fish to change shape and form at our will. Just as vision, sight and touch have their own dedicated neural pathways, we could create novel "search organs" to navigate the internet or large databases, to "feel" molecular structures or social network information.

While we can learn to pay attention to multiple things simultaneously, there appears to be an upper limit to our moment-to-moment information processing capacity after which performance on any given sub-task breaks down (Busse et al., 2005; Dugué et al., 2014). Our brains operate as if having a single attentional spotlight for conscious perception—even if multiple items may be continuously processed in parallel in the unconscious background, reaching conscious perception only when called upon or relevant (Müller et al., 2003; McAlonan et al., 2006).The use of shortcuts or macros are ubiquitous in computer use; by recording a complex series of steps and providing a rule, a macro can allow a computer to blindly repeat the steps and free the human operator. Yet the problem is precisely that the computer is blind: if a file name or operation

Edited by:
Manuel Fernando Casanova, University of Louisville, USA

Reviewed by:
Yu Liu, The University of Tennessee Health Science Center, USA
Mikhail Lebedev, Duke University, USA
Ioan Opris, Wake Forest University School of Medicine, USA

***Correspondence:**
Mijail D. Serruya, mijail.serruya@jefferson.edu

Received: *14 October 2014*
Accepted: *12 March 2015*
Published: *14 April 2015*

Citation:
Serruya MD (2015) As we may think and be: brain-computer interfaces to expand the substrate of mind. Front. Syst. Neurosci. 9:53. doi: 10.3389/fnsys.2015.00053

does not precisely fit a predefined grammar, the performance will grind to a halt, and the previously liberated computer user will have her spotlight forced back to illuminate the problem at hand. A primary goal of expanding the neural substrate will be to enable the brain-computer hybrid to conduct these computerized macro tasks with great speed and efficiency and with just enough conscious awareness of context and content to enable them to proceed. One way to achieve this might be to create a hierarchy of attentional spotlights, or miniature conscious selves, all subsumed by the primary conscious self that one identifies as oneself. One may imagine having avatars: quasi-independent replicas of your own mind created to perform tasks that require a minimum of conscious attention, and which, once trained, could operate without your conscious awareness. These sub-selves, or avatars, could be implemented in tiny constructs of bioengineered autologous neural tissue directly linked to our brain. Just as an individual mouse has his own tiny consciousness devoted to his innumerable mouse tasks, so too could a mouse-brain-sized module of neural tissue be designed to perform the kind of "mindless" computer chores that we would rather not relegate to our primary conscious self. Arrayed with a chain of these interlinked mini-selves, we could entrain each to perform complex tasks that required this minimum of conscious attention, and assign priority flags to which module would know to alert the next level of consciousness up that more attentional consciousness resources were needed for the assigned task. Such abilities to navigate and access information might speed translational science efforts and push the boundaries of human knowledge in an unprecedented manner.

If we can identify the neural signatures of meditative states then we can, both with traditional techniques of breathing and posture ubiquitous to prayer and meditation the world over, and with neurofeedback facilitated by neural modules designed to allow the conscious mind to gain unprecedented perception of the power spectral and ensemble unit firing activity patterns of the brain itself, move our brains into meditative states with improved attentional and integrative capacity (Dickenson et al., 2013; Astrand et al., 2014; Steiner et al., 2014; Strenziok et al., 2014; deBettencourt et al., 2015). By learning to perceive and control the aspects of our brain that give rise to conscious effort and distress we could likewise steer our internal state toward compassion and equanimity; a seamless computer-brain hybrid could be trained to identify when too much information was overwhelming, to steer us to tasks or priority flags that would be best integrated, and also to lay off such automation entirely and let the naked brain be itself. Truly integrated at multiple levels into the brain, these sub-selves- and super-selves born of interfaces linking multiple people—would sleep and dream along with us, and perhaps enter other states of consciousness to promote exchange of information, integration of a unitary consciousness, and the promotion of self-awareness, self-discipline, critical thinking, and compassion.

Acknowledgments

The author would like to thank Abdolmohammed Rostami and Thomas Jefferson University for financial support.

References

Astrand, E., Wardak, C., and Ben Hamed, S. (2014). Selective visual attention to drive cognitive brain-machine interfaces: from concepts to neurofeedback and rehabilitation applications. *Front. Syst. Neurosci.* 8:144. doi: 10.3389/fnsys.2014.00144

Bush, V. (1945). As we may think. *The Atlantic* (Boston, MA).

Busse, L., Roberts, K. C., Crist, R. E., Weissman, D. H., and Woldorff, M. G. (2005). The spread of attention across modalities and space in a multisensory object. *Proc. Natl. Acad. Sci. U.S.A.* 102, 18751–18756. doi: 10.1073/pnas.0507704102

Deadwyler, S. A., Berger, T. W., Sweatt, A. J., Song, D., Chan, R. H., Opris, I., et al. (2013). Donor/recipient enhancement of memory in rat hippocampus. *Front. Syst. Neurosci.* 7:120. doi: 10.3389/fnsys.2013.00120

deBettencourt, M. T., Cohen, J. D., Lee, R. F., Norman, K. A., and Turk-Browne, N. B. (2015). Closed-loop training of attention with real-time brain imaging. *Nat. Neurosci.* 18, 470–475. doi: 10.1038/nn.3940

Dickenson, J., Berkman, E. T., Arch, J., and Lieberman, M. D. (2013). Neural correlates of focused attention during a brief mindfulness induction. *Soc. Cogn. Affect. Neurosci.* 8, 40–47. doi: 10.1093/scan/nss030

Dugué, L., Marque, P., and VanRullen, R. (2014). Theta oscillations modulate attentional search performance periodically. *J. Cogn. Neurosci.* 12, 1–14. doi: 10.1162/jocn_a_00755

McAlonan, K., Cavanaugh, J., and Wurtz, R. H. (2006). Attentional modulation of thalamic reticular neurons. *J. Neurosci.* 26, 4444–4450. doi: 10.1523/JNEUROSCI.5602-05.2006

Müller, M. M., Malinowski, P., Gruber, T., and Hillyard, S. A. (2003). Sustained division of the attentional spotlight. *Nature* 424, 309–312. doi: 10.1038/nature01812

O'Doherty, J. E., Lebedev, M. A., Ifft, P. J., Zhuang, K. Z., Shokur, S., Bleuler, H., et al. (2011). Active tactile exploration using a brain-machine-brain interface. *Nature* 479, 228–231. doi: 10.1038/nature10489

Schalk, G. (2008). Brain-computer symbiosis. *J. Neural Eng.* 5, P1–P15. doi: 10.1088/1741-2560/5/1/P01

Serruya, M. D., and Kahana, M. J. (2008). Techniques and devices to restore cognition. *Behav. Brain Res.* 192, 149–165. doi: 10.1016/j.bbr.2008.04.007

Steiner, N. J., Frenette, E. C., Rene, K. M., Brennan, R. T., and Perrin, E. C. (2014). In-school neurofeedback training for ADHD: sustained improvements from a randomized control trial. *Pediatrics* 133, 483–492. doi: 10.1542/peds.2013-2059

Strenziok, M., Parasuraman, R., Clarke, E., Cisler, D. S., Thompson, J. C., and Greenwood, P. M. (2014). Neurocognitive enhancement in older adults: comparison of three cognitive training tasks to test a hypothesis of training transfer in brain connectivity. *Neuroimage* 85(Pt 3), 1027–1039. doi: 10.1016/j.neuroimage.2013.07.069

Vidu, R., Rahman, M., Mahmoudi, M., Enachescu, M., Poteca, T. D., and Opris, I. (2014). Nanostructures: a platform for brain repair and augmentation. *Front. Syst. Neurosci.* 8:91. doi: 10.3389/fnsys.2014.00091

Conflict of Interest Statement: The author declares that the research was conducted in the absence of any commercial or financial relationships that could be construed as a potential conflict of interest.

frontiers in
SYSTEMS NEUROSCIENCE

REVIEW ARTICLE
published: 29 April 2014
doi: 10.3389/fnsys.2014.00068

What limits the performance of current invasive brain machine interfaces?

Gytis Baranauskas*

Neurophysiology Laboratory, Neuroscience Institute, Lithuanian University of Health Sciences, Kaunas, Lithuania

Edited by:
Mikhail Lebedev, Duke University, USA

Reviewed by:
Mikhail Lebedev, Duke University, USA
Imran Khan Niazi, Aalborg University, Denmark
Philip Kennedy, Neural Signals Inc., USA

****Correspondence:***
Gytis Baranauskas, Neurophysiology Laboratory, Neuroscience Institute, Lithuanian University of Health Sciences, Eiveniu g. 4, LT-50009 Kaunas, Lithuania
e-mail: gytis11@yahoo.com

The concept of a brain-machine interface (BMI) or a computer-brain interface is simple: BMI creates a communication pathway for a direct control by brain of an external device. In reality BMIs are very complex devices and only recently the increase in computing power of microprocessors enabled a boom in BMI research that continues almost unabated to this date, the high point being the insertion of electrode arrays into the brains of 5 human patients in a clinical trial run by Cyberkinetics with few other clinical tests still in progress. Meanwhile several EEG-based BMI devices (non-invasive BMIs) were launched commercially. Modern electronics and dry electrode technology made possible to drive the cost of some of these devices below few hundred dollars. However, the initial excitement of the direct control by brain waves of a computer or other equipment is dampened by large efforts required for learning, high error rates and slow response speed. All these problems are directly related to low information transfer rates typical for such EEG-based BMIs. In invasive BMIs employing multiple electrodes inserted into the brain one may expect much higher information transfer rates than in EEG-based BMIs because, in theory, each electrode provides an independent information channel. However, although invasive BMIs require more expensive equipment and have ethical problems related to the need to insert electrodes in the live brain, such financial and ethical costs are often not offset by a dramatic improvement in the information transfer rate. Thus the main topic of this review is why in invasive BMIs an apparently much larger information content obtained with multiple extracellular electrodes does not translate into much higher rates of information transfer? This paper explores possible answers to this question by concluding that more research on what movement parameters are encoded by neurons in motor cortex is needed before we can enjoy the next generation BMIs.

Keywords: brain machine interface, brain computer interface, extracellular recordings, information, throughput, multichannel recordings

Although the idea of a direct control of devices by human mind can be tracked down to the first experiments relating brain signals to behavior (Humphrey et al., 1970; Kennedy et al., 1992; Kennedy and Bakay, 1998; Wolpaw et al., 2002; Mussa-Ivaldi and Miller, 2003), only the advent of more powerful computer technologies in the last few decades enabled routine testing of these ideas in the environment of a scientific laboratory and, in some cases, in real life (Chapin et al., 1999; Taylor et al., 2002; Carmena et al., 2003; Velliste et al., 2008). This lead to the use of term "brain machine interface" (BMI) for such devices and in the last 15 years the number of papers published per year in the field of BMI increased exponentially (**Figure 1**). During this period it has been demonstrated that not only rats (Chapin et al., 1999) and monkeys (Wessberg et al., 2000) but also humans can control both a computer cursor and a prosthetic arm by their brain activity (Kennedy et al., 2000; Wolpaw and McFarland, 2004; Hochberg et al., 2006, 2012; Kim et al., 2008). Although already in late '90s Kennedy and his colleagues employed a single electrode in human patients to conditionally control activity of single units (Kennedy and Bakay, 1998) and then a computer cursor (Kennedy et al., 2000), usually only experiments with multiple electrodes are considered to be relevant to BMIs of today and the tests with a robotic lever in rats are viewed as the birth of the modern BMI concept (Chapin et al., 1999; Lebedev and Nicolelis, 2006). Thus for electrode arrays it is possible to claim that in less than a decade the idea of BMI made a jump from the animal research to the tests in humans (Hochberg et al., 2006), a spectacular achievement.

However, did we achieve a qualitative improvement in invasive BMIs? This paper tries to answer this question by applying a single measure- information transfer rate. Although it may be viewed as a rather narrow-minded approach to evaluate the progress in a large field of science and technology by applying a single measure, the author believes that such a unified approach can be very useful in determining the strategy for future development of research and technology. This view is shared by a number of researchers as attested by a recent focused review on the topic (Tehovnik et al., 2013), a few reviews on EEG-based non-invasive BMIs (Wolpaw et al., 2000, 2002; Haselager, 2013), some papers on invasive BMIs (Gilja et al., 2012) and the position taken by the Defense Advanced Research Project Agency (DARPA), which funded many outstanding labs in the field of invasive BMI during

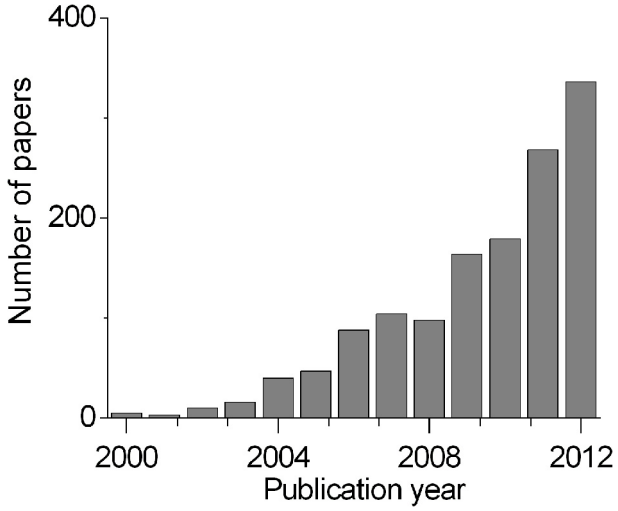

FIGURE 1 | The number of papers published each year with terms "Brain Machine Interface," PubMed search data.

the last few decades (Judy, 2012). The agency states that higher information transfer rates and increased durability/stability of BMI devices are the primary goals for this field of research (Judy, 2012). The information transfer rate is directly related to the ability to control a device (Tonet et al., 2008; Haselager, 2013; also see below) and may not be easily applied to some recently proposed new applications of BMIs such as restoration of neuronal function (Grosse-Wentrup et al., 2011). Nevertheless, device control remains the mainstream of BMI research and in these applications the information transfer rates can be used as the main quantitative measure to evaluate the overall system performance (Tonet et al., 2008; Haselager, 2013; Tehovnik et al., 2013).

Originally the mathematical information theory was developed to help optimize the communication line capacity (Shannon, 1948); these lines were mainly used for telegraph at that time, however, the theory is sufficiently general to be applied to any communication line, including the one used for a device control in BMI and the theory provides a quantitative measure, information content, that is independent of how BMI functions.

Even though to quantify BMI performance we employ just a single measure, the information transfer rate, we are still facing a daunting task to estimate information content in behavioral tasks that are used for BMI capability demonstration. The mathematical information theory determines what it takes to reproduce "at one point either exactly or approximately a message selected at another point" in space and time (Shannon, 1948). Shannon talks about a message selected from a set of messages and it is not important what is actually written in the message, the only thing that matters is how many such messages can be chosen, the number of possible selections. In a center-out reaching behavioral task, which is frequently used for BMI demonstrations (Taylor et al., 2002; Wolpaw and McFarland, 2004; Mulliken et al., 2008) and in which typically a subject has to choose several targets on the screen by moving a cursor from a central location, one message can correspond to one target. If during all runs 8 different targets were presented, we have 8 different messages. The information content is measured as a logarithm of number of choices to base of 2; for 8 messages with an equal probability to be presented the information content will be $\log_2(8) = 3$. By taking into account the error rates and the time needed to accomplish the task one can obtain the information transfer rate values (Tonet et al., 2008; Tehovnik et al., 2013). However, this approach has caveats and such a simple information content estimate is insufficient when we evaluate BMI performance. In this task the target relative size affects the subject performance and the larger target size will lead to higher information transfer rate even though no actual change in BMI performance will be present. The question of such task difficulty has been investigated in a number of papers on human-computer interactions (Fitts, 1954; MacKenzie and Buxton, 1992) and the Fitts' law is probably the best for evaluation of information content in such tasks. For other types of tasks, such as reaching and grasping (Carmena et al., 2003), the parameters determining task difficulty can be only guessed and there is a need of experimental data that information content of such tasks is evaluated. As long as no such experimental data exist, we are limited to these BMI studies that employ center-out reaching task. Luckily, this behavioral task is, probably, the most frequently used behavioral task in invasive BMI research from early on and even by limiting analysis to the center-out reaching task a trend in invasive BMI performance can be detected and few conclusions made.

In this review the author will try to show that the fundamental issues of biology but not computer power or electronic circuit capabilities are the limiting factors in achieving higher information transfer rates in invasive BMIs of today. More specifically, the author believes that, to increase invasive BMI performance, a more profound understanding about what neurons encode in motor areas of our brain is necessary and, actually, such BMIs can be a testing ground for new ideas on what kind of information is present in neuronal signals.

The paper is organized as follows. First, differences between invasive and non-invasive BMIs will be explained in brief. Second, the relationship between the information transfer rates and practical applications is discussed; examples from both invasive and non-invasive BMI will be presented. Third, technological factors that affect information rates in invasive BMIs will be evaluated. Finally, two examples of high information transfer rates in invasive BMIs will be analyzed and the strategies to improve information transfer rates will be suggested.

Today the term BMI can be applied to very different devices, from head caps with electrodes for electro-encephalogram (EEG) recording, in which EEG signal is transformed to commands for letter selection on a computer screen (Wolpaw et al., 2002; Krusienski et al., 2008) to implanted electrode arrays in monkey or, less frequently, rat and human brains, enabling a robotic arm control (Hochberg et al., 2006; Nicolelis and Lebedev, 2009). Since there are vast technological differences between a head-cap with electrodes for EEG and an array of wires inserted into the brain to record single neurons or field potentials of neuronal assemblies, usually all BMIs are broadly divided into two groups (Wolpaw et al., 2002; Tonet et al., 2008):

(1) Non-invasive BMIs, mainly EEG-based, although there are also systems that use muscle signals (EMG), gaze direction (Surakka et al., 2004; Oskoei and Hu, 2007; Tuisku et al., 2012) and other signals that do not require a surgical intervention.
(2) Invasive BMIs, these systems require a surgical intervention for electrode insertion and include not only electrode arrays inserted into the cortex but also electrodes implanted into the body for peripheral nerve activity detection (Navarro et al., 2005) or any other type of BMI that require extensive surgical procedure, for instance, cochlear implants (Moller, 2006).

These two classes of BMIs can be separated not only on the basis of technological differences but also on the basis of ethical problems associated with surgery in invasive BMIs. Invasive BMIs always require at least some surgery, which could be painful and, possibly, risky and there is always a question if such risks are offset by the benefits of BMI. In addition, invasive BMIs are usually much more expensive than non-invasive ones. Therefore, the expectation bar for invasive BMIs is higher than for non-invasive BMIs.

In spite of differences, all BMIs can be defined as devices that process information detected in the brain activity; the extracted information is used to determine the subject's intent and to control a computer cursor or a prosthesis. Thus, from information theory point of view the key characteristic of such a device is the amount of information transferred per unit of time, or channel capacity if we use Shannon's terms (Shannon, 1948) or throughput as it is called in many recent papers (Tonet et al., 2008; Gilja et al., 2012). An attempt to take a unified approach in the BMI research dates back to at least the first international meeting on non-invasive BMIs (Wolpaw et al., 2000). However, the use of information transfer rates became more common in the field of invasive BMIs only recently (Simeral et al., 2011; Gilja et al., 2012; Flint et al., 2013). Thus it is not an accident that the mentioned above DARPA initiative aimed to advance significantly the development of the upper-limb prosthesis technology places the information transfer rates at the center of its stated goals. The main reason for such an emphasis on information transfer rates is that in the design of neuroprosthesis this rate determines the functionality of a device (Tonet et al., 2008; Haselager, 2013). To understand that, we can take a wheelchair controlled by BMI as an example. One of the most important features of a wheelchair is the ability to stop it in case of emergency. The information transfer rate can be directly translated into the time required for such a command, because the command has 1 bit of information. Since typical EEG-based BMIs have information transfer rates of 0.25–0.5 bits/s (Wolpaw et al., 2002; Allison et al., 2012), for a EEG-based BMI it will take at least 2–4 s to stop a wheelchair. This is hardly acceptable because even at a very moderate speed of 0.5–1 m/s the wheelchair will move 1–2 m before it will stop. Although for non-emergency cases one can anticipate when to stop but if something unexpected happens there is no time for preparation, thus at least two-fold faster information transfer rates are needed for efficient stopping of a wheelchair in case of emergency.

More complex behaviors such as an arm movement correspond to much higher information transfer rates. To give an example, Paul Fitts in his famous paper (Fitts, 1954) estimated that in a simple tapping task human subject routinely achieve ∼10 bit/s information transfer rates. It is likely that the control of a robotic arm with many degrees of freedom will require even higher information transfer rates. Human speech can be used as another example of a typical information rate routinely achieved by our brains. In a slow human speech ∼100 words are produced each minute, or 1–2 words per second. If we use word recognition perplexity to estimate information content of each word (Brown et al., 1992), then each English word contains ∼7.5 bits of information on average, corresponding to 7–15 bit/s of information transfer rates in a slow human speech. These examples show that fluent interactions with human beings require information transfer rates of $\geq\sim$10 bit/s and, keeping in mind that information unit, a bit, is defined in a logarithmic scale, this information transfer rate is several orders of magnitude higher than achieved by most BMIs today, usually <3 bit/s (see below). It may be argued that some human patients could benefit even from such low information transfer rates (Wolpaw et al., 2002) but an example with a wheelchair shows that even for such patients increasing these rates is critical for at least some functions.

Lower information transfer rates mean less fun as it has been discovered by companies making EEG-based devices for entertainment. A number of devices are already on the market such as several toys made by Neurosky, Mindball made by Interactive Productline and few others. Although Neurosky claims that several of its toys had "a phenomenal success," all these devices, according to their users, share one thing in common- they are difficult to control. More specifically, not only it takes time to learn to use them but also the achieved control is unreliable. Some users even claimed that actually no control was achieved by such devices, in many cases brain signals are of low quality because of the presence of artifacts (Fatourechi et al., 2007). Thus in spite of relatively low prices of some of these devices, the lowest being approximately 100$, the user experience is still somehow limited in spite of attractiveness of the idea to directly control a device by thought.

From the point view of information theory, unreliable control is equivalent to low information transfer rates. Today EEG-based BMIs are limited to information transfer rates of <0.5 bit/s (Klobassa et al., 2009; Townsend et al., 2010). To put this number in perspective, we can take as a benchmark information transfer rates achieved by human subjects in a simple motor task of tapping (Fitts, 1954) and in speech recognition employing cochlear implants, the first BMIs used in large numbers (Mussa-Ivaldi and Miller, 2003). The gap between the EEG-based BMI information transfer rate of 0.5 bit/s and the 10 bit/s rate achieved in both cochlear implants used for human speech recognition (Dunn et al., 2010), and the tapping task is frightening. Since the bit scale is logarithmic, a difference of 10 bits in information content corresponds to 1000 times higher information content. It is true that cochlear implants, so far the only invasive BMIs in wide use, started slowly in 50 and 60 s. The first users of cochlear implants were able to have only some comprehension of sounds but not speech, corresponding to very low information transfer rates, probably of the order of few bits per second (Moller, 2006). However, the ability to recognize human speech

was, almost certainly, a key to their widespread use and today >40,000 (by some estimates >20,000) of these devices have been implanted (Rauschecker and Shannon, 2002).

These considerations should suffice to convince the reader that, at least to some degree, progress in the development of BMIs can be evaluated by looking at how much information transfer rates were improved over the years of research. In non-invasive BMIs there is a consensus that current limit is ∼0.5 bit/s and it is largely unchanged in the last 10–15 years (Wolpaw et al., 2002; Krusienski et al., 2008; Townsend et al., 2010). This notion is less obvious for invasive BMIs. One problem in this field is that only recently the need for a uniform measure of information content has been more widely recognized and employed in the result description (Li et al., 2009; Simeral et al., 2011; Gilja et al., 2012; Flint et al., 2013). Although to calculate the information content of a behavioral task the information theory allows the use of almost any movement parameter such as the target number or the target coordinate (Tonet et al., 2008; Tehovnik et al., 2013), to have a meaningful comparison of BMI performance in different tasks, the comparison that permits to decide which algorithm, parameter choice or configuration of BMI is better, we need to take into account the difficulty of task. The concept of difficulty can be easily explained in a center-out reaching task (Taylor et al., 2002; Hochberg et al., 2006), in which a subject has to reach from the monitor center a target located some distance from the initial position. Although it is possible to take the logarithm of the number of targets as the information content of such a task, intuitively it seems obvious that larger targets are easier to reach. Fitts' studies for one-dimensional tasks of this type confirmed that target size but not number of targets determines how long it takes to reach the target (Fitts, 1954). He introduced an index of difficulty, defined as

$$I_d = -log_2 \frac{W_s}{2A}\ bits/response,$$

where W_s is the target size ("tolerance range" in the original paper) and A is the average amplitude of movements, corresponding to the average distance to the target. Importantly, Fitts showed that for this measure of difficulty the limit of human performance was always the same, 10 bits/s, independent of target size, distance to the target etc. Thus, if this index of difficulty is used as the information content of the task, then differences in center-out task performance should indicate differences in the BMI performance but not the task difficulty. Although attempts were made to extend this method to 2D and 3D tasks (MacKenzie and Buxton, 1992), there is no consensus what difficulty measure should be used in such cases. Recently an alternative approach has been suggested, SNR, a logarithm of the ratio of the actual value variance to the mean squared error of the predicted values (Li et al., 2009). It is reminiscent of the index of difficulty, where target size is substituted by the mean square of the predicted values and the average amplitude of movements by the actual value variance. However, first it has to be demonstrated experimentally that SNR evaluates correctly the difficulty of a behavioral task. SNR is only one possible measure to evaluate BMI performance in motor tasks, one can invent many other measures and the question is what these measures tell us. If exactly the same task is performed by different BMIs, it is straightforward to compare the performance of these BMIs. However, if tasks differ even in a single parameter, be it target presentation time or movement speed, it is much more difficult to compare the performance of these BMIs. We need a measure that represents BMI performance in a task-independent manner, something what Fitts demonstrated for human performance in several different tasks: his difficulty measure returned similar performance values (<20% change) for movement distances covering more than one order of magnitude (Fitts, 1954). If SNR is an objective measure of BMI performance it should produce the same or similar value for all tasks performed by the same BMI; to verify this statement we need experimental data.

For a symmetrical center-out reaching task the above Fitts' formula can be easily applied because distance to all targets is the same. Therefore in this review the analysis of BMI performance is limited to a single behavioral task, the center-out reaching task. Luckily, a sufficiently large number of studies employed this task over the span of more than one decade and the results from probably the best laboratories in the field of BMI can be included (**Figure 2**). The results presented in **Figure 2** show little or no improvement in the information transfer rates over ∼10 years of research except for two data points, marked in red and black (**Figure 2**). These two outliers will be discussed below. If we neglect the outliers, the obvious question is why so much effort resulted in not much improvement in probably the main parameter determining the performance of invasive BMIs? A number of brilliant people were involved in this type of research and there must be a serious reason why we see little progress toward improvement in this key parameter. The next few paragraphs will be devoted to an attempt to answer this question. First the issues of technology will be very briefly explained, with a focus on the question if the current state of computer power, electrode technology impedes to achieve higher information transfer rates. Then an answer to the main question of this paper, how to improve the performance of invasive BMIs, will be sought.

In invasive devices typically >20 of electrodes are used to pick up extracellularly brain signals (Schwartz et al., 2006, 2001). Usually, these brain signals are the so-called "single units," representing action potentials of one or few neurons (Harris et al., 2000). When more than one single-unit is present in the trace from one electrode, spike sorting procedure is employed for their separation (Lewicki, 1998). In some cases local field potentials and multi-unit signals are also used for BMIs, these signals represent large populations of neurons (Andersen et al., 2004; Buzsáki et al., 2012; Aggarwal et al., 2013). How much information can be present in such recordings and how does the recording technology limit this amount of information?

It is much debated how much information a single action potential encodes. In visual system information rates up to ∼1 bit/spike and >10 bit/s have been reported (Buracas et al., 1998). If all recorded single neurons were independent with no correlation between their action potential firing times, 10 neurons would correspond to 10 independent information channels and suffice to achieve information transfer rates of >100 bit/s (10 × 10). This rate is many orders of magnitude higher than typical rates of 1–2 bit/s achieved in invasive BMIs (**Figure 2**). In visual system

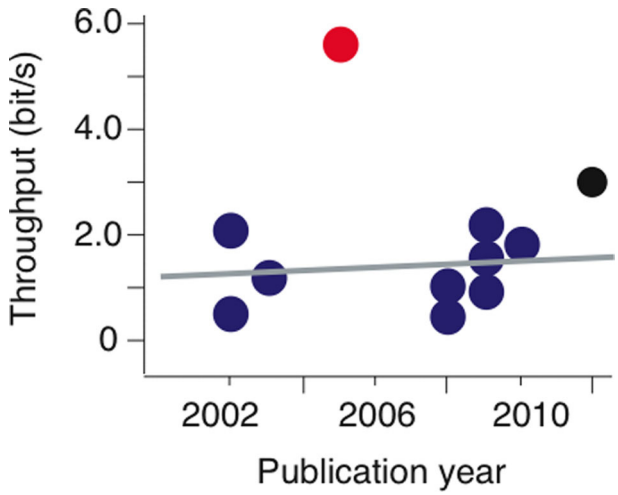

FIGURE 2 | Information transfer rates or throughput estimated for center-out reaching task (blue and black circles) and for "GO" cue task (red circle) in BMI papers. Most data were taken from supplemental material of Gilja et al. (2012) while the "GO" cue data are for Santhanam et al. (2006) study. The line represents a linear fit for all blue data points; there was no significant increase in information transfer rates in this time period.

neurons seem to be rather independent in information coding (Ecker et al., 2010), suggesting that potentially the information transfer rates that can be achieved with tens of recorded neurons in invasive BMIs is huge, well above the required 10 bits/s for fluent interaction with humans (see above) and magnitudes of order higher than currently achieved rates. One explanation for low information transfer rates achieved in current invasive BMIs could be that in motor systems only relatively few neurons encode large amounts of information and correlation between neurons is sufficiently high to reduce the amount of information encoded by the whole neuronal population (Carmena et al., 2003; Lebedev et al., 2008; Ecker et al., 2010). This inference is supported by the fact that for BMI control the pooled single unit information content is not much higher than the one found in the local field potential and multiunit signals, which are presumably the averages of large neuronal populations and individual differences of neurons are canceled out (Buzsáki et al., 2012; Aggarwal et al., 2013). In fact one of the best BMI performances in the terms of information transfer rates was achieved with no spike sorting, i.e., no neuron separation at each single electrode was used (Gilja et al., 2012).

One may argue that, since spike sorting procedure requires relatively high signal-to-noise ratio (Lewicki, 1998), low signal-to-noise ratio obtained with electrode arrays may result in poorly-separated single units, containing action potentials from more than one neuron, and the real independence of single neurons will be masked by such a contaminated single neuron signal (Ecker et al., 2010). However, in electrode arrays each recording site is sufficiently distant ($>150\,\mu m$) from the other recording sites to ensure that no action potentials from the same neuron will be recorded by two recordings sites (Henze et al., 2000). Nevertheless, in electrode arrays correlation has been observed even for single units from different recording sites, corresponding to distinct, non-overlapping neuronal signals, thus it is unlikely that signal quality can account for relatively strong correlation between single units in motor system (Nicolelis and Lebedev, 2009; Ifft et al., 2013). These correlations between single units changed during learning to perform motor tasks, a clear indication that they are genuine and related to the motor control (Ifft et al., 2013). Finally, one of the best BMI performances in the terms of information transfer rates was achieved with no spike sorting, indicating that recorded single unit signal quality was not a limiting factor (Gilja et al., 2012). Thus it can be concluded that it is unlikely that insufficient quality of the electrode signal or amplification and filtration of the electrode signal limits the performance of current BMIs.

Another limitation of current technology is the number of simultaneously supported channels, usually it is the number of electrodes employed and the number of signal channels amplified and processed. The largest current systems can support up to 256 independent channels (Blackrock Microsystems, Salt Lake City, USA) while the largest electrode arrays may contain up to 96 electrodes. In one of the first papers on invasive BMIs it has been claimed that an almost unlimited accuracy of limb movement predictions could be achieved by increasing the number of recorded neurons (Wessberg et al., 2000). It was estimated that 400–500 of simultaneously recorded neurons would permit to achieve 90% accuracy. However, as the number of electrodes and simultaneously recorded neurons increased, the obtained data suggest no dramatic improvement beyond the first 40–100 neurons (Carmena et al., 2003; supplementary material in Gilja et al., 2012). Recently, based on a more extensive dataset, a logarithmic dependence of BMI performance (measured as SNR, see above) on the number of recorded neurons has been proposed (Lebedev and Nicolelis, 2011). It can be shown that essentially it is the same relationship suggested previously (Wessberg et al., 2000). It is asserted that with >10,000 of neurons the BMI performance would be on par with native hand (Lebedev and Nicolelis, 2011). Obviously the final proof of this claim will be an experiment with >10,000 recorded neurons. For now, several cautionary remarks can be made. The log/log scale is deceiving when a relatively narrow range of values is used, less than two orders of magnitude for recorded neuron numbers (from 2–3 to <200) and less than one order for SNR (from 0 to ~8 in $10^*\log_{10}$ scale, corresponding to 1–6.3, Figure 2 in Lebedev and Nicolelis, 2011); we still need to see if the same relationship holds for additional >2 orders for neuronal numbers and ~2 orders for SNR. Second, the graph is based on data tracking monkey walking, it is a stereotyped repetitive movement and it is not clear if the same relationship will hold for voluntary movements. One more note on the neuronal numbers regards neuron selection process in planar electrode arrays that are employed in most invasive BMIs of today. Since in such an array all electrodes are permanently fixed to the same platform it is impossible to adjust the penetration depth individually resulting in suboptimal location of electrode tips. It has been claimed that this is a serious issue that may compromise dramatically the BMI performance (Mulliken et al., 2008). In this paper it is shown that a better selection of <10 neurons in BMI with

a flexible array with movable electrodes permits to achieve the same or even better performance than in a BMI with a rigid array and 10 times more recorded single units (∼80). Nevertheless, the achieved performance is not better than reported previously; and probably it is safe to say that at least for the foreseeable future we will not achieve significantly higher information transfer rates by employing much larger arrays if no other changes are introduced.

The final note in support of the statement that currently technology is not a limiting factor in achieving higher information transfer rates in invasive BMIs is the absence of a clear increase in the information transfer rates in the last 10 years although the computer technology and electronics improved significantly, there were also advances in the electrode technology.

Clearly, this analysis on how the recording technology limits the amount of information present in the traces of extracellular electrodes is very brief. Nevertheless, it should be sufficient to state that electrode design, signal amplification and filtration, spike detection and sorting is unlikely to limit the information content present in these traces and there is a hope that the information content could be increased if the number of electrodes is increased >10 times. Then we have to accept the fact that in invasive BMI papers the recorded neurons probably encode only the reported amount of information about the predicted movement parameters. This conclusion is based in part on the fact that, for a given pair of parameters, let's say the neuronal spike rate and the cursor coordinate x, the information theory provides a precise formula to calculate the mutual information which is directly related to the maximal ability to estimate the value of one parameter when we know the value of the second parameter; in our example it would be the ability of the neuronal spike rate to predict the cursor coordinate x (Nelken and Chechik, 2007). Most algorithms that are used for movement control such as Kalman filters are known to efficiently utilize available information and it is unlikely that these algorithms dramatically limit the performance of BMIs. An example of an algorithm that does improve BMI performance nearly two-fold provided here below (Gilja et al., 2012) is largely based on a change of the movement parameters that are used for prediction but not the filters itself, the filters in the study were essentially a modified version of Kalman filter used by others also. We should remember that the information content is always calculated for a certain set of parameters that we want to predict and the information theory does not provide a recipe which parameters we should choose. It is possible in the same neuronal data set to find larger information quantity encoded by neurons if another movement parameter is chosen. To give an example, motor neurons may encode both the velocity and the position of a hand and but more velocity information is usually found in these neurons (Kim et al., 2011; Simeral et al., 2011). Thus, it is crucial to determine behavioral task or movement parameters for which the information quantity encoded by neurons is the highest. Essentially it is equivalent to asking what information the recorded neurons encode.

The presence of significant correlation between the measured parameter and the recorded neuronal activity does not mean that the recorded neuronal population is involved in determination of that parameter; correlation alone does not prove the presence of a causal link (Cramer, 2003; MacKinnon et al., 2007; Guilford and Fruchter, 1973). Actually in one of the papers considered to be a forerunner of the BMI concept (Fetz and Finocchio, 1971; Mussa-Ivaldi and Miller, 2003) the authors were asking very similar question: if we see a correlation between neuronal activity and muscle activity and movements, do these neurons participate in the generation of these movements? Since it was possible to force some neurons to be active when no muscle activity was present, even though just minutes before their activity correlated with the muscle activity, the answer was that correlation alone is not sufficient for such a claim.

BMIs may offer a new way to explore this issue. Intuitively it seems that the most efficient BMI will employ for the device control those parameters that are associated with the highest information content in the recorded neurons; this notion is confirmed by the information theory (Nelken and Chechik, 2007). Below two examples will be discussed to demonstrate how an unorthodox choice of parameters used for prediction enabled a dramatic increase in the information transfer rates in BMI.

One such an example has been reported by Shenoy group for the standard center-out reaching task (Gilja et al., 2012). Although in this case, similarly to the previous BMIs employing the center-out reaching task, the population of recorded neurons predicted the continuous movement parameters such as cursor position and velocity, there was a change in the coordinate system. Instead of trying to predict the cursor velocity with the respect to the observer, in other words instead of using a coordinate system fixed to the observer, it was assumed that the monkey always aims to the target, thus the coordinate axis was rotating toward the target as the cursor moved on. Although this modification was used only to predict cursor movements during algorithm training with brain control, the key fact is that such a modification of training introduced a coordinate system transformation for the velocity estimates. This modification alone significantly improved the information transfer rate in this task by <1 bit/s (less than two-fold). Although a relatively modest improvement, it was sufficient to achieve the best performance in this type of task (black circle in **Figure 2**) and to bring the target reach time to the range similar of the native hand (Gilja et al., 2012). A possible critique of this particular paper can be that apparently no limb fixation was used. In a number of studies it has been shown that there is a decrease in BMI performance following limb fixation (reviewed in Tehovnik et al., 2013). Nevertheless, it should be noted that Gilja and his colleagues demonstrated an improvement in BMI performance that resulted following the introduction of the new algorithm while all other conditions including hand fixation remained unchanged. Hence, the modification of coordinate system for algorithm training was sufficient to improve BMI performance by almost two fold. In addition, the same algorithm was used in an ALS patient with very limited hand movements and the achieved information transfer rate was well above the reported rates for similar patients (Henderson et al., 2013).

In invasive BMIs based on electrode arrays implanted in monkeys, the maximal reported information transfer rate was obtained in a 2006 study performed by the same Shenoy group (red circle in **Figure 2**, Santhanam et al., 2006). In contrast to all previous and most subsequent invasive BMI embodiments in monkeys, in this BMI the recorded neuronal population did

not predict a parameter related to the continuous movement of a cursor such as velocity or coordinates, instead the recorded neuronal population was used to directly predict which target was chosen by the monkey. In the task employed in the study a monkey had to choose a limited number of targets following the "GO" cue and the algorithm predicted which target was chosen, no attempt to identify the movement trajectory was made. This change alone permitted to increase the information transfer rate from typical 0.8–1.5 bit/s to >6 bit/s. Such a >4 bit/s increase corresponds to more than one order increase in the information content. Although care was taken to have no eye movements during the period used to predict which target was chosen, it is clear that the signal used in this study is related to vision- the monkey had first to see the location of the target and then in one way or another this target location in the visual field of the monkey was reflected in the activity of neurons in the pre-motor area of the cortex.

This approach is somehow similar to the one taken in one of the most efficient forms of non-invasive BMIs in the terms of information transfer rates- row-column flickering based spellers (Wolpaw et al., 2002; Krusienski et al., 2008). In these spellers a subject watches a matrix of letters and symbols on a computer screen and each column or row increases in intensity for a brief period of time, 60–100 ms. Following 3–15 repetitions an accuracy >90% can be achieved. In non-invasive BMIs such an approach can routinely achieve information transfer rates of 0.25–0.5 bit/s, only two times less than it is achieved in standard center-out reaching tasks of invasive BMIs (**Figure 2**). Similarly to (Santhanam et al., 2006); most spellers use a vision related signal, either steady state evoked potentials (SSVEPs, reviewed in Vialatte et al., 2010) or P300, which in case of the EEG-based spellers is likely to be related to gaze (Brunner et al., 2010) and is clearly triggered by a visual signal. In spite of this similarity in the origins of the control signal, assuming that the "GO" cue task in Santhanam et al. (2006) and the speller tasks are similar, the invasive BMI is a clear winner with information transfer rates higher by >5 bit/s. This difference (>6 bit/s and 0.5 bit/s) correspond to a >∼40 fold increase in the information transfer rates and only 3–4 bit/s shy of the rates typical for cochlear implants, ∼10 bit/s. Thus, although the signal used by Santhanam and his colleagues is somehow similar to the non-invasive, EEG-based BMI signals P300 and SSVEP (Wolpaw et al., 2002), there is a dramatic difference in information transfer rates between invasive and non-invasive BMIs. May be we are not that far from electrode-array based invasive BMIs suitable for clinical applications?

The last example of an efficient invasive BMI presented here (Santhanam et al., 2006) suggests that the type of information encoded by the recorded neuronal signals in the cortical pre-motor areas is actually very different from what we usually think it is. This cortical area was used by many invasive BMIs although primary motor cortex may better predict upper limb movements (Wessberg et al., 2000; Carmena et al., 2003). It is difficult to compare information content in reaching and grasping tasks because we need to know the statistics of movements with and without BMI control, correlation coefficients alone cannot be directly translated into information content and, as explained above, the new suggested measure SNR (Li et al., 2009; Fitzsimmons et al., 2009) has not been validated experimentally. Although intuitively it may seem that, because of the 3-dimensionality and many degrees of freedom involved, 3D tasks correspond to large information transfer rates, Fitts' and subsequent studies on information content of human reaching movements suggest that a simple ratio of the target size (determined by the variability of the hand movement at the end point) to the distance to the target defines the information content of these movements (Fitts, 1954; MacKenzie and Buxton, 1992). Thus even for 3D tasks the information transfer rates may be similar to the ones present in 1D and 2D tasks, the data on which are shown in **Figure 2**.

If in the 3D-tasks the achieved information transfer rates are similar to the 2D-tasks, few bits per second, then may be these pre-motor neurons encode something that is not directly related to the movement trajectory? At least one study suggests that the answer is yes. It is clear that in Santhanam et al. (2006), study the pre-motor cortex neuronal signal that predicted targets was related to vision even though eyes were fixed during the period used for prediction; this choice of signal permitted to achieve the information transfer rates higher by >3–4 bit/s or by one order of magnitude compared to BMIs predicting movement. If such high information transfer rates can be achieved for a vision-related signal, maybe there is something fundamental that we are missing from the motor signal in primary and pre-motor areas? The "GO" cue permitted synchronization of all neuronal responses and a very brief time window of 250 ms could be used for decoding (Santhanam et al., 2006), something that is impossible to apply for a continuous movement decoding. It has been shown that the first few hundreds of milliseconds contain most information about the movement in the center-out reaching task (Taylor et al., 2003), indicating that after these first moments something is changed. The results of Gilja et al. (2012), suggest that the trick could be the changing coordinate system, in other words neurons encode in a coordinate system that is not fixed with respect to the subject's body/torso but moves together with the hand approaching the target.

It should be noted that, at least in theory, there is an entirely different method to achieve high information transfer rates, at least when we deal with very few neurons. It is the so-called conditional modulation that was used in 70 s (Fetz and Finocchio, 1971; Schmidt et al., 1978). It has been shown that rates up to >1 bit/s can be achieved with a single neuron (in an 8-target task the average time to target was 1.35 s, 97.5% correct, p. 359 in Schmidt et al., 1978). Similar approach was used by Kennedy and his colleagues when a single electrode was implanted in a human patient though much lower information transfer rates were achieved (<0.5 bit/s, Kennedy and Bakay, 1998). In a direct test of this idea in BMI the information transfer rates of 0.2–0.5 bit/s were achieved (Moritz and Fetz, 2011). A further modification of this approach is to directly stimulate muscles by a signal generated by such modulated neuronal activity (Moritz et al., 2008). The main question for this method is, can several neurons or groups of neurons be simultaneously modulated in independent fashion? It is known that monkeys are capable to voluntary modify the firing rates of neighboring neurons in opposite direction (Fetz and Baker, 1973); however it has yet to be shown if the same principle can be applied in BMI with at least 5–10 neurons.

Nevertheless, potentially, such a method could offer very high information transfer rates even with a limited number of channels offered by current recording technologies.

As a final note, it should be added that there are new directions in BMI research that are difficult to evaluate from the point of view of information transfer rates. One such an example can be the recent demonstration that electrical stimulation of sensory areas may provide a sensation of a surface texture (O'Doherty et al., 2011). The difficulty of the task was low- the target size was almost the same as the distance between the targets and the estimated Fitts' difficulty of the task is <1.5 bit. For the achieved travel times between targets >1 s, the estimated information transfer rate was <1.5 bit/s, no improvement over typical rates in the center-out reaching task. However, this analysis misses the fact that in some case, due to brain stimulation, a monkey was able to determine if the target touched by the monkey was correct in less than <0.35 s. Even though it is only a yes or no decision and errors were present, the estimated information transfer rate is >2.5 bit/s. In addition one has to take into account that stimulation was performed in packets at 10 Hz, thus in reality the information transfer rates of >3 bit/s could be present. Furthermore, the texture sensation may be extremely valid for human patients to improve their comfort level with new BMI devices that would make this new technology more acceptable for the patients. The information transfer rates alone cannot be used to evaluate the performance of BMI also in an entirely new trend in BMI research- neuronal restoration (Grosse-Wentrup et al., 2011). Nevertheless, for device control information transfer rates offer a universal measure of BMI performance and may prove to be very useful in better understanding of our brain function.

In summary, the provided examples suggest that we still don't have sufficient understanding about what is encoded in premotor and motor areas of the cortex in order to achieve high rates of information transfer in invasive BMIs. Probably more effort should be devoted to understanding what kind of information is represented in recorded neuronal populations while technology issues seem to be secondary, at least for now. Research on invasive BMIs provides an unparalleled opportunity to test hypothesis on how movements are encoded in the brain. It seems that neurons in cortical pre-motor areas process a significant component of vision- or/and intention-related information that can be used to better predict movements; probably future BMIs should take into account this type of information. It is known that visual feedback is important for accurate hand movements (Saunders and Knill, 2003); in all invasive BMIs subjects can see the position of a cursor or a device. However, during decoding of neuronal signals vision-related or intention-related information is almost never used for invasive BMI control; probably, because it seems to contradict the idea of BMI, namely to predict movements from neuronal activity without other additional information. Since by far the best result in the center-out or similar tasks was achieved in an invasive BMI that does use intention- or/and vision- related information, maybe it is an indication that our brains never tries to predict limb coordinates alone but always combines different types of information and these different types of information are processed by neurons in cortical pre-motor areas and used to reach the desired target. There is nothing new in this idea (Hoshi and Tanji, 2004) and it should be no surprise that the use of intention or vision-related information permitted to Santhanam et al. to achieved maximal rate of 6 bit/s in invasive BMI, not much worse than it is achieved in natural movements, ∼10 bit/s, thus assuring us that one day we will have prosthetic arms, controlled by brain almost as efficiently as we can control our own hands.

ACKNOWLEDGMENTS

This work was funded by the European Social Fund under the Global Grant measure.

REFERENCES

Aggarwal, V., Mollazadeh, M., Davidson, A. G., Schieber, M. H., and Thakor, N. V. (2013). State-based decoding of hand and finger kinematics using neuronal ensemble and LFP activity during dexterous reach-to-grasp movements. *J. Neurophysiol.* 109, 3067–3081. doi: 10.1152/jn.01038.2011

Allison, B. Z., Dunne, S., Leeb, R., Millan, J. D. R., and Nijholt, A. (2012). *Towards Practical Brain-computer Interfaces*. Heidelberg; New York, NY; Dordrecht, London: Springer.

Andersen, R. A., Musallam, S., and Pesaran, B. (2004). Selecting the signals for a brain-machine interface. *Curr. Opin. Neurobiol.* 14, 720–726. doi: 10.1016/j.conb.2004.10.005

Brown, P. F., Pietra, V. J. D., Mercer, R. L., Pietra, S. A. D., and Lai, J. C. (1992). An estimate of an upper bound for the entropy of english. *Comput. Linguist.* 18, 31–40.

Brunner, P., Joshi, S., Briskin, S., Wolpaw, J. R., Bischof, H., and Schalk, G. (2010). Does the "P300" speller depends on eye gaze? *J. Neural. Eng.* 7, 056013. doi: 10.1088/1741-2560/7/5/056013

Buracas, G. T., Zador, A. M., DeWeese, M. R., and Albright, T. D. (1998). Efficient discrimination of temporal patterns by motion-sensitive neurons in primate visual cortex. *Neuron* 20, 959–969. doi: 10.1016/S0896-6273(00)80477-8

Buzsáki, G., Anastassiou, C. A., and Koch, C. (2012). The origin of extracellular fields and currents–EEG, ECoG, LFP and spikes. *Nat. Rev. Neurosci.* 13, 407–420. doi: 10.1038/nrn3241

Carmena, J. M., Lebedev, M. A., Crist, R. E., O'Doherty, J. E., Santucci, D. M., Dimitrov, D. F., et al. (2003). Learning to control a brain-machine interface for reaching and grasping by primates. *PLoS Biol.* 1:E42. doi: 10.1371/journal.pbio.0000042

Chapin, J. K., Moxon, K. A., Markowitz, R. S., and Nicolelis, M. A. (1999). Real-time control of a robot arm using simultaneously recorded neurons in the motor cortex. *Nat. Neurosci.* 2, 664–670. doi: 10.1038/10223

Cramer, D. (2003). A cautionary tale of two statistics: partial correlation and standardized partial regression. *J. Psychol.* 137, 507–511. doi: 10.1080/00223980309600632

Dunn, C. C., Noble, W., Tyler, R. S., Kordus, M., Gantz, B. J., and Ji, H. (2010). Bilateral and unilateral cochlear implant users compared on speech perception in noise. *Ear Hear.* 31, 296–298. doi: 10.1097/AUD.0b013e3181c12383

Ecker, A. S., Berens, P., Keliris, G. A., Bethge, M., Logothetis, N. K., and Tolias, A. S. (2010). Decorrelated neuronal firing in cortical microcircuits. *Science* 327, 584–587. doi: 10.1126/science.1179867

Fatourechi, M., Bashashati, A., Ward, R. K., and Birch, G. E. (2007). EMG and EOG artifacts in brain computer interface systems: a survey. *J. Clin. Neurophysiol.* 118, 480–494. doi: 10.1016/j.clinph.2006.10.019

Fetz, E. E., and Baker, M. A. (1973). Operantly conditioned patterns on precentral unit activity and correlated responses in adjacent cells and contralateral muscles. *J. Neurophysiol.* 36, 179–204.

Fetz, E. E., and Finocchio, D. V. (1971). Operant conditioning of specific patterns of neural and muscular activity. *Science* 174, 431–435. doi: 10.1126/science.174.4007.431

Fitts, P. M. (1954). The information capacity of the human motor system in controlling the amplitude of movement. *J. Exp. Psychol.* 47, 381–391. doi: 10.1037/h0055392

Fitzsimmons, N. A., Lebedev, M. A., Peikon, I. D., and Nicolelis, M. A. (2009). Extracting kinematic parameters for monkey bipedal walking from cortical neuronal ensemble activity (2009). *Front. Integr. Neurosci.* 3:3. doi: 10.3389/neuro.07.003.2009

Flint, R. D., Wright, Z. A., Scheid, M. R., and Slutzky, M. W. (2013). Long term, stable brain machine interface performance using local field potentials and multiunit spikes. *J. Neural Eng.* 10, 056005. doi: 10.1088/1741-2560/10/5/056005

Gilja, V., Nuyujukian, P., Chestek, C. A., Cunningham, J. P., Yu, B. M., Fan, J. M., et al. (2012). A high-performance neural prosthesis enabled by control algorithm design. *Nat. Neurosci.* 15, 1752–1757. doi: 10.1038/nn.3265

Grosse-Wentrup, M., Mattia, D., and Oweiss, K. (2011). Using brain-computer interfaces to induce neural plasticity and restore function. *J. Neural Eng.* 8:025004. doi: 10.1088/1741-2560/8/2/025004

Guilford, J. P., and Fruchter, B. (1973). *Fundamental Statistics in Psychology and Education*. 5th Edn. New York, NY: McGraw-Hill Book Co.

Harris, K. D., Henze, D. A., Csicsvari, J., Hirase, H., and Buzsáki, G. (2000). Accuracy of tetrode spike separation as determined by simultaneous intracellular and extracellular measurements. *J. Neurophysiol.* 84, 401–414.

Haselager, P. (2013). Did I do that? Brain–computer interfacing and the sense of agency. *Minds Mach.* 23, 405–418. doi: 10.1007/s11023-012-9298-7

Henderson, J. M., Giljam V., Pandarinath, C., Blabe, C., Hochberg, L. R., and Shenoy, K. V. (2013). High performance computer cursor control using neuronal ensemble recordings from the motor cortex of a person with ALS. *Neurosurgery* 60, 184. doi: 10.1227/01.neu.0000432784.58847.74

Henze, D. A., Borhegyi, Z., Csicsvari, J., Mamiya, A., Harris, K. D., and Buzsáki, G. (2000). Intracellular features predicted by extracellular recordings in the hippocampus *in vivo*. *J. Neurophysiol.* 84, 390–400.

Hochberg, L. R., Bacher, D., Jarosiewicz, B., Masse, N. Y., Simeral, J. D., Vogel, J., et al. (2012). Reach and grasp by people with tetraplegia using a neurally controlled robotic arm. *Nature* 485, 372–375. doi: 10.1038/nature11076

Hochberg, L. R., Serruya, M. D., Friehs, G. M., Mukand, J. A., Saleh, M., Caplan, A. H., et al. (2006). Neuronal ensemble control of prosthetic devices by a human with tetraplegia. *Nature* 442, 164–171. doi: 10.1038/nature04970

Hoshi, E., and Tanji, J. (2004). Functional specialization in dorsal and ventral premotor areas. *Prog. Brain Res.* 143, 507–511. doi: 10.1016/S0079-6123(03)43047-1

Humphrey, D. R., Schmidt, E. M., and Thompson, W. D. (1970). Predicting measures of motor performance from multiple cortical spike trains. *Science* 170, 758–762. doi: 10.1126/science.170.3959.758

Ifft, P. J., Shokur, S., Lebedev, M. A., and Nicolelis, M. A. (2013). A brain-machine interface enables bimanual arm movements in monkeys. *Sci. Transl. Med.* 5, 210ra154. doi: 10.1126/scitranslmed.3006159

Judy, J. W. (2012). Neural interfaces for upper-limb prosthesis control: opportunities to improve long-term reliability. *IEEE Pulse* 3, 57–60. doi: 10.1109/MPUL.2011.2181026

Kennedy, P. R., and Bakay, R. A. (1998). Restoration of neural output from a paralyzed patient by a direct brain connection. *Neuroreport* 9, 1707–1711. doi: 10.1097/00001756-199806010-00007

Kennedy, P. R., Bakay, R. A., Moore, M. M., and Adams, K. (2000). Direct control of a computer from the human central nervous system. *IEEE Trans. Rehabil. Eng.* 8, 198–202. doi: 10.1109/86.847815

Kennedy, P. R., Bakay, R. A., and Sharpe, S. M. (1992). Behavioral correlates of action potentials recorded chronically inside the Cone Electrode. *Neuroreport* 3, 605–608. doi: 10.1097/00001756-199207000-00015

Kim, S.-P., Simeral, J. D., Hochberg, L. R., Donoghue, J. P., and Black, M. J. (2008). Neural control of computer cursor velocity by decoding motor cortical spiking activity in humans with tetraplegia. *J. Neural Eng.* 5, 455–476. doi: 10.1088/1741-2560/5/4/010

Kim, S.-P., Simeral, J. D., Hochberg, L. R., Donoghue, J. P., Friehs, G. M., and Black, M. J. (2011). Point-and-click cursor control with an intracortical neural interface system by humans with tetraplegia. *IEEE Trans. Neural Syst. Rehabil. Eng.* 19, 193–203. doi: 10.1109/TNSRE.2011.2107750

Klobassa, D. S., Vaughan, T. M., Brunner, P., Schwartz, N. E., Wolpaw, J. R., Neuper, C., et al. (2009). Toward a high-throughput auditory P300-based brain-computer interface. *Clin. Neurophysiol.* 120, 1252–1261. doi: 10.1016/j.clinph.2009.04.019

Krusienski, D. J., Sellers, E. W., McFarland, D. J., Vaughan, T. M., and Wolpaw, J. R. (2008). Toward enhanced P300 speller performance. *J. Neurosci. Methods* 167, 15–21. doi: 10.1016/j.jneumeth.2007.07.017

Lebedev, M. A., and Nicolelis, M. A. L. (2006). Brain-machine interfaces: past, present and future. *Trends Neurosci.* 29, 536–546. doi: 10.1016/j.tins.2006.07.004

Lebedev, M. A., and Nicolelis, M. A. L. (2011). Toward a whole-body neuroprosthetic. *Prog. Brain Res.* 194, 47–60. doi: 10.1016/B978-0-444-53815-4.00018-2

Lebedev, M. A., O'Doherty, J. E., and Nicolelis, M. A. (2008). Decoding of temporal intervals from cortical ensemble activity. *J. Neurophysiol.* 99, 166–186. doi: 10.1152/jn.00734.2007

Lewicki, M. S. (1998). A review of methods for spike sorting: the detection and classification of neural action potentials. *Netw. Bristol Engl.* 9, R53–R78. doi: 10.1088/0954-898X/9/4/001

Li, Z., O'Doherty, J. E., Hanson, T. L., Lebedev, M. A., Henriquez, C. S., and Nicolelis, M. A. L. (2009). Unscented Kalman filter for brain-machine interfaces. *PLoS ONE* 4:e6423. doi: 10.1371/journal.pone.0006243

MacKenzie, I. S., and Buxton, W. (1992). "Extending Fitts Law to two-dimensional tasks," in *Proceedings of the SIGCHI Conference on Human Factors in Computing Systems, series CHI '92*, (New York, NY: ACM), 219–226. doi: 10.1145/142750.142794

MacKinnon, D. P., Fairchild, A. J., and Fritz, M. S. (2007). Mediation analysis. *Annu. Rev. Psychol.* 58, 593–614. doi: 10.1146/annurev.psych.58.110405.085542

Moller, A. R. (2006). "History of cochlear impalnts and auditory brainstem implants," in *Cohlear and Brainstem Implants. Adv. Otorhinolaryngology.* (Basel: Karger), 1–10.

Moritz, C. T., and Fetz, E. E. (2011). Volitional control of single cortical neurons in a brain machine interface. *J. Neural. Eng.* 8, 025017. doi: 10.1088/1741-2560/8/2/025017

Moritz, C. T., Perlmutter, S. I., and Fetz, E. E. (2008). Direct control of paralyzed muscles by cortical neurons. *Nature* 456, 639–643. doi: 10.1038/nature07418

Mulliken, G. H., Musallam, S., and Andersen, R. A. (2008). Decoding trajectories from posterior parietal cortex ensembles. *J. Neurosci.* 28, 12913–12926. doi: 10.1523/JNEUROSCI.1463-08.2008

Mussa-Ivaldi, F. A., and Miller, L. E. (2003). Brain-machine interfaces: computational demands and clinical needs meet basic neuroscience. *Trends Neurosci.* 26, 329–334. doi: 10.1016/S0166-2236(03)00121-8

Navarro, X., Krueger, T. B., Lago, N., Micera, S., Stieglitz, T., and Dario, P. (2005). A critical review of interfaces with the peripheral nervous system for the control of neuroprostheses and hybrid bionic systems. *J. Peripher. Nerv. Syst.* 10, 229–258. doi: 10.1111/j.1085-9489.2005.10303.x

Nelken, I., and Chechik, G. (2007). Information theory in auditory research. *Hear. Res.* 229, 94–105. doi: 10.1016/j.heares.2007.01.012

Nicolelis, M. A. L., and Lebedev, M. A. (2009). Principles of neural ensemble physiology underlying the operation of brain-machine interfaces. *Nat. Rev. Neurosci.* 10, 530–540. doi: 10.1038/nrn2653

O'Doherty, J. E., Lebedev, M. A., Ifft, P. J., Zhuang, K. Z., Shokur, S., Bleuler, H. et al. (2011). Active tactile exploration using a brain-machine-brain interface. *Nature* 479, 228–231. doi: 10.1038/nature10489

Oskoei, M. A., and Hu, H. (2007). Myoelectric control systems- a survey. *Biomed. Signal Process. Control* 2, 275–294. doi: 10.1016/j.bspc.2007.07.009

Rauschecker, J. P., and Shannon, R. V. (2002). Sending sound to the brain. *Science* 295, 1025–1029. doi: 10.1126/science.1067796

Santhanam, G., Ryu, S. I., Yu, B. M., Afshar, A., and Shenoy, K. V. (2006). A high-performance brain-computer interface. *Nature* 442, 195–198. doi: 10.1038/nature04968

Saunders, J. A., and Knill, D. C. (2003). Humans use continuous visual feedback from the hand to control fast reaching movements. *Exp. Brain Res.* 152, 341–352. doi: 10.1007/s00221-003-1525-2

Schmidt, E. M., McIntosh, J. S., Durelli, L., and Bak, M. J. (1978). Fine control of operantly conditioned firing patterns of cortical neurons. *Exp. Neurol.* 61, 349–369. doi: 10.1016/0014-4886(78)90252-2

Schwartz, A. B., Cui, X. T., Weber, D. J., and Moran, D. W. (2006). Brain-controlled interfaces: movement restoration with neural prosthetics. *Neuron* 52, 205–220. doi: 10.1016/j.neuron.2006.09.019

Schwartz, A. B., Taylor, D. M., and Tillery, S. I. (2001). Extraction algorithms for cortical control of arm prosthetics. *Curr. Opin. Neurobiol.* 11, 701–707. doi: 10.1016/S0959-4388(01)00272-0

Shannon, C. E. (1948). Mathematical theory of communication. *Bell Syst. Tech. J.* 27, 379–423, 623–656. doi: 10.1002/j.1538-7305.1948.tb00917.x

Simeral, J. D., Kim, S.-P., Black, M. J., Donoghue, J. P., and Hochberg, L. R. (2011). Neural control of cursor trajectory and click by a human with tetraplegia 1000 days after implant of an intracortical microelectrode array. *J. Neural Eng.* 8, 025027. doi: 10.1088/1741-2560/8/2/025027

Surakka, V., Illi, M., and Isokoski, P. (2004). Gazing and frowning as a new human-computer interaction technique. *ACM Trans. Appl. Percept.* 1, 40–56. doi: 10.1145/1008722.1008726

Taylor, D. M., Tillery, S. I. H., and Schwartz, A. B. (2002). Direct cortical control of 3D neuroprosthetic devices. *Science* 296, 1829–1832. doi: 10.1126/science.1070291

Taylor, D. M., Tillery, S. I. H., and Schwartz, A. B. (2003). Information conveyed through brain-control: cursor versus robot. *IEEE Trans. Neural. Syst. Rehab. Eng.* 11, 195–199. doi: 10.1109/TNSRE.2003.814451

Tehovnik, E. J., Woods, L. C., and Slocum, W. M. (2013). Transfer of information by BMI. *Neuroscience* 255, 134–146. doi: 10.1016/j.neuroscience.2013.10.003

Tonet, O., Marinelli, M., Citi, L., Rossini, P. M., Rossini, L., Megali, G., et al. (2008). Defining brain-machine interface applications by matching interface performance with device requirements. *J. Neurosci. Methods* 167, 91–104. doi: 10.1016/j.jneumeth.2007.03.015

Townsend, G., LaPallo, B. K., Boulay, C. B., Krusienski, D. J., Frye, G. E., Hauser, C. K., et al. (2010). A novel P300-based brain-computer interface stimulus presentation paradigm: moving beyond rows and columns. *Clin. Neurophysiol.* 121, 1109–1120. doi: 10.1016/j.clinph.2010.01.030

Tuisku, O., Surakka, V., Vanhala, T., Rantanen, V., and Lekkala, J. (2012). Wireless Face Interface: using voluntary gaze direction and facial muscle activations for human–computer interaction. *Interact. Comput.* 24, 1–9. doi: 10.1016/j.intcom.2011.10.002

Velliste, M., Perel, S., Spalding, M. C., Whitford, A. S., and Schwartz, A. B. (2008). Cortical control of a prosthetic arm for self-feeding. *Nature* 453, 1098–1101. doi: 10.1038/nature06996

Vialatte, F.-B., Maurice, M., Dauwels, J., and Cichocki, A. (2010). Steady state visually evoked potentials: focus on essential paradigms and future perspectives. *Prog. Neurobiol.* 90, 418–438. doi: 10.1016/j.neurobio.2009.11.005

Wessberg, J., Stambaugh, C. R., Kralik, J. D., Beck, P. D., Laubach, M., Chapin, J. K., et al. (2000). Real-time prediction of hand trajectory by ensembles of cortical neurons in primates. *Nature* 408, 361–365. doi: 10.1038/35042582

Wolpaw, J. R., Birbaumer, N., Heetderks, W. J., McFarland, D. J., Peckham, P. H., Schalk, G., et al. (2000). Brain-computer interface technology: a review of the first international meeting. *IEEE Trans. Rehabil. Eng.* 8, 164–173.

Wolpaw, J. R., Birbaumer, N., McFarland, D. J., Pfurtscheller, G., and Vaughan, T. M. (2002). Brain-computer interfaces for communication and control. *Clin. Neurophysiol.* 113, 767–791. doi: 10.1016/S1388-2457(02)00057-3

Wolpaw, J. R., and McFarland, D. J. (2004). Control of a two-dimensional movement signal by a noninvasive brain-computer interface in humans. *Proc. Natl. Acad. Sci. U.S.A.* 101, 17849–17854. doi: 10.1073/pnas.0403504101

Conflict of Interest Statement: The author declares that the research was conducted in the absence of any commercial or financial relationships that could be construed as a potential conflict of interest.

Received: 31 January 2014; accepted: 09 April 2014; published online: 29 April 2014.
Citation: Baranauskas G (2014) What limits the performance of current invasive brain machine interfaces? Front. Syst. Neurosci. ***8****:68. doi: 10.3389/fnsys.2014.00068*
This article was submitted to the journal Frontiers in Systems Neuroscience.

frontiers in
SYSTEMS NEUROSCIENCE

OPINION ARTICLE
published: 19 November 2013
doi: 10.3389/fnsys.2013.00080

Inter-laminar microcircuits across neocortex: repair and augmentation

Ioan Opris*

Department of Physiology and Pharmacology, Wake Forest University School of Medicine, Winston-Salem, NC, USA
**Correspondence: ioopris@wfubmc.edu*

Edited by:
Mikhail Lebedev, Duke University, USA

Reviewed by:
Manuel Casanova, University of Louisville, USA

Keywords: cortical minicolumn, cortical layer, cortical module, microcircuit, neocortex, repair, brain machine interface, prosthetics

INTRODUCTION

Repair and brain augmentation approaches, such as brain-machine interfaces, neural stimulation and other neural prostheses, have experienced a rapid development during the last decade (Nicolelis et al., 2003; Lebedev and Nicolelis, 2006). Still, only few of these methods target the fine microcircuitry of the brain (Jones and Rakic, 2010; Opris et al., 2012a). Here, it is highlighted the potential employing of inter-laminar recording and microstimulation of cortical microcircuits to build neural prostheses for repair and augmentation of cognitive function. In the future, such microcircuit-based prostheses will provide efficient therapies for patients with neurological and psychiatric disorders. Moreover, it is implied that neural enhancement approaches can be applied to inter-laminar microcircuits across the entire cortex.

CORTICAL MICROCIRCUITS

As proposed by Mountcastle, the primate neocortical circuitry has a modular architecture that subserves a multitude of sensory (visual, auditory, touch), motor, cognitive (attention, memory, decision) and emotional functions (Mountcastle, 1957, 1997; Opris and Bruce, 2005; Shepherd and Grillner, 2010). These modules are composed of elementary building blocks formed by vertical arrangements of cortical neurons, called minicolumns (Szentágothai and Arbib, 1975; Mountcastle, 1997). Within minicolumns, cortical neurons are aggregated into six horizontal layers (or laminae): three supra-granular layers (L1-L3), a granular layer (L4) and two infra-granular layers (L5/L6) (**Figure 1A**). The granular layer receives sensory input from thalamus (Constantinople and Bruno, 2013). The supra-granular layers consist of small pyramidal neurons that form a complex network of intra-cortical connections, particularly the connections to the infra-granular layers of larger pyramidal neurons that generate most of the output from cerebral cortex to other parts of the brain (Buxhoeveden and Casanova, 2002). According to this three stratum functional module, infra-granular layers execute the associative computations elaborated in supra-granular layers (Buxhoeveden and Casanova, 2002; Casanova et al., 2011).

Here, the focus is on inter-laminar cortical microcircuits formed by interconnected pyramidal neurons from the supra-granular and infra-granular layers (Thomson and Bannister, 2003; Opris et al., 2011, 2012a,b, 2013). These microcircuits receive input from neurons in layer L4, which project to L2/3, or through direct thalamic projections to the supragranular layers in the higher-order cortical areas. Neurons in L2/3 then project top-down to L5, where they target specific types of pyramidal cells and inhibitory interneurons. Some L5 neurons project back to L2/3 neurons, forming an inter-laminar loop (Weiler et al., 2008) or back to L4, targeting mostly interneurons (Thomson and Bannister, 2003). The outputs from cortical microcircuits, cortico-striatal projections arise mostly from L5, whereas cortico-thalamic projections arise from L6.

Cortical microcircuits are strikingly similar across the neocortex (hence the term "canonical microcircuits"). It has been suggested that such repeatability in the microcircuit pattern plays a key role in reducing the errors of encoding (Bastos et al., 2012). Some characteristics of microcolumns are specific to particular cortical areas. For example, the thickness of L4 is different across areas (DeFelipe et al., 2012). It is most prominent in sensory areas and the thinnest in the motor cortex. There are also area-specific differences in the topographic connectivity of microcircuits with their cortical and subcortical projection areas (Das and Gilbert, 1995; Kritzer and Goldman-Rakic, 1995; Opris et al., 2013).

INTER-AREA CONNECTIVITY

Cortical microcircuits are connected into a macro-network by cortico-cortical connections, which link areas within the same hemisphere, as well as between hemispheres (Van Essen et al., 1982). This super network subserves the "perception-to-action" cycle—a group of processes that handle environmental stimuli and convert them into actions (Romo et al., 2002; Fuster and Bressler, 2012). Microcircuits within the same hemisphere are interconnected (from low level sensory to high level associative processes) through horizontal connections in lamina 2/3, spanning over many cortical areas (Das and Gilbert, 1995; Kritzer and Goldman-Rakic, 1995; Fuster and Bressler, 2012).

Inter-area connectivity of cortical microcircuits preserves spatial topography suggesting a column-to-column match from one area to another (e.g., **Figure 1B** schematics of V1 projections to prefrontal area 46 through the dorsal visual stream; Goldman-Rakic, 1996). Additionally, the topography is preserved within minicolumns owing to the inter-laminar projections (Opris et al., 2013). Interhemispheric connectivity is formed by neural interconnections of lamina 3b (Jones et al., 1979; Van Essen et al., 1982).

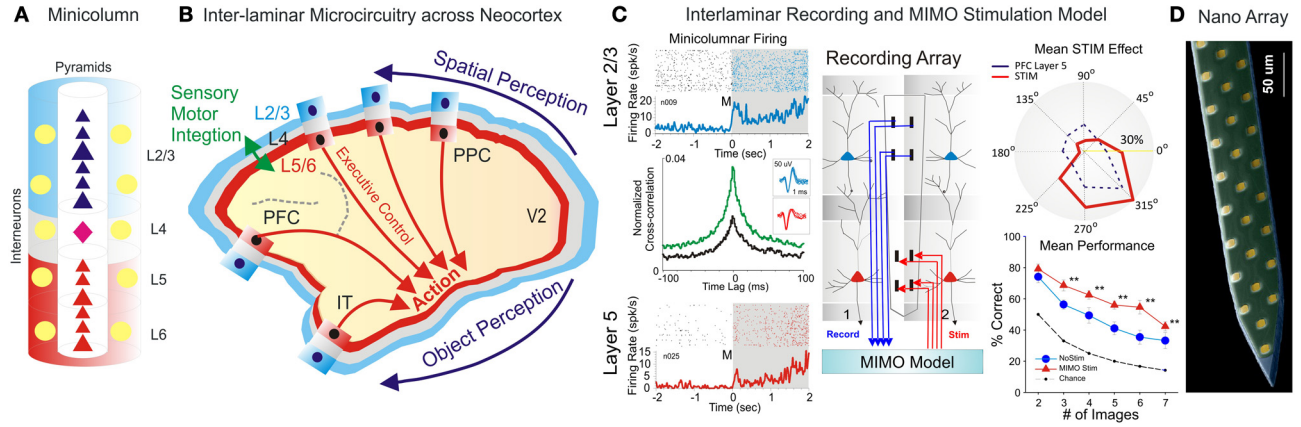

FIGURE 1 | Inter-Laminar Microcircuits across the Neocortex. (A) Cortical minicolumn with pyramidal cells labeled in dark blue for supra-granular layers and red for infra-granular layers. Stellate cells in layer 4 are colored in pink. The "curtain of inhibition" is depicted by interneurons, colored in yellow. **(B)** Primate brain showing the cortical mantle split in cortical layers and minicolumns. Minicolumn across neocortex work cooperatively to translate perception into complex action. **(C)** Interlaminar recording of pyramidal cells and MIMO stimulation model. Rasters and peri-event histograms in blue and red depict the activity of supra-and infra-granular layers. Cross-correlation show that inter-laminar firing increased following the presentation of targets compared to pre-target epoch. Recording array with the MIMO model for recording in layer 2/3 and stimulation in layer 5. Stimulation effect compare the population tuning for MIMO stim (red) vs. layer 5 prefrontal cortical activity (dark blue dotted line). Overall MIMO stimulation effect (red) is significantly greater than no-stim and the chance level (with permission from Opris et al., 2012a,b, 2013). **(D)** Nanoarray for recording neural activity in cortical layers and minicolumns (with permission from Alivisatos et al., 2013). $^{**}p < 0.001$, ANOVA.

MICROCIRCUITS AND COGNITION

Recent research conducted in non-human primates indicates that a variety of sensory, motor and executive functions emerge from the interactions between frontal, parietal, temporal and occipital cortical microcircuits (Atencio and Schreiner, 2010; Buffalo et al., 2011; Takeuchi et al., 2011; Hansen et al., 2012; Opris et al., 2012a,b, 2013; Hirabayashi et al., 2013a,b; Mahan and Georgopoulos, 2013). Moreover, several augmentation approaches based on microcircuits have been implemented. These advances have been possible owing to the development of new multi-electrode arrays (MEA) fitted for recordings from neural elements of cortical columns (Moxon et al., 2004). Thus, MEAs with linear or bi-linear geometry have been successfully employed for simultaneous recordings from supra- and infragranular cortical laminae in adjacent minicolumns, resulting in unprecedented insights into the function of cortical microcircuits (Mo et al., 2011; Opris et al., 2011, 2012a,b, 2013).

A number of recent publications suggest that cortical microcircuits perform elementary computations while cognitive functions are sub-served by a broader network comprising multiple cortical areas (Fuster and Bressler, 2012). For example, elementary computations related to executive control are performed by microcircuits in the prefrontal cortex (Opris et al., 2012a,b), whereas microcircuits of the temporal cortex maintain long term memory (Takeuchi et al., 2011; Hirabayashi et al., 2013a). Prefrontal microcircuits are in a unique and privileged position at the top of sensory-to-motor hierarchy network because they coordinate a multitude of stimuli, perceptions, biases and actions related to such functions as attention, decision making, and working memory. As such, prefrontal microcicuits integrate and synthetize signals over a broad spectrum of perceptual stimuli and various modalities. This integration is performed in supragranular layers, whereas the output of the infra-granular layers provides selection-related signals, which are sent back to the infra-granular layers and the other areas comprising the network. As a matter of fact, signals can reverberate within inter-laminar loops. Thus, cortical microcircuits for long term memory in entorhinal cortex and hippocampal formation employ such reverberating signals (Takeuchi et al., 2011) to integrate relevant information over time (Fuster, 2001).

Our group at Wake Forest University in collaboration with Dr. Berger's team at USC and Dr. Gerhard's group at University of Kentucky, examined the executive function of prefrontal microcircuits (Opris et al., 2012a,b, 2013). We trained rhesus monkeys to select a target (spatial or object) for hand movement, after a memory delay, while the neural activity in prefrontal microcircuits was recorded (**Figure 1C**). Our electrode arrays were specifically designed to record from neurons located in both supra- & infra-granular layers of adjacent minicolumns. We analyzed correlated firing in neurons from the supra- and infra-granular layers. Interestingly, the extent of correlated firing was linked to the accuracy of monkey performance. Correlated firing between cell pairs within single minicolumns was higher during correct selections and reduced in error trials (Opris et al., 2012a). Thus, we discovered that animals make errors when their prefrontal cortical microcircuits do not function properly when handle task relevant information. Additionally, we discovered that during the presentation of the target and during the executive selection of the correct target, assemblies of cell firing in prefrontal layers exhibited similar tuning to target locations on behavioral trials in which this information was important. These studies provided a direct demonstration of real-time

inter-laminar processing of information in prefrontal microcircuits during decision-making (Opris and Bruce, 2005; Opris et al., 2012a).

COGNITIVE ENHANCEMENT APPROACHES BASED ON MICROCIRCUITS

Recent studies have demonstrated that cognitive enhancement can be achieved by microstimulation of specific elements of cortical microcircuits (Opris et al., 2001, 2013; Hampson et al., 2012). These enhancement methods employed a multi-input/multi-output (MIMO) Volterra kernel-based non-linear dynamic model, which was applied to the spatiotemporal patterns of neuronal firing recorded in prefrontal cortical layers L2/3 and L5 to convert the firing of neurons in layer 2/3 into microstimulation patterns applied to layer 5 (Berger et al., 2011; Hampson et al., 2012). MIMO model is based on the principle of multiplexing, where a high rate signal is split into several low rate signals, which are then sent to multiple recipients via multiple channels. Using multiple channels of information transfer MIMO model provides a more reliable communication (**Figure 1C**, right panel).

To perform cognitive augmentation, inter-laminar recordings are analyzed via a non-linear MIMO model, whose output is then converted into patterns of microstimulation (Berger et al., 2011). In these studies, MIMO models used a precise *topographically matched stimulation* by extracting the patterns of firing that relate to the successful behavioral performance. This allowed the substitution of task-related laminar L5 neuron firing patterns with electrical stimulation in the same recording regions during columnar transmission from lamina L2/3 at the time of target selection. Such stimulation improved normal task performance, but more importantly, recovered performance after being impaired by a pharmacological disruption of decision making (Hampson et al., 2012). Moreover, the fact that stimulation-induced spatial preference (in percent correct performance) on spatial trials that was similar to neural tuning indicated that inter-laminar prefrontal microcircuits played causal roles to the executive function (Opris et al., 2005, 2013). These findings provided the first successful demonstration of a microcircuit-based neuroprosthesis designed specifically to restore or repair disrupted cognitive function.

NEUROLOGICAL DISEASES AND MICROCIRCUITS

Disruption of inter-laminar microcircuits within cortical minicolums is a signature of a broad spectrum of neurological and psychiatric disorders, such as autism (Casanova, 2013), schizophrenia (Di Rosa et al., 2009), Alzheimer's disease (Chance et al., 2011) drug addiction (Opris et al., 2012a) and other disorders. The use of both invasive MIMO stimulation (Hampson et al., 2012) and non-invasive transcranial magnrtic stimulation (TMS; Sokhadze et al., 2012) are valuable potential options to repair or treat such dysfunctions. The multitude of deficits in a cortical microcircuit involve the micro-anatomic disconnections between layers or within minicolumns (autism, schizophrenia, Alzheimer), the intra- and inter-laminar neuromodulation (drug addiction, aging), the lack or excess of inhibition (ADHD, depression), etc.

Microcircuit-based neuroprostheses, such as MIMO based memory implants (Berger et al., 2011), and decision chips (Hampson et al., 2012) hold the promise to provide treatment for neurological conditions that result from compromised microcircuits. Targeting cortical microcircuitry may be key to the development of next-generation enhancement methods and medical treatments.

FUTURE DIRECTIONS FOR MICROCIRCUIT-BASED APPROACHES

An emerging approach with broad implications for basic and clinical neuroscience is based on optogenetic stimulation (Gradinaru et al., 2007; Tye and Deisseroth, 2012). Recent developments in optogenetics based on optical manipulation of activity in neural circuits with light-sensitive rhodopsins, such as the *Chlamydomonas* channelrhodopsin-2 (ChR2) are now capable to stimulate the inter-laminar microcircuits at millisecond-scale, with cell type-specific effects of optical perturbations in non-human primates (Diester et al., 2011; Han, 2012), opening up new possibilities for repair and augmentation.

Recent developments in nanotechnological tools and in the design and synthesis of nano-materials have generated optical, electrical, and chemical methods that can readily be adapted for use in neuroscience. Nanotechnology was instrumental to nanofabricated planar electrode array (**Figure 1D**) for high-density neuronal voltage recording (Du et al., 2011; Suyatin et al., 2013). Leveraging micro- and nanofabrication technology raises the prospect for creating vastly greater numbers of electrodes and smaller, less invasive implantable devices. A promising category for brain microcircuits is the planar electrode array (Viventi et al., 2011; Alivisatos et al., 2013), which is patterned on a crystalline, ceramic, or polymer support structure (**Figure 1D**). The recording of neuronal activity with three-dimensional (3D) microelectrode arrays (Zorzos et al., 2012) represents a major advance in brain activity mapping techniques, by providing a tool to probe how intra and inter-laminar/regional neural circuits cooperate to process information. Building prosthetic minicolumns as basic modules to repair the damaged cortical tissue will become a valuable approach in the cognitive neuroprosthetics.

To trace the flow of neural signals in the cortical microcircuits across neocortex, or in the large scale brain networks, analytical tools based on dynamic Bayesian networks and Granger causality are available (Granger, 1969; Smith et al., 2006). These methods allow to identify putative causal interactions and population codes within the neural circuits involved in perception and behavior (Yu et al., 2004; Beck et al., 2008).

Microcircuit-based augmentation could be implemented in several cortical areas, where different functions could be enhanced. Thus, the prefrontal cortical microcircuits involved in attention, working memory, executive decisions and conflict monitoring may be augmented for autism (Casanova et al., 2010), schizophrenia (Chance et al., 2011), drug addiction (Opris et al., 2012a), Alzheimer's or attention deficit disorders.

In conclusion, a better understanding of the function of inter-laminar microcircuits across the neocortex is needed for the

development of treatments for neurological disorders, as well as for the development of methods of brain augmentation.

ACKNOWLEDGMENTS

The author would like to thank Drs. Samuel A. Deadwyler, Mikhail A. Lebedev and Manuel F. Casanova for reading the manuscript and for the valuable insights provided.

REFERENCES

Alivisatos, A. P., Andrews, A. M., Boyden, E. S., Chun, M., Church, G. M., Deisseroth, K., et al. (2013). Nanotools for neuroscience and brain activity mapping. *Nano Focus* 7, 1850–1866. doi: 10.1021/nn4012847

Atencio, C. A., and Schreiner, C. E. (2010). Columnar connectivity and laminar processing in cat primary auditory cortex. *PLoS ONE* 5:e9521. doi: 10.1371/journal.pone.0009521

Bastos, A. M., Usrey, W. M., Adams, R. A., Mangun, G. R., Fries, P., and Friston, K. J. (2012). Canonical microcircuits for predictive coding. *Neuron* 76, 695–711. doi: 10.1016/j.neuron.2012.10.038

Beck, J. M., Ma, W. J., Kiani, R., Hanks, T., Churchland, A. K., Roitman, J., et al. (2008). Probabilistic population codes for Bayesian decision making. *Neuron* 60, 1142–1152. doi: 10.1016/j.neuron.2008.09.021

Berger, T. W., Hampson, R. E., Song, D., Goonawardena, A., Marmarelis, V. Z., and Deadwyler, S. A. (2011). A cortical neural prosthesis for restoring and enhancing memory. *J. Neural Eng.* 8, 046017. doi: 10.1088/1741-2560/8/4/046017

Buffalo, E. A., Fries, P., Landman, R., Buschman, T. J., and Desimone, R. (2011). Laminar differences in gamma and alpha coherence in the ventral stream. *Proc. Natl. Acad. Sci. U.S.A.* 108, 11262–11267. doi: 10.1073/pnas.1011284108

Buxhoeveden, D. P., and Casanova, M. F. (2002). The minicolumn hypothesis in neuroscience. *Brain* 125, 935–951. doi: 10.1093/brain/awf110

Casanova, M. F. (2013). *Neural Mechanisms in Autism, Encyclopedia of autism spectrum disorders.* Heidelberg: Springer.

Casanova, M. F., Ayman El-Baz, A., Vanbogaert, E., Narahari, P., and Switala, A. (2010). A topographic study of minicolumnar core width by lamina comparison between autistic subjects and controls: Possible minicolumnar disruption due to an anatomical element in common to multiple laminae. *Brain Pathol.* 20, 451–458. doi: 10.1111/j.1750-3639.2009.00319.x

Casanova, M. F., Ayman El-Baz., and Switala, A. E. (2011). Laws of conservation as related to brain growth, aging, and evolution: symmetry of the minicolumn. *Front. Neuroanat.* 5:66. doi: 10.3389/fnana.2011.00066

Chance, S. A., Clover, L., Cousijn, H., Currah, L., Pettingill, R., and Esiri, M. M. (2011). Microanatomical correlates of cognitive ability and decline: normal ageing, MCI, and Alzheimer's disease. *Cereb. Cortex* 21, 1870–1878. doi: 10.1093/cercor/bhq264

Constantinople, C. M., and Bruno, R. M. (2013). Deep cortical layers are activated directly from thalamus. *Science* 340, 1591–1594. doi: 10.1126/science.1236425

Das, A., and Gilbert, C. D. (1995). Long-range horizontal connections and their role in cortical reorganization revealed by optical recording of cat primary visual cortex. *Nature* 375, 780–784. doi: 10.1038/375780a0

DeFelipe, J., Markram, H., and Rockland, K. S. (2012). The neocortical column. *Front Neuroanat.* 6, 22. doi: 10.3389/fnana.2012.00005

Di Rosa, E., Crow, T. J., Walker, M. A., Black, G., and Chance, S. A. (2009). Reduced neuron density, enlarged minicolumn spacing and altered ageing effects in fusiform cortex in schizophrenia. *Psychiatry Res.* 166, 102–115. doi: 10.1016/j.psychres.2008.04.007

Diester, I., Kaufman, M. T., Mogri, M., Pashaie, R., Goo, W., Yizhar, O., et al. (2011). An optogenetic toolbox designed for primates. *Nat. Neurosci.* 14, 387–397. doi: 10.1038/nn.2749

Du, J., Blanche, T. J., Harrison, R. R., Lester, H. A., and Masmanidis, S. C. (2011). Multiplexed high density electrophysiology with nanofabricated neural probes. *PLoS ONE* 6:e26204. doi: 10.1371/journal.pone.0026204

Fuster, J. M. (2001). The prefrontal cortex-an update: time is of the essence. *Neuron* 2, 319–333. doi: 10.1016/S0896-6273(01)00285-9

Fuster, J. M., and Bressler, S. L. (2012). Cognit activation: a mechanism enabling temporal integration in working memory. *Trends Cogn. Sci.* 16, 207–218. doi: 10.1016/j.tics.2012.03.005

Goldman-Rakic, P. S. (1996). The prefrontal landscape: implications of functional architecture for understanding human mentation and the central executive. *Philos. Trans. R Soc. Lond. B Biol. Sci.* 351, 1445–1453. doi: 10.1098/rstb.1996.0129

Gradinaru, V., Thompson, K. R., Zhang, F., Mogri, M., Kay, K., Schneider, M. B., et al. (2007). Targeting and readout strategies for fast optical neural control *in vitro* and *in vivo*. *J. Neurosci.* 27, 14231–14238. doi: 10.1523/JNEUROSCI.3578-07.2007

Granger, C. W. J. (1969). Investigating causal relations by econometric models and cross-spectral methods. *Econometrica* 37, 424–438. doi: 10.2307/1912791

Hampson, R. E., Gerhardt, G. A., Marmarelis, V., Song, D., Opris, I., Santos, L., et al. (2012). Facilitation and restoration of cognitive function in primate prefrontal cortex by a neuroprosthesis that utilizes minicolumn-specific neural firing. *J. Neural Eng.* 9:056012. doi: 10.1088/1741-2560/9/5/056012

Han, X. (2012). *In vivo* application of optogenetics for neural circuit analysis. *ACS Chem. Neurosci.* 3, 577–584. doi: 10.1021/cn300065j

Hansen, B. J., Chelaru, M. I., and Dragoi, V. (2012). Correlated variability in laminar cortical circuits. *Neuron*. 76, 590–602. doi: 10.1016/j.neuron.2012.08.029

Hirabayashi, T., Takeuchi, D., Tamura, K., and Miyashita, Y. (2013a). Microcircuits for hierarchical elaboration of object coding across primate temporal areas. *Science.* 341, 191–195. doi: 10.1126/science.1236927

Hirabayashi, T., Takeuchi, D., Tamura, K., and Miyashita, Y. (2013b). Functional microcircuit recruited during retrieval of object association memory in monkey perirhinal cortex. *Neuron* 77, 192–203. doi: 10.1016/j.neuron.2012.10.03

Jones, E. G., Coulter, J. D., and Wise, S. P. (1979). Commissural columns in the sensory-motor cortex of monkeys. *J. Comp. Neurol.* 188, 113–135. doi: 10.1002/cne.901880110

Jones, E. G., and Rakic, P. (2010). Radial columns in cortical architecture: it is the composition that counts. *Cereb. Cortex* 20, 2261–2264. doi: 10.1093/cercor/bhq127

Kritzer, M. F., and Goldman-Rakic, P. S. (1995). Intrinsic circuit organization of the major layers and sublayers of the dorsolateral prefrontal cortex in the rhesus monkey. *J. Comp. Neurol.* 359, 131–143. doi: 10.1002/cne.903590109

Lebedev, M. A., and Nicolelis, M. A. L. (2006). Brain-machine interfaces: past, present and future. *Trends Neurosci.* 29, 536–546. doi: 10.1016/j.tins.2006.07.004

Mahan, M. Y., and Georgopoulos, A. P. (2013). Motor directional tuning across brain areas: directional resonance and the role of inhibition for directional accuracy. *Front. Neural. Circuits* 7:92. doi: 10.3389/fncir.2013.00092

Mo, J., Schroeder, C. E., and Ding, M. (2011). Attentional modulation of alpha oscillations in macaque inferotemporal cortex. *J. Neurosci.* 31, 878–882. doi: 10.1523/JNEUROSCI.5295-10.2011

Mountcastle, V. B. (1957). Modality and topographic properties of single neurons of cat's somatic sensory cortex. *J. Neurophysiol.* 20, 408–434.

Mountcastle, V. B. (1997). The columnar organization of the neocortex. *Brain* 120, 701–722. doi: 10.1093/brain/120.4.701

Moxon, K. A., Leiser, S. C., Gerhardt, G. A., Barbee, K. A., and Chapin, J. K. (2004). Ceramic-based multisite electrode arrays for chronic single-neuron recording. *IEEE Trans. Biomed. Eng.* 51, 647–656. doi: 10.1109/TBME.2003.821037

Nicolelis, M. A., Dimitrov, D., Carmena, J. M., Crist, R., Lehew, G., Kralik, J. D., et al. (2003). Chronic, multisite, multielectrode recordings in macaque monkeys. *Proc. Natl. Acad. Sci. U.S.A.* 100, 11041–11046. doi: 10.1073/pnas.1934665100

Opris, I., Barborica, A., and Ferrera, V. P. (2001). A gap effect during microstimulation in the prefrontal cortex of monkey. *Exp. Brain Res.* 138, 1–7. doi: 10.1007/s002210100686

Opris, I., Barborica, A., and Ferrera, V. P. (2005). Microstimulation of dorsolateral prefrontal cortex biases saccade target selection. *J. Cogn. Neurosci.* 17, 893–904. doi: 10.1162/0898929054021120

Opris, I., and Bruce, C. J. (2005). Neural circuitry of judgment and decision mechanisms. *Brain Res. Rev.* 48, 509–528. doi: 10.1016/j.brainresrev.2004.11.001

Opris, I., Hampson, R. E., Gerhardt, G. A., Berger, T. W., and Deadwyler, S. A. (2012a). Columnar processing in primate pFC: evidence for executive control microcircuits. *J. Cogn. Neurosci.* 24, 2334–2347. doi: 10.1162/jocn_a_00307

Opris, I., Fuqua, J. L., Huettl, P. F., Gerhardt, G. A., Berger, T. W., Hampson, R. E., et al. (2012b). Closing the loop in primate prefrontal cortex: inter-laminar processing. *Front. Neural Circuits* 6:88. doi: 10.3389/fncir.2012.00088

Opris, I., Hampson, R. E., Stanford, T. R., Gerhardt, G. A., and Deadwyler, S. A. (2011). Neural activity in frontal cortical cell layers: evidence for columnar sensorimotor processing. *J. Cogn. Neurosci.* 23, 1507–1521. doi: 10.1162/jocn.2010.21534

Opris, I., Santos, L. M., Song, D., Gerhardt, G. A., Berger, T. W., Hampson, R. E., et al. (2013). Prefrontal cortical microcircuits bind perception to executive control. *Sci. Rep.* 3:2285. doi: 10.1038/srep02285

Romo, R., Hernández, A., Salinas, E., Brody, C. D., Zainos, A., Lemus, L., et al. (2002). From sensation to action. *Behav. Brain Res.* 135, 105–118. doi: 10.1016/S0166-4328(02)00161-4

Shepherd, G., and Grillner, S. (2010). *Handbook of Brain Microcircuits.* Oxford: Oxford University Press.

Smith, V. A., Yu, J., Smulders, T. V., Hartemink, A. J., and Jarvis, E. D. (2006). Computational inference of neural information flow networks. *PLoS Comput. Biol.* 2:e161. doi: 10.1371/journal.pcbi.0020161

Sokhadze, E. M., Baruth, J. M., Sears, L., Sokhadze, G. E., El-Baz, A. S., and Casanova, M. F. (2012). Prefrontal neuromodulation using rTMS improves error monitoring and correction function in autism. *Appl. Psychophysiol. Biofeedback* 37, 91–102. doi: 10.1007/s10484-012-9182-5

Suyatin, D. B., Wallman, L., Thelin, J., Prinz, C. N., Jorntell, H., Samuelson L., et al. (2013). Nanowire-based electrode for acute *in vivo* neural recordings in the brain. *PLoS ONE* 8:e56673. doi: 10.1371/journal.pone.0056673

Szentágothai, J., and Arbib, M. A. (1975). *Conceptual Models of Neural Organization*. Cambridge, MA: MIT Press.

Takeuchi, D., Hirabayashi, T., Tamura, K., and Miyashita, Y. (2011). Reversal of interlaminar signal between sensory and memory processing in monkey temporal cortex. *Science* 331, 1443–1447. doi: 10.1126/science.1199967

Thomson, A. M., and Bannister, A. P. (2003). Interlaminar connections in the neocortex. *Cereb. Cortex* 13, 5–14. doi: 10.1093/cercor/13.1.5

Tye, K. M., and Deisseroth, K. (2012). Optogenetic investigation of neural circuits underlying brain disease in animal models. *Nat. Rev. Neurosci.* 13, 251–266. doi: 10.1038/nrn3171

Van Essen, D., Newsome, W. T., and Bixby, J. L. (1982). The pattern of interhemispheric connections and its relationship to the extrastriate visual area in the macaque monkey. *J. Neurosci.* 2, 265–283.

Viventi, J., Kim, D.-H., Vigeland, L., Frechette, E. S., Blanco, J. A., Kim, Y.-S., et al. (2011). Flexible, foldable, actively multiplexed, high-density electrode array for mapping brain activity *in vivo*. *Nat. Neurosci.* 14, 1599–1605. doi: 10.1038/nn.2973

Weiler, N., Wood, L., Yu, J., Solla, S. A., and Shepherd, G. M. (2008). Top-down laminar organization of the excitatory network in motor cortex. *Nat. Neurosci.* 11, 360–366. doi: 10.1038/nn2049

Yu, J., Smith, V. A., Wang, P. P., Hartemink, A. J., and Jarvis, E. D. (2004). Advances to Bayesian network inference for generating causal networks from observational biological data. *Bioinformatics* 20, 3594–3603. doi: 10.1093/bioinformatics/bth448

Zorzos, A. N., Scholvin, J., Boyden, E. S., and Fonstad, C. G. (2012). Three-dimensional multiwaveguide probe array for light delivery to distributed brain circuits. *Opt. Lett.* 37, 4841–4843. doi: 10.1364/OL.37.004841

Received: 12 October 2013; accepted: 19 October 2013; published online: 19 November 2013.

Citation: Opris I (2013) Inter-laminar microcircuits across neocortex: repair and augmentation. Front. Syst. Neurosci. 7:80. doi: 10.3389/fnsys.2013.00080

This article was submitted to the journal Frontiers in Systems Neuroscience.

frontiers in
SYSTEMS NEUROSCIENCE

OPINION ARTICLE
published: 08 November 2013
doi: 10.3389/fnsys.2013.00077

Canonical circuits of the cerebral cortex as enablers of neuroprosthetics

Manuel F. Casanova*

Gottfried and Gisela Kolb Endowed Chair in Psychiatry, University of Louisville, Louisville, KY, USA
**Correspondence: m0casa02@louisville.edu*

Edited by:
Ioan Opris, Wake Forest University, USA

Keywords: minicolumns, microcircuits, cerebral cortex, neuroprosthetics

> "*. . . each technical advance over the past century has reaffirmed that repeated patterns of structure and function are seen at every level, from molecule to cell to circuit, and that many of these patterns are common across cortical areas and species. In this context, the concept of a canonical circuit, like the concept of hierarchies of processing, offers a powerful unifying principle that links structural and functional levels of analysis across species and different areas of the cortex*"
>
> (Douglas and Martin, 2010, p. 20).

The traditional microscopic assessment by a neuropathologist is usually accomplished by first examining sampled sections at low magnification looking for abnormalities of tissue characteristics and then at higher magnification for abnormalities in the morphometry of individual cellular elements. The presence of pathology is usually ascertained if cells are missing, reduced in size or exhibit aberrant staining properties. These cellular characteristics are not salient findings in many psychiatric conditions such as schizophrenia, autism and bipolar disorders. Given the large number of symptoms that are localizable to the central nervous system, the paradoxical absence of neuropathology in many psychiatric disorders makes us wonder whether we are missing some abnormalities. In other words, it is justifiable to consider whether pathology in these conditions escapes the level of resolution usually assessed by the neuropathologist. Cerebral abnormalities in many psychiatric conditions may not be evident in single cells but rather in units of neurons working together as circuitry. In this regard it is tempting to suggest a chiasm between medical disciplines: that neuronal abnormalities define the pathology of neurological disorders (e.g., Alzheimer's or Parkinson's disease) while those involving circuitry define abnormalities in psychiatric disorders (e.g., autism, schizophrenia).

Some years ago the famous historian of science, Thomas S. Kuhn wrote a popular book and bestseller entitled "The Structure of Scientific Revolution" (Kuhn, 1970). In the book Kuhn made the case that in order for science to advance it needed a "paradigm shift," a change in our way of thinking or in our approach to a problem. In the case of air travel, faster airplanes are not the product of bigger propeller engines that generate increasing thrust; rather, different engines and physical principles account for advancement in air travel. Many modern airplanes are propelled by a gas turbine while rocket engines use the thrust of their own combustion exhaust gas. In similar fashion, major advancements in science are not the result of gradual increments applying the same technology (e.g., bigger propeller engines for air travel), but respond to the introduction of a new way of thinking on an older problem.

For many decades neuroscience has been dominated by the cell theory of Schwann and Schleiden that argued in favor of the existence of a unique type of cell exemplifying the holistic properties of each individual organ. Acceptance of this reductionist approach has been promoted by the explanatory powers derived from the work of such an eminent neuroscientist as Theodor Meynert who used cellular details, as to both form and spatial organization, in order to parcellate the cerebral cortex. Santiago Ramón y Cajal extended this neuronocentric view by providing evidence that favored what would later on be called the "neuronal doctrine." In essence Ramón y Cajal argued that the relationship between neurons was not one of continuity but of contiguity.

The existence of a generalizable neuron with a clear separation between its functional components is an oversimplification. Countless number of neurons exist within the brain differing from one another in terms of size, shape, location and neurotransmission. Contrary to Ramón y Cajal's law of dynamic polarization the dendrites of some neurons may occasionally generate an action potential and axons my bear receptive surfaces. Many neurons throughout the animal kingdom lack axons while others release their neurotransmitters through non-synaptic sites (Casanova, 2010). The plurality of neurons argues against their designation as "individual" elements of the brain (Casanova, 2010).

Although the anatomical evidence prevailed during the ensuing decades it flew against opposition emanating from physiological studies. Sir Charles Sherrington posited the interactive function of neural elements, both excitatory and inhibitory, the simplest of which was the reflex arc. Still, even within a reflex arc, simple actions require the coordinated efforts of many neurons: "The reflex arc consisting of just two neurons is an abstraction . . . Even in systems such as the monosynaptic myotatic reflex in mammals, in which there is one set of afferent and one set of efferent neurons, many neurons are involved" (Brown, 2001, p. 146).

Actions within the nervous system are the result of neuronal ensembles, not of single cellular entities. The concept of cell assemblies acting at any given moment within closed systems was popularized by Donald Hebb in his famous book "The Organization of Behavior" (Hebb, 1957). According to this view, groups of neurons are capable of acting as a closed system and, depending on functional requirements, its individuals components

can participate in different cell assemblies. This interdependence of neurons is evident both *in vivo* as well as *in vitro*.

Cultured neurons are usually derived from stem cells that, depending on need, are later on differentiated into neurons, astrocytes or oligodendrocytes. In the case of neurons scientist can manipulate the culture media to enable cells to generate synapses and myelination. Still, the initial cellular density is critical to the survival of the colony. This factor, called the seeding density, usually varies between 80 and 300 cells/mm^2. We can safely conclude that neurons can't survive and perform their function in isolation. According to Shepherd and Koch, "No matter how complicated a single neuron may be, it cannot play a role in the processing of information without interacting with other neurons" (Shepherd, 2004, p. 27).

It is clear that a single neuron does not represent the holistic properties of the brain nor can it represent the basic unit of function for this organ. Only networks of neurons achieve this distinction. According to the work of the American psychologist and behaviorist Karl Spencer Lashley these networks appear widely distributed throughout the brain. Lashley's work using rat's brains failed to localize the substratum of memory to a particular area of the brain. In effect, he was the first person to spouse, based on his experimental work, the principle of equipotentiality. This principle antedated claims from modern neuroplasticity experiments that if certain parts of the brain are damaged, other regions may take over the function. Equipotentiality in this regard suggests the presence of circuitry capable of performing the same generic operations throughout different parts of the cortex.

The existence of repetitive circuits carrying generic types of operations within the cerebral cortex has been well discussed within the field of neuroanatomy. The nomenclature for this reiterative circuit has shifted through the decades being called either a basic, local or canonical circuit by different authorities (Shepherd, 1974, 1978; Rakic, 1975; Douglas and Martin, 1991). Lorente de No was the first researcher to propose the existence of vertically oriented cellular elements within the cerebral cortex that conjointly acted as a circuit. Lorente de No described these vertically arranged cellular aggregates as follows: "All the elements of the cortex are represented in it, and therefore it may be called an elementary unit, in which, theoretically, the whole process of transmission of impulses from the afferent fiber to the efferent axon may be accomplished" (Lorente de No, 1938). Not surprisingly Lorente de No was honored by the American Philosophical Society with the first Karl Spencer Lashley Award in 1959.

It is noteworthy that most of Lashley's work was performed while at the Johns Hopkins School of Medicine. It was in this academic setting that Stephen Kuffler employed microelectrodes to investigate receptive fields of retinal ganglion cells and their center-surround inhibition. Mountcastle and colleagues refined Kuffler's technique in order to proclaim the landmark discovery of functional cortical columns in the somatosensory cortex of cats and monkeys. The columnar organization proclaimed by Mountcastle was confirmed in two early experiments wherein slanted penetrations, i.e., an angle of 45° to the surface of the brain, demonstrated changes in modality as the microelectrode transversed neighboring tissue (Mountcastle, 1957).

Mountcastle's work indicated the presence of vertically arranged cellular structures with similar electrophysiological properties in different parts of the brain. The findings suggested that the cerebral cortex was more homogenous in its function than previously thought. According to Bach-y-Rita, this meant that, "... any part of the cortex should be able to process whatever electrical signals were sent to it, and that our brain modules were not so specialized after all" (Doidge, 2007, p. 18). Otto Creutzfeld believed that these repetitive neocortical microcircuits processed information in similar manner with the resultant output depending on both the source of information and modulatory influences peculiar to each brain region (Creutzfeldt, 1977). The seminal observations of Mountcastle's were later on expanded upon by two of his disciples: Apostolos Georgopolous and Michael Merzenich.

In the 1980s Apostolos Georgopolous used a population vector model to describe how groups of neurons act as voting circuits by using their firing rates as ballots to define the activity of individual components (Georgopolous et al., 1988). The final vote is tabulated by the vectorial sum of each cell's preferred orientation weighed by their firing rates. This model enabled the encoding of programs in monkeys that translated visual stimuli into reach direction.

Michael Merzenich used microelectrode techniques to show the rapidly changing nature of somatotopic and tonotopic maps in response to environmental exigencies. His notion about how the brain is capable of modifying itself (plasticity) enabled him to lead the cochlear implant team at UCSF (Merzenich et al., 1977). Merzenich's work has shown how artificial stimuli can be used to retrain cortical circuitry respective of brain region. In this regard the plasticity of the brain is dependent on the existence of "on-demand" event-based processing circuits. These cortical circuits are connected in a series of nested positive and negative feedback loops called repetitive or recurrent circuits (Douglas and Martin, 2010).

In recent years, Opris et al. (2012) implemented the use of a unique conformal multielectrode recording array to define the role of interlaminar circuitry within prefrontal cortex minicolumns in task-related target selection in non-human primates. Activation of innate prefrontal cortex minicolumns via the encoded interlaminar correlated firing sequences resulted in improved performance on trials where specific information was required depending on context (Opris et al., 2013). The results indicate interlaminar correlated firing during the decision phase of target selection and provide a direct demonstration of real-time minicolumnar processing during an executive function task. The discovery holds important promise for using minicolumnar circuitry in cognitive prosthetics.

In summary, brain plasticity holds the promise of restoring cognitive functions even when brain tissue has been lost. The use of neuroprosthetics is largely predicated on the existence of generic circuits which can be exapted by artificial stimuli, or in the case of cognitive neuroprosthetics, replaced by integrated circuits capable of processing stimuli in a manner similar

to that normally done by the diseased area of the brain. In this regard, our ability to provide brain-machine interfaces is grounded on a large body of knowledge from pioneering anatomists and physiologists in regards to the microcircuitry of the brain.

REFERENCES

Brown, A. G. (2001). *Nerve Cells and Nervous System: an Introduction to Neuroscience.* 2nd Edn. London: Springer. doi: 10.1007/978-1-4471-0237-3

Casanova, M. F. (2010). Cortical organization: anatomical findings based on systems theory. *Transl. Neurosci.* 1, 62–71. doi: 10.2478/v10134-010-0002-2

Creutzfeldt, O. D. (1977). Generality of the functional structure of the neocortex. *Naturwissenschaften* 64, 507–517. doi: 10.1007/BF00483547

Doidge, N. (2007). *The Brain that Changes Itself.* New York, NY: Viking Penguin.

Douglas, R. J., and Martin, K. A. C. (1991). A functional microcircuit for cat visual cortex. *J. Physiol.* 440, 735–769.

Douglas, R. J., and Martin, K. A. C. (2010). "Canonical cortical circuits," in *Handbook of Brain Microcircuits, Chapter 2,* eds G. M. Shepherd and S. Grillner (Oxford: Oxford University Press), 15–21. doi: 10.1093/med/9780195389883.003.0002

Georgopolous, A. P., Kettner, R. E., and Schwartz, A. B. (1988). Primate motor cortex and free arm movements to visual targets in three-dimensional space. II. Coding of the direction of movement by a neuronal population. *J. Neurosci.* 8, 2928–2937.

Hebb, D. (1957). *The Organization of Behavior: a Neurophysiological Theory.* New York, NY: J Wiley.

Kuhn, T. S. (1970). *The Structure of Scientific Revolution.* 2nd Edn. University of Chicago, IL: Chicago Press. doi: 10.1063/1.1684230

Lorente de No, R. (1938). "The cerebral cortex: architecture, intracortical connections, motor projections," in *Physiology of the Nervous System,* ed J. F. Fulton, (London: Oxford University Press), 274–301.

Merzenich, M. M., White, M. W., Leake, P. A., Schindler, R. A., and Michelson, R. P. (1977). Further progress in the development of multichannel cochlear implants. *Trans. Sect. Otolaryngol. Am. Acad. Ophthalmol. Otolaryngol.* 84, 181–182.

Mountcastle, V. B. (1957). Modality and topographic properties of single neurons of cat's somatic sensory cortex. *J. Neurophysiol.* 20, 408–434.

Opris, I., Hampson, R. E., Gerhardt, G. A., Berger, T. W., and Deadwyler, S. A. (2012). Columnar processing in primate pFC: evidence for executive control microcircuits. *J. Cogn. Neurosci.* 24, 2334–2347. doi: 10.1162/jocn_a_00307

Opris, I., Santos, L., Gerhardt, G. A., Song, D., Berger, T. W., Hampson, R. E., et al. (2013). Prefrontal cortical microcircuits bind perception to executive control. *Sci. Rep.* 3:2285. doi: 10.1038/srep02285

Rakic, P. (ed.). (1975). Local circuit neurons. *NRP Bull.* 3, 291–446.

Shepherd, G. M. (1974). *The Synaptic Organization of the Brain.* New York, NY: Oxford University Press.

Shepherd, G. M. (1978). Microcircuits in the nervous system. *Sci. Am.* 238, 93–103. doi: 10.1038/scientificamerican0278-92

Shepherd, G. M. (ed.). (2004). "Introduction to synaptic circuits," in *The Synaptic Organization of the Brain*, Chapter 1, 5th Edn (New York, NY: Oxford University Press), 1–38.

Received: 16 October 2013; accepted: 16 October 2013; published online: 08 November 2013.

Citation: Casanova MF (2013) Canonical circuits of the cerebral cortex as enablers of neuroprosthetics. Front. Syst. Neurosci. 7:77. doi: 10.3389/fnsys.2013.00077

This article was submitted to the journal Frontiers in Systems Neuroscience.

frontiers in
SYSTEMS NEUROSCIENCE

PERSPECTIVE ARTICLE
published: 06 May 2014
doi: 10.3389/fnsys.2014.00082

Understanding entangled cerebral networks: a prerequisite for restoring brain function with brain-computer interfaces

Emmanuel Mandonnet*[1,2,3] *and Hugues Duffau*[4,5]

[1] *Department of Neurosurgery, Hôpital Lariboisière, Paris, France*
[2] *Department of Neurosurgery, Université Paris Diderot, Paris, France*
[3] *IMNC, UMR 8165, Orsay, France*
[4] *Department of Neurosurgery, Gui de Chauliac Hospital, Montpellier University Medical Center, Montpellier, France*
[5] *Team "Plasticity of Central Nervous System, Stem Cells and Glial Tumors," INSERM U1051, Institute for Neuroscience of Montpellier, Montpellier University Medical Center, Montpellier, France*

Edited by:
Mikhail Lebedev, Duke University, USA

Reviewed by:
Yoshio Sakurai, Kyoto University, Japan
Philip Kennedy, Neural Signals Inc., USA

****Correspondence:***
Hugues Duffau, Department of Neurosurgery, Gui de Chauliac Hospital, Montpellier University Medical Center, 80 Av. Augustin Fliche, 34295 Montpellier, France
e-mail: h-duffau@chu-montpellier.fr

Historically, cerebral processing has been conceptualized as a framework based on statically localized functions. However, a growing amount of evidence supports a hodotopical (delocalized) and flexible organization. A number of studies have reported absence of a permanent neurological deficit after massive surgical resections of eloquent brain tissue. These results highlight the tremendous plastic potential of the brain. Understanding anatomo-functional correlates underlying this cerebral reorganization is a prerequisite to restore brain functions through brain-computer interfaces (BCIs) in patients with cerebral diseases, or even to potentiate brain functions in healthy individuals. Here, we review current knowledge of neural networks that could be utilized in the BCIs that enable movements and language. To this end, intraoperative electrical stimulation in awake patients provides valuable information on the cerebral functional maps, their connectomics and plasticity. Overall, these studies indicate that the complex cerebral circuitry that underpins interactions between action, cognition and behavior should be throughly investigated before progress in BCI approaches can be achieved.

Keywords: brain networks, movement, language, anatomo-functional connectivity, functional restoration, brain-computer interface

INTRODUCTION

Technological advances in electrodes design have opened a number of new possibilities for brain-computer interfaces (BCIs) that decode large-scale neuronal activity (Lebedev and Nicolelis, 2006). It is now feasible to simultaneously record single-unit activity of hundreds of brain neurons, or record local field potentials (LFPs) from several relatively small brain areas. However, these technological achievements are insufficient for a BCI that restores a specific function, unless the *network* of brain areas involved in that function is well understood.

Although localizationist theories of brain function have been influential in the past, it is becoming increasingly clear that they are, out of date and of little use for BCIs (Nicolelis and Lebedev, 2009). Instead of assigning a fixed function to each discrete brain area, the current hodotopical and plastic view on cerebral organization states that brain functions are subserved by multiple cortical areas. These densely areas, interconnected by white matter pathways, work together rather than representing isolated processing units, and constitute a functional network.

Many fundamental issues of such functional networks are under debate. For example, is it possible to subdivide a cognitive task into separate elementary subtasks (performed successively or simultaneously), each associated with a spatially distinct subnetwork? Such spatial separability is supported by the observation of dissociation and double dissociations in patients with focal lesions (Shadmehr and Krakauer, 2008). Direct electrical stimulation (DES) is a powerful methodology for the investigation of spatial separability. For this purpose, DES is applied in awake subjects to induce transient deficits in particular components of cognitive tasks. Here, we review DES studies of motor and language functions and we discuss the relevance of these results to BCIs.

Abbreviations: EMG, electromyogram; BCI, brain computer interface; SMA, supplementary motor area; CMAr, rostral cingulate motor area; CMAv, ventral cingulate motor area; CMAd, dorsal cingulate motor area; PMd, premotor dorsal; PMv, premotor ventral; RCZa, anterior rostral cingulate zone; RCZp, posterior rostral cingulate zone; CCZ, caudal cingulate zone; NMA, negative motor area; IFG, inferior frontal gyrus; VAC, vertical anterior commissure; BMMP, bimanual modulatory motor pathway; DES, direct electrical stimulation; PPTT, pyramid palm tree test; GPi, internal globus pallidum; GPe, external globus pallidum; STN, subthalamic nucleus; SLF, superior longitudinal fasciculus; IFOF, inferior fronto-occipital fasciculus; BCBI, brain-computer-brain interface; BCIm, multiple brain computer interface; DBS, deep brain stimulation; vSMG, ventral supramarginal gyrus.

NETWORKS FOR VOLUNTARY MOVEMENTS

Since the seminal work of Penfield (Penfield and Bolchey, 1937), it has been well known that, under local anesthesia, cortical stimulation of the precentral gyrus evokes movements on the

contra-lateral side of the body. This method reveals a cortical somatotopic map of the body, which is often called a "homunculus". A similar homunculus can be reconstructed from cortical lesion studies. Based on these results, many neurological textbooks have adopted a simplified model of brain function and connectivity, which maps each brain area to a body part and assigns it a fixed function. For example, motor functions are assigned to an area located in the precentral gyrus and called the primary motor cortex (M1). M1 is considered as the lowest level of cortical motor hierarchy because all cortical motor signals converge. M1 then utilizes its somatotopic map to issue commands to spinal motoneurons, to which it is connected through the corticospinal tract, as well as less direct projections relayed by subcortical nuclei.

This model of M1 function is often mimicked by BCIs (Lebedev and Nicolelis, 2006). For example, Hochberg and his colleagues employed a 96-channel microelectrode array implanted in M1 of tetraplegic patients to interface cortical activity and a robotic arm (Hochberg et al., 2012). This study provided an important proof-of-concept demonstration, but the patients were unable to achieve good accuracy in the control of the robotic arm. This observation suggested that recording from M1 only may not be sufficient to capture all details of voluntary movements. One way to improve the performance of such neural prosthesis would be to implant multiple brain areas with recording arrays (BCIm for multiple brain computer interface), coding for distinct subparts of intentional movement, instead of just M1 (Lebedev and Nicolelis, 2006; Nicolelis and Lebedev, 2009). The performance would improve because neuronal signals provided by multiple areas better capture a diversity of neuronal mechanisms involved in programming and execution of voluntary movements. Hence, there is a growing understanding that BCIs may benefit from the recordings of large-scale motor networks and the utilization of such networks' principles.

Important insights on the mechanisms of brain motor networks are provided by DES studies in humans. DES studies are conducted under three types of conditions: (i) pre-operative mapping with 50–60 Hz DES in pharmacoresistant epileptic patients; (ii) 60 Hz bipolar DES of gray and white matter during glioma surgery; and (iii) high-frequency deep brain stimulation (DBS) utilized for treatment of motor and psychiatric disorders. Motor responses can be evoked by DES of various cortical sites. Historically, Penfield and Bolchey (1937) reported that motor responses were not exclusively evoked from the precentral gyrus. For instance, they observed motor responses for about 25% of stimulated locations in the postcentral gyrus. Furthermore, they found that somatosensory responses were not localized to the postcentral gyrus either. They observed sensory responses in 25% of precentral recordings. Thus, these early experiments already questioned the segregation of sensory and motor functions in cortical areas traditionally believed to be purely motor or purely sensory. These results were somehow forgotten, but decisively rediscovered in 1996 (Nii et al., 1996). The functional significance of the mosaic pattern of sensory and motor representations within the primary motor and sensory areas remains to be elucidated.

Adding more sophistication to the function of somatosensory cortex, neurons in the primary motor and sensory areas exhibited responses to visual stimuli (Shokur et al., 2013). One influential theory explains such cross-modal responses in terms of a system of mirror neuron, first described in the premotor cortex of non-human primates and then in humans (Rizzolatti and Craighero, 2004). Mirror neurons respond to actions performed by a different person. Even in M1, neurons respond when a subject watches movement performed by somebody else (Vigneswaran et al., 2013). Despite these neurons having corticospinal projecting axons (pyramidal tract neurons), these M1 modulations do not evoke EMGs during observation only. This is possibly due to the fact that activation of M1 mirror neurons is accompanied by an inhibition of unwanted movement, for example unwanted imitation of the observed movements. Overall, these results indicate that M1 is not exclusively dedicated to motor execution. It has been suggested that M1 neurons that modulate their activity without producing overt movements can be utilized in BCIs (Schieber, 2011).

Apart from M1, motor responses can be evoked by DES applied to premotor areas. Premotor areas have direct connections to M1 *and* to the spinal cord (Dum and Strick, 1991). Premotor areas include four mesial (SMA proper, CMAr, CMAv, CMAd) and two lateral (PMd, PMv) areas (Dum and Strick, 2002). In humans, homologs of the mesial areas have been identified, and named SMA proper, RCZa, RCZp, and CCZ (Picard and Strick, 2001). DES of premotor areas induces movements, sometimes with complex pattern (Fried et al., 1991; Lim et al., 1996; Chassagnon et al., 2008; Basha et al., 2013).

The homologs of PMd and PMv are not clearly defined in humans, and stimulation of these areas often results in movement suppressions, called negative motor effects (Lüders et al., 1995; Mikuni et al., 2006). In negative motor areas (NMA), DES suppresses an ongoing movement on the contralateral side of the body. Such suppression can occur with or without associated speech arrest, and does not result in a loss of consciousness. As recently reviewed (Filevich et al., 2012), cortical NMA in humans have two epicenters: the pre-SMA (bilaterally) and the posterior part of the inferior frontal gyrus (right predominance). Additionally, several studies reported NMAs in PMd and PMv (Mikuni et al., 2006).

The physiological role of cortical NMAs is still debated. The classical interpretation is that 60 Hz stimulation may disturb neuronal networks responsible for sustained execution of movements. In this view, cortical NMAs would sustain the coding of (positive) motor programs that become jammed by DES. An alternative explanation is that these NMAs are physiologically involved in the inhibition of motor action; therefore their activation by DES inhibits movements. Note that pre-SMA and the IFG are not considered as premotor areas, meaning that this inhibition is probably not processed through direct projections to the spinal cord. We suggest that both interpretations are valid. In particular, the negative motor effect commonly elicited by the stimulation of the foot of the pre-central gyrus is likely due to a perturbation in the coding of the motor programs. This area is located just above the sylvian fissure, where Rizzolatti and Craighero reported the mirror neuron area of the ventral premotor cortex (vPMC; Rizzolatti and Craighero, 2004), as suggested in Mikuni et al. (2006). Because of the connections with parietal areas

(Matsumoto et al., 2012, 2007), this site is an ideal candidate for the storage of *state estimation* (see the model of optimal feedback control, Shadmehr and Krakauer (2008)). Hence, 60 Hz signals can be viewed as an increase of the noise in this system, causing motor action to stop (by some yet undiscovered mechanism). On the other hand, there is also evidence that pre-SMA and IFG stimulation effect could be mediated by a direct activation of an inhibiting area (Filevich et al., 2012). In support of such dual mechanism, resection of vPMC induces definitive articulatory deficits if the underlying connectivity is not preserved (van Geemen et al., 2014), while no permanent deficits are observed following a resection of pre-SMA and right IFG.

We next ask how is DES-induced inhibition enacted: is there a decrease in the firing of M1 neurons or is there an increase in the firing in some inhibitory circuits? These details have been recently clarified using white matter stimulation in awake patients undergoing glioma resection. Stimulation within the depth of the posterior SMA and posterior part of middle frontal gyrus (dorsal premotor areas)—more or less at the level of the VAC line in a sagittal plane—stopped an on-going movement (Schucht et al., 2013). It was proposed that the effect was mediated by a direct activation of corticospinal neurons that inhibit motoneurons at the level of a spinal circuitry. This mechanism should not come as a surprise because cortical control over fine movements requires both supra-spinal excitatory and inhibitory modulation of the spinal motoneurons (Filevich et al., 2012). The cortical origin of these fibers fits well with the depth of the pre-central sulcus.

A second pathway, distinct from the previous one, has been shown to generate a specific disruption of bimanual movements, performed either in phase or in anti-phase (Rech et al., 2014). The spatial distribution of the corresponding DES sites is very close to the one cited above for unilateral negative motor responses. They lie close to the VAC line in the sagittal plane and could take their origin in the caudal cingulate zone or in the depth of the pre-central sulcus, and running towards the head of caudate nucleus and the anterior arm of internal capsule (Rech et al., 2014). Based on these studies, the concept of bimanual modulatory motor pathway was introduced, and it was suggested that the stimulated fibers could belong to the subcallosal fasciculus (Kinoshita et al., 2012), also called frontal aslant tract (Catani et al., 2012). But again, it remains currently speculative whether this bilateral inhibitory effect should be interpreted as noise that perturbs the normal functioning of the BMMP or whether DES triggers the physiological inhibitory mechanism of the BMMP.

In addition to DES studies, similar questions have been regarding the action of DBS, stimulation approach widely used to treat movement disorders, such as Parkinson's disease. Here, computer modeling recently provided new insights. In these models, motor signs in parkinsonism are presumed to arise from the *bursting* activity of the GPi, which exerts an inhibitory effect onto the thalamus and compromises the fidelity of thalamocortical relay cells. This mechanism agrees with the recent suggestion that the thalamus is not simply a relay station but rather an active filter of the signals passing through cortico-thalamo-cortical loops, whose function is modulated by the basal ganglia output (Sherman and Guillery, 2011; Crosson, 2013). Computational simulations of the GPe-STN-GPi direct and indirect pathways showed that DBS can restore the thalamocortical transmission through *tonic* inhibition of the thalamocortical cells by GPi inputs, due to the prevention of the low-threshold calcium rebound bursts (Rubin and Terman, 2004; Guo et al., 2008; Rubin et al., 2012). Note that the pathological state is evoked by the *pattern* of activity within the network and not simply an average spiking neuronal rate in an area that correlates with the pathological state. Overall, computer simulation proved to be very helpful for better understanding of such networks.

In summary, we have a relatively good understanding of the motor system in non-human primates, but know very little about the organization and function of motor system in humans. Inferences from non-humans studies do not always hold true in humans. However, there is a growing understanding that motor systems in all primates function as distributed network of areas, each involved in multiple levels of motor control, rather than a collection of areas with specialized functions. Interestingly, DES studies in awake neurosurgical patients have provided important information on the organization of motor system in humans. Additional insights have been provided by computer modeling. We suggest that further research on the motor system in humans will be very beneficial for BCIs.

LANGUAGE NETWORKS

Unraveling the complex neural mechanisms of language is a real challenge. This challenge is even more difficult than the one for motor functions, because non-human primates cannot serve as a model. For many years, our knowledge came from the observations on speech deficits caused by brain lesions. These studies lead to the well-known model that describes a center of speech production (Broca's area), a center of speech comprehension (Wernicke's area), and a putative link between them made by the arcuate fasciculus. Following this model, the first BCI for language function utilized an array of microelectrodes implanted in the speech motor cortex (Kennedy et al., 2011).

Advances in non-invasive functional neuroimaging greatly enhanced our understanding of brain networks involved in language. It is now well recognized that distinct networks can be identified for different language aspects. In particular, a dual stream model of language has been proposed (Hickok and Poeppel, 2007). In this model, a left-lateralized dorsal stream is in charge of articulatory and phonological processes, whereas a bilateral ventral stream plays a central role in semantics. Observations of speech disturbances induced by axonal DES offer a unique tool to validate the model and to refine its axonal anatomical correlates. Indeed, errors induced by DES during a simple picture naming task, in awake patients operated for a glioma, allow to detect which subnetwork is transiently knocked out by the stimulation (Mandonnet et al., 2010). In these experiments, a speech therapist reports on-line the types of errors, e.g., dys- or anarthria, phonemic paraphasia, semantic paraphasia (Duffau et al., 2014). Dysarthria was observed when stimulating the opercular fronto-parietal loop that corresponds to the most lateral branch of superior longitudinal fasciculus (SLF III; Duffau et al., 2003). Phonemic paraphasia were elicited by

stimulation of the arcuate branch of the SLF (Maldonado et al., 2011). Finally, semantic paraphasias were caused by stimulation of the inferior fronto-occipital fasiculus (IFOF; Duffau et al., 2005). On top of that, supramodal semantic abilities can also be tested by adding a semantic association test (PPTT) in the set of intraoperative tasks (Gatignol et al., 2004). Double dissociation patterns can be evidenced by alternating the picture naming test with the PPTT: during stimulation of deepest part of the IFOF, the patient can name the picture without being able to answer the PPTT, and conversely, during stimulation of a more superficial part of the IFOF, the patient has anomia while performing correctly the PPTT (Duffau et al., 2013; Moritz-Gasser et al., 2013). This disruption of semantic association can be viewed in the broader framework of an impairment of the noetic consciousness (Moritz-Gasser et al., 2013). Last but not least, the contextual rule linked to a given task is equally important. For example, the picture naming is not a *per-se* task: one could ask the patient to tell the color of the item, or to categorize items as animate/inanimate. The anatomical correlates of this contextual role and its interplay with the networks mentioned above still have to be discovered, although one can reasonably assume a major role of the deep gray nuclei (Gil Robles et al., 2005) and thalamus (Hebb and Ojemann, 2013).

Finally, studies in glioma patients provide important insights on the plasticity of language networks. Atlases of functional resectability provide a simple way to assign a quantitative value of plastic potential for each brain voxel (Mandonnet et al., 2007; Ius et al., 2011; De Witt Hamer et al., 2013) emphasizing the fundamental role of long-range connections for language processing, especially for the IFOF and SLF on the dominant side.

We suggest that future BCI applications for language function should take into consideration the new views on the neural mechanism of language function. In particular, it is important to consider that language processing is subserved by plastic, delocalized and synchronized networks that handle distinct language components. For example, in a locked-in patient with intact language networks, is it possible to decode words by interfacing a unique site or is it mandatory to use several recording devices, for example, in the phonological and semantic areas? At a first glance, it might seem advantageous to place the device in the speech motor cortex, which is the final encoding stage that generates speech output signal. However, the paradox is that this type of decoding may be way too complex. Indeed, since speech motor cortex encodes words at the level of muscles activity, this encoding includes information indirectly related to the targeted word (the speed, volume, timber at which the word is pronounced), which makes the decoding task very challenging. Hence, it might be much more efficient to interface areas that encode words at a higher level of abstraction, for instance its phonological (sequence of ordered phonemes) or semantic (either language modality dependant or even at the level of an amodal concept) representations. The problem when dealing with the higher level of coding is that the information is distributed over several interconnected areas, and one might not be able to retrieve the target word by recording a single area belonging to the network. One possibility would be to change the design of the electrodes so that we could record the area of convergence of the IFOF or arcuate fasciculus.

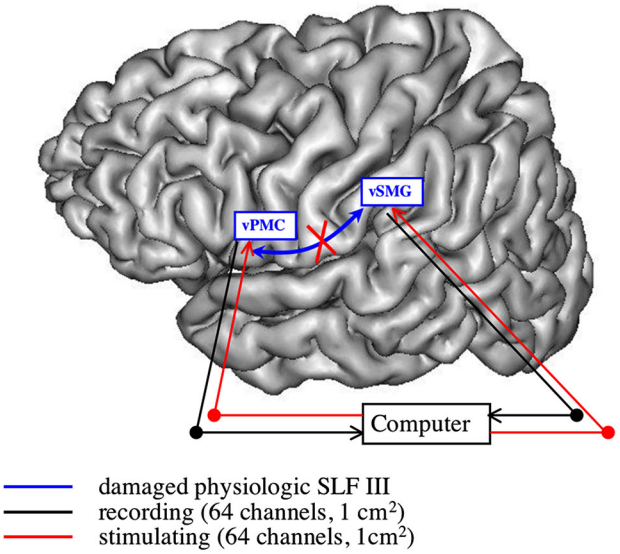

FIGURE 1 | Restoring the articulatory loop following white matter damage. This subnetwork is constituted by the ventral premotor cortex (vPMC) (BA 6) and the (antero-)ventral supramarginal gyrus (vSMG), linked through the third branch of the superior longitudinal fasciculus (SLF III). When this pathway is damaged, with cortical areas still intact, one has to recreate a bidirectional synchronized link: stimulation pattern over one area is computed from the recorded activity in the other area, introducing a time lag (see for example Jackson et al., 2006 for a short-range unidirectional version of such device).

Taking a different perspective, one can also envision BCI devices in aphasic patients following a stroke lesion, especially when one has to restore the long-range communication destroyed by the ischemia of the white matter. One possibility would be to build a brain-computer-brain interface (BCBI): two recording devices would be put in two distant disconnected areas still functional, and the activity of one area would shape the stimulation pattern over the other one, thus restoring a bidirectional synchronized link between both areas (see **Figure 1**).

CONCLUSION

DES studies greatly contributed to unravel the complex issue of separability of motor and language functions. Of note, neural networks subserving mentalizing and emotion can also be mapped with this method (Herbet et al., 2014). Combining this methodology with neuronal recordings (cortico-cortical evoked potentials (Matsumoto et al., 2004, 2007, 2012; Swann et al., 2012; Enatsu et al., 2013)) is currently the best way to characterize anatomically and electrophysiologically each subnetwork underlying an elementary subfunction. However, it is anticipated that computer modeling will play an essential role in the analysis of experimental data. In turn, better knowledge of the electrophysiological activity within a subnetwork will pave the way towards new BCI concepts, including mBCI and BCBI. In summary, the entangled circuits underpinning interactions between action, cognition and

behavior should need to be better understood for BCIs to take a full advantage of brain modulations in a reliable and reasonable way for patients.

REFERENCES

Basha, M. M., Fernández-Baca Vaca, G., and Lüders, H. O. (2013). Mapping of cingulate motor function by cortical stimulation. *Epileptic Disord.* 15, 333–337. doi: 10.1684/epd.2013.0595

Catani, M., Dell'acqua, F., Vergani, F., Malik, F., Hodge, H., Roy, P., et al. (2012). Short frontal lobe connections of the human brain. *Cortex* 48, 273–291. doi: 10.1016/j.cortex.2011.12.001

Chassagnon, S., Minotti, L., Kremer, S., Hoffmann, D., and Kahane, P. (2008). Somatosensory, motor, and reaching/grasping responses to direct electrical stimulation of the human cingulate motor areas. *J. Neurosurg.* 109, 593–604. doi: 10.3171/JNS/2008/109/10/0593

Crosson, B. (2013). Thalamic mechanisms in language: a reconsideration based on recent findings and concepts. *Brain Lang.* 126, 73–88. doi: 10.1016/j.bandl.2012.06.011

De Witt Hamer, P. C., Hendriks, E. J., Mandonnet, E., Barkhof, F., Zwinderman, A. H., and Duffau, H. (2013). Resection probability maps for quality assessment of glioma surgery without brain location bias. *PLoS One* 8:e73353. doi: 10.1371/journal.pone.0073353

Duffau, H., Gatignol, P., Denvil, D., Lopes, M., and Capelle, L. (2003). The articulatory loop: study of the subcortical connectivity by electrostimulation. *Neuroreport* 14, 2005–2008. doi: 10.1097/00001756-200310270-00026

Duffau, H., Gatignol, P., Mandonnet, E., Peruzzi, P., Tzourio-Mazoyer, N., and Capelle, L. (2005). New insights into the anatomo-functional connectivity of the semantic system: a study using cortico-subcortical electrostimulations. *Brain* 128, 797–810. doi: 10.1093/brain/awh423

Duffau, H., Herbet, G., and Moritz-Gasser, S. (2013). Toward a pluri-component, multimodal and dynamic organization of the ventral semantic stream in humans: lessons from stimulation mapping in awake patients. *Front. Syst. Neurosci.* 7:44. doi: 10.3389/fnsys.2013.00044

Duffau, H., Moritz-Gasser, S., and Mandonnet, E. (2014). A re-examination of neural basis of language processing: proposal of a dynamic hodotopical model from data provided by brain stimulation mapping during picture naming. *Brain Lang.* 131, 1–10. doi: 10.1016/j.bandl.2013.05.011

Dum, R. P., and Strick, P. L. (1991). The origin of corticospinal projections from the premotor areas in the frontal lobe. *J. Neurosci.* 11, 667–689.

Dum, R. P., and Strick, P. L. (2002). Motor areas in the frontal lobe of the primate. *Physiol. Behav.* 77, 677–682. doi: 10.1016/s0031-9384(02)00929-0

Enatsu, R., Matsumoto, R., Piao, Z., O'Connor, T., Horning, K., Burgess, R. C., et al. (2013). Cortical negative motor network in comparison with sensorimotor network: a cortico-cortical evoked potential study. *Cortex* 49, 2080–2096. doi: 10.1016/j.cortex.2012.08.026

Filevich, E., Kühn, S., and Haggard, P. (2012). Negative motor phenomena in cortical stimulation: implications for inhibitory control of human action. *Cortex* 48, 1251–1261. doi: 10.1016/j.cortex.2012.04.014

Fried, I., Katz, A., McCarthy, G., Sass, K. J., Williamson, P., Spencer, S. S., et al. (1991). Functional organization of human supplementary motor cortex studied by electrical stimulation. *J. Neurosci.* 11, 3656–3666.

Gatignol, P., Capelle, L., Le Bihan, R., and Duffau, H. (2004). Double dissociation between picture naming and comprehension: an electrostimulation study. *Neuroreport* 15, 191–195. doi: 10.1097/00001756-200401190-00037

Gil Robles, S., Gatignol, P., Capelle, L., Mitchell, M.-C., and Duffau, H. (2005). The role of dominant striatum in language: a study using intraoperative electrical stimulations. *J. Neurol. Neurosurg. Psychiatry* 76, 940–946. doi: 10.1136/jnnp.2004.045948

Guo, Y., Rubin, J. E., McIntyre, C. C., Vitek, J. L., and Terman, D. (2008). Thalamocortical relay fidelity varies across subthalamic nucleus deep brain stimulation protocols in a data-driven computational model. *J. Neurophysiol.* 99, 1477–1492. doi: 10.1152/jn.01080.2007

Hebb, A. O., and Ojemann, G. A. (2013). The thalamus and language revisited. *Brain Lang.* 126, 99–108. doi: 10.1016/j.bandl.2012.06.010

Herbet, G., Lafargue, G., Bonnetblanc, F., Moritz-Gasser, S., Menjot de Champfleur, N., and Duffau, H. (2014). Inferring a dual-stream model of mentalizing from associative white matter fibers disconnection. *Brain* 137, 944–959. doi: 10.1093/brain/awt370

Hickok, G., and Poeppel, D. (2007). The cortical organization of speech processing. *Nat. Rev. Neurosci.* 8, 393–402. doi: 10.1038/nrn2113

Hochberg, L. R., Bacher, D., Jarosiewicz, B., Masse, N. Y., Simeral, J. D., Vogel, J., et al. (2012). Reach and grasp by people with tetraplegia using a neurally controlled robotic arm. *Nature* 485, 372–375. doi: 10.1038/nature11076

Ius, T., Angelini, E., Thiebaut de Schotten, M., Mandonnet, E., and Duffau, H. (2011). Evidence for potentials and limitations of brain plasticity using an atlas of functional resectability of WHO grade II gliomas: towards a "minimal common brain". *Neuroimage* 56, 992–1000. doi: 10.1016/j.neuroimage.2011.03.022

Jackson, A., Mavoori, J., and Fetz, E. E. (2006). Long-term motor cortex plasticity induced by an electronic neural implant. *Science* 444, 56–60. doi: 10.1038/nature05226

Kennedy, P., Andreasen, D., Bartels, J., Ehirim, P., Mao, H., Velliste, M., et al. (2011). Making the lifetime connection between brain and machine for restoring and enhancing function. *Prog. Brain Res.* 194, 1–25. doi: 10.1016/B978-0-444-53815-4.00020-0

Kinoshita, M., Shinohara, H., Hori, O., Ozaki, N., Ueda, F., Nakada, M., et al. (2012). Association fibers connecting the Broca center and the lateral superior frontal gyrus: a microsurgical and tractographic anatomy. *J. Neurosurg.* 116, 323–330. doi: 10.3171/2011.10.JNS11434

Lebedev, M. A., and Nicolelis, M. A. (2006). Brain-machine interfaces: past, present and future. *Trends Neurosci.* 29, 536–546. doi: 10.1016/j.tins.2006.07.004

Lim, S. H., Dinner, D. S., and Lüders, H. O. (1996). Cortical stimulation of the supplementary sensorimotor area. *Adv. Neurol.* 70, 187–197.

Lüders, H. O., Dinner, D. S., Morris, H. H., Wyllie, E., and Comair, Y. G. (1995). Cortical electrical stimulation in humans. The negative motor areas. *Adv. Neurol.* 67, 115–129.

Maldonado, I. L., Moritz-Gasser, S., de Champfleur, N. M., Bertram, L., Moulinié, G., and Duffau, H. (2011). Surgery for gliomas involving the left inferior parietal lobule: new insights into the functional anatomy provided by stimulation mapping in awake patients. *J. Neurosurg.* 115, 770–779. doi: 10.3171/2011.5.JNS112

Mandonnet, E., Jbabdi, S., Taillandier, L., Galanaud, D., Benali, H., Capelle, L., et al. (2007). Preoperative estimation of residual volume for WHO grade II glioma resected with intraoperative functional mapping. *Neuro Oncol.* 9, 63–69. doi: 10.1215/15228517-2006-015

Mandonnet, E., Winkler, P. A., and Duffau, H. (2010). Direct electrical stimulation as an input gate into brain functional networks: principles, advantages and limitations. *Acta Neurochir. (Wien)* 152, 185–193. doi: 10.1007/s00701-009-0469-0

Matsumoto, R., Nair, D. R., Ikeda, A., Fumuro, T., Lapresto, E., Mikuni, N., et al. (2012). Parieto-frontal network in humans studied by cortico-cortical evoked potential. *Hum. Brain Mapp.* 33, 2856–2872. doi: 10.1002/hbm.21407

Matsumoto, R., Nair, D. R., LaPresto, E., Bingaman, W., Shibasaki, H., and Lüders, H. O. (2007). Functional connectivity in human cortical motor system: a cortico-cortical evoked potential study. *Brain* 130, 181–197. doi: 10.1093/brain/awl257

Matsumoto, R., Nair, D. R., LaPresto, E., Najm, I., Bingaman, W., Shibasaki, H., et al. (2004). Functional connectivity in the human language system: a cortico-cortical evoked potential study. *Brain* 127, 2316–2330. doi: 10.1093/brain/awh246

Mikuni, N., Ohara, S., Ikeda, A., Hayashi, N., Nishida, N., Taki, J., et al. (2006). Evidence for a wide distribution of negative motor areas in the perirolandic cortex. *Clin. Neurophysiol.* 117, 33–40. doi: 10.1016/j.clinph.2005.08.021

Moritz-Gasser, S., Herbet, G., and Duffau, H. (2013). Mapping the connectivity underlying multimodal (verbal and non-verbal) semantic processing: a brain electrostimulation study. *Neuropsychologia* 51, 1814–1822. doi: 10.1016/j.neuropsychologia.2013.06.007

Nicolelis, M. A., and Lebedev, M. A. (2009). Principles of neural ensemble physiology underlying the operation of brain-machine interfaces. *Nat. Rev. Neurosci.* 10, 530–540. doi: 10.1038/nrn2653

Nii, Y., Uematsu, S., Lesser, R. P., and Gordon, B. (1996). Does the central sulcus divide motor and sensory functions? Cortical mapping of human hand areas as revealed by electrical stimulation through subdural grid electrodes. *Neurology* 46, 360–367. doi: 10.1212/wnl.46.2.360

Penfield, W., and Bolchey, E. (1937). Somatic motor and sensory representation in the cerebral cortex of man as studied by electrical stimulation. *Brain* 60, 389–443. doi: 10.1093/brain/60.4.389

Picard, N., and Strick, P. L. (2001). Imaging the premotor areas. *Curr. Opin. Neurobiol.* 11, 663–672. doi: 10.1016/s0959-4388(01)00266-5

Rech, F., Herbet, G., Moritz-Gasser, S., and Duffau, H. (2014). Disruption of bimanual movement by unilateral subcortical electrostimulation. *Hum. Brain Mapp.* doi: 10.1002/hbm.22413. [Epub ahead of print].

Rizzolatti, G., and Craighero, L. (2004). The mirror-neuron system. *Annu. Rev. Neurosci.* 27, 169–192. doi: 10.1146/annurev.neuro.27.070203.144230

Rubin, J. E., and Terman, D. (2004). High frequency stimulation of the subthalamic nucleus eliminates pathological thalamic rhythmicity in a computational model. *J. Comput. Neurosci.* 16, 211–235. doi: 10.1023/b:jcns.0000025686.47117.67

Rubin, J. E., McIntyre, C. C., Turner, R. S., and Wichmann, T. (2012). Basal ganglia activity patterns in parkinsonism and computational modeling of their downstream effects. *Eur. J. Neurosci.* 36, 2213–2228. doi: 10.1111/j.1460-9568.2012.08108.x

Schieber, M. H. (2011). Dissociating motor cortex from the motor. *J. Physiol.* 589, 5613–5624. doi: 10.1113/jphysiol.2011.215814

Schucht, P., Moritz-Gasser, S., Herbet, G., Raabe, A., and Duffau, H. (2013). Subcortical electrostimulation to identify network subserving motor control. *Hum. Brain Mapp.* 34, 3023–3030. doi: 10.1002/hbm.22122

Shadmehr, R., and Krakauer, J. W. (2008). A computational neuroanatomy for motor control. *Exp. Brain Res.* 185, 359–381. doi: 10.1007/s00221-008-1280-5

Sherman, S. M., and Guillery, R. W. (2011). Distinct functions for direct and transthalamic corticocortical connections. *J. Neurophysiol.* 106, 1068–1077. doi: 10.1152/jn.00429.2011

Shokur, S., O'Doherty, J. E., Winans, J. A., Bleuler, H., Lebedev, M. A., and Nicolelis, M. A. (2013). Expanding the primate body schema in sensorimotor cortex by virtual touches of an avatar. *Proc. Natl. Acad. Sci. U S A* 110, 15121–15126. doi: 10.1073/pnas.1308459110

Swann, N. C., Cai, W., Conner, C. R., Pieters, T. A., Claffey, M. P., George, J. S., et al. (2012). Roles for the pre-supplementary motor area and the right inferior frontal gyrus in stopping action: electrophysiological responses and functional and structural connectivity. *Neuroimage* 59, 2860–2870. doi: 10.1016/j.neuroimage.2011.09.049

van Geemen, K., Herbet, G., Moritz-Gasser, S., and Duffau, H. (2014). Limited plastic potential of the left ventral premotor cortex in speech articulation: evidence From intraoperative awake mapping in glioma patients. *Hum. Brain Mapp.* 35, 1587–1596. doi: 10.1002/hbm.22275

Vigneswaran, G., Philipp, R., Lemon, R. N., and Kraskov, A. (2013). M1 corticospinal mirror neurons and their role in movement suppression during action observation. *Curr. Biol.* 23, 236–243. doi: 10.1016/j.cub.2012.12.006

Conflict of Interest Statement: The authors declare that the research was conducted in the absence of any commercial or financial relationships that could be construed as a potential conflict of interest.

Received: 25 December 2013; accepted: 20 April 2014; published online: 06 May 2014.
*Citation: Mandonnet E and Duffau H (2014) Understanding entangled cerebral networks: a prerequisite for restoring brain function with brain-computer interfaces. Front. Syst. Neurosci. **8**:82. doi: 10.3389/fnsys.2014.00082*
This article was submitted to the journal Frontiers in Systems Neuroscience.

frontiers in Systems Neuroscience

REVIEW
published: 01 April 2015
doi: 10.3389/fnsys.2015.00044

Brain enhancement through cognitive training: a new insight from brain connectome

*Fumihiko Taya[1], Yu Sun[1], Fabio Babiloni[2], Nitish Thakor[1,3,4] and Anastasios Bezerianos[1]**

[1] Centre for Life Sciences, Singapore Institute for Neurotechnology (SINAPSE), National University of Singapore, Singapore, Singapore, [2] Department of Molecular Medicine, University "Sapienza" of Rome, Rome, Italy, [3] Department of Electrical and Computer Engineering, National University of Singapore, Singapore, Singapore, [4] Department of Biomedical Engineering, Johns Hopkins University, Baltimore, MD, USA

Owing to the recent advances in neurotechnology and the progress in understanding of brain cognitive functions, improvements of cognitive performance or acceleration of learning process with brain enhancement systems is not out of our reach anymore, on the contrary, it is a tangible target of contemporary research. Although a variety of approaches have been proposed, we will mainly focus on cognitive training interventions, in which learners repeatedly perform cognitive tasks to improve their cognitive abilities. In this review article, we propose that the learning process during the cognitive training can be facilitated by an assistive system monitoring cognitive workloads using electroencephalography (EEG) biomarkers, and the brain connectome approach can provide additional valuable biomarkers for facilitating leaners' learning processes. For the purpose, we will introduce studies on the cognitive training interventions, EEG biomarkers for cognitive workload, and human brain connectome. As cognitive overload and mental fatigue would reduce or even eliminate gains of cognitive training interventions, a real-time monitoring of cognitive workload can facilitate the learning process by flexibly adjusting difficulty levels of the training task. Moreover, cognitive training interventions should have effects on brain sub-networks, not on a single brain region, and graph theoretical network metrics quantifying topological architecture of the brain network can differentiate with respect to individual cognitive states as well as to different individuals' cognitive abilities, suggesting that the connectome is a valuable approach for tracking the learning progress. Although only a few studies have exploited the connectome approach for studying alterations of the brain network induced by cognitive training interventions so far, we believe that it would be a useful technique for capturing improvements of cognitive functions.

Keywords: cognitive training, brain connectome, electroencephalography (EEG), functional magnetic resonance imaging (fMRI), biomarkers

OPEN ACCESS

Edited by:
Mikhail Lebedev, Duke University, USA

Reviewed by:
Yong He, Beijing Normal University, China
Joydeep Bhattacharya, Goldsmiths, University of London, UK
Tal Dotan Ben-Soussan, Research Institute for Neuroscience, Italy

***Correspondence:**
Anastasios Bezerianos, Centre for Life Sciences, Singapore Institute for Neurotechnology (SINAPSE), National University of Singapore, 28 Medical Drive, #05-Cor, 117456 Singapore, Singapore
tassos.bezerianos@nus.edu.sg

Received: *31 December 2014*
Accepted: *06 March 2015*
Published: *01 April 2015*

Citation:
Taya F, Sun Y, Babiloni F, Thakor N and Bezerianos A (2015) Brain enhancement through cognitive training: a new insight from brain connectome. Front. Syst. Neurosci. 9:44. doi: 10.3389/fnsys.2015.00044

Introduction

Recent developments in neuroimaging techniques and related mathematical tools have extended our understanding of neural mechanisms underlying brain cognitive functions. As such, enhancement of cognitive performance or speeding-up learning process through a brain

enhancement system is a tangible target of contemporary research. Thus, the enhancement of brain functions has been studied for a wide range of cognitive functions using a variety of techniques (Clark and Parasuraman, 2014).

Such a system for brain enhancement would be beneficial for a wide variety of people and can be based on several techniques. Firstly, patients with neurological disorders (e.g., Alzheimer's disease, dementia, stroke) or psychiatric disorder (e.g., schizophrenia, major depression, bipolar disorder) would be greatly benefitted if undesirable symptoms can be diminished or rehabilitation can be speeded up by the system (Farah et al., 2004). So far, two enhancement approaches, psychopharmacology and the brain stimulation, have a long history of researches and medical applications. Secondly, healthy elderly people with declined cognitive functions due to aging can be benefited from such a system, as the quality of their daily life would be improved. It is known that aging has detrimental effects on several cognitive functions such as processing speed, working memory (WM) function, executive function, reasoning, and long-term memory (LTM; Park et al., 2002) although some other cognitive functions such as vocabulary (Schaie, 1994) and implicit memory (Fleischman et al., 2004) remain relatively stable or even get improved. Also, substantial evidences have emerged to show that brain can be modified or reorganized throughout the lifespan (Gutchess, 2014). Thirdly, people who are working under extreme circumstances, such as traffic controllers, military personnel, and surveillance system operators, will have a great profit from the brain enhancement system as they need to engage in operations for a long duration with high workloads and pressure, and even a small error in the operations could result in fatal accidents (Pop et al., 2012). Fourthly, struggling students could be benefited from a system that accelerates their learning performance when they are cramming for their examinations, and thus improving their chances for a good job status and salary, which are often dependent on their educational backgrounds (Deary et al., 2007). In fact, it is known that a psychostimulant called methylphenidate (MPH), also known as Ritalin, is sometimes misused by students for boosting cognitive abilities (Talbot, 2009). Finally, even ordinary people can be benefitted from the advantages of such a system, since their quality of life, their reputation in public community, or their performance at workplace could be improved along with the enhancement of the memory function, the attention levels, or emotional states. For the purpose, a variety of interventions such as cognitive training (Klingberg, 2010), neurofeedback (Sulzer et al., 2013), or more directly by brain stimulations, e.g., TMS, tDCS (Hamilton et al., 2011), or psychopharmacological drugs, e.g., MPH, modafini (Repantis et al., 2010) have extensively been studied.

In this review article, we will mainly focus on the brain enhancement through the cognitive training interventions, in which people perform specific cognitive tasks for improving their cognitive functions (Klingberg, 2010). We will propose that electroencephalography (EEG) biomarkers of cognitive workload can be used for a brain enhancement system to improve the outcome of cognitive training interventions, and the connectome approach can provide further valuable metrics for the assessment of effectiveness of the interventions. For this purpose, three general topics will be covered: cognitive training interventions, EEG biomarkers for cognitive workload, and the brain connectome approach (**Figure 1**). The purpose of this review article is to bridge between these three different topics. A similar attempt has been made for the combination of brain stimulation and connectome, which will not be covered here (Luft et al., 2014).

Firstly, we will introduce studies on cognitive training interventions, and their effects on the brain activities (Klingberg, 2010). Generally, the cognitive training interventions without any physical or pharmacological interventions would be more desirable for most people because of its relatively low-costs and lower potential risks—undesirable side effects (e.g., headache, dizziness, nervousness, sleep disturbances) can be avoided. Neurofeedback, in which individuals are presented with a feedback signal derived from brain activity that indicates their learning goals, is another technique for brain enhancement which requires no physical interventions and has several common characteristics with the cognitive training. However a significant difference might be the fact that while cognitive training goals include improvements of behavioral performance and accompanying modifications in brain activations, neurofeedback is targeting directly in improving brain activations and consequently increasing cognitive performance.

Secondly, we will introduce EEG biomarkers for cognitive workload, and propose that an adaptive training system using EEG biomarkers based on real-time monitoring of cognitive workload can improve gains of the cognitive training interventions as cognitive overload or mental fatigue during the course of training would reduce or even eliminate the gains of cognitive training (Baldwin and Penaranda, 2012). Owing to recent developments and spreads of neuroimaging techniques such as EEG and MRI, tremendous amounts of studies have been done for investigating associations between mental states and brain activities. Meanwhile, a lot of researchers have developed mathematical methods for revealing biomarkers of brain functions mainly based on advances in signal processing and machine learning techniques (Kothe and Makeig, 2011). The combination of extended knowledge of the mechanism underlying brain cognitive functions and the advanced mathematical techniques would provide more elaborated ways for boosting learning processes during cognitive training.

Finally, we will propose that the brain connectome approach, mainly based on graph theory (Sporns, 2014), would provide further valuable biomarkers for monitoring mental states to accelerate learning process by optimizing cognitive workload during the performance of training tasks. The brain connectome is a relatively new approach for investigating topological architecture of the brain network. Because the brain is a complex network consisting of a number of brain areas dedicated to different functions, it has been suggested that cognitive functions emerged from the dynamic interactions of the distributed areas in large-scale network (Bressler and Menon, 2010). Therefore, brain network analysis would provide further

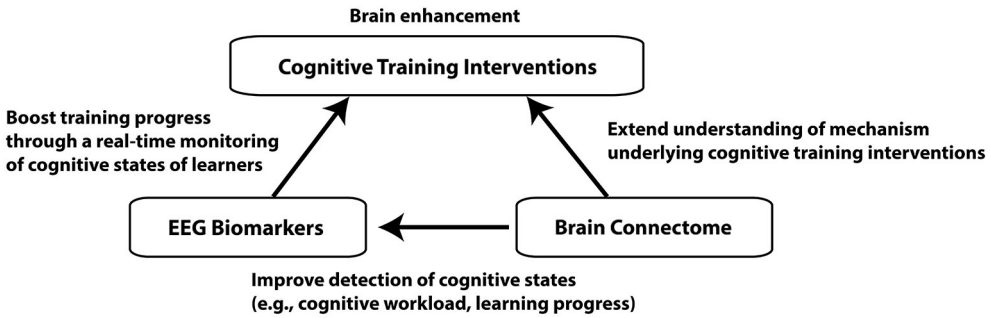

FIGURE 1 | A schematic diagram depicting connections between the three different topics. Improvement of cognitive functions through cognitive training interventions is the ultimate goal of the brain enhancement system we propose. EEG biomarkers can facilitate learners' learning process through a real-time monitoring of cognitive states while brain connectome approach can improve detection of cognitive states as well as understanding of neural mechanism underlying cognitive training.

insights into the mechanism underlying the cognitive training, and the graph theoretical network metrics would be useful for discriminating different brain states during the training. We will first provide a general introduction of the network science, and then introduce studies applying the connectome approach to the brain connectivity. Next, we will present our attempts to employ the connectome approach for discriminating different cognitive states as well as relevant studies that demonstrated cognitive state dependent differences in brain networks or changes in brain network evoked by prior experience or cognitive training. Although so far only one study directly examined the changes in network metrics induced by cognitive training interventions (Langer et al., 2013), the studies showing changes of brain connectivity and differences in graph theoretical network metrics would suggest a potential use of the network metrics for the brain enhancement system assisting learners' learning processes.

Cognitive Training

Cognitive Training Interventions

Cognitive training has emerged as a promising alternative to improve cognitive abilities (Lustig et al., 2009; Karbach and Schubert, 2013; Moreau and Conway, 2013). Several studies have been performed to explore the effectiveness of the cognitive training and its effects on neural activities (Klingberg, 2010; Jolles and Crone, 2012). It has also been suggested that even just playing video games could improve perceptual or cognitive abilities (Green and Bavelier, 2003). Because of its ease of use and the numerous potential applications, the cognitive training has attracted substantial public attention, and a lot of computer software for "brain training" are available on web, PCs or smartphones, e.g., Lumosity,[1] CogniFit,[2] Cogmed.[3]

In this section, we will introduce neuroimaging studies on cognitive training, which demonstrated changes of brain activations or morphological changes in the brain induced by the cognitive training interventions. Understanding the neural process underlying the cognitive training interventions is of great importance in order to develop the brain enhancement system facilitating learners' learning processes. The theoretical framework capturing the neural plasticity behind cognitive training is introduced by Hebb, known as Hebbian learning theory (Hebb, 1949). According to this theory, any two neurons or group of neurons that are repeatedly active at the same time they will tend to form stronger associations, and consequently, activity in one will be facilitating activity in the other. Briefly, when neurons fire together, the connection between them is strengthened. This means that when executing a cognitive task repeatedly, the brain areas associated with the cognitive functions engaged in the task will form stronger associations. Hence, we could improve our cognitive abilities through modifications of the brain activations induced by cognitive training interventions.

Major criticism on the cognitive training is about the transferability of training-related performance gain (Lustig et al., 2009). It is likely that performance of the trained task would be improved by the training, but its effects could be limited to the particular trained task (Jaeggi et al., 2008). What most of the people expect of the cognitive training is an improvement of their general cognitive abilities useful in everyday life, not just a better performance specific to the trained task. Therefore, it is of great importance to succeed in reproducing the improved performance gained from training in one task, on another, different task with no prior training on the second (Karbach and Schubert, 2013). Improved performance on untrained, but directly related tasks to the trained task is called "near transfer", while improvements on untrained tasks which are related, but not directly related to the cognitive abilities is called "far transfer". In fact, several studies have shown the possibility of such far transfer of practice effect beyond task-specific performance (Klingberg et al., 2002), although its generality remains controversial (Colom et al., 2010). The basic theory behind the transfer is also simple. If a brain sub-network that is engaged in a trained task overlaps with

[1]www.lumosity.com
[2]www.cognifit.com
[3]www.cogmed.com

networks related to untrained tasks, these networks will be also strengthened following the Hebbian learning rule, and consequently result in improved cognitive performance on the untrained tasks.

In search of training schemes that can induce transfer effects, WM training has been studied intensively. It is believed that the WM is essential for a variety of higher cognitive functions such as reasoning, problem solving, and decision making (Klingberg, 2010), and moreover, it is considered to be the basis for the general intelligence (Conway et al., 2003). Additionally, WM capacity is crucial for knowledge and skill acquisition, and is closely related to academic achievements and educational success, engaging intense interest from a broad range of people. For this reason, many programs for cognitive training including commercial products such as Cogmed WM Training[4] or Jungle Memory Program[5] (Shipstead et al., 2012), are designed to target on the WM capacity. Some studies have demonstrated that the gain of WM oriented cognitive training can be transferred to cognitive control mechanisms (Klingberg et al., 2002), the WM updating process (Dahlin et al., 2008), reading comprehension (Chein and Morrison, 2010), and even to measures of fluid intelligence, a cognitive ability of abstract thinking and adaptation to novel problems (Jaeggi et al., 2008). The fluid intelligence is known to be closely related to professional and educational success (Neisser et al., 1996). Although it is believed that the fluid intelligence is unsusceptible to influences of education, Halford et al. proposed a hypothesis that the WM and reasoning share a common mechanism, providing a framework for improvements of the general intelligence through WM oriented cognitive training (Halford et al., 2007). To verify the hypothesis, Jaeggi et al. trained subjects for 8–19 days with an adaptive dual *n*-back task, in which subjects were required to update the information about spatial locations of visual stimuli and auditory information concurrently, and found the improvements of the fluid intelligence measured by Raven's Advanced Progressive Matrices test and the Bochumer Matrizen-Test (Jaeggi et al., 2008). Stephenson et al. also found improved scores in two out of four tests for the fluid intelligence by the dual *n*-back task training (Stephenson and Halpern, 2013). Despite a number of successful observations of transfer effects of WM training gain, neural mechanism underlying the WM training interventions remains elusive. Some studies have suggested that the improvements of fluid intelligence could be achieved through cognitive training other than WM training. Colom et al. found similar improvements in two out of four scores measuring fluid intelligence induced by simple speed tasks (Colom et al., 2010). Also the improvement of fluid intelligence was observed only for participants who underwent cognitive training with visuospatial components, and even a visuospatial short-term memory (STM) training improved the fluid intelligence (Stephenson and Halpern, 2013). One promising account for the effects of WM training is that participants' short-term storage capacity, which is a common factor among STM, WM, executive function, attention, and general fluid intelligence, is expanded through intensive performance of the cognitive training (Colom et al., 2013).

[4]www.cogmed.com/program
[5]junglememory.com/

Effects of Cognitive Training on Brain Activations

In order to develop the brain enhancement system which facilitates cognitive training processes, it is also of great importance to investigate the effects of cognitive training on the brain and to understand what is actually accomplished by the cognitive training. Modulation of brain activation has been demonstrated with a variety of cognitive training interventions, such as the WM training (Hempel et al., 2004; Olesen et al., 2004; Jolles et al., 2010), an attentional training (Mozolic et al., 2010), dual tasks (Erickson et al., 2007), video games training (Maclin et al., 2011), and even meditation training (Tang and Posner, 2014).

A number of studies using functional magnetic resonance imaging (fMRI) have shown that besides improving behavioral performance, intense cognitive training resulted also in changes of the brain activations that were related to the cognitive functions implicated in the tasks used as cognitive interventions were changed by intense cognitive training, accompanying with improvements of behavioral performance (Hempel et al., 2004). Olesen et al. found an increase of brain activity in the areas related to the WM induced by 5 weeks practice of WM tasks (Olesen et al., 2004) while Hempel et al. showed increased activations after 2 weeks of training on a WM task and decreased activations after 4 weeks, suggesting two distinct mechanisms mediating the training effects: an enhancement mechanism for WM and a suppressive mechanism related to automation of processing (Hempel et al., 2004). Furthermore, a training of multi-task processing revealed training-induced reductions in activity of brain areas responsible for stimulus-response associations, attentional control, and response selection process as well as an increase of activity in a region related to executive control (Erickson et al., 2007). Such reductions in brain activity induced by training may reflect increased task selectivity within the areas (Dux et al., 2009). Even thirty hours of training on a video game can induce reduction of activation in attentional control areas, suggesting a reduction of attentional demands after the training (Lee et al., 2012). Interestingly, a WM training has also induced less deactivation in "default-mode network", which is usually deactivated during cognitive tasks, suggesting more automatic processing after practice (Jolles et al., 2010).

In addition to the changes of activation at brain regions specific to trained tasks, several neuroimaging studies demonstrated transfer effects of cognitive interventions (Dahlin et al., 2008). Dahlin et al. examined whether transfer effect was induced by training on a task that involved "updating", which is a basic executive function relating to intelligence, WM, and manipulation of information (Dahlin et al., 2008). After 5 weeks of training on a letter memory task, young subjects showed improved performance on 3-back task, but no improvement in the Stroop task. A comparison between pre- and post-changes in the fMRI data that were collected during the training task showed increased activity in the left striatum and decreased activity in fronto-parietal network. As

far as the transfer task is concerned, training-induced increases in brain activations were found in the left striatum and the frontal cortex for the 3-back task, but no significant changes were detected for the Stroop task. Additionally, a conjunction analysis revealed that overlap region exclusive to letter memory and 3-back was the left striatum, which is associated with updating, suggesting that the activation of the overlapping brain region during the training induced the transfer to the untrained 3-back task. No transfer was observed in older adults who showed no significant activation in the striatum during the letter memory task. Transfer effect was also examined for affective cognitive control (Schweizer et al., 2013). They found that twenty days of a dual *n*-back task with emotional stimuli (eWM task) induced improved emotional regulation and increased activations in the fronto-parietal demand network, including the dorsal and subgenual anterior cingulate (sgACC), on another task that required emotional regulation. Furthermore, several studies have examined cross-modal transfer effects of WM training (Schneiders et al., 2011, 2012; Buschkuehl et al., 2014). Buschkuel et al. have examined cross-modal transfer effects of 7 days of training of a visuospatial *n*-back task to an auditory *n*-back task, and investigated longitudinal changes of brain activities using perfusion (arterial spin labeling; ASL) (Buschkuehl et al., 2014). They found a transfer effects across modalities, and observed increased perfusion in right superior frontal gyrus, which is thought to be involved in executive control and WM processing. On the contrary, Schneiders et al. failed to observe cross-modal transfer effects for a visual and an auditory WM tasks (Schneiders et al., 2011, 2012). They found a modality-specific training effect for the visual WM training in the right middle frontal gyrus, which is to some extent specific to the maintenance of visual objects in WM, (Schneiders et al., 2011), and that for the auditory WM training in the right inferior frontal gyrus responsible for maintaining auditory information (Schneiders et al., 2012). However, no across-modal transfer effects were detected. One possible account for this discrepancy is that WM training would once increase brain activations in areas associated with executive control, which is shared between WM tasks with different modalities, but further training would decrease the brain activation along with a decrease in cognitive efforts necessary for the performance of the WM tasks (Chein and Schneider, 2005).

Furthermore, such modifications of brain activations induced by cognitive training can also be captured by EEG as well (Maclin et al., 2011). Changes in activtions related to attentional processes triggered by complex game learning were detected in P3 ERP component as well as in δ and α EEG spectral power (Maclin et al., 2011). Moreover, frontal EEG α power during early phase of the game training predicted subsequent learning rates (Mathewson et al., 2012). An improvement of the fluid intelligence induced by WM training and increases in θ and α synchronization have suggested that the WM training has improved not only WM maintenance functions, but also central executive and attentional control (Jaušovec and Jaušovec, 2012). A first-person shooter (FPS) video game enhanced neural processes that support spatial selective attention, as it was shown by increased amplitudes of the later visual ERPs in high-performing FPS players (Wu et al., 2012). Improvements of visual attention allocation, executive attention, and updating function in WM representation has been indicated by increases in ERP components (N160, P200 and P300) after training on a WM task that engaged updating function (Zhao et al., 2013). Modifications of EEG signals induced by training on a game involving dual tasks or a WM task along with behavioral improvements were also observed for elderly adults (Anguera et al., 2013) and dysphoric participants (Owens et al., 2013). Moreover, a meditation training such as integrative body-mind training (IBMT) improved attention, mood, and stress regulation, while it increased frontal midline θ power, where the anterior cingulate cortex (ACC) is suggested to be the generator of the activity (Tang et al., 2009). Thus, several cognitive training programs have shown alterations in brain activities as well as their effectiveness in improvements of cognitive performance. In **Table 1**, we provide a summary of existing neuroimaging studies showing changes in brain activations induced by cognitive training interventions.

Structural Brain Changes Induced by Cognitive Training Interventions

In addition to the training-induced changes in brain activity, morphological changes can be induced by cognitive practice in the adult brain despite a belief that changes in brain structure are limited to the critical period of development (Draganski and May, 2008). Repeated practice of skills during professional career can induce long-lasting changes in structure of the brain: i.e., London taxi drivers who have substantial experiences to use spatial knowledge for navigation in the complex city were found to have larger gray matter volumes in hippocampus (Maguire et al., 2006), professional typists devoted to the prolonged practice of typing show increased gray matter volume in brain regions related to programming of motor tasks such as supplementary motor area, prefrontal cortex and cerebellum (Cannonieri et al., 2007), violinists and other string players who use the second to the fifth digits of the left hand for fingering the string have larger cortical representation of the digits of the left hand in the primary somatosensory cortex (Elbert et al., 1995).

More directly, several studies have examined the effects of training on the structure of the brain. Modulations of neural structures and functions of the brain can occur for a relatively short period of time as demonstrated by MR-based morphology in conjunction with longitudinal design. Three months of training on juggling task induced a transient expansion of gray matter in the brain areas associated with the processing and storage of complex visual motion for both young and older participants (Draganski et al., 2004; Boyke et al., 2008). Even seven days of the juggling training induced a change in gray matter (Driemeyer et al., 2008) and 6 weeks of the training induced changes in white matter measured with diffusion tensor imaging (DTI) as well as in gray matter density (Scholz et al., 2009). Additionally, real-life intervention such as an intensive preparation for the medical examination, which requires acquisition of substantial amount of new information,

TABLE 1 | Studies showing changes in brain activations induced by cognitive interventions.

Study	Modality	Training task	Control group	Population	Training period
McKendrick et al. (2014)	NIRS	a dual verbal and spatial WM task	a yoked condition group	YA	5 days
Heinzel et al. (2014)	fMRI	an adaptive *n*-back task	-	OA and YA	4 weeks
Buschkuehl et al. (2014)	ASL	adaptive visuaospatial *n*-back	vocabulary and general knowledge questions	YA	7 days
Zhao et al. (2013)	EEG	Three memory tasks	no training	YA	21–23 days
Schweizer et al. (2013)	fMRI	adaptive emotional dual *n*-back	a feature match training	YA	20 days
Owens et al. (2013)	EEG	an online dual *n*-back task	a nonadaptive dual 1-back task	YA (dysphoric)	2 weeks
Anguera et al. (2013)	EEG	NeuroRacer (a dual task)	single task and no-contact control	OA	4 weeks
Wu et al. (2012)	EEG	a FPS video game	nonaction game control group	YA	10 h
Schneiders et al. (2012)	fMRI	adaptive auditory *n*-back	-	YA	2 weeks
Prakash et al. (2012)	fMRI	Space Fortress vidoegame	only limited game experience	YA	30 h
Mathewson et al. (2012)	EEG	Space Fortress vidoegame	-	YA	20 h
Lee et al. (2012)	fMRI	Space Fortress videogame	only limited game experience	YA	30 h
Jaušovec and Jaušovec (2012)	EEG, NIRS	Five different WM tasks	communication and social skills	YA	30 h
Schneiders et al. (2011)	fMRI	adaptive visual or auditory *n*-back	no training	YA	2 weeks
Maclin et al. (2011)	EEG	Space Fortress vidoegame	-	YA	20 h
Jolles et al. (2010)	fMRI	a verbal WM task	no training	YA	6 weeks
Dux et al. (2009)	fMRI	sensory-motor task (single or dual task trials)	-	YA	2 weeks
Tang et al. (2009)	EEG	a meditation training	a relaxation training	YA	5 days
Dahlin et al. (2008)	fMRI	a letter memory task	no training	OA and YA	5 weeks
Erickson et al. (2007)	fMRI	a dual tasks and a single task	no training	YA	2–3 weeks
Olesen et al. (2004)	fMRI	WM tasks	-	YA	5 weeks
Hempel et al. (2004)	fMRI	*n*-back	-	YA	4 weeks

Note: EEG: electroencephalography, fMRI: functional magnetic resonance imaging, NIRS: near-infrared spectroscopy, ASL: arterial spin labeling, YA: young adults, OA: old adults.

could also induce the increment of gray matter in the brain areas known to be involved in memory processes (Draganski et al., 2006). Furthermore, a variety of training tasks other than the juggling training have induced alterations in brain structures. A Morse code training, a sort of language learning, induced a gray matter increase in the left occipitotemporal cortex, which projects to the area involved in language perception (Schmidt-Wilcke et al., 2010). A complex motor skill learning task induced an increase in gray matter volume in the prefrontal cortex, which was positively correlated with performance improvements over time, and a decrease in white matter volume in the prefrontal cortex (Taubert et al., 2010). A memory training induced cortical thickness changes in the right fusiform and lateral orbitofrontal cortex correlated with improvements in memory performance (Engvig et al., 2010). A WM training increased myelination measured by fractional anisotropy (FA) of fiber tracts in the white matter regions adjacent to the intraparietal sulcus and the anterior part of the body of the corpus callosum, both of which are considered to be critical in WM (Takeuchi et al., 2010). A mental calculation training that required WM function induced a decrease in regional gray matter volume in the WM-related regions, which could be attributed to the usage-dependent selective elimination of synapses (Takeuchi et al., 2011). A meditation training increased white matter efficiency in areas surrounding the ACC that is implicated in cognitive control (Tang et al., 2012). Furthermore, a logical reasoning training gain to fluid intelligence was associated with an increase in structural integrity in corpus and genu of the corpus callosum, which connect between homologous cortical areas of the two hemispheres and are considered to be involved in executive functions and WM (Wolf et al., 2014). Taken together, structural brain changes in response to cognitive training interventions were observed for a variety of training schemes, and such changes were mainly found in the brain areas that were supposed to be involved in the training tasks. These observed structural plasticity can be a basis of improvements in cognitive functions through the interventions, suggesting a potential effectiveness of the cognitive training. We provide a brief summary of structural changes in the brain induced by training intervention in **Table 2**.

Summary of Effects of Cognitive Training

In summary, cognitive training can modify activations or the structure of the brain regions directly related to the training tasks along with improvements in behavioral performance of the tasks. As different training tasks can induce changes of brain activations at different brain areas, the selection of training tasks is also an important issue. Although the brain areas engaged by the training tasks can be different dependent on sensory modality, the cognitive tasks recruiting

TABLE 2 | Studies showing structural brain changes induced by training interventions.

Study	Modality	Training task	Control group	Population	Training period
Wolf et al. (2014)	DTI	logical reasoning training	-	OA	4 weeks
Tang et al. (2012)	DTI	a meditation training	a relaxation training	YA	4 weeks
Takeuchi et al. (2011)	gray matter volume	mental calculation	placebo, no training	YA	5 days
Takeuchi et al. (2010)	DTI	WM program	-	YA	2 months
Engvig et al. (2010)	cortical thickness	memory training	no training	OA	8 weeks
Taubert et al. (2010)	DTI, gray matter volume	a complex motor skill learning	-	YA	6 weeks
Schmidt-Wilcke et al. (2010)	gray matter density	a Morse code learning	no training	YA	2.5–8 months
Scholz et al. (2009)	DTI, gray matter	juggling	no training	YA	6 weeks
Driemeyer et al. (2008)	gray matter density	juggling	-	YA	7 days
Boyke et al. (2008)	gray matter density	juggling	-	OA	3 months
Draganski et al. (2006)	gray matter density	studying for medical exam	-	YA (medical students)	3 months
Draganski et al. (2004)	gray matter density	juggling	jugglers vs. non-jugglers	YA	3 months

Notes: DTI: diffusion tensor imaging, YA: young adults, OA: old adults.

higher cognitive functions, such as WM training or attentional training, are likely to show some transfer effects. Most of the demanding tasks usually recruit higher cognitive functions such as executive function, cognitive control, and attentional control (Buschkuehl et al., 2014). For example, WM training is supposed to induce changes in brain activity in frontal and parietal cortex, both of which are associated with WM capacity (Klingberg, 2010), a WM task that demands emotional regulation evoked increased activation in a part of the ACC, which has been shown to be involved in cognitive control and emotional regulation (Schweizer et al., 2013), an attention training program altered a part of the attentional control system in the prefrontal cortex (Mozolic et al., 2010), sensory motor tasks such as a juggling and a videogame modified cortical regions involved in spatial attention (Prakash et al., 2012) or visual areas specific to motion processing (Draganski and May, 2008), and meditation training program changed brain activities associated with attention, mood, and stress regulation (Tang and Posner, 2014). These results suggest that higher cognitive functions can be improved by cognitive training interventions regardless of sensory modality involved, and the changes in brain activations after cognitive training can be captured by a variety of neuroimaging techniques including fMRI, EEG, fNIRS and structural MRI. Although it is difficult to utilize functional or structural MRI for real-time tracking of training-induced changes of the brain due to their costs and portability, some of the neuroimaging techniques such as EEG can be useful for monitoring alterations in brain activity during the course of cognitive training.

EEG Biomarkers for Cognitve Workload

In the previous section, we introduced studies showing functional and structural changes of the brain induced by cognitive training interventions. These studies have shown that human cognitive functions could be improved through cognitive interventions if the brain regions implicated in trained tasks overlap between trained and untrained target tasks. In the cognitive training, subjects are required to repeatedly perform behavioral tasks such as WM tasks or video games. As a result of intense involvements of the brain regions during the course of the training, connections among the regions would be enhanced, leading to improved cognitive performance. To engage the brain regions effectively, individualized adaptive training platforms can be useful tools. Also, the neuroimaging techniques including EEG can capture changes in cognitive performance which could be potentially used as biomarkers for the brain enhancement system and facilitate learners' learning process through tracking learning progress or monitoring mental states.

For example, cognitive overload would induce a reduction of learner's motivation and mental fatigue, both of which hamper the effectiveness of cognitive training interventions. Thus, the cognitive training can be facilitated using passive Brain-Computer Interface (BCI) system, which utilizes biomarkers derived from the brain signal and adapts to the user's performance without the purpose of voluntary control of the system (Zander and Kothe, 2011). Through a real-time monitoring of cognitive workload of learners, the system can flexibly be adjusted to avoid overloading learners' cognitive resources and to keep the learners' engagement and motivation, speeding up the learning progress (Baldwin and Penaranda, 2012). Additionally, individual differences in learners' learning rate can be predicted by EEG biomarker (Mathewson et al., 2012), suggesting that combinations with other cognitive training or neurofeedback training which improve the EEG biomarker could optimize training of targeted cognitive functions. In this section, we will first provide a general introduction of EEG biomarkers, which have been studied mainly for BCI and Neurofeedback, and discuss a potential use of biomarkers for increasing effectiveness of cognitive training interventions. As it is practically difficult to use fMRI or structural MRI to monitor learners' learning process in real-time due to its costs and portability, we will focus on EEG biomarkers here. Then, examples of neurophysiological biomarkers for cognitive workload will be introduced, which can be used for optimizing cognitive workload of a training task to keep learners' concentration and motivation.

EEG Biomarkers: BCI and Neurofeedback

The biomarkers based on EEG have been studied extensively for the BCI, which enables users to control computers

or devices through the neurophysiological signals, mainly because of ease of use and low cost (Graimann et al., 2010). Mathematical techniques developed for the BCI system can also be employed for the assistive system of cognitive training interventions. In general, the detection of mental states consists of three stages: pre-processing, feature extraction and selection, and classification. The pre-processing can include artifact removals, spatial filtering, and temporal filtering. After the pre-processing, specific properties of the signal will be extracted over window, useful features will be selected for dimensional reduction, and the selected features will be subjected to classification, which accounts for difference in mental states. Classification enables the system to adapt to individual difference in learners, but the selection of feature space to be extracted is critical for detection of cognitive states, and requires understanding of mechanism behind the cognitive states.

In the BCI systems, various types of EEG signals such as modulations of sensorimotor rhythms (SMR) during motor imagery (Pfurtscheller et al., 1997), event-related potentials (Farwell and Donchin, 1988) or slow cortical potentials (SCPs; Birbaumer et al., 1999) are utilized for discriminating mental states. In any case, it is well known that users often have to be trained to control the BCI system properly, suggesting a need of adjustments to individual difference in signals (Neuper and Pfurtscheller, 2010). In the course of the training for the control of BCI, the user is repeatedly presented with feedbacks indicating performance of the system, and needs to learn voluntarily generating specific patterns of brain signal, which is detectable by the BCI system. Thus, a kind of neurofeedback training for the BCI control is necessary. Actually, the only difference between typical BCI systems and neurofeedback training is how to use biomarkers. For the BCI system, detected mental states would be used for controlling devices and the training would be done through improvements of behavioral performance in the control while the neurofeedback training would be achieved through direct modulations of brain signal.

EEG-neurofeedback has been examined with various types of EEG biomarkers, e.g., up- or down-training of the SMR, the β1 ratio, the θ/α ratio, γ, etc., and improved cognitive functions including sustained attention, orienting, executive functions, spatial rotation, procedural memory, recognition memory have been repeatedly reported through the EEG-neurofeedback training (Gruzelier, 2014). The successful outcomes of the neurofeedback training suggest that the mental state revealed by the EEG biomarkers could provide quantitative metrics for guiding learners to obtain certain mental state suitable for efficient learning or performing specific tasks. In the neurofeedback training, the desired brain state would be achieved through associative learning, in which the association between the desired state and reinforcing feedback stimulus revealing the brain activity is learned (Sulzer et al., 2013). For the adaptive system for effective training, such neurofeedback techniques could be used to optimize learners' mental state to facilitate their learning progress.

Neurophysiological Biomarkers for Cognitive Workload

The assessment of cognitive workload based on neurophysiological biomarkers, particularly EEG biomarker has been of great interest and been extensively studied (Kothe and Makeig, 2011), and the spectral analysis of the EEG waveforms is a powerful tool for the assessment of the mental states during performance of cognitive tasks (Kohlmorgen et al., 2007).

To search for features of EEG signals associated with task demands, an increase of the EEG power-spectrum in the θ bands (4–7 Hz) at frontal sites and a decrease in the α bands (8–12 Hz) over parietal sites have been investigated (Borghini et al., 2014). The increase of frontal θ activity has been observed for high cognitive demand or high mental effort (Berka et al., 2007), and is considered to reflect attentional process to allocate cognitive resources (Gomarus et al., 2006) while the decrease of α power may reflect semantic LTM processing (Klimesch, 1999).

These kinds of neurophysiological biomarkers can be used for on-line monitoring of mental states. Aricò et al. developed a framework for classification of multiple levels of mental workload during a simulated flight based on EEG and ECG signals (Aricò et al., 2014). In this study, subjects performed the Multi Attribute Task Battery (MATB; Comstock and Arnegard, 1992), which includes a variety of simulated tasks involved in a flight scene, over three different difficulty levels (cruise flight phase, flight level maintaining, and emergencies) during recordings of EEG and ECG signals. The classifiers were trained offline for discriminating cognitive workload, and then tested with the other data where difficulty levels were changed dynamically. The stability of the classifier parameters was tested as well. The workload was assessed based on fusion workload index: a combination of EEG and ECG based workload indices. For the EEG-based workload index, the power spectral density (PSD) was evaluated, and the stepwise linear discrimination analysis (SWLDA) was used to select the most relevant spectral features to discriminate workload levels. For the ECG-based workload index, the PSD was estimated for R-peaks extracted from the ECG signal, and the relevant features were selected using the SWLDA. The derived workload indices were subjected to the SWLDA to calculate the best estimation of coefficients of a linear combination of the EEG and ECG-based workload indices for discriminating the workload levels. The authors demonstrated that the proposed system was able to evaluate multiple levels of mental workload, and the classification parameters were stable within a week.

The frontal θ and parietal α power can be changed along with a change of cognitive efforts induced by training of a task. In the study by Borghini et al., subjects trained on the MATB for 5 days while EEG signals were recorded at first (T1), third (T3) and fifth (T5) day of the training (Borghini et al., 2015). The frontal θ power increased from T1 to T3, and then decreased at T5 and the parietal α power showed an opposite pattern while performances of the MATB task continued to improve during the training. This result seems to reflect changes in attentional demands in the

course of the training. We may be able to monitor the progress of cognitive training through such biomarkers associated with allocation of attentional resources.

In summary, there exist several evidences showing that neurophysiological biomarkers can discriminate between different levels of cognitive workload. Although further developments would be necessary for applications based on integration of such biomarkers into an adaptive training system, classification of cognitive workload can be a useful measure for assisting cognitive training and increase its effectiveness by controlling the difficulty levels of the training task. Actually, as mentioned above, some studies have shown changes in frontal θ power after WM training (Jaušovec and Jaušovec, 2012) or training that uses a complex video game (Anguera et al., 2013), suggesting that these EEG biomarkers can be useful for tracking the progress of cognitive training.

Brain Connectome Approach

The brain connectome is a useful approach not only for understanding brain cognitive functions, but also for extracting biomarkers that could discriminate between different brain states. By using network metrics to represent a feature space for classification, detection of mental states of learners could be enhanced. In this section, we will introduce the network science and its application to brain networks. Firstly, a general introduction of the network science will be provided. Secondly, prior studies using brain connectome approach will be introduced. Then, we will discuss why the connectome approach is beneficial to the brain enhancement system and how it can boost the learning progress. Finally, we will introduce prior studies showing differences or modifications of the brain connectivity patterns, which suggest potential use of brain connectome approach for the brain enhancement system.

Network Science

It is widely known that brain is a complex network consisting of brain regions dedicated to different kinds of cognitive functions. Furthermore, accumulating evidences support that cognitive functions emerge from the dynamic interactions of distributed brain areas in large-scale networks (Bressler and Menon, 2010). Thus, in order to understand the neural mechanism behind the cognitive training interventions, it would also be important to study alterations in the brain network. The network science, largely based on graph theory, is a useful methodology for investigating an architecture of a complex network and has been employed for studying the brain network (Bullmore and Sporns, 2009; Sporns, 2014). Graph theory is a field of mathematics, aiming at studying topological architecture of networks, and has a long history, dating back to 1736 when a pioneering Swiss mathematician, Leonhard Euler, published the paper on the famous "Seven Bridges of Königsberg" problem. More recently, Watts and Strogatz employed graph theoretical approach to show "small-world" structure of complex networks derived from empirical data (Watts and Strogatz, 1998), leading to the rise of network science as a mathematical tool for studying structure and functions of a wide variety of complex systems from neuroscience, social science, physics, biology, computer science, etc.

In graph theory, networks are represented as "graphs" that consist of objects ("nodes" or "vertices") and connections or relationships between them ("edges"). The topological properties of complex network are quantified by a wide variety of measures, such as small-worldness, modularity, hierarchy, centrality, and the distribution of network hubs (Bullmore and Sporns, 2009). For example, the degree of a node is the number of connections linking to the other nodes, and the probability distribution of the node degree over the whole network is called the degree distribution: a useful measure for investigating a global architecture of a network. Clustering coefficients quantify the degree of mutual connections between the nearest neighbors of a node. High clustering leads to high efficiency of local interactions and robustness. Shortest path length is the minimum number of edges necessary for a node to reach to another. The inverse of the path length can be used to quantify global efficiency of information transfer of the network. Connection density is a proportion of actual connections to the total possible connections. High connection density indicates high physical cost of a network. The centrality of a node represents its importance in communication, and several measures for node centrality has been proposed, such as degree centrality, eigenvector centrality, closeness centrality, betweennes centrality, and so on. For example, the degree centrality is the simplest centrality measure: the degree of a node, while Betweenness centrality is measured by counting the number of paths between the other nodes passing through the node for taking the shortest route. Nodes with high centrality are called hubs, and can be used for assessing robustness of the network by deleting them. Complex networks often consist of a number of modules composed of locally interconnected nodes with few connections to those in different modules. Hubs can have different roles in this complex network architecture. Provincial hubs are connected mainly to nodes inside their own modules while connector hubs have connections with nodes in other modules. Further details about the formulation of these network metrics and their interpretation can be found in recent reviews of this topic (e.g., Rubinov and Sporns, 2010).

Graph theoretical network analysis allows us to quantitatively study topology of networks. A number of studies utilizing graph theoretical measures have revealed that most real world networks including brain network had non-trivial topological features. Watts and Storogatz have shown that a variety of networks have "small-world" properties, based on empirical examples including social network of film actors, power grid, and the neural network of the worm Caenorhabditis elegans (C. elegans) (Watts and Strogatz, 1998). The "small-world" network, by analogy with the small-world phenomenon (popularly known as six degrees in separation), has topological properties somewhere between two extreme cases, i.e., regular and random networks. The small-world network can be characterized by two independent graph theoretical measures introduced above, namely the clustering coefficients and average shortest path length. Regular network is highly clustered, but has a large path length: it is robust,

yet inefficient in information transfer. Random network, on the other hand, has a small path length along with a small clustering coefficient, indicating that it is efficient, but is not robust. Small-world network is the intermediate between the regular and the random network, and consists of a number of clusters or modules, interlinking with each other via hubs. Such modular architecture of the small-world network enables global efficiency of information transfer and robustness to perturbations at the same time. It is believed that the small-world architecture is a fundamental principle of a diversity of complex networks, e.g., social, economical, biological, and neurological networks.

Scale-free network, whose degree distribution follows a power law, is also an important concept in the network science (Barabási, 2013). The scale-free property of the network means that some "hub" nodes have a large number of connections while a majority of nodes have only a few connections, which is considered to enable rapid information transfer, minimal wiring costs, and balancing between local and global communications. Such scale-free property has also been found in a variety of networks in the natural world.

Brain Connectome Approach to Large-Scale Human Brain Network

A number of studies have attempted to employ graph theoretical approaches for the brain network analysis (Sporns, 2014). For large-scale human brain networks, the nodes are usually considered to be brain regions or sensors (e.g., voxels for fMRI and electrodes for EEG/magnetoencephalography (MEG)) while the edges can be derived from different, but relevant forms of connectivity, i.e., anatomical connectivity (AC), functional connectivity (FC), or effective connectivity (EC). AC, also called structural connectivity, is the axonal-fibers (white matter) pathways usually acquired by DTI or diffusion spectrum imaging (DSI). FC is defined as temporal dependency between activities of distributed and often spatially distant brain regions without explicit reference to causal effects, normally monitored via fMRI. EC represents causal interactions between brain regions, defined as an influence of one system on another. The causality can be inferred through network perturbations, or the temporal ordering of events. As estimations of EC usually require high temporal resolution, signals from EEG, electrocorticogram (ECoG) or MEG are used. The distinction between FC and EC in neuroimaging studies is important when considering several aspects of functional organization (Friston, 1994). Once the connectivity pattern is provided, regardless of which modality is employed for deriving the network, graph theoretical approaches can be applied for investigating its network architecture. The functional and EC derived from functional data can dynamically change even at rest and do not necessarily match with the AC and should not be interpreted as it is (Honey et al., 2009; Hermundstad et al., 2013).

To obtain connectivity patterns of the large-scale network from brain activity, a variety of techniques have been proposed. For FC, correlation analysis can be used regardless of the modality of signals while several techniques have been proposed for EC, depending on modality of signals. To derive EC from electrophysiological signals such as EEG and ECoG, the Granger causality analysis based on multivariate autoregressive model (MVAR) can be used to determine the directional interaction among electrophysiological signals (Astolfi et al., 2007). The directed transfer function (DTF; Kamiński and Blinowska, 1991) and the partial directed coherence (PDC; Baccalá and Sameshima, 2001) have been used to estimate such causal relationships. To derive EC from fMRI data, Granger Causality Modeling (GCM) and Dynamic Causal Modeling (DCM) have been proposed (Valdes-Sosa et al., 2011). Approximately, GCM is data-driven while DCM is hypothesis-driven. Once connectivity maps are obtained regardless of techniques used for deriving connectivity patterns, graph theoretical approaches can be employed to investigate the network properties.

Graph theoretical network metrics demonstrate topological architecture of the brain network, such as global or local efficiency of information transfer, small-worldness, and a modular structure of the network. Studies employing graph theoretical metrics on human large-scale structural brain network have exhibited robust small-world properties, i.e., high clustering coefficients with relatively small mean path length, for structural brain networks derived from diffusion MRI (Hagmann et al., 2007) as well as those from cortical thickness (He et al., 2007). Similarly, the small-world properties have also been shown for human brain functional networks based on neurophysiological data, such as a task fMRI (Eguíluz et al., 2005; Kinnison et al., 2012; Breckel et al., 2013), resting-state fMRI (Salvador et al., 2005; Achard et al., 2006; Achard and Bullmore, 2007; van den Heuvel et al., 2008), EEG (Micheloyannis et al., 2006, 2009; Stam et al., 2007; Smit et al., 2008; Boersma et al., 2011; Langer et al., 2012; Sun et al., 2014a), and MEG (Stam, 2004; Deuker et al., 2009). Also, the scale-free organization has been reported for the functional network derived from fMRI (Eguíluz et al., 2005; Achard et al., 2006; van den Heuvel et al., 2008) and EEG (Lee et al., 2010). These findings consistent among structural and functional brain network reveal that the small-world and scale-free property are fundamental principles of the brain networks, suggesting that the brain networks have evolved to achieve high efficiency of information transfer between nodes at low connection cost with robustness to perturbations.

Furthermore, several studies have shown that the human brain network has some "hub" regions that work as core regions linking between brain regions (van den Heuvel and Sporns, 2013b). The hub regions were identified for both structural brain networks (He et al., 2007; Hagmann et al., 2008; Iturria-Medina et al., 2008; Gong et al., 2009; van den Heuvel and Sporns, 2011, 2013a; Nijhuis et al., 2013) and functional brain networks (Achard et al., 2006; Cole et al., 2010b; Tomasi and Volkow, 2011a,b; Zuo et al., 2012). The identified hub areas were relatively consistent among the studies regardless of the modality used for obtaining the brain networks, and mostly included parietal and prefrontal regions, such as precuneus, anterior and posterior cingulate gyrus, and the superior frontal gyrus (Bullmore and Sporns, 2009; van den Heuvel and Sporns, 2013b). These hub regions are believed to be responsible for multimodal or integrative function. In fact, the precuneus is a part of the

default mode network, and has been suggested to be involved in visuospatial imagery, episodic memory retrieval, self-processing, and consciousness (Cavanna and Trimble, 2006), while the superior frontal gyrus contributes to various cognitive functions, such as WM and attention (Petrides, 2005). The damage to these regions could result in drastic changes of stability and efficiency of the network (Sporns and Zwi, 2004). Such hub regions, in particular the fronto-parietal brain network (FPN), may work as a flexible hub, which implement cognitive control by biasing information flow across sub-networks depending on task demands (Cole et al., 2013).

As revealed by the graph theoretical approach, the brain has a modular architecture with small-world network attributes. Each module, probably corresponding to anatomically or functionally defined brain regions, has dense connections within the module for local processing of information, and is implicated in a particular function, exhibiting functional segregation of local areas. On the other hand, the modules are interconnected with each other through short- or long-range connections through hubs, implying functional integration of globally distributed brain areas. In fact, human brain structural network derived from co-variation of regional gray matter volumes measured using MRI and DSI exhibited hierarchical modular architecture with 2–3 levels (Bassett et al., 2010). It is likely that such hierarchical small-world network architecture enables the coexistence of functional segregation and functional integration within a single brain network. Also, these findings are consistent with those for the resting-state FC, which have shown the existence of a number of sub-networks consisting of functionally linked brain regions (Cole et al., 2010a). Therefore, the brain has an inhomogeneous architecture, and each brain region has different functions with different degree of importance. As such, brain regions dedicated to the relevant cognitive functions are engaged depending on cognitive demands, and work together as a network to communicate and influence one-another to produce coherent experiences and behavior. Such sub-networks could be divided into "intrinsic" and "evoked" functional network architecture, where the intrinsic network serves as a standard state of the brain and relatively small changes of the task-evoked networks support task-specific demands (Cole et al., 2014).

In summary, functional and structural connectivity patterns of the human large-scale brain network can be obtained by means of a variety of neuroimaging and mathematical techniques. A number of studies have been conducted to investigate the topological architecture of the brain network using graph theoretical network metrics, and have shown that the human brain network had small-world network characteristics, scale-free organization, and a modular structure, suggesting applicability of network analysis for elucidating neural underpinnings of human cognitive functions.

For the brain enhancement through cognitive training, elucidation of the brain network architecture is of great importance for several reasons. Firstly, cognitive training can affect sub-network consisting of spatially distributed, but functionally relevant brain regions even when improvement of activation in a single brain region is targeted. Secondly, a degree of impact of cognitive intervention can differ among brain regions, depending on its topological property of the brain network. To be specific, hub regions that link with other sub-network can have greater influence compared to other brain areas. Thirdly, the graph theoretical network metrics can simply be additional biomarkers for monitoring mental states of learners during the training, enabling the adaptive learning system depending on the learner's mental state to facilitate the learning progress. Finally, although reduced activation in brain regions responsible for attentional control and mental efforts has been observed after the cognitive training and is considered to indicate relative automaticity of behavior induced by the training (Prakash et al., 2012), it cannot be accounted for in terms of the improved "efficiency" of neural function (Poldrack, 2015). The connectome approach can provide another perspective for the effects of the cognitive training in terms of changes in cost of information transfer within the network. Additionally, FC strength was spatially correlated with regional cerebral blood flow (rCBF), particularly in the default mode network and executive control network, and the coupling between blood supply and FC in the lateral-parietal lobe was modulated with task demands (Liang et al., 2013), suggesting that FC analysis would provide effective tools for measuring changes of energy consumption induced by cognitive training interventions. Therefore, it is getting more important to consider about modulations of the brain network architecture induced by the cognitive training in order to develop the assistance system for the cognitive training.

We have introduced graph theory as a tool for investigating the topological architecture of complex networks, and its applications to the human large-scale brain network. In the studies introduced above, the graph theoretical network metrics have been used to show prevailing attributes of the brain network, such as small-world architecture, scale-free organization, or hub brain regions. In the next section, we will discuss its applicability for demonstrating difference in the brain functional network architecture, which could discriminate cognitive states.

Difference in the Brain Functional Network

The FC patterns of the brain network can be different depending on cognitive states or states of mind, suggesting that functional brain network can be used as biomarkers for detecting mental states. For example, the functional interaction between cell assemblies revealed by the human EEG coherence, which is the correlation coefficient in the frequency domain, was higher during memory encoding phase for subsequently recalled words compared to forgotten words (Weiss and Rappelsberger, 2000). In one study, Astolfi et al. showed different cortical connectivity pattern during observations of TV commercials between subsequently remembered and forgotten ones (Astolfi et al., 2008). They also demonstrated that the parietal areas received a larger amount of the incoming flow of information during the observation of TV commercials that were remembered than that of forgotten ones. Even more precise differences in cognitive states can be predicted by connectivity patterns of the brain network. Through calculating

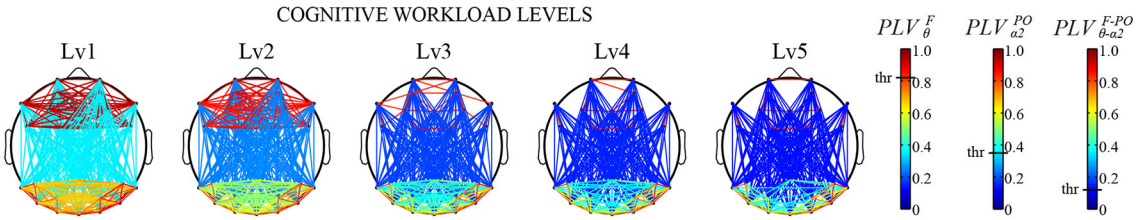

FIGURE 2 | Cross-frequency causal interactions revealed by Phase Locking Values (PLV) for multiple cognitive workload levels during a mental arithmetic task. Three different thresholds have been applied to each type of coupling (F/θ, POα2, CFC) (Adapted from Dimitriadis et al., 2014). a permission will be obtained from the publisher after acceptance, the image will be replaced with high-resolution version.

the cross-frequency causal interactions (Canolty and Knight, 2010) between frontal and parieto-occipital sites, Dimitriadis et al. estimated effective networks derived from EEG signals during a mental arithmetic task with different cognitive workload levels (Dimitriadis et al., 2014). The tensor subspace analysis (TSA) based learning was then used to extract features that can discriminate different cognitive workload levels based on FC patterns. These features achieved a remarkable high correct-recognition-rate (96%) for classification of the task difficulties, suggesting that the FC patterns based on cross-frequency couplings between subregions can become powerful biomarkers for measuring cognitive workload levels (**Figure 2**). Also, multivariate pattern analysis (MVPA) on EEG FC patterns demonstrated successful classification of mental fatigue states from vigilant state at an accuracy of 81.5% (Sun et al., 2014b). These results have suggested that a combination of FC patterns and advanced mathematical tools could provide powerful biomarkers of cognitive states.

In addition to the FC pattern itself, differences in the topological architecture of the brain functional network can be quantified in terms of graph theoretical network metrics. Kitzbichler et al. have found that the brain functional network derived from human MEG data became more globally efficient, less clustered, and less modular network configuration as cognitive efforts got greater during a WM task (Kitzbichler et al., 2011). Furthermore, Sun et al. employed the graph theoretical metrics on FC patterns derived from lower α band (8–10 Hz) of EEG data to investigate small-world network properties due to a decline in vigilance caused by performing an attention demanding task (Psychomotor Vigilance Test; PVT; Sun et al., 2014a). They found a decrease in efficiency of global information transfer revealed by increased weighted characteristic path length, and an asymmetrical pattern of connectivity (right > left) in fronto-parietal regions due to mental fatigue (**Figure 3**). Such difference in graph theoretical network metrics was found between rest and a task performance for the functional network derived from MEG (Bassett et al., 2006) and fMRI (Cao et al., 2014; Taya et al., 2014). Also, the graph theoretical metrics on fMRI functional network could discriminate between resting-state and sensory stimulation (Moussa et al., 2011), different cognitive load during a WM task (Ginestet and Simmons, 2011), different cognitive states in an emotional and a motivational task (Kinnison et al., 2012), and between an intentional and an incidental learning of words during neuropsychological tests (Kuhnert et al., 2013). The small-worldness of EEG functional network was different between during rest and mathematical thinking (Micheloyannis et al., 2009) and some network metrics of a combined EEG and MEG functional network was different between low- and high-memory load during a visual WM retention period (Palva et al., 2010). Furthermore, graph theoretical network metrics or network modularity of fMRI functional network were different depending on sleep levels or conscious levels (Ferri et al., 2007; Spoormaker et al., 2010; Tagliazucchi et al., 2013; Uehara et al., 2014).

The graph theoretical network metrics can be effective in discriminating individual differences in mental or cognitive abilities as well. Van den Heuvel et al. have demonstrated a strong negative association between the normalized characteristic path length of the intrinsic brain network derived from resting-state fMRI data and intelligence quotient (IQ), suggesting that human intellectual performance is related to how efficiently the brain integrates information between brain regions (van den Heuvel et al., 2009). Moreover Langer et al. have shown that clustering coefficient and path length of the functional network derived from resting EEG were strongly related to general intelligence evaluated by Ravens advanced progressive matrices: higher small-worldness for higher general intelligence (Langer et al., 2012). Although the network metrics can also be useful biomarkers for diagnosis of mental disorders (Bassett and Bullmore, 2009), we will not discuss about this case here.

In summary, the brain functional network can show different connectivity patterns depending on cognitive states such as cognitive workloads or sleep stages, and such difference can be extracted and be classified using advanced mathematical techniques. Furthermore, the graph theoretical metrics that quantify topological architecture of complex networks can also discriminate between cognitive states and individual differences in intelligence. These results have suggested that graph theoretical network metrics on functional network can be useful biomarkers for monitoring and optimizing cognitive states of learners during cognitive training.

Modulations of the Brain Network Induced by Cognitive Training Interventions

We have introduced a number of examples showing that the brain FC patterns could be different depending on cognitive

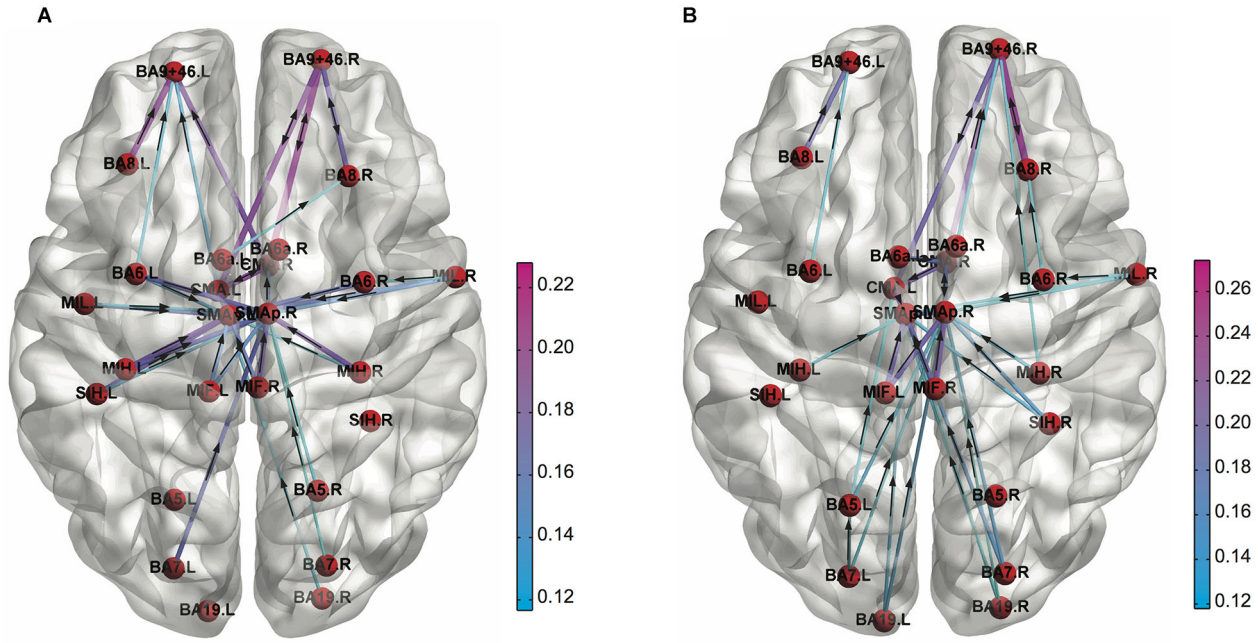

FIGURE 3 | Functional connectivity patterns in the low alpha (8–10 Hz) frequency band obtained for (A) 1st and (B) 4th quartile during the PVT task performance. The cortical connections are weaker at left prefrontal cortex compared to right one in the 4th quartile (Adapted from Sun et al., 2014a).

states or even individual cognitive abilities. For assisting the cognitive training, it is important to know whether the brain functional network could be changed through cognitive interventions. Although only one study has directly examined the effect of cognitive training interventions on topological architecture of the brain functional network so far (Langer et al., 2013), a number of studies have examined the effect of cognitive interventions on the brain network in different time scales, and found the modulation of the brain network induced by prior experiences including the cognitive training, as introduced below.

There are a number of studies showing modifications of the brain FC induced by cognitive or perceptual task performance. Albert et al. (2009) have shown that a motor learning could modulate subsequent neural activity during rest and the changes in resting activity were not limited to immediately after the learning, but persisted after 4 min of unrelated task. Stevens et al. (2010) have examined the effects of preceding exposure of visual stimuli from distinct categories (i.e., faces or scenes) on FC between frontal networks and category-preferential visual regions during rest. They found that increased couplings between a frontal brain region (rIFG) and category-preferential visual regions after each task, and subsequent memory performance was predicted by the degree of modulation of the couplings. These findings have indicated that resting-state FC could be modulated by perceptual or cognitive tasks at least in a short-term (minutes).

Such modulations of resting-state connectivity induced by prior experience can last for longer duration (days or weeks). Lewis et al. (2009) have investigated the effects of intense training (2–9 days) on a visual perceptual task on resting-state FC, and found that the FC between trained visual cortex and dorsal attention regions became more negatively correlated while that between untrained visual cortex and several default regions became less negatively correlated after learning. Changes of resting-state FC were found for WM training as well. Six weeks of a verbal WM training induced modifications in resting-state FC and the change of frontoparietal connectivity was positively related to performance improvement while that of default network connectivity was negatively correlated (Jolles et al., 2013). Also, 27 days of the WM training program increased FC between mPFC and precuneus and that between mPFC and right posterior parietal cortex and right lPFC (Takeuchi et al., 2013). Even some weeks of training of video games changed FC during game playing (Voss et al., 2012) and rest (Strenziok et al., 2014).

The changes in brain network induced by cognitive training interventions can be observed in structural connectivity as well. Takeuchi et al. have demonstrated that 2 months of WM training increased FA in the white matter regions, possibly attributable to increased myelination after training (Takeuchi et al., 2010). Additionally, Wolf et al. investigated the transfer capability of general fluid intelligence related cognitive training in elderly subjects (Wolf et al., 2014). They examined structural integrity measured by DTI immediately after a 4-week training and a 3-month follow-up period. Although only 22% of subjects showed successful long-term transfer effects, transfer of training gains was associated with a higher degree of structural integrity.

In addition to the individual connectivity between brain regions, the graph theoretical approaches can be employed to

TABLE 3 | Neuroimaging studies showing changes in brain FC induced by cognitive interventions.

Study	Modality	Training task	Control group	Population	Training period
Strenziok et al. (2014)	fMRI, DTI	Rise of Nations, Brain Fitness, Space Fortress	-	OA	6 weeks
Jolles et al. (2013)	fMRI	a verbal WM task	-	YA and CH	6 weeks
Takeuchi et al. (2013)	fMRI, ASL	WMT program	no training	YA	27 days
Langer et al. (2013)	EEG	Tatool (adaptive WM training)	tasks with low WM demand	YA	4 weeks
Heitger et al. (2012)	fMRI	a motor learning task	-	YA	4 days
Voss et al. (2012)	fMRI	Space Fortress	-	YA	20 h
Bassett et al. (2011)	fMRI	a motor learning task	-	YA (musical instruments)	5 days
Stevens et al. (2010)	fMRI	visual semantic classification tasks	-	YA	15 min
Albert et al. (2009)	fMRI	a motor learning task	a motor performance task	YA	11 min
Lewis et al. (2009)	fMRI	a shape-identification task	-	YA	2–9 days

YA: young adults, OA: old adults, CH: children.

examine changes in global characteristics of the brain network. Bassett et al. investigated reconfiguration of modular structure of the FC induced by 3 days of a motor learning task (Bassett et al., 2011). They found that some of the brain regions showed consistent community allegiance (low-flexibility nodes) while other regions constantly shift allegiance (high-flexibility nodes). Additionally, the network flexibility first increased and then decreased during the learning process. The authors have also examined changes of modular structure over thirty-day of a motor skill training, and demonstrated that the separation between core and periphery nodes decreased over the course of training, and good learners tend to have greater separation than poor learners (Bassett et al., 2013). Even 4 days of learning of complex hand coordination pattern induced changes in topological architecture of the fMRI functional network (Heitger et al., 2012). Additionally, Breckel et al. have demonstrated prolonged changes in the global architecture of the resting-state brain network during a series of task performance (Breckel et al., 2013). They compared topological properties of the functional brain network derived from fMRI data before a sustained attentional task performance and those after the task, and showed that the post-task functional network had more clustering, less global efficiency, and less long-distance connections, suggesting a reduction in network integration due to the task performance. These changes in network architecture were still observed after 6 min of resting state. Interestingly, such changes in information transfer efficiency of the brain functional network were induced by a cognitive training intervention (Langer et al., 2013). Langer et al. investigated effects of intensive WM training on the EEG functional network. They first confirmed that WM performance was correlated with power in the θ frequency band, and the WM training increased the θ power. Then, they found the global efficiency of the functional network in the θ band was correlated with higher WM performance before training, and WM training induced increase of small-world topology revealed by an increase of the clustering coefficient and a decrease of the path length in the majority of the subjects.

Taken together, prior sensory or cognitive experience and cognitive training interventions can have even prolonged effects on the brain structural and FC. In addition, motor training and WM training induced changes in topological architecture of the brain network. Although only one study has directly examined the effect of cognitive training interventions using brain connectome approach so far (Langer et al., 2013), alterations in the brain connectivity patterns can also be captured by graph theoretical network metrics such as clustering coefficients or path length. Such changes in topological architecture and information transfer efficiency of the brain functional network can be attributed to improvements in cognitive processing related to the trained tasks, enhancements of general intelligence, changes in attentional levels, difference in cognitive workload, or reconfiguration of brain sub-networks involved. These results have suggested that the network metrics can be useful biomarkers, not only for monitoring cognitive states, but also for tracking effects of the cognitive training interventions. A summary for existing studies showing changes in functional brain connectivity induced by cognitive training interventions is given in **Table 3**.

Conclusion

In this review article, we proposed that biomarkers based on brain connectome approach could be useful for a brain enhancement system by optimizing effectiveness of cognitive training interventions on learners' learning process. For this purpose, we first introduced studies on cognitive training interventions. A number of studies have shown that the brain cognitive functions could be improved through cognitive training interventions such as WM training or video game training, and brain activities were modulated as a result of the training (Klingberg, 2010). Although such cognitive interventions are effective, their effectiveness can be different among individuals and they may even vary depending on mental state at the moment of the training. If the task that

the learner is performing is too difficult or too demanding, it would be difficult for them to keep the motivation and concentration on the facing task and some of them can be exhausted from the excess of cognitive workload, resulting in a poor or a lack of improvement in cognitive functions. An adaptive assistance system for cognitive training through monitoring the learners' mental states such as cognitive workload using objective biomarkers is a useful approach to facilitation and optimization of the learning progress. As introduced above, a number of biomarkers have been proposed for monitoring mental states including cognitive workloads. Most of the biomarkers are based on spectral properties of EEG signals or ERPs, and the extracted features are often subjected to cutting-edge mathematical tools based on machine learning theory to discriminate mental states (Kothe and Makeig, 2011). Additionally, some biomarkers can be used to predict individuals' intelligence or learners' subsequent learning rate (Langer et al., 2012). If optimal mental states for ongoing training can be replicated in the brain through the adjustment of the cognitive workload, neurofeedback, or other cognitive training scheme, we could optimize the effectiveness of the training process.

Furthermore, we have introduced the functional connectome approach, which is mainly based on the graph theory (Sporns, 2014). The brain is a complex network consisting of spatially distributed regions dedicated to different functions, and it is proposed that cognitive functions emerge from dynamic interactions of several brain areas, not a result of an activation of a single brain region (Bressler and Menon, 2010). As such, the number of publications regarding brain network is drastically increasing (Friston, 2011). We have proposed here that the brain connectome can be a useful approach not only for elucidating mechanisms underlying brain cognitive functions, but also for detection of mental states. The graph theoretical network metrics can be biomarkers of cognitive states, as shown in previous studies on cognitive workload (Ginestet and Simmons, 2011; Kitzbichler et al., 2011) or mental fatigue (Breckel et al., 2013; Sun et al., 2014a). Several studies have shown that the brain functional and structural network connectivity can be altered through cognitive interventions, and the graph theoretical network metrics have shown the reorganization of topological architecture of the brain functional network over multiple temporal scales (i.e., minutes, days, weeks). These results suggest that the functional connectome approach as well as conventional biomarkers would be effective methods for boosting learning progress of learners during the course of cognitive training.

Acknowledgments

The authors appreciate the National University of Singapore for supporting the Cognitive Engineering Group at the Singapore Institute for Neurotechnology (SINAPSE) under WBS Number R-719-001-102-232 and Ministry of Education of Singapore for funding support under the grant number MOE2014-T2-1-115.

References

Achard, S., and Bullmore, E. (2007). Efficiency and cost of economical brain functional networks. *PLoS Comput. Biol.* 3:e17. doi: 10.1371/journal.pcbi.0030017

Achard, S., Salvador, R., Whitcher, B., Suckling, J., and Bullmore, E. (2006). A resilient, low-frequency, small-world human brain functional network with highly connected association cortical hubs. *J. Neurosci.* 26, 63–72. doi: 10.1523/jneurosci.3874-05.2006

Albert, N. B., Robertson, E. M., and Miall, R. C. (2009). The resting human brain and motor learning. *Curr. Biol.* 19, 1023–1027. doi: 10.1016/j.cub.2009.04.028

Anguera, J. A., Boccanfuso, J., Rintoul, J. L., Al-Hashimi, O., Faraji, F., Janowich, J., et al. (2013). Video game training enhances cognitive control in older adults. *Nature* 501, 97–101. doi: 10.1038/nature12486

Aricò, P., Borghini, G., Graziani, I., Taya, F., Sun, Y., Bezerianos, A., et al. (2014). Towards a multimodal bioelectrical framework for the online mental workload evaluation. *Conf. Proc. IEEE Eng. Med. Biol. Soc.* 2014, 3001–3004. doi: 10.1109/EMBC.2014.6944254

Astolfi, L., Cincotti, F., Mattia, D., Marciani, M. G., Baccala, L. A., de Vico Fallani, F., et al. (2007). Comparison of different cortical connectivity estimators for high-resolution EEG recordings. *Hum. Brain Mapp.* 28, 143–157. doi: 10.1002/hbm.20263

Astolfi, L., De Vico Fallani, F., Cincotti, F., Mattia, D., Bianchi, L., Marciani, M. G., et al. (2008). Neural basis for brain responses to TV commercials: a high-resolution EEG study. *IEEE Trans. Neural Syst. Rehabil. Eng.* 16, 522–531. doi: 10.1109/TNSRE.2008.2009784

Baccalá, L. A., and Sameshima, K. (2001). Partial directed coherence: a new concept in neural structure determination. *Biol. Cybern.* 84, 463–474. doi: 10.1007/pl00007990

Baldwin, C. L., and Penaranda, B. N. (2012). Adaptive training using an artificial neural network and EEG metrics for within- and cross-task workload classification. *Neuroimage* 59, 48–56. doi: 10.1016/j.neuroimage.2011.07.047

Barabási, A. L. (2013). Network science. *Philos. Trans. A Math. Phys. Eng. Sci.* 371:20120375. doi: 10.1098/rsta.2012.0375

Bassett, D. S., and Bullmore, E. T. (2009). Human brain networks in health and disease. *Curr. Opin. Neurol.* 22, 340–347. doi: 10.1097/WCO.0b013e32832d93dd

Bassett, D. S., Greenfield, D. L., Meyer-Lindenberg, A., Weinberger, D. R., Moore, S. W., and Bullmore, E. T. (2010). Efficient physical embedding of topologically complex information processing networks in brains and computer circuits. *PLoS Comput. Biol.* 6:e1000748. doi: 10.1371/journal.pcbi.1000748

Bassett, D. S., Meyer-Lindenberg, A., Achard, S., Duke, T., and Bullmore, E. (2006). Adaptive reconfiguration of fractal small-world human brain functional networks. *Proc. Natl. Acad. Sci. U S A* 103, 19518–19523. doi: 10.1073/pnas.0606005103

Bassett, D. S., Wymbs, N. F., Porter, M. A., Mucha, P. J., Carlson, J. M., and Grafton, S. T. (2011). Dynamic reconfiguration of human brain networks during learning. *Proc. Natl. Acad. Sci. U S A* 108, 7641–7646. doi: 10.1073/pnas.1018985108

Bassett, D. S., Wymbs, N. F., Rombach, M. P., Porter, M. A., Mucha, P. J., and Grafton, S. T. (2013). Task-based core-periphery organization of human brain dynamics. *PLoS Comput. Biol.* 9:e1003171. doi: 10.1371/journal.pcbi.1003171

Berka, C., Levendowski, D. J., Lumicao, M. N., Yau, A., Davis, G., Zivkovic, V. T., et al. (2007). EEG correlates of task engagement and mental workload in vigilance, learning and memory tasks. *Aviat. Space Environ. Med.* 78, B231–B244.

Birbaumer, N., Ghanayim, N., Hinterberger, T., Iversen, I., Kotchoubey, B., Kübler, A., et al. (1999). A spelling device for the paralysed. *Nature* 398, 297–298. doi: 10.1038/18581

Boersma, M., Smit, D. J. A., de Bie, H. M. A., Van Baal, G. C. M., Boomsma, D. I., de Geus, E. J. C., et al. (2011). Network analysis of resting state EEG in the developing young brain: structure comes with maturation. *Hum. Brain Mapp.* 32, 413–425. doi: 10.1002/hbm.21030

Borghini, G., Aricò, P., Graziani, I., Salinari, S., Sun, Y., Taya, F., et al. (2015). Quantitative assessment of the training improvement in a motor-cognitive task by using EEG, ECG and EOG signals. *Brain Topogr.* doi: 10.1007/s10548-015-0425-7. [Epub ahead of print].

Borghini, G., Astolfi, L., Vecchiato, G., Mattia, D., and Babiloni, F. (2014). Measuring neurophysiological signals in aircraft pilots and car drivers for the assessment of mental workload, fatigue and drowsiness. *Neurosci. Biobehav. Rev.* 44, 58–75. doi: 10.1016/j.neubiorev.2012.10.003

Boyke, J., Driemeyer, J., Gaser, C., Büchel, C., and May, A. (2008). Training-induced brain structure changes in the elderly. *J. Neurosci.* 28, 7031–7035. doi: 10.1523/JNEUROSCI.0742-08.2008

Breckel, T. P. K., Thiel, C. M., Bullmore, E. T., Zalesky, A., Patel, A. X., and Giessing, C. (2013). Long-term effects of attentional performance on functional brain network topology. *PLoS One* 8:e74125. doi: 10.1371/journal.pone.0074125

Bressler, S. L., and Menon, V. (2010). Large-scale brain networks in cognition: emerging methods and principles. *Trends Cogn. Sci.* 14, 277–290. doi: 10.1016/j.tics.2010.04.004

Bullmore, E., and Sporns, O. (2009). Complex brain networks: graph theoretical analysis of structural and functional systems. *Nat. Rev. Neurosci.* 10, 186–198. doi: 10.1038/nrn2575

Buschkuehl, M., Hernandez-Garcia, L., Jaeggi, S. M., Bernard, J. A., and Jonides, J. (2014). Neural effects of short-term training on working memory. *Cogn. Affect. Behav. Neurosci.* 14, 147–160. doi: 10.3758/s13415-013-0244-9

Cannonieri, G. C., Bonilha, L., Fernandes, P. T., Cendes, F., and Li, L. M. (2007). Practice and perfect: length of training and structural brain changes in experienced typists. *Neuroreport* 18, 1063–1066. doi: 10.1097/wnr.0b013e3281a030e5

Canolty, R. T., and Knight, R. T. (2010). The functional role of cross-frequency coupling. *Trends Cogn. Sci.* 14, 506–515. doi: 10.1016/j.tics.2010.09.001

Cao, H., Plichta, M. M., Schäfer, A., Haddad, L., Grimm, O., Schneider, M., et al. (2014). Test-retest reliability of fMRI-based graph theoretical properties during working memory, emotion processing and resting state. *Neuroimage* 84, 888–900. doi: 10.1016/j.neuroimage.2013.09.013

Cavanna, A. E., and Trimble, M. R. (2006). The precuneus: a review of its functional anatomy and behavioural correlates. *Brain* 129, 564–583. doi: 10.1093/brain/awl004

Chein, J. M., and Morrison, A. B. (2010). Expanding the mind's workspace: training and transfer effects with a complex working memory span task. *Psychon. Bull. Rev.* 17, 193–199. doi: 10.3758/PBR.17.2.193

Chein, J. M., and Schneider, W. (2005). Neuroimaging studies of practice-related change: fMRI and meta-analytic evidence of a domain-general control network for learning. *Brain Res. Cogn. Brain Res.* 25, 607–623. doi: 10.1016/j.cogbrainres.2005.08.013

Clark, V. P., and Parasuraman, R. (2014). Neuroenhancement: enhancing brain and mind in health and in disease. *Neuroimage* 85(Pt. 3), 889–894. doi: 10.1016/j.neuroimage.2013.08.071

Cole, M. W., Bassett, D. S., Power, J. D., Braver, T. S., and Petersen, S. E. (2014). Intrinsic and task-evoked network architectures of the human brain. *Neuron* 83, 238–251. doi: 10.1016/j.neuron.2014.05.014

Cole, M. W., Pathak, S., and Schneider, W. (2010b). Identifying the brain's most globally connected regions. *Neuroimage* 49, 3132–3148. doi: 10.1016/j.neuroimage.2009.11.001

Cole, M. W., Reynolds, J. R., Power, J. D., Repovs, G., Anticevic, A., and Braver, T. S. (2013). Multi-task connectivity reveals flexible hubs for adaptive task control. *Nat. Neurosci.* 16, 1348–1355. doi: 10.1038/nn.3470

Cole, D. M., Smith, S. M., and Beckmann, C. F. (2010a). Advances and pitfalls in the analysis and interpretation of resting-state FMRI data. *Front. Syst. Neurosci.* 4:8. doi: 10.3389/fnsys.2010.00008

Colom, R., Quiroga, M. Á., Shih, P. C., Martínez, K., Burgaleta, M., Martínez-Molina, A., et al. (2010). Improvement in working memory is not related to increased intelligence scores. *Intelligence* 38, 497–505. doi: 10.1016/j.intell.2010.06.008

Colom, R., Román, F. J., Abad, F. J., Shih, P. C., Privado, J., Froufe, M., et al. (2013). Adaptive n-back training does not improve fluid intelligence at the construct level: gains on individual tests suggest that training may enhance visuospatial processing. *Intelligence* 41, 712–727. doi: 10.1016/j.intell.2013.09.002

Comstock, J. R., and Arnegard, R. J. (1992). *The Multi-Attribute Task Battery for Human Operator Workload and Strategic Behavior Research.* Hampton, VA: National Aeronautics and Space Administration, Langley Research Center.

Conway, A. R., Kane, M. J., and Engle, R. W. (2003). Working memory capacity and its relation to general intelligence. *Trends Cogn. Sci.* 7, 547–552. doi: 10.1016/j.tics.2003.10.005

Dahlin, E., Neely, A. S., Larsson, A., Bäckman, L., and Nyberg, L. (2008). Transfer of learning after updating training mediated by the striatum. *Science* 320, 1510–1512. doi: 10.1126/science.1155466

Deary, I. J., Strand, S., Smith, P., and Fernandes, C. (2007). Intelligence and educational achievement. *Intelligence* 35, 13–21. doi: 10.1016/j.intell.2006.02.001

Deuker, L., Bullmore, E. T., Smith, M., Christensen, S., Nathan, P. J., Rockstroh, B., et al. (2009). Reproducibility of graph metrics of human brain functional networks. *Neuroimage* 47, 1460–1468. doi: 10.1016/j.neuroimage.2009.05.035

Dimitriadis, S. I., Sun, Y., Kwok, K., Laskaris, N. A., Thakor, N., and Bezerianos, A. (2014). Cognitive workload assessment based on the tensorial treatment of EEG estimates of cross-frequency phase interactions. *Ann. Biomed. Eng.* doi: 10.1007/s10439-014-1143-0. [Epub ahead of print].

Draganski, B., Gaser, C., Busch, V., Schuierer, G., Bogdahn, U., and May, A. (2004). Neuroplasticity: changes in grey matter induced by training. *Nature* 427, 311–312. doi: 10.1038/427311a

Draganski, B., Gaser, C., Kempermann, G., Kuhn, H. G., Winkler, J., Büchel, C., et al. (2006). Temporal and spatial dynamics of brain structure changes during extensive learning. *J. Neurosci.* 26, 6314–6317. doi: 10.1523/jneurosci.4628-05.2006

Draganski, B., and May, A. (2008). Training-induced structural changes in the adult human brain. *Behav. Brain Res.* 192, 137–142. doi: 10.1016/j.bbr.2008.02.015

Driemeyer, J., Boyke, J., Gaser, C., Büchel, C., and May, A. (2008). Changes in gray matter induced by learning–revisited. *PLoS One* 3:e2669. doi: 10.1371/journal.pone.0002669

Dux, P. E., Tombu, M. N., Harrison, S., Rogers, B. P., Tong, F., and Marois, R. (2009). Training improves multitasking performance by increasing the speed of information processing in human prefrontal cortex. *Neuron* 63, 127–138. doi: 10.1016/j.neuron.2009.06.005

Eguíluz, V. M., Chialvo, D. R., Cecchi, G. A., Baliki, M., and Apkarian, A. V. (2005). Scale-free brain functional networks. *Phys. Rev. Lett.* 94:018102. doi: 10.1103/physrevlett.94.018102

Elbert, T., Pantev, C., Wienbruch, C., Rockstroh, B., and Taub, E. (1995). Increased cortical representation of the fingers of the left hand in string players. *Science* 270, 305–307. doi: 10.1126/science.270.5234.305

Engvig, A., Fjell, A. M., Westlye, L. T., Moberget, T., Sundseth, Ø., Larsen, V. A., et al. (2010). Effects of memory training on cortical thickness in the elderly. *Neuroimage* 52, 1667–1676. doi: 10.1016/j.neuroimage.2010.05.041

Erickson, K. I., Colcombe, S. J., Wadhwa, R., Bherer, L., Peterson, M. S., Scalf, P. E., et al. (2007). Training-induced functional activation changes in dual-task processing: an FMRI study. *Cereb. Cortex* 17, 192–204. doi: 10.1093/cercor/bhj137

Farah, M. J., Illes, J., Cook-Deegan, R., Gardner, H., Kandel, E., King, P., et al. (2004). Neurocognitive enhancement: what can we do and what should we do? *Nat. Rev. Neurosci.* 5, 421–425. doi: 10.1038/nrn1390

Farwell, L. A., and Donchin, E. (1988). Talking off the top of your head: toward a mental prosthesis utilizing event-related brain potentials. *Electroencephalogr. Clin. Neurophysiol.* 70, 510–523. doi: 10.1016/0013-4694(88)90149-6

Ferri, R., Rundo, F., Bruni, O., Terzano, M. G., and Stam, C. J. (2007). Small-world network organization of functional connectivity of EEG slow-wave activity during sleep. *Clin. Neurophysiol.* 118, 449–456. doi: 10.1016/j.clinph.2006.10.021

Fleischman, D. A., Wilson, R. S., Gabrieli, J. D., Bienias, J. L., and Bennett, D. A. (2004). A longitudinal study of implicit and explicit memory in old persons. *Psychol. Aging* 19, 617–625. doi: 10.1037/0882-7974.19.4.617

Friston, K. J. (1994). Functional and effective connectivity in neuroimaging: a synthesis. *Hum. Brain Mapp.* 2, 56–78. doi: 10.1002/hbm.460020107

Friston, K. J. (2011). Functional and effective connectivity: a review. *Brain Connect.* 1, 13–36. doi: 10.1089/brain.2011.0008

Ginestet, C. E., and Simmons, A. (2011). Statistical parametric network analysis of functional connectivity dynamics during a working memory task. *Neuroimage* 55, 688–704. doi: 10.1016/j.neuroimage.2010.11.030

Gomarus, H. K., Althaus, M., Wijers, A. A., and Minderaa, R. B. (2006). The effects of memory load and stimulus relevance on the EEG during a visual selective memory search task: an ERP and ERD/ERS study. *Clin. Neurophysiol.* 117, 871–884. doi: 10.1016/j.clinph.2005.12.008

Gong, G., He, Y., Concha, L., Lebel, C., Gross, D. W., Evans, A. C., et al. (2009). Mapping anatomical connectivity patterns of human cerebral cortex using *in vivo* diffusion tensor imaging tractography. *Cereb. Cortex* 19, 524–536. doi: 10.1093/cercor/bhn102

Graimann, B., Pfurtscheller, G., and Allison, B. Z. (2010). *Brain-Computer Interfaces: Revolutionizing Human-Computer Interaction.* Heidelberg, Berlin: Springer.

Green, C. S., and Bavelier, D. (2003). Action video game modifies visual selective attention. *Nature* 423, 534–537. doi: 10.1038/nature01647

Gruzelier, J. H. (2014). EEG-neurofeedback for optimising performance. I: a review of cognitive and affective outcome in healthy participants. *Neurosci. Biobehav. Rev.* 44, 124–141. doi: 10.1016/j.neubiorev.2013.09.015

Gutchess, A. (2014). Plasticity of the aging brain: new directions in cognitive neuroscience. *Science* 346, 579–582. doi: 10.1126/science.1254604

Hagmann, P., Cammoun, L., Gigandet, X., Meuli, R., Honey, C. J., Wedeen, V. J., et al. (2008). Mapping the structural core of human cerebral cortex. *PLoS Biol.* 6:e159. doi: 10.1371/journal.pbio.0060159

Hagmann, P., Kurant, M., Gigandet, X., Thiran, P., Wedeen, V. J., Meuli, R., et al. (2007). Mapping human whole-brain structural networks with diffusion MRI. *PLoS One* 2:e597. doi: 10.1371/journal.pone.0000597

Halford, G. S., Cowan, N., and Andrews, G. (2007). Separating cognitive capacity from knowledge: a new hypothesis. *Trends Cogn. Sci.* 11, 236–242. doi: 10.1016/j.tics.2007.04.001

Hamilton, R., Messing, S., and Chatterjee, A. (2011). Rethinking the thinking cap: ethics of neural enhancement using noninvasive brain stimulation. *Neurology* 76, 187–193. doi: 10.1212/WNL.0b013e318205d50d

He, Y., Chen, Z. J., and Evans, A. C. (2007). Small-world anatomical networks in the human brain revealed by cortical thickness from MRI. *Cereb. Cortex* 17, 2407–2419. doi: 10.1093/cercor/bhl149

Hebb, D. (1949). *The Organization of Behavior: A Neuropsychological Theory.* New York: John Wiley and Sons.

Heinzel, S., Lorenz, R. C., Brockhaus, W. R., Wustenberg, T., Kathmann, N., Heinz, A., et al. (2014). Working memory load-dependent brain response predicts behavioral training gains in older adults. *J. Neurosci.* 34, 1224–1233. doi: 10.1523/JNEUROSCI.2463-13.2014

Heitger, M. H., Ronsse, R., Dhollander, T., Dupont, P., Caeyenberghs, K., and Swinnen, S. P. (2012). Motor learning-induced changes in functional brain connectivity as revealed by means of graph-theoretical network analysis. *Neuroimage* 61, 633–650. doi: 10.1016/j.neuroimage.2012.03.067

Hempel, A., Giesel, F. L., Garcia Caraballo, N. M., Amann, M., Meyer, H., Wüstenberg, T., et al. (2004). Plasticity of cortical activation related to working memory during training. *Am. J. Psychiatry* 161, 745–747. doi: 10.1176/appi.ajp.161.4.745

Hermundstad, A. M., Bassett, D. S., Brown, K. S., Aminoff, E. M., Clewett, D., Freeman, S., et al. (2013). Structural foundations of resting-state and task-based functional connectivity in the human brain. *Proc. Natl. Acad. Sci. U S A* 110, 6169–6174. doi: 10.1073/pnas.1219562110

Honey, C. J., Sporns, O., Cammoun, L., Gigandet, X., Thiran, J. P., Meuli, R., et al. (2009). Predicting human resting-state functional connectivity from structural connectivity. *Proc. Natl. Acad. Sci. U S A* 106, 2035–2040. doi: 10.1073/pnas.0811168106

Iturria-Medina, Y., Sotero, R. C., Canales-Rodríguez, E. J., Alemán-Gómez, Y., and Melie-García, L. (2008). Studying the human brain anatomical network via diffusion-weighted MRI and graph theory. *Neuroimage* 40, 1064–1076. doi: 10.1016/j.neuroimage.2007.10.060

Jaeggi, S. M., Buschkuehl, M., Jonides, J., and Perrig, W. J. (2008). Improving fluid intelligence with training on working memory. *Proc. Natl. Acad. Sci. U S A* 105, 6829–6833. doi: 10.1073/pnas.0801268105

Jaušovec, N., and Jaušovec, K. (2012). Working memory training: improving intelligence–changing brain activity. *Brain Cogn.* 79, 96–106. doi: 10.1016/j.bandc.2012.02.007

Jolles, D. D., and Crone, E. A. (2012). Training the developing brain: a neurocognitive perspective. *Front. Hum. Neurosci.* 6:76. doi: 10.3389/fnhum.2012.00076

Jolles, D. D., Grol, M. J., Van Buchem, M. A., Rombouts, S. A. R. B., and Crone, E. A. (2010). Practice effects in the brain: changes in cerebral activation after working memory practice depend on task demands. *Neuroimage* 52, 658–668. doi: 10.1016/j.neuroimage.2010.04.028

Jolles, D. D., van Buchem, M. A., Crone, E. A., and Rombouts, S. A. (2013). Functional brain connectivity at rest changes after working memory training. *Hum. Brain Mapp.* 34, 396–406. doi: 10.1002/hbm.21444

Kamiński, M. J., and Blinowska, K. J. (1991). A new method of the description of the information flow in the brain structures. *Biol. Cybern.* 65, 203–210. doi: 10.1007/bf00198091

Karbach, J., and Schubert, T. (2013). Training-induced cognitive and neural plasticity. *Front. Hum. Neurosci.* 7:48. doi: 10.3389/fnhum.2013.00048

Kinnison, J., Padmala, S., Choi, J. M., and Pessoa, L. (2012). Network analysis reveals increased integration during emotional and motivational processing. *J. Neurosci.* 32, 8361–8372. doi: 10.1523/JNEUROSCI.0821-12.2012

Kitzbichler, M. G., Henson, R. N., Smith, M. L., Nathan, P. J., and Bullmore, E. T. (2011). Cognitive effort drives workspace configuration of human brain functional networks. *J. Neurosci.* 31, 8259–8270. doi: 10.1523/JNEUROSCI.0440-11.2011

Klimesch, W. (1999). EEG alpha and theta oscillations reflect cognitive and memory performance: a review and analysis. *Brain Res. Brain Res. Rev.* 29, 169–195. doi: 10.1016/s0165-0173(98)00056-3

Klingberg, T. (2010). Training and plasticity of working memory. *Trends Cogn. Sci.* 14, 317–324. doi: 10.1016/j.tics.2010.05.002

Klingberg, T., Forssberg, H., and Westerberg, H. (2002). Training of working memory in children with ADHD. *J. Clin. Exp. Neuropsychol.* 24, 781–791. doi: 10.1076/jcen.24.6.781.8395

Kohlmorgen, J., Dornhege, G., Braun, M., Blankertz, B., Müller, K.-R., Curio, G., et al. (2007). "Improving human performance in a real operating environment through real-time mental workload detection," in *Toward Brain-Computer Interfacing*, eds G. Dornhege, J. D. R. Millán, T. Hinterberger, D. J. Mcfarland and K.-R. Müller (Cambridge, MA: MIT Press), 409–422.

Kothe, C. A., and Makeig, S. (2011). Estimation of task workload from EEG data: new and current tools and perspectives. *Conf. Proc. IEEE Eng. Med. Biol. Soc.* 2011, 6547–6551. doi: 10.1109/IEMBS.2011.6091615

Kuhnert, M.-T., Bialonski, S., Noennig, N., Mai, H., Hinrichs, H., Helmstaedter, C., et al. (2013). Incidental and intentional learning of verbal episodic material differentially modifies functional brain networks. *PLoS One* 8:e80273. doi: 10.1371/journal.pone.0080273

Langer, N., Pedroni, A., Gianotti, L. R., Hänggi, J., Knoch, D., and Jäncke, L. (2012). Functional brain network efficiency predicts intelligence. *Hum. Brain Mapp.* 33, 1393–1406. doi: 10.1002/hbm.21297

Langer, N., von Bastian, C. C., Wirz, H., Oberauer, K., and Jäncke, L. (2013). The effects of working memory training on functional brain network efficiency. *Cortex* 49, 2424–2438. doi: 10.1016/j.cortex.2013.01.008

Lee, U., Oh, G., Kim, S., Noh, G., Choi, B., and Mashour, G. A. (2010). Brain networks maintain a scale-free organization across consciousness, anesthesia and recovery: evidence for adaptive reconfiguration. *Anesthesiology* 113, 1081–1091. doi: 10.1097/ALN.0b013e3181f229b5

Lee, H., Voss, M. W., Prakash, R. S., Boot, W. R., Vo, L. T., Basak, C., et al. (2012). Videogame training strategy-induced change in brain function during a complex visuomotor task. *Behav. Brain Res.* 232, 348–357. doi: 10.1016/j.bbr.2012.03.043

Lewis, C. M., Baldassarre, A., Committeri, G., Romani, G. L., and Corbetta, M. (2009). Learning sculpts the spontaneous activity of the resting human brain. *Proc. Natl. Acad. Sci. U S A* 106, 17558–17563. doi: 10.1073/pnas.0902455106

Liang, X., Zou, Q., He, Y., and Yang, Y. (2013). Coupling of functional connectivity and regional cerebral blood flow reveals a physiological basis for network hubs of the human brain. *Proc. Natl. Acad. Sci. U S A* 110, 1929–1934. doi: 10.1073/pnas.1214900110

Luft, C. D., Pereda, E., Banissy, M. J., and Bhattacharya, J. (2014). Best of both worlds: promise of combining brain stimulation and brain connectome. *Front. Syst. Neurosci.* 8:132. doi: 10.3389/fnsys.2014.00132

Lustig, C., Shah, P., Seidler, R., and Reuter-Lorenz, P. A. (2009). Aging, training and the brain: a review and future directions. *Neuropsychol. Rev.* 19, 504–522. doi: 10.1007/s11065-009-9119-9

Maclin, E. L., Mathewson, K. E., Low, K. A., Boot, W. R., Kramer, A. F., Fabiani, M., et al. (2011). Learning to multitask: effects of video game practice on electrophysiological indices of attention and resource allocation. *Psychophysiology* 48, 1173–1183. doi: 10.1111/j.1469-8986.2011.01189.x

Maguire, E. A., Woollett, K., and Spiers, H. J. (2006). London taxi drivers and bus drivers: a structural MRI and neuropsychological analysis. *Hippocampus* 16, 1091–1101. doi: 10.1002/hipo.20233

Mathewson, K. E., Basak, C., Maclin, E. L., Low, K. A., Boot, W. R., Kramer, A. F., et al. (2012). Different slopes for different folks: alpha and delta EEG power predict subsequent video game learning rate and improvements in cognitive control tasks. *Psychophysiology* 49, 1558–1570. doi: 10.1111/j.1469-8986.2012.01474.x

McKendrick, R., Ayaz, H., Olmstead, R., and Parasuraman, R. (2014). Enhancing dual-task performance with verbal and spatial working memory training: continuous monitoring of cerebral hemodynamics with NIRS. *Neuroimage* 85(Pt. 3), 1014–1026. doi: 10.1016/j.neuroimage.2013.05.103

Micheloyannis, S., Pachou, E., Stam, C. J., Vourkas, M., Erimaki, S., and Tsirka, V. (2006). Using graph theoretical analysis of multi channel EEG to evaluate the neural efficiency hypothesis. *Neurosci. Lett.* 402, 273–277. doi: 10.1016/j.neulet.2006.04.006

Micheloyannis, S., Vourkas, M., Tsirka, V., Karakonstantaki, E., Kanatsouli, K., and Stam, C. J. (2009). The influence of ageing on complex brain networks: a graph theoretical analysis. *Hum. Brain Mapp.* 30, 200–208. doi: 10.1002/hbm.20492

Moreau, D., and Conway, A. R. (2013). Cognitive enhancement: a comparative review of computerized and athletic training programs. *Int. Rev. Sport Exerc. Psychol.* 6, 155–183. doi: 10.1080/1750984x.2012.758763

Moussa, M. N., Vechlekar, C. D., Burdette, J. H., Steen, M. R., Hugenschmidt, C. E., and Laurienti, P. J. (2011). Changes in cognitive state alter human functional brain networks. *Front. Hum. Neurosci.* 5:83. doi: 10.3389/fnhum.2011.00083

Mozolic, J. L., Hayasaka, S., and Laurienti, P. J. (2010). A cognitive training intervention increases resting cerebral blood flow in healthy older adults. *Front. Hum. Neurosci.* 4:16. doi: 10.3389/neuro.09.016.2010

Neisser, U., Boodoo, G., Bouchard, T. J. Jr., Boykin, A. W., Brody, N., Ceci, S. J., et al. (1996). Intelligence: knowns and unknowns. *Am. Psychol.* 51, 77–101. doi: 10.1037/0003-066X.51.2.77

Neuper, C., and Pfurtscheller, G. (2010). "Neurofeedback training for BCI control," in *Brain-Computer Interfaces*, eds B. Graimann, G. Pfurtscheller, and B. Allison (London: Springer), 65–78.

Nijhuis, E. H., van Cappellen van Walsum, A. M., and Norris, D. G. (2013). Topographic hub maps of the human structural neocortical network. *PLoS One* 8:e65511. doi: 10.1371/journal.pone.0065511

Olesen, P. J., Westerberg, H., and Klingberg, T. (2004). Increased prefrontal and parietal activity after training of working memory. *Nat. Neurosci.* 7, 75–79. doi: 10.1038/nn1165

Owens, M., Koster, E. H., and Derakshan, N. (2013). Improving attention control in dysphoria through cognitive training: transfer effects on working memory capacity and filtering efficiency. *Psychophysiology* 50, 297–307. doi: 10.1111/psyp.12010

Palva, S., Monto, S., and Palva, J. M. (2010). Graph properties of synchronized cortical networks during visual working memory maintenance. *Neuroimage* 49, 3257–3268. doi: 10.1016/j.neuroimage.2009.11.031

Park, D. C., Lautenschlager, G., Hedden, T., Davidson, N. S., Smith, A. D., and Smith, P. K. (2002). Models of visuospatial and verbal memory across the adult life span. *Psychol. Aging* 17, 299–320. doi: 10.1037//0882-7974.17.2.299

Petrides, M. (2005). Lateral prefrontal cortex: architectonic and functional organization. *Philos. Trans. R. Soc. Lond. B Biol. Sci.* 360, 781–795. doi: 10.1098/rstb.2005.1631

Pfurtscheller, G., Neuper, C., Flotzinger, D., and Pregenzer, M. (1997). EEG-based discrimination between imagination of right and left hand movement. *Electroencephalogr. Clin. Neurophysiol.* 103, 642–651. doi: 10.1016/s0013-4694(97)00080-1

Poldrack, R. A. (2015). Is "efficiency" a useful concept in cognitive neuroscience? *Dev. Cogn. Neurosci.* 11, 12–17. doi: 10.1016/j.dcn.2014.06.001

Pop, V. L., Stearman, E. J., Kazi, S., and Durso, F. T. (2012). Using engagement to negate vigilance decrements in the nextgen environment. *Int. J. Hum. Comput. Interact.* 28, 99–106. doi: 10.1080/10447318.2012.634759

Prakash, R. S., De Leon, A. A., Mourany, L., Lee, H., Voss, M. W., Boot, W. R., et al. (2012). Examining neural correlates of skill acquisition in a complex videogame training program. *Front. Hum. Neurosci.* 6:115. doi: 10.3389/fnhum.2012.00115

Repantis, D., Schlattmann, P., Laisney, O., and Heuser, I. (2010). Modafinil and methylphenidate for neuroenhancement in healthy individuals: a systematic review. *Pharmacol. Res.* 62, 187–206. doi: 10.1016/j.phrs.2010.04.002

Rubinov, M., and Sporns, O. (2010). Complex network measures of brain connectivity: uses and interpretations. *Neuroimage* 52, 1059–1069. doi: 10.1016/j.neuroimage.2009.10.003

Salvador, R., Suckling, J., Coleman, M. R., Pickard, J. D., Menon, D., and Bullmore, E. (2005). Neurophysiological architecture of functional magnetic resonance images of human brain. *Cereb. Cortex* 15, 1332–1342. doi: 10.1093/cercor/bhi016

Schaie, K. W. (1994). The course of adult intellectual development. *Am. Psychol.* 49, 304–313. doi: 10.1037//0003-066x.49.4.304

Schmidt-Wilcke, T., Rosengarth, K., Luerding, R., Bogdahn, U., and Greenlee, M. W. (2010). Distinct patterns of functional and structural neuroplasticity associated with learning Morse code. *Neuroimage* 51, 1234–1241. doi: 10.1016/j.neuroimage.2010.03.042

Schneiders, J. A., Opitz, B., Krick, C. M., and Mecklinger, A. (2011). Separating intra-modal and across-modal training effects in visual working memory: an fMRI investigation. *Cereb. Cortex* 21, 2555–2564. doi: 10.1093/cercor/bhr037

Schneiders, J. A., Opitz, B., Tang, H., Deng, Y., Xie, C., Li, H., et al. (2012). The impact of auditory working memory training on the fronto-parietal working memory network. *Front. Hum. Neurosci.* 6:173. doi: 10.3389/fnhum.2012.00173

Scholz, J., Klein, M. C., Behrens, T. E., and Johansen-Berg, H. (2009). Training induces changes in white-matter architecture. *Nat. Neurosci.* 12, 1370–1371. doi: 10.1038/nn.2412

Schweizer, S., Grahn, J., Hampshire, A., Mobbs, D., and Dalgleish, T. (2013). Training the emotional brain: improving affective control through emotional working memory training. *J. Neurosci.* 33, 5301–5311. doi: 10.1523/JNEUROSCI.2593-12.2013

Shipstead, Z., Redick, T. S., and Engle, R. W. (2012). Is working memory training effective? *Psychol. Bull.* 138, 628–654. doi: 10.1037/a0027473

Smit, D. J. A., Stam, C. J., Posthuma, D., Boomsma, D. I., and de Geus, E. J. C. (2008). Heritability of "small-world" networks in the brain: a graph theoretical analysis of resting-state EEG functional connectivity. *Hum. Brain Mapp.* 29, 1368–1378. doi: 10.1002/hbm.20468

Spoormaker, V. I., Schröter, M. S., Gleiser, P. M., Andrade, K. C., Dresler, M., Wehrle, R., et al. (2010). Development of a large-scale functional brain network during human non-rapid eye movement sleep. *J. Neurosci.* 30, 11379–11387. doi: 10.1523/JNEUROSCI.2015-10.2010

Sporns, O. (2014). Contributions and challenges for network models in cognitive neuroscience. *Nat. Neurosci.* 17, 652–660. doi: 10.1038/nn.3690

Sporns, O., and Zwi, J. D. (2004). The small world of the cerebral cortex. *Neuroinformatics* 2, 145–162. doi: 10.1385/ni:2:2:145

Stam, C. J. (2004). Functional connectivity patterns of human magnetoencephalographic recordings: a 'small-world' network? *Neurosci. Lett.* 355, 25–28. doi: 10.1016/j.neulet.2003.10.063

Stam, C. J., Jones, B. F., Nolte, G., Breakspear, M., and Scheltens, P. (2007). Small-world networks and functional connectivity in Alzheimer's disease. *Cereb. Cortex* 17, 92–99. doi: 10.1093/cercor/bhj127

Stephenson, C. L., and Halpern, D. F. (2013). Improved matrix reasoning is limited to training on tasks with a visuospatial component. *Intelligence* 41, 341–357. doi: 10.1016/j.intell.2013.05.006

Stevens, W. D., Buckner, R. L., and Schacter, D. L. (2010). Correlated low-frequency BOLD fluctuations in the resting human brain are modulated by recent experience in category-preferential visual regions. *Cereb. Cortex* 20, 1997–2006. doi: 10.1093/cercor/bhp270

Strenziok, M., Parasuraman, R., Clarke, E., Cisler, D. S., Thompson, J. C., and Greenwood, P. M. (2014). Neurocognitive enhancement in older adults: comparison of three cognitive training tasks to test a hypothesis of training

transfer in brain connectivity. *Neuroimage* 85(Pt. 3), 1027–1039. doi: 10.1016/j.neuroimage.2013.07.069

Sulzer, J., Haller, S., Scharnowski, F., Weiskopf, N., Birbaumer, N., Blefari, M. L., et al. (2013). Real-time fMRI neurofeedback: progress and challenges. *Neuroimage* 76, 386–399. doi: 10.1016/j.neuroimage.2013.03.033

Sun, Y., Lim, J., Kwok, K., and Bezerianos, A. (2014a). Functional cortical connectivity analysis of mental fatigue unmasks hemispheric asymmetry and changes in small-world networks. *Brain Cogn.* 85, 220–230. doi: 10.1016/j.bandc.2013.12.011

Sun, Y., Lim, J., Meng, J., Kwok, K., Thakor, N., and Bezerianos, A. (2014b). Discriminative analysis of brain functional connectivity patterns for mental fatigue classification. *Ann. Biomed. Eng.* 42, 2084–2094. doi: 10.1007/s10439-014-1059-8

Tagliazucchi, E., von Wegner, F., Morzelewski, A., Brodbeck, V., Borisov, S., Jahnke, K., et al. (2013). Large-scale brain functional modularity is reflected in slow electroencephalographic rhythms across the human non-rapid eye movement sleep cycle. *Neuroimage* 70, 327–339. doi: 10.1016/j.neuroimage.2012.12.073

Takeuchi, H., Sekiguchi, A., Taki, Y., Yokoyama, S., Yomogida, Y., Komuro, N., et al. (2010). Training of working memory impacts structural connectivity. *J. Neurosci.* 30, 3297–3303. doi: 10.1523/JNEUROSCI.4611-09.2010

Takeuchi, H., Taki, Y., Nouchi, R., Hashizume, H., Sekiguchi, A., Kotozaki, Y., et al. (2013). Effects of working memory training on functional connectivity and cerebral blood flow during rest. *Cortex* 49, 2106–2125. doi: 10.1016/j.cortex.2012.09.007

Takeuchi, H., Taki, Y., Sassa, Y., Hashizume, H., Sekiguchi, A., Fukushima, A., et al. (2011). Working memory training using mental calculation impacts regional gray matter of the frontal and parietal regions. *PLoS One* 6:e23175. doi: 10.1371/journal.pone.0023175

Talbot, M. (2009). Brain gain: the underground world of neuroenhancing drugs. *New Yorker* 27, 32–43.

Tang, Y. Y., Lu, Q., Fan, M., Yang, Y., and Posner, M. I. (2012). Mechanisms of white matter changes induced by meditation. *Proc. Natl. Acad. Sci. U S A* 109, 10570–10574. doi: 10.1073/pnas.1207817109

Tang, Y. Y., Ma, Y., Fan, Y., Feng, H., Wang, J., Feng, S., et al. (2009). Central and autonomic nervous system interaction is altered by short-term meditation. *Proc. Natl. Acad. Sci. U S A* 106, 8865–8870. doi: 10.1073/pnas.0904031106

Tang, Y.-Y., and Posner, M. I. (2014). Training brain networks and states. *Trends Cogn. Sci.* 18, 345–350. doi: 10.1016/j.tics.2014.04.002

Taubert, M., Draganski, B., Anwander, A., Müller, K., Horstmann, A., Villringer, A., et al. (2010). Dynamic properties of human brain structure: learning-related changes in cortical areas and associated fiber connections. *J. Neurosci.* 30, 11670–11677. doi: 10.1523/JNEUROSCI.2567-10.2010

Taya, F., Sun, Y., Thakor, N., and Bezerianos, A. (2014). "Information transfer efficiency during rest and task a functional connectome approach," in *IEEE Biomedical Circuits and Systems Conference* (Lausanne).

Tomasi, D., and Volkow, N. D. (2011a). Association between functional connectivity hubs and brain networks. *Cereb. Cortex* 21, 2003–2013. doi: 10.1093/cercor/bhq268

Tomasi, D., and Volkow, N. D. (2011b). Functional connectivity hubs in the human brain. *Neuroimage* 57, 908–917. doi: 10.1016/j.neuroimage.2011.05.024

Uehara, T., Yamasaki, T., Okamoto, T., Koike, T., Kan, S., Miyauchi, S., et al. (2014). Efficiency of a "small-world" brain network depends on consciousness level: a resting-state FMRI study. *Cereb. Cortex* 24, 1529–1539. doi: 10.1093/cercor/bht004

Valdes-Sosa, P. A., Roebroeck, A., Daunizeau, J., and Friston, K. (2011). Effective connectivity: influence, causality and biophysical modeling. *Neuroimage* 58, 339–361. doi: 10.1016/j.neuroimage.2011.03.058

van den Heuvel, M. P., and Sporns, O. (2011). Rich-club organization of the human connectome. *J. Neurosci.* 31, 15775–15786. doi: 10.1523/JNEUROSCI.3539-11.2011

van den Heuvel, M. P., and Sporns, O. (2013a). An anatomical substrate for integration among functional networks in human cortex. *J. Neurosci.* 33, 14489–14500. doi: 10.1523/JNEUROSCI.2128-13.2013

van den Heuvel, M. P., and Sporns, O. (2013b). Network hubs in the human brain. *Trends Cogn. Sci.* 17, 683–696. doi: 10.1016/j.tics.2013.09.012

van den Heuvel, M. P., Stam, C. J., Boersma, M., and Hulshoff Pol, H. E. (2008). Small-world and scale-free organization of voxel-based resting-state functional connectivity in the human brain. *Neuroimage* 43, 528–539. doi: 10.1016/j.neuroimage.2008.08.010

van den Heuvel, M. P., Stam, C. J., Kahn, R. S., and Hulshoff Pol, H. E. (2009). Efficiency of functional brain networks and intellectual performance. *J. Neurosci.* 29, 7619–7624. doi: 10.1523/JNEUROSCI.1443-09.2009

Voss, M. W., Prakash, R. S., Erickson, K. I., Boot, W. R., Basak, C., Neider, M. B., et al. (2012). Effects of training strategies implemented in a complex videogame on functional connectivity of attentional networks. *Neuroimage* 59, 138–148. doi: 10.1016/j.neuroimage.2011.03.052

Watts, D. J., and Strogatz, S. H. (1998). Collective dynamics of 'small-world' networks. *Nature* 393, 440–442. doi: 10.1038/30918

Weiss, S., and Rappelsberger, P. (2000). Long-range EEG synchronization during word encoding correlates with successful memory performance. *Brain Res. Cogn. Brain Res.* 9, 299–312. doi: 10.1016/s0926-6410(00)00011-2

Wolf, D., Fischer, F. U., Fesenbeckh, J., Yakushev, I., Lelieveld, I. M., Scheurich, A., et al. (2014). Structural integrity of the corpus callosum predicts long-term transfer of fluid intelligence-related training gains in normal aging. *Hum. Brain Mapp.* 35, 309–318. doi: 10.1002/hbm.22177

Wu, S., Cheng, C. K., Feng, J., D'Angelo, L., Alain, C., and Spence, I. (2012). Playing a first-person shooter video game induces neuroplastic change. *J. Cogn. Neurosci.* 24, 1286–1293. doi: 10.1162/jocn_a_00192

Zander, T. O., and Kothe, C. (2011). Towards passive brain-computer interfaces: applying brain-computer interface technology to human-machine systems in general. *J. Neural Eng.* 8:025005. doi: 10.1088/1741-2560/8/2/025005

Zhao, X., Zhou, R., and Fu, L. (2013). Working memory updating function training influenced brain activity. *PLoS One* 8:e71063. doi: 10.1371/journal.pone.0071063

Zuo, X. N., Ehmke, R., Mennes, M., Imperati, D., Castellanos, F. X., Sporns, O., et al. (2012). Network centrality in the human functional connectome. *Cereb. Cortex* 22, 1862–1875. doi: 10.1093/cercor/bhr269

Conflict of Interest Statement: The authors declare that the research was conducted in the absence of any commercial or financial relationships that could be construed as a potential conflict of interest.

frontiers in
SYSTEMS NEUROSCIENCE

OPINION ARTICLE
published: 12 December 2014
doi: 10.3389/fnsys.2014.00233

The relationship between local field potentials (LFPs) and the electromagnetic fields that give rise to them

Colin G. Hales[1]* and Susan Pockett[2]

[1] *Neuroengineering Laboratory, Department of Electrical and Electronic Engineering, University of Melbourne, Carlton, VIC, Australia*
[2] *School of Psychology, University of Auckland, Auckland, New Zealand*
**Correspondence: cghales@unimelb.edu.au*

Edited by:
Mikhail Lebedev, Duke University, USA

Reviewed by:
Zoltan Nadasdy, Seton Brain and Spine Institute, USA
Dimitris Pinotsis, University College London, UK

Keywords: brain electromagnetism, local field potential, Maxwell's equations, scalar potential, vector potential

Recently there has been a call (Reimann et al., 2013) for a re-evaluation of the genesis of local field potentials (LFPs), a measurement deeply correlated with normal and pathological excitable cell tissue operation (Einevoll et al., 2013; Friston et al., 2014). The lack of a full scientific account of LFP origins additionally means that brain augmentation hardware, a primary tool for which is the manipulation of LFPs, is in effect pulling unmarked levers. How can we knowledgeably control LFPs when LFP origin itself is a mystery? Here we investigate how the task of revisiting LFP origins might best be approached.

LFPs originate in the two deeply interconnected fundamental physical fields of the brain: the vector electric field [$\mathbf{E}(\mathbf{r},t)$, V/m] and the vector magnetic field [$\mathbf{B}(\mathbf{r},t)$, V-s/m^2]. Each of these can be Helmholtz-decomposed into the gradient of a scalar potential [say $\Phi(\mathbf{r},t)$] and the curl of a vector potential [say $\mathbf{A}(\mathbf{r},t)$] (Groot and Suttorp, 1972; Landau et al., 1984; Malmivuo and Plonsey, 1995; Jackson, 1999). This means in practice that there are three "potential fields" operating in the brain[1]. At present it is technologically impossible to directly measure the vector electric field or magnetic field at the resolution of tissue fine structure. Therefore neuroscientists rely on a technically straightforward measurement of voltage (call it LFP($\mathbf{r}$,t)) that imperfectly accesses the "potential fields" and within which **E** and **B** are only indirectly represented.

Empirical work over many decades has converged on transmembrane ionic current as the ultimate origin of the LFP (Buzsaki et al., 2012; Destexhe and Bedard, 2013). This means we must address the finest details of the formidably complex tissue ultra-structure typified by **Figure 1A** (Nicholson and Sykova, 1998; Briggman and Denk, 2006; Kinney et al., 2013)[2]. This is because the ionic currents originate in the membrane micro-environment indicated by the generic sources d1$\cdots$d4 in **Figure 1A**. Fundamental field theory tells us that **E** and **B** actually mediate LFP expression. This requires us to look at how membrane-related sources first cause **E** and **B** and through them, the LFP. We must treat transmembrane currents and their supporting systems of charge as electromagnetic (EM) field sources.

LFP($\mathbf{r}$,t) measurement arose as a lab technique nearly 70 years ago (Brooks and Eccles, 1947) and still involves insertion of electrodes that are huge compared to the cyto-architectural scale of the tissue. These electrodes inevitably disrupt the structure around their insertion routes and the eventual measurement points, homogenizing the tissue to some extent and causing an inflammatory response that adds to the disruption. Thus a localized artificial medium is created around each electrode tip, which forms the actual context of the LFP($\mathbf{r}$,t) measurement. The measurement reveals a spatial average (dependent on the electrode tip geometry) and a temporal average (dependent on sample rate and filters in the measurement equipment) voltage differential relative to a reference electrode elsewhere in the tissue. LFP($\mathbf{r}$,t) cannot be automatically claimed to access the scalar electric potential $\Phi(\mathbf{r},t)$ in the natural tissue. Even if contributions from tissue damage can be ignored, we are not directly measuring Φ. Rather, we are measuring some spatiotemporal average of Φ, the nature of which is not obvious and gets little attention in the literature. This LFP $\Leftrightarrow$ Φ mapping needs to be revisited as part of a campaign of elucidating LFP origins.

Another important factor affecting the ability to infer EM fields from voltage measurements is that there are an infinity of different **E** and **B** fields that can give rise to the same Φ (and therefore the same LFP). This degeneracy of Φ owes its mathematical origin to what is called, in classical electromagnetism, electromagnetic gauge (Jackson, 1999). **E** and **B** are not uniquely revealed by Φ. Scalar electric potential Φ is like a height measurement. The lack of specificity that scalar potential has as a reflection of the electric field generating it is analogous to the degeneracy that height has to the terrain. If I have a height of 20 m, am I on my balcony or up a tree? Thus LFPs cannot be properly interpreted or understood without a good theoretical foundation for the origins of **E** and **B** based on real tissue ultra-structure knowledge. The LFP is a one-way lens. **E** and

[1]The lack of a "magnetic monopole/charge" eliminates the scalar magnetic potential component of $\mathbf{B}(\mathbf{r},t)$, leaving **B** entirely characterized by a "vector potential," which can be mathematically related to the electric vector potential decomposition of the electric field **E** (Jackson, 1999).

[2]Tissue ultra-structure refers to tissue details as revealed when imaged at Angstrom (10^{-10} m) resolution, usually with electron microscopy.

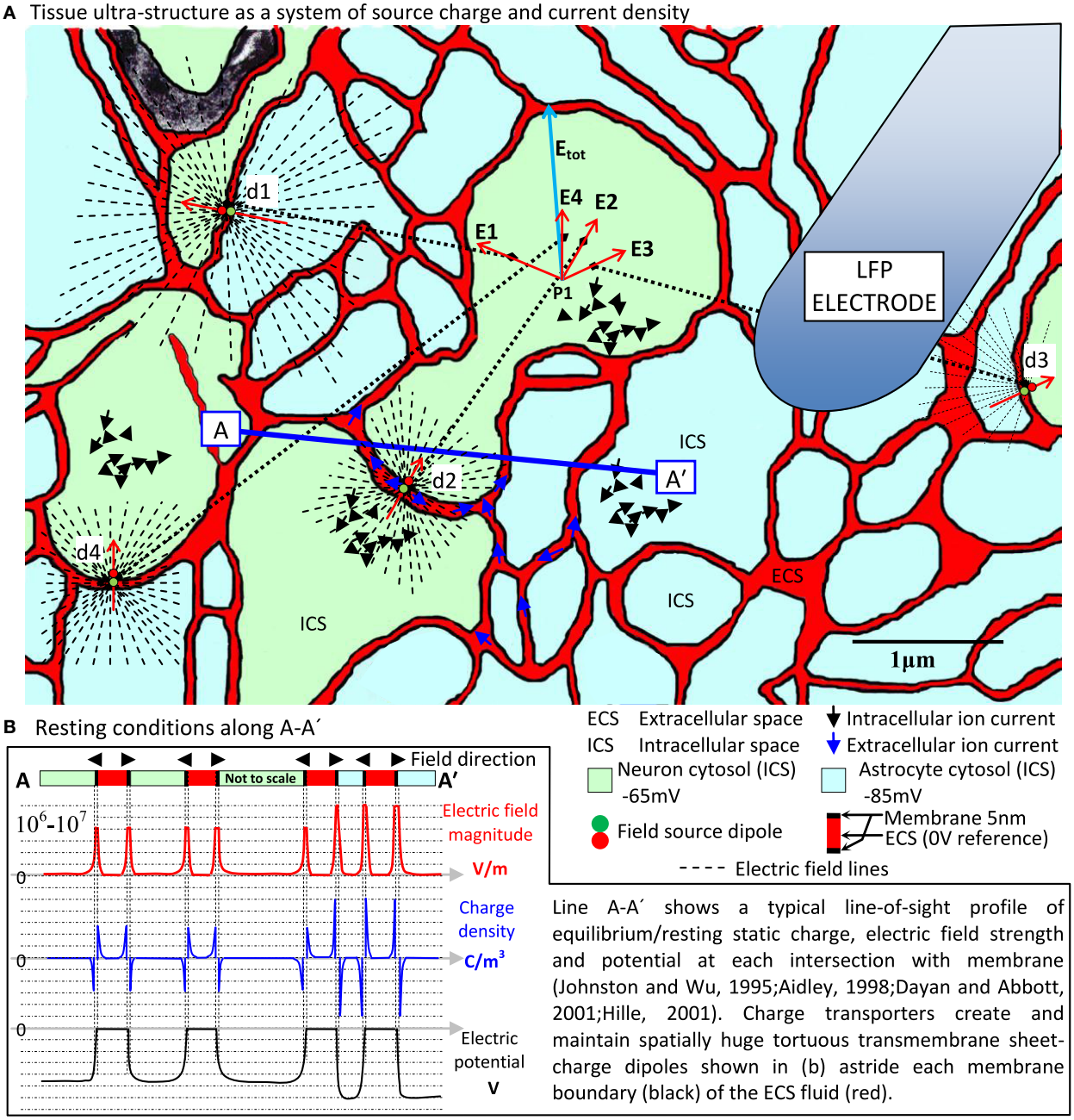

FIGURE 1 | EM field origins in nervous tissue ultra-structure. (A) Electron micrograph colored to reveal neuron/glia ultra-structure with **(B)** the resting state source charge density characteristic centered on the huge transmembrane electric field (10^6–10^7 V/m) across all neural and glial cell membrane and maintained by charge transporters not shown. This massive sheet-charge dipole lines the tortuous, narrow sheet/tunnel ECS (Kinney et al., 2013), which is the only tissue medium actually outside all cells. Spatially and temporally coherent ion channel activity in neuronal membranes produces fast, coherent, dynamic current sources that locally modulate (even reverse) the planar dipole field, expressing dynamic electric and magnetic field systems far into the surrounding tissue. This is the primary source that originates all other activity in the tissue. At any given point (say P1) there is a total electric and magnetic field expressed line-of-sight through the tissue at the speed of light. This total field exerts its influence on local charge populations via the Lorentz force. Secondary current systems in the ECS (blue arrows) and ICS (black arrows) resulting from this activity are hugely diluted, diffuse and randomized, traveling at speeds 10,000 times slower than through the membrane (Hille, 2001). Such a small, randomized current density cannot be argued to contribute anything more than field noise at the scale of tissue ultra-structure. However, long term persistent charge transport can support regional polarization and thereby cause the tissue as a whole to exhibit a macroscopic electric field system. In this way, an ultra-structured EM field system and a large-scale slow electric field system can operate simultaneously in the tissue. It is also a natural expectation of such a system that all EM field sources (probably minutely) influence, through the tissue at the speed of light, all other field sources. This is the probable origin of the recently revealed EM field coupling mechanism (Frohlich and Mccormick, 2010; Anastassiou et al., 2011). **(A)** Based on (Nicholson and Sykova, 1998; Kinney et al., 2013), neuron/astrocyte allocation notional.

B can "see" Φ but Φ cannot "see" **E** and **B**. A practical example of the degeneracy of Φ is in the use of lumped-element circuit models of neurons. These models accurately replicate voltages and currents even though the field (**E** and **B**) system of the model is totally unlike that of real tissue. This technique confers a degree of useful predictive utility, but loses contact with the actual underlying tissue physics. The degeneracy in potentials is the reason we can abstract-away **E** and **B** physics and is central to the success of circuit theory (Plonsey and Collin, 1961, p. 326). However, degeneracy in electric potentials means that the EM field system implicit in a tissue's circuit-element model cannot be claimed to be the EM field system of the tissue.

FROM CHARGES TO EM FIELDS TO LFPs

E and **B** sources are simply expressed by Maxwell's equations. An aggregate primary source "charge density (scalar) field" $\rho(\mathbf{r},t)$ (C/m^3) impresses an electric field system on space well beyond its bounds (notionally to infinity) by line of sight and at the speed of light. If a subset of that *same set of charges* happens to move and thereby create a primary "current density (vector) field," $\mathbf{J}(\mathbf{r},t)$ (A/m^2), then this charge motion (1) disturbs the charge density field, modulating the electric field commensurate with the spatial and temporal scale and detail of the changes, and (2) creates a magnetic field by virtue of the current density field. This is a universal property of Maxwell's equations.

In tissue, **E** and **B** owe their origins to the massive transmembrane sheet-charge density dipole astride all cell boundaries (**Figure 1B**), which dominates all other atomic/molecular sources. Neuron transmembrane disturbances in the sheet dipole charge density then dominate EM field dynamics. So at least at this level, **E** and **B** origins are easy to find. Detailing them, however, is the big challenge.

When attempting to meet this challenge, it is important to remember that in tissue, **E** and **B** are causally *prior*. Every kind of current and voltage elsewhere in the tissue is secondary. For example, consider the primary sources d1⋯ d4 shown in **Figure 1A**. Vector superposition creates electric field $\mathbf{E_{tot}}$ at point P1 and via the Lorentz force this produces a *secondary* current in the tissue at P1, which has nothing directly to do with the current at the sources d1⋯ d4. Independent vector superposition of **E** and **B** means each field is a unified, emergent single entity with a spatiotemporal life and a causal influence of its own.

SOURCES: DENSITY, COHERENCE AND PERSISTENCE ARE MASTERS

In Maxwell's equations **E** and **B** are intrinsically connected to current *density*, not current. Consider a single current that is first in the form of (i) fast, highly aligned transmembrane current filaments that then become (ii) slow, randomized and diffuse in the intracellular space (**Figure 1A**, black arrows). At some distant point the current operating in form (i) will impress a dominant, coherent EM field system whereas form (ii) will only create relative field "noise." The spatial (tightly co-located ion channels) and temporal (all firing at once) coherence of the transmembrane part of the ion transport means that field contribution (i) will dominate. This is how charge and current densities co-located and aligned in space, and aligned in time will result in dominant $\mathbf{E_{tot}}$ and $\mathbf{B_{tot}}$ vectors with functional consequences (consistent pointing, rotating, pulsing). Non-coherent source contributions result in $\mathbf{E_{tot}}$ and $\mathbf{B_{tot}}$ noise.

Additionally, persistent synchronous vector electric field expression by cells and cell assemblies can slowly move large populations of charge to create regional charge densities. The resultant electric field "atmosphere" superposes (feeds back) vectorially onto all endogenous EM field ultra-structure sources. Yet none of it would exist were it not for the source systems and dynamics expressed at the level of the **Figure 1A** tissue ultra-structure. The electric and magnetic field system therefore has an extraordinarily deep spatial and temporal structure, all of which involves itself in what is seen as the LFP. We are thereby forced to accept that cell and cell assembly signaling is deeply involved at the ultra-structure level of EM field expression. This means the EM fields have 6–8 orders of magnitude of spatiotemporal detail (neural membrane to whole tissue) and that fully understanding LFP means characterizing tissue with models incorporating that level of depth.

CONFIGURING MAXWELL'S EQUATIONS

The configuration of Maxwell's equations applicable at the level of the **Figure 1A** neuron transmembrane microenvironment, where **E** and **B** originate, also needs to be revised. This is necessary because the applicable charge transport equations are, technically, convection (Kirby, 2010). Convection current occurs when charge flows through an insulating medium such as liquid, rarefied gas or a vacuum (Sadiku, 2001, p. 163). ECS/ICS electrolyte currents are ions (charge) flowing in water, which is an extremely good insulator. Transmembrane ions travel through protein pores that have the same status as water at the time. Therefore convection is the applicable form of charge transport in ECS, ICS and through the membrane. How convection differs from formal conduction can be understood in terms of how charge density involves itself in charge transport dynamics. Convection involves using charge-density-dependent ion mobility properties and diffusion rather than charge-density-independent conductivity (Hille, 2001). Formal conduction involves charge motion under conditions of zero charge density maintained at the atomic scale. This happens in crystalline solid electron/hole conduction (Jackson, 1999, p. 706). In contrast, convective atomic ion transport can express a net charge density as it flows.

Yet conduction formalisms such as Ohm's Law are effective at quantifying currents and voltages in an overall sense of action potential signaling and LFP usage in the lab. This is because at spatial scales above the neuron membrane microenvironment, the regional average charge density asymptotes to zero. In the brain this is called "electro-neutrality" (Johnston and Wu, 1995; Nunez and Srinivasan, 2006). There is an overall balance in ion charge species in the brain. But that overall balance includes a radically dynamic imbalance around the membrane—otherwise there would be no resting potential, no neuronal signaling and no EM field expression.

Therefore any form of reconfigured Maxwell's equations must include a formal reconciliation between (1) the non-Ohmic nano-scale convection/diffusion charge transport proximal to/inside the

membrane that originates the **E** and **B** fields, with (2) the charge-neutral conditions obviously amenable to conduction formalisms that exist at scales above the membrane/ECS microenvironment, which have no bearing on **E** and **B** origination, but are consistent with it in a voltage/current sense. A future accurate formalism is one that originates both **E** and **B** using convection/diffusion processes, which then asymptotes seamlessly to the more familiar conduction formalisms at some spatio-temporal scale to be determined. The new view and the old can thereby meet in a familiar way.

With microscopic **E** and **B** formalized and the important LFP $\Leftrightarrow$ Φ mapping (electrode/tissue interaction) understood, years of LFP measurements become a revitalized body of evidence. Historically challenging concepts such as "open/closed field" (Nadasdy et al., 1998; Buzsaki et al., 2012), "neural field" (Coombes, 2006; Pinotsis and Friston, 2014), "power law spectra" (Buzsáki and Draguhn, 2004) and "ephaptic coupling" (Frohlich and Mccormick, 2010; Anastassiou et al., 2011) may take their mature form.

CONCLUSION

The critical path to successful hardware-based brain augmentation requires us to heed a recent call to revisit the genesis of the LFP. In the present paper, a broad-brush review reveals ways for physicists and neuroscientists to meet productively to that end. The primary need is to attend to the genesis of the electric and magnetic fields of the brain at the level of tissue ultra-structure, via spatiotemporally coherent systems of source charge density and source current density centered on the neural membrane. The configuration of Maxwell's equations also needs rework. The degeneracy in potentials inherent in Maxwell's equations has been a historical misdirection in EM field understanding. The ultra-structural basis of the EM fields, embedded in cell and cell assembly activity, is a productive route to understanding EM field effects at all the usual spatiotemporal scales examined in the lab. Only then can these fields reveal the true nature of the measurement we call the LFP.

REFERENCES

Aidley, D. J. (1998). *The Physiology of Excitable Cells*. New York, NY: Cambridge University Press.

Anastassiou, C. A., Perin, R., Markram, H., and Koch, C. (2011). Ephaptic coupling of cortical neurons. *Nat. Neurosci.* 14, 217–223. doi: 10.1038/nn.2727

Briggman, K. L., and Denk, W. (2006). Towards neural circuit reconstruction with volume electron microscopy techniques. *Curr. Opin. Neurobiol.* 16, 562–570. doi: 10.1016/j.conb.2006.08.010

Brooks, C., and Eccles, J. (1947). Electrical investigation of the monosynaptic pathway through the spinal cord. *J. Neurophysiol.* 10, 251–273.

Buzsaki, G., Anastassiou, C. A., and Koch, C. (2012). The origin of extracellular fields and currents - EEG, ECoG, LFP and spikes. *Nat. Rev. Neurosci.* 13, 407–420. doi: 10.1038/nrn3241

Buzsáki, G., and Draguhn, A. (2004). Neuronal oscillations in cortical networks. *Science* 304, 1926–1929. doi: 10.1126/science.1099745

Coombes, S. (2006). Neural fields. *Scholarpedia* 1:1373. doi: 10.4249/scholarpedia.1373

Dayan, P., and Abbott, L. F. (2001). *Theoretical Neuroscience: Computational and Mathematical Modeling of Neural Systems*. Cambridge, MA; London: MIT Press.

Destexhe, A., and Bedard, C. (2013). Local field potential. *Scholarpedia* 8:10713. doi: 10.4249/scholarpedia.10713

Einevoll, G. T., Kayser, C., Logothetis, N. K., and Panzeri, S. (2013). Modelling and analysis of local field potentials for studying the function of cortical circuits. *Nat. Rev. Neurosci.* 14, 770–785. doi: 10.1038/nrn3599

Friston, K. J., Bastos, A. M., Pinotsis, D., and Litvak, V. (2014). LFP and oscillations—what do they tell us? *Curr. Opin. Neurobiol.* 31, 1–6. doi: 10.1016/j.conb.2014.05.004

Frohlich, F., and Mccormick, D. A. (2010). Endogenous electric fields may guide neocortical network activity. *Neuron* 67, 129–143. doi: 10.1016/j.neuron.2010.06.005

Groot, S. R. D., and Suttorp, L. G. (1972). *Foundations of Electrodynamics*. Amsterdam: Noord-Hollandsche U.M.

Hille, B. (2001). *Ion Channels of Excitable Membranes*. Sunderland, MA: Sinauer Associates, Inc.

Jackson, J. D. (1999). *Classical Electrodynamics*. New York, NY: Wiley.

Johnston, D., and Wu, S. M.-S. (1995). *Foundations of Cellular Neurophysiology*. Cambridge, MA: MIT Press.

Kinney, J. P., Spacek, J., Bartol, T. M., Bajaj, C. L., Harris, K. M., and Sejnowski, T. J. (2013). Extracellular sheets and tunnels modulate glutamate diffusion in hippocampal neuropil. *J. Compar. Neurol.* 521, 448–464. doi: 10.1002/cne.23181

Kirby, B. (2010). *Micro- and Nanoscale Fluid Mechanics Transport in Microfluidic Devices*. Leiden: Cambridge University Press.

Landau, L. D., Lifshitz, E. M., and Pitaevskii, L. P. (1984). *Electrodynamics of Continuous Media*. Oxford; New York: Pergamon.

Malmivuo, J., and Plonsey, R. (1995). *Bioelectromagnetism: Principles and Applications of Bioelectric and Biomagnetic Fields*. New York, NY: Oxford University Press.

Nadasdy, Z., Csicsvari, J., Penttonen, M., Hetke, J., Wise, K., and Buzsaki, G. (1998). "Extracellular recording and analysis of neuronal activity: from single cells to ensembles," in *Neuronal Ensembles: Strategies for Recording and Decoding*, eds H. B. Eichenbaum and J. L. Davis (New York, NY: Wiley-Liss), 17–55.

Nicholson, C., and Sykova, E. (1998). Extracellular space structure revealed by diffusion analysis. *Trends Neurosci.* 21, 207–215. doi: 10.1016/S0166-2236(98)01261-2

Nunez, P. L., and Srinivasan, R. (2006). *Electric Fields of the Brain: the Neurophysics of EEG*. New York, NY: Oxford University Press.

Pinotsis, D. A., and Friston, K. J. (2014). Extracting novel information from neuroimaging data using neural fields. *EPJ Nonlin. Biomed. Phys.* 2, 5. doi: 10.1140/epjnbp18

Plonsey, R., and Collin, R. (1961). *Principles and Applications of Electromagnetic Fields*. New York, NY: McGraw Hill.

Reimann, M. W., Anastassiou, C. A., Perin, R., Hill, S. L., Markram, H., and Koch, C. (2013). A biophysically detailed model of neocortical local field potentials predicts the critical role of active membrane currents. *Neuron* 79, 375–390. doi: 10.1016/j.neuron.2013.05.023

Sadiku, M. N. O. (2001). *Elements of Electromagnetics*. New York, NY: Oxford University Press.

Conflict of Interest Statement: The authors declare that the research was conducted in the absence of any commercial or financial relationships that could be construed as a potential conflict of interest.

Received: 01 November 2014; accepted: 24 November 2014; published online: 12 December 2014.

*Citation: Hales CG and Pockett S (2014) The relationship between local field potentials (LFPs) and the electromagnetic fields that give rise to them. Front. Syst. Neurosci. **8**:233. doi: 10.3389/fnsys.2014.00233*

This article was submitted to the journal Frontiers in Systems Neuroscience.

frontiers in
SYSTEMS NEUROSCIENCE

PERSPECTIVE ARTICLE
published: 30 September 2014
doi: 10.3389/fnsys.2014.00152

"Messing with the mind": evolutionary challenges to human brain augmentation

Arthur Saniotis[1,2]*, Maciej Henneberg[1,2], Jaliya Kumaratilake[1] and James P. Grantham[1]

[1] *Biological Anthropology and Comparative Anatomy Unit, School of Medical Sciences, The University of Adelaide, Adelaide, SA, Australia*
[2] *Centre for Evolutionary Medicine, University of Zürich, Zürich, Switzerland*

Edited by:
Ioan Opris, Wake Forest University, USA

Reviewed by:
Victor Manuel Pulgar, Wake Forest University, USA
Daniel James Miller, Vanderbilt University, USA

****Correspondence:***
Arthur Saniotis, Biological Anthropology and Comparative Anatomy Unit, School of Medical Sciences, The University of Adelaide, North Terrace, Adelaide, SA 5005, Australia
e-mail: arthur.saniotis@adelaide.edu.au

The issue of brain augmentation has received considerable scientific attention over the last two decades. A key factor to brain augmentation that has been widely overlooked are the complex evolutionary processes which have taken place in evolving the human brain to its current state of functioning. Like other bodily organs, the human brain has been subject to the forces of biological adaptation. The structure and function of the brain, is very complex and only now we are beginning to understand some of the basic concepts of cognition. Therefore, this article proposes that brain-machine interfacing and nootropics are not going to produce "augmented" brains because we do not understand enough about how evolutionary pressures have informed the neural networks which support human cognitive faculties.

Keywords: brain size, hominin brain, memory formation, brain-machine interfaces, nootropic agents

INTRODUCTION

The issue of brain augmentation has received considerable scientific attention over the last two decades. Much of this focus has been prompted by the increase in human aging population and the concomitant rise in dementiae and neuro-degenerative disease. Moreover, brain augmentation has become a central theme for transhumanists who argue for the creation of various biotechnologies in order to transcend the limitations of the biological body (Drexler, 1992; Roco and Bainbridge, 2002; Bostrom, 2003; Ramez, 2005). Kurzweil (2000) has suggested that development of brain-machine interfaces will be necessary to cope with the informational demands of future high tech societies. He even proposes the supplanting of a "cognitively superior" nanotech brain to supplement the biological human brain (Kurzweil, 2000). Transhumanists have overlooked the complex and plural selective pressures which have led to the human brain's current functioning. Like other bodily organs, the human brain has been subject to the forces of biological adaptation (Hawks et al., 2007; Henneberg and Saniotis, 2009), thus it is continuously changing. The challenges that humans are faced with are the continuously changing living environment and to a very much lesser extent the "technological advancement". Being a result of the trial-and-error processes of biological adaptation the structure and function of the human brain are very complex and only now we are beginning to understand some of the basic concepts of cognition (i.e., in relation to memory, memory consolidation and retrieval). Therefore, this article proposes that brain-machine interfacing is not going to produce "augmented" brains because we do not understand enough about how evolutionary pressures have informed the neural networks which support human cognitive faculties.

EVOLUTION OF HUMAN BRAIN SIZE AND INTELLIGENCE

There is no doubt that humans display behavioral complexity greater than other mammals, and there is ample archeological evidence for the historical development of human mind that is a system of informational processes manifesting itself in symbolic communication transmissible from one individual to others (Bednarik, 1997; Butler, 2005; Bar-Yosef, 2007; Burke, 2010; Lycett and Chauhan, 2010). However, it is still difficult to pinpoint and identify what is special about a biological substrate that led to the evolution of human complex behaviors.

Human brain is a mammalian organ that in no single particular way is exceptional. Its anatomy is very similar to that of other primate brains (Radinsky, 1979). For the long time it has been widely accepted that during several million years of hominin evolution the human brain became especially large, thus indicating anatomical basis for our unusual abilities. This, however, turns out not to be true at closer scrutiny of the fossil record of hominin evolution. True enough, the volume of hominin braincase tripled in the last, approximately, 3 million years (from about 450 ml to current 1350 ml, De Miguel and Henneberg, 2001). During that time, however, hominin body size increased, too. Body size is measured either as the linear height, or weight, that in humans scales approximately to the second power of height (Henneberg et al., 1989), a fact generally recognized by the construction of the Body Mass index as a ratio of weight to height squared. When the size of human brain is expressed as a linear dimension (a cube root of volume), its increases over the last 3 million years are comparable to those of height (Henneberg and Saniotis, 2009) and weight (**Figure 1**). The size of the human brain is proportional to the size of musculoskeletal system mass (Rogers, 1992); scaling of

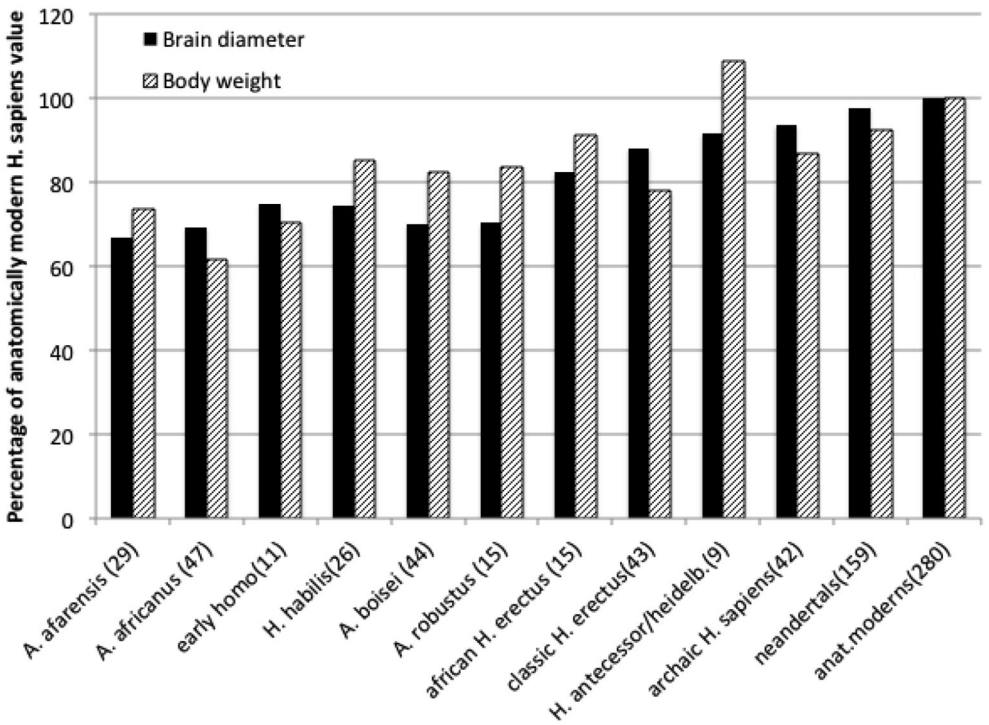

FIGURE 1 | Average brain diameters (a cubic root of endocranial capacity) and estimated body weights of hominids expressed as percentages of anatomically modern human averages. Data from De Miguel and Henneberg (2001) and Mathers and Henneberg supplemented with newer finds. Numbers in brackets are numbers of individual estimates taken into account.

human brain size to body size, in contrast to other vertebrates and mammals, where brain size increases allometrically at a fraction of body size (Jerison, 1973; Martin, 1990) is isometric, due to changes of body structure related to erect bipedalism, high quality diet and extraoral food processing together reducing body size (Henneberg, 1998). Physiological regulation of the human brain by endocrine exchanges follows the same principles as that of all other mammals, but the quantities of specific active substances may differ (Previc, 1999, 2009).

The size of the human brain does not correlate meaningfully with the mental abilities (Henneberg et al., 1985; McDaniel, 2005); the size explains at best about 10% of the variation in "intelligence" and even this number is debatable. Higher intellectual functions are difficult to localize precisely to specific regions of the brain compared to processing of sensory inputs and motor outputs (Power et al., 2011), while many tasks controlled by brains are processed in complex networks widely distributed across the cortex (Bullmore and Sporns, 2009). Researchers have tried to justify human uniqueness, since the rise of modern scientism by quoting various "exceptional" human brain characteristics. These were mostly associated with anatomical character due to the slow progress in physiological research on the human brain (because of ethical constraints), especially those related to neurotransmitter and hormone regulation of the central nervous system functions (i.e., primarily, synaptic function). The most common among the indices defining the uniqueness of the human brain are variously constructed "encephalization" indices. They combine in various forms information on brain size and body size, with the assumption that mammalian brains need to have a certain number of neurons to receive sensory information and process it to control functions of the body. The prevailing hypothesis states that the larger the brain in relation to body size, the greater the ability to process information. Averages of encephalization indices calculated in various ways (**Table 1**) place humans clearly above other mammals and human ancestors. However, when the range of variability in human brain size and the body size is taken into account differences between individual humans may be greater than those between Australopithecines and modern *Homo sapiens*. South African *Australopithecus robustus* had 4.3×10^9 extraneurons, while modern *Homo sapiens* have 8.2×10^9 extraneurons (McHenry, 1976, extra-neuron numbers were calculated using Jerison, 1973 formula). The large difference of 3.9×10^9, however, is smaller than the differences between some modern humans (see range in **Table 1**). When normal intraspecies variation is taken into account, it follows that individual members of our species, *H. sapiens*, do not differ from some individuals of *H. erectus* since the ranges of encephalization indices of these two species overlap widely.

Brains of different species have different neuronal densities and different levels of myelination in various regions (Haug, 1987; Glasser et al., 2014), which means that bigger brain does not necessarily contain more neurons. Usually neuronal density decreases with increasing brain size (Haug, 1987).

Table 1 | Ranges of various indices of encephalization in modern humans expressed as the lower and upper limits of 99% confidence intervals and their midpoints compared with *Homo erectus* midpoints (data from Henneberg, 1990) supplemented by *H. erectus* ranges calculated in a similar way using data from Henneberg and Thackeray, 1995.

Index (Author)	*H. erectus* lower limit	*H. erectus* midpoint	*H. erectus* upper limit	*H. sapiens* lower limit	*H. sapiens* midpoint	*H. sapiens* upper limit
Extraneurons (Jerison, 1973)	5.96×10^9	7.02×10^9	8.38×10^9	6.94×10^9	9.17×10^9	11.39×10^9
Encephalization Quotient (Jerison, 1973)	3.70	5.51	8.11	5.64	8.51	11.38
Index of Progression (Stephan, 1972)	18.59	23.0	32.33	23.6	35.0	46.4

Note that H. erctus midpoints are close to H. sapiens lower limits while H. sapiens midpoints are close to H. erectus upper limits. There is an obvious overlap between ranges of the two taxa.

BRAIN-MACHINE INTERFACES: EVOLUTIONARY CHALLENGES

Animal research in brain-machine interfaces has led to an improved understanding of memory and sensory processes and neural firing patterns, leading to possible prosthetic therapies for the restoration of motor function (Nicolelis, 2003; Nicolelis and Srinivasan, 2003; Sanchez et al., 2003; Lebedev and Nicolelis, 2006; Moritz et al., 2008; Ethier et al., 2012). These developments have prompted some thinkers to suggest that humans are on the verge of a "technological cognitive revolution" (Nicolelis and Srinivasan, 2003). Current research is focusing on the use of computers to ascertain information on a user's cognitive state by observing their physiology (Tan and Nijholt, 2010), thus therapeutically directed brain-machine interfaces appear to be promising (Collinger et al., 2012; Shih et al., 2012; Borton et al., 2013; Ifft et al., 2013; Thakor, 2013; Raspopovic et al., 2014). Recent developments have focussed on stimulation of ulner and median nerve fascicles using transversal multichannel intrafascicular electrodes, which enables an amputee to adapt their grasping force (Raspopovic et al., 2014). In another recent study a bimanual BMI has been developed that enables rhesus monkeys to simultaneously control two avatar arms. The bimanual BMI is based on extracellular activity of 374 to 497 neurons monitored from various parietal and cortical areas (Ifft et al., 2013). These developments should assist in the design of BMIs which enable human patients better manual control.

While neuroscience research is advancing BMI therapeutic capabilities, there is yet no existing brain-machine interface based on exchange of electrical (electromagnetic) signals that would improve human cognitive abilities above and beyond what a natural brain can do. We do not have yet a theory correctly approximating physical substrate of higher cognitive processes. Brain did not evolve by adding defined units for more complex functions, it improved its performance by physiological modulation enabled by biochemical alterations of neuroactive substances.

Therefore, the belief that brain-machine interfaces offer a viable method for augmenting cognitive processes lacks scientific credibility (Kurzweil, 2000). The mainstay of this rhetoric has come via futurists who have generally ignored evolutionary processes, which have produced the current structure and functions of the human brain. What we have to remember is that our advanced technology that is in use in society is not the product of the brain of one person, who generated it in a short time. Rather it is the combined effect of multitudinous brains over a long historical period (i.e., learning, processing of learned information, researching and planning) together or separately over a long period of time. The brain is a unique organ that "changes" with learning and processing of the learned material to generate novel ideas that could be researched or tested. In short, the brain is continuously changing to generate the complex technological advances of the modern world. Therefore, a normal brain does not need a brain-machine interface to cope with the ever increasing technology or new information; what the brain needs is continuous input of the new information (i.e., learning). Furthermore, when an individual executes an action (mental or physical), it results from the complex interactions of information inputs and outputs from many regions of the brain (e.g., a muscular action—sensory cortex, motor cortex, basal nuclei, cerebellum, etc.) and the level and type of interaction from each region vary (Blumenfeld, 2010; Michael-Titus et al., 2010). Therefore, proper understanding of all these process is critical, before manufacturing "brain-machine" interfaces to augment brain functions. If this path is not taken, brain-machine interfaces could cause more harm than benefits.

We may infer from this that any attempts to augment human intelligence via brain-machine interfaces will be problematic due to evolutionary dynamics underpinning the human brain. Furthermore, the incredibly complex nature of neural networks, chemical complexity of nerve signals conduction and individual anatomical and physiological variation pose enormous challenges for interaction of engineered devices with association networks in the human brain. However, in the current environment, brain-machine interfaces may have some therapeutic benefits in individuals developing dementiae, neuro-degenerative diseases and sensory input inadequacies (blindness, deafness). For example, neuromodulation using deep brain stimulation (DBS) is currently being used to reduce Parkinsonian symptoms in selected patients. A goal of DBS is not merely to slow down cognitive decline, but also to lead to a restoration of function, thereby increasing life quality (Zibly et al., 2014). Advantages of DBS surgery are its low complication rates and comparatively higher safety levels when performed by expert neurosurgeons (Zibly et al., 2014).

Since complex cognitive tasks rely on widely dispersed intersecting neural networks involving various parts of the brain, it is thought to be difficult to connect to the brain an engineered device that would assist or augment complex thoughts. Since transmission of signal from one neuron to other neurons is mediated chemically, it may be more feasible to introduce into brains

substances that alter the efficiency of neurotransmission. Chemical engineering may be more efficient than electronic engineering.

NOOTROPIC AGENTS AND EVOLUTION

There are a number of chemically based methods of augmenting the human brain, forming an important element of cosmetic neurology (Dees, 2004). The field of cosmetic neurology is increasingly dependent on the development and application of nootropic agents (Cakic, 2009). A nootropic agent is a substance that may alter, nourish or augment cognitive performance, predominantly through the stimulation or inhibition of certain neurotransmitters (Nishizaki et al., 1999). These agents may occur in nature or be synthetically derived (Dielenberg, 2013). These substances have been proven to increase concentration, harness memory potential and expedite cognitive functioning (Turner et al., 2003, 2004). Many of these agents act under the premise of manipulating neurochemistry in a targeted fashion and are predominantly stimulatory in nature (Copani et al., 1992). Most traditional and modern nootropics activate an excitatory neurotransmitter or suppress the action of its inhibitory counterpart (Ito et al., 1990; Nicoletti et al., 1991; Staubli et al., 1994; Lynch and Gall, 2006; Huff, 2012).

Many authors support the co-evolution of early hominins with the use of nootropic substances and the attainment of altered states of consciousness (Winkelman, 2000, 2001; Sullivan and Hagen, 2002; Saniotis, 2010). Indeed, the desire to augment cognitive performance through the consumption of particular substances predates antiquity.

There is evidence to support the long-standing and widespread use of nootropic agents on every inhabited continent. For example Aboriginal Australians have used the stimulatory effects of *Nicotiani gossei* for millennia (Watson, 1983; Sullivan and Hagen, 2002). The use of tobacco throughout North and Central America has been well established and coca, the pre-cursor of cocaine, was cultivated along the western coast of South America as long as 7,000 years ago (Balick and Cox, 1996; Sullivan and Hagen, 2002). This cultivation ran contemporaneously with the use of cannabis in Europe (Schultes and Hofmann, 1979). The modest potency of organically derived substances and the long-standing, stable use of the aforementioned products in these ancient cultures proved to be beneficial (Saniotis and Henneberg, 2011). The strongest evidence to support this development is the presence of encoding DNA specific for the metabolization of these substances, such as the cytochrome P450 2D6 (CYP2D6) gene (Saniotis and Henneberg, 2011). These examples illustrate the inextricable involvement of environmental substances in altering or augmenting cognitive performance.

The affiliation with biological neuro-stimulants has continued through to recent history. The industrial revolution permitted the production of mind-altering substances on an unprecedented scale. Throughout the 20th century, there was a proliferation of synthetically derived substances applicable to cosmetic neurology. Today, nootropic agents are used to intentionally augment cognitive performance. University students appear to be amongst major perpetrators as they complete assignments and prepare for examinations (Greely et al., 2008). Prescription medications such as methylphenidate (Ritalin) and dextroamphetamine (Adderall) are being increasingly used and modafinil, an analeptic prescription medication has been used as a study aid by one-fifth of UK university students (Ghahremani et al., 2011; Fitzsimons and McDonald, 2014). Modafinil is believed to increase concentrations of glutamate and decrease GABA within the posterior hypothalamus, producing an overall neuro-excitatory effect (Ferraro et al., 1999). The drug has been shown to improve attention and working memory in medical practitioners and aviators and may be used in other challenging professions (Turner et al., 2003; Chatterjee, 2004; Müller et al., 2004; Walsh et al., 2004; Czeisler et al., 2005; Warren et al., 2009; Garcia et al., 2013).

However, the over-application of modern cosmetic neurology is fraught with danger and has been proven deleterious in many instances. In the short term, modafinil is known to produce nausea, vomiting, diarrhea, dyspepsia, headache, insomnia and anxiety with its long-term complications remaining largely unknown (Ballon and Feifel, 2006; Sahakian and Morein-Zamir, 2007). More alarmingly, the consumption of commonly used psycho-stimulants, including Ritalin and Adderall, has been linked to the precipitation or exacerbation of underlying mental illness, sleep disturbances and cerebrovascular disease (Cakic, 2009). This is likely due to the modern human brain being maladaptive to the exaggerated pharmacological alteration of neurochemistry (Sullivan and Hagen, 2002). Increased drug potency associated with synthetic production has outpaced the brain's capacity to metabolize and clear toxic substances, leading to prolonged exposure to these potentially harmful products (Sullivan and Hagen, 2002). This may be an example of evolutionary mismatch (Sullivan and Hagen, 2002). Whatever the mechanism, it appears these ill-adapted responses to modern nootropic agents may account for the bulk of the observed negative outcomes.

The potential scope of application for nootropic agents is vast. Mind-altering substances have the capacity to optimize cognitive performance and maximize human achievement. However, the limits of pharmacologically aided human cognition should not exceed the capacities of the brain. The human brain is a complex organ, thus pushing its performance beyond its adaptive capacity using pharmacological products could lead to failure. Therefore, caution must be taken when approaching the inherent risks of exacerbating the existing evolutionary mismatch in order to avoid deleterious outcomes. The majority of these outcomes are likely to relate to unbalancing salubrious and delicate neurochemical concentrations. Many psychiatric conditions, including schizophrenia, bipolar disorder and major depression, have illustrated neurochemical etiologies (Knable and Weinberger, 1997; Hirschfeld, 2000; López-Figueroa et al., 2004; Berk et al., 2007). Evolutionary challenges aside, there are also unresolved ethical and practical issues related to the intentional consumption of nootropic agents, not the least of which being whether it is fair, ethical and sensible to do so.

CONCLUSION

Many believe it to be evident that the human brain has a tremendous propensity for technologically driven augmentation. Several authors have discussed the potential for anatomical and physiological enhancement via brain-machine interfaces and cosmetic

neurology. Despite the hypothetical applications of cognitive improvement, this article has argued that human brain augmentation possesses a number of inherent challenges, many of which are informed during prehistory. The daunting complexity of neurological processes which inform cognitive abilities, combined with a current lack of understanding will likely confound any attempts in creating "smarter" minds. In fact, any attempt to circumvent the archaic substructures of the human brain may only serve to exacerbate the already existing maladaptive responses. For this reason, great caution must be adopted in approaching further attempts to go "messing with the mind".

REFERENCES

Balick, M. J., and Cox, P. A. (1996). *Plants, People and Culture: The Science of Ethnobotany.* New York: Scientific American Library.

Ballon, J. S., and Feifel, D. (2006). A systematic review of modafinil: potential clinical uses and mechanisms of action. *J. Clin. Psychiatry* 67, 554–566. doi: 10.4088/jcp.v67n0406

Bar-Yosef, O. (2007). The archaeological framework of the upper paleolithic revolution. *Diogenes* 54, 3–18. doi: 10.1177/0392192107076869

Bednarik, R. G. (1997). The global evidence of early human symboling behaviour. *Hum. Evol.* 12, 147–168. doi: 10.1007/bf02438065

Berk, M., Dodd, S., Kauer-Sant Anna, M., Malhi, G. S., Bourin, M., Kapczinski, F., et al. (2007). Dopamine dysregulation syndrome: implications for a dopamine hypothesis of bipolar disorder. *Acta Psychiatr. Scand. Suppl.* 116, 41–49. doi: 10.1111/j.1600-0447.2007.01058.x

Blumenfeld, H. (2010). *Neuroanatomy Through Clinical Cases.* 2nd Edn. Sunderland, Massachusetts: Sinauer Associates, Inc.

Borton, D., Silvestro Micera, S., Millán, J. R., and Courtine, G. (2013). Robotics and neuroprosthetics: personalizsed neuroprosthetics. *Sci. Transl. Med.* 5:210rv2. doi: 10.1126/scitranslmed.3005968

Bostrom, N. (2003). Are you living in a computer simulation?. *Philos. Q.* 53, 243–255. doi: 10.1111/1467-9213.00309

Bullmore, E., and Sporns, O. (2009). Complex brain networks: graph theoretical analysis of structural and functional systems. *Nat. Rev. Neurosci.* 10, 186–198. doi: 10.1038/nrn2575

Burke, A. (2010). Spatial abilities, cognition and the pattern of Neanderthal and modern human dispersals. *Quat. Int.* 247, 230–235. doi: 10.1016/j.quaint.2010.10.029

Butler, C. (2005). *Prehistoric Flintwork.* Tempus: Stroud.

Cakic, V. (2009). Smart drugs for cognitive enhancement: ethical and pragmatic considerations in the era of cosmetic neurology. *J. Med. Ethics* 35, 611–615. doi: 10.1136/jme.2009.030882

Chatterjee, A. (2004). Cosmetic neurology: the controversy over enhancing movement, mentation and mood. *Neurology* 63, 968–974. doi: 10.1212/01.wnl.0000138438.88589.7c

Collinger, J. L., Wodlinger, B., Downey, J. E., Wang, W., Tyler-Kabara, E. C., Weber, D. J., et al. (2012). High-performance neuroprosthetic control by an individual with tetraplegia. *Lancet* 381, 557–564. doi: 10.1016/S0140-6736(12)61816-9

Copani, A., Genazzani, A. A., Aleppo, G., Casabona, G., Canonico, P. L., Scapagnini, U., et al. (1992). Nootropic drugs positively modulate α-amino-3-hydroxy-5-methyl-4-isoxazolepropionic acid-sensitive glutamate receptors in neuronal cultures. *J. Neurochem.* 58, 1199–1204. doi: 10.1111/j.1471-4159.1992.tb11329.x

Czeisler, C. A., Walsh, J. K., Roth, T., Hughes, R. J., Wright, K. P., Kingsbury, L., et al. (2005). Modafinil for excessive sleepiness associated with shift-work sleep disorder. *N. Engl. J. Med.* 353, 476–486. doi: 10.1056/nejm200509083531028

Dees, R. H. (2004). Slippery slopes, wonder drugs and cosmetic neurology the neuroethics of enhancement. *Neurology* 63, 951–952. doi: 10.1212/01.wnl.0000140733.62305.af

De Miguel, C., and Henneberg, M. (2001). Variation in hominid brain size: how much is due to method? *Homo* 52, 3–58. doi: 10.1078/0018-442x-00019

Dielenberg, R. A. (2013). The speculative neuroscience of the future human brain. *Humanities* 2, 209–252. doi: 10.3390/h2020209

Drexler, K. E. (1992). *Nanosystems: Molecular Machinery, Manufacturing and Computation.* New York: John Wiley and Sons, Inc.

Ethier, C., Oby, E. R., Bauman, M. J., and Miller, L. E. (2012). Restoration of grasp following paralysis through brain-controlled stimulation of muscles. *Nature* 485, 368–371. doi: 10.1038/nature10987

Ferraro, L., Antonelli, T., Tanganelli, S., O'Connor, W. T., Perez de la Mora, M., Mendez-Franco, J., et al. (1999). The vigilance promoting drug modafinil increases extracellular glutamate levels in the medial preoptic area and the posterior hypothalamus of the conscious rat: prevention by local GABAA receptor blockade. *Neuropsychopharmacology* 20, 346–356. doi: 10.1016/s0893-133x(98)00085-2

Fitzsimons, S., and McDonald, M. (2014). *One in Five Students have Used Modafinil: Study Drug Survey Results.* Cambrige: The Tab.com (Online).

Garcia, V. A., Hirotsu, C., Matos, G., Alvarenga, T., Pires, G. N., Kapczinski, F., et al. (2013). Modafinil ameliorates cognitive deficits induced by maternal separation and sleep deprivation. *Behav. Brain Res.* 253, 274–279. doi: 10.1016/j.bbr.2013.07.029

Ghahremani, D. G., Tabibnia, G., Monterosso, J., Hellemann, G., Poldrack, R. A., and London, E. D. (2011). Effect of modafinil on learning and task-related brain activity in methamphetamine-dependent and healthy individuals. *Neuropsychopharmacology* 36, 950–959. doi: 10.1038/npp.2010.233

Glasser, M. F., Goyal, M. S., Preuss, T. M., Raichle, M. E., and Van Essen, D. C. (2014). Trends and properties of human cerebral cortex: correlations with cortical myelin content. *Neuroimage* 93, 165–175. doi: 10.1016/j.neuroimage.2013.03.060

Greely, H., Sahakian, B., Harris, J., Kessler, R. C., Gazzaniga, M., Campbell, P., et al. (2008). Towards responsible use of cognitive-enhancing drugs by the healthy. *Nature* 456, 702–705. doi: 10.1038/456702a

Haug, H. (1987). Brain sizes, surfaces and neuronal sizes of the cortex cerebri: a stereological investigation of man and his variability and a comparison with some mammals (primates, whales, marsupials, insectivores and one elephant). *Am. J. Anat.* 180, 126–142. doi: 10.1002/aja.1001800203

Hawks, J., Wang, E. T., Cochran, G. M., Harpending, H. C., and Moyzis, R. K. (2007). Recent acceleration of human adaptive evolution. *Proc. Natl. Acad. Sci. U S A* 104, 20753–20758. doi: 10.1073/pnas.0707650104

Henneberg, M. (1990). Brain size/body weight variability in Homo sapiens: consequences for interpreting hominid evolution. *Homo* 39, 121–130.

Henneberg, M. (1998). Evolution of the human brain: is bigger better? *Clin. Exp. Pharmacol. Physiol.* 25, 745–749. doi: 10.1111/j.1440-1681.1998.tb02289.x

Henneberg, M., Budnik, A., Pezacka, M., and Puch, A. E. (1985). Head size body size and intelligence intraspecific correlation in Homo sapiens species. *Homo* 36, 207–218.

Henneberg, M., Hugg, J., and Townsend, E. J. (1989). Body weight/height relationship an exponential solution. *Am. J. Hum. Biol.* 1, 483–491. doi: 10.1002/ajhb.1310010412

Henneberg, M., and Saniotis, A. (2009). Evolutionary origins of human brain and spirituality. *Anthropol. Anz.* 67, 427–438. doi: 10.1127/0003-5548/2009/0032

Henneberg, M., and Thackeray, J. F. (1995). A single-lineage hypothesis of hominid evolution. *Evol. Theory* 13, 31–38.

Hirschfeld, R. M. A. (2000). History and evolution of the monoamine hypothesis of depression. *J. Clin. Psychiatry* 61, 4–6.

Huff, M. M. (2012). *Cosmetic Neurology: Enhancement of the Mind and Attention Deficit Hyperactive Disorder Medication Abuse among College Students.* Lynchburg: Liberty University.

Ifft, P. J., Shokur, S., Li, Z., Lebedev, M. A., and Nicolelis, M. A. L. (2013). A brain-machine interface enables bimanual arm movements in monkeys. *Sci. Transl. Med.* 5:210ra154. doi: 10.1126/scitranslmed.3006159

Ito, I., Tanabe, S., Kohda, A., and Sugiyama, H. (1990). Allosteric potentiation of receptors by a nootropic drug aniracetam. *J. Physiol.* 424, 533–543.

Jerison, H. J. (1973). *Evolution of the Brain and Intelligence.* New York: Academic Press.

Knable, M. B., and Weinberger, D. R. (1997). Dopamine, the pre-frontal cortex and schizophrenia. *J. Psychopharmacol.* 11, 123–131. doi: 10.1177/026988119701100205

Kurzweil, R. (2000). *The Age of Spiritual Machines: When Computers Exceed Human Intelligence.* New York: Penguin Books.

Lebedev, M., and Nicolelis, M. A. L. (2006). Brain-machine interfaces: past, present and future. *Trends Neurosci.* 29, 536–546. doi: 10.1016/j.tins.2006.07.004

López-Figueroa, A. L., Norton, C. S., Lopez-Figueroa, M. O., Armellini-Dodel, D., Burke, S., Akil, H., et al. (2004). Serotonin 5-HT1A, 5-HT1B and 5-HT2A receptor mRNA expression in subjects with major depression, bipolar disorder

and schizophrenia. *Biol. Psychiatry* 55, 225–233. doi: 10.1016/j.biopsych.2003.09.017

Lycett, S. P., and Chauhan, P. eds. (2010). *Newperspectives on Old Stones: Analytical Approaches to Palaeolithic Techniques.* New York: Springer.

Lynch, G., and Gall, C. M. (2006). Ampakines and the threefold path to cognitive enhancement. *Trends Neurosci.* 29, 554–562. doi: 10.1016/j.tins.2006.07.007

Martin, R. D. (1990). *Primate Origins and Evolution.* New Jersey: Princeton University Press.

McDaniel, M. A. (2005). Big-brained people are smarter: a meta-analysis of the relationship between in vivo brain volume and intelligence. *Intelligence* 33, 337–346. doi: 10.1016/j.intell.2004.11.005

McHenry, H. M. (1976). Early hominid body weight and encephalisation. *Am. J. Phys. Anthropol.* 45, 77–83. doi: 10.1002/ajpa.1330450110

Michael-Titus, A., Revest, P., and Shortland, P. (2010). *Systems of the Body: The Nervous System—Basic Science and Clinical Conditions.* 2nd Edn. New York, Oxford: Elsevier.

Moritz, C. T., Perlmutter, S. I., and Fetz, E. E. (2008). Direct control of paralysed muscles by cortical neurons. *Nature* 456, 639–642. doi: 10.1038/nature07418

Müller, U., Steffenhagen, N., Regenthal, R., and Bublak, P. (2004). Effects of modafinil on working memory processes in humans. *Psychopharmacology (Berl)* 177, 161–169. doi: 10.1007/s00213-004-1926-3

Nicolelis, M. A. L. (2003). Brain-machine interfaces to restore motor function and probe neural circuits. *Nat. Rev. Neurosci.* 4, 417–422. doi: 10.1038/nrn1105

Nicolelis, M. A. L., and Srinivasan, M. (2003). "Human-machine interactions: potential impact of nanotechnology in the design of neuroprosthetic devices aimed at restoring or augmenting human performance," in *Converging Technologies for Improving Human Performance: Nanotechnology, Biotechnology, Information Technology and Cognitive Science*, eds M. C. Roco and W. S. Bainbridge (Dordrecht, The Netherlands: Kluwer Academic Press), 251–255.

Nicoletti, F., Casabona, G., Genazzani, A. A., Copani, A., Aleppo, G., Canonico, P. L., et al. (1991). Excitatory amino acids and neuronal plasticity: modulation of AMPA receptors as a novel substrate for the action of nootropic drugs. *Funct. Neurol.* 7, 413–422.

Nishizaki, T., Matsuoka, T., Nomura, T., Matsuyama, S., Watabe, S., Shiotani, T., et al. (1999). A 'long-term-potentiation-like' facilitation of hippocampal synaptic transmission induced by the nootropic nefiracetam. *Brain Res.* 826, 281–288. doi: 10.1016/s0006-8993(99)01312-8

Power, J. D., Alexander, J., Cohen, L., Nelson, S. M., Wig, G. S., Barnes, K. A., et al. (2011). Functional network organization of the human brain. *Neuron* 72, 665–678. doi: 10.1016/j.neuron.2011.09.006

Previc, F. (1999). Dopamine and the origins of human intelligence. *Brain Cogn.* 41, 299–350. doi: 10.1006/brcg.1999.1129

Previc, F. (2009). *The Dopaminergic Mind in Human Evolution and History.* New York: Cambridge University Press.

Radinsky, L. B. (1979). *The Fossil Record of Primate Brain Evolution. 49th James Arthur Lecture, 1979.* New York: American Museum of Natural History.

Ramez, N. (2005). *More Than Human: Enhancing the Promise of Biological Enhancement.* New York: Broadway Books.

Raspopovic, S., Capogrosso, M., Petrini, F. M., Bonizzato, M., Rigosa, J., Di Pino, G., et al. (2014). Restoring natural sensory feedback in real-time bidirectional hand prostheses. *Sci. Transl. Med.* 6:222ra19. doi: 10.1126/scitranslmed.3006820

Roco, M. C., and Bainbridge, W. S. (2002). *Nanotechnology, Biotechnology, Information Technology and Cognitive Science.* Washington, DC: National Science Foundation.

Rogers, A. W. (1992). *A Textbook of Anatomy.* Edinburgh: Churchill Livingstone.

Sahakian, B., and Morein-Zamir, S. (2007). Professor's little helper. *Nature* 450, 1157–1159. doi: 10.1038/4501157a

Sanchez, J. C., Erdogmus, D., Rao, Y. N., Principe, J. C., Nicolelis, M., and Wessberg, J. (2003). "Learning the contributions of the motor, premotor and posterior parietal cortices for hand trajectory reconstruction in a brain machine interface," in Presented at the *IEEE EMBS Neural Engineering Conference*. Capri, Italy.

Saniotis, A. (2010). Evolutionary and anthropological approaches towards understanding human need for psychotropic and mood altering substances. *J. Psychoactive Drugs* 42, 477–484. doi: 10.1080/02791072.2010.10400710

Saniotis, A., and Henneberg, M. (2011). An evolutionary approach to exploring altered states of consciousness, mind-body techniques and non-local mind. *World Futures* 67, 182–200. doi: 10.1080/02604027.2011.555250

Schultes, R., and Hofmann, A. (1979). "An overview of hallucinogens in the western hemisphere," in *Flesh of the Gods*, ed P. Furst (New York: Praeger), 3–54.

Shih, J. J., Krusienski, D. J., and Wolpaw, J. R. (2012). Brain-computer interfaces in medicine. *Mayo Clin. Proc.* 87, 268–279. doi: 10.1016/j.mayocp.2011.12.008

Staubli, U., Rogers, G., and Lynch, G. (1994). Facilitation of glutamate receptors enhances memory. *Proc. Natl. Acad. Sci. U S A* 91, 777–781. doi: 10.1073/pnas.91.2.777

Stephan, H. (1972). "Evolution of primate brains: a comparative anatomical invesitigation," in *Functional and Evolutionary Biology of Primates*, ed R. Tuttle (Chicago: Aldine Atherton), 155–174.

Sullivan, R. J., and Hagen, E. H. (2002). Psychotropic substance-seeking: evolutionary pathology or adaptation?. *Addiction* 97, 389–400. doi: 10.1046/j.1360-0443.2002.00024.x

Tan, D. S., and Nijholt, A. (2010). "Brain-computer interfaces and human-computer interaction," in *Brain-Computer Interfaces*, eds D. S. Tan and A. Nijholt (London: Springer-Verlag Limited), 3–19.

Thakor, N. V. (2013). Translating the brain-machine interface. *Sci. Transl. Med.* 5:210ps17. doi: 10.1126/scitranslmed.3007303

Turner, D. C., Clark, L., Dowson, J., Robbins, J., and Sahakian, B. J. (2004). Modafinil improves cognition and response inhibition in adult attention-deficit/hyperactivity disorder. *Biol. Psychiatry* 55, 1031–1040. doi: 10.1016/j.biopsych.2004.02.008

Turner, D. C., Robbins, T. W., Clark, L., Aron, A. R., Dowson, J., and Sahakian, B. J. (2003). Cognitive enhancing effects of modafinil in healthy volunteers. *Psychopharmacology (Berl)* 165, 260–269.

Walsh, J. K., Randazzo, A. C., Stone, K. L., and Schweitzer, P. K. (2004). Modafinil improves alertness, vigilance and executive function during simulated night shifts. *Sleep* 27, 434–439.

Warren, O. J., Leff, D. R., Athanasiou, T., Kennard, C., and Darzi, A. (2009). The neurocognitive enhancement of surgeons: an ethical perspective. *J. Surg. Res.* 152, 167–172. doi: 10.1016/j.jss.2007.12.761

Watson, P. L. (1983). *This Precious Foliage: A Study of the Aboriginal Psycho-Active Drug Pituri.* Sydney: University of Sydney.

Winkelman, M. (2000). *The Neural Ecology of Consciousness and Healing.* Westport, Conneticut, London: Bergin and Garvey.

Winkelman, M. (2001). Alternative and traditional medicine approaches for substance abuse programs: a shamanic approach. *Int. J. Drug Policy* 12, 337–351. doi: 10.1016/s0955-3959(01)00100-1

Zibly, Z., Shawa, A., Harnof, S., Sharma, M., Graves, C., and Deogaonkar, M. (2014). Modulation of mind: therapeutic neuromodulation for cognitive disability. *J. Clin. Neurosci.* doi: 10.1016/j.jocn.2013.11.040. [Epub ahead of print].

Conflict of Interest Statement: The authors declare that the research was conducted in the absence of any commercial or financial relationships that could be construed as a potential conflict of interest.

Received: 30 May 2014; accepted: 04 August 2014; published online: 30 September 2014.

Citation: Saniotis A, Henneberg M, Kumaratilake J and Grantham JP (2014) "Messing with the mind": evolutionary challenges to human brain augmentation. Front. Syst. Neurosci. ***8****:152. doi: 10.3389/fnsys.2014.00152*

This article was submitted to the journal Frontiers in Systems Neuroscience.

frontiers in
SYSTEMS NEUROSCIENCE

REVIEW ARTICLE
published: 02 April 2014
doi: 10.3389/fnsys.2014.00046

Sleep for cognitive enhancement

Susanne Diekelmann*

Institute of Medical Psychology and Behavioral Neurobiology, University Tübingen, Tübingen, Germany

Edited by:
Mikhail Lebedev, Duke University, USA

Reviewed by:
Jessica Payne, University of Notre Dame, USA
Daniel Bendor, University College London, UK
Ivan N. Pigarev, Russian Academy of Sciences, Russia

****Correspondence:***
Susanne Diekelmann, Institute of Medical Psychology and Behavioral Neurobiology, University Tübingen, Otfried-Müller-Str. 25, CIN Building, 72076 Tübingen, Germany
e-mail: susanne.diekelmann@uni-tuebingen.de

Sleep is essential for effective cognitive functioning. Loosing even a few hours of sleep can have detrimental effects on a wide variety of cognitive processes such as attention, language, reasoning, decision making, learning and memory. While sleep is necessary to ensure normal healthy cognitive functioning, it can also enhance performance beyond the boundaries of the normal condition. This article discusses the enhancing potential of sleep, mainly focusing on the domain of learning and memory. Sleep is known to facilitate the consolidation of memories learned before sleep as well as the acquisition of new memories to be learned after sleep. According to a widely held model this beneficial effect of sleep relies on the neuronal reactivation of memories during sleep that is associated with sleep-specific brain oscillations (slow oscillations, spindles, ripples) as well as a characteristic neurotransmitter milieu. Recent research indicates that memory processing during sleep can be boosted by (i) cueing memory reactivation during sleep; (ii) stimulating sleep-specific brain oscillations; and (iii) targeting specific neurotransmitter systems pharmacologically. Olfactory and auditory cues can be used, for example, to increase reactivation of associated memories during post-learning sleep. Intensifying neocortical slow oscillations (the hallmark of slow wave sleep (SWS)) by electrical or auditory stimulation and modulating specific neurotransmitters such as noradrenaline and glutamate likewise facilitates memory processing during sleep. With this evidence in mind, this article concludes by discussing different methodological caveats and ethical issues that should be considered when thinking about using sleep for cognitive enhancement in everyday applications.

Keywords: sleep, cognitive enhancement, memory, learning, reactivation, brain stimulation, pharmacology, ethics

INTRODUCTION

Sleep is vital to ensure normal human cognitive performance. Not obtaining enough sleep diminishes a wide variety of cognitive functions such as attention, language, reasoning, decision making, learning and memory (for reviews see Durmer and Dinges, 2005; Killgore, 2010; Jackson et al., 2013). Acute sleep deprivation of one or more nights without sleep can slow down reaction times (Van Dongen et al., 2003), increase perseveration (Retey et al., 2006), reduce focused attention (Thomas et al., 2000), impair risk assessment (Killgore et al., 2006) and strategic planning (Harrison and Horne, 1999), and deteriorate divergent thinking (Harrison and Horne, 2000) as well as language and communication skills (Harrison and Horne, 1998). Yet, does an impairment of cognition due to the loss of sleep in turn indicate that sleep *enhances* cognition? The answer is no. Evidence for deleterious effects of sleep loss demonstrates that sleep is necessary to enable normal healthy cognitive functioning. Cognitive enhancement, however, is defined as "the amplification or extension of core capacities of the mind" that go beyond the normal healthy condition (Sandberg, 2011). In this way, enhancement contrasts with therapy, which is understood as the treatment and prevention of diseases with the goal to restore or maintain the normal healthy condition (Bostrom and Roache, 2008). A number of methods have proven effective to enhance cognition in the state of wakefulness, such as pharmaceutical drugs, brain stimulation and meditation practices. Sleep is a state of the organism that differs fundamentally from the wake state with regard to the neurochemical milieu, brain activity patterns and mental states. This article reviews evidence for methods of cognitive enhancement during sleep. Sleep-specific manipulations have been found to effectively boost cognitive functions beyond the boundaries of the normal condition.

Cognition is not a unitary process but involves different functions and components. Sleep is effective in facilitating several of these functions such as language processing (Dumay and Gaskell, 2007), working memory (Kuriyama et al., 2008), creativity (Ritter et al., 2012) and decision making (Pace-Schott et al., 2012a). The largest amount of research on enhancing cognition during sleep, however, has focused on the domain of learning and memory (Rasch and Born, 2013). Memory is one of the most essential cognitive functions involved in almost all other cognitive processes. The ability to remember past experiences is not only critical for appropriate behavior in the present but it also allows us to anticipate and predict future events and situations. Our individual memories and our ability to learn new things are an integral part of our identity and influence our prospects of a successful and happy life. Considering that memory is of critical importance for individuals as well as for societies (e.g., in education, professional

occupation, economic productivity, personal relationships), the possibility of enhancing memory has received increasing attention (Alberini and Chen, 2012; Collingridge et al., 2013; Stern and Alberini, 2013). Although sleep is widely neglected in the discussion of memory enhancement, the sleep state might be particularly well suited as a target for the enhancement of memory capacities.

Sleep is well known to facilitate memory consolidation, that is, the strengthening and stabilization of new memories acquired before sleep (Maquet, 2001; Walker and Stickgold, 2006; Rasch and Born, 2013). Subjects who are allowed to sleep after learning typically perform better on a subsequent retrieval test than subjects who spend a comparable amount of time awake following learning. Sleep actively promotes the reprocessing of fresh memories as well as their integration into the pre-existing network of long-term memories (Diekelmann and Born, 2010; Lewis and Durrant, 2011; Stickgold and Walker, 2013). Apart from its beneficial effect on the consolidation of previously learned memories, sleep also benefits the subsequent acquisition of new learning material (Van Der Werf et al., 2009). Even a short period of sleep prior to learning can enhance the capacity to encode new information (Mander et al., 2011).

Two main theories have been proposed to explain the beneficial effect of sleep for learning and memory. According to the active system consolidation theory, new memories become reactivated and reorganized on the system-level during sleep, with selected neuronal representations being potentiated and thereby strengthened (Lewis and Durrant, 2011; Inostroza et al., 2013; Rasch and Born, 2013). The synaptic homeostasis hypothesis, on the other hand, assumes that synaptic connections become widely depotentiated during sleep, whereby selected memory representations are depotentiated less or are spared from depotentiation so that these memories come out relatively stronger (Tononi and Cirelli, 2006, 2014). Both theories are well supported by experimental evidence and, importantly, are not mutually exclusive. Although this article is principally biased towards the active system consolidation theory, the reviewed evidence for cognitive enhancement during sleep is largely independent of mechanistic considerations and is also consistent with the synaptic homeostasis hypothesis in its most recent version (Tononi and Cirelli, 2014).

There are two ways in which sleep can be used to facilitate memory. First, sleep can be timed in relation to learning in such a way as to optimally support encoding and memory consolidation processes. In this way, the normal healthy function of sleep for memory can be optimized. For example, introducing short naps before learning of new information fosters the initial acquisition and encoding of new memory traces (Mander et al., 2011). Likewise, sleep episodes that follow shortly after the encoding session benefit the consolidation of fresh memories to preserve these memories for the long-term and protect them from subsequent interfering inputs (Gais et al., 2006b; Ellenbogen et al., 2009; Payne et al., 2012a,b). The second and more intriguing way to actually enhance memory during sleep (in the sense of augmenting memory beyond the normal condition) is to manipulate memory and/or sleep directly. Such manipulations target either the processing of specific memory representations during sleep or particular sleep features that are known to be implicated in memory processing. Additionally, pharmacological interventions can be applied to modulate the processing of memories during sleep.

The following sections Manipulation of Memory Reactivation During Sleep, Manipulation of Sleep-Specific Brain Oscillations and Manipulation of Neurotransmitter Systems outline examples of how memory representations and sleep processes can be directly or indirectly manipulated to enhance memory. Section Considerations and Caveats discusses possible considerations and caveats relating to methodological and ethical issues in the potential use of sleep for cognitive enhancement. Finally, section Conclusions presents general conclusions and an outlook on possible future research directions and practical applications.

MANIPULATION OF MEMORY REACTIVATION DURING SLEEP

The beneficial effect of sleep on memory is believed to rely on the neuronal reactivation of activity patterns that were present during the initial learning experience (Diekelmann and Born, 2010; Lewis and Durrant, 2011; Rasch and Born, 2013). In rats, firing sequences of hippocampal place cells that are observed during training, spontaneously re-express ("replay") in a coordinated fashion during subsequent sleep periods (Wilson and McNaughton, 1994; Skaggs and McNaughton, 1996). Such replay mainly occurs during slow wave sleep (SWS; Lee and Wilson, 2002), sometimes at a faster firing rate than that of the original pattern (Nádasdy et al., 1999), and happens also in other brain regions such as the ventral striatum, visual cortex and prefrontal cortex (Euston et al., 2007; Ji and Wilson, 2007; Lansink et al., 2008). Reactivation of learning-associated brain activation patterns during sleep is also observed in humans, for example following training on a spatial navigation task (Peigneux et al., 2004) as well as a procedural serial reaction time task (Maquet et al., 2000). It is believed that these sleep reactivations strengthen the underlying memory traces and integrate them into long-term associative memory networks.

Intriguingly, memory reactivation does not only occur spontaneously during sleep but can be induced and/or intensified using externally applied reminder cues, a procedure that has been termed "targeted memory reactivation" (Oudiette and Paller, 2013). A ground-breaking study by Rasch et al. showed that memories for object locations can be reactivated during sleep by re-exposing subjects to odor cues that were previously associated with the learned object locations (Rasch et al., 2007). In this study, subjects learned to associate everyday objects and their locations in a 2D object location task, a task also commonly known as the game "concentration". Throughout learning, subjects were presented with puffs of the scent of roses. Subjects went to bed after learning and during ensuing SWS the odor was presented again. When tested on their memory for the object locations in the next morning, subjects showed superior memory for the object locations when they had slept with the odor compared to another night in which they did not receive the odor during sleep (**Figure 1**). Odor re-exposure during rapid eye movement (REM) sleep as well as during wakefulness was not effective in enhancing memory performance. Also, presenting odor cues during SWS without prior odor exposure during learning had no effect on memory. Subsequent studies showed that odor-induced

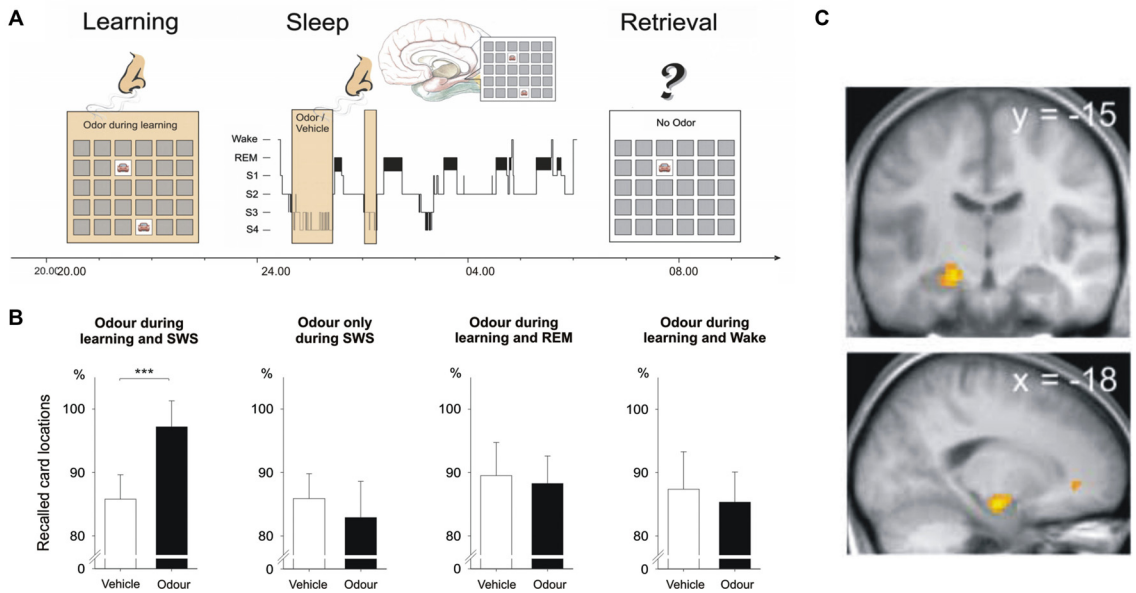

FIGURE 1 | Cueing reactivation during sleep by odors enhances memory. (A) Subjects learned card pair locations in the presence of an odor. The same odor or an odor-less vehicle was then presented during subsequent slow wave sleep (SWS). **(B)** Recall of card pair locations in the next morning was significantly better when subjects had received the odor during SWS. Odor presentation during REM sleep and during wakefulness remained ineffective. Memory was also not enhanced when the odor was omitted during learning. **(C)** Presentation of the learning-associated odor during SWS activated hippocampal regions (activation in the left anterior hippocampus shown here). From Rasch et al. (2007). Reprinted with permission from the American Association for the Advancement of Science.

reactivation during SWS does not only strengthen memories but also transforms them into a more stable form making them resistant to subsequent interfering inputs (Diekelmann et al., 2011). Furthermore, memory reactivation triggered by external odor cues accelerates memory consolidation processes leading to stable memory representations after a short sleep interval of only 40 min—a process that takes roughly double that time without odor cueing (Diekelmann et al., 2012).

Triggering reactivation during sleep to enhance memory performance not only works with odor cues; auditory stimuli seem to be comparably effective. Although auditory memory cues have the disadvantage that they can potentially disrupt sleep patterns, they also provide an important advantage: while odors represent rather broad context cues that presumably reactivate the entire learning experience, tones and sounds are more specific and can be used to reactivate individual memory contents. Rudoy et al. presented pictures at specific locations that were paired with corresponding sounds (Rudoy et al., 2009). Subjects learned the location for each picture (e.g., cat) and listened to the associated sound (e.g., meow) during training. Half of the sounds were then presented again during a nap following the training session. After sleep, subjects were asked to place each picture in its original position. Subjects performed significantly better for those pictures whose associated sounds they had heard during sleep compared to the pictures for which sounds were not presented during sleep. Recent evidence suggests that similar memory enhancing effects can be obtained by cueing vocabulary during sleep. Schreiner et al. presented half of a previously learned set of Dutch-German vocabulary to their participants during post-learning SWS. In the next morning participants correctly remembered more of the words that had been cued during sleep compared to the vocabulary that had not been cued (Schreiner et al., submitted manuscript).

External reactivation during sleep can also enhance procedural memories of sequential finger tapping skills. In a study by Antony et al. subjects were trained to tap two different sequences repeatedly on a keyboard. The tapped sequences corresponded to a melody of specific tones presented simultaneously during sequence tapping training. During a post-training nap of about 90 min the melody of one of the sequences was presented again in SWS. When tested on both sequences after the nap participants showed better tapping performance in the sequence for which the corresponding melody had been played during sleep (Antony et al., 2012). Interestingly, this cueing effect is strongly specific for the individual tones presented during sleep. Cueing only parts of the trained melody sequence results in very specific enhancements of performance in the respective cued sequence finger transitions (Schönauer et al., 2014).

Triggering memory reactivation during sleep cannot only improve subsequent retrieval performance for desired memories but can also help to forget undesired memories. In a study by Hauner et al. human subjects underwent a contextual fear conditioning procedure in which pictures of faces were paired with mild electric shocks while specific odors were presented as contextual background. Presenting one of the contextual odor cues again during subsequent sleep reduced fear responses to the face images in the next morning (Hauner et al., 2013). A similar study in mice used an odor as conditioned stimulus

that was systematically paired with foot shocks (Rolls et al., 2013). However, when mice were re-exposed to the odor during post-training sleep, subsequent fear responses to the odor were increased rather than decreased. Injection of a protein synthesis inhibitor in the amygdala before presentation of the odor during sleep resulted in fear extinction, i.e., reduced fear responses to the conditioned odor stimulus. These results demonstrate that subtle methodological differences in the experimental procedure can produce very different outcomes. For example, whether the reminder that is presented during sleep represents a context cue (as in Hauner et al.) or the conditioned stimulus itself (as in Rolls et al.) might determine whether fear memories are reduced or strengthened by reactivation during sleep (Oudiette et al., 2014).

Although the exact neurophysiological mechanisms underlying the effects of targeted memory reactivation during sleep are largely unknown, a seminal study by Bendor and Wilson indicates that external memory cueing during sleep can bias neuronal replay towards the firing patterns that were observed during prior learning (Bendor and Wilson, 2012). In this study, rats were trained on a linear track to run to the left side in response to sound L or to the right side in response to sound R. During subsequent sleep the sounds were presented again and sound L was found to elicit hippocampal firing patterns similar to those observed previously when the rats had been running to the left side during training, while sound R induced firing patterns similar to those observed when the rats had been running to the right side. Similarly, in humans the presentation of learning-associated cues during sleep activated task-specific brain regions in functional magnetic resonance imaging (fMRI). Re-exposure of a memory-associated odor during SWS activated hippocampal and neocortical brain regions (Rasch et al., 2007; Diekelmann et al., 2011), and presenting memory-related sounds during SWS increased activation in the parahippocampal cortex which predicted subsequent recall performance (van Dongen et al., 2012). Furthermore, epileptic patients who suffer from sclerosis in both hippocampi did not show a memory cueing effect with sounds during sleep, while in healthy controls as well as in patients with one functional hippocampus sound cueing enhanced memory consolidation (Fuentemilla et al., 2013). Thus, external memory reactivation biases neuronal replay and essentially depends on the integrity of the hippocampus. A recent study found that external memory cues (odors in this case) also alter sleep-specific brain oscillations presumably associated with memory replay. Odor cues presented during SWS increased slow wave activity (1–4 Hz) and fast spindle activity (13–15 Hz) and induced steeper slopes of slow oscillations, the latter being associated with memory improvement (Rihm et al., 2014).

MANIPULATION OF SLEEP-SPECIFIC BRAIN OSCILLATIONS

Considering that specific field potential oscillations in the sleeping brain have been associated with memory consolidation during sleep, targeting these phenomena directly is another promising road to enhance memory. Several lines of research have implicated SWS as the sleep stage that is most prominently involved in memory consolidation (since the role of REM sleep and stage 2 sleep for memory is less clear, these sleep stages will not be considered here, but see for example Genzel et al., 2013; Ackermann and Rasch, 2014). Neocortical slow oscillations, thalamo-cortical spindles and hippocampal ripples are the hallmark oscillations of SWS that are associated with memory processing. Slow oscillations (<1 Hz) are characterized by global up-states (neuronal firing) and down-states (neuronal silence) and are believed to orchestrate the dialogue between hippocampus and neocortex for long-term memory storage (Sirota and Buzsaki, 2005). Specifically, spindles and ripples occur preferentially during the slow oscillation up-state (Steriade, 2006), which is a state of widespread neuronal activity. Spindles are characteristic waxing and waning oscillations (∼10–15 Hz) that seem to prime cortical networks for neuronal plasticity. Hippocampal ripples, on the other hand, are high-frequency oscillations of ∼100–300 Hz that accompany memory replay in the hippocampal networks and are believed to carry the actual "memory information". The fine-tuned temporal interplay between slow oscillations, spindles and ripples presumably mediates the redistribution of new memories from the hippocampus, serving as a temporary store, to neocortical regions for longer-term storage (Diekelmann and Born, 2010).

A seminal study by Marshall et al. found that intensifying slow oscillations by electrical transcranial direct current stimulation (tDCS) enhances memory consolidation (Marshall et al., 2006). Subjects studied a list of word pairs in the evening and during subsequent sleep an electrical current that oscillated at the peak frequency of the endogenous slow oscillations (i.e., ∼0.75 Hz) was applied to the subjects' forehead. This electrical stimulation boosted endogenous slow oscillation activity and produced superior word recall in the next morning compared to a sleep condition without electrical stimulation (**Figure 2**). Importantly, the stimulation-induced memory improvement is specific for stimulation with the slow oscillation frequency: tDCS oscillating at 5 Hz (i.e., within the theta range) applied during SWS decreases slow oscillations and impairs memory consolidation (Marshall et al., 2011). Inducing slow oscillations can also be achieved with short auditory stimuli presented at the same frequency as endogenous slow oscillations (Ngo et al., 2013a). Presenting such an auditory stimulation closed-loop with endogenous slow oscillation up-states enhances memory consolidation of previously learned word pairs (Ngo et al., 2013b).

The stimulation of slow oscillations during sleep does not only enhance the consolidation of previously learned memories but can also augment the subsequent acquisition of new information. Antonenko et al. applied the previously described electrical slow oscillation stimulation during a midday nap in humans and tested their capacity to learn new word pairs, word lists and pictures thereafter (Antonenko et al., 2013). When subjects had slept with the slow oscillation stimulation, they were able to learn more new words and pictures after the nap compared to a nap without stimulation. Similar findings were observed in rats: electrical stimulation of slow oscillations via tDCS over several days improved the acquisition of task-inherent rules in a radial arm maze task (Binder et al., 2014). Intensifying slow oscillations might speed up processes that enable new learning in the hippocampus, possibly by down-scaling saturated neuronal networks or by shifting old

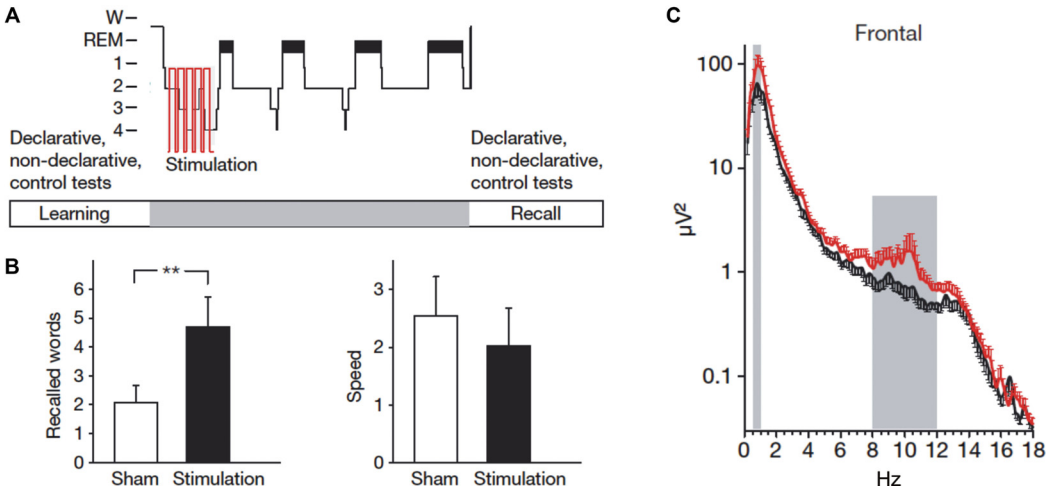

FIGURE 2 | Stimulating slow oscillations during sleep enhances memory. (A) Following learning of word pairs and finger sequence tapping, subjects received electrical stimulation of slow oscillations (tDCS at 0.75 Hz) during ensuing sleep. **(B)** Compared to a sham condition, subjects remembered more word pairs after slow oscillation stimulation. Speed in finger sequence tapping was not affected by the stimulation. **(C)** The stimulation increased activity in the slow oscillation (0.5–1 Hz) and the slow spindle frequency band (8–12 Hz) at frontal sites. Reprinted by permission from Macmillan Publishers Ltd.: Marshall et al. (2006).

memories from hippocampal to neocortical sites for long-term storage thereby freeing space for new memories.

Although spindles have frequently been associated with memory consolidation during sleep, it is unclear whether sleep spindles can be externally manipulated. There are numerous studies showing that spindle activity as well as spindle density increase following learning (e.g., Gais et al., 2002; Schabus et al., 2004; Schmidt et al., 2006) and the number and activity of sleep spindles correlates with subsequent memory performance (e.g., Clemens et al., 2005; Nishida and Walker, 2007). Furthermore, reactivating memories with learning-associated odors enhances spindle activity during odor cue presentation in SWS (Rihm et al., 2014). Increasing slow oscillations by electrical and auditory stimulation likewise induces a concurrent increase in spindle activity (Marshall et al., 2006; Ngo et al., 2013b). Yet, whether the relationship between spindles and memory is a causal one is unclear. It remains to be elucidated whether spindles can be externally triggered and whether such triggered spindles prove effective in enhancing memory.

Like sleep spindles, hippocampal ripple events are commonly associated with memory consolidation during sleep. During SWS in rats, ripples are observed during the replay of hippocampal neuron ensembles (Wilson and McNaughton, 1994; Peyrache et al., 2009) and their occurrence increases following learning (Eschenko et al., 2008). Moreover, during a nap in humans the number of ripples correlated with the consolidation of previously learned picture memories (Axmacher et al., 2008). Suppressing hippocampal ripples by electrical stimulation during post-learning sleep impairs memory for previously learned tasks in rats (Girardeau et al., 2009; Ego-Stengel and Wilson, 2010). However, it is hitherto unknown whether ripples can be induced or increased by external stimulation and whether this would enhance memory consolidation and/or acquisition.

MANIPULATION OF NEUROTRANSMITTER SYSTEMS

A number of different neurotransmitters and hormones modulates and influences the formation of memories. Most of these neurotransmitters and hormones are differentially regulated during sleep and wakefulness. SWS in particular is characterized by a decrease in levels of acetylcholine, noradrenaline and cortisol as well as by a distinct increase in growth hormone concentrations compared to periods of wakefulness (Marrosu et al., 1995; Born and Fehm, 2000). Other neurotransmitters such as glutamate, dopamine and GABA exhibit changes in concentrations across the sleep-wake cycle as well (Sowers and Vlachakis, 1984; Dash et al., 2009; Vanini et al., 2012). The exact mechanisms underlying the specific role of neurotransmitters in memory processing during sleep are not well understood. It is believed that the different levels of the respective neurotransmitters allow for and mediate the replay of firing patterns in neuronal circuits as well as the associated electrophysiological brain oscillations during sleep.

Several neurotransmitters have been found suitable for memory enhancement during sleep. For example, increasing the availability of noradrenaline during sleep with the noradrenaline reuptake inhibitor reboxetine enhances performance in an odor recognition task (Gais et al., 2011). In this study, subjects learned a set of odors and received reboxetine or placebo before a night of sleep. Two days later subjects recognized more of the previously learned odors when they had received reboxetine as compared to the night with placebo administration. In another study, reboxetine enhanced the consolidation of procedural memories in a finger sequence tapping task, which was associated with an increase in the number of sleep spindles (Rasch et al., 2009). The role of noradrenaline in sleep-dependent memory consolidation is further supported by findings showing that reducing the availability of noradrenaline by administering the α2-autoreceptor agonist clonidine blocks the improvement of memory for odors

(Gais et al., 2011) as well as the enhancement of emotional over neutral memories that is typically observed after sleep (Groch et al., 2011).

Enhancing glutamatergic neurotransmission during sleep likewise boosts the consolidation of previously acquired memories. Feld et al. performed a study in which subjects learned a set of word pairs in the evening and received the NMDA receptor coagonist D-cycloserine during subsequent sleep (Feld et al., 2013a). At retrieval testing 1 day later subjects remembered significantly more of the learned words when they had received D-cycloserine during sleep compared to a night of sleep without substance administration. D-cycloserine is assumed to facilitate synaptic plastic changes resulting from reactivation of glutamatergic neuronal ensembles (Feld et al., 2013a).

Other substances that target different neurotransmitter systems can enhance the consolidation of particular memories during sleep. For instance, the dopamine D2-like receptor agonist pramipexole enhances the consolidation of memories that had been associated with low reward during learning before sleep but does not affect memories associated with a high reward (Feld et al., in press). The cytokine interleukin-6, administered intranasally shortly before sleep, increases slow wave activity and enhances the consolidation of emotional but not neutral memories (Benedict et al., 2009). And while reboxetine increases the consolidation of finger sequence tapping skills it does not affect mirror tracing performance (Rasch et al., 2009).

Studies on the effect of GABA for memory enhancement during sleep revealed mixed results (Hall-Porter et al., 2014). Increasing spindle density with the $GABA_A$ positive modulator zolpidem enhances memory for word pairs and emotionally negative pictures but impairs perceptual learning and has no effect on finger sequence tapping and memory for emotionally neutral pictures (Kaestner et al., 2013; Mednick et al., 2013). Intensifying SWS and slow wave activity with the GABA reuptake inhibitor tiagabine did not have an enhancing effect on memory consolidation (Feld et al., 2013b), which was possibly due to a non-functional increase of slow oscillations that was accompanied by a decrease in spindle activity phase-locked to slow oscillations. Growth hormone, another important neuromodulator, had long been suspected to play a role in sleep-dependent memory consolidation as it is mainly secreted during SWS and is involved in hippocampal memory formation (Nyberg and Hallberg, 2013). Yet, effectively blocking growth hormone release during SWS by infusion of somatostatin left memory consolidation unaffected (Gais et al., 2006a). Whether it is possible to enhance memory by increasing the availability of growth hormone during sleep is unclear.

Low levels of the neurotransmitter acetylcholine are known to be critical for SWS-dependent memory consolidation (Buzsáki, 1986; Hasselmo, 1999). Increasing cholinergic activity during SWS by administering the choline esterase inhibitor physostigmine impairs memory consolidation (Gais and Born, 2004). It is unclear, however, whether a reduction of cholinergic activity during SWS can further boost memory. Findings of studies that manipulated the stress hormone cortisol during SWS suggest otherwise. Cortisol shows secretion patterns very similar to those of acetylcholine, with very low concentration levels during SWS. Similar to acetylcholine, increasing cortisol during SWS by infusion of hydrocortisone or dexamethasone blocks the beneficial effect of sleep for memory consolidation (Plihal and Born, 1999; Plihal et al., 1999; Wilhelm et al., 2011). Yet, further decreasing cortisol levels during SWS with the cortisol synthesis inhibitor metyrapone did not enhance but paradoxically reduced the consolidation of hippocampus-dependent memories (Wagner et al., 2005). Thus, the neurochemical milieu of neurotransmitters and hormones during sleep, particularly during SWS, might be intricately optimized to support memory consolidation such that pharmacological manipulations of this finely tuned balance often do not have the expected results.

Overall, manipulating neurotransmitter systems to enhance memory during sleep has revealed inconsistent results. Future research will have to replicate and specify the key findings in this field. At present, these findings should therefore be interpreted with caution.

CONSIDERATIONS AND CAVEATS

Several different manipulations of sleep and memory have been proven effective to enhance learning and memory consolidation. Yet, there are a number of central questions that are still unknown, both in the experimental study of sleep to enhance memory as well as for possible applications of these new methods in everyday life. Among these questions are important issues relating to methodological intricacies, such as possible boundary conditions, potential unintended effects, the actual effect size of the improvement, as well as the practicability for everyday use. Besides these methodological problems, the possibility of enhancing cognitive functions during sleep raises certain ethical questions. Apart from the ethical questions that are discussed in relation to cognitive enhancement in general, applying cognition-altering manipulations during sleep—a state of unconsciousness, reduced voluntary control, and heightened vulnerability of the individual—might pose additional ethical concerns.

METHODOLOGY

Although we know that normal sleep facilitates learning and memory and that specific manipulations of memory during sleep can further boost this effect, we still don't understand the exact conditions under which the memory enhancement occurs (Diekelmann et al., 2009; Diekelmann, 2013). Memory cueing, stimulation of sleep oscillations as well as pharmacological interventions enhance some memories but not others depending on the particular methods used. For example, using odors as context cues to reactivate associated memories during sleep enhances declarative memories for object locations but not procedural memories in the finger sequence tapping task (Rasch et al., 2007). Stimulating slow oscillations via tDCS likewise enhances declarative word pair memories but not procedural finger sequence tapping (Marshall et al., 2006). Yet, cueing memories for finger sequence tapping directly by tones associated with specific finger movements does in fact enhance finger tapping performance (Antony et al., 2012; Schönauer et al., 2014).

Furthermore, increasing the availability of noradrenaline during sleep by reboxetine enhances odor memory (Gais et al., 2011) and finger sequence tapping (Rasch et al., 2009) but does not

enhance memory for word pairs and performance in a mirror tracing task (Rasch et al., 2009). Intranasal interleukin-6 improves memory for emotional stories but not for neutral stories, object locations and finger sequence tapping (Benedict et al., 2009). And while the modulation of GABA transmission with zolpidem enhances emotional picture memory and verbal memory, it does not affect neutral picture memory and motor memory, and it even impairs perceptual learning.

Considering that some memories can be enhanced during sleep under some conditions but not under others suggests that there are certain boundary conditions for the enhancing effect of sleep. For cueing memory reactivation with odors, for example, it was found that the same odor needs to be presented during learning and subsequent sleep to enhance memory; presenting a different odor during sleep than during learning remains ineffective (Rihm et al., 2014). Generally, it is unclear how many different odors can be associated with different memories and how many times a single odor can be associated with new learning material before it produces interference rather than enhancement. Olfactory cues presumably represent general context cues that reactivate the entire learning context when presented during sleep, increasing the risk of interference when different memories are learned in the same context. In order to target individual memories, auditory cues might be better suited; yet these cues have the disadvantage to change the natural sleep cycle by inducing arousals and awakenings if the sound level is not optimally adjusted. The effectiveness of memory cueing during sleep might generally depend on whether or not the learning information is relevant for the individual, which can be signaled for example by associated low or high rewards (Oudiette et al., 2013). Furthermore, when trying to reduce undesired memories by cueing during sleep, different methods can produce fundamentally different results. Whether fear memories are weakened or even strengthened during sleep, for instance, depends on methodological subtleties such as contingencies in the conditioning procedure and the nature of the reactivation cue (Oudiette et al., 2014).

Similar boundary conditions are presumably relevant in the stimulation of sleep-specific brain oscillations as well as in pharmacological manipulations of neurotransmitters and hormones. Importantly, sleep oscillations, neurotransmitter concentrations and memory replay during sleep are intricately interlinked. Targeting one or the other component of this interwoven net of factors might produce unexpected adverse effects and can even be harmful to memory. For example, the GABA agonist tiagabine increases slow wave activity but does not enhance memory consolidation, possibly due to a concurrent decrease in functionally coupled spindle activity (Feld et al., 2013b). Likewise, low levels of cortisol during SWS are known to be essential for memory consolidation processes, yet further decreasing cortisol concentrations paradoxically impairs memory rather than further enhancing it (Wagner et al., 2005). These examples show that it is essential to consider the functional role of single components and processes in sleep-dependent memory consolidation as well as their inter-dependencies when trying to manipulate particular aspects of this complex system. However, the way in which the different processes and components interact is not well understood.

Apart from its enhancing effect on memory, manipulations of memory processing during sleep can have side effects and unintended effects. It has been shown, for instance, that the reprocessing and integration of information during sleep can qualitatively change memories. Although in many cases this a positive effect, for example generating insight (Wagner et al., 2004), drawing relational inferences (Ellenbogen et al., 2007) and abstracting schemas (Lewis and Durrant, 2011), it can also lead to the generation of memory distortions and false memories (Payne et al., 2009; Diekelmann et al., 2010). Up to now it is unclear whether and how external manipulations of memory during sleep affect the veridicality of memories. Furthermore, there might be a trade-off between different memories: enhancing one memory could come at the cost of impairing others. For example, sleep increases memory for emotional components of a scene but concurrently decreases memory for the neutral background (Payne et al., 2008, 2012a; Payne and Kensinger, 2010, 2011). Although trade-off effects in sleep-dependent memory consolidation have not been studied directly, indirect evidence suggests that there might be a limited capacity for memory replay during sleep such that increasing reactivation of one memory decreases reactivation of other memories (Antony et al., 2012; Bendor and Wilson, 2012; Kelemen and Born, 2012). It is generally unknown how targeted manipulations of memory during sleep are. The discussed manipulations might not only affect other memories but also other cognitive functions and even other bodily functions. Slow oscillation stimulation with tDCS, for example, was found to improve mood, though the mechanisms for this effect are unclear (Marshall et al., 2006; Göder et al., 2013). Also pharmacological treatments for memory enhancement during sleep are typically "dirty" interventions that affect numerous other functions and can also produce unwanted side effects.

Although the effects of memory enhancement during sleep are reproducible and statistically significant, the practical significance of these effects is unclear. In humans, the estimated performance improvement in studies manipulating memory during sleep (either by cueing memory replay, stimulating sleep oscillations or applying pharmacological substances) is usually in the margins of 5–15% compared to sleep conditions without treatment. Considering that natural sleep without any manipulations produces a memory improvement of about 10–20% compared to wakefulness, the combined improvement of sleep with external manipulations adds up to an enhancement of 15–35% as compared to wake intervals without manipulations. Even taking into account that this number might eventually turn out to be smaller, considering that effect sizes are typically overestimated in the first studies of a new field of research, the true effect size might still be high enough to warrant practical applications. Experimental studies on sleep and memory usually test for enhancing effects of sleep manipulations during one night of sleep only. The long-term effects of using sleep applications for cognitive enhancement on a regular basis are presently unclear. Generally, the effect of sleep and the need for sleep is rather variable between individuals. Considering that current activity schedules, in schools and at work, do not provide an ideal environment for adequate sleep, the most straight forward method to optimize normal cognitive

function by sleep in a first step may be a policy change towards more flexible timing of activity and rest.

The practicability of memory enhancing methods during sleep for applications in everyday life depends on the type of method. Odors are relatively easy to apply during learning and subsequent sleep in the home environment. For auditory cues, home applications are likewise relatively easy to conceive. Stimulation of sleep-specific brain oscillations and pharmacological substance administration, however, is more difficult to do in everyday life. Although apparatuses for home use of tDCS in the wake state are already available on the market, their potential for the stimulation of specific sleep oscillations is unclear. Also safety and potential side effects of long-term tDCS treatment is completely unknown. The optimal stimulation of sleep-specific brain oscillations as well as the application of odors and sounds to reactivate memories during specific sleep stages is further complicated by the lack of easy-to-use sleep recording systems for the home environment. Finally, the pharmacological substances that (so far) have been shown to enhance memory during sleep are not available for use outside their medical indication at the moment.

ETHICAL ISSUES

On the one hand, ethical questions regarding the use of sleep for cognitive enhancement relate to the general ethical issues that are discussed in the context of cognitive enhancement and biomedical enhancement at large (for overview see for example Farah et al., 2004; Buchanan, 2011). The enhancement of cognitive capacities can potentially have substantial positive effects for individuals as well as for societies by increasing productivity and overall quality of life through more personally and financially rewarding occupations, more fulfilling personal relationships, and less suffering from cognitively impairing diseases (Buchanan, 2008, 2011; Bostrom and Roache, 2011). Yet, cognitive enhancement might also have direct or indirect negative consequences. Just to name a few, through the enhancement of our cognitive capabilities we could lose our sense of giftedness (Sandel, 2007), we might no longer appreciate the effort to achieve something, we could become inauthentic by changing central features of our identity such as our memories, we might be coerced to use cognitive enhancers if others do it, the use of cognitive enhancers might be seen as cheating, and an unfair access to cognitive enhancers could potentially increase social injustice.

Ethical issues that are specific to manipulations of cognitive capacities by targeting sleep relate to the specific nature of sleep as an exceptional state of the organism. Sleep is characterized by immobility and muscle relaxation, greatly diminished processing and perception of external stimuli as well as greatly limited or even absent voluntary control. These characteristics make the sleeping individual particularly vulnerable for all kinds of external influences. Manipulations of cognitive processes during sleep are designed in such a way that the individual does not notice the treatment. In studies using memory cueing during sleep, subjects typically report not to have noticed any presentation of the cues. Likewise, following stimulation of brain oscillations during sleep as well as after the administration of pharmacological substances, participants usually cannot tell whether they received the treatment or not. Thus, subjects not only have no control over such manipulations but they don't even know whether they have been manipulated at all. This constellation can give rise to a certain misuse potential. In Aldous Huxley's science fiction novel "Brave new world", indoctrination of infants and children during sleep is used to shape how these children will think, feel and behave as members of their respective caste. Huxley calls this procedure "hypnopaedia" and describes it as "the greatest moralizing and socializing force of all time". Although it is unclear whether sleep goes along with an enhanced suggestibility, Huxley's fictitious idea illustrates that sleep is a highly sensitive state in which we are relatively unprotected against external influences.

Such worries and premonitions are legitimate and important to discuss in the context of cognitive enhancement during sleep. However, they do not provide conclusive reasons against the use of sleep for cognitive enhancement. What is needed is a balanced account to weigh possible risks against the benefits to allow for a well-informed and all-things-considered judgment about the responsible use of sleep for cognitive enhancement (Buchanan, 2011). Even if negative consequences were to be expected, the numerous positive effects could be so desirable as to outweigh possible negative effects. The question is not whether or not to use sleep for cognitive enhancement—cognitive enhancers of all sorts are already there and their use will increase even more in the near future—the question is rather how to enhance cognitive capacities responsibly, how to deal with issues of distributive justice and how to prevent misuse and malpractice.

CONCLUSION

This article has focused on the function of sleep to augment cognitive capacities, a function that will arguably receive more and more attention in the next few years, both in research as well as in practical applications. The reviewed evidence shows that targeted manipulations of memory processing during sleep can be used to enhance learning and memory. Sleep can thereby be considered a cognitive enhancer as this state provides optimal conditions to augment memory capacities above and beyond the normal level. It is important to note that the discussed effects of manipulations to enhance memory during sleep are specific for the sleep state. Identical methods applied during wakefulness have no enhancing effect on memory or can even impair memory processing. For instance, reactivating memories by odors during wakefulness does not affect memory for object locations (Rasch et al., 2007) or even renders these memory representations unstable making them more vulnerable for disruptive interfering inputs (Diekelmann et al., 2011). Manipulating sleep-specific brain oscillations is naturally confined to the sleep state. Except for ripples, which also occur during wakefulness (O'Neill et al., 2010), slow oscillations and sleep spindles selectively occur during sleep. Interestingly, stimulating the brain during wakefulness with frequencies oscillating in the slow oscillation range has no effect on memory consolidation but increases theta activity resulting in better encoding of new information (Kirov et al., 2009). Furthermore, the neurochemical milieu of neurotransmitters and hormones is very different during sleep and wakefulness such that administration of certain substances can have fundamentally different effects on memory. For example, while an infusion of cortisol impairs memory consolidation during sleep it facilitates

consolidation processes when administered in the wake state (Wilhelm et al., 2011).

Importantly, memory enhancement in the context of cognitive enhancement should not be confused with the term "enhancement" that has sometimes been used in the sleep and memory literature to describe actual sleep-dependent gains in performance. Initial research on memory consolidation during sleep, particularly with respect to procedural memory, showed that performance levels after sleep can exceed performance levels observed before sleep (Walker, 2005). We know now that this is not true (see for example Rickard et al., 2008). Even external manipulations of memory during sleep cannot produce anything that was not previously encoded; rather sleep as well as memory manipulations during sleep enhance memory in the sense of less forgetting (to the point of no forgetting) and higher memory stability (i.e., resistance to subsequent interference). Related to this, only a very few reports show that conditioned responses can be acquired during sleep (Arzi et al., 2012), but new learning of declarative and procedural memories during sleep seems to be impossible. Nevertheless, sleep can produce new knowledge from previously encoded memories through processes of generalization, integration, schema abstraction, and conversion of implicit into explicit knowledge (Wagner et al., 2004; Gomez et al., 2006; Ellenbogen et al., 2007; Durrant et al., 2011; Wilhelm et al., 2013).

It is of note that sleep is not only effective as a cognitive enhancer to boost memory performance, but it can also be applied in clinical settings to restore normal cognitive functioning. A number of disorders and diseases are accompanied by changes in sleep patterns and dysfunctions of memory, such as depression (Steiger et al., 2013), post-traumatic stress disorder (Germain, 2013), Alzheimer's disease (Wang et al., 2011) and schizophrenia (Lu and Goder, 2012). In patients with schizophrenia, stimulation of slow oscillations with tDCS during sleep was found to improve memory for words (Göder et al., 2013). Furthermore, administration of the atypical antipsychotic olanzapine increased SWS, and the GABA agonist eszopiclone enhanced the number of sleep spindles in schizophrenia; yet both treatments failed to normalize memory consolidation in these patients (Göder et al., 2008; Wamsley et al., 2013). Future studies will have to test new methods for the treatment of memory dysfunctions during sleep in different clinical settings, which could also potentially improve the outcome of standard therapeutic treatments. For the treatment of spider phobia, for example, sleep after exposure therapy was found to increase therapeutic effectiveness (Pace-Schott et al., 2012b; Kleim et al., 2013). It remains to be elucidated whether manipulations of memory processing during sleep, such as memory reactivation or sleep oscillation stimulation, can boost this effect further.

Manipulating memory during sleep is a very new field of research and we are only beginning to understand which methods are best suited to use sleep for memory enhancement. Much more research is needed to determine the optimal procedures to unravel this effect and to understand its underlying mechanisms and principles. Future research will have to extend the knowledge obtained from findings in the domain of learning and memory to other cognitive functions such as creativity, executive functions and decision making. This research could not only provide us with new means to augment our cognitive capabilities in different domains but could also help to change the image of sleep as a useless waste of time to being a beneficial state that supports our wake performance.

ACKNOWLEDGMENTS

The author would like to thank Jan Born and Gordon Feld for helpful discussions and comments on an earlier draft of this article. This work was funded by the Deutsche Forschungsgemeinschaft (DFG, TR-SFB 654).

REFERENCES

Ackermann, S., and Rasch, B. (2014). Differential effects of non-REM and REM sleep on memory consolidation? *Curr. Neurol. Neurosci. Rep.* 14:430. doi: 10.1007/s11910-013-0430-8

Alberini, C. M., and Chen, D. Y. (2012). Memory enhancement: consolidation, reconsolidation and insulin-like growth factor 2. *Trends Neurosci.* 35, 274–283. doi: 10.1016/j.tins.2011.12.007

Antonenko, D., Diekelmann, S., Olsen, C., Born, J., and Molle, M. (2013). Napping to renew learning capacity: enhanced encoding after stimulation of sleep slow oscillations. *Eur. J. Neurosci.* 37, 1142–1151. doi: 10.1111/ejn.12118

Antony, J. W., Gobel, E. W., O'Hare, J. K., Reber, P. J., and Paller, K. A. (2012). Cued memory reactivation during sleep influences skill learning. *Nat. Neurosci.* 15, 1114–1116. doi: 10.1038/nn.3152

Arzi, A., Shedlesky, L., Ben-Shaul, M., Nasser, K., Oksenberg, A., Hairston, I. S., et al. (2012). Humans can learn new information during sleep. *Nat. Neurosci.* 15, 1460–1465. doi: 10.1038/nn.3193

Axmacher, N., Elger, C. E., and Fell, J. (2008). Ripples in the medial temporal lobe are relevant for human memory consolidation. *Brain* 131, 1806–1817. doi: 10.1093/brain/awn103

Bendor, D., and Wilson, M. A. (2012). Biasing the content of hippocampal replay during sleep. *Nat. Neurosci.* 15, 1439–1444. doi: 10.1038/nn.3203

Benedict, C., Scheller, J., Rose-John, S., Born, J., and Marshall, L. (2009). Enhancing influence of intranasal interleukin-6 on slow-wave activity and memory consolidation during sleep. *FASEB J.* 23, 3629–3636. doi: 10.1096/fj.08-122853

Binder, S., Rawohl, J., Born, J., and Marshall, L. (2014). Transcranial slow oscillation stimulation during NREM sleep enhances acquisition of the radial maze task and modulates cortical network activity in rats. *Front. Behav. Neurosci.* 7:220. doi: 10.3389/fnbeh.2013.00220

Born, J., and Fehm, H. L. (2000). The neuroendocrine recovery function of sleep. *Noise Health* 2, 25–38.

Bostrom, N., and Roache, N. (2008). "Ethical issues in human enhancement," in *New Waves in Applied Ethics*, eds J. Ryberg, T. Petersen and C. Wolf (Basingstoke: Palgrave Macmillan), 120–152.

Bostrom, N., and Roache, N. (2011). "Smart policy: cognitive enhancement and the public interest," in *Enhancing Human Capacities*, eds J. Savulescu, R. ter Muelen and G. Kahane (Oxford: Wiley-Blackwell), 138–152.

Buchanan, A. (2008). Enhancement and the ethics of development. *Kennedy Inst. Ethics J.* 18, 1–34. doi: 10.1353/ken.0.0003

Buchanan, A. (2011). *Beyond Humanity? The Ethics of Biomedical Enhancement.* New York: Oxford University Press.

Buzsáki, G. (1986). Hippocampal sharp waves: their origin and significance. *Brain Res.* 398, 242–252. doi: 10.1016/0006-8993(86)91483-6

Clemens, Z., Fabo, D., and Halasz, P. (2005). Overnight verbal memory retention correlates with the number of sleep spindles. *Neuroscience* 132, 529–535. doi: 10.1016/j.neuroscience.2005.01.011

Collingridge, G. L., Volianskis, A., Bannister, N., France, G., Hanna, L., Mercier, M., et al. (2013). The NMDA receptor as a target for cognitive enhancement. *Neuropharmacology* 64, 13–26. doi: 10.1016/j.neuropharm.2012.06.051

Dash, M. B., Douglas, C. L., Vyazovskiy, V. V., Cirelli, C., and Tononi, G. (2009). Long-term homeostasis of extracellular glutamate in the rat cerebral cortex across sleep and waking states. *J. Neurosci.* 29, 620–629. doi: 10.1523/jneurosci.5486-08.2009

Diekelmann, S. (2013). Open questions in sleep and memory research. *Somnologie* 17, 21–27. doi: 10.1007/s11818-013-0600-6

Diekelmann, S., Biggel, S., Rasch, B., and Born, J. (2012). Offline consolidation of memory varies with time in slow wave sleep and can be accelerated by cuing memory reactivations. *Neurobiol. Learn. Mem.* 98, 103–111. doi: 10.1016/j.nlm.2012.07.002

Diekelmann, S., and Born, J. (2010). The memory function of sleep. *Nat. Rev. Neurosci.* 11, 114–126. doi: 10.1038/nrn2762

Diekelmann, S., Born, J., and Wagner, U. (2010). Sleep enhances false memories depending on general memory performance. *Behav. Brain Res.* 208, 425–429. doi: 10.1016/j.bbr.2009.12.021

Diekelmann, S., Buchel, C., Born, J., and Rasch, B. (2011). Labile or stable: opposing consequences for memory when reactivated during waking and sleep. *Nat. Neurosci.* 14, 381–386. doi: 10.1038/nn.2744

Diekelmann, S., Wilhelm, I., and Born, J. (2009). The whats and whens of sleep-dependent memory consolidation. *Sleep Med. Rev.* 13, 309–321. doi: 10.1016/j.smrv.2008.08.002

Dumay, N., and Gaskell, M. G. (2007). Sleep-associated changes in the mental representation of spoken words. *Psychol. Sci.* 18, 35–39. doi: 10.1111/j.1467-9280.2007.01845.x

Durmer, J. S., and Dinges, D. F. (2005). Neurocognitive consequences of sleep deprivation. *Semin. Neurol.* 25, 117–129. doi: 10.1055/s-2005-867080

Durrant, S. J., Taylor, C., Cairney, S., and Lewis, P. A. (2011). Sleep-dependent consolidation of statistical learning. *Neuropsychologia* 49, 1322–1331. doi: 10.1016/j.neuropsychologia.2011.02.015

Ego-Stengel, V., and Wilson, M. A. (2010). Disruption of ripple-associated hippocampal activity during rest impairs spatial learning in the rat. *Hippocampus* 20, 1–10. doi: 10.1002/hipo.20707

Ellenbogen, J. M., Hu, P. T., Payne, J. D., Titone, D., and Walker, M. P. (2007). Human relational memory requires time and sleep. *Proc. Natl. Acad. Sci. U S A* 104, 7723–7728. doi: 10.1073/pnas.0700094104

Ellenbogen, J. M., Hulbert, J. C., Jiang, Y., and Stickgold, R. (2009). The sleeping brain's influence on verbal memory: boosting resistance to interference. *PLoS One* 4:e4117. doi: 10.1371/journal.pone.0004117

Eschenko, O., Ramadan, W., Molle, M., Born, J., and Sara, S. J. (2008). Sustained increase in hippocampal sharp-wave ripple activity during slow-wave sleep after learning. *Learn. Mem.* 15, 222–228. doi: 10.1101/lm.726008

Euston, D. R., Tatsuno, M., and McNaughton, B. L. (2007). Fast-forward playback of recent memory sequences in prefrontal cortex during sleep. *Science* 318, 1147–1150. doi: 10.1126/science.1148979

Farah, M. J., Illes, J., Cook-Deegan, R., Gardner, H., Kandel, E., King, P., et al. (2004). Neurocognitive enhancement: what can we do and what should we do? *Nat. Rev. Neurosci.* 5, 421–425. doi: 10.1038/nrn1390

Feld, G. B., Besedovsky, L., Kaida, K., Münte, T. F., and Born, J. (in press). Dopamine D2-like receptor activation wipes out preferential consolidation of high over low reward memories in human sleep. *J. Cogn. Neurosci.*

Feld, G. B., Lange, T., Gais, S., and Born, J. (2013a). Sleep-dependent declarative memory consolidation–unaffected after blocking NMDA or AMPA receptors but enhanced by NMDA coagonist D-cycloserine. *Neuropsychopharmacology* 38, 2688–2697. doi: 10.1038/npp.2013.179

Feld, G. B., Wilhelm, I., Ma, Y., Groch, S., Binkofski, F., Molle, M., et al. (2013b). Slow wave sleep induced by GABA agonist tiagabine fails to benefit memory consolidation. *Sleep* 36, 1317–1326. doi: 10.5665/sleep.2954

Fuentemilla, L., Miro, J., Ripolles, P., Vila-Ballo, A., Juncadella, M., Castaner, S., et al. (2013). Hippocampus-dependent strengthening of targeted memories via reactivation during sleep in humans. *Curr. Biol.* 23, 1769–1775. doi: 10.1016/j.cub.2013.07.006

Gais, S., and Born, J. (2004). Low acetylcholine during slow-wave sleep is critical for declarative memory consolidation. *Proc. Natl. Acad. Sci. U S A* 101, 2140–2144. doi: 10.1073/pnas.0305404101

Gais, S., Hullemann, P., Hallschmid, M., and Born, J. (2006a). Sleep-dependent surges in growth hormone do not contribute to sleep-dependent memory consolidation. *Psychoneuroendocrinology* 31, 786–791. doi: 10.1016/j.psyneuen.2006.02.009

Gais, S., Lucas, B., and Born, J. (2006b). Sleep after learning aids memory recall. *Learn. Mem.* 13, 259–262. doi: 10.1101/lm.132106

Gais, S., Molle, M., Helms, K., and Born, J. (2002). Learning-dependent increases in sleep spindle density. *J. Neurosci.* 22, 6830–6834.

Gais, S., Rasch, B., Dahmen, J. C., Sara, S., and Born, J. (2011). The memory function of noradrenergic activity in non-REM sleep. *J. Cogn. Neurosci.* 23, 2582–2592. doi: 10.1162/jocn.2011.21622

Genzel, L., Ahrberg, K., Roselli, C., Niedermaier, S., Steiger, A., Dresler, M., et al. (2013). Sleep timing is more important than sleep length or quality for medical school performance. *Chronobiol. Int.* 30, 766–771. doi: 10.3109/07420528.2012.763132

Germain, A. (2013). Sleep disturbances as the hallmark of PTSD: where are we now? *Am. J. Psychiatry* 170, 372–382. doi: 10.1176/appi.ajp.2012.12040432

Girardeau, G., Benchenane, K., Wiener, S. I., Buzsaki, G., and Zugaro, M. B. (2009). Selective suppression of hippocampal ripples impairs spatial memory. *Nat. Neurosci.* 12, 1222–1223. doi: 10.1038/nn.2384

Göder, R., Baier, P. C., Beith, B., Baecker, C., Seeck-Hirschner, M., Junghanns, K., et al. (2013). Effects of transcranial direct current stimulation during sleep on memory performance in patients with schizophrenia. *Schizophr. Res.* 144, 153–154. doi: 10.1016/j.schres.2012.12.014

Göder, R., Fritzer, G., Gottwald, B., Lippmann, B., Seeck-Hirschner, M., Serafin, I., et al. (2008). Effects of olanzapine on slow wave sleep, sleep spindles and sleep-related memory consolidation in schizophrenia. *Pharmacopsychiatry* 41, 92–99. doi: 10.1055/s-2007-1004592

Gomez, R. L., Bootzin, R. R., and Nadel, L. (2006). Naps promote abstraction in language-learning infants. *Psychol. Sci.* 17, 670–674. doi: 10.1111/j.1467-9280.2006.01764.x

Groch, S., Wilhelm, I., Diekelmann, S., Sayk, F., Gais, S., and Born, J. (2011). Contribution of norepinephrine to emotional memory consolidation during sleep. *Psychoneuroendocrinology* 36, 1342–1350. doi: 10.1016/j.psyneuen.2011.03.006

Hall-Porter, J. M., Schweitzer, P. K., Eisenstein, R. D., Ahmed, H. A., and Walsh, J. K. (2014). The effect of two benzodiazepine receptor agonist hypnotics on sleep-dependent memory consolidation. *J. Clin. Sleep Med.* 10, 27–34. doi: 10.5664/jcsm.3352

Harrison, Y., and Horne, J. A. (1998). Sleep loss impairs short and novel language tasks having a prefrontal focus. *J. Sleep Res.* 7, 95–100. doi: 10.1046/j.1365-2869.1998.00104.x

Harrison, Y., and Horne, J. A. (1999). One night of sleep loss impairs innovative thinking and flexible decision making. *Organ. Behav. Hum. Decis. Process.* 78, 128–145. doi: 10.1006/obhd.1999.2827

Harrison, Y., and Horne, J. A. (2000). The impact of sleep deprivation on decision making: a review. *J. Exp. Psychol. Appl.* 6, 236–249. doi: 10.1037/1076-898x.6.3.236

Hasselmo, M. E. (1999). Neuromodulation: acetylcholine and memory consolidation. *Trends Cogn. Sci.* 3, 351–359. doi: 10.1016/s1364-6613(99)01365-0

Hauner, K. K., Howard, J. D., Zelano, C., and Gottfried, J. A. (2013). Stimulus-specific enhancement of fear extinction during slow-wave sleep. *Nat. Neurosci.* 16, 1553–1555. doi: 10.1038/nn.3527

Inostroza, M., Binder, S., and Born, J. (2013). Sleep-dependency of episodic-like memory consolidation in rats. *Behav. Brain Res.* 237, 15–22. doi: 10.1016/j.bbr.2012.09.011

Jackson, M. L., Gunzelmann, G., Whitney, P., Hinson, J. M., Belenky, G., Rabat, A., et al. (2013). Deconstructing and reconstructing cognitive performance in sleep deprivation. *Sleep Med. Rev.* 17, 215–225. doi: 10.1016/j.smrv.2012.06.007

Ji, D., and Wilson, M. A. (2007). Coordinated memory replay in the visual cortex and hippocampus during sleep. *Nat. Neurosci.* 10, 100–107. doi: 10.1038/nn1825

Kaestner, E. J., Wixted, J. T., and Mednick, S. C. (2013). Pharmacologically increasing sleep spindles enhances recognition for negative and high-arousal memories. *J. Cogn. Neurosci.* 25, 1597–1610. doi: 10.1162/jocn_a_00433

Kelemen, E., and Born, J. (2012). Sleep tight, wake up bright. *Nat. Neurosci.* 15, 1327–1329. doi: 10.1038/nn.3227

Killgore, W. D. (2010). Effects of sleep deprivation on cognition. *Prog. Brain Res.* 185, 105–129. doi: 10.1016/b978-0-444-53702-7.00007-5

Killgore, W. D., Balkin, T. J., and Wesensten, N. J. (2006). Impaired decision making following 49 h of sleep deprivation. *J. Sleep Res.* 15, 7–13. doi: 10.1111/j.1365-2869.2006.00487.x

Kirov, R., Weiss, C., Siebner, H. R., Born, J., and Marshall, L. (2009). Slow oscillation electrical brain stimulation during waking promotes EEG theta activity and memory encoding. *Proc. Natl. Acad. Sci. U S A* 106, 15460–15465. doi: 10.1073/pnas.0904438106

Kleim, B., Wilhelm, F. H., Temp, L., Margraf, J., Wiederhold, B. K., and Rasch, B. (2013). Sleep enhances exposure therapy. *Psychol. Med.* doi: 10.1017/s0033291713001748. [Epub ahead of print].

Kuriyama, K., Mishima, K., Suzuki, H., Aritake, S., and Uchiyama, M. (2008). Sleep accelerates the improvement in working memory performance. *J. Neurosci.* 28, 10145–10150. doi: 10.1523/jneurosci.2039-08.2008

Lansink, C. S., Goltstein, P. M., Lankelma, J. V., Joosten, R. N., McNaughton, B. L., and Pennartz, C. M. (2008). Preferential reactivation of motivationally relevant information in the ventral striatum. *J. Neurosci.* 28, 6372–6382. doi: 10.1523/jneurosci.1054-08.2008

Lee, A. K., and Wilson, M. A. (2002). Memory of sequential experience in the hippocampus during slow wave sleep. *Neuron* 36, 1183–1194. doi: 10.1016/s0896-6273(02)01096-6

Lewis, P. A., and Durrant, S. J. (2011). Overlapping memory replay during sleep builds cognitive schemata. *Trends. Cogn. Sci.* 15, 343–351. doi: 10.1016/j.tics.2011.06.004

Lu, W., and Goder, R. (2012). Does abnormal non-rapid eye movement sleep impair declarative memory consolidation?: Disturbed thalamic functions in sleep and memory processing. *Sleep Med. Rev.* 16, 389–394. doi: 10.1016/j.smrv.2011.08.001

Mander, B. A., Santhanam, S., Saletin, J. M., and Walker, M. P. (2011). Wake deterioration and sleep restoration of human learning. *Curr. Biol.* 21, R183–R184. doi: 10.1016/j.cub.2011.01.019

Maquet, P. (2001). The role of sleep in learning and memory. *Science* 294, 1048–1052. doi: 10.1016/b978-012370509-9.00181-9

Maquet, P., Laureys, S., Peigneux, P., Fuchs, S., Petiau, C., Phillips, C., et al. (2000). Experience-dependent changes in cerebral activation during human REM sleep. *Nat. Neurosci.* 3, 831–836. doi: 10.1038/77744

Marrosu, F., Portas, C., Mascia, M. S., Casu, M. A., Fa, M., Giagheddu, M., et al. (1995). Microdialysis measurement of cortical and hippocampal acetylcholine release during sleep-wake cycle in freely moving cats. *Brain Res.* 671, 329–332. doi: 10.1016/0006-8993(94)01399-3

Marshall, L., Helgadottir, H., Molle, M., and Born, J. (2006). Boosting slow oscillations during sleep potentiates memory. *Nature* 444, 610–613. doi: 10.1038/nature05278

Marshall, L., Kirov, R., Brade, J., Molle, M., and Born, J. (2011). Transcranial electrical currents to probe EEG brain rhythms and memory consolidation during sleep in humans. *PLoS One* 6:e16905. doi: 10.1371/journal.pone.0016905

Mednick, S. C., McDevitt, E. A., Walsh, J. K., Wamsley, E., Paulus, M., Kanady, J. C., et al. (2013). The critical role of sleep spindles in hippocampal-dependent memory: a pharmacology study. *J. Neurosci.* 33, 4494–4504. doi: 10.1523/jneurosci.3127-12.2013

Nádasdy, Z., Hirase, H., Czurko, A., Csicsvari, J., and Buzsaki, G. (1999). Replay and time compression of recurring spike sequences in the hippocampus. *J. Neurosci.* 19, 9497–9507.

Ngo, H. V., Claussen, J. C., Born, J., and Molle, M. (2013a). Induction of slow oscillations by rhythmic acoustic stimulation. *J. Sleep Res.* 22, 22–31. doi: 10.1111/j.1365-2869.2012.01039.x

Ngo, H. V., Martinetz, T., Born, J., and Molle, M. (2013b). Auditory closed-loop stimulation of the sleep slow oscillation enhances memory. *Neuron* 78, 545–553. doi: 10.1016/j.neuron.2013.03.006

Nishida, M., and Walker, M. P. (2007). Daytime naps, motor memory consolidation and regionally specific sleep spindles. *PLoS One* 2:e341. doi: 10.1371/journal.pone.0000341

Nyberg, F., and Hallberg, M. (2013). Growth hormone and cognitive function. *Nat. Rev. Endocrinol.* 9, 357–365. doi: 10.1038/nrendo.2013.78

O'Neill, J., Pleydell-Bouverie, B., Dupret, D., and Csicsvari, J. (2010). Play it again: reactivation of waking experience and memory. *Trends Neurosci.* 33, 220–229. doi: 10.1016/j.tins.2010.01.006

Oudiette, D., Antony, J. W., Creery, J. D., and Paller, K. A. (2013). The role of memory reactivation during wakefulness and sleep in determining which memories endure. *J. Neurosci.* 33, 6672–6678. doi: 10.1523/jneurosci.5497-12.2013

Oudiette, D., Antony, J. W., and Paller, K. A. (2014). Fear not: manipulating sleep might help you forget. *Trends Cogn. Sci.* 18, 3–4. doi: 10.1016/j.tics.2013.10.003

Oudiette, D., and Paller, K. A. (2013). Upgrading the sleeping brain with targeted memory reactivation. *Trends Cogn. Sci.* 17, 142–149. doi: 10.1016/j.tics.2013.01.006

Pace-Schott, E. F., Nave, G., Morgan, A., and Spencer, R. M. (2012a). Sleep-dependent modulation of affectively guided decision-making. *J. Sleep Res.* 21, 30–39. doi: 10.1111/j.1365-2869.2011.00921.x

Pace-Schott, E. F., Verga, P. W., Bennett, T. S., and Spencer, R. M. (2012b). Sleep promotes consolidation and generalization of extinction learning in simulated exposure therapy for spider fear. *J. Psychiatr. Res.* 46, 1036–1044. doi: 10.1016/j.jpsychires.2012.04.015

Payne, J. D., Chambers, A. M., and Kensinger, E. A. (2012a). Sleep promotes lasting changes in selective memory for emotional scenes. *Front. Integr. Neurosci.* 6:108. doi: 10.3389/fnint.2012.00108

Payne, J. D., and Kensinger, E. A. (2010). Sleep's role in the consolidation of emotional episodic memories. *Curr. Dir. Psychol. Sci.* 19, 290–295. doi: 10.1177/0963721410383978

Payne, J. D., and Kensinger, E. A. (2011). Sleep leads to changes in the emotional memory trace: evidence from FMRI. *J. Cogn. Neurosci.* 23, 1285–1297. doi: 10.1162/jocn.2010.21526

Payne, J. D., Schacter, D. L., Propper, R. E., Huang, L. W., Wamsley, E. J., Tucker, M. A., et al. (2009). The role of sleep in false memory formation. *Neurobiol. Learn. Mem.* 92, 327–334. doi: 10.1016/j.nlm.2009.03.007

Payne, J. D., Stickgold, R., Swanberg, K., and Kensinger, E. A. (2008). Sleep preferentially enhances memory for emotional components of scenes. *Psychol. Sci.* 19, 781–788. doi: 10.1111/j.1467-9280.2008.02157.x

Payne, J. D., Tucker, M. A., Ellenbogen, J. M., Wamsley, E. J., Walker, M. P., Schacter, D. L., et al. (2012b). Memory for semantically related and unrelated declarative information: the benefit of sleep, the cost of wake. *PLoS One* 7:e33079. doi: 10.1371/journal.pone.0033079

Peigneux, P., Laureys, S., Fuchs, S., Collette, F., Perrin, F., Reggers, J., et al. (2004). Are spatial memories strengthened in the human hippocampus during slow wave sleep? *Neuron* 44, 535–545. doi: 10.1016/j.neuron.2004.10.007

Peyrache, A., Khamassi, M., Benchenane, K., Wiener, S. I., and Battaglia, F. P. (2009). Replay of rule-learning related neural patterns in the prefrontal cortex during sleep. *Nat. Neurosci.* 12, 919–926. doi: 10.1038/nn.2337

Plihal, W., and Born, J. (1999). Memory consolidation in human sleep depends on inhibition of glucocorticoid release. *Neuroreport* 10, 2741–2747. doi: 10.1097/00001756-199909090-00009

Plihal, W., Pietrowsky, R., and Born, J. (1999). Dexamethasone blocks sleep induced improvement of declarative memory. *Psychoneuroendocrinology* 24, 313–331. doi: 10.1016/s0306-4530(98)00080-8

Rasch, B., and Born, J. (2013). About sleep's role in memory. *Physiol. Rev.* 93, 681–766. doi: 10.1152/physrev.00032.2012

Rasch, B., Buchel, C., Gais, S., and Born, J. (2007). Odor cues during slow-wave sleep prompt declarative memory consolidation. *Science* 315, 1426–1429. doi: 10.1126/science.1138581

Rasch, B., Pommer, J., Diekelmann, S., and Born, J. (2009). Pharmacological REM sleep suppression paradoxically improves rather than impairs skill memory. *Nat. Neurosci.* 12, 396–397. doi: 10.1038/nn.2206

Retey, J. V., Adam, M., Gottselig, J. M., Khatami, R., Durr, R., Achermann, P., et al. (2006). Adenosinergic mechanisms contribute to individual differences in sleep deprivation-induced changes in neurobehavioral function and brain rhythmic activity. *J. Neurosci.* 26, 10472–10479. doi: 10.1523/jneurosci.1538-06.2006

Rickard, T. C., Cai, D. J., Rieth, C. A., Jones, J., and Ard, M. C. (2008). Sleep does not enhance motor sequence learning. *J. Exp. Psychol. Learn. Mem. Cogn.* 34, 834–842. doi: 10.1037/0278-7393.34.4.834

Rihm, J., Diekelmann, S., Born, J., and Rasch, B. (2014). Reactivating memories during sleep by odors: odor-specificity and associated changes in sleep oscillations. *J. Cogn. Neurosci.* doi: 10.1162/jocn_a_00579. [Epub ahead of print].

Ritter, S. M., Strick, M., Bos, M. W., van Baaren, R. B., and Dijksterhuis, A. (2012). Good morning creativity: task reactivation during sleep enhances beneficial effect of sleep on creative performance. *J. Sleep Res.* 21, 643–647. doi: 10.1111/j.1365-2869.2012.01006.x

Rolls, A., Makam, M., Kroeger, D., Colas, D., de Lecea, L., and Heller, H. C. (2013). Sleep to forget: interference of fear memories during sleep. *Mol. Psychiatry* 18, 1166–1170. doi: 10.1038/mp.2013.121

Rudoy, J. D., Voss, J. L., Westerberg, C. E., and Paller, K. A. (2009). Strengthening individual memories by reactivating them during sleep. *Science* 326:1079. doi: 10.1126/science.1179013

Sandberg, A. (2011). "Cognition enhancement: upgrading the brain," in *Enhancing Human Capacities*, eds J. Savulescu, R. ter Muelen and G. Kahane (Oxford: Wiley-Blackwell), 71–91.

Sandel, M. (2007). *The Case Against Perfection: Ethics in the Age of Genetic Engineering*. Cambridge, MA: Harvard University Press.

Schabus, M., Gruber, G., Parapatics, S., Sauter, C., Klosch, G., Anderer, P., et al. (2004). Sleep spindles and their significance for declarative memory consolidation. *Sleep* 27, 1479–1485.

Schmidt, C., Peigneux, P., Muto, V., Schenkel, M., Knoblauch, V., Munch, M., et al. (2006). Encoding difficulty promotes postlearning changes in sleep spindle activity during napping. *J. Neurosci.* 26, 8976–8982. doi: 10.1523/jneurosci.2464-06.2006

Schönauer, M., Geisler, T., and Gais, S. (2014). Strengthening procedural memories by reactivation in sleep. *J. Cogn. Neurosci.* 26, 143–153. doi: 10.1162/jocn_a_00471

Sirota, A., and Buzsaki, G. (2005). Interaction between neocortical and hippocampal networks via slow oscillations. *Thalamus Relat. Syst.* 3, 245–259. doi: 10.1017/s1472928807000258

Skaggs, W. E., and McNaughton, B. L. (1996). Replay of neuronal firing sequences in rat hippocampus during sleep following spatial experience. *Science* 271, 1870–1873. doi: 10.1126/science.271.5257.1870

Sowers, J. R., and Vlachakis, N. (1984). Circadian variation in plasma dopamine levels in man. *J. Endocrinol. Invest.* 7, 341–345.

Steiger, A., Dresler, M., Kluge, M., and Schussler, P. (2013). Pathology of sleep, hormones and depression. *Pharmacopsychiatry* 46(Suppl. 1), S30–S35. doi: 10.1055/s-0033-1337921

Steriade, M. (2006). Grouping of brain rhythms in corticothalamic systems. *Neuroscience* 137, 1087–1106. doi: 10.1016/j.neuroscience.2005.10.029

Stern, S. A., and Alberini, C. M. (2013). Mechanisms of memory enhancement. *Wiley Interdiscip. Rev. Syst. Biol. Med.* 5, 37–53. doi: 10.1002/wsbm.1196

Stickgold, R., and Walker, M. P. (2013). Sleep-dependent memory triage: evolving generalization through selective processing. *Nat. Neurosci.* 16, 139–145. doi: 10.1038/nn.3303

Thomas, M., Sing, H., Belenky, G., Holcomb, H., Mayberg, H., Dannals, R., et al. (2000). Neural basis of alertness and cognitive performance impairments during sleepiness. I. Effects of 24 h of sleep deprivation on waking human regional brain activity. *J. Sleep Res.* 9, 335–352. doi: 10.1046/j.1365-2869.2000.00225.x

Tononi, G., and Cirelli, C. (2006). Sleep function and synaptic homeostasis. *Sleep Med. Rev.* 10, 49–62. doi: 10.1016/j.smrv.2005.05.002

Tononi, G., and Cirelli, C. (2014). Sleep and the price of plasticity: from synaptic and cellular homeostasis to memory consolidation and integration. *Neuron* 81, 12–34. doi: 10.1016/j.neuron.2013.12.025

Van Der Werf, Y. D., Altena, E., Schoonheim, M. M., Sanz-Arigita, E. J., Vis, J. C., De Rijke, R. W., et al. (2009). Sleep benefits subsequent hippocampal functioning. *Nat. Neurosci.* 12, 122–123. doi: 10.1038/nn.2253

Van Dongen, H. P., Maislin, G., Mullington, J. M., and Dinges, D. F. (2003). The cumulative cost of additional wakefulness: dose-response effects on neurobehavioral functions and sleep physiology from chronic sleep restriction and total sleep deprivation. *Sleep* 26, 117–126.

van Dongen, E. V., Takashima, A., Barth, M., Zapp, J., Schad, L. R., Paller, K. A., et al. (2012). Memory stabilization with targeted reactivation during human slow-wave sleep. *Proc. Natl. Acad. Sci. U S A* 109, 10575–10580. doi: 10.1073/pnas.1201072109

Vanini, G., Lydic, R., and Baghdoyan, H. A. (2012). GABA-to-ACh ratio in basal forebrain and cerebral cortex varies significantly during sleep. *Sleep* 35, 1325–1334. doi: 10.5665/sleep.2106

Wagner, U., Degirmenci, M., Drosopoulos, S., Perras, B., and Born, J. (2005). Effects of cortisol suppression on sleep-associated consolidation of neutral and emotional memory. *Biol. Psychiatry* 58, 885–893. doi: 10.1016/j.biopsych.2005.05.008

Wagner, U., Gais, S., Haider, H., Verleger, R., and Born, J. (2004). Sleep inspires insight. *Nature* 427, 352–355. doi: 10.1038/nature02223

Walker, M. P. (2005). A refined model of sleep and the time course of memory formation. *Behav. Brain Sci.* 28, 51–64. doi: 10.1017/s0140525x05000026

Walker, M. P., and Stickgold, R. (2006). Sleep, memory and plasticity. *Annu. Rev. Psychol.* 57, 139–166. doi: 10.1146/annurev.psych.56.091103.070307

Wamsley, E. J., Shinn, A. K., Tucker, M. A., Ono, K. E., McKinley, S. K., Ely, A. V., et al. (2013). The effects of eszopiclone on sleep spindles and memory consolidation in schizophrenia: a randomized placebo-controlled trial. *Sleep* 36, 1369–1376. doi: 10.5665/sleep.2968

Wang, G., Grone, B., Colas, D., Appelbaum, L., and Mourrain, P. (2011). Synaptic plasticity in sleep: learning, homeostasis and disease. *Trends Neurosci.* 34, 452–463. doi: 10.1016/j.tins.2011.07.005

Wilhelm, I., Rose, M., Imhof, K. I., Rasch, B., Buchel, C., and Born, J. (2013). The sleeping child outplays the adult's capacity to convert implicit into explicit knowledge. *Nat. Neurosci.* 16, 391–393. doi: 10.1038/nn.3343

Wilhelm, I., Wagner, U., and Born, J. (2011). Opposite effects of cortisol on consolidation of temporal sequence memory during waking and sleep. *J. Cogn. Neurosci.* 23, 3703–3712. doi: 10.1162/jocn_a_00093

Wilson, M. A., and McNaughton, B. L. (1994). Reactivation of hippocampal ensemble memories during sleep. *Science* 265, 676–679. doi: 10.1126/science.8036517

Conflict of Interest Statement: The author declars that the research was conducted in the absence of any commercial or financial relationships that could be construed as a potential conflict of interest.

Received: 31 January 2014; accepted: 13 March 2014; published online: 02 April 2014.
*Citation: Diekelmann S (2014) Sleep for cognitive enhancement. Front. Syst. Neurosci. **8**:46. doi: 10.3389/fnsys.2014.00046*
This article was submitted to the journal Frontiers in Systems Neuroscience.

frontiers in
SYSTEMS NEUROSCIENCE

HYPOTHESIS AND THEORY ARTICLE
published: 01 May 2014
doi: 10.3389/fnsys.2014.00075

Partial sleep in the context of augmentation of brain function

Ivan N. Pigarev[1]* and Marina L. Pigareva[2]

[1] *Institute for Information Transmission Problems (Kharkevich Institute), Russian Academy of Sciences, Moscow, Russia*
[2] *Institute of Higher Nervous Activity and Neurophysiology, Russian Academy of Sciences, Moscow, Russia*

Edited by:
Mikhail Lebedev, Duke University, USA

Reviewed by:
Manuel Casanova, University of Louisville, USA
Mikhail Lebedev, Duke University, USA
György Benedek, Szegedi Tudományegyetem, Hungary
Elena Budkevich, North Caucasus Federal University, Russia

****Correspondence:***
Ivan N. Pigarev, Institute for Information Transmission Problems (Kharkevich Institute), Russian Academy of Sciences, Bol'shoy Karetny Lane 19, Moscow 127994, Russia
e-mail: pigarev@iitp.ru

Inability to solve complex problems or errors in decision making is often attributed to poor brain processing, and raises the issue of brain augmentation. Investigation of neuronal activity in the cerebral cortex in the sleep-wake cycle offers insights into the mechanisms underlying the reduction in mental abilities for complex problem solving. Some cortical areas may transit into a sleep state while an organism is still awake. Such local sleep would reduce behavioral ability in the tasks for which the sleeping areas are crucial. The studies of this phenomenon have indicated that local sleep develops in high order cortical areas. This is why complex problem solving is mostly affected by local sleep, and prevention of local sleep might be a potential way of augmentation of brain function. For this approach to brain augmentation not to entail negative consequences for the organism, it is necessary to understand the functional role of sleep. Our studies have given an unexpected answer to this question. It was shown that cortical areas that process signals from extero- and proprioreceptors during wakefulness, switch to the processing of interoceptive information during sleep. It became clear that during sleep all "computational power" of the brain is directed to the restoration of the vital functions of internal organs. These results explain the logic behind the initiation of total and local sleep. Indeed, a mismatch between the current parameters of any visceral system and the genetically determined normal range would provide the feeling of tiredness, or sleep pressure. If an environmental situation allows falling asleep, the organism would transit to a normal total sleep in all cortical areas. However, if it is impossible to go to sleep immediately, partial sleep may develop in some cortical areas in the still behaviorally awake organism. This local sleep may reduce both the "intellectual power" and the restorative function of sleep for visceral organs.

Keywords: local sleep, cerebral cortex, slow wave sleep, sleep function, visceral control

SLEEP AND "HUMAN FACTOR"

The modern industrial style of life and necessity to live in non-natural environments often leads to dramatic errors in human behavior. Usually these errors are included in the general term "human factor" and are attributed to reduced attention, inability to predict consequences of an action in complex conditions and, finally, to reduced brain ability. Thus, the intention to augment the brain function can be considered a challenging goal for Neuroscience.

It was noticed that industrial anthropogenic disasters, traffic accidents, and medical errors often occur during the night, suggesting a probable link between sleepiness and reduced quality of brain functioning (Mitler et al., 1988; Dinges, 1995; Dinges et al., 1997; Cajochen et al., 1999; Barger et al., 2006; Akerstedt et al., 2011). Given the importance of this issue, many special studies devoted to investigation of the possible link between sleep disturbances and mental abilities were undertaken.

It was demonstrated that short-term total sleep deprivation results in cognitive impairments, especially in learning, and memory tasks (Maquet, 2001; Stickgold, 2005; Born et al., 2006; Walker, 2008, 2009; Diekelmann and Born, 2010; McCoyand and Strecker, 2011; Diekelmann et al., 2012, 2013).

In some studies, authors concluded that periods of slow wave sleep (SWS) played a particular role in these processes (Fowler et al., 1973; Plihal and Born, 1997; Diekelmann et al., 2011). Others maintained a rapid eye movement (REM) sleep dependency (Empson and Clarke, 1970), although in some studies REM sleep deprivation had no effect on different aspects of memory function (Hornung et al., 2007; Saxvig et al., 2008).

In addition to the function of memory consolidation, sleep has been proposed to benefit the encoding of new information during succeeding periods of wakefulness (McDermott et al., 2003; Yoo et al., 2007; Mander et al., 2011).

PECULIARITIES OF SLEEP DEPRIVATION EFFECTS

The impact of sleep deprivation on memory formation did not appear to be universal, but instead, differed on the basis of many factors such as the types of tasks used for learning,

and personal characteristics of subjects, including their emotionality. It has been shown that sleep-dependent motor skill memory improvement was dependent on the nature of the skill to be learned (Cohen et al., 2005; Cohen and Robertson, 2007; Siengsukon and Boyd, 2008). In another study, perception, attention and memory were impaired by sleep deprivation, but visual search and logical reasoning tasks were not (Williamson et al., 2001). A deficit in perceptual classification ability in an information-integration task was observed for some, but not all, sleep-deprived individuals (Maddox et al., 2009).

In their review of the sleep deprivation literature, Harrison and Horne (2000) concluded that sleep deprivation has little effect on simple rule-following tasks, but it obstructs decision making in complex integration tasks requiring flexibility, innovation or plan revision. However, other researchers observed performance decrements in relatively simple tasks such as identification and vigilance tasks (Chee et al., 2008; Ratcliff and Van Dongen, 2009). Sleep deprived subjects exhibited decreased performance in the taking advantage task (Glass et al., 2011).

Genzel et al. (2009) used different deprivation conditions throughout the experiment and did not find that an intense decrease in the total amount of REM sleep or SWS of their volunteers led to the inhibition of learning. They even proposed that sleep-dependent memory consolidation did not rely only on intact amounts of SWS or REM sleep across a night, but required different EEG microstructures, e.g., sleep spindles, δ-waves, and PGO waves.

It was proposed that reduced visual short-term memory after sleep deprivation may be connected, not with impairment of memory consolidation mechanisms but, rather, with a decline in visual attention and/or visual processing (Chuah and Chee, 2008).

An important factor was the length of time between training and test or amount of skill practice, independent of whether there was sleep or not (Shadmehr and Brashers-Krug, 1997; Robertson et al., 2004; Keisler et al., 2007; Song et al., 2007; Criscimagna-Hemminger and Shadmehr, 2008; Doyon et al., 2009; Debas et al., 2010; Borich et al., 2011; Borich and Kimberley, 2011; Voderholzer et al., 2011; Reis et al., 2013). In a nap study (Mander et al., 2011) no differences were observed between the sleep and no sleep groups in a specific alertness control task.

Results of sleep deprivation experiments were often rather contradictory. According to Lo et al. (2012), influence of sleep deprivation depends on the task domain, prior sleep debt, circadian phase at which performance is assessed, and genetically determined subject characteristics. Degree of task difficulty and the subject's emotionality influence the outcome of experiments concerning the connection between sleep and memory (Smith, 2001; Walker and Stickgold, 2006). Small differences in test design can cause large discrepancies in the studies of sleep dependency of memory processes. This may explain why some results are regularly found only by the same groups of scientists (Genzel et al., 2009).

Even in those experiments where positive effects of sleep on memory consolidation were demonstrated, these effects were very small. It seemed unlikely to us that the only function of sleep was simply to provide such a modest improvement in memory. On the other hand, the probable connection of sleepiness with the rare but dramatic consequences of anthropogenic disasters, as well as the fantastic pictures of dreams, support the general belief that the first function of sleep is for efficient functioning of the brain.

MODERN THEORIES OF SLEEP

Several modern theories concerning the function of sleep offer hypothetical mechanisms, which could be used by the brain for this purpose, e.g., the theory of neuronal groups (Krueger and Obál, 1993; Krueger et al., 2008) or the theory of synaptic homeostasis (Tononi and Cirelli, 2003, 2006). All theories, which were based on the assumption that sleep first of all is important for efficient brain function referred to numerous studies which demonstrated, both in humans and animals, "local use dependent processes". It was shown that δ-power during the first hours of sleep is higher in those cortical areas, which were more active immediately before sleep (Kattler et al., 1994; Rector et al., 2005; Huber et al., 2006). δ-power was considered therefore as an indicator and measure of recuperative processes in the brain.

However, if to accept an idea that function of sleep is to keep the efficient brain function it would be logical to expect that the brain would be the organ most vulnerable to sleep deprivation. However, the results of fundamental studies of A. Rechtshaffen and his colleagues (Everson et al., 1989; Cirelli et al., 1999; Rechtshaffen and Bergmann, 2002) do not confirm this suggestion. Their experiments demonstrated that total sleep deprivation led first of all to multiple visceral disorders (hair loss, skin and gastro-intestinal ulcerations and so on) and, finally, to unavoidable death of animals. A striking finding was that in rats that died after several days of total sleep deprivation, the only organ, which did not have any obvious degenerative changes, was the brain (Cirelli et al., 1999). This observation is surprising, since the negative effects of sleep deprivation on mental ability are well known. However, investigation of neuronal activity in the cerebral cortex in the sleep-wake cycle offers insights into the other sleep dependent mechanisms which can explain the reduction of mental abilities for complex problem solving, even in the normally working brain.

PHENOMENON OF LOCAL (PARTIAL) SLEEP

It was generally assumed for a long time that sleep develops synchronously in all areas of the mammalian cortex. The only exception has been reported for dolphins, whose EEG show periods of deep SWS in either the right or left hemisphere alone. Such periods of unilateral sleep may last for more than 2 h. Even in dolphins, however, EEG activity in different areas of one hemisphere was always found to be synchronized, or desynchronized simultaneously (Mukhametov et al., 1977; Mukhametov, 1984).

However, later it was shown that in terrestrial animals, in particular conditions, sleep developed only in some cortical areas during behavioral wakefulness. Thus, such partial sleep might be especially dangerous, because neither the person himself nor other individuals could notice its appearance and development. At the same time, dangerous consequences of temporal disengagement of some cortical areas from the control of behavior potentially can be rather dramatic. That is why understanding

the physiological mechanisms involved in initiation of sleep, and particularly of local sleep, can be considered an important element in attempts to augment brain functionality.

The phenomenon, which later was called "local sleep" was described in a study of the cat's frontal eye field (Pigarev, 1984). Neurons in this frontal cortical area strongly responded to visual stimulation only during periods of high behavioral alertness, and often became visually unresponsive during subsequent periods of quiet wakefulness. However, any sensory stimulation raising alertness (visual, auditory or olfactory), restored visual responses in this cortical area.

More detailed description of such unusual neuronal behavior in the cerebral cortex, and the term "local or partial sleep" appeared in the investigation of cortical visual area V4 in experiments with behaviorally awake monkeys (Pigarev et al., 1996, 1997; Pigarev, 1997). It was demonstrated in long-running experiments, that when a monkey had to perform a monotonic visual discrimination task, neurons became less responsive to the same visual stimuli and finally stopped responding at all, while the monkey continued to work in the task. If the task was interrupted, the monkey fell asleep for 10–20 min. After the nap, neuronal responses to visual stimuli often recovered. Neuronal background firing during such periods of temporal inactivity resembled that which these neurons demonstrated during periods of natural sleep of the animal. The monkey's performance in the visual task during periods of local sleep in the area V4 was rather high, although it was slightly reduced in comparison with that at the beginning of the experiment. Thus, one could conclude that at least visual area V1 still was working. In the same study it was noticed that, even within the area V4, local sleep developed not simultaneously but started from the periphery of the visual field. The last neurons, which were recruited in sleep, were neurons in the region of the foveal representation.

It was obvious that spread of sleep started from the "higher order" sensory areas most likely crucial for the most complicated behavioral situations. Taking all those considerations into account, one could expect to observe local sleep more often in organisms with better expressed multiple sensory representations, and most of all in primates. Indeed, the fronto-occipital trend in δ-power most pronounced during beginning of sleep was discovered in human subjects by the group of A. Borbély (Werth et al., 1996, 1997). Extensive studies of sleep spread dynamics are presented and discussed in the review of Ferrara and De Gennaro (2011).

We would like to remind here that since 1993 (Krueger and Obál, 1993; Kattler et al., 1994) the mentioned above idea concerning local use dependent sleep was widely discussed in sleep literature. Although experiments demonstrated local use dependent sleep, and observations of local sleep in behaviorally awake animals were mutually supportive, they were not absolutely identical. In the first case it was shown that in sleeping brain the depth of sleep can locally vary from region to region dependent on the previous history of activation. In the second case sleep in some cortical areas appeared during behavioral wakefulness. Namely this second case we will have in mind using the term "local sleep" in future.

Unexpected results obtained by Drummond et al. (2001, 2004) most likely were also connected with dynamics of local sleep spread over the human cerebral cortex. Investigating the effects of 35 h total sleep deprivation on memory impairments in verbal learning tasks using fMRI, these researchers demonstrated increased activity in frontal and parietal cortical regions, absent in the control non-deprived group. This can reflect partial sleep development in these high order associative cortical areas caused by sleep deprivation.

It seemed less likely that local sleep would be found in animals with more simple cortical organization and a limited number of sensory areas. However, recently, local sleep was described in behaviorally active rats, and again in the frontal cortical area (Vyazovskiy et al., 2011).

LOCAL SLEEP AND COGNITIVE IMPAIRMENTS AFTER SLEEP DEPRIVATION

Taking into account the phenomenon of local sleep, the cognitive impairments after sleep deprivation can be explained not by the general deterioration of brain efficiency, but by switching of several cortical areas from those functions, which they have to perform in wakefulness.

At first sight, the hypothesis that local sleep is responsible for a reduction of brain functionality looks similar to the proposal that after a long period of wakefulness, the brain needs recuperation during sleep. The difference is only in the temporal sequence of events. After prolonged wakefulness, all regions of the brain may fall asleep for recovery simultaneously, or certain areas may do so at first, while others remain awake for some time.

However, it is possible to consider another, fundamentally different, scenario. What if the brain, as all other visceral organs of an organism, does not need any special recuperative rest connected with total interruption of functionality? What if the brain, like a computer, can work efficiently for long periods of time, and observed "sensory isolation" of the brain during sleep just reflects switching over for processing of another flow of incoming information?

We should not forget that sleep-deprived animals die not because they become blind, deaf, have forgotten the ways to a food tray or because of serious problems with decision making. They die mainly because of multiple visceral disorders in virtually all life supporting systems, including the immune system (Rechtshaffen and Bergmann, 2002). At the same time, the brain appears to be the most resistant organ.

Our observations of the neuronal activity in the sleep-wake cycle also did not convince us that during long periods of wakefulness there were crucial pathological changes of the neuronal state, which forced a brain to switch into a sleeping "restorative" mode. Nevertheless, one can argue that it is generally recognized that the pattern of SWS EEG is very specific for this state, and differs from the pattern of EEG in wakefulness. However, interpretation of this observation also is equivocal. The EEG pattern of active SWS was usually compared with the EEG pattern in a state of very passive wakefulness, when human subjects or animals were immobile and without intensive sensory stimulation.

WHETHER CORTICAL EEG REFLECTS PECULIARITY OF BRAIN ACTIVITY IN WAKEFULNESS AND SLEEP, OR JUST PATTERN OF THE CORTICAL AFFERENT FLOW?

We proposed that difference of cortical afferentation in wakefulness and sleep might define the observed difference of neuronal activity in SWS and wakefulness. To check this proposal, general EEG and eye movements were recorded in behaviorally awake cats during SWS and active wakefulness between electrodes located over temporal and frontal cortical areas. In addition, we recorded neuronal activity and local field potentials (local EEG) from visual (**Figure 1**) and somatosensory (**Figure 2**) cortical areas using bipolar tungsten microelectrodes with distances of about 300 μm between the tips of the electrodes. During SWS the animal eyes were always deviated upward, and this allowed us to easily distinguish periods of sleep from active wakefulness in the obtained recordings. For every group of recorded neurons we applied the optimal parameters of stimulation (either visual or somatosensory), and delivered these stimuli in a rhythmic manner. We called this procedure "sleep EEG imitation in wakefulness". Using this procedure (right column), in actively awake cats, we got burst neuronal firing (not shown) and EEG slow waves, which were indistinguishable from, or even higher than, those which we had observed during the periods of natural SWS (left column). These sleep-like waves were especially well visible in the channel of the local field potentials (**Figures 1C** and **2C**, right columns) because the local EEG reflected activity of the neurons for which we used the optimal stimulation. The general EEG reflected averaged activity collected from the large cortical territory, including those neurons for which applied stimuli were not optimal. Nevertheless, some sleep-like waves were seen even in the general EEG (**Figures 1B** and **2B**, right columns). In row D in **Figures 1** and **2** we present power spectrums calculated for the 10 s fragments of the local EEG shown in row C of the corresponding column. It is seen that spectral compositions of the local EEG for SWS (left column) and imitation of sleep EEG in wakefulness (right column) were rather similar, and both differed from the usual spectrum of quiet wakefulness (central column).

The presented observations supported an idea that patterns of the cortical afferentation, rather than the state of vigilance,

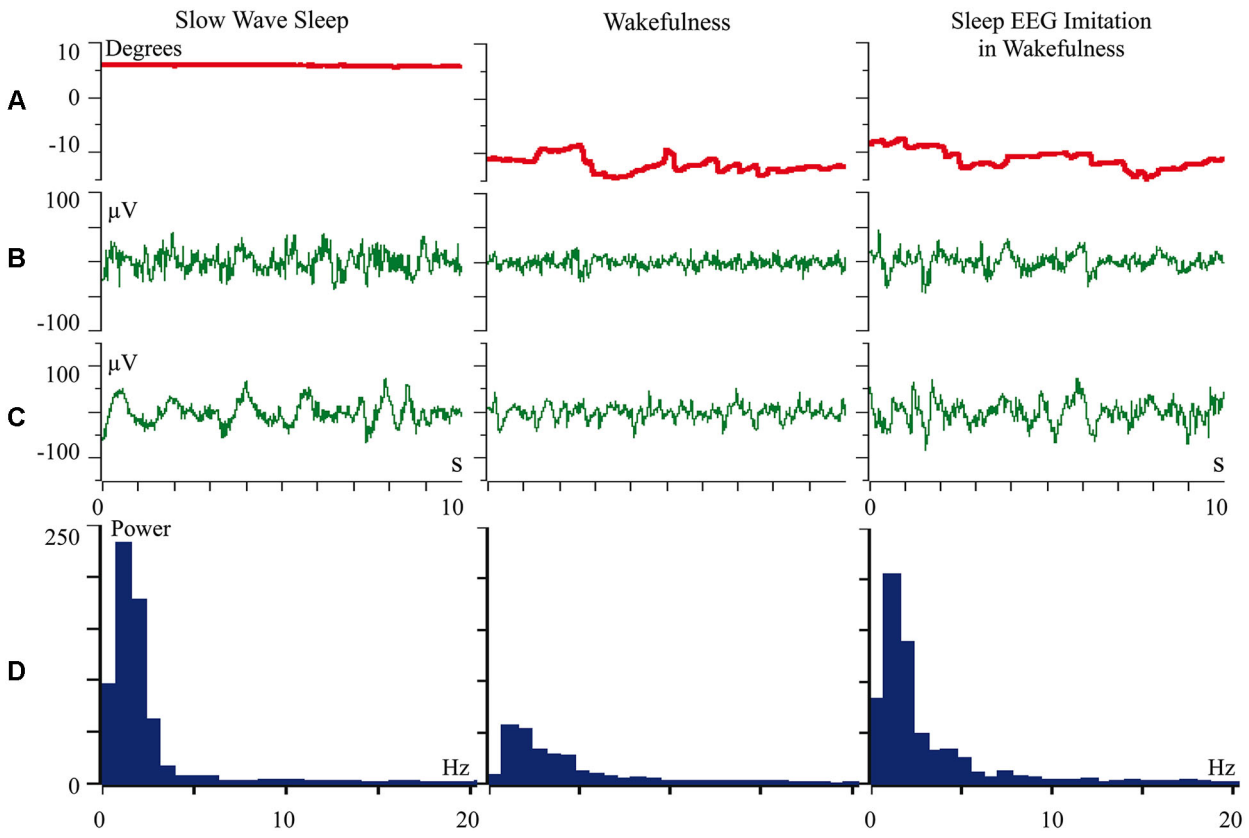

FIGURE 1 | Rhythmic stimulation by the optimal visual stimulus during wakefulness evokes sleep like slow wave activity in the cat visual cortex. The rows: **(A)** vertical component of eye movements which helps to distinguish sleep (upward deviation) from wakefulness (downward deviation); **(B)** general EEG recorded between electrodes over temporal and frontal cortical areas of the cat; **(C)** local field potentials (local EEG) recorded between two tungsten microelectrodes located 300 μm one from another within the cortical visual area V1; **(D)** power spectrum of the local EEG presented above in **panel C**. All parameters were collected during SWS (left column), during passive wakefulness (middle column), and during the procedure of "sleep EEG imitation" by visual stimulation in wakefulness, which produced strong excitation of the cortical neurons recorded by the microelectrodes (right column). Technical details of the study in Pigarev et al. (2013).

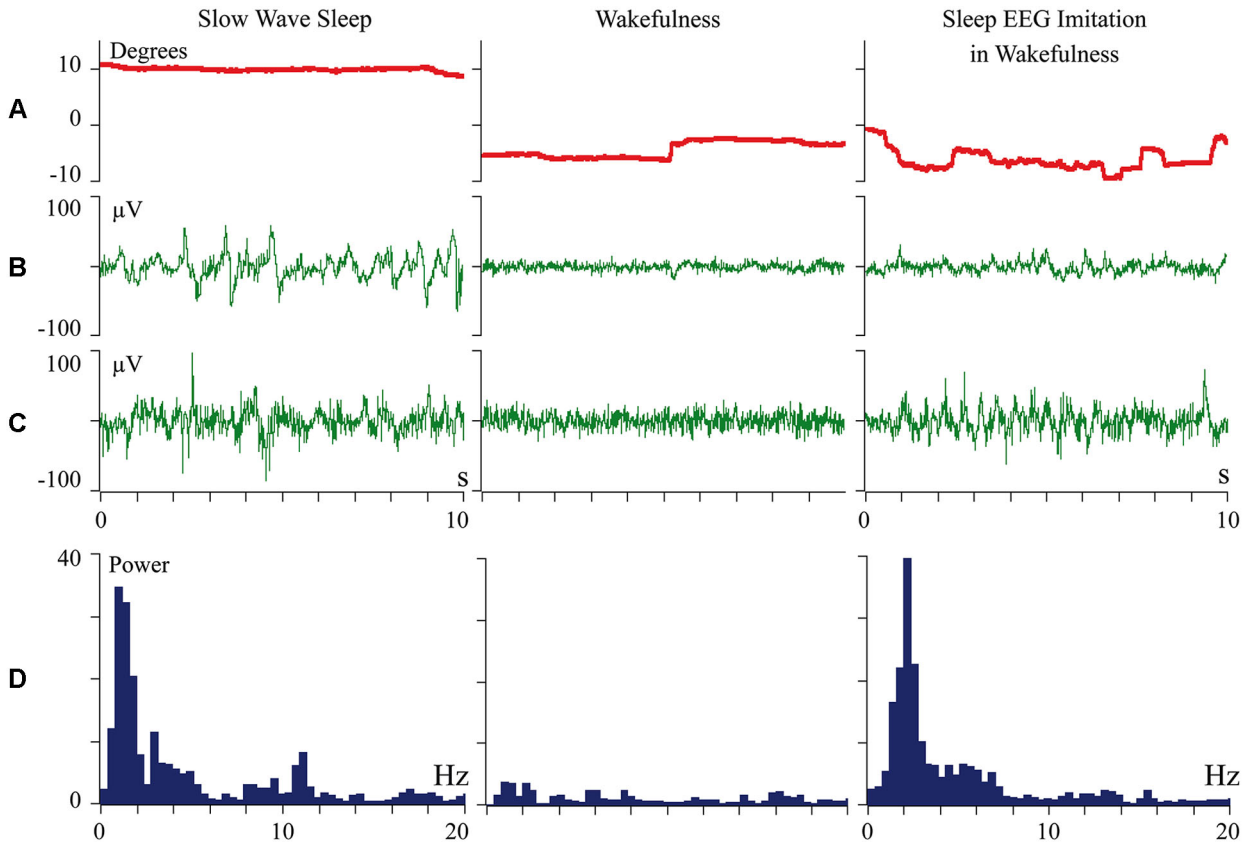

FIGURE 2 | Periodic optimal somatic stimulation during wakefulness evokes sleep like slow wave activity in the cat somatosensory cortex. The rows: **(A)** vertical component of eye movements which helps to distinguish sleep (upward deviation) from wakefulness (downward deviation); **(B)** general EEG recorded between electrodes over temporal and frontal cortical areas of the cat; **(C)** local field potentials (local EEG) recorded between two tungsten microelectrodes located 300 mm one from another within the cortical somatosensory area 5; **(D)** power spectrum of the local EEG presented above in **panel C**. All parameters were collected during SWS (left column), during passive wakefulness (middle column) and during the procedure of "sleep EEG imitation" in wakefulness by rhythmic stimulation of the contralateral forepaw, which produced strong excitation of the cortical neurons recorded by the microelectrodes. Technical details of the study in Pigarev et al. (2013).

determine the pattern of cortical activity. All above-mentioned considerations inclined us to conclude that switching to analysis of another flow of incoming information would be able to better explain the phenomenology of transition from wakefulness to sleep. The temporal organization of these incoming signals, specific for the state of sleep, will define the pattern of cortical activity during sleep.

WHICH SIGNALS COULD PROVIDE PERIODIC AND SYNCHRONOUS AFFERENTATION DURING SLEEP?

Animal physiology offered the answer on this question; that it can be periodic activity of various visceral systems, e.g., gastrointestinal peristalsis, heart and respiratory activities. We proposed that during sleep the same brain neurons that in wakefulness process exteroceptive information of various modalities switch over to the analysis of interoceptive information coming from visceral systems. Rhythmic activities of different visceral systems define this periodic afferent flow towards the cortical areas, which is reflected in cortical SWS activity. Thus, the central nervous system during sleep might be involved in the process of visceral regulation (Pigarev, 2014).

According to this proposal, periods of local sleep are not the periods when "tired" brain areas stop processing of exteroceptive information in favor of self-recuperation. During periods of local sleep, normally working brain areas respond to warning messages from the internal organs and switch to the processing of the alarming visceral afferentation. Within the frame of this hypothesis, we should "think differently" about the nature of sleep and local sleep.

This suggestion may be too fantastic for the brain paradigm generally accepted at present. This paradigm was established mainly on the basis of data collected for the state of wakefulness. On the other hand, our "fantastic" proposal opened the way for its experimental validation in simple experiments, which could not be conducted without this theoretical background. Below, we offer a short review of the experiments performed to investigate such nontrivial predictions of the visceral hypothesis of sleep.

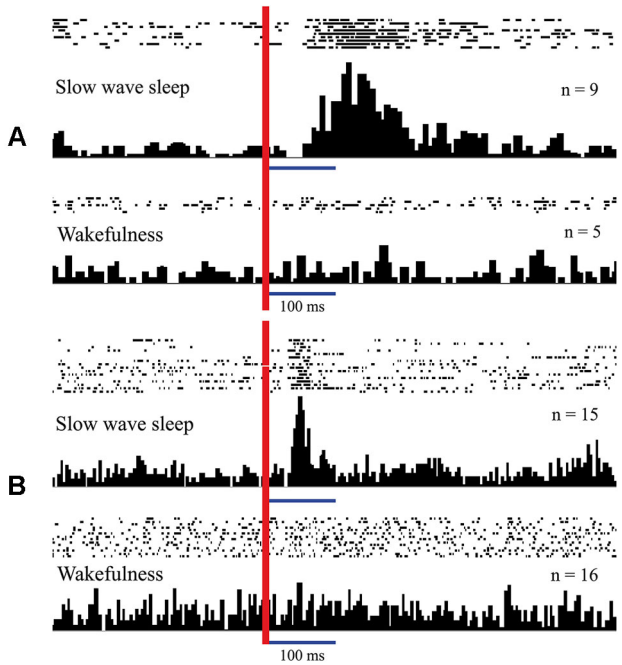

FIGURE 3 | Responses of neurons in the cat cortical visual area V1 (A) and somatosensory area 5 (B) to intraperitoneal electrical stimulation delivered in sleep and in wakefulness. Responses presented as rasters where every line corresponds to single stimulation trial. Dots represent single spikes. Below are averaged histograms. Vertical red line–moment of intraperitoneal stimulation. n—number of averaged trials. Technical details of the study in Pigarev (1994).

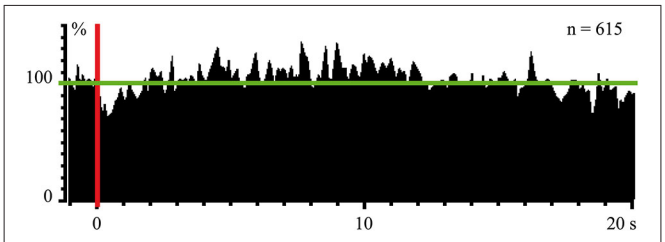

FIGURE 4 | Population response of 61 neurons (615 trials) in monkey's cortical visual area V4 to magnetic stimulation of stomach during SWS. Vertical red line–moment of stimulation. Horizontal green line indicate mean background firing rate before stimulation taken as 100%. Technical details of the study in Pigarev et al. (2008).

EXPERIMENTAL VALIDATION OF THE VISCERAL HYPOTHESIS OF SLEEP

First of all, to check this hypothesis responses of different cortical regions to extero- and interoceptive stimulation during sleep and wakefulness were compared. These experiments were started from the visual cortical areas. Visual areas were selected for these experiments because they were well studied, and it was generally recognized that in behaviorally awake animals neurons of these areas were responding exclusively to visual stimulation. In addition, one of us (Ivan N. Pigarev) had considerable experience in investigation of various visual areas in behaviorally awake animals. Later, similar experiments were conducted with neurons not only in occipital, but also in frontal and parietal cortical areas.

In **Figure 3** (adopted from Pigarev, 1994; Pigarev and Pigareva, 2012) we show responses of complex neurons in visual cortical area V1 (**panel A**) and somatosensory area 5 (**panel B**) of cats to electrical intraperitoneal stimulation delivered in SWS and in wakefulness. These neurons in the state of wakefulness responded to visual and somatosensory stimuli respectively. During SWS both neurons responded to electrical stimulation of the area of the small intestine, and these apparent responses immediately disappeared in REM sleep and after awakening.

Similar experiments were conducted with monkeys, where evoked responses to intraperitoneal electrical stimulation were recorded above the cortical visual area V1 (Pigarev et al., 2006). Evoked responses were again obtained only during SWS, and disappeared during REM sleep and in the state of wakefulness.

In experiments with one monkey we used magnetic stimulation, with the coil located close to the surface of the monkey's stomach. In response to magnetic pulses, which did not wake the animal, we obtained cortical evoked responses, recorded by the electrodes above the occipital pole of the skull. These responses were observed again only during SWS (Pigarev et al., 2008). Simultaneous recording of the neuronal activity in the visual area V4 revealed a strong short latency inhibition in response to these magnetic pulses, which was obviously visible even in the population response of 61 neurons (**Figure 4**). After this short latency inhibition, the delayed (5–15 s) activation of the background firing took place. This result deserves attention because receptive fields in area V4 had small excitatory areas and huge inhibitory surrounds. The applied magnetic pulses could activate those parts of visceral organs, which projected to this huge inhibitory periphery of the studied receptive fields. On the other hand, after some delay, peristaltic waves provoked by the stimulation could reach regions, which projected to the central excitatory part of the receptive fields, causing the observed delayed activation. All these responses to magnetic stimulation again disappeared in wakefulness.

In experiments with rabbits (Pigarev et al., 2004), we also recorded evoked responses to electrical intraperitoneal stimulation in visual and somatosensory cortical areas, which appeared again exclusively during SWS.

It has been argued that electrical and magnetic stimuli are not natural, and that observed effects could have a non-specific origin. Although the main information concerning organization of the nervous system was obtained using electrical stimulation, it would be much more important to demonstrate a functional link between visceral organs and cortical areas during sleep in natural conditions, without any artificial stimulation.

Such experiments were conducted with the help of our colleagues from the Pavlov Institute of Physiology (St. Petersburg), prof. V. A. Bagaev and I. I. Busigina. Recording electrodes were implanted in the walls of the small intestine and stomach of cats, together with stomach fistula. With this approach, in addition to cortical neuronal activity, EEG, and ocular movements we could record myoelectrical activity of small intestine and stomach, and to change intragastric contents.

In **Figure 5** we present a spectrogram of cat cortical EEG (A) recorded simultaneously with myoelectrical activity of the stomach (B) during an episode of SWS. In the spectrogram, yellow colors indicate higher power, and periodic vertical blue fragments indicate moments of short desynchronizations connected with lack of low frequency components. These desynchronized intervals are well known to anybody who has recorded EEG during SWS. It was previously demonstrated (Oniani et al., 1974) that, behaviorally, sleep was not interrupted during these periods, and thresholds for awakening during such short desynchronizations still were very high. What was new in the presented figure was a surprising coincidence of these EEG desynchronizations with the appearance of periodic migrating myoelectrical complexes in the stomach (short vertical inclinations in B). There was no need for any special analysis in order to notice such coincidence. Simultaneous appearance of the migrating myoelectrical complexes in stomach activity and short desynchronizations in the cortical EEG usually happened during intervals of 10–20 min of SWS. The observed coincidence of these effects can disappear for a while and appear again later. This was a very robust effect, observed in most of our sleep recordings, which included the periods of corresponding stomach activity.

More impressive were results of those experiments where we have studied interaction of the neuronal activity in various cortical visual areas and myoelectrical activity from the wall of the duodenum (Pigarev et al., 2013). It was demonstrated that about one third of more than 200 of the studied cortical neurons during SWS established a causal relationship with the activity of the duodenum during SWS. Even more, these neurons demonstrated selectivity to particular types of duodenal rhythmicity. Some neurons preferred simple duodenal waves, and others responded only to waves with spike potentials. Such a relationship was never observed in wakefulness.

Finally it was found that changes of the intragastric medium (water infusion via fistula into the stomach) performed in the period of SWS lead to changes in the EEG pattern and temporal reorganization of the background neuronal spiking, revealed by Fano factor analysis (Pigarev et al., 2010).

We do not imply that only the structures of the digestive system are represented in the cerebral cortex during sleep. In other experiments we recorded evoked responses to heartbeats during sleep (Pigarev and Feodorov, 2012). An example of neuronal firing and local field potentials in the visual area V1, which synchronized with respiration during SWS, is shown in **Figure 6**. Dr. M. Lebedev, during experiments with monkeys under anesthesia, also observed unexpected neuronal activity synchronized with respiration in somatosensory cortical areas within the representation of the hind paw (personal communication).

THE VISCERAL SLEEP THEORY AND OBSERVATIONS OF "SLOW WAVE" ACTIVITY IN THE CORTICAL SLABS AND SLICES

According to the visceral sleep theory, patterns of periodic activation coming from the visceral organs determine the oscillating picture of cortical activity during SWS. The desynchronized pattern of cortical EEG during REM sleep can be connected with afferentation coming to the cerebral cortex from visceral systems lacking obvious rhythmic activity, e.g., liver, kidneys, reproductive organs and, finally, the brain itself. The brain's status within this theory is obviously dual. On the one hand, the brain is the central processor which controls behavior in the environment during wakefulness and defines recovery of all visceral organs during sleep. However, on the other hand, the brain itself is an enormously complicated visceral organ, which certainly should be in need of service. How and when such brain self-service is realized is a challenging question. It may happen, for example, during particular phases of REM or SWS, or it may be organized as a permanent service, e.g., by glial cells. The recently discovered "glymphatic" mechanism may reflect elements of such brain self-servicing (Nedergaard, 2013; Xie et al., 2013). Various other options can be offered, but that is a topic for future studies.

Our approach to sleep function supposes that cortical activity during sleep is defined by the afferent flow coming to the cerebral cortex from various visceral organs. On the other hand, there is substantial evidence that sleep-like activity can be generated in cortical slabs (Timofeev et al., 2000) and isolated cortical slices (Sanchez-Vives and McCormick, 2000) without any interoceptive inputs. However, we do not think that these observations are inconsistent with our theoretical proposal. Of relevance is the

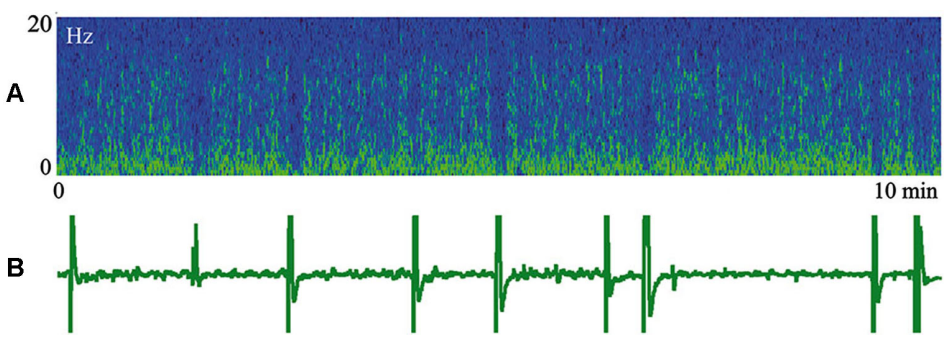

FIGURE 5 | Episode of SWS. **(A)** Spectrogram of the cat cortical EEG. Yellow color indicates higher power. **(B)** Myoelectrical activity of stomach. Technical details of the study in Pigarev et al. (2013).

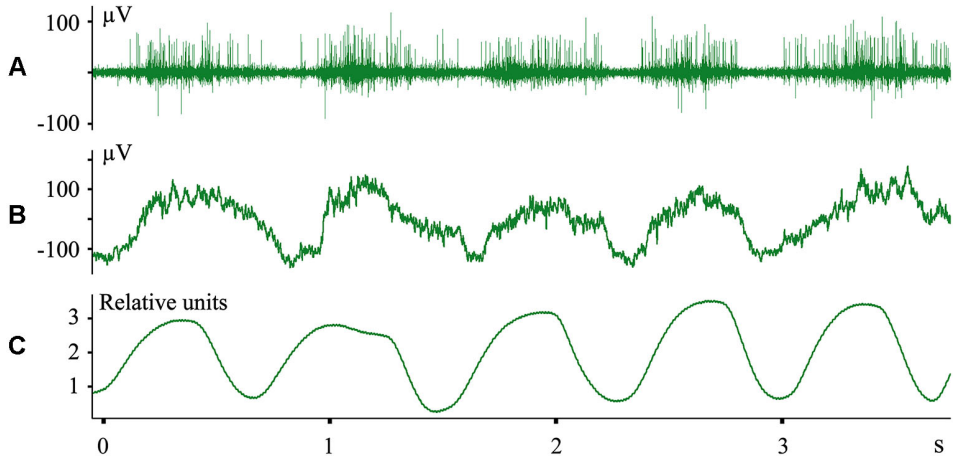

FIGURE 6 | Neuronal activity in the cat primary visual cortex synchronized with respiration during SWS. (A) Multiunit activity; **(B)** local field potentials (local EEG); **(C)** nasal air flow in relative units. Technical details of the study in Pigarev et al. (2013).

important discovery of Steriade et al. (2001), who performed the first intracellular recordings of neuronal cortical activity in naturally sleeping cats. They found that waves of hyperpolarization reflected as periodic silent pauses in neuronal firing during SWS were connected not with active inhibition, but with disfacilitation caused by the lack of excitatory inputs to these cortical neurons. At the time of their study it was generally recognized that, during sleep, the cerebral cortex was disconnected from any afferent inputs, and they had to conclude that, "during SWS, neocortical neurons may be engaged in information processing of internally generated signals...", which provided such excitatory inputs. As a source of such "internally generated signals" they considered intracortical excitation (Steriade et al., 2001).

The studies performed on the isolated cortical slices demonstrated that, in certain conditions, it was possible to evoke periodic neuronal discharges, which had some features of similarity with real SWS oscillations. Later it was shown in experiments on thalamo-cortical slices that activation of the thalamo-cortical neurons dominates in triggering such cortical oscillations (Contreras and Steriade, 1995; Rigas and Castro-Alamancos, 2007). In a review (Crunelli and Hughes, 2010) it was recognized that most likely several mechanisms might elicit the cortical slow waves. We propose that "internally generated signals", which define cortical waves during SWS, are actually coming from various visceral systems using the same thalamo-cortical pathways, which activate cortical neurons during wakefulness.

THE PATHWAYS FOR THE VISCERAL AFFERENTATION TO THE CEREBRAL CORTEX DURING SLEEP

One may inquire about the ways by which the information from various visceral systems may reach "the same thalamo-cortical pathways". For the somatosensory system it is well investigated. It is known since early anatomical studies in the 19th century (Head, 1896), that visceral and somatosensory afferents terminate at the same neurons in the spinal cord, and thus visceral information may travel to the cerebral cortex through the fibers of the somatosensory columns. The fact of such combined projections was confirmed in many studies (e.g., Kuo et al., 1981; Cervero, 1983; Cervero et al., 1984; Akeyson and Schramm, 1994; Perry and Lawson, 1998) and this overlap is regarded as the most probable mechanism of the referred pains (Head, 1896; Arendt-Nielsen and Svensson, 2001; Peles et al., 2004; Hobson et al., 2010).

However, this overlap created a yet unresolved problem–how the central nervous system manages to distinguish spikes coming by a single fiber from so different sources. Our hypothesis offers a solution to this problem. The transmission of the somatosensory information happens during wakefulness, while visceral information is transmitted to the central nervous system during sleep, when muscles are relaxed and movements are excluded.

To our knowledge, pathways of the visceral information to the visual cortical areas have never been investigated. Here we offer only some considerations. It is well known that, in the main thalamic visual relay (lateral geniculate nucleus), retinal synaptic terminals form only one third of all synaptic terminals. Another third of terminals belong to backward cortico-thalamic projections. The remaining one third of terminals is of non-visual origin, and come from the pontine and the brain stem regions (Hughes and Mullikin, 1984). Activation from pontine nuclei reaches the lateral geniculate nucleus during sleep, especially during REM sleep, and reflects in the visual cortical areas as well known ponto-geniculo-occipital waves (Brooks and Bizzi, 1963). The origin of this pontine activity has not yet been investigated. On the other hand, pontine and brain stem projections to the lateral geniculate nucleus come from the regions of entering and passage of various visceral nerves. Therefore, their link with visceral information is very probable.

K-COMPLEXES AND VISCERAL AFFERENTATION, USE DEPENDENCY AND SLEEP HOMEOSTASIS

In discussions of cortical visceral activation during sleep, one often argues that these visceral responses can be of nonspecific origin, resembling sensory-triggered K-complexes. This topic was

investigated in detail in our special study (Pigarev et al., 2011). It was shown that visually induced K-complexes had absolutely specific origin. Even more, K-complexes could be induced by sensory stimuli only during short intervals of developing sleep. In contrast, cortical visceral responses could be recorded during periods of deep SWS, when K-complexes could not be induced by any sensory stimulation. In addition, we presented arguments indicating that visually induced K-complexes were also of visceral origin.

The attempts to link various visceral events with the elements of EEG recorded during sleep, e.g., K-complexes, has been undertaken in many studies (Pampiglione and Ackner, 1958; Johnson and Karpan, 1968; Halász et al., 1985; Heald et al., 1989; Hornyak et al., 1991; Okada et al., 1991; Niiyama et al., 1996; Monstad and Guilleminault, 1999; Tank et al., 2003). The same idea was expressed in a study of Cash et al. (2009), where it was suggested that spontaneous K-complexes appearing in the EEG during transition from wakefulness to sleep could be induced by a "sensory stimulus occult to the investigator (e.g., gastric)".

In the middle of the previous century, cortical responses to the stimulation of various visceral nerves were described and intensively investigated in several laboratories (e.g., Bailey and Bremer, 1938; Amassian, 1951; Patton and Amassian, 1952; Gardner et al., 1955; Chernigovskiy, 1960). These studies were performed in acute experiments under anesthesia. However, in later experiments without anesthesia, these results could not be reproduced. In wakefulness, neurons in these areas responded only to visual or somatosensory stimulation. Thus, cortical responses to visceral stimulation were regarded as probable artifacts of anesthesia.

In our studies we have demonstrated that without any anesthesia, in natural conditions, cortical areas do establish connections with visceral organs, but this link is functionally active only during sleep. Involvement of the highest levels of the central nervous system, up to the cerebral cortex in mammals, in the processing of visceral information during periods of sleep may be the main, if not the exclusive, function of sleep.

Here we should come back to the above-mentioned effect of "use dependency", which is widely explored now as an experimental argument in favor of the concepts that sleep is necessary for brain recovery (Kattler et al., 1994; Rector et al., 2005; Huber et al., 2006). This effect can also be explained by the visceral sleep theory. High activation of some cortical areas by intensive exteroceptive stimulation during wakefulness will lower the neuronal thresholds of the neurons in these areas (e.g., due to the LTP mechanism). As a result, during sleep, these neurons will respond more strongly to visceral stimulation, coming to the same neurons through the same synaptic connections. Consequently the δ-power of the EEG will grow.

Discussing the visceral sleep theory we would like to draw attention to the distinguished theory of A. Borbély—the two-process model of sleep regulation (Borbély, 1982; Borbély and Achermann, 1999). This model proposes that sleep is regulated by the interaction of two processes—homeostatic and circadian. The homeostatic process allows for a constant amount of sleep during 24 h. Visceral sleep theory offers the physiological framework of this homeostatic mechanism. Homeostasis of all visceral systems is supported during sleep due to the involvement of all the cerebral cortex in the processing of information from internal organs. These informational processes define the total length of sleep.

MECHANISM OF SLEEP INITIATION AND FEATURES OF LOCAL SLEEP

The visceral sleep theory explains the logic behind the initiation of sleep. Indeed, a mismatch between the current parameters of any visceral system and the genetically determined range for these parameters would provide the feeling of tiredness, or sleep pressure. If an environmental situation allows sleep, an organism would transit to normal total sleep in all cortical areas. Actually the chain of events for sleep initiation is more complicated. Evaluation of the visceral problems may need engagement of the mechanisms of emotions and such structures as hippocampus, amygdala and prefrontal cortex. All those questions were discussed in our recent article (Pigarev and Pigareva, 2013), and we will not continue this topic here. Now we would like to go back to the phenomenon of local sleep and to discuss it within the frame of the presented visceral sleep theory.

In the cases when, because of visceral problems, the need for sleep is dramatically increased, but environmental conditions do not allow sleep to occur, sleep may progress only in some cortical areas in still behaviorally active organisms. According to the information cited above, the development of sleep starts from the most recent, "high order" cortical areas. The proportion of such areas is highest in the frontal pole of the brain. This might underlie the reported fronto-occipital trend in the development of sleep.

It is logical to propose that those behavioral tasks, which do not need engagement of the highest cortical resources would be normally realized even in conditions when part of the brain is sleeping. However, in the situation when all cortical computational ability is required for decision making in a complicated problem, local sleep may lead to severe and often dramatic behavioral errors.

Conditions of local sleep development indicate that local sleep is very probable when it is necessary to remain awake during periods of high (natural) sleep pressure. For humans this might happen during work at the time of the maximal sleepiness. For rats, local sleep can accompany experiments during the light phase of the day, if the rats are caged in animal houses with non-inverted conditions of illumination.

People with habitual or forced short length of night sleep are at permanent risk of partial sleep development. For some professions partial sleep provoked by such chronic sleep deprivation may not cause any troubles. However, for professions connected with responsible and complex decision making, especially during night shifts, the dangerous consequences of local sleep are very high. For these professions, any visceral disorders, especially in the gastro-intestinal system, may dramatically increase the risk of wrong decisions.

Besides the negative effects of partial sleep for mental ability due to the disengagement of some cortical areas from the intellectual work, one should also not neglect the possible negative consequences of this phenomenon for the visceral health of an

organism. As participation of all cortical areas in information processing is essential for the efficient solution of complex problems in wakefulness, for efficient management of visceral systems, all cortical areas should be involved into the processing of visceral information. Appearance of local sleep during wakefulness means that the length of total sleep during the nighttime was not sufficient, and may indicate hidden problems in some visceral systems.

CONCLUSION

The detailed investigation of brain involvement in the regulation of the various visceral systems during sleep is a goal for further studies. At present, following the visceral theory of sleep, we can state that efficient and sufficient sleep, together with visceral health, might be the cheapest, safest and most pleasant way to augment brain function.

AUTHOR CONTRIBUTIONS

Both co-authors have equal contribution to all steps of preparation of this article and both approved the version to be published.

ACKNOWLEDGMENTS

We are very thankful to Dr. Denys Garden for critical reading of the manuscript and many helpful comments. The study was supported by Russian Foundation for Basic Researches grants 13-04-00941 and 13-04-00741.

REFERENCES

Akerstedt, T., Philip, P., Capelli, A., and Kecklun, G. (2011). Sleep loss and accidents–work hours, life style and sleep pathology. *Prog. Brain Res.* 190, 169–188. doi: 10.1016/b978-0-444-53817-8.00011-6

Akeyson, E. W., and Schramm, L. P. (1994). Splanchnic and somatic afferent convergence on cervical spinal neurons of the rat. *Am. J. Physiol.* 266(Suppl. 1), R268–R276.

Amassian, V. E. (1951). Cortical representation of visceral afferents. *J. Neurophysiol.* 14, 435–446.

Arendt-Nielsen, L., and Svensson, P. (2001). Referred muscle pain: basic and clinical findings. *Clin. J. Pain* 17, 11–19. doi: 10.1097/00002508-200103000-00003

Bailey, P., and Bremer, F. (1938). A sensory cortical representation of the vagus nerve. With a note on the effects of low blood pressure on the cortical electrogramm. *J. Neurophysiol.* 1, 405–414.

Barger, L. K., Ayas, N. T., Cade, B. E., Cronin, J. W., Rosner, B., Speizer, F. E., et al. (2006). Impact of extended-duration shifts on medical errors, adverse events and attentional failures. *PLoS Med.* 3:e487. doi: 10.1371/journal.pmed.0030487

Borbély, A. A., and Achermann, P. (1999). Sleep homeostasis and models of sleep regulation. *J. Biol. Rhythms* 14, 557–568.

Borbély, A. A. (1982). A two process model of sleep regulation. *Hum. Neurobiol.* 1, 195–204. doi: 10.1007/978-3-540-29678-2_6166

Borich, M., Furlong, M., Holsman, D., and Kimberley, T. J. (2011). Goal-directed visuomotor skill learning: off-line enhancement and the importance of the primary motor cortex. *Restor. Neurol. Neurosci.* 29, 105–113. doi: 10.3233/RNN-2011-0584

Borich, M. R., and Kimberley, T. J. (2011). Both sleep and wakefulness support consolidation of continuous, goal-directed, visuomotor skill. *Exp. Brain Res.* 214, 619–630. doi: 10.1007/s00221-011-2863-0

Born, J., Rasch, B., and Gais, S. (2006). Sleep to remember. *Neuroscientist* 12, 410–424. doi: 10.1177/1073858406292647

Brooks, D. C., and Bizzi, E. (1963). Brain stem electrical activity during deep sleep. *Arch. Ital. Biol.* 101, 648–665.

Cajochen, C., Foy, R., and Dijk, D. J. (1999). Frontal predominance of a relative increase in sleep delta and theta EEG activity after sleep loss in humans. *Sleep Res. Online* 2, 65–69.

Cash, S. S., Halgren, E., Dehghani, N., Rossetti, A. O., Thesen, T., Wang, C., et al. (2009). The human K-complex represents an isolated cortical down-state. *Science* 324, 1084–1087. doi: 10.1126/science.1169626

Cervero, F. (1983). Somatic and visceral inputs to the thoracic spinal cord of the cat: effects of noxious stimulation of the biliary system. *J. Physiol.* 337, 51–67.

Cervero, F., Connell, L. A., and Lawson, S. N. (1984). Somatic and visceral primary afferents in the lower thoracic dorsal root ganglia of the cat. *J. Comp. Neurol.* 228, 422–431. doi: 10.1002/cne.902280309

Chee, M. W., Tan, J. C., Zheng, H., Parimal, S., Weissman, D. H., Zagorodnov, V., et al. (2008). Lapsing during sleep deprivation is associated with distributed changes in brain activation. *J. Neurosci.* 28, 5519–5528. doi: 10.1523/jneurosci.0733-08.2008

Chernigovskiy, V. N. (1960). *Interoceptors.* Moscow: Medgiz. 650.

Chuah, L. Y., and Chee, M. W. (2008). Cholinergic augmentation modulates visual task performance in sleep-deprived young adults. *J. Neurosci.* 28, 11369–11377. doi: 10.1523/jneurosci.4045-08.2008

Cirelli, C., Shaw, P. J., Rechtschaffen, A., and Tononi, G. (1999). No evidence of brain cell degeneration after long-term sleep deprivation in rats. *Brain Res.* 840, 184–193. doi: 10.1016/s0006-8993(99)01768-0

Cohen, D. A., Pascual-Leone, A., Press, D. Z., and Robertson, E. M. (2005). Off-line learning of motor skill memory: a double dissociation of goal and movement. *Proc. Nat. Acad. Sci. U S A* 102, 18237–18241. doi: 10.1073/pnas.0506072102

Cohen, D. A., and Robertson, E. M. (2007). Motor sequence consolidation: constrained by critical time windows or competing components. *Exp. Brain Res.* 177, 440–446. doi: 10.1007/s00221-006-0701-6

Contreras, D., and Steriade, M. (1995). Cellular basis of EEG slow rhythms: a study of dynamic cortico-thalamic relationships. *J. Neurosci.* 15, 604–622.

Criscimagna-Hemminger, S. E., and Shadmehr, R. (2008). Consolidation patterns of human motor memory. *J. Neurosci.* 28, 9610–9618. doi: 10.1523/jneurosci.3071-08.2008

Crunelli, V., and Hughes, S. W. (2010). The slow (<1 Hz) rhythm of non-REM sleep: a dialogue between three cardinal oscillators. *Nat. Neurosci.* 13, 9–17. doi: 10.1038/nn.2445

Debas, K., Carrier, J., Orban, P., Barakat, M., Lungu, O., Vandewalle, G., et al. (2010). Brain plasticity related to the consolidation of motor sequence learning and motor adaptation. *Proc. Natl. Acad. Sci. U S A* 107, 17839–17844. doi: 10.1073/pnas.1013176107

Diekelmann, S., and Born, J. (2010). The memory function of sleep. *Nat. Rev. Neurosci.* 11, 114–126. doi: 10.1038/nrn2762

Diekelmann, S., Biggel, S., Rasch, B., and Born, J. (2012). Offline consolidation of memory varies with time in slow wave sleep and can be accelerated by cuing memory reactivations. *Neurobiol. Learn. Mem.* 98, 103–111. doi: 10.1016/j.nlm.2012.07.002

Diekelmann, S., Büchel, C., Born, J., and Rasch, B. (2011). Labile or stable: opposing consequences for memory when reactivated during waking and sleep. *Nat. Neurosci.* 14, 381–386. doi: 10.1038/nn.2744

Diekelmann, S., Wilhelm, I., Wagner, U., and Born, J. (2013). Sleep to implement an intention. *Sleep* 36, 149–153. doi: 10.5665/sleep.2322

Dinges, D. F. (1995). An overview of sleepiness and accidents. *J. Sleep Res.* 4, 4–14. doi: 10.1111/j.1365-2869.1995.tb00220.x

Dinges, D. F., Pack, F., Williams, K., Gillen, K. A., Powell, J. W., Ott, G. E., et al. (1997). Cumulative sleepiness, mood disturbance and psychomotor vigilance performance decrements during a week of sleep restricted to 4–5 hours per night. *Sleep* 20, 267–277.

Doyon, J., Korman, M., Morin, A., Dostie, V., Hadj Tahar, A., Benali, H., et al. (2009). Contribution of night and day sleep vs. simple passage of time to the consolidation of motor sequence and visuomotor adaptation learning. *Exp. Brain Res.* 195, 15–26. doi: 10.1007/s00221-009-1748-y

Drummond, S. P., Brown, G. G., Salamat, J. S., and Gillin, J. C. (2004). Increasing task difficulty facilitates the cerebral compensatory response to total sleep deprivation. *Sleep* 27, 445–451.

Drummond, S. P. A., Gillin, J. C., and Brown, G. G. (2001). Increased cerebral response during divided attention task following sleep deprivation. *J. Sleep Res.* 10, 85–92. doi: 10.1046/j.1365-2869.2001.00245.x

Empson, J. A. C., and Clarke, P. (1970). Rapid eye movements and remembering. *Nature* 227, 287–288. doi: 10.1038/227287a0

Everson, C. A., Bergmann, B. M., and Rechtschaffen, A. (1989). Sleep deprivation in the rat. III. Total sleep deprivation. *Sleep* 12, 13–21.

Ferrara, M., and De Gennaro, L. (2011). Going local: insights from EEG and stereo-EEG studies of the human sleep-wake cycle. *Curr. Top. Med. Chem.* 11, 2423–2437. doi: 10.2174/156802611797470268

Fowler, M., Sullivan, M., and Ekstrand, B. (1973). Sleep and memory. *Science* 179, 302–304. doi: 10.1126/science.179.4070.302

Gardner, E. D., Thomas, L. M., and Morin, F. (1955). Cortical projections of fast visceral afferents in the cat and monkey. *Am. J. Physiol.* 183, 438–444.

Genzel, L., Dresler, M., Wehrle, R., Grözinger, M., and Steiger, A. (2009). Slow wave sleep and REM sleep awakenings do not affect sleep dependent memory consolidation. *Sleep* 32, 302–310.

Glass, B. D., Maddox, W. T., Bowen, C., Savarie, Z. R., Mattews, M. D., Markman, A. B., et al. (2011). The effects of 24-hour sleep deprivation on the exploration-exploitation trade-off. *Biol. Rhythm Res.* 42, 99–110. doi: 10.1080/09291011003726532

Halász, P., Pál, I., and Rajna, P. (1985). K-complex formation of the EEG in sleep. A survey and new examinations. *Acta Physiol. Hung.* 65, 3–35.

Harrison, Y., and Horne, J. A. (2000). The impact of sleep deprivation on decision making: a review. *J. Exp. Psychol. Appl.* 6, 236–249. doi: 10.1037/1076-898x.6.3.236

Head, H. (1896). On disturbances of sensation with especial reference to the pain of visceral disease. *Brain* 19, 211–276. doi: 10.1093/brain/19.2-3.153

Heald, S., Siebers, R. W., and Maling, T. J. (1989). K-complex vasoconstrictor response: evidence for central vasomotor downregulation in borderline hypertension. *J. Hypertens. Suppl.* 7, S28–S29. doi: 10.1097/00004872-198900076-00011

Hobson, A. R., Chizh, B., Hicks, K., Aziz, Q., Worthen, S., Lawrence, P., et al. (2010). Neurophysiological evaluation of convergent afferents innervating the human esophagus and area of referred pain on the anterior chest wall. *Am. J. Physiol. Gastrointest. Liver Physiol.* 298, G31–G36. doi: 10.1152/ajpgi.00288.2009

Hornung, O. P., Regen, F., Danker-Hopfe, H., Schredl, M., and Heuser, I. (2007). The relationship between REM sleep and memory consolidation in old age and effects of cholinergic medication. *Biol. Psychiatry* 61, 750–757. doi: 10.1016/j.biopsych.2006.08.034

Hornyak, M., Cejnar, M., Elam, M., Matousek, M., and Wallin, B. G. (1991). Sympathetic muscle nerve activity during sleep in man. *Brain* 114, 1281–1295. doi: 10.1093/brain/114.3.1281

Huber, R., Ghilardi, M. F., Massimini, M., Ferrarelli, F., Riedner, B. A., Peterson, M. J., et al. (2006). Arm immobilization causes cortical plastic changes and locally decreases sleep slow wave activity. *Nat. Neurosci.* 9, 1169–1176. doi: 10.1038/nn1758

Hughes, H. C., and Mullikin, W. H. (1984). Brainstem afferents to the lateral geniculate nucleus of the cat. *Exp. Brain Res.* 54, 253–258. doi: 10.1007/bf00236224

Johnson, L. C., and Karpan, W. E. (1968). Autonomic correlates of the spontaneous K-complex. *Psychophysiology* 4, 444–452. doi: 10.1111/j.1469-8986.1968.tb02785.x

Kattler, H., Dijk, D. J., and Borbély, A. A. (1994). Effect of unilateral somatosensory stimulation prior to sleep on the sleep EEG in humans. *J. Sleep Res.* 3, 159–164. doi: 10.1111/j.1365-2869.1994.tb00123.x

Keisler, A., Ashe, J., and Willingham, D. T. (2007). Time of day accounts for overnight improvement in sequence learning. *Learn. Mem.* 14, 669–672. doi: 10.1101/lm.751807

Krueger, J. M., and Obál, F. (1993). A neuronal group theory of sleep function. *J. Sleep Res.* 2, 63–69. doi: 10.1111/j.1365-2869.1993.tb00064.x

Krueger, J. M., Rector, D. M., Roy, S., Van Dongen, H. P., Belenky, G., and Panksepp, J. (2008). Sleep as a fundamental property of neuronal assemblies. *Nat. Rev. Neurosci.* 9, 910–919. doi: 10.1038/nrn2521

Kuo, D. C., Krauthamer, G. M., and Yamasaki, D. S. (1981). The organization of visceral sensory neurons in thoracic dorsal root ganglia (DRG) of the cat studied by horseradish peroxidase (HRP) reaction using the cryostat. *Brain Res.* 208, 187–191. doi: 10.1016/0006-8993(81)90630-2

Lo, J. C., Groeger, J. A., Santhi, N., Arbon, E. L., Lazar, A. S., Hasan, S., et al. (2012). Effects of partial and acute total sleep deprivation on performance across cognitive domains, individuals and circadian phase. *PLoS One* 7:e45987. doi: 10.1371/journal.pone.0045987

Maddox, W. T., Glass, B. D., Wolosin, S. M., Savarie, Z. R., Bowen, C., Matthews, M. D., et al. (2009). The effects of sleep deprivation on information-integration categorization performance. *Sleep* 32, 1439–1448.

Mander, B. A., Santhanam, S., Saletin, J. M., and Walker, M. P. (2011). Wake deterioration and sleep restoration of human learning. *Curr. Biol.* 21, R183–R184. doi: 10.1016/j.cub.2011.01.019

Maquet, P. (2001). The role of sleep in learning and memory. *Science* 294, 1048–1052. doi: 10.1126/science.1062856

McCoyand, G., and Strecker, R. E. (2011). The cognitive cost of sleep lost. *Neurobiol. Learn. Mem.* 96, 564–582. doi: 10.1016/j.nlm.2011.07.004

McDermott, C. M., LaHoste, G. J., Chen, C., Musto, A., Bazan, N. G., and Magee, J. C. (2003). Sleep deprivation causes behavioral, synaptic and membrane excitability alterations in hippocampal neurons. *J. Neurosci.* 23, 9687–9695.

Mitler, M. M., Carskadon, M. A., Czeisler, C. A., Dement, W. C., Dinges, D. F., and Graeber, R. C. (1988). Catastrophes, sleep, and public policy: consensus report. *Sleep* 11, 100–109.

Monstad, P., and Guilleminault, C. (1999). Cardiovascular changes associated with spontaneous and evoked K-complexes. *Neurosci. Lett.* 263, 211–213. doi: 10.1016/s0304-3940(99)00142-1

Mukhametov, L. M. (1984). Sleep in marine mammals. *Exp. Brain Res.* 8, 227–238. doi: 10.1007/978-3-642-69554-4_17

Mukhametov, L. M., Supin, A. Y., and Polyakova, I. G. (1977). Interhemispheric asymmetry of the electroencephalographic sleep patterns in dolphins. *Brain Res.* 134, 581–584. doi: 10.1016/0006-8993(77)90835-6

Nedergaard, M. (2013). Garbage truck of the brain. *Science* 340, 1529–1530. doi: 10.1126/science.1240514

Niiyama, Y., Sato, N., Katsuzava, O., and Hishikawa, Y. (1996). Electrophysiological evidence suggesting that sensory stimuli of unknown origin induced spontaneous K-complexes. *Electroencephalogr. Clin. Neurophysiol.* 98, 394–400. doi: 10.1016/0013-4694(96)95103-2

Okada, H., Iwase, S., Mano, T., Sugiyama, Y., and Watanabe, T. (1991). Changes in muscle sympathetic nerve activity during sleep in humans. *Neurology* 41, 1961–1966. doi: 10.1212/wnl.41.12.1961

Oniani, T. N., Koridze, M. G., Kavkasidze, M. G., and Gvetadze, L. B. (1974). "The dynamics in excitability of various brain structures during different phases of wakefulness-sleep cycle," in *Neirofiziologia Emotsii I Tsikla Bodrstvovanie-Son*, ed T. N. Oniani (Tbilisi: Metsniereba), 120–159.

Pampiglione, G., and Ackner, B. (1958). The effects of repeated stimuli upon EEG and vasomotor activity during sleep in man. *Brain* 81, 64–74. doi: 10.1093/brain/81.1.64

Patton, H. D., and Amassian, V. E. (1952). Cortical projection zone of chorda tympany nerve in cat. *J. Neurophysiol.* 15, 245–254.

Peles, S. H., Miranda, A., Shaker, R., and Sengupta, J. N. (2004). Acute nociceptive somatic stimulus sensitizes neurones in the spinal cord to colonic distension in the rat. *J. Physiol.* 560, 291–302. doi: 10.1113/jphysiol.2004.069070

Perry, M. J., and Lawson, S. N. (1998). Differences in expression of oligosaccharides, neuropeptides, carbonic anhydrase and neurofilament in rat primary afferent neurons retrogradely labelled via skin, muscle or visceral nerves. *Neuroscience* 85, 293–310. doi: 10.1016/s0306-4522(97)00629-5

Pigarev, I. N., Almirall, H., Marimon, J., and Pigareva, M. L. (2004). Dynamic pattern of the viscero-cortical projections during sleep. Study in New Zealand rabbits. *J. Sleep Res.* 13(Suppl. 1), 574–575.

Pigarev, I. N. (1984). New visual area on the inferior bank of the cruciate sulcus of the cat brain. *Neirofiziologiia* 16, 766–773.

Pigarev, I. N. (1994). Neurons of visual cortex respond to visceral stimulation during slow wave sleep. *Neuroscience* 62, 1237–1243. doi: 10.1016/0306-4522(94)90355-7

Pigarev, I. N. (1997). Partial sleep in cortical areas. *WFSRS Newsletters* 5, 7–8.

Pigarev, I. N. (2014). The visceral theory of sleep. *Neurosci. Behav. Physiol.* 44, 421–434. doi: 10.1007/s11055-014-9928-z

Pigarev, I. N., Almirall, H., and Pigareva, M. L. (2008). Cortical evoked responses to magnetic stimulation of macaque's abdominal wall in sleep-wake cycle. *Acta Neurobiol. Exp. (Wars)* 68, 91–96.

Pigarev, I. N., Almirall, H., Pigareva, M. L., Bautista, V., Sánchez-Bahillo, A., Barcia, C., et al. (2006). Visceral signals reach visual cortex during slow wave sleep: study in monkeys. *Acta Neurobiol. Exp. (Wars)* 66, 69–73.

Pigarev, I. N., Bagaev, V. A., Busigina, I. I., and Bibikov, N. G. (2010). "The state of sleep – period of the cortical control of the visceral functions," in *The Regulation of Physiological Functions During Adaptation to Environmental Changes*, (St.-Petersburg: I.P. Pavlov Institute of Physiology), 228.

Pigarev, I. N., Bagaev, V. A., Levichkina, E. V., Fedorov, G. O., and Busigina, I. I. (2013). Cortical visual areas process intestinal information during the periods slow-wave sleep. *Neurogastroenterol. Motil.* 25, 268–275, e169. doi: 10.1111/nmo.12052

Pigarev, I. N., Fedorov, G. O., Levichkina, E. V., Marimon, J. M., Pigareva, M. L., and Almirall, H. (2011). Visually triggered K-complexes: a study in New Zealand rabbits. *Exp. Brain Res.* 210, 131–142. doi: 10.1007/s00221-011-2606-2

Pigarev, I. N., and Feodorov, G. O. (2012). "Reflection of the heart beats in the cortical electrical activity during sleep," in *Physiology of the Visceral Systems*, eds E. L. Poliakov and V. N. Shouvaeva (S.-Petersbourg: Pavlov Inst. Physiology Press), 182.

Pigarev, I. N., Nothdurft, H.-Ch., Rodionova, E. I., and Kastner, S. (1996). Asynchronous sleep development in cortical areas. *J. Sleep Res.* 5(Suppl. 1), 176.

Pigarev, I. N., Nothdurft, H.-Ch., and Kastner, S. (1997). Evidence for asynchronous development of sleep in cortical areas. *Neuroreport* 8, 2557–2560. doi: 10.1097/00001756-199707280-00027

Pigarev, I. N., and Pigareva, M. L. (2013). Sleep, emotions and visceral control. *Hum. Physiol.* 39, 590–601. doi: 10.1134/s036211971306008x

Pigarev, I. N., and Pigareva, M. L. (2012). Sleep and control of visceral functions. *Neurosci. Behav. Physiol.* 42, 948–956. doi: 10.1007/s11055-012-9661-4

Plihal, W., and Born, J. (1997). Effects of early and late nocturnal sleep on declarative and procedural memory. *J. Cogn. Neurosci.* 9, 534–547. doi: 10.1162/jocn.1997.9.4.534

Ratcliff, R., and Van Dongen, H. P. A. (2009). Sleep deprivation affects multiple distinct cognitive processes. *Psychon. Bull. Rev.* 16, 742–751. doi: 10.3758/pbr.16.4.742

Rechtshaffen, A., and Bergmann, B. M. (2002). Sleep deprivation in the rat: an update of the 1989 paper. *Sleep* 25, 18–24.

Rector, D. M., Topchiy, I. A., Carter, K. M., and Rojas, M. J. (2005). Local functional state differences between rat cortical columns. *Brain Res.* 1047, 45–55. doi: 10.1016/j.brainres.2005.04.002

Reis, J., Fischer, J. T., Prichard, G., Weiller, C., Cohen, L. G., and Fritsch, B. (2013). Time–but not sleep-dependent consolidation of tDCS-enhanced visuomotor skills. *Cereb. Cortex* doi: 10.4324/9780080473321. [Epub ahead of print].

Rigas, P., and Castro-Alamancos, M. A. (2007). Thalamo-cortical Up states: different effects of intrinsic and extrinsic cortical inputs on persistent activity. *J. Neurosci.* 27, 4261–4272. doi: 10.1523/jneurosci.0003-07.2007

Robertson, E. M., Pascual-Leone, A., and Press, D. Z. (2004). Awareness modifies the skill-learning benefits of sleep. *Curr. Biol.* 14, 208–212. doi: 10.1016/s0960-9822(04)00039-9

Sanchez-Vives, M. V., and McCormick, D. A. (2000). Cellular and network mechanisms of rhythmic recurrent activity in neocortex. *Nat. Neurosci.* 3, 1027–1034. doi: 10.1038/79848

Saxvig, I. W., Lundervold, A. J., Gronli, J., Ursin, R., Bjorvatn, B., and Portas, C. M. (2008). The effect of a REM sleep deprivation procedure on different aspects of memory function in humans. *Psychophysiology* 45, 309–317. doi: 10.1111/j.1469-8986.2007.00623.x

Shadmehr, R., and Brashers-Krug, T. (1997). Functional stages in the formation of human long-term motor memory. *J. Neurosci.* 17, 409–419.

Siengsukon, C. F., and Boyd, L. A. (2008). Sleep enhances implicit motor skill learning in individuals poststroke. *Top. Stroke Rehabil.* 15, 1–12. doi: 10.1310/tsr1501-1

Smith, C. (2001). Sleep states and memory processes in humans: procedural versus declarative memory systems. *Sleep Med. Rev.* 5, 491–506. doi: 10.1053/smrv.2001.0164

Song, S., Howard, J. H., and Howard, D. V. (2007). Sleep does not benefit probabilistic motor sequence learning. *J. Neurosci.* 27, 12475–12483. doi: 10.1523/jneurosci.2062-07.2007

Steriade, M., Timofeev, I., and Grenier, F. (2001). Natural waking and sleep states: a view from inside neocortical neurons. *J. Neurophysiol.* 85, 1969–1985.

Stickgold, R. (2005). Sleep-dependent memory consolidation. *Nature* 437, 1272–1278. doi: 10.1038/nature04286

Tank, J., Diedrich, A., Hale, N., Niaz, F. E., Furlan, R., Robertson, R. M., et al. (2003). Relationship between blood pressure, sleep K-complexes and muscle sympathetic nerve activity in humans. *Am. J. Physiol. Regul. Integr. Comp. Physiol.* 285, R208–R214.

Timofeev, I., Grenier, F., and Bazhenov, M. (2000). Origin of slow cortical oscillations in deafferented cortical slabs. *Cereb. Cortex* 10, 1185–1199. doi: 10.1093/cercor/10.12.1185

Tononi, G., and Cirelli, C. (2003). Sleep and synaptic homeostasis: a hypothesis. *Brain Res. Bull.* 62, 143–150. doi: 10.1016/j.brainresbull.2003.09.004

Tononi, G., and Cirelli, C. (2006). Sleep function and synaptic homeostasis. *Sleep Med. Rev.* 10, 49–62. doi: 10.1016/j.smrv.2005.05.002

Voderholzer, U., Piosczyk, H., Holz, J., Landmann, N., Feige, B., Loessl, B., et al. (2011). Sleep restriction over several days does not affect long-term recall of declarative and procedural memories in adolescents. *Sleep Med.* 12, 170–178. doi: 10.1016/j.sleep.2010.07.017

Vyazovskiy, V. V., Olcese, U., Hanlon, E. C., Nir, Y., Cirelli, C., and Tononi, G. (2011). Local sleep in awake rats. *Nature* 472, 443–447. doi: 10.1038/nature10009

Walker, M. P. (2008). Cognitive consequences of sleep and sleep loss. *Sleep Med.* 9, S29–S34. doi: 10.1016/s1389-9457(08)70014-5

Walker, M. P. (2009). The role of sleep in cognition and emotion. *Ann. N Y Acad. Sci.* 1156, 168–197. doi: 10.1111/j.1749-6632.2009.04416.x

Walker, M. P., and Stickgold, R. (2006). Sleep, memory, and plasticity. *Annu. Rev. Psychol.* 57, 139–166. doi: 10.1146/annurev.psych.56.091103.070307

Werth, E., Achermann, P., and Borbely, A. A. (1996). Brain topography of the human sleep EEG: antero-posterior shifts of spectral power. *Neuroreport* 8, 123–127. doi: 10.1097/00001756-199612200-00025

Werth, E., Achermann, P., and Borbely, A. A. (1997). Fronto-occipital EEG power gradients on human sleep. *J. Sleep Res.* 6, 102–112. doi: 10.1046/j.1365-2869.1997.d01-36.x

Williamson, A. M., Feyer, A., Mattick, R. P., Friswell, R., and Finlay-Brown, S. (2001). Developing measures of fatigue using an alcohol comparison to validate the effects of fatigue on performance. *Accid. Anal. Prev.* 33, 313–326. doi: 10.1016/s0001-4575(00)00045-2

Xie, L., Kang, H., Xu, Q., Chen, M. J., Liao, Y., Thiyagarajan, M., et al. (2013). Sleep drives metabolite clearance from the adult brain. *Science* 342, 373–377. doi: 10.1126/science.1241224

Yoo, S. S., Hu, P. T., Gujar, N., Jolesz, F. A., and Walker, M. P. (2007). A deficit in the ability to form new human memories without sleep. *Nat. Neurosci.* 10, 385–392. doi: 10.1038/nn1851

Conflict of Interest Statement: The authors declare that the research was conducted in the absence of any commercial or financial relationships that could be construed as a potential conflict of interest.

Received : 23 January 2014; accepted: 14 April 2014; published online: 01 May 2014.
Citation: Pigarev IN and Pigareva ML (2014) Partial sleep in the context of augmentation of brain function. Front. Syst. Neurosci. ***8****:75. doi: 10.3389/fnsys.2014.00075*
This article was submitted to the journal Frontiers in Systems Neuroscience.

frontiers in
SYSTEMS NEUROSCIENCE

REVIEW ARTICLE
published: 03 November 2014
doi: 10.3389/fnsys.2014.00206

Should I stay or should I go? Conceptual underpinnings of goal-directed actions

***Giovanni Mirabella*[1,2] ***

[1] *Istituto Neurologico Mediterraneo, IRCCS Neuromed, Pozzilli, Italy*
[2] *Department of Physiology and Pharmacology 'V. Erspamer,' La Sapienza University, Rome, Italy*

Edited by:
Manuel Casanova, University of Louisville, USA

Reviewed by:
Satoshi Tsujimoto, Kobe University, Japan
Mikhail Lebedev, Duke University, USA

***Correspondence:**
Giovanni Mirabella, Istituto Neurologico Mediterraneo, IRCCS Neuromed, via Atinense 18, 86077 Pozzilli, Italy
e-mail: giovanni.mirabella@uniroma1.it

All actions, even the simplest like moving an arm to grasp a pen, are associated with energy costs. Thus all mobile organisms possess the ability to evaluate resources and select those behaviors that are most likely to lead to the greatest accrual of valuable items (reward) in the near or, especially in the case of humans, distant future. The evaluation process is performed at all possible stages of the series of decisions that lead to the building of a goal-directed action or to its suppression. This is because all animals have a limited amount of energy and resources; to survive and be able to reproduce they have to minimize the costs and maximize the outcomes of their actions. These computations are at the root of behavioral flexibility. Two executive functions play a major role in generating flexible behaviors: (i) the ability to predict future outcomes of goal-directed actions; and (ii) the ability to cancel them when they are unlikely to accomplish valuable results. These two processes operate continuously during the entire course of a movement: during its genesis, its planning and even its execution, so that the motor output can be modulated or suppressed at any time before its execution. In this review, functional interactions of the extended neural network subserving generation and inhibition of goal-directed movements will be outlined, leading to the intriguing hypothesis that the performance of actions and their suppression are not specified by independent sets of brain regions. Rather, it will be proposed that acting and stopping are functions emerging from specific interactions between largely overlapping brain regions, whose activity is intimately linked (directly or indirectly) to the evaluations of pros and cons of an action. Such mechanism would allow the brain to perform as a highly efficient and flexible system, as different functions could be computed exploiting the same components operating in different configurations.

Keywords: decision-making, reward, voluntary motor control, behavioral flexibility, countermanding task, reaching arm movements

INTRODUCTION

Our survival depends on the ability to gather, parse and evaluate the stream of constantly changing environmental stimuli and to flexibly adapt our behavioral responses according to the context in which we are embedded. This is because all animals operate with limited resources, and thus the way they value their internal states, sensory experience, and behavioral output influences directly how they will invest their time and energy (Rangel et al., 2008). The bottom line is that the opportunity of executing any action needs to be continuously evaluated in order to minimize its costs and to maximize its payoffs. In fact, the value associated with a certain stimulus is not an intrinsic property of the stimulus, but can change as a function of the internal states of the agent at the time the stimulus is encountered and as a function of agent's previous experience with that stimulus. For instance, for a thirsty gazelle the water of a pond might represent a highly valuable stimulus, unless it perceives the presence of hungry lions.

Central to this process are two executive functions: (i) the ability to predict the future outcomes of a given action; and (ii) the ability to suppress inappropriate, i.e., not sufficiently valuable, actions. Importantly, these two executive functions operate not only during the genesis of an action, but also during the planning of an already selected action. In fact, during the temporal gap between the time when an action has been chosen and the moment when the motor output is going to be generated, the context might have changed, altering the computed value of the action and thus requiring a radical change of the planned motor strategy. For instance, the sight of a tasty cake is likely to drive a child to plunge his fingers into the cream, but if, when he is about to act, he suddenly feels he is observed by his parents, he will refrain from executing the planned movement. In this instance, the fear of being punished has overcome the potential reward of a sweet food, causing the suppression of the pending action.

Conceptually, a goal-directed action can be modeled as multi-step decision process to which several brain regions contribute (see **Figure 1**; **Table 1**). The different stages leading up to the execution or the inhibition of an action are described in the next sections. The model I propose has been inspired by that suggested by Haggard (2008). However, there are two key differences between the former and the latter. First of all, the new model does not necessarily subserve human volition (see paragraph 'Concluding Thoughts'). Secondly, in this new

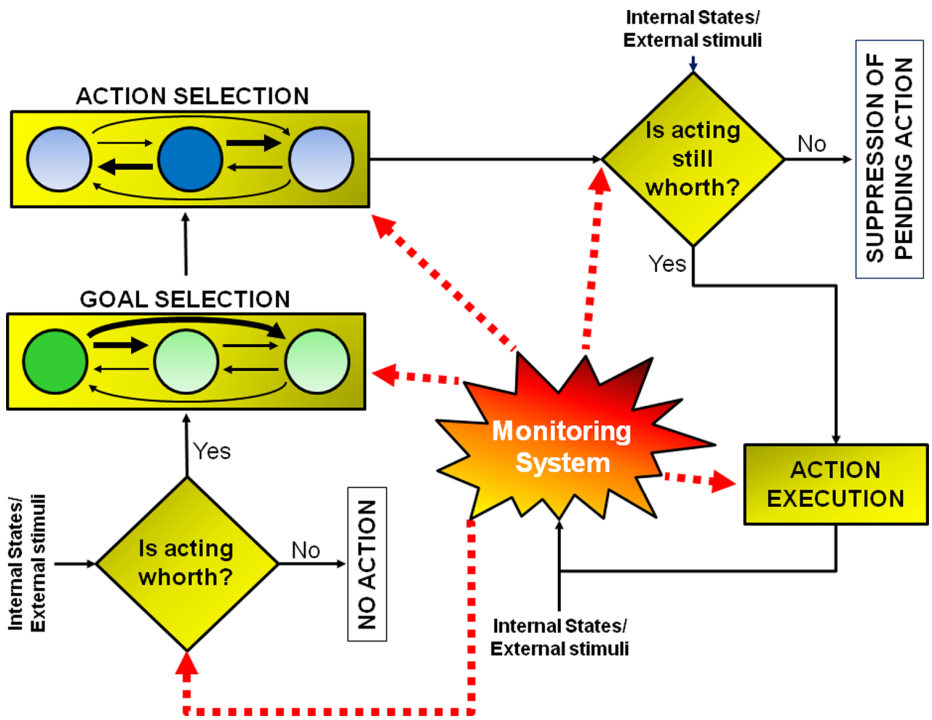

FIGURE 1 | Model of goal-directed actions. The model consists of a set of a multi-step decision processes leading either to the execution or to the inhibition of an action, according to the evaluation of its pros and cons. This model does not have a strictly serial or parallel architecture. Some processes must occur before others (e.g., the early "should-I-stay-or-should-I-go" decision aimed at evaluating whether acting is worthwhile must occur before goal or action selection), but other processes occur in parallel (e.g., the monitoring system, whose role is to compute predictions about future reward and to measure discrepancies between expected and actual outcomes, is active during all the steps). See text for further details.

model, each stage of the process can be influenced by a component named monitoring system, according to the results of the outcomes of previous decisions (see paragraph 'The Monitoring System'). As a consequence the model I propose does not work strictly in a serial fashion, but both serially and in parallel.

Before proceeding, I want to remark that I will mostly deal with upper limb action control, leaving aside saccadic eye movement control. This is because the saccadic system has a different functional organization from that controlling arm and hand movements (e.g., see Churchland and Shenoy, 2007; Schall and Godlove, 2012). For instance, a number of studies have provided evidence that the inhibitory controls of eye and hand movements are independent (e.g., Logan and Irwin, 2000; Boucher et al., 2007; Sumner et al., 2007; Mirabella et al., 2011). Interestingly, Mirabella et al. (2009) and Stevenson et al. (2009) studied the effect of introducing a temporal gap between the end of the fixation and target presentation on the reaction times (RTs) and on the speed of inhibition of reaching movements and saccades, respectively. They found contrasting results: in the former study the gap produced a decrease in the inhibitory speed and in the latter an increase. This is not odd, as saccades have a different ecological relevance from hand and arm movements in primates. In fact, outside neurophysiology laboratories, they allow physical interactions with the environment, thus leading to material outcomes such as acquisition of food or tools. Nevertheless, it is likely that the very general principles, not the fine details, of the genesis of eye and limb movements are rather similar.

THE MOTIVATION TO ACT (EARLY "SHOULD-I-STAY-OR-SHOULD-I-GO" DECISION)

The first step is represented by the motivation to act (early "should-I-stay-or-should-I-go" decision). This is determined by an evaluation process which is aimed at determining whether or not the individual's current needs are satisfied. The evaluative process can be primed because of a change in either the external environment (e.g., the sight of a cake) or the internal states (e.g., a sudden hungry feeling), or both (e.g., the sight of a cake prompts a hungry feeling). Thus, these first computations would evaluate whether or not the current state has to be changed to pursue a desire (e.g., eating) against several possible constraints (e.g., eating too much might cause weight gain). If the motivation is considered worthwhile then movement preparation will jump to the next stage, otherwise it will be canceled.

This is an essential process and one which is continuously performed by our motor system. In fact, in most places where we live, if not all, we are surrounded by tools whose sight automatically activates motor schemas that would normally be employed to interact with those objects. These actions are prompted by the features of the objects, the so-called affordances (Gibson,

Table 1 | Summary of the main brain regions involved in each stage of the model describing the genesis of an arm goal oriented action, together with the most relevant references.

Early "should-I-stay-or-should-I-go" decision	SMA/pre-SMA	Boccardi et al. (2002), Grezes and Decety (2002), Biran and Chatterjee (2004), Sumner et al. (2007), Forstmann et al. (2008), Ridderinkhof et al. (2011), van Gaal et al. (2011)
	Sector F5 (subregion of PMv)/PPC	Murata et al. (1997), Rizzolatti and Luppino (2001)
	Basal ganglia (dopaminergic neurons; putamen and pallidum)	Mazzoni et al. (2007), Schmidt et al. (2008), Bonanni et al. (2010), for a review see Turner and Desmurget (2010)
Goal selection	OFC	Damasio (1994), Padoa-Schioppa and Assad (2006), Fellows and Farah (2007), Padoa-Schioppa and Assad (2008), for a review see Wallis (2007)
	LPFC	Hoshi et al. (2000), Barraclough et al. (2004), Genovesio et al. (2005, 2012), for a review see Wise (2008)
Action selection	PMd	Cisek and Kalaska (2005), Klaes et al. (2011), for a review see Cisek and Kalaska (2010)
	PRR	Calton et al. (2002), Cui and Andersen (2007), Scherberger and Andersen (2007)
Late "should-I-stay-or-should-I-go" decision	IFG/DLPFC (subregions of LPFC)	Aron et al. (2003), Aron and Poldrack (2006), Chambers et al. (2006), Aron et al. (2007), Zheng et al. (2008), Zandbelt and Vink (2010), Jahfari et al. (2012), Zandbelt et al. (2013), for a review see Aron et al. (2014)
	Pre-SMA	Aron et al. (2007), Li et al. (2008), Chen et al. (2010), Zandbelt and Vink (2010), Jahfari et al. (2012), Zandbelt et al. (2013)
	Basal ganglia (striatum, STN)	Aron and Poldrack (2006), Van den Wildenberg et al. (2006), Aron et al. (2007), Li et al. (2008), Zandbelt and Vink (2010), Swann et al. (2011), Mirabella et al. (2012)
	PMd and M1	Coxon et al. (2006), Swann et al. (2009), Mirabella et al. (2011), Mattia et al. (2012), Mattia et al. (2013)
	PPC	Chikazoe et al. (2009), Jahfari et al. (2010), Zandbelt et al. (2013)
Action execution	PMd and M1	Tanji and Evarts (1976), Georgopoulos et al. (1982), Weinrich et al. (1984), Riehle and Requin (1989), Hoshi and Tanji (2000), Hoshi and Tanji (2002), Churchland et al. (2006), for a review see Shenoy et al. (2013)
	Spinal cord	Prut and Fetz (1999)
	Basal ganglia (STN)	Paradiso et al. (2003), Loukas and Brown (2004), Mirabella et al. (2013)
Monitoring system	ACC	Bernstein et al. (1995), Brown and Braver (2005), Kennerley et al. (2006), Sheth et al. (2012)
	Basal ganglia (dopaminergic neurons; ventral striatum)	Schultz et al. (1997), O'Doherty et al. (2003), Montague et al. (2004), Bayer and Glimcher (2005), Chikazoe et al. (2009), Zandbelt and Vink (2010), Jahfari et al. (2012), Zandbelt et al. (2013)
	Frontal pole cortex (subregion of PFC)	Tsujimoto et al. (2010), for a review see Tsujimoto et al. (2011)
	SMA/pre-SMA	Chikazoe et al. (2009), Chen et al. (2010), Scangos and Stuphorn (2010), Zandbelt and Vink (2010), Jahfari et al. (2012), Zandbelt et al. (2013), Bonini et al. (2014)

SMA, supplementary motor area; pre-SMA, pre-supplementary motor area; PMv, ventral premotor cortex; PPC, posterior parietal cortex; LPFC, lateral prefrontal cortex; DLPFC, dorsolateral prefrontal cortex; PMd, dorsal premotor cortex; PRR, parietal reach region; IFG, inferior frontal gyrus; STN, subthalamic nucleus; M1, primary motor cortex; ACC, anterior cingulate cortex; FPC, frontal pole cortex.

1979). It has been shown that even the simple observation of pictures depicting affordable objects (such as graspable objects) activates a sub-region of the medial frontal cortex, the supplementary motor area (SMA; see **Figure 2**), even when there is no requirement to actually act on those stimuli (Grezes and Decety, 2002). These stimulus-driven activations are rapid, involuntary, and unconscious.

Sumner et al. (2007), using subliminal stimuli to prime movements in a direction opposite to the requested one, showed that while control subjects were able to withhold unwanted actions, patients with microlesions of the SMA or the supplementary eye fields (SEFs) were impaired during the execution of hand or eye movements, respectively. They concluded that the SMA and SEF mediate automatic effector-specific suppression of motor plans.

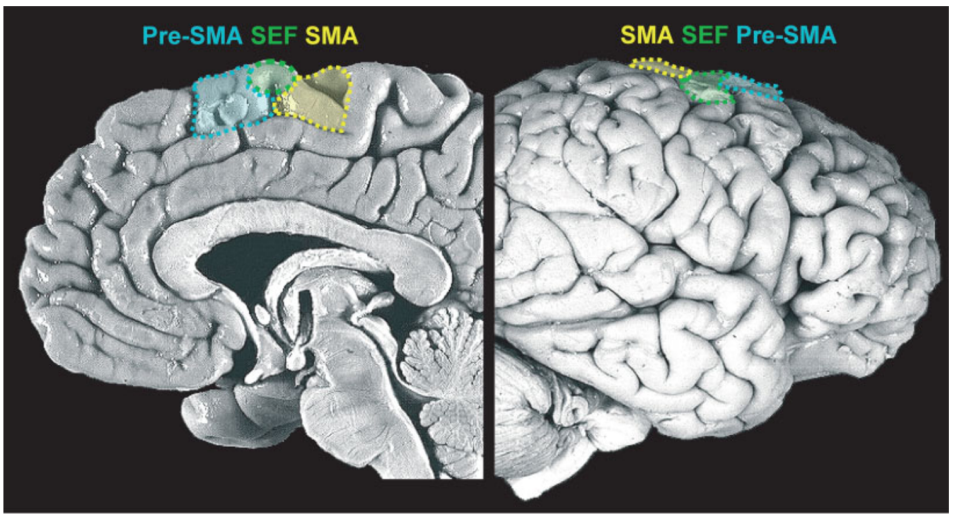

FIGURE 2 | Medial frontal cortex (details of the medial portion of Brodmann areas 6 and 8). Midsagittal view of the medial wall **(left)** and lateral prefrontal cortex (LPFC) surface **(right)**, delineating the supplementary motor area (SMA), supplementary eye field (SEF) and pre-supplementary motor area (pre-SMA). Reproduced with permission from Ridderinkhof et al. (2011).

However, there is another way to look at those automatic activations: they might represent the activity of the network subserving the evaluative process which is at the base of the early "should-I-stay-or-should-I-go" decision. In other words, affordances might increase the motivation to act, but to execute an action they have to be coupled with an internal state congruent with the primed action (e.g., the sight of a glass of water will prime the action if and only if an individual is thirsty; see **Figure 1**).

From this perspective the suppression of a triggered action might be seen not as an active process, but rather as an automatic consequence of the evaluative procedure. Using this framework, is possible to put forward a functional hypothesis underling two rare neuropsychological disorders, the alien limb syndrome and the utilization behavior. Both diseases are characterized by the fact that patients cannot resist objects' affordance, and they are automatically forced to perform stimulus-driven motor responses even when they do not need those objects (Humphreys and Riddoch, 2000). Patients with the alien hand syndrome perform involuntary actions with the limb contralateral to a focal brain lesion most frequently located in the medial frontal cortex, usually involving the SMA (Della Sala et al., 1991; Biran and Chatterjee, 2004). Patients suffering from utilization behavior compulsively grasp and use objects placed within their reach. This syndrome has been linked to bilateral damage to the medial frontal region involving the SMA, pre-SMA, and cingulate motor areas (Boccardi et al., 2002). Therefore, at least to some extent, the sites of the lesions causing those syndromes are largely overlapping, with the difference that in the former case it is located just in one hemisphere whereas in the latter case it affects both hemispheres. Possibly what is affected in both syndromes is the circuitry underlying the early "should-I-stay-or-should-I-go" evaluation, so that most stimulus-driven activations are no longer matched with our internal needs and thus they cannot be filtered out.

The discovery of the so-called canonical neurons in monkeys' lateral premotor area F5 may represent the neural mechanisms underlying responsiveness to object affordances (Murata et al., 1997). These neurons become active both when grasping an object and when seeing the same object without moving (Murata et al., 1997), and they are likely to feed the neural network of the medial frontal region which presides over the evaluation of whether to act. In fact, the lateral premotor area F5 receives projections from several regions of the posterior parietal cortex (PPC; Rizzolatti and Luppino, 2001), which is the end point of a crucial pathway for the visual guidance of actions toward objects, named the dorsal stream (Milner and Goodale, 1995). As such, PPC and F5 are likely to play a key role in visuomotor transformations, providing a neurophysiological correlate of stimulus-driven action affordance.

Several lines of evidence indicate that the fate of these activations might be decided in pre-SMA, which would act as a gate through which the available action affordances might be translated into actual actions (Ridderinkhof et al., 2011). First of all, a functional magnetic imaging (fMRI) study has shown that the strength of activation in pre-SMA covaries with the extent of inappropriate responses driven by stimulus-action association, i.e., the selection of appropriate action engages stronger activation of the pre-SMA in the face of many competing alternatives (Forstmann et al., 2008). Second, a strong negative correlation has been demonstrated between pre-SMA gray-matter volume and the inability to efficiently deal with competing response tendencies (van Gaal et al., 2011).

It would be very reductive to limit this first stage to the filtering of stimulus-driven action affordances and to the medial frontal regions. In fact, a role is surely also played by those brain regions that underlie arousal regulation (in particular the dopaminergic system), increasing or decreasing the readiness of animals to react. There are a wide variety of stimuli that can trigger arousal, from relatively simple sensory stimuli (e.g., the smell of blood or the

sound of a mating call) to much more complex situations (e.g., the feeling of social exclusion or the feeling of being idolized). These signals prompt some basic instincts or learned memories which, according to the current contextual situation, might change the internal state of the animals, triggering an alert state. In these instances, animals do not yet have a goal, but they are more ready to act. The dopaminergic system is likely to play an important role in this stage of action genesis as witnessed by one of the symptoms of the most severe form Parkinson's disease (PD), the akinesia, i.e., the inability to initiate any goal-directed movement. Akinesia is not a pure motor disturbance, because it has been shown that in situations of great emergency (e.g., a missile attack, an earthquake) otherwise akinetic PD patients can show a sudden transient ability to move (paradoxical kinesia; Glickstein and Stein, 1991; Schlesinger et al., 2007; Bonanni et al., 2010). Evidently, when dopamine neurons are remarkably reduced in number, all behavioral options or internal mental states would appear to have the same value as the current state. In the face of this flat value function, the best choice for PD patients is to freeze. In extreme situations, salient stimuli may elicit stronger discharge of dopaminergic cells than normal, driving the patient to act. Recently, Mazzoni et al. (2007) suggested that even in less dramatic situations the slowness of movements (bradikinesia) in PD patients may be attributable to an improper evaluation of movement energy costs. In these experiments, PD patients and healthy controls were asked to move their arm to a previously specified target at different speeds a given number of times. Both were able to make required movements with the same accuracy, but PD patients needed significantly more trials before reaching the required number of repetitions. As the accuracy of patients was the same as that of controls, authors concluded that the loss of dopamine did not cause bradykinesia through a speed-accuracy trade-off. Rather, it affected decision-making through a faulty evaluation of the costs of movements, i.e., allocation of the correct amount of energy to meet the demands of the task. In other words, PD weakened the key link between motivation and movement gain. In fact, the dopaminergic system has been shown to play a major role in reward-dependent learning (e.g., Schultz et al., 1997; Montague et al., 2004).

Other evidence indicates that the regulation of action motivation based on previous experiences is one of the main functions of the basal ganglia, not just of the dopaminergic system (Turner and Desmurget, 2010). This hypothesis is supported by one symptom which often accompanies focal damage of the basal ganglia, the so-called auto-activation deficit or abulia (Habib, 2004), in which patients suffer from a marked deficit in motivation to perform spontaneous acts despite an absence of overt motor impairment. In particular, Schmidt et al. (2008) asked patients suffering from auto-activation deficit, due to bilateral lesions of the putamen or pallidum, to control grip forces in response either to explicit sensory instructions or to monetary incentives. Although they fully understood the instructions, patients were capable of modulating their movement only in the former, not in the latter, condition.

All in all, it is clear that there are several brain regions that regulate the willingness to act. This early "should-I-stay-or-should-I-go" decision should play a key role because it would activate (or stop) the chain of other decisions that will potentially lead to action execution. While many other subsequent stages might be performed in parallel, this first one is likely to be a stand-alone process during which no actions are planned and thus there is no need for any neural signal to inhibit them.

GOAL SELECTION

Once performance of an action is considered worthwhile, because a need has to be satisfied, the next set of decisions will be devoted to the selection of the most opportune goal among the several different alternatives usually available (e.g., to satisfy the feeling of hunger we might decide to eat the cake in front of us or to leave the room and go to a restaurant). This process possibly entails two stages: first, values are assigned to each available option and subsequently a decision is taken weighting these values according to the behavioral context (e.g., Glimcher et al., 2005). Even though this schema is conceptually logical, it is very unlikely that neural processing would be strictly organized in distinct serial stages. As depicted in **Figure 1**, it is very likely that multiple potential goals are simultaneously represented. To each goal a given value would be assigned and weighted according to the situation. As multiple goals cannot be pursued at the same time, these representations probably start to compete with each other, perhaps through mutual inhibition (**Figure 1**). This competition can be biased by several factors which ultimately influence the expected outcome of the action[1]. In this review I will argue that these biasing signals might come from the brain regions of the "monitoring system," i.e., the system that evaluates and stores the outcome of past actions (see **Figure 1** and see The Monitoring System). Value assignment and the competition might occur at the same time, probably in different sectors of the prefrontal cortex (PFC). PFC is not a homogeneous structure but is composed of multiple areas that differ in terms of cytoarchitecture and anatomical connections with other areas (Petrides and Pandya, 1999, 2002; **Figure 3**). Thus, it is likely that each area might perform its own function; however, their exact roles are not yet clear. Part of the reason is that the PFC contributes to a bewildering array of functions (Wise, 2008).

Nevertheless, converging evidence argues that orbitofrontal cortex (OFC) plays a key role in linking stimuli to their values (for a review see Wallis, 2007). Indeed, lesions to the OFC impair choice behavior, leading to unreliable choices (e.g., Damasio, 1994; Fellows and Farah, 2007) or abnormal gambling (e.g., Camille et al., 2004; Koenigs and Tranel, 2007). Padoa-Schioppa and Assad (2006), recording single-units in monkeys, demonstrated that a particular class of neurons of the OFC ("chosen neurons") encode the subjective value of two different drinks (juice and water) irrespective of their taste, volume or the action that needs to be taken to obtain them. Thus these cells encoded value *per se*, allowing a comparison for qualitatively different goods. Later on, Padoa-Schioppa and Assad (2008) also showed that the discharge of these neurons was independent of the presence of other goods. These findings indicate that the OFC produces stable value representations, i.e., a key trait of choices, because it allows abstract comparisons such as

[1]An exception to this model might occur when the number of potential goals exceeds the capacity of working memory. In these instances goals might be processed differently.

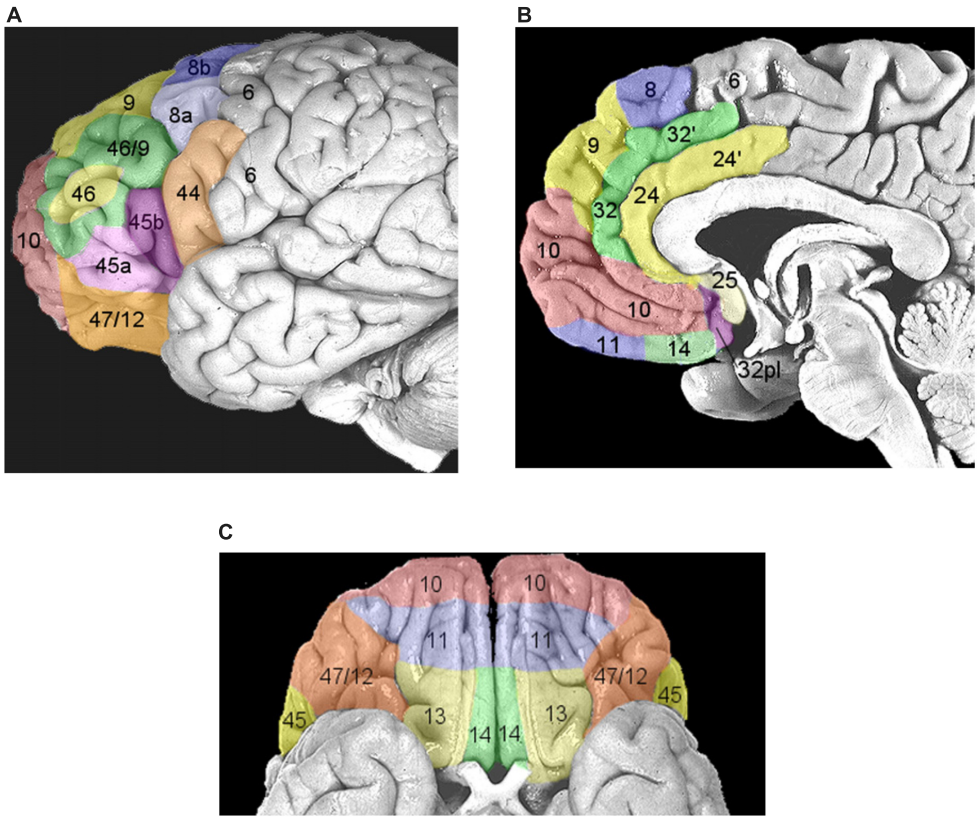

FIGURE 3 | Areas composing the prefrontal cortex (PFC) according to the parcellation of Petrides and Pandya (1999, 2002). (A) Areas of the lateral PFC. The inferior frontal gyrus (IFG) corresponds to Brodmann area (BA) 44, or pars opercolaris, to BA45, or pars triangularis, and to BA47/12, or pars orbitalis. The dorsolateral prefrontal cortex (DLPFC) corresponds to BA9/46 and BA46. **(B)** Areas of the medial wall of the PFC. The anterior cingulate cortex (ACC) corresponds to BA32, BA24, and BA25 (dorsocaudal portions are indicated with a hyphen). BA10 corresponds to the frontopolar cortex. The orbitofrontal cortex (OFC) corresponds to BA11 and BA14. **(C)** Areas of ventral orbital surface of the PFC. BA10 corresponds to the frontopolar cortex. Area BA47/12 corresponds to the pars orbitalis of the IFG. The OFC corresponds to BA11, BA13, and BA14. Reproduced with permission from Ridderinkhof et al. (2004).

transitivity between different goods which are not available at the same time.

On the other hand, to select properly the more appropriate goal, the values of the options must be evaluated in light of the situation which an animal has to face (e.g., if an animal is starving even a non-preferred food represents a good choice). Therefore, to represent value efficiently in different situations, a neuronal representation should flexibly adapt to the current context. These computations are probably carried on in lateral prefrontal cortex (LPFC). Several studies have shown that neural activities of those areas specify the so-called task sets. A task set is a configuration of perceptual, attentional, mnemonic, and motor processes that is actively maintained to perform a given task. It specifies the rules needed to solve the specific task, but it is independent of the stimuli as long as they have to be processed in the same way. Therefore it is not surprising that the PFC contributes to an enormous array of functions ranging from selective attention (Lebedev et al., 2004) to working memory (Funahashi et al., 1989), problem-solving strategies (Genovesio et al., 2005) and categorization of sensory stimuli (Freedman et al., 2002). This list is by no means exhaustive, but it is intended to give an idea of the several kinds of knowledge that are processed in the LPFC. Recently, a series of studies has provided evidence about the way in which this array of cognitive processes can be combined to produce sophisticated behavior (Genovesio et al., 2005, 2006, 2012). The logic underlying all these experiments was that of setting tasks which require several kinds of long-term and short-term knowledge, while recording single-unit activity in the LPFC. For instance, Genovesio et al. (2005) trained monkeys to make a saccade to the left, right, or upward direction in response to a visual object, depending on the cue and on the goal that had occurred on the previous trial (**Figure 4**). This way the monkeys could not learn a fixed stimulus-response association. Instead, they had to adopt repeat-stay and change-shift strategies, i.e., if the cue was the same as in the previous successful trial the monkeys repeated the response, while if the cue was different they had to change their response. Genovesio et al. (2005) found that the activity of some single-neurons in the dorsolateral prefrontal cortex (DLPFC) represent different strategies, that is, special kinds of abstract rules acquired on the basis of task performance history. Similarly, Barraclough et al. (2004) found that DLPFC neurons encoded monkeys' past decisions and payoffs, providing crucial

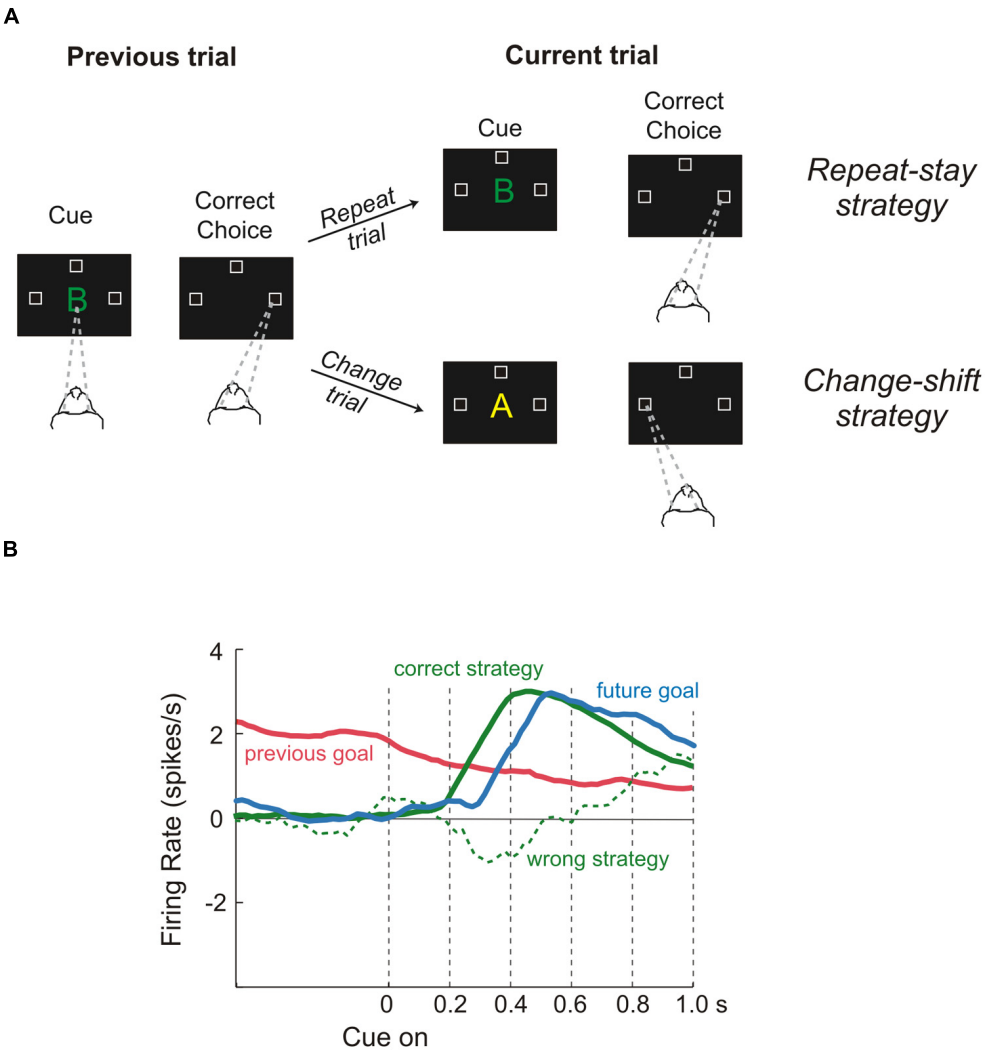

FIGURE 4 | Role of dorsolateral prefrontal cortex during a "strategy task." (A) Temporal sequence of the visual displays during the task and behavioral responses required of the monkeys. Each trial began when monkeys fixated on a spot at the center of the display (gaze direction is indicated by the dashed lines). After a delay, a cue appeared. When it disappeared, the monkeys had to make a saccadic eye movement to one of three positions (unfilled squares). Monkeys were required to remember both the cue and the goal of the trial just performed because the response on the next trial (current trial) depended on the previous choice, i.e., if the cue was the same as in the previous successful trial, the monkeys repeated the response (repeat trial), while if the cue was different they had to change their response (change trial). Thus, monkeys were forced to change strategy according to the past trial history, adopting either a repeat-stay strategy or a change-shift strategy **(B)** Neural activity reflecting the previous goal (red), the future goal (blue), the correct strategy (solid green line), and the wrong strategy (dashed green line). Previous-goal signal decreased after cue onset as the signals for the correct strategy and future goal increased. In contrast, when monkeys chose the wrong strategy, a weak or absent strategy signal occurred during the time of goal selection. Reproduced with permission from Wise (2008).

signals to update estimates of expected reward. Thus, according to the authors the activity of these cells subserves the optimization of decision-making strategies. Other neurons in the same area represented fixed stimulus–response mappings learned previously (Hoshi et al., 2000).

All in all it seems that the different subregions of the LPFC process several types of knowledge and, taking into account the context in which the animals operate and the outcome of the action performed, allow the performance of non-routine, i.e., flexible, behaviors (Wise, 2008). Clearly such complex elaborations cannot be done in isolation. In fact, it has been recently proposed that information about several different metrics of available resources in the surrounding environment (e.g., numerosity, duration, distance) are provided to the LPFC by the PPC (Genovesio et al., 2014). Certainly, along the fronto-parietal network attentive signals flow bidirectionally, allowing the selection of salient stimuli during visually guided movements (e.g., Lebedev and Wise, 2001; for reviews see Corbetta and Shulman, 2002; Reynolds and Chelazzi, 2004). Two other relevant sources of information are the OFC, which, as described at the beginning of this paragraph, delivers knowledge about the value of the stimuli, and the anterior cingulate cortex (ACC) and/or the pre-SMA, which

deliver signals dealing with prediction of expected outcome (see The Monitoring System). In addition, sensory areas could also contribute to this process. For instance, it has been found that activity of neurons in macaque area V4 can underlie the selection of elemental object features and their translation into a response-related format that can directly contribute to the control of the animal's actions (Mirabella et al., 2007).

These are just a few examples; many cortical and subcortical structures are connected with the PFC, which is optimally situated to gather and synthesize information to select the more appropriate goal, and the best task set to achieve it in a given context.

ACTION SELECTION

Even though goal and strategies are selected in the PFC, there are several lines of evidence indicating that choosing between alternative actions to achieve an identified goal and the generation of specific motor commands (i.e., motor plans) are accomplished by neural populations in the dorsal premotor cortex (PMd; Cisek and Kalaska, 2005; Klaes et al., 2011), in the primary motor cortex (Tanji and Evarts, 1976) and in the so-called parietal reach region (PRR), a subregion of the PPC (Cui and Andersen, 2007; Scherberger and Andersen, 2007). Therefore goal selection and the selection of movements to reach them are two separate processes that, to some extent, are likely to occur one after the other.

As most goals can be achieved in any of several ways, multiple potential actions are possibly represented at the same time and start to compete for implementation[2]. That this was the case was demonstrated by Cisek and Kalaska (2005) in a seminal experiment. While recording from PMd, they set a task in which two spatial cues indicated two opposite potential reaching actions. After a delay, a non-spatial cue specified the correct choice (**Figure 5**). Soon after the presentation of the two cues, the neural activity of PMd specified both directions of potential reach targets simultaneously. When information for selecting the correct action became available, its neural representation was strengthened while the other was suppressed.

On these grounds, the authors hypothesized that PMd prepares multiple actions in parallel and selects between them through a process of biased competition taking place within the same neural substrate that guides the execution of those actions (Cisek, 2006; Cisek and Kalaska, 2010). Thus, the mechanism of action selection is likely to occur in a similar way to that underlying goal selection (**Figure 1**).

Dorsal premotor cortex is not the only site where multiple potential actions can be represented. In fact, it has been shown that if a monkey is presented with a spatial target, but not instructed about whether an arm or a saccadic eye movement is required, neurons begin to discharge simultaneously in different regions of the PPC, the lateral and the medial intraparietal sulcus (LIP and MIP, respectively; Calton et al., 2002; Cui and Andersen, 2007). These discharges represent the simultaneous coding of saccade and reach plans. Later, if an arm movement is cued (Calton et al., 2002) or freely chosen (Cui and Andersen, 2007), the activity of MIP becomes stronger than that of LIP, and vice versa if a saccade is instructed or chosen.

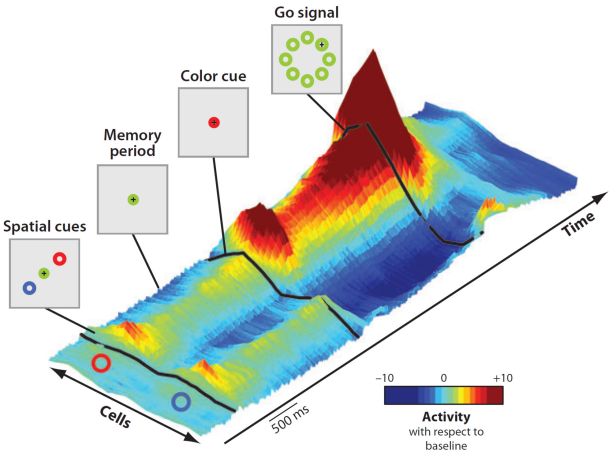

FIGURE 5 | Time course of population activity in the dorsal premotor cortex during a reach-selection task. The diagrams on the left replicate the temporal sequence of the visual displays during the task. Each trial began with the monkeys moving the cursor (+) into a central green circle. Next, a red and a blue cue circle appeared at two of eight possible target positions, in opposite directions from the center for about a second (first display, "Spatial cues"). Then the cues disappeared (second display, "Memory period") and after a variable period the central circle changed color to red or blue (third display, "Color cue"). Finally, the go signal was delivered (fourth display). The central circle disappeared and green circles appeared at all eight positions. To perform correctly the monkeys had to move the cursor from the central circle to the target indicated by the color cue. The 3-D colored surface on the right depicts changes of neural activity along time with respect to baseline, with cells sorted by their preferred direction along the bottom edge. Note that during the entire period of ambiguity until the presentation of the color cue, the population encoded both potential directions. When the color cue provided the information for selecting the correct action, its neural representation was strengthened while the other was suppressed. Reproduced with permission from Cisek and Kalaska (2010).

Recently, Klaes et al. (2011) confirm and extended these findings by demonstrating that in situations of uncertain choice, the frontoparietal reach areas (PRR and PMd) construct all potential motor alternatives. However, Klaes et al. (2011) made a further step showing that that potential actions were also biased by the monkeys' subjective desirability, confirming the model proposed by Cisek (2006).

All in all, these findings seem to indicate that in the frontoparietal reach areas there is a continuous and simultaneous processing of multiple movement options. Possibly, as some computational models predict (e.g., Smith and Ratcliff, 2004), neural activity related to response choices, i.e., the motor plans, builds up in separate accumulators as a function of the evidence for or against them until one reaches a threshold, winning the competition.

What a motor plan is or what it represents is a very debated issue. It is generally accepted that the motor plan is formed in the premotor cortex and in M1 (Tanji and Evarts, 1976; Weinrich et al., 1984), but what is encoded by the neural activity of the motor cortices and how it relates to movement activity are matters of some

[2]As previously stated for the representation of multiple goals, even in this instance the representation of multiple potential movements may be limited by the capacity of working memory.

controversy. It has been proposed that the discharge of single-unit might represent a subthreshold version of movement (Tanji and Evarts, 1976) or that population activity represents some movement parameters (e.g., reach direction and distance Georgopoulos et al., 1982; Riehle and Requin, 1989) or even the combination between information about the target and about the effector used (Hoshi and Tanji, 2000, 2002). However, all these approaches have been proven to be inconsistent or equivocal in fully explaining the activity in the motor system (for a review see Shenoy et al., 2013).

An alternative proposal is that this activity reflects a mix of signals: "*some will be outputs to drive the spinal cord and muscles, but many will be internal processes that help to compose the outputs, but are themselves only poorly described in terms of the movement*" (Shenoy et al., 2013, p. 339). In other words, the activity that precedes a movement would represent the initial state of a dynamic system which will determine the temporal patterns needed to drive actions. Under this hypothesis the motor plan does not explicitly represent movement parameters; it is still closely related to movement activity, but the reciprocal relationship is not transparent at the level of the individual cells. This framework seems to reconcile several past, apparently contradictory, findings and to provide a wider comprehension of the functioning of the cortical motor system (Shenoy et al., 2013). One possible limit of the dynamic system hypothesis, that future studies will have to overcome, is that most of the data come from experiments in which there is a delay between the appearance of the target and the go signal (delayed-reach task, e.g., Churchland et al., 2006). Clearly, to be fully validated the hypothesis should be tested in tasks featuring performance or inhibition of reaching movements in different contexts (but see Mattia et al., 2013).

In conclusion, the same substrates where the action selections occur are also those that are used to prepare and guide the execution of the movement that is ultimately selected.

THE FINAL EVALUATION (LATE "SHOULD-I-STAY-OR-SHOULD-I-GO" DECISION)

By the end of the previous stages, what had been evaluated as the best action to achieve the desired goal is planned, but before the corresponding motor plan can be executed it has to pass a further final check (late "should-I-stay-or-should-I-go" decision). This is a fundamental step, because from the moment at which the decision to act has been taken to the time when the motor output is about to be generated, the continuous flow of information might signal that something has changed in the external environment, in the internal states or in both. These changes might impact on the previous evaluations as the selected action might turn out to be no longer appropriate (Haggard, 2008). A common experience might be that of a person about to cross a road but, just before stepping onto the road, he hears the sound of an ambulance siren clearly approaching. In the most common instance, the person would halt his step to avoid being hit. However, the evaluation might be radically different if his/her child is already in the middle of the road. In the former case suppressing the action is clearly the most valuable decision but, in the latter, the risk of losing the parental investment might trigger the person to act even faster in order to secure the child. The evaluation could be also influenced by endogenous signals, for instance the same person in the above example could take the risk of crossing the road because he suddenly remembers that his plane is leaving.

Computationally this last check could be realized by comparing the output of a predictive forward model with a goal description (e.g., see Wolpert and Miall, 1996). When the mismatch between the predicted result and the goal becomes too large, i.e., the action is unlikely to allow the achievement of the desired result, the pending action is canceled. There are several tasks that are currently exploited to study the inhibitory function and each has some advantages over the others (for a review see Ridderinkhof et al., 2011); however, in order to design a potential neural network capable of augmenting inhibition of pending actions, I will focus on the stop-signal paradigm (Logan and Cowan, 1984). There are two reasons to choose this as a paradigmatic task. Firstly it is the only one which allows study of the suppression of ongoing movements, and secondly it has been widely used exploiting several effectors (the eyes, e.g., see Hanes and Schall, 1996; the finger, e.g., see Logan and Cowan, 1984; the arm, e.g., see Mirabella et al., 2006); thus a wealth of data are available. The stop-signal (or countermanding) paradigm probes a subject's ability to withhold a planned movement triggered by a go signal when an infrequent stop-signal is presented after a variable delay (see **Figure 6A**).

Starting from the behavioral performance during the countermanding task it is possible to yield an estimate of the duration of the suppression process [stop-signal reaction time (SSRT); Logan and Cowan, 1984; Band et al., 2003; Boucher et al., 2007]. The SSRT is a key behavioral parameter for uncovering the neural substrates of inhibition. In fact, those brain regions showing a change in activity when a movement is produced with respect to when it is suppressed, and where the onset of this shift precedes the end of the SSRT, can be assumed to be causally related to the suppression process.

Thus the stop-signal task allows to study of the way subjects react to an unexpected imperative stop instruction. This is referred to as "reactive inhibition." At the same time, this approach also allows assessment of changes in the response strategies of individuals embedded in such an experimental context. In fact, the rules of the countermanding task create a conflict on all no-stop trials because subjects are instructed to move as fast as possible, but, at the same time, they tend to delay movement initiation to wait for the occurrence of a possible stop-signal. As a consequence, healthy subjects had longer RTs when executing go-trials intermixed with stop-trials than when executing go-trials alone (e.g., Mirabella et al., 2006; Verbruggen and Logan, 2009). In addition, the occurrence of stop trials induces a lengthening of the RTs of responses produced in the immediately subsequent no-stop trials (Mirabella et al., 2006, 2012; Verbruggen and Logan, 2009; Zandbelt and Vink, 2010). This form of control over response execution in anticipation of known task demands, driven by endogenous signals, i.e., the awareness of the possible presentation of stop-signals, has been called "proactive control/inhibition." In the following, I will describe results mainly related to reactive inhibition, while I will mainly focus on proactive inhibition in the next paragraph where

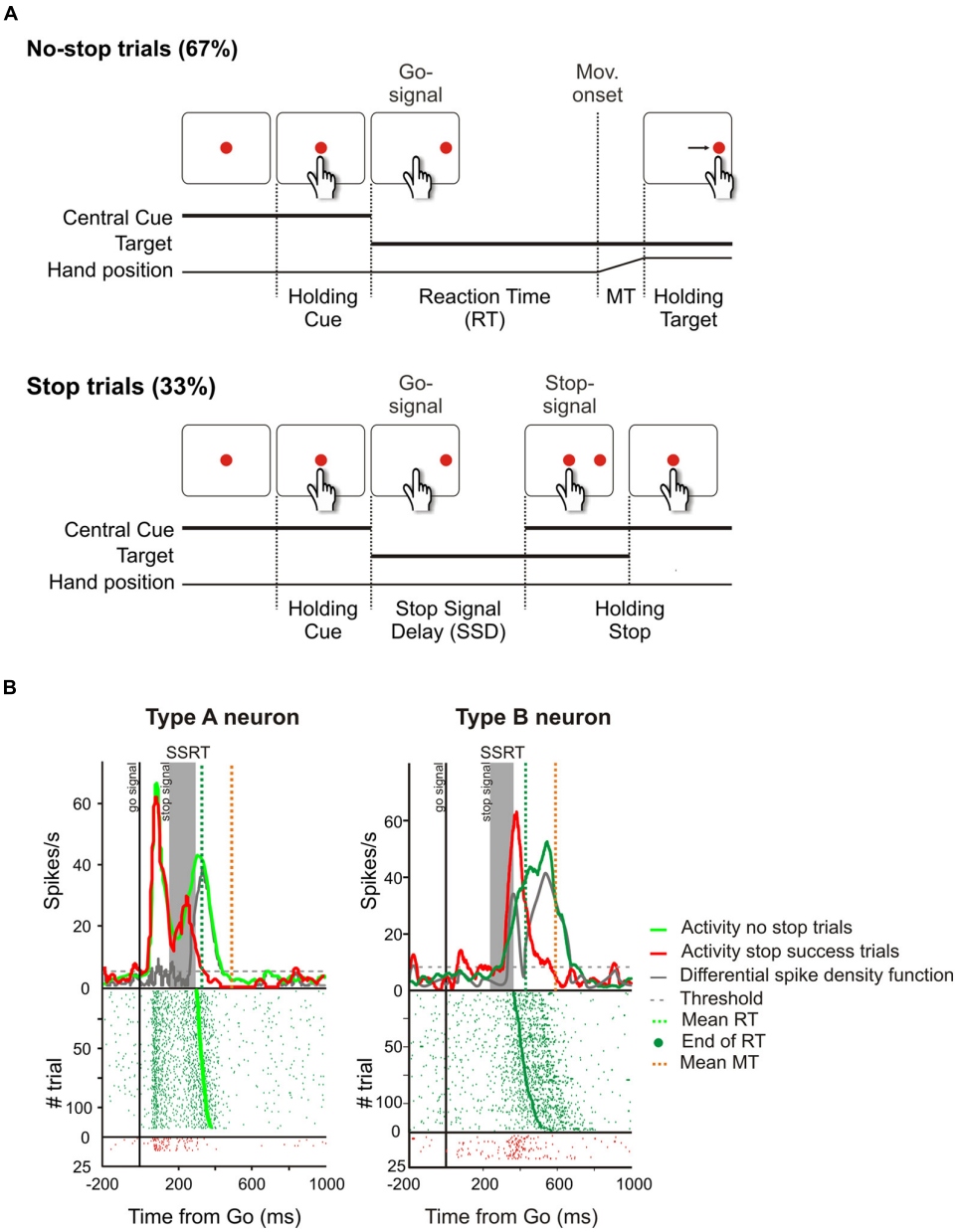

FIGURE 6 | Causal role of neurons of the dorsal premotor cortex (PMd) in reactive inhibition. (A) Temporal sequence of the visual displays for no-stop and stop trials in the reaching version of the countermanding task. All trials began with the presentation of a central stimulus. After a variable holding delay (500–800 ms) it disappeared and simultaneously a target appeared to the right, acting as a go-signal. In the no-stop trials subjects had to start a speeded reaching movement toward the peripheral target. Randomly, on a fraction of interleaved trials (33%), the central stimulus reappeared after variable delays (SSDs), instructing subjects to inhibit movement initiation. In these stop trials, if subjects countermanded the planned movement keeping the arm on the central stimulus the trial was scored as a stop-success trial. Otherwise, if subjects executed the reaching movement the trial was scored as a stop-failure trial (not shown). Reproduced with permission from Mattia et al. (2012). **(B)** Changes of activity driven by the stop-signal onset in PMd neurons modulated during the preparation of the movement. In each panel the upper graph represents the average spike density function while the lower graph shows the raster plots of neural activity in no-stop trials (green tick-marks) and stop-success trials (red tick-marks). Neural activity was always aligned to the go-signal onset (first vertical line). The gray band represents the estimated duration of the stop-signal reaction time (SSRT) in that session. The gray line represents the differential spike density function, while the dashed gray line represents the threshold value for significant divergence. The green and the orange vertical dotted lines in the top panels indicate the average RT and the average end of MT, respectively. The green dots in the rasters represent the end of the RTs. On the right, the activity of a representative "type A" countermanding neuron is shown. In this cell, neural activity during stop-success trials (red line) initially resembles that of no-stop trials (green line) but, with a delay after the stop-signal presentation, it suddenly starts to decrease and the differential spike density function crosses the threshold 34.4 ms before the end of the SSRT. On the left, the activity of a representative "type B" countermanding neuron is shown. In this instance, the activity in stop-success trials increases after stop-signal presentation with respect to that recorded during no-stop trials 39.9 ms before the end of the SSRT. Therefore both these two types of neurons exhibit a modulation of activity sufficient to control the suppression of an ongoing arm movement.

I will deal with the monitoring system (but see also Action Execution). Clearly, all proactive strategies necessarily derive from these computations. This does not mean the neural substrates of reactive and proactive inhibition have to be different. In fact, it has been shown that there is an overlap between them (e.g., Jahfari et al., 2012; Zandbelt et al., 2013; for a review see Aron, 2011); however, reactive and proactive inhibition might derive from two conceptually different modules (the late "should-I-stay-or-should-I-go" decision module and the monitoring system; see **Figure 1**).

Variants of the stop-signal task have been used several times in association with different techniques [e.g., single-unit recordings, fMRI, electroencephalographic scalp recordings (EEG), intracranial electroencephalographic recordings (iEEF), lesions, transcranial magnetic stimulation (TMS), deep brain stimulation (DBS)], different effectors (the eyes, the arm, and the fingers), and different pathologies (e.g., PD, attention deficit and hyperactivity disorder, Tourette syndrome, obsessive–compulsive disorder). From this large number of studies, a network of brain regions that seem to be involved in implementing inhibition has been identified. To this network belong both cortical and subcortical structures, that largely overlap with those involved in movement generation, planning, and even movement execution.

One of the prefrontal regions that more frequently has been reported to have an inhibitory role is the inferior frontal gyrus (IFG), especially in the right hemisphere (see Aron et al., 2014 for a recent review). For instance, Aron et al. (2003) have shown that humans with a lesion to the right, but not to the left IFG exhibit longer SSRTs than healthy subjects. Furthermore they showed that the lengthening of the SSRT was proportional to the extent of damage in the right IFG. Less frequently, the DLPFC has also been claimed to participate in this executive function (e.g., Zheng et al., 2008). However, its role is controversial. In fact, while Zheng et al. (2008) showed that individuals who were more proficient at inhibition had a greater activation in DLPF, Chambers et al. (2006) found that temporary deactivation of the same region, with repetitive TMS, did not significantly alter the speed of inhibition.

Imagining studies revealed the involvement in this form of inhibition of the pre-SMA (e.g., Aron et al., 2007; Li et al., 2008; Zandbelt and Vink, 2010; Jahfari et al., 2012) as well as of the striatum (Li et al., 2008; Zandbelt and Vink, 2010). Even in this instance the exact role of these structures is unclear and debated. Li et al. (2008) compared the fMRI brain activation of individuals with short versus long SSRTs who were identical in all other aspects of stop-signal performance. Their aim was to isolate the neural correlates of response inhibition from those of response monitoring and/or attentional control. Under these experimental conditions, Li et al. (2008) found that the caudate head had greater activation in individuals with short than with long SSRT, and the extent of its activation was positively correlated with activity in the pre-SMA. In contrast, Scangos and Stuphorn (2010), by recording single-neuron activity of SMA and pre-SMA of monkeys during an arm countermanding task, found that these cells could not contribute directly to response inhibition as most of them modulate after the SSRT. Instead, the majority of neurons signaled expectation of reward, as they were modulated by the amount of expected reward.

Another basal ganglion implicated in stopping ongoing actions is the subthalamic nucleus (STN; see Aron and Poldrack, 2006). Mirabella et al. (2012) demonstrated that bilateral STN DBS selectively improves inhibitory functions as its electrical stimulation significantly shortened the SSRT, but did not influence the RTs of no-stop trials. These results agree with those of Van den Wildenberg et al. (2006) and Swann et al. (2011), but not with those of Li et al. (2008). In the above-described study, they found that neither the STN nor the IFG were active during reactive stop and thus concluded that both structures had a role in attentional monitoring of the stop-signal. Similarly, Zandbelt and Vink (2010) did not find evidence of STN activation during movement cancelation.

Finally, two other areas have been found to be involved in inhibitory function, i.e., the PMd (Mirabella et al., 2011; Mattia et al., 2012, 2013) and the primary motor cortex (M1; Coxon et al., 2006; Swann et al., 2009; Mattia et al., 2012). Mirabella et al. (2011) showed that about 30% of PMd cells changed their discharge before the end of the SSRT when the monkey had to stop a reaching movement. Thus these neurons seem to be causally involved in reactive inhibition (see **Figure 6B**). These findings were confirmed and extended by a subsequent study (Mattia et al., 2012), in which epicortical event-related potentials (ERPs) were recorded from the lateral surface of the fronto-temporal lobes of epileptic patients performing the countermanding task. It was found that an ERP complex was selectively expressed before the end of the SSRT in M1, and in the premotor cortex (**Figure 7**). Thus, Mattia et al. (2012) deduced that motor cortices are causally involved in inhibitory control. In conclusion, even though the exact role of each of the brain regions involved in the stop task remains controversial, it clearly emerges a considerable overlap between brain region subserving the preparation of an action and its suppression (see **Table 1**).

To summarize, the late "should-I-stay-or-should-I-go" decision represents a hinge of our goal-directed behavior because it allows crucial, last-minute changes of strategies when the cost of an action overcomes the benefits. Unlike the early "should-I-stay-or-should-I-go" decision, which does not require active suppression, in this instance some neural signals aiming to halt the activity linked to the ongoing action have to be produced by the nervous system (**Figure 1**). Given this, it should not come as a surprise that such a large network of brain regions has to be involved.

ACTION EXECUTION

Once the last check is passed, the motor commands are sent to the spinal cord, activate the muscles, and produce the movement. It must be remarked that it is very unlikely that even the spinal cord would be a passive relay of "higher directives." In fact, Prut and Fetz (1999) have shown that spinal interneurons show pre-movement activity during a delayed task, similarly to PMd (Wise et al., 1983). This indicates that, at least under some experimental conditions, movement preparation may occur simultaneously over widely distributed regions, including spinal levels.

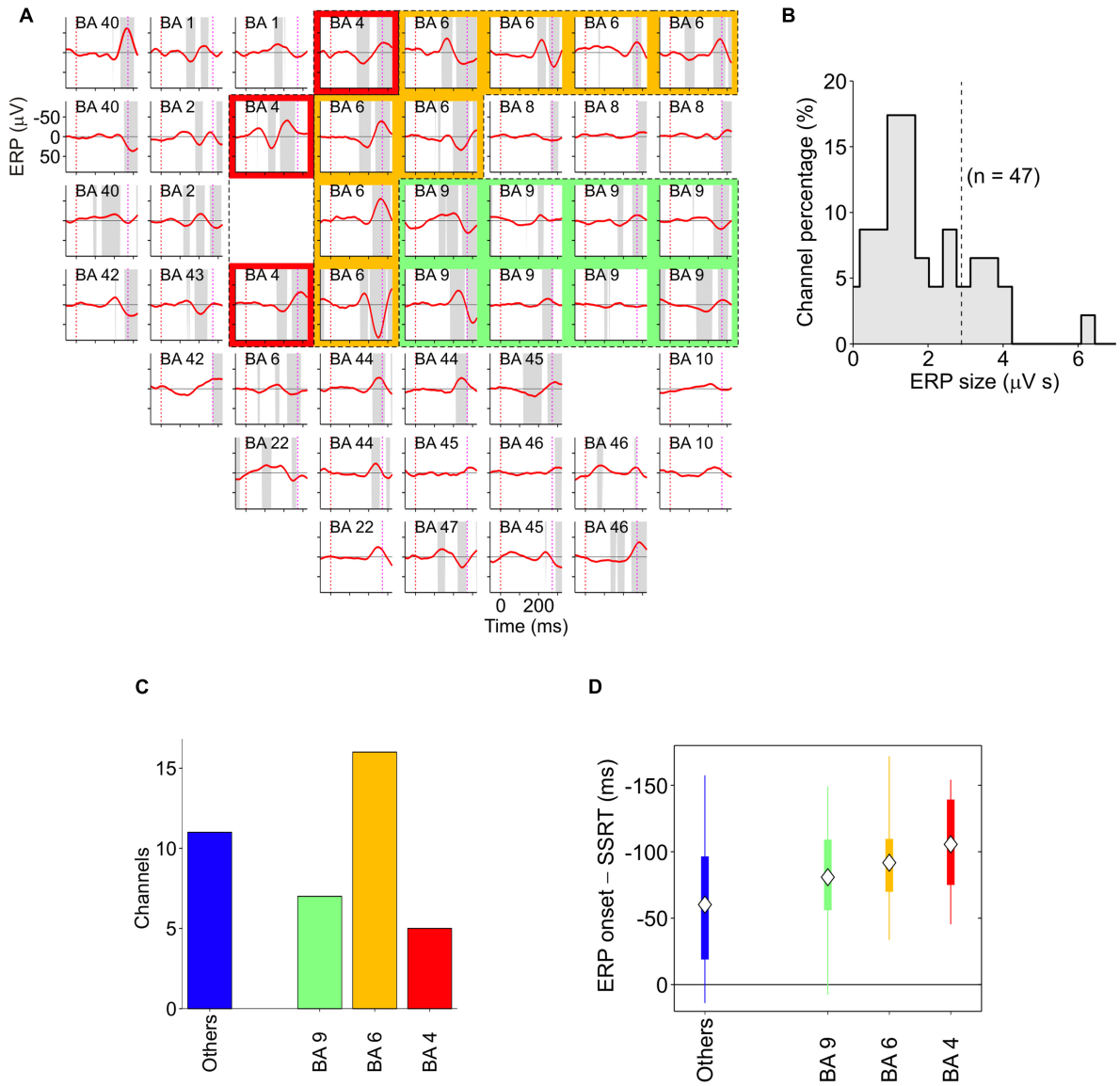

FIGURE 7 | Spatiotemporal distribution of stop-event related potentials (ERPs) in successful-stop (SS) trials. (A) Average stop-ERPs (solid red curves) of SS trials centered on stop-signal appearance corresponding to the selected channels for one pharmacoresistant epileptic patient. Gray areas, time intervals at which the stop-ERP was significantly different from 0 (Wilcoxon signed-rank test, $P < 0.01$). Subplot labels: Brodmann areas (BAs) over which electrodes were positioned. Colored areas: electrodes placed over the primary motor cortex (red, BA4), the premotor cortex (yellow, BA6) and the DLPFC (green, BA9). **(B)** Histogram of the stop-ERP sizes of panel **(A)**. Stop-ERP sizes were computed as the integral of absolute values of stop-ERP voltage deflections in the interval periods marked by gray areas within SSRT. Dashed line: threshold value for selecting the subset of channels with large enough stop-ERPs used for population analyses (see Mattia et al., 2012 for details). **(C)** Number of channels showing large enough average stop-ERPs across five patients ($n = 39$) grouped by BA. Blue bar (others) represents those areas where channels were not selected more than twice across all patients. **(D)** Box plot of stop-ERP onsets measured with respect to the end of SSRT across all selected channels in all patients. Stop-ERP onset was defined as the first time that an electrode voltage was significantly different from 0. Diamonds indicate average onset times. Tick bars indicate the first and the third quartile. Vertical lines indicate the extreme time lags in the channel group. Freely adapted from Mattia et al. (2012), with permission.

Additionally, it must be taken into account that arm movements, unlike saccades, are not ballistic movements as they can be stopped at any point along their path (De Jong et al., 1990; Scangos and Stuphorn, 2010). As a consequence, their planning can be modified even during the execution phase. This is in line with the findings of Mirabella et al. (2008), who compared RTs and movement times (MTs) of reaching movements toward visual targets executed either during an RT task (go-only task) or during a countermanding task. In both tasks subjects executed the same movements, but in the countermanding task subjects were aware that a stop-signal could randomly appear during movement preparation, indicating that the pending action should be suppressed. The awareness of the possible appearance of the stop-signal creates a conflict on all no-stop trials because, despite the

instructions to always move as fast as possible, subjects spontaneously tend to delay movement initiation to wait for the possible occurrence of a stop-signal (e.g., Mirabella et al., 2006, 2012). This is a common proactive strategy that subjects implicitly adopt to have a greater chance of stopping their movements. However, the proactive strategy was also found to affect the MTs, which were shorter during the no-stop trials and longer during the go-only trials. Probably the increased length of RTs during the no-stop trials allowed subjects to fully process movement parameters and thus to move faster. In contrast, in go-only trials the absence of a proactive brake allows a shortening of RTs, at the cost of leaving some details of the motor program uncompleted, so that the planning must be completed during the movement. This strategy represents an optimization of costs versus benefits because shorter RTs are compensated by longer MTs and vice versa.

Interestingly, Mirabella et al. (2013) demonstrated that STN takes part in this process. In fact PD patients in which both DBS were turned on behaved similarly to healthy subjects, whereas when both DBS were off the same patients had both RTs and MTs longer in no-stop trials than in go-only trials (**Figure 8**). Therefore this study demonstrated the existence of a causal link between the DBS of STN and the motor strategy exploited. Once again this evidence favors the hypothesis that STN is not involved in a single function (e.g., reactive inhibition); instead, more generally, it can compute the payoff of an ongoing action.

THE MONITORING SYSTEM

In order to learn how to make good decisions, the brain needs to compute, learn, and store the results of the outcomes that were generated by its previous decisions. To this end the ability of computing predictions about future reward and the ability of measuring discrepancies between attended and actual outcomes are fundamental. These functions are performed by a set of brain regions that collectively I will call the "monitoring system" (**Figure 1**). This system is composed of a set of cortical and subcortical structures that allow coding of reward expectations, detection of errors and implementation of behavioral adjustments, aiming to cope with more or less demanding context in order to optimize future choices. Therefore signals produced by the monitoring system can influence any stage of action implementation.

A key role in this set of processes is played by the ACC, located in the frontal medial wall (**Figure 3**). It has been known for

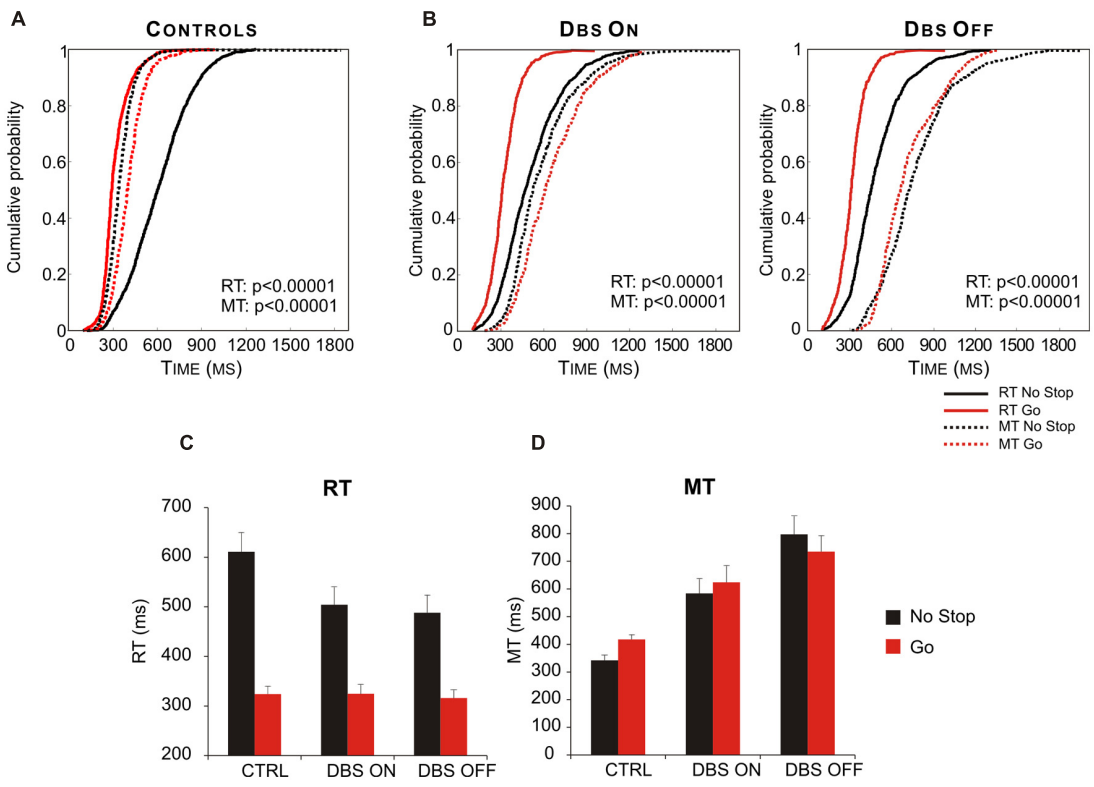

FIGURE 8 | Deep brain stimulation (DBS) of subthalamic nucleus (STN) partially restores the appropriate motor strategy according to the contexts. (A) Cumulative distribution of RTs (solid lines) and MTs (dotted lines) of healthy subjects (n = 13) for go-only (red lines) and no-stop (black lines) trials. **(B)** Cumulative distributions of RTs (solid lines) and MTs (dotted lines) of DBS patients (n = 12) in DBS-ON and DBF-OFF conditions for both go-only (red lines) and no-stop (black lines) trials. For each condition the P-value of Kolmogorov–Smirnov test is given, both for RTs and for MTs. **(C)** Histograms of average RTs of no-stop and go-only trials in DBS-ON and DBF-OFF conditions. Bars represent the standard error of the mean. **(D)** Histograms of average MTs of no-stop and go-only trials in each DBS-ON and DBF-OFF condition. Bars represent the standard error of the mean. Reproduced from Mirabella et al. (2013), with permission from PLOS.

a long time that this area is involved in cognitive control over behavior (e.g., Bernstein et al., 1995; Botvinick et al., 1999); however, its precise role remains considerably debated. One influential hypothesis is that the activity of ACC might represent the likelihood of obtaining or losing reward in response to particular actions. Evidence in support of this idea comes from the results of Brown and Braver (2005). They administered to human volunteers a stop-change task while recording the fMRI BOLD signal. The task, (**Figure 9**), required participants to make rapid left- or right-hand button-press responses according to the direction of an arrow. In 33% of cases, during the RTs, a second arrow pointing in the opposite direction was presented and the responses had to be reversed. Using a staircase algorithm, authors adjusted the time of presentation of the second arrow, hence controlling the likelihood of making mistakes (either 10 or 50%). At the beginning of each trial, participants were informed of the error likelihood by a color cue: a blue bar indicated 50% error probability, while a white bar indicated 10% error probability. The activity of ACC was greater during the high error than during the low error conditions. This held true not only during change trials, but also during trials in which participants did not have to change the responses (**Figure 9**). Therefore ACC does not simply indicate response conflict (occurring when the two arrows are presented) or error occurrence; instead more generally it signals the perceived likelihood of potential errors. Crucially, Brown and Braver (2005) exploiting a neural-network model, showed that this pattern of response gradually emerged over the course of the experimental session, i.e., after individuals learned the associations between color cue and error likelihood.

Other studies point to a slightly different role for the ACC. According to these accounts, ACC would provide a continuously updated prediction of expected cognitive demand which will be used to optimize future behavior. For instance, Sheth et al. (2012) showed that ACC activity speeds up behavioral responses when cognitive demand remain stable, but, in more challenging situations, it slows down responses to allow a greater accuracy. Kennerley et al. (2006), studying the behavioral responses of monkeys before and after ACC lesions, confirmed that this region adaptively guides future behaviors, but exploiting a different mechanism. In a key experiment, monkeys were rewarded when performing a certain action (e.g., lifting a lever) until the rewarded action was changed (e.g., to get the reward it had to turn the lever). Non-lesioned monkeys had no difficult in this task, while ACC-lesioned monkeys following an unrewarded lift response switched to turning, but could not sustain this response on subsequent trials. Thus, the lesion compromised the ability to associate payoffs with the outcome of past actions to adaptively guide future behavior.

Whatever the exact role of ACC in monitoring behavioral performance, it appears that this capability develops through experience. It is very probable that the knowledge of past experiences is built through reinforcement-learning processes, mediated by the discharge of midbrain dopamine neurons. The discharge of these neurons measures deviations from individuals' previous reward expectations, i.e., they compute the so-called prediction errors (Schultz et al., 1997; O'Doherty et al., 2003; Bayer and Glimcher, 2005). Every time an event is better than expected, dopaminergic neurons phasically increase their discharge. In contrast, they do not change firing rate when an event occurs as predicted, while they decrease their discharge if something worse than expected takes place. Prediction errors are thought to play a key role in guiding decision-making by signaling the need to adjust future behavior, i.e., they are fundamental to learning processes (Schultz et al., 1997; Montague et al., 2004).

Dopaminergic neurons project widely to the striatum and to several regions of PFC including the ACC (Freund et al., 1984; Smith et al., 1994). The activity of ventral striatum seems to correlate with prediction error computation (Bray and O'Doherty, 2007; Hare et al., 2008) and thus it is likely to contribute to some further elaboration of action-outcome predictions. However, ACC plays a different role from ventral striatum, exploiting prediction errors as training signals to build extended action-outcome histories, that later could be exploited to adapt goal-directed behaviors (Holroyd and Coles, 2002; Brown and Braver, 2005; Kennerley et al., 2006). Given such a complex function, it is unlikely that ACC would rely solely on signals coming from dopaminergic neurons. In fact, other brain regions have been shown to produce signals promoting learning. For instance, it has been shown that neurons of the frontal pole cortex code the outcome of actions (Tsujimoto et al., 2010; for a review see Tsujimoto et al., 2011). Also, neurons in SMA and pre-SMA of monkeys have been shown to be modulated by the amount of expected reward and thus these regions might, among other things, be signaling expectation of reward too (Scangos and Stuphorn, 2010). Not all studies point to this conclusion, e.g., recently Bonini et al. (2014), by recording evoked field potentials in pharmacoresistant epileptic patients, claimed that SMA continuously assesses ongoing actions and, when an error occurs, it signals to ACC.

Whatever the exact role of each of these components, they form a system that is capable of monitoring actions, evaluating their behavioral outcomes, and learning the association between a certain environmental context and the likelihood that a certain action or strategy will lead to the desired goal. Thus, the monitoring system is the ideal candidate for implementing proactive preparation of action plans in anticipation of known task demands. Such advance preparation has been studied in the context of response inhibition, in particular when the countermanding task is employed. This is because the rules of this paradigm produce a conflict every time subjects have to execute no-stop trials (see **Figure 6A**). As described above, this context induces a lengthening of the RTs and at the same time a shortening of MTs with respect to situations in which the same movements have to be performed, but stop-signals are never presented (e.g., Mirabella et al., 2008, 2013).

The study of the neural underpinnings of proactive control revealed that the network of brain regions that subserve this function largely overlaps with those subserving reactive inhibition. This conclusion stems from several fMRI studies which employed a probabilistic stop task with cues indicating the likelihood of stop trial occurrence (e.g., Chikazoe et al., 2009; Zandbelt and Vink, 2010; Jahfari et al., 2012; Zandbelt et al., 2013). Some cues indicate that go-signals are never followed by a stop-signal (certain go-signals), whereas others indicate that go-signals have a

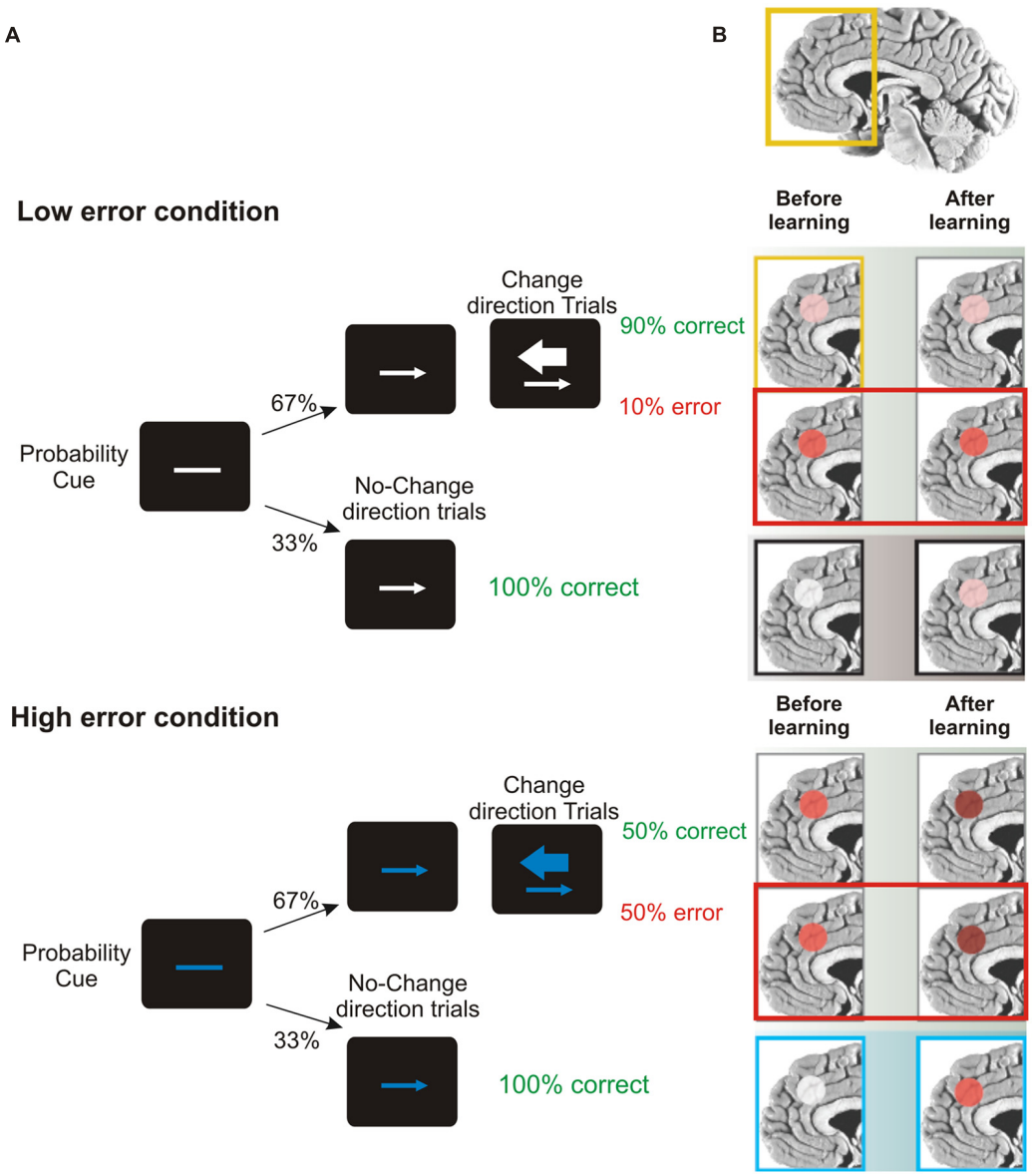

FIGURE 9 | Role of ACC in predicting error likelihood. (A) Temporal sequence of the visual displays for the change-signal task. Initially a probability cue (plain line) was displayed. The cue could be either white or blue, predicting low or high error likelihood respectively. After a delay, a go signal was presented (left or right pointing arrow) indicating the required button-press response (left or right index press for left or right pointing arrow, respectively). Randomly on 33% of the trials a change signal was displayed (a larger arrow pointing in the opposite direction with respect to that presented as go signal). To this signal, subjects had to reverse the response from that indicated by the go signal. Error rates were controlled by a staircase procedure so that in the low error condition the delay between the go signal and the change signal was kept shorter and subjects made around 90% of correct responses. In the high error condition the delay was kept longer and subjects made around 50% correct responses. **(B)** Brain regions highlighted indicate the activation of ACC during the stop-change before and after learning (the greater the activation, the deeper the red color) for correct, wrong change-direction trials and for no-change trials (for the top to the bottom row) in the low and high error conditions. Interestingly, during no-change trials ACC activity increased with practice, especially in response to blue color cues, reflecting an improved ability to predict the likelihood of making an error. Freely adapted from Ridderinkhof and van den Wildenberg (2005), with permission.

certain likelihood of being followed by a stop-signal (uncertain go-signals). By comparing brain activity between these conditions, it has been possible to uncover the neural substrate of advanced action preparation. Overall it emerged that when subjects expect the occurrence of a stop-signal, they proactively engage the network subserving reactive inhibition in a progressively increasing fashion according to the likelihood of stop presentation. A lower stop probability would correspond to a weaker activation of the network and to less marked slowing of responses, while when the stop is presented the activation is much stronger and the motor output is completely blocked (Aron, 2011).

These studies did not show clear activations of either of ACC or midbrain dopaminergic neurons in the ventral tegmental area and in the substantia near pars compacta (but see Zandbelt et al., 2013). However, these might be due either to the fact that commonly a region-of-interest approach had been chosen or because of limitations of the fMRI technique. Nevertheless, the activation of other components of the monitoring system, i.e., striatum, SMA and pre-SMA, has been shown several times (Chikazoe et al., 2009; Zandbelt and Vink, 2010; Jahfari et al., 2012; Zandbelt et al., 2013). This activity might reflect the computations which underlie learning of the association between the experimental context and the likelihood of performing (or stopping) an action. Thus, these signals should drive the proactive network so as to maximize the probability of moving without missing stop trials. Further studies are needed to test this hypothesis.

CONCLUDING THOUGHTS

On the whole, it seems clear that the neural network subserving goal-directed actions is very extensive, encompassing both frontal and parietal area as well as subcortical brain structures. This does not come as a surprise, as we live in a complex and ever-changing environment, which continuously offers an enormous variety of opportunities for potential actions. Thus, our motor system is called on to perform a continuous evaluation of alternative actions that may become available, in order to decide whether to persist in a given activity or to stop it and switch to a different one. This is the hinge of our behavioral flexibility. Central to this feature are the abilities of predicting the likelihood of achieving the desired goal with a certain action or strategy, and of canceling pending actions when they are no longer valuable. These two processes operate continuously during the entire course of a movement, during its genesis, its planning, and even its execution, so that the motor output can be modulated or suppressed at any time before its execution.

These considerations are clearly at odds with the old-fashioned serial framework according to which "*we sense the world, think about it, and then act upon it*" (Cisek and Kalaska, 2010, p. 271). Instead, they are compatible with the idea of parallel processing. Thus, one or more goals or actions can be coded at the same time, so that alternatives can be ready for release at short notice. Importantly, the evaluation of an action can also lead to its suppression when it has already been selected. Very probably the neural machinery underling action preparation and the neural substrates underling action inhibition are simultaneously active. From what is stated above, it is not too surprising that many of the regions mediating the decisions to act appear to be involved also in decisions to refrain from acting (Coxon et al., 2006; Mirabella et al., 2011; Mattia et al., 2012; see **Table 1**). This leads to the main point of the present review. Many, if not all, brain regions belonging to the network which controls goal-oriented movements are involved in more stages of this process. For instance, the SMA and the pre-SMA are involved in the early "should-I-stay-or-should-I-go" decision as they are involved in gating action affordances (e.g., Sumner et al., 2007; Ridderinkhof et al., 2011). However, they are also part of the monitoring system (see The Monitoring System) and they contribute to the late "should-I-stay-or-should-I-go" decision (Aron and Poldrack, 2006; Aron et al., 2007). In addition it has been shown that stimulation of SMA generates a feeling of an urge to move a particular body part, without necessarily causing any actual movement (Fried et al., 1991). The involvement of SMA in the feeling of volition has recently been confirmed by Fried et al. (2011) who recorded single-neuron activity in epileptic pharmacoresistant patients. Both PMd and M1 are involved both in the genesis of motor plans (Tanji and Evarts, 1976; Weinrich et al., 1984; Hoshi and Tanji, 2000, 2002; Churchland et al., 2006; Mattia et al., 2013; Shenoy et al., 2013) and also in their inhibition (Coxon et al., 2006; Mirabella et al., 2011; Mattia et al., 2012). Most of the network subserving reactive inhibition is also involved in proactive inhibition (see Action Execution).

Some other brain regions are involved not solely in motor controls, but also in very different tasks. The ACC has been shown to be involved in monitoring behavioral performance (see The Monitoring System), but also in pain processing (Singer et al., 2004). The role of the IFG is even more controversial as it seems to perform several different functions, some of which are lateralized (see Liakakis et al., 2011 for a review). The left IFG is implicated in both perceptive and productive aspects of language (see Uddén and Bahlmann, 2012 for a review). Some studies indicate that the right IFG plays a key role in redirecting selective attention toward unexpected stimuli (Corbetta and Shulman, 2002); others suggest that it has a specific role in motor inhibition (Aron et al., 2014) or in suppression of unwanted memories (Benoit and Anderson, 2012). In addition, the IFG of both hemispheres are involved in processing of symbolic gestures used for social non-verbal communication (Lindenberg et al., 2012), and they are regions belonging to the core of the human mirror-neuron system, i.e., of the system that is thought to allow the ability of understanding the intentions of others (for a review see Rizzolatti and Craighero, 2004). Finally, the PFC contribute to an enormous array of functions (for a review see Wise, 2008).

Given this picture, I believe that is rather hard to assign a very specific role to most of those regions when performing complex cognitive functions, such as the augmentation of adaptive behaviors. Possibly, complex cognitive functions are not performed by a unique structure. Rather, they might emerge from the coordinated activity of large-scale neuronal networks that are dynamically configured on fixed anatomical connections (von der Malsburg et al., 2010). The mechanisms underlying the dynamic coordination of neural populations are poorly understood. Nevertheless, it has been suggested that the formation of functional networks is achieved by modulating the degree of coherence among temporally structured responses of widely distributed neurons. In its turn, coherence might be modulated by rhythmic modulation of activity and synchronization among these populations (see Fries, 2005 for a review). According to this framework a given brain region can perform specific operations, e.g., the right IFG might subserve the reorienting of selective attention (Corbetta and Shulman, 2002) or the ACC might compute the likelihood of a successful action, but its functional features can be exploited in a variety of tasks. Thus the outcome of complex processes would depend not upon the activation of one or a few brain regions, but on the specific interactions of the network activated during

the ongoing task. This hypothesis would explain why the same regions are active under many different contexts, and it might also help to understand the limited success achieved by brain–machine interfaces (BMIs; for reviews see Baranauskas, 2014; Bensmaia and Miller, 2014).

The large majority of BMI interfaces are aimed at restoring body mobility in patients suffering from motor deficits caused by brain injury, neurologic diseases and limb loss (Bensmaia and Miller, 2014). BMIs record brain signals, decode movement-related information and use these to control external devices (e.g., prosthetic limbs, wheelchairs). Although at present the BMI approach had been fruitful (e.g., Hatsopoulos and Donoghue, 2009) it has also shown several limitations. Patients have to undergo a long period of training before learning how to use the BMIs, and signals extracted from the brain are noisy and difficult to interpret so the error rate is rather high and the response speed is slow. All in all, the guidance of external devices is still far from approximating natural behaviors. This applies to both non-invasive and invasive BMIs. Non-invasive BMIs are mainly based on EEG signals recorded from the scalp. Activity recorded at the scalp level lacks selectivity; it is made up of a mix of signals coming from different cortical regions and thus the amount of useable information conveyed is likely to be too low (Baranauskas, 2014). On the other hand, invasive BMIs employ multiple electrodes surgically inserted into the brain (usually in M1 and/or the somatosensory cortex). Even though the quality of the recorded signals is definitely better, information transfer rate is still not dramatically improved (Baranauskas, 2014). The BMI approach has been shown to reproduce relatively simple behaviors such as two-dimensional center-out reaching tasks (e.g., Wolpaw and McFarland, 2004). Other much more complex tasks, e.g., those entailing suppression of pending actions (Mirabella, 2012), have almost never been tested (but see Ifft et al., 2012). The relatively low degree of success of invasive BMI might be due to the fact that, due to ethical reasons, it has been possible to capture only a very limited amount of the activity of the neural network underling goal-directed actions. However, as stated above, flexible control of behavior can be achieved only through the functional interactions of several brain regions, so it is possible that signals recorded from a limited cortical area fail to provide enough information to reproduce natural movements. To overcome these limitations, it would be necessary to find a way to record simultaneously from several key regions underlying goal-directed actions. Clearly, this is currently not feasible on humans beings, though it could be tested on non-human primates.

Before concluding, I would like to make an important remark: all processes described in the present review, i.e., genesis and suppression of goal-directed actions, do not require either intention, volition, or awareness. These computations can be performed by most animals, and surely by all primates. Not by chance, many of the data described here come from studies on non-human primates. What exactly volition or free will is and how and when it is generated from brain activity is, at best, unclear. There is a consensus around the idea originally proposed by Libet et al. (1983) that the awareness of intention precedes movements by some 100s of milliseconds. Thus, it is possible that the brain generates a action and, only subsequently, some pre-motor processes produce the subjective experience of willing to execute that action, which is perceived as being freely chosen (Hallett, 2007). To overcome the impasse of these findings, Libet (1985) proposed that because awareness of intention precedes movements, our free will should rely on the ability to withhold upcoming actions (see Mirabella, 2007; Haggard, 2008 for reviews). However, it has been shown that action suppression can be implemented unintentionally and unconsciously (see van Gaal et al., 2008). Furthermore, both monkeys (e.g., Mirabella et al., 2011) and rats (e.g., Eagle et al., 2008) can cancel pending movements. It has to be recognized that most studies on action inhibition in humans rely on externally and not on internally triggered stops (see Brass and Haggard, 2007 for an original approach), so further evidence has to be collected before venturing conclusions around the relationship between the veto power and willingness. As Roskies (2010) stated: "*For now, [. . .], the most significant contribution neuroscience has made has been in allowing us to formulate novel questions about the nature of voluntary behavior, and in providing new ways of addressing them.*" I hope that the present review will also help to circumscribe what free will is not.

ACKNOWLEDGMENTS

I thank Maurizio Mattia, Leonardo Chelazzi, and Richard Ridderinkhof for valuable comments and helpful discussions.

REFERENCES

Aron, A. R. (2011). From reactive to proactive and selective control: developing a richer model for stopping inappropriate responses. *Biol. Psychiatry* 69, e55–e68. doi: 10.1016/j.biopsych.2010.07.024

Aron, A. R., Behrens, T. E., Smith, S., Frank, M. J., and Poldrack, R. A. (2007). Triangulating a cognitive control network using diffusion-weighted magnetic resonance imaging (MRI) and functional MRI. *J. Neurosci.* 27, 3743–3752. doi: 10.1523/JNEUROSCI.0519-07.2007

Aron, A. R., Fletcher, P. C., Bullmore, E. T., Sahakian, B. J., and Robbins, T. W. (2003). Stop-signal inhibition disrupted by damage to right inferior frontal gyrus in humans. *Nat. Neurosci.* 6, 115–116. doi: 10.1038/nn1003

Aron, A. R., and Poldrack, R. A. (2006). Cortical and subcortical contributions to stop signal response inhibition: role of the subthalamic nucleus. *J. Neurosci.* 26, 2424–2433. doi: 10.1523/JNEUROSCI.4682-05.2006

Aron, A. R., Robbins, T. W., and Poldrack, R. A. (2014). Inhibition and the right inferior frontal cortex: one decade on. *Trends Cogn. Sci.* 18, 177–185. doi: 10.1016/j.tics.2013.12.003

Band, G. P., van der Molen, M. W., and Logan, G. D. (2003). Horse-race model simulations of the stop-signal procedure. *Acta Psychol. (Amst.)* 112, 105−142. doi: 10.1016/S0001-6918(02)00079-3

Baranauskas, G. (2014). What limits the performance of current invasive brain machine interfaces? *Front. Syst. Neurosci.* 8:68. doi: 10.3389/fnsys.2014.00068

Barraclough, D. J., Conroy, M. L., and Lee, D. (2004). Prefrontal cortex and decision making in a mixed-strategy game. *Nat. Neurosci.* 7, 404–410. doi: 10.1038/nn1209

Bayer, H. M., and Glimcher, P. W. (2005). Midbrain dopamine neurons encode a quantitative reward prediction error signal. *Neuron* 47, 129–141. doi: 10.1016/j.neuron.2005.05.020

Benoit, R. G., and Anderson, M. C. (2012). Opposing mechanisms support the voluntary forgetting of unwanted memories. *Neuron* 76, 450–460. doi: 10.1016/j.neuron.2012.07.025

Bensmaia, S. J., and Miller, L. E. (2014). Restoring sensorimotor function through intracortical interfaces: progress and looming challenges. *Nat. Rev. Neurosci.* 15, 313–325. doi: 10.1038/nrn3724

Bernstein, P. S., Scheffers, M. K., and Coles, M. G. (1995). "Where did I go wrong?" A psychophysiological analysis of error detection. *J. Exp. Psychol. Hum. Percept. Perform.* 21, 1312–1322. doi: 10.1037/0096-1523.21.6.1312

Biran, I., and Chatterjee, A. (2004). Alien hand syndrome. *Arch. Neurol.* 61, 292–294. doi: 10.1001/archneur.61.2.292

Boccardi, E., Della Sala, S., Motto, C., and Spinnler, H. (2002). Utilisation behaviour consequent to bilateral SMA softening. *Cortex* 38, 289–308. doi: 10.1016/S0010-9452(08)70661-0

Bonanni, L., Thomas, A., and Onofrj, M. (2010). Paradoxical kinesia in parkinsonian patients surviving earthquake. *Mov. Disord.* 25, 1302–1304. doi: 10.1002/mds.23075

Bonini, F., Burle, B., Liégeois-Chauvel, C., Régis, J., Chauvel, P., and Vidal, F. (2014). Action monitoring and medial frontal cortex: leading role of supplementary motor area. *Science* 343, 888–891. doi: 10.1126/science.1247412

Botvinick, M., Nystrom, L. E., Fissell, K., Carter, C. S., and Cohen, J. D. (1999). Conflict monitoring versus selection-for-action in anterior cingulate cortex. *Nature* 402, 179–181. doi: 10.1038/46035

Boucher, L., Palmeri, T. J., Logan, G. D., and Schall, J. D. (2007). Inhibitory control in mind and brain: an interactive race model of countermanding saccades. *Psychol. Rev.* 114, 376–397. doi: 10.1037/0033-295X.114.2.376

Brass, M., and Haggard, P. (2007). To do or not to do: the neural signature of self-control. *J. Neurosci.* 27, 9141–9145. doi: 10.1523/JNEUROSCI.0924-07.2007

Bray, S., and O'Doherty, J. (2007). Neural coding of reward-prediction error signals during classical conditioning with attractive faces. *J. Neurophysiol.* 97, 3036–3045. doi: 10.1152/jn.01211.2006

Brown, J. W., and Braver, T. S. (2005). Learned predictions of error likelihood in the anterior cingulate cortex. *Science* 307, 1118–1121. doi: 10.1126/science.1105783

Calton, J. L., Dickinson, A. R., and Snyder, L. H. (2002). Non-spatial, motor-specific activation in posterior parietal cortex. *Nat. Neurosci.* 5, 580–588. doi: 10.1038/nn0602-862

Camille, N., Coricelli, G., Sallet, J., Pradat-Diehl, P., Duhamel, J. R., and Sirigu, A. (2004). The involvement of the orbitofrontal cortex in the experience of regret. *Science* 304, 1167–1170. doi: 10.1126/science.1094550

Chambers, C. D., Bellgrove, M. A., Stokes, M. G., Henderson, T. R., Garavan, H., Robertson, I. H., et al. (2006). Executive "brake failure" following deactivation of human frontal lobe. *J. Cogn. Neurosci.* 18, 444–455. doi: 10.1162/089892906775990606

Chen, X., Scangos, K. W., and Stuphorn, V. (2010). Supplementary motor area exerts proactive and reactive control of arm movements. *J. Neurosci.* 30, 14657–14675. doi: 10.1523/JNEUROSCI.2669-10.2010

Chikazoe, J., Jimura, K., Hirose, S., Yamashita, K., Miyashita, Y., and Konishi, S. (2009). Preparation to inhibit a response complements response inhibition during performance of a stop-signal task. *J. Neurosci.* 29, 15870–15877. doi: 10.1523/JNEUROSCI.3645-09.2009

Churchland, M. M., and Shenoy, K. V. (2007). Delay of movement caused by disruption of cortical preparatory activity. *J. Neurophysiol.* 97, 348–359. doi: 10.1152/jn.00808.2006

Churchland, M. M., Yu, B. M., Ryu, S. I., Santhanam, G., and Shenoy, K. V. (2006). Neural variability in premotor cortex provides a signature of motor preparation. *J. Neurosci.* 26, 3697–3712. doi: 10.1523/JNEUROSCI.3762-05.2006

Cisek, P. (2006). Integrated neural processes for defining potential actions and deciding between them: a computational model. *J. Neurosci.* 26, 9761–9770. doi: 10.1523/JNEUROSCI.5605-05.2006

Cisek, P., and Kalaska, J. F. (2005). Neural correlates of reaching decisions in dorsal premotor cortex: specification of multiple direction choices and final selection of action. *Neuron* 45, 801–814. doi: 10.1016/j.neuron.2005.01.027

Cisek, P., and Kalaska, J. F. (2010). Neural mechanisms for interacting with a world full of action choices. *Annu. Rev. Neurosci.* 33, 269–298. doi: 10.1146/annurev.neuro.051508.135409

Corbetta, M., and Shulman, G. L. (2002). Control of goal-directed and stimulus-driven attention in the brain. *Nat. Rev. Neurosci.* 3, 201–215. doi: 10.1038/nrn755

Coxon, J. P., Stinear, C. M., and Byblow, W. D. (2006). Intracortical inhibition during volitional inhibition of prepared action. *J. Neurophysiol.* 95, 3371–3383. doi: 10.1152/jn.01334.2005

Cui, H., and Andersen, R. A. (2007). Posterior parietal cortex encodes autonomously selected motor plans. *Neuron* 56, 552–559. doi: 10.1016/j.neuron.2007.09.031

Damasio, A. R. (1994). *Descartes' Error: Emotion, Reason, and the Human Brain.* New York: Putman.

De Jong, R., Coles, M. G., Logan, G. D., and Gratton, G. (1990). In search of the point of no return: the control of response processes. *J. Exp. Psychol. Hum. Percept. Perform.* 16, 164–182. doi: 10.1037/0096-1523.16.1.164

Della Sala, S., Marchetti, C., and Spinnler, H. (1991). Right-sided anarchic (alien) hand: a longitudinal study. *Neuropsychologia* 29, 1113–1127. doi: 10.1016/0028-3932(91)90081-I

Eagle, D. M., Baunez, C., Hutcheson, D. M., Lehmann, O., Shah, A. P., and Robbins, T. W. (2008). Stop-signal reaction-time task performance: role of prefrontal cortex and subthalamic nucleus. *Cereb. Cortex* 18, 178–188. doi: 10.1093/cercor/bhm044

Fellows, L. K., and Farah, M. J. (2007). The role of ventromedial prefrontal cortex in decision making: judgment under uncertainty or judgment per se? *Cereb. Cortex* 17, 2669–2674. doi: 10.1093/cercor/bhl176

Forstmann, B. U., van den Wildenberg, W. P. M., and Ridderinkhof, K. R. (2008). Neural mechanisms, temporal dynamics, and individual differences in interference control. *J. Cogn. Neurosci.* 20, 1854–1865. doi: 10.1162/jocn.2008.20122

Freedman, D. J., Riesenhuber, M., Poggio, T., and Miller, E. K. (2002). Visual categorization and the primate prefrontal cortex: neurophysiology and behavior. *J. Neurophysiol.* 88, 929–941.

Freund, T. F., Powell, J. F., and Smith, A. D. (1984). Tyrosine hydroxylase-immunoreactive boutons in synaptic contact with identified striatonigral neurons, with particular reference to dendritic spines. *Neuroscience* 13, 1189–1215. doi: 10.1016/0306-4522(84)90294-X

Fried, I., Katz, A., McCarthy, G., Sass, K. J., Williamson, P., Spencer, S. S., et al. (1991). Functional organization of human supplementary motor cortex studied by electrical stimulation. *J. Neurosci.* 11, 3656–3666.

Fried, I., Mukamel, R., and Kreiman, G. (2011). Internally generated preactivation of single neurons in human medial frontal cortex predicts volition *Neuron* 69, 548–562. doi: 10.1016/j.neuron.2010.11.045

Fries, P. (2005). A mechanism for cognitive dynamics: neuronal communication through neuronal coherence. *Trends Cogn. Sci.* 9, 474–480. doi: 10.1016/j.tics.2005.08.011

Funahashi, S., Bruce, C. J., and Goldman-Rakic, P. S. (1989). Mnemonic coding of visual space in the monkey's dorsolateral prefrontal cortex. *J. Neurophysiol.* 61, 331–349.

Genovesio, A., Brasted, P. J., Mitz, A. R., and Wise, S. P. (2005). Prefrontal cortex activity related to abstract response strategies. *Neuron* 47, 307–320. doi: 10.1016/j.neuron.2005.06.006

Genovesio, A., Brasted, P. J., and Wise, S. P. (2006). Representation of future and previous spatial goals by separate neural populations in prefrontal cortex. *J. Neurosci.* 26, 7305–7316. doi: 10.1523/JNEUROSCI.0699-06.2006

Genovesio, A., Tsujimoto, S., and Wise, S. P. (2012). Encoding goals but not abstract magnitude in the primate prefrontal cortex. *Neuron* 74, 656–662. doi: 10.1016/j.neuron.2012.02.023

Genovesio, A., Wise, S. P., and Passingham, R. E. (2014). Prefrontal-parietal function: from foraging to foresight. *Trends Cogn. Sci.* 18, 72–81. doi: 10.1016/j.tics.2013.11.007

Georgopoulos, A. P., Kalaska, J. F., Caminiti, R., and Massey, J. T. (1982). On the relations between the direction of two-dimensional arm movements and cell discharge in primate motor cortex. *J. Neurosci.* 2, 1527–1537.

Gibson, J. J. (1979). *The Ecological Approach to Visual Perception.* Boston, MA: Houghton-Mifflin.

Glickstein, M., and Stein, J. (1991). Paradoxical movement in Parkinson's disease. *Trends Neurosci.* 14, 480–482. doi: 10.1016/0166-2236(91)90055-Y

Glimcher, P. W., Dorris, M. C., and Bayer, H. M. (2005). Physiological utility theory and the neuroeconomics of choice. *Games Econ. Behav.* 52, 213–256. doi: 10.1016/j.geb.2004.06.011

Grezes, J., and Decety, J. (2002). Does visual perception of object afford action? Evidence from a neuroimaging study. *Neuropsychologia* 40, 212–222. doi: 10.1016/S0028-3932(01)00089-6

Habib, M. (2004). Athymhormia and disorders of motivation in basal ganglia disease. *J. Neuropsychiatry Clin. Neurosci.* 16, 509–524. doi: 10.1176/appi.neuropsych.16.4.509

Haggard, P. (2008). Human volition: towards a neuroscience of will. *Nat. Rev. Neurosci.* 9, 934–946. doi: 10.1038/nrn2497

Hallett, M. (2007). Volitional control of movement: the physiology of free will. *Clin. Neurophysiol.* 118, 1179–1192. doi: 10.1016/j.clinph.2007.03.019

Hanes, D. P., and Schall, J. D. (1996). Neural control of voluntary movement initiation. *Science* 274, 427–430. doi: 10.1126/science.274.5286.427

Hare, T. A., O'Doherty, J., Camerer, C. F., Schultz, W., and Rangel, A. (2008). Dissociating the role of the orbitofrontal cortex and the striatum in the computation of goal values and prediction errors. *J. Neurosci.* 28, 5623–5630. doi: 10.1523/JNEUROSCI.1309-08.2008

Hatsopoulos, N. G., and Donoghue, J. P. (2009). The science of neural interface systems. *Annu. Rev. Neurosci.* 32, 249–266. doi: 10.1146/annurev.neuro.051508.135241

Holroyd, C. B., and Coles, M. G. (2002). The neural basis of human error processing: reinforcement learning, dopamine, and the error-related negativity. *Psychol. Rev.* 109, 679–709. doi: 10.1037/0033-295X.109.4.679

Hoshi, E., Shima, K., and Tanji, J. (2000). Neuronal activity in the primate prefrontal cortex in the process of motor selection based on two behavioral rules. *J. Neurophysiol.* 83, 2355–2373.

Hoshi, E., and Tanji, J. (2000). Integration of target and body-part information in the premotor cortex when planning action. *Nature* 408, 466–470. doi: 10.1038/35044075

Hoshi, E., and Tanji, J. (2002). Contrasting neuronal activity in the dorsal and ventral premotor areas during preparation to reach. *J. Neurophysiol.* 87, 1123–1128.

Humphreys, G. W., and Riddoch, M. J. (2000). One more cup of coffee for the road: object-action assemblies, response blocking and response capture after frontal lobe damage. *Exp. Brain Res.* 133, 81–93. doi: 10.1007/s002210000403

Ifft, P. J., Lebedev, M. A., and Nicolelis, M. A. (2012). Reprogramming movements: extraction of motor intentions from cortical ensemble activity when movement goals change. *Front. Neuroeng.* 5:16. doi: 10.3389/fneng.2012.00016

Jahfari, S., Stinear, C. M., Claffey, M., Verbruggen, F., and Aron, A. R. (2010). Responding with restraint: what are the neurocognitive mechanisms? *J. Cogn. Neurosci.* 22, 1479–1492. doi: 10.1162/jocn.2009.21307

Jahfari, S., Verbruggen, F., Frank, M. J., Waldorp, L. J., Colzato, L., Ridderinkhof, K. R., et al. (2012). How preparation changes the need for top-down control of the basal ganglia when inhibiting premature actions. *J. Neurosci.* 32, 10870–10878. doi: 10.1523/JNEUROSCI.0902-12.2012

Kennerley, S. W., Walton, M. E., Behrens, T. E. J., Buckley, M. J., and Rushworth, M. F. S. (2006). Optimal decision making and the anterior cingulate cortex. *Nat. Neurosci.* 9, 940–947. doi: 10.1038/nn1724

Klaes, C., Westendorff, S., Chakrabarti, S., and Gail, A. (2011). Choosing goals, not rules: deciding among rule-based action plans. *Neuron* 70, 536–548. doi: 10.1016/j.neuron.2011.02.053

Koenigs, M., and Tranel, D. (2007). Irrational economic decision-making after ventromedial prefrontal damage: evidence from the Ultimatum Game. *J. Neurosci.* 27, 951–956. doi: 10.1523/JNEUROSCI.4606-06.2007

Lebedev, M. A., Messinger, A., Kralik, J. D., and Wise, S. P. (2004). Representation of attended versus remembered locations in prefrontal cortex. *PLoS Biol.* 2:e365. doi: 10.1371/journal.pbio.0020365

Lebedev, M. A., and Wise, S. P. (2001). Tuning for the orientation of spatial attention in dorsal premotor cortex. *Eur. J. Neurosci.* 13, 1002–1008. doi: 10.1046/j.0953-816x.2001.01457.x

Li, C. S., Yan, P., Sinha, R., and Lee, T. W. (2008). Subcortical processes of motor response inhibition during a stop signal task. *Neuroimage* 41, 1352–1363. doi: 10.1016/j.neuroimage.2008.04.023

Liakakis, G., Nickel, J., and Seitz, R. J. (2011). Diversity of the inferior frontal gyrus – a meta-analysis of neuroimaging studies. *Behav. Brain Res.* 225, 341–347. doi: 10.1016/j.bbr.2011.06.022

Libet, B. (1985). Unconscious cerebral initiative and the role of conscious will in voluntary action. *Behav. Brain Sci.* 8, 529–566. doi: 10.1017/S0140525X00044903

Libet, B., Gleason, C. A., Wright, E. W., and Pearl, D. K. (1983). Time of conscious intention to act in relation to onset of cerebral activity (readiness-potential). The unconscious initiation of a freely voluntary act. *Brain* 106, 623–642. doi: 10.1093/brain/106.3.623

Lindenberg, R., Uhlig, M., Scherfeld, D., Schlaug, G., and Seitz, R. J. (2012). Communication with emblematic gestures: shared and distinct neural correlates of expression and reception. *Hum. Brain Mapp.* 33, 812–823. doi: 10.1002/hbm.21258

Logan, G. D., and Cowan, W. B. (1984). On the ability to inhibit thought and action: a theory of an act of control. *Psychol. Rev.* 91, 295–327. doi: 10.1037/0033-295X.91.3.295

Logan, G. D., and Irwin, D. E. (2000). Don't look! Don't touch! Inhibitory control of eye and hand movements. *Psychon. Bull. Rev.* 7, 107–112. doi: 10.3758/BF03210728

Loukas, C., and Brown, P. (2004). Online prediction of self-paced hand-movements from subthalamic activity using neural networks in Parkinson's disease. *J. Neurosci. Methods* 137, 193–205. doi: 10.1016/j.jneumeth.2004.02.017

Mattia, M., Pani, P., Mirabella, G., Costa, S., Del Giudice, P., and Ferraina, S. (2013). Heterogeneous attractor cell assemblies for motor planning in premotor cortex. *J. Neurosci.* 33, 11155–11168. doi: 10.1523/JNEUROSCI.4664-12.2013

Mattia, M., Spadacenta, S., Pavone, L., Quarato, P., Esposito, V., Sparano, A., et al. (2012). Stop-event-related potentials from intracranial electrodes reveal a key role of premotor and motor cortices in stopping ongoing movements. *Front. Neuroeng.* 5:12. doi: 10.3389/fneng.2012.00012

Mazzoni, P., Hristova, A., and Krakauer, J. W. (2007). Why don't we move faster? Parkinson's disease, movement vigor, and implicit motivation. *J. Neurosci.* 27, 7105–7116. doi: 10.1523/JNEUROSCI.0264-07.2007

Milner, D., and Goodale, M. (1995). *The Visual Brain in Action.* Oxford: Oxford University press.

Mirabella, G. (2007). Endogenous Inhibition and the neural basis of "free won't." *J. Neurosci.* 27, 13919–13920. doi: 10.1523/JNEUROSCI.4943-07.2007

Mirabella, G. (2012). Volitional inhibition and brain-machine interfaces: a mandatory wedding. *Front. Neuroeng.* 5:20. doi: 10.3389/fneng.2012.00020

Mirabella, G., Bertini, G., Samengo, I., Kilavik, B. E., Frilli, D., Della Libera, C., et al. (2007). Neurons in area V4 of the macaque translate attended features into behaviorally relevant categories. *Neuron* 54, 303–318. doi: 10.1016/j.neuron.2007.04.007

Mirabella, G., Iaconelli, S., Modugno, N., Giannini, G., Lena, F., and Cantore, G. (2013). Stimulation of subthalamic nuclei restores a near normal planning strategy in Parkinson's patients. *PLoS ONE* 8:e62793. doi: 10.1371/journal.pone.0062793

Mirabella, G., Iaconelli, S., Romanelli, P., Modugno, N., Lena, F., Manfredi, M., et al. (2012). Deep brain stimulation of subthalamic nuclei affects arm response inhibition in Parkinson's patients. *Cereb. Cortex* 22, 1124–1132. doi: 10.1093/cercor/bhr187

Mirabella, G., Pani, P., and Ferraina, S. (2008). Context influences on the preparation and execution of reaching movements. *Cogn. Neuropsychol.* 25, 996–1010. doi: 10.1080/02643290802003216

Mirabella, G., Pani, P., and Ferraina, S. (2009). The presence of visual gap affects the duration of stopping process. *Exp. Brain Res.* 192, 199–209. doi: 10.1007/s00221-008-1570-y

Mirabella, G., Pani, P., and Ferraina, S. (2011). Neural correlates of cognitive control of reaching movements in the dorsal premotor cortex of rhesus monkeys. *J. Neurophysiol.* 106, 1454–1466. doi: 10.1152/jn.00995.2010

Mirabella, G., Pani, P., Paré, M., and Ferraina, S. (2006). Inhibitory control of reaching movements in humans. *Exp. Brain Res.* 174, 240–255. doi: 10.1007/s00221-006-0456-0

Montague, P. R., Hyman, S. E., and Cohen, J. D. (2004). Computational roles for dopamine in behavioural control. *Nature* 431, 760–767. doi: 10.1038/nature03015

Murata, A., Fadiga, L., Fogassi, L., Gallese, V., Raos, V., and Rizzolatti, G. (1997). Object representation in the ventral premotor cortex (area F5) of the monkey. *J. Neurophysiol.* 78, 2226–2230.

O'Doherty, J. P., Dayan, P., Friston, K., Critchley, H., and Dolan, R. J. (2003). Temporal difference models and reward-related learning in the human brain. *Neuron* 38, 329–337. doi: 10.1016/S0896-6273(03)00169-7

Padoa-Schioppa, C., and Assad, J. A. (2006). Neurons in the orbitofrontal cortex encode economic value. *Nature* 441, 223–226. doi: 10.1038/nature04676

Padoa-Schioppa, C., and Assad, J. A. (2008). The representation of economic value in the orbitofrontal cortex is invariant for changes of menu. *Nat. Neurosci.* 11, 95–102. doi: 10.1038/nn2020

Paradiso, G., Saint-Cyr, J. A., Lozano, A. M., Lang, A. E., and Chen, R. (2003). Involvement of the human subthalamic nucleus in movement preparation. *Neurology* 61, 1538–1545. doi: 10.1212/01.WNL.0000096021.28967.57

Petrides, M., and Pandya, D. N. (1999). Dorsolateral prefrontal cortex: comparative cytoarchitectonic analysis in the human and the macaque brain and corticocortical connection patterns. *Eur. J. Neurosci.* 11, 1011–1136. doi: 10.1046/j.1460-9568.1999.00518.x

Petrides, M., and Pandya, D. N. (2002). Comparative cytoarchitectonic analysis of the human and the macaque ventrolateral prefrontal cortex and corticocortical connection patterns in the monkey. *Eur. J. Neurosci.* 16, 291–310. doi: 10.1046/j.1460-9568.2001.02090.x

Prut, Y., and Fetz, E. E. (1999). Primate spinal interneurons show pre-movement instructed delay activity. *Nature* 401, 590–594. doi: 10.1038/44145

Rangel, A., Camerer, C., and Montague, P. R. (2008). A framework for studying the neurobiology of value-based decision making. *Nat. Rev. Neurosci.* 9, 545–556. doi: 10.1038/nrn2357

Reynolds, J. H., and Chelazzi, L. (2004). Attentional modulation of visual processing. *Annu. Rev. Neurosci.* 27, 611–647. doi: 10.1146/annurev.neuro.26.041002.131039

Ridderinkhof, K. R., Forstmann, B. U., Wylie, S. A., Burle, B., and van den Wildenberg, W. P. M. (2011). Neurocognitive mechanisms of action control: resisting the call of the sirens. *Cogn. Sci.* 2, 174–192. doi: 10.1002/wcs.99

Ridderinkhof, K. R., and van den Wildenberg, W. P. (2005). Adaptive coding. *Science* 307, 1059–1060. doi: 10.1126/science.1109837

Ridderinkhof, K. R., van den Wildenberg, W. P., Segalowitz, S. J., and Carter, C. S. (2004). Neurocognitive mechanisms of cognitive control: the role of prefrontal cortex in action selection, response inhibition, performance monitoring, and reward-based learning. *Brain Cogn.* 56, 129–140. doi: 10.1016/j.bandc.2004.09.016

Riehle, A., and Requin, J. (1989). Monkey primary motor and premotor cortex: single-cell activity related to prior information about direction and extent of an intended movement. *J. Neurophysiol.* 61, 534–549.

Rizzolatti, G., and Craighero, L. (2004). The mirror-neuron system. *Annu. Rev. Neurosci.* 27, 169–192. doi: 10.1146/annurev.neuro.27.070203.144230

Rizzolatti, G., and Luppino, G. (2001). The cortical motor system. *Neuron* 31, 889–901. doi: 10.1016/S0896-6273(01)00423-8

Roskies, A. L. (2010). How does neuroscience affect our conception of volition? *Annu. Rev. Neurosci.* 33, 109–130. doi: 10.1146/annurev-neuro-060909-153151

Scangos, K. W., and Stuphorn, V. (2010). Medial frontal cortex motivates but does not control movement initiation in the countermanding task. *J. Neurosci.* 30, 1968–1982. doi: 10.1523/JNEUROSCI.4509-09.2010

Schall, J. D., and Godlove, D. C. (2012). Current advances and pressing problems in studies of stopping. *Curr. Opin. Neurobiol.* 22, 1012–1021. doi: 10.1016/j.conb.2012.06.002

Scherberger, H., and Andersen, R. A. (2007). Target selection signals for arm reaching in the posterior parietal cortex. *J. Neurosci.* 27, 2001–2012. doi: 10.1523/JNEUROSCI.4274-06.2007

Schlesinger, I., Erikh, I., and Yarnitsky, D. (2007). Paradoxical kinesia at war. *Mov. Disord.* 22, 2394–2397. doi: 10.1002/mds.21739

Schmidt, L., d'Arc, B. F., Lafargue, G., Galanaud, D., Czernecki, V., Grabli, D., et al. (2008). Disconnecting force from money: effects of basal ganglia damage on incentive motivation. *Brain* 131, 1303–1310. doi: 10.1093/brain/awn045

Schultz, W., Dayan, P., and Montague, P. R. (1997). A neural substrate of prediction and reward. *Science* 275, 1593–1599. doi: 10.1126/science.275.5306.1593

Shenoy, K. V., Sahani, M., and Churchland, M. M. (2013). Cortical control of arm movements: a dynamical systems perspective. *Annu. Rev. Neurosci.* 36, 337–359. doi: 10.1146/annurev-neuro-062111-150509

Sheth, S. A., Mian, M. K., Patel, S. R., Asaad, W. F., Williams, Z. M., Dougherty, D. D., et al. (2012). Human dorsal anterior cingulate cortex neurons mediate ongoing behavioural adaptation. *Nature* 488, 218–221. doi: 10.1038/nature11239

Singer, T., Seymour, B., O'Doherty, J., Kaube, H., Dolan, R. J., and Frith, C. D. (2004). Empathy for pain involves the affective but not sensory components of pain. *Science* 303, 1157–1162. doi: 10.1126/science.1093535

Smith, P. L., and Ratcliff, R. (2004). Psychology and neurobiology of simple decisions. *Trends Neurosci.* 27, 161–168. doi: 10.1016/j.tins.2004.01.006

Smith, Y., Bennett, B. D., Bolam, J. P., Parent, A., and Sadikot, A. F. (1994). Synaptic relationships between dopaminergic afferents and cortical or thalamic input in the sensorimotor territory of the striatum in monkey. *J. Comp. Neurol.* 344, 1–19. doi: 10.1002/cne.903440102

Stevenson, S. A., Elsley, J. K., and Corneil, B. D. (2009). A "gap effect" on stop signal reaction times in a human saccadic countermanding task. *J. Neurophysiol.* 101, 580–590. doi: 10.1152/jn.90891.2008

Sumner, P., Nachev, P., Morris, P., Jackson, S. R., Kennard, C., and Husain, M. (2007). Human medial frontal cortex mediates unconscious inhibition of voluntary action. *Neuron* 54, 697–711. doi: 10.1016/j.neuron.2007.05.016

Swann, N., Poizner, H., Houser, M., Gould, S., Greenhouse, I., Cai, W., et al. (2011). Deep brain stimulation of the subthalamic nucleus alters the cortical profile of response inhibition in the beta frequency band: a scalp EEG study in Parkinson's disease. *J. Neurosci.* 31, 5721–5729. doi: 10.1523/JNEUROSCI.6135-10.2011

Swann, N., Tandon, N., Canolty, R., Ellmore, T. M., McEvoy, L. K., Dreyer, S., et al. (2009). Intracranial EEG reveals a time-and frequency-specific role for the right inferior frontal gyrus and primary motor cortex in stopping initiated responses. *J. Neurosci.* 29, 12675–12685. doi: 10.1523/JNEUROSCI.3359-09.2009

Tanji, J., and Evarts, E. V. (1976). Anticipatory activity of motor cortex neurons in relation to direction of an intended movement. *J. Neurophysiol.* 39, 1062–1068.

Tsujimoto, S., Genovesio, A., and Wise, S. P. (2010). Evaluating self-generated decisions in frontal pole cortex of monkeys. *Nat. Neurosci.* 13, 120–126. doi: 10.1038/nn.2453

Tsujimoto, S., Genovesio, A., and Wise, S. P. (2011). Frontal pole cortex: encoding ends at the end of the endbrain. *Trends Cogn. Sci.* 15, 169–176. doi: 10.1016/j.tics.2011.02.001

Turner, R. S., and Desmurget, M. (2010). Basal ganglia contributions to motor control: a vigorous tutor. *Curr. Opin. Neurobiol.* 20, 704–716. doi: 10.1016/j.conb.2010.08.022

Uddén, J., and Bahlmann, J. (2012). A rostro-caudal gradient of structured sequence processing in the left inferior frontal gyrus. *Philos. Trans. R. Soc. Lond. B Biol. Sci.* 367, 2023–2032. doi: 10.1098/rstb.2012.0009

Van den Wildenberg, W. P., van Boxtel, G. J., van der Molen, M. W., Bosch, D. A., Speelman, J. D., and Brunia, C. H. (2006). Stimulation of the subthalamic region facilitates the selection and inhibition of motor responses in Parkinson's disease. *J. Cogn. Neurosci.* 18, 626–636. doi: 10.1162/jocn.2006.18.4.626

van Gaal, S., Ridderinkhof, K. R., Fahrenfort, J. J., Scholte, H. S., and Lamme, V. A. (2008). Frontal cortex mediates unconsciously triggered inhibitory control. *J. Neurosci.* 28, 8053–8062. doi: 10.1523/JNEUROSCI.1278-08.2008

van Gaal, S., Scholte, H. S., Lamme, V. A., Fahrenfort, J. J., and Ridderinkhof, K. R. (2011). Pre-SMA graymatter density predicts individual differences in action selection in the face of conscious and unconscious response conflict *J. Cogn. Neurosci.* 23, 382–390. doi: 10.1162/jocn.2010.21444

Verbruggen, F., and Logan, G. D. (2009). Proactive adjustments of response strategies in the stop-signal paradigm. *J. Exp. Psychol. Hum. Percept. Perform.* 35, 835–854. doi: 10.1037/a0012726

von der Malsburg, C., Phillips, W. A., and Singer, W. (2010). *Dynamic Coordination in the Brain: From Neurons to Mind.* Cambridge, MA: The MIT Press. doi: 10.7551/mitpress/9780262014717.001.0001

Wallis, J. D. (2007). Orbitofrontal cortex and its contribution to decision-making. *Annu. Rev. Neurosci.* 30, 31–56. doi: 10.1146/annurev.neuro.30.051606.094334

Weinrich, M., Wise, S. P., and Mauritz, K. H. (1984). A neurophysiological study of the premotor cortex in the rhesus monkey. *Brain* 107, 385–414. doi: 10.1093/brain/107.2.385

Wise, S. P. (2008). Forward frontal fields: phylogeny and fundamental function. *Trends Neurosci.* 31, 599–608. doi: 10.1016/j.tins.2008.08.008

Wise, S. P., Weinrich, M., and Mauritz, K. H. (1983). Motor aspects of cue-related neuronal activity in premotor cortex of the rhesus monkey. *Brain Res.* 260, 301–305. doi: 10.1016/0006-8993(83)90685-6

Wolpaw, J. R., and McFarland, D. J. (2004). Control of a two-dimensional movement signal by a noninvasive brain-computer interface in humans. *Proc. Natl. Acad. Sci. U.S.A.* 101, 17849–17854. doi: 10.1073/pnas.0403504101

Wolpert, D. M., and Miall, R. C. (1996). Forward models for physiological motor control. *Neural Netw.* 9, 1265–1279. doi: 10.1016/S0893-6080(96)00035-4

Zandbelt, B. B., Bloemendaal, M., Neggers, S. F., Kahn, R. S., and Vink, M. (2013). Expectations and violations: delineating the neural network of proactive inhibitory control. *Hum. Brain Mapp.* 34, 2015–2024. doi: 10.1002/hbm.22047

Zandbelt, B. B., and Vink, M. (2010). On the role of the striatum in response inhibition. *PLoS ONE* 5:e13848. doi: 10.1371/journal.pone.0013848

Zheng, D., Oka, T., Bokura, H., and Yamaguchi, S. (2008). The key locus of common response inhibition network for nogo and stop signals. *J. Cogn. Neurosci.* 20, 1–9. doi: 10.1162/jocn.2008.20100

Conflict of Interest Statement: The author declares that the research was conducted in the absence of any commercial or financial relationships that could be construed as a potential conflict of interest.

Received: 01 August 2014; accepted: 01 October 2014; published online: 03 November 2014.

Citation: Mirabella G (2014) Should I stay or should I go? Conceptual underpinnings of goal-directed actions. Front. Syst. Neurosci. ***8****:206. doi: 10.3389/fnsys.2014.00206*

This article was submitted to Frontiers in Systems Neuroscience.

frontiers in Neuroscience

ORIGINAL RESEARCH
published: 05 August 2016
doi: 10.3389/fnins.2016.00336

Neostriatal Neuronal Activity Correlates Better with Movement Kinematics under Certain Rewards

Ioan Opris[1], Mikhail A. Lebedev[2] and Randall J. Nelson[3]*

[1] Miami Project, University of Florida, Miami, FL, USA, [2] Department of Neurobiology, Duke University, Durham, NC, USA, [3] Department of Anatomy and Neurobiology, The University of Tennessee Health Science Center, Memphis, TN, USA

This study investigated how the activity of neostriatal neurons is related to the kinematics of movement when monkeys performed visually and vibratory cued wrist extensions and flexions. Single-unit recordings of 142/236 neostriatal neurons showed pre-movement activity (PMA) in a reaction time task with unpredictable reward. Monkeys were pseudo-randomly (75%) rewarded for correct performance. A regression model was used to determine whether the correlation between neostriatal neuronal activity and the kinematic variables (position, velocity, and acceleration) of wrist movement changes as a function of reward contingency, sensory cues, and movement direction. The coefficients of determination (CoD) representing the proportion of the variance in neuronal activity explained by the regression model on a trial by trial basis, together with their temporal occurrences (time of best regression/correlation, ToC) were compared across sensory modality, movement direction, and reward contingency. The best relationship (correlation) between neuronal activity and movement kinematic variables, given by the average coefficient of determination (CoD), was: (a) greater during trials in which rewards were certain, called "A" trials, as compared with those in which reward was uncertain called ("R") trials, (b) greater during flexion (Flex) trials as compared with extension (Ext) trials, and (c) greater during visual (VIS) cued trials than during vibratory (VIB) cued trials, for the same type of trial and the same movement direction. These results are consistent with the hypothesis that predictability of reward for correct performance is accompanied by faster linkage between neostriatal PMA and the vigor of wrist movement kinematics. Furthermore, the results provide valuable insights for building an upper-limb neuroprosthesis.

Keywords: basal ganglia, neostriatum, neuronal activity, movement preparation, hand movement, multilinear regression, reward uncertainty, motivation

OPEN ACCESS

Edited by:
Yoshio Sakurai, Doshisha University, Japan

Reviewed by:
Vassiliy Tsytsarev, University of Maryland School of Medicine, USA
Christian K. E. Moll, University Medical Center Hamburg-Eppendorf, Germany

****Correspondence:***
Ioan Opris
ioanopris.phd@gmail.com; ixo82@med.miami.edu

Specialty section:
This article was submitted to Neural Technology, a section of the journal Frontiers in Neuroscience

Received: *20 April 2016*
Accepted: *04 July 2016*
Published: *05 August 2016*

Citation:
Opris I, Lebedev MA and Nelson RJ (2016) Neostriatal Neuronal Activity Correlates Better with Movement Kinematics under Certain Rewards. Front. Neurosci. 10:336. doi: 10.3389/fnins.2016.00336

INTRODUCTION

A significant proportion of neurons from neostriatum (NS) modulate their firing rate in response to environmental stimuli and/or fire before movement initiation and/or execution (Aldridge et al., 1980; Liles, 1985; Schultz and Romo, 1988; Alexander and Crutcher, 1990; Kimura, 1990; Romo and Schultz, 1990; Gardiner and Nelson, 1992; Lebedev and Nelson, 1999; Opris et al., 2011a). Several studies indicate that NS neurons may also participate in associating task stimuli with rewards (Schultz and Romo, 1990; Apicella et al., 1991; Robbins and Everitt, 1996; Opris et al., 2009; Schultz, 2010) or in modulating movement vigor (Opris et al., 2011a).

This connection between reinforcement and behavior may be mediated by the dopaminergic system at either sub-cortical or cortical levels (Robbins and Everitt, 1996; Schultz et al., 1997). After behaviors are learned, a state of expectation about the time of occurrence of reward delivery relative to requested behaviors is created (Apicella et al., 1991, 1992; Schultz et al., 1992, 1993).

It has also been suggested that during goal-oriented behavior NS neurons exhibit context-dependent behavioral responses that may vary depending on changes in the predictability of the linkage between stimuli and rewards (Schultz and Romo, 1990; Apicella et al., 1992; Schultz et al., 1992; Mirenowicz and Schultz, 1994). Moreover, several lines of evidence indicate that the NS neuronal activity may become better related to movements and sensory cues when behavioral conditions are novel (Mirenowicz and Schultz, 1994; Nelson et al., 1996; Berns et al., 1997). Sensitivity to novelty seems to be a property of neurons in the substantia nigra, the ventral striatum, and the prefrontal cortex (Apicella et al., 1991; Schultz et al., 1992, 1993; Watanabe, 1996; Berns et al., 1997; Schultz, 2010). Surmeier and Kitai (1997) indicated that the dopaminergic inputs to neostriatum may "shape" the activity of NS neurons involved in motor behavior. Therefore, the substantia nigra, ventral striatum and prefrontal cortex may influence segments of the so-called "motor loop" (which includes the dorsal striatum) where pre-movement activity (PMA) often occurs (Alexander et al., 1986; Hoover and Strick, 1993; Graybiel et al., 1994; Watanabe, 1996; Berns et al., 1997).

We hypothesize that primate dorsal striatum (Putamen and Caudate Nucleus) is part of a system that modulates the behavioral parameters (i.e., movement kinematics: position, speed, and acceleration), depending on the probability of the expected reward (Fu et al., 1995; Fiorillo et al., 2003; Lee and Assad, 2003; Stark et al., 2007; Pekny et al., 2015; Reppert et al., 2015). Dorsal striatum may be responsible for enhancing movement vigor when rewards are certain and decreasing the vigor when rewards become uncertain (Turner and Desmurget, 2010; Opris et al., 2011a). This hypothesis is supported by the finding that changes in dorsal striatal activity occur shortly after go cues and clearly earlier than the movements (100–200 ms before movements). Therefore, *certain rewards* may mediate a stronger correlation (Opris et al., 2011a) between neostriatal PMA and the kinematics of wrist movements.

Below, we describe the changes in NS neuronal activity in relation to movement kinematics by using a multilinear regression analysis (Ashe and Georgopoulos, 1994). Furthermore, we believe that striatal modulations can provide a good motor signal for neuroprosthetics (Lebedev and Nicolelis, 2006; Nicolelis and Lebedev, 2009). The goals of this study was to: (a) determine if the correlation between NS firing rates and the movement kinematics varies as a function of go-cue modality, movement directions, behavioral contexts; and (b) quantify the occurrence and timing of best relationship/correlation between NS neuronal activity and hand movement kinematics. Moreover, since changes in movement related NS activity often occur 100–200 ms before movements, it is possible that unpredictable behavioral conditions modify NS activity that is involved in movement preparation and initiation. The results are relevant for the decoding of wrist kinematics for building an upper-limb neuroprosthesis (Lebedev et al., 2005; Aggarwal et al., 2009).

MATERIALS AND METHODS

Experimental Apparatus and Behavioral Paradigm

Two adult male rhesus monkeys (*Macaca mulatta*: E, N) were trained to make wrist flexion and extension movements in response to vibratory or visual stimuli (Lebedev and Nelson, 1995; Liu et al., 2005; Opris et al., 2011a). The monkeys were cared for in accordance with the National Research Council Guide for the Care and Use of Laboratory Animals. Experimental protocols were approved by the Animal Care and Use Committee of The University of Tennessee Health Science Center, Memphis. Detailed descriptions of the experimental apparatus have been provided elsewhere (Gardiner and Nelson, 1992; Lebedev and Nelson, 1995; Liu et al., 2005, 2008). A brief description is provided below.

Each monkey sat in an acrylic monkey chair, with its right palm on a movable plate (**Figure 1A**). One end of the plate was attached to the axle of a brushless D.C. torque motor (Colburn and Evarts, 1978). A load of 0.07 Nm was applied to the plate. The load assisted wrist extensions and opposed wrist flexions. Feedback of current wrist position was provided by a visual display consisting of 31 light-emitting diodes (LEDs), located 35 cm in front of the animal. The middle, red LED corresponded to a centered wrist position. Yellow LEDs (above and below the middle LED) indicated successive angular deviations of 1°. Two instructional LEDs were located in the upper left corner of the visual display. When the first red LED was illuminated at the start of a trial, it indicated that extension movements should be made; otherwise flexions were required. When the second, green LED was illuminated, it informed the monkey that the go-cue for that trial would be a palmar vibration; otherwise, the go-cue was the illumination of one of two LEDs which were each 5° from the center. Vibratory go-cues of 27, 57, and 127 Hz were routinely used. In this paper we consider only records of neuronal activity triggered by vibratory cues at 57 Hz and/or visual go-cues.

The behavioral paradigm is illustrated schematically in **Figure 1B** and the partition of reaction time (RT) interval in **Figure 1C**. Each trial began when the monkey centered the plate. At this time a movement direction request was given by the instructional LED as described above. The monkey was required to hold the plate in the centered position for 0.5, 1.0, 1.5, 2.0 s (pseudo-randomized) without moving, until a go cue (visual or vibrotactile) was presented. If the animal moved prior to the completion of the hold period, the trial was canceled. If the monkey made the requested movement of 5° or greater, he received a fruit juice reward. The reward delivery for blocks of 10 trials per direction was pseudorandom with correct performance being rewarded on average 75% of the time. Two unrewarded trials were never imposed sequentially. The type of trials under this pseudorandom reward schedule included: (i) rewarded trials, for which the current and the immediately

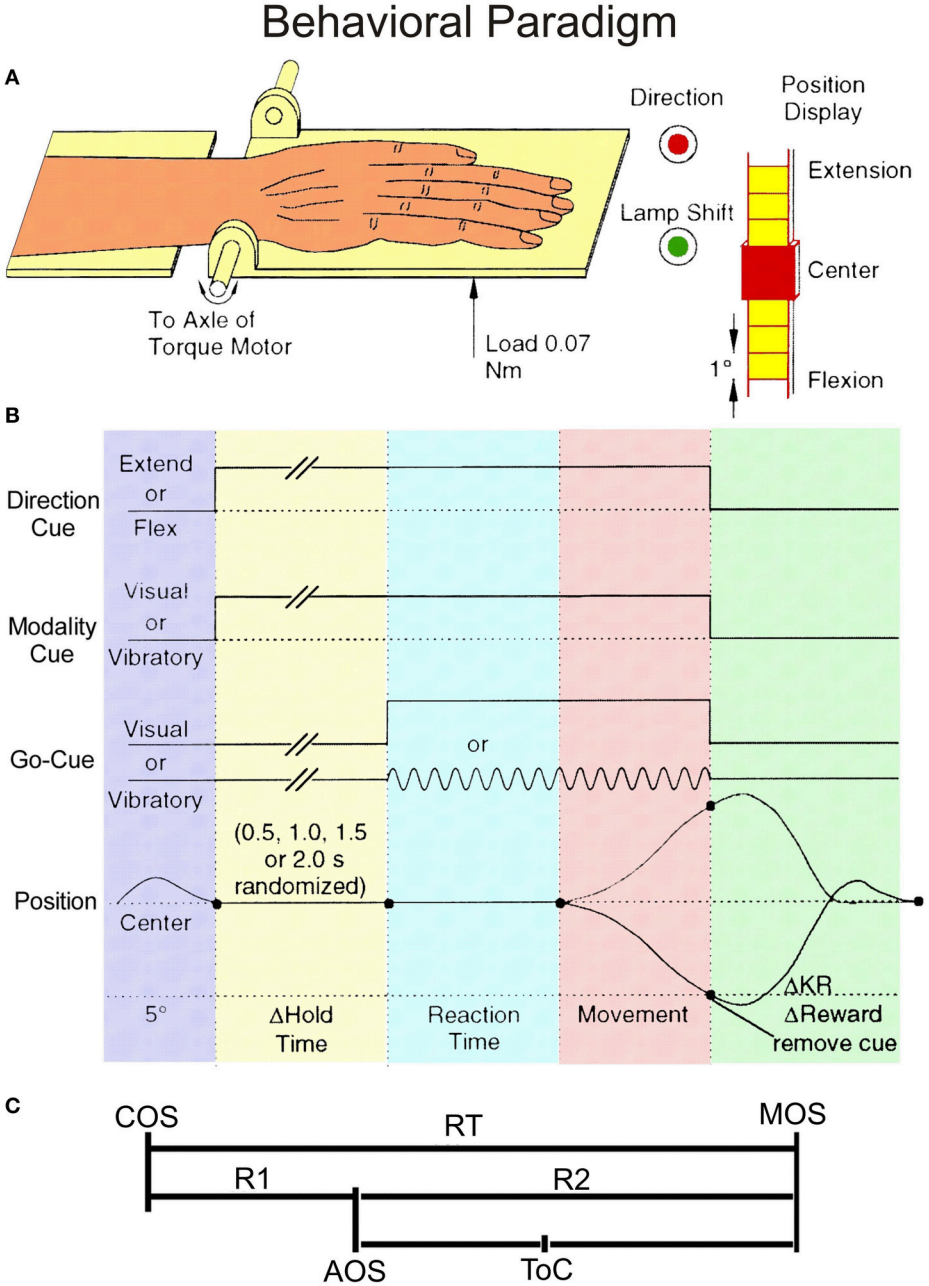

FIGURE 1 | Behavioral paradigm. (A) The experimental setup showing monkey's hand on the handle together with the instruction LEDs. **(B)** Schematic diagram of the unpredictable task. The direction cue was given by a red LED that was illuminated during extension trials, but not during flexion trials. The modality cue was a green LED that was illuminated during vibratory cued trials but not during visually cued trials. The onset of these instructional cues was coincident with the onset of the hold period. They remained lit until the end of the trial, coincident with reward delivery. Go-cues that signaled the monkeys could initiate wrist movements were presented after a variable time delay of 0.5, 1.0, 1.5, or 2.0 s (pseudo-randomized). **(C)** Divisions of the Reaction Time (RT) interval. RT has been split into two intervals: R1, the latency from cue onset (COS) to premovement activity onset (AOS), and R2, the time from AOS until movement onset (MOS). ToC represents the time of best correlation (time at best CoD).

preceding trial were rewarded, called regular ("R") trials, (ii) unrewarded trials, and (iii) trials immediately following withheld rewards, called after ("A") trials or *certain reward* trials (while reward in all other trials was *uncertain*). In some instances there were trials in which the animal failed to perform properly (i.e., made a movement in the wrong direction). For analyses we required that each neuron must have at least 4 valid trials per condition. If any single group of records had fewer than 4 trials, the data from that group were not included in the analyses.

Electrophysiological Recordings and Histology

Once an animal reached a stable daily performance level (∼2000 rewarded trials per experimental session), it was prepared for recording. A stainless steel recording chamber was surgically implanted over the skull to allow for extracellular recordings of the activity of basal ganglia neurons by using platinum-iridium microelectrodes with impedances of 1–2 MOhms (see Nelson et al., 1991; Gardiner and Nelson, 1992). Transdural penetrations began no sooner than 1 week after the chamber implantation. In each recording session, a microelectrode was lowered into the striatum and the activity of single units was amplified, discriminated, and stored in a computer by conventional means (Lebedev and Nelson, 1995; Liu et al., 2005). Neuronal receptive fields (RFs) were examined by lightly touching punctuate skin surfaces, manipulating joints, and palpating muscles. On occasion, the electromyographic (EMG) activity patterns of forearm muscles acting across the wrist were recorded using intramuscular EMG wires (see Nelson, 1987). EMG activity was converted into pulse data (Nelson, 1987; Vaadia et al., 1988). On the last recording day, electrolytic lesions were made to mark some recording locations by passing 10 μA of current for 10–20 s. These lesions provided references for the histological reconstruction of the recording sites. The animal was then deeply anesthetized with sodium pentobarbital and transcardially perfused with 10% buffered formol-saline. The brain was removed from the skull, and cut on a freezing microtome into 50 μm thick coronal sections. Histological sections of the basal ganglia (**Figure 2**) were stained for Nissl substance. Recording sites were reconstructed based on the depth of each electrode penetration and its location with respect to the marking lesions (Nelson, 1988; Nelson et al., 1991).

Data Analysis

Neuronal activity data, recorded on-line (Lebedev and Nelson, 1995, 1996; Liu et al., 2005; Opris et al., 2011a), were processed by off-line analysis programs and displayed as rasters, peri-event time histogram (PETH), fractional interspike interval (ISI) histogram (FISIH; Ashe and Georgopoulos, 1994), and traces of position, velocity, and acceleration, aligned on important events in the animal's behavior. A multilinear regression analysis (Ashe and Georgopoulos, 1994) has been used to regress low-pass filtered single trial spike functions coming from a FISIH, against position, velocity, and acceleration traces.

Multilinear Regression Analysis

An important step in our implementation of the regression analysis is the formulation of a FISIH from single trial neuronal activity records. We followed almost precisely the published methods (Ashe and Georgopoulos, 1994; Taira et al., 1996). This type of histogram is a filtered version of a binned PETH, in which the fraction of each ISI that is distributed across a given bin is calculated. The whole ISI is equal to unity, whereas each bin receives fractional contributions relative to the interval of that bin. We have employed single trial FISIHs, as well as, composite FISIH representing up to 40 trials. Each spike train was binned in 5 ms bins and the time-varying frequency of cell discharge, d(t), was computed from FISIHs. The resulting spike function, f(t), was smoothed using a 5-point low-pass filter, then the squared root of each point comprising the function was taken (Cox and Lewis, 1966; Ashe and Georgopoulos, 1994) and the resultant was divided by the binwidth (bw; in seconds), to convert this function to units proportional to the instantaneous firing rate:

$$f(t) = \mathrm{sqrt}(d(t))/bw \quad (1)$$

The position trace was smoothed using a single 5-point low-pass filter while the velocity and acceleration were obtained from the smoothed position trace as single or double discrete time derivatives.

A multilinear regression algorithm (Sokal and Rohlf, 1981) was applied to epochs of single trials so that portion of the single trial FISIH was expressed as a function of the animal's hand position, velocity, and acceleration during the initial phase of the movement. The regression analysis compares, on a trial-by-trial basis (**Figure 3A**), the frequency of cell discharge, f, at time $t_0 + \tau$, where τ is the variable time shift of a "sliding window" (**Figure 3B**), relative to movement onset, and the duration of t_0 is equal to the movement time. The window was advanced in time steps of 5 ms over the behaviorally important epoch T (the number of steps being T/bw). The variable T is defined as the interval that begins 50 ms after the cue onset, and ends at the time at which the movement reached amplitude of 5° from center. The square root of the discharge frequency, f, at time $t_0 + \tau$, was expressed as a function of the position (°), velocity (°/sec), and acceleration (°/sec^2) of monkey's hand at time t_1, where t_1 always began at movement onset (MOS). The regression equation is:

$$f(t_0 + t) = \mathrm{const} + c1\varphi1(t1) + c2\varphi2(t1) + c3\varphi3(t1) + \varepsilon,\ t_0 + \tau < T \text{ and} |t_0| = |t1| \quad (2)$$

where c1, c2, and c3 are the regression coefficients of position, velocity, and acceleration. The terms φ1(t1), φ2(t1) and φ3(t1) are the time-dependent variables of position, velocity, and acceleration, and ε is an error term. The coefficient of determination (CoD) is defined as the proportion of variance accounted for by the neuronal activity-to-movement correlation. Average CoDs were calculated only for valid trials having significant activity changes within the period of consideration.

The output of the regression analysis program provided averaged values of the CoD together with the time shift representing the time of best correlation (ToC) at which the best CoD occurred, as well as the partial regression coefficients at that point. The values of CoD ranged from 0 (the absence of correlation) to 1, where a full correlation of spike function and movement variables occurs. The analysis has been performed on single trial basis, but the results are displayed in normalized composite histograms for convenience and clarity (**Figures 3A,C**).

The changes in neuronal activity and their relationship to movement initiation and/or execution can be easily appreciated by visually estimating the outline of the composite histogram. FISIH patterns depict the activity of a cell, as indicated by the shape of the composite histogram and the site ToC relative to the shape of the composite histogram.

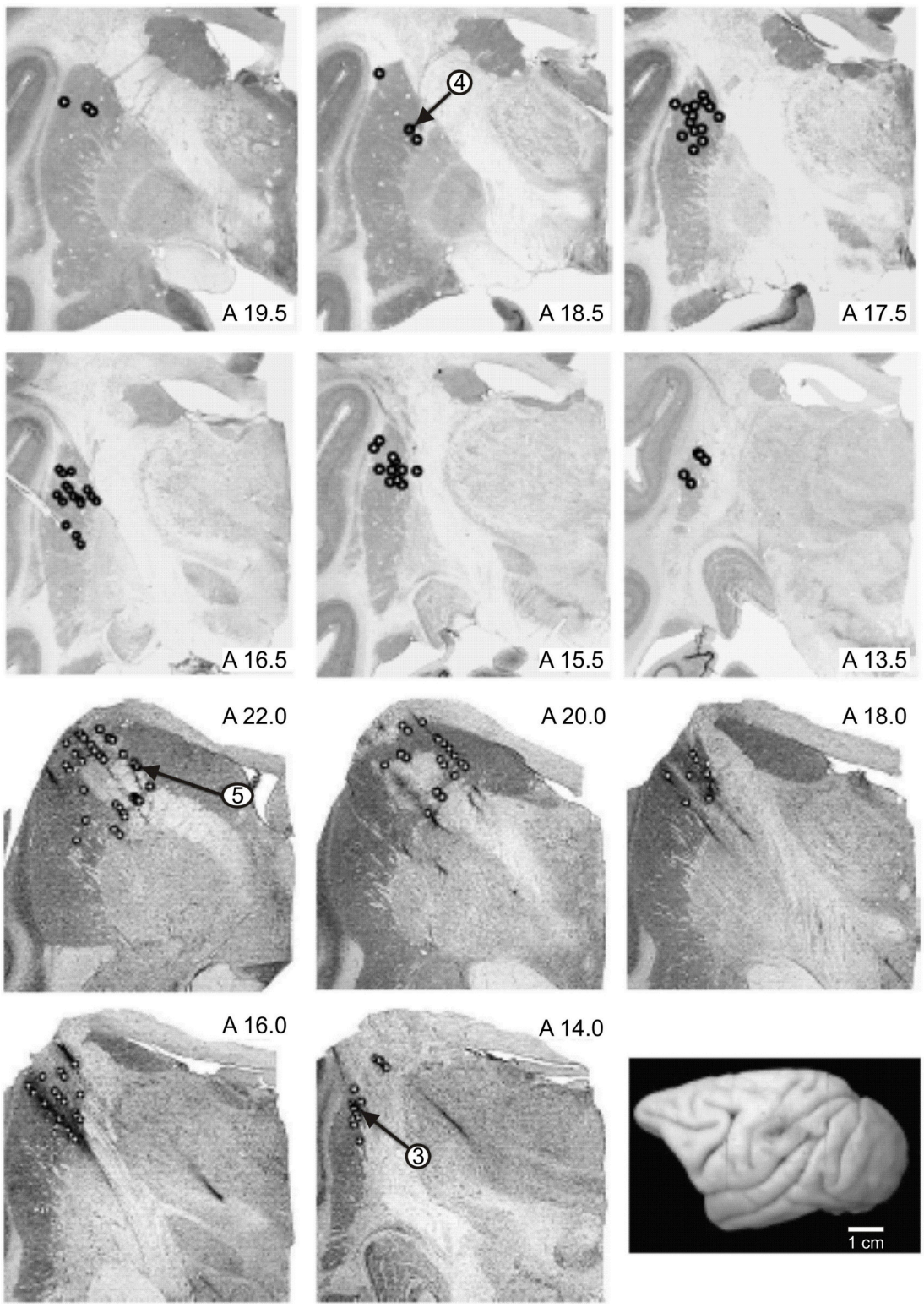

FIGURE 2 | Reconstructed locations of recorded neurons. Location of recorded neurons from monkeys E (panels in the upper row) and N (panels in the lower row) are shown. Small open circles indicate the locations in the basal ganglia at which records were taken. The recording locations of cells whose records have been illustrated are indicated by the arrows. A drawing of the dorsolateral surface of monkey E is shown in the lower right panel.

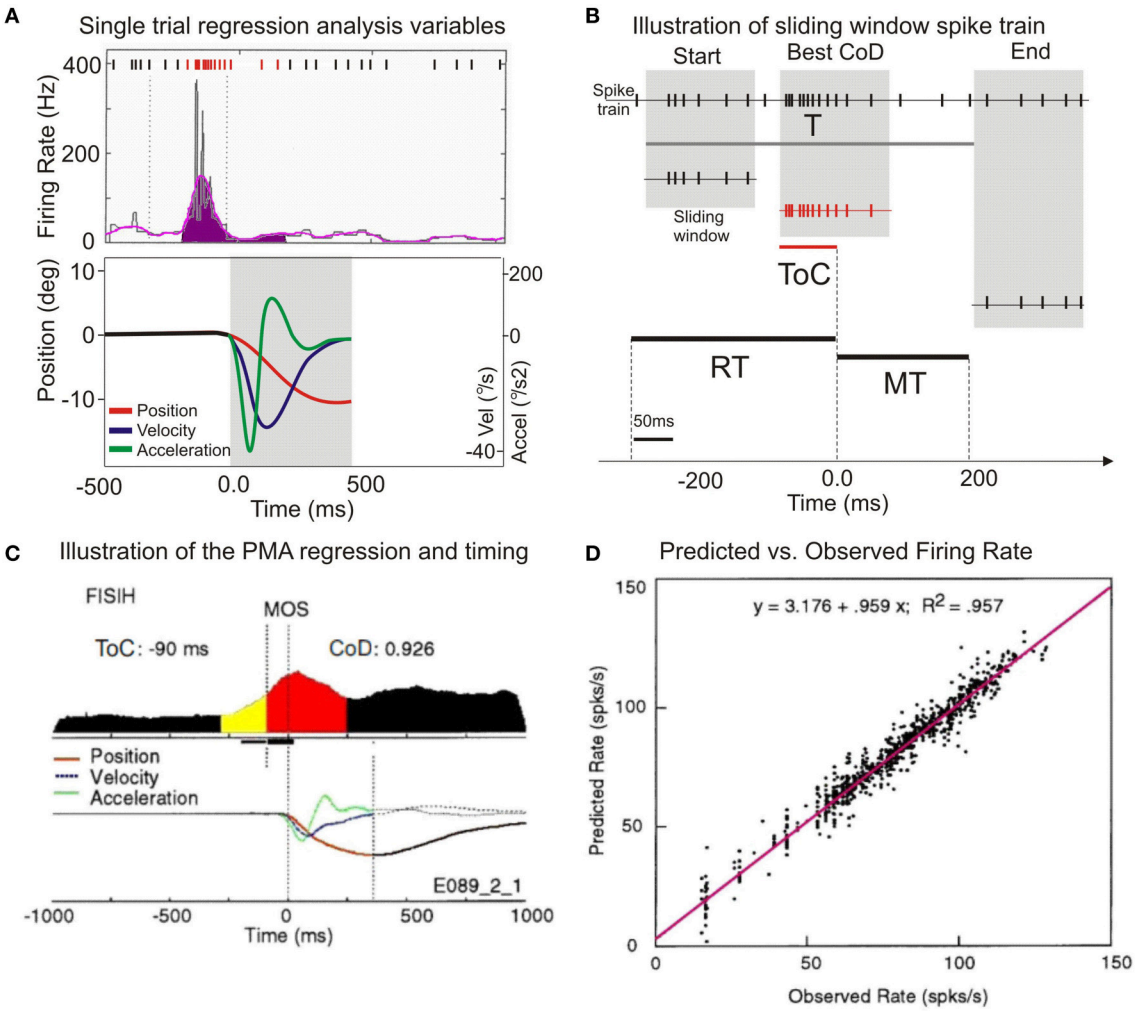

FIGURE 3 | Illustration of the application of multilinear regression analysis. (A) A single trial histogram of the neuronal activity expressed as mean firing rate (in spikes/s), together with the kinematic variables of position, velocity, and accelaration. **(B)** Illustration of the sliding window regression analysis. RT, reaction time; MT, movement time; ToC is the time of best correlation (at best CoD). **(C)** A typical putamen neuron with increased premovement activity during vibratory cued trials is shown. The display of the average kinematics for uncertain reward flexion trials R, are centered on MOS, on both panels. **(D)** The scatter diagram of the predicted discharge rate plotted against the observed rate. Regression equation of predicted vs. observed mean firing rates and the regression coefficient in the upper part of the panel.

Analysis of Changes in Neuronal Activity

The changes of neuronal activity associated with wrist movement were analyzed using multilinear regression in single trial (**Figure 3A**). Data from a putamen neuron, recorded during vibratory cued "R" trials, is presented in **Figure 3C**. The baseline activity (Bkg) of each recorded neuron was calculated as its mean firing rate during the 250 ms prior to the presentation of go-cues, while the animal held his wrist in a centered position. The first change in the cumulative sum of more than three standard deviations (SDs), lasting for at least 40 ms, was designated as the activity onset (Onset or AOS). The total number of spikes occurring from AOS until movement onset (**Figure 3C** the yellow segment) divided by the interval divided by the number of trials was designated as the cell's pre-movement firing response (Resp). Mean firing rates of Bkg and Resp (4.9 and 24.7 spikes/s) together with the AOS (−147 ms) are further compared across cells and conditions (see **Figure 6B**). The period between AOS and MOS (R2) is defined in **Figure 1C**.

The regression analysis describes the covariant relationship between changes in NS activity and movement variables. The best covariance between activity and kinematics (cT) occurred ∼90 ms before MOS. The average CoD of this cell was 0.926 and indicates that the neuronal activity has 92.6% of the variance explained by the multilinear regression analysis. This implies that the correlation between neuronal activity and the subsequent movement occurred at a time that proceeds the average onset time of electromyographic activity in this task (Gardiner and Nelson, 1992; Lebedev and Nelson, 1995). The time course of position, velocity, and acceleration are displayed beneath the FISIH; the regression analysis is described by Equation (2). To

compare the actual firing properties with those predicted by the regression model, **Figure 3D** shows a scatter-gram of the predicted discharge rate plotted against the observed rate. Each column of dots is a trial, and each window shift is a dot. The plot indicates a consistent linear relationship between the predicted firing rate as calculated by the regression model and the rate recorded during experiments. This relationship suggests that the methods are reliable and compatible with those used by other investigators (Ashe and Georgopoulos, 1994; Taira et al., 1996).

Quantitative Criteria for PMA Directionality

To determine the directionality of PMA, we calculated the difference between the Resp and the Bkg, and dubbed this difference the activity change (Act). In the cases in which Act was <1 spike/s, Act was recorded as 0 spike/s. If the sign of Act for a neuron differed as a function of movement direction, then that neuron was classified as "reciprocal" (encoding both flexions and extensions). In addition, we compared Act for flexion and extension movements and calculated their difference and sum. The ratio between difference and sum yields a scalar that should theoretically range between −1 and +1. Cases in which the ratio was −1 or +1, corresponded to those in which there was no change in activity for one direction of movement. These were coded as "directional." Cases in which the scalar was $> +1$ or < -1 were instances in which PMA had the opposite sign as a function of movement direction, and were thus "reciprocal." For those cases with scalars between −1 and +1, we took the standard score of the mean value, (about zero) and then defined cases that were between ±2 SDs from the mean and the extremes as being "directional." Cases with values falling within the ±2 SD limits were classified as non-directional. The distribution of PMA directionality of NS neurons by location is shown in **Table 1**.

TABLE 1 | The distribution of recorded neurons by location.

Category	Putamen		Caudate		Bridge		Total	
Recorded cells	104	73%	20	14%	18	13%	142	100%
RFs tested	81	78%	16	80%	16	89%	113	80%
Cutaneous	7	9%	1	6%	2	13%	10	7%
Deep	27	33%	3	19%	4	25%	34	24%
No Clear RF	47	58%	12	75%	10	62%	69	49%
PMA								
Cue	11	11%	2	10%	1	6%	14	10%
Movement	85	82%	17	85%	17	94%	119	84%
Intermediate	8	8%	1	5%	0	0%	9	6%
PMA DIR R Trials								
Reciprocal	36	35%	6	30%	5	28%	47	13%
Directional	4	4%	0	0%	0	0%	4	3%
Non-Directional	64	62%	14	70%	13	72%	91	64%
PMA DIR A Trials								
Reciprocal	35	34%	5	25%	3	17%	43	30%
Directional	2	2%	1	5%	0	0%	3	2%
Non-Directional	67	67%	14	70%	15	83%	96	68%

RF type and RF location. PMA relationship to cue and movement. PMA changes during certain/uncertain "A" and "R" trials.

Statistical Analysis

Analyses of the characteristics of activity-to-movement relationships for different NS neurons were examined for statistical significance using repeated measures ANOVA, including Scheffe's *post hoc* test and *t*-test. The observations were also checked using the nonparametric Mann Whitney *U*-test and Kruskal–Wallis tests to determine the significance levels of the differences in CoDs and ToCs, for groups separated by trial type (regular or after), go-cue (visual or vibratory), and movement direction (flexion or extension).

RESULTS

Database

A total of 236 recorded neurons, 142 (∼60%) were selected, because each neuron: (i) had activity changes (PMA) following the vibratory or visual go-cue onset and prior to MOS, (ii) had a PMA firing rate that was at least 3 SDs different from the Bkg activity firing rate, and (iii) was held long enough to record at least 25 trials for each movement direction. Of these, 102/142 (∼72%) also had a complete set of recordings during visually cued trials. Of the selected NS neurons, 104/142 (∼73%) neurons were located in putamen, 20/142 (∼14%) in the caudate nucleus, and 18/142 (∼13%) in the cellular bridges in between these structures. We eliminated 3/142 neurons from consideration because their activity was completely suppressed during the PMA interval. Also, the activity of 3/142 neurons during flexion movements and of 7/142 neurons during extension movements had CoDs outside the range that included ±4 SDs from the distribution of the main population and were thus excluded as outliers. This left for statistical consideration the records of 136/142 (96%) cells for flexion movements and 130/142 (92%) cells for extensions. Receptive fields (RF) were found for 44/142 (∼31%) NS neurons; 69/136 (∼49%) had no clear RFs and 29/142 (∼20%) were not tested. Of the cells exhibiting RFs, 10/44 had cutaneous RFs and 34/44 had deep RFs. **Table 1** shows the distribution of NS neurons by location and RF type.

The activity patterns of the striatal neurons could not be defined as a homogeneous group. Separation was required because these neurons had significant differences in their activity-to-movement relationship as a function of trial type, cue, movement direction, and location revealed by factorial ANOVA and Scheffe's *post hoc* comparisons. Therefore, our data were grouped by these variables.

PMA and Movement Initiation

Significant changes in neuronal activity, defined as a deviation of at least ±3 SDs from the baseline that lasted more than 40 ms (see Nelson and Douglas, 1989; Gardiner and Nelson, 1992) were commonly related either to the go-cue or to the movement. Neuronal firing changes were considered to be cue-related if they occurred in a consistent temporal relationship with the cue and followed its presentation after a relatively short latency (<100 ms). Of the total number, 14/142 (∼10%) had cue-related activity, while 9/142 (∼6%) had very early PMA

which we termed "intermediate" responses. Each of these also had movement related activity as did the 119/142 (∼84%) which show activity changes only in relationship to movement onset (see **Table 1** for their distribution by location). Significant changes in firing rate that were time locked with MOS, but that preceded MOS, were considered to be PMA (Gardiner and Nelson, 1992; Lebedev et al., 1994; Lebedev and Nelson, 1995; Opris et al., 2011a). Changes in neuronal firing rates that occurred during the execution of wrist movement (i.e., from MOS until potential reward delivery) were classified as "movement-associated activity." Movement related cells exhibiting PMA may be involved in either movement initiation or execution, depending on the time of occurrence of their activity changes.

Neural Activity to Movement Kinematics Relationship

Consistent with the motor role of dorsal striatum, the firing rate of a subpopulation of neurons in putamen reflect the encoding of hand kinematics (position, velocity, and acceleration).

Examples of Differential Firing during Encoding of Hand Position

Figure 4A shows the PMA of a putamen neuron classified as "reciprocal" that exhibits a strong suppression during flexion trials while during extension trials this cell's firing is substantially increased. This differential mean firing rate during flexion and extension movements likely reflects the encoding of hand position in the two opposite movement directions (flexions and extensions). At the population level, the encoding of position occurred in 47/142 (33%) VIB cued neurons during uncertain reward "R" trials and 43/142 (30%) during certain reward "A" trials, and in 32/102 VIS cued neurons during uncertain reward "R" trials and of 38/102 NS neurons during certain reward "A" trials. Only 4 NS neurons were "directional" during "R" trials and three cells were "directional" during "A" trials. A minority of the population changed the type of direction-related activity between "R" and "A" trials.

The non-directional NS cell subpopulation which included the vast majority of the studied neurons (*vibration cues*: 91/142 neurons during "R" trials and 96/142 neurons during "A" trials; *visual cues*: 66/102 neurons during "R" trials and 60/102 neurons during "A" trials) had characteristics consistent with the encoding of the magnitude of the position (distance from the center) shown for the population, as a whole, in **Tables 1, 2**. This type of non-directional modulation was noticed in most of the cells, regardless of go-cue modality. That is, the sign of the activity changes of these neurons was the same regardless of the direction of the movements that followed the onset of this activity (Gardiner and Nelson, 1992).

Examples of Differential Firing with Hand Velocity and Acceleration Encoding

In **Figure 4B** is shown the PMA of a putamen neuron, cued by vibratory stimuli ("A" trials) with firing rate mimicking the velocity profile (on the left). On the other hand, **Figure 4C** shows a sharper PMA modulation of a putamen neuron, cued by visual stimuli ("A" trials) with firing rate mimicking the acceleration profile (on the right). It is noticeable a sharper firing peak encoding acceleration that is accompanied by a deeper inhibition trough than in the case of cell encoding velocity. Bkg and Resp firing rates (**Figures 4B,C**) were again slightly higher during "A" trials (not shown) than in "R" trials.

Neural Activity-to-Movement Kinematics Analysis

The regression analysis described above was used to investigate changes in NS activity associated with movement initiation under two conditions. Comparisons were made between trials with uncertain rewards ("R" trials) and trials with certain rewards ("A" trials). We illustrate the activity patterns of a representative putamen neuron recorded during vibratory go-cue trials, in **Figure 5A**, and the pattern of the same neuron recorded during visual go-cue trials, in **Figure 5B**. The records of "R" trials (left panel, **Figure 5A**) and "A" trials (right panel, **Figure 5A**) are illustrated for flexion movements. This cell exhibited an increased discharge, before MOS (**Figure 5A**), and thus PMA preceding wrist flexion (position traces displayed for both "R" and "A" conditions). The neuron was more active in the blocks of vibratory cued "A" trials than during R trials (left panel, **Figure 5A**). Bkg and Resp were also higher when rewards were certain. In addition to PMA changes associated with unpredictable reward conditions, this putamen neuron's activity became better correlated with animal's movement. This is accompanied by changes in the average CoDs, which were greater during "A" trials than during "R" trials (0.941 vs. 0.920). The time occurrence of the best correlation (ToC) was ∼117 ms before MOS during "A" trials and ∼99 ms, during regular reward.

This same putamen neuron, whose visually cued trial records are shown in **Figure 5B** exhibited a higher firing rate during the "A" trials for flexion movement under this cueing condition, as well. The Bkg and Resp are higher during "A" trials (26.8 and 52.2 spks/s) than during regularly "R" rewarded ones (21.3 and 49.3 spks/s). The PMA changes occur quite early, before MOS. The increase in CoDs in "A" trials, as compared with "R" trials, indicates that PMA becomes better correlated with the movement after withheld rewards (0.954 vs. 0.942). Comparing the neuronal activity during visual go-cue trials with vibratory go-cue trials, one can note an average increase (of 10 spks/s) in the mean firing rate of PMA that occurred during the former. However, average CoDs during visually cued A trials were greater than during cued trials (0.954 vs. 0.941).

At the population level, NS firing was significantly higher in the Resp vs. Bkg conditions for the majority of cells ($p < 0001$, *post hoc*). However, when comparing mean firing rate across trial type, go-cue type or movement direction the effects varied (see **Table 2**). Bkg and Resp firing rates were slightly higher during "A" vs. "R" trials (**Figure 5C**) and during VIS vs. VIB trials ($P < 0.001$, *post hoc*; $n = 91$ vs. 66).

Additional information about the timing of this relationship can be derived from the examination of the time of occurrence of best CoDs i.e., (ToCs), which indicate the time of best CoDs at either MOS or AOS, respectively (see **Table 2**). A comparison of PMA onsets and ToCs for vibratory cued trials

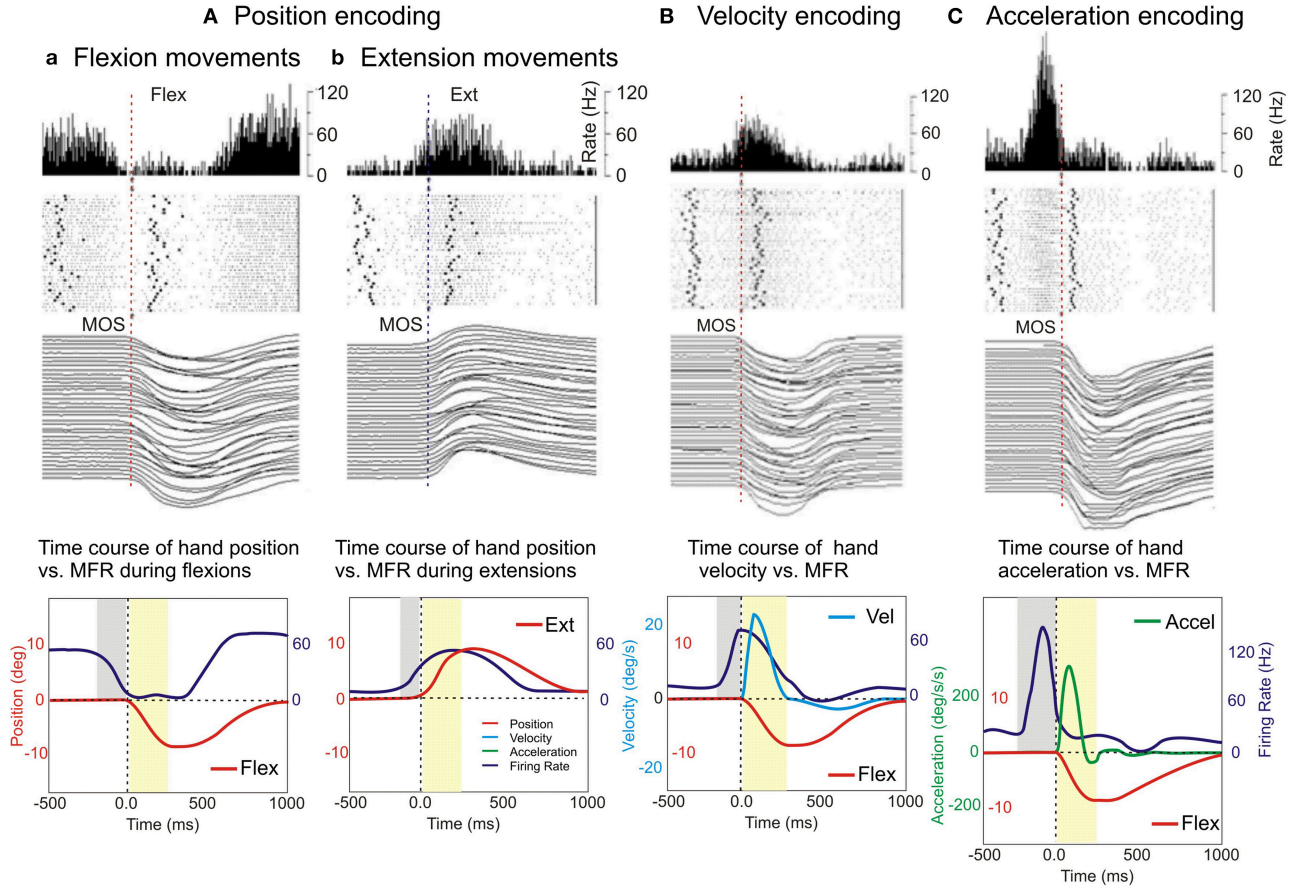

FIGURE 4 | Examples of encoding the variables of movement kinematics. Putamen neurons show encoding of hand position (**Aa**, flexions and **b**, for extensions) movement velocity **(B)** and acceleration **(C)**. Peri-event histograms (PEHs), rasters, and movement trajectories were plotted for R flexions and extensions **(Aa,b)**, velocity **(B)**, and acceleration **(C)**. The PEHs of the neuronal activity expressed as mean firing rate (in spikes/s), with a bin size equal to 5 ms and a raster display. In the raster display, rows represent individual trials, dots represent single spikes, while the left and right bold dots represent vibratory cue onset and reward delivery, respectively.

TABLE 2 | The means and standard deviations for Bkg and Resp neural activity, premovement onset R2s, time of best regression/correlation ToC, and the coefficients of determination CoD for flexions and extensions trials, under certain vs. uncertain rewards.

Go Cue	Vibratory				Visual			
Direction	Flexions		Extensions		Flexions		Extensions	
Trial Type	R Trials	A Trials	R Trials	A Trials	R Trials	A Trials	R Trials	A Trials
Bkg (Hz)	21 ± 14	21 ± 14	20 ± 14	21 ± 13	19 ± 13	20 ± 14	20 ± 14	20 ± 13
Resp (Hz)	25 ± 16	26 ± 16	24 ± 14	25 ± 14	24 ± 15	24 ± 16	24 ± 14	24 ± 14
R2 (ms)	187 ± 74	160 ± 54	173 ± 52	158 ± 49	228 ± 70	215 ± 60	185 ± 42	185 ± 50
ToC (ms)	88 ± 70	84 ± 60	73 ± 62	68 ± 58	154 ± 59	161 ± 52	121 ± 51	121 ± 46
CoD	0.871 ± 0.054	0.888 ± 0.056	0.861 ± 0.054	0.867 ± 0.054	0.902 ± 0.04	0.908 ± 0.033	0.903 ± 0.039	0.908 ± 0.033

Comparison between values for certain vs. uncertain rewards, in respectively, "A" and "R" trials. Statistical significance was determined using repeated measures ANOVA, including Scheffe's post hoc test and t-test (See Text for abbreviations).

is shown in **Figure 5D**. The ToCs during visually cued trials occur much earlier than during vibratory cue trials. The ToCs in "A" vs. "R" trials for flexion movements were significantly different only with visual go-cues (see **Table 2**). There was also a statistical significance in the ToCs for flexions and extensions triggered by visual cues (not shown). Although we were unable to distinguish between direction and load effects (since monkeys always performed the movements against a load which assisted

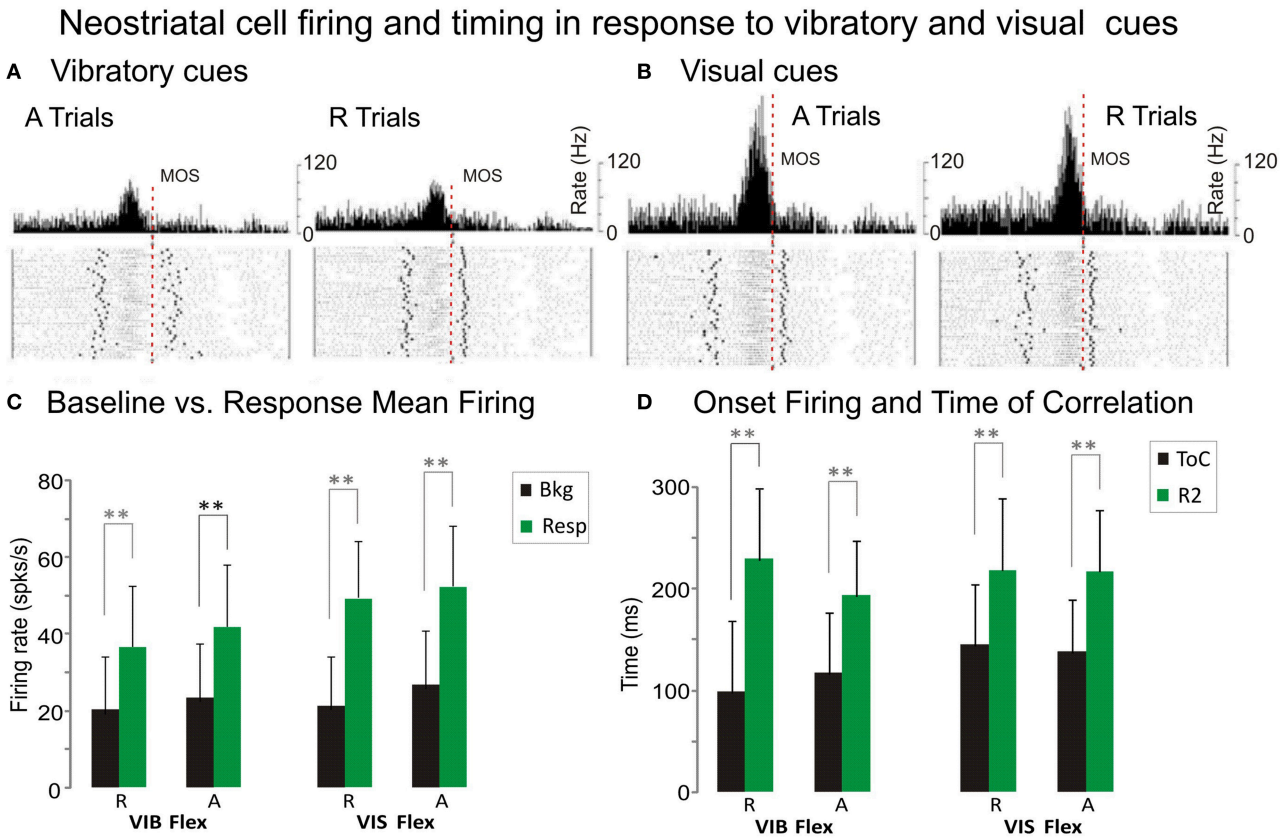

FIGURE 5 | Premovement firing and timing. (A,B) Example of putaminal cell that exhibited PMA under vibratory **(A)** and visual **(B)** stimuli. Each histogram illustrates neuronal activity expressed as mean firing rate together with raster displays aligned on MOS. The left panels display the NS activity during "A" flexion trials and the right panels represent the activity during "R" flexion trials. Wrist position traces for each trial are presented at the bottom of each panel. Coefficients of Determination (CoDs) which quantify the best relationship, are: 0.920 ± 0.044 during R trials and 0.941 ± 0.024 during "A" trials (**Figure 4A**). CoDs for R and A trials are: 0.942 ± 0.021 and 0.954 ± 0.021, (**Figure 4B**) respectively. This cell exhibited increased discharge during flexion movements that occurred well before MOS. Baseline firing BKG and RESP are higher during trials following withheld rewards than during R trials. PMA onsets together with ToCs suggest that the cell may have been involved in movement initiation. **(C)** Comparison of premovement mean firing rates of NS cells during baseline BKG and response RESP for flexions and extensions under vibratory and visual cues. **(D)** Comparison of the premovement activity timing for response onsets and of best correlation time ToC for flexions and extensions under vibratory and visual cues. Statistical significance was determined using repeated measures. $^{**}p < 0.001$ ANOVA, including Scheffe's *post hoc* test and *t*-test.

wrist extensions and opposed flexions), the effects of direction and load were evident through the fact that interfered with each other.

PMA onsets for single trials were measured relative to two events: go-cue onsets (COS) and movement onsets (MOS; see **Figure 1**). R1s, measured from COS, during vibrotactile stimulation, for both flexion and extension movements were significantly shorter in the A trials (see **Table 2**). R2s, measured from MOS, were calculated by subtracting the R1 from the RT (**Figure 1**). Flexion movements had R2s that were significantly shorter during "A" trials regardless of go-cue modality. Thus, PMA during vibratory cued trials started ∼27 ms closer to MOS in the "A" trials when compared with "R" trials. During visually cued flexion trials, it started closer to MOS by ∼13 ms. R2s were significantly different during visually cued flexion and extension movements, but not different during vibratory cued trials.

Statistical analyses of the activity-movement kinematics relation under unpredictable reward conditions are presented in **Table 2**. We have considered the trial type as a repeated measure and split each of the PMA-related variables by the go cue type and movement direction. Significant differences in the variables between conditions ("R" and "A" trials) were obtained by repeated measures ANOVA.

Coefficients of Determination

A measure of the correlation's strength in "R" and "A" trials is provided by the average CoDs. In general, the average CoDs showed a tight relationship between NS neuronal activity and monkey's kinematics (see **Table 2**). Flexion movement CoDs were significantly greater during "A" trials than during "R" trials ($p < 0.01$; ANOVA) regardless of the modality of go cues (see **Table 2**). The occurrence of enhanced activity-to-movement correlation in trials following withheld rewards is illustrated in

Figure 6. Cumulative sum plots of CoDs for "R" and "A" trials show a consistent shift to the right for the "A" trials ($p < 0.001$ for vibratory flexions; $p < 0.01$ for vibratory extensions; $p < 0.01$ for visual flexions; $p \sim$ ns for visual extensions; ANOVA), independent of go-cue modality.

There was also a directional effect, in that CoDs after withheld rewards were significantly greater during flexion trials than during extension trials ($p < 0.001$ for flexions; $p < 0.01$, for extensions, ANOVA), for both vibratory cued trials and visually cued trials (**Table 2**). In general, there was a better correlation of NS neuronal activity with kinematics in visual go-cue trials compared with that in vibratory go-cue trials ($p < 0.001$ for flexions). The average CoDs for visually cued flexions during "A" trials were greater during vibratory go-cued flexion "A" trials.

Given the existence of the activity-to-movement relationship (measured by the CoD) during trials following withheld rewards, we noticed three distinct effects: first, an effect of unpredictable reward which results in a better activity-to-movement correlation for certain rewarded "A" trials than for "R" trials; second, a directional effect which results in a better correlation for flexion than for extension movements for both cues, and third, a modality effect as indicated by better relationship for visually cued as compared with vibratory cued movements.

Electromyographic Activity

We compared average onsets of electromyographic (EMG) activity between flexion (**Figure 7A**) and extension (**Figure 7B**) movements for both "Regular" and "After" trials. With few exceptions, for most muscles the EMG activity starts earlier in the "After" trials than in "Regular" trials. Brachioradialis has the opposite trend in the "After" vs. "Regular" trials for both flexions and extensions. All together the EMG and behavioral measures seem to have a consistent agreement with NS pre-movement neural activity supporting the hypothesis that under certain rewards NS neuronal activity becomes better correlated to movement kinematics.

DISCUSSION

In the present study we recorded the activity of neostriatal neurons in two rhesus monkeys performing wrist movements in a pseudo-random reward task. We examined the relationship between PMA and kinematic variables (position, velocity, and acceleration) under three conditions: (a) reward contingency, (b) vibratory vs. visual go-cues, and (c) flexions vs. extensions movements (Opris et al., 2011a).

The results of this study indicate that NS neurons have PMA which is functionally correlated with movement kinematics. This correlation varies as a function of reward contingency (unpredictable vs. predictable delivery of reward for correct performance). Our goal was to determine whether there is a relationship between NS PMA and movement kinematics and to quantify this relationship in terms of coefficients of determination (CoDs) and relationship occurrence times (ToCs). These parameters varied significantly not only as a function of rewarding conditions, but also with variations in the modality of sensory triggering stimuli and with the direction of movement. In addition, we found that reaction times RTs and PMA onsets are also significantly different as a function of reward schedule and go-cue modality. These results suggest that it is likely that the NS is involved in sensorimotor-related activity that is combined with attentional, decision, and motivational influences (Schultz, 1997, 2010; Schultz et al., 1997; Opris and Bruce, 2005; Samejima et al., 2005).

Neural Firing to Movement Correlation Under Unpredictable Task

The statistically significant differences in CoDs for "R" and "A" trials may be related to attention and motivational factors associated with reward (Watanabe, 1996; Ueda and Kimura, 2003). Changes in the predictability of reward delivery, assumed to occur after withheld rewards, are accompanied by increases in CoDs and decreases in reaction times. Furthermore, changes in the predictability of reward delivery are accompanied by increases in CoDs, suggesting that the changes in CoDs are related to an animal's increased attention.

Differences in CoDs as a function of go-cue modality may be related to the gating of somatosensory inputs that often accompanies sensory-triggered movements. Our results indicate that the CoDs associated with NS neural activity during vibratory cued trials have significantly lower values as compared with those occurring during visual go-cued trials. Vibratory stimuli are one type of peripheral input to SI neurons that may be gated before active movements (Lebedev and Nelson, 1995). Because somatosensory cortex projects extensively to the neostriatum (see Parent and Hazrati, 1995 for review), it seems reasonable to suggest that gating in the cortex could ultimately result in modulation of NS activity. Changes in CoDs as a function of go-cue modality may be a reflection of alterations in cortical inputs to NS, as well as modulatory effects by dopaminergic systems (Lebedev and Nelson, 1995; Kiyatkin and Rebec, 1996). It has been suggested that changes in behavioral motivation may be mediated by dopaminergic neurons (Apicella et al., 1991; Schultz et al., 1992, 1993). Therefore, the dopaminergic pathways arising from the pars compacta of substantia nigra (SNc) and projecting to dorsal striatum (Lynd-Balta and Haber, 1994; Parent and Hazrati, 1995) may be involved in the motivational process underlying the learning and maintenance of goal driven behavior (Mirenowicz and Schultz, 1994; Schultz et al., 1997).

Statistically significant differences in CoDs between trials involving flexion and extension movements may be due to the fact that the movements were performed against a load which assisted wrist extensions and opposed flexions. Flexion trials had CoDs that were significantly higher than those during extension movements. The presence of the load may add a small contribution to the relationship during flexion movements or subtract that contribution when moving with the load (Liles, 1985; Alexander and Crutcher, 1990; Gardiner and Nelson, 1992). Sensorimotor territories of NS may also show differential firing as a result of cortical load effects, since it has been suggested that there are several parallel pathways of somatotopic input to NS (Alexander et al., 1986; Graybiel et al., 1994). Therefore, the difference in CoDs as a function of movement direction may be influenced by load, the movement direction itself, or both.

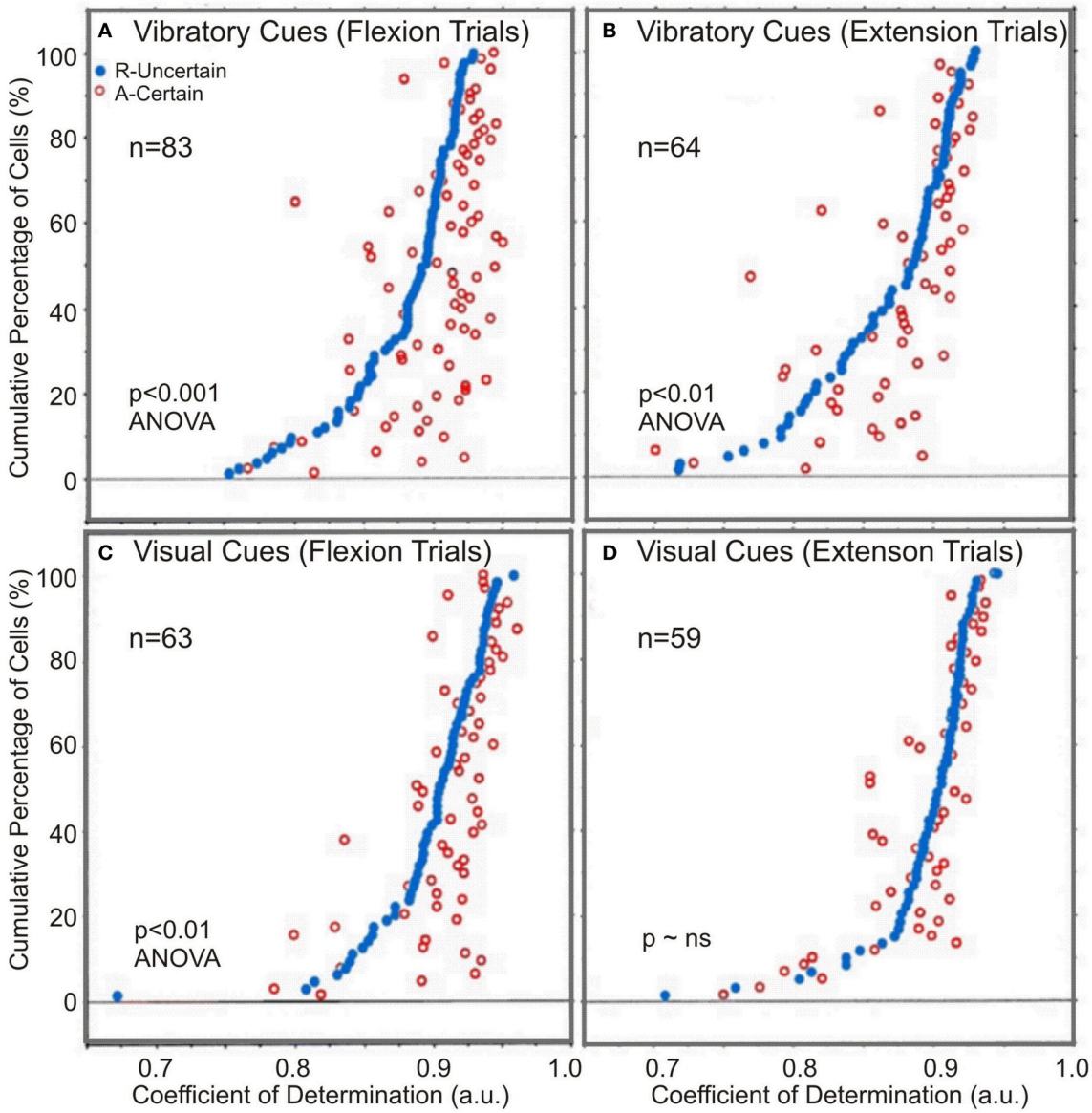

FIGURE 6 | The comparison of regression coefficients. Paired coefficients of determination, CoDs, for both vibratory and visually cued trials: **(A,B)** Certain "A" and uncertain "R" rewarded trials for vibratory cued trials and **(C,D)** for visually cued trials. In both instances, CoDs of the uncertain R trials (black dots) were arranged in ascending order from left to right. The certain trial CoDs corresponding to each uncertain trial CoDs were plotted at the appropriate height. Open dots to the right of the black dots indicate instances where the neuronal activity was better related (CoDs were greater) for movements made in the certain reward A trials.

Pre-movement Activity and Regression Times as a Function of Reward Schedule

In general, PMA activity was well correlated with wrist movement variables. The average CoD of the whole NS neuronal population was >0.85 for each modality, movement direction, recording location, and rewarding schedule. During vibratory cued trials which follow withheld rewards, there is a shift in PMA onset toward MOS despite the fact that reaction times become shorter. Schultz and co-workers have demonstrated that leftward shifts in the onset of activity occur in the firing patterns of dopaminergic neurons when tasks become more predictable (Schultz et al., 1992, 1993). The corollary of this would be that if the process was reversed and task requirements become more unpredictable, rightward shifts in activity onsets might be observed as was indeed observed in this study. Similar shifts in PMA were seen by Kimura (1990) when the amount of prior task information about behavioral requirements was varied. In our task, shifts in reaction times and PMA onsets, as shown in **Figure 6A**, occur after withheld rewards (Kimura et al., 2003; Churchland et al., 2006; Hori et al., 2009). Despite these shifts, the onsets of PMA and ToCs are early enough to suggest that the activity of NS neurons may be associated with the initiation

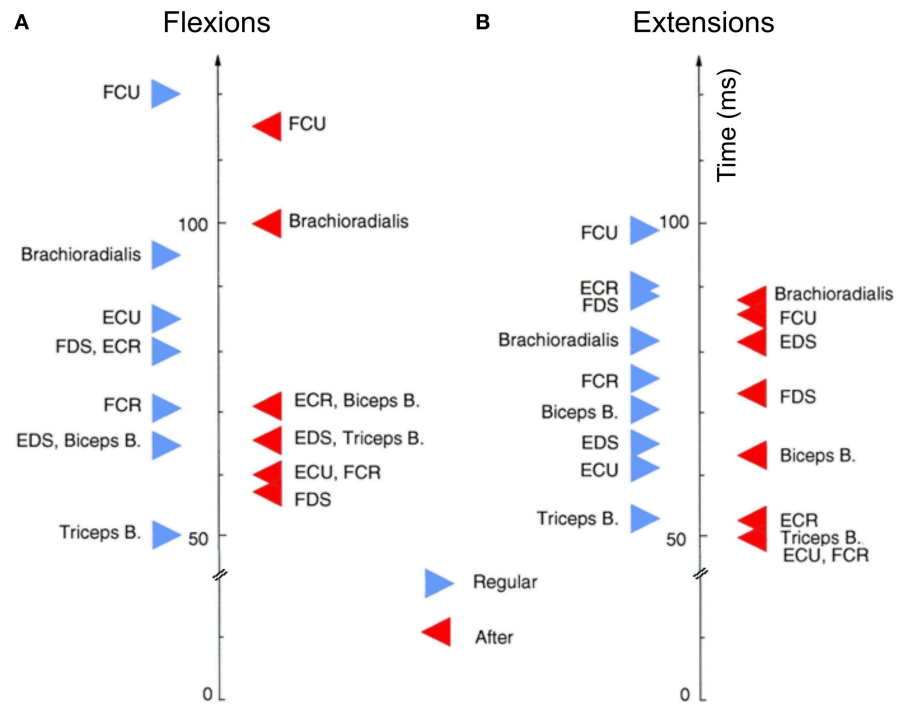

FIGURE 7 | Average onsets of electromyographic (EMG) activity. EMG activity between flexion **(A)** and extension **(B)** movements for both certain and uncertain reward trials. Each triangle (red for certain and blue for uncertain reward trials) represents the average EMG onset for at least 40 trials recorded consecutively. Biceps B, biceps brachii; BR, brachioradialis; ECR, extensor carpi radialis; ECU, extensor carpi ulnaris; EDS, extensor digitorum superficialis; FCR, flexorcarpi radialis; FDS, flexor digitorum superficialis; FCU, flexor carpi ulnaris; FDS, flexor digitorium superficialis; Triceps B, triceps brachii.

of wrist movements, as well as its execution (Graybiel, 1990; Romo et al., 1992; Nelson et al., 1996). The onset of PMA in NS occurred earlier than did PMA onset for somatosensory cortical neurons when monkeys performed the same task (unpublished observations).

Functional Consequences of Unpredictable Reward

The mechanisms contributing to sensorimotor integration in the NS, as perhaps indicated by PMA, are not completely understood. However, part of a mechanism necessary for the shaping of NS activity during the initiation and execution of motor behavior has been suggested to involve the dopaminergic (DA) modulation (Surmeier and Kitai, 1997). There are several relevant features of DA modulation. DA modulation is a dynamic process that, depending on the level of membrane depolarization, causes an increase in the NS neuron firing rate if the membrane is in an "up" state or a decrease in firing rate if the membrane is in the "down" state (Hernández-López et al., 1997).

According to Berns et al. (1997) the withholding of rewards may be considered to be a context violation which may be thought of as a breach in expectation. These authors suggest that ventral striatum becomes activated when contexts are violated by stimuli that appear unexpectedly. It is reasonable to assume that the absence of reward, when it is expected, is itself, an unexpected stimulus. Dopamine neurons become activated during unpredictable behavioral conditions, thereby providing contrast to previously fully predicted stimuli (Mirenowicz and Schultz, 1994). As a working hypothesis, we suggest that the dopamine system, through its projections to NS, may influence neuronal activity (Schultz and Romo, 1988; Pasquereau et al., 2007), resulting in an increase of covariant relationship between PMA neuronal activity and movement variables (Nelson et al., 1996). Moreover, learning theories suggest that the learning process is driven by the unpredictability of reward, and that little or no further learning takes place when reward is entirely predicted (see Schultz et al., 1997 for review). Dealing with unpredictable aspects of behavior seems to involve a higher order processing of information in basal ganglia and require multiple processing channels (Hoover and Strick, 1993).

The results presented in this work are consistent with the view that NS may provide an "interface" between sensorimotor, limbic and association subcortical territories and cortical areas involved in higher brain functions such as motivation, attention, and memory (Evarts and Wise, 1984; Schultz et al., 1997; Opris et al., 2011a,b, 2013; Santos et al., 2014). The complete understanding of these functions requires more experimental and theoretical work. However, it is likely that cerebral cortex and basal ganglia structures utilize different modular subsets at any given time

during highly dynamic processing involved in sensorimotor integration (Evarts et al., 1984).

SUMMARY

When monkeys are rewarded pseudo-randomly (75% of the correct trials) in a task requiring either vibratory or visually-cued wrist movements, neostriatal PMA is tightly correlated with movement kinematics. There are two different modes of this activity-to-movement correlation. The correlation between neuronal activity and movement, during flexion trials but not extension trials, was higher in trials with certain rewards as compared to the trials with uncertain rewards. The improvement in the activity-to-movement correlation was accompanied by shifts in PMA onsets so that they occurred closer to movement onset and by shorter reaction times (Opris et al., 2011a). Thus, the changes in the predictability of behavioral requirements are reflected in the correlation between neostriatal PMA and the kinematics of wrist movements. These observations are consistent with the hypothesized modulation of neostriatal activity by the dopaminergic systems during certain vs. uncertain behavioral situations.

AUTHOR CONTRIBUTIONS

IO performed the data analyses and wrote the manuscript. ML collected the data. RN supervised all aspects of the research.

ACKNOWLEDGMENTS

The authors wish to thank John M. Denton who assisted during the gathering of data that was presented in this manuscript and Ben Bennet, D. James Surmeier, and Charles J. Wilson for detailed comments on versions of this manuscript. This work was supported by NIH Program Project Grant NS26473.

REFERENCES

Aggarwal, V., Tenore, F., Acharya, S., Schieber, M. H., and Thakor, N. V. (2009). Cortical decoding of individual finger and wrist kinematics for an upper-limb neuroprosthesis. *Conf. Proc. IEEE Eng. Med. Biol. Soc.* 2009, 4535–4538. doi: 10.1109/iembs.2009.5334129

Aldridge, J. W., Anderson, R. J., and Murphy, J. T. (1980). The role of basal ganglia in controlling a movement initiated by a visually presented cue. *Brain Res.* 192, 3–16. doi: 10.1016/0006-8993(80)91003-3

Alexander, G. E., and Crutcher, M. D. (1990). Preparation for movement: neural representations of intended direction in three motor areas of the monkey. *J. Neurophysiol.* 64, 133–150.

Alexander, G. E., DeLong, M. E., and Strick, P. L. (1986). Parallel organization of functionally segregated circuits linking basal ganglia and cortex. *Ann. Rev. Neurosci.* 9, 357–381. doi: 10.1146/annurev.ne.09.030186.002041

Apicella, P., Ljungberg, T., Scarnati, E., and Schultz, W. (1992). Neuronal activity in the monkey striatum related to the expectation of predictable environmental events. *J. Neurophysiol.* 68, 945–960.

Apicella, P., Scarnati, E., and Schultz, W. (1991). Tonically discharging neurons of monkey striatum respond to preparatory and rewarding stimuli. *Exp. Brain Res.* 84, 672–675. doi: 10.1007/BF00230981

Ashe, J., and Georgopoulos, A. P. (1994). Movement parameters and neural activity in motor cortex and area 5. *Cereb. Cortex* 6, 590–600. doi: 10.1093/cercor/4.6.590

Berns, G. S., Cohen, J. D., and Mintun, M. A. (1997). Brain regions responsive to novelty in the absence of awareness. *Science* 276, 1272–1275.

Churchland, M. M., Santhanam, G., and Shenoy, K. V. (2006). Preparatory activity in premotor and motor cortex reflects the speed of the upcoming reach. *J. Neurophysiol.* 96, 3130–3146. doi: 10.1152/jn.00307.2006

Colburn, T. R., and Evarts, E. V. (1978). "Long-loop adjustments during intended movements: use of brushless DC. torque motors in studies of neuromuscular function," in *Progress in Clinical Neurophysiology*, Vol. 4, ed J. E. Desmedt (New York, NY: Karger), 153–166.

Cox, D. R., and Lewis, P. A. W. (1966). *The Statistical Analysis of Series of Events*. London: Chapman and Hall.

Evarts, E. V., Kimura, M., Wurtz, R. H., and Hikosaka, O. (1984). Behavioral correlates of activity in basal ganglia neurons. *Trends Neurosci.* 7, 447–453. doi: 10.1016/S0166-2236(84)80151-4

Evarts, E. V., and Wise, S. P. (1984). Basal ganglia outputs and motor control. *Ciba Found. Symp.* 107, 83–102. doi: 10.1002/9780470720882.ch6

Fiorillo, C. D., Tobler, P. N., and Schultz, W. (2003). Discrete coding of reward probability and uncertainty by dopamine neurons. *Science* 299, 1898–1902. doi: 10.1126/science.1077349

Fu, Q. G., Flament, D., Coltz, J. D., and Ebner, T. J. (1995). Temporal encoding of movement kinematics in the discharge of primate primary motor and premotor neurons. *J. Neurophysiol.* 73, 836–854.

Gardiner, T. W., and Nelson, R. J. (1992). Striatal neuronal activity during the initiation of hand movements made in response to visual and vibratory cues. *Exp. Brain Res.* 92, 15–26. doi: 10.1007/BF00230379

Graybiel, A. M. (1990).The basal ganglia and the initiation of movement. *Rev. Neurol. (Paris)* 146, 570–574.

Graybiel, A. M., Aosaki, T., Flaherty, A. W., and Kimura, M. (1994). The basal ganglia and adaptive motor control. *Science* 265, 1826–1831. doi: 10.1126/science.8091209

Hernández-López, S., Bargas, J., Surmeier, D. J., Reyes, A., and Galarraga, E. (1997). D1 receptor activation enhances evoked discharge in neostriatal medium spiny neurons by modulating an L-type Ca2+ conductance. *J. Neurosci.* 17, 3334–3342.

Hoover, J. E., and Strick, P. L. (1993). Multiple output channels in the basal ganglia. *Science* 259, 819–821. doi: 10.1126/science.7679223

Hori, Y., Minamimoto, T., and Kimura, M. (2009). Neuronal encoding of reward value and direction of actions in the primate putamen. *J. Neurophysiol.* 102, 3530–3543. doi: 10.1152/jn.00104.2009

Kimura, M. (1990). Behaviorally contingent property of movement-related activity of the primate putamen. *J. Neurophysiol.* 63, 1277–1296.

Kimura, M., Yamada, H., and Matsumoto, N. (2003). Tonically active neurons in the striatum encode motivational contexts of action. *Brain Dev.* 25(Suppl. 1), S20–S23. doi: 10.1016/S0387-7604(03)90003-9

Kiyatkin, E. A., and Rebec, G. V. (1996). Dopaminergic modulation of glutamate-induced excitations of neurons in the neostriatum and nucleus accumbens of awake unrestrained rats. *J. Neurophysiol.* 75, 142–152.

Lebedev, M. A., Carmena, J. M., O'Doherty, J. E., Zacksenhouse, M., Henriquez, C. S., Principe, J. C., et al. (2005). Cortical ensemble adaptation to represent velocity of an artificial actuator controlled by a brain-machine interface. *J. Neurosci.* 25, 4681–4693. doi: 10.1523/JNEUROSCI.4088-04.2005

Lebedev, M. A., Denton, J. M., and Nelson, R. J. (1994). Vibration-entrained and premovement activity in monkey primary somatosensory cortex. *J. Neurophysiol.* 72, 1654–1673.

Lebedev, M. A., and Nelson, R. J. (1995). Rhythmically firing, 20-50 Hz neurons in monkey primary somatosensory cortex: activity patterns during initiation of vibratory-cued hand movements. *J. Comp. Neurosci.* 2, 313–334. doi: 10.1007/BF00961443

Lebedev, M. A., and Nelson, R. J. (1996). High-frequency vibratory neurons in monkey primary somatosensory cortex: entrained and nonintrained responses to vibration during the performance of vibratory-cued hand movements. *Exp. Brain Res.* 111, 313–325. doi: 10.1007/BF00228721

Lebedev, M. A., and Nelson, R. J. (1999). Rhythmically firing neostriatal neurons in monkey: activity patterns during reaction-time hand movements. *J. Neurophysiol.* 82, 1832–1842.

Lebedev, M. A., and Nicolelis, M. A. (2006). Brain-machine interfaces: past, present and future. *Trends Neurosci.* 29, 536–546. doi: 10.1016/j.tins.2006.07.004

Lee, H., and Assad, J. (2003). Putaminal activity for simple reactions or self-timed movements. *J. Neurophysiol.* 89, 2528–2537. doi: 10.1152/jn.01055.2002

Liles, S. L. (1985). Activity of neurons in putamen during active and passive movements of the wrist. *J. Neurophysiol.* 53, 217–235.

Liu, Y., Denton, J. M., and Nelson, R. J. (2005). Neuronal activity in primary motor cortex differs when monkeys perform somatosensory and visually guided wrist movements. *Exp. Brain Res.* 167, 571–586. doi: 10.1007/s00221-005-0052-8

Liu, Y., Denton, J. M., and Nelson, R. J. (2008). Monkey primary somatosensory cortical activity during the early reaction time period differs with cues that guide movements. *Exp. Brain Res.* 187, 349–358. doi: 10.1007/s00221-008-1307-y

Lynd-Balta, E., and Haber, S. N. (1994). The organization of midbrain projections to the ventral striatum in the primate: a comparison of the sensorimotor-related striatum and the ventral striatum. *J. Comp. Neurol.* 345, 562–578. doi: 10.1002/cne.903450407

Mirenowicz, J., and Schultz, W. (1994). Importance of unpredictability for reward responses in primate dopamine neurons. *J. Neurophysiol.* 72, 1024–1027.

Nelson, R. J. (1987). Activity of monkey primary somatosensory cortical neurons changes prior to active moment. *Brain Res.* 406, 402–407. doi: 10.1016/0006-8993(87)90815-8

Nelson, R. J. (1988). Set related and premovement related activity of primate somatosensory cortical neurons depends upon stimulus modality and subsequent movement. *Brain Res. Bull.* 21, 411–424. doi: 10.1016/0361-9230(88)90153-0

Nelson, R. J., and Douglas, V. D. (1989). Changes in premovement activity in primary somatosensory cortex differ when monkey make hand movements in response to visual vs. vibratory cues. *Brain Res.* 484, 43–56. doi: 10.1016/0006-8993(89)90346-6

Nelson, R. J., Lebedev, M. A., Opris, I., and Denton, J. M. (1996). Neostriatal neuronal activity becomes better related to movements when conditions become unpredictable. *Soc. Neurosci. Abstr.* 22, 1085.

Nelson, R. J., Smith, B. N., and Douglas, V. D. (1991). Relationship between sensory responsiveness and premovement activity of quickly adapting neurons in areas 3b and 1 of monkey primary somatosensory cortex. *Exp. Brain Res.* 71, 431–436. doi: 10.1007/bf00231763

Nicolelis, M. A., and Lebedev, M. A. (2009). Principles of neural ensemble physiology underlying the operation of brain-machine interfaces. *Nat. Rev. Neurosci.* 10, 530–540. doi: 10.1038/nrn2653

Opris, I., and Bruce, C. J. (2005). Neural circuitry of judgment and decision mechanisms. *Brain Res. Rev.* 48, 509–528. doi: 10.1016/j.brainresrev.2004.11.001

Opris, I., Hampson, R. E., and Deadwyler, S. A. (2009). The encoding of cocaine vs. natural rewards in the striatum of nonhuman primates: categories with different activations. *Neuroscience* 163, 40–54. doi: 10.1016/j.neuroscience.2009.06.002

Opris, I., Hampson, R. E., Stanford, T. R., Gerhardt, G. A., and Deadwyler, S. A. (2011b). Neural activity of frontal cortical layers: evidence for columnar sensorimotor processing. *J. Cogn. Neurosci.* 23, 1507–1521 doi: 10.1162/jocn.2010.21534

Opris, I., Santos, L., Gerhardt, G. A., Song, D., Berger, T. W., Hampson, R. E., et al. (2013). Prefrontal cortical microcircuits bind perception to executive control. *Sci. Rep.* 3:2285. doi: 10.1038/srep02285

Opris, I., Lebedev, M., and Nelson, R. J. (2011a). Motor planning under unpredictable reward: Modulations of movement vigor and primate striatum activity. *Front. Neurosci.* 5:61. doi: 10.3389/fnins.2011.00061

Parent, A., and Hazrati, L.-N. (1995). Functional anatomy of the basal ganglia. I. The cortico-basal ganglia-thalamo-cortical loop. *Brain Res. Rev.* 20, 91–127. doi: 10.1016/0165-0173(94)00007-C

Pasquereau, B., Nadjar, A., Arkadir, D., Bezard, E., Goillandeau, M., Bioulac, B., et al. (2007). Shaping of motor responses by incentive values through the basal ganglia. *J. Neurosci.* 27, 1176–1183. doi: 10.1523/JNEUROSCI.3745-06.2007

Pekny, S. E., Izawa, J., and Shadmehr, R. (2015). Reward-dependent modulation of movement variability. *J. Neurosci.* 35, 4015–4024. doi: 10.1523/JNEUROSCI.3244-14.2015

Reppert, T. R., Lempert, K. M., Glimcher, P. W., and Shadmehr, R. (2015). Modulation of Saccade Vigor during Value-Based Decision Making. *J. Neurosci.* 35, 15369–15378. doi: 10.1523/JNEUROSCI.2621-15.2015

Robbins, T. W., and Everitt, B. J. (1996). Neurobehavioral mechanisms of reward and motivation. *Curr. Opin. Neurobiol.* 6, 228–236. doi: 10.1016/S0959-4388(96)80077-8

Romo, R., Scarnati, E., and Schultz, W. (1992). Role of primate basal ganglia and frontal cortex in the internal generation of movements. *Exp. Brain Res.* 91, 385–395. doi: 10.1007/BF00227835

Romo, R., and Schultz, W. (1990). Dopamine neurons of the monkey midbrain: Contingencies of responses to active touch during self-initiated arm movements. *J. Neurophysiol.* 63, 592–606.

Samejima, K. Ueda, Y., Doya, K., and Kimura, M. (2005). Representation of action-specific reward values in the striatum. *Science* 310, 1337–1340. doi: 10.1126/science.1115270

Santos, L. M., Opris, I., Hampson, R. E., Godwin, D. W., Gerhardt, G. A., and Deadwyler, S. A. (2014). Functional dynamics of primate cortico-striatal networks during volitional movements. *Front. Syst. Neurosci.* 8:27. doi: 10.3389/fnsys.2014.00027

Schultz, W. (1997). Dopamine neurons and their role in reward mechanisms. *Curr. Opin. Neurobiol.* 7, 191–197. doi: 10.1016/S0959-4388(97)80007-4

Schultz, W. (2010). Dopamine signals for reward value and risk: basic and recent data. *Behav. Brain Funct.* 6:24. doi: 10.1186/1744-9081-6-24

Schultz, W., Apicella, P., and Ljungberg, T. (1993). Response of monkey dopamine neurons to reward and conditioned stimuli during successive steps of learning a delayed response task. *J. Neurosci.* 13, 900–913.

Schultz, W., Apicella, P., Scarnati, E., and Ljungberg, T. (1992). Neuronal activity in monkey ventral striatum related to the expectation of reward. *J. Neurosci.* 12, 4595–4610.

Schultz, W., Dayan, P., and Read-Montague, P. (1997). A neural substrate of prediction and reward. *Science* 275, 1593–1599. doi: 10.1126/science.275.5306.1593

Schultz, W., and Romo, R. (1988). Neuronal activity in the monkey striatum during the initiation of movements. *Exp. Brain Res.* 71, 431–436. doi: 10.1007/BF00247503

Schultz, W., and Romo, R. (1990). Dopamine neurons of the monkey midbrain: contingencies of responses to active touch during self-initiated arm movements. *J. Neurophysiol.* 63, 607–624.

Sokal, R. R., and Rohlf, F. J. (eds.). (1981). *Biometry: The Principles and Practice of Statistics in Biological Research.* San Francisco, CA: W. H. Freeman. Available online at: https://books.google.com/books/about/Biometry.html?id=C-OTQgAACAAJ

Stark, E., Drori, R., Asher, I., Ben-Shaul, Y., and Abeles, M. (2007). Distinct movement parameters are represented by different neurons in the motor cortex. *Eur. J. Neurosci.* 2007, 1055–1066. doi: 10.1111/j.1460-9568.2007.05711.x

Surmeier, D. J., and Kitai, S. T. (1997). State-dependent regulation of neuronal excitability by dopamine. *Jpn. J. Psychopharmacol.* 17, 105–110.

Taira, M., Boline, J., Smyrnis, N., Georgopoulos, A. P., and Ashe, J. (1996). On the relations between single cell activity in the motor cortex and the direction and magnitude of three-dimensional static force. *Exp. Brain Res.* 109, 367–376. doi: 10.1007/BF00229620

Turner, R. S., and Desmurget, M. (2010). Basal ganglia contributions to motor control: a vigorous tutor. *Curr. Opin. Neurobiol.* 20, 704–716. doi: 10.1016/j.conb.2010.08.022

Ueda, Y., and Kimura, M. (2003). Encoding of direction and combination of movements by primate putamen neurons. *Eur. J. Neurosci.* 18, 980–994. doi: 10.1046/j.1460-9568.2003.02814.x

Vaadia, E., Kurata, K., and Wise, S. P. (1988). Neuronal activity preceding directional and nondirectional cues in the premotor cortex of rhesus monkeys. *Somatosens. Motor Res.* 6, 207–230. doi: 10.3109/08990228809144674

Watanabe, M. (1996). Reward expectancy in primate prefrontal neurons. *Nature* 382, 629–632. doi: 10.1038/382629a0

Conflict of Interest Statement: The authors declare that the research was conducted in the absence of any commercial or financial relationships that could be construed as a potential conflict of interest.

frontiers in
SYSTEMS NEUROSCIENCE

PERSPECTIVE ARTICLE
published: 29 September 2014
doi: 10.3389/fnsys.2014.00171

On the need to better specify the concept of "control" in brain-computer-interfaces/neurofeedback research

Guilherme Wood[1,2]*, Silvia Erika Kober[1,2], Matthias Witte[1,2] and Christa Neuper[1,2]

[1] *Department of Psychology, Karl-Franzens-University Graz, Graz, Austria*
[2] *BioTechMed, Graz, Austria*

Edited by:
Mikhail Lebedev, Duke University, USA

Reviewed by:
Andrea Kübler, University of Würzburg, Germany
Kenji Kansaku, Research Institute of National Rehabilitation Center for Persons with Disabilities, Japan
Annette Sterr, University of Surrey, UK

****Correspondence:***
Guilherme Wood, Department of Neuropsychology, Institute of Psychology, University of Graz, Brandhofgasse 5 (Palais Apfaltrem), A-8010 Graz, Austria
e-mail: guilherme.wood@uni-graz.at

Aiming at a better specification of the concept of "control" in brain-computer-interfaces (BCIs) and neurofeedback (NF) research, we propose to distinguish "self-control of brain activity" from the broader concept of "BCI control", since the first describes a neurocognitive phenomenon and is only one of the many components of "BCI control". Based on this distinction, we developed a framework based on dual-processes theory that describes the cognitive determinants of self-control of brain activity as the interplay of automatic vs. controlled information processing. Further, we distinguish between cognitive processes that are necessary and sufficient to achieve a given level of self-control of brain activity and those which are not. We discuss that those cognitive processes which are not necessary for the learning process can hamper self-control because they cannot be completely turned-off at any time. This framework aims at a comprehensive description of the cognitive determinants of the acquisition of self-control of brain activity underlying those classes of BCI which require the user to achieve regulation of brain activity as well as NF learning.

Keywords: BCI, neurofeedback, executive functions, dual-process theory, rumination, meta-cognition, cognitive strategies

INTRODUCTION

Brain computer interfaces (BCIs) make possible the direct communication pathway between the brain and an external device. BCIs are often directed at assisting, augmenting, or repairing human cognitive or sensory-motor functions. Individuals learn how to induce certain patterns of brain activity, which can be detected and transcoded into some form of action or feedback in the external device. One special case of BCI is neurofeedback (NF), in which the aim is not to control an external device but rather to use external feedback to modulate specific aspects of physiological signal intrinsic to the brain. Both human and nonhuman animals are able to learn to use BCI/NF with a short amount of training (Sterman, 1977; Nicolelis and Lebedev, 2009; Phillippens and Vanwersch, 2010).

Generally, the term "BCI control" has been used interchangeably to refer to two different processes. On the one side, "BCI control" refers to the ability to control an external device and can be seen mainly as a complex problem of neuroengineering (Donoghue, 2008). This definition simultaneously involves neuro-bio-psychological, data analytical and ergonomical aspects (see Kübler et al., 2011). On the other side, "BCI control" may refer to the much more specific ability of an individual to control some aspects of his/her own brain activity (Hinterberger et al., 2003; Halder et al., 2011), which is clearly a neurocognitive topic that is central but not restricted to BCI/NF. Broadly speaking, not only BCI/NF but many other processes such as meditation techniques (Tang et al., 2014), emotion regulation (Thayer and Lane, 2000) and even psychotherapy (Beauregard, 2007) also induce some form of self-control of brain activity. Since the definition of "BCI control" from either a neuroengineering perspective or from a neurocognitive perspective fundamentally differs, it is necessary to disentangle both views. The topic of the present article is "BCI control" as self-regulation of neuronal activity and, for the sake of transparency, it will be called hereafter "self-control of brain activity".

With the aim of better understanding BCI/NF learning, the first step to characterize "self-control of brain activity" is to specify the cognitive mechanisms responsible for learning control. The more popular models of BCI/NF discuss "operant conditioning" and a "motor skill learning" as these mechanisms (Hammer et al., 2012). However, many studies indicate that other cognitive mechanisms such as locus of control towards technology (Burde and Blankertz, 2006; Ninaus et al., 2013; Witte et al., 2013), aptitude towards BCI (Hammer et al., 2012; Halder et al., 2013), motivation (Kleih et al., 2010) and spontaneous strategies (Kober et al., 2013) also influence BCI or NF learning. As a consequence, these predictors may either constitute a secondary correlate of self-control of brain activity or may represent key cognitive processes in addition to conditioning and skill learning. Given the high variety of cognitive and emotional processes apparently associated with self-control of brain activity and BCI learning, it is particularly useful to define a simple but comprehensible framework to evaluate the common and unique contributions of each one of these processes.

A dual-processes theory has been related to BCI/NF learning (Lacroix, 1986; Hammer et al., 2012). In the following, we shortly point out how this theory can be employed to better understand how the processes mentioned above might determine self-control of brain activity.

TWO TYPES OF MENTAL ACTIVITY

The dual-processes theory categorizes the whole mental activity into two main types of processing: more automatic and capacity-free processes (i.e., type I processes) vs. more controlled and capacity-limited processes (i.e., type II processes). Type I processes reflect the automatic, capacity-free, effortless and context-specific information processing such as for instance trying to open the office door with the home key because one has been thinking about dinner. Moreover, type I processes are usually unconscious and difficult to control by self-instruction. Type II processes reflect the activity of a supervisory attention system, specialized in monitoring and regulating the activity in other cognitive systems (Shallice and Cooper, 2011). Type II processes are usually in the center of our focus of attention (but see Horga and Maia, 2012 for an exception), are regulated mainly by self-instruction and are fundamental for executive functions and metacognitive abilities (Bewick et al., 1995). Accordingly, control beliefs are much more related to the function of the type II processes while the heuristics regulating most of our cognitive activity and behavior are type I processes.

A central aspect of the dual-processes theory is that both automatic and controlled processes have control of behavior as well as of different aspects of cognition (Alos Ferrer, 2013) but both learn from and react to different aspects of the task at hand. Automatic systems learn only through cumulative reward while controlled systems are more flexible, context-oriented and learn fast from instructions. It is beyond the scope of this perspective article to review every single manifestation of automatic vs. controlled processing to each one of the predictors of self-control of brain activity. Instead, we present one example regarding motivation, which may suffice to make our point: motivation consists of a more controlled component called intrinsic motivation, which is highly sensitive to self-instruction and self-efficacy beliefs, and a more automatic component called extrinsic motivation, which is more sensitive to the current amount of reward received (Ryan and Deci, 2000). Accordingly, as long as some reward can be obtained during BCI/NF learning, automatic processing will predominate. Controlled processing will be engaged when negative feedback predominates over longer periods of time and will have a larger impact, if the participant shows high levels of intrinsic motivation. In summary, dual-process models such as Lacroix (1986) make clear that self-regulation is not a unitary process but rather the result of the conjoint action of type I and type II processes.

A FRAMEWORK OF SELF-CONTROL OF BRAIN ACTIVITY

Automatic and controlled processes determine self-control of brain activity in very different ways. Even more, not every cognitive process is necessary and sufficient to perform a specific BCI/NF task, but instead a small subset may play a key role. The remaining mental activity -that is neither necessary nor sufficient for a specific BCI/NF task -will act on BCI/NF learning in one of two ways: firstly, this activity can interfere with the learning process, if it hampers self-control of the specific aspect of brain activity being targeted in a specific BCI/NF task. Secondly, activations can promote the learning process indirectly, if they do not interfere with the activity in that small subset of both automatic and controlled processes necessary and sufficient to perform the BCI/NF task at hand. Although in some BCI classes such as those employing electrocorticogram or other kinds of stable and specific brain signals such as SSVEP the influence of unspecific processes signal is barely important, cognitive BCIs (Astrand et al., 2014) or BCI classes based on cognitive tasks such as mental calculation and motor imagery (Halder et al., 2011; Hammer et al., 2012) should be more subjected to the effects of different forms of self-control over brain activity. Based on the differentiation between automatic vs. controlled processing as well as necessary vs. unnecessary processes, we define a framework of self-control of brain activity.

We start with the automatic and controlled processes both necessary and sufficient to perform BCI/NF tasks: both are subsumed under *local control network*. The more the feedback provided by BCI/NF reflects the activity in these networks, the more efficient is the learning process. The role of automatic and controlled processes in the *local control network* is complementary: automatic processes are driven directly by the amount and quality of feedback obtained whereas controlled processes are driven by the verbalizations and self-instruction (Lacroix, 1986), that are largely under conscious control of the individual and subjected to beliefs and expectations. While automatic learning is very insensitive to verbal instructions and only takes place when some pattern of reaction is systematically rewarded, controlled processes are mainly driven by direct verbal instructions. Efficient BCI/NF learning reflects the timely combination of both processes depending on the present learning rates: when a steep learning curve is forming, automatic processes take the lead, when the learning curve temporarily flattens, controlled processes correct the course by means of self-instruction (Lacroix, 1986). The optimal level of self-control of brain activity in the *local control network* is achieved under two main conditions: (i) avoidance of irrelevant associations between internal states and external reward; and (ii) staying engaged and focused on the task at hand without distractions. As we will discuss below, condition (i) can be achieved when activity in the *organismic control network* is reduced to a minimum and condition (ii), when the *central control network* frees the most of its limited resources for the *local control network*.

We define a framework of three concentric circles (**Figure 1**) representing three sources of self-control. First, the outmost and thus most unspecific level of response to feedback reflects basically automatic processes. Second, the middle circle depicts central control networks performing controlled processing. Finally, in the innermost level, we describe networks responding specifically to the BCI/NF learning protocol. This local control relies on both automatic and controlled processes.

We define those *automatic* processes unnecessary to perform a given BCI/NF task as the *organismic control network*. We call them organismic control because it reflects the activity of the

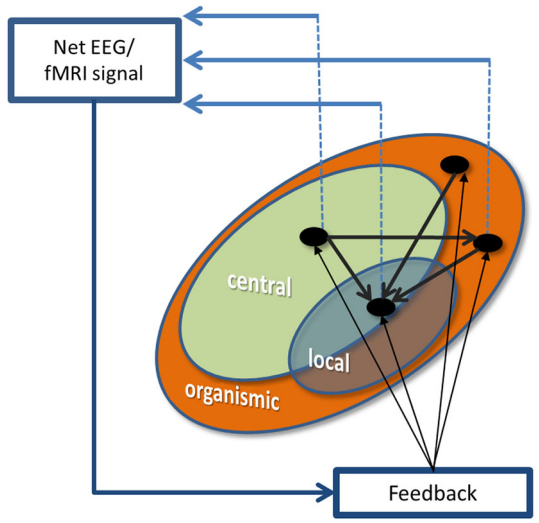

FIGURE 1 | A schema of different types of self-control of the brain activity. Specific cognitive processes such as for instance motivation, mood, attention and executive functions are represented by black dots. Black arrows connecting the dots represent the interactions between the different cognitive functions. Two dots are depicted over the domain of organismic control network to illustrate that these processes are largely independent from one another. The contribution of the three types of self-control to physiological signals is represented by the dashed lines linking the specific cognitive processes to the physiological signals being recorded for BCI/NF learning.

thousands of automatic and unconscious mental processes regulating the largest part of cognitive activity (Dijksterhuis and Nordgren, 2006). The interference of these processes is high when unnecessary automatic reactions to feedback are triggered, which compete with the learning process taking place in the *local control network*. Rumination, for instance, describes the intrusion of negative feelings about past experiences in the stream of thoughts and emerges primarily during relaxation (Nolen-Hoeksema et al., 2008). The intrusion of ruminative thoughts is an example of the negative impact of the *organismic control network* on self-control of brain activity during BCI/NF learning. Cognitive processes subsumed under *organismic control network* are not easily influenced by direct instructions and mostly not even conscious to the participant. Therefore, it may be very important to monitor any signs of negative influences originating in organismic control networks. This unwanted activity should be fed back in a timely manner during training. As a consequence, processes like increased anxiety or intrusive thoughts are accessible to BCI/NF users and can trigger appropriate learning mechanisms capable to control or suppress these processes.

Finally, we define the *central control network* as those *controlled* processes not strictly necessary to perform a given BCI/NF task. Controlled processes have limited capacity, so that every bit of irrelevant information being employed in the *central control network* will be missed by the *local control network*. The negative impact of *central control network* is high when improper strategies, self-instruction, over-instruction or excessive attention to the self (Leary et al., 2006) withdraw resources from the *local control network* and hamper the regulation of the learning process in a similar way as a dual-task (Logan and Gordon, 2001) drains resources. In contrast to the *organismic control network*, controlled processing is largely under conscious control and can be modulated directly by instructions (Dijksterhuis and Nordgren, 2006).

In summary, the aim of any BCI/NF learning is to magnify the signal produced by *local control networks* and suppress as much as possible the activity elsewhere. To do that, it is in our view necessary to take into consideration the specificities of two types of cognitive activity subsumed under *organismic control networks* and *central control networks*, since they imply very different learning mechanisms sensitive to different types of cues and reward. On the one side, participants should learn to decouple irrelevant from those relevant automatic processes. One way to achieve this is to monitor the automatic processes regulating for instance negative emotional reactions and anxiety as well as with a more selective schedule of reward and punishment. On the other side, participants should learn to use the *central control networks* to suppress irrelevant cognitive activity operating under conscious control such as excessive attention to the self (Leary et al., 2006). This can be achieved by direct instruction or self-instruction. Once this balance is achieved, the outcome of BCI/NF learning should be improved. Among many other possibilities, one simple experiment to investigate how the suppression of irrelevant cognitive activity could improve BCI/NF learning would involve the monitoring of inner speech (Perrone-Bertolotti et al., 2014). Extra feedback requiring focus on the concrete task is presented when an increase in the levels of inner speech is detected in combination with a local flattening of the learning curve. As suggested by Leary et al. (2006), this extra feedback should help to reduce excessive attention to the self and improve learning.

FINAL REMARKS

We propose that self-regulation of brain activity should be distinguished from the more general process of "BCI learning", since the latter one is more of a neuroengineering problem whereas the former is mainly a neurocognitive problem. To better understand how self-regulation of brain activity works, we propose to look at the cognitive predictors of BCI/NF performance from the point of view of a framework which organizes them according to the main type of cognitive processing required: more automatic or more controlled processing. Further on, we distinguish between cognitive resources necessary and sufficient for BCI/NF learning and other cognitive processes, which should be suppressed or down-regulated to improve learning. Finally, we argue that our framework can be very useful to optimize BCI learning, since it predicts the most suitable tools to modulate the activation generated by automatic and controlled cognitive processes.

ACKNOWLEDGMENTS

This work is supported by the European STREP Program—Collaborative Project no. FP7-287320—CONTRAST. Possible inaccuracies of information are under the responsibility of the project team. The text reflects solely the views of its authors. The European Commission is not liable for any use that may be made of the information contained therein.

REFERENCES

Alos Ferrer, C. (2013). "Think, but not too much: a dual-process model of willpower and self-control," in *Annual Conference 2013 (Duesseldorf): Competition Policy and Regulation in a Global Economic Order 80019* (Verein für Socialpolitik/German Economic Association).

Astrand, E., Wardak, C., and Ben Hamed, S. (2014). Selective visual attention to drive cognitive brain-machine interfaces: from concepts to neurofeedback and rehabilitation applications. *Front. Syst. Neurosci.* 8:144. doi: 10.3389/fnsys.2014.00144

Beauregard, M. (2007). Mind does really matter: evidence from neuroimaging studies of emotional self-regulation, psychotherapy and placebo effect. *Prog. Neurobiol.* 81, 218–236. doi: 10.1016/j.pneurobio.2007.01.005

Bewick, K. C., Raymond, M. J., Malia, K. B., and Bennett, T. L. (1995). Metacognition as the ultimate executive: techniques and tasks to facilitate executive functions. *NeuroRehabilitation* 5, 367–375. doi: 10.3233/NRE-1995-5411

Burde, W., and Blankertz, B. (2006). "Is the locus of control of reinforcement a predictor of brain-computer interface performance?," in *Proceedings of the 3rd International Brain-Computer Interface Workshop and Training Course* (Graz, Austria), 76–77.

Dijksterhuis, A., and Nordgren, L. F. (2006). A theory of unconscious thought. *Perspect. Psychol. Sci.* 1, 95–109. doi: 10.1111/j.1745-6916.2006.00007.x

Donoghue, J. P. (2008). Bridging the brain to the world: a perspective on neural interface systems. *Neuron* 60, 511–521. doi: 10.1016/j.neuron.2008.10.037

Halder, S., Agorastos, D., Veit, R., Hammer, E. M., Lee, S., Varkuti, B., et al. (2011). Neural mechanisms of brain-computer interface control. *Neuroimage* 55, 1779–1790. doi: 10.1016/j.neuroimage.2011.01.021

Halder, S., Hammer, E. M., Kleih, S. C., Bogdan, M., Rosenstiel, W., Birbaumer, N., et al. (2013). Prediction of auditory and visual p300 brain-computer interface aptitude. *PLoS One* 8:e53513. doi: 10.1371/journal.pone.0053513

Hammer, E. M., Halder, S., Blankertz, B., Sannelli, C., Dickhaus, T., Kleih, S., et al. (2012). Psychological predictors of SMR-BCI performance. *Biol. Psychol.* 89, 80–86. doi: 10.1016/j.biopsycho.2011.09.006

Hinterberger, T., Veit, R., Strehl, U., Trevorrow, T., Erb, M., Kotchoubey, B., et al. (2003). Brain areas activated in fMRI during self-regulation of slow cortical potentials (SCPs). *Exp. Brain Res.* 152, 113–122. doi: 10.1007/s00221-003-1515-4

Horga, G., and Maia, T. V. (2012). Conscious and unconscious processes in cognitive control: a theoretical perspective and a novel empirical approach. *Front. Hum. Neurosci.* 6:199. doi: 10.3389/fnhum.2012.00199

Kleih, S. C., Nijboer, F., Halder, S., and Kübler, A. (2010). Motivation modulates the P300 amplitude during brain-computer interface use. *Clin. Neurophysiol.* 121, 1023–1031. doi: 10.1016/j.clinph.2010.01.034

Kober, S. E., Witte, M., Ninaus, M., Neuper, C., and Wood, G. (2013). Learning to modulate one's own brain activity: the effect of spontaneous mental strategies. *Front. Hum. Neurosci.* 7:695. doi: 10.3389/fnhum.2013.00695

Kübler, A., Blankertz, B., Müller, K. R., and Neuper, C. (2011). "A model of BCI control," in *Proceedings of the 5th International Brain-Computer Interface Conference, September 22–24 2011*, eds G. R. Müller-Putz, R. Scherer, M. Billinger, A. Kreilinger, V. Kaiser and C. Neuper (Austria: Graz University of Technology), 100–103.

Lacroix, J. M. (1986). "Mechanisms of biofeedback control: on the importance of verbal (conscious) processing," in *Consciousness and Self-Regulation: Vol. 4, Chapter Mechanisms of Biofeedback Control*, eds R. J. Davidson, G. E. Schwartz and D. Shapiro (New York: Plenum), 137–162.

Leary, M. R., Adams, C. E., and Tate, E. B. (2006). Hypo-egoic self-regulation: exerting self-control by diminishing the influence of the self. *J. Pers.* 74, 1803–1832. doi: 10.1111/j.1467-6494.2006.00429.x

Logan, G. D., and Gordon, R. D. (2001). Executive control of visual attention in dual-task situations. *Psychol. Rev.* 108, 393–434. doi: 10.1037//0033-295x.108.2.393

Nicolelis, M. A., and Lebedev, M. A. (2009). Principles of neural ensemble physiology underlying the operation of brain-machine interfaces. *Nat. Rev. Neurosci.* 10, 530–540. doi: 10.1038/nrn2653

Ninaus, M., Kober, S. E., Witte, M., Koschutnig, K., Stangl, M., Neuper, C., et al. (2013). Neural substrates of cognitive control under the belief of getting neurofeedback training. *Front. Hum. Neurosci.* 7:914. doi: 10.3389/fnhum.2013.00914

Nolen-Hoeksema, S., Wisco, B. E., and Lyubomirsky, S. (2008). Rethinking rumination. *Perspect. Psychol. Sci.* 3, 400–424. doi: 10.1111/j.1745-6924.2008.00088.x

Perrone-Bertolotti, M., Rapin, L., Lachaux, J. P., Baciu, M., and Loevenbruck, H. (2014). What is that little voice inside my head? Inner speech phenomenology, its role in cognitive performance and its relation to self-monitoring. *Behav. Brain Res.* 261, 220–239. doi: 10.1016/j.bbr.2013.12.034

Phillippens, I. H. C. H. M., and Vanwersch, R. A. P. (2010). Neurofeedback training on sensorimotor rhythm in marmoset monkeys. *Neuroreport* 21, 328–332. doi: 10.1097/wnr.0b013e3283360ba8

Ryan, R., and Deci, E. L. (2000). Intrinsic and extrinsic motivations: classic definitions and new directions. *Contemp. Educ. Psychol.* 25, 54–67. doi: 10.1006/ceps.1999.1020

Shallice, T., and Cooper, R. (2011). *The Organisation of Mind.* Oxford: Oxford University Press.

Sterman, M. B. (1977). Sensorimotor EEG operant conditioning: experimental and clinical effects. *Pavlov. J. Biol. Sci.* 12, 63–92.

Tang, Y. Y., Posner, M. I., and Rothbart, M. K. (2014). Meditation improves self-regulation over the life span. *Ann. N Y Acad. Sci.* 1307, 104–111. doi: 10.1111/nyas.12227

Thayer, J. F., and Lane, R. D. (2000). A model of neurovisceral integration in emotion regulation and dysregulation. *J. Affect. Disord.* 61, 201–216. doi: 10.1016/s0165-0327(00)00338-4

Witte, M., Kober, S. E., Ninaus, M., Neuper, C., and Wood, G. (2013). Control beliefs can predict the ability to up-regulate sensorimotor rhythm during neurofeedback training. *Front. Hum. Neurosci.* 7:478. doi: 10.3389/fnhum.2013.00478

Conflict of Interest Statement: The authors declare that the research was conducted in the absence of any commercial or financial relationships that could be construed as a potential conflict of interest.

Received: 30 May 2014; accepted: 31 August 2014; published online: 29 September 2014.

Citation: Wood G, Kober SE, Witte M and Neuper C (2014) On the need to better specify the concept of "control" in brain-computer-interfaces/neurofeedback research. Front. Syst. Neurosci. ***8****:171. doi: 10.3389/fnsys.2014.00171*

This article was submitted to the journal Frontiers in Systems Neuroscience.

frontiers in
SYSTEMS NEUROSCIENCE

ORIGINAL RESEARCH ARTICLE
published: 17 February 2015
doi: 10.3389/fnsys.2014.00252

Hemodynamic responses on prefrontal cortex related to meditation and attentional task

Singh Deepeshwar*, Suhas Ashok Vinchurkar, Naveen Kalkuni Visweswaraiah and Hongasandra RamaRao Nagendra

ANVESANA Research Laboratory, Department of Yoga and Life Sciences, Swami Vivekananda Yoga Research Foundation, Bangalore, Karnataka, India

Edited by:
Mikhail Lebedev, Duke University, USA

Reviewed by:
José M. Delgado-García, University Pablo de Olavide, Seville, Spain
Laura Marzetti, University "G. d'Annunzio" of Chieti-Pescara, Italy

****Correspondence:***
Singh Deepeshwar, ANVESANA Research Laboratory, Department of Yoga and Life Sciences, Swami Vivekananda Yoga Research Foundation, #19 Eknath Bhavan, Gavipuram Circle, K.G. Nagar, Bangalore – 560019, Karnataka, India
e-mail: deepeshwar.singh@gmail.com

Recent neuroimaging studies state that meditation increases regional cerebral blood flow (rCBF) in the prefrontal cortex (PFC). The present study employed functional near infrared spectroscopy (fNIRS) to evaluate the relative hemodynamic changes in PFC during a cognitive task. Twenty-two healthy male volunteers with ages between 18 and 30 years (group mean age ± SD; 22.9 ± 4.6 years) performed a color-word stroop task before and after 20 min of meditation and random thinking. Repeated measures ANOVA was performed followed by a *post hoc* analysis with Bonferroni adjustment for multiple comparisons between the mean values of "During" and "Post" with "Pre" state. During meditation there was an increased in oxy-hemoglobin (ΔHbO) and total hemoglobin (ΔTHC) concentration with reduced deoxy-hemoglobin (ΔHbR) concentration over the right prefrontal cortex (rPFC), whereas in random thinking there was increased ΔHbR with reduced total hemoglobin concentration on the rPFC. The mean reaction time (RT) was shorter during stroop color word task with concomitant reduction in ΔTHC after meditation, suggestive of improved performance and efficiency in task related to attention. Our findings demonstrated that meditation increased cerebral oxygenation and enhanced performance, which was associated with activation of the PFC.

Keywords: meditation, attention task, Stroop task, fNIRS, cerebral blood flow

INTRODUCTION

Meditation is a complex mental process that aims to calm the fluctuations of the mind and improve cognitive functions. Several meditation techniques from diverse traditions (e.g., Transcendental meditation, Buddhists, Zen, Yoga, Vipassana, Brahmakumari, Mindfulness-based stress reduction (MBSR) etc.,) demonstrated that regular practice of meditation develops awareness to the contents of subjective experience, including thoughts, sensations, intentions, and emotions (Saggar et al., 2012). It is considered as a voluntary means of mental training to achieve greater control of higher mental functions. Traditional yoga texts like Patanjali's Yoga *Sutras* (the Sage Patanjali', *Circa* 900 B.C.) and *Bhagavad Gita* (*Circa* 400–600 B.C.) very well describe the connection between meditation and mental modifications. Traditionally, two states of meditation have been described, viz., (i) focused meditation (*dharana* in Sanskrit, Patanjali's Yoga *Sutras*, Chapter III, Verse 1), and this state is supposed to lead to the next stage of effortless mental expansion i.e., (iii) meditation (*dhyana* in Sanskrit; Patanjali's Yoga *Sutras*, Chapter III, Verse 2). When not in meditation, it is said that the mind may be in two other states (Telles et al., 2012). These are (i) random thinking (*cancalata* in Sanskrit; *Bhagavad Gita*, chapter VI, *verse* 34); and (ii) non-meditative focused thinking (*ekagrata* in Sanskrit; *Bhagavad Gita*, chapter VI, *verse* 12) (Telles et al., 2014).

In recent years, there have been a number of neuroimaging studies showing that meditation improves cognitive performance as signified by behavioral and neurophysiological measures (Tang et al., 2007; Lutz et al., 2009). Previous studies have shown that the practice of meditation enhances behavioral performance viz., perceptual discrimination and sustained attention during visual discrimination task (MacLean et al., 2010). Meditation practice develops the ability to engage the attention onto an object for extended periods of time (Carter et al., 2005; Jha et al., 2007; Lutz et al., 2008). It improves the control over the distribution of limited brain resources in the temporal domain, as measured by the attentional blink task (van Leeuwen et al., 2009; Slagter et al., 2011). Long term meditation practice has been found to enhance cognitive performance (Cahn and Polich, 2006), attentional focus, alerting (Jha et al., 2007), processing speed (Lutz et al., 2009; Slagter et al., 2009), and overall information processing (van Vugt and Jha, 2011). In a study, Buddhist meditation practitioners showed mindfulness meditation was positively correlated with sustained attention, when compared to non-meditation practitioners (Moore and Malinowski, 2009). Improvements in sustained attention and attentional error monitoring demonstrated a positive correlation with increased activation in executive attention networks in meditators (Short et al., 2010). Other studies have shown that meditation is associated with improved conflict scores on the attention network test (Tang et al., 2007), reduced interference (Chan and Woollacott, 2007) and enhanced attentional performance during the stroop task compared to meditation-naïve control

group (Moore and Malinowski, 2009). These studies provide significant evidence of meditation promoting the higher-order cognitive processing (Zeidan et al., 2010), particularly, the features of conflict monitoring and cognitive control processes.

The stroop task is one of the most frequently used models of the conflict processing (Szűcs et al., 2012) in cognitive neuroscience. Stroop color word task performance evaluates flexibility in the purview of cognitive processes and behavior which requires both attention and impulse control. The simultaneous presentation of the prime color and a written word stimulus will either facilitate (when the color and word stimuli are congruent, e.g., "b-l-u-e" written in the color blue) or interfere (the incongruent stroop trial, e.g., "blue" written in red) with color naming (MacLeod, 1991; Peterson et al., 1999). Previous studies on stroop test have consistently shown that responses in naming the ink color of incongruent color word are much slower than in naming the ink color of neutral (Zysset et al., 2007), and responses are often, but not always, faster when color and word are congruent than in the neutral condition. It supports the hypothesis that, both the task relevant and task irrelevant dimensions of stroop task activate the same response in the congruent condition, in contrast, these dimensions stimulate opposing response tendencies in the incongruent condition (Morton and Chambers, 1973; Posner and Snyder, 1975; Szűcs et al., 2012).

Recent studies reported that regular practice of meditation may alter brain structure and function related to attention (Lazar et al., 2005; Holzel et al., 2011; Kozasa et al., 2012). A study on 20 experienced participants of extensive Insight meditation, that involves focused attention to internal experiences, reported increased cortical thickness in prefrontal cortex (PFC) and right anterior insula associated with attention, interoception and sensory processing in meditation participants compared with matched controls (Lazar et al., 2005).

In order to examine neuronal activity and hemodynamic changes in the brain regions during meditation, the application of different neuroimaging techniques (viz., fMRI and MEG) would be beneficial. The neuronal activity during meditation has been reported in several electroencephalography (EEG) and magnetoencephalography (MEG) studies. Experienced meditators showed an increased EEG power in lower frequency bands (theta, delta and alpha) (Kubota et al., 2001; Takahashi et al., 2005) compared to controls. An EEG study on Transcendental Meditation, showed intermittent prominent bursts of frontally dominant theta activity at an average maximal amplitude of 135 μV in 21 practitioners (Hebert and Lehmann, 1977). Zen meditators showed fast theta and slow alpha power during meditation (Takahashi et al., 2005) demonstrating enhanced automatic memory and reduction in conceptual thinking following meditation (Faber et al., 2014). In a single MEG study on twelve long term Buddhist meditators were assessed in two distinct types of self-awareness, i.e., "narrative" and "minimal" in mindfulness-induced selflessness awareness (Dor-Ziderman et al., 2013). It was found that there was a reduction in gamma band (60–80 Hz) power in frontal, and medial prefrontal areas, and reduced beta band (13–25 Hz) power in ventral medial prefrontal, medial posterior and lateral parietal regions (Dor-Ziderman et al., 2013) and right inferior parietal lobules. These studies are consistent with fMRI and NIRS findings. Functional magnetic resonance imaging (fMRI) poses several challenges such as high sensitivity to participant's motion, a loud, restrictive environment, low temporal resolution, and relatively high cost (Cui et al., 2011). Some of these challenges are overcome with new optical imaging technique: NIRS measure's changes in oxy-hemoglobin and deoxy-hemoglobin (ΔHbO and ΔHbR) concentration changes from the cortical surface and less invasive and expensive than fMRI (Bunce et al., 2006). Functional near infrared spectroscopy (fNIRS) is a compact and portable optical technique to monitor hemodynamics of the brain in real time (Son and Yazici, 2006; Lin et al., 2009).

Brain hemodynamic responses during meditation, i.e., ΔHbO, ΔHbR and total hemoglobin changes (ΔTHC) are in its infancy. In fact, there is only one study that assessed deoxyhemoglobin changes with a single wavelength probe placed over the left PFC during Qigong meditation (Cheng et al., 2010). Practitioners showed decrease in deoxy-hemoglobin and increase in oxy-hemoglobin concentration that suggest, meditation lead to left prefrontal activation during meditation.

With this background, the present study was designed to assess the bilateral prefrontal hemodynamic responses in meditation and random thinking. Additionally, we investigated the hemodynamic changes and performance during a stroop color word task before and after meditation and random thinking. Since, stroop color word task is known to measure attention, interference, processing speed, and executive attention, we expected that this task to be the most sensitive to the effects of meditation.

MATERIALS AND METHODS

PARTICIPANTS

A total of 25 right handed healthy male participants with ages ranging from 19 and 30 years (Mean, SD; 23.4 ± 3.7 years) were recruited from S-VYASA (a Yoga University), South India. All participants had a minimum of 12-month experience in meditation (group average experience ± S.D., 15.6 ± 14.2 months) on the Sanskrit syllable "*OM*". Three participants were excluded from the study because of large motion artifacts in the signals due to head movements or because of failure in probe placement due to obstruction by hair (Taga et al., 2003; Minagawa-Kawai et al., 2011). Thus, only data from 22 participants (mean age 22.9 ± 4.6 years) were included in the final analysis. Participants fulfilling the following criteria were included in the study: (i) the participants with at least 12 months of meditation experience; (ii) male participants alone were studied as cognitive abilities and cerebral blood flow (Brackley et al., 1999) have been shown to fluctuate which the phases of menstrual cycle (Yadav et al., 2002); and (iii) no history of smoking; and (iv) normal health on a routine clinical examination. Participants with following criteria were excluded from the study: (i) persons on any

Table 1 | Characteristics of 22 participants.

Characteristics	
Age (in years) (group mean ± S.D.)	22.9 ± 4.6 years
Years of education	
17 years and more	6 (27.3%)
Upto 15 years	10 (45.5%)
Upto 12 years	6 (27.3%)
Type of meditation	Meditation on the Sanskrit syllable "*OM*"
Experience of meditation practice (in months)	
6–12 months	4 (18.2%)
13–24 months	3 (13.6%)
25–36 months	7 (31.8%)
37–48 months	6 (27.3%)
48–60 months	2 (9.1%)

medication or herbal remedy; (ii) participants having clinical evidence of medical, neuropsychological, or drug abuse that would potentially alter cerebral blood flow (Liddle et al., 1992; Newberg et al., 2010a,b; Goldstein and Volkow, 2011); and (iii) any visual deficit; and (iv) any cognitive impairment. None of the potential participants were involved in any other ongoing research activity. The characteristics of participants are given in **Table 1**.

The study was approved by the Institutional Ethics Committee of S-VYASA, a Yoga University (No.-RES/IEC-S-VYASA/11/2011). The study protocol, nature of the experiments and the operating mode of the instrument was explained to the subjects before obtaining signed informed consent.

DESIGN

The protocol utilized in the present study consisted of two sessions i.e., random thinking (*cancalata*) and meditation (*dhyana*), and eight States (Pre, Stroop_Pre, During (D1-D4 each of 5 min), Stroop_Post, and Post). Each participant was assessed for both the meditation and control session on two separate consecutive days. The sessions were randomized online with randomization software.[1] During the acquisition and analysis of data, researcher was blinded to the session of the individual. The total duration of the each session was 60 min: Pre (5 min), Stroop_Pre (15 min), During (20 min), Stroop_Post (15 min), and Post (5 min). The schematic presentation of the design has been given in **Figure 1**.

Apart from their prior experience of meditation on "*OM*", all participants were given a 3 month orientation, 5 days a week under the guidance of an experienced meditation teacher. The purpose of this orientation was for to ensure uniformity among all practitioners based on specific instructions.

INTERVENTIONS

Each participant sat cross-legged with eyes closed and followed pre-recorded instructions throughout meditation and random thinking sessions. An emphasis was placed on slowly, practice with awareness of physical and mental sensations, and relaxation. The duration of each session was 20 min between 06:00 to 06:30 h conducted 5 days a week. The theoretical aspects of the meditation were detailed by the meditation teacher on the first day. Following this, the practice of each session began with pre-recorded instructions. The practice of meditation was evaluated based on their self-reporting and by consultations with the meditation teacher. The two phases—random thinking (Rand) and meditative defocusing were as follows:

1. ***Random thinking***:
   Participants were asked to listen a compiled audio CD consisting of brief periods of random conversation, announcements, various advertisements and non-connected talks recorded from a local radio station transmission and allow their thoughts to wander freely. All these non-connected conversations could induce the state of random thinking.
2. ***Meditative de-focusing or effortless meditation***:
   In effortless meditation session, each participant was instructed to dwell effortlessly on thoughts of "*OM*", particularly on the subtle (rather than physical) attributes and connotations of the syllable with closed eyes. This involved combined mental chanting with effortless defocusing on syllable "*OM*". This gradually allowed the participants to experience brief periods of silence, which they reported after the session.

ASSESSMENTS PROCEDURE

Laboratory environment

All Participants were assessed in a sound and light dampening Faraday cage. Participants' were monitored using a closed circuit television outside the cabin to detect if they moved or fell asleep during a session. During the session, instructions were passed through a two-way intercom, so that participants could remain uninterrupted. The recording room temperature was maintained at 24.0 ± 1.0°C with 56 percent average humidity during the conduct of experiments. The background noise level was 26 dB of the acoustically shielded chamber. For each participant, the data acquisition session lasted 60 min.

Functional near infrared spectroscopy (fNIRS)

A 16-channel continuous wave fNIRS imager system (FNIR1000-ACK-W, BIOPAC Systems, Inc., U.S.A) was employed to map changes in ΔHbO, ΔHbR and ΔTHC over bilateral PFC. The system consisted of a flexible probe to match contour of the human forehead (see **Figure 2**). The probe embedded with four LED diodes as light sources (at λ_1 = 730 nm, λ_2 = 830 nm, λ_3 = 850 nm) and ten photodiodes as detectors that were symmetrically arranged in an area of 3.5 × 14 cm^2, conducing to 16 nearest source—detector (i.e., channels) at 2.5 cm separation displayed in **Figure 3**. A source-detector distance provides a penetration depth of 1.25 cm (León-Carrion et al., 2008; Kim et al., 2010; Leon-Dominguez et al., 2014). The description of the probe setting is detailed in earlier studies (Krawczyk, 2002; Izzetoglu et al., 2005; Leon-Dominguez et al., 2014). During the experiment, the probe was firmly held with a velcro band on the forehead, and stretched from hairline to eyebrow in a sagittal

[1]http://www.randomizer.org

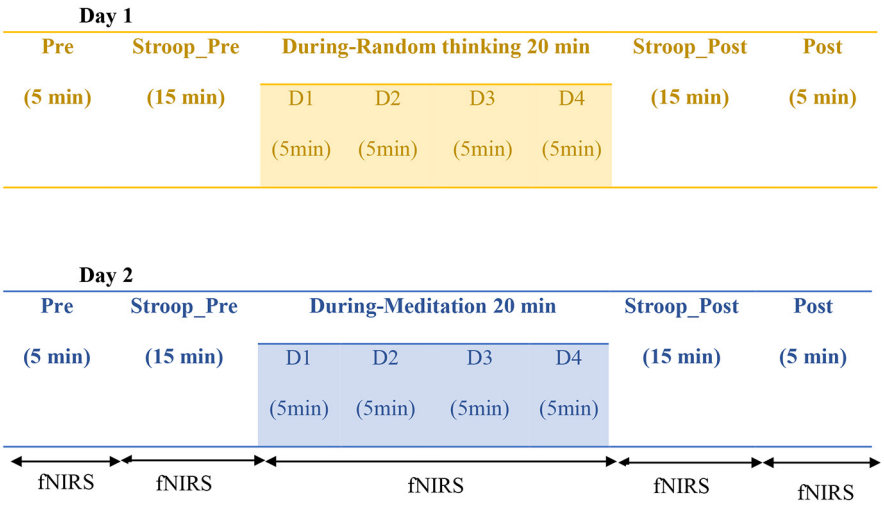

FIGURE 1 | Schematic representation of the study design. Note: Sessions were modified for each participant D1: During 1; D2: During 2; D3: During 3; D4: During 4.

direction and from ear to ear in axial direction (Tian et al., 2009). The probes were positioned bilaterally on forehead, over the left and right frontal poles, a part of dorsolateral PFC, and a portion of the ventrolateral PFC. Regional cerebral blood flow (rCBF), ΔHbO, ΔHbR, and ΔTHC for each hemisphere were updated every 0.5 s. The four LEDs flashed in sequence; the reflected light from the brain as detected with the nearest photodiodes of each LED and converted into digital signals using an analog-digital converter (ADC) card in the control box. The digital data were sent to the laptop though a serial port. The sampling rate was 3 Hz across all 16 channels. The principles of measurement were based on the modified Beer-Lambert law for highly scattering media (Plichta et al., 2006) that agrees assessing changes in ΔHbO and ΔHbR at a certain measured point (Hoshi and Tamura, 1993). Increases in ΔHbO and corresponding decrease in ΔHbR can be interpreted as a sign of functional brain activation.

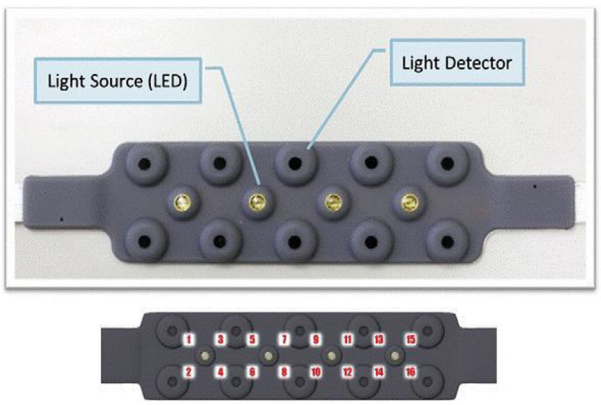

FIGURE 2 | The complete setup employed is herein presented. The fNIRS sensor is displayed with 4 light sources and 10 detectors (top) and 16 optode (channel) measurement locations registered on the sensor.

Stroop color word task

Subjects were seated comfortably on a reclining chair in a Faraday cage, facing a 21 inch LCD monitor placed at a distance of 70 cm from their eyes. Participants were required to focus on the center of the screen which was guided by a fixation object "+" followed by stimuli. Participants did a modified multiple-trial stroop task and were confronted with neutral, congruent, and incongruent stimuli on a black background using E-Prime 2.0.8.90 (Psychological Software Tools, Inc., Pittsburgh, PA, USA). The stroop color word task consisted of red, green and blue colored boxes and the corresponding written words "RED", "BLUE" and "GREEN". The color was presented as color square (4.5 × 4.5 cm) boxes on a black background. The duration of the presented square boxes and words was 500 ms each. Congruent trials comprised of square color boxes followed by words describing the color of the box written in the same color (e.g., the BLUE square box and the printed word "BLUE" in blue ink); incongruent trials comprised of words describing the color of the box written in a color other than that of the box (e.g., the RED square box and word RED written in blue ink); neutral trials comprised words written in white (e.g., the BLUE square box and word BLUE printed in white ink). Participants were instructed to reply as speedily and accurately as possible to the name of the color word (while ignoring the color itself) consistent to the color of the Box with a button press of the response key using the thumb of their right hand. To increase the potency of the conflict stimulus, 20% of trials were congruent (approximately 45 trials), 20% were incongruent (approximately 45 trials) and 50% were neutral (90 trials). The duration of the stimulus was 500 ms, with a variable interstimulus interval (ISI) of 1000–2500 ms the experimental steps are illustrated in **Figure 4**.

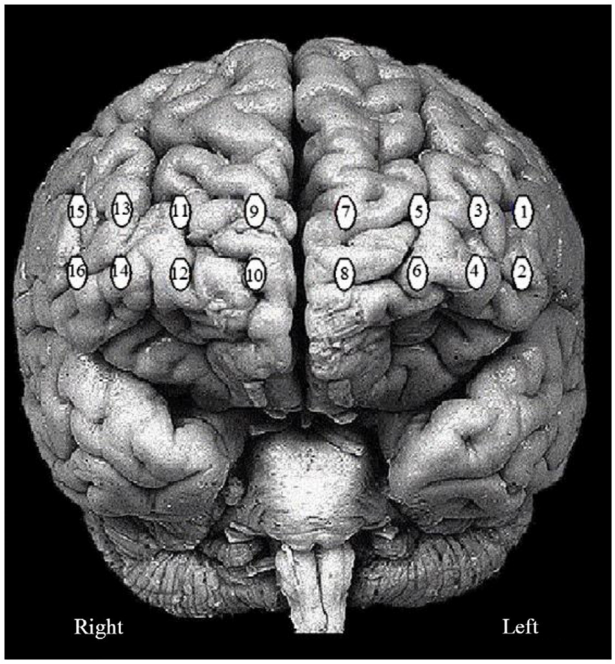

FIGURE 3 | The 16 fNIRS optode (channel) measurement locations registered on the brain surface image are presented.

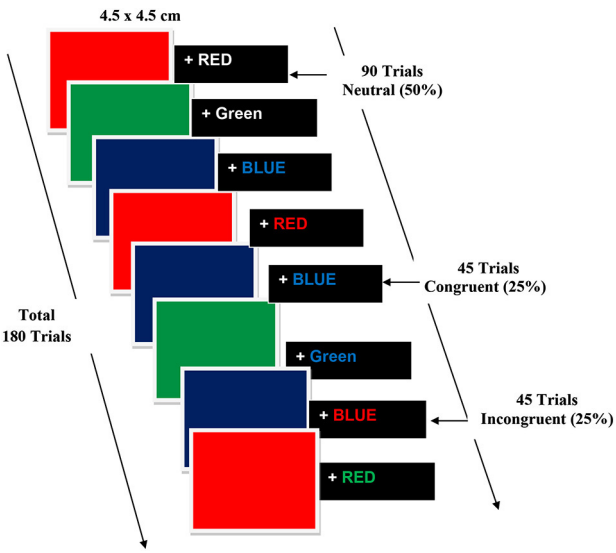

FIGURE 4 | Experimental steps of Color word Stroop Task.

Data acquisition

The participants were assessed in two separate sessions i.e., random thinking and meditation while recording hemodynamic activity on the PFC using 16-channel continuous wave fNIRS system. On the preceding day and on the day of the recording, participants were asked to avoid tea and coffee which are known to influence cognitive performance (Nehlig, 2010) and cerebral blood flow (Addicott et al., 2009). Where this was unavoidable the session was engaged on another day. The participants wore a flexible sensor pad over prefrontal region and covered with a black cloth. The probable artifacts such as heart rate pulsation, respiration and high frequency noise in raw data, which may possibly be induced by autonomic arousal caused during stroop task, was eliminated with pre designed finite impulse response (FIR) filters based on type, order, window function and cut-off frequency. For the present study, raw data were acquired from the probe, which is pre-filtered by two filters and processed in the data processing unit using COBI filter module. The first filter is a 10th order low-pass filter with cutoff frequency of 0.1 Hz with Blackman window. The second filter is a 20th order low-pass, with the normalized cut-off frequency of 0.1 Hz which uses a Hamming window. The filtered data were averaged according to the tasks and conditions for further statistical analysis.

Data analysis

The hemodynamic responses of bilateral PFC were recorded and data were averaged according to the task condition (pre, stroop_pre, during, stroop_post and post). Statistical analysis has been carried out on these differential values. Filtered data were tested with Kolmogorov-Smirnov test for normality. Repeated measures analysis of variance (RM-ANOVA) was used because the same individuals were assessed in repeated sessions on two separate days (i.e., random thinking and meditation). RM-ANOVA was performed with three "within subjects" factors, i.e., Factor 1: Sessions (random thinking and meditation); Factor 2: PFC (right and left). Factor 3: States ("Pre", "Stroop_Pre", "During" (D1 to D4), "Stroop_Post" and "Post"). The repeated measures ANOVAs were carried out for concentration changes of oxygenated and deoxygenated hemoglobin and total hemoglobin change (ΔHbO, ΔHbR and ΔTHbC) across the right and left PFC. This was followed by a *post hoc* analysis with Bonferroni adjustment for multiple comparisons between the mean values of different states ("During" and "Post") and all comparisons were made with the respective "Pre" state.

Moreover, for analysis of stroop task we compared the mean reaction time (ms) of neutral, congruent and incongruent conditions and hemodynamic responses of stroop color word task before and after the sessions (random thinking and meditation). The results were averaged for each side of PFC (right and left), parameter and subject separately to compare between different conditions and sessions. A repeated measures ANOVA was carried for multiple comparisons following Bonferroni adjustment. Statistical analyses were carried out using the Statistical software SPSS version 20.0 (SPSS Inc., Chicago, USA). The alpha level was set at $p < 0.05$. The effect size (d) defined by Cohen (1988), as the mean change score divided by the standard deviation of change, calculated for further statistical analysis.

RESULTS

BEHAVIORAL RESULTS

Reaction times (RTs) were computed solely from the correctly answered trials. With respect to RT, a repeated—measures 3 way ANOVA with Sessions (random thinking and meditation) × States ("Stroop_Pre", "Stroop_Post") × Conditions (neutral vs. congruent vs. incongruent). Repeated

measures ANOVA demonstrated a significant main effect for Sessions ($F_{(1,21)}$ = 4.862, p = 0.039, η^2p = 0.188); Conditions ($F_{(2,42)}$ = 24.12, $p < 0.001$, η^2p = 0.535); States ($F_{(1,21)}$ = 6.696, $p < 0.023$, η^2p = 0.242), and the significant interaction between Sessions × States ($F_{(1,21)}$ = 45.36, $p < 0.001$, η^2p = 0.684).

Post hoc analysis revealed that there was a significant improvement in cognitive performance after meditation in all three conditions (neutral, congruent and incongruent) compared to random thinking session given in **Table 1**. The RTs differed in all the conditions (neutral vs. congruent vs. incongruent) in both the sessions. These findings verify that our attentional manipulation was indeed effective.

The RTs were compared using two-tailed paired sample *t*-test, revealed significant differences among all three conditions (neutral, congruent and incongruent) in two different sessions (meditation and random thinking). In random thinking session, there were significant differences in neutral vs. congruent: $t_{(21)}$ = −3.86, p = 0.001; congruent vs. incongruent: $t_{(21)}$ = −2.31, p = 0.031; neutral vs. incongruent: $t_{(21)}$= −5.92, $p < 0.001$ whereas in meditation session, there was a significant difference in neutral—congruent: $t_{(21)}$ = −4.47, $p < 0.001$; congruent—incongruent: $t_{(21)}$ = −1.85, $p > 0.05$ (NS); neutral—incongruent: $t_{(21)}$ = −6.148, $p < 0.001$. The mean RTs were significantly shorter in the neutral (p = 0.002), congruent ($p < 001$) and incongruent ($p < 0.003$) conditions after meditation session whereas after the random thinking session, mean RTs were delayed in the neutral (p = 0.034) and incongruent (p = 0.008) conditions. The average RTs for neutral, congruent, and incongruent trials of the stroop color word task are given in **Table 2**. Subjects made negligible errors during the color word matching stroop task. For error rates, we did not make any statistical test, since their distributions are clearly not Gaussian. However, it can be supposed that interference effect also reveals itself in error rates. In summary, behavioral results of the stroop color word task are in accordance with the literature, as demonstrated by a clear interference effect in the participants for meditation and random thinking sessions.

HEMODYNAMIC RESPONSES IN STROOP COLOR WORD TASK

In the present study, the 16 channel fNIRS device provided a set of time series recorded over the PFC. The locations of the probed regions are shown in **Figure 2**. The order of the channels is from left to right, i.e., "1" is on the left and "16" is on the right as depicted in **Figure 3**. Analysis of hemoglobin signals i.e., ΔHbO or ΔHbR is still a controversial issue, specifically which hemoglobin signal is more reliably associated with brain activity still remain unclear (Schroeter et al., 2002). In this study, we have utilized three wavelengths (i.e.,750, 803 and 850 nm). This combination is suitable only for detecting ΔHbO signal. Therefore we used ΔHbO, ΔHbR and ΔTHC signals for statistical analysis. The groups mean values ± S.D. for the ΔHbO, ΔHbR and ΔTHC in stroop task and the two sessions (random thinking and meditation) in "Pre", "During" and "Post" states are given in **Table 3**.

For ΔHbO, the repeated—measures ANOVA for Sessions (Random thinking and Meditation) × PFC (Left and Right) × States ("Stroop_Pre", "Stroop_Post") revealed no significant main effect for Sessions, States and PFC. There was a significant interaction between PFC × States ($F_{(1,175)}$ = 9.87, $p < 0.01$, η^2p = 0.053); Sessions × PFC × States ($F_{(1,175)}$ = 3.17, $p < 0.01$, η^2p = 0.040).

For ΔHbR, the repeated—measures ANOVA demonstrated significant main effect for Sessions ($F_{(1,175)}$ = 9.99, $p < 0.01$, η^2p = 0.054); PFC ($F_{(1,175)}$ = 4.57, $p < 0.05$, η^2p = 0.025). Also, there was a significant interaction between Sessions × PFC (F = 5.11, $p < 0.05$, η^2p = 0.028); Sessions × States ($F_{(1,175)}$ = 22.13, $p < 0.001$, η^2p = 0.112); Sessions × PFC × States ($F_{(1,175)}$ = 9.81, $p < 0.01$, η^2p = 0.053).

For total hemoglobin (ΔTHC), the repeated—measures ANOVA revealed that there was a significant main effect for PFC ($F_{(1,175)}$ = 9.71, $p < 0.01$, η^2p = 0.053), and the significant interaction between Sessions × PFC ($F_{(1,175)}$ = 5.33, $p < 0.01$, η^2p = 0.03); Sessions × States ($F_{(1,175)}$ = 19.87, $p < 0.001$, η^2p = 0.102); PFC × States ($F_{(1,175)}$ = 5.96, $p < 0.05$, η^2p = 0.033); Sessions × PFC × States ($F_{(1,175)}$ = 14.20, $p < 0.001$, 0.075).

The *post hoc* analysis with Bonferroni corrections demonstrated forehead hemodynamic responses during stroop task related to random thinking and meditation sessions are given in **Table 3**. The results demonstrated a significant decrease in the concentration of ΔHbO in left PFC (p = 0.016) and in the right PFC (p = 0.032) after random thinking session during stroop color word task, whereas, there was a significant improvement in ΔHbO in left PFC (p = 0.006) and right PFC (p = 0.046) following the meditation session.

From the above observations, it can be concluded that meditation enhances bilaterally activation of the anterior PFC

Table 2 | Group mean values ± S.D. of the reaction time scores (ms) of Stroop color word Task.

Sessions	States	Pre	Post	*t*-value	*P* value	% Change
Rand	Neutral	643.18 ± 130.654	660.00 ± 113.641	−2.274	**0.034***	2.62
	Congruent	783.64 ± 117.333	790.91 ± 119.440	−0.876	0.391	0.93
	Incongruent	871.41 ± 136.070	892.73 ± 136.004	−2.920	**0.008****	2.45
Med	Neutral	638.64 ± 118.615	617.73 ± 121.653	3.533	**0.002****	−3.27
	Congruent	794.55 ± 118.029	764.55 ± 112.238	6.205	**<0.001*****	−3.78
	Incongruent	865.00 ± 137.797	819.09 ± 133.627	3.302	**0.003****	−5.31

*$p < 0.05$; $p <$ **0.01; ***$p < 0.001$; repeated measures of ANOVA with Bonferroni adjustment comparing Post values with Pre values. Values are group means ± S.D. Rand—Random Thinking; Med—Meditation.*

Table 3 | Group mean values ± S.D. of the oxyhemoglobin (ΔHbO), deoxyhemoglobin (ΔHbR) and total hemoglobin change (ΔTHC) of Stroop color word task before, during and after random thinking (rand) and meditation (Med).

Sessions	Voxels	Pre	Stroop_Pre	During				Stroop_Post	Post
				D1	D2	D3	D4		
					Oxyhemoglobin (ΔHbO)				
Rand	**Left PFC**	−0.71 ± 3.71	−0.64 ± 7.39	0.51 ± 7.58	0.15 ± 6.69	0.25 ± 7.16	0.21 ± 7.61	0.83 ± 7.41	0.80 ± 7.22
	Right PFC	−2.65 ± 5.56	0.81 ± 4.59	−2.21 ± 12.47	−1.30 ± 12.45	−1.69 ± 12.67	−1.65 ± 12.49	−1.56 ± 11.90	−1.00 ± 10.02
Med	**Left PFC**	−0.43 ± 6.53	−0.93 ± 2.55	−1.13 ± 3.17	−0.79 ± 3.22	−0.64 ± 3.54	−0.77 ± 3.98	−0.09 ± 5.15	0.44 ± 5.25
	Right PFC	−2.45 ± 7.18	−1.30 ± 2.64	**−0.71 ± 4.07***	**−0.44 ± 3.84***	**−0.19 ± 3.86****	−0.89 ± 3.70	−0.79 ± 3.89	**0.35 ± 4.41*****
					Deoxyhemoglobin (ΔHbR)				
Rand	**Left PFC**	−0.20 ± 15.36	−1.70 ± 4.23	−2.03 ± 5.27	−0.98 ± 5.94	−0.73 ± 6.45	−0.73 ± 6.57	−0.32 ± 8.80	−0.91 ± 8.10
	Right PFC	−5.18 ± 10.80	−2.86 ± 3.65	−3.22 ± 6.89	**−1.78 ± 5.75*****	**−0.48 ± 8.08*****	**0.01 ± 8.05*****	**1.22 ± 8.18*****	**0.19 ± 10.25*****
Med	**Left PFC**	−1.57 ± 6.61	−1.27 ± 8.85	−2.82 ± 18.20	−2.25 ± 18.82	−2.38 ± 19.15	−2.29 ± 18.82	−2.28 ± 19.80	−2.23 ± 17.63
	Right PFC	−3.90 ± 8.22	−3.00 ± 7.93	−7.19 ± 23.46	−8.16 ± 23.09	−8.14 ± 23.43	**−8.15 ± 22.72***	−7.28 ± 23.56	−7.04 ± 19.93
					Total hemoglobin change (ΔTHC)				
Rand	**Left PFC**	−1.70 ± 5.39	−1.83 ± 9.87	−1.58 ± 20.98	−1.39 ± 21.02	−1.73 ± 21.40	−1.66 ± 21.16	−1.71 ± 21.56	−1.02 ± 19.70
	Right PFC	−4.29 ± 6.67	−3.28 ± 9.05	−8.85 ± 28.49	**−9.07 ± 27.55***	**−10.41 ± 26.99*****	**−10.28 ± 26.52*****	**−10.26 ± 26.89****	**−8.41 ± 21.55****
Med	**Left PFC**	−0.78 ± 17.63	−2.98 ± 7.98	−3.50 ± 9.7	−2.18 ± 10.23	−1.82 ± 10.74	−1.98 ± 11.34	−1.21 ± 14.27	−1.15 ± 13.88
	Right PFC	−5.11 ± 11.97	−4.36 ± 5.29	−4.37 ± 7.48	**−2.83 ± 7.18****	**−1.94 ± 8.48*****	**−2.16 ± 9.14****	**−1.45 ± 10.11****	**−0.57 ± 11.07*****

***p < 0.01; repeated measures of ANOVA with Bonferroni adjustment comparing During and Post values with Pre values. Values are group means ± S.D.*

and consequently, a stronger increase of oxygenation and cerebral blood flow during stroop task at the right PFC due to interference reduction.

HEMODYNAMICS RESPONSES IN MEDITATION AND RANDOM THINKING

For ΔHbO, the repeated—measures ANOVA for Sessions (Random thinking and Meditation) × PFC (Left and Right) × States (Pre Stroop_Pre, D1-D4, Stroop_Post, Post) demonstrated a significant main effects for States ($F_{(7,1225)} = 5.23$, $p < 0.001$, $\eta^2 p = 0.029$). There was a significant interaction between the PFC × States ($F_{(7,1225)} = 2.42$, $p < 0.001$, $\eta^2 p = 0.014$); Sessions × Hemispheres × States ($F_{(7,1225)} = 7.32$, $p < 0.05$, $\eta^2 p = 0.040$).

For ΔHbO, the repeated—measures ANOVA showed there was a significant main effect for Sessions ($F_{(1,175)} = 12.20$, $p < 0.001$, $\eta^2 p = 0.065$); PFC ($F_{(1,175)} = 7.89$, $p < 0.01$, $\eta^2 p = 0.043$) and States ($F_{(7,1225)} = 3.55$, $p < 0.001$, $\eta^2 p = 0.019$). There was a significant interaction between the Sessions × PFC ($F_{(1,175)} = 4.13$, $p < 0.001$, $\eta^2 p = 0.023$); Sessions × States ($F_{(7,1225)} = 9.99$, $p < 0.001$, $\eta^2 p = 0.054$); Sessions × PFC × States ($F_{(7,1225)} = 10.37$, $p < 0.001$, $\eta^2 p = 0.056$).

For total hemoglobin change (ΔTHC), there was a significant main effect for Sessions ($F_{(1,175)} = 5.07$, $p < 0.05$, $\eta^2 p = 0.028$); PFC ($F_{(1,175)} = 12.20$, $p < 0.001$, $\eta^2 p = 0.065$); and States ($F_{(1,175)} = 2.79$, $p < 0.01$, $\eta^2 p = 0.016$) and a significant interaction between the Sessions × PFC ($F_{(1,175)} = 6.45$, $p < 0.05$, $\eta^2 p = 0.036$); Sessions × States ($F_{(7,1225)} = 9.06$, $p < 0.001$, $\eta^2 p = 0.049$); PFC × States ($F_{(7,1225)} = 2.34$, $p < 0.05$, $\eta^2 p = 0.036$]; Session × PFC × State ($F_{(7,1225)} = 14.51$, $p < 0.001$).

Post hoc analyses with Bonferroni corrections were performed on ΔHbO, ΔHbR and ΔTHC and all comparisons were made with respective "Pre" state. These have been summarized in **Table 3**. There was a significant increase in ΔHbR at the right PFC ($p = 0.005$) after random thinking session whereas there was a significant increase in the left PFC ($p = 0.02$) and in right PFC ($p < 0.001$) after meditation session. Similarly, in ΔTHC, there was a significant decrease in blood flow change in the right PFC ($p < 0.001$) after the random thinking session whereas there was a significant increase in blood flow change in the left ($p = 0.03$) and in right PFC ($p < 0.001$) after meditation session.

In summary, as described in **Table 3** and in Line diagrams (**Figures 5–7**), there was a positive trend to show a significant increase in the concentration of oxyhemoglobin change (ΔHbO) during meditation session at right PFC (as shown in **Figure 5**). There was a significant decrease in deoxyhemoglobin change (ΔHbR) (as shown in **Figure 6**) during meditation session whereas there was a significant increase in the concentration of deoxyhemoglobin change during random thinking session at the right PFC. Additionally, there was also a significant increase in the total hemoglobin change (ΔTHC) during and after meditation sessions (**Figure 7**) and decrease in the total hemoglobin change (ΔTHC) during and after random thinking session.

DISCUSSION

The primary goal of the present study was to ascertain whether meditation increases rCBF at bilateral PFC, measured with fNIRS, compared to random thinking. Our secondary goal was to observe the RT scores and relative changes in cerebral blood flow, and to determine if there are persistent effects following meditation session compared to random thinking session. Results as confirmed with recent studies on meditation with spectroscopy (Cheng et al., 2010), SPECT imaging (Newberg et al., 2001, 2010a,b; Cohen et al., 2009) and fMRI (Short et al., 2010; Guleria et al., 2013; Zeidan et al., 2014) have revealed that meditation program resulted in significant increases in baseline CBF ratios in the prefrontal, superior, inferior and orbital frontal cortex, dorsolateral prefrontal cortex (DLPFC), right dorsal medial frontal lobe, cingulate gyrus and right sensorimotor cortex. In present study, we found that brain activation, measured by changes in ΔHbO and ΔTHC concentration in the right prefrontal area was followed by a strong decrease in ΔHbR concentration during meditation. Additionally, the rCBF significantly increased in the right frontal lobe during stroop task after meditation, which suggest the improvement in the participant's performance (reaction time) during the task. The total blood oxygenation (ΔTHC) level in the PFC could rise with increasing task load from neutral to congruent, and then incongruent; this would demonstrate a positive correlation with performance measures. The changes in regional blood flow is mediated by changes in neural activity in a single region or in several selective regions of the brain (Lauritzen, 2001).

Earlier studies have demonstrated that the PFC is activated particularly on the right PFC and anterior cingulate cortex (ACC) in willful act and tasks that require intense focused and sustained attention (Frith et al., 1991; Pardo et al., 1991; Vogt et al., 1992; Petersen and Posner, 2012). A study on eight Tibetan Buddhist meditators demonstrated improved activity in the PFC bilaterally (though greater on the right hemisphere) and the cingulate gyrus during meditation (Newberg and Iversen, 2003). This suggests that meditation begins with activation of the PFC and anterior cingulate gyrus associated with the will or intent to clear the mind of thoughts or to focus on an object (Edwards et al., 2012).

Meditation increases CBF and decreases cerebrovascular resistance (CVR) suggesting a contributing vascular mechanism (Jevning et al., 1996) which reflect cerebral activation. The CVR reduction being associated with cognitive improvement which suggests a vascular contribution to cognitive enhancement (Nation et al., 2013). During meditation, the activation of right PFC is theoretically associated with the activity in the reticular nucleus of the thalamus. This activation may be accomplished by the PFC's production and distribution of glutamate, a known excitatory neurotransmission (Cheramy et al., 1987; Finkbeiner, 1987), which communicate with other brain structures such as lateral geniculate and lateral posterior nuclei of the thalamus (Portas et al., 1998). An early study on meditation with single photon emission computed tomography (SPECT) demonstrated a general increase in thalamic activity that was proportional to the activity levels in the PFC (Newberg et al., 2001; Edwards et al., 2012). The activation on the right PFC causes increased activity in the reticular nucleus during meditation, the results may be decreased sensory input entering into the posterior superior parietal lobule which is involved in the analysis and integration of higher order visual, auditory, and somesthetic information (Adair et al., 1995).

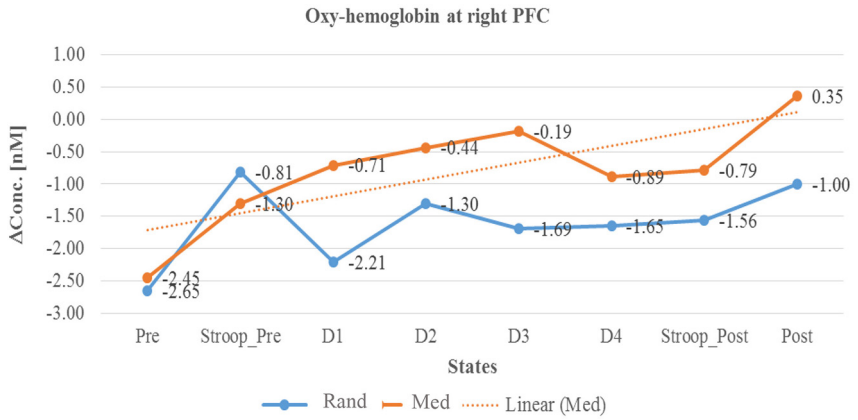

FIGURE 5 | Line graph represents averaged Oxy-hemoglobin change at right prefrontal cortex (rPFC) in two sessions i.e., random thinking and meditation and Stroop task. Note: Line graph represents comparisons between baseline, stroop_pre, during sessions (random thinking and meditation), stroop_post, and post. Stroop Pre showed higher Oxy-hemoglobin change compared to baseline. During and after meditation, the cerebral oxygenation was higher in rPFC compared to random thinking.

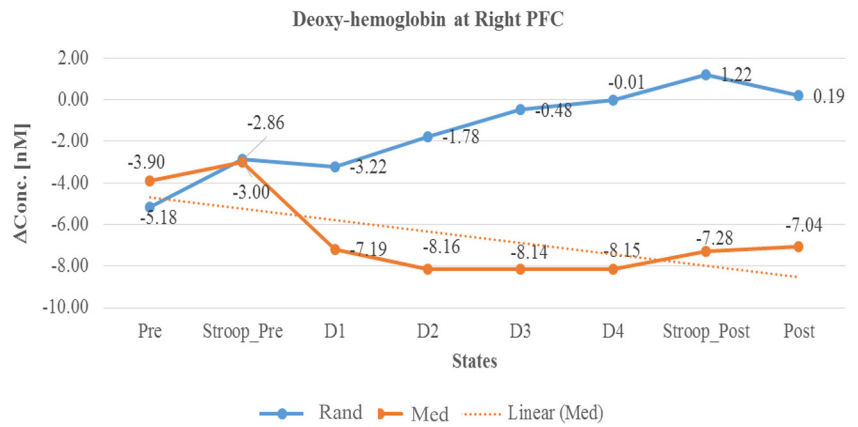

FIGURE 6 | Line graph represents averaged Deoxy-hemoglobin change at right PFC in two sessions i.e., random thinking and meditation and Stroop task. Note: Line graph represents de-oxyhemoglobin changes was higher in right PFC during random thinking (D2, D3, and D4), stroop task and after random thinking. In other hand, during meditation, there was a decrease in de-oxyhemoglobin in D3 level in rPFC.

A major strength of the present study was to examine the states of meditation and random thinking related hemodynamic responses in cerebral oxygenation during performance of the stroop color word task. It is a well established phenomenon that executive processes are facilitated by the frontal lobe and due to stroop interference brain activity may depend on increased ability to recruit frontal neural resources (Schroeter et al., 2004b). This allowed us to examine whether there is an increase in oxygenation with meditation corresponding to an ability to recruit appropriate resources for task performance or a decrease in activation corresponding to better optimization and possible reduction in task difficulty with meditation. In a study, fNIRS showed stroop interference is consistently associated with the ACC and the lateral prefrontal cortex (LPFC), especially the DLPFC, where the ACC is considered to be susceptible to conflict, and the DLPFC is purported to implement cognitive control (Carter et al., 2000; Leung et al., 2000). DLPFC may involve attentional maintenance while ACC monitors performance (MacDonald et al., 2000). Another similar study suggested meditation may enhance specific subcomponents of attention such as conflict monitoring or performance (Jha et al., 2007). Although fNIRS cannot monitor the cortical activation in the ACC because its measurement is limited to lateral cortical surfaces, it has successfully monitored the activation of the LPFC associated with stroop interference (Schroeter et al., 2002, 2003, 2004a,b; Ehlis et al., 2005).

There have been several neuroimaging studies evaluating the cerebral blood flow and performance of different meditation practices using behavioral, EEG and (Carter et al., 2005) fMRI imaging. Previous studies on meditation and EEG reported, greater midline theta power and slow alpha power in the frontal area during meditation (Takahashi et al., 2005; Chan

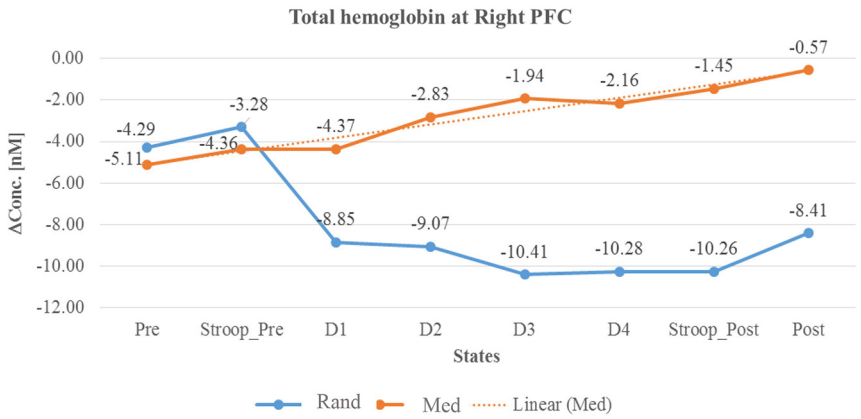

FIGURE 7 | Line graph represents averaged total hemoglobin change at rPFC in two sessions i.e., random thinking and meditation and Stroop task. Note: Line graph represents total hemoglobin change was higher in rPFC during meditation (D2, D3, and D4), in stroop task, and in post session. In other hand, there was a decrease in rPFC during random thinking (D2, D3, and D4), in stroop task and in post session.

et al., 2008). Zazen meditation showed increased alpha-1 and alpha-2 frequency activity of EEG in right prefrontal areas including insula, parts of the somatosensory, motor cortices and temporal areas (Faber et al., 2014). A subsequent study, on Satyananda Yoga meditation practice, showed greater source activity in low frequencies (particularly theta and alpha 1) during mental calculation, body-steadiness and mantra meditation (Thomas et al., 2014). Additionally, body-steadiness and mantra meditation showed greatest activity in right side of superior frontal and precentral gyri, parietal and occipital lobes. Similarly, neuroimaging studies on meditation practice, when compared to the control session showed significantly increased oxy-hemoglobin and CBF in the medial PFC which was associated with the intense focus-based component of the practice (Wang et al., 2011). Meditation involves attentional regulation and leads to increased activity in brain regions associated with attention such as DLPFC and ACC. The long-term practitioners had significantly more consistent and sustained activation in the DLPFC and the ACC during meditation vs. control in comparison to short-term practitioners (Baron Short et al., 2010). These studies suggest that willful acts and tasks that require sustained attention are initiated via activity in the PFC, particularly in the right hemisphere (Posner and Petersen, 1990; Frith et al., 1991; Pardo et al., 1991; Ingvar, 1994). Meditation requires focus of attention on objects which thereby activates PFC, particularly in the right hemisphere (Cohen et al., 2009), as well as the cingulate gyrus (Herzog et al., 1990; Lazar et al., 2000; Newberg et al., 2001). This demonstrated that during meditation there was an increased activity in the PFC bilaterally (greater on the right) and the cingulate gyrus (Newberg and Iversen, 2003). Therefore, the process of meditation seems to happen by activation of the prefrontal and cingulate cortex which are associated with the will or intent to clear one's mind of thoughts or to focus on an object.

In other imaging studies on meditation, there have been inconsistent results regarding the frontal cortex. A recent study showed decreased frontal activity during externally guided word generation compared to internal or volitional word generation (Cross et al., 2012). Thus, prefrontal and cingulate activation may be associated with the volitional aspects of meditation. Meditation with fluorodeoxyglucose (FDG) PET in eight subjects undergoing Yoga meditative relaxation (Herzog et al., 1990) reported increased rCBF in the frontal: occipital ratio of cerebral metabolism. Specifically, there was a mild increase in the frontal lobe, but marked decreases in metabolism in the occipital and superior parietal lobes. In addition to these studies, the PFC is reported to have a crucial role in social cognitive skills and along with the cingulate gyrus governs social behavior tasks related to Theory of Mind, empathy, moral reasoning, and evaluation of emotional states (Declerck et al., 2006). The PFC is essential for flexible behavior because it inhibits the habitual responses that have become inappropriate (Mesulam, 1998). But, an increase in the activity of PFC (determined by fNIRS) is not necessarily beneficial always. For example, animal experimentation has shown that the electrical activation of the medial PFC prevent the proper sequence of pressing the lever and collecting the reward (a pellet of food) in an operant condition task (Cross et al., 2012; Jurado-Parras et al., 2012) and also prevent the expression of an already acquired classically conditioned eyelid response (Leal-Campanario et al., 2007, 2013). However, in our study we infer that activation of prefrontal cortices after meditation had beneficial effects on cognition as manifested by improved performance in stroop color word task.

The present study reported increased oxy-hemoglobin concentration because of enhanced neural activity and cerebral blood flow in the prefrontal area during meditation compared to random thinking. In such studies, it is very important to understand the influences of systemic artifacts such as those from the heart, breathing, superficial perfusion, etc., which may be induced by the cognitive tasks related stress and autonomic responses. For example, a recent study performed on peripheral physiological measurements with temporal correlations of fNIRS and fMRI signals concluded that the physiological

basis of the systemic artifact is a task-evoked sympathetic arterial vasoconstriction monitored by a decrease in venous volume and these artifacts are fairly common (Kirilina et al., 2012). They also suggested that the separation of fNIRS signals originating from activated brain and from scalp is a necessary precondition for unbiased fNIRS brain activation maps and pre-processing of the raw data using high definition filters is necessary.

In summary, the results of the present study provided first evidence that the oxygenation levels are increased in the PFC during meditation compared with random thinking in the same practitioners. Further event-related NIRS studies may apply well-tested fMRI paradigms in studies with children and patients, utilizing the advantages of the method.

ACKNOWLEDGMENTS

This research work was supported by the Center for Advanced Research in Yoga and Neurophysiology, Swami Vivekananda Yoga Research Foundation, Bangalore, India. We are gateful to Dr. Shirley Telles, Dr. Manjunath N.K. and Dr. Hemant Bhargav for their support and guidelines with regards to data acquisition and analysis.

REFERENCES

Adair, J. C., Gilmore, R. L., Fennell, E. B., Gold, M., and Heilman, K. M. (1995). Anosognosia during intracarotid barbiturate anesthesia: unawareness or amnesia for weakness. *Neurology* 45, 241–243. doi: 10.1212/wnl.45.2.241

Addicott, M. A., Yang, L. L., Peiffer, A. M., Burnett, L. R., Burdette, J. H., Chen, M. Y., et al. (2009). The effect of daily caffeine use on cerebral blood flow: how much caffeine can we tolerate? *Hum. Brain Mapp.* 30, 3102–3114. doi: 10.1002/hbm.20732

Baron Short, E., Kose, S., Mu, Q., Borckardt, J., Newberg, A., George, M. S., et al. (2010). Regional brain activation during meditation shows time and practice effects: an exploratory FMRI study. *Evid. Based Complement. Alternat. Med.* 7, 121–127. doi: 10.1093/ecam/nem163

Brackley, K. J., Ramsay, M. M., Broughton Pipkin, F., and Rubin, P. C. (1999). The effect of the menstrual cycle on human cerebral blood flow: studies using Doppler ultrasound. *Ultrasound Obstet. Gynecol.* 14, 52–57. doi: 10.1046/j.1469-0705.1999.14010052.x

Bunce, S., Izzetoglu, M., Izzetoglu, K., Onaral, B., and Pourrezaei, K. (2006). Functional near infrared spectroscopy: an emerging neuroimaging modality. *IEEE Eng. Med. Biol. Mag. Spec. Issue Clin. Neuroengineering* 25, 54–62. doi: 10.1109/MEMB.2006.1657788

Cahn, B. R., and Polich, J. (2006). Meditation states and traits: EEG, ERP and neuroimaging studies. *Psychol. Bull.* 132, 180–211. doi: 10.1037/0033-2909.132.2.180

Carter, C. S., Macdonald, A. M., Botvinick, M., Ross, L. L., Stenger, V. A., Noll, D., et al. (2000). Parsing executive processes: strategic vs. evaluative functions of the anterior cingulate cortex. *Proc. Natl. Acad. Sci. U S A* 97, 1944–1948. doi: 10.1073/pnas.97.4.1944

Carter, O. L., Presti, D. E., Callistemon, C., Ungerer, Y., Liu, G. B., and Pettigrew, J. D. (2005). Meditation alters perceptual rivalry in Tibetan Buddhist monks. *Curr. Biol.* 15, R412–R413. doi: 10.1016/j.cub.2005.05.043

Chan, A. S., Han, Y. M. Y., and Cheung, M.-C. (2008). Electroencephalographic (EEG) measurements of mindfulness-based Triarchic body-pathway relaxation technique: a pilot study. *Appl. Psychophysiol. Biofeedback* 33, 39–47. doi: 10.1007/s10484-008-9050-5

Chan, D., and Woollacott, M. (2007). Effects of level of meditation experience on attentional focus: is the efficiency of executive or orientation networks improved? *J. Altern. Complement. Med.* 13, 651–657. doi: 10.1089/acm.2007.7022

Cheng, R. W. F., Borrett, D. S., Cheng, W., Kwan, H. C., and Cheng, R. S. S. (2010). Human prefrontal cortical response to the meditative state: a spectroscopy study. *Int. J. Neurosci.* 120, 483–488. doi: 10.3109/00207454.2010.483650

Cheramy, A., Romo, R., and Glowinski, J. (1987). "Role of corticostriatal glutamatergic neurons in the presynaptic control of dopamine release," in *Neurotransmitter Interactions in the Basal Ganglia*, eds M. Sandler, C. Feuerstein and B. Scatton (New York: Raven), 131–133.

Cohen, J. (1988). *Statistical Power Analysis for the Behavioral Sciences*. 2nd Edn. Hillsdale, NJ: Erlbaum.

Cohen, D. L., Wintering, N., Tolles, V., Townsend, R. R., Farrar, J. T., Galantino, M. L., et al. (2009). Cerebral blood flow effects of yoga training: preliminary evaluation of 4 cases. *J. Altern. Complement. Med.* 15, 9–14. doi: 10.1089/acm.2008.0008

Cross, L., Brown, M. W., Aggleton, J. P., and Warburton, E. C. (2012). The medial dorsal thalamic nucleus and the medial prefrontal cortex of the rat function together to support associative recognition and recency but not item recognition. *Learn. Mem.* 20, 41–50. doi: 10.1101/lm.028266.112

Cui, X., Bray, S., Bryant, D. M., Glover, G. H., and Reiss, A. L. (2011). A quantitative comparison of NIRS and fMRI across multiple cognitive tasks. *Neuroimage* 54, 2808–2821. doi: 10.1016/j.neuroimage.2010.10.069

Declerck, C. H., Boone, C., and De Brabander, B. (2006). On feeling in control: a biological theory for individual differences in control perception. *Brain Cogn.* 62, 143–176. doi: 10.1016/j.bandc.2006.04.004

Dor-Ziderman, Y., Berkovich-Ohana, A., Glicksohn, J., and Goldstein, A. (2013). Mindfulness-induced selflessness: a MEG neurophenomenological study. *Front. Hum. Neurosci.* 7:582. doi: 10.3389/fnhum.2013.00582

Edwards, J., Peres, J., Monti, D., and Newberg, A. (2012). "The neurobiological correlates of meditation and mindfulness," in *Exploring Frontiers of the Mind-Brain Relationship SE - 6 Mindfulness in Behavioral Health*, eds A. Moreira-Almeida and F. Santana Santos (New York: Springer), 97–112.

Ehlis, A.-C., Herrmann, M. J., Wagener, A., and Fallgatter, A. J. (2005). Multi-channel near-infrared spectroscopy detects specific inferior-frontal activation during incongruent Stroop trials. *Biol. Psychol.* 69, 315–331. doi: 10.1016/j.biopsycho.2004.09.003

Faber, P. L., Lehmann, D., Gianotti, L. R. R., Milz, P., Pascual-Marqui, R. D., Held, M., et al. (2014). Zazen meditation and no-task resting EEG compared with LORETA intracortical source localization. *Cogn. Process.* doi: 10.1007/s10339-014-0637-x. [Epub ahead of print].

Finkbeiner, S. M. (1987). Neurotransmitter interactions in the basal ganglia. *Yale J. Biol. Med.* 60:483.

Frith, C. D., Friston, K. J., Liddle, P. F., and Frackowiak, R. S. (1991). Willed action and the prefrontal cortex in man: a study with PET. *Proc. Biol. Sci.* 244, 241–246. doi: 10.1098/rspb.1991.0077

Goldstein, R. Z., and Volkow, N. D. (2011). Dysfunction of the prefrontal cortex in addiction: neuroimaging findings and clinical implications. *Nat. Rev. Neurosci.* 12, 652–669. doi: 10.1038/nrn3119

Guleria, A., Kumar, U., Kishan, S. S. K., and Khetrapal, C. L. (2013). Effect of "SOHAM" meditation on the human brain: an fMRI study. *Psychiatry Res.* 214, 462–465. doi: 10.1016/j.pscychresns.2013.06.012

Hebert, R., and Lehmann, D. (1977). Theta bursts: an EEG pattern in normal subjects practising the transcendental meditation technique. *Electroencephalogr. Clin. Neurophysiol.* 42, 397–405. doi: 10.1016/0013-4694(77)90176-6

Herzog, H., Lele, V. R., Kuwert, T., Langen, K. J., Rota Kops, E., and Feinendegen, L. E. (1990). Changed pattern of regional glucose metabolism during yoga meditative relaxation. *Neuropsychobiology* 23, 182–187. doi: 10.1159/000119450

Holzel, B. K., Lazar, S. W., Gard, T., Schuman-Olivier, Z., Vago, D. R., and Ott, U. (2011). How does mindfulness meditation work? Proposing mechanisms of action from a conceptual and neural perspective. *Perspect. Psychol. Sci.* 6, 537–559. doi: 10.1177/1745691611419671

Hoshi, Y., and Tamura, M. (1993). Dynamic multichannel near-infrared optical imaging of human brain activity. *J. Appl. Physiol. (1985)* 75, 1842–1846.

Ingvar, D. H. (1994). The will of the brain: cerebral correlates of willful acts. *J. Theor. Biol.* 171, 7–12. doi: 10.1006/jtbi.1994.1206

Izzetoglu, M., Izzetoglu, K., Bunce, S., Ayaz, H., Devaraj, A., Onaral, B., et al. (2005). Functional near-infrared neuroimaging. *IEEE Trans. Neural Syst. Rehabil. Eng.* 13, 153–159. doi: 10.1109/TNSRE.2005.847377

Jevning, R., Anand, R., Biedebach, M., and Fernando, G. (1996). Effects on regional cerebral blood flow of transcendental meditation. *Physiol. Behav.* 59, 399–402. doi: 10.1016/0031-9384(95)02006-3

Jha, A. P., Krompinger, J., and Baime, M. J. (2007). Mindfulness training modifies subsystems of attention. *Cogn. Affect. Behav. Neurosci.* 7, 109–119. doi: 10.3758/cabn.7.2.109

Jurado-Parras, M. T., Gruart, A., and Delgado-García, J. M. (2012). Observational learning in mice can be prevented by medial prefrontal cortex stimulation and enhanced by nucleus accumbens stimulation. *Learn. Mem.* 19, 99–106. doi: 10.1101/lm.024760.111

Kim, M. N., Durduran, T., Frangos, S., Edlow, B. L., Buckley, E. M., Moss, H. E., et al. (2010). Noninvasive measurement of cerebral blood flow and blood oxygenation using near-infrared and diffuse correlation spectroscopies in critically brain-injured adults. *Neurocrit. Care* 12, 173–180. doi: 10.1007/s12028-009-9305-x

Kirilina, E., Jelzow, A., Heine, A., Niessing, M., Wabnitz, H., Brühl, R., et al. (2012). The physiological origin of task-evoked systemic artefacts in functional near infrared spectroscopy. *Neuroimage* 61, 70–81. doi: 10.1016/j.neuroimage.2012.02.074

Kozasa, E. H., Sato, J. R., Lacerda, S. S., Barreiros, M. A. M., Radvany, J., Russell, T. A., et al. (2012). Meditation training increases brain efficiency in an attention task. *Neuroimage* 59, 745–749. doi: 10.1016/j.neuroimage.2011.06.088

Krawczyk, D. C. (2002). Contributions of the prefrontal cortex to the neural basis of human decision making. *Neurosci. Biobehav. Rev.* 26, 631–664. doi: 10.1016/s0149-7634(02)00021-0

Kubota, Y., Sato, W., Toichi, M., Murai, T., Okada, T., Hayashi, A., et al. (2001). Frontal midline theta rhythm is correlated with cardiac autonomic activities during the performance of an attention demanding meditation procedure. *Brain Res. Cogn. Brain Res.* 11, 281–287. doi: 10.1016/s0926-6410(00)00086-0

Lauritzen, M. (2001). Relationship of spikes, synaptic activity and local changes of cerebral blood flow. *J. Cereb. Blood Flow Metab.* 21, 1367–1383. doi: 10.1097/00004647-200112000-00001

Lazar, S. W., Bush, G., Gollub, R. L., Fricchione, G. L., Khalsa, G., and Benson, H. (2000). Functional brain mapping of the relaxation response and meditation. *Neuroreport* 11, 1581–1585. doi: 10.1097/00001756-200005150-00041

Lazar, S. W., Kerr, C. E., Wasserman, R. H., Gray, J. R., Greve, D. N., Treadway, M. T., et al. (2005). Meditation experience is associated with increased cortical thickness. *Neuroreport* 28, 1893–1897. doi: 10.1097/01.wnr.0000186598.66243.19

Leal-Campanario, R., Delgado-García, J. M., and Gruart, A. (2013). The rostral medial prefrontal cortex regulates the expression of conditioned eyelid responses in behaving rabbits. *J. Neurosci.* 33, 4378–4386. doi: 10.1523/jneurosci.5560-12.2013

Leal-Campanario, R., Fairén, A., Delgado-García, J. M., and Gruart, A. (2007). Electrical stimulation of the rostral medial prefrontal cortex in rabbits inhibits the expression of conditioned eyelid responses but not their acquisition. *Proc. Natl. Acad. Sci. U S A* 104, 11459–11464. doi: 10.1073/pnas.0704548104

León-Carrion, J., Damas-López, J., Martín-Rodríguez, J. F., Domínguez-Roldán, J. M., Murillo-Cabezas, F., Barroso Y Martin, J. M., et al. (2008). The hemodynamics of cognitive control: the level of concentration of oxygenated hemoglobin in the superior prefrontal cortex varies as a function of performance in a modified Stroop task . *Behav. Brain Res.* 193, 248–256. doi: 10.1016/j.bbr.2008.06.013

Leon-Dominguez, U., Izzetoglu, M., Leon-Carrion, J., Solís-Marcos, I., Garcia-Torrado, F. J., Forastero-Rodríguez, A., et al. (2014). Molecular concentration of deoxyHb in human prefrontal cortex predicts the emergence and suppression of consciousness. *Neuroimage* 85(Pt. 1), 616–625. doi: 10.1016/j.neuroimage.2013.07.023

Leung, H. C., Skudlarski, P., Gatenby, J. C., Peterson, B. S., and Gore, J. C. (2000). An event-related functional MRI study of the stroop color word interference task. *Cereb. Cortex* 10, 552–560. doi: 10.1093/cercor/10.6.552

Liddle, P. F., Friston, K. J., Frith, C. D., Hirsch, S. R., Jones, T., and Frackowiak, R. S. (1992). Patterns of cerebral blood flow in schizophrenia. *Br. J. Psychiatry* 160, 179–186. doi: 10.1192/bjp.160.2.179

Lin, P. Y., Lin, S. I., Penney, T., and Chen, J. J. J. (2009). Review: applications of near infrared spectroscopy and imaging for motor rehabilitation in stroke patients. *Time* 29, 210–221.

Lutz, A., Slagter, H. A., Dunne, J. D., and Davidson, R. J. (2008). Attention regulation and monitoring in meditation. *Trends Cogn. Sci.* 12, 163–169. doi: 10.1016/j.tics.2008.01.005

Lutz, A., Slagter, H. A., Rawlings, N. B., Francis, A. D., Greischar, L. L., and Davidson, R. J. (2009). Mental training enhances attentional stability: neural and behavioral evidence. *J. Neurosci.* 29, 13418–13427. doi: 10.1523/jneurosci.1614-09.2009

MacDonald, A. W., Cohen, J. D., Stenger, V. A., and Carter, C. S. (2000). Dissociating the role of the dorsolateral prefrontal and anterior cingulate cortex in cognitive control. *Science* 288, 1835–1838. doi: 10.1126/science.288.5472.1835

MacLean, K. A., Ferrer, E., Aichele, S. R., Bridwell, D. A., Zanesco, A. P., Jacobs, T. L., et al. (2010). Intensive meditation training improves perceptual discrimination and sustained attention. *Psychol. Sci.* 21, 829–839. doi: 10.1177/0956797610371339

MacLeod, C. M. (1991). Half a century of research on the Stroop effect: an integrative review. *Psychol. Bull.* 109, 163–203. doi: 10.1037//0033-2909.109.2.163

Mesulam, M. (1998). From sensation to cognition. *Brain* 121, 1013–1052. doi: 10.1093/brain/121.6.1013

Minagawa-Kawai, Y., van der Lely, H., Ramus, F., Sato, Y., Mazuka, R., and Dupoux, E. (2011). Optical brain imaging reveals general auditory and language-specific processing in early infant development. *Cereb. Cortex* 21, 254–261. doi: 10.1093/cercor/bhq082

Moore, A., and Malinowski, P. (2009). Meditation, mindfulness and cognitive flexibility. *Conscious. Cogn.* 18, 176–186. doi: 10.1016/j.concog.2008.12.008

Morton, J., and Chambers, S. M. (1973). Selective attention to words and colours. *Q. J. Exp. Psychol.* 25, 387–397. doi: 10.1080/14640747308400360

Nation, D., Clark, L., Wierenga, C., Delano-Wood, L., Dev, S., Bangen, K., et al. (2013). Cerebrovascular resistance and cognitive decline: modulating effects of age. *Neurology* 80, P07.135.

Nehlig, A. (2010). Is caffeine a cognitive enhancer? *J. Alzheimers Dis.* 20(Suppl. 1), S85–S94. doi: 10.3233/JAD-2010-091315

Newberg, A., Alavi, A., Baime, M., Pourdehnad, M., Santanna, J., and d'Aquili, E. (2001). The measurement of regional cerebral blood flow during the complex cognitive task of meditation: a preliminary SPECT study. *Psychiatry Res.* 106, 113–122. doi: 10.1016/s0925-4927(01)00074-9

Newberg, A. B., and Iversen, J. (2003). The neural basis of the complex mental task of meditation: neurotransmitter and neurochemical considerations. *Med. Hypotheses* 61, 282–291. doi: 10.1016/s0306-9877(03)00175-0

Newberg, A. B., Wintering, N., Khalsa, D. S., Roggenkamp, H., and Waldman, M. R. (2010a). Meditation effects on cognitive function and cerebral blood flow in subjects with memory loss: a preliminary study. *J. Alzheimers Dis.* 20, 517–526. doi: 10.3233/JAD-2010-1391

Newberg, A. B., Wintering, N., Waldman, M. R., Amen, D., Khalsa, D. S., and Alavi, A. (2010b). Cerebral blood flow differences between long-term meditators and non-meditators. *Conscious. Cogn.* 19, 899–905. doi: 10.1016/j.concog.2010.05.003

Pardo, J. V., Fox, P. T., and Raichle, M. E. (1991). Localization of a human system for sustained attention by positron emission tomography. *Nature* 349, 61–64. doi: 10.1038/349061a0

Petersen, S. E., and Posner, M. I. (2012). The attention system of the human brain: 20 years after. *Annu. Rev. Neurosci.* 35, 73–89. doi: 10.1146/annurev-neuro-062111-150525

Peterson, B. S., Skudlarski, P., Gatenby, J. C., Zhang, H., Anderson, A. W., and Gore, J. C. (1999). An fMRI study of Stroop word-color interference: evidence for cingulate subregions subserving multiple distributed attentional systems. *Biol. Psychiatry* 45, 1237–1258. doi: 10.1016/s0006-3223(99)00056-6

Plichta, M. M., Herrmann, M. J., Baehne, C. G., Ehlis, A.-C., Richter, M. M., Pauli, P., et al. (2006). Event-related functional near-infrared spectroscopy (fNIRS): are the measurements reliable? *Neuroimage* 31, 116–124. doi: 10.1016/j.neuroimage.2005.12.008

Portas, C. M., Rees, G., Howseman, A. M., Josephs, O., Turner, R., and Frith, C. D. (1998). A specific role for the thalamus in mediating the interaction of attention and arousal in humans. *J. Neurosci.* 18, 8979–8989.

Posner, M. I., and Petersen, S. E. (1990). The attention system of the human brain. *Annu. Rev. Neurosci.* 13, 25–42. doi: 10.1146/annurev.ne.13.030190.000325

Posner, M. I., and Snyder, C. R. R. (1975). "Attention and cognitive control," in *Information Processing and Cognition: The Loyola Symposium*, ed R. L. SolSo (Hillsdale, NJ: Erlbaum, Lawrence Associates, Inc), 55–85.

Saggar, M., King, B. G., Zanesco, A. P., Maclean, K. A., Aichele, S. R., Jacobs, T. L., et al. (2012). Intensive training induces longitudinal changes in meditation state-related EEG oscillatory activity. *Front Hum Neurosci* 6:256. doi: 10.3389/fnhum.2012.00256

Schroeter, M. L., Zysset, S., Kruggel, F., and von Cramon, D. Y. (2003). Age dependency of the hemodynamic response as measured by functional near-infrared spectroscopy. *Neuroimage* 19, 555–564. doi: 10.1016/s1053-8119(03)00155-1

Schroeter, M. L., Zysset, S., Kupka, T., Kruggel, F., and Yves von Cramon, D. (2002). Near-infrared spectroscopy can detect brain activity during a color-word matching Stroop task in an event-related design. *Hum. Brain Mapp.* 17, 61–71. doi: 10.1002/hbm.10052

Schroeter, M. L., Zysset, S., and Von Cramon, D. Y. (2004a). Shortening intertrial intervals in event-related cognitive studies with near-infrared spectroscopy. *Neuroimage* 22, 341–346. doi: 10.1016/j.neuroimage.2003.12.041

Schroeter, M. L., Zysset, S., Wahl, M., and von Cramon, D. Y. (2004b). Prefrontal activation due to Stroop interference increases during development—an event-related fNIRS study. *Neuroimage* 23, 1317–1325. doi: 10.1016/j.neuroimage.2004.08.001

Short, E. B., Kose, S., Mu, Q., Borckardt, J., Newberg, A., George, M. S., et al. (2010). Regional brain activation during meditation shows time and practice effects: an exploratory FMRI study. *Evid. Based Complement. Altern. Med.* 7, 121–127. doi: 10.1093/ecam/nem163

Slagter, H. A., Davidson, R. J., and Lutz, A. (2011). Mental training as a tool in the neuroscientific study of brain and cognitive plasticity. *Front. Hum. Neurosci.* 5:17. doi: 10.3389/fnhum.2011.00017

Slagter, H. A., Lutz, A., Greischar, L. L., Nieuwenhuis, S., and Davidson, R. J. (2009). Theta phase synchrony and conscious target perception: impact of intensive mental training. *J. Cogn. Neurosci.* 21, 1536–1549. doi: 10.1162/jocn.2009.21125

Son, I.-Y., and Yazici, B. (2006). Near infrared imaging and spectroscopy for brain activity monitoring. *Adv. Sens. with Secur. Appl.* 2, 341–372. doi: 10.1007/1-4020-4295-7_15

Szűcs, D., Killikelly, C., and Cutini, S. (2012). Event-related near-infrared spectroscopy detects conflict in the motor cortex in a Stroop task. *Brain Res.* 1477, 27–36. doi: 10.1016/j.brainres.2012.08.023

Taga, G., Asakawa, K., Maki, A., Konishi, Y., and Koizumi, H. (2003). Brain imaging in awake infants by near-infrared optical topography. *Proc. Natl. Acad. Sci. U S A* 100, 10722–10727. doi: 10.1073/pnas.1932552100

Takahashi, T., Murata, T., Hamada, T., Omori, M., Kosaka, H., Kikuchi, M., et al. (2005). Changes in EEG and autonomic nervous activity during meditation and their association with personality traits. *Int. J. Psychophysiol.* 55, 199–207. doi: 10.1016/j.ijpsycho.2004.07.004

Tang, Y.-Y., Ma, Y., Wang, J., Fan, Y., Feng, S., Lu, Q., et al. (2007). Short-term meditation training improves attention and self-regulation. *Proc. Natl. Acad. Sci. U S A* 104, 17152–17156. doi: 10.1073/pnas.0707678104

Telles, S., Deepeshwar, S., Naveen, K. V., and Pailoor, S. (2014). Long latency auditory evoked potentials during meditation. *Clin. EEG Neurosci.* doi: 10.1177/1550059414544737. [Epub ahead of print].

Telles, S., Raghavendra, B. R., Naveen, K. V., Manjunath, N. K., and Subramanya, P. (2012). Mid-latency auditory evoked potentials in 2 meditative states. *Clin. EEG Neurosci.* 43, 154–160. doi: 10.1177/1550059412439963

Thomas, J., Jamieson, G., and Cohen, M. (2014). Low and then high frequency oscillations of distinct right cortical networks are progressively enhanced by medium and long term Satyananda Yoga meditation practice. *Front. Hum. Neurosci.* 8:197. doi: 10.3389/fnhum.2014.00197

Tian, F., Chance, B., and Liu, H. (2009). Investigation of the prefrontal cortex in response to duration-variable anagram tasks using functional near-infrared spectroscopy. *J. Biomed. Opt.* 14:054016. doi: 10.1117/1.3241984

van Leeuwen, S., Müller, N. G., and Melloni, L. (2009). Age effects on attentional blink performance in meditation. *Conscious. Cogn.* 18, 593–599. doi: 10.1016/j.concog.2009.05.001

van Vugt, M. K., and Jha, A. P. (2011). Investigating the impact of mindfulness meditation training on working memory: a mathematical modeling approach. *Cogn. Affect. Behav. Neurosci.* 11, 344–353. doi: 10.3758/s13415-011-0048-8

Vogt, B. A., Finch, D. M., and Olson, C. R. (1992). Functional heterogeneity in cingulate cortex: the anterior executive and posterior evaluative regions. *Cereb. Cortex* 2, 435–443. doi: 10.1093/cercor/2.6.435-a

Wang, D. J. J., Rao, H., Korczykowski, M., Wintering, N., Pluta, J., Khalsa, D. S., et al. (2011). Cerebral blood flow changes associated with different meditation practices and perceived depth of meditation. *Psychiatry Res.* 191, 60–67. doi: 10.1016/j.pscychresns.2010.09.011

Yadav, A., Tandon, O. P., and Vaney, N. (2002). Auditory evoked responses during different phases of menstrual cycle. *Indian J. Physiol. Pharmacol.* 46, 449–456.

Zeidan, F., Johnson, S. K., Diamond, B. J., David, Z., and Goolkasian, P. (2010). Mindfulness meditation improves cognition: evidence of brief mental training. *Conscious. Cogn.* 19, 597–605. doi: 10.1016/j.concog.2010.03.014

Zeidan, F., Martucci, K. T., Kraft, R. A., McHaffie, J. G., and Coghill, R. C. (2014). Neural correlates of mindfulness meditation-related anxiety relief. *Soc. Cogn. Affect. Neurosci.* 9, 751–759. doi: 10.1093/scan/nst041

Zysset, S., Schroeter, M. L., Neumann, J., and von Cramon, D. Y. (2007). Stroop interference, hemodynamic response and aging: an event-related fMRI study. *Neurobiol. Aging* 28, 937–946. doi: 10.1016/j.neurobiolaging.2006.05.008

Conflict of Interest Statement: The authors declare that the research was conducted in the absence of any commercial or financial relationships that could be construed as a potential conflict of interest.

Received: 01 November 2014; accepted: 22 December 2014; published online: 17 February 2015.

Citation: Deepeshwar S, Vinchurkar SA, Visweswaraiah NK and Nagendra HR (2015) Hemodynamic responses on prefrontal cortex related to meditation and attentional task. Front. Syst. Neurosci. ***8****:252. doi: 10.3389/fnsys.2014.00252*

This article was submitted to the journal Frontiers in Systems Neuroscience.

frontiers in Systems Neuroscience

OPINION
published: 08 October 2015
doi: 10.3389/fnsys.2015.00141

Augmenting brain function with meditation: can detachment coincide with empathy?

*Shirley Telles *, Nilkamal Singh and Acharya Balkrishna*

Patanjali Research Foundation, Haridwar, India

Keywords: meditation, detachment, empathy, dmPFC, vmPFC

Background and Aim

Meditation practices aim at modifying the emotions by reducing reactivity to both pleasant and unpleasant emotions (Sperduti et al., 2012; Reva et al., 2014). Meditation also regulates the attention by reducing distractibility and directing focused attention to the object of meditation (Sperduti et al., 2012). In many meditation techniques attention is directed to ongoing experiences without the intention to analyze, judge, get involved, or expect anything which can lead to detachment (Tei et al., 2009). Detachment here was taken to mean reducing or removing the need to control, possess, and be influenced by the actions of people or circumstances. Detachment or remaining dispassionate is ideally combined with empathy. The aim of the present article is to discuss the neurophysiological basis by which detachment and empathy may co-exist in meditation.

OPEN ACCESS

Edited by:
Mikhail Lebedev,
Duke University, USA

Reviewed by:
Maria V. Sanchez-Vives,
ICREA-Institut d'Investigacions Biomèdiques August Pi i Sunyer, Spain
Mikhail Lebedev,
Duke University, USA
Jooseph John Loizzo,
Weill Cornell Medical College, USA
Michael Stephen Ball,
Northumbria University, UK

****Correspondence:***
Shirley Telles
shirleytelles@gmail.com

Received: *31 October 2014*
Accepted: *22 September 2015*
Published: *08 October 2015*

Citation:
Telles S, Singh N and Balkrishna A (2015) Augmenting brain function with meditation: can detachment coincide with empathy? Front. Syst. Neurosci. 9:141. doi: 10.3389/fnsys.2015.00141

Review of Relevant Articles

Tei et al. (2009) found differences between Qigong meditators and controls in the resting state using standardized low resolution electromagnetic tomography (sLORETA; *t*-tests for unpaired data, Tei et al., 2009). The Qigong meditation includes practices for self-regulation of the body and mind (Pan et al., 1994). In the study by Tei et al. (2009) differences between groups were seen in the delta EEG band. In meditators brain areas involved in detecting and integrating internal and external sensory information were activated, whereas appraisal systems were inhibited. In non-meditators film generated emotion which is emotion in response to external stimuli was associated with activity in the occipitotemporoparietal cortex, lateral cerebellum, hypothalamus, and regions involving the anterior temporal cortex, amygdala, and hippocampal formation; whereas recall generated emotion, associated with the response to interoceptive sensory stimuli was associated with activation in the anterior insular cortex (Reiman et al., 1997).

A quantitative meta-analysis of 10 neuroimaging studies with 91 meditators, tested the hypothesis that a common neural network exists for different meditations since all meditations aim at inducing relaxation, regulating attention, and developing detachment from one's thoughts (Sperduti et al., 2012). An activation likelihood estimation (ALE) of the 10 fMRI studies showed activation during meditation in the left caudate nucleus (body of the caudate), entorhinal cortex and medial prefrontal cortex. This suggests that a common neural network may exist for meditation techniques which have comparable regulation of attention and goals. Changes in activity in the medial prefrontal cortex (MPFC) can be associated with mental activity during introspection (Gusnard et al., 2001). The ventral MPFC shows task-induced decreases in activity even when the task consists, for example, of lying quietly (Shulman et al., 1997). Hence, the ventral MPFC is believed to be engaged in actively maintaining a default state, which gets attenuated even by

passive activities (e.g., lying quietly with eyes closed or passively viewing a stimulus; Raichle et al., 2001). In addition as detailed below the ventral MPFC, along with the temporo-parietal junction and medial temporal lobe are involved in cognitive aspects of empathy (Shamay-Tsoory, 2011). In contrast to the ventral MPFC, changes in the dorsal MPFC include both increases and decreases in activity (Pardo et al., 1993; Shulman et al., 1997). Increased activity was found in BA 8, 9, and 10 and the adjacent paracingulate sulcus of the dorsal MPFC (Castelli et al., 2000). Gusnard and others showed increased activity in the dorsal MPFC during mental activity associated with introspection (Gusnard et al., 2001).

Mental activity associated with introspection is possibly part of a continuum in the mental state induced by meditation which could lead to detachment (Atchley, 1997).

This is supported by a sLORETA study of experienced meditators practicing five types of techniques, viz., Tibetan-Buddhist, Qigong, Sahaja-Yoga, Ananda Marga Yoga, and Zen (Lehmann et al., 2012). Eight EEG frequency bands (delta through gamma) were computed for 171 functional connectivities between regions (*t*-tests for unpaired data), and showed "lagged coherence." All significant differences between meditation and before/after states showed lower coherence during meditation for the five meditations and eight EEG bands. This suggested that functional interdependence between brain regions was globally reduced. The reduced functional interdependence was considered to be related to minimized interaction and constraints on the self process (which includes self-awareness and embodiment), leading to non-involvement and detachment (Lehmann et al., 2012). Detachment can help an individual to get mental peace (Sonnetag et al., 2010). However, in order to contribute usefully to society empathy and compassion are essential. Empathy and compassion are seemingly similar social emotions, however they alter brain activation in distinct, non-overlapping neural networks, and change affective responses with opposite valence (Klimecki et al., 2014).

Empathy is the ability to understand other's feelings (Bird et al., 2010). However, when faced with the suffering of others, intense sharing of the pain experiences by others can cause empathic distress, and reduce helping behavior (Batson et al., 1987; Eisenberg et al., 1989). It was speculated by Klimecki et al. (2014) that compassion could be a potential remedy. Compassion has been defined as a feeling of concern for the suffering of others, associated with the motivation to help (Keltner and Goetz, 2007). Klimecki et al. (2014) demonstrated that after empathy training viewing videos depicting suffering resulted in negative affect and brain activation in regions previously associated with empathy for pain. The areas were the anterior insula, and anterior mid cingulate cortex (Fan et al., 2011; Lamm et al., 2011). When the same individuals (Klimecki et al., 2014) were subsequently given training in compassion and asked to view videos depicting comparable suffering, the negative affect was reversed and brain activations occurred in non-overlapping areas including the ventral striatum, pregenual anterior cingulate cortex, and medial orbito frontal cortex. Klimecki et al. (2014) concluded that compassion training could actually reduce empathic distress and increase emotional resilience. Compassion is an inherent part of a meditation technique called compassion-meditation (CM), which is closely related to two other widely studied meditation techniques, that is, mindfulness-based meditation (MM) and Loving-Kindness meditation (LKM; Hofmann et al., 2011).

There is evidence which supports two separate systems for cognitive and for emotional aspects of empathy apart from the areas involved in empathy training described earlier (Klimecki et al., 2014). The areas involved in cognitive empathy, are particularly relevant to this article. They are the ventral MPFC, temporo-parietal junction, and medial temporal lobe (Shamay-Tsoory, 2011). As discussed above the dorsal MPFC is associated with detachment (Gusnard et al., 2001). Hence, the MPFC in addition to other functions, is concerned with both empathy (the ventral MPFC) and with detachment (the dorsal MPFC).

Brain activity using fMRI was assessed while novice and experienced meditators practiced loving-kindness-compassion meditation (LKCM; Lutz et al., 2008). Affective reactivity was probed by presenting emotional and neutral sounds during meditation and control periods. When emotional sounds were presented there was activation in the insula and cingulate cortices during meditation compared to rest (ANOVA; paired *t*-tests). Also, during meditation (compared to rest), in response to emotional and neutral sounds, there was increased activation in the amygdala, right temporo-parietal junction, and right posterior superior temporal sulcus. The results support the speculation that LKCM activates brain circuits related to empathy in response to emotional stimuli.

The studies cited above suggest that LKM causes functional changes in specific areas and in inter-connections between areas, to generate social consciousness and empathy. However, as the names suggest, LKM and CM emphasize loving kindness and compassion, respectively, in addition to empathy.

A study was designed to examine the effects of focused-attention meditation (FAM) and loving-kindness meditation (LKM) during the performance of cognitive and affective tasks (Lee et al., 2012). There were 22 practitioners of FAM (11 experts and 11 novices) and similarly for LKM, 11 experts and 11 novices. Comparisons were between states (meditation vs. baseline) and expertise (experts vs. novices; paired and unpaired *t*-tests). A conjunction approach was used to reveal regions common to the expert meditation state. Both FAM and LKM appeared to influence the neural responses to affective pictures.

The difference between FAM and LKM was apparent when participants were given emotion-processing tasks, involving viewing affective pictures. When viewing sad faces the FAM practitioners showed activation in areas related to attention whereas in the LKM practitioners changes occurred in areas associated with compassion and emotional regulation.

Summary

These findings showed that different meditations are associated with distinct neural activity during sustained attention and

processing emotions. Hence, meditation causes changes in parts of the brain and modifies brain activity, in distinct ways based on the meditation technique.

To our knowledge no study has checked whether detachment and empathy can co-exist as a result of meditation; and the pathway has not been determined. The dorsal MPFC showed increased activation associated with mental activity during introspection (Gusnard et al., 2001), which is believed to lead to detachment (Raichle et al., 2001). The ventral MPFC has been associated with cognitive empathy (Shamay-Tsoory, 2011). The ventral and dorsal MPFC are functionally connected via the amygdala (Kim et al., 2011). It is speculated that this neural circuit, involving the dorsal and ventral MPFC and the amygdala, a circuit which could be the basis for simultaneous detachment and empathy. It hence appears that detachment and empathy are associated with activation in closely connected areas of the brain.

Recommendations for Future Studies

The above discussion suggests that detachment and empathy can be experienced simultaneously through meditation. A study of the effects of meditation would be interesting to test whether detachment and empathy can indeed co-exist. It would also be of interest to understand whether following the necessary training empathy could lead to compassion. The present speculation suggests that through meditation an individual can reach a mental state which is disengaged and detached, but retains the choice to engage with specific situations based on empathy.

References

Atchley, R. C. (1997). Everyday mysticism: spiritual development in later adulthood. *J. Adult Dev.* 4, 123–134.

Batson, C. D., Fultz, J., and Schoenrade, P. A. (1987). Distress and empathy: two qualitatively distinct vicarious emotions with different motivational consequences. *J. Pers.* 55, 19–39.

Bird, G., Silani, G., Brindley, R., White, S., Frith, U., and Singer, T. (2010). Empathic brain responses in insula are modulated by levels of alexithymia but not autism. *Brain* 133, 1515–1525. doi: 10.1093/brain/awq060

Castelli, F., Happé, F., Frith, U., and Frith, C. (2000). Movement and mind: a functional imaging study of perception and interpretation of complex intentional movement patterns. *Neuroimage* 12, 314–325. doi: 10.1006/nimg.2000.0612

Eisenberg, N., Fabes, R. A., Miller, P. A., Fultz, J., Shell, R., Mathy, R. M., et al. (1989). Relation of sympathy and personal distress to prosocial behavior: a multimethod study. *J. Pers. Soc. Psychol.* 57, 55–66.

Fan, Y., Duncan, N. W., de Greck, M., and Northoff, G. (2011). Is there a core neural network in empathy? an fMRI based quantitative meta-analysis. *Neurosci. Biobehav. Rev.* 35, 903–911. doi: 10.1016/j.neubiorev.2010.10.009

Gusnard, D. A., Akbudak, E., Shulman, G. L., and Raichle, M. E. (2001). Medial prefrontal cortex and self-referential mental activity: relation to a default mode of brain function. *Proc. Natl. Acad. Sci. U.S.A.* 98, 4259–4264. doi: 10.1073/pnas.071043098

Hofmann, S. G., Grossman, P., and Hinton, D. E. (2011). Loving-kindness and compassion meditation: potential for psychological interventions. *Clin. Psychol. Rev.* 31, 1126–1132. doi: 10.1016/j.cpr.2011.07.003

Keltner, D., and Goetz, J. L. (2007). "Compassion," in *Encyclopedia of Social Psychology,* eds R. F. Baumeister and K. D. Vohs (Thousand Oaks, CA: Sage Publications), 159–161.

Kim, M. J., Gee, D. G., Loucks, R. A., Davis, F. C., and Whalen, P. J. (2011). Anxiety dissociates dorsal and ventral medial prefrontal cortex functional connectivity with the amygdale at rest. *Cereb. Cortex*21, 1667–1673. doi: 10.1093/cercor/bhq237

Klimecki, O. M., Leiberg, S., Ricard, M., and Singer, T. (2014). Differential pattern of functional brain plasticity after compassion and empathy training. *Soc. Cogn. Affect. Neurosci.* 9, 873–879. doi: 10.1093/scan/nst060

Lamm, C., Decety, J., and Singer, T. (2011). Meta-analytic evidence for common and distinct neural networks associated with directly experienced pain and empathy for pain. *Neuroimage* 54, 2492–2502. doi: 10.1016/j.neuroimage.2010.10.014

Lee, T. M, Leung, M. K., Hou, W. K., Tang, J. C., Yin, J., So, K. F., et al. (2012). Distinct neural activity associated with focused-attention meditation and loving-kindness meditation. *PLoS ONE*7:e40054. doi: 10.1371/journal.pone.0040054

Lehmann, D., Faber, P. L., Tei, S., Pascual-Marqui, R. D., Milz, P., Kochi, K., et al. (2012). Reduced functional connectivity between cortical sources in five meditation traditions detected with lagged coherence using EEG tomography. *Neuroimage* 60, 1574–1586. doi: 10.1016/j.neuroimage.2012.01.042

Lutz, A., Brefczynski-Lewis, J., Johnstone, T., and Davidson, R. J. (2008). Regulation of the neural circuitry of emotion by compassion meditation: effects of meditative expertise. *PLoS ONE*3:e1897. doi: 10.1371/journal.pone.0001897

Pan, W., Zhang, L., and Xia, Y. (1994). The difference in EEG theta waves between concentrative and non-concentrative Qi-Gong states – a power spectrum and topographic mapping study. *J. Tradit. Chin. Med.* 14, 212–218.

Pardo, J. V., Pardo, P. J., and Raichle, M. E. (1993). Neural correlates of self-induced dysphoria. *Am. J. Psychiatry* 150, 713–719.

Raichle, M. E., MacLeod, A. M., Snyder, A. Z., Powers, W. J., Gusnard, D. A., and Shulman, G. L. (2001). A default mode of brain function. *Proc. Natl. Acad. Sci. U.S.A.* 98, 676–682. doi: 10.1073/pnas.98.2.676

Reiman, E. M., Lane, R. D., Ahern, G. L., Schwartz, G. E., Davidson, R. J., Friston, K. J., et al. (1997). Neuroanatomical correlates of externally and internally generated human emotion. *Am. J. Psychiatry* 154, 918–925.

Reva, N. V., Pavlov, S. V., Loktev, K. V., Korenyok, V. V., and Aftanas, L. I. (2014). Influence of long-term Sahaja Yoga meditation practice on emotional processing in the brain: an ERP study. *Neuroscience* 281, 195–201. doi: 10.1016/j.neuroscience.2014.09.053

Shamay-Tsoory, S. G. (2011). The neural bases for empathy. *Neuroscientist* 17, 18–24. doi: 10.1177/1073858410379268

Shulman, G. L., Fiez, J. A., Corbetta, M., Buckner, R. L., Miezin, F. M., Raichle, M. E., et al. (1997). Common blood flow changes across visual tasks: II. decreases in cerebral cortex. *J. Cogn. Neurosci.* 9, 648–663.

Sonnetag, S., Kuttler, I., and Fritz, C. (2010). Job stressor, emotional exhaustion, and need for recovery: a multi-source study on the benefits of psychological detachment. *J. Vocat. Behav.* 76, 355–365. doi: 10.1016/j.jvb.2009.06.005

Sperduti, M., Martinelli, P., and Piolino, P. (2012). A neurocognitive model of meditation based on activation likelihood estimation (ALE) meta-analysis. *Conscious. Cogn.* 21, 269–276. doi: 10.1016/j.concog.2011.09.019

Tei, S., Faber, P. L., Lehmann, D., Tsujiuchi, T., Kumano, H., Pascual-Marqui, R. D., et al. (2009). Meditators and non-meditators: EEG source imaging during resting. *Brain Topogr.* 22, 158–165. doi: 10.1007/s10548-009-0107-4

Conflict of Interest Statement: The authors declare that the research was conducted in the absence of any commercial or financial relationships that could be construed as a potential conflict of interest.

frontiers in
SYSTEMS NEUROSCIENCE

REVIEW ARTICLE
published: 11 June 2014
doi: 10.3389/fnsys.2014.00109

Augmentation-related brain plasticity

Giovanni Di Pino[1,2], Angelo Maravita[3], Loredana Zollo[2], Eugenio Guglielmelli[2] and Vincenzo Di Lazzaro[1]*

[1] Institute of Neurology and Fondazione Alberto Sordi - Research Institute for Ageing, Campus Bio Medico University of Rome, Rome, Italy
[2] Laboratory of Biomedical Robotics and Biomicrosystems CIR - Centre for Integrated Research, Campus Bio Medico University of Rome, Rome, Italy
[3] Department of Psycology, Università di Milano-Bicocca, Milano, Italy

Edited by:
Mikhail Lebedev, Duke University, USA

Reviewed by:
Arvid Guterstam, Karolinska Institutet, Sweden
Bérangère Thirioux, Unité de Recherche Clinique - Centre Hospitalier Henri Laborit, France

****Correspondence:***
Giovanni Di Pino, Institute of Neurology and Fondazione Alberto Sordi - Research Institute for Ageing, Campus Bio Medico University of Rome, Via Alvaro del Portillo 21, Rome 00128, Italy
e-mail: g.dipino@unicampus.it

Today, the anthropomorphism of the tools and the development of neural interfaces require reconsidering the concept of human-tools interaction in the framework of human augmentation. This review analyses the plastic process that the brain undergoes when it comes into contact with augmenting artificial sensors and effectors and, on the other hand, the changes that the use of external augmenting devices produces in the brain. Hitherto, few studies investigated the neural correlates of augmentation, but clues on it can be borrowed from logically-related paradigms: sensorimotor training, cognitive enhancement, cross-modal plasticity, sensorimotor functional substitution, use and embodiment of tools. Augmentation modifies function and structure of a number of areas, i.e., primary sensory cortices shape their receptive fields to become sensitive to novel inputs. Motor areas adapt the neuroprosthesis representation firing-rate to refine kinematics. As for normal motor outputs, the learning process recruits motor and premotor cortices and the acquisition of proficiency decreases attentional recruitment, focuses the activity on sensorimotor areas and increases the basal ganglia drive on the cortex. Augmentation deeply relies on the frontoparietal network. In particular, premotor cortex is involved in learning the control of an external effector and owns the tool motor representation, while the intraparietal sulcus extracts its visual features. In these areas, multisensory integration neurons enlarge their receptive fields to embody supernumerary limbs. For operating an anthropomorphic neuroprosthesis, the mirror system is required to understand the meaning of the action, the cerebellum for the formation of its internal model and the insula for its interoception. In conclusion, anthropomorphic sensorized devices can provide the critical sensory afferences to evolve the exploitation of tools through their embodiment, reshaping the body representation and the sense of the self.

Keywords: supernumerary limbs, sensory substitution, cognitive enhancement, embodiment, brain machine interface (BMI), cross-modal plasticity, hand prostheses, sensorimotor abilities

INTRODUCTION

Humans have always tried to augment their able-body abilities with the help of tools; lenses have been exploited to see further afield or to look at tiny objects, vehicles to travel long distances quicker and pincers and tongs to tightly manipulate objects. Tools use is a unique feature that humans and primates share, whit a loud influence in evolutionary processes, allowing them to push their abilities beyond the boundaries set by evolution and better interact with the environment (Ambrose, 2001).

Today's achievements in biological sciences and engineering might need to reconsider the concept of human-tools interaction in the framework of human augmentation. Human augmentation is a newborn domain of investigation that aims to exploit methodologies proper of medical therapeutic intervention and rehabilitative medicine, such as strategies, drugs and external artificial devices originally designed to compensate for the loss of functions, to increase physical and cognitive ability of able-bodied individuals, beyond the level characteristic of the normal physiological health status. Hence, the health status of the population targeted by the intervention critically sets the difference between rehabilitative functional restoration and human augmentation.

Actually, the idea of augmenting human abilities is not brand new, since, for instance, almost half a century ago, Von Gierke stated that it was among the goals of bionics "to extend man's physical and intellectual capabilities by prosthetic devices in the most general sense" (Von Gierke, 1970). However, more recently, the field of human augmentation started to capture the attention of scientists worldwide and to raise the level of awareness on its ethical and societal implications (for a deep analysis of ethical and societal implications of human augmentation see Clark, 2007; Blanke and Aspell, 2009). Indeed, several features of modern functional prostheses signed a sharp discontinuity with any device previously aimed at enhancing the ability of able-bodied: (i) the achieved high level of anthropomorphism of the tool; (ii) the intimate contact that the tool establishes with the user; and (iii) the absence of bottlenecks in the flow of information from the brain to the environment on which the tool operates. In summary, in recent years we are assisting to the first true attempts to

create Hybrid Bionic Systems (HBSs), containing both technical and biological components arranged in a tight complex, where the robotic artifact is directly interfaced with the brain of a human being (Dario et al., 1993). This scenario encompasses, for example, modern cybernetic hand prostheses that exploit neural signals taken by electrodes implanted invasively into the cortex or into peripheral nerves to decode the user's intention of movement (Hochberg et al., 2006; Rossini et al., 2010). This modern approach could eventually lead to an unprecedented degree of man-machine integration.

The development of invasive (Lebedev and Nicolelis, 2006) and non-invasive (Birbaumer and Cohen, 2007) Brain-Machine Interfaces (BMI) and neural interfaces with peripheral nerves (Navarro et al., 2005) allowed to bypass the activity of the muscles and the physical transduction of cutaneous/proprioceptive sensory organs, while directly picking up motor signals from, or delivery sensory inputs to the nervous system. Hitherto, this has been the main determinant of the functional continuity between man and machines and represents the biggest milestone in the enquiry of the human augmentation. Prostheses that the user operates through neural interfaces are often named neuroprostheses. Although this term literally means a prosthesis for replacing a function of the nervous system, as it was originally conceived in the domain of cochlear implant (Terr et al., 1987) and in the stimulation of the sacral roots for bladder control (Brindley, 1974), it was lately used for motor functional electrical stimulation (Popovic et al., 2002) and more recently started to be used also for prostheses interfaced with the nervous system (Lebedev and Nicolelis, 2006). This extended meaning seems to be sufficiently accurate in operational terms and will be use from now on.

The recent advancements in robotics and BMIs are key enabling technologies for the creation of an augmented bionic man. However, can humans adapt themselves to effectively control external additional limbs and other body parts by learning and integrating them into a new sensorimotor representation? In the attempt to answer the question, it might be helpful to make a simple parallelism with the operation of adding a printer or an external hard-drive to our personal computer. The compatibility of the hardware is *conditio sine qua non, moreover* printer and laptop must share, for instance, the same I/O port. However, for a new device to be proficiently controlled the presence of its "representation" in the software that manages external devices is mandatory. In the case the software was not originally designed to allocate that device, it needs to be reprogrammed, often by means of supplemental drivers that plastically adapt it to the new condition. Analogously, human brain can be trained to expand its motor control to a supernumerary, artificial limb or else to receive sensory information from an external accessory sensor and plastically embed them into its representation of the body.

Most of the advancements in the field of human-machine interface have been achieved by pursuing two strategies in parallel: on one hand, the development of devices for restoring sensorimotor functions in disabled and, on the other hand, the development of devices for augmenting sensorimotor capabilities of able-bodied, allowing for instance to operate in impervious environments. However, it is worth considering that a further possible field of application of such technology, located in between rehabilitative functional restoration and human augmentation, is aging. The augmenting technology can be aimed indeed at supporting sensorimotor and cognitive abilities that are lost day-by-day with normal aging. The existence of a net border between therapeutic and augmenting applications seems to be overestimated, since the continuous distribution of individual human performance and its extreme variability could make exploitable for augmentation what has been developed for restoration and vice versa. Along this line, as we will see in the following paragraphs, most brain processes subtending functional restoration match the ones subtending augmentation and can be exploited to understand this phenomenon.

This review is aimed to analyze the neural correlates of human augmentation and, in particular, the plastic process that the brain undergoes when it comes into contact with artificial sensors and effectors meant as external aids and, on the other hand, the changes that the use of external augmenting devices produces in the brain.

BRAIN PLASTICITY: GENERAL CONSIDERATIONS

Brain plasticity is the ability of the brain to adapt its structural and functional connectivity in response to an external condition promoting a novel function, or a new way to perform an old function, or else the suppression of a sensorimotor ability. Plasticity has widely been considered the neural substrate of early development (Hensch, 2005), of the acquisition of new skills (Pascual-Leone et al., 1995) and of the recovery from brain injuries (Chen et al., 2002). It may be intended as an inner property of neural networks that results from the exposure of the system to physiological or pathological conditions (Pascual-Leone et al., 2005).

The Hebb and Paillard's theoretical hypothesis of brain plasticity (Hebb, 1949; Paillard, 1976), postulating that a long lasting strengthening of the connection between two neurons is induced by the simultaneous activation of those cells, has found its neural correlate in the phenomenon of associative learning mediated by long-term potentiation/depression (Bliss and Lomo, 1973; Bailey and Kandel, 2008).

Most of the findings regarding brain plasticity first came from lesion study in animals and, later on, from non-invasive functional imaging in humans. Plastic changes have been widely described in sensorimotor cortices that undergo deep remodeling with an extension of cortical representation of the still functionally active projections (Kaas, 1991). An initial unmasking of already present, but inactive, connections is the effect of increased cortical excitability due to a reduction of GABA-mediated inhibition (Jones, 1993) and an increase of NMDA-mediated activation (Buonomano and Merzenich, 1998). More stable changes often underlie structural modifications, characterized by axonal regeneration and sprouting (Kaas, 1991).

Hitherto, the amount of studies on ability augmentation, nearly all in animals, which investigating the recruited neural networks and/or on the plastic processes involved, are not enough to build a comprehensive body of knowledge on this topic. However, clues about augmentation-related plasticity can be obtained by borrowing insights gained from similar logically-related paradigms, i.e., sensorimotor training, cognitive

enhancement, cross-modal plasticity, sensory and motor output functional substitution, use of tools and embodiment.

For instance, sensorimotor abilities can be enhanced by specific training and are boosted in athletes, while cognitive training enhances memory and attentive functions in healthy and brain-damaged, or aged, individuals. Artificial devices for etero-modal sensory substitution are exploited in the deaf and blind and rely on cross-modal plasticity, but the same devices can be exploited for sensory augmentation in sighted and normal hearing people. Motor augmentation, as well as motor functional substitution, involves the use of external effectors, including prostheses. Their optimal functionality relays on their integration in the user body schema, like any other kind of hand-held tool. Starting from those considerations, we will briefly describe the aforementioned paradigms and revise their implications for augmentation-related plasticity.

SENSORIMOTOR TRAINING-INDUCED PLASTICITY

Several effects of sensory motor training have been demonstrated in both the sensory and the motor domains, as well as at cellular level and at the level of whole brain areas or brain networks. Within the sensory domain, the acquisition or improvement of sensory functions is accompanied by plastic changes in the brain. Sensory discrimination training is able to induce changes in primary sensory cortices. Frequency discrimination training in adult owl monkeys results in increased performance and an enlargement of the stimulated skin representation in the primary somatosensory cortex, where the receptive fields of sensory neurons were significantly expanded (Recanzone et al., 1992). For example, monkeys trained in a visual orientation task showed a refined tuning of V1 neurons towards the trained orientation (Schoups et al., 2001).

Within the motor domain, a huge body of literature is devoted to the motor system plasticity induced by training. In rats, practicing a reaching task produced an enlarged representation of the wrist and digit movements in the primary motor cortex (M1) with an increase of the number of synapses per neurons (Kleim et al., 2002). The improvement seen in a reaction task can be well inferred from the activity of the motor neuronal ensemble in charge of the task (Laubach et al., 2000). In awake monkeys, skills acquisition modulates the activity of M1 neurons as assessed through cortical invasive recordings (Germain and Lamarre, 1993). Furthermore, the enlargement of M1 depends more on motor skill acquisition (Nudo et al., 1996) than on the simple repetitive use (Plautz et al., 2000). Long-term training-induced plastic changes in neuronal properties seem to be the substrate for the internal storage of motor skills (Matsuzaka et al., 2007). M1 changes during motor sequence learning, as evidenced by functional magnetic resonance imaging (fMRI), present an initial reduced area of M1 activation, following short-term repetition, but a progressive increased of the extension of M1 activation following motor training. Such a pattern of activation may be the neural substrate underpinning a three-phase motor skill acquisition: initial habituation, consolidation and long-lasting plasticity (Karni et al., 1998). A model that has been largely used to assess sensorimotor plasticity is that of studying the brain of people that hold (or else acquire) peculiar sensorimotor skills, such as sport or music expertise. For example, learning a one-hand piano exercise produces an enlargement of the motor representation of the hand and a facilitation of the corticospinal tract devoted to the muscles of the trained fingers (Pascual-Leone et al., 1995). Expert tennis players have an asymmetry of hand motor cortex with an enlarged representations and increased motor cortex excitability as evaluated by measuring the threshold for motor-evoked potential (MEP) after transcranial brain stimulation, in the cortex controlateral to the hand using the racket (Pearce et al., 2000). Plastic changes take place in the somatosensory system as well. In violin players, the somatosensory cortical representation of the fingers used to play the strings are enlarged and the amount of enlargement correlates with the years of practice (Elbert et al., 1995).

As far as the neurobiological mechanisms of sensorimotor plasticity, evidence from both animal (Rioult-Pedotti et al., 1998, 2000) and human (Ziemann et al., 2004) studies attributes training-induced motor plasticity to long-term potentiation (LTP)-like mechanisms involving the synaptic strength of cortical horizontal connections. However, structural plasticity, in parallel with the modulation of synaptic strength, plays a crucial role even after a few days of training. In humans, learning to juggle induced a bilateral increase in the gray matter of the occipito-temporal cortex, especially in the middle temporal motion-sensitive area (Draganski et al., 2004), after only a week of practice. Such plastic changes were no more present after the training ceased, although the performance did not decrease (Driemeyer et al., 2008). Structural modifications have been reported also for the white matter underlying the intraparietal sulcus (Scholz et al., 2009). Moreover, exercise showed to stimulate neurogenesis in the dentate gyrus of the hippocampus in mice and humans (Pereira et al., 2007).

Sensorimotor plasticity also manifests as a change in the pattern of activation of different brain areas and circuits. Motor skill acquisition recruits brain regions that are not recruited during simple motor task execution (Grafton et al., 1992). Several factors influence which network is recruited by practice, such as the specific task domain and the behavioral and cognitive load required. In general, practice of sensorimotor tasks determines an increased reliance on sensorimotor areas and a decreased recruitment of attentional control exerted by prefrontal, anterior cingulate and posterior parietal cortex (Kelly and Garavan, 2005). Motor practice not only affects the pattern of brain activation involved in the execution of the movement, but also its preparation. It has been shown that during stroke preparation expert golf players, compared to novices, show higher levels of activity in areas involved in visuomotor integration (superior parietal lobule, the dorsal lateral premotor cortex and the occipital area), and decreased activation in attentional/emotional basal ganglia and limbic structures (Milton et al., 2007). In the same paradigm, electroencephalographic (EEG) recordings demonstrated higher frontal theta and parietal alpha power, probably due to attention focusing for sensory processing (Baumeister et al., 2008). Skilled motor performance refines also the activity of the mirror system and goes in parallel with enhanced ability to anticipate the outcome of actions executed by others by resonant motor activation (Aglioti et al., 2008).

In summary, augmentation of sensorimotor skills, and sensorimotor training produce, an enhancement of performance, which is paralleled by specific neurobiological changes in the brain tissue and a change in the pattern of cortical activity, mainly by the focalization of brain activity on sensorimotor cortex both during movement execution and preparation (Yarrow et al., 2009).

COGNITIVE ENHANCEMENT

Cognitive enhancement is the attempt to improve cognitive functions (memory, working memory, attention, fluid intelligence) through training, psychological strategies, drugs or other medical interventions and last, but not least, external technological supports. Today's human augmentation targets cognitive enhancement *per se*, or can affect it as a consequence of sensorimotor augmentation. However, pursuing cognitive enhancement can be considered a foundational goal of humans. For instance, the aim of education always went beyond the mere learning of specific information; even pencil and paper can be regarded as primitive forms of external memory enhancement, while the use of nicotine and caffeine to focus attention, increase alertness and reduce the sense of fatigue can be dated far back in time (Bostrom and Sandberg, 2009).

The amount and quality of the stimuli offered by the environment are main determinants of cognitive development (Taffoni et al., 2014) and can be used to burst cognition. Indeed, in rats, an enriched environment produces an improvement of spatial memory and increases neurogenesis in the dentate gyrus (Nilsson et al., 1999) in a comparable way to chronic cholinergic treatment (Murphy et al., 2006). Also sensorimotor exercise, further than in sensorimotor processes, has a deep impact on cognition and promotes brain plasticity by modulating regional bloody flow and neurotrophic support, especially by releasing brain derived neurotrophic factor (BDNF; Vaynman and Gomez-Pinilla, 2005).

Cognitive enhancement by can be achieved with drugs. These molecules mostly target neurotransmitters of ascending systems from the brainstem nuclei, and have been directed to treat cognitive impairments of attention deficit hyperactivity disorder (ADHD), Parkinson's disease, schizophrenia, while acetylcholinesterase inhibitors are currently used as a the therapy in Alzheimer's disease (Husain and Mehta, 2011). Memory enhancing drugs are of two main classes: (i) LTP inducing drugs, mostly modulating AMPA (α-amino-3-hydroxy-5-methyl-4-isoxazole propionic acid receptors); and (ii) molecules increasing the cAMP response element-binding protein that enhances synapses, stabilizing proteins to allow memory consolidation (Farah et al., 2004). Effects of those drugs can go beyond the cognitive domains and influence non-cognitive symptoms of those clinical conditions. In this line, the acetylcholinesterase inhibitor rivastigmine reversed the abnormality of sensorimotor integration, as evaluated by testing short-latency afferent inhibition, in patients affected by Alzheimer's disease (Di Lazzaro et al., 2005).

It is worth noting that memory enhancement techniques have been developed to counteract memory decline of Alzheimer's and other neurodegenerative disorders, but they are currently extended to the healthy elder population in order to counteract age-related involution. Here again the borders between therapy and augmentation are weak. Similarly, methylphenidate (Ritalin), a catecolamine-like drug that represents the treatment of choice for ADHD and is known to improve cognitive performance also in healthy volunteers, is largely assumed even by children without diagnosed AHDH (Farah et al., 2004). The use of drugs for cognitive enhancement produces structural and functional changes in the brain. In healthy volunteers, the cognitive improvement seen after a single dose of modafinil, a monoamminergic stimulator, goes in parallel with an increased functional connectivity at rest in the anterior cingulate cortex, part of the left fronto-parietal control network and in the bilateral occipito-parietal node of the dorsal attention network (Esposito et al., 2013). Structural changes have been also described following drug treatment. In a rat model of stroke the administration of D-amphetamine induced an amelioration of motor and working memory performance and a significant increase of neurites growth and synaptogenesis in the neocortex (Stroemer et al., 1998).

Does superior memory ability rely on higher Q.I. or particularly developed brain structures or alternatively does it mostly rely on a specific functional engaging strategy? Evidence is in favor of the latter. During memory tasks, people with exceptional memory activate different neural networks involved in spatial learning and navigation, especially the hippocampus. This luckily reflects a "method of loci" memorizing strategy based on the association of each object to memorize with a location in an imagined physical pathway (Maguire et al., 2002). In healthy subjects, spatial memory can be dramatically increased by training, as happens for London taxi drivers that aim to acquire the license. A voxel-based morphometry study documented an increased gray-matter volume of the posterior hippocampus, which correlates with years of works and that can represent the plastic substrate for the allocation of spatial representations (Maguire et al., 2000).

Several attempts to achieve cognitive enhancement target the working memory. Working memory is the ability of retaining information over a brief time. It plays a pivotal role in most cognitive functions and is strictly linked with inhibitory functions, reasoning and intentional allocation of self-attention (Klingberg, 2010). In particular, spatial working memory improvement exerted by methylphenidate has been associated to a task-related activity refinement in the posterior parietal cortex and dorsolateral prefrontal cortex, especially on the left hemisphere, (Mehta et al., 2000); the former locus seems to relate to online organization and storage of information and the latter to their active manipulation and monitoring. Working memory can be enhanced by training. Several training programs have been developed, for instance computerized training devoted to ADHD children (Klingberg et al., 2005), that showed long-term efficacy (Holmes et al., 2009). Training working memory shapes the brain (Klingberg, 2010) by increasing the activity in the middle frontal gyrus, in the superior and inferior parietal cortices (Olesen et al., 2004) and in the caudate nucleus (Dahlin et al., 2008) and decreasing the number of cortical D1 dopamine receptors (McNab et al., 2009). Training affecting the intraparietal-prefrontal network yields effects that are not modality specific and that can be transferred to any different task requiring working memory (Thorell et al., 2009). Indeed, the positive effect in the retention of instrumental activities of daily-living in older

adults produced by cognitive training have been documented even after 5 years from the initial intervention (Willis et al., 2006). The extension of performance improvement to untrained domains has a deep impact in the translation to human cognitive augmentation.

Being brain plasticity the base of cognitive enhancement, training programs specifically designed to target its mechanisms gave very promising results. It has been shown in healthy adults over 60, in whom a training program comprising stimulus recognition, discrimination, sequencing, and memory tasks under strict attentional control, high reward, and novelty has been used to target age-related degraded sensory processing and the down-regulation of neuromodulatory control nuclei. The training produced a memory improvement, which generalized to untrained tasks and was maintained over 3 months (Mahncke et al., 2006). Similar findings were demonstrated in children affected by dyslexia. A program composed by auditory and oral language training produced an increased activity during language processing in the right fronto-temporal regions and anterior cingulate cortex and, similarly to unaffected children, in the left inferior frontal gyrus and left temporo-parietal cortex. Activity in the latter area positively correlated with language recovery (Temple et al., 2003).

Currently, the wide diffusion of computer and videogames-based technology for cognitive training gives the opportunity to proficiently self-train cognitive abilities (Jak et al., 2013). Recently, a multitasking performance training videogame has proved effective in restoring, in elder adults, the same brain activity pattern found in younger controls, with an increase in the midline EEG theta band power over the frontal regions and a higher coherence with the posterior regions. EEG changes predicted the improvement of sustained attention and working memory and their maintenance after 6 months (Anguera et al., 2013).

Meditation, in its various forms, is a kind of mental training with a diverse and long-lasting history, that can be exploited as a strategy for cognitive enhancement (So and Orme-Johnson, 2001). It is able to enhance pre-attentive processes, as evidenced by an increase of the amplitude of auditory mismatch negativity waves (Srinivasan and Baijal, 2007) and of the functional activity of anterior cingulate cortex, prefrontal cortex, hippocampus and insula (Lazar et al., 2000; Farb et al., 2007; Hölzel et al., 2008; Lutz et al., 2008). Indeed, meditation induces short and long-term plasticity. High amplitude gamma-band activity has been described during meditation, especially over the lateral fronto-parietal electrodes, and long-distance phase-synchrony, while resting state EEG shows higher gamma/theta+alpha ratio which burst during meditation and persists after it (Lutz et al., 2004). Several studies demonstrated that meditation is able to induce structural changes especially in the prefrontal cortex, hippocampus and the right anterior insula (Lazar et al., 2005; Pagnoni and Cekic, 2007; Hölzel et al., 2008; Luders et al., 2009). Those areas are involved in the regulation of emotions and in their integration with cognition. Changes have been also evidenced in the brainstem (Vestergaard-Poulsen et al., 2009). Recently, a longitudinal follow-up after 8 weeks of meditation documented an increase of gray matter in the left hippocampus, in the posterior cingulate cortex, the temporo-parietal junction, and in the cerebellum (Hölzel et al., 2011).

Brain activity can be voluntarily modulated to pursue cognitive enhancement with the help of neurofeedback, an operant conditioning paradigm, in which participants exploit a feedback of their brain electrical activity to learn to influence it. Several neurofeedback protocols have been attempted so far. For instance, increase of beta/theta+alpha ratio (Rasey et al., 1995) and increase of sensorimotor (12–15 Hz) rhythm to achieve improvement of working memory and attention (Vernon et al., 2003) or perceptual sensitivity and reduced omission errors (Egner and Gruzelier, 2004), beta rhythm to improve reaction time (Egner and Gruzelier, 2004), increase peak of alpha to improve speed of processing and executive function (Angelakis et al., 2007) and frontal-midline theta activity to improve attention and working memory (Wang and Hsieh, 2013). However, changes of EEG rhythm and improvement of cognitive performance have to be taken with caution: in subject exposed to sham neurofeedback the sole attempt to control a bar, that they believed to be driven by EEG rhythm, produced a wide engagement of fronto-parietal and cingulo-opercular network, which are known to be involved in cognitive control (Ninaus et al., 2013).

Further than with the above mentioned drugs, trainings and strategies, cognitive enhancement can be achieved through external technological support and invasive brain stimulation. For instance, computer based memory aids are interactive diaries that can be embedded in portable or wearable devices and that help patients to remind everyday tasks such as calling a relative or taking a medication (Schulze, 2004). As regard as the stimulation, deep brain stimulation of the septal nucleus (Jiang et al., 1997) and high frequency stimulation of caudate and striatum (Williams and Eskandar, 2006) ameliorate learning and memory in humans and rodents, similarly to vagal nerve stimulation (Clark et al., 1999). Coupled cortical stimulating/recordings arrays can be exploited to trigger and support cortical plasticity (Jackson et al., 2006) and to burst inter-regional functional connectivity at the base of cognitive enhancement, or to substitute lost white matter in demyelinating lesions and subcortical atrophies (Serruya and Kahana, 2008). In theory, cognitive enhancement could, one day, completely rely on external modules. Indeed, artificially interfacing a cortical area with a different one is not very dissimilar from interfacing it with external ectopic (namely located in an abnormal position or environment respecting to the one for which they were originally developed) neural modules. Technology could provide surrogates of cortical or basal ganglia circuitries externally grown *in vitro* (Pfister et al., 2007) or hybrid neuron-chips where neurons grow in a silico support (Zeck and Fromherz, 2001; Serruya and Kahana, 2008).

In conclusion, cognitive enhancement can be achieved through appropriate training strategies and drugs and it mostly relies on plastic processes modulating neurotrasmitters ascending systems and involving the frontoparietal network and, in the case of working memory enhancement, the hippocampus.

CROSS-MODAL PLASTICITY AND SENSORY SUBSTITUTION

Literature on plasticity across the systems has been focused on the investigation of the changes that a disrupted sensory modality

evokes on different sensorial networks, as occurring in sensory-deprived animals and humans. However, cross-modal plasticity can be considered as an example of the propensity of some brain areas to manage functions that they have not been originally aimed at.

Reading Braille produces an expansion of the S1 representation of the reading fingers in the blind (Pascual-Leone and Torres, 1993), but in parallel, a task-specific activation of V1 (Sadato et al., 1996), which is critically not present if the hand is used for motor tasks others than Braille reading (Gizewski et al., 2003).

Although basic parameters of spared sensory functions, such as visual contrast sensitivity (Finney and Dobkins, 2001), absolute auditory or tactile threshold (Niemeyer and Starlinger, 1981) may not be affected, cross-modal plasticity results in more complex behavioral advantages, as in the case of blind that process sounds faster and better and have enhanced tactile accuracy (Roder and Neville, 2003). This sustains the localization of this plasticity to be primarily in associative cortices. In this line, functional neuroimaging studies documented an increased recruitment of posterior superior temporal sulcus and inferior parietal lobe in the processing of stimuli processed by spared senses in the blind (Büchel et al., 1998) and deaf (Bavelier et al., 2001). However, even primary sensory areas are targets of cross-modal plasticity and in animals the artificial transposition of fibers from the retina to S1 makes S1 responding to light stimulation (Métin and Frost, 1989), while disruptive transcranial magnetic stimulation (TMS) targeting V1 cortex impairs a tactile discrimination task in blind humans (Cohen et al., 1997).

To understand the impact of cross-modal plasticity in augmentation, a first question is whether cross-modal plasticity is active only in response to brain damage or sensory deprivation. Intracortical invasive recordings in animals documented activity in V1 evoked by non-visual stimuli also in non-deprived animals (Murata et al., 1965) and tactile stimulation enhance V1 activity of healthy subjects (Macaluso et al., 2000), thus raising the intriguing possibility that even primary sensory cortices, in physiological conditions, are not completely unimodal. Indeed data support the idea of the existence of heteromodal connection between primary sensory cortices, as found between primary visual and somatosensory cortices in the monkey. Furthermore, connections between primary sensory areas through multisensory cortices may provide feedback projections that may enhance the response to a stimulus presented in one sensory modality when a spatially-temporally congruent stimulus is delivered in a different sensory modality (Macaluso and Maravita, 2010).

The mechanisms at play during cross-modal plasticity are likely the same of intra-modal plasticity and involve changes in local connectivity that warrant for the rearrangements of sensory maps, stabilization of transient long-range connections during development and changes in cortico-cortical feedback (Bavelier and Neville, 2002) and are mostly driven by activity-dependent inputs competition. Those changes are easier during childhood, but still possible along the adult life and may be the consequences of plasticity of subcortical structures, as in the thalamus and/or brainstem nuclei (Jones and Pons, 1998). Cortical feedback exerts also an important role in determining cross-modal changes, involving direct long range connections between primary sensory areas or connections through associative cortices, in line with the finding of enhanced fMRI connectivity between visual and parietal areas in deaf individuals (Bavelier et al., 2000).

Taking together the premises that sensory brain areas that are classically considered unimodal may be not strictly unimodal and that the mechanisms behind cross-modal plasticity are mostly the same at the base of intra-modal plasticity, would raise the hypothesis that the main determinants of plasticity are the features of the experienced stimulus, its timing along the development of the nervous system and the neurobiological features of the targeted system (Bavelier and Neville, 2002). This would happen mostly independently from any a priori restriction related to the modality of the stimulus, allowing therefore to easily conceive, and practically achieve, an artificial heteromodal sensory substitution.

It deserves to be mentioned that cross-modal plasticity could, in some circumstances, be detrimental for sensory-replacement implants, because it sustains a rewiring of the target orphan cortex from areas controlling other modalities, that could compete with inputs coming from the implant (Lee et al., 2001).

Little evidence sustains so far that also the motor system can undergo changes prompted by the incorporation of functions of different modalities: for instance motor cortex representation of the reading fingers is enhanced in Braille-readers far more than the extent only ascribable to its mere increased use (Pascual-Leone et al., 1993). As far as the effect of multi-modal plasticity induced by the introduction of devices offering new motor efferences, it would be extremely interesting to look at widespread brain plastic modifications in primates experiencing the control of a third arm.

Prostheses designed for sensory substitution, rely on cross-modal plasticity where afferences from a sensory modality are employed to guide the accomplishment of tasks that in able-bodied are primarily executed by means of a diverse sense (Bach-y-Rita and W Kercel, 2003). For instance, an electrotactile array laying on the tongue, has been exploited to deliver information coming from two head-mounted accelerometers, in order to stabilize the posture of subjects with bilateral vestibular deficiency (Tyler et al., 2003) or to transfer visual information taken by a camera in blind people (Sampaio et al., 2001).

Direct demonstrations of cross-modal plasticity after training with non-invasive sensory substitution prostheses have been provided. Blind experiencing auditory-to-vision sensory substitution via an ultrasonic echolocation device showed increased occipital cortex activity compared to trained blindfolded sighted control (De Volder et al., 1999), while replacing vision with somesthesis increased the activation of occipital cortex, which correlated with that of posterior parietal cortex (Ptito et al., 2005). Hence, tactile-dependent activation of occipital cortex may occur through feedback projections from multisensory parietal areas.

Heteromodal sensory substitution, relying on cross-modal plasticity, forces the brain towards changes to fulfill the gap between old and new sensory modality. This may involve to fell the replacement as not enough direct and intuitive. An interface able to feedback sensitive information respecting the site and the modality of the cutaneous hand touching and proprioceptive sensations will overcome this issue. We recently demonstrated that the translation of the output of sensors embedded in the prosthesis into patterns of intraneural stimulation allows recognizing

shape and stiffness of different objects and consequently choose the appropriate grasp and strength (Raspopovic et al., 2014).

To summarize, cross-modal plasticity has been found to significantly occur in associative areas, such as the parietal cortex, as well as primary sensory areas. Moreover, its occurrence does not only follow compensative mechanisms following brain damage, but may also act as at the basis of sensory substitution.

TOOLS USE INDUCED PLASTICITY

When we think of human augmentation the image that more probably arises is the one of a man, with additional arm-like devices endowed with tools, who operates in hostile or complex environments. Thus, understanding how brain interacts with tools is mandatory to the present paper.

In the late Seventies Gibson defined the concept of affordance of an object or an environment as "a specific combination of the properties of its substance and its surfaces taken with reference to an animal" in Gibson (1977). "It implies the complementarity of the animal and the environment" (Gibson, 1986). The very external appearance of the tool suggest its unique role in enhancing man-environment relationship: one end of the tool is typically, devoted to the interaction with humans and defines their affordance (i.e., the handle of the hammer) and the other is designed for the interaction with the environment (i.e., the weighted head of the hammer).

Critically, the brain encodes different aspects of the tool, from its more perceptual features to its conceptual meaning and its motor feature. Early knowledge on the cognitive representation of the use of tools in the human brain, and on the putative underlying brain areas, comes from reports of patients affected by brain lesions and suffering from apraxia (Goldenberg, 2003), while only more recently functional imaging studies allowed to infer those processes in healthy subjects (Moll et al., 2000). Moreover, much has been inferred capitalizing on findings from non-human primates. However, humans and monkeys exhibit interspecific differences in the way that their brain deals with tools. In monkey, the mirror neuron system, activated when the animal observes an action performed with the hand, is activated very weakly if the same action is performed through a pincer (Gallese et al., 1996). Visuomotor neurons of premotor area F5 are activated by the visual presentation of a specific tool, or by a subclass of objects, and probably code the motor features of the object (Murata et al., 1997). Visual features of the objects are instead coded by the inferior parietal lobe (Shikata et al., 1996) and in the anterior intraparietal area (Murata et al., 2000). Peculiarly in humans, but not in monkey, the inferior parietal lobule, and in particular the anterior supramarginal gyrus, seems to take part in this network by associating the function of the tool with the required action of the hand (Peeters et al., 2009). Human premotor cortex seems instead to host category-specific representation of tools (Perani et al., 1995), probably as a consequence of the precocious exposition to tools during human motor development.

Either observing, performing or only imagining a task recruits different regions when this is done by means of a tool. A task performed with a tool activates the ipsilateral intraparietal sulcus to a greater extent than the same task performed with the hands (Inoue et al., 2001). Furthermore, the imagination of grasping with tools is accompanied by specific activation of premotor and parietal cortices as well as middle temporal and fusiform gyri (Creem-Regehr and Lee, 2005). In humans, observation of tool use produces a suppression of 20 Hz magnetoencephalographic activity, an hallmark of bilateral primary motor cortex function, which is stronger if the tool is involved in goal-directed actions and if the subject is familiar with the use of that specific tool (Järveläinen et al., 2004).

The neural substrates for the representation of the conceptual knowledge of tools, the ones affected in conceptual or ideational apraxia, are different from the ones hosting the representation of dexterous tool use, affected instead in ideomotor apraxia. Both of them are mainly represented in partially dissociable neural networks, primarily of the left hemisphere (Johnson-Frey, 2004), even in left-handed subjects (Lausberg et al., 1999) and converge in the premotor and parietal areas where the conceptual knowledge of the tool is coupled with the motor program to operate it. Key areas of the tool conceptual knowledge network are the fusiform and the middle temporal gyrus, middle and inferior gyrus, and ventral premotor cortex of the frontal lobe, while dorsal premotor cortex, anterior supramarginal gyrus and intraparietal sulcus of the parietal lobe are activated only if conceptual knowledge is mediated by attention. The network dealing with the motor representation of tools comprises the dorsal premotor and middle frontal gyrus plus the posterior parietal cortex and the intraparietal sulcus (Johnson-Frey, 2004).

Cortical structural changes induced by learning to use a tool can take place rapidly. Learning to retrieve food with a rake in a monkey naive for any tool use produced after only 2 weeks a gray matter increase in the superior temporal sulcus, and in the intraparietal sulcus and bilaterally in white matter underlying the cerebellar cortex (Quallo et al., 2009). On a similar token, gene expression was induced while macaque monkeys learned to use a rake. In particular, during the 2 week period necessary for the acquisition of skillful tool use, but not after the learning phase, an increased level of BDNF and its cellular receptors was found in the anterior bank of intraparietal sulcus, witnessing a learning-induced gene expression, which was linked to the reorganization of visuo-tactile integration in parietal cortex following tool use (Ishibashi et al., 2002).

Finally, as in the case of sensory-motor plasticity reviewed above, the pattern of brain recruitment seems to be specific for a given tool and dependent on previous experience. Imagination of tasks performed with a familiar tool, i.e., a tennis racquet in experienced tennis players, produces a facilitation of corticospinal fibers devoted to the muscles needed to operate the tool, which become more excitable. This process does not take place if the subject imagines motor tasks involving similar tools, either a tennis table-paddle or a golf club, or if the subject is an athlete but not an expert tennis player (Fourkas et al., 2008).

Overall, the above reviewed evidence, speaks in favor of a large representation of tool-use in the cortex. Such representation critically depends upon the conceptual categorization of the tool, its motor mechanics and, importantly, the motor goal that it allows to reach. Such a reach coding of tools and tool-mediated actions is particularly important when it comes to include in the

brain representation external augmentation devices. The brain is in facts ready to code for the more conceptual, to the more perceptual and motor features of the newly acquired device for optimal performance.

PLASTICITY INDUCED BY ARTIFACT EMBODIMENT

The expansion of the possible interaction between the organism and the environment has been ascribed to the use of tools, while the settlement of the boundary has been ascribed to its practice (Smitsman, 1997). In absence of tools, the part of space where the subject is able to act through his hands and limbs without locomotion, namely the peripersonal space, is coded by dedicated neural structures in the primate brain. A particular relevant role is exerted by visuotactile neurons located in the frontal area 6 and in the inferior parietal lobule (Fogassi et al., 1996). The visual receptive fields of some of those bimodal neurons are arm-centered (Graziano et al., 1994) and surprisingly, following repetitive reaching tasks performed with a rake, increase to cover the expanded range of action of the hand wielding the rake, or increase to encompass the whole length of the tool (Iriki et al., 1996). This seminal finding demonstrated that the human body schema, a mainly unconscious representation of the body arising from the integration of sensory afferences, is not rigid, but maintains a certain plastic flexibility and by integrating sensorimotor inputs (Maravita et al., 2003) can be modulated to embed a tool. Several behavioral data document that how the brain computes tool-use has much more in common with the control of the hands themselves, than that of other objects. Crossing tools affects performance as crossing hands does by producing similar cross-modal interferences and reaching tasks performed with tools are affected in patients with neglect as much as are tasks performed with hands, while, for instance, are spared tasks with pointing devices (Maravita and Iriki, 2004). Moreover a training performed with a grabber extending the range of action, alters the kinematics of subsequent free-hand grasping movements, also reshapes the sensory representation of the arm, inducing subject to localize touch more distally then where it is actually delivered (Cardinali et al., 2009).

Further than body-space interactions, also the sense of ownership towards external objects may be modulated through experience and external interventions (**Figure 1**). The rubber hand illusion is a striking example of how our body image can be tricked to embody a replica of a body segment. The vision of a fake hand stroked with a paintbrush synchronously with the stroking of the hidden real hand induces a sense of ownership of the rubber hand and a proprioceptive drift of the perceived position of the real hand towards the fake one (Botvinick and Cohen, 1998; **Figure 1A**). This process seems to be based on a Bayesian bottom-up integration of convergent multisensory inputs that determines what, within the peripersonal space, belongs to our body (Armel and Ramachandran, 2003) and may involve the activity of multimodal neurons that are activated by proprioceptive, tactile and visual inputs presented in spatial and temporal congruency (Makin et al., 2008). Those neurons have been extensively investigated in non-human primates (Graziano et al., 1994; Fogassi et al., 1996) and their presence has been also documented in humans (Bremmer et al., 2001).

In humans, the rubber hand illusion has been found to activate areas in the premotor cortex (Ehrsson et al., 2004) in the posterior parietal cortex (Ehrsson et al., 2005). Specifically to the mechanisms underlying the illusion, while somatosensory cortex was activated by the rubber-hand situations (comprising asynchronous visuo-tactile stimulation) not inducing embodiment (as assessed by the proprioceptive drift), the occurrence of the RHI was linked to the activation of the posterior insula and frontal operculum (Tsakiris et al., 2007). According to such a different brain substrate, proprioceptive drift and illusory sense of ownership for the rubber hand have been often found to have a low level of correlation (e.g., see Makin et al., 2008; Tsakiris, 2010; Rohde et al., 2011). In particular, the remapping of self body part to the position of an alien hand in external space would include premotor cortex, for the sense of ownership aspect, and the posterior parietal cortex for the monitoring of limb position (Brozzoli et al., 2012). Strikingly, the sense of ownership can be extended even to an empty portion of peripersonal space, thus literally expanding the boundaries of the self, following spatially and temporally congruent visual-proprioceptive signals activating a premotor-intraparietal neural substrate (Guterstam et al., 2013). Finally, brain damage affecting subcortical structures disrupting fronto-parietal connections, may lead to the loss of contralesonal or ipsilesional sensitivity to the RHI (Zeller et al., 2011).

The level of gamma band synchrony over the parietal regions (Kanayama et al., 2009) and a medial shift of the hand representation have also been associated with the strength of the illusion (Schaefer et al., 2009).

When a protocol of repetitive transcranial brain stimulation producing inhibitory effect is delivered over the inferior parietal lobule, it impairs the perceptual component of the illusion, but not the action-oriented component (Kammers et al., 2009), while stroke patients with damage in the white matter connected with prefrontal, premotor and parietal areas have a consistently higher odd to be unable to experience this illusion (Zeller et al., 2011).

However, subjects tested with the rubber hand illusion may experience that the fake hand substitutes their own (Lewis and Lloyd, 2010; Tsakiris et al., 2010) and a sense of disownership toward the real hand (Guterstam et al., 2011). Thus, since the paradigm of augmentation involves the presence of extra-effectors that are controlled in parallel with one's own limbs, an open question is to what extend the brain may show the ability to host a vivid representation of an extra-limb, while preserving that of the physiological ones.

The mirror box illusion was initially developed to give to amputees a normal, though artificial, visual feedback of their lost limb by reflecting the controlateral healthy one in a mirror. This has been shown to readdress amputees' aberrant brain plasticity and improve their phantom limb pain (Ramachandran et al., 1995; Ramachandran and Altschuler, 2009). However, also healthy subjects can be induce to feel the sense of ownership for the reflected image by hiding their intact limb inside the mirror box (**Figure 1B**; Romano et al., 2013).

Reports of humans that, mostly affected by brain lesions located to the right hemisphere, perceive a supernumerary limb in the controlesional side (Halligan and Marshall, 1995) seem to support this possibility. More recently, few modified rubber

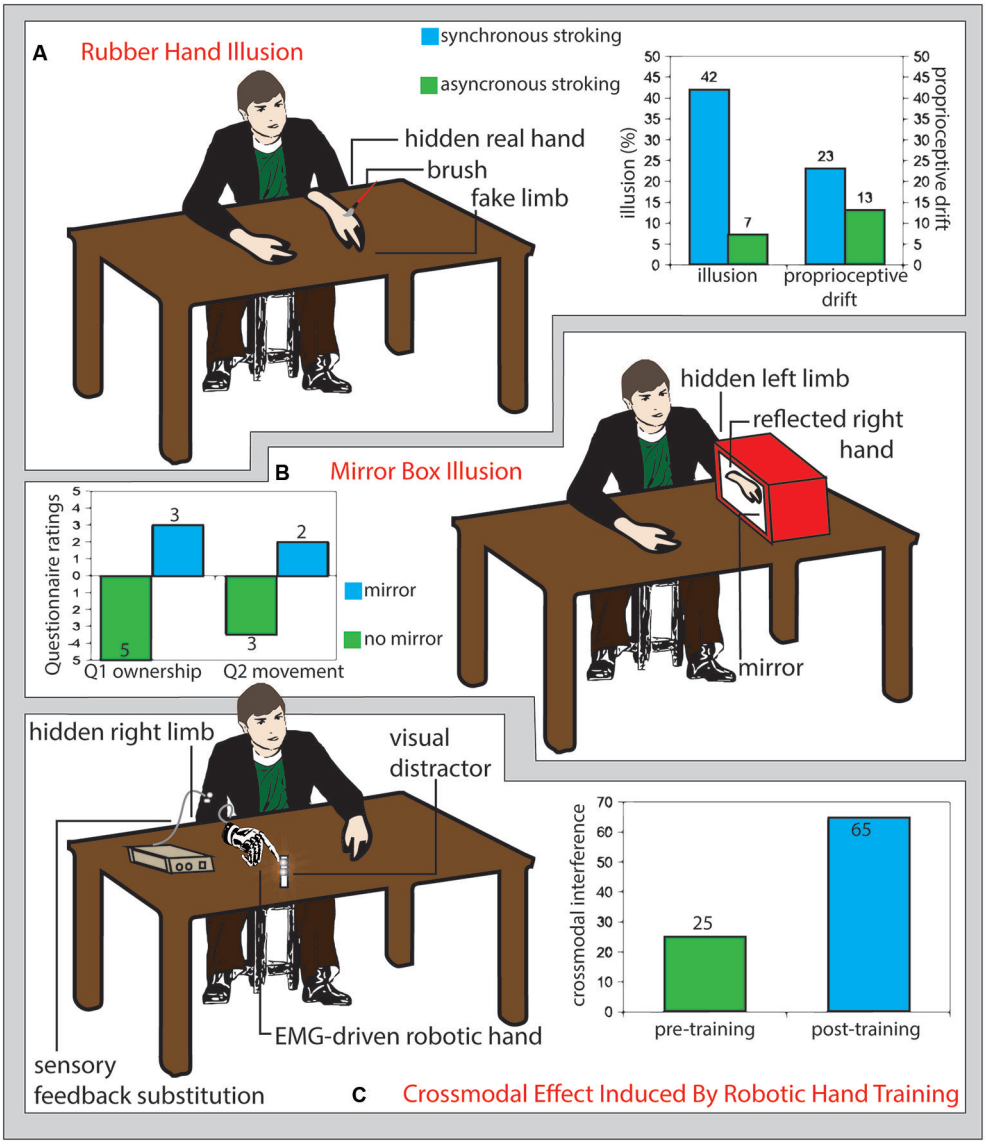

FIGURE 1 | (A) Rubber hand illusion. Participants sit in front of a table with their left hand hidden under the table and a fake limb (white detached arm in figure) placed on the table in front of them. If the fake limb is visibly stroked (schematic red brush in figure) together with the real limb (not visible), participants experience the illusion that the touch is referred to the fake limb (illusion) and that their real limb posture shits toward the fake limb (proprioceptive drift). The size of such effects is greater if the touches on the real and fake limb are delivered synchronously (right panel, light blue columns) than asynchronous (right panel, green columns) (Redrawn from the original data of: Botvinick and Cohen, 1998). **(B)** Mirror box illusion. Participant execute right-hand movements while the left arm is hidden from view and kept still inside a box, the right wall of which is replaced by a mirror (Ramachandran et al., 1995). As compared with a no-mirror condition (left panel, green columns), the mirror reflection of the right hand mimics the movements of the left hand inside the mirror box, biasing the participants feeling (assessed through a questionnaire) of ownership (Question 1: "The reflection in the mirror looks like the hand behind the mirror", left panel, left light blue column) and inducing the illusion of apparent movement (or a true, involuntary, unconscious movement) of the hand inside the box (Question 2: It seems as though the hand behind the mirror is moving; left panel right light blue column) (Romano et al., 2013). **(C)** Crossmodal effects induced by robotic hand training. Prolonged use of an electromyography-driven, detached robot hand (drawn in gray on the right side of the table) providing sensory feedback referred to the participant's arm (white circles), increased the interference from visual distracter leds located near the robot hand fingers (reddish shadowed circles) tested with the crossmodal congruency paradigm (right panel, light blue columns), as compared to the pre-training assessment (right panel, green columns). This pattern of results suggests a training-dependent expansion of crossmodal integration properties, typical of the peripersonal space near the body, to the space surrounding the robot hand (Marini et al., 2014).

hand paradigms documented the embodiment of supernumerary limbs, being them two rubber hands for which the subject proved increased protective autonomic response (Ehrsson, 2009) or two virtual copies of the subject real hand (Newport et al., 2010). In

the latter case, subjects integrated the perception of both hands into the body image, but were able to control the movement of only one of them, as if only that limb fully integrated in the body representation for action. Incongruence between efferent and proprioceptive signals and between body image and body schema may sustain the possibility to feel a sense of ownership for both the real and the supernumerary limb (Giummarra et al., 2008). Indeed, aberrant plastic modifications of the hand cortical representation that are common in the amputees' brain (Ramachandran et al., 1992; Flor et al., 1995; Pascual-Leone et al., 1996; Di Pino et al., 2009), not only still allow amputees to experience the rubber hand illusion (Ehrsson et al., 2008), but also to easily embody more than one fake limb at a time (Giummarra et al., 2011). An explanation advanced for this surprising phenomenon is that, in front of multiple, anatomically plausible limbs, the nervous system gradually assigns an equal probability that own limbs may be located at one of the different locations where the fake limbs are, due to multisensory integration (Guterstam et al., 2011).

Which features have to be implemented in the artificial limb to facilitate the process of its embodiment? The level of anthropomorphism of the artifact seems to be a key factor. In front of several objects only realistic prosthetic hands generated strong illusions (Tsakiris et al., 2010), which is prevented by rotating the hand into anatomically implausible postures (Ehrsson et al., 2004). Also proprioceptive afferences play a pivotal role and synchronous active movements of both the real and the fake hand make the embodiment stronger (Tsakiris et al., 2006). Furthermore, the embodiment of virtual hands providing realistic visual input (Slater et al., 2008; Newport et al., 2010).

The embodiment of the supernumerary artificial limb seems like the counterpart of deficit shown by brain-damaged patients who fail to recognize the ownership of their own limbs, attributing them to someone else, and even failing to show anticipatory responses to threatening incoming stimuli (Romano et al., 2014). To the same token, the inclusion of an alien limb in the patient's body representation could provide several advantages that go well beyond the mere improvement of motor control, including an extend sense of protection against forthcoming threats to the artifact. Indeed, it has been shown that, once a rubber hand is embodied, its threatening induces the activation of the insula and the anterior cingulate cortex that is due to interoception and anxiety, together with a motor activation that reflects the replay of the motor properties of the lost limb. Activity in these regions correlates with the level of embodiment (Ehrsson et al., 2007).

Recently, intracortical recordings in primates have revealed that S1 and M1 are involved in the plastic processes responsible for the embodiment of a virtual hand. The time delay of those responses was compatible with an indirect activation of primary sensorimotor areas by visual cortices, probably trough the fronto-parietal cortical circuitry (Shokur et al., 2013).

In order the rubber hand illusion to arise, congruent tactile and visual afferences are needed. Hence, it is plausible to suppose that to enrich the user experience of prosthesis control with a sensory feedback could be a main determinant to prompt the embodiment of prosthetic limbs. Whole nerve electrical stimulation (Mulvey et al., 2012) and vibrotactile stimulation (brushstroke or stick tapping) (D'Alonzo and Cipriani, 2012) of the real hand are able to substitute a real touch in the processes needed to evoke the rubber hand illusion. A pressure stimulator that translated the data acquired by a load cell mounted on a prosthesis into tactile stimulation of the skin reinnervated with nerves originally devoted to the lost hand was able to evoke the rubber hand illusion for a prosthetic device in patients undergoing target muscle reinnervation (Marasco et al., 2011). Moreover, as it happens for the real hands, the embodiment of the prosthesis should produce a cross-modal integration of tactile afferences with visual stimuli coming from the surroundings of the prosthesis, in order to ameliorate manipulation and sensory anticipation of stimuli in its surrounding environment. In healthy participants, long-term use of an electromyographic signal-driven detached robotic hand, able to provide substitutionary sensory feedback from its fingers via vibrotactile stimulation, produces a pattern of visuo-tactile interference from visual stimuli close to the prosthesis fingers, over tactile stimuli referred to the same fingers, in the cross-modal congruency effect, as typically shown when testing the real hand (**Figure 1C**; Marini et al., 2014).

However, a lesson learned from the rubber hand illusion is that, further than its intuitive consequences in a more dexterous control of the prosthesis, the more the afferent feedback from a prosthesis is veridical and close to normal physiology, the more the eventual embodiment of the artifact is likely. This has strong implications for the strategy to adopt for prosthesis-user interfacing.

Finally, the integration of neuroprostheses into the dynamic body image of the users, would likely change the body representation in a proficient, but also unnatural way, giving rise to a potential side effect of the prosthesis (Dobkin, 2007). Indeed, the risk of the arising of perceptual distortions of the body image could produce also detrimental effects due to the possible mismatch between the mental body image and the physical body. For example, psychological/psychiatric symptoms may occur, similar to those suffered by teens affected by body dysmorphic disorders, with consequent severe emotional distress, anxiety and depression or to those reported in the body integrity identity disorders or even somatoparaphrenia, where the subject reports extreme discomfort for a body segment that he feel as not belonging to him (Blom et al., 2012; Romano et al., 2014).

PLASTICITY INDUCED BY THE FUNCTIONAL REPLACEMENT OF MOTOR OUTPUT

Amputation is a straightforward model of deprivation-dependent plasticity and the consequences of the use of prostheses may be taken as a model of brain reorganization following the replacement of sensation and motor output. The interruption of incoming and outgoing flow between the lost segment and the brain triggers, in amputees, a plastic rearrangement of pathways and relays, especially in the cortical sensorimotor representation (Ramachandran et al., 1992; Pascual-Leone et al., 1996). The neural underpinning of phantom limb pain has been primarily ascribed to such an aberrant cortical reorganization (Flor et al., 1995). Long-term use of myoelectric (Lotze et al., 1999) or even body-powered (Weiss et al., 1999) prostheses somehow reduces the maladaptive cortical reorganization and the

associated phantom limb pain. The right ventral premotor cortex is strongly activated during the control of an EMG-guided prosthesis, while the right posterior parietal cortex activation may underlie its perceptual assimilation in the body schema (Maruishi et al., 2004).

However, interfacing systems relying on the contraction of far spared muscles transmitted through hidden pulleys and cables or superficial electromyographic sensors, may be inadequate for the control of novel multifingered sensorized prostheses and to effectively readdress the aberrant plasticity. To this aim invasive multicontact electrodes have been developed to be implanted in the peripheral nerves (Navarro et al., 2005) and to reopen a bunch of input/output channels directly toward the nervous system of amputees (Micera et al., 2009, 2010). The surgery needed to implant the electrodes, if performed by experts respecting few restrictions, could be considered a low-risk procedure (Di Pino et al., 2013), that may be eventually available in the near future also for healthy people aiming at augmentation.

In parallel with the anthropomorphism and the manipulative skills own by the prosthesis, a key factor that plays a major role in driving the brain reshaping accompanying the employment of a motor substitution device is the achievement of proper solutions for effective and natural bidirectional human–machine interfacing (Di Pino et al., 2009). Indeed, the training for the control of an anthropomorphic dexterous robotic hand interfaced with intraneural multielectrodes with the forearm nerves of the user, induced consistent reversion of the amputation-induced aberrant cortical plasticity. In particular, it can unmask the motor cortical representation of the lost hand (Rossini et al., 2010) and normalize the EEG activation pattern during movement of the phantom hand (Tombini et al., 2012), the functional interhemispheric interaction (Di Pino et al., 2012c) and the cortico-cortical functional connectivity (Ferreri et al., 2014). Those plastic changes are accompanied by a modulation of patient body image, who referred the reshaping of the perceived phantom of the lost limb, now resembling more closely the healthy real arm, and an improvement of his phantom limb pain (Di Pino et al., 2012a,b).

Also targeted muscle reinnervation, the relocation of sensory and motors nerve fibers once devoted to the missing hand toward spared muscles above the line of amputation, could represent a good solution for human–machine interfacing devoted to prosthesis control (Kuiken et al., 2007). Indeed, in amputees this solution results in the return of motor task execution that reversed the previous shift of lost limb cortical motor representation (Chen et al., 2013).

The readdressing of aberrant cortical changes described so far well matches those produced by the transplantation of biological functional body parts. Recovered intracortical and corticospinal excitability was found in patients undergoing toe-to-thumb transfer for their lost thumb (Ni et al., 2010) or for the correct relocation of the functional sensorimotor representation of the grafted hands in bilateral amputees who underwent transplantation of both hands (Giraux et al., 2001). Reacquiring a lost or a new motor output drives brain plasticity also in case of central nervous system damage. Indeed, stroke patients exploiting a mu rhythm-driven magnetoencephalographic brain computer interface (BCI) to operate an orthesis controlling their paretic hand improved their ability to modulate mu rhythm (Buch et al., 2008).

Therefore, the evidence is in favor of a normalization of the aberrant motor cortical plasticity pushed by the reacquisition of a viable motor efference: The more the regained output resembles the previous physiologic condition, the more the normalization of cortical plasticity.

AUGMENTATION-INDUCED PLASTICITY

Although strictly inherent to human augmentation, the evidence on the evolution of neural plastic processes reviewed so far, is mainly inferred from parallel knowledge acquired from logically related paradigms. From now on, we will focus our discussion on the brain mechanisms that lie behind enhancing able-bodied ability. Augmentation is achieved through BMI, invasive or not, as well as with more traditional devices such as haptic manipulators and vibrotactile stimulators.

Humans have been shown able to acquire new, not-previously experienced, sensory modalities that are instead typical of other animal species. Vibrotactile stimulation can deliver inputs through gyroscopes, accelerometers and magnetometers-embedded in a belt, to be used for space orientation, (Nagel et al., 2005) or for "whisking" through an ad-hoc developed artificial whisker (Saig et al., 2010). Devices for haptic augmented reality are based on the same rationale. Artificial sensors mounted on a fingernail (Ando et al., 2002), on a pen-like tool (Nojima et al., 2002) or directly on an artificial skin layer (Kajimoto et al., 2003) extract from the environment visual information that a tactile display converts mostly into vibrations. A proficient interaction with those devices primarily relies on cross-modal plasticity in the user's brain. They have been designed to touch the untouchable and can find, for instance, in the enhancement of manipulative skills inside particular surgical theaters their operating field. Surgery under microscope and through robotic effectors can be considered a sort of human augmented scenario, as shown by the ability of transfer to the surgical tool, even a virtual one, multisensory integration properties that are proper of the body itself (Sengül et al., 2012). In humans exposed to an augmented task, the features of the tool adopted for functional augmentation influence the activation pattern of the brain. Indeed, surgeons involved in a laparoscopic procedure manifested higher intrahemispheric sensorimotor EEG coherence, probably because operating straight instruments in a bi-dimensional view requests an enhanced activation of primary and high-order areas. Surgeons performing the same task with the da Vinci® robotic surgical system, which offers more dexterous surgical instruments (EndoWrist) articulated like a wrist in a tridimensional view, had instead higher interhemispheric coherence and a more robust alpha and beta activity, perhaps underlying the enhanced exploitation of bimanuality accomplishing robotic-aided surgery (Bocci et al., 2013).

Proves of the acquisition of unnatural new sensory modalities through invasive brain machine interfaces have been documented in rodents. Rats reorganized their foraging behavior in function of infrared cues sensed by an IR detector directly interfaced with their barrel cortex. Here again, cross-modal plasticity

demonstrated to be the key of sensory augmentation. Remarkably, as previously described for the artificial transposition of retinal afferences to S1 that makes S1 responding to light (Métin and Frost, 1989), S1 neurons developed bimodal tactile-IR receptive fields. Unfortunately, it is impossible to disentangle if new inputs were perceived by rats as unnatural stimuli coming from the whiskers or as stimuli arising from a brand new sensory modality (Thomson et al., 2013).

Human augmentation realized some of its best potentialities, also starting to attract a wide attention from non-specialists since brain to machine interfaces have been employed to control artificial limbs, assistive grabbers or wheelchairs. Brain-machine (or computer) interfaces are intrinsic promoters of brain plasticity by forcing an unnatural function of cortical neurons that, instead of modulating the inferior spinal motor neuron, start to be the final nervous element of the motor output chain (Wolpaw, 2007). Moreover, brain machine interfaces give to users the opportunity to have a novel feedback of their brain activity, namely neurofeedback, which would be otherwise unavailable. Such a new form of awareness is a further determinant of brain plastic processes (Dobkin, 2007). The more the feedback on the state of the brain is given in an optimal modality and relayed with good accuracy and delay, the more it is able to support the process of reorganization (Grosse-Wentrup et al., 2011).

The execution of actions through brain machine interface is intentional and goal-directed, since those actions are learned worse if the action-reward contingency is altered or the weight of the reward is reduced (Koralek et al., 2012).

Controlling the output of a BCI, although the controlled task has not prevalent motor features, such as in the case of the control of a visual cursor or the modulation of the pitch of an auditory cursor, seems to be resolved by the brain similarly to a motor task. In this line, the achievement of proficiency is not dissimilar to the one involved in motor skills learning with an initial fast improvement of performance and a later phase of slower learning. In epileptic patients undergoing electrocorticography-monitoring, the control of a one degree-of-freedom BCI by volitional modulation of high gamma band produced a diffuse cortical activation, especially sensorimotor and visuomotor areas. The refinement of performance, achieved through the training, corresponded to a focalization of cortical recruitment, akin to what often seen following motor non-BMI training (Kelly and Garavan, 2005), with a decrement of activity in prefrontal, premotor and parietal cortex, probably due to the shift from a fully cognitive towards a more automatic control of the task (Wander et al., 2013). In a similar paradigm, an increase in non REM spindles has been reported, which witness a facilitation of synaptic plasticity (Johnson et al., 2012). Improvement of BMI control is strongly sustained by an increased striatal to M1 functional coupling (enhanced lower band coherence) and increased firing rate of the cortical-striatal projection. It is based on LTP-dependent plasticity, since mice with defective NMDA striatal receptors exhibit impaired ability to refine their performance (Koralek et al., 2012). The finding of a very similar enhancement of cortico-striatal functional coupling in normal subjects who learn to response with the most appropriate motor behavior to given visual stimuli (Toni et al., 2002) strongly supports the neural correlate correspondence of learning tasks executed exploiting physiological motor outputs or BMI.

A key issue explored in the present paper is whether the brain expand its motor control to a supernumerary limb. In monkeys, several studies documented the ability of the brain to control supernumerary, artificial limbs. Monkey implanted in their primary motor cortex were able to control a 5 degrees of freedom actuated arm for self-feeding, while their own real hand was restrained (Velliste et al., 2008). In a previous study, a significant performance decrease took place when the monkey independently used its own hand (Carmena et al., 2003). To the best of the authors' knowledge, so far, these findings have not been replicated in humans.

As far as the independency of real and artificial limb control is concerned, cortical motor neurons with augmented outputs, even if still devoted to the control of the natural arm, are able to arrange their activity in order to create what somehow may be considered as the cortical map of the neuroprosthesis. Indeed, in the presence of a constant transformation function of the recorded activity into movement of the external actuator, the learning process results in the formation of a functional neuronal compound, defined by the refinement of tuning parameters such as, preferred directions, mean firing rates and the depth of modulation (Ganguly and Carmena, 2009). The ensemble of neurons controlling the position of a cursor in a 3D space can also plastically adapt its behavior in front of a modification of the transformation function that produces a visuomotor rotation. Both rotated and especially non-rotated units shift their tuning toward the applied perturbation, but rotated units decrease their modulation depth in order to lower their influence on the preferred direction (Jarosiewicz et al., 2008), showing a relative selectivity of response in different subpopulation of neurons. A similar approach, but scaled at the level of entire brain, has been taken by Imamizu and colleagues, that demonstrated an activation of the posterior superior fissure of the cerebellum in subjects relearning to use a computer mouse that underwent a rotational transformation (Imamizu et al., 2000). Learning the use of two mice with alterations of different parameters (rotation and velocity) of their transformation functions activated contiguous, yet different, cerebellar areas (Imamizu et al., 2003). Authors explain cerebellar activity as the result of the formation of a tool-use internal model, a neural process mimicking the input-output flow of tool motor (and probably cognitive) constraints characterizing the interaction.

Amelioration of the intracortical BMI performance also affects the modulation of neuronal firing rate in motor, premotor supplementary motor and parietal regions to a level not directly correlated with the refinement of cursor kinematic. This firing-rate variance showed an inverse *u*-shape trend, increasing in the initial training and decreasing with the acquisition of proficiency, as if it was driven by a progressive reduction of prediction and execution error due, to a progressive refinement of the internal model of the external controlled device (Zacksenhouse et al., 2007). Such a progressive cortical representation of the neuroprosthesis seems to be stable, and ready to use at each new recording session, critical for task accuracy, (since the removal of neurons from the ensemble deeply impairs performance) and resistant

to interference since it keeps working even in parallel with the formation of new maps (Ganguly and Carmena, 2009). This body of evidence has enormous implications in favor of the relative stability of the neurons-behavioral links in neuroprosthetic as well as in natural control.

"To resume the section in a few words, controlling external augmenting devices through neural interfaces is resolved by the brain as it does by controlling normal motor output; in particular by building a cortical map of the motor efferences which change its features to achieve, day after day, a more proficient control".

MODULATING AUGMENTATION RELATED PLASTICITY

Along the present manuscript we showed how the propensity of the brain to be plastic can be considered as the fertile soil needed for a proficient implant of new input/output external aid. This implies that any attempt to increase the efficiency of any plastic brain changes or even to redirect them towards the desired direction could result in a more effective blend between the biological and the artificial component of any hybrid bionic system.

In this view, it is known that brain plasticity can be modulated through drugs. Especially noradrenergic agonists have been exploited to enhance M1 excitability (Ziemann et al., 2002), improve motor skill acquisition (Plewnia et al., 2004), learning language (Breitenstein et al., 2004) and in the motor recovery from stroke and other brain lesions (Gladstone and Black, 2000; Schuster et al., 2011). Recently, it has been hypothesized that motor improvement after the administration of amphetamine-like drugs may be due to a better visuomotor integration, with an increased functional coupling between right intraparietal and superior frontal premotor cortex (Grefkes et al., 2010). We already discussed the primary role that the right fronto-parietal circuit plays in augmentation-related plasticity.

Recently, non-invasive neuromodulatory techniques, mostly based on repetitive transcranial magnetic stimulation and transcranial direct current stimulation, have been introduced and showed to effectively inhibit or facilitate the excitability of the motor cortex, possibly through LTP/LTD-like mechanisms (Ziemann et al., 2008). For instance, in humans, transcranial direct current stimulation showed to be able to enhance not only motor skills (Nitsche et al., 2003) and movement speed accuracy (Reis et al., 2009), but also visuomotor coordination (Antal et al., 2004b), learning (Antal et al., 2004a) and frontal functions (Capone et al., 2014). Stimulation of motor cortex has been also successfully used to control chronic neuropatic pain of different etiology, possibly enhancing descending analgesic effects that limit aberrant afferent noxious signals and overall limiting maladaptive plasticity (Andrade et al., 2013; Bolognini et al., 2013a,b). However not invasive neuromodulation can be used also for modulating plasticity of frontal and associative cortices with the aim of cognitive enhancement in the domain of working memory (Andrews et al., 2011; Cantone et al., 2014), problem solution (Chi and Snyder, 2012) and creative intelligence (Cerruti and Schlaug, 2009). Paired associative stimulation is a neuromodulation paradigm that targets specifically sensorimotor integration process by repeating the coupled electrical stimulus to a peripheral nerve and a time-locked TMS pulse to the contralateral M1 (Stefan et al., 2002). Neither paired associative stimulation nor other non-invasive neuromodulatory techniques, perhaps targeting premotor of posterior parietal cortices have been applied, to our knowledge, to attempt to facilitate the embodiment of tools and prostheses. This should definitely deserve our future efforts.

Also less conventional non-invasive brain stimulation can improve augmentation plasticity, as for alpha frequency visual flickering that improves word recall (Williams, 2001). Sleep is a physiological prolonged activity, taking almost a third of our life, when the brain is extremely prone to undergo plastic remodeling especially linked with consolidation of memories (Diekelmann and Born, 2010). A bad sleep is known to negatively impact plastic processes, such as, for instance, those at the base of the recovery from stroke (Zunzunegui et al., 2011). Therefore its modulation could also enhance learning processes related to augmentation. Indeed, it has been shown how sleep-related plasticity can be modulated with transcranial stimulation (Marshall et al., 2006), or simply by delivering external odors (Rasch et al., 2007), with a significant impact on consolidated memory. The tight relation among BCI-related plasticity and sleep is sustained by the local increase of spindles, signs of a cortical state conductive to synaptic plasticity, in subjects trained to control a computer cursor via an electrocorticographic interface (Johnson et al., 2012).

Furthermore, different genetic substrates could have an impact in the individual propensity to be augmented. This can be inferred from the effect of different haplotypes on plasticity related paradigms. Indeed, The Val66Met polymorphism of the brain derived neurotrophic factor, present in about a third of the Caucasian population, has been associated with reduced sensitivity to plasticity-inducing neuromodulation (Cheeran et al., 2008) and with a worse recovery from stroke (Kim et al., 2012). The response of ADHD children to methylphenidate seems to be affected by the Val158Met polymorphism in the Catechol-O-methyltransferase (Kereszturi et al., 2008) and by the genotype of the dopamine transporter (Winsberg and Comings, 1999), which affects also the outcome of working memory training (Brehmer et al., 2009).

Also age-related effect could be taken into consideration as modulating factors for augmentation-related plasticity. Although the rate of enhancement of motor and cognitive ability is maximal at younger ages, when sensorimotor areas express their critical plastic period (Hensch, 2005), there is also evidence that augmentation-related plasticity can take place throughout the entire life span. Plasticity in primary visual (Kaas et al., 1990), auditory (Recanzone et al., 1993) and somatosensory cortices (Merzenich et al., 1984) has been described at later ages and cats deprived of vision during adulthood showed cross-modal improvement of the ability to localize sound, albeit lower than earlier deprived cats do (Rauschecker and Kniepert, 1994).

Finally, can augmentation-related plasticity always be enhanced or it may suffer from ceiling effects that limit the ability to be further augmented? Overtrained athletes can undergo the burnout syndrome (Winsley and Matos, 2011) and excessive use and training can be responsible of aberrant plasticity in sensorimotor areas and in the basal ganglia at the base of the focal

dystonia of expert players and musicians (Defazio et al., 2007). There are also reports of ceiling effect in cognitive enhancement (Kwok et al., 2011) and London taxi drivers, whit exceptional navigation ability, acquired worse new spatial memory as if the hyper-representation of posterior hippocampus may undermined new plasticity in the anterior hippocampus (Maguire et al., 2006). However, sometimes improvement can undergo false ceiling effects due to precocious delegation of not yet consolidated functions to brain networks in charge of automaticity (Ericsson, 2007).

CONCLUSION

SUMMARY OF THE EVIDENCE ON AUGMENTING-RELATED PLASTICITY

From the body of literature reviewed in the present paper, a few conclusions can be drawn.

First, augmentation-related plasticity takes place at the cellular level, likely through synaptic signals, as evidenced by changes of gray matter thickness and even with neurogenesis in the dentate gyrus.

Second, a number of brain areas have been identified as likely actors of augmentation-based plasticity, playing a role at different stage of the process (**Figure 2**). The representation of the external world in primary sensory areas is extremely sensitive to activity that modulates their tuning parameters. These cortices are able to accept afferences from different physiological or artificial sensory modalities by shaping the receptive fields of their neurons to make them sensitive to novel kinds of sensory input.

Also M1 is highly susceptible to modulation of cortical representation and corticospinal excitability. The control of neuroprostheses recruits motor and premotor areas, and the acquisition of the skillful use of them promotes the recovery of the cortical representation of a lost limb and its functional interplay with related regions. Training-based skill acquisition gradually decreases attentional recruitment, focusing the activity on sensorimotor areas and increasing the basal ganglia drive of cortical activity. Indeed, the brain can learn to deal with neuroprostheses as it does with normal motor outputs, producing similar learning curves in both conditions.

The frontoparietal network is another functional actor that plays the key role in augmentation-related plasticity. It is strongly recruited in the initial phase of the acquisition of a new motor ability. Premotor cortex is also activated to learn to control an external effector, controls tool motor representation and together with the intraparietal sulcus, which contributes to extracting the visual features of the tool, is the main substrate for artifact embodiment. In these areas, neurons responsible for multisensory integration can be modified to extend their receptive fields and assimilate a supernumerary limb. An anthropomorphic sensorized prosthesis provides the critical sensory afferences needed for a full, comfortable embodiment, and thus optima efficiency, of the artifact. By operating a neuroprosthesis, the brain builds up a cortical representation of the device. This process selectively involves subgroup of interfaced neurons that plastically adapt their firing rate to refine the kinematic parameters and reduce the execution error.

The mirror system of premotor and parietal areas may exert a role in understanding the meaning of an action performed with anthropomorphic augmentation devices and in learning to operate them. Furthermore, plasticity in posterior parietal cortex is responsible also for the assimilation of artificial sensory modalities and for the complex behavioral advantages that from this derive.

Finally, plasticity in the attentional frontoparietal network is the main target of cognitive enhancement, achieved as a corollary effect of sensorimotor augmentation or, selectively, by modulating the neurochemical signals ascending from the brainstem. The hippocampus contributes by undergoing memory-induced changes. The insula and the cerebellum are involved in augmentation-related plasticity too. The cerebellar cortex is activated during the learning of a tool or a neuroprosthesis, contributing to their embodiment; furthermore its activation is related to the formation of an internal model of the external effector. The insula plays a role in the interoception of the embodied artifact and in the relationship of augmented skills with emotions.

FUTURE PERSPECTIVES

The evidence provided in this review, unmasks the ability of the central nervous system of primates and humans, not only to master the use of external tools, but also to plastically reshape the body representation and the very sense of the self in favor of a more affordable sensing, and operating in the environment (Clark, 2007).

Central to the topic of the present review is the integration of any augmentative device in the global sense of the self of the user. Operatively, the sense that conscious experience is bound to the self has been defined to emerge from a series of elements including the feeling of body ownership, the perception of self-location in space and the observation of our own body and outside world according to a first-person perspective (Blanke, 2012). The sense of self can be notably disrupted in pathological conditions affecting a single body part such as somatoparaphrenia (the denial of ownership of contralesional limbs, following brain damage) (Vallar and Ronchi, 2009) or the whole body, such as in the out-of-the-body experience phenomena (Blanke and Mohr, 2005). An experimental modulation of the sense of the self for the whole body has been famously demonstrated using the "full body illusion" procedures, in which participants receive tactile strokes, while seeing their own body, filmed by a camera, receiving synchronous or asynchronous strokes of homologous body regions (back/chest). Following this procedure, a variety of illusions of self-identification with the virtual body (Lenggenhager et al., 2007), with the camera viewpoint (as if looking to an alien body), as well as modulation of sensory experience (Aspell et al., 2009; Romano et al., 2014) have been obtained. Different aspects of corporeal self consciousness have been linked to the activation of different brain structures, including premotor, parietal (somatosensory and IPS), extrastriate (EBA) and putaminal regions, as well as the temporoparietal junction, as the result of a process of multisensory integration involving visual, somatosensory and vestibular input (see Blanke, 2012 for review).

The knowledge acquired on the mechanisms of body ownership and, in general, self identification, may put the basis for understanding how plasticity-induced brain augmentation may contribute to the recovery or the enhancement of the sense of

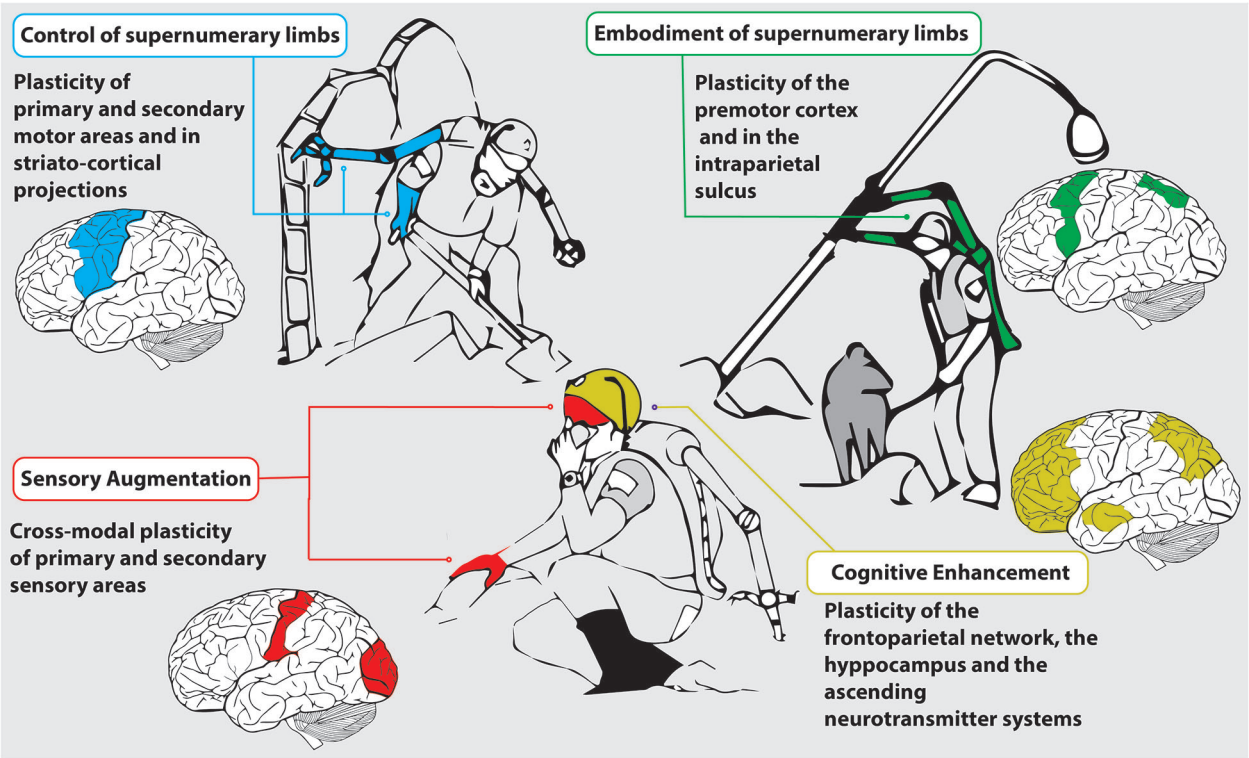

FIGURE 2 | Possible applicative scenario of human augmentation. Rescuers dug through the rubble of collapsed buildings looking for survivors in the wake of an earthquake exploiting artificial supernumerary limbs (light blue and green), artificial organs of sense (red) and cognitive enhancement (yellow). The most relevant areas of the brain recruited by the task are drown on the side. Control of supernumerary limbs mostly relies on primary and secondary sensorimotor areas and on the facilitation of striato-cortical projection, their embodiment in changes especially taking place in the premotor cortex and in the intraparietal sulcus. Sensory augmentation is enabled by cross-modal plasticity of sensory areas, while cognitive enhancement has in the neural plasticity of the frontoparietal network, of the hippocampus and in the facilitation of the ascending neurotransmitter system its neurobiological substrate.

the self. The more straightforward situation to think about is certainly the case of amputation. As discussed previously, a key role of functional prostheses is to allow the rebuilt of a full sense of ownership and agency of the prosthesis through a process of training-induced, embodiment (Ehrsson et al., 2008; Marasco et al., 2011; D'Alonzo and Cipriani, 2012; Mulvey et al., 2012). In this respect, the plasticity induced by functional prostheses (Di Pino et al., 2009; Rossini et al., 2010; Maruishi et al., 2004), targets similar sensorimotor brain areas as those modulated by paradigms inducing illusory sense of ownership for alien body parts and could constitute the basis of a full inclusion of external devices into the self as well as the extension of visuo-tactile integration properties to an external augmentation device (Marini et al., 2014).

Indeed, the evaluation of whole brain activity, and the monitoring of cortico-cortical connectivity, for instance by means of functional magnetic resonance, in primates undergoing motor output augmentation through BMI, of which literature to the best of authors knowledge is still wanting, would be of utmost value to depict a comprehensive picture of brain processes underlying augmentation. Such studies could be of out-breaking relevance in order to understand the interplay among different brain structures in the buildup of plasticity, as well as for the monitoring of the neural substrates of possible conditions (pain, emotional distress) that may co-occur as severe side effects.

Finally, we saw how the plastic changes resulting from the interaction with external devices are the necessary neural correlates of functional augmentation, of learning new skills and exploiting artificial senses. Plasticity allows evolving the exploitation of tools through their embodiment and it is strongly correlated with how much the interface constituting the hybrid bionic system is direct and intuitive. We thus propose that, in parallel with more classical instruments for performance monitoring, methods for the functional evaluation of the augmentation-related plasticity, can provide reliable and comprehensive measures of the effectiveness achieved by the hybrid bionic system in accomplishing augmentation.

AUTHOR AND CONTRIBUTORS

Giovanni Di Pino chose the topic, conceived the design of the manuscript and wrote the main text. Angelo Maravita was in charge of the sections on tools use and embodiment. Loredana Zollo took care of the section on prostheses. Eugenio Guglielmelli and Vincenzo Di Lazzaro deeply revised the manuscript. All the

authors checked and approved the final submitted version of the manuscript.

ACKNOWLEDGMENTS

This work was partially supported by the National Project of the Italian Ministry of Research, PRIN 2010, HANDBOT—Biomechatronic and Prostheses Endowed with Bio-inspired Tactile Perception, Bi-directional Neural Interfaces and Distributed Sensorymotor Control, CUP: B81J12002680008".

REFERENCES

Aglioti, S. M., Cesari, P., Romani, M., and Urgesi, C. (2008). Action anticipation and motor resonance in elite basketball players. *Nat. Neurosci.* 11, 1109–1116. doi: 10.1038/nn.2182

Ambrose, S. H. (2001). Paleolithic technology and human evolution. *Science* 291, 1748–1753. doi: 10.1126/science.1059487

Ando, H., Miki, T., Inami, M., and Maeda, T. (2002). The nail-mounted tactile display for the behavior modeling. Proceedings of the ACM SIGGRAPH 2002. conference abstracts and applications; ACM.

Andrade, D. C., Borges, I., Bravo, G. L., Bolognini, N., and Fregni, F. (2013). Therapeutic time window of noninvasive brain stimulation for pain treatment: inhibition of maladaptive plasticity with early intervention. *Expert Rev. Med. Devices* 10, 339–352. doi: 10.1586/erd.12.90

Andrews, S. C., Hoy, K. E., Enticott, P. G., Daskalakis, Z. J., and Fitzgerald, P. B. (2011). Improving working memory: the effect of combining cognitive activity and anodal transcranial direct current stimulation to the left dorsolateral prefrontal cortex. *Brain Stimul.* 4, 84–89. doi: 10.1016/j.brs.2010.06.004

Angelakis, E., Stathopoulou, S., Frymiare, J. L., Green, D. L., Lubar, J. F., and Kounios, J. (2007). EEG neurofeedback: a brief overview and an example of peak alpha frequency training for cognitive enhancement in the elderly. *Clin. Neuropsychol.* 21, 110–129. doi: 10.1080/13854040600744839

Anguera, J. A., Boccanfuso, J., Rintoul, J. L., Al-Hashimi, O., Faraji, F., Janowich, J., et al. (2013). Video game training enhances cognitive control in older adults. *Nature* 501, 97–101. doi: 10.1038/nature12486

Antal, A., Nitsche, M. A., Kincses, T. Z., Kruse, W., Hoffmann, K. P., and Paulus, W. (2004a). Facilitation of visuo-motor learning by transcranial direct current stimulation of the motor and extrastriate visual areas in humans. *Eur. J. Neurosci.* 19, 2888–2892. doi: 10.1111/j.1460-9568.2004.03367.x

Antal, A., Nitsche, M. A., Kruse, W., Kincses, T. Z., Hoffmann, K.-P., and Paulus, W. (2004b). Direct current stimulation over V5 enhances visuomotor coordination by improving motion perception in humans. *J. Cogn. Neurosci.* 16, 521–527. doi: 10.1162/089892904323057263

Armel, K. C., and Ramachandran, V. S. (2003). Projecting sensations to external objects: evidence from skin conductance response. *Proc. Biol. Sci.* 270, 1499–1506. doi: 10.1098/rspb.2003.2364

Aspell, J. E., Lenggenhager, B., and Blanke, O. (2009). Keeping in touch with one's self: multisensory mechanisms of self-consciousness. *PLoS One* 4:e6488. doi: 10.1371/journal.pone.0006488

Bach-y-Rita, P., and W Kercel, S. (2003). Sensory substitution and the human–machine interface. *Trends Cogn. Sci.* 7, 541–546. doi: 10.1016/j.tics.2003.10.013

Bailey, C. H., and Kandel, E. R. (2008). Synaptic remodeling, synaptic growth and the storage of long-term memory in Aplysia. *Prog. Brain Res.* 169, 179–198. doi: 10.1016/s0079-6123(07)00010-6

Baumeister, J., Reinecke, K., Liesen, H., and Weiss, M. (2008). Cortical activity of skilled performance in a complex sports related motor task. *Eur. J. Appl. Physiol.* 104, 625–631. doi: 10.1007/s00421-008-0811-x

Bavelier, D., Brozinsky, C., Tomann, A., Mitchell, T., Neville, H., and Liu, G. (2001). Impact of early deafness and early exposure to sign language on the cerebral organization for motion processing. *J. Neurosci.* 21, 8931–8942.

Bavelier, D., and Neville, H. J. (2002). Cross-modal plasticity: where and how? *Nat. Rev. Neurosci.* 3, 443–452. doi: 10.1038/nrn848

Bavelier, D., Tomann, A., Hutton, C., Mitchell, T., Corina, D., Liu, G., et al. (2000). Visual attention to the periphery is enhanced in congenitally deaf individuals. *J. Neurosci.* 20, RC93.

Birbaumer, N., and Cohen, L. G. (2007). Brain-computer interfaces: communication and restoration of movement in paralysis. *J. Physiol.* 579, 621–636. doi: 10.1113/jphysiol.2006.125633

Blanke, O. (2012). Multisensory brain mechanisms of bodily self-consciousness. *Nat. Rev. Neurosci.* 13, 556–571. doi: 10.1038/nrn3292

Blanke, O., and Aspell, J. E. (2009). Brain technologies raise unprecedented ethical challenges. *Nature* 458, 703–703. doi: 10.1038/458703b

Blanke, O., and Mohr, C. (2005). Out-of-body experience, heautoscopy, and autoscopic hallucination of neurological origin: implications for neurocognitive mechanisms of corporeal awareness and self-consciousness. *Brain Res. Brain Res. Rev.* 50, 184–199. doi: 10.1016/j.brainresrev.2005.05.008

Bliss, T. V., and Lomo, T. (1973). Long-lasting potentiation of synaptic transmission in the dentate area of the anaesthetized rabbit following stimulation of the perforant path. *J. Physiol.* 232, 331–356.

Blom, R. M., Hennekam, R. C., and Denys, D. (2012). Body integrity identity disorder. *PLoS One* 7:e34702. doi: 10.1371/journal.pone.0034702

Bocci, T., Moretto, C., Tognazzi, S., Briscese, L., Naraci, M., Leocani, L., et al. (2013). How does a surgeon's brain buzz? An EEG coherence study on the interaction between humans and robot. *Behav. Brain Funct.* 9:14. doi: 10.1186/1744-9081-9-14

Bolognini, N., Olgiati, E., Maravita, A., Ferraro, F., and Fregni, F. (2013a). Motor and parietal cortex stimulation for phantom limb pain and sensations. *Pain* 154, 1274–1280. doi: 10.1016/j.pain.2013.03.040

Bolognini, N., Spandri, V., Olgiati, E., Fregni, F., Ferraro, F., and Maravita, A. (2013b). Long-term analgesic effects of transcranial direct current stimulation of the motor cortex on phantom limb and stump pain: a case report. *J. Pain Symptom Manage.* 46, e1–e4. doi: 10.1016/j.jpainsymman.2013.06.014

Bostrom, N., and Sandberg, A. (2009). Cognitive enhancement: methods, ethics, regulatory challenges. *Sci. Eng. Ethics.* 15, 311–341. doi: 10.1007/s11948-009-9142-5

Botvinick, M., and Cohen, J. (1998). Rubber hands "feel" touch that eyes see. *Nature* 391, 756–756. doi: 10.1038/35784

Brehmer, Y., Westerberg, H., Bellander, M., Fürth, D., Karlsson, S., and Bäckman, L. (2009). Working memory plasticity modulated by dopamine transporter genotype. *Neurosci. Lett.* 467, 117–120. doi: 10.1016/j.neulet.2009.10.018

Breitenstein, C., Wailke, S., Bushuven, S., Kamping, S., Zwitserlood, P., Ringelstein, E. B., et al. (2004). D-amphetamine boosts language learning independent of its cardiovascular and motor arousing effects. *Neuropsychopharmacology* 29, 1704–1714. doi: 10.1038/sj.npp.1300464

Bremmer, F., Schlack, A., Shah, N. J., Zafiris, O., Kubischik, M., Hoffmann, K.-P., et al. (2001). Polymodal motion processing in posterior parietal and premotor cortex: a human fMRI study strongly implies equivalencies between humans and monkeys. *Neuron* 29, 287–296. doi: 10.1016/s0896-6273(01)00198-2

Brindley, G. S. (1974). Emptying the bladder by stimulating sacral ventral roots. *J. Physiol.* 237, 15P–16P.

Brozzoli, C., Gentile, G., and Ehrsson, H. H. (2012). That's near my hand! parietal and premotor coding of hand-centered space contributes to localization and self-attribution of the hand. *J. Neurosci.* 32, 14573–14582. doi: 10.1523/jneurosci.2660-12.2012

Buch, E., Weber, C., Cohen, L. G., Braun, C., Dimyan, M. A., Ard, T., et al. (2008). Think to move: a neuromagnetic brain-computer interface (BCI) system for chronic stroke. *Stroke* 39, 910–917. doi: 10.1161/strokeaha.107.505313

Büchel, C., Price, C., Frackowiak, R., and Friston, K. (1998). Different activation patterns in the visual cortex of late and congenitally blind subjects. *Brain* 121, 409–419. doi: 10.1093/brain/121.3.409

Buonomano, D. V., and Merzenich, M. M. (1998). Cortical plasticity: from synapses to maps. *Annu. Rev. Neurosci.* 21, 149–186. doi: 10.1146/annurev.neuro.21.1.149

Cantone, M., Di Pino, G., Capone, F., Piombo, M., Chiarello, D., and Cheeran, B. (2014). The contribution of transcranial magnetic stimulation in the diagnosis and in the management of dementia. *Clin. Neurophysiol.* doi: 10.1016/j.clinph.2014.04.010. [Epub ahead of print].

Capone, F., Capone, G., Ranieri, F., Di Pino, G., Oricchio, G., and Di Lazzaro, V. (2014). The effect of practice on random number generation task: a transcranial direct current stimulation study. *Neurobiol. Learn. Mem.* 114C, 51–57. doi: 10.1016/j.nlm.2014.04.013

Cardinali, L., Frassinetti, F., Brozzoli, C., Urquizar, C., Roy, A. C., and Farnè, A. (2009). Tool-use induces morphological updating of the body schema. *Curr. Biol.* 19, R478–R479. doi: 10.1016/j.cub.2009.05.009

Carmena, J. M., Lebedev, M. A., Crist, R. E., O'Doherty, J. E., Santucci, D. M., Dimitrov, D. F., et al. (2003). Learning to control a brain-machine interface for

reaching and grasping by primates. *PLoS Biol.* 1:E42. doi: 10.1371/journal.pbio.0000042

Cerruti, C., and Schlaug, G. (2009). Anodal transcranial direct current stimulation of the prefrontal cortex enhances complex verbal associative thought. *J. Cogn. Neurosci.* 21, 1980–1987. doi: 10.1162/jocn.2008.21143

Cheeran, B., Talelli, P., Mori, F., Koch, G., Suppa, A., Edwards, M., et al. (2008). A common polymorphism in the brain-derived neurotrophic factor gene (BDNF) modulates human cortical plasticity and the response to rTMS. *J. Physiol.* 586, 5717–5725. doi: 10.1113/jphysiol.2008.159905

Chen, A., Yao, J., Kuiken, T., and Dewald, J. P. (2013). Cortical motor activity and reorganization following upper-limb amputation and subsequent targeted reinnervation. *Neuroimage Clin.* 3, 498–506. doi: 10.1016/j.nicl.2013.10.001

Chen, R., Cohen, L. G., and Hallett, M. (2002). Nervous system reorganization following injury. *Neuroscience* 111, 761–773. doi: 10.1016/s0306-4522(02)00025-8

Chi, R. P., and Snyder, A. W. (2012). Brain stimulation enables the solution of an inherently difficult problem. *Neurosci. Lett.* 515, 121–124. doi: 10.1016/j.neulet.2012.03.012

Clark, A. (2007). Re-inventing ourselves: the plasticity of embodiment, sensing and mind. *J. Med. Philos.* 32, 263–282. doi: 10.1080/03605310701397024

Clark, K. B., Naritoku, D. K., Smith, D. C., Browning, R. A., and Jensen, R. A. (1999). Enhanced recognition memory following vagus nerve stimulation in human subjects. *Nat. Neurosci.* 2, 94–98. doi: 10.1038/4600

Cohen, L. G., Celnik, P., Pascual-Leone, A., Corwell, B., Faiz, L., Dambrosia, J., et al. (1997). Functional relevance of cross-modal plasticity in blind humans. *Nature* 389, 180–183. doi: 10.1038/38278

Creem-Regehr, S. H., and Lee, J. N. (2005). Neural representations of graspable objects: are tools special? *Brain Res. Cogn. Brain Res.* 22, 457–469. doi: 10.1016/j.cogbrainres.2004.10.006

D'Alonzo, M., and Cipriani, C. (2012). Vibrotactile sensory substitution elicits feeling of ownership of an alien hand. *PLoS One* 7:e50756. doi: 10.1371/journal.pone.0050756

Dahlin, E., Nyberg, L., Bäckman, L., and Neely, A. S. (2008). Plasticity of executive functioning in young and older adults: immediate training gains, transfer and long-term maintenance. *Psychol. Aging* 23, 720–730. doi: 10.1037/a0014296

Dario, P., Sandini, G., and Aebischer, P. (1993). "Robots and biological systems: towards a new bionics?," in *Proceedings of the NATO Advanced Workshop on Robots and Biological Systems*. Available at http://www.springer.com/computer/ai/book/978-3-540-56158-3

De Volder, A. G., Catalan-Ahumada, M., Robert, A., Bol, A., Labar, D., Coppens, A., et al. (1999). Changes in occipital cortex activity in early blind humans using a sensory substitution device. *Brain Res.* 826, 128–134. doi: 10.1016/s0006-8993(99)01275-5

Defazio, G., Berardelli, A., and Hallett, M. (2007). Do primary adult-onset focal dystonias share aetiological factors? *Brain* 130, 1183–1193. doi: 10.1093/brain/awl355

Di Lazzaro, V., Oliviero, A., Pilato, F., Saturno, E., Dileone, M., Marra, C., et al. (2005). Neurophysiological predictors of long term response to AChE inhibitors in AD patients. *J. Neurol. Neurosurg. Psychiatry* 76, 1064–1069. doi: 10.1136/jnnp.2004.051334

Di Pino, G., Benvenuto, A., Cavallo, G., Denaro, L., Denaro, V., Ferreri, F., et al. (2012a). "In human implant of intraneural multielectrodes for controlling a 5-fingered hand prosthesis and delivering sensorial feedback," in *Grasping the Future: Advances in Powered Upper Limb Prosthetics*, eds V. P. Castelli and M. Troncossi (Beijing, P. R. China: Bentham Science Publishers), 28–38.

Di Pino, G., Benvenuto, A., Tombini, M., Cavallo, G., Denaro, L., Denaro, V., et al. (2012b). Overview of the implant of intraneural multielectrodes in human for controlling a 5-fingered hand prosthesis, delivering sensorial feedback and producing rehabilitative neuroplasticity. Proceedings of the Biomedical Robotics and Biomechatronics (BioRob), 4th IEEE RAS and EMBS International Conference on 2012.

Di Pino, G., Denaro, L., Vadala, G., Marinozzi, A., Tombini, M., Ferreri, F., et al. (2013). Invasive neural interfaces: the perspective of the surgeon. *J. Surg. Res.* 188, 77–87. doi: 10.1016/j.jss.2013.12.014

Di Pino, G., Guglielmelli, E., and Rossini, P. M. (2009). Neuroplasticity in amputees: main implications on bidirectional interfacing of cybernetic hand prostheses. *Prog. Neurobiol.* 88, 114–126. doi: 10.1016/j.pneurobio.2009.03.001

Di Pino, G., Porcaro, C., Tombini, M., Assenza, G., Pellegrino, G., Tecchio, F., et al. (2012c). A neurally-interfaced hand prosthesis tuned inter-hemispheric communication. *Restor. Neurol. Neurosci.* 30, 407–418. doi: 10.3233/RNN-2012-120224

Diekelmann, S., and Born, J. (2010). The memory function of sleep. *Nat. Rev. Neurosci.* 11, 114–126. doi: 10.1038/nrn2762

Dobkin, B. H. (2007). Brain-computer interface technology as a tool to augment plasticity and outcomes for neurological rehabilitation. *J. Physiol.* 579, 637–642. doi: 10.1113/jphysiol.2006.123067

Draganski, B., Gaser, C., Busch, V., Schuierer, G., Bogdahn, U., and May, A. (2004). Neuroplasticity: changes in grey matter induced by training. *Nature* 427, 311–312. doi: 10.1038/427311a

Driemeyer, J., Boyke, J., Gaser, C., Büchel, C., and May, A. (2008). Changes in gray matter induced by learning—revisited. *PLoS One* 3:e2669. doi: 10.1371/journal.pone.0002669

Egner, T., and Gruzelier, J. (2004). EEG biofeedback of low beta band components: frequency-specific effects on variables of attention and event-related brain potentials. *Clin. Neurophysiol.* 115, 131–139. doi: 10.1016/s1388-2457(03)00353-5

Ehrsson, H. H., Holmes, N. P., and Passingham, R. E. (2005). Touching a rubber hand: feeling of body ownership is associated with activity in multisensory brain areas. *J. Neurosci.* 25, 10564–10573. doi: 10.1523/jneurosci.0800-05.2005

Ehrsson, H. H., Rosen, B., Stockselius, A., Ragno, C., Kohler, P., and Lundborg, G. (2008). Upper limb amputees can be induced to experience a rubber hand as their own. *Brain* 131, 3443–3452. doi: 10.1093/brain/awn297

Ehrsson, H. H., Spence, C., and Passingham, R. E. (2004). That's my hand! Activity in premotor cortex reflects feeling of ownership of a limb. *Science* 305, 875–877. doi: 10.1126/science.1097011

Ehrsson, H. H., Wiech, K., Weiskopf, N., Dolan, R. J., and Passingham, R. E. (2007). Threatening a rubber hand that you feel is yours elicits a cortical anxiety response. *Proc. Natl. Acad. Sci. U S A* 104, 9828–9833. doi: 10.1073/pnas.0610011104

Ehrsson, H. H. (2009). How many arms make a pair? Perceptual illusion of having an additional limb. *Perception* 38, 310–312. doi: 10.1068/p6304

Elbert, T., Pantev, C., Wienbruch, C., Rockstroh, B., and Taub, E. (1995). Increased cortical representation of the fingers of the left hand in string players. *Science* 270, 305–307. doi: 10.1126/science.270.5234.305

Ericsson, K. A. (2007). Deliberate practice and the modifiability of body and mind: Toward a science of the structure and acquisition of expert and elite performance. *Int. J. Sport. Psychol.* 38, 4–34.

Esposito, R., Cilli, F., Pieramico, V., Ferretti, A., Macchia, A., Tommasi, M., et al. (2013). Acute effects of modafinil on brain resting state networks in young healthy subjects. *PLoS One* 8:e69224. doi: 10.1371/journal.pone.0069224

Farah, M. J., Illes, J., Cook-Deegan, R., Gardner, H., Kandel, E., King, P., et al. (2004). Neurocognitive enhancement: what can we do and what should we do? *Nat. Rev. Neurosci.* 5, 421–425. doi: 10.1038/nrn1390

Farb, N. A., Segal, Z. V., Mayberg, H., Bean, J., McKeon, D., Fatima, Z., et al. (2007). Attending to the present: mindfulness meditation reveals distinct neural modes of self-reference. *Soc. Cogn. Affect. Neurosci.* 2, 313–322. doi: 10.1093/scan/nsm030

Ferreri, F., Ponzo, D., Vollero, L., Guerra, A., Di Pino, G., Petrichella, S., et al. (2014). Does an intraneural interface short-term implant for robotic hand control modulate sensorimotor cortical integration? An EEG-TMS co-registration study on a human amputee. *Restor. Neurol. Neurosci.* 32, 281–292. doi: 10.3233/RNN-130347

Finney, E. M., and Dobkins, K. R. (2001). Visual contrast sensitivity in deaf versus hearing populations: exploring the perceptual consequences of auditory deprivation and experience with a visual language. *Brain Res. Cogn. Brain Res.* 11, 171–183. doi: 10.1016/s0926-6410(00)00082-3

Flor, H., Elbert, T., Knecht, S., Wienbruch, C., Pantev, C., Birbaumer, N., et al. (1995). Phantom-limb pain as a perceptual correlate of cortical reorganization following arm amputation. *Nature* 375, 482–484. doi: 10.1038/375482a0

Fogassi, L., Gallese, V., Fadiga, L., Luppino, G., Matelli, M., and Rizzolatti, G. (1996). Coding of peripersonal space in inferior premotor cortex (area F4). *J. Neurophysiol.* 76, 141–157.

Fourkas, A. D., Bonavolontà, V., Avenanti, A., and Aglioti, S. M. (2008). Kinesthetic imagery and tool-specific modulation of corticospinal representations in expert tennis players. *Cereb. Cortex* 18, 2382–2390. doi: 10.1093/cercor/bhn005

Gallese, V., Fadiga, L., Fogassi, L., and Rizzolatti, G. (1996). Action recognition in the premotor cortex. *Brain* 119, 593–609. doi: 10.1093/brain/119.2.593

Ganguly, K., and Carmena, J. M. (2009). Emergence of a stable cortical map for neuroprosthetic control. *PLoS Biol.* 7:e1000153. doi: 10.1371/journal.pbio.1000153

Germain, L., and Lamarre, Y. (1993). Neuronal activity in the motor and premotor cortices before and after learning the associations between auditory stimuli and motor responses. *Brain Res.* 611, 175–179. doi: 10.1016/0006-8993(93)91792-q

Gibson, J. J. (1977). "The theory of affordances," in *Perceiving, Acting and Knowing. Towards an Ecological Psychology*, eds R. Shaw and J. Bransford (Hoboken, NJ: John Wiley and Sons Inc.), 67–82.

Gibson, J. J. (1986). *The Ecological Approach to Visual Perception.* Hillsdale, NJ: Psychology Press.

Giraux, P., Sirigu, A., Schneider, F., and Dubernard, J.-M. (2001). Cortical reorganization in motor cortex after graft of both hands. *Nat. Neurosci.* 4, 691–692. doi: 10.1038/89472

Giummarra, M. J., Georgiou-Karistianis, N., Nicholls, M. E., and Bradshaw, J. L. (2011). The third hand: ownership of a rubber hand in addition to the existing (phantom) hand. *Cortex* 47, 998–1000. doi: 10.1016/j.cortex.2011.02.010

Giummarra, M. J., Gibson, S. J., Georgiou-Karistianis, N., and Bradshaw, J. L. (2008). Mechanisms underlying embodiment, disembodiment and loss of embodiment. *Neurosci. Biobehav. Rev.* 32, 143–160. doi: 10.1016/j.neubiorev.2007.07.001

Gizewski, E., Gasser, T., de Greiff, A., Boehm, A., and Forsting, M. (2003). Cross-modal plasticity for sensory and motor activation patterns in blind subjects. *Neuroimage* 19, 968–975. doi: 10.1016/s1053-8119(03)00114-9

Gladstone, D. J., and Black, S. E. (2000). Enhancing recovery after stroke with noradrenergic pharmacotherapy: a new frontier? *Can. J. Neurol. Sci.* 27, 97–105.

Goldenberg, G. (2003). Apraxia and beyond: life and work of Hugo Liepmann. *Cortex* 39, 509–524. doi: 10.1016/s0010-9452(08)70261-2

Grafton, S. T., Mazziotta, J. C., Presty, S., Friston, K. J., Frackowiak, R., and Phelps, M. E. (1992). Functional anatomy of human procedural learning determined with regional cerebral blood flow and PET. *J. Neurosci.* 12, 2542–2548.

Graziano, M. S., Yap, G. S., and Gross, C. G. (1994). Coding of visual space by premotor neurons. *Science* 266, 1054–1057. doi: 10.1126/science.7973661

Grefkes, C., Wang, L. E., Eickhoff, S. B., and Fink, G. R. (2010). Noradrenergic modulation of cortical networks engaged in visuomotor processing. *Cereb. Cortex* 20, 783–797. doi: 10.1093/cercor/bhp144

Grosse-Wentrup, M., Mattia, D., and Oweiss, K. (2011). Using brain-computer interfaces to induce neural plasticity and restore function. *J. Neural Eng.* 8:025004. doi: 10.1088/1741-2560/8/2/025004

Guterstam, A., Gentile, G., and Ehrsson, H. H. (2013). The invisible hand illusion: multisensory integration leads to the embodiment of a discrete volume of empty space. *J. Cogn. Neurosci.* 25, 1078–1099. doi: 10.1162/jocn_a_00393

Guterstam, A., Petkova, V. I., and Ehrsson, H. H. (2011). The illusion of owning a third arm. *PLoS One* 6:e17208. doi: 10.1371/journal.pone.0017208

Halligan, P., and Marshall, J. (1995). Supernumerary phantom limb after right hemispheric stroke. *J. Neurol. Neurosurg. Psychiatry* 59, 341–342. doi: 10.1136/jnnp.59.3.341-a

Hebb, D. O. (1949). *The Organization of Behavior.* New York: Wiley.

Hensch, T. K. (2005). Critical period plasticity in local cortical circuits. *Nat. Rev. Neurosci.* 6, 877–888. doi: 10.1038/nrn1787

Hochberg, L. R., Serruya, M. D., Friehs, G. M., Mukand, J. A., Saleh, M., Caplan, A. H., et al. (2006). Neuronal ensemble control of prosthetic devices by a human with tetraplegia. *Nature* 442, 164–171. doi: 10.1038/nature04970

Holmes, J., Gathercole, S. E., and Dunning, D. L. (2009). Adaptive training leads to sustained enhancement of poor working memory in children. *Dev. Sci.* 12, F9–F15. doi: 10.1111/j.1467-7687.2009.00848.x

Hölzel, B. K., Carmody, J., Vangel, M., Congleton, C., Yerramsetti, S. M., Gard, T., et al. (2011). Mindfulness practice leads to increases in regional brain gray matter density. *Psychiatry Res.* 191, 36–43. doi: 10.1016/j.pscychresns.2010.08.006

Hölzel, B. K., Ott, U., Gard, T., Hempel, H., Weygandt, M., Morgen, K., et al. (2008). Investigation of mindfulness meditation practitioners with voxel-based morphometry. *Soc. Cogn. Affect. Neurosci.* 3, 55–61. doi: 10.1093/scan/nsm038

Husain, M., and Mehta, M. A. (2011). Cognitive enhancement by drugs in health and disease. *Trends Cogn. Sci.* 15, 28–36. doi: 10.1016/j.tics.2010.11.002

Imamizu, H., Kuroda, T., Miyauchi, S., Yoshioka, T., and Kawato, M. (2003). Modular organization of internal models of tools in the human cerebellum. *Proc. Natl. Acad. Sci. U S A* 100, 5461–5466. doi: 10.1073/pnas.0835746100

Imamizu, H., Miyauchi, S., Tamada, T., Sasaki, Y., Takino, R., Pütz, B., et al. (2000). Human cerebellar activity reflecting an acquired internal model of a new tool. *Nature* 403, 192–195. doi: 10.1038/35003194

Inoue, K., Kawashima, R., Sugiura, M., Ogawa, A., Schormann, T., Zilles, K., et al. (2001). Activation in the ipsilateral posterior parietal cortex during tool use: a PET study. *Neuroimage* 14, 1469–1475. doi: 10.1006/nimg.2001.0942

Iriki, A., Tanaka, M., and Iwamura, Y. (1996). Coding of modified body schema during tool use by macaque postcentral neurones. *Neuroreport* 7, 2325–2330. doi: 10.1097/00001756-199610020-00010

Ishibashi, H., Hihara, S., Takahashi, M., Heike, T., Yokota, T., and Iriki, A. (2002). Tool-use learning selectively induces expression of brain-derived neurotrophic factor, its receptor *trk*B and neurotrophin 3 in the intraparietal multisensorycortex of monkeys. *Brain Res. Cogn. Brain Res.* 14, 3–9. doi: 10.1016/s0926-6410(02)00056-3

Jackson, A., Mavoori, J., and Fetz, E. E. (2006). Long-term motor cortex plasticity induced by an electronic neural implant. *Nature* 444, 56–60. doi: 10.1038/nature05226

Jak, A. J., Seelye, A. M., and Jurick, S. M. (2013). Crosswords to computers: a critical review of popular approaches to cognitive enhancement. *Neuropsychol. Rev.* 23, 13–26. doi: 10.1007/s11065-013-9226-5

Jarosiewicz, B., Chase, S. M., Fraser, G. W., Velliste, M., Kass, R. E., and Schwartz, A. B. (2008). Functional network reorganization during learning in a brain-computer interface paradigm. *Proc. Natl. Acad. Sci. U S A* 105, 19486–19491. doi: 10.1073/pnas.0808113105

Järveläinen, J., Schuermann, M., and Hari, R. (2004). Activation of the human primary motor cortex during observation of tool use. *Neuroimage* 23, 187–192. doi: 10.1016/j.neuroimage.2004.06.010

Jiang, F., Racine, R., and Turnbull, J. (1997). Electrical stimulation of the septal region of aged rats improves performance in an open-field maze. *Physiol. Behav.* 62, 1279–1282. doi: 10.1016/s0031-9384(97)00306-5

Johnson, L. A., Blakely, T., Hermes, D., Hakimian, S., Ramsey, N. F., and Ojemann, J. G. (2012). Sleep spindles are locally modulated by training on a brain–computer interface. *Proc. Natl. Acad. Sci. U S A* 109, 18583–18588. doi: 10.1073/pnas.1207532109

Johnson-Frey, S. H. (2004). The neural bases of complex tool use in humans. *Trends Cogn. Sci.* 8, 71–78. doi: 10.1016/j.tics.2003.12.002

Jones, E. G., and Pons, T. P. (1998). Thalamic and brainstem contributions to large-scale plasticity of primate somatosensory cortex. *Science* 282, 1121–1125. doi: 10.1126/science.282.5391.1121

Jones, E. G. (1993). GABAergic neurons and their role in cortical plasticity in primates. *Cereb. Cortex* 3, 361–372. doi: 10.1093/cercor/3.5.361-a

Kaas, J. H., Krubitzer, L. A., Chino, Y. M., Langston, A. L., Polley, E. H., and Blair, N. (1990). Reorganization of retinotopic cortical maps in adult mammals after lesions of the retina. *Science* 248, 229–231. doi: 10.1126/science.2326637

Kaas, J. H. (1991). Plasticity of sensory and motor maps in adult mammals. *Annu. Rev. Neurosci.* 14, 137–167. doi: 10.1146/annurev.neuro.14.1.137

Kajimoto, H., Inami, M., Kawakami, N., and Tachi, S. (2003). Smarttouch-augmentation of skin sensation with electrocutaneous display. Proceedings of the Haptic Interfaces for Virtual Environment and Teleoperator Systems, 2003 HAPTICS 2003 Proceedings 11th Symposium on; IEEE.

Kammers, M. P., Verhagen, L., Dijkerman, H. C., Hogendoorn, H., De Vignemont, F., and Schutter, D. J. (2009). Is this hand for real? Attenuation of the rubber hand illusion by transcranial magnetic stimulation over the inferior parietal lobule. *J. Cogn. Neurosci.* 21, 1311–1320. doi: 10.1162/jocn.2009.21095

Kanayama, N., Sato, A., and Ohira, H. (2009). The role of gamma band oscillations and synchrony on rubber hand illusion and crossmodal integration. *Brain Cogn.* 69, 19–29. doi: 10.1016/j.bandc.2008.05.001

Karni, A., Meyer, G., Rey-Hipolito, C., Jezzard, P., Adams, M. M., Turner, R., et al. (1998). The acquisition of skilled motor performance: fast and slow experience-driven changes in primary motor cortex. *Proc. Natl. Acad. Sci. U S A* 95, 861–868. doi: 10.1073/pnas.95.3.861

Kelly, A. C., and Garavan, H. (2005). Human functional neuroimaging of brain changes associated with practice. *Cereb. Cortex* 15, 1089–1102. doi: 10.1093/cercor/bhi005

Kereszturi, E., Tarnok, Z., Bognar, E., Lakatos, K., Farkas, L., Gadoros, J., et al. (2008). Catechol-O-methyltransferase Val158Met polymorphism is associated with methylphenidate response in ADHD children. *Am. J. Med. Genet. B Neuropsychiatr. Genet.* 147B, 1431–1435. doi: 10.1002/ajmg.b.30704

Kim, J. M., Stewart, R., Park, M. S., Kang, H. J., Kim, S. W., Shin, I. S., et al. (2012). Associations of BDNF genotype and promoter methylation with acute and long-term stroke outcomes in an East Asian cohort. *PLoS One* 7:e51280. doi: 10.1371/journal.pone.0051280

Kleim, J. A., Barbay, S., Cooper, N. R., Hogg, T. M., Reidel, C. N., Remple, M. S., et al. (2002). Motor learning-dependent synaptogenesis is localized to functionally reorganized motor cortex. *Neurobiol. Learn. Mem.* 77, 63–77. doi: 10.1006/nlme.2000.4004

Klingberg, T., Fernell, E., Olesen, P. J., Johnson, M., Gustafsson, P., Dahlström, K., et al. (2005). Computerized training of working memory in children with ADHD–a randomized, controlled trial. *J. Am. Acad. Child Adolesc. Psychiatry* 44, 177–186. doi: 10.1097/00004583-200502000-00010

Klingberg, T. (2010). Training and plasticity of working memory. *Trends Cogn. Sci.* 14, 317–324. doi: 10.1016/j.tics.2010.05.002

Koralek, A. C., Jin, X., Long, J. D. 2nd, Costa, R. M., and Carmena, J. M. (2012). Corticostriatal plasticity is necessary for learning intentional neuroprosthetic skills. *Nature* 483, 331–335. doi: 10.1038/nature10845

Kuiken, T. A., Miller, L. A., Lipschutz, R. D., Lock, B. A., Stubblefield, K., Marasco, P. D., et al. (2007). Targeted reinnervation for enhanced prosthetic arm function in a woman with a proximal amputation: a case study. *Lancet* 369, 371–380. doi: 10.1016/s0140-6736(07)60193-7

Kwok, T. C., Chau, W. W., Yuen, K. S., Wong, A. Y., Li, J. C., Shiu, R. Y., et al. (2011). Who would benefit from memory training? A pilot study examining the ceiling effect of concurrent cognitive stimulation. *Clin. Interv. Aging* 6, 83–88. doi: 10.2147/CIA.S16802

Laubach, M., Wessberg, J., and Nicolelis, M. A. (2000). Cortical ensemble activity increasingly predicts behaviour outcomes during learning of a motor task. *Nature* 405, 567–571. doi: 10.1038/35014604

Lausberg, H., Göttert, R., Münninger, U., Boegner, F., and Marx, P. (1999). Callosal disconnection syndrome in a left-handed patient due to infarction of the total length of the corpus callosum. *Neuropsychologia* 37, 253–265. doi: 10.1016/s0028-3932(98)00079-7

Lazar, S. W., Bush, G., Gollub, R. L., Fricchione, G. L., Khalsa, G., and Benson, H. (2000). Functional brain mapping of the relaxation response and meditation. *Neuroreport* 11, 1581–1585. doi: 10.1097/00001756-200005150-00041

Lazar, S. W., Kerr, C. E., Wasserman, R. H., Gray, J. R., Greve, D. N., Treadway, M. T., et al. (2005). Meditation experience is associated with increased cortical thickness. *Neuroreport* 16, 1893–1897. doi: 10.1097/01.wnr.0000186598.66243.19

Lebedev, M. A., and Nicolelis, M. A. (2006). Brain-machine interfaces: past, present and future. *Trends Neurosci.* 29, 536–546. doi: 10.1016/j.tins.2006.07.004

Lee, D. S., Lee, J. S., Oh, S. H., Kim, S.-K., Kim, J.-W., Chung, J.-K., et al. (2001). Deafness: cross-modal plasticity and cochlear implants. *Nature* 409, 149–150. doi: 10.1038/35051653

Lenggenhager, B., Tadi, T., Metzinger, T., and Blanke, O. (2007). Video ergo sum: manipulating bodily self-consciousness. *Science* 317, 1096–1099. doi: 10.1126/science.1143439

Lewis, E., and Lloyd, D. M. (2010). Embodied experience: a first-person investigation of the rubber hand illusion. *Phenomenology Cogn. Sci.* 9, 317–339. doi: 10.1007/s11097-010-9154-2

Lotze, M., Grodd, W., Birbaumer, N., Erb, M., Huse, E., and Flor, H. (1999). Does use of a myoelectric prosthesis prevent cortical reorganization and phantom limb pain? *Nat. Neurosci.* 2, 501–502. doi: 10.1038/9145

Luders, E., Toga, A. W., Lepore, N., and Gaser, C. (2009). The underlying anatomical correlates of long-term meditation: larger hippocampal and frontal volumes of gray matter. *Neuroimage* 45, 672–678. doi: 10.1016/j.neuroimage.2008.12.061

Lutz, A., Brefczynski-Lewis, J., Johnstone, T., and Davidson, R. J. (2008). Regulation of the neural circuitry of emotion by compassion meditation: effects of meditative expertise. *PLoS One* 3:e1897. doi: 10.1371/journal.pone.0001897

Lutz, A., Greischar, L. L., Rawlings, N. B., Ricard, M., and Davidson, R. J. (2004). Long-term meditators self-induce high-amplitude gamma synchrony during mental practice. *Proc. Natl. Acad. Sci. U S A* 101, 16369–16373. doi: 10.1073/pnas.0407401101

Macaluso, E., Frith, C. D., and Driver, J. (2000). Modulation of human visual cortex by crossmodal spatial attention. *Science* 289, 1206–1208. doi: 10.1126/science.289.5482.1206

Macaluso, E., and Maravita, A. (2010). The representation of space near the body through touch and vision. *Neuropsychologia* 48, 782–795. doi: 10.1016/j.neuropsychologia.2009.10.010

Maguire, E. A., Gadian, D. G., Johnsrude, I. S., Good, C. D., Ashburner, J., Frackowiak, R. S., et al. (2000). Navigation-related structural change in the hippocampi of taxi drivers. *Proc. Natl. Acad. Sci. U S A* 97, 4398–4403. doi: 10.1073/pnas.070039597

Maguire, E. A., Valentine, E. R., Wilding, J. M., and Kapur, N. (2002). Routes to remembering: the brains behind superior memory. *Nat. Neurosci.* 6, 90–95. doi: 10.1038/nn988

Maguire, E. A., Woollett, K., and Spiers, H. J. (2006). London taxi drivers and bus drivers: a structural MRI and neuropsychological analysis. *Hippocampus* 16, 1091–1101. doi: 10.1002/hipo.20233

Mahncke, H. W., Connor, B. B., Appelman, J., Ahsanuddin, O. N., Hardy, J. L., Wood, R. A., et al. (2006). Memory enhancement in healthy older adults using a brain plasticity-based training program: a randomized, controlled study. *Proc. Natl. Acad. Sci. U S A* 103, 12523–12528. doi: 10.1073/pnas.0605194103

Makin, T. R., Holmes, N. P., and Ehrsson, H. H. (2008). On the other hand: dummy hands and peripersonal space. *Behav. Brain Res.* 191, 1–10. doi: 10.1016/j.bbr.2008.02.041

Marasco, P. D., Kim, K., Colgate, J. E., Peshkin, M. A., and Kuiken, T. A. (2011). Robotic touch shifts perception of embodiment to a prosthesis in targeted reinnervation amputees. *Brain* 134, 747–758. doi: 10.1093/brain/awq361

Maravita, A., and Iriki, A. (2004). Tools for the body (schema). *Trends Cogn. Sci.* 8, 79–86. doi: 10.1016/j.tics.2003.12.008

Maravita, A., Spence, C., and Driver, J. (2003). Multisensory integration and the body schema: close to hand and within reach. *Curr. Biol.* 13, R531–R539. doi: 10.1016/s0960-9822(03)00449-4

Marini, F., Tagliabue, C. F., Sposito, A. V., Hernandez-Arieta, A., Brugger, P., Estevez, N., et al. (2014). Crossmodal representation of a functional robotic hand arises after extensive training in healthy participants. *Neuropsychologia* 53, 178–186. doi: 10.1016/j.neuropsychologia.2013.11.017

Marshall, L., Helgadóttir, H., Mölle, M., and Born, J. (2006). Boosting slow oscillations during sleep potentiates memory. *Nature* 444, 610–613. doi: 10.1038/nature05278

Maruishi, M., Tanaka, Y., Muranaka, H., Tsuji, T., Ozawa, Y., Imaizumi, S., et al. (2004). Brain activation during manipulation of the myoelectric prosthetic hand: a functional magnetic resonance imaging study. *Neuroimage* 21, 1604–1611. doi: 10.1016/j.neuroimage.2003.12.001

Matsuzaka, Y., Picard, N., and Strick, P. L. (2007). Skill representation in the primary motor cortex after long-term practice. *J. Neurophysiol.* 97, 1819–1832. doi: 10.1152/jn.00784.2006

McNab, F., Varrone, A., Farde, L., Jucaite, A., Bystritsky, P., Forssberg, H., et al. (2009). Changes in cortical dopamine D1 receptor binding associated with cognitive training. *Science* 323, 800–802. doi: 10.1126/science.1166102

Mehta, M. A., Owen, A. M., Sahakian, B. J., Mavaddat, N., Pickard, J. D., and Robbins, T. W. (2000). Methylphenidate enhances working memory by modulating discrete frontal and parietal lobe regions in the human brain. *J. Neurosci.* 20, RC65, 1–6.

Merzenich, M. M., Nelson, R. J., Stryker, M. P., Cynader, M. S., Schoppmann, A., and Zook, J. M. (1984). Somatosensory cortical map changes following digit amputation in adult monkeys. *J. Comp. Neurol.* 224, 591–605. doi: 10.1002/cne.902240408

Métin, C., and Frost, D. O. (1989). Visual responses of neurons in somatosensory cortex of hamsters with experimentally induced retinal projections to somatosensory thalamus. *Proc. Natl. Acad. Sci. U S A* 86, 357–361. doi: 10.1073/pnas.86.1.357

Micera, S., Citi, L., Rigosa, J., Carpaneto, J., Raspopovic, S., Di Pino, G., et al. (2010). Decoding information from neural signals recorded using intraneural electrodes: towards the development of a neurocontrolled hand prosthesis. *Proceedings of the IEEE* 98, 407–417. doi: 10.1109/jproc.2009.2038726

Micera, S., Rigosa, J., Carpaneto, J., Citi, L., Raspopovic, S., Guglielmelli, E., et al. (2009). On the control of a robot hand by extracting neural signals from the PNS: Preliminary results from a human implantation. *Conf. Proc. IEEE Eng. Med. Biol. Soc.* 2009, 4586–4589. doi: 10.1109/IEMBS.2009.5332764

Milton, J., Solodkin, A., Hluštík, P., and Small, S. L. (2007). The mind of expert motor performance is cool and focused. *Neuroimage* 35, 804–813. doi: 10.1016/j.neuroimage.2007.01.003

Moll, J., de Oliveira-Souza, R., Passman, L., Cunha, F. C., Souza-Lima, F., and Andreiuolo, P. (2000). Functional MRI correlates of real and imagined tool-use pantomimes. *Neurology* 54, 1331–1336. doi: 10.1212/wnl.54.6.1331

Mulvey, M. R., Fawkner, H. J., Radford, H. E., and Johnson, M. I. (2012). Perceptual embodiment of prosthetic limbs by transcutaneous electrical nerve stimulation. *Neuromodulation* 15, 42–46; discussion 47. doi: 10.1111/j.1525-1403.2011.00408.x

Murata, A., Fadiga, L., Fogassi, L., Gallese, V., Raos, V., and Rizzolatti, G. (1997). Object representation in the ventral premotor cortex (area F5) of the monkey. *J. Neurophysiol.* 78, 2226–2230.

Murata, A., Gallese, V., Luppino, G., Kaseda, M., and Sakata, H. (2000). Selectivity for the shape, size and orientation of objects for grasping in neurons of monkey parietal area AIP. *J. Neurophysiol.* 83, 2580–2601.

Murata, K., Cramer, H., and Bach-y-Rita, P. (1965). Neuronal convergence of noxious, acoustic and visual stimuli in the visual cortex of the cat. *J. Neurophysiol.* 28, 1223–1239.

Murphy, K. J., Foley, A. G., O'Connell, A. W., and Regan, C. M. (2006). Chronic exposure of rats to cognition enhancing drugs produces a neuroplastic response identical to that obtained by complex environment rearing. *Neuropsychopharmacology* 31, 90–100. doi: 10.1038/sj.npp.1300810

Nagel, S. K., Carl, C., Kringe, T., Martin, R., and Konig, P. (2005). Beyond sensory substitution—learning the sixth sense. *J. Neural. Eng.* 2, R13–R26. doi: 10.1088/1741-2560/2/4/r02

Navarro, X., Krueger, T. B., Lago, N., Micera, S., Stieglitz, T., and Dario, P. (2005). A critical review of interfaces with the peripheral nervous system for the control of neuroprostheses and hybrid bionic systems. *J. Peripher. Nerv. Syst.* 10, 229–258. doi: 10.1111/j.1085-9489.2005.10303.x

Newport, R., Pearce, R., and Preston, C. (2010). Fake hands in action: embodiment and control of supernumerary limbs. *Exp. Brain Res.* 204, 385–395. doi: 10.1007/s00221-009-2104-y

Ni, Z., Anastakis, D. J., Gunraj, C., and Chen, R. (2010). Reversal of cortical reorganization in human primary motor cortex following thumb reconstruction. *J. Neurophysiol.* 103, 65–73. doi: 10.1152/jn.00732.2009

Niemeyer, W., and Starlinger, I. (1981). Do the blind hear better? Investigations on auditory processing in congenital or early acquired blindness II. central functions. *Int. J. Audiol.* 20, 510–515. doi: 10.3109/00206098109072719

Nilsson, M., Perfilieva, E., Johansson, U., Orwar, O., and Eriksson, P. S. (1999). Enriched environment increases neurogenesis in the adult rat dentate gyrus and improves spatial memory. *J. Neurobiol.* 39, 569–578. doi: 10.1002/(sici)1097-4695(19990615)39:4<569::aid-neu10>3.0.co;2-f

Ninaus, M., Kober, S. E., Witte, M., Koschutnig, K., Stangl, M., Neuper, C., et al. (2013). Neural substrates of cognitive control under the belief of getting neurofeedback training. *Front. Hum. Neurosci.* 7:914. doi: 10.3389/fnhum.2013.00914

Nitsche, M. A., Schauenburg, A., Lang, N., Liebetanz, D., Exner, C., Paulus, W., et al. (2003). Facilitation of implicit motor learning by weak transcranial direct current stimulation of the primary motor cortex in the human. *J. Cogn. Neurosci.* 15, 619–626. doi: 10.1162/089892903321662994

Nojima, T., Sekiguchi, D., Inami, M., and Tachi, S. (2002). The smarttool: a system for augmented reality of haptics. Proceedings of the Virtual Reality, 2002 Proceedings IEEE.

Nudo, R., Milliken, G., Jenkins, W. M., and Merzenich, M. (1996). Use-dependent alterations of movement representations in primary motor cortex of adult squirrel monkeys. *J. Neurosci.* 16, 785–807.

Olesen, P. J., Westerberg, H., and Klingberg, T. (2004). Increased prefrontal and parietal activity after training of working memory. *Nat. Neurosci.* 7, 75–79. doi: 10.1038/nn1165

Pagnoni, G., and Cekic, M. (2007). Age effects on gray matter volume and attentional performance in Zen meditation. *Neurobiol. Aging* 28, 1623–1627. doi: 10.1016/j.neurobiolaging.2007.06.008

Paillard, J. (1976). [Neural coding of motor commands]. *Rev. Electroencephalogr. Neurophysiol. Clin.* 6, 453–472. doi: 10.1016/s0370-4475(76)80006-8

Pascual-Leone, A., Amedi, A., Fregni, F., and Merabet, L. B. (2005). The plastic human brain cortex. *Annu. Rev. Neurosci.* 28, 377–401. doi: 10.1146/annurev.neuro.27.070203.144216

Pascual-Leone, A., Cammarota, A., Wassermann, E. M., Brasil-Neto, J. P., Cohen, L. G., and Hallett, M. (1993). Modulation of motor cortical outputs to the reading hand of braille readers. *Ann. Neurol.* 34, 33–37. doi: 10.1002/ana.410340108

Pascual-Leone, A., Nguyet, D., Cohen, L. G., Brasil-Neto, J. P., Cammarota, A., and Hallett, M. (1995). Modulation of muscle responses evoked by transcranial magnetic stimulation during the acquisition of new fine motor skills. *J. Neurophysiol.* 74, 1037–1045.

Pascual-Leone, A., Peris, M., Tormos, J. M., Pascual, A. P., and Catala, M. D. (1996). Reorganization of human cortical motor output maps following traumatic forearm amputation. *Neuroreport* 7, 2068–2070. doi: 10.1097/00001756-199609020-00002

Pascual-Leone, A., and Torres, F. (1993). Plasticity of the sensorimotor cortex representation of the reading finger in Braille readers. *Brain* 116, 39–52. doi: 10.1093/brain/116.1.39

Pearce, A. J., Thickbroom, G. W., Byrnes, M. L., and Mastaglia, F. L. (2000). Functional reorganisation of the corticomotor projection to the hand in skilled racquet players. *Exp. Brain Res.* 130, 238–243. doi: 10.1007/s002219900236

Peeters, R., Simone, L., Nelissen, K., Fabbri-Destro, M., Vanduffel, W., Rizzolatti, G., et al. (2009). The representation of tool use in humans and monkeys: common and uniquely human features. *J. Neurosci.* 29, 11523–11539. doi: 10.1523/JNEUROSCI.2040-09.2009

Perani, D., Cappa, S., Bettinardi, V., Bressi, S., Gorno-Tempini, M., Matarrese, M., et al. (1995). Different neural systems for the recognition of animals and man-made tools. *Neuroreport* 6, 1637–1641. doi: 10.1097/00001756-199508000-00012

Pereira, A. C., Huddleston, D. E., Brickman, A. M., Sosunov, A. A., Hen, R., McKhann, G. M., et al. (2007). An in vivo correlate of exercise-induced neurogenesis in the adult dentate gyrus. *Proc. Natl. Acad. Sci. U S A* 104, 5638–5643. doi: 10.1073/pnas.0611721104

Pfister, B. J., Huang, J. H., Kameswaran, N., Zager, E. L., and Smith, D. H. (2007). Neural engineering to produce in vitro nerve constructs and neurointerface. *Neurosurgery* 60, 137–141; discussion 141–142. doi: 10.1227/01.neu.0000249197.61280.1d

Plautz, E. J., Milliken, G. W., and Nudo, R. J. (2000). Effects of repetitive motor training on movement representations in adult squirrel monkeys: role of use versus learning. *Neurobiol. Learn. Mem.* 74, 27–55. doi: 10.1006/nlme.1999.3934

Plewnia, C., Hoppe, J., Cohen, L. G., and Gerloff, C. (2004). Improved motor skill acquisition after selective stimulation of central norepinephrine. *Neurology* 62, 2124–2126. doi: 10.1212/01.wnl.0000128041.92710.17

Popovic, M. R., Popovic, D. B., and Keller, T. (2002). Neuroprostheses for grasping. *Neurol. Res.* 24, 443–452. doi: 10.1179/016164102101200311

Ptito, M., Moesgaard, S. M., Gjedde, A., and Kupers, R. (2005). Cross-modal plasticity revealed by electrotactile stimulation of the tongue in the congenitally blind. *Brain* 128, 606–614. doi: 10.1093/brain/awh380

Quallo, M., Price, C., Ueno, K., Asamizuya, T., Cheng, K., Lemon, R., et al. (2009). Gray and white matter changes associated with tool-use learning in macaque monkeys. *Proc. Natl. Acad. Sci. U S A* 106, 18379–18384. doi: 10.1073/pnas.0909751106

Ramachandran, V. S., and Altschuler, E. L. (2009). The use of visual feedback, in particular mirror visual feedback, in restoring brain function. *Brain* 132, 1693–1710. doi: 10.1093/brain/awp135

Ramachandran, V. S., Rogers-Ramachandran, D., and Cobb, S. (1995). Touching the phantom limb. *Nature* 377, 489–490. doi: 10.1038/377489a0

Ramachandran, V. S., Rogers-Ramachandran, D., and Stewart, M. (1992). Perceptual correlates of massive cortical reorganization. *Science* 258, 1159–1160. doi: 10.1126/science.1439826

Rasch, B., Büchel, C., Gais, S., and Born, J. (2007). Odor cues during slow-wave sleep prompt declarative memory consolidation. *Science* 315, 1426–1429. doi: 10.1126/science.1138581

Rasey, H. W., Lubar, J. F., McIntyre, A., Zoffuto, A. C., and Abbott, P. L. (1995). EEG biofeedback for the enhancement of attentional processing in normal college students. *J. Neurother.* 1, 15–21. doi: 10.1300/j184v01n03_03

Raspopovic, S., Capogrosso, M., Petrini, F. M., Bonizzato, M., Rigosa, J., Di Pino, G., et al. (2014). Restoring natural sensory feedback in real-time bidirectional hand prostheses. *Sci. Transl. Med.* 6:222ra219. doi: 10.1126/scitranslmed.3006820

Rauschecker, J. P., and Kniepert, U. (1994). Auditory localization behaviour in visually deprived cats. *Eur. J. Neurosci.* 6, 149–160. doi: 10.1111/j.1460-9568.1994.tb00256.x

Recanzone, G. A., Schreiner, C., and Merzenich, M. M. (1993). Plasticity in the frequency representation of primary auditory cortex following discrimination training in adult owl monkeys. *J. Neurosci.* 13, 87–103.

Recanzone, G. H., Merzenich, M. M., Jenkins, W. M., Grajski, K. A., and Dinse, H. R. (1992). Topographic reorganization of the hand representation in cortical area 3b owl monkeys trained in a frequency-discrimination task. *J. Neurophysiol.* 67, 1031–1056.

Reis, J., Schambra, H. M., Cohen, L. G., Buch, E. R., Fritsch, B., Zarahn, E., et al. (2009). Noninvasive cortical stimulation enhances motor skill acquisition over multiple days through an effect on consolidation. *Proc. Natl. Acad. Sci. U S A* 106, 1590–1595. doi: 10.1073/pnas.0805413106

Rioult-Pedotti, M.-S., Friedman, D., and Donoghue, J. P. (2000). Learning-induced LTP in neocortex. *Science* 290, 533–536. doi: 10.1126/science.290.5491.533

Rioult-Pedotti, M.-S., Friedman, D., Hess, G., and Donoghue, J. P. (1998). Strengthening of horizontal cortical connections following skill learning. *Nat. Neurosci.* 1, 230–234. doi: 10.1038/678

Roder, B., and Neville, H. (2003). Developmental functional plasticity. *Handbook of Neuropsychology* 9, 231–270.

Rohde, M., Di Luca, M., and Ernst, M. O. (2011). The rubber hand illusion: feeling of ownership and proprioceptive drift do not go hand in hand. *PLoS One* 6:e21659. doi: 10.1371/journal.pone.0021659

Romano, D., Bottini, G., and Maravita, A. (2013). Perceptual effects of the mirror box training in normal subjects. *Restor. Neurol. Neurosci.* 31, 373–386. doi: 10.3233/RNN-120273

Romano, D., Gandola, M., Bottini, G., and Maravita, A. (2014). Arousal responses to noxious stimuli in somatoparaphrenia and anosognosia: clues to body awareness. *Brain* 137, 1213–1223. doi: 10.1093/brain/awu009

Rossini, P. M., Micera, S., Benvenuto, A., Carpaneto, J., Cavallo, G., Citi, L., et al. (2010). Double nerve intraneural interface implant on a human amputee for robotic hand control. *Clin. Neurophysiol.* 121, 777–783. doi: 10.1016/j.clinph.2010.01.001

Sadato, N., Pascual-Leone, A., Grafman, J., Ibanez, V., Deiber, M.-P., Dold, G., et al. (1996). Activation of the primary visual cortex by Braille reading in blind subjects. *Nature* 380, 526–528. doi: 10.1038/380526a0

Saig, A., Arieli, A., and Ahissar, E. (2010). "What is it like to be a rat? sensory augmentation study," in *Haptics: Generating and Perceiving Tangible Sensations*, eds A. M. L. Kappers, J. B. F. van Erp, W. M. Bergmann Tiest and F. C. T. van der Helm (Berlin Heidelberg: Springer), 298–305.

Sampaio, E., Maris, S., and Bach-y-Rita, P. (2001). Brain plasticity: 'visual' acuity of blind persons via the tongue. *Brain Res.* 908, 204–207. doi: 10.1016/S0006-8993(01)02667-1

Schaefer, M., Heinze, H. J., and Rotte, M. (2009). My third arm: shifts in topography of the somatosensory homunculus predict feeling of an artificial supernumerary arm. *Hum. Brain Mapp.* 30, 1413–1420. doi: 10.1002/hbm.20609

Scholz, J., Klein, M. C., Behrens, T. E. J., and Johansen-Berg, H. (2009). Training induces changes in white-matter architecture. *Nat. Neurosci.* 12, 1370–1371. doi: 10.1038/nn.2412

Schoups, A., Vogels, R., Qian, N., and Orban, G. (2001). Practising orientation identification improves orientation coding in V1 neurons. *Nature* 412, 549–553. doi: 10.1038/35087601

Schulze, H. (2004). MEMOS: a mobile extensible memory aid system. *Telemed. J. E Health* 10, 233–242. doi: 10.1089/1530562041641228

Schuster, C., Maunz, G., Lutz, K., Kischka, U., Sturzenegger, R., and Ettlin, T. (2011). Dexamphetamine improves upper extremity outcome during rehabilitation after stroke: a pilot randomized controlled trial. *Neurorehabil. Neural Repair* 25, 749–755. doi: 10.1177/1545968311405674

Sengül, A., van Elk, M., Rognini, G., Aspell, J. E., Bleuler, H., and Blanke, O. (2012). Extending the body to virtual tools using a robotic surgical interface: evidence from the crossmodal congruency task. *PLoS One* 7:e49473. doi: 10.1371/journal.pone.0049473

Serruya, M. D., and Kahana, M. J. (2008). Techniques and devices to restore cognition. *Behav. Brain Res.* 192, 149–165. doi: 10.1016/j.bbr.2008.04.007

Shikata, E., Tanaka, Y., Nakamura, H., Taira, M., and Sakata, H. (1996). Selectivity of the parietal visual neurones in 3D orientation of surface of stereoscopic stimuli. *Neuroreport* 7, 2389–2394. doi: 10.1097/00001756-199610020-00022

Shokur, S., O'Doherty, J. E., Winans, J. A., Bleuler, H., Lebedev, M. A., and Nicolelis, M. A. (2013). Expanding the primate body schema in sensorimotor cortex by virtual touches of an avatar. *Proc. Natl. Acad. Sci. U S A* 110, 15121–15126. doi: 10.1073/pnas.1308459110

Slater, M., Perez-Marcos, D., Ehrsson, H. H., and Sanchez-Vives, M. V. (2008). Towards a digital body: the virtual arm illusion. *Front. Hum. Neurosci.* 2:6. doi: 10.3389/neuro.09.006.2008

Smitsman, A. W. (1997). "The development of tool use: changing boundaries between organism and environment," in *Evolving Explanations of Development: Ecological Approaches to Organism-Environment Systems*, eds C. Dent-Read and P. Zukow-Goldring (Washington DC: American Psychological Association).

So, K.-T., and Orme-Johnson, D. W. (2001). Three randomized experiments on the longitudinal effects of the Transcendental Meditation technique on cognition. *Intelligence* 29, 419–440. doi: 10.1016/s0160-2896(01)00070-8

Srinivasan, N., and Baijal, S. (2007). Concentrative meditation enhances preattentive processing: a mismatch negativity study. *Neuroreport* 18, 1709–1712. doi: 10.1097/wnr.0b013e3282f0d2d8

Stefan, K., Kunesch, E., Benecke, R., Cohen, L. G., and Classen, J. (2002). Mechanisms of enhancement of human motor cortex excitability induced by interventional paired associative stimulation. *J. Physiol.* 543, 699–708. doi: 10.1113/jphysiol.2002.023317

Stroemer, R. P., Kent, T. A., Hulsebosch, C. E., and Feeney, D. M. (1998). Enhanced neocortical neural sprouting, synaptogenesis and behavioral recovery with d-amphetamine therapy after neocortical infarction in rats editorial comment. *Stroke* 29, 2381–2395. doi: 10.1161/01.str.29.11.2381

Taffoni, F., Tamilia, E., Focaroli, V., Formica, D., Ricci, L., Di Pino, G., et al. (2014). Development of goal-directed action selection guided by intrinsic motivations: an experiment with children. *Exp. Brain Res.* doi: 10.1007/s00221-014-3907-z. [Epub ahead of print].

Temple, E., Deutsch, G. K., Poldrack, R. A., Miller, S. L., Tallal, P., Merzenich, M. M., et al. (2003). Neural deficits in children with dyslexia ameliorated by behavioral remediation: evidence from functional MRI. *Proc. Natl. Acad. Sci. U S A* 100, 2860–2865. doi: 10.1073/pnas.0030098100

Terr, L. I., Sinha, U. K., and House, W. F. (1987). Anatomical relationships of the cochlear nuclei and the pontobulbar body: possible significance for neuroprosthesis placement. *Laryngoscope* 97, 1009–1011. doi: 10.1288/00005537-198709000-00001

Thomson, E. E., Carra, R., and Nicolelis, M. A. (2013). Perceiving invisible light through a somatosensory cortical prosthesis. *Nat. Commun.* 4:1482. doi: 10.1038/ncomms2497

Thorell, L. B., Lindqvist, S., Bergman Nutley, S., Bohlin, G., and Klingberg, T. (2009). Training and transfer effects of executive functions in preschool children. *Dev. Sci.* 12, 106–113. doi: 10.1111/j.1467-7687.2008.00745.x

Tombini, M., Rigosa, J., Zappasodi, F., Porcaro, C., Citi, L., Carpaneto, J., et al. (2012). Combined analysis of cortical (EEG) and nerve stump signals improves robotic hand control. *Neurorehabil. Neural Repair* 26, 275–281. doi: 10.1177/1545968311408919

Toni, I., Rowe, J., Stephan, K. E., and Passingham, R. E. (2002). Changes of cortico-striatal effective connectivity during visuomotor learning. *Cereb. Cortex* 12, 1040–1047. doi: 10.1093/cercor/12.10.1040

Tsakiris, M., Carpenter, L., James, D., and Fotopoulou, A. (2010). Hands only illusion: multisensory integration elicits sense of ownership for body parts but not for non-corporeal objects. *Exp. Brain Res.* 204, 343–352. doi: 10.1007/s00221-009-2039-3

Tsakiris, M., Hesse, M. D., Boy, C., Haggard, P., and Fink, G. R. (2007). Neural signatures of body ownership: a sensory network for bodily self-consciousness. *Cereb. Cortex* 17, 2235–2244. doi: 10.1093/cercor/bhl131

Tsakiris, M., Prabhu, G., and Haggard, P. (2006). Having a body *versus* moving your body: How agency structures body-ownership. *Conscious. Cogn.* 15, 423–432. doi: 10.1016/j.concog.2005.09.004

Tsakiris, M. (2010). *My* body in the brain: a neurocognitive model of body-ownership. *Neuropsychologia* 48, 703–712. doi: 10.1016/j.neuropsychologia.2009.09.034

Tyler, M., Danilov, Y., and Bach-y-Rita, P. (2003). Closing an open-loop control system: vestibular substitution through the tongue. *J. Integr. Neurosci.* 2, 159–164. doi: 10.1142/s0219635203000263

Vallar, G., and Ronchi, R. (2009). Somatoparaphrenia: a body delusion. A review of the neuropsychological literature. *Exp. Brain Res.* 192, 533–551. doi: 10.1007/s00221-008-1562-y

Vaynman, S., and Gomez-Pinilla, F. (2005). License to run: exercise impacts functional plasticity in the intact and injured central nervous system by using neurotrophins. *Neurorehabil. Neural Repair* 19, 283–295. doi: 10.1177/1545968305280753

Velliste, M., Perel, S., Spalding, M. C., Whitford, A. S., and Schwartz, A. B. (2008). Cortical control of a prosthetic arm for self-feeding. *Nature* 453, 1098–1101. doi: 10.1038/nature06996

Vernon, D., Egner, T., Cooper, N., Compton, T., Neilands, C., Sheri, A., et al. (2003). The effect of training distinct neurofeedback protocols on aspects of cognitive performance. *Int. J. Psychophysiol.* 47, 75–85. doi: 10.1016/s0167-8760(02)00091-0

Vestergaard-Poulsen, P., van Beek, M., Skewes, J., Bjarkam, C. R., Stubberup, M., Bertelsen, J., et al. (2009). Long-term meditation is associated with increased gray matter density in the brain stem. *Neuroreport* 20, 170–174. doi: 10.1097/wnr.0b013e328320012a

Von Gierke, H. (1970). Principles and Practice of Bionics. Proceedings of the Proc 44th AGARD—Conference Brüssel.

Wander, J. D., Blakely, T., Miller, K. J., Weaver, K. E., Johnson, L. A., Olson, J. D., et al. (2013). Distributed cortical adaptation during learning of a brain-computer interface task. *Proc. Natl. Acad. Sci. U S A* 110, 10818–10823. doi: 10.1073/pnas.1221127110

Wang, J. R., and Hsieh, S. (2013). Neurofeedback training improves attention and working memory performance. *Clin. Neurophysiol.* 124, 2406–2420. doi: 10.1016/j.clinph.2013.05.020

Weiss, T., Miltner, W. H., Adler, T., Bruckner, L., and Taub, E. (1999). Decrease in phantom limb pain associated with prosthesis-induced increased use of an amputation stump in humans. *Neurosci. Lett.* 272, 131–134. doi: 10.1016/s0304-3940(99)00595-9

Williams, J. H. (2001). Frequency-specific effects of flicker on recognition memory. *Neuroscience* 104, 283–286. doi: 10.1016/s0306-4522(00)00579-0

Williams, Z. M., and Eskandar, E. N. (2006). Selective enhancement of associative learning by microstimulation of the anterior caudate. *Nat. Neurosci.* 9, 562–568. doi: 10.1038/nn1662

Willis, S. L., Tennstedt, S. L., Marsiske, M., Ball, K., Elias, J., Koepke, K. M., et al. (2006). Long-term effects of cognitive training on everyday functional outcomes in older adults. *JAMA* 296, 2805–2814. doi: 10.1001/jama.296.23.2805

Winsberg, B. G., and Comings, D. E. (1999). Association of the dopamine transporter gene (*DAT1*) with poor methylphenidate response. *J. Am. Acad. Child Adolesc. Psychiatry* 38, 1474–1477. doi: 10.1097/00004583-199912000-00006

Winsley, R., and Matos, N. (2011). Overtraining and elite young athletes. *Med. Sport Sci.* 56, 97–105. doi: 10.1159/000320636

Wolpaw, J. R. (2007). Brain-computer interfaces as new brain output pathways. *J. Physiol.* 579, 613–619. doi: 10.1113/jphysiol.2006.125948

Yarrow, K., Brown, P., and Krakauer, J. W. (2009). Inside the brain of an elite athlete: the neural processes that support high achievement in sports. *Nat. Rev. Neurosci.* 10, 585–596. doi: 10.1038/nrn2672

Zacksenhouse, M., Lebedev, M. A., Carmena, J. M., O'Doherty, J. E., Henriquez, C., and Nicolelis, M. A. (2007). Cortical modulations increase in early sessions with brain-machine interface. *PLoS One* 2:e619. doi: 10.1371/journal.pone.0000619

Zeck, G., and Fromherz, P. (2001). Noninvasive neuroelectronic interfacing with synaptically connected snail neurons immobilized on a semiconductor chip. *Proc. Natl. Acad. Sci. U S A* 98, 10457–10462. doi: 10.1073/pnas.181348698

Zeller, D., Gross, C., Bartsch, A., Johansen-Berg, H., and Classen, J. (2011). Ventral premotor cortex may be required for dynamic changes in the feeling of limb ownership: a lesion study. *J. Neurosci.* 31, 4852–4857. doi: 10.1523/jneurosci.5154-10.2011

Ziemann, U., Iliać, T. V., Pauli, C., Meintzschel, F., and Ruge, D. (2004). Learning modifies subsequent induction of long-term potentiation-like and long-term depression-like plasticity in human motor cortex. *J. Neurosci.* 24, 1666–1672. doi: 10.1523/JNEUROSCI.5016-03.2004

Ziemann, U., Paulus, W., Nitsche, M. A., Pascual-Leone, A., Byblow, W. D., Berardelli, A., et al. (2008). Consensus: motor cortex plasticity protocols. *Brain Stimul.* 1, 164–182. doi: 10.1016/j.brs.2008.06.006

Ziemann, U., Tam, A., Butefisch, C., and Cohen, L. G. (2002). Dual modulating effects of amphetamine on neuronal excitability and stimulation-induced plasticity in human motor cortex. *Clin. Neurophysiol.* 113, 1308–1315. doi: 10.1016/s1388-2457(02)00171-2

Zunzunegui, C., Gao, B., Cam, E., Hodor, A., and Bassetti, C. L. (2011). Sleep disturbance impairs stroke recovery in the rat. *Sleep* 34, 1261–1269. doi: 10.5665/sleep.1252

Conflict of Interest Statement: The authors declare that the research was conducted in the absence of any commercial or financial relationships that could be construed as a potential conflict of interest.

Received: 14 March 2014; accepted: 23 May 2014; published online: 11 June 2014.
*Citation: Di Pino G, Maravita A, Zollo L, Guglielmelli E and Di Lazzaro V (2014) Augmentation-related brain plasticity. Front. Syst. Neurosci. **8**:109. doi: 10.3389/fnsys.2014.00109*
This article was submitted to the journal Frontiers in Systems Neuroscience.

frontiers in
SYSTEMS NEUROSCIENCE

PERSPECTIVE ARTICLE
published: 26 May 2014
doi: 10.3389/fnsys.2014.00104

Brain-machine interfaces can accelerate clarification of the principal mysteries and real plasticity of the brain

Yoshio Sakurai*

Department of Psychology, Graduate School of Letters, Kyoto University, Kyoto, Japan

Edited by:
Mikhail Lebedev, Duke University, USA

Reviewed by:
Mikhail Lebedev, Duke University, USA
Ioan Opris, Wake Forest University, USA

*****Correspondence:***
Yoshio Sakurai, Department of Psychology, Graduate School of Letters, Kyoto University, Yoshida-honmachi, Sakyo-ku, Kyoto 606-8501, Japan
e-mail: ysakurai@bun.kyoto-u.ac.jp

This perspective emphasizes that the brain-machine interface (BMI) research has the potential to clarify major mysteries of the brain and that such clarification of the mysteries by neuroscience is needed to develop BMIs. I enumerate five principal mysteries. The first is "how is information encoded in the brain?" This is the fundamental question for understanding what our minds are and is related to the verification of Hebb's cell assembly theory. The second is "how is information distributed in the brain?" This is also a reconsideration of the functional localization of the brain. The third is "what is the function of the ongoing activity of the brain?" This is the problem of how the brain is active during no-task periods and what meaning such spontaneous activity has. The fourth is "how does the bodily behavior affect the brain function?" This is the problem of brain-body interaction, and obtaining a new "body" by a BMI leads to a possibility of changes in the owner's brain. The last is "to what extent can the brain induce plasticity?" Most BMIs require changes in the brain's neuronal activity to realize higher performance, and the neuronal operant conditioning inherent in the BMIs further enhances changes in the activity.

Keywords: brain-machine interface, neuronal coding, cell assembly, functional localization, ongoing activity, brain-body interaction, brain plasticity

INTRODUCTION

A brain-machine interface (BMI) is used to enable the neuroprosthetic control of external devices by neuronal activity instead of body parts movements (Lebedev and Nicolelis, 2006; Berger et al., 2008; Hatsopoulos and Donoghue, 2009; Nicolelis and Lebedev, 2009; Andersen et al., 2010; Moran, 2010; Green and Kalaska, 2011; Lebedev, 2014). Although the development of invasive BMIs has been making a steady progress and holds promises for future clinical use (Lebedev and Nicolelis, 2011; Lebedev et al., 2011; Nicolelis, 2011; Ethier et al., 2012; Hochberg et al., 2012; Collinger et al., 2013), currently available BMIs are limited in terms of accuracy and efficiency with which they can be controlled. As described in the papers referenced above, it is possible to indicate some technical factors affecting the limited performance of current BMIs. However, as also emphasized in some of the papers (e.g., Nicolelis and Lebedev, 2009; Andersen et al., 2010), improvements in the technical factors alone cannot solve all the problems preventing the realization of an ideal BMI, i.e., a system controlling external neuroprosthetic devices freely as intended by the brain without any special training. The ideal BMI required rich and precise information that depends on the activity and function of the brain. Therefore, as Nicolelis (2003), Baranauskas (2014), and Mandonnet and Duffau (2014) has discussed, knowledge of what the brain is and how it works, the ultimate goals of neuroscience research, are essential for BMI research. To achieve these goals, the present paper enumerates five principal mysteries of the brain that must be clarified. It should be emphasized that BMI research has the potential to clarify these principal mysteries and, at the same time, their clarification by neuroscience research is necessary to realize the ideal BMI.

HOW IS INFORMATION ENCODED IN THE BRAIN?

As the final goal of a BMI is to detect neuronal activity representing information in the brain, BMI research inevitably faces the problem of how is information encoded in the working brain. Neuronal coding (e.g., Calvin, 1996; Abbott and Sejnowski, 1999; Nicolelis, 2001; Nicolelis and Ribeiro, 2006; Holscher and Munk, 2009) is one of the principal mysteries of the brain and may be the ultimate problem of neuroscience, because its final goal is to bridge the mind and brain and detect the mind from brain activity. The early studies of BMIs (Chapin et al., 1999; Wessberg et al., 2000; Nicolelis and Chapin, 2002) have already produced very important and instructive findings demonstrating the nature of the neuronal coding of information. They reported that the activity of only a limited number of neurons randomly sampled from the motor cortex of an animal provided sufficient information to predict arm kinematics during reaching, as well as hand gripping force. In addition, the accuracy of prediction increased as the number of recorded randomly sampled neurons increased. These results indicate that kinematic and kinetic parameters are coded not by the activities of specific motor-related neurons but by the activity of many neurons distributed in the motor cortex. Subsequent BMI studies more or less supported this notion of neuronal coding in the motor cortex (e.g., Carmena et al., 2003). Therefore, as Nicolelis (2003) and Nicolelis and Lebedev (2009) have suggested, a BMI both utilizes population coding

by cell assemblies (Hebb, 1949), functionally connected neurons acting as codes representing information in the working brain (Eichenbaum, 1993; Sakurai, 1996b, 1999; Harris, 2005; Sakurai and Takahashi, 2006, 2008; Buzsáki, 2010; Wallace and Kerr, 2010; Sakurai et al., 2013), and provides new insights on this coding. In other words, the theory of cell assembly has been further verified by BMI studies and is approaching an answer to the mystery of neuronal coding.

Although recent neuroscience studies have often reported small populations of neurons related to information processing (e.g., Takahashi and Sakurai, 2009a,b; Opris et al., 2012, 2013) and BMI research has clearly supported the cell assembly theory, the existence of cell assemblies as carriers of neuronal codes has not yet been directly proven, because current BMIs have a bias in the firing rate or amplitude of neuronal activity used as the source signals. This bias may be a factor affecting the limited performance of current BMIs (Sakurai et al., 2014). According to the notion of cell assembly, synchronous and oscillatory activities among many neurons may have the potential to be informative signals for BMIs. It is expected to construct a BMI system which uses ensemble and correlated firing of distributed many neurons, in addition to their firing rates, as neuronal source signals.

HOW IS INFORMATION DISTRIBUTED IN THE BRAIN?

BMI studies have revealed the fact that the neurons whose activity can be used as signals representing information of motor movements are distributed in the motor cortex. Concerning the range of distribution of such neurons, some BMI studies have obtained an optimal basis for brain control of devices by recording the activity of neurons in the precentral (motor) cortical area associated with actual limb movement (Chapin et al., 1999; Taylor et al., 2002; Carmena et al., 2003; Hochberg et al., 2006; Koike et al., 2006; Choi et al., 2009). However, some other studies on BMIs demonstrated their ability to predict movements from neurons in the postcentral (parietal) as well as the precentral cortical areas (Wessberg et al., 2000; Carmena et al., 2003). Although precentral motor neurons can provide accurate predictions of force and displacement even in small numbers (Koike et al., 2006; Choi et al., 2009), many neurons from the parietal and other cortical areas could also have the potential to provide significant predictions. The prediction accuracy increased with the number of neurons included, even when the included neurons were randomly selected from the non-motor area and unrelated to motor movement in nature (Wessberg et al., 2000; Carmena et al., 2003). This indicates that neuronal information on motor movements and forces is widely distributed in cortical areas.

These findings by BMI studies could challenge the classical and conservative view of functional localization based on functional divisions in the brain. Constructing functional divisions is a major problem of neuroscience and many researchers are investigating what functions are localized in what brain areas. The results of BMI studies indicate that the functional boundaries are not definite and fixed but obscure and dynamic. Some BMIs do not necessarily require the selection of functionally specific motor neurons (e.g., Moritz et al., 2008) or, as described above, a specific motor area in the brain to improve their performance in brain control of devices. This notion may be related to the theory of multipotentiality of the brain (John, 1980). This theory suggests that any neuron and region may contribute to the mediation of a diversity of functions and that many neurons and regions contribute to many functions, although it does not imply that different neurons and regions have complete equivalence of functions or that different functions depend equally on diverse neurons and regions. BMI research may again direct the spotlight on the theory of multipotentiality and push back the view of too rigid and too subdivided functional maps. On the other hand, regarding the use of a BMI as a neuroprosthetic system, it is advantageous for it to have the potential to utilize any neuron and any brain region unrelated to the target functions replaced by the BMI.

WHAT IS THE FUNCTION OF THE ONGOING ACTIVITY OF THE BRAIN?

Invasive BMIs will be continuously introduced to use in daily life and should function to voluntarily control moving and resting external devices. Therefore, a principal mystery that BMI research requires present neuroscience to solve is, as Velliste et al. (2014) has discussed, how the brain is active during lengthy periods of behavioral inactivity when no specific tasks are, at least consciously, being performed. This is the problem of the "ongoing" or "intrinsic" activity of the brain (Vincent et al., 2007). Most neuroscience studies have not paid any attention to this problem and have devoted themselves to recording and analyzing neural activity only during the performance of various behavioral tasks. In such recording studies using behavioral tasks, most researchers have implicitly assumed that the spontaneous neural activity prior to the presentation of stimuli or motor responses is an independent random process and have treated it as "baseline activity" or "background noise" unrelated to information processing.

However, this view of spontaneous activity was challenged as early as the 1990s. For example, Arieli et al. (1995) reported that collective ensembles of activity of many neurons of the visual cortex occurred not only during stimulus-evoked periods but also during spontaneous non-stimulus periods. They suggested that the population activity of neurons is not an independent random process even during baseline periods. The correlated activity was detected among neurons comprising a population and among separate populations of neurons. It can be considered that these temporally correlated neurons and populations are cell assemblies, and the ongoing spontaneous activity of cell assemblies may reflect the processing of the context, which affects the processing of incoming sensory stimuli or motor responses (Arieli et al., 1995). The result of Sakurai (1996a) supports this notion, because the correlated activity of hippocampal and auditory cortical neurons, recorded during non-stimulus intertrial intervals, represented the context, i.e., the type of tasks that the animal was currently engaged in. These studies strongly indicate that important mechanisms underlying the higher integrative processing of perception, cognition, attention, and memory depend on the spatiotemporal interactions between ongoing and event-evoked activities of neurons and cell assemblies.

The significant role of the spontaneous activity of neuronal populations may be related to the assumption of "default mode network" suggested by noninvasive imaging (PET, fMRI) studies on human (Raichle, 2010) and monkey (Mantini et al., 2011) brains. The noninvasive images, which represent the activity of large populations of neurons, often show periodic synchronous activation across several close and distant cortical areas during periods of rest with no tasks. Raichle (2010, 2011) suggests that such periodic activation in multiple areas, the "default mode", has a preparatory function to process incoming sensory stimuli or motor responses. Therefore, the default mode and the ongoing activity have the same features and functions and indicate the significant role of the synchronous activity during periods with no tasks. Further clarification of its functional role must contribute to further development of BMIs that can be mounted continuously in daily life.

HOW DOES THE BODILY BEHAVIOR AFFECT THE BRAIN FUNCTION?

The brain controls behavioral functions of the body and, at the same time, the behavior of the body affects the activity of the brain (Chiel and Beer, 1997). In this notion of brain-body interaction, the problem of how bodily movements constrain brain activity is closely related to BMIs, because BMIs require the replacement of bodily movements with machine devices. Typical evidence of the bodily effect on brain activity and function is the "phantom limb" (Ramachandran and Hirstein, 1998). A sudden loss of parts of the body often causes drastic changes in tactile and movement-related perception and generates hallucinations of body images. This confused representation of perceptual information is considered to be due to the reorganization of neuronal networks and the following confused coding of sensory information (Melzack, 1990). Accordingly, a BMI might change functions of the brain, especially the neuronal coding of perceptual information.

The phenomenon of the phantom limb indicates that stable and precise coding in the brain requires stable and precise inputs of sensory information generated from the body. This is not restricted to tactile and movement-related sensations but also applicable to other sensory inputs. "Charles Bonnet syndrome" (Menon et al., 2003) is a typical case of visual hallucinations, i.e., the confused and spontaneous coding of perceptual information caused by the complete and long-lasting deprivation of visual inputs. In addition, isolation experiments cutting off visual, auditory, and tactile sensory inputs, originally discussed by Hebb (1949), showed that several types of hallucination can be generated even in short periods of sensory deprivation (Heron, 1957). If stable and precise sensory inputs are essential for the normal coding of information, the artificial operation of sensory inputs may correct the abnormal hallucinations caused by sensory deprivation. This assumption is supported by the "virtual reality box" experiment (Ramachandran and Hirstein, 1998), in which the artificial presentation of mirror images of lost parts of the body often changes or erases hallucinations that involve body images.

All these findings indicating the importance of sensory inputs consistent with bodily behaviors recommend the further development of BMIs equipped with sensory feedback contingent with the behaviors of brain-controlling devices. Recently, Tabot et al. (2013) have succeeded in restoring tactile feedback using a brain-controlled prosthetic hand. O'Doherty et al. (2011) have developed a BMBI (brain-machine-brain interface), which can provide a monkey with not only visual but also tactile feedback from a brain-controlled device (virtual hand). Further neuroscience research on brain-body interaction will contribute to development of BMBIs, and progress in BMBI research will clarify how the brain interacts with the body, encodes sensory information, and constructs body images (Shokur et al., 2013).

TO WHAT EXTENT CAN THE BRAIN INDUCE PLASTICITY?

This final section further discusses the BMI-induced plasticity of the brain and emphasizes why it is inevitable in all BMIs. Some studies have reported clear changes in the plasticity of neuronal activities and functions induced by the use of BMIs (e.g., Zacksenhouse et al., 2007; Ganguly et al., 2011). Such plastic changes can be thought to be induced to some extent in most BMI experiments, in which the conversion of neuronal signals is aided by appropriate transform algorithms to generate suitable control parameters. The conversion parameters obtained for one set of trials provided increasingly poor predictions of future responses, indicating the drift of neuronal signals over tens of minutes. Therefore, accurate device control under BMI conditions inevitably requires the neuronal activity to be volitionally modulated to become more suitable signals for device control, and the brain surely responds to the request for activity modulation. The BMI-induced changes in neuronal activity are not restricted to the regions from which signals used for device control are recorded. Koralek et al. (2012, 2013) investigated the role of corticostriatal plasticity, usually involved in learning physical skills, in abstract skill learning by a BMI using motor cortical neurons. During the learning of control by the BMI, an alteration of activity was observed in the striatal neurons, and strong correlations, reflected in oscillatory coupling, between the neuronal activity in the motor cortex and the striatum emerged. The authors concluded that temporally precise coherence develops specifically in motor output-related neuronal populations during learning and that the oscillatory activity serves to synchronize widespread brain networks to produce appropriate behaviors.

Discussion of the mechanisms of BMI-induced plastic changes in neuronal activity also requires a psychological view, i.e., operant conditioning. In most BMI situations, the successful control of devices can function as a reward and reinforces the occurrence of volitionally modulated neuronal activity to control the devices. This process of reinforcing the volitional modulation of activity is the operant conditioning of neuronal activity (Fetz, 1969). All BMIs are thought to include this process of conditioning (Fetz, 2007; Sakurai et al., 2014), making plastic changes in neuronal activity inevitable. This leads to the argument that the investigation of neuronal operant conditioning (neurofeedback)

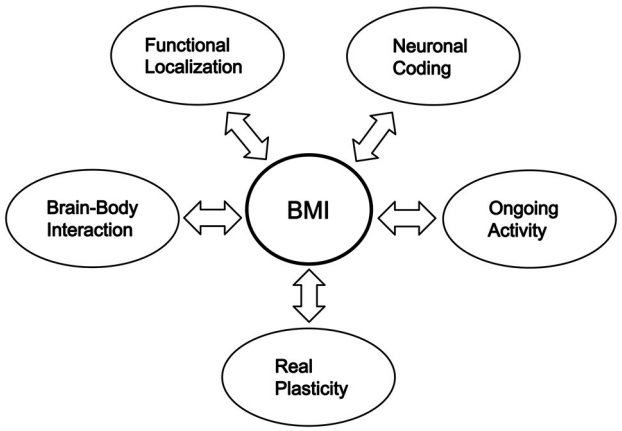

FIGURE 1 | Interactive advancement of researches on BMIs and the principal mysteries of the brain.

will inevitably contribute to the realization of higher-performing BMIs (Fetz, 2007; Moritz et al., 2008; Sakurai et al., 2014). In addition, research on the operant conditioning of synchrony and oscillation of neurons (Engelhard et al., 2013; Fetz, 2013; Sakurai and Takahashi, 2013), i.e., the activity of cell assemblies, will also significantly contribute to the development of BMIs (Sakurai et al., 2014).

It should be noted that the neuronal plasticity inherent in BMI experiments is not always an obstacle for the development of higher-performing BMIs and can be actively applied to research on the extent to which the brain can change and how the brain can be changed efficiently. The former means that BMI studies are able to classify the real plasticity of the brain. The latter suggests that the development of BMIs will lead to the development of better methods of neurorehabilitation to induce changes in neuronal activities and connections for functional compensation (Dobkin, 2007; Fetz, 2007; Jackson and Fetz, 2011; Miller and Weber, 2011).

CONCLUSION

Although research in modern neuroscience has made great progress, BMI research has shown that we still do not fully understand even the major properties of the brain, i.e., the principal mysteries enumerated in the present paper. BMI research has the role of impelling present neuroscience to clarify the major properties, including the real plasticity, of the brain, and further progress in neuroscience in uncovering the properties of the brain contributes to the further development of BMIs (**Figure 1**).

ACKNOWLEDGMENTS

This work was supported by JST Core Research for Evolution Science and Technology (CREST) program and JSPS KAKENHI grant Nos. 24223004 and 24243069 (Yoshio Sakurai).

REFERENCES

Abbott, L., and Sejnowski, T. J. (1999). *Neural Codes and Distributed Representations.* Cambridge: MIT Press.

Andersen, R. A., Hwang, E. J., and Mulliken, G. H. (2010). Cognitive neural prosthetics. *Annu. Rev. Psychol.* 61, 169–190. doi: 10.1146/annurev.psych.093008.100503

Arieli, A., Shoham, D., Hildesheim, R., and Grinvald, A. (1995). Coherent spatiotemporal patterns of ongoing activity revealed by real-time optical imaging coupled with single-unit recording in the cat visual cortex. *J. Neurophysiol.* 73, 2072–2093.

Baranauskas, G. (2014). What limits the performance of current invasive brain machine interfaces? *Front. Sys. Neurosci.* 8:68. doi: 10.3389/fnsys.2014.00068

Berger, T. W., Chapin, J. K., Gerhardt, G. A., McFarland, D. J., Principe, J. C., Soussou, W. V., et al. (2008). *Brain-Computer Interfaces.* New York: Springer.

Buzsáki, G. (2010). Neural syntax: cell assemblies, synapsembles, and readers. *Neuron* 68, 362–385. doi: 10.1016/j.neuron.2010.09.023

Calvin, W. H. (1996). *The Cerebral Code—Thinking a Thought in the Mosaics of the Mind.* Cambridge: MIT Press.

Carmena, J. M., Lebedev, M. A., Crist, R. E., O'Doherty, J. E., Santucci, D. M., Dimitrov, D. F., et al. (2003). Learning to control a brain-machine interface for reaching and grasping by primates. *PLoS Biol.* 1:E42. doi: 10.1371/journal.pbio.0000042

Chapin, J. K., Moxon, K. A., Markowitz, R. S., and Nicolelis, M. A. (1999). Real-time control of a robot arm using simultaneously recorded neurons in the motor cortex. *Nat. Neurosci.* 2, 664–670. doi: 10.1038/10223

Chiel, H. J., and Beer, R. D. (1997). The brain has a body: adaptive behavior emerges from interactions of nervous system, body and environment. *Trends Neurosci.* 20, 553–557. doi: 10.1016/s0166-2236(97)01149-1

Choi, K., Hirose, H., Sakurai, Y., Iijima, T., and Koike, Y. (2009). Prediction of arm trajectory from the neural activities of the primary motor cortex with modular connectionist architecture. *Neural Netw.* 22, 1214–1223. doi: 10.1016/j.neunet.2009.09.003

Collinger, J. L., Wodlinger, B., Downey, J. E., Wang, W., Tyler-Kabara, E. C., Weber, D. J., et al. (2013). High-performance neuroprosthetic control by an individual with tetraplegia. *Lancet* 381, 557–564. doi: 10.1016/s0140-6736(12)61816-9

Dobkin, B. H. (2007). Brain-computer interface technology as a tool to augment plasticity and outcomes for neurological rehabilitation. *J. Physiol.* 579, 637–642. doi: 10.1113/jphysiol.2006.123067

Eichenbaum, H. (1993). Thinking about brain cell assemblies. *Science* 261, 993–994. doi: 10.1126/science.8351525

Engelhard, B., Ozeri, N., Israel, Z., Bergman, H., and Vaadia, E. (2013). Inducing gamma oscillations and precise spike synchrony by operant conditioning via brain-machine interface. *Neuron* 77, 361–375. doi: 10.1016/j.neuron.2012.11.015

Ethier, C., Oby, E. R., Bauman, M. J., and Miller, L. E. (2012). Restoration of grasp following paralysis through brain-controlled stimulation of muscles. *Nature* 485, 368–371. doi: 10.1038/nature10987

Fetz, E. E. (1969). Operant conditioning of cortical unit activity. *Science* 163, 955–958. doi: 10.1126/science.163.3870.955

Fetz, E. E. (2007). Volitional control of neural activity: implications for brain-computer interfaces. *J. Physiol.* 579, 571–579. doi: 10.1113/jphysiol.2006.127142

Fetz, E. E. (2013). Volitional control of cortical oscillations and synchrony. *Neuron* 77, 216–218. doi: 10.1016/j.neuron.2013.01.003

Ganguly, K., Domitrov, D. F., Wallis, J. D., and Carmena, J. M. (2011). Reversible large-scale modification of cortical networks during neuroprosthetic control. *Nat. Neurosci.* 14, 662–667. doi: 10.1038/nn.2797

Green, A. M., and Kalaska, J. F. (2011). Learning to move machines with the mind. *Trends Neurosci.* 34, 61–75. doi: 10.1016/j.tins.2010.11.003

Harris, K. D. (2005). Neural signatures of cell assembly organization. *Nat. Rev. Neurosci.* 6, 399–407. doi: 10.1038/nrn1669

Hatsopoulos, N. G., and Donoghue, J. P. (2009). The science of neural interface systems. *Annu. Rev. Neurosci.* 32, 249–266. doi: 10.1146/annurev.neuro.051508.135241

Hebb, D. O. (1949). *The Organization of Behavior—A Neuropsychological Theory.* New York: Wiley.

Heron, W. (1957). The pathology of boredom. *Sci. Am.* 196, 52–56. doi: 10.1038/scientificamerican0157-52

Hochberg, L. R., Bacher, D., Jarosiewicz, B., Masse, N. Y., Simeral, J. D., Vogel, J., et al. (2012). Reach and grasp by people with tetraplegia using a neurally controlled robotic arm. *Nature* 485, 372–375. doi: 10.1038/nature11076

Hochberg, L. R., Serruya, M. D., Friehs, G. M., Mukand, J. A., Saleh, M., Caplan, A. H., et al. (2006). Neuronal ensemble control of prosthetic devices by a human with tetraplegia. *Nature* 442, 164–171. doi: 10.1038/nature04970

Holscher, C., and Munk, M. (2009). *Information Processing by Neuronal Populations.* New York: Cambridge University Press.

Jackson, A., and Fetz, E. E. (2011). Interfacing with the computational brain. *IEEE Trans. Neural Syst. Rehabil. Eng.* 19, 534–541. doi: 10.1109/tnsre.2011.2158586

John, E. R. (1980). "Multipotentiality: a statistical theory of brain function–evidence and implications," in *The Psychobiology of Consciousness*, ed D. Richard (New York: Springer), 129–146.

Koike, Y., Hirose, H., Sakurai, Y., and Iijima, T. (2006). Prediction of arm trajectory from a small number of neuron activities in the primary motor cortex. *Neurosci. Res.* 55, 146–153. doi: 10.1016/j.neures.2006.02.012

Koralek, A. C., Costa, R. M., and Carmena, J. M. (2013). Temporally precise cell-specific coherence develops in corticostriatal networks during learning. *Neuron* 79, 865–872. doi: 10.1016/j.neuron.2013.06.047

Koralek, A. C., Jin, X., Long, J. D. II., Costa, R. M., and Carmena, J. M. (2012). Corticostriatal plasticity is necessary for learning intentional neuroprosthetic skills. *Nature* 483, 331–335. doi: 10.1038/nature10845

Lebedev, M. A. (2014). Brain-machine interfaces: an overview. *Trans. Neurosci.* 5, 99–110. doi: 10.2478/s13380-014-0212-z

Lebedev, M. A., and Nicolelis, M. A. L. (2006). Brain-machine interfaces: past, present and future. *Trends Neurosci.* 29, 536–546. doi: 10.1016/j.tins.2006.07.004

Lebedev, M. A., and Nicolelis, M. A. L. (2011). Toward a whole body neuroprosthetic. *Prog. Brain Res.* 194, 47–60. doi: 10.1016/b978-0-444-53815-4.00018-2

Lebedev, M. A., Tate, A. J., Hanson, T. L., Li, Z., O'Doherty, J. E., Winans, J. A., et al. (2011). Future developments in brain-machine interface research. *Clinics (Sao Paulo)* 66(Suppl. 1), 25–32. doi: 10.1590/s1807-59322011001300004

Mandonnet, E., and Duffau, H. (2014). Understanding entangled cerebral networks: a prerequisite for restoring brain function with brain-computer interfaces. *Front. Sys. Neurosci.* 8:82. doi: 10.3389/fnsys.2014.00082

Mantini, D., Gerits, A., Neilssen, K., Durand, J.-B., Joly, O., Simone, L., et al. (2011). Default mode of brain function in monkeys. *J. Neurosci.* 31, 12954–12962. doi: 10.1523/JNEUROSCI.2318-11.2011

Melzack, R. (1990). Phantom limbs and the concept of a neuromatrix. *Trends Neurosci.* 13, 88–92. doi: 10.1016/0166-2236(90)90179-e

Menon, G. J., Rahman, I., Menon, S. J., and Dutton, G. N. (2003). Complex visual hallucinations in the visually impaired: the Charles Bonnet Syndrome. *Surv. Ophthalmol.* 48, 58–72. doi: 10.1016/S0039-6257(02)00414-9

Miller, L. E., and Weber, D. J. (2011). Brain training: cortical plasticity and afferent feedback in brain-machine interface system. *IEEE Trans. Neural Syst. Rehabil. Eng.* 19, 465–467. doi: 10.1109/tnsre.2011.2168989

Moran, D. (2010). Evolution of brain-computer interface: action potentials, local field potentials and electrocorticograms. *Cur. Opin. Neurobiol.* 20, 741–745. doi: 10.1016/j.conb.2010.09.010

Moritz, C. T., Perimutter, S. I., and Fetz, E. E. (2008). Direct control of paralysed muscles by cortical neurons. *Nature* 456, 639–642. doi: 10.1038/nature07418

Nicolelis, M. A. L. (2001). *Advances in Neural Population Coding (Progress in Brain Research)* (Vol. 130). New York: Elsevier.

Nicolelis, M. A. L. (2003). Brain–machine interfaces to restore motor function and probe neural circuits. *Nat. Rev. Neurosci.* 4, 417–422. doi: 10.1038/nrn1105

Nicolelis, M. A. L. (2011). Mind out of body. *Sci. Am.* 304, 80–83. doi: 10.1038/scientificamerican0211-80

Nicolelis, M. A. L., and Chapin, J. K. (2002). Controlling robots with the mind. *Sci. Am.* 287, 46–53. doi: 10.1038/scientificamerican1002-46

Nicolelis, M. A. L., and Lebedev, M. A. (2009). Principles of neural ensemble physiology underlying the operation of brain-machine interfaces. *Nat. Rev. Neurosci.* 10, 530–540. doi: 10.1038/nrn2653

Nicolelis, M. A. L., and Ribeiro, S. (2006). Seeking the neural code. *Sci. Am.* 295, 70–77. doi: 10.1038/scientificamerican1206-70

O'Doherty, J. E., Lebedev, M. A., Ifft, P. J., Zhuang, K. Z., Shokur, S., Bleuler, H., et al. (2011). Active tactile exploration enabled by a brain-machine-brain interface. *Nature* 479, 228–231. doi: 10.1038/nature10489

Opris, I., Fuqua, J. L., Huettl, P. F., Gerhardt, G. A., Berger, T. W., Hampson, R. E., et al. (2012). Closing the loop in primate prefrontal cortex: inter-laminar processing. *Front. Neural Circuits* 6:88. doi: 10.3389/fncir.2012.00088

Opris, I., Santos, L., Gerhardt, G. A., Song, D., Berger, T. W., Hampson, R. E., et al. (2013). Prefrontal cortical microcircuits bind perception to executive control. *Sci. Rep.* 3:2285. doi: 10.1038/srep02285

Raichle, M. E. (2010). Two views of brain function. *Trends Cogn. Sci.* 14, 180–190. doi: 10.1016/j.tics.2010.01.008

Raichle, M. E. (2011). The restless brain. *Brain Connect.* 1, 3–12. doi: 10.1089/brain.2011.0019

Ramachandran, V. S., and Hirstein, W. (1998). The perception of phantom limbs. The D. O. Hebb lecture. *Brain* 121, 1603–1630. doi: 10.1093/brain/121.9.1603

Sakurai, Y. (1996a). Hippocampal and neocortical cell assemblies encode memory processes for different types of stimuli in the rat. *J. Neurosci.* 16, 2809–2819.

Sakurai, Y. (1996b). Population coding by cell assemblies—what it really is in the brain. *Neurosci. Res.* 26, 1–16. doi: 10.1016/0168-0102(96)01075-9

Sakurai, Y. (1999). How do cell assemblies encode information in the brain? *Neurosci. Biobehav. Rev.* 23, 785–796. doi: 10.1016/s0149-7634(99)00017-2

Sakurai, Y., and Takahashi, S. (2006). Dynamic synchrony of firing in the monkey prefrontal cortex during working memory tasks. *J. Neurosci.* 26, 10141–10153. doi: 10.1523/jneurosci.2423-06.2006

Sakurai, Y., and Takahashi, S. (2008). Dynamic synchrony of local cell assembly. *Rev. Neurosci.* 19, 425–440. doi: 10.1515/revneuro.2008.19.6.425

Sakurai, Y., and Takahashi, S. (2013). Conditioned enhancement of firing rates and synchrony of hippocampal neurons and firing rates of motor cortical neurons in rats. *Eur. J. Neurosci.* 37, 623–639. doi: 10.1111/ejn.12070

Sakurai, Y., Nakazono, T., Ishino, S., Terada, S., Yamaguchi, K., and Takahashi, S. (2013). Diverse synchrony of firing reflects diverse cell-assembly coding in the prefrontal cortex. *J. Physiol. Paris* 107, 459–470. doi: 10.1016/j.jphysparis.2013.05.004

Sakurai, Y., Song, K., Tachibana, S., and Takahashi, S. (2014). Volitional enhancement of firing synchrony and oscillation by neuronal operant conditioning: interaction with neurorehabilitation and brain-machine interface. *Front. Sys. Neurosci.* 8:11. doi: 10.3389/fnsys.2014.00011

Shokur, S., O'Doherty, J. E., Winans, J. A., Bleuler, H., Lebedev, M. A., and Nicolelis, M. A. L. (2013). Expanding the primate body schema in sensorimotor cortex by virtual touches of an avatar. *Proc. Natl. Acad. Sci. U S A* 110, 15121–15126. doi: 10.1073/pnas.1308459110

Tabot, G. A., Dammann, J. F., Berg, J. A., Tenore, F. V., Boback, J., Vogelstein, R. J., et al. (2013). Restoring the sense of touch with a prosthetic hand through a brain interface. *Proc. Natl. Acad. Sci. U S A* 110, 18279–18284. doi: 10.1073/pnas.1221113110

Takahashi, S., and Sakurai, Y. (2009a). Information in small neuronal ensemble activity in the hippocampal CA1 during delayed non-matching to sample performance in rats. *BMC Neurosci.* 10:115. doi: 10.1186/1471-2202-10-115

Takahashi, S., and Sakurai, Y. (2009b). Sub-millisecond firing synchrony of closely neighboring pyramidal neurons in hippocampal CA1 of rats during delayed non-matching to sample task. *Front. Neural Circuits* 3:9. doi: 10.3389/neuro.04.009.2009

Taylor, D. M., Tillery, S. I., and Schwartz, A. B. (2002). Direct cortical control of 3D neuroprosthetic devices. *Science* 296, 1829–1832. doi: 10.1126/science.1070291

Velliste, M., Kennedy, S. D., Schwartz, A. B., Whitford, A. S., Sohn, J.-W., and McMorland, A. J. C. (2014). Motor cortical correlates of arm resting in the context of a reaching task and implications for prosthetic control. *J. Neurosci.* 34, 6011–6022. doi: 10.1523/jneurosci.3520-13.2014

Vincent, J. L., Patel, G. H., Fox, M. D., Snyder, A. Z., Baker, J. T., Van Essen, D. C., et al. (2007). Intrinsic functional architecture in the anaesthetized monkey brain. *Nature* 447, 83–86. doi: 10.1038/nature05758

Wallace, D. J., and Kerr, J. N. (2010). Chasing the cell assembly. *Curr. Opin. Neurobiol.* 20, 296–305. doi: 10.1016/j.conb.2010.05.003

Wessberg, J., Stambaugh, C. R., Kralik, J. D., Beck, P. D., Laubach, M., Chapin, J. K., et al. (2000). Real-time prediction of hand trajectory by ensembles of cortical neurons in primates. *Nature* 408, 361–365. doi: 10.1038/35042582

Zacksenhouse, M., Lebedev, M. A., Carmena, J. M., O'Doherty, J. E., Henriquez, C., and Nicolelis, M. A. L. (2007). Cortical modulations increase in early sessions with brain-machine interface. *PLoS One* 2:e629. doi: 10.1371/journal.pone.0000619

Conflict of Interest Statement: The author declares that the research was conducted in the absence of any commercial or financial relationships that could be construed as a potential conflict of interest.

Received: 26 April 2014; accepted: 13 May 2014; published online: 26 May 2014.
*Citation: Sakurai Y (2014) Brain-machine interfaces can accelerate clarification of the principal mysteries and real plasticity of the brain. Front. Syst. Neurosci. **8**:104. doi: 10.3389/fnsys.2014.00104*
This article was submitted to the journal Frontiers in Systems Neuroscience.

frontiers in
SYSTEMS NEUROSCIENCE

REVIEW ARTICLE
published: 06 February 2014
doi: 10.3389/fnsys.2014.00011

Volitional enhancement of firing synchrony and oscillation by neuronal operant conditioning: interaction with neurorehabilitation and brain-machine interface

Yoshio Sakurai[1]*, Kichan Song[1], Shota Tachibana[1] and Susumu Takahashi[2]

[1] *Department of Psychology, Graduate School of Letters, Kyoto University, Kyoto, Japan*
[2] *Laboratory of Neural Circuitry, Graduate School of Brain Science, Doshisha University, Kizugawa, Japan*

Edited by:
Mikhail Lebedev, Duke University, USA

Reviewed by:
Mikhail Lebedev, Duke University, USA
Valerie Ego-Stengel, Centre national de la recherche scientifique, France

****Correspondence:***
Yoshio Sakurai, Department of Psychology, Graduate School of Letters, Kyoto University, Yoshida-honmachi, Sakyo-ku, Kyoto 606-8501, Japan
e-mail: ysakurai@bun.kyoto-u.ac.jp

In this review, we focus on neuronal operant conditioning in which increments in neuronal activities are directly rewarded without behaviors. We discuss the potential of this approach to elucidate neuronal plasticity for enhancing specific brain functions and its interaction with the progress in neurorehabilitation and brain-machine interfaces. The key to-be-conditioned activities that this paper emphasizes are synchronous and oscillatory firings of multiple neurons that reflect activities of cell assemblies. First, we introduce certain well-known studies on neuronal operant conditioning in which conditioned enhancements of neuronal firing were reported in animals and humans. These studies demonstrated the feasibility of volitional control over neuronal activity. Second, we refer to the recent studies on operant conditioning of synchrony and oscillation of neuronal activities. In particular, we introduce a recent study showing volitional enhancement of oscillatory activity in monkey motor cortex and our study showing selective enhancement of firing synchrony of neighboring neurons in rat hippocampus. Third, we discuss the reasons for emphasizing firing synchrony and oscillation in neuronal operant conditioning, the main reason being that they reflect the activities of cell assemblies, which have been suggested to be basic neuronal codes representing information in the brain. Finally, we discuss the interaction of neuronal operant conditioning with neurorehabilitation and brain-machine interface (BMI). We argue that synchrony and oscillation of neuronal firing are the key activities required for developing both reliable neurorehabilitation and high-performance BMI. Further, we conclude that research of neuronal operant conditioning, neurorehabilitation, BMI, and system neuroscience will produce findings applicable to these interrelated fields, and neuronal synchrony and oscillation can be a common important bridge among all of them.

Keywords: operant conditioning, synchrony, oscillation, neurorehabilitation, brain-machine interface

OPERANT CONDITIONING OF NEURONAL FIRING

When we require learning of volitional enhancement of a certain behavior, operant conditioning (Skinner, 1974; Reynolds, 1975) should be the first choice. The voluntary behavior immediately followed by reward, i.e., having contingency of reward, soon becomes more frequent, and humans and animals volitionally conduct the behavior more frequently to get more reward. Based on such methodology, an intriguing method of learning of volitional enhancement in neuronal firing has been developed and called neuronal operant conditioning, in which rewards are given for modulations of neuronal firing which are not linked to overt behaviors. Since Olds (1965) and Fetz (1969) published their pioneering research, conditioned enhancement of neuronal firing has been frequently reported in animals and humans. In particular, Fetz and collaborators (Fetz, 1969; Fetz and Finocchio, 1971; Fetz and Baker, 1973) had established the methodology of neuronal operant conditioning and reported that monkeys could control firing rates of individual neurons in the motor cortex (**Figure 1**). Following these pioneering and memorable experiments, several intriguing studies by Fetz and other researchers have been published.

Recently, for example, Kobayashi et al. (2010) has demonstrated a remarkable capacity of single neurons to be driven by volition by adapting to specific operant requirements. This experiment set variable relationships between levels of single-neuron activity in the monkey prefrontal cortex and rewarding outcomes. Prefrontal neurons changed firing rates according to the specific requirements for gaining reward, without the monkeys making a motor response, and indicated that neuronal firings constituted a volitional operant response enhanced by reward. The control task of the experiment suggested that these changes of firing were unlikely to reflect simple reward predictions. In humans, Cerf et al. (2010) demonstrated that subjects can regulate firing rates of single neurons in the medial temporal lobe (MTL) to

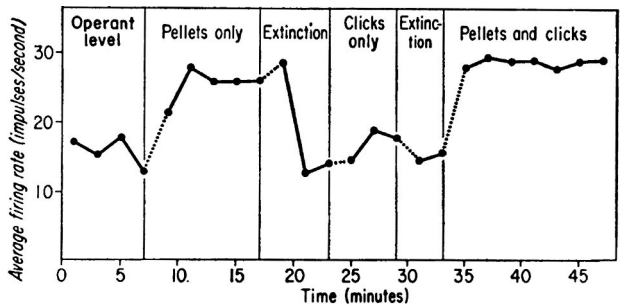

FIGURE 1 | Data showing firing rate of a motor cortex neuron of the monkey as a function of reinforcement schedule of neuronal operant conditioning. During operant level and extinction periods neither food nor click feedback was presented. During "Pellets only" period, the highest firing rates were reinforced with delivery of a food pellet without click feedback. During "Click only" period, a click was presented for each firing of the neuron; finally, both pellets and clicks were provided. (From Fetz, 1969, with permission).

obtain the rewarding outcome that visual images they liked to see became clearer on the computer screen in front of them. The study recorded from single neurons in patients implanted with intracranial electrodes for clinical reasons. The subjects looked at a hybrid superposition of two images representing familiar individuals, landmarks, objects, or animals and had to enhance one image at the expense of the other, competing one. Simultaneously, the firing of MTL neurons was decoded in real time to control the content of the hybrid, i.e., making one of the superposed images clearer than the other. The subjects reliably regulated the firing rate of these neurons, increasing the rate of some while simultaneously decreasing the rate of others. The subjects achieved this by focusing onto one image, which gradually became clearer on the computer screen, thereby overriding sensory input. On the basis of the firing of these MTL neurons, visual images in the subject's mind were visualized on an external display, which functioned as reward.

The most recent progress is reported by Arduin et al. (2013). They employed a strategy of accessing reward by controlling a prosthetic device with self-generated neuronal firing from a single neuron. They recorded multiple neurons from motor cortical areas in rats for controlling a linear actuator with a water bottle. To receive reward of water, the rats had to move the bottle until it reached a zone for drinking by raising and maintaining firing rate of each neuron above a high threshold. They defined the time the bottle took to reach the drinking zone after trial onset as time-to-reward. If the time-to-reward distribution during trials significantly differed from that during waiting periods, the single neuron was considered an operantly conditioned neuron (Opris et al., 2011b).

The firing rates of conditioned neurons increased instantaneously after a trial onset and the bottle entered the drinking zone within a very short time. The time-to-reward for the conditioned neurons soon decreased and exhibited significant difference compared to that for non-conditioned neurons. The majority of the conditioned neurons increased firing rates reliably and instantaneously after trial onset despite the absence of any temporal requisition. Furthermore, the conditioned neurons fired more frequently, instantaneously, and strongly than the neighboring neurons that were simultaneously recorded around the conditioned neurons (**Figure 2**). The authors concluded that only the operant-conditioned neurons possessing significantly increased firing rates take the lead as "master neurons", that exhibit most prominent volitionally driven modulations in a small neural network.

Such on-going progress of research into neuronal operant conditioning confirms the possibility of volitional enhancement of activity for specific individual neurons. However, possibility of chance reinforcement of a body movement rather than neuronal activity should always be checked. The question is whether operantly conditioned neuronal firing is directly controlled in certain central pathways or through an accidentally reinforced body movement which generates activity in the whole pathways leading to the muscles, including corollary discharge and proprioceptive and sensory feedbacks. Concerning involvement of the proprioceptive feedback, Wyler et al. (1979) reported that section of pyramidal tract and ventral rhizotomies disrupted operant conditioning of firing of precentral neurons and suggested that the precentral neurons were operantly controlled through the proprioceptive feedback from the peripheral mechanoreceptors. However, such lesions of nerve fibers could yield neuronal death and/or reorganization of neuronal networks, which may disrupt normal neuronal activity and/or potential for learning and conditioning. Intact brains and input-output pathways should be employed to answer the question of central pathways vs. body movements. Using the intact brains and pathways, several former and recent studies (Fetz and Finocchio, 1971; Koralek et al., 2012; Engelhard et al., 2013; Sakurai and Takahashi, 2013) reported the absence of specific body movements or muscle activity during the operant conditioning of neuronal firing. Although precise and detailed mechanisms that make neuronal operant conditioning possible are not clear yet, it is apparent that neuronal activity can be operantly conditioned without body movement and enhanced volitionally by setting direct contingency between changes of neuronal activity and delivery of reward.

OPERANT CONDITIONING OF FIRING SYNCHRONY AND OSCILLATION

The previous studies surely have confirmed robustness of operant conditioning of neuronal activity. Most of them, however, had a bias due to an exclusive focus on the firing rates of individual neurons of neocortices. Neuronal operant conditioning should be used to explore the extent to which synchronous activity in neurons can be volitionally enhanced. Synchronous neuronal activity reflects functional connectivity among multiple neurons and had not been the target of neuronal operant conditioning, though the brain functions can be considered to be realized by activities not of individual neurons but of ensembles of populations of neurons interrelated with each other. Therefore, enhancement of neuronal activity related to brain functions could be realized more reliably by operant conditioning of such ensemble activity of neuronal populations typically reflected by synchronized firing of multiple neurons.

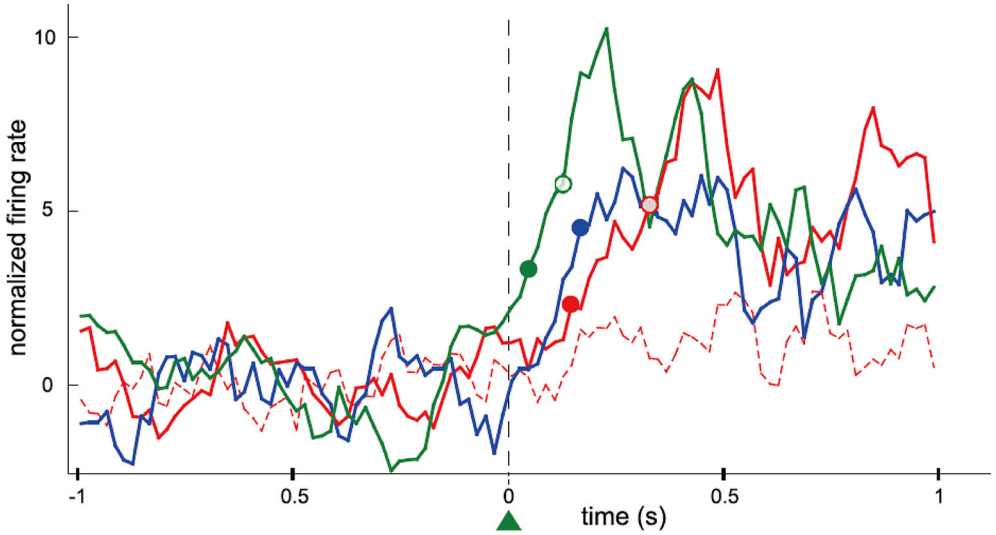

FIGURE 2 | Data showing differences in the rank of activation between conditioned neurons and simultaneously recorded neighboring neurons. Firing rate of motor cortex neurons in the rat was operantly conditioned. This presents perievent time histogram of neuronal activity normalized and centered on trial onset, for four neurons simultaneously recorded during the same session (green: the conditioned neuron; blue: a previously conditioned neuron; red: two neighboring neurons never conditioned). Filled and empty circles of different colors represent the latency of the neurons until their firings exceeded the thresholds at 2 and 5 standard deviations (SD), respectively. One of the neurons (red dashed line) did not have a measurable latency for that recording session. The latency of the blue neuron could only be defined for the 2 SD threshold. Additional (n = 20) neurons that were simultaneously recorded during that recording session have not been included for sake of clarity. Bin size: 20 ms; each value is the z-transform of the firing rate integrated over a sliding window of 100 ms. Latencies were calculated using a 20 ms bin scale. (From Arduin et al., 2013, with permission).

Engelhard et al. (2013) has recently reported that periodically synchronized activity, i.e., oscillatory activity, of motor cortical neurons can be enhanced by operant conditioning. The study has succeeded to train monkeys to increase motor cortex low-gamma waves of local field potential (LFP) (**Figure 3**). Single-neuron firing was recorded, and the enhancement of operantly conditioned oscillatory waves was accompanied by a correlated increase in the synchrony of the entrained neurons. This relation of LFP and neuronal firing can be explained by the fact that LFPs are produced by postsynaptic potentials, and periodicity in neuronal firing would be associated with periodicity in LFPs. They also documented the spatial extent of neurons entrained with the operantly conditioned oscillatory activity. Over the extent of 4 × 4 mm electrode grids, enhanced gamma power in the LFP and phase locking of neuronal firings occurred in a broad range (approximately 500 μm), and depth of entrained modulation decreased as a function of distance from the operant conditioning sites of electrodes. The study also confirmed that the enhancement of oscillatory activity was not associated with any observed movements or increases in muscle activity. From these findings, the authors argue that the findings link volitional control of LFP oscillations and neuronal-firing synchrony.

The low-gamma oscillations have been found in many different brain areas and are considered to be associated with different functions such as attention, perception, cognition, and computation (Herrmann et al., 2010) and to play as neural synchrony both within (Salinas and Sejnowski, 2001) and between (Siegel et al., 2012) brain areas. Therefore, the results of Engelhard et al. (2013) are ground breaking, whereby monkeys demonstrated the ability to directly modulate and enhance specific patterns of synchrony of many neurons in somewhat broad ranges, which may be related to several motor functions of the brain.

On the other hand, it is desirable to directly demonstrate operant enhancement of firing synchrony among individual neurons located closely in restricted smaller ranges. For such experiments, precise separation of extracellular firing from closely neighboring neurons in real time is required. It had been difficult, however, for traditional spike-sorting techniques (Lewicki, 1994; Fee et al., 1996), primarily because spike waveforms overlap on a common electrode when nearby neurons fire coincidently. To address this problem, we (Takahashi et al., 2003a,b) developed a unique method of spike-sorting using independent component analysis (ICA; Comon, 1994) with a specific multielectrode (Takahashi and Sakurai, 2005, 2007, 2009a,b). The method allows sorting of the firings of closely neighboring neurons in real time and the detection of firing synchrony. Using this technique, we have recently reported that synchronized firing of closely neighboring neurons in rat hippocampus can be enhanced by neuronal operant conditioning (Sakurai and Takahashi, 2013).

We trained rats to engage in a free-operant task in which nose-poke behavior was rewarded in session 1, and firing rates and synchrony of multiple neighboring neurons above preset criteria were rewarded in sessions 2 and 3, respectively. Placing contingency of reward on firing synchrony in session 3 resulted in selective enhancement of firing synchrony of the hippocampal neurons (**Figure 4**). Control experiments revealed that the enhancement of firing synchrony was not attributable to increments of behaviors

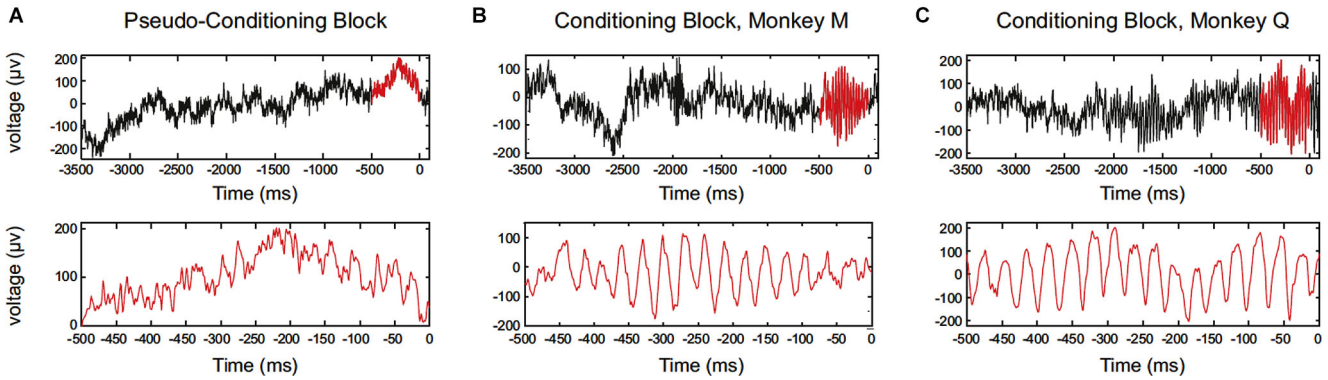

FIGURE 3 | Data showing single-trial examples of LFP aligned to reward delivery (0). Oscillatory firing of motor cortical neurons of the monkey was operantly conditioned. **(A)** Data for monkey M (session #20). Upper panel shows a raw LFP trace in the pseudoconditioning block. The 500 ms period before reward is highlighted in red. Lower panel is an expanded view of the 500 ms period before reward. **(B)** The same as in **(A)**, but for a trial in the conditioning block. **(C)** The same as in **(A)**, but for a trial in the conditioning block, monkey Q (session #17). (From Engelhard et al., 2013, with permission).

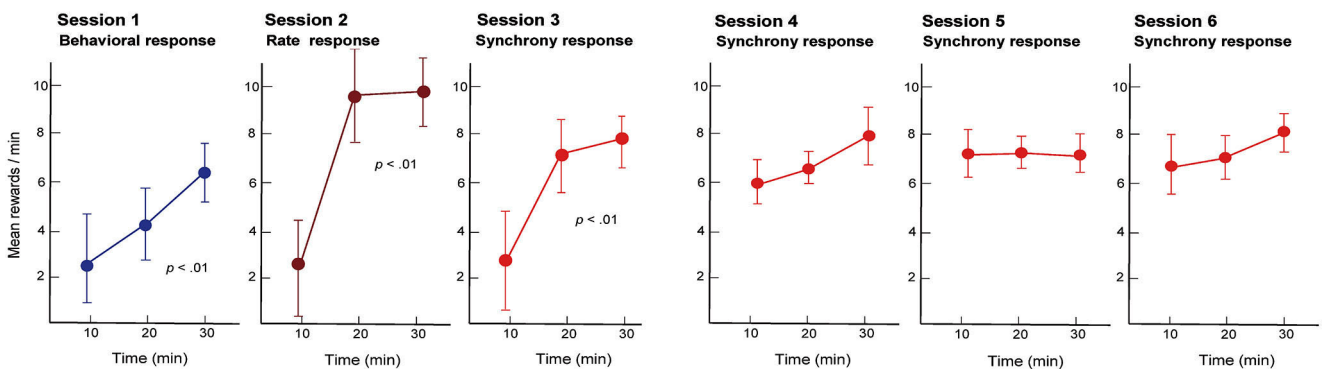

FIGURE 4 | Mean quantities of pellets, reward in the operant conditioning, delivered by behavior (session 1), firing rate above preset criteria (session 2) and firing synchrony above preset criteria (sessions 3–6) during each 30 min conditioning session. Neuronal firing rate and synchrony were obtained from a group of neighboring neurons in the hippocampal CA1 of the rat and operantly conditioned. In sessions 1–3, means were calculated for three periods (10–20, 21–30 and 31–40 min) of each session. Data recorded for the first 10 min of each session are not presented because the first 10 min were used to perform behavioral shaping (session 1) and selection of criteria for the neuronal activities (sessions 2 and 3). In sessions 4–6, means were calculated for periods of 0–10, 11–20 and 21–30 min of each session because criterion selection had been conducted in session 3 and was thus unnecessary. (From Sakurai and Takahashi, 2013, with permission).

or excitation caused by reward delivery. Analysis of the firing rates and synchrony of individual neurons and neuron pairs during the conditioning revealed that the firing rates and synchrony of some but not all neurons and neuron pairs increased in each group of neighboring neurons (**Figures 5**, **6**). No firing enhancement was observed in any neurons and neuron pairs recorded by closely placed electrodes not used for the conditioning. From all these findings, we conclude that neuronal operant conditioning can lead to volitional enhancement of firing synchrony in a small group of neurons in a small restricted area in the hippocampus.

In that study, operant conditioning of firing synchrony was obtained in the hippocampus but not in the motor cortex. One explanation might be that the hippocampus has the high level of plasticity causing learning-related changes of firing synchrony among the neurons (e.g., Sakurai, 1996a, 2002). This explanation, however, does not exclude the possibility of motor cortical neurons to be conditioned in their firing synchrony. The hippocampal synchrony functions could be revealed at small timescales such as the bin (2–4 ms) used for the operant conditioning in our study (Sakurai and Takahashi, 2013), whereas in the motor cortex synchrony could be best functional at longer timescales such as that of low gamma oscillations. This assumption is apparently supported by the result of Engelhard et al. (2013) introduced above.

It should be noted that, as Fetz (2013) suggested, synchronous neuronal firing was detected not only as lasting and periodic, e.g., oscillations, but also as temporal and episodic. For example, Riehle et al. (1997) has reported that such temporally short and episodic synchrony of firing of motor cortical neurons can be detected during some specific behavior. Such synchrony was termed "unitary event" which appeared consistently at particular times in relation to an expected cue at times unrelated to sensory

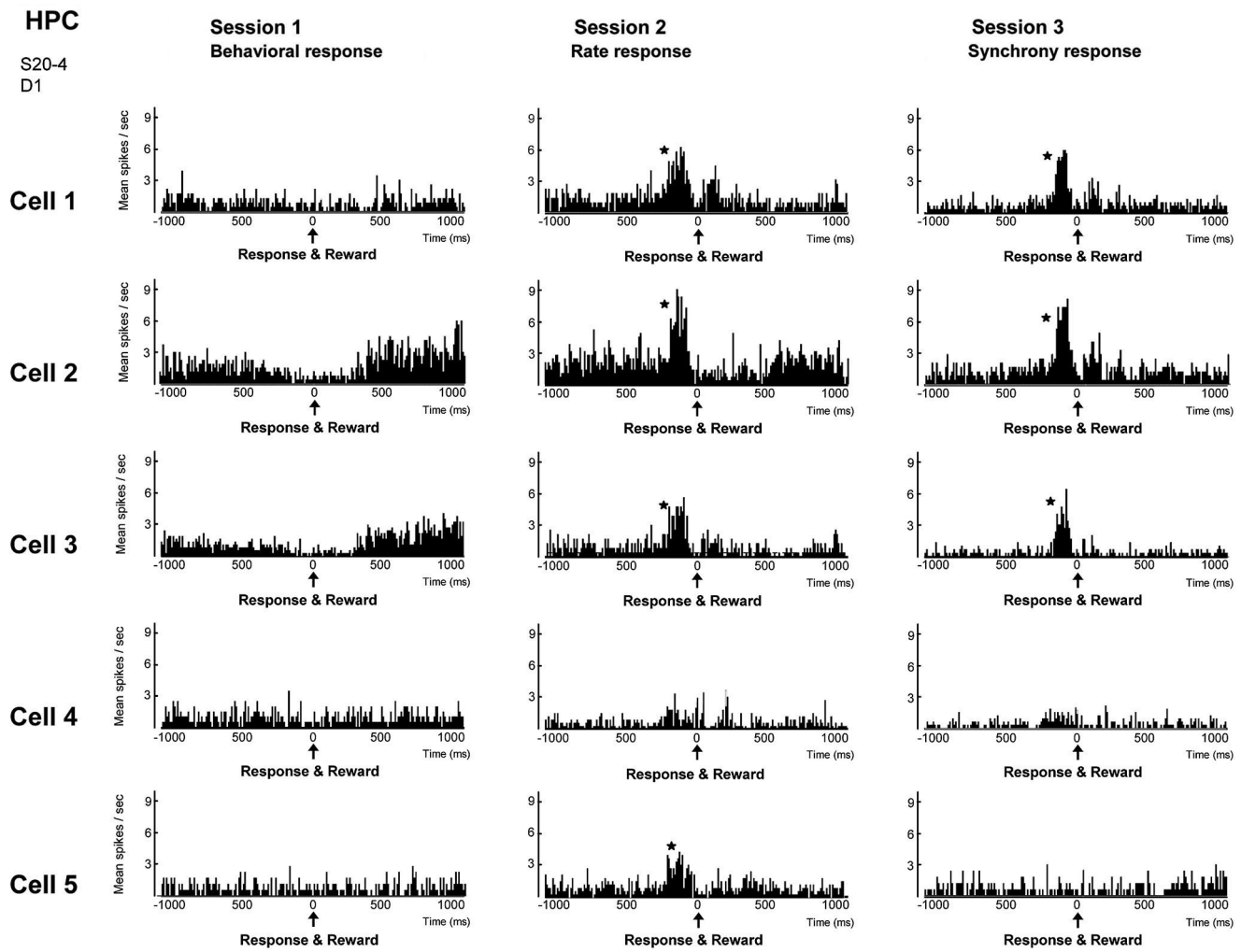

FIGURE 5 | Firing-rate histograms of five individual neurons comprising a group of neighboring neurons in the hippocampal CA1 in sessions 1–3. The center (0) of each histogram means the time when behavior (session 1), firing rate above preset criteria (session 2) and firing synchrony above preset criteria (session 3) immediately followed by reward delivery were conducted. A bin is 10 ms and an asterisk indicates a significant increment of firing (confidence limit, $p < 0.005$). (From Sakurai and Takahashi, 2013, with permission).

or motor events. Such episodic synchrony of firing should be a target of neuronal operant conditioning. Schmied et al. (1993) reported that humans could be operantly conditioned to increase some episodic synchrony of groups of motor cortical neurons. However, because synchronized firings can be caused by common synaptic inputs, such demonstration may be essentially equivalent to demonstrating enhancement of firing of the common input neurons. In contrast, periodic synchrony of firing represents a rhythmic phenomenon involving a different mechanism generating more prolonged circuit resonance (Fetz, 2013).

WHY SYNCHRONY AND OSCILLATION?—VIEW ON "CELL ASSEMBLY"

As described above, operant conditioning of oscillation and synchrony of multiple neurons can be indispensable to enhancing brain functions because they are realized by ensemble activities of populations of neurons that are functionally connected with each other. Such a functional population of neurons has been proposed to be "cell assembly" (Hebb, 1949), postulated to act as a functional unit that represents information in the working brain and underlie perception, learning, and memory for adaptive behavior (Eichenbaum, 1993; Sakurai, 1996b, 1999; Harris, 2005; Opris et al., 2013). The original concept of cell assembly was a theoretical notion and it could have value and be substantial when it accounts for experimentally observed phenomena. The experimental observations showing major properties of the cell assembly are, as Sakurai (1999) suggested, the task-related functional overlapping of individual neurons (Sakurai, 1994) and the task-dependent dynamics of the functional connectivity among the neurons (Sakurai, 1993). In particular, the latter phenomena, reflected as dynamically changing synchrony of firing of multiple neurons, has often been reported and regarded as the popular operational definition or indirect evidence of the activity of cell assemblies (Sakurai, 1996a, 2002; Riehle et al., 1997; Engel

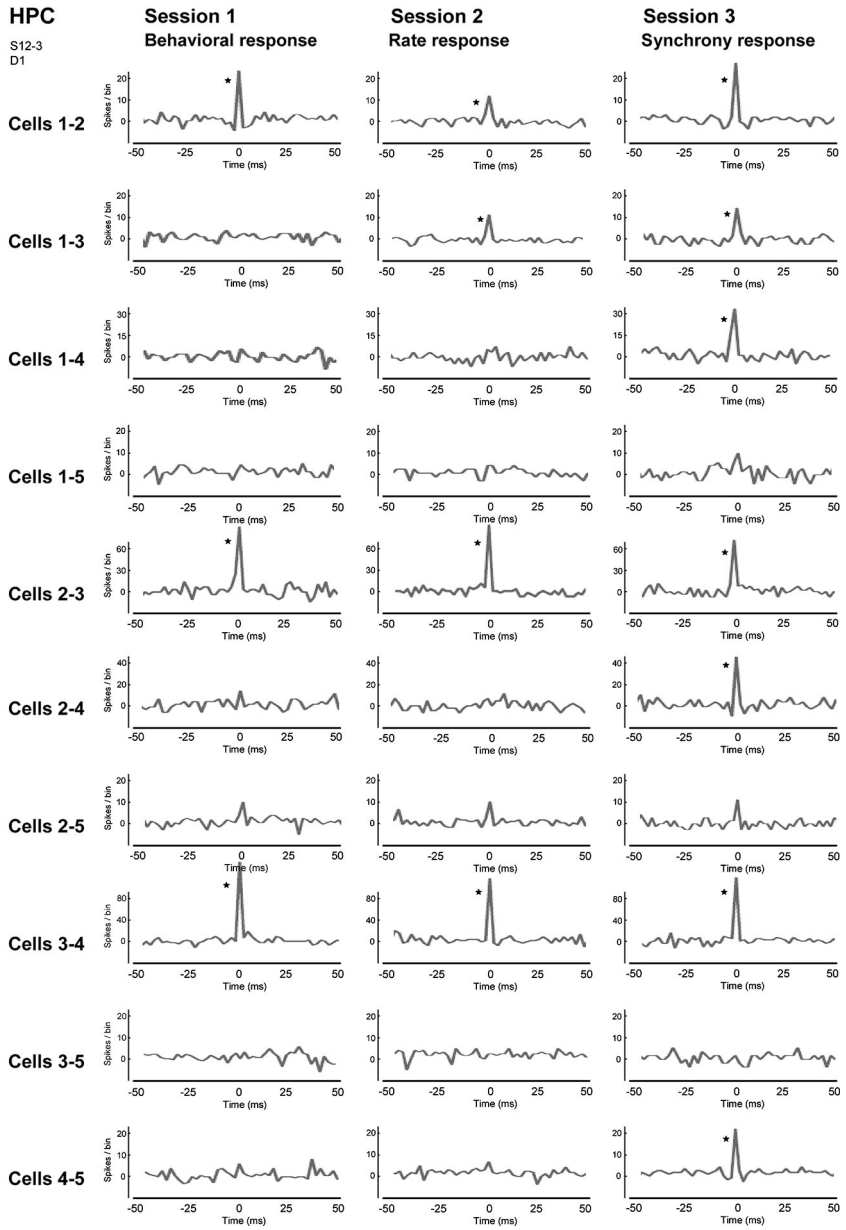

FIGURE 6 | Correlograms of all neuron pairs of five neighboring neurons in the hippocampal CA1 in sessions 1–3. The center (0) of each correlogram means the time when two neurons fired simultaneously, i.e., achieved firing synchrony. A bin is 2 ms and an asterisk indicates a significant increment in firing synchrony (confidence limit, $p < 0.005$). (From Sakurai and Takahashi, 2013, with permission).

et al., 2001). Therefore, the target activity of neuronal operant conditioning should include not only firing rates but also firing synchrony of multiple neurons, as reported in Engelhard et al. (2013) and Sakurai and Takahashi (2013).

However, operant conditioning of the activity of cell assemblies is not an easy task because the ranges in the patterns of activation of cell assemblies, i.e., sizes of cell assemblies, have been postulated to be diverse (Sakurai et al., 2013). A cell assembly could be comprised of a small number of localized neurons or a large number of broadly distributed neurons (Eichenbaum, 1993). Therefore, neurons in the neocortices and the limbic structures, particularly the hippocampus, are expected to show various forms of firing synchrony, which represent dynamic and diverse representation by cell assemblies, in various behavioral tasks. Actually, several former studies have reported the task- and behavior-dependent dynamic synchrony of neurons in the wide ranges (Abeles et al., 1993; Vaadia et al., 1995; Seidemann et al., 1996; Engel et al., 2001; Opris et al., 2011a, 2012a,b) and the local ranges (Funahashi and Inoue, 2000; Constantinidis et al., 2001; Sakurai and Takahashi, 2008). We have reported task-dependent sharp synchrony of firing among the neighboring neurons, reflecting the small and localized cell assemblies, in the

monkey prefrontal cortex, but at the same time, we have also found dynamically changing broad synchrony of firing among the distant neurons (Sakurai and Takahashi, 2006). The sizes of cell assemblies are certainly diverse and dependent on information representation and processing in behavioral tasks.

The diversity in the sizes of cell assemblies should be considered when neuronal operant conditioning is applied to enhance synchronized neuronal activity. Our study (Sakurai and Takahashi, 2013) has operantly enhanced firing synchrony of the small and localized groups of neighboring neurons, using the specific electrode and the spike sorting, in the rat hippocampus. Such synchronized firing among close neurons has been shown to be valid for some information processes. For example, Fujisawa et al. (2008) has reported clear synchrony of firing among neighboring neurons in the rat prefrontal cortex. The authors focused on the sharp peaks in cross-correlograms between pyramidal neurons and interneurons with millisecond time lags that were consistent with monosynaptic delays. The temporal relationships of the activities of neurons were examined during a working memory task. Numerous monosynaptic pairs between the pyramidal neurons and interneurons dynamically varied their peaks in the cross-correlograms across various phases of the task beyond the statistical accounting for the effects of covarying the firing rates of the neurons. This indicates that functional interplay among the close neurons linked by monosynaptic connections is working during the behavioral task. This finding was consistent with those of previous studies that have observed variance in the short-term synchrony between neuronal pairs as a function of behavioral performance and learning (Constantinidis et al., 2002; Baeg et al., 2007; Opris et al., 2011a, 2012a).

On the other hand, the study of Engelhard et al. (2013), introduced above, can be considered to have succeeded to operantly enhance activity of broader cell assemblies reflected by oscillatory low-gamma waves of LFP, because the oscillatory LFPs are produced by synchronized postsynaptic potentials of many neurons in broader ranges. Oscillatory activity in the motor cortex has been observed in many experiments and led various hypotheses about its possible functions, such as motor preparation and attention to aspects of movement (Murthy and Fetz, 1996; Donoghue et al., 1998). Oscillatory activity has also been documented most thoroughly in the visual system, where many experiments have suggested that the widespread periodicity is involved in top-down processing (Engel et al., 2001) and plays a role in long-range interactions between different cortical regions (Siegel et al., 2012).

Discussion is still ongoing about the actual functional role of oscillatory and synchronous activities. But with neuronal operant conditioning, as Fetz (2013) suggested, those activities become the independent variable in the experiments, and their effects on behavior are more compelling evidence of their functions. Actually, Keizer et al. (2010) has shown that volitionally increased gamma oscillation at occipital and frontal sites in humans surely improved performance on cognitive tests of sensory binding and memory. This result supports the notion that various information processes are generated by oscillatory activity in the motor and sensory cortices.

In addition to the findings of oscillation, synchrony of firings among individual neurons in broader ranges has been reported. Pipa and Munk (2011) trained monkeys to perform a short-term visual memory task and simultaneously recorded multi-neuronal activity from the prefrontal cortex with electrodes that were arranged in a square-shaped 4×4 grid with a distance between the nearest neighbors of 500 μm. The authors found firing synchrony of neurons with high temporal precision across the electrode sites. The frequency of synchrony was modulated depending on the behavioral performance and the specific stimuli that were presented. In particular, during the delay period, larger groups of up to 7 electrode sites showed performance-dependent modulation of the synchronous firings. These findings indicate dynamic activity of broad populations of distributed neurons that underlie the higher temporal organization of information being processed for the task performance.

Recent technological advances have made it possible to record from larger neuronal populations. New principal component analysis (PCA) methods (Peyrache et al., 2009; Lopes-dos-Santos et al., 2011) are suitable for detecting larger cell assemblies that are constructed from larger number of distributed neurons. However, classical methods, such as cross-correlation analyses, have merit in detection of detailed structures of functional connectivity between neighboring neurons. A combination of the new methods of PCA and the classical methods may be ideal in detecting diverse synchrony of neuronal activity and useful to selectively enhance activities of cell assemblies with different sizes.

RELEVANCE TO NEUROREHABILITATION AND BRAIN-MACHINE INTERFACE

NEUROREHABILITATION

Neuronal operant conditioning can elucidate the potential of neuronal plasticity (Dobkin, 2007) induced by conditioning of neuronal activity including synchronous and oscillatory activities. Such elucidation contributes to progress in the development of neurorehabilitation methods (Raskin, 2011), the majority of which attempt artificial enhancement of neuronal activity to compensate for loss of brain motor functions. A turning point of neuronal operant conditioning to be applicable may be the fact that it does not require selection of functionally specific neurons for the conditioning. It would not be possible to condition and enhance inherent motor neurons for compensation of motor functions because most motor-function losses are accompanied by loss of inherent motor neurons. Therefore, neuronal operant conditioning should have the potential to enhance any neuron and hopefully any brain region unrelated to the target functions to be compensated. This could be related to the theory of multipotentiality of the brain (John, 1980). That theory suggests that any neuron and region may contribute to the mediation of a diversity of functions and that many neurons and regions contribute to every function, but it does not imply that different neurons and regions are functionally equivalent or that different functions depends equally on diverse neurons and regions.

Actually in our study (Sakurai and Takahashi, 2013), the neurons showing rapid enhancement in firing rates and synchrony during the neuronal operant conditioning had been selected randomly and originally manifested no behavior-related activity responsible for motor responses. This finding indicates that neurons not initially involved in behavioral performance can

be enhanced by the conditioning and subsequently utilized to compensate for loss of motor functions responsible for behavior. Such an indication had previously emerged from the findings of Moritz et al. (2008), who observed that monkeys could learn to use task-unrelated neurons to control an external device if they were provided with operant control training.

Besides the notion of non-selectivity of neurons, it is again noted that conditioning of oscillatory and synchronous activities are expected to lead to more effective neurorehabilitation. Synchronous oscillations in motor cortical neurons have been observed in many behavioral experiments, leading to hypotheses about its possible function. For example, it has been reported to occur during an instructed delay period prior to movement and then disappear during the overt movement, suggesting a role in motor preparation (Donoghue et al., 1998). Oscillations have also been observed to appear during a maintained precision grip (Baker et al., 1999) and free exploratory hand movements (Murthy and Fetz, 1996). It should be emphasized that these oscillations entrained both task-related and unrelated neurons equally, and coherent oscillations occurred over widespread cortical areas, including both hemispheres, but correlations between different cortical sites did not depend on the site's relation to the task (Fetz, 2013). Consequently, inducing such oscillatory activity by operant conditioning could thus enhance several motor-related functions.

In addition to the motor-related functions, synchrony and oscillations are considered to be associated with attention, perception, cognition, and computation (Fries, 2009; Herrmann et al., 2010) and active both within (Salinas and Sejnowski, 2001) and between (Siegel et al., 2012; Terada et al., 2013) brain locations, as described previously. These indicate the possibility of enhancing such higher functions by conditioning of synchrony and oscillations of firing. An issue to be addressed is whether any neuron can be available for the conditioning to enhance the higher functions in the sensory and higher brain regions, as motor functions in the motor-related regions. Addressing this issue involves testing the validity of the view of multipotentiality of the brain (John, 1980) briefly introduced above.

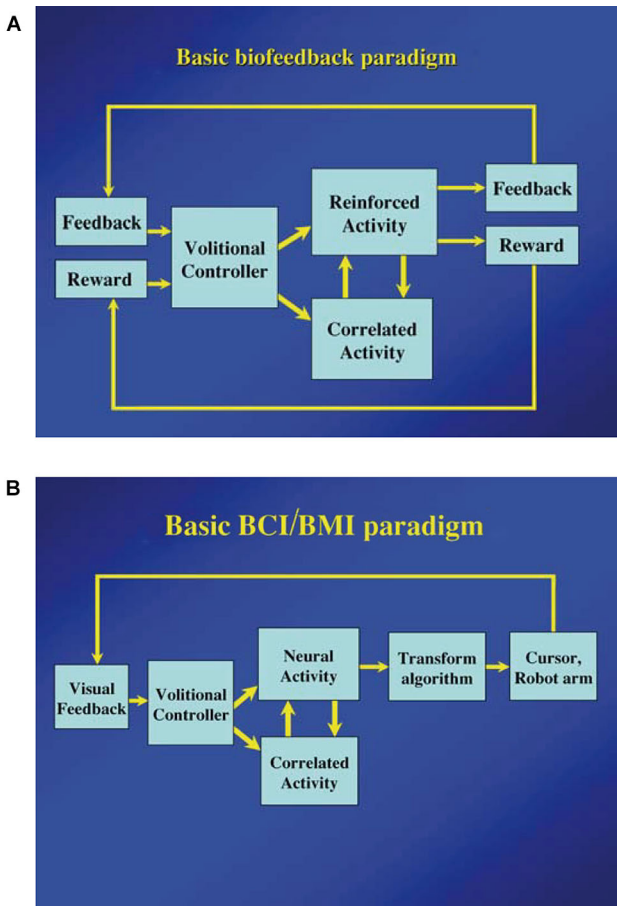

FIGURE 7 | (A) Basic components of neuronal operant conditioning (biofeedback) paradigm. Feedback and reward are contingent on the reinforced activity and provided to the brain of the "volitional controller". The correlated activity consists of additional neural or physiological activity either causally or adventitiously associated with the reinforced activity. (From Fetz, 2007, with permission). **(B)** Basic components of the brain–computer interface (BCI) or brain-machine interface (BMI) paradigms. Essential components are identical to those of the neuronal operant conditioning, except that feedback (usually visual) is provided by the controlled device or cursor, and a more sophisticated transform algorithm is typically used to convert neural activity to the requisite control signals. (From Fetz, 2007, with permission).

BRAIN-MACHINE INTERFACE

As Fetz (2007) suggested, the basic paradigm for neuronal operant conditioning (neural biofeedback) is essentially identical to the paradigm for brain-machine interface (BMI) (**Figure 7**). BMI is for neuroprosthetic control of external devices by neuronal activity instead of behavior (Berger et al., 2008; Hatsopoulos and Donoghue, 2009; Nicolelis and Lebedev, 2009; Andersen et al., 2010; Green and Kalaska, 2011). Neuronal operant learning can elucidate the possibility of volitional control of neuronal activity and contribute to the development of BMI. One difference is the transform algorithm converting neural activity to the control signals operating the external device to get reward. Though this interposes an intermediate stage that may complicate the relationship between neural activity and device control, the final outcome is identical with that of neuronal operant conditioning, i.e., getting reward. The device control in BMI finally results in getting of reward and sometimes, particularly in humans, being able to control the device itself functions as reward. This leads to the conclusion that the basic strategy—volitional activity associated with getting reward is enhanced by reinforcement feedback—is identical between BMI and neuronal operant conditioning. **Figure 8** summarizes the common and different stages in BMI and neuronal operant conditioning.

Although the development of invasive BMI is promising (Lebedev and Nicolelis, 2006), currently available BMIs are limited in terms of accuracy and the facility with which they can be controlled. The most significant factor to which these limits may be attributable may be changes in the plasticity of neuronal activities and functions induced by the use of BMI (Zacksenhouse et al., 2007; Ganguly et al., 2011). In most BMI experiments based on the decoding approach, conversion of neuronal signals is aided by appropriate transform algorithms to generate the adequate

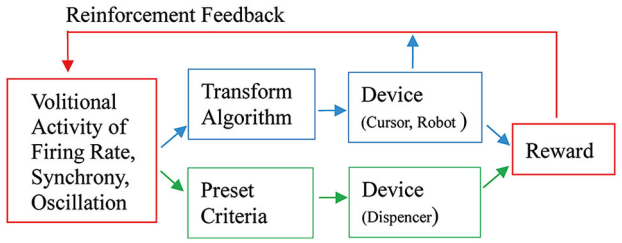

FIGURE 8 | An integrated view of basic components of neuronal operant conditioning (Figure 7A) and BMI (Figure 7B) paradigms. The different stages are shown in blue and green parts, the former for BMI and the latter for neuronal operant conditioning, and the common stages are shown in red parts. See the text for detail.

control parameters. However, the conversion parameters obtained for one set of trials provided increasingly poor predictions of future responses, indicating a source of drift over tens of minutes. Therefore, accurate device control under BMI conditions depends significantly on the degree to which the neuronal activity can be volitionally modulated even for experiments not based on neuronal operant conditioning. Research on such volitional modulation of neuronal activity can be conducted by investigating neuronal operant conditioning, which contributes to realization of a higher performing BMI. The other significant factor affecting the limited performance of the current BMIs may be the bias on firing rate or amplitude of neuronal activity as the source signals. As emphasized in the present paper, synchronous and oscillatory activities have the potential to be neuronal signals constantly representing valid information in the brain. Research for volitional modulation of neuronal synchrony and oscillation by neuronal operant conditioning may contribute much to development of a higher performing BMI.

The issue of neuron selectivity and multipotentiality in the study of neuronal operant conditioning is also a significant issue in BMI studies. Many BMI studies first obtain an optimal basis for brain control by recording the neural activity associated with real limb movement from precentral motor cortex and deriving appropriate transform algorithms (Chapin et al., 1999; Taylor et al., 2002; Carmena et al., 2003; Hochberg et al., 2006; Koike et al., 2006; Choi et al., 2009). However, several other studies demonstrated the ability to extract movement predictions from neurons in postcentral as well as precentral cortical areas (Wessberg et al., 2000; Carmena et al., 2003). Precentral motor neurons could provide the accurate predictions of force and displacement even in small numbers (Koike et al., 2006; Choi et al., 2009), but many neurons from other areas also had potential to provide significant predictions (Wessberg et al., 2000; Carmena et al., 2003). The prediction accuracy increased with the number of neurons included, even when the included neurons were randomly selected and not related to motor movement in nature (Wessberg et al., 2000; Carmena et al., 2003).

Neuronal plasticity, which is inherent in BMI experiments, is not always an obstacle but can be actively applied to induce changes in neuronal connections for functional compensation. For example, Mavoori et al. (2005) investigated the operation of a small computer chip in conjunction with wire electrodes implanted in monkey motor cortex. This "neurochip", useful for invasive BMI, can convert firings of a cortical neuron not to control signals for external devices but to stimuli directly delivered to other neurons and regions to appropriately modify the neural activity in these regions. Jackson et al. (2006) configured the neurochip as action potentials recorded at one site triggered synchronous stimulation at the neighboring site in the monkey motor cortex. Continuous operation for a day or more resulted in long-term changes in the output effects evoked from the recording site and the changes remained stable for more than a week of testing after the conditioning had terminated. Such conditioning effects were related to time-dependent plasticity and obtained only when the delays between neuronal firings and stimuli were less than 50 ms, indicating that firing synchrony could be involved as an effective factor in such plastic changes.

Finally, we introduce the recent findings that learning to operate BMI induces synchronous and oscillatory activity in other brain regions related to specific functions. Koralek et al. (2012) investigated the role of corticostriatal plasticity, usually involved in learning physical skills, in abstract skill learning using BMI. The authors trained rats to learn to control the pitch of an auditory cursor to reach one of two targets by modulating firing activity in the motor cortex independently of physical movement. During the learning of BMI, alteration of activity was observed in striatal neurons, with more neurons modulating activity in relation to the progress in learning to reach the targets. Concurrently, strong correlations, reflected in oscillatory coupling, between the neuronal activity in the motor cortex and the striatum emerged. This suggests that corticostriatal plasticity and oscillatory interaction underlying physical skill learning is also necessary for abstract skill learning using BMI and that neuroprosthetic movements capitalize on the neural circuitry involved in natural motor learning. Most recently, Koralek et al. (2013) also reported that coherence of activity between motor cortex and striatum during learning of the BMI task is selectively increased in neurons controlling behavioral output relative to adjacent neurons. The temporal offset of these oscillatory interactions aligned closely with corticostriatal conduction delays, demonstrating highly precise timing. Firings from either region were followed by a consistent phase in the other region, suggesting that network feedback reinforces the coherent activity. The authors conclude that temporally precise coherence develops during learning specifically in motor output-related neuronal populations and oscillatory activity serves to synchronize widespread brain networks to produce adequate behavior. This confirms that selective temporal coordination between neurons leading to development of cell assemblies is fundamental in learning to control behavior. Koralek et al. (2012, 2013) reliably indicate that research using BMI can be research of system neuroscience and can provide significant data to reveal normal brain functions and their mechanisms.

In conclusion, research into neuronal operant conditioning, neurorehabilitation, BMI, and system neuroscience will produce findings applicable to all these interrelated fields, and synchrony and oscillation of neuronal activity can be a common key bridge interrelating these disciplines.

ACKNOWLEDGMENTS

This work was supported by JST Core Research for Evolution Science and Technology (CREST) program and JSPS KAKENHI grant Nos. 24223004 and 24243069 (Yoshio Sakurai) and 24300148 and 25560435 (Susumu Takahashi).

REFERENCES

Abeles, M., Bergman, H., Margalit, E., and Vaadia, E. (1993). Spatiotemporal firing patterns in the frontal cortex of behaving monkeys. *J. Neurophysiol.* 70, 1629–1638.

Andersen, R. A., Hwang, E. J., and Mulliken, G. H. (2010). Cognitive neural prosthetics. *Annu. Rev. Psychol.* 61, 169–190. doi: 10.1146/annurev.psych.093008.100503

Arduin, P., Fregnac, Y., Shulz, D. E., and Ego-Stengel, V. (2013). "Master" neurons induced by operant conditioning in rat motor cortex during a brain-machine interface task. *J. Neurosci.* 33, 8308–8320. doi: 10.1523/JNEUROSCI.2744-12.2013

Baeg, E. H., Kim, Y. B., Ghim, J. W., Kim, J. J., and Jung, M. W. (2007). Learning-induced enduring changes in functional connectivity among prefrontal cortical neurons. *J. Neurosci.* 27, 909–918. doi: 10.1523/jneurosci.4759-06.2007

Baker, S. N., Kilner, J. M., Pinches, E. M., and Lemon, R. N. (1999). The role of synchrony and oscillations in the motor output. *Exp. Brain Res.* 128, 109–117. doi: 10.1007/s002210050825

Berger, T. W., Chapin, J. K., Gerhardt, G. A., McFarland, D. J., Principe, J. C., Soussou, W. V., et al. (2008). *Brain-Computer Interfaces*. New York: Springer.

Carmena, J. M., Lebedev, M. A., Crist, R. E., O'Doherty, J. E., Santucci, D. M., Dimitrov, D. F., et al. (2003). Learning to control a brain-machine interface for reaching and grasping by primates. *PLoS Biol.* 1:E42. doi: 10.1371/journal.pbio.0000042

Cerf, M., Thiruvengadam, N., Mormonn, F., Kraskov, A., Quiroga, R. Q., Koch, C., et al. (2010). On-line, voluntary control of human temporal lobe neurons. *Nature* 467, 1104–1108. doi: 10.1038/nature09510

Chapin, J. K., Moxon, K. A., Markowitz, R. S., and Nicolelis, M. A. (1999). Real-time control of a robot arm using simultaneously recorded neurons in the motor cortex. *Nat. Neurosci.* 2, 664–670. doi: 10.1038/10223

Choi, K., Hirose, H., Sakurai, Y., Iijima, T., and Koike, Y. (2009). Prediction of arm trajectory from the neural activities of the primary motor cortex with modular connectionist architecture. *Neural Netw.* 22, 1214–1223. doi: 10.1016/j.neunet.2009.09.003

Comon, P. (1994). Independent component analysis, a new concept? *Signal Process.* 36, 287–314. doi: 10.1016/0165-1684(94)90029-9

Constantinidis, C., Franowicz, M. N., and Goldman-Rakic, P. S. (2001). Coding specificity in cortical microcircuits: a multiple-electrode analysis of primate prefrontal cortex. *J. Neurosci.* 21, 3646–3655.

Constantinidis, C., Williams, G. V., and Goldman-Rakic, P. S. (2002). A role for inhibition in shaping the temporal flow of information in prefrontal cortex. *Nat. Neurosci.* 5, 175–180. doi: 10.1038/nn799

Dobkin, B. H. (2007). Brain-computer interface technology as a tool to augment plasticity and outcomes for neurological rehabilitation. *J. Physiol.* 597, 637–642. doi: 10.1113/jphysiol.2006.123067

Donoghue, J. P., Sanes, J. N., Hatsopoulos, N. G., and Gaál, G. (1998). Neural discharge and local field potential oscillations in primate motor cortex during voluntary movements. *J. Neurophysiol.* 79, 159–173.

Eichenbaum, H. (1993). Thinking about brain cell assemblies. *Science* 261, 993–994. doi: 10.1126/science.8351525

Engel, A. K., Fiees, P., and Singer, W. (2001). Dynamic predictions: oscillations and synchrony in top-down processing. *Nat. Rev. Neurosci.* 2, 704–716. doi: 10.1038/35094565

Engelhard, B., Ozeri, N., Israel, Z., Bergman, H., and Vaadia, E. (2013). Inducing gamma oscillations and precise spike synchrony by operant conditioning via brain-machine interface. *Neuron* 77, 361–375. doi: 10.1016/j.neuron.2012.11.015

Fee, M., Mitra, P., and Kleinfeld, D. (1996). Variability of extracellular spike waveforms of cortical neurons. *J. Neurophysiol.* 76, 3823–3833.

Fetz, E. E. (1969). Operant conditioning of cortical unit activity. *Science* 163, 955–958. doi: 10.1126/science.163.3870.955

Fetz, E. E. (2007). Volitional control of neural activity: implications for brain-computer interfaces. *J. Physiol.* 579, 571–579. doi: 10.1113/jphysiol.2006.127142

Fetz, E. E. (2013). Volitional control of cortical oscillations and synchrony. *Neuron* 77, 216–218. doi: 10.1016/j.neuron.2013.01.003

Fetz, E. E., and Baker, M. A. (1973). Operantly conditioned patterns on precentral unit activity and correlated responses in adjacent cells and contralateral muscles. *J. Neurophysiol.* 36, 179–204.

Fetz, E. E., and Finocchio, D. V. (1971). Operant conditioning of specific patterns of neural and muscular activity. *Science* 174, 431–435. doi: 10.1126/science.174.4007.431

Fries, P. (2009). Neuronal gamma-band synchronization as a fundamental process in cortical computation. *Annu. Rev. Neurosci.* 32, 209–224. doi: 10.1146/annurev.neuro.051508.135603

Fujisawa, S., Amarasingham, A., Harrison, M. T., and Buzsaki, G. (2008). Behavior-dependent short-term assembly dynamics in the medial prefrontal cortex. *Nat. Neurosci.* 11, 823–833. doi: 10.1038/nn.2134

Funahashi, S., and Inoue, M. (2000). Neuronal interactions related to working memory processes in the primate prefrontal cortex revealed by cross-correlation analysis. *Cereb. Cortex* 10, 535–551. doi: 10.1093/cercor/10.6.535

Ganguly, K., Domitrov, D. F., Wallis, J. D., and Carmena, J. M. (2011). Reversible large-scale modification of cortical networks during neuroprosthetic control. *Nat. Neurosci.* 14, 662–667. doi: 10.1038/nn.2797

Green, A. M., and Kalaska, J. F. (2011). Learning to move machines with the mind. *Trends Neurosci.* 34, 61–75. doi: 10.1016/j.tins.2010.11.003

Harris, K. D. (2005). Neural signatures of cell assembly organization. *Nat. Rev. Neurosci.* 6, 399–407. doi: 10.1038/nrn1669

Hatsopoulos, N. G., and Donoghue, J. P. (2009). The science of neural interface systems. *Annu. Rev. Neurosci.* 32, 249–266. doi: 10.1146/annurev.neuro.051508.135241

Hebb, D. O. (1949). *The Organization of Behavior—A Neuropsychological Theory*. New York: Wiley.

Herrmann, C. S., Frund, I., and Lenz, D. (2010). Human gamma-band activity: a review on cognitive and behavioral correlates and network models. *Neurosci. Biobehav. Rev.* 34, 981–992. doi: 10.1016/j.neubiorev.2009.09.001

Hochberg, L. R., Serruya, M. D., Friehs, G. M., Mukand, J. A., Saleh, M., Caplan, A. H., et al. (2006). Neuronal ensemble control of prosthetic devices by a human with tetraplegia. *Nature* 442, 164–171. doi: 10.1038/nature04970

Jackson, A., Mavoori, J., and Fetz, E. E. (2006). Long-term motor cortex plasticity induced by an electronic neural implant. *Nature* 444, 56–60. doi: 10.1038/nature05226

John, E. R. (1980). "Multipotentiality: a statistical theory of brain function–evidence and implications" in *The Psychobiology of Consciousness*, ed D. Richard (New York: Springer), 129–146.

Keizer, A. W., Verment, R. S., and Hommel, B. (2010). Enhancing cognitive control through neurofeedback: a role of gamma-band activity in managing episodic retrieval. *Neuroimage* 49, 3404–3413. doi: 10.1016/j.neuroimage.2009.11.023

Kobayashi, S., Schultz, W., and Sakagami, M. (2010). Operant conditioning of primate prefrontal neurons. *J. Neurophysiol.* 103, 1843–1855. doi: 10.1152/jn.00173.2009

Koike, Y., Hirose, H., Sakurai, Y., and Iijima, T. (2006). Prediction of arm trajectory from a small number of neuron activities in the primary motor cortex. *Neurosci. Res.* 56, 146–153. doi: 10.1016/j.neures.2006.02.012

Koralek, A. C., Costa, R. M., and Carmena, J. M. (2013). Temporally precise cell-specific coherence develops in corticostriatal networks during learning. *Neuron* 79, 865–872. doi: 10.1016/j.neuron.2013.06.047

Koralek, A. C., Jin, X., Long, J. D. II., Costa, R. M., and Carmena, J. M. (2012). Corticostriatal plasticity is necessary for learning intentional neuroprosthetic skills. *Nature* 483, 331–335. doi: 10.1038/nature10845

Lebedev, M. A., and Nicolelis, M. A. L. (2006). Brain-machine interfaces: past, present and future. *Trends Neurosci.* 29, 536–546. doi: 10.1016/j.tins.2006.07.004

Lewicki, M. (1994). Bayesian modelling and classification of neural signals. *Neural Comput.* 6, 1005–1030. doi: 10.1162/neco.1994.6.5.1005

Lopes-dos-Santos, V., Conde-Ocazionez, S., Nicolelis, M. L., Ribeiro, S. T., and Tort, A. B. L. (2011). Neuronal assembly detection and cell membership specification by principal component analysis. *PLoS One* 6:e20996. doi: 10.1371/journal.pone.0020996

Mavoori, J., Jackson, A., Diorio, C., and Fetz, E. (2005). An autonomous implantable computer for neural recording and stimulation in unrestrained primates. *J. Neurosci. Meth.* 148, 71–77. doi: 10.1016/j.jneumeth.2005.04.017

Moritz, C. T., Perimutter, S. I., and Fetz, E. E. (2008). Direct control of paralysed muscles by cortical neurons. *Nature* 456, 639–642. doi: 10.1038/nature 07418

Murthy, V. N., and Fetz, E. E. (1996). Oscillatory activity in sensorimotor cortex of awake monkeys: synchronization of local field potentials and relation to behaviour. *J. Neurophysiol.* 76, 3949–3967.

Nicolelis, M. A. L., and Lebedev, M. A. (2009). Principles of neural ensemble physiology underlying the operation of brain-machine interfaces. *Nat. Rev. Neurosci.* 10, 530–540. doi: 10.1038/nrn2653

Olds, J. (1965). Operant conditioning of single unit responses. *Excerpta. Med. Int. Cong. Ser.* 87, 372–380.

Opris, I., Fuqua, J. L., Huettl, P. F., Gerhardt, G. A., Berger, T. W., Hampson, R. E., et al. (2012a). Closing the loop in primate prefrontal cortex: interlaminar processing. *Front. Neural Circuits* 6:88. doi: 10.3389/fncir.2012. 00088

Opris, I., Hampson, R. E., Gerhardt, G. A., Berger, T. W., and Deadwyler, S. A. (2012b). Columnar processing in primate pFC: evidence for executive control microcircuits. *J. Cog. Neurosci.* 24, 2334–2347. doi: 10.1162/jocn_a_00307

Opris, I., Hampson, R. E., Stanford, T. R., Gerhardt, G. A., and Deadwyler, S. A. (2011a). Neural activity in frontal cortical cell layers: evidence for columnar sensorimotor processing. *J. Cog. Neursci.* 23, 1507–1521. doi: 10.1162/jocn.2010. 21534

Opris, I., Lebedev, M., and Nelson, R. (2011b). Motor planning under unpredictable reward: modulations of movement vigor and primate striatum activity. *Front. Neurosci.* 5:61. doi: 10.3389/fnins.2011.00061

Opris, I., Santos, L., Gerhardt, G. A., Song, D., Berger, T. W., Hampson, R. E., et al. (2013). Prefrontal cortical microcircuits bind perception to executive control. *Sci. Rep.* 3:2285. doi: 10.1038/srep02285

Peyrache, A., Khamassi, M., Benchenane, K., Wiener, S. I., and Battaglia, F. P. (2009). Replay of rule-learning related neural patterns in the prefrontal cortex during sleep. *Nat. Neurosci.* 12, 919–926. doi: 10.1038/nn.2337

Pipa, G., and Munk, M. H. (2011). Higher order spike synchrony in prefrontal cortex during visual memory. *Front. Comput. Neurosci.* 5:23. doi: 10.3389/fncom. 2011.00023

Raskin, S. A. (2011). *Neuroplasticity and Rehabilitation*. New York: Guilford.

Reynolds, G. S. (1975). *A Primer of Operant Conditioning*. Glenview: Scott Foresman.

Riehle, A., Grün, S., Diesmann, M., and Aertsen, A. (1997). Spike synchronization and rate modulation differentially involved in motor cortical function. *Science* 278, 1950–1953. doi: 10.1126/science.278.5345.1950

Sakurai, Y. (1993). Dependence of functional synaptic connections of hippocampal and neocortical neurons on types of memory. *Neurosci. Lett.* 158, 181–184. doi: 10.1016/0304-3940(93)90259-n

Sakurai, Y. (1994). Involvement of auditory cortical and hippocampal neurons in auditory working memory and reference memory in the rat. *J. Neurosci.* 14, 2606–2623.

Sakurai, Y. (1996a). Hippocampal and neocortical cell assemblies encode memory processes for different types of stimuli in the rat. *J. Neurosci.* 16, 2809–2819.

Sakurai, Y. (1996b). Population coding by cell assemblies—what it really is in the brain. *Neurosci. Res.* 26, 1–16. doi: 10.1016/0168-0102(96)01075-9

Sakurai, Y. (1999). How do cell assemblies encode information in the brain? *Neurosci. Biobehav. Rev.* 23, 785–796. doi: 10.1016/s0149-7634(99)00017-2

Sakurai, Y. (2002). Coding of auditory temporal and pitch information by hippocampal individual cells and cell assemblies in the rat. *Neurosci.* 115, 1153–1163. doi: 10.1016/s0306-4522(02)00509-2

Sakurai, Y., and Takahashi, S. (2006). Dynamic synchrony of firing in the monkey prefrontal cortex during working memory tasks. *J. Neurosci.* 26, 10141–10153. doi: 10.1523/jneurosci.2423-06.2006

Sakurai, Y., and Takahashi, S. (2008). Dynamic synchrony of local cell assembly. *Rev. Neurosci.* 19, 425–440. doi: 10.1515/revneuro.2008.19.6.425

Sakurai, Y., and Takahashi, S. (2013). Conditioned enhancement of firing rates and synchrony of hippocampal neurons and firing rates of motor cortical neurons in rats. *Eur. J. Neurosci.* 37, 623–639. doi: 10.1111/ejn.12070

Sakurai, Y., Nakazono, T., Ishino, S., Terada, S., Yamaguchi, K., and Takahashi, S. (2013). Diverse synchrony of firing reflects diverse cell-assembly coding in the prefrontal cortex. *J. Physiol. Paris* 107, 459–470. doi: 10.1016/j.jphysparis.2013. 05.004

Salinas, E., and Sejnowski, T. J. (2001). Correlated neuronal activity and the flow of neural information. *Nat. Rev. Neurosci.* 2, 539–550. doi: 10.1038/35086012

Schmied, A., Ivarsson, C., and Fetz, E. E. (1993). Short-term synchronization of motor units in human extensor digitorum communis muscle: relation to contractile properties and voluntary control. *Exp. Brain Res.* 97, 159–172. doi: 10.1007/bf00228826

Seidemann, E., Meilijson, I., Abeles, M., Bergman, H., and Vaadia, E. (1996). Simultaneously recorded single units in the frontal cortex go through a sequence of discrete and stable states in monkeys performing a delayed localization task. *J. Neurosci.* 16, 752–768.

Siegel, M., Donner, T. H., and Engel, A. K. (2012). Spectral fingerprints of large-scale neuronal interactions. *Nat. Rev. Neurosci.* 13, 121–134. doi: 10. 1038/nrn3137

Skinner, B. F. (1974). *About Behaviorism*. New York: Alfred A. Knopf.

Takahashi, S., and Sakurai, Y. (2005). Real-time and automatic sorting of multineuronal activity for sub-millisecond interactions in vivo. *Neurosci.* 134, 301–315. doi: 10.1016/j.neuroscience.2005.03.031

Takahashi, S., and Sakurai, Y. (2007). Coding of spatial information by soma and dendrite of pyramidal cells in the hippocampal CA1 of behaving rats. *Eur. J. Neurosci.* 26, 2033–2045. doi: 10.1111/j.1460-9568.2007.05827.x

Takahashi, S., and Sakurai, Y. (2009a). Information in small neuronal ensemble activity in the hippocampal CA1 during delayed non-matching to sample performance in rats. *BMC Neurosci.* 10:115. doi: 10.1186/1471-2202-10-115

Takahashi, S., and Sakurai, Y. (2009b). Sub-millisecond firing synchrony of closely neighboring pyramidal neurons in hippocampal CA1 of rats during delayed non-matching to sample task. *Front. Neural Circuits* 3:9. doi: 10.3389/neuro.04. 009.2009

Takahashi, S., Anzai, Y., and Sakurai, Y. (2003a). Automatic sorting for multi-neuronal activity recorded with tetrodes in the presence of overlapping spikes. *J. Neurophysiol.* 89, 2245–2258. doi: 10.1152/jn.00827.2002

Takahashi, S., Anzai, Y., and Sakurai, Y. (2003b). New approach to spike sorting for multi-neuronal activities recorded with a tetrode—how ICA can be practical. *Neurosci. Res.* 46, 265–272. doi: 10.1016/s0168-0102(03)00103-2

Taylor, D. M., Tillery, S. I., and Schwartz, A. B. (2002). Direct cortical control of 3D neuroprosthetic devices. *Science* 296, 1829–1832. doi: 10.1126/science.107 0291

Terada, S., Takahashi, S., and Sakurai, Y. (2013). Oscillatory interaction between amygdala and hippocampus coordinates behavioral modulation based on reward expectation. *Front. Behav. Neurosci.* 7:177. doi: 10.3389/fnbeh.2013. 00177

Vaadia, E., Haalman, I., Abeles, M., Bergman, H., Prut, Y., Slovin, H., et al. (1995). Dynamics of neuronal interactions in monkey cortex in relation to behavioural events. *Nature* 373, 515–518. doi: 10.1038/373515a0

Wessberg, J., Stambaugh, C. R., Kralik, J. D., Beck, P. D., Laubach, M., Chapin, J. K., et al. (2000). Real-time prediction of hand trajectory by ensembles of cortical neurons in primates. *Nature* 408, 361–365. doi: 10.1038/35042582

Wyler, A. R., Burchiel, K. J., and Robbins, C. A. (1979). Operant control of precentral neurons in monkeys: evidence against open loop control. *Brain Res.* 171, 29–39.

Zacksenhouse, M., Lebedev, M. A., Carmena, J. M., O'Doherty, J. E., Henriquez, C., and Nicolelis, M. A. L. (2007). Cortical modulations increase in early sessions with brain-machine interface. *PLoS One* 2:e629. doi: 10.1371/journal.pone. 0000619

Conflict of Interest Statement: The authors declare that the research was conducted in the absence of any commercial or financial relationships that could be construed as a potential conflict of interest.

Received: 13 November 2013; accepted: 16 January 2014; published online: 06 February 2014.

Citation: Sakurai Y, Song K, Tachibana S and Takahashi S (2014) Volitional enhancement of firing synchrony and oscillation by neuronal operant conditioning: interaction with neurorehabilitation and brain-machine interface. Front. Syst. Neurosci. ***8****:11. doi: 10.3389/fnsys.2014.00011*

This article was submitted to the journal Frontiers in Systems Neuroscience.

frontiers in Systems Neuroscience

HYPOTHESIS AND THEORY
published: 19 May 2015
doi: 10.3389/fnsys.2015.00071

Optimal feedback control successfully explains changes in neural modulations during experiments with brain-machine interfaces

Miri Benyamini and Miriam Zacksenhouse *

Brain-computer Interfaces for Rehabilitation Laboratory, Department of Mechanical Engineering, Technion - Israel Institute of Technology, Haifa, Israel

Recent experiments with brain-machine-interfaces (BMIs) indicate that the extent of neural modulations increased abruptly upon starting to operate the interface, and especially after the monkey stopped moving its hand. In contrast, neural modulations that are correlated with the kinematics of the movement remained relatively unchanged. Here we demonstrate that similar changes are produced by simulated neurons that encode the relevant signals generated by an optimal feedback controller during simulated BMI experiments. The optimal feedback controller relies on state estimation that integrates both visual and proprioceptive feedback with prior estimations from an internal model. The processing required for optimal state estimation and control were conducted in the state-space, and neural recording was simulated by modeling two populations of neurons that encode either only the estimated state or also the control signal. Spike counts were generated as realizations of doubly stochastic Poisson processes with linear tuning curves. The model successfully reconstructs the main features of the kinematics and neural activity during regular reaching movements. Most importantly, the activity of the simulated neurons successfully reproduces the observed changes in neural modulations upon switching to brain control. Further theoretical analysis and simulations indicate that increasing the process noise during normal reaching movement results in similar changes in neural modulations. Thus, we conclude that the observed changes in neural modulations during BMI experiments can be attributed to increasing process noise associated with the imperfect BMI filter, and, more directly, to the resulting increase in the variance of the encoded signals associated with state estimation and the required control signal.

Keywords: brain-machine interfaces, neural modulations, optimal feedback control, computational motor control, process noise

OPEN ACCESS

Edited by:
Manuel Fernando Casanova, University of Louisville, USA

Reviewed by:
Ferran Galán, Newcastle University, UK
Frédéric Crevecoeur, Queen's University, Canada
Yuki Ueyama, Research Institute of National Rehabilitation Center for Persons with Disabilities, Japan

***Correspondence:**
Miriam Zacksenhouse, Brain-computer interfaces for rehabilitation Laboratory, Department of Mechanical Engineering, Technion - Israel Institute of Technology, Haifa 32000, Israel
mermz@technion.ac.il

Received: *31 December 2014*
Accepted: *20 April 2015*
Published: *19 May 2015*

Citation:
Benyamini M and Zacksenhouse M (2015) Optimal feedback control successfully explains changes in neural modulations during experiments with brain-machine interfaces. Front. Syst. Neurosci. 9:71. doi: 10.3389/fnsys.2015.00071

1. Introduction

Brain-Machine Interfaces (BMIs) have been developed to provide a direct communication link between the brain and external devices, bypassing the remaining, potentially injured

neuro-muscular system (Nicolelis, 2001; Taylor et al., 2002; Lebedev et al., 2005). Additionally, BMIs provide a unique window into information representation and processing in the brain. In particular, it was observed that the extent of neural modulations (during BMI experiments reported in Carmena et al., 2003) increased abruptly upon starting to operate the interface, and especially after the monkey stopped moving its hand (Zacksenhouse et al., 2007). In contrast, neural modulations that are correlated with the movement kinematics remained relatively unchanged. Here we develop an optimal feedback control model (OFC) of BMI experiments to explain the observed changes in neural modulations and to investigate how they are related to changes in state estimation during brain control.

OFC was recently proposed as a viable model for motor control during reaching movements (Todorov and Jordan, 2002; Todorov, 2005; Shadmehr and Krakauer, 2008). While the term "optimal feedback control" emphasizes the optimality of the control gains given the cost function, the main component of interest here is optimal state estimation. This component is hypothesized to integrate visual and proprioceptive information with prior state estimation from an internal model to optimize the posterior state estimate (Miall and Wolpert, 1996; Wolpert and Ghahramani, 2000). The relative weights given to the sensory measurements versus the internal estimation depend on the relative variance of measurement and process noise, and, for linear systems corrupted by Gaussian noise, are determined by the Kalman filter (Schwartz, 2004; Stengel, 2012). The main hypothesis of this paper is that changes in process and measurement noise caused by the switch to brain control can explain the observed changes in neural modulations.

OFC is adopted here, instead of alternative computational motor control models, such as feedback error learning (Kawato et al., 1987), active inference (Friston et al., 2010, 2011) and distal teacher (Jordan and Rumelhart, 1992), for three main reasons. First, OFC does not require explicit specification of the desired trajectory of movement. While the desired trajectory can be assumed to follow the minimum jerk profile, its specification during brain control, when the initial stroke does not reach the target, is not straightforward. In contrast, OFC generates the trajectory implicitly, rather than following an externally specified trajectory. Secondly, the optimization inherent in OFC constrains the parameters of the state estimation filter and the control gains, so the model has fewer free parameters that need to be tuned. Thus, OFC provides a coherent and principled framework for investigating possible mechanisms underlying changes in neural modulations following the transition to brain control. Finally, OFC explicitly accounts for the variance of the process and measurement noise, which are assumed to change when switching to brain control, and thus is most appropriated for investigating how these mechanisms may contribute to the observed changes in neural modulations.

The processing required for optimal state estimation and control are conducted in the state-space. Neural recording is simulated by modeling two populations of neurons that encode the relevant signals, including either just the estimated state or also the resulting control signal. Thus, the approach presented here combines the dynamical perspective, which focuses on how the brain commands movements, with the representational perspective, which investigates what the neurons encode (Shenoy et al., 2013), by suggesting that they encode the signals that are relevant for the computations that underlie state estimation and control. The goal of this work is to investigate whether the resulting neural activity would produce the observed changes in neural modulations during BMI experiments.

The above OFC framework for investigating the changes in neural modulations during BMI experiments should be distinguished from recent applications of state estimation (Schwartz, 2004; Wu et al., 2006; Cunningham et al., 2011) and OFC (Shanechi et al., 2013a,b) to improve neural decoders for BMIs. BMI decoders estimate the state by integrating the observed neural activity, which is assumed to encode the state of the movement, with a presumed or learned model of reaching movement dynamics. Advanced models (Shanechi et al., 2013a,b) account for the effect of the control signal generated by the brain on the movement dynamics by modeling the sensory motor system in the brain as OFC. However, since the focus of such models is the BMI decoder, the brain is assumed to know the actual state of the movement via noise-free sensory measurements, thereby eliminating the need for state estimation. In contrast, our focus is on state estimation in the brain, which is assumed to integrate noisy visual and proprioception observations with an internal model of movement dynamics (Miall and Wolpert, 1996; Wolpert and Ghahramani, 2000), and how the changes in sensory and process noise affect those estimations and the resulting neural activity.

In summary, this work investigates the hypothesis that the observed changes in neural modulations following the transition to brain control can be explained in the context of OFC model of motor control. We hypothesize that neurons in cortical motor areas, and in particular in primary motor area, M1, and premotor dorsal, PMd, encode the relevant signals for OFC of reaching movements, i.e., the estimated state and the resulting control signal, as depicted in **Figure 1**. Thus, the observed changes in neural rate modulations are hypothesized to reflect corresponding changes in the variance of these signals. Furthermore, we hypothesize that the increase in the variance of the estimated state and control signal is due to the higher process noise during brain control caused by the imperfect BMI filter. These hypotheses are investigated in three levels: (i) simulations of pole control and brain control, and evaluation of the corresponding changes in neural modulations (Section 3.2), (ii) theoretical analysis of the effect of increasing process noise during pole control (Section 2.4), and (iii) simulations of the effect of increasing process noise on neural modulations during pole control (Section 3.3). Other aspects of the model are investigated in Sections 3.1, 3.4–3.6.

2. Materials and Methods

2.1. Experimental Methods

The proposed model is evaluated by comparing the different properties of the simulated neural activity to those observed during the BMI experiments described in Carmena et al. (2003). The BMI experiments were conducted with macaque monkeys whose goal was to move the cursor to randomly appearing

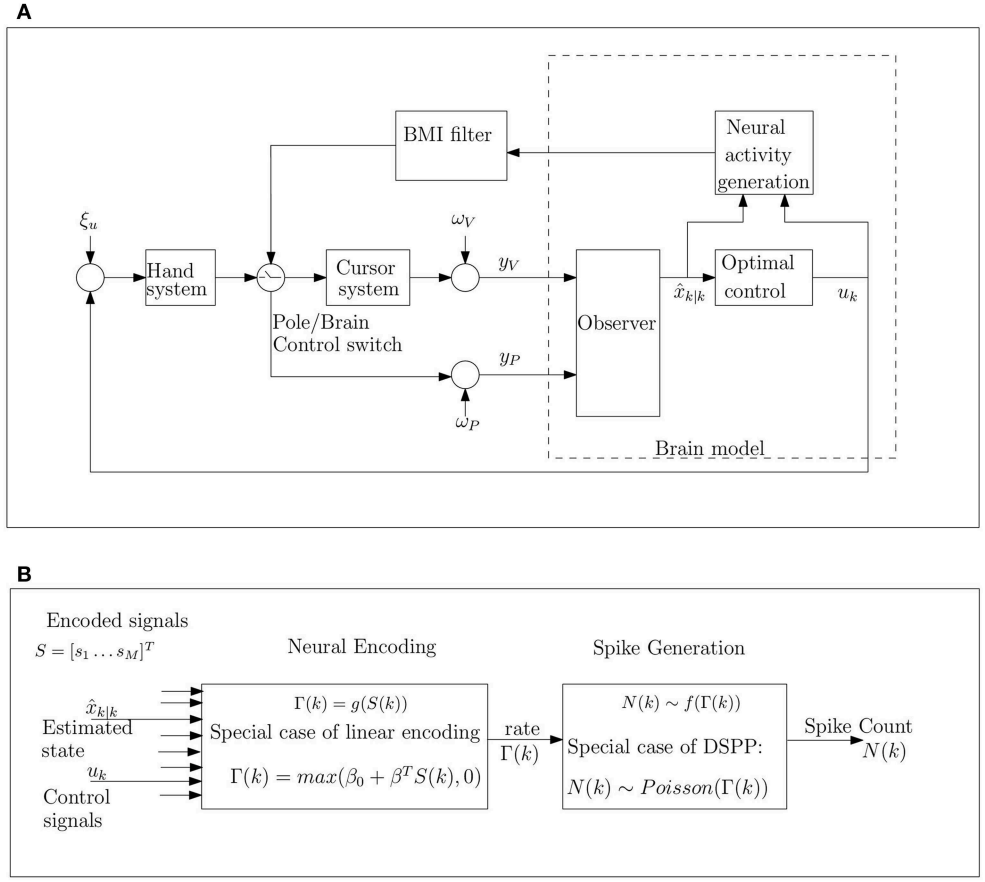

FIGURE 1 | Schematic model of movement control during BMI experiments under the hypothesis that the brain implements OFC (A), and detailed block diagram of neural activity generation (B). **(A)** The brain model receives noisy proprioceptive (y_P) and visual (y_C) measurements from the hand and cursor, corrupted by proprioceptive and visual measurement noise, ω_P and ω_V, respectively. These noisy measurements are integrated with prior predictions from the internal model to generate optimal state estimates $\hat{x}_{k|k}$ and control signal u_k, which are encoded by the neural activity. The control signal is corrupted by hand process noise ξ_U. The BMI filter is trained based on the neural activity in pole control and then used to move the cursor in brain control. **(B)** The cumulative bin rate, $\Gamma(k)$, at time step k, is modulated by the encoded signals $S = \left[s_1, \quad \cdots \quad, s_M\right]^T$ including the estimated state $\hat{x}_{k|k}$ and control signals u_k. The spike-count $N(k)$ is generated as a doubly stochastic Point process given the rate parameter $\Gamma(k)$. Here we consider the special case of linear encoding, where $\Gamma(k)$ is a linear combination of the encoded signals (including the estimated speed and the magnitude of the control signal), and doubly stochastic Poisson processes (DSPP), where the spike count $N(k)$ has a Poisson distribution with rate $\Gamma(k)$.

targets and hold the cursor on the target for 150 ms to accept a juice reward. Each experiment included three control modes: (i) pole control during which the monkey controlled the cursor using hand-held pole, (ii) brain control with hand movements (BCWHM), during which the cursor was controlled by the output of the BMI interface while the monkey continued moving the pole and (iii) brain control without hand movements (BCWOHM), during which the cursor was controlled by the BMI interface even though the monkey stopped moving the pole.

Neural activity was recorded from multiple brain area, but mostly from the primary motor area (M1) and the dorsal premotor area (PMd). The BMI interface binned the recorded spike trains in 100 ms bins, to generate the input to a linear filter. The linear BMI filter was trained with data recorded during the last 10 min of pole control, and held fixed during brain control.

2.2. Analysis Methods

2.2.1. Percent Overall Modulations

Spike-trains can be considered as realizations of point processes (Johnson, 1996). The number of spikes recorded in a bin, N, depends on the cumulative spike-rate during the bin, Γ (Zacksenhouse et al., 2007), which can be modulated by the encoded signals as outlined in **Figure 1B**. Since this dependence is stochastic, the variance of the spike-count $var(N)$ is higher than the variance of the cumulative spike-rate $var(\Gamma)$ (Zacksenhouse et al., 2007). While the variance of the spike-count can be measured directly, it is the variance of the cumulative spike-rate that captures the effect of the encoded signals on rate modulations. In order to quantify these rate modulations, the percent overall modulation (POM) is defined as Zacksenhouse et al. (2007)

$$POM = \frac{var[\Gamma]}{var[N]} \cdot 100\% \quad (1)$$

Since the variance of the bin-rate cannot be measured directly, the POM cannot be estimated without further assumptions. Consider first the simplest point process that can describe stochastic rate modulations, i.e., the doubly stochastic Poisson processes (DSPP), for which Snyder (1975), Zacksenhouse et al. (2007)

$$\begin{aligned} E(N_{DSPP}) &= E(\Gamma) \\ Var(N_{DSPP}) &= var(\Gamma) + E(\Gamma) \end{aligned} \quad (2)$$

In this case, the POM can be estimated form the mean and variance of the spike count as

$$\hat{POM}[N] = \frac{var[N] - E[N]}{var[N]} \cdot 100\% \quad (3)$$

where $\hat{POM}$ denotes the estimated POM. When applied to the analysis of spike trains recorded during BMI experiments, we assume that the movement is composed of an asynchronous sequence of reaching movements (Zacksenhouse et al., 2014) so the cumulative spike-rate and the binned spike-counts are stationary processes. Hence, the POM is estimated from Equation (3) using the temporal mean and variance rather than ensemble mean and variance.

In the general case of doubly stochastic Point processes (not necessarily Poisson distributed), the variance of the spike-counts can be decomposed into Churchland et al. (2011)

$$var(N) = var[E[N|\Gamma]] + E[var[N|\Gamma]] \quad (4)$$

The first term on the right reflects the variance of the cumulative spike-rate Γ, though is equal to it only for DSPPs. The second term can be interpreted as the Point process noise, since it contributes to the variance of the spike-counts even if Γ is constant. While this term equals the mean rate only for DSPPs, evidence suggests that in many cases it is proportional to the mean rate (Tolhurst et al., 1983; Geisler and Albrecht, 1995), i.e., $var[N|\Gamma] = \gamma E[N|\Gamma]$, $(\gamma > 0)$ and hence $E[var[N|\Gamma]] = \gamma E[N]$. Hence, a revised definition of POM quantifies the ratio between the first term on the right, which reflects the variance of the cumulative spike-rate Γ, and the total variance in the spike counts

$$POM_{REV}(N) = \frac{var[E[N|\Gamma]]}{var(N)} \cdot 100\% \quad (5)$$

This can be related to the POM estimated by Equation (3) by inserting the expression for the point process noise in Equation (4) and Equation (5) to get

$$\hat{POM}_{REV}(N) = \frac{var[N] - \gamma E[N]}{var(N)} \cdot 100\% = (\gamma \hat{POM} - (1-\gamma)) \cdot 100\% \quad (6)$$

Thus, changes in the POM estimated by Equation (3) reflect proportional changes in the revised POM of Equation (5) up to a positive scaling and positive or negative offset. Having established this connection, the revised POM will not be used any further.

All the POM results described in Section 3 and shown in the Figures are $\hat{POM}$ (Equation 3), estimated from temporal statistics, while the theoretical analysis in Section 2.4 is based on the definition of POM in Equation (1).

2.2.2. Percent Kinematics Modulations

Numerous studies suggested that the neural activity can be related to the kinematics of the movement, including position, velocity and speed, via a linear model (Georgopoulos et al., 1986; Ashe and Georgopoulos, 1994; Moran and Schwartz, 1999; Todorov, 2000; Zacksenhouse and Nemets, 2008; Chang et al., 2014)

$$\begin{aligned} N(k) = &\sum_{l=-L_1}^{L_2} \omega_{p_{cx}}(l) p_{cx}(k+l) + \sum_{l=-L_1}^{L_2} \omega_{p_{cy}}(l) p_{cy}(k+l) \\ &+ \sum_{l=-L_1}^{L_2} \omega_{v_{cx}}(l) v_{cx}(k+l) + \sum_{l=-L_1}^{L_2} \omega_{v_{cy}}(l) v_{cy}(k+l) \\ &+ \sum_{l=-L_1}^{L_2} \omega_S(l) S_{pc}(k+l) + \omega_0 + \epsilon(k) \end{aligned} \quad (7)$$

where k is the index of the current bin, $N(k)$ is the binned spike count, p_{cx} and p_{cy} are the x and y components of the cursor position, v_{cx} and v_{cy} are the x and y components of the cursor velocity, $S_{pc} = \sqrt[2]{v_{cx}^2 + v_{cy}^2}$ is the cursor's speed, l is the relative lag, L_1 and L_2 are the number of preceding and succeeding lags, $\omega_{p_{cx}}$, $\omega_{p_{cy}}$, $\omega_{v_{cx}}$, $\omega_{v_{cy}}$ and ω_S are the corresponding regression weights, ω_0 is the bias parameters and $\epsilon(k)$ is the residual error.

The coefficient of determination of the spatio-temporal regression, R^2, describes the fraction of the variance in the binned spike-count that is linearly related to variations in the temporal profile of the kinematic signals in the surrounding temporal window. Expressed as a percentage, R^2 is referred to as the percent kinematic-related modulation, or PKM (Zacksenhouse et al., 2007).The PKM results reported here are computed with L1 = L2 = 9.

2.3. Modeling methods

The simplifying assumptions on which the proposed OFC model for BMI experiments is based are explicitly stated in Section 2.3.1. As depicted in **Figure 1A**, the model includes three main parts: (1) Hand and cursor model, (2) Brain model, and (3) BMI filter, as briefly explained in Sections 2.3.2–2.3.5, and detailed in Appendices A and B. Model parameters are detailed in Section 2.3.6, and the effect of process noise in pole control is investigated in Section 2.3.7.

2.3.1. Simplifying Assumptions

The goal of this work is to construct a simple model that can capture the observed abrupt changes in neural modulations following the transition to brain control, and to assess if those changes can be attributed to increasing process and measurement noise. Hence, within the framework of OFC (Todorov and Jordan, 2002; Todorov, 2005; Shadmehr and Krakauer, 2008) we made the following simplifying assumptions (SA):

SA1: Absolute delays are ignored, thought the relative time-shift between the command to the muscle and the force

it produces is captured by a second order muscle model (Section 2.3.2). Thus, the model successfully reproduces the observed time-lag in the cross-correlation between the neural activity and the movement velocity (Lebedev et al., 2005) as detailed in Section 3.1. The effect of sensory delays on movement variability and bias can be accounted for by sensory noise, at least when the perturbations are not abrupt (Todorov and Jordan, 2002; Crevecoeur and Scott, 2013).

SA2: The process noise during pole control is assumed to be signal independent white Gaussian noise. This assumption is justified since the resulting velocity profile agrees well with the commonly observed minimum jerk velocity profile (Flash and Hogan, 1985). While evidence suggests that the variance of the process noise increases with the control signal (Harris and Wolpert, 1998; Wolpert and Ghahramani, 2000), this was not modeled in order to focus on the effect of brain control on process noise and neural modulations.

SA3: The internal forward model is assumed to be identical to the actual hand and cursor system in pole control. Adaptation to brain control is ignored since the focus is on the abrupt changes in neural modulations immediately after the transition to brain control. Adaptation is expected to be important in explaining the subsequent gradual decrease in neural modulations with BMI sessions (Zacksenhouse et al., 2007), and will be explored in future work.

SA4: Spike counts are generated as realization of doubly stochastic Poisson process with linear tuning curves (as detailed in Section 2.3.4) (Zacksenhouse and Nemets, 2008; Cunningham et al., 2011; Chang et al., 2014).

2.3.2. Simplified Hand and Cursor Model

Following Todorov (2005) the hand is modeled as a point mass driven by an over damped second order muscle model that responds to the control signal from the brain. An additional friction term is introduced to model the friction of the hand held pole, as described by Equation (A2) in Supplementary Material.

As in the BMI experiments (Carmena et al., 2003), the cursor position during brain control is generated by integrating the velocity predicted by the BMI interface and filtering it with a high pass filter (HPF) to remove low frequency drifts, as described by Equation (A7) in Supplementary Material. During pole control, the cursor position is determined in the same way, using the actual hand velocity instead of the predicted velocity.

The simulation is updated at 100 Hz, and the discrete dynamics of the combined system, including the hand, cursor and target along a single degree of freedom, can be expressed as (see Equation A10 in Supplementary Material)

$$x(k+1) = Ax(k) + B_u u(k) + B_{BMI} v_{BMI}(k) + \xi_p(k) \qquad (8)$$

where x is the combined state (specified by Equation A9 in Supplementary Material), A, B_u, and B_{BMI} are the matrices describing the system dynamics, the effect of the control signal u generated by the optimal feedback controller implemented by the brain, and the integration of the velocity predictions v_{BMI} during brain control, respectively, as detailed in Equations (A11–A13 in Supplementary Material). The 2-degrees of freedom simulations are performed by evolving two independent systems for the x and y directions, respectively.

During normal simulations of pole and brain control, the process noise, ξ_p, stems only from the noise in the control signal ξ_u (Equation A3 in Supplementary Material), i.e., $\xi_p = B_u \xi_u$. Under assumption SA2, ξ_u is a white Gaussian noise, whose variance (note that in the single dimension case ξ_u is a scalar) is denoted by α_u^2. Hence the covariance matrix of the process noise can be expressed as

$$\Omega^p = \alpha_u^2 B_u B_u' \qquad (9)$$

The position and velocity of the cursor are measured via visual (V) feedback, while the position and velocity of the hand are measured via proprioceptive (P) feedback. Both visual and proprioceptive measurements are assumed to be corrupted by zero mean white Gaussian measurement noise and the covariance matrix of the combined measurement is denoted by Ω^m.

2.3.3. Brain Model

Following current computational motor control theories, the brain is assumed to implement optimal state estimation and feedback control (Kuo, 1995; Wolpert et al., 1995; Todorov and Jordan, 2002). However, for simplicity, the computations are performed in the state space, rather than their neural representations. Neural recording is simulated by modeling neurons that encode the relevant signals including the estimated state and control signal (as detailed in Section 2.3.4). The brain model includes three parts as depicted in **Figure 1A** and further detailed in Appendix B (Supplementary Materials)(first two parts) and Section 2.3.4 (third part):

A: Observer that implements optimal state estimation by integrating the sensory feedback and internal model predictions. Under assumption (SA2), optimal estimation is achieved with Kalman filter (Wolpert et al., 1995; Stengel, 2012), as specified in Equation (B1 in Supplementary Material). During simulations of normal reaching movements (pole control) the internal model is assumed to be accurate and the Kalman filter is based on the actual covariance matrices of the process and measurements noise. By assumption (SA3), the same covariance matrices are also used for computing the Kalman filter when simulating brain control.

B: Optimal controller that, under assumption (SA2), reduces to Linear Quadratic Gaussian (LQG) controller (Stengel, 2012), as specified in Equations (B5–B8 in Supplementary Material). The controller gains were computed off-line to minimize a standard cost function that includes penalty for the control effort and for deviations from the target, as specified in Equations (B2–B4 in Supplementary Material) (Kuo, 1995; Wolpert et al., 1995; Todorov and Jordan, 2002).

C: Neural activity generator that converts the relevant signals i.e., the internally estimated cursor state and the control signal, into neural activity of a population of N_n simulated neurons using linear multi-variable tuning functions (as

detailed in Section 2.3.4). This population of neurons simulates the population of neurons recorded during the BMI experiments, so their activity is used to train and drive the BMI filter during simulated pole and brain control, respectively, as detailed in 2.3.5. By assumption (SA4), spike-counts are generated as realizations of *doubly stochastic* Poisson processes.

2.3.4. Neural Activity Generator

Many studies (Georgopoulos et al., 1986; Moran and Schwartz, 1999) demonstrated that during reaching movements the neural activity is linearly correlated with several motor parameters, including hand position, velocity, speed and gripping force. One of the main hypotheses in this work is that the neurons encode the estimated state and control signal, and that the observed correlations with the above motor parameters result from this encoding. Since we are interested in the statistics of the binned spike-count (in bins of 100 ms), we generate the binned spike-counts directly (instead of simulating the spike-train, and then binning the data). As outlined in **Figure 1B**, the binned spike-counts of each neuron are generated as a realization of a DSPP (Johnson, 1996; Dayan and Abbott, 2001) whose cumulative rate Γ is a linear function of the encoded signals. Specifically, the cumulative spike-rate of neuron i during the k-th bin, $\Gamma^i(k)$, is given by

$$\Gamma^i(k) = max(\beta_{i,0} + \beta_i^T S(k), 0) \tag{10}$$

where $S(k)$ is the vector of encoded signals at time step k, $\beta_{i,0}$ is the bias of neuron $i = 1 \ldots N_n$ and β_i is the vector of its tuning weights.

Since the monkey is rewarded when the cursor is at the target, independent of the position of the hand, we assume that only the estimated cursor-state is encoded. Thus, the vector of encoded signals

$$S = \begin{bmatrix} \hat{p}_{cx} & \hat{p}_{cy} & \hat{v}_{cx} & \hat{v}_{cy} & \hat{S}_p & u_x & u_y & u_e \end{bmatrix}' \tag{11}$$

includes three 2-dimensional vectors: the estimated cursor position $\hat{p} = \begin{bmatrix} \hat{p}_{cx} & \hat{p}_{cy} \end{bmatrix}'$ velocity $\hat{v} = \begin{bmatrix} \hat{v}_{cx} & \hat{v}_{cy} \end{bmatrix}'$, and control signal $u = \begin{bmatrix} u_x & u_y \end{bmatrix}'$, and the magnitude of the last two (estimated speed $\hat{S}_p = ||\hat{v}||$ and control effort $u_e = ||u||$). The representation of the speed of movement in the neural activity, beyond the representation of the velocity vector, is well documented (Moran and Schwartz, 1999), and here we assume it reflects the encoding of the estimated speed $\hat{S}_p$. Similarity, we assume that the magnitude of the control signal u_e is also encoded.

The tuning weights β_i to the kinematic parameters (position, velocity and speed) were selected to obtain PKM levels similar to the PKM observed in the BMI experiments during pole control. Specifically, the tuning weights for each kinematic parameter were selected from a uniform distribution whose variance was proportional to the destined PKM associated with that kinematic parameter and inversely proportionally to its variance. The tuning weights for the control signal were also selected from a uniform distribution, but its variance was adjusted to get the proper time-shift in the cross-correlation between the neural activity and the velocity, which are described in Section 3.1. The tuning vectors for the position, velocity and control parameters define the respective, and in general different, preferred directions (PD) and modulation depths.

The literature on cortical motor units suggests that neurons in different areas in the brain encode different information.The activity of M1 neurons has been shown to correlate with both the kinematics, including velocity, speed and direction of movement (Georgopoulos et al., 1982; Ashe and Georgopoulos, 1994) and with the applied forces (Evarts, 1968; Ashe, 1997; Todorov, 2000). PMd neurons are modulated mainly by the direction and amplitude of the movement (Messier and Kalaska, 2000; Hendrix et al., 2009). In agreement with those studies, the activity of M1 units recorded during the BMI experiments considered here were shown to predict well hand position, velocity and gripping force (73, 66, and 83% of variance, respectively), while the activity of the recorded PMd units predicted well hand position and velocity (48 and 46% of variance, respectively), but not the gripping force (29% of variance) (Carmena et al., 2003). Considering the above evidence, we simulate the activity of two sub-populations of neurons encoding either: (i) only the estimated cursor state (position, velocity and speed), or (ii) both the estimated cursor state and the control signal (vector and magnitude). Based on the evidence in the literature, we expect that the behavior of simulated neurons in those two sub-populations would be similar to the behavior of recorded PMd and M1 units, respectively, and hence refer to them as PMd-like and M1-like neurons. Such similarities are demonstrated in Section 3.1, where the cross-correlations between the movement velocity and either the recorded or simulated neural activity are compared.

2.3.5. BMI Filter

As in the BMI experiments (Carmena et al., 2003), the velocity in simulated brain control was predicted from the simulated spike-counts by a linear multi-lag multi-variable BMI filter

$$v_{BMI}(k) = \theta_0 + \sum_{j=1}^{N_n} \sum_{l=-L}^{0} \theta_j(l) N_j(k+l) \tag{12}$$

where N_n is the number of simulated neurons, $L = 10$ the number of lags used for prediction and $N_j(k)$ the spike count of neuron j in bin k. The filter parameters θ_0 and $\theta_j(l)$, (where l is the index of the lag) were computed using truncated Singular Value Decomposition (Zacksenhouse et al., 2007). Two BMI filters were trained to reconstruct the velocity in x and y, respectively, using the last 10 min of simulated pole control.

The performance of the experimental BMI filter (similarly trained on the last 10 min of pole control) was assessed by testing its predictions on a different section of pole control and was quantified by a coefficient of correlation of $R(\hat{v}, v) = 0.755 \pm 0.02$. We expect that this imperfect performance is critical for generating the observed changes in neural modulations. Hence, this performance served as a benchmark for tuning the number of neurons and the process noise in the simulation to obtain a similar performance (as detailed in Section 2.3.6).

2.3.6. Model Parameters

Model parameters are detailed in **Table 1**. The basic parameters of the hand model, visual measurement noise and cost function were taken from Todorov (2005) as noted in **Table 1**. The basic hand model was extended with a friction term to model the friction of the hand held pole. The basic cost function was augmented to describe the requirement for holding the cursor on the target as described in Appendix B (Equations B2–B4 in Supplementary Material) using the same weight parameters. The reaching time t_f (in Supplementary Equation B3) is uniformly distributed between 1.7-2.2 s in pole control and 2.4-6 s in brain control.

As detailed in our simplifying assumption SA2, the process noise during pole control is assumed to be signal independent, and its magnitude is quantified by of α_u in Equation (9). Initial simulations revealed that the performance of the experimental BMI filter, quantified by $R(\hat{v}, v)$ (Section 2.3.5), is highly sensitive to the process noise during simulated pole control, as shown in **Figures 2A,B**. The magnitude of the process noise was normalized by the equivalent signal-independent process noise suggested in Todorov (2005), signal-independent process noise suggested in the process noise factor defined as $k_u = \frac{\alpha_u}{4.6N}$. **Figures 2A,C** also depicts the effect of the total number of simulated neurons N_n on $R(\hat{v}, v)$, while the ratio between the two populations of simulated neurons, the M1-like and PMd-like neurons, was kept constant (1:1). The results in **Figure 2** are based on 15 simulated sessions of 20 min pole control, each with a different, randomly selected targets, but all with the same set of neural tuning weights. In each session the coefficient of correlation between the actual and predicted velocity $R(\hat{v}, v)$ was computed from the first 10 min, while training was conducted on the last non-overlapping 10 min. Each data point and error bar (in (B-C)) depict the average and standard deviation of $R(\hat{v}, v)$ across the 15 sessions. **Figure 2** suggests that with $N_n = 50$ and $k_u = 0.1$ the average performance of the BMI filter trained on simulated activity is $R(\hat{v}, v) = 0.77$, close to the observed BMI filter performance. Hence, these are the default values used in all other standard simulations as indicated in **Table 1**.

While proprioceptive measurement noise has little effect on $R(\hat{v}, v)$ it has significant effect on the resulting changes in neural modulations. This effect is investigated in Section 3.5 and motivated the selection of a common 10-fold factor between the diagonal covariance matrices of the proprioceptive and visual measurements noise, as specified in **Table 1**. This proprioceptive noise factor, denoted by k_m, was used during simulations of pole control and BCWHM, while during simulations of BCWOHM it was increased to infinity to reflect the lack of relevant proprioception measurements in this mode.

2.3.7. Effect of Process Noise

Following our primary hypothesis that the observed changes in neural modulations can be explained in the framework OFC, we further hypothesize that these changes result from the higher process noise generated by the imperfect BMI filter that reconstructs the cursor velocity. This hypothesis is investigated both by simulations of noisy pole control, as outlined here, and by theoretical analysis in Section 2.4. Noisy pole control is simulated by using Equation (8) with the matrices associated with pole control (Equations A11–A13 in Supplementary Material), but with process noise that includes also the simulated effect of the BMI filter reconstruction error (as further explained in Appendix A2, Supplementary Material). Thus, instead of Equation (9) the covariance matrix of the process noise during noisy pole control simulations is

$$\Omega^{p}_{noisy} = \alpha_u^2 B_u B_u' + \alpha_{rec}^2 B_{BMI} B_{BMI}' \tag{13}$$

TABLE 1 | Model Parameters table.

Parameter	Description	Value	References
Δ	Discretization time of the hand model	0.01[s]	Todorov, 2005
m	Hand mass	1[kg]	Todorov, 2005
γ	Coefficient of friction	$7.7[\frac{kg}{s}]$	-
τ	Time constant of the muscle model	0.04[s]	Todorov, 2005
w_v	Velocity cost function weight	0.2	Todorov, 2005
w_f	Energy cost function weight	0.02	Todorov, 2005
t_f	Reaching time in pole control (range)	$1.7 - 2.2$[s]	Carmena et al., 2003
t_f	Reaching time in brain control (range)	$2.4 - 6$[s]	Carmena et al., 2003
σ^2_{Vp}	Variance of the visual (V) position measurement noise	$(0.01\text{m})^2$	Todorov, 2005
σ^2_{Vv}	Variance of the visual (V) velocity measurement noise	$(0.1\frac{m}{s})^2$	Todorov, 2005
σ^2_{Pp}	Variance of the proprioception (P) position measurement noise	$k_m(0.01\text{m})^2$	Section 2.3.6/3.5
σ^2_{Pv}	Variance of the proprioception (P) velocity measurement noise	$k_m(0.1\frac{m}{s})^2$	Section 2.3.6/3.5
k_m	Proprioception measurement noise factor	10	Section 2.3.6/3.5
α_u	Magnitude of the hand process noise	$k_u \cdot (4.6[N])$	Section 2.3.6
k_u	Hand process noise factor	0.1	Section 2.3.6
N_n	Number of neurons	50	Section 2.3.6
T	Bin size	0.1[s]	Carmena et al., 2003

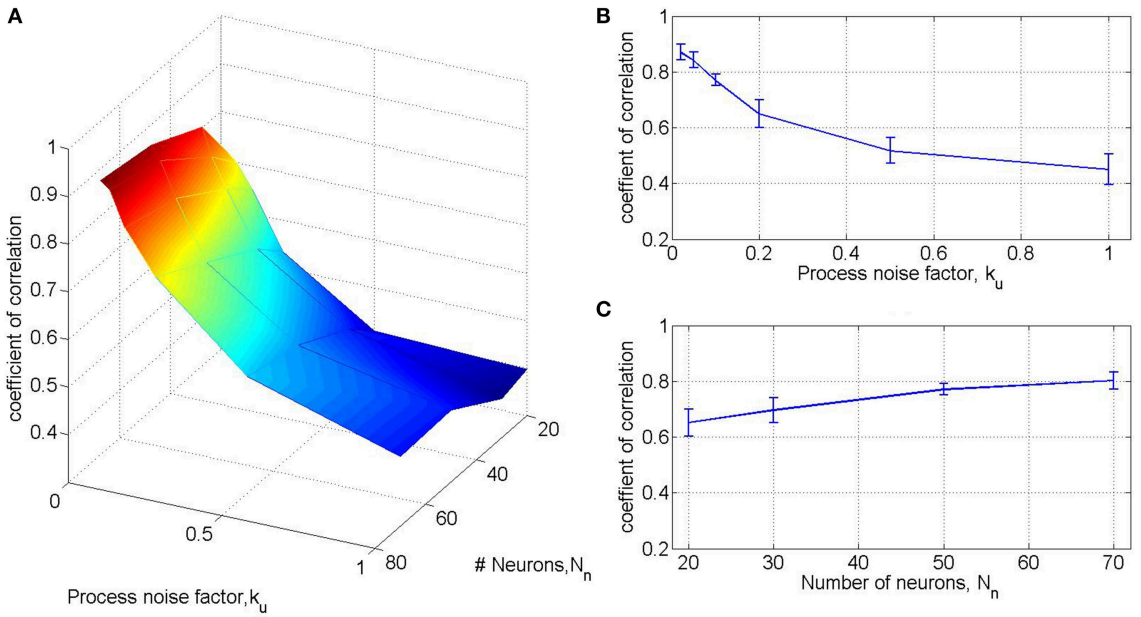

FIGURE 2 | BMI filter performance as a function of the number of neurons and the process noise factor. Results are based on 15 simulated sessions of 20 min pole control, each with a different, randomly selected targets, but all with the same set of neural tuning weights. In each session the BMI filter was trained on the last 10 min and its performance was quantified by the coefficient of correlation between the actual and predicted velocity in the first 10 min. Each data point and error bar (in **B,C**) depict the average and standard deviation of the coefficient of correlations across the 15 sessions for a specific process noise factor k_u and total number of neurons N_n. The effect of k_u is evaluated with $N_n = 50$ **(B)**, while the effect of N_n is evaluated with $k_u = 0.1$ **(C)**. A fixed 1:1 ratio is kept between the M1-like and PMd-like simulated neurons.

The first term represents the contribution of the noise in the control signal, and is the same as during regular pole control (Equation 9). The second term represents the additional noise introduced by the imperfect BMI filter, and its magnitude is quantified by α_{rec}. The effect of varying the magnitude α_{rec} on neural modulations is investigated in Section 3.4.

2.4. Theoretical Analysis of POM

As detailed in Section 2.3.7, we hypothesize that the observed changes in neural modulations following the transition to brain control result from the higher process noise introduced by the imperfect BMI filter. Here we investigate theoretically the effect of increasing process noise during simulations of normal reaching movements on POM defined theoretically in Equation (1), and show that under the assumptions of linear decoding and invariant internal model (see theoretical assumptions 1 and 2 below), the POM indeed increases with the process noise. The covariance matrix of the process noise, Ω^p, is assumed to increase from a nominal low level Ω^p_L to a high level Ω^p_H such that the difference $\Omega^p_H - \Omega^p_L$ is positive semi-definite (psd) (Horn and Johnson, 2012) and is denoted by $\Omega^p_H - \Omega^p_L \succcurlyeq 0$ or equivalently by $\Omega^p_H \succcurlyeq \Omega^p_L$. Note that this analysis is general and does not rely on the specific structures of Ω^p_L and Ω^p_H suggested by Equations (9, 13), respectively.

We make the following simplifying theoretical assumptions (TA):

TA1: The cumulative spike-rate Γ encodes a linear combination of the estimated state. Since the optimal control signal is proportional to the estimated state, this includes also the control signal. However, non-linear functions, and in particular the estimated speed $\hat{S}_p$ and the magnitude of the control effort u_e, which are included in Equation (11), are not considered here.

TA2: The internal model of the process noise does not change. This assumption follows directly from the simplifying assumption (SA3) that there is no adaptation to brain control.

Within the framework of state estimation and OFC, (TA1) implies that Γ can be expressed as the output of an extended linear system whose state $\tilde{x} = \begin{bmatrix} x_k & \hat{x}_{k|k} & 1 \end{bmatrix}^T$ includes both the actual and estimated states (of the hand and cursor). Following the details in Equations (C2–C5 in Supplementary Material), the extended system can be described as:

$$\begin{aligned} \tilde{x}_k &= \tilde{A}_k \tilde{x}_{k-1} + \tilde{\xi}_k \\ \Gamma_k &= \tilde{H}_k \tilde{x}_k \end{aligned} \tag{14}$$

where $\tilde{\xi}$ is the process noise of the extended system, which captures both the process noise of the actual system and the estimation error (Equation C4 in Supplementary Material). Since both are assumed to be white Gaussian noise, so is $\tilde{\xi}$, and its covariance matrix $E[\tilde{\xi}_i \tilde{\xi}_j] = \Omega^{\tilde{p}}_i \delta_{ij}$ is given by (see Equation C6 in Supplementary Material):

$$\Omega_k^{\tilde{p}} = \begin{bmatrix} \Omega_k^p & 0 & 0 \\ 0 & K_{k+1}H\Omega_k^p H^T K_{k+1}^T + K_{k+1}\Omega^m K_{k+1}^T & 0 \\ 0 & 0 & 0 \end{bmatrix} \quad (15)$$

Given (TA2), the Kalman gains K_k are optimized for the nominal system with the low process noise and are not updated to reflect the higher process noise.

Proposition: Let Γ_k^L and Γ_k^H be the outputs of two systems described by Equations (14,15) with the same parameters except for the process noise that is either Ω_L^p or Ω_H^p, respectively, where $\Omega_H^p \succcurlyeq \Omega_L^p$. Let POM^L and POM^H be the POM (Equation 1) of the resulting spike counts generated by DSPPs from Γ_k^L and Γ_k^H, respectively, then $POM^H \geq POM^L$.

Proof: Proposition C1 in Appendix C (Supplementary Material) proves that under the conditions of the proposition, the cumulative spike-rates Γ_k^L and Γ_k^H satisfy two conditions: (i) $E_m[\Gamma_k^L] = E_m[\Gamma_k^H]$ and (ii) $E_m[(\Gamma_k^H)^2] \geq E_m[(\Gamma_k^L)^2]$, where $E_m[\cdot]$ denotes ensemble average over different movements starting from the same distribution of initial conditions. Proposition C2 indicates that those two conditions assure that the POMs of the spike counts generated by DSPPs from Γ_k^L and Γ_k^H, i.e., POM^L and POM^H, respectively, satisfy $POM^H \geq POM^L$.

3. Results

The OFC model detailed in Section 2.3 was used to simulate 60 min sessions of BMI experiments equally divided into pole control, BCWHM and BCWOHM. Unless otherwise specified, new neural tuning weights and targets were randomly generated (as detailed in Sections 2.3.4 and 2.3.6) for each session. Since the performance of the BMI filter, quantified by $R(\hat{v}, v)$ (see Sections 2.3.5, 2.3.6), depends on the specific set of the neural tuning weights, only simulated sessions for which $R(\hat{v}, v)$ was between 0.65 and 0.85 were considered for further analysis (as further detailed in Section 3.2).

Simulated reaching movements under pole control resulted in an average speed profile that agrees well with the expected minimum jerk velocity profile (Flash and Hogan, 1985). Representative traces of the cursor during simulated pole control and BCWHM are shown in **Figure 3**. In order to facilitate comparison, the same sets of targets and desired reaching times were used. While in both phases the depicted traces reach the targets, they differ considerably, and are more variable in simulated BCWHM than in simulated pole control. In particular, the variance of the velocity (estimated over 2 min intervals) is significantly higher in simulated BCWHM than in simulated pole control (Wilcoxon rank sum test, $p < 0.0001$). This reproduces well the significant increase in the variance of the velocity from the experimental pole control to experimental BCWHM (Wilcoxon rank sum test, $p < 0.0002$).

The resulting cross correlations between the cursor velocity and neural activity generated during simulated pole control are investigated in Section 3.1 and compared with the cross-correlations derived from the BMI experiments. The main results regarding the changes in neural modulations are reported in Section 3.2. In Section 3.3 we investigate the effect of process noise on neural modulations during pole control, to support our hypothesis that increasing process noise introduced by the imperfect BMI filter contributes to the observed changes in neural modulations in brain control. Sections 3.4 and 3.5 evaluate the effect of the baseline measurement and process noise on estimated POM, respectively, and Section 3.6 investigates the effect of imperfect internal model. The $\hat{POM}$ results described in this section and shown in the Figures were estimated from temporal statistics as detailed in Section 2.2.1 using Equation (3).

3.1. Cross Correlation between Cursor Velocity and Neural Activity

The average cross correlations between the recorded cursor velocity and the recorded neural activity of either PMd

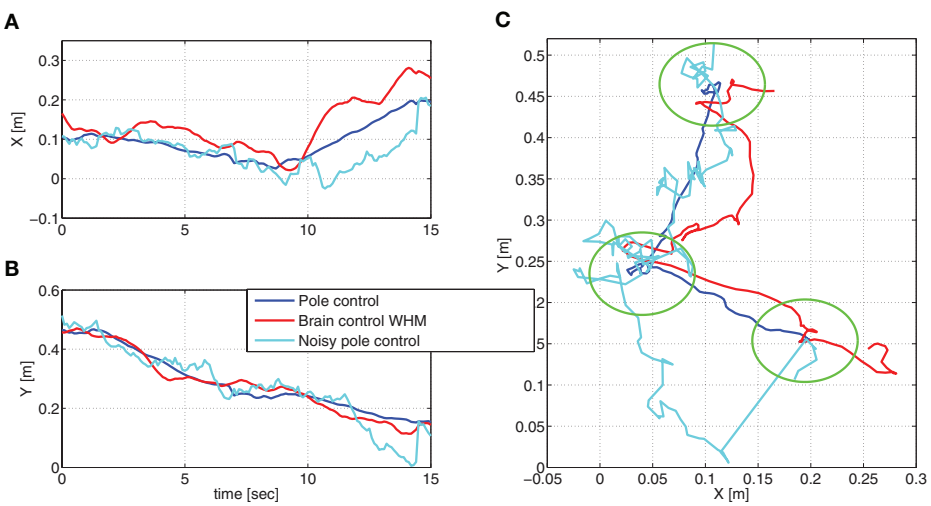

FIGURE 3 | Movement trajectories. Representative traces of the cursor during simulated pole control, brain control and noisy pole control (with $\alpha_{rec} = 0.035$). To facilitate comparison, the same set of targets (marked by green circles) and desired reaching times was used in these three simulations.

(**Figure 4A**) or M1 units (**Figure 4B**), demonstrate different temporal relationships. While there is no dominant time shift between the recorded neural activity of PMd neurons and the cursor velocity, the neural activity of M1 neurons clearly precede the velocity (Lebedev et al., 2005). The average cross correlations were computed by first calculating the cross-correlation for each unit from each non-overlapping 2-min interval, then averaging across units to get the ensemble-mean cross correlation, and finally averaging across intervals. Error bars depict the standard deviations of the ensemble-means across the non-overlapping 2-min intervals. Lags at which the cross correlation is significantly lower than the peak at either 0 s in (A) or −0.2 s in (B) are marked with open circles and stars, for significance level of p = 0.05 (standard) or p = 0.005 (Bonferroni corrected for 10 multiple comparisons), respectively (Wilcoxon rank sum test). It is evident that for M1 units, the peak at −0.2 s in **Figure 4B** is significantly higher than the cross-correlation at zero lag. In contrast, for PMd units, the cross-correlation at negative or positive lags are either significantly lower than the peak at 0 s or at least not significantly different (**Figure 4A**).

Similar temporal relationships are also observed in the simulations, depending on whether the simulated neurons encode only the estimated state or also the control signal. **Figure 4C** demonstrates that the activity of neurons that encode only the estimated state do not exhibit any dominant time shift with respect to the velocity, in agreement with the temporal relationship depicted by the recorded PMd units. As detailed in Section 2.3.4, this agreement is in line with the literature on PMd neural encoding (Messier and Kalaska, 2000; Hendrix et al., 2009), so we refer to these simulated neurons as PMd-like neurons.

In contrast, the activity of simulated neurons that encode both the estimated state and the control signal, precedes the simulated cursor velocity, as demonstrated in **Figure 4D**. In particular, the peak cross correlation at −0.2 s is significantly higher than the cross correlation at zero-lag.This is in agreement with the cross correlation depicted by the recorded M1 units. Given this agreement, and the literature on M1 neural encoding (Evarts, 1968; Kalaska et al., 1989; Todorov, 2000), we refer to these simulated neurons as M1-like neurons. The delay in the cursor velocity can be attributed to the effect of the muscles, which are modeled as a second order over-damped filter, and thus introduce a delay in the forces and eventually the movements that are generated in response to the control signal.

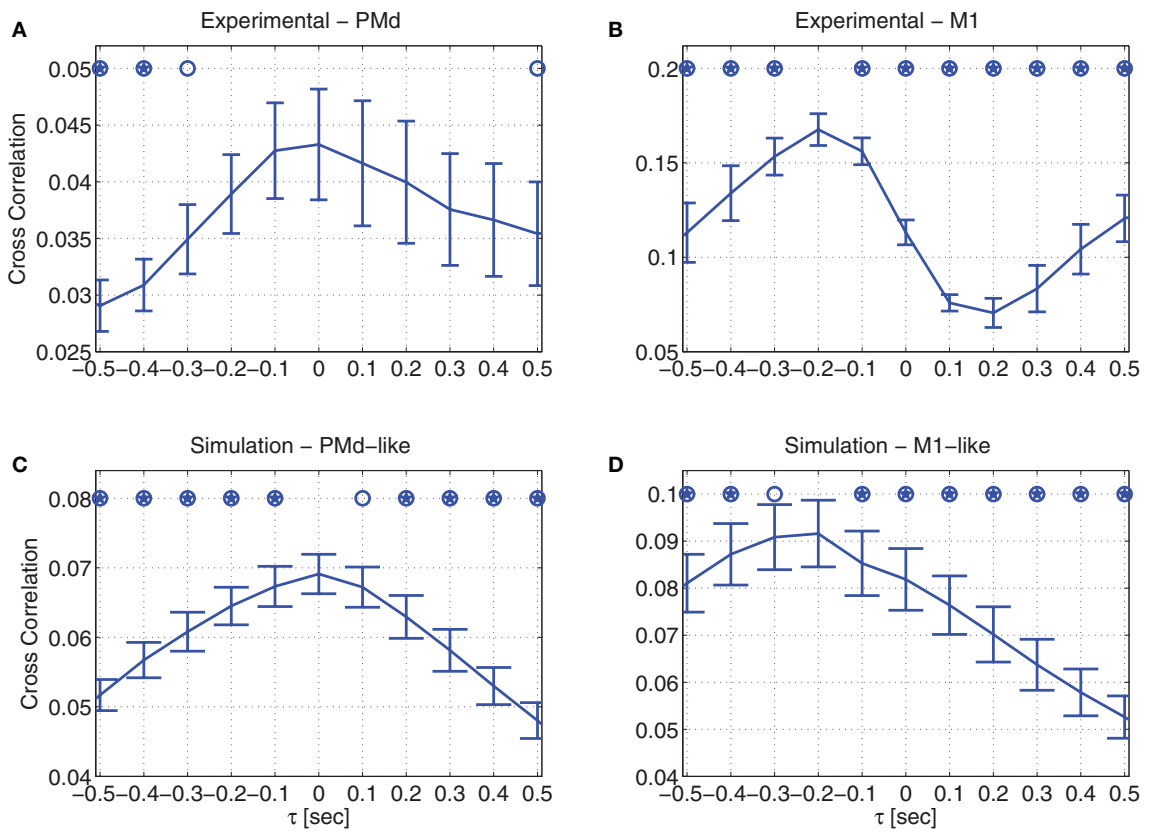

FIGURE 4 | Cross correlation between velocity and neural activity during pole control. Averaged cross correlation of: **(A)** recorded data from PMd units **(B)** recorded data from M1 units **(C)** simulated PMd-like neurons **(D)** simulated M1-like neurons. Error bars depict standard deviations across non-overlapping 2-min intervals. Open circles and stars indicate cross-correlations that are significantly lower than the peak at 0 s in **(A,C)**, and at −0.2 s at **(B,D)** with significance level of either $p = 0.05$ (standard) or $p = 0.005$ (Bonferroni corrected for 10 multiple comparisons), respectively.

3.2. Neural Modulations in Simulated Pole and Brain Control

Simulated neural activity generated by the model described in Section 2.3, based on the framework of OFC, successfully depicts the observed changes in neural modulations, as shown in **Figure 5**. **Figures 5A,B** depicts the results from a single session to facilitate direct comparison with the experimental results, while **Figures 5C,D** demonstrates the robustness of the results across a number of sessions with different sets of random tuning weights. As in Zacksenhouse et al. (2007), mean $\hat{POM}$ and PKM were computed by first estimating the $\hat{POM}$ and PKM from non-overlapping 2-min intervals of the binned spike-counts of individual neurons, then averaging across the relevant neurons to get the ensemble mean, and finally averaging across the 10 intervals of each control mode. Error bars in **Figures 5A,B** depict the standard deviations across the 10 intervals.

Figure 5 demonstrates that the $\hat{POM}$ estimated from a single simulated session increases significantly when switching to brain control, with no matching increase in PKM. Focusing first on the detailed results from a single session in **Figures 5A,B**, the ensemble-mean $\hat{POM}$ during simulated brain control is significantly higher than of ensemble-mean $\hat{POM}$ during simulated pole control (Wilcoxon rank sum test, $p = 0.001$ for both BCWHM and BCWOHM), while the ensemble mean PKM did not differ significantly ($p > 0.55$). This behavior is evident in the simulated neural activity of both PMd-like and M1-like simulated neurons. This reproduces well the significant increase in the ensemble mean $\hat{POM}$ from experimental pole control to BCWHM or BCWOHM (Wilcoxon rank sum test, $p < 0.008$), with no significant increase in the ensemble mean PKM ($p > 0.39$).

The robustness of the changes in neural modulations following the transition to brain control was investigated by simulating 100 sessions, each with a different set of tuning weights. Pole control was simulated first, while brain control was conducted only in the 78 sessions in which the performance of the BMI filter was within the constraint described above ($0.65 < R(\hat{v}, v) < 0.85$). The scatter plot in **Figure 5C** demonstrates that in these cases the $\hat{POM}$ in BCWHM and BCWOHM are significantly higher than the $\hat{POM}$ in pole control (Wilcoxon rank sum test, $p < 10^{-10}$). In contrast, the scatter plot in **Figure 5D** demonstrates that the PKM in BCWHM and BCWOHM are not significantly higher than the PKM in pole control ($p = 0.13$ and $p = 0.08$, respectively).

3.3. Effect of Process Noise on Neural Modulations

Our main hypothesis is that the higher $\hat{POM}$ in brain control, without matching increase in PKM, results from higher process noise introduced by the imperfect performance of the BMI filter.

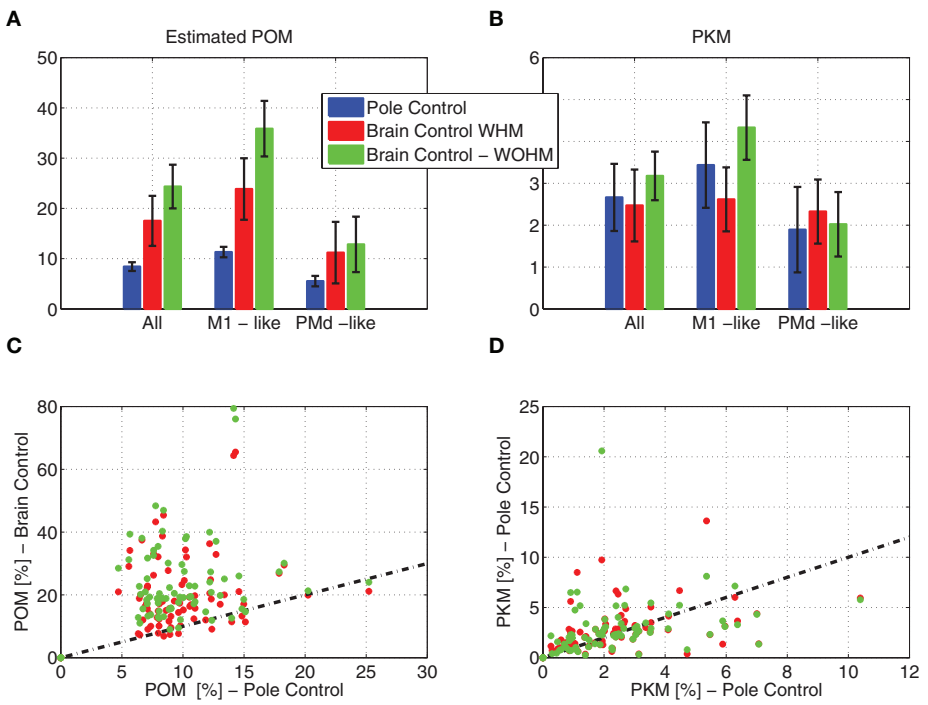

FIGURE 5 | Estimated POM and PKM of simulated neural activity. Estimated POM and PKM were computed by first estimating the POM and PKM of the binned spike-counts of individual neurons in 2-min intervals, and then averaging across the relevant neurons and across the 10 intervals of each control mode. Mean estimated POM **(A)** and PKM **(B)** across all neurons and across neurons that encode only the estimated state (PMd-like) or also the control signals (M1-like). Error bars depict the standard deviations across the 10 intervals. Scatter plot of estimated POM **(C)** and PKM **(D)** in brain vs. pole control for 78 out of 100 sessions (each with a different set of tuning weights) in which the performance of the BMI filter satisfied $0.65 < R(\hat{v}, v) < 0.85$. Dashed lines depict the identity relationship.

As detailed in Section 2.3.7, this hypothesis is investigated here by simulating noisy pole control in which the covariance of the process noise is characterized by Equation (13) instead of Equation (9). The additional term in Equation (13) describes the equivalent noise introduced by the imperfect BMI filter with magnitude that is quantified by α_{rec}. **Figure 3** demonstrates that indeed the cursor movements during noisy pole control (with $\alpha_{rec} = 0.035$) are more similar to those during brain control than those during pole control. In particular, the variance of the velocity in the simulated trajectories generated with $\alpha_{rec} = 0.0035$ was $88 \pm 7[(\frac{\text{cm}}{\text{sec}})^2]$, comparable with the variance of the velocity in the simulated trajectories during BCWHM ($75 \pm 29[(\frac{\text{cm}}{\text{sec}})^2]$), and significantly higher than the variance of the velocity in the simulated trajectories during pole control (Wilcoxon rank sum test, $p < 0.0001$).

The effects of α_{rec} on PÔM and PKM are depicted in **Figure 6** both when the internal model of the noise is not updated (in line with simplifying assumption SA3 that there is no adaptation) and when it is updated to match the actual process noise. All simulated sessions analyzed in **Figure 6** were performed with the same set of randomly selected targets and neural tuning weights. At each α_{rec}, the average PÔM and PKM and their standard deviations were computed from a singe simulated session as detailed in Section 3.2.

Figure 6 demonstrates that as the process noise increases, due to increasing α_{rec}, PÔM increases while PKM does not change or even decreases. This is evident by the high positive (> 0.99) and negative (< -0.96) cross correlations between α_{rec} and either PÔM or PKM, respectively. Furthermore, at all the noisy pole control cases analyzed in **Figure 6**, the PÔM was significantly higher than the PÔM with the standard process noise (i.e., with $\alpha_{rec} = 0$, Wilcoxon rank sum test, with Bonferroni corrected significance level of $p = 0.005$, corrected for the 10 multiple comparisons), as marked by stars in **Figure 6**. The effect is similar whether the internal model of the process noise is updated to match the actual process noise or not. The results shown in **Figure 6** are averaged PÔM and PKM across all the simulated neurons, but similar trends were also observed when averaging across PMd-like and M1-like simulated neurons separately.

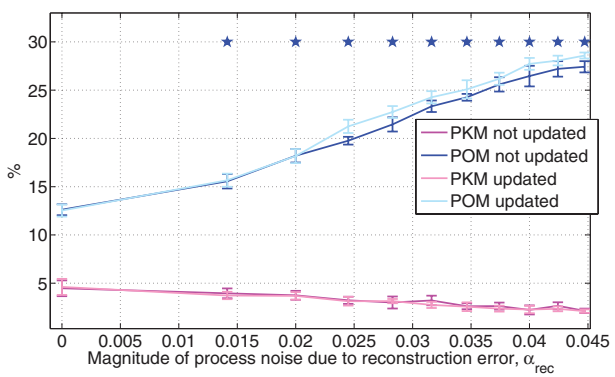

FIGURE 6 | Estimated POM and PKM during simulated noisy pole control. Noisy pole control includes both the baseline process noise due to the control signal, and an additional process noise, simulating the contribution of the BMI filter reconstruction error, as quantified by the magnitude of α_{rec} in Equation (13). At each α_{rec} and for each adaptation option (updated or not), the average estimated POM and PKM were computed from a single 20 min session of simulated pole control as detailed in the caption of **Figure 5**. Standard deviations were computed across the 10 2-min intervals and stars indicate the estimated POM (for not-updated case) that are significantly larger than the estimated POM at the standard process noise ($\alpha_{rec} = 0$) as determined by Wilcoxon rank sum test, with Bonferroni corrected significance level $p = 0.005$, corrected for 10 multiple comparisons. All sessions were performed with the same randomly selected targets and neural tuning weights.

3.4. Sensitivity to Baseline Measurement Noise

In this and the next section we investigate the sensitivity of PÔM to the baseline covariance matrices of the different sources of noise, i.e., the covariance matrices of the measurement and process noise during pole control. Since the internal model is assumed to be well-adapted for pole control, these are also the covariance matrices of the internal model of the noise. Each sensitivity analysis is conducted with 15 sessions simulated with the same set of neurons but different sets of targets. This is equivalent to simulating longer sessions, which improves the accuracy of the estimated POM. In particular, the mean PÔM across all the simulated neurons was estimated from each session and the average and standard deviations were computed across the 15 sessions.

The Kalman filter depends on the relative size of these covariance matrices, so the value of one of the elements can be kept constant. Furthermore, since we found that the PÔM is insensitive to the ratio between visual position and velocity measurements noise, we kept the diagonal covariance matrix of the visual measurement noise fixed and equals to the one suggested in Todorov (2005).

Focusing first on the sensitivity of PÔM to the baseline proprioceptive measurement noise, we found that the PÔM is insensitive to the proprioceptive position measurement noise. Hence, **Figure 7A** depicts only the effect of a common scaling factor between the covariance matrices of the visual and proprioceptive measurements noise, i.e., the effect of the proprioceptive measurement noise factor k_m in **Table 1**. **Figure 7A** indicates that the PÔM is sensitive to k_m only in BCWHM. When the covariance matrices of the proprioceptive and visual measurement noise are comparable ($0.5 < k_m < 2$), the PÔM in simulated BCWHM is significantly larger than the PÔM during the experimental BCWHM (Wilcoxon rank sum test, $p < 0.004$) and even larger than the PÔM in BCWOHM, in contrast with the observed relationship in the BMI experiments (Zacksenhouse et al., 2007). When the proprioceptive measurement noise is 10-fold larger than the visual measurement noise ($k_m = 10$), the PÔM in simulated BCWHM does not differ significantly from the PÔM during the experimental BCWHM and is lower than the PÔM in BCWOHM, as in the BMI experiments. Further increase in the the proprioceptive measurement noise has little effect on the PÔM even in BCWHM. These observations motivated the

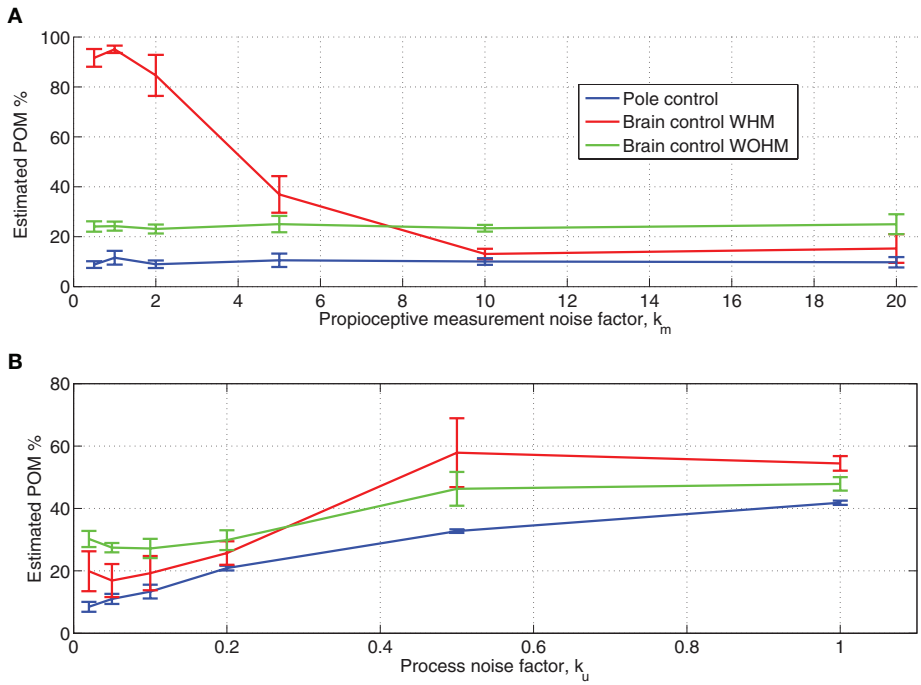

FIGURE 7 | Sensitivity of estimated POM to proprioceptive measurement noise (A) and magnitude of baseline process noise (B). The proprioceptive measurement noise factor k_m quantifies the ratio between the variance of the proprioceptive and the visual measurement noise (same factor for both position and velocity measurements). The process noise factor k_U quantifies the magnitude of hand process noise, as specified in **Table 1**. Each sensitivity analysis was conducted by simulating 15 sessions with the same set of neurons but different sets of targets. The mean estimated POM over the simulated neurons was computed for each session and the average and standard deviations across the 15 sessions are plotted.

selection of $k_m = 10$ as the default factor in all other simulations (**Table 1**).

The lack of sensitivity to proprioceptive measurement noise during pole control can be attributed to the perfect internal model and low baseline process noise, which cause state-estimation to be based mainly on the internal model. The high $\hat{\text{POM}}$ during BCWHM when the baseline proprioceptive and visual measurements noise are comparable can be attributed to the resulting similar Kalman gains for those two modalities. Due to the imperfect BMI filter, the estimation measurement error in brain control is high, and during BCWHM the proprioceptive measurement may differ from the visual measurement. When both modalities are given similar Kalman gains, the deviation between the proprioceptive and visual measurements contributes to higher variance in the resulting estimated state. Finally, during BCWOHM the proprioceptive measurement noise is increased to infinity to model the lack of relevant proprioceptive feedback in this mode, and hence the $\hat{\text{POM}}$ in this mode does not depend on the baseline proprioceptive measurement noise.

3.5. Sensitivity to Baseline Process Noise

During regular pole control, the covariance of the process noise is described by Equation (9) and its magnitude is quantified by α_u , or alternatively by the process noise factor k_u, as described in Section 2.3.6 and **Table 1**. As noted in Section 2.3.6 and **Figure 2**, adequate performance of the BMI filter in the simulated BMI sessions can be achieved with $k_u = 0.1$. Here we investigate the effect of k_u on $\hat{\text{POM}}$.

Figure 7B depicts the changes in the $\hat{\text{POM}}$ as a function of the process noise factor k_u. It is apparent that $\hat{\text{POM}}$ in brain control is always higher than $\hat{\text{POM}}$ in pole control, in agreement with the observed changes in the $\hat{\text{POM}}$ during the BMI experiments. However, for $k_u = 1$, the $\hat{\text{POM}}$ in each of control mode is too large compared with the experimentally observed $\hat{\text{POM}}$ (Wilcoxon rank sum test, $p < 0.002$ for each control mode). This further supports the selection of a smaller process noise factor, and in particular $k_u = 0.1$, made in section 2.3.6 based on the performance of the BMI filter. For this process noise, the relation between the $\hat{\text{POM}}$ in BCWHM versus BCWOHM agrees well with the experimental observations.

Figure 7B also shows that $\hat{\text{POM}}$ increases with the magnitude of the process noise. This is in agreement with the results described in Section 3.4, though in that section the magnitude of the process noise described by Equation (13) was manipulated by changing of α_{rec} instead of α_u (via k_u).

3.6. Internal Model Variations

The simulations presented so far were based on simplifying assumption SA3, so the internal model did not change due to transition to brain control. Since the monkey stopped moving its hand in BCWOHM, the internal model may change to account

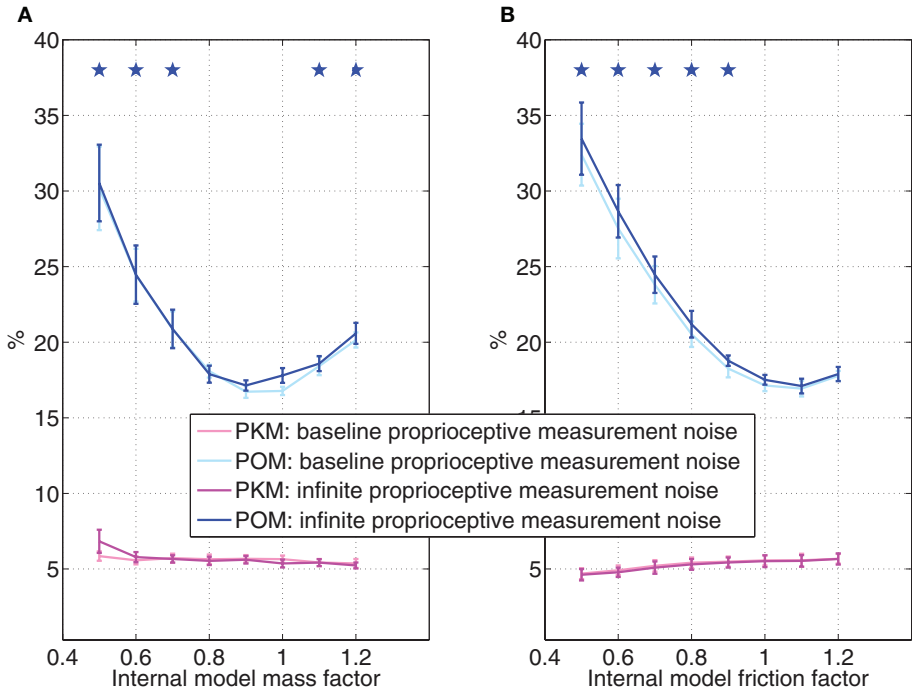

FIGURE 8 | Effect of internal model variations during pole control. The value of the mass **(A)** or the coefficient of friction **(B)** in the internal model is normalized to the value of the actual parameter. Simulations are conducted with either the baseline proprioceptive measurement noise characteristic of pole control or infinite proprioceptive measurement noise characteristic of BCWOHM. At each parameter value, and for each level of the proprioceptive measurement noise, the average estimated POM and PKM were computed from a single 20 min session of simulated pole control as detailed in the caption of **Figure 5**. Standard deviations were computed across the 10 2-min intervals and stars indicate estimated POMs that are significantly larger than the estimated POM at the nominal parameter (internal model factor = 1), as determined by Wilcoxon rank sum test with Bonferroni corrected significance level $p = 0.007$, corrected for 7 multiple comparisons. All sessions were performed with the same randomly selected targets and neural tuning weights.

for the lack of hand movements. **Figure 8** evaluates the effect of changing the parameters of the internal model, and in particular the mass (**Figure 8A**), or the coefficient of friction (**Figure 8B**), during pole control while keeping the external model the same. In both cases, the x-axis is the normalized parameter of the internal model (mass or coefficient of friction) relative to the nominal value of the parameter of the external model. The effect is evaluated both with the baseline proprioceptive measurement noise characteristic of pole control and BCWHM, and with infinite proprioceptive measurement noise characteristic of BCWOHM. All simulated sessions analyzed in **Figure 8** were performed with the same set of randomly selected targets and neural tuning weights, but not the same set used in other sections. At each parameter value, and for each level of the proprioceptive measurement noise, the average $\hat{\text{POM}}$ and PKM in **Figure 8** and their standard deviations were computed from a single simulated session as detailed in Section 3.2.

Figure 8 indicates that when the internal model deviates from the external model, the $\hat{\text{POM}}$ increases significantly, while the PKM does not change significantly or even decease over most of the range. Parameter values at which the $\hat{\text{POM}}$ (generated in simulations with infinite process noise) is significantly higher than the $\hat{\text{POM}}$ at the nominal parameter are marked by stars (Wilcoxon rank sum test with Bonferroni corrected significance level $p = 0.007$, corrected for 7 multiple comparisons). The effect of increasing the covariance matrix of the proprioceptive measurement noise to infinity, as in BCWOHM, is negligible. Hence, changes in the parameters of the internal model may further contribute the observed change in $\hat{\text{POM}}$ upon switching to brain control, and especially to BCWOHM.

4. Discussion

4.1. Modeling

The implemented OFC model successfully moves the hand and cursor in simulated pole control to reach randomly selected targets. Neural activity is generated to simulate neural recording and perform brain control. The simulated neurons are assumed to encode the signals that are relevant for OFC, i.e., the estimated state and the control signal, and spike-counts are generated as doubly stochastic Poisson processes. The model parameters were taken from the literature or selected to match the experimental observations. In particular, the magnitude of the process noise and the number of neurons were selected so the performance of the BMI filter trained on the simulated neural activity matches the performance of the BMI filter trained on the recorded neural activity. The resulting model successfully generates the main

phenomena that it was developed to explain: the POM of the neural activity in brain control is higher than the POM in pole control with no matching increase in PKM.

OFC involves different computational tasks that can be mapped to different brain regions. In particular, it has been suggested (Shadmehr and Krakauer, 2008) that expected costs and rewards are evaluated by the basal ganglia, the forward model is implemented by the cerebellum, and the predicted sensory feedback is combined with the actual sensory feedback at the parietal cortex to estimate the state. Given the estimated state, the pre-motor and primary motor cortices are hypothesized to generate the control signals associated with visual and proprioceptive feedback, respectively. As mentioned above (Introduction and Section 2.3.3) the OFC is simulated in the state space, so all these computational tasks are included regardless of where they are implemented in the brain. In contrast, neural activity is generated to simulate neural recording from M1 and PMd only, since those are the main brain regions recorded in the BMI experiments considered here.

4.2. Neural Encoding

Neural encoding is an open and important research question. Common strategies to investigate this issue involve quantifying the correlation between the neural activity and different relevant signals, or assessing how well those signals can be predicted by the neural activity. However, those strategies are usually restricted to measurable signals. In particular, many studies investigated the correlation between the activity of cortical motor units and different kinematics and kinetics signals (Georgopoulos et al., 1984, 1986, 1992; Kalaska et al., 1989; Ashe and Georgopoulos, 1994; Ashe, 1997; Moran and Schwartz, 1999; Paninski et al., 2004; Kalaska, 2009). Since correlations do not imply causality, the observed correlations with any of the measurable signals do not imply that the neurons indeed encode these signals. Instead, the neurons may encode internal, hidden signals, which are also correlated with the measurable signals (Zacksenhouse et al., 2014) including, for example, muscle activation patterns (Todorov, 2000).

Here we suggest that cortical motor neurons encode signals that are relevant for performing state estimation and control, i.e., the estimated state and the control signal. Since these signals are internal signals generated by the brain, direct correlation cannot be evaluated. Nevertheless, during normal reaching movements, the actual movement should agree well with the estimated state, and thus the neural activity would appear to be correlated with the movement. However, in other conditions, and in particular during brain control, the estimated state may deviate from the measured state. This work suggests that the higher POM during brain control with no matching increase in PKM may arise from such deviations.

We noted that the neural activity recorded from M1 and PMd units exhibited different cross-correlations with the velocity. In particular, the average cross-correlations between the velocity and the recorded neural activity during pole control indicate that there is no time-shift between the neural activity of PMd units and the cursor velocity, while the neural activity of M1 neurons precedes the velocity. These temporal relationships are reproduced well by simulated neurons that encode only the estimated state or also the control signal, respectively. The time shift in the latter case can be ascribed to the delay in the response of the muscles. Hence, the different types of observed cross-correlations, with and without time shift, can be attributed to encoding different signals within the framework OFC, including and excluding the control signal, respectively. Encoding the control signal in M1 but not in PMd neurons agrees well with evidence that the activity of PMd neurons is modulated mainly by the direction and magnitude of movements while the activity of M1 neurons is correlated also with the forces (Evarts, 1968; Kalaska et al., 1989). Further support is provided by previous investigation of the BMI experiments considered here, which indicated that PMd neurons can predict well the position and velocity but not the force, while M1 neurons can predict well the force too (Carmena et al., 2003). While this specific distinction between M1 and PMd neurons may result from the specific sample of units recorded during the BMI experiments considered here, it is well reproduced by the simulated model based on OFC.

4.3. Process Noise

Our main hypothesis is that the observed increase in POM following the transition to brain control reflects increasing variance of the encoded signals due to higher process noise. The latter is assumed to occur in brain control due to the limited accuracy of the BMI filter. This hypothesis was proved theoretically and by simulations. Theoretical proof was limited to the case when the estimated process noise in the internal model is not updated, and the neurons encode linear combinations of the estimated state. The simulations demonstrate that increasing process noise during pole control results in higher POM even when neurons encode non-linear functions of the estimated state (e.g., speed and magnitude of the control signal) and regardless of whether the internal model is updated or not.

4.4. Implications for BMI

The proposed model attributes the increase in POM following the transition to brain control to the higher process noise introduced by the imperfect performance of the BMI filter. This suggests that the POM is a proxy for the performance of the BMI filter: High POM indicates that the BMI filter performs poorly while low POM indicates that the BMI filter performs well. As a proxy signal for the performance of the BMI filer, the POM could be used to adapt the BMI filter using reinforcement learning (DiGiovanna et al., 2009; Mahmoudi et al., 2013), especially in cases when an error signal cannot be determined (Bensmaia and Miller, 2014). Furthermore, the proposed model developed here, provides a framework for investigating this and other suggestion for improving BMIs. Finally, the proposed model can be used to investigate other changes that occur following the transition to brain control and in particular the changes in neural tuning (Lebedev et al., 2005).

4.5. Alternative Hypotheses

Our main hypothesis is that the observed changes in neural modulations following the transition to brain control are related to changes in the process and measurement noise induced by

the transition, and in particular, the increase in process noise due to the imperfect BMI filter. OFC provides a coherent and concise framework for relating the changes in process and measurement noise to changes in the estimated state and control signals, and finally to changes in neural modulations. However, the key elements are state estimation and the encoding of the estimated state, so other models that include those components may produce similar results. In particular, state estimation and control may not be optimal, but only satisficing (Simon, 1956; Brown et al., 2004). The OFC framework was adopted here since optimization constrains the parameters of the estimation filter and the gains of the control law, resulting in fewer free parameters to be tuned, thus granting the resulting model higher credibility.

An alternative hypothesis that may contribute to the changes in neural modulations involve changes in the internal model. As was shown in Section 3.6, deviations between the internal model and the external system, and in particular deviations in the mass or the coefficient of friction, result in higher PÔM with no matching increase in PKM. Thus, changes in the internal model of the mass or coefficient of friction, may contribute to the increase in PÔM beyond what is attributed to the increase in process noise. Since the transition to BCWOHM involves stopping hand movements, it is conceivable that it is associated with a switch to a different internal model, with lower mass and coefficient of friction. However, the change in the internal model is not justified in the transition to BCWHM, when the monkey continues to make hand movements.

Alternative frameworks for explaining the changes in neural modulations may be provided by intermittent predictive control (Doeringer and Hogan, 1998; Gawthrop et al., 2011) and active inference (Friston et al., 2010, 2011). Intermittent predictive control alleviates the computational load of prediction that is necessary to address time delays (Doeringer and Hogan, 1998; Gawthrop et al., 2011). Due to the imperfect BMI filter, the transition to brain control is expected to result in more frequent updates of the predictor, and hence in higher variability in the predicted state. Since intermittent predictive control is based on OFC, this is an extension of the current model, and will be considered in future work. Indeed it could be argued that due to the inaccurate movements of the cursor during brain control, the monkey is making explorative movements to adapt to the new environment. While the explorative movements may contribute to higher POM, they are expected to also increase the PKM, in contrast with the observation.

In summary, we demonstrated that the observed changes in neural modulations following the transition to brain control can be successfully explained under the assumption that the neurons encode the estimated state and control signal. To be concrete we used the framework of OFC, but similar results are expected even if the controller is not optimal, as long as it relies on state estimation that deteriorates upon switching to brain control.

Acknowledgments

The BMI experiments were conducted at Nicolelis' lab, Duke University, and we thank MAL Nicolelis, J Carmena and M Lebedev for sharing the data. The research was supported by Fund C for research at the Technion's Autonomous Systems Program, under grant numbers 2018172. We thank Prof. Y. halevi for his suggestions on the theoretical analysis.

Supplementary Material

The Supplementary Material for this article can be found online at: http://journal.frontiersin.org/article/10.3389/fnsys.2015.00071/abstract

References

Ashe, J. (1997). Force and the motor cortex. *Behav. Brain Res.* 87, 255–269. doi: 10.1016/S0166-4328(97)00752-3

Ashe, J., and Georgopoulos, A. P. (1994). Movement parameters and neural activity in motor cortex and area 5. *Cereb. Cortex* 4, 590–600. doi: 10.1093/cercor/4.6.590

Bensmaia, S. J., and Miller, L. E. (2014). Restoring sensorimotor function through intracortical interfaces: progress and looming challenges. *Nat. Rev. Neurosci.* 15, 313–325. doi: 10.1038/nrn3724

Brown, E. N., Kass, R. E., and Mitra, P. P. (2004). Multiple neural spike train data analysis: state-of-the-art and future challenges. *Nat. Neurosci.* 7, 456–461. doi: 10.1038/nn1228

Carmena, J. M., Lebedev, M. A., Crist, R. E., O'Doherty, J. E., Santucci, D. M., Dimitrov, D. F., et al. (2003). Learning to control a brain-machine interface for reaching and grasping by primates. *PLoS Biol.* 1:E42. doi: 10.1371/journal.pbio.0000042

Chang, Y. H., Chen, M., Shanechi, M., Carmena, J. M., and Tomlin, C. (2014). "A design of neural decoder by reducing discrepancy between Manual Control (MC) and Brain Control (BC)," in *2014 European Control Conference (ECC)* (Strasbourg), 516–521.

Churchland, A. K., Kiani, R., Chaudhuri, R., Wang, X.-J., Pouget, A., and Shadlen, M. N. (2011). Variance as a signature of neural computations during decision making. *Neuron* 69, 818–831. doi: 10.1016/j.neuron.2010.12.037

Crevecoeur, F., and Scott, S. H. (2013). Priors engaged in long-latency responses to mechanical perturbations suggest a rapid update in state estimation. *PLoS Comput. Biol.* 9:e1003177. doi: 10.1371/journal.pcbi.1003177

Cunningham, J. P., Nuyujukian, P., Gilja, V., Chestek, C. A., Ryu, S. I., and Shenoy, K. V. (2011). A closed-loop human simulator for investigating the role of feedback control in brain-machine interfaces. *J. Neurophysiol.* 105, 1932–1949. doi: 10.1152/jn.00503.2010

Dayan, P., and Abbott, L. F. (2001). *Theoretical Neuroscience*. Cambridge, MA: MIT Press.

DiGiovanna, J., Mahmoudi, B., Fortes, J., Principe, J. C., and Sanchez, J. C. (2009). Coadaptive brain–machine interface via reinforcement learning. *Biomed. Eng. IEEE Trans.* 56, 54–64. doi: 10.1109/TBME.2008.926699

Doeringer, J. A., and Hogan, N. (1998). Intermittency in preplanned elbow movements persists in the absence of visual feedback. *J. Neurophysiol.* 80, 1787–1799.

Evarts, E. V. (1968). Relation of pyramidal tract activity to force exerted during voluntary movement. *J. Neurophysiol.* 31, 14–27.

Flash, T., and Hogan, N. (1985). The coordination of arm movements: an experimentally confirmed mathematical model. *J. Neurosci.* 5, 1688–1703.

Friston, K., Mattout, J., and Kilner, J. (2011). Action understanding and active inference. *Biol. Cybern.* 104, 137–160. doi: 10.1007/s00422-011-0424-z

Friston, K. J., Daunizeau, J., Kilner, J., and Kiebel, S. J. (2010). Action and behavior: a free-energy formulation. *Biol. Cybern.* 102, 227–260. doi: 10.1007/s00422-010-0364-z

Gawthrop, P., Loram, I., Lakie, M., and Gollee, H. (2011). Intermittent control: a computational theory of human control. *Biol. Cybern.* 104, 31–51. doi: 10.1007/s00422-010-0416-4

Geisler, W., and Albrecht, D. (1995). Bayesian analysis of identification performance in monkey visual cortex: nonlinear mechanisms and stimulus certainty. *Vis. Res.* 35, 2723–2730. doi: 10.1016/0042-6989(95)00029-Y

Georgopoulos, A., Caminiti, R., and Kalaska, J. (1984). Static spatial effects in motor cortex and area 5: quantitative relations in a two-dimensional space. *Exp. Brain Res.* 54, 446–454. doi: 10.1007/BF00235470

Georgopoulos, A. P., Ashe, J., Smyrnis, N., and Taira, M. (1992). The motor cortex and the coding of force. *Science* 256, 1692–1695. doi: 10.1126/science.256.5064.1692

Georgopoulos, A. P., Kalaska, J. F., Caminiti, R., and Massey, J. T. (1982). On the relations between the direction of two-dimensional arm movements and cell discharge in primate motor cortex. *J. Neurosci.* 2, 1527–1537.

Georgopoulos, A. P., Schwartz, A. B., and Kettner, R. E. (1986). Neuronal population coding of movement direction. *Science* 233, 1416–1419. doi: 10.1126/science.3749885

Harris, C. M., and Wolpert, D. M. (1998). Signal-dependent noise determines motor planning. *Nature* 394, 780–784. doi: 10.1038/29528

Hendrix, C. M., Mason, C. R., and Ebner, T. J. (2009). Signaling of grasp dimension and grasp force in dorsal premotor cortex and primary motor cortex neurons during reach to grasp in the monkey. *J. Neurophysiol.* 102, 132–145. doi: 10.1152/jn.00016.2009

Horn, R. A., and Johnson, C. R. (2012). *Matrix Analysis*. Cambridge, MA: Cambridge University Press. doi: 10.1017/CBO9781139020411

Johnson, D. H. (1996). Point process models of single-neuron discharges. *J. Comput. Neurosci.* 3, 275–299. doi: 10.1007/BF00161089

Jordan, M. I., and Rumelhart, D. E. (1992). Forward models: supervised learning with a Distal teacher. *Cogn. Sci.* 16, 307–354. doi: 10.1207/s15516709cog1603_1

Kalaska, J. F. (2009). "From intention to action: motor cortex and the control of reaching movements," in *Progress in Motor Control,* ed D. Sternad (Springer US), 139–178.

Kalaska, J. F., Cohen, D., Hyde, M. L., and Prud'Homme, M. (1989). A comparison of movement direction-related versus load direction-related activity in primate motor cortex, using a two-dimensional reaching task. *J. Neurosci.* 9, 2080–2102.

Kawato, M., Furukawa, K., and Suzuki, R. (1987). A hierarchical neural-network model for control and learning of voluntary movement. *Biol. Cybern.* 57, 169–185. doi: 10.1007/BF00364149

Kuo, A. D. (1995). An optimal control model for analyzing human postural balance. *Biomed. Eng. IEEE Trans.* 42, 87–101. doi: 10.1109/10.362914

Lebedev, M. A., Carmena, J. M., O'Doherty, J. E., Zacksenhouse, M., Henriquez, C. S., Principe, J. C., et al. (2005). Cortical ensemble adaptation to represent velocity of an artificial actuator controlled by a brain-machine interface. *J. Neurosci.* 25, 4681–4693. doi: 10.1523/JNEUROSCI.4088-04.2005

Mahmoudi, B., Pohlmeyer, E. A., Prins, N. W., Geng, S., and Sanchez, J. C. (2013). Towards autonomous neuroprosthetic control using hebbian reinforcement learning. *J. Neural Eng.* 10, 66005. doi: 10.1088/1741-2560/10/6/066005

Messier, J., and Kalaska, J. F. (2000). Covariation of primate dorsal premotor cell activity with direction and amplitude during a memorized-delay reaching task. *J. Neurophysiol.* 84, 152–165.

Miall, R., and Wolpert, D. M. (1996). Forward models for physiological motor control. *Neural Netw.* 9, 1265–1279. doi: 10.1016/S0893-6080(96)00035-4

Moran, D. W., and Schwartz, A. B. (1999). Motor cortical representation of speed and direction during reaching. *J. Neurophysiol.* 82, 2676–2692.

Nicolelis, M. A. (2001). Actions from thoughts. *Nature* 409, 403–407. doi: 10.1038/35053191

Paninski, L., Fellows, M. R., Hatsopoulos, N. G., and Donoghue, J. P. (2004). Spatiotemporal tuning of motor cortical neurons for hand position and velocity. *J. Neurophysiol.* 91, 515–532. doi: 10.1152/jn.00587.2002

Schwartz, A. B. (2004). Cortical neural prosthetics. *Annu. Rev. Neurosci.* 27, 487–507. doi: 10.1146/annurev.neuro.27.070203.144233

Shadmehr, R., and Krakauer, J. W. (2008). A computational neuroanatomy for motor control. *Exp. Brain Res.* 185, 359–381. doi: 10.1007/s00221-008-1280-5

Shanechi, M. M., Williams, Z. M., Wornell, G. W., Hu, R. C., Powers, M., and Brown, E. N. (2013a). A real-time brain-machine interface combining motor target and trajectory intent using an optimal feedback control design. *PLoS ONE* 8:e59049. doi: 10.1371/journal.pone.0059049

Shanechi, M. M., Wornell, G. W., Williams, Z. M., and Brown, E. N. (2013b). Feedback-controlled parallel point process filter for estimation of goal-directed movements from neural signals. *Neural Syst. Rehabil. Eng. IEEE Trans.* 21, 129–140. doi: 10.1109/TNSRE.2012.2221743

Shenoy, K. V., Sahani, M., and Churchland, M. M. (2013). Cortical control of arm movements: a dynamical systems perspective. *Annu. Rev. Neurosci.* 36, 337–359. doi: 10.1146/annurev-neuro-062111-150509

Simon, H. A. (1956). Rational choice and the structure of the environment. *Psychol. Rev.* 63, 129. doi: 10.1037/h0042769

Snyder, D. L. (1975). *Random Point Processes*. New York, NY: J. Willey & Sons.

Stengel, R. F. (2012). *Optimal Control and Estimation*. London: Courier Dover Publications.

Taylor, D. M., Tillery, S. I. H., and Schwartz, A. B. (2002). Direct cortical control of 3d neuroprosthetic devices. *Science* 296, 1829–1832. doi: 10.1126/science.1070291

Todorov, E. (2000). Direct cortical control of muscle activation in voluntary arm movements: a model. *Nat. Neurosci.* 3, 391–398. doi: 10.1038/73964

Todorov, E. (2005). Stochastic optimal control and estimation methods adapted to the noise characteristics of the sensorimotor system. *Neural Comput.* 17, 1084–1108. doi: 10.1162/0899766053491887

Todorov, E., and Jordan, M. I. (2002). Optimal feedback control as a theory of motor coordination. *Nat. Neurosci.* 5, 1226–1235. doi: 10.1038/nn963

Tolhurst, D. J., Movshon, J., and Dean, A. (1983). The statistical reliability of signals in single neurons in cat and monkey visual cortex. *Vis. Res.* 23, 775–785. doi: 10.1016/0042-6989(83)90200-6

Wolpert, D., Ghahramani, Z., and Jordan, M. (1995). Are arm trajectories planned in kinematic or dynamic coordinates? An adaptation study. *Exp. Brain Res.* 103, 460–470. doi: 10.1007/BF00241505

Wolpert, D. M., and Ghahramani, Z. (2000). Computational principles of movement neuroscience. *Nat. Neurosci.* 3, 1212–1217. doi: 10.1038/81497

Wu, W., Gao, Y., Bienenstock, E., Donoghue, J. P., and Black, M. J. (2006). Bayesian population decoding of motor cortical activity using a Kalman filter. *Neural Comput.* 18, 80–118. doi: 10.1162/089976606774841585

Zacksenhouse, M., Lebedev, M. A., Carmena, J. M., O'Doherty, J. E., Henriquez, C., and Nicolelis, M. a. L. (2007). Cortical modulations increase in early sessions with brain-machine interface. *PLoS ONE* 2:e619. doi: 10.1371/journal.pone.0000619

Zacksenhouse, M., Lebedev, M. A., and Nicolelis, M. A. L. (2014). Signal-independent timescale analysis (SITA) and its application for neural coding during reaching and walking. *Front. Comput. Neurosci.* 8:91. doi: 10.3389/fncom.2014.00091

Zacksenhouse, M., and Nemets, S. (2008). "Strategies for neural ensemble data analysis for brain-machine interface (BMI) applications," in *Methods Neural Ensemble Record*, 2nd Edition, Chapter 4, ed M. Nicolelis (Boca Raton, FL: CRC Press), 57–82. doi: 10.1201/9781420006414.ch4

Conflict of Interest Statement: The authors declare that the research was conducted in the absence of any commercial or financial relationships that could be construed as a potential conflict of interest.

frontiers in
SYSTEMS NEUROSCIENCE

REVIEW ARTICLE
published: 12 May 2014
doi: 10.3389/fnsys.2014.00084

The reactivation of somatosensory cortex and behavioral recovery after sensory loss in mature primates

Hui-Xin Qi*, Jon H. Kaas and Jamie L. Reed

Department of Psychology, Vanderbilt University, Nashville, TN, USA

Edited by:
Mikhail Lebedev, Duke University, USA

Reviewed by:
Preston E. Garraghty, Indiana University, USA
Ioan Opris, Wake Forest University, USA

****Correspondence:***
Hui-Xin Qi, Department of Psychology, Vanderbilt University, 111 21st Ave. S., Nashville, TN 37240, USA
e-mail: huixin.qi@vanderbilt.edu

In our experiments, we removed a major source of activation of somatosensory cortex in mature monkeys by unilaterally sectioning the sensory afferents in the dorsal columns of the spinal cord at a high cervical level. At this level, the ascending branches of tactile afferents from the hand are cut, while other branches of these afferents remain intact to terminate on neurons in the dorsal horn of the spinal cord. Immediately after such a lesion, the monkeys seem relatively unimpaired in locomotion and often use the forelimb, but further inspection reveals that they prefer to use the unaffected hand in reaching for food. In addition, systematic testing indicates that they make more errors in retrieving pieces of food, and start using visual inspection of the rotated hand to confirm the success of the grasping of the food. Such difficulties are not surprising as a complete dorsal column lesion totally deactivates the contralateral hand representation in primary somatosensory cortex (area 3b). However, hand use rapidly improves over the first post-lesion weeks, and much of the hand representational territory in contralateral area 3b is reactivated by inputs from the hand in roughly a normal somatotopic pattern. Quantitative measures of single neuron response properties reveal that reactivated neurons respond to tactile stimulation on the hand with high firing rates and only slightly longer latencies. We conclude that preserved dorsal column afferents after nearly complete lesions contribute to the reactivation of cortex and the recovery of the behavior, but second-order sensory pathways in the spinal cord may also play an important role. Our microelectrode recordings indicate that these preserved first-order, and second-order pathways are initially weak and largely ineffective in activating cortex, but they are potentiated during the recovery process. Therapies that would promote this potentiation could usefully enhance recovery after spinal cord injury.

Keywords: area 3b, cuneate nucleus, monkey, plasticity, spinal cord, ventroposterior nucleus, somatosensory system

INTRODUCTION

The last 30 years of intensive research has led to a greatly improved understanding of how the somatosensory system of mature primates and other mammals responds to sensory loss, as reviewed by others (Buonomano and Merzenich, 1998; Jones, 2000; Wall et al., 2002; Kaas et al., 2008; Darian-Smith, 2009; Xerri, 2012). The types of sensory loss that have been experimentally studied have varied, ranging from the loss of peripheral nerves, especially the median nerve to the glabrous skin of the hand (Merzenich et al., 1983a,b; Silva et al., 1996; Florence et al., 1998; Xu and Wall, 1999), the sectioning of dorsal roots of peripheral nerve afferents as they enter the spinal cord (Pons et al., 1991; Jones and Pons, 1998; Darian-Smith and Brown, 2000; Darian-Smith, 2004; Darian-Smith and Ciferri, 2005, 2006), the loss of a digit or part of forelimb (Kelahan and Doetsch, 1984; Crockett et al., 1993; Florence and Kaas, 1995; Sengelaub et al., 1997; Florence et al., 1998; Li et al., 2013), the section of peripheral nerve afferents as they travel in the dorsal columns of spinal cord (Jain et al., 1997, 1998, 2000, 2008; Weng et al., 2003; Graziano and Jones, 2009; Qi et al., 2011a), or spinal cord injury in rodents (Ghosh et al., 2009; Aguilar et al., 2010; Humanes-Valera et al., 2013). All these types of sensory loss deactivate topographically matched parts of the somatosensory system, including parts of the ipsilateral dorsal column-trigeminal complex in lower brainstem and the contralateral ventroposterior nucleus (VP) of the thalamus, and the primary (area 3b) and other areas (1 and 2) of contralateral somatosensory cortex. These extensive deactivations were expected from the somatotopic organization and hierarchical arrangement of these processing stations.

What was not expected, at least by most investigators, was that over various amounts of time, the deactivated parts of the somatosensory system became responsive to tactile stimulation again, based on the somatosensory inputs that remained. Some changes in the receptive fields of neurons in the somatosensory system were apparent as soon as they could be measured after sensory loss (Wall, 1977; Calford and Tweedale, 1988; Faggin et al., 1997; Xu and Wall, 1997, 1999; Krupa et al., 1999), and these immediate changes could be attributed to the removal of the excitatory drive on central inhibitory neurons that normally constrain the receptive fields of relay neurons by keeping some of the excitatory inputs subthreshold. Other reactivations with greater changes in the receptive field locations of central neurons occurred over hours to weeks, such as the reactivation of cortical neurons previously activated from the glabrous skin of

the hand by touch on the back of the hand after sectioning of the median nerve to the glabrous skin of digits 1–3 (Merzenich et al., 1983a,b). Such rapid reactivations may largely result from the potentiation of previously existing subthreshold inputs, especially in the cuneate nucleus representing the hand in the lower brainstem, by homeostatic mechanisms (Garraghty et al., 1991; Turrigiano, 1999; Wellman et al., 2002), and possibly by new axon growth over short distances (Darian-Smith and Gilbert, 1994; Jain et al., 2000; Darian-Smith, 2004; Hickmott and Steen, 2005; Cheetham et al., 2008; Yamahachi et al., 2009; Marik et al., 2010, 2014). Other reactivations that follow the loss or denervation of the forelimb, including invasion by inputs from the face (Pons et al., 1991; Jain et al., 1997, 2000; Wu and Kaas, 1999; Florence et al., 2000), may take many months to emerge (Jain et al., 1997), and depend on longer distances of new axon growth at subcortical and cortical levels (Florence et al., 1998; Jain et al., 2000). Cortical reorganization after limb amputations in humans can be found in several studies (Flor et al., 1995, 1998; Elbert et al., 1997; Davis et al., 1998; Lotze et al., 1999; Brugger et al., 2000; Moore et al., 2000; Curt et al., 2002). Thus, reactivations commonly occur in humans and other primates after a total loss of a subset of peripheral nerve inputs. In part, the reactivations after injury involve activity-dependent homeostatic cellular mechanisms, but also require the growth of new connections for greater changes in somatotopy. Because of the need for longer axon growth, greater changes in somatotopy take a longer time to emerge. Finally, somatotopic reorganization in cortex may usefully compensate for some of the sensory loss, but extensive reorganizations appear to lead to persisting mislocalization of sensory stimuli, such that the activation of hand cortex by inputs from the face leads to sensation felt on a phantom hand (Ramachandran, 1993; Davis et al., 1998; Ramachandran and Rogers-Ramachandran, 2000). Hence, somatosensory reactivations that restore much of normal somatotopy may be the most useful in restoring lost functions after sensory system damage. For example, highly somatotopic reactivations may occur when a loss of peripheral nerve afferents from any given region of skin is incomplete, as the subsequent potentiation of remaining weak or subthreshold inputs allows aspects of normal somatotopic order in central representations to be restored, at least partially. This may happen after selective sections of the dorsal roots of peripheral nerves as they enter the spinal cord (Darian-Smith and Brown, 2000; Darian-Smith and Ciferri, 2005, 2006), as similar inputs from a region of skin may enter over several dorsal roots (Welker, 1973), including roots left intact. In a similar manner, sectioning of peripheral nerve afferents as they ascend in the dorsal column of the spinal cord may leave a scattering of afferents that can restore some of the normal somatotopy of the deactivated somatosensory cortex (Jain et al., 1997). Alternatively, the information provided by cutting dorsal column afferents may not be totally lost, because these afferents branch as they enter the spinal cord. One branch ascends in the dorsal columns and the other terminates on the dorsal horn neurons in the spinal cord. As this sensory information is preserved, a more useful somatotopic reactivation of cortex may emerge based on the connections of the spinal cord neurons. The remainder of this review mainly focuses on the consequences of dorsal column lesions of the spinal cord in primates, including characteristics of natural recoveries and potential for augmented recoveries, but it is not intended to be a comprehensive literature review of other types of injuries and recovery mechanisms.

DORSAL COLUMN LESIONS IN PRIMATES

Dorsal column lesions in monkeys and other primates provide a number of advantages in studies of central nervous system reorganization after sensory loss. Most importantly, the loss is selective for the afferents that convey low-threshold, rapidly conducting tactile inputs from the slowly adapting and rapidly adapting receptors in the skin, while less rapidly conducting afferents for pain, temperature, and crude touch are left intact, as these afferents bypass the dorsal columns (Kaas, 2012). In addition, proprioceptive information from receptors located in muscles and joints travels in peripheral nerve afferents that ascend lateral to the dorsal column afferents in the spinal cord, where they are damaged only if the dorsal column lesion includes the fibers of the lateral spinal cord. Furthermore, the peripheral nerve afferents that contribute to the dorsal columns branch, such that one branch terminates in the dorsal horn of the spinal cord while another branch ascends in the dorsal columns to terminate in the brainstem. Although one branch is cut by the dorsal column lesion, the other branch may still function in the dorsal horn, where the afferents continue to contribute to spinal cord reflexes and other spinal cord functions, and possibly to ascending sensory pathways that compensate for dorsal column lesions. Studies of the effects of dorsal column lesions in rats have produced useful information (for reviews, see Kaas et al., 2008; Onifer et al., 2011); however, unlike the separation between the sensory and motor pathways in primates, corticospinal (motor) projections course in the dorsal columns in rodents (Hicks and D'Amato, 1975; D'Amato and Hicks, 1978; Vahlsing and Feringa, 1980; Paxino and Watson, 2007). Therefore, dorsal column lesions in rodents involve a direct motor loss in addition to the sensory loss. Thus, the use of dorsal column lesions in primates has the advantages of producing a rather specific loss of tactile capacities, while leaving other functions intact. Importantly, these specific lesions in primates are followed by unexpected levels of behavioral recovery (see below). While the lesions do not mimic the typical types of injury that occur in most cases of spinal cord injury in humans, where damage may be extensive and somewhat non-specific, the lesions can be made with precision and consistency so that useful results can be obtained from a few subjects. Consistent results from similar lesions allow therapeutic procedures to be evaluated. Thus, experimental results from monkeys have the potential of providing information that can usefully guide the interpretations and predictions of consequences of spinal cord damage in humans, and hopefully guide the development of therapeutic procedures.

Our experiments typically involve a unilateral lesion of the dorsal columns at a C4–C5 level of the spinal cord (**Figure 1**). This removes the primary afferent tactile inputs to the cuneate nucleus from one hand, while leaving the inputs from the other hand intact. All inputs to the dorsal horn neurons of the spinal cord are preserved, as are the primary proprioceptive afferents in the lateral spinal cord pathway. Neurons in the elongated cuneate nucleus project to the hand and forelimb subnucleus of

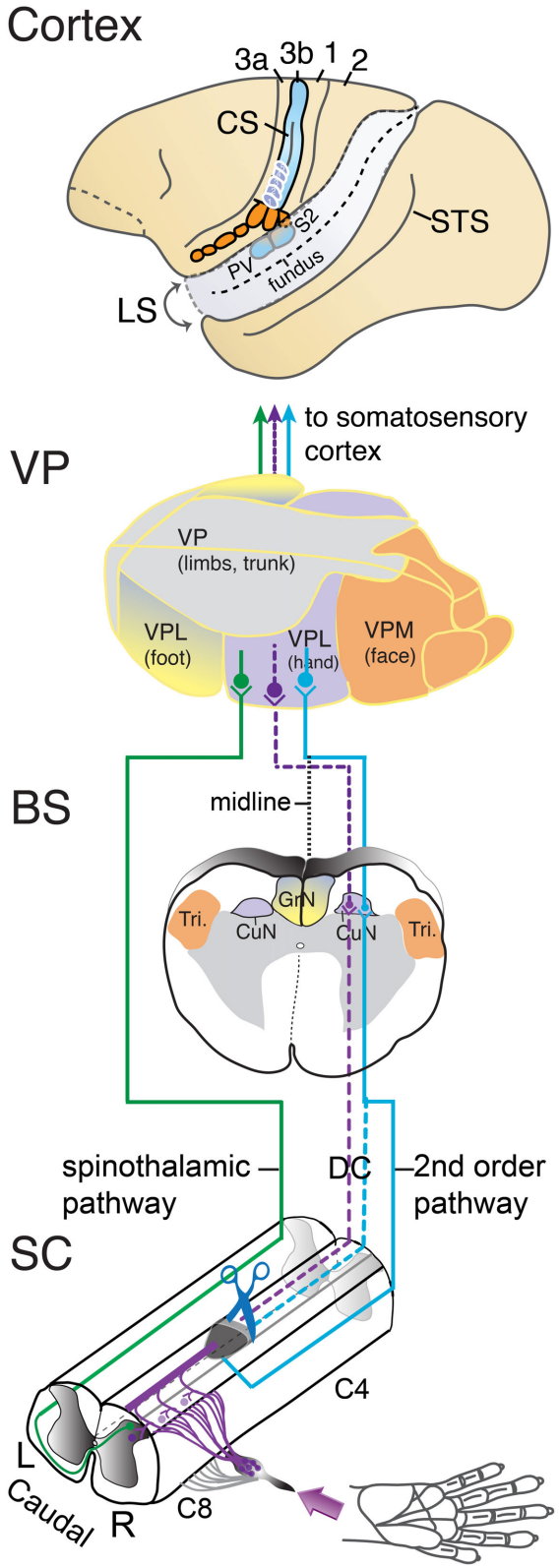

FIGURE 1 | Somatosensory pathways from the spinal cord to cortex of a squirrel monkey. Cutaneous afferents from the hand that enter the cervical spinal cord between C4 and C8 levels via the dorsal roots are *(Continued)*

FIGURE 1 | Continued
shown in the lower panel. In the spinal cord (SC), one branch of the afferents enters the ascending dorsal column pathway to terminate in the ipsilateral cuneate nucleus (violet line). The other branch terminates in the dorsal horn of the spinal cord. Second-order neurons activated in the dorsal horn by cutaneous primary afferents project to the ipsilateral cuneate nucleus via dorsal column, the dorsolateral pathway, or other pathways (blue line). Other dorsal horn neurons send axons to the contralateral spinal cord and form the spinothalamic pathway (green line). Cutting (scissors) the dorsal column pathway at a C4–C5 level deactivates the cuneate nucleus by removing the direct primary afferent inputs from the hand. The dashed lines mark the partially deafferented pathways from spinal cord to cortex after the spinal cord lesion. Most of the afferents of second-order tactile neurons in the dorsal horn that course in the dorsal columns may be preserved as well, but others may join the dorsal columns above the lesions, or travel outside the lesion in the dorsal lateral fiber tracts. The spinothalamic afferents may contribute to the reactivation of the ventroposterior nucleus and somatosensory cortex. The location of the elongated cuneate nucleus at the junction of the upper spinal cord with the lower brainstem (BS) is shown to represent how the pathways for touch on the hand travel. CuN, cuneate nucleus; Tri, trigeminal nucleus; ECN, external cuneate nucleus of the contralateral (left) somatosensory thalamus. In the somatosensory thalamus (VP), the larger ventroposterior lateral division, VPL, contains subnuclei for the hand and foot, which is capped by a region for the upper (proximal) portions of the limbs and trunk. The medial division, VPM, separates the face. Inputs from the hand are relayed to the hand subnucleus of VPL. The spinothalamic pathway terminates in the ventroposterior inferior nucleus (not shown) as well as VP. In cortex, somatosensory areas of the left cerebral hemisphere are shown. Squirrel monkeys have a short, shallow central sulcus, CS, so that the primary cortical area for touch, area 3b of Brodmann, is largely exposed on the brain surface. The region of the hand representation is indicated below the central tip of the central sulcus. Area 3b receives tactile information from VP. Area 1 contains a higher-order representation of touch just caudal to area 3b. Area 3a receives proprioceptive information from the ventroposterior superior nucleus of the thalamus (not shown). Area 2 is a higher-order somatosensory area just caudal to area 1. The second somatosensory area, S2, and the posterior ventral area, PV, are located on the upper bank of the lateral sulcus, LS. The superior temporal sulcus, STS, is shown for reference.

the ventroposterior nucleus (VP) of the contralateral thalamus. VP is commonly divided into a lateral "nucleus" (VPL) representing the contralateral upper and lower body, and a medial "nucleus" (VPM) representing the contralateral face and both the contralateral and ipsilateral tongue and teeth (Kaas et al., 2006). VP projects to primary somatosensory cortex, area 3b, in a somatotopic pattern, so that the hand subnucleus projects to the hand representation in area 3b just medial to that of the face and lateral to that of the arm and trunk. The VP inputs activate area 3b neurons, while VP provides subthreshold projections to area 1 (e.g., Nelson and Kaas, 1981; Garraghty et al., 1990a), which has a somatotopic organization that parallels and mirrors that in area 3b (Kaas et al., 1979).

In our experiments, we typically determine the effects of dorsal column lesions by recording from the hand subdivision of contralateral area 3b in squirrel monkeys or owl monkeys with microelectrodes. Squirrel monkeys have only a short, shallow central sulcus, and owl monkeys have only a short central dimple. For both of these primates, the representations of the hand in area 3b and in adjoining areas 3a and 1 are exposed on the surface of the brain. This exposure of the cortical areas allows activity patterns to be mapped in detail with densely spaced

microelectrode penetrations. Microelectrode mapping can also be done at thalamic and brainstem levels, but not under visual guidance. Therefore, the somatotopy of these subcortical representations is both harder to determine in detail, and harder to illustrate compared to the two-dimensional cortical maps. In addition, reorganized area 3b maps reflect both subcortical alterations and those that originate in area 3b. Thus, area 3b is a key location for investigation in most experiments. We and others have also studied area 3b reorganization in macaque monkey (Pons et al., 1991; Florence and Kaas, 1995; Florence et al., 1998; Darian-Smith and Brown, 2000; Jain et al., 2008), where area 3b is hidden on the caudal bank of a deep central fissure, as in humans. These more difficult studies are important because macaques are used as a more common model for human brain organization, as macaque brains have some features of the somatosensory system that more closely resemble those of humans.

Neurons in the hand portion of area 3b typically have small excitatory receptive fields, mostly located on the glabrous skin of the hand, especially on the distal phalanges of digits, and they are often confined to part of a single phalange of a digit or pad of the palm. Nearby neurons have similar receptive fields, and a systematic partial map of the hand representation in area 3b can be reconstructed from a dense array of microelectrode recordings across the hand region by outlining all electrode penetration sites with receptive fields centered on any digit phalanges or pad of the palm, or part of the body (Merzenich et al., 1978; Nelson et al., 1980; Sur et al., 1982; Krubitzer and Kaas, 1990). Such maps are extremely consistent in somatotopy across individuals, and they conform to the orderly arrangement of projections from VP to area 3b (Jones et al., 1982; Kaas et al., 1984; Cusick and Gould, 1990; Qi et al., 2011b; Liao et al., 2013). In addition, narrow cell-poor septa separate the representations of digits in area 3b so that digit territories are histologically visible (Qi and Kaas, 2004). The most apparent of these cortical septa separates the representation of digit 1, the thumb, from that of the face; and this septum serves as a highly useful landmark when recording sites are related to cortical histology (Jain et al., 1998, 2001).

THE REACTIVATION AND REORGANIZATION OF SOMATOSENSORY CORTEX AFTER DORSAL COLUMN LESIONS

As the primary somatosensory cortical area for tactile stimuli, area 3b has been the most studied area after dorsal column injury. Most of the results have been obtained from multiple microelectrode recordings where receptive fields for cortical neurons have been defined by stimulating the skin with hand-held probes. Traditionally, near-threshold skin indentations are used to define the "minimal excitatory receptive field" (Merzenich et al., 1983a). In reactivated regions of cortex deprived of their normal sources of activation, neuron responses are subjectively classified as good or excellent, meaning that the neuron responses to light touch closely resemble those in normal cortex, or as poor, or non-responsive. Recordings in deprived cortex immediately after a dorsal column lesion reveal that this cortex is totally unresponsive to light tactile stimuli. Thus, no neuronal spikes are evoked in deprived cortex, while neurons in un-deprived cortex, such as face cortex, respond normally. After a dorsal column lesion at a high cervical level above C4, the hand cortex in area 3b is completely deprived and unresponsive. Over a period of 3–4 weeks, much of the deprived hand cortex starts to respond to touch on the hand, with a distorted but crudely normal somatotopy. Thus, neurons responsive to touch on digit 1 (thumb) are in cortex lateral to those for digit 2, and digits 1–5 are represented in a lateral to medial order. However, this pattern is often disrupted by displaced islands of neurons that represent the same digit, patches of cortex that remain unresponsive, and neurons with discontinuous receptive fields that represent more than one location on the hand. Such results have been reported in a number of studies, including those from owl monkeys, squirrel monkeys, marmosets, and macaque monkeys (Jain et al., 1997, 1998, 2008; Qi et al., 2011a; Bowes et al., 2012, 2013).

Studies of the reactivation process in monkeys with dorsal column lesion using imaging methods, such as fMRI, optical imaging, and radiographic imaging, have been limited but informative (Tommerdahl et al., 1996; Chen et al., 2012; Dutta et al., 2013; Yang et al., under revision). As an example, results from one squirrel monkey from Chen et al. (2012) are shown in **Figure 2**. Before a dorsal column lesion, tactile stimulation of each of the five digits resulted in a focus of activity in the hand region of area 3b, with foci for digits 1–5 in the expected lateral to medial order (**Figure 2A**. In this anesthetized monkey, responses in area 1 were not reliably obtained. Four weeks after a dorsal column lesion at the C4–C5 level, area 3b was responsive to touch on the digits, and the somatotopic order of foci activated from each digit was roughly in the normal order, but distorted from the normal pattern (**Figure 2B**). After 8 weeks, the cortex was more responsive, and the somatotopic pattern appeared more normal (**Figure 2C**). When the final somatotopic pattern from fMRI was compared to an optical imaging pattern and a microelectrode map in the same monkey, there was good agreement between the activation patterns from the three methods, but optical imaging produced a more detailed map than the fMRI imaging, and greatest detail was provided by the microelectrode maps. Although the fMRI mapping provides less sensitive somatotopic detail than the microelectrode recordings or the optical imaging, fMRI allows the same cortex to be imaged multiple times non-invasively. Over an eight-week or even longer period of recovery, there was no evidence that the deprived hand cortex was reactivated by any other part of the body, including the face. However, after longer periods of 6–8 months to years, face inputs from the region of the chin often activate parts of the hand cortex (Jain et al., 1997).

When the dorsal column lesion is incomplete, perhaps as an unintended result, or because the lesion was intentionally placed at a lower C5–C6 level in order to preserve some inputs from digit 1 and a few from digit 2, then these preserved inputs come to represent larger than normal territories in area 3b after 5–8 weeks of recovery with sensorimotor training and testing. However, much of the activation is in the normal territories for those digits. Somatotopic organization of reactivated cortex after recovery is likely dependent on the level and extent of the lesion, as indicated by studies using single microelectrodes to map the cortex (Qi et al., 2011a; Chen et al., 2012) and using multi-electrode arrays implanted in cortex (Qi et al., 2014). For example, receptive field mapping of neurons recorded with a 100-electrode array

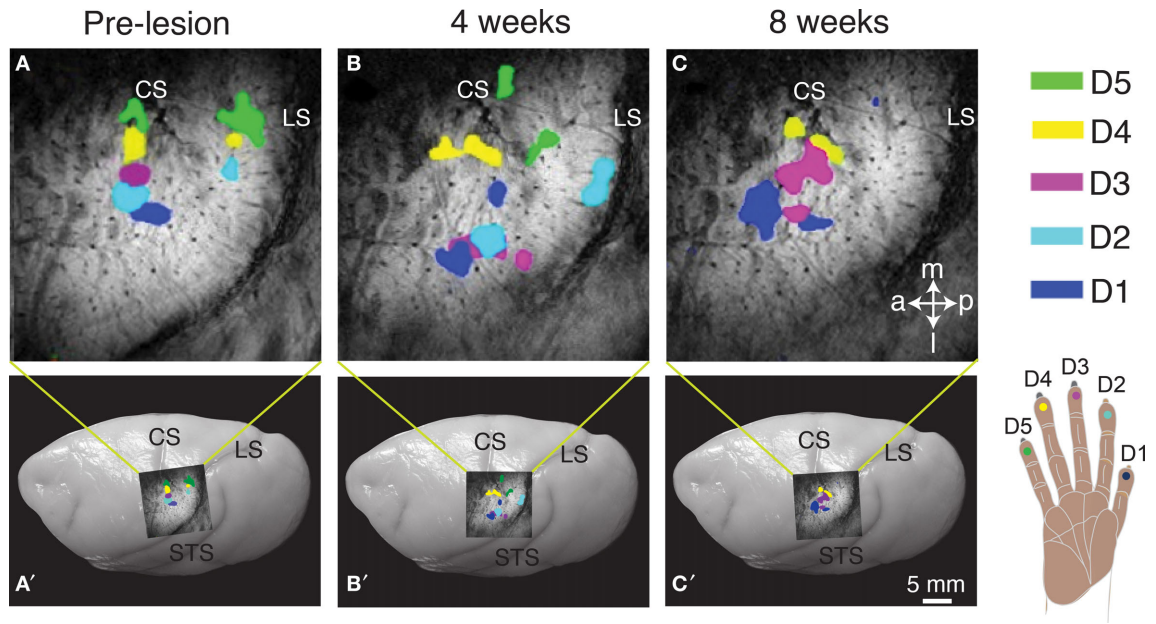

FIGURE 2 | Longitudinal mapping of fMRI activation to vibrotactile stimulation on digits 1–5 pre-lesion (A) and after 4-weeks (B) and 8-weeks (C) post-lesion following unilateral dorsal column section in a squirrel monkey (SM-O). Activation foci from trial blocks of stimulation on individual digits were superimposed for the composite images **(A–C)**. The location of the top panel on the brain is shown for each panel below. Dots on the hand schematic (lower right) are color-coded to represent the activation in cortex when that digit location was stimulated **(A–C)**. Superimposed images of the fMRI activation on photograph of a squirrel monkey brain indicates the approximate location of the region of interest **(A′–C′)**. Abbreviations: a, anterior; CS, central sulcus; D1–5, digits 1–5; l, lateral; LS, lateral sulcus; m, medial; p, posterior; STS, superior temporal sulcus. Adapted from Chen et al. (2012).

in area 3b in a squirrel monkey showed that somatotopic organization in reactivated cortex was largely normal after behavioral recovery from a dorsal column lesion at the C6 level (compare **Figures 3B,C**). However, the cortical territories occupied by spared inputs for digits 1 and 2 encroached into regions deprived of input by the C6 lesion (digits 3–5). This monkey received sensorimotor training and testing for use of the impaired hand over the course of 6 weeks prior to recording with the array, and it is unknown what effect this behavioral intervention may have had on the cortical reactivation beyond what would have occurred spontaneously. In this case, preserved inputs activated their normal locations in cortex, but also came to activate larger than normal territories.

Finally, the reactivation of area 3b hand cortex should result in the reactivation of the hand territories of other cortical areas that depend on area 3b for activation, such as areas 1, S2, and PV, as reported previously (Pons et al., 1987; Burton et al., 1990; Garraghty et al., 1990b). Indeed, the area 1 representation of touch is restored in a somatotopic pattern that generally parallels that in area 3b, but it is less precise in detailed somatotopy, and the neuronal responses tend to be weaker in the reactivated regions (Merzenich et al., 1983a; Jain et al., 2008; Qi et al., 2011a). Responses to tactile stimuli also return to areas 3a and 2 (Garraghty et al., 1990a; Bowes et al., 2013) and the hand region of areas S2 and PV (Pons et al., 1987, 1992; Burton et al., 1990; Garraghty et al., 1990b; Tandon et al., 2009; Wang et al., 2013; Yang et al., under revision). Areas 3a and 2 receive proprioceptive input from the ventroposterior superior nucleus of the thalamus (Kaas, 2012), so neurons in these areas may remain responsive to hand manipulation after dorsal column lesions that spare the proprioceptive axons in the lateral spinal cord. As all these areas recover responsiveness to tactile stimuli and provide direct and indirect inputs to motor and premotor cortex (Krubitzer and Kaas, 1990; Stepniewska et al., 1993; Disbrow et al., 2003; Fang et al., 2005; Qi et al., 2010; Kambi et al., 2011; see Wise et al., 1997 for review), considerable sensory guidance of motor behavior is restored.

THE RESPONSE PROPERTIES OF REACTIVATED NEURONS IN AREA 3b

Reactivated cortical neurons may have disorganized excitatory receptive fields, or larger than normal receptive fields, but these responses to light touch on the hand appear to range from subjectively normal amplitude to weak responses (Qi et al., 2014). Over recovery periods longer than 4–8 weeks, more neurons likely become capable of stronger responses. Quantifying response properties beyond receptive field organization is a growing focus of study in the somatosensory system (Doetsch et al., 1996; Wang et al., 2013; Qi et al., 2014), but some support for these studies comes from studies of reactivated neurons in primary visual cortex after retinal lesions (Chino et al., 1995, 2001; Darian-Smith and Gilbert, 1995). Our quantitative studies of the response properties of reactivated cortical neurons after dorsal column lesions have been limited (Wang et al., 2013; Qi et al., 2014), but there is already evidence that reactivated neurons have responses to tactile stimuli (indentation of the skin with an electromechanical

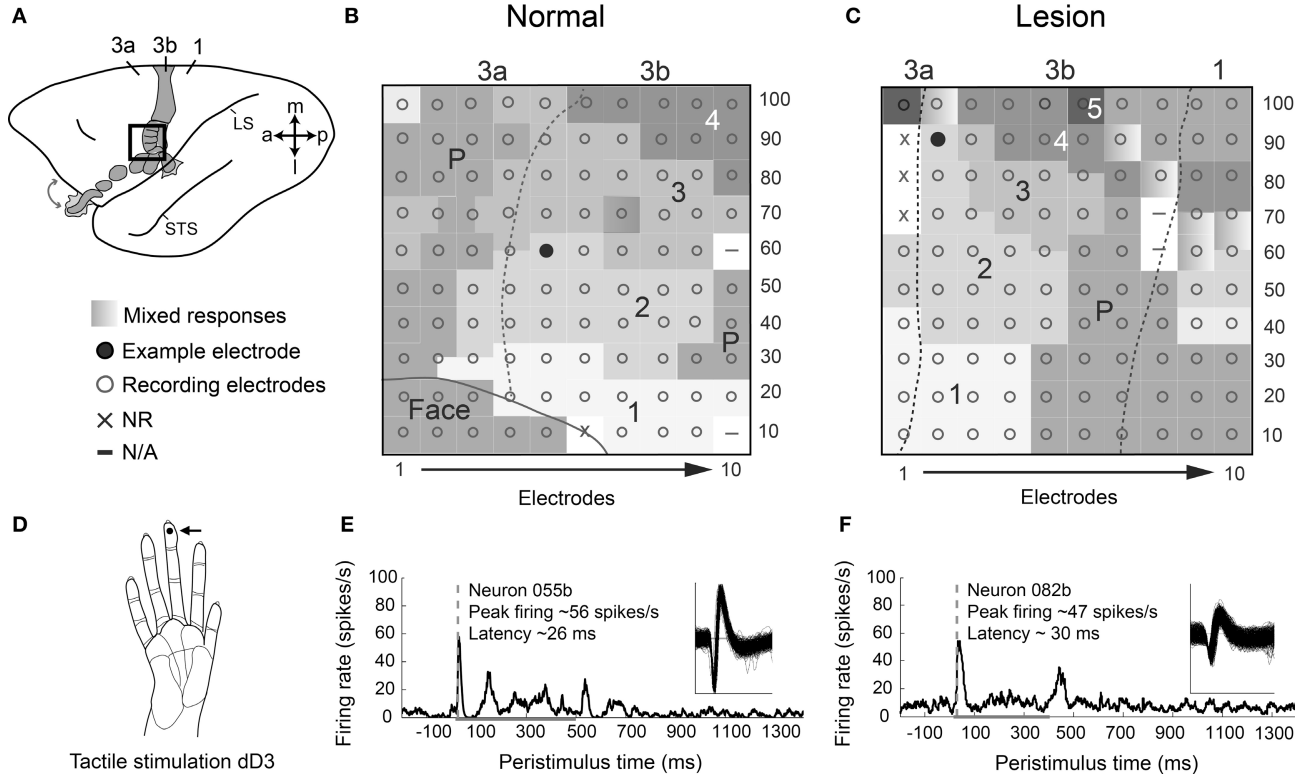

FIGURE 3 | Response properties of area 3b neurons after behavioral recovery from dorsal column lesion are similar to those in a monkey with no lesion. (A) A schematic of the left hemisphere of an owl monkey brain with area 3b shaded shows the approximate placement of a 100-electrode array for monkey OM-A with no lesion (see **B**). The array placement for a monkey SM-G with a dorsal column lesion was similar, but slightly more medial and posterior (see **C**). Note the key for the somatotopic mapping of the array applies to **(B)** and **(C)**. **(B)** Representation of coverage of 100-electrode array in cortex for a normal monkey with somatotopic map reconstructed from locations of receptive fields for neurons at each electrode. Coverage included part of the area 3b hand and face representation as well as area 3a, with somatotopy consistent with previous reports from normal monkeys. The electrode location from which the example neuron for the lower panel **(E)** was recorded is indicated by the filled circle. **(C)** Representation of coverage of 100-electrode array in cortex for monkey SM-G after behavioral recovery from partial DC lesion at the C6 spinal cord level. This lesion preserved many of the dorsal column afferents from digits 1 and 2. SM-G experienced sensorimotor training and testing using the impaired hand for 6 weeks following DC lesion prior to recording with the multi-electrode array. All digits are represented within expected somatotopic locations, but D1 and D2 appear to be represented in more territory than D3–D5. Electrode location for the example neuron in the lower panel **(F)** is indicated by the filled circle. **(D)** Activities of neurons from monkeys with and without a lesion in **(B–C)** are shown in **(E–F)** during tactile stimulation on right distal digit 3 (dD3). The stimulation site is indicated by a dot (see arrow) on drawing of a monkey hand. **(E)** Example of a single unit 055b shows typical peak firing rates and latencies for an example normal case, monkey OM-A. Spikes during 100 trials of tactile stimulation on dD3 are averaged in the peristimulus-time histogram (PSTH). Waveforms of the recorded unit are shown (inset). **(F)** Example of a single unit 082b shows typical responses for a case with a dorsal column lesion, monkey SM-G, following recovery of reaching behavior with the impaired hand. Activity during 150 trials of tactile stimulation on dD3 is shown in the PSTH. In **(B–C)**, dashed lines indicate area 3b borders based on receptive field topography and myelin architecture. In **(E–F)**, dashed gray line indicates the latency of the peak firing response that exceeds 2 times the standard deviation of the average baseline firing. Peak firing value listed is baseline-subtracted. Horizontal gray line indicates stimulus duration in each trial (500 ms in OM-A, 400 ms in SM-G). Abbreviations: 1–5, digits 1–5; 3a, 3b, 1, area 3a, area 3b, area 1; a, anterior; dD3, distal digit 3; l, lateral; LS, lateral sulcus; m, medial; p, posterior; STS, superior temporal sulcus. Modified from Reed et al. (2010) and Qi et al. (2014).

probe) that are in the normal or near-normal range, as indicated by examples of cortical activity (**Figure 3**) from an intact monkey (Reed et al., 2010) and a monkey 6 weeks after mid-cervical dorsal column lesion (Qi et al., 2014).

Qi et al. (2014) found that fewer neurons in area 3b responded to tactile stimulation on the hand in monkeys after sensory loss followed by behavioral training compared to normal monkeys. However, peak firing rates of responsive neurons were similar in monkeys with and without lesions. An example neuron from a normal monkey (**Figure 3E**) maintained low levels of spontaneous firing and increased firing to about 56 spikes/s in response to the onset of a 500 ms depression of the skin on distal digit 3. This example showed some increased firing during the sustained indentation of the stimulus and a response to the removal of the stimulus from the skin. Such "off responses" are common in normal animals (Sur et al., 1984; Pei et al., 2009). The neuron's response with some maintained discharge during the duration of skin indentation is common in area 3b neurons, as these neurons can show mixtures of properties reflecting both rapidly-adapting and slowly-adapting afferents (Sur et al., 1984; Pei et al., 2009). The example neuron in the reactivated cortex after nearly complete dorsal column lesion (**Figure 3F**) responded to both

stimulus onset and removal, while maintaining some firing during the sustained skin indentation on distal digit 3. Notably, the neuron in reactivated cortex had somewhat lower peak firing rates during tactile stimulation at about 47 spikes/s, but still greater than the median response rates reported previously (about 18 spikes/s) and seemingly close to rates expected normally (Reed et al., 2010; Qi et al., 2014). In 3 monkeys with dorsal column lesions and after hand use in a reaching task recovered to normal levels, response latencies of neurons in reactivated area 3b to skin indentation were similar to normal or slightly longer than normal, averaging about 31 ms [Reed et al., 2012 (abstract)]. Using similar recording methods and data analysis, Reed et al. (2010) found that response latencies of area 3b neurons in normal monkeys averaged about 21 ms. The example of neuronal activity in **Figure 3** shows a neuron in a lesioned monkey with a response latency to skin indentation that was slightly longer than the latency of a normal neuron (compare **Figure 3E** to **Figure 3F**). Similar response rates with slightly longer latencies than normal may suggest that some sensory input reaches area 3b after dorsal column lesions through alternative pathways that require additional synapses to reach the target. More study is needed, but the reactivated neurons clearly have response properties that could usefully guide behavior.

THE EFFECTS OF DORSAL COLUMN LESION ON BEHAVIOR

There is no doubt that spinal cord injuries often have devastating consequences for functional outcomes. A large number of studies in rodents (e.g., Anderson et al., 2005; Courtine et al., 2008; Zorner et al., 2010) and monkeys (e.g., Schmidlin et al., 2011; Nout et al., 2012a,b) have investigated the behavioral deficits that occur after spinal cord injury. Other studies have focused on the effects of a restricted interruption of the ascending dorsal column somatosensory pathway on the dexterity of the forepaws in rodents (e.g., McKenna and Whishaw, 1999; Ballermann et al., 2001) and monkeys (e.g., Beck, 1976; Glendinning et al., 1992; Leonard et al., 1992; Cooper et al., 1993; Vierck, 1998; Vierck and Cooper, 1998; Qi et al., 2013). In humans and monkeys, the effects of dorsal column lesions on sensory behavior have been interpreted in two quite different ways in early reports. Thus, Rose and Mountcastle (1959) concluded that the "destruction of the posterior columns in man leads to a loss of the capacity to appreciate the position and movement of the limbs," and "severe"—"disturbance in tactile sensations." Later, Mountcastle further stated, "What remains in the mechanoreceptive sphere after…dorsal column lesion is the capacity to recognize that a mechanical stimulus has occurred; it is no longer possible to specify it exactly as to location, intensity or shape" (Mountcastle and Darian-Smith, 1968). These pronouncements clearly reflect what would be expected after damage of such a major sensory pathway. However, Wall (1970) quite differently concluded that "no sensory defect has been shown to follow isolated dorsal column lesion" in human, and "animals with complete dorsal column section can carry out discriminations of weight, texture, vibration, two points and position." Later, Azulay and Schwartz (1975) summarized the effects of dorsal column lesion in monkeys by stating that "surprisingly little, if any, tactile functions are impaired after extensive damage to the dorsal funiculus." Subsequent to these early reports, several studies have reported impairments of hand use after lesion of the dorsal columns in macaque monkeys (Glendinning et al., 1992; Leonard et al., 1992), and sensory alterations have been described in macaques (Vierck, 1973, 1974) and humans (Nathan et al., 1986).

How can we explain these great differences in conclusions about the effects of dorsal column lesion in primates? There are several possible reasons for differences in findings and conclusions. (1) One possibility is that different lesions produce different results. For performance with the hand, the dorsal column lesion should be at the C4–C5 level or higher to remove all afferents from the hand, the lower lesions at C5–C6 of the cervical spinal cord spare some afferents from digit 1 and 2, and still lower lesions would spare inputs from most of the hand. Even with C4–C5 lesions or higher, various afferents in the dorsal columns could be spared. (2) Compensations likely occur. As described below for our study of the effects of dorsal column lesions on behavior, vision appears to supplement tactile feedback in food retrieval tasks after dorsal column lesions. Other compensations for sensory impairments are likely to be rapidly acquired as well. (3) Plasticity of the somatosensory system, even in mature primates appears to be a major source of recovery after dorsal column lesions. Recoveries of activation within the system and use of the hand may result from the potentiation of the activating effects of preserved dorsal columns afferents, even when they are very few. This possibility is well demonstrated by the effects of cutting most of the dorsal sensory roots of nerves of the forearm in monkeys, while leaving a few inputs from that hand that initially fail to activate cortex. However, several months later cortex responded to cutaneous stimulation of the largely deafferented digits. **Figure 4** illustrates such an example reprinted from Figure 10 of Darian-Smith (2004; see also, Darian-Smith and Brown, 2000; Darian-Smith and Ciferri, 2005, 2006; Darian-Smith, 2009). This reactivation of cortex is due in part to the potentiation of preserved afferents likely through axon growth and the formation of new synaptic contacts on deactivated neurons occurring at brainstem, thalamic, and cortical levels (Darian-Smith and Gilbert, 1994, 1995; Florence et al., 1998; Jain et al., 2000; Darian-Smith et al., 2010). A related possibility is that after dorsal column lesion second-order spinal cord neuron inputs to the cuneate nucleus are also potentiated and thereby come to reactivate that nucleus by touch on the hand, effectively replacing some of the lost direct dorsal column inputs to the cuneate nucleus. We return to this possibility in the last section of this review. (4) Finally, some of the effects attributed to damage to the dorsal columns in previous studies may reflect damage to other afferents, as motor impairments may occur when the lesions extend into the lateral spinal cord where the dorsal lateral funiculus with proprioceptive afferents and the lateral corticospinal motor tract are located.

The results of our recent study of hand use in squirrel monkeys after a unilateral dorsal column lesion provide evidence that the sensory loss produced by lesions confined to the dorsal columns do produce impairments in a food retrieval task (Qi et al., 2013). Monkeys were trained to reach for and retrieve small sugar pellets from wells that ranged from easy (shallow) to difficult (deep). Several results are presented in **Figure 5**. Before the spinal cord

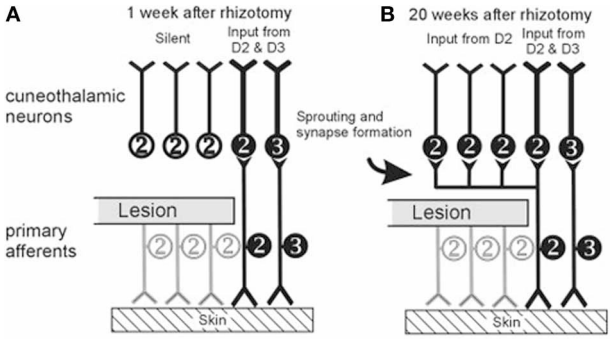

FIGURE 4 | Schematics represent hypothesized effects of a dorsal rootlet section that blocks sensory input from digit 1 (thumb) and digit 2 (index finger) in a macaque monkey after 1 week (A) and after 20 weeks (B). Inputs from digits 1 and 2 are labeled together as 2. After cutting the dorsal rootlet, some fraction of neurons innervating digits 1 and 2 may be spared, but a population of cuneate (and dorsal horn) neurons will be left without peripheral input. By 20 weeks after the dorsal rootlet section, terminals of the spared neurons innervating digits 1 and 2 have sprouted collaterals to innervate the previously deafferented target neurons in the cuneate nucleus. Similar mechanisms are hypothesized to occur at all levels of processing hierarchy from the brainstem to cortex. (From Darian-Smith, 2004, Figure 10, Copyright©2004 Wiley-Liss, Inc.. Reprinted with permission from John Wiley & Sons).

lesion, monkeys were very good at the task, even for the most difficult well. They quickly reached to grasp the pellet after briefly visualizing it, and retrieved it with one or sometimes 2 flexes of the digits to bring the pellet from the well to the mouth. When behavioral testing was continued two weeks after a complete or nearly complete lesion of the dorsal columns, the behavior was clearly impaired in that it took more than one attempt to successfully grasp objects from the difficult wells, and more flexes of the digits were needed. The video recordings of the task performance revealed another change in the behavior. Before the dorsal column lesion, the monkey looked at the pellet in the well only briefly as the monkey started the reach, and instead watched the investigator during the grasp and retrieval. This may seem strange, but extensive visual guidance was unnecessary, and the monkey may regard the investigator as a potential competitor for the food, as it would another monkey, or as potentially dangerous and in need of watching. In contrast, after the lesion, the monkey acted as if it could not sense by touch if the pellet was in the hand, and always looked to see if the pellet was there. During the retrieval, the palm was turned up so the presence of the pellet could be visually confirmed. Overall, we think that the deficits in the retrieval behavior were due to the sensory loss, as they occurred when the lesions did not include motor axons lateral to the dorsal columns. Early successes likely related to behavioral compensations, especially the visual assurance that the pellet had been grasped. In addition, sensory perception likely improved as early as 3–4 weeks after the lesion, as cortex became progressively more responsive to touch on the hand due to cortical reactivation.

MECHANISMS OF CORTICAL REACTIVATION AND THE POTENTIAL FOR THERAPEUTIC TREATMENTS

The reactivation of deprived hand cortex weeks to months after high cervical dorsal column lesion depends on the potentiation

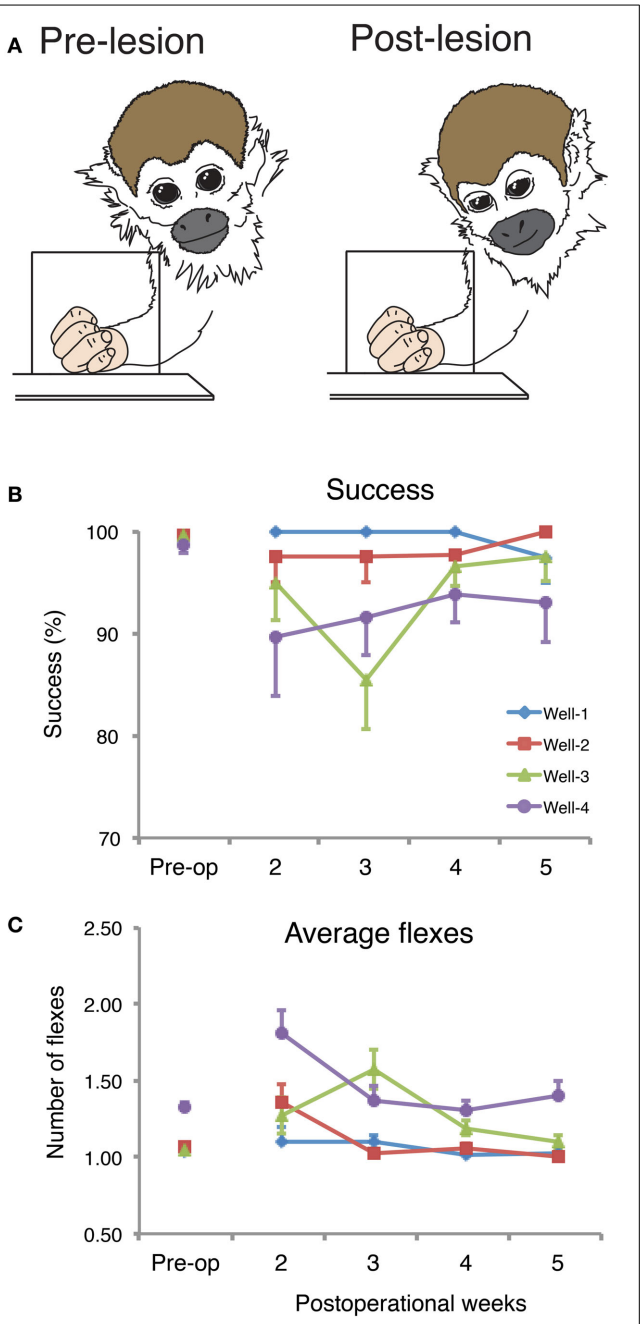

FIGURE 5 | Spontaneous recoveries after dorsal column injury can be incomplete or incorporate various compensations. (A) Drawings from the captured photo-frames taken from a squirrel monkey (SM-O) during the reach-to-grasp task pre-lesion (left) and on post-op Day 15 (right). The schematic summarizes observations that after the spinal cord lesion, monkeys compensate for reduced tactile sensation by relying more often on vision. **(B)** Post-operational changes in the percentage of successful retrievals (mean, ± *SD*) in the reach-to-grasp task. Success scores in percent of the retrieval success for summed trials from each of the 4 testing wells per post-op week for monkey SM-O. Pre-op final week trials were summed. **(C)** Post-operational changes in mean number of flexes (mean, ± *SD*) for monkey SM-O. Each data point within each panel is the averaged number of flexes from the sum of the trials from each of the 4 wells over each testing week. Adapted from Qi et al. (2013).

of preserved sensory pathways through axon growth and the formation of new synapses. We have previously suggested that dorsal column lesions are often incomplete, and that preserved but subthreshold dorsal column inputs to the cuneate nucleus gain strength by forming more synapses on more neurons as the result of reduced competition for synaptic space (Rasmusson and Northgrave, 1997; Xu and Wall, 1997; Darian-Smith, 2004; Darian-Smith and Ciferri, 2006). Similar changes likely occur at the levels of the ventroposterior nucleus and somatosensory cortex (Garraghty et al., 1991, 2006; Rasmusson, 1996; Wellman et al., 2002). Under conditions of extreme loss of afferents to the cuneate nucleus, we had evidence that even afferents from the adjacent trigeminal complex for the face could sprout and grow to innervate the cuneate nucleus (Jain et al., 2000), providing relays to the hand subnucleus of the contralateral ventroposterior nucleus and then to the hand territory of primary somatosensory cortex. While such reactivations of the cuneate nucleus by inputs from the hand that were preserved after the dorsal column lesion, as well as those that grow into the cuneate nucleus from the face, do occur, we have observed reactivations of hand cortex after lesions of the dorsal columns that were 95–100% complete (Qi et al., 2011a). Although it can be difficult to accurately determine the completeness of a lesion of the dorsal columns from histological sections through the lesion site, we feel confident about the completeness of experimental lesions because we injected tracers into the fingers of both hands in monkeys with unilateral lesions to demonstrate the loss of labeled axon terminations in the cuneate nucleus on the lesioned compared to the non-lesioned side (Qi et al., 2011a). Thus, we have strong evidence that there are reactivations that do not depend on preserved dorsal column first-order afferents, and thus depend mostly on other afferents from the hand.

The most likely alternative pathway is from neurons in the dorsal horn of the spinal cord that project to the dorsal column nuclei (Perl et al., 1962; Rustioni et al., 1979; Bennett et al., 1983). These neurons are directly activated by one of the bifurcated branches of peripheral nerve axons that terminates in the dorsal horn, while the other branch ascends in the dorsal columns and terminates in the dorsal column nuclei (Wall, 1970; Willis and Coggeshall, 2004). These dorsal column neurons would receive the same information for the skin of the hand that the cuneate nucleus directly receives, although there may be differences in the amounts of convergence of inputs and inhibitory mechanisms so that receptive field sizes may differ for neurons in the dorsal horn or cuneate nucleus (Dykes and Craig, 1998; Witham and Baker, 2011). However, the normal role of second-order spinal cord inputs to the cuneate nucleus most likely would be to provide subthreshold activation, because cortical reactivation after a loss of the primary inputs to the cuneate nucleus takes weeks to emerge.

In order to be effective, the projections to the cuneate nucleus by second-order dorsal horn neurons must survive the dorsal column lesion. Some axons from second-order neurons might enter the dorsal columns below the lesion and be lost. Others might enter above the lesion, or travel in some other pathway, such as the lateral funiculus, which is dominated by proprioceptive afferents (Rustioni et al., 1979). This possibility seems likely in that larger

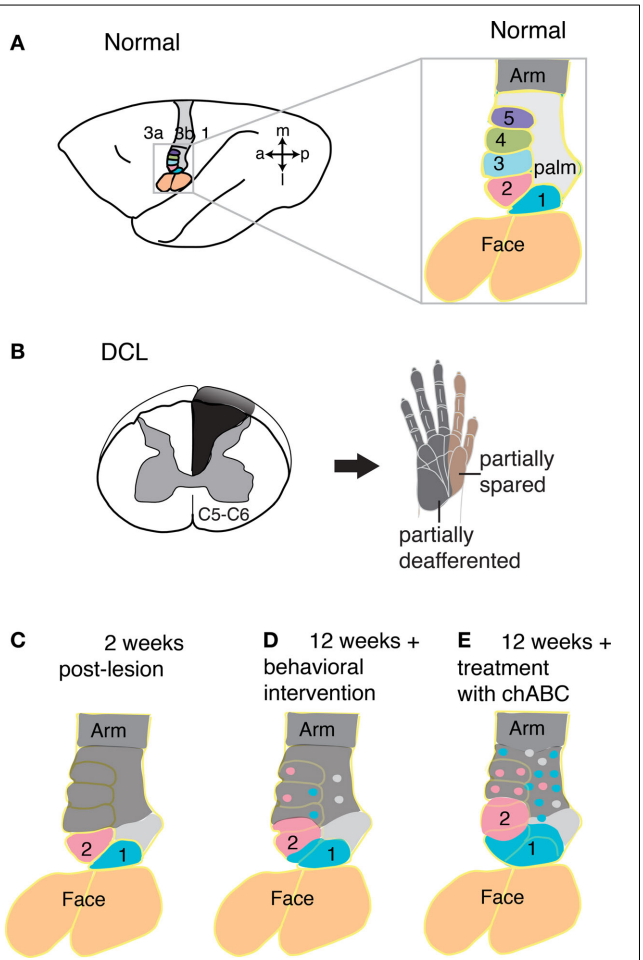

FIGURE 6 | Spontaneous and augmented recoveries from sensory loss in monkey cortex. (A) Schematic view of the left hemisphere of an owl monkey brain with area 3b highlighted in color and expanded (right) to focus on the hand representation. **(B)** When afferents devoted to the hand are cut in the cervical spinal cord at the C5 or C6 level in squirrel monkeys and owl monkeys (left), inputs from much of digit 1 and digit 2 are spared, while inputs from most of the rest of the hand are disrupted, as indicated by the hand schematic (right). **(C)** After such a lesion **(B)**, the hand representation in primary somatosensory cortex is immediately rendered largely unresponsive to tactile stimuli (gray shading), with the exception of much of the digit 1 and digit 2 representations (blue and pink shading, respectively), for which the majority of axons enter the spinal cord above the level of the lesion. Over weeks of spontaneous post-lesion recovery without augmentation, the deactivated cortex becomes partly reactivated by inputs from the hand with activation from the spared dorsal column inputs (digits 1 and 2), and possibly other pathways (not shown). **(D)** This schematic summarizes expected results in monkeys with dorsal column lesions that received behavioral intervention when the cortex is studied 12 weeks after the lesion. Sensorimotor training and testing for use of the impaired hand appears to promote reactivation of cortex, but further study is needed to determine how effective behavioral intervention is beyond spontaneous recoveries and in comparison with other types of treatments. Based on previous findings and ongoing research, we expect that the representations of spared digits will expand their territories and islands of responsiveness will emerge in previously unresponsive zones. **(E)** The effectiveness of a few preserved dorsal column afferents for activating cortex can be enhanced by treatment of the target site in the cuneate nucleus with the enzyme chondroitinase ABC shortly after the spinal cord injury. Digestion of

(Continued)

FIGURE 6 | Continued
components of the extracellular matrix in the cuneate that inhibit axon sprouting allows axons spared from the lesion to sprout collaterals and innervate additional territory, which is reflected at the cortical level (examined 12 weeks after lesion and enzyme treatment). Thus, augmentation in this way produces expanded representations of the spared inputs from digits 1 and 2 in cortex, and possibly enhances ability of axons of second-order spinal cord neurons to sprout and innervate islands of the deprived cuneate nucleus. Abbreviations: 1–5, digits 1–5; 1, 3a and 3b, areas 1, 3a and 3b; a, anterior; C5–6, cervical spinal cord segments 5–6; chABC, chondroitinase ABC; DCL, dorsal column lesion; l, lateral; m, medial; p, posterior. Based on Jain et al. (1997), Bowes et al. (2012), and Qi et al. (2014).

lesions of the dorsal column that extend into the lateral fiber tracts appear to reduce the extent of the reactivation of the hand cortex from inputs from the hand.

Given the evidence that the reactivation of the cortex by inputs from the hand is important for the recovery of manual dexterity, what can be done to promote these reactivations? Recently, we have investigated two interventions for promoting reactivations. First, we found promising evidence that behavioral training after sensory loss improved the recovery of hand use in a retrieval task and correlated with cortical reorganization [Qi et al., 2010, 2012 (abstracts)]. Second, we found that an injection of an enzyme, chondroitinase ABC, into the cuneate nucleus after the lesion of the dorsal columns promotes the reactivation of hand cortex by preserved dorsal column afferents (Bowes et al., 2012). This enzyme digests chondroitin sulphate proteoglycans, which make up the extracellular matrix around neurons and glia. Treatment with chondroitinase ABC was first shown to promote recovery after spinal cord injury in rats by Bradbury et al. (2002). The extracellular matrix around neurons in the cuneate nucleus provide a chemical and physiological barrier that appears to inhibit new axon growth into and within the nucleus, thereby limiting the reactivation of deprived neurons in the nucleus, and the relay of driven activity to higher levels of the somatosensory system. By intentionally sparing dorsal column afferents from the thumb (digit 1) in squirrel monkeys by placing the dorsal column lesion at a lower cervical level (C6), and using the chondroitinase ABC enzyme injections near the targets for new growth from the spinal cord into the brainstem, more of the hand representation in contralateral somatosensory cortex was activated than in monkeys without this injection (**Figure 6**). Chondroitinase ABC has been used by others in a number of different experiments to increase axon sprouting, including the growth of dorsal column axons past a lesion site in rats (Massey et al., 2006, see reviews by Onifer et al., 2011; Garcia-Alias and Fawcett, 2012). Other promising treatments for recovery after sensory loss or spinal cord injury include the use of antibodies to a major myelin-associated neurite growth inhibitor, named Nogo-A (see Fawcett et al., 2012). The local placement of factors that promote growth and provide attraction to a target may also be useful (Schnell et al., 1994). Additional treatments for spinal cord injury have been reviewed by others (He and Koprivica, 2004; Buchli and Schwab, 2005; Bradbury and McMahon, 2006; Cafferty et al., 2008; Giger et al., 2010; Cregg et al., 2014; Silva et al., 2014). Sensorimotor training and testing for use of the impaired hand in monkeys (Qi et al., 2013, 2014) or impaired limbs in rodent (Kao et al., 2009; Krajacic et al., 2010; Graziano et al., 2013), appears to promote functional recovery and reactivation of cortex, but further study is needed to determine how effective behavioral intervention is beyond spontaneous recoveries or in relation to pharmacological treatments such as chondroitinase ABC. Combining pharmacological and behavioral interventions may promote even more useful recoveries in primates, as promising results have been reported in rodent models (Tetzlaff et al., 2009; Garcia-Alias and Fawcett, 2012; Zhao et al., 2013). In conclusion, we stress that much progress has been made over the last several years in understanding the recovery process that occurs after sensory loss following dorsal column injury. Much of this plasticity was unexpected, but the spontaneous recovery accounts for the early misinterpretations that the dorsal column pathway has little sensory significance. In addition to the unexpected spontaneous recovery, there are also hopeful signs that various therapeutic treatments have the potential of greatly improving the course of recovery.

AUTHOR CONTRIBUTIONS

All authors contributed to the writing of the manuscript. The findings reviewed are those of the authors, as well as those of other investigators.

ACKNOWLEDGMENTS

Our research was supported by NIH grants NS057399 and NS067017 to Hui-Xin Qi; NIH grant NS16446 to Jon H. Kaas, and awards from the Christopher and Dana Reeve Foundation to Jamie L. Reed and to Jon H. Kaas.

REFERENCES

Aguilar, J., Humanes-Valera, D., Alonso-Calvino, E., Yague, J. G., Moxon, K. A., Oliviero, A., et al. (2010). Spinal cord injury immediately changes the state of the brain. *J. Neurosci.* 30, 7528–7537. doi: 10.1523/JNEUROSCI.0379-10.2010

Anderson, K. D., Gunawan, A., and Steward, O. (2005). Quantitative assessment of forelimb motor function after cervical spinal cord injury in rats: relationship to the corticospinal tract. *Exp. Neurol.* 194, 161–174. doi: 10.1016/j.expneurol.2005.02.006

Azulay, A., and Schwartz, A. S. (1975). The role of the dorsal funiculus of the primate in tactile discrimination. *Exp. Neurol.* 46, 315–332. doi: 10.1016/0014-4886(75)90138-7

Ballermann, M., McKenna, J., and Whishaw, I. Q. (2001). A grasp-related deficit in tactile discrimination following dorsal column lesion in the rat. *Brain Res. Bull.* 54, 237–242. doi: 10.1016/S0361-9230(01)00431-2

Beck, C. (1976). Forelimb performance by squirrel monkeys (Saimiri sciureus) before and after dorsal column lesions. *J. Comp. Physiol. Psychol.* 90, 353–362. doi: 10.1037/h0077206

Bennett, G. J., Seltzer, Z., Lu, G. W., Nishikawa, N., and Dubner, R. (1983). The cells of origin of the dorsal column postsynaptic projection in the lumbosacral enlargements of cats and monkeys. *Somatosens Res.* 1, 131–149. doi: 10.3109/07367228309144545

Bowes, C., Burish, M., Cerkevich, C., and Kaas, J. (2013). Patterns of cortical reorganization in the adult marmoset after a cervical spinal cord injury. *J. Comp. Neurol.* 521, 3451–3463. doi: 10.1002/cne.23360

Bowes, C., Massey, J. M., Burish, M., Cerkevich, C. M., and Kaas, J. H. (2012). Chondroitinase ABC promotes selective reactivation of somatosensory cortex in squirrel monkeys after a cervical dorsal column lesion. *Proc. Natl. Acad. Sci. U.S.A.* 109, 2595–2600. doi: 10.1073/pnas.1121604109

Bradbury, E. J., and McMahon, S. B. (2006). Spinal cord repair strategies: why do they work? *Nat. Rev. Neurosci.* 7, 644–653. doi: 10.1038/nrn1964

Bradbury, E. J., Moon, L. D., Popat, R. J., King, V. R., Bennett, G. S., Patel, P. N., et al. (2002). Chondroitinase ABC promotes functional recovery after spinal cord injury. *Nature* 416, 636–640. doi: 10.1038/416636a

Brugger, P., Kollias, S. S., Muri, R. M., Crelier, G., Hepp-Reymond, M. C., and Regard, M. (2000). Beyond re-membering: phantom sensations of congenitally absent limbs. *Proc. Natl. Acad. Sci. U.S.A.* 97, 6167–6172. doi: 10.1073/pnas.100510697

Buchli, A. D., and Schwab, M. E. (2005). Inhibition of Nogo: a key strategy to increase regeneration, plasticity and functional recovery of the lesioned central nervous system. *Ann. Med.* 37, 556–567. doi: 10.1080/07853890500407520

Buonomano, D. V., and Merzenich, M. M. (1998). Cortical plasticity: from synapses to maps. *Annu. Rev. Neurosci.* 21, 149–186. doi: 10.1146/annurev.neuro.21.1.149

Burton, H., Sathian, K., and Shao, D. H. (1990). Altered responses to cutaneous stimuli in the second somatosensory cortex following lesions of the postcentral gyrus in infant and juvenile macaques. *J. Comp. Neurol.* 291, 395–414. doi: 10.1002/cne.902910307

Cafferty, W. B., McGee, A. W., and Strittmatter, S. M. (2008). Axonal growth therapeutics: regeneration or sprouting or plasticity? *Trends Neurosci.* 31, 215–220. doi: 10.1016/j.tins.2008.02.004

Calford, M. B., and Tweedale, R. (1988). Immediate and chronic changes in responses of somatosensory cortex in adult flying-fox after digit amputation. *Nature* 332, 446–448. doi: 10.1038/332446a0

Cheetham, C. E., Hammond, M. S., McFarlane, R., and Finnerty, G. T. (2008). Altered sensory experience induces targeted rewiring of local excitatory connections in mature neocortex. *J. Neurosci.* 28, 9249–9260. doi: 10.1523/JNEUROSCI.2974-08.2008

Chen, L. M., Qi, H. X., and Kaas, J. H. (2012). Dynamic reorganization of digit representations in somatosensory cortex of nonhuman primates after spinal cord injury. *J. Neurosci.* 32, 14649–14663. doi: 10.1523/JNEUROSCI.1841-12.2012

Chino, Y., Smith, E. L. 3rd., Zhang, B., Matsuura, K., Mori, T., and Kaas, J. H. (2001). Recovery of binocular responses by cortical neurons after early monocular lesions. *Nat. Neurosci.* 4, 689–690. doi: 10.1038/89469

Chino, Y. M., Smith, E. L. 3rd., Kaas, J. H., Sasaki, Y., and Cheng, H. (1995). Receptive-field properties of deafferentated visual cortical neurons after topographic map reorganization in adult cats. *J. Neurosci.* 15, 2417–2433.

Cooper, B. Y., Glendinning, D. S., and Vierck, C. J. Jr. (1993). Finger movement deficits in the stumptail macaque following lesions of the fasciculus cuneatus. *Somatosens Mot. Res.* 10, 17–29. doi: 10.3109/08990229309028820

Courtine, G., Song, B., Roy, R. R., Zhong, H., Herrmann, J. E., Ao, Y., et al. (2008). Recovery of supraspinal control of stepping via indirect propriospinal relay connections after spinal cord injury. *Nat. Med.* 14, 69–74. doi: 10.1038/nm1682

Cregg, J. M., Depaul, M. A., Filous, A. R., Lang, B. T., Tran, A., and Silver, J. (2014). Functional regeneration beyond the glial scar. *Exp. Neurol.* 253C, 197–207. doi: 10.1016/j.expneurol.2013.12.024

Crockett, D. P., Maslany, S., Harris, S. L., and Egger, M. D. (1993). Enhanced cytochrome-oxidase staining of the cuneate nucleus in the rat reveals a modifiable somatotopic map. *Brain Res.* 612, 41–55. doi: 10.1016/0006-8993(93)91642-6

Curt, A., Alkadhi, H., Crelier, G. R., Boendermaker, S. H., Hepp-Reymond, M. C., and Kollias, S. S. (2002). Changes of non-affected upper limb cortical representation in paraplegic patients as assessed by fMRI. *Brain* 125, 2567–2578. doi: 10.1093/brain/awf250

Cusick, C. G., and Gould, H. J. 3rd. (1990). Connections between area 3b of the somatosensory cortex and subdivisions of the ventroposterior nuclear complex and the anterior pulvinar nucleus in squirrel monkeys. *J. Comp. Neurol.* 292, 83–102. doi: 10.1002/cne.902920106

D'Amato, C. J., and Hicks, S. P. (1978). Normal development and post-traumatic plasticity of corticospinal neurons in rats. *Exp. Neurol.* 60, 557–569. doi: 10.1016/0014-4886(78)90010-9

Darian-Smith, C. (2004). Primary afferent terminal sprouting after a cervical dorsal rootlet section in the macaque monkey. *J. Comp. Neurol.* 470, 134–150. doi: 10.1002/cne.11030

Darian-Smith, C. (2009). Synaptic plasticity, neurogenesis, and functional recovery after spinal cord injury. *Neuroscientist* 15, 149–165. doi: 10.1177/1073858408331372

Darian-Smith, C., and Brown, S. (2000). Functional changes at periphery and cortex following dorsal root lesions in adult monkeys. *Nat. Neurosci.* 3, 476–481. doi: 10.1038/74852

Darian-Smith, C., and Ciferri, M. (2006). Cuneate nucleus reorganization following cervical dorsal rhizotomy in the macaque monkey: its role in the recovery of manual dexterity. *J. Comp. Neurol.* 498, 552–565. doi: 10.1002/cne.21088

Darian-Smith, C., and Ciferri, M. M. (2005). Loss and recovery of voluntary hand movements in the macaque following a cervical dorsal rhizotomy. *J. Comp. Neurol.* 491, 27–45. doi: 10.1002/cne.20686

Darian-Smith, C., and Gilbert, C. D. (1994). Axonal sprouting accompanies functional reorganization in adult cat striate cortex. *Nature* 368, 737–740. doi: 10.1038/368737a0

Darian-Smith, C., and Gilbert, C. D. (1995). Topographic reorganization in the striate cortex of the adult cat and monkey is cortically mediated. *J. Neurosci.* 15, 1631–1647.

Darian-Smith, C., Hopkins, S., and Ralston, H. J. 3rd. (2010). Changes in synaptic populations in the spinal dorsal horn following a dorsal rhizotomy in the monkey. *J. Comp. Neurol.* 518, 103–117. doi: 10.1002/cne.22216

Davis, K. D., Kiss, Z. H., Luo, L., Tasker, R. R., Lozano, A. M., and Dostrovsky, J. O. (1998). Phantom sensations generated by thalamic microstimulation. *Nature* 391, 385–387. doi: 10.1038/34905

Disbrow, E., Litinas, E., Recanzone, G. H., Padberg, J., and Krubitzer, L. (2003). Cortical connections of the second somatosensory area and the parietal ventral area in macaque monkeys. *J. Comp. Neurol.* 462, 382–399. doi: 10.1002/cne.10731

Doetsch, G. S., Harrison, T. A., Macdonald, A. C., and Litaker, M. S. (1996). Short-term plasticity in primary somatosensory cortex of the rat: rapid changes in magnitudes and latencies of neuronal responses following digit denervation. *Exp. Brain Res.* 112, 505–512. doi: 10.1007/BF00227956

Dutta, A., Kambi, N., Raghunathan, P., Khushu, S., and Jain, N. (2013). Large-scale reorganization of the somatosensory cortex of adult macaque monkeys revealed by fMRI. *Brain Struct. Funct.* doi: 10.1007/s00429-013-0569-8. [Epub ahead of print].

Dykes, R. W., and Craig, A. D. (1998). Control of size and excitability of mechanosensory receptive fields in dorsal column nuclei by homolateral dorsal horn neurons. *J. Neurophysiol.* 80, 120–129.

Elbert, T., Sterr, A., Flor, H., Rockstroh, B., Knecht, S., Pantev, C., et al. (1997). Input-increase and input-decrease types of cortical reorganization after upper extremity amputation in humans. *Exp. Brain Res.* 117, 161–164. doi: 10.1007/s002210050210

Faggin, B. M., Nguyen, K. T., and Nicolelis, M. A. (1997). Immediate and simultaneous sensory reorganization at cortical and subcortical levels of the somatosensory system. *Proc. Natl. Acad. Sci. U.S.A.* 94, 9428–9433. doi: 10.1073/pnas.94.17.9428

Fang, P. C., Stepniewska, I., and Kaas, J. H. (2005). Ipsilateral cortical connections of motor, premotor, frontal eye, and posterior parietal fields in a prosimian primate, Otolemur garnetti. *J. Comp. Neurol.* 490, 305–333. doi: 10.1002/cne.20665

Fawcett, J. W., Schwab, M. E., Montani, L., Brazda, N., and Muller, H. W. (2012). Defeating inhibition of regeneration by scar and myelin components. *Handb. Clin. Neurol.* 109, 503–522. doi: 10.1016/B978-0-444-52137-8.00031-0

Flor, H., Elbert, T., Knecht, S., Wienbruch, C., Pantev, C., Birbaumer, N., et al. (1995). Phantom-limb pain as a perceptual correlate of cortical reorganization following arm amputation. *Nature* 375, 482–484. doi: 10.1038/375482a0

Flor, H., Elbert, T., Muhlnickel, W., Pantev, C., Wienbruch, C., and Taub, E. (1998). Cortical reorganization and phantom phenomena in congenital and traumatic upper-extremity amputees. *Exp. Brain Res.* 119, 205–212. doi: 10.1007/s002210050334

Florence, S. L., Hackett, T. A., and Strata, F. (2000). Thalamic and cortical contributions to neural plasticity after limb amputation. *J. Neurophysiol.* 83, 3154–3159.

Florence, S. L., and Kaas, J. H. (1995). Large-scale reorganization at multiple levels of the somatosensory pathway follows therapeutic amputation of the hand in monkeys. *J. Neurosci.* 15, 8083–8095.

Florence, S. L., Taub, H. B., and Kaas, J. H. (1998). Large-scale sprouting of cortical connections after peripheral injury in adult macaque monkeys. *Science* 282, 1117–1121. doi: 10.1126/science.282.5391.1117

Garcia-Alias, G., and Fawcett, J. W. (2012). Training and anti-CSPG combination therapy for spinal cord injury. *Exp. Neurol.* 235, 26–32. doi: 10.1016/j.expneurol.2011.09.009

Garraghty, P. E., Arnold, L. L., Wellman, C. L., and Mowery, T. M. (2006). Receptor autoradiographic correlates of deafferentation-induced reorganization

in adult primate somatosensory cortex. *J. Comp. Neurol.* 497, 636–645. doi: 10.1002/cne.21018

Garraghty, P. E., Florence, S. L., and Kaas, J. H. (1990a). Ablations of areas 3a and 3b of monkey somatosensory cortex abolish cutaneous responsivity in area 1. *Brain Res.* 528, 165–169. doi: 10.1016/0006-8993(90)90213-U

Garraghty, P. E., Lachica, E. A., and Kaas, J. H. (1991). Injury-induced reorganization of somatosensory cortex is accompanied by reductions in GABA staining. *Somatosens Mot. Res.* 8, 347–354. doi: 10.3109/08990229109144757

Garraghty, P. E., Pons, T. P., and Kaas, J. H. (1990b). Ablations of areas 3b (SI proper) and 3a of somatosensory cortex in marmosets deactivate the second and parietal ventral somatosensory areas. *Somatosens Mot. Res.* 7, 125–135. doi: 10.3109/08990229009144703

Ghosh, A., Sydekum, E., Haiss, F., Peduzzi, S., Zorner, B., Schneider, R., et al. (2009). Functional and anatomical reorganization of the sensory-motor cortex after incomplete spinal cord injury in adult rats. *J. Neurosci.* 29, 12210–12219. doi: 10.1523/JNEUROSCI.1828-09.2009

Giger, R. J., Hollis, E. R. 2nd., and Tuszynski, M. H. (2010). Guidance molecules in axon regeneration. *Cold Spring Harb. Perspect. Biol.* 2, a001867. doi: 10.1101/cshperspect.a001867

Glendinning, D. S., Cooper, B. Y., Vierck, C. J. Jr., and Leonard, C. M. (1992). Altered precision grasping in stumptail macaques after fasciculus cuneatus lesions. *Somatosens Mot. Res.* 9, 61–73. doi: 10.3109/08990229209144763

Graziano, A., Foffani, G., Knudsen, E. B., Shumsky, J., and Moxon, K. A. (2013). Passive exercise of the hind limbs after complete thoracic transection of the spinal cord promotes cortical reorganization. *PLoS ONE* 8:e54350. doi: 10.1371/journal.pone.0054350

Graziano, A., and Jones, E. G. (2009). Early withdrawal of axons from higher centers in response to peripheral somatosensory denervation. *J. Neurosci.* 29, 3738–3748. doi: 10.1523/JNEUROSCI.5388-08.2009

He, Z., and Koprivica, V. (2004). The Nogo signaling pathway for regeneration block. *Annu. Rev. Neurosci.* 27, 341–368. doi: 10.1146/annurev.neuro.27.070203.144340

Hickmott, P. W., and Steen, P. A. (2005). Large-scale changes in dendritic structure during reorganization of adult somatosensory cortex. *Nat. Neurosci.* 8, 140–142. doi: 10.1038/nn1384

Hicks, S. P., and D'Amato, C. J. (1975). Motor-sensory cortex-corticospinal system and developing locomotion and placing in rats. *Am. J. Anat.* 143, 1–42. doi: 10.1002/aja.1001430102

Humanes-Valera, D., Aguilar, J., and Foffani, G. (2013). Reorganization of the intact somatosensory cortex immediately after spinal cord injury. *PLoS ONE* 8:e69655. doi: 10.1371/journal.pone.0069655

Jain, N., Catania, K. C., and Kaas, J. H. (1997). Deactivation and reactivation of somatosensory cortex after dorsal spinal cord injury. *Nature* 386, 495–498. doi: 10.1038/386495a0

Jain, N., Catania, K. C., and Kaas, J. H. (1998). A histologically visible representation of the fingers and palm in primate area 3b and its immutability following long-term deafferentations. *Cereb. Cortex* 8, 227–236. doi: 10.1093/cercor/8.3.227

Jain, N., Florence, S. L., Qi, H. X., and Kaas, J. H. (2000). Growth of new brainstem connections in adult monkeys with massive sensory loss. *Proc. Natl. Acad. Sci. U.S.A.* 97, 5546–5550. doi: 10.1073/pnas.090572597

Jain, N., Qi, H. X., Catania, K. C., and Kaas, J. H. (2001). Anatomic correlates of the face and oral cavity representations in the somatosensory cortical area 3b of monkeys. *J. Comp. Neurol.* 429, 455–468. doi: 10.1002/1096-9861(20010115)429:3%3C455::AID-CNE7%3E3.0.CO;2-F

Jain, N., Qi, H. X., Collins, C. E., and Kaas, J. H. (2008). Large-scale reorganization in the somatosensory cortex and thalamus after sensory loss in macaque monkeys. *J. Neurosci.* 28, 11042–11060. doi: 10.1523/JNEUROSCI.2334-08.2008

Jones, E. G. (2000). Cortical and subcortical contributions to activity-dependent plasticity in primate somatosensory cortex. *Annu. Rev. Neurosci.* 23, 1–37. doi: 10.1146/annurev.neuro.23.1.1

Jones, E. G., Friedman, D. P., and Hendry, S. H. (1982). Thalamic basis of place- and modality-specific columns in monkey somatosensory cortex: a correlative anatomical and physiological study. *J. Neurophysiol.* 48, 545–568.

Jones, E. G., and Pons, T. P. (1998). Thalamic and brainstem contributions to large-scale plasticity of primate somatosensory cortex. *Science* 282, 1121–1125. doi: 10.1126/science.282.5391.1121

Kaas, J. H. (2012). "Somatosensory system," in *The Human Nervous System.* 3rd Edn, eds J. K. Mai and G. Paxinos. (London: ElsevierAcademic Press), 1064–1099.

Kaas, J. H., Nelson, R. J., Sur, M., Dykes, R. W., and Merzenich, M. M. (1984). The somatotopic organization of the ventroposterior thalamus of the squirrel monkey, Saimiri sciureus. *J. Comp. Neurol.* 226, 111–140. doi: 10.1002/cne.902260109

Kaas, J. H., Nelson, R. J., Sur, M., Lin, C. S., and Merzenich, M. M. (1979). Multiple representations of the body within the primary somatosensory cortex of primates. *Science* 204, 521–523. doi: 10.1126/science.107591

Kaas, J. H., Qi, H. X., Burish, M. J., Gharbawie, O. A., Onifer, S. M., and Massey, J. M. (2008). Cortical and subcortical plasticity in the brains of humans, primates, and rats after damage to sensory afferents in the dorsal columns of the spinal cord. *Exp. Neurol.* 209, 407–416. doi: 10.1016/j.expneurol.2007.06.014

Kaas, J. H., Qi, H. X., and Iyengar, S. (2006). Cortical network for representing the teeth and tongue in primates. *Anat. Rec. A Discov. Mol. Cell Evol. Biol.* 288, 182–190. doi: 10.1002/ar.a.20267

Kambi, N., Tandon, S., Mohammed, H., Lazar, L., and Jain, N. (2011). Reorganization of the primary motor cortex of adult macaque monkeys after sensory loss resulting from partial spinal cord injuries. *J. Neurosci.* 31, 3696–3707. doi: 10.1523/JNEUROSCI.5187-10.2011

Kao, T., Shumsky, J. S., Murray, M., and Moxon, K. A. (2009). Exercise induces cortical plasticity after neonatal spinal cord injury in the rat. *J. Neurosci.* 29, 7549–7557. doi: 10.1523/JNEUROSCI.2474-08.2009

Kelahan, A. M., and Doetsch, G. S. (1984). Time-dependent changes in the functional organization of somatosensory cerebral cortex following digit amputation in adult raccoons. *Somatosens Res.* 2, 49–81.

Krajacic, A., Weishaupt, N., Girgis, J., Tetzlaff, W., and Fouad, K. (2010). Training-induced plasticity in rats with cervical spinal cord injury: effects and side effects. *Behav. Brain Res.* 214, 323–331. doi: 10.1016/j.bbr.2010.05.053

Krubitzer, L. A., and Kaas, J. H. (1990). The organization and connections of somatosensory cortex in marmosets. *J. Neurosci.* 10, 952–974.

Krupa, D. J., Ghazanfar, A. A., and Nicolelis, M. A. (1999). Immediate thalamic sensory plasticity depends on corticothalamic feedback. *Proc. Natl. Acad. Sci. U.S.A.* 96, 8200–8205. doi: 10.1073/pnas.96.14.8200

Leonard, C. M., Glendinning, D. S., Wilfong, T., Cooper, B. Y., and Vierck, C. J. Jr. (1992). Alterations of natural hand movements after interruption of fasciculus cuneatus in the macaque. *Somatosens Mot. Res.* 9, 75–89. doi: 10.3109/08990229209144764

Li, C. X., Yang, Q., Vemulapalli, S., and Waters, R. S. (2013). Forelimb amputation-induced reorganization in the cuneate nucleus (CN) is not reflected in large-scale reorganization in rat forepaw barrel subfield cortex (FBS). *Brain Res.* 1526, 26–43. doi: 10.1016/j.brainres.2013.05.049

Liao, C. C., Gharbawie, O. A., Qi, H., and Kaas, J. H. (2013). Cortical connections to single digit representations in area 3b of somatosensory cortex in squirrel monkeys and prosimian galagos. *J. Comp. Neurol.* 521, 3768–3790. doi: 10.1002/cne.23377

Lotze, M., Grodd, W., Birbaumer, N., Erb, M., Huse, E., and Flor, H. (1999). Does use of a myoelectric prosthesis prevent cortical reorganization and phantom limb pain? *Nat. Neurosci.* 2, 501–502. doi: 10.1038/9145

Marik, S. A., Yamahachi, H., McManus, J. N., Szabo, G., and Gilbert, C. D. (2010). Axonal dynamics of excitatory and inhibitory neurons in somatosensory cortex. *PLoS Biol.* 8:e1000395. doi: 10.1371/journal.pbio.1000395

Marik, S. A., Yamahachi, H., Meyer Zum Alten Borgloh, S., and Gilbert, C. D. (2014). Large-Scale Axonal Reorganization of Inhibitory Neurons following Retinal Lesions. *J. Neurosci.* 34, 1625–1632. doi: 10.1523/JNEUROSCI.4345-13.2014.

Massey, J. M., Hubscher, C. H., Wagoner, M. R., Decker, J. A., Amps, J., Silver, J., et al. (2006). Chondroitinase ABC digestion of the perineuronal net promotes functional collateral sprouting in the cuneate nucleus after cervical spinal cord injury. *J. Neurosci.* 26, 4406–4414. doi: 10.1523/JNEUROSCI.5467-05.2006

McKenna, J. E., and Whishaw, I. Q. (1999). Complete compensation in skilled reaching success with associated impairments in limb synergies, after dorsal column lesion in the rat. *J. Neurosci.* 19, 1885–1894.

Merzenich, M. M., Kaas, J. H., Sur, M., and Lin, C. S. (1978). Double representation of the body surface within cytoarchitectonic areas 3b and 1 in "SI" in the owl monkey (*Aotus trivirgatus*). *J. Comp. Neurol.* 181, 41–73. doi: 10.1002/cne.901810104

Merzenich, M. M., Kaas, J. H., Wall, J., Nelson, R. J., Sur, M., and Felleman, D. (1983a). Topographic reorganization of somatosensory cortical areas 3b and 1 in adult monkeys following restricted deafferentation. *Neuroscience* 8, 33–55. doi: 10.1016/0306-4522(83)90024-6

Merzenich, M. M., Kaas, J. H., Wall, J. T., Sur, M., Nelson, R. J., and Felleman, D. J. (1983b). Progression of change following median nerve section in the cortical representation of the hand in areas 3b and 1 in adult owl and squirrel monkeys. *Neuroscience* 10, 639–665. doi: 10.1016/0306-4522(83)90208-7

Moore, C. I., Stern, C. E., Dunbar, C., Kostyk, S. K., Gehi, A., and Corkin, S. (2000). Referred phantom sensations and cortical reorganization after spinal cord injury in humans. *Proc. Natl. Acad. Sci. U.S.A.* 97, 14703–14708. doi: 10.1073/pnas.250348997

Mountcastle, V. B., and Darian-Smith, I. (1968). "Neural mechanisms in somesthesia," in *Medical Physiology,* ed V. B. Mountcastle (St. Louis, MO: C. V. Mosby), 1372–1423.

Nathan, P. W., Smith, M. C., and Cook, A. W. (1986). Sensory effects in man of lesions of the posterior columns and of some other afferent pathways. *Brain* 109(Pt. 5), 1003–1041.

Nelson, R. J., and Kaas, J. H. (1981). Connections of the ventroposterior nucleus of the thalamus with the body surface representations in cortical areas 3b and 1 of the cynomolgus macaque, (*Macaca fascicularis*). *J. Comp. Neurol.* 199, 29–64. doi: 10.1002/cne.901990104

Nelson, R. J., Sur, M., Felleman, D. J., and Kaas, J. H. (1980). Representations of the body surface in postcentral parietal cortex of Macaca fascicularis. *J. Comp. Neurol.* 192, 611–643. doi: 10.1002/cne.901920402

Nout, Y. S., Ferguson, A. R., Strand, S. C., Moseanko, R., Hawbecker, S., Zdunowski, S., et al. (2012b). Methods for functional assessment after C7 spinal cord hemisection in the rhesus monkey. *Neurorehabil. Neural Repair* 26, 556–569. doi: 10.1177/1545968311421934

Nout, Y. S., Rosenzweig, E. S., Brock, J. H., Strand, S. C., Moseanko, R., Hawbecker, S., et al. (2012a). Animal models of neurologic disorders: a nonhuman primate model of spinal cord injury. *Neurotherapeutics* 9, 380–392. doi: 10.1007/s13311-012-0114-0

Onifer, S. M., Smith, G. M., and Fouad, K. (2011). Plasticity after spinal cord injury: relevance to recovery and approaches to facilitate it. *Neurotherapeutics* 8, 283–293. doi: 10.1007/s13311-011-0034-4

Paxino, G., and Watson, C. (2007). *The Rat Brain in Stereotaxic Coordinates.* Amsterdam: Elsevier.

Pei, Y. C., Denchev, P. V., Hsiao, S. S., Craig, J. C., and Bensmaia, S. J. (2009). Convergence of submodality-specific input onto neurons in primary somatosensory cortex. *J. Neurophysiol.* 102, 1843–1853. doi: 10.1152/jn.00235.2009

Perl, E. R., Whitlock, D. G., and Gentry, J. R. (1962). Cutaneous projection to second-order neurons of the dorsal column system. *J. Neurophysiol.* 25, 337–358.

Pons, T. P., Garraghty, P. E., Friedman, D. P., and Mishkin, M. (1987). Physiological evidence for serial processing in somatosensory cortex. *Science* 237, 417–420. doi: 10.1126/science.3603028

Pons, T. P., Garraghty, P. E., and Mishkin, M. (1992). Serial and parallel processing of tactual information in somatosensory cortex of rhesus monkeys. *J. Neurophysiol.* 68, 518–527.

Pons, T. P., Garraghty, P. E., Ommaya, A. K., Kaas, J. H., Taub, E., and Mishkin, M. (1991). Massive cortical reorganization after sensory deafferentation in adult macaques. *Science* 252, 1857–1860. doi: 10.1126/science.1843843

Qi, H. X., Chen, L. M., and Kaas, J. H. (2011a). Reorganization of somatosensory cortical areas 3b and 1 after unilateral section of dorsal columns of the spinal cord in squirrel monkeys. *J. Neurosci.* 31, 13662–13675. doi: 10.1523/JNEUROSCI.2366-11.2011

Qi, H. X., Gharbawie, O. A., Wong, P., and Kaas, J. H. (2011b). Cell-poor septa separate representations of digits in the ventroposterior nucleus of the thalamus in monkeys and prosimian galagos. *J. Comp. Neurol.* 519, 738–758. doi: 10.1002/cne.22545

Qi, H. X., Gharbawie, O. A., Wynne, K. W., and Kaas, J. H. (2013). Impairment and recovery of hand use after unilateral section of the dorsal columns of the spinal cord in squirrel monkeys. *Behav. Brain Res.* 252, 363–376. doi: 10.1016/j.bbr.2013.05.058

Qi, H. X., Jain, N., Collins, C. E., Lyon, D. C., and Kaas, J. H. (2010). Functional organization of motor cortex of adult macaque monkeys is altered by sensory loss in infancy. *Proc. Natl. Acad. Sci. U.S.A.* 107, 3192–3197. doi: 10.1073/pnas.0914962107

Qi, H. X., and Kaas, J. H. (2004). Myelin stains reveal an anatomical framework for the representation of the digits in somatosensory area 3b of macaque monkeys. *J. Comp. Neurol.* 477, 172–187. doi: 10.1002/cne.20247

Qi, H. X., Reed, J. L., Bui, T., Chen, L. M., and Kaas, J. H. (2012). Longitudinal fMRI and behavioral recovery after sensory loss from the hand of adult monkeys. *Fed. Euro. Neurosci. Soc. Forum Abstr.* A-471-0142-02394.

Qi, H. X., Reed, J. L., Gharbawie, O. A., Burish, M. J., and Kaas, J. H. (2014). Cortical neuron response properties are related to lesion extent and behavioral recovery after sensory loss from spinal cord injury in monkeys. *J. Neurosci.* 34, 4345–4363. doi: 10.1523/JNEUROSCI.4954-13.2014

Ramachandran, V. S. (1993). Behavioral and magnetoencephalographic correlates of plasticity in the adult human brain. *Proc. Natl. Acad. Sci. U.S.A.* 90, 10413–10420. doi: 10.1073/pnas.90.22.10413

Ramachandran, V. S., and Rogers-Ramachandran, D. (2000). Phantom limbs and neural plasticity. *Arch. Neurol.* 57, 317–320. doi: 10.1001/archneur.57.3.317

Rasmusson, D. D. (1996). Changes in the response properties of neurons in the ventroposterior lateral thalamic nucleus of the raccoon after peripheral deafferentation. *J. Neurophysiol.* 75, 2441–2450.

Rasmusson, D. D., and Northgrave, S. A. (1997). Reorganization of the raccoon cuneate nucleus after peripheral denervation. *J. Neurophysiol.* 78, 2924–2936.

Reed, J. L., Qi, H. X., and Kaas, J. H. (2012). Ipsilateral responses and interhemispheric interactions in area 3b after dorsal column spinal cord injury in New World monkeys. *Soc. Neurosci. Abstr.* 42.

Reed, J. L., Qi, H. X., Zhou, Z., Bernard, M. R., Burish, M. J., Bonds, A. B., et al. (2010). Response properties of neurons in primary somatosensory cortex of owl monkeys reflect widespread spatiotemporal integration. *J. Neurophysiol.* 103, 2139–2157. doi: 10.1152/jn.00709.2009

Rose, J. E., and Mountcastle, V. B. (1959). "Touch and kinesthesis," in *Handbook of Physiology,* ed H. W. Magoun (Washington, DC: American Physiology Society), 387–429.

Rustioni, A., Hayes, N. L., and O'Neill, S. (1979). Dorsal column nuclei and ascending spinal afferents in macaques. *Brain* 102, 95–125. doi: 10.1093/brain/102.1.95

Schmidlin, E., Kaeser, M., Gindrat, A. D., Savidan, J., Chatagny, P., Badoud, S., et al. (2011). Behavioral assessment of manual dexterity in non-human primates. *J. Vis. Exp.* 57, 3258–3270. doi: 10.3791/3258

Schnell, L., Schneider, R., Kolbeck, R., Barde, Y. A., and Schwab, M. E. (1994). Neurotrophin-3 enhances sprouting of corticospinal tract during development and after adult spinal cord lesion. *Nature* 367, 170–173. doi: 10.1038/367170a0

Sengelaub, D. R., Muja, N., Mills, A. C., Myers, W. A., Churchill, J. D., and Garraghty, P. E. (1997). Denervation-induced sprouting of intact peripheral afferents into the cuneate nucleus of adult rats. *Brain Res.* 769, 256–262. doi: 10.1016/S0006-8993(97)00708-7

Silva, A. C., Rasey, S. K., Wu, X., and Wall, J. T. (1996). Initial cortical reactions to injury of the median and radial nerves to the hands of adult primates. *J. Comp. Neurol.* 366, 700–716. doi: 10.1002/(SICI)1096-9861(19960318)366:4<700::AID-CNE9>3.0.CO;2-8

Silva, N. A., Sousa, N., Reis, R. L., and Salgado, A. J. (2014). From basics to clinical: a comprehensive review on spinal cord injury. *Prog. Neurobiol.* 114, 25–57. doi: 10.1016/j.pneurobio.2013.11.002

Stepniewska, I., Preuss, T. M., and Kaas, J. H. (1993). Architectonics, somatotopic organization, and ipsilateral cortical connections of the primary motor area (M1) of owl monkeys. *J. Comp. Neurol.* 330, 238–271. doi: 10.1002/cne.903300207

Sur, M., Nelson, R. J., and Kaas, J. H. (1982). Representations of the body surface in cortical areas 3b and 1 of squirrel monkeys: comparisons with other primates. *J. Comp. Neurol.* 211, 177–192. doi: 10.1002/cne.902110207

Sur, M., Wall, J. T., and Kaas, J. H. (1984). Modular distribution of neurons with slowly adapting and rapidly adapting responses in area 3b of somatosensory cortex in monkeys. *J. Neurophysiol.* 51, 724–744.

Tandon, S., Kambi, N., Lazar, L., Mohammed, H., and Jain, N. (2009). Large-scale expansion of the face representation in somatosensory areas of the lateral sulcus after spinal cord injuries in monkeys. *J. Neurosci.* 29, 12009–12019. doi: 10.1523/JNEUROSCI.2118-09.2009

Tetzlaff, W., Fouad, K., and Kwon, B. (2009). Be careful what you train for. *Nat. Neurosci.* 12, 1077–1079. doi: 10.1038/nn0909-1077

Tommerdahl, M., Whitsel, B. L., Vierck, C. J. Jr., Favorov, O., Juliano, S., Cooper, B., et al. (1996). Effects of spinal dorsal column transection on the response of monkey anterior parietal cortex to repetitive skin stimulation. *Cereb. Cortex* 6, 131–155. doi: 10.1093/cercor/6.2.131

Turrigiano, G. G. (1999). Homeostatic plasticity in neuronal networks: the more things change, the more they stay the same. *Trends Neurosci.* 22, 221–227. doi: 10.1016/S0166-2236(98)01341-1

Vahlsing, H. L., and Feringa, E. R. (1980). A ventral uncrossed corticospinal tract in the rat. *Exp. Neurol.* 70, 282–287. doi: 10.1016/0014-4886(80)90027-8

Vierck, C. J. Jr. (1973). Alterations of spatio-tactile discrimination after lesions of primate spinal cord. *Brain Res.* 58, 69–79. doi: 10.1016/0006-8993(73)90824-X

Vierck, C. J. Jr. (1974). Tactile movement detection and discrimination following dorsal column lesions in monkeys. *Exp. Brain Res.* 20, 331–346. doi: 10.1007/BF00237379

Vierck, C. J. Jr. (1998). Impaired detection of repetitive stimulation following interruption of the dorsal spinal column in primates. *Somatosens Mot. Res.* 15, 157–163. doi: 10.1080/08990229870880

Vierck, C. J. Jr., and Cooper, B. Y. (1998). Cutaneous texture discrimination following transection of the dorsal spinal column in monkeys. *Somatosens Mot. Res.* 15, 309–315. doi: 10.1080/08990229870718

Wall, J. T., Xu, J., and Wang, X. (2002). Human brain plasticity: an emerging view of the multiple substrates and mechanisms that cause cortical changes and related sensory dysfunctions after injuries of sensory inputs from the body. *Brain Res. Brain Res. Rev.* 39, 181–215. doi: 10.1016/S0165-0173(02)00192-3

Wall, P. D. (1970). The sensory and motor role of impulses travelling in the dorsal columns towards cerebral cortex. *Brain* 93, 505–524. doi: 10.1093/brain/93.3.505

Wall, P. D. (1977). The presence of ineffective synapses and the circumstances which unmask them. *Philos. Trans. R. Soc. Lond. B Biol. Sci.* 278, 361–372. doi: 10.1098/rstb.1977.0048

Wang, Z., Qi, H. X., Kaas, J. H., Roe, A. W., and Chen, L. M. (2013). Functional signature of recovering cortex: dissociation of local field potentials and spiking activity in somatosensory cortices of spinal cord injured monkeys. *Exp. Neurol.* 249, 132–143. doi: 10.1016/j.expneurol.2013.08.013

Welker, W. I. (1973). Principles of organization of the ventrobasal complex in mammals. *Brain Behav. Evol.* 7, 253–336. doi: 10.1159/000124417

Wellman, C. L., Arnold, L. L., Garman, E. E., and Garraghty, P. E. (2002). Acute reductions in GABAA receptor binding in layer IV of adult primate somatosensory cortex after peripheral nerve injury. *Brain Res.* 954, 68–72. doi: 10.1016/S0006-8993(02)03343-7

Weng, H. R., Lenz, F. A., Vierck, C., and Dougherty, P. M. (2003). Physiological changes in primate somatosensory thalamus induced by deafferentation are dependent on the spinal funiculi that are sectioned and time following injury. *Neuroscience* 116, 1149–1160. doi: 10.1016/S0306-4522(02)00796-0

Willis, W. D., and Coggeshall, R. E. (2004). "Sensory pathways in the Dorsal Funiculus," in *Sensory Mechanisms of the Spinal cord: Ascending Sensory Tracts And Their Descending Control.* 3rd Edn, eds W. D. Willis and R. E. Coggeshall (New York, NY: Kluwer Academy/Plenum Publisher), 597–664. doi: 10.1007/978-1-4615-0035-3_9

Wise, S. P., Boussaoud, D., Johnson, P. B., and Caminiti, R. (1997). Premotor and parietal cortex: corticocortical connectivity and combinatorial computations. *Annu. Rev. Neurosci.* 20, 25–42. doi: 10.1146/annurev.neuro.20.1.25

Witham, C. L., and Baker, S. N. (2011). Modulation and transmission of peripheral inputs in monkey cuneate and external cuneate nuclei. *J. Neurophysiol.* 106, 2764–2775. doi: 10.1152/jn.00449.2011

Wu, C. W., and Kaas, J. H. (1999). Reorganization in primary motor cortex of primates with long-standing therapeutic amputations. *J. Neurosci.* 19, 7679–7697.

Xerri, C. (2012). Plasticity of cortical maps: multiple triggers for adaptive reorganization following brain damage and spinal cord injury. *Neuroscientist* 18, 133–148. doi: 10.1177/1073858410397894

Xu, J., and Wall, J. T. (1997). Rapid changes in brainstem maps of adult primates after peripheral injury. *Brain Res.* 774, 211–215. doi: 10.1016/S0006-8993(97)81706-4

Xu, J., and Wall, J. T. (1999). Evidence for brainstem and supra-brainstem contributions to rapid cortical plasticity in adult monkeys. *J. Neurosci.* 19, 7578–7590.

Yamahachi, H., Marik, S. A., McManus, J. N., Denk, W., and Gilbert, C. D. (2009). Rapid axonal sprouting and pruning accompany functional reorganization in primary visual cortex. *Neuron* 64, 719–729. doi: 10.1016/j.neuron.2009.11.026

Zhao, R. R., Andrews, M. R., Wang, D., Warren, P., Gullo, M., Schnell, L., et al. (2013). Combination treatment with anti-Nogo-A and chondroitinase ABC is more effective than single treatments at enhancing functional recovery after spinal cord injury. *Eur. J. Neurosci.* 38, 2946–2961. doi: 10.1111/ejn.12276

Zorner, B., Filli, L., Starkey, M. L., Gonzenbach, R., Kasper, H., Rothlisberger, M., et al. (2010). Profiling locomotor recovery: comprehensive quantification of impairments after CNS damage in rodents. *Nat. Methods* 7, 701–708. doi: 10.1038/nmeth.1484

Conflict of Interest Statement: The authors declare that the research was conducted in the absence of any commercial or financial relationships that could be construed as a potential conflict of interest.

Received: 06 March 2014; accepted: 22 April 2014; published online: 12 May 2014.
Citation: Qi H-X, Kaas JH and Reed JL (2014) The reactivation of somatosensory cortex and behavioral recovery after sensory loss in mature primates. Front. Syst. Neurosci. ***8****:84. doi: 10.3389/fnsys.2014.00084*
This article was submitted to the journal Frontiers in Systems Neuroscience.

frontiers in
SYSTEMS NEUROSCIENCE

ORIGINAL RESEARCH ARTICLE
published: 21 April 2014
doi: 10.3389/fnsys.2014.00060

The pregnane xenobiotic receptor, a prominent liver factor, has actions in the midbrain for neurosteroid synthesis and behavioral/neural plasticity of female rats

***Cheryl A. Frye*[1,2,3,4,5,6,7]*, Carolyn J. Koonce[1,6,7] and Alicia A.Walf[1,6,7]**

[1] *Department of Psychology, The University at Albany-SUNY, Albany, NY, USA*
[2] *Department of Biological Sciences, The University at Albany-SUNY, Albany, NY, USA*
[3] *The Center for Neuroscience Research, The University at Albany-SUNY, Albany, NY, USA*
[4] *The Center for Life Sciences Research, The University at Albany-SUNY, Albany, NY, USA*
[5] *Department of Chemistry and Biochemistry, The University of Alaska–Fairbanks, Fairbanks, AK, USA*
[6] *Institute of Arctic Biology, The University of Alaska–Fairbanks, Fairbanks, AK, USA*
[7] *IDeA Network of Biomedical Excellence (INBRE), The University of Alaska–Fairbanks, Fairbanks, AK, USA*

Edited by:
Mikhail Lebedev, Duke University, USA

Reviewed by:
Raúl G. Paredes, National University of Mexico, Mexico
Mikhail Lebedev, Duke University, USA
Graziano Pinna, University of Illinois at Chicago, USA
Nico Mitro, Università degli Studi di Milano, Italy

****Correspondence:***
Cheryl A. Frye, Department of Chemistry and Biochemistry, Institute of Arctic Biology, The University of Alaska–Fairbanks, 223 Murie Life Sciences Building, 982 Koyukuk Drive, Fairbanks, AK 99775, USA
e-mail: cheryl.a.frye@gmail.com

A novel factor of interest for growth/plasticity in the brain is pregnane xenobiotic receptor (PXR). PXR is a liver factor known for its role in xenobiotic clearance and cholesterol metabolism. It is expressed in the brain, suggesting a potential role for plasticity, particularly involving cholesterol-based steroids and neurosteroids. Mating induces synthesis of neurosteroids in the midbrain Ventral Tegmental Area (VTA) of female rodents, as well as other "plastic" regions of the brain, including the hippocampus, that may be involved in the consolidation of the mating experience. Reducing PXR in the VTA attenuates mating-induced biosynthesis of the neurosteroid, 5α-pregnan-3α-ol-20-one (3α,5α-THP). The 18 kDA translocator protein (TSPO) is one rate-limiting factor for 3α,5α-THP neurosteroidogenesis. The hypothesis tested was that PXR is an upstream factor of TSPO for neurosteroidogenesis of 3α,5α-THP in the VTA for lordosis, independent of peripheral glands. First, proestrous rats were administered a TSPO blocker (PK11195) and/or 3α,5α-THP following infusions of PXR antisense oligonucleotides (AS-ODNs) or vehicle to the VTA. Inhibiting TSPO with PK11195 reduced 3α,5α-THP levels in the midbrain and lordosis, an effect that could be reversed with 3α,5α-THP administration, but not AS-ODN+3α,5α-THP. Second, proestrous, ovariectomized (OVX), or ovariectomized/adrenalectomized (OVX/ADX) rats were infused with a TSPO enhancer (FGIN 1-27) subsequent to AS-ODNs or vehicle to the VTA. PXR AS-ODNs blocked actions of FGIN 1–27 for lordosis and 3α,5α-THP levels among proestrous > OVX > OVX/ADX rats. Thus, PXR may be upstream of TSPO, involved in neurosteroidogenesis of 3α,5α-THP in the brain for plasticity. This novel finding of a liver factor involved in behavioral/neural plasticity substantiates future studies investigating factors known for their prominent actions in the peripheral organs, such as the liver, for modulating brain function and its augmentation.

Keywords: midbrain ventral tegmental area, allopregnanolone, progesterone, cognition, reproduction

INTRODUCTION

Steroid hormones are well-recognized for their role for growth processes in the body. For example, physiological roles of steroids hormones for growth are apparent during puberty, with the onset of the patterned secretion of these steroids from the gonads, and morphological differences (secondary sex characteristics), and during pregnancy, with substantial changes in many systems modulated by steroid hormones (e.g., the progestogens—progesterone and its metabolites), as two examples. In these two examples there are obvious physical changes, but the effects, mechanisms, and brain targets of steroids, such as the progestogens, for cognitive and behavioral processes, in relation to the body, are starting to become better understood. Data from large clinical trials conducted of hormone replacement therapies (HRTs) (which typically include synthetic compounds to mimic hormones lost during menopause, estradiol and progesterone), do not entirely support the basic literature on the beneficial role of these hormones for brain functions, like enhancements in learning/memory (described below) and reduction in stroke- and injury-related pathology (Roof et al., 1992, 1993; Chen et al., 1999; He et al., 2004; Shapiro, 2006; Billeci et al., 2007). Moreover, these trials were halted early due to increased cardiovascular and cancer risks and there was a subsequent backlash against clinical use of HRTs that did not take into account individual patient characteristics and risk (Rossouw et al., 2002; Shumaker et al., 2003; Maki and Henderson, 2012). Together, these examples substantiate the importance of understanding the role and mechanisms of steroids in the body and brain.

In addition to the controversy of whether the potential benefits of hormones outweigh their risks, there has been controversy of the role of progestogens for benefiting brain function *per se*. Historically, the basic experimental design to understand whether a particular hormone was necessary and sufficient for a physiological process was to assess co-variation in the hormone of interest and a process and remove the gland that produced the hormone (extirpation) and replace back the hormone (to see if the process is abrogated and then reinstated, respectively). In rodent models of cognitive function, studies assessing natural increases in progestogens over the estrous cycle, or during and after pregnancy, support the mnemonic effects of these high, physiological levels of progestogens in spatial and object recognition tasks (Lambert et al., 2005; Walf et al., 2006; Kinsley and Lambert, 2008; Paris and Frye, 2008; Macbeth and Luine, 2010). Moreover, ovariectomy (surgical removal of the ovaries) of young, adult female rats produces performance deficits in the object recognition and placement tasks, which can be abrogated with replacement back with progesterone or its neuroactive metabolite, 5α-pregnan-3α-ol-20-one (3α,5α-THP, a.k.a. allopregnanolone; Walf et al., 2006; Frye et al., 2007). However, these beneficial effects of progestogens are not uniformly observed in other studies, using different tasks, or dosing and formulation of progestogens, or involving investigations in aged rodents (Murphy et al., 2002; Toung et al., 2004; see review by Acosta et al., 2013). Together, these data suggest that progestogens' effects for cognitive function may be influenced by task, dosing and formulation of progestogen administered, age and likely many other factors.

Given that there are many factors that can influence responses to progestogens for neural processes, an approach that we have taken is to use the well-characterized behavioral model of reproductive behavior of rodents to investigate progestogens' mechanisms. The notion is that we can begin to understand the mechanisms of progestogens in regions that have been investigated for decades (hypothalamus and midbrain) for this basic, hormone-dependent behavior (lordosis, or mating posture of female rodents), substantiating subsequent studies on such mechanisms in corticolimbic structures underlying complex cognitive processes. Lordosis only occurs in appropriate neuroendocrine and environmental context, with reductions in the response supported by effects of ovariectomy, steroid blockers or environmental stressors (Uphouse et al., 2005, 2013; reviewed in Frye, 2011; Frye et al., 2013). From studies using this approach, the effects of progesterone and/or its metabolite, 3α,5α-THP, in the midbrain ventral tegmental area (VTA), through novel neurotransmitter targets (e.g., GABA, dopamine, glutamate, and second messenger cascades) have been supported (reviewed in Frye and Walf, 2008). Interestingly, there is high expression of factors involved in the metabolism and synthesis of 3α,5α-THP in the VTA (from precursor of all steroids, cholesterol; reviewed in Frye, 2011), suggesting the importance of 3α,5α-THP production and action in this region.

Another consideration is that experience can alter hormone levels (and thereby modify the CNS). An example of this is mating-induced neurosteroid synthesis. Mating induces synthesis of neurosteroids in the midbrain VTA of female rodents, as well as other "plastic" regions of the brain, including the hippocampus and prefrontal cortex, that may be involved in the consolidation of the mating experience in rodents. There can be dynamic changes in 3α,5α-THP production in midbrain and corticolimbic structures following mating or other social and environmental challenges (Purdy et al., 1991; Barbaccia et al., 2001; Agís-Balboa et al., 2007; Pinna et al., 2008; Pinna and Rasmusson, 2012). In further support, midbrain 3α,5α-THP levels are higher after female rats are tested in the paced mating task, compared to standard mating task (which does not involve females temporally controlling the frequency of contacts with males), compared to no mating (reviewed in Frye, 2011). Thus, our model system is to use lordosis as a bioassay to further understand mechanisms involved in 3α,5α-THP synthesis and actions for neural/behavioral plasticity.

Studies focused on mechanistic questions about progestogens' actions and production in the VTA, using lordosis as the bioassay, have been extended to understand novel targets, such as the pregnane xenobiotic receptor (PXR), for these responses. PXR has a well-established role as a ubiquitous and promiscuous nuclear receptor in the liver and other excretory organs (kidneys, intestines) for metabolism and xenobiotic clearance (Geick et al., 2001; Dussault and Forman, 2002; Francis et al., 2002; Kliewer et al., 2002). Its role in the CNS was not understood until more recently. Some of the first studies examining PXR's role were those focused on its function in the blood-brain-barrier, which was similar to other excretory organs in the body (Bauer et al., 2004, 2006; Xu et al., 2005; Harmsen et al., 2007; Ma et al., 2008; Zhang et al., 2008; Ott et al., 2009). However, PXR is also expressed in the brain itself, suggesting a potential role for plasticity, particularly involving steroids (which are cholesterol-based hormones) and neurosteroids (which are produced from metabolism of cholesterol in the central nervous system itself). For example, for synthesis of 3α,5α-THP, cholesterol is transported into the mitochondria by way of the 18-kDa translocator protein (TSPO) on the outer mitochondrial membrane. Inside the mitochondria, cholesterol interacts with steroidogenic acute regulatory protein and cytochrome P450-dependent side chain cleavage (P450scc) enzymes (Mellon and Deschepper, 1993; King et al., 2002; Papadopoulos et al., 2006), as well downstream steroidogenic enzymes (5α-reductase, 3α-hydroxysteroid dehydrogenase) to produce pregnenolone, progesterone, dihydroprogesterone, and, ultimately, 3α,5α-THP. A question is the role of PXR in this pathway. Our interest in PXR as a novel target was supported by a microarray study in which the gene for this receptor was expressed in the midbrain following paced mating of female rodents (reviewed in Frye, 2011). We subsequently characterized the expression of this receptor in the midbrain across the estrous cycle of rats (in which we found higher expression associated with higher progestogen levels; Frye et al., 2012, 2013). Moreover, knocking down PXR expression in the VTA reduces mating-induced biosynthesis of 3α,5α-THP in the VTA. Given that TSPO is one rate-limiting factor for 3α,5α-THP neurosteroidogenesis, a question is whether metabolism at TSPO involves, or requires, PXR for production of 3α,5α-THP. The hypothesis was that PXR is a necessary upstream factor of TSPO for neurosteroidogenesis of 3α,5α-THP in the VTA for lordosis, independent of peripheral glands. We assessed the role of

PXR, and TSPO manipulations in different hormonal contexts (i.e., over the estrous cycle with extirpation of the ovaries and/or adrenal glands). First, proestrous rats were administered a TSPO blocker (PK11195) and/or 3α,5α-THP following infusions of PXR antisense oligonucleotides (AS-ODNs) or vehicle to the VTA in Experiment 1. We aimed to determine the extent to which the TSPO inhibitor may have effects similar to PXR knockdown and whether this may be reversed with 3α,5α-THP replacement. Second, proestrous (Experiment 2), ovariectomized (OVX; Experiment 3), or ovariectomized/adrenalectomized (OVX/ADX; Experiment 4) rats were infused with a TSPO enhancer (FGIN 1–27) subsequent to AS-ODNs or vehicle to the VTA. We aimed to determine the extent to which the TSPO enhancer may reverse effects of PXR knockdown and whether this may be related to hormonal milieu. Results from these experiments supported the notion that PXR (traditionally considered a liver factor), may be upstream of TSPO, acting as a homeostatic regulator involved in neurosteroidogenesis of 3α,5α-THP in the brain and behavioral plasticity.

MATERIALS AND METHODS

SUBJECTS AND HOUSING

Adult, Long–Evans female rats ($n = 236$), approximately 55 days of age, were bred in the Life Sciences Laboratory Animal Care Facility at The University at Albany–SUNY (original stock: Taconic Farms, Germantown, NY, USA) and/or shipped from Taconic. Rats were group-housed in polycarbonate cages with woodchip bedding (45 × 24× 21 cm) in a temperature- (21 ± 1°C) and humidity- (50 ± 5%) controlled room in the Laboratory Animal Care Facility. Rats were maintained on a 12:12 h reversed light cycle (lights off at 0800 hours) with continuous access to Purina Rat Chow and tap water in their home cages.

GENERAL PROCEDURE

Four experiments were run, using a between- and within-subjects design. All experimental rats had stereotaxic surgery to implant cannulae aimed at the VTA, 7 days before drug manipulations were initiated. Experimental rats were randomly-assigned to one treatment condition (between-subjects) within a single experiment, and then were tested in a single battery of behavioral tasks (within-subjects). The general procedure utilized is depicted in **Figure 1**. All experimental techniques in rats were approved by the Institutional Animal Care and Use Committee at the University at Albany, where the experiments were conducted.

SURGICAL MANIPULATIONS

All rats in Experiments 1–4 were stereotaxically implanted with bilateral guide cannulae aimed at the VTA (from bregma: AP = −5.3, ML = ±0.4, DV = −7.0; Paxinos and Watson, 1986) under xylazine (12 mg/kg) and ketamine (80 mg/kg) anesthesia per prior methods (Frye et al., 2013). Immediately following stereotaxic surgery, rats were OVX ($n = 49$; Experiment 3) and/or OVX/ADX ($n = 48$; Experiment 4). For OVX/ADX, dorsal incisions were made between the ribs and hip, so that the ovaries and the adrenals could be isolated. The ovaries were ligated and removed, and the adrenals were isolated and removed. As ADX rats are sodium deficient, all rats received a bottle of 0.9% saline and a bottle of tap water in their home cages to maintain water/salt balance. Following surgery and prior to testing, animals were monitored for loss of weight, righting response, flank stimulation response, and/or muscle tone. Only rats that passed neurological evaluations and gained weight following surgery until behavioral testing commenced were continued in the experiment. All rats that underwent ADX were validated to have complete ADX surgery via *post-hoc* assessment of corticosterone in plasma. Rats were administered ibuprofen (once per oral, and daily in

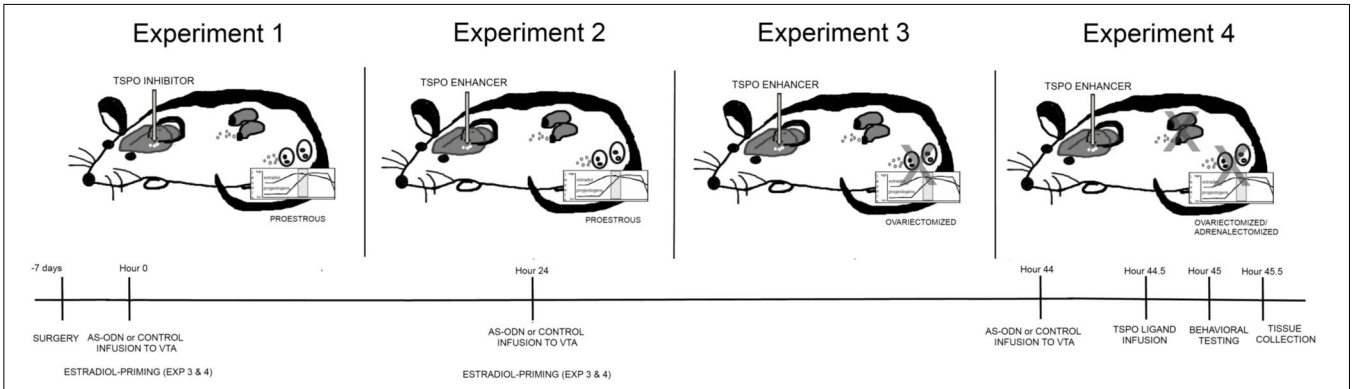

FIGURE 1 | Depicts different hormonal conditions and TSPO ligand infusions in rats (top) and timeline of experimental protocol (bottom). In Experiment 1, all rats were in the proestrous phase of the estrous cycle and administered via infusions to the VTA, placebo or PXR AS-ODNs (at hour 0, 24, and 44), followed by an inhibitor of TSPO (PK11195) or saline vehicle and/or 3α,5α-THP (at hour 44.5). In Experiment 2, all rats were in the proestrous phase of the estrous cycle and administered via infusions to the VTA, placebo or PXR AS-ODNs (at hour 0, 24, and 44), followed by an enhancer of TSPO (FGIN) or saline vehicle (at hour 44.5). In Experiment 3, all rats were ovariectomized (OVX) and administered subcutaneous injections of E_2 at hour 0 and 24 and then administered via infusions to the VTA, placebo or PXR AS-ODNs (at hour 0, 24, and 44), followed by an enhancer of TSPO (FGIN) or saline vehicle (at hour 44.5). In Experiment 4, all rats were OVX and adrenalectomized (OVX/ADX), and administered subcutaneous injections of E_2 at hour 0 and 24 and then administered via infusions to the VTA, placebo or PXR AS-ODNs (at hour 0, 24, and 44), followed by an enhancer of TSPO (FGIN) or saline vehicle (at hour 44.5). All rats were tested at hour 45, and euthanized for tissue collection immediately after behavioral testing was complete. In all experiments, knockdown of PXR expression in the VTA was validated and levels of 3α,5α-THP were measured in the midbrain.

the recovery period in drinking water; 30 mg/kg) as post-surgical analgesia.

ESTROUS CYCLE

Vaginal epithelium of each rat was collected and examined daily under a light microscope (between 0800–1000). Rats were cycled through two normal estrous cycles (4–5 days cycle) prior to testing. Rats were tested on proestrus (epithelium characterized by nucleated cells, 4–5 days after the previous occurrence) for Experiments 1 ($n = 68$) and 2 ($n = 71$).

INFUSIONS

For Experiments 1–4, rats received either sterile saline (0.9% w/v) or PXR AS-ODN infusions. AS-ODNs by (5′ CTTGCGGAAGGGGCACCTCA 3′; made in a concentration of 100 ng/μl; Frye et al., 2012, 2013, 2014, in press) were synthesized and desalted Invitrogen Life Technologies (Carlsbad, CA). This PXR AS-ODN strategy decreases expression of PXR in the midbrain, as measured by quantitative polymerase chain reaction (qPCR) (which was utilized here to validate) and western blotting (Frye, 2011; Frye et al., 2012, 2013). In Experiment 1, PK11195 (Tocris Biosciences, R&D Systems, Minneapolis, MN) was utilized as a TSPO antagonist (compounded by adding crystalline drug to sterile saline at a concentration of 50 ng per μl; Bitran et al., 2000; Frye et al., 2006, 2009). 3α,5α-THP (purchased from Dr. Robert Purdy, Scripps Institute, CA) was prepared to a concentration of 100 ng per μl in β-cyclodextran (with 5% concentration of β-cyclodextran in sterile water; Frye and Rhodes, 2006; Frye et al., 2008a, 2014). In Experiments 2–4, a neurosteroidogenesis enhancer, FGIN 1–27, an agonist of TSPO was utilized (Petralia and Frye, 2005; Frye et al., 2009, used in Experiments 2–4). Crystalline FGIN was compounded in a concentration of 50 ng per μl (Tocris) in sterile saline. Rats received bilateral infusions of each compound or placebo vehicle. This infusion protocol has been utilized without any indication of damaging effects as assessed by behavioral changes, or estradiol levels (given damage can induce aromatase activity, and thereby local estradiol levels; Azcoitia et al., 2003); this was determined by comparing rats that were sham surgerized, had stereotaxic implantation of cannulae to the VTA, but were not administered infusions, and those that were administered infusions of saline vehicle in the same volumes as drugs are administered (Frye et al., 2013).

ESTRADIOL PRIMING

For Experiment 3 and 4, OVX and OVX/ADX rats were primed with subcutaneous administration of estradiol(10 μg in 0.2 cc vegetable oil) at 0 and 24 h before behavioral testing.

BEHAVIORAL MEASURES

Our primary interest was in the role of PXR and TSPO for reproductive responding (as measured in the paced mating task); however, control measures of exploration, anxiety, and social interaction were also collected. Behavioral data were simultaneously collected by using the Any-maze behavioral assessment computer program (Stoelting Inc., Wood Lawn, IL; for open field, elevated plus maze, and social interaction) or a digital video camera (for paced mating) and trained experimenters.

Control measures- exploration, anxiety, non-sexual social interaction

Immediately before assessment in the paced mating task, rats were tested sequentially in the open field for 5 min, the elevated plus maze for 5 min, and the social interaction tasks, as per established methods (see Frye et al., 2013). Across experiments, there were no differences between comparisons groups in rats that were tested for exploratory behavior in the open field, anxiety behavior in the elevated plus maze, or social interaction with a female conspecific.

Paced mating

Paced mating was conducted per previous methods (Erskine, 1985; Frye et al., 2013) in an apparatus (37.5 × 75 × 30 cm) that was divided down the center by a Plexiglas partition. An experimental female has access to both sides of the pacing chamber, while a stimulus male was confined to one side for a 15-min test period. Standard measures of mating behavior (lordosis quotients, proceptivity quotients, and aggression quotients) are being reported herein. Lordosis quotients are the percentage of total number of lordosis responses per total number of sexual contacts by the male. Aggression/rejection (aggression quotients) are defined as behaviors such as boxing and kicking the male during contacts.

TISSUE COLLECTION AND PREPARATION

Immediately after testing, rats were euthanized by rapid decapitation and whole brain and trunk blood was collected, frozen, and stored in a freezer. For brain dissections, punches from the midbrain, around the VTA, were taken from coronal frozen slices (approximately 60 microns thick), made anterior and posterior to the VTA, and used for analyses of PXR expression (described below). At this time of collecting these slices, whether cannulae/infusion tracks were aimed at the VTA was determined (as per Frye et al., 2013, 2014). There were a total of $n = 17$ rats that had placement outside of the VTA; their data was excluded from analyses of the data from rats with placement to the VTA. Not all experimental groups were represented in rats that had missed sites, precluding systematic analyses of the data from these rats to those with placement to the VTA. However, in comparing the data available, the pattern that emerged was that rats with placement outside of the VTA had responses similar to control groups.

VALIDATION OF PXR KNOCKDOWN FOLLOWING PXR AS-ODNs

Standard qPCR methods were utilized on VTA punches to determine whether PXR AS-ODN infusions reduced PXR expression (described in Frye et al., 2013, 2014). Data were analyzed by comparing PXR values to actin control, and PXR expression is described as fold-change of the rats infused with PXR AS-ODNs to those infused with control (saline; Livak and Schmittgen, 2001; Schmittgen and Livak, 2008; Frye et al., 2013, 2014).

STEROID HORMONE MEASUREMENT

Plasma levels of corticosterone, estradiol, and progesterone were measured to validate adequacy of ADX, estrous cycle stage and/or OVX and hormone-priming, respectively. Concentrations of corticosterone, estradiol, progesterone and 3α,5α-THP were assessed using standard steroid extraction and radioimmunoassay (primarily for corticosterone and 3α,5α-THP) or

commercially-available enzyme-linked immunosorbent assays (estradiol, progesterone) techniques used by our laboratory (Frye and Bayon, 1999; Frye et al., 2008a, 2013, 2014, in press). Concentrations were determined for each sample based upon concurrent standard curves run in duplicate for each of the assays. Concentrations reflect the approximate concentrations of the volume of plasma, or protein concentrations determined in midbrain homogenate samples measured by a NanoDrop spectrometer.

STATISTICAL ANALYSES

Analyses of variances (ANOVAs) were used to examine effects of PXR AS-ODN condition (control, PXR AS-ODN), PK11195 condition (control, PK11195) and 3α,5α,-THP condition (β-cyclodextrin, 3α,5α,-THP for Experiment 1) and for Experiment 2–4, PXR AS-ODN condition (control, PXR AS-ODN) and FGIN condition (control, FGIN), and/or testing condition (non tested, tested) on behavioral and endocrine measures. The assumptions of homogeneity of variance were supported, suggesting that parametric ANOVA tests be utilized as the most appropriate statistic across experiments. When the α level for statistical significance was reached ($p = 0.05$) for main effects and interactions, Fisher's Least Significant Differences *post-hoc* tests were used to determine group differences.

RESULTS

EXPERIMENT 1: EFFECTS OF TSPO BLOCKER, PK11195, IN PROESTROUS RATS

Validation of PXR AS-ODNs for PXR expression in the midbrain

Rats infused with PXR AS-ODN had 1.5 fold lower PXR expression in the midbrain VTA compared to rats infused with control condition [$F_{(1,29)} = 11.9, P < 0.001$].

3α,5α-THP levels in the midbrain (Figure 2A)

There was significant interaction between PXR AS-ODN condition and 3α,5α-THP condition [$F_{(1,\ 60)} = 10.7,\ P < 0.002$] for 3α,5α-THP levels in the midbrain VTA, such that control rats infused with 3α,5α-THP had higher levels of 3α,5α-THP levels in the midbrain compared to PXR AS-ODN infusions. There were significant main effects of PXR AS-ODN [$F_{(1,\ 60)} = 29.7,\ P < 0.0001$], 3α,5α-THP [$F_{(1,\ 60)} = 13.1,\ P = 0.0007$], and PK11195 [$F_{(1,\ 60)} = 7.3,\ P = 0.01$] conditions for 3α,5α-THP levels in the midbrain. Infusions of PXR AS-ODNs reduced, 3α,5α-THP increased, and PK11195 reduced 3α,5α-THP levels in midbrain compared to control infusions for each manipulation.

Lordosis quotients (Figure 2B)

There was an interaction between 3α,5α-THP condition and PK11195 condition [$F_{(1,\ 60)} = 11.4,\ P = 0.001$] for lordosis quotients, such that PK11195 reduced lordosis quotients, but not when co-administered with 3α,5α-THP. There was significant interaction between PXR AS-ODN condition and 3α,5α-THP condition [$F_{(1,\ 60)} = 4.7,\ P = 0.03$] for lordosis quotients, such that control rats infused with 3α,5α-THP had increased lordosis quotients, but not when co-administered PXR AS-ODNs. There was a significant main effect of PXR AS-ODN condition [$F_{(1,\ 60)} = 12.5,\ P = 0.0008$] to reduce lordosis quotients compared to those infused with control.

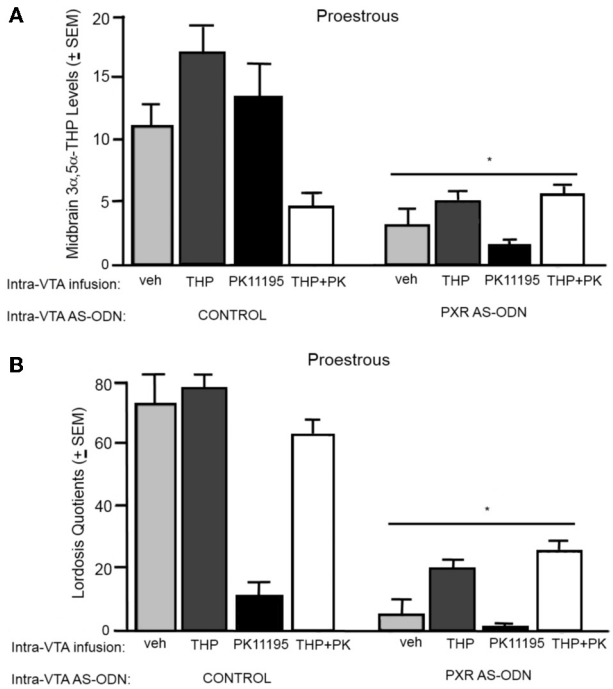

FIGURE 2 | (A) Depicts the mean (+s.e.m.) 3α,5α-THP levels in the midbrain of proestrous rats infused first with control and vehicle (veh, n = 5), 3α,5α-THP ($n = 7$), PK11195 ($n = 12$), PK11195+3α,5α-THP ($n = 11$), or pregnane xenobiotic receptor (PXR) antisense deoxynucleotides (AS-ODNs) and veh ($n = 10$), PXR AS-ODN +3α,5α-THP ($n = 8$), PXR AS-ODN+ PK11195 ($n = 7$), PXR AS-ODN + PK11195+ 3α,5α-THP ($n = 8$) in Experiment 1. **(B)** Depicts the mean (+s.e.m.) lordosis quotient of proestrous rats in these conditions. Rats infused with PXR AS-ODN had a mean 1.5 fold lower PXR expression in the midbrain compared to control infusions in Experiment 1 (data not shown). *above a line indicates a significant effect of PXR AS-ODNs compared to control infusion ($P < 0.05$). *above a bar indicates a significant effect of PK11195 and PK1195+3α,5α-THP compared to vehicle infusions ($P < 0.05$).

Aggression quotients (Table 1)

There was significant main effect of PXR AS-ODN condition [$F_{(1,\ 60)} = 19.9,\ P = 0.0003$] and PK11195 condition [$F_{(1,\ 60)} = 3.9,\ P = 0.05$] for aggression quotients. Rats infused with PXR AS-ODN or PK11195 had increased aggression quotients compared to respective control infusions.

EXPERIMENT 2: EFFECTS OF TSPO ENHANCER, FGIN 1–27, IN PROESTROUS RATS

Validation of PXR AS-ODNs for PXR expression in the midbrain

Rats infused with PXR AS-ODN had 1.8 fold lower PXR expression in the midbrain VTA compared to rats administered control infusions [$F_{(1,\ 37)} = 36.4, P < 0.0001$].

3α,5α-THP levels in the midbrain (Figure 3A)

There was a significant main effect of PXR AS-ODN condition [$F_{(1,\ 52)} = 14.4,\ P = 0.0004$] for 3α,5α-THP levels in the midbrain. Rats infused with PXR AS-ODN had significantly lower

Table 1 | Depicts mean (± s.e.m.) aggression quotients (AQ) of rats during the paced mating task In Experiments 1–4.

EXPERIMENT 1								
Hormone condition	Proestrous							
AS-ODN condition	Control				PXR AS-ODN			
Infusion condition	Veh	3α,5α-THP	PK11195	PK11195 + 3α,5α-THP	Veh	3α,5α-THP	PK11195	PK11195 + 3α,5α-THP
AQ	33.9 ± 10.6	14.4^ ± 8.8	49.2 ± 9.1	12.5 ± 5.1	51.8* ± 18.2	37.9*^ ± 7.5	58.3* ± 8.3	46.4* ± 9.7
EXPERIMENT 2								
Hormone condition	Proestrous							
AS-ODN condition	Control				PXR AS-ODN			
FGIN condition	Veh		FGIN		Veh		FGIN	
AQ	26.5 ± 9.0		30.9 ± 7.6		34.2 ± 12.6		46.5 ± 9.2	
EXPERIMENT 3								
Hormone condition	OVX, E_2-primed							
AS-ODN condition	Control				PXR AS-ODN			
FGIN condition	Veh		FGIN		Veh		FGIN	
AQ	40.6 ± 11.6		74.2 ± 10.4		75.2 ± 12.1		66.2 ± 7.9	
EXPERIMENT 4								
Hormone condition	OVX/ADX, E_2-primed							
AS-ODN condition	Control				PXR AS-ODN			
FGIN condition	Veh		FGIN		Veh		FGIN	
AQ	39.6 ± 12.9		23.0 ± 10.1		61.1* ± 10.3		66.6* ± 16.0	

** Indicates a significant difference of pregnane xenobiotic receptor (PXR) PXR antisense oliodeoxynucleotides (AS-ODN) from control (P > 0.05).*

^ Indicates significant interaction between AS-ODN, PK11195, and 3 α, 5 α-THP (P > 0.05).

3α,5α-THP in the midbrain compared to those infused with control; effects of testing and FGIN infusions did not reach statistical significance.

Lordosis Quotients (Figure 4A)

There was a significant interaction between PXR AS-ODN condition and FGIN condition [$F_{(1,\ 47)} = 3.8$, $P < 0.05$] for lordosis quotients, such that PXR AS-ODNs reduced lordosis, but not when co-administered with FGIN. There was a significant main effect of PXR AS-ODN condition [$F_{(1,\ 47)} = 3.8$, $P = 0.05$] for lordosis quotients. Rats infused with PXR AS-ODN had significantly lower lordosis quotients compared to those infused with control condition.

Aggression quotients (Table 1)

There were no statistically significant effects of conditions for aggression quotients in this experiment.

EXPERIMENT 3: EFFECTS OF TSPO ENHANCER, FGIN 1–27, IN OVX RATS

Validation of PXR AS-ODNs for PXR expression in the midbrain

Rats infused with PXR AS-ODN had 1.5 fold lower PXR expression in the midbrain VTA compared to control infusions [$F_{(1,\ 41)} = 14.2$, $P = 0.0005$].

3α,5α-THP levels in the midbrain (Figure 3B)

There was a main effect for testing condition [$F_{(1,\ 41)} = 16.9$, $P = 0.002$] for 3α,5α-THP levels in the midbrain, such that tested rats had higher levels of 3α,5α-THP inmidbrain compared to non-tested rats; effects of PXR AS-ODN and FGIN infusions did not reach statistical significance.

Lordosis quotients (Figure 4B)

There was a significant main effect of PXR AS-ODN condition [$F_{(1,\ 24)} = 18.9$, $P = 0.0002$] and FGIN condition [$F_{(1,\ 24)} = 9.3$, $P = 0.005$] for lordosis quotients. Rats infused with PXR AS-ODN had significantly lower, and those infused with FGIN had significantly higher, lordosis quotients, compared to those infused with respective control conditions.

Aggression quotients (Table 1)

There were no significant main effects for AS-ODN condition or FGIN condition for aggression quotients.

EXPERIMENT 4: EFFECTS OF TSPO ENHANCER, FGIN 1–27, IN OVX/ADX RATS

Validation of PXR AS-ODNs for PXR expression in the midbrain

Rats infused with PXR AS-ODN had 1.4 fold lower PXR expression in the midbrain VTA compared to control infusions [$F_{(1,\ 24)} = 6.4$, $P = 0.01$].

3α,5α-THP levels in the midbrain (Figure 3C)

There was main effect of testing condition [$F_{(1,\ 38)} = 10.3$, $P = 0.002$] and PXR AS-ODN condition [$F_{(1,\ 38)} = 4.4$, $P = 0.04$] for 3α,5α-THP levels in the midbrain. Tested rats had higher levels of 3α,5α-THP in midbrain compared tonon-tested rats, and rats

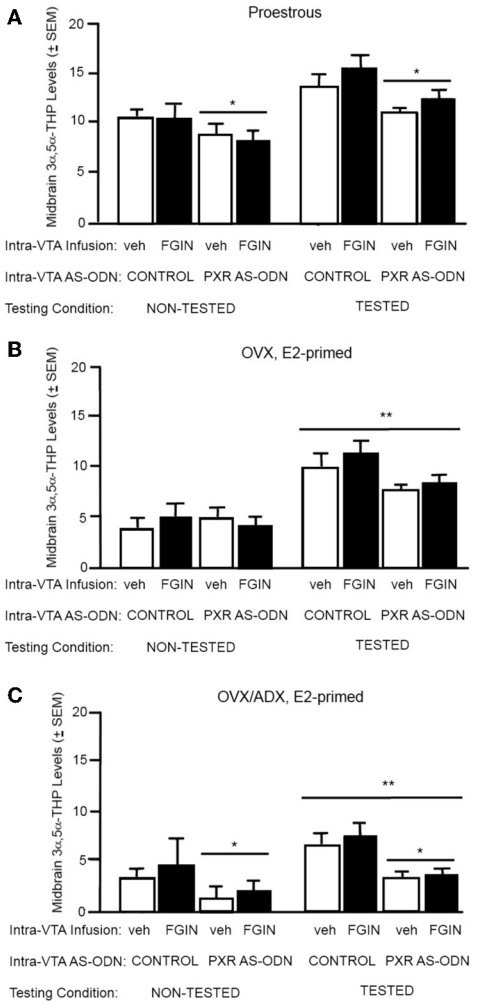

FIGURE 3 | (A) Depicts the mean (±s.e.m.) 3α,5α-THP levels in the midbrain of proestrous non tested rats infused with control and vehicle (veh, $n = 5$) or control+FGIN ($n = 4$), or pregnane xenobiotic receptor (PXR) antisense deoxynucleotides (AS-ODNs) and veh ($n = 6$), or PXR AS-ODN+FGIN ($n = 6$) or behaviorally-tested rats infused with control+veh ($n = 15$), control+FGIN ($n = 15$), PXR AS-ODN+veh ($n = 8$), or PXR AS-ODN+FGIN ($n = 13$) in Experiment 2. Rats infused with PXR AS-ODN had a mean 1.8 fold lower PXR expression in the midbrain compared to control infusions in Experiment 2 (data not shown). **(B)** Depicts the mean (±s.e.m.) 3α,5α-THP levels in the midbrain of ovariectomized (OVX) estradiol (E2)-primed non tested rats infused with control+veh ($n = 5$), control+FGIN ($n = 6$), PXR AS-ODN+veh ($n = 5$), PXR AS-ODN+FGIN ($n = 5$), or behaviorally-tested rats infused with control+veh ($n = 8$), control+FGIN ($n = 7$), PXR AS-ODN+veh ($n = 7$), or PXR AS-ODN+FGIN ($n = 6$) in Experiment 3. Rats infused with PXR AS-ODN had a mean 1.5 fold lower PXR expression in the midbrain compared to control infusions in Experiment 3 (data not shown). **(C)** Depicts the mean (±s.e.m.) 3α,5α-THP levels in the midbrain of OVX/adrenalectomized (ADX), E2-primed rats that were non tested and infused with control+veh ($n = 6$), control+FGIN ($n = 5$), PXR AS-ODN+veh ($n = 5$), PXR AS-ODN+FGIN ($n = 5$), or behaviorally-tested and infused with control+veh ($n = 9$), control+FGIN ($n = 5$), PXR AS-ODN+veh ($n = 8$), or PXR AS-ODN+FGIN ($n = 5$) in Experiment 4. Rats infused with PXR AS-ODN had a mean 1.4 fold lower PXR expression in the midbrain compared to control infusions in Experiment 4 (data not shown). *above a line indicates a significant effect of PXR AS-ODNs compared to control. **above a line indicates significant effect of testing compared to non-tested rats ($P < 0.05$).

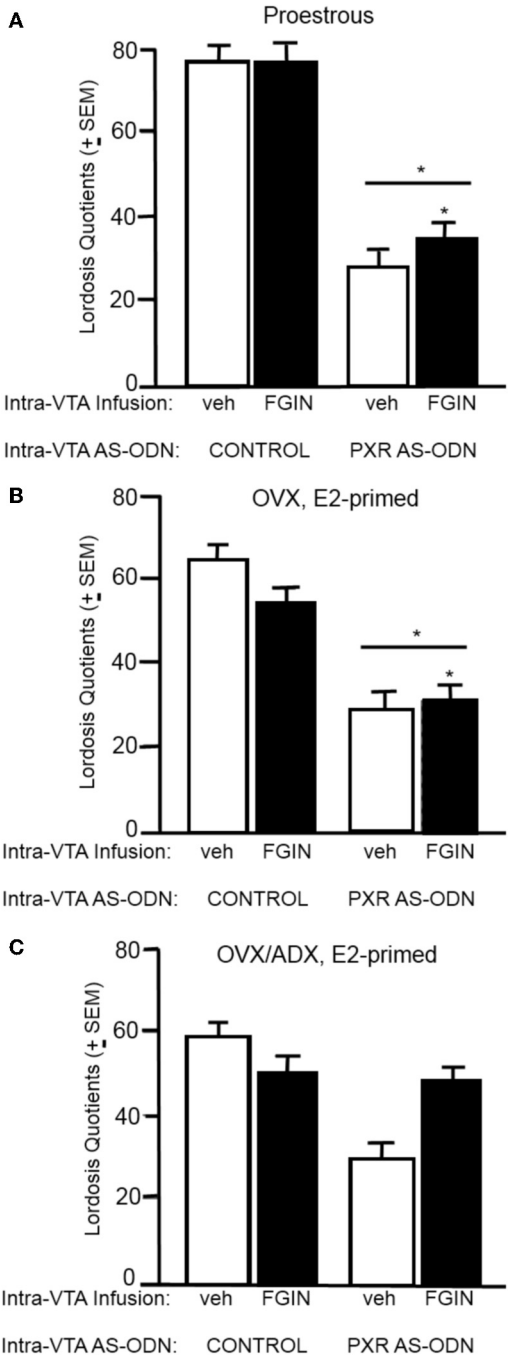

FIGURE 4 | (A) Depicts the mean (±s.e.m.) lordosis quotients of proestrous rats infused with control and vehicle (veh, $n = 15$), control+FGIN ($n = 15$), pregnane xenobiotic receptor (PXR) antisense deoxynucleotides (AS-ODNs)+vehicle ($n = 8$), or PXR AS-ODN+FGIN ($n = 13$) in Experiment 2. **(B)** Depicts the mean (±s.e.m.) lordosis quotients of ovariectomized (OVX) estradiol (E2)-primed rats infused with control+veh ($n = 8$), control+FGIN ($n = 7$), PXR AS-ODN+veh ($n = 7$), or PXR AS-ODN+FGIN ($n = 6$) in Experiment 3. **(C)** Depicts the mean (±s.e.m.) lordosis quotients of OVX/adrenalectomized (ADX), E2-primed rats infused with control+veh ($n = 9$), control+FGIN ($n = 5$), PXR AS-ODN+veh ($n = 8$), or PXR AS-ODN+FGIN ($n = 5$) in Experiment 4. *above a line indicates a significant effect of PXR AS-ODNs compared to control. ($P < 0.05$).

infused with PXR AS-ODNs had lower levels compared to control infusions.

Lordosis quotients (Figure 4C)

There was main effect of PXR AS-ODN condition [$F_{(1, 25)} = 5.8$, $P = 0.02$] for lordosis quotients, such that infusions of PXR AS-ODN decreased lordosis quotients compared to control infusions; effects of FGIN infusions did not reach statistical significance.

Aggression quotients (Table 1)

There was main effect of PXR AS-ODN condition [$F_{(1, 25)} = 4.9$, $P = 0.03$] for aggression quotients, such that infusions of PXR AS-ODN decreased aggression quotients compared to control infusions; effects of FGIN infusions did not reach statistical significance.

DISCUSSION

The data support, in part, the hypothesis tested that PXR is an upstream factor of TSPO for neurosteroidogenesis of 3α,5α-THP in the VTA for lordosis, independent of peripheral glands. First, proestrous rats administered a TSPO blocker (PK11195), subsequent to AS-ODNs to the VTA, had lower 3α,5α-THP levels in the midbrain and lordosis; the effects on lordosis could be reversed with replacement with 3α,5α-THP administration alone, but not when co-administered with PXR AS-ODN. Second, proestrous, OVX, or OVX/ADX rats infused with a TSPO enhancer (FGIN 1–27), subsequent to AS-ODNs to the VTA, had lower 3α,5α-THP levels in the midbrain and lordosis particularly among proestrous rats, compared to those that were OVX or OVX/ADX. Comparisons with removal of the main peripheral sources of steroids, ovaries and adrenals, were completed to address the role of PXR and TSPO for steroid synthesis in the brain. These data with a greater response in proestrous compared to rats with glands surgically removed suggest that there is not complete independence of these peripheral sources for PXR's actions in the midbrain VTA, which are likely upstream of TSPO. Thus, PXR may be acting as a homeostatic regulator, upstream of TSPO in the pathway for production of 3α,5α-THP in the midbrain VTA, and behavioral responses of female rats.

The present data confirm the importance of PXR in the midbrain for 3α,5α-THP and lordosis. Inhibiting PXR with the same AS-ODN approach used here reduces 3α,5α-THP in the midbrain VTA concomitant with reductions in lordosis and enhancements in aggressive responding toward males during paced mating of proestrous rats, or those that were OVX and estradiol-primed (Frye et al., 2013, 2014). Additionally, activating PXR with ligands infused to the midbrain VTA enhances reproductive responding of female rats (Frye, 2011). Moreover, the present data confirm the role of biosynthesis of 3α,5α-THP from cholesterol in the midbrain VTA for lordosis. Inhibitors of TSPO, as well as downstream factors involved in biosynthesis, StAR or P450scc, infused to the midbrain VTA of female rats attenuates progestogen-facilitated lordosis (Petralia et al., 2005; Frye et al., 2008a; Frye, 2009; Frye and Paris, 2011). An opposite effect is observed with TSPO agonist, such as FGIN, when infused to the midbrain VTA as was observed here (Frye et al., 2009; Frye and Paris, 2011).

It should be noted that FGIN infusions in this study did not produce the same pattern of reduction for 3α,5α-THP levels in the midbrain as was observed in lordosis quotients. A consideration is that this experiment was conducted in proestrous rats, with peripheral sources of steroids, as well as typical steroid feedback mechanisms in place; a more robust response may have been observed with this FGIN dosing in OVX and/or OVX/ADX rats. Another consideration is that comparisons with non-tested rats in this experiment may have provided an indication of mating-induced 3α,5α-THP production from metabolism of progesterone from the ovaries, which could account for little difference in 3α,5α-THP levels in the midbrain after mating, albeit low lordosis responding with this manipulation. A third consideration is that measurement of dihydroprogesterone, or other steroids, were not assessed in the midbrain. Indeed, in the group that was co-administered PK11195 and 3α,5α-THP, the enhancements in lordosis were more robust than post-mating levels of 3α,5α-THP on the midbrain that were measured; whether this could have been due to back-conversion of administered 3α,5α-THP or 3α,5α-THP from other sources is not known. Together, these data extends previous findings to suggest that PXR, which is known to act as a transcription factor for P450 enzymes involved in steroid metabolism, such as CYP11A1 (Ma et al., 2008; Zhang et al., 2008), may be another important neuroregulatory factor in the biosynthesis of 3α,5α-THP in the midbrain, upstream of TSPO, and resulting actions on lordosis in the adult. Moreover, the data that there were differences between proestrous, OVX, and OVX/ADX rats suggest that biosynthesis in the brain, as well as metabolism from peripheral sources of progesterone, are involved in PXR's modulation of 3α,5α-THP. Alternatively, the removal of the glands disrupts multiple negative feedback loops of steroids, and thereby disrupts typical responses to steroids for behavior. We have observed that effects of PXR AS-ODN infusions to reduce lordosis and 3α,5α-THP levels in the midbrain of OVX rats only when they were estradiol-primed (Frye et al., 2014). Thus, hormonal milieu provides a significant context for interactions between neuroendocrine and behavioral responses.

The pattern of results here confirms prior studies showing a greater influence of PXR knockdown in the midbrain for behavior in the paced mating task, compared to the other behavioral tasks assessed (even when the order of testing in these tasks is altered as in Frye et al., in press). There were very few animals that received infusions outside the targeted area, and all experimental groups were not represented. The data from these subjects suggest that manipulations to other midbrain sites (e.g., substantia nigra, or central gray) did not produce the same pattern of effects as did infusions to the VTA, but rather produced responses similar to the control groups. Manipulations of 3α,5α-THP from exposure to mating, or infusions of 3α,5α-THP directly to this the midbrain (but not substantia nigra or central gray), increase levels of 3α,5α-THP in corticolimbic structures and reduce anxiety-like responding; however, manipulations of PXR typically produce less robust effects on these other measures, as was observed here. A question for future studies is the expression patterns and actions of PXR beyond the midbrain for reproduction-relevant behaviors, such as cognition, exploration, anxiety, and interactions with conspecifics. Mating-induced neurosteroidogenesis

occurs beyond the midbrain to the hippocampus, cortex, and striatum (Frye and Rhodes, 2006; Frye et al., 2009). Indeed, we have observed that manipulating PXR in the midbrain of proestrous rats reduces 3α,5α-THP levels in the midbrain and the hippocampus, as well as a growth factor (brain-derived neurotrophic factor; BDNF) in the hippocampus (Frye et al., 2013, in press). It is plausible that PXR is having effects beyond those involving progestogen-facilitated lordosis through actions in the midbrain.

Beyond facilitating successful mating, progestogens are considered to have organizing effects on the nervous system during gestation/perinatally to influence later adult behaviors that ultimately are adaptive (reducing stress/anxiety, enhancing cognition, and conferring protection to neural insults/aging; Frye, 2009; Brinton, 2013; Brunton et al., 2014; Bali and Jaggi, 2014). We have focused on using lordosis as a bioassay to understand progestogens' mechanisms and effects in the central nervous system; albeit, other models support a role of progestogens for motivated, and cognitive processes. One example is mating-induced conditioned placed preference, where females will change their initial preference to spend time in a context associated with mating (González-Flores et al., 2004; Camacho et al., 2009; Arzate et al., 2011). Beneficial effects of progesterone or 3α,5α-THP administration to ovariectomized rats or mice has been described for spatial and object recognition memory tasks (Sandstrom and Williams, 2001; Tanabe et al., 2004; Walf et al., 2006; Frye et al., 2007, 2013). Furthermore, the capacity for *de novo* steroid synthesis in the prefrontal cortex and hippocampus (Cheng and Karavolas, 1975; Li et al., 1997; Furukawa et al., 1998; Frye, 2001a,b) suggests that PXR may also be a factor to investigate systematically in these regions for behaviors that contribute to successful mating. For example, in recent studies assessing the requirement of PXR for mating-induced 3α,5α-THP synthesis in the midbrain and the hippocampus, knocking down PXR attenuated effects of paced mating experience to increase 3α,5α-THP in these regions, as well as increase BDNF in the hippocampus, of proestrous rats (Frye et al., in press). Given the role of progestogens throughout the lifespan, the importance of PXR-mediated 3α,5α-THP production and other measures of neural plasticity (e.g., BDNF) and behavioral plasticity (e.g., mating) are of continued interest.

In addition to further understanding potential downstream factors, such as TSPO and BDNF, the contributory role of other "liver" factors in the same nuclear receptor super family as PXR, such as liver X receptor (LXR), for neural and behavioral plasticity needs to be explored. Although the present experiment focused on the role of PXR, it would be of interest to consider the respective roles of these factors, which were first described in the liver, but both have received a greater focus on their effects in the nervous system more recently (Mellon et al., 2008). One focus of the effects of these receptors is their role in cholesterol clearance, which is related to diet and cardiovascular function, as well as important for neurodegenerative disorders, such as Alzheimer's disease, and neurodevelopmental disorders, such as Niemann-Pick disease (Whitney et al., 2002; Repa et al., 2007; Ma et al., 2008; Tang et al., 2008). As one example, mouse models of Niemann-Pick disease show deficits in cholesterol metabolism and 3α,5α-THP production in the brain, and such deficits could be reversed with administration of PXR ligands, one of them being 3α,5α-THP (Frye and Rhodes, 2006; Frye, 2009; Brinton, 2013).

Early developmental effects of LXR in the brain have also been described. For example, protective effects similar to those described for PXR have been noted with LXR modulation in a Niemann-Pick disease mouse model (Repa et al., 2007) as well as promoting neurosteroidogenesis and protective effects in animal models of diabetic neuropathy and multiple sclerosis (Cermenati et al., 2010, 2012; Mitro et al., 2012). As well, the role of LXR in typical neurodevelopmental processes, such as neurogenesis, in the VTA of mice, using an *in vitro* model, has been recently described (Theofilopoulos et al., 2013). Additionally, knockout of the beta form of LXR that is highly expressed in the central nervous system increases anxiety-like responding of female mice and alters GABA in the cortex (Tan et al., 2012). In the present study, the role of PXR in the VTA for 3α,5α-THP production from cholesterol and subsequent behavioral effects was assessed. A consideration for future studies is elucidating how PXR and LXR may act synergistically for efficient cholesterol metabolism and clearance in neurons and glia, respectively, supporting neural and behavioral plasticity. Another important question is the role of PXR for neurosteroidogenesis in males; production of androstane neurosteroids, such as 3α-androstanediol, occurs after mating of male rodents and has robust behavioral actions (Edinger and Frye, 2007; Frye et al., 2008b). Although proestrous female rats have higher expression of PXR in the midbrain than do males (Frye et al., 2013), the expression of PXR in males and females in other brain regions with high capacity for neurosteroidogenesis is not completely known. Together, these results involving liver factors, such as PXR, substantiate further studies of an interaction between peripheral and brain factors for behavior.

In summary, inhibiting TSPO with PK11195 reduced 3α,5α-THP levels in the midbrain and lordosis, an effect that could be reversed with 3α,5α-THP administration, but not AS-ODN+3α,5α-THP. PXR AS-ODNs blocked actions of FGIN 1–27 for lordosis and 3α,5α-THP levels among proestrous > OVX > OVX/ADX rats. Together, these data suggest the liver factor, PXR, may be upstream of TSPO, acting as a homeostatic regulator involved in neurosteroidogenesis of 3α,5α-THP in the brain for behavior. Understanding these basic mechanisms of how steroids are involved, and what factors are necessary for their production, for behavioral/neural plasticity supports future work on how a prominent peripheral factor, such as PXR, may have actions in the brain and, ultimately, find use in brain augmentation approaches.

AUTHOR CONTRIBUTIONS

All authors on this paper substantially contributed to the work described herein. Carolyn J. Koonce was involved in acquisition, analysis, and interpretation of data, and drafting of figures for paper and Results and Methods section. Alicia A.Walf was involved in acquisition, analysis, and interpretation of data, and drafting and revising of all sections of the paper. Cheryl A. Frye was involved in the conception and study design, acquisition, analysis, and interpretation of data, reviewing drafts of the work, and giving final approval of the paper to be submitted.

ACKNOWLEDGMENTS

This research was supported by grants from the National Institute of Mental Health (MH0676980; RMH067698B). Technical assistance, provided by Drs. Paris and Rusconi, and Anthony Santarelli, Jennifer Torgersen, and Zhenhong Zhao, is greatly appreciated. Experiments described herein comply with the current laws of the United States. All authors report that they have no conflicts of interest (financial or otherwise) that would bias them to the outcome of these experiments.

REFERENCES

Acosta, S. A., Tajiri, N., Shinozuka, K., Ishikawa, H., Grimmig, B., Diamond, D., et al. (2013). Long-term upregulation of inflammation and suppression of cell proliferation in the brain of adult rats exposed to traumatic brain injury using the controlled cortical impact model. *PLoS ONE* 8:e53376. doi: 10.1371/journal.pone.0053376

Agís-Balboa, R. C., Pinna, G., Pibiri, F., Kadriu, B., Costa, E., and Guidotti, A. (2007). Down-regulation of neurosteroid biosynthesis in corticolimbic circuits mediates social isolation-induced behavior in mice. *Proc. Natl. Acad. Sci. U.S.A.* 104, 18736–18741. doi: 10.1073/pnas.0709419104

Arzate, D. M., Portillo, W., Rodríguez, C., Corona, R., and Paredes, R. G. (2011). Extended paced mating tests induces conditioned place preference without affecting sexual arousal. *Horm. Behav.* 59, 674–680. doi: 10.1016/j.yhbeh.2010.08.016

Azcoitia, I., Sierra, A., Veiga, S., and Garcia-Segura, L. M. (2003). Aromatase expression by reactive astroglia is neuroprotective. *Ann. N. Y. Acad. Sci.* 1007, 298–305. doi: 10.1196/annals.1286.028

Bali, A., and Jaggi, A. S. (2014). Multifunctional aspects of allopregnanolone in stress and related disorders. *Prog. Neuropsychopharmacol. Biol. Psychiatry* 48, 64–78. doi: 10.1016/j.pnpbp.2013.09.005

Barbaccia, M. L., Serra, M., Purdy, R. H., and Biggio, G. (2001). Stress and neuroactive steroids. *Int. Rev. Neurobiol.* 246, 243–272. doi: 10.1016/S0074-7742(01)46065-X

Bauer, B., Hartz, A. M., Fricker, G., and Miller, D.S. (2004). Pregnane X receptor up-regulation of P-glycoprotein expression and transport function at the blood-brain barrier. *Mol. Pharmacol.* 66, 413–419. doi: 10.1124/mol.66.3

Bauer, B., Yang, X., Hartz, A. M., Olson, E. R., Zhao, R., Kalvass, J. C., et al. (2006). *In vivo* activation of human pregnane X receptor tightens the blood-brain barrier to methadone through P-glycoprotein up-regulation. *Mol. Pharmacol.* 70, 1212–1219. doi: 10.1124/mol.106.023796

Billeci, A., Caso, V., Paciaroni, M., Palmerini, F., and Agnelli, G. (2007). Hormone-replacement therapy, dementia and stroke. *Womens Health* 3, 699–710. doi: 10.2217/17455057.3.6.699

Bitran, D., Foley, M., Audette, D., Leslie, N., and Frye, C. A. (2000). Activation of peripheral mitochondrial benzodiazepine receptors in the hippocampus stimulates allopregnanolone synthesis and produces anxiolytic-like effects in the rat. *Psychopharmacology* 151, 64–71. doi: 10.1007/s002130000471

Brinton, R. D. (2013). Neurosteroids as regenerative agents in the brain: therapeutic implications. *Nat. Rev. Endocrinol.* 9, 241–250. doi: 10.1038/nrendo.2013.31

Brunton, P. J., Russell, J. A., and Hirst, J. J. (2014). Allopregnanolone in the brain: Protecting pregnancy and birth outcomes. *Prog. Neurobiol.* 113, 106–136. doi: 10.1016/j.pneurobio.2013.08.005

Camacho, F. J., García-Horsman, P., and Paredes, R. G. (2009). Hormonal and testing conditions for the induction of conditioned place preference by paced mating. *Horm. Behav.* 56, 410–415. doi: 10.1016/j.yhbeh.2009.07.007

Cermenati, G., Abbiati, F., Cermenati, S., Brioschi, E., Volonterio, A., Cavaletti, G., et al. (2012). Diabetes-induced myelin abnormalities are associated with an altered lipid pattern: protective effects of LXR activation. *J. Lipid Res.* 53, 300–310. doi: 10.1194/jlr.M021188

Cermenati, G., Giatti, S., Cavaletti, G., Bianchi, R., Maschi, O., Pesaresi, M., et al. (2010). Activation of the liver X receptor increases neuroactive steroid levels and protects from diabetes-induced peripheral neuropathy. *J. Neurosci.* 30, 11896–11901. doi: 10.1523/JNEUROSCI.1898-10.2010

Chen, J., Chopp, M., and Li, Y. (1999). Neuroprotective effects of progesterone after transient middle cerebral artery occlusion in rat. *J. Neurol. Sci.* 171, 24–30. doi: 10.1016/S0022-510X(99)00247-6

Cheng, Y. J., and Karavolas, H. J. (1975). Subcellular distribution and properties of progesterone (delta4-steroid) 5a-reductase in rat medial basal hypothalamus. *J. Biol. Chem.* 250, 7997–8003.

Dussault, I., and Forman, B. M. (2002). The nuclear receptor PXR: a master regulator of "homeland" defense. *Crit. Rev. Eukaryot. Gene Expr.* 12, 53–64. doi: 10.1615/CritRevEukaryotGeneExpr.v12.i1.30

Edinger, K. L., and Frye, C. A. (2007). Sexual experience of male rats influences anxiety-like behavior and androgen levels. *Physiol. Behav.* 92, 443–453. doi: 10.1016/j.physbeh.2007.04.018

Erskine, M. S. (1985). Effects of paced coital stimulation on estrus duration in intact cycling rats and ovariectomized and ovariectomized-adrenalectomized hormone-primed rats. *Behav. Neurosci.* 99, 151–161. doi: 10.1037/0735-7044.99.1.151

Francis, G. A., Fayard, E., Picard, F., and Auwerx, J. (2002). Nuclear receptors and the control of metabolism. *Annu. Rev. Physiol.* 65, 261–311. doi: 10.1146/annurev.physiol.65.092101.142528

Frye, C. A. (2001a). The role of neurosteroids and nongenomic effects of progestins in the ventral tegmental area in mediating sexual receptivity of rodents. *Horm. Behav.* 40, 226–233. doi: 10.1006/hbeh.2001.1674

Frye, C. A. (2001b). The role of neurosteroids and non-genomic effects of progestins and androgens in mediating sexual receptivity of rodents. *Brain Res. Brain Res. Rev.* 37, 201–222. doi: 10.1016/S0165-0173(01)00119-9

Frye, C. A. (2009). Neurosteroids' effects and mechanisms for social, cognitive, emotional, and physical functions. *Psychoneuroendocrinology* 34, S143–S161. doi: 10.1016/j.psyneuen.2009.07.005

Frye, C. A. (2011). Novel substrates for, and sources of, progestogens for reproduction. *J. Neuroendocrinol.* 23, 961–973. doi: 10.1111/j.1365-2826.2011.02180.x

Frye, C. A., and Bayon, L. E. (1999). Mating stimuli influence endogenous variations in the neurosteroids 3α,5α-THP and 3α-Diol. *J. Neuroendocrinol.* 11, 839–847. doi: 10.1046/j.1365-2826.1999.00379.x

Frye, C. A., Duffy, C. K., and Walf,A. A. (2007). Estrogens and progestins enhance spatial learning of intact and ovariectomized rats in the object placement task. *Neurobiol. Learn. Mem.* 88, 208–216. doi: 10.1016/j.nlm.2007.04.003

Frye, C. A., Koonce, C. J., Edinger, K. L., Osborne, D. M., and Walf, A. A. (2008b). Androgens with activity at estrogen receptor beta have anxiolytic and cognitive-enhancing effects in male rats and mice. *Horm. Behav.* 54, 726–734. doi: 10.1016/j.yhbeh.2008.07.013

Frye, C. A., Koonce, C. J., and Walf, A. A. (2014). Role of pregnane xenobiotic receptor in the midbrain ventral tegmental area for estradiol- and 3α,5α-THP-facilitated lordosis of female rats. *Psychopharmacology*. doi: 10.1007/s00213-013-3406-0. [Epub ahead of print].

Frye, C. A., Koonce, C. J., and Walf, A. A. (in press). Involvement of pregnane xenobiotic receptor in mating-induced allopregnanolone formation in the midbrain and hippocampus and brain-derived neurotrophic factor in the hippocampus among female rats. *Psychopharmacology*. doi: 10.1007/s00213-014-3569-3

Frye, C. A., Koonce, C. J., Walf, A. A., and Rusconi, J. C. (2013). Motivated behaviors and levels of 3α,5α-THP in the midbrain are attenuated by knocking down expression of pregnane xenobiotic receptor in the midbrain ventral tegmental area of proestrous rats. *J. Sex. Med.* 10, 1692–1706. doi: 10.1111/jsm.12173

Frye, C. A., and Paris, J. J. (2011). Progesterone turnover to its 5α-reduced metabolites in the ventral tegmental area of the midbrain is essential for initiating social and affective behavior and progesterone metabolism in female rats. *J. Endocrinol. Invest.* 34, e188–e199. doi: 10.3275/7334

Frye, C. A., Paris, J. J., and Rhodes, M. E. (2008a). Exploratory, anti-anxiety, social, and sexual behaviors of rats in behavioral estrus is attenuated with inhibition of 3α,5α-THP formation in the midbrain ventral tegmental area. *Behav. Brain Res.* 193, 269–276. doi: 10.1016/j.bbr.2008.06.005

Frye, C. A., Paris, J. J., and Rhodes, M. E. (2009). Increasing 3α, 5α-THP following inhibition of neurosteroid biosynthesis in the ventral tegmental area reinstates anti-anxiety, social, and sexual behavior of naturally receptive rats. *Reproduction* 137, 119–128. doi: 10.1530/REP-08-0250

Frye, C. A., Paris, J. J., Walf, A. A., and Rusconi, J. C. (2012). Effects and mechanisms of 3α,5α,-THP on emotion, motivation, and reward functions involving pregnane xenobiotic receptor. *Front. Neurosci.* 195:136. doi: 10.3389/fnins.2011.00136

Frye, C. A., and Rhodes, M. E. (2006). Progestin concentrations are increased following paced mating in midbrain, hippocampus, diencephalon, and

cortex of rats in behavioral estrus, but only in midbrain of diestrous rats. *Neuroendocrinology* 83, 336–347. doi: 10.1159/000096051

Frye, C. A., Rhodes, M. E., Petralia, S. M., Walf, A. A., Sumida, K., and Edinger, K. L. (2006). 3alpha-hydroxy-5alpha-pregnan-20-one in the midbrain ventral tegmental area mediates social, sexual, and affective behaviors. *Neuroscience* 138, 1007–1014. doi: 10.1016/j.neuroscience.2005.06.015

Frye, C. A., and Walf, A. A. (2008). Membrane actions of progestins at dopamine type 1-like and GABAA receptors involve downstream signal transduction pathways. *Steroids* 73, 906–913. doi: 10.1016/j.steroids.2008.01.020

Furukawa, A., Miyatake, A., Ohnishi, T., and Ichikawa, Y. (1998). Steroidogenic acute regulatory protein (StAR) transcripts constitutively expressed in the adult rat central nervous system: colocalization of StAR, cytochrome P-450SCC (CYP XIA1), and 3β-hydroxysteroid dehydrogenase in the rat brain. *J. Neurochem.* 71, 2231–2238. doi: 10.1046/j.1471-4159.1998.71062231.x

Geick, A., Eichelbaum, M., and Burk, O. (2001). Nuclear receptor response elements mediate induction of intestinal MDR1 by rifampin. *J. Biol. Chem.* 276, 14581–14587. doi: 10.1074/jbc.M010173200

González-Flores, O., Camacho, F. J., Domínguez-Salazar, E., Ramírez-Orduna, J. M., Beyer, C., and Paredes, R. G. (2004). Progestins and place preference conditioning after paced mating. *Horm. Behav.* 46, 151–157. doi: 10.1016/j.yhbeh.2004.02.006

Harmsen, S., Meijerman, I., Beijnen, J. H., and Schellens, J. H. (2007). The role of nuclear receptors in pharmacokinetic drug-drug interactions in oncology. *Cancer Treat. Rev.* 33, 369–380. doi: 10.1016/j.ctrv.2007.02.003

He, J., Hoffman, S. W., and Stein, D. G. (2004). Allopregnanolone, a progesterone metabolite, enhances behavioral recovery and decreases neuronal loss after traumatic brain injury. *Restor. Neurol. Neurosci.* 22, 19–31.

King, S. R., Manna, P. R., Ishii, T., Syapin, P. J., Ginsberg, S. D., Wilson, K., et al. (2002). An essential component in steroid synthesis, the steroidogenic acute regulatory protein, is expressed in discrete regions of the brain. *J. Neurosci.* 22, 10613–10620.

Kinsley, C. H., and Lambert, K. G. (2008). Reproduction-induced neuroplasticity: natural behavioural and neuronal alterations associated with the production and care of offspring. *J. Neuroendocrinol.* 20, 515–525. doi: 10.1111/j.1365-2826.2008.01667.x

Kliewer, S. A., Goodwin, B., and Willson, T. M. (2002). The nuclear pregnane X receptor: a key regulator of xenobiotic metabolism. *Endocr. Rev.* 23, 687–702. doi: 10.1210/er.2001-0038

Lambert, K. G., Berry, A. E., Griffins, G., Amory-Meyers, E., Madonia-Lomas, L., Love, G., et al. (2005). Pup exposure differentially enhances foraging ability in primiparous and nulliparous rats. *Physiol. Behav.* 84, 799–806. doi: 10.1016/j.physbeh.2005.03.012

Li, X., Bertics, P. J., and Karavolas, H. J. (1997). Regional distribution of cytosolic and particulate 5a-dihydroprogesterone 3a-hydroxysteroid oxidoreductases in female rat brain. *J. Steroid Biochem. Mol. Biol.* 60, 311–318. doi: 10.1016/S0960-0760(96)00195-1

Livak, K. J., and Schmittgen, T. D. (2001). Analysis of relative gene expression data using real-time quantitative PCR and the 2(-Delta Delta C(T)). *Methods* 25, 402–408. doi: 10.1006/meth.2001.1262

Ma, X., Idle, J. R., and Gonzalez, F. J. (2008). The pregnane X receptor: from bench to bedside. *Expert Opin. Drug Metab. Toxicol.* 4, 895–908. doi: 10.1517/17425255.4.7.895

Macbeth, A. H., and Luine, V. N. (2010). Changes in anxiety and cognition due to reproductive experience: a review of data from rodent and human mothers. *Neurosci. Biobehav. Rev.* 34, 452–467. doi: 10.1016/j.neubiorev.2009.08.011

Maki, P. M., and Henderson, V. W. (2012). Hormone therapy, dementia, and cognition: the Women's Health Initiative 10 years on. *Climacteric* 15, 256–262. doi: 10.3109/13697137.2012.660613

Mellon, S. H., and Deschepper, C. F. (1993). Neurosteroid biosynthesis: genes for adrenal steroidogenic enzymes are expressed in the brain. *Brain Res.* 629, 283–292. doi: 10.1016/0006-8993(93)91332-M

Mellon, S. H., Gong, W., and Schonemann, M. D. (2008). Endogenous and synthetic neurosteroids in treatment of Niemann-Pick Type C disease. *Brain Res. Rev.* 57, 410–420. doi: 10.1016/j.brainresrev.2007.05.012

Mitro, N., Cermenati, G., Giatti, S., Abbiati, F., Pesaresi, M., Calabrese, D., et al. (2012). LXR and TSPO as new therapeutic targets to increase the levels of neuroactive steroids in the central nervous system of diabetic animals. *Neurochem. Int.* 60, 616–621. doi: 10.1016/j.neuint.2012.02.025

Murphy, S. J., Littleton-Kearney, M. T., and Hurn, P. D. (2002). Progesterone administration during reperfusion, but not preischemia alone, reduces injury in ovariectomized rats. *J. Cereb. Blood Flow Metab.* 22, 1181–1188. doi: 10.1097/00004647-200210000-00005

Ott, M., Fricker, G., and Bauer, B. (2009). Pregnane X receptor (PXR) regulates P-glycoprotein at the blood-brain barrier: functional similarities between pig and human PXR. *J. Pharmacol. Exp. Ther.* 329, 141–149. doi: 10.1124/jpet.108.149690

Papadopoulos, V., Baraldi, M., Guilarte, T. R., Knudsen, T. B., Lacapère, J. J., Lindemann, P., et al. (2006). Translocator protein (18kDa): new nomenclature for the peripheral-type benzodiazepine receptor based on its structure and molecular function. *Trends Pharmacol. Sci.* 27, 402–409. doi: 10.1016/j.tips.2006.06.005

Paris, J. J., and Frye, C. A. (2008). Estrous cycle, pregnancy, and parity enhance performance of rats in object recognition or object placement tasks. *Reproduction* 136, 105–115. doi: 10.1530/REP-07-0512

Paxinos, G., and Watson, C. (1986). *The Rat Brain*. New York, NY: Academic Press.

Petralia, S. M., and Frye, C. A. (2005). In the ventral tegmental area picrotoxin blocks FGIN 1-27-induced increases in sexual behavior of rats and hamsters. *Psychopharmacology* 178, 174–182. doi: 10.1007/s00213-004-2001-9

Petralia, S. M., Jahagirdar, V., and Frye, C. A. (2005). Inhibiting biosynthesis and/or metabolism of progestins in the ventral tegmental area attenuates lordosis of rats in behavioural oestrus. *J. Neuroendocrinol.* 17, 545–552. doi: 10.1111/j.1365-2826.2005.01342.x

Pinna, G., Agis-Balboa, R. C., Pibiri, F., Nelson, M., Guidotti, A., and Costa, E. (2008). Neurosteroid biosynthesis regulates sexually dimorphic fear and aggressive behavior in mice. *Neurochem. Res.* 33, 1990–2007. doi: 10.1007/s11064-008-9718-5

Pinna, G., and Rasmusson, A. M. (2012). Up-regulation of neurosteroid biosynthesis as a pharmacological strategy to improve behavioural deficits in a putative mouse model of post-traumatic stress disorder. *J. Neuroendocrinol.* 24, 102–116. doi: 10.1111/j.1365-2826.2011.02234.x

Purdy, R. H., Morrow, A. L., Moore, P. H. Jr., and Paul, S. M. (1991). Stress-induced elevations of gamma-aminobutyric acid type A receptor-active steroids in the rat brain. *Proc. Natl. Acad. Sci. U.S.A.* 88, 4553–4557. doi: 10.1073/pnas.88.10.4553

Repa, J. J., Li, H., Frank-Cannon, T. C., Valasek, M. A., Turley, S. D., Tansey, M. G., and Dietschy, J. M. (2007). Liver X receptor activation enhances cholesterol loss from the brain, decreases neuroinflammation, and increases survival of the NPC1 mouse. *J. Neurosci.* 27, 14470–14480. doi: 10.1523/JNEUROSCI.4823-07.2007

Roof, R. L., Duvdevani, R., and Stein, D. G. (1992). Progesterone treatment attenuates brain edema following contusion injury in male and female rats. *Restor. Neurol. Neurosci.* 4, 425–427.

Roof, R. L., Duvdevani, R., and Stein, D.G. (1993). Gender influences outcome of brain injury: progesterone plays a protective role. *Brain Res.* 607, 333–336. doi: 10.1016/0006-8993(93)91526-X

Rossouw, J. E., Anderson, G. L., Prentice, R. L., LaCroix, A. Z., Kooperberg, C., Stefanick, M. L., et al. (2002). Risks and benefits of estrogen plus progestin in healthy postmenopausal women: Principal results from the Women's Health Initiative randomized controlled trial. *JAMA* 288, 321–333. doi: 10.1001/jama.288.3.321

Sandstrom, N. J., and Williams, C. L. (2001). Memory retention is modulated by acute estradiol and progesterone replacement. *Behav. Neurosci.* 115, 384–393. doi: 10.1037/0735-7044.115.2.384

Schmittgen, T. D., and Livak, K. J. (2008). Analyzing real-time PCR data by the comparative C(T) method. *Nat. Protoc.* 3, 1101–1108. doi: 10.1038/nprot.2008.73

Shapiro, S. (2006). Risk of cardiovascular disease in relation to the use of combined postmenopausal hormone therapy: detection bias and resolution of discrepant findings in two Women's Health Initiative studies. *Climacteric* 9, 416–420. doi: 10.1080/13697130601012061

Shumaker, S. A., Legault, C., Rapp, S. R., Thal, L., Wallace, R. B., Ockene, J. K., et al. (2003). Estrogen plus progestin and the incidence of dementia and mild cognitive impairment in postmenopausal women: the Women's Health Initiative Memory Study: a randomized controlled trial. *JAMA* 289, 2651–2662. doi: 10.1001/jama.289.20.2651

Tan, X. J., Dai, Y. B., Wu, W. F., Warner, M., and Gustafsson, J. Å. (2012). Anxiety in liver X receptor β knockout female mice with loss of glutamic acid decarboxylase

in ventromedial prefrontal cortex. *Proc. Natl. Acad. Sci. U.S.A.* 109, 7493–7498. doi: 10.1073/pnas.1205189109

Tanabe, F., Miyasaka, N., Kubota, T., and Aso, T. (2004). Estrogen and progesterone improve scopolamine-induced impairment of spatial memory. *J. Med. Dent. Sci.* 51, 89–98.

Tang, W., Ma, Y., Jia, L., Ioannou, Y. A., Davies, J. P., and Yu, L. (2008). Niemann-Pick C1-like 1 is required for an LXR agonist to raise plasma HDL cholesterol in mice. *Arterioscler. Thromb. Vasc. Biol.* 28, 448–454. doi: 10.1161/ATVBAHA.107.160465

Theofilopoulos, S., Wang, Y., Kitambi, S. S., Sacchetti, P., Sousa, K. M., Bodin, K., et al. (2013). Brain endogenous liver X receptor ligands selectively promote midbrain neurogenesis. *Nat. Chem. Biol.* 9, 126–133. doi: 10.1038/nchembio.1156

Toung, T. J., Chen, T. Y., Littleton-Kearney, M. T., Hurn, P. D., and Murphy, S. J. (2004). Effects of combined estrogen and progesterone on brain infarction in reproductively senescent female rats. *J. Cereb. Blood Flow Metab.* 24, 1160–1166. doi: 10.1097/01.WCB.0000135594.13576.D2

Uphouse, L., Adams, S., Miryala, C. S., Hassell, J., and Hiegel, C. (2013). RU486 blocks effects of allopregnanolone on the response to restraint stress. *Pharmacol. Biochem. Behav.* 103, 568–572. doi: 10.1016/j.pbb.2012.09.024

Uphouse, L., Selvamani, A., Lincoln, C., Morales, L., and Comeaux, D. (2005). Mild restraint reduces the time hormonally primed rats spend with sexually active males. *Behav. Brain Res.* 157, 343–350. doi: 10.1016/j.bbr.2004.08.001

Walf, A. A., Rhodes, M. E., and Frye, C. A. (2006). Ovarian steroids enhance object recognition in naturally cycling and ovariectomized, hormone-primed rats. *Neurobiol. Learn. Mem.* 86, 35–46. doi: 10.1016/j.nlm.2006.01.004

Whitney, K. D., Watson, M. A., Collins, J. L., Benson, W. G., Stone, T. M., Numerick, M. J., et al. (2002). Regulation of cholesterol homeostasis by the liver X receptors in the central nervous system. *Mol. Endocrinol.* 16, 1378–1385. doi: 10.1210/mend.16.6.0835

Xu, D. X., Wei, W., Sun, M. F., Wei, L. Z., and Wang, J.P. (2005). Melatonin attenuates lipopolysaccharide-induced down-regulation of pregnane X receptor and its target gene CYP3A in mouse liver. *J. Pineal Res.* 38, 27–34. doi: 10.1111/j.1600-079X.2004.00171.x

Zhang, B., Xie, W., and Krasowski, M.D. (2008). PXR: a xenobiotic receptor of diverse function implicated in pharmacogenetics. *Pharmacogenomics* 9, 1695–1709. doi: 10.2217/14622416.9.11.1695

Conflict of Interest Statement: The authors declare that the research was conducted in the absence of any commercial or financial relationships that could be construed as a potential conflict of interest.

Received: 23 January 2014; accepted: 31 March 2014; published online: 21 April 2014. Citation: Frye CA, Koonce CJ and Walf AA (2014) The pregnane xenobiotic receptor, a prominent liver factor, has actions in the midbrain for neurosteroid synthesis and behavioral/neural plasticity of female rats. Front. Syst. Neurosci. ***8****:60. doi: 10.3389/fnsys.2014.00060*

This article was submitted to the journal Frontiers in Systems Neuroscience.

frontiers in Neuroscience

DATA REPORT
published: 13 May 2016
doi: 10.3389/fnins.2016.00196

The Temple University Hospital EEG Data Corpus

Iyad Obeid and Joseph Picone*

Electrical and Computer Engineering, Temple University, Philadelphia, PA, USA

Keywords: EEG, database, machine learning, clinical trials as topic, big data

INTRODUCTION

The electroencephalogram (EEG) is an excellent tool for probing neural function, both in clinical and research environments, due to its low cost, non-invasive nature, and pervasiveness. In the clinic, the EEG is the standard test for diagnosing and characterizing epilepsy and stroke, as well as a host of other trauma and pathology related conditions (Tatum et al., 2007; Yamada and Meng, 2009). In research laboratories, EEG is used to study neural responses to external stimuli, motor planning and execution, and brain-computer interfaces (Lebedev and Nicolelis, 2006; Wang et al., 2013). While human interpretation is still the gold standard for EEG analysis in the clinic, a host of software tools exist to facilitate the process or to make predictive analyses such as seizure prediction.

Recently, a confluence of events has underscored the need for robust EEG tools. First, there has been a renewed push via the White House BRAIN initiative to understand neural function and disease (Weiss, 2013). Secondly, there is an increased awareness on brain injury owing to both the influx of injured warfighters and numerous high-profile athletes found to have chronic brain damage (McKee et al., 2009; Stern et al., 2011). And thirdly, a wave of consumer grade scalp sensors has entered the market, allowing end users to monitor sleep, arousal, and mood (Liao et al., 2012).

In all these applications, there is a need for robust signal processing tools to analyze the EEG data. Historically, EEG signal processing tools have been devised using either ad hoc heuristic methods, or by training pattern recognition engines on small data sets (Gotman, 1982). These methods have yielded limited results, owing mostly to the fact that brain signals (and EEG in particular) are characterized by great variability, which can only be properly interpreted by building statistical models using massive amounts of data (Alotaiby et al., 2014; Ramgopal et al., 2014). Unfortunately, despite EEG being perhaps the most pervasive modality for acquiring brain signals, there is a severe lack of data in the public domain. For example, the "EEG Motor Movement/Imagery Dataset" (http://www.physionet.org/pn4/eegmmidb/) contains ∼1500 recordings of 1 or 2 min duration apiece from 109 subjects (Goldberger et al., 2000; Schalk et al., 2004). The CHB-MIT database contains data from 22 subjects, mostly pediatric (Shoeb, 2009). A database from Karunya University contains 175 16-channel EEGs of duration 10 s (Selvaraj et al., 2014). One of the most extensive databases for supporting epilepsy research is the European Epilepsy Database (http://epilepsy-database.eu/), which contains 250 datasets from 30 unique patients, but sells for €3000. Other databases, such as ieee.org, contain a wealth of data from more invasive modalities such as electrocorticogram, but little or no EEG.

This lack of publically available data is ironic considering that hundreds of thousands of EEGs are administered annually in clinical settings around the world. Relatively little of this data is publicly available to the research community in a form that is useful to machine learning research. Massive amounts of EEG data would allow the use of state-of-the-art machine learning algorithms to discover new diagnostics and validate clinical practice. Furthermore, it is desirable that such data be collected in clinical settings, as opposed to tightly controlled research environments, since "clinical-grade" data is inherently more variable with respect to parameters such as electrode location, clinical environment, equipment, and noise. Capturing this variability is critical to the development of robust, high performance technology that has real-world impact.

OPEN ACCESS

Edited by:
Mikhail Lebedev,
Duke University, USA

Reviewed by:
Duygu Kuzum,
University of California, San Diego, USA
Ervin Sejdic,
University of Pittsburgh, USA
Ivan Selesnick,
New York University, USA
Xiaomu Song,
Widener University, USA
Zhanpeng Jin,
Binghamton University, USA

****Correspondence:***
Iyad Obeid
iobeid@temple.edu

Specialty section:
This article was submitted to Neural Technology, a section of the journal Frontiers in Neuroscience

Received: *29 February 2016*
Accepted: *20 April 2016*
Published: *13 May 2016*

Citation:
Obeid I and Picone J (2016) The Temple University Hospital EEG Data Corpus. Front. Neurosci. 10:196. doi: 10.3389/fnins.2016.00196

In this work, we describe a new corpus, the TUH-EEG Corpus, which is an ongoing data collection effort that has recently released 14 years of clinical EEG data collected at Temple University Hospital. The records have been curated, organized, and paired with textual clinician reports that describe the patients and scans. The corpus is publicly available from the Neural Engineering Data Consortium (www.nedcdata.org) (Picone and Obeid, 2016).

METHODS

Clinical EEG data were collected from archival records at Temple University Hospital (TUH). All work was performed in accordance with the Declaration of Helsinki and with the full approval of the Temple University IRB. All personnel in contact with privileged patient information were fully trained on patient privacy and were certified by the Temple IRB.

Archival EEG signal data were recovered from CD-ROMs. Files were converted from their native proprietary file format (Nicolet's NicVue) to an open format EDF standard. Data was then rigorously de-identified to conform to the HIPAA Privacy Rule by eliminating 18 potential identifiers including patient names and dates of birth. Patient medical record numbers were replaced with randomized database identifiers, with a key to that mapping being saved to a secure off-line location. Importantly, our process captured instances in which the same patient received multiple EEGs over time and assigned database IDs accordingly. Data de-identification was performed by combining automated custom-designed software tools with manual editing and proofreading. All storage and manipulation of source files was conducted on dedicated non-network connected computers that were physically located within the TUH Department of Neurology.

We also manually paired each retrieved EEG with its corresponding clinician report. These reports are generated by the neurologist after analyzing the EEG scan and are the official hospital summary of the clinical impression. These reports are comprised of unstructured text that describes the patient, relevant history, medications, and clinical impression. Reports were mined from the hospital's central electronic medical records archives and typically consisted of image scans of printed reports. Various levels of image processing were employed to improve the image quality before applying optical character recognition (OCR) to convert the images into text. A combination of software and manual editing was used to scrub protected health information (PHI) from the reports and to correct errors in OCR transcription. Only sessions with both an EEG and a corresponding clinician report were included in the final corpus.

The corpus was defined with a hierarchical Unix-style filetree structure. The top folder, `edf`, contains 109 numbered folders, each of which contain numbered folders for up to 100 patients. Each of these patient folders contains sub-folders that correspond to individual recording sessions. Those folder names reflect the session number and date of recording. Finally, each session folder includes one or more EEG (`.edf`) data files as well as the clinician report in `.txt` format. **Figure 1** summarizes the corpus file structure and gives examples of text and signal data.

RESULTS

The completed corpus comprises 16,986 sessions from 10,874 unique subjects. Each of these sessions contains at least one EDF file (more in the case of long term monitoring sessions that were broken into multiple files) and one physician report. Corpus metrics are summarized in **Figure 2**. Subjects were 51% female and ranged in age from less than 1 year to over 90 (average 51.6, stdev 55.9; see **Figure 2** bottom left). The average number of sessions per patient was 1.56, although as many as 37 EEGs were

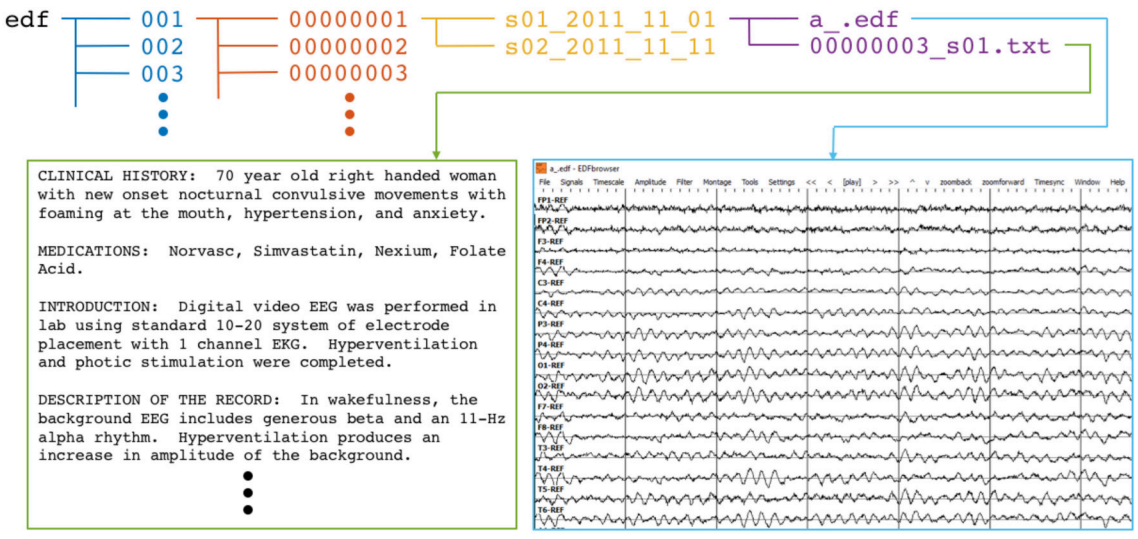

FIGURE 1 | Directory and file structure of the TUH-EEG database. Data is organized by patient (orange) and then by session (yellow). Each session contains one or more signal (edf) and physician report (txt) files. To accommodate file system management issues, patients are grouped into sets of about 100 (blue).

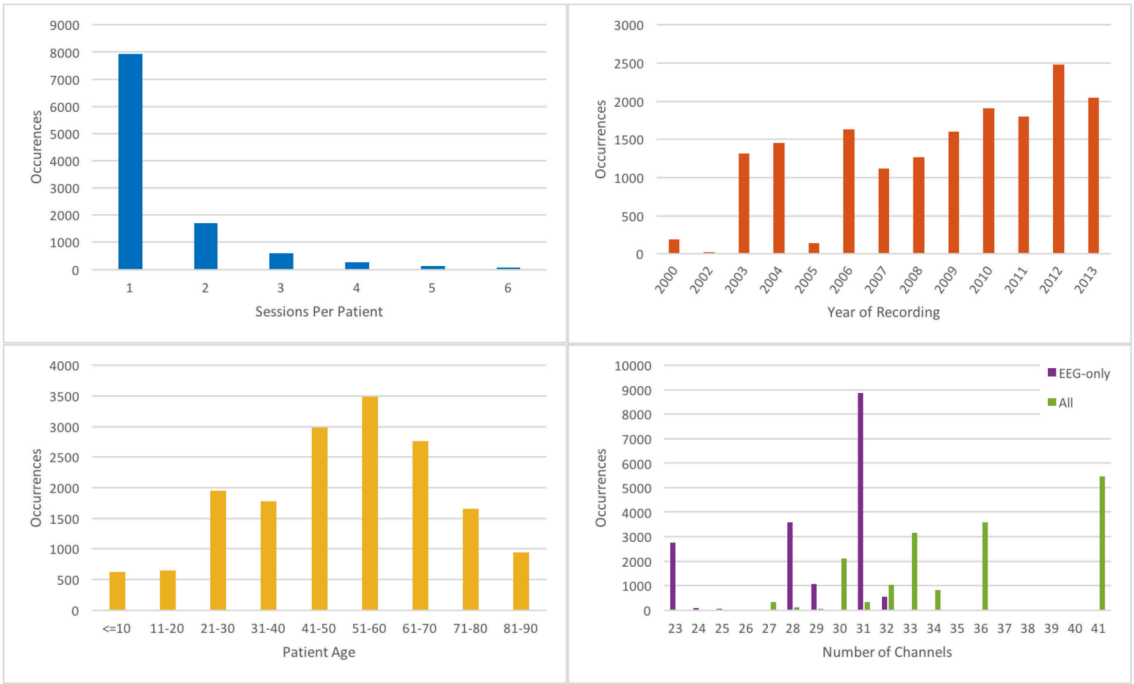

FIGURE 2 | Metrics describing the TUH-EEG corpus. [**Top left**] histogram showing number of sessions per patient; [**top right**] histogram showing number of sessions recorded per calendar year; [**bottom left**] histogram of patient ages; [**bottom right**] histogram showing number of EEG-only channels (purple); and total channels (green).

recorded for a single patient over an 8-month period (**Figure 2** top left). The number of sessions per year varies from ∼1000 to 2500 (with the exception of years 2000–2002, and 2005, in which limited numbers of complete reports were found in the various electronic medical record archives; see **Figure 2** top right).

There was a substantial degree of variability with respect to the number of channels included in the corpus (see **Figure 2** bottom right). EDF files typically contained both EEG-specific channels as well as supplementary channels such as detected bursts, EKG, EMG, and photic stimuli. The most common number of EEG-only channels per EDF file was 31, although there were cases with as few as 20. A majority of the EEG data was sampled at 250 Hz (87%) with the remaining data being sampled at 256 Hz (8.3%), 400 Hz (3.8%), and 512 Hz (1%).

An initial analysis of the physician reports reveals a wide range of medications and medical conditions. Unsurprisingly, the most common listed medications were anti-convulsants such as Keppra and Dilantin, as well as blood thinners such as Lovenox and heparin. Approximately 87% of the reports included the text string "`epilep`," and about 12% included "`stroke`." Only 48 total reports included the string "`concus`."

The TUH-EEG corpus v0.6.0 has been released and is freely available online at www.nedcdata.org. Users must register with a valid email address. The uncompressed EDF files and reports together comprise 572 GB. For convenience, the website stores all data from each patient as individual `gzip` files with a median filesize of 4.1 MB; all 10,874 `gzips` together comprise 330GB. Users wanting to access the entire database are encouraged to physically mail a USB hard drive to the authors in order to avoid the downloading process.

DISCUSSION

This work presents the world's largest publically available corpus of clinical EEG data, representing a grand total of 29.1 years (total duration summed over all EEG channels) of EEG data. In addition to its size, this corpus features a wide variation of patient ages, diagnoses, medications, channel counts, and sampling rates. Furthermore, the corpus continues to be expanded at a rate of ∼2500 new sessions per year.

Biomedicine is entering a new age of data-driven discovery driven by ubiquitous computing power, inexpensive data storage, the machine learning revolution, and high speed internet connections. Access to massive quantities of properly curated data is now the critical bottleneck to advancement in many areas of biomedical research. Ironically, doctors and clinicians generate enormous quantities of data every day, but that information is almost exclusively sequestered in secure archives where it cannot be used for research by the biomedical research community. The quantity, quality, and variability of such data represent a significant unrealized potential, which is doubly unfortunate considering that the cost of generating that data has already been borne. Although, there has been some advancement with respect to publishing databases of patient metadata, curated *signal* databases are much less commonly available, especially in quantities that would be sufficient to train most contemporary machine learning engines.

In this work, we have endeavored to achieve two goals. The first is to create a corpus of clinical EEG signals and their corresponding physician reports. The second is to establish best practices for the curation and publication of clinical signal data, which is an inherently different entity than discrete metadata. The EEG corpus we present here is the first of its kind, both in terms of volume and heterogeneity, both of which are critical factors for training machine learning engines. Typically, "research-grade" data is created by tightly controlling as many external factors as possible. In contrast, "clinical-grade" data is inherently heterogeneous with respect to those same external factors. Whereas certain classes of research questions can only be answered using well-controlled data, others benefit from variability. For example, an epilepsy detection algorithm that is trained using 31 specific EEG channels may not be effective if one or more of those channels are not connected, or if the electrodes are improperly located or affixed to the scalp. Algorithms that must be sufficiently robust to function under a plurality of conditions must be trained with data that is sufficiently heterogeneous.

Our work has shown that, although clinical signal data is ubiquitous and inherently valuable to the research community, it requires substantial manipulation before it can be released as an adequately curated data corpus. This effort is non-trivial, both in terms of time and cost. Our team's activities ranged from the mundane (e.g., manually copying archival hospital data from over 1500 CD-ROMs) to more technical challenges (e.g., developing software for detecting data entry errors in the clinical records). Physician reports had to be located through one of five different EMR portals, often manually. A battery of tests was created to validate that each record was complete, unique, error-free, and completely free of privileged patient information. A rigorous accounting system was created to track and organize the tens of thousands of files and their status.

The cost to develop the TUH EEG Corpus has been relatively low, totaling less than $100 K in direct charges. As medical record technology improves, the cost of this collection can be reduced even further. On the balance, these types of large-scale collections are a worthwhile investment, since costs are minor relative to the cost of acquiring the data or conducting research on the data. In general, the authors expect that a dedicated community-wide data facility would be best suited to curate data of the magnitude and complexity described here because there are significant on-going costs associated with such an activity.

An example of these on-going costs is annotation of the data—a critical issue for machine learning research. In most semi-supervised machine learning applications, one of the first steps is to annotate the data, a process in which important elements of the signal are marked as such. This can be performed either manually by a human domain expert, or automatically with a bootstrap-style algorithm. In addition to the EEG data itself, we are releasing a collection of annotations which may be downloaded separately if they are of interest to the user. The annotations contain the start and stop time and an event label and are specific to each channel. Six classes of events are included: (1) spike and/or sharp waves (SPSW), (2) periodic lateralized epileptiform discharges (PLED), and (3) generalized periodic epileptiform discharges (GPED). SPSW events are epileptiform transients that are typically observed in patients with epilepsy. PLED events are indicative of EEG abnormalities and often manifest themselves with repetitive spike or sharp wave discharges that can be focal or lateralized over one hemisphere. These signals display quasi-periodic behavior. GPED events are similar to PLEDs, and manifest themselves as periodic short-interval diffuse discharges, periodic long-interval diffuse discharges and suppression-burst patterns according to the interval between the discharges. Triphasic waves, which manifest themselves as diffuse and bilaterally synchronous spikes with bifrontal predominance, typically at a rate of 1–2 Hz, are also included in this class.

Three events are used to model background noise: (1) artifacts (ARTF) are recorded electrical activity that is not of cerebral origin, such as those due to the equipment, patient behavior or the environment; (2) eye movement (EYEM) are common events that can often be confused with a spike; (3) background (BCKG) is used for all other signals.

These six classes (three signal classes and three noise classes) were arrived at through several iterations of a study conducted with Temple University Hospital neurologists. Automatic labeling of these events allows a neurologist to rapidly search long-term EEG recordings for anomalous behavior. However, there are many more annotations that need to be developed for this data. For example, we are currently developing technology to automatically annotate seizures. There are many other events of interest that need annotation (e.g., sleep states). We expect to be continually enhancing the value of the TUH EEG Corpus.

AUTHOR CONTRIBUTIONS

JP led the database creation effort and co-wrote the manuscript. IO contributed to the database creation effort, performed data metrics, and co-wrote the manuscript.

FUNDING

This work has been supported by DARPA award D13AP00065, NSF awards 1305190 and 1458411, and by the Research Office and Dean of Engineering at Temple University.

REFERENCES

Alotaiby, T. N., Alshebeili, S. A., Alshawi, T., Ahmad, I., and Abd El-Samie, F. E. (2014). EEG seizure detection and prediction algorithms: a survey. *EURASIP J. Adv. Signal Process.* 2014:183. doi: 10.1186/1687-6180-2014-183

Goldberger, A. L., Amaral, L. A., Glass, L., Hausdorff, J. M., Ivanov, P. C., Mark, R. G., et al. (2000). Physiobank, physiotoolkit, and physionet components of a new research resource for complex physiologic signals. *Circulation* 101, e215–e220. doi: 10.1161/01.CIR.101.23.e215

Gotman, J. (1982). Automatic recognition of epileptic seizures in the EEG. *Electroencephalogr. Clin. Neurophysiol.* 54, 530–540. doi: 10.1016/0013-4694(82)90038-4

Lebedev, M., and Nicolelis, M. (2006). Brain–machine interfaces: past, present and future. *Trends Neurosci.* 29, 536–546. doi: 10.1016/j.tins.2006.07.004

Liao, L. D., Lin, C. T., McDowell, K., Wickenden, A. E., Gramann, K., Jung, T. P., et al. (2012). Biosensor technologies for augmented brain – computer interfaces in the next decades. *Proceed. IEEE* 100, 1553–1566. doi: 10.1109/JPROC.2012.2184829

McKee, A. C., Cantu, R. C., Nowinski, C. J., Hedley-Whyte, E. T., Gavett, B. E., Budson, A. E., et al. (2009). Chronic traumatic encephalopathy in athletes: progressive tauopathy after repetitive head injury. *J. Neuropathol. Exp. Neurol.* 68, 709–35. doi: 10.1097/NEN.0b013e3181a9d503

Picone, J., and Obeid, I. (2016). *Temple University Hospital EEG Corpus, Neural Engineering Data Consortium, v0.6.3*. Available online at: www.nedcdata.org

Ramgopal, S., Thome-Souza, S., Jackson, M., Kadish, N. E., Sánchez Fernández, I., Klehm, J., et al. (2014). Seizure detection, seizure prediction, and closed-loop warning systems in Epilepsy. *Epilepsy Behav.* 37, 291–307. doi: 10.1016/j.yebeh.2014.06.023

Schalk, G., McFarland, D. J., Hinterberger, T., Birbaumer, N., and Wolpaw, J. R. (2004). BCI2000: a general-purpose Brain-Computer Interface (BCI) system. *IEEE Trans. Bio Med. Eng.* 51, 1034–1043. doi: 10.1109/TBME.2004.827072

Selvaraj, T. G., Ramasamy, B., Jeyaraj, S. J., and Suviseshamuthu, E. S. (2014). EEG database of seizure disorders for experts and application developers. *Clin. EEG Neurosci.* 45, 304–309. doi: 10.1177/1550059413500960

Shoeb, A. (2009). *Application of Machine Learning to Epileptic Seizure Onset Detection and Treatment*. Cambridge, MA: MIT.

Stern, R. A., Riley, D. O., Daneshvar, D. H., Nowinski, C. J., Cantu, R. C., and McKee, A. C. (2011). Long-term consequences of repetitive brain trauma: chronic traumatic encephalopathy. *PM R* (10 Suppl. 2), S460–S467. doi: 10.1016/j.pmrj.2011.08.008

Tatum, W., Husain, A., Benbadis, S., and Kaplan, P. (2007). *Handbook of EEG Interpretation*. New York, NY: Demos Medical Publishing.

Wang, W., Collinger, J. L., Degenhart, A. D., Tyler-Kabara, E. C., Schwartz, A. B., Moran, D. W., et al. (2013). An electrocorticographic brain interface in an individual with tetraplegia. *PLoS ONE* 8:e55344. doi: 10.1371/journal.pone.0055344

Weiss, P. S. (2013). President obama announces the BRAIN initiative. *ACS Nano* 7, 2873–2874. doi: 10.1021/nn401796f

Yamada, T., and Meng, E. (2009). *Practical Guide for Clinical Neurophysiologic Testing: EEG*. Philadelphia, PA: Lippincott Williams & Wilkins.

Conflict of Interest Statement: The authors declare that the research was conducted in the absence of any commercial or financial relationships that could be construed as a potential conflict of interest.

frontiers in
SYSTEMS NEUROSCIENCE

ORIGINAL RESEARCH ARTICLE
published: 17 February 2015
doi: 10.3389/fnsys.2015.00011

Classification of single-trial auditory events using dry-wireless EEG during real and motion simulated flight

Daniel E. Callan[1,2]*, Gautier Durantin[3] and Cengiz Terzibas[2]

[1] Center for Information and Neural Networks (CiNet), National Institute of Information and Communications Technology (NICT), Osaka University, Osaka, Japan
[2] Multisensory Cognition and Computation Laboratory Universal Communication Research Institute, National Institute of Information and Communications Technology, Kyoto, Japan
[3] Centre Aéronautique et Spatial, Institut Supérieur de l'Aéronautique et de l'Espace, Université de Toulouse, Toulouse, France

Edited by:
Mikhail Lebedev, Duke University, USA

Reviewed by:
Alistair McEwan, The University of Sydney, Australia
Raja Parasuraman, George Mason University, USA

****Correspondence:***
Daniel E. Callan, Center for Information and Neural Networks (CiNet), National Institute of Information and Communications Technology (NICT), Osaka University, 1-4 Yamadaoka, Suita City, Osaka 565-0871, Japan
e-mail: dcallan@nict.go.jp

Application of neuro-augmentation technology based on dry-wireless EEG may be considerably beneficial for aviation and space operations because of the inherent dangers involved. In this study we evaluate classification performance of perceptual events using a dry-wireless EEG system during motion platform based flight simulation and actual flight in an open cockpit biplane to determine if the system can be used in the presence of considerable environmental and physiological artifacts. A passive task involving 200 random auditory presentations of a chirp sound was used for evaluation. The advantage of this auditory task is that it does not interfere with the perceptual motor processes involved with piloting the plane. Classification was based on identifying the presentation of a chirp sound vs. silent periods. Evaluation of Independent component analysis (ICA) and Kalman filtering to enhance classification performance by extracting brain activity related to the auditory event from other non-task related brain activity and artifacts was assessed. The results of permutation testing revealed that single trial classification of presence or absence of an auditory event was significantly above chance for all conditions on a novel test set. The best performance could be achieved with both ICA and Kalman filtering relative to no processing: Platform Off (83.4% vs. 78.3%), Platform On (73.1% vs. 71.6%), Biplane Engine Off (81.1% vs. 77.4%), and Biplane Engine On (79.2% vs. 66.1%). This experiment demonstrates that dry-wireless EEG can be used in environments with considerable vibration, wind, acoustic noise, and physiological artifacts and achieve good single trial classification performance that is necessary for future successful application of neuro-augmentation technology based on brain-machine interfaces.

Keywords: EEG, dry EEG, brain machine interface, independent component analysis, Kalman filter, auditory evoked response, single trial, classification

INTRODUCTION

Technology capable of augmenting human performance by means of feedback of decoded neural states has potential for many types of neuroergonimic applications. Neuroergonomics is the study of the human brain in relation to performance at work, at home, in transportation, and in everyday settings with the goal of using this knowledge to design technologies and work environments to augment human behavior to enhance safety, usability, efficiency and enjoyment (Parasuraman, 2003; Parasuraman and Rizzo, 2008). Because of the inherent dangers in aviation and space operations these fields may be particularly well suited for neuroergonomic applications to increase performance and safety. There are many challenges for effective implementation of neuroergonomic technology in real-world situations. Unlike the laboratory where brain recordings can be made under controlled conditions, in real world situations there is considerable additional physiological and environmental noise that must be dealt with. In addition it is likely the case that brain dynamics differ in real-world environments compared to those of the laboratory (McDowell et al., 2013; Lin et al., 2014).

Pilots' often face periods of excessive workload, stress, fatigue, attentional deficits, etc... during flight operations that may affect performance. The ability to decode the mental state of the pilot and augment these states by neuro- adaptive feedback and/or automation has great potential in improving training, performance, and safety. In this article we are particularly interested in investigating brain potentials that occur as a result of passive presentation of an auditory stimulus during flight. This research has relevance to the phenomenon of inattentional deafness in which pilots' sometimes miss audio alarms. Missed audio alarms are responsible for a significant number of aviation accidents (Bliss, 2003; Scannella et al., 2013; Dehais et al., 2014).

There have been a number of studies in which brain activity has been measured with electroencephalography EEG during aviation (Sem-Jacobsen et al., 1959; Blanc et al., 1966; Caldwell

and Lewis, 1995) and space operations (Maulsby, 1966; Cheron et al., 2009). EEG has been successfully collected in flight since the late 1950's (Sem-Jacobsen et al., 1959). These studies showed that although the in flight environment is subject to noise caused by vibration and greater physical movement of the pilot that are not present during laboratory based experiments, the EEG signals recorded are able to show changes in various frequency bands and additional specific features that are associated with flight performance (Sterman et al., 1987) as well as workload (Howitt et al., 1978; Hankins and Wilson, 1998; Dussault et al., 2005) and fatigue (Howitt et al., 1978; Sauvet et al., 2014). Experiments conducted aboard the International Space Station have shown changes in the rhythmic brain activity of astronauts as a result of microgravity (Cheron et al., 2009). In an experiment conducted during parabolic flight it was found that a mental imagery (Thinking of moving arm vs. thinking of words) based brain machine interface (BMI) task could achieve between 72%–79% single trial classification performance across the various g-force conditions ranging from 0 to 2 g (Millàn Jdel et al., 2009).

A BMI is a device that provides for the ability to transfer and use information from distinct brain states for communicating with a machine (Blankertz et al., 2010). BMI based on electroencephalography EEG have been used in many applications including, but not limited to, modulating brain rhythms to control movement of a cursor on a screen (Wolpaw et al., 2002) as well as a quadrocopter in the real world (LaFleur et al., 2013), decoding brain states such as attention, performance capability, workload, etc. . . (Dornhege et al., 2007; Müller et al., 2008; Blankertz et al., 2010), decoding various perceptual events (Birbaumer et al., 1999; Wang et al., 2006; Bin et al., 2009). A primary goal of BMI research is to augment human behavior to allow for enhanced performance. Notably, there are considerable improvements in performance for some medical applications of BMI when the user's motor system is severely incapacitated. For example patients with locked-in syndrome who are not able to communicate through standard pathways or assistive technology can learn to spell and initiate dialogs using P300 based BMI (Sellers et al., 2014). Non-medical application of the BMI P300 speller in normal healthy individuals is not practical since normal channels of communication are considerably better.

There are several limitations for the practical neuroergonomic application of many of these BMIs in real-world situations (Blankertz et al., 2010). Many of these BMIs take a considerable amount of time for operator training, on the order of months. This is true especially for implementations when the user needs to learn how to modulate various brain rhythms (Wolpaw et al., 2002; LaFleur et al., 2013). For practical application there should be very little if any operator training in control of the BMI. Many BMIs require considerable mental workload to operate, such as those requiring mental imagery and those utilizing focused attention away from the primary task environment. The amount of cognitive resources required to operate such BMI can be so high, that the operator's usual channels of perceptual, motor, and cognitive processing are greatly impaired. For example, it is obvious that if one is actively involved with mentally imaging movement of their left hand to move a vehicle left, mentally imaging movement of both arms to move a vehicle right, mentally imaging walking to move forward, and mental word association to move back, that this will drastically compromise the operators ability to speak, walk, and move their hands while engaged in operating the BMI. However, if one uses a joystick to move a vehicle the operator will still be able to speak, walk, and move their hands around without drastically compromising performance depending on the difficulty of the task at hand. While P300 based BMI have advantages in that they do not require extensive subject training, they often require directed attention away from the environment in which they are suppose to operate in. For example subjects using a P300 based BMI to control various items in a virtual apartment reported a far lower sense of presence, which they attributed to increased workload, in interacting in the environment than did control subjects not using BMI (Groenegress et al., 2010). In order for a BMI to be effective it is necessary to utilize naturally occurring brain states for control. Another limitation of many of these BMI implementations is that they utilize rather bulky EEG systems that are not portable and use gel that takes a considerable amount of time and assistance to apply.

Practical application of EEG in real-world situations requires the use of technology that is easy to wear without the use of gel and one that is wireless to transmit data to a computer for real-time processing. There are many dry-wireless EEG systems available that have been used for many different applications including drowsiness detection (Park et al., 2011), gaming (Liao et al., 2012; Zao et al., 2014), and detection of perceptual events (Lin et al., 2014). Of particular interest in relation to real-world application of BMI is the study conducted by Lin et al. (2014) investigating the impact of walking locomotion on the ability to detect steady state visual evoked potentials (SSVEP) using a dry-wireless EEG system. The SSVEP is a frequency coded neural response that is modulated by the presentation frequency of the visual stimuli (Lin et al., 2014). The classification performance was good but decreased as a result of walking speed from 84.87% for standing to 83.03% for 1 MPH walking, 79.47% for 2 MPH walking, and 75.26% for 3 MPH walking (Lin et al., 2014). The decrease in performance as a function of walking speed may result from increasingly larger artifacts in the EEG as well as to greater difficulty in fixated attention to the visual stimuli as one moves more. Dry electrodes are more susceptible to movement related artifacts than gel based EEG recording (Guger et al., 2012; Lin et al., 2014). One limitation for utilization of the SSVEP for many BMI applications is that the task requires the subject to attend to the visual stimuli presented on the computer screen. This requirement is not practical in many real-world situations where perceptual motor control requires the use of the visual system such as in aviation and space operations.

The goal of this study is to determine the extent to which perceptually evoked brain related EEG signals, recorded with a dry-wireless system in noisy real-world environments can be decoded for potential use in BMIs to augment human performance. With a focus on aviation related applications we conducted our experiment in two environmental conditions.

One environmental condition was the use of a motion platform based flight simulator the other was an open cockpit biplane. In order to avoid practical problems in controlling the airplane by using a visual based perceptual presentation task, an auditory stimulus presentation task was used to assess single trial classification performance. The advantage of using an audio stimulus presentation task (100 ms chirp sound) is that it can be played passively in the background while the pilot attends to flying the plane. The goal for the classifier was to determine from the EEG data the presentation of the audio stimulus (chirp) from periods of no audio stimulus (silence) presentation.

A control condition was used for both environmental conditions. In the motion platform condition the experiment was conducted with the platform and flight simulator off (a relatively noise free condition) and with the motion platform on while flying aerobatic maneuvers in the flight simulator (Platform Off and Platform On conditions). In the platform on condition there is considerable movement of the individuals arms, legs, eyes, neck, and entire body as well as potential electrical noise from the motion platform motors. In the biplane condition the experiment was conducted with the engine and avionics off while sitting on the tarmac (a relatively noise free condition) and with the engine and avionics on while piloting the plane in cruise flight. The open cockpit biplane may constitute one of the most challenging environments for EEG recording in which there is an incredible amount of vibration, wind, acoustic noise, as well as considerable movement of the individual's arms, legs, eyes, neck, and entire body.

There are considerable sources of noise that make recording of EEG in real-world environments challenging including non-neurological electrophysiological signals (e.g., muscle activity), electronic noise, and mechanical vibrations. In order to be able to clean the data of the artifacts and extract brain activity related to the auditory evoked responses several procedures within EEGLAB (Swartz Center for Computational Neuroscience, Delorme and Makeig, 2004) are used including independent component analysis (ICA). In addition to these artifact-cleaning procedures a Kalman (1960) filter implementing a dynamical model of the single-trial auditory evoked responses was also used to help extract brain activity related to presentation of the audio stimuli. Based on the results of Lin et al. (2014) using a similar dry-wireless EEG system it is predicted that above chance classification performance in detecting single trial audio stimulus presentation will be achieved in all conditions. Furthermore, it is predicted that both ICA and Kalman filtering will improve classification performance across all conditions.

METHODS

SUBJECTS

The same subject was used for all studies. The subject was male, right handed, 45 years old, with normal hearing. One of the authors served as the subject in this experiment. He has 5 years of flying experience with more than 250 h total time and 200 h in biplanes of the same make and model. The subject gave informed consent for experimental procedures approved by the ethics committee of the National Institute of Information and Communications Technology in accordance with the principles expressed in the Declaration of Helsinki.

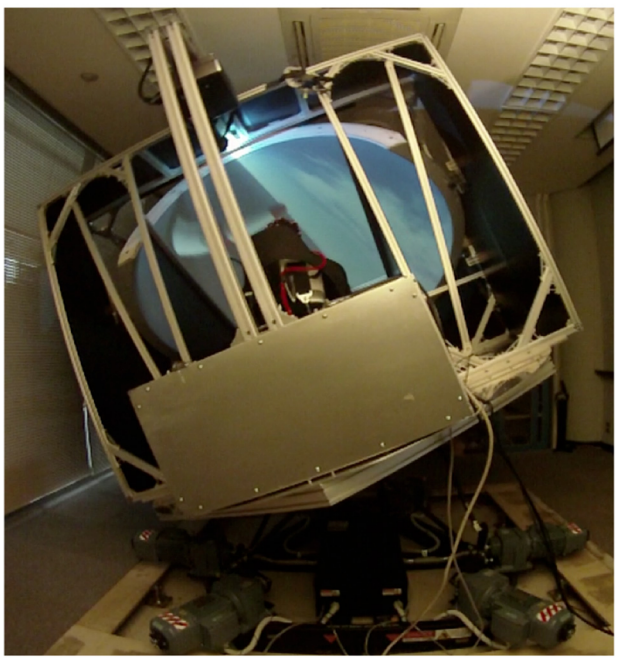

FIGURE 1 | Motion Platform Flight Simulator composed of the CKAS V7 6 degree of freedom Motion System (CKAS Mechatronics, Melborn, Australia) with a custom built cockpit utilizing dome projection for video. The flight controls consist of 1. A control stick to manipulate the elevator (pitch) and ailerons (roll), 2. Rudder pedals to manipulate the rudder (yaw), and 3. A Throttle to manipulate thrust. Single-trial auditory events using dry-wireless EEG were evaluated while the subject was flying through a simulated Redbull Air Race course.

PROCEDURE

The experimental task consisted of passively listening to a chirp sound (0.1 s duration) in different environmental settings while recording brain activity using the Cognionics 64 channel dry wireless EEG system. The chirp sound was presented 200 times spaced randomly by at least 0.6–2.5 s of silence. Within these periods of silence 200 independent 0.5 s segments were randomly extracted. The different environmental settings and conditions are as follows: Electric Motion Platform (Platform Off, Platform On) and open cockpit Biplane (Engine Off, Engine On).

The CKAS V7 6 degree of freedom Motion System (CKAS Mechatronics, Melborn, Australia) with a custom built cockpit utilizing dome projection for video was used (see **Figure 1**). In the motors off condition the subject was sitting still in the chair mounted on the platform. In the motors on condition the subject was engaging in aerobatic flight simulation (X-Plane Laminar Research) through the same Redbull Air Race course as used in a previous fMRI study (Callan et al., 2012). See Callan et al. (2012, 2013) for details on the implementation of the flight simulator system for brain imaging experiments. Just as in a

FIGURE 2 | Open Cockpit Starduster SA300 Biplane used for in flight and ground testing of single-trial auditory events using dry-wireless EEG. **(A)** View off the biplane on the ground. **(B)** View of the biplane in the air. **(C)** Picture of the subject wearing the Cognionics 64 channel dry-wireless EEG under the leather flight helmet. This is the same EEG system pictured in **Figure 3**.

real airplane, the subject controlled the ailerons and elevator by stick with the right hand, the throttle lever with the left hand, and the rudders with foot pedals. The motors of the motion platform moved in relation to the accelerations of the aircraft in the flight simulator. No sound was presented from the flight simulator. In both the platform off and platform on conditions the audio stimuli were presented using the Clarity Aloft Pro aviation headset using the same sound level. The experiment took approximately 10 min for each condition. The platform on condition was conducted first followed by the platform off condition.

The biplane used in the experiment was an open cockpit two passenger Starduster SA300 (see **Figure 2**). In the engine off condition the subject was sitting in the front seat of the biplane on the tarmac with avionics off. In the engine on condition the subject was piloting the plane during cruise flight from the front seat with avionics on. In the engine on condition there was extreme vibration, acoustic noise, and wind. In both the engine off and engine on conditions the Cognionics EEG system was worn underneath a leather flight cap. The audio stimuli were presented using the Bose A20 active noise canceling aviation headset using the same sound level. The experiment took approximately 10 min for each condition. The engine off condition was conducted first followed by the engine on condition.

EEG RECORDING AND ANALYSIS

EEG was recorded using the Cognionics HD-72 dry wireless EEG headset (Cognionics, Inc., San Diego[1]). The same 64-channel EEG system was used by Mullen et al. (2013) and shares the same underlying technology as the 32-channel system reported in Chi et al. (2013) and Lin et al. (2014).

The EEG headset consists of a mechanically flexible spine to provide structure and ease of handling. Each segment of the spine contains a row of electrodes. The 64 electrodes provide full scalp coverage. An internal active shield, covering all sensor positions, spans the entire headset to minimize external noise pickup and

[1]http://www.cognionics.com/

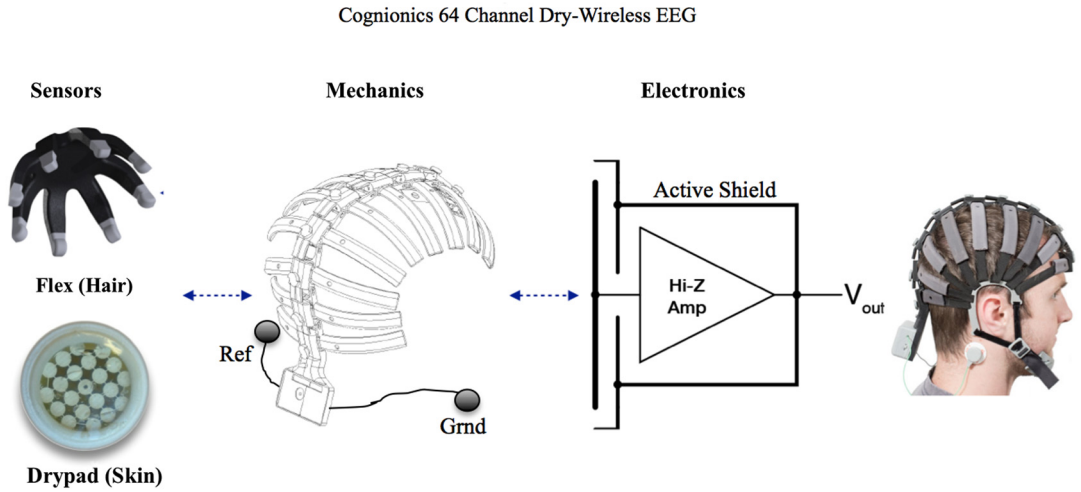

FIGURE 3 | Cognionics 64 Channel Dry-Wireless EEG Headset. Two types of dry sensors are used: The flex sensors are placed over hair and the Drypad sensors are laced over bearskin, such as the forehead. In our setup, we utilized 7 Drypad sensors on the forehead (first band) and 54 flex sensors across the rest of the array. Each band of the headset is user adjustable to enable proper fit and sensor pressure over different head sizes and shapes. An internal flexible conductive layer forms an active shield, which spans the entire headset, to minimize external noise pickup even with high-impedance dry electrodes. Ground (Grnd) and reference (Ref) electrodes are placed under the ear as shown in the figure. The same cap pictured here is in **Figure 2** underneath the leather flight helmet. See the text in the Methods section for further details.

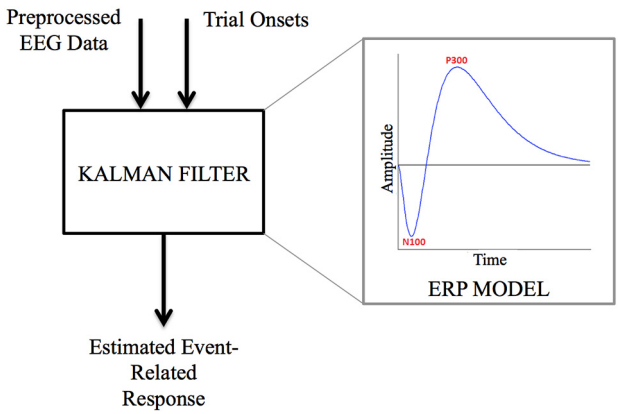

FIGURE 4 | Kalman filter functional model. Kalman filter is designed from an Event Related Potential (ERP) dynamical model (on the right), and uses both preprocessed EEG data and trial onsets to estimate the instantaneous event-related response.

artifacts. Reference and ground are placed on the mastoids with by two standard ECG adhesive electrodes (see **Figure 3**).

Two sensor options are compatible with the headset and connect via a miniature snap receptacle. In the setup, seven Drypad sensors were placed on the forehead (**Figure 3**). The Drypad electrode is a cushioned membrane that is optimized for bare skin contact. For the remaining 57 positions, we used the Flex sensors designed for thru-hair measurements. The Flex sensor is specifically designed to brush aside hair and make direct scalp contact with legs that gently bend and deform under modest pressure. Compared to previous metal pin sensors (e.g., Liao et al., 2011), the Flex sensors offer improved comfort and safety since the sensors can completely flatten under hard impacts. Contact impedances with both sensors typically range from 100 k to 1 MOhm (Mullen et al., 2013) on unprepared skin.

To adequately acquire EEG signals with high electrode impedances, the Cognionics system utilizes a combination of active shielding, high input impedance amplifiers and active grounding to cancel and minimize environmental noise. Data is sampled at 300 Hz (DC-80 Hz bandwidth) with 24-bit ADCs to maximize dynamic range and quickly recover from overload artifacts. Total noise within the EEG band (1–50 Hz) is 0.7 microVolts RMS. The signal quality of the sensors, electrodes, and the data acquisition circuitry has been shown to be comparable to wet electrode based EEG systems with a correlation between simultaneously recorded evoked potentials of $r > 0.9$ (Chi et al., 2013; Mullen et al., 2013).

All electronics are housed in a miniature box at the base of the headset, which weighs a total of only 350 g making the entire system lightweight, portable and wearable. Data transmission is accomplished by a custom 5 GHz WiFi module. The headset radio communicates directly to an embedded WiFi host, in a point-to-point network, running on a USB dongle to minimize the overhead associated with a typical access point and PC-based software protocol stack, thereby minimizing latency and jitter. The receiving computer was a Panasonic CF-AX2 running Ubuntu Linux operating system. The average delay in receiving the signal was less than 1 ms. Audio stimuli were presented from the same computer as used to record the EEG by means of the auxiliary input to the aviation headset. The presentation of the audio signals was given time stamps in correspondence with the time stamps given for each of the recorded EEG samples. The high temporal precision of the

wireless link and the presentation software allows for accurate time registration between stimulus and EEG without the use of wire-line markers.

The EEG data was preprocessed using artifact-cleaning procedures available in EEGLAB (Delorme and Makeig, 2004). The data was first filtered using a FIR band pass filter between 2 and 30 Hz with a filter order of 496. The data was separated into a training set of 75% of the stimuli (150 chirp stimuli and 150 silent stimuli) and a testing set of 25% of the stimuli (50 chirp stimuli and 50 silent stimuli) for the platform off and on conditions and the biplane engine off and on conditions. The rational for choosing 75% of the trials for training and 25% for testing is that we believed this division would provide enough training data to generalize to a novel testing set while maintaining enough trials in the testing set to be a reasonable representation of the population. Although we did not attempt to train and test on a 50% split of the data we believed that the amount of training data may not have been sufficient for generalization to the novel test set. The artifact cleaning procedures were applied only to the training sets. The results of which were then applied to the corresponding test sets. The exact same cleaning procedures were then applied to the corresponding testing sets, with the same parameters.

Channels were considered to be bad and were removed from the training data based on the following: Maximum amplitude in the channel is greater than 100 microvolts; Channel flatline duration is greater than 5 s; Channel is correlated at less than 0.8 to its robust estimate based on other channels; Channel has more line noise relative to its signal than 4 standard deviations from the channel population mean. These same channels were then removed from the corresponding test sets.

The next step was to clean the multi-channel training data with the artifact subspace reconstruction (ASR) method using the defaults given in the clean_artifacts software within EEGLAB. ASR allows for the removal of non-stationary high-variance signals from EEG and reconstructs missing data using a spatial mixing matrix (See EEGLAB software by Christian Kothe and the following for details[2]). Calibration data from clean segments of the training data were used to determine the ASR filters separately for each of the four conditions. The ASR filter was then applied to the corresponding test data.

Following cleaning of the data by ASR, ICA using the extended infomax algorithm (Bell and Sejnowski, 1995) in EEGLAB was applied in order to separate brain activity related to the auditory evoked potentials from other brain and artifact related components. The weights of the ICA were determined only from the training data separately for each of the four conditions (platform off, platform on, engine off, engine on). These weights were then applied to the corresponding test data to determine the ICA activation waveforms. See **Figure 5** for an example of the continuous data before ASR, after ASR, and after ICA.

Kalman filtering (Kalman, 1960) was applied to the ASR filtered data both before and after ICA, to produce an estimate of the single-trial auditory evoked response. Kalman filtering is a linear quadratic estimation method, which relies on both the measurements and a modelization of the Event-Related Potential (ERP) dynamics to product an estimate in real-time. This method has been successfully applied to single-trial event related potentials estimation (Georgiadis et al., 2005). In our case, the parameters used as a model for the Kalman filter design were the N100 and P300 waves, generic features of the auditory evoked potential (see **Figure 4**). Both waves were modeled by a third-order impulse response with peaks respectively at 100 ms and 300 ms. The state noise was considered as white noise (Georgiadis et al., 2005), and the measurement noise covariance to state noise covariance ratio was fixed to 0.001, so that the Kalman estimate would put confidence in the measurements (Grewal and Andrews, 2008).

TRAINING AND TESTING THE CLASSIFIER

The Matlab Least Squares Probabilistic Classification (LSPC) toolbox (Sugiyama, 2010) was used to determine how well single trial audio presented stimuli could be identified in the EEG signal from periods of audio silence. LSPC uses a linear combination of kernel function to model the class-posterior probability. Regularized least-squares fitting of the true class-posterior probability is used to learn its parameters (Sugiyama, 2010). The use of least-squares fitting to determine a linear model allows for a global solution to be made analytically providing a considerable speedup in computational time. The default parameters were used in training of the LSPC models (see Matlab code: Sugiyama, 2010).

The features used to train the classifier consisted of the samples from onset to 500 ms after stimulus onset (150 samples) for both chirp and silent stimuli. In the case of ICA data the components selected to be included in the LSPC model were determined by visual inspection of the mean of the activation waveform of the chirp training data stimuli that showed a characteristic auditory evoked potential. For the pre-ICA data all of the channels were included in the LSPC model. The large number of features relative to the number of trials used to train the classifiers has the potential for over-fitting, resulting in poor generalization to the novel test data. We utilized inner cross-validation procedures for model selection in part to assess and protect against potential over-fitting.

The following inner cross-validation procedures were used for model selection and testing: Randomized ten fold cross-validation was used on the training data and the trained model with the best performance was selected for evaluating performance on the test data. One fold of the training data consisted of 135 chirp and 135 silent stimuli and one fold upon which the model was evaluated for selection consisted of 15 chirp and 15 silent stimuli. The final test data consisted of 50 chirp and 50 silent stimuli. This procedure was conducted 100 times to determine the distribution of performance of the model given random aspects of training (e.g., the trials selected for training and their order into the model).

Several conditions were evaluated to assess the efficacy of ICA and Kalman filtering in improving classification performance on the data. These conditions included the four environmental

[2]http://sccn.ucsd.edu/eeglab/plugins/ASR.pdf

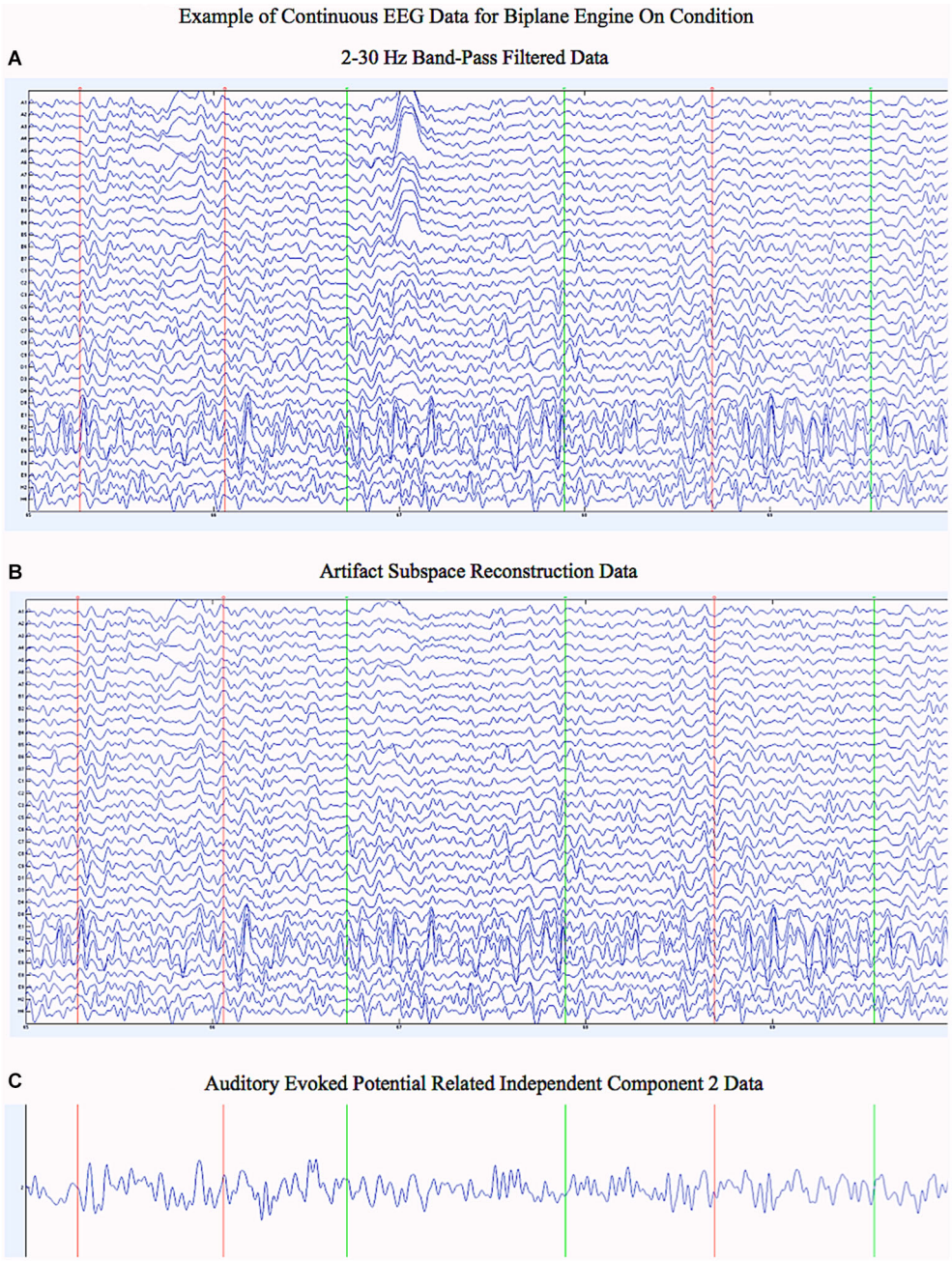

FIGURE 5 | Example of Continuous EEG Data for the Biplane Engine On Condition. **(A)** Five seconds of continuous data from the test set that has been band pass filtered from 2–30 Hz for the 34 electrodes included. **(B)** Five seconds of continuous data from the test set that has undergone artifact subspace reconstruction as well as band pass filtered from 2–30 Hz for the 34 electrodes included. Notice how ASR has cleaned up the artifact present in many of the channels (compare with **(A)** above). **(C)** Five seconds of continuous data from the test set for auditory evoked potential related independent component number 2. The ICA was carried out over the data in **(B)**. Green lines denote the onset of audio stimuli and Red lines denote the onset of silent trials.

conditions (Platform Off, Platform On, biplane Engine Off, biplane Engine On) and four preprocessing conditions (pre-ICA constituting the baseline no processing condition, ICA, pre-ICA Kalman filtered, ICA Kalman filtered) for a total of 16 analyses.

The statistical significance between the various conditions was determined by repeating the nested cross-validation process ten times for each condition. The nested cross-validation procedure is commonly used to estimate the stability of the model across conditions (Shenoy et al., 2008). At each step, we computed the

Table 1 | Classification performance for the platform condition on the test data.

	Platform off				Platform on			
	Accuracy (%)	False positive rate (%)	False negative rate (%)	d'	Accuracy (%)	False positive rate (%)	False negative rate (%)	d'
Pre-ICA	78.3 (0.33)	19.8 (0.20)	23.6 (0.65)	1.69 (0.01)	71.6 (0.56)	35.4 (1.52)	21.4 (0.60)	0.75 (0.08)
ICA	81.0 (0.49)	21.4 (0.99)	16.6 (0.73)	1.59 (0.07)	73.7 (0.52)	26.8 (1.91)	25.8 (1.75)	1.26 (0.12)
Pre-ICA + Kalman Filter	77.8 (0.55)	20.2 (1.05)	24.2 (1.94)	1.68 (0.07)	72.8 (0.53)	36.6 (1.58)	17.8 (1.94)	0.69 (0.08)
ICA + Kalman Filter	83.4 (0.27)	17.2 (0.53)	16.0 (0.60)	1.90 (0.04)	73.1 (0.8)	28.4 (2.61)	25.4 (1.79)	1.18 (0.16)

The standard error is given in parentheses below each mean value of the 10 nested cross-validation iterations.

Table 2 | Classification performance for the biplane condition on the test data.

	Biplane engine off				Biplane engine on			
	Accuracy	False positive rate	False negative rate	d'	Accuracy	False positive rate	False negative rate	d'
Pre-ICA	77.4 (1.01)	20.2 (2.72)	25.0 (2.20)	1.75 (0.21)	66.1 (0.75)	38.0 (1.23)	29.8 (1.31)	0.61 (0.06)
ICA	78.5 (0.72)	20.0 (1.58)	23.0 (0.68)	1.71 (0.11)	77.3 (0.45)	23.6 (1.26)	21.8 (0.81)	1.45 (0.08)
Pre-ICA + Kalman Filter	77.0 (0.97)	14.6 (1.16)	31.4 (2.53)	2.13 (0.1)	65.3 (0.96)	35.4 (2.78)	34.0 (2.40)	0.78 (0.17)
ICA + Kalman Filter	81.1 (0.35)	10.0 (1.19)	27.8 (1.35)	2.65 (0.18)	79.2 (0.39)	22.6 (1.12)	19.0 (1.16)	1.51 (0.07)

The standard error is given in parentheses below each mean value of the 10 nested cross-validation iterations.

classification accuracy, false positive rate and false negative rate. The differences between the classification results obtained from each of the preprocessing conditions were then compared using Wilcoxon sign-rank test.

RESULTS

The number of channels not rejected out of the 64 by the preprocessing steps for the various conditions are as follows: Platform Off (46), Platform On (20), Biplane Engine Off (30), Biplane Engine On (34). The independent components showing auditory evoked potentials used to train the LSPC models were the following for the various conditions: Platform Off (2, 3), Platform On (1, 3), Biplane Engine Off (2, 3), Biplane Engine On (2, 16). The components are sorted in descending order of mean projected variance. Therefore, the lower the component number the larger is the projected variance. Parentheses.

The results of the single trial classification performance for audio chirp verses silent stimuli for all environmental and analysis method conditions were significantly above chance ($p < 0.05$) based on permutation testing of 100 random shuffling of the labels compared to the mean performance of the respective models trained with correct labels. The accuracy, false positive rate, false negative rate, and d' (sensitivity) along with the standard errors in parentheses for the platform off and platform on conditions for the four analysis conditions (Pre-ICA, ICA Pre-ICA + Kalman Filter, and ICA + Kalman Filter) are given in **Table 1**. The corresponding results for the biplane Engine Off and Engine On conditions are given in **Table 2**. The statistical significance of model stability for accuracy on the contrasts of pre-ICA vs. ICA, Off vs. On, and No Kalman filter vs. Kalman filter are given in **Tables 3A–C**. Testing for significance based on the 100 trials of the test set across the various contrasts using the Wilcoxon sign-rank test is given in **Tables 4A–D**.

DISCUSSION

The primary objective of this experiment was to show as a proof of concept that a dry-wireless EEG system could be used in extremely noisy real-world environments while the operator is carrying out complex perceptual motor tasks and still show good classification performance of a perceptual event. Both the motion platform based flight simulation and the open cockpit biplane environments produced considerable artifacts challenging the ability for accurate classification of a perceptual event from EEG data. In the platform on condition the subject was flying through a Redbull Air Race course making abrupt banks to go through the cones in the correct orientation (Callan et al., 2013). The movement of the platform and the head and body to these banks produces large artifacts in the EEG trace. In the open cockpit biplane there is considerable vibration, wind, acoustic noise, and physiological noise resulting from control of the plane and movement of the body that produces large artifacts in the EEG trace.

Despite these challenging environments our study showed that far above chance classification performance can be achieved for all environmental conditions (Platform Off, Platform On, Biplane Engine Off, Biplane Engine On) and for all analysis conditions (Pre-ICA, Pre-ICA Kalman filtered, ICA, and ICA Kalman filtered) (See **Tables 1–4**). The classification performance was the best when applying both ICA and Kalman filtering to the data. This was especially true in the Biplane Engine On condition in which classification performance improved from 66.1% in the baseline pre-ICA no processing condition to 79.2% in the ICA Kalman filtering condition (See **Tables 2–4**). This

Table 3 | Statistical significance of the various contrasts using nested cross-validation to evaluate model stability.

A. ICA vs. Baseline Pre-ICA								
Overall	Platoff	Platon	Engoff	Engon	Platoff + Kalman	Platon + Kalman	Engoff + Kalman	Engon + Kalman
***		**		**		**		**
B. Off vs. On								
Overall	Platform Pre-ICA	Engine Pre-ICA	Platform Pre-ICA + Kalman	Engine Pre-ICA + Kalman	Platform ICA	Engine ICA	Platform ICA + Kalman	Engine ICA + Kalman
***	**	**	**	**	**		**	*
C. Kalman Filter vs. no Kalman Filter								
Overall	Platform Off Pre-ICA	Platform On Pre-ICA	Engine Off Pre-ICA	Engine On On Pre-ICA	Platform Off ICA	Platform On ICA	Engine Off ICA	Engine On ICA
*					**		*	**

*Significance (one-tailed) is determined using the Wilcoxon sign-rank test. * = $p < 0.05$; ** = $p < 0.01$; *** = $p < 0.001$.*

Table 4 | Statistical significance evaluated across trials of the test set for the various contrasts.

A. ICA vs. Baseline Pre-ICA						
Overall	Platform	Biplane	Platoff	Platon	Engoff	Engon
**		**				**
B. ICA + Kalman vs. Baseline Pre-ICA						
Overall	Platform	Biplane	Platoff	Platon	Engoff	Engon
**		**			*	**
C. Off vs. On						
Overall	Platform	Biplane				
***	**	*				
D. ICA + Kalman vs. ICA						
Overall	Platform	Biplane	Platoff	Platon	Engoff	Engon
		*			*	

*Significance (one-tailed) is determined using the Wilcoxon sign-rank test. * = $p < 0.05$; ** = $p < 0.01$; *** = $p < 0.001$.*

classification performance was comparable to that of the Engine Off condition (81.1%) in which the biplane was sitting on the tarmac. It is unclear why the Platform On condition did not show the same beneficial effects of ICA Kalman filtering vs. the baseline no processing condition (73.1% vs. 71.6% respectively), as did the Biplane Engine On condition (See **Tables 1–4**). One possibility is that the abrupt movement of the body and head during the flight task produced non-stationary artifacts that could not be separated by the EEGLAB artifact cleaning methods or by ICA and Kalman filtering. In the future utilizing data from an accelerometer mounted on the head as a regressor of non-interest may be able to extract possible movement related artifacts and improve classification performance. The significantly greater accuracy for the Off over the On conditions is to be expected (See **Tables 1–4**) not only because of the much greater artifacts present in the On conditions but also because auditory responses are decreased depending on attention (Paul et al., 2014). It is likely that the attention needed for piloting in the On conditions reduced attention to the auditory stimuli.

The use of Kalman filtering was most effective when conducted on ICA processed data. Kalman filtering on pre-ICA data did not show improvement in performance compared to that of ICA processed data (See **Tables 1–4**). One possible explanation for these results is that ICA is able to separate the brain activity related to the auditory event from other brain activity and artifacts allowing for better estimation by the Kalman filter that utilizes generic information about the auditory evoked response as a dynamical model. In the pre-ICA data the brain activity for various processes as well as artifacts are mixed within all the channels and estimation of the auditory events by the Kalman filter model may be more difficult for these signals.

Because the results are only of a single subject it is not clear how well they generalize to other individuals. It is likely that different individuals with different levels of flight experience may show more/or less movement and physiological artifacts that may decrease/increase classification performance. The Cognionics dry wireless EEG system has already been shown to give good classification performance on a SSVEP test across a number of subjects (Lin et al., 2014). The Lin et al. (2014) study demonstrates that the Cognionics EEG system is able to extract from a group of individuals and is not just limited to a few special individuals. ICA has additionally been shown to be very good at extracting artifacts and task related components from EEG data (Delorme et al., 2007). This was also demonstrated

for the data collected in this study and it is unlikely that it is only applicable to the single subject that participated. Despite these limitations the results do stand as a demonstration that it is possible to collect data in real-world environments that have considerable noise, both environmental and physiological, using dry-wireless EEG and obtain classification performance sufficient for some BMI augmentive neuroscience based applications. The research presented here lays a foundation for future aviation based studies where subject variability in EEG responses can be evaluated.

For effective use in implementing BMI in real-world applications it is necessary that the processes used for classification be fast enough for online control either in terms of manipulating robotic devices, giving feedback to the operator, and/or utilizing adaptive automation to augment human performance (Byrne and Parasuraman, 1996; Wilson and Russell, 2007). One of the key elements of this study was that the training set came from the first 75% of the data and the novel test set came from the last 25% of the data. All of the artifact-cleaning methods were applied to the training set and the same criteria and weights were then applied to the testing set. ASR, ICA, and LSPC classifier model selection by cross-validation requires some processing time depending on computer speed. In our case running the programs in Matlab on a MacBook Pro took around 10 min. The largest portion of time was spent computing the ICA. Therefore, implementation of a BMI would require a delay of approximately 10 min after the training data is collected before it could be applied if ICA is used. Just a couple minutes for model selection and training are required if ICA is not used. The extraction of channels, the ASR model, and the ICA weights from the training data as well as the Kalman filter can be applied without delay (the delay is the same as the sampling rate) to the test set. In this case the features used in the classification model were samples for 500 ms after stimulus onset. Therefore, depending on the type of initial band-pass filtering, the processing delay to control the BMI could be around 515 ms. Although the initial band-pass filter order for processing this data set was 496 samples, which would create a considerable delay it is possible to implement different types of filters with a lower order to decrease the processing delay. A delay of less than a second could certainly be used in a BMI to give a warning signal to the pilot or engage adaptive automation (Byrne and Parasuraman, 1996; Wilson and Russell, 2007), however, it is not sufficient for closed-loop control.

Given the significant number of aviation accidents that result from missed auditory alarms (Bliss, 2003; Scannella et al., 2013; Dehais et al., 2014), a BMI based on detection of auditory events could be quite important in giving alternate forms of feedback to warn the pilot when necessary. It is well known that high workload decreases the ability to perceive task-irrelevant and/or unattended visual and auditory information (Lavie, 1995, 2005, 2010). This phenomenon is called inattentional blindness with respect to vision (Mack and Rock, 1998) and inattentional deafness with respect to audition (Wood and Cowan, 1995; Macdonald and Lavie, 2011; Dehais et al., 2014). Inattentional deafness is known to be a critical factor in missing of auditory alarms in aeronautics (Dehais et al., 2014). It is interesting that although task irrelevant auditory stimuli can be presented in the background without any decrement in task related performance, the evoked brain potentials to these auditory events is modulated by workload on the primary task (Krammer et al., 1995). As such, it may be possible to assess the workload of the pilot and likely occurrences of inattentional deafness by investigating brain response to auditory events. An EEG based BMI system could potentially be used to decode the mental state of the pilot for occurrence of inattantional deafness and augment their mental state by feedback through a different modality or engage adaptive automation. Considerably more research needs to be conducted to determine on a single event basis whether an incidence of inattentional deafness is present or not before such a system can be implemented.

When one considers that brain dynamics are different while undergoing complex tasks in natural environments from that of the laboratory (McDowell et al., 2013; Lin et al., 2014) and that dry EEG systems are susceptible to movement-based artifacts (Guger et al., 2012; Lin et al., 2014) the single-trial classification performance of auditory perceptual events by a dry-wireless EEG system in the robust flight conditions of our study are quite impressive. This research demonstrates the feasibility of new avenues for investigating brain processes in real-world situations that cannot be conducted in the laboratory. In addition the research presented here also demonstrates that plausible BMI using dry-wireless EEG can be implemented in real-world settings to augment human performance.

ACKNOWLEDGMENTS

I would like to thank Makoto Miyakoshi and John Iversen for assistance with pre-processing techniques in EEGLAB and Mike Chi for assistance with the Cognionics EEG system. I would also like to thank James Zapata for piloting assistance in carrying out the experiment in the biplane. In addition I would like to give special thanks to Wayne Spani and sons for all their great work on the Starduster.

REFERENCES

Bell, A. J., and Sejnowski, T. J. (1995). An information-maximization approach to blind separation and blind deconvolution. *Neural Comput.* 7, 1129–1159. doi: 10.1162/neco.1995.7.6.1129

Bin, G., Gao, X., Yan, Z., Hong, B., and Gao, S. (2009). An online multichannel SSVEP-based brain-computer interface using a canonical correlation analysis method. *J. Neural Eng.* 6:046002. doi: 10.1088/1741-2560/6/4/046002

Birbaumer, N., Ghanayim, N., Hinterberger, T., Iversen, I., Kotchoubey, B., Kübler, A., et al. (1999). A spelling device for the paralysed. *Nature* 398, 297–298. doi: 10.1038/18581

Blanc, C., Lafontain, E., and Medvadeff, M. (1966). Radiotelemetric recordings of the electroencephalograms of civil aviation pilots during flight. *Aerosp. Med.* 37, 1060–1065.

Blankertz, B., Tangermann, M., Vidaurre, C., Fazli, S., Sannelli, C., Haufe, S., et al. (2010). The Berlin brain-computer interface: non-medical uses of BCI technology. *Front. Neurosci.* 4:198. doi: 10.3389/fnins.2010.00198

Bliss, J. P. (2003). Investigation of alarm-related accidents and incidents in aviation. *Int. J. Aviat. Psychol.* 13, 249–268. doi: 10.1207/s15327108ijap1303_04

Byrne, E. A., and Parasuraman, R. (1996). Psychophysiology and adaptive automation. *Biol. Psychol.* 42, 249–268. doi: 10.1016/0301-0511(95)05161-9

Caldwell, J. A., and Lewis, J. A. (1995). The feasibility of collecting in-flight EEG data from helicopter pilots. *Aviat. Space Environ. Med.* 66, 883–889.

Callan, D. E., Gamez, M., Cassel, D. B., Terzibas, C., Callan, A., Kawato, M., et al. (2012). Dynamic visuomotor transformation involved with remote flying of a plane utilizes the 'Mirror neuron' system. *PLoS One* 7:e33873. doi: 10.1371/journal.pone.0033873

Callan, D. E., Terzibas, C., Cassel, D. B., Callan, A., Kawato, M., and Sato, M. A. (2013). Differential activation of brain regions involved with error-feedback and imitation based motor simulation when observing self and an expert's actions in pilots and non-pilots on a complex glider landing task. *Neuroimage* 72, 55–68. doi: 10.1016/j.neuroimage.2013.01.028

Cheron, G., Cebolla, A. M., Petieau, M., Bengoetxea, A., Palmero-Soler, E., Leroy, A., et al. (2009). Chapter 13 adaptive changes of rhythmic EEG oscillations in space: implications for brain-machine interface applications. *Int. Rev. Neurobiol.* 86, 171–187. doi: 10.1016/s0074-7742(09)86013-3

Chi, Y. M., Wang, Y., Wang, Y.-T., Jung, T.-P., Kerth, T., and Cao, Y. (2013). "A practical mobile dry EEG system for human computer interfaces," in *Foundations of Augmented Cognition*, eds D. Schmorrow and C. Fidopiastis (Berlin, Heidelberg: Springer), 649–655.

Dehais, F., Causse, M., Vachon, F., Régis, N., Menant, E., and Tremblay, S. (2014). Failure to detect critical auditory alerts in the cockpit: evidence for inattentional deafness. *Hum. Factors* 56, 631–644. doi: 10.1177/0018720813510735

Delorme, A., and Makeig, S. (2004). EEGLAB: an open source toolbox for analysis of single-trial EEG dynamics including independent component analysis. *J. Neurosci. Methods* 134, 9–21. doi: 10.1016/j.jneumeth.2003.10.009

Delorme, A., Sejnowski, T., and Makeig, S. (2007). Improved rejection of artifacts from EEG data using high-order statistics and independent component analysis. *Neuroimage* 34, 1443–1449. doi: 10.1016/j.neuroimage.2006.11.004

Dornhege, G., del, R., Millan, J., Hinterberger, T., McFarland, D. J., and Muller, K. (eds) (2007). *Toward Brain-Computer Interfacing.* Cambridge, MA: MIT Press.

Dussault, C., Jouanin, J. C., and Guezennec, C. Y. (2005). EEG and ECG changes during selected flight sequences. *Aviat. Space Environ. Med.* 75, 889–897.

Georgiadis, S. D., Ranta-aho, P. O., Tarvainen, M. P., and Karjalainen, P. A. (2005). Single-trial dynamical estimation of event-related potentials: a Kalman filter-based approach. *IEEE Trans. Biomed. Eng.* 52, 1397–1406. doi: 10.1109/tbme.2005.851506

Grewal, M. S., and Andrews, A. P. (2008). *Kalman Filtering: Theory and Practice using MATLAB.* Hoboken, NJ: John Wiley and Sons.

Groenegress, C., Holzner, C., Guger, C., and Slater, M. (2010). Effects of P300-based BCI use on reported presence in a virtual environment. *Presence* 19, 1–11. doi: 10.1162/pres.19.1.1

Guger, C., Ktausz, G., Allison, B. Z., and Edlinger, G. (2012). Comparison of dry and gel based electrodes for p300 brain-computer interfaces. *Front. Neurosci.* 6:60. doi: 10.3389/fnins.2012.00060

Hankins, T. C., and Wilson, G. F. (1998). A comparison of heart rate, eye activity, EEG and subjective measures of pilot mental workload during flight. *Aviat. Space Environ. Med.* 69, 360–367.

Howitt, J. S., Hay, A. E., Shergold, G. R., and Ferres, H. M. (1978). Workload and fatigue–in-flight EEG changes. *Aviat. Space Environ. Med.* 49, 1197–1202.

Kalman, R. E. (1960). A new approach to linear filtering and prediction problems. *J. Fluids Eng.* 82, 35–45. doi: 10.1115/1.3662552

Krammer, A. F., Trejo, L. J., and Humphrey, D. (1995). Assessment of mental workload with task-irrelevant auditory probes. *Biol. Psychol.* 40, 83–100. doi: 10.1016/0301-0511(95)05108-2

LaFleur, K., Cassady, K., Doud, A., Shades, K., Rogin, E., and He, B. (2013). Quadcopter control in three-dimensional space using a noninvasive motor imagery-based brain-computer interface. *J. Neural Eng.* 10:046003. doi: 10.1088/1741-2560/10/4/046003

Lavie, N. (1995). Perceptual load as a necessary condition for selective attention. *J. Exp. Psychol. Hum. Percept. Perform.* 21, 451–468. doi: 10.1037//0096-1523.21.3.451

Lavie, N. (2005). Distracted and confused?: selective attention under load. *Trends Cogn. Sci.* 9, 75–82. doi: 10.1016/j.tics.2004.12.004

Lavie, N. (2010). Attention, distraction and cognitive control under load. *Curr. Dir. Psychol. Sci.* 19, 143–148. doi: 10.1177/0963721410370295

Liao, L. D., Chen, C. Y., Wang, I. J., Chen, S. F., Li, S. Y., Chen, B. W., et al. (2012). Gaming control using a wearable and wireless EEG-based brain-computer interface device with novel dry foam-based sensors. *J. Neuroeng. Rehabil.* 9:5. doi: 10.1186/1743-0003-9-5

Liao, L. D., Wang, I. J., Chen, S. F., Chang, J. Y., and Lin, C. T. (2011). Design, fabrication and experimental validation of a novel dry-contact sensor for measuring electroencephalography signals without skin preparation. *Sensors* 11, 5819–5834. doi: 10.3390/s110605819

Lin, Y. P., Wang, Y., Wei, C. S., and Jung, T. P. (2014). Assessing the quality of steady-state visual-evoked potentials for moving humans using a mobile electroencephalogram headset. *Front. Hum. Neurosci.* 8:182. doi: 10.3389/fnhum.2014.00182

Macdonald, J. S., and Lavie, N. (2011). Visual perceptual load induces inattentional deafness. *Atten. Percept. Psychophys.* 73, 1780–1789. doi: 10.3758/s13414-011-0144-4

Mack, A., and Rock, I. (1998). *Inattentional Blindness.* Cambridge: MIT Press.

Maulsby, R. (1966). Electroencephalogram during orbital flight. *Aerosp. Med.* 37, 1022–1026.

McDowell, K., Chin-Teng, L., Oie, K. S., Jung, T. P., Gordon, S., Whitaker, K., et al. (2013). Real-world neuroimaging technologies. *IEEE Access* 1, 131–149. doi: 10.1109/access.2013.2260791

Millàn Jdel, R., Ferrez, P. W., and Seidl, T. (2009). Chapter 14 validation of brain-machine interfaces during parabolic flight. *Int. Rev. Neurobiol.* 86, 189–197. doi: 10.1016/s0074-7742(09)86014-5

Mullen, T., Kothe, C., Chi, Y. M., Ojeda, A., Kerth, T., Makeig, S., et al. (2013). "Real-time modeling and 3D visualization of source dynamics and connectivity using wearable EEG," in *EMBC, 25th Annual International Conference of the IEEE* (Osaka: IEEE), 2184–2187.

Müller, K., Tangermann, M., Dornhege, G., Krauledat, M., Curio, G., and Blankertz, B. (2008). Machine learning for real-time single-trial EEG-analysis: from brain-computer interfacing to mental state monitoring. *J. Neurosci. Methods* 167, 82–90. doi: 10.1016/j.jneumeth.2007.09.022

Parasuraman, R. (2003). Neuroergonomics; research and practice. *Theor. Issues Ergon. Sci.* 4, 5–20. doi: 10.1080/14639220210199753

Parasuraman, R., and Rizzo, M. (2008). *Neuroergonomics: The Brain at Work.* New York, NY: Oxford University Press.

Park, J., Xu, L., Sridhar, V., Chi, M., and Cauwenberghs, G. (2011). "Wireless dry EEG for drowsiness detection," in *33rd Annual International Conference of the IEEE EMBS* (Boston, Massachusetts USA: IEEE).

Paul, B. T., Bruce, I. C., Bosnyak, D. J., Thompson, D. C., and Roberts, L. E. (2014). Modulation of electrocortical brain activity by attention in individuals with and without Tinnitus. *Neural Plast.* 2014:127824. doi: 10.1155/2014/127824

Sauvet, F., Baugard, C., Coroenne, M., Lely, L., Van Beers, P., Elbaz, M., et al. (2014). In-flight automatic detection of vigilance states using a single EEG channel. *IEEE Trans. Biomed. Eng.* 61, 2840–2847. doi: 10.1109/TBME.2014.2331189

Scannella, S., Causse, M., Chauveau, N., Pastor, J., and Dehais, F. (2013). Effects of the audiovisual conflict on auditory early processes. *Int. J. Psychophysiol.* 89, 115–122. doi: 10.1016/j.ijpsycho.2013.06.009

Sellers, E. W., Ryan, D. B., and Hauser, C. K. (2014). Noninvasive brain-computer interface enables communication after brainstem stroke. *Sci. Transl. Med.* 6:257re7. doi: 10.1126/scitranslmed.3007801

Sem-Jacobsen, C. W., Nilseng, O., Patten, C., and Eriksen, O. (1959). Electroencephalographic recording in simulated combat flight in a jet fighter plane. *Electroencephalogr. Clin. Neurophysiol.* 11, 154–155. doi: 10.1016/0013-4694(59)90018-5

Shenoy, P., Miller, K. J., Ojemann, J. G., and Rao, R. P. (2008). Generalized features for electrocorticographic BCIs. *IEEE Trans. Biomed. Eng.* 55, 273–280. doi: 10.1109/tbme.2007.903528

Sterman, M., Schummer, G., Dushenko, T., and Smith, J. (1987). "Electroencephalographic correlates of pilot performance: simulation and in-flight studies," in *Electrical and Magnetic Activity of the Central Nervous System: Research and Clinical Applications in Aerospace Medicine* (Neuilly Sur Seine, France: Nato. AGARD CP No. 432), 1–16.

Sugiyama, M. (2010). Superfast-trainable multi-class probabilistic classifier by least-squares posterior fitting. *IEICE Trans. Inf. Syst.* 93-D, 2690–2701.

Wang, Y., Wang, R., Gao, X., Hong, B., and Gao, S. (2006). A practical VEP-based brain-computer interface. *IEEE Trans. Neural Syst. Rehabil. Eng.* 14, 234–239. doi: 10.1109/tnsre.2006.875576

Wilson, G. F., and Russell, C. A. (2007). Performance enhancement in an uninhabited air vehicle task using psychophysiologically determined adaptive aiding. *Hum. Factors* 49, 1005–1018. doi: 10.1518/001872007x249875

Wolpaw, J. R., McFarland, D. J., and Vaughan, T. M. (2002). Brain computer interface research at the Wadsworth center. *IEEE Trans. Rehabil. Eng.* 8, 222–226. doi: 10.1109/86.847823

Wood, N. L., and Cowan, N. (1995). The cocktail party phenomenon revisited: attention and memory in the classic selective listening procedure of Cherry (1953). *J. Exp. Psychol. Gen.* 124, 243–262. doi: 10.1037/0096-3445.124.3.243

Zao, J. K., Gan, T. T., You, C. K., Chung, C. E., Wang, Y. T., Rodríguez Méndez, S. J., et al. (2014). Pervasive brain monitoring and data sharing based on multi-tier distributed computing and linked data technology. *Front. Hum. Neurosci.* 8:370. doi: 10.3389/fnhum.2014.00370

Conflict of Interest Statement: The authors declare that the research was conducted in the absence of any commercial or financial relationships that could be construed as a potential conflict of interest.

Received: 01 November 2014; accepted: 23 January 2015; published online: 17 February 2015.

Citation: Callan DE, Durantin G and Terzibas C (2015) Classification of single-trial auditory events using dry-wireless EEG during real and motion simulated flight. Front. Syst. Neurosci. ***9****:11. doi: 10.3389/fnsys.2015.00011*

This article was submitted to the journal Frontiers in Systems Neuroscience.

frontiers in Neuroscience

REVIEW
published: 21 November 2016
doi: 10.3389/fnins.2016.00530

The Berlin Brain-Computer Interface: Progress Beyond Communication and Control

Benjamin Blankertz[1,2], Laura Acqualagna[1], Sven Dähne[3], Stefan Haufe[2,3], Matthias Schultze-Kraft[1,2], Irene Sturm[1], Marija Ušćumlic[1], Markus A. Wenzel[1], Gabriel Curio[2,4] and Klaus-Robert Müller[2,3,5]**

[1] Neurotechnology Group, Technische Universität Berlin, Berlin, Germany, [2] Bernstein Focus: Neurotechnology, Berlin, Germany, [3] Machine Learning Group, Technische Universität Berlin, Berlin, Germany, [4] Neurophysics Group, Department of Neurology, Campus Benjamin Franklin, Charité - University Medicine Berlin, Berlin, Germany, [5] Department of Brain and Cognitive Engineering, Korea University, Seoul, South Korea

The combined effect of fundamental results about neurocognitive processes and advancements in decoding mental states from ongoing brain signals has brought forth a whole range of potential neurotechnological applications. In this article, we review our developments in this area and put them into perspective. These examples cover a wide range of maturity levels with respect to their applicability. While we assume we are still a long way away from integrating Brain-Computer Interface (BCI) technology in general interaction with computers, or from implementing neurotechnological measures in safety-critical workplaces, results have already now been obtained involving a BCI as research tool. In this article, we discuss the reasons why, in some of the prospective application domains, considerable effort is still required to make the systems ready to deal with the full complexity of the real world.

Keywords: Brain-Computer Interfacing (BCI), electroencephalography (EEG), covert user states, machine learning, mental workload, video quality, implicit information, cognitive neuroscience

OPEN ACCESS

Edited by:
Mikhail Lebedev, Duke University, USA

Reviewed by:
Surjo R. Soekadar, University Hospital of Tübingen, Germany
Sue Becker, McMaster University, Canada
Gert Cauwenberghs, University of California, San Diego, USA

****Correspondence:***
Benjamin Blankertz
benjamin.blankertz@tu-berlin.de
Klaus-Robert Müller
klaus-robert.mueller@tu-berlin.de

Specialty section:
This article was submitted to Neuroprosthetics, a section of the journal Frontiers in Neuroscience

Received: *21 April 2016*
Accepted: *31 October 2016*
Published: *21 November 2016*

Citation:
Blankertz B, Acqualagna L, Dähne S, Haufe S, Schultze-Kraft M, Sturm I, Ušćumlic M, Wenzel MA, Curio G and Müller K-R (2016) The Berlin Brain-Computer Interface: Progress Beyond Communication and Control. Front. Neurosci. 10:530. doi: 10.3389/fnins.2016.00530

1. INTRODUCTION

Since the discovery of electrical brain activity and the invention of the Electroencephalogram (EEG), by Hans Berger in 1924 (Berger, 1929), there have been many ideas and dreams about how to exploit this access to the center of human thoughts and emotions and the control of actions. Gray Walter developed the toposcope in 1951 which visualized rhythmic brain activity in 22 spatially laid out cathode ray tubes, each of which showing amplitude and phase in spiral displays (Walter and Shipton, 1951; Bladin, 2006). In the 1960s, realtime EEG was used in artistic performances (e.g., Lucier, 1965; Straebel and Thoben, 2014) and for neurofeedback training (Kamiya, 1969). The latter laid the foundation for possible clinical applications by neurofeedback (Sterman and Friar, 1972). This research led to the idea that human intentions could be transmitted directly from brain to computer (Vidal, 1973). By voluntarily acquiring certain mental states, the user of such a Brain-Computer Interface (BCI) could communicate or control a technical device while circumventing the need for any muscular activity (Dornhege et al., 2007; Wolpaw and Wolpaw, 2012). Clinical application has been the principal goal of BCI research for about four decades (Elbert et al., 1980; Kübler et al., 2005; Shih et al., 2012; Faller et al., 2014; Gallegos-Ayala et al., 2014; Hill et al., 2014; Morone et al., 2015; Soekadar et al., 2015).

In the last decade, the potential of *non*-medical applications of BCI technology has increasingly drawn renewed attention (Müller et al., 2008; Blankertz et al., 2010; van Erp et al., 2012). Two of

the five application scenarios defined in the roadmap of brain/neural-computer interaction (BNCI Horizon 2020, 2015; Brunner et al., 2015), primarily target non-medical areas. The *enhance* scenario comprises applications that enhance human functions or user interactivity by adapting the device to their momentary mental state, for example, and by exploiting implicit information about the user's intention. The *research tool* scenario utilizes real-time analysis of neural signals to investigate and understand brain and cognitive functions.

In this review, we deliberately focus on certain developments that we discuss in some detail. We hope that this focused view on our own work will nevertheless be of use to the interested reader and still provide a broad account of the developments of BCI-enhanced neurotechnology. We leave aside a wide range of other relevant research, though it is no less important, pointing here exemplarily just at a few: One potentially interesting aspect for enhancing human-computer interaction is the possibility of predicting the subject confidence of participants (Graziano et al., 2015). Research on memory encoding processes is converging toward the feasibility of predicting the success of memorization by observing brain signals before and/or during encoding (Noh et al., 2014; Cohen et al., 2015). An elaboration of these techniques toward online prediction based on single-trial data would have interesting applications in adaptive learning software. A collective computer game was used to collect data sets from 523 participants in a single night who controlled an immersive art environment with the mental states of relaxation and concentration (Kovacevic et al., 2015).

2. OVERVIEW OF THE APPLICATIONS

Since our first review (Blankertz et al., 2010), 6 years have passed, bringing a wealth of novel developments. In this article, we review a selection of our research in this direction. Unlike in most medical applications, these approaches do not employ BCIs to let the user consciously transmit information to the computer. Instead, they use BCIs to infer covert user states and implicit information.

2.1. Types and Components of Brain Signals Being Exploited

Brain signals are either of the *exogenous* type, in which corresponding processes are elicited by external stimuli, or they are *endogenous*, originating from the participant independently of external events. Examples of endogenous brain signals include preparatory signals, such as the readiness potential (RP) and ongoing oscillations, like the alpha rhythm of the visual cortex. The exogenous signals that originate from the cortex can be roughly divided into those that are as being perception related, e.g., the visual evoked potential (VEP), the N1–P2 complex, and the steady-state visual evoked potential (SSVEP) or as being related to cognitive processes such as the P300 or the late positive component. The BCI applications that are reviewed here exploit all of these different types of brain signals—sometimes they are used in combination, sometimes just one alone.

2.2. Stratification of Use Cases

2.2.1. Type I: BCI as a Tool for Research

BCIs can provide an instantaneous estimate of the mental state and processing of an experimental subject. This possibility offers novel opportunities for (notably non-BCI-related) research. In Section 7, we show how closed-loop technology can be harnessed to study the relationship between preparatory signals (the RP) and corresponding actions—particularly the vetoing of such actions—and how it can thereby contribute to a fundamental question in cognitive neuroscience. The studies reviewed in Section 8 similarly target research questions in a different domain: the cognition and processing of music. In contrast to previous studies, it is not the real-time aspect that is exploited here, but rather the increased sensitivity to the methods that have been developed in BCI contexts. These algorithms enable a step forward in the analysis of music perception from fundamental studies with artificial and repeated stimuli toward investigating more natural behavior in music listening.

2.2.2. Type II: BCI as a Tool to Improve Devices, Interfaces, or Infrastructure

By providing brain-based measures while a participant is using a certain interface or product, or is interacting in a certain environment, one can assess and compare different variants and settings. A navigation system for a car may be tested and optimized with respect to how little it distracts the driver from the driving task as quantified by neural measures of workload or focused attention (Kohlmorgen et al., 2007; Blankertz et al., 2010). This is an example of an effect about which it is difficult to obtain reliable and unbiased measures through means such as questionnaires. The quantification of mental workload under real world conditions, however, is still a challenge for neurotechnologies. This ability would open an attractive range of applications. Section 5 presents some novel data analysis techniques that can be useful in this context. A workload index could also be employed to assess safety-critical aspects of infrastructure, such as harbors and bridges that require demanding maneuvers (Miklody et al., 2016).

An example of this application type in a quite different domain is given in Section 4. Visual perception of slight distortions in videos is probed and quantified as SSVEP amplitude, giving rise to a potential means of assessing the quality of video codecs. We contrast this approach with alternatives that employ cognitive event-related potential (ERP) components.

2.2.3. Type III: BCI as a Device to Enhance or Facilitate Human Actions

The direct control of computer applications with a BCI does not seem to be a realistic objective for healthy users. Yet some mileage could well be gained from using a BCI to obtain implicit information from a user during computer use. Added to the explicit information the computer obtains during an interaction, such implicit information should enable computers to understand human users better. We summarize studies dealing with various aspects of such implicit interactions in Section 6.

Section 3 explores the potential of BCI technology to provide information about an intended action before its execution. This

potential is exemplified in the prediction of emergency braking when driving. A similar methodology is used in Section 7 as described above. But whereas the allter[PS1] use case exploits endogenous signals only, the prediction of emergency braking is based on a combination of different components, including perceptual and cognitive exogenous signals. For potential applications of the possibility of speeding up actions with BCIs, however, one needs to consider that this by-pass bears the risk of triggering actions on premature intentions and that it eliminates the possibility of vetoing the respective action in the last moment. This aspect is backed by the results reviewed in Section 7. The techniques for establishing a neural workload index, as mentioned above, may also be employed in a closed-loop fashion. Section 7 demonstrates such a type of application in the context of adapting working environments to the human factor.

2.3. Comparisons of the Categories of Use Cases

Type I. The use of BCIs as a tool for research is an easier case, in several ways. Experiments are conducted under laboratory conditions, complexity is often reduced to one variable of interest, standard EEG equipment with lengthy preparation times does not pose a serious problem, and it is not problematic if the system does not work for all participants. Still, specific requirements of a given use case can make the enterprise a challenge. In this category, the end users of the BCI are the researchers.

Type II. Using BCI technology in this way seems realistic in the medium term. The scenarios are often complex (e.g., driving a car), with mingled interactions between various perceptual and cognitive processes, calling for advanced decoding methods. On the other hand, there is no strict requirement for an easily deployable setup, the experimental conditions are somewhat controlled, and the experimental subjects can be selected according to the decodability of the given brain processes (provided that the selection criterion does not imply a bias with respect to the subject of investigation). Applications in this category mostly do not critically rely on the real-time aspect. In this case, the end users are the companies that develop the devices or interfaces, as well as the institutions that are responsible for the infrastructure.

Type III. BCI applications in this category are mostly rather far-reaching. The concepts are not yet ready for the dynamics and complexity of the real world, the measurement devices need to be easily deployable, yet also to provide robust signals, and the system should work preferably for anyone, as all human beings[PS3] are the end users in this category.

3. DETECTION OF EMERGENCY BRAKING INTENTION DURING DRIVING

This section summarizes two studies that investigate the possibility of predicting upcoming emergency braking from neural signals. The method makes use of exogenous ERPs related to perception and cognition in combination with an endogenous signal that indicates the preparation of a movement. We discuss potential benefits and caveats.

3.1. Context: Neurotechnology in the Context of Driving a Car

Neurotechnology can detect specific brain states before they reach consciousness and before they trigger behavioral actions (Section 7). Neuroergonomic approaches are therefore of interest for increasing our understanding of physiological aspects in time- and safety-critical applications, because a potentially dangerous situation may be detected before the user is aware of it and/or able to respond to it. In this section, we explore the feasibility and utility of this approach in driving a car. Kohlmorgen et al. (2007) and Dijksterhuis et al. (2013) study EEG correlates of mental workload during real-world and simulated driving, while (Kecklund and Åkerstedt, 1993; Papadelis et al., 2007; Schmidt et al., 2007, 2009; Gugler et al., 2010; Simon et al., 2011; Sonnleitner et al., 2012) study fatigue and attention during monotonous real-world driving. Reaction time in lane changing tasks has been investigated with EEG (Zhang et al., 2015a). Further studies demonstrate the detection of error and anticipatory potentials that could potentially be harnessed to increase driving safety (Khaliliardali et al., 2015; Zhang et al., 2015b). In emergency situations caused by obstacles on the road, drivers need to react quickly by braking. Such events lead to a cascade of mental responses from the perception and evaluation of the emergency-inducing stimulus to the activation of the lower limb muscles initiating the release of the gas pedal and the activation of the brake pedal. Due to the latencies inherent in motor responses, and due to the complexity of the required movement, the time spent between the stimulus and an effective deceleration of the vehicle can easily be on the order of 1 s, even if the decision to brake is made several hundred milliseconds earlier. This delay has led to attempts to retrieve the driver's braking intent earlier, which can be done by considering additional behavioral inputs such as gas pedal release, steering angle, foot position, and head movements (McCall and Trivedi, 2007; Trivedi and Cheng, 2007). Neuroergonomic approaches have the potential to prompt the user's decision even earlier—at the time of its very emergence—by tapping directly into the brain. This extra time might in principle either be used to prevent crashes through automatic braking, or to perform preparatory measures aimed at mitigating the impact of a crash through an automated response such as tightening the seat belts.

3.2. Two Studies on Predicting Emergency Braking

The first study to describe such a system was Haufe et al. (2011). In a driving simulator, $N = 18$ participants were instructed to follow a computer-controlled vehicle. The distance between vehicles was 20 m; the speed was 100 km/h. Occasionally (20–40 s inter-stimulus-interval, randomized), a rapid braking of the leading vehicle would induce an emergency braking situation. In order to avoid a crash, participants were required to perform immediate emergency braking in these situations. The onset of the lead vehicle's braking (and brake light flashing) is here

referred to as the *stimulus*. The experiment comprised three blocks (45 min each) of driving with 10–15 min periods of rest in-between.

The authors measured myoelectric (EMG) activity using two bipolar electrodes located at the *M. tibialis anterior* and the knee of the right leg, as well as electroencephalography (EEG) from 64 scalp sites (nose reference). Behavioral and technical data—including brake and gas pedal deflections, the acceleration of the participant's vehicle, and the distance between vehicles—were also measured and synchronized with the physiological data. This yielded a multivariate, multi-modal time series from which the segments reflecting induced emergency situations and normal driving periods, respectively, were extracted.

Using univariate analysis, the authors discovered a characteristic event-related potential (ERP) signature preceding executed emergency braking in the EEG data. They then used multivariate machine learning to compare the predictive power (derived by distinguishing emergency braking from normal driving episodes) of a system utilizing all measurement modalities to systems either omitting EEG, EMG, or both. The study was later replicated with $N = 20$ subjects in a real car on a non-public test track (Haufe et al., 2014a).

Figure 1 depicts the event-related potentials that are characteristic of forced emergency braking. In both studies, a spatio-temporal ERP complex composed of the three overlapping subcomponents was observed: an early symmetric negative deflection in occipito-temporal areas, a negativity at central scalp sites, and a positive deflection in centro-parietal areas. The early occipital negativity is a visual-evoked potential (VEP) that can be attributed to low-level processing of the flashing of the brake light of the leading vehicle, which initiates the emergency situation. Higher-level processing of the importance of this flashing is reflected in the later centro-parietal positivity (P300). The late central negativity amounts to the readiness potential (RP), which reflects the motor preparation and execution related to pressing the brake pedal.

Figure 2 shows the detection accuracy of single-trial braking intention using a multivariate classifier as achieved on hold-out data and measured using the area under the curve (AUC) score. The classifier was evaluated at each stage of emergency braking between 0 and 1200 ms post-stimulus using data from the preceding 1500 ms. Without the EEG and EMG channels, the performance significantly dropped between approximately 200 and 1000 ms post-stimulus in both studies, indicating that EEG and EMG contain important information about the driver's intention that is not available in the combined remaining channels in the early stage of dealing with an emergency.

3.3. Conclusion and Outlook

Summarizing, Haufe et al. (2011) showed that EEG and EMG recordings reach the predictive accuracy of behavioral channels at earlier stages of the emergency situation. Their laboratory results were reproduced during real-world driving (Haufe et al., 2014a), demonstrating that well-designed simulator studies can be a useful proxy for real world studies. The results have also been confirmed under more diversified traffic conditions (Kim et al., 2014; Khaliliardali et al., 2015).

The robustness of our findings motivates the use of neuroergonomic approaches to driving assistance. Such a system may detect a driver's intention to brake before any of their actions become observable, and may thereby reduce the time after which appropriate action can be carried out. Haufe et al. (2011) evaluated a simplistic implementation of an online emergency braking detector in their simulation environment, and estimated that the time that can be saved by the system is around 130 ms. At 100 km/h, this amounts to a reduction of the braking

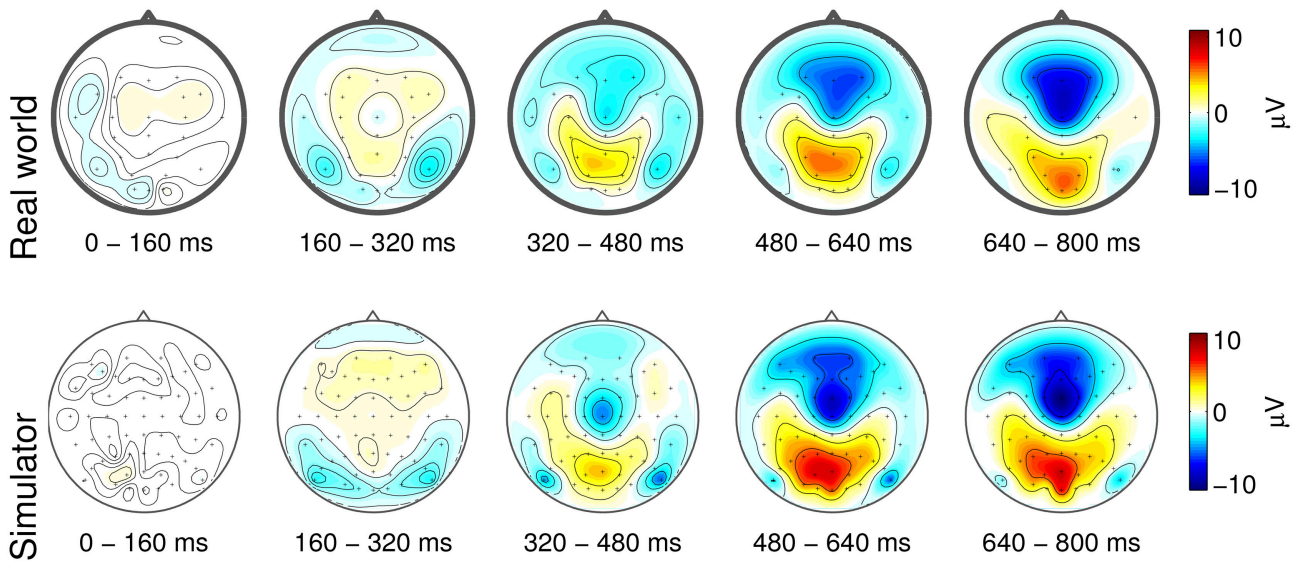

FIGURE 1 | Grand-average stimulus-aligned EEG responses to forced emergency braking during real-world (upper panel) and laboratory driving (lower panel). Potentials are visualized as topographical maps of grand-average ERPs in five temporal intervals. The stimulus onset ($t = 0$ ms) is the time of the brake lightbrake light flashing of the lead vehicle. Figure taken from Haufe et al. (2014a) with permission.

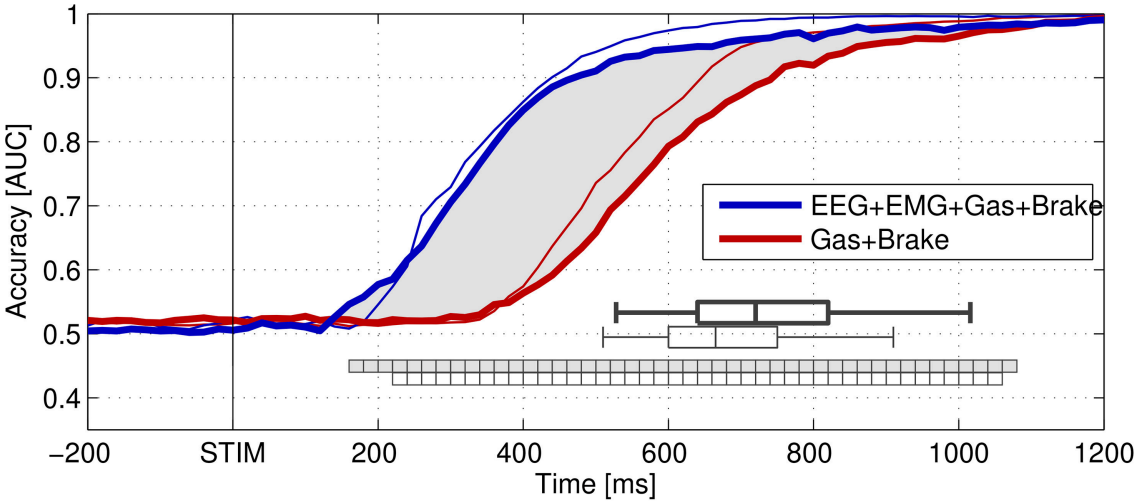

FIGURE 2 | Grand-average area under the curve (AUC) scores calculated from the outputs of linear classifiers that were optimized to distinguish normal driving intervals from stimulus-aligned target intervals representing different stages of emergency braking situations. STIM denotes the onset of braking (brake light flashing) of the lead vehicle. Thick lines represent the results of the real-world driving study (Haufe et al., 2014a), while thin lines represent results obtained in the driving simulator study of Haufe et al. (2011). The distribution of pooled braking response times in both datasets is indicated by box plots showing the 5th, 25th, 50th (median), 75th, and 95th percentiles. Classification was based on (spatio-) temporal features observed prior to the decision points. Performance of combinations of modalities. Blue: EEG+EMG+Gas+Brake (electrophysiological and behavioral channels). Red: Gas+Brake (only behavioral channels). The intervals, in which the inclusion of electrophysiological channels significantly improved classification accuracy are marked as square boxes (no filling for simulated driving, light gray filling for real-world driving). Figure taken from Haufe et al. (2014a) with permission.

distance by 3.66 m. With respect to practical implementation, another aspect has also to be considered. While anticipatory brain signals allow for an early prediction of an action, they do not necessarily reflect the final decision as shown in the study discussed in Section 7. In the presence of motor predictive brain signals, the participant may still change their mind and cancel the movement or act differently. In the scenario of emergency situations, this could be caused by the insight that under the given condition the avoidance of an obstruction might be a better option than braking.

4. EEG-BASED CLASSIFICATION OF VIDEO QUALITY PERCEPTION

By the virtue of a specific experimental paradigm, the watchers' SSVEP amplitudes were modulated by degradations in the quality of videos. Classification methods derived neural indices that correlated with the mean opinion scores (MOS) given by the participants in the standard behavioral assessment, giving rise to a new approach to video quality assessment.

4.1. Context: Brain-Guided Quality Assessment

As we elaborated in our first review (Blankertz et al., 2010), there is a good outlook for using neurotechnology in usability studies because it allows for an effortless continuous acquisition of usability parameters without requiring any action on the part of the user. It may also include aspects that are difficult to quantify objectively with conventional methods and access variables unknown to the test subjects themselves. In a similar vein, neurotechnology may prove useful for the quality assessment of such multi-media content (Moldovan et al., 2013; Antons et al., 2014). Such an approach may capitalize on neural correlates of perceptual or cognitive processes. The assessment of audio quality based on EEG was pioneered in Porbadnigk et al. (2010). Their results showed that the methodology taken from BCI research has the potential to detect changes in the brain signals of listeners, who were presented with audio signals that had quality degradations below the threshold of perception, (cf. also Antons et al., 2012; Porbadnigk et al., 2013). This demonstrated an increased sensitivity compared to behavioral measures, which was also found in studies on the visual domain (Porbadnigk et al., 2011). In this section, we review studies investigating the neurotechnology-based assessment of video quality with the aim of improving video codecs.

4.2. Studies on Neural Measures of Video Quality

For the transmission of video signals at today's high bit rates, video codecs usually employ high levels of compression, which might introduce distortions visible to the human eye. It is therefore desirable to measure the perceived distortions through the assessment of the visual quality of compressed video. This assessment is usually done through so-called mean opinion scores (MOS) that are obtained through questionnaires, in which participants are asked to rate the quality of a visual stimulus on a rating scale (ITU, 2002, 2008). These behavioral tests have many limitations, including large inter-subject variance and

the requirement of a high number of participants to achieve statistical significance. The judgment of the participants can also be biased by several factors not related to the quality of the stimulus itself. In recent years, therefore, there has been increasing interest in investigating novel paradigms for video quality assessment through the direct measurement of neural activity via EEG (Hayashi et al., 2000; Babiloni et al., 2006; Arndt et al., 2011; Lindemann et al., 2011; Mustafa et al., 2012; Arndt et al., 2014; Kroupi et al., 2014).

The authors of Scholler et al. (2012) used an experimental design that capitalized on the ERP component P3 to quantify the perception of the human observer when being confronted with a change in video quality. As stimuli, they showed 8 s video clips based on a synthetic image of a textured checkerboard, which was deformed over time by simulating a swaying water surface on the top. The quality change was introduced by lossy compression, while its magnitude was controlled by the quantization parameter of the video coder. Participants had to acknowledge the perception of the quality change via button press. They found that quality changes elicited a P3 component that was positively correlated with the magnitude of the change, which could be classified on a single-trial basis using LDA. They report a single-trial classification with AUC-values close to 1 for the highest level of distortion in most subjects, referring only to trials correctly identified by the participants at the behavioral level. They also report, for three participants, an average 65% accuracy in classifying the trials in which the quality change was present but not detected by the subjects, advancing the hypothesis of higher sensitivity of the EEG compared to the behavioral response.

All the previously mentioned studies are based on the detection of the P3 component, which is a cognitive ERP not directly linked to sensory processing. Complementarily, we investigated a paradigm based on Steady-State Visual Evoked Potentials (SSVEPs) that reflect perceptual processes. The basic suitability of the SSVEP-based design for video quality assessment has been demonstrated (Norcia et al., 2014). Here, we review a systematic follow-up study (Acqualagna et al., 2015).

As stimuli, six gray-level natural images in six levels of degradation (corresponding to six compression rates) were used. The degradation levels were controlled by the quantization parameter, as in Scholler et al. (2012). The experiment comprised 51 videos in which all the textures in all the levels of degradation were displayed (**Figure 3**). The original and distorted textures were presented in alternating order with a stimulus onset asynchrony (SOA) of 333 ms (i.e., at a frequency of 3 Hz). The flickering effect of the sequence of quality changes caused the elicitation of SSVEPs in the occipital cortex, the amplitude of which increased with increased distortion levels.

In the first approach, single VEPs of the steady-state signal were classified using spatio-temporal features (Blankertz et al., 2011) applied to epochs without and with a time-lag of 160 ms (**Figure 4**, left). Single-trial classification achieved an average maximum AUC of 0.84 for the maximum distortion level. **Figure 4** (right) shows that the first three distortion levels (D1–D3), which were chosen to be below the threshold of perception, did not modulate the SSVEPs and classification stayed at chance level. Further on, classification performance linearly increases with the distortion level. AUC scores significantly linearly correlated with MOS-values for all the participants ($p < 0.01$).

The same trend was obtained for the classification of spectral features at 3 and 6 Hz (i.e., the frequencies of the EEG spectrum that showed the highest modulation). CSP filters were calculated on the training data between the epochs referred to the maximum distortion level (D6) and those referred to the original textures (D0). CSP filters were then applied on the test data for all distortion levels. Features consisted of the log-variance of the CSP filtered data. Epochs locked to the distorted textures (D1–D6) were classified vs. epochs locked to D0 using LDA, achieving the maximum average AUC of 0.74 for D6.

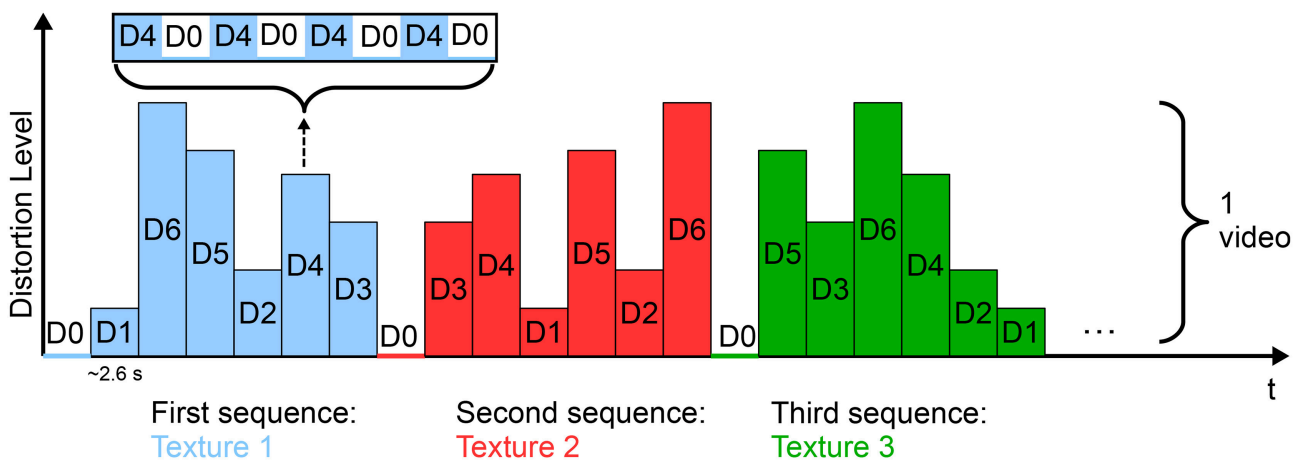

FIGURE 3 | SSVEP-based paradigm for video quality assessment. Each video comprised the six textures presented in all the levels of distortion (D1, ... , D6) in random order. Each texture was displayed distorted for 333 ms, followed by the undistorted form for 333 ms (D0) and the same succession was repeated four times for each level. Figure adapted from Acqualagna et al. (2015) with permission.

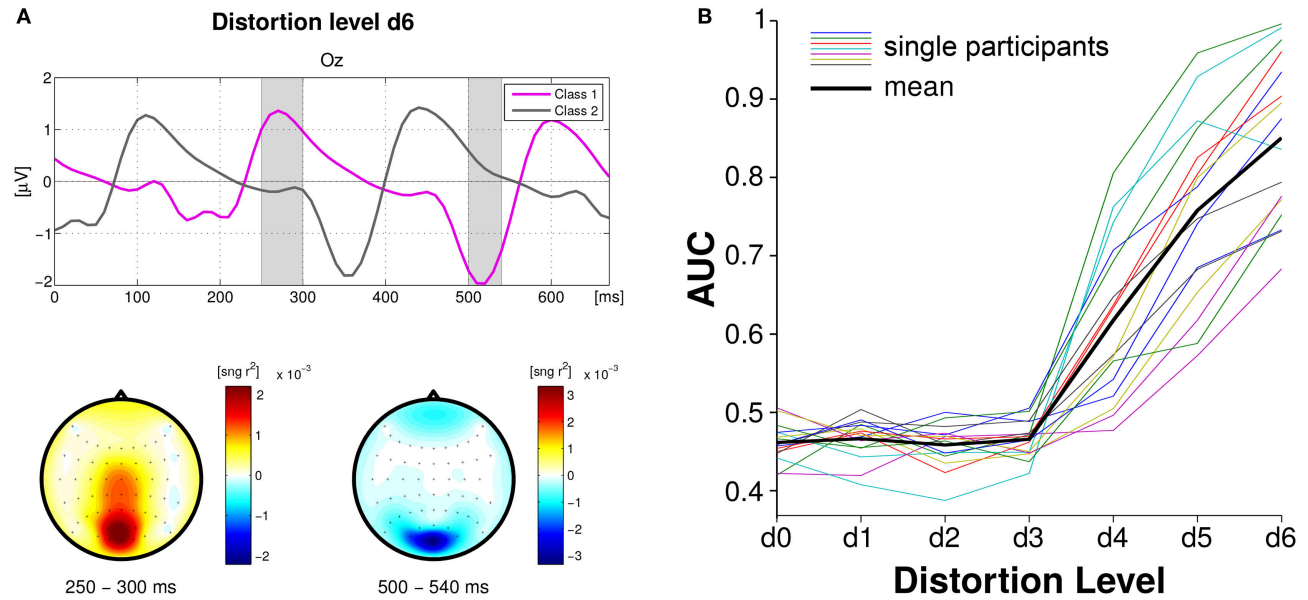

FIGURE 4 | Single-trial classification of VEPs based on spatio-temporal features. (A) Grand average brain activity over all participants at channel Oz, at maximum distortion level D6. The magenta line represents "Class 1" and the gray line "Class 2." Scalp plots underneath refer to the shaded areas in the time plot and display the magnitude of the *sign* $- r^2$ for each channel. **(B)** Classification performances using shrinkage LDA for all participants (colored lines) and mean (black thick line). Figure adapted from Acqualagna et al. (2015) with permission.

4.3. Concluding Remarks

Importantly, this study showed that an SSVEP-based paradigm allows a much quicker collection of trials than previous P3-based paradigms for quality assessment. The results of the neural assessment also correlated significantly with the MOS-values. The study thus demonstrated that an SSVEP-based video quality assessment can be considered a viable complement to behavioral-based assessments and a presumably faster alternative to methods based on the P3 component. For further details about the study and complementary analysis, please refer to Bosse et al. (2014, 2015) and Acqualagna et al. (2015). More generally, the results indicate the utility of the brain-based approach for usability testing and related quality assessment.

5. ADVANCED MONITORING OF WORKLOAD

This section reports methodological advancements in the context of brain-based mental state monitoring (Blankertz et al., 2010) and neuroergonomics (Mehta and Parasuraman, 2013). We take the estimation of the so-called operator workload as an application scenario, although the methodology is much more widely applicable. We explored estimates based on spectral features of endogenous brain rhythms that differ with respect to the label information required for training, including entirely unsupervised approaches. The explored estimators also differed with respect to the level at which the spectral features are extracted, thereby comparing traditional single-channel based approaches to approaches that employ recent advances in spatial filtering methods (Schultze-Kraft et al., 2016b).

5.1. Context: Neuroergonomics and Physiology of Operator Workload

Many work places with high levels of automation require human operators to perform monotonous but attention-demanding tasks, such as driving and air traffic control, or as in industrial contexts. In such work environments, the demand for high levels of alertness can lead to an overload of the human operator, which in turn can have critical consequences for health, safety, and efficiency. An assessment of the operator's workload (Gevins et al., 1995; Gevins and Smith, 2003) can be utilized to prevent overload and can lead to adaptive systems that automatically self-regulate the level of human-machine interaction (Pope et al., 1995; Prinzel et al., 2003; Parasuraman and Wilson, 2008). Another area of application is in training procedures, in which displaying the current workload level to the trainer as well as to the trainee her/himself is expected to facilitate learning or to make the alignment of difficulty levels to the trainee's progress more efficient (Borghini et al., 2016). This possibility has been explored for pilots (Borghini et al., 2013), air traffic controllers (Di Flumeri et al., 2015), and shipmasters (Miklody et al., 2016). The technique could similarly be used to improve infrastructure, by testing, for example, which features of streets, harbors, and the like require maneuvers that are likely to induce high workload.

The human EEG has been shown to provide reliable estimators of workload, based on the fact that changes in workload are associated with characteristic modulations in the power of oscillatory activity in particular frequency bands of the EEG (Buzsáki and Draguhn, 2004). The most prominent frequency bands with power changes related to workload are theta (4–7 Hz) and alpha (8–12 Hz). Theta power has been shown

to be positively correlated with workload, most notably in frontal regions (Gevins et al., 1998; Smith et al., 2001; Holm et al., 2009), whereas alpha power is typically found to be negatively correlated with workload, in parietal regions in particular (Gevins and Smith, 2003; Holm et al., 2009). This effect cannot be expected in general, however, as these results refer to the visual modality only (see the discussion Section 9).

5.2. Study Comparing Methodologies for Estimating Workload

The experiment setup in Schultze-Kraft et al. (2016b) was designed to emulate an industrial working scenario in which an operator performs tasks requiring a continuous effort of visual and motor processing with alternating difficulty. Ten healthy male subjects, aged 26–40, participated in the experiments. Subjects were instructed to carry out a task on a 21-inch touch screen lying on a table in front of them (**Figure 5A**).

The task was designed as a computer game in which objects consisting of three vertically aligned screws (screw triplets) were falling from random positions at top of the screen and had to be caught in a bucket at the bottom of the screen. Subjects could move the bucket horizontally by sliding it with one of their index fingers. The coloring of the bucket could be adjusted by touching colored buttons that were positioned on either side of the screen. The catching task was further complicated by the constraint that the coloring of the bucket had to match the coloring of a screw triplet before catching it. Not catching a screw triplet was considered an error and so was catching a triplet with a color scheme that did not match the color scheme of the bucket. In the low workload condition (L), the interval between falling screw triples was constant, whereas in the high workload condition (H) the intervals were shorter and were randomly varied. The experiment was conducted in four runs, where each run lasted 24 min and consisted of alternating low and high workload blocks, with each block lasting 90 s. See **Figure 5B** for the experimental design.

In addition to 64-channel EEG, we also determined task performance (error rate) and measured the following peripheral physiological measures (PPM): respiratory frequency, cardiac frequency, and electrodermal response. See **Figures 5C–F** for the task-induced effects on error rate and PPMs. Switching from low to high workload induced consistent and significant increases in error rate and all PPMs.

In order to classify (or predict) workload levels, we compared six different predictive models. Three of them are based on spectral features at *channel-level*, whereas the other three used specific data-driven *spatial filters*. In the channel-level approaches, spectral features are computed for each recording

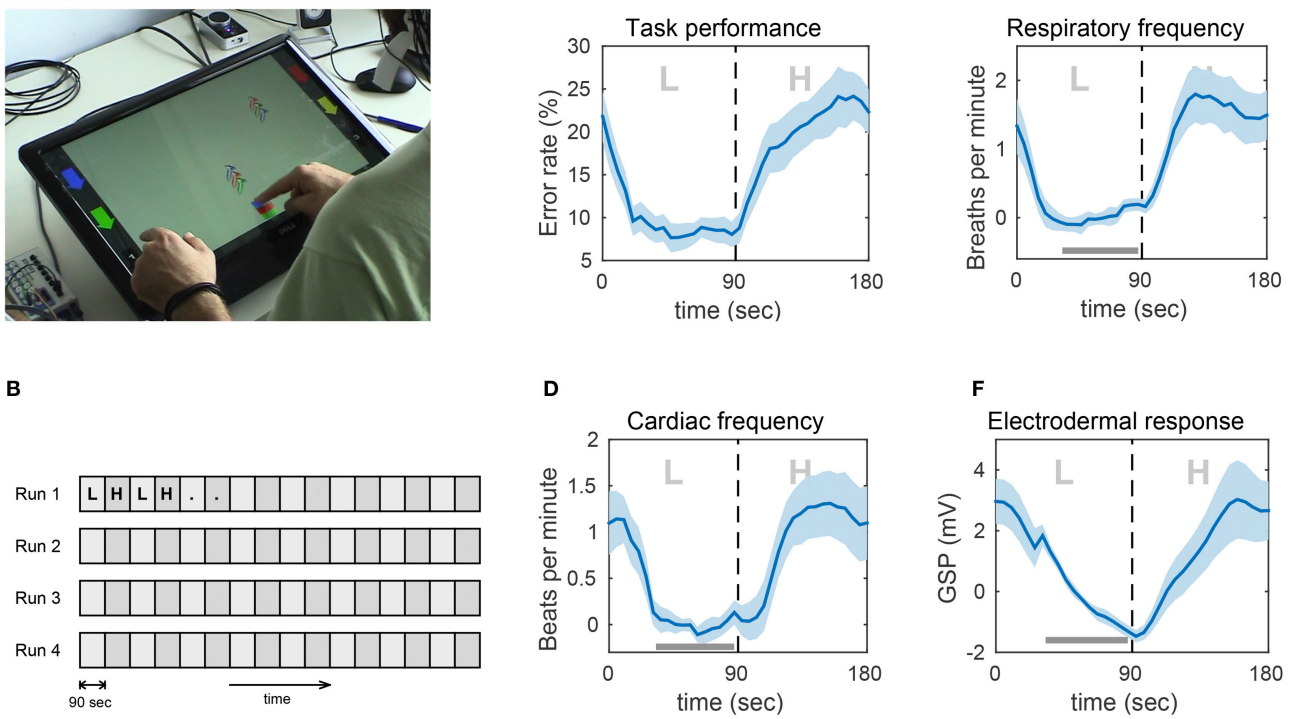

FIGURE 5 | Experimental task and impact of the experimental paradigm on task performance and peripheral physiological measures (PPM). (A) Snapshot from one of the experiments showing a subject playing the game on the touch screen. **(B)** Block structure of the experiment. Participants performed four runs of 24 min, each consisting of 90-s blocks of alternating low (*L*) and high (*H*) workload conditions. **(C)** Error rate. **(D)** Respiratory frequency in breaths per minute. **(E)** Cardiac frequency in beats per minute. **(F)** Electrodermal response in Galvanic skin potential. Shown are the grand averages of the mean over all L–H block pairs. The light blue shadings indicate the standard error of the mean. Due to large inter-subject differences in the average of the PPMs, the grand average and standard error were computed after subtracting the mean in the indicated bar. Thus, the plotted values represent changes from this baseline. Figure taken from Schultze-Kraft et al. (2016b) with permission.

channel separately. In the spatial-filter-level approaches, the data are first projected onto a set of optimized spatial filters. Spectral features are then computed based on the output of the spatial filters. Each of the channel-level and spatial-filter-level approaches fall into one out of three sub-categories, depending on the amount of information required by the approach. These sub-categories include (a) use of binary class labels (classification models, tag *cfy*), (b) use of a continuous error measure (regression models, tag *regr*), and (c) no use of a supervision signal at all (unsupervised models, tag *unsup*). In the classification models, spectral features were combined using regularized linear discriminant analysis (LDA) in combination with binary labels. In the regression models, spectral features were combined using regularized least-squares regression (LSR) in combination with the subject's error rate as a supervision signal. Finally, the output of the unsupervised models was simply the difference between theta and alpha features (Power diff). These three sub-categories represent a progression from (a) controlled laboratory conditions in which full label information is available to more realistic settings in which either (b) only a proxy-variable, such as the error rate is available, or (c) no external information about the variable of interest is available at all. This last scenario requires assumptions about the nature of the expected spectral changes in the EEG, which, in our case, is associated with workload (Gevins et al., 1998; Gevins and Smith, 2003; Holm et al., 2009).

Matching the level of additional information provided, we employed the following spatial filter methods. For the classification model, we used the Common Spatial Pattern (CSP) algorithm (Fukunaga, 1990; Koles, 1991; Blankertz et al., 2008) to train the spatial filters. For the regression model, we used the Source Power Co-modulation (SPoC) algorithm (Dähne et al., 2014a). For the unsupervised model, we used the canonical Source Power Co-modulation (cSPoC) algorithm (Dähne et al., 2014b). While CSP is a well-established method in the field of BCI, SPoC, and cSPoC represent recent advances in the development of spatial filtering methods. See Dähne et al. (2015) and Fazli et al. (2015) for further information on the background of these methods.

Figure 6A shows the mean classification accuracies for the six models, averaged across subjects. Both groups of models, with and without spatial filtering, show a decrease of performance with a decreasing amount of exploited label information. Between the groups, models using spatial filtering show a clear advantage that becomes greater the smaller the amount of label information that is available: 3.8% (CSP), 4.2% (SPoC), and 8.2% (cSPoC), compared to the respective channel-based method.

Given the modulation of PPMs by the workload condition (**Figures 5C,D**) and given that PPM features can be extracted from the data as an unsupervised signal, we assessed whether PPM features constitute an added value to the features extracted in the unsupervised models. We first of all found that the mean classification accuracy using only PPM features was 81.8% (**Figure 6B**, white bar). We then repeated the analysis with unsupervised models. This time, however, we augmented the EEG features with PPM features. This resulted in enhanced classification accuracies: a 3.6% increase for the channel-based (n.s.) and a significant increase of 4.3% for the spatial filtering-based method. Note that the unsupervised but PPM-augmented model outperformed the supervised channel-based model and even nearly equaled the performance of the supervised model, which used spatial filters. These results support the assumption that peripheral physiology can indeed provide an added value to the unsupervised model for the classification of workload.

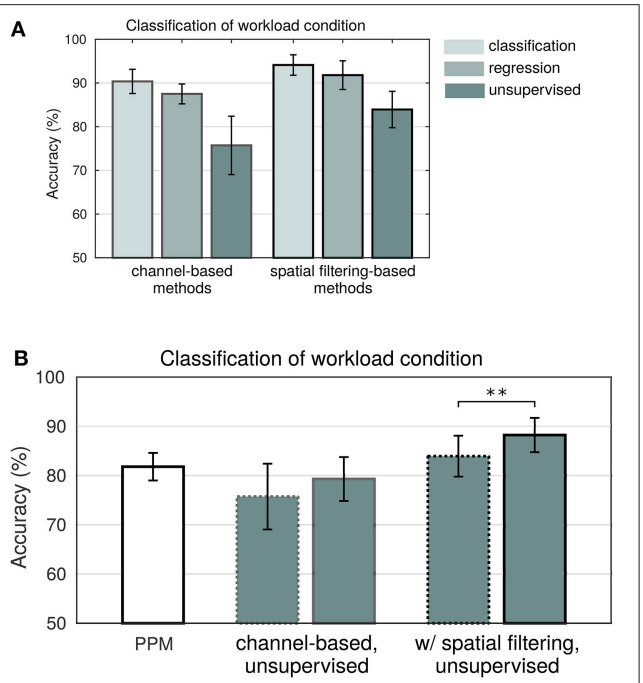

FIGURE 6 | Results. (A) Mean classification accuracy and standard error of the six models across subjects. **(B)** Added value of peripheral physiological measures. Mean classification accuracy and standard error across subjects when using only PPM features (white) and comparison to the two unsupervised predictive models before (dotted) and after (solid) augmenting with PPM features. Figure taken from Schultze-Kraft et al. (2016b) with permission. **Indicates a significance level of $p < 0.01$.

Next to an increased signal-to-noise ratio, a further benefit of using spatial filtering methods is that they allow for the inspection and interpretation of spatial activation patterns, which are associated with the extracted signals (Haufe et al., 2014b). It is thus possible to verify that the signals extracted by the CSP, SPoC, and cSPoC filters were of cortical origin, as opposed to possibly stemming from ocular or other artifactual sources. For this purpose, we examined the spatial activation patterns that correspond to the components found using the three methods, as well as the corresponding power envelopes of the components' time series. **Figure 7** shows the activation patterns and corresponding power envelopes for one example subject. The activation patterns indicate that frontal theta activity and parietal/occipital alpha activity are the sources of workload modulated signals.

5.3. Conclusion and Outlook

In summary, we find that using established and, in particular, recently developed spatial filtering methods, it has become

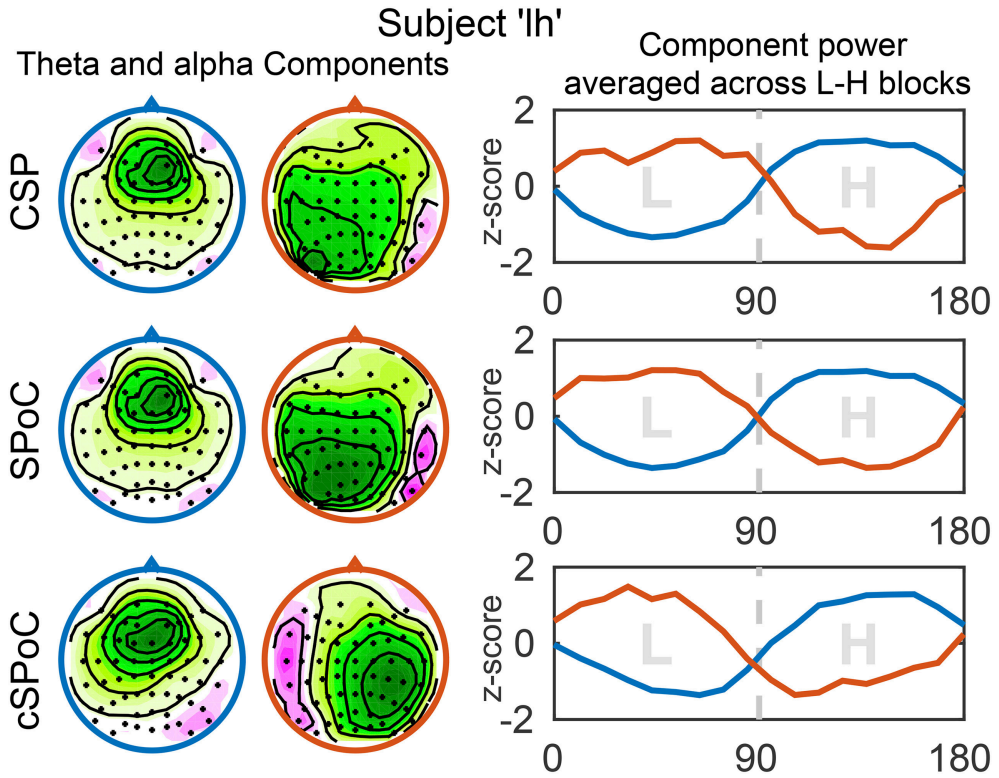

FIGURE 7 | Spatial activation patterns and power envelopes of components extracted by the three EEG spatial filtering methods. The shown activation patterns (scalp maps) and power envelopes correspond to the components with the highest value of the optimization criterion of the respective method. The left and middle column show the activation patterns of components obtained from the theta (blue) and alpha (red) bandpassed data, respectively. The color coding and sign of the activation patterns were adjusted to be consistent across methods, but are arbitrary otherwise. The power envelopes (right column) are color-coded accordingly (theta: blue; alpha: red), the x-axis shows time in seconds. Due to standardizing to *z*-scores, the amplitudes of the curves do not relate to discriminative power. Figure taken from Schultze-Kraft et al. (2016b) with permission.

possible to estimate an operator's workload based on brain signals and peripheral measures. Additionally, we would like to point out that we observed similarly promising results in a workload-related study (Naumann et al., 2016) in which subjects played the classical Tetris video game. In contrast to most workload-related studies, the task in Naumann et al. (2016) was not to classify workload into one of two categories (typically high vs. low workload). Instead, we aimed to predict the player's current game level, purely on the basis of spectral features from the brain. We employed the model outlined above (SPoC combined with regression) and we were able to predict the current gaming level with high precision (Naumann et al., 2016), results that are comparable with the findings presented in Schultze-Kraft et al. (2016b).

6. BRAIN-COMPUTER INTERFACES FOR HUMAN-COMPUTER INTERACTION

While intentional control of computer applications is the target of classic BCI research for patients, this approach does not seem promising for general users. Instead, it seems worthwhile to employ BCIs to infer implicit information during software usage and to use that information to augment the explicit interaction. In other words, to make the computer better at understanding the human user on the basis of soft skills. In view of this far-reaching goal, we have investigated several studies that pave the way.

6.1. Context: BCIs for General Human-Computer Interaction

The interaction with a complex interface might be facilitated if the system is able to exploit implicit information about the cognitive state of its user inferred from physiological signals. Measures from eye movement patterns, pupil size, electrodermal activity (EDA), facial electromyography (fEMG), and other peripheral physiological signals can provide insights into the user's mind with respect to relevance, attention, or intent (Oliveira et al., 2009; Hardoon and Pasupa, 2010; Cole et al., 2011a,b; Gwizdka and Cole, 2011; Haji Mirza et al., 2011; Hajimirza et al., 2012; Barral et al., 2015). However, electrophysiology may provide a more direct access to the cognition of the user in comparison to eye tracking or peripheral physiology (Zander and Kothe, 2011; Eugster et al., 2014; Ušćumlić and Blankertz, 2016; Wenzel et al., 2016).

Transferring the decoding results from the classic (fixed-gaze) BCI systems toward general human-computer interaction (HCI) applications, in which complex displays are explored in

an unconstrained free-viewing manner, holds a number of challenges that we discuss in this section. These scenarios, which allow natural behavior, essentially require co-registration of eye-movements and EEG, since free viewing implies self-paced scene exploration. The emerging research on eye fixation-related potentials has shown that fixations on the object of search evoke EEG responses similar to the one evoked in the classical visual oddball paradigm with fixed gaze (Rämä and Baccino, 2010; Kamienkowski et al., 2012; Brouwer et al., 2013; Kaunitz et al., 2014), which motivated an expansion of potential BCI applications. The joint EEG and eye-tracking studies, such as those addressing active visual search of the target face in images of crowds (Kaunitz et al., 2014), or during navigation of 3D naturalistic environments (Jangraw et al., 2014), provide evidence for the feasibility of EEG-based intention decoding in realistic active visual search tasks. Both studies, however, impose certain constraints, either in terms of subjects' behavior (i.e., promoting longer fixations Kaunitz et al., 2014) or in terms of stimuli that prevent the overlap of target responses (Jangraw et al., 2014). Neither of these studies, moreover, address the system's performance with respect to the content of scenes, i.e., its semantic and spatial distribution, clutter, and temporal dynamic.

We conducted various experiments to approach these issues, taking as a guiding example the assessment of the relevance of the items on screen with regard to the user's task (e.g., information seeking). The goal is to obtain implicit information about the user's intention from the brain signals (as co-registered eye-tracker data) to supplement the explicit interaction with computer software via mouse and keyboard. Implicit relevance measures can be captured unobtrusively in the background and consume less time and effort in comparison to a laborious manual evaluation of the relevance of each item. In this transfer of BCI technology to realistic settings of human-computer interaction, we face a number of challenges that we address in the following section.

6.2. Variable Neural Latency in Dynamic Scenes

On the one hand, applications for information seeking and retrieval are nowadays characterized by rich and dynamic visual interfaces. Such interfaces inevitably engage different attentional and perceptual brain processes (e.g., covert attention and peripheral vision) to sample the relevant content of scenes through consecutive eye-fixations. On the other hand, information is typically provided as semantic concepts that are richer than a simple symbol or a plain word; they may be contained in data of different modalities (e.g., text, image, and video). While a semantic concept may be ambiguous or vague, its recognition may require integration of evidence over time. Typical examples of the latter case are action and behavior recognition, or the recognition of new content on a screen when transition visual effects are applied, as it is often the case in visual interfaces. Altogether, in real world applications the cognitive processing may vary in both duration and onset time with reference to fixations. Our recently published study (Ušćumlić and Blankertz, 2016), which was motivated by the non-stationarity of our natural visual environment, addressed the EEG correlates of visual recognition while participants overtly performed visual search in non-stationary scenes. Our research particularly concerned whether scene dynamics might intensify the temporal uncertainty of ERPs with reference to fixations, introducing an extra challenge for state-of-the-art EEG decoding methods. We designed three free-view visual search tasks mimicking the type of visual effects that may appear in real world human-computer visual interfaces. Alongside popping-up stimuli, two composite appearance styles based on fading-in, enlarging, and motion effects were considered (**Figure 8**). In the Pop-Up (PU) and Smooth Appearance (SA) conditions, stimuli appear at random but fixed positions on the screen. In the Motion Appearance (MA) condition, the constant stimuli motion causes the entire scene to continuously change (for details, see Ušćumlić and Blankertz, 2016). First, we investigated the performance of the state-of-the-art EEG decoding method *hierarchical discriminant components analysis (HDCA)* (Gerson et al., 2006) across different conditions. The results confirmed our concerns, indicating a drop in decoding performance when facing less certain timing of visual events (i.e., the appearance of new content in a scene) due to the transitional changes (cf. **Figure 9** upper panel). We showed, however, that the knowledge obtained from the paradigm characterized by less temporal uncertainty (i.e., popping-up stimuli) can be exploited to boost the EEG decoding performance in more challenging conditions. This is done by estimating posterior probabilities across different time lags with reference to fixation onset, using the classifier trained on popping-up condition, and by making the final decision based on a maximum of the estimated posteriors. The improved decoding performance, estimated in a 10-fold validation setting, is presented in **Figure 9** (lower panel), for fading-in and motion conditions, respectively.

6.3. Variable Neural Latency Due to Variable Saliency

In typical BCI experiments, different stimuli are flashed one-by-one (cf. **Figure 10A**) and the EEG is segmented in stimulus-aligned epochs that are used to predict the selected stimulus of interest (e.g., Treder et al., 2011). In regular software applications, several items are usually presented in parallel, rather than one-by-one. In this case, the saccades to the items, as measured with an eye tracker, can serve as time points of reference for the EEG segmentation (cf. **Figure 10B**). Using this approach, it is possible to estimate which items displayed on the screen are task-relevant and which are not (e.g., Brouwer et al., 2013; Kaunitz et al., 2014; Ušćumlić and Blankertz, 2016; Wenzel et al., 2016).

Pictograms and words shown in real software applications are usually diverse and feature different colors, shapes, and sizes. Saliency, which enables the recognition of relevant items, varies accordingly, such that recognition can happen either before the saccade (when the item is still in peripheral vision) or after the saccade to the item (when the item is in foveal vision; cf. **Figure 10C**). Accordingly, neural activity related to recognition can exhibit a temporal variability with respect to the saccades, which are used as time point of reference for the EEG

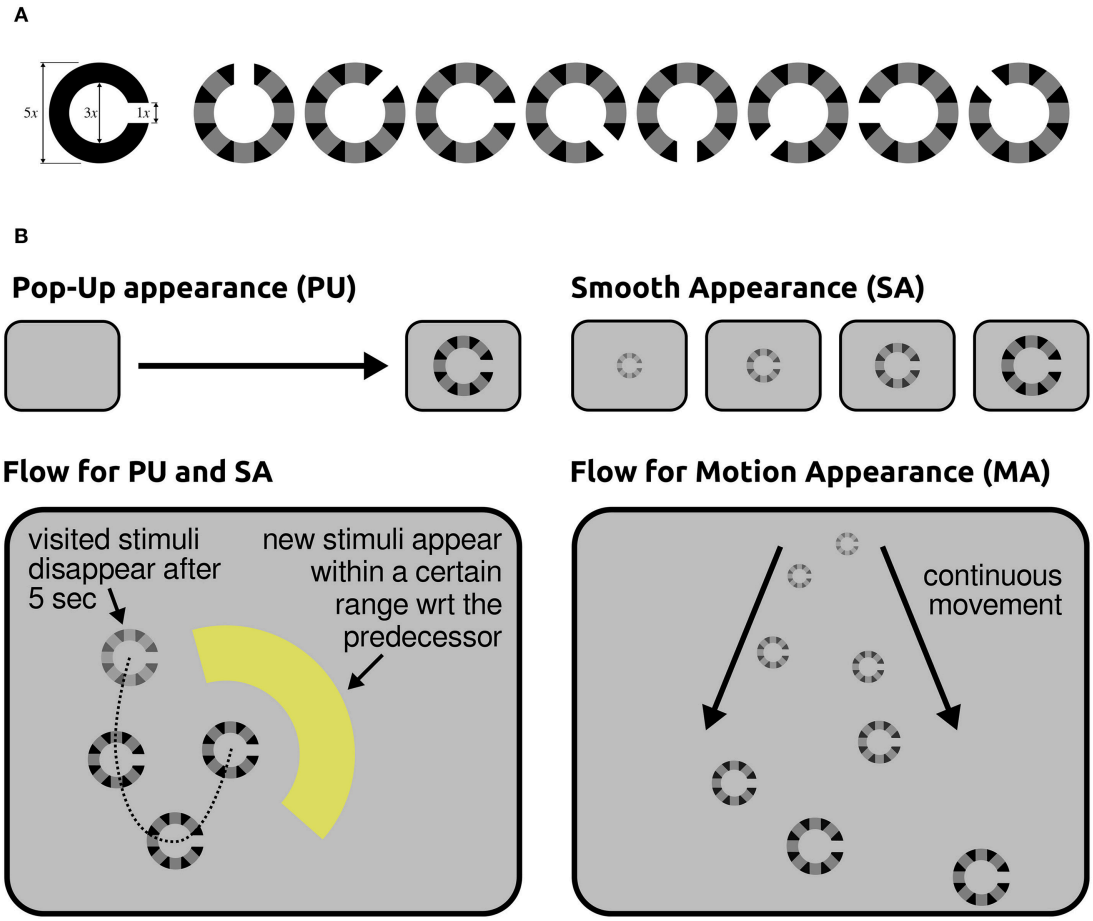

FIGURE 8 | (A) Left: A standard Landolt broken ring. **Right:** Eight modified Landolt rings that we used in our study. **(B)** Illustration of the stimuli presentation flow for different conditions. **Top-left:** In the PU condition, stimuli appear in one step. **Top-right:** Three intermediate steps of stimulus evolution in time are presented for the SA condition, followed by a completely revealed stimulus. **Bottom-right** The dashed line indicates the order of the appearance of stimuli in the PU and SA conditions. **Bottom-left** Several intermediate steps in the evolution of two successive stimuli are illustrated for the MA condition. The arrows indicate the direction of their continuous motion. This illustration is simplified, since multiple objects were present on the screen during the motion condition (MA). Stimuli are enlarged in comparison to the real screen dimensions. Figure taken from Uščumlić and Blankertz (2016) with permission.

segmentation. BCI prediction algorithms are not required to deal with this temporal variability because the stimulus onset serves as reference and the eyes are not moved in typical BCI experiments. An experiment with unrestricted eye gaze was performed in order to systematically investigate whether the algorithms can cope with this issue, which can be expected in realistic HCI settings (Wenzel et al., 2016). The participants were asked to find and count certain items that were presented in parallel on the screen and that were sometimes more and sometimes less salient. The continuous EEG data were segmented in epochs aligned to the (ends of the) saccades toward the items. Salient task-relevant items evoked an earlier neural response in comparison to less salient task-relevant items, presumably because recognition was possible already in peripheral vision. Nevertheless, even when the item saliency was mixed, a typical BCI prediction algorithm was suited to deal with the resulting temporal variability and was able to detect the task-relevant items in this search task.

6.4. Interference of Eye Movements with the EEG

EEG epochs used for the predictions in BCI experiments are usually set at several hundred milliseconds long in order to capture the P300 wave. But fixations often last only few hundred milliseconds and the subsequent saccade can occur during the same EEG epoch. This is problematic because eye movements can interfere with the EEG data. Yet, even when the eye movements were unrestricted, it was possible to capture neural signals related to recognition when the discriminative information was not (primarily) a result of eye movements (Wenzel et al., 2016). Interestingly, information from the two modalities of EEG and eye tracking were found to be complementary. An investigation of target detection with moving objects that require smooth-pursuit eye-movements showed no decrease of decoding performance if the timing of the event was known (Uščumlić et al., 2015).

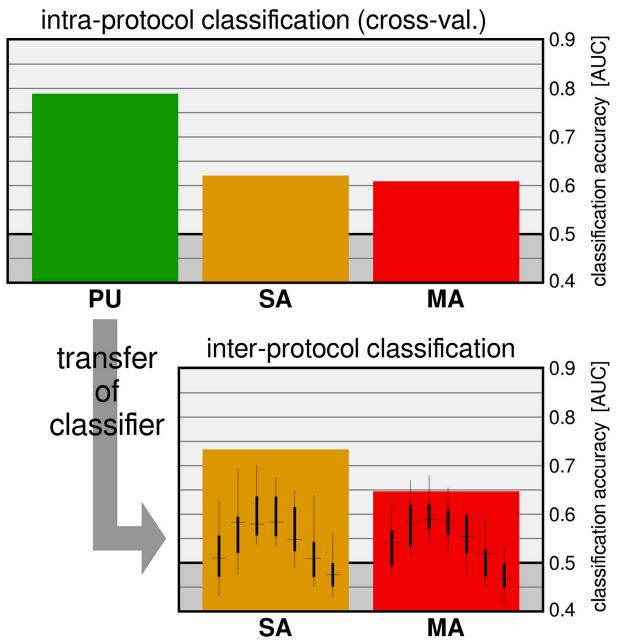

FIGURE 9 | Upper plot: Intra-protocol classification with an HDCA was cross-validated on the three conditions. **Lower plot:** For the inter-protocol classifier transfer, the HDCA was trained on the training data (PU condition) on a fixed time interval. The intermediate results of the testing datasets (conditions SA and MA), obtained for different positions of the sliding window (small boxplots), are combined to give the results indicated by the broad bars. Figure adapted from Uščumlić and Blankertz (2016).

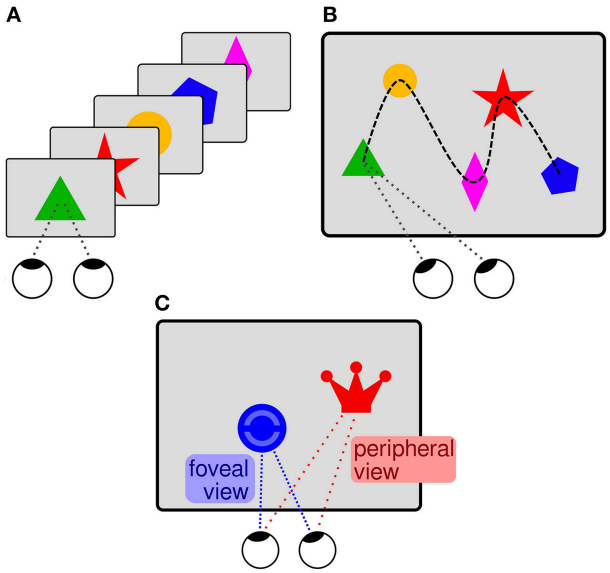

FIGURE 10 | (A) Sequential centered "BCI presentation." A simplified "mental typewriter" serves as example for an ERP-based BCI (cf. Treder et al., 2011). Different items (square, triangle, disc, pentagon) are flashed one-by-one, on the same spot on the screen. Each item stands for a (group of) letter(s). The subject selects a letter and silently counts the flashes of the corresponding item in order to direct their attention toward it. The selected (group of) letter(s) can be decoded from the EEG data using the flashes as time points of reference. **(B)** Item scanning in free-viewing. In an HCI scenario, words or pictograms (symbolized in the illustration) are displayed in parallel on the screen and are not flashed one-by-one. Items of particular interest for the user shall be decoded from the EEG data. The saccades (white arrow) to the items, as measured with an eye tracker, can serve as time points of reference for the EEG analysis. **(C)** The stimulus saliency may vary in HCI settings. An item of little saliency (here represented by a blue disc with indistinct interior) can only be recognized after a saccade when the item is in foveal vision. In contrast, a salient item (red crown) can be recognized already in peripheral vision, before a saccade toward it. A variable timing of recognition can therefore be expected with respect to the saccades, which are used as time points of reference for the EEG analysis.

6.5. Insufficient Accuracy in Single-Trials

EEG and eye tracking data can be informative about item relevance, but they are not sufficient for a reliable relevance estimate after a single fixation of an item. Brain-Computer Interfaces have to deal with a similar uncertainty and address this problem usually by combining predictions from several EEG epochs for class selection. The same strategy could be followed for the transfer to human-computer interaction. Practical applications should be designed such that evidence about user relevance is accumulated over time. This approach is favored naturally, because humans frequently move their eyes, which may result in a large number of saccade-aligned EEG epochs. For instance, when subjects scanned a mosaic of images that belonged to two classes, it was possible to reliably estimate, based on EEG and eye tracking data, which of the two classes of images was more relevant for the user, even if the predictions for the single images were not accurate. This strategy allowed the implicit resolution of ambiguities in an image web search (Golenia et al., 2015).

6.6. Conclusion and Outlook

Taken together, these results indicate the basic feasibility of exploiting implicit information through the use of BCI techniques for human-computer interaction. This holds also if the targets are not previously known stimuli, but rather semantically described categories consisting of a large variety of previously unseen stimuli (Acqualagna and Blankertz, 2015).

Apart from relevance, estimating the "depth of cognitive processing" would be useful in HCI when, for example, interfaces can adapt according to whether displayed information was adequately processed by the user or not. Recent work indicates that this variable can also be estimated sufficiently from the EEG (Nicolae et al., 2015a,b).

For a realistic perspective of using BCI technology in general human-computer interaction, the extraction of implicit information needs to be further improved, as in the context of, for example, more complex visual stimuli (Wenzel et al., 2015). Moreover, the co-registered acquisition of EEG and eye tracking data needs to be simplified to a deployable setup. We briefly discuss this aspect in a paragraph in the concluding Section 9.

7. BCI AS A RESEARCH TOOL IN COGNITIVE NEUROSCIENCE

Employing a BCI to obtain early predictions of motor intentions in a gaming scenario required participants to cancel self-initiated

button presses upon seeing a stop signal. By virtue of this paradigm, conclusions about the deterministic coupling between preparatory brain signals and the corresponding motor actions could be drawn that have a number of important implications ranging from the debate over free will to ethical considerations about applications that potentially speed up human behavior.

7.1. Context: Preparatory Signals and Research Questions in Cognitive Neuroscience

The readiness potential (RP) is a slow, negative cortical potential that is observed over motor areas in the EEG and can start more than one second before voluntary, self-initiated movements (Kornhuber and Deecke, 1965). It gained particular fame in the work of Libet et al. (1983), who found that the conscious decision to move occurs several hundred milliseconds after the onset of the RP, thereby initiating a still-ongoing heated debate about free will (Libet, 1985). One particular question that has remained unanswered is whether a person can still exert a veto by inhibiting a voluntary movement after onset of the RP (Haynes, 2011). One possibility is that once that RP begins to build up the planned movement must occur and cannot be canceled (De Jong et al., 1990). Another possibility is that people can still exert a veto by canceling or altering the movement after the onset of the RP. If the latter is the case, a follow-up question is whether there exists a point of no return along the time course of the RP, after which people cannot stop the planned movement. In order to test this, we devised an experiment that required subjects to cancel a self-paced movement once an RP had been detected by a BCI in real time.

7.2. Study on the Coupling of Preparatory Signals and Corresponding Actions

The experimental task was designed as a "duel" between the subject and the computer. Subjects ($N = 10$) were confronted with a floor-mounted button and a light presented on a computer screen. If the subject pressed the button while the light on the screen was green, they would win a point. If they pressed the button after the computer had turned the light red (stop signal), they would lose a point. The experiment had three consecutive stages. In stage I, stop signals were elicited at random onset times. The EEG data from stage I were then used to train a classifier to predict upcoming movements. In stages II and III, movement predictions were made in real time by the BCI with the aim of turning on the stop signal in time to interrupt the subject's movement. EEG signals were continuously classified by the Berlin Brain-Computer Interface toolbox (https://github.com/bbci/bbci_public) in order to control the stop signal. Additionally, EMG was recorded from the calf muscle of the moving foot in order to determine the time of movement onset. For details on experimental procedures, please refer to Schultze-Kraft et al. (2016a).

Each trial could end in one of four possible ways (**Figure 11A**): In "missed button press" trials subjects, won a point when they pressed the button while the light was green, whereas in "predicted button press" trials, they lost a point when they pressed the button after the stop signal had been turned on. Another possibility is that the BCI indicated an RP, elicited a stop signal, and the subject started to move (as indicated by EMG activity), but canceled the movement early enough ("aborted button press" trials). In the last case, the stop signal was elicited, but the participant showed no overt sign of movement. This trial type is ambiguous because it could either result from a prepared movement being terminated at an early stage ("early cancelation") or it could reflect false positive detections by the classifier ("false alarm").

We first of all examined the efficiency of the BCI predictor to detect RPs and elicit stop signals in real time. **Figure 11B** shows that while during stage I (random predictions), roughly 2 out of 3 trials were "missed button press" trials, during stages II and III only 1 out of 3 button presses were missed. Furthermore, predicted or aborted button press trials occurred very rarely during stage I, while during stages II and III they occurred in roughly 20 and 15% of trials, respectively. "Early cancelation/false alarm" trials occurred at comparable rates in all three stages.

Next, we assessed how the timing of stop signals was related to movement onsets (as assessed by EMG). The distribution of stop signals in "predicted button press" trials (**Figure 12A**, red, top panel) shows that the vast majority of stop signals occurred after EMG onset. Since the movement was completed by pressing the button, the stop signal presumably came too late for a veto. Stop signals in "aborted button press" trials (**Figure 12A**, green, middle panel) occurred earlier (starting around 200 ms before EMG). Thus, when stop signals were presented at late stages of movement, preparation subjects could not stop themselves from beginning to move, even though they could abort the movement, once started. There was a gradual transition between stop signal times in which movements could be aborted and those in which they could not be aborted (**Figure 12A**, bottom panel).

It is interesting that there were rarely any cases in which subjects moved despite seeing stop signals earlier than 200 ms before EMG, even though RP onset occurred more than 1000 ms before EMG onset. We therefore examined the timing of predictions in "silent trials," which occurred in 40% of trials during stages II and III. Here, when the BCI predicted a movement, the time was silently recorded, but the stop signal was not turned on and the trial continued until the button was pressed. As a detailed investigation of those silent trials shows (cf., Schultze-Kraft et al., 2016a), although a majority of predictions also in silent trials occurred around movement onset, many silent predictions occurred more than 200 ms before movement onset. The fact that these early predictions were absent for predicted button press trials or aborted button press trials suggests that the BCI was indeed able to predict movements at such early stages and that subjects were caught early enough to cancel their decision without any overt sign of movement.

In order to further investigate this assumption and assert whether predictions in the ambiguous trial type were early cancelations or false alarms, we looked for the occurrence of event-related desynchronization (ERD) in these ambiguous trials at the time of prediction. ERD occurs before and during movements in particular frequency bands in the EEG and has been shown to have a different generator in the brain than the

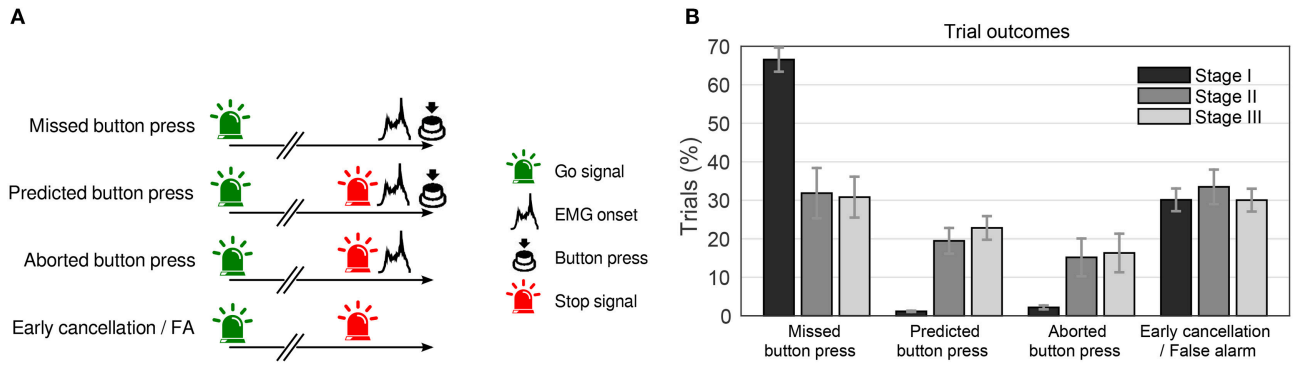

FIGURE 11 | (A) Possible trial outcomes during the experiment. See text for details. **(B)** Percentage of trial outcomes across stages for the four trial categories (as in panel **(A)**). All trial categories in one stage (bars of same color) add up to 100%. Shown is the average across subjects (error bars = SEM). Figure taken from Schultze-Kraft et al. (2016a) with permission.

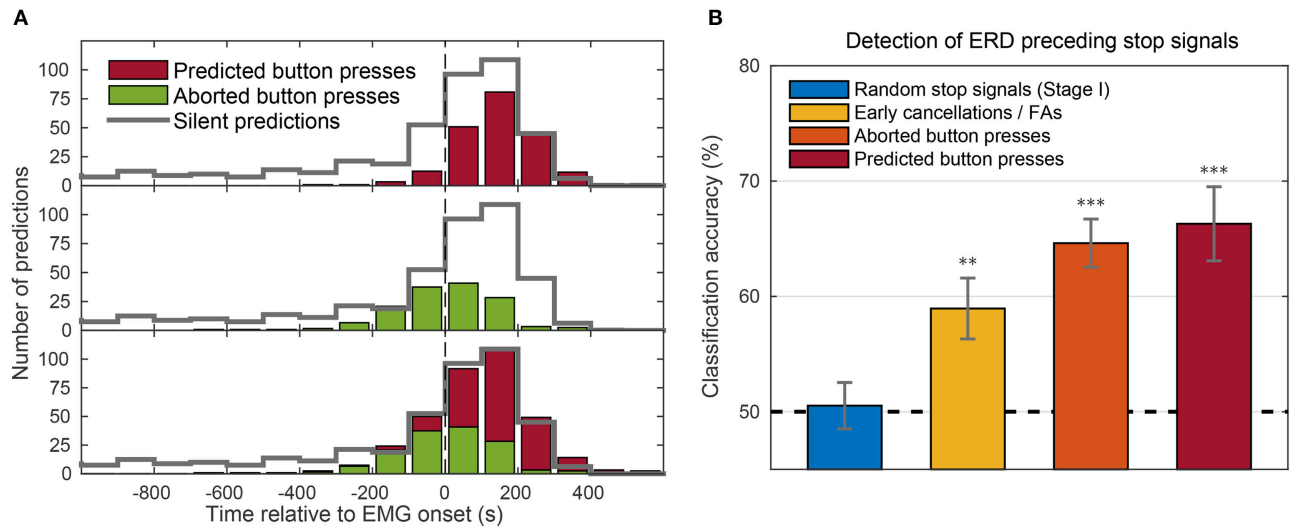

FIGURE 12 | (A) Distribution of BCI predictions time-locked to EMG onset (vertical line). The three panels show the distribution of stop signal timings in predicted button press trials (top, red) and in aborted button press trials (middle, green). The bottom panel (red and green) shows their joint distribution. The gray distribution superimposed as outline in all three panels shows the stop signal distribution in silent trials, adjusted to account for the imbalanced probability of a trial being silent (40%) or not (60%). All bins comprised intervals of 100 ms and counts were pooled across stages II and III of all subjects. **(B)** Accuracies of a classifier trained to detect an impending movement based on event-related desynchronization (ERD) occurring before stop signals. Bars show the mean accuracies of subjects (error bars = SEM) for four different trial types. Figure taken from Schultze-Kraft et al. (2016a) with permission. Significance above chance level is indicated by $^{**}p < 0.01$ and $^{***}p < 0.0001$.

RP, therefore making ERD an index for motor preparation that is independent of the RP (Pfurtscheller and Aranibar, 1979; Bai et al., 2006). The analyses revealed that ERD was detected in ambiguous trials, but not in the random stop signal trials from stage I (**Figure 12B**). Thus, at least a subset of ambiguous trials had likely already reached movement preparation and were not false alarms, but rather early cancelations.

7.3. Conclusion

Our findings suggest that subjects were able to cancel self-initiated movements, even after onset of the readiness potential. If a stop signal is elicited before a *point of no return* around 200 ms before movement onset, subjects are able to veto the prepared movement, while subjects cannot avoid moving when a stop signal occurs after that time point. Note, however, that the point of no return can be expected to vary from trial to trial, and that it might be impossible to determine when the point of no return has passed in single trials. This has the important implication that no critical actions should be triggered in this way, because the speed-up comes at the price of losing the opportunity to reevaluate the situation and possibly veto the action.

BCI technology offers the unique possibility of intervening in an experimental paradigm based on the momentary mental state (including intention and decision processes) of the test subject. This intriguing opportunity opens the potential for employing real-time BCIs as a research tool. While this perspective was

mentioned already in the BNCI Roadmap (BNCI Horizon 2020, 2015), the presented study (Schultze-Kraft et al., 2016a) is, to the best of our knowledge, its first realization. The key point in our study is the capability of allowing for instantaneous feedback of motor intentions to subjects in real time (Blankertz et al., 2006; Salvaris and Haggard, 2014), thereby extending the important line of experimental work on the nature of predictive brain activity preceding self-initiated movements (Haggard and Eimer, 1999). This novel approach allowed us to elucidate a fundamental question in cognitive neuroscience, thereby demonstrating the potential of a Brain-Computer Interface as a powerful research tool.

8. ANALYZING NATURAL MUSIC LISTENING

In this section, we show how BCI technology can be applied to the study of the processing of music. In particular, we propose a regression-based method that enables the extraction of cortical responses to note onsets in music from the continuous EEG. The extracted continuous brain responses are used to assess the brain-stimulus synchronization with a measure called Cortico-Acoustic Correlation (CACor). Several examples show the application of CACor in a range of analysis scenarios related to music perception.

8.1. Context: Neural Processes in Real World Experiences

Brain states during real-word experiences have attracted growing research interest in the past decade (Hasson, 2004; Hasson et al., 2010; Dmochowski et al., 2012; Hasson and Honey, 2012; Gaebler et al., 2014); Listening to music is one example of an ongoing real world experience that relies on structured auditory input that can be subject to many forms of audio signal analysis. At the same time, listening to music is one of the richest human experiences (Altenmüller and Schlaug, 2013) encompassing sensory, sensorimotor, cognitive, affective, and memory-related processes. Studying how brain dynamics underlying perceptual and cognitive processes unfold along the structure of a naturalistic music stimulus has therefore been recognized as a fruitful approach for deepening the understanding of the transformation of sensory input into human experience (Alluri et al., 2012, 2013; Sturm et al., 2014; Jäncke et al., 2015).

In the music domain, linear classification methods have, beyond measures of discriminability, provided knowledge about the neural representations of complex musical sounds (Schaefer et al., 2011; Treder et al., 2014). Unsupervised ICA-based approaches identified common features in the EEG of music listeners (Cong et al., 2012, 2013; Thompson, 2013). The results support the idea that the waveform envelope (which contains information about the timing of note onsets) is reflected in EEG and therefore provides a good starting point for linking music signals and brain signals. Likewise, in the domain of speech processing, cortical onset responses that reflect changes in the waveform envelope (termed Envelope Following Responses or EFRs), have been a target of interest for a long time (Purcell et al., 2004; Aiken and Picton, 2006, 2008).

8.2. Two Studies Investigating Continuous Listening Experience

Here, we review a novel approach that utilizes the relationship of the EEG signal to the audio waveform envelope in an analysis framework that is applicable in any experimental setting in which EEG recordings and stimulus waveforms are available. As shown schematically in **Figure 13** Linear Ridge Regression with the audio power slope as a target function is used to extract continuous cortical onset responses from the EEG signal of the music listener. Note that regression with the audio power *slope* capitalizes on the brain's sensitivity to change and represents a further refinement of previous EFR-related methods. Two examples of EEG projections and the respective power slope are given in **Figure 14**. Based on the extracted EEG projections, a measure of brain-stimulus synchronization called Cortico-Acoustic correlation (CACor) is developed (for details of the method see Sturm et al., 2015a; Sturm, 2016). We demonstrate

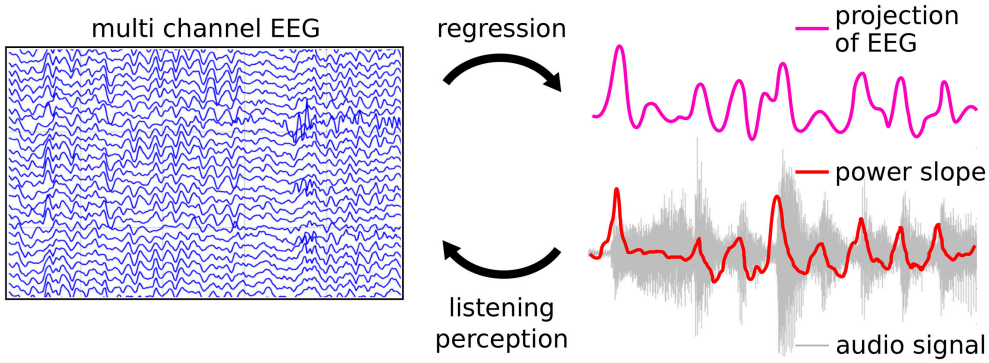

FIGURE 13 | Regression approach for extracting neural correlates of music perception. The perception of sound is reflected in the brain signals, the power slope of the sound waves being a crucial factor. Linear Ridge Regression is applied to the temporally embedded multichannel EEG signal using the audio power slope as a target function. This results in a spatio-temporal filter (regression weight matrix) that can be applied to new data. It reduces the multichannel EEG to a one-dimensional projection that can subsequently be examined with respect to Cortico-Acoustic correlation (CACor).

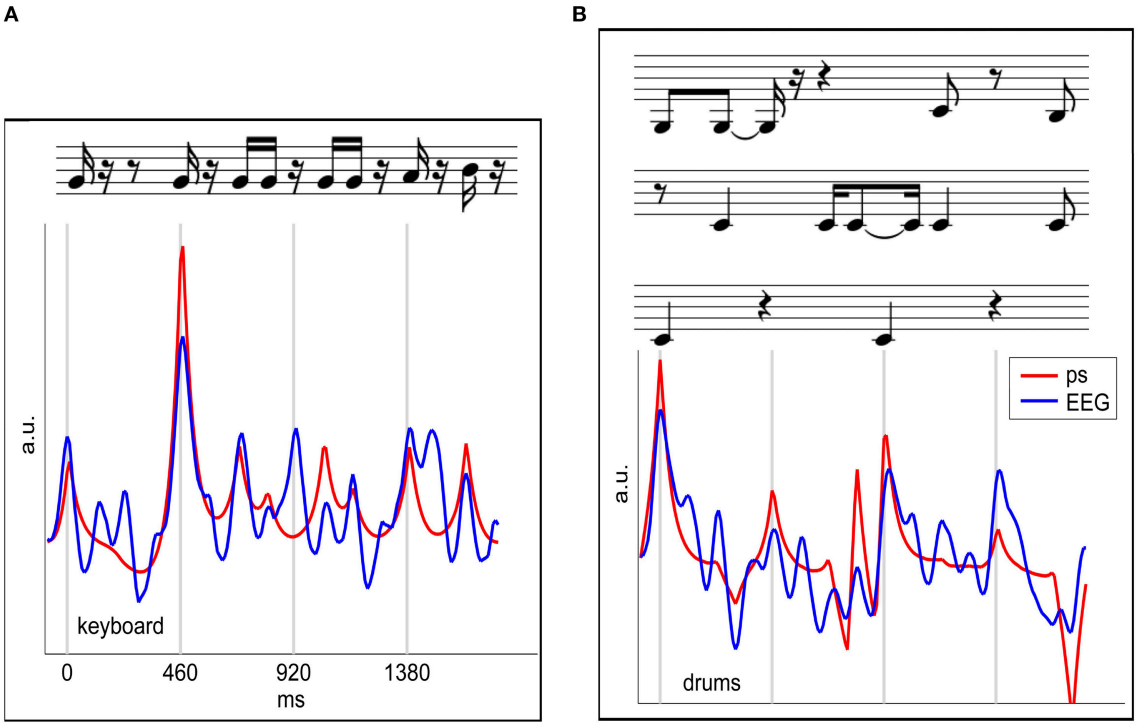

FIGURE 14 | EEG projections reflecting cortical responses to note onsets. The two examples of keyboard **(A)** and bass **(B)** show segments of an extracted EEG projection (blue) for a single stimulus presentation and a single subject and the respective audio power slope (red). Note that in the optimization procedure a time lag between stimulus and brain response is integrated in the spatio-temporal filter, and that, consequently, the EEG projections shown here are not delayed with respect to the audio power slope. Figure adapted from Sturm et al. (2015b).

that CACor can be applied for investigating brain-stimulus synchronization in experimental settings related to different aspects of music perception (Sturm et al., 2015b). We also provide examples of how CACor can be employed in the complementary analysis of EEG signals, behavioral measures, and audio signal analysis (Sturm et al., 2015a).

In a first study that explored the perception of naturalistic music, nine subjects passively listened to auditory stimuli from various sound categories, including full-length romantic piano pieces as well as simple tone sequences and natural (non-music) soundscapes (Sturm et al., 2015a). In a separate behavioral experiment, continuous ratings of the perceived tension in the same stimuli were obtained from an independent listener group. The regression approach (**Figure 13**) reduced the 61-channel EEG to one-time course optimally reflecting note onsets. The EEG projection was utilized to determine the Cortico-Acoustic Correlation (CACor). Significant CACor was detected in the individual listener's EEG signals of single presentations of full-length complex naturalistic music stimuli. The reliability of the occurrence of significant CACor in the group of participants differed among stimuli. It co-varied with the stimuli's average magnitudes of sharpness, spectral centroid, and rhythmic complexity. In particular, the subset of stimuli effecting a consistently strong CACor in the EEG participants (indicated by a high CACor score in **Figure 15**) also produced strongly coordinated tension ratings in the (independent) group of participants of the behavioral experiment. This relation between CACor and behavioral measures provides a first tentative link between neurophysiological responses to low-level acoustic events and the more cognitive-affective experience of tension in music. It is a first step toward bridging the gap between behavioral studies related to the perception of complex music and electrophysiological studies that use simplified musical stimulus material. If CACor scores are viewed as a measure of neural reliability, our findings add an interesting novel aspect to previous findings in which between-subject reliability of neural processing of naturalistic audiovisual stimuli indicates arousing and threatening passages (Dmochowski et al., 2012) and predicts the behavioral responses of large audiences (Dmochowski et al., 2014). Within this scope, our results indicate a more global, but very specific link between neural reliability and music stimulus features that might be useful for predicting listener behavior in the future.

In a second EEG study, music clips representing "rudimentary music" were presented to 11 subjects (Sturm et al., 2015b). These clips featured three instruments (keyboard, drums, and bass) playing repetitive music sound patterns, either in an ensemble version (resembling minimalistic electro-pop) or in the corresponding three solo versions (for details on stimuli and paradigm see also Treder et al., 2014). In the ensemble presentations, subjects were instructed to focus on just one of the instruments during each clip. For each instrument, a Linear

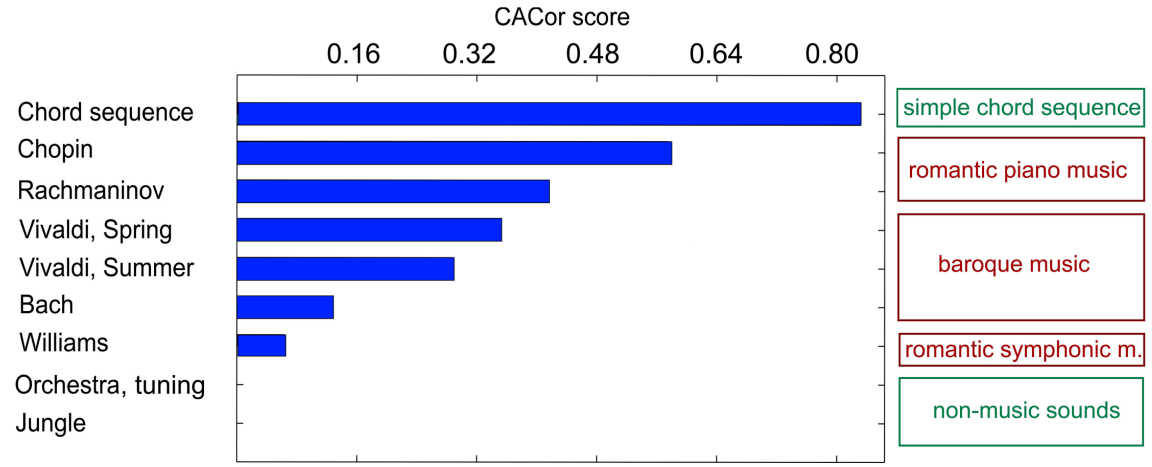

FIGURE 15 | The CACor score profile for the set of nine stimuli can be interpreted as a measure of reliability of the occurrence of significant CACor that can be compared across stimuli. The distribution of CACor scores for the set of nine stimuli is significantly correlated ($r = 0.9, p = 0.005$) with the distribution of coordination scores (not shown here) that quantify how strongly coordinated behavioral responses a stimulus produces (for details on the calculation of CACor and coordination scores see Sturm et al. (2015a)). The description on the right suggests that stimuli from the same category have similar CACor measures. Figure adapted from Sturm et al. (2015a) with permission.

Ridge Regression model was trained that extracted the EEG projection that represented the sequence of note onsets in the audio signal of the respective solo voice in an optimal way. In a second step, these instrument-specific filters were applied to EEG recorded during the ensemble presentations. CACor of the extracted EEG projections and the solo version of the music clip were assessed in order to probe whether a neural representation of the solo parts is present that is congruent to the natural ability of the subjects to perceive the single instrument's "voices" within the ensemble. Our results showed that the reflection of the melody instrument keyboard in the EEG exceeds that of the other instruments by far, suggesting a high-voice superiority effect in the neural representation of note onsets. The results further indicate that focusing attention on a particular instrument can enhance this reflection. We conclude that, in principle, the neural representation of tone onsets at the level of early auditory ERPs can parallel the perceptual segregation of ensemble music.

8.3. Conclusion and Outlook

In summary, the machine learning based multivariate methods for EEG analysis obviates the need to present a high number of stimulus repetitions, thereby paving the avenue for studying the physiological effect of long, complex stimuli, such as full-length pieces of natural music. The approach can provide a neural representation that parallels the separate streams a listener perceives in multi-voiced music. The proposed method therefore represents a promising tool for investigating auditory stream segregation in naturalistic listening scenarios. While the investigations discussed in this section do not require the real-time capability of BCI technology, closely related research may profit from the techniques presented here. EEG-enhanced assistive listening technology aims at recognizing cortical responses to the sound envelope as a promising way to determine the attended speech stream in complex listening situations (Ding and Simon, 2012; O'Sullivan et al., 2015; Akram et al., 2016). Through this, the function of hearing aids/auditory prostheses may be adapted in a situation-dependent manner (Mirkovic et al., 2015; O'Sullivan et al., 2015).

9. DISCUSSION

Most of the work on applications of BCI technology beyond communication and control is based on fundamental studies in cognitive science, psychophysics, and neuroscience. The results have been achieved in experimental studies that were confined to carefully controlled situations that limit fluctuating factors of natural tasks and behavior in order to exclude confounding variables. This is a reasonable approach for a rigorous investigation of fundamental concepts. In order to pave the way for incorporating neurotechnology into real-life applications, however, there needs to be a paradigm shift toward allowing more complex scenarios in neurocognitive studies. In this respect, it is important to note that increased noise (e.g., movement artifacts) is just one of the problems being faced.

To illustrate a more severe kind of challenge, we take the example of monitoring cognitive workload. There is a wealth of literature on the fundamental aspects of this topic, and a reliable system for real-time estimation of the current level of the user's workload would have useful applications in many areas. Studies have shown that the power of parietal alpha activity is negatively correlated with cognitive workload in visual tasks (Gevins and Smith, 2003; Holm et al., 2009). But in a complex scenario with a continuously changing visual background (such as driving a car), the alpha rhythm might be completely blocked already, such that no further decrease due to additional workload can be detected (Kohlmorgen et al., 2007). Other studies have shown that the parietal alpha amplitude *increases* with workload in non-visual tasks (Legewie et al., 1969; Galin et al., 1978; Markand, 1990),

presumably as a cause of inhibition in order to focus resources to the relevant neural processes (Klimesch et al., 1999). In a natural task of high workload, the demands can change between the modalities. There might be phases when retrieving experience from memory or motor programs is critical, while in other phases the focus is on the analysis of the visual scene. The expected effect on parietal alpha is then reversed, such that this feature might be difficult to exploit in a natural task context.

A related challenge in the transfer to more complex scenarios is the sensitivity vs. specificity trade-off. Fundamental studies with confined settings have repeatedly demonstrated the high sensitivity of EEG for retrieving certain aspects of perception or cognition. Potential applications of neurotechnology often refer to this fact, e.g., when promising higher precision compared to behavioral measures. The effects found in the EEG, however, are often not very specific; the interpretation of the effect is only valid under the highly constrained experimental setting. In situations of more complex scenes or tasks there might be other factors, unrelated to the variable of interest, that can cause either the same or a reversed effect, potentially annihilating the usability of the EEG-based measure that was previously found viable in a laboratory setting.

This review excluded the aspect of a deployable setup for acquiring the brain signals. For some of the discussed applications the usual EEG hardware is appropriate (BCI as research tool, Section 7), for others a less intrusive setup is desirable (Neurousability, Section 4), while still others critically depend on the future availability of truly deployable devices (HCI applications, Section 6). Developments in this directions are the recently developed, invisible (Nikulin et al., 2010), and easy to set up, gel-free EEG electrodes (Zander et al., 2011; Guger et al., 2012; Mullen et al., 2015). Electrodes can also be placed so that they are barely visible in the ear (Looney et al., 2014; Goverdovsky et al., 2016), on the ear (Norton et al., 2015), or, as printed electrode arrays, around the ears (Debener et al., 2015). In addition, miniaturized mobile EEG systems (De Vos et al., 2014; Stopczynski et al., 2014) and NIRS systems are presently being developed (Piper et al., 2014; Von Lühmann et al., 2015). New affordable eye trackers (Dalmaijer, 2014) and the increasing commercial interest in wearable physiological sensors, such as heart-rate sensors in smart watches or a glucose sensor in a contact lens ("Google Contact Lens"), likewise promise to be beneficial for further development.

The (potential) applications of BCI technology beyond communication and control presented here have different levels of maturity. BCIs are ready for use as research tools (Sections 7 and 8). Using BCI technology to access certain user variables based on neural signals within a development cycle in order to optimize devices and interfaces is within reach for some application areas (Section 4). For other fields of applications (Sections 5 and 6), we expect that intense and challenging research is still necessary to pave the way to actual applications. The studies reviewed in this article are just the beginning (resp. already the second step) in this enterprise, which will hopefully be interesting and attractive to many researchers.

AUTHOR CONTRIBUTIONS

BB made the concept of the review, wrote Abstract, Introduction, Overview, and Conclusion, and revised all sections. SH wrote Section 3, LA Section 4, SD Section 5, MU, MW, and BB Section 6, MS Section 7, and IS Section 8. GC contributed to the research reviewed in Sections 3–5 and 8. KM contributed to the research reviewed in Section 4. All authors read, revised, and approved the manuscript.

FUNDING

This work was supported by a grant from the German Federal Ministry of Education and Research (BMBF) under contract No. 01GQ0850. Furthermore, some of the reviewed research has received funding from the European Union Seventh Framework Programme (FP7/2007-2013) under grant agreement No. 611570. SH was supported by a Marie Curie International Outgoing Fellowship (grant No. 625991) within the 7th European Community Framework Program. IS's work was supported by the Berlin School of Mind and Brain and by the Christiane-Nüsslein-Volhard Foundation. KM gratefully acknowledges funding by the Federal Ministry of Education and Research (BMBF) under the projects Adaptive BCI (FKZ 01GQ1115) and Berlin Big Data Center BBDC (01IS14013A), in part by the German Research Foundation (GRK 1589/1), and by the Brain Korea 21 Plus Program through the National Research Foundation of Korea funded by the Ministry of Education.

ACKNOWLEDGMENTS

We acknowledge inspiring and fruitful discussions with many researchers, with whom we discussed novel applications of BCI technology and advanced data analysis methods. Moreover, we would like to thank our coauthors for allowing us to use materials from former joint publications.

REFERENCES

Acqualagna, L., and Blankertz, B. (2015). "Neural correlates of relevant stimuli processing for brain computer interfaces," in *Engineering in Medicine and Biology Society (EMBC), 2015 37th Annual International Conference of the IEEE* (Milano: IEEE).

Acqualagna, L., Bosse, S., Porbadnigk, A. K., Curio, G., Müller, K.-R., Wiegand, T., et al. (2015). EEG-based classification of video quality perception using steady state visual evoked potentials (SSVEPs). *J. Neural Eng.* 12:026012. doi: 10.1088/1741-2560/12/2/026012

Aiken, S. J., and Picton, T. W. (2006). Envelope following responses to natural vowels. *Audiol. Neurotol.* 11, 213–232. doi: 10.1159/000092589

Aiken, S. J., and Picton, T. W. (2008). Human cortical responses to the speech envelope. *Ear Hear.* 29, 139–157. doi: 10.1097/AUD.0b013e31816453dc

Akram, S., Presacco, A., Simon, J. Z., Shamma, S. A., and Babadi, B. (2016). Robust decoding of selective auditory attention from MEG in a competing-speaker

environment via state-space modeling. *Neuroimage* 124, 906–917. doi: 10.1016/j.neuroimage.2015.09.048

Alluri, V., Toiviainen, P., Jääskeläinen, I. P., Glerean, E., Sams, M., and Brattico, E. (2012). Large-scale brain networks emerge from dynamic processing of musical timbre, key and rhythm. *Neuroimage* 59, 3677–3689. doi: 10.1016/j.neuroimage.2011.11.019

Alluri, V., Toiviainen, P., Lund, T. E., Wallentin, M., Vuust, P., Nandi, A. K., et al. (2013). From Vivaldi to Beatles and back: predicting lateralized brain responses to music. *Neuroimage* 83, 627–636. doi: 10.1016/j.neuroimage.2013.06.064

Altenmüller, E., and Schlaug, G. (2013). Neurologic music therapy: the beneficial effects of music making on neurorehabilitation. *Acoust. Sci. Technol.* 34, 5–12. doi: 10.1250/ast.34.5

Antons, J.-N., Arndt, S., Schleicher, R., and Möller, S. (2014). "Brain activity correlates of quality of experience," in *Quality of Experience*, eds S. Möller and A. Raake (Berlin: Springer), 109–119.

Antons, J.-N., Schleicher, R., Arndt, S., Möller, S., Porbadnigk, A. K., and Curio, G. (2012). Analyzing speech quality perception using electroencephalography. *IEEE J. Sel. Top. Signal Process.* 6, 721–731. doi: 10.1109/JSTSP.2012.2191936

Arndt, S., Antons, J.-N., Schleicher, R., Moller, S., and Curio, G. (2014). Using electroencephalography to measure perceived video quality. *IEEE J. Sel. Top. Signal Process.* 8, 366–376. doi: 10.1109/JSTSP.2014.2313026

Arndt, S., Antons, J.-N., Schleicher, R., Möller, S., Scholler, S., and Curio, G. (2011). "A physiological approach to determine video quality," in *2011 IEEE International Symposium on Multimedia (ISM)* (IEEE), 518–523.

Babiloni, C., Vecchio, F., Bultrini, A., Romani, G. L., and Rossini, P. M. (2006). Pre-and poststimulus alpha rhythms are related to conscious visual perception: a high-resolution EEG study. *Cereb. Cortex* 16, 1690–1700. doi: 10.1093/cercor/bhj104

Bai, O., Vorbach, S., Hallett, M., and Floeter, M. K. (2006). Movement-related cortical potentials in primary lateral sclerosis. *Ann. Neurol.* 59, 682–690. doi: 10.1002/ana.20803

Barral, O., Eugster, M. J., Ruotsalo, T., Spapé, M. M., Kosunen, I., Ravaja, N., et al. (2015). "Exploring peripheral physiology as a predictor of perceived relevance in information retrieval," in *Proceedings of the 20th International Conference on Intelligent User Interfaces, IUI '15* (New York, NY: ACM), 389–399. doi: 10.1145/2678025.2701389

Berger, H. (1929). Über das elektroenkephalogramm des menschen. *Arch. Psychiatr. Nervenkr.* 87, 527–570. doi: 10.1007/BF01797193

Bladin, P. F. (2006). W. Grey Walter, pioneer in the electroencephalogram, robotics, cybernetics, artificial intelligence. *J. Clin. Neurosci.* 13, 170–177. doi: 10.1016/j.jocn.2005.04.010

Blankertz, B., Dornhege, G., Lemm, S., Krauledat, M., Curio, G., and Müller, K.-R. (2006). The Berlin Brain-Computer Interface: machine learning based detection of user specific brain states. *J. Univ. Comput. Sci.* 12, 581–607. doi: 10.3217/jucs-012-06-0581

Blankertz, B., Lemm, S., Treder, M. S., Haufe, S., and Müller, K.-R. (2011). Single-trial analysis and classification of ERP components – a tutorial. *Neuroimage* 56, 814–825. doi: 10.1016/j.neuroimage.2010.06.048

Blankertz, B., Tangermann, M., Vidaurre, C., Fazli, S., Sannelli, C., Haufe, S., et al. (2010). The Berlin Brain-Computer Interface: non-medical uses of BCI technology. *Front. Neurosci.* 4:198. doi: 10.3389/fnins.2010.00198

Blankertz, B., Tomioka, R., Lemm, S., Kawanabe, M., and Müller, K.-R. (2008). Optimizing spatial filters for robust EEG single-trial analysis. *IEEE Signal Process. Mag.* 25, 41–56. doi: 10.1109/MSP.2008.4408441

BNCI Horizon 2020 (2015). *Roadmap - The Future in Brain/Neural-Computer Interaction: Horizon 2020*. BNCI Horizon 2020.

Borghini, G., Arico, P., Astolfi, L., Toppi, J., Cincotti, F., Mattia, D., et al. (2013). "Frontal EEG theta changes assess the training improvements of novices in flight simulation tasks," in *Engineering in Medicine and Biology Society (EMBC), 2013 35th Annual International Conference of the IEEE* (Osaka: IEEE), 6619–6622.

Borghini, G., Aricò, P., Graziani, I., Salinari, S., Sun, Y., Taya, F., et al. (2016). Quantitative assessment of the training improvement in a motor-cognitive task by using EEG, ECG and EOG signals. *Brain Topogr.* 29, 149–161. doi: 10.1007/s10548-015-0425-7

Bosse, S., Acqualagna, L., Porbadnigk, A. K., Blankertz, B., Curio, G., Muller, K.-R., et al. (2014). "Neurally informed assessment of perceived natural texture image quality," in *2014 IEEE International Conference on Image Processing (ICIP)* (IEEE), 1987–1991.

Bosse, S., Acqualagna, L., Porbadnigk, A. K., Curio, G., Müller, K.-R., Blankertz, B., et al. (2015). "Neurophysiological assessment of perceived image quality using steady-state visual evoked potentials," in *SPIE Optical Engineering+ Applications*, ed A. G. Tescher (International Society for Optics and Photonics), 959914–959914.

Brouwer, A., Reuderink, B., Vincent, J., van Gerven, M., and van Erp, J. (2013). Distinguishing between target and nontarget fixations in a visual search task using fixation-related potentials. *J. Vis.* 13:17. doi: 10.1167/13.3.17

Brunner, C., Birbaumer, N., Blankertz, B., Guger, C., Kübler, A., Mattia, D., et al. (2015). BNCI Horizon 2020: towards a roadmap for the BCI community. *Brain Comput. Interf.* 2, 1–10. doi: 10.1080/2326263X.2015.1008956

Buzsáki, G., and Draguhn, A. (2004). Neuronal oscillations in cortical networks. *Science* 304, 1926–1929. doi: 10.1126/science.1099745

Cohen, N., Pell, L., Edelson, M. G., Ben-Yakov, A., Pine, A., and Dudai, Y. (2015). Peri-encoding predictors of memory encoding and consolidation. *Neurosci. Biobehav. Rev.* 50, 128–142. doi: 10.1016/j.neubiorev.2014.11.002

Cole, M. J., Gwizdka, J., and Belkin, N. J. (2011a). "Physiological data as metadata," in *SIGIR 2011 Workshop on Enriching Information Retrieval (ENIR 2011)* (Beijing).

Cole, M. J., Gwizdka, J., Liu, C., Bierig, R., Belkin, N. J., and Zhang, X. (2011b). Task and user effects on reading patterns in information search. *Interact. Comput.* 23, 346–362. doi: 10.1016/j.intcom.2011.04.007

Cong, F., Alluri, V., Nandi, A. K., Toiviainen, P., Fa, R., Abu-Jamous, B., et al. (2013). Linking brain responses to naturalistic music through analysis of ongoing EEG and stimulus features. *IEEE Trans. Multimedia* 15, 1060–1106. doi: 10.1109/TMM.2013.2253452

Cong, F., Phan, A. H., Zhao, Q., Nandi, A. K., Alluri, V., Toiviainen, P., et al. (2012). "Analysis of ongoing EEG elicited by natural music stimuli using nonnegative tensor factorization," in *Signal Processing Conference (EUSIPCO)*, 494–498.

Dähne, S., Bießman, F., Samek, W., Haufe, S., Goltz, D., Gundlach, C., et al. (2015). Multivariate machine learning methods for fusing functional multimodal neuroimaging data. *Proc. IEEE* 103, 1507–1530. doi: 10.1109/JPROC.2015.2425807

Dähne, S., Meinecke, F. C., Haufe, S., Höhne, J., Tangermann, M., Müller, K.-R., et al. (2014a). SPoC: a novel framework for relating the amplitude of neuronal oscillations to behaviorally relevant parameters. *Neuroimage* 86, 111–122. doi: 10.1016/j.neuroimage.2013.07.079

Dähne, S., Nikulin, V. V., Ramírez, D., Schreier, P. J., Müller, K.-R., and Haufe, S. (2014b). Finding brain oscillations with power dependencies in neuroimaging data. *Neuroimage* 96, 334–348. doi: 10.1016/j.neuroimage.2014.03.075

Dalmaijer, E. (2014). *Is the Low-cost Eyetribe Eye Tracker Any Good for Research?* Technical report, PeerJ PrePrints. Available online at: https://peerj.com/preprints/585/

De Jong, R., Coles, M. G., Logan, G. D., and Gratton, G. (1990). In search of the point of no return: the control of response processes. *J. Exp. Psychol. Hum. Percept. Perform.* 16, 164–182. doi: 10.1037/0096-1523.16.1.164

De Vos, M., Gandras, K., and Debener, S. (2014). Towards a truly mobile auditory brain–computer interface: exploring the P300 to take away. *Int. J. Psychophysiol.* 91, 46–53. doi: 10.1016/j.ijpsycho.2013.08.010

Debener, S., Emkes, R., De Vos, M., and Bleichner, M. (2015). Unobtrusive ambulatory EEG using a smartphone and flexible printed electrodes around the ear. *Sci. Rep.* 5:16743. doi: 10.1038/srep16743

Di Flumeri, G., Borghini, G., Aricò, P., Colosimo, A., Pozzi, S., Bonelli, S., et al. (2015). "On the use of cognitive neurometric indexes in aeronautic and air traffic management environments," in *Symbiotic Interaction, Vol. 9359, Lecture Notes in Computer Science*, eds B. Blankertz, G. Jacucci, L. Gamberini, A. Spagnolli, and J. Freeman (Berlin: Springer), 45–56. doi: 10.1007/978-3-319-24917-9_5

Dijksterhuis, C., de Waard, D., Brookhuis, K., Mulder, B., and de Jong, R. (2013). Classifying visuomotor workload in a driving simulator using subject specific spatial brain patterns. *Front. Neurosci.* 7:149. doi:10.3389/fnins.2013.00149

Ding, N., and Simon, J. Z. (2012). Emergence of neural encoding of auditory objects while listening to competing speakers. *Proc. Natl. Acad. Sci. U.S.A.* 109, 11854–11859. doi: 10.1073/pnas.1205381109

Dmochowski, J. P., Bezdek, M. A., Abelson, B. P., Johnson, J. S., Schumacher, E. H., and Parra, L. C. (2014). Audience preferences are predicted by temporal reliability of neural processing. *Nat. Commun.* 5:4567. doi: 10.1038/ncomms5567

Dmochowski, J. P., Sajda, P., Dias, J., and Parra, L. C. (2012). Correlated components of ongoing EEG point to emotionally laden attention–a possible marker of engagement? *Front. Hum. Neurosci.* 6:112. doi: 10.3389/fnhum.2012.00112

Dornhege, G., del R. Millán, J., Hinterberger, T., McFarland, D., and Müller, K.-R. (eds.) (2007). *Toward Brain-Computer Interfacing*. Cambridge, MA: MIT Press.

Elbert, T., Rockstroh, B., Lutzenberger, W., and Birbaumer, N. (1980). Biofeedback of slow cortical potentials. I. *Electroencephalogr. Clin. Neurophysiol.* 48, 293–301. doi: 10.1016/0013-4694(80)90265-5

Eugster, M. J., Ruotsalo, T., Spapé, M. M., Kosunen, I., Barral, O., Ravaja, N., et al. (2014). "Predicting term-relevance from brain signals," in *Proceedings of the 37th International ACM SIGIR Conference on Research & Development in Information Retrieval, SIGIR '14* (New York, NY: ACM), 425–434. doi: 10.1145/2600428.2609594

Faller, J., Scherer, R., Costa, U., Opisso, E., Medina, J., and Müller-Putz, G. R. (2014). A co-adaptive brain-computer interface for end users with severe motor impairment. *PLoS ONE* 9:e101168. doi: 10.1371/journal.pone.0101168

Fazli, S., Dähne, S., Samek, W., Bießmann, F., and Müller, K.-R. (2015). Learning from more than one data source: data fusion techniques for sensorimotor rhythm-based Brain-Computer Interfaces. *Proc. IEEE* 103, 891–906. doi: 10.1109/JPROC.2015.2413993

Fukunaga, K. (1990). *Introduction to Statistical Pattern Recognition, 2nd Edn*. Boston, MA: Academic Press.

Gaebler, M., Bießmann, F., Lamke, J. P., Müller, K. R., Walter, H., and Hetzer, S. (2014). Stereoscopic depth increases intersubject correlations of brain networks. *Neuroimage* 100, 427–434. doi: 10.1016/j.neuroimage.2014.06.008

Galin, D., Johnstone, J., and Herron, J. (1978). Effects of task difficulty on EEG measures of cerebral engagement. *Neuropsychologia* 16, 461–472. doi: 10.1016/0028-3932(78)90069-6

Gallegos-Ayala, G., Furdea, A., Takano, K., Ruf, C. A., Flor, H., and Birbaumer, N. (2014). Brain communication in a completely locked-in patient using bedside near-infrared spectroscopy. *Neurology* 82, 1930–1932. doi: 10.1212/WNL.0000000000000449

Gerson, A., Parra, L., and Sajda, P. (2006). Cortically-coupled computer vision for rapid image search. *IEEE Trans. Neural Syst. Rehabil. Eng.* 2, 174–179. doi: 10.1109/TNSRE.2006.875550

Gevins, A., Leong, H., Du, R., Smith, M. E., Le, J., DuRousseau, D., et al. (1995). Towards measurement of brain function in operational environments. *Biol. Psychol.* 40, 169–186. doi: 10.1016/0301-0511(95)05105-8

Gevins, A., and Smith, M. E. (2003). Neurophysiological measures of cognitive workload during human-computer interaction. *Theor. Issues Ergon. Sci.* 4, 113–131. doi: 10.1080/14639220210159717

Gevins, A., Smith, M. E., Leong, H., McEvoy, L., Whitfield, S., Du, R., et al. (1998). Monitoring working memory load during computer-based tasks with EEG pattern recognition methods. *Hum. Factors* 40, 79–91. doi: 10.1518/001872098779480578

Golenia, J.-E., Wenzel, M., and Blankertz, B. (2015). "Live demonstrator of EEG and eye-tracking input for disambiguation of image search results," in *Symbiotic Interaction, Vol. 9359, Lecture Notes in Computer Science*, eds B. Blankertz, G. Jacucci, L. Gamberini, A. Spagnolli, and J. Freeman (Berlin: Springer International Publishing), 81–86. doi: 10.1007/978-3-319-24917-9_8

Goverdovsky, V., Looney, D., Kidmose, P., and Mandic, D. P. (2016). In-ear EEG from viscoelastic generic earpieces: robust and unobtrusive 24/7 monitoring. *IEEE Sensors J.* 16, 271–277. doi: 10.1109/JSEN.2015.2471183

Graziano, M., Parra, L. C., and Sigman, M. (2015). Neural correlates of perceived confidence in a partial report paradigm. *J. Cogn. Neurosci*. 27, 1090–1103. doi: 10.1162/jocn_a_00759

Guger, C., Krausz, G., Allison, B. Z., and Edlinger, G. (2012). Comparison of dry and gel based electrodes for P300 brain-computer interfaces. *Front. Neurosci.* 6:60. doi: 10.3389/fnins.2012.00060

Gugler, M., Sannelli, C., Haufe, S., Schubert, R., Schrauf, M., Kincses, W. E., et al. (2010). "Intramodal attentional processing during a monotonous car driving simulation: an EEG study," in *Annual Meeting of the Cognitive Neuroscience Society* (Montreal, QC), 17:20.

Gwizdka, J., and Cole, M. J. (2011). "Inferring cognitive states from multimodal measures in information science," in *ICMI 2011 Workshop on Inferring Cognitive and Emotional States from Multimodal Measure* (Alicante), 1–4.

Haggard, P., and Eimer, M. (1999). On the relation between brain potentials and the awareness of voluntary movements. *Exp. Brain Res.* 126, 128–133. doi: 10.1007/s002210050722

Haji Mirza, S. N. H., Proulx, M., and Izquierdo, E. (2011). "Gaze movement inference for user adapted image annotation and retrieval," in *Proceedings of the 2011 ACM Workshop on Social and Behavioural Networked Media Access , SBNMA '11* (New York, NY: ACM), 27–32. doi: 10.1145/2072627.2072636

Hajimirza, S., Proulx, M., and Izquierdo, E. (2012). Reading users' minds from their eyes: a method for implicit image annotation. *IEEE Trans. Multimedia* 14, 805–815. doi: 10.1109/TMM.2012.2186792

Hardoon, D. R., and Pasupa, K. (2010). "Image ranking with implicit feedback from eye movements," in *Proceedings of the 2010 Symposium on Eye-Tracking Research & Applications , ETRA '10* (New York, NY: ACM), 291–298. doi: 10.1145/1743666.1743734

Hasson, U. (2004). Intersubject synchronization of cortical activity during natural vision. *Science* 303, 1634–1640. doi: 10.1126/science.1089506

Hasson, U., and Honey, C. J. (2012). Future trends in neuroimaging: neural processes as expressed within real-life contexts. *NeuroImage* 62, 1272–1278. doi: 10.1016/j.neuroimage.2012.02.004

Hasson, U., Malach, R., and Heeger, D. J. (2010). Reliability of cortical activity during natural stimulation. *Trends Cogn. Sci.* 14, 40–48. doi: 10.1016/j.tics.2009.10.011

Haufe, S., Kim, J.-W., Kim, I.-H., Sonnleitner, A., Schrauf, M., Curio, G., et al. (2014a). Electrophysiology-based detection of emergency braking intention in real-world driving. *J. Neural Eng.* 11:056011. doi: 10.1088/1741-2560/11/5/056011

Haufe, S., Meinecke, F., Görgen, K., Dähne, S., Haynes, J.-D., Blankertz, B., et al. (2014b). On the interpretation of weight vectors of linear models in multivariate neuroimaging. *NeuroImage* 87, 96–110. Neuroimage single best paper of 2014 Award. doi: 10.1016/j.neuroimage.2013.10.067

Haufe, S., Treder, M. S., Gugler, M. F., Sagebaum, M., Curio, G., and Blankertz, B. (2011). EEG potentials predict upcoming emergency brakings during simulated driving. *J. Neural Eng.* 8:056001. doi: 10.1088/1741-2560/8/5/056001

Hayashi, H., Shirai, H., Kameda, M., Kunifuji, S., and Miyahara, M. (2000). "Assessment of extra high quality images using both eeg and assessment words on high order sensations," in *2000 IEEE International Conference on Systems, Man, and Cybernetics*, Vol. 2 (Nashville, TN: IEEE), 1289–1294. doi: 10.1109/icsmc.2000.886031

Haynes, J. D. (2011). Decoding and predicting intentions. *Ann. N. Y. Acad. Sci.* 1224, 9–21. doi: 10.1111/j.1749-6632.2011.05994.x

Hill, N. J., Ricci, E., Haider, S., McCane, L. M., Heckman, S., Wolpaw, J. R., et al. (2014). A practical, intuitive brain–computer interface for communicating 'yes' or 'no' by listening. *J. Neural Eng.* 11:035003. doi: 10.1088/1741-2560/11/3/035003

Holm, A., Lukander, K., Korpela, J., Sallinen, M., and Muller, K. M. (2009). Estimating brain load from the EEG. *ScientificWorldJournal* 9, 639–651. doi: 10.1100/tsw.2009.83

ITU (2002). "Methodology for the subjective assessment of the quality of television pictures," in *Rec. ITU-R BT 500-11*. Available online at: https://www.itu.int/rec/R-REC-BT.500

ITU (2008). "Subjective video quality assessmentmethods formultimedia applications," in *Rec. ITU-T P.910*. Available online at: https://www.itu.int/rec/T-REC-P.910/en

Jäncke, L., Kühnis, J., Rogenmoser, L., and Elmer, S. (2015). Time course of EEG oscillations during repeated listening of a well-known aria. *Front. Hum. Neurosci.* 9:401. doi: 10.3389/fnhum.2015.00401

Jangraw, D. C., Wang, J., Lance, B. J., and Chang, S.-F. (2014). Neurally and ocularly informed graph-based models for searching 3d environments. *J. Neural Eng.* 11:046003. doi: 10.1088/1741-2560/11/4/046003

Kamienkowski, J. E., Ison, M. J., Quiroga, R. Q., and Sigman, M. (2012). Fixation-related potentials in visual search: a combined EEG and eye tracking study. *J. Vis.* 12:4. doi: 10.1167/12.7.4

Kamiya, J. (1969). "Operant control of the EEG alpha rhythm and some of its reported effects," in *Altered States of Consciousness: A Book of Readings*, ed C. Tart (New York, NY: Wiley), 489–501.

Kaunitz, L., Kamienkowski, J., Varatharajah, A., Sigman, M., Quiroga, R., and Ison, M. (2014). Looking for a face in the crowd: fixation-related potentials in an eye-movement visual search task. *Neuroimage* 89, 297–305. doi: 10.1016/j.neuroimage.2013.12.006

Kecklund, G., and Åkerstedt, T. (1993). Sleepiness in long distance truck driving: an ambulatory EEG study of night driving. *Ergonomics* 36, 1007–1017. doi: 10.1080/00140139308967973

Khaliliardali, Z., Chavarriaga, R., Gheorghe, L. A., and del R Millán, J. (2015). Action prediction based on anticipatory brain potentials during simulated driving. *J. Neural Eng.* 12:066006. doi: 10.1088/1741-2560/12/6/066006

Kim, I.-H., Kim, J.-W., Haufe, S., and Lee, S.-W. (2014). Detection of braking intention in diverse situations during simulated driving based on EEG feature combination. *J. Neural Eng.* 12:016001. doi: 10.1088/1741-2560/12/1/016001

Klimesch, W., Doppelmayr, M., Schwaiger, J., Auinger, P., and Winkler, T. (1999). Paradoxical'alpha synchronization in a memory task. *Cogn. Brain Res.* 7, 493–501. doi: 10.1016/S0926-6410(98)00056-1

Kohlmorgen, J., Dornhege, G., Braun, M., Blankertz, B., Müller, K.-R., Curio, G., et al. (2007). "Improving human performance in a real operating environment through real-time mental workload detection," in *Toward Brain-Computer Interfacing*, eds G. Dornhege, J. del R. Millán, T. Hinterberger, D. McFarland and K.-R. Müller (Cambridge, MA: MIT Press), 409–422.

Koles, Z. J. (1991). The quantitative extraction and topographic mapping of the abnormal components in the clinical EEG. *Electroencephalogr. Clin. Neurophysiol.* 79, 440–447. doi: 10.1016/0013-4694(91)90163-X

Kornhuber, H. H., and Deecke, L. (1965). Hirnpotentialänderungen bei willkürbewegungen und passiven bewegungen des menschen: bereitschaftspotential und reafferente potentiale. *Pflugers Arch.* 284, 1–17. doi: 10.1007/BF00412364

Kovacevic, N., Ritter, P., Tays, W., Moreno, S., and McIntosh, A. R. (2015). 'virtual dream': collective neurofeedback in an immersive art environment. *PLoS ONE* 10:e0130129. doi: 10.1371/journal.pone.0130129

Kroupi, E., Hanhart, P., Lee, J.-S., Rerabek, M., and Ebrahimi, T. (2014). "EEG correlates during video quality perception," in *European Sign Process Conference* (Lisbon).

Kübler, A., Nijboer, F., Mellinger, J., Vaughan, T. M., Pawelzik, H., Schalk, G., et al. (2005). Patients with ALS can use sensorimotor rhythms to operate a brain-computer interface. *Neurology* 64, 1775–1777. doi: 10.1212/01.WNL.0000158616.43002.6D

Legewie, H., Simonova, O., and Creutzfeldt, O. (1969). EEG changes during performance of various tasks under open-and closed-eyed conditions. *Electroencephalogr. Clin. Neurophysiol.* 27, 470–479. doi: 10.1016/0013-4694(69)90187-4

Libet, B. (1985). Unconscious cerebral initiative and the role of conscious will in voluntary action. *Behav. Brain Sci.* 8, 529–539. doi: 10.1017/S0140525X00044903

Libet, B., Gleason, C. A., Wright, E. W., and Pearl, D. K. (1983). Time of conscious intention to act in relation to onset of cerebral activity (readiness-potential). *Brain* 106, 623–642. doi: 10.1093/brain/106.3.623

Lindemann, L., Wenger, S., and Magnor, M. (2011). "Evaluation of video artifact perception using event-related potentials," in *Proc ACM SIGGRAPH Symp Appl Percept in Graph and Visualiz* (Toulouse), 53–58.

Looney, D., Kidmose, P., and Mandic, D. P. (2014). "Ear-EEG: user-centered and wearable BCI," in *Brain-Computer Interface Research*, eds C. Guger, B. Allison, and E. C. Leuthardt (Berlin: Springer), 41–50.

Lucier, A. (1965). *Music for Solo Performer for Enormously Amplified Brain Waves and Percussion, Score.* in *Chambers: Scores by Alvin Lucier. Interviews with the composer by Douglas Simon* (Middletown, CT: Wesleyan University Press), 67. The piece was premiered on 5 May 1965 at the Rose Art Museum of Brandeis University in Waltham, MA.

Markand, O. N. (1990). Alpha rhythms. *J. Clin. Neurophysiol.* 7, 163–190. doi: 10.1097/00004691-199004000-00003

McCall, J., and Trivedi, M. (2007). Driver behavior and situation aware brake assistance for intelligent vehicles. *Proc. IEEE* 95, 374–387. doi: 10.1109/JPROC.2006.888388

Mehta, R. K., and Parasuraman, R. (2013). Neuroergonomics: a review of applications to physical and cognitive work. *Front. Hum. Neurosci.* 7:889. doi: 10.3389/fnhum.2013.00889

Miklody, D., Uitterhoeve, W., v. Heel, D., Klinkenberg, K., and Blankertz, B. (2016). "Maritime cognitive workload assessment," in *Symbiotic Interaction, Vol. 9961, Lecture Notes in Computer Science*, eds L. Gamberini, A. Spagnolli, G. Jacucci, B. Blankertz, and J. Freeman (Springer International Publishing).

Mirkovic, B., Debener, S., Jaeger, M., and De Vos, M. (2015). Decoding the attended speech stream with multi-channel EEG: implications for online, daily-life applications. *J. Neural Eng.* 12:046007. doi: 10.1088/1741-2560/12/4/046007

Moldovan, A.-N., Ghergulescu, I., Weibelzahl, S., and Muntean, C. (2013). "User-centered eeg-based multimedia quality assessment," in *2013 IEEE International Symposium on Broadband Multimedia System and Broadcasting (BMSB)*, 1–8. doi: 10.1109/BMSB.2013.6621743

Morone, G., Pisotta, I., Pichiorri, F., Kleih, S., Paolucci, S., Molinari, M., et al. (2015). Proof of principle of a brain-computer interface approach to support poststroke arm rehabilitation in hospitalized patients: design, acceptability, and usability. *Arch. Phys. Med. Rehabil.* 96, S71–S78. doi: 10.1016/j.apmr.2014.05.026

Mullen, T. R., Kothe, C. A., Chi, Y. M., Ojeda, A., Kerth, T., Makeig, S., et al. (2015). Real-time neuroimaging and cognitive monitoring using wearable dry EEG. *IEEE Trans. Biomed. Eng.* 62, 2553–2567. doi: 10.1109/TBME.2015.2481482

Müller, K.-R., Tangermann, M., Dornhege, G., Krauledat, M., Curio, G., and Blankertz, B. (2008). Machine learning for real-time single-trial EEG-analysis: from brain-computer interfacing to mental state monitoring. *J. Neurosci. Methods* 167, 82–90. doi: 10.1016/j.jneumeth.2007.09.022

Mustafa, M., Guthe, S., and Magnor, M. (2012). Single-trial EEG classification of artifacts in videos. *ACM Trans. Appl. Percept.* 9:12. doi: 10.1145/2325722.2325725

Naumann, L., Schultze-Kraft, M., Dähne, S., and Blankertz, B. (2016). "Prediction of difficulty levels in video games from ongoing EEG," in *Symbiotic Interaction, Vol. 9961, Lecture Notes in Computer Science*, eds L. Gamberini, A. Spagnolli, G. Jacucci, B. Blankertz, and J. Freeman (Springer International Publishing).

Nicolae, I., Acqualagna, L., and Blankertz, B. (2015a). "Neural indicators of the depth of cognitive processing for user-adaptive neurotechnological applications," in *Engineering in Medicine and Biology Society (EMBC), 2015 37th Annual International Conference of the IEEE* (Milano: IEEE), 1484–1487.

Nicolae, I.-E., Acqualagna, L., and Blankertz, B. (2015b). "Tapping neural correlates of the depth of cognitive processing for improving human computer interaction," in *Symbiotic Interaction, Vol. 9359, Lecture Notes in Computer Science*, eds B. Blankertz, G. Jacucci, L. Gamberini, A. Spagnolli, and J. Freeman (Springer International Publishing), 126–131. doi: 10.1007/978-3-319-24917-9_13

Nikulin, V. V., Kegeles, J., and Curio, G. (2010). Miniaturized electroencephalographic scalp electrode for optimal wearing comfort. *Clin. Neurophysiol.* 121, 1007–1014. doi: 10.1016/j.clinph.2010.02.008

Noh, E., Herzmann, G., Curran, T., and de Sa, V. R. (2014). Using single-trial EEG to predict and analyze subsequent memory. *Neuroimage* 84, 712–723. doi: 10.1016/j.neuroimage.2013.09.028

Norcia, A., Ales, J., Cooper, E., and Wiegand, T. (2014). Measuring perceptual differences between compressed and uncompressed video sequences using the swept-parameter visual evoked potential. *J. Vis.* 14, 649–649. doi: 10.1167/14.10.649

Norton, J. J., Lee, D. S., Lee, J. W., Lee, W., Kwon, O., Won, P., et al. (2015). Soft, curved electrode systems capable of integration on the auricle as a persistent brain–computer interface. *Proc. Natl. Acad. Sci. U.S.A.* 112, 3920–3925. doi: 10.1073/pnas.1424875112

Oliveira, F. T., Aula, A., and Russell, D. M. (2009). "Discriminating the relevance of web search results with measures of pupil size," in *Proceedings of the SIGCHI Conference on Human Factors in Computing Systems, CHI '09* (New York, NY: ACM), 2209–2212. doi: 10.1145/1518701.1519038

O'Sullivan, J. A., Power, A. J., Mesgarani, N., Rajaram, S., Foxe, J. J., Shinn-Cunningham, B. G., et al. (2015). Attentional selection in a cocktail party environment can be decoded from single-trial EEG. *Cereb. Cortex* 25, 1697–1706. doi: 10.1093/cercor/bht355

Papadelis, C., Chen, Z., Kourtidou-Papadeli, C., Bamidis, P. D., Chouvarda, I., Bekiaris, E., et al. (2007). Monitoring sleepiness with on-board electrophysiological recordings for preventing sleep-deprived traffic accidents. *Clin. Neurophysiol.* 118, 1906–1922. doi: 10.1016/j.clinph.2007.04.031

Parasuraman, R., and Wilson, G. (2008). Putting the brain to work: Neuroergonomics past, present, and future. *Hum. Factors* 50:468. doi: 10.1518/001872008X288349

Pfurtscheller, G., and Aranibar, A. (1979). Evaluation of event-related desynchronization preceding and following voluntary self-paced movement. *Electroencephalogr. Clin. Neurophysiol.* 46, 138–146. doi: 10.1016/0013-4694(79)90063-4

Piper, S. K., Krueger, A., Koch, S. P., Mehnert, J., Habermehl, C., Steinbrink, J., et al. (2014). A wearable multi-channel fNIRS system for brain imaging in freely moving subjects. *Neuroimage* 85, 64–71. doi: 10.1016/j.neuroimage.2013.06.062

Pope, A. T., Bogart, E. H., and Bartolome, D. S. (1995). Biocybernetic system evaluates indices of operator engagement in automated task. *Biol. Psychol.* 40, 187–195. doi: 10.1016/0301-0511(95)05116-3

Porbadnigk, A. K., Antons, J.-N., Blankertz, B., Treder, M. S., Schleicher, R., Möller, S., et al. (2010). "Using ERPs for assessing the (sub)conscious perception of noise," in *Conference of Proceedings IEEE Engineering in Medicine and Biology Society* (Buenos Aires), 2690–2693.

Porbadnigk, A. K., Scholler, S., Blankertz, B., Ritz, A., Born, M., Scholl, R., et al. (2011). "Revealing the neural response to imperceptible peripheral flicker with machine learning," in *Conference of Proceedings IEEE Engineering in Medicine and Biology Society* (Boston, MA), 3692–3695.

Porbadnigk, A. K., Treder, M. S., Blankertz, B., Antons, J.-N., Schleicher, R., Möller, S., et al. (2013). Single-trial analysis of the neural correlates of speech quality perception. *J. Neural Eng.* 10:056003. doi: 10.1088/1741-2560/10/5/056003

Prinzel, L. J., Freeman, F. G., Scerbo, M. W., Mikulka, P. J., and Pope, A. T. (2003). Effects of a psychophysiological system for adaptive automation on performance, workload, and the event-related potential P300 component. *Hum. Factors* 45, 601–613. doi: 10.1518/hfes.45.4.601.27092

Purcell, D. W., John, S. M., Schneider, B. A., and Picton, T. W. (2004). Human temporal auditory acuity as assessed by envelope following responses. *J. Acoust. Soc. Am.* 116, 3581–3593. doi: 10.1121/1.1798354

Rämä, P., and Baccino, T. (2010). Eye-Fixation Related Potentials (efrps) during object identification. *Vis. Neurosci.* 27, 187–192. doi: 10.1017/S0952523810000283

Salvaris, M., and Haggard, P. (2014). Decoding intention at sensorimotor timescales. *PLoS ONE* 9:e85100. doi: 10.1371/journal.pone.0085100

Schaefer, R. S., Farquhar, J., Blokland, Y., Sadakata, M., and Desain, P. (2011). Name that tune: decoding music from the listening brain. *Neuroimage* 56, 843–849. doi: 10.1016/j.neuroimage.2010.05.084

Schmidt, E. A., Kincses, W. E., Schrauf, M., Haufe, S., Schubert, R., and Curio, G. (2007). "Assessing drivers' vigilance state during monotonous driving," in *Proceedings of the Fourth International Symposium on Human Factors in Driving Assessment, Training, and Vehicle Design* (Washington, DC), 138–145.

Schmidt, E. A., Schrauf, M., Simon, M., Fritzsche, M., Buchner, A., and Kincses, W. E. (2009). Drivers' misjudgement of vigilance state during prolonged monotonous daytime driving. *Accid. Anal. Prev.* 41, 1087–1093. doi: 10.1016/j.aap.2009.06.007

Scholler, S., Bosse, S., Treder, M. S., Blankertz, B., Curio, G., Müller, K.-R., et al. (2012). Towards a direct measure of video quality perception using EEG. *IEEE Trans. Image Process.* 21, 2619–2629. doi: 10.1109/TIP.2012.2187672

Schultze-Kraft, M., Birman, D., Rusconi, M., Allefeld, C., Görgen, K., Dähne, S., et al. (2016a). The point of no return in vetoing self-initiated movements. *Proc. Natl. Acad. Sci. U.S.A.* 113, 1080–1085. doi: 10.1073/pnas.1513569112

Schultze-Kraft, M., Dähne, S., Gugler, M., Curio, G., and Blankertz, B. (2016b). Unsupervised classification of operator workload from brain signals. *J. Neural Eng.* 13:036008. doi:10.1088/1741-2560/13/3/036008

Shih, J. J., Krusienski, D. J., and Wolpaw, J. R. (2012). Brain-computer interfaces in medicine. *Mayo Clin. Proc.* 87, 268–279. doi: 10.1016/j.mayocp.2011.12.008

Simon, M., Schmidt, E. A., Kincses, W. E., Fritzsche, M., Bruns, A., Aufmuth, C., et al. (2011). EEG alpha spindle measures as indicators of driver fatigue under real traffic conditions. *Clin. Neurophysiol.* 122, 1168–1178. doi: 10.1016/j.clinph.2010.10.044

Smith, M. E., Gevins, A., Brown, H., Karnik, A., Du, R., and Gevins, A. S. (2001). Monitoring task loading with multivariate EEG measures during complex forms of human-computer interaction. *Hum. Factors* 43, 366–380. doi: 10.1518/001872001775898287

Soekadar, S. R., Birbaumer, N., Slutzky, M. W., and Cohen, L. G. (2015). Brain-machine interfaces in neurorehabilitation of stroke. *Neurobiol. Dis.* 83, 172–179. doi: 10.1016/j.nbd.2014.11.025

Sonnleitner, A., Simon, M., Kincses, W. E., Buchner, A., and Schrauf, M. (2012). Alpha spindles as neurophysiological correlates indicating attentional shift in a simulated driving task. *Int. J. Psychophysiol.* 83, 110–118. doi: 10.1016/j.ijpsycho.2011.10.013

Sterman, M., and Friar, L. (1972). Suppression of seizures in an epileptic following sensorimotor {EEG} feedback training. *Electroencephalogr. Clin. Neurophysiol.* 33, 89–95. doi: 10.1016/0013-4694(72)90028-4

Stopczynski, A., Stahlhut, C., Larsen, J. E., Petersen, M. K., and Hansen, L. K. (2014). The smartphone brain scanner: a portable real-time neuroimaging system. *PLoS ONE* 9:e86733. doi: 10.1016/0013-4694(72)90028-4

Straebel, V., and Thoben, W. (2014). Alvin Lucier's music for solo performer: experimental music beyond sonification. *Organ. Sound* 19:17. doi: 10.1017/S135577181300037X

Sturm, I. (2016). *Analyzing the perception of natural music with EEG and ECoG*. Ph.D. thesis, Berlin Institute of Technology.

Sturm, I., Blankertz, B., Potes, C., Schalk, G., and Curio, G. (2014). ECoG high gamma activity reveals distinct cortical representations of lyrics passages, harmonic and timbre-related changes in a rock song. *Front. Hum. Neurosci.* 8:798. doi: 10.3389/fnhum.2014.00798

Sturm, I., Dähne, S., Blankertz, B., and Curio, G. (2015a). Multi-variate EEG analysis as a novel tool to examine brain responses to naturalistic music stimuli. *PLoS ONE* 10:e0141281. doi: 10.1371/journal.pone.0141281

Sturm, I., Treder, M., Miklody, D., Purwins, H., Dähne, S., Blankertz, B., et al. (2015b). Extracting the neural representation of tone onsets for separate voices of ensemble music using multivariate EEG analysis. *Psychomusicol. Music Mind Brain* 25, 366–379. doi: 10.1037/pmu0000104

Thompson, J. (2013). *Neural Decoding of Subjective Music Listening Experiences*. Ph.D. thesis, Dartmouth College Hanover, New Hampshire, Hanover.

Treder, M. S., Purwins, H., Miklody, D., Sturm, I., and Blankertz, B. (2014). Decoding auditory attention to instruments in polyphonic music using single-trial EEG classification. *J. Neural Eng.* 11:026009. doi: 10.1088/1741-2560/11/2/026009

Treder, M. S., Schmidt, N. M., and Blankertz, B. (2011). Gaze-independent brain-computer interfaces based on covert attention and feature attention. *J. Neural Eng.* 8:066003. doi: 10.1088/1741-2560/8/6/066003

Trivedi, M. M., and Cheng, S. Y. (2007). Holistic sensing and active displays for intelligent driver support systems. *Computer* 40, 60–68. doi: 10.1109/MC.2007.170

Ušćumlić, M., and Blankertz, B. (2016). Active visual search in non-stationary scenes: coping with temporal variability and uncertainty. *J. Neural Eng.* 13:016015. doi: 10.1088/1741-2560/13/1/016015

Ušćumlić, M., Hägele, M., and Blankertz, B. (2015). "EEG correlates of visual recognition while overtly tracking a moving object," in *Symbiotic Interaction, Vol. 9359, Lecture Notes in Computer Science*, eds B. Blankertz, G. Jacucci, L. Gamberini, A. Spagnolli, and J. Freeman (Berlin: Springer International Publishing), 166–171. doi: 10.1007/978-3-319-24917-9_18

van Erp, J., Lotte, F., and Tangermann, M. (2012). Brain-computer interfaces: beyond medical applications. *Computer* 45, 26–34. doi: 10.1109/MC.2012.107

Vidal, J. J. (1973). Toward direct brain-computer communication. *Annu. Rev. Biophys.* 2, 157–180. doi: 10.1146/annurev.bb.02.060173.001105

Von Lühmann, A., Herff, C., Heger, D., and Schultz, T. (2015). Towards a wireless open source instrument: functional near-infrared spectroscopy in mobile neuroergonomics and BCI applications. *Front. Hum. Neurosci.* 9:617. doi: 10.3389/fnhum.2015.00617

Walter, W., and Shipton, H. (1951). A toposcopic display system applied to neurophysiology. *J. Br. Inst. Radio Eng.* 11, 260–273. doi: 10.1049/jbire.1951.0040

Wenzel, M., Moreira, C., Lungu, I.-A., Bogojeski, M., and Blankertz, B. (2015). "Neural responses to abstract and linguistic stimuli with variable recognition latency," in *Symbiotic Interaction, Vol. 9359, Lecture Notes in Computer Science*, eds B. Blankertz, G. Jacucci, L. Gamberini, A. Spagnolli, and J. Freeman (Springer International Publishing), 172–178. doi: 10.1007/978-3-319-24917-9_19

Wenzel, M. A., Golenia, J.-E., and Blankertz, B. (2016). Classification of eye fixation related potentials for variable stimulus saliency. *Front. Neurosci.* 10:23. doi: 10.3389/fnins.2016.00023

Wolpaw, J. R., and Wolpaw, E. W., (eds.). (2012). *Brain-Computer Interfaces: Principles and Practice*. New York, NY: Oxford University Press.

Zander, T. O., and Kothe, C. (2011). Towards passive brain-computer interfaces: applying brain-computer interface technology to human-machine systems in general. *J. Neural Eng.* 8:025005. doi: 10.3389/fnins.2011.00053

Zander, T. O., Lehne, M., Ihme, K., Jatzev, S., Correia, J., Kothe, C., et al. (2011). A dry EEG-system for scientific research and brain–computer interfaces. *Front. Neurosci.* 5:53. doi: 10.3389/fnins.2011.00053

Zhang, H., Chavarriaga, R., Gheorghe, L. A., and Millán, J. d. R. (2015a). "Brain correlates of lane changing reaction time in simulated driving," in *2015 IEEE International Conference on Systems, Man, and Cybernetics (SMC2015)* (Hong Kong).

Zhang, H., Chavarriaga, R., Khaliliardali, Z., Gheorghe, L., Iturrate, I., and d R Millan, J. (2015b). EEG-based decoding of error-related brain activity in a real-world driving task. *J. Neural Eng.* 12:066028. doi: 10.1088/1741-2560/12/6/066028

Conflict of Interest Statement: The authors declare that the research was conducted in the absence of any commercial or financial relationships that could be construed as a potential conflict of interest.

frontiers in
SYSTEMS NEUROSCIENCE

ORIGINAL RESEARCH ARTICLE
published: 07 August 2014
doi: 10.3389/fnsys.2014.00139

An electrocorticographic BCI using code-based VEP for control in video applications: a single-subject study

Christoph Kapeller[1,2,3], Kyousuke Kamada[4], Hiroshi Ogawa[4], Robert Prueckl[1,2,3], Josef Scharinger[3] and Christoph Guger[1,2]*

[1] *Guger Technologies OG, Graz, Austria*
[2] *g.tec medical engineering GmbH, Schiedlberg, Austria*
[3] *Department of Computational Perception, Johannes Kepler University, Linz, Austria*
[4] *Department of Neurosurgery, Asahikawa Medical University, Asahikawa, Japan*

Edited by:
Mikhail Lebedev, Duke University, USA

Reviewed by:
Duk Shin, Tokyo Institute of Technology, Japan
Martin Spüler, University of Tübingen, Germany

****Correspondence:***
Christoph Guger, g.tec medical engineering GmbH, Sierningstrasse 14, Schiedlberg 4521, Austria
e-mail: guger@gtec.at

A brain-computer-interface (BCI) allows the user to control a device or software with brain activity. Many BCIs rely on visual stimuli with constant stimulation cycles that elicit steady-state visual evoked potentials (SSVEP) in the electroencephalogram (EEG). This EEG response can be generated with a LED or a computer screen flashing at a constant frequency, and similar EEG activity can be elicited with pseudo-random stimulation sequences on a screen (code-based BCI). Using electrocorticography (ECoG) instead of EEG promises higher spatial and temporal resolution and leads to more dominant evoked potentials due to visual stimulation. This work is focused on BCIs based on visual evoked potentials (VEP) and its capability as a continuous control interface for augmentation of video applications. One 35 year old female subject with implanted subdural grids participated in the study. The task was to select one out of four visual targets, while each was flickering with a code sequence. After a calibration run including 200 code sequences, a linear classifier was used during an evaluation run to identify the selected visual target based on the generated code-based VEPs over 20 trials. Multiple ECoG buffer lengths were tested and the subject reached a mean online classification accuracy of 99.21% for a window length of 3.15 s. Finally, the subject performed an unsupervised free run in combination with visual feedback of the current selection. Additionally, an algorithm was implemented that allowed to suppress false positive selections and this allowed the subject to start and stop the BCI at any time. The code-based BCI system attained very high online accuracy, which makes this approach very promising for control applications where a continuous control signal is needed.

Keywords: electrocorticography, brain-computer-interface, code-based stimulation, VEP, augmented control

INTRODUCTION

People have long sought to extract users' intentions from brain signals to give impaired persons a communication channel or optimize interaction between users and their environments. Such a brain-computer-interface (BCI) allows the user to control a device or software with brain activity (Wolpaw et al., 2002). People can use a BCI to interact with their environments even if they have limited or no muscle control. Various data acquisition techniques like electroencephalography (EEG) (Wolpaw et al., 2002), electrocorticography (ECoG) (Leuthardt et al., 2004), functional magnetic resonance imaging (fMRI) (Weiskopf et al., 2004), and near infrared spectroscopy (NIRS) (Coyle et al., 2004) can be used as a BCI system.

The EEG is the most common brain imaging method in BCI research because it is inexpensive, portable, non-invasive, and has excellent temporal resolution (Mason et al., 2007). However, the EEG has only a limited spatial resolution, as each channel is influenced by the activation of millions of neurons, and the signal is smeared and filtered during passage through the scalp. ECoG signals recorded from the brain's surface are more robust against electromyographic (EMG) artifacts and provide a higher spatial and temporal resolution compared to EEG signals (Leuthardt et al., 2004). Several groups investigated the reliability of electrocorticographic signals for real-time applications, like 2D movement control based on motor imagery tasks (Schalk et al., 2008) or a P300 spelling device (Brunner et al., 2011).

Most BCIs rely on one of three kinds of brain signals: event related desynchronization (ERD) associated with motor-imagery, P300 and steady-state visual evoked potentials (SSVEP) (Wolpaw et al., 2002). While P300 based systems typically rely on discrete control, which is excellent for selecting commands to control a spelling device (Mason et al., 2007; Guger et al., 2009), the motor imagery and SSVEP based systems often give a continuous control signal that could be used to steer a wheelchair in different directions. The performance of a BCI

relying on motor imagery has already been comprehensively investigated using EEG (Müller-Gerking et al., 1999; Guger et al., 2000, 2003; Krausz et al., 2003; Blankertz et al., 2010) and ECoG recordings (Leuthardt et al., 2004; Schalk et al., 2008; Miller et al., 2010). Recently, an ECoG BCI was presented that decoded attempted arm and hand movements for 3D cursor control using activation of the high-frequency band between 40 and 200 Hz, which were mapped to velocity control signals (Wang et al., 2013).

This work is focused on BCIs based on visual evoked potentials (VEP) derived from subdural ECoG signals over the visual cortex. Two methods are generally used to distinguish different visual targets: phase coding and frequency coding (Wang et al., 2008). In SSVEPs, the brain waves derived from the scalp contain sinusoidal signals with the same frequency as the visual stimuli. The so called Bremen BCI used a minimum energy based feature extraction applied on EEG data including SSVEPs and reached a mean ITR of 61.70 bits/min and a mean accuracy of 96.79% (Volosyak, 2011). Another SSVEP BCI study presented a grand average accuracy of 95.50% for EEG recordings from 53 subjects (Guger et al., 2012). An alternative type of stimulation that combines the phase and frequency coded VEPs is based on code sequences, producing code-based VEPs (c-VEP) (Bin et al., 2009). This type of BCI was initially proposed by Erich Sutter as a spelling device and tested with an ALS patient having epidural implants over 11 months (Sutter, 1992). The subject achieved a spelling rate of 10–12 words per minute. In a more recent paper, a multi-channel c-VEP BCI was tested with EEG signals (Bin et al., 2011). A spatial filter was computed from a canonical correlation analysis (CCA) and then applied on multiple EEG channels over the visual cortex. The authors developed a 32 target system with a stimulation sequence of 1.05 s. The resulting mean online accuracy was 85.00%, which led to an ITR of 108 bits/min. An even faster version of this c-VEP speller application led to an average accuracy of 96.00% and an ITR of 144 bit/min (Spüler et al., 2012). Although the code-based stimulation approach is not the same as a conventional steady state stimulus, BCIs based on c-VEP are often grouped together with SSVEP BCIs for convenience.

BCIs relying on VEPs could benefit from on-screen solutions, which do not need additional hardware like LEDs and can be embedded into a virtual environment. This was achieved inside a 2D or 3D gaming environments, as well as virtual reality scenarios (Lalor et al., 2005; Martinez et al., 2007; Faller et al., 2010). In a previous study we tested a c-VEP BCI for robotic control with EEG on 11 subjects showing a grand average online accuracy of 98.18% (Kapeller et al., 2013). Specifically, the control interface was embedded inside a video application showing the moving robot, while the user was steering the robot along a given path.

The main goal of this study is to investigate an intracranial c-VEP BCI designed as a continuous control interface for augmentation of video applications.

MATERIALS AND METHODS

SUBJECT DESCRIPTION

The subject, a 35 year old woman suffering from intractable epilepsy underwent subdural grid implantation prior to resective brain surgery, which was part of the clinical treatment. After full explanation of the experimental procedure and its possible risks, a written informed consent was obtained from the subject. This work was approved by the institutional review board of the Asahikawa Medical University (No. 693) before the study. She had corrected-to-normal vision and a Japanese Wechsler Memory Scale—Revised Edition (WMS-R) test showed normal memory function (average score 100, $SD = 15$). As the epileptic focus did not overlap with the visual cortex, there was no reason to reject the subject from the study.

In order to localize epileptic foci, four grids and five strips containing 100 subdural electrodes were temporarily implanted widely across the right hemisphere. **Figure 1** shows the grid alignment on the cortex and the numbering of the electrodes. The clinical electrodes were made of platinum and had an inter-electrode distance of 10 mm and a conductive area of about 7.1 mm^2.

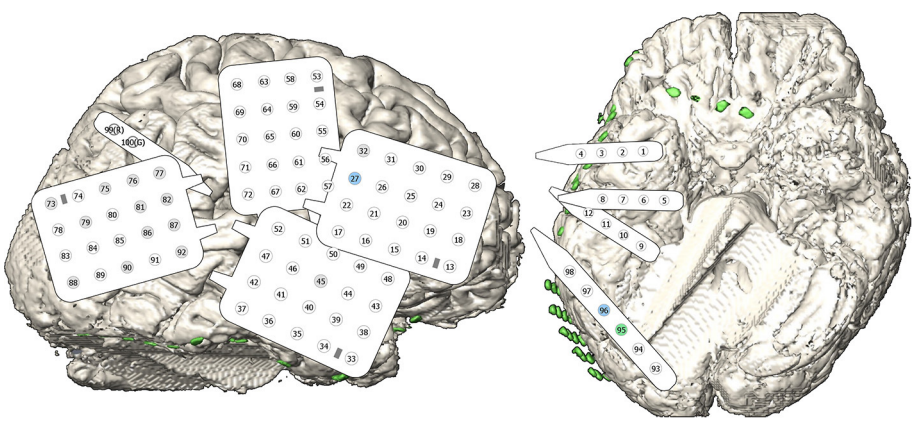

FIGURE 1 | Implanted electrodes. The subject had 100 electrodes on **four** grids and **five** strips located implanted over the frontal, temporal, parietal, and occipital lobe of the right hemisphere. The schematic views of the grids and strips contain electrodes represented by a circle and their number in the montage. An additional strip on the frontal base region was not recorded and is not included into the electrode numbering. The gray highlighted electrodes represent very noisy channels which were recorded, but not considered for signal processing. The green/blue colored channels indicate high/medium contribution during feature extraction.

DATA ACQUISITION

The electrodes were connected to a g.HIamp (g.tec medical engineering GmbH, Austria) biosignal data acquisition device, which digitized the data with 24 bit resolution and 256 Hz sampling frequency. The data were band-pass filtered between 1 and 30 Hz and notch filtered at 50 Hz to suppress power line interference. This pass band was designed to maximize the signal-to-noise ratio (SNR) of the recorded VEPs for a maximum stimulation frequency of 30 Hz using a monitor with a refresh rate of 60 Hz. The grounding strip covering the superior parietal lobule contained the electrodes number 99 and 100, which were used as reference (REF) and ground (GND) electrode, respectively. Therefore, 98 signal channels were recorded during the experiment.

The biosignal data acquisition device transferred the data via USB to the computer system, which was used for data acquisition, online processing, experimental paradigm control, data visualization and data storage.

SYSTEM CONFIGURATION

The design of the BCI system is based on the work of Bin et al. (2011) and modified for continuous control input from the user. The stimulation unit, a 60 Hz LCD monitor, presents visual targets that each occupy 4.2 × 2.4 cm of the screen. These targets are embedded inside an OpenGL based video application and remotely connected with the BCI system, which controls the visual stimulation and the feedback to the user.

The stimulus definition is based on a pseudo-random binary code sequence, a so called m-sequence. These binary sequences are used for nonlinear signal analysis and also in multi input systems (Golomb et al., 1982). Therefore, black and white stimulation is applied using a 63 bit m-sequence, where 1 and 0 are represented by white and black, respectively. Due to the stimulation rate of 60 Hz, one stimulation sequence lasts 1.05 s. The BCI presented in this work contains four visual targets (C1, C2, C3, and C4), which can be selected by the user. This is a well-suited number of classes for a continuous control task, e.g., moving a robotic device or a virtual avatar forward, backward, left or right (Kapeller et al., 2013). As the autocorrelation function of the m-sequence is approximating the unit impulse function (Zierler, 1959), we can use the same modulation sequence for all visual targets. Only a phase shift of the sequence onset is necessary to distinguish between the resultant VEPs inside the synchronized processing unit of the BCI. The phase shift for each target is equally distributed along the m-sequence and then rounded to the next lower integer value. This leads to a phase shift in bits of $\rho_1 = 0$, $\rho_2 = 15$, $\rho_3 = 30$, and $\rho_4 = 45$ for class C1 to C4, respectively.

In order to synchronize the visual stimulation with the recorded ECoG signals, a trigger signal representing the sequence onset of C1 is sent via UDP connection to the BCI system. Once the stimulation is synchronized, the BCI is processing the resultant VEPs using a signal buffer that is updated each 51 samples (∼200 ms). The processing system is running in the MATLAB/Simulink rapid prototyping environment.

SCREEN OVERLAY CONTROL INTERFACE (SOCI)

The visual targets are presented on the monitor through the SOCI module. The SOCI module is a C++ library based on OpenGL that is loadable at runtime and can be used by OpenGL based host applications to embed visual stimulation. The host applications could be virtual reality environments or simple real-world videos that are acquired from a camera. The SOCI works as a remote visual stimulator and provides a network interface that can be used to load visual targets, start or stop the flickering, and synchronize the stimulation with the signal processing. Since it is a multi-threaded application, the communication with the BCI model and the OpenGL drawing commands are handled within separate threads. The host graphics application has to initialize and control the SOCI. This utilizes an abstract interface class that provides public functions to embed the module.

The visual targets can be configured very flexibly using an XML description provided from a configuration file or an external application (Putz et al., 2011). Users can change the number, position, size, and content of the icons and modify other parameters.

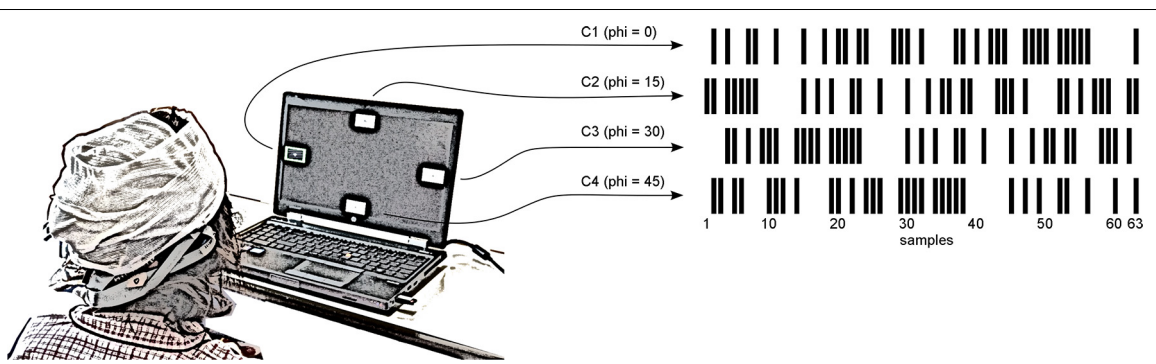

FIGURE 2 | Experimental design. A notebook presented **four** visual targets to the subject, who sat around 80 cm in front of the monitor. The size of **one** target was 4.2 × 2.4 cm leading to a visual angle of 3.0 × 1.7°. Each visual target (C1, C2, C3, and C4) was flickering with a phase shifted version of the same m-sequence. The subject was asked to focus the cued target or to choose an arbitrary target if the cue was disabled. In unsupervised mode, the selected target was surrounded by a green border.

EXPERIMENTAL DESIGN

The subject was seated ∼80 cm in front of the stimulation monitor visualizing the BCI targets during the experiment (see **Figure 2**), which was separated into three phases. Specifically, the subject participated in a calibration run to compute a classifier, an evaluation run to estimate the accuracy of the BCI and a free run to let the subject experience unsupervised interaction with the system in combination with online feedback of the selected target.

After a pre-run delay of 10 s (to avoid settling effects of the filters), the subject performed the calibration run. The subject's task was to focus on target C1 for 200 stimulation cycles, while all other targets were not visible. Since one cycle lasts 1.05 s, the entire calibration took less than 4 min.

In the evaluation run, all targets were displayed on the monitor and the online accuracy of the BCI system was tested across 20 trials. Specifically, the SOCI displayed four rectangles on the top, bottom, left, and right of the monitor (see **Figure 2**). During each trial, the subject focused on the target that was highlighted by a visual cue (green border around the target). Each trial consisted of a 3.0 s long resting phase with no visual stimulation, followed by a 7.0 s long stimulation period showing all targets flickering simultaneously. This trial definition was based on previous studies about BCIs using SSVEP or c-VEP (Guger et al., 2012; Kapeller et al., 2013). Since the stimulation period exceeded the longest buffer size and the signal buffer was updated each 200 ms, we decided to keep a trial duration that is not a multiple of the stimulation sequence. No feedback about the classification result was given to the subject at any time during the evaluation run.

Finally, the subject performed the free run to experience the interaction with the BCI by getting feedback about the selected target. Again, all four targets were flickering simultaneously with the m-sequence and corresponding phase shift. No cue was presented on the screen to indicate the current target, and all targets continued flickering throughout the free run. The subject could select any target at any time. Feedback reflecting the current selection was presented as a green border around the selected target. After the free run, the subject was asked about her impression of the system's accuracy.

OFFLINE ANALYSES

The recorded data set from the calibration run was used for offline analyses. As we had to exclude bad channels from the offline analyses, all channels that did not pass visual inspection of the raw data were set to zero. After checking the signal quality, the 200 recorded sequences were epoched and DC corrected for each trial. Then the trials were averaged to a set of templates for each signal channel and phase shift. These templates were used for waveform detection of the c-VEP inside the ECoG signals. Therefore, a CCA was used to maximize the correlation coefficient of all templates and the raw data.

Compared to ordinary correlation, the CCA is independent from the used coordinate system. It provides the maximum correlation of the variables, which is also called the canonical correlation (Borga, 2001). The correlation coefficient ρ is maximized, with respect to the normalized base vectors for canonical correlation ($\hat{w}_x$ and $\hat{w}_y$):

$$\max_{\widehat{w}_x \widehat{w}_y} \rho = \max_{\widehat{w}_x \widehat{w}_y} \left(\frac{E\left[\widehat{w}_x^T X Y^T \widehat{w}_y\right]}{E\left[\widehat{w}_x^T X X^T \widehat{w}_x\right] E\left[\widehat{w}_y^T Y Y^T \widehat{w}_y\right]} \right)$$

X and Y are the analyzed multidimensional variables. In our case, X contained the raw ECoG data of 200 sequences and Y consisted of 200 concatenated templates for each channel.

The calculation of the maximum correlation is based on the eigenvalue equations below, where C is the covariance matrix of the multidimensional variables. In these equations, multiple non-zero eigenvalues are possible. As the eigenvalues represent the squared correlation coefficients, the highest eigenvalue leads to the canonical correlation. The corresponding eigenvectors are the base vectors from:

$$C_{xx}^{-1} C_{xy} C_{yy}^{-1} C_{yx} \widehat{w}_x = \rho^2 \widehat{w}_x$$

$$C_{yy}^{-1} C_{yx} C_{xx}^{-1} C_{xy} \widehat{w}_y = \rho^2 \widehat{w}_y.$$

The resultant vectors $\hat{w}_x$ and $\hat{w}_y$ were interpreted as spatial filters, where $\hat{w}_x$ was applied on the raw ECoG signals and $\hat{w}_y$ was applied on the template data. **Figure 3** shows the averaged c-VEP templates for each channel together with the weight for the individual channel.

The spatial filtered calibration data was then used for computing a linear classifier using a multi-class linear discriminant analysis (m-LDA) (Duda et al., 2000). The features were extracted by computing the correlation coefficients of the spatially filtered templates and the spatially filtered raw data. In order to extract features for each class, the data set of the calibration run was epoched four times. Before each epoching step, the signals were shifted with respect to the trigger channel and the phase shift of the current class. Hence, the correlation coefficients were maximized for the corresponding phase shift.

A zero class provided an idle state that occurred when no target was selected by the user. Based on the classification scores only, it is not possible to determine whether the user has selected any target. This entails rejecting any classification result for which the residual error probability is larger than a predefined limit. A Softmax function is used, which transforms the output of the discrimination function into a value p between 0 and 1:

$$p_i = \frac{e^{q_{i/\tau}}}{\sum_{b=1}^{N} e^{q_{b/\tau}}}$$

Where q_i is the distance to class i and τ is called the temperature, which is used to adjust the gap between the resultant probabilities (Sutton and Barto, 1998). N is the total number of possible classes.

SETUP FOR THE ONLINE EXPERIMENT

During the online experiments a Simulink model was processing incoming data with an update rate of 256 Hz driven by the data acquisition device. After the preprocessing step described in Section Data Acquisition, the recorded ECoG signals were buffered and DC corrected. The size of the signal buffer was set to a multiple of the template length and was updated every 51

processing steps. In order to extract characteristic features for each individual class, this buffer was then compared with the templates for each phase shift. Therefore, two processing steps were required. First, the spatial filter from the offline analysis was applied to the signal buffer and the templates and led to a combined channel with maximized correlation with respect to the spatially filtered templates. Second, the spatially filtered signal was correlated with each spatially filtered template leading to one feature channel for each class.

Before starting the free run, the data from the evaluation run was used to investigate the system's accuracy and latency. Different settings were tested to provide the best configuration for the free run.

As the length of the ECoG signal buffer could heavily influence the performance of the BCI, we tested the system accuracy for multiple buffer lengths. The signal buffer has to be a multiple of the m-sequence length, where the minimum length is the duration of one m-sequence cycle. We explored buffer lengths of 1.05, 2.10, and 3.15 s. Longer buffer lengths were not considered in this work, since this would not proper to our previously proposed BCI applications.

In order to stabilize the features, a 1.0 s moving window filter was used before applying the linear classifier. If the classification result was below a 97–100% confidence interval, the output was assigned to the zero class.

The mean online accuracy of the BCI was determined by averaging all classifier outputs at the last 2 s of each trial. This gives a measure about the performance of the BCI, when the feature values reached their maximum with respect to the selected target.

RESULTS

CLASSIFICATION ACCURACY

Figure 4A shows the mean on-line accuracy for three buffer lengths (1.05, 2.10, and 3.15 s) after 20 trials. The shortest window length resulted in the lowest accuracy, but fastest reaction of the BCI system. The classification accuracies for growing buffer length were 86.76, 92.96, and 99.21%, respectively. **Figure 4B** illustrates the BCI latency that was necessary to reach 80% classification accuracy. Specifically, this latency consisted of the moving average window length (1.0 s), the signal buffer length and the time that was necessary for the user to locate and focus on the

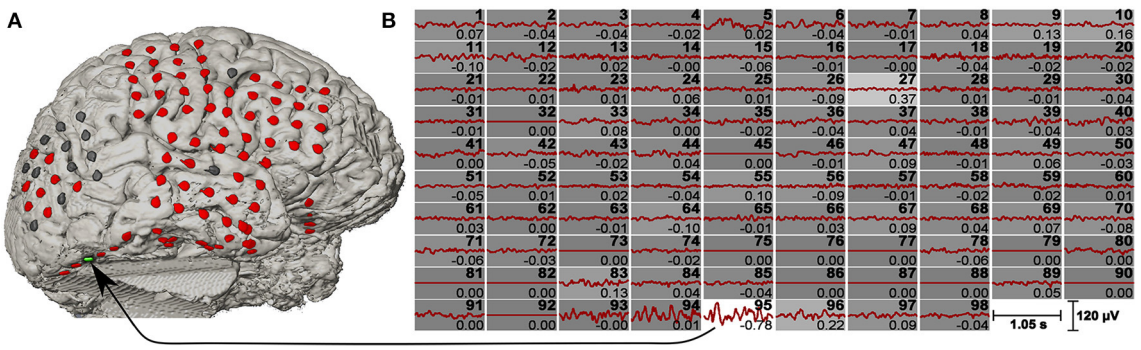

FIGURE 3 | c-VEP templates and spatial filter. (A) Co-registered brain model of a pre-surgical T1-weighted MRI and a post-implantation CT scan. The channels are highlighted in different colors (bad channels are gray, normal channels are red, and the maximum weighted channel of the CCA is green). **(B)** Signals of all 98 channels were averaged over 200 stimulation sequences. Channel numbers are shown on the top right corner of each plot, while the spatial filter coefficients are shown on the bottom right corner. Beside the numeric value, the spatial filter coefficients are also represented by the background intensity of each channel (the highest weight is plotted on white background). Bad channels were set to zero.

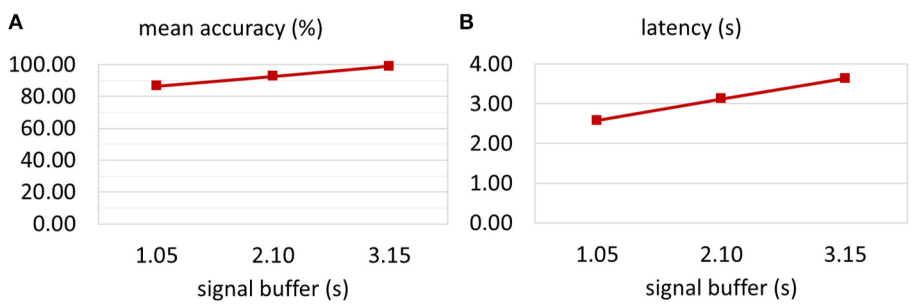

FIGURE 4 | Optimization of the signal buffer. The classification accuracy for **three** different signal buffer sizes was tested. **(A)** Increasing the buffer size from **one** to **three** stimulation sequence lengths (1.05–3.15 s) led to an increase in mean accuracy from 86.76 to 99.21%. **(B)** Of course, the latency of the system depends on the signal buffer length. However, small buffer might reduce the quality of the extracted features. Hence, the latency presented here shows the time that is necessary to achieve classification accuracy above 80%. Increasing the signal buffer size increased the latency from 2.59 to 3.65 s.

target and then produce clear ECoG activity. The exact latencies were 2.59, 3.14, and 3.65 s for a buffer length of 1.05, 2.10, and 3.15 s, respectively.

EVALUATION OF THE ZERO CLASS

Figure 5 shows as an example the effect of the zero class for a signal buffer window length of 2.10 s. The highest classification accuracy could be reached when no zero class was applied. However, if the subject was not attending to any target, the resultant false positive (FP) rate was very high and showed random target selection. If the threshold for the zero class was set to a confidence level of 97%, then the classification accuracy was about 30–40% lower, but also FP rate dropped down to less than 5% if the subject was not attending to one of the targets (second 0.0 to 3.0 in **Figure 5**). Once the subject was focusing a target and the signal buffer contained the corresponding c-VEPs, the FP rate even dropped down to 0%, which means that only reliable features were accepted for classification. The period from second −3.0 to 0.0 represented a period, in which the subject was intended to stop the selection of the previous target. From second −3.0 to −2.0 the FP rate rose up to 50–60%. This period was characterized by high feature values from the last classification leading to an FP rate similar to the classification accuracy with enabled zero class. After another 1.5 s the signal buffer did not contain any target related VEPs anymore.

UNSUPERVISED ONLINE EXPERIMENT

During the free run, the subject performed 17 unsupervised selections. She reported that the feedback of the selected targets was correct throughout the whole run.

DISCUSSION

This work successfully showed that a continuous control signal can be extracted from ECoG data with c-VEPs. The c-VEP approach has an advantage over SSVEPs: there is no single frequency that flashes. Instead, a certain code is embedded, and therefore the risk of inducing seizures is reduced, which is especially important for subjects with increased photosensitivity. SSVEP studies showed that the area of the flashing item, the intensity and the frequency are important parameters for improving the performance. But increasing area and intensity are especially problematic for these persons. SSVEP BCIs work best in a frequency range between about 8–25 Hz, which is a sensitive range for inducing seizures. The c-VEPs contain a mixture of frequencies with lower intensity, comparable to watching TV, and are therefore better suited for these persons.

A big problem of ECoG BCI studies is the rapid selection of appropriate channels coding the necessary information. This can either be done offline with channel selection algorithms like distinction sensitive learning vector quantization (DSLVQ) (Pregenzer and Pfurtscheller, 1995) or by observing reactive frequency spectra or similar parameters. But all these procedures require manual optimization and are time consuming. In the presented work, a spatial filter was automatically obtained using the calibration data during the offline analyses. The result is a spatial filter that selects the most important channels according to their importance for the discrimination task. This is comparable to common spatial patterns (CSP) that are used for motor imagery based BCI system to automatically weight the channels (Guger et al., 2000). For this patient, one of the electrodes (channel 95) mostly contributed to the classification task, two more channels showed medium weights for the spatial filter (channel number

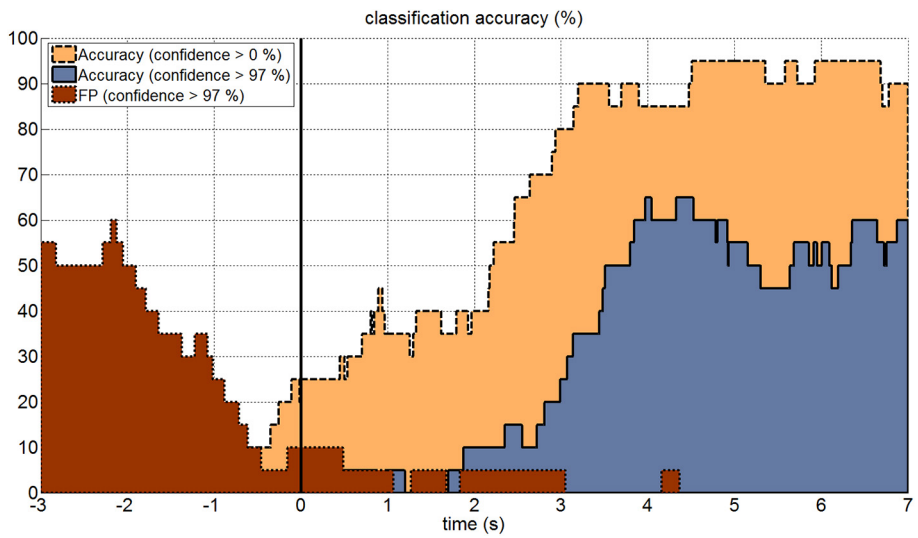

FIGURE 5 | Online accuracy and zero class. The figure shows the online classification accuracy for a 10 s long trial. The black vertical line indicates the onset of the visual stimulation for each trial. Classification was performed using a 2.10 s signal buffer and a confidence interval for classification of 0–100% (yellow area with dashed line) and 97–100% (blue area with solid line). The false positive rate (red area with dotted line) was very high before the stimulation onset, because of the buffer overlap from previous trials. Once the signal buffer did not contain any c-VEPs anymore, the false positive rate dropped down to around 5% and then to 0%, when the signal buffer was again filled with c-VEPs.

27 and 96 ordered by priority). This is similar to CSP, where the weights of the electrodes are also ordered according to the eigenvalues obtained with the algorithm (Müller-Gerking et al., 1999). Interestingly, electrodes 95 and 96 were neighbors located at occipital base (green/blue channel in **Figure 1**), but electrode 27 was located at lateral frontal lobe (blue channel in **Figure 1**). However, as the amplitude of the VEPs of the electrodes 95 and 96 were much higher than for electrode 27, the contribution of electrode 27 to the feature values was very small.

The spatial filter also allows easy system configuration updating with new calibration data. Previous publications with EEG data showed that subjects were trained multiple times to increase the classification accuracy (Guger et al., 2012). In an SSVEP group study with EEG recordings from 53 subjects, the classification accuracy could be increased from a grand average accuracy of 87.9–95.5% after only 20 min of training (Guger et al., 2012). In the current study the used c-VEP algorithm showed a high mean classification accuracy of 99.21% that was achieved with only 200 s of calibration data and after only a single training run lasting less than 4 min in total.

In comparison, the group study of Guger et al. (2012) showed that 27 out of 53 subjects achieved perfect accuracy of 100% and only seven subjects achieved less than 90% accuracy. Another study with a c-VEP BCI including 11 subjects reported a grand average classification accuracy of 98.18% with nobody below 90% accuracy (Kapeller et al., 2013). This study showed that a BCI using c-VEPs works even for subjects who could not use an SSVEP BCI. The c-VEP BCI using ECoG showed similar results compared to the EEG study. This might be an indicator that the SNR of the recorded VEPs was similar in both setups. However, it is important to note that the ECoG setup is much more robust against eye blinks or EMG artifacts. Moreover, in this study the signals were recorded from the right hemisphere only and it is unclear if the electrode positions were optimal with respect to the amplitude of the VEPs.

Notably, the mean classification accuracy from second 5 to 7 is 99.21%, which shows that the subject could continue attending to a certain target for a longer time window. This is important for generating a continuous control signal, unlike discrete selection BCI systems such as a typical P300 BCI. Sutter tested an approach similar to the present system with ECoG data in 1992. He used also c-VEPs with 64 icons on a screen for a spelling system. The study showed that 64 targets could be successfully selected by the ALS patient, who reached about 10–12 words a minute with this setup. Nowadays, the P300 is used for most BCI spellers because these BCI systems support a very high number of targets and can work even better if more targets are used (Allison and Pineda, 2003; Sellers et al., 2006; Guger et al., 2009; Brunner et al., 2011). The SSVEP and c-VEP principles are limited by the number of different targets that can be generated. While the screen refresh rate is a limiting factor for an SSVEP BCI, the sequence length defines the number of possible targets in a c-VEP BCI.

Although, the c-VEP principle allows fast switching from one target to another target, the latency of at least 1.05 s requires anticipation of the user, e.g., while steering an avatar or a robotic system in real-time. Previous studies using ECoG showed very short latencies during 3D cursor control (Wang et al., 2013) or movement of a prosthetic arm (Yanagisawa et al., 2012). In these studies the subjects either performed real or attempted movements in order to detect changes in power of different frequency bands, especially in the frequency band >70 Hz. However, such a BCI system that is independent from motor execution usually requires a much longer training period than the calibration time presented in this work. While using the c-VEP BCI, the subject learned very easily and quickly how to control the system. She was able perform a calibration run, a testing run and a free run within 30 min.

In combination with a goal-oriented BCI system, this allows for full control of humanoid robotic systems. For such applications, it is important to embed the BCI controls into a control display that is either a computer screen or a head-mounted display. Such a humanoid robotic system might have also cameras with 2D or 3D vision embedded for online transmission of a video stream to the BCI feedback monitor, so that the BCI user is also embedded in its avatar for optimizing the control behavior (Gergondet et al., 2012). In this case a big advantage is the zero class property, because it ensures that the humanoid robotic system does not make movements if the user is not attending to one of the controls.

We plan to integrate and test different target shapes and patterns and increase the number of targets. Since the number of targets for the c-VEP configuration is only limited by the sequence length and the minimum phase shift between the sequences, the system can be optimized in terms of number of decisions and reaction time.

ACKNOWLEDGMENT

This research is supported by the European Union FP7 integrated project VERE (No. 257695) and the ENIAC JU project DeNeCor (No. 324257).

REFERENCES

Allison, B. Z., and Pineda, J. A. (2003). ERPs evoked by different matrix sizes: implications for a brain computer interface (BCI) system. *IEEE Trans. Neural Syst. Rehabil. Eng.* 11, 110–113. doi: 10.1109/TNSRE.2003.814448

Bin, G., Gao, X., Wang, Y., Hong, B., and Gao, S. (2009). VEP-based brain-computer interfaces: time, frequency, and code modulations [Research Frontier]. *IEEE Comput. Intell. Mag.* 4, 22–26. doi: 10.1109/MCI.2009.934562

Bin, G., Gao, X., Wang, Y., Li, Y., Hong, B., and Gao, S. (2011). A high-speed BCI based on code modulation VEP. *J. Neural Eng.* 8:025015. doi: 10.1088/1741-2560/8/2/025015

Blankertz, B., Tangermann, M., Vidaurre, C., Fazli, S., Sannelli, C., Haufe, S., et al. (2010). The Berlin brain–computer interface: non-medical uses of BCI technology. *Front. Neurosci.* 4:198. doi: 10.3389/fnins.2010.00198

Borga, M. (2001). *Canonical Correlation: A Tutorial*. On line tutorial. Available online at: http://people.imt.liu.se/magnus/cca

Brunner, P., Ritaccio, A. L., Emrich, J. F., Bischof, H., and Schalk, G. (2011). Rapid communication with a "P300" matrix speller using electrocorticographic signals (ECoG). *Front. Neurosci.* 5:5. doi: 10.3389/fnins.2011.00005

Coyle, S., Ward, T., Markham, C., and McDarby, G. (2004). On the suitability of near-infrared (NIR) systems for next-generation brain–computer interfaces. *Physiol. Meas.* 25:815. doi: 10.1088/0967-3334/25/4/003

Duda, R. O., Hart, P. E., and Stork, D. G. (2000). "Component analysis and discriminations," in *Pattern Classification* (New York, NY: John Wiley & Sons), 117–124.

Faller, J., Müller-Putz, G., Schmalstieg, D., and Pfurtscheller, G. (2010). An application framework for controlling an avatar in a desktop-based virtual environment via a software ssvep brain-computer interface. *Presence Teleoper. Virtual Environ.* 19, 25–34. doi: 10.1162/pres.19.1.25

Gergondet, P., Petit, D., and Kheddar, A. (2012). "Steering a robot with a brain-computer interface: impact of video feedback on BCI performance," in *RO-MAN, 2012 International Symposium on Robot and Human Interactive Communication* (Paris), 271–276.

Golomb, S. W., Welch, L. R., Goldstein, R. M., and Hales, A. W. (1982). *Shift Register Sequences,* Vol. 78. Laguna Hills, CA: Aegean Park Press.

Guger, C., Allison, B. Z., Grosswindhager, B., Prückl, R., Hintermüller, C., Kapeller, C., et al. (2012). How many people could use an SSVEP BCI? *Front. Neurosci.* 6:169. doi: 10.3389/fnins.2012.00169

Guger, C., Daban, S., Sellers, E., Holzner, C., Krausz, G., Carabalona, R., et al. (2009). How many people are able to control a P300-based brain–computer interface (BCI)? *Neurosci. Lett.* 462, 94–98. doi: 10.1016/j.neulet.2009.06.045

Guger, C., Edlinger, G., Harkam, W., Niedermayer, I., and Pfurtscheller, G. (2003). How many people are able to operate an EEG-based brain-computer interface (BCI)? *IEEE Trans. Neural Syst. Rehabil. Eng.* 11, 145–147. doi: 10.1109/TNSRE.2003.814481

Guger, C., Ramoser, H., and Pfurtscheller, G. (2000). Real-time EEG analysis with subject-specific spatial patterns for a brain-computer interface (BCI). *IEEE Trans. Rehabil. Eng.* 8, 447–456. doi: 10.1109/86.895947

Kapeller, C., Hintermuller, C., Abu-Alqumsan, M., Pruckl, R., Peer, A., and Guger, C. (2013). "A BCI using VEP for continuous control of a mobile robot," in *2013 35th Annual International Conference of the IEEE Engineering in Medicine and Biology Society (EMBC)* (Osaka), 5254–5257. doi: 10.1109/EMBC.2013.6610734

Krausz, G., Scherer, R., Korisek, G., and Pfurtscheller, G. (2003). Critical decision-speed and information transfer in the "Graz Brain–Computer Interface." *Appl. Psychophysiol. Biofeedb.* 28, 233–240. doi: 10.1023/A:1024637331493

Lalor, E. C., Kelly, S. P., Finucane, C., Burke, R., Smith, R., Reilly, R. B., et al. (2005). Steady-state VEP-based brain-computer interface control in an immersive 3D gaming environment. *EURASIP J. Appl. Signal Process.* 2005, 3156–3164. doi: 10.1155/ASP.2005.3156

Leuthardt, E. C., Schalk, G., Wolpaw, J. R., Ojemann, J. G., and Moran, D. W. (2004). A brain–computer interface using electrocorticographic signals in humans. *J. Neural Eng.* 1:63. doi: 10.1088/1741-2560/1/2/001

Martinez, P., Bakardjian, H., and Cichocki, A. (2007). Fully online multicommand brain-computer interface with visual neurofeedback using SSVEP paradigm. *Comput. Intell. Neurosci.* 2007:13. doi: 10.1155/2007/94561

Mason, S. G., Bashashati, A., Fatourechi, M., Navarro, K. F., and Birch, G. E. (2007). A comprehensive survey of brain interface technology designs. *Ann. Biomed. Eng.* 35, 137–169. doi: 10.1007/s10439-006-9170-0

Miller, K. J., Schalk, G., Fetz, E. E., den Nijs, M., Ojemann, J. G., and Rao, R. P. (2010). Cortical activity during motor execution, motor imagery, and imagery-based online feedback. *Proc. Natl. Acad. Sci. U.S.A.* 107, 4430–4435. doi: 10.1073/pnas.0913697107

Müller-Gerking, J., Pfurtscheller, G., and Flyvbjerg, H. (1999). Designing optimal spatial filters for single-trial EEG classification in a movement task. *Clin. Neurophysiol.* 110, 787–798. doi: 10.1016/S1388-2457(98)00038-8

Pregenzer, M., and Pfurtscheller, G. (1995). "Distinction Sensitive Learning Vector Quantization (DSLVQ) application as a classifier based feature selection method for a brain computer interface," in *Fourth International Conference on Artificial Neural Networks* (Cambridge), 433–436.

Putz, V., Guger, C., Holzner, C., Torrellas, S., and Miralles, F. (2011). "A unified XML based description of the contents of brain computer interfaces," in *Proceedings of the 5th International BCI Conference* (Graz), 22–24.

Schalk, G., Miller, K. J., Anderson, N. R., Wilson, J. A., Smyth, M. D., Ojemann, J. G., et al. (2008). Two-dimensional movement control using electrocorticographic signals in humans. *J. Neural. Eng.* 5, 75–84. doi: 10.1088/1741-2560/5/1/008

Sellers, E. W., Krusienski, D. J., McFarland, D. J., Vaughan, T. M., and Wolpaw, J. R. (2006). A P300 event-related potential brain–computer interface (BCI): the effects of matrix size and inter stimulus interval on performance. *Biol. Psychol.* 73, 242–252. doi: 10.1016/j.biopsycho.2006.04.007

Spüler, M., Rosenstiel, W., and Bogdan, M. (2012). Online adaptation of a c-VEP Brain-computer Interface (BCI) based on error-related potentials and unsupervised learning. *PLoS ONE* 7:e51077. doi: 10.1371/journal.pone.0051077

Sutter, E. E. (1992). The brain response interface: communication through visually-induced electrical brain responses. *J. Microcomp. Appl.* 15, 31–45. doi: 10.1016/0745-7138(92)90045-7

Sutton, R. S., and Barto, A. G. (1998). "Softmax action selection," in *Reinforcement Learning: An Introduction*, eds R. S. Sutton and A. G. Barto (Cambridge: The MIT Press), 1998.

Volosyak, I. (2011). SSVEP-based Bremen–BCI interface—boosting information transfer rates. *J. Neural Eng.* 8:036020. doi: 10.1088/1741-2560/8/3/036020

Wang, W., Collinger, J. L., Degenhart, A. D., Tyler-Kabara, E. C., Schwartz, A. B., Moran, D. W., et al. (2013). An electrocorticographic brain interface in an individual with tetraplegia. *PLoS ONE* 8:e55344. doi: 10.1371/journal.pone.0055344

Wang, Y., Gao, X., Hong, B., Jia, C., and Gao, S. (2008). Brain-computer interfaces based on visual evoked potentials. *IEEE Eng. Med. Biol. Mag.* 27, 64–71. doi: 10.1109/MEMB.2008.923958

Weiskopf, N., Mathiak, K., Bock, S. W., Scharnowski, F., Veit, R., Grodd, W., et al. (2004). Principles of a brain-computer interface (BCI) based on real-time functional magnetic resonance imaging (fMRI). *IEEE Trans. Biomed. Eng.* 51, 966–970. doi: 10.1109/TBME.2004.827063

Wolpaw, J. R., Birbaumer, N., McFarland, D. J., Pfurtscheller, G., and Vaughan, T. M. (2002). Brain–computer interfaces for communication and control. *Clin. Neurophysiol.* 113, 767–791. doi: 10.1016/S1388-2457(02)00057-3

Yanagisawa, T., Hirata, M., Saitoh, Y., Kishima, H., Matsushita, K., Goto, T., et al. (2012). Electrocorticographic control of a prosthetic arm in paralyzed patients. *Ann. Neurol.* 71, 353–361. doi: 10.1002/ana.22613

Zierler, N. (1959). Linear recurring sequences. *J. Soc. Ind. Appl. Math.* 7, 31–48. doi: 10.1137/0107003

Conflict of Interest Statement: The authors declare that the research was conducted in the absence of any commercial or financial relationships that could be construed as a potential conflict of interest.

Received: 31 May 2014; accepted: 17 July 2014; published online: 07 August 2014.
Citation: Kapeller C, Kamada K, Ogawa H, Prueckl R, Scharinger J and Guger C (2014) An electrocorticographic BCI using code-based VEP for control in video applications: a single-subject study. Front. Syst. Neurosci. ***8****:139. doi: 10.3389/fnsys.2014.00139*
This article was submitted to the journal Frontiers in Systems Neuroscience.

frontiers in Systems Neuroscience

ORIGINAL RESEARCH
published: 12 May 2015
doi: 10.3389/fnsys.2015.00073

A novel wireless recording and stimulating multichannel epicortical grid for supplementing or enhancing the sensory-motor functions in monkey (*Macaca fascicularis*)

Antonio G. Zippo[1], *Pantaleo Romanelli*[2]*, *Napoleon R. Torres Martinez*[3], *Gian C. Caramenti*[4], *Alim L. Benabid*[3] and *Gabriele E. M. Biella*[1]*

[1] Institute of Molecular Bioimaging and Physiology, National Research Council, Segrate, Italy, [2] Ab Medica, Lainate, Italy, [3] Commissariat à l'Energie Atomique et aux Energies Alternatives, Laboratoire d' Électronique des Technologies de l'Information, CLINATEC, Grenoble, France, [4] Institute of Biomedical Technology, Segrate, Italy

OPEN ACCESS

Edited by:
Mikhail Lebedev,
Duke University, USA

Reviewed by:
Yoshio Sakurai,
Kyoto University, Japan
Kazutaka Takahashi,
University of Chicago, USA
Ioan Opris,
Wake Forest University School of Medicine, USA

***Correspondence:**
Pantaleo Romanelli,
Via Nerviano 31, 20020 Lainate, Milan, Italy
radiosurgery2000@yahoo.com
Gabriele E. M. Biella,
Via Nerviano 31, Lainate, Milan, Italy
gembiella@gmail.com

Received: 19 December 2014
Accepted: 22 April 2015
Published: 12 May 2015

Citation:
Zippo AG, Romanelli P, Torres Martinez NR, Caramenti GC, Benabid AL and Biella GEM (2015) A novel wireless recording and stimulating multichannel epicortical grid for supplementing or enhancing the sensory-motor functions in monkey (Macaca fascicularis). Front. Syst. Neurosci. 9:73. doi: 10.3389/fnsys.2015.00073

Artificial brain-machine interfaces (BMIs) represent a prospective step forward supporting or replacing faulty brain functions. So far, several obstacles, such as the energy supply, the portability and the biocompatibility, have been limiting their effective translation in advanced experimental or clinical applications. In this work, a novel 16 channel chronically implantable epicortical grid has been proposed. It provides wireless transmission of cortical recordings and stimulations, with induction current recharge. The grid has been chronically implanted in a non-human primate (*Macaca fascicularis*) and placed over the somato-motor cortex such that 13 electrodes recorded or stimulated the primary motor cortex and three the primary somatosensory cortex, in the deeply anaesthetized animal. Cortical sensory and motor recordings and stimulations have been performed within 3 months from the implant. In detail, by delivering motor cortex epicortical single spot stimulations (1–8 V, 1–10 Hz, 500 ms, biphasic waves), we analyzed the motor topographic precision, evidenced by tunable finger or arm movements of the anesthetized animal. The responses to light mechanical peripheral sensory stimuli (blocks of 100 stimuli, each single stimulus being <1 ms and interblock intervals of 1.5–4 s) have been analyzed. We found 150–250 ms delayed cortical responses from fast finger touches, often spread to nearby motor stations. We also evaluated the grid electrical stimulus interference with somatotopic natural tactile sensory processing showing no suppressing interference with sensory stimulus detection. In conclusion, we propose a chronically implantable epicortical grid which can accommodate most of current technological restrictions, representing an acceptable candidate for BMI experimental and clinical uses.

Keywords: brain-machine interface, sensory-motor recordings, sensory-motor stimulation, *Macaca fascicularis*, epicortical grid, chronic implantation

Introduction

It is now almost 50 years that brain-machine interfaces (BMI) are used both in research and in the clinics (Lebedev and Nicolelis, 2006; Graimann et al., 2010; Borton et al., 2013; Wenger et al., 2014) with an expanding range of applications and a growing complexity of exploited tasks. BMIs have been originally devoted to create implantable devices or external frames able to substitute failing brain functions by invasive surgery with e.g., stimulating electrodes (Hochberg et al., 2006; George et al., 2007; Schulze-Bonhage, 2009; Géléoc and Holt, 2014) or by peripheral auxiliary tutors such as cochlear or motor prostheses (Esquenazi and Packel, 2012; Jackson and Zimmermann, 2012). A further issue is represented by the signal quality: the higher the signal to noise ratio, the better the signal representation and the better the output will be presented. Novel applications are also gradually introduced with the aim to enhance brain functions (Deca and Koene, 2014). BMIs are, however, progressively refining on emergent knowledge of brain dynamics and in particular on the assessment that neuronal populations better tune outputs than the activity modulation of single neurons (Nicolelis and Lebedev, 2009). A cooperative, not merely additive, model of brain operation modes turns to be a greater hurdle in completing integrative devices upscaling in complexity, a matter still far from a rigorous understanding (Baranauskas, 2014) though promising preliminary results (Ifft et al., 2012). Along with these functional requirements, a compliant neural interface has also to meet constraints of biological tolerability in order to reduce or block adverse responses from hosting tissues (Groothuis et al., 2014). These prerequisites appear crucial for lifelong neuromorpho implants. In summary, a sort of BMI "ecology" to interlace to local structures and activities appears necessary (Freire et al., 2011; Andersen et al., 2014; Orsborn et al., 2014). Indeed, promising solutions have been since successively proposed in these years (Lebedev and Nicolelis, 2006). From then now, a further new research path has grown related to exploring possible enhancements of brain functions (Deca and Koene, 2014), virtually enabling expanded aptitudes (in strength, fatigue resistance, sensory perspicuity a.s.o.) or working in special or hostile environments (Lebedev et al., 2011). As from the above description, planning a new brain stimulating device settles as a strongly demanding topic, with a large front of vital requirements. In an earlier work on another monkey a prototype grid had been previously implanted with no additional feature for stimulating and recording (Piangerelli et al., 2014). In this paper we tried to focus, beyond the experimental application of stimulation and recording we further checked two of those themes mentioned above, namely the noiseless data transmission accompanied to high biological compatibility and the biological tolerance during long term experiments. We show here the electrophysiological results obtained by the epicortical grid in the monkey. The grid has a matrix of 16 recording and stimulating channels mounted over a thinnest (15 μm) plastic support and connected with a subcutaneously implantable wireless and power supply. The final goal of this device is meant to sense and counteract anomalous excitation in epilepsy with easier localization of epileptic foci or to balance activity disorders in chronic pain. Two experimental series, with recording and stimulating sessions, have been performed, while checking long term performance of the grid within 3 months from the device placement analysing the single channel resistance. In the first experimental series an analysis of the fine grained stimulation of single fingers by the epicortical probes has been evaluated. In the second series the recording properties from the sensory cortical potentials elicited by peripheral electrical and natural stimuli, as well as the electrical interference on the naturally evoked stimuli have been estimated.

Methods

Surgical Procedure and Implanted Device

The grid was implanted by one of the authors (Pantaleo Romanelli) in a non-human primate (*Macaca fascicularis*) over the sensorimotor cortex to record somatosensory potentials, to check the grid efficiency in eliciting fine finger or gross arm movements through remotely-driven cortical stimulation. Briefly, a male macaque monkey, weighting 7.07 kg, was used in this study. The experimental protocol was approved by the regional committee (Cometh Grenoble) and registered to the national committee under the number 12/136 Clinatec-NTM-01 and complied with the EU directive 22nd September 2010 (2010/63/EU) on the care and use of laboratory animals (for an extensive description of the surgical preparation used in former experiments on a prototype of this grid see Piangerelli et al., 2014 on a different monkey). The new grid was equipped with the technical facilities for wireless recording and stimulating to and to from each of its channels. This enabled us to program experimental sessions with diverse protocols. The protocols aimed, to map the cortical responsiveness to light sensory stimuli delivered onto somatotopically competent peripheral areas, and explored the interference of stimuli delivered by the grid electrodes on the epicortical foci with the peripheral stimuli. Briefly, the animal was anesthetized using Xylazine (5 mg/kg), and Ketamine hydrochloride (20 mg/kg), intramuscular (IM), and then a maintenance dose of 1.25 mg/kg, 5 mg/kg Xylazine/Ketamine. All the vital parameters (Heart rate, ECG, respiration, oxygenation, and body temperature) were constantly monitored by the veterinary staff (monitor Infinity® Delta XL; DRAGER, Luebeck, Germany). Surgical procedures took place in standard aseptic conditions. In deep anesthesia with the animal secured to a stereotaxic frame, a craniotomy was performed over the left motor cortex (M1) in Brodmann area 4 and, posteriorly, gyrus of the corresponding primary somatosensory cortex (SS1) removing a rectangular (3×2.5 cm) bone tile. After bone removal, the epidural site was tested using ISIS IOM Neuromonitoring© cortical stimulator (INOMED Medizintechnik; Emmendingen, GERMANY) which delivered biphasic train pulses between poles, to identify the hand area. The *dura mater* was then opened by a Y-shaped cut, exposing the surface of M1 and the anterior margin of the corresponding primary somatosensory cortex (SS1). The location of the grid electrodes was determined by identifying topic anatomical landmarks (the central, the intraparietal, and

the arcuate sulci). Retesting was conducted and hand area identification was refined with the same INOMED stimulator directly in contact to the cortex and EMG of the right hand (Cortical stimulation parameters were 100 μs, 5 mA, 7 Hz). The device was positioned orthogonally and the grid was centered above the hand knob of the left motor cortex. The grid Channels 1, 2, and 3 were placed over the sensory cortex in correspondence of cortical stations responsive to light peripheral stimuli on contralateral thumb, index and middle fingers. Channels 4 to 16 covered the motor cortex able to generate fine movements in the contralateral upper limb. The electrode impedance has been measured during the months of the experiment, allowing for comparisons among the experimental recording or stimulating procedures in time. The signals were recorded using commercial software for Epicortical Grid (EcoG) recording provided by Micromed, Treviso, Italy. The technical characteristics of this new grid, different from those shown in the previous work by Piangerelli et al., are summarized in **Table 1**. In detail, the grid was made by a thin (15 μm) foil of flexible polyimide with printed platinum (Pt) small plaquettes (16 plaques in a 4 × 4 matrix, 200 nm thick, interplaque distance of slightly less than 3 mm). Two reference Pt electrodes were printed posteriorly to the plan of application of the grid. The grid was built with direct connection with a battery (Li ions, rechargeable) case (Peek polymer, 800 μm thick) including the electronic components for wireless transmission. The recording features were realized with a detection range of ±780 μV in a bandwidth of 0–500 Hz at gain 12. The available variable gains were (1, 2, 3, 4, 6, 8, 10, 12). The programmable waveforms were between ±3 V at impedance of 10Ω (**Figure 2E**).

The Cortical Recordings and Stimulations

Recordings and stereoselective somatic stimulations (13 electrodes placed over the primary motor cortex and 3 on the primary somatosensory cortex) were performed within 3 months from the implant. A sampling rate of 512 Hz (@16 bit) was used for the grid recordings. Electrical stimulations were delivered on the spontaneous activity background either *per se*, to evaluate the magnitude of the elicited motor responses or concurrently to peripheral light threshold stimuli to check the spatiotemporal electrical interference of artificial inputs over the sensory responses. In **Figure 1** the elements of the grid and of the wireless transmitting and recharging device are shown. **Figure 1A**: the constructive elements of the grid and of the power supply are reported. **Figure 1B**: a view in detail of the grid circuitry is shown. The recording and stimulating plaquettes and their schematized circuitry along with the analytic spatial measures of its architecture are also shown. **Figure 1C**: the grid to be implanted is shown. **Figure 1D**: the apparatuses for wireless recording and stimulus delivery with the anesthetized monkey are shown. During the experiments the monkey was covered with a blanket to avoid loss of temperature of the animal. In **Figure 1E**, the recording device alone is shown. The grid was recharged by induction into a dedicated cage (not shown here). Thirteen electrodes (4–16) were placed over the motor fields. Electrodes 1–3 face the sensory cortical surface. In **Figure 2** the technical details of the grid stimulating output and the Arduino driven sensory stimuli device are shown. In detail, in **Figures 2A,B** the electrical scheme and the controller with optic insulator for the electrical grid stimulus control are respectively displayed. In **Figure 2C** the home-made device able to release point-like (1 mm^2) sub-millisecond random stimuli (see Zippo et al., 2014) are shown. **Figure 2D**: The overall 16 channel impedance profiles during the implantation period. **Figure 2E**: The peripheral signal as delivered by the microcontroller. As evident from the reported trace, sensory inputs are elicited in random sequence.

The Peripheral Stimulator

The peripheral stimulation device is composed by an Arduino® electronic card able to deliver 1 kHz outputs in random sequences (See **Figures 2C,D**). The output device is composed by a woofer with a pipette tip mounted vertically over the cusp of the woofer dust cap. The stimuli had to be as fast and spatially selective as possible in order to reduce the "background noise" and sharpen the signals of interest. To this purpose, we used the stimulation device together with a novel stimulus delivery protocol and a predictive computational framework. The protocol of randomizing stimuli offered the advantage of paired pulses and reduced the possibility of spurious locking between stimuli and spontaneous periodical bursts of neuronal activity and sensory habituation with waning responses to equal subsequent stimuli (Zippo et al., 2013, 2014).

The Grid Stimulation

Bipolar stimulations were delivered by rectangular 0.5 ms pulses and anodal monophasic current. This stimulation technique consists of a train of five pulses delivered at 1 Hz with an interstimulus interval of 100 ms. The stimulus intensity was regulated between 1 and 3 mA at constant voltage of 3.3 V.

In **Tables 1, 2**, the technical data of the EcoG pads and of the Grid (Cyberbrain, AB Medica) electronic properties are reported.

We followed three experimental protocols to analyze, respectively, the stability of the spontaneous activity with the cortical responses to peripheral light threshold stimuli, the spontaneous activity with the responses to grid driven electrical stimuli, and, finally, the interference induced by the grid electrical stimuli on the sensory patterns elicited by the sensory peripheral stimuli.

Protocols

(1) Protocol 1

   (a) 15 min (three sessions of 5 min each) of spontaneous activity recording have been performed from all the available channels
   (b) Natural Peripheral Stimulations: Short, non-nociceptive, point-like sensory stimuli have been delivered on the finger tips by the pipette tip mounted over a woofer dust-cap driven by an Arduino electronically controlled output (Zippo et al., 2014). Each finger-tip was stimulated by trains of light touches (100 stimuli randomised in order to avoid habituation). Each 100 stimulus train lasted 90 s. An trigger to the recording

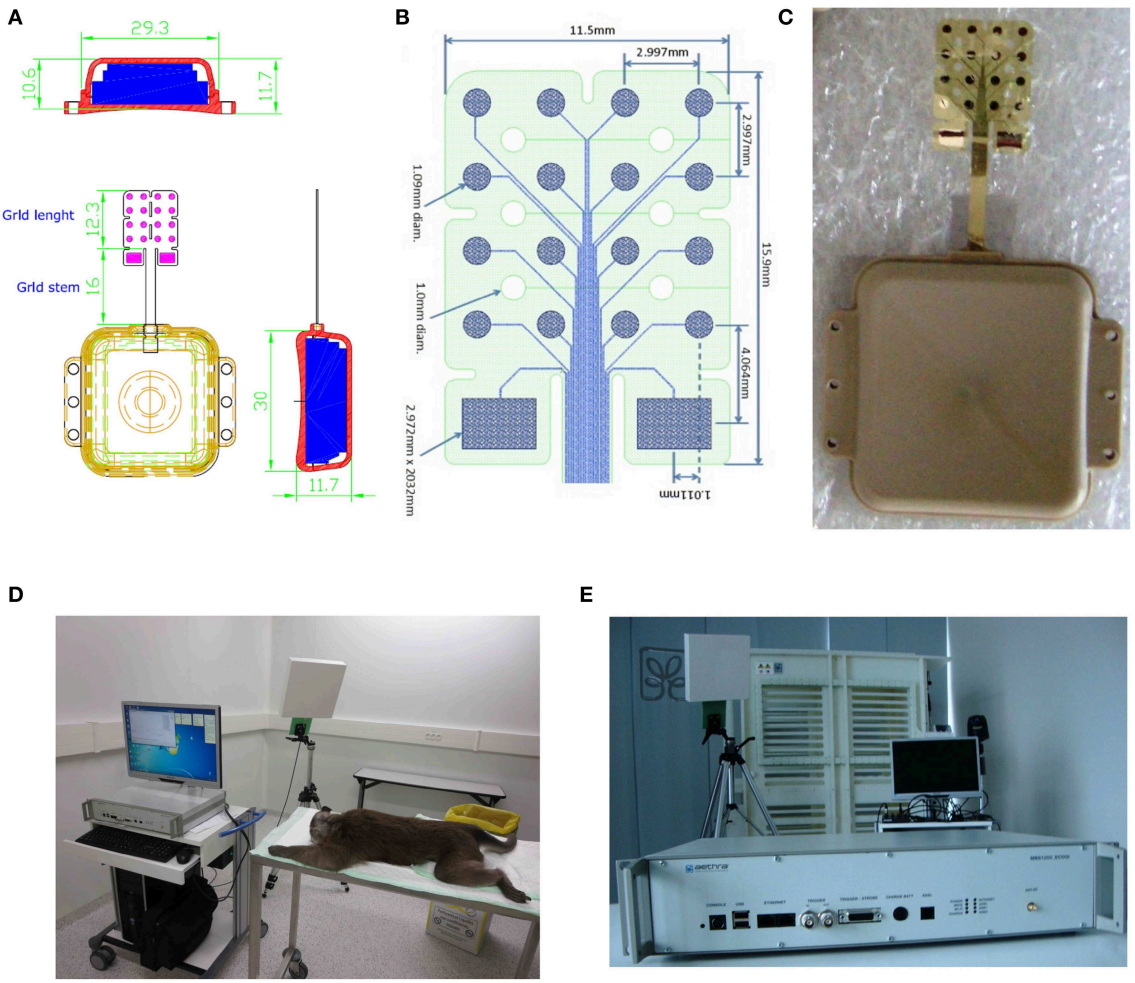

FIGURE 1 | Characteristics of the epicortical grid. (A,B) Shape and measures of the grid. **(C)** Picture of the grid. **(D)** Experimental configuration with wireless data transmission device. **(E)** Wireless data transmission device in detail.

device from the Arduino card was provided in order to synchronize the stimulus signals with the recorded electrocorticographic activities.

(2) Protocol 2

   (a) 15 min (three sessions of 5 min each) of spontaneous activity recording from all the available channels
   (b) Grid Stimulations: Stimuli have been delivered by the ECoG device. Stimuli will be separately delivered at each electrode placed over the sensory cortex. 2 min of 1, 7, and 30 Hz of 100 to 500 μs stimulation cycles have been recorded from the other two sensory electrodes. Some 5 min of resting activity recordings among the stimulation trains was left.

(3) Protocol 3

   (a) Concurrent Grid and peripheral stimulations: The peripheral stimuli were delivered with comparable scheme (see above) to the responsive fingers after 1 min of Grid electrical stimuli. Plaquette current sources were chosen with the criterion of proximity to those showing maximal sensory responses. These observations have been done in order to evaluate the effects of central electrical stimuli on the peripheral natural stimuli cortical estimates.

Analysis of Epicortical Evoked Potentials

The effects of the different stimulation protocols were evaluated by averaging the recorded potentials among all trials (100) and all experimental sessions (2). Each recording session was split into 100 time windows taking into account 125 ms before the onset of the stimulus (both tactile peripheral and electrical) and 1 s after the onset of the stimulus. Therefore we had 1125 ms windows in all stimulation protocols. To evaluate the null hypothesis, that the observed potentials were not due to our stimulation protocols (SHAM), we randomized the time occurrences of the stimuli and we repeated the same averaging technique used in the previous description.

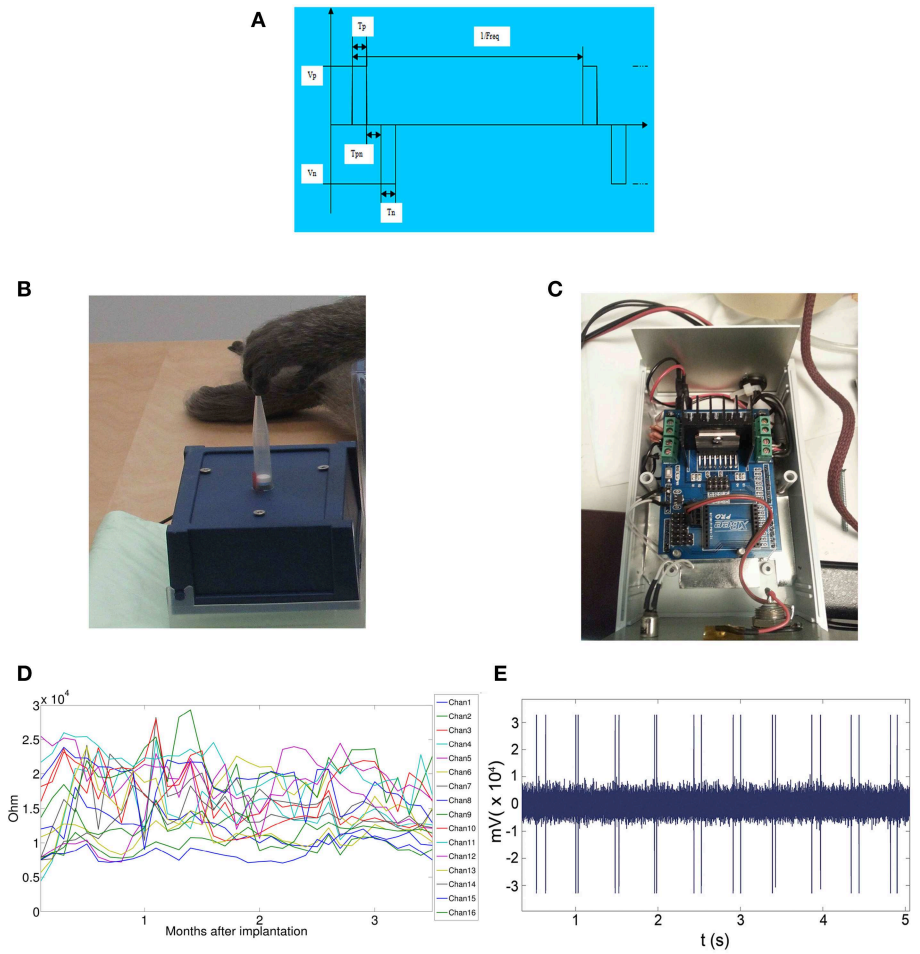

FIGURE 2 | Features of the electrical and tactile stimulation setups. **(A)** Wave-front of the Arduino delivered stimuli. **(B)** The stimulus delivery device. The pipette base is sealed on a midrange loudspeaker dust-cap moved at 1 kHz. The tip was placed just on hand fingertips, *thenar* or *hypothenar* eminences or on foot fingertips. **(C)** The electronic card Arduino driving the woofer dustcap. **(D)** Impedences of the grid during the period of the experimental sensory-motor measurements. **(E)** Stimulus artifacts over the magnified trace of the stimulus recording channel.

Statistical Tests

To assess statistical differences between evoked potential patterns we used an *ad hoc* hypothesis test. Given the evoked potentials by N trials of all the 16 electrodes in two sites, A $= A_{1,\cdots,}A_N$ and B $= B_{1,\cdots,}B_N$, we computed the correlation coefficient (R) between A_i and B_j, $\forall i, j \in \{1, \ldots, N\}$.

Subsequently we arbitrarily set a threshold of 0.5 for the correlation coefficient: A_i and B_j are considered different matrices if R was below the threshold, similar otherwise. An exploratory analysis revealed that R values (99.87%) were clustered into two groups: those in the range [0, 0.23] and those in the range [0.7, 1]. Therefore the arbitrary choice of the used threshold (0.5) did not produce effects on results. Finally, to estimate the p-value we computed the ratio of comparisons with a R value above the threshold among the set of all comparisons between the trials of two stimulation sites.

To establish the statistical significance of the impedance measures (16 electrodes per day of sampling) over time, we used the Kruskal-Wallis test avoiding the assumption of normality of the data.

Results

We performed repeated the same experimental protocol (see Methods Section) in two dates: the first, approximately 1 month after (D34) the day of surgical implantation and the second after 3 months (D92). In each session we applied the same experimental protocol divided into parts: in the first we produced tactile stimulations through the Arduino microntroller in five different sites, namely the thumb, the index, the middle and the anular fingers of the right forelimb, and the big toe finger of the right hindlimb. In the second part we combined the tactile stimulations with trains of direct current stimulations delivered by the epicortical grid.

Prior to analyze the electrical potentials evoked by stimulation protocols we wondered whether the electrode impedance

TABLE 1 | Physical features of the epicortical grid.

EcoG 16 PADS MATERIALS		
Components	**Materials**	**Characteristics**
Grid	Flexible polymide	15 μm thickness
Electrodes	Platinum	200 nm thickness
Case	Peek (invibio)	0.8 mm thickness
Adhesives	Fast-cure silicone adhesives (Nusil)	MED1-4213, MED2-4213, MED3-4213
	Solicon primer (Nasil)	MED-163
	Epoxy resin (Epoxy Technology)	EPO-TEK 301-2
EMC	Alumina thick film	0.5 mm thickness
Battery	Rechargeable lithium ion polymer cell	
Electronic circuits	Electronics components	

TABLE 2 | Technical features of the grid.

ANALOG FRONT END	
Numer of channels	16
Variable Gain	1, 2, 3, 4, 6, 8, 12
Detection range	± 780 μV (@ Gain 12)
Bandwidth	0–500 Hz (@ 2 Ksps)
Resolution	16 bit $\sum/\Delta$
Input noise	1 μVrms (G = 12 @ 500 Hz BW)
Sampling frequency	250 Hz to 2 KHz
Lead off detection	DC and 250 Hz @ 24 nA
MICROCONTROLLER AND PERIPHERAL	
Microcontroller	Kinetic MK40N512K 100 MHz Freescale
External SRAM	16 Mbits (2 M × 8 bit)
Sensors	3 Axis g, Temperature, Charge current
STIMULUS	
Waveform	Programmable waveforms
Amplitude	± 3V and ± 1.65 V (between Ref and Pad)
Impedance	10 Ω
INDUCTIVE WIRELESS POWER	
Inductive local coil frequency	145 KHz (Charge current 20 mA @ 3.7 V
Magnetic cage	145 KHz (Charge current 20 mA @ 3.7 V)
BATTERY	
Li Ion rechargeable	3.6 V 140 mA/h
	Battery Life ∼3h @38 mA
	Recharging Period >12 h (Cage)
POWER CONSUMPTION	
16CH @ 500SPS + TX_RF	38 mA
16CH @ 500SPS	33 mA

(measured once a day) changed along the 3 months (104 days). We found that no significant modifications of the electrode impedance emerged during these months ($P = 0.591$, $N = 1664$, Kruskal-Wallis test). Furthermore, no conspicuous immune response or evident grid rejection signs were noticed neither at the interface with the cortical surface nor by the removed *dura mater* during the period of electrophysiological observation.

From the electrophysiological point of view the grid efficiently detected the fine-grain tactile information from peripheral stimuli and the central electrically evoked potentials. By using a specific statistical hypothesis test we evaluated the stability of the evoked potentials in a stimulation site or the statistical difference between the responses of two different sites. We found that evoked potentials of each of the five sites corresponded to stable response patterns (see the diagonal of the **Table 3**, all *P*-values are close to 1). In addition we wondered if each stimulation site produced a specific response pattern and we found that this was the case. Indeed, each site evoked a particular and an unequivocal potential along the recording electrodes that fully identified the stimulus location (non-diagonal values of **Table 3** that are all smaller than 0.1). Here below are reported the results of the three experimental conditions we tested the grid. In **Figure 3** are reported the recorded somatosensory responses to the peripheral point-like stimuli delivered by the Arduino driven device. Stimuli were delivered on four fingertips of the right arm (**Figures 3B–D**), contralateral to the stimulated cortex as well to the homologous big toe (**Figure 3A**). Clear patterns of responses are reported in color-code raster images (Blue to Brick Red representing a scale from no to "strong" cortical response, normalized on these maxima). It is interesting to note that the four stimulated fingers produced four different patterns of response. Namely, index and thumb showed precocious responses within 125 ms while the responses to the big toe and the hand middle finger had delayed response onset latency around 250 ms.

Eventually, we investigated the potential effects of epicortical current stimulations (whose effects are shown in **Video 1**) on the somatosensory processing caused by tactile stimulations. This has been planned in order to examine the effects of repeated electrical stimulations over the timing and patterning of the natural peripheral stimuli. For this reason we applied the same statistical framework to verify whether the responses from a given site were statistically similar or different. Taking into consideration the large variability of the responses to peripheral stimuli, no significant influence after the discontinuation of the grid electrical stimuli was noticed in the response profile of sensory peripheral stimuli. As expected by a first visual inspection, electrical stimulation did not interfere with the normal somatosensory processing (see *P*-values in the last column of **Table 3**, all close to 1).

In **Figure 4** are reported the results from the concurrent electrical vs. natural peripheral stimuli. Left column—Above: the picture shows an example of cortical responses to low-threshold peripheral stimuli delivered to a finger. Bottom: the peripheral stimuli have been delivered after a cycle of grid driven electrical stimuli on the same recording plaquettes. Where the fine grain of the responses was slightly interfered, there was no gross suppression or distortion of sensory signaling after the electrical stimuli delivery.

Discussion

In this paper we propose a novel ultrathin 16 channel grid apparatus to record/stimulate the cerebral cortex in

TABLE 3 | Statistical comparisons among the tactile stimulation sites.

Site	Thumb (Forelimb)	Index (Forelimb)	Middle (Forelimb)	Anular (Forelimb)	Big Toe (Forelimb)	DCS
Thumb (Forelimb)	$P = 0.872$, $N = 200$	$P = 0.012$, $N = 40{,}000$	$P = 0.015$, $N = 40{,}000$	$P = 0.013$, $N = 40{,}000$	$P = 0.058$, $N = 40{,}000$	$P = 0.992$, $N = 200$
INdex (Forelimb)	$P = 0.013$, $N = 40{,}000$	$P = 0.939$, $N = 200$	$P = 0.017$, $N = 40{,}000$	$P = 0.015$, $N = 40{,}000$	$P = 0.017$, $N = 40{,}000$	$P = 0.988$, $N = 200$
Middle (Forelimb)	$P = 0.079$, $N = 40{,}000$	$P = 0.125$, $N = 40{,}000$	$P = 0.973$, $N = 200$	$P = 0.127$, $N = 40{,}000$	$P = 0.013$, $N = 40{,}000$	$P = 0.975$, $N = 200$
Anular (Forelimb)	$P = 0.014$, $N = 40{,}000$	$P = 0.099$, $N = 40{,}000$	$P = 0.124$, $N = 40{,}000$	$P = 0.994$, $N = 200$	$P = 0.014$, $N = 40{,}000$	$P = 0.966$, $N = 200$
Big Toe (Hindlimb)	$P = 0.015$, $N = 40{,}000$	$P = 0.018$, $N = 40{,}000$	$P = 0.010$, $N = 40{,}000$	$P = 0.016$, $N = 40{,}000$	$P = 0.894$, $N = 200$	$P = 0.981$, $N = 200$

We exerted each stimulation site of the right forelimb and hindlimb 200 times: 100 times in the first experimental session after 1 month and 100 in the second experimental session after 3 months of the grid surgical implantation. P-values toward 1 on the table diagonal ensured that the response patterns were stable both within each experimental session and between the experimental sessions. Instead, small p-values indicated that each stimulation site produces an unequivocal activation pattern detected by the epicortical grid that characterized the somatosensory response. The similarity between responses was asserted by computing the correlation coefficient between the resulting matrices (see Methods section).

diverse clinical conditions such as epilepsy or chronic pain. Brain Machine Interfaces (BMIs) are multipurpose devices instrumental in a number of brain pathological conditions from replacement of injured brain circuits to sustenance of weakened functions or of circuitry intermittent failures or again to their supervision (Nicolelis, 2012; Rao, 2013).

The BMI Puzzle

More recently the concept of brain function augmentation has also been set forth with the aim of supporting particularly demanding performances as for instance actions in adverse environments (e.g., in outer space missions or in memory challenging assignments) (Hampson et al., 2012; Deca and Koene, 2014). Most of these applications come from practice on "normal" experimental animals and prospected to find application in pathology (as for instance to vascular, degenerative or traumatic pathologies). Hence, it is advisable to point-out that resident "functional engrams" simply activated in "normal conditions" don't overlap pathological conditions where exogenous "neural programs" are to be re-assigned *ab-externo* (Birbaumer et al., 2006; Andersen et al., 2014; Grahn et al., 2014; Hu et al., 2014; Lebedev, 2014). The grid presented in this paper has been planned to evolve in a frame apt to intercept anomalous insurgence of seizure signals, to localize them on the cortical thread and ultimately generate interfering or blocking hyper-synchronization codes of epileptic waves. Eventually, it has been, as well, designed to balance the electrical anomalies steadily present in chronic pain. Along a theoretic approach stemmed in our labs, chronic pain relates to a collapse of information transmission within supraspinal sensory networks (Zippo et al., 2011). As prediction, an admittance of coherent information to the involved networks is critical to reestablish natural conditions abating stereotyped signal recursions. Cortically applied magnetic fields or electrical currents have been indeed shown to control chronic pain symptoms (Passard et al., 2007; Fricová et al., 2013; Lefaucheur et al., 2014; Moreno-Duarte et al., 2014). Instead, diversely from these settings, the disruption of epileptic hyper-synchronizations meets less "refined" problems, the goal being to stop abruptly diffuse and "sudden" excitatory wave fronts. Currently, there are no clear indications on "prospective" electrodynamical solutions to balance or cancel these anomalies but thinking of electrical interferences halting the anomalous signal regeneration with different DBS or peripheral stimulation approaches (Goodman, 2004; Boon et al., 2009; Fisher and Velasco, 2014). On a theoretic ground, these devices should subserve fast "interpretations" of degeneracy codes and deliver tuned outputs or re-drive networks within normal ranges. The "interference" over epileptic backgrounds, presents, thus, distinct aims from the "ecological coherences" needed by BMIs in other contexts (e.g., trial and error routines to drive external prostheses; Dromerick et al., 2008; Bongers et al., 2011). A provisional measure counteracting the epileptic surge is expected to either provide rough "antagonistic" currents or to generate "seizure contextual" outputs, a very remote goal because of the poor decoding of epileptic waves achieved until now, but for snapshots of non-deterministic analyses of ictal and interictal epochs (Knowlton et al., 2004a,b; Dwyer et al., 2010).

Function Restorations

A different planning would be obviously to be provided for substitutive tasks, such as in motor and motor-like functions, requiring to re-allocating lost abilities within a (slow) trial-and-error learning context. Surprisingly, in these experiments carried on normal experimental animals, it has been shown that the number of involved neurons seemingly sufficient in prosthesis motion appears notably small with consistent conservation of the collective neuronal frequency (with multiple single unit and unit ensemble tuning; Nicolelis and Lebedev, 2009). These features may hypostatize future synthetic bases enriched with multiple network activation loci where the recruitment of a limited number of neurons for each locus may facilitate textured activations. However these assumptions may be biased by the mismatch between experimental trials on healthy circuits and those providing restitutive implants for lost functions. Namely, in the former conditions, long

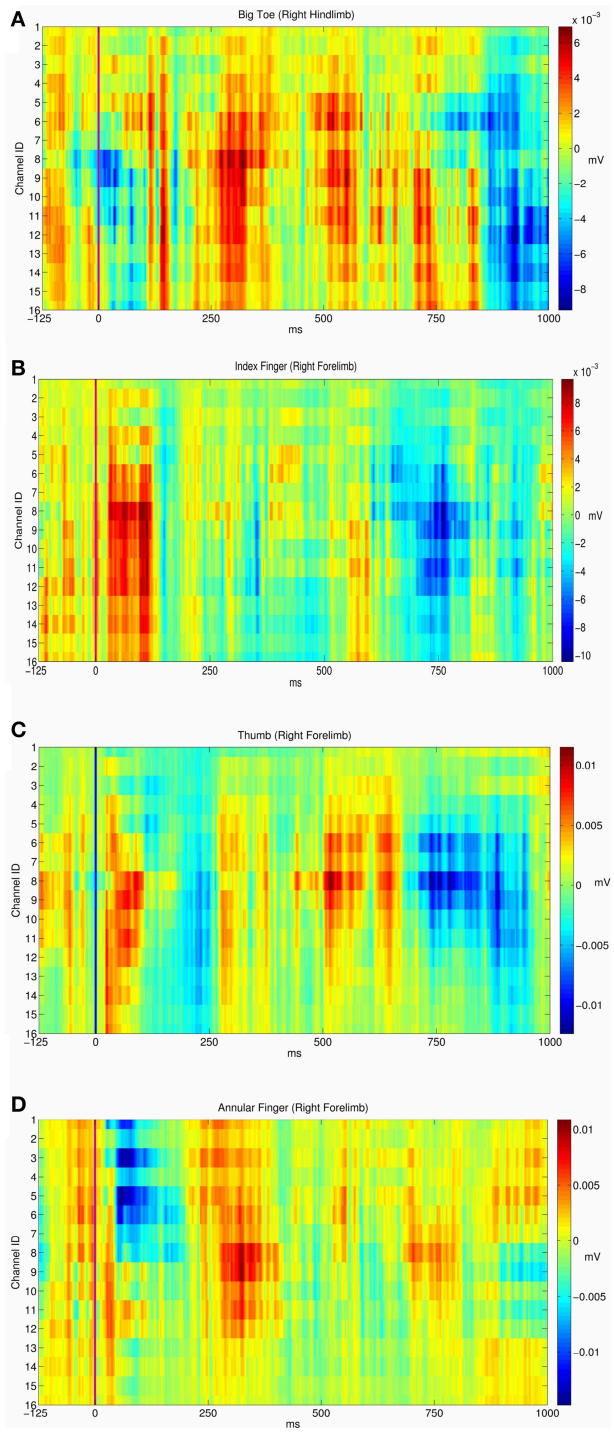

FIGURE 3 | Average evoked potentials of the cortical recorded responses to the peripheral sensory stimuli (Arduino driven fingertip stimuli) on four regions. Responses from respectively **(A)** the right big toe. **(B)** The right index fingertip. **(C)** The right index fingertip. **(D)** The right ring (or annular) fingertip.

processes of environmental adaptation and learning may have reduced the network dimensionality by gradual pruning of prototypal neuronal ensembles in conjunction to budding memories and plasticity processes (Koralek et al., 2012; Di Pino et al., 2014) to realize complex outputs with parsimonious expenditures and scaled modulations (Ganguly et al., 2011; Marblestone et al., 2013). In case of brain damages, machines have to be merged within erratic environment connectivity, hardly an achievable context by current devices (Mandonnet and Duffau, 2014). Cutting edge technologies, now, prompt to deep functional refinements such as interventions on cortical minicolumn coherence or stabilization of engrams generated by the prosthetic devices or again able to spot not only surface but also intrasulcal electrocorticographic signals (Ganguly and Carmena, 2009; Matsuo et al., 2011; Opris and Casanova, 2014) or again on intrinsic oscillatory circuit properties to coordinate dispersed neuronal populations (Canolty et al., 2010). These issues don't change even in functional disorders accompanied by cortical microstructural misalignments, such as chronic pain. It has been shown that exogenous transcranial magnetic or epicortical inputs significantly reduce chronic pain symptoms and these results go along with our theory on chronic pain as the result of collapsed information and the assumed symptom conversion by reinstatement of information. This strengthens the idea to adopt implantable brain machine devices injecting opportune or comparable currents to durably control chronic pain.

Advancement of Interface Material

All the above hints highlight the technical novelties to be imported onto future devices. Technical novelties grow significantly and allow for a wide range of applications with constructive (as for instance in sensory-motor supply), modulatory (as in chronic pain control) or disruptive (to counteract epileptic foci dynamic anomalies) scopes. Basic requirements are, obviously, features like adjustable intensity of output and functional coherence with the extant tissue. Examples have been realized recently for extreme flexibility of newly conceived devices (Yin et al., 2011) as well as for even neuroprosthetic device learning reactivation (Gulati et al., 2014). A further step has, been recently done by an organic material–based, biocompatible neural interface array apt to record both local field potentials (LFPs) and action potentials from superficial cortical neurons without penetrating the brain surface, a crucial leap forward in the technique of cortical grids when enabled to be mounted on human patients (Khodagholy et al., 2015). The grid we present here delivers strength enough to provoke sudden gross arm displacements as well as tunings able to elicit fine movements of single fingers. This suggests that, in the first mode, a "stop" sequence might be generated strong enough to halt even a generalized seizure (where a mere quantitative criterion could be held). On the other side the grid, selectively arousing smooth and independent finger movements, prospectively adapts to generate finest motor plans in suitable contexts. The subject becomes even more delicate with future BMIs applied on sensory compartments. Aside from the delivery of conventional stimulus sequences to elicit raw sensory information, BMIs would be loaded by semantics apt to encode the environment information features and keep into account corollary problems such as the forward effects of sensory

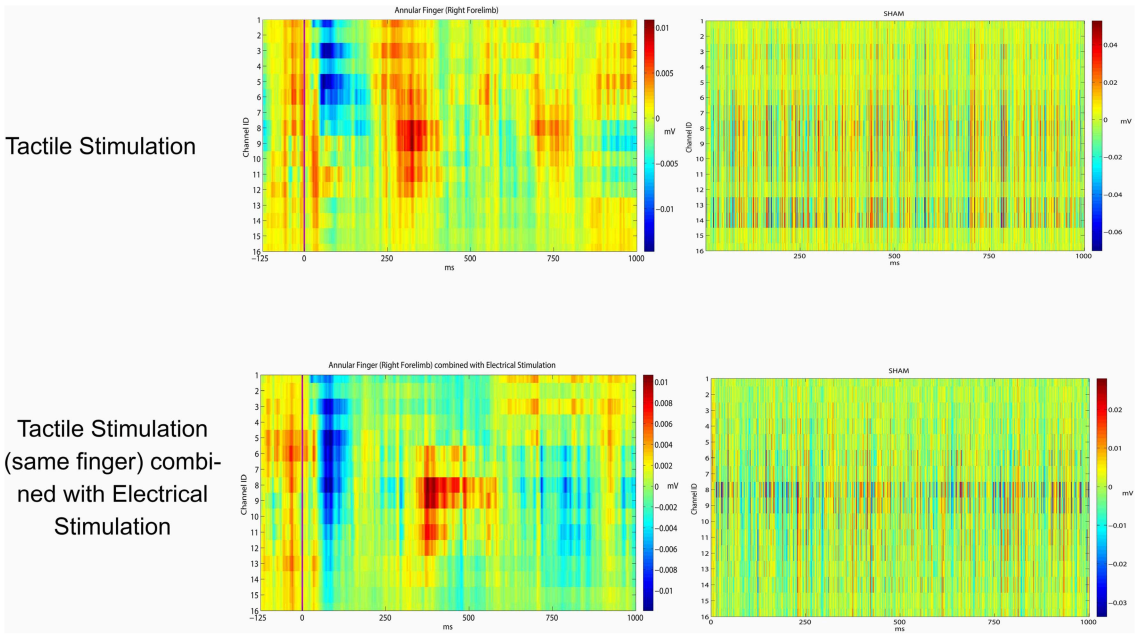

FIGURE 4 | Average evoked potentials from the ring (annular) finger. Row above: peripheral Arduino driven sensory stimuli (left). With no peripheral stimuli (right). Bottom row: peripheral Arduino driven sensory stimuli just after the central grid driven electrical stimuli on the most responding channels (left). Recording just after the central grid driven electrical stimuli with no peripheral Arduino driven sensory stimuli (right).

generated motor activations (O'Doherty et al., 2011; Opris et al., 2013), or input induced sensory learning (Koralek et al., 2012; Tabot et al., 2014). In fact, in experiments on rats, repetitive sensory or prefrontal cortical stimuli have shown coherent motor learning enhancements (Opris et al., 2013).

The Sensorimotor Pathway

Along these lines, we then explored the effect of epicortical stimulus patterns and their potential spreading to nearby grid plaquettes and, in conjunction, we analyzed the interferences of epicortical stimuli with concurrent peripheral sensory stimuli, in keeping with the core idea that local synthetic activations could drift natural stimuli. Indeed, in experiments on rats, mismatches between active and passive activations of the sensory cortex have been reported (Krupa et al., 2004). In our experiments, epicortical stimuli, although disturbing parallel natural sensory stimuli, once discontinued, did not show any extra interference with the responses to those stimuli. The natural stimuli were very light threshold sensory touches, repeatedly presented on single fingertips by a device delivering less than one millisecond-long inputs over some 1 mm^2 (Zippo et al., 2014). They were apt to elicit extremely evident responses on a significant cluster of recording electrodes with evident stereotactical distribution. On the other side, artificial grid stimuli were of low or mean intensity (see **Table 2**) and suitably delivered in turn from one single of the 16 plaquette. As noted above, the four stimulated fingers produced four different patterns of response. Namely, index and thumb showed precocious responses within 125 ms while the responses to the big toe and the hand middle finger had delayed response onset latency around 250 ms. These discrepancies may be explained by potential somatotopic coherence of the stimulated regions with the responding electrode. If the epicortical plaquette was place over the correct somatotopic projection area of the stimulated finger, the response could be clearly and quickly identified. If a mismatch between the projection field and the finger was relevant, it is conceivable to hypothesize that intra-cortical ("horizontal") paths could transport delayed activations from sources in the focus of inputs but far from the plaquettes. An alternative explanation could hold and namely that the stimulus competent (but non-recorded) cortex could recruit the thalamus (backward recruitment within local recurrent thalamic-cortico-thalamic loops). The thalamus could, in turn, forwardly recruit non-competent (but recorded) cortical areas. The mechanism could simply generate there a "warning sensory condition" in non-somatotopic areas declining in case of stimulus cessation. A balance between specific and non-specific (or core and matrix) thalamic activations could also be prospected. Whatever the origin, a delayed response was well detectable. Handiness and precision thus provide a path for future complex input constructs, meeting at least a number of requirements.

Limitations and Conclusions

As further note, the BMI driven function enhancement deserves some additional reflection. Supplementary feature integrations within natural networks urge questioning on the essence of the envisioned functional increment and, in greater detail, on how and what to achieve it. The increments themselves appear planned imbalances within however "normal" circuitries, well far from the conventional BMI roles in circuit degeneracies

(Hu et al., 2014), devoted to achievements in shorter time or with higher efficiency, time endurance or, again, by helping fatigued brain circuitries in defiant conditions. All in all, in a "connectome" perspective, both subsidiary and vicarious devices must recognize spatio-temporal alignments in hosting tissue to avoid anomalous avalanches and signal propagation within the biological environment (Deca, 2012). Finally, biologically-oriented manufacture and dedicated architectures are required to circumvent or strongly reduce immuno-rejection or inflammatory foci hampering the implanted devices by responses such as partial or complete connective encapsulation (McConnell et al., 2009). For instance, gelatine (Lind et al., 2010) or other treatments provided interesting experimental results to counter these effects and, more recently special probe shaping showed improvements in tissue tolerance by reducing the effects of sustained trauma (Sohal et al., 2014). No particular treatment has been operated over the grid, yet obtaining satisfying results during period of the electrophysiological study, due to the particularly suited polymer material surrounding the plaquettes (no apparent reaction observed during the period of the electrophysiological observations). Interesting results have also been obtained with other materials, however only in laboratory experiments and not in surgical epicortical implants (Chou et al., 2013). As a rule, however, the epicortical devices are usually placed for short or very short periods for diagnostic aims and then quickly removed. A long-term placement with negligible or no cortical damage could overcome the conventional diagnostic limits to switch them to long term application. The grid has been in-site showing no generalized rejection signs from an electrophysiological point of view and no blinding of the local electrical cortical contacts. The subtlety of the plastic contact carrier appears, then, contributing to its good tolerance. A prospective suitably engineered grid conformation could extend its application range, by encompassing more than one single cortical region and allow for the accurate studies of intra-cortical stimuli conduction and the careful activations of collection or single mini-electrodes exploring selected subsets of cortical regions.

In conclusion, the grid used in these experiments enabled the fine detail recordings and the conveyance of long-term fine-grain information from and to cortical surfaces. These features will potentially help for future therapeutic applications in sensorimotor and neurodegenerative diseases.

Supplementary Material

The Supplementary Material for this article can be found online at: http://journal.frontiersin.org/article/10.3389/fnsys.2015.00073/abstract

Video 1 | Movements elicited by electrical grid stimulation: Fine (little finger) and gross (arm) movements elicited by changing the grid current intensity in the same recording session.

References

Andersen, R. A., Kellis, S., Klaes, C., and Aflalo, T. (2014). Toward more versatile and intuitive cortical brain-machine interfaces. *Curr. Biol.* 24, R885–R897. doi: 10.1016/j.cub.2014.07.068

Baranauskas, G. (2014). What limits the performance of current invasive brain machine interfaces? *Front. Syst. Neurosci.* 8:68. doi: 10.3389/fnsys.2014.00068

Birbaumer, N., Weber, C., Neuper, C., Buch, E., Haagen, K., and Cohen, L. (2006). "Physiological regulation of thinking: brain–computer interface (BCI) research, Chap. 24," in *Progress in Brain Research,* Vol. 159, eds Neuper and Klimesch, 369–391. doi: 10.1016/S0079-6123(06)59024-7

Bongers, R. M., Bouwsema, H., and van der Sluis, C. K. (2011). "Motor control processes when learning to use a prosthetic device. MEC 11 raising the standard," in *Proceedings of the 2011 MyoElectric Controls/Powered Prosthetics Symposium Fredericton August 14-19, 2011* (New Brunswick, NJ: Copyright University of New Brunswick).

Boon, P., Raedt, R., de Herdt, V., Wyckhuys, T., and Vonck, K. (2009). Electrical stimulation for the treatment of epilepsy. *Neurotherapeutics* 6, 218–227. doi: 10.1016/j.nurt.2008.12.003

Borton, D. A., Yin, M., Juan, A., and Nurmikko, A. (2013). An implantable wireless neural interface for recording cortical circuit dynamics in moving primates. *J. Neural Eng.* 10:026010. doi: 10.1088/1741-2560/10/2/026010

Canolty, R., Ganguly, K., Kennerley, S., Cadieu, C., Koepsell, K., Wallis, J., et al. (2010). Oscillatory phase coupling coordinates anatomically-dispersed functional cell assemblies. *Proc. Natl. Acad. Sci. U.S.A.* 107, 17356–17361. doi: 10.1073/pnas.1008306107

Chou, N., Yoo, S., and Sohee Kim, S. (2013). A largely deformable surface type neural electrode array based on PDMS. *IEEE Trans. Neural. Syst. Rehabil. Eng.* 21, 544–553. doi: 10.1109/TNSRE.2012.2210560

Deca, D. (2012). The Connectome, WBE and AGI. *Artif. Gen. Intell. Lect. Notes Comp. Sci.* 7716, 41–49. doi: 10.1007/978-3-642-35506-6_5

Deca, D., and Koene, R. A. (2014). Experimental enhancement of neurphysiological function. *Front. Syst. Neurosci.* 8:189. doi: 10.3389/fnsys.2014.00189

Di Pino, G., Maravita, A., Zollo, L., Guglielmelli, E., and Di Lazzaro, V. (2014). Augmentation-related brain plasticity. *Front. Syst. Neurosci.* 8:109. doi: 10.3389/fnsys.2014.00109

Dromerick, A. W., Schabowsky, C. N., Holley, R. J., Monroe, B., Markotic, A., and Lum, P. S. (2008). Effect of training on upper-extremity prosthetic performance and motor learning: a single-case study. *Arch. Phys. Med. Rehabil.* 89, 1199–1204. doi: 10.1016/j.apmr.2007.09.058

Dwyer, J., Lee, H., Martell, A., Stevens, R., Hereld, M., and van Drongelen, W. (2010). Oscillation in a network model of neocortex. *Neurocomputing* 73, 1051–1056. doi: 10.1016/j.neucom.2009.12.021

Esquenazi, A., and Packel, A. (2012). Robotic-assisted gait training and restoration. *Am. J. Phys. Med. Rehabil.* 91(11 Suppl. 3), S217–S227. doi: 10.1097/PHM.0b013e31826bce18

Fisher, R. S., and Velasco, A. L. (2014). Electrical brain stimulation for epilepsy. *Nat. Rev. Neurol.* 10, 261–270. doi: 10.1038/nrneurol.2014.59

Freire, M. A., Morya, E., Faber, J., Santos, J. R., Guimaraes, J. S., Lemos, N. A., et al. (2011). Comprehensive analysis of tissue preservation and recording quality from chronic multielectrode implants. *PLoS ONE* 6:e27554. doi: 10.1371/journal.pone.0027554

Fricová, J., Klírová, M., Masopust, V., Novák, T., Vérebová, K., and Rokyta, R. (2013). Repetitive transcranial magnetic stimulation in the treatment of chronic orofacial pain. *Physiol Res.* 62(Suppl. 1), S125–S134.

Ganguly, K., and Carmena, J. M. (2009). Emergence of a stable cortical map for neuroprosthetic control. *PLoS Biol.* 7:e1000153. doi: 10.1371/journal.pbio.1000153

Ganguly, K., Dimitrov, D. F., Wallis, J. D., and Carmena, J. M. (2011). Reversible large-scale modification of cortical networks during neuroprosthetic control. *Nat. Neurosci.* 14, 662–667. doi: 10.1038/nn.2797

Géléoc, G. S., and Holt, J. R. (2014). Sound strategies for hearing restoration. *Science* 344:1241062. doi: 10.1126/science.1241062

George, M. S., Nahas, Z., Borckardt, J. J., Anderson, B., Burns, C., Kose, S., et al. (2007). Vagus nerve stimulation for the treatment of depression and other neuropsychiatric disorders. *Expert Rev. Neurother.* 7, 63–74. doi: 10.1586/14737175.7.1.63

Goodman, J. H. (2004). Brain stimulation as a therapy for epilepsy. *Adv. Exp. Med. Biol.* 548, 239–247. doi: 10.1007/978-1-4757-6376-8_17

Grahn, P. J., Mallory, G. W., Berry, B. M., Hachmann, J. T., Lobel, D. A., and Lujan, J. L. (2014). Restoration of motor function following spinal cord injury via optimal control of intraspinal microstimulation: toward a next generation closed-loop neural prosthesis. *Front. Neurosci.* 8:296. doi: 10.3389/fnins.2014.00296

Graimann, B., Allison, B., and Pfurtscheller, G. (2010). Brain–computer interfaces: a gentle introduction. *Brain Comput. Interfaces* 1–27. doi: 10.1007/978-3-642-02091-9_1

Groothuis, J., Ramsey, N. F., Ramakers, G. M., and van der Plasse, G. (2014). Physiological challenges for intracortical electrodes. *Brain Stimul.* 7, 1–6. doi: 10.1016/j.brs.2013.07.001

Gulati, T., Ramanathan, D. S., Wong, C. C., and Ganguly, K. (2014). *Nat. Neurosci.* 17, 1107–1113. doi: 10.1038/nn.3759

Hampson, R. E., Gerhardt, G. A., Marmarelis, V., Song, D., Opris, I., Santos, L., et al. (2012). Facilitation and restoration of cognitive function in primate prefrontal cortex by a neuroprosthesis that utilizes minicolumn-specific neural firing. *J. Neural. Eng.* 9:056012. doi: 10.1088/1741-2560/9/5/056012

Hochberg, L. R., Serruya, M. D., Friehs, G. M., Mukand, J. A., Saleh, M., Caplan, A. H., et al. (2006). Neuronal ensemble control of prosthetic devices by a human with tetraplegia. *Nature* 442, 164–171. doi: 10.1038/nature04970

Hu, X., Wang, Y., Zhao, T., and Gunduz, A. (2014). Neural coding for effective rehabilitation. *Biomed Res. Int.* 2014:286505. doi: 10.1155/2014/286505

Ifft, P. J., Lebedev, M. A., and Nicolelis, M. A. L. (2012). Reprogramming movements: extraction of motor intentions from cortical ensemble activity when movement goals change. *Front. Neuroeng.* 5:16. doi: 10.3389/fneng.2012.00016

Jackson, A., and Zimmermann, J. B. (2012). Neural interfaces for the brain and spinal cord–restoring motor function. *Nat. Rev. Neurol.* 8, 690–699. doi: 10.1038/nrneurol.2012.219

Khodagholy, D., Gelinas, J. N., Thesen, T., Doyle, W., Devinsky, O., Malliaras, G. et al. (2015). NeuroGrid: recording action potentials from the surface of the brain. *Nat. Neurosci.* 18, 310–315. doi: 10.1038/nn.3905

Knowlton, R. C., Lawn, N. D., Mountz, J. M., Buddhiwardhan, O., Miller, S., Burneo, J. G., et al. (2004b). Ictal single-photon emission computed tomography imaging in extra temporal lobe epilepsy using statistical parametric mapping. *J. Neuroimaging* 14, 324–330. doi: 10.1177/1051228404268570

Knowlton, R. C., Lawn, N. D., Mountz, J. M., and Kuzniecky, R. I. (2004a). Ictal SPECT analysis in epilepsy: subtraction and statistical parametric mapping techniques. *Neurology* 63, 10–15. doi: 10.1212/01.WNL.0000132885.83350.45

Koralek, A., Jin, X., Long, J., Costa, R., and Carmena, J. M. (2012). Corticostriatal plasticity is necessary for learning intentional neuroprosthetic skills. *Nature* 483, 331–335. doi: 10.1038/nature10845

Krupa, D. J., Wiest, M. C., Shuler, M. G., Laubach, M., and Nicolelis, M. A. (2004). Layer-specific somatosensory cortical activation during active tactile discrimination. *Science* 304, 1989–1992. doi: 10.1126/science.1093318

Lebedev, M. (2014). Brain-machine interfaces: an overview. *Transl. Neurosci.* 5, 99–110. doi: 10.2478/s13380-014-0212-z

Lebedev, M. A., and Nicolelis, M. A. (2006). Brain-machine interfaces: past, present and future. *Trends Neurosci.* 29, 536–46. doi: 10.1016/j.tins.2006.07.004

Lebedev, M. A., Tate, A. J., Hanson, T. L., Li, Z., O'Doherty, J. E., Winans, J. A., et al. (2011). Future developments in brain-machine interface research. *Clinics* 66, 25–32. doi: 10.1590/S1807-59322011001300004

Lefaucheur, J. P., André-Obadia, N., Antal, A., Ayache, S. S., Baeken, C., Benninger, D. H., et al. (2014). Evidence-based guidelines on the therapeutic use of repetitive transcranial magnetic stimulation (rTMS). *Clin. Neurophysiol.* 125, 2150–2206. doi: 10.1016/j.clinph.2014.05.021

Lind, G., Eriksson Linsmeier, C., Thelin, J., and Schouenborg, J. (2010). Gelatine-embedded electrodes—a novel biocompatible vehicle allowing implantation of highly flexible microelectrodes. *J. Neural Eng.* 7:046005. doi: 10.1088/1741-2560/7/4/046005

Mandonnet, E., and Duffau, H. (2014). Understanding entangled cerebral networks: a prerequisite for restoring brain function with brain-computer interfaces. *Front. Syst. Neurosci.* 8:82. doi: 10.3389/fnsys.2014.00082

Marblestone, A. H., Zamft, B. M., Maguire, Y. G., Shapiro, M. G., Cybulski, T. R., Glaser, J. I., et al. (2013). Physical principles for scalable neural recording. *Front. Comput. Neurosci.* 7:137. doi: 10.3389/fncom.2013.00137

Matsuo, T., Kawasaki, K., Osada, T., Sawahata, H., Suzuki, T., Shibata, M., et al. (2011). Intrasulcal electrocorticography in macaque monkeys with minimally invasive neurosurgical protocols. *Front. Syst. Neurosci.* 5:34. doi: 10.3389/fnsys.2011.00034

McConnell, G. C., Rees, H. D., Levey, A. I., Gutekunst, C. A., Gross, R. E., and Bellamkonda, R. V. (2009). Implanted neural electrodes cause chronic, local inflammation that is correlated with local neurodegeneration. *J. Neural Eng.* 6:056003. doi: 10.1088/1741-2560/6/5/056003

Moreno-Duarte, I., Morse, L. R., Alam, M., Bikson, M., Zafonte, R., and Fregni, F. (2014). Targeted therapies using electrical and magnetic neural stimulation for the treatment of chronic pain in spinal cord injury. *Neuroimage* 85(Pt 3), 1003–113. doi: 10.1016/j.neuroimage.2013.05.097

Nicolelis, M. A. L. (2012). *Beyond Boundaries: The New Neuroscience of Connecting Brains with Machines and How It Will Change Our Lives*. New York, NY: Times Books; Henry Holt and Company.

Nicolelis, M. A., and Lebedev, M. A. (2009). Principles of neural ensemble physiology underlying the operation of brain-machine interfaces. *Nat. Rev.* 10, 530–540. doi: 10.1038/nrn2653

O'Doherty, J. E., Lebedev, M. A., Ifft, P. J., Zhuang, K. Z., Shokur, S., Bleuler, H., et al. (2011). Active tactile exploration enabled by a brain-machine-brain interface. *Nature* 479, 228–231. doi: 10.1038/nature10489

Opris, I., and Casanova, M. F. (2014). Prefrontal cortical minicolumn: from executive control to disrupted cognitive processing. *Brain* 137(Pt 7), 1863–1875. doi: 10.1093/brain/awt359

Opris, I., Santos, L. M., Song, D., Gerhardt, G. A., Berger, T. W., Hampson, R. E., et al. (2013). Prefrontal cortical microcircuits bind perception to executive control. *Sci. Rep.* 3:2285. doi: 10.1038/srep02285

Orsborn, A., Moorman, H., Overduin, S., Shanechi, M., Dimitrov, D., and Carmena, J. M. (2014). Closed-loop decoder adaptation shapes neural plasticity for skillful neuroprosthetic control. *Neuron* 82, 1–14. doi: 10.1016/j.neuron.2014.04.048

Passard, A., Attal, N., Benadhira, R., Brasseur, L., Saba, G., Sichere, P., et al. (2007). Effects of unilateral repetitive transcranial magnetic stimulation of the motor cortex on chronic widespread pain in fibromyalgia. *Brain* 130(Pt 10), 2661–2670. doi: 10.1093/brain/awm189

Piangerelli, M., Ciavarro, M., Paris, A., Marchetti, S., Cristiani, P., Puttilli, C., et al. (2014). A fully integrated wireless system for intracranial direct cortical stimulation, real-time electrocorticography data transmission, and smart cage for wireless battery recharge. *Front. Neurol.* 5:156. doi: 10.3389/fneur.2014.00156

Rao, R. P. N. (2013). *Brain-Computer Interfacing: An Introduction.* New York, NY: Cambridge University Press

Schulze-Bonhage, A. (2009). Deep brain stimulation: a new approach to the treatment of epilepsy. *Dtsch Arztebl Int.* 106, 407–412. doi: 10.3238/arztebl.2009.0407

Sohal, H. S., Jackson, A., Jackson, R., Clowry, G. J., Vassilevski, K., O'Neill, A., et al. (2014). The sinusoidal probe: a new approach to improve electrode longevity. *Front. Neuroeng.* 7:10. doi: 10.3389/fneng.2014.00010

Tabot, G. A., Kim, S. S., Winberry, J. E., and Bensmaia, S. J. (2014). Restoring tactile and proprioceptive sensation through a brain interface. *Neurobiol. Dis.* 260–265. doi: 10.1016/j.nbd.2014.08.029

Wenger, N., Moraud, E. M., Raspopovic, S., Bonizzato, M., DiGiovanna, J., Musienko, P., et al. (2014). Closed-loop neuromodulation of spinal sensorimotor circuits controls refined locomotion after complete spinal cord injury. *Sci. Transl. Med.* 6, 255. doi: 10.1126/scitranslmed.3008325

Yin, M., Borton, D. A., Komar, J., Agha, N., Lu, Y., Li, H., et al. (2011). Wireless Neurosensor for Full-Spectrum Electrophysiology Recordings during Free Behavior. *Neuron* 84, 1170–1182. doi: 10.1016/j.neuron.2014.11.010

Zippo, A. G., Nencini, S., Caramenti, G. C., Valente, M., Storchi, R., and Biella, G. E. M. (2014). A simple stimulatory device for evoking point-like tactile stimuli: a searchlight for LFP to spike transitions. *J. Vis. Exp. 25, 85* doi: 10.3791/50941

Zippo, A. G., Storchi, R., Nencini, S., Caramenti, G. C., Valente, M., and Biella, G. E. M. (2013). Neuronal functional connection graphs among multiple areas of the rat somatosensory system during spontaneous and evoked activities. *PLoS Comput. Biol.* 9:e1003104. doi: 10.1371/journal.pcbi.1003104

Zippo, A. G., Storchi, R., Valente, M., Caramenti, G. C., and Biella, G. E. M. (2011). Neural substrates of chronic pain in the thalamocortical circuit. *Nat. Preceed.*

Conflict of Interest Statement: The authors declare that the research was conducted in the absence of any commercial or financial relationships that could be construed as a potential conflict of interest.

frontiers in Neuroscience

OPINION
published: 24 March 2016
doi: 10.3389/fnins.2016.00117

Self-Regulation of Blood Oxygenation Level Dependent Response: Primary Effect or Epiphenomenon?

Andrea Caria [1, 2]*

[1] Department of Psychology and Cognitive Science, University of Trento, Rovereto, Italy, [2] Institute of Medical Psychology and Behavioral Neurobiology, Eberhard-Karls-University of Tübingen, Tübingen, Germany

Keywords: real-time fMRI, BOLD signal, neurofeedback, self-regulation

In the last decade, several studies indicated that neuronal activity can be volitionally modulated using real-time fMRI (rtfMRI) based neurofeedback. Human participants through rtfMRI paradigms can learn to regulate the blood oxygenation level dependent (BOLD) response in several localized cortical and subcortical regions (for extended reviews see Caria et al., 2012; Weiskopf, 2012; Sulzer et al., 2013). Increasing evidence also indicated that strengthening or weakening specific BOLD activity using rtfMRI training leads to significant changes in cognitive, emotional and motor behavior (Caria et al., 2012; Weiskopf, 2012; Sulzer et al., 2013). These findings suggested that rtfMRI might represent an important novel approach in cognitive neuroscience by potentially providing indications of cause-and-effect relationships between brain and behavior, and also in clinical applications (Subramanian et al., 2011; Linden et al., 2012; Ruiz et al., 2013; Sitaram et al., 2014).

Although rtfMRI studies extend and enrich a large body of literature demonstrating operant learning of neuronal oscillations, skepticism still exists on the validity and reliability of studies showing learned control of the BOLD response. In particular, it is still debated whether this phenomenon is a primary effect of learning or it just an epiphenomenon resulting, for instance, from repeated execution of some mental processes.

Here, I will discuss specific psychophysiological and neurophysiological mechanisms presumably underlying learned regulation of the BOLD response to attempt to clarify its nature.

OPEN ACCESS

Edited by:
Manuel Fernando Casanova, University of Louisville, USA

Reviewed by:
Hari S. Sharma, Uppsala University, Sweden
Victor Manuel Pulgar, Wake Forest School of Medicine, USA

***Correspondence:**
Andrea Caria
andrea.caria@unitn.it

Specialty section:
This article was submitted to Neural Technology, a section of the journal Frontiers in Neuroscience

Received: *28 January 2016*
Accepted: *09 March 2016*
Published: *24 March 2016*

Citation:
Caria A (2016) Self-Regulation of Blood Oxygenation Level Dependent Response: Primary Effect or Epiphenomenon? Front. Neurosci. 10:117. doi: 10.3389/fnins.2016.00117

OPERANT LEARNING OF THE BOLD RESPONSE

Direct manipulation of brain activity grounds on the principles of operant conditioning that describe the relationship between changes in behavior (in this case the neurophysiological response) as consequence of contingent environmental events. Reinforcement is the mechanism that allows participants to increase the frequency of specific brain activity and to shape the desired pattern of neuronal activations. During operant learning of the BOLD response participants are reinforced proportionally to how much the ongoing metabolic signal approach or resemble the target level of activation in single or multiple regions of interest. The information of the ongoing signal fluctuations, provided as explicit visual feedback to the participants, represents the intrinsic reward.

Operant learning is an important approach for manipulating brain functions (Birbaumer and Kimmel, 1979) acting on intrinsic physiological properties of neuronal activity, which have been extensively shown to undergo classical and operant conditioning (Kandel and Schwartz, 1982).

The application of operant control principles to metabolic signals builds on several previous experiments demonstrating operant control of neuroeletric activity in non-human and human

animals (Birbaumer and Kimmel, 1979; Fetz, 2007). Studies on volitional control of neural activity dates back to the late sixties and seventies when operant conditioning of central nervous system activity was demonstrated (Olds, 1965; Fetz, 1969; Shinkman et al., 1974). CNS unit conditioning was shown by operantly rewarding rats to increase the activity of midbrain neurons using intracranial stimulation (Olds, 1965). In 1969, Fetz demonstrated conditioning of the activity of single neurons in precentral cortex in anesthetized monkeys by reinforcing high rates of neuronal discharge with food reward and auditory or visual feedback of unit firing rates (Fetz, 1969). More recently, Brain-Computer Interface and Brain-Machine interface studies reported volitional control of cortical cell activity, in particular in the motor cortex, in both animals and humans (Serruya et al., 2002; Taylor et al., 2002; Carmena et al., 2003; Moritz et al., 2008), with food reward and visual feedback of neuronal ensembles' activity. Altogether these findings robustly proved that neuronal activity from localized brain areas can be manipulated through operant conditioning.

On the other hand, there are unclear aspects of operant conditioning of the BOLD response in humans that make rtfMRI neurofeedback paradigms not fully established. Among these is the role of mental and cognitive processes for learning. Some rtfMRI studies indicated that successful BOLD regulation relies on the use of mental imagery (Chiew et al., 2012; Banca et al., 2015; Blefari et al., 2015). In particular, these studies suggested that strategies based on mental imagery are important for learning BOLD control considering the partial common substrates for internal representations and overt behavior, which holds in particular for the primary motor (Jeannerod, 1995; Roth et al., 1996; Jeannerod and Frak, 1999; Niyazov et al., 2005) and visual areas (Kosslyn and Thompson, 2003; Klein et al., 2004; Slotnick et al., 2005). On the contrary, other studies indicated that a combination of cognitive strategies (mental imagery) and feedback information is critical for participants to learn BOLD regulation, and that cognitive and imagery alone is not sufficient (decharms et al., 2005; Bray et al., 2007; Caria et al., 2010; Scharnowski et al., 2012). In particular, mere repetition of mental strategies leads to an initial increase of BOLD signal but to a rapid decrease in the following consecutive runs (Caria et al., 2010). In fact, fMRI adaptation paradigms (Kourtzi and Kanwisher, 2001) show that task repetition leads to a decrease of the BOLD signal.

In addition, while it is true that imagery and cognitive processing certainly affect learning and physiological regulation, studies on operant control of brain oscillations suggest that feedback is more important than instructions for successful slow cortical potentials regulation (Roberts et al., 1989; Birbaumer et al., 1990). There are indications from EEG based neurofeedback studies that mental imagery is efficacious initially but it would be then dropped when participants become more confident with self-regulation (Leuthardt et al., 2004). Ultimately, control of neuroelectric activity turns to a highly implicit process over training, and the contribution of higher order cognitive processes becomes negligible. Indeed, control of neurophysiological signals can even be attained when participants have little or no direct experience of it (Rockstroh et al., 1984). However, until now there exist no clear demonstrations that these mechanisms, although plausible, hold also for learned metabolic signals.

In most rtfMRI studies participants were aware of the responses leading to reward. Only one study reported to have employed implicit visual task and feedback to learn BOLD control in V1/V2 areas, however participants still reported to have used explicit mental strategies (Shibata et al., 2011).

In short, the fact that operant control of brain activity, even single cell responses is possible also in animals speaks against a fundamental influence of cognitive factors on the effect of operant brain regulation. On the other hand, it is conceivable that in human participants the combination of specific conscious processes and operant strategies might support retention of learned BOLD control out of the laboratory setting, and might facilitate the (re-)activation of impaired or dormant mechanisms, in particular in patients.

WHAT NEUROPHYSIOLOGICAL MECHANISMS MEDIATE LEARNED BOLD CONTROL?

A further issue of rtfMRI experiments is the unclear neurophysiology of the BOLD signal, which prevents us to univocally interpret the behavioral changes induced by operant learning of the metabolic signal. We know from previous investigations on instrumental learning of neuroelectric signals that the brain has intrinsic neurophysiological processes allowing regulation of neural activity even in the absence of external stimuli (Wolpaw et al., 2002; Birbaumer and Cohen, 2007; Fetz, 2007). While no specific receptors directly support regulation of brain oscillations, it exists a complex neurovascular system that regulates and controls the BOLD signal.

At least three main blood flow regulatory mechanisms have been described: cerebral autoregulation—the brain ability to maintain a constant flow through changes of cerebral perfusion pressure—neurogenic regulation—the cerebral blood flow modulation through extensive arborization of perivascular nerves—and flow-metabolism coupling, or functional hyperemia—the brain capacity to vary blood flow to match metabolic activity (Peterson et al., 2011). Endothelial cells and astrocytes play a central role in all these regulatory mechanisms (Iadecola and Nedergaard, 2007): the former by providing several vasoactive factors for the regulation of cerebral blood flow and the latter because of their anatomical position that physically links the cerebral microvasculature with synapses.

Learned increase and decrease of BOLD activity might indeed be associated with variations in the flow-metabolism coupling. Local changes in neural activity have been shown to influence BOLD signal (Buxton et al., 2004; Logothetis and Wandell, 2004; Lee et al., 2010) through variations in cerebral blood flow (CBF), cerebral blood volume (CBV) and cerebral metabolic rate of oxygen consumption (CMRO2). It has been also demonstrated that changes in the coupling ratio of CBF and CMRO2 in response to neural activity strongly affect the BOLD response (Kim and Ogawa, 2012; Buxton et al., 2014). Considering such complexity of the neurovascular system, it is thus conceivable

that learned control of the BOLD response might be based on these sophisticated regulatory mechanisms.

An intriguing perspective for rtfMRI neurofeedback arises from the hypothesis proposing that modulation of brain activity is directly and causally affected by changes of metabolic signals (Moore and Cao, 2008). Specifically, it has been conjectured that the brain vascular system, being a complex and interconnected network under tight regulatory control that occurs in close communication with neurons and glia, might directly contribute to information processing (Moore and Cao, 2008). Accordingly, the hemodynamic processes would not only support metabolic demand but also directly shape brain functions; self-regulation of metabolic signals might thus induce changes of neuronal activations. In line with this perspective non-invasive direct electrical stimulation (e.g., using transcranial direct electric stimulation, tDCS) targeting cerebral microvessels has been proposed to enhance brain functions trough changes of cerebrovascular function (Dutta, 2015; Pulgar, 2015).

So far, despite the increasing number of hypotheses and studies aiming to clarify the nature of the BOLD response, the neurometabolic coupling of this signal remains unclear. It has been shown that the BOLD fMRI response correlates with local field potentials (Logothetis et al., 2001; Viswanathan and Freeman, 2007), with spiking activity (Heeger and Ress, 2002), and with both LFP and spiking activity (Mukamel et al., 2005). In addition, BOLD signal can reflect different brain processing such as excitatory and inhibitory activity, neuromodulation, and bottom-up and top-down signals (Viswanathan and Freeman, 2007; Logothetis, 2008; Lee et al., 2010).

On the basis of this evidence it is difficult to infer whether the net effect of self-regulation of BOLD signal is excitatory, inhibitory or a combination or both. On the other hand, rtfMRI studies, although sometimes controversial, often reported an improvement of subjects' performance associated with increased amplitude of the BOLD response (decharms et al., 2005; Bray et al., 2007; Rota et al., 2009; Caria et al., 2010; Scharnowski et al., 2012, 2015; Zhang et al., 2013; Blefari et al., 2015). For instance, studies showed a decrease in reaction times for task execution associated with increase activity of the primary motor cortex (M1), and for task initiation after up-regulation of the SMA (Scharnowski et al., 2015). M1 activity was also positively correlated with accuracy improvement of performance during an isometric pinching task (Blefari et al., 2015) In the visual domain, increased visual perception was induced by increased BOLD response in the visual cortex (Scharnowski et al., 2012). Moreover, enhanced emotional response was associated with increased percentage BOLD signal change in the left anterior insula (Caria et al., 2010). Importantly, these studies reported poorer performance either during initial regulation runs or after down-regulation. Altogether these findings suggest that learned increase of the BOLD response might be associated with increased excitatory activity. This assumption would be also supported by studies showing improved memory performance associated with decreased BOLD activity in the parahippocampal cortex (Yoo et al., 2012; Scharnowski et al., 2015), which was then interpreted as result of increased brain resources for memory encoding because of decreased cortical processing (Yoo et al., 2012). Indeed, increased BOLD signal might occur from increased net excitation associated with glutamatergic activity (Logothetis, 2008). However, this represents only one possible interpretation, as larger BOLD signal can also be induced by concurrent increase of both glutamatergic and GABAergic activity, with changes in hemodynamic responses reflecting balanced local recurrent activity (Logothetis, 2008). In line with this alternative mechanism, it has been shown that enhanced perceptual sensitivity induced by fMRI feedback training results from a mixture of positive and negative activated voxels in the targeted regions of interest rather than from uniform positive or negative activity (Shibata et al., 2011).

Therefore, fMRI neurofeedback might also rely on, and possibly alter, the capacity of the cerebral cortex to generate persistent activity in the absence of sensory stimulation (Haider et al., 2006), which would in turn influence neuronal responsiveness to a wide range of inputs (Shu et al., 2003a). In addition, as the ongoing network activity can be turned on and off by synaptic inputs via electrical stimulation (Shu et al., 2003b), it can also be postulated its self-regulation via operant conditioning.

CONCLUSIONS

In short, the observed behavioral changes induced by rtfMRI training might be related to several plausible neurophysiological processes, and it is still not possible to conclusively ascertain the actual mechanism on the basis of the current results. Multimodal measurements such as simultaneous EEG-rtfMRI acquisition, as well as alternative real-time functional imaging methods such as MR perfusion and MR spectroscopy, might help to clarify the neurophysiological mechanisms underlying learned control of the BOLD response. Nevertheless, there exist clear indications that self-regulation of BOLD signal is not an epiphenomenon but a primary effect of operant learning, which can rely on precise neurovascular regulatory mechanisms.

AUTHOR CONTRIBUTIONS

The author confirms being the sole contributor of this work and approved it for publication.

ACKNOWLEDGMENTS

This work is part of the BRAINTRAIN European research network (Collaborative Project) supported by the European Commission under the Health Cooperation Work Programme of the 7th Framework Programme (Grant agreement n° 602186).

REFERENCES

Banca, P., Sousa, T., Catarina Duarte, I., and Castelo-Branco, M. (2015). Visual motion imagery neurofeedback based on the hMT+/V5 complex: evidence for a feedback-specific neural circuit involving neocortical and cerebellar regions. *J. Neural Eng.* 12:066003. doi: 10.1088/1741-2560/12/6/066003

Birbaumer, N., and Cohen, L. G. (2007). Brain-computer interfaces: communication and restoration of movement in paralysis. *J. Physiol.* 579, 621–636. doi: 10.1113/jphysiol.2006.125633

Birbaumer, N., Elbert, T., Canavan, A. G., and Rockstroh, B. (1990). Slow potentials of the cerebral cortex and behavior. *Physiol. Rev.* 70, 1–41.

Birbaumer, N., and Kimmel, H. (1979). *Biofeedback and Self-Regulation.* Hillsdale, NJ: Erlbaum.

Blefari, M. L., Sulzer, J., Hepp-Reymond, M. C., Kollias, S., and Gassert, R. (2015). Improvement in precision grip force control with self-modulation of primary motor cortex during motor imagery. *Front. Behav. Neurosci.* 9:18. doi: 10.3389/fnbeh.2015.00018

Bray, S., Shimojo, S., and O'doherty, J. P. (2007). Direct instrumental conditioning of neural activity using functional magnetic resonance imaging-derived reward feedback. *J. Neurosci.* 27, 7498–7507. doi: 10.1523/JNEUROSCI.2118-07.2007

Buxton, R. B., Griffeth, V. E., Simon, A. B., Moradi, F., and Shmuel, A. (2014). Variability of the coupling of blood flow and oxygen metabolism responses in the brain: a problem for interpreting BOLD studies but potentially a new window on the underlying neural activity. *Front. Neurosci.* 8:139. doi: 10.3389/fnins.2014.00139

Buxton, R. B., Uludag, K., Dubowitz, D. J., and Liu, T. T. (2004). Modeling the hemodynamic response to brain activation. *Neuroimage* 23(Suppl. 1), S220–S233. doi: 10.1016/j.neuroimage.2004.07.013

Caria, A., Sitaram, R., and Birbaumer, N. (2012). Real-time fMRI: a tool for local brain regulation. *Neuroscientist* 18, 487–501. doi: 10.1177/1073858411407205

Caria, A., Sitaram, R., Veit, R., Begliomini, C., and Birbaumer, N. (2010). Volitional control of anterior insula activity modulates the response to aversive stimuli. A real-time functional magnetic resonance imaging study. *Biol. Psychiatry* 68, 425–432. doi: 10.1016/j.biopsych.2010.04.020

Carmena, J. M., Lebedev, M. A., Crist, R. E., O'doherty, J. E., Santucci, D. M., Dimitrov, D. F., et al. (2003). Learning to control a brain-machine interface for reaching and grasping by primates. *PLoS Biol.* 1:E42. doi: 10.1371/journal.pbio.0000042

Chiew, M., Laconte, S. M., and Graham, S. J. (2012). Investigation of fMRI neurofeedback of differential primary motor cortex activity using kinesthetic motor imagery. *Neuroimage* 61, 21–31. doi: 10.1016/j.neuroimage.2012.02.053

decharms, R. C., Maeda, F., Glover, G. H., Ludlow, D., Pauly, J. M., Soneji, D., et al. (2005). Control over brain activation and pain learned by using real-time functional MRI. *Proc. Natl. Acad. Sci. U.S.A.* 102, 18626–18631. doi: 10.1073/pnas.0505210102

Dutta, A. (2015). Bidirectional interactions between neuronal and hemodynamic responses to transcranial direct current stimulation (tDCS): challenges for brain-state dependent tDCS. *Front. Syst. Neurosci.* 9:107. doi: 10.3389/fnsys.2015.00107

Fetz, E. E. (1969). Operant conditioning of cortical unit activity. *Science* 163, 955–958. doi: 10.1126/science.163.3870.955

Fetz, E. E. (2007). Volitional control of neural activity: implications for brain-computer interfaces. *J. Physiol.* 579, 571–579. doi: 10.1113/jphysiol.2006.127142

Haider, B., Duque, A., Hasenstaub, A. R., and Mccormick, D. A. (2006). Neocortical network activity *in vivo* is generated through a dynamic balance of excitation and inhibition. *J. Neurosci.* 26, 4535–4545. doi: 10.1523/JNEUROSCI.5297-05.2006

Heeger, D. J., and Ress, D. (2002). What does fMRI tell us about neuronal activity? *Nat. Rev. Neurosci.* 3, 142–151. doi: 10.1038/nrn730

Iadecola, C., and Nedergaard, M. (2007). Glial regulation of the cerebral microvasculature. *Nat. Neurosci.* 10, 1369–1376. doi: 10.1038/nn2003

Jeannerod, M. (1995). Mental imagery in the motor context. *Neuropsychologia* 33, 1419–1432. doi: 10.1016/0028-3932(95)00073-C

Jeannerod, M., and Frak, V. (1999). Mental imaging of motor activity in humans. *Curr. Opin. Neurobiol.* 9, 735–739. doi: 10.1016/S0959-4388(99)00038-0

Kandel, E. R., and Schwartz, J. H. (1982). Molecular biology of learning: modulation of transmitter release. *Science* 218, 433–443. doi: 10.1126/science.6289442

Kim, S. G., and Ogawa, S. (2012). Biophysical and physiological origins of blood oxygenation level-dependent fMRI signals. *J. Cereb. Blood Flow Metab.* 32, 1188–1206. doi: 10.1038/jcbfm.2012.23

Klein, I., Dubois, J., Mangin, J. F., Kherif, F., Flandin, G., Poline, J. B., et al. (2004). Retinotopic organization of visual mental images as revealed by functional magnetic resonance imaging. *Brain Res. Cogn. Brain Res.* 22, 26–31. doi: 10.1016/j.cogbrainres.2004.07.006

Kosslyn, S. M., and Thompson, W. L. (2003). When is early visual cortex activated during visual mental imagery? *Psychol. Bull.* 129, 723–746. doi: 10.1037/0033-2909.129.5.723

Kourtzi, Z., and Kanwisher, N. (2001). Representation of perceived object shape by the human lateral occipital complex. *Science* 293, 1506–1509. doi: 10.1126/science.1061133

Lee, J. H., Durand, R., Gradinaru, V., Zhang, F., Goshen, I., Kim, D. S., et al. (2010). Global and local fMRI signals driven by neurons defined optogenetically by type and wiring. *Nature* 465, 788–792. doi: 10.1038/nature09108

Leuthardt, E. C., Schalk, G., Wolpaw, J. R., Ojemann, J. G., and Moran, D. W. (2004). A brain-computer interface using electrocorticographic signals in humans. *J. Neural Eng.* 1, 63–71. doi: 10.1088/1741-2560/1/2/001

Linden, D. E., Habes, I., Johnston, S. J., Linden, S., Tatineni, R., Subramanian, L., et al. (2012). Real-time self-regulation of emotion networks in patients with depression. *PLoS ONE* 7:e38115. doi: 10.1371/journal.pone.0038115

Logothetis, N. K. (2008). What we can do and what we cannot do with fMRI. *Nature* 453, 869–878. doi: 10.1038/nature06976

Logothetis, N. K., Pauls, J., Augath, M., Trinath, T., and Oeltermann, A. (2001). Neurophysiological investigation of the basis of the fMRI signal. *Nature* 412, 150–157. doi: 10.1038/35084005

Logothetis, N. K., and Wandell, B. A. (2004). Interpreting the BOLD signal. *Annu. Rev. Physiol.* 66, 735–769. doi: 10.1146/annurev.physiol.66.082602.092845

Moore, C. I., and Cao, R. (2008). The hemo-neural hypothesis: on the role of blood flow in information processing. *J. Neurophysiol.* 99, 2035–2047. doi: 10.1152/jn.01366.2006

Moritz, C. T., Perlmutter, S. I., and Fetz, E. E. (2008). Direct control of paralysed muscles by cortical neurons. *Nature* 456, 639–642. doi: 10.1038/nature07418

Mukamel, R., Gelbard, H., Arieli, A., Hasson, U., Fried, I., and Malach, R. (2005). Coupling between neuronal firing, field potentials, and FMRI in human auditory cortex. *Science* 309, 951–954. doi: 10.1126/science.1110913

Niyazov, D. M., Butler, A. J., Kadah, Y. M., Epstein, C. M., and Hu, X. P. (2005). Functional magnetic resonance imaging and transcranial magnetic stimulation: effects of motor imagery, movement and coil orientation. *Clin. Neurophysiol.* 116, 1601–1610. doi: 10.1016/j.clinph.2005.02.028

Olds, J. (1965). Operant conditioning of single unit responses. *Excerpta Med. Int. Cong. Series* 87, 372–380.

Peterson, E. C., Wang, Z., and Britz, G. (2011). Regulation of cerebral blood flow. *Int. J. Vasc. Med.* 2011:823525. doi: 10.1155/2011/823525

Pulgar, V. M. (2015). Direct electric stimulation to increase cerebrovascular function. *Front. Syst. Neurosci.* 9:54. doi: 10.3389/fnsys.2015.00054

Roberts, L. E., Birbaumer, N., Rockstroh, B., Lutzenberger, W., and Elbert, T. (1989). Self-report during feedback regulation of slow cortical potentials. *Psychophysiology* 26, 392–403. doi: 10.1111/j.1469-8986.1989.tb01941.x

Rockstroh, B., Birbaumer, N., Elbert, T., and Lutzenberger, W. (1984). Operant control of EEG and event-related and slow brain potentials. *Biofeedback Self Regul.* 9, 139–160. doi: 10.1007/BF00998830

Rota, G., Sitaram, R., Veit, R., Erb, M., Weiskopf, N., Dogil, G., et al. (2009). Self-regulation of regional cortical activity using real-time fMRI: the right inferior frontal gyrus and linguistic processing. *Hum. Brain Mapp.* 30, 1605–1614. doi: 10.1002/hbm.20621

Roth, M., Decety, J., Raybaudi, M., Massarelli, R., Delon-Martin, C., Segebarth, C., et al. (1996). Possible involvement of primary motor cortex in mentally simulated movement: a functional magnetic resonance imaging study. *Neuroreport* 7, 1280–1284. doi: 10.1097/00001756-199605170-00012

Ruiz, S., Lee, S., Soekadar, S. R., Caria, A., Veit, R., Kircher, T., et al. (2013). Acquired self-control of insula cortex modulates emotion recognition and brain network connectivity in schizophrenia. *Hum. Brain Mapp.* 34, 200–212. doi: 10.1002/hbm.21427

Scharnowski, F., Hutton, C., Josephs, O., Weiskopf, N., and Rees, G. (2012). Improving visual perception through neurofeedback. *J. Neurosci.* 32, 17830–17841. doi: 10.1523/JNEUROSCI.6334-11.2012

Scharnowski, F., Veit, R., Zopf, R., Studer, P., Bock, S., Diedrichsen, J., et al. (2015). Manipulating motor performance and memory through real-time fMRI neurofeedback. *Biol. Psychol.* 108, 85–97. doi: 10.1016/j.biopsycho.2015.03.009

Serruya, M. D., Hatsopoulos, N. G., Paninski, L., Fellows, M. R., and Donoghue, J. P. (2002). Instant neural control of a movement signal. *Nature* 416, 141–142. doi: 10.1038/416141a

Shibata, K., Watanabe, T., Sasaki, Y., and Kawato, M. (2011). Perceptual learning incepted by decoded fMRI neurofeedback without stimulus presentation. *Science* 334, 1413–1415. doi: 10.1126/science.1212003

Shinkman, P. G., Bruce, C. J., and Pfingst, B. E. (1974). Operant conditioning of single-unit response patterns in visual cortex. *Science* 184, 1194–1196. doi: 10.1126/science.184.4142.1194

Shu, Y., Hasenstaub, A., Badoual, M., Bal, T., and Mccormick, D. A. (2003a). Barrages of synaptic activity control the gain and sensitivity of cortical neurons. *J. Neurosci.* 23, 10388–10401.

Shu, Y., Hasenstaub, A., and Mccormick, D. A. (2003b). Turning on and off recurrent balanced cortical activity. *Nature* 423, 288–293. doi: 10.1038/nature01616

Sitaram, R., Caria, A., Veit, R., Gaber, T., Ruiz, S., and Birbaumer, N. (2014). Volitional control of the anterior insula in criminal psychopaths using real-time fMRI neurofeedback: a pilot study. *Front. Behav. Neurosci.* 8:344. doi: 10.3389/fnbeh.2014.00344

Slotnick, S. D., Thompson, W. L., and Kosslyn, S. M. (2005). Visual mental imagery induces retinotopically organized activation of early visual areas. *Cereb. Cortex* 15, 1570–1583. doi: 10.1093/cercor/bhi035

Subramanian, L., Hindle, J. V., Johnston, S., Roberts, M. V., Husain, M., Goebel, R., et al. (2011). Real-time functional magnetic resonance imaging neurofeedback for treatment of Parkinson's disease. *J. Neurosci.* 31, 16309–16317. doi: 10.1523/JNEUROSCI.3498-11.2011

Sulzer, J., Haller, S., Scharnowski, F., Weiskopf, N., Birbaumer, N., Blefari, M. L., et al. (2013). Real-time fMRI neurofeedback: progress and challenges. *Neuroimage* 76, 386–399. doi: 10.1016/j.neuroimage.2013.03.033

Taylor, D. M., Tillery, S. I., and Schwartz, A. B. (2002). Direct cortical control of 3D neuroprosthetic devices. *Science* 296, 1829–1832. doi: 10.1126/science.1070291

Viswanathan, A., and Freeman, R. D. (2007). Neurometabolic coupling in cerebral cortex reflects synaptic more than spiking activity. *Nat. Neurosci.* 10, 1308–1312. doi: 10.1038/nn1977

Weiskopf, N. (2012). Real-time fMRI and its application to neurofeedback. *Neuroimage* 62, 682–692. doi: 10.1016/j.neuroimage.2011.10.009

Wolpaw, J. R., Birbaumer, N., Mcfarland, D. J., Pfurtscheller, G., and Vaughan, T. M. (2002). Brain-computer interfaces for communication and control. *Clin. Neurophysiol.* 113, 767–791. doi: 10.1016/S1388-2457(02)00057-3

Yoo, J. J., Hinds, O., Ofen, N., Thompson, T. W., Whitfield-Gabrieli, S., Triantafyllou, C., et al. (2012). When the brain is prepared to learn: enhancing human learning using real-time fMRI. *Neuroimage* 59, 846–852. doi: 10.1016/j.neuroimage.2011.07.063

Zhang, G., Yao, L., Zhang, H., Long, Z., and Zhao, X. (2013). Improved working memory performance through self-regulation of dorsal lateral prefrontal cortex activation using real-time fMRI. *PLoS ONE* 8:e73735. doi: 10.1371/journal.pone.0073735

Conflict of Interest Statement: The author declares that the research was conducted in the absence of any commercial or financial relationships that could be construed as a potential conflict of interest.

frontiers in
SYSTEMS NEUROSCIENCE

REVIEW ARTICLE
published: 20 June 2014
doi: 10.3389/fnsys.2014.00091

Nanostructures: a platform for brain repair and augmentation

Ruxandra Vidu[1]*, Masoud Rahman[1], Morteza Mahmoudi[2†], Marius Enachescu[3,4], Teodor D. Poteca[5] and Ioan Opris[6]

[1] *Department of Chemical Engineering and Materials Science, University of California Davis, Davis, CA, USA*
[2] *Department of Nanotechnology and Nanotechnology Research Center, Faculty of Pharmacy, Tehran University of Medical Sciences, Tehran, Iran*
[3] *Center for Surface Science and Nanotechnology, University "Politehnica" Bucharest, Bucharest, Romania*
[4] *Academy of Romanian Scientists, Bucharest, Romania*
[5] *Carol Davila University of Medicine and Pharmacy, Bucharest, Romania*
[6] *Wake Forest University Health Sciences, Winston-Salem, NC, USA*

Edited by:
Mikhail Lebedev, Duke University, USA

Reviewed by:
Dong Song, University of Southern California, USA
Randal A. Koene, Boston University, USA

****Correspondence:***
Ruxandra Vidu, Department of Chemical Engineering and Materials Science, University of California Davis, One Shields Avenue, Davis, CA 95616, USA
e-mail: rvidu@ucdavis.edu

†Present address:
Morteza Mahmoudi, Division of Cardiology, Department of Pediatrics, School of Medicine, Stanford University, Stanford, USA

Nanoscale structures have been at the core of research efforts dealing with integration of nanotechnology into novel electronic devices for the last decade. Because the size of nanomaterials is of the same order of magnitude as biomolecules, these materials are valuable tools for nanoscale manipulation in a broad range of neurobiological systems. For instance, the unique electrical and optical properties of nanowires, nanotubes, and nanocables with vertical orientation, assembled in nanoscale arrays, have been used in many device applications such as sensors that hold the potential to augment brain functions. However, the challenge in creating nanowires/nanotubes or nanocables array-based sensors lies in making individual electrical connections fitting both the features of the brain and of the nanostructures. This review discusses two of the most important applications of nanostructures in neuroscience. First, the current approaches to create nanowires and nanocable structures are reviewed to critically evaluate their potential for developing unique nanostructure based sensors to improve recording and device performance to reduce noise and the detrimental effect of the interface on the tissue. Second, the implementation of nanomaterials in neurobiological and medical applications will be considered from the brain augmentation perspective. Novel applications for diagnosis and treatment of brain diseases such as multiple sclerosis, meningitis, stroke, epilepsy, Alzheimer's disease, schizophrenia, and autism will be considered. Because the blood brain barrier (BBB) has a defensive mechanism in preventing nanomaterials arrival to the brain, various strategies to help them to pass through the BBB will be discussed. Finally, the implementation of nanomaterials in neurobiological applications is addressed from the brain repair/augmentation perspective. These nanostructures at the interface between nanotechnology and neuroscience will play a pivotal role not only in addressing the multitude of brain disorders but also to repair or augment brain functions.

Keywords: nanotechnology, brain repair and augmentation, brain activity mapping, blood brain barrier, carbon nanotube, multi-electrode array, nano-imprint lithography, inter-laminar microcircuit

INTRODUCTION

NeuroNanoTechnology (NNT) is an emerging approach in science and engineering not only to assess the unique properties, structures and functions of brain circuits, but also to manipulate or to heal damaged neural circuits. This is largely because the brain functions operate at the nanoscale level, and therefore, in order to access and communicate with the entities of interest, we need tools and techniques that work at nano-scale level as well. The synthesis and characterization, as well as the design of materials with functional organization at nanoscale give us the possibility to engineer and control functional bio-integrated systems. Importantly, the ability to manipulate atoms and molecules, induce unique properties, increase stability, and communicate signals is opening up incredible opportunities for a broad spectrum of scientists. The purpose of this review is to highlight recent engineering advances in the rapidly developing field and its clinical applications, including augmenting brain function. NNT as applied nanotechnology to engineered sensing platforms has the ultimate goal of developing interdisciplinary nanotechnology strategies that can directly investigate specific neural interactions and circuits for treating the broad spectrum of neurological and psychiatric disorders.

The foundation of the "nanoworld" was established in 1980's when for the first time, scientists were able to see the atom (i.e., the tiny "brick" of matter) in 3D real space. This was primarily due to the invention of the scanning tunneling microscope (Binning et al., 1982; Binnig et al., 1983), followed by additional techniques, such as atomic force microscopy (Binnig et al., 1986).

The "nanoworld" in science consists of several nano "chapters" such as nanomaterials—materials at nanoscale; nanoarrays—arrays of nanowires; nanotools—tools needed to characterize the nanomaterials; and nanodevices—new devices, many of them using quantum effects. The miniaturization trend and the high output of integrated circuits have stimulated the development of both nanostructured materials and new synthesis methods. Thus, nano-tools bring at the table the "internal" or "external" "nano-surgeons" for operating at the nano- and micro-level in neuronal circuits. The most promising "nano-surgeons" are the carbon nanotubes (CNTs) and nanowires (NWs). Carbon nanotubes and nanowires demonstrate new and/or enhanced functions crucial to neuroscience, offering a bottom-up approach in assembling nanoscale arrays and devices.

Research efforts are concentrated towards increasing the number and the density of extracellular electrodes while decreasing the device size. Acting as "on-site" laboratories, nanostructures arrays can be integrated into sensing, stimulating, monitoring and recording devices for nano-neuroscience. For example, microelectrode arrays use nanomaterials produced for various applications including *in vivo* penetration for recording, neurostimulation and optogenetic manipulations, surface electrodes measuring event related potentials in human brain, as well as fluidic, *in vitro* chemical sensing. Although these microelectrodes are made of platinum and iridium oxide, electrochemical degradation and delamination of the coating layer of the electrode may occur in time, recent advances are resolving these problems. Neural probes and micro-devices are currently used for recording activity of large neuronal assemblies (Wise, 2007; Chang-Hsiao et al., 2010; Amaral et al., 2013). For instance, low noise 64-channel neural probes made of silicon with nanoscale leads have been demonstrated feasible by Du et al. (2011). The creation of the nanomaterials—carbon nanotubes in particular—and a general approach to the preparation and applications of nanomaterials using template synthesis are also presented in this article.

Additionally, recent developments in the application of nanotechnological neuroscience to the study of human brain are reviewed (**Figure 1**). NNT research aims to regenerate and protect the central nervous system (CNS) by developing nanoengineered substrates, for example, to help guide axon growth after damage or degeneration. Other therapeutic strategies for CNS disorders require getting a device or drug to a specific site in the CNS. Acute compression in spinal cord injury, for example, requires laminectomy and *in vivo* delivery of peptide amphiphile molecules for nanofiber network formation (in rat models) (Silva, 2005). Nanomaterials used as vessels to deliver drugs are discussed in conjunction with methods that help nanoparticles to transfer across the blood brain barrier. Finally, we review exciting advances in various clinical applications to stimulate nerve cells for regeneration and even augmentation of brain function. NNT's promise is to provide chips that will interface with the brain and allowing to detect and correcting online any potential miss-function of the brain's microcircuits bridging the perception with the executive control of behavior.

NANOMATERIALS

CARBON NANOTUBES

Nanotechnology of carbon nanotubes and nanowires junctions

Nanotubes and nanowires are nanomaterials that basically represent the quasi-one-dimensional (1D) conductors and semiconductors available for nanotechnology to use. The nanotechnology rush, currently in progress, was generated by nanotubes and

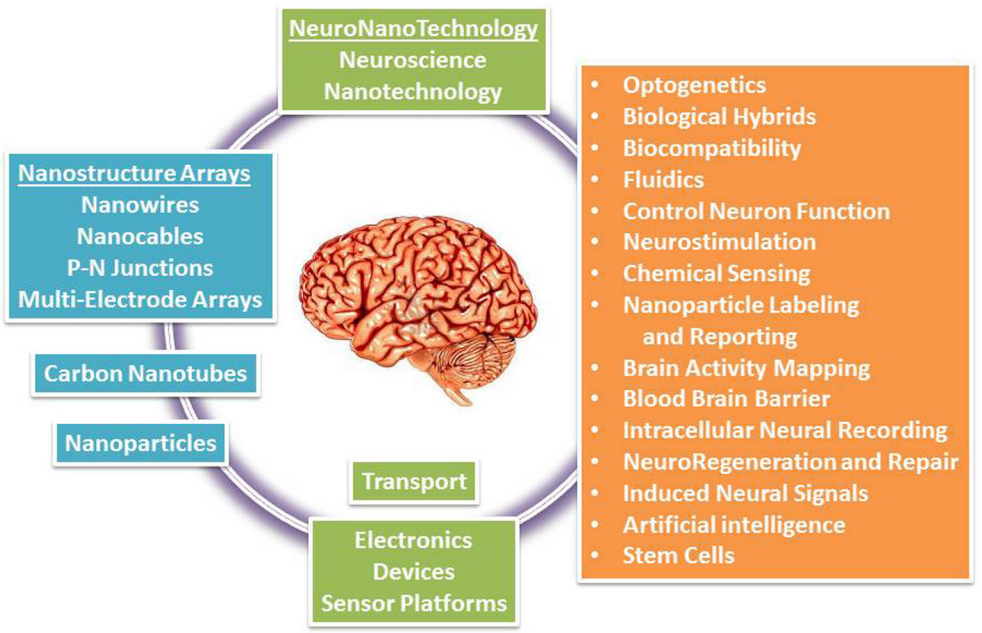

FIGURE 1 | Illustration of nanotechnology integration into the brain research.

nanowires that have evolved into some of the most intensively studied materials (Mao et al., 2013). Carbon nanotubes (CNTs), discovered by Iijima (1991), are exhibiting outstanding mechanical, thermal, and conductive properties. Rolling-up one or more graphene sheets generates CNTs with excellent chemical and thermal stability, extreme electronic properties, large surface area and high mechanical strength while carrying ultralight weight (Ajayan, 1999).

Under well-defined conditions of synthesis, two forms of CNTs can efficiently be prepared: single-wall carbon nanotubes (SWCNTs) or nested multiwall carbon nanotubes (MWCNTs) (**Figure 2**). Being so close to graphene, CNTs are usually near to atomic-scale perfection making CNTs chemically inert (Enachescu et al., 1999; Bota et al., 2014a,b). Although the CNTs have 1/6th of the weight of steel, similar to graphene under tension, nanotubes are two orders of magnitude stronger than steel. Computer simulations estimation of melting point of nanotubes of about 3700°C is higher than that of any metal, but close to that of graphite. SWCNTs can act as very good conductors of electrons or can show semiconducting behavior, depending on their diameter and the atomic structure of nanotubes. Even the very high thermal conductivity of isotopically pure diamond is expected to be exceeded by that of CNTs (CNTs being excellent conductors of heat) that can be perfectly positioned in the devices to dissipate heat from PC chips. Additionally, CNTs are biocompatible in many environments, similar to the related graphite.

Different technological fields are witnessing great developments in CNTs devices based on their unique properties: probes, conductive composites, nanometer sized semiconductor devices, field emission displays and radiation sources, hydrogen storage media, sensors, energy storage, and energy conversion devices (Sharma and Ahuja, 2008). Functionalization of the CNTs surface was performed during the last decade using many different approaches, some of which focused on increasing CNTs solubility and lowering their toxic effects in order to fit biomedical applications (Bianco et al., 2011), because CNTs were showing poor solubility and apparently high toxicity (Fabbro et al., 2012). CNTs have been proposed either by themselves or as components for biosensors (Wenrong et al., 2010), ion channel blockers (Park et al., 2003), biocatalysts (Feng and Ji, 2011), photothermal probes in cancer therapy (Moon et al., 2009), nanovectors (Klumpp et al., 2006) and imaging applications (Kam et al., 2005a; Wu et al., 2005; Klumpp et al., 2006).

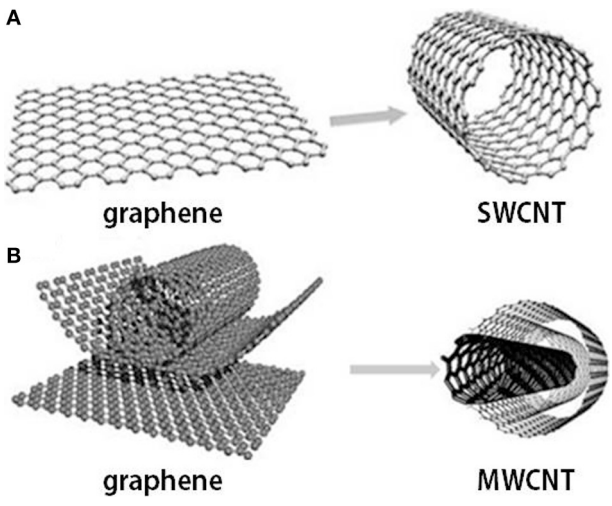

FIGURE 2 | Graphene and carbon nanotubes as (A) single wall carbon nanotube (SWCNT) and (B) multi-wall carbon nanotube (MWCNT) structures.

A nanotube can be conjugated with multi-functional agents (Wu et al., 2005). The particularity of CNTs to have a higher surface area to volume ratio compared to spheres allows high loads of therapeutic agents (Kam et al., 2005a). CNTs are very good candidates for new delivery vehicles as well increasing the therapeutic effect of drugs. Viral vectors, lipids (positive charged), polymers, liposomes, and NPs represent the previous delivery vehicles. However, reduced penetration into the cell of certain therapeutic agents is one issue of concern despite the versatility of shape, size and materials of non-viral vehicles (Endo et al., 1990). After surface modification via functionalization, CNTs show low cytotoxicity as measured over a few days (Kam et al., 2004; Lu et al., 2004; Pantarotto et al., 2004a,b; Cai et al., 2005; Kam and Dai, 2005; Kam et al., 2005a; Wu et al., 2005) while CNTs are readily internalized by cells.

In addition, single-walled carbon nanotubes (SWCNTs) show confined heating at near infrared (NIR) absorption because SWCNTs absorb strongly in NIR wavelengths range (Endo et al., 1990). In his work, Kam et al. (2005b) showed that SWCNTs released DNA upon exposure to NIR radiation, which permits its translocation into the cell nucleus. Cell death was demonstrated in the same study by using the same technique. SWCNTs were adopted by folate labeled cells, increasing the CNTs functionalization using a folate moiety.

The transport of nanotubes into cells is of fundamental importance for the biomedical applications mentioned above and below. As yet, the way in which CNTs enter cells is still under hot debate, generating both controversy and confusion about the mechanism of entering cells. Bianco et al. (Pantarotto et al., 2004b) suggested that ammonium-functionalized SWCNTs and MWCNTs are formed via a passive, endocytosis-independent mechanism; however, Dai et al. (Kam et al., 2004) came to the conclusion that the mechanism of the acid-functionalized SWCNTs entering the cell involves an endocytosis pathway. Another mechanism proposed for MWCNTs, which cannot use the endocytosis pathway due to their size takes into consideration the flipping of lipid molecules of the membrane to allow CNTs to enter the cell (Kam et al., 2004; Lopez et al., 2004; Lu et al., 2004; Pantarotto et al., 2004a,b; Cai et al., 2005; Kam and Dai, 2005). The communication between cell and nanotube is constrained by the type of coating on the nanotube surface. By transferring CNTs into cells, proteins are absorbed to the nanotube surface, coating the nanotube with serum-containing proteins, such as albumin and fibronectin. It has been suggested that the CNT transfer into cells has a natural switching mechanism of lipids in the membrane (Lopez et al., 2004; Pantarotto et al., 2004a) and to not exceed an endocytotic pathway for the MWCNTs that are 200 nm in length with 10 nm radius.

An open subject remains regarding what happens to CNTs once they have entered the cell and also about when or how they would be exocytosed by the cells (Sakhtianchi et al., 2013). The possibility for the nanotubes to be subsequently expelled from the cell would be advantageous for most biological applications; however, as yet, this has not been reported in the literature. There is still much work necessary to understand the CNTs cellular transport in order to be able to control the CNTs placement inside cells.

Nanowires junctions

In biology the range of length scale varies by orders of magnitudes—from nanometer sized nucleic or amino acids to several centimeters for organs and neuronal circuits. There is a need for interfaces with nanoscale spatial resolution in order to investigate processes at the subcellular level. Besides carbon nanotubes, these interfaces can be achieved through the use of other nanostructures, such as semiconductor nanowires (NWs). With dimensions that are as small as a protein molecule, CNTs and NWs present the building blocks for nanoscale electronics (McEuen et al., 2002; Lieber, 2003). The critical feature sizes (atomic scale) of these building blocks can be well-controlled during synthesis, in contrast with nanostructures fabricated by "top-down" process. Even for isolated CNTs transistors that have shown exceptional properties (Javey et al., 2003), large scale integration challenges remain due to difficulties in preparing pure semiconductor nanotubes. The issues faced by CNTs could be overcome by nanowires because of the reproducible control over size and electronic properties that current growth methods enable (Cui and Lieber, 2001; Cui et al., 2001a, 2003; Wu et al., 2004). A wide class of NWs have been developed, ranging from NWs based on classic semiconductors, such as silicon NWs (Chen et al., 2006a; Goncher et al., 2006; Yajie et al., 2008), GaP (Dujavova-Laurencikova et al., 2013), GaN (Lee et al., 2007), CdS and ZnS (Barrelet et al., 2003), heterostructures as Ge-Si (Xiang et al., 2006a,b), InAs-InP (Jiang et al., 2007), oxide nanowires MgO (Yin et al., 2002), Cu_2O (Jiang et al., 2002), SiO_2 (Yu et al., 1998; Liu et al., 2001; Zheng et al., 2002), Ga_2O_3 (Wu et al., 2000; Sharma and Sunkara, 2002), Al_2O_3 (Valcarcel et al., 1998; Xiao et al., 2002), In_2O_3 (Li et al., 2003), SnO_2 (Dai et al., 2001), MnO_2 (Wang and Li, 2002), Sb_2O_3 (Guo et al., 2000), TiO_2 (Seraji et al., 2000; Miao et al., 2002), ZnO (Tian et al., 2003; Vayssieres, 2003), and $LiNiO_2$ (Zhou et al., 2002).

The field-effect transistors (FETs) configuration of semiconductor NWs is one of the most appropriate detection schemes (Cui and Lieber, 2001; Cui et al., 2001b, 2003; Zheng et al., 2004; Xiang et al., 2006a). Binding to the dielectric gate of a polar/charged species appears analogous to applying a voltage to a gate electrode. For example, accumulation of positive carriers (holes) together with an increase/variation in device conductance can be generated by binding a protein with negative charge to the surface of a *p*-type FET. Silicon based NWs (or composed of other types of semiconductors) also may function as FET devices (Cui and Lieber, 2001; Cui et al., 2003; Lieber, 2003; Zheng et al., 2004; Li et al., 2006; Xiang et al., 2006a). One-dimensional morphology of NWs is the main feature that determines overcoming sensitivity limitations for planar FET devices. Thus, a more substantial change in device conductance for the NW vs. a planar FET will take place if any analyte binding event will happen (this event leads to accumulation or depletion of carriers).

One of the most powerful and versatile platforms based on NWs devices has emerged to build functional interfaces for biological (including neurons) systems. NWs are non-invasive (highly local) probes of neuronal projections; individual NWs devices are becoming optimal for interfacing with neurons due to the fact that the contact length along the axon (or the dendrite projection crossing a NW) is just about 20 nm. Compared to other electrophysiological methods, with micro-fabricated electrodes and planar FETs, the active junction area for NWs devices is orders of magnitude smaller and is quite similar to natural synapses. This small size creates advantages, such as: (a) spatially resolved signal detection without complicated averaging of extracellular potentials that change over a large portion of a given neuron, and (b) integration of axon's elements together with the dendrite projections from a single cell. The stimulation of neuronal activity through NW/axon junctions is also achievable using NWs devices. Somatic action potential spikes detected with intracellular electrodes, are generated by applying excitatory sequences of biphasic pulses to the NWs of NW/axon junctions (Patolsky et al., 2007).

Also, NW-based FET device can be designed into a device array; neuron growth over dense NWs device arrays is usually achievable nowadays (Patolsky et al., 2007). Thus, interfacing ensembles of NWs inputs and outputs to different neural networks and neurons enables the implementation of stimulation, inhibition, or reversibly blocking signal propagation through specific pathways (while the signal flow is simultaneously mapped throughout the network). Besides single NW-based FET devices or arrays of NW-based FET devices used for investigating neuronal activity, the NWs are also used to design and build NWs-based electrodes for neural recordings in the brain.

The potential to revolutionize neuroscience research and clinical therapy (Benabid, 2007; Kipke et al., 2008; Vaadia and Birbaumer, 2009; Suyatin et al., 2013) is represented even by implantable neural interfaces (Rutten, 2002; Fromherz, 2003; Cogan, 2008). However, the recorded neurons and tissue reactions that encapsulate and insulate the implant are still presenting instability results (Schouenborg, 2011). The nanostructured electrodes are considered as a promising alternative to conventional neuronal interfaces because the recording properties depend, primarily on electrode surface properties and tissue reactions to the surface (Kotov et al., 2009; Timko et al., 2010; Dvir et al., 2011; Voge and Stegemann, 2011; Suyatin et al., 2013). Nanostructured electrodes provide additional advantages such as improved electrical properties (Keefer et al., 2008; Cellot et al., 2009; Martin et al., 2010; Ansaldo et al., 2011; Duan et al., 2012), shorter cell-to-electrode distance (Tian et al., 2010; Duan et al., 2012; Xie et al., 2012), as well as a better spatial resolution. They also have a potential for less tissue damage (Almquist and Melosh, 2010; Martin et al., 2010; Tian et al., 2010; Duan et al., 2012), better biocompatibility (Hallstrom et al., 2007; Kim et al., 2007; Martin et al., 2010; Berthing et al., 2011) and new functionalities, such as selective guidance of neuronal fibers (Hallstrom et al., 2009). Importantly, recent cell signal recordings with different nanowire-based electrodes have been achieved *in vitro* (Tian

et al., 2010; Timko et al., 2010; Brueggemann et al., 2011; Dvir et al., 2011; Duan et al., 2012; Robinson et al., 2012; Xie et al., 2012), demonstrating the epitaxially grown wires of small diameter may provide minimally invasive tissue penetration (Kawano et al., 2010; Takei et al., 2010; Tian et al., 2010; Duan et al., 2012; Xie et al., 2012). Up to now, using mainly carbon nanotubes without structural feature control and in combination with rather big surfaces has been performed with *in vivo* studies using nanostructured neuronal electrodes (Keefer et al., 2008; Ansaldo et al., 2011; Suyatin et al., 2013). However, recently, it has been shown that with neuronal interfaces for improved cell survival (Hallstrom et al., 2007) and improved cell adhesion with focal adhesions forming specifically on the nanowires, the epitaxially grown gallium phosphide (GaP) NWs have beneficial properties (Prinz et al., 2008). Compared to other material NWs, GaP NWs can be synthesized with very little tapering and exceptional control over their position and geometry, and with a high aspect ratio (over 50) (Suyatin et al., 2009). Also recently, the design and fabrication of a first generation of GaP NW-based electrode with a controllable nanomorphology was reported (Suyatin et al., 2013). The first functional testing *in vivo* of a NWs-based device was performed during acute recordings in the rat cerebral cortex, where the NWs were used as a backbone for a metal nanostructured electrode with a three-dimensional (3D) structure. This electrode design opened the development of a new model system, with the prospect of enabling more reliable tissue anchoring as well as a more intimate contact between the electrode and the neurons, Xie et al. (2010) furthering research on the functionality of nanostructure-based neuronal interfaces *in vivo*, given the better electrode-cell electrical coupling (Hai et al., 2010; Robinson et al., 2012; Xie et al., 2012).

In recent years, a broad platform for electronic interfaces with cells and tissue using CNTs and NWs devices has been implemented. Compared to standard techniques used to measure, record and observe extracellular signals from individual tissues and cells, CNTs and NWs devices have orders of magnitude smaller recording area. The mV range signals of CNT/NW platforms device are significantly larger than those measured using planar devices or multiple electrode arrays, likely due to enhanced coupling between the cell membrane and nanoscale device. CNTs and NWs represent also the natural building blocks for biological-nanomaterial interfaces; the creation of hybrid nanoelectronic-neuronal devices is permitting novel directions in neuronal research and applications. The possibility of tuning their material composition and corresponding properties at the time of synthesis is opening up the design of ultra-high sensitivity devices at nanoscale for future opportunities.

Carbon nanotubes use in neuroscience

Carbon nanotubes have an arsenal of properties (electrical, mechanical, and chemical) that make them very promising materials for applications in neuroscience. The ease with which carbon nanotubes can be patterned makes them very useful for studying the organization of neural networks while the electrical conductivity of nanotubes can provide a vital mechanism to monitor or stimulate neurons. Carbon nanotubes themselves can interact with and affect neuronal function, most likely at the level of ion channels (Malarkey and Parpura, 2007, 2010). Both SWCNTs and MWCNTs have been increasingly used as "scaffolds for neuronal growth." Lately, CNTs were used in the research of neural stem cell growth and differentiation. Additionally, CNTs were applied as interface materials with neurons, where they deliver electrical stimulation to these cells and detect electrical activity. Here are just few applications of the CNTs:

Interfacing cultured neurons with carbon nanotubes. To demonstrate that the electrical simulation produced by single-wall carbon nanotubes (SWCNTs) can indeed induce neuronal signaling, Mazzatenta et al. (2007) developed an integrated SWCNTs neuronal system and demonstrated that hippocampal cells can be grown on pure SWCNTs substrates. Their experimental results point to the fact that SWCNTs can be directly used to stimulate brain circuit activity. These results may have a remarkable impact on the future developments and architectural design of microsystems for neural prosthetics (Mazzatenta et al., 2007).

Intracellular neural recording with pure carbon nanotubes probes. A novel millimeter-long electrode, remarkably simple, can be used to produce extracellular and intracellular recordings from vertebrate neurons *in vitro* and *in vivo* experiments, when it is terminated with a tip fabricated from self-entangled pure CNTs with sub-micron dimensions (Yoon et al., 2013). Assembling intracellular electrodes from CNTs using the self-entangled CNTs fabrication technology is opening a new opportunity to harness nanotechnology for neuroscience applications.

Carbon nanotubes in neuro-regeneration and repair. CNTs based technologies are emerging as particularly innovative tools for tissue repair and functional recovery after brain damage, due to their ability to interface neuronal circuits, synapses and membranes (Sakhtianchi et al., 2013). Carbon nanotube technology can now be applied to develop new devices that are capable to drive repair of nerve tissue, neuronal differentiation, growth and network reconstruction.

Analog neuromorphic modules based on carbon nanotube synapses. Shen et al. (2013) recently reported an analog neuromorphic module consisting of an integrate-and-fire circuit and *p*-type carbon nanotubes (CNTs) synapses. The CNTs synapse resembles a FET structure using as its gate an aluminum oxide dielectric layer implanted with indium ions and as its channel a random CNTs network. Electrons are attracted into the defect sites of the gate aluminum oxide layer by a positive voltage pulse applied to the gate, followed by a gradual release of the trapped electrons after the pulse is removed. Thus, the electrons induce a dynamic postsynaptic current in the CNTs channel by modifying the holes' concentration. The excitatory or inhibitory postsynaptic currents generated by the multiple input pulses via excitatory or inhibitory CNTs synapses flow toward an integrate-and-fire circuit which triggers output pulses. Further, the analysis of the dynamic transfer functions between the input and output pulses of the neuromorphic module are performed. An emulation of

biological neural networks and their functions could be implemented by scaling up such a neuromorphic module.

Nanotechnology and nanocomputing. The last decade in nanotechnology research witnessed an increasing use of artificial intelligence tools (Sacha and Varona, 2013). Current and future perspectives in the nanocomputing hardware development can boost the field of artificial-intelligence-based applications. Moreover, convergence of the two sciences, i.e., nanocomputing and nanotechnology, has the potential to shape research directions and technological developments in medical and information sciences. The great potential of combining nanotechnology and nanocomputing is also shown by hybrid technologies (i.e., nanodevice and biological entities), neuroscience, bioengineering combined with new data representations and computer architectures and a large variety of other related disciplines.

Carbon nanotubes platform for regeneration, stroke, brain tumors, and neoplasm

Carbon nanotubes present a broad regenerative spectrum from nerve tissue repair to bone tissue engineering (Newman et al., 2013).

Neuroregeneration and repair. Development of future strategies for tissue repair in order to promote functional recovery after brain damage is one of the main aims of nanotech studies (Fabbro et al., 2012). In this framework, particularly innovative tools are emerging based on CNTs technologies due to their ability to interface with neuronal circuits, synapses and membranes, as well as due to the outstanding physical properties of these nanomaterials. CNTs technology is now applied to the development of devices able to drive nerve tissue engineering, focusing in particular on growth and nerve network reconstruction, neuronal differentiation and nerve tissue repair.

Arslantunali et al. (2014) constructed a nerve conduit from poly (2-hydroxyethyl methacrylate) (pHEMA) that was loaded with MWCNTs. This pHEMA guide was more hydrophobic and more conductive than pristine pHEMA hydrogel when loaded with relatively high concentrations of MWCNTs (6%, w/w in hydrogels). The neuroblastoma cells seeded on pure pHEMA lost their viability when an electrical potential was applied, while MWCNTs carrying pHEMA maintained their viability, demonstrating that MWCNTs are conducting electricity, making them more suitable as nerve conduits. CNTs are instrumental in regeneration and reparation of irreversibly diseased or damaged nerve tissues in the peripheral and central nervous system of the human body (Stankova et al., 2014).

A class of ideal biomaterials for a wide range of regenerative medicine applications is MWCNTs polymer composites because they are hybrid materials combining numerous electrical, mechanical and chemical properties. Using a composite as a substrate to increase electronic interfacing between neurons and micro-machined electrodes (Antoniadou et al., 2011) reported the synthesis and characterization of a novel biomaterial for the development of nerve guidance channels in order to promote nerve regeneration, opening up potential applications for prosthetic devices, neural probes, and brain implants.

Stroke damage repair. Disruption of tissue architecture happens as a result of a stroke. However, in a rat stroke model, amine-modified SWCNTs protect neurons from injury. CNTs used as scaffolds in brain tissues and neural cells have shown promising results, supporting the treatment strategy based on transferring stem cells containing scaffolds to damaged regions of the brain. In rats with induced stroke, protection of neurons and enhanced recovery of behavioral functions were observed for the rats pretreated with amine-modified SWCNTs (Lee et al., 2011a). Also, the amine-modified SWCNTs protected the brains of treated rats, as indicated by the low levels of apoptotic, angiogenic and inflammation markers. In another study, it was shown that CNTs promote recovery from stroke when they are impregnated with neural progenitor cells in subventricular zones. The improvement of stem cell differentiation to heal stroke damage assisted by CNTs was first demonstrated by Moon et al. (2012).

Cancer and brain tumors therapy. It has been shown that the intratumoral delivery of low-dose of free CpG is less effective than immunostimulatory CpG oligodeoxynucleotides conjugated with (CNT-CpG) (Adeli et al., 2012). Moreover, CpG oligodeoxynucleotides conjugated with (CNT-CpG) was shown to induce antitumor immunity that protect mice from subsequent systemic or intracranial (i.c.) tumor rechallenge as well as eradicating i.c. gliomas. Also, it was shown that the treatment of metastatic brain tumors could be more efficient using the same "intracerebral immunotherapy" strategy. Thus, compared to systemic therapy generating antitumor responses that target both brain and systemic melanomas, the intracerebral CNT-CpG immunotherapy is more effective. Moreover, CNTs potentiate CpG.

A novel type of nanoprobe employs SWCNTs as a photosensitizer for application in cancer cell imaging and therapy. Ou and Wu (2013) developed a nanoprobe based on SWCNTs and a fluorescent photosensitizer pyropheophorbide (PPa) for use in cancer cell imaging and therapy *in vitro*. Phospholipids bearing polyehylene-glycol modified SWCNTs which provide an interface for the conjugation of PPa were prepared by ultrasonication. The polyehylene-glycol modified SWCNTs were then conjugated with PPa using covalent functionalization methods to construct a SWCNTs-PEG-PPa nanoprobe. The functionalization of SWCNTs was evidenced by UV-vis absorption spectra and fluorescence spectra. Imaging cancer cells with SWCNTs-PEG-PPa nanoprobe was confirmed using two cancer cell lines via laser scanning confocal microscope tests, and killing cancer cells with SWCNTs-PEG-PPa was demonstrated using cytotoxicity tests. This indicated that the resulting SWCNTs-PEG-PPa nanoprobe has great potential to be a potent candidate for cancer imaging and therapy. Also, CNTs-polymer interactions play a key role in cancer therapy (Adeli et al., 2012).

NANOMATERIALS AND BLOOD BRAIN BARRIER

Transportation mechanisms through the brain barrier

One of the major challenges for nanotechnology deals with the diagnosis and treatment of BBB-related dysfunctions involving stroke, brain tumors and cancer. Tight junction (TJ) barriers protect the CNS. These barriers are located in three main locations inside CNS: the brain endothelium, the arachnoid epithelium,

and the choroid plexus epithelium (**Figure 3**, Abbott et al., 2006). BBB consists of endothelial cells connected by close fitting junctions that separate the flowing blood from the brain extracellular fluid. Therefore, BBB controls the entrance of biomolecules into the brain and protects the brain from many common bacterial infections. However, the BBB presents a few limitations for nanomedicine approaches. For instance, due to the presence of BBB, the drug delivery to the brain area for tumor therapy or other neurodegenerative diseases such as Alzheimer's is a crucial challenge. The majority of diagnosed brain tumors are currently treated with surgery, radiation, and chemotherapy; nanoscience and technology could be a promising solution to this challenge. There are several comprehensive reviews on the interaction of BBB with nanomaterials that focus on various methods to transfer nanomaterials across BBB (Chen and Liu, 2012; Khawli and Prabhu, 2013; Krol et al., 2013).

Figure 4 (Chen and Liu, 2012) presents the main, well-recognized, transport pathways across BBB, which are commonly used for carrying solute molecules. Among all the pathways shown in **Figure 4**, the "g" route is the most suitable for drug delivery via liposomes or nanoparticles. A summary of the conventional methods used for BBB permeability assessment is given in Stam's work (Stam, 2010).

Different approaches and routes possible for transport of drugs across the BBB as summarized in **Table 1**. Biocompatible nanomaterials such as nanoparticles, liposomes, and supramolecular aggregates are promising drug carriers since their size can be tuned to fit the BBB transport. In addition, their surfaces can be functionalized to facilitate their transport through the BBB. It should be mentioned that the cytotoxicity of NPs must be precisely monitored, using various well-recognized methodologies (Mahmoudi et al., 2010, 2011a; Mao et al., 2013), to ensure their biocompatibility. The surface functional groups enhance the BBB permeability by various mechanisms such as adsorptive-mediated transcytosis and receptor-mediated transcytosis. As an example, Lactoferrin is a receptor located on cerebral endothelial cells that facilitates the transport of NPs across BBB by receptor-mediated transcytosis (Qiao et al., 2012).

In addition to the brain tumors which require drug delivery to the brain, there are some diseases which are related to dysfunctional BBB (Azhdarzadeh et al., 2013). The BBB diseases are epilepsy, Meningitis, Alzheimer's disease, multiple sclerosis (MS), brain abscess, Neuromyelitisoptica, Progressive Multifocal Leukoencephalopathy (PML), late-stage neurological trypanosomiasis (Sleeping sickness) and *De Vivo* disease (Mahmoudi et al., 2011b, 2012a; Amiri et al., 2013a). Nanomaterials show promising results for treatment of these diseases. Some of the recent nanomaterials investigations in BBB-related disease are summarized in **Table 2**.

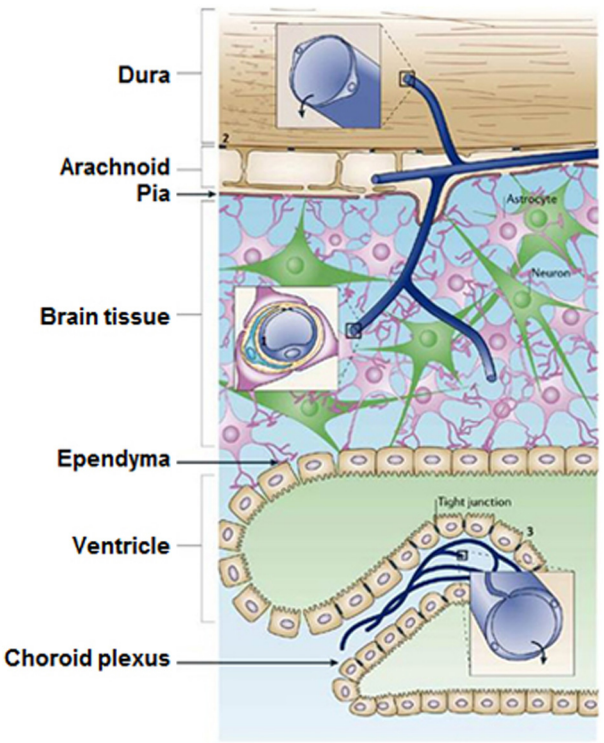

FIGURE 3 | The locations of tight junction barriers in the central nervous system. (1) brain endothelium forming the BBB, **(2)** the arachnoid epithelium forming the middle layer of the meninges, and **(3)** the choroid plexus epithelium which secretes cerebrospinal fluid. (Reprinted by permission from Macmillan Publishers Ltd: Abbott et al., 2006.)

Hidden factors

Several "ignored" factors exist at the nano-bio-interface such as the effects of protein corona, cell "vision," gradient plasma concentration, and temperature (Laurent et al., 2012; Mahmoudi et al., 2012b; Amiri et al., 2013b; Ghavami et al., 2013). In order to have high-yield NP delivery to the brain environment, these crucial hidden factors should be carefully considered. The protein corona is a tightly formed layer of proteins at the surface of nanomaterials at their entrance into the biological fluids (such as blood plasma) (Monopoli et al., 2012). Thus, the biological species (e.g., cells) interact with the corona-coated NPs, rather than the pristine surface-coated one. In this case, *in vitro* models evaluating NPs for brain-related diseases should use the corona-coated NPs to reflect the real *in vivo* situation (Mahmoudi et al., 2012c, 2013a,b, 2014). As mentioned earlier, engineering the surface of drug carriers with functional groups to enhance BBB targeting and transport is one of the main approaches to reach therapeutic agents to the brain environment (as confirmed by *in vitro* BBB models) (Ragnaill et al., 2011). However, the protein corona may cover the designed functional groups and significantly reduce the ability of NPs to cross through cell barriers (Laurent and Mahmoudi, 2011; Mirshafiee et al., 2013; Salvati et al., 2013). Thus, in order to design NPs with high BBB crossability yield, one should control the corona composition *in vivo*. As the composition and the structure of protein corona depend on the chemistry and the physics of the nanostructured materials (e.g., shape, size and distribution, crystallinity, surface composition, surface functional groups, surface roughness/smoothness, and surface charges), one can tune these characteristics to have desired proteins in the corona composition. For instance, association of apolipoprotein-E in the corona composition could enhance NPs transport across BBB (Wagner et al., 2012). Another

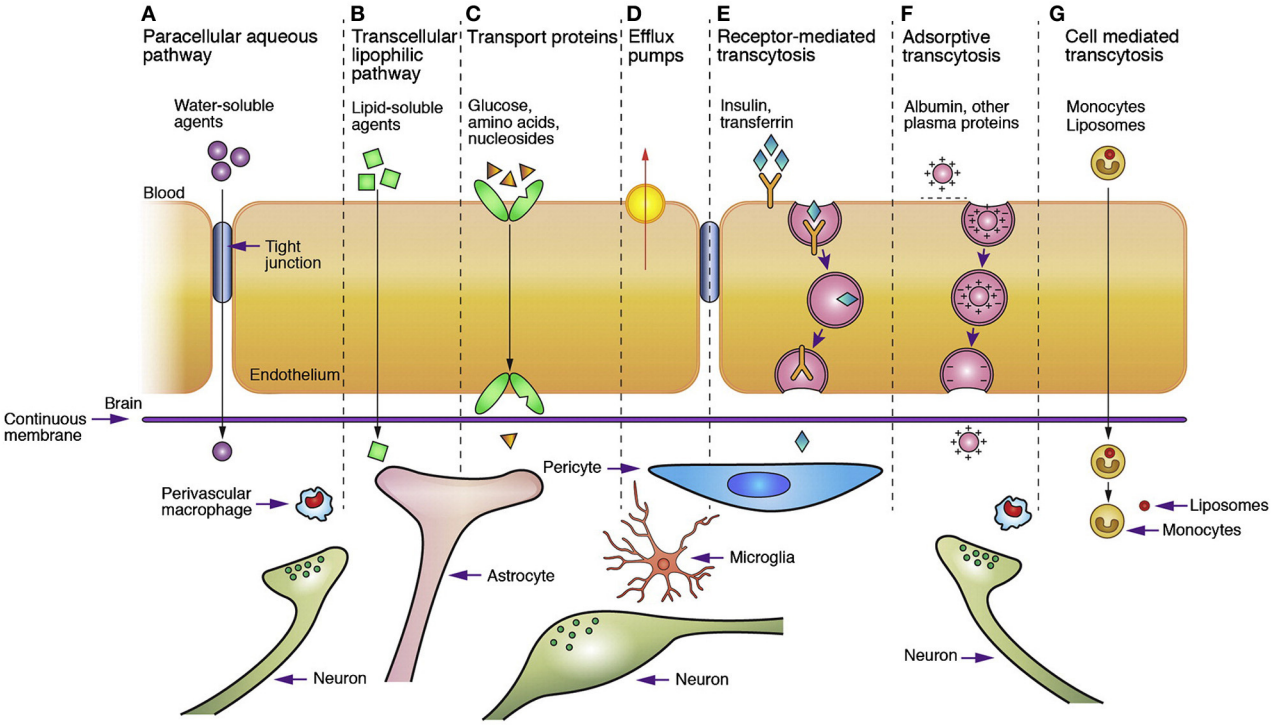

FIGURE 4 | Transport pathways across blood brain barrier. (Reprinted by permission from Macmillan Publishers Ltd: Chen and Liu, 2012.)

important but ignored matter is the effect of temperature on the protein corona. Slight temperature changes may cause considerable variation of protein corona composition at the surface of NPs (Ghavami et al., 2012; Amiri et al., 2013a; Mahmoudi et al., 2013c, 2014). The mean body temperature varies slightly for healthy individuals (mainly in the range of 35.8–37.2°C) but will vary in different parts of the body in different circumstances.

For instance, in the case of disease, the body temperature may have significant variations (e.g., it can reach to 41°C in the case of fever). Therefore, one can expect to have different corona composition at the surface of the injected NPs for different individuals, leading to the various therapeutic effects. In order to have high-yield therapeutic results, the body temperature of the individuals must be tightly monitored/controlled. Additionally, local temperature changes near the surface of NPs (e.g., by laser activation of plasmonic NPs) can change the composition of protein corona (Mahmoudi et al., 2014). Therefore, one can expect that the potential changes in the protein corona following hyperthermia or laser treatment of magnetic and plasmonic NPs may change *in vivo* toxicity or biodistribution in clinical applications.

Emerging new therapies for stroke, tumors, and cancer

By far the best therapy is to prevent damaging/degenerative effects of any kind. For example, rare earth NPs prevent retinal degeneration (Chen et al., 2006b). It is believed that in blinding diseases such as macular degeneration or retinitis pigmentosa, as well as stroke, Alzheimer's, atherosclerosis, diabetes and other disorders, these NPs could efficiently inhibit cell death. Therefore, a unique technology for multiple diseases can be created by using NPs as a novel strategy to direct therapy for various disorders. Other applications of NPs are as follows:

Improvement in cerebrovascular dysfunction following traumatic brain injury. Cerebrovascular dysfunction that is characterized by a decrease in cerebral blood flow (CBF) is a critical factor that worsens after traumatic brain injury (TBI). To improve cerebral dysfunction, a new class of antioxidants (nontoxic carbon particles) based on poly(ethylene glycol)-functionalized hydrophilic carbon clusters (PEG-HCCs) has been developed. This was demonstrated in a mild TBI/hypotension/resuscitation in rat when administered during a clinical relevant event: the resuscitation (Bitner et al., 2012). A concomitant normalization of superoxide and nitric oxide levels was also noticed. This is highly relevant for patient health improvement under clinical conditions requiring resuscitative care as well as in circumstances of stroke and organ transplantation.

Primary brain tumors: diagnosis and treatment. Since glial tumors seem to be able to create a favorable environment for the invasion of neoplastic cells into the cerebral parenchyma when they interact with the extracellular matrix via cell surface receptors, the prognosis in patients affected by primary brain tumors is still very unfavorable. The major problem for drug delivery into the brain is due to the presence of BBB as discussed above. NP systems can represent ideal devices for delivery of specific compounds to brain tumors, across the BBB.

Table 1 | Possible methods and routes for drug transport across BBB.

Method	Examples of studied drug/marker	Remarks	References
Ultrasound-assisted TJ opening	(1) Evans Blue Dye transport through BBB of white rabbits (2) fluorescent-tagged dextrans at different molecular weights in mice	(1) Transient, localized, reversible disrupt of BBB by ultrasonic (2) High-frequency focused ultrasound results in skull overheating and skull-induced beam distortion (3) low-frequency ultrasounds may produce standing waves inside the human skull, which might result in intra-cerebral hemorrhage (4) low-frequency ultrasound require longer exposure time (5) Drug can be loaded inside micro-bubbles	Choi et al., 2010; Liu et al., 2010; O'Reilly and Hynynen, 2012; Ting et al., 2012; Beccaria et al., 2013; Burgess and Hynynen, 2013
Electromagnetic field-assisted TJ opening	Markers such as Fluorescein, Albumin, Mannitol, Evans Blue, Sucrose, horseradish peroxidase	(1) Pulse wave is more effective than continuous wave in BBB permeability (2) Macromolecule permeability can be reversibly increased by high electromagnetic fields (EMF), which also increase by more than 1°C the brain temperature (3) Data on low frequency EMF (without tissue heating) is sparse and does not depend on permeability changes (4) EMF could induce overexpression of beta amyloid	Qiu et al., 2010; Stam, 2010; Jiang et al., 2013
Macrophage-assisted TJ opening	(1) HIV-1 encephalitis rodent model (2) macrophage bearing liposomal doxorubicin	(1) Monocytes/macrophages can reach the tumor sites across BBB by acting as Trojan horses carrying drug cargoes	Dou et al., 2009; Choi et al., 2012
Protein-assisted TJ opening	(1) Fluorescein isothiocyanate-dextran	(1) Twin-arginine translocation (Tat) translocase proteins TatB and TatC disrupt the BBB integrity	Gandhi et al., 2010
Peptide-assisted TJ opening	(1) Small interfering RNA for gene silencing	(1) There is a 29-amino-acid peptide that can be bound specifically to the acetylcholine receptor, i.e., neuronal cells	Kumar et al., 2007
Surfactant-assisted TJ opening	(1) Digoxin	(1) Pluronic block copolymer P85 inhibited the drug efflux from brain via P-glycoprotein efflux mechanism	Batrakova et al., 2001
Functionalized Nanocarriers	Nanomaterials as drug carriers has been reviewed in several papers. The requirements for this application are: (1) Stable in blood and long blood circulation time, (2) tunable drug release, (3) BBB-targeting mechanism		Tysseling and Kessler, 2011; Chen and Liu, 2012; Wohlfart et al., 2012
Amphiphilicsupramolecular aggregates	(1) Beta-galactosidase as a model protein	Vesicles, micelles, and liposomes are frequently used in drug delivery (1) Pluronic has also been used as nanocarrier which upon conjugation with Chitosan is effective for delivery of proteins to the brain (2) Polyethylene glycol increase the life time of liposome by preventing interaction/exchange with cell membranes as well as protection against Phagocytes	Kumari et al., 2010; Kim et al., 2013; Kreuter, 2013
Transport vectors	L-DOPA	The route for transport of nutrients to brain can be used as successful strategy. But this method is limited to peptide drugs with similar molecular structure to nutrients	Wade and Katzman, 1975
Adsorptive-mediated transcytosis (AMT)	siRNA	Cell penetrating peptide and cationic proteins use AMT to enter the brain	Adenot et al., 2007; Sharma et al., 2012; Kanazawa et al., 2013
Endogenous receptor-mediated transcytosis (RMT)	RMT has the advantage of BBB targeting. The targeting starts with endocytosis after receptor-ligand binding which is followed by exocytosis to the brain side. Different receptors employed are: (1) Insulin receptor, (2) Transferrin receptor, (3) Lipoprotein receptors, (4) Diphtheria toxin receptor		Qiao et al., 2012; Wang et al., 2013; Wiley et al., 2013
Cell-mediated transport	Cells such as macrophages and monocytes act like Trojan horse to transport the drug		Jain et al., 2003

Table 2 | Some of the recent investigations of NPs in the treatment of BBB-related diseases.

Type of NP/Disease	Physicochemical properties	Results	Remarks	References
Cationic antimicrobial peptide/meningitis	CG3R6TAT, the short amphiphilic peptide forms micelles with TAT molecules toward the external medium, having the hydrophilic peptide shell and hydrophobic cholesterol core	NPs crossed the BBB and inhibited the evolution of bacteria in the infected parts of brain, a high therapeutic index (50) against S. aureus infection in a rabbit model was noticed. NPs also showed the same efficiency in decreasing the growth rate of C. neoformans in brain compared to amphotericin B as they do not damage the kidney and liver and do not change the blood electrolyte balance	TAT peptides (YGRKKRRQRRR) help the NP to cross the BBB	Liu et al., 2009; Wang et al., 2010
Amphotericin B-polybutylcyanoacrylate NPs (AmB-PBCA-NPs)/cryptococcal meningitis	NPs with mean particle diameter of 69 nm were modified with polysorbate 80	The NPs path through BBB was perceived after 30 min. Mice treated by AmB-PBCA-NPs lived more than 4 days. Up to 80% survived to the day 10 remaining constant until day 20th		Xu et al., 2011
Anti-body conjugated iron oxide NPs/ multiple sclerosis	Iron oxide macroparticles of around 1 μm conjugated with rat antibody of vascular cell adhesion molecule-1 (VACAM-1)	Enhanced detection resolution of VACAM-1 at early stage	Early stage MRI molecular imaging of disease activity with contrast agent	McAteer et al., 2007
Melarsoprolnanosuspension/ cerebral stage of African trypanosomiasis	Sizes of 324 and 427 nm	Decreasing the concentration of melarsoprol in brain but increasing the concentration at bone marrow, the nanosuspension decreases the brain toxicity, which may not be useful for Trypanosomiasis; nevertheless, it might be helpful for Leukemia treatment	*In vitro* data also showed that nanosuspension concentration in the bone is very much higher	Ben Zirar et al., 2008
Porous cationic NP having oily core (70DGNP+)/ Trypanosomabrucei. African trypanosomiasis	NPs with zeta potential of 29 mV and an average diameter of 74 nm	*In vitro* tests proved efficacy	Loading the diminazene inside NPs after the synthesis of NPs resulted in better entrapment with a stability up to 6 months and about 80% entrapment efficiency	Kroubi et al., 2010
Lipid–diminazene conjugate NPs/Trypanosomiasis	Multiple particle sizes within the range of 285–442 nm and zeta potential around −35 mV	The adsorption pattern of plasma protein indicates a higher uptake chance of the receptors at BBB		Olbrich et al., 2004
Ag-nanotriangles on the surface of functionalized mica/Alzheimer's Disease	Ag NPs with width and length of 90 and 25 nm, respectively	Quantitative detection of amyloid-β at physiologically monomer concentration	Use of localized surface plasmon resonance for optical biosensor	Haes et al., 2005
Amine-modified single-walled carbon nanotube (a-SWCNT)/Stroke	a-SWCNT prepared from SWCNT (4–10 nm in diameter and 500–1500 nm in length)	There is a low damage of the tissue in treated rats. SWCNT can protect from ischemic injury due to the low levels of apoptotic, antigenic and inflammation markers	Carbon nanotubes as scaffold of neural cells	Lee et al., 2011b

The results described by Caruso et al. (2010) shed light on the emerging novel applications of NP systems in diagnosis and treatment of primary brain tumors, and also on the NP systems as drug delivery carriers in brain tumor diagnosis and therapy.

Applications of boron-enriched nanocomposites in cancer therapy. Nanocomposites have stirred much attention due to their applicability in cancer therapy. In particular the isotope ^{10}B, has a unique ability to absorb a slow neutron in order to initiate a nuclear reaction with release of energetic Li-particles that was not observed in the carbon analogs. The nuclear capture reaction principle has been successfully applied in radiation therapy and further used in boron neutron capture therapy (BNCT). Thus, BNCT may be applied as a promising treatment for malignant brain tumors and in other types of cancer, regardless of the limitation in neutron sources (Yinghuai and Hosmane, 2013). Recent research demonstrated that such development of "boron-based therapeutic nanomaterials" based on BNCT agents holds promise for cancer therapy.

NANOWIRE SYNTHESIS AND INTEGRATION

TEMPLATE SYNTHESIS

Through the years, novel technologies were developed to create nanostructures with a defined set of properties for a particular application. Template synthesis is one of the technologies that emerged in the quest for better nano-electronics. Nanostructure synthesis with a template offers the possibility to grow nanostructures with complex compositions (Quach et al., 2010; Vidu et al., 2012), high aspect ratios, and integrated junctions, such as nanocable structures with integrated p-n junctions (Vidu, 2000; Vidu et al., 2007). The nanosize of these structures, and the diameter in particular, impose a series of interesting properties to this material (Piraux et al., 1999). More importantly, template synthesis offers the direct integration of nanostructures into electronic devices. Once the template is created, nanostructures can be produced by either chemical (electroless deposition), electrochemical, or physical methods. After the nanostructures are synthesized, the template can be removed to expose the nanostructure arrays.

Presently, only polycarbonate track-etch membranes (PCTE) and porous alumina membranes (AAO) have been largely used for template synthesis. The track-etch method is a well-established way to produce micro and nanoporous polymeric filtration membranes (Martin, 1994, 1996; Martin and Mitchell, 1999; Apel, 2001; Vidu et al., 2007). Track-etch polymeric membranes are obtained by bombarding a polymeric sheet of a given thickness (between 6 and 20 μm) with heavy ions to generate tracks that are then etched with acids to form pores in the tracks. The resulting membrane contains transversal pores of uniform diameter that are randomly distributed (Nkosi, 2005). On the other hand, alumina membranes are prepared by electrochemical methods, i.e., by anodization of aluminum foil in acidic solution (Despic and Parkhutik, 1989). Unlike track-etch membranes, the pores in the AAO membrane are almost parallel to the surface normal. Typical membrane thickness is up to 100 μm but more limited in pore sizes compared to PCTE (Foss et al., 1992, 1994; Pang et al., 2002, 2003a,b,c; Tian et al., 2004).

Other nanoporous materials and membrane templates include mesoporous zeolites (Miller et al., 1988; Tierney and Martin, 1989; Beck et al., 1992), nanochannel array glass (Tonucci et al., 1992), polypeptide tubules (Ye et al., 2001), surface relief grating (SRG) templates (Ye et al., 2001; Yi et al., 2002a,b,c), and other nanoporous membrane (Ozin, 1992; Schollhorn, 1996). For example, SRG patterns can be used as a template for nanowire fabrication and colloid self-assembly. Titanium nanowires have been fabricated using a spin-on process on both flat substrates of epoxy-based azobenzene functionalized polymer (AFP) templates and on one-dimensional (1D) SRG patterns (Yi et al., 2002a,b,c).

Template synthesis involves the creation of nanowires or nanotubes inside a template using various deposition techniques. In the following, the electroless and electrochemical deposition will be discussed. In particular, the electrochemical deposition permits the synthesis of nanostructures with unique properties in an integrated approach that allows us to design the sensing device and to control the architecture of the array while reducing fabrication costs.

Electroless deposition

Electroless deposition can be used to create nanoelectrodes in templates that generally speaking are not conductive. Electroless deposition can be used to create nanotubes or nanowires by coating the nanopore wall or by filling up the pore with the material of interest. Nanocables with radial junctions can also be produced (e.g., Au/Te, Ku et al., 2005; Vidu et al., 2006). Slow electroless plating (no mass transfer limitations) allows for a uniform metallic film, where the metal deposition occurs uniformly at the pore walls creating hollow metallic nanotubes inside the pores (Hou et al., 1998; Bergquist et al., 2001; Bercu et al., 2004; Yuan et al., 2004a,b,c).

Electrochemical deposition

In recent years, electrochemical nanotechnology (nanoelectrochemistry) has become a key technology due to the scale up potential and low energy consumption. Typically, a decrease in the size of an electrode causes changes in the diffusion layer from linear to spherical form. For multiscale nanostructures such as nanotubes, nanofibers, and nanocables, it is important to know which characteristic length scale, nm or μm, governs the deposition process (Lebedev et al., 2005). For the μm scale, diffusion limitations can be important if the surface deposition processes are relatively fast.

Electrochemical template synthesis is mainly used to create arrays of nanoelectrodes (Wirtz et al., 2002a,b; Wirtz and Martin, 2003; Ku et al., 2004; Quach et al., 2010; Vidu et al., 2012). Both axial and longitudinal growth of nanocables with p-n junctions can be produced. **Figure 5** illustrates the process of creating nanocable structures using a combination of electroless and electrochemical deposition. There are several advantages associated with nanoelectrode arrays, which usually display a small potential drop. This behavior makes possible electrochemical measurements at low electrolyte concentrations. The small size of the nanoelectrodes array maintains a steady-state current and has a high ratio of signal to noise. This property is mainly used in sensors, where the sensitivity of the device could increase more

than 100 times. Furthermore, one of the many advantages for preparing multilayered nano-sized materials is that the electrodeposition can be performed at room temperature, which is very important for systems in which undesirable interdiffusion occurs between the adjacent layers.

Electrochemical deposition can also be used to synthesize conductive polymer nanotubes and nanowires, such as polypyrrole, polyaniline, or poly(3-methylthiophene). In this case, the pore walls are favorable sites for nucleation and growth, resulting in polymeric tubules. Various polymeric structures such as thin-walled tubules, thick-walled tubules or solid fibrils can be obtained by simply controlling the polymerization time (Brendel et al., 1997; Cepak et al., 1997; Demoustier-Champagne et al., 1998, 1999; Demoustier-Champagne and Legras, 1998; Demoustier-Champagne and Stavaux, 1999).

However, more recent developments have suggested that a more sophisticated architecture of the NCs arrangement cannot be achieved using commercial templates. More complex NCs or NWs configurations for certain applications in neuroscience can use other technologies to create particular nanostructured arrays for nanoelectrodes, such as nano-imprinting. This is particularly important in designing new nanoelectronics for applications in neuroscience.

NANO-IMPRINTING TECHNOLOGY

The ability to replicate patterns is of crucial importance to the advancement of micro- and nano-devices, and to induce the development of stem cells into the desired cell types (Mahmoudi et al., 2013b).

Recently, nanoimprint technology (NIL, **Figure 6**), has reproduced nanopatterns on large areas at a much lower cost than e-beam lithography by using mechanical embossing of a polymer at processing temperatures above glass transition temperature. Moreover, NIL technique can resolve patterns beyond light diffraction or beamscattering limitations as in other lithography techniques (**Figure 7**, Radha et al., 2012). Since it was demonstrated that NIL can achieve a sub-10 nm resolution and alignment (Chou and Krauss, 1997; Chou et al., 1997) with high fidelity on a large area pattern (Khang and Lee, 1999; Perret et al., 2004), this imprinting technique has been applied to produce microfluidics and microelectromechanical system (MEMS) devices, compact disks, field effect transistors, patterned magnetic disks, micro-optics, etc. Additionally, using NIL to create templates offers the benefit of creating templates of desired geometry for further optimization if needed.

Using NIL to create nanoelectrodes allows control of the nanostructure size (height, diameter), density, distribution and integration (Kuo et al., 2003; Torres et al., 2003; Hu et al., 2005; Konijn et al., 2005; Tormen et al., 2005; Cui and Veres, 2006; Le et al., 2006; Nakamatsu et al., 2006; Park et al., 2006; Sandison and Cooper, 2006; Zhang et al., 2006). Nanostructure fabrication is flexible in terms of choices of deposition techniques and the substrates on which the deposition takes place (insulators, semiconductors or conductors) and standard thin film fabrication techniques can be used. There is a need for new device architecture that requires less power and uses smaller surface than the multi-channel devices produced by lithographic patterning. Recently, Rehman and Kamboh (2013) reported a novel architecture to amplify the neural signal in implantable brain machine interfaces, which is able to manage both components of the neural signals, i.e., the action potentials, also known as neural spikes, and the local field potentials. Performance metrics could be improved if nanotechology is used to create novel architectures with nanosize features.

Although the template synthesis has been successfully used to create nanostructures such as nanorods and nanocable structures (see **Figure 5**), the integration of multiple junctions in a nanocable format is more challenging. Because this technology works for more simple nanostructures, the challenge is to finely tune the deposition conditions for creating multi-junction nanostructures using a diameter-controlled synthesis inside the nanopores of a custom made template. The unique properties of these metal core/multi-shell nanocable heterostructures combined with the possibility of building 3D interface between electrodes and neural tissue has great potential for applications at smaller scale than was previously possible.

An example is the nanofabrication of extracellular electrode array with high density electrical leads such as the low noise multi-channel silicone system (Du et al., 2011) presented in **Figure 8**. These results were obtained in awake, behaving, mice by using nanoarrays with a 64 channel silicone-based neural probe. In the quest to minimize the size and the noise of the system, researchers are searching to decrease the size of neural probes. NIL could be a useful tool to increase the density of recording channels and to achieve high performance recording devices at small scale.

Engineering a nanostructure-integrated neuroelectrode represents a particularly difficult challenge: characterization by conventional methods reveals the complexity of materials while in fact the devices are quite simple. Unconventional physical

FIGURE 5 | (A) Metal-nanotube membrane formed by electroless deposition of metal nanotubes inside the PCTE membrane. **(B)** Electrochemical deposition radially fills in the nanopores (the arrows show growth direction). **(C)** Nanocables obtained inside nanoporous PCTE membranes.

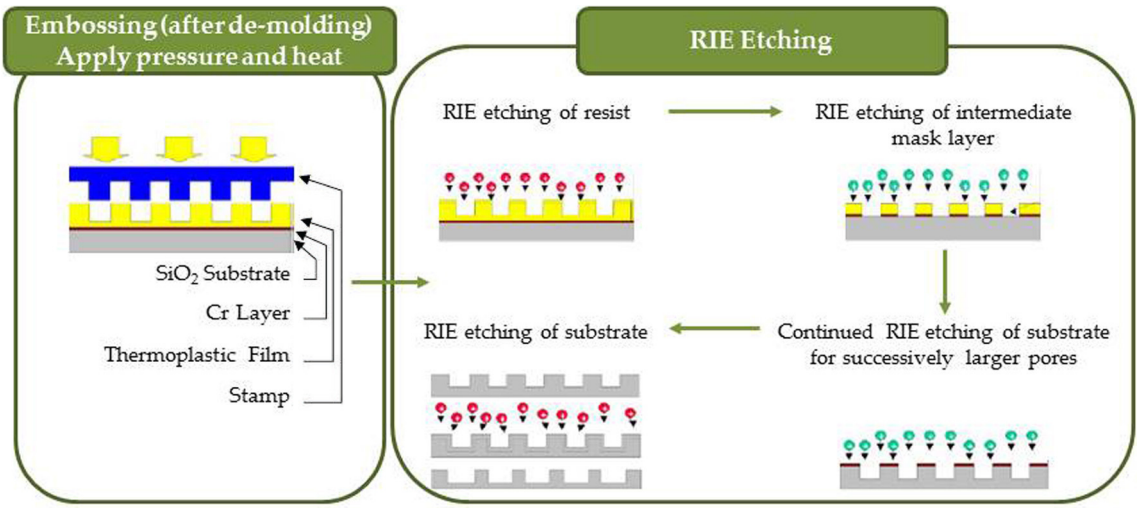

FIGURE 6 | Nanoimprinting process consisting of embossing and RIE etching into resist, intermediate mask layers and substrate.

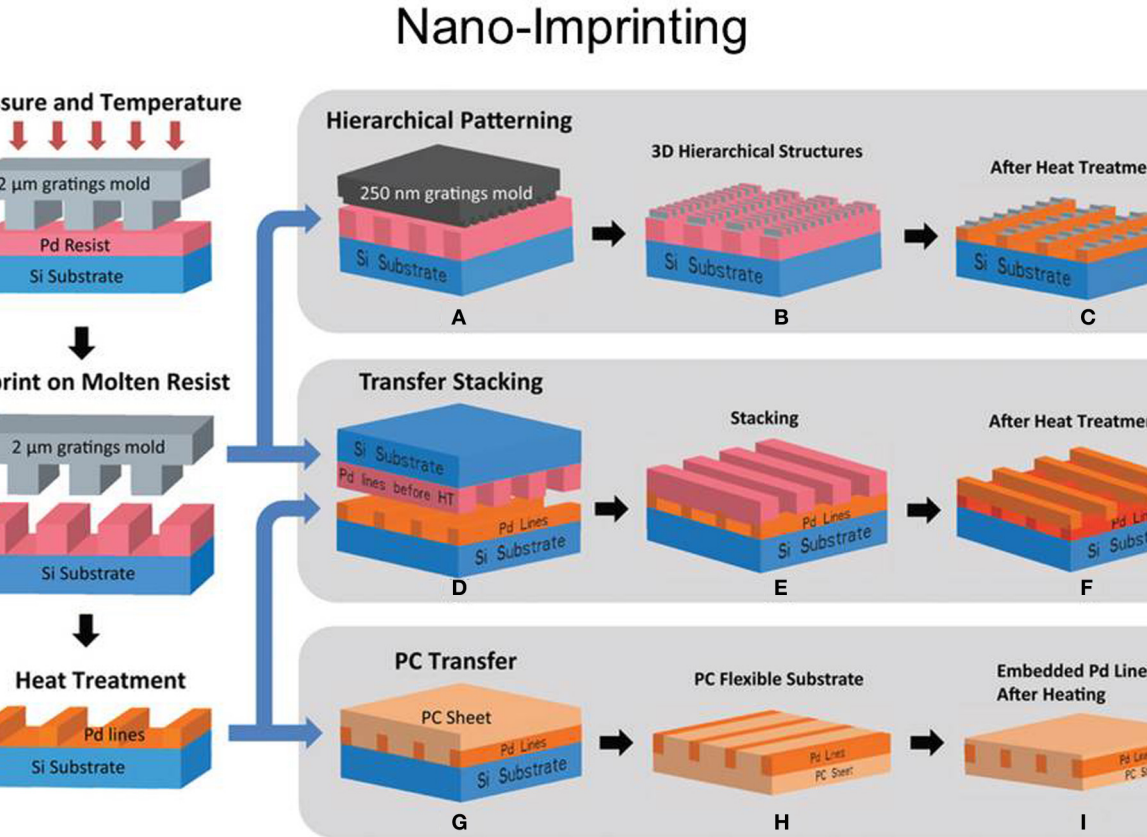

FIGURE 7 | Illustration of imprinting technique using a Si mold. A Pd benzylthiolate film was spin coated on Si substrate and imprinted at temperatures close to its melting point (120řC) by applying pressure. During this process, the pattern of the mold is imprinted (2) and cooled down. After de-molding (3), the patterns on the Si substrate were heat treated to obtain the final Pd patterns. During stage 2, there are a few other patterning possibilities: (A–C) hierarchical patterning can be obtained by using a different Si mold with smaller feature sizes on top of the imprinted Pd benzylthiolate patterns; (D–F) transfer stacking that is realized by using the Pd pattern and (3) as a substrate; (G–I) polycarbonate (PC) transfer that is obtained by using (3) as mold and PC as substrate. (Reprinted by permission from Macmillan Publishers Ltd: Radha et al., 2012).

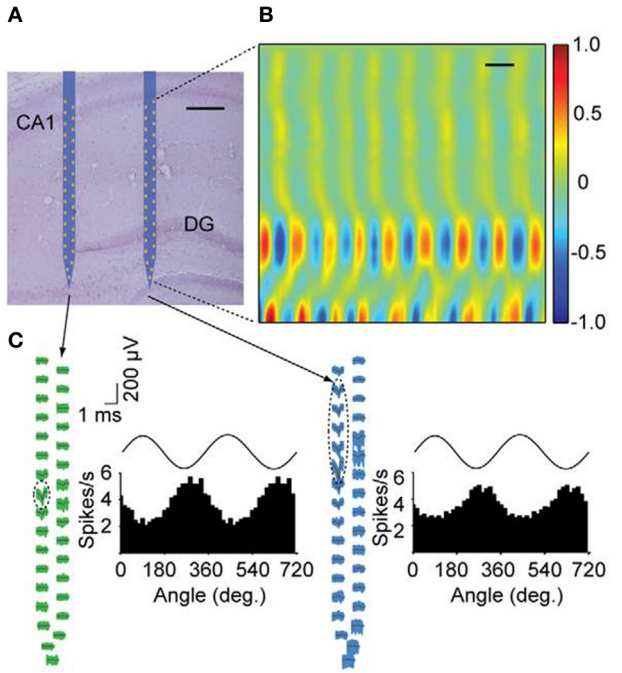

FIGURE 8 | Simultaneous recordings of neurons with nanofabricated probes in awake behaving mice. (A) Nissl-stained brain section overlaid with a schematic of the probe at its stereotaxically implanted location. Each silicon shaft is 60 mm wide. Scale bar, 200 mm. **(B)** Current source density analysis of local field potentials across the hippocampus with a vertical resolution of 28 mm. DG, dentate gyrus. Neural data was collected during home cage exploratory behavior. Current source density is normalized to ś 1. Scale bar, 100 ms. **(C)** Waveforms of two putative single cells recorded with the nano-probe across all sites together with histograms showing theta phase locking of spikes. Dashed ellipses indicate the sites exhibiting the highest extracellular action potentials for these units. Theta oscillations shown on top of the histograms are for reference. Theta oscillations were measured from the upper rightmost electrode near the CA1 pyramidal cell layer (Adapted with permission from Du et al., 2011).

properties are expected since the crystalline structure depends on the direction of growth. Device performance cannot be exclusively defined by taking the properties of each component and then applying junction theory to them. Instead, a multidisciplinary approach is required. Given the ability of nanoelectrodes to interact with physiological systems, there is a still work to be done in understanding the relationship between the nanostructure properties and the device properties made from them. Cooperative efforts of many techniques and approaches are required to gain a comprehensive understanding of this relationship. Additionally, many surface-sensitive techniques have been developed for flat and ultraflat surfaces but not for nanostructures.

NANOSTRUCTURES: A PLATFORM FOR BRAIN REPAIR AND AUGMENTATION

The tools needed to study the brain must operate at the same nanoscale as brain functions. Nanoscience together with nanotechnology bring together a "rich toolkit" of unique methods useful for realizing the complexity of brain functions by allowing concurrent recording of thousands of neurons with manipulation of the activity of millions of cells. Huge effort is now devoted to the decoding of specific neural interactions and circuits, a goal that has emerged as the Brain Activity Mapping Project (Alivisatos et al., 2013). Several examples of the synergy between nanoscience and neuroscience contributions to brain study and brain augmentation are given as follows:

MULTI-ELECTRODE ARRAY (MEA) TECHNOLOGIES FOR NEUROSCIENCE

Using "substrate-integrated" microelectrode arrays (MEAs) is the finest approach to study brain circuitry, connectivity, neurophysiology, or pathology both *in vivo* and *in vitro*. MEAs add versatility to the real-time, long-term recording of chemical fluctuations in the extra-cellular micro-environment along with neurophysiological activity while being minimally invasive (Wise, 2007; Chang-Hsiao et al., 2010; Amaral et al., 2013). The organization of neural network, its neuronal excitability, and synaptic plasticity, together with drug responses may be monitored by MEAs.

Carbon nanotubes MEAs

Carbon nanotubes (CNTs) array chips are now used for non-invasive measurement of action potentials, real-time concentration of dopamine, and postsynaptic potentials. Suzuki et al. (Suzuki et al., 2013) developed MEA chips of planar CNTs that can measure both the electrophysiological responses (such as action potentials and field postsynaptic potentials) and release of the dopamine neurotransmitter. These CNTs-MEA chips have been fabricated directly on the microelectrode surfaces by electroplating an indium-tin oxide. Chronoamperometric measurements based on such CNTs-MEA chips detected dopamine concentration at nanomolar level with high temporal resolution and a 100-fold better signal to noise ratio. MEA chips may be useful for various applications such as drug screening and toxicity, *in vitro* stem cell differentiation, synaptic plasticity, or pathogenic processes associated with stroke, epilepsy, Alzheimer's and other neurodegenerative diseases.

Multi-walled carbon nanotubes MEAs

MEAs using MWCNTs have the advantage of decreased physical size of microelectrode with increased impedance and decreased charge-transfer capability (Gacem et al., 2013). To decrease impedance, the effective surface area for recording of the electrode needs to be increased. With a steam-plasma treatment the surface of MWCNTs becomes converted from super-hydrophobic to super-hydrophilic. This hydrophilic property is attributed to the OH bonding on the surface of MWCNTs. A multi-walled MEA was employed to record neural signals from a lateral giant cell of an American crayfish. This electrode type allows the separation of neural signals with their distinct shapes for long-term recordings and improved recording performance.

Multiplexed high density MEA

Recent neural probes based on silicon (Du et al., 2011) employed nanofabricated, high-density electrical leads that can read out multichannel data. MEA uses an application-specific integrated

circuit (ASIC) to intensify signals, multiplexing functions and band-pass filtering. Multiplex high density devices with a fully integrated low noise, 64-channel system can perform high spatial resolution extracellular measurements and weighs just 330 mg (Du et al., 2011). These on-chip multiplexers allow recordings with "substantially fewer external wires than the number of input channels." The combination of ASICs and nanofabricated probes that is both "minimally invasive and highly scalable" (Du et al., 2011) was employed for carrying out large-scale, high-density electrophysiology in small animals.

Similarly, Viventi et al. (2011) integrated "ultrathin and flexible silicon nanomembrane transistors" into a MEA, enabling "dense arrays" of thousands of amplified and multiplexed sensors to be connected with fewer wires. This system was employed to record in cat the spatial properties of brain activity *in vivo*, including patterns of activity like sleep spindles, single-trial visual evoked responses or electrographic seizures. These developments might provide diagnostic and therapeutic brain-machine interface devices.

Nanowire-based electrode for acute neural recordings in the brain

A new kind of electrode is based on "structurally controlled nanowires," for neurophysiological measurements *in vivo* (Xie et al., 2010). This electrode has a sensing part made of a thin metal layer deposited on epitaxial grown GaP nanowires. Suyatin et al. (Xie et al., 2010) realized the first functional NWs-based electrode. The team also has successfully tested the electrode by *in vivo* recordings in the cortex of rat in multiple brain implantations. This kind of electrode with a controllable geometry of nanowires now can be further used for the investigation of many *in vivo* functional properties in nanostructured neuronal interfaces.

Substrate-integrated microelectrode arrays

Current methodologies permit the simultaneous, long-term non-invasive recordings of extracellular field potentials, but not the sub-threshold synaptic potentials that are generated by single cells. Because intracellular recordings of the electrophysiological properties (sub-threshold action potentials, synaptic potentials and membrane oscillations) can be acquired only by sharp (or patch) microelectrodes, these recordings may be limited to very short durations and single cells at a time. An emerging approach in a number of laboratories is based on the merging of the advantages of extracellular microelectrode arrays with those of intracellular microelectrodes (Spira and Hai, 2013).

BRAIN-MACHINE INTERFACES AND NEUROPROSTHETICS

The neural prostheses that successfully help patients increase their daily living activities are quite simple implants that yield some definite tissue response and are well recognized as foreign body (Stieglitz, 2007). Based on the latest developments in materials science, new avenues for highly advanced systems to interface the human brain have emerged. Nanotechnology is opening the door to employing macromolecular approaches to implants that mimic the "biologic topology" and take into account the surface interaction of biologic cells. Combinations of neural cells with micro-implants can become the platform of stable bio-hybrid interfaces. Furthermore, converging technologies that exploit synergies between computer sciences and engineering, neuroscience and psychology are envisioned to completely change the understanding of the entire field.

Artificial synapses in neuromorphic circuits based on nanoscale memory devices have been recently accepted as a promising route for creating novel circuit architectures that tolerate variability and/or defects (Gacem et al., 2013). Still, the implementation of the neural network type of circuits that are based on non-CMOS (complementary metal-oxide-semiconductor) memory devices with learning capabilities are rare. Gacem et al. (2013) showed that memory elements based on CNTs may be used as "artificial synapses" combined with "conventional neurons" further "trained" to perform several functions (by applying a supervised learning algorithm). This is possible because the same device ensemble can be trained many times to code successively any type of 3-input combination of Boolean logic functions despite the variability among devices. This approach has huge potential for application to parallel learning of several devices with more complex function.

Carbon nanowires used as interface material in contact with neurons can both deliver electrical stimulation to these cells and detect neuronal electrical activity. Carbon nanowires or nanotubes emerge as materials that do not have recognizable adverse effects. Consequently, they can be successfully used in brain-machine interfaces (Malarkey and Parpura, 2010). In recent years, research on growing CNT substrates has been used to examine *in vivo* formation of neurons and neuronal networks during guided growth by artificial nano-scaled cues. Additionally, prostheses for monitoring brain activity were developed using interfaces based on nanotube architecture (Stankova et al., 2014). Fabbro et al. (2012) demonstrating the alteration of various hippocampal neurons responses by the CNT substrates in cultures. This observation highlighted the exceptional ability of the CNT substrate to induce nerve tissue growth. They confirmed that CNT scaffolds promote the development of immature neurons isolated from the neonatal rat spinal cord and maintained *in vitro*. by performing electrophysiological studies associated with gene expression analysis. Results indicated that spinal neurons plated on electro-conductive CNTs show an assisted expansion. These microarray experiments suggest that CNT platforms activate healing activities involving microglia in the absence of reactive gliosis.

APPLICATION OF CARBON NANOTUBES IMAGING

Imaging applications of CNTs to living cells and tissues bring promising advantages to biological applications based on optical properties of nanotubes. Due to the high photostability of SWCNTs' photoluminescence, a longer excitation time is attainable at higher laser fluency compared to quantum dots or organic fluorophores. Also, attenuated absorption combined with autofluorescence and scattering characteristics makes visible the opaque tissue in the range of 700–1400 nm, while nanotubes allow imaging of the whole blood and thick tissue (Heller et al., 2006). This is mainly because the fluorescence profiles of many semiconducting NTs overlaps with the wavelength range. Imaging SWCNTs in tissue sections and the nanotubes concentration measured in blood was also based on nanotube fluorescence

(Cherukuri et al., 2006). In addition, CNTs can be detected due to their large resonance-enhanced Raman scattering (Heller et al., 2005).

INTER-LAMINAR MICROCIRCUITS ACROSS NEOCORTEX: REPAIR AND AUGMENTATION

Repair and brain augmentation approaches, such as brain-machine interfaces (Nicolelis et al., 2003; Lebedev and Nicolelis, 2006; Opris, 2013), neural stimulation and other neural prostheses, have experienced rapid development during the last decade (Opris and Bruce, 2005; Lebedev and Nicolelis, 2006; Opris et al., 2013). However, few of these methods target the inter-laminar micro-circuitry of the brain (Jones and Rakic, 2010; Opris et al., 2011, 2012a,b). The potential for employing inter-laminar recording and micro-stimulation of cortical microcircuits with CNT-MEAs to build neural prostheses for repair and augmentation of cognitive function is now being considered. Thus, nanotechnology is instrumental to nanofabricate planar electrode arrays (**Figure 9**) to be used in high-density neuronal voltage recording (Du et al., 2011; Suyatin et al., 2013). Micro/nano-fabrication technologies raise the prospect for increasing the numbers of electrodes for smaller, less invasive implantable devices. A promising nano-array for brain microcircuits is the new planar electrode array (Viventi et al., 2011; Alivisatos et al., 2013), which is configured on a crystalline, ceramic, or polymer support structure (**Figure 9**). Recording neural firing with 3-dimensional microelectrode arrays (Zorzos et al., 2012) represents a major advance in brain activity mapping techniques, by providing a tool to demonstrate how intra and inter-laminar/regional neural circuits cooperate together to process information. Building prosthetic minicolumns (Mountcastle, 1957, 1997; Buxhoeveden and Casanova, 2002; Mahan and Georgopoulos, 2013; Opris and Casanova, 2014) as basic modules to repair the damaged cortical tissue will become a valuable approach for cognitive neuroprosthetics. This may be accomplished by designing artificial minicolumns that can be inserted by minor surgery into the human brain, or the use of nanowire contacts to place a device with minicolumn function within the damaged circuitry (Lebedev and Nicolelis, 2006; Bokara et al., 2013; Marmarelis et al., 2014). Moreover, neural enhancement approaches may be applied to inter-laminar microcircuits across the entire cortex (Opris, 2013). In the future, such microcircuit based prostheses will provide efficient therapies for patients with neurological and psychiatric disorders (Casanova, 2007, 2013; Casanova et al., 2008; Chance et al., 2011).

ASSOCIATIVE MEMORIES WITH ENHANCED STORAGE CAPACITY

The modeling of associative memories with non-monotonic neural networks (Nishimori and Opris, 1993) was demonstrated by Monte Carlo computer simulations to yield an enhanced storage capacity. Recent experiments employing MIMO microstimulation (based on multiplexing principle) of prefrontal cortical inter-laminar microcircuits was shown to enhance cognitive performance and memory in non-human primates performing a behavioral task (Hampson et al., 2012; Opris et al., 2012a,b). Future use of multiplexed high density MEAs (Du et al., 2011) holds the promise to provide an unprecedented enhancement of memory for both artificial intelligence and humans with implanted chips.

BIOCOMPATIBILITY BETWEEN CARBON NANOTUBES AND STEM CELLS

Regenerative medicine, especially for CNS, has looked extensively into the possibility to use stem cell therapy to replace lost cells during CNS injuries (Bokara et al., 2013). However, the survival rate of the transplanted stem cells affecting tissue restoration may be limited by the toxic byproducts and the complexity of the CNS injuries. CNTs are a novel class of nanomaterials that show encouraging results in various areas of nanomedicine including therapy, diagnosis, and prevention of CNS diseases. The use of CNTs as substrates or scaffolds in the study of stem cell differentiation has recently become a dynamic research area. Both SWCNTs and MWCNTs are being used more often as scaffolds for neural stem cell differentiation and for neuronal growth. The

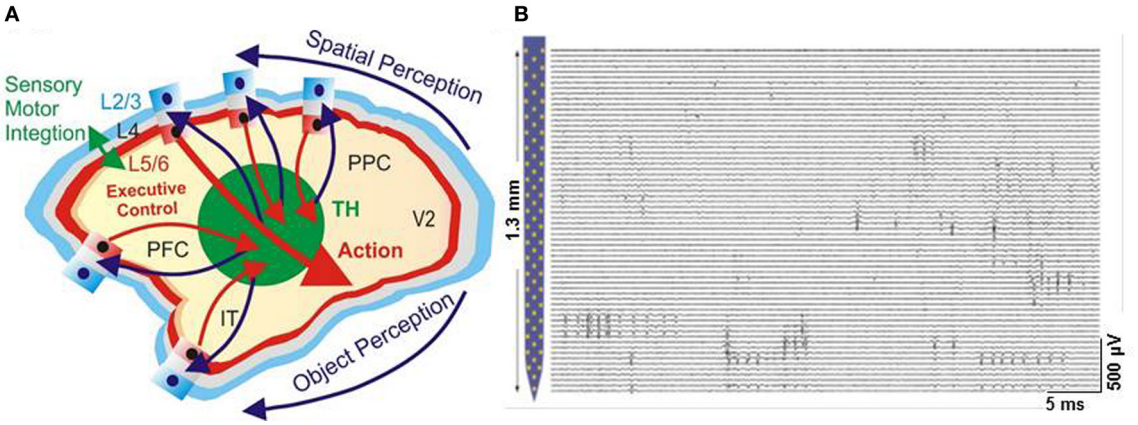

FIGURE 9 | Cortical modularity and parallel recording capabilities of the multiplexed neurophysiological system. (A) Cortical modularity showing laminar anc columnar arrangements of neurons in the primate neocortex (L2/3 is layer 2/3, L5/6, layer 5/6, V2, visual cortical area 2, PPC, posterior parietal cortex, PFC, prefrontal cortex, IT, inferotemporal cortex, TH, thalamus). **(B)** Parallel recording with nano-array in the mouse brain (Adapted with permission from Du et al., 2011).

use of CNTs-based materials was shown to affect the differentiation of progenitor and stem cells and to guide them in the direction of specific neurons. In addition, they enhanced synaptogenesis and axon regeneration, while being effective in the treatment of brain injuries. Moreover, increasing evidence supports the great potential of CNTs in neurobiological research and their use as a tolerant and biocompatible substrate/scaffold for neural cells.

NANOTECHNOLOGIES USED FOR STEM CELLS

Nanotechnologies have emerged as useful platforms for understanding, measuring, and manipulating stem cells (Ferreira et al., 2008). Examples include: (i) magnetic nanoparticles (NPs) and quantum dots for labeling stem cell and *in vivo* tracking, (ii) NPs, CNTs, and polyplexes used for the intracellular delivery of genes (i.e., oligonucleotides) and protein (i.e., peptides), (iii) nanometer-scale engineered scaffolds for stem cell differentiation and transplantation, and (iv) nanotechnological use for tracking, differentiation, and transplantation of stem cells.

CONCLUSION

Nanostructures are platforms that can be used in many ways for brain repair and augmentation. In addition, these nanostructures play a crucial role in the study of brain disorders. One exciting approach is to integrate them into arrays for developing sensors and biomarkers. Due to the unique electrical and optical properties of nanowires, nanotubes, and nanocables assembled on sensing platforms, they also hold the potential to augment brain functions. There are many challenges in creating nanowires/nanotubes/nanocables arrays-based sensors, but the goal is to make individual electrical connections between brain microcircuits and nanostructures of interest. Finally, nanostructures represent the interface between nanotechnology and neuroscience, making them promising aids in neurology for the diagnosis and treatment of brain disorders.

ACKNOWLEDGMENT

The authors would like to thank Dr. Cheryl Ann Sexton for comments on earlier versions of this manuscript.

REFERENCES

Abbott, N. J., Ronnback, L., and Hansson, E. (2006). Astrocyte-endothelial interactions at the blood-brain barrier. *Nat. Rev. Neurosci.* 7, 41–53. doi: 10.1038/nrn1824

Adeli, M., Beyranvand, S., and Hamid, M. (2012). Noncovalent interactions between linear-dendritic copolymers and carbon nanotubes lead to liposome-like nanocapsules. *J. Mater. Chem.* 22, 6947–6952. doi: 10.1039/c2jm16919c

Adenot, M., Merida, P., and Lahana, R. (2007). Applications of a blood-brain barrier technology platform to predict CNS penetration of various chemotherapeutic agents. 2. Cationic peptide vectors for brain delivery. *Chemotherapy* 53, 73–76. doi: 10.1159/000098422

Ajayan, P. M. (1999). Nanotubes from carbon. *Chem. Rev.* 99, 1787–1799. doi: 10.1021/cr970102g

Alivisatos, A. P., Andrews, A. M., Boyden, E. S., Chun, M., Church, G. M., Deisseroth, K., et al. (2013). Nanotools for neuroscience and brain activity mapping. *ACS Nano* 7, 1850–1866. doi: 10.1021/nn4012847

Almquist, B. D., and Melosh, N. A. (2010). Fusion of biomimetic stealth probes into lipid bilayer cores. *Proc. Natl. Acad. Sci. U.S.A.* 107, 5815–5820. doi: 10.1073/pnas.0909250107

Amaral, J., Pinto, V., Costa, T., Gaspar, J., Ferreira, R., Paz, E., et al. (2013). Integration of TMR sensors in silicon microneedles for magnetic measurements of neurons. *IEEE Trans. Magn.* 49, 3512–3515. doi: 10.1109/TMAG.2013.2239274

Amiri, H., Bordonali, L., Lascialfari, A., Wan, S., Monopoli, M. P., Lynch, I., et al. (2013b). Protein corona affects the relaxivity and MRI contrast efficiency of magnetic nanoparticles. *Nanoscale* 5, 8656–8665. doi: 10.1039/c3nr00345k

Amiri, H., Saeidi, K., Borhani, P., Manafirad, A., Ghavami, M., and Zerbi, V. (2013a). Alzheimer's disease: pathophysiology and applications of magnetic nanoparticles as mri theranostic agents. *ACS Chem. Neurosci.* 4, 1417–1429. doi: 10.1021/cn4001582

Ansaldo, A., Castagnola, E., Maggiolini, E., Fadiga, L., and Ricci, D. (2011). Superior electrochemical performance of carbon nanotubes directly grown on sharp microelectrodes. *ACS Nano* 5, 2206–2214. doi: 10.1021/nn103445d

Antoniadou, E. V., Ahmad, R. K., Jackman, R. B., Seifalian, A. M. (2011). Next generation brain implant coatings and nerve regeneration via novel conductive nanocomposite development. *Conf. Proc. IEEE Eng. Med. Biol. Soc.* 2011, 3253–3257. doi: 10.1109/IEMBS.2011.6090884

Apel, P. (2001). Track etching technique in membrane technology. *Radiat. Meas.* 34, 559–566. doi: 10.1016/S1350-4487(01)00228-1

Arslantunali, D., Budak, G., and Hasirci, V. (2014). Multiwalled CNT-pHEMA composite conduit for peripheral nerve repair. *J. Biomed. Mater. Res. A* 102, 828–841. doi: 10.1002/jbm.a.34727

Azhdarzadeh, M., Noroozian, M., Aghaverdi, H., Akbari, S. M., Baum, L., and Mahmoudi, M. (2013). Serum multivalent cationic pattern: speculation on the efficient approach for detection of alzheimer's disease. *Sci. Rep.* 3:2782. doi: 10.1038/srep02782

Barrelet, C. J., Wu, Y., Bell, D. C., and Lieber, C. M. (2003). Synthesis of CdS and ZnS nanowires using single-source molecular precursors. *J. Am. Chem. Soc.* 125, 11498–11499. doi: 10.1021/ja036990g

Batrakova, E. V., Miller, D. W., Li, S., Alakhov, V. Y., Kabanov, A. V., and Elmquist, W. F. (2001). Pluronic P85 enhances the delivery of digoxin to the brain: *in vitro* and *in vivo* studies. *J. Pharmacol. Exp. Ther.* 296, 551–557.

Beccaria, K., Canney, M., Goldwirt, L., Fernandez, C., Adam, C., Piquet, J., et al. (2013). Opening of the blood-brain barrier with an unfocused ultrasound device in rabbits. *J. Neurosurg.* 119, 887–898. doi: 10.3171/2013.5.JNS122374

Beck, J. S., Vartuli, J. C., Roth, W. J., Leonowicz, M. E., Kresge, C. T., Schmitt, K. D., et al. (1992). A new family of mesoporous molecular-sieves prepared with liquid-crystal templates. *J. Am. Chem. Soc.* 114, 10834–18043. doi: 10.1021/ja00053a020

Benabid, A. L. (2007). What the future holds for deep brain stimulation. *Expert. Rev. Med. Devices* 4, 895–903. doi: 10.1586/17434440.4.6.895

Ben Zirar, S., Astier, A., Muchow, M., and Gibaud, S. (2008). Comparison of nanosuspensions and hydroxypropyl-beta-cyclodextrin complex of melarsoprol: pharmacokinetics and tissue distribution in mice. *Eur. J. Pharm. Biopharm.* 70, 649–656. doi: 10.1016/j.ejpb.2008.05.012

Bercu, B., Enculescu, I., and Spohr, R. (2004). Copper tubes prepared by electroless deposition in ion track templates. *Nuclear Instrum. Methods Phys. Res. B Beam Interact. Mater. Atoms* 225, 497–502. doi: 10.1016/j.nimb.2004.06.011

Bergquist, J., Gobom, J., Blomberg, A., Roepstorff, P., and Ekman, R. (2001). Identification of nuclei associated proteins by 2D-gel electrophoresis and mass spectrometry. *J. Neurosci. Methods* 109, 3–11. doi: 10.1016/S0165-0270(01)00395-8

Berthing, T., Bonde, S., Sorensen, C. B., Utko, P., Nygard, J., and Martinez, K. L. (2011). Intact mammalian cell function on semiconductor nanowire arrays: new perspectives for cell-based biosensing. *Small* 7, 640–647. doi: 10.1002/smll.201001642

Bianco, A., Kostarelos, K., and Prato, M. (2011). Making carbon nanotubes biocompatible and biodegradable. *Chem. Commun.* 47, 10182–10188. doi: 10.1039/c1cc13011k

Binnig, G., Quate, C. F., and Gerber, C. (1986). Atomic force microscope. *Phys. Rev. Lett.* 56, 930–933. doi: 10.1103/PhysRevLett.56.930

Binnig, G., Rohrer, H., Gerber, C., and Weibel, E. (1983). 7X7 Reconstruction on SI(111) resolved in real space. *Phys. Rev. Lett.* 50, 120–123. doi: 10.1103/PhysRevLett.50.120

Binning, G., Rohrer, H., Gerber, C., and Weibel, E. (1982). Surface studies by scanning tunneling microscopy. *Phys. Rev. Lett.* 49, 57–61. doi: 10.1103/PhysRevLett.49.57

Bitner, B. R., Marcano, D. C., Berlin, J. M., Fabian, R. H., Cherian, L., Culver, J. C., et al. (2012). Antioxidant carbon particles improve cerebrovascular dysfunction following traumatic brain injury. *ACS Nano* 6, 8007–8014. doi: 10.1021/nn302615f

Bokara, K. K., Kim, J. Y., Lee, Y. I., Yun, K., Webster, T. J., and Lee, J. E. (2013). Biocompatability of carbon nanotubes with stem cells to treat CNS injuries. *Anat. Cell Biol.* 46, 85–92. doi: 10.5115/acb.2013.46.2.85

Bota, P. M., Dorobantu, D., Boerasu, I., Bojin, D., and Enachescu, M. (2014a). New laser ablation chamber for producing carbon nanomaterials using excimer laser. *Mater. Res. Innov.* (in press).

Bota, P. M., Dorobantu, D., Boerasu, I., Bojin, D., and Enachescu, M. (2014b). Synthesis of single wall carbon nanotubes by excimer laser ablation. *Surf. Eng. Appl. Electrochem.* (in press).

Brendel, R., Gier, A., Mennig, M., Schmidt, H., and Werner, J. H. (1997). Sol-gel coatings for light trapping in crystalline thin film silicon solar cells. *J. Non Cryst. Solids* 218, 391–394. doi: 10.1016/S0022-3093(97)00170-1

Brueggemann, D., Wolfrum, B., Maybeck, V., Mourzina, Y., Jansen, M., and Offenhaeusser, A. (2011). Nanostructured gold microelectrodes for extracellular recording from electrogenic cells. *Nanotechnology* 22:265104. doi: 10.1088/0957-4484/22/26/265104

Burgess, A., and Hynynen, K. (2013). Noninvasive and targeted drug delivery to the brain using focused ultrasound. *ACS Chem. Neurosci.* 4, 519–526. doi: 10.1021/cn300191b

Buxhoeveden, D. P., and Casanova, M. F. (2002). The minicolumn hypothesis in neuroscience. *Brain* 125, 935–951. doi: 10.1093/brain/awf110

Cai, D., Mataraza, J. M., Qin, Z. H., Huang, Z. P., Huang, J. Y., Chiles, T. C., et al. (2005). Highly efficient molecular delivery into mammalian cells using carbon nanotube spearing. *Nat. Methods* 2, 449–454. doi: 10.1038/nmeth761

Caruso, G., Raudino, G., Caffo, M., Alafaci, C., Granata, F., Lucerna, S., et al. (2010). Nanotechnology platforms in diagnosis and treatment of primary brain tumors. *Recent Pat. Nanotechnol.* 4, 119–124. doi: 10.2174/187221010791208786

Casanova, M. F. (2007). Schizophrenia seen as a deficit in the modulation of cortical minicolumns by monoaminergic systems. *Int. Rev. Psychiatry* 19, 361–372. doi: 10.1080/09540260701486738

Casanova, M. F. (2013). "Neural mechanisms in autism," in *Encyclopedia of Autism Spectrum Disorders* (Heidelberg: Springer), 1994–2007.

Casanova, M. F., Kreczmanski, P., and Trippe, J., Ii (2008). Neuronal distribution in the neocortex of schizophrenic patients. *Psychiatry Res.* 158, 267–277. doi: 10.1016/j.psychres.2006.12.009

Cellot, G., Cilia, E., Cipollone, S., Rancic, V., Sucapane, A., Giordani, S., et al. (2009). Carbon nanotubes might improve neuronal performance by favouring electrical shortcuts. *Nat. Nanotechnol.* 4, 126–133. doi: 10.1038/nnano.2008.374

Cepak, V. M., Hulteen, J. C., Che, G. L., Jirage, K. B., Lakshmi, B. B., Fisher, E. R., et al. (1997). Chemical strategies for template syntheses of composite micro- and nanostructures. *Chem. Mater.* 9, 1065–1067. doi: 10.1021/cm970014c

Chance, S. A., Clover, L., Cousijn, H., Currah, L., Pettingill, R., and Esiri, M. M. (2011). Microanatomical correlates of cognitive ability and decline: normal ageing, mci, and alzheimer's disease. *Cereb. Cortex* 21, 1870–1878. doi: 10.1093/cercor/bhq264

Chang-Hsiao, C., Shih-Chang, C., Yu-Tao, L., Yen-Chung, C., Shih-Rung, Y., and Da-Jeng, Y. (2010). Three-dimensional flexible microprobe for recording the neural signal. *J. Micro* 9:031007. doi: 10.1117/1.3455409

Chen, J., Patil, S., Seal, S., and McGinnis, J. F. (2006b). Rare earth nanoparticles prevent retinal degeneration induced by intracellular peroxides. *Nat. Nanotechnol.* 1, 142–150. doi: 10.1038/nnano.2006.91

Chen, Y., Barrelet, C. J., Capasso, F., and Lieber, C. M. (2006a). Single p-type/intrinsic/n-type silicon nanowires as nanoscale avalanche photodetectors. *Nano Lett.* 6, 6–6. doi: 10.1021/nl062314b

Chen, Y., and Liu, L. (2012). Modern methods for delivery of drugs across the blood-brain barrier. *Adv. Drug Deliv. Rev.* 64, 640–665. doi: 10.1016/j.addr.2011.11.010

Cherukuri, P., Gannon, C. J., Leeuw, T. K., Schmidt, H. K., Smalley, R. E., Curley, S. A., et al. (2006). Mammalian pharmacokinetics of carbon nanotubes using intrinsic near-infrared fluorescence. *Proc. Natl. Acad. Sci. U.S.A.* 103, 18882–18886. doi: 10.1073/pnas.0609265103

Choi, J., Kim, H. Y., Ju, E. J., Jung, J., Park, J., Chung, H. K., et al. (2012). Use of macrophages to deliver therapeutic and imaging contrast agents to tumors. *Biomaterials* 33, 4195–4203. doi: 10.1016/j.biomaterials.2012.02.022

Choi, J. J., Wang, S., Tung, Y. S., Morrison, B. 3rd., and Konofagou, E. E. (2010). Molecules of various pharmacologically-relevant sizes can cross the ultrasound-induced blood-brain barrier opening *in vivo*. *Ultrasound Med. Biol.* 36, 58–67. doi: 10.1016/j.ultrasmedbio.2009.08.006

Chou, S. Y., and Krauss, P. R. (1997). Imprint lithography with sub-10 nm feature size and high throughput. *Microelectron. Eng.* 35, 237–240. doi: 10.1016/S0167-9317(96)00097-4

Chou, S. Y., Krauss, P. R., Zhang, W., Guo, L., and Zhang, L. (1997). Sub-10 nm imprint lithography and applications. *J. Vac. Sci. Technol. B* 15, 2897–2904. doi: 10.1116/1.589752

Cogan, S. F. (2008). Neural stimulation and recording electrodes. *Annu. Rev. Biomed. Eng.* 10, 275–309. doi: 10.1146/annurev.bioeng.10.061807.160518

Cui, B., and Veres, T. (2006). Pattern replication of 100 nm to millimeter-scale features by thermal nanoimprint lithography. *Microelectron. Eng.* 83, 902–905. doi: 10.1016/j.mee.2006.01.013

Cui, Y., Lauhon, L. J., Gudiksen, M. S., Wang, J. F., and Lieber, C. M. (2001a). Diameter-controlled synthesis of single-crystal silicon nanowires. *Appl. Phys. Lett.* 78, 2214–2216. doi: 10.1063/1.1363692

Cui, Y., and Lieber, C. M. (2001). Functional nanoscale electronic devices assembled using silicon nanowire building blocks. *Science* 291, 851–853. doi: 10.1126/science.291.5505.851

Cui, Y., Wei, Q. Q., Park, H. K., and Lieber, C. M. (2001b). Nanowire nanosensors for highly sensitive and selective detection of biological and chemical species. *Science* 293, 1289–1292. doi: 10.1126/science.1062711

Cui, Y., Zhong, Z. H., Wang, D. L., Wang, W. U., and Lieber, C. M. (2003). High performance silicon nanowire field effect transistors. *Nano Lett.* 3, 149–152. doi: 10.1021/nl025875l

Dai, Z. R., Pan, Z. W., and Wang, Z. L. (2001). Ultra-long single crystalline nanoribbons of tin oxide. *Solid State Commun.* 118, 351–354. doi: 10.1016/S0038-1098(01)00122-3

Demoustier-Champagne, S., Duchet, J., and Legras, R. (1999). Chemical and electrochemical synthesis of polypyrrole nanotubules. *Synth. Met.* 101, 20–21. doi: 10.1016/S0379-6779(98)00813-3

Demoustier-Champagne, S., Ferain, E., Jerome, C., Jerome, R., and Legras, R. (1998). Electrochemically synthesized polypyrrole nanotubules: effects of different experimental conditions. *Eur. Polym. J.* 34, 1767–1774. doi: 10.1016/S0014-3057(98)00034-2

Demoustier-Champagne, S., and Legras, R. (1998). Electrosynthesis of polypyrrole nanotubules using particle track-etched membranes as template. *J. Chim. Phys. Phys. Chim. Biol.* 95, 1200–1203. doi: 10.1051/jcp:1998235

Demoustier-Champagne, S., and Stavaux, P. Y. (1999). Effect of electrolyte concentration and nature on the morphology and the electrical properties of electropolymerized polypyrrole nanotubules. *Chem. Mater.* 11, 829–834. doi: 10.1021/cm9807541

Despic, A., and Parkhutik, V. P. (1989). *Modern Aspects of Electrochemistry.* New York, NY: Plenum Press.

Dou, H., Grotepas, C. B., McMillan, J. M., Destache, C. J., Chaubal, M., Werling, J., et al. (2009). Macrophage delivery of nanoformulated antiretroviral drug to the brain in a murine model of neuroAIDS. *J. Immunol.* 183, 661–669. doi: 10.4049/jimmunol.0900274

Du, J., Blanche, T. J., Harrison, R. R., Lester, H. A., and Masmanidis, S. (2011). Multiplexed, high density electrophysiology with nanofabricated neural probes. *PLoS ONE* 6:e26204. doi: 10.1371/journal.pone.0026204

Duan, X., Gao, R., Xie, P., Cohen-Karni, T., Qing, Q., Choe, H. S., et al. (2012). Intracellular recordings of action potentials by an extracellular nanoscale field-effect transistor. *Nat. Nanotechnol.* 7, 174–179. doi: 10.1038/nnano.2011.223

Dujavova-Laurencikova, A., Hasenoehrl, S., Elias, P., Stoklas, R., Blaho, M., Novotny, I., et al. (2013). Ohmic contacts to p-GaP/n-ZnO core/shell nanowires based on Au metallization. *Appl. Surf. Sci.* 269, 60–64. doi: 10.1016/j.apsusc.2012.10.051

Dvir, T., Timko, B. P., Kohane, D. S., and Langer, R. (2011). Nanotechnological strategies for engineering complex tissues. *Nat. Nanotechnol.* 6, 13–22. doi: 10.1038/nnano.2010.246

Enachescu, M., Schleef, D., and Ogletree, D. F. (1999). Integration of point-contact microscopy and atomic-force microscopy: application to characterization of graphite/Pt(111). *Phys. Rev. B* 60, 16913–16919. doi: 10.1103/PhysRevB.60.16913

Endo, M., Strano, M. S., and Ajayan, P. M. (1990). *Potential Applications of Carbon Nanotubes.* Orlando, FL: American Electroplaters and Surface Finishers Society.

Fabbro, A., Bosi, S., Ballerini, L., and Prato, M. (2012). Carbon nanotubes: artificial nanomaterials to engineer single neurons and neuronal networks. *ACS Chem. Neurosci.* 3, 611–618. doi: 10.1021/cn300048q

Feng, W., and Ji, P. (2011). Enzymes immobilized on carbon nanotubes. *Biotechnol. Adv.* 29, 889–895. doi: 10.1016/j.biotechadv.2011.07.007

Ferreira, L., Squier, T., Park, H., Choe, H., Kohane, D. S., and Langer, R. (2008). Human embryoid bodies containing nano- and microparticulate delivery vehicles. *Adv. Mater.* 20, 2285– 2291. doi: 10.1002/adma.200702404

Foss, C. A. Jr., Hornyak, G. L., Stockert, J. A., and Martin, C. R. (1992). Optical properties of composite membranes containing arrays of nanoscopic gold cylinders. *J. Phys. Chem.* 96, 7497–7499. doi: 10.1021/j100198a004

Foss, C. A. Jr., Hornyak, G. L., Stockert, J. A., and Martin, C. R. (1994). Template-synthesized nanoscopic gold particles - optical-spectra and the effects of particle-size and shape. *J. Phys. Chem.* 98, 2963–2971. doi: 10.1021/j100062a037

Fromherz, P. (2003). "Semiconductor chips with ion channels, nerve cells and brain slices," in *1st International Ieee Embs Conference on Neural Engineering 2003, Conference Proceedings*, eds L. J. Wolf and J. L. Strock (Capri Island), 1–1.

Gacem, K., Retrouvey, J.-M., Chabi, D., Filoramo, A., Zhao, W., Klein, J.-O., et al. (2013). Neuromorphic function learning with carbon nanotube based synapses. *Nanotechnology* 24:384013. doi: 10.1088/0957-4484/24/38/384013

Gandhi, N., Saiyed, Z. M., Napuri, J., Samikkannu, T., Reddy, P. V., Agudelo, M., et al. (2010). Interactive role of human immunodeficiency virus type 1 (HIV-1) clade-specific Tat protein and cocaine in blood-brain barrier dysfunction: implications for HIV-1-associated neurocognitive disorder. *J. Neurovirol.* 16, 294–305. doi: 10.3109/13550284.2010.499891

Ghavami, M., Rezaei, M., Ejtehadi, R., Lotfi, M., Shokrgozar, M. A., Abd Emamy, B., et al. (2012). Physiological temperature has a crucial role in amyloid beta in the absence and presence of hydrophobic and hydrophilic nanoparticles. *ACS Chem. Neurosci.* 4, 375–378. doi: 10.1021/cn300205g

Ghavami, M., Saffar, S., Abd Emamy, B., Peirovi, A., Shokrgozar, M. A., Serpooshan, V., et al. (2013). Plasma concentration gradient influences the protein corona decoration on nanoparticles. *RSC Adv.* 3, 1119–1126. doi: 10.1039/c2ra22093h

Goncher, G., Solanki, R., Carruthers, J. R., Conley, J. Jr., and Ono, Y. (2006). p-n junctions in silicon nanowires. *J. Electron. Mater.* 35, 1509–1512. doi: 10.1007/s11664-006-0140-y

Guo, L., Wu, Z. H., Liu, T., Wang, W. D., and Zhu, H. S. (2000). Synthesis of novel Sb2O3 and Sb2O5 nanorods. *Chem. Phys. Lett.* 318, 49–52. doi: 10.1016/S0009-2614(99)01461-X

Haes, A. J., Chang, L., Klein, W. L., and Van Duyne, R. P. (2005). Detection of a biomarker for Alzheimer's disease from synthetic and clinical samples using a nanoscale optical biosensor. *J. Am. Chem. Soc.* 127, 2264–2271. doi: 10.1021/ja044087q

Hai, A., Shappir, J., and Spira, M. E. (2010). In-cell recordings by extracellular microelectrodes. *Nat. Methods* 7, U200–U250. doi: 10.1038/nmeth.1420

Hallstrom, W., Martensson, T., Prinz, C., Gustavsson, P., Montelius, L., Samuelson, L., et al. (2007). Gallium phosphide nanowires as a substrate for cultured neurons. *Nano Lett.* 7, 2960–2965. doi: 10.1021/nl070728e

Hallstrom, W., Prinz, C. N., Suyatin, D., Samuelson, L., Montelius, L., and Kanje, M. (2009). Rectifying and sorting of regenerating axons by free-standing nanowire patterns: a highway for nerve fibers. *Langmuir* 25, 4343–4346. doi: 10.1021/la900436e

Hampson, R. E., Gerhardt, G. A., Marmarelis, V., Song, D., Opris, I., Santos, L., et al. (2012). Facilitation and restoration of cognitive function in primate prefrontal cortex by a neuroprosthesis that utilizes minicolumn-specific neural firing. *J. Neural Eng.* 9:056012. doi: 10.1088/1741-2560/9/5/056012

Heller, D. A., Baik, S., Eurell, T. E., and Strano, M. S. (2005). Single-walled carbon nanotube spectroscopy in live cells: towards long-term labels and optical sensors. *Adv. Mater.* 17, 2793–2799. doi: 10.1002/adma.200500477

Heller, D. A., Jeng, E. S., Yeung, T. K., Martinez, B. M., Moll, A. E., Gastala, J. B., et al. (2006). Optical detection of DNA conformational polymorphism on single-walled carbon nanotubes. *Science* 311, 508–511. doi: 10.1126/science.1120792

Hou, Z. Z., Abbott, N. L., and Stroeve, P. (1998). Electroless gold as a substrate for self-assembled monolayers. *Langmuir* 14, 3287–3297. doi: 10.1021/la971327p

Hu, W., Yim, E. K. F., Reano, R. M., Leong, K. W., and Pang, S. W. (2005). Effects of nanoimprinted patterns in tissue-culture polystyrene on cell behavior. *J. Vac. Sci. Technol. B* 23, 2984–2989. doi: 10.1116/1.2121729

Iijima, S. (1991). Helical microtubules of graphitic carbon. *Nature* 354, 56–58. doi: 10.1038/354056a0

Jain, S., Mishra, V., Singh, P., Dubey, P. K., Saraf, D. K., and Vyas, S. P. (2003). RGD-anchored magnetic liposomes for monocytes/neutrophils-mediated brain targeting. *Int. J. Pharm.* 261, 43–55. doi: 10.1016/S0378-5173(03)00269-2

Javey, A., Guo, J., Wang, Q., Lundstrom, M., and Dai, H. J. (2003). Ballistic carbon nanotube field-effect transistors. *Nature* 424, 654–657. doi: 10.1038/nature01797

Jiang, D. P., Li, J., Zhang, J., Xu, S. L., Kuang, F., Lang, H. Y., et al. (2013). Electromagnetic pulse exposure induces overexpression of beta amyloid protein in rats. *Arch. Med. Res.* 44, 178–184. doi: 10.1016/j.arcmed.2013.03.005

Jiang, X., Xiong, Q., Nam, S., Qian, F., Li, Y., and Lieber, C. M. (2007). InAs/InP radial nanowire heterostructures as high electron mobility devices. *Nano Lett.* 7, 3214–3218. doi: 10.1021/nl072024a

Jiang, X. C., Herricks, T., and Xia, Y. N. (2002). CuO nanowires can be synthesized by heating copper substrates in air. *Nano Lett.* 2, 1333–1338. doi: 10.1021/nl0257519

Jones, E. G., and Rakic, P. (2010). Radial columns in cortical architecture: it is the composition that counts. *Cereb. Cortex* 20, 2261–2264. doi: 10.1093/cercor/bhq127

Kam, N. W. S., and Dai, H. J. (2005). Carbon nanotubes as intracellular protein transporters: generality and biological functionality. *J. Am. Chem. Soc.* 127, 6021–6026. doi: 10.1021/ja050062v

Kam, N. W. S., Jessop, T. C., Wender, P. A., and Dai, H. J. (2004). Nanotube molecular transporters: internalization of carbon nanotube-protein conjugates into mammalian cells. *J. Am. Chem. Soc.* 126, 6850–6851. doi: 10.1021/ja0486059

Kam, N. W. S., Liu, Z., and Dai, H. J. (2005a). Functionalization of carbon nanotubes via cleavable disulfide bonds for efficient intracellular delivery of siRNA and potent gene silencing. *J. Am. Chem. Soc.* 127, 12492–12493. doi: 10.1021/ja053962k

Kam, N. W. S., O'Connell, M., Wisdom, J. A., and Dai, H. J. (2005b). Carbon nanotubes as multifunctional biological transporters and near-infrared agents for selective cancer cell destruction. *Proc. Natl. Acad. Sci. U.S.A.* 102, 11600–11605. doi: 10.1073/pnas.0502680102

Kanazawa, T., Akiyama, F., Kakizaki, S., Takashima, Y., and Seta, Y. (2013). Delivery of siRNA to the brain using a combination of nose-to-brain delivery and cell-penetrating peptide-modified nano-micelles. *Biomaterials* 34, 9220–9226. doi: 10.1016/j.biomaterials.2013.08.036

Kawano, T., Harimoto, T., Ishihara, A., Takei, K., Kawashima, T., Usui, S., et al. (2010). Electrical interfacing between neurons and electronics via vertically integrated sub-4 mu m-diameter silicon probe arrays fabricated by vapor-liquid-solid growth. *Biosens. Bioelectron.* 25, 1809–1815. doi: 10.1016/j.bios.2009.12.037

Keefer, E. W., Botterman, B. R., Romero, M. I., Rossi, A. F., and Gross, G. W. (2008). Carbon nanotube coating improves neuronal recordings. *Nat. Nanotechnol.* 3, 434–439. doi: 10.1038/nnano.2008.174

Khang, D.-Y., and Lee, H. H. (1999). Wafer-scale sub-micron lithography. *Appl. Phys. Lett.* 75, 2599. doi: 10.1063/1.125090

Khawli, L. A., and Prabhu, S. (2013). Drug delivery across the blood-brain barrier. *Mol. Pharm.* 10, 1471–1472. doi: 10.1021/mp400170b

Kim, J. Y., Choi, W. I., Kim, Y. H., and Tae, G. (2013). Brain-targeted delivery of protein using chitosan- and RVG peptide-conjugated, pluronic-based nano-carrier. *Biomaterials* 34, 1170–1178. doi: 10.1016/j.biomaterials.2012.09.047

Kim, W., Ng, J. K., Kunitake, M. E., Conklin, B. R., and Yang, P. (2007). Interfacing silicon nanowires with mammalian cells. *J. Am. Chem. Soc.* 129, 7228–7229. doi: 10.1021/ja071456k

Kipke, D. R., Shain, W., Buzsaki, G., Fetz, E., Henderson, J. M., Hetke, J. F., et al. (2008). Advanced neurotechnologies for chronic neural interfaces: new horizons and clinical opportunities. *J. Neurosci.* 28, 11830–11838. doi: 10.1523/JNEUROSCI.3879-08.2008

Klumpp, C., Kostarelos, K., Prato, M., and Bianco, A. (2006). Functionalized carbon nanotubes as emerging nanovectors for the delivery of therapeutics. *Biochim. Biophys. Acta* 1758, 404–412. doi: 10.1016/j.bbamem.2005.10.008

Konijn, M., Alkaisi, M. M., and Blaikie, R. J. (2005). Nanoimprint lithography of sub-100 nm 3D structures. *Microelectron. Eng.* 78–79, 653–658. doi: 10.1016/j.mee.2004.12.081

Kotov, N. A., Winter, J. O., Clements, I. P., Jan, E., Timko, B. P., Campidelli, S., et al. (2009). Nanomaterials for neural interfaces. *Adv. Mater.* 21, 3970–4004. doi: 10.1002/adma.200801984

Kreuter, J. (2013). Mechanism of polymeric nanoparticle-based drug transport across the blood-brain barrier (BBB). *J. Microencapsul.* 30, 49–54. doi: 10.3109/02652048.2012.692491

Krol, S., Macrez, R., Docagne, F., Defer, G., Laurent, S., Rahman, M., et al. (2013). Therapeutic benefits from nanoparticles: the potential significance of nanoscience in diseases with compromise to the blood brain barrier. *Chem. Rev.* 113, 1877–1903. doi: 10.1021/cr200472g

Kroubi, M., Daulouede, S., Karembe, H., Jallouli, Y., Howsam, M., Mossalayi, D., et al. (2010). Development of a nanoparticulate formulation of diminazene to treat African trypanosomiasis. *Nanotechnology* 21:505102. doi: 10.1088/0957-4484/21/50/505102

Ku, J. R., Vidu, R., and Stroeve, P. (2005). Mechanism of film growth of tellurium by electrochemical deposition in the presence and absence of cadmium ions. *J. Phys. Chem. B* 109, 21779–21787. doi: 10.1021/jp053833q

Ku, J. R., Vidu, R., Talroze, R., and Stroeve, P. (2004). Fabrication of nanocables by electrochemical deposition inside metal nanotubes. *J. Am. Chem. Soc.* 126, 15022–15023. doi: 10.1021/ja0450657

Kumar, P., Wu, H., McBride, J. L., Jung, K. E., Kim, M. H., Davidson, B. L., et al. (2007). Transvascular delivery of small interfering RNA to the central nervous system. *Nature* 448, 39–43. doi: 10.1038/nature05901

Kumari, A., Yadav, S. K., and Yadav, S. C. (2010). Biodegradable polymeric nanoparticles based drug delivery systems. *Colloids Surf. B Biointerfaces* 75, 1–18. doi: 10.1016/j.colsurfb.2009.09.001

Kuo, C. W., Shiu, J. Y., Cho, Y. H., and Chen, P. (2003). Fabrication of large-area periodic nanopillar arrays for nanoimprint lithography using polymer colloid masks. *Adv. Mater.* 15, 1065–1068. doi: 10.1002/adma.200304824

Laurent, S., Burtea, C., Thirifays, C., Haefeli, U. O., and Mahmoudi, M. (2012). Crucial ignored parameters on nanotoxicology: the importance of toxicity assay modifications and "Cell Vision." *PLoS ONE* 7:e29997. doi: 10.1371/journal.pone.0029997

Laurent, S., and Mahmoudi, M. (2011). Superparamagnetic iron oxide nanoparticles: promises for diagnosis and treatment of cancer. *Int. J. Mol. Epidemiol. Genet.* 2, 367–390.

Le, N. V., Dauksher, W. J., Gehoski, K. A., Nordquist, K. J., Ainley, E., and Mangat, P. (2006). Direct pattern transfer for sub-45 nm features using nanoimprint lithography. *Microelectron. Eng.* 83, 839–842. doi: 10.1016/j.mee.2006.01.254

Lebedev, K., Mafe, S., and Stroeve, P. (2005). Modeling electrochemical deposition inside nanotubes to obtain metal-semiconductor multiscale nanocables or conical nanopores. *J. Phys. Chem. B* 109, 14523–14528. doi: 10.1021/jp051133f

Lebedev, M. A., and Nicolelis, M. A. L. (2006). Brain-machine interfaces: past, present and future. *Trends Neurosci.* 29, 536–546. doi: 10.1016/j.tins.2006.07.004

Lee, G.-J., Choi, S. K., Choi, S., Park, J. H., and Park, H.-K. (2011a). "Enzyme-immobilized CNT network probe for *in vivo* neurotransmitter detection," in *Nanoscale Biocatalysis: Methods and Protocols*, ed P. Wang (Springer), 65–75.

Lee, H. J., Park, J., Yoon, O. J., Kim, H. W., Lee Do, Y., Kim Do, H., et al. (2011b). Amine-modified single-walled carbon nanotubes protect neurons from injury in a rat stroke model. *Nat. Nanotechnol.* 6, 121–125. doi: 10.1038/nnano.2010.281

Lee, S. Y., Kim, T. H., Suh, D. I., Park, J. E., Kim, J. H., Youn, C. J., et al. (2007). An electrical characterization of a hetero-junction nanowire (NW) PN diode (n-GaN NW/p-Si) formed by dielectrophoresis alignment. *Phys. E-Low Dimens. Syst. Nanostruct.* 36, 194–198. doi: 10.1016/j.physe.2006.10.019

Li, C., Zhang, D. H., Han, S., Liu, X. L., Tang, T., and Zhou, C. W. (2003). Diameter-controlled growth of single-crystalline In2O3 nanowires and their electronic properties. *Adv. Mat.* 15, 143. doi: 10.1002/adma.200390029

Li, Y., Qian, F., Xiang, J., and Lieber, C. M. (2006). Nanowire electronic and optoelectronic devices. *Mater. Today* 9, 18–27. doi: 10.1016/S1369-7021(06)71650-9

Lieber, C. M. (2003). Nanoscale science and technology: building a big future from small things. *MRS Bull.* 28, 486–491. doi: 10.1557/mrs2003.144

Liu, H. L., Pan, C. H., Ting, C. Y., and Hsiao, M. J. (2010). Opening of the blood-brain barrier by low-frequency (28-kHz) ultrasound: a novel pinhole-assisted mechanical scanning device. *Ultrasound Med. Biol.* 36, 325–335. doi: 10.1016/j.ultrasmedbio.2009.10.004

Liu, L., Xu, K., Wang, H., Tan, P. K. J., Fan, W., Venkatraman, S. S., et al. (2009). Self-assembled cationic peptide nanoparticles as an efficient antimicrobial agent. *Nat. Nanotechnol.* 4, 457–463. doi: 10.1038/nnano.2009.153

Liu, Z. Q., Xie, S. S., Sun, L. F., Tang, D. S., Zhou, W. Y., Wang, C. Y., et al. (2001). Synthesis of alpha-SiO2 nanowires using Au nanoparticle catalysts on a silicon substrate. *J. Mater. Res.* 16, 683–686. doi: 10.1557/JMR.2001.0102

Lopez, C. F., Nielsen, S. O., Moore, P. B., and Klein, M. L. (2004). Understanding nature's design for a nanosyringe. *Proc. Natl. Acad. Sci. U.S.A.* 101, 4431–4434. doi: 10.1073/pnas.0400352101

Lu, Q., Moore, J. M., Huang, G., Mount, A. S., Rao, A. M., Larcom, L. L., et al. (2004). RNA polymer translocation with single-walled carbon nanotubes. *Nano Lett.* 4, 2473–2477. doi: 10.1021/nl048326j

Mahan, M. Y., and Georgopoulos, A. P. (2013). Motor directional tuning across brain areas: directional resonance and the role of inhibition for directional accuracy. *Front. Neural. Circuits* 7:92. doi: 10.3389/fncir.2013.00092

Mahmoudi, M., Abdelmonem, A. M., Behzadi, S., Clement, J. H., Dutz, S., Ejtehadi, M. R., et al. (2013c). Temperature: the "Ignored" factor at the nanobio interface. *ACS Nano* 7, 6555–6562. doi: 10.1021/nn305337c

Mahmoudi, M., Akhavan, O., Ghavami, M., Rezaee, F., and Ghiasi, S. M. A. (2012c). Graphene oxide strongly inhibits amyloid beta fibrillation. *Nanoscale* 4, 7322–7325. doi: 10.1039/c2nr31657a

Mahmoudi, M., Bonakdar, S., Shokrgozar, M. A., Aghaverdi, H., Hartmann, R., Pick, A., et al. (2013b). Cell-imprinted substrates direct the fate of stem cells. *ACS Nano* 7, 8379–8384. doi: 10.1021/nn403844q

Mahmoudi, M., Hofmann, H., Rothen-Rutishauser, B., and Petri-Fink, A. (2011a). Assessing the *in vitro* and *in vivo* toxicity of superparamagnetic iron oxide nanoparticles. *Chem. Rev.* 112, 2323–2338. doi: 10.1021/cr2002596

Mahmoudi, M., Lohse, S. E., Murphy, C. J., Fathizadeh, A., Montazeri, A., and Suslick, K. S. (2014). Variation of protein corona composition of gold nanoparticles following plasmonic heating. *Nano Lett.* 14, 6–12. doi: 10.1021/nl403419e

Mahmoudi, M., Monopoli, M. P., Rezaei, M., Lynch, I., Bertoli, F., McManus, J. J., et al. (2013a). The protein corona mediates the impact of nanomaterials and slows amyloid beta fibrillation. *Chembiochem* 14, 568–572. doi: 10.1002/cbic.201300007

Mahmoudi, M., Quinlan-Pluck, F., Monopoli, M. P., Sheibani, S., Vali, H., Dawson, K. A., et al. (2012a). Influence of the physiochemical properties of superparamagnetic iron oxide nanoparticles on amyloid β protein fibrillation in solution. *ACS Chem. Neurosci.* 4, 475–485. doi: 10.1021/cn300196n

Mahmoudi, M., Saeedi-Eslami, S. N., Shokrgozar, M. A., Azadmanesh, K., Hassanlou, M., Kalhor, H. R., et al. (2012b). Cell "vision:" complementary factor of protein corona in nanotoxicology. *Nanoscale* 4, 5461–5468. doi: 10.1039/c2nr31185b

Mahmoudi, M., Sahraian, M. A., Shokrgozar, M. A., and Laurent, S. (2011b). Superparamagnetic iron oxide nanoparticles: promises for diagnosis and treatment of multiple sclerosis. *ACS Chem. Neurosci.* 2, 118–140. doi: 10.1021/cn100100e

Mahmoudi, M., Simchi, A., Imani, M., Shokrgozar, M. A., Milani, A. S., Häfeli, U. O., et al. (2010). A new approach for the *in vitro* identification of the cytotoxicity of superparamagnetic iron oxide nanoparticles. *Colloids Surf. B Biointerfaces* 75, 300–309. doi: 10.1016/j.colsurfb.2009.08.044

Malarkey, E. B., and Parpura, V. (2007). Applications of carbon nanotubes in neurobiology. *Neurodegener. Dis.* 4, 292–299. doi: 10.1159/000101885

Malarkey, E. B., and Parpura, V. (2010). "Carbon nanotubes in neuroscience," in *Brain Edema XIV*, eds Z. Czernicki, A. Baethmann, U. Ito, Y. Katayama, T. Kuroiwa, and D. Mendelow (Springer), 337–341.

Mao, H. Y., Laurent, S., Chen, W., Akhavan, O., Imani, M., Ashkarran, A. A., et al. (2013). Graphene: promises, facts, opportunities, and challenges in nanomedicine. *Chem. Rev.* 113, 3407–3424. doi: 10.1021/cr300335p

Marmarelis, V. Z., Shin, D. C., Song, D., Hampson, R. E., Deadwyler, S. A., and Berger, T. W. (2014). On parsing the neural code in the prefrontal cortex of primates using principal dynamic modes. *J. Comput. Neurosci.* 36, 321–337. doi: 10.1007/s10827-013-0475-3

Martin, C. R. (1994). Nanomaterials: a membrane-based synthetic approach. *Science* 266, 1961–1966. doi: 10.1126/science.266.5193.1961

Martin, C. R. (1996). Membrane-based synthesis of nanomaterials. *Chem. Mater.* 8, 1739–1746. doi: 10.1021/cm960166s

Martin, C. R., and Mitchell, D. T. (1999). Template-synthesized nanomaterials in electrochemistry. *Electroanal. Chem.* 21, 1–74. doi: 10.1201/9780203909492.ch1

Martin, D. C., Wu, J., Shaw, C. M., King, Z., Spanninga, S. A., Richardson-Burns, S., et al. (2010). The morphology of poly(3,4-Ethylenedioxythiophene). *Polymer Rev.* 50, 340–384. doi: 10.1080/15583724.2010.495440

Mazzatenta, A., Giugliano, M., Campidelli, S., Gambazzi, L., Businaro, L., Markram, H., et al. (2007). Interfacing neurons with carbon nanotubes: electrical signal transfer and synaptic stimulation in cultured brain circuits. *J. Neurosci.* 27, 6931–6936. doi: 10.1523/JNEUROSCI.1051-07.2007

McAteer, M. A., Sibson, N. R., Von Zur Muhlen, C., Schneider, J. E., Lowe, A. S., Warrick, N., et al. (2007). *In vivo* magnetic resonance imaging of acute brain inflammation using microparticles of iron oxide. *Nat. Med.* 13, 1253–1258. doi: 10.1038/nm1631

McEuen, P. L., Fuhrer, M. S., and Park, H. K. (2002). Single-walled carbon nanotube electronics. *IEEE Trans. Nanotechnol.* 1, 78–85. doi: 10.1109/TNANO.2002.1005429

Miao, Z., Xu, D. S., Ouyang, J. H., Guo, G. L., Zhao, X. S., and Tang, Y. Q. (2002). Electrochemically induced sol-gel preparation of single-crystalline TiO2 nanowires. *Nano Lett.* 2, 717–720. doi: 10.1021/nl025541w

Miller, C. J., Widrig, C. A., Charych, D. H., and Majda, M. (1988). Microporous aluminum oxide films at electrodes. 4. Lateral charge transport in self-organized bilayer assemblies. *J. Phys. Chem.* 92, 1928–1936. doi: 10.1021/j100318a044

Mirshafiee, V., Mahmoudi, M., Lou, K., Cheng, J., and Kraft, M. L. (2013). Protein corona significantly reduces active targeting yield. *Chem. Commun.* 49, 2557–2559. doi: 10.1039/c3cc37307j

Monopoli, M. P., Åberg, C., Salvati, A., and Dawson, K. A. (2012). Biomolecular coronas provide the biological identity of nanosized materials. *Nat. Nanotechnol.* 7, 779–786. doi: 10.1038/nnano.2012.207

Moon, H. K., Lee, S. H., and Choi, H. C. (2009). *In vivo* near-infrared mediated tumor destruction by photothermal effect of carbon nanotubes. *ACS Nano* 3, 3707–3713. doi: 10.1021/nn900904h

Moon, S. U., Kim, J., Bokara, K. K., Kim, J. Y., Khang, D., Webster, T. J., et al. (2012). Carbon nanotubes impregnated with subventricular zone neural progenitor cells promotes recovery from stroke. *Int. J. Nanomedicine* 7, 2751–2765. doi: 10.2147/IJN.S30273

Mountcastle, V. B. (1957). Modality and topographic properties of single neurons of cats somatic sensory cortex. *J. Neurophysiol.* 20, 408–434.

Mountcastle, V. B. (1997). The columnar organization of the neocortex. *Brain* 120, 701–722. doi: 10.1093/brain/120.4.701

Nakamatsu, K., Tone, K., and Matsui, S. (2006). Room-temperature nanoimprint lithography using photosensitive dry film. *Jpn. J. Appl. Phys.* 45, 4290–4292. doi: 10.1143/JJAP.45.4290

Newman, P., Minett, A., Ellis-Behnke, R., and Zreiqat, H. (2013). Carbon nanotubes: their potential and pitfalls for bone tissue regeneration and engineering. *Nanomedicine* 9, 1139–1158. doi: 10.1016/j.nano.2013.06.001

Nicolelis, M. A., Dimitrov, D., Carmena, J. M., Crist, R., Lehew, G., and Kralik, J. D. (2003). Chronic, multisite, multi-electrode recordings in macaque monkeys. *Proc. Natl. Acad. Sci. U.S.A.* 100, 11041–11046. doi: 10.1073/pnas.1934665100

Nishimori, H., and Opris, I. (1993). Retrieval process of an associative memory with a general input-output function. *Neural Netw.* 6, 1061–1067. doi: 10.1016/S0893-6080(09)80017-8

Nkosi, M. M. (2005). *Preparation of Physico-Chemical Properties of Nickel Nanostructured Materials Deposited in Etched Ion-Track Membrane*. Ph.D. thesis, Cape Town, 162.

Olbrich, C., Gessner, A., Schroder, W., Kayser, O., and Muller, R. H. (2004). Lipid-drug conjugate nanoparticles of the hydrophilic drug diminazene-cytotoxicity testing and mouse serum adsorption. *J. Control. Release* 96, 425–435. doi: 10.1016/j.jconrel.2004.02.024

Opris, I. (2013). Inter-laminar microcircuits across the neocortex: repair and augmentation. *Front. Syst. Neurosci.* 7:80. doi: 10.3389/fnsys.2013.00080

Opris, I., and Bruce, C. J. (2005). Neural circuitry of judgment and decision mechanisms. *Brain Res. Rev.* 48, 509–526. doi: 10.1016/j.brainresrev.2004.11.001

Opris, I., and Casanova, M. F. (2014). Prefrontal cortical minicolumn: from executive control to disrupted cognitive processing. *Brain*. doi: 10.1093/brain/awt359. [Epub ahead of print].

Opris, I., Fuqua, J. L., Huettl, P. F., Gerhardt, G. A., Berger, T. W., Hampson, R. E., et al. (2012a). Closing the loop in primate prefrontal cortex: inter-laminar processing. *Front. Neural Circ.* 6:88. doi: 10.3389/fncir.2012.00088

Opris, I., Hampson, R. E., Gerhardt, G. A., Berger, T. W., and Deadwyler, S. A. (2012b). Columnar processing in primate pFC: evidence for executive control microcircuits. *J. Cogn. Neurosci.* 24, 2334–2347. doi: 10.1162/jocn_a_00307

Opris, I., Hampson, R. E., Stanford, T. R., Gerhardt, G. A., and Deadwyler, S. A. (2011). Neural activity in frontal cortical cell layers: evidence for columnar sensorimotor processing. *J. Cogn. Neurosci.* 23, 1507–1521. doi: 10.1162/jocn.2010.21534

Opris, I., Santos, L., Gerhardt, G. A., Song, D., Berger, T. W., Hampson, R. E., et al. (2013). Prefrontal cortical microcircuits bind perception to executive control. *Sci. Rep.* 3:2285. doi: 10.1038/srep02285

O'Reilly, M. A., and Hynynen, K. (2012). Ultrasound enhanced drug delivery to the brain and central nervous system. *Int. J. Hyperthermia* 28, 386–396. doi: 10.3109/02656736.2012.666709

Ou, Z., and Wu, B. (2013). A novel nanoprobe based on single-walled carbon nanotubes/photosensitizer for cancer cell imaging and therapy. *J. Nanosci. Nanotechnol.* 13, 1212–1216. doi: 10.1166/jnn.2013.6086

Ozin, G. A. (1992). Nanochemistry—synthesis in diminishing dimensions. *Adv. Mater.* 4, 612–649. doi: 10.1002/adma.19920041003

Pang, Y. T., Meng, G. W., Shan, W. J., Fang, Q., and Zhang, L. D. (2003a). Micropolarizer of ordered Ni nanowire arrays embedded in porous anodic alumina membrane. *Chin. Phys. Lett.* 20, 144–147. doi: 10.1088/0256-307X/20/1/343

Pang, Y. T., Meng, G. W., Shan, W. J., Zhang, L. D., Gao, X. Y., Zhao, A. W., et al. (2003b). Arrays of ordered Ag nanowires with different diameters in different areas embedded in one piece of anodic alumina membrane. *Appl. Phys. A Mater. Sci. Process.* 77, 717–720. doi: 10.1007/s00339-002-1920-8

Pang, Y. T., Meng, G. W., Zhang, L. D., Shan, W. J., Gao, X. Y., Zhao, A. W., et al. (2002). Arrays of ordered Pb nanowires with different diameters in different areas embedded in one piece of anodic alumina membrane. *J. Phys. Condens. Matter* 14, 11729–11736. doi: 10.1088/0953-8984/14/45/314

Pang, Y. T., Meng, G. W., Zhang, Y., Fang, Q., and Zhang, L. D. (2003c). Copper nanowire arrays for infrared polarizer. *Appl. Phys. A Mater. Sci. Process.* 76, 533–536. doi: 10.1007/s00339-002-1483-8

Pantarotto, D., Briand, J. P., Prato, M., and Bianco, A. (2004a). Translocation of bioactive peptides across cell membranes by carbon nanotubes. *Chem. Commun.* 16–17. doi: 10.1039/b311254c

Pantarotto, D., Singh, R., McCarthy, D., Erhardt, M., Briand, J. P., Prato, M., et al. (2004b). Functionalized carbon nanotubes for plasmid DNA gene delivery. *Angew. Chem. Int. Ed. Engl.* 43, 5242–5246. doi: 10.1002/anie.200460437

Park, J. H., Pham, T. A., Lee, J. J., and Kim, D. P. (2006). Fabrication of ceramic line pattern by UV-nanoimprint lithography of inorganic polymers. *Polymer* 30, 407–411.

Park, K. H., Chhowalla, M., Iqbal, Z., and Sesti, F. (2003). Single-walled carbon nanotubes are a new class of ion channel blockers. *J. Biol. Chem.* 278, 50212–50216. doi: 10.1074/jbc.M310216200

Patolsky, F., Timko, B. P., Zheng, G., and Lieber, C. M. (2007). Nanowire-based nanoelectronic devices in the life sciences. *MRS Bull.* 32, 142–149. doi: 10.1557/mrs2007.47

Perret, C., Gourgon, C., Lazzarino, F., Tallal, J., Landis, S., and Pelzer, R. (2004). Characterization of 8-in. wafers printed by nanoimprint lithography. *Microelectron. Eng.* 73–74, 172–177. doi: 10.1016/S0167-9317(04)00094-2

Piraux, L., Dubois, S., Duvail, J. L., Radulescu, A., Demoustier-Champagne, S., Ferain, E., et al. (1999). Fabrication and properties of organic and metal nanocylinders in nanoporous membranes. *J. Mater. Res.* 14, 3042–3050. doi: 10.1557/JMR.1999.0408

Prinz, C., Haellstroem, W., Martensson, T., Samuelson, L., Montelius, L., and Kanje, M. (2008). Axonal guidance on patterned free-standing nanowire surfaces. *Nanotechnology* 19:345101. doi: 10.1088/0957-4484/19/34/345101

Qiao, R., Jia, Q., Huwel, S., Xia, R., Liu, T., Gao, F., et al. (2012). Receptor-mediated delivery of magnetic nanoparticles across the blood-brain barrier. *ACS Nano* 6, 3304–3310. doi: 10.1021/nn300240p

Qiu, L. B., Ding, G. R., Li, K. C., Wang, X. W., Zhou, Y., Zhou, Y. C., et al. (2010). The role of protein kinase C in the opening of blood-brain barrier induced by electromagnetic pulse. *Toxicology* 273, 29–34. doi: 10.1016/j.tox.2010.04.013

Quach, D. V., Vidu, R., Groza, J. R., and Stroeve, P. (2010). Electrochemical Deposition of Co-Sb Thin Films and Nanowires. *Ind. Eng. Chem. Res.* 49, 11385–11392. doi: 10.1021/ie101173u

Radha, R., Lim, S. H., Saifullah, M., and Kulkarni, G. U. (2012). Metal hierarchical patterning by direct nanoimprint lithography. *Sci. Rep.* 3:1078. doi: 10.1038/srep01078

Ragnaill, M. N., Brown, M., Ye, D., Bramini, M., Callanan, S., Lynch, I., et al. (2011). Internal benchmarking of a human blood–brain barrier cell model for screening of nanoparticle uptake and transcytosis. *Eur. J. Pharm. Biopharm.* 77, 360–367. doi: 10.1016/j.ejpb.2010.12.024

Rehman, S. U., and Kamboh, A. M. (2013). "A new architecture for neural signal amplification in implantable brain machine interfaces," in *2013 35th Annual International Conference of the IEEE Engineering in Medicine and Biology Society (EMBC)* (Osaka), 2744–2747.

Robinson, J. T., Jorgolli, M., Shalek, A. K., Yoon, M.-H., Gertner, R. S., and Park, H. (2012). Vertical nanowire electrode arrays as a scalable platform for intracellular interfacing to neuronal circuits. *Nat. Nanotechnol.* 7, 180–184. doi: 10.1038/nnano.2011.249

Rutten, W. L. C. (2002). Selective electrical interfaces with the nervous system. *Annu. Rev. Biomed. Eng.* 4, 407–452. doi: 10.1146/annurev.bioeng.4.020702.153427

Sacha, G. M., and Varona, P. (2013). Artificial intelligence in nanotechnology. *Nanotechnology* 24:452002. doi: 10.1088/0957-4484/24/45/452002

Sakhtianchi, R., Minchin, R. F., Lee, K.-B., Alkilany, A. M., Serpooshan, V., and Mahmoudi, M. (2013). Exocytosis of nanoparticles from cells: role in cellular retention and toxicity. *Adv. Colloid Interface Sci.* 201, 18–29. doi: 10.1016/j.cis.2013.10.013

Salvati, A., Pitek, A. S., Monopoli, M. P., Prapainop, K., Bombelli, F. B., Hristov, D. R., et al. (2013). Transferrin-functionalized nanoparticles lose their targeting capabilities when a biomolecule corona adsorbs on the surface. *Nat. Nanotechnol.* 8, 137–143. doi: 10.1038/nnano.2012.237

Sandison, M. E., and Cooper, J. M. (2006). Nanofabrication of electrode arrays by electron-beam and nanoimprint lithographies. *Lab Chip* 6, 1020–1025. doi: 10.1039/b516598a

Schollhorn, R. (1996). Intercalation systems as nanostructured functional materials. *Chem. Mater.* 8, 1747–1757. doi: 10.1021/cm960142l

Schouenborg, J. (2011). Biocompatible multichannel electrodes for long-term neurophysiological studies and clinical therapy-Novel concepts and design. *Brain Mach. Interfaces* 194, 61–70. doi: 10.1016/B978-0-444-53815-4.00017-0

Seraji, S., Wu, Y., Jewell-Larson, N. E., Forbess, M. J., Limmer, S. J., Chou, T. P., et al. (2000). Patterned microstructure of sol-gel derived complex oxides using soft lithography. *Adv. Mater.* 12, 1421–1424. doi: 10.1002/1521-4095(200010)12:19<1421::AID-ADMA1421>3.0.CO;2-4

Sharma, G., Modgil, A., Sun, C., and Singh, J. (2012). Grafting of cell-penetrating peptide to receptor-targeted liposomes improves their transfection efficiency and transport across blood-brain barrier model. *J. Pharm. Sci.* 101, 2468–2478. doi: 10.1002/jps.23152

Sharma, P., and Ahuja, P. (2008). Recent advances in carbon nanotube-based electronics. *Mater. Res. Bull.* 43, 2517–2526. doi: 10.1016/j.materresbull.2007.10.012

Sharma, S., and Sunkara, M. K. (2002). Direct synthesis of gallium oxide tubes, nanowires, and nanopaintbrushes. *J. Am. Chem. Soc.* 124, 12288–12293. doi: 10.1021/ja027086b

Shen, A. M., Chen, C.-L., Kim, K., Cho, B., Tudor, A., and Chen, Y. (2013). Analog neuromorphic module based on carbon nanotube synapses. *ACS Nano* 7, 6117–6122. doi: 10.1021/nn401946s

Silva, G. A. (2005). Nanotechnology approaches for the regeneration and neuroprotection of the central nervous system. *Surg. Neurol.* 63, 301–306. doi: 10.1016/j.surneu.2004.06.008

Spira, M. E., and Hai, A. (2013). Multi-electrode array technologies for neuroscience and cardiology. *Nat. Nanotechnol.* 8, 83–94. doi: 10.1038/nnano.2012.265

Stam, R. (2010). Electromagnetic fields and the blood-brain barrier. *Brain Res. Rev.* 65, 80–97. doi: 10.1016/j.brainresrev.2010.06.001

Stankova, L., Fraczek-Szczypta, A., Blazewicz, M., Filova, E., Blazewicz, S., Lisa, V., et al. (2014). Human osteoblast-like MG 63 cells on polysulfone modified with carbon nanotubes or carbon nanohorns. *Carbon* 67, 578–591. doi: 10.1016/j.carbon.2013.10.031

Stieglitz, T. (2007). Restoration of neurological functions by neuroprosthetic technologies: future prospects and trends towards micro-, nano-, and biohybrid systems. *Acta Neurochir. Suppl.* 97, 435–442. doi: 10.1007/978-3-211-33079-1_57

Suyatin, D. B., Hallstram, W., Samuelson, L., Montelius, L., Prinz, C. N., and Kanje, M. (2009). Gallium phosphide nanowire arrays and their possible application in cellular force investigations. *J. Vac. Sci. Technol. B* 27, 3092–3094. doi: 10.1116/1.3264665

Suyatin, D. B., Wallman, L., Thelin, J., Prinz, C. N., Jorntell, H., Samuelson, L., et al. (2013). Nanowire-based electrode for acute *in vivo* neural recordings in the brain. *PLoS ONE* 8:e56673. doi: 10.1371/journal.pone.0056673

Suzuki, I., Fukuda, M., Shirakawa, K., Jiko, H., and Gotoh, M. (2013). Carbon nanotube multi-electrode array chips for noninvasive real-time measurement of dopamine, action potentials, and postsynaptic potentials. *Biosens. Bioelectron.* 49, 270–275. doi: 10.1016/j.bios.2013.05.023

Takei, K., Kawano, T., Kawashima, T., Sawada, K., Kaneko, H., and Ishida, M. (2010). Microtube-based electrode arrays for low invasive extracellular recording with a high signal-to-noise ratio. *Biomed. Microdevices* 12, 41–48. doi: 10.1007/s10544-009-9356-y

Tian, B., Cohen-Karni, T., Qing, Q., Duan, X., Xie, P., and Lieber, C. M. (2010). Three-dimensional, flexible nanoscale field-effect transistors as localized bioprobes. *Science* 329, 830–834. doi: 10.1126/science.1192033

Tian, Y. T., Meng, G. W., Gao, T., Sun, S. H., Xie, T., Peng, X. S., et al. (2004). Alumina nanowire arrays standing on a porous anodic alumina membrane. *Nanotechnology* 15, 189–191. doi: 10.1088/0957-4484/15/1/036

Tian, Z. R. R., Voigt, J. A., Liu, J., McKenzie, B., McDermott, M. J., Rodriguez, M. A., et al. (2003). Complex and oriented ZnO nanostructures. *Nat. Mater.* 2, 821–826. doi: 10.1038/nmat1014

Tierney, M. J., and Martin, C. R. (1989). Transparent metal microstructures. *J. Phys. Chem.* 93, 2878–2880. doi: 10.1021/j100345a005

Timko, B. P., Cohen-Karni, T., Qing, Q., Tian, B., and Lieber, C. M. (2010). Design and implementation of functional nanoelectronic interfaces with biomolecules, cells, and tissue using nanowire device arrays. *IEEE Trans. Nanotechnol.* 9, 269–280. doi: 10.1109/TNANO.2009.2031807

Ting, C. Y., Fan, C. H., Liu, H. L., Huang, C. Y., Hsieh, H. Y., Yen, T. C., et al. (2012). Concurrent blood-brain barrier opening and local drug delivery using drug-carrying microbubbles and focused ultrasound for brain glioma treatment. *Biomaterials* 33, 704–712. doi: 10.1016/j.biomaterials.2011.09.096

Tonucci, R. J., Justus, B. L., Campillo, A. J., and Ford, C. E. (1992). Nanochannel array glass. *Science* 258, 783–785. doi: 10.1126/science.258.5083.783

Tormen, M., Carpentiero, A., Vaccari, L., Altissimo, M., Ferrari, E., Cojoc, D., et al. (2005). Fabrication of three-dimensional stamps for embossing techniques by lithographically controlled isotropic wet etching. *J. Vac. Sci. Technol. B* 23, 2920–2924. doi: 10.1116/1.2130348

Torres, C. M. S., Zankovych, S., Seekamp, J., Kam, A. P., Cedeno, C. C., Hoffmann, T., et al. (2003). Nanoimprint lithography: an alternative nanofabrication approach. *Mater. Sci. Eng. C Biomimetic Supramol. Syst.* 23, 23–31. doi: 10.1016/S0928-4931(02)00221-7

Tysseling, V. M., Kessler, J. A., (2011). "Chapter 185: biomaterials for central nervous system regeneration," in *Comprehensive Biomaterials*, ed P. Ducheyne (Major Reference Works, Elsevier Ltd.), 455–466.

Vaadia, E., and Birbaumer, N. (2009). Grand challenges of brain computer interfaces in the years to come. *Front. Neurosci.* 3, 151–154. doi: 10.3389/neuro.01.015.2009

Valcarcel, V., Souto, A., and Guitian, F. (1998). Development of single-crystal alpha-Al2O3 fibers by vapor-liquid-solid deposition (VLS) from aluminum and powdered silica. *Adv. Mater.* 10, 138–140. doi: 10.1002/(SICI)1521-4095(199801)10:2<138::AID-ADMA138>3.0.CO;2-A

Vayssieres, L. (2003). Growth of arrayed nanorods and nanowires of ZnO from aqueous solutions. *Adv. Mater.* 15, 464–466. doi: 10.1002/adma.200390108

Vidu, R. (2000). *Electrochemical Atomic Force Microscopy Studies of Te, Cd and CdTe Electrodeposition Processes on Au Single Crystal*. Ph.D. thesis, Osaka University.

Vidu, R., Ku, J.-R., and Stroeve, P. (2006). Growth of ultrathin films of cadmium telluride and tellurium as studied by electrochemical atomic force

microscopy. *J. Colloid Interface Sci.* 300, 404–412. doi: 10.1016/j.jcis.2006.03.078

Vidu, R., Ku, J.-R., and Stroeve, P. (2007). "Fabrication of multiscale nanostructures from polymeric membrane templates," in *Polymeric Nanostructures and Their Applications*, ed H. S. Nalwa (American Scientific Publishers), 124–149.

Vidu, R., Li, S., Quach, D. V., and Stroeve, P. (2012). Electrochemical deposition of Co-Sb thin films on nanostructured gold. *J. Appl. Electrochem.* 42, 333–339. doi: 10.1007/s10800-012-0401-9

Viventi, J., Kim, D.-H., Vigeland, L., Frechette, E. S., Blanco, J. A., Kim, Y.-S., et al. (2011). Flexible, foldable, actively multiplexed, high-density electrode array for mapping brain activity *in vivo*. *Nat. Neurosci.* 14, U1599–U1605. doi: 10.1038/nn.2973

Voge, C. M., and Stegemann, J. P. (2011). Carbon nanotubes in neural interfacing applications. *J. Neural Eng.* 8:011001. doi: 10.1088/1741-2560/8/1/011001

Wade, L. A., and Katzman, R. (1975). 3-0-Methyldopa uptake and inhibition of L-dopa at the blood-brain barrier. *Life Sci.* 17, 131–136. doi: 10.1016/0024-3205(75)90248-9

Wagner, S., Zensi, A., Wien, S. L., Tschickardt, S. E., Maier, W., Vogel, T., et al. (2012). Uptake mechanism of ApoE-modified nanoparticles on brain capillary endothelial cells as a blood-brain barrier model. *PLoS ONE* 7:e32568. doi: 10.1371/journal.pone.0032568

Wang, D., El-Amouri, S. S., Dai, M., Kuan, C. Y., Hui, D. Y., Brady, R. O., et al. (2013). Engineering a lysosomal enzyme with a derivative of receptor-binding domain of apoE enables delivery across the blood-brain barrier. *Proc. Natl. Acad. Sci. U.S.A.* 110, 2999–3004. doi: 10.1073/pnas.1222742110

Wang, H., Xu, K., Liu, L., Tan, J. P. K., Chen, Y., Li, Y., et al. (2010). The efficacy of self-assembled cationic antimicrobial peptide nanoparticles against Cryptococcus neoformans for the treatment of meningitis. *Biomaterials* 31, 2874–2881. doi: 10.1016/j.biomaterials.2009.12.042

Wang, X., and Li, Y. D. (2002). Selected-control hydrothermal synthesis of alpha- and beta-MnO2 single crystal nanowires. *J. Am. Chem. Soc.* 124, 2880–2881. doi: 10.1021/ja0177105

Wenrong, Y., Ratinac, K. R., Ringer, S. P., Thordarson, P., Gooding, J. J., and Braet, F. (2010). Carbon nanomaterials in biosensors: should you use nanotubes or graphene? *Angew. Chem. Int. Ed.* 49, 2114–2138. doi: 10.1002/anie.200903463

Wiley, D. T., Webster, P., Gale, A., and Davis, M. E. (2013). Transcytosis and brain uptake of transferrin-containing nanoparticles by tuning avidity to transferrin receptor. *Proc. Natl. Acad. Sci. U.S.A.* 110, 8662–8667. doi: 10.1073/pnas.1307152110

Wirtz, M., and Martin, C. R. (2003). Template-fabricated gold nanowires and nanotubes. *Adv. Mater.* 15, 455–458. doi: 10.1002/adma.200390106

Wirtz, M., Parker, M., Kobayashi, Y., and Martin, C. R. (2002b). Molecular sieving and sensing with gold nanotube membranes. *Chem. Rec.* 2, 259–267. doi: 10.1002/tcr.10027

Wirtz, M., Yu, S. F., and Martin, C. R. (2002a). Template synthesized gold nanotube membranes for chemical separations and sensing. *Analyst* 127, 871–879. doi: 10.1039/b201939f

Wise, K. D. (2007). Integrated sensors, MEMS, and microsystems: reflections on a fantastic voyage. *Sens. Actuators A Phys.* 136, 39–50. doi: 10.1016/j.sna.2007.02.013

Wohlfart, S., Gelperina, S., and Kreuter, J. (2012). Transport of drugs across the blood-brain barrier by nanoparticles. *J. Control. Release* 161, 264–273. doi: 10.1016/j.jconrel.2011.08.017

Wu, W., Wieckowski, S., Pastorin, G., Benincasa, M., Klumpp, C., Briand, J. P., et al. (2005). Targeted delivery of amphotericin B to cells by using functionalized carbon nanotubes. *Angew. Chem. Int. Ed. Engl.* 44, 6358–6362. doi: 10.1002/anie.200501613

Wu, X. C., Song, W. H., Huang, W. D., Pu, M. H., Zhao, B., Sun, Y. P., et al. (2000). Crystalline gallium oxide nanowires: intensive blue light emitters. *Chem. Phys. Lett.* 328, 5–9. doi: 10.1016/S0009-2614(00)00899-X

Wu, Y., Cui, Y., Huynh, L., Barrelet, C. J., Bell, D. C., and Lieber, C. M. (2004). Controlled growth and structures of molecular-scale silicon nanowires. *Nano Lett.* 4, 433–436. doi: 10.1021/nl035162i

Xiang, J., Lu, W., Hu, Y. J., Wu, Y., Yan, H., and Lieber, C. M. (2006a). Ge/Si nanowire heterostructures as high-performance field-effect transistors. *Nature* 441, 489–493. doi: 10.1038/nature04796

Xiang, J., Vidan, A., Tinkham, M., Westervelt, R. M., and Lieber, C. M. (2006b). Ge/Si nanowire mesoscopic Josephson junctions. *Nat. Nanotechnol.* 1, 208–213. doi: 10.1038/nnano.2006.140

Xiao, Z. L., Han, C. Y., Welp, U., Wang, H. H., Kwok, W. K., Willing, G. A., et al. (2002). Fabrication of alumina nanotubes and nanowires by etching porous alumina membranes. *Nano Lett.* 2, 1293–1297. doi: 10.1021/nl025758q

Xie, C., Hanson, L., Xie, W., Lin, Z., Cui, B., and Cui, Y. (2010). Noninvasive neuron pinning with nanopillar arrays. *Nano Lett.* 10, 4020–4024. doi: 10.1021/nl101950x

Xie, C., Lin, Z., Hanson, L., Cui, Y., and Cui, B. (2012). Intracellular recording of action potentials by nanopillar electroporation. *Nat. Nanotechnol.* 7, 185–190. doi: 10.1038/nnano.2012.8

Xu, N., Gu, J., Zhu, Y., Wen, H., Ren, Q., and Chen, J. (2011). Efficacy of intravenous amphotericin B-polybutylcyanoacrylate nanoparticles against cryptococcal meningitis in mice. *Int. J. Nanomedicine* 6, 905–913. doi: 10.2147/IJN.S17503

Yajie, D., Guihua, Y., McAlpine, M. C., Wei, L., and Lieber, C. M. (2008). Si/a-Si core/shell nanowires as nonvolatile crossbar switches. *Nano Lett.* 8, 386–391. doi: 10.1021/nl073224p

Ye, Y.-H., Badilescu, S., Truong, V.-V., Rochon, P., and Natansohn, A. (2001). Self-assembly of colloidal spheres on patterned substrates. *Appl. Phys. Lett.* 79, 872. doi: 10.1063/1.1391234

Yi, D. K., Kim, M. J., and Kim, D. Y. (2002a). Surface relief grating induced colloidal crystal structures. *Langmuir* 18, 2019–2023. doi: 10.1021/la011340g

Yi, D. K., Seo, E. M., and Kim, D. Y. (2002b). Surface-modulation-controlled three-dimensional colloidal crystals. *Appl. Phys. Lett.* 80, 225. doi: 10.1063/1.1434313

Yi, D. K., Yoo, S. J., and Kim, D. Y. (2002c). Spin-on-based fabrication of titania nanowires using a sol-gel process. *Nano Lett.* 2, 1101–1104. doi: 10.1021/nl0257115

Yin, Y. D., Zhang, G. T., and Xia, Y. N. (2002). Synthesis and characterization of MgO nanowires through a vapor-phase precursor method. *Adv. Funct. Mater.* 12, 293–298. doi: 10.1002/1616-3028(20020418)12:4<293::AID-ADFM293>3.0.CO;2-U

Yinghuai, Z., and Hosmane, N. S. (2013). Applications and perspectives of boron-enriched nanocomposites in cancer therapy. *Future Med. Chem.* 5, 705–714. doi: 10.4155/fmc.13.47

Yoon, I., Hamaguchi, K., Borzenets, I. V., Finkelstein, G., Mooney, R., and Donald, B. R. (2013). Intracellular neural recording with pure carbon nanotube probes. *PLoS ONE* 8:e65715. doi: 10.1371/journal.pone.0065715

Yuan, X. Y., Wu, G. S., Xie, T., Lin, Y., Meng, G. W., and Zhang, L. D. (2004a). Autocatalytic redox fabrication and magnetic studies of Co-Ni-P alloy nanowire arrays. *Solid State Commun.* 130, 429–432. doi: 10.1016/j.ssc.2003.12.028

Yuan, X. Y., Wu, G. S., Xie, T., Lin, Y., and Zhang, L. D. (2004b). Self-assembly synthesis and magnetic studies of Co-P alloy nanowire arrays. *Nanotechnology* 15, 59–61. doi: 10.1088/0957-4484/15/1/011

Yuan, X. Y., Xie, T., Wu, G. S., Lin, Y., Meng, G. W., and Zhang, L. D. (2004c). Fabrication of Ni-W-P nanowire arrays by electroless deposition and magnetic studies. *Phys. E-Low Dimens. Syst. Nanostruct.* 23, 75–80. doi: 10.1016/j.physe.2004.01.011

Yu, D. P., Hang, Q. L., Ding, Y., Zhang, H. Z., Bai, Z. G., Wang, J. J., et al. (1998). Amorphous silica nanowires: intensive blue light emitters. *Appl. Phys. Lett.* 73, 3076–3078. doi: 10.1063/1.122677

Zhang, Y. J., Li, W., Meng, X. D., Yang, J. H., Hua, Z., Li, W., et al. (2006). Fabrication of nanoimprint mold by multilayer film deposition technique. *Acta Phys. Sin.* 55, 2033–2037.

Zhao, D., Alizadeh, D., Zhang, L., Liu, W., Farrukh, O., Manuel, E., et al. (2011). Carbon nanotubes enhance CpG uptake and potentiate antiglioma immunity. *Clin. Cancer Res.* 17, 771–782. doi: 10.1158/1078-0432.CCR-10-2444

Zheng, B., Wu, Y. Y., Yang, P. D., and Liu, J. (2002). Synthesis of ultra-long and highly oriented silicon oxide nanowires from liquid alloys. *Adv. Mater.* 14, 122–124. doi: 10.1002/1521-4095(20020116)14:2<122::AID-ADMA122>3.0.CO;2-V

Zheng, G. F., Lu, W., Jin, S., and Lieber, C. M. (2004). Synthesis and fabrication of high-performance n-type silicon nanowire transistors. *Adv. Mater.* 16, 1890–1893. doi: 10.1002/adma.200400472

Zhou, Y. K., Huang, J., Shen, C. M., and Li, H. L. (2002). Synthesis of highly ordered LiNiO2 nanowire arrays in AAO templates and their structural properties. *Mater. Sci. Eng.* 335, 260–267. doi: 10.1016/S0921-5093(01)01938-4

Zorzos, A. N., Scholvin, J., Boyden, E. S., and Fonstad, C. G. (2012). Three-dimensional multiwaveguide probe array for light delivery to distributed brain circuits. *Opt. Lett.* 37, 4841–4843. doi: 10.1364/OL.37.004841

Conflict of Interest Statement: The Reviewer Dr Song declares that despite having collaborated with the author, Dr Opris, the review process was handled objectively. The authors declare that the research was conducted in the absence of any commercial or financial relationships that could be construed as a potential conflict of interest.

Received: 04 March 2014; accepted: 30 April 2014; published online: 20 June 2014.
Citation: Vidu R, Rahman M, Mahmoudi M, Enachescu M, Poteca TD and Opris I (2014) Nanostructures: a platform for brain repair and augmentation. Front. Syst. Neurosci. ***8****:91. doi: 10.3389/fnsys.2014.00091*
This article was submitted to the journal Frontiers in Systems Neuroscience.

frontiers in Neuroscience

METHODS
published: 25 September 2015
doi: 10.3389/fnins.2015.00331

An array of highly flexible electrodes with a tailored configuration locked by gelatin during implantation—initial evaluation in cortex cerebri of awake rats

Johan Agorelius[1,2], Fotios Tsanakalis[1], Annika Friberg[1], Palmi T. Thorbergsson[1], Lina M. E. Pettersson[1]*† and Jens Schouenborg[1,2]*†*

[1] Department of Experimental Medical Science, Neuronano Research Centre, Lund University, Lund, Sweden, [2] The Nanometer Structure Consortium, Lund University, Lund, Sweden

OPEN ACCESS

Edited by:
Manuel Fernando Casanova, University of Louisville, USA

Reviewed by:
Jit Muthuswamy, Arizona State University, USA
Ulrich G. Hofmann, Albert-Ludwigs-University Freiburg, Germany

***Correspondence:**
Johan Agorelius, Lina M. E. Pettersson and Jens Schouenborg, Department of Experimental Medical Science, Neuronano Research Center, Lund University, BMC F10, SE-221 84 Lund, Sweden
johan.agorelius@med.lu.se; lina.pettersson@med.lu.se; jens.schouenborg@med.lu.se

† *These authors jointly directed this work.*

Specialty section:
This article was submitted to Neural Technology, a section of the journal Frontiers in Neuroscience

Received: *05 January 2015*
Accepted: *04 September 2015*
Published: *25 September 2015*

Citation:
Agorelius J, Tsanakalis F, Friberg A, Thorbergsson PT, Pettersson LME and Schouenborg J (2015) An array of highly flexible electrodes with a tailored configuration locked by gelatin during implantation—initial evaluation in cortex cerebri of awake rats. Front. Neurosci. 9:331. doi: 10.3389/fnins.2015.00331

Background: A major challenge in the field of neural interfaces is to overcome the problem of poor stability of neuronal recordings, which impedes long-term studies of individual neurons in the brain. Conceivably, unstable recordings reflect relative movements between electrode and tissue. To address this challenge, we have developed a new ultra-flexible electrode array and evaluated its performance in awake non-restrained animals.

Methods: An array of eight separated gold leads (4 × 10 μm), individually flexible in 3D, were cut from a gold sheet using laser milling and insulated with Parylene C. To provide structural support during implantation into rat cortex, the electrode array was embedded in a hard gelatin based material, which dissolves after implantation. Recordings were made during 3 weeks. At termination, the animals were perfused with fixative and frozen to prevent dislocation of the implanted electrodes. A thick slice of brain tissue, with the electrode array still in situ, was made transparent using methyl salicylate to evaluate the conformation of the implanted electrode array.

Results: Median noise levels and signal/noise remained relatively stable during the 3 week observation period; 4.3–5.9 μV and 2.8–4.2, respectively. The spike amplitudes were often quite stable within recording sessions and for 15% of recordings where single-units were identified, the highest-SNR unit had an amplitude higher than 150 μV. In addition, high correlations (>0.96) between unit waveforms recorded at different time points were obtained for 58% of the electrode sites. The structure of the electrode array was well preserved 3 weeks after implantation.

Conclusions: A new implantable multichannel neural interface, comprising electrodes individually flexible in 3D that retain its architecture and functionality after implantation has been developed. Since the new neural interface design is adaptable, it offers a versatile tool to explore the function of various brain structures.

Keywords: brain machine interface, flexible electronic implant, neural probe, embedding material, brain micro-motions, stable neural recordings, mechanical compliance, neuromodulation

Introduction

A major challenge in the field of Brain-Machine Interfaces (BMIs) is that the stability of neuronal recordings often is insufficient for studies of single neuronal activity over long periods of time. Unstable electrode position in the tissue can occur if the implant is too rigid to follow the movements of the brain during for example the respiratory and cardiac cycles (Britt and Rossi, 1982) but can also be caused by body movements (Jackson and Fetz, 2007; Santhanam et al., 2007). Moreover, the quality, i.e., signal-to-noise ratio, commonly gradually deteriorates over time (Rousche and Normann, 1998; Williams et al., 1999; Polikov et al., 2005). This deterioration may in part also be due to instability, since micro-motions between probe and tissue are likely to cause continuous irritation or indeed injury of the tissue that result in long-term glial activation and unfavorable effects on nearby neurons (Turner et al., 1999; Williams et al., 1999; Szarowski et al., 2003; Biran et al., 2005; Gilletti and Muthuswamy, 2006; Seymour and Kipke, 2007; Thelin et al., 2011; Lind et al., 2013). These glial reactions and effects on nearby neurons are known to impair recording quality (Nolta et al., 2015).

The largest micro-motions occur between the brain and the skull in the awake freely moving animals (Kim et al., 2004; Gilletti and Muthuswamy, 2006; Biran et al., 2007). For this reason, flexible leads on the cortical surface connecting the implanted rather stiff electrodes to the electronics have been developed (Rousche and Normann, 1998; Jackson and Fetz, 2007; Musallam et al., 2007). However, there are also significant micro-motions inside the brain caused by propagating waves of blood inside the vessels (Eide, 2008; Wagshul et al., 2011). The propagating nature of these movements implies that the movements inside the brain are not uniform. On top of these movements, there are movements caused by respiration. If the implanted electrodes cannot follow these tissue movements in all three dimensions, micro-forces/micro-movements between tissue and the recording sites on the electrodes will ensue. Indeed, it is a common experience, when performing acute electrophysiological experiments using stiff microelectrodes for extracellular recordings, that substantial pulsative movements inside the brain can occur as an effect of e.g., heart beats despite stabilization of the surface. As a result, such recordings tend to be short lived if the electrode is too close to the recorded neurons. Hence, to allow close contacts with neurons for longer periods of time, a high degree of mechanical compliance between electrodes and tissue is likely to be beneficial.

To improve mechanical compliance between electrodes and tissue, efforts have been made to increase the flexibility of the implanted electrodes themselves (Rousche et al., 2001; Kipke et al., 2002; Takeuchi et al., 2005; Stice et al., 2007; Bae et al., 2008; Krüger et al., 2010; Andrei et al., 2012; Felix et al., 2012; Lee et al., 2012; Kuo et al., 2013; Ejserholm et al., 2014; Kozai et al., 2014; Sohal et al., 2014). However, some of them are too flexible to be implanted on their own, and thus structural support in the form of a stiff guide or cannula (Kipke et al., 2002; Felix et al., 2012; Kuo et al., 2013; De Faveri et al., 2014; Sohal et al., 2014) has been used. These guides/cannulae cause additional stab wound-like injuries on their own, and on removal risk perturbing the position of the implanted flexible electrodes. Many of these flexible electrodes embed the conductive leads in a polymer sheet. However, this reduces their flexibility to one dimension only, and since the electrode leads are fixed in the polymer they cannot move independently of each other. In addition, such chip-like constructions also permanently split the tissue into two halves, causing an irreversible disruption of communication between neural networks on the two sides and therefore create a less than ideal situation when analyzing the function of neuronal networks. Hence, the challenge of providing an implantable array of independent highly flexible electrodes and that can be provided with an architecture adapted to the target tissue still remains.

The aim of the present project was thus to develop a fully functional and implantable array of ultra-thin electrodes, individually flexible in three dimensions after implantation. We present a new type of array of ultra-flexible electrodes which by being embedded in a hard but dissolvable gelatin based material retains its conformation and arrangement during implantation. Preliminary performance tests in awake rats showed encouraging results.

Materials and Methods

Design and Fabrication of the Electrode Array

We designed an array of eight wavy electrodes, thus flexible/extendable in three dimensions, each equipped with a distal protruding branch from where neuronal recordings could be made (**Figure 1**). The electrode array conformation was designed to allow recordings from different cortical laminae. The design was created using AutoCAD 2011 software and digitally imported into a Laser Machining System (Laser mill 50, standard micro-milling system, Nd:YAG laser system, New Wave Research, Inc., Fremont, CA). A 4 μm-thick sheet of gold foil (Rosenobel-Doppelgold 23 ¾ karat, J.G. Eytzinger GmbH, Germany) was fastened onto a microscope glass slide using polyethylene glycol (Sigma-Aldrich). Gold leads, 10 μm in width were milled under a fixed 20X objective using pulsed green laser light (wavelength 532 nm, energy density 10 J/cm^2).

The glass slide containing the milled electrodes was mounted with silicon (Elastosil A07) and aligned on a metal frame to which a printed circuit board (PCB) was attached. The individual leads were manually soldered to the PCB one by one using a flux mixture solution (62% Sn, 36% Pb, 2% Ag) applied between the electrodes to be soldered and the contacts on the PCB. This process was performed under a stereomicroscope (SMZ1500, Nikon Instruments Europe BV, The Netherlands). To wash away the remaining flux mixture from between the PCB leads and to release the electrode leads from the glass slide, the metal frame was immersed in 70% ethanol, after which the glass slide was carefully removed manually.

An acrylic coating (HumiSeal advanced protective coating for electronics) was applied as protection over the soldered leads and over the bottom part of the PCB. The electrode array, including the PCB, was then coated with Parylene C (4 μm thick) using a Compact Bench Top Coating System (Labtop 3000, Para Tech Coating Inc., CA, US).

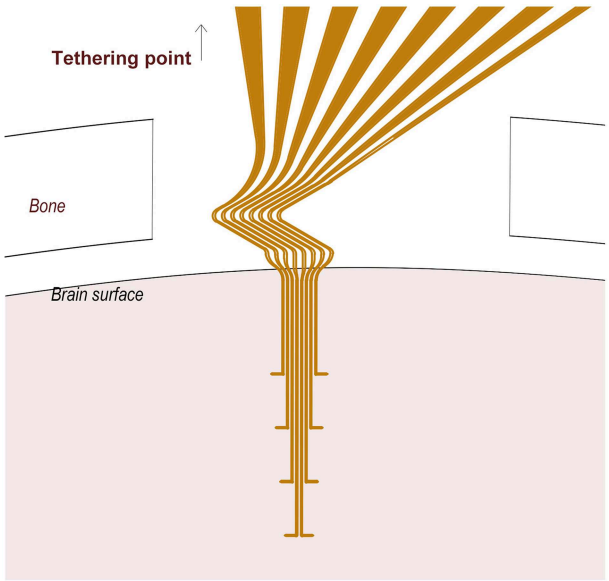

FIGURE 1 | A schematic of the 3D flexible electrode array. Note the Z-shaped proximal part of the electrode array located between the cranium and the brain surface, and the tips (10 μm) of the distal protrusions which serve as recording sites.

There were no obvious inherent strain forces in the construct since the gold electrodes were not displaced after being cut out from the gold sheet and also kept their conformation when insulated with parylene C.

To prepare the active recording sites on the protruding tips, the parylene coating was photo-ablated on both sides, over an area extending 10 μm from each electrode lead tip, using focused UV radiation (wavelength 355 nm, energy density 1.4 J/cm^2) under a 20x objective. The successful exposure of the lead recording sites was monitored in real time during the ablation process and subsequently carefully confirmed with Scanning Electron Microscopy (SEM).

A ∼40 mm long, 150 μm thick, un-insulated silver wire (Advent research Materials Ltd, England) was attached to the chip in the assigned "ground" position in order to be used as animal ground for the recordings. The electrode, connected to the chip, was finally released from the frame.

Impedance Spectroscopy

The electrical properties of each electrode lead were evaluated by impedance spectroscopy (Gamry Instruments, Series G 300, USA). After immersion in 0.9% saline solution, the impedance of the individual channels was measured by applying a 10 mV AC voltage with a frequency of 1 KHz, using a large Pt wire as counter electrode and an Ag/AgCl electrode in phosphate buffer as reference. The mean impedance of the individual channels was 832 kΩ (SD = 230 kΩ). It should be noted that repeated impedance measurements did not significantly change the impedance of the electrodes.

Embedding of the Electrodes

The gold electrodes used in this study are highly flexible, for instance they cannot be inserted into water without bending. To provide structural support during implantation, the ultra-flexible electrode array was embedded in a hard, but dissolvable, gelatin B based matrix material. The gelatin matrix was prepared by slowly heating a mixture of 3 g gelatin (Gelatin powder Ph.Eur., 24360.368, WWR International AB, Sweden), 750 mg PEG 400 (81172-1L, Sigma-Aldrich Chemie GmbH, Germany), 150 mg glycerol 98% (GRP Rectapur, 24 387.361, VWR, BDH Prolabo, France), and 7 mL Millipore water (Millipak-20 Filter Unit 0.22 μm 1/4 in), to 70°C, giving a final concentration of 27.5% gelatin, 1.4% glycerol and 6.9% PEG. The mixture was then placed on a hot plate while stirring. The electrode array was placed inside a custom made Poly Methyl Methacrylate (PMMA) mold and the gelatin mixture was injected. The humidity during drying was held at 21%, and the gelatin was dried first 24 h inside the mold, and then 24 h with the top lid of the mold removed. The remaining water content after drying was estimated to be below 4% (by measuring the weight of the probes (n = 5) before and after drying). This method enabled production of a probe embedded in a gelatin matrix with a sharp rigid tip that allowed for penetration of the brain tissue (**Figure 3B**).

Finally, a thin coat of a water retardation material was applied in order to delay dissolution of the matrix material until the implant was fully implanted. In short, the gelatin-embedded electrode array was dip-coated in a 5% (w/w) solution of kollicoat (Fluka, Sigma-Aldrich Sweden AB) in 99.7% ethanol, two times with a drying interval of 24 h in between each coat, and at least 1 h between the last coating and implantation.

Animal Surgery

Approval for the experiments was obtained in advance from the Malmö/Lund Animal Ethics Committee on Animal Experiments (ethical permit M60-13) and all experiments in this work conform to the regulatory standards of this approval. All rats had free access to food and water and were kept in a 12-h light/dark cycle at a constant environmental temperature of 21°C and 65% humidity.

Female Sprague-Dawley rats were implanted with the embedded ultra-flexible electrode array in the hind paw area of the primary somatosensory (SI) cortex at the following stereotactic coordinates; 1.5 mm rostral and 2.0 mm lateral from Bregma. The rats weighed 222.5 g (SD = 3.8 g) at the time of surgery, corresponding to approximately 9–10 weeks. In short, anesthesia was induced by placing the rat in a chamber of 2% isoflurane (Isoba®vet., Apoteksbolaget, Sweden) with 40% oxygen and 60% nitrous oxide (Granmo et al., 2013). The animal was placed on a heating pad and its body temperature was monitored and kept at a stable level. The head was shaved and the rat was mounted in a stereotactic frame (KOPF Instruments, USA). After disinfection of the skin with 70% ethanol, the skull was exposed with a midline incision. The skin was retracted and the skull was cleaned from connective tissue under a stereomicroscope (Leica Microsystems, M651, Germany). Two holes (0.8 mm) were drilled anterior to bregma and one posterior to the SI cortex using a high-speed stereotaxic drill (Dest 300

IN, model MM 323IN, Silfradent, Italy). Small custom-made titanium screws with a length of 1900 μm were screwed ∼570 μm into the holes. The choice of material was based on the fact that titanium is a well-known biocompatible material commonly used in implants and which has the potential to integrate into the bone of the skull, yielding increased screw stability and thus adherence of the implant to the skull. The screws were used as anchoring sites for the dental cement (FujuCEM, GC, Europe, Belgium), which was applied at a later stage to attach the electrode/PCB to the skull. The ground wire was wired around the screw and inserted in a separate hole so as to be in contact with the CSF, see below.

A craniotomy, ∼2 mm in the rostro-caudal direction, and ∼3.5 mm in the medio-lateral dimension was made in the bone of the skull at the SI cortex coordinates, while leaving the underlying dura mater intact. The hind paw area in the S1 cortex was targeted using stereotactical implantation (Kalliomäki et al., 1993). Onset latencies of tactile response were measured from the stimulation artifact. The hole was rinsed with 0.9 % sterile saline solution to clear away any possible debris and prevent tissues from drying.

The embedded electrode was mounted in a hydraulic micromanipulator (KOPF Instruments, USA) and positioned above the SI cortex coordinates. The dura mater was carefully incised and deflected. Care was taken to always keep a thin layer of saline on the cortical surface to prevent it from drying. The electrode was implanted at the above mentioned coordinates to a depth of 1800 μm with a speed of 50 μm/s. After implantation, the ground wire was looped around one of the screws, and subsequently inserted under the bone on top of the dura on the contralateral side of the skull. A small piece of collagen biomatrix for dura regeneration (TissuDura, Baxter International Inc., USA) was positioned in the hole on top of the animal ground wire. The wire was secured and the hole was protected by application of dental cement. To increase the adherence of the PCB and dental cement to the skull, a primer, RelyX™ Unicem, Aplicap™ (3M, Sollentuna; Sweden) was applied prior to dental cement application.

In order to roughly estimate how long after implantation a neural signal could be obtained from the electrodes, a short-lasting recording was made in the anesthetized animal after implantation. In the three animals used for recordings (on 2–4 out of 8 electrode sites in each animal), neuronal activity was detectable already 30–40 min after implantation.

During surgery, the eyes were shielded with a compress which was continually refreshed with physiological saline. In addition, care was taken to make absolutely sure that ethanol or disinfectant was not applied anywhere in the vicinity of the eyes.

After surgery the rat was given subcutaneous injections of 0.01 mg/kg of temgesic (buprenorfin; Schering-Plough, Belgium) to relieve postoperative pain and animals were monitored during the awakening phase. At the end of the experimental period, (3 weeks post implantation), animals were killed by an intraperitoneal injection overdose of pentobarbital and transcardially perfused with saline (0.9%) followed by ice-cold 4% paraformaldehyde (PF) in 0.1 M phosphate buffer, pH 7.4. The brains were post fixed in PF overnight.

Tissue Clarification

To evaluate how well the flexible electrode array maintains its conformation after implantation, the head and brain with the probe still in situ was sectioned and processed according to the clarification protocol described below.

In short, after fixation, the whole head was snap frozen in isopentane on dry ice and stored at −80°C. This preparation method was developed in order to prevent distortion or removal of the electrode from the brain during sectioning of the skull and brain tissue. The top part of the skull bone including the upper part of the electrode was cut off using a circular diamond saw blade mounted on a high-speed dental drill (Desk 200 In, Silfradent, Italy) at 10,000 rpm. After this, the frozen head was cut in 4.5–5.5 mm thick slices with a tissue-slicing machine (ABW 300 GM, 242 W, Avery Berkel, UK), while still kept deep frozen. Care was taken to make sure that the entire electrode array was contained within a single tissue slice (**Figure 3C**).

For clarification the tissue slice was rinsed in 0.1 M phosphate buffered saline (3 × 5 min) to remove the fixative, dehydrated through ethanol of increased concentration (50, 70, and 99.5%, 3–4 h in each), and finally cleared in increasing concentrations (50, 70 in ethanol and 100%) of methyl salicylate (Sigma-Aldrich, Stockholm, Sweden) at least 5 h in each immersion. The conformation of the electrode within the brain slice was examined after clarification and compared with the conformation of the same gelatin embedded electrode before implantation, using 11.5 × magnification stereo microscope (SMZ 1500, Nikon, Japan) with 0.5x WD 136 objective (Nikon, Japan).

In-vivo Electrophysiology in Awake Animals

To evaluate the functionality and stability of the 3D electrode, *in vivo* recordings of single unit activity were made, in awake and non-restrained animals. Neural recordings were performed 2–5 times a week, starting day 1 (1 day after implantation) up to the end point at day 21.

The *in-vivo* recordings were performed in a faraday cage to eliminate external electromagnetic interference. Rats were briefly anesthetized with isoflurane (as per above) to connect the PCB to a 64 channel Plexon data acquisition system via a 20X head stage, a commutator and pre-amplifier (OmniPlex, Plexon Inc, Texas, USA) with a 60 cm long cable. The anesthetic gas was discontinued and signals were recorded from awake and non-restrained rats enclosed in a cage-like container.

To verify the physiological nature of the recorded activity, tactile stimulations of the glabrous skin of the contralateral hind paw were performed by triggering a tactile stimulator connected to a Master 8 stimulator (A.M.P.I., Jerusalem, Israel). At least one session of tactile stimulations was performed per animal. For each session a minimum of 150 tactile stimulations were performed and event time stamps were registered together with the electrophysiological recordings.

Data Analysis

The performance of the developed electrode arrays was evaluated by analyzing the noise levels, signal-to-noise ratio (SNR), yield (ratio of active electrodes that recorded single units and total

number of electrodes) and stability of the neural recordings over a period of 3 weeks.

Recording Parameters

The electrophysiological data were sampled at 16 bit and 40 kHz per channel using a Plexon data acquisition system (Plexon Inc., Texas, USA). The signals were bandpass-filtered (0.25–8 kHz) using a noncausal filter (Quian Quiroga, 2009) and re-referenced using Common Median Referencing (Rolston et al., 2009) to eliminate common-mode artifacts. All post-acquisition analysis was performed automatically using in-house written Matlab (Mathworks Inc.) programs.

Unit-identification

Putative single-units were identified using an unsupervised algorithm consisting of a simple amplitude-threshold detector (Quiroga et al., 2004) and clustering with Gaussian Mixture Models (GMM) (Pouzat et al., 2002; Ludwig et al., 2006). The threshold for spike detection was set as minus four times the estimated noise level (standard deviation of background noise) and spikes were aligned temporally at the point of maximum amplitude of the detected valley (Mitra and Bokil, 2008). The noise level was estimated using the maximum absolute deviation (MAD) estimator for standard deviation (Quiroga et al., 2004), given by:

$$\widehat{\sigma}_N = median\frac{|signal|}{0.6745}. \quad (1)$$

As features for spike sorting, the first six principal component analysis (PCA) weights were used (Lewicki, 1998). To estimate the number of units, the feature-distributions were fitted to GMMs with one to six components and the model for which the Bayesian Information Criterion (BIC) converged (BIC < 10% of the BIC-range for all models) was selected. The spikes were assigned to the unit (mixture-component) according to their maximum posterior membership-probability. Spikes that did not have a posterior membership-probability above 0.8 for any unit were classified as outliers (Ludwig et al., 2006).

Signal-to noise ratio (SNR) of units was defined as:

$$SNR = \frac{s_{pp}}{2 \cdot \sigma_N} \quad (2)$$

where s_{pp} is the peak-to-peak amplitude of the unit-waveform and σ_N is the standard deviation of residuals after subtracting the unit-waveform from each detected spike waveform. ISI (inter-spike interval) violation rate was defined as the percentage of ISIs that were shorter than 1 ms.

An automatic unit-validation procedure largely based on the manual procedure described in Suner et al. (2005) was implemented to identify putative units that could be reasonably assumed to represent neuronal activity. In Suner et al. (2005), this validation was performed by visual inspection of unit-waveforms, and by rejecting units that did not have at least a biphasic component. In order to do this in an objective and consistent manner, we extracted several descriptive features of the unit-waveforms related to this criterion. Those were: (1) polarity of the pre- and post-peak phases of the waveform (identifies strictly monophasic waveforms), (2) the amplitude-difference between waveform endpoints relative to the maximum amplitude (rejecting strongly unbalanced waveforms likely to be artifacts), (3) the number of zero-crossings of pre- and post-peak phases of the waveform (rejecting waveforms with more than 3 zero-crossings in one of the phases) and (4) temporal location of the waveform-peak (rejecting slowly varying waveforms, usually representing artifacts). In addition to these waveshape-related features, we used (5) SNR (rejecting units with SNR < 2 and SNR > 20, representing noise and artifacts, respectively), (6) ISI violation rate (rejecting units with $>0.5\%$ ISI violation rate), (7) amplitude-threshold-rate (rejecting units that only marginally crossed the detection threshold), and (8) amplitude (rejecting units with amplitude < 25 uV). The thresholds for the individual metrics were set empirically to obtain consistent rejection of units that would have been likely to be rejected by a manual procedure.

The SNR was further used to classify units as good (SNR ≥ 4), fair ($2 \leq$ SNR < 4), poor ($1 \leq$ SNR < 2), and no-signal (SNR < 1). In addition to these classes, we introduced a fifth class containing very-high SNR units (SNR > 6).

Recording Performance Over Time

To make a preliminary assessment of the recording performance over time, we measured noise level (Equation 1), SNR of valid units (Equation 2), yield, and relative difference in amplitude between units with highly correlated unit-waveforms recorded on the same channel but on different days. When evaluating performance, the SNR of recordings was taken as the SNR of the highest-SNR valid single-unit identified in the recording. Yield was defined as the percentage of electrode-sites on which at least one valid unit with SNR ≥ 2 (at least fair) or SNR ≥ 4 (at least good) was identified (Ludwig et al., 2006) and was quantified both on a per-week basis and with all days pooled together. To identify units recorded on the same channel but on different days, that might represent the same neuron, we used a method similar to that described in Fraser and Schwartz (2012) in which both the shapes of unit-waveforms and firing statistics were compared between recording sessions. However, since our experiments were performed mainly during spontaneous behavior, no measures related to firing statistics were included in our procedure. Hence, we emphasize that while suggestive, the analysis applied here does not allow safe conclusion on whether or not pairs of valid units with a high correlation between waveform shapes between different recording sessions indeed represent the same neuron.

For all pairs of valid units with SNR ≥ 2 (at least fair) identified on different days, the similarity-measure was taken as the Fisher-transformed maximum value of the cross-correlation between the unit-waveforms. The waveform-correlation threshold for what to consider as units with highly similar waveforms was set as the 90th percentile limit of the distribution of Fisher-transformed waveform-correlations for pairs consisting of units from separate animals. This resulted in a waveform-correlation threshold of 0.96. The correlation threshold was then applied to all same-animal, same-channel, different-day unit-pairs, and pairs with correlation above 0.96 were assumed to putatively represent the

same neuron. When multiple unit-pairs were found, only the pair with the highest waveform-correlation was considered.

Results

Design Features

The resulting electrode array comprised a Z-shaped suspension in the upper part of the shank designed to absorb the major part of the motions between the brain and the skull (Supplementary Video 1). Each of the electrode leads was equipped with a 100 μm long protrusion perpendicular to the main axis, which served a dual function of adding to the flexibility and anchorage in the tissue close to the recording sites. The electrode array was designed to obtain recordings from four different depths, each 400 μm apart, corresponding to layer IV–VI of the rat primary somatosensory cortex. SEM examination of the probe confirmed that a ~100 μm^2 area of gold surface was de-insulated at the recording sites. To assess the thickness necessary to allow implantation we implanted probes with a thickness of 75 μm (one animal), 100 μm (4 animals), and 125 μm (3 animals). While a thickness of 75–100 μm was deemed to thin to avoid bending during implantation, 125 um thick vehicles did not bend. From these tests we deduced the minimal thickness.

A compression test (Zwick GmbH & Co. KG, Materials Testing Machine with load cell Zwick/Roell KAP-Z (0.04-4N), zero-point deviation 0.02% and pre-load 0.08 N. Acquisition system Zwick/Roell testXpert II) was performed on five gelatin embedded and coated, dummy probes (gold-sheet corresponding to the total area of all 8 leads before individual cut out). The average maximum deformation force (Fmax, force at which the probe begins to bend) was equal to 0.373 N ($SD = 0.18$). This stiffness combined with a needle shaped tip was enough to allow implantation of the electrodes into the tissue with only minor dimpling of the surface.

The shape of the gelatin matrix after molding resulted in a probe with a needle shaped tip and an oval shank diameter (~400 μm wide and ~130 μm thick). To avoid dimpling of the cortical surface during implantation, a sharp tip angle (mean tip angle 41.3°, $SD = 3.2°$) and a tapering distal part is important. The shape used here was therefore a trade-off between the need for stabilization during implantation and a need to keep the size of the probe as small as possible.

Evaluation of Implantation and Electrode Conformation

The implantation into rat cortex proved to be smooth, without bleeding ($n = 15$) or visible conformational changes of the flexible electrode array. The gelatin matrix remained stiff enough to withstand implantation to the intended depth of 1800 μm. To investigate whether any gelatin is likely to remain non-dissolved around the implanted electrode array, gelatin embedded electrode arrays were implanted into the brains of four animals. The brain surface was kept exposed and monitored for 3.5 h. During this time the brain surface was covered by a thin layer of saline to mimic the conditions of the normal implantation procedure in which the skull opening is sealed with dental cement. These experiments showed that the brain surface had contracted around the implant with no visual trace of gelatin in any of the four animals after 3.5 h (**Figure 2**). Clarification of brain tissue slices with the electrode array still in situ (3 rats) confirmed that the electrode array could be implanted into the brain and remain in the brain for 3 weeks with preserved conformation (**Figure 3**).

Quality of Recordings in Non-restrained Awake Animals

Evaluation of electrode functionality showed that single unit activity was readily recorded during the full length of the experiment (3 weeks in 3 rats). Single units often remained quite stable both in amplitude and waveform during individual

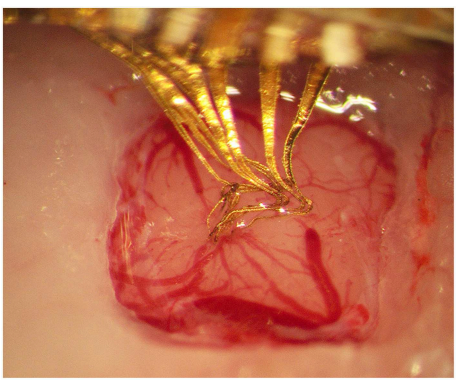

FIGURE 2 | Photograph taken 3.5 h after implantation of the gelatin embedded electrode, showing that the gelatin has dissolved and the brain surface contracted around the electrode array.

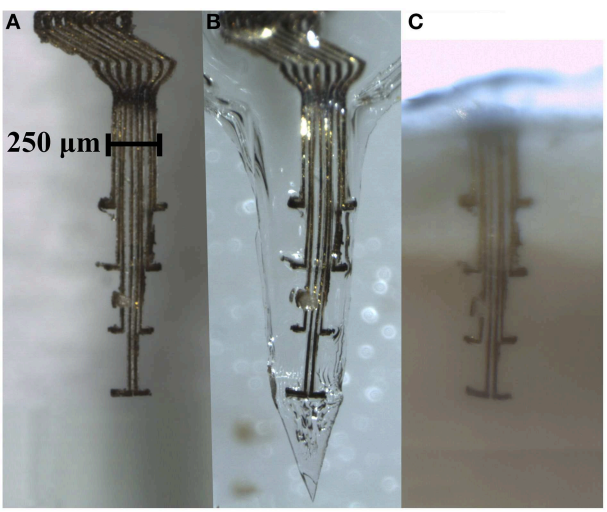

FIGURE 3 | Electrode array comprising eight thin (4 × 10 μm) gold leads insulated with Parylene C, except for an area (10 × 10 μm) at the tip of the 100 μm long protrusions. (A) An electrode array before embedding into a gelatin based matrix. **(B)** The same electrode array after being embedded into a gelatin matrix shaped as a needle, and in **(C)**, same electrode array inside a section of clarified brain tissue 3 weeks post implantation. Note that the conformation of the electrode array is well preserved inside the gelatin matrix as well as after implantation in the brain.

recording sessions (up to 50 min) as shown in **Figure 4**, indicating that the electrode recording sites remained relatively stable in the tissue during the time-course of individual recordings.

In order to verify the physiological nature of the detected spike activity tactile stimulations of the hind paw were performed and correlated to evoked spike activity through the calculation of a peri-stimulus time histogram (PSTH). An example of a single unit with high correlation to tactile stimulation is shown in **Figure 5**.

The signal quality was good throughout the experiment with an overall median noise level of 5.42 μV (IQR[1] = 2.16 μV) and overall median single-unit SNR of 3.30 (IQR = 2.30), respectively. As can be seen in **Figure 6A**, the noise level increased significantly (Mann-Whitney test, $p < 0.001$) between weeks 1 and 2, or from 4.27 to 5.95 μV (median) but remained stable ($p > 0.05$) between weeks 2 and 3. The SNR remained stable ($p > 0.05$) between weeks 1 and 2, but increased significantly ($p < 0.01$) between weeks 2 and 3, from 2.78 to 4.21 (median) (**Figure 6B**). In some cases, units with very high SNR (SNR > 6) were identified, indicating that the corresponding electrode sites in these cases were located very close to active neurons. In many cases, several single units with lower SNR were identified on the same channel, indicating that signals from more distant or electrically isolated neurons were also recorded.

Out of all electrode sites, 87.5% yielded at least one fair unit (SNR > 2), and 29.2% at least one good unit (SNR > 4) at some point in time. Over the course of the experiment, the weekly yield for both good and fair units showed a clear tendency to increase (**Figure 6C**).

On the Stability of Unit Recordings

To assess the positional stability of electrodes within the time-span of individual recording sessions, we measured the variation in mean spike-amplitude for every identified single-unit within a 1-s long moving window applied to the entire recording session. The sliding window was applied in order to diminish the influence of noise on the assessment of amplitude-variation. The amplitude-variation for a given unit was quantified as the standard deviation of relative amplitude deviations across all window positions. This analysis showed that the spike-amplitude remained relatively stable during the time-span of individual recordings, with an overall median standard deviation of 8.65% (IQR = 6.21%) across all identified single-units. Thus, for example, a single-unit with average peak-to-peak amplitude of approximately 130 μV (**Figure 4**) would be expected to vary around 130 μV by approximately 11.2 μV (8.65% of 130 μV).

Single-unit recordings obtained during different recording sessions with a waveform correlation higher than 0.96 [see

[1]IQR = Interquartile-range.

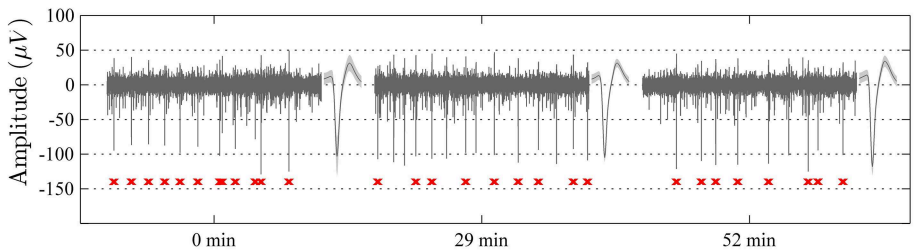

FIGURE 4 | Samples of 1 s long recordings extracted at 0, 29, and 52 min from one electrode channel in an awake non-restrained rat. The unit spike with the highest signal to noise ratio in each segment is shown to the right of respective sample (mean waveform ± standard deviation). Note the high level of stability of the recordings with respect to spike-waveforms (waveform correlation > 0.99 between the indicated unit waveforms of all three segments) and amplitude, as well as the overall recording qualities. The spike-times of the indicated single-unit are marked in red below the sweeps.

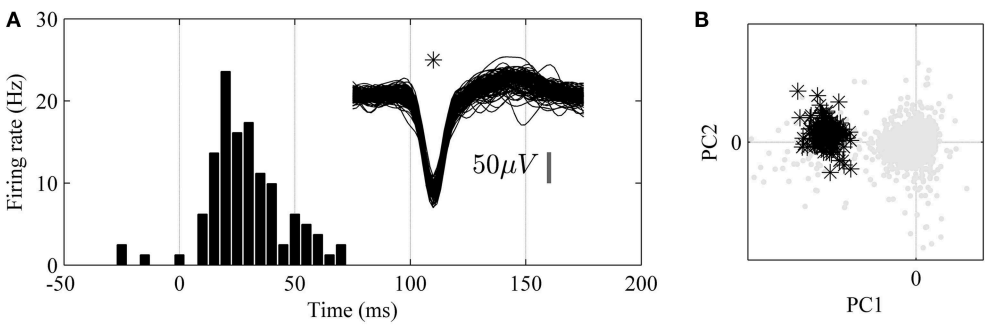

FIGURE 5 | Analysis of unit responses to tactile stimulation of the hind paw in awake, non-restrained rat. (A) Peristimulus-Time-Histogram (PSTH) for an identified single-unit (superimposed 1.6 ms long spike wave-forms for the unit are shown to the right, $n = 150$). **(B)** Principal component analysis (PCA). Note that the single unit (black stars) is well isolated from the background noise (gray dots) in the principal component (PC1 and PC2) feature space.

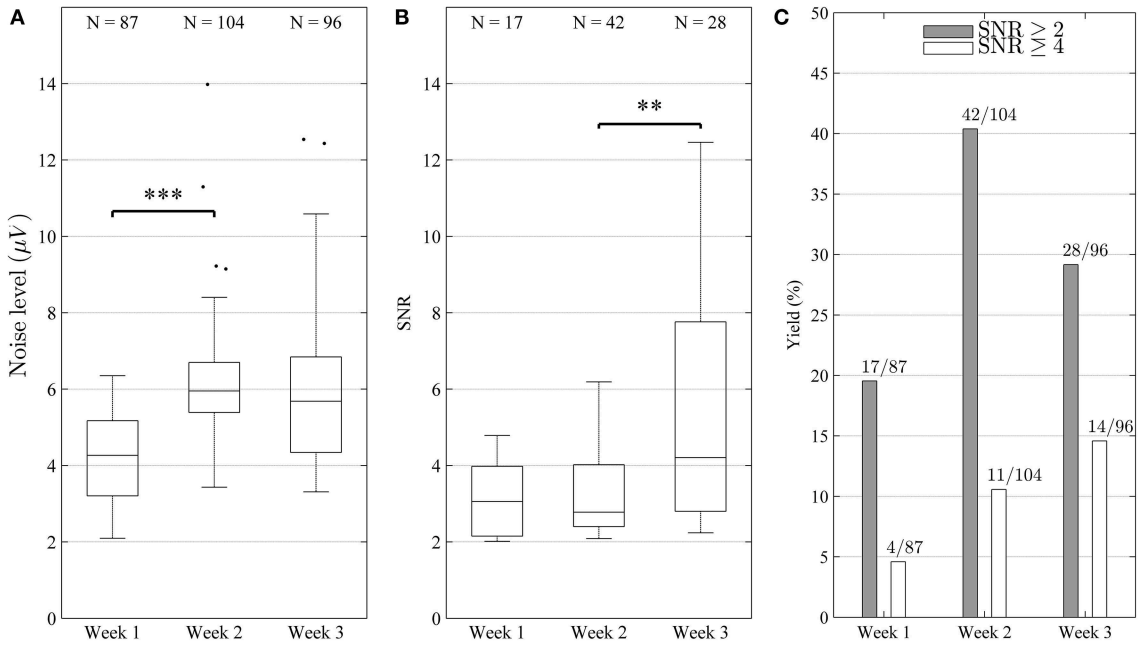

FIGURE 6 | Characterization of electrode performance over time. (A) Noise level estimated by Equation (1) (distributions shown as median and percentiles values) including all electrode channels. The noise increased significantly (***$p < 0.001$) between weeks 1 and 2, but remained stable between weeks 2 and 3 ($p > 0.05$). **(B)** Signal to noise ratio (SNR) of single-units (distribution including all identified units shown as median and percentile values) remained stable ($p > 0.05$) between week 1 and 2, but increased significantly between week 2 and 3 (**$p < 0.01$). This reflects the fact that high amplitude units were added during week 3. The increase in SNR and yield suggest that the overall recording conditions improved during the course of the experiment. **(C)** Bar diagram depicting yield in percentage (number of channels with units divided by number of channels is shown on top of each bar). It can be seen that yield increased for both good (SNR $\geq$ 4) and fair (SNR $\geq$ 2) units **(C)**, although the increase was not strictly monotonic for fair units (peaked during week 2).

Section Materials and Methods (subsection Recording Performance Over Time)] were obtained during the larger part of the experimental period in all animals. The relative difference in amplitude for such correlated waveforms was close to 1 (median = 1.22, IQR = 0.72) during the whole experiment (**Figure 7A**). No significant ($p > 0.05$) difference in relative amplitude difference was observed between week 1 and 2, and week 2 and 3. However, the relative difference in amplitude tended to be smaller (closer to 1) between week 2 and 3. Despite this relatively low overall difference in amplitude, we did observe some cases where the amplitude (and thus SNR) differed significantly (up to a factor of around 3) while the waveform remained relatively unchanged (correlation > 0.96) (**Figures 7B,C**).

In 13 out of 87 recordings where single-units were identified, the units with the highest-SNR had amplitudes greater than 150 μV. The maximum amplitude obtained for a unit was 424 uV. When comparing the waveforms of those units only, and with a stricter fixed waveform-correlation threshold of 0.99, 8 putative same-neuron pairs were identified, extending across a period of 1 day to 1 week, all within the period from day 13 and onward. Given that units with spike amplitudes >150 μV are likely to originate from units that are positioned close to the recordings electrodes (Pettersen and Einevoll, 2008; Thorbergsson et al., 2012), the high waveform correlations between recording sessions in these 8 putative same-neuron pairs is consistent with a high level of positional stability between electrode and neuron. It should be kept in mind, however, that when comparing single-units from discontinuous sessions exhibiting a high correlation of waveform shape (even for cases with correlations >0.99), it cannot be excluded that the recordings derive from different neurons since only spontaneous activity was recorded.

Discussion

In the present study, we provide a viable solution to the long-standing problem of how to implant electrode arrays, which are too flexible to be implanted without support, with retained conformation during and after implantation. The advantage of this new method is that it allows a tailored architecture of ultra-thin, and therefore more biocompatible electrodes, to be implanted in the brain. In other words, the electrode array can be designed to match the architecture of the tissue. In addition, electrodes individually flexible in all dimensions are expected to reduce the effects of micromotions/microforces which are likely to trigger tissue reactions. Furthermore, the free space between individual leads allows for electrode-tissue integration and prevents the array from creating a significant diffusion barrier. Preliminary tests in 3 animals also demonstrate that high quality recordings from single neurons can indeed by obtained using these electrodes, which is very encouraging.

We chose a rather simple array design with relatively few curved ultrathin leads as our first version. However, it should

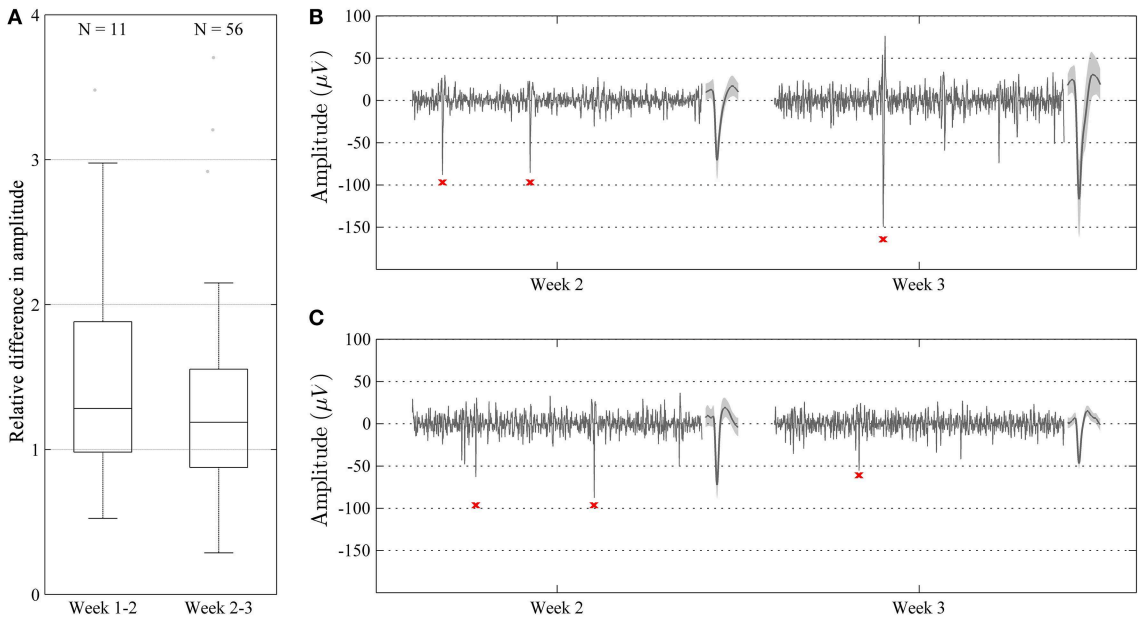

FIGURE 7 | Characterization of relative amplitudes of single unit spikes with high waveform correlation (>0.96) during two consecutive weeks. (A) Relative difference in amplitude shown as median and percentile values. The amplitude of units showed a tendency to increase over time, but this difference was not significant ($p > 0.05$). **(B,C)** Representative recordings (100 ms long) during week 2 and 3 in two different animals. Recordings are made from the same channel and show highly correlated units (waveform correlation > 0.96). Mean waveform ± standard deviation is shown to the right of each recording. In some cases, the amplitude of the units increased from week 2 to 3 **(B)**, whereas in some other cases, the amplitude decreased **(C)**.

be noted that the gelatin based vehicle can harbor practically any design of electrode array, including individual leads in the nanometer scales (Witteveen et al., 2010; Suyatin et al., 2013), as well as a larger number of individual channels. The design of the electrode array and hence relative position of recording sites can be adapted to the anatomical structure of various target areas demonstrating its potential for a wide range of applications in neuroscience research and in the clinic (Schouenborg, 2013).

On the Quality and Stability of the Obtained Recordings

The SNR and noise levels found in the present study appear to be similar to data from other current electrodes (Ludwig et al., 2006). A fair comparison of signal quality with the performance of other electrodes would, however, require standardized conditions (Ward et al., 2009). The SNR (Equation 2) was defined on a per-unit basis, using the noise level estimation for each unit individually and not the recording noise-level as defined by Equation (1). The reason for this choice was to ensure compatibility with the SNR-classes defined in Suner et al. (2005). In general, the noise-level estimate in Equation (2) was higher than that of Equation (1). Also, the factor 2 in the denominator of Equation (2) is based on the assumption of bipolar unit-waveforms with positive and negative phases of equal amplitude. However, this was very seldom the case for the units reported here, also suggesting a general underestimation of SNR. Moreover, the generally small variation in spike amplitude within the recording-sessions shows that good recording stability can be obtained in the freely moving animal.

For the majority of electrode sites, single-units were detected at different points in time that, according to the waveform shape criterion (waveform correlation > 0.96), might represent the same neurons. For all three animals, such units were detected over the major part of the observation-period of 3 weeks. Some of those units had high spike amplitudes (>150 μV) indicating that the de-insulated electrode recording sites were located close to the neurons. These findings are consistent with the assumption that good positional stability can be obtained when electrodes flexible in 3D are used. Note, however, that while a high correlation is a necessary criterion for classifying unit pairs as originating from same neurons it is not a sufficient criterion. Since recordings were discontinued between sessions it is still possible that unit pairs with a high correlation and with small changes in amplitudes could originate from different neurons (Fraser and Schwartz, 2012).

The presence of small amplitude fluctuations of unit spikes during the recording sessions suggests that micro-motions, while presumably being significantly reduced by the flexible design of the neural interface, still remain between electrodes and recorded neurons. Moreover, due to the embedding technology used here, it is expected that displacement of neurons relative to the electrodes will occur during the initial period after implantation when the tissue retracts as the gelatin gel is dissolved. Characterization of gelatin dissolution showed that gelatin dissolved and the brain contracted around the implant within 3.5 h. The inevitable loss of cells during the implantation procedure, as well as accompanying glial activation (Biran et al., 2005; Polikov et al., 2005; Leach et al., 2010) will also cause

some displacement of nearby neurons, and thus instability in recordings, during the initial week (Ludwig et al., 2006). The findings that the SNR and yield of neurons recorded per channel in fact increased over time may be related to such structural changes in the tissue. This also suggests that longer periods of stable and high quality recordings from the same neurons are within reach. Nevertheless, this remains to be evaluated in long-term studies.

Gel Embedded Electrode Arrays—Comparison with Chip-based Electrode Arrays

In this study, we demonstrate that the overall configuration of the array was well preserved after implantation. This implies there were no significant inherent strain forces in the electrode construction, which could have resulted in non-intended changes in electrode conformation after dissolution of the gelatin. Importantly, the individually separated channels (as in contrast to electrodes embedded into a sheet of polymer) allow for better diffusion inside the tissue and the opportunity for the tissue to integrate with the implant thereby creating a seamless integration of electronics and neural networks.

Gelatin was chosen as the main embedding material due to its biocompatible properties. For example, it is well known that neurons thrive on gelatin in cultures (Abranches et al., 2009) and cells embedded in gelatin have been implanted with no adverse signs reported in humans (Watts et al., 2003; Stover and Watts, 2008). Gelatin is also known to minimize bleeding, presumably due the hemostatic properties of collagen, which is the main constituent of gelatin (Marieb and Hoehn, 2010). There was no visual bleeding during and after any of the implantations of these electrodes (total number of implantations in this study $n = 15$). Thus, the minimal bleeding observed during implantation in this study could be due to the hemostatic properties of collagen.

Moreover, in a previous study in our lab we found that the brain is capable of eliminating implanted pure gelatin needles without forming a permanent scar (Lind et al., 2010). By contrast, a "stab wound" scar was clearly present after 12 weeks when using a non-gelatin embedded needle. More recently, we also found that gelatin coating of flexible probes not only significantly reduces microglial activation but also appears to preserve a normal neuronal density in the area adjacent to the electrode, i.e., a 50 μm wide zone around flexible probes (Köhler et al., 2015). This is in sharp contrast to previous studies reporting a reduction in neuronal density ranging between 20 and 60% in this inner zone (Biran et al., 2005; McConnell et al., 2009; Winslow and Tresco, 2010).

Limitations and Future Directions

The development of biocompatible neural interfaces is a very time consuming process, involving multiple cycles of design changes followed by *in vivo* testing. In fact, the present study took several years of developmental work. The present work was focused on evaluating the performance *in vivo* during a relatively short period of time. This short-term study shows that the proposed method makes it possible to manufacture and implant arrays of ultra-flexible, individually separated electrodes whose recording quality is improved after 2 weeks. Given these promising results, long-term studies are a logical next step. Such long-term studies are also needed to compare long-term performance with current neural interfaces and to evaluate several potential improvements of the developed neural interface. For example, the exposed de-insulated tips may be provided with surface enlargements to reduce the impedance and thereby the noise level, e.g., by electroplating procedures (Desai et al., 2010; Ludwig et al., 2011; Ejserholm et al., 2014). Also, the flexibility, and thereby presumably stability, can be further improved by e.g., using thinner leads and/or more curvy shapes of the leads. However, thinner electrodes are more prone to break during manufacturing and implantation procedures and this may thus limit the feasibility of such attempts. Notably, the previous assumption that the size of the electrodes *per se* is critical for long-term glial reactions (Stice et al., 2007; Thelin et al., 2011) may however be erroneous since also large implanted probes elicit very small chronic reactions provided they are truly floating in the brain, i.e., that their specific weight is close to that of the tissue (Lind et al., 2013).

While the present results are encouraging, future long-term studies of probe functions would benefit from being performed during well-defined behavioral tasks to permit an analysis of possible probe induced alterations in neuronal activity. Moreover, more frequent recording sessions would make the unit-tracking procedure more reliable due to the possibility to include measures related to firing-characteristics (Fraser and Schwartz, 2012) and facilitate a more precise quantification of the day-to-day changes of the relative position of the electrode.

It should also be noted that, while a primary purpose of embedding the electrodes in a hard but dissolvable matrix material was to provide the necessary support for fragile electrodes during implantation, the possibility of adding drugs to the embedding material could potentially also provide new opportunities in e.g., pharmacology (Ek et al., 2010). Moreover, by incorporating drugs in the embedding matrix material, e.g., neurotrophic factors, which are released locally in the brain during and after the implantation, it may be possible to promote restitution of the neuronal circuits after the injury caused by the implantation (Gámez et al., 2004; Chang, 2009).

Concluding Remarks

While this first design of gelatin embedded electrode arrays most likely can be improved as discussed above, the present results are encouraging since they suggests that stable long-term communications with the same neurons are indeed attainable. From a research perspective, the importance of stable communication lies in that it will open up for an extraordinarily detailed analysis of how the neuronal circuits in the brain functions under physiological and pathological conditions (Schouenborg, 2011). In particular, the identification and analysis of plastic long-term alterations in neural networks, e.g., during learning or during neurodegenerative diseases, would benefit considerably by stable long-term recordings from the same neurons.

From a clinical perspective, stable recordings of neural activity is a prerequisite for developing robust and interactive protocols for enhancing efficacy and safety of stimulation based treatment (for example deep brain stimulation). In addition, the finding

that the configuration of the highly flexible electrode array was retained inside the cortex cerebri after 3 weeks, indicate that a seamless integration of electronics and neural circuits is possible in the near future. Such integration, in particular if stability can be achieved over long periods of time, has the potential of enabling highly interesting neuroengineering development in the future, aiming at, for example, restitution of neural circuits after injury.

Acknowledgments

This project was sponsored by a Linnaeus grant (project number 60012701) and project 01013 from the Swedish Research Council, The Knut and Alice Wallenberg Foundation (project number: KAW 2004.0119), grants from Skåne County Council (ALF), 2014/354 and the Nanometer Structure Consortium (nmC@LU) at Lund University. The authors would like to thank Petter Pettersson, Peter Paulander and Suzanne Rosander-Jönsson for their skillful technical assistance.

Supplementary Material

The Supplementary Material for this article can be found online at: http://journal.frontiersin.org/article/10.3389/fnins.2015.00331

References

Abranches, E., Silva, M., Pradier, L., Schulz, H., Hummel, O., Henrique, D., et al. (2009). Neural differentiation of embryonic stem cells *in vitro*: a road map to neurogenesis in the embryo. *PLoS ONE* 4:6286. doi: 10.1371/journal.pone.0006286

Andrei, A., Tutunjyan, N., Verbinnen, G., Vanput, S., Krylychkina, O., Eberle, W., et al. (2012). "Fabrication and successful *in-vivo* implantation of a flexible neural implant with a hybrid polyimide-silicon design," in *Proceedings of the Annual International Conference of the IEEE Engineering in Medicine and Biology Society, EMBS* (San Diego, CA), 3890–3893.

Bae, W. J., Ruddy, B. P., Richardson, A. G., Hunter, I. W., and Bizzi, E. (2008). "Cortical recording with polypyrrole microwire electrodes," in *Conference Proceedings?: Annual International Conference of the IEEE Engineering in Medicine and Biology Society* (Vancouver, BC), 5794–5797.

Biran, R., Martin, D. C., and Tresco, P. A. (2005). Neuronal cell loss accompanies the brain tissue response to chronically implanted silicon microelectrode arrays. *Exp. Neurol.* 195, 115–126. doi: 10.1016/j.expneurol.2005.04.020

Biran, R., Martin, D. C., and Tresco, P. A. (2007). The brain tissue response to implanted silicon microelectrode arrays is increased when the device is tethered to the skull. *J. Biomed. Mat. Res. Part A* 82, 169–178. doi: 10.1002/jbm.a.31138

Britt, R. H., and Rossi, G. T. (1982). Quantitative analysis of methods for reducing physiological brain pulsations. *J. Neurosci. Methods* 6, 219–229. doi: 10.1016/0165-0270(82)90085-1

Chang, C.-J. (2009). The effect of pulse-released nerve growth factor from genipin-crosslinked gelatin in schwann cell-seeded polycaprolactone conduits on large-gap peripheral nerve regeneration. *Tissue Eng. Part A*, 15, 547–557. doi: 10.1089/ten.tea.2007.0342

De Faveri, S., Maggiolini, E., Miele, E., De Angelis, F., Cesca, F., Benfenati, F., et al. (2014). Bio-inspired hybrid microelectrodes: a hybrid solution to improve long-term performance of chronic intracortical implants. *Front. Neuroeng.* 7:7. doi: 10.3389/fneng.2014.00007

Desai, S. A., Rolston, J. D., Guo, L., and Potter, S. M. (2010). Improving impedance of implantable microwire multi-electrode arrays by ultrasonic electroplating of durable platinum black. *Front. Neuroeng.* 3:5. doi: 10.3389/fneng.2010.00005

Eide, P. K. (2008). Comparison of simultaneous continuous intracranial pressure (ICP) signals from ICP sensors placed within the brain parenchyma and the epidural space. *Med. Eng. Phys.* 30, 34–40. doi: 10.1016/j.medengphy.2007.01.005

Ejserholm, F., Köhler, P., Granmo, M., Schouenborg, J., and Bengtsson, M., W. L. (2014). μ-Foil polymer electrode array for intracortical neural recordings. *IEEE J. Trans. Eng. Health Med.* 2, 1–7. doi: 10.1109/JTEHM.2014.2326859

Ek, F., Danielsen, N., Eriksson, J., Petersson, P., and Schouenborg, J. (2010). *Microelectrode and multiple microelectrodes.* Patent US 8954142 B2. PCT/SE2010/000152.

Felix, S., Shah, K., George, D., Tolosa, V., Tooker, A., Sheth, H., et al. (2012). "Removable silicon insertion stiffeners for neural probes using polyethylene glycol as a biodissolvable adhesive," in *Proceedings of the Annual International Conference of the IEEE Engineering in Medicine and Biology Society, EMBS* (San Diego, CA), 871–874.

Fraser, G. W., and Schwartz, A. B. (2012). Recording from the same neurons chronically in motor cortex. *J. Neurophysiol.* 107, 1970–1978. doi: 10.1152/jn.01012.2010

Gámez, E., Goto, Y., Nagata, K., Iwaki, T., Sasaki, T., and Matsuda, T. (2004). Photofabricated gelatin-based nerve conduits: nerve tissue regeneration potentials. *Cell Transp.* 13, 549–564. doi: 10.3727/000000004783983639

Gilletti, A., and Muthuswamy, J. (2006). Brain micromotion around implants in the rodent somatosensory cortex. *J. Neural Eng.* 3, 189–195. doi: 10.1088/1741-2560/3/3/001

Granmo, M., Jensen, T., and Schouenborg, J. (2013). Nociceptive transmission to rat primary somatosensory cortex – comparison of sedative and analgesic effects. *PLoS ONE* 8:e53966. doi: 10.1371/journal.pone.0053966

Jackson, A., and Fetz, E. E. (2007). Compact movable microwire array for long-term chronic unit recording in cerebral cortex of primates. *J. Neurophysiol.* 98, 3109–3118. doi: 10.1152/jn.00569.2007

Kalliomäki, J., Weng, H.-R., Nilsson, H.-J., and Schouenborg, J. (1993). Nociceptive C fibre input to the primary somatosensory cortex (SI). A field potential study in the rat. *Brain Res.* 622, 262–270. doi: 10.1016/0006-8993(93)90827-A

Kim, Y. T., Hitchcock, R. W., Bridge, M. J., and Tresco, P. A. (2004). Chronic response of adult rat brain tissue to implants anchored to the skull. *Biomaterials* 25, 2229–2237. doi: 10.1016/j.biomaterials.2003.09.010

Kipke, D. R., Pellinen, D. S., and Vetter, R. J. (2002). "Advanced neural implants using thin-film polymers," in *2002 IEEE International Symposium on Circuits and Systems. Proceedings (Cat. No.02CH37353)* (Phoenix-Scottsdale, AZ), 4.

Köhler, P., Wolff, A., Ejserholm, F., Wallman, L., Schouenborg, J., and Linsmeier, C. E. (2015). Influence of probe flexibility and gelatin embedding on neuronal density and glial responses to brain implants. *PLoS ONE* 10:e0119340. doi: 10.1371/journal.pone.0119340

Kozai, T. D. Y., Gugel, Z., Li, X., Gilgunn, P. J., Khilwani, R., Ozdoganlar, O. B., et al. (2014). Chronic tissue response to carboxymethyl cellulose based dissolvable insertion needle for ultra-small neural probes. *Biomaterials* 35, 9255–9268. doi: 10.1016/j.biomaterials.2014.07.039

Krüger, J., Carulana, F., Volta, R. D., and Rizzolatti, G. (2010). Seven years of recording from monkey cortex with a chronically implanted multiple microelectrode. *Front. Neuroeng.* 3:6. doi: 10.3389/fneng.2010.00006

Kuo, J. T. W., Kim, B. J., Hara, S. A., Lee, C. D., Gutierrez, C. A., Hoang, T. Q., et al. (2013). Novel flexible Parylene neural probe with 3D sheath structure for enhancing tissue integration. *Lab. Chip.* 13, 554–561. doi: 10.1039/c2lc40935f

Leach, J. B., Achyuta, A. K. H., and Murthy, S. K. (2010). Bridging the divide between neuroprosthetic design, tissue engineering and neurobiology. *Front. Neuroeng.* 2:18. doi: 10.3389/neuro.16.018.2009

Lee, S. E., Jun, S. B., Lee, H. J., Kim, J., Lee, S. W., Im, C., et al. (2012). A flexible depth probe using liquid crystal polymer. *IEEE Trans. Biomed. Eng.* 59, 2085–2094. doi: 10.1109/TBME.2012.2196274

Lewicki, M. S. (1998). A review of methods for spike sorting: the detection and classification of neural action potentials. *Netw. (Bristol, England)* 9, R53–R78. Available online at: http://www.ncbi.nlm.nih.gov/pubmed/10221571

Lind, G., Linsmeier, C. E., and Schouenborg, J. (2013). The density difference between tissue and neural probes is a key factor for glial scarring. *Sci. Rep.* 3:2942. doi: 10.1038/srep02942

Lind, G., Linsmeier, C. E., Thelin, J., and Schouenborg, J. (2010). Gelatine-embedded electrodes–a novel biocompatible vehicle allowing implantation of highly flexible microelectrodes. *J. Neural Eng.* 7:046005. doi: 10.1088/1741-2560/7/4/046005

Ludwig, K. A., Langhals, N. B., Joseph, M. D., Richardson-Burns, S. M., Hendricks, J. L., and Kipke, D. R. (2011). Poly(3,4-ethylenedioxythiophene) (PEDOT) polymer coatings facilitate smaller neural recording electrodes. *J. Neural Eng.* 8:014001. doi: 10.1088/1741-2560/8/1/014001

Ludwig, K. A., Uram, J. D., Yang, J., Martin, D. C., and Kipke, D. R. (2006). Chronic neural recordings using silicon microelectrode arrays electrochemically deposited with a poly(3,4-ethylenedioxythiophene) (PEDOT) film. *J. Neural Eng.* 3, 59–70. doi: 10.1088/1741-2560/3/1/007

Marieb, E. N., and Hoehn, K. (2010). Human anatomy and physiology. *Physiology* 7, 664–668. doi: 10.1038/nnano.2011.234

McConnell, G. C., Rees, H. D., Levey, A. I., Gutekunst, C.-A., Gross, R. E., and Bellamkonda, R. V. (2009). Implanted neural electrodes cause chronic, local inflammation that is correlated with local neurodegeneration. *J. Neural Eng.* 6:056003. doi: 10.1088/1741-2560/6/5/056003

Mitra, P., and Bokil, H. (2008). *Observed Brain Dynamics*. Oxford University Press. Available online at: http://www.amazon.com/Observed-Brain-Dynamics-Partha-Mitra/dp/0195178084

Musallam, S., Bak, M. J., Troyk, P. R., and Andersen, R. A. (2007). A floating metal microelectrode array for chronic implantation. *J. Neurosci. Methods* 160, 122–127. doi: 10.1016/j.jneumeth.2006.09.005

Nolta, N. F., Christensen, M. B., Crane, P. D., Skousen, J. L., and Tresco, P. A. (2015). BBB leakage, astrogliosis, and tissue loss correlate with silicon microelectrode array recording performance. *Biomaterials* 53, 753–762. doi: 10.1016/j.biomaterials.2015.02.081

Pettersen, K. H., and Einevoll, G. T. (2008). Amplitude variability and extracellular low-pass filtering of neuronal spikes. *Biophys. J.* 94, 784–802. doi: 10.1529/biophysj.107.111179

Polikov, V. S., Tresco, P. A., and Reichert, W. M. (2005). Response of brain tissue to chronically implanted neural electrodes. *J. Neurosci. Methods* 148, 1–18. doi: 10.1016/j.jneumeth.2005.08.015

Pouzat, C., Mazor, O., and Laurent, G. (2002). Using noise signature to optimize spike-sorting and to assess neuronal classification quality. *J. Neurosci. Methods* 122, 43–57. doi: 10.1016/S0165-0270(02)00276-5

Quian Quiroga, R. (2009). What is the real shape of extracellular spikes? *J. Neurosci. Methods* 177, 194–198. doi: 10.1016/j.jneumeth.2008.09.033

Quiroga, R. Q., Nadasdy, Z., and Ben-Shaul, Y. (2004). Unsupervised spike detection and sorting with wavelets and superparamagnetic clustering. *Neural Comput.* 16, 1661–1687. doi: 10.1162/089976604774201631

Rolston, J. D., Gross, R. E., and Potter, S. M. (2009). "Common median referencing for improved action potential detection with multielectrode arrays," in *Conference Proceedings: Annual International Conference of the IEEE Engineering in Medicine and Biology Society* (Minneapolis, MN), 1604–1607.

Rousche, P. J., and Normann, R. A. (1998). Chronic recording capability of the utah intracortical electrode array in cat sensory cortex. *J. Neurosci. Methods* 82, 1–15. doi: 10.1016/S0165-0270(98)00031-4

Rousche, P. J., Pellinen, D. S., Pivin, D. P. Jr., Williams, J. C., Vetter, R. J., and Kipke, D. R. (2001). Flexible polyimide-based intracortical electrode arrays with bioactive capability. *IEEE Trans. Biomed. Eng.* 48, 361–370. doi: 10.1109/10.914800

Santhanam, G., Linderman, M. D., Gilja, V., Afshar, A., Ryu, S. I., Meng, T. H., et al. (2007). HermesB: A continuous neural recording system for freely behaving primates. *IEEE Trans. Biomed. Eng.* 54, 2037–2050. doi: 10.1109/TBME.2007.895753

Schouenborg, J. (2011). Biocompatible multichannel electrodes for long-term neurophysiological studies and clinical therapy-Novel concepts and design. *Progr. Brain Res.* 194, 61–70. doi: 10.1016/B978-0-444-53815-4.00017-0

Schouenborg, J. (2013). *Medical Electrode, Electrode Bundle and Electrode Bundle Array*. US 8,386,006 B2, Feb 2013.

Seymour, J. P., and Kipke, D. R. (2007). Neural probe design for reduced tissue encapsulation in CNS. *Biomaterials* 28, 3594–3607. doi: 10.1016/j.biomaterials.2007.03.024

Sohal, H. S., Jackson, A., Jackson, R., Clowry, G. J., Vassilevski, K., O'Neill, A., et al. (2014). The sinusoidal probe: a new approach to improve electrode longevity. *Front. Neuroeng.* 7:10. doi: 10.3389/fneng.2014.00010

Stice, P., Gilletti, A., Panitch, A., and Muthuswamy, J. (2007). Thin microelectrodes reduce GFAP expression in the implant site in rodent somatosensory cortex. *J. Neural Eng.* 4, 42–53. doi: 10.1088/1741-2560/4/2/005

Stover, N. P., and Watts, R. L. (2008). Spheramine for treatment of Parkinson's disease. *Neurotherapeutics* 5, 252–259. doi: 10.1016/j.nurt.2008.02.006

Suner, S., Fellows, M. R., Vargas-Irwin, C., Nakata, G. K., and Donoghue, J. P. (2005). Reliability of signals from a chronically implanted, silicon-based electrode array in non-human primate primary motor cortex. *IEEE Trans. Neural Syst. Rehabil. Eng.* 13, 524–541. doi: 10.1109/TNSRE.2005.857687

Suyatin, D. B., Wallman, L., Thelin, J., Prinz, C. N., Jörntell, H., Samuelson, L., et al. (2013). Nanowire-based electrode for acute *in vivo* neural recordings in the brain. *PLoS ONE* 8:56673. doi: 10.1371/journal.pone.0056673

Szarowski, D. H., Andersen, M. D., Retterer, S., Spence, A. J., Isaacson, M., Craighead, H. G., et al. (2003). Brain responses to micro-machined silicon devices. *Brain Res.* 983, 23–35. doi: 10.1016/S0006-8993(03)03023-3

Takeuchi, S., Ziegler, D., Yoshida, Y., Mabuchi, K., and Suzuki, T. (2005). Parylene flexible neural probes integrated with microfluidic channels. *Lab. Chip.* 5, 519–523. doi: 10.1039/b417497f

Thelin, J., Jörntell, H., Psouni, E., Garwicz, M., Schouenborg, J., Danielsen, N., et al. (2011). Implant size and fixation mode strongly influence tissue reactions in the CNS. *PLoS ONE* 6:16267. doi: 10.1371/journal.pone.0016267

Thorbergsson, P. T., Garwicz, M., Schouenborg, J., and Johansson, A. J. (2012). Computationally efficient simulation of extracellular recordings with multielectrode arrays. *J. Neurosci. Methods* 211, 133–144. doi: 10.1016/j.jneumeth.2012.08.011

Turner, J. N., Shain, W., Szarowski, D. H., Andersen, M., Martins, S., Isaacson, M., et al. (1999). Cerebral astrocyte response to micromachined silicon implants. *Exp. Neurol.* 156, 33–49. doi: 10.1006/exnr.1998.6983

Wagshul, M. E., Eide, P. K., and Madsen, J. R. (2011). The pulsating brain: a review of experimental and clinical studies of intracranial pulsatility. *Fluids Barriers CNS* 8:5. doi: 10.1186/2045-8118-8-5

Ward, M. P., Rajdev, P., Ellison, C., and Irazoqui, P. P. (2009). Toward a comparison of microelectrodes for acute and chronic recordings. *Brain Res.* 1282, 183–200. doi: 10.1016/j.brainres.2009.05.052

Watts, R. L., Raiser, C. D., Stover, N. P., Cornfeldt, M. L., Schweikert, A. W., Allen, R. C., et al. (2003). Stereotaxic intrastriatal implantation of human retinal pigment epithelial (hRPE) cells attached to gelatin microcarriers: a potential new cell therapy for Parkinson's disease. *J. Neural Transm. Suppl.* 65, 215–227. doi: 10.1007/978-3-7091-0643-3_14

Williams, J. C., Rennaker, R. L., and Kipke, D. R. (1999). Long-term neural recording characteristics of wire microelectrode arrays implanted in cerebral cortex. *Brain Res. Protoc.* 4, 303–313. doi: 10.1016/S1385-299X(99)00034-3

Winslow, B. D., and Tresco, P. A. (2010). Quantitative analysis of the tissue response to chronically implanted microwire electrodes in rat cortex. *Biomaterials* 31, 1558–1567. doi: 10.1016/j.biomaterials.2009.11.049

Witteveen, J. A., Suyatin, D. B., Gällentoft, L., Schouenborg, J., Danielsen, N., and Prinz, C. N. (2010). Gelatin/glycerol coating to preserve mechanically compliant nanowire electrodes from damage during brain implantation. *J. Vac. Sci. Technol. B* 28, C6K13–C6K16. doi: 10.1116/1.3498764

Conflict of Interest Statement: Jens Schouenborg is an inventor of issued patents or patent applications on flexible electrodes embedded in dissolvable matrix materials and cofounder of Neuronano AB that owns the patents. Jens Schouenborg did not take part in the actual data handling. The other authors have no competing financial interests. There has been no significant financial support for this work that could have influenced its outcome.

frontiers in Neuroscience

ORIGINAL RESEARCH
published: 18 November 2016
doi: 10.3389/fnins.2016.00528

EEG Negativity in Fixations Used for Gaze-Based Control: Toward Converting Intentions into Actions with an Eye-Brain-Computer Interface

Sergei L. Shishkin[1], Yuri O. Nuzhdin[1], Evgeny P. Svirin[1], Alexander G. Trofimov[2], Anastasia A. Fedorova[1], Bogdan L. Kozyrskiy[1,3] and Boris M. Velichkovsky[1,4,5]*

[1] Department of Neurocognitive Technologies, Kurchatov Complex of NBICS Technologies, National Research Centre "Kurchatov Institute," Moscow, Russia, [2] Department of Cybernetics, National Research Nuclear University MEPhI, Moscow, Russia, [3] Department of Computer Systems and Technologies, National Research Nuclear University MEPhI, Moscow, Russia, [4] Centre for Cognitive Programs and Technologies, Russian State University for Humanities, Moscow, Russia, [5] Department of Psychology, Technische Universität Dresden, Dresden, Germany

OPEN ACCESS

Edited by:
Mikhail Lebedev, Duke University, USA

Reviewed by:
George C. McConnell, Stevens Institute of Technology, USA
Witali Dunin-Barkowski, Scientific Research Institute of System Analysis (RAS), Russia

***Correspondence:**
Sergei L. Shishkin
sergshishkin@mail.ru

Specialty section:
This article was submitted to Neuroprosthetics, a section of the journal Frontiers in Neuroscience

Received: *06 September 2016*
Accepted: *31 October 2016*
Published: *18 November 2016*

Citation:
Shishkin SL, Nuzhdin YO, Svirin EP, Trofimov AG, Fedorova AA, Kozyrskiy BL and Velichkovsky BM (2016) EEG Negativity in Fixations Used for Gaze-Based Control: Toward Converting Intentions into Actions with an Eye-Brain-Computer Interface. Front. Neurosci. 10:528. doi: 10.3389/fnins.2016.00528

We usually look at an object when we are going to manipulate it. Thus, eye tracking can be used to communicate intended actions. An effective human-machine interface, however, should be able to differentiate intentional and spontaneous eye movements. We report an electroencephalogram (EEG) marker that differentiates gaze fixations used for control from spontaneous fixations involved in visual exploration. Eight healthy participants played a game with their eye movements only. Their gaze-synchronized EEG data (fixation-related potentials, FRPs) were collected during game's control-on and control-off conditions. A slow negative wave with a maximum in the parietooccipital region was present in each participant's averaged FRPs in the control-on conditions and was absent or had much lower amplitude in the control-off condition. This wave was similar but not identical to stimulus-preceding negativity, a slow negative wave that can be observed during feedback expectation. Classification of intentional vs. spontaneous fixations was based on amplitude features from 13 EEG channels using 300 ms length segments free from electrooculogram contamination (200–500 ms relative to the fixation onset). For the first fixations in the fixation triplets required to make moves in the game, classified against control-off data, a committee of greedy classifiers provided 0.90 ± 0.07 specificity and 0.38 ± 0.14 sensitivity. Similar (slightly lower) results were obtained for the shrinkage Linear Discriminate Analysis (LDA) classifier. The second and third fixations in the triplets were classified at lower rate. We expect that, with improved feature sets and classifiers, a hybrid dwell-based Eye-Brain-Computer Interface (EBCI) can be built using the FRP difference between the intended and spontaneous fixations. If this direction of BCI development will be successful, such a multimodal interface may improve the fluency of interaction and can possibly become the basis for a new input device for paralyzed and healthy users, the EBCI "Wish Mouse."

Keywords: brain-computer interfaces, human-computer interfaces, gaze interaction, assistive technology, eye tracking, detection of intention, slow cortical potentials, stimulus-preceding negativity

INTRODUCTION

A brain-computer interface (BCI) is a tool of control and communication without using muscles or peripheral nerves, through the use of brain signals only (Wolpaw et al., 2002). The lay public often expects that such tools should directly and effortlessly converts internal intents into actions in the outside physical world. In reality, however, BCIs provide much slower interaction comparing to traditional human-machine interfaces, such as mouse and keyboard computer input. Most of mental operations and states cannot be detected from the electroencephalogram (EEG) or other non-invasive brain signals on single-trial basis within seconds. A typical BCI does not recognize the user's whishes or action plans directly; to send a command, a user needs to execute one of a limited range of motor imagery, cognitive or perceptual tasks that can evoke recognizable brain signals. Such tasks are typically unrelated to the current activity and their use imposes additional mental load and decreases the fluency of BCI use. Invasive BCIs are promising, but high risks and costs associated with brain surgery require further efforts to make this technology acceptable even for severely paralyzed patients (Lahr et al., 2015; Bowsher et al., 2016; Waldert, 2016).

Can a machine recognize our intentions more directly at least in certain situations? Consider, for example, using a computer Graphical User Interface (GUI) by a healthy person. When he or she decides to click a screen button or a link, they need to take a mouse with their hand, move the cursor to the screen button or link and then click the mouse button (**Figure 1**, **upper panel**). Imagine that the computer analyzes his or her brain signals and can detect signal patterns related to the intention to make an action, so that the mouse is no longer needed. It is likely that, under these settings, the user could better focus on their main activity, because they would not need to switch to any motor task (**Figure 1**, **bottom panel**).

In this case, gaze positioning would play important role, and eye muscles need to be used intensively. However, the same is true for the operation of any non-invasive BCI when high information transfer rate is demonstrated: it is always a gaze-dependent operation, in a partial contradiction to Wolpaw et al. (2002) strict definition of a BCI. The user of such BCIs (the Steady State Visual Evoked Potential based BCI, SSVEP BCI; the codebook Visual Evoked Potential based BCI, cVEP BCI; the P300 wave based BCI, P300 BCI, when it is used by healthy people and some of the EEG electrodes are placed over the visual areas) selects one of a number of spatially distinct stimuli with his or her gaze, and the BCI task is actually to find where the user is looking by analyzing the brain's fully automatic response to stimulation.

In other words, these BCIs play the role of an eye tracker, and the brain's response to stimuli is used in such BCIs somewhat similarly to the use of the corneal reflection in a video based eye tracker. Moreover, a BCI that uses spatially distinct visual stimuli is an eye tracker with limited capabilities: unlike the usual eye trackers, it cannot determine coordinates of an arbitrary gaze position, but only indicate at which one of the stimuli the user is looking. Although attention is involved, and attempts were made to use overt and covert attention as separate BCI control channels, its direct (not gaze-mediated) effect is low comparing to gaze dependent effects. This is one of the main reasons why performance of the same BCI systems is, unfortunately, much lower in severely paralyzed users who do not control their gaze well (e.g., Sellers et al., 2010). In addition, as these BCIs depend on repetitive presentation of visual stimuli, GUIs should be significantly modified to become compatible with them.

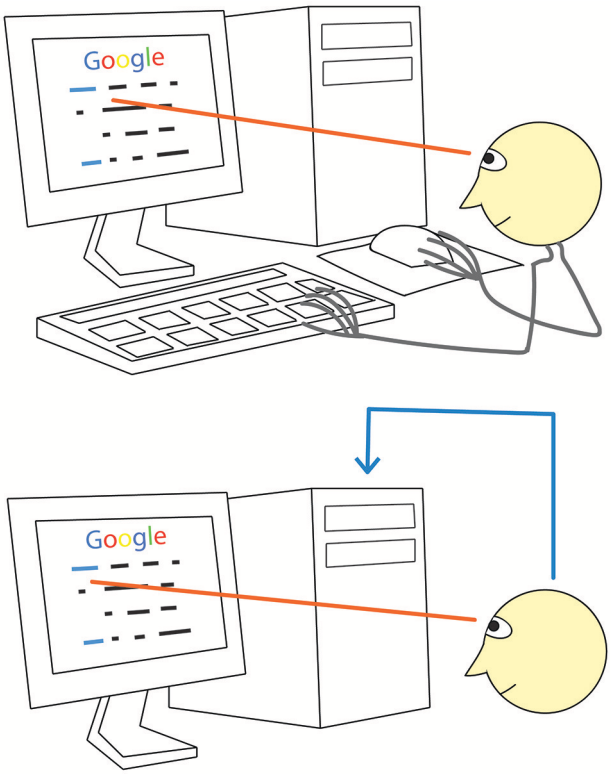

FIGURE 1 | A direct way to convey your desire to a computer: just look! When using a monitor, we normally look at a screen button or a link before clicking on them (upper panel). Between looking and clicking, we take the mouse (if we are not holding it all time), locate the cursor, move the cursor to the button or link, check if it reached the target. Gaze fixation at a given monitor location, however, can be promptly recognized with an eye tracker. If our intention to click would be recognized with some technology based on brain signal analysis (**lower panel, blue line**), computer control could be obtained without the above listed range of motor and sensory activities. (Generally, detection of gaze fixations alone is not enough due to the Midas touch problem, see text for details).

The technology that enables direct interaction with computers using eye gaze also exists and is already used to assist paralyzed people in such tasks as typing and web browsing, with better performance than typical BCIs offer (Bolt, 1982; Jacob, 1990, 1991; Velichkovsky et al., 1997; Majaranta and Bulling, 2014). In a frequent variant of this technology, a video based eye tracker captures gaze direction. Intentionally prolonged gaze fixations (dwells) on elements of GUI, such as screen buttons, are detected and converted into equivalents of mouse clicks. It was, however, recognized early in the development of gaze-based interaction that the eye movements and fixations used for sending commands in such interfaces are similar to eye

movements and fixations that are a part of normal eye behavior unrelated to interaction, such as viewing (Jacob, 1990, 1991). The interaction systems that are based on gaze direction, therefore, cannot distinguish between attempts to issue a command and the visual gaze fixations, and this leads to the Midas touch problem (Jacob, 1990, 1991): wherever the user looks, a command is activated, even if he or she has no intention to produce any command.

It was also stated at that early stage of developing gaze-base interaction with computers that the main issue in this field is "appropriate interaction techniques that incorporate eye movements into the user-computer dialogue in a convenient and natural way" (Jacob, 1990, p. 11). Such techniques have not been developed so far, despite many attempts to solve the Midas touch problem. For example, if only fixations on screen buttons exceeding a long (1000 ms or longer) threshold produce "clicks," erroneous command activations will be rare, but the need to use such long fixation will slow down the control and make it tiresome. Impressive speed of interaction was recently achieved with dwell-free typing approach (Kristensson and Vertanen, 2012; Sarcar et al., 2013; Pedrosa et al., 2015), however, it seems to impose high attentional demands. Another recently developed approach to increase the speed is to use, as a marker of control, a saccade to a new position of interest that naturally occurs immediately after the feedback at the position where the user currently looks for control (Publicover et al., 2016). In this case, short fixation duration thresholds can be used because unintended selection are typically not confirmed by such well-timed saccades. This system, by definition, cannot work when the user does not respond to feedback quickly enough. Thus, attentional demands imposed by this system can also be high. Other attempts to provide markers for command-related gaze fixations or eye movements (see, e.g., Velichkovsky et al., 1997; Majaranta and Bulling, 2014, for reviews) possessed the same or other drawbacks.

One may expect that brain state and/or course of brain activity differs strongly during gaze fixations related to attempts to send a command and gaze fixations related to other activities, such as free viewing or mind wandering. A "click" on a fixated GUI element could be made on the basis of fast detection of brain activity patterns that correlate with the intention to activate a command (**Figure 1**, **bottom panel**). The joint use of the information from "eyes and brains" for GUI control ("point with your eye and click with your mind!") was proposed as early as in 1996 (Velichkovsky and Hansen, 1996).

Several attempts to enhance gaze based control with a "mental click" recognized by BCI has been made. However, the use of additional mental tasks, such as motor imagery (e.g., in Zander et al., 2010) or mental concentration (Kim et al., 2015) does not seem to be effective, because BCIs cannot reliably recognize such activity within a fixation unless it is very long. Moreover, the use of additional mental task may itself interfere with the main mental activity. It is, therefore, not surprising that in a recent extensive review of hybrid BCIs only 3 of 55 reviewed journal papers addressed the Midas touch problem (Banville and Falk, 2016; see also other reviews on hybrid BCIs by Pfurtscheller et al., 2010; Müller-Putz et al., 2015). It seems that mechanistically combining gaze based technologies with existing BCIs cannot lead to the development of an efficient input system.

Zander and colleagues (Ihme and Zander, 2011; Protzak et al., 2013) proposed to make use of the EEG patterns that naturally accompany gaze based control. Their works were based on the "passive BCI" approach, i.e., the detection of brain signal patterns that naturally accompany the brain activities of interest, without the need from the user to do anything voluntarily to evoke these patterns (Zander and Kothe, 2011). The passive BCI approach seems to be exactly what is needed for detecting intentions in the most unobtrusive way, while gaze dwells effectively reveal the time intervals where the markers of intentions can be searched for in the brain signals. The EEG was collected during fixations intentionally used for control and during non-controlling fixations and successfully classified off-line (Ihme and Zander, 2011; Protzak et al., 2013). However, gaze dwell time thresholds were again quite long, 2000 ms in Ihme and Zander (2011) and 1000 ms in Protzak et al. (2013). Moreover, the participant task in both studies involved visual search, and the classification could rely mainly on fixation-related potential (FRP) components related to finding a target, rather than to intention to act.

When a target is searched for among a range of distractors, one may use the EEG potentials that accompany target detection, such as the P300 wave. Recent studies of the FRPs in the visual search tasks demonstrated that finding an object, area or position of interest can be detected using a combination of eye tracking and EEG (Healy and Smeaton, 2011; Kamienkowski et al., 2012; Brouwer et al., 2013; Kaunitz et al., 2014; Devillez et al., 2015; Finke et al., 2016; Ušćumlić and Blankertz, 2016; Wenzel et al., 2016). In particular, Finke et al. (2016) reported high performance, with area under ROC curve (AUC) of about 0.9, for classification of short target vs. non-target fixations. Similar phenomena could be a basis of classification in studies by Ihme and Zander (2011) and Protzak et al. (2013). This approach, however, is limited, because a click on a screen button or link is not always required immediately after they are found. In many applications, the user should be at least given an option to execute control in less automatic way. The P300 wave, which plays important role in this approach, can decrease and even vanish under many conditions, for example, when the target is always found at the same position. Classification of FRPs can be also related to the effects from planning a saccade to a new location of interest (Graupner et al., 2011; Nikolaev et al., 2013), but its possible use in BCI is limited for similar reasons. An effective general-purpose interface may include algorithms for supporting fast responses to just-found targets, but has to be primarily focused on more direct procedures of intention detection.

The current study followed the proposals of Zander and colleagues (Ihme and Zander, 2011; Protzak et al., 2013), i.e., it relied on finding EEG (FRP) markers for gaze dwells intentionally used for control. However, we aimed on investigating the possibility to find the FRP markers of controlling fixations when relatively short (500 ms) dwell time threshold is used. Fixations of this length are frequently observed in normal viewing, and do not require significant effort when they should

be produced voluntarily. Special attention was paid to equalizing irrelevant factors that could confound the difference between the fixations used for control and spontaneous fixations. We took a straightforward approach of collecting the synchronized gaze and EEG data from the participants in a realistic scenario, when they played a game with their gaze only. The gaze controlled variant of a known, sufficiently engaging computer game was designed for this study, to make possible obtaining a large number of fixations of required duration, both intentionally used for control and spontaneous ones.

Results from a pilot study of the FRP markers of controlling fixations and summaries of the current work were presented at a few conferences (Shishkin et al., 2015, 2016b,c). This publication provides the detailed description of the approach, methodology and results.

METHODS

Participants

The study was conducted in 8 healthy participants (age 21–48, mean 29, one female) in accordance with the Declaration of Helsinki and the local institutional regulations. All participants gave written informed consent. They had normal or corrected to normal vision. Two of them (participants 6 and 7) had no previous experience with gaze based control. The others already participated in a few pilot experiments with the same gaze controlled game as in this study.

Apparatus and Software Used in Online Experiments

Electroencephalogram (EEG) was recorded at 500 Hz and 24 bit voltage resolution with an *actiCHamp* amplifier and *actiCAP* active electrodes (Brain Products, Germany) from 19 positions (Fz, F3, F4, Cz, C3, C4, Pz, P1, P2, P3, P4, POz, PO3, PO4, PO7, PO8, Oz, O1, and O2). More electrodes were placed in the posterior area than in the anterior one, because our pilot studies indicated that the marker for controlling fixations was likely to be found in the occipitoparietal region. Reference EEG electrodes were located at earlobes. Electrooculogram (EOG) was captured with the same amplifier and active electrode set. For horizontal EOG, electrodes were placed about 1 cm from the outer canthi. Vertical EOG was recorded with an electrode about 2 cm below the right eye and another one at Fp2 position (this location was preferred to more standard lower locations to avoid interference with the forehead rest). Ground electrode was located at AFz. Electrode impedances were kept below 20 KOhm. Gaze coordinates were recorded monocularly at 500 Hz sampling rate with the *EyeLink 1000 Plus* video based eye tracker (SR Research, Canada).

Recording of EEG and EOG, their synchronization with the eye gaze data, online processing of the eye gaze data and running the gaze controlled game were made with custom programs under *Resonance*, a framework for prototyping multimodal (hybrid) BCIs being developed by one of the authors of this study (Y.O.N.). For offline synchronization of the data, markers were sent from the eye tracker computer's parallel port to the EEG amplifier's TTL port in the beginning of each game. To control the stability of synchronization, this procedure was repeated in the end of the games (the time difference was typically no larger than two samples).

Dwells were detected online using a spatial (dispersion-based) criterion: gaze position range on each of X and Y coordinates should not exceed 2° for the specified dwell time (500 or 1000 ms, depending on condition). This criterion was chosen for two practical reasons: first, it could be easily implemented in the online software; secondly, it provided subjective experience of reliable control, according to our observations in the pilot experiments with the gaze controlled game used in this study. Several additional criteria had also to be met: no dwell detected in a $3 \times 3^{\circ}$ squared region centered around the previous click's position for previous 3000 ms, and no dwell detected in any position for 500 ms or 1000 ms (depending on condition). Each time all these criteria were met, a "click" was produced in the game (an event with the same effect as of a computer mouse click), and this time minus 500 or 1000 ms (for 500 or 1000 ms conditions, relatively) was designated as the beginning of the dwell event. The location of each "click" was computed as medians of X and Y coordinates of the gaze within the dwell time interval (excluding subintervals corresponding to the blinks reported by the eye tracker).

For simplicity, we call in this paper all the detected intentional and spontaneous dwell events "fixations." Although the criteria for their detection were rather loose and, theoretically, small amplitude saccades and re-fixations could happen within the dwell interval, it seemed unlikely that they could bias our analysis results.

The Gaze Controlled Game

To collect the EEG during diverse, intensive and realistic gaze-mediated interaction with a computer, we designed a gaze controlled game *EyeLines*. It was based on a computer game *Lines* (or *Color Lines*) ("Color Lines," in Wikipedia. Retrieved June 27, 2016, from http://en.wikipedia.org/wiki/ColorLines). Like the original game, the *EyeLines* is a simple computer puzzle game, with the goal to construct as many "lines" from colored balls as possible. The player is presented with a square board on which three colored balls appear in the beginning of the game. On each turn, the player has to move one ball to a free cell on the board. When the required or higher number of balls with the same color form a "full" line, either horizontal, vertical or diagonal, these balls disappear. If no such line is formed, three new balls randomly selected out of seven different colors are put on random cells. The game is over when the board is full.

In *Lines*, a move is typically made with a mouse click first on a ball and then on a free cell where it should be moved. In *EyeLines* (**Figure 2**), gaze dwells are used as an equivalent to mouse clicks, following the approach most often used in gaze controlled software. To avoid unwanted actions resulting from spontaneous long fixations and also to make possible collecting sufficient number of such fixations, gaze based control in the game board was off by default. After deciding which ball to move and to which free cell, a participant had to switch control on by gaze dwell on the only location where control was permanently

on. This location was an additional cell (the *button*) positioned outside the game board either left, as in **Figure 2**, or right to it.

The participants were instructed to make the moves in the game by three subsequent *controlling fixations*: on the *button*, on a *ball* and on a *free cell* where the ball should be moved. A 500 or 1000 ms dwell time threshold was used (same in all games that constituted one experiment block) for all these actions. When fixation duration exceeded the threshold, a visual feedback was given. It was specific to each action: dwell on the button led to appearing, in this separate cell, a ball of color different from the board balls (the participants were told that this indicates switching the board control on); dwell on a ball within the board led to ball selection indicated by a gray square frame that appeared around the ball; dwell on a free cell led to moving the selected ball into this cell.

When control was off, fixations on the balls made no effect. They were considered as presumably spontaneous fixations (used for viewing or related to mind wandering) and constituted a separate type of *non-controlling fixations*.

To ensure more reliable gaze based control and to reduce complexity of the gameplay (so that even novices could make sufficient number of moves per game without long practice), we made some features of *EyeLines* simpler comparing to typical implementations of *Lines*. In particular, the board size was made 7×7 instead of 9×9 in "classical" *Lines*, and the minimal number of balls required to form a full line was decreased from five to four. To support more detectable gaze fixations, a dot was put in the center of each ball and each free cell, the balls were drawn as plane circles (not as "3d like" spheres, to avoid asymmetrical features that could significantly shift the gaze from the center), and cells were designed as small squares with substantial spaces between them (**Figure 2**).

The game was presented on a 27″ LCD monitor positioned at the distance of 60 cm from participant's eyes. The game board subtended $18 \times 18^{\circ}$ on the monitor screen.

Procedure

Participants were seated in a chair in front of the monitor. Chin and forehead rest was used to ensure stable head positioning. Participants were asked to relax and make no bodily movements during calibration and playing the game. They were instructed to make moves in the game by still looking sequentially at the button, the ball and the free cell, each time until they saw the feedback. After a move was completed, they could freely look at the board and fixate any ball or free cell for any time without evoking any action, until they dwelled at the button again for a time exceeding the threshold.

Participants were told to refrain from hurrying up with each move and to find "better" moves whenever possible, but not to think for too long time. In the preliminary experiments, however, we found that the *EyeLines* players often tend to makes moves as fast as possible even when they were urged not to do so. Due to this, sufficient number of non-controlling fixations could be not always collected. Therefore, an additional feature was introduced to *EyeLines*: after each 4–8 moves the cell outside the board that indicated the button's position disappeared from the screen for 10 s and the dwell on its former position had no effect, so that the participant could not make moves during this time. The participants were told that they had to use this time for planning the further moves. In addition to encouraging higher number of long fixations within this time, this trick presumably could help to prevent the participants from playing the game at too fast pace.

To those participants who had no prior experience with *EyeLines* or *Lines*, rules of the game were explained prior to EEG electrode mounting. They played two games with short duration (2 min) for practice.

In the main part of the experiment, all the participants played, in total, eight games with maximum duration of 5 min. The session was divided into two blocks of equal size, differed by the dwell time threshold, which was set at either 500 or 1000 ms. The order of the blocks was randomly assigned to the participants (three of the eight started with the 500 ms threshold block). The switch-on button position (left or right to the board) was alternated every game throughout the session. Its position in the first game was also chosen randomly (counterbalanced over the group). A 5 to 10 min rest was offered between the blocks, and shorter (typically up to minute) rest intervals were inserted between the games. Prior to each game, a nine-point calibration of the eye tracker was run.

Offline Data Analysis

In this study, all EEG analysis, including classification, was made offline using the EEG data collected during the online gaze-based control. However, to make single-trial FRP classification performance evaluation realistic, the procedures for signal processing, feature extraction and application of the classifier to the new data were designed so that they could be used online without introducing any significant delay.

Signal preprocessing and segmentation were made mainly with *R*, while *MATLAB* (*MathWorks*) was used for visualization and classification. EEGLAB (Delorme and Makeig, 2004) routines *eegplot* and *topoplot* were used, relatively, for manual checking the quality of EEG/EOG epochs and for plotting scalp topographies. MANOVA was performed using *STATISTICA 7* (*StatSoft*).

Electroencephalogram (EEG) was re-referenced offline to linked earlobes, and bipolar EOG was calculated as the difference of amplitude in right/left and upper/lower channels, respectively. Line noise in EEG and EOG was reduced with 50 Hz notch filter (2nd order Butterworth). For creating the ERP time plots (but not for the other types of analysis), low-pass 7 Hz filter (2nd order Butterworth) was also applied.

For EEG and EOG analysis, $[-500\ +1500]$ ms epochs were extracted related to the start of four types of fixations exceeding the dwell time threshold: three types of controlling fixations (button, ball and free cell) and one type of non-controlling fixations. As non-controlling fixations, only fixations on balls made without fixating the button prior to them were considered; fixations of this kind on free cells were very rare and could not be used in the analysis. Data were analyzed separately for 500 and 1000 ms dwell threshold conditions. In some cases, they were also divided into subconditions related to left and right position of the button.

Fixation-related potentials (FRPs), by definition, are synchronized with the eye movements and, therefore, can be systematically contaminated by EOG artifacts. To deal with

FIGURE 2 | An example screenshot of the *EyeLines* display. The participants moved the color balls in order to construct lines from balls of the same color. Each move was made with gaze fixations only. A participant could make any number of spontaneous fixations (S) without any visible effect; however, their time was recorded. A dwell on the button (1) lead to appearing a ball in the button position, indicating that "control is on." After this, a dwell on any ball in the game board (2) led to its "selection" (a frame appeared around it), and then the ball could be placed to a new position by a dwell on a free cell (3). (The digits 1, 2, 3, and the letter "S" were not a part of the actual display and were added to the screenshot for illustrative purposes).

this problem, we set the baseline interval and borders of the EEG time intervals used for analysis and classification within the fixation. Our pilot studies suggested that the difference between the EEG amplitude in controlling and non-controlling fixations in the *EyeLines* game was most pronounced in the late part of fixation. In contrast, the amplitude of the lambda wave, the component of the fixation-related potentials with the latency of about 100 ms from fixation start, did not exhibit pronounced dependence on gaze-based control. To make the baseline less sensitive to the lambda wave and other visual components that could be irrelevant for control detection, we decided to use as the baseline 200–300 ms interval relative to the fixation start. No high-pass filter was used (the EEG amplifier used in this study allowed for DC recording), so the amplitude shifts related to eye movements could not influence the fixation interval through the transient response of the filter. Because our study was focused on the EEG features that could be used in fast online classification of the controlling and non-controlling fixations, the upper border of the analyzed interval was set at 500 ms both in 500 ms and 1000 ms dwell threshold conditions.

After baseline subtraction, we checked the number of epochs with amplitude higher than 70 μV in 200–500 ms interval in any channel, per fixation type, condition and participant. The highest incidence of such epochs was only five, while in most cases no such epochs were observed at all. Therefore, no artifact rejection procedure was applied to the data.

Feature Extraction and Classification

Electroencephalogram (EEG) features were extracted from only 13 posterior channels (P1, P2, P3, P4, Pz, PO3, PO4, PO7, PO8, POz, O1, O2, and Oz). Due to low number of non-controlling fixations exceeding 1000 ms threshold, the classifier was trained using only the data from the condition where this threshold was used. Therefore, the right border of the interval for feature selection was set as the lowest dwell threshold in our experiment, i.e., 500 ms. (In online mode, not implemented in this study but supposed to be the main application of its results, a fixation exceeding this threshold should be classified as soon as possible, thus features could be taken only before the threshold.) The left border was set at 200 ms after the fixation start, to exclude the EOG artifacts. As in the EEG analysis described above, mean amplitude of the 200–300 ms baseline interval was subtracted from the EEG amplitudes channelwise, and no filter was used (except for the 50 Hz notch filter during EEG recording).

To capture the development of the negative wave, we used overlapping windows of 50 ms length and time step 20 ms (200–250, 220–270, and 440–490 ms, total $n = 13$ windows). The feature vector (169 features) for each fixation k was composed of the mean values of EEG amplitude $m_k(i, c)$ computed for each of these windows ($i = 1$–8) in each channel ($c = 1$–13).

One class of the data was the non-controlling fixations. The other class was formed either from the button fixations only (Trainset 1) or from all controlling fixations (Trainset 2). Trainset

1 was used because button FRPs differed most strongly from the non-controlling fixations, so their classification could provide an upper estimate of the performance. It is also possible that only the first fixation in a controlling sequence of fixations should be detected in the EBCI. Trainset 2 was used to explore how well the classifier could be used with different type of controlling fixations without additional tuning to each of them.

Two classification approaches were applied to the data separately. The first one was the Linear Discriminate Analysis (LDA) with shrinkage regularization (Blankertz et al., 2011) implemented in Fieldtrip toolbox for EEG/MEG-analysis (Oostenveld et al., 2011, http://www.ru.nl/neuroimaging/fieldtrip), further referred to as Shrinkage LDA. The second approach, the Committee of Greedy Classifiers, further referred to as Committee, was to create a pool of weak threshold classifiers performing in one-dimensional feature spaces (one classifier per feature), to select classifiers with a greedy algorithm and to use them in a classifier committee. More specifically, each weak classifier was trained independently on one of the 169 features, and a greedy algorithm was used to select 15 features and corresponding classifiers from the pool (at the first iteration, the classifier which had the minimal classification error was chosen to become a committee member; at each of further iterations, the classifier which minimized the error of committee was added to it). The Committee classified fixations by simple voting of the selected weak classifiers (Trofimov et al., 2015).

Thresholds for the classifiers were adjusted using validation subsets to obtain at least 0.90 specificity. The reason to aim on relatively high specificity in expense of sensitivity was that in EBCIs, i.e., interfaces based on combining gaze based control and the BCI technology, low sensitivity of an EEG classifier can be partly compensated by additional gaze based control routines. In particular, if users found that the interface does not respond to their intention as fast as they expect, they can simply dwell longer, so that the interface may recognize the intention without the EEG, just with an additional, longer dwell time threshold. In contrast, the specificity of the interface should be kept high in most cases, because too frequent false alarms can be annoying and even dangerous (e.g., in robotic applications).

For each classifier, performance was estimated separately for training and testing using either Trainset 1 or Trainset 2, and for testing on data from either 500 ms or 1000 ms dwell threshold conditions, to estimate if the same classifier could be used effectively for different types of data.

Five-fold cross-validation was used for estimation of the classifiers' performance, except for the cases when training and testing was done on different subtypes of fixations. Details on how the data were divided into training, validating and testing subsets are given in notes under relevant tables (**Tables 2**–**5**) in the *Results* section.

RESULTS

Behavioral Data

Each participant was able to play *EyeLines* with gaze control only, i.e., without any manual input. The control was very stable: participants reported that they encountered from 1 to 4 errors per session, including ball selections or free cell selection incorrectly recognized by the software, as well as their own errors. Offline analysis of gaze data showed that there were also rare cases when the participants dwelled on two or more balls in a row when control was on, or attempted to make a move that violated the rules and therefore was not actually executed; these cases were excluded from the analysis, except for some of the rarest cases which were difficult to separate due to technical reasons (the latter lead to slightly higher number of ball selections comparing to button activation events). On average, a participant made about 150 moves in the condition with 500 ms dwell threshold and about 120 moves in the condition with 1000 ms dwell threshold.

The number of controlling and non-controlling threshold-exceeding fixations collected in the experiment is given in **Table 1**. About 160 spontaneous fixations of 500 ms or longer duration were collected with 500 ms threshold, while the number of 1000 ms or longer spontaneous fixations was about 15 times lower. Except for these long spontaneous fixations, the number of collected fixations was sufficient for analysis, varying from 74 for free cell selection with 1000 ms threshold (in participant 2), to 208 for non-controlling fixation with 500 ms threshold (in the same participant). The number of controlling fixations was higher in every participant in the 500 ms compared to 1000 ms threshold conditions (see **Table 1**), possibly due to the restriction of the total game duration that was same in both conditions. However, the size of this difference was small in all participants (varying from 20 to 34%), therefore, no correction of the EEG analysis procedure was needed.

Overview of the Fixation-Related Potentials (FRPs)

Our main interest was to characterize the EEG features that can be used for online detection of the dwell-based gaze control and, therefore, should appear earlier than the dwell time threshold. In the current study, for the sake of simplicity, we focused only on amplitude (not spectral and not synchrony based) features, on current fixation (not the preceding one) and only on the features that could not be affected by eye movement artifacts.

Before starting to analyze the FRPs, we had to check if the EEG at the output of our preprocessing algorithm was sufficiently free from the EOG contamination. The highest contamination could be expected in the case of button fixations, when the gaze fixated an extreme position and the horizontal EOG could be added to the EEG signal especially strongly and systematically. **Figure 3** shows FRPs (as a "butterfly plot") and EOG for the button events averaged separately for left and right button positions. While the EOG contamination was evident in the FRP waveforms before the start of the fixation (0 on the time scale) and after approximately 250 ms following the dwell threshold at 500 ms (right vertical line), the horizontal EOG had very low amplitude in the 200–500 ms range. This interval was used for the analysis of EEG amplitude in both 500 and 1000 ms dwell time threshold conditions.

Figure 3 reveals a nearly linear negative trend in most of the EEG channels used in the study, possibly related to the

TABLE 1 | Number of controlling and non-controlling (spontaneous) fixations exceeding the dwell time threshold in the 500 ms and 1000 ms threshold conditions (collapsed over left-button and right-button conditions).

Sbj.	500 ms fixation threshold					1000 ms fixation threshold				
	Non-controlling fixations	Controlling fixations				Non-controlling fixations	Controlling fixations			
		All	Button	Ball	Free cell		All	Button	Ball	Free cell
1	114	444	150	148	146	9	369	124	123	122
2	208	364	120	128	116	15	271	101	96	74
3	144	408	138	139	131	13	325	109	108	108
4	200	549	184	184	181	24	446	150	148	148
5	162	435	147	148	140	4	338	113	113	112
6	124	527	176	180	171	5	428	145	142	141
7	123	442	151	153	138	7	358	122	121	115
8	194	517	171	175	171	9	378	125	127	126
Mean	158.6	460.8	154.6	156.9	149.3	10.8	364.1	123.6	122.3	118.3
Std.	38.0	64.1	21.2	20.4	22.7	6.5	56.0	16.9	17.1	22.6

expectation of the visual feedback (note that the experiment was organized in such a way that the gaze dwells intentionally used for control led to an equivalent of mouse click on the fixated position of the screen). Since we already used an interval near the start of this trend (200–300 ms) as the baseline, an average over an interval near the threshold can be used as a robust estimate of the trend. To view the topography of this negativity, we averaged EEG amplitude over 400–500 ms interval and plotted the results. **Figure 4** shows grand average maps (individual maps had a similar pattern). According to this figure, the negativity was prominent in the parietooccipital area in all conditions. The maps also demonstrate a left-right asymmetry in Button condition that depended on button position: it was slightly stronger in the hemisphere contralateral to the gaze controlled switch-on button position where gaze dwelled in these fixations. Specifically, the difference between PO4 and PO3 amplitude in Button fixations with 500 ms dwell threshold was $-0.4 \pm 1.7\ \mu V$ ($M \pm SD$) in left button condition and $+2.2 \pm 1.3\ \mu V$ in right button condition. The difference was significant, according to paired Student's *t*-test [$t_{(7)} = -3.2$, $p = 0.02$]. In Ball fixations, no difference between the two positions of the button was observed [the corresponding values were $+ 0.5 \pm 0.9\ \mu V$ and $+ 0.3 \pm 0.8\ \mu V$, $t_{(7)} = 0.5$, $p = 0.6$].

Note that Button fixations were the most extreme fixations required for playing the game (the switch-on button was positioned left or right to the game board), while Ball fixations were all within the game board. The presence of the laterality effect in the Button but not in the Ball fixations means that it was not related to the direction of the previous saccade but is not sufficient to decide whether it was related to the current fixation or to the direction of the saccade to the next position that could be planned within this fixation. Nevertheless, the laterality effect is interesting because it was not reported so far for the Stimulus-Preceding Negativity (SPR) that could be the closest "relative" of the observed negative variation in the psychophysiological literature (see Discussion for more details).

In the rest of the amplitude analysis, POz electrode was used, because it the negativity that marked control-on fixations was typically highest at this location.

Factors Influencing the FRPs

Generally, FRPs may depend on many factors that may vary significantly during gaze interaction. These effects may negatively affect the stability of EBCI classifiers built using the FRPs or can be used for increasing the amplitude of the FRPs markers and, thus, for improving the EBCI performance. Detailed analysis of such effects could not be performed within the current study. However, we were interested to estimate if the negativity in the intentional fixation can be influenced by several factors which were well controlled in our experiment: left or right position of the switch-on "button" (which was already shown to produce a laterality effect), dwell time threshold (low effect of this factor would suggest that varying time of the feedback can be applied in online operation of EBCI likely without strong reduction of performance) and fixation type (it was most important to confirm the difference between spontaneous (non-controlling) and controlling fixations, but the difference between different types of controlling fixations should also be taken into account in EBCI development).

For this analysis, each participant's POz amplitudes averaged over 400–500 ms interval (with 200–300 ms baseline) for each fixation type and dwell time threshold were submitted to a 3-way MANOVA, with the following repeated measures factors:

- Button Position, with 2 levels: Left and Right,
- Dwell Threshold, with 2 levels: 500 ms and 1000 ms dwell time,
- Fixation Type, with 4 levels: Button, Ball, Free Cell, No-Control.

Significant effect was found for Fixation Type [Wilk's $\lambda = 0.06$, $F_{(3, 5)} = 24.6$, $p = 0.002$], whereas the Button Position effect [Wilk's $\lambda = 0.96$, $F_{(1, 7)} = 0.32$, $p = 0.6$], Dwell Threshold effect [Wilk's $\lambda = 0.99$, $F_{(1, 7)} = 0.02$, $p = 0.9$] and all interactions

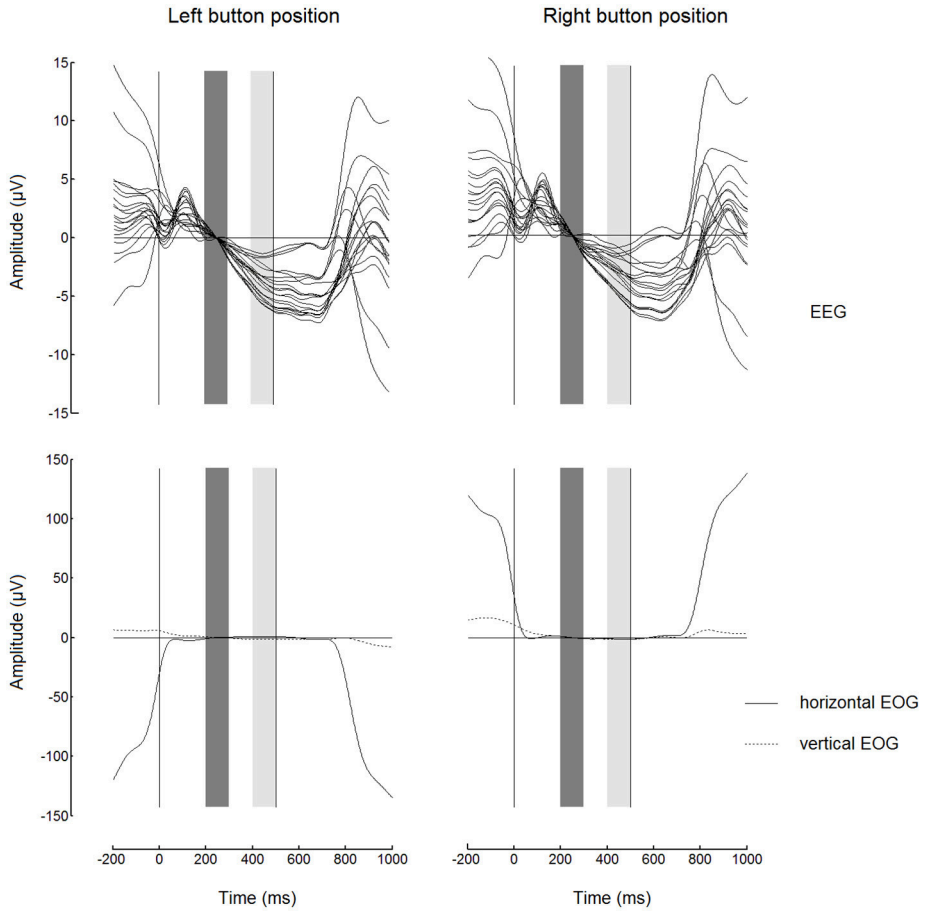

FIGURE 3 | Butterfly plots showing grand average ($n = 8$) superimposed channels with fixation-related potentials (FRPs, upper panels) and corresponding electrooculogram (EOG, lower panels) for fixations on button. The signals were low-pass filtered at 7 Hz and baseline corrected (high-pass filtering was not used). Note the similarity between the waveforms for left and right button positions (in the left and in the right, respectively) within most of the fixation interval. Zero millisecond corresponds to the beginning of fixation. The baseline interval (200–300 ms) is shown by dark gray bars. The light gray bars show 400–500 ms interval from which the EEG amplitudes were averaged to obtain estimates of the trend over the fixation used in the subsequent analysis (**Figures 4**, **5**). Dwell time threshold was 500 ms (marked with the vertical lines in the right edges of the light gray bars).

between factors were not significant. According to *post-hoc* Tukey HSD test, amplitude at POz in 400–500 ms interval was significantly more negative in Button comparing to No-Control fixations ($p = 0.0002$), in Ball comparing to No-Control fixations ($p = 0.01$) and in Button comparing to Free Cell fixations ($p = 0.0007$). In Ball fixations, POz was nearly significantly more negative than in Free Cell fixations ($p = 0.064$), while the difference between No-Control and Free Cell fixation as well as between Button and Ball fixations was not significant ($p = 0.18$ and $p = 0.8$, respectively).

Mean amplitudes and confidence intervals are shown in **Figure 5**. Individual data generally followed the same pattern, with largest POz amplitude in Button fixations. With 500 ms dwell threshold, POz amplitude ranged −3.6 to −10.3 μV in the Left button condition (−5.5 ± 2.1 μV) and −3.4 to −7.4 μV (5.1 ± 1.4 μV) in the Right button condition (the values in the parenthesis are M ± SD). POz amplitude in No-Control fixations, however, tended to be also negative (Left button: −0.4 to −4.0 μV, −2.0 ± 1.3 μV; Right button: +0.6 to −3.2 μV, −1.1 ± 1.2 μV).

Individual and averaged over the groups FRPs at POz for Button fixations and both 500 ms and 1000 ms thresholds are shown, separately for the left and right button conditions, in **Figure 6**. Note that in the 200–500 ms interval the signal pattern was similar for all the compared conditions, and the amplitudes and time courses were, in general, very similar in different dwell threshold and button position conditions (**Figure 6**). Importantly, during Button and Ball fixations the negativity at POz was developed over the first 500 ms in all participants (this was not the case only in the Free cell fixations for several participants).

FRPs time courses for all fixation types averaged over the left and right button positions are presented in **Figure 7** (only for the 500 ms dwell threshold condition). This figure confirms the difference between fixation types: subsequent fixations were progressively weaker within the triplets used to make moves.

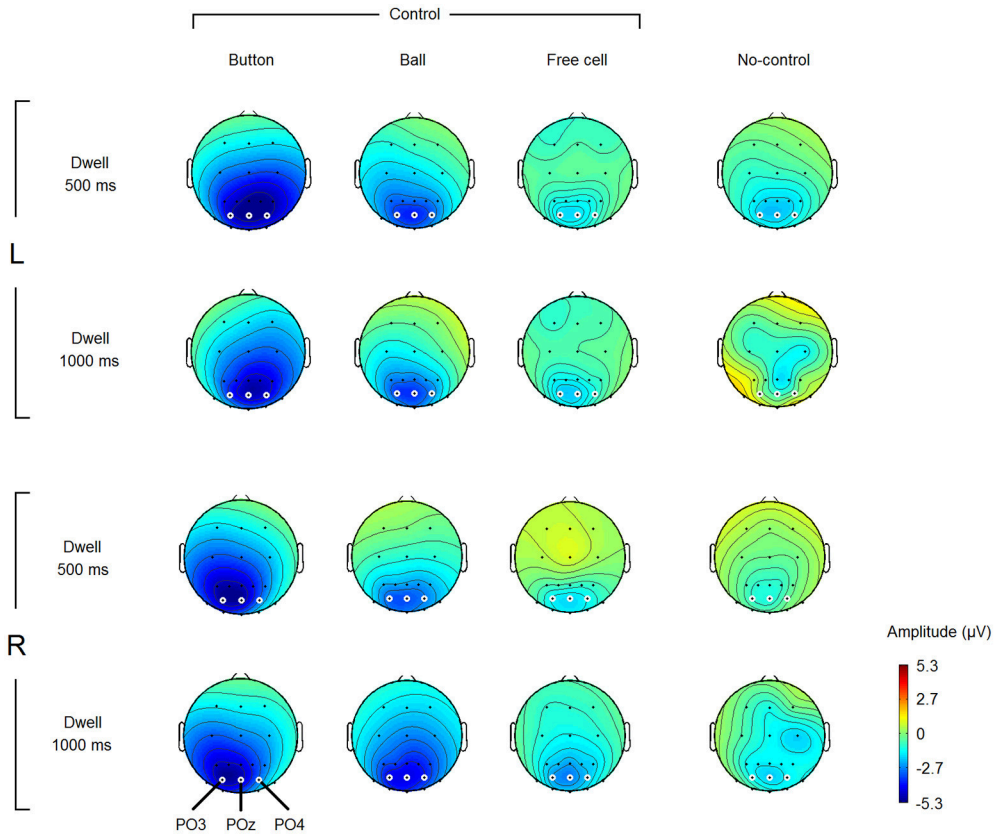

FIGURE 4 | Grand average ($n = 8$) amplitude topography of the negative potential developed within different types of fixations and different dwell time thresholds. L, left button position; R, right button position (note that the switch-on button was "clicked" not manually but by gaze fixations only). Amplitude estimates were obtained by averaging over 400–500 ms interval relative to fixation start (baseline 200–300 ms). Small white circles highlight the electrodes which were used in statistical analysis (POz, PO3, and PO4). Note that non-controlling fixations were rare in Dwell 1000 ms condition (see **Table 1**), thus the corresponding maps can be considered only as a rough estimate.

More detailed analysis is needed to estimate possible impact of the negativity from previous fixation(s) on the baseline, that could, theoretically, cause this progressive decrease. Also, additional experiments and analysis are needed to rule out the possibility that it was an extreme eye position that enabled high effect in Button fixations and to rule out possible effects that the preceding high-amplitude saccade could have on it or (through its effect on the lambda wave) even on the beginning of the baseline (cf. Nikolaev et al., 2016).

Figure 7 shows that, although No-Control fixations were accompanied by the negativity at POz in some participants, its growth tended to terminate in these fixations earlier than in the controlling fixations. It was possible that the participants sometimes forgot to switch control on before fixating a ball and quickly recognized their fault but could made a saccade before the dwell time threshold, so such fixations were erroneously considered as non-controlling ones in our analysis.

Classification

Finally, we estimated the possibilities to use the EEG marker of the gaze dwells used for intentional control by training statistical classifiers on the collected data and testing their performance offline under different settings that could be generally reproduced in online operation of the hybrid gaze interaction/BCI system (EBCI). Only 300 ms long EEG segments corresponding to fixations (200–500 ms relative to fixation onset) were used for single-trial classification.

The classifiers were trained using non-controlling fixations as the non-target class. The target class was represented either by Button fixations only (Trainset 1), or by all controlling fixations (Trainset 2). For the LDA classifier with the shrinkage regularization, performance results are provided in **Table 2** (Trainset 1) and **Table 3** (Trainset 2). For the committee of weak classifiers selected by the greedy algorithm, performance results are presented in **Table 4** (Trainset 1) and **Table 5** (Trainset 2).

As follows from **Tables 2–5**, the procedure for setting the classifier threshold using the validation subset provided a good approximation to the target specificity value of 0.90. Insufficient number of the non-controlling fixations in the 1000 ms dwell threshold condition (see **Table 1**) made calculation of specificity for this condition impossible. For the 500 ms dwell threshold data and LDA classifier, specificity was almost the same for

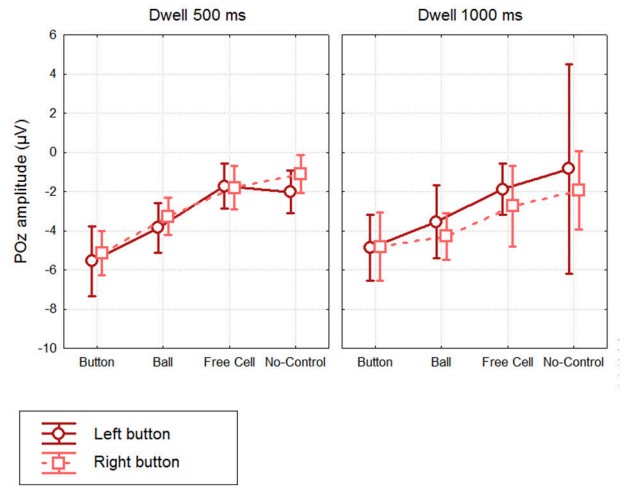

FIGURE 5 | Grand mean ($n = 8$) values and 95% confidence intervals of the negative potential at POz developed within different types of fixations, using different dwell time thresholds and button positions. Amplitude estimates were obtained by averaging over 400.500 ms interval relative to fixation start (baseline 200. 300 ms). Note that No-Control fixations were rare in Dwell 1000 ms condition (see **Table 1**), thus the average for these data can be considered only as a rough estimate.

Trainset 1 and Trainset 2: M ± SD was 0.87 ± 0.11 and 0.86 ± 0.15, respectively. A similar pattern was observed in the case of the committee of classifiers, but the mean values were slightly higher comparing to LDA: 0.90 ± 0.07 and 0.91 ± 0.07, respectively, for Trainset 1 and Trainset 2. Since the average number of non-controlling fixations in 4 games with the 500 ms dwell threshold was about 160 (**Table 1**) and one game lasted 5 min or (rarely) slightly less, the rate of 500 ms or longer non-controlling fixations was about $160/(4 \times 5) = 8$ min^{-1}, and the specificity of 0.9 corresponded to $8 \times (1–0.9) = 0.8$ false alarms per minute.

It was not possible to compare the two classifiers using ROC AUC values (the index which integrates performance estimates for different thresholds), because they could be computed not in all cases. However, given that the specificity values did not strongly differ between the classifiers and the training sets, we decided to compare the sensitivity values directly between different settings (**Figure 8**). We run a single 4-way MANOVA analysis on all sensitivity data, with the following repeated measures factors:

- Classifier, with 2 levels: Shrinkage LDA, Committee of Greedy Classifiers,
- Training Set, with 2 levels: Trainset 1 (only fixations on button as controlling fixations), Trainset 2 (all controlling fixations),
- Threshold, with 2 levels: 500 ms dwell time, 1000 ms dwell time,
- Fixation Type, with 3 levels: Button, Ball, Free Cell.

MANOVA results are presented in **Table 6**. They generally followed the effects observed in the analysis of EEG amplitudes reported above, such as significant main effect for Fixation Type factor (sensitivity was significantly higher for Button fixations, according to *post-hoc* analysis). Main effect and almost all interactions were not significant for Classifier, except for Classifier × Training Set × Dwell Threshold interaction ($p = 0.04$). There was a tendency of better sensitivity provided by the committee of classifiers comparing to the LDA in the case of training on all types of fixations and applying the classifier to 1000 ms data ($p = 0.08$, *post-hoc* Tukey test).

Although main effect was not significant for Training Set ($p = 0.32$), its interaction with Fixation Type was significant ($p = 0.012$). *Post-hoc* analysis revealed that the classifiers that were trained using all controlling fixations (Trainset 2) overperformed the classifiers trained on Button fixations only (Trainset 1) in the case of Ball and Free Cell fixations ($p = 0.005$ for both of them). With Trainset 1, sensitivity for the fixations not used for training (Button and Free Cell) was close to random level, especially with LDA classifier (**Table 2**), while improvement for Button fixations in the case of Trainset 1 did not reached statistical significance ($p = 0.09$, *post-hoc* Tukey test).

As one could expect, the classifier was more sensitive when the train and test data were recorded with the same dwell time threshold ($p = 0.0002$ for main effect of the factor Threshold). However, as follows from **Tables 2, 3**, the average difference was relatively small (on average, not higher than 0.03 for Trainset 1 and not higher than 0.06 for Trainset 2).

DISCUSSION

This study, for the first time, demonstrated that gaze fixations used for the interaction with a computer can be differentiated from spontaneous fixations using EEG markers from short time intervals (here, 200–500 ms relative to fixation start). This result opens the perspective of developing a hybrid "eye-brain computer interface," the EBCI, as an unobtrusive communication and control tool both for paralyzed patients with preserved gaze control and for healthy users.

In addition, with special measures taken to obtain the fixation-related EEG potentials (FRPs) free from contamination with EOG artifacts, we revealed and quantitatively characterized a pattern differentiating the controlling and no-controlling (spontaneous) fixations in each of the eight participants.

The analysis of FRPs is challenging due to the systematic contamination of the EEG from electrical potential shifts accompanying the eyeball movements. Such contamination cause problems either when the EOG artifacts appear in the time intervals that are the main focus of analysis or when they are present during intervals used for baseline correction (Finke et al., 2016; Nikolaev et al., 2016). In addition, EEG components within the first 200 ms after fixation onset depend on the size of saccade preceding the fixation (Nikolaev et al., 2016). In our study, only the 200–500 ms interval relative to fixation start was used for FRP analysis and classification of fixations to avoid any interference. Moreover, we did not filter out low frequencies, to avoid contamination that can extend into this interval due to strong transient response after saccade-related shift of the EOG potential, and set the baseline intervals borders within the analyzed interval, i.e., at 200–300 ms relative

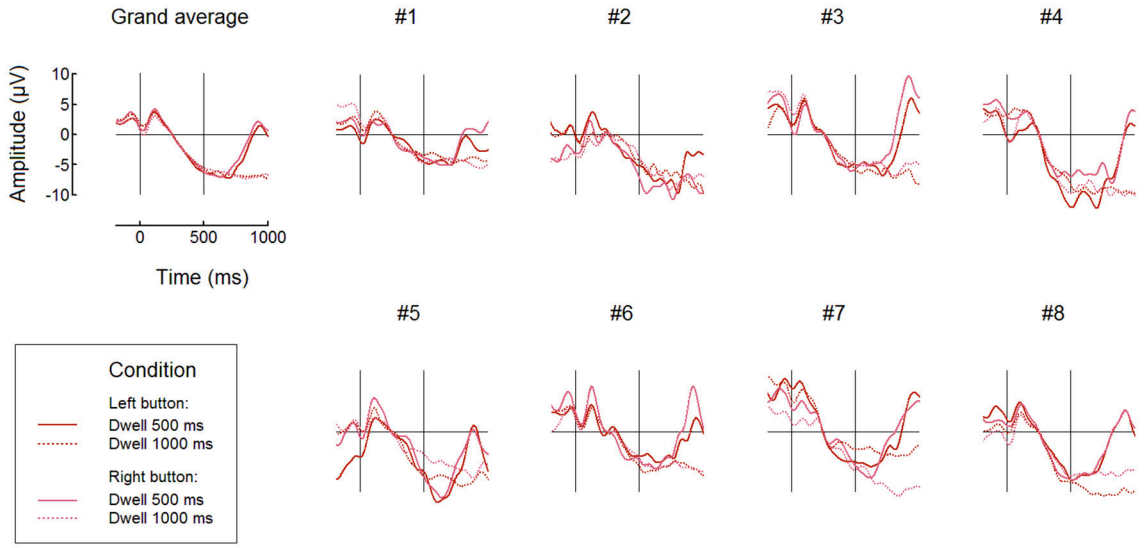

FIGURE 6 | Comparing different dwell time thresholds and button positions: grand average ($n = 8$) and individual FRP waveforms observed at POz in Button fixations. Fixation start and the 500 ms dwell time threshold are denoted by vertical lines. Filtering and baseline as in **Figure 3**.

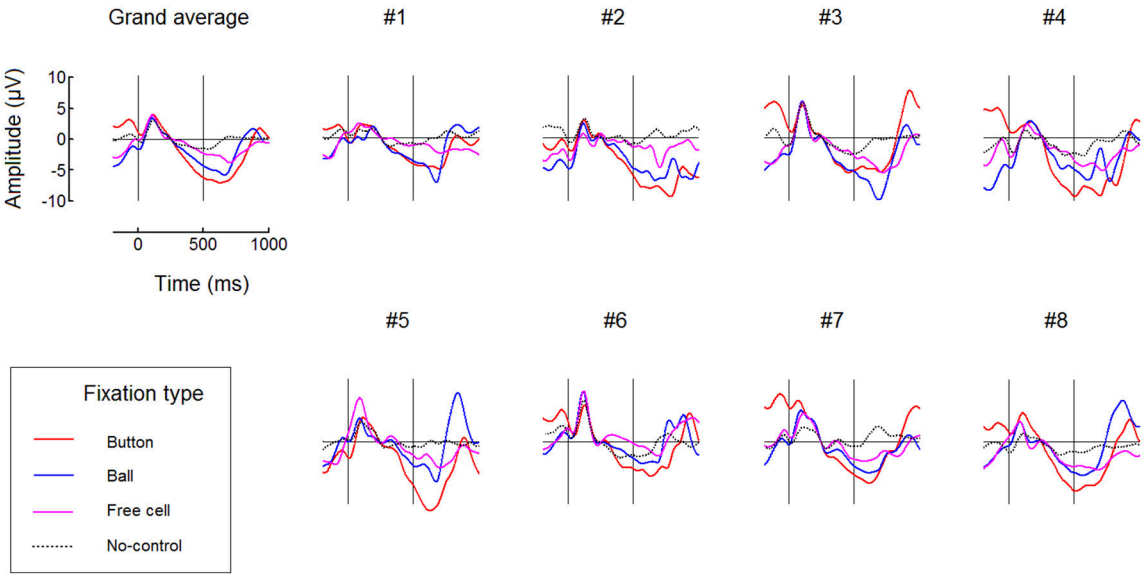

FIGURE 7 | Comparing different types of fixations: grand average ($n = 8$) and individual FRP waveforms observed at POz with 500 ms dwell time threshold. Here, left and right button data were averaged. Fixation start and the dwell time threshold are denoted by vertical lines. Filtering and baseline as in **Figure 3**.

to fixation onset. Positioning of the baseline in this interval means that results should be interpreted with care taking into account possible dampening of the activity of interest due to its presence in the subtracted signal. However, for demonstrating the possibility of developing an EBCI it was more important to prove that we obtained an EEG marker that was free from EOG contamination. As **Figure 3** shows, the EOG contamination indeed was absent in the 200–500 ms interval of the analyzed data that could be affected by it most strongly, i.e., in Button fixations.

The Negative EEG Wave

The topography of the EEG amplitudes in the 400–500 ms interval relative to fixation onset revealed a negativity focused at POz (**Figure 4**). Surprisingly, it was already developed in this interval even when the dwell threshold was 1000 ms. In the first and second of the three dwells used to make a move in the game (Button and Ball fixations), the EEG negativity at POz was strong in the 400–500 ms interval in all participants and significantly differed from the values in long non-controlling (spontaneous) fixations.

TABLE 2 | Performance of the LDA classifier with shrinkage regularization trained using only fixations on button as target fixations (Trainset 1).

Sbj.	Test on fixations with 500 ms threshold					Test on fixations with 1000 ms threshold		
	Specificity	Sensitivity			AUC	Sensitivity		
		Button	Ball	Free cell	Button	Button	Ball	Free cell
1	0.87 ± 0.13	0.23 ± 0.17	0.05	0.12	0.64 ± 0.06	0.16	0.07	0.09
2	0.85 ± 0.10	0.29 ± 0.22	0.15	0.09	0.67 ± 0.09	0.28	0.08	0.05
3	0.84 ± 0.09	0.51 ± 0.24	0.26	0.29	0.76 ± 0.07	0.41	0.20	0.30
4	0.92 ± 0.12	0.29 ± 0.21	0.08	0.08	0.70 ± 0.08	0.30	0.05	0.11
5	0.83 ± 0.14	0.38 ± 0.11	0.20	0.29	0.77 ± 0.03	0.45	0.30	0.28
6	0.87 ± 0.09	0.23 ± 0.06	0.09	0.11	0.64 ± 0.07	0.19	0.12	0.13
7	0.93 ± 0.05	0.15 ± 0.09	0.03	0.02	0.57 ± 0.03	0.07	0.04	0.04
8	0.86 ± 0.11	0.43 ± 0.18	0.05	0.15	0.76 ± 0.04	0.34	0.13	0.10
Mean	0.87	0.31	0.11	0.14	0.69	0.28	0.12	0.14
Std.	0.11	0.20	0.08	0.10	0.09	0.13	0.09	0.10

For training, recordings with 500 ms dwell threshold were used. On these recordings, 5-fold cross-validation was used to estimate, as M ± SD over folds, sensitivity and Area Under [ROC] Curve (AUC) for Button fixations, as well as specificity, in the 500 ms dwell threshold data. For each fold, the classifier was trained on 80% of the set, its threshold was adjusted on 8% aiming to obtain 90% specificity, and testing was done on 12%. In the case of testing on Ball and Free cell fixations, as well as for all 1000 ms dwell threshold data, the train and test sets were not overlapped and, therefore, the classifier was applied to all test data. Sensitivity is the same as True Positive Rate (TPR), here, the rate of correct classification of the intentional dwells. Specificity is equal to one minus the False Positive Rate (FPR); FPR is the same as the rate of false alarms, and in this work it corresponds to incorrectly classifying a spontaneous fixation as the controlling one (i.e., an intentional dwell).

The EEG negativity that was characteristic for the fixations used for control in our study was growing along the course of fixations, while Ihme and Zander (2011) and Protzak et al. (2013) reported EEG markers (also in the form of negativity) early within the controlling fixations. This difference could be caused by the differences in study design and processing approaches. In particular, the FRP in the study by Ihme and Zander (2011) could be influenced by EOG (although it unlikely influenced the classification results, according to the classifier weight scalp maps), while Protzak et al. (2013) focused on a time interval that immediately followed finding the target by the participants and could contain related activity. However, the FRPs presented in the latter work also showed, in the later part of the fixation intervals (mostly not used for classification), a deflection in negative direction, that could resemble the negative wave observed in our study if the authors would choose the baseline in the same time interval as we did it.

When a fixation is intentionally used for sending a command to computer, a user is expecting a feedback signal. In such situations, Stimulus Preceding Negativity (SPN) is observed. This EEG phenomenon can have a form of sustained negativity in anterior areas (unlikely to be detected with our baseline) and a sharp growth of negativity in parietal areas (Brunia, 1988; Brunia and Van Boxtel, 2001; Van Boxtel and Böcker, 2004; Brunia et al., 2011; Kotani et al., 2015). However, in our study the negativity was shifted to the hemisphere contralateral to the fixated location in the condition where the gaze was strongly shifted to the left or to the right (dwell on the switch-on button), an effect not known for SPN. Saccade preparation (possibly accompanying Button and Ball fixations, and, in some cases, even Free cell fixations) is characterized by a similar negative wave in the parietal area and is stronger in the hemisphere contralateral to saccade direction (Klostermann et al., 1994; Berchicci et al., 2012; Krebs et al., 2012). However, in our experiment the saccades following dwell on the button should be made in the direction opposite to the fixation location, i.e., the negativity had higher amplitude in the hemisphere ipsilateral to the direction of the saccade that followed the dwell; one may hypothesize that the mechanism enabling an intentional fixation at some location may have something in common with planning a saccade to this location, but we failed to find an evidence for this in the literature. Other slow negative EEG components related to preparation for action, Contingent Negative Variation (CNV) and Readiness Potential (RP), have more anterior localization.

Thus, we could not reliably identify the nature of the negative wave that marked the intentionally used gaze fixations, and additional studies are needed to clarify this question. In particular, it will be of practical importance to understand if the amplitude decreases within the controlling triplets (Button–Ball–Free cell) was just the order effect (the feedback for the second and especially third fixations in the sequence could be less informative, or affected by a refractory effect, etc.), or it resulted from factors specific to gaze position and object properties. Note, however, that when the classifier was trained on all types of data its performance was nonrandom even for Free cell fixations. If the EEG markers of intention to act will turn to be sensitive to various factors (properties of fixations, fixated objects, visual context, previous fixations, previous or planned saccades, variations in difficulty of maintaining a fixation intentionally, etc.; see, e.g., Nikolaev et al., 2016), different classifiers could be used for each specific case.

TABLE 3 | Performance of the LDA classifier with shrinkage regularization trained using all controlling fixations as target fixations (Trainset 2).

Sbj.	Test on fixations with 500 ms threshold							Test on fixations with 1000 ms threshold		
	Specificity	Sensitivity			AUC			Sensitivity		
		All	Button	Ball	Free cell	All	Button	Ball	Free cell	But-ton	Ball	Free cell
1	0.90 ± 0.16	0.18 ± 0.19	0.21 ± 0.21	0.17 ± 0.18	0.18 ± 0.18	0.63 ± 0.06	0.64 ± 0.10	0.61 ± 0.05	0.64 ± 0.06	0.13	0.09	0.08
2	0.85 ± 0.07	0.28 ± 0.10	0.34 ± 0.17	0.30 ± 0.08	0.20 ± 0.13	0.63 ± 0.02	0.66 ± 0.06	0.64 ± 0.02	0.58 ± 0.05	0.30	0.24	0.16
3	0.96 ± 0.05	0.19 ± 0.12	0.24 ± 0.21	0.15 ± 0.10	0.15 ± 0.11	0.63 ± 0.04	0.70 ± 0.10	0.60 ± 0.06	0.59 ± 0.08	0.20	0.10	0.09
4	0.83 ± 0.17	0.32 ± 0.18	0.41 ± 0.19	0.26 ± 0.21	0.27 ± 0.17	0.64 ± 0.02	0.69 ± 0.07	0.62 ± 0.03	0.60 ± 0.03	0.34	0.24	0.32
5	0.83 ± 0.09	0.21 ± 0.08	0.25 ± 0.14	0.19 ± 0.08	0.21 ± 0.11	0.64 ± 0.03	0.67 ± 0.03	0.61 ± 0.03	0.66 ± 0.05	0.19	0.16	0.14
6	0.70 ± 0.25	0.32 ± 0.23	0.36 ± 0.27	0.30 ± 0.23	0.37 ± 0.28	0.59 ± 0.06	0.59 ± 0.06	0.56 ± 0.05	0.63 ± 0.07	0.31	0.21	0.27
7	0.90 ± 0.09	0.12 ± 0.09	0.19 ± 0.11	0.12 ± 0.06	0.13 ± 0.11	0.56 ± 0.01	0.60 ± 0.02	0.55 ± 0.03	0.56 ± 0.05	0.07	0.07	0.09
8	0.92 ± 0.05	0.26 ± 0.16	0.24 ± 0.15	0.28 ± 0.15	0.30 ± 0.19	0.71 ± 0.06	0.68 ± 0.07	0.72 ± 0.05	0.74 ± 0.06	0.26	0.27	0.21
Mean	0.86	0.24	0.28	0.22	0.23	0.63	0.65	0.61	0.63	0.23	0.17	0.17
Std.	0.15	0.17	0.08	0.07	0.19	0.04	0.04	0.05	0.06	0.09	0.08	0.09

For training, recordings with 500 ms dwell threshold were used. On these recordings, 5-fold cross-validation was used to estimate, as M ± SD over folds, all the performance indices. For each fold, the classifier was trained on 80% of the set, its threshold was adjusted on 8% aiming to obtain 90% specificity, and testing was done on 12%. In the case of testing on 1000 ms dwell threshold data, the train and test sets were not overlapped and, therefore, the classifier was applied to all test data.

EBCI Performance

To enable fluent interaction, an EBCI should use short EEG segments. Our results demonstrated, for the first time, that EEG segments as short as 300 ms were sufficient to detect gaze fixations intentionally used for control.

In this study, the classifier threshold was adjusted for achieving specificity of about 0.9, that corresponded to false alarm rate of about 0.8 per minute. This rate is far from perfect, but can be acceptable in certain situations provided that the errors can be easily corrected. For example, in a game like *EyeLines*, if it was controlled on-line with an EBCI always switched on (with no need for the switch-on button), the player could simply attempt to choose another ball if a wrong one was selected, so the wrong selection would go harmless. (To complete the move, a free cell should be selected after the selection of a ball, but spontaneous dwells on free cells are not frequent even if the player do not make any effort to refrain from them, and can be easily avoided intentionally in the case of erroneous ball selection).

The best group average value of sensitivity, among all conditions and processing schemas, was only 0.38 ± 0.14 (in one participant, it was 20, and in others, ranged 0.31 to 0.47). This value was obtained for Button fixations using Trainset 1 (only Button fixations as the target class, non-controlling fixations as the non-target class) and the committee of greedy classifiers. Such sensitivity, of course, is not sufficient if the command always should be issued using the classifier.

However, as Protzak et al. (2013) suggested, an additional gaze dwell threshold can be used to ensure issuing a command even if it was not recognized by the BCI component of the system. We observed the high similarity of the FRPs before the 500 ms from the fixation onset under the 500 ms and 1000 ms dwell threshold conditions (**Figures 4**, **6**) and the relatively small decrease of the 500 ms trained classifier sensitivity when it was applied to the data from the 1000 ms condition (**Figure 8**). These results are in accordance with the recommendation by Protzak et al. (2013), demonstrating that the use of two thresholds will not likely lead to substantial drop in the classifier performance.

Classifier sensitivity followed the pattern observed for the amplitude of the negative wave that served as the marker of the controlling fixations, tending to decrease within the triplets of gaze dwells (Button–Ball–Free cell). The factors that are responsible for this decrease are yet to be determined, but it is likely that the key role was played by the order of dwells that closely followed each other. There are serious alternatives for the dwell-based EBCI in fast serial operation, such as dwell-free (Kristensson and Vertanen, 2012; Sarcar et al., 2013; Pedrosa et al., 2015) or response-based control (Publicover et al., 2016). The EBCI, thus, can be more suitable for single "clicks" or for starting a sequence, so that the rest of it will be entered using one of these alternative approaches.

Although the LDA classifier with shrinkage regularization is one of the methods of choice for ERP based BCIs (see, e.g., Blankertz et al., 2011), a simple classification approach based on the committee of greedy classifiers demonstrated at least comparable performance with our FRP data. In future studies, other classification approaches should be tested for the

TABLE 4 | Performance of the committee of 15 greedy classifiers trained using only fixations on button as target fixations (Trainset 1).

Sbj.	Test on fixations with 500 ms threshold				Test on fixations with 1000 ms threshold		
	Specificity	Sensitivity			Sensitivity		
		Button	Ball	Free cell	Button	Ball	Free cell
1	0.92 ± 0.04	0.31 ± 0.08	0.16	0.14	0.23	0.24	0.13
2	0.92 ± 0.03	0.40 ± 0.16	0.17	0.12	0.17	0.17	0.16
3	1.00 ± 0.00	0.20 ± 0.06	0.06	0.02	0.07	0.05	0.06
4	0.83 ± 0.04	0.44 ± 0.08	0.28	0.18	0.36	0.27	0.17
5	0.85 ± 0.06	0.45 ± 0.10	0.20	0.17	0.31	0.19	0.17
6	0.90 ± 0.06	0.39 ± 0.12	0.14	0.14	0.20	0.13	0.11
7	0.86 ± 0.06	0.47 ± 0.16	0.33	0.25	0.34	0.31	0.27
8	0.95 ± 0.04	0.41 ± 0.06	0.17	0.17	0.35	0.13	0.07
Mean	0.90	0.38	0.19	0.15	0.25	0.19	0.14
Std.	0.07	0.14	0.08	0.07	0.10	0.08	0.07

For training, recordings with 500 ms dwell threshold were used. On these recordings, 5-fold cross-validation was used to estimate, as M ± SD over folds, sensitivity for Button fixations and specificity in the 500 ms dwell threshold data. For each fold, the classifier was trained on 80% and tested on 20% of the set. In the case of testing on Ball and Free cell fixations, as well as for all 1000 ms dwell threshold data, the train and test sets were not overlapped and, therefore, the classifier was applied to all test data.

TABLE 5 | Performance of the committee of 15 greedy classifiers trained using all controlling fixations as target fixations (Trainset 2).

Sbj.	Test on fixations with 500 ms threshold					Test on fixations with 1000 ms threshold		
	Specificity	Sensitivity				Sensitivity		
		All	Button	Ball	Free cell	Button	Ball	Free cell
1	0.92 ± 0.08	0.22 ± 0.02	0.28 ± 0.07	0.22 ± 0.05	0.15 ± 0.03	0.25	0.27	0.17
2	0.91 ± 0.05	0.24 ± 0.08	0.30 ± 0.06	0.23 ± 0.09	0.18 ± 0.12	0.21	0.17	0.14
3	0.96 ± 0.04	0.18 ± 0.03	0.18 ± 0.04	0.19 ± 0.05	0.18 ± 0.09	0.11	0.10	0.12
4	0.91 ± 0.04	0.20 ± 0.02	0.30 ± 0.06	0.19 ± 0.01	0.10 ± 0.05	0.21	0.20	0.09
5	0.93 ± 0.06	0.26 ± 0.06	0.23 ± 0.11	0.24 ± 0.06	0.30 ± 0.09	0.22	0.24	0.19
6	0.93 ± 0.03	0.33 ± 0.06	0.34 ± 0.12	0.29 ± 0.04	0.36 ± 0.09	0.24	0.19	0.32
7	0.92 ± 0.08	0.26 ± 0.04	0.31 ± 0.11	0.27 ± 0.02	0.19 ± 0.06	0.29	0.21	0.17
8	0.84 ± 0.06	0.45 ± 0.07	0.50 ± 0.10	0.42 ± 0.12	0.43 ± 0.09	0.46	0.39	0.37
Mean	0.91	0.27	0.31	0.26	0.24	0.25	0.22	0.20
Std.	0.07	0.10	0.09	0.07	0.13	0.10	0.08	0.10

For training, recordings with 500 ms dwell threshold were used. On these recordings, 5-fold cross-validation was used to estimate, as M ± SD over folds, all the performance indices. For each fold, the classifier was trained on 80% and tested on 20% of the set. In the case of testing on 1000 ms dwell threshold data, the train and test sets were not overlapped and, therefore, the classifier was applied to all test data.

EBCI, especially those that were successful with similar data patterns, such as Locality Preserving Projections algorithm that provided good results for movement-related potentials (Xu et al., 2014). A relatively low intersubject variability of the negativity that marked the controlling fixations suggests that the classifier training can provide higher results when trained on the same data with priors obtained from other participants.

A thorough search for better feature sets can result in even higher improvement in performance. For example, in a preliminary study adding wavelet features extracted from the same data to the amplitude features provided significant increase of AUC up to 0.75 ± 0.04 (M ± SD for the same group) for shrinkage LDA classifier (Shishkin et al., 2016a). Note that in the current study we avoided using any data from the EEG earlier than 200 ms after fixation onset for most reliable exclusion of any contamination by artifacts, although earlier EEG samples from the fixation interval and pre-saccadic activity may include additional useful information. Moreover, our baseline choice could prevent extraction of any activity that was stable within our interval (e.g., the anterior component of SPN). Non-EEG information, especially gaze data and data about the fixated objects, their environment, possible types of current activity of the user and so on can be used as additional features, or, in some cases, for selecting a classifier (e.g., specific classifiers

can be trained for different steps in sequences of actions, as in action triplets in our game). If sufficiently large amounts of gaze-synchronized EEG data will be harvested during the use of EBCIs, it will become possible to apply deep learning algorithms (LeCun et al., 2015; see also Nurse et al., 2016, on deep learning implementation at TrueNorth chip for EEG/ECoG/LFP data) that are able to find hidden patterns in the data and strongly improve classification performance.

However, it is possible that the sensitivity will not be improved to values close to 100%. What can be the added value of the BCI component if its sensitivity would be, for example, about 0.7, and the long dwells (without a BCI!) should be yet used in the rest of trials? We expect that even in this case the hybrid EBCI can provide advantage over usual gaze-based interaction when the interaction should require as little effort as possible. Indeed, the user will not need to take care about his or her attention and gaze to prevent unwanted "clicks," to confirm the command, etc., except to be ready to fixate slightly longer in certain cases. Moreover, it is possible that many of the misses are caused by low attentional concentration. In such cases, it might be even useful to avoid too fast interface response.

It is also possible that practice will lead to more stable and higher EEG marker amplitude through the operant conditioning mechanism. Practice can improve intentional regulation of the slow cortical potentials when they are used for BCI-based communication (Neumann et al., 2004), and the same may appear to be also true for the EBCI based on SPN-like slow activity. To test this hypothesis, the FRP dynamics and EBCI performance can be studied during prolonged use of the online EBCI. The use of additional, longer dwell time threshold makes possible intensive practice even with low sensitivity of the classifier. It was thus important that the study demonstrated high similarity of the 200–500 ms interval of FRPs of controlling fixations with 500 ms and 1000 ms dwell time thresholds.

Fast Fixation-Based EBCIs: An Emerging Class of Effective Hybrid BCIs

The gaze fixation and FRP data complement each other when used as an input to a hybrid interface: the fixation onset provides the temporal marker required for EEG segmentation and FRP extraction, the FRP provides features for a passive BCI classifier that automatically recognizes target finding (in the case of visual search) or issuing a command (in intentional dwell-based control), and the gaze position indicates the target (Protzak et al., 2013; Finke et al., 2016). This combination may enable fluent interaction both in visual search (Finke et al., 2016; see also Introduction) and in intentional dwell-based control (Protzak et al., 2013, and the current study).

These two types of interaction are rather different. In a visual search, the user typically makes the decision about what target he or she is looked for in advance, but the target location is not known and should be found during exploration of a scene. In intentional control, the scene and all objects in it can be well known to the user, who should be given an option not to evoke any interaction even when looking at them until the decision to interact will be made. Moreover, it is not unlikely that such an EBCI will be able to make "clicks" even at freely chosen places without any defined objects, for example, when used for drawing. While the P300 wave is important in the search tasks (Finke et al., 2016), in the intentional dwell-based interaction a negative SPN-like wave and no signs of P300 were observed (**Figures 6**, **7** in the current paper). Nevertheless, in both cases the BCI task is the same: to detect a target fixation among non-target fixations, in other words, just to provide "yes" or "no" answer for each fixation. Given the limitations of non-invasive brain signals and

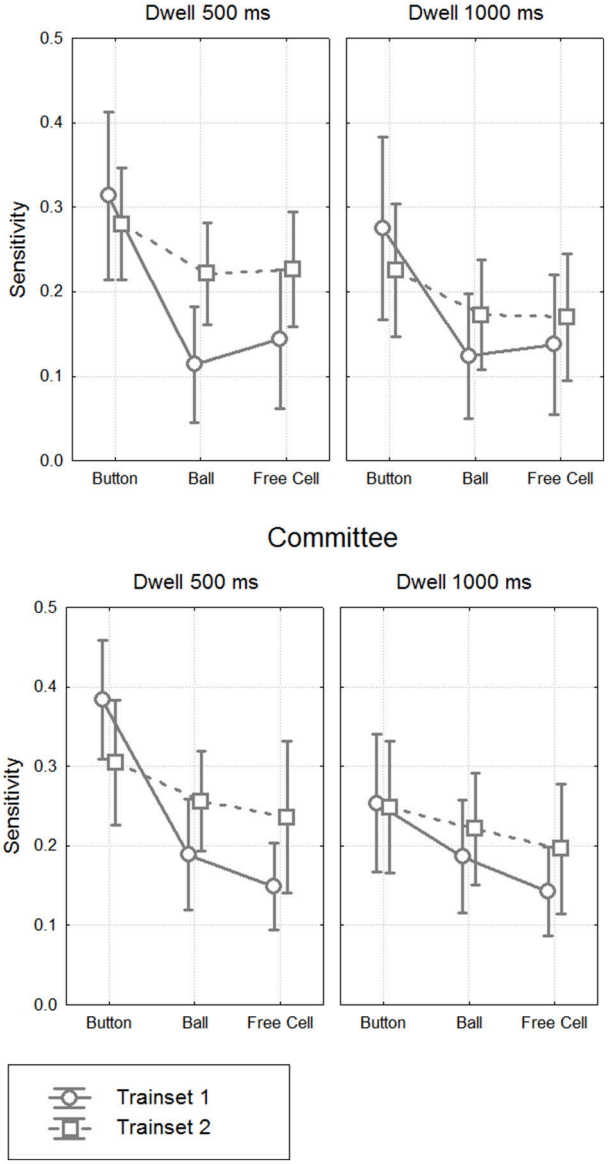

FIGURE 8 | Classifier sensitivity on the test data. Grand mean ($n = 8$) values and 95% confidence intervals for different classifiers, different types of fixations and different dwell time thresholds. The target (controlling) class in the train data was either button fixations (Trainset 1) only or all controlling fixations (Trainset 2).

TABLE 6 | Four-way MANOVA results for sensitivity.

Factor	*Wilks' λ*	*F*	*df*	*p*
Classifier	0.90	0.80	1, 7	0.40
Training Set	0.86	1.15	1, 7	0.32
Dwell Threshold	**0.12**	**52.06**	**1, 7**	**0.0002**
Fixation Type	**0.06**	**44.68**	**2, 6**	**0.0002**
Classifier × Training Set	1.00	0.01	1, 7	0.94
Classifier × Dwell Threshold	0.87	1.05	1, 7	0.34
Training Set × Dwell Threshold	**0.46**	**8.23**	**1, 7**	**0.024**
Classifier × Fixation Type	0.54	2.55	2, 6	0.16
Training Set × Fixation Type	**0.23**	**10.18**	**2, 6**	**0.012**
Dwell Threshold × Fixation Type	**0.06**	**44.71**	**2, 6**	**0.0002**
Classifier × Training Set × Dwell Threshold	**0.52**	**6.34**	**1, 7**	**0.040**
Classifier × Training Set × Fixation Type	0.47	3.45	2, 6	0.10
Classifier × Dwell Threshold × Fixation Type	0.53	2.68	2, 6	0.15
Training Set × Dwell Threshold × Fixation Type	**0.35**	**5.62**	**2, 6**	**0.042**
Classifier × Training Set × Dwell Threshold × Fixation Type	0.77	0.91	2, 6	0.45

Significant effects ($p < 0.05$) are shown in bold. Factors and their levels are described in the text.

the need to use single-trial data, it is important that the BCI task is made as simple as this. Gaze single-trial data provide much more reach information, but they lack the modalities that can be extracted from brain signals. Therefore, it is natural to combine the gaze and brain state data in a multimodal (hybrid) human-machine interface (Velichkovsky and Hansen, 1996).

It seems possible that some other psychophysiological paradigms of interaction with computer GUI elements (and, possibly, with other visual media, virtual and real objects, robot parts, etc.) can be also useful for evoking brain activity that can be quickly recognized and used to act at a fixated location. Due to similarity of the input data, all such tasks can be implemented in interfaces, for the use in different situations, with the same hardware and even software. A "second-order-hybrid" BCI built in this way may provide a highly fluent and natural means of interaction. Other functions of passive BCI (Zander and Kothe, 2011) and brain state monitoring (Van Erp et al., 2012), such as based on estimation of attention level for different objects or using error potential detection, also can benefit from fixation-based EEG segmentation and can be easily incorporated into the same system to support adaptation (immediate or based on long-term data analysis) of the interface and connected machines to the user's attentive states and interests.

Augmentation of Human-Computer Interaction with Passive Dwell-Based EBCIs

Although in most cases computers assist people in their mental, not physical activities, for every interaction with a computer the motor system should be used. Effects of physical workload on mental activity have not been much studied (DiDomenico and Nussbaum, 2011), and effects of light physical load on some specific kinds of mental activity, such as creative and/or highly focused, seems not been investigated at all. It is not unlikely that even a light physical load can interfere with mental work, at least in certain individuals, and that full freeing from physical activity can provide certain benefits, at least in certain cases of high focus on a mental task. In addition, certain forms of computer use, e.g., viewing artistic images, may benefit from enabling this activity in a highly relaxed state, without any use of skeletal muscles. To test the hypothesis that the non-motor interaction with computers can provide special benefits for the intellectual activities requires an interface enabling such interaction in unobtrusive way. Such an interface must have much better performance than the existing BCIs and without the burden of the Midas touch problem (or of existing solutions to it) associated with the gaze control technologies. EBCIs may become the first type of interface suitable for this.

With a tool for the separation of intentional and spontaneous fixations, potential benefits of the gaze based interaction could be high, due to the natural co-ordination between gaze and action. A user often fixates their gaze on a GUI button or a link earlier than approaches them with the mouse cursor (Huang et al., 2012; Liebling and Dumais, 2014) or before manually touching it on a touchscreen (Weill-Tessier et al., 2016). Fixating gaze at action location prior to reaching it or prior to the action is also observed when locations or objects in the physical world are reached and manipulated (Land et al., 1999; Neggers and Bekkering, 2000; Johansson et al., 2001). Gaze leadership should not be overemphasized: for known locations, the mouse typically leads the gaze, and the gaze often goes to a new location before the mouse click occurs (Liebling and Dumais, 2014), a behavior that is impossible with a dwell-based EBCI. In addition, it is not likely that it will not be possible to significantly reduce the dwell duration in dwell-based EBCIs comparing to our settings, where it was at least 500 ms plus the time of reaction to feedback. For serial operation and automatized actions, dwell-free approaches seem more relevant to optimize gaze based interaction. However, gaze dwells are a natural mean to convey intentions in social

interactions, and it seems natural to use them in interaction with computers as well. What the dwell-based passive EBCI may offer is not speed but fluency of operation: it could become a tool to convert intentions into actions seamlessly and without any involvement of motor system. Ideally, such an EBCI will not require from the user anything more than just looking and willing to act.

The use of passive BCIs can be not the only way to enable such a fluent interaction. For example, for the interaction with anthropomorphic robots that could be considered as partners rather than tools, we proposed to use "joint attention" gaze patterns (gaze gesture sequences) that are developed in infancy and can be automatically used by adults. Most of our participants easily found the ways to interact with a simple model of an anthropomorphic robot which responded to such patterns, although no information was provided to them about these patterns (Fedorova et al., 2015). However, we believe that for a certain range of tasks the use of dwell-based EBCIs will be optimal.

From the Wish Switch to the Wish Mouse

Gray Walter, who discovered the CNV, created the first BCI, the "wish switch" (Regan, 1989, p. 218) as early as in 1964. It sent a command to a projector to present the next picture when the patient was just going to press the button to advance the projector. The BCI was directly connected to the patient's motor cortex and could detect "the wish" even before the actual button press (Graimann et al., 2010). Later, Gray Walter proposed separate use of the CNV components, the Expectancy Wave (for direct control) and earlier Intention Wave ("so that the subject has the desired experience before any action has been taken"—Walter, 1966), but it seems that such experiments were never made.

Later on, slow negative potentials that could be related to expectation and intention (but possibly to other mental activities as well) were used, together with positive deflections, by Birbaumer and his colleagues in their "Thought Translation Device" (e.g., Neumann et al., 2003, 2004), and the Lateralized Readiness Potential (LRP) was used in the Berlin BCI group's early works (Blankertz et al., 2002, 2003). Computer screen color control through a BCI, that presumably responded to individual's wishes (here, unconscious ones), was demonstrated by Kaplan et al. (2005) with the use of rhythmic EEG components instead of the negative deflections. The majority of BCI studies were focused on techniques that do not respond to wishes and intents directly, such as motor imagery and responses to stimuli. Recently, slow premotor potentials were employed for developing neurorehabilitation BCIs (Niazi et al., 2011; Ibáñez et al., 2014; Lew et al., 2014; Xu et al., 2014; Jiang et al., 2015; Shakeel et al., 2015). But probably only the works by Zander's group (Ihme and Zander, 2011; Protzak et al., 2013) addressed the direct conversion of intentions into actions in line with the elegant approach by Gray Walter, now also enhanced with gaze capabilities. In the current work, we demonstrated that this combination can be efficient in realistic settings, and described an EEG marker for the controlling gaze fixations. As we discussed above, this marker is similar to SPN, the phenomenon that is again a member of the family of slow negative cortical potentials related to anticipation (Van Boxtel and Böcker, 2004).

Gaze is an ideal complement to brain activity in an interface aiming on a direct conversion of intentions into actions: it is itself driven by interest and wishes, but is able to convey the information about location, not easily available even from invasive brain signal recordings. Thus, combining eye tracking with the detection of FRP correlates of the wish to make a click at the fixated location will lead to creation of a "wish mouse," a tool that will possibly provide unusually fluent interaction with computers both for people with motor disabilities and for healthy individuals.

CONCLUSION

This study demonstrated that intentional gaze fixations for 500 ms, used to control a computer interface through eye tracking technology, can be discriminated from spontaneous gaze fixations of the same duration using only 300 ms EEG segments. This was done by recording EEG from healthy participants who played a game with real-time control by 500 ms gaze fixations and by running an offline BCI simulation. We also described an EEG marker for the controlling gaze fixations, which was prominent in all our 8 participants. The marker was a negativity with occipitoparietal focus, similar to Stimulus-Preceding Negativity (SPN) but differed from it by its lateralization. In the subsequent work, we plan to test the online version of the Eye-Brain-Computer Interface (EBCI) using this EEG marker.

AUTHOR CONTRIBUTIONS

SS designed the study. SS, YN, AT, ES, and AF developed the methodology. AF, ES, and YN collected the data. SS, AT, ES, BK, YN, and AF analyzed the data. SS wrote the first draft. AF and SS drew the picture for **Figure 1**. SS and BV wrote the final draft. BV and SS supervised all aspects of the research.

FUNDING

This work was partly supported by the Russian Science Foundation, grant 14-28-00234 (all parts of the work except for the literature analysis and the development of the greedy classifier committee) and by the Russian Foundation for Basic Research, grant ofi-m 15-29-01344 (the development of the greedy classifier committee).

ACKNOWLEDGMENTS

The authors would like to thank Alex Ossadtchi and Andrey Nikolaev for useful comments and suggestions.

REFERENCES

Banville, H., and Falk, T. H. (2016). Recent advances and open challenges in hybrid brain-computer interfacing: a technological review of non-invasive human research. *Brain Comput. Interfaces* 3, 9–46. doi: 10.1080/2326263X.2015.1134958

Berchicci, M., Stella, A., Pitzalis, S., Spinelli, D., and Di Russo, F. (2012). Spatio-temporal mapping of motor preparation for self-paced saccades. *Biol. Psychol.* 90, 10–17. doi: 10.1016/j.biopsycho.2012.02.014

Blankertz, B., Curio, G., and Muller, K. R. (2002). Classifying single trial EEG: Towards brain computer interfacing. *Adv. Neural Inf. Process. Syst.* 14, 157–164.

Blankertz, B., Dornhege, G., Schäfer, C., Krepki, R., Kohlmorgen, J., Müller, K. R., et al. (2003). Boosting bit rates and error detection for the classification of fast-paced motor commands based on single-trial EEG analysis. *IEEE Trans. Neural Syst. Rehabil. Eng.* 11, 127–131. doi: 10.1109/TNSRE.2003.814456

Blankertz, B., Lemm, S., Treder, M., Haufe, S., and Müller, K. R. (2011). Single-trial analysis and classification of ERP components—a tutorial. *Neuroimage* 56, 814–825. doi: 10.1016/j.neuroimage.2010.06.048

Bolt, R. A. (1982). "Eyes at the interface," in *Proceedings of the 1982 Conference on Human Factors in Computing Systems (CHI '82)*, (New York, NY: ACM), 360–362. doi: 10.1145/800049.801811

Bowsher, K., Civillico, E. F., Coburn, J., Collinger, J., Contreras-Vidal, J. L., Denison, T., et al. (2016). Brain–computer interface devices for patients with paralysis and amputation: a meeting report. *J. Neural Eng.* 13:023001. doi: 10.1088/1741-2560/13/2/023001

Brouwer, A. M., Reuderink, B., Vincent, J., van Gerven, M. A., and van Erp, J. B. (2013). Distinguishing between target and nontarget fixations in a visual search task using fixation-related potentials. *J. Vis.* 13:17. doi: 10.1167/13.3.17

Brunia, C. H., Hackley, S. A., van Boxtel, G. J., Kotani, Y., and Ohgami, Y. (2011). Waiting to perceive: reward or punishment? *Clin. Neurophysiol.* 122, 858–868. doi: 10.1016/j.clinph.2010.12.039

Brunia, C. H. M. (1988). Movement and stimulus preceding negativity. *Biol. Psychol.* 26, 165–178. doi: 10.1016/0301-0511(88)90018-X

Brunia, C. H. M., and Van Boxtel, G. J. M. (2001). Wait and see. *Int. J. Psychophysiol.* 43, 59–75. doi: 10.1016/S0167-8760(01)00179-9

Delorme, A, and Makeig, S. (2004). EEGLAB: an open source toolbox for analysis of single-trial EEG dynamics including independent component analysis. *J. Neurosci. Methods* 134, 9–21. doi: 10.1016/j.jneumeth.2003.10.009

Devillez, H., Guyader, N., and Guérin-Dugué, A. (2015). An eye fixation–related potentials analysis of the P300 potential for fixations onto a target object when exploring natural scenes. *J. Vis.* 15:20. doi: 10.1167/15.13.20

DiDomenico, A., and Nussbaum, M. A. (2011). Effects of different physical workload parameters on mental workload and performance. *Int. J. Ind. Ergon.* 41, 255–260. doi: 10.1016/j.ergon.2011.01.008

Fedorova, A. A., Shishkin, S. L., Nuzhdin, Y. O., and Velichkovsky, B. M. (2015). "Gaze based robot control: the communicative approach," in *2015 7th International IEEE/EMBS Conference on Neural Engineering (NER)*, 751–754.

Finke, A., Essig, K., Marchioro, G., and Ritter, H. (2016). Toward FRP-based brain-machine interfaces–single-trial classification of fixation-related potentials. *PLoS ONE* 11:e0146848. doi: 10.1371/journal.pone.0146848

Graimann, B., Allison, B., and Pfurtscheller, G. (eds.). (2010). "Brain–Computer Interfaces: A Gentle Introduction," in *Brain–Computer Interfaces, The Frontiers Collection* (Berlin: Springer-Verlag), 1–27.

Graupner, S.-T., Pannasch, S., and Velichkovsky, B. M. (2011). Saccadic context indicates information processing within visual fixations: evidence from event-related potentials and eye-movements analysis of the distractor effect. *Int. J. Psychophysiol.* 80, 54–62. doi: 10.1016/j.ijpsycho.2011.01.013

Healy, G., and Smeaton, A. F. (2011). "Eye fixation related potentials in a target search task," in *33rd Annual International Conference of the IEEE Engineering in Medicine and Biology Society (EMBC'11)* (Boston, MA), 4203–4206.

Huang, J., White, R., and Buscher, G. (2012). "User see, user point: gaze and cursor alignment in web search," in *Proceedings of the SIGCHI Conference on Human Factors in Computing Systems (CHI '12)* (New York, NY: ACM), 1341–1350. doi: 10.1145/2207676.2208591

Ibáñez, J., Serrano, J. I., Del Castillo, M. D., Monge-Pereira, E., Molina-Rueda, F., Alguacil-Diego, I., et al. (2014). Detection of the onset of upper-limb movements based on the combined analysis of changes in the sensorimotor rhythms and slow cortical potentials. *J. Neural Eng.* 11:056009. doi: 10.1088/1741-2560/11/5/056009

Ihme, K., and Zander, T. O. (2011). "What you expect is what you get? Potential use of contingent negative variation for passive BCI systems in gaze-based HCI," in *International Conference on Affective Computing and Intelligent Interaction* (Berlin, Heidelberg: Springer), 447–456.

Jacob, R. J. (1990). "What you look at is what you get: eye movement-based interaction techniques," in *Proceedings of the SIGCHI Conference on Human Factors in Computing Systems (CHI '90)*, eds J. Carrasco Chew and J. Whiteside (New York, NY: ACM), 11–18. doi: 10.1145/97243.97246

Jacob, R. J. (1991). The use of eye movements in human-computer interaction techniques: what you look at is what you get. *ACM Trans. Inf. Syst.* 9, 152–169. doi: 10.1145/123078.128728

Jiang, N., Gizzi, L., Mrachacz-Kersting, N., Dremstrup, K., and Farina, D. (2015). A brain–computer interface for single-trial detection of gait initiation from movement related cortical potentials. *Clin. Neurophysiol.* 126, 154–159. doi: 10.1016/j.clinph.2014.05.003

Johansson, R. S., Westling, G., Bäckström, A., and Flanagan, J. R. (2001). Eye–hand coordination in object manipulation. *J. Neurosci.* 21, 6917–6932.

Kamienkowski, J. E., Ison, M. J., Quiroga, R. Q., and Sigman, M. (2012). Fixation-related potentials in visual search: a combined EEG and eye tracking study. *J. Vis.* 12:4. doi: 10.1167/12.7.4

Kaplan, A. Y., Lim, J. J., Jin, K. S., Park, B. W., Byeon, J. G., and Tarasova, S. U. (2005). Unconscious operant conditioning in the paradigm of brain-computer interface based on color perception. *Intern. J. Neuroscience.* 115, 781–802. doi: 10.1080/00207450590881975

Kaunitz, L. N., Kamienkowski, J. E., Varatharajah, A., Sigman, M., Quiroga, R. Q., and Ison, M. J. (2014). Looking for a face in the crowd: fixation-related potentials in an eye-movement visual search task. *Neuroimage* 89, 297–305. doi: 10.1016/j.neuroimage.2013.12.006

Kim, M., Kim, B. H., and Jo, S. (2015). Quantitative evaluation of a low-cost noninvasive hybrid interface based on EEG and eye movement. *IEEE Trans. Neural Syst. Rehabil. Eng.* 23, 159–168. doi: 10.1109/TNSRE.2014.2365834

Klostermann, W., Kömpf, D., Heide, W., Yerleger, R., Wauschkuhn, B., and Seyfert, T. (1994). The presaccadic cortical negativity prior to self-paced saccades with and without visual guidance. *Electroencephalogr. Clin. Neurophysiol.* 91, 219–228. doi: 10.1016/0013-4694(94)90072-8

Kotani, Y., Ohgami, Y., Ishiwata, T., Arai, J. I., Kiryu, S., and Inoue, Y. (2015). Source analysis of stimulus-preceding negativity constrained by functional magnetic resonance imaging. *Biol. Psychol.* 111, 53–64. doi: 10.1016/j.biopsycho.2015.08.005

Krebs, R. M., Boehler, C. N., Zhang, H. H., Schoenfeld, M. A., and Woldorff, M. G. (2012). Electrophysiological recordings in humans reveal reduced location-specific attentional-shift activity prior to recentering saccades. *J. Neurophysiol.* 107, 1393–1402. doi: 10.1152/jn.00912.2010

Kristensson, P. O., and Vertanen, K. (2012). "The potential of dwell-free eye-typing for fast assistive gaze communication," in *Proceedings of the Symposium on Eye Tracking Research and Applications (ETRA '12)*, eds S. N. Spencer (New York, NY: ACM), 241–244. doi: 10.1145/2168556.2168605

Lahr, J., Schwartz, C., Heimbach, B., Aertsen, A., Rickert, J., and Ball, T. (2015). Invasive brain–machine interfaces: a survey of paralyzed patients' attitudes, knowledge and methods of information retrieval. *J. Neural Eng.* 12:043001. doi: 10.1088/1741-2560/12/4/043001

Land, M., Mennie, N., and Rusted, J. (1999). The roles of vision and eye movements in the control of activities of daily living. *Perception* 28, 1311–1328. doi: 10.1068/p2935

LeCun, Y., Bengio, Y., and Hinton, G. (2015). Deep learning. *Nature* 521, 436–444. doi: 10.1038/nature14539

Lew, E.Y., Chavarriaga, R., Silvoni, S., and Millán, J. D. R. (2014). Single trial prediction of self-paced reaching directions from EEG signals. *Front. Neurosci.* 8:222. doi: 10.3389/fnins.2014.00222

Liebling, D. J., and Dumais, S. T. (2014). "Gaze and mouse coordination in everyday work," in *Proceedings of the 2014 ACM International Joint Conference on Pervasive and Ubiquitous Computing: Adjunct Publication (UbiComp '14 Adjunct)* (New York, NY: ACM), 1141–1150. doi: 10.1145/2638728.2641692

Majaranta, P., and Bulling, A. (2014). "Eye tracking and eye-based human–computer interaction," in *Advances in Physiological Computing: Human–Computer Interaction Series*, eds S. H. Fairclough and K. Gilleade (London: Springer-Verlag), 39–65.

Müller-Putz, G., Leeb, R., Tangermann, M., Höhne, J., Kübler, A., Cincotti, F., et al. (2015). Towards noninvasive hybrid brain–computer interfaces: framework, practice, clinical application, and beyond. *Proc. IEEE* 103, 926–943. doi: 10.1109/JPROC.2015.2411333

Neggers, S. F. W., and Bekkering, H. (2000). Ocular gaze is anchored to the target of an ongoing pointing movement. *J. Neurophysiol.* 83, 639–651.

Neumann, N., Hinterberger, T., Kaiser, J., Leins, U., Birbaumer, N., and Kübler, A. (2004). Automatic processing of self-regulation of slow cortical potentials: evidence from brain-computer communication in paralysed patients. *Clin. Neurophysiol.* 115, 628–635. doi: 10.1016/j.clinph.2003.10.030

Neumann, N., Kübler, A., Kaiser, J., Hinterberger, T., and Birbaumer, N. (2003). Conscious perception of brain states: mental strategies for brain–computer communication. *Neuropsychologia* 41, 1028–1036. doi: 10.1016/S0028-3932(02)00298-1

Niazi, I. K., Jiang, N., Tiberghien, O., Nielsen, J. F., Dremstrup, K., and Farina, D. (2011). Detection of movement intention from single-trial movement-related cortical potentials. *J. Neural Eng.* 8:066009. doi: 10.1088/1741-2560/8/6/066009

Nikolaev, A. R., Jurica, P., Nakatani, C., Plomp, G., and van Leeuwen, C. (2013). Visual encoding and fixation target selection in free viewing: presaccadic brain potentials. *Front. Syst. Neurosci.* 7:26. doi: 10.3389/fnsys.2013.00026

Nikolaev, A. R., Meghanathan, R. N., and van Leeuwen, C. (2016). Combining EEG and eye movement recording in free viewing: Pitfalls and possibilities. *Brain Cogn.* 107, 55–83. doi: 10.1016/j.bandc.2016.06.004

Nurse, E., Mashford, B. S., Yepes, A. J., Kiral-Kornek, I., Harrer, S., and Freestone, D. R. (2016). "Decoding EEG and LFP signals using deep learning: heading TrueNorth," in *Proceedings of the ACM International Conference on Computing Frontiers* (Boulder, CO). 259–266.

Oostenveld, R., Fries, P., Maris, E., and Schoffelen, JM (2011). FieldTrip: open source software for advanced analysis of MEG, EEG, and Invasive electrophysiological data. *Comput. Intell. Neurosci.* 2011:156869. doi: 10.1155/2011/156869

Pedrosa, D., Pimentel, M. D. G., Wright, A., and Truong, K. N. (2015). Filteryedping: design challenges and user performance of dwell-free eye typing. *ACM Trans. Accessible Comput.* 6:3. doi: 10.1145/2724728

Pfurtscheller, G., Allison, B. Z., Bauernfeind, G., Brunner, C., Solis-Escalante, T., Scherer, R., et al. (2010). The hybrid BCI. *Front. Neurosci.* 4:3. doi: 10.3389/fnpro.2010.00003

Protzak, J., Ihme, K., and Zander, T. O. (2013). "A passive brain-computer interface for supporting gaze-based human-machine interaction," in *International Conference on Universal Access in Human-Computer Interaction* (Heidelberg, Berlin: Springer), 662–671.

Publicover, N. G., Marggraff, L. J., and Drake, E. F. (2016). *Systems and Methods for Biomechanically-Based Eye Signals for Interacting with Real and Virtual Objects*. U.S. Patent Application No. 20160085302.

Regan, D. (1989). *Human Brain Electrophysiology: Evoked Potentials and Evoked Magnetic Fields in Science and Medicine*. Amsterdam: Elsevier.

Sarcar, S., Panwar, P., and Chakraborty, T. (2013). "EyeK: an efficient dwell-free eye gaze-based text entry system," in *Proceedings of the 11th Asia Pacific Conference on Computer Human Interaction (APCHI '13)* (New York, NY: ACM), 215–220. doi: 10.1145/2525194.2525288

Sellers, E. W., Vaughan, T. M., and Wolpaw, J. R. (2010). A brain-computer interface for long-term independent home use. *Amyotroph. Lateral Scler.* 11, 449–455. doi: 10.3109/17482961003777470

Shakeel, A., Navid, M. S., Anwar, M. N., Mazhar, S., Jochumsen, M., and Niazi, I. K. (2015). A review of techniques for detection of movement intention using movement-related cortical potentials. *Comput. Math. Methods Med.* 2015:346217. doi: 10.1155/2015/346217

Shishkin, S. L., Kozyrskiy, B. L., Trofimov, A. G., Nuzhdin, Y. O., Fedorova, A. A., Svirin, E. P., et al. (2016a). Improving eye-brain-computer interface performance by using electroencephalogram frequency components. *Bull. RSMU* 2, 36–41.

Shishkin, S. L., Nuzhdin, Y. O., Svirin, E. P., Fedorova, A. A., Slobodskoy-Plusnin, Y. Y., Trofimov, A. G., et al. (2015). "Toward a fluent eye-brain-computer interface: EEG negativity marks visual fixations used to control a game," in *7th International IEEE EMBS Conference on Neural Engineering (IEEE/EMBS NER2015)* (Montpellier: Late Breaking Research Papers), 055–0463.

Shishkin, S. L., Nuzhdin, Y. O., Svirin, E. P., Trofimov, A. G., Fedorova, A. A., Dubynin, I. A., et al. (2016b). "Semi-direct mind-to-machine interface using gaze and intention markers," in *7th International Conference on Cognitive Science* (Svetlogorsk), 68-69.

Shishkin, S. L., Nuzhdin, Y. O., Trofimov, A. G., Svirin, E. P., Fedorova, A. A., Dubynin, I. A., et al. (2016c). Fixation-based eye-brain-computer interfaces: approaching a better human-computer symbiosis. *OperaMed. Physiol.* 2016(Suppl. S2), 83–84. Proceedings of Volga Neuroscience Meeting 2016. doi: 10.20388/OMP2016.00S2.005

Trofimov, A. G., Ivanitsky, I. I., and Velichkovsky, B. M. (2015). [*A greedy algorithm for constructing a committee of classifiers for the EEG signal.*] Vestnik Natsional'nogo Issledovatel'skogo Yadernogo Universiteta "MIFI" [Herald of the National Research Nuclear University MEPhI] 4, 537–544.

Ušćumlić, M., and Blankertz, B. (2016). Active visual search in non-stationary scenes: coping with temporal variability and uncertainty. *J. Neural Eng.* 13:016015. doi: 10.1088/1741-2560/13/1/016015

Van Boxtel, G. J., and Böcker, K. B. (2004). Cortical measures of anticipation. *J. Psychophysiol.* 18, 61–76. doi: 10.1027/0269-8803.18.23.61

Van Erp, J. B., Lotte, F., and Tangermann, M. (2012). Brain-computer interfaces: beyond medical applications. *Computer* 45, 26–34. doi: 10.1109/MC.2012.107

Velichkovsky, B. M., and Hansen, J. P. (1996). "New technological windows into mind: there is more in eyes and brains for human-computer interaction," in *Proceedings of the SIGCHI Conference on Human Factors in Computing Systems (CHI '96)*, ed M. J. Tauber (New York, NY: ACM), 496–503. doi: 10.1145/238386.238619

Velichkovsky, B., Sprenger, A., and Unema, P. (1997). "Towards gaze-mediated interaction: collecting solutions of the "Midas touch problem," in *Proceedings of IFIP TC13 International Conference on Human-Computer Interaction (INTERACT'97)*, eds S. Howard, J. Hammond, and G. Lindgaard (London: Chapman and Hall), 509–516.

Waldert, S. (2016). Invasive vs. non-invasive neuronal signals for brain-machine interfaces: Will one prevail? *Front. Neurosci.* 10:295. doi: 10.3389/fnins.2016.00295

Walter, W. G. (1966). Expectancy waves and intention waves in the human brain and their application to the direct cerebral control of machines. *Electroenceph. Clin. Neurophysiol.* 21, 616.

Weill-Tessier, P., Turner, J., and Gellersen, H. (2016). "How do you look at what you touch? A study of touch interaction and gaze correlation on tablets," in *Proceedings of the Ninth Biennial ACM Symposium on Eye Tracking Research & Applications (ETRA '16)* (New York, NY: ACM), 329–330. doi: 10.1145/2857491.2888592

Wenzel, M. A., Golenia, J. E., and Blankertz, B. (2016). Classification of eye fixation related potentials for variable stimulus saliency. *Front. Neurosci.* 10:23. doi: 10.3389/fnins.2016.00023

Wolpaw, J. R., Birbaumer, N., McFarland, D. J., Pfurtscheller, G., and Vaughan, T. M. (2002). Brain–computer interfaces for communication and control. *Clin. Neurophysiol.* 113, 767–791. doi: 10.1016/S1388-2457(02)00057-3

Xu, R., Jiang, N., Lin, C., Mrachacz-Kersting, N., Dremstrup, K., and Farina, D. (2014). Enhanced low-latency detection of motor intention from EEG for closed-loop brain-computer interface applications. *IEEE Trans. Biomed. Eng.* 61, 288–296. doi: 10.1109/TBME.2013.2294203

Zander, T. O., Gaertner, M., Kothe, C., and Vilimek, R. (2010). Combining eye gaze input with a brain–computer interface for touchless human–computer interaction. *Int. J. Hum. Comput. Interact.* 27, 38–51. doi: 10.1080/10447318.2011.535752

Zander, T. O., and Kothe, C. (2011). Towards passive brain–computer interfaces: applying brain–computer interface technology to human–machine systems in general. *J. Neural Eng.* 8:025005. doi: 10.1088/1741-2560/8/2/025005

Conflict of Interest Statement: The authors declare that the research was conducted in the absence of any commercial or financial relationships that could be construed as a potential conflict of interest.

frontiers in Systems Neuroscience

MINI REVIEW
published: 30 November 2015
doi: 10.3389/fnsys.2015.00162

Control Capabilities of Myoelectric Robotic Prostheses by Hand Amputees: A Scientific Research and Market Overview

Manfredo Atzori and Henning Müller*

Information Systems Institute, University of Applied Sciences Western Switzerland (HES-SO Valais), Sierre, Switzerland

Hand amputation can dramatically affect the capabilities of a person. Cortical reorganization occurs in the brain, but the motor and somatosensorial cortex can interact with the remnant muscles of the missing hand even many years after the amputation, leading to the possibility to restore the capabilities of hand amputees through myoelectric prostheses. Myoelectric hand prostheses with many degrees of freedom are commercially available and recent advances in rehabilitation robotics suggest that their natural control can be performed in real life. The first commercial products exploiting pattern recognition to recognize the movements have recently been released, however the most common control systems are still usually unnatural and must be learned through long training. Dexterous and naturally controlled robotic prostheses can become reality in the everyday life of amputees but the path still requires many steps. This mini-review aims to improve the situation by giving an overview of the advancements in the commercial and scientific domains in order to outline the current and future chances in this field and to foster the integration between market and scientific research.

Keywords: electromyography, prosthetics, rehabilitation robotics, machine learning

OPEN ACCESS

Edited by:
Mikhail Lebedev,
Duke University, USA

Reviewed by:
Ning Jiang,
University of Waterloo, Canada
Kianoush Nazarpour,
Newcastle University, UK
Agamemnon Krasoulis,
University of Edinburgh, UK

****Correspondence:***
Manfredo Atzori
manfredo.atzori@hevs.ch

Received: *20 July 2015*
Accepted: *09 November 2015*
Published: *30 November 2015*

Citation:
Atzori M and Müller H (2015) Control Capabilities of Myoelectric Robotic Prostheses by Hand Amputees: A Scientific Research and Market Overview.
Front. Syst. Neurosci. 9:162.
doi: 10.3389/fnsys.2015.00162

INTRODUCTION

It is estimated that 41,000 persons were living with a major loss of an upper limb in 2005 (Ziegler-Graham et al., 2008). A hand amputation is one of the most impairing injuries and it can dramatically affect the capabilities of a person. Recent scientific and commercial advances in man-machine interfaces are promising and suggest that dexterous, naturally controlled, proportional and simultaneous robotic prostheses could be reality in the future of amputees. Nevertheless, the outline of the situation in the market and scientific field is complex and the path to naturally controlled prostheses still requires several steps.

Man-machine interfaces have been developed to control hand prostheses via the brain (Lebedev and Nicolelis, 2006), peripheral nerves (Navarro et al., 2005) or the muscles (Cipriani et al., 2011). The first two methods are promising but they usually require invasive procedures to obtain robust performance, thus they are currently applied only in scientific research. The third method (surface electromyography, sEMG) is probably the most widely used both in commercial settings and in scientific research.

Myoelectric hand prostheses with many degrees of freedom and very good mechanical capabilities are now commercially available. However, prosthetics companies target most of their communication efforts to end users. Thus they highlight the practical capabilities

of the hands, but they usually do not provide information regarding the technical functionalities and specifications of the prostheses that can be exploitable by academic researchers. Previous papers presented some hand prostheses in detail (Belter et al., 2013) but the market changes quickly.

The scientific research field is even more complex and quickly changing. Many papers have been written in scientific research about the natural control of robotic hands by intact and transradial hand amputated subjects. Most of the methods rely on the use of sEMG and of pattern recognition or proportional control algorithms. The first commercial products exploiting pattern recognition to recognize the movements have recently been released. Targeted muscle reinnervation (TMR) can allow the exploitation of these methods even on subjects with above-elbow amputations. Benchmark databases to compare the performance of different methods and setups have been released (Atzori et al., 2014a). However, several steps are still required to obtain proportional, naturally controlled, robust and usable robotic hand prostheses (bionic hands).

Since the market and the scientific field are so complex and changing so quickly, it can be difficult to have a complete overview of them and to remain constantly updated in both fields. This mini-review aims to be a resource for young and experienced researchers in academia and prosthetic companies by providing a synthetic but complete overview of the current level of advancement in the commercial and scientific reality.

MARKET OUTLINE

A relatively wide choice of devices is available to restore the capabilities of hand amputees by myoelectric robotic prostheses. Such devices are continuously evolving according to technology, scientific research, market needs and user requirements. The devices usually include two main parts: prosthetic hands and control systems.

Prosthetic Hands

Currently, hand prostheses include cosmetic prostheses, kinematic prostheses and myoelectric prostheses. Cosmetic prostheses offer esthetical and psychological support. Kinematic prostheses also have functional capabilities, since the user can control the opening and closing of a gripper hand through the motion of the shoulder. Myoelectric prosthesis users can control a battery-powered hand through the electrical signal emitted by the remnant muscles, usually located in the forearm.

The continuous improvements in the field and the different targets and aims of the papers published by the companies can make it difficult for researchers to remain updated with the capabilities of available prostheses. For example, Belter et al. (2013) performed a very thorough description of the mechanical properties of prosthetic hands produced by four companies, but in less than 2 years several companies produced new versions or made substantial changes to the products from a mechanical or electronic point of view. Thus, the market and research achievements often remain disconnected.

Many prosthetic hands are commercially available. However, few have the capability to reproduce many movements. The following selection represents some of the currently most advanced hand prostheses and gives a representation of different companies and approaches: (1) Touch Bionics i-limb Quantum; (2) Otto Bock Michelangelo; (3) Steeper Bebionic v3; and (4) Vincent hand Evolution 2. **Table 1** summarizes the most important features that can be useful in a laboratory. The features are grouped into the following four categories: general technical data, dexterity related features, force related features and control related features.

Control Systems

Usually two or three sEMG electrodes are located in the socket in correspondence to specific muscles (**Figure 1**). A myoelectric impulse (i.e., an increase in the amplitude of the electrical signal emitted by the muscles) is used to open and close the prosthetic hand. The number of movements can be increased employing specific (e.g., sequential) control strategies. Such control strategies are usually still far from being natural, thus controlling prostheses requires a high level of skill and a training procedure. Control problems contribute to the scarce capabilities and acceptance of sEMG prostheses (Atkins et al., 1996), but they are likely promising for improvements in a near future.

In **Table 1** we summarize some of the most important control related features for the considered prosthetic hands including: number of electrodes, movement control type, movement command and particular features of each control system. As can be noticed in **Table 1**, despite the mechanical characteristics of the prosthesis allowing to reproduce up to 24 hand movements, the control systems rely in most cases on few (1–3) electrodes and on sequential control strategies or on specific movement triggers (in some cases tunable through a mobile app or other strategies). In sequential control strategies, a specific signal (for example, a simultaneous activation of two sEMG electrodes, usually called co-contraction) is used to switch between a set of predefined movements. In movement triggers on the other hand specific patterns of electrode activation are related to specific movements of the prosthesis. The mentioned methods are not natural, in the sense that they do not correspond to the movement that the subject would have thought to do before the amputation. However, they offer robust results, which is one of the main needs in real life.

Several of the considered prostheses include external sources of information as well. In particular, Touch Bionics i-limb Quantum recently introduced gesture control (recorded via gyroscope, accelerometer and magnetometer) and grip chips (that use blue-tooth chips attached to specific objects) to perform movement selection, while Steeper Bebionic exploits finger position encoders to perform falling object prevention. Sometimes research achievements translate to clinical practice too. In 2013 a pattern recognition system similar to the ones described in the scientific literature was made commercially available (http://www.coaptengineering.com/).

TABLE 1 | Characteristics of the examined prosthetic hands.

	Company name Prosthesis model	Touch Bionics i-limb Quantum	Otto Bock Michelangelo with Axon Bus Technology	Steeper Bebionic v3	Vincent GmbH Evolution 2
General technical data	Weight (without battery)	474–515 g	∼510 g	550–598 g (365–390 g small hand)	380–410g
	Operating voltage	7.4 V	11.1 V	7.4 V	6–8 V
	Battery type	Lithium polymer	Li-Ion	Li-Ion	Li-Pol
	Battery capacity	1300–2400 mAh	1500 mAh	1300–2200 mAh	1300–2600 mAh
	Number of actuators	6	2	5	6
Dexterity	Active fingers	5 independent	3	5 independent	5 (+12 *active joints*)
	Thumb rotation	Powered	Powered	Manual	Powered
	Total number of grip patterns	24	7	14	20
	Grip patterns available at any moment	7	7	11	20
	Flexible wrist	Available	Included	Available	Available
	Rotating wrist	Available	Available	Available	Available
	Rotating wrist	*(active or passive)*	*(active or passive)*	*(active or passive)*	*(only passive)*
	Full closing time	0.8 s (0.7 s small hand)	0.37 s	0.5–1 s	0.8 s
	Finger position encoders	No	2 *motor position encoders*	5 *(one in each actuator)*	2 *(in thumb actuators)*
Force	Power grip	100–136 N	∼70 N	140.1 N (280 N small hand)	60 N
	Lateral pinch	40 N (60 N small hand)	∼60 N	26.5 N (53 N small hand)	15 N
	Adaptive Grip	Yes	Yes	Yes	Yes
	Falling object prevention	Active *(auto-grasp, based on accidental sEMG signal detection)*	No	Active *(auto-grip, based on finger position encoders)*	Passive *(spring load)*
	Proportional control	Yes	Yes	Yes	Yes
	N° of electrodes	1–2	1–2–3	1–2	1–2 wired
Control	Movement control type	Movement triggers, mobile app, bluetooth grip chips, favorite environment, gesture control	Sequential, 4-channel control	Sequential, Morph RFId GRIP selection compatible	Single trigger or Vincent Morse code
	Movement command	Hold open, double impulse, triple impulse, co-contraction	Different switching modes available, fast and high signal controls rotation in 4-channel control	Co-contraction/ open-open signal	Hold signal (opening or closing), double signal, co-contraction, alternating signal
	Particular features	Various control methods thumb rotating manually and automatically	Sensor hand speed *(stiff and harder finger tips)*; Fragile objects grasping	Fully free flexing fingers	Very low weight
	Feedback	No	No	Audible beeps and/or vibration *(grip changes)*	Vibration *(force detected via motor current and DMS sensors)*

The Coapt system can include up to eight sEMG electrodes. It is generic and it is typically set up to control the number of powered DOFs the patient's prosthesis has. That is, if a powered elbow, wrist, and terminal device are built into the prosthesis then the Coapt system is set to control these. If, however the prosthesis only has a powered terminal device and/or wrist, the Coapt system is set up for those DOFs. Wherever possible, Coapt performs natural control. The technician is encouraged to work with the patient to determine which are the most physiological, repeatable, consistent, and intuitive movements to use for control. Slight variations can be attempted if necessary, also through re-calibration procedures. The number of natural grasping patterns that can be achieved varies. According to Coapt, typically users can select between 3–6 naturally. It should be noted that the physical interconnection of the Coapt system and several prostheses has yet to be implemented. An example of movement-triggered control that we received by Coapt is the following one:

1. Hand closing: closing prosthesis.
2. Hand opening: opening prosthesis.
3. Wrist clockwise/counterclockwise rotation: powered wrist clockwise/counterclockwise rotation.
4. Double impulse of natural hand opening: grip A.
5. Triple impulse of natural hand opening: grip B.
6. Holding the hand open: grip C.
7. Single impulse of natural hand opening: grip D.

SCIENTIFIC RESEARCH OUTLINE

Many papers have been written in scientific research about the control of robotic hands and prostheses by intact and hand amputated subjects.

Usually several electrodes are placed on the forearm of the subject to record the myoelectric signals (**Figure 1**) with a dense sampling approach (Fukuda et al., 2003; Tenore et al., 2009; Li et al., 2010) or a precise anatomical positioning strategy (De Luca, 1997; Castellini et al., 2009a). The most common control procedures can be subdivided into pattern recognition or proportional control approaches, which can be applied to sEMG and multimodal signals.

Pattern recognition algorithms are used to classify the movement that the subject aims to perform according to a label (Scheme and Englehart, 2011). Pattern recognition results provided in several cases classification accuracy over 90–95% on less than 10 classes (e.g., Castellini et al., 2009b), however average results are usually below 80–90% (Peerdeman et al., 2011). Movement classification methods require movement labeling and they are restricted to a predetermined set of hand movements. Simultaneous pattern recognition has been studied recently (Jiang et al., 2013b; Ortiz-Catalan et al., 2013; Young et al., 2013), however usually such procedures consider simultaneous motions as new classes, thus they can reduce the robustness of the classifier.

Proportional and simultaneous control of a large number of degrees of freedom of the prosthesis can allow achieving more natural and dexterous control using unsupervised or supervised methods (Fougner et al., 2012; Farina et al., 2014). Unsupervised methods are usually based on signal factorization (e.g., through Non-Negative Matrix Factorization, NMF), they require a short calibration phase and they are relatively independent on the number and exact location of the electrodes (Jiang et al., 2009, 2014a,b; Muceli et al., 2014). Supervised methods (Nielsen et al., 2011; Muceli and Farina, 2012; Ameri et al., 2014a,b; Gijsberts et al., 2014b; Hahne et al., 2014) are usually based on regression techniques (e.g., Linear Regression, LR, Artificial Neural Networks, ANN, Support Vector Machines, SVM) that require a reliable ground truth for hand kinematics. This is easy for intact subjects (e.g., using data gloves), but it can be difficult for amputees, for whom the ground truth can be acquired only via bilateral mirrored contractions (Nielsen et al., 2011) or via visual cues (Ameri et al., 2014a,b). Recently, semi-supervised methods (NMF) and supervised methods (LR, ANN) were compared to evaluate the impact of precise kinematics estimation for accurately completing goal-directed tasks (Jiang et al., 2014b). The results showed that, although the three algorithms' mapping accuracies were significantly different, their online performance was similar. These results underline the hypothesis that good proportional myoelectric control can be achieved by the interaction and adaptation of the user with the myoelectric controller through closed-loop feedback. The same hypothesis is also demonstrated in other recent papers on multiple degrees of freedom for intact subjects (Pistohl et al., 2013; Antuvan et al., 2014) and hand amputees (Jiang et al., 2014a). Despite most of the proportional studies concentrating on full hand movements (e.g., hand supination, pronation, rotation, flexion, extension), proportional and simultaneous control has a strong potential for decoding finger kinematics as well. In particular, recent work described average correlation coefficients of up to 0.9 for the estimation of single finger movements (Smith et al., 2008) and 0.8 for the estimation of simultaneous and complex movements (Ngeo et al., 2014).

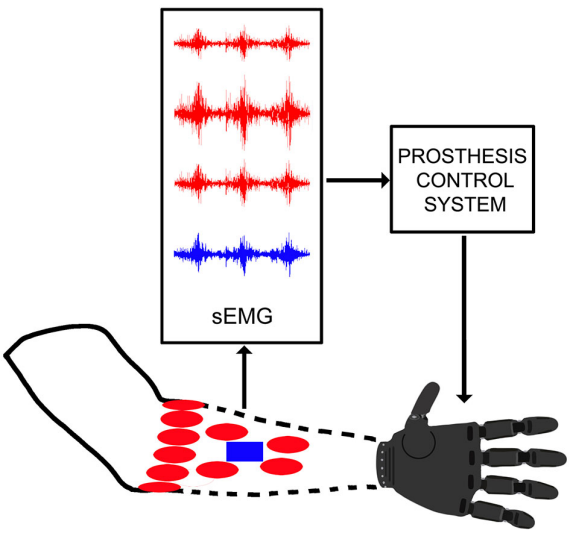

FIGURE 1 | Scheme of a generic myoelectric control system: (i) for commercial prosthesis without pattern recognition (blue rectangle); and (ii) for research (or control system with pattern recognition; red ellipses). The same architecture is assumed in the external forearm.

Also in scientific research, additional sources of information can be used to improve the performance of myoelectric control. Computer vision has been integrated to predetermine the type and size of the required grasp in relation to the object (Došen et al., 2010; Markovic et al., 2014). Accelerometers showed excellent capabilities to recognize hand movements using pattern recognition and regression methods, both alone and in combination with sEMG electrodes (Atzori et al., 2014b; Gijsberts et al., 2014a; Krasoulis et al., 2015).

A common problem in the field is that often the studies are highly specific and they are not directly comparable, due to different acquisition setups, protocols and analysis pipelines. Moreover, often the datasets are not publicly available. The NinaPro project (Atzori et al., 2015) released a publicly available benchmark with EMG, kinematic and dynamic data sources from intact and amputated subjects to help the scientific community to overcome control problems (http://ninaweb.hevs.ch/). Ninapro was recently used to evaluate regression methods for the continuous decoding of finger movements from sEMG and accelerometry (Krasoulis et al., 2015), to apply Dynamic time warping (DTW) in the context of myoelectric control (AbdelMaseeh et al., 2015) and to present the *Movement Error Rate*, an alternative to the standard window-based accuracy in pattern recognition (Gijsberts et al., 2014a).

Many factors can theoretically influence sEMG controlled prosthesis, including anatomical characteristics of the subjects

(Farina et al., 2002), training in using myoelectric prostheses (Cipriani et al., 2011), clinical parameters of the subjects (e.g., level of the amputation, phantom limb sensation intensity; Atzori et al., in press), fatigue, sweating, changes in electrode or arm positioning, surgical procedures used during the amputation and even cortical reorganization. However, few studies addressed these effects.

Implanting intramuscular EMG-recording devices reduces the number of parameters affecting the EMG signal and it can improve simultaneous control of multi-DOF prosthetic wrist and hand (Smith et al., 2014, 2015).

TMR is a surgical procedure that redirects the nerves that used to control the muscles of the hand to innervate accessory muscles from which surface sEMG is recorded. Impressive results have been obtained with this method, especially in persons with above-elbow or shoulder amputations (Kuiken et al., 2009). The same technique has also been applied on muscles transferred to the forearm to better integrate with traditional commercial prostheses (Aszmann et al., 2015).

The opposite neural direction, i.e., transferring information from the hand prosthesis to the brain, has been studied in several papers as well. Several attempts have been performed using non-invasive or invasive methods. Electrocutaneous and vibratory stimulation channels have been extensively studied in the past Szeto and Saunders (1982). TMR represents a promising solution also in this case, since it theoretically allows a certain amount of sensory feedback (Marasco et al., 2009). However, to date, the only example of real-time use of neural interfaces for the effective bidirectional control of dexterous prosthetic hands performing different grasping tasks is given by Raspopovic et al. (2014).

Despite the achievements described in this article, there are still several challenges before amputees can benefit from the mentioned signal processing developments (Jiang et al., 2012). First, robustness is probably the most important and challenging problem, in particular for simultaneous and proportional control. Second, the sensory-motor loop should be closed with proper feedback systems, thus opening new possibilities for effective and intuitive prosthetic control. Third, most of the studies are performed in controlled laboratory conditions with non-amputated subjects, which do not adapt to several different real life conditions of amputees (Fougner et al., 2011; Jiang et al., 2013a; He et al., 2015a,b).

CONCLUSIONS

Hand amputation can dramatically affect the capabilities of a person. The augmentation of the functionalities of the nervous and muscular system through external devices can already improve the situation of amputees. The market and the scientific field are complex and changing quickly, thus it is often difficult for young researchers to have a complete overview of them, as well as for experienced researchers to remain constantly updated in both the fields. In this mini review, we provide a synthetic but complete overview of the current level of advancement in the commercial and scientific reality, addressing each field in a specific section.

The commercial outline highlights the existence of very advanced prosthetic hands and control systems. Four of the most advanced prosthetic hands were analyzed, showing important mechanical and control differences. In particular, the number of actuators ranges between 2 (Otto Bock Michelangelo), 5 (Steeper Bebionic 3) and 6 (Touch Bionics i-limb Quantum and Vincent Evolution 2) while the number of finger position encoders ranges between 0 (Touch Bionics i-limb Quantum), 2 (Otto Bock Michelangelo, Vincent Evolution 2) and 5 (Steeper Bebionic 3). The first commercial control system based on pattern recognition has been released and it seems a great advancement with respect to previous ones. However natural, proportional and simultaneous control of a large number of degrees of freedom is currently not available.

The scientific research outline shows a large variety of control methods and several possible improvements. Pattern recognition, proportional control and TMR are extremely promising. Common sEMG data resources and benchmarks have been proposed recently to compare different sEMG analysis methods. Most of the factors that can theoretically affect the control of myoelectric prostheses, such as clinical data (e.g., level of the amputation, phantom limb sensation intensity) were recently studied. Finally sensorial feedback recently showed very promising advancements.

In conclusion, the path to proportional, naturally controlled, robust and usable robotic hand prostheses with sensorial feedback (bionic hands) seems to be well initiated and extremely promising for the coming years even though it is still a challenging work in progress.

ACKNOWLEDGMENTS

We would like to thank Valentina Baruchello and Hugh Gill at Touch Bionics, Bruce Rattray at Steeper, Stefan Schultz at Vincent, Blair Lock at Coapt Engineering, Martin Wehrle, Amsüss Sebastian and Karsten Ley at Otto Bock, and their teams for their helpfulness in providing information for this study.

REFERENCES

AbdelMaseeh, M., Chen, T.-W., and Stashuk, D. (2015). Extraction and classification of multichannel electromyographic activation trajectories for hand movement recognition. *IEEE Trans. Neural Syst. Rehabil. Eng.* doi: 10.1109/tnsre.2015.2447217 [Epub ahead of print].

Ameri, A., Kamavuako, E. N., Scheme, E. J., Englehart, K. B., and Parker, P. A. (2014a). Real-time, simultaneous Myoelectric control using visual target-based training paradigm. *Biomed. Signal Process. Control* 13, 8–14. doi: 10.1016/j.bspc.2014.03.006

Ameri, A., Kamavuako, E. N., Scheme, E. J., Englehart, K. B., and Parker, P. (2014b). Support vector regression for improved real-time, simultaneous

Myoelectric control. *IEEE Trans. Neural Syst. Rehabil. Eng.* 22, 1198–1209. doi: 10.1109/TNSRE.2014.2323576

Antuvan, C. W., Ison, M., and Artemiadis, P. (2014). Embedded human control of robots using Myoelectric interfaces. *IEEE Trans. Neural Syst. Rehabil. Eng.* 22, 820–827. doi: 10.1109/TNSRE.2014.2302212

Aszmann, O. C., Roche, A. D., Salminger, S., Paternostro-Sluga, T., Herceg, M., Sturma, A., et al. (2015). Bionic reconstruction to restore hand function after brachial plexus injury: a case series of three patients. *Lancet* 385, 2183–2189. doi: 10.1016/s0140-6736(14)61776-1

Atkins, D. J., Heard, D. C. Y., and Donovan, W. H. (1996). Epidemiologic overview of individuals with upper-limb loss and their reported research priorities. *J. Prosthet. Orthot.* 8, 2–11. doi: 10.1097/00008526-199600810-00003

Atzori, M., Gijsberts, A., Castellini, C., Caputo, B., Hager, A.-G. M., Elsig, S., et al. (2014a). Electromyography data for non-invasive naturally-controlled Robotic hand prostheses. *Sci. Data* 1:140053. doi: 10.1038/sdata.2014.53

Atzori, M., Gijsberts, A., Müller, H., and Caputo, B. (2014b). Classification of hand movements in amputated subjects by sEMG and accelerometers, in *Annual International Conference of the IEEE Engineering in Medicine and Biology Society (EMBC)* (Chicago, IL: IEEE), 3545–3549.

Atzori, M., Gijsberts, A., Castellini, C., Caputo, B., Mittaz Hager, A.-G., Elsig, S., et al. (in press). Clinical parameter effect on the capability to control Myoelectric Robotic prosthetic hands. *J. Rehabil. Res. Dev.* [Epub ahead of print].

Atzori, M., Gijsberts, A., Kuzborskij, I., Elsig, S., Mittaz Hager, A.-G., Deriaz, O., et al. (2015). Characterization of a benchmark database for Myoelectric movement classification. *IEEE Trans. Neural Syst. Rehabil. Eng.* 23, 73–83. doi: 10.1109/TNSRE.2014.2328495

Belter, J. T., Segil, J. L., Dollar, A. M., and Weir, R. F. (2013). Mechanical design and performance specifications of anthropomorphic prosthetic hands: a review. *J. Rehabil. Res. Dev.* 50, 599–618. doi: 10.1682/jrrd.2011.10.0188

Castellini, C., Fiorilla, A. E., and Sandini, G. (2009a). Multi-subject/daily-life activity EMG-based control of mechanical hands. *J. Neuroeng. Rehabil.* 6:41. doi: 10.1186/1743-0003-6-41

Castellini, C., Gruppioni, E., Davalli, A., and Sandini, G. (2009b). Fine detection of grasp force and posture by amputees via surface electromyography. *J. Physiol. Paris* 103, 255–262. doi: 10.1016/j.jphysparis.2009.08.008

Cipriani, C., Antfolk, C., Controzzi, M., Lundborg, G., Rosen, B., Carrozza, M. C., et al. (2011). Online Myoelectric control of a dexterous hand prosthesis by transradial amputees. *IEEE Trans. Neural Syst. Rehabil. Eng.* 19, 260–270. doi: 10.1109/TNSRE.2011.2108667

De Luca, C. J. (1997). The use of surface electromyography in biomechanics. *J. Appl. Biomech.* 13, 135–163.

Došen, S., Cipriani, C., Kostić, M., Controzzi, M., Carrozza, M. C., and Popović, D. B. (2010). Cognitive vision system for control of dexterous prosthetic hands: experimental evaluation. *J. Neuroeng. Rehabil.* 7:42. doi: 10.1186/1743-0003-7-42

Farina, D., Cescon, C., and Merletti, R. (2002). Influence of anatomical, physical and detection-system parameters on surface EMG. *Biol. Cybern.* 86, 445–456. doi: 10.1007/s00422-002-0309-2

Farina, D., Jiang, N., Rehbaum, H., Holobar, A., Graimann, B., Dietl, H., et al. (2014). The extraction of neural information from the surface EMG for the control of upper-limb prostheses: emerging avenues and challenges. *IEEE Trans. Neural Syst. Rehabil. Eng.* 22, 797–809. doi: 10.1109/TNSRE.2014.2305111

Fougner, A., Scheme, E., Chan, A. D. C., Englehart, K., and Stavdahl, O. (2011). Resolving the limb position effect in Myoelectric pattern recognition. *IEEE Trans. Neural Syst. Rehabil. Eng.* 19, 644–651. doi: 10.1109/TNSRE.2011.2163529

Fougner, A., Stavdahl, Ø., Kyberd, P. J., Losier, Y. G., and Parker, P. A. (2012). Control of upper limb prostheses: terminology and proportional Myoelectric control-a review. *IEEE Trans. Neural Syst. Rehabil. Eng.* 20, 663–677. doi: 10.1109/TNSRE.2012.2196711

Fukuda, O., Tsuji, T., Kaneko, M., Otsuka, A., and Tsuji, O. F. T. (2003). A human-assisting manipulator teleoperated by EMG signals and arm motions. *IEEE Trans. Robot. Autom.* 19, 210–222. doi: 10.1109/tra.2003.808873

Gijsberts, A., Atzori, M., Castellini, C., Muller, H., and Caputo, B. (2014a). The movement error rate for evaluation of machine learning methods for sEMG-based hand movement classification. *IEEE Trans. Neural Syst. Rehabil. Eng.* 22, 735–744. doi: 10.1109/TNSRE.2014.2303394

Gijsberts, A., Bohra, R., González, D. S., Werner, A., Nowak, M., Caputo, B., et al. (2014b). Stable Myoelectric control of a hand prosthesis using non-linear incremental learning. *Front. Neurorobot.* 8:8. doi: 10.3389/fnbot.2014.00008

Hahne, J. M., BieBmann, F., Jiang, N., Rehbaum, H., Farina, D., Meinecke, F. C., et al. (2014). Linear and nonlinear regression techniques for simultaneous and proportional Myoelectric control. *IEEE Trans. Neural Syst. Rehabil. Eng.* 22, 269–279. doi: 10.1109/TNSRE.2014.2305520

He, J., Zhang, D., Jiang, N., Sheng, X., Farina, D., and Zhu, X. (2015a). User adaptation in long-term, open-loop Myoelectric training: implications for EMG pattern recognition in prosthesis control. *J. Neural Eng.* 12:046005. doi: 10.1088/1741-2560/12/4/046005

He, J., Zhang, D., Sheng, X., Li, S., and Zhu, X. (2015b). Invariant surface EMG feature against varying contraction level for Myoelectric control based on muscle coordination. *IEEE J. Biomed. Health Inform.* 19, 874–882. doi: 10.1109/JBHI.2014.2330356

Jiang, N., Dosen, S., Muller, K., and Farina, D. (2012). Myoelectric control of artificial limbs-is there a need to change focus? *IEEE Signal Process. Mag.* 29, 150–152. doi: 10.1109/msp.2012.2203480

Jiang, N., Englehart, K. B., Parker, P. A., and Englehart, K. B. (2009). Extracting simultaneous and proportional neural control information for multiple degree of freedom prostheses from the surface electromyographic signal. *IEEE Trans. Biomed. Eng.* 56, 1070–1080. doi: 10.1109/TBME.2008.2007967

Jiang, N., Muceli, S., Graimann, B., and Farina, D. (2013a). Effect of arm position on the prediction of kinematics from EMG in amputees. *Med. Biol. Eng. Comput.* 51, 143–151. doi: 10.1007/s11517-012-0979-4

Jiang, N., Tian, L., Fang, P., Dai, Y., and Li, G. (2013b). Motion recognition for simultaneous control of multifunctional transradial prostheses, in *Engineering in Medicine and Biology Society (EMBC), 2013 35th Annual International Conference of the IEEE* (Osaka: IEEE), 1603–1606.

Jiang, N., Rehbaum, H., Vujaklija, I., Graimann, B., and Farina, D. (2014a). Intuitive, online, simultaneous and proportional Myoelectric control over two degrees-of-freedom in upper limb amputees. *IEEE Trans. Neural Syst. Rehabil. Eng.* 22, 501–510. doi: 10.1109/TNSRE.2013.2278411

Jiang, N., Vujaklija, I., Rehbaum, H., Graimann, B., and Farina, D. (2014b). Is accurate mapping of EMG signals on kinematics needed for precise online Myoelectric control? *IEEE Trans. Neural Syst. Rehabil. Eng.* 22, 549–558. doi: 10.1109/tnsre.2013.2287383

Krasoulis, A., Vijayakumar, S., and Nazarpour, K. (2015). Evaluation of regression methods for the continuous decoding of finger movement from surface EMG and accelerometry, in *Neural Engineering (NER), 2015 7th International IEEE/EMBS Conference on* (Montpellier: IEEE), 631–634.

Kuiken, T. A., Li, G., Lock, B. A., Lipschutz, R. D., Miller, L. A., Stubblefield, K. A., et al. (2009). Targeted muscle reinnervation for real-time Myoelectric control of multifunction artificial arms. *JAMA* 301, 619–628. doi: 10.1001/jama.2009.116

Lebedev, M. A., and Nicolelis, M. A. L. (2006). Brain-machine interfaces: past, present and future. *Trends Neurosci.* 29, 536–546. doi: 10.1016/j.tins.2006.07.004

Li, G., Schultz, A. E., and Kuiken, T. A. (2010). Quantifying pattern recognition-based Myoelectric control of multifunctional transradial prostheses. *IEEE Trans. Neural Syst. Rehabil. Eng.* 18, 185–192. doi: 10.1109/TNSRE.2009.2039619

Marasco, P. D., Schultz, A. E., and Kuiken, T. A. (2009). Sensory capacity of reinnervated skin after redirection of amputated upper limb nerves to the chest. *Brain* 132, 1441–1448. doi: 10.1093/brain/awp082

Markovic, M., Dosen, S., Cipriani, C., Popovic, D., and Farina, D. (2014). Stereovision and augmented reality for closed-loop control of grasping in hand prostheses. *J. Neural Eng.* 11:046001. doi: 10.1088/1741-2560/11/4/046001

Muceli, S., and Farina, D. (2012). Simultaneous and proportional estimation of hand kinematics from EMG during mirrored movements at multiple degrees-of-freedom. *IEEE Trans. Neural Syst. Rehabil. Eng.* 20, 371–378. doi: 10.1109/TNSRE.2011.2178039

Muceli, S., Jiang, N., and Farina, D. (2014). Extracting signals robust to electrode number and shift for online simultaneous and proportional Myoelectric control by factorization algorithms. *IEEE Trans. Neural Syst. Rehabil. Eng.* 22, 623–633. doi: 10.1109/TNSRE.2013.2282898

Navarro, X., Krueger, T. B., Lago, N., Micera, S., Stieglitz, T., and Dario, P. (2005). A critical review of interfaces with the peripheral nervous system for the control of neuroprostheses and hybrid bionic systems. *J. Peripher. Nerv. Syst.* 10, 229–258. doi: 10.1111/j.1085-9489.2005.10303.x

Ngeo, J. G., Tamei, T., and Shibata, T. (2014). Continuous and simultaneous estimation of finger kinematics using inputs from an EMG-to-muscle activation model. *J. Neuroeng. Rehabil.* 11:122. doi: 10.1186/1743-0003-11-122

Nielsen, J. L. G., Holmgaard, S., Jiang, N., Englehart, K. B., Farina, D., and Parker, P. A. (2011). Simultaneous and proportional force estimation for multifunction Myoelectric prostheses using mirrored bilateral training. *IEEE Trans. Biomed. Eng.* 58, 681–688. doi: 10.1109/TBME.2010.2068298

Ortiz-Catalan, M., Branemark, R., and Hakansson, B. (2013). Evaluation of classifier topologies for the real-time classification of simultaneous limb motions. *Conf. Proc. IEEE Eng. Med. Biol. Soc.* 2013, 6651–6654. doi: 10.1109/EMBC.2013.6611081

Peerdeman, B., Boere, D., Witteveen, H., Huis in 't Veld, R., Hermens, H., Stramigioli, S., et al. (2011). Myoelectric forearm prostheses: state of the art from a user-centered perspective. *J. Rehabil. Res. Dev.* 48, 719–738. doi: 10.1682/jrrd.2010.08.0161

Pistohl, T., Cipriani, C., Jackson, A., and Nazarpour, K. (2013). Abstract and proportional Myoelectric control for multi-fingered hand prostheses. *Ann. Biomed. Eng.* 41, 2687–2698. doi: 10.1007/s10439-013-0876-5

Raspopovic, S., Capogrosso, M., Petrini, F. M., Bonizzato, M., Rigosa, J., Di Pino, G., et al. (2014). Restoring natural sensory feedback in real-time bidirectional hand prostheses. *Sci. Transl. Med.* 6:222ra19. doi: 10.1126/scitranslmed.3006820

Scheme, E., and Englehart, K. (2011). Electromyogram pattern recognition for control of powered upper-limb prostheses: state of the art and challenges for clinical use. *J. Rehabil. Res. Dev.* 48, 643–659. doi: 10.1682/jrrd.2010.09.0177

Smith, L. H., Kuiken, T. A., and Hargrove, L. J. (2014). Real-time simultaneous and proportional Myoelectric control using intramuscular EMG. *J. Neural Eng.* 11:066013. doi: 10.1088/1741-2560/11/6/066013

Smith, L. H., Kuiken, T. A., and Hargrove, L. J. (2015). Linear regression using intramuscular EMG for simultaneous Myoelectric control of a wrist and hand system, in *Neural Engineering (NER), 2015 7th International IEEE/EMBS Conference on* (Montpellier: IEEE), 619–622.

Smith, R. J., Tenore, F., Huberdeau, D., Cummings, R. E., and Thakor, N. V. (2008). Continuous decoding of finger position from surface EMG signals for the control of powered prostheses. *Conf. Proc. IEEE Eng. Med. Biol. Soc.* 2008, 197–200. doi: 10.1109/IEMBS.2008.4649124

Szeto, A. Y. J., and Saunders, F. A. (1982). Electrocutaneous stimulation for sensory communication in rehabilitation engineering. *IEEE Trans. Biomed. Eng.* 4, 300–308. doi: 10.1109/tbme.1982.324948

Tenore, F. V. G., Ramos, A., Fahmy, A., Acharya, S., Etienne-Cummings, R., and Thakor, N. V. (2009). Decoding of individuated finger movements using surface electromyography. *IEEE Trans. Biomed. Eng.* 56, 1427–1434. doi: 10.1109/TBME.2008.2005485

Young, A. J., Smith, L. H., Rouse, E. J., and Hargrove, L. J. (2013). Classification of simultaneous movements using surface EMG pattern recognition. *IEEE Trans. Biomed. Eng.* 60, 1250–1258. doi: 10.1109/TBME.2012.2232293

Ziegler-Graham, K., MacKenzie, E. J., Ephraim, P. L., Travison, T. G., and Brookmeyer, R. (2008). Estimating the prevalence of limb loss in the United States: 2005 to 2050. *Arch. Phys. Med. Rehabil.* 89, 422–429. doi: 10.1016/j.apmr.2007.11.005

Conflict of Interest Statement: The authors declare that the research was conducted in the absence of any commercial or financial relationships that could be construed as a potential conflict of interest.

frontiers in Neuroscience

ORIGINAL RESEARCH
published: 29 October 2015
doi: 10.3389/fnins.2015.00389

A dynamical model improves reconstruction of handwriting from multichannel electromyographic recordings

Elizaveta Okorokova[1], *Mikhail Lebedev*[2], *Michael Linderman*[3] *and Alex Ossadtchi*[1,4]*

[1] Centre for Cognition and Decision Making, National Research University Higher School of Economics, Moscow, Russia, [2] Department of Neurobiology, Duke University, Durham, NC, USA, [3] Department of Biomedical Engineering, Norconnect Inc., Ogdensburg, NY, USA, [4] Laboratory of Control of Complex Systems, Institute of Problems of Mechanical Engineering, Russian Academy of Sciences, St. Petersburg, Russia

In recent years, several assistive devices have been proposed to reconstruct arm and hand movements from electromyographic (EMG) activity. Although simple to implement and potentially useful to augment many functions, such myoelectric devices still need improvement before they become practical. Here we considered the problem of reconstruction of handwriting from multichannel EMG activity. Previously, linear regression methods (e.g., the Wiener filter) have been utilized for this purpose with some success. To improve reconstruction accuracy, we implemented the Kalman filter, which allows to fuse two information sources: the physical characteristics of handwriting and the activity of the leading hand muscles, registered by the EMG. Applying the Kalman filter, we were able to convert eight channels of EMG activity recorded from the forearm and the hand muscles into smooth reconstructions of handwritten traces. The filter operates in a causal manner and acts as a true predictor utilizing the EMGs from the past only, which makes the approach suitable for real-time operations. Our algorithm is appropriate for clinical neuroprosthetic applications and computer peripherals. Moreover, it is applicable to a broader class of tasks where predictive myoelectric control is needed.

Keywords: handwriting, electromyography, pattern recognition, dynamical modeling, the Kalman Filter, the Wiener Filter

OPEN ACCESS

Edited by:
Giovanni Mirabella, Sapienza University of Rome, Italy

Reviewed by:
Giancarlo Ferrigno, Politecnico di Milano, Italy
Giuseppe D'Avenio, Istituto Superiore di Sanità, Italy

***Correspondence:**
Alex Ossadtchi
ossadtchi@gmail.com

Specialty section:
This article was submitted to Neural Technology, a section of the journal Frontiers in Neuroscience

Received: *20 July 2015*
Accepted: *05 October 2015*
Published: *29 October 2015*

Citation:
Okorokova E, Lebedev M, Linderman M and Ossadtchi A (2015) A dynamical model improves reconstruction of handwriting from multichannel electromyographic recordings. Front. Neurosci. 9:389. doi: 10.3389/fnins.2015.00389

1. INTRODUCTION

Handwriting is a unique development of human culture. A skill learned during the early childhood, it remains among the primary means of communication and self-expression throughout the course of life. From the physiological point of view, handwriting is a complex interplay between the nervous system and the numerous muscles of the upper extremity. Despite several attempts to study this intricate activity theoretically (Plamondon and Maarse, 1989; McKeague, 2005) and experimentally (Linderman et al., 2009; Huang et al., 2010; Li et al., 2013), it is still not well understood and can not be reliably replicated in prostheses.

The relationship between the muscle force and the pen trajectory is complicated by the motor redundancy phenomenon (Bernstein, 1967; Guigon et al., 2006). One and the same movement can be accomplished via basically infinite number of muscle activation patterns. Relatively fine spatial

scale inherent to the handwriting process and the natural variations of the limb's kinematic variables further complicate the issue.

Additional obstacle in studying the physiology of handwriting is the difficulty of measuring the muscle force directly. Surface and intramuscular Electromyography (EMG) are the common methods to register neuromuscular activity during a motor task. Surface EMG is a non-invasive method which implies placing the electrodes on the skin above the muscles of interest. Being easy and safe to implement, this technique, however, does not yield sufficiently accurate biomechanical measurements, due to the complex relationship between the EMG and muscle force, complicated anatomy of muscles and the inability to record from all the muscles involved, especially from the deep muscles. Intramuscular EMG (iEMG) is invasive and uses needle electrodes inserted into the muscle tissue to yield more spatially specific measurements with less leakage and disturbance. The invasive nature of iEMG limits its utility.

Both EMG registration methods posit several substantial difficulties, primarily related to signal quality and associated issues of noise filtering and source extraction from the observed data. Nonetheless, it was shown that even the surface EMG carries valuable information about the neuromuscular interactions and can therefore be used effectively in modeling and interpreting movements (Reaz et al., 2006; Ahsan et al., 2009).

Despite the evident difficulties of measuring and interpreting neuromuscular activity with the currently available techniques, understanding such complex motor tasks as handwriting is important for both theoretical and practical reasons. Once we learn how to model the relationship between EMG patterns and pen movements during handwriting, we can introduce this knowledge to many rapidly expanding fields and practices, including biomedical engineering, robotics and biofeedback therapy. For instance, we can substantially improve the existing treatment and rehabilitation techniques for patients with a loss or an injury of an upper limb (Xiao and Menon, 2014), create rules for diagnostics of motor diseases based on handwriting (Van Gemmert et al., 1999; Stanford, 2004; Silveri et al., 2007), and even assist young children in learning how to write (Carter and Russell, 1985). Besides, an accurate model and methodolgies for building such models, establishing the correspondence between the handwriting and muscle activation patterns has a potential to become a foundation for creating intelligent neural prosthesis with a substantial number of degrees of freedom and fine spatial scale (Chan et al., 2000; Ohnishi et al., 2007; Shenoy et al., 2008; Bu et al., 2009; Castellini and van der Smagt, 2009).

However, such appealing advances and practices are still in their infancy. To date, the existing research on decoding of handwriting from electromyography is small and restricted to laboratory conditions. Several papers addressed the question of written character classification based on surface EMG, which involved implementation of machine-learning techniques to distinguish between muscle activation patterns for different written characters, such as digits, alphabet letters or simple geometric shapes. Linderman et al. (2009) classified symbols from 0 to 9, using eight bipolar surface electrodes placed on the hand and the forearm muscles. They implemented Fisher Linear Discriminant Analysis to obtain, on average, 90% accuracy of classification across subjects. Huang et al. (2010) used Dynamic Time Warping (DTW) to classify symbols based on 6-channel EMG recordings. Their average classification accuracy was 98.25% for digits, 97.89% for Chinese symbols and 84.29% for Latin capital letters. Li et al. (2013) improved the DTW algorithm by substituting Euclidean Distance with Mahalanobis Distance, to increase classification precision to almost 95%. In their experiment, subjects were instructed to write lower-case letters, while 4-channel EMG signals were recorded from their forearm.

The other studies considered a rather complex task of on-line decoding of the pen traces, based on the incoming EMG signals from the measurement electrodes. Among the most successful methods known to the authors, is the Wiener Filter (Linderman et al., 2009), which allows to attain accuracy of reconstruction of 47 $\pm$ 2% for X-coordinate and 63 $\pm$ 15% for Y-coordinate, measured by the coefficient of determination. However, the method used the data samples from the future, which would lead to extra delays in cases when used in the on-line mode.

In this paper, we consider the same multisubject data-set as in Linderman et al. (2009) and present our approach to EMG-based pen tracking that by taking into account the dynamic model of the pen coordinate process allows to outperform the previously reported techniques. The main idea behind our method is to fuse two information sources available about the process of handwriting. The first information source comes from the physical and the kinematic characteristics of handwriting. The second information source comes from the multichannel electromyography that indirectly measures the strength of the upper extremity muscles, activated to move the pen. To perform the fusion of the two sources optimally, we employ the Linear Kalman Filter (Kalman, 1960), which is a well-known recursive algorithm for dynamic statistical model-based inference.

2. MATERIALS AND METHODS

2.1. The Kalman Filter

2.1.1. Preliminary Remarks

In its classical formulation the Kalman Filter (KF) (Kalman, 1960) is an algorithm that fuses several (usually two) noisy sources of information to produce an estimate of the dynamical system's state vector, which is optimal in the "minimum squared error" sense. The method is over 50 years old, but it is still very popular, due to its intuitive structure, ease of implementation and computational efficiency.

In our application, the first information source is the dynamical model that captures the physical properties of the arm-wrist-pen device and is formalized as a multivariate autoregressive (MVAR) process, whose parameters are estimated from the data. The noisy vector of EMG measurements is the second source of information, whose relation to the pen coordinate is modeled via multivariate linear regression equation with coefficients determined from the training data-set.

For simplicity, the derivations provided in this section are based on the assumption of multivariate normality of the fused

sources (Faragher, 2012), which is essential for the Kalman Filter to be the optimal estimator (the best among all other kinds). However, in the general Kalman Filter framework, this does not have to be the case (Arulampalam et al., 2002). When the assumption of normality does not hold, it is still possible to derive the KF equations based on the orthogonality principle (e.g., Jazwinski, 2007), which would guarantee the KF to be the best linear estimator, but not necessarily be optimal. In this case, it might be possible to increase accuracy by employing non-linear techniques that exploit higher order dependencies in the data, such as the Extended Kalman Filter (Julier and Uhlmann, 1997) or its "distribution-free" version, called Unscented Kalman Filter (Wan and Van Der Merwe, 2000). However, since the majority of trials in our multisubject dataset appear to test positively for the normality (see Appendix, Section Testing the Assumptions of the Model) the extent of improvement furnished by the use of the non-linear approaches is hard to predict theoretically. This leaves the question in the empirical realm to be addressed in the future studies.

As demonstrated by the statistical tests described in the Appendix (Section Testing the Assumptions of the Model), we could not reject the hypothesis of independence for the majority of trials. Based on this and, for the simplicity reasons, we base our developments in this paper on the assumption of independence of the two fused sources. In case the independence assumption is violated, the performance gained by taking into account the dynamics of the reconstructed process could have been more sizable should we use a slightly modified form of equations (Shimkin, 2009) to account for the non-trivial cross-covariance structure of the residuals. However, the extent to which modeling the cross-covariance structure of residuals would improve the performance is not entirely clear, due to the inherent non-stationarity and the associated estimation errors.

2.1.2. State Transition Model

As the first information source, we assume that, at each time moment t, the system evolves from the previous state at time $t-1$, according to the rule:

$$\boldsymbol{s}_t = \boldsymbol{A}\boldsymbol{s}_{t-1} + \boldsymbol{v}_t \tag{1}$$

where

- $\boldsymbol{s}_t = [\boldsymbol{x}_t, \boldsymbol{y}_t, \dot{\boldsymbol{x}}_t, \dot{\boldsymbol{y}}_t, \ddot{\boldsymbol{x}}_t, \ddot{\boldsymbol{y}}_t, ..., \boldsymbol{x}_{t-K+1}, \boldsymbol{y}_{t-K+1}, \dot{\boldsymbol{x}}_{t-K+1}, \dot{\boldsymbol{y}}_{t-K+1}, \ddot{\boldsymbol{x}}_{t-K+1}, \ddot{\boldsymbol{y}}_{t-K}]^T$ is a $6K \times 1$ state vector containing pen coordinates and their first and second rates of change for the window of K time moments starting from t;
- $\boldsymbol{A}$ is a $[6K \times 6K]$ state transition matrix, which performs the mapping between the state vectors at the two consecutive time moments;
- $\boldsymbol{v}_t$ is a $[6K \times 1]$ vector containing process noise, which is assumed to be drawn from a multivariate Gaussian distribution with zero mean and covariance matrix $\boldsymbol{Q}$.

Based on Equation (1), we can derive the following expressions connecting the mean and the covariance matrix of the state vector at the two consecutive time moments.

- $\boldsymbol{\mu}_{1t} = \boldsymbol{A}\boldsymbol{\mu}_{1(t-1)}$ is a 6K-dimensional mean state vector at time t;
- $\boldsymbol{\Sigma}_{1t} = \boldsymbol{A}\boldsymbol{\Sigma}_{1(t-1)}\boldsymbol{A}^T + \boldsymbol{Q}$ is a $6K \times 6K$ positive-definite covariance matrix of the state vector at time t.

Detailed derivations of the model parameters can be found in the Appendix (Section Testing the Assumptions of the Model).

2.1.3. Measurement Model

Usually, in the KF framework, the measurement equation appears in the $\boldsymbol{z} = F(\boldsymbol{s})$ form, describing the way the process to be estimated ($\boldsymbol{s}$) is related to the available vector of indirect measurements ($\boldsymbol{z}$). However, in our application, due to causal and physiological reasons, it is more natural to think that the EMG registered muscle activity gives rise to the pen movement. Therefore, we use the "inverse" form of what is usually called the observation equation in the KF framework and write

$$\boldsymbol{s}_t = \boldsymbol{H}\boldsymbol{z}_t + \boldsymbol{w}_t \tag{2}$$

where

- $\boldsymbol{z}_t$ is a $[8L \times 1]$ observation vector containing L groups of eight EMG measurements corresponding to the $[t-L+1, t]$ window of L most recent samples;
- $\boldsymbol{H}$ is a $[6K \times 8L]$ measurement transformation matrix, mapping the measurement domain to the state vector domain;
- $\boldsymbol{w}_t$ is a $[8L \times 1]$ vector of measurement noise with zero mean and covariance matrix $\boldsymbol{R}$. Additionally, the measurement noise $\boldsymbol{w}_t$ is assumed to be independent from the process noise $\boldsymbol{v}_t$.

The $6K$-dimensional state mean vector at time t is given by

$$\boldsymbol{\mu}_{2t} = \boldsymbol{E}[\boldsymbol{s}_t] = \boldsymbol{H}\boldsymbol{z}_t. \tag{3}$$

Since we do not model $\boldsymbol{z}_t$ as a stochastic process, the covariance matrix of $\boldsymbol{s}_t$ reduces to covariance matrix of the measurement noise, so that $\boldsymbol{\Sigma}_{2t} = \boldsymbol{E}[\boldsymbol{w}_t\boldsymbol{w}_t^T] = \boldsymbol{R}$. Note that this noise is assumed to be stationary.

2.1.4. Information Fusion

As outlined in the previous two subsections, we have two independent sources of information about the state vector. The first endogenous source bases its predictions on the dynamical characteristics of the pen coordinates during the handwriting and yields $f_1(\boldsymbol{s}_t|\boldsymbol{s}_{t-1})$ as the state vector distribution (red distribution in **Figure 1**). The second source is exogenous and uses externally registered EMG signals to suggest $f_2(\boldsymbol{s}_t|\boldsymbol{z}_t)$ as the state vector distribution (blue distribution in **Figure 1**). In order to reconstruct the state vector, optimally taking into account the predictions from both sources, we perform the statistical fusion of the estimates based on the dynamical and the measurement models. The schematic procedure of the source fusion is illustrated in **Figure 1**.

The joint conditional estimate of the state vector is distributed as $f_{fused}(\boldsymbol{s}_t|\boldsymbol{s}_{t-1}, \boldsymbol{z}_t)$ (green distribution in **Figure 1**). Assuming independence of the sources, the problem of finding $f(\boldsymbol{s}_t|\boldsymbol{s}_{t-1}, \boldsymbol{z}_t)$

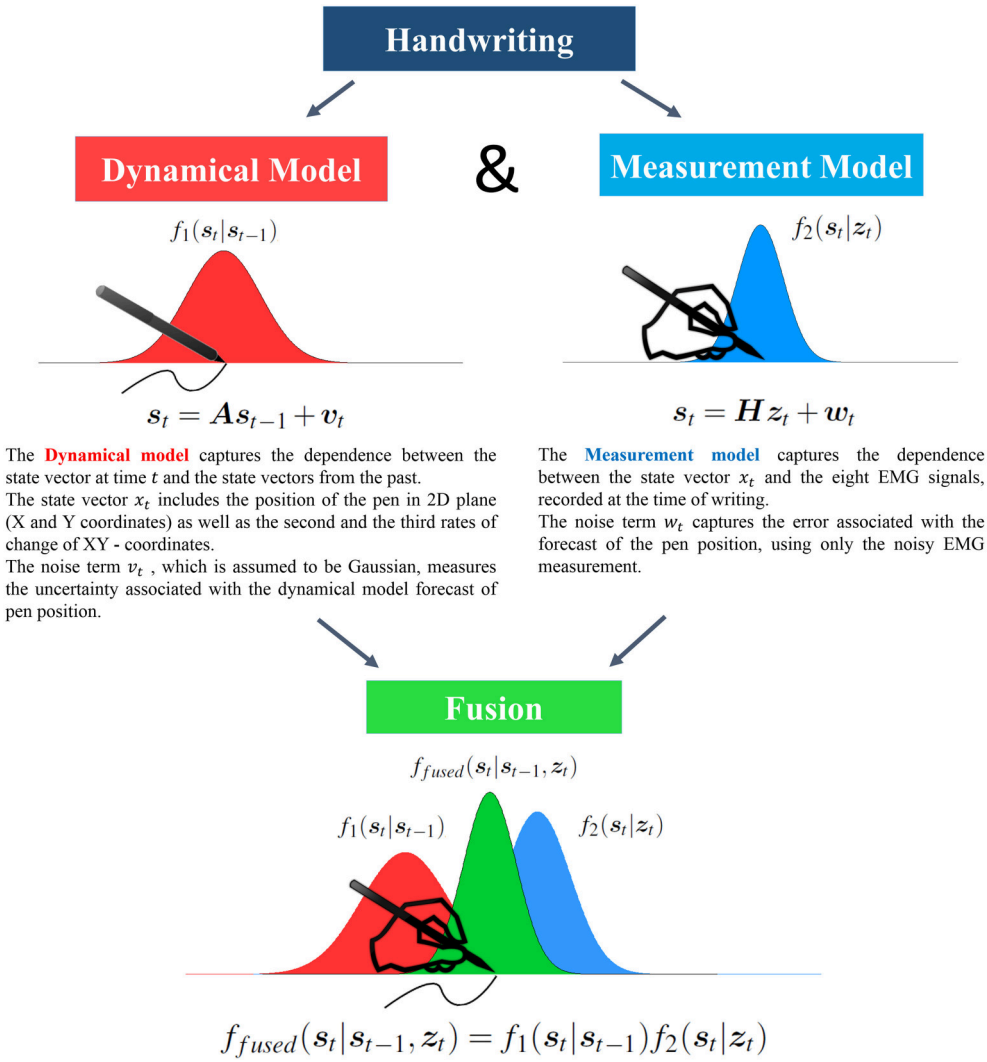

FIGURE 1 | Information Fusion by means of the Kalman Filter allows to improve reconstruction accuracy by adaptively balancing the contribution from the two information sources.

reduces to a simple multiplication of the two probability density functions, i.e.,

$$f_{fused}(s_t|s_{t-1}, z_t) = f_1(s_t|s_{t-1})f_2(s_t|z_t) \quad (4)$$

The product of two multivariate normal distributions is also a multivariate normal (Rencher, 2003). Its mean and covariance can be easily expressed in terms of the mean vectors and the covariance matrices of each of the two normal multipliers.

Specifically, Σ_{fused} is the covariance matrix of the fused distribution can be computed as

$$\Sigma_{fused} = (\Sigma_{1t}^{-1} + \Sigma_{2t}^{-1})^{-1}, \quad (5)$$

and the $6K$-dimensional mean vector of the fused distribution is found to be the following weighted sum of the two mean vectors of the fused information sources:

$$\mu_{fused} = \Sigma_{fused}(\Sigma_{1t}^{-1}\mu_{1t} + \Sigma_{2t}^{-1}\mu_{2t}), \quad (6)$$

It is instructive to reformulate the expressions for the mean and the covariance matrix of the new distribution and to separate the influence of the two distributions being fused.

Using the matrix inversion lemma (Henderson and Searle, 1981), and setting

$$K_t = \Sigma_{1t}(\Sigma_{1t} + \Sigma_{2t})^{-1} \quad (7)$$

we can rewrite Equations (5) and (6) as

$$\boldsymbol{\Sigma}_{fused} = \boldsymbol{\Sigma}_{1t} - \boldsymbol{K}_t\boldsymbol{\Sigma}_{1t}. \quad (8)$$

and

$$\boldsymbol{\mu}_{fused} = (\boldsymbol{I} - \boldsymbol{K}_t)\boldsymbol{\mu}_{1t} + \boldsymbol{K}_t\boldsymbol{\mu}_{2t}. \quad (9)$$

For detailed derivation of the parameters see the Appendix.

The term $\boldsymbol{K}_t$ in Equation (7), commonly known as the Kalman Gain, plays a crucial role of the dynamic scaling factor reflecting the distribution of trust in each of the two information sources. It depends on the relative amount of uncertainty present in the estimates by each of the information sources alone, and varies over time.

Since covariance matrices are positive definite, Equation (8) shows that by fusing the two distributions we reduce the variation associated with the state estimate, proportionally to the Kalman gain. At the same time, the fused mean (Equation 9) becomes the weighted average of the endogenously predicted and the measurements-based mean estimates.

2.1.5. The Algorithm

Based on the above equations we are now ready to formulate the algorithm for calculating the Kalman Filter estimate. At each time moment the computation can be split into three consecutive steps.

1. Endogenous state prediction and error covariance update:

$$\hat{\boldsymbol{s}}_{t|t-1} = \boldsymbol{\mu}_{1t} = \boldsymbol{A}\hat{\boldsymbol{s}}_{t-1|t-1} \quad (10)$$

$$\boldsymbol{P}_{t|t-1} = \boldsymbol{\Sigma}_{1t} = \boldsymbol{A}\boldsymbol{P}_{t-1|t-1}\boldsymbol{A}^T + \boldsymbol{Q} \quad (11)$$

2. Kalman Gain Calculation:

$$\boldsymbol{K}_t = \boldsymbol{\Sigma}_{1t}(\boldsymbol{\Sigma}_{1t} + \boldsymbol{\Sigma}_{2t})^{-1} = P_{t|t-1}(\boldsymbol{P}_{t|t-1} + \boldsymbol{R})^{-1} \quad (12)$$

3. Measurement Update:

$$\hat{\boldsymbol{s}}_{t|z} = \boldsymbol{\mu}_{2t} = \boldsymbol{H}\boldsymbol{z}_t \quad (13)$$

$$\hat{\boldsymbol{s}}_{t|t} = \hat{\boldsymbol{s}}_{t|t-1} + \boldsymbol{K}_t(\hat{\boldsymbol{s}}_{t|z} - \hat{\boldsymbol{s}}_{t|t-1}) \quad (14)$$

$$\boldsymbol{P}_{t|t} = \boldsymbol{P}_{t|t-1} - \boldsymbol{K}_t\boldsymbol{P}_{t|t-1} \quad (15)$$

In order to relate our approach to the classical KF paradigm in the equations above, we assigned the variables used in the previous subsection to the standard symbols, commonly employed in the KF literature. In the above algorithm, the first step is to use the State Transition Equation only and to calculate the so-called *a priori* estimate $\hat{\boldsymbol{s}}_{t|t-1}$, with associated variance $\boldsymbol{P}_{t|t-1}$ (Equations 10 and 11).

Then, we calculate the Kalman Gain based on the *a priori* covariance matrix and the covariance matrix of the Measurement Model (Equation 12).

Finally, the *a posteriori* estimate $\hat{\boldsymbol{s}}_{t|t}$ is computed by adjusting the endogenous *a priori* estimate with the EMG measurements. The amount of adjustment is governed by the time-varying Kalman Gain (Equation 14) and the innovations process $\hat{\boldsymbol{s}}_{t|z} - \hat{\boldsymbol{s}}_{t|t-1}$, informing the algorithm on the amount of mismatch between the endogenous and exogenous estimates. The *a posteriori* uncertainty, associated with the prediction, based on the two models, is given by $\boldsymbol{P}_{t|t}$ (Equation 15), which shows that, in the final estimate, the *a priori* uncertainty gets reduced proportionally to the Kalman Gain.

2.2. The Experiment

2.2.1. Data

Six healthy participants were instructed to write symbols from 0 to 9, repeating each symbol approximately 50 times. At the same time, muscle activity was recorded with eight bipolar-surface EMG electrodes, placed on each participants leading hand muscles: *opponens pollicis*, *abductor pollicis brevis*, *medial and lateral heads of first dorsal interrosseus*, and four forearm muscles: *flexor carpi radialis*, *extensor digitorum*, *extensor carpi ulnaris*, and *extensor carpi radialis*. The reference electrode was placed on each subject's forehead. Position of the pen was recorded using the special digitizing tablet, yielding a pair of coordinates in the two-dimensional space. For a detailed illustration of the experiment set-up, see Linderman et al. (2009).

2.2.2. Preprocessing

Before applying the algorithm, we preprocessed EMG signals to extract the envelope via the standard rectification procedure. For each channel separately, we first calculated the absolute value of the EMG signals and then low-pass filtered the result with a second-order Butterworth Filter with the cut-off frequency of F_c. We optimized the value of the cut-off frequency based on the training subset of the recorded data to obtain the best reconstruction performance. In the final results reported here $F_c = 2$ Hz. Additionally, we have applied square-root transformation to each signal's envelope, obtained via the described rectification procedure.

2.2.3. Training and Testing

Half of the trials of each symbol was randomly assigned to training the parameters of the model, while the remaining half was used for testing the performance (**Figure 2**). During training, the parameters of the dynamical model (Equation 1) and the measurement model (Equation 2) were estimated. We applied Ordinary Least Squares Method to estimate matrix $\boldsymbol{A}$ in the state transition equation and matrix $\boldsymbol{H}$ in the measurement equation. Covariance matrices $\boldsymbol{R}$ and $\boldsymbol{Q}$ were estimated based on the residuals of the two fitted models. Note that estimation of the covariance matrices of the error processes is particularly simple here, since, at the model identification step, we have the direct access to both state vector and the actual EMG measurements, thanks to the experimental setup described in Linderman et al. (2009). **Figure 2** shows the data flow diagram in the model identification and coordinate reconstruction modes.

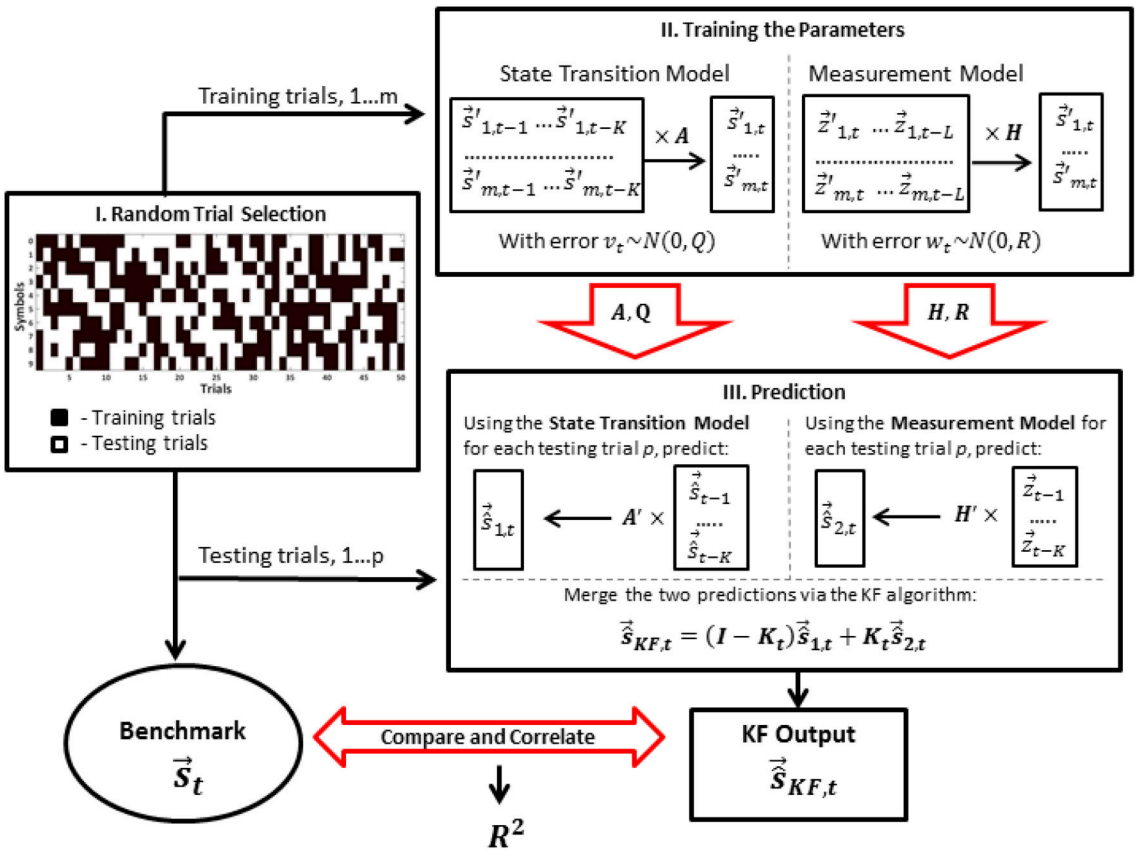

FIGURE 2 | Implementation of the Kalman Filter algorithm. For each participant of the experiment, the trials are randomly divided into training trials (black) and testing trials (white). Then, the training trials are used for learning of the parameters of the state transition model (matrices A and Q) and the measurement model (matrices H and R). The EMG data from the testing trials and the learned matrices are then used for the prediction of the state vector in both models. Finally, the predictions of the two models are merged via the Kalman filter algorithm and the result of the filter is compared to the actual state vector. The squared correlation coefficient (R^2) is used as a measure of efficiency of reconstruction.

We used two basic experimental designs to calibrate our pen tracking algorithm.

1. Within-Group Design
   A single set of parameters ($\boldsymbol{A}$, $\boldsymbol{H}$, $\boldsymbol{R}$, and $\boldsymbol{Q}$) was estimated using the training trials from all symbols at the same time and then tested on the remaining test trials.
2. Between-Group Design
   A separate set of parameters ($\boldsymbol{A^n}$, $\boldsymbol{H^n}$, $\boldsymbol{R^n}$ and $\boldsymbol{Q^n}$, $n \in 0, ..9$) was estimated for each symbol and then tested within the data from the trials of the same symbol.

Note that for Within-Group Design, only one set of matrices was estimated by pooling all the training samples together, while in Between-Group Design the four matrices were estimated separately for each of the ten symbols. Then, the out-of-training sample measurements were used to reconstruct handwriting via the recursive process outlined in Section 2.1.5.

The testing procedure was the same within each experimental design (see **Figure 2**). For each trial, the starting pen location point was set to zero vector. Then, the estimate of the pen position was computed recursively (Section 2.1.5). Reconstruction accuracy was measured by the squared correlation coefficient $\boldsymbol{R^2}$ between the actual coordinate and its fused estimate (**Figure 2**). This criterion corresponds to the percentage of energy in the actual pen traces (Total Sum of Squares - $\boldsymbol{SS_t}$) explained by the reconstructed ones (Explained Sum of Squares $\boldsymbol{SS_e}$), i.e.,

$$\boldsymbol{R^2} = \frac{\boldsymbol{SS_e}}{\boldsymbol{SS_t}} = \frac{\sum_{i=1}^{N} (\hat{s}_i - \bar{s})^2}{\sum_{i=1}^{N} (s_i - \bar{s})^2} \tag{16}$$

The accuracy was computed within each trial, and then averaged across trials for each symbol. Confidence intervals were computed to account for the standard errors associated with the variation across the participants.

2.2.4. Comparison with Other Models

We compared the accuracy of our model to the accuracy of the Wiener Filter (WF) estimate, which was originally tested

on the same data-set by Linderman et al. (2009). The Wiener Filter approach is directly equivalent to predicting the pen coordinates, using only the measurement equation of the KF-framework alone (Equation 2). In other words, the Kalman filter is the Wiener filter, accompanied by information about the system's physical properties. Therefore, a comparison between the two models would not only show the possible improvement associated with the Kalman Filter, but also highlight the isolated benefit furnished by employing the dynamical properties of the system.

In the framework of handwriting recognition from electromyography reported in Linderman et al. (2009), the pen trace at time t was represented as a linear combination of EMG signals recorded in the non-causal interval of t: $[t - \delta_1, t + \delta_2]$. The unknown weights, mapping rectified EMG signals into the pen-tip coordinate vector, were estimated using the Ordinary Least Squares Method. It is important to stress that, in contrast to the approach reported in Linderman et al. (2009), our reconstruction procedures (both Kalman Filter and Wiener Filter based) operate causally and use only the samples from the immediate past. For each time moment t, only the samples from the $[t - \delta_1, t]$ interval were used. It is, therefore, interesting and instructive to test, whether or not the use of the dynamical model compensates for the reduced amount of information in the external measurements. In the situation when both methods use the same amount of exogenously registered data, the Kalman Filter is expected to outperform the Wiener Filter. To test the hypothesis, we performed the coordinate reconstruction with the two filters, fixing all other external parameters related to the data preprocessing step and compared their performance on the testing set of trials.

3. RESULTS

3.1. Finding Optimal Model Order

The dynamical model (Equation 1) and the measurement model (Equation 2) contain model order parameters K and L, corresponding to the number of past samples used. In order to find the optimal values of these parameters, we applied the cross-validation procedure. We used $\boldsymbol{R}^2$ as a metric of the goodness of reconstruction achieved (**Figure 3**).

To search for the combination of K and L that delivers the highest performance, we looked for the values of these parameters that maximize the $g = E(\boldsymbol{R}^2)/std(\boldsymbol{R}^2)$ ratio. The expected value $E(\boldsymbol{R}^2)$ and the standard deviation $std(\boldsymbol{R}^2)$ were computed over the trials in the data-set used for cross-validation. Therefore, high values of g correspond to the combination of high accuracy and stability of the reconstruction quality. **Figure 4** shows the average over all subjects value of g and $\boldsymbol{R}^2$.

Based on these maps, we set $K = 1$ and $L = 2$ to obtain the results reported in this paper. Note that the number of optimal measurement lags was reduced from 20 to 2, comparing to the original paper by Linderman et al. (2009), which significantly reduces computational complexity of the problem and reduces the response time of the system and potentially allows to track brisker movements.

3.2. Within-Group Design

We first trained one set of parameters for all symbols and used it to reconstruct pen traces from the EMG data in the testing set. **Figure 5** shows the result of reconstruction of several trials of each character for one of the participants. Despite being noisy

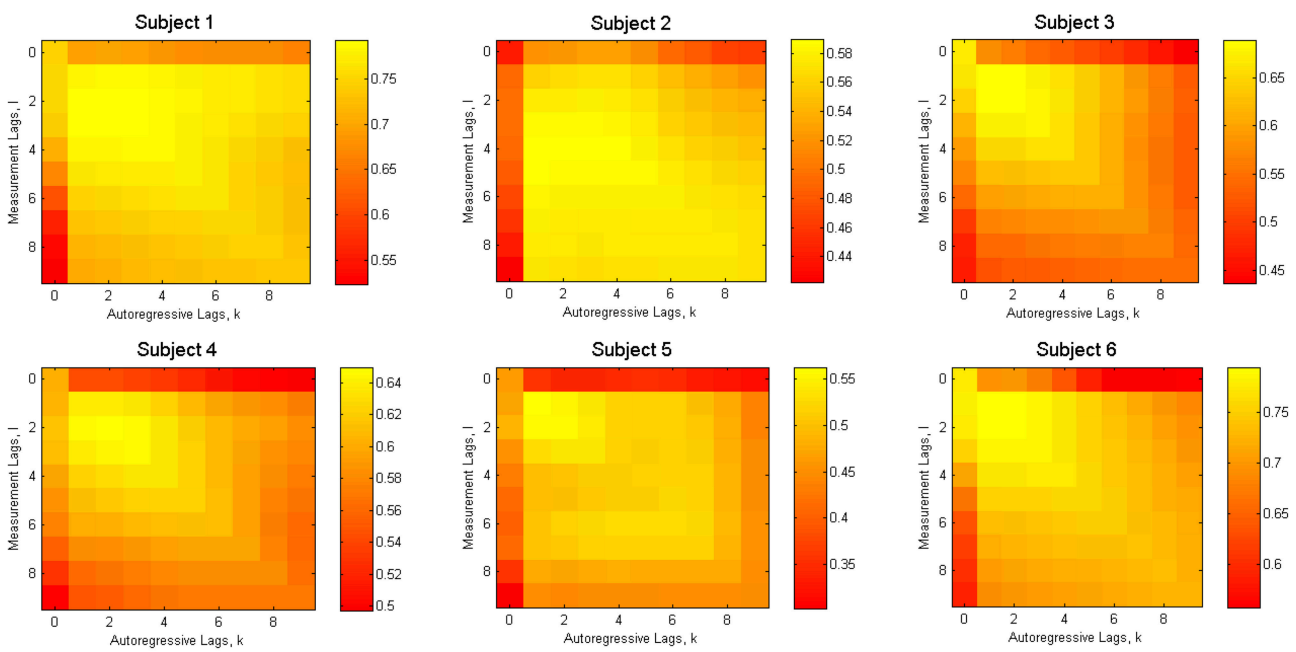

FIGURE 3 | Reconstruction accuracy as a function of model order parameters (*K* and *L*) for 6 subjects separately.

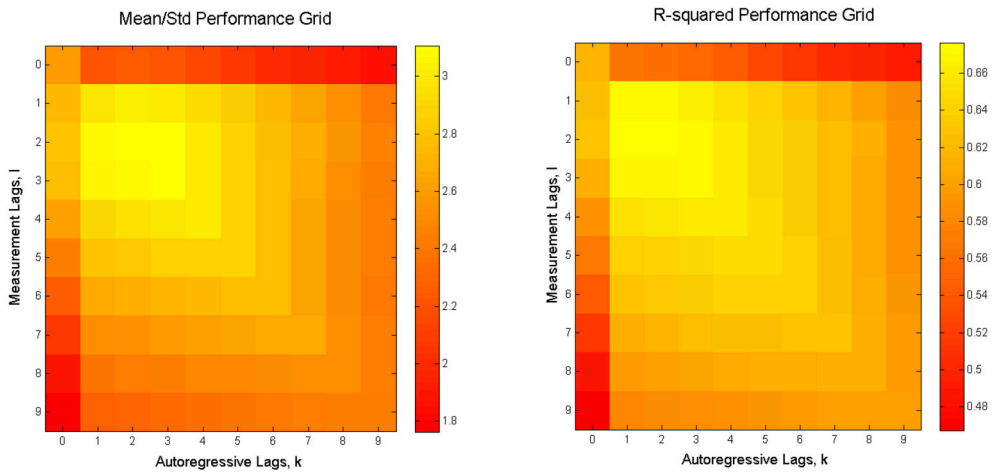

FIGURE 4 | Average reconstruction accuracy as a function of model order parameters (K and L). Left: average over all 6 subjects value of g. **Right:** Average over all 6 subjects value of R^2 for the mean reconstruction accuracy in the two coordinates $(X + Y)//2$.

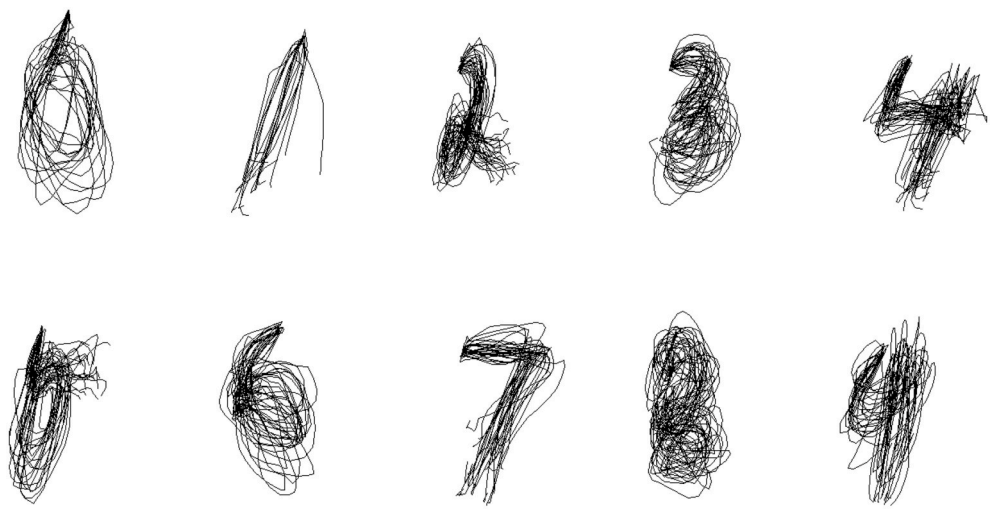

FIGURE 5 | Within-Group Reconstruction: several reconstructed trials of each symbol from cross-validation sample of one of the participants.

and, at times, inaccurate, the symbols are still identifiable and reproducible between trials.

Table 1 gives a detailed accuracy distribution for all symbols. Each of the entries in the table were found as follows: we computed accuracy of reconstruction for each test trial available for each symbol, then calculated the statistics within trial of the same symbol to determine the reported mean and standard deviation. Finally, we computed 95% confidence intervals for the average accuracy of every symbol reconstruction, based on the sample of 6 participants. We report reconstruction accuracy by coordinates independently, and as an average between the two coordinates.

Statistically speaking, we managed to achieve the average accuracy of 63 ± 17% and 73 ± 14% with 95% confidence, for the two reconstructed coordinates, as estimated for the six participants of the experiment. Note that the average accuracy in both coordinates is higher than that found by Linderman et al. (2009) (47 ± 2% and 63 ± 15% for the two coordinates, respectively), where non-causal Wiener Filter based reconstruction was employed. Additional improvement over that pioneering work lies in the use of the smaller number of measurement lags (L) (2 instead of 20, see Section 3.1) which reduces the response time of the system. These observations demonstrate the benefits brought in by the use of the dynamical properties of the process being identified.

3.3. Between-Group Design

In the Between-group design, we attempted to learn the parameters of the Kalman Filter for each symbol separately, and then reconstruct the traces of the same symbol. **Figure 6** shows

the results of reconstruction of several trials of each symbol for one of the participants. As predicted, the separate Kalman Filters for each symbol perform a more specific and accurate reconstruction, which is visually evident from the figure.

The average reconstruction in the two coordinates between subjects was 78 ± 13% and 88 ± 7%, respectively. **Table 2** reports 95% confidence intervals for the average reconstruction accuracy of each symbol with separate Kalman Filters.

3.4. Comparison with the Wiener Filter

In the previous subsection we have shown that, as expected, the Kalman Filter improves the reconstruction performance, as compared to the previously proposed method (Linderman et al., 2009). The parameter search (Section 3.1) shows that adding non-zero autoregressive lag(s) to the model, and as a result, capturing the dynamical properties of the system, leads to the increase in accuracy of reconstruction for all subjects (**Figures 3**, **4**).

To consider the increase in accuracy, specifically associated with the dynamical model, we reconstructed pen traces of several symbols by Within-group design (one set of parameters for all symbols), and then repeated the procedure on the same samples using the Wiener Filter, fixing all other external parameters, including those related to the training-testing split of the data and data preprocessing techniques.

On average, introduction of the KF framework leads to a significant increase in accuracy for both reconstructed coordinates across the six participants (**Figure 7**). The increase is more or less homogeneous between different symbols. **Figure 8** shows the distribution of the difference between the Kalman Filter accuracy and the Wiener Filter accuracy for separate symbols. For all symbols, the difference is significantly greater

TABLE 1 | Within-Group Reconstruction Performance: 95% confidence intervals for the average reconstruction accuracy of each symbol between the 6 participants.

	Average performance, R^2		
Symbol	**X-coordinate**	**Y-coordinate**	**Average: (X+Y)/2**
"0"	0.65 ± 0.15	0.57 ± 0.17	0.61 ± 0.15
"1"	0.49 ± 0.08	0.85 ± 0.08	0.67 ± 0.05
"2"	0.71 ± 0.14	0.75 ± 0.12	0.73 ± 0.13
"3"	0.59 ± 0.20	0.79 ± 0.09	0.69 ± 0.13
"4"	0.71 ± 0.15	0.63 ± 0.17	0.67 ± 0.13
"5"	0.67 ± 0.15	0.72 ± 0.05	0.70 ± 0.08
"6"	0.68 ± 0.18	0.71 ± 0.11	0.70 ± 0.12
"7"	0.59 ± 0.28	0.69 ± 0.22	0.63 ± 0.25
"8"	0.61 ± 0.15	0.74 ± 0.12	0.77 ± 0.11
"9"	0.62 ± 0.22	0.71 ± 0.15	0.67 ± 0.17
All	0.63 ± 0.17	0.73 ± 0.14	0.68 ± 0.13

TABLE 2 | Between-Group Reconstruction Performance: 95% confidence intervals for the average reconstruction accuracy of each symbol between the 6 participants.

	Average performance, R^2		
Symbol	**X-coordinate**	**Y-coordinate**	**Average: (X+Y)/2**
"0"	0.84 ± 0.06	0.86 ± 0.05	0.85 ± 0.05
"1"	0.63 ± 0.15	0.97 ± 0.01	0.80 ± 0.08
"2"	0.82 ± 0.11	0.92 ± 0.06	0.87 ± 0.09
"3"	0.75 ± 0.12	0.93 ± 0.06	0.84 ± 0.08
"4"	0.81 ± 0.11	0.81 ± 0.03	0.81 ± 0.05
"5"	0.80 ± 0.10	0.86 ± 0.06	0.83 ± 0.07
"6"	0.83 ± 0.05	0.88 ± 0.05	0.85 ± 0.05
"7"	0.76 ± 0.20	0.88 ± 0.08	0.82 ± 0.14
"8"	0.76 ± 0.12	0.86 ± 0.07	0.81 ± 0.09
"9"	0.81 ± 0.09	0.84 ± 0.08	0.83 ± 0.08
All	0.78 ± 0.13	0.88 ± 0.07	0.83 ± 0.08

FIGURE 6 | Between-Group Reconstruction: several reconstructed trials of each symbol from cross-validation sample of one of the participants.

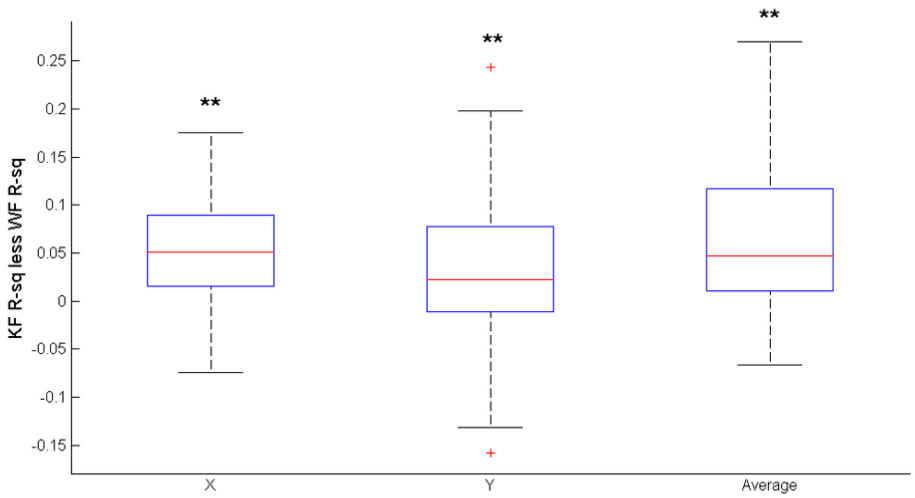

FIGURE 7 | Distribution of the difference in the average performance of the Kalman Filter (KF) and the average performance of the Wiener Filter (WF) for all written characters across subjects. Statistical Difference between the average KF and the average WF performance is measured by one-sided Wilcoxon matched-pair test for X-coordinate, Y-coordinate and the average of the two, i.e., (X+Y)/2: **significantly greater than zero at 1% significance level.

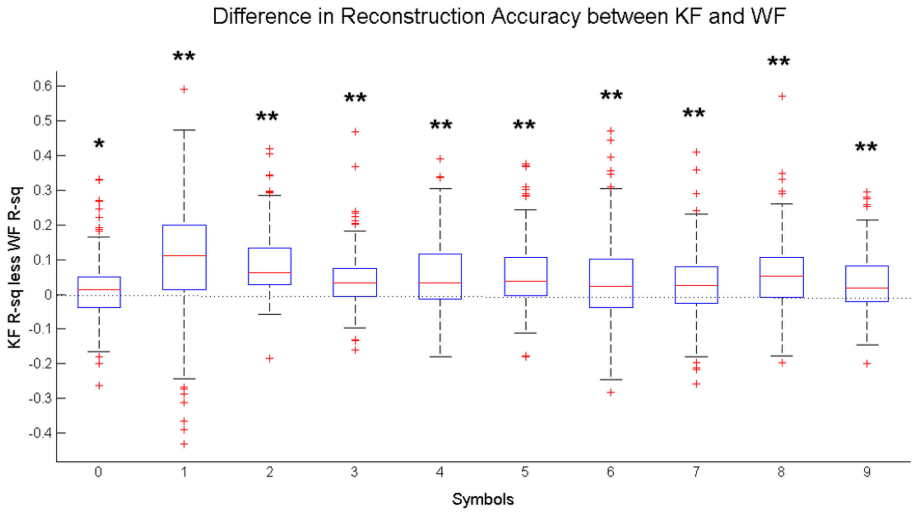

FIGURE 8 | Distribution of the difference between the Kalman Filter Accuracy (KF R^2) and the Wiener Filter Accuracy (WF R^2) between subjects, measured for each written character independently. Statistical Difference between the KF and the WF performance is measured by one-sided Wilcoxon matched-pair test for each character: *significantly greater than zero at 5% significance level, **significantly greater than zero at 1% significance level.

than zero with at least 95% confidence, guaranteed by the one-sided Wilcoxon test for matched pairs.

The ergonomics of the reconstructed handwriting traces plays an important role. The use of the dynamical model to enforce natural smoothness of handwriting yielded improved ergonomics of the recovered traces. **Figure 9** allow to visually compare the reconstruction of the pen traces for each symbol obtained with the two methods (left—the Kalman Filter reconstruction, right—the Wiener Filter reconstruction). As we can see from the figures, the use of the Kalman filter furnishes a smoother coordinate reconstruction than that based exclusively on the measurements. While both filters make it possible to visually discriminate between different symbols, the smoothness of the traces, obtained with the Kalman filter, makes them more natural and ergonomically plausible.

4. DISCUSSION

In this work we applied the Kalman Filter approach to reconstruction of handwritten pen traces on the basis of EMG

FIGURE 9 | Pen trace reconstruction of digits zero to nine with the Kalman Filter (left) and the Wiener Filter (right), Within-Group Method for several cross-validation trials of one of the participants.

measurements. We have demonstrated that it is possible to obtain accurate and ergonomic reconstruction of pen traces and still remain in the linear framework to utilize all the benefits associated with it. Our results show a significant improvement over the figures, previously reported by Linderman et al. (2009). In contrast to that pioneering work, we used only causal filtering and exploited fewer past samples of the EMG signals.

Although the accuracy of reconstruction does not generally go above 90%, in terms of the coefficient of determination, the method still offers a reliable and ergonomic reconstruction for all symbols. Approximately 25 trials of each symbol were enough to learn the parameters of the filter and yield comparable results in testing samples.

The method works well for both specific (Between-Group design) and general (Within-Group design) models, which reveals its potential for a wide range of applications. The Between-group design, although quite limited at first sight, is not entirely unrealistic, due to the fact that handwritten figures are very well discriminated between each other on the basis of EMG signals (Linderman et al., 2009; Huang et al., 2010). It means that separate Kalman filters can be applied as a second-stage algorithm in the off-line experiments, after another algorithm (such as the Hidden Markov Model of Linear Discriminant Analysis) is used to classify the symbols into groups.

The Within-group design, on the other hand, is more applicable to on-line handwriting reconstruction, when no prior information about the class of the symbol being written is available. In this framework the causality of our approach offers additional benefits and makes the EMG-controlled handwriting feel natural to the user. Also, the natural smoothness of the traces, recovered with the use of the KF, provides for an improved feedback, which is crucial in the real-life on-line scenario.

While our method has shown improvement over the previously proposed technique, it still requires thorough consideration before it can be reliably applied in neuroprosthetic devices and rehabilitation practices. One of the main difficulties in applying the Linear Kalman filter is the high variability of results across subjects. The confidence intervals in **Tables 1**, **2** clearly show very high margins of error, which indicate that handwriting is very person-specific.

Such heterogeneous performance across individuals apparently stems from a combination of behavioral and physiological factors, which we could not control in this study. Participants vary in the style and neatness of handwriting, including the way they hold and press the pen, and the strategies they apply to write the same symbol. Anatomical differences, such as the individual muscle length, muscle size and attachment to the bones and the differences in the amount of subcutaneous fat might be significant factors influencing the patterns of the recorded neuromuscular activity (EMGs). Additional source of variability may come from the variation in electrode placement sites.

The problem of EMG variability has received significant attention in the recent experimental literature (Linssen et al., 1993; Araújo et al., 2000; Nordander et al., 2003). Fundamentally, one and the same movement can be reproduced by different force patterns in multiple agonist and antagonist muscles. This phenomenon, called *motor redundancy* (Bernstein, 1967; Guigon et al., 2008) allows a certain kinematic pattern to be reproduced by virtually infinite number of distinct muscular activation patterns (Amis et al., 1979). The EMG recordings which we used captured relatively consistent EMG patterns in individual subjects, which were, however, different from subject to subject. The approach proposed in this paper appears to have sufficient generalization power to capture the within subject variability (both natural and the one that stems from instructed variations of symbol writings to be produced). However, initial training of the algorithm is required for each individual subject independently.

Additionally, the results can be further improved by individually tuning the latent parameters, such as the model orders, filter cut-off frequency and sensor locations. In this work, however, we intentionally used a single set of latent variable values in order to emulate the out-of-box performance of such a system. Methods for non-supervised on-line adaptation and individual tuning of the latent variables need to be developed to address these issues and make the fine-tuning seamless to the user.

The linear framework of the filter offers significant benefits, such as stability and good generalization ability. However, the non-linear nature of the relation between the recorded EMG signals and the actuator trajectory prompts to explore the use of non-linear models in this application. The benefits brought in by the non-linearity, however, have to be leveraged against the additional complexity and potential instability associated with the use of such models.

5. CONCLUSIONS

In this paper we investigated the relationship between handwriting and neuromuscular activity measured by electromyography. We built and optimized the Kalman filter in order to reconstruct the pen coordinates based on the dynamical characteristics of handwriting and the corresponding EMG measurements.

We showed that the Kalman filter significantly outperforms previously proposed method (Linderman et al., 2009) and yields a mean accuracy of 68% in Within-Group design and 83% in Between-Group design, measured by the coefficient of determination, averaged for the two reconstructed coordinates. Our method is suitable for real-time applications as it is causal and utilizes only the EMGs from the past. The dynamical nature of the Kalman filter provides for the time-varying optimal fusion of the information and allows to take into account not only the EMG activity, but also the physical properties of handwriting.

The main attraction of the proposed method is its ability to smooth the noise and, as a result, provide a comprehensible and realistic reconstruction. Further progress in this field would potentially create intelligent rehabilitation techniques for patients with hand injuries, as well as become useful in human-computer interfaces, associated with handwriting.

ACKNOWLEDGMENTS

The authors are grateful for the fruitful comments of Dr. Igor Furtat related to the algorithmic portion of the work. The experimental portion (Section 3) was funded by the government subsidy for improving competitiveness of National Research University Higher School of Economics among the leading world centers for research and education. The data fusion algorithm for reconstruction of pen traces (Section 2) was adapted to the use with the EMG data solely under support of RNF (grant 14-29-00142) in IPME RAS.

REFERENCES

Ahsan, M. R., Ibrahimy, M. I., and Khalifa, O. O. (2009). Emg signal classification for human computer interaction: a review. *Eur. J. Sci. Res.* 33, 480–501.

Amis, A., Dowson, D., and Wright, V. (1979). Muscle strengths and musculoskeletal geometry of the upper limb. *Eng. Med.* 8, 41–48. doi: 10.1243/EMED/JOUR/1979/008/010/02

Araújo, R. C., Duarte, M., and Amadio, A. C. (2000). On the inter-and intra-subject variability of the electromyographic signal in isometric contractions. *Electromyogr. Clin. Neurophysiol.* 40, 225–230.

Arulampalam, M. S., Maskell, S., Gordon, N., and Clapp, T. (2002). A tutorial on particle filters for online nonlinear/non-gaussian bayesian tracking. *Signal Process. IEEE Trans.* 50, 174–188. doi: 10.1109/78.978374

Bernstein, N. (1967). *The Coordination and Regulation of Movements*. Oxford: Pergamon Press.

Bu, N., Okamoto, M., and Tsuji, T. (2009). A hybrid motion classification approach for EMG-based human–robot interfaces using bayesian and neural networks. *Robot. IEEE Trans.* 25, 502–511. doi: 10.1109/TRO.2009.2019782

Carter, J. L., and Russell, H. L. (1985). Use of EMG biofeedback procedures with learning disabled children in a clinical and an educational setting. *J. Learn. Disabil.* 18, 213–216. doi: 10.1177/002221948501800406

Castellini, C., and van der Smagt, P. (2009). Surface EMG in advanced hand prosthetics. *Biol. Cybern.* 100, 35–47. doi: 10.1007/s00422-008-0278-1

Chan, F. H., Yang, Y.-S., Lam, F. K., Zhang, Y.-T., and Parker, P. A. (2000). Fuzzy emg classification for prosthesis control. *Rehabil. Eng. IEEE Trans.* 8, 305–311. doi: 10.1109/86.867872

Faragher, R. (2012). Understanding the basis of the kalman filter via a simple and intuitive derivation. *IEEE Signal Process. Mag.* 29, 128–132. doi: 10.1109/MSP.2012.2203621

Guigon, E., Baraduc, P., and Desmurget, M. (2006). Computational motor control: redundancy and invariance. *J. Neurophysiol.* 97, 331–347. doi: 10.1152/jn.00290.2006

Guigon, E., Baraduc, P., and Desmurget, M. (2008). Optimality, stochasticity, and variability in motor behavior. *J. Comput. Neurosci.* 24, 57–68. doi: 10.1007/s10827-007-0041-y

Henderson, H. V., and Searle, S. R. (1981). On deriving the inverse of a sum of matrices. *Siam Rev.* 23, 53–60. doi: 10.1137/1023004

Huang, G., Zhang, D., Zheng, X., and Zhu, X. (2010). "An EMG-based handwriting recognition through dynamic time warping," in *Engineering in Medicine and Biology Society (EMBC), 2010 Annual International Conference of the IEEE* (Shanghai: IEEE), 4902–4905.

Jazwinski, A. H. (2007). *Stochastic Processes and Filtering Theory*. Mineola, NY: Courier Corporation.

Julier, S. J., and Uhlmann, J. K. (1997). "New extension of the kalman filter to nonlinear systems," in *AeroSense'97*, ed I. Kadar (Orlando, FL: International Society for Optics and Photonics), 182–193.

Kalman, R. E. (1960). A new approach to linear filtering and prediction problems. *J. Fluids Eng.* 82, 35–45. doi: 10.1115/1.3662552

Li, C., Ma, Z., Yao, L., and Zhang, D. (2013). "Improvements on emg-based handwriting recognition with dtw algorithm," in *Engineering in Medicine and Biology Society (EMBC), 2013 35th Annual International Conference of the IEEE* (IEEE), 2144–2147.

Linderman, M., Lebedev, M. A., and Erlichman, J. S. (2009). Recognition of handwriting from electromyography. *PLoS ONE* 4:e6791. doi: 10.1371/journal.pone.0006791

Linssen, W. H., Stegeman, D. F., Joosten, E. M., Binkhorst, R. A., van't Hof, M. A., and Notermans, S. L. (1993). Variability and interrelationships of surface emg parameters during local muscle fatigue. *Muscle Nerve* 16, 849–856. doi: 10.1002/mus.880160808

McKeague, I. W. (2005). A statistical model for signature verification. *J. Am. Stat. Assoc.* 100, 231–241. doi: 10.1198/016214504000000827

Nordander, C., Willner, J., Hansson, G.-Å., Larsson, B., Unge, J., Granquist, L., et al. (2003). Influence of the subcutaneous fat layer, as measured by ultrasound, skinfold calipers and bmi, on the emg amplitude. *Eur. J. Appl. Physiol.* 89, 514–519. doi: 10.1007/s00421-003-0819-1

Ohnishi, K., Weir, R. F., and Kuiken, T. A. (2007). Neural machine interfaces for controlling multifunctional powered upper-limb prostheses. *Expert Rev. Med. Devices* 4, 43–53. doi: 10.1586/17434440.4.1.43

Plamondon, R., and Maarse, F. J. (1989). An evaluation of motor models of handwriting. *Syst. Man Cybern. IEEE Trans.* 19, 1060–1072. doi: 10.1109/21.44021

Reaz, M., Hussain, M., and Mohd-Yasin, F. (2006). Techniques of EMG signal analysis: detection, processing, classification and applications. *Biol. Proced. Online* 8, 11–35. doi: 10.1251/bpo115

Rencher, A. C. (2003). *Methods of Multivariate Analysis*, Vol. 492. John Wiley & Sons. Available online at: https://books.google.ru/books?hl=ru&lr=&id=SpvBd7IUCxkC&oi=fnd&pg=PR5&dq=methods+of+multivariate+analysis&ots=ItWFsHM9w3&sig=K7-D_CG8CgdDkrVrYX0wFYmBY-8&redir_esc=y#v=onepage&q=methods%20of%20multivariate%20analysis&f=false

Shenoy, P., Miller, K. J., Crawford, B., and Rao, R. P. N. (2008). Online electromyographic control of a robotic prosthesis. *Biomed. Eng. IEEE Trans.* 55, 1128–1135. doi: 10.1109/TBME.2007.909536

Shimkin, N. (2009). Derivations of the discrete-time kalman filter. *Estim. Ident. Dyn. Syst.*

Silveri, M. C., Corda, F., and Di Nardo, M. (2007). Central and peripheral aspects of writing disorders in alzheimer's disease. *J. Clin. Exp. Neuropsychol.* 29, 179–186. doi: 10.1080/13803390600611351

Stanford, V. (2004). Biosignals offer potential for direct interfaces and health monitoring. *Pervas. Comput. IEEE* 3, 99–103. doi: 10.1109/MPRV.2004.1269140

Van Gemmert, A., Teulings, H.-L., Contreras-Vidal, J., and Stelmach, G. (1999). Parkinsons disease and the control of size and speed in handwriting. *Neuropsychologia* 37, 685–694. doi: 10.1016/S0028-3932(98)00122-5

Wan, E., and Van Der Merwe, R. (2000). "The unscented kalman filter for nonlinear estimation," in *Adaptive Systems for Signal Processing, Communications, and Control Symposium 2000. AS-SPCC. The IEEE 2000* (Beaverton, OR: IEEE), 153–158.

Xiao, Z. G., and Menon, C. (2014). Towards the development of a wearable feedback system for monitoring the activities of the upper-extremities. *J. Neuroeng. Rehabil.* 11, 1–13. doi: 10.1186/1743-0003-11-2

Conflict of Interest Statement: The authors declare that the research was conducted in the absence of any commercial or financial relationships that could be construed as a potential conflict of interest.

APPENDIX

Parameters of the State Transition Model

Equation (A3) shows the distribution of the estimate of the State Transition Model given by Equation (1).

The mean of the distribution is

$$\boldsymbol{\mu}_{1t} = \boldsymbol{E}[\boldsymbol{s}_t] = \boldsymbol{A}\hat{\boldsymbol{s}}_{t-1} = \boldsymbol{A}\boldsymbol{\mu}_{1(t-1)}. \tag{A1}$$

The covariance matrix is derived the following way:

$$\begin{aligned}
\boldsymbol{\Sigma}_{1t} &= \boldsymbol{E}[(\boldsymbol{s}_t - \boldsymbol{\mu}_{1t})(\boldsymbol{s}_t - \boldsymbol{\mu}_{1t})^T] = \\
&= \boldsymbol{E}[(\boldsymbol{A}\boldsymbol{s}_{t-1} + \boldsymbol{v}_t - \boldsymbol{A}\hat{\boldsymbol{s}}_{t-1})(\boldsymbol{A}\boldsymbol{s}_{t-1} + \boldsymbol{v}_t - \boldsymbol{A}\hat{\boldsymbol{s}}_{t-1})^T] = \\
&= \boldsymbol{E}[(\boldsymbol{A}(\boldsymbol{s}_{t-1} - \hat{\boldsymbol{s}}_{t-1}) + \boldsymbol{v}_t)(\boldsymbol{A}(\boldsymbol{s}_{t-1} - \hat{\boldsymbol{s}}_{t-1}) + \boldsymbol{v}_t)^T] = \\
&= \boldsymbol{E}[(\boldsymbol{A}(\boldsymbol{s}_{t-1} - \hat{\boldsymbol{s}}_{t-1}) + \boldsymbol{v}_t)((\boldsymbol{s}_{t-1} - \hat{\boldsymbol{s}}_{t-1})^T\boldsymbol{A}^T + \boldsymbol{v}_t^T)] = \\
&= \boldsymbol{A}\boldsymbol{E}[(\boldsymbol{s}_{t-1} - \hat{\boldsymbol{s}}_{t-1})(\boldsymbol{s}_{t-1} - \hat{\boldsymbol{s}}_{t-1})^T]\boldsymbol{A}^T + \boldsymbol{A}\boldsymbol{E}[(\boldsymbol{s}_{t-1} - \hat{\boldsymbol{s}}_{t-1})\boldsymbol{v}_t^T] \\
&\quad + \boldsymbol{E}[\boldsymbol{v}_t(\boldsymbol{s}_{t-1} - \hat{\boldsymbol{s}}_{t-1})^T]\boldsymbol{A}^T + \boldsymbol{E}[\boldsymbol{v}_t\boldsymbol{v}_t^T].
\end{aligned}$$

Since the state estimate noise $\boldsymbol{v}_t$ is uncorrelated with the estimate,

$$\boldsymbol{E}[\boldsymbol{v}_t(\boldsymbol{s}_{t-1} - \hat{\boldsymbol{s}}_{t-1})^T] = \boldsymbol{E}[(\boldsymbol{s}_{t-1} - \hat{\boldsymbol{s}}_{t-1})\boldsymbol{v}_t^T] = 0$$

and the covariance matrix reduces to:

$$\begin{aligned}
\boldsymbol{\Sigma}_{1t} &= \boldsymbol{A}\boldsymbol{E}[(\boldsymbol{s}_{t-1} - \hat{\boldsymbol{s}}_{t-1})(\boldsymbol{s}_{t-1} - \hat{\boldsymbol{s}}_{t-1})^T]\boldsymbol{A}^T + \boldsymbol{E}[\boldsymbol{v}_t\boldsymbol{v}_t^T] = \\
&= \boldsymbol{A}\boldsymbol{\Sigma}_{1(t-1)}\boldsymbol{A}^T + \boldsymbol{Q}.
\end{aligned} \tag{A2}$$

The Fusion

Under the normality assumption the probability density function (pdf) of the state space vector $\boldsymbol{s}_t$ can be written as

$$f_1(\boldsymbol{s}_t|\boldsymbol{s}_{t-1}) = (2\pi)^{-3K}|\boldsymbol{\Sigma}_{1t}|^{-1/2}\exp\left(-\frac{1}{2}(\boldsymbol{s}_t - \boldsymbol{\mu}_{1t})^T \boldsymbol{\Sigma}_{1t}^{-1}(\boldsymbol{s}_t - \boldsymbol{\mu}_{1t})\right) \tag{A3}$$

Since the additive noise term $\boldsymbol{w}_t$ in Equation (2) is assumed to be Gaussian, while each of the observed EMG signals are not modeled as stochastic processes, the state vector follows the Gaussian distribution

$$f_2(\boldsymbol{s}_t|\boldsymbol{z}_t) = (2\pi)^{-4L}|\boldsymbol{\Sigma}_{2t}|^{-1/2}\exp\left(-\frac{1}{2}(s_t - \boldsymbol{\mu}_{2t})^T\boldsymbol{\Sigma}_{2t}^{-1}(s_t - \boldsymbol{\mu}_{2t})\right). \tag{A4}$$

By multiplying pdf in Equation (A3) by pdf in Equation (A4) we get a scaled fused Distribution of the state estimate:

$$\begin{aligned}
&f_{fused}(s_t|s_{t-1}, z_t) = f_1(s_t|s_{t-1})f_2(s_t|z_t) = \\
&\mathcal{N}(\boldsymbol{\mu}_{1t}, \boldsymbol{\Sigma}_{1t}) \cdot \mathcal{N}(\boldsymbol{\mu}_{2t}, \boldsymbol{\Sigma}_{2t}) = c\mathcal{N}(\boldsymbol{\mu}_{fused}, \boldsymbol{\Sigma}_{fused}),
\end{aligned} \tag{A5}$$

with parameters

$$\boldsymbol{\Sigma}_{Fused} = (\boldsymbol{\Sigma}_{1t}^{-1} + \boldsymbol{\Sigma}_{2t}^{-1})^{-1} \tag{A6}$$

$$\boldsymbol{\mu}_{Fused} = \boldsymbol{\Sigma}_{Fused}(\boldsymbol{\Sigma}_{1t}^{-1}\boldsymbol{\mu}_{1t} + \boldsymbol{\Sigma}_{2t}^{-1}\boldsymbol{\mu}_{2t}) \tag{A7}$$

and a normalization constant

$$c = \frac{1}{(2\pi)^{k/2}}\frac{|\boldsymbol{\Sigma}_{Fused}|^{1/2}}{|\boldsymbol{\Sigma}_{1t}|^{1/2}|\boldsymbol{\Sigma}_{2t}|^{1/2}}\exp\left(-\frac{1}{2}\left(\boldsymbol{\mu}_{1t}^T\boldsymbol{\Sigma}_{1t}^{-1}\boldsymbol{\mu}_{1t} + \boldsymbol{\mu}_{2t}^T\boldsymbol{\Sigma}_{2t}^{-1}\boldsymbol{\mu}_{2t} + \boldsymbol{\mu}_{Fused}^T\boldsymbol{\Sigma}_{Fused}^{-1}\boldsymbol{\mu}_{Fused}\right)\right) \tag{A8}$$

Let us reformulate the expressions for the mean and Covariance matrix of the new distribution in such a way that they separate the influence of the two fused distributions.

Using the Matrix Inversion lemma (the Woodbury matrix identity) for two matrices of the same dimension ($\boldsymbol{\Sigma}_{1t}$ and $\boldsymbol{\Sigma}_{2t}$) and setting $\boldsymbol{K}_t = \boldsymbol{\Sigma}_{1t}(\boldsymbol{\Sigma}_{1t} + \boldsymbol{\Sigma}_{2t})^{-1}$ the parameters of the fused Gaussian can be neatly rewritten in the form of Equations (8) and (9), i.e.,

$$\boldsymbol{\Sigma}_{Fused} = \boldsymbol{\Sigma}_{1t} - \boldsymbol{\Sigma}_{1t}(\boldsymbol{\Sigma}_{1t} + \boldsymbol{\Sigma}_{2t})^{-1}\boldsymbol{\Sigma}_{1t} = \boldsymbol{\Sigma}_{1t} - \boldsymbol{K}_t\boldsymbol{\Sigma}_{1t}. \tag{A9}$$

$$\begin{aligned}
\boldsymbol{\mu}_{Fused} &= (\boldsymbol{\Sigma}_{1t} - \boldsymbol{K}_t\boldsymbol{\Sigma}_{1t})(\boldsymbol{\Sigma}_{1t}^{-1}\boldsymbol{\mu}_{1t} + \boldsymbol{\Sigma}_{2t}^{-1}\boldsymbol{\mu}_{2t}) = \\
&= \boldsymbol{\mu}_{1t} + \boldsymbol{\Sigma}_{1t}\boldsymbol{\Sigma}_{2t}^{-1}\boldsymbol{\mu}_{2t} - \boldsymbol{K}_t\boldsymbol{\mu}_1 - \boldsymbol{K}_t\boldsymbol{\Sigma}_{1t}\boldsymbol{\Sigma}_{2t}\boldsymbol{\mu}_{2t} = \\
&= \boldsymbol{\mu}_{1t} + \boldsymbol{K}_t(\boldsymbol{K}_t^{-1}\boldsymbol{\Sigma}_{1t}\boldsymbol{\Sigma}_{2t}^{-1}\boldsymbol{\mu}_{2t} - \boldsymbol{\mu}_{1t} - \boldsymbol{\Sigma}_{1t}\boldsymbol{\Sigma}_{2t}^{-1}\boldsymbol{\mu}_{2t}) = \\
&= \boldsymbol{\mu}_{1t} + \boldsymbol{K}_t((\boldsymbol{\Sigma}_{1t} + \boldsymbol{\Sigma}_{2t})\boldsymbol{\Sigma}_{1t}^{-1}\boldsymbol{\Sigma}_{1t}\boldsymbol{\Sigma}_{2t}^{-1}\boldsymbol{\mu}_{2t} - \boldsymbol{\mu}_{1t} - \boldsymbol{\Sigma}_{1t}\boldsymbol{\Sigma}_{2t}^{-1}\boldsymbol{\mu}_{2t}) = \\
&= \boldsymbol{\mu}_{1t} + \boldsymbol{K}_t(\boldsymbol{\Sigma}_{1t}\boldsymbol{\Sigma}_{2t}^{-1}\boldsymbol{\mu}_{2t} + \boldsymbol{\mu}_{2t} - \boldsymbol{\mu}_{1t} - \boldsymbol{\Sigma}_{1t}\boldsymbol{\Sigma}_{2t}^{-1}\boldsymbol{\mu}_{2t}) = \\
&= \boldsymbol{\mu}_{1t} + \boldsymbol{K}_t(\boldsymbol{\mu}_{2t} - \boldsymbol{\mu}_{1t}) = (\boldsymbol{I} - \boldsymbol{K}_t)\boldsymbol{\mu}_{1t} + \boldsymbol{K}_t\boldsymbol{\mu}_{2t}.
\end{aligned} \tag{A10}$$

Testing the Assumptions of the Model

We ran the Royston test for multivariate normality on the residuals of each training sample and concluded that for most samples the assumption of normality is not violated (at 1% significance level). **Table A1** summarized the percentages of

TABLE A1 | Percentages of trials across participants, in which the assumption of multivariate normality of the error term is not violated at 1% significance level.

	Participants						
	1 (%)	2 (%)	3 (%)	4 (%)	5 (%)	6 (%)	Average (%)
State transition model	92	79	92	96	83	73	86
Measurement model	93	85	92	94	80	77	87
Joint model	89	72	89	93	76	67	81

TABLE A2 | Percentages of trials across participants, in which the test for uncorrelatedness of residuals of the two fused models was not rejected at 5% significance level.

	Participants						
	1 (%)	2 (%)	3 (%)	4 (%)	5 (%)	6 (%)	Average (%)
Independent trials	83	72	76	80	67	68	74

samples, in which the assumption of normality of the error term holds in the two reconstructed models and in the joint model.

The fusion of the two information sources described in this paper is heavily based on the assumption that the two merged sources are independent.

Then, we checked to what extent the two information sources can be considered independent. Taking into account the results of the test for multivariate normality, we checked for the absence of correlation between the error terms of the two merged models (Equations 1 and 2). We used the residuals of the two models to calculate the sample cross-correlation matrix and assessed the significance of its elements for each trial.

Given the sample size and the multiplicity of the tested hypothesis (36), we could not reject the null-hypothesis of no-correlation at 5% group level significance for the majority of trials (74%). Detailed distribution of the test performance across the participants is given in **Table A2.**

frontiers in
SYSTEMS NEUROSCIENCE

ORIGINAL RESEARCH ARTICLE
published: 09 April 2014
doi: 10.3389/fnsys.2014.00052

Effect of biased feedback on motor imagery learning in BCI-teleoperation system

***Maryam Alimardani*[1,2]*, *Shuichi Nishio*[2] *and Hiroshi Ishiguro*[1,2]**

[1] *Department of System Innovation, Graduate school of Engineering science, Osaka University, Osaka, Japan*
[2] *Advanced Telecommunications Research Institute International, Kyoto, Japan*

Edited by:
Mikhail Lebedev, Duke University, USA

Reviewed by:
Duk Shin, Tokyo Institute of Technology, Japan
W. Geoffrey Wright, Temple University, USA

***Correspondence:**
Maryam Alimardani, HIL, Advanced Telecommunications Research Institute International, 2-2 Hikaridai, Seika-cho, Soraku-gun, Kyoto 619-0288, Japan
e-mail: maryam@atr.jp

Feedback design is an important issue in motor imagery BCI systems. Regardless, to date it has not been reported how feedback presentation can optimize co-adaptation between a human brain and such systems. This paper assesses the effect of realistic visual feedback on users' BCI performance and motor imagery skills. We previously developed a tele-operation system for a pair of humanlike robotic hands and showed that BCI control of such hands along with first-person perspective visual feedback of movements can arouse a sense of embodiment in the operators. In the first stage of this study, we found that the intensity of this ownership illusion was associated with feedback presentation and subjects' performance during BCI motion control. In the second stage, we probed the effect of positive and negative feedback bias on subjects' BCI performance and motor imagery skills. Although the subject specific classifier, which was set up at the beginning of experiment, detected no significant change in the subjects' online performance, evaluation of brain activity patterns revealed that subjects' self-regulation of motor imagery features improved due to a positive bias of feedback and a possible occurrence of ownership illusion. Our findings suggest that in general training protocols for BCIs, manipulation of feedback can play an important role in the optimization of subjects' motor imagery skills.

Keywords: body ownership illusion, BCI-teleoperation, motor imagery learning, feedback effect, training

INTRODUCTION

Brain computer interfaces (BCIs) have widely become popular in many fields as a new communication and control channel between the human brain and an external device. However, the application of this technology is not as simple and intuitive as its concept suggests. To operate a BCI, subjects need to perform certain tasks and learn how to intentionally modulate certain characteristics of their brain activities in order to express their intentions. The motor imagery method, for instance, is one of the most commonly employed methods for BCI control of intended motions (Curran and Stokes, 2003). Subjects imagine the movement of a certain limb of their own body to induce changes in mu and beta rhythms over the corresponding sub-region of sensorimotor cortex. These changes are detected by BCI and translated into control commands. Motor imagery task requires relatively longer training compared to other BCI paradigms such as P300 or steady state visually evoked potential (SSVEP) since the mental rehearsal of a movement without actual execution is not a normal and daily practice for subjects and hence the task of motor imagery is an unfamiliar experience to most of them.

While the importance of subject's motor imagery skills in BCIs is well recognized, most studies have focused on the computer side and improving classification algorithms and very few have attended the human side and training paradigms that can facilitate the skill acquisition process for subjects (Lotte et al., 2013). As in any form of interface, users of BCIs learn to co-adapt with the system through the feedback they receive of their performance. Therefore feedback design is particularly influential in the process of motor imagery learning and performance improvement. Standard BCI protocols typically provide online visual feedback in the form of a moving cursor or target on the computer screen. Neuper et al. compared realistic presentation of feedback, in form of a grasping hand vs. abstract feedback in the form of an extending bar, on a computer screen (Neuper et al., 2009). However, they found no evidence of a significant difference between the performances of two feedback groups. In another study, the influence of motivation on BCI performance was also investigated by biasing the feedback accuracy (Barbero and Grosse-Wentrup, 2010). The results indicated that subjects with poor performance benefitted from positive biasing while those with better performance were impeded by inaccurate feedback. In a similar work (Gonzalez-Franco et al., 2011), authors provided subjects fake negative and positive feedback of their performance and reported that negative feedback had a greater learning effect on motor imagery BMIs.

Although in the above works, the effect of feedback presentation and accuracy has been probed, none of them has actually discussed the direct interaction between subject and BCI system. When performing a motor imagery task, subjects are asked to imagine their own body movements while the output is fed back in the form of movement for objects other than their own body. This mismatch and dissociation between subject's life experience and BCI task can in fact interfere with the imagination and impair the performance of motor imagery especially for novice users.

The goal of the present study is to explore the influence of feedback design on enhancement of user's performance and interaction with a BCI system. Previously we showed that BCI-operation of a pair of humanlike robotic hands by motor imagery while watching first-person perspective images of robot's movement could induce an illusion of body ownership transfer (BOT) for the operators (Alimardani et al., 2013). In post-experiment interviews, some subjects stated that when the robot moved as they intended, it felt like their own hand was moving and motor imagery became easier. We hypothesize that inducement of such feeling of ownership and the sense of agency driven toward the seen motions may have a positive loop effect on execution of motor imagery during BCI-operation. In other words, we speculate that once the thought of "I am the one moving the hands" raises the feeling of "These hands are mine," the illusion of owning hands enhances the imagery ability in subjects and boosts the inverse thought of "These are my hands so I can move them."

To that end, in this study we used the same BCI-teleoperation paradigm while exposing naïve subjects to different feedback conditions in order to probe the relationship between subject's experience of BOT and BCI-performance. Two experiments are presented. In the first experiment, by manipulating the presentation of misperformance, we surveyed how subjects' perception of their own performance could affect the intensity of BOT. In the second experiment, we then examined how this effect can be influential on subjects' real performance and trend of motor imagery learning.

Both experiments in this study were approved by the Ethics Committee of Advanced Telecommunications Research Institute International (12-506-3). All subjects read and signed a written consent form prior to experiment and received payment for their participation.

EXPERIMENT 1

This experiment was designed to investigate the inducement of body ownership illusion for a pair of BCI-operated human-like robotic hands under different presentations of feedback.

PARTICIPANTS

Forty healthy participants (26 male, 14 female, age $M = 21.13$, $SD = 1.92$) were selected for the experiment. Thirty eight participants were right-handed and 2 left-handed. All participants were naive to the research topic and received explanation prior to the experiment.

METHOD

Participants sat in a comfortable chair and were asked to remain motionless. They wore an EEG electrode cap and 27 EEG electrodes were placed over their primary sensori-motor cortex according to the international 10–20 system (FT7, FC5, FC3, FC1, FCz, FC2, FC4, FC6, FT8, T7, C5, C3, C1, Cz, C2, C4, C6, T8, TP7, CP5, CP3, CP1, CPz, CP2, CP4, CP6, TP8). A reference electrode was mounted on the right ear and a ground electrode on the forehead. Participants were asked to imagine a grasp or squeeze motion for their own hand while their cerebral activities were recorded by g.USBamp biosignal amplifiers (Guger Technologies). In an initial training session, they practiced a motor imagery task by extending a feedback bar to left or right side on a 15-inch laptop computer screen. A visual cue in the form of a horizontal pointing arrow specified the timing and the hand they were supposed to hold image for. Each trial lasted 7.5 s and started with the presentation of a fixation cross on the display. After 2 s an acoustic warning was given in the form of a "beep." From second 3 to 4.25, an arrow pointing to the left or right side randomly was shown. Depending on the arrow's direction participants were instructed to perform motor imagery. They watched the feedback bar and continued the imagery task until the fixation cross was erased. After a short pause, which took 1 second, the next trial started. The first run consisting of 40 trials (20 trials per class left/right presented in a randomized order) was conducted without feedback and lasted 5 min. The recorded brain activities in the initial non-feedback run were used to set up a subject specific classifier for the classification in the following feedback runs. In the feedback runs, participants performed similar trials but received online classification results of their performance in form of a horizontal feedback bar on the screen. Subjects' task was to extend the feedback bar in the correct direction.

The classification of recorded signals was conducted under Simulink/MATLAB (Mathworks) for offline and online parameter extraction. This process included bandpass filtering between 0.5 and 30 Hz, sampling at 128 Hz, cutting off artifacts by notch filter at 60 Hz, and adopting the Common Spatial Pattern (CSP) algorithm for discrimination of Event Related Desynchronization (ERD) and Event Related Synchronization (ERS) patterns associated with the motor imagery task (Guger et al., 2000). The classifier was trained using CSP analysis of calibration measurements. CSP found weight vectors that weighed each electrode based on its importance for the discrimination task. The spatial filters were designed such that the resulting signal had maximum variance for left trials and minimum variance for right trials. Therefore, the difference between left and right populations was maximized to show where the EEG variance fluctuated the most. Finally, when the discrimination between left and right imaginations was made, the classifier outputted a linear array signal in the range of $[-1,1]$, where -1 denotes the extreme left and 1 denotes the extreme right. Negative values were then translated as the robot's left hand grasp motions and positive values as the robot's right hand grasp motions. A threshold of ± 0.1 was considered in the system, in order to avoid multiple movements of both hands for subjects with unstable classification results.

Following training sessions the main test sessions commenced, in which subjects wore a head mounted display (Vuzix iWear VR920) and tele-operated the robot's hands using the same BCI system. They performed a motor imagery task for their right or left hand while they watched first-person images of the robot's hands performing the motions respectively (**Figure 1A**). Two LED-embedded balls were installed in the robot's grasp and provided motor imagery cues by randomly lighting. During the experiment subjects were told to look down as if they were watching their own hands and the same blankets were laid on both the robot's and participants' legs to give a similar view. Participants placed their arms in a similar position and orientation as the robot's arms. In order to measure subjects' physiological reactions to a threatening stimulus, skin conductance response (SCR)

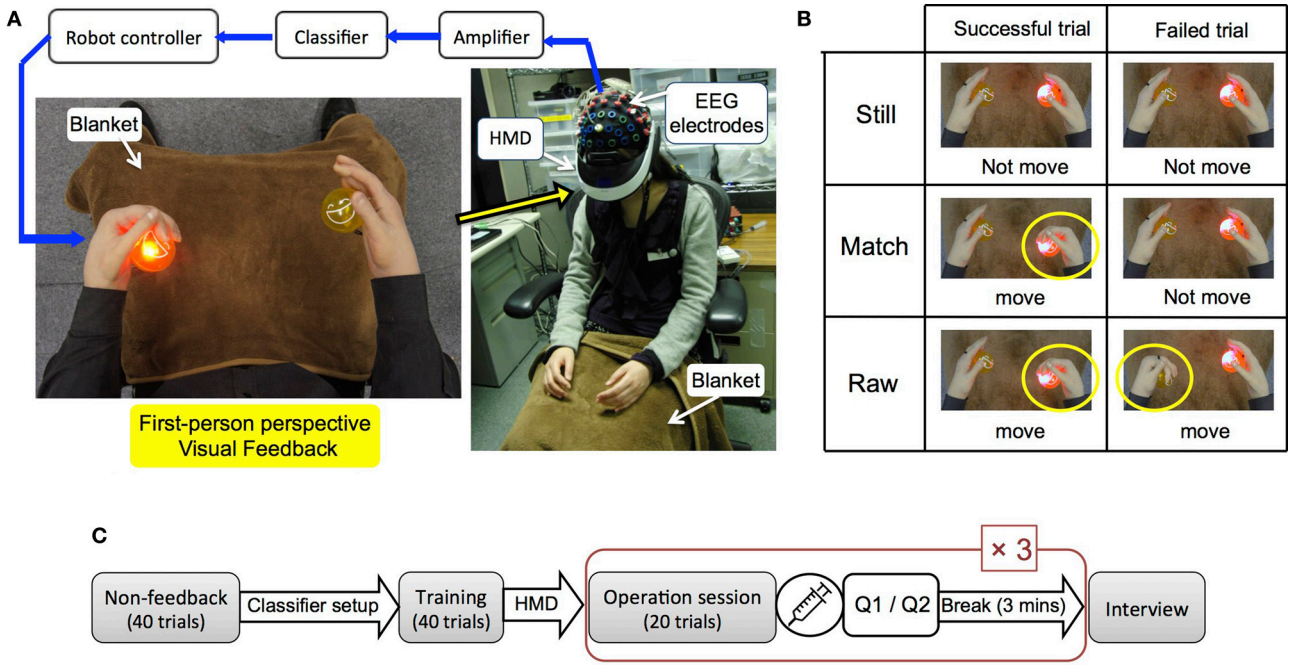

FIGURE 1 | Experiment setup. (A) EEG electrodes installed on a subject's sensorimotor cortex recorded brain activities during a motor imagery task. Subjects watched first-person images from a robot's perspective through a head mounted display. A lighting ball in front of each of the robot's hands gave motor imagery cues and subjects imagined grasping their corresponding hands. The classifier detected two classes of results (right or left) and motion command was sent to the robot's hand. **(B)** Subjects repeated the experiment under three different conditions: Still, where the robot's hand didn't move at all. Match in which the robot's hand only moved in successful trials, and Raw where the robot's hand also performed failed trials using the wrong hand. **(C)** Experimental procedure consisted of a non-feedback session for classifier setup, training sessions and three operational sessions.

electrodes were installed on their left palms. A bio-amplifier recording device (Polymate II AP216, TEAC, Japan) with sampling rate of 1000 Hz was used to record SCR measurements. Prior to the testing sessions, participants watched an act of injection via a syringe to the robot's hand (painful stimulus) through the head mounted display, which was explained to them as a necessary procedure for preparing the robot. The injection was continued until subjects' SCR responses disappeared (Armel and Ramachandran, 2003). Afterwards, testing sessions were carried out in a random order under three conditions (**Figure 1B**):

(1) Still (no feedback): The robot's hands did not move at all throughout the whole session although a subject performed motor imagery according to cues.
(2) Match (no negative feedback): The robot's hands moved only in those trials that the classification result was correct and in accordance with cue.
(3) Raw: The robot's hands moved according to the classification results in all trials. In case of wrong result that was not in accordance with cue, the robot's opposite hand moved.

Still was designed as control condition where visual images of hands without motion feedback were expected to raise no body ownership illusion. The last session is called Raw since we inputted the unprocessed values obtained from the classifier as the robot's motion parameter. In all conditions above, participants performed trials that were designed to be identical to the trials in training sessions regarding duration and stimulus timing. Each session was followed by a break of 3 min. Test sessions comprised 20 trials, lasting 2 min and 40 s each (**Figure 1C**). Following the last trial, an injection was applied to the robot's left hand to examine if the illusion of ownership could cause a response to a pain-causing stimulus (Nishio et al., 2012). Immediately after injecting the session was terminated and participants were orally asked the following questions: (Q1) When the robot's hand was injected, did it feel as if your own hand was receiving the injection? (Q2) Throughout the entire session while you were operating the robot's hands, did it feel as if they were your own hands? Participants scored Q1 and Q2 based on the seven-point Likert Scale, 1 meaning, "Didn't feel such thing at all" and 7 meaning, "Felt it very strongly." In addition to the self-assessment, we physiologically measured the body ownership illusion by recording the SCRs.

RESULT

The response variables for 40 participants were obtained from questionnaires and SCR recordings. Participants' responses in three conditions of Still, Match and Raw were averaged and compared. The mean value, standard deviation, and *p*-value are depicted on each graph (**Figure 2**).

For both Q1 and Q2, the Match condition showed a higher average value compared to the other two conditions (**Figures 2A,B**). Non-parametric statistical analysis was used

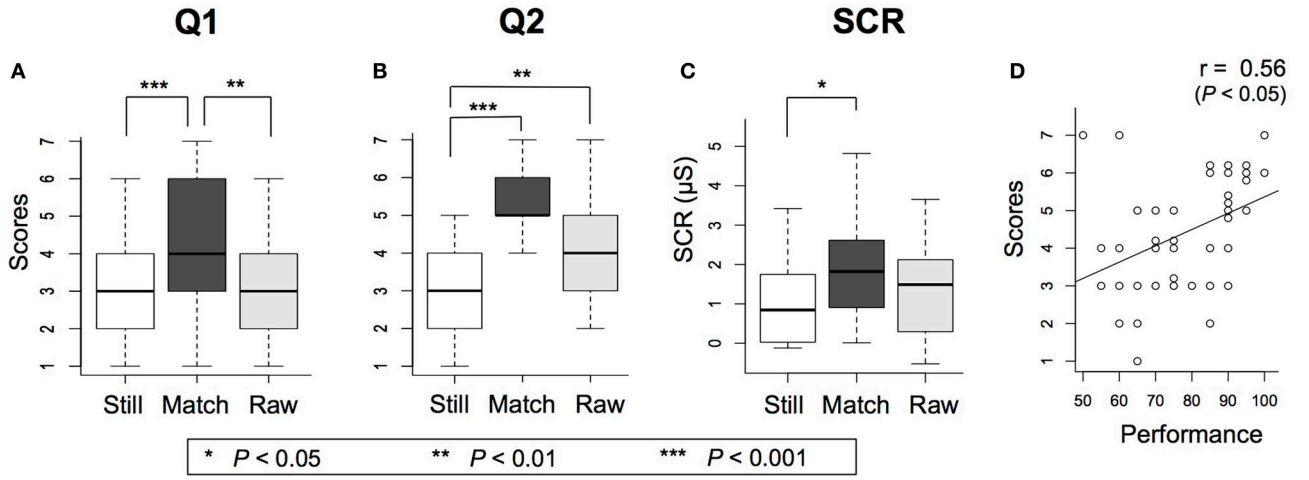

FIGURE 2 | Results for experiment 1 (A) Mean values and standard deviations for Q1 in each session, with Match significantly higher than Still and Raw **(B)** Mean values and standard deviations for Q2 in each session, with Match and Raw significantly higher than Still **(C)** Mean values and standard deviations of SCR values for 35 subjects, with Match associated with significantly higher responses to injection than Still **(D)** Subjects' performances vs. their scores of illusion in the Match condition. For those with the same performance and score, the score has been slightly modified to a non-integer neighbor value to avoid the overlap of the markers. A significantly positive correlation was found between BCI-performance and intensity of illusion.

to compare as Shapiro-Wilks test rejected the normal distribution for the Likert scores. Kruskal-Wallis tests showed a significant effect of BCI tele-operation on the level of BOT between the three Still, Match and Raw conditions for Q1 scores [$\chi^2_{(2)} = 19.11$, $p < 0.0001$] and for Q2 scores [$\chi^2_{(2)} = 34.52$, $p < 10^{-6}$]. *Post-hoc* Mann-Whitney *U*-tests for comparison with Bonferroni adjustment indicated that in Q1 Match ($M = 4.38$, $SD = 1.51$) raised BOT significantly higher than Still ($M = 2.83$, $SD = 1.43$); [Match > Still, $p < 0.0001$] and than Raw ($M = 3.15$, $SD = 1.57$); [Match > Raw, $p < 0.01$]. Similarly, Mann-Whitney *U*-tests with Bonferroni adjustment for Q2 scores showed significant difference between Match ($M = 5.15$, $SD = 1.10$) and Still ($M = 2.93$, $SD = 1.25$); [Match > Still, $p < 10^{-6}$] and also between Raw ($M = 4.18$, $SD = 1.38$) and Still; [Raw > Still, $p < 0.01$].

The SCR peak value within a 6-s interval (1 s after the appearance of syringe in the participant's view to 5 s after the injection) was selected as the reaction value (Alimardani et al., 2013). In this experiment, we only evaluated the response values of 35 participants, since five participants showed unchanged responses during the experiment and were excluded from analysis. Results showed a higher mean value for the Match condition compared to the other two conditions (**Figure 2C**). Due to non-normal distribution of SCR values revealed by Shapiro-Wilks test, we performed Kruskal-Wallis tests on participants' reaction values and the analysis was significant, [$\chi^2_{(2)} = 8.39$, $p < 0.01$]. *Post-hoc* comparisons by Mann-Whitney *U*-tests with Bonferroni adjustment confirmed significant differences only between Match ($M = 1.68$, $SD = 1.98$) and Still ($M = 0.90$, $SD = 1.42$); [Match > Still, $p < 0.05$]. Moreover, a significantly positive correlation was found between subjects' performances and the Q1 scores only in the Match condition (Pearson correlation coefficient $r = 0.56$, $p < 0.05$, **Figure 2D**). The term performance here refers to the rate of trials subjects could successfully grasp the lightened ball out of the total 20 trials in each run scaled in percentage.

DISCUSSION

In study 1, we investigated the inducement of body ownership illusion for a pair of BCI-operated human-like robotic hands under different feedback conditions. Results from both measurement methods (Q1 and SCR) indicated significantly high responses to the injection in the Match condition, where robot's hands moved only if the classification result was correct and same as the cue. This shows that the feeling of receiving an injection was significantly stronger when the robot's hands moved exclusively in agreement with the operator's intentions than when the robot made no motion (Still) or performed a wrong motion in the case of errors (Raw). Since this is a feeling aroused due to the illusion of ownership over robot's body, we can state that the transfer of body ownership could be evoked more reliably by precise mind-control of a robot's hands.

On the other hand, in Q2 participants directly scored their sensation of ownership for robot's body during the entire operation time. Based on participants' assessments, the feeling of ownership was significantly stronger in both the Match and Raw conditions, when the robot dynamically moved and reacted to the participant's intentions, compared to the control condition, Still, when the robot did not show any motion at all. Although Match showed a higher average response compared to Raw, no significant difference between these two conditions was confirmed in Q2. This can imply that in both the Raw and Match conditions the robot's successive motions following the participant's act of motor imagery raised a sense of agency during the session that led to a perception of owning the hands in participants.

Meanwhile, the results of this experiment showed a wide dispersion over the response values of illusion in each condition,

which we presumed is due to the difference of performance level among subjects. A positive correlation was confirmed between participants' performances and their indicated scores for Q1 (**Figure 2D**), which indicates that participants with a better operational performance experienced a stronger illusion of BOT. Therefore, we can tell that subjects' skill in a motor imagery task and BCI performance are associated with the intensity of ownership illusion in such a tele-operational system.

From the obtained results in this experiment, we conclude that in a BCI-teleoperation system for humanlike hands, the feedback presentation could affect the eliciting of ownership illusion over the controlled hands; the illusion was augmented when negative feedback of subject's misperformance was eliminated. Also, a positive correlation was found between the intensity of BOT and subjects' performance, which suggests that subjects with better BCI-performance experienced a stronger illusion. Therefore BOT could be affected both by subjects' BCI-performance, and feedback design, which regulated subjects' perceptions of their own performance. On the other hand, although an intuitive conclusion of this experiment could be that better BCI-performance caused a stronger perception of illusion in subjects, the reverse thought could also be claimed; that is, higher BOT motivated subjects to perform better on the motor imagery task. Therefore, it remains to be clarified how the mutual interaction between performance and BOT is formed and how feedback design contributes to improvement of each element and their interaction (**Figure 3**). Thus, in experiment 2 we focused on the effect of feedback design on a subject's BCI-performance and examined how manipulation of subjects' perceptions of self-performance can affect the trend of their motor imagery learning and BCI-performance.

EXPERIMENT 2

From experiment 1 we found that subjects' perceptions of their own performance was important for the inducement of ownership illusion. Moreover, a close relationship between the intensity of illusion and a subject's performance was found. We were further interested in knowing how the subjects' self-evaluations and subsequent inducement of BOT can directly affect their skills in a motor imagery operational system. Therefore in this experiment, by manipulating the presentation and accuracy of subjects' performances we designed four different feedback conditions including two in which each subjects' performance was positively and negatively biased in the first half of each session. We then examined how conditioning feedback can affect the trend of learning by two methods; (1) measuring subjects' online performance in the second half of sessions and (2) comparing time-variant distribution of EEG features regarding right and left hand imagery in each half of the session.

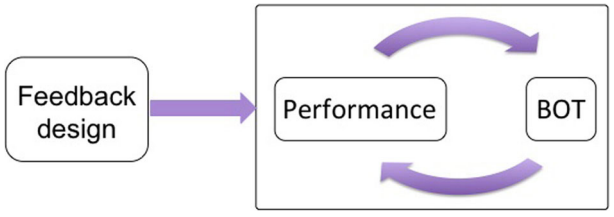

FIGURE 3 | Model diagram for effect of feedback design. Feedback bias can affect the interaction between BCI-performance and BOT illusion.

PARTICIPANTS

Sixteen healthy subjects (6 male and 10 female, age $M = 21.1$, $SD = 1.4$) participated in this experiment. 15 participants were right-handed and one left-handed. None of them had participated in our previous experiments and they were all unfamiliar with the research topic. Participants received explanation prior to the experiment.

METHOD

The BCI devices, preparation procedure and session paradigms of Experiment 2 were identical with Experiment 1, except in this experiment we used a new type of head mounted display (Sony HMZ-T1) for the real time first-person visual feedback (**Figure 1A**).

Participants performed 4 experimental sessions each consisting of 40 imagery trials which lasted 5 min. Each session was followed by a break of 3 min. The first half of each session (20 trials) was randomly conditioned as below:

(1) Raw: Participants' performance was not biased. The robot's hands grasped the ball according to the classification result.
(2) Match: Participants' performance was not biased. However, the robot's hands only grasped the lit ball when the classification results matched the cue.
(3) Positive Feedback (Fake-P): Participants' performance was biased positively. The robot's hands grasped the lit ball correctly in 90% of trials regardless of the subject's real performance.
(4) Negative Feedback (Fake-N): Participants' performance was biased negatively. The robot's hands grasped the lit ball correctly only in 20% of trials regardless of the subject's real performance.

In the first two conditions, Raw and Match (**Figure 1B**), a subject's performance was not biased although the robot's hand motion in mistaken trials differed—one with execution of wrong hand motion and one without robot motion. Raw is an equivalent feedback design of the one used in general motor imagery BCIs where subject's failure in executing motor imagery for one class results in feedbacks of the other class. However, since Raw and Match conditions previously revealed a different level of illusion (Experiment 1) we made the assumption that presentation of negative feedback affects subject's perception of self-performance and therefore influences subject's interaction with the system. To clarify this point, we respectively designed two more sessions (Fake-P and Fake-N) in which we deliberately biased feedback of performance regardless of subjects' real performance accuracy in order to extremely enhance or decrease their self-evaluation. In the second half of all sessions subjects received feedback of their real performance as they did in Raw. The goal was to seek changes in BCI-performance and motor imagery skills in the second half of each session due to the positive or negative bias of

feedback. Subjects' performance in the second half of all sessions was registered.

In addition to subjects' online performance, we conducted an offline re-analysis of data to extract the feature distribution of right and left motor imagery in each session. We speculated that by receiving biased feedback or experiencing illusion, subjects may consciously or unconsciously modify the generation of their brain activity patterns throughout the experiment, although the classifier could fail to detect these changes because it did not use a learning algorithm and once the classification boundary for the two classes, Right and Left, was defined within the feature space in the initial training session, the same classifier and parameters were used to the end of the experiment. Therefore, we used the original brain signals and ran the following offline processing to seek changes in motor imagery patterns.

After artifact removal and temporal filtering (Guger et al., 2000), the features used for classification were obtained by the method of CSP. Having N channels of EEG for each left and right trial $\boldsymbol{X}$, the CSP builds an $N \times N$ projection matrix $\boldsymbol{W}$. With the projection matrix $\boldsymbol{W}$, the mapping of a trial is given as

$$\boldsymbol{Z} = \boldsymbol{WX}$$

The columns of $\boldsymbol{W^{-1}}$ are the CSPs and can be seen as time-invariant EEG source distribution vectors. By design the variance for imagining left hand motion is largest in the first row of $\boldsymbol{Z}$ and decreases with the increasing number of subsequent rows. To obtain reliable features, it is not necessary to calculate the variances of all N time series. The optimal number of CSPs used to build the feature vector is four (Müller-Gerking et al., 1999). Therefore, only the first and last two rows ($p = 4$) of $\boldsymbol{W}$ were used to filter data $\boldsymbol{X}$ and build a new signal $\boldsymbol{Z_p}$ ($p = 1 \ldots 4$). The variance of the resulting four time series is obtained for a time window $T = (t_0, t_1)$

$$\boldsymbol{var_p} = \sum_{t=t_0}^{t_1} \left(\boldsymbol{Z_{p(t)}}\right)^2$$

where window length was set to be 1 s, starting 1500 ms after the presentation of the cue (Pfurtscheller and Neuper, 2001). Feature vectors were obtained after normalizing and log-transforming as following:

$$\boldsymbol{f_p} = \boldsymbol{log}\left(\frac{\boldsymbol{var}\left(\boldsymbol{Z_p}\right)}{\sum_{i=1}^{p} \boldsymbol{var}\left(\boldsymbol{Z_p}\right)}\right)$$

The online classifier uses each trial's feature vector $\boldsymbol{f_p}$ to categorize it into two classes of right and left. In order to estimate the goodness of this classification, we used Fisher's discriminant criterion measures in a linear discriminant analysis to observe the distribution of two classes feature vectors in a 4-dimential space. Fisher's parameter $\boldsymbol{J}$ is defined as

$$\boldsymbol{J} = \frac{\left|\widetilde{\boldsymbol{\mu}}_R - \widetilde{\boldsymbol{\mu}}_L\right|^2}{\widetilde{\boldsymbol{s}}_R^2 + \widetilde{\boldsymbol{s}}_L^2}$$

where $\widetilde{\mu}_R$ and $\widetilde{\mu}_L$ are the means of feature vectors for two right and left classes and the quantity $|\widetilde{\mu}_R - \widetilde{\mu}_L|^2$ is the distance between the two classes' means. For each class $\widetilde{s}_R^2$ and $\widetilde{s}_L^2$ were defined as the scatter, an equivalent of the variance, and obtained by

$$\widetilde{\boldsymbol{s}}_{\boldsymbol{i}}^{\boldsymbol{2}} = \sum_{\boldsymbol{x} \in \boldsymbol{f_i}} \left(\boldsymbol{x} - \widetilde{\boldsymbol{\mu}}_{\boldsymbol{i}}\right)^2$$

The quantity $\widetilde{\boldsymbol{s}}_{\boldsymbol{R}}^{\boldsymbol{2}} + \widetilde{\boldsymbol{s}}_{\boldsymbol{L}}^{\boldsymbol{2}}$ indicates the within-class scatter. When performing motor imagery a larger $\boldsymbol{J}$ corresponds to closer dispersion of feature vectors per each class and further distance between two class means, which represents better feature distribution for classification, and therefore better execution of motor imagery task.

In each session, the $\boldsymbol{J}$ parameter for the first 20 conditioned trials ($\boldsymbol{J_1}$) and for the second 20 test trials ($\boldsymbol{J_2}$) was calculated. Since subjects' initial skills were diverse, and for every subject the order of sessions was considerable in the amount of motor imagery skills, the ratio $\boldsymbol{\Delta J = J_2/J_1}$ was selected as a measurement of subjects' motor imagery learning in that session.

RESULT

Online performance

Performances of 16 subjects in the second half of each session were averaged and demonstrated in **Figure 4A**. The term performance refers to the percentage of successful trials among the post 20 trials. Fake-P ($M = 60.78$, $SD = 10.24$) showed the highest performance compared to Raw ($M = 49.22$, $SD = 9.07$), Match ($M = 54.37$, $SD = 10.89$) and Fake-P ($M = 50.47$, $SD = 10.58$). However, One-Way ANOVA test did not reject the null hypothesis, [$F_{(3,\ 60)} = 2.51, p = 0.07$].

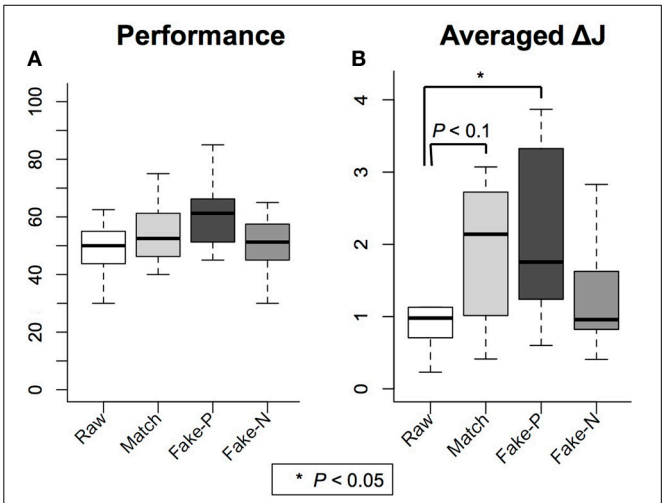

FIGURE 4 | Results for experiment 2 (A) Mean value of subjects' performances in the second half of each session is demonstrated. No significant difference was found. **(B)** Mean value of the ratio $\boldsymbol{J_2/J_1}$, an identifier of motor imagery quality, showed significantly higher values in the Fake-P and Match conditions compared to Raw.

Offline classification

We calculated ΔJ for 16 subjects. Using interquartile range (IQR) for statistical dispersion in each condition (Moore and McCabe, 1998), two outliers were detected in the Fake-N condition (S2 and S4) and one outlier was detected in the Raw condition (S15). The data of these three subjects were discarded from further analysis. The mean value of ΔJ for the remaining 13 subjects was highest in the Fake-P condition ($M = 2.12$, $SD = 1.78$) compared to the other three conditions, Raw ($M = 1.07$, $SD = 0.75$), Match ($M = 1.87$, $SD = 0.95$) and Fake-N ($M = 1.35$, $SD = 0.84$) (**Figure 4B**). A One-Way ANOVA test yielded a significant effect of feedback design for the four conditions, [$F_{(3,\ 48)} = 3.53$, $p < 0.05$]. Using Tukey *post-hoc* comparisons, a significance difference was obtained between Fake-P and Raw; [Fake-P > Raw, $p < 0.05$] and between Match and Raw; [Fake-P > Raw, $p = 0.08$].

DISCUSSION

In experiment 2, we biased the visual feedback of performance in a BCI-teleoperation system of a human-like robot in order to probe the effect of positive and negative feedback on subjects' BCI-performance and motor imagery skills.

Online results demonstrated no significant changes in the subjects' real time performances and the mean value of subjects' performances remained in the chance level for all conditions. On the other hand, results from offline classification revealed that the ratio J_2/J_1, an identifier of class separation between the two halves of sessions, was significantly higher in the Fake-P than in the Raw condition. This indicates that subjects could generate motor patterns that are more classifiable by CSP algorithm by receiving positive feedback of their performance in the Fake-P condition. Using a statistical significance level of 10%, a similar relation was confirmed between Match and Raw conditions, indicating that in the Match condition where subjects did not receive negative feedback of their failed performance, motor imagery improved and they could produce more separable activity patterns for two classes of right and left hand movement. Both results imply that positive bias of feedback had an enhancing effect on motor imagery learning which is consistent with some previous reports (Lotte et al., 2013). One probable cause could be the inducement of a stronger BOT due to biased feedback, which facilitated imagination of movement in motor imagery task and eventually enhanced self-regulation of brain patterns in subjects (**Figure 3**).

Unlike previous reports on biased BCI feedback, no significant improvement (Gonzalez-Franco et al., 2011) or impediment (Barbero and Grosse-Wentrup, 2010) was found in the Fake-N condition compared to other conditions. However, S2 and S4 who were discarded from analysis as outliers showed drastic ΔJ increase in Fake-N. Since subjects majorly received enhanced learning in Fake-P condition, we assume that the effect of biasing is closely relevant to the subject's personality and the influence of motivation on different individuals. While there are learners who benefit from encouragement and positive feedback of their performance, there are a few who benefit more from negative feedback and try harder when the feedback informs them that they are not performing well. In future experiments, a personality test could be used in order to categorize subjects into groups, so that results can be analyzed according to stratified personality groups.

Lastly, although in this experiment we hypothetically assume that enhancement of motor imagery learning due to positive bias of feedback was associated with ownership illusion over the controlled robot's hands (**Figure 3**), further study is required to veritably measure the intensity of illusion at the end of each conditioned section. In this experiment we suspected that pausing the sessions and asking assessment questions could shatter the illusion. In the future, comparison between human-like and non-human-like visual feedback under biased feedback is necessary to precisely verify whether illusion of body ownership influences the trend of motor imagery learning.

CONCLUSION

In this study, we designed two experiments to answer the following questions: (1) How can presentation of visual feedback affect the inducement of body ownership illusion in the BCI-operators of human-like hands, and (2) How can positively and negatively biased feedback in such a system influence operators' interaction with the system and improve their BCI performances. Results of the first experiment revealed that negative feedback of subjects' errors impeded the intensity of ownership illusion. Also BOT was correlated with subjects' performance in BCI and how well subjects felt they were in control of the hands. In the second experiment, we realized that biasing feedback could not immediately boost subjects' performance in the same session. However, the analysis of brain patterns showed that in fact it could change the trend of motor imagery learning.

In terms of feedback design for future BCI systems, it is conceivable that a more realistic feedback presentation can assist novice users to train and adapt to a system faster and more efficiently. Also, BCI users may benefit from positive bias of feedback in training sessions, although their personality should be taken into account. Meanwhile, since subjects motor imagery skills dynamically change during a session based on their state of mind, further development of sophisticated classifiers that customize classification parameters in an online session are required.

ACKNOWLEDGMENTS

This work was partially supported by JSPS KAKENHI Grant Number 25220004 and 24650114.

REFERENCES

Alimardani, M., Nishio, S., and Ishiguro, H. (2013). Humanlike robot hands controlled by brain activity arouse illusion of ownership in operators. *Sci. Rep.* 3:2396. doi: 10.1038/srep02396

Armel, K. C., and Ramachandran, V. S. (2003). Projecting sensations to external objects: evidence from skin conductance response. *Proc. Biol. Sci.* 270, 1499–1506. doi: 10.1098/rspb.2003.2364

Barbero, Á., and Grosse-Wentrup, M. (2010). Biased feedback in brain-computer interfaces. *J. Neuroeng. Rehabil.* 7, 1–4. doi: 10.1186/1743-0003-7-34

Curran, E. A., and Stokes, M. J. (2003). Learning to control brain activity: a review of the production and control of EEG components for driving brain–computer interface (BCI) systems. *Brain Cogn.* 51, 326–336. doi: 10.1016/S0278-2626(03)00036-8

Gonzalez-Franco, M., Peng, Y., Dan, Z., Bo, H., and Shangkai, G. (2011). "Motor imagery based brain-computer interface: a study of the effect of positive and negative feedback," in *Engineering in Medicine and Biology Society (EMBC), Annual International Conference of the IEEE* (Boston, MA), 6323–6326.

Guger, C., Ramoser, H., and Pfurtscheller, G. (2000). Real-time EEG analysis with subject-specific spatial patterns for a brain-computer interface (BCI). *IEEE Trans. Rehabil. Eng.* 8, 447–456. doi: 10.1109/86.895947

Lotte, F., Larrue, F., and Muhl. C. (2013). Flaws in current human training protocols for spontaneous brain-computer interfaces: lessons learned from instructional design. *Front. Hum. Neurosci.* 7:568. doi: 10.3389/fnhum.2013.00568

Moore, D. S., and McCabe, G. P. (1998). *Introduction to the Practice of Statistics, 3rd Edn*. New York, NY: W. H. Freeman.

Müller-Gerking, J., Pfurtscheller, G., and Flyvbjerg, H. (1999). Designing optimal spatial filters for single-trial EEG classification in a movement task. *Clin. Neurophysiol.* 110, 787–798. doi: 10.1016/S1388-2457(98)00038-8

Neuper, C., Scherer, R., Wriessnegger, S., and Pfurtscheller, G. (2009). Motor imagery and action observation: modulation of sensorimotor brain rhythms during mental control of a brain–computer interface. *Clin. Neurophysiol.* 120, 239–247. doi: 10.1016/j.clinph.2008.11.015

Nishio, S., Watanabe, T., Ogawa, K., and Ishiguro, H. (2012). "Body ownership transfer to teleoperated android robot," in *International Conference on Social Robotics* (*ICSR* 2012) (Chengdu), 398–407.

Pfurtscheller, G., and Neuper, C. (2001). Motor imagery and direct brain-computer communication. *Proc. IEEE* 89, 1123–1134. doi: 10.1109/5.939829

Conflict of Interest Statement: The authors declare that the research was conducted in the absence of any commercial or financial relationships that could be construed as a potential conflict of interest.

Received: 02 February 2014; accepted: 21 March 2014; published online: 09 April 2014.
Citation: Alimardani M, Nishio S and Ishiguro H (2014) Effect of biased feedback on motor imagery learning in BCI-teleoperation system. Front. Syst. Neurosci. ***8****:52. doi: 10.3389/fnsys.2014.00052*
This article was submitted to the journal Frontiers in Systems Neuroscience.

frontiers in
SYSTEMS NEUROSCIENCE

ORIGINAL RESEARCH ARTICLE
published: 08 September 2014
doi: 10.3389/fnsys.2014.00143

Gaze-independent ERP-BCIs: augmenting performance through location-congruent bimodal stimuli

Marieke E. Thurlings[1,2]*, Anne-Marie Brouwer[2], Jan B. F. Van Erp[2] and Peter Werkhoven[1]

[1] *Information and Computing Sciences, Utrecht University, Utrecht, Netherlands*
[2] *Perceptual and Cognitive Systems, TNO, Soesterberg, Netherlands*

Edited by:
Mikhail Lebedev, Duke University, USA

Reviewed by:
Dewen Hu, National University of Defense Technology, China
Betts Peters, Oregon Health and Science University, USA

****Correspondence:***
Marieke E. Thurlings, Information and Computing Sciences, Utrecht University, P. O. Box 80.089, 3508 TB Utrecht, Netherlands
e-mail: marieke.thurlings@gmail.com

Gaze-independent event-related potential (ERP) based brain-computer interfaces (BCIs) yield relatively low BCI performance and traditionally employ unimodal stimuli. Bimodal ERP-BCIs may increase BCI performance due to multisensory integration or summation in the brain. An additional advantage of bimodal BCIs may be that the user can choose which modality or modalities to attend to. We studied bimodal, visual-tactile, gaze-independent BCIs and investigated whether or not ERP components' tAUCs and subsequent classification accuracies are increased for (1) bimodal vs. unimodal stimuli; (2) location-congruent vs. location-incongruent bimodal stimuli; and (3) attending to both modalities vs. to either one modality. We observed an enhanced bimodal (compared to unimodal) P300 tAUC, which appeared to be positively affected by location-congruency (p = 0.056) and resulted in higher classification accuracies. Attending either to one or to both modalities of the bimodal location-congruent stimuli resulted in differences between ERP components, but not in classification performance. We conclude that location-congruent bimodal stimuli improve ERP-BCIs, and offer the user the possibility to switch the attended modality without losing performance.

Keywords: BCI, ERP, gaze-independent, bimodal, tactile, multisensory, location-congruency, selective attention

INTRODUCTION

Event-related potential (ERP) based brain-computer interfaces (BCIs) can be used to actively and voluntarily control a system, e.g., for communication (Farwell and Donchin, 1988) or navigation (Bell et al., 2008; Thurlings et al., 2010). ERP-BCIs make use of stimuli that correspond to control options (e.g., "left" or "right"). The user can select an option by attending to the corresponding stimulus (target) while ignoring other stimuli (nontargets). Stimulus-locked brain responses (ERPs) differ between the attended targets and ignored nontargets.

Most ERP-BCIs employ visual stimuli and require the user to gaze at the target stimulus, i.e., such a BCI is *gaze-dependent*. When the user does not directly gaze at the target but only covertly attends to it, the high-level endogenous ERP components but not the low-level perceptual ERP-components differ from those of nontargets. This results in a reduced BCI performance in terms of classification accuracy (and hence bitrate) (Brunner et al., 2010; Treder and Blankertz, 2010). BCIs for which users do not have to gaze at the stimuli or to shift focus (alter viewing direction) in order to control it are called *gaze-independent*. An example is the Hex-o-Spell of Treder and Blankertz (2010). The importance of developing BCIs independent of the ability to shift focus has been expressed in studies investigating the rapid serial visual presentation paradigm (Orhan et al., 2012; Acqualagna and Blankertz, 2013). Yet, in that paradigm participants are required to directly focus at the visual stimuli.

When users cannot reliably direct their gaze, or when other tasks interfere with gaze, stimuli can also be presented in other modalities like the auditory modality (Schreuder et al., 2010, 2011; Höhne et al., 2011). In application domains such as driving and gaming, BCIs must be gaze-independent as gaze is required for control and navigation tasks and the visual (and auditory) channel is already heavily loaded (Van Erp and Van Veen, 2004). The tactile channel has also been suggested as a viable alternative for these situations, and Brouwer and Van Erp (2010) demonstrated the feasibility of employing tactile stimuli around the waist in a tactile ERP-BCI. The natural correspondence of tactile stimuli around the waist with navigation directions (Van Erp, 2005) makes a tactile ERP-BCI especially interesting for navigation applications.

BCI performance of tactile ERP-BCIs (Brouwer et al., 2010; Thurlings et al., 2012a,b) is generally lower than that of gaze-dependent BCIs (Thurlings et al., 2012a,b). In addition, when a BCI is used as a control device in the context of a dual-task, for example to navigate in a game, BCI performance is even lower than in BCI-only tasks (Thurlings et al., 2013). Therefore, in order to achieve effective use of BCI outside the lab, it is highly important to increase BCI performance of gaze-independent BCIs.

This study focusses on potential benefits regarding brain activity resulting from stimulus presentation in multiple sensory modalities, using a gaze-independent setup, and addresses

three main research questions which are introduced in the next sections.

THE BIMODAL ERP-BCI

The processing and integration of multisensory stimuli is likely to cause additional neuronal activity (Ernst and Bülthoff, 2004; Driver and Noesselt, 2008; Stein and Stanford, 2008). Integration may take place at perceptual stages (Molholm et al., 2002; Philippi et al., 2008), higher cognitive stages (Schröger and Widmann, 1998), and/or during motor preparation and execution (Giray and Ulrich, 1993). Bimodal stimuli generally yield faster behavioral responses and more accurate perceptual discrimination (Gondan et al., 2005; Teder-Sälejärvi et al., 2005; Philippi et al., 2008).

Multisensory integration has extensively been investigated in cognitive science, but has barely received attention in the field of BCI. In a recent BCI-study, we showed that an additional (early) ERP component was present when participants were presented with and attended to stimuli in two modalities rather than one, due to multisensory interaction (Thurlings et al., 2012a). To the best of our knowledge, only two other BCI-related studies investigated bimodal stimuli: visual-tactile stimuli (Brouwer et al., 2010), and audio-visual stimuli (Belitski et al., 2011). In both studies the authors reported increased classification accuracies (i.e., the percentage of correctly classified target responses) for bimodal compared to unimodal conditions, which is in line with the trend we reported in Thurlings et al. (2012a).

Multisensory or bimodal ERP-BCIs can be regarded as a type of hybrid BCIs (Pfurtscheller et al., 2010a). Hybrid BCIs are BCIs that "can either process their inputs simultaneously, or operate two systems sequentially". By allowing the processing of two inputs simultaneously, the second input could improve the classification accuracy of the first BCI (Pfurtscheller et al., 2010a; Yin et al., 2013).

As motivated in the beginning of the introduction, we are interested in multisensory BCIs, as a way to potentially increase BCI performance of (traditional) unimodal ERP-BCIs, in particularly the gaze-independent variants. From the three above mentioned bimodal studies, only Brouwer and Van Erp (2010) used a gaze-independent setup with visual-tactile stimuli. However in that study the effects on target and non-target responses of endogenous (voluntary) attention and exogenous (stimulus driven) attention were confound. Both endogenous and exogenous attention can affect ERP components (Woldorff and Hillyard, 1991), but only endogenous attention is relevant for BCI operation. Thus, the question whether or not gaze-independent ERP-BCIs benefit from bimodal stimulus presentation remains unanswered.

Multisensory integration has been shown to start as early as 80–120 ms after stimulus onset for visual-tactile stimuli (Sambo and Forster, 2009), but is modulated by endogenous attention at different stages of processing (Talsma and Woldorff, 2005). As reported in Thurlings et al. (2012a), positive effects of bimodal stimulus attending have been shown on an early stage of processing, i.e., early negative activity (N1) in the difference ERP (target minus nontarget ERP) was stronger for the bimodal compared to the unimodal conditions. However, we observed negative effects of bimodal stimulus attending on a late stage of the ERP, i.e., positive late activity (P300) in the difference ERP was stronger for one of the unimodal conditions (visual) compared to the bimodal condition. We hypothesized that the latter effect was caused by the spatial relation of the two unimodal stimuli that formed a bimodal stimulus pair. More specifically, although the spatial relation unambiguously indicated which unimodal stimuli formed a pair, those stimuli were not co-located. Possibly, this affected spatial attention and top-down stimulus processing. Therefore in the present study we focus on co-located (i.e., location-congruent) bimodal stimuli, with the expectation to lose the negative effects on late ERP components.

Thus, our first research question is: Are ERP components (quantified in the topographic Area Under the Curve or tAUC; Thurlings et al., 2012a,b) and corresponding classification accuracies of a bimodal visual-tactile ERP-BCI enhanced compared to its unimodal counterparts? We hypothesize enhanced bimodal ERP tAUCs both on early and late stages of processing when employing location-congruent bimodal stimuli in a gaze-independent setup, which should result in enhanced classification accuracies.

EFFECTS OF LOCATION-CONGRUENCY ON THE BIMODAL ERP-BCI

In case we find a benefit of bimodal compared to unimodal stimulus presentation and attending, as hypothesized in the previous section, it is relevant to know whether or not that effect depends (partly) on the spatial relation within the bimodal stimulus pairs. This is important for the designing of bimodal ERP-BCIs, especially since the most straightforward design might employ location incongruent bimodal stimulus pairs as in Thurlings et al. (2012a). In that study, a display presented visual navigation information and included visual stimuli located at the possible navigation directions. Tactile stimuli were presented around the waist, corresponding with navigation directions around us. To make the spatial relation as congruent as possible in that setup, the display was oriented in the horizontal plane, to match the horizontal lay-out of the tactile stimuli (Thurlings et al., 2012b). Therefore the bimodal stimulus pairs were directional-congruent, but not location-congruent. We showed in Thurlings et al. (2012a) that location-incongruency resulted in negative effects of bimodal (compared to unimodal) stimulus attending on a late stage, while effects on the early stage were positive (see previous section).

Literature on the effects of location-congruency is not unequivocal. According to the spatial rule (Meredith and Stein, 1986), stimuli from different modalities are only integrated when stimuli are spatially co-located (or proximate). Stein et al. (1989) showed for example that the performance of animals that were trained to approach visual stimuli is improved when matched with (unattended) auditory stimuli, but only if the visual-auditory stimulus pairs were spatially co-located (or proximate). Frassinetti et al. (2002) replicated these results in humans. However, also when bimodal stimulus-pairs are not location-congruent, behavior performance has been found to be enhanced (Gondan et al., 2005; Teder-Sälejärvi et al., 2005; Philippi et al., 2008). These studies differ in tasks, but have in common that

the task does not enforce selective attention to one modality (as in the studies of Meredith and Stein), but rather both modalities need to be attended. Apparently the role of the spatial relation within multisensory information and if and how it affects multisensory integration depends on the specific circumstances (We address the role of selective attention to modality in the next section). Nevertheless, also when bimodal benefits are found for location-incongruent bimodal stimuli, behavioral performance may be further improved by location-congruency (Gondan et al., 2005). Teder-Sälejärvi et al. (2005) did not observe such a behavioral benefit, but did report differences in the ERP for location-congruent and location-incongruent bimodal stimuli after 100 ms. They concluded that there are overlapping and distinct processes involved in processing of location-congruent and incongruent stimuli.

Multisensory studies typically involve a task that requires participants to distinguish targets from nontargets based on physical stimulus characteristics, instead of on (only) spatial differences such as is the case in a BCI-setup (which uses spatial selective attention). Possibly, the role of the spatial relation is larger when the task is only based on spatial discrimination. Therefore it is important to study the role of the spatial relation of bimodal stimuli in ERP-BCIs.

Our second research question is: What is the effect of location-congruent compared to location-incongruent bimodal stimuli on the ERP tAUCs and corresponding classification accuracies in an ERP-BCI? We hypothesize positive effects for location congruent bimodal stimuli at late stages (e.g., P300 tAUC) of stimulus processing, which should correspond to enhanced classification accuracies.

EFFECTS OF SELECTIVE ATTENTION TO MODALITY ON THE BIMODAL ERP-BCI

Both exogenous and endogenous attention affect the ERP (Eimer et al., 2001). When participants are presented with bimodal stimuli, but they endogenously attend to either one or both modalities, exogenous attention involved in both cases is the same (as the physical characteristics have not changed). However, the amount of attentional resources allocated endogenously for processing the stimulus information of the two modalities involved differs between these cases (Macaluso, 2010). For example, when participants are precued and (pre)attending to the visual rather than the auditory modality, audio-visual stimuli are processed differently, resulting in enhanced early activity starting around 110 ms and peaking around 150 ms (Foxe and Simpson, 2005). Talsma et al. (2007) showed that for the earliest multisensory integration effect (a superadditive effect) of audiovisual stimuli to occur, both modalities need to be attended. Nevertheless, if only a single modality was attended integration still occurred but the process appeared to start later (after 250 ms after stimulus onset) and was dependent on which modality was attended.

Users of a bimodal ERP-BCI could choose to attend to either one or both modalities, which could affect the resulting ERP and may require modality-specific trained classifiers for optimal performance. In this study, we investigated the trade-off between possibly affected classification accuracies (when a bimodal classifier trained with attending to both modalities is used also when only one modality is attended to) and the advantage of the flexibility offered to the user to choose the modality to attend to.

Our third research question is: Does, and if so how does, attending to the visual or tactile modality, or both modalities affect ERP components' tAUCs and corresponding classification accuracies in a bimodal ERP-BCI? We hypothesize that when both modalities (as opposed to either one alone) of bimodal (location-congruent) stimuli are attended, the early stage of the bimodal ERP tAUC is enhanced. Such an enhancement of the ERP tAUC could also result in enhanced classification accuracies.

Following up on the third main research question, a subquestion is: (3a) How do these classification accuracies depend on the degree of overlap in the attended modalities of the datasets during training and classification. That is, would it be possible to switch the attended modality during use, or does the classifier then need to be retrained? We hypothesize that classification accuracies are negatively affected if the applied classifier is trained on data with a different attended modality than the data that are being classified. When attended modalities during training and classifying partly overlap (i.e., visual and bimodal, or tactile and bimodal) higher classification accuracies are expected than when they do not overlap (i.e., visual and tactile).

MATERIALS AND METHODS

PARTICIPANTS

Ten students voluntarily participated in this study. Participants were aged between 22 and 26 years (mean age 23.5 years). All participants were male and had normal or corrected-to-normal vision. None had previously participated in a BCI-experiment and one was left-handed. The participants signed informed consent forms.

TASK

The task was to select one of two possible control options: left or right. In this study we used the index fingers to present stimulus information, in contrast to locations around the waist (corresponding to navigation directions around us) used in our previous tactile studies. The reason is that we here focus on a gaze-independent and location-congruent setup of bimodal stimuli, and participants should be able to comfortably perceive visual and tactile information from the same location(s). Because the bimodal stimuli should in addition be located at equal distances and angles from fixation, we opted to only employ two bimodal stimuli.

The two control options were presented sequentially in random order, at the left and right index finger through a tactile actuator, an LED, or both. To select an option, participants had to attend to a target stimulus location and modality, and count the number of tactile, visual or visual–tactile activations at that location. At the beginning of each trial the current target (i.e., a combination of finger and modality) was indicated by means of a short activation of the particular target stimulus. Participants were instructed to attend to all targets (and count them internally), and ignore nontargets. Within one trial, each control option (target and nontarget) was activated 10 times.

Note that although ERP-BCIs typically make use of more than two control options (i.e., more than one nontarget), Brouwer and Van Erp (2010) have shown that the P300 is also elicited in a 2-class tactile BCI and operation is not significantly reduced compared to a 4- or 6-class BCI.

DESIGN

The experiment involved six conditions, named after the type of stimuli and attended modality involved. In four conditions targets had to be attended in the modalities that the stimuli of that condition were presented in (no selective attention to modality): Visual, Tactile, Bimodal, Bimodal-Incongr (i.e., short for "Incongruent"). In the Bimodal condition a control option consisted of the simultaneous activation of a visual and tactile actuator at the same finger, while for Bimodal-Incongr a visual and tactile actuator of opposite fingers were matched. In the two other conditions, only one modality had to be attended, while bimodal (location-congruent) stimuli were presented. For attending the visual or tactile modality, the conditions were named: Bimodal-Att-V and Bimodal-Att-T, respectively. The order of the conditions was counterbalanced over participants.

Each condition consisted of three sets. In each set, each of the two control options was designated as the target three times, i.e., there were six trials. Each trial consisted of 10 consecutive repetitions of the control options in random order, i.e., in each set there were 60 target and 60 nontarget activations. The data of the first two sets (the training sets) were used for the training of a classifier, which was applied to classify the data in the third set (the test set). Online BCI-feedback was given to participants in the test set about which stimulus was classified as the target. The training (but not the test) set was also used for the analysis of participants' ERP components.

MATERIALS

General

An actuator pair, consisting of a tactile vibrator and a visual LED, was attached with Velcro to each index finger (22 degrees from a fixation cross). The target and nontarget stimuli consisted of a single pulse with a pulse duration of 187.5 ms. The interval between pulses was 437.5 ms. To indicate the designated target control option at the beginning of a trial and the classified control option for BCI-feedback at the end of a trial, a 2 s and a 1 s single pulse were presented, respectively.

Stimuli

Tactile stimuli: The tactile stimuli were presented through a vibrating element called a tactor. The tactors were custom built and consisted of a plastic case with a contact area of 1 × 2 cm containing a 160 Hz electromotor (TNO, The Netherlands, model JHJ-3, see: Van Erp et al., 2007). To prevent participants from perceiving auditory information from the tactors, they listened to pink noise via speakers during the experiment in all conditions.

Visual stimuli: Visual stimuli were presented through two white LEDs of 5 mm, 3.2 V.

Bimodal stimuli: For all bimodal conditions, except for Bimodal-Incongr, bimodal stimuli consisted of the simultaneous activation of the visual and tactile stimulus on the same index finger (location-congruent). For the Bimodal-Incongr condition, the visual stimulus of one index finger and the tactile stimulus of the other index finger were activated simultaneously.

EEG recording equipment

EEG was recorded from eight linked-mastoids-referenced scalp electrodes (F_z, C_z, P_z, O_z, P_3, P_4, PO_7, PO_8) that used a common forehead ground (g.Tec medical engineering, GmbH). The impedance of each electrode was below 5 kΩ, as was confirmed prior to and during the measurements. EEG data were recorded with a hardware filter (bandpass 0.1–60 Hz, notch at 50 Hz) and sampled at a frequency of 256 Hz.

DATA ANALYSIS

EEG preprocessing and selection

To prepare the recorded EEG for ERP-analysis, we followed similar procedures as taken in Thurlings et al. (2012a,b): selecting (non)target responses, baseline correction, threshold rejection of responses, and computation of a difference ERP. However, the data were not additionally low-pass filtered (the relatively large band was chosen because of potential multisensory effects in the 30–60 Hz band).

Selecting (non)target responses: For ERP-analysis, both target and nontarget responses were used when preceded by a nontarget. Responses preceded by a target were discarded (i.e., there were no (other) targets presented between −625 and 625 ms relative to (non)target onset) (see also Treder and Blankertz, 2010).

Baseline correction: For the selected targets and nontargets, epochs from all electrodes were extracted from −100 to 625 ms relative to stimulus onset and baseline corrected relative to the average voltage during the 100 ms preceding the stimulus onset.

Threshold rejection of responses: We discarded epochs from all electrodes belonging to a certain stimulus, if any epoch contained amplitude differences exceeding 100 μV, indicating movement artifacts. On average, the previous steps left us with 58.8 target epochs (with a range over participants and conditions from 35 to 70) and 54.0 nontarget epochs (with a range over participants and conditions from 32 to 67). Subsequently, the selected target and nontarget epochs were averaged per participant, per condition and per electrode.

Difference ERP: We subtracted the averaged clean nontarget epochs from the averaged clean target epochs for each participant, each condition and each electrode. With this step, we removed exogenous (involuntary or automatic) attention effects. Further analyses were performed regarding this difference ERP (or endogenous ERP).

Identifying and quantifying ERP components

To identify and quantify ERP components triggered by endogenously attended stimuli, we applied the detection method as reported in Thurlings et al. (2012a,b). Only data of the training set was used, to prevent influence of BCI feedback. We identified significant effects of attending stimuli by performing a sample-by-sample *t*-test on the difference ERP (between 0 and 625 ms relative to (non)target onset) for each electrode and condition and clustered the stable segments (i.e., in this case at least seven consecutive significant samples; see also: Guthrie and Buchwald,

1991). Clusters were considered robust if they contained segments of at least two electrodes. These robust clusters defined the topographic distribution and the interval of the endogenous ERP components, taking the beginning of the earliest segment and the ending of the latest segment in the clusters as ERP component intervals.

We quantified the endogenous ERP components by using the tAUC-value (topographic Area Under the Curve), as described in Thurlings et al. (2012a,b). The tAUC reflects the magnitude of an ERP component not only by taking the averaged amplitude and duration of the component into account but also by considering the topographic distribution.

Online and offline BCI performance

Classification accuracies were calculated both online and offline. Online analysis was performed using BCI2000 (Schalk et al., 2004), which made use of SWLDA (stepwise linear discriminant analysis) on epochs from 0–797 ms after stimulus onset, decimation factor 4 (i.e., 64 Hz), and other standard parameters (maximum of 60 features, p-values initially included and backward excluded from the model <0.1 and >0.15 respectively; see Krusienski et al., 2008). The classifier was trained using the training set for each participant and for each condition.

We investigated classification accuracies more detailed offline. Standard classification parameters are based on visual ERP-BCI research. We established potentially more appropriate parameters for bimodal BCIs, and using those parameters assessed the results of the research questions in practical use. To this end, for all conditions we executed a parameter sweep with all combinations of decimation factors (between 4 and 26), and the number of blocks of downsampled windows (between 1 block and the maximum number of blocks approaching a correspondence of 800 ms). The parameter-pair resulting in the highest overall classification accuracies (averaged over all six conditions) after 10 repetitions was selected for further analyses. Then for each condition, we calculated accuracies after each repetition and established the number of repetitions which is expected most appropriate in practical use. We considered the number of repetitions the most appropriate, when classification accuracies of 70% or higher were achieved using a minimal number of repetitions (Kubler et al., 2004; Birbaumer and Cohen, 2007; Pfurtscheller et al., 2010b).

For all conditions, classification accuracies were determined by classifying the test set using a classifier trained on the training set. Additionally, to assess what the costs on BCI performance are of switching attended modality during BCI operation, analysis was done cross-conditionally: that is, for each of the conditions Bimodal, Bimodal-Att-V, and Bimodal-Att-T, the test set was classified using a classifier trained on the test set of each of the other two conditions. From the nine resulting classes of responses, we clustered three categories: (1) trained and tested on data of the same condition ("Equal"); (2) trained and tested on data of two different conditions, but with an overlap in the attended modality (e.g., trained on Bimodal, tested on Bimodal-Att-V; attending of the visual modality is overlapping) ("Overlap"); and (3) trained and tested on data of two different conditions, but without an overlap in the attended modality (e.g., trained on Bimodal-Att-V, tested on Bimodal-Att-T ("No Overlap"). Within each category the included classes were averaged per participant.

Statistical analysis

ERP components' tAUC-values and classification accuracies were statistically analyzed using Statistica 8.0 (StatSoft, Tulsa, USA). To test for normality Shapiro-Wilk tests were applied, and when normality could not be assumed the data were log-transformed. We used separate one-way repeated-measures ANOVAs to examine different subsets of data appropriate to answer each of the three research questions when comparing three conditions, and paired t-tests when comparing two conditions. The dependent variables were tAUCs and classification accuracies. For the three main research questions, the independent variables were: (1) Bimodality (three levels: Visual, Tactile, Bimodal); (2) Location-Congruency (two levels: Bimodal, Bimodal-Incongr); and (3) Attending Modality (three levels: Bimodal, Bimodal-Att-V, Bimodal-Att-T). For sub-question (3a) the dependent variable was classification accuracies, and the independent variable was Cross-training (three levels: Equal, Overlap, No Overlap). Tukey *post-hoc* tests were applied when appropriate.

PROCEDURE

After the participant was verbally instructed and had read and signed the informed consent form, we attached the visual-tactile actuator pairs on his index-fingers using Velcro. The participant was seated in a dimly lit, electromagnetically shielded room and positioned his arms on the desk in front of him. We allowed the participant to become accustomed to the stimuli, by activating them for several minutes. The participant was asked to gaze at the fixation cross in front of him on the table.

During EEG preparation, we repeated the outline of the experiment and instructed the participant to move as little as possible during stimulus presentations. Before each condition, we informed the participant about the oncoming condition. When the participant indicated to be ready to begin, we started the condition. In the test sets, online BCI feedback was given after each trial (i.e., the 10th repetition). Each condition (including two training and one test recording) took approximately 3.8 min recording time. Conditions followed each other with 1–15 min breaks in between, depending on the participant's preferences.

RESULTS

First we describe the general observed results (General) considering ERP components and BCI performance for each condition. Subsequently, the effects for each of the three main research questions (regarding the effects of bimodality (The effect of Bimodality), location-congruency (The effect of Location-Congruency), and selective attention to modality (The effect of Selective Attention to Modality)) are reported both with respect to ERP components and classification accuracy. Additionally, the effect of the sub-question of the third main research (addressing the effect of Cross-training) is presented in terms of classification accuracies (Classification accuracies of Cross-training (attended modality cross classifier)).

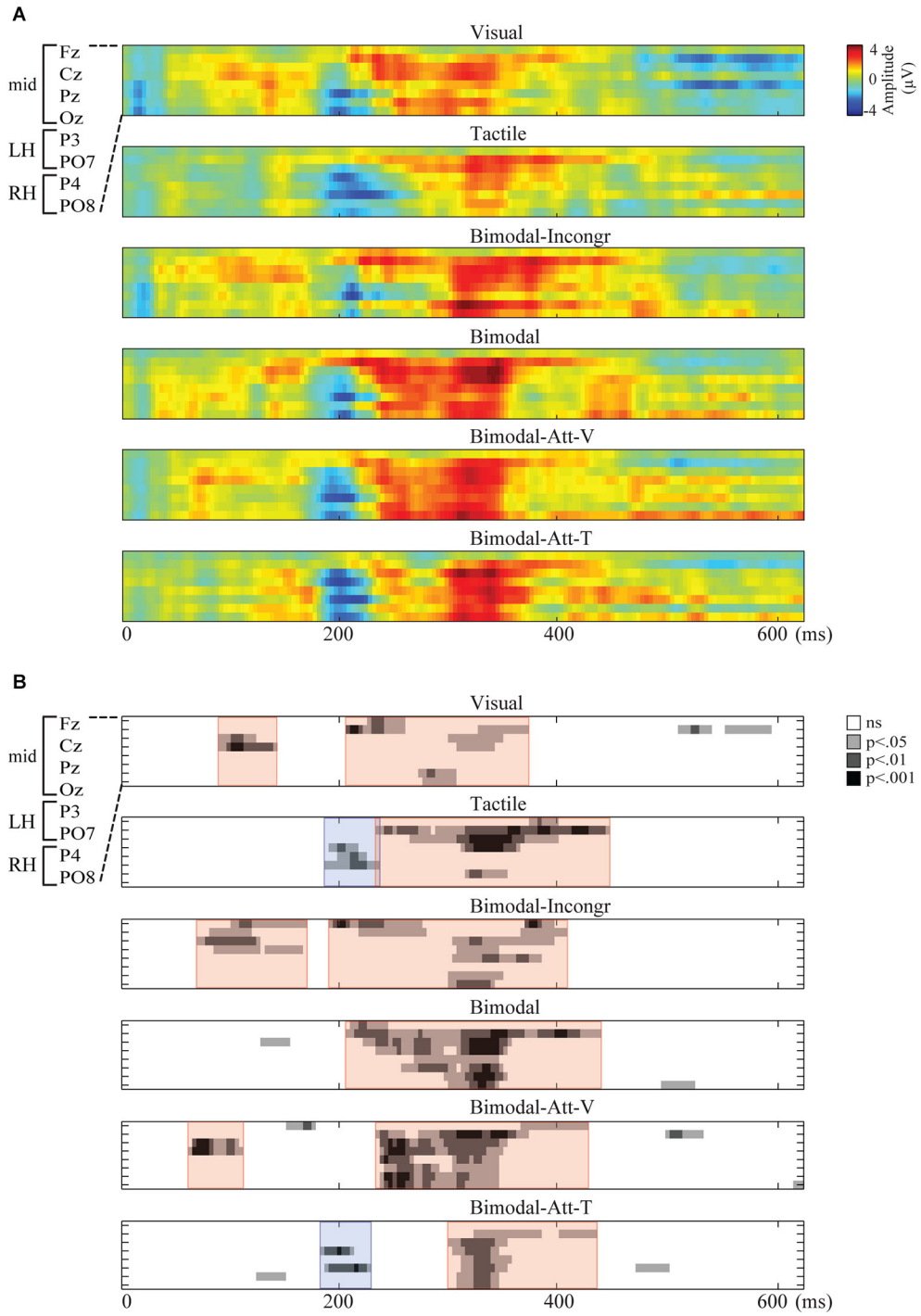

FIGURE 1 | Spatiotemporal representations of the endogenous ERP for each condition, with time (ms) on the x-axis and electrodes on the y-axis. Electrodes from top to bottom: F_z, C_z, P_z, O_z, P_3, P_4, PO_7, PO_8. **(A)** The Grand Average of the amplitudes of the endogenous ERP (μV) for each condition. **(B)** The statistical significance of the endogenous ERP (*p*-values) resulting in stable segments, clustered in ERP components. ERP components are marked by colored overlays in red and blue for positive and negative components, respectively.

GENERAL

Endogenous ERP components

Spatiotemporal presentations of the amplitudes of the endogenous ERPs are presented in **Figure 1A**. For all conditions, endogenous activity was observed during one or two periods within the analyzed interval from 0 until 625 ms after stimulus onset. In **Figure 1B**, spatiotemporal plots show the significant stable segments. The red and blue areas in that figure indicate

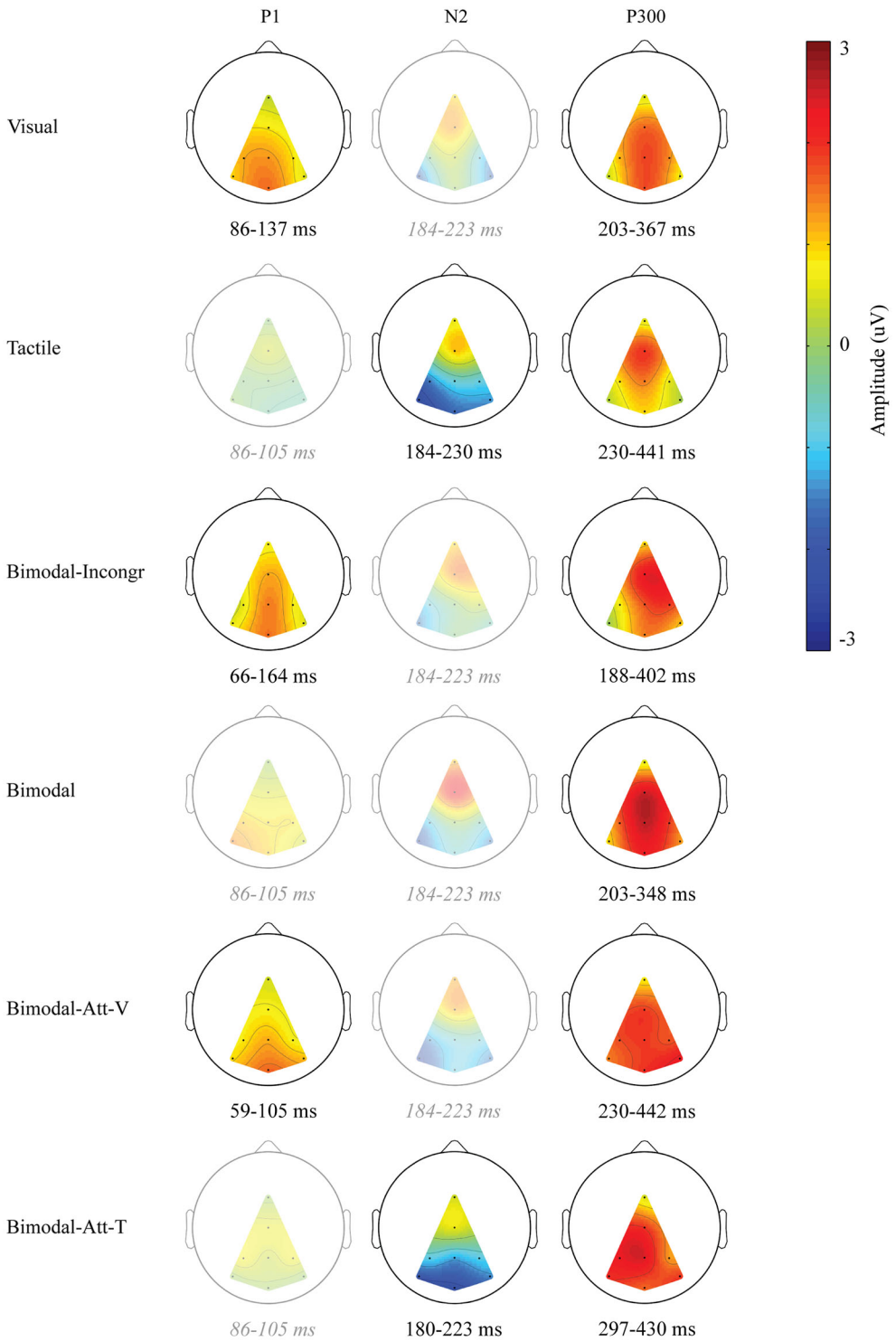

FIGURE 2 | Scalp distributions of the endogenous ERP for the identified endogenous ERP components. Only that part of the scalp is visualized, in which electrode information could be interpolated. Amplitudes (μV) are averages calculated within each ERP component's interval, averaged over participants. If no ERP component was identified, the overlapping interval (of the windows of the ERP component for conditions in which it was identified) was used to visualize that activity for comparison. In that case, the scalp plot is left semitransparent, and the corresponding interval is shown in gray and italics.

the polarities (positive and negative, respectively) of the clustered segments that were found to be robust and were thus identified as endogenous ERP components.

As apparent from **Figure 1B**, only one endogenous ERP component was identified in all six conditions: the P300. In **Figure 2**, the ERP components are visualized by means of scalp plots (averaged amplitudes of the endogenous ERP at all electrodes, within the ERP components' intervals). The P300 amplitudes were largest in the central-parietal area, it appeared to be the strongest in the Bimodal and Bimodal-Att-V conditions, and the weakest for the Visual condition. The windows in which the P300 was detected were: 203–367 ms (Visual), 230–441 ms (Tactile), 188–402 ms (Bimodal-Incongr), 203–348 ms (Bimodal), 230–442 ms (Bimodal-Att-V), and 297–430 ms (Bimodal-Att-T) after stimulus onset.

Furthermore, early positive activity was detected and identified as P1 for the Visual, Bimodal-Att-V and Bimodal-Incongr conditions, in the windows 86–137 ms, 59–105 ms, and 66–164 ms respectively, after stimulus onset. For the Tactile and Bimodal-Att-T conditions a different early component was detected. Early negative activity was identified as an N2 in the windows 184–230 ms, and 180–223 ms respectively after stimulus onset.

The complete ERPs are visualized for each condition for electrode P_z in **Figure 3** (grouped per research question). The main effect of conditions on the ERP components' tAUC-values are visualized in **Figures 5A–C**.

BCI performance

A parameter-sweep was performed for combinations of decimation factors and the length of the epoch used (divided into blocks of downsampled windows). The parameter-pair of decimation factor 5 (i.e., 51.2 Hz) and epoch length of 625 ms resulted in the highest overall classification accuracies of 82.2% (SD: 11.1) over conditions. Thus, these parameters were further used for offline analysis.

Both online and offline classification accuracies are visualized in **Figure 4**. Overall classification accuracies (averaged over participants) are highest for all bimodal conditions employing location-congruent stimuli (i.e., Bimodal, Bimodal-Att-V, and Bimodal-Att-T). For all conditions offline classification accuracies increase with each repetition, except for the Bimodal-Incongr condition. After six repetitions, the averaged classification accuracies for five out of the six conditions exceeded the threshold of 70% necessary for effective control. For the Bimodal-Incongr condition this threshold was not reached at all. Therefore the sixth repetition is considered the most appropriate to assess effects of all research questions in a practical setting, and was used for statistical analysis.

THE EFFECT OF BIMODALITY

ERP components' tAUCs

The P300 tAUC (**Table 1**) was significantly affected by Bimodality ($F_{(2,18)} = 23.93$, $p < 0.001$). The P300 tAUC was larger for the Bimodal condition compared to both unimodal conditions (both $p < 0.001$), and did not differ significantly between the unimodal conditions (**Figure 5A**).

The P1 was only identified for the Visual condition (neither for Tactile nor for Bimodal) and the P1's tAUC (**Table 1**) differed significantly from 0 ($t_{(9)} = 6.69$, $p < 0.001$).

The N2 was only identified for the Tactile condition (neither for Visual nor for Bimodal) and the N2's tAUC (**Table 1**) differed significantly from 0 ($t_{(9)} = 6.41$, $p < 0.001$).

Classification accuracies

The effect of Bimodality on classification accuracies was significant ($F_{(2,18)} = 7.30$, $p < 0.01$), with higher accuracies for Bimodal compared to Visual ($p < 0.05$) and Tactile ($p < 0.01$) (**Figure 5D**).

THE EFFECT OF LOCATION-CONGRUENCY

ERP components' tAUCs

An increased P300 tAUC (**Table 1**) for Bimodal compared to Bimodal-Incongr approached significance ($t_{(9)} = 2.19$, $p = 0.056$) (**Figure 5B**).

The P1 was only identified for the Bimodal-Incongr condition (not for Bimodal) and the P1's tAUC (**Table 1**) differed significantly from 0 ($t_{(9)} = 5.91$, $p < 0.001$).

Classification accuracies

An effect of Location-Congruency on classification accuracies was found, with higher accuracies for Bimodal compared to Bimodal-Incongr ($t_{(9)} = 3.88$, $p < 0.01$) (**Figure 5E**).

THE EFFECT OF SELECTIVE ATTENTION TO MODALITY

ERP components' tAUCs

The P300 tAUC was significantly affected by Modality ($F_{(2,18)} = 7.50$, $p < 0.01$). The P300 was stronger for the Bimodal and Bimodal-Att-V conditions compared to the Bimodal-Att-T condition ($p < 0.05$ and $p < 0.01$, respectively) (**Figure 5C**).

The P1 was only identified for the Bimodal-Att-V condition (neither for Bimodal-Att-T nor for Bimodal) and the P1's tAUC (**Table 1**) differed significantly from 0 ($t_{(9)} = 8.19$, $p < 0.001$).

The N2 was only identified for the Bimodal-Att-T condition (neither for Bimodal-Att-V nor for Bimodal) and the N2's tAUC (**Table 1**) differed significantly from 0 ($t_{(9)} = 6.20$, $p < 0.001$).

Classification accuracies (attended modality specific classifier)

For the attended modality specific classifier, the data used for training of the classifier and for the actual classification are recorded under the same attending-modality conditions (using bimodal location-congruent stimuli only).

No effect of Attending Modality on classification accuracies was found (**Figure 5F**).

Classification accuracies of Cross-training (attended modality cross classifier)

In this subsection the results of sub-question 3a are reported. For the attended modality cross classifier, training of the classifier occurred for each of the attending-modality conditions, and the resulting classifier was used to cross-classify the data of each of the attending-modality conditions.

FIGURE 3 | Grand average of the endogenous ERP. The averaged endogenous ERP is visualized for electrode P_z for each condition included in the comparison for each research question.

Table 1 | Mean and standard errors averaged over participants of the tAUC-values (μV*ms) of all identified ERP components for each condition.

ERP Component	Visual	Tactile	Bimodal-Incongr	Bimodal	Bimodal-Att-V	Bimodal-Att-T
P1	37.6 (17.8)		92.3 (49.4)		36.4 (14.1)	
N2		56.5 (27.9)				44.4 (22.7)
P300	168.9 (63.5)	237.0 (73.4)	351.3 (140.9)	526.7 (223.3)	534.7 (125.4)	265.2 (168.0)

Table 2 shows the results of the cross-condition classification analyses. In **Figure 5G** the effect of Cross-training on the clustered categories is visualized. Cross-training affected classification accuracies ($F_{(2,18)} = 4.86$, $p < 0.05$), with higher accuracies for Equal compared to No Overlap ($p < 0.05$).

DISCUSSION

THE EFFECT OF BIMODALITY

The first and main research question addressed in this study was: Are ERP components' tAUCs and corresponding classification accuracies of a bimodal visual-tactile ERP-BCI enhanced

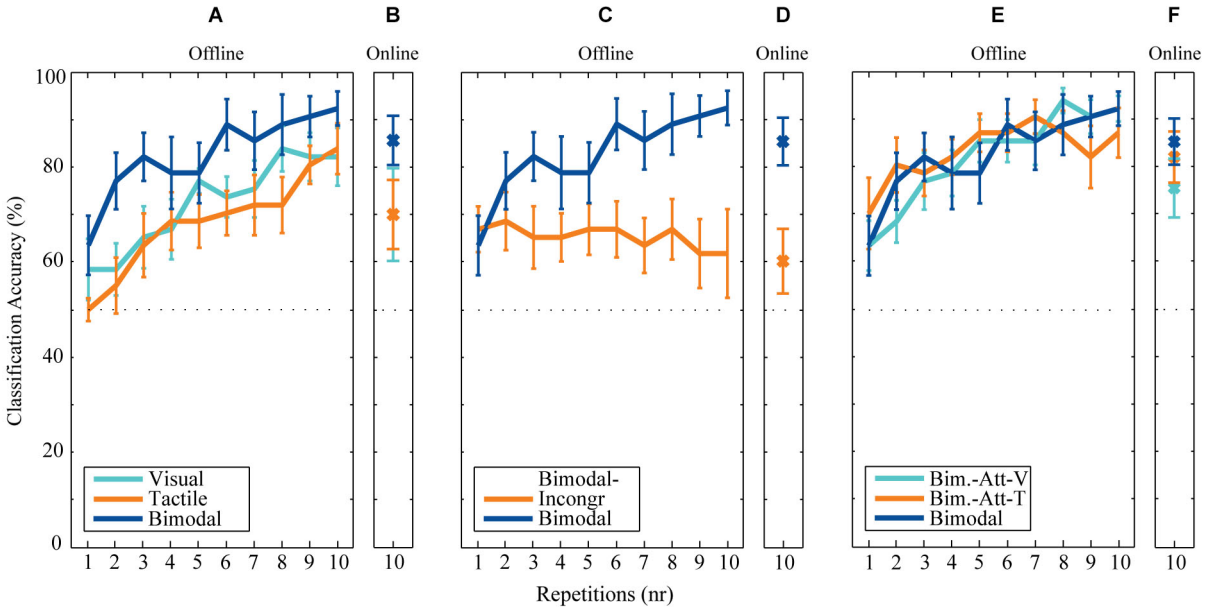

FIGURE 4 | Offline and online classification accuracies. (A) Offline and **(B)** online classification accuracies after each repetition for the conditions involved in the analysis of the first research question (the effect of Bimodality). **(C)** Offline and **(D)** online classification accuracies after each repetition for the conditions involved in the analysis of the second research question (the effect of Location Congruency). **(E)** Offline and **(F)** online classification accuracies after each repetition for the conditions involved in the analysis of the third research question (the effect of Attending Modality).

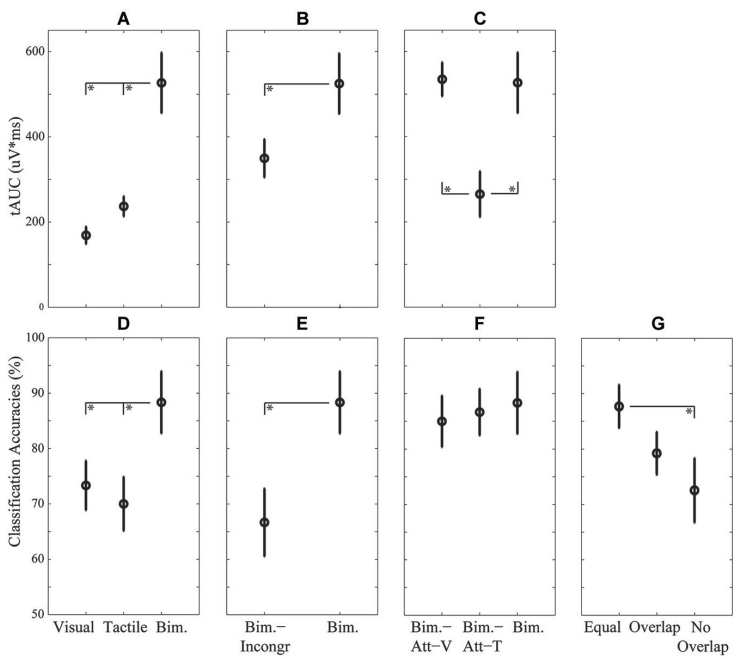

FIGURE 5 | Mean and standard errors over participants of the P300 (A–C) and classification accuracies (D–G), for each research question: the effect of modality (A,D), the effect of location-congruency (B,E), the effect of selective attention to modality (C,F), and the effect of cross-training (G). Condition pairs that significantly differed from each other are indicated by an asterisk (*) symbol.

Table 2 | Classification accuracies (averages and standard deviations) for each class of cross-conditional classification.

Tested on	Trained on Bimodal	Bimodal-Att-V	Bimodal-Att-T
Bimodal	83.33 (17.66)*	76.67 (21.08)^	80.00 (18.92)^
Bimodal-Att-V	81.67 (12.30)^	85.00 (14.59)*	73.33 (14.05)#
Bimodal-Att-T	76.67 (17.92)^	71.67 (26.12)#	86.67 (13.15)*

*Symbols ∗∧# indicate which classes are categorized together, with * for Equal, ^ for Overlap, and # for No Overlap.*

compared to its unimodal counterparts? As we hypothesized, we found an enhanced late effect on the ERP (P300 tAUC) and corresponding enhanced classification accuracies for the location-congruent bimodal compared to the unimodal conditions, using a gaze-independent setup. In our previous bimodal work (Thurlings et al., 2012a), we did not find an enhanced bimodal P300. Instead, the bimodal P300 was even decreased compared to the visual P300. We hypothesized that effect to be a result of location-incongruent bimodal stimuli, as the P300 is affected by spatial attention (Kramer and Strayer, 1988). In this study, we showed that attending to (location-congruent) bimodal (compared to unimodal) stimuli does indeed result in an increasement of the P300 tAUC. The different findings in these two studies hint that location-congruency may indeed affect the processing of bimodal stimuli, which we will further discuss in the next section (The effect of Location-Congruency).

In contrast to our expectations, we did not find positive effects of attending to bimodal stimuli on the early stage of processing. In fact, we did not detect an early bimodal ERP component at all for location-congruent stimuli when both modalities were attended. However we did observe early ERP components for both unimodal conditions: a visual P1 and a tactile N2. Because the unimodal conditions resulted in early ERP components with opposite polarities, the lack of a bimodal early ERP component in this study may be explained by counterbalanced activity. In Thurlings et al. (2012a) we did find a bimodal early ERP component (N1), which was not detected in either of the unimodal conditions. The early ERPs of those unimodal conditions, however, appeared much more alike and already showed a slight negative drift. Also in Talsma and Woldorff (2005)—in which positive effects of audiovisual stimulus attending on early and late stages of processing are reported- the unimodal early ERPs were quite alike. The same is the case in other bimodal studies (e.g., Gondan et al., 2005; Teder-Sälejärvi et al., 2005; Philippi et al., 2008). In multisensory literature there is an on-going debate about whether or not superadded activity is elicited when multisensory integration takes place, and how integration effects can be measured (Barth et al., 1995; Gondan and Röder, 2006; Boll and Berti, 2009; Senkowski et al., 2011). Perhaps ERP summation is the driving factor behind enhanced effects of bimodal compared to unimodal ERPs in our study.

If unimodal ERP components need to be alike to elicit bimodal effects usable in BCI, it is relevant to understand why in the current study this was not the case. For the tactile condition the early ERP component (N1) resembles the tactile N2 described in Thurlings et al. (2012a), but occurred slightly (∼25 ms) earlier in this study. The P1 from the visual condition also occurs ∼25 ms earlier compared to the visual N2 in Thurlings et al. (2012a), but has a reversed polarity. Possibly, these visual early components do have the same generator: The polarity of the P1 can be reversed if the concerning electrode is measured in reference to for example the nose instead of linked-mastoids (Chiappa and Chiappa, 1997). Indeed in this study linked-mastoid references were used (with which a visual P1 is expected: Mangun, 1995) while in Thurlings et al. (2012a) a nose-reference was used. Not every ERP component has to be affected by such a difference: depending on the generator of a certain ERP component and the recorded electrode(s) this can affect polarity.

Attending to bimodal compared to unimodal stimuli may have increased exogenous as well as endogenous attention. Therefore the cause of the bimodality effect here could theoretically be either bottom-up, or top-down driven, or by an interaction between the two. In this study Bimodality affected the ERP positively at the late stage. Since Hopfinger and West (2006) found the P300 to be unaffected by increased exogenous attention, we think that top-down controlled endogenous attention caused the Bimodality effect. While this study does not map out the exact mechanism behind the effect, it is clear that BCI performance was much higher when congruent bimodal stimuli were used compared to unimodal stimuli. We therewith provide a way to improve performance of a gaze-independent ERP-BCI.

THE EFFECT OF LOCATION-CONGRUENCY

The second research question concerned the effect of location-congruent compared to location-incongruent bimodal stimuli on the ERP components' tAUC and corresponding classification accuracies in an ERP-BCI. As we hypothesized, we found an indication that location-congruency positively affects the late ERP component tAUC in response to bimodal stimuli ($p = 0.056$), and this trend corresponded to increased classification accuracies.

Although we only expected location-congruency to influence the late stage of the ERP, we also found a difference at the early stage: A P1 was observed for the Bimodal-Incongr condition, whereas we did not detect early ERP components for the Bimodal condition at all. This P1 resembles the P1 from the conditions in which the visual modality was relevant (Visual and Bimodal-Att-V). Therefore the occurrence of the P1 in the Bimodal-Incongr condition could be due to (stronger) attending to the visual modality. Although for that condition, participants were instructed to attend both modalities equally, the task may have been too difficult as the locations of the visual and tactile parts of the bimodal incongruent stimuli were rather far apart, and even in opposite hemifields. This could have caused participants to attend more to one of the modalities, in this case, the visual modality. The P1 seems even stronger in the Bimodal-Incongr compared to the Visual condition and compared to the Bimodal-Att-V condition, suggesting that in the Bimodal-Incongr condition participants tried to focus even more on the visual part of the stimulus to not have themselves distracted by the tactile stimulus.

BCI performance was clearly affected by location-congruency. Therefore bimodal BCIs (based on spatial attention) should be

based on location-congruent bimodal stimuli for optimal performance. The performance drop caused by location-incongruent bimodal stimuli is expected to depend on the degree of incongruency.

THE EFFECT OF SELECTIVE ATTENTION TO MODALITY

The third research question was does, and if so how does, attending to the visual or tactile modality, or both modalities affect ERP components' tAUCs and corresponding classification accuracies in a bimodal ERP-BCI? We hypothesized a positive effect on the late ERP component tAUC when both modalities of bimodal (location-congruent) stimuli were attended rather than just one. Indeed attending to both modalities resulted in a stronger P300 compared to attending to the tactile modality alone, but it was equally strong as attending to the visual modality alone. Possibly, and in line with our interpretation of effects on the P1 as discussed in the previous section (processing of), the visual stimulus was dominant over (processing of) the tactile stimulus.

Selectively attending modality also had an effect on the early ERP components' tAUCs. When the visual modality was attended in a bimodal BCI, a P1 was detected, similar as in the visual BCI. Likewise, when the tactile modality was attended in a bimodal BCI, an N2 was detected, similar as for the tactile BCI. Thus, these early ERP effects appear unrelated to multisensory interaction and solely explainable by unisensory (bottom-up) effects of stimulus processing at attended locations and within attended modalities.

The effect of Cross-training

BCI performance in terms of classification accuracies was equally good for the three bimodal attention conditions. This means that users can choose a preferred modality to attend to for operating a bimodal BCI when training and classifying occurs using the same attended modalities (attended modality specific classifier). We additionally assessed the effect of switching the attended modality during BCI operation by cross-classifying each one of the three bimodal attention conditions (sub-question 3a). The results indicate that when the attended modalities are different during bimodal BCI operation and training of the bimodal classifier (attended modality cross classifier), this causes a drop in BCI performance. The size of this drop depends on the degree of overlap in the attended modalities. However, even if there is no overlap, operation of the bimodal BCI is still feasible and performance is similar to that of unimodal BCIs. That means that bimodal BCIs offer the option to be used flexibly, i.e., users can switch the modality to attend to during operation.

CONCLUSION

Multisensory effects can be used to enhance BCI performance (as reflected by classification accuracies) by employing bimodal stimuli. In this study we investigated bimodal effects in gaze-independent ERP-BCIs, using visual-tactile stimuli. The P300 tAUC and corresponding classification accuracies were enhanced when participants were attending to (location-congruent) bimodal vs. unimodal stimuli. Unexpectedly, we did not observe early bimodal effects for the specific condition where stimuli were location-congruent and both modalities were attended. This is possibly due to reversed polarities of early unimodal ERP components. We suggest that bimodal BCI performance may further be improved when the early unimodal ERP components are more similar, which may be achieved with different locations of the EEG reference electrode.

Furthermore, bimodal classification accuracies were improved when bimodal stimuli were location-congruent. Thus bimodal BCIs should be designed location-congruent for optimal performance.

Additionally, BCI performance was invariant for the specific modality attended, although the underlying ERP components' tAUCs were affected. When the bimodal classifier was not trained for the specific modality attended, the drop in BCI performance depends on the degree of overlap in attended modalities between training and classifying, but was still at least as good as for the unimodal ERP-BCIs. Thus bimodal BCIs may increase BCI performance and offer more flexibility in use. This implies that for the practical use of BCIs, people who are either restricted physically or by the context of use (e.g., sensory overload of the visual channel while driving) to attend to a certain modality may benefit from using bimodal BCIs.

ACKNOWLEDGMENTS

This research has been supported by the GATE project, funded by the Netherlands Organization for Scientific Research (NWO) and the Netherlands ICT Research and Innovation Authority (ICT Regie). The authors gratefully acknowledge the support of the BrainGain Smart Mix Programme of the Netherlands, the Ministry of Economic Affairs and the Netherlands Ministry of Education, Culture and Science.

We also like to thank the students of the elective course "Multimodal Perception and Interaction" at the Utrecht University, and Antoon Wennemers.

REFERENCES

Acqualagna, L., and Blankertz, B. (2013). Gaze-independent BCI-spelling using rapid serial visual presentation (RSVP). *Clin. Neurophysiol.* 124, 901–908. doi: 10.1016/j.clinph.2012.12.050

Barth, D. S., Goldberg, N., Brett, B., and Di, S. (1995). The spatiotemporal organization of auditory, visual and auditory-visual evoked potentials in rat cortex. *Brain Res.* 678, 177–190. doi: 10.1016/0006-8993(95)00182-p

Belitski, A., Farquhar, J., and Desain, P. (2011). P300 audio-visual speller. *J. Neural Eng.* 8:025022. doi: 10.1088/1741-2560/8/2/025022

Bell, C. J., Shenoy, P., Chalodhorn, R., and Rao, R. P. N. (2008). Control of a humanoid robot by a noninvasive brain-computer interface in humans. *J. Neural Eng.* 5, 214–220. doi: 10.1088/1741-2560/5/2/012

Birbaumer, N., and Cohen, L. G. (2007). Brain-computer interfaces: communication and restoration of movement in paralysis. *J. Physiol.* 579, 621–636. doi: 10.1113/jphysiol.2006.125633

Boll, S., and Berti, S. (2009). Distraction of task-relevant information processing by irrelevant changes in auditory, visual and bimodal stimulus features: a behavioral and event-related potential study. *Psychophysiology* 46, 645–654. doi: 10.1111/j.1469-8986.2009.00803.x

Brouwer, A.-M., and Van Erp, J. B. F. (2010). A tactile P300 brain-computer interface. *Front. Neurosci.* 4:19. doi: 10.3389/fnins.2010.00019

Brouwer, A.-M., Van Erp, J. B. F., Aloise, F., and Cincotti, F. (2010). Tactile, visual and bimodal P300s: could bimodal P300s boost BCI performance? *SRX Neurosci.* 2010. doi: 10.3814/2010/967027

Brunner, P., Joshi, S., Briskin, S., Wolpaw, J. R., Bischof, H., and Schalk, G. (2010). Does the 'P300' speller depend on eye gaze? *J. Neural Eng.* 7:056013. doi: 10.1088/1741-2560/7/5/056013

Chiappa, K. H., and Chiappa, K. H. (1997). Pattern-shift visual evoked potentials: methodology. *Evoked Potentials Clin. Med.* 2, 37–109.

Driver, J., and Noesselt, T. (2008). Multisensory interplay reveals crossmodal influences on 'sensory-specific' brain regions, neural responses and judgments. *Neuron* 57, 11–23. doi: 10.1016/j.neuron.2007.12.013

Eimer, M., Cockburn, D., Smedley, B., and Driver, J. (2001). Cross-modal links in endogenous spatial attention are mediated by common external locations: evidence from event-related brain potentials. *Exp. Brain Res.* 139, 398–411. doi: 10.1007/s002210100773

Ernst, M. O., and Bülthoff, H. H. (2004). Merging the senses into a robust percept. *Trends Cogn. Sci.* 8, 162–169. doi: 10.1016/j.tics.2004.02.002

Farwell, L. A., and Donchin, E. (1988). Talking off the top of your head—toward a mental prosthesis utilizing event-related brain potentials. *Electroencephalogr. Clin. Neurophysiol.* 70, 510–523. doi: 10.1016/0013-4694(88)90149-6

Foxe, J. J., and Simpson, G. V. (2005). Biasing the brain's attentional set: II. Effects of selective intersensory attentional deployments on subsequent sensory processing. *Exp. Brain Res.* 166, 393–401. doi: 10.1007/s00221-005-2379-6

Frassinetti, F., Bolognini, N., and Ladavas, E. (2002). Enhancement of visual perception by crossmodal visuo-auditory interaction. *Exp. Brain Res.* 147, 332–343. doi: 10.1007/s00221-002-1262-y

Giray, M., and Ulrich, R. (1993). Motor coactivation revealed by response force in divided and focused attention. *J. Exp. Psychol. Hum. Percept. Perform.* 19, 1278–1291. doi: 10.1037/0096-1523.19.6.1278

Gondan, M., Niederhaus, B., Rösler, F., and Röder, B. (2005). Multisensory processing in the redundant-target effect: a behavioral and event-related potential study. *Percept. Psychophys.* 67, 713–726. doi: 10.3758/bf03193527

Gondan, M., and Röder, B. (2006). A new method for detecting interactions between the senses in event-related potentials. *Brain Res.* 1073–1074, 389–397. doi: 10.1016/j.brainres.2005.12.050

Guthrie, D., and Buchwald, J. S. (1991). Significance testing of difference potentials. *Psychophysiology* 28, 240–244. doi: 10.1111/j.1469-8986.1991.tb00417.x

Höhne, J., Schreuder, M., Blankertz, B., and Tangermann, M. (2011). A novel 9-class auditory erp paradigm driving a predictive text entry system. *Front. Neurosci.* 5:99. doi: 10.3389/fnins.2011.00099

Hopfinger, J. B., and West, V. M. (2006). Interactions between endogenous and exogenous attention on cortical visual processing. *Neuroimage* 31, 774–789. doi: 10.1016/j.neuroimage.2005.12.049

Kramer, A. F., and Strayer, D. L. (1988). Assessing the development of automatic processing: an application of dual-task and event-related brain potential methodologies. *Biol. Psychol.* 26, 231–267. doi: 10.1016/0301-0511(88)90022-1

Krusienski, D. J., Sellers, E. W., McFarland, D. J., Vaughan, T. M., and Wolpaw, J. R. (2008). Toward enhanced P300 speller performance. *J. Neurosci. Methods* 167, 15–21. doi: 10.1016/j.jneumeth.2007.07.017

Kubler, A., Neumann, N., Wilhelm, B., Hinterberger, T., and Birbaumer, N. (2004). Brain-computer predictability of brain-computer communication. *J. Psychophysiol.* 18, 121–129. doi: 10.1027/0269-8803.18.23.121

Macaluso, E. (2010). Orienting of spatial attention and the interplay between the senses. *Cortex* 46, 282–297. doi: 10.1016/j.cortex.2009.05.010

Mangun, G. R. (1995). Neural mechanisms of visual selective attention. *Psychophysiology* 32, 4–18. doi: 10.1111/j.1469-8986.1995.tb03400.x

Meredith, M. A., and Stein, B. E. (1986). Spatial factors determine the activity of multisensory neurons in cat superior colliculus. *Brain Res.* 365, 350–354. doi: 10.1016/0006-8993(86)91648-3

Molholm, S., Ritter, W., Murray, M. M., Javitt, D. C., Schroeder, C. E., and Foxe, J. J. (2002). Multisensory auditory-visual interactions during early sensory processing in humans: a high-density electrical mapping study. *Brain Res. Cogn. Brain Res.* 14, 115–128. doi: 10.1016/s0926-6410(02)00066-6

Orhan, U., Ii, K. E. H., Erdogmus, D., Roark, B., Oken, B., and Fried-oken, M. (2012). RSVP keyboard: an EEG based typing interface. *Acoustics, Speech and Signal Processing (ICASSP), 2012 IEEE International Conference on* (Kyoto), 645–648.

Pfurtscheller, G., Allison, B. Z., Brunner, C., Bauernfeind, G., Solis-Escalante, T., Scherer, R., et al. (2010a). The hybrid BCI. *Front. Neurosci.* 4:30. doi: 10.3389/fnpro.2010.00003

Pfurtscheller, G., Solis-Escalante, T., Ortner, R., Linortner, P., and Muller-Putz, G. R. (2010b). Self-paced operation of an ssvep-based orthosis with and without an imagery-based "brain switch:" a feasibility study towards a hybrid BCI. *IEEE Trans. Neural Syst. Rehabil. Eng.* 18, 409–414. doi: 10.1109/tnsre.2010.2040837

Philippi, T. G., Van Erp, J. B. F., and Werkhoven, P. J. (2008). Multisensory temporal numerosity judgment. *Brain Res.* 1242, 116–125. doi: 10.1016/j.brainres.2008.05.056

Sambo, C. F., and Forster, B. (2009). An ERP investigation on visuotactile interactions in peripersonal and extrapersonal space: evidence for the spatial rule. *J. Cogn. Neurosci.* 21, 1550–1559. doi: 10.1162/jocn.2009.21109

Schalk, G., McFarland, D. J., Hinterberger, T., Birbaumer, N., and Wolpaw, J. R. (2004). BCI2000: a general-purpose, brain-computer interface (BCI) system. *IEEE Trans. Biomed. Eng.* 51, 1034–1043. doi: 10.1109/tbme.2004.827072

Schreuder, M., Blankertz, B., and Tangermann, M. (2010). A new auditory multi-class brain-computer interface paradigm: spatial hearing as an informative cue. *PLoS One* 5:e9813. doi: 10.1371/journal.pone.0009813

Schreuder, M., Rost, T., and Tangermann, M. (2011). Listen, you are writing! speeding up online spelling with a dynamic auditory BCI. *Front. Neurosci.* 5:112. doi: 10.3389/fnins.2011.00112

Schröger, E., and Widmann, A. (1998). Speeded responses to audiovisual signal changes result from bimodal integration. *Psychophysiology* 35, 755–759. doi: 10.1111/1469-8986.3560755

Senkowski, D., Saint-Amour, D., Hofle, M., and Foxe, J. J. (2011). Multisensory interactions in early evoked brain activity follow the principle of inverse effectiveness. *Neuroimage* 56, 2200–2208. doi: 10.1016/j.neuroimage.2011.03.075

Stein, B. E., Meredith, M. A., Huneycutt, W. S., and McDade, L. (1989). Behavioral indices of multisensory integration: orientation to visual cues is affected by auditory stimuli. *J. Cogn. Neurosci.* 1, 12–24. doi: 10.1162/jocn.1989.1.1.12

Stein, B. E., and Stanford, T. R. (2008). Multisensory integration: current issues from the perspective of the single neuron. *Nat. Rev. Neurosci.* 9, 255–266. doi: 10.1038/nrn2377

Talsma, D., Doty, T. J., and Woldorff, M. G. (2007). Selective attention and audiovisual integration: is attending to both modalities a prerequisite for early integration? *Cereb. Cortex* 17, 679–690. doi: 10.1093/cercor/bhk016

Talsma, D., and Woldorff, M. G. (2005). Selective attention and multisensory integration: multiple phases of effects on the evoked brain activity. *J. Cogn. Neurosci.* 17, 1098–1114. doi: 10.1162/0898929054475172

Teder-Sälejärvi, W. A., Di Russo, F., McDonald, J. J., and Hillyard, S. A. (2005). Effects of spatial congruity on audio-visual multimodal integration. *J. Cogn. Neurosci.* 17, 1396–1409. doi: 10.1162/0898929054985383

Thurlings, M. E., Brouwer, A. M., Van Erp, J. B. F., Blankertz, B., and Werkhoven, P. J. (2012a). Does bimodal stimulus presentation increase ERP components usable in BCIs? *J. Neural Eng.* 9:045005. doi: 10.1088/1741-2560/9/4/045005

Thurlings, M. E., Van Erp, J. B. F., Brouwer, A.-M., Blankertz, B., and Werkhoven, P. J. (2012b). Control-display mapping in brain-computer interfaces. *Ergonomics* 55, 564–580. doi: 10.1080/00140139.2012.661085

Thurlings, M. E., Van Erp, J. B. F., Brouwer, A.-M., and Werkhoven, P. J. (2010). "EEG-based navigation from a human factors perspective," in *Brain-Comput. Interfaces*, eds D. S. Tan and A. Nijholt (London: Springer), 71–86.

Thurlings, M. E., Van Erp, J. B. F., Brouwer, A.-M., and Werkhoven, P. (2013). Controlling a tactile ERP-BCI in a multimodal dual-task. *IEEE Trans. Comput. Intell. AI in Games* 5, 129–140. doi: 10.1109/tciaig.2013.2239294

Treder, M. S., and Blankertz, B. (2010). (C)overt attention and visual speller design in an ERP-based brain-computer interface. *Behav. Brain Funct.* 6:28. doi: 10.1186/1744-9081-6-28

Van Erp, J. B. F. (2005). Presenting directions with a vibrotactile torso display. *Ergonomics* 48, 302–313. doi: 10.1080/0014103042000327670

Van Erp, J. B. F., Eriksson, L., Levin, B., Carlander, O., Veltman, J. A., and Vos, W. K. (2007). Tactile cueing effects on performance in simulated aerial combat with

high acceleration. *Aviat. Space Environ. Med.* 78, 1128–1134. doi: 10.3357/asem.2133.2007

Van Erp, J. B. F., and Van Veen, H. A. H. C. (2004). Vibrotactile in-vehicle navigation system. *Transp. Res. Part F Traffic Psychol. Behav.* 7, 247–256. doi: 10.1016/j.trf.2004.09.003

Van Erp, J. B. F., Veltman, J. A., and Grootjen, M. (2010). "Brain-based indices for user system symbiosis," in *Brain Computer Interfaces, Human-Computer Interaction Series*, eds D. S. Tan and A. Nijholt (London: Spinger-Verlag), 201–219.

Woldorff, M. G., and Hillyard, S. A. (1991). Modulation of early auditory processing during selective listening to rapidly presented tones. *Electroencephalogr. Clin. Neurophysiol.* 79, 170–191. doi: 10.1016/0013-4694(91)90136-r

Yin, E., Zhou, Z., Jiang, J., Chen, F., Liu, Y., and Hu, D. (2013). A novel hybrid BCI speller based on the incorporation of SSVEP into the P300 paradigm. *J. Neural Eng.* 10:026012. doi: 10.1088/1741-2560/10/2/026012

Conflict of Interest Statement: The authors declare that the research was conducted in the absence of any commercial or financial relationships that could be construed as a potential conflict of interest.

Received: 03 February 2014; accepted: 23 July 2014; published online: 08 September 2014.

Citation: Thurlings ME, Brouwer A-M, Van Erp JBF and Werkhoven P (2014) Gaze-independent ERP-BCIs: augmenting performance through location-congruent bimodal stimuli. Front. Syst. Neurosci. ***8****:143. doi: 10.3389/fnsys.2014.00143*

This article was submitted to the journal Frontiers in Systems Neuroscience.

frontiers in
SYSTEMS NEUROSCIENCE

REVIEW ARTICLE
published: 06 October 2014
doi: 10.3389/fnsys.2014.00190

Time-interval for integration of stabilizing haptic and visual information in subjects balancing under static and dynamic conditions

Jean-Louis Honeine*[1] *and Marco Schieppati*[1,2]

[1] *Department of Public Health, Experimental and Forensic Medicine, University of Pavia, Pavia, Italy*
[2] *Centro Studi Attività Motorie (CSAM), Fondazione Salvatore Maugeri (IRCSS), Scientific Institute of Pavia, Pavia, Italy*

Edited by:
Mikhail Lebedev, Duke University, USA

Reviewed by:
Yoshio Sakurai, Kyoto University, Japan
Robert Peterka, Oregon Health and Science University, USA
David A. E. Bolton, Queen's University Belfast, UK

***Correspondence:**
Marco Schieppati, Centro Studi Attività Motorie (CSAM), Fondazione Salvatore Maugeri (IRCSS), Scientific Institute of Pavia, Via Salvatore Maugeri 4, Pavia 27100, Italy
e-mail: marco.schieppati@unipv.it

Maintaining equilibrium is basically a sensorimotor integration task. The central nervous system (CNS) continually and selectively weights and rapidly integrates sensory inputs from multiple sources, and coordinates multiple outputs. The weighting process is based on the availability and accuracy of afferent signals at a given instant, on the time-period required to process each input, and possibly on the plasticity of the relevant pathways. The likelihood that sensory inflow changes while balancing under static or dynamic conditions is high, because subjects can pass from a dark to a well-lit environment or from a tactile-guided stabilization to loss of haptic inflow. This review article presents recent data on the temporal events accompanying sensory transition, on which basic information is fragmentary. The processing time from sensory shift to reaching a new steady state includes the time to (a) subtract or integrate sensory inputs; (b) move from allocentric to egocentric reference or vice versa; and (c) adjust the calibration of motor activity in time and amplitude to the new sensory set. We present examples of processes of integration of posture-stabilizing information, and of the respective sensorimotor time-intervals while allowing or occluding vision or adding or subtracting tactile information. These intervals are short, in the order of 1–2 s for different postural conditions, modalities and deliberate or passive shift. They are just longer for haptic than visual shift, just shorter on withdrawal than on addition of stabilizing input, and on deliberate than unexpected mode. The delays are the shortest (for haptic shift) in blind subjects. Since automatic balance stabilization may be vulnerable to sensory-integration delays and to interference from concurrent cognitive tasks in patients with sensorimotor problems, insight into the processing time for balance control represents a critical step in the design of new balance- and locomotion training devices.

Keywords: sensory integration, sensory reweighting, haptic, vision, equilibrium, quiet stance, dynamic balance

INTRODUCTION

Maintaining balance involves complex sensorimotor transformations that continually integrate several sensory inputs and coordinate multiple motor outputs to muscles throughout the body (Ting, 2007). The control of quiet-standing posture consists in the maintenance of the center of mass (CoM) of the body within narrow limits. Also under dynamic balance conditions, like riding a platform periodically moving in the antero-posterior direction (Buchanan and Horak, 1999; Corna et al., 1999), the body requires accurate control of the CoM displacement within the range of the platform displacement. In both cases, the spatio-temporal activity of the agonist postural muscles (Schieppati et al., 1994, 1995; Tokuno et al., 2007; Kelly et al., 2012; Wright et al., 2012; Sozzi et al., 2013) is orchestrated by the central nervous system (CNS) based on one or multiple frames of reference (Peterka, 2002; Mergner et al., 2003; Schmid et al., 2007) upon which the body scheme is constructed (Haggard and Wolpert, 2005).

While keeping our body stable during the so-called "quiet stance" condition, feed-forward mechanisms are paramount in modulating the tonic activity in our antigravity extensor muscles and the correcting bursts in the antagonist muscles, which together control the displacement of the center of foot pressure (CoP; Morasso and Schieppati, 1999; Jacono et al., 2004; Bottaro et al., 2005, 2008; Loram et al., 2011; Vieira et al., 2012). In turn, these spatio-temporal patterns of activity rely on the knowledge of our orientation in space and of the relative position of our body segments during stance. This knowledge is built on multiple sensory inputs, which concur in the more or less accurate construction of the "internal model" of our body and of its relationship with the environment (van der Kooij and Peterka, 2011). The accuracy depends on the number and quality of the inflow from the various sensory modalities that

have access to the centers integrating and using such information. Feedback obviously contributes to the instant-to-instant control of the stabilizing effort both by engaging reflex responses and by continuously updating the internal model (van Emmerik and van Wegen, 2002). Under steady-state conditions, the feedback contribution may be down-weighted by the brain (Peterka and Loughlin, 2004; Assländer and Peterka, 2014). Under dynamic but stabilized conditions, as when standing on a tilting platform and holding onto a still frame, the proprioceptive feedback from the legs is also down-weighted (Nardone et al., 1990; Schieppati and Nardone, 1991). During locomotion, alteration of the proprioceptive input from the leg muscle produces little effects on gait variables (Courtine et al., 2001). Thus, under predictable, steady-state conditions and tasks, be they static or dynamic, voluntary or produced in response to equilibrium perturbation, the excitability of the circuits ultimately called forth in the control of equilibrium may be tuned down. In general, sensory gating optimizes the execution of ongoing motor tasks (Clarac et al., 1992) by minimizing the effects on the motor command due to the inescapable delay from detection of the relevant information to its transmission to the neural generators of muscle activity (Suzuki et al., 2011). In this context, it is helpful to introduce an operative definition of postural set as it applies to both the control of body orientation in space and to the particular temporary level of excitability of the sensorimotor circuits underpinning the actual state of the body in its environment: "sensorimotor set is a state in which transmission parameters in various sensorimotor pathways have been adjusted to suit a particular task or context" (Prochazka, 1989). As such, the postural set, and in particular the neural circuits' excitability to impending stimuli, is modifiable by the intention to change motor task and by the prediction of a change in the environment.

Stance stability depends on the availability and accuracy of the afferent stimuli that are integrated by the brain. The time-period whereby a sensory input is integrated and incorporated in the control of equilibrium is critical. For example, when the CoM is close to the border of its fixed support base (Schieppati et al., 1994), a handful of milliseconds can be enough to pass this limit and reach a condition that prevents any useful reaction. Any stabilizing information (e.g., vision) must therefore be rapidly integrated and rapidly produce corrective actions. Further, when we maintain the equilibrium during repeated and predictable perturbations of balance, anticipatory postural adjustments occur and in this context changes in visual conditions can quickly lead to appropriate modification in the anticipatory activities with appropriate changes in the balancing strategy (Corna et al., 1999; Schieppati et al., 2002).

The dependence of the control of human stance on sensory information has been the object of a great deal of investigations (Paulus et al., 1984; Day et al., 1993; Bronstein and Buckwell, 1997; Maurer et al., 2006; Guerraz and Bronstein, 2008). Much attention has been devoted to the central integration of afferent input from visual, somatosensory and vestibular receptors (Massion, 1994; Mergner and Rosemeier, 1998; Meyer et al., 2004; Borel et al., 2008). Changes in these sensory inputs lead the CNS to re-evaluate the respective contribution of the different sources of information for regulating posture (Oie et al., 2002; Peterka and Loughlin, 2004).

Ultimately, the more rapid the gain modulation on the insertion (or withdrawal) of a new stabilizing input, the shorter the time-period to reach the new appropriate postural set. Any information from the environment and from the body itself would concur in creating the better condition for the release of the postural muscle bursts apt to brake the displacement of the body's CoM. It would be therefore appropriate if the CNS could integrate the stabilizing information within the shortest possible period of time.

The effects of changing sensory inflow during the performance of a coordinated complex motor task such as maintaining balance under quiet stance or dynamic conditions have received little attention so far (Rabin et al., 2006; Tax et al., 2013). The likelihood that sensory inflow changes during a complex movement is high, not only because of the obvious movement-related changes in proprioceptive input, but also because movement can imply passing from a dark to a lit environment, or from a stationary to a moving visual flow, or from a tactile-guided body displacement to an abrupt loss of such haptic-stabilized condition (Bove et al., 2006). The basic information for addressing these aspects of sensorimotor integration is fragmentary. Hence, the purpose of this review is to discuss sensory reweighting during static or dynamic balancing tasks. Particularly, the review focuses on the time-interval necessary for integration of balance stabilizing haptic or visual inputs, since this topic area is still relatively unexplored with most of the most relevant work having occurred in recent years.

VISUAL INFORMATION AND STANCE STABILIZATION

Vision affects both body sway during quiet stance (Schieppati et al., 1994; Nougier et al., 1998; Slobounov et al., 1998) and postural synergies when balancing on an oscillating platform (Buchanan and Horak, 1999; Corna et al., 1999; De Nunzio et al., 2005; Schmid et al., 2007). In a variety of situations, vision dominates over the proprioceptive input from a great number of postural muscles, the activity of which necessarily accompanies the standing task (Nardone et al., 1990; Bronstein and Buckwell, 1997; Redfern et al., 2001; van Emmerik and van Wegen, 2002; Hagura et al., 2007; Schmid et al., 2008; Carpenter et al., 2010; Murnaghan et al., 2011).

INTERACTION OF VISION AND PROPRIOCEPTION

Regardless of the weight assigned to vision and proprioception by the brain, the interaction between the two sensory inputs may not be based on a simple algebraic sum, not least because of the different time-period necessary for the two inputs to access the brain, as shown by the different latency of their primary components in the cortical evoked potentials (Schieppati and Ducati, 1984; Bodis-Wollner, 1992; Shokur et al., 2013) or to reach consciousness (Barnett-Cowan and Harris, 2009). Further, the ultimate functional effects of either input or of their interaction over time relates to the particular current balance or movement constraints. For example, anticipatory muscle action preceding a

predictable perturbation of quiet stance eyes-open is delayed by vibration of leg muscles (Mohapatra et al., 2012). On the other hand, relatively minor effects of muscle vibration are induced on the balancing behavior on a continuously oscillating platform in spite of vision being denied (De Nunzio et al., 2005). These findings open the issue of the effectiveness of leg muscle tendon vibration *per se* in modifying the control of balance, i.e., of a task strongly dependent on proprioception. This is not a matter of interest for this present review. Suffice it to mention here the intriguing finding that tendon vibration operates by triggering a vibration-frequency entrained discharge of the primary afferent fibers from the spindles (Hagbarth et al., 1973; Burke et al., 1976; Roll and Vedel, 1982; Matthews, 1988; Naito, 2002), while quiet stance relies mostly on the inflow of the secondary spindle afferent fibers (Schieppati and Nardone, 1995, 1999; Marque et al., 2001; Nardone and Schieppati, 2004; see also Pettorossi and Schieppati, under review).

Postural control provides an experimental context appropriate to highlight the interaction of multiple sensory inputs originating from different sensory systems (Hatzitaki et al., 2004). Body stability strongly depends on the non-linear aspects of the sensory fusion process and its temporal dynamics (Black and Nashner, 1984; Jeka et al., 2000; Horak and Hlavačka, 2002; Barnett-Cowan and Harris, 2009; Rowland and Stein, 2014). In turn, this depends to a large extent on the nature of the signals involved and their spatiotemporal relationship (Hlavačka et al., 1999). Experiments on the ability of young and elderly subjects to reconfigure their mode of stance control when submitted to successive reduced and augmented visual sensory conditions have shown a deficit in the operation of their central integrative mechanisms responsible for promptly modifying their postural control in the elderly (Teasdale et al., 1991). Young and elderly subjects' body sway increased when occluding vision, while adding vision had a better effect on sway in young than the elderly, suggesting that elderly persons have a deficit in exploiting the stabilizing effect of vision (Jeka et al., 2010).

In a recent study, it was assumed that the sensory organization and the consequent postural set were influenced by the temporal relationship between visual and neck input (Bove et al., 2009), on the premise that re-weighting sensory inputs and re-shaping the postural reference frame must be a time-consuming process. In that paper, the authors investigated whether a given visual condition affects the postural response to neck vibration, and for how long does vision need to be absent prior to perturbation, before its stabilizing contribution be fully abolished. To this aim, the visual condition was time-manipulated to study its effects on the postural response to a balance-perturbing stimulus produced by neck muscle vibration. Notably, neck muscle vibration produces whole-body postural effects under both static and dynamic conditions (Lund, 1980; Roll et al., 1989; Lekhel et al., 1997; Ivanenko et al., 1999, 2000; Kavounoudias et al., 1999; Bove et al., 2001, 2002). The smallest postural response to vibration was observed when the eyes were open with respect to eyes-closed. This shows that vision is sufficient to significantly attenuate sway evoked by neck vibration. Conversely, the postural response to vibration eyes-closed that followed a period during which vision was allowed was significantly smaller than when vision was denied in the foreperiod. This indicated that the postural response to vibration is influenced not only by the visual condition during the administration of the vibratory stimulus, but also by the visual condition immediately preceding the vibration. A second finding was that, in the complete absence of visual references, the amplitude of the postural responses to vibration became progressively larger as a function of the repetition of the stimuli: in spite of the recovery to the initial position after each vibration pulse, the center of pressure moved forward to an increasingly larger extent during the successive neck vibration pulses, as if each vibration pulse found the postural control system progressively more susceptible to the abnormal proprioceptive input, when the absence of vision persisted. In a sense, the repeated proprioceptive perturbation eyes-closed progressively reinstated a heavy dependence of the postural control on proprioception or cancelled any postural reference constructed by visuo-somatosensory integration (Bottini et al., 2001). This sway-increasing phenomenon was not observed under eyes-open/eyes-closed condition, independently of the number of successive vibration pulses in the sequence. Clearly, presence of vision up to the beginning of vibration allows the CNS to define, and retain for a while, a stable postural reference able to cope with the threat represented by the abnormal proprioceptive inflow.

EFFECTS OF VISION ON BALANCING BEHAVIOR DURING A CONTINUOUS PREDICTABLE PERTURBATION OF STANCE

Standing upright quietly can hardly be considered a real balance challenge. Surprisingly, balance control under dynamic conditions (such as standing on a back-and-forth continuously translating platform) is not much more challenging either, at least as based on the observation that neither sensory nor motor impairment represent an unsustainable challenge to the elderly and patients with peripheral neuropathy or movement disorder (Nardone et al., 2000, 2006, 2007, 2008; Nardone and Schieppati, 2005, 2006). Certainly, subjects put in much more cognitive effort to sustain the performance level than under quiet stance (Beckley et al., 1991). Dynamic balancing behavior is an excellent experimental condition for assessing the role of vision in dynamic with respect to static equilibrium. There is indeed a remarkable difference in strategy depending on the availability of vision, whereby the balancing behavior shifts from that of a pendulum to an inverted-pendulum, passing from "head-fixed-in-space" behavior with eyes open to maximal body compliance to the perturbation with eyes closed (Corna et al., 1999). Incidentally, when blind subjects perform the task of balancing while riding a periodically moving platform, their strategy matches that of the sighted subjects performing eyes-closed (Schmid et al., 2007). This shows that long-term absence of visual information cannot be substituted by other sensory inputs (e.g., proprioception) for the selection of the balancing strategy in the control of equilibrium, in spite of the demonstrated cross-modal plasticity in blind subjects (Cohen et al., 1997; Kupers and Ptito, 2014). The findings point to the obligatory (though not unique, e.g., Panichi et al., 2011) role of vision in the processing and integration of other sensory inputs.

Schmid et al. (2008) investigated two competing hypotheses regarding the relationship between visual acuity and balance

control strategy. One hypothesis referred to the existence of a threshold value of visual acuity as a turning point between the eyes-open and eyes-closed strategy. The other assumed that the change from eyes-open to eyes-closed balancing behavior is continuous and varies progressively with the worsening of the visual acuity. The findings showed that, in order to stabilize the head in space, visual information of the environment must be distinct. Reducing visual acuity leads to a graded modification of the "head-fixed-in-space" behavior. Thus, the body can produce a continuous mode of balancing patterns as a function of visual acuity. In a sense, this had already been shown by Paulus et al. (1984) for visual control of quiet stance. The findings suggest the notion that the central mechanisms for head and body stabilization operate through linear integration of the visual input with the general somesthetic feedback.

ABRUPT CHANGES IN VISION DURING THE CONTINUOUS PERTURBATION OF BALANCE

The previously mentioned studies have considered balancing behaviors to periodic balance-perturbing stimuli, under stationary sensory conditions (e.g., vision, reduced vision, or no-vision). They ignored relevant aspects of the postural behavior connected to transient sensory events. In subsequent studies, the time interval between the occurrence of a change in the sensory (visual) condition and the corresponding change in the motor behavior was investigated (De Nunzio and Schieppati, 2007). This interval includes the time to (a) integrate subtraction or addition of the sensory inputs; (b) shift from an allocentric reference (vision) to an egocentric reference (no-vision) or vice versa; and (c) adjust the calibration of the motor activity in time and amplitude to reach the best control appropriate to the new sensory set. A related question of adaptation to transient conditions had been previously addressed by Schweigart and Mergner (2008), who described a "sensory reweighting switch", by which subjects change from a control that is referenced to the support to one that is referenced to space. Under optimal visual-acuity levels, on changing visual inflow during the trial (from eyes open to eyes closed or vice versa), the pattern of head and hip movement and of muscle activity turned into that appropriate for the new visual condition in a time-interval broadly ranging from about 1–2.5 s (De Nunzio et al., 2007). On the one hand, the findings indicate that subjects can rapidly adapt their balancing behavior to the new visual condition. On the other hand, the ample range of latencies across trials suggests that subjects refrained from releasing the new behavior when it was inappropriate, but rather released it at an appropriate time in the next platform translation cycle.

ABRUPT CHANGES IN VISION DURING CONTINUOUS PERTURBATION OF BALANCE IN PATIENTS WITH PD

Processing of sensory information and timing operations could be affected in Parkinson's disease (PD) patients, who show abnormal calibration of postural responses (Schieppati and Nardone, 1991) or impaired flexibility of motor strategies (Horak et al., 1992). The capacity and swiftness to pass from a kinesthetic- to a vision-dependent behavior of these patients was investigated during the dynamic balancing task on the same continuously moving platform mentioned above. It turned out that both patients and normal subjects changed kinematics and EMG patterns to those appropriate for the new visual condition. However, PD patients were generally slower in changing their behavior under the eyes-closed to eyes-open condition (De Nunzio et al., 2007). These findings show abnormal temporal features in balancing strategy adaptation when shifting from kinesthetic only to kinesthetic plus visual reference in PD. The delay in the implementation of the vision-dependent behavior was unexpected, given the advantage vision is supposed to confer to motor performance in PD (Cooke et al., 1978). The delay on addition of vision in PD might be connected to an insufficient integration of a new sensory information in their body scheme, or to a delay in the implementation of the change in the appropriate balancing strategy (Bandini et al., 2001; Contreras-Vidal and Buch, 2003). This state might play a role in the instability of patients performing dynamic postural tasks under changing sensory conditions. Although static visual feedback reduces the walking patients' reliance on kinesthetic feedback thereby favoring gait execution (Azulay et al., 1999; Lewis and Byblow, 2002), fast shifting to a new sensory reference may not be adequately exploited in everyday postural tasks. Venkatakrishnan et al. (2011) have suggested that *gradual* shifting of a new afferent input allows PD to better process the sensory input in a pointing movement.

MEASURING THE DELAY BETWEEN VISUAL SHIFT AND IMPLEMENTATION OF THE NEW BALANCING BEHAVIOR IN STATIC CONDITION

The great variability under the dynamic balancing conditions described above (Schieppati et al., 2002) does not allow to adequately address the issue of the sensori-motor processing time during sensory reweighting, owing to the complex motor task at hand. In a much simpler balancing condition, unaffected by the continuously variable kinesthetic inflow and relevant mechanical instability, the onset and time course of postural adjustments may be more clearly detected following abrupt sensory changes (from no-vision to vision or vice versa). Under these conditions, the stabilizing effect of vision is much less conspicuous than under more complex, balance challenging conditions (Buchanan and Horak, 1999; Corna et al., 1999; Ravaioli et al., 2005; Schmid et al., 2007); but it is definitely present (Paulus et al., 1984). The simple question was how long does it take for vision (eyes-closed to eyes-open) to stabilize posture, or how long does it take for the body to become less stable when vision is withdrawn?

The promptness of adaptation of stance control mechanisms was quantified by the latency at which body oscillation and postural muscle activity varied after a shift in visual condition. In a study aimed at estimating the promptness of adaptation to changes in visual conditions (Sozzi et al., 2011), volunteers stood on a force platform with feet parallel or in tandem. Shifts in visual condition were produced by electronic spectacles (LCD goggles that allowed or removed vision on receiving a TTL impulse). On allowing or occluding vision, decrements and increments in the CoP oscillation start occurring within about 2 s. These were preceded by appropriate changes in muscle activity, regardless of the visual-shift direction and the foot position during the standing task (feet parallel or in tandem). After the initial

changes, EMG and CoP oscillations slowly reached the steady-state level corresponding to the new sensory condition within about 3 s. These figures were not dependent of the position of the feet, in spite of the overall larger sway under tandem condition, pointing to a constant duration of the sensorimotor integration process, hardly affected by the particular stance conditions at hand.

HAPTIC INFORMATION AND STANCE STABILIZATION

Very much as with vision, contact of the index finger with a stationary surface (Lederman and Klatzky, 2009) attenuates postural sway during quiet stance, even if the applied force itself (1 N) cannot provide mechanical stabilization. It has been proposed that slight changes in contact force at the fingertip give sensory cues about the direction of body sway (Holden et al., 1994; Jeka and Lackner, 1994; Jeka et al., 1997; Rabin et al., 1999, 2006; Krishnamoorthy et al., 2002; Kouzaki and Masani, 2008). Under steady state conditions, the effect of passive tactile cues during standing has been evaluated (Rogers et al., 2001) and the conclusion drawn that, if passive sensory input is available, the postural control process adapts to this input, better so the more cranial the point of application of the stimulus.

Sensory information from light fingertip touch (LFT) on a stationary surface can help in the case of loss of vestibular function (Lackner et al., 1999; Creath et al., 2002; Horak and Hlavačka, 2002). Therefore, LFT is relevant in the control of body orientation in space. Fingertip somatosensory input from an external reference provides spatial cues, which, akin to vision, facilitate the control of body equilibrium (see Wing et al., 2011). LFT has also been shown to suppress the destabilizing effect on posture induced by lower limb muscle vibration (Lackner et al., 2000). Of note, light touch contact between two individuals induced interpersonal stance symmetry (Johannsen et al., 2012). In other terms, the sway of the persons oscillating more would be reduced while the sway of the one oscillating less would be increased.

Stabilizing effects of LFT have been also described in normal subjects after lower-limb muscular fatigue (Vuillerme and Nougier, 2003), in healthy older adults (Tremblay et al., 2004; Baccini et al., 2007), in patients with peripheral neuropathy (Dickstein et al., 2001, 2003) or multiple sclerosis (Kanekar et al., 2013), and in patients with PD (Rabin et al., 2013) or bilateral vestibular loss (Lackner et al., 1999). Interestingly, LFT is able to relieve the perturbing effects of vibration-induced proprioceptive input from the neck, a segment central to postural control and orientation. LFT during neck vibration also attenuates vibration post-effects, further suggesting that its action is not merely mechanical (Bove et al., 2006). All these findings point to a paramount effect of the sensory inflow from light haptic touch on balance control.

HAPTIC EFFECTS ON REFLEX RESPONSES OF POSTURAL MUSCLES

Haptic information from a stable structure not only reduces the sway of the CoP during quiet stance, therefore of the CoM of the body, but also deeply modifies the excitability of the spinal proprioceptive reflexes that normally subserve the reaction to postural perturbations. By using a conditioning-test protocol, major effects of the haptic stabilization on reflex responses to postural perturbations have been observed (Nardone et al., 1990; Schieppati and Nardone, 1991). It was shown that stabilization of stance induced by holding onto a stable frame had a profound depressive action on the size of the medium-latency response to stretch of the postural leg muscles. This phenomenon was attributed to the change in the postural set. Interestingly, the reflex responses began to decrease about 200 ms before subjects touched the frame, but were not fully expressed until well after contact. The initial changes in amplitude of leg muscle responses are therefore not triggered by the go-signal or the contact with the frame itself, suggesting that the modulation is related at least in part to the central command to transition to a new stabilized postural set.

ACTIVE AND PASSIVE INSERTION OR WITHDRAWAL OF HAPTIC INFORMATION DURING STANCE

Thus, touch helps stabilize our standing body very much as vision does, but little is known about the time-interval necessary for the brain to process the haptic inflow (or its removal) and exploit the new information (or counteract its removal). Moreover, under conditions in which haptic information plays a stabilizing role, it would be interesting, on the basis of both basic and applied research data, to assess whether active touch or passive touch are equally effective (Chapman, 1994; Winter et al., 2008; Smith et al., 2009; Sciutti et al., 2010; Waszak et al., 2012), or significant differences exist, since our sensory systems are simultaneously activated as the result of our own actions and of changes in the external word (Von Holst and Mittelstaedt, 1950; Cullen, 2004). Active touch refers to the event where the subject would deliberately touch a surface, while passive touch refers to the event where contact with the surface would be established by external action without movement or anticipation of the stimulus by the subject.

Sozzi et al. (2012) estimated the latency of onset and the time-course of the changes in postural control mode following addition or withdrawal of haptic information produced by touching (eyes-closed) with the tip of the index finger a strain-gauge instrumented touch-pad. Subjects were asked to actively touch the pad, or it was suddenly lowered or raised permitting to study the passive condition. The EMG of postural muscles during tandem stance was also recorded (in order to enhance muscle activity and body sway), to try to get as close as possible to the neural processing of the sensory information by eliminating the effect of the electromechanical delay. It had been shown previously that light touch stabilizes stance under both tandem stance and feet parallel 12 cm apart (Clapp and Wing, 1999). A summary representation of the modification in the medio-lateral and antero-posterior axes occurring around the instant of visual or haptic information shift is reported in **Figure 1**.

Muscle activity and sway adaptively decreased in amplitude on adding stabilizing haptic information. Across the subjects, the time-interval from the sensory shift to decrease in EMG and sway was ∼0.5–2 s (Rabin et al., 2006). CoP followed the changes in tibialis anterior muscle EMG by ∼0.2 s. Only slightly

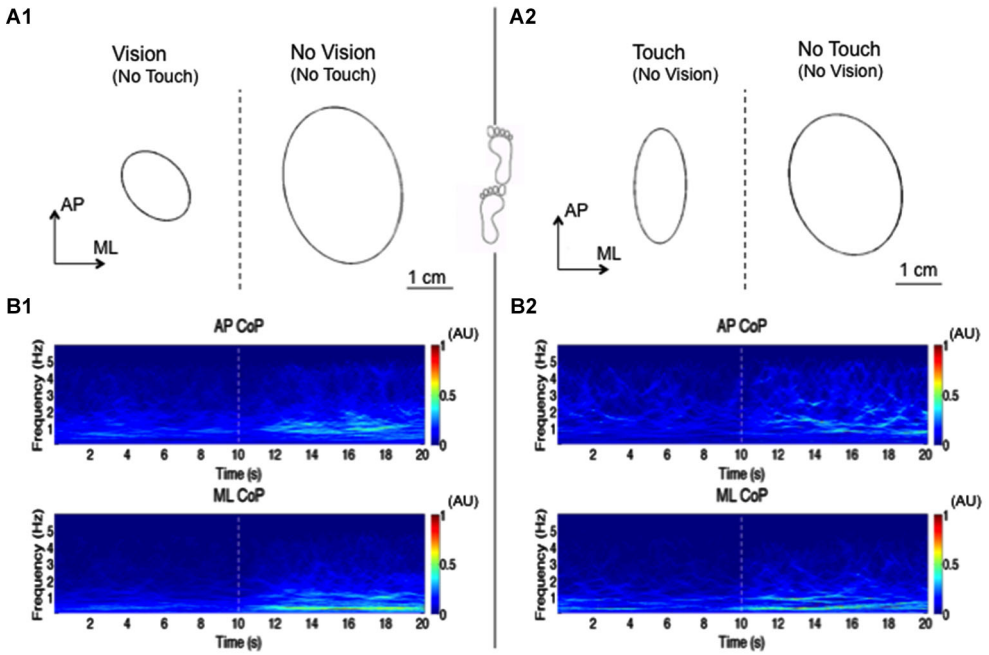

FIGURE 1 | Reweighting of visual or haptic information during tandem stance. This figure shows an elaboration of the results obtained by Sozzi et al. (2011) in one subject standing upright under tandem-stance condition. In this experiment, the subjects' visual sensory information was shifted from vision to no-vision (no touch), while haptic simulation was from touch to no-touch (blindfolded). The sensory shifts occurred at 10 s and were involuntary. The upper panel shows the ellipses of 95% confidence interval of CoP position (mean of 50 trials) during the vision/no-vision shift **(A1)** and touch/no-touch shift **(A2)**. Vision as well as haptic inflow decrease the area of the ellipse. The lower panel shows the "synchro-squeezed" (Daubechies et al., 2011) wavelet transform using a Morlet wavelet of AP CoP (upper traces) and ML CoP (lower traces) between 0.2 and 6 Hz. **(B1)** shows the transform during the vision/no-vision shift, **(B2)** during the touch/no-touch shift. The wavelet transform seen here is the mean of the transforms of 50 trials. The colors in the Figure represent the amplitude of the wavelet coefficient. Dark red represent the highest while dark blue is the lowest wavelets coefficient. Bins of 0.1 s have been chosen in order to better highlight the temporal changes in the coefficients after the sensory shift. Occluding vision or haptic information increases the wavelet coefficients in the frequencies ranging from 0.2 to 3 Hz, which indicates increase in the amplitude of the ML and AP oscillations. Higher frequency components were added up to the spectrum when sensory information was lost. The changes in the wavelets coefficient start increasing after a delay of approx. 1 s, to reach a stationary state in a few more seconds.

shorter intervals were observed following active sensory shifts (Pais-Vieira et al., 2013), in line with the conclusions by Winter et al. (2008) based on a stimulus timing-matching paradigm, who found no advantage on the perceived timing of an active over a passive touch. Latencies of EMG and postural changes were the shortest on removal of haptic information. Following the earliest detectable changes in amplitude, EMG and body sway reached the steady-state corresponding to the new sensory condition within ∼1–3 s, under both active and passive tasks. Under control conditions, when subjects were asked to produce deliberate muscle activation in response to the sensory shift in a reaction-time mode, EMG bursts and CoP changes appeared at ∼200 ms from the haptic shift, therefore much earlier than the adaptive postural changes seen during stance, signifying the operation of a different order of magnitude of the time scale of these events. Therefore, as much as for the visual information shifts mentioned above, changes in postural behavior require a finite amount of time from haptic shift. In particular, this delay from the sensory shift to the change in postural control mode was significantly longer for haptic than visual cues, the difference being much longer than that between the reaction times to the respective stimuli (Barnett-Cowan and Harris, 2009), indicating a modality-dependence and a heavier computational load for haptic information processing (Vuillerme et al., 2006; Tommerdahl et al., 2010; Bolton et al., 2011a).

The output of the sensory integration process seems to be issued to all relevant muscles. However, the latency of the change was shorter for the tibialis anterior muscle than soleus, likely because the latter rather plays a weight-bearing role (Schmid et al., 2011) while the former, along with peroneus longus, is responsible for providing medial-lateral stability in tandem-stance (Sozzi et al., 2013). Consistent with this role, the cortical projection to the tibialis anterior is stronger than to soleus (Valls-Solé et al., 1994). In this light, the shorter latency of the tibialis anterior changes would be an expression of a prominent supraspinal sensorimotor integration (Bolton et al., 2012) and fast cortical descending control. This finding would be in keeping with the proposals that the cerebral cortex plays a non-negligible role in the control of stance (Tokuno et al., 2009; Pasalar et al., 2010; Murnaghan et al., 2014).

It should be recalled here that the above delays are the result of a statistical estimation. Using statistics to document when a change occurs relies on assumptions and depends on the number of the cases upon which statistics is performed and the data variability, and cannot detect the "true" time at which a change at the CNS level occurs. Rather, the procedure will likely overestimate the true temporal locus of this change at the level of the CNS. Changes at the CNS level in response to visual or tactile inflow certainly occur before a value determined by using statistical tests (Soto-Faraco and Azañón, 2013; Heed and Azañón, 2014; Quinn et al., 2014). However, the same statistics and the same number of cases had been used in Sozzi et al. (2011) and Sozzi et al. (2012) when assessing both addition and withdrawal of information, and when comparing the time-periods to integration of haptic and visual addition (or withdrawal) in body stabilization, allowing a fair comparison to be made between the findings obtained with different sensory modalities and conditions. Admittedly, the "fuzziness" around when actual sensory events influence postural responses requires caution to be exercised to avoid precise claims on absolute times for when sensory signals play their role.

On reflection, one might wonder whether, in spite of all other things being equal, it was legitimate to compare the effect of the haptic sense from a minimal body surface (the tip of the index finger) with the visual information coming from a full binocular visual-field stimulation by the lighted and structured environment. Surprisingly, in spite of these disparities, the duration of the time-periods behind these sensory integrations and the extent of body-sway stabilization was remarkably consistent under both circumstances (Rogers et al., 2001), pointing to a sensory re-weighting phenomenon underpinning a change in reference frame rather than a central detailed analysis of the incoming information. Based on another analytical approach, Riley et al. (1997) had suggested an equivalent time-structure of the haptic and visual effects on the trajectory of the CoP.

HAPTIC INTEGRATION IN BLIND SUBJECTS

Major reorganization of brain areas and reduced cross-modal interaction at the behavioral level follow congenital visual deprivation (Hötting and Röder, 2009; Fiehler and Rösler, 2010; Renier et al., 2014). Vision and touch rapidly lead to postural stabilization in sighted subjects, but is touch-induced stabilization more rapid in blind than in sighted subjects, owing to cross-modal reorganization of function in the blind? In people with impaired visual function, only minor differences in quiet stance control compared to sighted people have been reported (Rougier and Farenc, 2000). Jeka et al. (1996) found no differences between sighted and blind subjects on postural stability while using a cane, a task to which blind people are accustomed. Moreover, when exposed to sudden stance perturbation, the automatic postural responses of the blind are not substantially different from those of sighted persons (Nakata and Yabe, 2001). The same is true also for balancing while riding a periodically moving platform, where the balancing strategy of the blind subjects is similar to that of the sighted subjects performing eyes-closed (Schmid et al., 2007). The sensorimotor integration time of blind subjects should therefore be validly compared to that of sighted people under equal stance conditions. The aim of the Schieppati et al. (2014) study was to assess whether, in spite of known deficits in the processing speed of visual stimuli in the intact visual field of patients with visual system damage (Bola et al., 2013), blind subjects are more prompt than sighted subjects eyes-closed in reducing body sway in response to a haptic cue, based on their past experience and acquired skill in the use of their remaining senses (Pascual-Leone et al., 2005; Cattaneo et al., 2011).

Blind and sighted subjects, standing eyes closed with feet in tandem position, touched a pad with their index finger (LFT) and withdrew the finger from the pad in sequence. Steady-state body sway (with or without contact) did not differ between blind and sighted subjects. On adding the haptic stimulus, postural muscle activity and sway diminished in both groups, but at a significantly shorter latency (by about 0.5 s) in the blind (Schieppati et al., 2014). These data showed that blind are rapid in implementing adaptive postural modifications when granted an external haptic reference. Interestingly, the short delays appeared to be, at least in part, the consequence of a rapid learning process at the beginning of the series of trials, whereby the differences with respect to sighted subjects became obvious after some 10 task repetitions or so.

These findings show that fast processing of the stabilizing haptic spatial-orientation cues may be favored by neural plasticity in the blind, and add new information to the field of sensory-guided dynamic control of equilibrium in man. Under steady-state conditions, the balance control of blind subjects is not superior to that of sighted subjects eyes-closed. However, the former are considerably more rapid than the latter in implementing the appropriate modifications in postural set when confronted with a change in the relationship between body and environment. Coping with the haptic transient (rather than body stabilization *per se* under steady-state condition) seems to be favored by the loss of vision, perhaps through increased reliance on the sense of touch (Wong et al., 2011) and the enhanced functional connectivity between sensory and visual cortex (Ioannides et al., 2013; Ricciardi et al., 2014). The fact that the early-blind subjects showed a more prompt stabilization than late-blind subjects and that the latter were faster than in sighted subjects (Schieppati et al., 2014) suggests a progressive modification over time of the sensorimotor integration processes controlling body orientation in space, as part of their adaptation implying increased attention to non-visual events (Burton et al., 2014). Perhaps, the relatively lesser problems encountered by early-blind subjects in their activities of daily life compared to elderly, low-vision subjects (Chen et al., 2012) may be related to the early onset of plastic changes. In the view of these findings, protocols may be developed for enhancing both postural capacities and tactual object exploration and recognition (Tzovaras et al., 2004).

WHAT DETERMINES THE LENGTH OF THE SENSORIMOTOR PROCESSING TIME?

What mechanisms contribute to the rapid decline in body sway following access to stabilizing haptic or visual sensory inflow? In stance control, under both static and dynamic conditions, we not only track with the CoP the random displacement of the CoM, but

we bypass its instantaneous position, in the presumed direction along which it moves, in order to create the torque necessary for braking and reverting its displacement. Indeed, we act on the movement of the CoM, in order to constrain its displacement within a relatively narrow space. In doing so, we rely on the operation of complex processes, whereby ongoing sensory information may be able to inform about future states of instability in a predictive manner (Slobounov et al., 1997, 2009). This may not be dissimilar from the sheepdog task, promptly gathering and fetching moving animals to a pre-defined goal position (Vaughan et al., 1998). The narrower the surface of the ellipse within which the center of feet pressure—the flock—moves, the smaller the energy spent, and the more stable the CoM of the body. In the sheepdog model, the size of the overshoot can be greatly reduced by appropriately tuning the gain parameter—or increasing the dog's anticipatory capacities.

Reducing the overshoot of the CoP with respect to the instantaneous position of the CoM to the extent sufficient for balancing with the minimal possible energy and computation costs would be achieved by increasing the gain of the system controlling the reciprocal positions of the CoM and of CoP, as if the sheepdog became "smarter" in controlling the flock. Changing the gain is likely operating by successive approximations, therefore time consuming, which might explain the relatively long delay of the onset of the changes in postural control mode and the slow time constant of the reduction in sway. Under different conditions (a computer-generated expanding visual field), likely requiring more complex processing than the simple abrupt change in haptic and visual information mentioned above, Jeka et al. (2008) measured the delay necessary for the nervous system to determine the most relevant sensory information for successful control of semi-tandem stance. Seconds from the change were necessary before a steady state was reached. Additionally, their data indicate a low speed for reweighting, when the visual scene motion was reduced, suggesting a temporal asymmetry (a slower process) whenever the change in the information does not threaten balance. Differences in the same sense (longer times to reach steady-state) have been also found on addition compared to withdrawal of stabilizing haptic and visual information, as mentioned above (Sozzi et al., 2012). Notably, under the condition of withdrawal of visual or haptic information, our nervous system could rely on its capacity for sustaining a working memory trace of recent information about the environment for guiding the reaction to postural perturbation (Bove et al., 2009; King et al., 2010; Cheng et al., 2012). Such a memory trace appears to explain our ability to guide targeted compensatory arm responses in the absence of online vision when a postural perturbation occurs (Cheng et al., 2013). However, this mechanism would not justify the *shorter* latencies of sway oscillation changes on withdrawal than addition of visual and haptic information under conditions of maintenance of unperturbed stance.

The timing of sensory modulation may differ when the task demands it and if the threat of an imminent fall increases the rate of gain modulation. For instance, threat of falling (Bolton et al., 2011b) or startling stimuli (Valls-Solé et al., 1999; Alibiglou and MacKinnon, 2012; Stevenson et al., 2014) can drive cortical motor responses faster than expected under normal conditions of voluntary control. Sensorimotor processes could as well be quickened when the task demands it. The slightly shorter latency of postural changes on *withdrawal* than addition of visual and haptic information would be affected by a similar event, since standing in tandem is more demanding in the absence of stabilizing information. Overall, one might note here that, however difficult the task of tandem standing, there is no urgent need to drive a rapid (and possibly metabolically costly) reweighting on the CNS, if a sufficient result can be managed with slower modulation.

CONCLUSIONS AND PERSPECTIVES: BRAIN AUGMENTATION AND NEUROPROSTHESES

The likelihood that the inflow from different senses changes concurrently, or within a short time-interval, is non-negligible. This gives rise to new questions. Do concurrent changes in the "stabilizing" direction (e.g., from no-vision to vision and from no-touch to touch) summate and ultimately assure a "better", more rapid performance? Are there differences when both changes occur in the opposite condition? Each stage of processing sensory information takes a certain amount of time, unique for each sensory modality (Barnett-Cowan and Harris, 2009): do these differences have an impact on the performance? Does the CNS, faced with a movement-balance integration problem, "select" one modality over the other in case of both changing? If so, are there "rules" for this selection? To what extent does the temporal order prevail over the modality? In this context, the expectation that the sensory condition(s) changes during the maintenance of a given (more or less critical) posture or in the preparation of a movement can play a role in the selection of the leading sensory information.

These questions should be taken into account when considering problems of sensorimotor integration in elderly subjects or patients, and when designing simulation models of human balance. In perspective, aged persons (Nardone et al., 1995), Parkinsonian patients, and patients affected by peripheral neuropathies, and blind subjects (Bugnariu and Fung, 2007; Striem-Amit et al., 2012; Maidenbaum et al., 2014) represent examples of different conditions liable to affect the variable at hand, i.e., the sensori-motor processing time, due to progressive losses in function across multiple systems, including sensation, cognition, memory, motor control (Mahncke et al., 2006; De Nunzio et al., 2007; Nardone et al., 2007; Konczak et al., 2008, 2012; Schmid et al., 2008; Aman et al., 2014). A rough attempt at identifying possible steps of the sensorimotor integration process is reported in graphic form in **Figure 2**, where different reweighting coefficients are assumed for different modalities of posture-stabilizing information. Whether the coefficients also affect the delays should be checked by further investigations.

These mechanisms should have an impact on both basic knowledge and applied science: (1) The duration of the process of integration of a change in sensory information is an important variable in the field of sensory-motor coordination. It can be affected by various sensory and motor conditions, and be a marker of a normal state under a given condition. (2) Cognitive processing and integration of sensory inputs for balance require time, and attention influences this processing

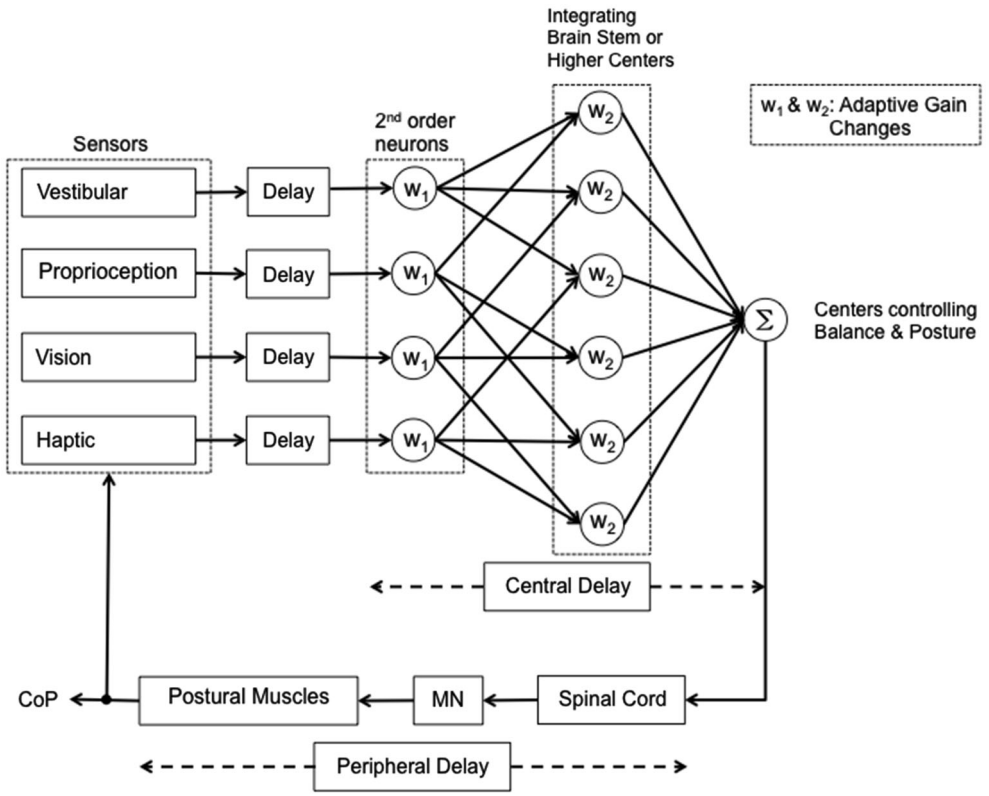

FIGURE 2 | Simplified scheme of the reweighting process during quiet stance. Vestibular, proprioceptive, visual and haptic signals are coded by the peripheral receptors and reach the brain after a corresponding delay. The information is first processed in 2nd order neurons. The afferent information then diverges to higher integrating centers and may be then reweighted according to the availability and accuracy of the other sensory inputs and balance constraints. Then information converges again (Σ) in the centers responsible for the control of balance. Following a short delay the information is transferred to the spinal cord interneuronal circuitry that generates the appropriate spatio-temporal pattern of muscle activity. This implies activation of MN activity and relevant muscle force, the effect of which is measured as displacement of the center of pressure (CoP). Most likely, the main part of the interval between the shift in sensory condition and the change in CoP displacement (approx. 1–2 s) conditional to active or passive addition or withdrawal of sensory information) depends on the operation of the central mechanisms generating the adaptive gain changes.

time, as well as sensory selection by facilitating specific sensory channels. Since performing a concurrent information-processing task may have an effect on the time delay, balance processes in older adults (Papegaaij et al., 2014) or sensory-impaired patients may be vulnerable to sensory-integration delays and to interference from concurrent cognitive tasks (Lacour et al., 2008). (3) Implementation of an appropriate time-lag between changes in a sensory modality, including its effects on balance, seems to represent an important aspect of the design of the control system for humanoid robots (Mahboobin et al., 2008, 2009; Peterka, 2009; Klein et al., 2011; Lebedev et al., 2011; O'Doherty et al., 2011; Rincon-Gonzalez et al., 2011; Demain et al., 2013). Biologically-inspired computational architectures, which are continuous in time and parallel in nature, do not map well onto conventional processors, which are discrete in time and serial in operation (Higgins, 2001). The findings briefly mentioned here would probably foster power- and space-efficient implementation technology. (4) "Rehabilitation robotics" is a new field of investigation between science and technology (Volpe et al., 2003; Casadio et al., 2008). Robots are being used to understand (Mergner, 2007; Mergner et al., 2009) and assist in maintaining balance and equilibrium (Forrester et al., 2014), or in helping movement practice following neurological injury (Krebs and Volpe, 2013), also providing insight into movement recovery. (5) Augmentation protocols of brain function offer enhancements for sensorimotor functions (this issue). For instance, appropriate patterns of vibratory stimulation to the dorsal axial trunk muscles easily reproduce functional medio-lateral oscillations of the standing body (De Nunzio et al., 2007) as well as enhance walking cadence and velocity in PD patients (De Nunzio et al., 2010). Moreover, evolved neuroprostheses employing functional neuromuscular stimulation (FNS) can restore basic standing function (Mushahwar et al., 2007; Braz et al., 2009; Capogrosso et al., 2013). Cochlear implants providing vestibular electrodes can enhance the function of the vestibulo-ocular reflex (Perez-Fornos et al., 2014).

Robots can haptically assess sensorimotor performance, administer training, and improve motor recovery. In addition to providing insight into motor control, robotic paradigms and sensory augmentation devices may eventually enhance motor

learning and motor recovery beyond the levels possible with conventional training techniques (Steffin, 1997; Bach-y-Rita, 2004; Kärcher et al., 2012; Proulx et al., 2014; Wright, 2014). We hope that defining the sensorimotor processing time for balance can represent a small but critical step in the direction of building new, smarter balance and locomotion training devices.

ACKNOWLEDGMENTS

This study was supported in part by the "Ricerca Finalizzata" grants (GR-2009-1471033 and RF-2011-02352379) from the Italian Ministry of Health and by the "PRIN" grants (2009JMMYFZ and 2010MEFNF7) from the Italian Ministry of University. We would like to sincerely thank the reviewers for their valuable comments and suggestions on our original manuscript.

REFERENCES

Alibiglou, L., and MacKinnon, C. D. (2012). The early release of planned movement by acoustic startle can be delayed by transcranial magnetic stimulation over the motor cortex. *J. Physiol.* 590, 919–936. doi: 10.1113/jphysiol.2011.219592

Aman, J. E., Abosch, A., Bebler, M., Lu, C. H., and Konczak, J. (2014). Subthalamic nucleus deep brain stimulation improves somatosensory function in Parkinson's disease. *Mov. Disord.* 29, 221–228. doi: 10.1002/mds.25731

Assländer, L., and Peterka, R. J. (2014). Sensory reweighting dynamics in human postural control. *J. Neurophysiol.* 111, 1852–1864. doi: 10.1152/jn.00669.2013

Azulay, J. P., Mesure, S., Amblard, B., Blin, O., Sangla, I., and Pouget, J. (1999). Visual control of locomotion in Parkinson's disease. *Brain* 122, 111–120. doi: 10.1093/brain/122.1.111

Baccini, M., Rinaldi, L. A., Federighi, G., Vannucchi, L., Paci, M., and Masotti, G. (2007). Effectiveness of fingertip light contact in reducing postural sway in older people. *Age Ageing* 36, 30–35. doi: 10.1093/ageing/afl072

Bach-y-Rita, P. (2004). Tactile sensory substitution studies. *Ann. N Y Acad. Sci.* 1013, 83–91. doi: 10.1196/annals.1305.006

Bandini, F., Pierantozzi, M., and Bodis-Wollner, I. (2001). Parkinson's disease changes the balance of onset and offset visual responses: an evoked potential study. *Clin. Neurophysiol.* 112, 976–983. doi: 10.1016/s1388-2457(01)00531-4

Barnett-Cowan, M., and Harris, L. R. (2009). Perceived timing of vestibular stimulation relative to touch, light and sound. *Exp. Brain Res.* 198, 221–231. doi: 10.1007/s00221-009-1779-4

Beckley, D. J., Bloem, B. R., Remler, M. P., Roos, R. A., and Van Dijk, J. G. (1991). Long latency postural responses are functionally modified by cognitive set. *Electroencephalogr. Clin. Neurophysiol.* 81, 353–358. doi: 10.1016/0168-5597(91)90024-r

Black, F. O., and Nashner, L. M. (1984). Vestibulo-spinal control differs in patients with reduced versus distorted vestibular function. *Acta Otolaryngol. Suppl.* 406, 110–114. doi: 10.3109/00016488309123015

Bodis-Wollner, I. (1992). Sensory evoked potentials: PERG, VEP and SEP. *Curr. Opin. Neurol. Neurosurg.* 5, 716–726.

Bola, M., Gall, C., and Sabel, B. A. (2013). The second face of blindness: processing speed deficits in the intact visual field after pre- and post-chiasmatic lesions. *PLoS One* 8:e63700. doi: 10.1371/journal.pone.0063700

Bolton, D. A., Brown, K. E., McIlroy, W. E., and Staines, W. R. (2012). Transient inhibition of the dorsolateral prefrontal cortex disrupts somatosensory modulation during standing balance as measured by electroencephalography. *Neuroreport* 23, 369–372. doi: 10.1097/WNR.0b013e328352027c

Bolton, D. A., McIlroy, W. E., and Staines, W. R. (2011a). The impact of light fingertip touch on haptic cortical processing during a standing balance task. *Exp. Brain Res.* 212, 279–291. doi: 10.1007/s00221-011-2728-6

Bolton, D. A. E., Patel, R., Staines, W. R., and McIlroy, W. E. (2011b). Transient inhibition of primary motor cortex suppresses hand muscle responses during a reactive reach to grasp. *Neurosci. Lett.* 504, 83–87. doi: 10.1016/j.neulet.2011.09.001

Borel, L., Lopez, C., Péruch, P., and Lacour, M. (2008). Vestibular syndrome: a change in internal spatial representation. *Neurophysiol. Clin.* 38, 375–389. doi: 10.1016/j.neucli.2008.09.002

Bottaro, A., Casadio, M., Morasso, P. G., and Sanguineti, V. (2005). Body sway during quiet standing: is it the residual chattering of an intermittent stabilization process? *Hum. Mov. Sci.* 24, 588–615. doi: 10.1016/j.humov.2005.07.006

Bottaro, A., Yasutake, Y., Nomura, T., Casadio, M., and Morasso, P. (2008). Bounded stability of the quiet standing posture: an intermittent control model. *Hum. Mov. Sci.* 27, 473–495. doi: 10.1016/j.humov.2007.11.005

Bottini, G., Karnath, H. O., Vallar, G., Sterzi, R., Frith, C. D., Frackowiak, R. S., et al. (2001). Cerebral representations for egocentric space: functional-anatomical evidence from caloric vestibular stimulation and neck vibration. *Brain* 124, 1182–1196. doi: 10.1093/brain/124.6.1182

Bove, M., Bonzano, L., Trompetto, C., Abbruzzese, G., and Schieppati, M. (2006). The postural disorientation induced by neck muscle vibration subsides on lightly touching a stationary surface or aiming at it. *Neuroscience* 143, 1095–1103. doi: 10.1016/j.neuroscience.2006.08.038

Bove, M., Courtine, G., and Schieppati, M. (2002). Neck muscle vibration and spatial orientation during stepping in place in humans. *J. Neurophysiol.* 88, 2232–2241. doi: 10.1152/jn.00198.2002

Bove, M., Diverio, M., Pozzo, T., and Schieppati, M. (2001). Neck muscle vibration disrupts steering of locomotion. *J. Appl. Physiol. (1985)* 91, 581–588.

Bove, M., Fenoggio, C., Tacchino, A., Pelosin, E., and Schieppati, M. (2009). Interaction between vision and neck proprioception in the control of stance. *Neuroscience* 164, 1601–1608. doi: 10.1016/j.neuroscience.2009.09.053

Braz, G. P., Russold, M., Smith, R. M., and Davis, G. M. (2009). Efficacy and stability performance of traditional versus motion sensor-assisted strategies for FES standing. *J. Biomech.* 42, 1332–1338. doi: 10.1016/j.jbiomech.2009.03.003

Bronstein, A. M., and Buckwell, D. (1997). Automatic control of postural sway by visual motion parallax. *Exp. Brain Res.* 113, 243–248. doi: 10.1007/bf02450322

Buchanan, J. J., and Horak, F. B. (1999). Emergence of postural patterns as a function of vision and translation frequency. *J. Neurophysiol.* 81, 2325–2339.

Bugnariu, N., and Fung, J. (2007). Aging and selective sensorimotor strategies in the regulation of upright balance. *J. Neuroeng. Rehabil.* 20, 4–19. doi: 10.1186/1743-0003-4-19

Burke, R. E., Rudomin, P., and Zajac, F. E. 3rd. (1976). The effect of activation history on tension production by individual muscle units. *Brain Res.* 109, 515–529. doi: 10.1016/0006-8993(76)90031-7

Burton, H., Snyder, A. Z., and Raichle, M. E. (2014). Resting state functional connectivity in early blind humans. *Front. Syst. Neurosci.* 8:51. doi: 10.3389/fnsys.2014.00051

Capogrosso, M., Wenger, N., Raspopovic, S., Musienko, P., Beauparlant, J., Bassi Luciani, L., et al. (2013). A computational model for epidural electrical stimulation of spinal sensorimotor circuits. *J. Neurosci.* 33, 19326–19340. doi: 10.1523/JNEUROSCI.1688-13.2013

Carpenter, M. G., Murnaghan, C. D., and Inglis, J. T. (2010). Shifting the balance: evidence of an exploratory role for postural sway. *Neuroscience* 171, 196–204. doi: 10.1016/j.neuroscience.2010.08.030

Casadio, M., Sanguineti, V., Morasso, P., and Solaro, C. (2008). Abnormal sensorimotor control, but intact force field adaptation, in multiple sclerosis subjects with no clinical disability. *Mult. Scler.* 14, 330–342. doi: 10.1177/1352458507085068

Cattaneo, Z., Fantino, M., Tinti, C., Pascual-Leone, A., Silvanto, J., and Vecchi, T. (2011). Spatial biases in peripersonal space in sighted and blind individuals revealed by a haptic line bisection paradigm. *J. Exp. Psychol. Hum. Percept. Perform.* 37, 1110–1121. doi: 10.1037/a0023511

Chapman, C. E. (1994). Active versus passive touch: factors influencing the transmission of somatosensory signals to primary somatosensory cortex. *Can. J. Physiol. Pharmacol.* 72, 558–570. doi: 10.1139/y94-080

Chen, N., Huang, T. L., Tsai, R. K., and Sheu, M. M. (2012). Prevalence and causes of visual impairment in elderly Amis aborigines in Eastern Taiwan (the Amis Eye Study). *Jpn. J. Ophthalmol.* 56, 624–630. doi: 10.1007/s10384-012-0178-8

Cheng, K. C., McKay, S. M., King, E. C., and Maki, B. E. (2012). Reaching to recover balance inunpredictable circumstances: is online visual control of the reach-to-grasp reaction necessary or sufficient? *Exp. Brain Res.* 218, 589–599. doi: 10.1007/s00221-012-3051-6

Cheng, K. C., Pratt, J., and Maki, B. E. (2013). Effects of spatial-memory decay and dual-task interference on perturbation-evoked reach-to-grasp reactions in the absence of online visual feedback. *Hum. Mov. Sci.* 32, 328–342. doi: 10.1016/j.humov.2012.11.001

Clapp, S., and Wing, A. M. (1999). Light touch contribution to balance in normal bipedal stance. *Exp. Brain Res.* 125, 521–524. doi: 10.1007/s002210050711

Clarac, F., el Manira, A., and Cattaert, D. (1992). Presynaptic control as a mechanism of sensory-motor integration. *Curr. Opin. Neurobiol.* 2, 764–769. doi: 10.1016/0960-9822(92)90095-r

Cohen, L. G., Celnik, P., Pascual-Leone, A., Corwell, B., Falz, L., Dambrosia, J., et al. (1997). Functional relevance of cross-modal plasticity in blind humans. *Nature* 389, 180–183. doi: 10.1038/38278

Contreras-Vidal, J. L., and Buch, E. R. (2003). Effects of Parkinson's disease on visuomotor adaptation. *Exp. Brain Res.* 150, 25–32. doi: 10.1007/s00221-003-1403-y

Cooke, J. D., Brown, J. D., and Brooks, V. B. (1978). Increased dependence on visual information for movement control in patients with Parkinson's disease. *Can. J. Neurol. Sci.* 5, 413–415.

Corna, S., Tarantola, J., Nardone, A., Giordano, A., and Schieppati, M. (1999). Standing on a continuously moving platform: is body inertia counteracted or exploited? *Exp. Brain Res.* 124, 331–341. doi: 10.1007/s002210050630

Courtine, G., Pozzo, T., Lucas, B., and Schieppati, M. (2001). Continuous, bilateral Achilles' tendon vibration is not detrimental to human walk. *Brain Res. Bull.* 55, 107–115. doi: 10.1016/s0361-9230(01)00504-4

Creath, R., Kiemel, T., Horak, F., and Jeka, J. J. (2002). Limited control strategies with the loss of vestibular function. *Exp. Brain Res.* 145, 323–333. doi: 10.1007/s00221-002-1110-0

Cullen, K. E. (2004). Sensory signals during active versus passive movement. *Curr. Opin. Neurobiol.* 14, 698–706. doi: 10.1016/j.conb.2004.10.002

Daubechies, I., Jianfeng, L., and Hau-Tiemg, W. (2011). Synchrosqueezed wavelet transforms: an empirical mode decomposition-like tool. *Appl. Comput. Harmon. Anal.* 30, 243–261. doi: 10.1016/j.acha.2010.08.002

Day, B. L., Steiger, M. J., Thompson, P. D., and Marsden, C. D. (1993). Effect of vision and stance width on human body motion when standing: implications for afferent control of lateral sway. *J. Physiol.* 469, 479–499.

Demain, S., Metcalf, C. D., Merrett, G. V., Zheng, D., and Cunningham, S. A. (2013). Narrative review on haptic devices: relating the physiology and psychophysical properties of the hand to devices for rehabilitation in central nervous system disorders. *Disabil. Rehabil. Assist. Technol.* 8, 181–189. doi: 10.3109/17483107.2012.697532

De Nunzio, A. M., Grasso, M., Nardone, A., Godi, M., and Schieppati, M. (2010). Alternate rhythmic vibratory stimulation of trunk muscles affects walking cadence and velocity in Parkinson's disease. *Clin. Neurophysiol.* 121, 240–247. doi: 10.1016/j.clinph.2009.10.018

De Nunzio, A. M., Nardone, A., and Schieppati, M. (2005). Head stabilization on a continuously oscillating platform: the effect of a proprioceptive disturbance on the balancing strategy. *Exp. Brain Res.* 165, 261–272. doi: 10.1007/s00221-005-2297-7

De Nunzio, A. M., Nardone, A., and Schieppati, M. (2007). The control of equilibrium in Parkinson's disease patients: delayed adaptation of balancing strategy to shifts in sensory set during a dynamic task. *Brain Res. Bull.* 74, 258–270. doi: 10.1016/j.brainresbull.2007.06.020

De Nunzio, A. M., and Schieppati, M. (2007). Time to reconfigure balancing behaviour in man: changing visual condition while riding a continuously moving platform. *Exp. Brain Res.* 178, 18–36. doi: 10.1007/s00221-006-0708-z

Dickstein, R., Peterka, R. J., and Horak, F. B. (2003). Effects of light fingertip touch on postural responses in subjects with diabetic neuropathy. *J. Neurol. Neurosurg. Psychiatry* 74, 620–626. doi: 10.1136/jnnp.74.5.620

Dickstein, R., Shupert, C. L., and Horak, F. B. (2001). Fingertip touch improves postural stability in patients with peripheral neuropathy. *Gait Posture* 14, 238–247. doi: 10.1016/s0966-6362(01)00161-8

Fiehler, K., and Rösler, F. (2010). Plasticity of multisensory dorsal stream functions: evidence from congenitally blind and sighted adults. *Restor. Neurol. Neurosci.* 28, 193–205. doi: 10.3233/RNN-2010-0500

Forrester, L. W., Roy, A., Krywonis, A., Kehs, G., Krebs, H. I., and Macko, R. F. (2014). Modular ankle robotics training in early subacute stroke: a randomized controlled pilot study. *Neurorehabil. Neural Repair* 28, 678–687. doi: 10.1177/1545968314521004

Guerraz, M., and Bronstein, A. M. (2008). Ocular versus extraocular control of posture and equilibrium. *Neurophysiol. Clin.* 38, 391–398. doi: 10.1016/j.neucli.2008.09.007

Hagbarth, K. E., Wallin, G., and Löfstedt, L. (1973). Muscle spindle responses to stretch in normal and spastic subjects. *Scand. J. Rehabil. Med.* 5, 156–159.

Haggard, P. D., and Wolpert (2005). "Disorders of body schema," in *High-Order Motor Disorders: From Neuroanatomy and Neurobiology to Clinical Neurology*, eds J. Freund, M. Jeannerod, M. Hallett and R. Leiguarda (Oxford: Oxford University Press), 261–271.

Hagura, N., Takei, T., Hirose, S., Aramaki, Y., Matsumura, M., Sadato, N., et al. (2007). Activity in the posterior parietal cortex mediates visual dominance over kinesthesia. *J. Neurosci.* 27, 7047–7053. doi: 10.1523/jneurosci.0970-07.2007

Hatzitaki, V., Pavlou, M., and Bronstein, A. M. (2004). The integration of multiple proprioceptive information: effect of ankle tendon vibration on postural responses to platform tilt. *Exp. Brain Res.* 154, 345–354. doi: 10.1007/s00221-003-1661-8

Heed, T., and Azañón, E. (2014). Using time to investigate space: a review of tactile temporal order judgments as a window onto spatial processing in touch. *Front. Psychol.* 5:76. doi: 10.3389/fpsyg.2014.00076

Higgins, C. M. (2001). Sensory architectures for biologically inspired autonomous robotics. *Biol. Bull.* 200, 235–242. doi: 10.2307/1543322

Hlavačka, F., Shupert, C. L., and Horak, F. B. (1999). The timing of galvanic vestibular stimulation affects responses to platform translation. *Brain Res.* 821, 8–16. doi: 10.1016/s0006-8993(98)01356-0

Holden, M., Ventura, J., and Lackner, J. R. (1994). Stabilization of posture by precision contact of the index finger. *J. Vestib. Res.* 4, 285–301.

Horak, F. B., and Hlavačka, F. (2002). Vestibular stimulation affects medium latency postural muscle responses. *Exp. Brain Res.* 144, 95–102. doi: 10.1007/s00221-002-1041-9

Horak, F. B., Nutt, J. G., and Nashner, L. M. (1992). Postural inflexibility in PD subjects. *J. Neurol. Sci.* 111, 46–58. doi: 10.1016/0022-510x(92)90111-w

Hötting, K., and Röder, B. (2009). Auditory and auditory-tactile processing in congenitally blind humans. *Hear. Res.* 258, 165–174. doi: 10.1016/j.heares.2009.07.012

Ioannides, A. A., Liu, L., Poghosyan, V., Saridis, G. A., Gjedde, A., Ptito, M., et al. (2013). MEG reveals a fast pathway from somatosensory cortex to occipital areas via posterior parietal cortex in a blind subject. *Front. Hum. Neurosci.* 7:429. doi: 10.3389/fnhum.2013.00429

Ivanenko, Y. P., Grasso, R., and Lacquaniti, F. (2000). Neck muscle vibration makes walking humans accelerate in the direction of gaze. *J. Physiol.* 525, 803–814. doi: 10.1111/j.1469-7793.2000.t01-1-00803.x

Ivanenko, Y. P., Talis, V. L., and Kazennikov, O. V. (1999). Support stability influences postural responses to muscle vibration in humans. *Eur. J. Neurosci.* 11, 647–654. doi: 10.1046/j.1460-9568.1999.00471.x

Jacono, M., Casadio, M., Morasso, P. G., and Sanguineti, V. (2004). The sway-density curve and the underlying postural stabilization process. *Motor Control* 8, 292–311.

Jeka, J. J., Allison, L. K., and Kiemel, T. (2010). The dynamics of visual reweighting in healthy and fall-prone older adults. *J. Mot. Behav.* 42, 197–208. doi: 10.1080/00222895.2010.481693

Jeka, J. J., Easton, R. D., Bentzen, B. L., and Lackner, J. R. (1996). Haptic cues for orientation and postural control in sighted and blind individuals. *Percept. Psychophys.* 58, 409–423. doi: 10.3758/bf03206817

Jeka, J. J., and Lackner, J. R. (1994). Fingertip contact influences human postural control. *Exp. Brain Res.* 100, 495–502. doi: 10.1007/bf00229188

Jeka, J., Oie, K. S., and Kiemel, T. (2000). Multisensory information for human postural control: integrating touch and vision. *Exp. Brain Res.* 134, 107–125. doi: 10.1007/s002210000412

Jeka, J. J., Oie, K. S., and Kiemel, T. (2008). Asymmetric adaptation with functional advantage in human sensorimotor control. *Exp. Brain Res.* 191, 453–463. doi: 10.1007/s00221-008-1539-x

Jeka, J. J., Schöner, G., Dijkstra, T., Ribeiro, P., and Lackner, J. R. (1997). Coupling of fingertip somatosensory information to head and body sway. *Exp. Brain Res.* 113, 475–483. doi: 10.1007/pl00005600

Johannsen, L., Wing, A. M., and Hatzitaki, V. (2012). Contrasting effects of finger and shoulder interpersonal light touch on standing balance. *J. Neurophysiol.* 107, 216–225. doi: 10.1152/jn.00149.2011

Kanekar, N., Lee, Y. J., and Aruin, A. S. (2013). Effect of light finger touch in balance control of individuals with multiple sclerosis. *Gait Posture* 38, 643–647. doi: 10.1016/j.gaitpost.2013.02.017

Kärcher, S. M., Fenzlaff, S., Hartmann, D., Nagel, S. K., and König, P. (2012). Sensory augmentation for the blind. *Front. Hum. Neurosci.* 6:37. doi: 10.3389/fnhum.2012.00037

Kavounoudias, A., Gilhodes, J. C., Roll, R., and Roll, J. P. (1999). From balance regulation to body orientation: two goals for muscle proprioceptive information processing? *Exp. Brain Res.* 124, 80–88. doi: 10.1007/s002210050602

Kelly, L. A., Kuitunen, S., Racinais, S., and Cresswell, A. G. (2012). Recruitment of the plantar intrinsic foot muscles with increasing postural demand. *Clin. Biomech. (Bristol, Avon)* 27, 46–51. doi: 10.1016/j.clinbiomech.2011.07.013

King, E. C., McKay, S. M., Cheng, K. C., and Maki, B. E. (2010). The use of peripheral vision to guide perturbation-evoked reach-to-grasp balance-recovery reactions. *Exp. Brain Res.* 207, 105–118. doi: 10.1007/s00221-010-2434-9

Klein, A., Jeka, J., Kiemel, T., and Lewis, M. A. (2011). Navigating sensory conflict in dynamic environments using adaptive state estimation. *Biol. Cybern.* 105, 291–304. doi: 10.1007/s00422-011-0466-2

Konczak, J., Li, K. Y., Tuite, P. J., and Poizner, H. (2008). Haptic perception of object curvature in Parkinson's disease. *PLoS One* 3:e2625. doi: 10.1371/journal.pone.0002625

Konczak, J., Sciutti, A., Avanzino, L., Squeri, V., Gori, M., Masia, L., et al. (2012). Parkinson's disease accelerates age-related decline in haptic perception by altering somatosensory integration. *Brain* 135, 3371–3379. doi: 10.1093/brain/aws265

Kouzaki, M., and Masani, K. (2008). Reduced postural sway during quiet standing by light touch is due to finger tactile feedback but not mechanical support. *Exp. Brain Res.* 188, 153–158. doi: 10.1007/s00221-008-1426-5

Krebs, H. I., and Volpe, B. T. (2013). Rehabilitation robotics. *Handb. Clin. Neurol.* 110, 283–294. doi: 10.1016/B978-0-444-52901-5.00023-X

Krishnamoorthy, V., Slijper, H., and Latash, M. L. (2002). Effects of different types of light touch on postural sway. *Exp. Brain Res.* 147, 71–79. doi: 10.1007/s00221-002-1206-6

Kupers, R., and Ptito, M. (2014). Compensatory plasticity and cross-modal reorganization following early visual deprivation. *Neurosci. Biobehav. Rev.* 41, 36–52. doi: 10.1016/j.neubiorev.2013.08.001

Lackner, J. R., DiZio, P., Jeka, J., Horak, F., Krebs, D., and Rabin, E. (1999). Precision contact of the fingertip reduces postural sway of individuals with bilateral vestibular loss. *Exp. Brain Res.* 126, 459–466. doi: 10.1007/s002210050753

Lackner, J. R., Rabin, E., and DiZio, P. (2000). Fingertip contact suppresses the destabilizing influence of leg muscle vibration. *J. Neurophysiol.* 84, 2217–2224.

Lacour, M., Bernard-Demanze, L., and Dumitrescu, M. (2008). Posture control, aging and attention resources: models and posture-analysis methods. *Neurophysiol. Clin.* 38, 411–421. doi: 10.1016/j.neucli.2008.09.005

Lebedev, M. A., Tate, A. J., Hanson, T. L., Li, Z., O'Doherty, J. E., Winans, J. A., et al. (2011). Future developments in brain-machine interface research. *Clinics (Sao Paulo)* 66, 25–32. doi: 10.1590/s1807-59322011001300004

Lederman, S. J., and Klatzky, R. L. (2009). Haptic perception: a tutorial. *Atten. Percept. Psychophys.* 71, 1439–1459. doi: 10.3758/app.71.7.1439

Lekhel, H., Popov, K., Anastasopoulos, D., Bronstein, A., Bhatia, K., Marsden, C. D., et al. (1997). Postural responses to vibration of neck muscles in patients with idiopathic torticollis. *Brain* 120, 583–591. doi: 10.1093/brain/120.4.583

Lewis, G. N., and Byblow, W. D. (2002). Altered sensorimotor integration in Parkinson's disease. *Brain* 125, 2089–2099. doi: 10.1093/brain/awf200

Loram, I. D., Gollee, H., Lakie, M., and Gawthrop, P. J. (2011). Human control of an inverted pendulum: is continuous control necessary? Is intermittent control effective? Is intermittent control physiological? *J. Physiol.* 589, 307–324. doi: 10.1113/jphysiol.2010.194712

Lund, S. (1980). Postural effects of neck muscle vibration in man. *Experientia* 36:1398. doi: 10.1007/bf01960120

Mahboobin, A., Loughlin, P., Atkeson, C. G., and Redfern, M. (2009). A mechanism for sensory re-weighting in postural control. *Med. Biol. Eng. Comput.* 47, 921–929. doi: 10.1007/s11517-009-0477-5

Mahboobin, A., Loughlin, P. J., Redfern, M. S., Anderson, S. O., Atkeson, C. G., and Hodgins, J. K. (2008). Sensory adaptation in human balance control: lessons for biomimetic robotic bipeds. *Neural Netw.* 21, 621–627. doi: 10.1016/j.neunet.2008.03.013

Mahncke, H. W., Bronstone, A., and Merzenich, M. M. (2006). Brain plasticity and functional losses in the aged: scientific bases for a novel intervention. *Prog. Brain Res.* 157, 81–109. doi: 10.1016/s0079-6123(06)57006-2

Maidenbaum, S., Abboud, S., and Amedi, A. (2014). Sensory substitution: closing the gap between basic research and widespread practical visual rehabilitation. *Neurosci. Biobehav. Rev.* 41, 3–15. doi: 10.1016/j.neubiorev.2013.11.007

Marque, P., Nicolas, G., Marchand-Pauvert, V., Gautier, J., Simonetta-Moreau, M., and Pierrot-Deseilligny, E. (2001). Group I projections from intrinsic foot muscles to motoneurones of leg and thigh muscles in humans. *J. Physiol.* 536, 313–327. doi: 10.1111/j.1469-7793.2001.t01-1-00313.x

Massion, J. (1994). Postural control system. *Curr. Opin. Neurobiol.* 4, 877–887. doi: 10.1016/0959-4388(94)90137-6

Matthews, P. B. (1988). Proprioceptors and their contribution to somatosensory mapping: complex messages require complex processing. *Can. J. Physiol. Pharmacol.* 66, 430–438. doi: 10.1139/y88-073

Maurer, C., Mergner, T., and Peterka, R. J. (2006). Multisensory control of human upright stance. *Exp. Brain Res.* 171, 231–250. doi: 10.1007/s00221-005-0256-y

Mergner, T. (2007). Modeling sensorimotor control of human upright stance. *Prog. Brain Res.* 165, 283–297. doi: 10.1016/s0079-6123(06)65018-8

Mergner, T., Maurer, C., and Peterka, R. J. (2003). A multisensory posture control model of human upright stance. *Prog. Brain Res.* 142, 189–201. doi: 10.1016/s0079-6123(03)42014-1

Mergner, T., and Rosemeier, T. (1998). Interaction of vestibular, somatosensory and visual signals for postural control and motion perception under terrestrial and microgravity conditions—a conceptual model. *Brain Res. Brain Res. Rev.* 28, 118–135. doi: 10.1016/s0165-0173(98)00032-0

Mergner, T., Schweigart, G., and Fennell, L. (2009). Vestibular humanoid postural control. *J. Physiol. Paris* 103, 178–194. doi: 10.1016/j.jphysparis.2009.08.002

Meyer, P. F., Oddsson, L. I., and De Luca, C. J. (2004). The role of plantar cutaneous sensation in unperturbed stance. *Exp. Brain Res.* 156, 505–512. doi: 10.1007/s00221-003-1804-y

Mohapatra, S., Krishnan, V., and Aruin, A. S. (2012). Postural control in response to an external perturbation: effect of altered proprioceptive information. *Exp. Brain Res.* 217, 197–208. doi: 10.1007/s00221-011-2986-3

Morasso, P. G., and Schieppati, M. (1999). Can muscle stiffness alone stabilize upright standing? *J. Neurophysiol.* 82, 1622–1626.

Murnaghan, C. D., Horslen, B. C., Inglis, J. T., and Carpenter, M. G. (2011). Exploratory behavior during stance persists with visual feedback. *Neuroscience* 195, 54–59. doi: 10.1016/j.neuroscience.2011.08.020

Murnaghan, C. D., Squair, J. W., Chua, R., Inglis, J. T., and Carpenter, M. G. (2014). Cortical contributions to control of posture during unrestricted and restricted stance. *J. Neurophysiol.* 111, 1920–1926. doi: 10.1152/jn.00853.2012

Mushahwar, V. K., Jacobs, P. L., Normann, R. A., Triolo, R. J., and Kleitman, N. (2007). New functional electrical stimulation approaches to standing and walking. *J. Neural Eng.* 4, S181–S197. doi: 10.1088/1741-2560/4/3/s05

Naito, E. (2002). Perceptual distortion of intrapersonal and near-personal space sensed by proprioception. *Percept. Mot. Skills* 94, 499–505. doi: 10.2466/pms.2002.94.2.499

Nakata, H., and Yabe, K. (2001). Automatic postural response systems in individuals with congenital total blindness. *Gait Posture* 14, 36–43. doi: 10.1016/s0966-6362(00)00100-4

Nardone, A., Galante, M., Grasso, M., and Schieppati, M. (2008). Stance ataxia and delayed leg muscle responses to postural perturbations in cervical spondylotic myelopathy. *J. Rehabil. Med.* 40, 539–547. doi: 10.2340/16501977-0214

Nardone, A., Galante, M., Pareyson, D., and Schieppati, M. (2007). Balance control in sensory neuron disease. *Clin. Neurophysiol.* 118, 538–550. doi: 10.1016/j.clinph.2006.11.012

Nardone, A., Giordano, A., Corrà, T., and Schieppati, M. (1990). Responses of leg muscles in humans displaced while standing. Effects of types of perturbation and of postural set. *Brain* 113, 65–84. doi: 10.1093/brain/113.1.65

Nardone, A., Grasso, M., and Schieppati, M. (2006). Balance control in peripheral neuropathy: are patients equally unstable under static and dynamic conditions? *Gait Posture* 23, 364–373. doi: 10.1016/j.gaitpost.2005.04.002

Nardone, A., Grasso, M., Tarantola, J., Corna, S., and Schieppati, M. (2000). Postural coordination in elderly subjects standing on a periodically moving platform. *Arch. Phys. Med. Rehabil.* 81, 1217–1223. doi: 10.1053/apmr.2000.6286

Nardone, A., and Schieppati, M. (2004). Group II spindle fibres and afferent control of stance. Clues from diabetic neuropathy. *Clin. Neurophysiol.* 115, 779–789. doi: 10.1016/j.clinph.2003.11.007

Nardone, A., and Schieppati, M. (2005). Reflex contribution of spindle group Ia and II afferent input to leg muscle spasticity as revealed by tendon vibration in hemiparesis. *Clin. Neurophysiol.* 116, 1370–1381. doi: 10.1016/j.clinph.2005.01.015

Nardone, A., and Schieppati, M. (2006). Balance in Parkinson's disease under static and dynamic conditions. *Mov. Disord.* 21, 1515–1520. doi: 10.1002/mds.21015

Nardone, A., Siliotto, R., Grasso, M., and Schieppati, M. (1995). Influence of aging on leg muscle reflex responses to stance perturbation. *Arch. Phys. Med. Rehabil.* 76, 158–165. doi: 10.1016/s0003-9993(95)80025-5

Nougier, V., Bard, C., Fleury, M., and Teasdale, N. (1998). Contribution of central and peripheral vision to the regulation of stance: developmental aspects. *J. Exp. Child Psychol.* 68, 202–215. doi: 10.1006/jecp.1997.2427

O'Doherty, J. E., Lebedev, M. A., Ifft, P. J., Zhuang, K. Z., Shokur, S., Bleuler, H., et al. (2011). Active tactile exploration using a brain-machine-brain interface. *Nature* 479, 228–231. doi: 10.1038/nature10489

Oie, K. S., Kiemel, T., and Jeka, J. J. (2002). Multisensory fusion: simultaneous reweighting of vision and touch for the control of human posture. *Brain Res. Cogn. Brain Res.* 14, 164–176. doi: 10.1016/s0926-6410(02)00071-x

Pais-Vieira, M., Lebedev, M. A., Wiest, M. C., and Nicolelis, M. A. (2013). Simultaneous top-down modulation of the primary somatosensory cortex and thalamic nuclei during active tactile discrimination. *J. Neurosci.* 33, 4076–4093. doi: 10.1523/JNEUROSCI.1659-12.2013

Panichi, R., Botti, F. M., Ferraresi, A., Faralli, M., Kyriakareli, A., Schieppati, M., et al. (2011). Self-motion perception and vestibulo-ocular reflex during whole body yaw rotation in standing subjects: the role of head position and neck proprioception. *Hum. Mov. Sci.* 30, 314–332. doi: 10.1016/j.humov.2010.10.005

Papegaaij, S., Taube, W., Baudry, S., Otten, E., and Hortobágyi, T. (2014). Aging causes a reorganization of cortical and spinal control of posture. *Front. Aging Neurosci.* 6:28. doi: 10.3389/fnagi.2014.00028

Pasalar, S., Ro, T., and Beauchamp, M. S. (2010). TMS of posterior parietal cortex disrupts visual tactile multisensory integration. *Eur. J. Neurosci.* 31, 1783–1790. doi: 10.1111/j.1460-9568.2010.07193.x

Pascual-Leone, A., Amedi, A., Fregni, F., and Merabet, L. B. (2005). The plastic human brain cortex. *Annu. Rev. Neurosci.* 28, 377–401. Review. doi: 10.1146/annurev.neuro.27.070203.144216

Paulus, W. M., Straube, A., and Brandt, T. (1984). Visual stabilization of posture. Physiological stimulus characteristics and clinical aspects. *Brain* 107, 1143–1163. doi: 10.1093/brain/107.4.1143

Perez-Fornos, A., Guinand, N., van de Berg, R., Stokroos, R., Micera, S., Kingma, H., et al. (2014). Artificial balance: restoration of the vestibulo-ocular reflex in humans with a prototype vestibular neuroprosthesis. *Front. Neurol.* 5:66. doi: 10.3389/fneur.2014.00066

Peterka, R. J. (2002). Sensorimotor integration in human postural control. *J. Neurophysiol.* 88, 1097–1118. doi: 10.1152/jn.00605.2001

Peterka, R. J. (2009). Comparison of human and humanoid robot control of upright stance. *J. Physiol.* 103, 149–158. doi: 10.1016/j.jphysparis.2009.08.001

Peterka, R. J., and Loughlin, P. J. (2004). Dynamic regulation of sensorimotor integration in human postural control. *J. Neurophysiol.* 91, 410–423. doi: 10.1152/jn.00516.2003

Prochazka, A. (1989). Sensorimotor gain control: a basic strategy of motor systems? *Prog. Neurobiol.* 33, 281–307. doi: 10.1016/0301-0082(89)90004-x

Proulx, M. J., Brown, D. J., Pasqualotto, A., and Meijer, P. (2014). Multisensory perceptual learning and sensory substitution. *Neurosci. Biobehav. Rev.* 41, 16–25. doi: 10.1016/j.neubiorev.2012.11.017

Quinn, B. T., Carlson, C., Doyle, W., Cash, S. S., Devinsky, O., Spence, C., et al. (2014). Intracranial cortical responses during visual-tactile integration in humans. *J. Neurosci.* 34, 171–181. doi: 10.1523/JNEUROSCI.0532-13.2014

Rabin, E., Bortolami, S. B., DiZio, P., and Lackner, J. R. (1999). Haptic stabilization of posture: changes in arm proprioception and cutaneous feedback for different arm orientations. *J. Neurophysiol.* 82, 3541–3549.

Rabin, E., Chen, J., Muratori, L., Di Francisco-Donoghue, J., and Werner, W. G. (2013). Haptic feedback from manual contact improves balance control in people with Parkinson's disease. *Gait Posture* 38, 373–379. doi: 10.1016/j.gaitpost.2012.12.008

Rabin, E., DiZio, P., and Lackner, J. R. (2006). Time course of haptic stabilization of posture. *Exp. Brain Res.* 170, 122–126. doi: 10.1007/s00221-006-0348-3

Ravaioli, E., Oie, K. S., Kiemel, T., Chiari, L., and Jeka, J. J. (2005). Nonlinear postural control in response to visual translation. *Exp. Brain Res.* 160, 450–459. doi: 10.1007/s00221-004-2030-y

Redfern, M. S., Yardley, L., and Bronstein, A. M. (2001). Visual influences on balance. *J. Anxiety Disord.* 15, 81–94. Review. doi: 10.1016/s0887-6185(00)00043-8

Renier, L., De Volder, A. G., and Rauschecker, J. P. (2014). Cortical plasticity and preserved function in early blindness. *Neurosci. Biobehav. Rev.* 41, 53–63. doi: 10.1016/j.neubiorev.2013.01.025

Ricciardi, E., Bonino, D., Pellegrini, S., and Pietrini, P. (2014). Mind the blind brain to understand the sighted one! Is there a supramodal cortical functional architecture? *Neurosci. Biobehav. Rev.* 41, 64–77. doi: 10.1016/j.neubiorev.2013.10.006

Riley, M. A., Wong, S., Mitra, S., and Turvey, M. T. (1997). Common effects of touch and vision on postural parameters. *Exp. Brain Res.* 117, 165–170. doi: 10.1007/s002210050211

Rincon-Gonzalez, L., Warren, J. P., Meller, D. M., and Tillery, S. H. (2011). Haptic interaction of touch and proprioception: implications for neuroprosthetics. *IEEE Trans. Neural Syst. Rehabil. Eng.* 19, 490–500. doi: 10.1109/tnsre.2011.2166808

Rogers, M. W., Wardman, D. L., Lord, S. R., and Fitzaptrick, R. C. (2001). Passive tactile sensory input improves stability during standing. *Exp. Brain Res.* 136, 514–522. doi: 10.1007/s002210000615

Roll, J. P., and Vedel, J. P. (1982). Kinaesthetic role of muscle afferents in man, studied by tendon vibration and microneurography. *Exp. Brain Res.* 47, 177–190. doi: 10.1007/bf00239377

Roll, J. P., Vedel, J. P., and Ribot, E. (1989). Alteration of proprioceptive messages induced by tendon vibration in man: a microneurographic study. *Exp. Brain Res.* 76, 213–222. doi: 10.1007/bf00253639

Rougier, P., and Farenc, I. (2000). Adaptative effects of loss of vision on upright undisturbed stance. *Brain Res.* 871, 165–174. doi: 10.1016/s0006-8993(00)02357-x

Rowland, B. A., and Stein, B. E. (2014). A model of the temporal dynamics of multisensory enhancement. *Neurosci. Biobehav. Rev.* 41, 78–84. doi: 10.1016/j.neubiorev.2013.12.003

Schieppati, M., and Ducati, A. (1984). Short-latency cortical potentials evoked by tactile air-jet stimulation of body and face in man. *Electroencephalogr. Clin. Neurophysiol.* 58, 418–425. doi: 10.1016/0013-4694(84)90138-x

Schieppati, M., and Nardone, A. (1991). Free and supported stance in Parkinson's disease. The effect of posture and postural set on leg muscle responses to perturbation and its relation to the severity of the disease. *Brain* 114, 1227–1244. doi: 10.1093/brain/114.3.1227

Schieppati, M., and Nardone, A. (1995). Time course of 'set'-related changes in muscle responses to stance perturbation in humans. *J. Physiol.* 487, 787–796.

Schieppati, M., and Nardone, A. (1999). Group II spindle afferent fibers in humans: their possible role in the reflex control of stance. *Prog. Brain Res.* 123, 461–472. doi: 10.1016/s0079-6123(08)62882-4

Schieppati, M., Giordano, A., and Nardone, A. (2002). Variability in a dynamic postural task attests ample flexibility in balance control mechanisms. *Exp. Brain Res.* 144, 200–210. doi: 10.1007/s00221-002-1028-6

Schieppati, M., Hugon, M., Grasso, M., Nardone, A., and Galante, M. (1994). The limits of equilibrium in young and elderly normal subjects and in parkinsonians. *Electroencephalogr. Clin. Neurophysiol.* 93, 286–298. doi: 10.1016/0168-5597(94)90031-0

Schieppati, M., Nardone, A., Siliotto, R., and Grasso, M. (1995). Early and late stretch responses of human foot muscles induced by perturbation of stance. *Exp. Brain Res.* 105, 411–422. doi: 10.1007/bf00233041

Schieppati, M., Schmid, M., and Sozzi, S. (2014). Rapid processing of haptic cues for postural control in blind subjects. *Clin. Neurophysiol.* 125, 1427–1439. doi: 10.1016/j.clinph.2013.11.011

Schmid, M., Bottaro, A., Sozzi, S., and Schieppati, M. (2011). Adaptation to continuous perturbation of balance: progressive reduction of postural muscle activity with invariant or increasing oscillations of the center of mass depending

on perturbation frequency and vision conditions. *Hum. Mov. Sci.* 30, 262–278. doi: 10.1016/j.humov.2011.02.002

Schmid, M., Casabianca, L., Bottaro, A., and Schieppati, M. (2008). Graded changes in balancing behavior as a function of visual acuity. *Neuroscience* 153, 1079–1091. doi: 10.1016/j.neuroscience.2008.03.024

Schmid, M., Nardone, A., De Nunzio, A. M., Schmid, M., and Schieppati, M. (2007). Equilibrium during static and dynamic tasks in blind subjects: no evidence of cross-modal plasticity. *Brain* 130, 2097–2107. doi: 10.1093/brain/awm157

Schweigart, G., and Mergner, T. (2008). Human stance control beyond steady state response and inverted pendulum simplification. *Exp. Brain Res.* 185, 635–653. doi: 10.1007/s00221-007-1189-4

Sciutti, A., Squeri, V., Gori, M., Masia, L., Sandini, G., and Konczak, J. (2010). Predicted sensory feedback derived from motor commands does not improve haptic sensitivity. *Exp. Brain Res.* 200, 259–267. doi: 10.1007/s00221-009-1996-x

Shokur, S., O'Doherty, J. E., Winans, J. A., Bleuler, H., Lebedev, M. A., and Nicolelis, M. A. (2013). Expanding the primate body schema in sensorimotor cortex by virtual touches of an avatar. *Proc. Natl. Acad. Sci. U S A* 110, 15121–15126. doi: 10.1073/pnas.1308459110

Slobounov, S., Cao, C., Jaiswal, N., and Newell, K. M. (2009). Neural basis of postural instability identified by VTC and EEG. *Exp. Brain Res.* 199, 1–16. doi: 10.1007/s00221-009-1956-5

Slobounov, S. M., Moss, S. A., Slobounova, E. S., and Newell, K. M. (1998). Aging and time to instability in posture. *J. Gerontol. A Biol. Sci. Med. Sci.* 53, B71–B78. doi: 10.1093/gerona/53a.1.b71

Slobounov, S. M., Slobounova, E. S., and Newell, K. M. (1997). Virtual time-to-collision and human postural control. *J. Mot. Behav.* 29, 263–281. doi: 10.1080/00222899709600841

Smith, A. M., Chapman, C. E., Donati, F., Fortier-Poisson, P., and Hayward, V. (2009). Perception of simulated local shapes using active and passive touch. *J. Neurophysiol.* 102, 3519–3529. doi: 10.1152/jn.00043.2009

Soto-Faraco, S., and Azañón, E. (2013). Electrophysiological correlates of tactile remapping. *Neuropsychologia* 51, 1584–1594. doi: 10.1016/j.neuropsychologia.2013.04.012

Sozzi, S., Do, M. C., Monti, A., and Schieppati, M. (2012). Sensorimotor integration during stance: processing time of active or passive addition or withdrawal of visual or haptic information. *Neuroscience* 212, 59–76. doi: 10.1016/j.neuroscience.2012.03.044

Sozzi, S., Honeine, J. L., Do, M. C., and Schieppati, M. (2013). Leg muscle activity during tandem stance and the control of body balance in the frontal plane. *Clin. Neurophysiol.* 124, 1175–1186. doi: 10.1016/j.clinph.2012.12.001

Sozzi, S., Monti, A., De Nunzio, A. M., Do, M. C., and Schieppati, M. (2011). Sensori-motor integration during stance: time adaptation of control mechanisms on adding or removing vision. *Hum. Mov. Sci.* 30, 172–189. doi: 10.1016/j.humov.2010.06.002

Steffin, M. (1997). Virtual reality therapy of multiple sclerosis and spinal cord injury: design consideration for a haptic-visual interface. *Stud. Health Technol. Inform.* 44, 185–208.

Stevenson, A. J., Chiu, C., Maslovat, D., Chua, R., Gick, B., Blouin, J. S., et al. (2014). Cortical involvement in the StartReact effect. *Neuroscience* 269, 21–34. doi: 10.1016/j.neuroscience.2014.03.041

Striem-Amit, E., Cohen, L., Dehaene, S., and Amedi, A. (2012). Reading with sounds: sensory substitution selectively activates the visual word form area in the blind. *Neuron* 76, 640–652. doi: 10.1016/j.neuron.2012.08.026

Suzuki, Y., Nomura, T., and Morasso, P. (2011). Stability of a double inverted pendulum model during human quiet stance with continuous delay feedback control. *Conf. Proc. IEEE Eng. Med. Biol. Soc.* 2011, 7450–7453. doi: 10.1109/iembs.2011.6091747

Tax, C. M., Bom, A. P., Taylor, R. L., Todd, N., Cho, K. K., Fitzpatrick, R. C., et al. (2013). The galvanic whole-body sway response in health and disease. *Clin. Neurophysiol.* 124, 2036–2045. doi: 10.1016/j.clinph.2012.12.041

Teasdale, N., Stelmach, G. E., Breunig, A., and Meeuwsen, H. J. (1991). Age differences in visual sensory integration. *Exp. Brain Res.* 85, 691–696. doi: 10.1007/bf00231755

Ting, L. H. (2007). Dimensional reduction in sensorimotor systems: a framework for understanding muscle coordination of posture. *Prog. Brain Res.* 165, 299–321. doi: 10.1016/s0079-6123(06)65019-x

Tokuno, C. D., Carpenter, M. G., Thorstensson, A., Garland, S. J., and Cresswell, A. G. (2007). Control of the triceps surae during the postural sway of quiet standing. *Acta Physiol. (Oxf.)* 191, 229–236. doi: 10.1111/j.1748-1716.2007.01727.x

Tokuno, C. D., Taube, W., and Cresswell, A. G. (2009). An enhanced level of motor cortical excitability during the control of human standing. *Acta Physiol. (Oxf)* 195, 385–395. doi: 10.1111/j.1748-1716.2008.01898.x

Tommerdahl, M., Favorov, O. V., and Whitsel, B. L. (2010). Dynamic representations of the somatosensory cortex. *Neurosci. Biobehav. Rev.* 34, 160–170. doi: 10.1016/j.neubiorev.2009.08.009

Tremblay, F., Mireault, A. C., Dessureault, L., Manning, H., and Sveistrup, H. (2004). Postural stabilization from fingertip contact: I. Variations in sway attenuation, perceived stability and contact forces with aging. *Exp. Brain Res.* 157, 275–285. doi: 10.1007/s00221-004-1830-4

Tzovaras, D., Nikolakis, G., Fergadis, G., Malasiotis, S., and Stavrakis, M. (2004). Design and implementation of haptic virtual environments for the training of the visually impaired. *IEEE Trans. Neural Syst. Rehabil. Eng.* 12, 266–278. doi: 10.1109/tnsre.2004.828756

Valls-Solé, J., Alvarez, R., and Tolosa, E. S. (1994). Responses of the soleus muscle to transcranial magnetic stimulation. *Electroencephalogr. Clin. Neurophysiol.* 93, 421–427. doi: 10.1016/0168-5597(94)90148-1

Valls-Solé, J., Rothwell, J. C., Goulart, F. R., Cossu, G., and Muñoz, E. (1999). Patterned ballistic movements triggered by a startle in healthy humans. *J. Physiol.* 516, 931–938. doi: 10.1111/j.1469-7793.1999.0931u.x

van der Kooij, H., and Peterka, R. J. (2011). Non-linear stimulus-response behavior of the human stance control system is predicted by optimization of a system with sensory and motor noise. *J. Comput. Neurosci.* 30, 759–778. doi: 10.1007/s10827-010-0291-y

van Emmerik, R. E., and van Wegen, E. E. (2002). On the functional aspects of variability in postural control. *Exerc. Sport Sci. Rev.* 30, 177–183. doi: 10.1097/00003677-200210000-00007

Vaughan, R., Sumpter, N., Frost, A., and Cameron, S. (1998). "Robot sheepdog project achieves automatic flock control," in *Proceedings of the Fifth International Conference on Simulation of Adaptive Behavior on From Animals to Animats 5* (Cambridge, MA: MIT Press), 489–493.

Venkatakrishnan, A., Banquet, J. P., Burnod, Y., and Contreras-Vidal, J. L. (2011). Parkinson's disease differentially affects adaptation to gradual as compared to sudden visuomotor distortions. *Hum. Mov. Sci.* 30, 760–769. doi: 10.1016/j.humov.2010.08.020

Vieira, T. M., Loram, I. D., Muceli, S., Merletti, R., and Farina, D. (2012). Recruitment of motor units in the medial gastrocnemius muscle during human quiet standing: is recruitment intermittent? What triggers recruitment? *J. Neurophysiol.* 107, 666–676. doi: 10.1152/jn.00659.2011

Volpe, B. T., Krebs, H. I., and Hogan, N. (2003). Robot-aided sensorimotor training in stroke rehabilitation. *Adv. Neurol.* 92, 429–433.

Von Holst, E., and Mittelstaedt, H. (1950). Das Reafferezprinzip. Wechselwirkungen zwischen Zentralnerven-System und Peripherie. *Naturwiss.* 37, 467–476. doi: 10.1007/BF00622503

Vuillerme, N., Isableu, B., and Nougier, V. (2006). Attentional demands associated with the use of a light fingertip touch for postural control during quiet standing. *Exp. Brain Res.* 169, 232–236. doi: 10.1007/s00221-005-0142-7

Vuillerme, N., and Nougier, V. (2003). Effect of light finger touch on postural sway after lower-limb muscular fatigue. *Arch. Phys. Med. Rehabil.* 84, 1560–1563. doi: 10.1016/s0003-9993(03)00235-1

Waszak, F., Cardoso-Leite, P., and Hughes, G. (2012). Action effect anticipation: neurophysiological basis and functional consequences. *Neurosci. Biobehav. Rev.* 36, 943–959. doi: 10.1016/j.neubiorev.2011.11.004

Wing, A. M., Johannsen, L., and Endo, S. (2011). Light touch for balance: influence of a time-varying external driving signal. *Philos. Trans. R. Soc. Lond. B Biol. Sci.* 366, 3133–3141. doi: 10.1098/rstb.2011.0169

Winter, R., Harrar, V., Gozdzik, M., and Harris, L. R. (2008). The relative timing of active and passive touch. *Brain Res.* 1242, 54–58. doi: 10.1016/j.brainres.2008.06.090

Wong, M., Gnanakumaran, V., and Goldreich, D. (2011). Tactile spatial acuity enhancement in blindness: evidence for experience-dependent

mechanisms. *J. Neurosci.* 31, 7028–7037. doi: 10.1523/jneurosci.6461-10.2011

Wright, W. G. (2014). Using virtual reality to augment perception, enhance sensorimotor adaptation and change our minds. *Front. Syst. Neurosci.* 8:56. doi: 10.3389/fnsys.2014.00056

Wright, W. G., Ivanenko, Y. P., and Gurfinkel, V. S. (2012). Foot anatomy specialization for postural sensation and control. *J. Neurophysiol.* 107, 1513–1521. doi: 10.1152/jn.00256.2011

Conflict of Interest Statement: The authors declare that the research was conducted in the absence of any commercial or financial relationships that could be construed as a potential conflict of interest.

Received: 21 July 2014; accepted: 17 September 2014; published online: 06 October 2014.

Citation: Honeine J-L and Schieppati M (2014) Time-interval for integration of stabilizing haptic and visual information in subjects balancing under static and dynamic conditions. Front. Syst. Neurosci. ***8****:190. doi: 10.3389/fnsys.2014.00190*

This article was submitted to the journal Frontiers in Systems Neuroscience.

frontiers in Systems Neuroscience

ORIGINAL RESEARCH
published: 31 March 2015
doi: 10.3389/fnsys.2015.00052

Comparison of haptic guidance and error amplification robotic trainings for the learning of a timing-based motor task by healthy seniors

*Amy E. Bouchard, Hélène Corriveau and Marie-Hélène Milot**

Centre de Recherche sur le Vieillissement, Université de Sherbrooke, Sherbrooke, QC, Canada

With age, a decline in the temporal aspect of movement is observed such as a longer movement execution time and a decreased timing accuracy. Robotic training can represent an interesting approach to help improve movement timing among the elderly. Two types of robotic training—haptic guidance (HG; demonstrating the correct movement for a better movement planning and improved execution of movement) and error amplification (EA; exaggerating movement errors to have a more rapid and complete learning) have been positively used in young healthy subjects to boost timing accuracy. For healthy seniors, only HG training has been used so far where significant and positive timing gains have been obtained. The goal of the study was to evaluate and compare the impact of both HG and EA robotic trainings on the improvement of seniors' movement timing. Thirty-two healthy seniors (mean age 68 ± 4 years) learned to play a pinball-like game by triggering a one-degree-of-freedom hand robot at the proper time to make a flipper move and direct a falling ball toward a randomly positioned target. During HG and EA robotic trainings, the subjects' timing errors were decreased and increased, respectively, based on the subjects' timing errors in initiating a movement. Results showed that only HG training benefited learning, but the improvement did not generalize to untrained targets. Also, age had no influence on the efficacy of HG robotic training, meaning that the oldest subjects did not benefit more from HG training than the younger senior subjects. Using HG to teach the correct timing of movement seems to be a good strategy to improve motor learning for the elderly as for younger people. However, more studies are needed to assess the long-term impact of HG robotic training on improvement in movement timing.

Keywords: haptic guidance, error amplification, timing, aging, learning

OPEN ACCESS

Edited by:
Mikhail Lebedev, Duke University, USA

Reviewed by:
Herbert Heuer, Leibniz Research Centre for Working Environment and Human Factors, Germany
Andrea Cristina De Lima-Pardini, University of São Paulo, Brazil
Jon Doan, University of Lethbridge, Canada

***Correspondence:**
Marie-Helene Milot, Centre de Recherche sur le Vieillissement, Université de Sherbrooke, 1036 Belvédère sud, Sherbrooke, QC J1H 4C4, Canada
marie-helene.milot@usherbrooke.ca

Received: *22 December 2014*
Accepted: *12 March 2015*
Published: *31 March 2015*

Citation:
Bouchard AE, Corriveau H and Milot M-H (2015) Comparison of haptic guidance and error amplification robotic trainings for the learning of a timing-based motor task by healthy seniors. Front. Syst. Neurosci. 9:52. doi: 10.3389/fnsys.2015.00052

Introduction

Movements are made up of spatial (e.g., direction of movement) and temporal (e.g., reaction time and timing of muscle activation) aspects, which can be controlled separately depending on the task that is to be performed (Georgopoulos, 2002). The temporal aspect of movement plays an important role in the accomplishment of many everyday activities like playing tennis (Marchal-Crespo et al., 2013) or using a motorized wheelchair (Marchal Crespo and Reinkensmeyer, 2008). With age, and as compared to younger individuals, a decline in the temporal aspect of movement occurs,

translating into a slowing of internalized timing processes, as highlighted by the synchronization-continuation paradigm, and by deficits in temporal predictions for accurate movement production (Carnahan et al., 1996; Wishart et al., 2000; McAuley et al., 2006; van Dijk et al., 2007; Marchal-Crespo et al., 2010; Seidler et al., 2010; Pietschmann et al., 2011; Turgeon and Wing, 2012; Hoogendam et al., 2014), negatively impacting daily activities. Explanations for this age-related timing deficit may be explained by changes in the nervous system (Seidler et al., 2010). For example, a decrease in the nigrostriatal region's dopamine (DA) functioning, important for motor learning, is observed with age (van Dijk et al., 2007). In fact, van Dijk et al. (2007) found that the availability of the DA transporters (DAT) was negatively correlated ($r = -0.40$) with older individuals' reaction times; in other words, the slower the reaction time, the higher the deficiency in DAT. Other studies have also found significant relations between decreased functional performance found with aging and decreased fractional anisotropy, a measure of fiber density (Zahr et al., 2009), or decreased volume in the cerebellum, which plays an essential role in movement timing (Raz et al., 2005; Seidler et al., 2010). In addition, it is suggested that elders strategically prioritize the spatial aspects of movement over the temporal aspects, in other words favoring a better control of movements over their speed in order to achieve a required task (Seidler-Dobrin et al., 1998).

Despite these drawbacks, seniors can still learn new motor skills (Voelcker-Rehage, 2008), although often at a significantly slower pace (Marchal-Crespo et al., 2010; Pietschmann et al., 2011). The fact that they have the potential for motor learning is important because the elderly population needs to be able to learn new timing tasks like driving a powered wheelchair, or playing sports such as golf in order to maintain a good quality of life as they age (Carnahan et al., 1996; Wishart et al., 2000; Marchal-Crespo et al., 2010). Yet, few studies have attempted to improve elderly movement timing.

One solution is robotic training (Patton and Mussa-Ivaldi, 2004; Marchal Crespo and Reinkensmeyer, 2008; Marchal-Crespo et al., 2010, 2013; Milot et al., 2010; Luttgen and Heuer, 2013). Two emerging types of robotic training, haptic guidance (HG) and error amplification (EA), are increasingly used as effective training methods for improving movement execution in both healthy persons and those having a pathology (Liu et al., 2006; Patton et al., 2006a,b; Cesqui et al., 2008; Marchal Crespo and Reinkensmeyer, 2008; Marchal-Crespo et al., 2010, 2013, 2014; Milot et al., 2010; Luttgen and Heuer, 2013). HG is based on the principle that guiding the person to make the correct movement would provide the nervous system with additional proprioceptive and somatosensory cues to allow for a better planning of movement and thus reducing timing errors and improving movement execution (Marchal-Crespo et al., 2010; Milot et al., 2010; Luttgen and Heuer, 2013). EA, on the other hand, is based on the theory that error is an essential neural signal for motor adaptation (Thoroughman and Shadmehr, 2000), where the nervous system detects and corrects these errors for future movements (Milot et al., 2010). By artificially increasing movement errors, EA training would then allow a faster and more complete learning (Emken and Reinkensmeyer, 2005). In a previous study, we evaluated and compared the immediate impact of HG and EA robotic trainings on movement timing for 20 young healthy participants, while they played a computerized pinball-like game (Milot et al., 2010). The results showed that both EA and HG training were effective in improving timing accuracy so that it was appropriate for hitting a target with the pinball. Moreover, the effectiveness of the robotic trainings was dependent on the participant's initial skill level, where less-skilled participants seemed to benefit more from HG and better-skilled participants from EA. The results of our study further supported studies that used HG or EA robotic trainings, where faster execution times (Feygin et al., 2002; Bluteau et al., 2008) and improved timed movement for the task (Marchal Crespo and Reinkensmeyer, 2008; Luttgen and Heuer, 2013; Marchal-Crespo et al., 2013, 2014) were noted following HG or EA training. However, these studies were conducted on young and healthy individuals. Very few studies have compared the effectiveness of both EA and HG to improve movement timing in the elderly, despite there being a negative impact of aging on movement timing. Only one study by Marchal-Crespo et al. (2010) trained elders with HG on a computerized steering task. The authors found that after receiving HG training, elders improved their timing by straightening their wheel faster after having just coming out of turns.

With respect to the benefits of HG and EA robotic training on the performance of timed movement in young healthy individuals, the goal of the study was to directly compare and evaluate the impact of both types of robotic trainings on improving movement timing accuracy in elders. Since learning can still take place with age (Carnahan et al., 1996; Wishart et al., 2000; Marchal-Crespo et al., 2010; Pietschmann et al., 2011) and following our previous results on young healthy individuals (Milot et al., 2010) which showed that timing error can be improved using HG and EA robotic trainings, we expected both EA and HG to be equally effective in improving seniors' timing errors. However, knowing that there is a decrease in motor skill observed with older age (Hoogendam et al., 2014), we hypothesized that our oldest senior participants would more likely have a poorer task performance and would thus benefit the most from HG, whereas our younger senior participants would not necessarily be bad performers and would therefore benefit more from EA.

Materials and Methods

Participants

Thirty-two healthy participants (10 male; 22 female) between the ages of 61 and 75 (mean age 68 $\pm$ 4 years) took part in the study. In order to participate in the study, individuals had to meet the following criteria: (1) be at least 60 years of age, (2) be right-handed [*Edinburgh Handedness Inventory* (Oldfield, 1971)], and (3) be able to flex the right wrist by at least 10° without any pain. The exclusion criteria were: having a cognitive impairment as evaluated by the *Montreal Cognitive Assessment* exam [score $<$ 26 on the Version 7.3 (Gluhm et al., 2013)]; having an active neurological (e.g., stroke) or orthopedic (e.g., fracture) problem in the right upper limb; having a visual problem (e.g., a

cataract) that was non-corrected and would prevent the proper viewing of a computer screen. This project was approved by the CSSS-IUGS ethics board and all participants signed the consent form.

Timing Exerciser Orthosis (TEO)

Timing exerciser orthosis (TEO) is a modified version of TAPPER, which was used in a previous study (Milot et al., 2010). TEO is a one degree of freedom robot that allows 10° of wrist flexion of both the left and right hands. It is mounted on an aluminum frame and is mechanically actuated by a Dynamixel MX-106 servomotor (*Robotis Inc*, USA), sampled at 1,000 Hz for the recording of the servomotor's torque and position data. A forearm brace also ensures the participant's comfort and safety. A button, placed on the frame, allows the participants to experience sensory feedback during each trial but pressing the button did not play a role in triggering the sequence of the timing task (see **Figure 1**).

Since the task was time dependent, a photodiode (*BPW21R*, Vishay, Germany), placed at the bottom right corner of the computer screen, was used as a time reference in order to detect the start of the task. This was done by the appearance of a luminous white dot at the bottom right corner of the computer screen, which was read by the photodiode, as a red ball appeared at the top of the computer screen simultaneously. This photodiode and TEO were plugged into a USB-6008 data acquisition card (*National Instruments*, USA), sampled at 5,000 Hz. This acquisition card allowed the synchronization between the photodiode and the servomotor for the timing task.

Pinball Simulation Game

The pinball-like game is similar to the one used in a previous study [for more details see (Milot et al., 2010)]. In sum, the goal of the game was to hit targets to earn as many points as possible. A total of five colored-targets located at specific positions across the computer screen were randomly presented to the participants. A red ball that fell toward a flipper could be seen on the computer screen during each trial. In order to hit a specific target, participants had to activate TEO with the correct timing (with a timing accuracy of 4 ms) so the flipper could rotate and have the ball to bounce upward toward the target. TEO was activated when the participants flexed their wrists at a torque $\geq$ 0.5 Nm. One out of three feedback messages were provided during each trial, depending on the participant's timing accuracy ("Wow! Just on time!," "Too early! Hit later!," and "Too late! Hit sooner!"). The pinball simulator was created using LabVIEW^{TM} 2013 software.

Haptic Guidance and Error Amplification Algorithms

The algorithms were slightly modified from those that we used in a previous study (Milot et al., 2010). To decrease participants' timing errors during HG, we wanted to delay or speed up the start of the robot when the participants initiated wrist movement too early or too late, respectively. The exact opposite was done to increase errors during EA. More specifically, $t = 0$ was defined as the time in which the ball began to fall toward the flipper. Tbp was defined as the time in which TEO was activated. So:

$$\mathrm{Tbp} = \mathrm{Tip} + \mathrm{Dc} \quad (1)$$

where Tip was the time in which the motor sensors detected the initiation of the participant's wrist flexion and Dc was defined as the programmed delay in which the participant initiated movement and TEO was commanded to move. The values that ensured success for hitting each target were defined as Tbd and Tid, therefore:

$$\mathrm{Tbd} = \mathrm{Tid} + \mathrm{Dcd} \quad (2)$$

where Tbd was defined as the time in which TEO needed to move in order for the ball to bounce back in time to hit the target, Tid was the desired time in which the participant should have initiated movement, and Dcd was a constant (0.5 s).

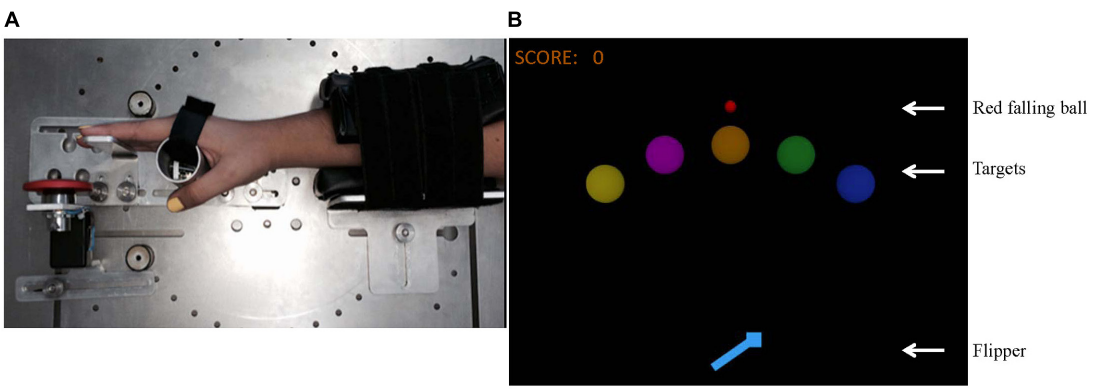

FIGURE 1 | (A) The Timing Exerciser Orthosis (TEO) robot; **(B)** Description of the computerized pinball-like game: a red ball appears at the top of the screen and falls toward the virtual flipper. Subjects flex their right wrist to activate TEO. TEO moves the wrist at an angle of 10°, allowing the subject's fingers to touch the button while rotating the flipper. The ball touches the flipper, and then bounces toward the target.

Next, Ep was defined as the timing error in which the participant initiated movement, thus:

$$\mathrm{Ep} = \mathrm{Tip} - \mathrm{Tid} \quad (3)$$

Furthermore, Eb represented TEO's timing error, where:

$$\mathrm{Eb} = \mathrm{Tbp} - \mathrm{Tbd} = \mathrm{Ep} + \mathrm{Dc} - \mathrm{Dcd} \quad (4)$$

We wanted Eb to be proportional to Ep, so:

$$\mathrm{Eb} = k\mathrm{Ep} \quad (5)$$

where k was defined as the EA gain. By substituting equation 4 into equation 5 and solving for Dc, we obtained the following equation for the programmed delay:

$$\mathrm{Dc} = \mathrm{Dcd} + \mathrm{Ep}(k-1) \quad (6)$$

Equation 6 was used to establish the delay between when the participant initiated wrist movement, and when TEO began to move, in order to proportionally decrease or increase the participant's timing errors. Note that no HG or EA trainings were provided when $k = 1$, where a $k > 1$ caused an increase in timing errors and a $k < 1$ resulted in a decrease in timing errors.

Furthermore, knowing that baseline skill level can influence motor learning during HG or EA (Milot et al., 2010), we wanted to adjust each participant's k-value to his own skill level. We did so during a 39-trial baseline adjustment phase (B2), where participants played at a constant game difficulty ($k = 0.4$). When the B2 phase was completed, we classified each participant's timing errors in an ascending order and chose the 12$^{\mathrm{th}}$ *Ep*-value. This 12$^{\mathrm{th}}$ *Ep*-value was chosen based on the fact that we wanted subjects to experience at least a 30% rate of success in the subsequent baseline (B3) and retention conditions (RCs). Afterward, taking the upper limit of timing accuracy in order to ensure a successful hit, that is 4 ms (corresponding to Eb), we calculated each participant's final k-value using equation 5.

$$k = 4/12^{\mathrm{th}}\mathrm{Ep} \quad (7)$$

The choice of a $k = 0.4$ was driven by our previous study, where the maximum k-value reached among the young participants was 0.27. It was reasonable to think that seniors would not reach a k-value higher than 0.27 at the end of the B2 adjustment phase. Thus, the robot was providing some help during B2 but to a much lower level than what the subjects really needed to be successful at least 30% of the time, just like during B3 and the RCs.

For each condition, the k-value was increased or decreased by 90%, in EA and HG, respectively, to increase and decrease the participant's timing errors. This 90% change in the k-value was sufficient to significantly produce a difference in error between both HG and EA training conditions (Milot et al., 2010).

Study Design

Participants were randomly assigned to the two testing conditions; those in Condition 1 experienced the EA training first and the HG second, whereas those in Condition 2 received the HG training first followed by EA (see **Figure 2**).

Before each condition, participants played a Baseline (B1) phase to gain familiarity with the task to be played. B1 was set at a fixed k-value of 1, meaning that no HG or EA trainings were provided for 40 trials. Next, a 39-trial adjustment phase (B2) served to determine each participant's k-value. After, participants played a B3 phase according to their k-value determined in B2, for 40 trials. Afterward, participants received the training phase (EA or HG), depending on which condition they were in. Each training phase had 75 trials and a 60 s pause after the first 40 trials. During both HG and EA, 20% of the trials were catch trials, meaning that the k-value unexpectedly returned to baseline to ensure that the participants would remain watchful throughout the training, especially during HG. A RC equal to B3 followed each training session to allow evaluating the impact of HG or EA robotic training. During HG and EA, three targets (yellow, orange, blue) were presented one at the time to the subjects whereas during B3 and the RC conditions, the two remaining targets were shown along with the three trained targets to assess generalization of the task to untrained targets.

Statistical Analysis

Subjects' timing errors were calculated for each trial of each condition. Then, for each subject, two values were computed: (1) mean absolute timing errors and (2) related SDs. Afterward, across subjects, the mean and SD of values #1 and #2 were computed and retained for analysis. The normality of data was assessed using Shapiro–Wilk W-test, where non-parametric statistical methods were used for non-normally distributed data that could not be transformed. An independent t-test was used to assess if the two groups (EA1 and HG1) were comparable at baseline in regards to age and baseline timing errors during B3. Also, Wilcoxon signed-rank tests were used to evaluate the stability of the learning curve for the timing task (comparison of the mean of the first and last 10 trials of B3 for the entire group of subjects) and introduction to HG and EA training (comparison of the last 10 trials of B3 to the first 10 trials of HG or EA for each training group). Next, a paired t-test was used to determine the efficacy of each training type (EA1−B3 and HG1−B3) on the improvement of the timing task, not taking into account the crossover study design, as well as a Wilcoxon signed-rank test to look at the SD of the absolute timing errors. The Hill–Armitage approach (Senn, 2002) to crossover study analysis was used to

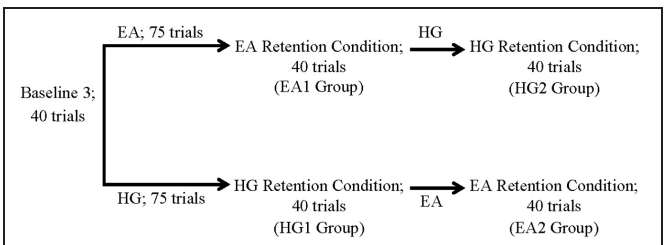

FIGURE 2 | Study design. EA, error amplification; HG, haptic guidance.

evaluate: (1) the difference in efficiency between the two types of trainings, by comparing the mean change (EA1 − HG2) of the EA1 group with that of the HG1 group (HG1 − EA2), and (2) whether there was no influence of training order administration, by comparing the mean of the sums (EA1 + HG2) and (HG1 + EA2) between groups. Finally, to evaluate the impact of age on the improvement in timing errors, two approaches were used. First, for each training group, a Pearson product moment correlation was performed to evaluate the relation between age and the change in absolute timing score following HG and EA, respectively. Second, following Senn (2002) procedure, a cross-over difference (mean change in absolute timing errors between the RCs of HG and EA, regardless of treatment order) was calculated and put in relation to age, using a Pearson product moment correlation. One-tailed tests were used and the significance level was set at 0.05. All statistical analyses were performed using IBM SPSS® software version 18.

Results

Success Rate, Learning Stability, and Baseline Group Comparison

At B1, where no robotic assistance was provided, the mean success rate of the entire group of subjects reached 2 ± 2%. However, at B3, when the game difficulty was adjusted to each subject's skill level, the overall mean success rate reached 25 ± 13%; confirming that the adjustment phase worked properly.

Also, when comparing the first and last 10 trials of B3 for the entire group, no difference in the subjects' absolute timing errors was noted (11.2 ± 5.6 ms vs. 10.1 ± 4.4 ms; $z = -0.88$; $p = 0.19$), meaning that a learning stability of the task has been reached before HG or EA trainings were introduced.

Finally, when comparing HG1 and EA1 training groups, no significant difference was noted in regards to age (68 ± 4 years vs. 68 ± 3 years, $t(30) = 0.24$; $p = 0.41$), and overall mean absolute timing errors at B3 (11.7 ± 4.3 ms vs. 9.8 ± 3.8 ms, $t(30) = -1.33$; $p = 0.10$).

Introduction to HG and EA

When introduced to HG, a significant decrease in the subjects' absolute timing errors was noted as compared to the last 10 trials of B3 (10.5 ± 4.8 ms vs. 1.4 ± 0.84 ms, $z = -3.52$; $p < 0.05$). On the contrary, when introduced to EA, a significant increase in the subjects' absolute timing errors was noted when comparing the last 10 trials of B3 to the first 10 trials of EA (9.8 ± 4.2 ms vs. 18.7 ± 6.5 ms, $z = -3.52$; $p < 0.05$). This means that HG and EA robotic training adequately decreased and increased subjects' timing errors, respectively.

Impact of Each Training Type on Timing Errors

When comparing the subjects' baseline performance on trained targets to that of their RC following HG training, a significant decrease in absolute timing errors was noted (11.7 ± 4.4 ms vs. 9.7 ± 3.4 ms, $t(15) = 1.76$; $p = 0.049$). At the same time, subjects were less variable in their timing errors as a significant improvement in the SD of their absolute timing errors was noted when comparing the value of B3 to that of the HG RC (9.5 ± 3.6 ms vs. 7.4 ± 3.2 ms; $z = -2.17$; $p = 0.01$; see **Figure 3**). In addition, when comparing the subjects' performance on untrained targets between B3 and HG RC, a trend toward a generalization of learning to untrained targets occurred with HG training (11.6 ± 3.2 ms vs. 10.4 ± 3.9 ms; $t(15) = 1.35$; $p = 0.09$). Further analysis also showed that during HG training, the subjects remained alert throughout the training, even though the robot provided them help, since no difference between the absolute timing errors of HG catch trials and B3 was observed (11.0 ± 3.9 ms vs. 11.7 ± 4.4 ms; $t(15) = 0.68$; $p = 0.25$).

Following training with EA, no difference in the subjects' absolute timing errors on trained targets was observed when comparing timing errors of B3 to that of the EA RC (9.8 ± 3.8 ms vs. 11.4 ± 5.9 ms; $t(15) = -1.16$; $p = 0.13$). In addition, a trend toward a worsening in the variability of the absolute timing errors was observed (7.9 ± 4.9 ms vs. 9.5 ± 7.2 ms; $z = -1.5$; $p = 0.07$; see **Figure 3**) as well as no generalization to untrained targets (10.6 ± 5.1 ms vs. 11.7 ± 5.6 ms; $t(15) = -1.08$; $p = 0.15$). Finally, like HG training, no difference between the subjects baseline performance at B3 and the one during EA catch trials was noted (9.8 ± 0.94 ms vs. 10.7 ± 5.3 ms; $t(15) = -1.02$; $p = 0.16$).

Finally, when comparing the change in absolute timing errors between HG1 and EA1 groups, a significant difference was noted (1.9 ± 4.5 ms vs. −1.6 ± 5.3 ms; $t(30) = -2.02$; $p = 0.03$). In other words, training with HG was more beneficial to learning the timed-based task than training with EA.

Comparison of the Efficacy of HG and EA Robotic Training on Improvement of Timing Errors and the Impact of Age

When looking at the subjects' absolute timing error on trained targets, the Hill–Armitage statistical analysis revealed no difference in the efficacy between HG and EA robotic trainings ($U = 102$; $p = 0.17$) and no effect of training order administration on the learning of the timing task ($U = 109$; $p = 0.25$). Although no significant difference in efficiency between the two types of training was noted, when looking at the change in absolute timing errors between RCs of both training groups (HG1/EA2 vs. and EA1/HG2), we performed further analyses by comparing the absolute timing errors of B3 to those of EA2 and HG2. Thus, if looking at the absolute timing errors of B3 to that of EA2, for the group that trained first with HG, a significant improvement in timing errors was noted (11.7 ± 4.4 ms vs. 9.9 ± 4.3 ms; $t(15) = 2.01$; $p = 0.03$). In addition, no difference in absolute timing errors between HG1 and EA2 was noted (9.7 ± 3.4 ms vs. 9.9 ± 4.3 ms; $t(15) = 0.14$; $p = 0.44$). This means that if training first with HG, no worsening in the subjects' performance occurred after training with EA. On the other hand, when looking at the absolute timing errors between B3 and HG2, for the group that trained first with EA, a trend toward a worsening in timing errors was noted (9.8 ± 3.8 ms vs. 11.7 ± 4.4 ms; $t(15) = -1.5$; $p = 0.08$). In addition, no difference between the absolute timing errors of EA1 and HG2 was observed (11.7 ± 4.4 ms vs.

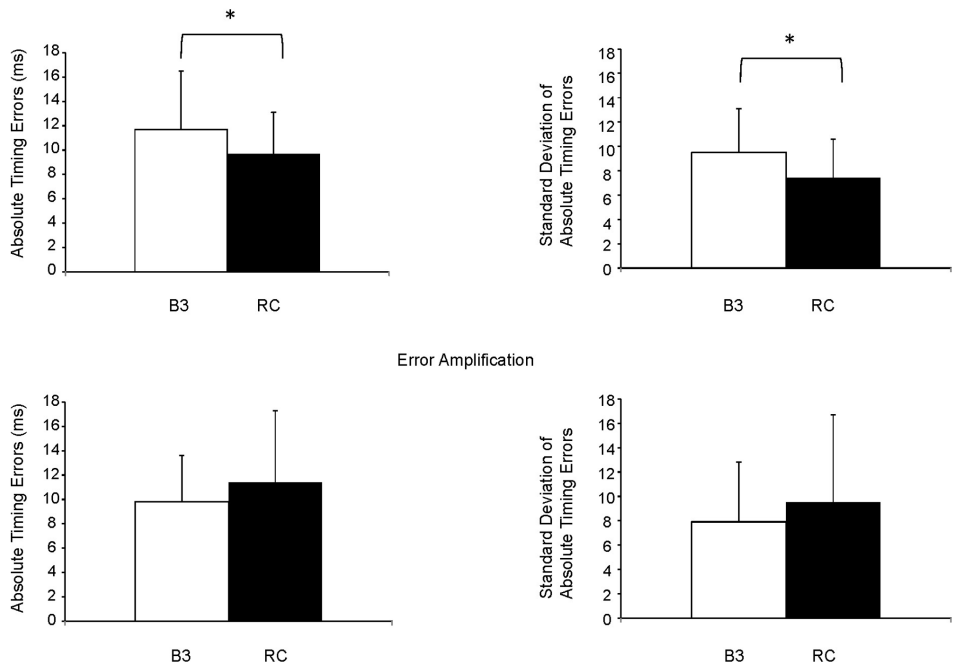

FIGURE 3 | Improvement in absolute timing errors and related SD following HG and EA robotic trainings. B3, baseline 3; RC, retention condition, $^*p < 0.05$.

12.6 ± 7.7ms; $t(15) = 0.81$; $p = 0.22$). This means that HG training was not effective, if given after EA training.

When looking at the impact of age on the subjects' absolute timing errors for each training group, no significant relation was found for the HG1 group ($r = 0.12$; $p = 0.33$). On the other hand, a significant relationship was obtained for the EA1 group ($r = -0.59$; $p = 0.008$); meaning that for the oldest subjects, training with EA was even more detrimental to learning. In addition, age was not related to the change in subjects' performance from HG RC to EA RC ($r = 0.04$, $p = 0.41$; see **Figure 4**).

Discussion

The results of the current study showed that a robotic hand device aimed at reducing healthy seniors timing errors was effective in improving learning a timing-based task, regardless of age. However, improved learning was mostly limited to trained targets. On the other hand, artificially increasing seniors' timing errors with the use of the robotic device did not promote learning and its generalization. It actually worsened performance with increasing age.

The fact that HG training did improve subjects' performance further supports the use of HG training for learning time-based tasks (Marchal-Crespo et al., 2010, 2013; Milot et al., 2010; Luttgen and Heuer, 2013). For example, the study of Marchal-Crespo et al. (2010) obtained a significant improvement in steering timing when healthy seniors trained with HG as compared to no guidance. Likewise, in our previous study on healthy young subjects using a similar pinball-like task (Milot et al., 2010), for subjects less-skilled at the task, that is having a k-value < 0.1, HG seemed to benefit learning more. Looking at the mean k-value of the current subjects (mean k-value of 0.06), they did fall within this less-skilled subcategory. As mentioned by Luttgen and Heuer (2013), if a task's characteristic is difficult to demonstrate either visually or verbally, such as the timing of a task, robotic guidance may provide a helpful role, especially for subjects who struggle with the task.

However, HG training did not translate into generalization of performance, although a trend was noted. Lack of generalization following HG training has been found in several other studies using a variety of tasks (Marchal Crespo and Reinkensmeyer, 2008; Marchal-Crespo et al., 2013). As mentioned by Marchal Crespo and Reinkensmeyer (2008), it could be thought that the current subjects relied too much on the robotic assistance during training with HG, hindering generalization of learning to other targets. Yet, this is not the case as the subjects' timing errors during HG catch trials did not increase when the robotic assistance was unexpectedly removed as compared to their B3 timing errors. Another explanation could come from the formation of an internal model of the task by the motor system. Indeed, formation of an internal model of the task is important to allow generalization of performance beyond the position (Grafton et al., 2008) or timing (Milot et al., 2010) of trained targets. In young healthy subjects, it was demonstrated that the

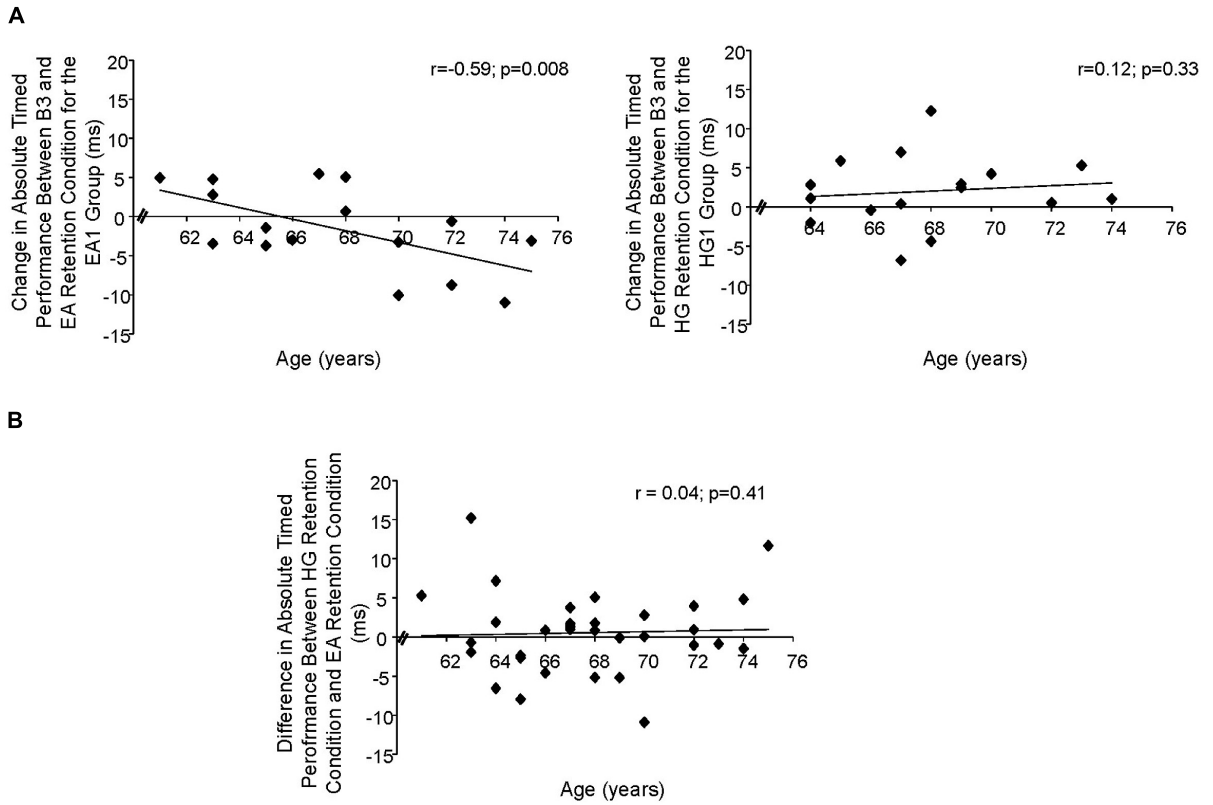

FIGURE 4 | Correlation between age and: (A) the change in absolute timed performance for EA1 group and HG1 group. Note that a negative value means a worsening of performance; **(B)** the cross-over difference between the absolute timing errors of the HG RC, and EA RC, $p < 0.05$.

motor system does indeed create an internal model of timing that can serve for generalization (Milot et al., 2010). However, the creation of an internal model is driven by errors (Thoroughman and Shadmehr, 2000) and because our subjects' *k*-values were small, they experienced a reduced range of timing errors (Marchal Crespo and Reinkensmeyer, 2008). This might have prevented the motor system to form an adequate internal model of the timing task to allow generalization of performance to untrained targets.

The fact that the subjects' timing errors decreased after HG training suggest that as one ages, learning can still occur, supporting results of previous studies on seniors' ability to learn new tasks (van Dijk et al., 2007; Marchal-Crespo et al., 2010; Pietschmann et al., 2011). Knowing that with age, motor performance usually worsens (Hoogendam et al., 2014) it was expected that HG would have been more beneficial for the oldest subjects. However, no relation with age and the change in timing errors following HG was obtained. Further looking at the data, no relation between age and *k*-value was also noted (data not shown); meaning that our oldest subjects did not systematically perform worst at the task to begin with and thus did not necessarily need more help from the robot while playing. To support, Marchal-Crespo et al. (2010) did not find an age dependent relation with motor performance while training with HG on their timing task. Age became an important factor when looking at the long-term retention of the learned task, which was not assessed in the current study.

When looking at the impact of EA training on improvement in timing errors, no significant change in either the absolute timing errors or related SDs was noted. This is not in line with studies on young healthy subjects where EA training translated into a significant improvement in learning various tasks (Patton and Mussa-Ivaldi, 2004; Milot et al., 2010; Marchal-Crespo et al., 2014). Consequently, it seems that exaggerating timing errors in the course of learning for individuals that are more prone to present baseline timing deficits because of normal aging might not be a good strategy to boost learning as for young individuals. Contrarily, following the results of our previous study, for young subjects that were less-skilled at the timing task, EA training did not improve learning (Milot et al., 2010). Explanation of this result was based on the challenge-point theory (Guadagnoli and Lee, 2004), which suggests that learning is a function of both skill level and task difficulty. Thus, for the less-skilled subgroup of young healthy subjects, it was thought that EA training was too challenging for their skill level, overwhelming the motor system with too much information to process and thus hindering any learning. This could be especially true for the current senior subjects knowing that slowness in information processing is observed in the elderly as compared to young individuals due to changes in structural

and functional features of the nervous system (Seidler et al., 2010). This is supported also by the significant negative relation found between age and deterioration of timing accuracy following EA training. Thus, with age, EA training could have a more pronounced detrimental effect on learning. On the other hand, it seems that if EA training is given after HG training, no worsening of performance occurs. It is possible that teaching seniors how to perform a timing-task first allows them to improve their skill level and thus makes EA training less challenging.

Although age had a significant negative impact on learning for the EA training group, it did not play an important role when related to the change in score between HG and EA RCs when taking into account all subjects. This could be related to the fact that even though HG training significantly improved subjects' timing errors, its efficacy was not superior to EA training, when looking at the mean change in absolute timing errors of the RCs between the two groups. The high variability in training responses, often observed with aging (Seidler-Dobrin et al., 1998; Marchal-Crespo et al., 2010), could have prevented the detection of the superiority of HG robotic training over EA when taking into account all subjects, and in parallel precluded to a significant impact of age on the change in score between both types of training.

Limits

Even though the task that was practiced in this study was similar to the one used in a previous study on young healthy subjects, it was difficult to directly compare the results of both studies since the robots, as well as the determination of each subject's skill level, differed. The inclusion of a control group with young healthy individuals in the current study would have helped to better interpret the impact of aging on the learning of movement timing. However, when looking at the *k*-value of both studies, representing each subject's baseline skill level, it is noticeable that the senior subjects did have on average lower *k*-values than young subjects (0.06 vs. 0.15), possibly suggesting a decline in motor timing ability with age. In addition, since no *k*-values reached a value greater than 1 during EA, one could say that no true EA was provided during EA. This fact was also acknowledged in a previous study with young healthy subjects, where it was hypothesized that providing true EA could have been too demanding and thus detrimental to learning. This is even truer with the elderly subjects of this study since, as opposed to young healthy subjects, no learning occurred with EA when the error gains were smaller than 1. Nevertheless, our elderly subjects experienced a significant increase in their timing errors when comparing their baseline performances to their performances when being introduced to EA. Also, one could ask about the relevance of using a pinball-like game to assess timing performance of seniors instead of a more meaningful timing task. The rationale behind the choice of this task was based on the study by Wishart et al. (2000) which suggested that to better evaluate the impact of age on learning, the task should be an unfamiliar one, requiring effortful processing, as opposed to a task that is automatic, involving almost unconscious processing. Thus, by choosing a pinball-like game, we thought that this task was unfamiliar enough to the subjects to properly assess the effect of age on learning. Finally, the long-term retention as well as the clinical importance of a 2-ms improvement in timing following HG training were not established in the current study. Was the improvement in timing maintained over time? Was the change in timing important enough to positively impact seniors' performance in their everyday activities? Because studies on motor timing in the elderly are scarce, these questions are yet to be answered and more studies are needed to explore these questions. Nevertheless, knowing that the current robotic training significantly and positively helped improve elderly timing, its use with neurologically impaired individuals, where timing deficits can be even more substantial, is worth evaluating. A study is underway to assess the impact of both HG and EA robotic trainings on timing improvement for post-stroke individuals.

Conclusion

This study evaluated the impact of both HG and EA robotic trainings on the improvement of motor timing in healthy seniors. The results showed that HG was beneficial to learning, with subjects improving their timing accuracy regardless of age. However, learning was restricted to the targets in which practice occurred. No improvement in seniors' timing errors was noted following EA training. Moreover, a worsening of performance was noted with age after EA training, suggesting that this type of training can be detrimental to learning as one age. Future research should look at the long-term impacts of HG and EA robotic trainings as well as the effects of these robotic trainings on the performance of daily activities to validate their clinical usefulness, particularly with impaired populations.

Authors Contributions

Conception and design the experiment: MHM, HC
Collection of data: AB
Analysis and interpretation: MHM
Writing of the manuscript: MHM, AB
Revising the manuscript: MHM, AB, HC

Acknowledgments

The authors would like to thank Mathieu Hamel and Antoine Guillerand for their technical support as well as Prof. David J. Reinkensmeyer for his input on the manuscript. The project was conducted at the Technological Innovations Lab at the Research Center on Aging of the CSSS-IUGS, Sherbrooke, Qc, Canada with the help of M-HM's start-up funds from the Faculté de médecine et des sciences de la santé of the Université de Sherbrooke.

References

Bluteau, J., Coquillart, S., Payan, Y., and Gentaz, E. (2008). Haptic guidance improves the visuo-manual tracking of trajectories. *PLoS ONE* 3:e1775. doi: 10.1371/journal.pone.0001775

Carnahan, H., Vandervoort, A. A., and Swanson, L. R. (1996). The influence of summary knowledge of results and aging on motor learning. *Res. Q. Exerc. Sport* 67, 280–287. doi: 10.1080/02701367.1996.10607955

Cesqui, B., Aliboni, S., Mazzoleni, S., Corrozza, M. C., Postoraro, F., and Micero, S. (2008). "On the use of divergent force fields in robot-mediated neurorehabilitation," in *Proceedings of the 2nd Biennial IEEE/RAS-EMBS International Conference on Biomedical Robotics and Biomechatronics*, Scottsdale, AZ.

Emken, J. L., and Reinkensmeyer, D. J. (2005). Robot-enhanced motor learning: accelerating internal model formation during locomotion by transient dynamic amplification. *IEEE Trans. Neural. Syst. Rehabil. Eng.* 13, 33–39. doi: 10.1109/TNSRE.2004.843173

Feygin, D., Keehner, M., and Tendick, F. (2002). "Haptic guidance: experimental evaluation of a haptic training method for a perceptual motor skill," in *Proceedings of the 10th Symp. On Haptic Interfaces For Virtual Environment and Teleoperator System*. (*HAPTICS'02*), Orlando, FL.

Georgopoulos, A. P. (2002). Cognitive motor control: spatial and temporal aspects. *Curr. Opin. Neurobiol.* 12, 678–683. doi: 10.1016/S0959-4388(02)00382-3

Gluhm, S., Goldstein, J., Loc, K., Colt, A., Liew, C. V., and Corey-Bloom, J. (2013). Cognitive performance on the mini-mental state examination and the montreal cognitive assessment across the healthy adult lifespan. *Cogn. Behav. Neurol.* 26, 1–5. doi: 10.1097/WNN.0b013e31828b7d26

Grafton, S. T., and Schmitt, P., Van Horn, J., Diedrichsen, J. (2008). Neural substrates of visuomotor learning based on improved feedback control and prediction. *Neuroimage* 39, 1383–1395. doi: 10.1016/j.neuroimage.2007.09.062

Guadagnoli, M. A., and Lee, T. D. (2004). Challenge point: a framework for conceptualizing the effects of various practice conditions in motor learning. *J. Mot. Behav.* 36, 212–224. doi: 10.3200/JMBR.36.2.212-224

Hoogendam, Y. Y., van der Lijn, F., Vernooij, M. W., Hofman, A., Niessen, W. J., van der Lugt, A., et al. (2014). Older age relates to worsening of fine motor skills: a population-based study of middle-aged and elderly persons. *Front. Aging Neurosci.* 6:259. doi: 10.3389/fnagi.2014.00259

Liu, J., Cramer, S. C., and Reinkensmeyer, D. J. (2006). Learning to perform a new movement with robotic assistance: comparison of haptic guidance and visual demonstration. *J. Neuroeng. Rehabil.* 3, 20. doi: 10.1186/1743-0003-3-20

Luttgen, J., and Heuer, H. (2013). The influence of robotic guidance on different types of motor timing. *J. Mot. Behav.* 45, 249–258. doi: 10.1080/00222895.2013.785926

Marchal-Crespo, L., McHughen, S., Cramer, S. C., and Reinkensmeyer, D. J. (2010). The effect of haptic guidance, aging, and initial skill level on motor learning of a steering task. *Exp. Brain Res.* 201, 209–220. doi: 10.1007/s00221-009-2026-8

Marchal Crespo, L., and Reinkensmeyer, D. J. (2008). Haptic guidance can enhance motor learning of a steering task. *J. Mot. Behav.* 40, 545–556. doi: 10.3200/JMBR.40.6.545-557

Marchal-Crespo, L., Schneider, J., Jaeger, L., and Riener, R. (2014). Learning a locomotor task: with or without errors? *J. Neuroeng. Rehabil.* 11, 25. doi: 10.1186/1743-0003-11-25

Marchal-Crespo, L., van Raai, M., Rauter, G., Wolf, P., and Riener, R. (2013). The effect of haptic guidance and visual feedback on learning a complex tennis task. *Exp. Brain Res.* 231, 277–291. doi: 10.1007/s00221-013-3690-2

McAuley, J. D., Jones, M. R., Holub, S., Johnston, H. M., and Miller, N. S. (2006). The time of our lives: life span development of timing and event tracking. *J. Exp. Psychol. Gen.* 135, 348–367. doi: 10.1037/0096-3445.135.3.348

Milot, M. H., Marchal-Crespo, L., Green, C. S., Cramer, S. C., and Reinkensmeyer, D. J. (2010). Comparison of error-amplification and haptic-guidance training techniques for learning of a timing-based motor task by healthy individuals. *Exp. Brain Res.* 201, 119–131. doi: 10.1007/s00221-009-2014-z

Oldfield, R. C. (1971). The assessment and analysis of handedness: the Edinburgh inventory. *Neuropsychologia* 9, 97–113. doi: 10.1016/0028-3932(71)90067-4

Patton, J. L., Kovic, M., and Mussa-Ivaldi, F. A. (2006a). Custom-designed haptic training for restoring reaching ability to individuals with poststroke hemiparesis. *J. Rehabil. Res. Dev.* 43, 643–656. doi: 10.1682/JRRD.2005.05.0088

Patton, J. L., Stoykov, M. E., Kovic, M., and Mussa-Ivaldi, F. A. (2006b). Evaluation of robotic training forces that either enhance or reduce error in chronic hemiparetic stroke survivors. *Exp. Brain Res.* 168, 368–383. doi: 10.1007/s00221-005-0097-8

Patton, J. L., and Mussa-Ivaldi, F. A. (2004). Robot-assisted adaptive training: custom force fields for teaching movement patterns. *IEEE Trans. Biomed. Eng.* 51, 636–646. doi: 10.1109/TBME.2003.821035

Pietschmann, M., Endrass, T., and Kathmann, N. (2011). Age-related alterations in performance monitoring during and after learning. *Neurobiol. Aging* 32, 1320–1330. doi: 10.1016/j.neurobiolaging.2009.07.016

Raz, N., Lindenberger, U., Rodrigue, K. M., Kennedy, K. M., Head, D., Williamson A., et al. (2005). Regional brain changes in aging healthy adults: general trends, individual differences and modifiers. *Cereb. Cortex* 15, 1676–1689. doi: 10.1093/cercor/bhi044

Seidler, R. D., Bernard, J. A., Burutolu, T. B., Fling, B. W., Gordon, M. T., Gwin, J. T., et al. (2010). Motor control and aging: links to age-related brain structural, functional, and biochemical effects. *Neurosci. Biobehav. Rev.* 34, 721–733. doi: 10.1016/j.neubiorev.2009.10.005

Seidler-Dobrin, R. D., He, J., and Stelmach, G. E. (1998). Coactivation to reduce variability in the elderly. *Motor. Control.* 2, 314–330.

Senn, S. (2002). *Cross-over Trials in Clinical Research*. Hoboken: John Wiley & Sons Ltd. doi: 10.1002/0470854596

Thoroughman, K. A., and Shadmehr, R. (2000). Learning of action through adaptive combination of motor primitives. *Nature* 407, 742–747. doi: 10.1038/35037588

Turgeon, M., and Wing, A. M. (2012). Late onset of age-related difference in unpaced tapping with no age-related difference in phase-shift error detection and correction. *Psychol. Aging* 27, 1152–1163. doi: 10.1037/a0029925

van Dijk, H., Mulder, T., and Hermens, H. J. (2007). Effects of age and content of augmented feedback on learning an isometric force-production task. *Exp. Aging Res.* 33, 341–353. doi: 10.1080/03610730701319194

Voelcker-Rehage, C. (2008). Motor-skill learning in older adults-a review of studies on age-related differences. *Eur. Rev. Aging Phys. Act.* 5, 5–16. doi: 10.1007/s11556-008-0030-9

Wishart, L. R., Lee, T. D., Murdoch, J. E., and Hodges, N. J. (2000). Effects of aging on automatic and effortful processes in bimanual coordination. *J. Gerontol. B Psychol. Sci. Soc. Sci.* 55, 85–94. doi: 10.1093/geronb/55.2.P85

Zahr, N. M., Rohlfing, T., Pfefferbaum, A., and Sullivan, E. V. (2009). Problem solving, working memory, and motor correlates of association and commissural fiber bundles in normal aging: a quantitative fiber tracking study. *Neuroimage* 44, 1050–1062. doi: 10.1016/j.neuroimage.2008.09.046

Conflict of Interest Statement: The authors declare that the research was conducted in the absence of any commercial or financial relationships that could be construed as a potential conflict of interest.

frontiers in Systems Neuroscience

ORIGINAL RESEARCH
published: 02 June 2015
doi: 10.3389/fnsys.2015.00084

Task-dependent calibration of auditory spatial perception through environmental visual observation

*Alessia Tonelli, Luca Brayda and Monica Gori**

Robotics, Brain and Cognitive Sciences Department, Fondazione Istituto Italiano di Tecnologia, Genoa, Italy

Visual information is paramount to space perception. Vision influences auditory space estimation. Many studies show that simultaneous visual and auditory cues improve precision of the final multisensory estimate. However, the amount or the temporal extent of visual information, that is sufficient to influence auditory perception, is still unknown. It is therefore interesting to know if vision can improve auditory precision through a short-term environmental observation preceding the audio task and whether this influence is task-specific or environment-specific or both. To test these issues we investigate possible improvements of acoustic precision with sighted blindfolded participants in two audio tasks [minimum audible angle (MAA) and space bisection] and two acoustically different environments (normal room and anechoic room). With respect to a baseline of auditory precision, we found an improvement of precision in the space bisection task but not in the MAA after the observation of a normal room. No improvement was found when performing the same task in an anechoic chamber. In addition, no difference was found between a condition of short environment observation and a condition of full vision during the whole experimental session. Our results suggest that even short-term environmental observation can calibrate auditory spatial performance. They also suggest that echoes can be the cue that underpins visual calibration. Echoes may mediate the transfer of information from the visual to the auditory system.

Keywords: audio, vision, bisection, multisensory, calibration, space perception, echoes

OPEN ACCESS

Edited by:
Mikhail Lebedev, Duke University, USA

Reviewed by:
Nicholas Altieri, Idaho State University, USA
Caterina Bertini, University of Bologna, Italy
Patrick Bruns, University of Hamburg, Germany

***Correspondence:**
Monica Gori, Robotics, Brain and Cognitive Sciences Department, Fondazione Istituto Italiano di Tecnologia, via Morego 30, 16163 Genoa, Italy
monica.gori@iit.it

Received: *30 January 2015*
Accepted: *18 May 2015*
Published: *02 June 2015*

Citation:
Tonelli A, Brayda L and Gori M (2015) Task-dependent calibration of auditory spatial perception through environmental visual observation. Front. Syst. Neurosci. 9:84. doi: 10.3389/fnsys.2015.00084

Introduction

The visual system is the most accurate sense to estimate spatial properties. Many studies involving adult individuals support this idea, showing that when the spatial locations of audio and visual stimuli are in conflict, vision usually dominates, generating the so-called "ventriloquist effect" (Warren et al., 1981; Mateeff et al., 1985). This effect is possibly due to an optimal combination of cues performed by the human brain, where modalities are weighted by their statistical reliability. Vision dominates over audition in localization tasks (Alais and Burr, 2004). When visual and auditory systems are simultaneously presented to get spatial information, the final multisensory estimate tends to be more precise than either unisensory estimate (Clarke and Yuille, 1990; Ghahramani et al., 1997; Ernst and Banks, 2002; Alais and Burr, 2004; Landy et al., 2011). Interestingly, vision can interact with audition even when a visual stimulus is not provided during an auditory task: specifically. For example, although the angle of incidence of a sound source can be estimated with the use of only auditory cues, performance improves when vision is also present (Jackson, 1953; Shelton and Searle, 1980). A recent study by Tabry et al. (2013) has shown that the

mere possibility of observing the setup by keeping eyes open during auditory horizontal and vertical localization tasks can improve audio accuracy, even if no visual cues of the stimuli are provided.

Another example of the connection between audio-spatial and visuo-spatial information is given by a technique used by some blind people, called echolocation. Some studies have shown that this technique can operate as a crude substitute for vision, because some purely visual phenomenona, such as size constancy (Milne et al., 2015) or size-weight illusion (Buckingham et al., 2015), are present in expert echolocators, who use echoes to navigate in unknown environments.

However, it is still unknown which are the visual cues that allow an improvement in audio-spatial tasks, nor it is understood how long visual cues should last to determine such improvement. As well, it is unknown whether this phenomenon can be task-specific, i.e., if audio-spatial abilities are improved in general or if the influence of vision depends on the complexity of the audio task. Can it be argued that increased audio-spatial abilities are due to a transfer of information from the visual to the auditory system? Which is the information that is transferred? Is vision more informative for some aspects than for others?

In this paper we tested two audio tasks under various environmental conditions and visual feedbacks to answer these questions. In particular we investigated: (i) whether the environmental visual cues (i.e., prior short observation of the environment and full vision during the tasks) can improve auditory precision; (ii) whether this improvement is task-specific; and (iii) which are the environmental cues that mediate the auditory improvement due to the interaction between vision and audition.

To investigate the first point about whether environmental visual cues can improve auditory precision we tested a sample of blindfolded sighted participants twice: the first time with no visual input of the environment where the auditory task was performed; the second time after they observed for 1 min the environment. We compared the performance with no visual input of the environment with that with 1 min observation. We also tested a different group of sighted participants, who performed the two tasks with a full vision of the room but without being blindfolded. We compared the performance of this last sample with the other. Our hypothesis was that if the visual cues coming from the environmental observation can help to improve the auditory precision, then the improvement should occur at least with full vision and possibly with short-term observation.

The second question was about whether auditory precision improvement was task-specific. We tested all participants in two audio tasks: the minimum audible angle (MAA) task and the spatial bisection. In the MAA task the participant had to judge which of the two sounds generated by an array of loudspeakers was more from the right. Instead, in the spatial bisection task the participant heard three sounds coming from three distinct locations and had to judge whether the second sound was closer to the first or third sound coming from the array. The difference between these two tasks is that the spatial bisection task requires subjects to encode the position of three sounds, remember them over a period of 1 s and compare their remembered positions. Contrarily, in the MAA task, the subject has to compare the position of the two sounds relatively to the subject's position. Moreover while MMA requires estimating a relation of order between two acoustic directions; bisection requires estimating a relation of order between two estimated acoustic distances. To summarize, while the space bisection requires a Euclidian representation of space and involves higher abstraction capabilities, for the MMA task a topological representation of space is sufficient.

Moreover, we chose these two tasks because we recently reported that the visual information is fundamental for the bisection task and not essential for the MAA task (Gori et al., 2014). A visual dominance over audition during development was observed for the space bisection task (Gori et al., 2012), while the absence of visual input in congenitally blind individuals negatively impacts their performance on audio space bisection tasks (Gori et al., 2014). However the absence of vision does not affect the ability of performing the MAA task in visually impaired individuals (Gori et al., 2014; in agreement with Lessard et al., 1998).

The apparent influence of the visuo-spatial knowledge on space bisection tasks leads to our second hypothesis: if the environmental visual information can improve acoustic spatial precision, then the improvement should be bigger for the space bisection task than for the MAA task.

With regard to the third point, which consists in investigating the environmental cues that possibly mediate the auditory improvement after observation, we replicated all audio tests in an anechoic room. In such a room, the walls absorb part of the sound energy; therefore the auditory system almost exclusively acquires the direct path of the sound, i.e., not reflected by walls. Conversely, in the normal room, a wall reflects sounds and generates echoes. Our hypothesis is that if the interpretation of echoes is triggered by visual observation, an improvement of acoustic precision should occur only in the normal room, while not in the anechoic chamber.

Materials and Methods

Participants

We measured auditory spatial discrimination in 33 sighted individuals with normal or corrected to normal vision (an average age of 28, 5 years, with 18 females and 15 males), all with normal hearing (assessed by Ear Test 1.0 software) and no cognitive impairment. All participants gave informed consent before starting the tests. The study was approved by the ethics committee of the local health service (*Comitato Etico, ASL3, Genova*).

Apparatus and Stimuli

The participants sat 180 cm away from the center of a bank of 23 speakers, 161 cm long (see **Figure 1**), and spanning $\pm 25°$ of visual angle.

During the auditory space bisection task, three stimuli, each having a duration of 75 ms, were presented at interval of

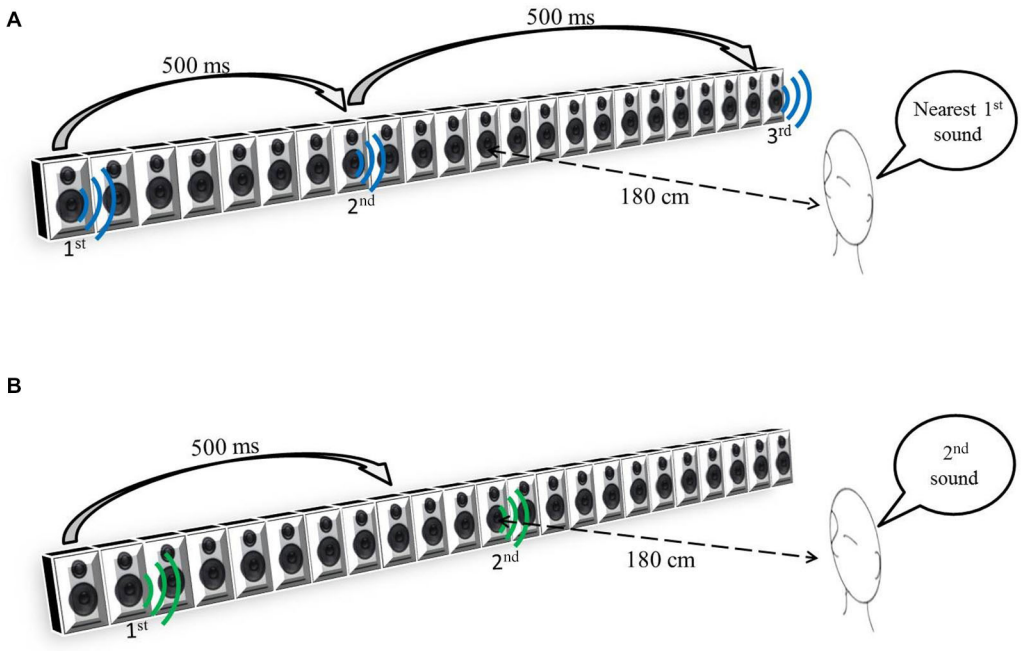

FIGURE 1 | (A) Space Bisection Task. **(B)** Minimum audible angle (MAA) task.

500 ms (see **Figure 1A**). The first stimulus was always at −25°, the third always at +25° and the second at an intermediate speaker position which was determined by QUEST (Watson and Pelli, 1983), an adaptive algorithm which estimates the best stimulus value to be presented after each trial, given the current participant's estimate. To ensure that a wide range of positions was sampled, that estimate was jittered by a random amount, drawn from a Gaussian distribution of space covering the full width of the loudspeaker's array, and the nearest speaker to that estimate chosen. In the MAA task, two 75 ms pink noise (Will and Berg, 2007) stimuli were presented with a 500 ms interval. One sound came from the central loudspeaker (12th speaker) and the other one at a random distance from center on its left or on its right (**Figure 1B**). Also in this case, the QUEST algorithm determined the position of the second stimulus. For both tasks, the proportion of rightward responses was calculated for each speaker distance. Gaussian functions by means of the Maximum Likelihood method were used to estimate both the mean, or PSE (Point of Subjective Equality), and the standard deviation, or JND (Just Noticeable Difference). The standard deviation of the fit was taken as an estimate of the threshold, indicating the precision of the task.

To better generalize our results, in 15 participants we used three different sound sources (randomized across trials), all with a 75 ms duration and a 60 dB SPL intensity (measured at the participant's position): a 500 Hz sound (for which interaural time differences are more important for sound localization); a 3000 Hz sound (for which interaural level differences are more important); and pink noise (ranging from 0 to 5 KHz) for which both are important. As the precision in sound localization varied very little among the three sounds, only pink noise burst data were considered.

Procedure

Two audio spatial tasks were considered: an auditory space bisection task and a MAA task. The entire group of participants were divided into three groups. The first group (composed of 11 participants) performed four audio tasks (two times the bisection task and two times the MMA task) in an anechoic chamber (3 m × 5 m), the second groups (composed of 11 participants) performed four audio tasks (two times the bisection task and two times the MAA task) in a normal room (7, 20 m × 3, 5 m). The participants of these two groups were blindfolded before entering the room; during the first two audio tasks (one audio bisection and one MAA task), they had no notion of the room or the acoustic stimulation setup. After having performed both the audio tasks, the participants were allowed to remove the blindfold and observe for 1 min the room: in one case an anechoic chamber (first group) and in the other case a normal room (second group). Afterwards they were blindfolded again to repeat both audio tasks again. The last group (composed of 11 participants) was not blindfolded, so they had a full vision of the room and the setup during the tasks. They performed two audio tasks (one time the bisection task and one time the MAA task) just on the normal room. For all the groups the bisection and MAA tasks were presented in a random order.

In the auditory space bisection, participants reported verbally whether the second sound was spatially closer to the first sound (produced by the first speaker on the left, number 1) than the last sound (produced by the last speaker on the right, number 23). Each subject performed 60 trials.

In the MAA task, the participants had to verbally report which sound was more from the right, choosing between the first or the second sound. Each subject performed 60 trials for each task.

Results

Figure 2 show psychometric functions of the proportion of trials judged "closer to the right sound source", plotted against speaker position (in cm). On the top of the figure are shown the results obtained by one of the participant took as an example of the global trend in the anechoic chamber for the space bisection (**Figure 2A**) and the MAA (**Figure 2C**). In the same way, on the bottom, the **Figure 2** show the results of one of the participant for the normal room in the space bisection (**Figure 2B**) and the MAA (**Figure 2D**).

Figure 3 shows the thresholds obtained before and after having observed the environment, it also shows the performance with eyes open for both the tasks: the MAA (**Figure 3A**) and the space bisection (**Figure 3B**). In both figures, the solid colors refer to the performance before room observation, while the colors with reticulus refer to the performance after the room observation.

We conducted a mixed model 2-way (2 × 2) ANOVA for both MAA and Space Bisection tasks with a between factor, *room kind* (normal room vs. anechoic chamber), and within factor, *room observation* (before environmental observation vs. after environmental observation). For the space bisection task the ANOVA revealed significant main effect for both factors, *room observation* ($F_{(2,22)} = 6.55$, $p < 0.02$) and *room kind* ($F_{(2,22)} = 7.35$, $p < 0.01$). It has been observed a significant *room observation* × *room kind* interaction ($F_{(4,11)} = 6.86$, $p < 0.01$). Then we ran Student's *t*-test that indicate a significant difference between the groups who performed the space bisection task in the normal room and anechoic chamber before observing the room (two tailed two-sample *t*-test, $t_{(20)} = 3.44$, $p < 0.01$) and in the normal room between before environmental observation and after environmental observation (two tailed pair-sample *t*-test, $t_{(10)} = 5.46$, $p < 0.001$). On the other hand, for the MAA, no significant effect was found (*room observation*, $F_{(2,22)} = 0.48$, $p = 0.49$; *room kind*, $F_{(2,22)} = 1.49$, $p = 0.28$; *room observation* × *room kind* $F_{(4,11)} = 0.506$, $p = 0.481$).

No significant difference was obtained in the precision after environmental observation and full vision (violet bars) for the space bisection task (two tailed two-sample *t*-test, $t_{(20)} = 1.279$,

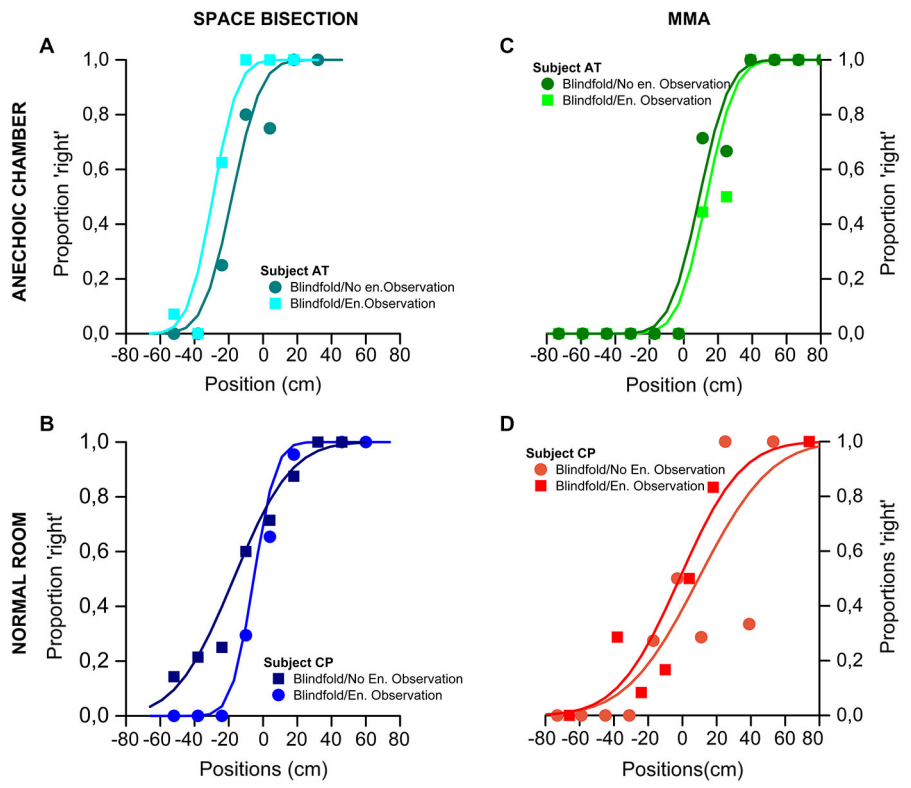

FIGURE 2 | Results of the Space Bisection Task and MAA of two participants, one for each group (normal room and anechoic chamber) as example. (A,B) Space bisection: proportion of trials judged "closer to the right sound source", plotted against speaker position (in cm). The area of the dots is the proportion of trials at that position, normalized by the total number of trials performed by each participants. At the top-left the results obtained in the anechoic chamber by participant AT **(A)**; at the bottom-left the results obtained in the normal room by participant CP **(B)**. Both sets of data are it with the Gaussian error function. **(C,D)** MAA: proportion of trials where the second of a two-sound sequence was reported to the right of the first, plotted against difference in speaker position. At the top-right the results obtained in the anechoic chamber by participant AT **(C)**; at the bottom-right the results obtained in the normal room by participant CP **(D)** Again the fits are the Gaussian error function.

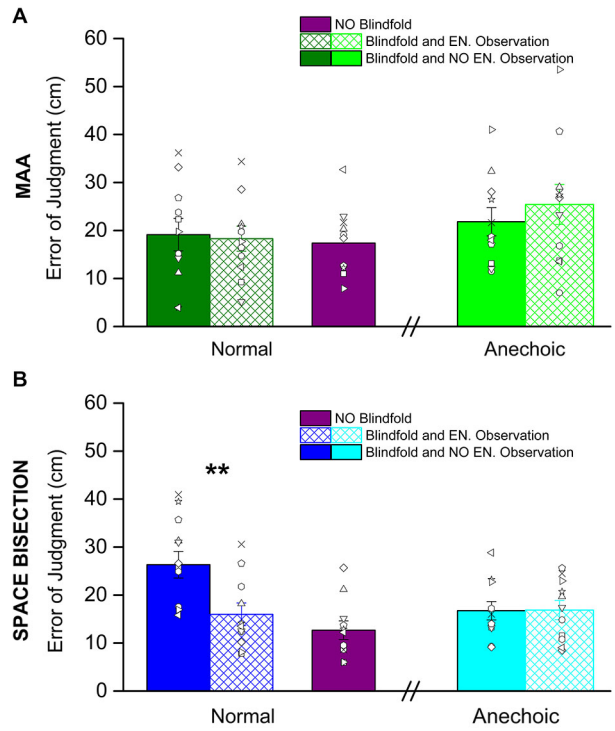

FIGURE 3 | Shown here are the average precision thresholds obtain in the MAA (A) and Space Bisection (B) tasks. (A) The dark green bars, on the left, represent the average precision thresholds obtained in the normal room before (fill in dark green bar) and after (reticulus dark green bar) environmental observation. On the right the light green bars are the average precision thresholds obtained in the anechoic chamber before (fill in light green bar) and after (reticulus light green bar) environmental observation. The violet bar is the average precision obtained by the subject in full vision in the normal room. The dots represent individual data. **(B)** For the space bisection, dark blue bars, on the left, represent the average precision thresholds obtained in the normal room before (fill in dark blue bar) and after (reticulus dark blue bar) environmental observation. On the right the light blue bars are the average precision thresholds obtained in the anechoic chamber before (fill in light blue bar) and after (reticulus light blue bar) environmental observation. Also in this case the violet bar represent the average precision obtained by the subject in full vision in the normal room. The dots represent individual data. (**) Indicates a significant difference of precision between before and after environmental observation in the normal room ($p < 0.01$).

$p = 0.27$) and for the MAA (two tailed two-sample t-test, $t_{(20)} = 0.257$, $p = 0.799$).

No change was observed in the localization bias (PSE) for both groups and tasks (bisection task: 2-ways (2 × 2) ANOVA with factors *room observation*—$F_{(2,22)} = 0.79$, $p = 0.38$—and *room kind*—$F_{(2,22)} = 1.48$, $p = 0.23$—and *room observation* × *room kind* interaction, $F_{(4,11)} = 0.088$, $p = 0.77$; MAA task: 2-ways (2 × 2) ANOVA with factors *room observation*—$F_{(2,22)} = 0.373$, $p = 0.545$—and *room kind*—$F_{(2,22)} = 1.91$, $p = 0.175$—, and *room observation* × *room kind* interaction, $F_{(4,11)} = 0.001$, $p = 0.97$).

Discussion

Recent works suggest that vision can interact with the auditory modality even when visual information is not useful for the auditory task, by improving the accuracy of auditory localization judgments (Jackson, 1953; Shelton and Searle, 1980; Tabry et al., 2013). For example acoustic performance has been found to be better when participants were allowed to observe the setup by keeping eyes open even if no visual cues were provided (Tabry et al., 2013). Thus even the simple observation of the setup and the environment during the task can improve auditory performance.

Why does this process occur? Which are the visual cues used by the visual system that allow for such an auditory improvement?

In this paper we investigated these issues by studying: (i) the environmental visual cues that are involved in auditory precision improvement; and (ii) whether this improvement is task related.

We tested the first point by asking the participants to perform two audio tasks twice. The first time the tasks were performed without observing the room; the second time, after having observed the room for 1 min. The results suggest that the observation of the environment for a brief period improves the auditory space precision and that the improvement is environment dependent. The improvement was only found after the observation of a natural environment, while, when the test was replicated in an anechoic chamber, no improvement was obtained. Besides, the improvement was task dependent. Two tasks were tested: a MAA task and an audio spatial bisection task; the improvement was observed only for the space bisection task but not for the MAA.

The first question that arises from these results is why the improvement is task-specific, giving that it occurs only for the audio space bisection task. We think that this specificity can be related to the role of visual information on the calibration of the auditory system.

Most recent works on multi-sensory interactions concentrated on sensory *fusion*, investigating the efficiency of the integration of information from different senses. Equally important, but somewhat neglected aspect, is sensory *calibration*.

Our idea is that, while *precision* has the highest weight for sensory integration, the most important property for sensory calibration is *accuracy*. Precision is a relative measure defined as the degree of reproducibility or repeatability between measurements, usually defined as the standard deviation of the distribution. Accuracy, conversely, is defined in absolute terms as the vicinity of a measurement to its true physical value.

We have recently observed that during an audio-visual bisection task, sighted children show a strong visual dominance before multisensory integration occurs (Gori et al., 2012). It is reasonable that for the audio bisection task, the sense of vision is the most accurate for estimating the space. Therefore, it may be used to calibrate the audio system for this spatial task. An important question inferring from our cross-modal calibration theory is: what happens when the calibrating sense is impaired or absent, as is the case of visually impaired adults? We recently tackled this question by testing blind adults in an spatial audio bisection task demonstrating that, in absence of visual input, they have deficits in understanding the spatial relationship between sounds (Gori et al., 2014). The audio deficit was not observed, in

agreement with previous studies (Lessard et al., 1998), for the MAA task.

Several physiological works confirm that vision is fundamental for some kind of auditory spatial localization: a series of experiments on animals have documented that displacing vision (Knudsen and Knudsen, 1985) or producing total visual deprivation (King and Carlile, 1993) often lead to systematic and persistent biases in auditory tasks. In the same way, transitory visual distortions in humans produce dramatic changes in auditory spatial maps (Recanzone, 1998; Zwiers et al., 2003).

On the basis of this evidence we can infer that the visual environmental information is not directly involved in the calibration of acoustic system in tasks such as the MAA. This idea would explain why we found a specific audio improvement after environment observation only for the audio bisection task and not for the MAA task.

A second interesting result is that: (i) before the environment observation, audio space bisection performance was worse in the normal room than in the anechoic room; and (ii) after the environment observation, an audio improvement was observed in the normal room and not in the anechoic room. Why performance for the space bisection task did not improve in the anechoic chamber and why it was worse before environment observation in the normal room than in the anechoic chamber? The observed null effect of the short environmental observation in the anechoic room might have been caused by a ceiling effect, i.e., performance was best already before room observation. However, this was not the case in the normal room, suggesting an alternative interpretation: in an anechoic chamber part of the energy of sounds produced by the loudspeakers is absorbed by the walls, therefore the hearing system acquires almost exclusively the direct sound. This is not true in the normal room, where the sound produced by the speakers is reflected by the walls, therefore producing echoes. This results in stimuli with scattering patterns or spectral coloration, or both, which are as much different as source locations are far apart. These echoes add perceptual information to the direct path of the sound, which may not be immediately interpretable without visual input, therefore causing a mismatch and worse performance in the normal room than in anechoic condition. However, the visual system could help the auditory system to compensate for such mismatch and obtain performance again comparable to those obtained in anechoic condition.

For similar reasons, observing an anechoic room does not improve acoustic precision because visual knowledge of the room structure is by no means related to any acoustic cue. Obtaining improvements in both rooms (or in the anechoic room only) would have supported the hypothesis that vision helps in estimating mainly the direction of arrival of acoustic direct paths, i.e., the only cue present in an anechoic room. However, this did not happen, supporting instead the hypothesis that visual cues related, even if implicitly, more to a global footprint given by room acoustics than to the local and specific acoustical feedback of our stimulation setup.

As discussed above, the fact that only the space bisection task results improved after room observation suggests that the transfer of information from the visual system toward the auditory one occurs only for those aspects for which the visual system can be used to calibrate the auditory one. In this vein, gaining knowledge about room acoustics through vision seems to be involved much more when estimating complex relationship between sound sources: while estimating audible angles requires comparison between the estimated direction of two sound sources, space bisection requires establishing a specific ordering relation between the direction of three sound sources, of which two are far apart in space. This operation may require Euclidian representation of space (Gori et al., 2014) and involve more spatial processing, possibly related to cues linked to the room structure that visual input helps to interpret.

A final interesting result is that no difference was observed between the performance obtained for the space bisection task after 1 min of environment observation and in the condition in which the eyes were maintained open for the entire experimental session. This suggests that the visual system needs only a brief period of environment observation to allow an improvement in this audio task.

In our past works we suggested that a process of cross-modal calibration might occur during development (Gori et al., 2008). During this process the visual system seems to be involved in the calibration of auditory space bisection (Gori et al., 2012, 2014). A possible interpretation of the results presented in this paper is that vision can calibrate audition also in a short-term form in adult individuals. It can indeed improve auditory space precision through a transfer of information about environmental cues from the visual system. In particular our results suggest that visual information might help the hearing system to compensate for the mismatch produced by echoes, and that visual knowledge of the room structure is linked to understanding of room acoustics.

If this interpretation is correct, then our results can be discussed in relation to the echolocation technique. Some blind individuals use the echoes produced by the environment to their advantage, thanks to echolocation. Human echolocation is an ability of humans to detect objects in their surroundings by sensing echoes from those objects. By actively creating sounds, such as clicks produced by rapidly moving the tongue in the palatal area behind the teeth (Rojas et al., 2009) or sounds produced by external mechanical means such as tapping a cane against the floor (Burton, 2000), people trained to orientate with echolocation can interpret the sound waves reflected by nearby objects. Many studies conducted under controlled experimental conditions have shown that echolocation improves blind people's spatial sensing ability.

For example a recent study (Vercillo et al., 2015) has compared the performance of expert echolocators, blind and sighted people with no previous experience of echolocation, in a space bisection task. It was found that blind expert echolocators performed the spatial bisection task with similar or even better precision than the sighted group. Moreover, in several studies were demonstrated that echolocation improves the ability to

determine other characteristics as distance (Kolarik et al., 2013), motion (Thaler et al., 2011, 2014), size (Teng and Whitney, 2011; Teng et al., 2012), shape (Thaler et al., 2011; Milne et al., 2014).

Therefore we can assume that echolocation could serve to recalibrate the ability of blind individuals to represent sounds in some spatial configurations and compensate the lack of vision. Our results support the idea that the visual system might in some form compensate for the mismatch produced by echoes in unknown environments by helping to interpret them. Visual information and spatio-acoustic representation appear therefore intertwined. If this is correct then the use of the echolocation technique can be a way of substituting the role of the visual system on this process. This would partially explain the improved spatial skills of blind expert echolocators. To conclude, the current findings suggest that vision is not only important for the auditory system during the development of space auditory representation, but also during adulthood. Although the mechanisms that subtend this process still have to be completely understood, our results suggest that the visual system can improve some forms of auditory spatial perception also in adults and after short-term environmental observation.

Acknowledgments

This research is partly funded by the FP7 EU STREP project BLINDPAD (www.blindpad.eu), under grant 611621, by the FP7 EU STREP project ABBI (www.abbiproject.eu), under grant 611452, and by the Fondazione Istituto Italiano di Tecnologia (www.iit.it). The authors would like to thank all the participants to this study.

References

Alais, D., and Burr, D. (2004). The ventriloquist effect results from near-optimal bimodal integration. *Curr. Biol.* 14, 257–262. doi: 10.1016/s0960-9822(04)00043-0

Buckingham, G., Milne, J. L., Byrne, C. M., and Goodale, M. A. (2015). The size-weight illusion induced through human echolocation. *Psychol. Sci.* 26, 237–242. doi: 10.1177/0956797614561267

Burton, G. (2000). The role of the sound of tapping for nonvisual judgment of gap crossability. *J. Exp. Psychol. Hum. Percept. Perform.* 26, 900–916. doi: 10.1037/0096-1523.26.3.900

Clarke, J. J., and Yuille, A. L. (1990). *Data Fusion for Sensory Information Processing*. Boston: Kluwer Academic.

Ernst, M. O., and Banks, M. S. (2002). Humans integrate visual and haptic information in a statistically optimal fashion. *Nature* 415, 429–433. doi: 10.1038/415429a

Ghahramani, Z., Wolpert, D. M., and Jordan, M. I. (1997). "Computational models of sensorimotor integration," in *Self-Organization, Computational Maps and Motor Control*, ed. P. G. M. A. V. Sanguineti (Amsterdam: Elsevier Science Publ), 117–147.

Gori, M., Del Viva, M., Sandini, G., and Burr, D. C. (2008). Young children do not integrate visual and haptic form information. *Curr. Biol.* 18, 694–698. doi: 10.1016/j.cub.2008.04.036

Gori, M., Giuliana, L., Sandini, G., and Burr, D. (2012). Visual size perception and haptic calibration during development. *Dev. Sci.* 15, 854–862. doi: 10.1111/j.1467-7687.2012.2012.01183.x

Gori, M., Sandini, G., Martinoli, C., and Burr, D. C. (2014). Impairment of auditory spatial localization in congenitally blind human subjects. *Brain* 137, 288–293. doi: 10.1093/brain/awt311

Jackson, C. (1953). Visual factors in auditory localization. *Q. J. Exp. Psychol.* 5, 52–65. doi: 10.1080/17470215308416626

King, A. J., and Carlile, S. (1993). Changes induced in the representation of auditory space in the superior colliculus by rearing ferrets with binocular eyelid suture. *Exp. Brain Res.* 94, 444–455. doi: 10.1007/bf00230202

Knudsen, E. I., and Knudsen, P. F. (1985). Vision guides the adjustment of auditory localization in young barn owls. *Science* 230, 545–548. doi: 10.1126/science.4048948

Kolarik, A. J., Cirstea, S., and Pardhan, S. (2013). Evidence for enhanced discrimination of virtual auditory distance among blind listeners using level and direct-to-reverberant cues. *Exp. Brain Res.* 224, 623–633. doi: 10.1007/s00221-012-3340-0

Landy, M. S., Banks, M. S., and Knill, D. C. (2011). "Ideal-observer models of cue integration," in *Book of Sensory Cue Integration*, ed. K. K. A. M. S. L. Julia Trommershauser (Sensory cue integration: Oxford University Press), 5–29.

Lessard, N., Paré, M., Lepore, F., and Lassonde, M. (1998). Early-blind human subjects localize sound sources better than sighted subjects. *Nature* 395, 278–280. doi: 10.1038/26228

Mateeff, S., Hohnsbein, J., and Noack, T. (1985). Dynamic visual capture: apparent auditory motion induced by a moving visual target. *Perception* 14, 721–727. doi: 10.1068/p140721

Milne, J. L., Anello, M., Goodale, M. A., and Thaler, L. (2015). A blind human expert echolocator shows size constancy for objects perceived by echoes. *Neurocase* 21, 465–470. doi: 10.1080/13554794.2014.922994

Milne, J. L., Goodale, M. A., and Thaler, L. (2014). The role of head movements in the discrimination of 2-D shape by blind echolocation experts. *Atten. Percept. Psychophys.* 76, 1828–1837. doi: 10.3758/s13414-014-0695-2

Recanzone, G. H. (1998). Rapidly induced auditory plasticity: the ventriloquism aftereffect. *Proc. Natl. Acad. Sci. U S A* 95, 869–875. doi: 10.1073/pnas.95.3.869

Rojas, J. A. M., Hermosilla, J. A., Montero, R. S., and Espí, P. L. L. (2009). Physical analysis of several organic signals for human echolocation: oral vacuum pulses. *Acta Acust. United Acust.* 95, 325–330. doi: 10.3813/aaa.918155

Shelton, B. R., and Searle, C. L. (1980). The influence of vision on the absolute identification of sound-source position. *Percept. Psychophys.* 28, 589–596. doi: 10.3758/bf03198830

Tabry, V., Zatorre, R. J., and Voss, P. (2013). The influence of vision on sound localization abilities in both the horizontal and vertical planes. *Front. Psychol.* 4:932. doi: 10.3389/fpsyg.2013.00932

Teng, S., Puri, A., and Whitney, D. (2012). Ultrafine spatial acuity of blind expert human echolocators. *Exp. Brain Res.* 216, 483–488. doi: 10.1007/s00221-011-2951-1

Teng, S., and Whitney, D. (2011). The acuity of echolocation: spatial resolution in the sighted compared to expert performance. *J. Vis. Impair. Blind.* 105, 20–32.

Thaler, L., Arnott, S. R., and Goodale, M. A. (2011). Neural correlates of natural human echolocation in early and late blind echolocation experts. *PLoS One* 6:e20162. doi: 10.1371/journal.pone.0020162

Thaler, L., Milne, J. L., Arnott, S. R., Kish, D., and Goodale, M. A. (2014). Neural correlates of motion processing through echolocation, source hearing and vision in blind echolocation experts and sighted echolocation novices. *J. Neurophysiol.* 111, 112–127. doi: 10.1152/jn.00501.2013

Vercillo, T., Milne, J. L., Gori, M., and Goodale, M. A. (2015). Enhanced auditory spatial localization in blind echolocators. *Neuropsychologia* 67C, 35–40. doi: 10.1016/j.neuropsychologia.2014.12.001

Warren, D. H., Welch, R. B., and McCarthy, T. J. (1981). The role of visual-auditory "compellingness" in the ventriloquism effect: implications for

transitivity among the spatial senses. *Percept. Psychophys.* 30, 557–564. doi: 10.3758/bf03202010

Watson, A. B., and Pelli, D. G. (1983). QUEST: a Bayesian adaptive psychometric method. *Percept. Psychophys.* 33, 113–120. doi: 10.3758/bf03202828

Will, U., and Berg, E. (2007). Brain wave synchronization and entrainment to periodic acoustic stimuli. *Neurosci. Lett.* 424, 55–60. doi: 10.1016/j.neulet.2007.07.036

Zwiers, M. P., Van Opstal, A. J., and Paige, G. D. (2003). Plasticity in human sound localization induced by compressed spatial vision. *Nat. Neurosci.* 6, 175–181. doi: 10.1038/nn999

Conflict of Interest Statement: The authors declare that the research was conducted in the absence of any commercial or financial relationships that could be construed as a potential conflict of interest.

frontiers in
SYSTEMS NEUROSCIENCE

REVIEW ARTICLE
published: 08 April 2014
doi: 10.3389/fnsys.2014.00054

Are videogame training gains specific or general?

Adam C. Oei and Michael D. Patterson*

Division of Psychology, School of Humanities and Social Sciences, Nanyang Technological University, Singapore, Singapore

Edited by:
Mikhail Lebedev, Duke University, USA

Reviewed by:
Richard Haier, University of California, USA
Kynan Eng, University of Zurich and ETH Zurich, Switzerland

****Correspondence:***
Michael D. Patterson, Division of Psychology, School of Humanities and Social Sciences, Nanyang Technological University, #04-13, 14 Nanyang Drive, Singapore 637332, Singapore
e-mail: mdpatterson@ntu.edu.sg

Many recent studies using healthy adults document enhancements in perception and cognition from playing commercial action videogames (AVGs). Playing action games (e.g., *Call of Duty*, *Medal of Honor*) is associated with improved bottom-up lower-level information processing skills like visual-perceptual and attentional processes. One proposal states a general improvement in the ability to interpret and gather statistical information to predict future actions which then leads to better performance across different perceptual/attentional tasks. Another proposal claims all the tasks are separately trained in the AVGs because the AVGs and laboratory tasks contain similar demands. We review studies of action and non-AVGs to show support for the latter proposal. To explain transfer in AVGs, we argue that the perceptual and attention tasks share common demands with the trained videogames (e.g., multiple object tracking (MOT), rapid attentional switches, and peripheral vision). In non-AVGs, several studies also demonstrate specific, limited transfer. One instance of specific transfer is the specific enhancement to mental rotation after training in games with a spatial emphasis (e.g., *Tetris*). In contrast, the evidence for transfer is equivocal where the game and task do not share common demands (e.g., executive functioning). Thus, the "common demands" hypothesis of transfer not only characterizes transfer effects in AVGs, but also non-action games. Furthermore, such a theory provides specific predictions, which can help in the selection of games to train human cognition as well as in the design of videogames purposed for human cognitive and perceptual enhancement. Finally this hypothesis is consistent with the cognitive training literature where most post-training gains are for tasks similar to the training rather than general, non-specific improvements.

Keywords: video games, transfer (psychology), cognition, perception, learning

INTRODUCTION

Over the last decade, effects of videogame play on human perception and cognition have been intensely studied and debated. Most studies have examined effects from action videogame (AVG) play. With a few exceptions (e.g., Boot et al., 2008; Irons et al., 2011), results from independent laboratories have shown experienced AVG players outperforming non-players in a variety of cognitive and perceptual tasks (e.g., Green and Bavelier, 2003; Colzato et al., 2010; Vallett et al., 2013).

What type of games can be considered an AVG? While the complexity and cross-fertilization across videogames makes pigeonholing each game into a distinct category difficult and somewhat arbitrary, AVGs contain many characteristics that make them unique. These include unpredictability, fast speed in presentation and response requirements, high perceptual load, the selection between multiple action plans and an emphasis on peripheral processing (Green et al., 2010a; Hubert-Wallander et al., 2011). Most of the games used in AVG studies have been first-person shooters (FPS) like *Call of Duty*, *Counterstrike*, *Unreal Tournament* and *Medal of Honor* (see also Latham et al., 2013 for more detailed descriptions of different AVGs). Although games of other genres like role-playing (e.g., *Final Fantasy*), puzzle (e.g., *Tetris*) may have one or two features in common with AVGs (e.g., speeded responses), they rarely, if ever, present these all the aforementioned demands in combination. Note that exactly what part of the AVG that leads to transfer is not yet clearly understood, and whether all or only some of the components are necessary for the transfer effects that have been observed.

Although cross-sectional comparisons suggest playing videogames leads to cognitive enhancements, they actually have little bearing on causality (Boot et al., 2011; Kristjánsson, 2013). Primary problems include issues of directionality (i.e., it is unclear whether people develop superior cognitive skills because of gaming or whether people with superior skills become gamers) and expectancy effects (people recruited for their gaming expertise are more motivated and expect to perform better) (Boot et al., 2011; Kristjánsson, 2013).

In contrast to cross-sectional studies, longitudinal-type training studies that show improved cognitive and perceptual abilities following a short bout of videogame training involving novice videogame players make stronger inferences for causality (e.g., Green and Bavelier, 2003; Wu and Spence, 2013). These games used for training are so intriguing because they were not specifically designed with the goal of training human cognition and perception (e.g., Klingberg et al., 2005; Jaeggi et al., 2011; Anguera et al., 2013). Rather, they are commercially available

games designed for entertainment. Hence, learning as a result of playing these games is incidental rather than intentional.

PURPOSE AND SCOPE OF THE REVIEW

While there are many studies documenting the effects of videogame play on cognitive and perceptual skills, the mechanism of transfer is not well understood. One proposal to explain the wide range of AVG-related transfer across multiple perceptual, attentional and executive measures is that the transfer is due to a general improvement in probabilistic inference. In other words, AVG trainees become better able to use evidence from repeated presentations of a task to guide their decision-making and allocation of cognitive resources (Green et al., 2010b; Bavelier et al., 2012b). Hence, AVG experience may enhance a general capacity to control top-down attention and learning of a new task, which in turn translates to improvement across many different tasks. This process is termed "learning to learn" (Bavelier et al., 2012b). Although intriguing, this suggestion is not without problems. First, it is unclear whether this transfer to a general statistical learning ability applies only to AVG or whether it can also be used to explain transfer effects from other videogames. If only applicable to AVG-based learning, it remains unclear what is special about AVG or the exact properties that would be required in an AVG to cause transfer. Second, this hypothesis is too general such that it is not clear which tasks AVG training can and cannot transfer to. Third and most importantly, although it has been demonstrated that AVG trainees do indeed improve probabilistic inference in a visual perceptual task (Green et al., 2010b), empirical evidence is currently lacking to show that this can also account for transfer to the other tasks seen in the AVG literature.

In contrast to the view of Bavelier et al. (2012b), we argue that transfer is task-specific and limited to perceptual and cognitive skills common to both the trained videogame and laboratory transfer task. The roots of this proposal go back to the theory of identical elements (Thorndike and Woodworth, 1901). Therefore, repeated playing of a videogame allows the player to hone the shared specific demands. We argue that the tasks used to test transfer have similar demands to what is trained by AVG. To demonstrate this, we will review each task that has been improved by AVG playing and explain how demands within the AVG are similar to the task itself. The hypothesis of common demands is also consistent with evidence showing that transfer from training is more likely if training and transfer task recruited common neural regions (Dahlin et al., 2008).

The review covers both cross-sectional comparisons between experienced videogame players as well as longitudinal-type training studies. Although videogame training has been studied across the lifespan from young children (Subrahmanyam and Greenfield, 1994; Yuji, 1996) to old adults (Basak et al., 2008), Due to limited space, we limit this review to young adults, which make up the majority of the samples used in the videogame literature.

The reader should note that because of the interest generated by the groundbreaking work that emerged from the Bavelier lab (Green and Bavelier, 2003), the majority of investigations over the last decade have been focused mainly on AVGs. In contrast, non-AVGs are rarely studied. Rather, non-AVG players and non-AVG training groups are often used as control groups. Hence, inevitably a large portion of the review will document cognitive and perceptual enhancements via AVG play. Nevertheless, where available, we review evidence for transfer effects arising from non-AVGs as these studies also provide evidence to support our common demands hypothesis. We review the evidence for videogame-related transfer starting from lower level perceptual skills to higher-order cognitive control.

EVIDENCE FOR VIDEOGAME-RELATED TRANSFER

Enhancements in many visual-perceptual skills have been demonstrated empirically in many AVG-training studies and those that compared non-AVG and habitual AVG players. The different demands described above in AVGs allow predictions on what abilities are trained and the plausible transfer effects using the common demands hypothesis. Consider what is expected in a typical AVG. In these games, players often are required to detect and respond to enemies quickly as well as keeping track of them as they move around the screen. These demands are coupled with the need to attend to several items simultaneously in both central and peripheral vision. These are similar to the demands in multiple object tracking (MOT) and Useful Field of View (UFOV) tasks. Moreover, as enemies appear rapidly one after another or simultaneously, there is great emphasis on the ability to rapidly switch attention from one target to another. This is similar to an attentional blink task. In addition, players have to resist being distracted by task irrelevant stimuli no matter how salient these distractors are. This may lead to improved performance in tasks that require suppressing distractors. Failure to successfully perform any of the above may result in failure in the game mission. Because of these special properties, one can imagine that hours spent on playing action AVG play can serve to exercise many of these perceptual and attentional skills that underpin successful gameplay.

CONTRAST SENSITIVITY

An important aspect of visual perception that is enhanced by AVG playing is the ability to detect subtle contrast differences. Specifically, Li et al. (2009) showed that habitual AVG players outperformed non-videogame players in the ability to detect a low contrast Gabor patch. Additionally, videogame novices also showed enhancements in this skill following 50 h training in a fast-paced FPS relative to playing a control non-action game (*The Sims*).

At first glance, it does not appear obvious that an AVG experience demands detecting contrast differences between objects. However, note that in many action games, a strong emphasis is on distinguishing targets from non-targets to allow rapid responding. The emphasis on rapid responding thus places a demand on distinguishing a target from a non-target based on even the subtlest differences (e.g., visual characteristics such as color or contrast).

PERIPHERAL VISION

AVGs make good candidates for training peripheral vision because of their heavy emphasis on detecting targets across different central and peripheral areas. For example, in many shooter games, enemies often appear at far areas of the periphery and

players must spot and dispatch them early to advance in the game. It is therefore likely that hours spent on AVG play would serve to enhance sensitivity to targets in the periphery.

One measure of peripheral vision is the UFOV, which is the total area of the visual field where useful information is captured at a glance without eye or head movements (Sanders, 1970; Ball et al., 1988). Comparisons of UFOV between regular AVG players and non-players have shown that the former exhibited superior ability to detect targets at peripheral areas of vision (10°, 20° and 30° eccentricity) (Green and Bavelier, 2003). Target detection at these eccentricities was also enhanced following AVG training for as short as 10 h relative to *Tetris* (Green and Bavelier, 2003). This enhanced target detection in regular AVG players and non-players trained to play an AVG was also found in more demanding UFOV tasks that included more distractors and a secondary task (Green and Bavelier, 2006a).

As the UFOV represents only an effective or functional field of view relevant to a particular visual task, videogame effects on peripheral vision have also been studied using clinical measures of central and peripheral visual fields. The results in Green and Bavelier (2003, 2006a), where videogame advantage extended to 30° eccentricity from fixation may have represented only the outer edges of central vision (Buckley et al., 2010). Hence, Buckley et al. (2010) tested regular AVG players and non-players on the Goldman Kinetic perimetry, a standard clinical measure of peripheral vision. Their results replicated Green and Bavelier (2003, 2006a) by showing enhanced central visual fields (30° eccentricity from fixation). Crucially, the AVG players also had, on average, a larger peripheral visual field (60° eccentricity from fixation). These results taken together provide strong evidence of AVG-related enhancements to peripheral vision, which may have ecological significance especially given that gender differences in UFOV can be reduced with AVG training (Feng et al., 2007).

Although the aforementioned studies show an AVG-related enhancement in UFOV, other studies have failed to replicate these results. Specifically, Boot et al. (2008) and Murphy and Spencer (2009) found equivalent UFOV performance in AVG and non-AVG players. Furthermore, no differences were found in UFOV improvement beyond test-retest effects in AVG trainees after 21.5 h of training relative to those trained in a strategy game and *Tetris* (Boot et al., 2008). The reason for the discrepancies in findings is unclear, but in cross-sectional comparisons, differences in selecting samples may have resulted in the null findings. For example, in Boot et al. participants in the AVG group did not exclusively play that genre but also reported playing other genres as well. As for the training study, Strobach et al. (2012) speculated that the large number of transfer tasks in their training study might have undermined any transfer effects due to test fatigue. Also, it is important to note that the transfer tasks in Boot et al. were administered three times at pre, mid and post-training. Presumably, multiple testing induced practice effects in the AVG and control groups that masked transfer effects.

DIVIDED ATTENTION

Given the nature of many fast-paced AVG, the ability to divide attention to several items confers a great advantage when playing these games. Hence, according to the common demands hypothesis playing fast-paced AVG should potentially enhance performance in tasks that require allocation of attention towards several items. Current evidence generally supports this claim (but see Boot et al., 2008).

Posner cueing

In one of the first studies that demonstrated spatial attentional advantages in videogame players, Greenfield et al. (1994) showed that expert players of the game *Robot Battle*, were superior in attending to more than one space relative to game novices using the Posner cueing task (Posner et al., 1980). Briefly, in the Posner cueing task, a cue was given to indicate the probable location of a target. There were three probabilities of the target appearing where the cue indicated—80% (high probability), 50% (neutral) or 20% (low). The speed of target detection was fastest in the high probability condition, and slowest in the low probability condition (Posner et al., 1980). In terms of overall response times, expert videogame players were faster in target detection in the high and low probability conditions compared to non-gamers. Furthermore, the videogame experts did not show an increased response time in the low probability relative to the neutral condition (Greenfield et al., 1994).

Demonstrating a causal effect, those trained to play a videogame, *Robotron*, for 5 h, where a player fended off robot attacks from many directions, showed greater improvement at the low probability condition whereas non-players showed no improvement. These results thus provided early and preliminary evidence of AVG-related advantage in attending to multiple locations in space, a demand common to many fast-paced AVG.

Flanker effects

Corroborating evidence for AVG-related superior attentional capacity to attend to more items in parallel has also been shown using different attentional tasks. In their groundbreaking work using a modified flanker task (Lavie and Cox, 1997), Green and Bavelier (2003) claimed that experienced AVG players had leftover attentional resources to attend to distractors when performing a demanding task, whereas non-gamers did not attend to them and thus were not distracted. This suggests that AVG players had greater attentional capacities to attend to multiple items in parallel. In contrast, Irons et al. (2011) failed to replicate these results. However, note that both studies were cross-sectional, not training studies. Hence, it is unclear whether the AVG advantage is causal. The discrepancy in findings may simply reflect sample differences. A training study is therefore needed to resolve this issue.

Multiple object tracking

Green and Bavelier (2006b) found that experienced AVG players were able to track on average two items more than non-gamers in an MOT task. In addition, following 30 h of training, non-players trained in an action game, *Unreal Tournament* improved accuracy rate when the number of objects to-be-tracked increased beyond four items. In contrast, accuracy rate for the control group trained in *Tetris* remained unchanged regardless of the number of targets shown. Similar enhancements were found after 20 h of training using a different measure of MOT (Oei and Patterson,

2013). Corroborating these results, Boot et al. (2008) showed that AVG players were able to track on average, at higher speeds than non-gamers.

The transfer to MOT appears confined to fast-paced FPS. In contrast, training using slower-paced AVGs or other types of AVG such as fast-paced sports game showed no such improvement (Cohen et al., 2008). Like MOT tasks, FPS have multiple fast moving objects that require simultaneous tracking. In contrast, games with multiple items on screen without requiring attention to-be-allocated to all items simultaneously (such as match-3 games) may not result in transfer after training (Oei and Patterson, 2013). However, this hypothesis remains tentative as Boot et al. (2008) failed to find evidence for enhanced MOT tracking speed in participants trained in a fast-paced FPS for 21.5 h compared to non-AVG trained participants.

Enumeration

Evidence for the enhanced ability of AVG players to attend to multiple items has also been corroborated using an enumeration task. Green and Bavelier (2006b) showed that experienced action gamers were more accurate in estimating the number of items displayed than non-action gamers. In addition, experienced action gamers were able to estimate about two items more than non-action gamers. This enhanced ability was also found after 10 h training using an FPS AVG relative to controls (*Tetris* training).

VISUAL SEARCH

FPS games are highly similar to a visual search paradigm because players must search for targets amidst distractors, such as an enemy in hiding (Wu and Spence, 2013). Indeed, converging evidence shows search advantages in habitual AVG players. First, AVG players searched faster and more efficiently overall (Hubert-Wallander et al., 2011) without sacrificing accuracy (Castel et al., 2005). Additionally, AVG players searched more accurately and faster in demanding conjunction conditions (Wu and Spence, 2013). Finally, AVG players were able to search more accurately when distracting objects were in close proximity to the target (Green and Bavelier, 2007), a condition known as crowding (Toet and Levi, 1992; Intriligator and Cavanagh, 2001).

Several longitudinal studies have corroborated the cross-sectional results. These studies used both FPS and other types of AVG training compared with non-AVG training. In a 30-h training study, Green and Bavelier (2007) found that players trained in an AVG (*Unreal Tournament*) were able to detect targets at reduced target-distractor separations compared to the non-AVG group (*Tetris*) at 0°, 10° and 25° eccentricity. Furthermore, following 10 h of training using an FPS, and a racing AVG compared to a control group (3D puzzle game, *Ballance*), Wu and Spence (2013) demonstrated greater accuracy and faster search time for both types of AVG players compared to the control game in a dual search task that involved searches in central and peripheral vision. Interestingly, the results for the FPS and racing game were equivalent. Although most racing games do not include visual search, Wu and Spence (2013) argued that for this particular racing game, the player was expected to also locate and identify several targets. Therefore, these results match the common demands hypothesis.

Demonstrating that not all AVG are alike, we failed to find an AVG-related enhancement in visual search following 20 h of FPS training (Oei and Patterson, 2013). The AVG game used in Oei and Patterson did not have search demands because enemies tended to pop out and engage the player rather than making the player search them out.

Importantly, Oei and Patterson (2013) showed that transfer is not dependent on the training game being an AVG. Instead, visual search time was significantly decreased following training in a hidden object game and a match-3 game (*Bejeweled*) that required searching a display for matching shapes. Therefore, the data in Oei and Patterson (2013) and Wu and Spence (2013) support the common demands hypothesis, such that training in games that included frequent search improved visual search performance. On the other hand, the failure to find evidence for AVG related transfer is inconsistent with a general transfer mechanism, which would lead to improvements across multiple tasks, including visual search.

CHANGE DETECTION

A fundamental requirement in any fast-paced AVG is the need to respond quickly to a sudden onset stimulus. This could be a visual anomaly such as an enemy that appears when the player is preoccupied by something else in the visual field. Given this requirement for successful gameplay, it is plausible that expert AVG players will exhibit superior ability to detect visual anomalies when they are focused on other features in their visual field.

Current evidence for enhanced change detection in AVG players remains mixed. On one hand, Murphy and Spencer (2009) showed that AVG and non-AVG players are equally as likely to miss a cross moving across their visual field while performing a counting task. On the other hand, Vallett et al. (2013), using a popular inattentional blindness task (Simons and Chabris, 1999), showed that AVG players have a significantly greater likelihood of detecting a visual anomaly (man in a gorilla suit) while performing a counting task than non-gamers. One possibility for the inconsistent finding is that the original task in Simons and Chabris presented a more salient visual anomaly than that in Murphy and Spencer. This is not unlike an AVG where a sudden-onset visual stimulus is likely to be a salient one that demands a response (e.g., enemy).

ATTENTIONAL BLINK

Attentional blink refers to a bottleneck in information processing whereby a second target (T2) presented close in time (200–500 ms) to an accurately detected first target (T1), fails to be detected (Raymond and Shapiro, 1992; Shapiro et al., 1994, 1997). Green and Bavelier (2003) reported that AVG players were less affected by attentional blink than non-gamers. Furthermore, non-gamers trained in an AVG for 10 h improved T2 detection during the intervals susceptible to the attentional blink effect (Green and Bavelier, 2003). This training-related enhancement specifically on a fast-paced FPS has generally been replicated following 12–20 h of training (Cohen et al., 2008; Oei and Patterson, 2013). Crucially, the enhancement is seen only following a fast-paced FPS, but not to other slower paced FPS, third-person shooters and sports games (Cohen et al., 2008). Compared to other

AVG, fast-paced FPS requires fast responses to rapidly presented successive targets which leads to these specific improvements (Cohen et al., 2008). This is consistent with the common demands hypothesis.

In contrast, Boot et al. (2008) and Murphy and Spencer (2009) failed to find AVG-related advantages in attentional blink performance. Importantly, no attentional blink enhancement was seen beyond test-retest effects in AVG trainees after 20 h of training (Boot et al., 2008). However, it is again important to place the findings in context of the criticisms of the study mentioned above.

SPATIAL COGNITION

Spatial cognition involves multiple components and broadly speaking refers to the skill in representing, transforming, generating and recalling symbolic, nonlinguistic information (Linn and Petersen, 1985). AVG, especially those with a first-person perspective, should be good training tools for some spatial skills due to navigation and rotation demands in 3D space (Spence and Feng, 2010; Sanchez, 2012). However, training may not transfer to other components if the relevant spatial cognitive demands are not present in the game (Okagaki and Frensch, 1994). For example, enhanced 3D mental rotation was found only following FPS training but not using games without demands to navigate in 3D space (Feng et al., 2007; Sanchez, 2012). Furthermore, the enhancement to spatial ability was specific only to mental rotation of 3D shapes but not to spatial visualization in a paper-folding task where no rotation was necessary (Sanchez, 2012).

Transfer is also seen using non-AVG training. Specifically, faster and more accurate mental rotation has been found in experienced and trained *Tetris* players (Okagaki and Frensch, 1994; Sims and Mayer, 2002; Boot et al., 2008). Unlike AVGs, *Tetris* does not involve fast responding except for the highest levels. Furthermore, new objects in *Tetris* always enter from one location (vertically from the top) and hence there is no requirement to track multiple moving objects in the periphery. There is also no requirement to construct a representation of a complex 3D environment in order to navigate. Finally, virtually no distractors appear in *Tetris*. Rather, participants must stack falling shapes efficiently using mental rotation and planning. These demands lead to different, specific effects compared to those commonly found from playing action games, indicating that *Tetris* should be classified a non-action game.

Three months of *Tetris* training was associated with decreased activation in right frontal (BA 32, 8, 9, 6, 46) as well as parietal (BA 40) areas (Haier et al., 2009). These areas have been previously been shown to be highly activated in mental rotation tasks (Cohen et al., 1996). This reduction in brain activation may suggest enhanced neural efficiency to perform mental rotation (cf. Haier et al., 1992).

Transfer effects from *Tetris* training were highly specific to mental rotation measures (Boot et al., 2008). Notably, the shapes used in the mental rotation task resembled shapes that appeared in *Tetris* (Boot et al., 2008). Conversely, no advantage was seen in skilled or trained players in mental rotation tests that did not involve *Tetris*-like shapes (Sims and Mayer, 2002; Boot et al., 2008). Furthermore, although 12 h of *Tetris* training did not result in transfer to spatial ability tests in general, examinations of the mental rotation strategies showed that *Tetris* trainees were more likely to use a Tetris-like mental rotation (clockwise rotation up to 225°) for *Tetris* shapes (Sims and Mayer, 2002).

These specific improvements thus add converging evidence to the proposal of a transfer being more likely if the game and transfer task share common demands. In contrast, a more general transfer mechanism would predict a general spatial ability or overall mental rotation enhancement. Moreover, the general learning proposal was originally proposed to explain AVG-related improvements only. Thus, the common demands theory allows explanation of more types of video-game related cognitive changes.

EXECUTIVE FUNCTIONS

Task switching

Both alternate-runs and random task switching paradigms have been employed to study the effects of videogame playing on task switching. In the former, a task-switch takes place after a fixed number of trials allowing preparation so that switching is less demanding and typically yields smaller switch costs (Monsell, 2003). In contrast, task-switches are random and unpredictable in the latter. The inability to prepare for a switch leads to greater conflicts, which in turn results in the switch cost being larger (Rogers and Monsell, 1995; Monsell, 2003).

Smaller switch costs in reaction time (RT) and accuracy have been demonstrated in regular AVG players compared to non-players in both alternate-runs and more demanding random task switches (Andrews and Murphy, 2006; Boot et al., 2008; Colzato et al., 2010; Cain et al., 2012; Green et al., 2012; Strobach et al., 2012). Greater switch cost reductions in alternate-runs task switching was found following 15 (Strobach et al., 2012) and 50 h (Green et al., 2012) of AVG training compared to controls that played non-AVGs (e.g., *Tetris* and *The Sims*).

Although task switching superiority in experienced AVG players is consistently reported, results of training studies for transfer to task switching remain equivocal. In contrast to Green et al. (2012) and Strobach et al. (2012), Boot et al. (2008) failed to find transfer effects following 21.5 h of AVG training. Different task-switching paradigms used in each study may explain the conflicting results. Specifically, while Green et al. (2012) and Strobach et al. (2012) utilized a predictable alternate-runs switch format, Boot et al. (2008) instead used a random task switching paradigm. Thus, AVG training may only improve the ability to prepare for upcoming switches but not more demanding mental flexibility measured by random task switching paradigms as these are supported by different neural and cognitive mechanisms (see Baddeley et al., 2001; Bryck and Mayr, 2005; Pereg et al., 2013).

Consistent with the argument of the common demands hypothesis, the transfer of predictable task switching may stem from the frequent practice in AVGs to switch between targets and between items during gameplay. Each activity has clear objectives with little conflict between them. Thus disengagement from a previous task to switch focus on an upcoming task is relatively easy. Take for instance switching rapidly between enemies where the switch can be planned or reactive. Either way, the action following a switch is similar. This is like a task-repeat and involves negligible response conflict. Even switching from an enemy to

collecting an item (e.g., health replenishments or bonus items) is unlikely to result in any decisional or response conflicts as the actions involved with either task are distinct. These are akin to the predictable task switching condition whereby any switch is predictable and an upcoming switch or task-repeat condition can be planned in advance. In contrast, decisional conflicts like the random task switching condition are rarely, if ever, encountered in such AVGs.

Distractor suppression

Several studies indicate that AVG players are less susceptible to attentional capture by task-irrelevant stimuli than non-players. Experienced AVG players and those trained to play an AVG for 20 h were faster in responding to targets in the presence of distractors (Chisholm et al., 2010; Oei and Patterson, 2013). This advantage may stem from improved top-down suppression of attentional capture rather than a faster recovery from capture (Chisholm and Kingstone, 2012). Support for better distractor suppression in AVG players comes from neuroimaging. Relative to non-gamers, action gamers showed increased suppression of steady state visually evoked potential (SSVEP) amplitudes to unattended peripheral stimuli in a target detection task where the goal was to detect targets at central fixation or when cued, at left and right peripheries (Mishra et al., 2011). Additionally, using a visual search task with moving distractors at central or peripheral vision, action gamers showed reduced blood-oxygenated level dependent (BOLD) response in visual motion-sensitive regions (Medial Temporal/Medial Superior Temporal areas) to moving distractors compared to non-gamers (Bavelier et al., 2012a). Moreover, 10 h of AVG training has been shown to increase P2 and P3 waves at occipital and occipito-parietal sites (Wu et al., 2012) when performing an attention visual field task where one is required indicate the direction of a target amidst distractors. Increases in P2 and P3 amplitudes may reflect adaptations to task demands on attentional control in attentional selection as well as inhibition of processing of task-irrelevant stimuli (Bledowski et al., 2004; Potts et al., 2004; Sawaki and Luck, 2010; Fritzsche et al., 2011). Taken together, these findings suggest that experienced AVG players are better than their non-AVG counterparts at applying top-down control to suppress attention for task-irrelevant distractors. Longitudinal training studies further show that the advantages displayed are causal.

SPECIFIC OR GENERAL TRANSFER? THE CASE FOR SPECIFIC TRANSFER GAINS

Over the last 10 years since the seminal work of Green and Bavelier (2003), the focus of videogame training has been directed towards AVGs. The growing literature suggests that AVGs enhance lower-level information processing skills ranging from visual perception to different aspects of attention (Green and Bavelier, 2003, 2006a,b, 2007; Chisholm et al., 2010). These include expanded peripheral vision (Green and Bavelier, 2003), target discrimination, identification and contrast (Green and Bavelier, 2007; Li et al., 2009), selective attention (Wu et al., 2012) and attentional blink (Cohen et al., 2008; Green and Bavelier, 2003). In contrast, evidence for transfer to some executive functions remains equivocal (e.g., Boot et al., 2008).

Given the differing characteristics of non-action games, one would expect different types of transfer from non-action game training compared to AVG. However, unlike AVGs, not much research has been conducted to determine the range of transfer. Nevertheless, a small number of studies also suggest some benefits from non-AVGs such as *Tetris*' transfer to mental rotation (Okagaki and Frensch, 1994; Sims and Mayer, 2002; Boot et al., 2008). Importantly, like AVG, transfer effects are also quite specific to skills that are common to the trained game and transfer task (Okagaki and Frensch, 1994; Sims and Mayer, 2002; Boot et al., 2008; Oei and Patterson, 2013).

A critical question we set out to answer in this review is whether transfer gains from videogames reflect a general or more specific enhancement. One hypothesis is that a general attentional control mechanism accounts for transfer effects seen in (action) videogames. This theory suggests that (action) videogame play enhances a general learning of task statistical patterns that supports perceptual decision-making and allocation of cognitive resources (Green et al., 2010b; Bavelier et al., 2012b). However, it has not been empirically demonstrated that this mechanism can indeed account for transfer across the wide range of tasks utilized in the videogame literature. Moreover, it is unclear if such a learning mechanism is applicable to non-action games. Furthermore, the data reviewed earlier do not support this hypothesis. Specifically, if a general learning mechanism really underlies AVG-related transfer, enhancements should be seen across multiple tasks, even those that do not share overlapping demands with the trained AVG. Unfortunately, as most current studies only included transfer tasks that share common demands with the trained AVG, it is difficult to assess the validity of this hypothesis. In the few studies that included tasks that do not appear to share common demands with AVG used for training, however, AVG playing did not transfer to all tasks (e.g., Boot et al., 2008; Murphy and Spencer, 2009; Oei and Patterson, 2013).

In contrast to a general transfer mechanism, the main proposal here is that transfer effects are specific to common demands shared between the trained videogame and transfer task. This hypothesis can explain both AVG and non-AVG training effects (Oei and Patterson, 2013).

Converging evidence from neuroimaging also appears to support the current hypothesis. For instance, transfer is more likely if training and transfer tasks recruit overlapping neural regions (Dahlin et al., 2008). Evidence from the working memory training literature also supports specific over general transfer. For instance, working memory training improved performance on working memory measures but not to measures of fluid intelligence (Harrison et al., 2013; Melby-Lervåg and Hulme, 2013; Redick et al., 2013). Hence, we feel that although working memory and videogame play are different activities, they share a common principle in relation to transfer of cognitive skill in that transfer is specific to what is practiced within the training regime. In contrast, little or no transfer can be expected for skills not explicitly practiced.

We do note that although the general transfer mechanism proposed by Bavelier et al. (2012b) contrasts with the common demand specific mechanism proposal, they added a caveat that "changes in knowledge produce benefits only to the extent to

which new tasks share structure with AVG. No benefits are expected in tasks that share no such structure" (Bavelier et al., 2012b). No study has yet been reported that systematically manipulates the demands contained in the AVG used for training because the definition of AVG has remained overly general, but there is some preliminary evidence that FPS AVG lead to different results than other types of AVG (Cohen et al., 2008).

CONCLUDING REMARKS AND FUTURE DIRECTIONS

Several gaps and unanswered questions still remain. First, it remains unclear how "closely-matched" the game and transfer task must be to maximize transfer. It is likely that the demands of the training game and transfer task must engage common neural networks (Dahlin et al., 2008). Nevertheless, quantitative metrics of how close a training game and the transfer tasks remains elusive and are worthy of further investigation. A quantifiable metric would be most useful especially in occupational settings in order to guide the selection of a training paradigm that maximizes transfer effects. For instance, in FPS, one could compare games with either progressively increasing speeds in which enemies appear or the number of enemies that appear simultaneously. We would predict that high-speed games would lead to a decrease in attentional blink, and faster RT, but would not have as large of an effect on MOT as the latter manipulation. To further test for the specificity of transfer effects, one could also conduct a study whereby games with different demands (or intensity) from the same genre are compared (see Cohen et al., 2008 for such an example). To determine whether general or specific transfer has occurred, it is important to include a wider variety of transfer tasks, some of which contain similar demands to the videogames and some of which measure more general learning. To test for general transfer, a videogame training regime could also target training visual attention or visual working memory and test whether improvements generalize across to the verbal or auditory modalities using material that was not trained during the games.

A second gap relates to which cognitive abilities can or cannot be improved by training. It will be important in the future to investigate which abilities are more resistant or amenable to be modified with training or whether improvement in one area will lead to worse performance in another (Takeuchi et al., 2011).

A third important issue is the durability of transfer effects. Thus far, many videogame studies have not tested whether the transfer effects remained after the laboratory tests have concluded (see Li et al., 2009; Anguera et al., 2013 for exceptions). Hence, it is unclear whether transfer effects remain after cessation of training. A main goal of a training task is the retention of skills in the long-term after the training has ceased (Schmidt and Bjork, 1992). As with any type of training, the effectiveness of videogame training should also be evaluated with this criterion.

Fourth, more research should examine individual differences in training-related transfer. It has been argued that the capacity for "cognitive modifiability" as a result of training varies from individual to individual (Calero and Navarro, 2007). It is thus unlikely that all individuals trained with a similar videogame improve similarly (see Wu et al., 2012). There are many factors that can influence plasticity and how well one responds to a training regime. Briefly, some examples of individual differences shown to influence training, cognition and transfer include age and baseline cognitive ability including intelligence (Yesavage et al., 1988, 1990; Haier et al., 1992; Verhaeghen et al., 1992; Bissig and Lustig, 2007; Calero and Navarro, 2007), gender (Feng et al., 2007) as well as lifestyle factors such as cardiovascular health and exercise (Gomez-Pinilla, 2008). Thus far, videogame training studies have not examined how these individual differences affect training-related transfer. Hence, investigating training-related transfer from an individual differences perspective is worthwhile as it can be critical for the implementation of a training regime to maximize transfer effects.

Finally, we feel that ultimately a training regime should translate to real-world applications outside of the laboratory. Thus far, the bulk of the studies have focused on laboratory tasks. Just like games have several demands in common with the cognitive tasks, we assume many everyday tasks have common demands that are trained by the videogames. Thus, we assume that playing videogames will lead to improvements in activities in everyday life. However, few studies have shown video game-related advantage in real-world activities. Videogame experience and skill has been shown to correlate with laparoscopic surgery skills (Rosser et al., 2007). Also, a short bout (10-h) of videogame training, albeit not a commercially available one, has been shown to improve flight performance in cadet pilots (Gopher et al., 1994). One potential area of future research may be to investigate whether videogame training in search skills can benefit performance in occupations that demand intense visual search skills (e.g., airport baggage scanners or air traffic controllers). Hence, the potential of videogame training advantages in real-world applications warrants further investigation.

In closing, over the last decade, we have seen considerable literature documenting the potential benefits of videogame training. With the increase in attention and effort dedicated to this area, intense debate, skepticism and scrutiny have also resulted (Boot et al., 2011, 2013; Kristjánsson, 2013). Nevertheless, such intense debate and scrutiny can only be beneficial to researchers as they strive to refine the methodology of videogame training research. Despite the increasing number of works and considerable progress, the field is still in its infancy and considerable advances are yet to be made. There are many advantages with training via a videogame. Training via videogame represents a departure from traditional learning activities in that it is highly arousing and motivating and has the potential to keep the player engaged for longer periods. With progress in computing power and artificial intelligence, there are arguably major leaps that can be made in game immersion and realism. Additionally, with input from psychologists and learning theory in videogame design, we can further tailor videogames for learning purposes. Hence, further investments in time and money to understand, research and improve transfer from videogame training to the work place, classroom and rehabilitation is surely worthwhile.

REFERENCES

Andrews, G., and Murphy, K. (2006). "Does video game playing improve executive functioning?," in *Frontiers in Cognitive Psychology*, ed M. A. Vachevsky (New York: Nova Science Publishers), 145–161.

Anguera, J. A., Boccanfuso, J., Rintoul, J. L., Al-Hashimi, O., Faraji, F., Janowich, J., et al. (2013). Video game training enhances cognitive control in older adults. *Nature* 501, 97–101. doi: 10.1038/nature12486

Baddeley, A. D., Chincotta, D., and Adlam, A. (2001). Working memory and the control of action: evidence from task switching. *J. Exp. Psychol. Gen.* 130, 641–657. doi: 10.1037/0096-3445.130.4.641

Ball, K. K., Beard, B. L., Roenker, D. L., Miller, R. L., and Griggs, D. S. (1988). Age and visual search: expanding the useful field of view. *J. Opt. Soc. Am. A* 5, 2210–2219. doi: 10.1364/josaa.5.002210

Basak, C., Boot, W. R., Voss, M. W., and Kramer, A. F. (2008). Can training in a real-time strategy video game attenuate cognitive decline in older adults? *Psychol. Aging* 23, 765–777. doi: 10.1037/a0013494

Bavelier, D., Achtman, R. L., Mani, M., and Föcker, J. (2012a). Neural bases of selective attention in action video game players. *Vision Res.* 61, 132–143. doi: 10.1016/j.visres.2011.08.007

Bavelier, D., Green, C. S., Pouget, A., and Schrater, P. (2012b). Brain plasticity through the life span: learning to learn and action video games. *Annu. Rev. Neurosci.* 35, 391–416. doi: 10.1146/annurev-neuro-060909-152832

Bissig, D., and Lustig, C. (2007). Who benefits from memory training? *Psychol. Sci.* 18, 720–726. doi: 10.1111/j.1467-9280.2007.01966.x

Bledowski, C., Prvulovic, D., Goebel, R., Zanella, F. E., and Linden, D. E. J. (2004). Attentional systems in target and distractor processing: a combined ERP and fMRI study. *Neuroimage* 22, 530–540. doi: 10.1016/j.neuroimage.2003.12.034

Boot, W. R., Blakely, D. P., and Simons, D. J. (2011). Do action video games improve perception and cognition? *Front. Psychol.* 2:226. doi: 10.3389/fpsyg.2011.00226

Boot, W. R., Kramer, A. F., Simons, D. J., Fabiani, M., and Gratton, G. (2008). The effects of video game playing on attention, memory and executive control. *Acta Psychol. (Amst)* 129, 387–398. doi: 10.1016/j.actpsy.2008.09.005

Boot, W. R., Simons, D. J., Stothart, C., and Stutts, C. (2013). The pervasive problem with placebos in psychology: why active control groups are not sufficient to rule out placebo effects. *Perspect. Psychol. Sci.* 8, 445–454. doi: 10.1177/1745691613491271

Bryck, R. L., and Mayr, U. (2005). On the role of verbalization during task set selection: switching or serial order control? *Mem. Cognit.* 33, 611–623. doi: 10.3758/bf03195328

Buckley, D., Codina, C., Bhardwaj, P., and Pascalis, O. (2010). Action video game players and deaf observers have larger Goldmann visual fields. *Vision Res.* 50, 548–556. doi: 10.1016/j.visres.2009.11.018

Cain, M. S., Landau, A. N., and Shimamura, A. P. (2012). Action video game experience reduces the cost of switching tasks. *Atten. Percept. Psychophys.* 74, 641–647. doi: 10.3758/s13414-012-0284-1

Calero, M. D., and Navarro, E. (2007). Cognitive plasticity as a modulating variable on the effects of memory training in elderly persons. *Arch. Clin. Neuropsychol.* 22, 63–72. doi: 10.1016/j.acn.2006.06.020

Castel, A. D., Pratt, J., and Drummond, E. (2005). The effects of action video game experience on the time course of inhibition of return and the efficiency of visual search. *Acta Psychol. (Amst)* 119, 217–230. doi: 10.1016/j.actpsy.2005.02.004

Chisholm, J. D., Hickey, C., Theeuwes, J., and Kingstone, A. (2010). Reduced attentional capture in action video game players. *Atten. Percept. Psychophys.* 72, 667–671. doi: 10.3758/APP.72.3.667

Chisholm, J. D., and Kingstone, A. (2012). Improved top-down control reduces oculomotor capture: the case of action video game players. *Atten. Percept. Psychophys.* 74, 257–262. doi: 10.3758/s13414-011-0253-0

Cohen, J. E., Green, C. S., and Bavelier, D. (2008). "Training visual attention with video games: not all games are created equal," in *Computer Games and Team and Individual Learning*, eds H. F. O'neil and R. S. Perez (Oxford, UK: Elsievier), 205–228.

Cohen, M. S., Kosslyn, S. M., Breiter, H. C., Digirolamo, G. J., Thompson, W. L., Anderson, A. K., et al. (1996). Changes in cortical activity during mental rotation A mapping study using functional MRI. *Brain* 119(Pt. 1), 89–100. doi: 10.1093/brain/119.1.89

Colzato, L. S., Van Leeuwen, P. J. A., Van Den Wildenberg, W. P. M., and Hommel, B. (2010). DOOM'd to switch: superior cognitive flexibility in players of first person shooter games. *Front. Psychol.* 1:8. doi: 10.3389/fpsyg.2010.00008

Dahlin, E., Neely, A. S., Larsson, A., Bäckman, L., and Nyberg, L. (2008). Transfer of learning after updating training mediated by the striatum. *Science* 320, 1510–1512. doi: 10.1126/science.1155466

Feng, J., Spence, I., and Pratt, J. (2007). Playing an action video game reduces gender differences in spatial cognition. *Psychol. Sci.* 18, 850–855. doi: 10.1111/j.1467-9280.2007.01990.x

Fritzsche, A.-S., Stahl, J., and Gibbons, H. (2011). An ERP study of target competition: individual differences in functional impulsive behavior. *Int. J. Psychophysiol.* 81, 12–21. doi: 10.1016/j.ijpsycho.2011.03.014

Gomez-Pinilla, F. (2008). The influences of diet and exercise on mental health through hormesis. *Ageing Res. Rev.* 7, 49–62. doi: 10.1016/j.arr.2007.04.003

Gopher, D., Weil, M., and Bareket, T. (1994). Transfer of skill from a computer game trainer to flight. *Hum. Factors* 36, 387–405. doi: 10.1177/001872089403600301

Green, C. S., and Bavelier, D. (2003). Action video game modifies visual selective attention. *Nature* 423, 534–537. doi: 10.1038/nature01647

Green, C. S., and Bavelier, D. (2006a). Effect of action video games on the spatial distribution of visuospatial attention. *J. Exp. Psychol. Hum. Percept. Perform.* 32, 1465–1478. doi: 10.1037/0096-1523.32.6.1465

Green, C. S., and Bavelier, D. (2006b). Enumeration versus multiple object tracking: the case of action video game players. *Cognition* 101, 217–245. doi: 10.1016/j.cognition.2005.10.004

Green, C. S., and Bavelier, D. (2007). Action-video-game experience alters the spatial resolution of vision. *Psychol. Sci.* 18, 88–94. doi: 10.1111/j.1467-9280.2007.01853.x

Green, C. S., Li, R., and Bavelier, D. (2010a). Perceptual learning during action video game playing. *Top. Cogn. Sci.* 2, 202–216. doi: 10.1111/j.1756-8765.2009.01054.x

Green, C. S., Pouget, A., and Bavelier, D. (2010b). Improved probabilistic inference as a general learning mechanism with action video games. *Curr. Biol.* 20, 1573–1579. doi: 10.1016/j.cub.2010.07.040

Green, C. S., Sugarman, M. A., Medford, K., Klobusicky, E., and Bavelier, D. (2012). The effect of action video game experience on task-switching. *Comput. Human Behav.* 28, 984–994. doi: 10.1016/j.chb.2011.12.020

Greenfield, P. M., Dewinstanley, P., Kilpatrick, H., and Kaye, D. (1994). Action video games and informal education: effects on strategies for dividing visual attention. *J. Appl. Dev. Psychol.* 15, 105–123. doi: 10.1016/0193-3973(94)90008-6

Haier, R. J., Karama, S., Leyba, L., and Jung, R. E. (2009). MRI assessment of cortical thickness and functional activity changes in adolescent girls following three months of practice on a visual-spatial task. *BMC Res. Notes* 2:174. doi: 10.1186/1756-0500-2-174

Haier, R. J., Siegel, B., Tang, C., Abel, L., and Buchsbaum, M. S. (1992). Intelligence and changes in regional cerebral glucose metabolic rate following learning. *Intelligence* 16, 415–426. doi: 10.1016/0160-2896(92)90018-m

Harrison, T. L., Shipstead, Z., Hicks, K. L., Hambrick, D. Z., Redick, T. S., and Engle, R. W. (2013). Working memory training may increase working memory capacity but not fluid intelligence. *Psychol. Sci.* 24, 2409–2419. doi: 10.1177/0956797613492984

Hubert-Wallander, B., Green, C. S., Sugarman, M., and Bavelier, D. (2011). Changes in search rate but not in the dynamics of exogenous attention in action videogame players. *Atten. Percept. Psychophys.* 73, 2399–2412. doi: 10.3758/s13414-011-0194-7

Intriligator, J., and Cavanagh, P. (2001). The spatial resolution of visual attention. *Cogn. Psychol.* 43, 171–216. doi: 10.1006/cogp.2001.0755

Irons, J. L., Remington, R. W., and Mclean, J. P. (2011). Not so fast: rethinking the effects of action video games on attentional capacity. *Aust. J. Psychol.* 63, 224–231. doi: 10.1111/j.1742-9536.2011.00001.x

Jaeggi, S. M., Buschkuehl, M., Jonides, J., and Shah, P. (2011). Short-and long-term benefits of cognitive training. *Proc. Natl. Acad. Sci. U S A* 108, 10081–10086. doi: 10.1073/pnas.1103228108

Klingberg, T., Fernell, E., Olesen, P. J., Johnson, M., Gustafsson, P., Dahlström, K., et al. (2005). Computerized training of working memory in children with ADHD–a randomized, controlled trial. *J. Am. Acad. Child Adolesc. Psychiatry* 44, 177–186. doi: 10.1097/00004583-200502000-00010

Kristjánsson, Á. (2013). The case for causal influences of action videogame play upon vision and attention. *Atten. Percept. Psychophys.* 75, 667–672. doi: 10.3758/s13414-013-0427-z

Latham, A. J., Patston, L. L. M., and Tippett, L. J. (2013). Just how expert are "expert" video-game players? Assessing the experience and expertise of video-game players across "action" video-game genres. *Front. Psychol.* 4:491. doi: 10.3389/fpsyg.2013.00941

Lavie, N., and Cox, S. (1997). On the efficiency of visual selective attention: efficient visual search leads to inefficient distractor rejection. *Psychol. Sci.* 8, 395–396. doi: 10.1111/j.1467-9280.1997.tb00432.x

Li, R., Polat, U., Makous, W., and Bavelier, D. (2009). Enhancing the contrast sensitivity function through action video game training. *Nat. Neurosci.* 12, 549–551. doi: 10.1038/nn.2296

Linn, M. C., and Petersen, A. C. (1985). Emergence and characterization of sex differences in spatial ability: a meta-analysis. *Child Dev.* 56, 1479–1498. doi: 10.2307/1130467

Melby-Lervåg, M., and Hulme, C. (2013). Is working memory training effective? A meta-analytic review. *Dev. Psychol.* 49, 270–291. doi: 10.1037/a0028228

Mishra, J., Zinni, M., Bavelier, D., and Hillyard, S. A. (2011). Neural basis of superior performance of action videogame players in an attention-demanding task. *J. Neurosci.* 31, 992–998. doi: 10.1523/jneurosci.4834-10.2011

Monsell, S. (2003). Task switching. *Trends Cogn. Sci.* 7, 134–140. doi: 10.1016/S1364-6613(03)00028-7

Murphy, K., and Spencer, A. (2009). Playing video games does not make for better visual attention skills. *J. Artic. Support Null Hypothesis* 6, 1–20.

Oei, A. C., and Patterson, M. D. (2013). Enhancing cognition with video games: a multiple game training study. *PLoS One* 8:e58546. doi: 10.1371/journal.pone.0058546

Okagaki, L., and Frensch, P. A. (1994). Effects of video game playing on measures of spatial performance: gender effects in late adolescence. *J. Appl. Dev. Psychol.* 15, 33–58. doi: 10.1016/0193-3973(94)90005-1

Pereg, M., Shahar, N., and Meiran, N. (2013). Task switching training effects are mediated by working-memory management. *Intelligence* 41, 467–478. doi: 10.1016/j.intell.2013.06.009

Posner, M. I., Snyder, C. R., and Davidson, B. J. (1980). Attention and the detection of signals. *J. Exp. Psychol.* 109, 160–174. doi: 10.1037/0096-3445.109.2.160

Potts, G. F., Patel, S. H., and Azzam, P. N. (2004). Impact of instructed relevance on the visual ERP. *Int. J. Psychophysiol.* 52, 197–209. doi: 10.1016/j.ijpsycho.2003.10.005

Raymond, J. E., and Shapiro, K. L. (1992). Temporary suppression of visual processing in an RSVP task: an attentional blink? *J. Exp. Psychol. Hum. Percept. Perform.* 18, 849–860. doi: 10.1037/0096-1523.18.3.849

Redick, T. S., Shipstead, Z., Harrison, T. L., Hicks, K. L., Fried, D. E., Hambrick, D. Z., et al. (2013). No evidence of intelligence improvement after working memory training: a randomized, placebo-controlled study. *J. Exp. Psychol. Gen.* 142, 357–379. doi: 10.1037/a0029082

Rogers, R. D., and Monsell, S. (1995). Costs of a predictable switch between simple cognitive tasks. *J. Exp. Psychol.* 124, 207–231.

Rosser, J. C., Lynch, P. J., Cuddihy, L., Gentile, D. A., Klonsky, J., and Merrell, R. (2007). The impact of video games on training surgeons in the 21st century. *Arch. Surg.* 142, 181–186. doi: 10.1001/archsurg.142.2.186

Sanchez, C. A. (2012). Enhancing visuospatial performance through video game training to increase learning in visuospatial science domains. *Psychon. Bull. Rev.* 19, 58–65. doi: 10.3758/s13423-011-0177-7

Sanders, A. F. (1970). Some aspects of the selective process in the functional visual field. *Ergonomics* 13, 101–117. doi: 10.1080/00140137008931124

Sawaki, R., and Luck, S. J. (2010). Capture versus suppression of attention by salient singletons: electrophysiological evidence for an automatic attend-to-me signal. *Atten. Percept. Psychophys.* 72, 1455–1470. doi: 10.3758/APP.72.6.1455

Schmidt, R. A., and Bjork, R. A. (1992). New conceptualizations of practice: common principles in three paradigms suggest new concepts for training. *Psychol. Sci.* 3, 207–217. doi: 10.1111/j.1467-9280.1992.tb00029.x

Shapiro, K. L., Raymond, J. E., and Arnell, K. M. (1994). Attention to visual pattern information produces the attentional blink in rapid serial visual presentation. *J. Exp. Psychol. Hum. Percept. Perform.* 20, 357–371. doi: 10.1037/0096-1523.20.2.357

Shapiro, K. L., Raymond, J. E., and Arnell, K. M. (1997). The attentional blink. *Trends Cogn. Sci.* 1, 291–296. doi: 10.1016/S1364-6613(97)01094-2

Simons, D. J., and Chabris, C. F. (1999). Gorillas in our midst: sustained inattentional blindness for dynamic events. *Perception* 28, 1059–1074. doi: 10.1068/p2952

Sims, V. K., and Mayer, R. E. (2002). Domain specificity of spatial expertise: the case of video game players. *Appl. Cogn. Psychol.* 16, 97–115. doi: 10.1002/acp.759

Spence, I., and Feng, J. (2010). Video games and spatial cognition. *Rev. Gen. Psychol.* 14, 92–104. doi: 10.1037/a0019491

Strobach, T., Frensch, P. A., and Schubert, T. (2012). Video game practice optimizes executive control skills in dual-task and task switching situations. *Acta Psychol. (Amst)* 140, 13–24. doi: 10.1016/j.actpsy.2012.02.001

Subrahmanyam, K., and Greenfield, P. M. (1994). Effect of video game practice on spatial skills in girls and boys. *J. Appl. Dev. Psychol.* 15, 13–32. doi: 10.1016/0193-3973(94)90004-3

Takeuchi, H., Taki, Y., Sassa, Y., Hashizume, H., Sekiguchi, A., Fukushima, A., et al. (2011). Working memory training using mental calculation impacts regional gray matter of the frontal and parietal regions. *PLoS One* 6:e23175. doi: 10.1371/journal.pone.0023175

Thorndike, E. L., and Woodworth, R. S. (1901). The influence of improvement in one mental function upon the efficiency of other functions. *Psychol. Rev.* 8, 247–261. doi: 10.1037/h0074898

Toet, A., and Levi, D. M. (1992). The two-dimensional shape of spatial interaction zones in the parafovea. *Vision Res.* 32, 1349–1357. doi: 10.1016/0042-6989(92)90227-a

Vallett, D. B., Lamb, R. L., and Annetta, L. A. (2013). The gorilla in the room: the impacts of video-game play on visual attention. *Comput. Human Behav.* 29, 2183–2187. doi: 10.1016/j.chb.2013.05.001

Verhaeghen, P., Marcoen, A., and Goossens, L. (1992). Improving memory performance in the aged through mnemonic training: a meta-analytic study. *Psychol. Aging* 7, 242–251. doi: 10.1037/0882-7974.7.2.242

Wu, S., Cheng, C. K., Feng, J., D'Angelo, L., Alain, C., and Spence, I. (2012). Playing a first-person shooter video game induces neuroplastic change. *J. Cogn. Neurosci.* 24, 1286–1293. doi: 10.1162/jocn_a_00192

Wu, S., and Spence, I. (2013). Playing shooter and driving videogames improves top-down guidance in visual search. *Atten. Percept. Psychophys.* 75, 673–686. doi: 10.3758/s13414-013-0440-2

Yesavage, J. A., Sheikh, J. I., Friedman, L., and Tanke, E. D. (1990). Learning mnemonics: roles of aging and subtle cognitive impairment. *Psychol. Aging* 5, 133–137. doi: 10.1037/0882-7974.5.1.133

Yesavage, J. A., Sheikh, J., Tanke, E. D., and Hill, R. (1988). Response to memory training and individual differences in verbal intelligence and state anxiety. *Am. J. Psychiatry* 145, 636–639.

Yuji, H. (1996). Computer games and information-processing skills. *Percept. Mot. Skills* 83, 643–647. doi: 10.2466/pms.1996.83.2.643

Conflict of Interest Statement: The authors declare that the research was conducted in the absence of any commercial or financial relationships that could be construed as a potential conflict of interest.

Received: 30 January 2014; accepted: 22 March 2014; published online: 08 April 2014.
Citation: Oei AC and Patterson MD (2014) Are videogame training gains specific or general? Front. Syst. Neurosci. ***8****:54. doi: 10.3389/fnsys.2014.00054*
This article was submitted to the journal Frontiers in Systems Neuroscience.

frontiers in
SYSTEMS NEUROSCIENCE

MINI REVIEW ARTICLE
published: 08 April 2014
doi: 10.3389/fnsys.2014.00056

Using virtual reality to augment perception, enhance sensorimotor adaptation, and change our minds

W. Geoffrey Wright*

Physical Therapy and Bioengineering, Motion Analysis and Perception Laboratory, Temple University, Philadelphia, PA, USA

Edited by:
Mikhail Lebedev, Duke University, USA

Reviewed by:
Christopher K. Rhea, University of North Carolina – Greensboro, USA
Mohammad Al-Amri, Cardiff University, UK

****Correspondence:***
W. Geoffrey Wright, Physical Therapy and Bioengineering, Motion Analysis and Perception Laboratory, 1301 Cecil B. Moore Ave., Ritter Annex, Room 992, Temple University, Philadelphia, PA 19122, USA
e-mail: wrightw@temple.edu

Technological advances that involve human sensorimotor processes can have both intended and unintended effects on the central nervous system (CNS). This mini review focuses on the use of virtual environments (VE) to augment brain functions by enhancing perception, eliciting automatic motor behavior, and inducing sensorimotor adaptation. VE technology is becoming increasingly prevalent in medical rehabilitation, training simulators, gaming, and entertainment. Although these VE applications have often been shown to optimize outcomes, whether it be to speed recovery, reduce training time, or enhance immersion and enjoyment, there are inherent drawbacks to environments that can potentially change sensorimotor calibration. Across numerous VE studies over the years, we have investigated the effects of combining visual and physical motion on perception, motor control, and adaptation. Recent results from our research involving exposure to dynamic passive motion within a visually-depicted VE reveal that short-term exposure to augmented sensorimotor discordance can result in systematic aftereffects that last beyond the exposure period. Whether these adaptations are advantageous or not, remains to be seen. Benefits as well as risks of using VE-driven sensorimotor stimulation to enhance brain processes will be discussed.

Keywords: virtual reality environment, vection, sensorimotor integration, motor adaptation, prism adaptation cross-modal processing, posture control, brain augmentation

INTRODUCTION

The use of technology to augment brain function has a nebulous history, in part, because the term *brain augmentation* can be defined in so many ways. It implies an enhancement of brain function, but how it is measured introduces some uncertainty. To clarify this further, it should be recognized that the function of the brain is nothing short of control of the entire body and all one's experiences, both internal processes and externally-directed actions. Therefore augmenting brain function could include a wide range of easy or difficult to identify enhancements, such as boosting immune system response, improving mood, memory, or perception, optimizing motor control, or increasing sub-optimal function after injury. To make brain augmentation even harder to define, sometimes the only measure we have of its effective implementation is through observation of external behavior.

A simple definition of brain augmentation could be enhancement of sensation, such as the use of spectacles to improve myopia. Most glasses wearers will be familiar with the initial adaptation to a slight magnification and/or shift in close-up visual space that occurs with new glasses. This type of adaptation is even more evident when using light-refracting prism glasses to intentionally shift the visually perceived world. Facilitation of adaptive processes could be considered another form of brain augmentation. For example, prism adaptation has been used to correct strabismus by helping the eyes accomplish perceptual convergence and reducing the angle of squint (Pigassou, 1972). In hemispatial neglect wearing prism glasses can augment the brain's ability to adapt its sensorimotor representation of the external world and reduce the perceptual deficit (Rossetti et al., 1998).

Augmenting brain function by enhancing perception or compensating for a deficit is an area in which virtual reality (VR) technology is also being applied. Similar to prism adaptation, VR technology can be used to alter the egocentric and allocentric representations of the world (Castiello et al., 2004). In this paper, the issue of identifying enhancement in the realm of sensory perception, motor control, and sensorimotor adaptation by using virtual environments (VE) will be reviewed. The sensorimotor and perceptual processes that may cause these changes will be examined while also highlighting the difficulty that goes along with defining, measuring, and quantifying enhancement. Not all changes are enhancement, since some are not adaptive or are accompanied by unwanted degradation of other functions or cause unintended responses.

AUGMENTING PERCEPTION

A fundamental aspect of creating an immersive experience within a VE is in creating a sense of three-dimensionality so that one believes one can move about within the virtual world. A common barrier to this is that one may wish to travel further in the VE than is possible in a limited space (e.g., a flight simulation).

Although the perception of self-motion typically occurs as a result of combined visual and physical motion stimuli, its long been known that visually-induced self-motion perception (i.e., vection) can occur in the absence of actual motion (Mach, 1875; Young et al., 1973; Pavard and Berthoz, 1977; Howard, 1986; Frigon and Delorme, 1992; Harris et al., 2000; Palmisano, 2002; Wright, 2002). However, optic flow when walking about the real world is different than when rotating the eyes or head while the body remains stationary (Gibson, 1954). That our central nervous system (CNS) can accurately detect this difference likely evolved as an essential part of navigating through the world searching for food or mates and avoiding danger. The exact selective pressures that shaped these neural processes can only be inferred, however, its very likely that in the pre-modern world earth-bound species (flightless and terrestrial) were less frequently exposed to the visual-vestibular discordance that occurs during passive motion to which we are often exposed in the modern world (e.g., during any vehicle transport). Although the multiple sensory inputs that occur during self-motion do not always have a prescribed relation, they co-occur with greater probability in certain relations to one another than others. For example, terrestrial animals experience sustained vection (very low frequency) in a direction orthogonal to vertical more frequently than parallel to it. Furthermore, the sensory organs are oriented upright relative to gravity more frequently than inverted. Despite this, it seems there was a strong selective advantage for omnidirectional sensory organs that could be mapped to each other rather flexibly. One need only don a pair of prism glasses to experience visuomotor remapping that makes even a completely inverted world eventually feel "normal" (Stratton, 1896). This sensorimotor lability can be used to induce a compelling sense of immersion in a VE even when sensory inputs are incongruent, sub-threshold, or absent.

The flexible, adaptable sensorimotor integration described above is how the brain's perceptual abilities can be augmented in a VE. For example, self-motion perception can be induced even when sensory input is below threshold. In a VE, the inertial stimulus is often sub-threshold or even absent, yet perception of self-motion is still experienced. In our VE studies, we have tested how this perception is affected by manipulating the concordance of visual and inertial sensory inputs (see **Table 1**; Wright, 2002, 2009; Wright and Glasauer, 2003, 2006; Wright and Schneider, 2009). To enhance the level of immersion, subjects viewed a high-fidelity, realistic visual scene from a first person perspective while wearing a head-mounted display (HMD; Wright et al., 2005, 2006, 2009). To further enhance the perceptual experience, we drew on previously established knowledge about motion perception. The visual system primarily transduces velocity information from the visual stimulus, and is less sensitive to acceleration (Berthoz et al., 1975; Telford et al., 1992; Warren and Kurtz, 1992). Acceleration information is primarily derived from the inertial stimulus, which even in the absence of vision plays an important part of the experience of motion (Wright et al., 2005). Gravitoinertial input resulting from physical motion and background gravity stimulate the vestibular and somatosensory systems (i.e., the graviceptors) which provide linear acceleration

Table 1 | Perceptual and/or motor behavior in immersive VE.

Study	Visual stimulus	Physical stimulus	Instructed response (DV)	Unintended response
Wright and Glasauer (2003)	Static or Roll tilting VE scene	Roll tilt of whole body while sitting	Subjective vertical (joystick/glass orientation)	Motor response depends on type of object wielded even if similar size and weight
Wright et al. (2005)	Up-down translation of VE scene depicting various amplitudes of motion	Up-down whole body translation either matching or mismatching visual amplitude	Subjective estimate of self-motion amplitude	Visual-vestibular weighting not always linear summation
Wright et al. (2009)	Left-right translation of VE scene	Roll tilt of whole body while sitting	Subjective vertical (joystick orientation)	Joystick Translations
Wright and Schneider (2009)	Left-right or up-down translation of VE scene	None	Subjective vertical (joystick orientation)	Joystick Translations
Wright (2009)	Left-right translation of VE scene	Up-down whole body translation of various amplitudes	Subjective estimate of self-motion amplitude	Left-right self-motion perception increased as physical up-down motion increased
Wright et al. (2013)	Left-right translation of VE scene	Fore-aft whole body translation while sitting	Stabilize head (yaw, pitch, roll angular velocity)	Yaw head movement
Wright (2013)	Fore-aft translation of VE scene in 3-walled, earth-fixed cave	Left-right whole-body translation while standing	Maintain balance (center of pressure)	Postural response to visual+physical stimulus. Postural aftereffects during post-adaptation visual stimulation

and rotation information (Guedry, 1974). But like the visual system, there is an overlap in what qualifies as an adequate stimulus, as suggested by the fact that graviceptors may also be sensitive to velocity cues (Jones and Young, 1978). Our investigations suggest that combinations of physical and visual stimulation can result in sensory summation. This can increase how compelling perceived self-motion is when stimuli are matched directionally and temporally (Wright et al., 2005). However, we have also found that perceived self-motion can be enhanced by adding together discordant stimuli, such as by combining physical tilt with visually-depicted translation (Wright et al., 2009). In fact, the "compellingness" of visually-induced self-motion can be enhanced in the direction of the visual stimulus by increasing the amplitude of a discordant inertial input. This is true even if the visual and inertial vectors are 90–180° out of alignment with each other (Wright et al., 2005; Wright, 2009; Ash et al., 2011).

Another contributing factor that augments the VE-user's immersion by enhancing the self-motion experience is predicated on the idea of tilt-translation ambiguity (Young et al., 1984; Parker et al., 1985; Merfeld et al., 2005; Holly et al., 2006). Accurate perception of tilt versus translation is obfuscated in part because gravitational and inertial accelerations are physically indistinguishable, and in part because the adequate stimulus for the visual system is velocity-dependent while the adequate stimulus for graviceptors is acceleration-dependent. Thus, tilt in a gravitational field could conceivably be perceived as translation. However, when multiple sensory inputs are combined, a unified sense of self-motion can be derived. Whether this perception is rotation or translation or some combination of both is, in part, determined by spatial, temporal, and cognitive factors (Wertheim et al., 2001; Wright et al., 2006; Holly and McCollum, 2008; Riecke, 2009). The perception also depends on the independence of the velocity and acceleration vectors. In nature, a positive velocity could be experienced with an infinite number of positive or negative acceleration vectors. This is important because the visual system's velocity-sensitive and the vestibular system's acceleration-sensitive. All these factors contribute to how VE can be used to induce unusual self-motion perceptions, despite the fact that the sensory pattern has never been experienced (Wright, 2009). This fact has been capitalized on by IMAX®-based rides for decades, where an individual can experience compelling self-motion while completely stationary; moreover, the perception can be further enhanced when subtle movements of the theater seat are added.

The phenomenological evidence above suggests that veridical self-motion perception is dependent on the integration of multiple sensory inputs that do not have a prescribed relation to one another. Moreover, perception can be extended beyond the normal limits of the senses by combining sensory inputs in VE to induce non-veridical self-motion perception. A sense of immersion in a VE can be enhanced by the belief that movement within the VE is actually happening. But if the VE is augmenting perception of a "false" reality, does this also alter one's actions? And more importantly, is there a real-world benefit? The first question has been brought up before (Stanney et al., 1998; Cohn et al., 2000) but lately the focus of attention has shifted to the latter question. Many researchers and clinicians have embarked upon systematic investigation of how VR can augment the brain's ability to recover from disease and injury (e.g., Liebermann et al., 2012). In the next sections we delve into these questions, first by determining whether motor behaviors are altered by VE immersion then by looking at sensorimotor adaptation within a VE.

THE PERCEPTION-ACTION LINK IN VE

Perception can be defined as the organization of sensory stimuli (both externally received or internally generated) resulting in a conscious awareness of a phenomenon. Perception and action are tightly linked processes, with the interaction of sensory input and motor output being fundamental to the calibration of fine and gross motor skills. Accurate perception of the body's movements is critical to fine-tuning motor skills. However, there are many examples of dissociations between perception and action (e.g., Goodale and Milner, 1992; Merfeld et al., 2005). Thus, even though perception of self-motion and orientation can be altered in a VE, how it affects motor output has required investigation. In a series of studies, we looked at manual motor control, head stabilization, and postural control while immersed in a VE to evaluate whether the perception-action link reliably occurs in VE.

Much like in the perceptual studies, we tested conditions that combined visually-depicted motion both with and without actual physical motion. Subjects performed a manual motor control task while sitting in a tiltable motion device and viewing a visual depiction of linear translation in an HMD (Wright and Glasauer, 2003, 2006; Wright et al., 2009; Wright and Schneider, 2009). During this VE immersion, subjects were instructed to align a handheld object to the perceived vertical. Perceptual reports confirmed self-translation to be more compelling when physical tilt of the subject was added to the linear visual motion (Wright et al., 2009; Wright and Schneider, 2009). But interestingly, despite being asked only to align the handheld object to vertical, subjects also showed automatic, unconscious translation of the unconstrained arm. These unintended motor actions were entrained with the visually-depicted motion, as if experiencing accelerations due to actual translation (see **Table 1**). Although its been shown that constant velocity visual rotation in a VE can affect the direction of reaching (Cohn et al., 2000; Dvorkin et al., 2009), our findings also revealed that vision could induce vection with both velocity and acceleration components. Automatic motor responses occurred as if a compensatory force was required to counter the illusory acceleration. Moreover, the more compelling the perceived self-motion, the larger the motor response.

We were also interested in determining how VE immersion might affect other motor control processes such as head stabilization (Wright et al., 2013) and whole-body postural control (Wright, 2013). In one study, subjects were exposed to physical accelerations while viewing a directionally discordant visual scene. Significant head stabilization responses were dependent on the direction of visual flow even though visual input was discordant with the physical stimulus (Wright et al., 2013). In another study applying a similar experimental test protocol to investigate posture control, we paired visually-depicted translation in one direction with an orthogonally directed translation

of the support surface. This cross-axis stimulation resulted in a postural response in standing humans that showed entrainment with both the visual and the support surface stimuli (Wright, 2013). These findings may not be unexpected, since studies predating VR technology have shown that postural control can be entrained to a visual stimulus by simulating movement of the entire room, when the floor is kept stationary (Lishman and Lee, 1973). Furthermore, the postural response can be influenced by the characteristics of the discordant visual input (Lestienne et al., 1977). If an immersive VE is used the postural response to a visual input can be potentiated even if the input is temporally discordant with surface movement (Keshner et al., 2004). Together these results suggest that VE can be used to induce a motor response to a non-veridical virtual input, even in the presence of a strong destabilizing physical stimulus that requires an appropriate postural response to keep from falling. Thus, VE can cause an unintended postural response leading to instability.

INDUCING SENSORIMOTOR ADAPTATION AND MALADAPTIVE AFTEREFFECTS

To study postural adaptation in VE, we exposed subjects to cross-axis postural stimulation for an extended period of time. By looking for aftereffects, as is often done in prism-adaptation research, we wished to see if the postural response seen during discordant stimulation involved adaption or was simply a transient response that would disappear as soon as one of the stimuli was removed (Wright, 2013). The plasticity of the CNS, which allows discordance to be reduced by sensorimotor re-mapping, is present at birth and plays an essential role in shaping motor development through interaction with the environment (Held and Freedman, 1963). Seminal work on visuospatial adaptation using light-refracting prism glasses dating back a century and a half (von Helmholtz, 1867; Stratton, 1896) has shown us that although neural plasticity may diminish with age, this form of plasticity does not have a critical period; rather to some extent it lasts well into adulthood (Hardt et al., 1971). Therefore, determining whether VE exposure will automatically cause sensorimotor adaptation is important. If one considers VE usage in everyday life, for training purposes, or for rehabilitation, one might expect very large exposure times, which could have long lasting aftereffects.

We exposed standing subjects for an extended period of time (5 min) to the cross-axis stimulation. After the adaptation period, we stopped the dynamic support stimulation while subjects continued to view the same visual translation stimulus as before. What was found in the post-adaptation phase is that subjects indeed showed an aftereffect in the COP, which was rotated as much as 45° from the direction of the visual stimulation. This finding is complementary to the finding which showed sensorimotor adaptation of the vestibulo-ocular reflex (VOR) in monkeys after prolonged pairing of physical rotation with an orthogonally directed optic flow (Wei and Angelaki, 2001). The evidence from our study on humans show that long lasting (>2 min) whole-body sensorimotor adaption can also be induced after prolonged exposure (<5 min) to discordant combinations of inertial and visual stimulation in a VE (Wright, 2013). Preliminary evidence suggests that these adaptations may even last for a few days. Specifically, after a few exposures staggered over multiple days, aftereffects appear immediately upon re-immersion into the VE without requiring a fresh dose of cross-axis adaptation.

This raises the question whether these residual aftereffects seen in healthy individuals who spend extended time in a VE are adaptive in the real world or unwanted aftereffects. Inaccurate automatic motor responses due to recalibration of visual, vestibular, and somatosensory coordination certainly involves a risk. However, for those with a perceptual or motor deficit, VE immersion may move them from a maladaptive state towards an adaptive one. Although this requires further investigation, what is apparent is that VE can be used to facilitate the brain's natural ability to adapt to changes in the sensory environment. In fact, VE-based brain augmentation applications have already begun to appear in clinical applications. They have been used to ameliorate hemi-neglect symptoms by remapping the neglected space (Castiello et al., 2004), thus reducing a perceptual deficit, and improving function.

CONCLUSIONS

The fidelity of immersive VE has increased with amazing speed over the last two decades. One need only play the latest release of any popular first person shooter or sports-themed video game to be astounded by its verisimilitude. Because of the level of immersion one can experience, the question arises as to how quickly our CNS adapts to such simulated reality. More importantly, how robust are these adaptations, not only to the accurate attributes of the manufactured environments, but also to their inaccuracies. Even if visual fidelity such as spatial resolution, update rates, perspective geometry, monocular and binocular cues, et cetera are all perfectly programmed to match reality in a VE, the absence of inertial cues to accompany simulated translation through such environments will affect how the CNS calibrates the perceptuomotor system to these non-veridicalities. In other words, exposure to a VE will automatically cause sensorimotor adaptation, whether desired or not. But hopefully, VE's ability to augment brain functions by enhancing perception, eliciting automatic motor behavior, and inducing sensorimotor adaptation can be applied in useful ways.

Trusting what we can measure as evidence of brain enhancement may not solve the problem of defining brain augmentation, when short-term benefits may accompany long-term deficits. Conversely, long-term enhancements may be overlooked because of a more immediate decrement in brain function that can happen as the brain adapts to or learns a new technology. What can be certain is that benefits from brain augmentation, if understood and applied, can be far-reaching. If used to recover loss of function following neurological damage, brain augmentation can potentially bring function back to healthy levels. The ways in which scientist, technologist, and clinicians are applying VR technology to rehabilitation is already happening and the hopes are that the individuals involved in this collective creative process will have the foresight to exploit the potential of neural plasticity, while recognizing that not all change is good.

ACKNOWLEDGMENTS

This work is supported, in part, by the US Army Medical Research and Materiel Command under Contract No. W81XWH-13-C-0189 (W. Geoffrey Wright).

REFERENCES

Ash, A., Palmisano, S., and Kim, J. (2011). Vection in depth during consistent and inconsistent multisensory stimulation. *Perception* 40, 155–174. doi: 10.1068/p6837

Berthoz, A., Pavard, B., and Young, L. R. (1975). Perception of linear horizontal self-motion induced by peripheral vision (linearvection): basic characteristics and visual-vestibular inter-actions. *Exp. Brain Res.* 23, 471–489. doi: 10.1007/bf00234916

Castiello, U., Lusher, D., Burton, C., Glover, S., and Disler, P. (2004). Improving left hemispatial neglect using virtual reality. *Neurology* 62, 1958–1962. doi: 10.1212/01.wnl.0000128183.63917.02

Cohn, J. V., DiZio, P., and Lackner, J. R. (2000). Reaching during virtual rotation: context specific compensations for expected coriolis forces. *J. Neurophysiol.* 83, 3230–3240.

Dvorkin, A. Y., Kenyon, R. V., and Keshner, E. A. (2009). Effects of roll visual motion on online control of arm movement: reaching within a dynamic virtual environment. *Exp. Brain Res.* 193, 95–107. doi: 10.1007/s00221-008-1598-z

Frigon, J.-Y., and Delorme, A. (1992). Roll, pitch, longitudinal and yaw vection visually induced by optical flow in flight simulation conditions. *Perceptual and Motor Skills* 74, 935–955.

Gibson, J. (1954). The visual perception of objective motion and subjective movement. *Psychol. Rev.* 61, 304–314. doi: 10.1037/h0061885

Goodale, M. A., and Milner, A. D. (1992). Separate visual pathways for perception and action. *Trends Neurosci.* 15, 20–25. doi: 10.1016/0166-2236(92)90344-8

Guedry, F. E. (1974). "Psychophysics of vestibular sensation," *Handbook of Sensory Physiology* (Vol. 6), ed H. H. Kornhuber (New York: Springer-Verlag), 1–154.

Hardt, M. E., Held, R., and Steinbach, M. J. (1971). Adaptation to displaced vision: a change in the central control of sensorimotor coordination. *J. Exp. Psychol.* 89, 229–239. doi: 10.1037/h0031159

Harris, L. R., Jenkin, M., and Zikovitz, D. C. (2000). Visual and non- visual cues in the perception of linear self motion. *Exp. Brain Res.* 135, 12–21. doi: 10.1007/s002210000504

Held, R., and Freedman, S. J. (1963). Plasticity in the human sensorimotor control. *Science* 142, 455–462. doi: 10.1126/science.142.3591.455

Holly, J. E., and McCollum, G. (2008). Constructive perception of self-motion. *J. Vestib. Res.* 18, 249–266.

Holly, J. E., Pierce, S. E., and McCollum, G. (2006). Head tilt-translation combinations distinguished at the level of neurons. *Biol. Cybern.* 95, 311–326.

Howard, I. P. (1986). "The perception of posture, self motion and the visual vertical," in *Sensory Processes and Perception, Handbook of Human Perception and Performance* (Vol. 1), eds K. R. Boff, L. Kaufman and J. P. Thomas (New York: Wiley), 18.1–18.62.

Jones, G. M., and Young, L. R. (1978). Subjective detection of vertical acceleration: a velocity-dependent response? *Acta Otolaryngol.* 85, 45–53. doi: 10.3109/00016487809121422

Keshner, E. A., Kenyon, R. V., and Langston, J. (2004). Postural responses exhibit multisensory dependencies with discordant visual and support surface motion. *J. Vestib. Res.* 14, 307–319.

Lestienne, F., Soechting, J., and Berthoz, A. (1977). Postural readjustments induced by linear motion of visual scenes. *Exp. Brain Res.* 28, 363–384. doi: 10.1007/bf00235717

Liebermann, D. G., Berman, S., Weiss, P. L., and Levin, M. F. (2012). Kinematics of reaching movements in a 2-D virtual environment in adults with and without stroke. *IEEE Trans. Neural Syst. Rehabil. Eng.* 20, 778–787. doi: 10.1109/tnsre.2012.2206117

Lishman, J. R., and Lee, D. N. (1973). The autonomy of visual kinaesthesis. *Perception* 2, 287–294. doi: 10.1068/p020287

Mach, E. (1875). *Grundlinien der Lehre von den Bewegungsempfindungen.* Leipzig: Engelmann.

Merfeld, D. M., Sukyung, P., Gianna-Poulin, C., Black, F. O., and Wood, S. (2005). Vestibular perception and action employ qualitatively different mechanisms. II. VOR and perceptual responses during combined Tilt and Translation. *J. Neurophysiol.* 94, 199–205. doi: 10.1152/jn.00905.2004

Palmisano, S. (2002). Consistent stereoscopic information increases the perceived speed of vection in depth. *Perception* 31, 463–480. doi: 10.1068/p3321

Parker, D. E., Reschke, M. F., Arrott, A. P., Homick, J. L., and Lichtenberg, B. K. (1985). Otolith tilt-translation reinterpretation following prolonged weightlessness: implications for preflight training. *Aviat. Space Environ. Med.* 56, 601–606.

Pavard, B., and Berthoz, A. (1977). Linear acceleration modifies the perceived velocity of a moving visual scene. *Perception* 6, 529–540. doi: 10.1068/p060529

Pigassou, R. (1972). The functional treatment of strabismus. *Can. J. Ophthalmol.* 7, 331–335.

Riecke, B. E. (2009). Cognitive and higher-level contributions to illusory self-motion perception ("vection"): does the possibility of actual motion affect vection? *Jpn. J. Psychon. Sci.* 28, 135–139.

Rossetti, Y., Rode, G., Pisella, L., Farne, A., Li, L., Boisson, D., et al. (1998). Prism adaptation to a rightward optical deviation rehabilitates left hemispatial neglect. *Nature* 395, 166–169. doi: 10.1038/25988

Stanney, K., Salvendy, G., Deisinger, J., DiZio, P., Ellis, S., Ellison, J., et al. (1998). Aftereffects and sense of presence in virtual environments: formulation of a research and development agenda. *Int. J. Hum. Comput. Interact.* 10, 135–187. doi: 10.1207/s15327590ijhc1002_3

Stratton, G. (1896). Some preliminary experiments on vision without inversion of the retinal image. *Psychol. Rev.* 3, 611–617. doi: 10.1037/h0072918

Telford, L., Spratley, J., and Frost, B. J. (1992). Linear vection in the central visual field facilitated by kinetic depth cues. *Perception* 21, 337–349. doi: 10.1068/p210337

von Helmholtz, H. (1867). *Handbuch der physiologischen Optik.* Leipzig: Voss.

Warren, W. H., and Kurtz, K. J. (1992). The role of central and peripheral vision in perceiving the direction of self-motion. *Percept. Psychophys.* 51, 443–454. doi: 10.3758/bf03211640

Wei, M., and Angelaki, D. E. (2001). Cross-axis adaptation of the translational vestibulo-ocular reflex. *Exp. Brain Res.* 138, 304–312. doi: 10.1007/s002210100695

Wertheim, A. H., Mesland, B. S., and Bles, W. (2001). Cognitive suppression of tilt sensations during linear horizontal self-motion in the dark. *Perception* 30, 733–741. doi: 10.1068/p3092

Wright, W. G. (2002). *Human Self-motion Perception During Vertical Linear Oscillation and Virtual Environment Exposure.* PhD Dissertation Waltham, MA: Brandeis University.

Wright, W. G. (2009). Linear vection in virtual environments can be strengthened by discordant inertial input. *Conf. Proc. IEEE Eng. Med. Biol. Soc.* 1157–1160. doi: 10.1109/iembs.2009.5333425

Wright, W. G. (2013). Using virtual reality to induce cross-axis adaptation of postural control: implications for rehabilitation. *IEEE Proc. ICVR2013* 289–294. doi: 10.1109/icvr.2013.6662095

Wright, W. G., Agah, M., Darvish, K., and Keshner, E. A. (2013). Head stabilization shows multisensory dependence on spatiotemporal characteristics of visual and inertial passive stimulation. *IEEE Trans. Neural Syst. Rehabil. Eng.* 21, 191–197. doi: 10.1109/icvr.2011.5971869

Wright, W. G., DiZio, P., and Lackner, J. R. (2005). Vertical linear self-motion perception during virtual visual and inertial stimulation: more than weighted summation of sensory inputs. *J. Vest. Res.* 15, 185–195.

Wright, W. G., DiZio, P., and Lackner, J. R. (2006). Apparent self-motion in two visual contexts: dissociable mechanisms underlie perception. *J. Vest. Res.* 16, 23–28.

Wright, W. G., and Glasauer, S. (2003). Haptic subjective vertical shows context dependence: task and vision play a role during dynamic tilt stimulation. *Ann. N Y Acad. Sci.* 1004, 531–535. doi: 10.1196/annals.1303.069

Wright, W. G., and Glasauer, S. (2006). Subjective somatosensory vertical during dynamic tilt is dependent on task, inertial condition and multisensory concordance. *Exp. Brain Res.* 172, 310–321. doi: 10.1007/s00221-006-0347-4

Wright, W. G., and Schneider, E. (2009). Manual motor control during "virtual" self-motion: implications for VR rehabilitation. *IEEE Proc. ICVR2009* 166–172. doi: 10.1109/icvr.2009.5174226

Wright, W. G., Schneider, E., and Glasauer, S. (2009). Compensatory motor responses of object-wielding during combined linear visual and physical

roll tilt stimulation. *Exp. Brain Res.* 192, 683–694. doi: 10.1007/s00221-008-1581-8

Young, L. R., Dichgans, J., Murphy, R., and Brandt, T. (1973). Interaction of optokinetic and vestibular stimuli in motion perception. *Acta Otolaryngol.* 76, 24–31. doi: 10.3109/00016487309121479

Young, L. R., Oman, C. M., Watt, D. G. D., Money, K. E., and Lichtenberg, B. K. (1984). Spatial orientation in weightlessness and readaptation to earth's gravity. *Science* 225, 205–208. doi: 10.1126/science.6610215

Conflict of Interest Statement: The author declares that the research was conducted in the absence of any commercial or financial relationships that could be construed as a potential conflict of interest.

Citation: Wright WG (2014) Using virtual reality to augment perception, enhance sensorimotor adaptation, and change our minds. Front. Syst. Neurosci. ***8****:56. doi: 10.3389/fnsys.2014.00056*

Received: 02 February 2014; accepted: 24 March 2014; published online: 08 April 2014.

This article was submitted to the journal Frontiers in Systems Neuroscience.

frontiers in Systems Neuroscience

ORIGINAL RESEARCH
published: 14 April 2015
doi: 10.3389/fnsys.2015.00056

Hearing colors: an example of brain plasticity

Arantxa Alfaro[1,2], *Ángela Bernabeu*[3], *Carlos Agulló*[3], *Jaime Parra*[4] *and Eduardo Fernández*[1,5]*

[1] CIBER-BBN, Madrid, Spain, [2] Hospital Vega Baja, Orihuela, Spain, [3] Department of Magnetic Resonance, INSCANER S.L., Alicante, Spain, [4] Hospital San Rafael, Madrid, Spain, [5] Institute of Bioengineering, Universidad Miguel Hernández, Elche, Spain

Sensory substitution devices (SSDs) are providing new ways for improving or replacing sensory abilities that have been lost due to disease or injury, and at the same time offer unprecedented opportunities to address how the nervous system could lead to an augmentation of its capacities. In this work we have evaluated a color-blind subject using a new visual-to-auditory SSD device called "Eyeborg", that allows colors to be perceived as sounds. We used a combination of neuroimaging techniques including Functional Magnetic Resonance Imaging (fMRI), Diffusion Tensor Imaging (DTI) and proton Magnetic Resonance Spectroscopy (^{1}H-MRS) to study potential brain plasticity in this subject. Our results suggest that after 8 years of continuous use of this device there could be significant adaptive and compensatory changes within the brain. In particular, we found changes in functional neural patterns, structural connectivity and cortical topography at the visual and auditive cortex of the Eyeborg user in comparison with a control population. Although at the moment we cannot claim that the continuous use of the Eyeborg is the only reason for these findings, our results may shed further light on potential brain changes associated with the use of other SSDs. This could help to better understand how the brain adapts to several pathologies and uncover adaptive resources such as cross-modal representations. We expect that the precise understanding of these changes will have clear implications for rehabilitative training, device development and for more efficient programs for people with disabilities.

Keywords: functional magnetic resonance imaging (fMRI), diffusion tensor imaging (DTI), magnetic resonance spectroscopy, sensory substitution device (SSD), neuroplasticity, blindness, visual cortex

OPEN ACCESS

Edited by:
Ioan Opris, Wake Forest University School of Medicine, USA

Reviewed by:
Jitendra Sharma, Massachusetts Institute of Technology, USA
Preston E. Garraghty, Indiana University, USA

***Correspondence:**
Eduardo Fernández, Institute of Bioengineering, Universidad Miguel Hernández, Avda. Universidad s/n, Elche 03202 Alicante, Spain
Tel: +34/ 96 522 2001, Fax: +34/ 96 591 9434
e.fernandez@umh.es

Received: *03 January 2015*
Accepted: *23 March 2015*
Published: *14 April 2015*

Citation:
Alfaro A, Bernabeu Á, Agulló C, Parra J and Fernández E (2015) Hearing colors: an example of brain plasticity. Front. Syst. Neurosci. 9:56. doi: 10.3389/fnsys.2015.00056

Introduction

Neuroplasticity is an intrinsic property of the brain, which allows us to adapt to environmental pressures, physiologic changes and experiences by dynamic shifts in the strength of pre-existing connections or by establishing new networks in response to changes in afferent inputs or efferent demands (Pascual-Leone et al., 2005). Consequently, the adult brain has a remarkable capacity to change and adapt throughout the development of lifetime, requiring changes at different levels (genes, molecules, synapses, etc.), and is associated with structural and functional reorganization of the brain (Cramer et al., 2011).

Plasticity can occur during development, learning, in response to the environment or disease, or in relation to therapy. As we interact with a rich multisensory world, our sensory experiences are the product of extensive and dynamic neural connections, which are highly influenced

by our experiences and developmental constraints. Such ability can be viewed as adaptivewhen associated with a gain in function (Cohen et al., 1997) or as maladaptive when linked to negative consequences such as loss of function or increased injury (Nudo, 2006). Consequently, the understanding of the nature of these changes is important not only in terms of establishing the brain's true adaptive potential but also in guiding future rehabilitation strategies (Merabet and Pascual-Leone, 2010).

Sensory substitution devices (SSDs) in people with severe visual impairment offer amazing opportunities to study how the nervous system reorganizes its structure, function and connections when one sensory modality is supplied by another modality. Efficient use of SSDs is based on the brain's ability to reorganize itself and it depends on the possibility of teaching the brain new complex perceptual skills as well as a different way to process sensory information (Proulx et al., 2014). Although, the most common modality to replace sight is touch, several authors proposed special devices for visual substitution by the auditory pathway in the context of real time reactivity (Meijer, 1992; Capelle et al., 1998; Cronly-Dillon et al., 1999; Striem-Amit et al., 2012; Abboud et al., 2014; Maidenbaum et al., 2014). Sound spatialization consists of virtually creating a three-dimensional auditory environment, where sound sources can be positioned all around the listener. However, these devices often generate unpleasant sensations and lack color information. This motivated the creation of new SSDs that encode color information such as Soundview (Nie et al., 2009), Haptic-Color Glove (Kahol et al., 2006), SeeColOr (Bologna et al., 2009) and EyeMusic (Abboud et al., 2014).

In this framework, our group has had the opportunity to evaluate the brain changes related to the continued use of a visual-to-auditory prosthetic device called *Eyeborg* specifically designed to help color-blind people. This device was developed by Neil Harbisson and Adam Montandon in 2003 and allows colors to be perceived as sound (Eyeborg, 2015). Briefly, it consists of a small video sensor placed at eye level of the head that transmits color information to a computer chip. Electromagnetic light waves are turned into sound frequencies that are heard as musical notes with distinct pitches in real-time (high frequency colors have high notes and low frequency colors have low notes). The computer chip is resting on the back of the head so the sound is heard through vibrations that are directly transmitted into the skull by bone conduction. It is thought that a proficient user of *Eyeborg* could perceive 360 different hues, one for each degree on the color wheel. Each hue is assigned to an audible frequency between 384 and 718 Hz, which allows differentiation between brighter and darker variations as well as color saturation (due to lighting conditions and the environment) and the recognition of the similarities and differences between hues.

In this work, we introduce the potential adaptive and compensatory changes within the brain associated with the continuous use of Eyeborg in a subject with achromatopsia (an irreversible visual impairment characterized by the inability to perceive colors). Our results suggest that after 8 years of continuous use of this device there could be significant changes in functional neural patterns, structural connectivity and cortical topography. Although there is still a lot of work to be done and we cannot claim that the continuous use of the Eyeborg is the only reason for these findings, our study offers the amazing opportunity to delve into the brain's potential for change by using SSDs. Moreover, it could contribute to a better understanding of the functional and crossmodal organization that supports the neuroenhancement.

Materials and Methods

Participants

Five non-synesthete adults (mean 32.2 ± 2.38 years old; males 3, females 2; 4 right handed, 1 left handed) participated in this study. All were enrolled as part of a broader study examining brain plasticity. One of them (the main subject of this study) had difficulty distinguishing colors from childhood and was diagnosed of achromatopsia when he was 11 years old. He is a proficient Eyeborg user that had been using the device, intensively, throughout the whole day during the past 8 years. The control group was an age matched population of healthy volunteers. None of them had absolute pitch. The protocol was approved by the institutional review board and all volunteers gave their written informed consent prior to entering the study.

Neuroimage Studies

All neuroimaging studies were performed in a Philips Achieva 3T (Philips Medical Systems, Netherlands) with a SENSE Neurovascular coil (18 elements) supplied by the manufacturer. No sedation or contrast agent was given. The protocol included a high-resolution T1-weighted gradient-echo scan: 212 slices, 0.8 mm isotropic voxels, field of view 250 × 250 mm, TR 11 ms and TE 4.9 ms. After the structural data was acquired, functional magnetic resonance (fMRI), diffusion tensor imaging (DTI) and single voxel MR Spectroscopy (^{1}H-MRS) studies were carried out.

Functional Magnetic Resonance Imaging (fMRI)

For the fMRI experiments four different block paradigms were carried out. The visual and auditive stimuli were presented with a special compatible system (VisuaStim Digital Glasses; Resonance Technology, Northridge, CA, USA). Subjects were instructed to keep their gaze fixed on the screen. The tasks were performed in the same order in all the subjects to reduce task interaction effects. No oral output was required avoiding overt movement. fMRI experiment were carried out in the dark.

For the first two paradigms retinotopic mapping stimuli were carried out following conventional procedures based on previously published studies (Engel et al., 1994). The stimuli consisted of high-contrast checkerboards in a rotating wedge and expanding ring. Both stimuli moved in a periodic pattern and completed a full cycle in 24 s with a total of 5 cycles per scanning run. Images were acquired throughout a blood oxygenation level-dependent (BOLD) sensitive T2-weighted multi-slice gradient echo EPI sequence (TE = 35 ms, TR = 2500 ms, FOV = 230 × 230, 64 × 64 matrix). Twentytwo contiguous 4-mm thick axial slices were prescribed parallel to the AC–PC ensuring a full coverage

of the occipital lobe. A total of 160 whole brain volumes were collected.

The third paradigm was a color test based on previously published studies (Beauchamp et al., 1999). The stimuli consisted of five wedges arranged around a central fixation bar, extending from one to four degrees of eccentricity. In the chromatic trials subjects were instructed to decide if the colors in the intervening wedges formed an orderly sequence or not. During achromatic trials, wedges of different luminance were presented and subjects decided if the sequence presented a regular luminance sequence or didn't. The functional scan parameters were as follows: TR = 3000 ms, TE = 35 ms, FOV: 230 × 230, 64 × 64 matrix. Thirty contiguous 4-mm thick axial slices were prescribed parallel to the AC–PC with a total of 84 whole brain volumes collected.

Finally, the forth paradigm consisted of studies where images and sounds were presented simultaneously (Tregellas et al., 2009). The subjects were instructed to look at the images and pay attention to their accompanying sounds, thinking about a putative color that could be assigned to the sound. To encode the sound we used specific algorithms provided by the *Eyeborg* designers. Therefore, we tried to simulate the usage of the Eyeborg inside the environment of the MRI machine. The test presented two condition blocks with a duration of 14 s for each condition. The functional scan parameters were as follows: time repetition = 2000 ms, time echo = 35 ms, FOV: 230 × 230, 64 × 64 matrix. Thirty contiguous 4-mm thick axial slices were prescribed parallel to the AC–PC with a total of 210 whole brain volumes collected.

For the fMRI data analysis, we used SPM8 (The Wellcome Trust Center for Neuroimaging)[1] implemented in MATLAB 2010a (MathWorks, Inc., Massachusetts). We initially performed motion correction, normalization to the Montreal Neurological Institute (MNI) template, and spatial smoothing (8 mm). After the realignment processes, we checked the head-movement parameters which were not used as covariates in the analyses. The task-related activation was evaluated statistically on a voxel-by-voxel basis using a general linear model at the individual level to generate contrast images, which then were incorporated into analysis at the group level. Statistically significant clusters of activity were recorded for each condition. Only those clusters with a corrected *P* value of 0.05 or less and clusters of 10 voxels or greater are reported. The coordinates reported by SPM (which were in "MNI space") were transformed to the stereotaxic coordinate frame developed by Talairach and Tournoux (available at http://macdownload.informer.com/talairach-client) and thus enabled comparison to a reference atlas for appropriate neuroanatomical localization. In order to test whether results obtained for our single subject are valid at the population level, we performed a random effects group analysis (RFX) with the help of BrainVoyager QX (Goebel et al., 2006). This neuroimaging software package was also used in same cases for visualization of anatomical and functional data sets.

[1]http://www.fil.ion.ucl.ac.uk/spm

Diffusion Tensor Imaging (DTI)

DTI-MR was performed in transversal slice orientation, using a single-shot EPI sequence with diffusion encoding in 32 directions (values 0 and 800 s/mm^2). The acquired voxel size was 2 × 2 × 2 mm^3 in 60 slices, with a SENSE factor of 1.9. The diffusion-weighted data were transferred to a workstation for analysis. Before DTI analysis eddy current compensation was applied by affine registration to B0 image. Tractography was then performed using the PRIDE fiber-tracking tool supplied by Philips Medical Systems, as described previously (Nilsson et al., 2007). The ROIs were drawn manually based on the anatomical images and on previously published atlases (Wakana et al., 2004). Tractography was performed based on the connection between two regions of interest (ROI) in order to minimize the risk of including other tracts. Fibers running through the 2 ROIs were computed automatically by the software taking into account a minimum fractional anisotropy value (FA) of 0.3, maximum fiber angle between fibers of 27° and minimum fiber length of 10 mm as stopping criteria.

Magnetic Resonance Spectroscopy (^{1}H-MRS)

For the ^{1}H-MRS study the volume of interest was placed based on anatomical structures. The aim was to get an overall spectroscopic representation of different areas within the visual cortex (V1, V2 and V4) avoiding contamination of the surrounding tissues. The resulted volume size was 14 cm^3 for V1, 12 cm^3 for V2 and 7 cm^3 for V4. Shimming and tuning were achieved with automated procedures before acquisition. Water signal was suppressed with selective water signal inversion. For the spectroscopic measurements a standard short-echo-time acquisition mode sequence (TR/TE/averages = 2000/32/128) was used. A total of 512 data points were collected over a spectral width of 1000 Hz. Assignment of the resonances of interest included N-acetylaspartate and other N-acetyl-containing compounds (NAA) at 2.02 ppm, glutamate and glutamine (Glx) at 2.35 ppm, creatine plus phosphocreatine (Cr) at 3.03 ppm, choline and other trimethylamine-containing compounds (Cho) at 3.20 ppm, and myo-inositol (mIno) at 3.55 ppm (Haga et al., 2009). Spectrum analysis was performed off-line with the help of jMRUI 3.0 package (Naressi et al., 2001) available through the MRUI Project[2] as documented in previous studies (Bernabeu et al., 2009; Poveda et al., 2010).

Results

All the subjects of the study presented normal MRI images of the brain with neither detectable degenerative changes nor any brain lesions.

Functional Magnetic Resonance Imaging (fMRI)

Basic visual retinotopic fMRI paradigms showed brain activation in the corresponding visual areas (BA17, BA18 and BA19) in all the subjects studied. No significant differences in the brain

[2]www.mrui.uab.es/mrui

activation pattern were observed between the Eyeborg user and the control subjects (data not shown).

The analysis of the color paradigm showed clear differences between the activated areas of the Eyeborg user and the controls. Particularly, during the chromatic phase of the test, the Eyeborg user showed activation in V1 (BA17) and other small clusters of activation located mainly in the left V2 (BA18). However, the control group showed strong bilateral activation with a great number of other brain areas involved (**Figure 1**). Thus the color-selective activation in the control group (chromatic blocks vs. fixation) was situated in occipital, temporal, parietal and frontal cortex. More specifically, these areas were located in: (1) occipital lobe (areas BA18 and BA19); (2) temporal lobe related to object and face recognition (BA37), language and auditory processing (BA21, BA22, BA42), memory (BA38) and high level object representation (visual stream BA20); and (3) parietal lobe related to stimulation and texture discrimination tasks (BA40), visuo-motor coordination (BA7, BA6, BA4), and somatosensory functions (BA2); and (4) prefrontal cortex, related with executive functions (BA9, BA10, BA11, 46) and semantic tasks (45, 44). During the achromatic stimulation blocks there was a significant decrease in the number of brain-activated areas in all subjects. In the Eyeborg user we only found activation in areas BA17 and left BA18. In contrast, the control group presented during this achromatic

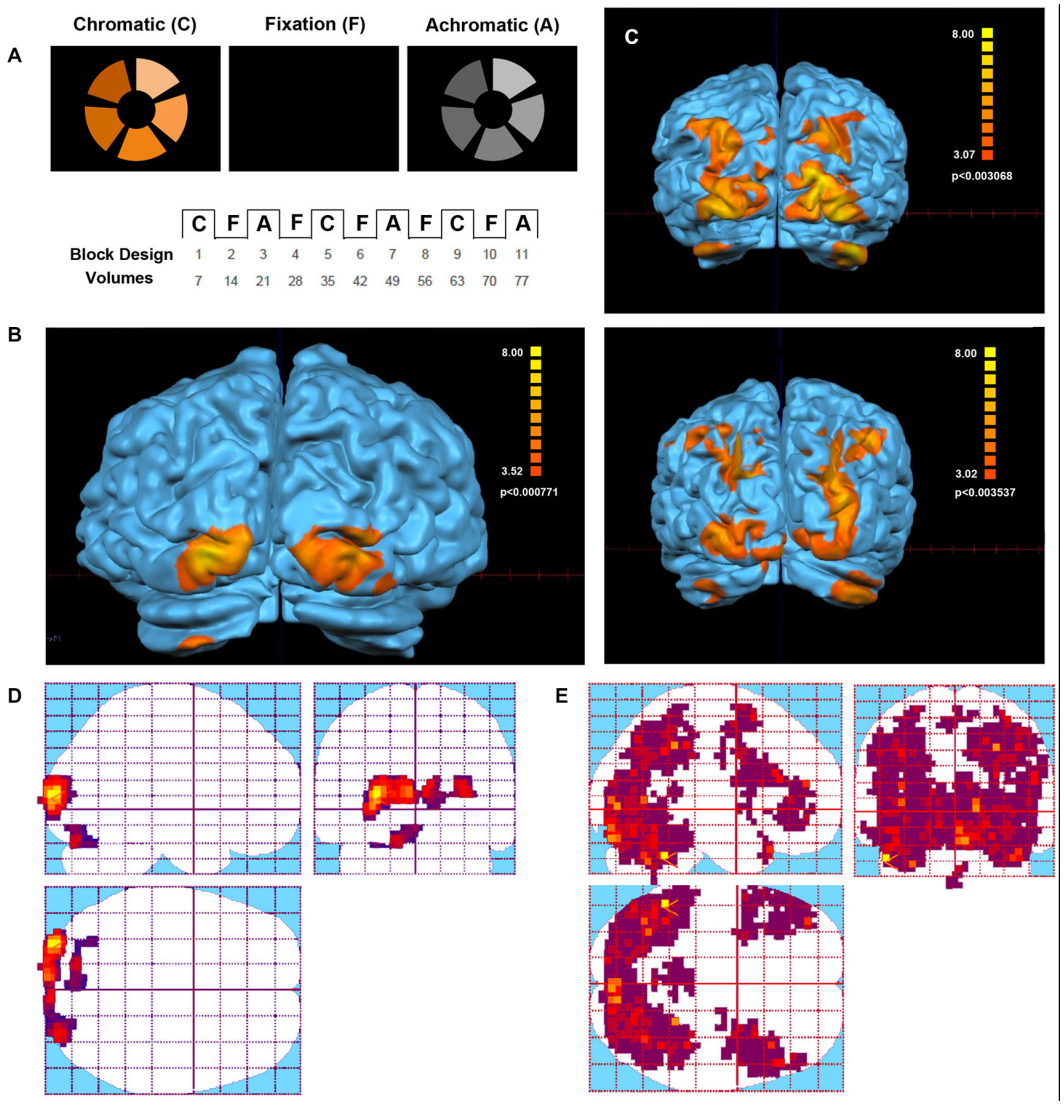

FIGURE 1 | Visual stimulus and Functional Magnetic Resonance Imaging (fMRI) activation in the Eyeborg user and the control group. **(A)** Protocol of the Farnsworth-Munsell test. Within each scan series, the stimulus alternated between blocks of chromatic or achromatic discrimination trials and fixation. **(B)** Areas showing a significant response to chromatic stimulation in the Eyeborg user. **(C)** Areas showing a significant response to chromatic stimulation in two representative controls (single subjects). **(D)** Statistical parametric maps of the Eyeborg user are shown in standard anatomical space. **(E)** Statistical parametric maps of the whole control population in standard anatomical space.

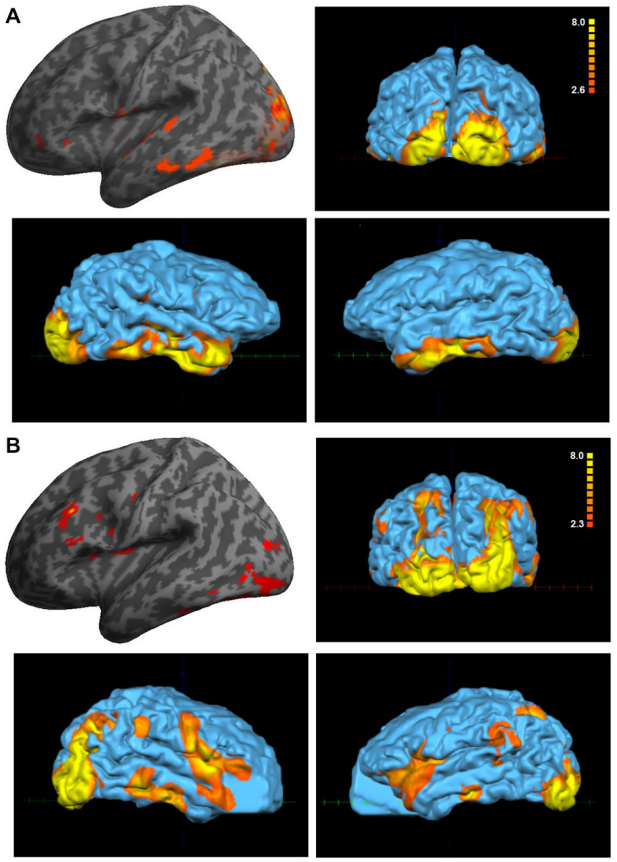

FIGURE 2 | Analysis of the paradigm involving the presentation of simultaneously visual and auditory stimulation. **(A)** Data corresponding to the Eyeborg user (single subject analysis) showing a strong effect on temporal and occipital cortex. **(B)** Averaged activation of the control group in response to the same paradigm of stimulation.

stimulation a higher number of occipital areas activated such as BA17, BA18 and BA19. Moreover, there was brain activation located in the temporal and parietal lobes (BA7 and BA37) and within the entorhinal cortex (BA28) of the right hemisphere.

The paradigm that comprised visual and auditory stimuli showed interesting and significant differences between the Eyeborg user and the controls. Particularly, the Eyeborg user displayed a wider brain activation of the auditory pathway and also involved frontal, temporal and occipital areas (**Figure 2**; **Table 1**). The frontal activated areas were mainly BA6, BA10 and BA11, which are related to motor and executive functions. The temporal activation was in primary auditory cortex (BA42) and also in areas related to language and auditory processing (BA21) and memory and emotion (BA38). Furthermore, in the Eyeborg user there was a robust activation located in the left BA22 area, which contains Wernicke's area, and bilateral activation in BA13 (located in the insula) when we presented simultaneously visual and auditory stimuli that were previously encoded by the Eyeborg algorithms.

Diffusion Tensor Imaging (DTI)

We used DTI to trace the microstructure of the main white matter tracts between the brain areas dedicated to auditory and visual processing (temporal and occipital cortices, respectively). By measuring diffusivity in multiple directions, we estimate the FA value. FA is a normalized measure used in diffusion neuroimaging studies which reflects fiber density, axonal diameter, and myelination in white matter (Yoshida et al., 2013). The more aligned fibers are within a tract, the higher the tract or regional FA value, therefore FA differences between groups can be regarded as a surrogate marker of structural adaptation in the white matter (Fabri et al., 2014; Kantarci, 2014).

When we compared the fiber tracts between the Eyeborg user and the controls we found higher FA values in the Eyeborg user in the corpus callosum (CC), and also (although they were not statistically significant) in both inferior longitudinal fasciculus (ILF) and in both inferior fronto-occipital fasciculus (IFOF) (see **Table 2**). Neither differences nor interhemispheric asymmetry in the FA or in the apparent diffusion coefficient (ADC) values were observed between groups (data not). In addition to this, by comparing the relative positions and properties of the estimated tracts we found more estimated fiber tracks in the temporal-callosal connections of the Eyeborg user. Furthermore, the IFOF of the Eyeborg user presented a region located in the temporal-basal area with a higher white matter density (**Figure 3**).

Magnetic Resonance Spectroscopy (^{1}H-MRS)

The mean values and the corresponding standard deviations of the estimated metabolite ratios for the Eyeborg user and the controls are reported in **Table 3**. There were some differences between the metabolite ratios mIno/Cr, NAA/Cr and Glx/Cr in the visual areas of the Eyeborg user when compared to controls although they were not statistically significant. Specifically, there was an increase in the levels of mIno, a putative marker of glia, in V4 which is the area involved in visual color processing. Furthermore, the Eyeborg user showed an increase in the neuronal integrity marker NAA (NAA/Cr ratio) in V2 and a higher Glx/Cr (Glutamate plus Glutamine) proportion in V1 and V2.

Discussion

This study represents the first attempt to directly assess the structural adjustments and neuroplastic changes related to the chronic use of the *Eyeborg*, an electronic device that allows colors to be perceived as sounds. This offers the amazing opportunity to investigate the link between brain activity, conscious perception and technological devices. Our results suggest that after 8 years of continuous use of this device, there could be some adaptive and compensatory changes within the brain. However, we should take into account that this is a very preliminary investigation that needs to be confirmed by further studies with a larger sample size. Thus, some of these changes could exist before the use of the Eyeborg and therefore we cannot claim that the continuous use of the Eyeborg is the only reason of these findings. Nonetheless, several studies have looked into differential activation before and

TABLE 1 | Talairach coordinates and Z-scores of the maximally activated voxels associated with the presentation of simultaneously visual and auditory stimulation.

	Left Hemisphere					Right Hemisphere				
	x	*y*	*z*	*T* value	Brodman Area	*x*	*y*	*z*	*T* value	Brodman Area
Eyeborg user	−9.59	−97.6	18.39	19.4	18	12	−94	22	25	19
	−63.59	−11.2	3.99	15.62	22	33.6	−79.6	−21.2	18.8	18
	−52.79	−0.4	−10.4	11.11	38	69.6	−14.8	0.39	22.58	21
	−34.79	−36.4	18.39	10.09	13	58.8	13.99	−6.8	15.65	38
	−34.79	57.2	−6.8	5.71	10	66	−18.4	18.4	14.69	42
	−27.6	57.2	−3.2	5.53	10	48	−36.4	25.6	8.8	13
						30	50	−14	7.55	11
						22.8	60.79	−6.8	4.74	10
						48	6.79	43.6	6.92	6
						48	3.2	36.4	5.54	6
Controls	−38.39	−35.59	−6.8	31.76	47	44.4	−32.8	3.9	181	41
	−45.6	−35.6	14.79	17.99	46	26.4	−79.6	−10.4	169.13	18
	−23.99	17.6	57.9	29.35	6	44.4	3.2	25.6	29.5	9
	−38.4	3.2	54.4	23.45	6	37.2	6.79	25.6	20.74	9
	−16.8	39.2	50.8	19.04	8	44.4	−4	29.2	7.96	6
	−34.79	13	29	24.2	9	40.8	35.6	−14	27	11
	−31.2	−0.4	18.4	16.93	13	44.4	42.79	−3.2	22.3	10
	−42	6	22	20.04	9	66	−40	−14	12.42	21
	−49.2	−54	43.6	9.37	40	48	−29.2	50.8	8.98	40
	−34.8	−54.4	54.4	3.23	7	55.2	−22	36.4	5.47	2
	−49.2	−4	36.4	8.85	6	48	−25	36	5.04	2
	−49.2	−11.2	47.2	6.21	4	33.6	3.2	−17.6	5.62	38
	−42	−7.6	43.6	5.78	6	40.8	28.4	22	7.78	46
	−49.2	28.4	32.8	6.25	9					
	−49.2	21.2	36.4	6.08	9					
	−52.79	13.99	32.79	3.5	9					

Specification of active clusters at $p < 0.001$ (cluster criterion: 10 voxels).

TABLE 2 | Diffusion Tensor Imaging results for white selected white matter tracts in the Eyeborg user and controls.

		FA value	ADC value ($10^{-3}MM^2/S$)
Corpus callosum	Eyeborg user	0.57 ± 0.02*	0.92 ± 0.03
	Controls	0.52 ± 0.03	0.88 ± 0.02
Inferior longitudinal fasciculus			
Left	Eyeborg user	0.53 ± 0.01	0.85 ± 0.02
	Controls	0.49 ± 0.03	0.84 ± 0.04
Right	Eyeborg user	0.51 ± 0.01	0.86 ± 0.02
	Controls	0.48 ± 0.02	0.82 ± 0.04
Inferior fronto-occipital fasciculus			
Left	Eyeborg user	0.51 ± 0.06	0.82 ± 0.02
	Controls	0.45 ± 0.08	0.85 ± 0.09
Right	Eyeborg user	0.50 ± 0.07	0.83 ± 0.01
	Controls	0.48 ± 0.01	0.89 ± 0.02

*FA = fractional anisotropy value; ADC = apparent diffusion coefficient; *$p < 0.05$. Diffusion Tensor Imaging results for white selected white matter tracts in the Eyeborg user and controls.*

after learning how to use a specific SSD (Ptito et al., 2005; Amedi et al., 2007; Poirier et al., 2007; Connell and Merabet, 2014) showing similar cognitive and neural changes.

The fMRI version of the Farnsworth-Munsell 100 Hue test, requires the use of color information to make perceptual decisions about the sequencing of colors and is able to circumvent the difficulties found in previous studies of color processing areas using passive viewing of colors or simple color discrimination (Beauchamp et al., 1999). Our results showed that the activation in our subject during both, the chromatic and achromatic phases in the color test paradigm, were very similar and constrained to V1 (BA17) and the left V2 area (BA18). This finding fits perfectly with his difficulty for distinguishing between colors and his vision in shades of gray and confirms the usefulness of this test for studying the organization of color-selective areas in normal subjects and in persons with achromatopsia.

The paradigm that comprised visual-auditory stimuli also displayed significant differences in the brain activation pattern of the Eyeborg user. Thus when we presented simultaneously visual images and their correspondent sounds encoded by the Eyeborg algorithms, the activated areas involved the temporal lobe and included the auditory cortex (BA42), Wernicke's area (BA22) and the rostral part of the superior and middle temporal gyri (BA38), which has been recently related to color and structural judgments of familiar objects (Kellenbach et al., 2005). A particular point of interest is the bilateral activation of BA13 in the Eyeborg user. This finding was not present in any of the control subjects. BA13 is located in the posterior insular cortex and several studies relate this area with phonation, pitch judgment and melodic perception (Zatorre et al., 1994; Kikuta et al., 2006). Moreover, there were

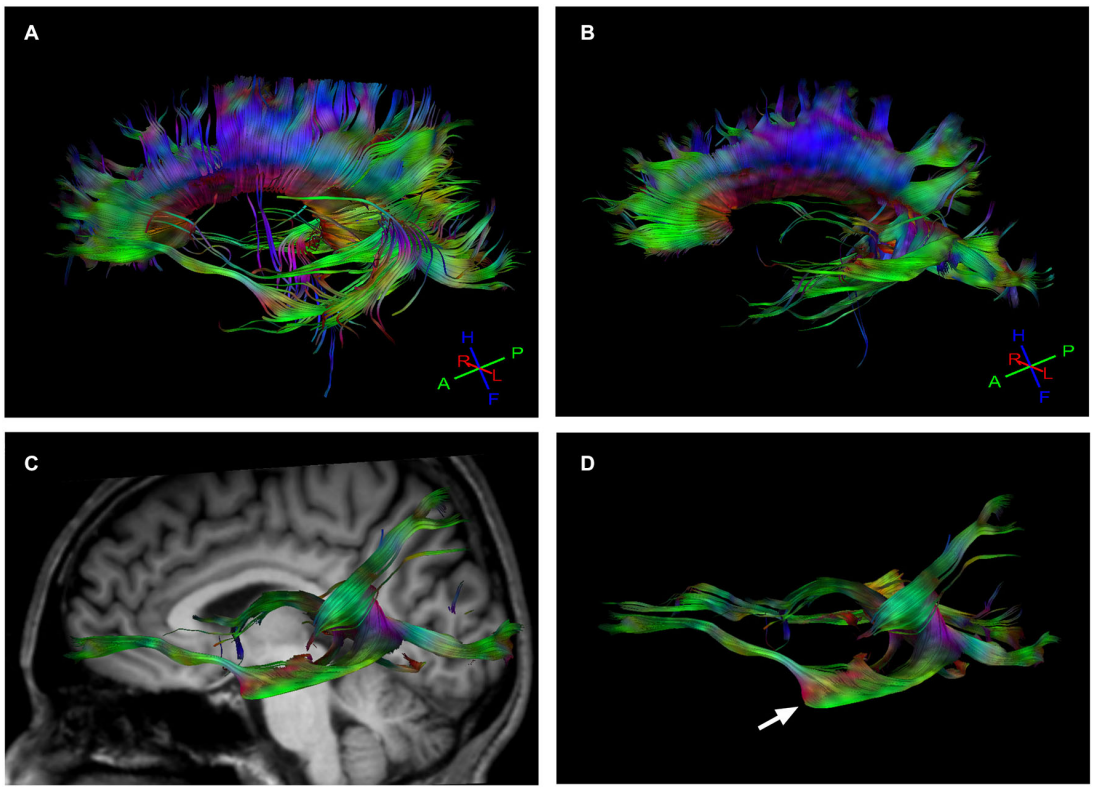

FIGURE 3 | Tractography results. **(A)** Callosal fiber tracks in the Eyeborg user. **(B)** Callosal fiber tracks in a representative control subject (matched in age and sex). **(C)** Left inferior fronto-occipital fasciculus (IFOF), which connects the ventral occipital lobe and the orbitofrontal cortex, in the Eyeborg user. **(D)** Enlargement of the IFOF displayed in panel **(C)**. The arrow points the region with increased myelin density related to the temporal lobe.

robust activations in prefrontal, orbito-frontal, premotor and supplementary motor cortex (BA10, BA11 and BA6). We think that the activation of the orbito-frontal cortex is highly relevant due to its robust connections not only with limbic and olfactory systems but also with the ventral visual pathways involved in the analysis of form and color of the visual information. However, it is also possible that it can be related to some ectopic changes due to other adaptive processes or even to some other preexisting anomalous connections in this particular subject.

The individual variability observed in functional imaging studies may also be related to underlying anatomical patterns that can be studied thanks to recent methodological advances in DTI and fiber tractography (DTI). Our results showed an enhanced structural connectivity between frontal lobe and auditory and visual association areas in the Eyeborg user. Thus, compared to controls, the Eyeborg user has an increased myelin density, which is probably related to a greater number of axons in the IFOF. This is a ventral associative bundle that connects the ventral occipital lobe and the orbitofrontal cortex. Furthermore, IFOF also constitutes one of the major efferent and afferent neuronal projections between the prefrontal cortex, auditory and visual association cortex (Catani et al., 2003; Catani and Mesulam, 2008).

As our subject reports seeing colors upon hearing sounds by using the *Eyeborg*, we hypothesized that the increased FA in IFOF might be related with a pattern of functional connectivity between frontal, auditory and visual association areas and could be involved in enhanced cross-modal associations to process the new information. In support of this idea, an increased structural connectivity in the right IFOF in people with color-music synesthesia has been recently described. This suggests that this perceptual experience could be linked to higher white matter connectivity in this pathway (Zamm et al., 2013). Presently, it

TABLE 3 | ^{1}H-MRS results showing the metabolite ratios for the Eyeborg user and the control subjects.

	Metabolite ratios			
Voxel Location	**NAA/Cr**	**Glx/Cr**	**Cho/Cr**	**mIno/Cr**
V1				
Eyeborg user	1.53	1.74	0.46	0.42
Controls	1.45 ± 0.12	1.33 ± 0.31	0.52 ± 0.06	0.55 ± 0.09
V2				
Eyeborg user	1.63	1.27	0.56	0.57
Controls	1.41 ± 0.12	1.05 ± 0.30	0.44 ± 0.01	0.58 ± 0.12
V4				
Eyeborg user	1.48	0.93	0.43	0.8
Controls	1.44 ± 0.10	1.07 ± 0.17	0.64 ± 0.18	0.62 ± 0.11

(NAA), N-acetylaspartate and other N-acetyl-containing compounds. (Glx), Glutamate and Glutamine. (Cr), Creatine. (Cho), Choline. (mIno), Myo-inositol. Data obtained at ^{1}H MR spectroscopy.

remains an open question as to whether, sensory substitution and synesthesia share similar neural mechanisms. In fact, some authors point out that sensory substitution shows properties of synesthesia, as both are associated with atypical perceptual experiences elicited by the processing of a qualitatively different stimulus to that which normally gives rise to that experience (Zamm et al., 2013). In this context, results from the current study seem to suggest that color-sound synesthesia as well as the continued use of the *Eyeborg* could potentially share a common underlying neuroanatomical basis where IFOF has a major role. Another important finding is the higher FA values in ILF in the Eyeborg user. ILF is a direct connection from the occipital cortex to the anterior part of the temporal lobe, running laterally and inferiorly above optic radiation fibers. However, it is important to note that in contrast to IFOF, which is known as a direct pathway (one that connects the occipital, posterior temporal, and the orbito-frontal areas), the ILF is considered to be an indirect pathway that essentially connects similar brain locations. This leads us to believe that IFOF and ILF are probably enhancing similar perceptive processes in our subject, which could be represented by a functional heightened network between frontal, auditory and visual association areas.

The DTI also reveals other structural differences in the Eyeborg user such as an increase of white matter tracts in the CC. The CC is the largest bundle of the human brain and connects left and right cerebral hemispheres. It allows the transfer of inputs from one hemisphere to the other and is involved in several motor, perceptual and cognitive functions (Catani and Thiebaut de Schotten, 2008). In the case of our subject, increased connectivity in CC could be ascribed to the use of *Eyeborg*, however future work will be needed to determine the exact meaning and repeatability of these connectivity changes.

On the other hand, the magnetic resonance spectroscopy (^{1}H-MRS) also revealed some changes in metabolic levels of mIno, NAA and Glx in the visual brain areas of the Eyeborg user. Myo-inositol is the most common biological stereoisomer of inositol, a sugar-like molecule synthesized mainly within astrocytes, which has been proposed as a marker of remodeling and plays an essential role in the mechanisms of brain adaptation and plasticity (Bernabeu et al., 2009; Weaver et al., 2013). Specifically, we found an increase in the levels of mIno/Cr in V4, which is mostly involved in color constancy and responds according to perceptual color space. Furthermore, we also found an increase in the NAA/Cr ratio in V2, that is particularly localized within neurons and considered as a major marker for neural integrity. This could reflect not only a higher neuronal and axonal density but also compensatory adjustments in which neurons could be actively implicated. Likewise, there is an increase in the Glx/Cr (Glutamate plus Glutamine) ratio in V1 and V2, in the Eyeborg user which could reflect changes in excitatory biochemical pathways in these areas and a higher synaptic activity (Hensch and Fagiolini, 2005; Bavelier et al., 2010). Taken together all these findings might suggest, the existence of an interconnected network in which glia and neurons work together to process and adapt to the novel sensory experience. In support of this idea, it has been recently proposed (Weaver et al., 2013) that continued use of SSDs might have an effect analogous to the environmental enrichment, resulting in an increase in the astrocyte population and its excitatory synapses that might lead to functional changes in brain activity.

In conclusion, we have tried to present some cues about the possible brain changes associated with the use of the Eyeborg. Our results suggest that there are metabolic, structural and functional changes, particularly in visual and auditive cortices, following the continuous use of this specific SSD device. However, we should emphasize that this is a preliminary work and that further studies, including the analysis of the same subjects before and after the continuous use of a SSD device such as the Eyeborg should be performed. We expect that the precise understanding of these plastic changes will have clear implications for new device development and for more efficient rehabilitative programs for people with disabilities. Furthermore, they could also be helpful in the framework of other approaches for restoring lost neural functions such as innovative artificial vision systems or novel cochlear implants (Fernández et al., 2005; Fernandez and Merabet, 2011).

Acknowledgments

We are very grateful to all our volunteers for their time and their help in supporting this study. This work has been supported in part by grant MAT2012-39290-C02-01, by the Bidons Egara Research Chair of the University Miguel Hernández and by a research grant of the Spanish Blind Organization (ONCE).

References

Abboud, S., Hanassy, S., Levy-Tzedek, S., Maidenbaum, S., and Amedi, A. (2014). EyeMusic: introducing a "visual" colorful experience for the blind using auditory sensory substitution. *Restor. Neurol Neurosci.* 32, 247–257. doi: 10.3233/RNN-130338

Amedi, A., Stern, W. M., Camprodon, J. A., Bermpohl, F., Merabet, L., Rotman, S., et al. (2007). Shape conveyed by visual-to-auditory sensory substitution activates the lateral occipital complex. *Nat. Neurosci.* 10, 687–689. doi: 10.1038/nn1912

Bavelier, D., Levi, D. M., Li, R. W., Dan, Y., and Hensch, T. K. (2010). Removing brakes on adult brain plasticity: from molecular to behavioral interventions. *J. Neurosci.* 30, 14964–14971. doi: 10.1523/JNEUROSCI.4812-10.2010

Beauchamp, M. S., Haxby, J. V., Jennings, J. E., and DeYoe, E. A. (1999). An fMRI version of the Farnsworth-Munsell 100-Hue test reveals multiple color-selective areas in human ventral occipitotemporal cortex. *Cereb. Cortex* 9, 257–263. doi: 10.1093/cercor/9.3.257

Bernabeu, A., Alfaro, A., García, M., and Fernández, E. (2009). Proton magnetic resonance spectroscopy (^{1}H-MRS) reveals the presence of elevated myo-inositol in the occipital cortex of blind subjects. *Neuroimage* 47, 1172–1176. doi: 10.1016/j.neuroimage.2009.04.080

Bologna, G., Deville, B., and Pun, T. (2009). On the use of the auditory pathway to represent image scenes in real-time. *Neurocomputing* 72, 839–849. doi: 10.1016/j.neucom.2008.06.020

Capelle, C., Trullemans, C., Arno, P., and Veraart, C. (1998). A real-time experimental prototype for enhancement of vision rehabilitation using auditory substitution. *IEEE Trans. Biomed. Eng.* 45, 1279–1293. doi: 10.1109/10.720206

Catani, M., Jones, D. K., Donato, R., and Ffytche, D. H. (2003). Occipito-temporal connections in the human brain. *Brain* 126, 2093–2107. doi: 10.1093/brain/awg203

Catani, M., and Mesulam, M. (2008). The arcuate fasciculus and the disconnection theme in language and aphasia: history and current state. *Cortex* 44, 953–961. doi: 10.1016/j.cortex.2008.04.002

Catani, M., and Thiebaut de Schotten, M. (2008). A diffusion tensor imaging tractography atlas for virtual *in vivo* dissections. *Cortex* 44, 1105–1132. doi: 10.1016/j.cortex.2008.05.004

Cohen, L. G., Celnik, P., Pascual-Leone, A., Corwell, B., Falz, L., Dambrosia, J., et al. (1997). Functional relevance of cross-modal plasticity in blind humans. *Nature* 389, 180–183. doi: 10.1038/38278

Connell, N., and Merabet, L. B. (2014). Uncovering the connectivity of the brain in relation to novel vision rehabilitation strategies. *Neurology* 83, 484–485. doi: 10.1212/WNL.0000000000000664

Cramer, S. C., Sur, M., Dobkin, B. H., O'Brien, C., Sanger, T. D., Trojanowski, J. Q., et al. (2011). Harnessing neuroplasticity for clinical applications. *Brain* 134, 1591–1609. doi: 10.1093/brain/awr039

Cronly-Dillon, J., Persaud, K., and Gregory, R. P. (1999). The perception of visual images encoded in musical form: a study in cross-modality information transfer. *Proc. Biol. Sci.* 266, 2427–2433. doi: 10.1098/rspb.1999.0942

Engel, S. A., Rumelhart, D. E., Wandell, B. A., Lee, A. T., Glover, G. H., Chichilnisky, E. J., et al. (1994). fMRI of human visual cortex. *Nature* 369:525. doi: 10.1038/369525a0

Eyeborg. (2015). Available online at: http://en.wikipedia.org/wiki/Eyeborg. Accessed on 2015.

Fabri, M., Pierpaoli, C., Barbaresi, P., and Polonara, G. (2014). Functional topography of the corpus callosum investigated by DTI and fMRI. *World J. Radiol.* 6, 895–906. doi: 10.4329/wjr.v6.i12.895

Fernandez, E., and Merabet, L. B. (2011). "Cortical plasticity and reorganization in severe vision loss," in *Visual Prosthetics*, ed G. Dagnelie (New York, NY: Springer), 77–92.

Fernández, E., Pelayo, F., Romero, S., Bongard, M., Marin, C., Alfaro, A., et al. (2005). Development of a cortical visual neuroprosthesis for the blind: the relevance of neuroplasticity. *J. Neural Eng.* 2, R1–R12. doi: 10.1088/1741-2560/2/4/r01

Goebel, R., Esposito, F., and Formisano, E. (2006). Analysis of functional image analysis contest (FIAC) data with brainvoyager QX: from single-subject to cortically aligned group general linear model analysis and self-organizing group independent component analysis. *Hum. Brain Mapp.* 27, 392–401. doi: 10.1002/hbm.20249

Haga, K. K., Khor, Y. P., Farrall, A., and Wardlaw, J. M. (2009). A systematic review of brain metabolite changes, measured with 1H magnetic resonance spectroscopy, in healthy aging. *Neurobiol. Aging* 30, 353–363. doi: 10.1016/j.neurobiolaging.2007.07.005

Hensch, T. K., and Fagiolini, M. (2005). Excitatory-inhibitory balance and critical period plasticity in developing visual cortex. *Prog. Brain Res.* 147, 115–124. doi: 10.1016/s0079-6123(04)47009-5

Kahol, K., French, J., Bratton, L., and Panchanathan, S. (2006). Learning and perceiving colors haptically. *Proc. ASSETS* 173–180. doi: 10.1145/1168987.1169017

Kantarci, K. (2014). Fractional anisotropy of the fornix and hippocampal atrophy in Alzheimer's disease. *Front. Aging Neurosci.* 6:316. doi: 10.3389/fnagi.2014.00316

Kellenbach, M. L., Hovius, M., and Patterson, K. (2005). A pet study of visual and semantic knowledge about objects. *Cortex* 41, 121–132. doi: 10.1016/s0010-9452(08)70887-6

Kikuta, K., Takagi, Y., Nozaki, K., Hanakawa, T., Okada, T., Miki, Y., et al. (2006). Early experience with 3-T magnetic resonance tractography in the surgery of cerebral arteriovenous malformations in and around the visual pathway. *Neurosurgery* 58, 331–337; discussion 331–337. doi: 10.1227/01.neu.0000195017.82776.90

Maidenbaum, S., Abboud, S., and Amedi, A. (2014). Sensory substitution: closing the gap between basic research and widespread practical visual rehabilitation. *Neurosci. Biobehav. Rev.* 41, 3–15. doi: 10.1016/j.neubiorev.2013.11.007

Meijer, P. B. (1992). An experimental system for auditory image representations. *IEEE Trans. Biomed. Eng.* 39, 112–121. doi: 10.1109/10.121642

Merabet, L. B., and Pascual-Leone, A. (2010). Neural reorganization following sensory loss: the opportunity of change. *Nat. Rev. Neurosci.* 11, 44–52. doi: 10.1038/nrn2758

Naressi, A., Couturier, C., Castang, I., de Beer, R., and Graveron-Demilly, D. (2001). Java-based graphical user interface for MRUI, a software package for quantitation of *in vivo*/medical magnetic resonance spectroscopy signals. *Comput. Biol. Med.* 31, 269–286. doi: 10.1016/s0010-4825(01)00006-3

Nie, M., Ren, J., Li, Z., Niu, J., Qiu, Y., Zhu, Y., et al. (2009). SoundView: an auditory guidance system based on environment understanding for the visually impaired people. *Conf. Proc. IEEE Eng. Med. Biol. Soc.* 2009, 7240–7243. doi: 10.1109/IEMBS.2009.5334754

Nilsson, C., Markenroth Bloch, K., Brockstedt, S., Lätt, J., Widner, H., and Larsson, E. M. (2007). Tracking the neurodegeneration of parkinsonian disorders–a pilot study. *Neuroradiology* 49, 111–119. doi: 10.1007/s00234-006-0165-1

Nudo, R. J. (2006). Plasticity. *NeuroRx* 3, 420–427. doi: 10.1016/j.nurx.2006.07.006

Pascual-Leone, A., Amedi, A., Fregni, F., and Merabet, L. B. (2005). The plastic human brain cortex. *Annu. Rev. Neurosci.* 28, 377–401. doi: 10.1146/annurev.neuro.27.070203.144216

Poirier, C., De Volder, A., Tranduy, D., and Scheiber, C. (2007). Pattern recognition using a device substituting audition for vision in blindfolded sighted subjects. *Neuropsychologia* 45, 1108–1121. doi: 10.1016/j.neuropsychologia.2006.09.018

Poveda, M. J., Bernabeu, A., Concepción, L., Roa, E., de Madaria, E., Zapater, P., et al. (2010). Brain edema dynamics in patients with overt hepatic encephalopathy a magnetic resonance imaging study. *Neuroimage* 52, 481–487. doi: 10.1016/j.neuroimage.2010.04.260

Proulx, M. J., Ptito, M., and Amedi, A. (2014). Multisensory integration, sensory substitution and visual rehabilitation. *Neurosci. Biobehav. Rev.* 41, 1–2. doi: 10.1016/j.neubiorev.2014.03.004

Ptito, M., Moesgaard, S. M., Gjedde, A., and Kupers, R. (2005). Cross-modal plasticity revealed by electrotactile stimulation of the tongue in the congenitally blind. *Brain* 128, 606–614. doi: 10.1093/brain/awh380

Striem-Amit, E., Guendelman, M., and Amedi, A. (2012). 'Visual' acuity of the congenitally blind using visual-to-auditory sensory substitution. *PLoS One* 7:e33136. doi: 10.1371/journal.pone.0033136

Tregellas, J. R., Ellis, J., Shatti, S., Du, Y. P., and Rojas, D. C. (2009). Increased hippocampal, thalamic and prefrontal hemodynamic response to an urban noise stimulus in schizophrenia. *Am. J. Psychiatry* 166, 354–360. doi: 10.1176/appi.ajp.2008.08030411

Wakana, S., Jiang, H., Nagae-Poetscher, L. M., van Zijl, P. C., and Mori, S. (2004). Fiber tract-based atlas of human white matter anatomy. *Radiology* 230, 77–87. doi: 10.1148/radiol.2301021640

Weaver, K. E., Richards, T. L., Saenz, M., Petropoulos, H., and Fine, I. (2013). Neurochemical changes within human early blind occipital cortex. *Neuroscience* 252, 222–233. doi: 10.1016/j.neuroscience.2013.08.004

Yoshida, S., Oishi, K., Faria, A. V., and Mori, S. (2013). Diffusion tensor imaging of normal brain development. *Pediatr. Radiol.* 43, 15–27. doi: 10.1007/s00247-012-2496-x

Zamm, A., Schlaug, G., Eagleman, D. M., and Loui, P. (2013). Pathways to seeing music: enhanced structural connectivity in colored-music synesthesia. *Neuroimage* 74, 359–366. doi: 10.1016/j.neuroimage.2013.02.024

Zatorre, R. J., Evans, A. C., and Meyer, E. (1994). Neural mechanisms underlying melodic perception and memory for pitch. *J. Neurosci.* 14, 1908–1919.

Conflict of Interest Statement: The authors declare that the research was conducted in the absence of any commercial or financial relationships that could be construed as a potential conflict of interest.

frontiers in
SYSTEMS NEUROSCIENCE

ORIGINAL RESEARCH ARTICLE
published: 25 September 2014
doi: 10.3389/fnsys.2014.00181

A little elastic for a better performance: kinesiotaping of the motor effector modulates neural mechanisms for rhythmic movements

Riccardo Bravi[1], Eros Quarta[1], Erez J. Cohen[1], Anna Gottard[2] and Diego Minciacchi[1]*

[1] *Department of Experimental and Clinical Medicine, University of Florence, Florence, Italy*
[2] *Department of Statistics, Informatics, Applications, University of Florence, Florence, Italy*

Edited by:
Mikhail Lebedev, Duke University, USA

Reviewed by:
Peter Praamstra, Radboud University Nijmegen, Netherlands
Yuri P. Ivanenko, IRCCS Fondazione Santa Lucia, Italy

***Correspondence:**
Diego Minciacchi, Department of Experimental and Clinical Medicine, University of Florence, Viale Morgagni 63, Florence I-50134, Italy
e-mail: diego@unifi.it

A rhythmic motor performance is brought about by an integration of timing information with movements. Investigations on the millisecond time scale distinguish two forms of time control, event-based timing and emergent timing. While event-based timing asserts the existence of a central internal timekeeper for the control of repetitive movements, the emergent timing perspective claims that timing emerges from dynamic control of nontemporal movements parameters. We have recently demonstrated that the precision of an isochronous performance, defined as performance of repeated movements having a uniform duration, was insensible to auditory stimuli of various characteristics (Bravi et al., 2014). Such finding has led us to investigate whether the application of an elastic therapeutic tape (Kinesio® Tex taping; KTT) used for treating athletic injuries and a variety of physical disorders, is able to reduce the timing variability of repetitive rhythmic movement. Young healthy subjects, tested with and without KTT, have participated in sessions in which sets of repeated isochronous wrist's flexion-extensions (IWFEs) were performed under various auditory conditions and during their recall. Kinematics was recorded and temporal parameters were extracted and analyzed. Our results show that the application of KTT decreases the variability of rhythmic movements by a 2-fold effect: on the one hand KTT provides extra proprioceptive information activating cutaneous mechanoreceptors, on the other KTT biases toward the emergent timing thus modulating the processes for rhythmic movements. Therefore, KTT appears able to render movements less audio dependent by relieving, at least partially, the central structures from time control and making available more resources for an augmented performance.

Keywords: sensory-motor integration, timing, isochronous movements, auditory imagery, music

INTRODUCTION

Considerable evidence suggest that the study of human motor rhythmic performance synchronized to auditory stimuli is useful in unraveling neural aspects of action timing. The effects of different types of audio information (i.e., metronome or music) on motor performance have been extensively investigated in studies of finger tapping (Repp, 1999a,b; del Olmo and Cudeiro, 2005) and of gait (see Wittwer et al., 2013). The interest for the effects of paced auditory stimuli on rhythmic activities stems from the proven notion that this design of sensorimotor integration is shown to be an effective tool for gross motor rehabilitation in neurological diseases by improving spatial-temporal parameters and decreasing temporal variability (Thaut et al., 1996; McIntosh et al., 1997; del Olmo and Cudeiro, 2005; del Olmo et al., 2006; Hausdorff et al., 2007; Arias and Cudeiro, 2008; de Dreu et al., 2012).

In a recent study we showed how do auditory stimuli with distinct characteristics, streams of clicks or excerpts of music, influence the precision of repeated isochronous wrist's flexion-extensions (IWFEs), performed with no direct surface opposition and minimizing visual information (Bravi et al., 2014). Some reports have described a reduction of temporal variability for rhythmic movements in the presence of paced auditory stimuli. Our data, however, displayed clearly that when both tactile and visual information are minimized, the listening alone to paced auditory stimuli does not improve the precision of an isochronous performance. Also, in a previous study on timing of rhythmic movements a lack of reduction in temporal variability was observed during paced tapping when compared to unpaced tapping (Schlerf et al., 2007). These findings have prompted us to investigate other tools that might augment the precision of rhythmic movement.

In addition, investigations on the millisecond time scale distinguish two forms of time control, explicit timing and implicit

Abbreviations: bpm, beats per minute; Cl, while listening to a stream of clicks; Cl2, after 2 min from the end of the Cl condition; CVs, coefficients of variation; Fr, free, in absence of auditory information; IWFEs, isochronous wrist's flexion-extensions; KTT, Kinesio® Tex taping; Mu, while listening to an excerpt of music; Mu2, after 2 min from the end of the Mu condition; N/KTT, no KTT; $w\gamma(1)$, windowed lag-one autocorrelations.

timing, later renamed as event-based timing and emergent timing, respectively, (Spencer and Ivry, 2005). Event-based timing has evolved from the information processing approach, asserting the existence of internal timekeepers for motor control, and is well represented by the two-level model proposed by Wing and Kristofferson (1973a,b). According to the Wing and Kristofferson model, temporal precision in a self-paced tapping is limited by variability in the central timekeeper and by variability arising from the peripheral motor system (Semjen et al., 2000). The emergent timing perspective is derived from the dynamic systems theory, claiming that there are no representational clocks (Kugler et al., 1980; Kelso, 1995) and that timing emerges from dynamic control of nontemporal movements parameters (Schoner, 2002; Huys et al., 2008) such as stiffness which is playing a major role for determining movement frequency (Turvey, 1977; Delignières et al., 2004). For the study of timing, the task most widely employed was the performance of repeated movements. Among the rhythmic motor tasks, tapping is thought to be under the control of the event-based timing while circle drawing is thought to be under the control of the emergent timing (Zelaznik et al., 2002). Air tapping, a motor task performed in the air with no surface contact, represents a more recent approach for the study of timing. This motor task possesses specific characteristics of both the event-based and emergently motor rhythmic tasks due to the presence of salient motor events and smooth effector trajectories (Delignières and Torre, 2011).

The participation of the cerebellum in timing was once a controversial issue (Leiner et al., 1993; Rao et al., 2001). To date, the cerebellar timing hypothesis, first formulated by Keele and Ivry (1990), is widely accepted. According to this hypothesis, the cerebellum functions as an internal timing device in the milliseconds range for both motor and non-motor processes (Ivry and Spencer, 2004). In particular, the involvement of the inferior olive and the climbing fiber system in timing was shown to take part in encoding temporal information independent of motor behavior (Xu et al., 2006). Investigations using rhythmic tapping tasks have provided evidences to support this hypothesis. In a study on individuals with unilateral cerebellar lesions, participants were asked to perform timed tapping, intermittent circle drawing, and continuous circle drawing tasks. Performances were impaired only when tasks were executed with the ipsilesional hand and involved movements theorized to require event-based but not emergent timing (Spencer et al., 2003).

The timing mode of rhythmic movements can change over time within a single task (Studenka and Zelaznik, 2008; Zelaznik and Rosenbaum, 2010; Delignières and Torre, 2011). The discrete or continuous character of movements performed in the rhythmic tasks is considered to be a key factor for the involvement of the event-based or the emergent timing mode (Robertson et al., 1999; Huys et al., 2008). In addition, neurophysiological and neuroanatomical studies provided bases to suggest that neural circuits are not completely independent of the timing functions. For discrete movements, it is proposed that explicit processes for timing arise as coordinated activity in the core striatal and olivo-cerebellar networks that are interconnected, with each other and with the cerebral cortex, through multiple synaptic pathways (Spencer et al., 2007; Teki et al., 2012). Conversely continuous movements, by nature, lack an event structure. For these movements timing may be achieved through the control of a secondary variable, such as angular velocity, which does not involve the cerebellum.

Kinesio® Tex Tape is an elastic cotton strip with an acrylic adhesive developed by Japanese chiropractor, Dr. Kenso Kase, in the 1970's (Kase et al., 2013). Kinesio® Tex taping (KTT) is a kinesthetic method commonly used in clinical practice for treating athletic injuries and a variety of physical disorders, with the purpose of mimicking the thickness and flexibility of the skin (Morris et al., 2013). It is claimed that the application of KTT causes micro convolutions, or folds, in the skin; it brings about a lifting of the skin away from the tissue beneath, favoring the release of pressure from tender tissues underneath and providing space for lymphatic fluid movement (Morris et al., 2013).

It was proposed that KTT is able to enhance somatosensory inputs and influence proprioception through stimulation of cutaneous mechanoreceptors (Callaghan et al., 2002; Kneeshaw, 2002; Halseth et al., 2004). We have, therefore, chosen KTT as a tool for possibly augmenting the precision of rhythmic movements. While little is known about the potential proprioceptive effect of KTT, the stimulation of cutaneous mechanoreceptors is believed to be induced by the pressure and stretching effect provoked by KTT application on the skin (Grigg, 1994).

In the current study we investigate whether the application of KTT on skin is able to reduce the timing variability of repetitive rhythmic movements. We also attempt to understand whether a causal relationship subsists between such reduction and functional augmentation of central structures involved, brought about by relieving, at least partially, these structures from time control.

We thus performed an experiment in which subjects, tested with and without KTT, participated in sessions in which sets of repeated IWFEs were performed under different conditions (i.e., without audio information, with paced audio in the form of clicks or music, and in the recall conditions; see Bravi et al., 2014). Our IWFEs performed with no direct surface opposition and while minimizing visual information, could potentially employ, as air finger tapping movements, both event-based and emergent timing processes. Participants were not instructed about the way to perform the IWFEs since it was showed that in the absence of specific instructions, the production of movements with no contact surface elicits alternatively different timing modes (Delignières and Torre, 2011).

We hypothesize that KTT, due to its aforementioned characteristics, is able to cause an improvement of the wrist joint proprioception due to augmented afferent input via the stimulation of cutaneous mechanoreceptors (Riemann and Lephart, 2002). The improvement in wrist joint proprioception would stabilize the motor effector during the performance, causing the IWFEs to be less discrete and thus smoother. Consequently this would entail the shifting from an event-based to emergent process to control the production of the IWFEs (Spencer et al., 2007; Huys et al., 2008). Therefore, by relieving, at least partially, the central structures from timing control, KTT would release resources and allow for a net augmentation of the central efficiency and, consequently, reduce the timing variability of IWFEs.

MATERIALS AND METHODS

PARTICIPANTS

A group of 25 right-handed volunteers (21 males, ages 20–27, mean 24.1 ± 2.4 years; 4 females, ages 18–27, mean 23.0 ± 2.7 years) took part in the recording sessions. All participants were naive to the purpose of the study; they were neither musically trained nor listeners of a classical music repertoire, and reported no auditory, motor, or other neurological impairments. The experimental protocol conformed to the requirements of the Federal Policy for the Protection of Human Subjects (U.S. Office of Science and Technology Policy) and of the Declaration of Helsinki, and has been approved by the Research Ethics Board of our Institution (Local Ethics Committee, Azienda Ospedaliero Universitaria Careggi, Florence, Italy). All participants provided an informed consent in written form.

SET UP

Each subject was tested individually, sitting upright on a chair with the legs comfortably positioned on leg-rest (**Figure 1A**). The participant's right forearm was placed on the armrest, in a relaxed horizontal position. The wrist and hand of the subject were free to move in mid-air with no direct opposition, thus minimizing tactile information. In order to reduce possible interference of visual information, the subject was requested to wear a blindfold. Environmental noise was reduced by the use of headphones (K 240 Studio, AKG Acoustics GmbH, Wien, AT), which were also used for the clean delivery of audio information. This setup was designed to minimize all information that is known to influence motor strategies (i.e., visual, tactile, and environmental noise) and that may result in a different motor performance (Bove et al., 2009; Saijo and Gomi, 2010). A triaxial accelerometer (ADXL330, Analog Devices Inc., Norwood, MA 02062) was placed on the dorsal aspect of the hand, over the proximal part of the 2nd–3rd metacarpal bones. The sensor, placed in a small pocket, was kept in position by an elastic band and secured by a Velcro strap. Sensor output was acquired and digitized at 200 Hz through PCI-6071E (12-Bit E Series Multifunction DAQ, National Instruments, Austin, TX, USA).

STIMULI

Audio stimuli were paced streams of clicks and excerpts of music. Music excerpts of 60 s duration were extracted from original professional productions. Selected fragments had a simple and explicit rhythmic structure and a tempo that remained constant throughout time. Music fragments were taken from musical styles popular among young people: rock, techno, dance, trance, hard rock, and film music. Three musical experts (professionals with musical experience) were asked to verify independently the tempo of the excerpts in order to be as accurate and sure as possible in the choice of unambiguous paced excerpts. It is known that the determination of perceptual musical tempo can be ambiguous (McKinney and Moelants, 2007) and that algorithms for music tempo extraction have several limitations (McKinney et al., 2007), although recent effort has been put into methods to possibly improve the evaluation metrics used for automatic tempo estimation (Levy, 2011). Only fragments for which the experts collectively agreed of having a single musical tempo were selected.

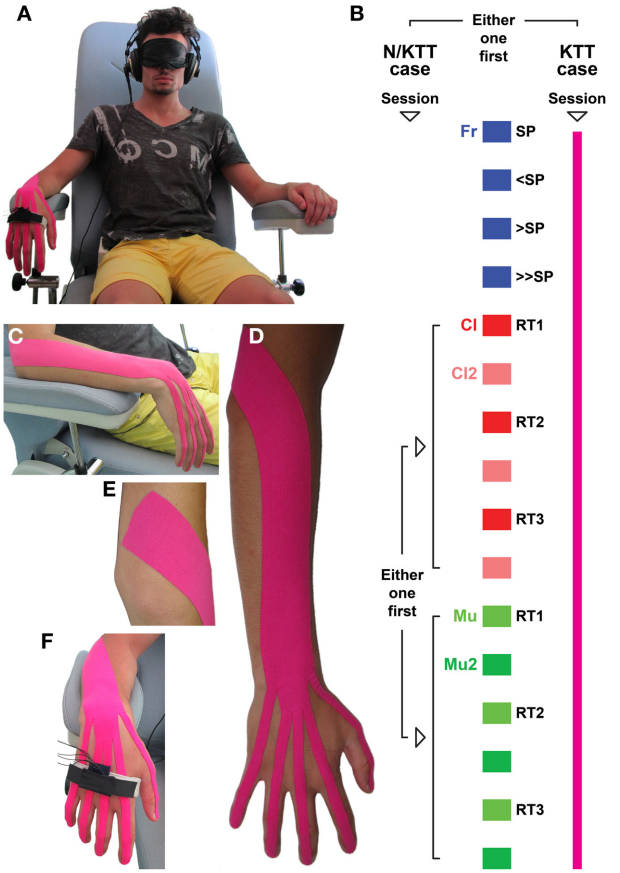

FIGURE 1 | (A) The subject is seated on a chair with armrests, wearing an eye-mask and headphones. The triaxial accelerometer is placed over the 2nd–3rd metacarpal bones. Subject is asked to perform sets of IWFEs. **(B)** The two sessions, one with N/KTT and one with KTT (color-coded in pink) are designed to record first IWFEs in condition free from auditory information (in the absence of auditory information, free = Fr, self-paced = SP; slower than SP = <SP; faster than SP = >SP; faster than >SP = >>SP) and then in conditions related to clicks (during the listening of clicks = Cl; recall after 2 min from the end of the Cl condition = Cl2; one block consisting of three pairs of Cl and Cl2 sets performed at three different reference tempi: RT1, RT2, and RT3) followed by those related to music (during the listening of music = Mu; recall after 2 min from the end of the Mu condition = Mu2; one block consisting of three pairs Mu and Mu2 sets performed at three different reference tempi: RT1, RT2, and RT3), or vice versa. In this and in the following figures the conditions and associated results are color-coded. **(C)** KTT was placed between the lateral epicondyle of the humerus and phalanges, at the position of maximum flexion. **(D)** KTT was applied over the extensor carpi ulnaris, extensor carpi radialis longus and brevis, extensor digitorum, extensor indicis, extensor digiti minimi, and extensor pollicis longus. **(E)** Proximally, KTT was placed from 5 cm proximal to muscles insertion. **(F)** Each branch of tape was applied down on the back of phalanx until the nail. As in the N/KTT set up, the accelerometer was placed on the dorsal aspect of the hand, over the proximal part of the 2nd–3rd metacarpal bones, into a pocket kept in position by an elastic band and secured by a Velcro strap.

All chosen fragments had small tempo variations due to live performance. Therefore, the tempo for each fragment was analyzed, beat-mapped, and set to fixed beats per minute (bpm, used as a measure of tempo in music) using the softwares Jackson

(http://vanaeken.com/; accuracy is within a 0.001 bpm margin) and Audacity (GNU/GPL, http://audacity.sourceforge.net/). Our time manipulations were all well below 5% deviation of the mean music tempo (professional performances have minimal deviations from mean tempo; Dannenberg and Mohan, 2011) and thus below the detection threshold for temporal changes in music (Ellis, 1991; Madison and Paulin, 2010). We didn't use fragments likely to be familiar to the listeners since it has been shown that high familiarity with a song installs an accurate long-term memory of its tempo (Levitin and Cook, 1996; Quinn and Watt, 2006). Streams of clicks of 60 s duration were produced using the audio editor Audacity, via the Generate Click Track function. The duration of an individual click was set to 10 ms and the click sound was set to white noise. The music and clicks stimuli were set to eight reference tempi ranging from 64 to 176 bpm (937.21 to 340.95 ms, **Table 1**). The same eight tempi were chosen for both streams of clicks and excerpts of music. Audio files were all normalized to −0.3 dB as the highest peak and stored as waveform (waveform audio file; 44.1 kHz; 16-bit depth) using Audacity. Fade in and fade out (10 ms) were placed at the beginning and end of each file. Audio stimuli were presented binaurally to the subjects through headphones (**Figure 1A**).

DATA FORMAT

Subjects were asked to perform sets of IWFEs and kinematic parameters were evaluated. Data from the sensor were stored and an off-line analysis of raw data from the triaxial accelerometer was implemented. The signal extracted from the accelerometer presented a minimum when the wrist reached the maximum flexion and a maximum when it reached the maximum extension. The duration of a single wrist's flexion-extension (i.e., IWFE duration) was calculated as the difference between two consecutive flexion-extension minima (custom software developed in Matlab®). To avoid initial and final transients, the first and last 5 s of each recording were excluded from analysis (Repp, 2005, 2011). Considering that tempi of the recorded IWFEs sets were remarkably variable, giving rise to a quantitative redundancy of tempi obtained in overall, we have decided to rank them as ranges (**Table 1**). IWFEs sets were then assigned to a defined range according to their tempo.

SESSION

Each subject had participated in two sessions, one with no KTT (N/KTT) and one with KTT (**Figure 1B**), that were performed at a week's distance. The order in which subjects performed the N/KTT or KTT sessions were set to obtain equivalent number of subjects that played first one or the other. The KTT session started approximately 10 min after mounting the tape since this interval is needed to overcome perception of tape on the skin (Kase et al., 2013). In each session the subject performed 16 sets of repeated IWFEs under various conditions. A single session was comprised of a baseline recording (4 sets) and 2 blocks (12 sets). In a single session the performance of the IWFEs sets was executed under five conditions: in absence of auditory information (free, Fr), while listening to a stream of clicks (Cl), after 2 min from the end of the Cl condition (Cl2), while listening to an excerpt of music (Mu), after 2 min from the end of the Mu condition (Mu2). Sets of IWFEs were recorded in all conditions. For each block IWFEs sets were performed using one type of auditory stimulus (Cl or Mu). One block consisted of three pairs of Cl and Cl2 sets, or Mu and Mu2 sets, performed at three different reference tempi, for the auditory Cl or Mu sets; the same tempi were then used for the auditory sets of the second block (**Figure 1B**). The order in which the clicks or music stimuli were presented was set to obtain equivalent number of subjects that received first one or the other.

The subject was instructed to restrain from listening to music during the day of the session. Each session began with instructions on how the sets of wrist's flexion-extensions were to be performed, followed by a short practice test. During the practice test, IWFEs were recorded and evaluated to assess whether the instructions were understood; after the practice test, the subject was asked if he/she felt comfortable with the task. Recordings from the practice test were not used for further analyses. The session started with recording in the Fr condition, which consisted of four IWFEs sets. In the first set, the subject was asked to perform IWFEs in a self-paced manner. In the second set, the subject was asked to perform IWFEs slower than those of the first set. In the third and fourth sets, the subject was asked to perform IWFEs faster than first recording and then faster than the third recording. The subject was then instructed to perform a set of repetitive IWFEs while listening to clicks or music at a similar pace concurrently with the tempo of the delivered audio

Table 1 | Musical names, ranking, and tempo equivalences between ranges of movement durations in Hertz and milliseconds.

Musical names	Rank	Tempo equivalences					
		Ranges (Hz)			Ranges (ms)		
		Reference	From	To	Reference	From	To
Adagio	1	1.067	1.017	1.133	937.21	983.28	882.61
Andante	2	1.333	1.283	1.400	750.19	779.42	714.29
	3	1.600	1.550	1.667	625.00	645.16	599.88
Moderato	4	1.867	1.817	1.933	535.62	550.36	517.33
	5	2.133	2.083	2.200	468.82	480.08	454.55
Allegro	6	2.400	2.350	2.467	416.67	425.53	405.35
	7	2.700	2.617	2.800	370.37	382.12	357.14
Presto	8	2.933	2.817	3.000	340.95	354.99	333.33

(i.e., maintaining an in-phase 1:1 relationship between repeated wrist's flexion-extensions and the tempo of the audio, conditions Cl or Mu). Then, instructions to subject for IWFEs performances in recalls were of the kind: "now, try to hear in your head the auditory stimulus just heard" (immediately after the end of the stimulus, see Zatorre and Halpern, 2005). After a 2 min break, the subject was asked to perform IWFEs as accurately as possible at the tempo of the auditory stimulus just heard while concurrently hearing mentally the stimulus itself (conditions Cl2 or Mu2). The session continued with the recordings of IWFEs in a reversed order (i.e., with the Mu conditions if Cl was recorded first, or vice versa). In order to obtain a balanced number of performances for the eight chosen reference tempi, the three tempi that were selected for the blocks were randomized for each single session.

KINESIO® TEX TAPE APPLICATION

The Kinesio® Tex Tape is comprised of a polymer elastic strand wrapped by 100% cotton fibers. It allow for a longitudinal stretch of 55–60% of its resting length. The Kinesio® Tex Tape is applied to the paper substrate with 25% of tension; the adhesive is 100% acrylic (Kase et al., 2013). For the KTT (Kinesio® Tex Gold™ FP—2″ Red) application the subject, already seated on the chair with own right forearm rested on the armrest, was asked to keep the wrist in a position of maximum flexion, and the distance between the lateral epicondyle of the humerus and the distal end of the third phalanx of the middle finger was measured. The purpose was to apply the tape over the open kinetic chain including wrist, metacarpal, and finger joints. During the application of KTT, between the lateral epicondyle of the humerus and phalanges, the wrist and forearm were maintained in full flexion and full pronation, respectively (**Figure 1C**). After manually assessing the origin and insertion of muscles, KTT was applied over the extensor carpi ulnaris, extensor carpi radialis longus and brevis, extensor digitorum, extensor indicis, extensor digiti minimi, and extensor pollicis longus (**Figures 1D–F**). The strip of Kinesio® Tex was cut 5 cm longer than the maximum length of the kinetic chain measured with the wrist in maximum flexion (Kase et al., 2013). The course of the tendons of the extensor muscles (for each finger) was then identified on the back of subject's hand and distances were measured between the distal end of each phalanx and the wrist. Measurements were used to cut the distal side of the elastic band into five branches to be placed over the metacarpal area and fingers following the course of the tendons. KTT was then applied from 5 cm proximal to muscles insertion to facilitate muscle function; the application tension was light, about 25%. From the lateral humeral epicondyle, KTT was applied—in a wave-like pattern—to wrap the wrist's extensors until reaching the wrist. Each branch was then applied down on the back of phalanx until the nail.

STATISTICAL ANALYSIS

To model directly the observed IWFEs durations we adopted random effect ANOVA models for repeated measurements (Pinheiro and Bates, 2000; Diggle et al., 2002). Separate models were adopted for different kinds of conditions and also the response variable was chosen differently according to the presence of audio. In particular, the differences between observed and the expected IWFEs durations were considered as response variable for performances under audio (Cl and Mu) and recall (Cl2 and Mu2) conditions. This response variable measures the error observed in the IWFEs durations, the observed IWFEs duration was instead considered as the response variable for performances in the Fr condition. As the response variables have been recorded several times for each performance and for each individual, a random effect part had to be included to take into account the lack of independence among the observations. Typically, in the random effect ANOVA models adopted for the analyses, the main effects concern the effect of the overall mean of the absence/presence of KTT (N/KTT vs. KTT) and of the tempo (fast if <517.33 ms, slow otherwise). The random effect part of the ANOVA models was specified in order to separately measure the variability within individuals and within performances. Moreover, the residual variance among observations, once taken into account for the main fixed and the random effects, was further modeled to take into account possible residual heteroscedasticity.

Moreover, in order to evaluate the precision of IWFEs, we used coefficients of variation (CVs = standard deviation/mean $\times$ 100). CVs of IWFEs durations were used to investigate whether the KTT influences the precision of IWFEs performances under different conditions and, if not indicated otherwise, are to be considered as the condition's and the range's means.

Lag-one autocorrelation analysis is used as statistical signature to investigate the processes for temporal regulation. It is assumed (see Wing and Kristofferson, 1973a,b) that series of produced time intervals regulated by the event-based process should have negative lag-one autocorrelation values (between -0.5 and 0). Conversely, emergent timing is characterized by positive lag-one autocorrelation values (between 0 and 0.5). To study the influence of KTT in the Cl and Cl2 conditions we computed series of windowed lag-one autocorrelations $w\gamma(1)$ (Delignières and Torre, 2011) for each set of IWFEs. Each windowed autocorrelation coefficient was computed as the mean of a set of 30 autocorrelations. Moving the set along the sequence, a series of windowed autocorrelation coefficients was computed for each performance, measuring autoregressive linear dependency within the IWFEs. Then, we calculated the mean of the obtained windowed lag series for each performance. We considered the mean $w\gamma(1)$ as an estimator of overall dependence in the performance. Furthermore, we calculated the percentage of positive and negative windowed $w\gamma(1)$ values for each performance. If not indicated otherwise, the mean of $w\gamma(1)$ and the percentage of positive and negative $w\gamma(1)$ are to be considered as the condition's and the range's means. To analyze the observed $w\gamma(1)$ we adopted random effects ANOVA model for repeated measurements. In order to allow an appropriate use of parametric statistical tests, the Fisher's Z-transformation was used to normalize the distribution of autocorrelation coefficients (Nolte et al., 2004; Freyer et al., 2012).

RESULTS

TIMING VARIABILITY

Examples of our datasets are illustrated in **Figure 2** as parallel box plots, for the Mu and Mu2 conditions. It is interesting to note that pairs of N/KTT—KTT plots are relatively analogous when compared for slow (≥ 517.33 ms) or fast (<517.33 ms) movements

durations. Also, it is easily appreciable that while median, upper and lower hinges and whiskers are visibly similar for pairs of N/KTT—KTT parallel box plots in the slow and fast collections of movements durations, the position and especially number of outside values is reduced when KTT is applied, with the lonely exception of a single far out value in the condition Mu2 for slow movements with KTT.

We estimated separate random effect ANOVA models for the different conditions: without audio information (Fr), with clicks (Cl), or music (Mu), and in the recall conditions (Cl2 and Mu2). The estimates for the main effects for the models in the two audio conditions Cl and Mu are reported in **Table 2**, together with their *p*-values and confidence intervals. As aforementioned, for these models the response variable is the difference between the observed and the expected IWFEs durations. As can be seen in **Table 2**, the overall mean is negative and significant in both models. This implies that, under a slow stimulus, observed IWFEs durations are, on mean, shorter than expected. The effect of tempo (movement duration) is significant in both Cl and Mu conditions, correcting the mean error toward zero. Conversely, KTT has no significant effect on the mean error.

The parameters concerning the random effects are also of interest. These parameters specifically shape the variability of the response variable. All the parameters for the random effects reported in **Table 2** are significant according to the appropriate likelihood ratio test. Remarkably, the most relevant result concerns the fact that the residual variability resulted heterogeneous between N/KTT or KTT cases. The KTT-specific residual variances (usually called factor-specific residual variances, see Muthén, 1989; for details on random effects model for heterogeneous population) result significantly different (**Table 3**). **Table 3** reports the estimate of the ratio between the residual variance for N/KTT and KTT cases. Both in the case of Mu and of Cl stimuli, this ratio is significantly less than one, assessing that the presence of the tape significantly help to decrease the variability of the errors in IWFEs durations. In particular, residual variance for KTT cases is about 14% less of the variance for N/KTT cases in Cl and 8% less in Mu.

A similar model was adopted for the recalls Cl2 and Mu2, recorded 2 min after the audio stimuli (**Table 4**). In this second model, the main effects are the overall mean, the condition and the movement duration, and the absence or presence of KTT. None of the estimates are significant, suggesting that, on mean, there is no evidence of a systematic error in IWFEs durations when movements are performed during recalls of music or clicks, recalls of fast or slow audio stimuli, and recalls with N/KTT or KTT. Interestingly, the presence of KTT still helps to significantly reduce the residual variance of about 6% (**Table 3**). The

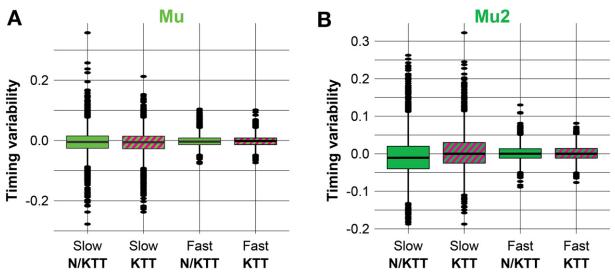

FIGURE 2 | (A,B) Box plots of the response variable, i.e., the difference between the observed and the expected interval durations, for datasets in the conditions Mu and Mu2, respectively. Pairs of N/KTT—KTT box plots are noticeably similar when compared for slow (≥517.33 ms) vs. fast (<517.33 ms) IWFEs durations. Also, easily appreciable is that the median, the upper and lower hinges and the whiskers are very similar for pairs of N/KTT—KTT parallel box plots in slow and fast collections of IWFEs durations. Conversely, the queues of the distributions are reduced when KTT is applied (the only exception is a single far out value in the condition Mu2 for slow IWFEs with KTT). KTT reduces the variability of IWFEs durations.

Table 3 | Factor specific residual variances (σ^2) for N/KTT vs. KTT movements.

Condition	N/KTT (σ^2)	KTT (σ^2)	N/KTT vs. KTT (*p*-value)
Cl	0.00076729	0.0006625549	< 0.0001
Mu	0.000772	0.000714	< 0.0001
Recalls (Cl2 and Mu2)	0.00085849	0.0008080108	< 0.0001
Fr	0.00082369	0.0007996383	0.005

Table 2 | Estimate, *p*-values (in parenthesis) and confidence intervals for model parameters in random effects ANOVA models for the Cl and Mu conditions.

	Cl		Mu	
Main fixed effects	**Estimate (*p*-value)**	**95% confidence interval**	**Estimate (*p*-value)**	**95% confidence interval**
Overall mean	−0.0063 (0.0000)	−0.0086; −0.0039	−0.0056 (0.0100)	−0.0099; −0.0013
Movement duration	0.0021 (0.0283)	0.0002; 0.0040	0.0042 (0.0401)	0.0002; 0.0083
N/KTT vs. KTT	−0.0009 (0.3349)	−0.0009; 0.0026	−0.0020 (0.3004)	−0.0058; 0.0018
Random effects	**Estimate**	**95% confidence interval**	**Estimate**	**95% confidence interval**
Within-individual SD	0.0045	0.0032; 0.0064	0.0066	0.0042; 0.0101
Within-set SD	0.0049	0.0042; 0.0057	0.0115	0.0101; 0.131
KTT residual variance ratio	0.8635	0.8440; 0.8835	0.9242	0.9036; 0.9452

Table 4 | Estimate, *p*-values (in parenthesis) and confidence intervals for model parameters in random effects ANOVA models for the Recalls and Fr conditions.

	Recalls (Cl2 and Mu2)		Fr	
Main fixed effects	**Estimate (*p*-value)**	**95% confidence interval**	**Estimate (*p*-value)**	**95% confidence interval**
Overall mean	−0.0014 (0.7492)	−0.0071; −0.0099	0.7218 (0.0000)	0.6865; 0.7571
Movement duration	−0.0034 (0.4347)	−0.0121; 0.0052	−0.3147 (0.0000)	−0.3571; −0.2723
N/KTT vs. KTT	0.0031 (0.4836)	−0.0055; 0.0117	0.0114 (0.5934)	−0.0306; 0.0533
Random effects	**Estimate**	**95% confidence interval**	**Estimate**	**95% confidence interval**
Within-individual SD	0.0031	1e-04; 0.0993	0.0127	1e-04; 1.2508
Within-set SD	0.0377	0.0347; 0.0410	0.1452	0.1306; 0.1614
KTT residual variance ratio	0.9412	0.9252; 0.9575	0.9708	0.9511; 0.9908

KTT residual variance ratio is estimated 0.9412 (95% confidence interval: 0.9252; 0.9575).

For the condition without audio stimulus (Fr), the model considers as the response variable directly the observed duration (**Table 4**). Consequently, the overall mean simply measures the mean movement duration chosen for performances of slow movements with N/KTT, while the main effect of movement duration measures the increment in bpm implied by a faster tempo. The overall mean and the main effect of tempo are then obviously significant by construction. The main effect of KTT is not significant. For this particular model, this result implies that individuals choose the tempo of the performance independently of the presence of the tape on their arm. Regarding the random part of the model, again it is worth to notice that the effect of the KTT in reducing the residual variability is still significant (**Table 3**). The residual variance, small but still present, is about the 3% less in KTT cases (estimate: 0.9708; 95% confidence interval: 0.9511; 0.9908).

The CV of IWFEs is used to normalize measures of temporal variability. We plotted the CVs of IWFEs as a function of the ranges of movement duration to visualize the rate dependent changes of the precision of isochronous performances and the interactions between these changes and the different experimental cases (N/KTT or KTT). The CVs of IWFEs, ranked per within-ranges of IWFEs durations, are illustrated in **Figure 3** for all conditions (**Figures 3A–E**). CVs values appear to change with movement duration. In particular, CVs of IWFEs become smaller as IWFEs become faster and, within the same condition and for the same range of movement duration, CVs values are very often smaller in KTT than in N/KTT cases. In **Figure 3F** the five within-condition CVs of IWFEs durations are compared for N/KTT and KTT cases. The CVs values of IWFEs are below 5% in all conditions and for both N/KTT and KTT cases. It is also noticeable that the within-condition CVs values are always smaller in KTT, when values for the same condition are compared, and that the difference is maximal for the condition Cl. Also, in **Figure 3G** are shown the percent reductions for the within-condition CVs in the case of KTT application. The percent reduction for the within-condition CVs values is maximal when IWFEs are performed while listening to an audio stimulus such as clicks (10.33%, for Cl). Impressively, a percent reduction for within-condition CVs values in KTT is visible in all other conditions (5.47%, for Mu; 4.03%, for Cl2; 5.96%, for Mu2; and 3.50%, for Fr; see **Figure 3G**).

THE PROCESSES FOR TEMPORAL REGULATION

To explore whether, and to what extent, the processes for temporal regulation are influenced by the application of KTT, the mean w$\gamma(1)$ values and the percentages of positive w$\gamma(1)$ of IWFEs computed in N/KTT and KTT cases are compared. We plot the mean w$\gamma(1)$ values and the percentages of positive w$\gamma(1)$ as function of ranges of movement durations of IWFEs. As an exemplar comparison, we here describe and analyze the Cl and Cl2 conditions since we already showed them to be the most subjective to the application of KTT.

The mean w$\gamma(1)$ values of IWFEs ranked per within-ranges of movement durations are displayed in **Figure 4** for the N/KTT and KTT cases of the Cl and Cl2 conditions. In all cases mean w$\gamma(1)$ values appear to change with movement durations. In the N/KTT case of the Cl condition (**Figure 4A**) mean w$\gamma(1)$ values are almost all negative with only one exception in range 5 (for this and the following references to ranges of movement durations see **Table 1**) whereas in the KTT case of the Cl condition (**Figure 4A**) mean w$\gamma(1)$ values are negative for only the half of eight ranges of movement durations. The highest peaks of mean w$\gamma(1)$ values are expressed within the moderato, allegro and presto tempi in the last four ranges of interval durations (Cl of N/KTT) and in the last five ranges of movement durations (Cl of KTT).

In the N/KTT case of the Cl2 condition (**Figure 4B**) mean w$\gamma(1)$ values are all negative with only one exception in range 6 whereas in the KTT case of the Cl2 condition (**Figure 4B**) mean w$\gamma(1)$ values are positive for more than half of ranges of movement durations. The highest peaks of mean w$\gamma(1)$ values for the Cl2 condition are expressed within the moderato, allegro and presto tempi in the last five ranges of movement durations in both N/KTT and KTT cases.

The percentages of positive and negative w$\gamma(1)$ values ranked per within-ranges of movement durations are displayed in **Figure 5** as radar charts for the N/KTT and KTT cases of the Cl and Cl2 conditions. Here also, it appears evident that the percentage of positive w$\gamma(1)$ values is sensitive to movement durations.

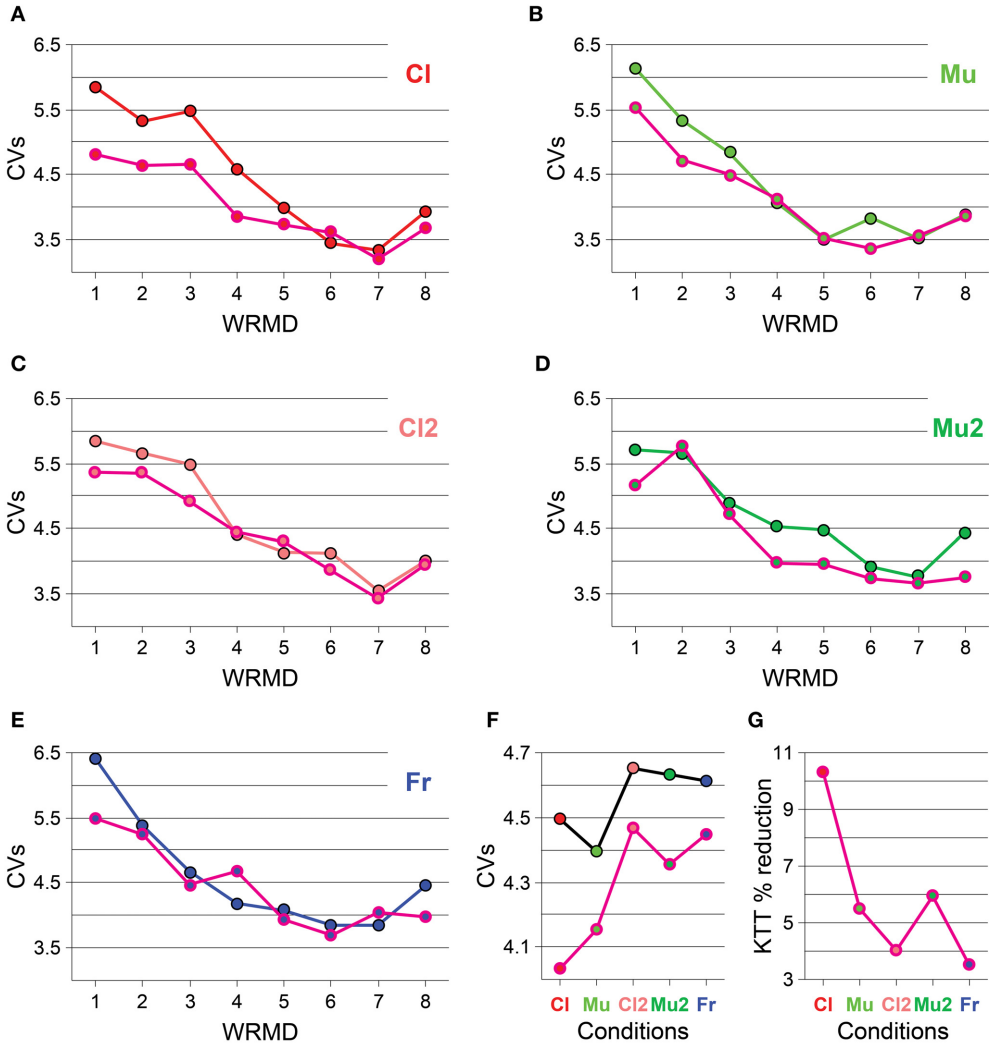

FIGURE 3 | (A–E) For each condition the CVs of IWFEs durations, ranked per within-ranges of durations, are illustrated. **(F)** The five within-condition CVs of IWFEs durations are compared for N/KTT and KTT. **(G)** The percent reduction of the within-condition CVs values when KTT is applied. The reduction is more than 3% in all conditions; the most evident reduction, more than 10%, is for the Cl condition. Values are plotted as black (N/KTT) and pink (KTT) outlined circles, filled-in color-coded per condition. Color-coded connecting lines are shown to ease reading. CVs = within-range or, in **(F)**, within-condition CVs values. WRMD, within-ranges movements durations.

The values of $w\gamma(1)$ of IWFEs in the Cl condition are mostly negative for the N/KTT case (75.27% of negative values and 24.73% of positive values). In the KTT case, although the amount of positive values increases, negative $w\gamma(1)$ values continue to outnumber positive ones (61.43% of negative values and 38.57% of positive values). In the N/KTT case of the Cl condition (**Figure 5A**), percentages of positive $w\gamma(1)$ values are extremely low in the first four ranges of movement durations. The highest peaks for percentages of positive $w\gamma(1)$ are evident in the last four ranges of movement durations. The highest peaks for percentages of positive $w\gamma(1)$ values are always less than 50%, with only one exception (range 6, 53.23%). In the KTT case of the Cl condition (**Figure 5C**), percentages of positive $w\gamma(1)$ values are extremely low only in the first two ranges of movement durations. However, the percentages of positive $w\gamma(1)$ values in the two successive ranges (3 and 4) increase from the 2.19 and 12.38% in the N/KTT case to the 34.38 and 49.93% in the KTT case, respectively. Also, in the last four ranges of movement durations of KTT case, the percentages of positive $w\gamma(1)$ values are similar to those in N/KTT case.

The values of $w\gamma(1)$ of IWFEs in the Cl2 condition are somewhat negative for the N/KTT case (61.09% of negative values and 38.91% of positive values) while in the KTT case negative $w\gamma(1)$ values slightly outnumber positive ones (54.74% of negative values and 45.26% of positive values). In the N/KTT case of the Cl2 condition (**Figure 5B**), percentages of positive $w\gamma(1)$ reach lowest values in the first and third ranges of movement durations. In the KTT case of the Cl2 condition (**Figure 5D**), percentages of positive $w\gamma(1)$ reach extremely low values only in the first three ranges of movement durations. The highest peaks for percentages

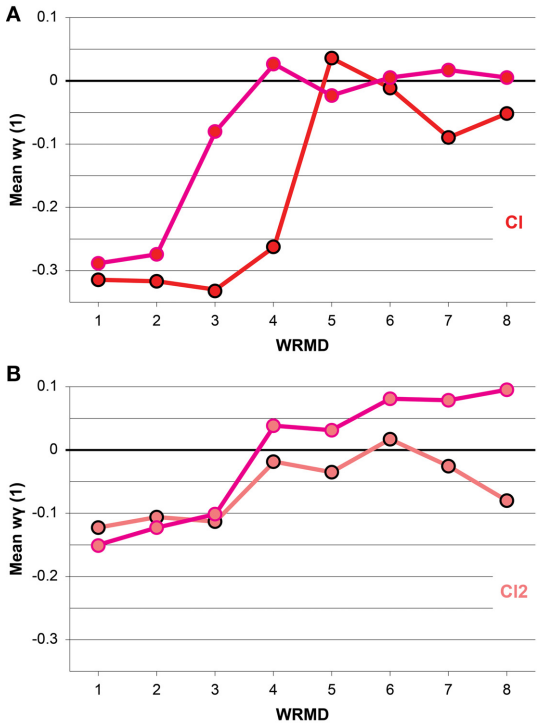

FIGURE 4 | (A,B) Mean windowed wγ(1) values, ranked per within-ranges of durations, are illustrated. The conditions Cl and Cl2 are compared for N/KTT and KTT. Note that mean wγ(1) values appear to change with movement durations and are, for both Cl and Cl2 conditions, biased toward more positive values when KTT is applied. Values are plotted as black (N/KTT) and pink (KTT) outlined circles, filled-in color-coded per condition. WRMD, within-ranges movements durations.

of positive wγ(1) values are in the five last ranges of movement durations both in the N/KTT and KTT case. It is also well perceivable that while in the N/KTT case only one of the within-range percentage of positive wγ(1) values is above the 50%, in the KTT case five of the eight within-range percentages of positive wγ(1) values are above the 50%.

In **Figures 5E,F** the percentages of positive wγ(1) values of N/KTT vs. KTT cases are compared separately for the Cl and the Cl2 conditions. As illustrated, the area generated by eight ranges percentages of positive wγ(1) values is wider in the KTT than in the N/KTT case, both for the Cl and the Cl2 conditions. For the Cl condition, the differential percent of positive wγ(1) values is of 13.84% (calculated as difference between the percentages of positive wγ(1) of 38.57% in KTT case and that of 24.73% in N/KTT case). This differential percent is equivalent to an increase of 55.96% of positive wγ(1) values in the KTT case (**Figure 5G**). Similarly, for the Cl2 condition, the differential percent of positive wγ(1) values is of 6.34% (calculated as difference between the percentages of positive wγ(1) of 45.26% in the KTT case and that of 38.91% in the N/KTT case). In the Cl2 condition, the differential percent is equivalent to an increase of 16.30% of positive wγ(1) values in the KTT case.

Finally, random effect ANOVA model for repeated measurements is performed for the wγ(1) values in Cl and Cl2 conditions, respectively. The model for Cl reveals a highly significant effect for the presence of KTT [$F_{(1,\ 98)} = 15.126, p < 0.001$] and tempo [$F_{(1,\ 98)} = 59.62,\ p < 0.001$]. The interaction between the presence of KTT and tempo shows also a significant effect [$F_{(1,\ 98)} = 5.05,\ p < 0.05$]. The model for Cl2 fails to reveal a significant effect of presence of KTT, [$F_{(1,\ 101)} = 0.34,\ p > 0.05$] and tempo, [$F_{(1,\ 101)} = 3.69,\ p > 0.05$]. Conversely, the interaction between the presence of KTT and tempo shows a significant effect [$F_{(1,\ 101)} = 5.05,\ p < 0.05$]. It should be remembered here that in the Cl2 condition mean within-range wγ(1) values become more positive in KTT than in N/KTT only for fast tempi (see **Figure 4B**).

DISCUSSION

In this study, we examined whether the application of KTT on skin is able to reduce the timing variability of repetitive rhythmic movements in healthy subjects.

Overall, our results indicate that the temporal variability of IWFEs is influenced by the application of KTT. Using a task of auditory-motor integration recently developed in our laboratory (see Bravi et al., 2014) we demonstrate that the timing variability is reduced in the KTT case, independently of the type of sensorimotor integration required from the participant to accomplish the motor performance (i.e., without audio information, with paced audio in the form of clicks or music, and in the recall conditions). Quantitatively, the reduction in the timing variability is different for the different conditions, and is greatest for the Cl and smallest for the Fr conditions. However, even though the reduction in timing variability for the Fr condition is quantitatively smaller than those estimated for the other conditions, the residual variance for KTT case is about 3% less than the variance of N/KTT case, which is of great importance. In fact, the residual variance evaluates the variability in the IWFEs durations when subjects are following their own tempo, which is mostly linked to the physical performance of the movement, without the effort of following or recalling a tempo proposed by others. Also, our analysis of the CVs of IWFEs show that, in general, when IWFEs are performed in presence of KTT the within-condition CVs values are smaller than those obtained in the N/KTT case. Here, again, the reduction in the CVs value is maximal when IWFEs are performed while listening to an audio stimulus such as clicks and minimal when performed in the Fr condition.

Our first experimental hypothesis is that KTT brings about an improvement of wrist joint proprioception due to augmented afferent input via the stimulation of cutaneous mechanoreceptors. This effect would, in turn, augment the coordination of the wrist joint during the rhythmic motor performance and consequently contribute to the reduction in timing variability of the IWFEs. The type of KTT application that we used allowed us to speculate about this possible effect provided by KTT: indeed, since the elastic band, placed between the lateral epicondyle of the humerus and the phalanges, is applied with the wrist positioned in maximum flexion, it cannot provide a facilitation of the ascent phase of the movement by means of elastic return to the starting position. This consents us to discard the possibility that the reduction of timing variability in the KTT condition is due to the dampening of gravity, but leads us toward an explanation

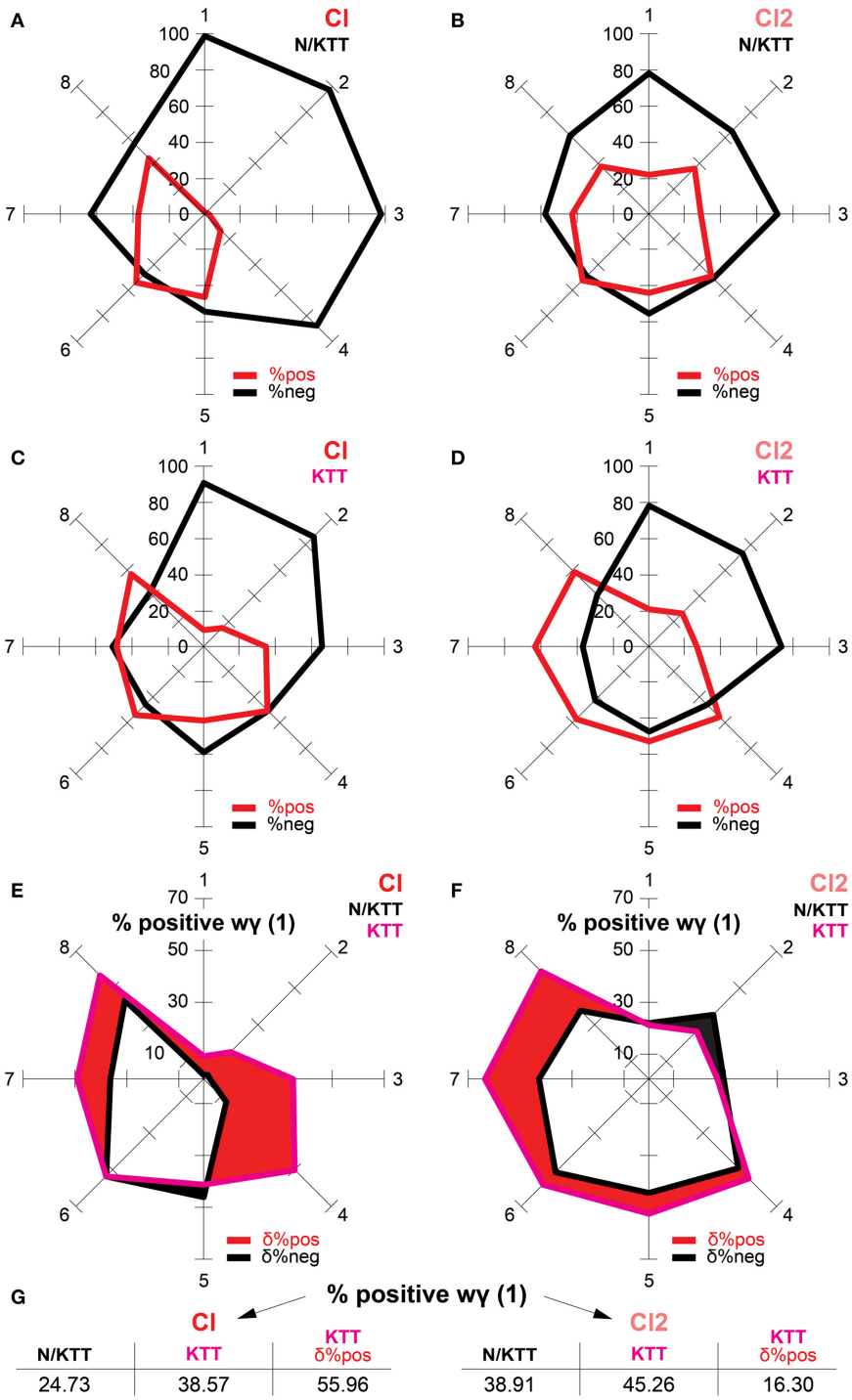

FIGURE 5 | (A–D) On the radar charts are illustrated, for the N/KTT and KTT cases of CI and CI2 conditions, the percentages of positive and negative wγ(1) values ranked per within-ranges of durations. Note that the areas generated by the eight within-range percentages of positive wγ(1) values are wider in the KTT than in N/KTT cases for both CI and CI2 conditions. **(E,F)** The percentages of N/KTT vs. KTT positive wγ(1) values are compared for the CI and the CI2 conditions, respectively. The red area indicates for each of the eight within-ranges of durations the differential percent of positive wγ(1) values. This area is wider in the KTT than in the N/KTT case, both for the CI and the CI2 conditions. Compound shapes are obtained by combination of areas of positive wγ(1) values in the N/KTT and KTT cases for both the CI and CI2 conditions. The overlapping area was excluded, turning the filled region into a hole. **(G)** The increase of positive wγ(1) values in the KTT case is comprehensively indicated as differential percent equivalent both for the CI and CI2 conditions (see text for more explanations). %pos (red) = percentages of positive wγ(1) values. %neg (black) = percentages of negative wγ(1) values. δ%pos (red) = differential percent equivalent for percentages of positive wγ(1) values. δ%neg (black) = differential percent equivalent for percentages of negative wγ(1) values.

that KTT might enhance proprioceptive information provided by activating cutaneous receptors.

Proprioception consists of a combination of joint position sense, i.e., the ability to sense the position and movement of a limb in space (Aydin et al., 2001), and the sense of muscular effort and tension (Proske and Gandevia, 2009). The joint position sense is a very important contributor to joint coordination, maintenance of muscle stiffness, and to the production of natural movements for appropriate task performance (Han and Lee, 2014). It was demonstrated that the principal muscle receptor in joint position sense is the muscle spindle; however, also cutaneous receptors have become recognized as playing an important role (Proske and Gandevia, 2009). The cutaneous receptors, subserving a sense of position and movement, respond to the stretching of skin (Proske and Gandevia, 2009). As proposed by Grigg (1994), it is plausible that the application of KTT induces, during the joint movement, a pressure and a stretching/deformation of the skin, thus activating cutaneous mechanoreceptors. Therefore, the mechanical effects of KTT applied to skin, augmenting skin receptor output, might enhance kinesthetic and joint position sense (Simoneau et al., 1997; Halseth et al., 2004).

Zelaznik and Rosenbaum (2010) performed an analysis in which timing precision was measured at different locations during both the performance of tapping and circle drawing tasks. Evidences showed that the highest values of CVs during the performance of the tapping task were at a location opposite to the specified timing location, that is, the maximum of the extension point. Earlier, Semjen and Garcia-Colera (1986) also noted that, in a tapping motor performance, timing variability showed smallest values at the instructed timing location. Hence, in tapping tasks the subject is timed to a location and the timing variability is best controlled at the corresponding event (e.g., the contact with the tap key); in circle drawing the subject is not timed to a place (i.e., is not required to rely on a target location or event) but is controlling evenly the entire movement trajectory (Spencer and Zelaznik, 2003). Our experimental design is not based on a tapping task, although the IWFEs, having clear turning points that provide salient sensory information (Elliott et al., 2009), are fairly similar. The KTT seemingly relieves, at least in part, from the need of a target or an event inherent with the kinematics of IWFEs. This is particularly evident in the Cl (see **Figure 3**) but also in the Mu audio conditions in which movements are performed with additional sensory cues. The extra proprioceptive information provided by KTT, augmenting the stability of wrist joint during the performance, could very well account for the reduction in IWFEs temporal variability that we observed as being more pronounced in our cued conditions.

In addition, we explore the possible influences of our KTT on the neural processes governing the temporal regulation for production of rhythmic movements. The mean $w\gamma(1)$ values and the percentages of positive $w\gamma(1)$ of IWFEs, calculated in N/KTT and KTT cases, and compared for the exemplar Cl and Cl2 conditions, show that the processes for temporal regulation can be influenced by the application of KTT. We demonstrate that the mean $w\gamma(1)$ and percentages of positive $w\gamma(1)$ are in fact biased toward values congruent with the emergent mode for control of timing.

Overall, these results have important implications for the event-emergent timing distinction. Heretofore, it was suggested that a task is controlled via event timing or via emergent timing depending on the kinematic of the performed movement (Zelaznik and Rosenbaum, 2010). Huys et al. (2008) using a rhythmic motor task, such as tapping, have demonstrated that discrete and continuous movements are two classes of movements topologically distinct. Indeed, it was shown that when finger flexion-extensions are performed as slow and discrete movements, the engagement of an explicit timing (event-based) process is required; whereas when the tapping is performed as rapid and smooth movements, the employment of a self-organized limit-cycle (emergent) process is necessary. The clarity with which such events are delineated in a particular experimental situation is considered to be the factor determining the weight of the event-based timing component. The continuity of the movement largely determines the strength of emergent timing component (Repp and Steinman, 2010). In addition, in a timing study on air finger tapping, participants performed discrete movements, being instructed to pause before each flexion cycle, and continuous movements, being instructed to move as smoothly as possible without pausing (Spencer et al., 2007). Despite the subtle difference between these discrete and continuous movements, activation in the cerebellum was greater when participants were instructed to perform discrete movements, suggesting that the engagement of the cerebellum may depend on how movements are produced or, even better, on how they are represented (Spencer et al., 2007).

Our experimental hypothesis is that the application of KTT, by stabilization of the motor effector during the performance, causes the IWFEs to be less discrete and thus more continuous. According to the dichotomic view of the event-based vs. emergent modes of temporal control (Delignières and Torre, 2011), KTT could promote the involvement of emergent timing control and, consequently, reduce the contribution of event-based timing. As a consequence, the control for timing would no longer need to refer to a nervous structure such as, for example, the cerebellum, in the building of an abstract representation of the time intervals to produce. Rather, the dynamics of the system could be sufficient *per se* to keep the movement cycle constant.

We demonstrate a reduction in timing variability with KTT, as seen by the CVs values and their dispersion, being very often smaller in the KTT than in the N/KTT cases (see **Figures 2**, **3**). Such reduction seemingly suggests a transition toward an emergent timing control. This emergence of the emergent timing strategy (see **Figures 4**, **5E–G**) appears to be by virtue of the KTT's to render movements less audio sensitive or dependent (compare, in **Figures 5A–C** vs. **B–D**). This mechanism ultimately results in a reduced variability and thus, in a better—more homogenous—performance. The same concept is analogous to a computer that allocates memory for a better performance; so do the cortical and subcortical circuits, which are usually required to bear the load of motor control and of other cognitive activities. Being less dependent on external/discrete events, central structures are partially relieved from timing control, thus freeing resources and allowing for a net augmentation of the central efficiency for motor control and cognition.

In conclusion, KTT was used in this study as a tool to possibly augment the precision of rhythmic movements. Our results show that KTT does, in fact, reduce the timing variability of rhythmic movements performed with no direct surface opposition and minimizing visual information. In particular, our results suggest that KTT—on the one hand by providing extra proprioceptive information, and on the other hand by relieving, at least partially, the central structures from time control—allows for a net augmentation of the central efficiency for motor control.

AUTHOR CONTRIBUTIONS

Riccardo Bravi: Substantial contributions to the conception of the work, the data acquisition, analysis, and the interpretation of data; Substantial contribution in drafting the work and revising it critically for important intellectual content; final approval of the version to be published; agreement to be accountable for accuracy and integrity of any part of the work. Eros Quarta: Substantial contributions to the design of the work and data acquisition; Substantial contribution in drafting the work; final approval of the version to be published; agreement to be accountable for accuracy and integrity of any part of the work. Erez J. Cohen: Substantial contributions to the design and the data acquisition of the work; Substantial contribution in drafting the work; final approval of the version to be published; agreement to be accountable for accuracy and integrity of any part of the work. Anna Gottard: Substantial contributions to the analysis and interpretation of data for the work; Substantial contribution in drafting the work; final approval of the version to be published; agreement to be accountable for accuracy and integrity of any part of the work. Diego Minciacchi: Substantial contributions to the conception of the work, analysis, and interpretation of data for the work; Substantial contribution in revising the work critically for important intellectual content; final approval of the version to be published; agreement to be accountable for accuracy and integrity of any part of the work.

ACKNOWLEDGMENTS

We are grateful for the seminal contribution of Dr. Giacomo Margiacchi, for the valuable contribution of Dr. Claudia del Tongo and Dr. Stefano Marletta during the setup of the experimental design and to the first experiments. We are also indebted with Mr. Filippo Cocchetti who kindly helped for the realization of the methodological Figure.

REFERENCES

Arias, P., and Cudeiro, J. (2008). Effects of rhythmic sensory stimulation (auditory, visual) on gait in Parkinson's disease patients. *Exp. Brain Res.* 186, 589–601. doi: 10.1007/s00221-007-1263-y

Aydin, T., Yildiz, Y., Yanmis, I., Yildiz, C., and Kalyon, T. A. (2001). Shoulder proprioception: a comparison between the shoulder joint in healthy and surgically repaired shoulders. *Arch. Orthop. Trauma Surg.* 121, 422–425. doi: 10.1007/s004020000245

Bove, M., Tacchino, A., Pelosin, E., Moisello, C., Abbruzzese, G., and Ghilardi, M. F. (2009). Spontaneous movement tempo is influenced by observation of rhythmical actions. *Brain Res. Bull.* 80, 122–127. doi: 10.1016/j.brainresbull.2009.04.008

Bravi, R., Del Tongo, C., Cohen, E. J., Dalle Mura, G., Tognetti, A., and Minciacchi, D. (2014). Modulation of isochronous movements in a flexible environment: links between motion and auditory experience. *Exp. Brain Res.* 232, 1663–1675. doi: 10.1007/s00221-014-3845-9

Callaghan, M. J., Selfe, J., Bagley, P. J., and Oldham, J. A. (2002). The effects of patellar taping on knee joint proprioception. *J. Athl. Train.* 37, 19–24. doi: 10.1016/S0031-9406(05)61377-6

Dannenberg, R. B., and Mohan, S. (2011). *Characterizing Tempo Change in Musical Performances*. Ann Arbor, MI: ICMC Proc.

de Dreu, M. J., van der Wilk, A. S. D., Poppe, E., Kwakkel, G., and van Wegen, E. E. H. (2012). Rehabilitation, exercise therapy and music in patients with Parkinson's disease: a meta-analysis of the effects of music-based movement therapy on walking ability, balance and quality of life. *Parkinsonism Relat. Disord.* 18(Suppl. 1), S114–S119. doi: 10.1016/S1353-8020(11)70036-0

Delignières, D., Lemoine, L., and Torre, K. (2004). Time intervals production in tapping and oscillatory motion. *Hum. Mov. Sci.* 23, 87–103. doi: 10.1016/j.humov.2004.07.001

Delignières, D., and Torre, K. (2011). Event-based and emergent timing: dichotomy or continuum? A reply to Repp and Steinman (2010). *J. Mot. Behav.* 43, 311–318. doi: 10.1080/00222895.2011.588274

del Olmo, M. F., Arias, P., Furio, M. C., Pozo, M. A., and Cudeiro, J. (2006). Evaluation of the effect of training using auditory stimulation on rhythmic movement in Parkinsonian patients–a combined motor and [18F]-FDG PET study. *Parkinsonism Relat. Disord.* 12, 155–164. doi: 10.1016/j.parkreldis.2005.11.002

del Olmo, M. F., and Cudeiro, J. (2005). Temporal variability of gait in Parkinson disease: effects of a rehabilitation programme based on rhythmic sound cues. *Parkinsonism Relat. Disord.* 11, 25–33. doi: 10.1016/j.parkreldis.2004.09.002

Diggle, P., Heagerty, P., Liang, K. Y., and Zeger, S. (2002). *Analysis of Longitudinal Data*. New York, NY: Oxford University Press.

Elliott, M. T., Welchman, A. E., and Wing, A. M. (2009). Being discrete helps keep to the beat. *Exp. Brain Res.* 192, 731–737. doi: 10.1007/s00221-008-1646-8

Ellis, M. (1991). Thresholds for detecting tempo change. *Psychol. Music* 19, 164–169. doi: 10.1177/0305735691192007

Freyer, F., Reinacher, M., Nolte, G., Dinse, H. R., and Ritter, P. (2012). Repetitive tactile stimulation changes resting-state functional connectivity-implications for treatment of sensorimotor decline. *Front. Hum. Neurosci.* 6:144. doi: 10.3389/fnhum.2012.00144

Grigg, P. (1994). Peripheral neural mechanisms in proprioception. *J. Sport Rehabil.* 3, 2–17.

Halseth, T., McChesney, J. W., Debeliso, M., Vaughn, R., and Lien, J. (2004). The effects of kinesio™ taping on proprioception at the ankle. *J. Sports Sci. Med.* 3, 1–7.

Han, J. T., and Lee, J. H. (2014). Effects of kinesiology taping on repositioning error of the knee joint after quadriceps muscle fatigue. *J. Phys. Ther. Sci.* 26, 921–923. doi: 10.1589/jpts.26.921

Hausdorff, J. M., Lowenthal, J., Herman, T., Gruendlinger, L., Peretz, C., and Giladi, N. (2007). Rhythmic auditory stimulation modulates gait variability in Parkinson's disease. *Eur. J. Neurosci.* 26, 2369–2375. doi: 10.1111/j.1460-9568.2007.05810.x

Huys, R., Studenka, B. E., Rheaume, N. R., Zelaznik, H. N., and Jirsa, V. K. (2008). Distinct timing mechanisms produce discrete and continuous movements. *PLoS Comput. Biol.* 4:e1000061. doi: 10.1371/journal.pcbi.1000061

Ivry, R. B., and Spencer, R. (2004). The neural representation of time. *Curr. Opin. Neurobiol.* 14, 225–232. doi: 10.1016/j.conb.2004.03.013

Kase, K., Wallis, J., and Kase, T. (2013). *Clinical Therapeutic Applications of the Kinesio Taping Method*, 3rd Edn. New Mexico: Kinesio Taping Ass.

Keele, S. W., and Ivry, R. (1990). Does the cerebellum provide a common computation for diverse tasks? A timing hypothesis. *Ann. N.Y. Acad. Sci.* 608, 179–207. doi: 10.1111/j.1749-6632.1990.tb48897.x

Kelso, J. A. S. (1995). *Dynamic Patterns*. Cambridge, MA: MIT Press.

Kneeshaw, D. (2002). Shoulder taping in the clinical setting. *J. Body Mov. Ther.* 6, 2–8. doi: 10.1054/jbmt.2001.0233

Kugler, P. N., Kelso, J. A. S., and Turvey, M. T. (1980). "On the concept of coordinative structures as dissipative structures I. Theoretical lines of convergence" in *Tutorials in Motor Behavior*, eds G. E. Stelmach and J. Requin (Amsterdam: North Holland), 3–47.

Leiner, H. C., Leiner, A. L., and Dow, R. S. (1993). Cognitive and language functions of the human cerebellum. *Trends Neurosci.* 16, 444–447. doi: 10.1016/0166-2236(93)90072-T

Levitin, D. J., and Cook, P. R. (1996). Memory for musical tempo: additional evidence that auditory memory is absolute. *Percept. Psychophys.* 58, 927–935. doi: 10.3758/BF03205494

Levy, M. (2011). "Improving perceptual tempo estimation with crowd-sourced annotations," in *12th International Society for Music Information Retrieval Conference (ISMIR 2011)* (Miami, FL), 317–322.

Madison, G., and Paulin, J. (2010). Ratings of speed in real music as a function of both original and manipulated beat tempo. *J. Acoust. Soc. Am.* 128, 3032–3040. doi: 10.1121/1.3493462

McIntosh, G. C., Brown, S. H., Rice, R. R., and Thaut, M. H. (1997). Rhythmic auditory-motor facilitation of gait patterns in patients with Parkinson's disease. *J. Neurol. Neurosurg. Psychiatry* 62, 22–26. doi: 10.1136/jnnp.62.1.22

McKinney, M. F., and Moelants, D. (2007). Ambiguity in tempo perception: what draws listeners to different metric levels? *Music Percept.* 24, 155–165. doi: 10.1525/mp.2006.24.2.155

McKinney, M. F., Moelants, D., Davies, E. P., and Klapuri, A. (2007). Evaluation of audio beat tracking and music tempo extraction algorithms. *J. New Music Res.* 36, 1–16. doi: 10.1080/09298210701653252

Morris, D., Jones, D., Ryan, H., and Ryan, C. G. (2013). The clinical effects of Kinesio® Tex taping: a systematic review. *Physiother. Theory Pract.* 29, 259–270. doi: 10.3109/09593985.2012.731675

Muthén, B. O. (1989). Latent variable modeling in heterogeneous populations. *Psychometrika* 54, 557–585. doi: 10.1007/BF02296397

Nolte, G., Bai, O., Wheaton, L., Mari, Z., Vorbach, S., and Hallett, M. (2004). Identifying true brain interaction from EEG data using the imaginary part of coherency. *Clin. Neurophysiol.* 115, 2292–2307. doi: 10.1016/j.clinph.2004.04.029

Pinheiro, J. C., and Bates, D. M. (2000). *Mixed Effects Models in S and S-PLUS*. New York, NY: Springer-Verlag.

Proske, U., and Gandevia, S. C. (2009). The kinaesthetic senses. *J. Physiol. (Lond.)* 587, 4139–4146. doi: 10.1113/jphysiol.2009.175372

Quinn, S., and Watt, R. (2006). The perception of tempo in music. *Perception* 35, 267–280. doi: 10.1068/p5353

Rao, S. M., Mayer, A. R., and Harrington, D. L. (2001). The evolution of brain activation during temporal processing. *Nat. Neurosci.* 4, 317–323. doi: 10.1038/85191

Repp, B. H. (1999a). Detecting deviations from metronomic timing in music: effects of perceptual structure on mental timekeeper. *Percept. Psychophys.* 61, 529–548. doi: 10.3758/BF03211971

Repp, B. H. (1999b). Control of expressive and metronomic timing in pianists. *J. Motor Behav.* 31, 145–164. doi: 10.1080/00222899909600985

Repp, B. H. (2005). Sensorimotor synchronization: a review of the tapping literature. *Psychon. Bull. Rev.* 12, 969–992. doi: 10.3758/BF03206433

Repp, B. H. (2011). Temporal evolution of the phase correction response in synchronization of taps with perturbed two-interval rhythms. *Exp. Brain Res.* 208, 89–101. doi: 10.1007/s00221-010-2462-5

Repp, B. H., and Steinman, S. R. (2010). Simultaneous event-based and emergent timing: synchronization, continuation, and phase correction. *J. Mot. Behav.* 42, 111–126. doi: 10.1080/00222890903566418

Riemann, B., and Lephart, S. (2002). The sensorimotor system, Part II: the role of proprioception in motor control and functional joint stability. *J. Athl. Train.* 37, 80–84.

Robertson, S. D., Zelaznik, H. N., Lantero, D. A., Bojczyk, K. G., Spencer, R. M., Doffin, J. G., et al. (1999). Correlations for timing consistency among tapping and drawing tasks: evidence against a single timing process for motor control. *J. Exp. Psychol. Hum. Percept. Perform.* 25, 1316–1330. doi: 10.1037/0096-1523.25.5.1316

Saijo, N., and Gomi, H. (2010). Multiple motor learning strategies in visuomotor rotation. *PLoS ONE* 5:e9399. doi: 10.1371/journal.pone.0009399

Schlerf, J. E., Spencer, R. M., Zelaznik, H. N., and Ivry, R. B. (2007). Timing of rhythmic movements in patients with cerebellar degeneration. *Cerebellum* 6, 221–231. doi: 10.1080/14734220701370643

Schoner, G. (2002). Timing, clocks, and dynamical systems. *Brain Cogn.* 48, 31–51. doi: 10.1006/brcg.2001.1302

Semjen, A., and Garcia-Colera, A. (1986). Planning and timing of finger- tapping sequences with a stressed element. *J. Mot. Behav.* 18, 287–322. doi: 10.1080/00222895.1986.10735383

Semjen, A., Schulze, H. H., and Vorberg, D. (2000). Timing precision in continuation and synchronization tapping. *Psychol. Res.* 63, 137–147. doi: 10.1007/PL00008172

Simoneau, G. G., Degner, R. M., Kramper, C. A., and Kittleson, K. H. (1997). Changes in ankle joint proprioception resulting from strips of athletic tape applied over the skin. *J. Athl. Train.* 32, 141–147.

Spencer, R. M. C., and Ivry, R. B. (2005). Comparison of patients with Parkinson's disease or cerebellar lesions in the production of periodic movements involving event-based or emergent timing. *Brain Cogn.* 58, 84–93. doi: 10.1016/j.bandc.2004.09.010

Spencer, R. M. C., Verstynen, T., Brett, M., and Ivry, R. (2007). Cerebellar activation during discrete and not continuous timed movements: an fMRI study. *Neuroimage* 36, 378–387. doi: 10.1016/j.neuroimage.2007.03.009

Spencer, R. M. C., and Zelaznik, H. N. (2003). Weber (slope) analyses of timing variability in tapping and drawing tasks. *J. Mot. Behav.* 35, 371–382. doi: 10.1080/00222890309603157

Spencer, R. M. C., Zelaznik, H. N., Diedrichsen, J., and Ivry, R. B. (2003). Disrupted timing of discontinuous but not continuous movements by cerebellar lesions. *Science* 300, 1437–1439. doi: 10.1126/science.1083661

Studenka, B. E., and Zelaznik, H. N. (2008). The influence of dominant versus nondominant hand on event and emergent motor timing. *Hum. Mov. Sci.* 27, 29–52. doi: 10.1016/j.humov.2007.08.004

Teki, S., Grube, M., and Griffiths, T. D. (2012). A unified model of time perception accounts for duration-based and beat-based timing mechanisms. *Front. Integr. Neurosci.* 5:90. doi: 10.3389/fnint.2011.00090

Thaut, M. H., McIntosh, G. C., Rice, R. R., Miller, R. A., Rathbun, J., and Brault, J. M. (1996). Rhythmic auditory stimulation in gait training for Parkinson's disease patients. *Mov. Disord.* 11, 193–200. doi: 10.1002/mds.870110213

Turvey, M. T. (1977). "Preliminaries to a theory of action with reference to vision," in *Perceiving, Acting and Knowing: Toward an Ecological Psychology*, eds R. Shaw and J. Bransford (Hillsdale, NJ: Erlbaum), 211–265.

Wing, A. M., and Kristofferson, A. B. (1973a). The timing of interresponse intervals. *Percept. Psychophys.* 13, 455–460. doi: 10.3758/BF03205802

Wing, A. M., and Kristofferson, A. B. (1973b). Response delays and timing of discrete motor responses. *Percept. Psychophys.* 14, 5–12. doi: 10.3758/BF03198607

Wittwer, J. E., Webster, K. E., and Hill, K. (2013). Music and metronome cues produce different effects on gait spatiotemporal measures but not gait variability in healthy older adults. *Gait Posture* 37, 219–222. doi: 10.1016/j.gaitpost.2012.07.006

Xu, D., Liu, T., Ashe, J., and Bushara, K. O. (2006). Role of the olivo-cerebellar system in timing. *J. Neurosci.* 26, 5990–5995. doi: 10.1523/JNEUROSCI.0038-06.2006

Zatorre, R. J., and Halpern, A. R. (2005). Mental concerts: musical imagery and auditory cortex. *Neuron* 47, 9–12. doi: 10.1016/j.neuron.2005.06.013

Zelaznik, H. N., and Rosenbaum, D. A. (2010). Timing processes are correlated when tasks share a salient event. *J. Exp. Psychol. Hum. Percept. Perform.* 36, 1565–1575. doi: 10.1037/a0020380

Zelaznik, H. N., Spencer, R. M. C., and Ivry, R. B. (2002). Dissociation of explicit and implicit timing in repetitive tapping and drawing movements. *J. Exp. Psychol. Hum. Percept. Perform.* 28, 575–588. doi: 10.1037/0096-1523.28.3.575

Conflict of Interest Statement: The authors declare that the research was conducted in the absence of any commercial or financial relationships that could be construed as a potential conflict of interest.

Received: 30 June 2014; accepted: 08 September 2014; published online: 25 September 2014.

Citation: Bravi R, Quarta E, Cohen EJ, Gottard A and Minciacchi D (2014) A little elastic for a better performance: kinesiotaping of the motor effector modulates neural mechanisms for rhythmic movements. Front. Syst. Neurosci. ***8****:181. doi: 10.3389/fnsys.2014.00181*

This article was submitted to the journal Frontiers in Systems Neuroscience.

frontiers in
SYSTEMS NEUROSCIENCE

ORIGINAL RESEARCH ARTICLE
published: 09 January 2015
doi: 10.3389/fnsys.2014.00247

Control of humanoid robot via motion-onset visual evoked potentials

***Wei Li*[1,2]*, Mengfan Li[2] and Jing Zhao[2]**

[1] *Department of Computer and Electrical Engineering and Computer Science, California State University, Bakersfield, CA, USA*
[2] *School of Electrical Engineering and Automation, Tianjin University, Tianjin, China*

Edited by:
Mikhail Lebedev, Duke University, USA

Reviewed by:
Ana-Maria Cebolla, Université Libre de Bruxelles, Belgium
Emmanuele Tidoni, Fondazione Santa Lucia, Italy
Arzu Güneysu, Bogaziçi University, Turkey

***Correspondence:**
Wei Li, Department of Computer and Electrical Engineering and Computer Science, California State University, 9001 Stockdale Highway, Bakersfield, CA 93311, USA
e-mail: wli@csub.edu

This paper investigates controlling humanoid robot behavior via motion-onset specific N200 potentials. In this study, N200 potentials are induced by moving a blue bar through robot images intuitively representing robot behaviors to be controlled with mind. We present the individual impact of each subject on N200 potentials and discuss how to deal with individuality to obtain a high accuracy. The study results document the off-line average accuracy of 93% for hitting targets across over five subjects, so we use this major component of the motion-onset visual evoked potential (mVEP) to code people's mental activities and to perform two types of on-line operation tasks: navigating a humanoid robot in an office environment with an obstacle and picking-up an object. We discuss the factors that affect the on-line control success rate and the total time for completing an on-line operation task.

Keywords: brain robot interaction, mind-controlled humanoid robot, N200 potentials, humanoid robot behavior, visual feedback

INTRODUCTION

Event related potentials (ERPs) are able to set up a communication between external stimuli and people's cognitive tasks. Assigning specific meanings to visual stimuli allows to "read" people's mind by identifying a target stimulus related with their attention (Lebedev and Nicolelis, 2006). A P300 model based on visual attention mechanism (Jin et al., 2012) is commonly used in the ERP-based brain-computer-interfaces (BCIs). When we evaluated the P300 model on Cerebot—a mind-controlled humanoid robot (Li et al., 2011, 2012), we noted some issues of this model (Li et al., 2013a,b). First, this model needs to flash a visual stimulus by growing its visual contrast, which easily causes people's visual fatigue (Hong et al., 2009). Second, the P300 potential is correlated with both the people's attention allocation (Farwell and Donchin, 1988) and the biological determinants of cognitive operation (Polich and Kok, 1995), so the people's states and experimental environments significantly affect the P300 signal quality. Considering the problems above, we investigate a N200 potential-based robot brain interaction (BRI) model.

The stimulus appearing in moving a bar through images instead of flashing the images (Heinrich, 2007) induces a N200 potential with a negative deflection occurring at 180–325 ms post-stimulus (Patel and Azzam, 2005). The N200 potential is an involuntary component that less depends on people's attention, and even people's fixation can induce this kind of potential (Frensel and Neubert, 2010). N200 potentials may promise a useful BCI model for controlling external devices due to the interface's low requirements of luminance and contrast, the large amplitude of the induced brain signal, and the low individual difference of mVEP (Schaeff et al., 2012). A N200-speller based Internet browser (Liu et al., 2010) reports that the N200 stimulus interface causes less visual discomfort and the induced N200 potential is more stable and less affected by the adaption effect. A BCI system is presented by combining mVEP and P300 potentials (Jin et al., 2012).

Comparing with manipulators and mobile robots, humanoid robots are more advanced as they are created to imitate some of the same physical and mental tasks that humans undergo daily (Hirai et al., 1998), but control of humanoid robots is much more complex. Humanoid robots are being developed to perform a wide range of complex tasks like personal assistance, where they should be able to assist the sick and elderly, and dirty or dangerous jobs. Recently, controlling a humanoid robot via brainwaves becomes more attractive. Bell et al. (2008) and Choi et al. (Choi and Jo, 2013) used ERPs to select an object as a target that a humanoid robot should reach, while our study focuses on telepresence control of humanoid robot behavior via the N200 potentials, including walking in an environment with obstacles and picking-up an object. The challenge to develop an ERP-based model is to make a trade-off between improving the classification accuracy and shortening the intervals between commands in controlling the humanoid robot in real time under the limited information transfer rate (ITR) (Wolpaw et al., 2000).

When investigating the P300-based BRI models (Li et al., 2013a,b), we noticed that the N200 components in brainwaves acquired from our experiments were stable and their amplitudes were relative high. The prominent shape of ERP is very helpful to build feature vectors for improving the classification accuracy. In this article, we propose a BRI model based on the N200 potentials. In order to acquire N200 potentials with high quality, we design an interface by replacing characters in a regular speller with robot images representing robot behaviors to be controlled with mind.

We evaluate this N200-based model by telepresence controlling a humanoid robot with live video feedback. We analyze the N200 potentials induced by the experiment procedure to suggest how to improve the proposed model.

The paper is organized as follows. In Section Materials and Methods, we present the materials and methods for this study, including our mind-controlled humanoid robot system-Cerebot, the detailed experiment procedure, and the method for analyzing and recognizing the N200 potentials. In section Results, we off-line analyze the N200 potentials elicited by the experiment procedure and present the model performance regarding the accuracy, the ITR and the practical bit rate (PBR) (Jin et al., 2012). In this section, we apply the N200-based model to telepresence control a humanoid robot to accomplish two types of tasks. In section Discussion, we discuss the factors that affect the performance of the on-line control operation tasks and draw some conclusions.

MATERIALS AND METHODS

CEREBOT

Cerebot is a mind-controlled humanoid robot platform (Li et al., 2011, 2012). Cerebus™ is the neural signal acquisition system in this platform. It is able to record both invasive and noninvasive neural signals and its processor can deal with on-line signal pre-processing, such as filtering and line noise removing. The platform uses two kinds of humanoid robots. The first one is a NAO humanoid robot made by Aldebaran in France [http://www.aldebaran.com/en]. The other one is a KT-X PC humanoid robot made by Kumotek in USA [http://kumotek.com]. Both of the humanoid robots with high degree of freedoms (DOFs) are equipped with microphones, a camera, a sonar rangefinder, etc., to provide environment information. The Cerebot platform can be used: first, to challenge brainwave-based methods since control of a humanoid robot with full body movements is difficult; second, to evaluate different methods for controlling a humanoid robot under a uniform platform; third, to testify neuroscience assumptions; fourth, to investigate the effect of telepresence control on the subject's mental activities. In this study, we implement the N200 model on Cerebot to on-line navigate a NAO humanoid robot in an office environment and to pick-up an object based on live videos sent back by the camera embedded in the robot.

The control architecture of Cerebot is developed under the OpenViBE-based programming environment. OpenViBE is a free and open-source software platform for designing, testing, and using brain-computer interfaces. It consists of a set of modules devoted to the acquisition, pre-processing, processing, and visualization of cerebral data, as well as to the interaction with Virtual Reality (VR) (Renard et al., 2010). It offers a powerful interface named "Virtual-Reality Peripheral Network (VRPN)" to communicate with other scripts programmed in Matlab or Python. In the Cerebot system (Zhao et al., 2013), OpenViBE integrates the signal acquisition section, the signal processing section, and the control section, as shown in **Figure 1**. In order to control the NAO robot via N200 potentials, an OpenViBE module generates a serial of visual stimuli in a random order to a subject who focuses on a target stimulus (a robot image) that codes the subject's mental activity. Cerebus™ records brainwaves and sends them to the signal processing section to pre-process them, to extract their features of N200 potentials, and to classify them according to the codes of the subject mental activities. Once the subject mental activity is identified, its corresponding control command is sent to the control section to activate the robot behavior.

N200 MODEL

Flow diagram

We implemented the N200 model on Cerebot under the OpenViBE programming environment. **Figure 2** shows the model flow diagram. The white boxes in the diagram are the toolboxes provided by the OpenViBE packages, while the colored boxes are modules developed in C++ or Matlab. The arrows in the diagram

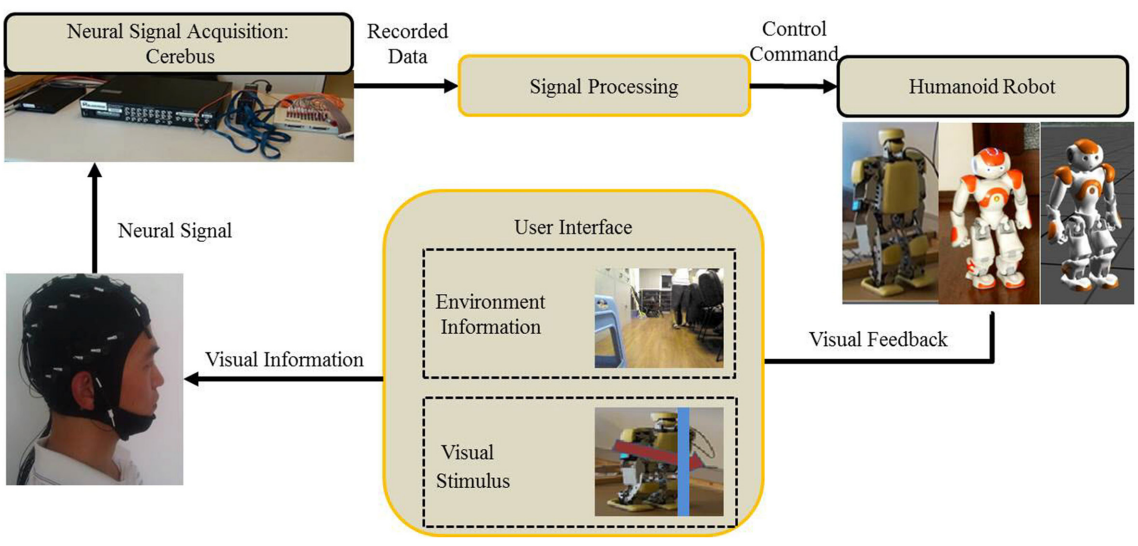

FIGURE 1 | A N200 model based mind-controlled humanoid robot.

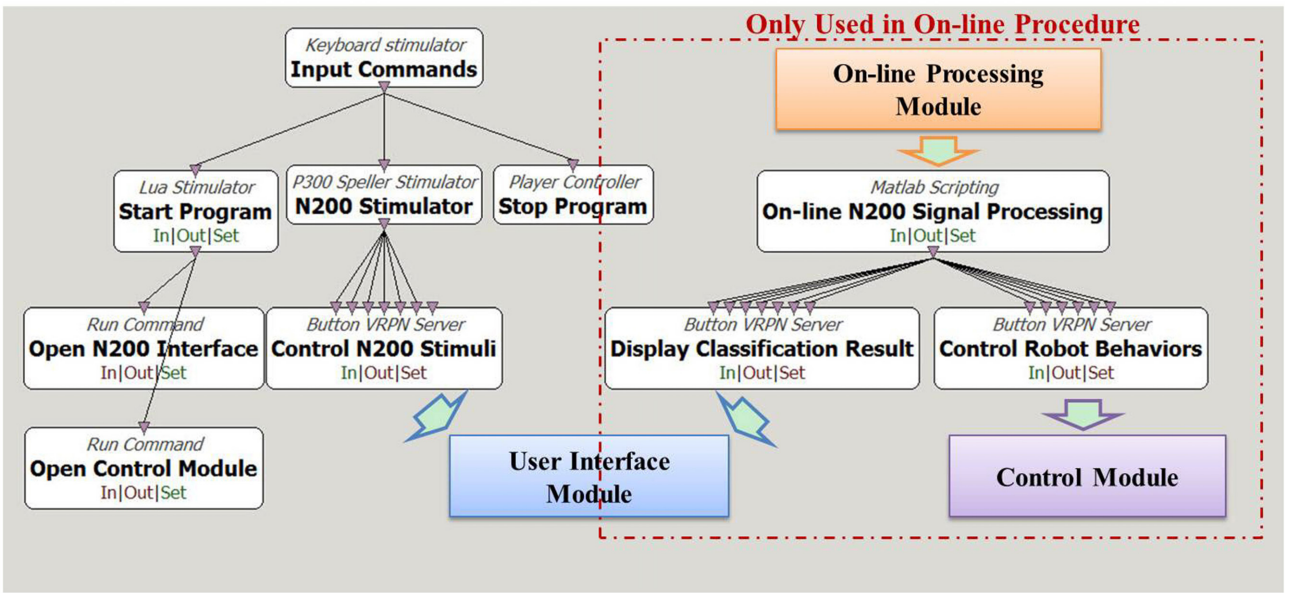

FIGURE 2 | Diagram of N200 model under the OpenViBE programming environment. The white boxes are functions provided by the OpenViBE software package, and the colored boxes are the modules for the N200 model. The boxes enclosed in the red dashed rectangle are only for the on-line control procedure.

indicate data flow paths. The N200 model uses the Start Program toolbox and the Open N200 Interface toolbox in **Figure 2** to start up the User Interface module programmed in C++. To start an experiment, the N200 model uses the N200 Stimulator toolbox provided by OpenViBE to determine the settings, e.g., the stimulating timeline of the visual stimuli, for the User Interface module. The communication from the N200 Stimulator toolbox to the User Interface module is established via VRPN. The User Interface module activates six robot images in random order as the visual stimuli to evoke N200 potentials and sends their event markers to Cerebus™ via serial port to lock the time point at which the relevant image is activated.

The model is designed for both off-line analyzing the acquired N200 potentials and on-line controlling the humanoid robot via brainwaves. The off-line procedure uses the Central software to record the brain signals acquired from the Cerebus™ system. The off-line N200 signal processing scripts developed in Matlab, which are not displayed in **Figure 2**, process the recorded data to analyze the brain signal features and to investigate classification algorithms. In the on-line procedure, the On-line N200 Signal Processing toolbox starts up the On-line Processing module via the Matlab engine to load the configured parameters, to acquire the brain signals from Cerebus™ in real-time and to classify them according to the N200 feature vectors generated during the off-line process. The Display Classification Result toolbox displays the hit visual stimulus on the user interface by framing the corresponding robot image. The Control Robot Behavior toolbox converts the classification result to its corresponding command for Control Module, which activates the behavior to be controlled with mind. **Figure 2** shows how the toolboxes and modules exchange data with each other under the OpenViBE environment.

Interface and protocol for acquiring N200 potentials

Figure 3A shows the user interface with a 2 × 3 matrix of images. These images taken from the real represent six robot behaviors: walking forward, walking backward, shifting left, shifting right, turning left and turning right. We attached red arrows on the images to make the meanings of the images more impressive. In order to induce N200 potentials, a blue bar scans an image from right to left. **Figure 3B** shows that the blue bar is moving on the image to activate the visual stimulus of robot working forward.

We applied the Single Character (SC) method (Guger et al., 2009) to randomly activate the images one by one with the probability of 1/6. The duration of the stimulus onset asynchrony (SOA) (Wei and Luo, 2010) is 220 ms consisting of 150 ms for scanning and 70 ms for a break between two consecutive activations. A repetition is defined as a process in which each image is scanned. The repetition duration is 220 ms × 6 = 1320 ms. **Figure 4** displays the entire process of a repetition. It uses the blue bar to scan the image of walking forward for 150 ms and takes a break for 70 ms, and afterward it uses the blue bar to scan the image of turning left, and so on. The repetition is completed after 1320 ms as the blue bar has scanned all the six images. Each image is randomly selected for scanning in a repetition, so the subject cannot predict which image will be the next visual stimulus. A number of repetitions constitute a trial in which the blue bar repeatedly scans each image for several times.

Experiment procedure

We conducted experiments in a quiet environment and asked subjects to sit in a comfortable armchair. The horizontal distance between the armchair and a monitor was 70 cm. The monitor was a 22-inch LCD one with a resolution of 1280×1024 pixels. The electroencephalogram (EEG) signals were recorded at

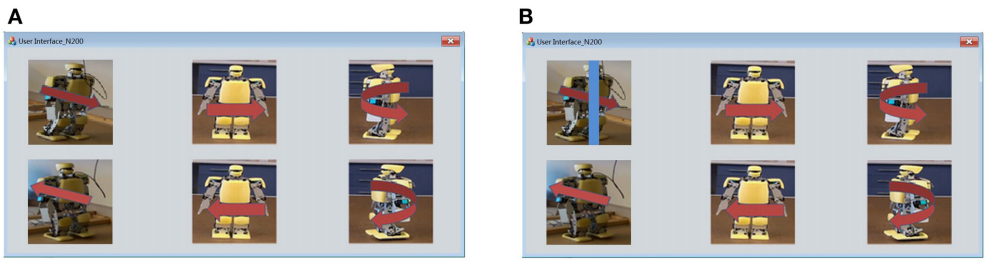

FIGURE 3 | (A) User interface of visual stimuli is a 2 × 3 matrix of six robot images depicting six humanoid robot behaviors. **(B)** The visual stimulus for walking forward is activated by using a blue bar to scan the robot walking forward image from left to right.

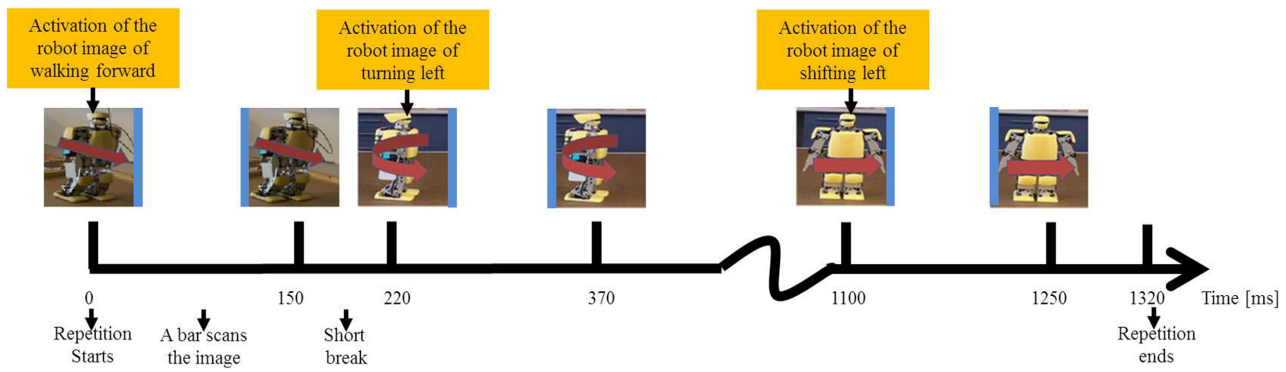

FIGURE 4 | Protocol of inducing N200 potentials activates the six visual stimuli one by one in a random order.

1000 Hz from 32 surface channels using an EEG cap according to the "International 10-20 system." The linked mastoids were reference channels and the channel AFz was the ground channel.

Five subjects (one female, four males, aged 26–28) signed a written informed consent to participate in experiments. Tianjin medical university general hospital ethics committee gives the oral approval of the consent form and experimental procedure before any subjects participated. All of their visual acuities were normal or corrected to normal. Three of them had no prior experience on the experiments. Each subject conducted 360 repetitions, i.e., 36 trials. In each trial, the subject selected a robot image as a target stimulus according to his/her mental activity. During a trial, the subject needed to focus on the target stimulus, tried his/her best to ignore the non-target stimuli, and had to avoid making any movements. Cerebus™ received the visual stimuli and simultaneously recorded the evoked potentials.

SIGNAL ANALYSIS AND FEATURE EXTRACTION

Signal analysis

We analyzed the recorded brain signals to extract their features. First, the brain signals were cut into epochs that were simultaneously with the visual stimuli. The length of each epoch was from post-stimulus 0 ms to post-stimulus 800 ms to cover the potentials. Because the delta (0.5–4 Hz) and theta (4–7.5 Hz) oscillation contribute to the N200 potentials (Karakas et al., 2000a) and the drift mainly appears in a low band, a digital band-pass filter with 1–10 Hz was chosen to process the epochs. Second, we removed the signal drift by the method of common average reference (CAR). Finally, the epochs were divided into two groups: the epochs induced by the target stimulus and the ones induced by the non-target stimulus, and then both the groups of the epochs were averaged, respectively.

Feature extraction and classification

Being able to represent the feature of brain signals in low dimension space can reduce the amount of computation (Bian and Zhang, 2000). According to Shannon's theorem, we were able to reduce the dimension of the feature vectors by down-sampling the data epochs from 1000 to 20 Hz (Krusienski et al., 2008). We used the N200 signal processing scripts to remove noises from the epoch from post-stimulus 100–500 ms and to average the epochs induced by the same visual stimulus in a trial. The brain signals from a single channel yielded an 8-dimension [(500-100)/1000 × 20] feature vector. If n channels were used to extract the features, the total dimension of a vector was $8 \times n$. The selected channel number depended on the characteristics of individual subject's brain signals.

We adopted the Fisher's linear discriminant analysis (FLDA) as a two-class classifier to discover which visual stimulus was the target one by checking each feature vector. The idea of this algorithm is to find the optimal direction of projections that groups the vectors with the same features into a class (Mika et al., 1999) as bellow:

$$\mathbf{w} = \mathbf{S}_w{}^{-1}(\mathbf{M}_1 - \mathbf{M}_2)$$
$$\mathbf{S}_w = \mathbf{S}_1 + \mathbf{S}_2$$
$$\mathbf{S}_i = \sum_{\mathbf{x}_k \in \mathrm{X}_i} (\mathbf{x}_k - \mathbf{M}_i)(\mathbf{x}_k - \mathbf{M}_i)^{\mathrm{T}}, i = 1, 2$$
$$\mathbf{M}_i = \frac{1}{n_i} \sum_{\mathbf{x}_k \in \mathrm{X}_i} \mathbf{x}_k, i = 1, 2$$

where $\mathbf{x}_k$ is the feature vector, X_i represents the class set and n_i is the number of feature vectors in the ith class.

We trained the FLDA classifier using the feature vectors and tested it by the brain signals recorded in a trial that established six feature vectors according to the six visual stimuli. The trained classifier processed each feature vector successively and outputted the classified value. The classifier outputted no control command if it classified the six features vectors as non-targets or outputted a control command if it classified one or more feature vectors as targets.

RESULTS

INDUCED N200 POTENTIALS

The solid and dotted curves in **Figure 5** represent the average brain signals induced by the target stimulus and non-target stimulus from channel P3, respectively. The brain signal induced by the target stimulus appears with a sharp negative deflection with amplitude of 5 uV at 258 ms and a positive deflection with amplitude of 3.5 uV at 358 ms. The negative deflection is known as the N200 potential that is the response to scanning over the target image by the blue bar. The positive deflection resembles the P300 potential. The brain signals induced by the non-target stimuli do not appear with obvious deflection. The results demonstrate that the designed interface can induce N200 potentials by scanning over a target image with the blue bar. The negative deflection provides a recognizable feature of the N200 potential for us to classify the brain signals.

We plot the average brain signals acquired from each subject through channels P3 and CP3 to discuss their individual difference, as shown in **Figures 6A,B**. The black thick curve is the average N200 potentials across the five subjects, while the other thin color curves are the N200 potentials from the individual subject. The N200 potential amplitudes acquired from the subj5, represented by the green curves in **Figures 6A,B**, are smaller than the others. The latencies of the N200 potentials acquired by the subj4, represented by the pink curves in **Figures 6A,B**, is 20 ms shorter than the average latency. The N200 potentials induced from the subjects show different amplitude distributions over channels P3 and CP3. For example, the N200 potential amplitude acquired from the subj2 through channel P3 is larger than the one through channel CP3, represented by the blue curves in **Figures 6A,B**, while the N200 potentials amplitudes acquired from the subj5 through channels P3 and CP3 are very close. The amplitude topographic maps show the distribution of the induced potentials. **Figures 6C,D** represent the amplitudes of average brain signals at 258 ms and 358 ms after the visual stimuli, respectively. The darker the red color indicates the positive amplitude the greater, and the darker the blue color indicates the negative amplitude the greater. **Figure 6C** shows that the largest amplitude of N200 potentials mainly appears in the temporal-parietal area near channel P3, while **Figure 6D** shows that the P300 potentials mainly distribute in the parietal area. We draw two following remarks. First, although the N200 potentials acquired from the subjects are slightly different, they exhibit the N200 potentials' features that are important to control the robot behavior. Second, the N200 and P300 potentials mainly appear in the parietal and temporal areas in a window of post-stimulus 100–500 ms and the channels from which the recognizable N200 potentials are acquired vary due to the individuality, so we determine time windows and select the best channels for the individual subject for processing N200 potentials to control the humanoid robot.

The electrical potentials caused by eye movement and blinking can be much larger than the ERPs (Joyce et al., 2004) and

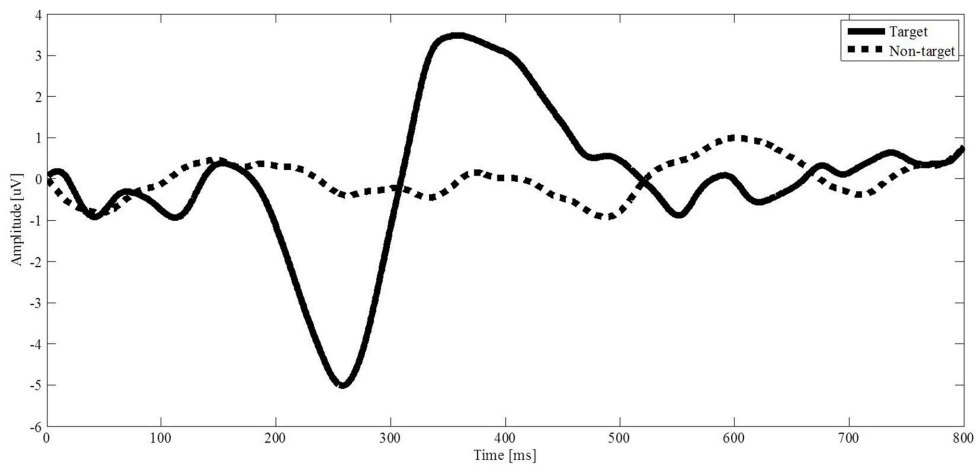

FIGURE 5 | Evoked potentials from channel P3 are averaged. The solid curve is the brainwave of a target stimulus, and the dotted curve is the brainwave of a non-target stimulus.

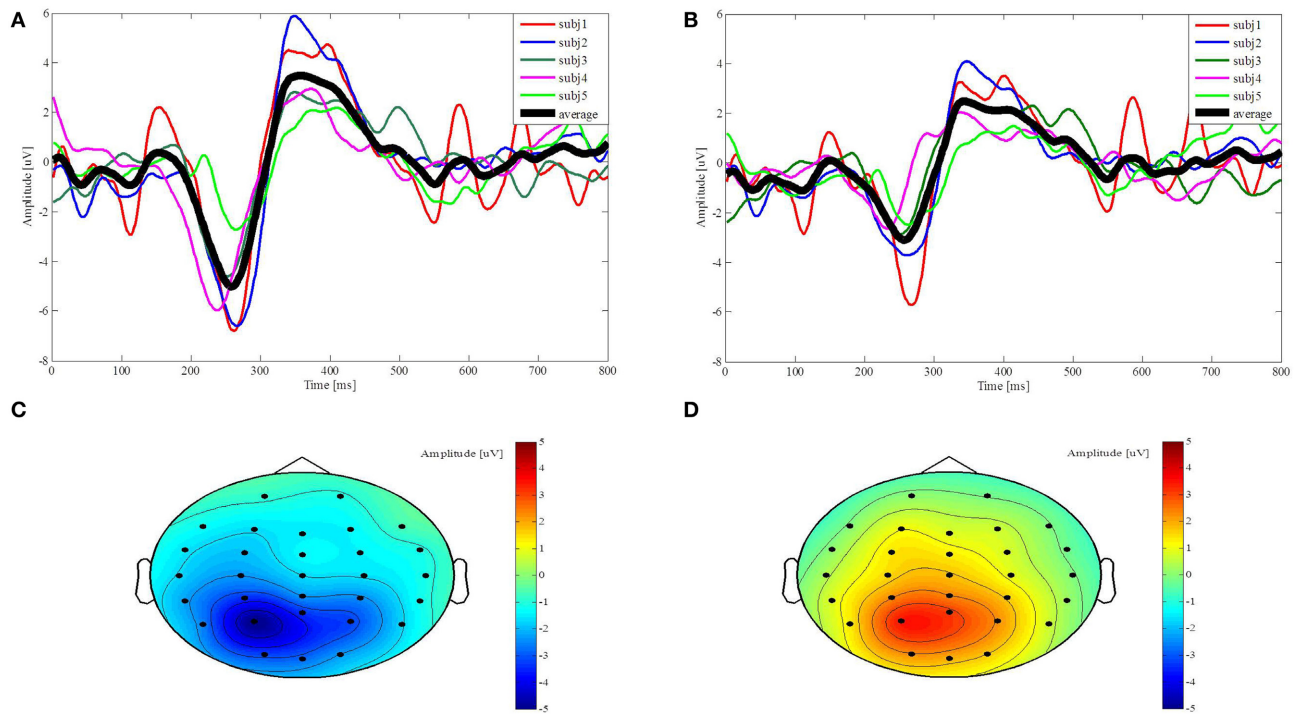

FIGURE 6 | Evoked potentials from channel P3 and CP3 and their topographies along with time points. (A,B) The colorful thin curves represent the five subjects' N200 and P300 potentials from post-stimulus 0–800 ms, respectively, and the black curve represents the average potentials over the five subjects. **(C,D)** The amplitude topographic maps of the average brain signals across five subjects are plotted at 258 ms and 358 ms.

propagate across the scalp, so these electrical potentials may distort the ERPs, but their impact on the ERPs decreases as a distance from the frontal increases. Because the induced N200 potentials mainly appear in the temporal—parietal area that is far from the frontal, the distortion of the N200 potentials induced by using a blue bar scanning visual stimulus images is irrelevant. In this study, therefore, we directly apply the induced N200 potentials to on-line control the humanoid robot.

However, the distortion of the P300 potentials induced by flashing stimulus images may be significant since the P300 potentials mainly appear in the parietal and central areas (Iturrate et al., 2009). Consequently, an additional algorithm has to be designed to remove eye artifacts to ensure high classification accuracy.

OFF-LINE EVALUATION

This subsection evaluates the off-line performance of the N200 model based on the classifier accuracy, which is the ratio between the trials detected correctly over the total trials, the ITR and the PBR.

We averaged the classified accuracy of each subject by the 10-fold cross-validation (Liu et al., 2010). The first step was to determine the candidate channels based on the subject's amplitude topographic map. The second step was to calculate the classified accuracy of each channel and their combinations. The third step was to select the combination that yielded the highest accuracy as the optimal channels for the individual subject, listed in **Table 1**. The three subjects denoted by **N** had no prior BCI experience on the experiments, while the other two subjects denoted by **Y** had prior BCI experience. **Figure 7** depicts the average accuracy for each subject vs. the number of repetitions. The accuracy is clearly increased when increasing the number from 1 to 10. The accuracies of the four subjects reach 100%, and three of them reach 100% with 6 repetitions. The accuracy of subj5 is slightly low. ITR measures the information rate per minute by taking the accuracy and the time needed to classify a visual stimulus described as

Table 1 | The off-line performance.

Subject	Optimal channels	Accuracy (%)	ITR (bits/min)	PBR (bits/min)
subj1 (Y)	P3, P4, Pz, CP3	98.6	22.22	21.58
subj2 (N)	P3, P4, Pz, CP3	98.6	22.22	21.58
subj3 (N)	P3, P7, CP3	92.9	18.61	15.95
subj4 (Y)	P3, P4, Pz,	97.1	21.19	19.98
subj5 (N)	P3, CPz	81.4	13.28	8.34
Mean	–	93.7	19.50	17.49

$$B = \left[\log_2 N + \log_2 P + (1-P) \times \log_2\left(\frac{1-P}{N-1}\right)\right] \times M$$

where $N = 6$ stands for 6 visual stimuli in the user interface, P is the classifier accuracy, M is the number of outputting commands in a minute (McFarland et al., 2003). The index,

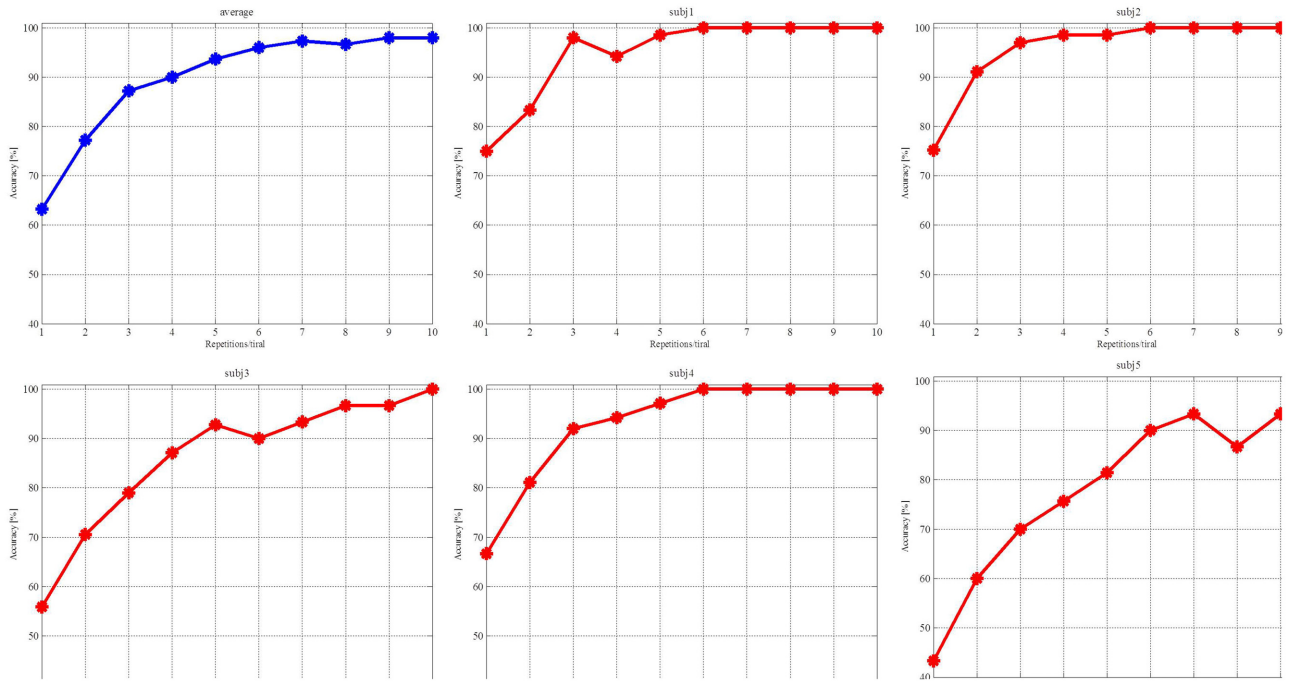

FIGURE 7 | Red curves are the accuracies achieved by the individual subjects and the blue curve is their average accuracy.

PBR, estimates the practical speed of a system, by considering each error classification that needs to be corrected by additional selections (Jin et al., 2012) as below:

$$PBR = B \times [1 - 2 \times (1 - P)]$$

PBR is meaningful only when $P \geq 50\%$. **Table 1** lists the five subjects' accuracies, ITRs and PBRs. For evaluating the off-line ITR, we set both the interval between the repetitions and the one between the trials as 0 ms (Jin et al., 2011), so M is 9.09 ($0.22 \times 6 \times 5 = 6.60$s, $60.00/6.60 \approx 9.09$) when the repetition number is 5. In **Table 1**, each subject's ITR is larger than 10 bits/min. ITR increases when the accuracy is increased. The highest accuracy of 98.57% yields the largest ITR of 22.22 bits/min. PBR is smaller than ITR due to $[1 - 2 \times (1 - P)] \leq 1$. The large accuracy reduces the difference between ITR and PBR. Clearly, a high accuracy allows the subject to correct the error quickly and to realize his/her intention accurately, while a low accuracy needs the subject to spend much time to correct an incorrect command. Improving the accuracy needs to increase the number of repetitions in a trial, i.e., to increase the control cycle, so a trade-off between the accuracy and control cycle speed must be considered according to a task requirement.

CASE STUDIES

In order to validate the developed N200 model, the subjects controlled on-line the NAO humanoid robot to accomplish two popular tasks in robotics research: to navigate the NAO robot to walk with obstacle avoidance and to control the NAO robot to pick up an object. These tasks are challenging because the subjects need live video feedback from a camera embedded in the NAO robot to activate appropriate robot behavior.

The experiments were carried out in a normal office without electromagnetic shielding. The subjects sat in a comfortable chair and 70 cm away from a 22-inch LCD monitor displaying the N200 interface and the live video feedback, as shown in **Figure 8A**. The live video window was placed above the interface window with a distance to reduce mutual influences on subjects' concentrations caused by visual stimuli and live video. During the experiments, the subjects needed to stabilize their heads since the head motion may cause noises. Once a trial began, the subjects relied on live video to observe the robot status and surroundings and focused on a visual stimulus depicting robot behavior whose meaning represented their intention. When a trial was ended, the classification result was transformed to a command to activate an appropriate robot behavior. For the on-line experiments, the interval between repetitions was set 600 ms, therefore the duration of outputting a command with 3 repetitions was 5.76 s; the duration was 9.60 s with 5 repetitions. The interval between trials was set 5 s as the subjects needed this interval to have a short rest and to decide the next behavior. **Figure 8B** shows an example of controlling the NAO robot to shift left with mind. The supplementary material (movie clip) that records the on-line control processes of navigating a humanoid robot in an office environment with an obstacle and picking-up an object is available.

For the navigation task, the subjects controlled the humanoid robot to walk from a start point to a destination by passing an obstacle as shown in **Figure 9A**. Based on the live video from the robot's camera, the subjects used N200 potentials to activate six

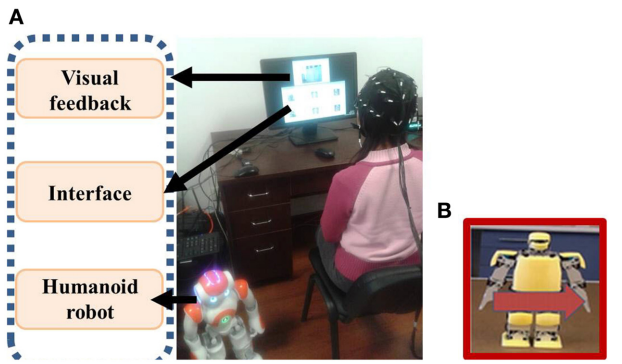

FIGURE 8 | (A) On-line control of the NAO humanoid robot with mind in an office environment **(B)** The visual stimulus of shifting left is classified as a target.

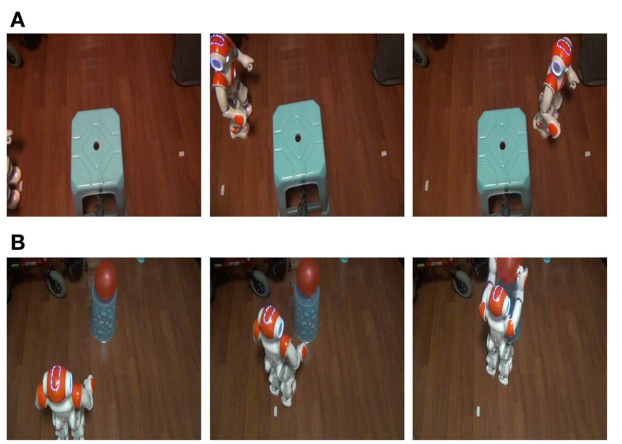

FIGURE 9 | On-line study cases of controlling the humanoid robot using the N200 model. (A) Robot navigation with obstacle avoidance. **(B)** Robot pick-up operation.

types of robot walking behaviors defined by: walking forward for 0.2 m, walking backward for 0.15 m, shifting left for 0.15 m, shifting right for 0.15 m, turning left for 30°, and turning right for 30°. We evaluate their control performance using the following criteria: the total commands for activating robot behaviors, the total time for completing the task, the on-line control success rates, and the number of collisions with an obstacle in the three experiments. The robot may collide with the obstacle when a subject cannot appropriately estimate the distance between the robot and the obstacle from the live video or his/her intention is incorrectly detected. **Table 2** lists the results herein averaged over the three experiments.

For the pick-up operation task, the subjects controlled the humanoid robot to approach a balloon and to pick up this target as shown in **Figure 9B**. The balloon was placed on a round table in the right front of the robot so the subjects had to move the robot to a position close enough to the table and to configure a proper orientation to pick up the balloon. For this task, the subjects used N200 potentials to activate the following defined behaviors: picking-up the target, walking forward for 0.1 m, shifting left/right for 0.1 m, and turning left/right for 15°. A task operation was classified as a failure if the pick-up behavior was activated before the robot reached the proper position. This task operation was repeated until each subject completed three successful experiments. In order to evaluate the on-line control performance, we recorded the total commands for activating robot behaviors in the three successful experiments, the average total time of completing a pick-up operation task, the average on-line success rate averaged over the three successful experiments, and the ratio of the successful experiments over the total ones.

Tables 2, **3** list the experimental results conducted by the five subjects. We compare their on-line control performance using 5 repetitions for a trial as defined in **Table 1** because this repetition number documents that all the subjects achieve their accuracies over 80%. For comparing the on-line control performance, **Tables 2**, **3** also list the test results with 3 repetitions of a trial. We address five remarks as follows.

(1) The on-line success rates differ from the off-line accuracies. The experiments of the navigation task documented that subj2, subj3, and subj5's on-line success rates (88.8, 78.4, 73.4%) were lower than their off-line accuracies (98.6, 92.8, 81.4%) when the repetition number was 5; while subj1 and subj4's success rates (100.0, 100.0%) were slightly higher than their off-line accuracies (98.6, 97.1%). The experiments of the pick-up operation task documented that subj1, subj2, and subj4's on-line success rates (95.2, 96.7, 92.3%) were slightly lower than their off-line accuracies (98.6, 98.6, 97.1%), while subj3 and subj5's success rates (100.0, 95.8%) were higher than the off-line accuracies (92.9, 81.4%).

(2) Most of the subjects achieved higher on-line success rates for the pick-up operation task than those for the navigation task. The subjects subj1, subj2, subj3, and subj4 achieved the higher on-line success rates (100.0, 96.3, 95.5, 100.0%) for the pick-up operation task than those (96.4, 84.5, 77.2, 90.9%) for the navigation task when the repetition number is 3. The subjects subj2, subj3, and subj5 achieved the higher on-line success rates (96.7, 100.0, 95.8%) for the pick-up operation task than those (88.8, 78.4, 73.4%) when the repetition number is 5.

(3) A lower success rate results in more total commands and longer total time for completing the operation tasks. For the navigation task, subj2 and subj3's success rates (84.5, 77.2%) with 3 repetitions were lower than the ones (88.8, 78.4%) with 5 repetitions, so their corresponding total commands for three successful experiments (49/3, 75/3) with 3 repetitions were more than ones (34/3, 51/3) with 5 repetitions and their average total times (180.8, 265.3 s) for completing each of the three successful experiments with 3 repetitions are longer than those (163.4, 245.5 s) with 5 repetitions although their duration of 5.76 s for outputting a command with 3 repetitions was shorter than the one of 9.60 s with 5 repetitions. For the pick-up operation task, when subj1, subj3, subj4, and subj5 achieved the higher success rates (100.0, 100.0, 100.0, 95.8%), they generated the fewer commands (19/3, 16/3, 20/3, 19/3). A low success rate increases the possibility

Table 2 | Performance of the navigation task.

Subject	Repetition number	Time/ command	Total time (s)	Total commands	On-line success rate (%)	Collisions
subj1 (Y)	3	5.76	99.8	28/3	96.4	0/3
	5	9.60	144.3	30/3	100.0	0/3
subj2 (N)	3	5.76	180.8	49/3	84.5	1/3
	5	9.60	163.4	34/3	88.8	0/3
subj3 (N)	3	5.76	265.3	75/3	77.2	0/3
	5	9.60	245.6	51/3	78.4	0/3
subj4 (Y)	3	5.76	116.1	33/3	90.9	0/3
	5	9.60	154.3	32/3	100.0	0/3
subj5 (N)	3	5.76	163.4	46/3	78.2	0/3
	5	9.60	229.7	45/3	73.4	4/3

Table 3 | Performance of the pick-up operation task.

Subject	Repetition number	Time/ command	Total time (s)	Total commands	On-line success rate (%) for successful experiments	Successful / total experiments
subj1 (Y)	3	5.76	65.4	19/3	100.0	3/4
	5	9.60	99.3	21/3	95.2	3/3
subj2 (N)	3	5.76	73.7	22/3	96.3	3/3
	5	9.60	105.0	23/3	96.7	3/3
subj3 (N)	3	5.76	70.4	20/3	95.8	3/4
	5	9.60	73.4	16/3	100.0	3/5
subj4 (Y)	3	5.76	69.1	20/3	100.0	3/5
	5	9.60	123.6	26/3	92.3	3/3
subj5 (N)	3	5.76	94.1	27/3	66.7	3/4
	5	9.60	85.0	19/3	95.8	3/5

of incorrectly detecting the subjects' intentions, so outputting additional commands to correct the false ones increases the number of total commands. For the three experiments, subj2 used 34 commands to navigate the NAO robot without collision with the obstacle under the success rate of 88.8%, while subj5 used 45 commands to navigate the NAO robot with 4 collisions with the obstacle under the success rate of 73.4%.

(4) A repetition number of a trial plays an important role in determining a total time for completing an operation task at a high success rate. For completing three successful navigation tasks, subj1, subj4, and subj5 varied slightly their numbers of total commands (from 28 to 30, from 33 to 32, from 46 to 45) when the repetition number increased from 3 to 5. For completing three successful pick-up operation tasks, subj1, subj2, and subj3 varied slightly their numbers of total commands (from 19 to 21, from 22 to 23, from 20 to 16) when the repetition number increased from 3 to 5. For the above cases, changing the repetition number does not affect the number of total commands very much, so the duration of a trial, i.e., the repetition number determines the total time for completing an operation task. Increasing the repetition number from 3 to 5, i.e., growing the duration of a trial from 5.76 to 9.60 s, increases the total times for completing the navigation tasks discussed above from 99.8 to 144.3 s, from 116.1 to 154.3 s, and from 163.4 to 229.7 s, and the total times for completing the pick-up operation tasks from 65.4 s to 99.3 s, from 73.7 to 105.0 s, from 70.4 to 73.4 s, as listed in **Tables 2**, **3**.

(5) The experience with the designed experimental procedure is an important factor that impacts the on-line success rates. The subjects subj1 and subj4 with prior experience on the experiments achieved the high on-line average success rates of 97.9 and 95.8%, while the subjects subj2, subj3, and subj5 without prior experience delivered the relatively low success rates of 91.6, 87.9, and 78.5%.

DISCUSSION

THE N200 MODEL

The work (Karakas et al., 2000b) shows that the ERP represents interplay between the oscillations that are mainly in the delta and theta frequencies. We assume that the moving bar scanning over the robot images may impact on event-related oscillations (EROs)

in the temporal-parietal area, because the brainwaves acquired from this area deliver the recognizable N200 potentials which may be contributed by the theta oscillation related with orientation and attention (Karakas et al., 2000a,b). We will verify this assumption in our further research.

The interface that we design for inducing the N200 potentials has three advantages. First, the robot images as the visual stimuli are more intuitive and help the subjects understand the meanings of the stimuli better. Second, scanning the static robot images by the blue bar, instead of flashing the robot images in the traditional P300 model, allows the subjects more intensively to concentrate on a target stimulus. The subjects reported that the moving bar could cause less visual fatigue than the flashing images. Third, the proposed visual stimulus mode also induces the P300 potentials, but the amplitudes of the N200 potentials are larger and more recognizable, so we use the N200 potentials to establish the features vector to achieve better classification accuracy.

EFFECTS ON THE ON-LINE SUCCESS RATES

We note that the on-line success rates vary for different operation tasks and their differences depend on the individual subjects. Here, we present the factors that affect the on-line success rates. The on-line success rates achieved in on-line control of the robot are usually lower than classification accuracies in the off-line evaluation. It would be a common fact because the off-line evaluation is an open-loop control, while the on-line task-driven control is a closed-loop control with live video feedback. Different from the off-line control, the on-line telepresence control needs a subject to coordinate his/her attention to both the live video and the visual stimuli, and especially the live video may divert a subject's attention away from the target stimulus, which decreases the on-line success rates (Gergondet et al., 2012). Especially, the poor quality of live videos may significantly deteriorate the subject's control performance. Auditory effect from the surrounding, e.g., the sound of robot's walking steps, may be another factor that distracts the subject's attention. Tidoni et al. (2014) reported that the sound of robot's walking steps delivered synchronously with the robot motion needs less time to control the robot than the asynchronous sound. In general, the success rates of the navigation task with noisy walking steps' sound are lower than those of the pick-up task. The subjects have to make a right decision based on the surrounding information sent by the live video to control the robot behavior. In addition, the subjects may get anxious when the robot falls down or collides with an obstacle caused by an incorrect command.

ANALYSIS OF THE ON-LINE CONTROLLED TASKS

We evaluate the total execution time of completing an on-line controlled task. Because the total time depends on the total commands generated by the induced N200 potentials, quickly and accurately outputting a command shortens the total time. The two factors mainly affect the total number of generated commands. The first factor is the on-line control success rate that indirectly indicates how many incorrect commands are outputted for the on-line control process. Each incorrect command causes an unexpected robot behavior that needs to be corrected by additional control commands. For the navigation task, subj2 and subj3 achieved the success rates with 3 repetitions lower than those with 5 repetitions and for the pick-up operation task subj5 achieved the success rates with 3 repetitions lower than those with 5 repetitions, so they spent more total time to complete their corresponding tasks since they outputted much more additional control commands. The second factor is the individuality of mental activities of planning in real-time to complete an operation task indicated by the following cases: 1. With 5 repetitions, subj5's brain activated fewer control commands than subj2's brain did to accomplish the pick-up operation task; 2. With 3 repetitions, subj3's brain activated fewer control commands than subj2's brain did to complete the pick-up operation task; 3. With 5 repetitions, subj5's brain activated fewer control commands than subj3's brain did to complete the navigation task.

The repetition number of a trial is a very important factor that affects the total time of an on-line task operation. The repetition number determines the duration of outputting a command. The large duration increases the total time. For example, subj1, subj4, and subj5 spent more time with 5 repetitions than with 3 repetitions to accomplish the navigation task, and subj1, subj2, and subj3 spent more time with 5 repetitions than 3 repetitions to complete the pick-up operation task, because each of them outputted the close number of total commands no matter the repetition number is 3 or 5. On the other hand, the large repetition number yields the high success rate. As discussed above, the high success rate reduces the incorrect outputs in the control process. Consequently, the few incorrect commands that need to be rectified shorten the total time. Usually, a high success rate needs the large repetition number to increase the reliability of the control system, but it increases the duration of a trial. How to determine the repetition number is an important issue because a balance between the reliability and the total time needs to be considered.

We used the robot images as the visual stimuli successfully to induce the N200 potentials with recognizable amplitudes. We implemented the proposed N200 model on the Cerebot platform to evaluate its off-line and on-line performances across five subjects. The off-line evaluations show that the average accuracy is 93.71% over the five subjects with 5 repetitions in a trial and two of the five subjects reach their accuracies of 98% with three repetitions. The five subjects participated in the navigation and pick-up operation tasks in an office environment in which the live video feedback provided surrounding information. The success rates affect the total number of commands outputted from the N200 model, the total time for completing an on-line operation task, and the number of collisions caused by the incorrect commands. Therefore achieving a high success rate has a priority using the N200 model to control the humanoid robot. As discussed above, the repetition number of a trial plays a prominent role in achieving the high success rate and shortening the duration of outputting a command. In the future work, we investigate the optimal repetition number according to a variety of on-line operation tasks.

Some research teams applied the steady state visually-evoked potential (e.g., Gergondet et al., 2012; Tidoni et al., 2014) to control a humanoid robot with live video or the motor imagery (e.g., Cohen et al., 2012) to control the robot behavior for a navigation task. In the future work, we will evaluate the performances of these models using the Cerebot platform.

ACKNOWLEDGMENTS

The authors would like to thank Mr. Guoxin Zhao, Mr. Hong Hu, and Ms. Wenxuan Li for their help in conducting the experiments. This work was supported in part by The National Natural Science Foundation of China (No. 61271321, No. 61473207), the Ph.D. Programs Foundation of the Ministry of Education of China (No. 20120032110068) and Tianjin Key Technology Research and Development Program (No. 14ZCZDSF00025).

SUPPLEMENTARY MATERIAL

The Supplementary Material for this article can be found online at: http://www.frontiersin.org/journal/10.3389/fnsys.2014.00247/abstract

REFERENCES

Bell, C. J., Shenoy, P., Chalodhorn, R., and Rao, R. P. N. (2008). Control of a humanoid robot by a noninvasive brain-computer interface in humans. *J. Neural Eng.* 5, 214–220. doi: 10.1088/1741-2560/5/2/012

Bian, Z., and Zhang, X. (2000). *Pattern Recognition*. Beijing: Tsinghua University Press.

Choi, B., and Jo, S. (2013). A low-cost EEG system-based hybrid brain-computer interface for humanoid robot navigation and recognition. *PLoS ONE* 8:e74583. doi: 10.1371/journal.pone.0074583

Cohen, O., Druon, S., Lengagne, S., Mendelsohn, A., Malach, R., Kheddar, A., et al. (2012). "fMRI robotic embodiment: a pilot study," in *4th IEEE RAS/EMBS International Conference on Robotics and Biomimetics* (Roma), 314–319.

Farwell, L. A., and Donchin, E. (1988). Talking off the top of your head: toward a mental prosthesis utilizing event-related brain potentials. *Electroencephalogr. Clin. Neurophysiol.* 70, 510–523. doi: 10.1016/0013-4694(88)90149-6

Frensel, S., and Neubert, E. (2010). *Is the P300 speller independent?* arXiv 1006.3688.

Gergondet, P., Petit, D., and Kheddar, A. (2012). "Steering a robot with a brain-computer interface: impact of video feedback on BCI performance," in *21st IEEE International Symposlum on Robot and Human Interactive Communication* (Paris), 271–276.

Guger, C., Daban, S., Sellers, E., Holzner, C., Krausz, G., and Carabalona, R. (2009). How many people are able to control a P300-based brain–computer interface (BCI)? *Neurosci. Lett.* 462, 94–98. doi: 10.1016/j.neulet.2009.06.045

Heinrich, S. P. (2007). A primer on motion visual evoked potentials. *Doc. Ophthalmol.* 114, 83–105. doi: 10.1007/s10633-006-9043-8

Hirai, K., Hirose, M., Haikawa, Y., and Takenaka, T. (1998). "The development of Honda humanoid robot," in *1998 IEEE International Conference on Robotics and Automation* (Leuven), 1321–1326.

Hong, B., Guo., F., Liu, T., and Gao, S. (2009). N200-speller using motion-onset visual response. *Clin. Neurophysiol.* 120, 1658–1666. doi: 10.1016/j.clinph.2009.06.026

Iturrate, I., Antelis, J. M., Kubler, A., and Minguez, J. (2009). A noninvasive brain-actuated wheelchair based on a P300 neurophysiological protocol and automated navigation. *IEEE Trans. Rob.* 25, 614–627. doi: 10.1109/TRO.2009.2020347

Jin, J., Allison, B. Z., Sellers, E. W., Brunner, C., Horki, P., Wang, X., et al. (2011). An adaptive P300-based control system. *J. Neural Eng.* 8:036006. doi: 10.1088/1741-2560/8/3/036006

Jin, J., Allison, B. Z., Wang, X., and Neuper, C. (2012). A combined brain–computer interface based on P300 potentials and motion-onset visual evoked potentials. *J. Neurosci. Methods* 205, 265–276. doi: 10.1016/j.jneumeth.2012.01.004

Joyce, C. A., Gorodnitsky, I. F., and Kutas, M. (2004). Automatic removal of eye movement and blink artifacts from EEG data using blind component separation. *Psychophysiology* 41, 313–325. doi: 10.1111/j.1469-8986.2003.00141.x

Karakas, S., Erzengin, O. U., and Basar, E. (2000a). The genesis of human event-related responses explained through the theory of oscillatory neural assemblies. *Neurosci. Lett.* 285, 45–48. doi: 10.1016/S0304-3940(00)01022-3

Karakas, S., Erzengin, O. U., and Basar, E. (2000b). A new strategy involving multiple cognitive paradigms demonstrates that ERP components are determined by the superposition of oscillatory responses. *Clin. Neurophysiol.* 111, 1719–1732. doi: 10.1016/S1388-2457(00)00418-1

Krusienski, D. J., Sellers, E. W., McFarland, T. M., Vaughan, T. M., and Wolpaw, J. R. (2008). Toward enhanced P300 speller performance. *J. Neurosci. Methods* 167, 15–21. doi: 10.1016/j.jneumeth.2007.07.017

Lebedev, M. A., and Nicolelis, M. A. L. (2006). Brain-machine interfaces: past, present and future. *Trends Neruosci.* 29, 536–546. doi: 10.1016/j.tins.2006.07.004

Liu, T., Goldberg, L., Gao, S., and Hong, B. (2010). An online brain-computer interface using non-flashing visual evoked potentials. *J. Neural Eng.* 7, 1–9. doi: 10.1088/1741-2560/7/3/036003

Li, W., Jaramillo, C., and Li, Y. (2011). "A brain computer interface based humanoid robot control system," in *IASTED International Conference on Robotics* (Pittsburgh, PA), 390–396.

Li, W., Jaramillo, C., and Li, Y. (2012). "Development of mind control system for humanoid robot through a brain computer interface," in *Intelligent System Design and Engineering Application (ISDEA)* (Hainan), 679–682.

Li, M., Li, W., Zhao, J., Meng, Q., Sun, F., and Chen, G. (2013a). "An adaptive P300 model for controlling a humanoid robot with mind," in *IEEE International Conference on Robotics and Biomimetics* (Guangdong), 1390–1395.

Li, M., Li, W., Zhao, J., Meng, Q., Zeng, M., and Chen, G. (2013b). "A P300 model for Cerebot- a mind –controlled humanoid robot," in *2nd International Conference on Robot Intelligent Technology and Applications* (Denver, CO), 495–502.

McFarland, D. J., Sarnacki, W. A., and Wolpaw, J. R. (2003). Brain-computer interface (BCI) operation: optimizing information transfer rates. *Biol. Psychol.* 63, 237–251. doi: 10.1016/S0301-0511(03)00073-5

Mika, S., Ratsch, G., Weston, J., Scholkopf, B., and Mullers, K. R. (1999). Fisher discriminant analysis with kernels. *Neural Netw. Signal Process.* IX, 41–48.

Patel, S. H., and Azzam, P. N. (2005). Characterization of N200 and P300: selected studies of the event-related potential. *Int. J. Med. Sci.* 2, 147–154. doi: 10.7150/ijms.2.147

Polich, J., and Kok, A. (1995). Cognitive and biological determinants of P300: an integrative review. *Biol Psychol.* 41, 103–146. doi: 10.1016/0301-0511(95)05130-9

Renard, Y., Lotte, F., Gibert, G., Congedo, M., Maby, E., Delannoy, V., et al. (2010). OpenViBE: an open-source software platform to design, test, and use brain-computer interfaces in real and virtual environments. *Presence (Camb.)* 19, 35–53. doi: 10.1162/pres.19.1.35

Schaeff, S., Treder, M. S., Venthur, B., and Blankertz, B. (2012). Exploring motion VEPs for gaze-independent communication. *J. Neural Eng.* 9, 045006. doi: 10.1088/1741-2560/9/4/045006

Tidoni, E., Gergondet, P., Kheddar, A., and Aglioti, S. M. (2014). Audio-visual feedback improves the BCI performance in the navigational control of a humanoid robot. *Front. Neurorobot.* 8:20. doi: 10.3389/fnbot.2014.00020

Wei, J. H., and Luo, Y. J. (2010). *Principle and Technique of Event-Related Brain Potentials*. Beijing: Science Press.

Wolpaw, J. R., Birbaumer, N., Heetderks, W. J., McFarland, D. J., Hunter Peckham, P., Schalk,G., et al. (2000). Brain-computer interface technology: a review of the first international meeting. *IEEE Trans. Rehabil. Eng.* 8, 164–173. doi: 10.1109/TRE.2000.847807

Zhao, J., Meng, Q., Li, W., Sun, F., and Chen, G. (2013). "An OpenViBE-based brainwave control system for Cerebot," in *IEEE International Conference on Robotics and Biomimetics* (Guangdong), 1169–1174.

Conflict of Interest Statement: The authors declare that the research was conducted in the absence of any commercial or financial relationships that could be construed as a potential conflict of interest.

Received: 25 October 2014; accepted: 17 December 2014; published online: 09 January 2015.

Citation: Li W, Li M and Zhao J (2015) Control of humanoid robot via motion-onset visual evoked potentials. Front. Syst. Neurosci. ***8****:247. doi: 10.3389/fnsys.2014.00247*

This article was submitted to the journal Frontiers in Systems Neuroscience.

frontiers in Systems Neuroscience

HYPOTHESIS AND THEORY
published: 28 July 2015
doi: 10.3389/fnsys.2015.00108

Advancing brain-machine interfaces: moving beyond linear state space models

Adam G. Rouse[1,2,3] *and Marc H. Schieber*[1,2,3]*

[1] Department of Neurology, University of Rochester, Rochester, NY, USA, [2] Department of Neurobiology and Anatomy, University of Rochester, Rochester, NY, USA, [3] Department of Biomedical Engineering, University of Rochester, Rochester, NY, USA

Advances in recent years have dramatically improved output control by Brain-Machine Interfaces (BMIs). Such devices nevertheless remain robotic and limited in their movements compared to normal human motor performance. Most current BMIs rely on transforming recorded neural activity to a linear state space composed of a set number of fixed degrees of freedom. Here we consider a variety of ways in which BMI design might be advanced further by applying non-linear dynamics observed in normal motor behavior. We consider (i) the dynamic range and precision of natural movements, (ii) differences between cortical activity and actual body movement, (iii) kinematic and muscular synergies, and (iv) the implications of large neuronal populations. We advance the hypothesis that a given population of recorded neurons may transmit more useful information than can be captured by a single, linear model across all movement phases and contexts. We argue that incorporating these various non-linear characteristics will be an important next step in advancing BMIs to more closely match natural motor performance.

Keywords: brain-computer interface, hand, kinematic synergy, motor cortex, movement phase, muscle synergy, neuroprosthetics, null space

OPEN ACCESS

Edited by:
Mikhail Lebedev, Duke University, USA

Reviewed by:
Ioan Opris, Wake Forest University School of Medicine, USA
Aaron Batista, University of Pittsburgh, USA

***Correspondence:**
Marc H. Schieber, Department of Neurology, University of Rochester Medical Center, 601 Elmwood Avenue, Box 673, Rochester, NY 14642, USA
mhs@cvs.rochester.edu

Received: *11 January 2015*
Accepted: *13 July 2015*
Published: *28 July 2015*

Citation:
Rouse AG and Schieber MH (2015) Advancing brain-machine interfaces: moving beyond linear state space models. Front. Syst. Neurosci. 9:108. doi: 10.3389/fnsys.2015.00108

Introduction

Research and development of brain-machine interfaces (BMIs) to restore lost motor function has expanded dramatically in recent years. Whereas, not long ago the state of the art in both non-human primates (Serruya et al., 2002; Taylor et al., 2002) and humans (Hochberg et al., 2006) consisted of controlling a cursor on a computer screen, recent advances in restoring upper limb function have incorporated robotic arms with the ability to grip and manipulate objects using either virtual (Carmena et al., 2003; Chadwick et al., 2011) or robotic (Velliste et al., 2008; Hochberg et al., 2012; Collinger et al., 2013; Wodlinger et al., 2015) hands and digits. In addition to restoring upper limb function, innovative exoskeletons are being used to restore trunk and leg function (Fitzsimmons et al., 2009; Lebedev and Nicolelis, 2011). Functional electrical stimulation also has made possible restoration of movement of the subject's own limbs (Moritz et al., 2008; Pancrazio and Peckham, 2009; Ethier et al., 2012). Many of these advances have transitioned from the research laboratory with non-human primates to the clinical world with human subjects.

Different but inter-related improvements have contributed to these advances. Better recording systems that allow chronically implanted electrodes to record an increasing number of channels of neural activity simultaneously have had a major impact (Stieglitz et al., 2009; Homer et al., 2013).

Better understanding of how to extract various neural signals, paradoxically including less focus on precise spike sorting and more use of simple detection methods like threshold crossings (Fraser et al., 2009; Chestek et al., 2011; Hochberg et al., 2012; Wodlinger et al., 2015), the application of statistical models to better estimate firing rates (Cunningham et al., 2010), and the implementation of Kalman filtering (Wu et al., 2003; Li et al., 2009), all have improved BMI performance as well. Better appreciation of the neural adaptation that occurs under BMI conditions has led to dynamic updating of decoding algorithms that enable BMI learning to be both faster and more robust to external changes (Gilja et al., 2012; Orsborn et al., 2012; Zhang and Chase, 2013; Shanechi et al., 2014). A focus on overcoming the technical challenges of chronically monitoring larger and larger amounts of neural activity and on controlling increasingly complex devices has advanced the field substantially and quickly.

Over the same period during which these advances have been made, relatively little has changed in how our understanding of natural motor physiology is applied to BMI control. Current BMI designs almost always assume that neural encoding is a linear, time-invariant system with independent degrees of freedom (DOFs), and therefore implement control algorithms that map neural inputs to a constant set of output variables with a fixed gain. Yet neural control of mammalian motor systems and the behaviors they produce cannot be explained fully with such an idealized model.

Here we examine selected aspects of motor behavior and physiology to explore ways in which current scientific understanding might be exploited to advance the design of BMIs toward achieving performance closer to that of natural human movement. We discuss four different topics. First, we consider differences in motor performance for very fast or very slow movements and examine how BMI decoding might better emulate similar principles. Second, we address evidence that cortical activity—even in areas with significant spinal projections—differs considerably from a veridical representation of actual movement of the body and we consider the implications of these differences for continuous BMI operation. Third, we explore the evidence that natural movement is not statistically independent across different joints or muscles but rather is coordinated and we ask how this might be incorporated more extensively in BMI design. And fourth, we explore the implications of having a large neuronal population to generate movement, examining whether such a system can be modeled effectively with a single, linear state space, and asking whether adhering to such a model has become a limiting oversimplification in current BMI designs. Although the four topics we explore may appear diverse and unrelated, they share the common theme that incorporating a deeper understanding of the non-linear dynamics of normal motor behavior and physiology—during different phases of movement and in different contexts—can advance BMI design. Whereas, scientists generally seek to identify the simplest explanation for the largest set of observations and engineers seek to provide the simplest design to achieve a specific function (Müller et al., 2003), here we argue that the next wave of advances in BMI technology will require incorporating additional levels of complexity.

Dealing with a Wide Dynamic Range of Movement

Humans are capable of performing skilled movements on a wide range of spatial and temporal scales, from the athletic prowess of throwing or kicking a ball at speeds approaching 100 miles per hour (44.7 m/s) to the fine motor skills required for watchmaking and surgery. But throwing a ball is not necessarily controlled in the same fashion as knotting a suture. We therefore consider how control might vary depending on the extent to which a subject intends to make a gross movement quickly vs. a fine movement accurately.

Dynamic Range of Movements

In natural movements, Fitts's law (Fitts, 1954) describes a tradeoff between speed and accuracy: The faster the movement, the less accurate it will be; greater accuracy is achieved with slower movement. This principle has been documented in numerous natural movement tasks and under many different conditions (Card et al., 1978; Jagacinski and Monk, 1985; Epps, 1986; MacKenzie, 1992), in neural correlates (Ifft et al., 2011), and in BMI tasks with direct neural control (Felton et al., 2009).

Current BMIs, however, do little to emulate the robust range of behavior observed to follow Fitts's law for either very fast or very accurate movements, relying instead on the designer to pick a fixed gain between input neural signals and output magnitude. This practice effectively limits good BMI performance to a narrow range of the speed/accuracy trade-off. Enabling the user's neural activity to select the movement speed and the associated accuracy dynamically depending on the current phase or context of the task could improve BMI control, providing a range of performance closer to that of natural movements.

Improving the Precision of BMIs

Fine, skilled movements presumably require more precise neural control signals than gross movements, whether the control signal is encoding muscle activation, force, joint position, or velocity. A study by Slifkin and Newell (1999) found, for example, that whereas the average maximum voluntary contraction (MVC) of the index finger against a load cell was 31.07 N with a standard deviation of ∼2.1 N, when producing forces of 5% MVC (∼1.55 N) the standard deviation was only ∼0.09 N. Variability in normal human force production thus scales with the magnitude of force being produced. Such signal-dependent noise appears in many natural motor behaviors (Harris and Wolpert, 1998). Smaller movements are made with smaller errors.

A system that linearly transforms an input to output with constant noise cannot be optimized for fine, accurate movement and for gross, fast movement simultaneously. Indeed, cortical microcircuits in the motor system recently have been proposed to adjust neuron tuning according to the level of precision required. By functionally varying the overall strength of excitatory/inhibitory drive and changing the tuning widths of individual M1 neurons, the accuracy and precision of movement

encoding by a population of neurons might be adjusted dynamically (Mahan and Georgopoulos, 2013; Georgopoulos, 2014). Although natural adjustment of neuronal tuning may be present in the input neurons, current BMIs that rely on the linear sum of neural activity nevertheless show poor adjustment of precision compared to that found in natural movements. Such suboptimal adjustment of precision might result from the small number of input neurons compared to the natural motor system and/or the lack of adjustment for precision in the tuning and decoding models used currently.

BMIs therefore might be improved by creating decoding schemes that more explicitly allow for encoding of the speed-accuracy tradeoff from a recorded subpopulation. If we construct a BMI model that uses instantaneous neuronal firing rates to encode velocity in a single dimension with a simple linear encoder, the magnitude of the error is uniform for all encoded velocities (**Figure 1A**). If instead the neurons in the model are assigned to encode a rescaling of velocity, the square root of velocity for example, the errors near zero velocity are smaller than those for high velocity (**Figure 1B**), more closely emulating the signal-dependent noise of natural behavior (**Figure 1C**). Applying such approaches to create noise profiles that more closely match natural behavior is likely to create BMI controlled movements that appear more natural by allowing greater precision for fine movements.

The Relationship of Cortical Activity to Physical Movement

The majority of current BMIs that control motor output use neural activity recorded from motor and premotor areas of the cerebral cortex as input for two reasons. First, many aspects of natural movements are represented in the activity of neurons in these cortical areas. Second, the cerebral cortex can be accessed for neural recording relatively easily compared to deeper parts of the brain and spinal cord. But using only cortical activity has other advantages and disadvantages for BMI control: (i) certain features of cortical activity are not output to physical movement of the body, (ii) the tuning of cortical neurons changes when controlling a BMI, and (iii) certain aspects of physical movement may not be controlled directly from the cortex.

Motor Imagery, Mirror Neurons, and BMI Control

During motor imagery, when humans imagine themselves performing movements without actually making any movement, activation appears in many of the same cortical motor areas that are activated during physical movement performance, including the primary motor cortex (Ersland et al., 1996; Grafton et al., 1996; Porro et al., 1996; Pfurtscheller and Neuper, 1997; Anderson et al., 2011; Ajiboye et al., 2012). Likewise during action observation, when a monkey observes another individual performing a particular movement, a large subpopulation of neurons discharges in a fashion similar to their discharge when the monkey executes the same action itself. These "mirror neurons," as well as other neurons that are activated when the monkey observes a cursor moved by the investigator, have been observed not only in premotor cortex but in primary motor cortex as well (Cisek and Kalaska, 2004; Tkach et al., 2007; Dushanova and Donoghue, 2010; Casile, 2013; Vigneswaran et al., 2013). Many neurons in motor cortex thus discharge during motor imagery and/or action observation, when subjects are not making any physical movement.

BMI experiments with normal subjects are perhaps the most clear-cut demonstration that neurons active during natural movements can also be activated voluntarily in the absence of

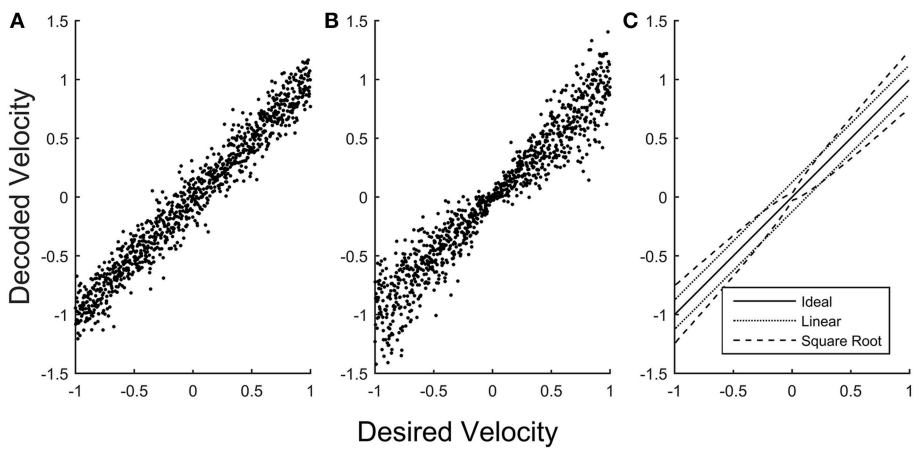

FIGURE 1 | Error in simulated velocity decoding. A simulated population of neurons was scaled to encode velocities (with a maximum system velocity equal to 1) using two different methods. **(A)** The simulated population encodes linear velocity, producing uniform error in the decoded velocity that is independent of the desired velocity. **(B)** The simulated population (with the same dynamic range and noise properties of the neurons) is now scaled to encode the square root of velocity, producing error in the decoded velocity that becomes smaller for velocities closer to zero. **(C)** The standard deviation of decoded velocity is plotted as a function of desired velocity for the linear model (**A**, dotted) and for the square root model (**B**, dashed), emphasizing that when decoding linear velocity the error is constant across desired velocities, whereas for the square root model the error is smaller close to zero velocity and larger for higher velocities.

physical movement. In such BMI experiments, normal monkeys typically first perform a task involving physical movement of their native limb while neural activity is recorded from the cortex. This activity then is used to calibrate a decoding algorithm that relates the recorded neuronal activity to the observed limb movements. But after switching to "brain-control"—now controlling a cursor or prosthesis directly through the decoding algorithm—the monkey often stops making any physical movement or producing any EMG activity, even though allowed to move freely (Taylor et al., 2002; Carmena et al., 2003). Meanwhile, the recorded neurons continue to modulate, voluntarily controlling the external BMI device. Like mirror neurons, these neurons are activated during physical movement of the native limb, but are not obligatorily coupled to physical movement. Though in most BMI experiments neurons have not been tested for such, many of them might have activity during action observation.

Indeed, we know that neurons activated during action observation can be used for voluntary BMI control, because in both normal monkeys and paralyzed humans neuronal activity recorded during action observation can be used effectively to develop the initial decoding algorithm (Velliste et al., 2008; Chadwick et al., 2011; Collinger et al., 2013). Although using neurons activated by action observation currently provides an advantage for calibrating BMIs in paralyzed or amputated subjects, using mirror neurons might have disadvantages as well. In one recent study, for example, having a particular object present during the initial calibration was needed to enable the subject subsequently to close the prosthetic hand optimally around that object (Wodlinger et al., 2015), possibly indicating that the recorded population included a substantial number of mirror neurons encoding that particular grasp shape. More detailed scientific understanding of the differences in neuronal activity during motor imagery vs. action observation vs. action execution may enable BMI decoding based on these differences to improve performance.

Changes in Cortical Activity during BMI Control

The change from "hand-control" to "brain-control" changes cortical activity. Many neurons, for example, show changes in their directional tuning (Taylor et al., 2002; Ganguly and Carmena, 2009). Such changes may result from alterations in proprioceptive feedback because a normal subject's native limb that moved during hand-control either moves differently or does not move at all during brain-control. Differences may exist as well in the descending regulation of sensory input to the spinal cord, which changes during voluntary movement as compared to rest (Seki et al., 2003). Visual inputs change too. If the subject is controlling a prosthetic arm, its visual representation obviously will differ from that of a native arm, as will incorporation of the prosthesis into the internal body schema (i.e., embodiment). Even if the subject is controlling a cursor on a computer screen, the visual motion of the cursor viewed by the subject will differ, being smoother and more accurate during hand-control but showing more jitter during brain-control. In addition, many changes in cortical activity may represent adaptation on the part of the subject to fit the linear model of the BMI decoder (Wolpaw, 2010; Chase and Schwartz, 2011). More detailed scientific understanding of such changes in cortical activity that occur upon switching to brain-control may improve BMI performance.

Transformations in the Spinal Cord and Phases of Motor Control

Though classically viewed as a simple communication channel between the brain and the motor periphery, the spinal cord now is known to contain complex circuits that make important contributions to natural movements. Beyond the basic reflex pathways that can elicit movement from sensory input through only one or two synapses without cortical interaction, central pattern generators in the spinal cord can produce complex rhythmic behaviors without patterned input from the brain or feedback from the periphery (Shik and Orlovsky, 1976; Stein, 1978; Grillner, 1985). Descending signals from the brain are likely to engage parts of this spinal circuitry for production of other, non-rhythmic movements as well (Georgopoulos and Grillner, 1989). Indeed, in most mammalian species, the descending fibers of the corticospinal tract end on spinal interneurons, not motoneurons. And in macaques, which do have direct cortico-motoneuronal (CM) projections, spinal interneurons output different information (Maier et al., 1998; Fetz et al., 2002). For example, whereas most CM-cells were active selectively when subjects exerted either flexion or extension wrist forces, a high percentage of spinal interneurons were active for both flexion and extension force production, as well as at rest. With such complexity in the spinal cord, it becomes apparent that spinal cord circuitry may be doing much more than simply relaying the current input of descending cortical signals to generate muscle activity.

An emerging distinction between motor signals in the cortex vs. those in the spinal cord has to do with relative degrees of dynamic vs. static function in controlling non-cyclical limb movements. Neurons in the motor cortex typically are relatively quiescent during maintenance of a steady posture, become intensely active leading limb movement, and then show declining activity as a new steady posture is established. In large part such observations are attributable to a stronger relationship to movement velocity than to position (Moran and Schwartz, 1999). Moreover, strong rotational dynamics of joint M1 neuron firing rate trajectories may reflect a complex, dynamical system responsible for the encoding of movement (Churchland et al., 2012; Hall et al., 2014). In comparison to cortical neurons, spinal interneurons show more static activity. In monkeys generating wrist forces isometrically and auxotonically, for example, cortical neurons produced relatively transient signals for ensuing motor actions while spinal neurons generated more sustained activity, suggesting that to some degree cortical signals to change state are integrated by spinal circuitry (Shalit et al., 2012). Indeed, recent models of spinal-like regulators have demonstrated that oversimplified step inputs from the brain could be transformed by spinal circuitry to replicate much of observed center-out reaching behavior (Tsianos et al., 2014). Implementing such spinal-like circuitry in BMIs may substantially improve the quality of the transitions between movement and posture.

The transition from movement to posture is but one example of what more generally might be considered different sequential phases of motor control. A single decoder cannot be expected to deal with all phases efficiently. Cortical neurons can be identified, for example, that are active specifically in relation to rest/posture in contrast to movement (Humphrey and Reed, 1983; Williams et al., 2013; Velliste et al., 2014). Including such neural activity in the same linear decoding algorithm that drives movement velocity would be counterproductive. But if one decoder used movement-related activity to drive motion during movement phases, and another decoder used posture-related activity to maintain position during postural phases, smoother and more efficient performance might be obtained. Such control would require yet another decoding algorithm to identify transitions between phases, sometimes referred to as changes of state (Kemere et al., 2008; Aggarwal et al., 2013; Kang et al., 2015). Sequential phases or states may include not just alternation between movement and posture, but also inattention, watchful waiting for an instructional cue, preparation of a specific motor plan, reaction time following a go cue, then reaching, grasping, manipulation, and others as well. Detecting these various phases and decoding them differently may be an important step toward achieving natural human performance with BMIs (see also section More Neurons than Controlled DOFs creates a Null Space, below).

Controlling Multiple Degrees of Freedom

Independent Degrees of Freedom

Analysis of voluntary movement consistently has shown that natural movement almost never occurs in isolation at a single joint or by activation of a single muscle, even the movement of a single finger (Hager-Ross and Schieber, 2000). For example, typists and pianists produce simultaneous movements of multiple digits even when striking a single key (Flanders and Soechting, 1992; Engel et al., 1997). Nevertheless, most of the variance of complex multi-joint movements can be reduced mathematically to a relatively small number of principal components, each of which captures a pattern of simultaneous motion at multiple joints (Santello et al., 1998; Mason et al., 2004). Such findings suggest that the number of DOFs being controlled actively during many natural movements might be less than the number of DOFs actually moving.

Bernstein (1967) first defined this problem of redundant DOFs in the musculoskeletal system: Many movements made in three-dimensional space engage more than three joint angles and more than three muscles. Mathematically, therefore, a given movement can be made in many different ways, i.e., infinite possible solutions can successfully accomplish a given movement task. Observing blacksmiths, for example, Bernstein noticed that while the joints of the arm might take quite different trajectories during a series of hammer strikes, the endpoint of contact was very consistent. This and other observations of considerable variation in certain DOFs while others are controlled precisely was formulated subsequently by Scholz and Schöner (1999) as the uncontrolled manifold hypothesis: Within the high dimensional configuration space that completely defines movements for a given task, there exists two orthogonal subspaces. Motion in a controlled subspace contains a set of actively controlled variables that are being monitored and controlled by the subject and are most important to completing the task. The other, uncontrolled subspace contains all motion orthogonal to the controlled variables and thus has no effect on successful task completion. Increased variability has been observed in the uncontrolled subspace compared to the controlled subspace in a wide variety of natural movement tasks (Scholz et al., 2001; Latash et al., 2002; Tseng et al., 2002; Kang et al., 2004), and recently in neuronal activity as well (Kaufman et al., 2014; Law et al., 2014).

Current BMI design, however, remains limited in strategies that take into account the relative importance of the various DOFs in different tasks, instead controlling the same fixed set of DOFs of the prosthetic device independently at all points in time. Likewise, regression and updating algorithms assume each DOF is encoded equally at all times. As the number of DOFs increase, BMI control becomes more difficult because more DOFs must be monitored and controlled by the subject. Models that more closely align BMI control at a given time with a subset of DOFs selected judiciously for the current task may enable more intuitive and precise control.

Kinematic and Muscular Synergies

One means of selecting subsets of multiple DOFs for BMI control is to look for naturally occurring patterns of simultaneous motion at multiple joints or patterns of simultaneous activation of multiple muscles. A small number of fixed patterns of multi-joint motion (Santello et al., 1998; Mason et al., 2004) or multi-muscle activity (d'Avella and Bizzi, 2005), each varying in amplitude and timing, in theory could produce a very large repertoire of smoothly coordinated motor output. Synergies that distribute forces across the fingers can also provide a balance between flexibility and stability (Latash et al., 2007).

Indeed, synergies identified with dimensionality reduction techniques—such as principal component analysis or non-negative matrix factorization—can provide a simplified view of complex movements. Two important scientific questions are (i) whether such synergies are, in fact, used by the nervous system in controlling natural movement, and if so, (ii) in what part(s) of the nervous system the synergies are instantiated. Recent studies indicate that many fundamental synergies may be organized in the brainstem and spinal cord, rather than the cortex (Buford and Davidson, 2004; Cheung et al., 2009; Baker, 2011; Roh et al., 2011; Giszter and Hart, 2013). Once these two questions have been answered, BMI performance might be enhanced by recording from these regions and using the decoded output to drive the relevant synergies rather than the individual degrees of freedom.

Whether or not synergies are used naturally by the nervous system, performance might be improved by incorporating synergies in BMI design. One synergy already in use involves control of arm endpoint in 3 dimensions (i.e., the location of the hand) with a robotic arm that has 4 rotational DOFs: 3 at the shoulder and 1 at the elbow (Lebedev et al., 2005; Velliste et al., 2008; Hochberg et al., 2012). Rather than providing the subject with independent control of all 4 DOFs, BMI output typically drives motion of the arm's endpoint in the

3 Cartesian coordinates (e.g., horizontal, vertical, depth), and this 3-dimensional output is partitioned across the 4 rotational DOFs by a fixed subroutine. Eliminating one DOF in this manner simplifies the control task for the subject at the cost of restricting the ways in which the robotic arm can move. Further incorporation of such simplifying synergies may enable the apparent complexity of movements achieved with BMIs to grow more rapidly than the complexity of control actually required of the subject.

Some synergies might be incorporated even in device hardware. For example, in the majority of hand motion for grasping, the four fingers extend roughly in parallel to open the hand. Rather than providing separate actuators (motors and cables) to extend each finger independently, a robotic hand could have one motor with a cable that divides to attach to each finger, reducing 4 DOFs to 1. Furthermore, extension of the fingers is rarely if ever used to apply substantial forces to objects, this being accomplished with finger flexion. If the extensor cable to each finger could be elastic, then independent flexion of each finger still could be achieved by independent flexion actuators for each finger.

Synergies may be especially useful in controlling a prosthetic hand. Whereas, motion of the shoulder, elbow, and wrist to transport and orient the hand involves 7 rotational DOFs, motion of the thumb and fingers involves 22. Yet even in sophisticated uses of the hand such as typing or piano playing, rarely if ever are individual DOFs moved independently (Soechting and Flanders, 1992, 1997; Engel et al., 1997). Current BMI decoding methods nevertheless assume separate channels for each individual digit, with no relationship between them. And state-of-the-art robotic hands now provide almost as many DOFs as are found in the natural hand (Dalley et al., 2010; Johannes et al., 2011; Resnik et al., 2013; Hutchinson, 2014). For most uses of the hand in activities of daily living, current BMI systems that attempt to control all the DOFs in the hand independently may, in fact, be overly complex.

Nevertheless, identifying an optimal set of synergies for controlling a prosthetic hand is far from simple. An orthogonal basis set of the multiple joints of the hand created with dimensionality reduction has obvious advantages both in its simplicity as well as straight-forward implementation in BMI applications (Ciocarlie et al., 2007; Vinjamuri et al., 2011; Velliste et al., 2012). Alternatively, observation can be used to select a limited set of basis functions. In one recent study, a human subject grasped a variety of objects by controlling a robotic hand through four independent basis functions identified by clinical observation of hand use: (i) pinch between the thumb and index, (ii) flexion and extension of the ring and little fingers in parallel, (iii) ab/adduction of all the fingers, and (iv) opposition of the thumb (Wodlinger et al., 2015). Yet such a simple, orthogonal basis set may fail to capture certain desirable features of hand motion. For example, while the flexion/extension of all five digits is a synergy commonly identified by analysis of hand movements, the thumb and index finger also move more independently than the other three digits. Thus, difficulty arises in trying to design a simple basis set that allows for a single degree of freedom that controls the opening and closing of all digits of the hand while also allowing independent control of the thumb and index finger.

While simplifying control, fixed synergies thus necessarily limit the ability to create all of the diverse movements of which humans are capable. An alternative model by Arbib and colleagues described "virtual fingers" and a schema that added or subtracted the number of digits to a central gripping controller depending on the size and shape of the object to be grasped (Arbib et al., 1985). This virtual fingers model essentially creates different synergies depending on the context of object size and shape. Extending the use of different sets of synergies depending on the particular task or context (e.g., throwing a ball vs. typing) may advance BMI control substantially toward normal human performance. Fully independent control of all the hand's DOFs may be valuable only for the most sophisticated uses of the hand.

More Inputs than Outputs

Redundancy in Neuron Populations

Of the roughly 100 billion neurons in the human cerebral cortex, approximately 1.4 million send axons through the corticospinal tract to synapse on motoneurons and interneurons in the spinal cord (Lassek, 1954). In achieving the remarkable performance of normal humans, these fibers convey much of natural cortical control to the "physical plant," which consists of approximately 600 muscles and 200 mechanical DOFs at the joints. At present, BMIs can sample only a small subset of any neuron population. As long as the sampling is reasonable, linear decoders can extract a representation of native limb motion and drive BMI end-effectors in multiple DOFs. A current trend, however, is to record increasing numbers of neural signals (Fitzsimmons et al., 2009; Lebedev and Nicolelis, 2011) with the goals not only of controlling more DOFs, but also of making the BMI more robust both to natural variability in neuron firing and to dropout of previously recorded neurons. How does the number of neurons used to control a BMI affect performance?

In the simplest BMI, a single neuron might be used to control each DOF (Fetz and Baker, 1973; Law et al., 2014). **Figure 2A** schematically illustrates 2 neurons (gray arrows) controlling 2 dimensions, using the familiar population vector approach. Each gray arrow represents a different neuron, the direction of the arrow represents that neuron's preferred direction, and the length of the arrow represents its firing rate. The black arrow represents the resulting population vector, and the cardioid curve indicates the idealized linear model of cosine tuning relative to the current output, i.e., the population vector. This arrangement has a major limitation: the noisiness of the individual neurons will produce equivalent noise in the resultant output.

Increasingly precise output can be obtained by linear summation of the observed firing rates of more neurons. **Figure 2B** illustrates such a situation, now using 20 neurons. In an idealized linear encoding model—where all neurons have the same noise properties and are independent—adding more neurons reduces error. Regardless of the specific partitioning of linear encoding across a population of n neurons, the predicted error decreases as $1/\sqrt{n}$, as follows from the central limit theorem. Adding more neurons thus progressively reduces

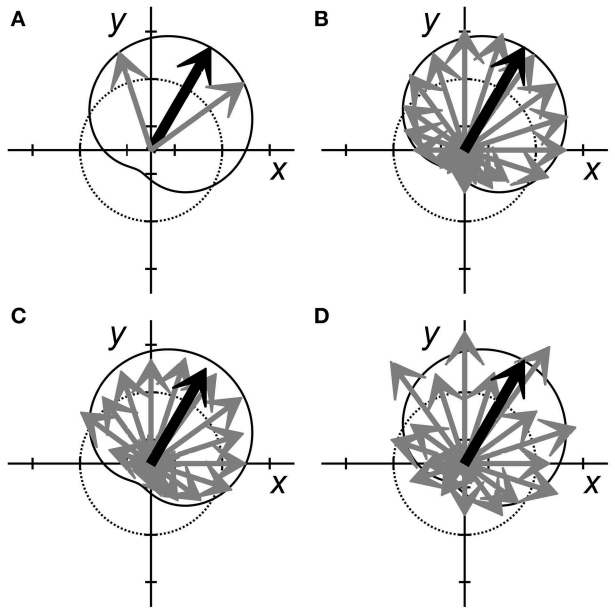

FIGURE 2 | Population vectors for neural encoding of two variables, *x* and *y*. Each neuron is represented by a gray arrow pointing in each cell's preferred direction. The length of each arrow represents the neuron's firing rate. The dotted circle represents a normalized baseline rate for each neuron, with arrow lengths greater than the dotted line representing increased firing rates and shorter lengths representing decreased firing rates. The black arrow represents the population vector sum that predicts the variables, *x* and *y*. The solid cardioid curve represents the expected firing rates of perfectly tuned neurons with various preferred directions when $x = 0.5$ and $y = 0.87$. **(A)** Two perfectly tuned neurons can encode *x* and *y* exactly, but the noise of the output will be equivalent to the noise of the two inputs. **(B)** More independently noisy neurons (here 20 neurons) can be combined to generate an accurate estimate of *x* and *y* with less noise. **(C)** When noise is correlated across neurons, adding more neurons to the population may not improve prediction. In this example, noise produced a correlated reduction in the firing rates of most neurons, resulting in a low amplitude prediction (small population vector). **(D)** In this example, although the neural activity does not match the tuning model (solid cardioid) as accurately as in **(B)**, the predicted *x* and *y* values nevertheless are similar. This departure from the tuning model for *x* and *y* might represent either increased noise, or the encoding of additional features.

error albeit requiring progressively increasing numbers of additional neurons for a given magnitude of reduction in error. In practice, as the number of neurons used for BMI control has increased, achieving BMI accuracy that matches idealized encoding behavior has become increasingly difficult. BMI performance tends to plateau once ∼50 recorded neurons have been incorporated, after which much less improvement occurs as more neurons are added (Homer et al., 2013; Tehovnik et al., 2013).

This departure from ideal encoding results in part from the fact that neurons typically are not entirely independent of one another. Sampled neurons often have correlations related not only to the encoded signal, but also to other signals. The correlations produced by these other signals—signals that typically are unknown, unmonitored, and not experimentally controlled—constitute noise with respect to the signal being encoded (Lee et al., 1998). When the noise is correlated, even weakly as is typically observed in cortical recordings (Zohary et al., 1994), perfectly accurate linear encoding becomes impossible. Noise correlations, for example, could cause the estimate for a given trial to converge to an incorrect value. **Figure 2C** illustrates such an example in which a correlated decrease in firing amongst many members of a neuron population causes the magnitude of the resulting population vector to be too small. Even as more and more neurons are added to the decoded population, such noise correlations prevent converging toward perfect decoding.

As more and more neurons are added, incorporating some individual neurons to decode a given variable may actually be detrimental to BMI performance. The relative strength of various signals among different neurons may make adding some neurons corrupted by correlated noise worse than using only those with strong, independent signals. In a BMI application, the ability to generalize control from an initial regression is critical and runs the risk of overfitting if the amount of sampled data is too small for the number of neurons. Also, the ability of the user and/or the decoder to adapt and learn quickly may be diminished as the neural space that must be explored becomes larger. Recognizing such issues, algorithms have been developed to identify those neurons that provide the most independent information, permitting more parsimonious selection of neurons for input to the decoding algorithm (Singhal et al., 2010; Kahn et al., 2011; Xu et al., 2013).

Additionally, the noise levels across a population related to a given variable may not be stationary with time. **Figure 2D** illustrates a situation in which the individual neurons appear to be relatively noisy. Though the population vector is similar to that of **Figure 2B**, in **Figure 2D** the individual neurons appear to deviate randomly from the idealized cosine tuning model indicated by the cardioid curve. Yet this apparent noisiness might represent another signal encoded by the same neuron population (see section Selective Encoding of Variables at Different Times below). How can we make judicious choices regarding the number of neurons used for BMIs?

More Neurons than Controlled DOFs Creates a Null Space

Although the optimal trade-off between the number of neurons recorded and the number of DOFs being controlled by linear BMIs has yet to be well understood, some insight can be gained by considering the simultaneous firing rates of a population of *n* recorded neurons as an *n*-dimensional space. When used as a linear signal to control *d* DOFs, the *n*-dimensional neural signal is projected into a smaller *d*-dimensional active control sub-space, leaving a null space of dimensionality $m = n–d$. Neural activity that projects along the *m* null-space dimensions has no effect on the *d* output DOFs. If the neurons are independent predictors, then most noise tends to result in changes in this null space of the joint neural state, allowing an ensemble of "noisy" neural signals to encode the output more precisely.

Yet the null space may be more than a repository for noise. Much of what appears to be noise related to a given signal may represent neural activity related to other signals encoded

by the same population of neurons. Below we explore two other potentially valuable aspects of the null space that permit: (i) motor learning with rapid flexibility, and (ii) non-linear encoding that repartitions the active control space vs. the null space depending on the phase of movement.

The Null Space and Motor Learning with Rapid Flexibility

While the null-space can be considered an "uncontrolled manifold" in a particular movement scenario (Scholz and Schöner, 1999; Latash et al., 2007), in the case of a neuronal state space, the uncontrolled manifold is not entirely uncontrolled. During both natural arm movements and BMI output, the joint neural state tends to follow a subset of preferred trajectories that use a subset of the null space, rather than using all possible trajectories distributed throughout the n-dimensional neural space that could provide an equivalent output (Kaufman et al., 2014; Law et al., 2014). Preferred trajectories through the neural state space may reflect the network architecture of pre-existing synaptic connections in which the neurons are embedded (Sadtler et al., 2014). Yet to control novel BMIs, monkeys can learn to use relatively novel neural trajectories (Jarosiewicz et al., 2008; Ganguly and Carmena, 2009; Ganguly et al., 2011; Law et al., 2014). A similar process of learning to use novel neural trajectories may underlie the natural process of learning new motor skills and then switching rapidly at will between one skill and another, according to the context. The relatively large number of neurons, $n > d$, is no longer entirely redundant when additional trajectories through the neural state space must be utilized in additional contexts. Finding and utilizing such additional trajectories might entail learning to associate a previously learned trajectory with a new context, modifying a previously learned trajectory for use in a new context, or learning an entirely new trajectory through the neural state space.

Some evidence that motor learning and rapid flexibility in various contexts involve changes in neural trajectories can be gleaned from studies that use spike-triggered averaging of EMG activity to assess functional connectivity among those neurons that provide last-order inputs to particular motoneuron pools. Broad synchrony facilitations in spike-triggered averages of EMG activity provide evidence that synchronous spikes are discharged by multiple neurons with inputs to the same motoneuron pool, indicating that groups of such neurons receive common or serial inputs (Baker and Lemon, 1998; Schieber and Rivlis, 2005). Among M1 cortico-motoneuronal (CM) cells, such spike synchronization is most common between CM-cells that have output effects in similar sets of muscles (muscle fields), suggesting that these groups of neurons may be recruited together to facilitate a particular set of muscles (Jackson et al., 2003). The prevalence of synchrony effects in M1 neurons increases with long-term training at an individuated finger movement task (Schieber, 2002), suggesting that such long-term training increases the common inputs to neurons that all input in turn to the same motoneuron pool. This change in common inputs will alter the neural trajectory during the practiced movements. Yet the size of synchrony effects also can change rapidly when novel motor behaviors are being performed (Davidson et al., 2007), suggesting that different common inputs to the population of neurons with last-order inputs to a given motoneuron pool become active in different contexts, again indicating different neural trajectories for different contexts. These rapid changes depending on context may involve processing in cortical minicolumns and corticostriatal circuits, where the level of functional connectivity (as measured by cross-correlations between simultaneously recorded spikes in layer 2/3 and layer 5 of a minicolumn, for example) has been found to vary with the type and difficulty of the task being performed (Opris et al., 2012, 2013; Santos et al., 2014). For optimal performance, BMIs will need to take into account such context-dependent changes in neuron activity and the changes in neural trajectories they represent.

Selective Encoding of Variables at Different Times

This idea that the firing of an individual neuron simultaneously carries representations of multiple motor parameters has been widely accepted in neurophysiological studies for some time (Humphrey et al., 1970; Thach, 1978). In general, however, neurophysiological studies make the implicit assumption that the relative weighting of the encoded motor variables remains stationary over the time course of single movements and entire sessions. The same assumption typically is made in current BMI controllers.

Yet some neurophysiological studies have indicated that the motor variables being encoded are not constant, even within a single movement. Time-resolved linear regression, for example, demonstrated that in single M1 and premotor cortex neurons, direction is represented most strongly early in the course of reaching movements, target position is represented most strongly later, and distance is represented most strongly still later in the same movements (Fu et al., 1995). Similarly, using time-resolved analysis of variance, we found recently that the firing rates of M1 neurons vary depending on location early in the course of reach-to-grasp movements, and then on the hand shape used to grasp the object later (Rouse and Schieber, 2014). Such changes in the strength of representation of different features can be viewed as rotations of the d controlled dimensions in the n-dimensional neural state space, which will repartition the m null-space dimensions across the time of a single movement. Hence different variables are represented more or less selectively at different phases of a single movement, and the apparent "null" space provides room for such rotations to occur.

Figure 3 and the Supplemental Video both illustrate this hypothetical repartitioning of the active control space vs. the null space, again using the familiar population vector approach. As in the 2-dimensional examples of **Figure 2**, each arrow represents a different neuron, the direction of the arrow represents that neuron's preferred direction, and the length of the arrow represents its firing rate. In **Figure 2**, the $d = 2$ active dimensions were represented as the ordinate and abscissa of the plot, and the output of the single, linear model depended only on the resulting population vector sum in those two dimensions. Similarly in **Figure 3A**, we plot a population of 20 neurons (colored arrows)

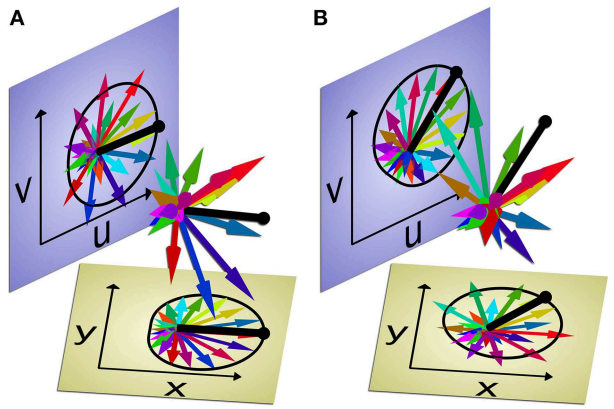

FIGURE 3 | Multi-dimensional population vector selectively encoding two pairs of variables at different times. Each of 20 neurons is represented by a colored arrow pointing in its preferred direction. The length of each arrow represents that neuron's firing rate. The two planes, $x \perp y$ (tan) and $u \perp v$ (blue), each show the individual neuron's firing rates and preferred directions projected into the two pairs of dimensions. The population vector sum (heavy black line) projected into each plane represents the population's estimate of the two pairs of variables: *x* and *y*, *u* and *v*. The black cardioid curve represents the predicted firing rates given the population vector if each neuron was ideally cosine-tuned to a given pair of variables (*x* and *y*, or *u* and *v*). The two panels **(A,B)** represent two different points in time. At the first time point **(A)**, the individual neuron firing rates are related most closely to *x* and *y*, matching the idealized cosine tuning to those two variables, as represented by the cardioid in that plane. But at the second time point **(B)**, the firing rates of the same 20 neurons are related most closely to *u* and *v*. The firing rates of these neurons may not be representing both pairs of variables equally at all points in time, but rather selectively encoding one pair of variables at each time. At either time point, if a single linear decoder were used to estimate all four dimensions—*x*, *y*, *u*, and *v*—simultaneously from the population, one pair would be estimated accurately and the other pair inaccurately. But using two different decoders—one to estimate *x* and *y*, the other to estimate *u* and *v*—and then selecting the currently decoded output by assessing which idealized model is better fit at the time, would enable more accurate decoding overall. The Supplemental Video provides an animated version of this Figure. (N.B. To illustrate a 4-dimensional space in 3-dimensions, we have made *u* linearly dependent on *x* and *y* in these images; but in the actual high-dimensional neural space, all four variables can be linearly independent).

projected into the plane of two output dimensions, *x* and *y*, and the resulting population vector (black). As in **Figure 2B**, at the point in time illustrated in **Figure 3A** each individual neuron's firing rate closely matches the idealized linear model represented by the cardioid curve drawn to indicate the cosine tuning of individual neurons to the variables *x* and *y* relative to the population vector.

The remaining $m = 20–2 = 18$-dimensional null space has no direct effect on the output (population vector) of this model in this $x \perp y$ plane. But consider the neural activity in two of these null dimensions, *u* and *v*. The neuron firing rates and resulting population vector projected in the $u \perp v$ plane also are illustrated in **Figure 3A**. A different cardioid curve is shown here to represent the cosine tuning that pertains when the population vector is calculated using a second idealized model based on the projections of the neuron firing rates in the $u \perp v$ plane. In the $u \perp v$ plane, the firing rates of the individual neurons match this second model poorly, not unlike the example of **Figure 2D**.

Now consider a different point in time when the individual neurons are firing at different rates, illustrated in **Figure 3B**. Now the firing rates match the cardioid in the $x \perp y$ plane poorly, but match the cardioid in the $u \perp v$ plane well. The same neuron population that encoded *x* and *y* previously, now is encoding *u* and *v*. We hypothesize that in this manner a given neuron population may encode different variables selectively during different phases of a single movement. In such a construct, treating the 20 neuron population as a 4-dimensional output space that continuously encodes *x*, *y*, *u*, and *v* plus a 16-dimensional null space would be suboptimal. For BMI purposes, decoding different variables at different points in time would provide more accurate output for the two variables as each becomes most relevant to the current phase (or context) of movement. At each point in time, the model most heavily weighted in the BMI output could be selected by having the computer assess which idealized model is better fit by the neuron firing rates currently being generated by the brain.

Such selective neural encoding of different sets of variables at different times might be dismissed as simply reflecting an inability to create a single linear model fitting all the observed firing rates well. An inaccurate single model might result from having insufficient data (numbers of trials), insufficient numbers of neurons (e.g., $n >> 20$ is needed), or insufficient sampling of the high-dimensional parameter space (…*u, v,* …*x, y*…). Yet if a given population of neurons does indeed represent different output features at different times, applying a single linear model cannot achieve high accuracy at all points in time regardless of how many neurons or how much data are incorporated. Non-linear models will be needed to repartition the active control space vs. the null space.

As reviewed above (section The Null Space and Motor Learning with Rapid Flexibility), we envision that during natural behavior the nervous system achieves the non-linear repartitioning that selects different controlled variables by coactivating, or even synchronizing, various subpopulations of neurons at different times. In view of the wide range of inputs that impinge on a single α-motoneuron (including Ia afferents, Ia-inhibitory interneurons, excitatory spinal interneurons, and CM-cells) or that affect a single M1 neuron (including inputs from the primary somatosensory cortex, ventral premotor cortex, dorsal premotor cortex, supplementary motor area, and thalamus), we hypothesize that non-linear repartitioning may involve various inputs predominating at different times, with synaptic summation that is not necessarily linear. The extent to which the nervous system naturally uses non-linear repartitioning to output different features from the same neuron population at different times remains an open scientific question.

In any case, BMI performance might be improved by implementing methods that allow for selective encoding of the variables most relevant to the current phase of movement. This could be achieved by applying different decoding algorithms to sequentially capture different features of complex movements (Ethier et al., 2011; Jiang et al., 2011; Srinivasan and da Silva, 2011; Shanechi et al., 2012; Aggarwal et al., 2013; Kang et al., 2015). Rather than continuously decoding all DOF simultaneously, the BMI controller might use population neural

activity to encode only a subset of variables while other variables are either passively dampened or even held constant by the BMI. Controlling a robotic arm and hand to reach and grasp, for example, might be improved by using neural activity sequentially, first to encode the reach location to which the arm transports the hand, and then as the hand arrives near the object, switching to encode the grasp while damping further movement of the arm. This could allow the user to focus on grasping the object precisely, without the distraction of simultaneously continuing to control the entire arm.

Conclusions

A general theme that emerges from our considerations is that natural motor control is not a single process that applies universally in all situations. The control of small, fine movements differs from that of large, gross movements. The control of posture is not achieved by producing movement with zero velocity. Many movements may be controlled through small numbers of synergies, and only the most sophisticated performances may require individuated control of large numbers of DOFs. In generating complex movements, the same neuronal population may transmit information on different sets of output variables sequentially rather than simultaneously. To advance the performance of BMIs further toward that of normal humans will require similar strategies that go beyond one-size-fits-all, linear state space models.

Achieving such advances necessarily will require increasing the complexity of BMI controllers. Decoding will need to be more flexible and applied differently at different times, possibly driven by inputs recorded from different parts of the nervous system. Moreover, supervisory algorithms will be needed to identify the contexts and movement phases that define this dynamic relationship between neural signals and output DOFs. Implementing such designs will go further to translate our knowledge of natural motor control physiology, advancing BMIs toward normal human performance.

Acknowledgments

This work was funded by National Institutes of Health R01s NS065902 and NS079664. The authors thank the anonymous reviewers for helpful suggestions and Marsha Hayles for editorial comments.

Supplementary Material

The Supplementary Material for this article can be found online at: http://journal.frontiersin.org/article/10.3389/fnsys.2015.00108

References

Aggarwal, V., Mollazadeh, M., Davidson, A. G., Schieber, M. H., and Thakor, N. V, (2013). State-based decoding of hand and finger kinematics using neuronal ensemble and LFP activity during dexterous reach-to-grasp movements. *J. Neurophysiol.* 109, 3067–3081. doi: 10.1152/jn.01038.2011

Ajiboye, A. B., Simeral, J. D., Donoghue, J. P., Hochberg, L. R., and Kirsch, R. F. (2012). Prediction of imagined single-joint movements in a person with high-level tetraplegia. *IEEE Trans. Biomed. Eng.* 59, 2755–2765. doi: 10.1109/TBME.2012.2209882

Anderson, W. S., Weiss, N., Lawson, H. C., Ohara, S., Rowland, L., and Lenz, F. A. (2011). Demonstration of motor imagery- and phantom-movement related neuronal activity in human thalamus. *Neuroreport* 22, 88–92. doi: 10.1097/WNR.0b013e328342c98a

Arbib, M. A., Iberall, T., and Lyons, D. (1985). "Coordinated control programs for movements of the hand," in *Hand Function and the Neocotex (Experimental Brain Research Series)*, eds A. W. Goodwin and I. Darian-Smith (Heidelberg: Springer–Verlag), 111–129.

Baker, S. N. (2011). The primate reticulospinal tract, hand function and functional recovery. *J. Physiol.* 589, 5603–5612. doi: 10.1113/jphysiol.2011.215160

Baker, S. N., and Lemon, R. N. (1998). Computer simulation of post-spike facilitation in spike-triggered averages of rectified EMG. *J. Neurophysiol.* 80, 1391–1406.

Bernstein, N. A. (1967). *The Co-ordination and Regulation of Movements,* 1st Edn. Oxford: Pergamon Press.

Buford, J. A., and Davidson, A. G. (2004). Movement-related and preparatory activity in the reticulospinal system of the monkey. *Exp. Brain Res.* 159, 284–300. doi: 10.1007/s00221-004-1956-4

Card, S. K., English, W. K., and Burr, B. J. (1978). Evaluation of mouse, rate-controlled isometric joystick, step keys, and text keys for text selection on a CRT. *Ergonomics* 21, 601–613. doi: 10.1080/00140137808931762

Carmena, J. M., Lebedev, M. A., Crist, R. E., O'Doherty, J. E., Santucci, D. M., Dimitrov, D. F., et al. (2003). Learning to control a brain-machine interface for reaching and grasping by primates. *PLoS Biol* 1:E42. doi: 10.1371/journal.pbio.0000042

Casile, A. (2013). Mirror neurons (and beyond) in the macaque brain: an overview of 20 years of research. *Neurosci. Lett.* 540, 3–14. doi: 10.1016/j.neulet.2012.11.003

Chadwick, E. K., Blana, D., Simeral, J. D., Lambrecht, J., Kim, S. P., Cornwell, A. S., et al. (2011). Continuous neuronal ensemble control of simulated arm reaching by a human with tetraplegia. *J. Neural Eng.* 8:034003. doi: 10.1088/1741-2560/8/3/034003

Chase, S. M., and Schwartz, A. B. (2011). "Inference from populations: going beyond models," in *Progress in Brain Research,* eds A. M. Green, C. E. Chapman, J. F. Kalaska, and F. Lepore (Amsterdam: Elsevier), 103–112. doi: 10.1016/B978-0-444-53355-5.00007-5

Chestek, C. A., Gilja, V., Nuyujukian, P., Foster, J. D., Fan, J. M., Kaufman, M. T., et al. (2011). Long-term stability of neural prosthetic control signals from silicon cortical arrays in rhesus macaque motor cortex. *J. Neural Eng.* 8:045005. doi: 10.1088/1741-2560/8/4/045005

Cheung, V. C. K., Piron, L., Agostini, M., Silvoni, S., Turolla, A., and Bizzi, E. (2009). Stability of muscle synergies for voluntary actions after cortical stroke in humans. *Proc. Natl. Acad. Sci. U. S. A.* 106, 19563–19568. doi: 10.1073/pnas.0910114106

Churchland, M. M., Cunningham, J. P., Kaufman, M. T., Foster, J. D., Nuyujukian, P., Ryu, S. I., et al. V (2012). Neural population dynamics during reaching. *Nature* 487, 51–56. doi: 10.1038/nature11129

Ciocarlie, M., Goldfeder, C., and Allen, P. (2007). Dimensionality reduction for hand-independent dexterous robotic grasping. *2007 IEEE/RSJ Int. Conf. Intell. Robot. Syst.* 20, 3270–3275. doi: 10.1109/IROS.2007.4399227

Cisek, P., and Kalaska, J. F. (2004). Neural correlates of mental rehearsal in dorsal premotor cortex. *Nature* 431, 993–996. doi: 10.1038/nature03005

Collinger, J. L., Wodlinger, B., Downey, J. E., Wang, W., Tyler-Kabara, E. C., Weber, D. J., et al. (2013). High-performance neuroprosthetic control by an individual with tetraplegia. *Lancet* 381, 557–564. doi: 10.1016/S0140-6736(12)61816-9

Cunningham, J. P., Gilja, V., Ryu, S. I., and Shenoy, K. V (2010). Methods for estimating neural firing rates, and their application to brain-machine interfaces. *Neural Netw.* 22, 249–266. doi: 10.1016/j.neunet.2009.02.004

Dalley, S. A., Wiste, T. E., Varol, H. A., and Goldfarb, M. (2010). A multigrasp hand prosthesis for transradial amputees. *Conf. Proc. IEEE Eng. Med. Biol. Soc.* 2010, 5062–5065. doi: 10.1109/iembs.2010.5626225

Davidson, A. G., Chan, V., O'Dell, R., and Schieber, M. H. (2007). Rapid changes in throughput from single motor cortex neurons to muscle activity. *Science* 318, 1934–1937. doi: 10.1126/science.1149774

d'Avella, A., and Bizzi, E. (2005). Shared and specific muscle synergies in natural motor behaviors. *Proc. Natl. Acad. Sci. U. S. A.* 102, 3076–3081. doi: 10.1073/pnas.0500199102

Dushanova, J., and Donoghue, J. P. (2010). Neurons in primary motor cortex engaged during action observation. *Eur. J. Neurosci.* 31, 386–398. doi: 10.1111/j.1460-9568.2009.07067.x

Engel, K. C., Flanders, M., and Soechting, J. F. (1997). Anticipatory and sequential motor control in piano playing. *Exp. brain Res.* 113, 189–199. doi: 10.1007/BF02450317

Epps, B. W. (1986). Comparison of six cursor control devices based on Fitts' law models. *Proc. Hum. Factors Ergon. Soc. Annu. Meet.* 30, 327–331. doi: 10.1177/154193128603000403

Ersland, L., Rosén, G., Lundervold, A., Smievoll, A. I., Tillung, T., Sundberg, H., et al. (1996). Phantom limb imaginary fingertapping causes primary motor cortex activation: an fMRI study. *Neuroreport* 8, 207–210. doi: 10.1097/00001756-199612200-00042

Ethier, C., Oby, E. R., Bauman, M. J., and Miller, L. E. (2012). Restoration of grasp following paralysis through brain-controlled stimulation of muscles. *Nature* 485, 368–371. doi: 10.1038/nature10987

Ethier, C., Sachs, N. A., Miller, L. E., and Collection, A. D. (2011). Continuous state-dependent decoders for brain machine interfaces. *Neural Eng. (NER), 2011 5th International IEEE/EMBS Conference on IEEE* (Cancun), 473–477. doi: 10.1109/NER.2011.5910589

Felton, E. A., Radwin, R. G., Wilson, J. A., and Williams, J. C. (2009). Evaluation of a modified Fitts law brain-computer interface target acquisition task in able and motor disabled individuals. *J. Neural Eng.* 6:056002. doi: 10.1088/1741-2560/6/5/056002

Fetz, E. E., and Baker, M. A. (1973). Operantly conditioned patterns of precentral unit activity and correlated responses in adjacent cells and contralateral muscles. *J. Neurophysiol.* 36, 179–204.

Fetz, E. E., Perlmutter, S. I., Prut, Y., Seki, K., and Votaw, S. (2002). Roles of primate spinal interneurons in preparation and execution of voluntary hand movement. *Brain Res. Rev.* 40, 53–65. doi: 10.1016/S0165-0173(02)00188-1

Fitts, P. M. (1954). The information capacity of human motor system in controlling the ampltude of movement. *J. Exp. Psychol.* 47, 381–391. doi: 10.1037/h0055392

Fitzsimmons, N. A., Lebedev, M. A., Peikon, I. D., and Nicolelis, M. A. L. (2009). Extracting kinematic parameters for monkey bipedal walking from cortical neuronal ensemble activity. *Front. Integr. Neurosci.* 3:3. doi: 10.3389/neuro.07.003.2009

Flanders, M., and Soechting, J. F. (1992). Kinematics of typing: parallel control of the two hands. *J. Neurophysiol.* 67, 1264–1274.

Fraser, G. W., Chase, S. M., Whitford, A., and Schwartz, A. B. (2009). Control of a brain-computer interface without spike sorting. *J. Neural Eng.* 6:055004. doi: 10.1088/1741-2560/6/5/055004

Fu, Q. G., Flament, D., Coltz, J. D., and Ebner, T. J. (1995). Temporal encoding of movement kinematics in the discharge of primate primary motor and premotor neurons. *J. Neurophysiol.* 73, 836–854.

Ganguly, K., and Carmena, J. M. (2009). Emergence of a stable cortical map for neuroprosthetic control. *PLoS Biol.* 7:e1000153. doi: 10.1371/journal.pbio.1000153

Ganguly, K., Dimitrov, D. F., Wallis, J. D., and Carmena, J. M. (2011). Reversible large-scale modification of cortical networks during neuroprosthetic control. *Nat. Neurosci.* 14, 662–667. doi: 10.1038/nn.2797

Georgopoulos, A. P. (2014). Cell directional spread determines accuracy, precision, and length of the neuronal population vector. *Exp. Brain Res.* 232, 2391–2405. doi: 10.1007/s00221-014-3936-7

Georgopoulos, A. P., and Grillner, S. (1989). Visuomotor coordination in reaching and locomotion. *Science* 245, 1209–1210. doi: 10.1126/science.2675307

Gilja, V., Nuyujukian, P., Chestek, C. A., Cunningham, J. P., Yu, B. M., Fan, J. M., et al. (2012). A high-performance neural prosthesis enabled by control algorithm design. *Nat. Neurosci.* 15, 1752–1757. doi: 10.1038/nn.3265

Giszter, S. F., and Hart, C. B. (2013). Motor primitives and synergies in the spinal cord and after injury–the current state of play. *Ann. N. Y. Acad. Sci.* 1279, 114–126. doi: 10.1111/nyas.12065

Grafton, S. T., Arbib, M. A., Fadiga, L., and Rizzolatti, G. (1996). Localization of grasp representations in humans by positron emission tomography. 2. Observation compared with imaginations. *Exp. Brain Res.* 112, 103–111. doi: 10.1007/BF00227183

Grillner, S. (1985). Neurobiological bases of rhythmic motor acts in vertebrates. *Science* 228, 143–149. doi: 10.1126/science.3975635

Hager-Ross, C., and Schieber, M. H. (2000). Quantifying the independence of human finger movements: comparisons of digits, hands, and movement frequencies. *J. Neurosci.* 20, 8542–8550.

Hall, T. M., de Carvalho, F., and Jackson, A. (2014). A common structure underlies low-frequency cortical dynamics in movement, sleep, and sedation. *Neuron* 83, 1185–1199. doi: 10.1016/j.neuron.2014.07.022

Harris, C. M., and Wolpert, D. M. (1998). Signal-dependent noise determines motor planning. *Nature* 394, 780–784. doi: 10.1038/29528

Hochberg, L. R., Bacher, D., Jarosiewicz, B., Masse, N. Y., Simeral, J. D., Vogel, J., et al. (2012). Reach and grasp by people with tetraplegia using a neurally controlled robotic arm. *Nature* 485, 372–375. doi: 10.1038/nature11076

Hochberg, L. R., Serruya, M. D., Friehs, G. M., Mukand, J. A., Saleh, M., Caplan, A. H., et al. (2006). Neuronal ensemble control of prosthetic devices by a human with tetraplegia. *Nature* 442, 164–171. doi: 10.1038/nature04970

Homer, M. L., Nurmikko, A. V., Donoghue, J. P., and Hochberg, L. R. (2013). Sensors and decoding for intracortical brain computer interfaces. *Annu. Rev. Biomed. Eng.* 15, 383–405. doi: 10.1146/annurev-bioeng-071910-124640

Humphrey, D. R., and Reed, D. J. (1983). Separate cortical systems for control of joint movement and joint stiffness: reciprocal activation and coactivation of antagonist muscles. *Adv. Neurol.* 39, 347–372.

Humphrey, D. R., Schmidt, E. M., and Thompson, W. D. (1970). Predicting measures of motor performance from multiple cortical spike trains. *Science* 170, 758–762. doi: 10.1126/science.170.3959.758

Hutchinson, D. T. (2014). The quest for the bionic arm. *J. Am. Acad. Orthop. Surg.* 22, 346–351. doi: 10.5435/JAAOS-22-06-346

Ifft, P. J., Lebedev, M. A., and Nicolelis, M. A. L. (2011). Cortical correlates of fitts' law. *Front. Integr. Neurosci.* 5:85. doi: 10.3389/fnint.2011.00085

Jackson, A., Gee, V. J., Baker, S. N., and Lemon, R. N. (2003). Synchrony between neurons with similar muscle fields in monkey motor cortex. *Neuron* 38, 115–125. doi: 10.1016/S0896-6273(03)00162-4

Jagacinski, R. J., and Monk, D. M. (1985). Fitts' law in two dimensions with hand and head movements. *J. Mot. Behav.* 17, 77–95. doi: 10.1080/00222895.1985.10735338

Jarosiewicz, B., Chase, S. M., Fraser, G. W., Velliste, M., Kass, R. E., and Schwartz, A. B. (2008). Functional network reorganization during learning in a brain-computer interface paradigm. *Proc. Natl. Acad. Sci. U.S.A.* 105, 19486–19491. doi: 10.1073/pnas.0808113105

Jiang, B., Wang, R., Zhang, Q., Zhang, J., Zheng, X., and Zhao, T. (2011). A pilot study on two stage decoding strategies. *Proc. IEEE EMBS Conf.* 2011, 3700–3703. doi: 10.1109/iembs.2011.6090627

Johannes, M. S., Bigelow, J. D., Burck, J. M., Harshbarger, S. D., and Kozlowski, M. V (2011). An overview of the developmental process for the modular prosthetic limb. *Johns Hopkins APL Tech. Dig.* 30, 207–216.

Kahn, K., Schieber, M. H., Thakor, N. V., and Sarma, S., V (2011). Neuron selection for decoding dexterous finger movements. *Conf. Proc. IEEE Eng. Med. Biol. Soc.* 2011, 4605–4608. doi: 10.1109/IEMBS.2011.6091140

Kang, N., Shinohara, M., Zatsiorsky, V. M., and Latash, M. L. (2004). Learning multi-finger synergies: an uncontrolled manifold analysis. *Exp. Brain Res.* 157, 336–350. doi: 10.1007/s00221-004-1850-0

Kang, X., Sarma, S., Santaniello, S., Schieber, M. H., and Thakor, N. (2015). Task-independent cognitive state transition detection from cortical neurons during 3D reach-to-grasp movements. *IEEE Trans. Neural Syst. Rehabil. Eng.* 23, 676–682. doi: 10.1109/TNSRE.2015.2396495

Kaufman, M. T., Churchland, M. M., Ryu, S. I., and Shenoy, K. V (2014). Cortical activity in the null space: permitting preparation without movement. *Nat. Neurosci.* 17, 440–448. doi: 10.1038/nn.3643

Kemere, C., Santhanam, G., Yu, B. M., Afshar, A., Ryu, S. I., Meng, T. H., et al. (2008). Detecting neural-state transitions using hidden Markov models for motor cortical prostheses. *J. Neurophysiol.* 100, 2441–2452. doi: 10.1152/jn.00924.2007

Lassek, A. M. (1954). *The Pyramidal Tract: Its Status in Medicine*. Springfield, IL: Charles C. Thomas.

Latash, M. L., Scholz, J. P., Danion, F., and Schöner, G. (2002). Finger coordination during discrete and oscillatory force production tasks. *Exp. Brain Res.* 146, 419–432. doi: 10.1007/s00221-002-1196-4

Latash, M. L., Scholz, J. P., and Schöner, G. (2007). Toward a new theory of motor synergies. *Motor Control* 11, 276–308.

Law, A. J., Rivlis, G., and Schieber, M. H. (2014). Rapid acquisition of novel interface control by small ensembles of arbitrarily selected primary motor cortex neurons. *J. Neurophysiol.* 112, 1528–1548. doi: 10.1152/jn.00373.2013

Lebedev, M. A., Carmena, J. M., O'Doherty, J. E., Zacksenhouse, M., Henriquez, C. S., Principe, J. C., et al. (2005). Cortical ensemble adaptation to represent velocity of an artificial actuator controlled by a brain-machine interface. *J. Neurosci.* 25, 4681–4693. doi: 10.1523/JNEUROSCI.4088-04.2005

Lebedev, M. A., and Nicolelis, M. A. L. (2011). Toward a whole-body neuroprosthetic. *Prog. Brain Res.* 194, 47–60. doi: 10.1016/B978-0-444-53815-4.00018-2

Lee, D., Port, N. L., Kruse, W., and Georgopoulos, A. P. (1998). Variability and correlated noise in the discharge of neurons in motor and parietal areas of the primate cortex. *J. Neurosci.* 18, 1161–1170.

Li, Z., O'Doherty, J. E., Hanson, T. L., Lebedev, M. A., Henriquez, C. S., and Nicolelis, M. A. L. (2009). Unscented Kalman filter for brain-machine interfaces. *PLoS ONE* 4:e6243. doi: 10.1371/journal.pone.0006243

MacKenzie, I. S. (1992). Fitts' law as a research and design tool in human-computer interaction. *Hum. Comput. Interact.* 7, 91–139. doi: 10.1207/s15327051hci0701_3

Mahan, M. Y., and Georgopoulos, A. P. (2013). Motor directional tuning across brain areas: directional resonance and the role of inhibition for directional accuracy. *Front. Neural Circuits* 7:92. doi: 10.3389/fncir.2013.00092

Maier, M. A., Perlmutter, S. I., and Fetz, E. E. (1998). Response patterns and force relations of monkey spinal interneurons during active wrist movement. *J. Neurophysiol.* 80, 2495–2513.

Mason, C. R., Theverapperuma, L. S., Hendrix, C. M., and Ebner, T. J. (2004). Monkey hand postural synergies during reach-to-grasp in the absence of vision of the hand and object. *J. Neurophysiol.* 91, 2826–2837. doi: 10.1152/jn.00653.2003

Moran, D. W., and Schwartz, A. B. (1999). Motor cortical representation of speed and direction during reaching. *J. Neurophysiol.* 82, 2676–2692.

Moritz, C. T., Perlmutter, S. I., and Fetz, E. E. (2008). Direct control of paralysed muscles by cortical neurons. *Nature* 456, 639–642. doi: 10.1038/nature07418

Müller, K., Anderson, C. W., and Birch, G. E. (2003). Linear and nonlinear methods for brain-computer interfaces. *IEEE Trans. Neural Syst. Rehabil. Eng.* 11, 165–169. doi: 10.1109/TNSRE.2003.814484

Opris, I., Fuqua, J. L., Huettl, P. F., Gerhardt, G. A., Berger, T. W., Hampson, R. E., et al. (2012). Closing the loop in primate prefrontal cortex: inter-laminar processing. *Front. Neural Circuits* 6:88. doi: 10.3389/fncir.2012.00088

Opris, I., Santos, L., Gerhardt, G. A., Song, D., Berger, T. W., Hampson, R. E., et al. (2013). Prefrontal cortical microcircuits bind perception to executive control. *Sci. Rep.* 3:2285. doi: 10.1038/srep02285

Orsborn, A. L., Dangi, S., Moorman, H. G., and Carmena, J. M. (2012). Closed-loop decoder adaptation on intermediate time-scales facilitates rapid BMI performance improvements independent of decoder initialization conditions. *IEEE Trans. Neural Syst. Rehabil. Eng.* 20, 468–477. doi: 10.1109/TNSRE.2012.2185066

Pancrazio, J. J., and Peckham, P. H. (2009). Neuroprosthetic devices: how far are we from recovering movement in paralyzed patients? *Expert Rev. Neurother.* 9, 427–430. doi: 10.1586/ern.09.12

Pfurtscheller, G., and Neuper, C. (1997). Motor imagery activates primary sensorimotor area in humans. *Neurosci. Lett.* 239, 65–68. doi: 10.1016/S0304-3940(97)00889-6

Porro, C. A., Francescato, M. P., Cettolo, V., Diamond, M. E., Baraldi, P., Zuiani, C., et al. (1996). Primary motor and sensory cortex activation during motor performance and motor imagery: a functional magnetic resonance imaging study. *J. Neurosci.* 16, 7688–7698.

Resnik, L., Klinger, S. L., and Etter, K. (2013). The DEKA Arm: Its features, functionality, and evolution during the Veterans Affairs Study to optimize the DEKA Arm. *Prosthet. Orthot. Int.* 38, 492–504. doi: 10.1177/0309364613506913

Roh, J., Cheung, V. C. K., and Bizzi, E. (2011). Modules in the brain stem and spinal cord underlying motor behaviors. *J. Neurophysiol.* 106, 1363–1378. doi: 10.1152/jn.00842.2010

Rouse, A. G., and Schieber, M. H. (2014). "Location then object representations sequentially predominate in the widely distributed activation of the primary motor cortex during reach to grasp," in *Society for Neuroscience Annual Meeting* (Washington, DC).

Sadtler, P. T., Quick, K. M., Golub, M. D., Chase, S. M., Ryu, S. I., Tyler-Kabara, E. C., et al. (2014). Neural constraints on learning. *Nature* 512, 423–426. doi: 10.1038/nature13665

Santello, M., Flanders, M., and Soechting, J. F. (1998). Postural hand synergies for tool use. *J. Neurosci.* 18, 10105–10115.

Santos, L., Opris, I., Hampson, R., Godwin, D. W., Gerhardt, G. A., and Deadwyler, S. (2014). Functional dynamics of primate cortico-striatal networks during volitional movements. *Front. Syst. Neurosci.* 8:27. doi: 10.3389/fnsys.2014.00027

Schieber, M. H. (2002). Training and synchrony in the motor system. *J. Neurosci.* 22, 5277–5281.

Schieber, M. H., and Rivlis, G. (2005). A spectrum from pure post-spike effects to synchrony effects in spike-triggered averages of electromyographic activity during skilled finger movements. *J. Neurophysiol.* 94, 3325–3341. doi: 10.1152/jn.00007.2005

Scholz, J. P., Reisman, D., and Schöner, G. (2001). Effects of varying task constraints on solutions to joint coordination in a sit-to-stand task. *Exp. Brain Res.* 141, 485–500. doi: 10.1007/s002210100878

Scholz, J. P., and Schöner, G. (1999). The uncontrolled manifold concept: identifying control variables for a functional task. *Exp. Brain Res.* 126, 289–306. doi: 10.1007/s002210050738

Seki, K., Perlmutter, S. I., and Fetz, E. E. (2003). Sensory input to primate spinal cord is presynaptically inhibited during voluntary movement. *Nat. Neurosci.* 6, 1309–1316. doi: 10.1038/nn1154

Serruya, M. D., Hatsopoulos, N. G., Paninski, L., Fellows, M. R., and Donoghue, J. P. (2002). Instant neural control of a movement signal. *Nature* 416, 141–142. doi: 10.1038/416141a

Shalit, U., Zinger, N., Joshua, M., and Prut, Y. (2012). Descending systems translate transient cortical commands into a sustained muscle activation signal. *Cereb. Cortex* 22, 1904–1914. doi: 10.1093/cercor/bhr267

Shanechi, M. M., Hu, R. C., Powers, M., Wornell, G. W., Brown, E. N., and Williams, Z. M. (2012). Neural population partitioning and a concurrent brain-machine interface for sequential motor function. *Nat. Neurosci.* 15, 1715–1722. doi: 10.1038/nn.3250

Shanechi, M. M., Orsborn, A., Moorman, H., Gowda, S., and Carmena, J. M. (2014). High-performance brain-machine interface enabled by an adaptive optimal feedback-controlled point process decoder. *Proc. IEEE EMBS Conf.* 36, 6493–6496. doi: 10.1109/embc.2014.6945115

Shik, M. L., and Orlovsky, G. N. (1976). Neurophysiology of locomotor automatism. *Physiol. Rev.* 56, 465–501.

Singhal, G., Aggarwal, V., Acharya, S., Aguayo, J., He, J., and Thakor, N. (2010). Ensemble fractional sensitivity: a quantitative approach to neuron selection for decoding motor tasks. *Comput. Intell. Neurosci.* 2010, 648202. doi: 10.1155/2010/648202

Slifkin, A. B., and Newell, K. M. (1999). Noise, information transmission, and force variability. *J. Exp. Psychol. Hum. Percept. Perform.* 25, 837–851. doi: 10.1037/0096-1523.25.3.837

Soechting, J. F., and Flanders, M. (1992). Organization of sequential typing movements. *J. Neurophysiol.* 67, 1275–1290.

Soechting, J. F., and Flanders, M. (1997). Flexibility and repeatability of finger movements during typing: analysis of multiple degrees of freedom. *J. Comput. Neurosci.* 4, 29–46. doi: 10.1023/A:1008812426305

Srinivasan, L., and da Silva, M. (2011). Breaking the fixed-arrival-time restriction in reaching movements of neural prosthetic devices. *IEEE Trans. Biomed. Eng.* 58, 1555–1564. doi: 10.1109/TBME.2010.2101599

Stein, P. S. G. (1978). Motor systems, with specific reference to the control of locomotion. *Annu. Rev. Neurosci.* 1, 61–81. doi: 10.1146/annurev.ne.01.030178.000425

Stieglitz, T., Rubehn, B., Henle, C., Kisban, S., Herwik, S., Ruther, P., et al. (2009). "Brain-computer interfaces: an overview of the hardware to record neural signals from the cortex," in *Progress in Brain Research*, eds J. Verhaagen, E. M. Hol, I. Huitenga, J. Wijholds, A. B. Bergen, G. J. Boer, and D. J. Swaab (Amsterdam: Elsevier), 297–315. doi: 10.1016/S0079-6123(09)17521-0

Taylor, D. M., Tillery, S. I. H., and Schwartz, A. B. (2002). Direct cortical control of 3D neuroprosthetic devices. *Science* 296, 1829–1832. doi: 10.1126/science.1070291

Tehovnik, E. J., Woods, L. C., and Slocum, W. M. (2013). Transfer of information by BMI. *Neuroscience* 255, 134–146. doi: 10.1016/j.neuroscience.2013.10.003

Thach, W. T. (1978). Correlation of neural discharge with pattern and force of muscular activity, joint position, and direction of intended next movement in motor cortex and cerebellum. *J. Neurophysiol.* 41, 654–676.

Tkach, D., Reimer, J., and Hatsopoulos, N. G. (2007). Congruent activity during action and action observation in motor cortex. *J. Neurosci.* 27, 13241–13250. doi: 10.1523/JNEUROSCI.2895-07.2007

Tseng, Y., Scholz, J. P., and Schöner, G. (2002). Goal-equivalent joint coordination in pointing: affect of vision and arm dominance. *Motor Control* 6, 183–204.

Tsianos, G. A., Goodner, J., and Loeb, G. E. (2014). Useful properties of spinal circuits for learning and performing planar reaches. *J. Neural Eng.* 11:056006. doi: 10.1088/1741-2560/11/5/056006

Velliste, M., McMorland, A. J. C., Diril, E., Clanton, S. T., and Schwartz, A. B. (2012). State-space control of prosthetic hand shape. *Conf. Proc. IEEE Eng. Med. Biol. Soc.* 2012, 964–967. doi: 10.1109/EMBC.2012.6346093

Velliste, M., Kennedy, S. D., Schwartz, A. B., Whitford, A. S., Sohn, J.-W., and McMorland, A. J. C. (2014). Motor cortical correlates of arm resting in the context of a reaching task and implications for prosthetic control. *J. Neurosci.* 34, 6011–6022. doi: 10.1523/JNEUROSCI.3520-13.2014

Velliste, M., Perel, S., Spalding, M. C., Whitford, A. S., and Schwartz, A. B. (2008). Cortical control of a prosthetic arm for self-feeding. *Nature* 453, 1098–1101. doi: 10.1038/nature06996

Vigneswaran, G., Philipp, R., Lemon, R. N., and Kraskov, A. (2013). M1 corticospinal mirror neurons and their role in movement suppression during action observation. *Curr. Biol.* 23, 236–243. doi: 10.1016/j.cub.2012.12.006

Vinjamuri, R., Weber, D. J., Mao, Z.-H., Collinger, J. L., Degenhart, A. D., Kelly, J. W., et al. (2011). Toward synergy-based brain-machine interfaces. *IEEE Trans. Inf. Technol. Biomed.* 15, 726–736. doi: 10.1109/TITB.2011.2160272

Williams, J. J., Rouse, A. G., Thongpang, S., Williams, J. C., and Moran, D. W. (2013). Differentiating closed-loop cortical intention from rest: building an asynchronous electrocorticographic BCI. *J. Neural Eng.* 10:046001. doi: 10.1088/1741-2560/10/4/046001

Wodlinger, B., Downey, J. E., Tyler-Kabara, E. C., Schwartz, A. B., Boninger, M. L., and Collinger, J. L. (2015). Ten-dimensional anthropomorphic arm control in a human brain-machine interface: difficulties, solutions, and limitations. *J. Neural Eng.* 12:016011. doi: 10.1088/1741-2560/12/1/016011

Wolpaw, J. R. (2010). Brain-computer interface research comes of age: traditional assumptions meet emerging realities. *J. Mot. Behav.* 42, 351–353. doi: 10.1080/00222895.2010.526471

Wu, W., Black, M. J., Gao, Y., Bienenstock, E., Serruya, M. D., Shaikhouni, A., et al. (2003). Neural decoding of cursor motion using a Kalman Filter. *Adv. Neural Inf. Process. Syst.* 133–140.

Xu, K., Wang, Y., Wang, Y., Wang, F., Hao, Y., Zhang, S., et al. (2013). Local-learning-based neuron selection for grasping gesture prediction in motor brain machine interfaces. *J. Neural Eng.* 10:026008. doi: 10.1088/1741-2560/10/2/026008

Zhang, Y., and Chase, S. M. (2013). A stabilized dual Kalman filter for adaptive tracking of brain-computer interface decoding parameters. *Conf. Proc. IEEE Eng. Med. Biol. Soc.* 2013, 7100–7103. doi: 10.1109/EMBC.2013.6611194

Zohary, E., Shadlen, M. N., and Newsome, W. T. (1994). Correlated neuronal discharge rate and its implications for psychophysical performance. *Nature* 370, 140–143. doi: 10.1038/370140a0

Conflict of Interest Statement: The authors declare that the research was conducted in the absence of any commercial or financial relationships that could be construed as a potential conflict of interest.

frontiers in
SYSTEMS NEUROSCIENCE

ORIGINAL RESEARCH ARTICLE
published: 03 April 2014
doi: 10.3389/fnsys.2014.00045

Large-scale resting state network correlates of cognitive impairment in Parkinson's disease and related dopaminergic deficits

Alexander V. Lebedev[1]*, Eric Westman[2], Andrew Simmons[3,4], Aleksandra Lebedeva[2], Françoise J. Siepel[1], Joana B. Pereira[2] and Dag Aarsland[1,2]

[1] *Department of Psychiatry, Centre for Age-Related Medicine, Stavanger University Hospital, Stavanger, Norway*
[2] *Department of Neurobiology, Care Sciences and Society, Karolinska Institutet, Stockholm, Sweden*
[3] *Department of Neuroimaging, Institute of Psychiatry, King's College London, London, UK*
[4] *NIHR Biomedical Research Centre for Mental Health and Biomedical Research Unit for Dementia, London, UK*

Edited by:
Mikhail Lebedev, Duke University, USA

Reviewed by:
Nicola B. Mercuri, University of Rome, Italy
Simon J. G. Lewis, Brain and Mind Research Institute, Australia
Andrew V. Poliakov, Seattle Children's Hospital, USA

****Correspondence:***
Alexander V. Lebedev, Department of Psychiatry, Centre for Age-Related Medicine, Stavanger University Hospital, Armauer Hansens vei 20, 4011 Stavanger, Norway
e-mail: alexander.vl.lebedev@gmail.com

Cognitive impairment is a common non-motor feature of Parkinson's disease (PD). Understanding the neural mechanisms of this deficit is crucial for the development of efficient methods for treatment monitoring and augmentation of cognitive functions in PD patients. The current study aimed to investigate resting state fMRI correlates of cognitive impairment in PD from a large-scale network perspective, and to assess the impact of dopamine deficiency on these networks. Thirty PD patients with resting state fMRI were included from the Parkinson's Progression Marker Initiative (PPMI) database. Eighteen patients from this sample were also scanned with ^{123}I-FP-CIT SPECT. A standardized neuropsychological battery was administered, evaluating verbal memory, visuospatial, and executive cognitive domains. Image preprocessing was performed using an SPM8-based workflow, obtaining time-series from 90 regions-of-interest (ROIs) defined from the AAL brain atlas. The Brain Connectivity Toolbox (BCT) was used to extract nodal strength from all ROIs, and modularity of the cognitive circuitry determined using the meta-analytical software Neurosynth. Brain-behavior covariance patterns between cognitive functions and nodal strength were estimated using Partial Least Squares. Extracted latent variable (LV) scores were matched with the performances in the three cognitive domains (memory, visuospatial, and executive) and striatal dopamine transporter binding ratios (SBR) using linear modeling. Finally, influence of nigrostriatal dopaminergic deficiency on the modularity of the "cognitive network" was analyzed. For the range of deficits studied, better executive performance was associated with increased dorsal fronto-parietal cortical processing and inhibited subcortical and primary sensory involvement. This profile was also characterized by a relative preservation of nigrostriatal dopaminergic function. The profile associated with better memory performance correlated with increased prefronto-limbic processing, and was not associated with presynaptic striatal dopamine uptake. SBR ratios were negatively correlated with modularity of the "cognitive network," suggesting integrative effects of the preserved nigrostriatal dopamine system on this circuitry.

Keywords: parkinson's disease, cognition, dopamine, resting state fMRI, SPECT, graph theory, nodal strength, modularity

INTRODUCTION

Cognitive impairment is a very important and common non-motor feature of Parkinson's disease (PD) with a major impact on patients' and caregivers' quality of life, as well as healthcare costs (Muslimovic et al., 2005; Vossius et al., 2011; Svenningsson et al., 2012). Approximately one-fifth of newly diagnosed PD patients fulfill clinical criteria for mild cognitive impairment (PD-MCI) (Aarsland et al., 2009) and about one-sixth develop dementia after 5 years (Williams-Gray et al., 2009).

Although the exact role and mechanisms of the dopaminergic system in cognition are still a matter of debate, there is no doubt that its preservation is crucial for cognitive functioning of PD patients. Thus, there is strong evidence suggesting that the impairment of at least 3 major dopaminergic pathways (nigrostriatal, mesocortical, mesolimbic) originating in the brainstem play a very important role in cognitive dysfunction associated with PD (Narayanan et al., 2013).

Previous neuroimaging studies assessing brain networks *in vivo* have shown impairment of the dopaminergic pathways and related neural circuits in PD. Numerous studies on cognitive dysfunction associated with PD have revealed structural and functional abnormalities within the

cortico-strio-thalamo-cortical circuits, known to be largely modulated by the dopaminergic system (Hirano et al., 2012; Christopher and Strafella, 2013).

Decreased 6-[^{18}F]-fluorodopa (^{18}F-DOPA) uptake in the anterior cingulate cortex, ventral striatum and right caudate nucleus has been found in PD patients with dementia (PDD) compared to PD (Ito et al., 2002). Studies employing Single Photon Emission Computed Tomography (SPECT) with the dopamine transporter-binding ligands (DaTSCAN) also suggest more severe striatal presynaptic dopaminergic deficiency in PDD compared to PD patients, especially in the caudate nuclei (O'Brien et al., 2004). In addition, there is also evidence suggesting an association between striatal ^{18}F-DOPA uptake and executive performance in PD patients (Bruck et al., 2001; Cheesman et al., 2005; Cropley et al., 2008).

Several ^{18}F-fludeoxyglucose Positron Emission Tomography (FDG-PET) studies analyzing brain networks in PD have identified partially overlapping patterns of brain metabolic changes associated with cognitive impairment in multiple domains, suggesting that the PD-related profile of cognitive impairment is associated with reduced glucose metabolism mainly in prefrontal, parietal, hippocampal, and striatal regions (Mentis et al., 2002; Huang et al., 2007a,b; Eidelberg, 2009). $H_2^{15}O$-PET studies have shown an impaired basal ganglia and dorsolateral prefrontal response during executive task performance in PD (Owen et al., 1998; Dagher et al., 2001; Cools et al., 2002).

Functional MRI studies have also revealed abnormalities within the frontal-subcortical circuits in patients with PD. For instance, an abnormal fronto-striatal response during executive task performance has been found in cognitively impaired PD patients compared to non-impaired ones (Lewis et al., 2003). Another fMRI study assessing working memory and motor functions in ON and OFF dopaminergic medication states in PD patients (Mattay et al., 2002) found increased prefrontal and parietal activations during the working memory task performance in the OFF state, which were positively correlated with errors during the task. Studies focusing on set-shifting paradigms have found a PD-associated pattern of prefrontal and parietal response characterized by either reduced or increased activation depending on whether the caudate nucleus was involved in the task (Monchi et al., 2004, 2007).

Notably, a pharmacological fMRI study in healthy subjects revealed a significant effect of L-dopa administration on striatal functional connectivity (Kelly et al., 2009). In addition to its effects on motor networks, L-dopa increased functional connectivity between the ventral striatum and ventrolateral prefrontal cortex, and disrupted connectivity of the striatum with components of the default mode network (Kelly et al., 2009). Impaired deactivation of the default mode network during executive task performance has been reported in several fMRI studies of PD (Tinaz et al., 2008; Van Eimeren et al., 2009). Resting state fMRI studies have reported abnormal cortico-striatal connectivity in PD (Wu et al., 2009; Helmich et al., 2010; Kwak et al., 2010), while L-DOPA administration has been shown to enhance functional connectivity in the frontal areas of the sensorimotor network (Esposito et al., 2013).

The brain is a complex biological system that demonstrates emergent network properties on different scales, even at a cellular and single-structure level (Welsh et al., 2010). At the cellular scale, neocortical neurons are organized into sets of structurally and physiologically merged modules (Mountcastle, 1997), which in turn, are grouped into functionally segregated hypercolumns, wired with inter-modular connections. At the larger scale, system-wide coordination of the brain networks give rise to the coherent dynamic states that support cognitive functions and behavior (Sporns, 2013). Large-scale network architecture of the human brain appears to combine two principles of structural and functional organization. On the one hand, densely connected network modules or communities promote specialized processing and *functional segregation*. On the other hand, these specialized communities are interconnected via long-distance pathways that ensure efficient *functional integration* across multiple functional domains. Maintaining the balance between segregation and integration is thought to be essential for establishing complex network dynamics that support cognition (Sporns, 2010).

Recent advances in neuroscience and mathematical modeling have made it possible to apply classical concepts of graph theory to the analysis of brain network structure and dynamics (Rubinov and Sporns, 2010; Sporns, 2010). Graph-theoretical studies of structural and functional networks of the brain have revealed "small-world" properties (Achard and Bullmore, 2007), i.e., the coexistence of dense local connectivity with relatively sparse long-range connections. Such small-world networks combine high clustering with a relatively short path length between any pair of the elements (e.g., brain regions). The "small-world" model may be of functional importance as it balances functional segregation (high modularity or clustering) and functional integration (short path length) and thus offers a network architecture that may be well-suited for neuronal information processing (Sporns and Zwi, 2004).

To date, there are very few studies of PD employing graph theoretical framework for fMRI data analysis. Skidmore et al. found reduced whole-brain global efficiency in PD (Skidmore et al., 2011). Compared to healthy controls, 14 PD patients included in the study demonstrated reduced local efficiency (nodal level) in the precentral regions, primary and secondary visual cortex. Another recent study found global reduction of network-level processing efficacy in PD. Analysis of network modules indicated decreased interaction of the visual network with other brain modules, but abnormally increased connectivity within the sensorimotor network. The authors interpreted the latter as a compensatory mechanism aimed at overcoming the striato-cortical functional deficit within the motor loops, which may also be associated with loss of mutual inhibition between brain networks (Gottlich et al., 2013).

To the best of our knowledge, there are no previous studies assessing brain correlates of PD-related cognitive impairment employing both dopamine transporter imaging and fMRI with graph theory metrics.

In the present study, we assessed global and local network-level correlates of cognitive dysfunction and related dopaminergic impairment in PD using the graph theory metrics of nodal strength and modularity.

We hypothesized that the PD-related profile of cognitive impairment would be associated mainly with abnormalities within the fronto-subcortical (impaired cortico-striatal connectivity) and fronto-parietal circuits, which are closely related to nigrostriatal deficiency.

METHODS

The main workflow steps are illustrated in **Figure S1**.

INCLUSION AND EXCLUSION CRITERIA

We included all 30 subjects (31 minus one subject excluded during quality control due to "cuts" of dorsal cortical areas) with rs-fMRI enrolled in the Parkinson's Progression Marker Initiative (PPMI) (in total 452 PD patients), a multicenter study launched in 2010 designed to identify progression biomarkers in newly diagnosed PD patients (www.ppmi-info.org/data).

Inclusion criteria required that subjects must have at least two of the following symptoms: resting tremor, bradykinesia, rigidity or either asymmetric resting tremor or asymmetric bradykinesia. In addition, the subjects had to be drug naïve, Hoehn and Yahr stage I or II at baseline, and a screening ^{123}I-FP-CIT SPECT scan, sensitive to the loss of striatal dopamine transporter (DaT) binding.

Exclusion criteria were atypical PD syndromes due to drugs or metabolic disorders, encephalitis, or other degenerative diseases. In addition, it was required that the subject was not taking levodopa, DA agonists, MAO-B inhibitors, amantadine, or other PD medication; or had taken levodopa or dopamine agonists prior to baseline for more than a total of 60 days.

NEUROPSYCHOLOGICAL ASSESSMENT

In addition to a cognitive screening test, the Montreal Cognitive Assessment (MoCA), all subjects underwent a neuropsychological test battery developed to assess major cognitive domains affected by PD.

Visuospatial function was evaluated using the 15-item version of the Benton's Judgment of Line Orientation Test, which examines the ability of a subject to estimate angular relationships between line segments by visually matching angled line pairs to 11 numbered radii forming a semi-circle (Benton et al., 1978).

Verbal memory was assessed using the Hopkins Verbal Learning Test-Revised (HVLT-R) (Shapiro et al., 1999), which consists of presenting a list of 12 words over three learning trials. With each repetition, subjects are expected to learn additional words on the list and increase their performance with each trial. Total immediate recall or encoding (sum of trial 1–3) and delayed recall (after 20–25 min) scores were included in this study.

Executive functions were evaluated using three semantic fluency tests (names of animals, fruits, and vegetables, in 1 min each), the MoCA subtests of phonemic fluency (words that start from the letter "F," in 1 min) and alternating trail making (drawing a line, going from a number to a letter, in ascending order; score 0–1).

Attention was assessed by the Letter-Number Sequencing Test (LNST), in which a combination of numbers and letters is read to the subject who is then asked to recall the numbers, first in ascending order and then the letters in alphabetical order. The Symbol Digit Modalities Test (SDMT) was also used to assess attention, in which specific numbers had to be paired with geometric figures based on a reference key within 90 s.

COGNITIVE DOMAINS

Three cognitive domains were calculated based on the standardized tests for memory, visuospatial, and attention/executive functioning. Raw values were converted to z-scores using the mean and standard deviation of the healthy control group. Domain composite scores were calculated by averaging z-scores of the standardized tests in each cognitive domain.

In the *memory domain*, three learning trials and the delayed recall of HVLT-R were included. The *visuospatial domain* included the Benton judgment of line orientation. The *attention/executive domain* included the LNST, SDMT, semantic fluency, and the phonemic fluency test. No corrections were performed to adjust the tests scores for age or gender given that the subsequent analyses included these variables as nuisances.

Since the calculated composite scores for cognitive domains were scaled and reflected positive cognitive performance (the higher the score, the better functioning in a corresponding domain), we defined the "motor" domain by inverting and scaling UPDRS-III raw scores in order to achieve the same variable scale and direction (higher scores correspond to better motor function) when assessing and plotting the results.

AUTOMATED META-ANALYSIS IN NEUROSYNTH

In order to support our hypotheses and to objectively identify regions that are relevant for cognitive functions, an automated search using the meta-analytical software Neurosynth (http://neurosynth.org) was undertaken. This approach utilizes text-mining and machine-learning techniques to perform probabilistic mapping between neural and cognitive states (Yarkoni et al., 2011). In the present study, the Python-based version (https://github.com/neurosynth/neurosynth) was used. The database was accessed on 24.10.13, searching for the key-words "executive" (237 studies), "visuospatial" ($n = 116$) and "memory" ($n = 1470$).

After the search overlapping patterns were found between cognitive domains. They were in line with the regions that have revealed an association with cognitive impairment in PD highlighted in the introduction. Thus, the profile of visuospatial functions included prefrontal, parietal, and occipital regions. The "executive" pattern contained prefrontal [with more extended involvement of dorsolateral prefrontal cortex (DLPFC)], cingulate, superior parietal, temporo-occipital, basal ganglia, and cerebellar regions. Finally, the "memory" profile, in addition to prefrontal and parietal regions, also included hippocampus, temporal areas, and basal ganglia.

Due to the observed overlap, the resulting statistical maps were merged and overlaid with the Automated Anatomical Labeling (AAL) atlas in order to have an unbiased definition of ROIs associated with cognitive functions for further network analysis. The main steps of the meta-analysis and the resulting maps are illustrated in **Figure S2**.

MRI

Image acquisition

A standardized MRI protocol included acquisition of whole-brain structural and functional scans on 3 Tesla Siemens Trio Tim MR system. More details can be found in the MRI technical operations manual at http://www.ppmi-info.org/.

3D T1 structural images were acquired in a sagittal orientation using a MPRAGE GRAPPA protocol with Repetition Time (TR) = 2300 ms, Echo Time (TE) = 2.98 ms, Field of View (FoV) = 256 mm, Flip Angle (FA) = 9° and 1 mm^3 isotropic voxel.

For each subject, 212 BOLD echo-planar rs-fMRI images (40 slices each, ascending direction) were acquired during a 8 min, 29 s scanning session (acquisition parameters: TR = 2400 ms, TE = 25 ms, FoV = 222 mm, FA = 80° and 3.3 mm^3 isotropic voxels). Subjects were instructed to rest quietly, keeping their eyes open and not to fall asleep.

^{123}I-FP-CIT SPECT

In the fMRI + DaTSCAN subgroup (n = 18), only those PD patients who had both fMRI and DaTSCAN acquired within less than a week interval were included.

Image acquisition was performed 4 ± 0.5 h after injection of ^{123}I-FP-CIT, a time-point at which striatal specific binding ratios are stable (Booij et al., 1999) with a target dose of 185 MBq. The radiopharmaceutical was provided as a unit dose and filled to a standard volume, which was re-assayed.

Raw projection data were acquired into a 128 × 128 matrix with steps of 3 or 4 degrees for the total projections. Image preprocessing (reconstruction, attenuation correction, spatial normalization) was performed using the Hermes software (Medical Solutions, Stockholm, Sweden) at a central SPECT Core lab in New Haven (Connecticut, United States). Specific binding ratios were calculated for the left and right caudate nuclei according to specific binding ratio = (L/R Caudate)/(Occipital area) − 1 and then averaged for further analysis.

IMAGE PREPROCESSING

As a first step, a population template was generated from the bias-corrected T1 structural images using the Diffeomorphic Anatomical Registration Through Exponentiated Lie Algebra (DARTEL) algorithm (Ashburner, 2007) in order to improve normalization quality.

For the fMRI data, two initial echo-planar volumes were automatically removed by the scanner software to minimize T1 effects on the T2* echo-planar images, and the remaining 210 volumes underwent preprocessing in the SPM8-based (http://www.fil.ion.ucl.ac.uk/spm) pipeline implemented in the Data Processing Assistant for Resting-State fMRI: Advanced Edition (DPARSFA, version 2.3) (Chao-Gan and Yu-Feng, 2010), installed within the MATLAB environment (Matlab 8.0 and Statistics Toolbox, 2012).

Next, functional images underwent the following preprocessing steps: spatial realignment and slice-timing correction, co-registration with the high-resolution structural scans. Finally, the co-registered BOLD volumes were normalized into standardized Montreal Neurological Institute (MNI) space using the DARTEL template and resampled to 3 mm^3 isotropic voxels. Spurious variance was reduced by a voxel-specific head motion correction (Satterthwaite et al., 2013) and by regressing-out time-series from the white matter and cerebrospinal fluid. Next, the images were band-pass filtered to eliminate biologically non-relevant signals (Biswal et al., 1995; Lowe et al., 1998) (it was not necessary to use large smoothing kernels due to a ROI-based framework implemented in the study), and the resulting low-frequency fluctuations were extracted from 90 regions-of-interest (ROIs) defined in the AAL atlas (Tzourio-Mazoyer et al., 2002) and were used in the subsequent network analysis (Rubinov and Sporns, 2010).

DATA ANALYSIS

Network analysis

The data analysis workflow was developed in order to assess both regional and global network-level correlates of presynaptic DAT uptake and cognitive functions. To do this, two metrics were selected: *nodal strength* (local measure) and *modularity* of a network (global measure).

Generalization of nodal strength and modularity for positive and negative connections

In binarized networks, the number of edges emanating from a particular node is known as its degree. For non-binarized networks, this metric has generalization called nodal strength (weighted degree), defined as the sum of neighboring link weights (Rubinov and Sporns, 2010).

Although the source of negative correlations in rs-fMRI is still a matter of debate (Fox et al., 2009; Murphy et al., 2009), there is strong evidence supporting a biological origin (Chang and Glover, 2009). In light of this, generalizations of several weighted graph theory metrics have been developed taking into account negative correlations (Rubinov and Sporns, 2011).

Thus, nodal strength can be calculated for positive and negative connections. The corresponding definition is straightforward:

$$S_i^{\pm} = \sum_{j \in N} w_{ij}^{\pm} \quad (1)$$

[Equation (1), adopted from Rubinov and Sporns, 2011] Where:

N—set of all nodes in the network;

(i, j)—link between nodes i and j ($i, j \in N$), associated with connection weights w_{ij} ($0 < |w| < 1$)

Nodal strength can therefore be computed for both positive and negative weights (±). In our analysis, the total strength of both positive and negative weights was used.

A widely used metric for network modularity is formally defined as the fraction of the edges that are within a given set of communities minus the expected fraction of edges if the network was randomly wired (Newman, 2006). The metric therefore serves as a global large-scale network measure that allows quantification of the community structure of the brain. Higher modularity values for a particular network are generally associated with denser within-modular connections, but sparser connections between nodes that are in different modules.

Generalization of the modularity to both positive and negative correlations is more complex than nodal strength due to the differences in significance of positive and negative weights when

determining modularity-partitions. Therefore, a non-symmetric generalization of network modularity has been proposed as:

$$Q^* = Q^+ + \frac{v^-}{v^+ + v^-} Q^- \quad (2a)$$

or more complete definition:

$$Q^* = \frac{1}{v^+} \sum_{ij} \left(w_{ij}^+ - e_{ij}^+ \right) \delta_{M_i M_j} - \frac{v^-}{v^+ + v^-} \sum_{ij} \left(w_{ij}^- - e_{ij}^- \right) \delta_{M_i M_j} \quad (2b)$$

Both equations are adopted from Rubinov and Sporns (2011)

Where:

$Q^{\pm}$—modularity;

$\left(w_{ij}^{\pm} - e_{ij}^{\pm} \right)$—difference between present within-module connection weights w and chance-expected within-module connection weights e;

$\delta_{M_i M_j} = 1$, when i and j are in the same module and $\delta_{M_i M_j} = 0$ otherwise.

$v^{\pm} = \sum_{i \in N} s_i^{\pm}$—total weight (the sum of all positive or negative weights)

The Brain Connectivity Toolbox (BCT, http://www.brain-connectivity-toolbox.net) (Rubinov and Sporns, 2010) was used to compute the described measures. Of note, connectivity matrices were neither thresholded nor binarized. Instead we employed a strategy that aimed to analyze weighted graphs by taking into account both positive and negative weights.

Next, the analysis proceeded in two directions with the aim of assessing local and global network-level correlates of cognitive functioning in PD and the impact of nigrostriatal dopaminergic deficiency on these networks.

All statistical analyses were performed using the R programming language, version 3.0.1 (R Core Team, 2013).

Dimensionality reduction: covariance patterns between nodal strength and cognitive functions

Partial Least Squares Regression (PLSR) was performed to reduce the dimensionality of the data, estimating latent components associated with composite scores for each domain (executive, memory, visuospatial).

PLSR is an effective data-driven method that allows high-dimensional associations between explanatory and response variables to be reduced into a small set of latent variables (LVs) (Wold et al., 1984). After decomposition, each of the LVs represents a distinct pattern of brain–behavior associations.

The following elements of these components were of particular interest in our study: (1) eigenvector (loadings) showing the degree to which a given LV contributes to the variance within the X-matrix (in our case, brain network measures), and (2) a set of scores representing a transform of a particular data-point into a latent component's space (the degree to which a given component is "represented" in a particular subject).

The models were assessed with leave-one-out cross-validation. As a result, 3 LVs minimizing total Root Mean Squared Error Prediction (RMSEP) for all 3 domains were selected. For details, see **Figure S3**. Individual LV scores were subsequently correlated with 3 cognitive domains using motor function, age, and sex as nuisance covariates.

GLM formula:

$$\begin{aligned} \mathrm{LV_N}-\mathrm{score} \sim\ & (\text{executive domain}) + (\text{memory domain}) \\ & + (\text{visuospatial domain}) + (\text{motor domain}) \\ & + (\text{age}) + (\text{sex}). \end{aligned} \quad (3)$$

Finally, the scores were correlated with mean caudate DaT binding ratios in order to investigate which of them were influenced by nigrostriatal dopamine deficiency. The analysis was focused only on the caudate nuclei (without putamen), as this striatal structure is well-documented to be involved in cognition.

Due to the concerns regarding potential influence of motion artifacts, in addition to a voxel-specific correction strategy (Satterthwaite et al., 2013), analysis of motion with respect to the variables of interest (cognitive, motor domains, and age) was also performed. For this purpose, first principal component extracted from the absolute mean displacement values (x, y, and z axes) as well as relative displacements were used.

None of our variables of interest (executive, memory, and visuospatial domains) demonstrated significant association. The only significant associations were found for the motor domain ($p_{\text{mean displacement}} = 0.036$; $p_{\text{relative displacement}} = 0.035$) and age ($p_{\text{mean displacement}} = 0.026$), as expected. These variables were included in the modes as nuisance covariates.

Impact of nigrostriatal deficiency on the modularity of cognitive brain circuitry

For the second part, adjacency matrices were constructed using 60 AAL ROIs identified during the meta-analysis step (see Meta-Analysis section and **Figure S2**). Next, modularity was estimated based on both negative and positive weights [as described in Equations 2a and 2b].

Finally, an association between network modularity and mean DaT uptake in the caudate nuclei was analyzed using linear modeling.

RESULTS

DEMOGRAPHICS AND CLINICAL DATA

Demographics and clinical characteristics are shown in **Table 1**.

The data were representative of the entire DaTSCAN cohort of PD patients (results not shown). Of note, visuospatial functions were relatively less affected than executive and memory domains.

GRAPH THEORETICAL ANALYSIS

Brain-behavior covariance patterns

The analysis was performed with PLS LV-scores determined after the dimensionality reduction step (see corresponding Methods section).

Nodal strength

The first PLS LV captured global effects. Its higher scores were associated with higher strength of all 90 nodes with largest effects on motor, prefrontal cortices, and striatum. On a behavioral level,

Table 1 | Demographics and clinical data.

	Complete sample ($n = 30$)		Subsample* ($n = 18$)	
	Mean [±SD]	Median (range)	Mean [±SD]	Median (range)
Age	61.67 [±9.46]	62 (40–75)	60.11 [±9.04]	61 (44–75)
MoCA	26.67 [±3]	27 (15–30)	26.72 [±3.5]	27 (15–30)
ExecDom	−0.254 [±0.73]	−0.125 (−1.37–1.26)	−0.297 [±0.67]	−0.125 (−1.35–0.99)
MemDom	−0.51 [±1.2]	−0.41 (−2.81–1.47)	−0.73 [±1.26]	−0.51 (−2.81–1.25)
VspDom	0.06 [±0.78]	−0.06 (−1.57–0.95)	0.08 [±0.84]	0.44 (−1.57–0.95)
UPDRS III	20.2 [±10.6]	17 (7–47)	19.83 [±10.9]	17 (7–47)

Male/Female ratio was 2:1.

**Subsample of subjects who had both fMRI and DaTSCAN acquired within less than a week interval.*

MoCA, the Montreal Cognitive Assessment; ExecDom, "Executive" domain; MemDom, "Memory" domain; VspDom, "Visuospatial" domain; UPDRS III, part III of the Unified Parkinson's Disease Rating Scale.

Table 2 | Associations between component scores and behavioral data: nodal strength.

	Executive			Memory			Visuospatial			Motor		
	T	DOF	*p*	*T*	DOF	*p*	*T*	DOF	*p*	*T*	DOF	*p*
LV I	0.782	29	0.442	1.35	29	0.19	−0.89	29	0.383	3	29	0.006
LV II	−0.656	29	0.518	−2.45	29	0.022	−1.74	29	0.094	1.327	29	0.127
LV III	3.21	29	0.004	−1.74	29	0.096	1.65	29	0.113	−2.02	29	0.055

The table shows associations between latent variable (LV) scores extracted from the nodal strength data and performance in 3 cognitive (executive, memory, visuospatial) and motor domains. Positive significant associations are depicted in red and negative ones in blue.

In total, 3 models were fitted with component scores as dependent variables, cognitive domains as independent variables (other covariates: motor domain score [also shown here as an important confounder], age and sex).

***T**, t-statistics; **DOF**, degrees of freedom.*

this component was positively associated with motor function (see **Table 2**, **Figure 1**).

The second LV was associated with higher degree of posterior (supramarginal, superior parietal, posterior cingulate, occipital regions) and striatal nodes, and lower prefronto-limbic (orbitofrontal, anterior cingulate, parahippocampal, temporopolar regions) nodal strength (except for operculo-triangular, middle frontal areas, and left hippocampus, which demonstrated positive associations). Behaviorally, this component displayed a negative association with memory function, that is to say that better memory performance was associated with reversed component pattern, favoring the involvement of prefronto-limbic nodes (see **Table 2**, **Figure 1**).

The third LV, in turn, favored cortical-subcortical segregation with positive associations found in dorsal cortical nodes (dorsolateral prefrontal, frontal and parietal areas) and negative in subcortical structures (hippocampi, striatum, globus pallidus), primary visual, middle temporal, and paralimbic (ventral prefrontal) areas. Higher scores of this component were associated with better executive performance (see **Table 2**, **Figure 1**).

Latent variable scores and caudate DaT uptake

Analysis of the effects of nigrostriatal dopaminergic deficiency on the LVs estimated from the nodal strength revealed significant positive associations of mean caudate SBR ratios with I and III LV-scores (See **Table 3**, **Figure 2**).

This means that higher caudate DaT binding is associated with global increase of nodal strength and segregation toward more active dorsal cortical processing when the subject is at rest.

Modularity of the cognitive circuitry and caudate DaT binding

The analysis revealed negative effects of the preserved dopaminergic function on modularity of the cognitive circuit ($T = -3.6$, 17 DOF, $p = 0.002$), suggesting greater integration among regions within this network (see **Figure 3**).

DISCUSSION

To the best of our knowledge, this is the first study to assess large-scale network correlates of PD-related cognitive impairment and presynaptic dopaminergic deficiency, combining rs-fMRI and DaTSCAN. Higher executive functional scores were associated with higher nodal strength of dorsal cortical nodes (predominantly in dorsolateral prefrontal, premotor, and superior parietal regions) and lower involvement of subcortical, occipital, temporal, and ventral cortical nodes, suggesting that relative preservation of executive functions in PD is linked to the dominance of dorsal cortical processing with inhibition of subcortical, paralimbic, and primary sensory circuitry when the subject is at resting state with eyes open. This pattern was positively influenced by higher nigrostriatal dopaminergic function.

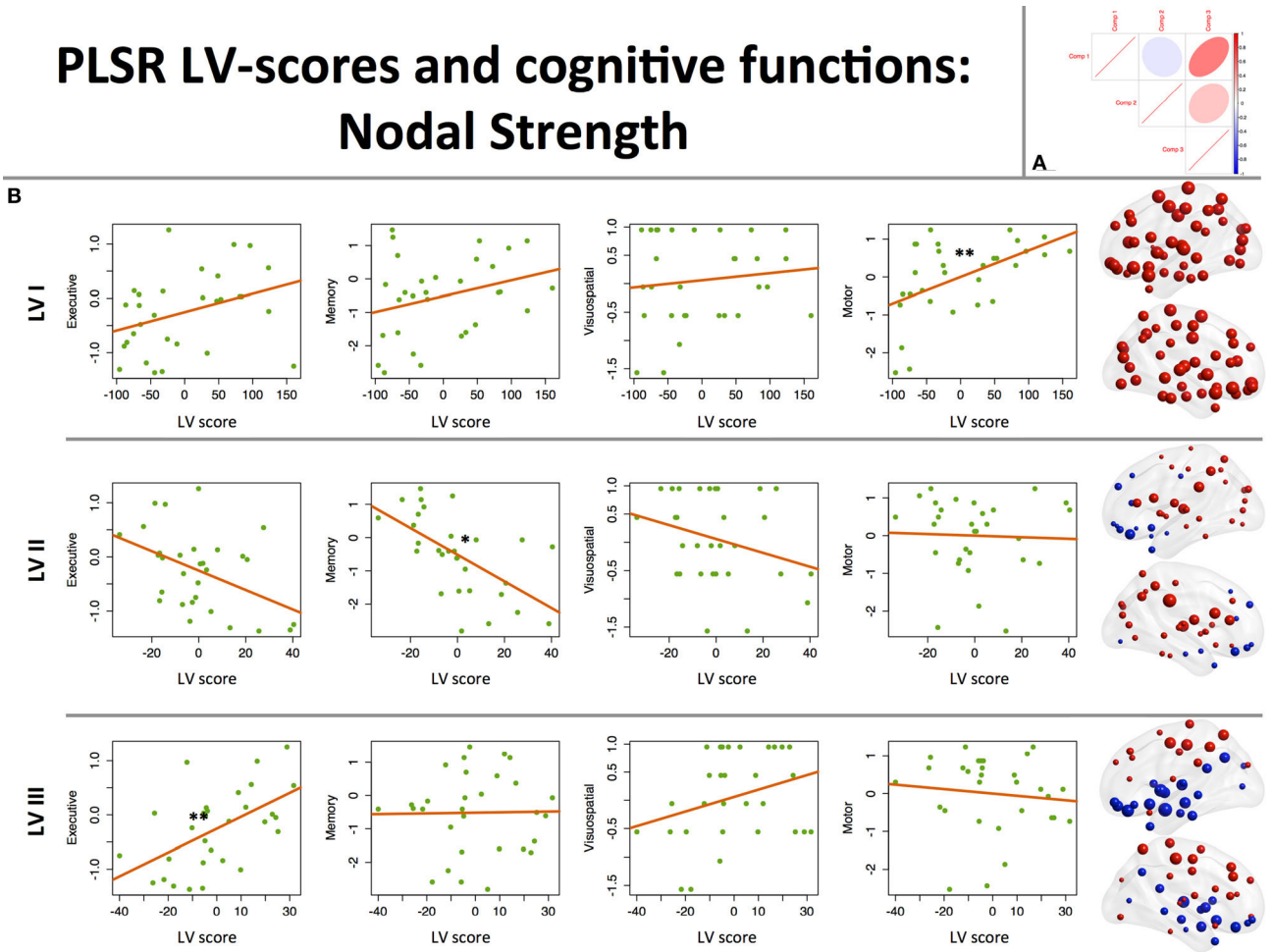

FIGURE 1 | Associations between component scores and behavioral data: nodal strength. (A) Between-component correlation plot. Positive association ($r = 0.5$) was found between latent variables (LVs) I and III. **(B)** Associations between LV scores extracted from the nodal strength data and performance in 3 cognitive (executive, memory, visuospatial) and motor domains. On the right-hand side of the graph, corresponding loading maps are depicted in brain space, reflecting the relevance of the nodes (spheres) for a particular LV, the magnitude of which is represented by nodal size. Positive loading values are depicted as red spheres, whereas negative ones are shown in blue. $^{*}p < 0.05$, $^{**}p < 0.01$.

Our results are consistent with an abnormally increased fronto-striatal connectivity found in a single-blind placebo-controlled rs-fMRI study of PD patients (Kwak et al., 2010), in which this hyperconnectivity was down-regulated by L-DOPA administration. Further analysis in this study revealed PD-related increase of power in the low-frequency band (0.02–0.05 Hz) in the striatum, which was also reduced after L-DOPA administration. Of note, this reduction correlated with L-DOPA-associated cognitive improvement. Apart from this, an increase in spontaneous oscillatory activity in the 10–35 Hz range (beta frequency band), occurring within the basal ganglia-thalamocortical networks and suppressed by dopaminergic treatment, is a well-replicated pathophysiological finding in PD (Brown et al., 2001; Levy et al., 2002; Gatev et al., 2006; Hammond et al., 2007), which provides additional support of our results converging from other imaging modalities.

The pattern associated with higher scores in the memory domain favoring prefronto-limbic processing did not reveal associations with presynaptic striatal dopamine uptake in the present study. The latter suggests that other mechanisms may be involved in the development of memory impairment associated with PD. The most likely ones are mesocortical dopaminergic deficiency (Narayanan et al., 2013) and impaired cortical cholinergic function (Bohnen et al., 2003), which in turn may at least be partly associated with concomitant cortical atrophy (Weintraub et al., 2012).

Of note, our study did not find any correlates of visuospatial impairment. However, this finding may be influenced by small sample size and due to the fact that visuospatial function was only mildly affected in the present cohort.

According to Mink's hypothesis (Mink, 1996), the basal ganglia play a crucial role in sustaining the balance between facilitation and suppression of movements. If we consider executive functions as the "movement of thoughts" a similar analogy can be drawn within this context. Indeed, cognitive frontal-subcortical loops is a widely accepted notion, where the DLPFC circuit has been

documented to mediate set-shifting, complex problem-solving, retrieval abilities, organizational strategies, concept-formation, working memory (Zgaljardic et al., 2006), and other executive functions that are known to be affected in PD. Preserved nigrostriatal dopamine function therefore not only allows effective execution and termination of motor activity, but may also implement smooth switching between cognitive patterns, controlling mutual inhibition and/or facilitation of fronto-subcortical circuits. This is also supported by computational models of the basal ganglia that highlight their routing role in various cognitive functions, such as for example action-selection (Stocco et al., 2010).

Table 3 | Latent variable scores and mean caudate DaT binding.

	CN DaT binding		
	T	**DOF**	***p***
LV I	2.87	17	0.011
LV II	−0.096	17	0.925
LV III	2.281	17	0.037

The table shows associations of the PLS latent variables (LVs) extracted during the dimensionality reduction step with nigrostriatal dopaminergic function measured by ^{123}I-FP-CIT SPECT (mean caudate SBR ratios). Positive significant associations (depicted in red) were found for LVs I ("global/motor") and III ("executive").

*CN, Caudate Nucleus; DaT, Dopamine Transporter; **T**, t-statistics; **DOF**, degrees of freedom.*

In general, higher DaT binding values were associated with global integrative effects on the brain (global increase of nodal strength). This was also confirmed for the cognitive circuitry (defined during meta-analysis), where higher DaT SBR ratios (relative preservation of dopaminergic function) were associated with lower network-level modularity, suggesting that dopamine favors integration of the cognitive network when the subject is at rest. These results are in line with previous fMRI studies that indicated globally impaired network-level processing in PD (Skidmore et al., 2011; Gottlich et al., 2013). Negative effects of the preserved dopaminergic function on the modularity of cognitive circuitry are also in line with previous literature. Thus, a recent randomized double-blind rs-fMRI study of healthy subjects with bromocriptine administration (dopamine agonist) revealed drug-induced decreases in modularity, estimated for the whole brain (White et al., 2013). Our results also suggest that preserved nigrostriatal dopaminergic system allows supporting integrity of the cognitive network when a subject is at rest. In

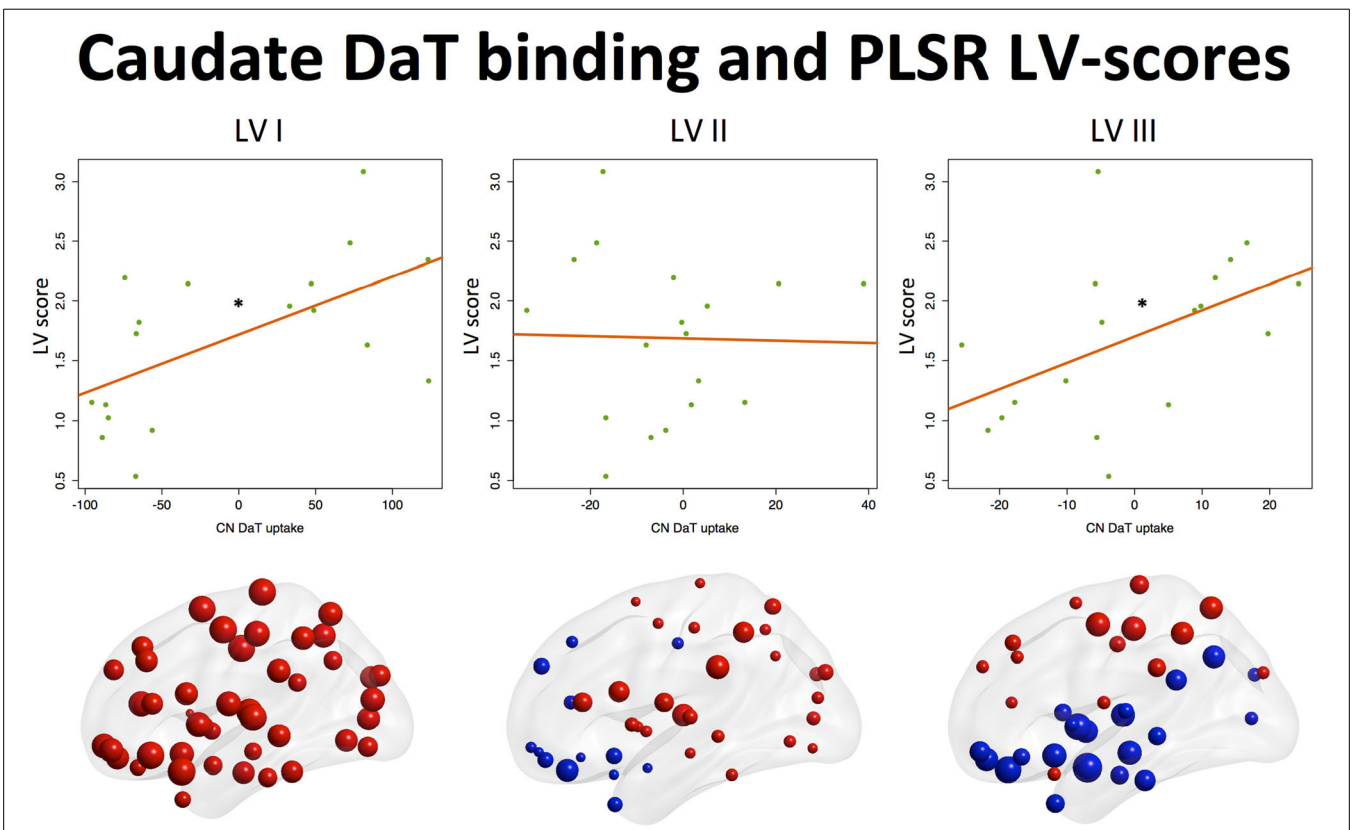

FIGURE 2 | Associations between component scores and mean caudate DaT binding. Associations of latent variable (LV) scores extracted from the nodal strength data with nigrostriatal dopaminergic function measured by ^{123}I-FP-CIT SPECT (mean caudate SBR ratios). Positive associations ($*p < 0.05$) were found for the Ist ("global/motor") and IIIrd ("executive") LVs. Corresponding loading maps are depicted in brain space, reflecting the relevance of the nodes (spheres) for a particular LV, the magnitude of which is represented by nodal size. Positive loading values are depicted as red spheres, whereas negative ones are shown in blue.

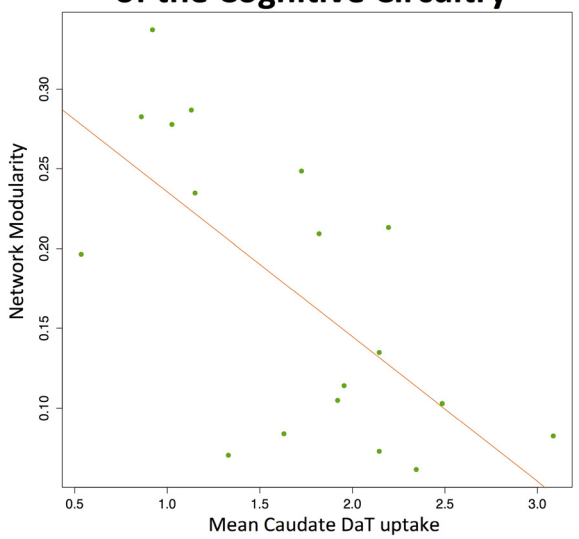

FIGURE 3 | Caudate DaT uptake and modularity of the cognitive circuitry at rest. The figure shows significant ($p < 0.01$) negative association between modularity of the cognitive circuitry (identified with automated meta-analysis) and nigrostriatal dopaminergic function measured by ^{123}I-FP-CIT SPECT (mean caudate SBR ratios).

the light of this, it would be interesting to assess the dynamics of cognitive circuitry during performance of particular executive tasks or multi-tasking, where dopamine may have different or even opposite effects on network modularity. This is supported by previous functional imaging studies of executive functions in PD, revealing that hypodopaminergic states are associated with increased prefrontal cortical responses during performance of corresponding tasks (Mattay et al., 2002), whereas L-dopa administration, in contrast, decreases it (Cools et al., 2002). In this context, it is also worth mentioning an event-related fMRI study that found PD-related brain abnormalities during performance of the set-shifting task specifically developed to elicit caudate responses (Monchi et al., 2007). Compared to the control group, patients demonstrated increased cortical activation in the condition not specifically requiring the caudate nucleus, whereas decreased cortical activation was observed in the task that involved the caudate nucleus. These studies, however, are not focused on any specific dopaminergic system, looking at general dopamine-related effects instead, and therefore do not necessarily confirm the role of exactly nigrostriatal dopaminergic system in these phenomena.

Finally, a recently published graph theoretical MEG study with longitudinal design found that progression of PD is associated with growing impairment of local integration (measured by clustering coefficient) in multiple frequency bands and loss of global brain network efficiency (based on path length) in the alpha2 frequency band. This deterioration was, in turn, correlated with cognitive and motor impairment observed during disease progression (Olde Dubbelink et al., 2014). These findings provide additional support for our results, also suggesting global positive effects of dopaminergic preservation on efficient functioning of the brain networks.

The main limitation of the present study is a relatively small sample size. In addition, the cross-sectional design complicates causal interpretation of the results. Apart from this, the resting state setting itself hampers direct interpretation of the findings with regard to the role of brain networks in cognitive task performance. Active cognitive processing is likely associated with patterns of brain dynamics that are different compared to the ones occurring when the subject is at rest. These patterns in turn may have different associations with altered dopaminergic function in PD. Therefore, this presents a need for further studies of brain dynamics underlying cognitive processing in PD and related dopaminergic deficits.

The main strengths are a multimodal approach and graph theoretical setting that have not yet been implemented together for clarifying brain mechanisms of PD-related cognitive impairment. Further strengths are a relatively broad cognitive evaluation combining multiple tests to assess three major functional domains and the drug-naïve status of the participants. Of note, although the present study specifically investigated the nigrostriatal system, the deficiency measured by ^{123}I-FP-CIT SPECT might also reflect indirect effects of neurodegeneration of dopaminergic neurons within other pathways, since the severity of dopaminergic deficits may correlate across different systems. Therefore, the results should be interpreted with caution.

To summarize, our study found that PD-related executive impairment is associated with altered balance between cortical and subcortical processing at rest, when contribution of the dorsal cortex is getting abnormally suppressed, and subcortical processing is disinhibited. This pattern (unlike brain profiles of visuospatial and memory impairment) is linked to nigrostriatal deficiency, which also has disruptive effects on cognitive circuitry at the network scale.

The results provide evidence for the contribution of the nigrostrital dopaminergic system in human cognition, and the described concept can potentially be utilized in future interventional studies to monitor the effects of treatments, including the approaches that augment cognitive functions.

ACKNOWLEDGMENTS

Data used in the preparation of this article were obtained from the Parkinson's Progression Markers Initiative (PPMI) database (www.ppmi-info.org/data). For up-to-date information on the study, visit www.ppmi-info.org. PPMI—a public-private partnership—is funded by the Michael J. Fox Foundation for Parkinson's Research and funding partners, including Abbott, Avid, Biogen Idec, Bristol-Myers Squibb, Covance, Elan, GlaxoSmithKline, Lilly, Merck, UCB, F. Hoffman-La Roche Ltd., GE Healthcare, Genentech, and Pfizer Inc. The authors are grateful to Dr. Olaf Sporns (Indiana University, USA) for the valuable discussions we had when working on the manuscript. Alexander V. Lebedev was supported by the Helse Vest Strategic Funding 2013 and MoodNet. Joana B. Pereira was funded by a Marie Curie fellowship for postdoctoral researchers (call FP7-PEOPLE-2012-IEF).

SUPPLEMENTARY MATERIAL

The Supplementary Material for this article can be found online at: http://www.frontiersin.org/journal/10.3389/fnsys.2014.00045/abstract

Figure S1 | Study Workflow. The study workflow consisted of IV main steps: (I) Selection of 30 PD subjects with fMRI data from the complete PPMI cohort and an fMRI + DaTSCAN subsample of 18 subjects; (II) Preparation of the data for further analysis that, in turn, included (IIa) calculation of composite scores for 3 cognitive domains, (IIb) automated meta-analysis to define "cognitive network," (IIc) image preprocessing and network measure extraction; (III) Dimensionality reduction with PLS followed by parametric tests evaluating associations between latent variable (LV) scores and cognitive functions; (IV) Final analysis assessing influence of caudate dopamine transporter (DaT) uptake on LV scores and modularity of the "cognitive network.

Figure S2 | Automated meta-analysis workflow. An automated search using the meta-analytical software Neurosynth (http://neurosynth.org) was undertaken in order to identify regions that are relevant for cognitive functions. The key-words "executive" (237 studies), "visuospatial" ($n = 116$) and "memory" ($n = 1470$). The profile of visuospatial functions included prefrontal, parietal, and occipital regions. The "executive" pattern contained prefrontal (with more extended involvement of DLPFC), cingulate, superior parietal, temporo-occipital, basal ganglia, and cerebellar regions. Finally, the "memory" profile, in addition to prefrontal and parietal regions, also included hippocampus, temporal areas, and basal ganglia. Due to the observed overlap, the resulting statistical maps were merged and overlaid with the Automated Anatomical Labeling (AAL) atlas defining cognitive circuitry, the modularity of which was then correlated with nigrostriatal function measured by ^{123}I-FP-CIT Single-Photon Emission Computed Tomography.

Figure S3 | Latent variable selection. The figure shows Root Mean Squared Error Prediction (RMSEP) as a function of a number of PLS latent variables (LVs). The maximum number of LVs was selected that minimized total training (red dashed line) and leave-one-out cross-validation (green solid line) errors for all the domains ($n = 3$).

REFERENCES

Aarsland, D., Bronnick, K., Larsen, J. P., Tysnes, O. B., Alves, G., and Norwegian Parkwest Study, G. (2009). Cognitive impairment in incident, untreated Parkinson disease: the Norwegian ParkWest study. *Neurology* 72, 1121–1126. doi: 10.1212/01.wnl.0000338632.00552.cb

Achard, S., and Bullmore, E. (2007). Efficiency and cost of economical brain functional networks. *PLoS Comput. Biol.* 3:e17. doi: 10.1371/journal.pcbi.0030017

Ashburner, J. (2007). A fast diffeomorphic image registration algorithm. *Neuroimage* 38, 95–113. doi: 10.1016/j.neuroimage.2007.07.007

Benton, A. L., Varney, N. R., and Hamsher, K. D. (1978). Visuospatial judgment. A clinical test. *Arch. Neurol.* 35, 364–367. doi: 10.1001/archneur.1978.00500300038006

Biswal, B., Yetkin, F. Z., Haughton, V. M., and Hyde, J. S. (1995). Functional connectivity in the motor cortex of resting human brain using echo-planar MRI. *Magn. Reson. Med.* 34, 537–541. doi: 10.1002/mrm.1910340409

Bohnen, N. I., Kaufer, D. I., Ivanco, L. S., Lopresti, B., Koeppe, R. A., Davis, J. G., et al. (2003). Cortical cholinergic function is more severely affected in parkinsonian dementia than in Alzheimer disease: an *in vivo* positron emission tomographic study. *Arch. Neurol.* 60, 1745–1748. doi: 10.1001/archneur.60.12.1745

Booij, J., Hemelaar, T. G., Speelman, J. D., De Bruin, K., Janssen, A. G., and Van Royen, E. A. (1999). One-day protocol for imaging of the nigrostriatal dopaminergic pathway in Parkinson's disease by [123I]FPCIT SPECT. *J. Nucl. Med.* 40, 753–761.

Brown, P., Oliviero, A., Mazzone, P., Insola, A., Tonali, P., and Di Lazzaro, V. (2001). Dopamine dependency of oscillations between subthalamic nucleus and pallidum in Parkinson's disease. *J. Neurosci.* 21, 1033–1038.

Bruck, A., Portin, R., Lindell, A., Laihinen, A., Bergman, J., Haaparanta, M., et al. (2001). Positron emission tomography shows that impaired frontal lobe functioning in Parkinson's disease is related to dopaminergic hypofunction in the caudate nucleus. *Neurosci. Lett.* 311, 81–84. doi: 10.1016/S0304-3940(01)02124-3

Chang, C., and Glover, G. H. (2009). Effects of model-based physiological noise correction on default mode network anti-correlations and correlations. *Neuroimage* 47, 1448–1459. doi: 10.1016/j.neuroimage.2009.05.012

Chao-Gan, Y., and Yu-Feng, Z. (2010). DPARSF: a MATLAB toolbox for "pipeline" data analysis of resting-state fMRI. *Front. Syst. Neurosci.* 4:13. doi: 10.3389/fnsys.2010.00013

Cheesman, A. L., Barker, R. A., Lewis, S. J., Robbins, T. W., Owen, A. M., and Brooks, D. J. (2005). Lateralisation of striatal function: evidence from 18F-dopa PET in Parkinson's disease. *J. Neurol. Neurosurg. Psychiatry* 76, 1204–1210. doi: 10.1136/jnnp.2004.055079

Christopher, L., and Strafella, A. P. (2013). Neuroimaging of brain changes associated with cognitive impairment in Parkinson's disease. *J. Neuropsychol.* 7, 225–240. doi: 10.1111/jnp.12015

Cools, R., Stefanova, E., Barker, R. A., Robbins, T. W., and Owen, A. M. (2002). Dopaminergic modulation of high-level cognition in Parkinson's disease: the role of the prefrontal cortex revealed by PET. *Brain* 125, 584–594. doi: 10.1093/brain/awf052

Cropley, V. L., Fujita, M., Bara-Jimenez, W., Brown, A. K., Zhang, X. Y., Sangare, J., et al. (2008). Pre- and post-synaptic dopamine imaging and its relation with frontostriatal cognitive function in Parkinson disease: PET studies with [11C]NNC 112 and [18F]FDOPA. *Psychiatry Res.* 163, 171–182. doi: 10.1016/j.pscychresns.2007.11.003

Dagher, A., Owen, A. M., Boecker, H., and Brooks, D. J. (2001). The role of the striatum and hippocampus in planning: a PET activation study in Parkinson's disease. *Brain* 124, 1020–1032. doi: 10.1093/brain/124.5.1020

Eidelberg, D. (2009). Metabolic brain networks in neurodegenerative disorders: a functional imaging approach. *Trends Neurosci.* 32, 548–557. doi: 10.1016/j.tins.2009.06.003

Esposito, F., Tessitore, A., Giordano, A., De Micco, R., Paccone, A., Conforti, R., et al. (2013). Rhythm-specific modulation of the sensorimotor network in drug-naive patients with Parkinson's disease by levodopa. *Brain* 136, 710–725. doi: 10.1093/brain/awt007

Fox, M. D., Zhang, D., Snyder, A. Z., and Raichle, M. E. (2009). The global signal and observed anticorrelated resting state brain networks. *J. Neurophysiol.* 101, 3270–3283. doi: 10.1152/jn.90777.2008

Gatev, P., Darbin, O., and Wichmann, T. (2006). Oscillations in the basal ganglia under normal conditions and in movement disorders. *Mov. Disord.* 21, 1566–1577. doi: 10.1002/mds.21033

Gottlich, M., Munte, T. F., Heldmann, M., Kasten, M., Hagenah, J., and Kramer, U. M. (2013). Altered resting state brain networks in Parkinson's disease. *PLoS ONE* 8:e77336. doi: 10.1371/journal.pone.0077336

Hammond, C., Bergman, H., and Brown, P. (2007). Pathological synchronization in Parkinson's disease: networks, models and treatments. *Trends Neurosci.* 30, 357–364. doi: 10.1016/j.tins.2007.05.004

Helmich, R. C., Derikx, L. C., Bakker, M., Scheeringa, R., Bloem, B. R., and Toni, I. (2010). Spatial remapping of cortico-striatal connectivity in Parkinson's disease. *Cereb. Cortex* 20, 1175–1186. doi: 10.1093/cercor/bhp178

Hirano, S., Shinotoh, H., and Eidelberg, D. (2012). Functional brain imaging of cognitive dysfunction in Parkinson's disease. *J. Neurol. Neurosurg. Psychiatry* 83, 963–969. doi: 10.1136/jnnp-2011-301818

Huang, C., Mattis, P., Tang, C., Perrine, K., Carbon, M., and Eidelberg, D. (2007a). Metabolic brain networks associated with cognitive function in Parkinson's disease. *Neuroimage* 34, 714–723. doi: 10.1016/j.neuroimage.2006.09.003

Huang, C., Tang, C., Feigin, A., Lesser, M., Ma, Y., Pourfar, M., et al. (2007b). Changes in network activity with the progression

of Parkinson's disease. *Brain* 130, 1834–1846. doi: 10.1093/brain/awm086

Ito, K., Nagano-Saito, A., Kato, T., Arahata, Y., Nakamura, A., Kawasumi, Y., et al. (2002). Striatal and extrastriatal dysfunction in Parkinson's disease with dementia: a 6-[18F]fluoro-L-dopa PET study. *Brain* 125, 1358–1365. doi: 10.1093/brain/awf134

Kelly, C., De Zubicaray, G., Di Martino, A., Copland, D. A., Reiss, P. T., Klein, D. F., et al. (2009). L-dopa modulates functional connectivity in striatal cognitive and motor networks: a double-blind placebo-controlled study. *J. Neurosci.* 29, 7364–7378. doi: 10.1523/JNEUROSCI.0810-09.2009

Kwak, Y., Peltier, S., Bohnen, N. I., Muller, M. L., Dayalu, P., and Seidler, R. D. (2010). Altered resting state cortico-striatal connectivity in mild to moderate stage Parkinson's disease. *Front. Syst. Neurosci.* 4:143. doi: 10.3389/fnsys.2010.00143

Levy, R., Ashby, P., Hutchison, W. D., Lang, A. E., Lozano, A. M., and Dostrovsky, J. O. (2002). Dependence of subthalamic nucleus oscillations on movement and dopamine in Parkinson's disease. *Brain* 125, 1196–1209. doi: 10.1093/brain/awf128

Lewis, S. J., Dove, A., Robbins, T. W., Barker, R. A., and Owen, A. M. (2003). Cognitive impairments in early Parkinson's disease are accompanied by reductions in activity in frontostriatal neural circuitry. *J. Neurosci.* 23, 6351–6356.

Lowe, M. J., Mock, B. J., and Sorenson, J. A. (1998). Functional connectivity in single and multislice echoplanar imaging using resting-state fluctuations. *Neuroimage* 7, 119–132. doi: 10.1006/nimg.1997.0315

Matlab 8.0 and Statistics Toolbox 8.1. (2012). T. M., Inc., Natick, MA, USA.

Mattay, V. S., Tessitore, A., Callicott, J. H., Bertolino, A., Goldberg, T. E., Chase, T. N., et al. (2002). Dopaminergic modulation of cortical function in patients with Parkinson's disease. *Ann. Neurol.* 51, 156–164. doi: 10.1002/ana.10078

Mentis, M. J., McIntosh, A. R., Perrine, K., Dhawan, V., Berlin, B., Feigin, A., et al. (2002). Relationships among the metabolic patterns that correlate with mnemonic, visuospatial, and mood symptoms in Parkinson's disease. *Am. J. Psychiatry* 159, 746–754. doi: 10.1176/appi.ajp.159.5.746

Mink, J. W. (1996). The basal ganglia: focused selection and inhibition of competing motor programs. *Prog. Neurobiol.* 50, 381–425. doi: 10.1016/S0301-0082(96)00042-1

Monchi, O., Petrides, M., Doyon, J., Postuma, R. B., Worsley, K., and Dagher, A. (2004). Neural bases of set-shifting deficits in Parkinson's disease. *J. Neurosci.* 24, 702–710. doi: 10.1523/JNEUROSCI.4860-03.2004

Monchi, O., Petrides, M., Mejia-Constain, B., and Strafella, A. P. (2007). Cortical activity in Parkinson's disease during executive processing depends on striatal involvement. *Brain* 130, 233–244. doi: 10.1093/brain/awl326

Mountcastle, V. B. (1997). The columnar organization of the neocortex. *Brain* 120(Pt 4), 701–722. doi: 10.1093/brain/120.4.701

Murphy, K., Birn, R. M., Handwerker, D. A., Jones, T. B., and Bandettini, P. A. (2009). The impact of global signal regression on resting state correlations: are anti-correlated networks introduced? *Neuroimage* 44, 893–905. doi: 10.1016/j.neuroimage.2008.09.036

Muslimovic, D., Post, B., Speelman, J. D., and Schmand, B. (2005). Cognitive profile of patients with newly diagnosed Parkinson disease. *Neurology* 65, 1239–1245. doi: 10.1212/01.wnl.0000180516.69442.95

Narayanan, N. S., Rodnitzky, R. L., and Uc, E. Y. (2013). Prefrontal dopamine signaling and cognitive symptoms of Parkinson's disease. *Rev. Neurosci.* 24, 267–278. doi: 10.1515/revneuro-2013-0004

Newman, M. E. (2006). Modularity and community structure in networks. *Proc. Natl. Acad. Sci. U.S.A.* 103, 8577–8582. doi: 10.1073/pnas.0601602103

O'Brien, J. T., Colloby, S., Fenwick, J., Williams, E. D., Firbank, M., Burn, D., et al. (2004). Dopamine transporter loss visualized with FP-CIT SPECT in the differential diagnosis of dementia with Lewy bodies. *Arch. Neurol.* 61, 919–925. doi: 10.1001/archneur.61.6.919

Olde Dubbelink, K. T., Hillebrand, A., Stoffers, D., Deijen, J. B., Twisk, J. W., Stam, C. J., et al. (2014). Disrupted brain network topology in Parkinson's disease: a longitudinal magnetoencephalography study. *Brain*. 137(Pt 1), 197–207. doi: 10.1093/brain/awt316

Owen, A. M., Doyon, J., Dagher, A., Sadikot, A., and Evans, A. C. (1998). Abnormal basal ganglia outflow in Parkinson's disease identified with PET. Implications for higher cortical functions. *Brain* 121(Pt 5), 949–965. doi: 10.1093/brain/121.5.949

R Core Team. (2013). *R: A Language and Environment for Statistical Computing*. Version 3.0.1. Vienna: R Foundation for Statistical Computing. ISBN: 3-900051-07-0. Available online at: http://www.R-project.org/ [Online] [Accessed].

Rubinov, M., and Sporns, O. (2010). Complex network measures of brain connectivity: uses and interpretations. *Neuroimage* 52, 1059–1069. doi: 10.1016/j.neuroimage.2009.10.003

Rubinov, M., and Sporns, O. (2011). Weight-conserving characterization of complex functional brain networks. *Neuroimage* 56, 2068–2079. doi: 10.1016/j.neuroimage.2011.03.069

Satterthwaite, T. D., Elliott, M. A., Gerraty, R. T., Ruparel, K., Loughead, J., Calkins, M. E., et al. (2013). An improved framework for confound regression and filtering for control of motion artifact in the preprocessing of resting-state functional connectivity data. *Neuroimage* 64, 240–256. doi: 10.1016/j.neuroimage.2012.08.052

Shapiro, A. M., Benedict, R. H., Schretlen, D., and Brandt, J. (1999). Construct and concurrent validity of the Hopkins Verbal Learning Test-revised. *Clin. Neuropsychol.* 13, 348–358. doi: 10.1076/clin.13.3.348.1749

Skidmore, F., Korenkevych, D., Liu, Y., He, G., Bullmore, E., and Pardalos, P. M. (2011). Connectivity brain networks based on wavelet correlation analysis in Parkinson fMRI data. *Neurosci. Lett.* 499, 47–51. doi: 10.1016/j.neulet.2011.05.030

Sporns, O. (2010). *Networks of the Brain, 1st Edn.* Cambridge, MA: The MIT Press.

Sporns, O. (2013). Network attributes for segregation and integration in the human brain. *Curr. Opin. Neurobiol.* 23, 162–171. doi: 10.1016/j.conb.2012.11.015

Sporns, O., and Zwi, J. D. (2004). The small world of the cerebral cortex. *Neuroinformatics* 2, 145–162. doi: 10.1385/NI:2:2:145

Stocco, A., Lebiere, C., and Anderson, J. R. (2010). Conditional routing of information to the cortex: a model of the basal ganglia's role in cognitive coordination. *Psychol. Rev.* 117, 541–574. doi: 10.1037/a0019077

Svenningsson, P., Westman, E., Ballard, C., and Aarsland, D. (2012). Cognitive impairment in patients with Parkinson's disease: diagnosis, biomarkers, and treatment. *Lancet Neurol.* 11, 697–707. doi: 10.1016/S1474-4422(12)70152-7

Tinaz, S., Schendan, H. E., and Stern, C. E. (2008). Fronto-striatal deficit in Parkinson's disease during semantic event sequencing. *Neurobiol. Aging* 29, 397–407. doi: 10.1016/j.neurobiolaging.2006.10.025

Tzourio-Mazoyer, N., Landeau, B., Papathanassiou, D., Crivello, F., Etard, O., Delcroix, N., et al. (2002). Automated anatomical labeling of activations in SPM using a macroscopic anatomical parcellation of the MNI MRI single-subject brain. *Neuroimage* 15, 273–289. doi: 10.1006/nimg.2001.0978

Van Eimeren, T., Monchi, O., Ballanger, B., and Strafella, A. P. (2009). Dysfunction of the default mode network in Parkinson disease: a functional magnetic resonance imaging study. *Arch. Neurol.* 66, 877–883. doi: 10.1001/archneurol.2009.97

Vossius, C., Larsen, J. P., Janvin, C., and Aarsland, D. (2011). The economic impact of cognitive impairment in Parkinson's disease. *Mov. Disord.* 26, 1541–1544. doi: 10.1002/mds.23661

Weintraub, D., Dietz, N., Duda, J. E., Wolk, D. A., Doshi, J., Xie, S. X., et al. (2012). Alzheimer's disease pattern of brain atrophy predicts cognitive decline in Parkinson's disease. *Brain* 135, 170–180. doi: 10.1093/brain/awr277

Welsh, D. K., Takahashi, J. S., and Kay, S. A. (2010). Suprachiasmatic nucleus: cell autonomy and network properties. *Annu. Rev. Physiol.* 72, 551–577. doi: 10.1146/annurev-physiol-021909-135919

White, R., Esther Aarts, E., and D'Esposito, M. (2013). Interactions of resting state brain networks, dopamine, and working memory behavior: a resting state functional MRI study. *Neurology* 80(Meeting Abstr. 1):S54.003.

Williams-Gray, C. H., Evans, J. R., Goris, A., Foltynie, T., Ban, M., Robbins, T. W., et al. (2009). The distinct cognitive syndromes of Parkinson's disease: 5 year follow-up of the CamPaIGN cohort. *Brain* 132, 2958–2969. doi: 10.1093/brain/awp245

Wold, S., Ruhe, A., Wold, H., and Dunn, W. J. III. (1984). The collinearity problem in linear regression. The Partial Least Squares (PLS) approach to generalized inverses. *SIAM J. Sci. Stat. Comput.* 5, 735–743. doi: 10.1137/0905052

Wu, T., Wang, L., Chen, Y., Zhao, C., Li, K., and Chan, P. (2009). Changes of functional connectivity of the motor network in the resting state in

Parkinson's disease. *Neurosci. Lett.* 460, 6–10. doi: 10.1016/j.neulet.2009.05.046

Yarkoni, T., Poldrack, R. A., Nichols, T. E., Van Essen, D. C., and Wager, T. D. (2011). Large-scale automated synthesis of human functional neuroimaging data. *Nat. Methods* 8, 665–670. doi: 10.1038/nmeth.1635

Zgaljardic, D. J., Borod, J. C., Foldi, N. S., Mattis, P. J., Gordon, M. F., Feigin, A., et al. (2006). An examination of executive dysfunction associated with frontostriatal circuitry in Parkinson's disease. *J. Clin. Exp. Neuropsychol.* 28, 1127–1144. doi: 10.1080/13803390500246910

Conflict of Interest Statement: The authors declare that the research was conducted in the absence of any commercial or financial relationships that could be construed as a potential conflict of interest.

Received: 28 January 2014; accepted: 11 March 2014; published online: 03 April 2014.
Citation: Lebedev AV, Westman E, Simmons A, Lebedeva A, Siepel FJ, Pereira JB and Aarsland D (2014) Large-scale resting state network correlates of cognitive impairment in Parkinson's disease and related dopaminergic deficits. Front. Syst. Neurosci. ***8****:45. doi: 10.3389/fnsys.2014.00045*
This article was submitted to the journal Frontiers in Systems Neuroscience.

Advantages of publishing in Frontiers

OPEN ACCESS
Articles are free to read for greatest visibility and readership

FAST PUBLICATION
Around 90 days from submission to decision

HIGH QUALITY PEER-REVIEW
Rigorous, collaborative, and constructive peer-review

TRANSPARENT PEER-REVIEW
Editors and reviewers acknowledged by name on published articles

Frontiers
Avenue du Tribunal-Fédéral 34
1005 Lausanne | Switzerland

Visit us: www.frontiersin.org
Contact us: info@frontiersin.org | +41 21 510 17 00

REPRODUCIBILITY OF RESEARCH
Support open data and methods to enhance research reproducibility

DIGITAL PUBLISHING
Articles designed for optimal readership across devices

FOLLOW US
@frontiersin

IMPACT METRICS
Advanced article metrics track visibility across digital media

EXTENSIVE PROMOTION
Marketing and promotion of impactful research

LOOP RESEARCH NETWORK
Our network increases your article's readership